MONASH University

# Biochemical pathways and molecular targets involved in the mechanism of action of ozonide antimalarials in *Plasmodium falciparum*

**Carlo Riccardo Giannangelo**

Bachelor of Pharmacy (Honours)

A thesis submitted for the degree of

**DOCTOR OF PHILOSOPHY**

at

Monash University

May 2018

Drug Delivery, Disposition and Dynamics

Monash Institute of Pharmaceutical Sciences

Monash University

Melbourne, Victoria, Australia

## Copyright notice

# Table of Contents

# Abstract

Malaria infections were responsible for 445 000 deaths in 2016, with more than 90% caused by the parasite species *Plasmodium falciparum*. Multi-drug resistant parasites now limit the efficacy of all available antimalarial drug classes, including front line artemisinin-based therapies, highlighting the urgent need for new drugs to treat malaria. One of the most advanced drug classes currently in clinical development is the synthetic peroxide antimalarials, known as ozonides. While the first-generation ozonide, OZ277, is already approved for use, and the second-generation compound, OZ439, is in phase IIb clinical trials, the mechanism of action of peroxide-based antimalarials is poorly understood. It is thought to involve haem-mediated reductive activation of the peroxide bond, generating toxic drug-derived radicals that alkylate intraparasitic targets. The aim of this thesis was to investigate the intraparasitic targets and parasite biochemical pathways involved in the mode of action of selected ozonides to better understand the mechanistic basis for activity in *P. falciparum*.

Quantitative assessment of parasite-mediated ozonide degradation, under varying *in vitro* conditions, was found to be positively correlated with parasitaemia, was parasite stage-specific and associated with a significant reduction in activity at high trophozoite parasitaemia. Furthermore, drug degradation could be reduced with the falcipain inhibitor, E64d. Taken together, these data indicate optimal *in vitro* activity requires a balance between haem-mediated activation and degradation processes and highlights the importance of considering stability and parasite load when investigating peroxide antimalarial mechanisms of action.

Untargeted LC-MS analysis of ozonide-treated parasites identified the ozonide-alkylated haem adduct and various oxidative degradation products from alkylated haem, suggesting haem alkylation may be involved in ozonide drug action. A novel 'click' chemistry-based metabolomics strategy identified no other ozonide-alkylated metabolites. Using ozonide

‘click’ chemistry probes, confocal microscopic analysis revealed a protein alkylation signature that does not co-localise with a specific parasite compartment, and which was inhibited by E64d, consistent with indiscriminate protein alkylation by ozonide-derived radicals.

The temporal biochemical response of ozonide-treated *P. falciparum* parasites was also investigated using an untargeted multi-omics-based approach. Metabolomics and peptidomics analysis identified rapid ozonide-induced disruption of haemoglobin catabolism, while activity-based protease probe studies revealed drug-dependent alterations in haemoglobin protease activity within 1 h of ozonide exposure. Proteomic experiments uncovered proteasomal and translation-related protein dysregulation, indicative of a cellular response to stress. Together these data indicate that peroxides initially disrupt haemoglobin catabolism and that parasites engage a stress response to manage peroxide-induced damage.

Peroxide exposure also induced perturbation to haemoglobin-derived peptide metabolism in paired *K13*-mutant artemisinin-resistant and -sensitive parasites, with more pronounced peptide depletion occurring in the sensitive line. In general, the peptides that were depleted following peroxide exposure were initially elevated in abundance in untreated resistant parasites compared with the sensitive controls, further emphasising the importance of haemoglobin catabolism in ozonide activity and *K13*-mediated peroxide resistance.

This thesis expands our current understanding of the modes of action and resistance of peroxide antimalarials in *P. falciparum*, demonstrating a central role for the parasite haemoglobin digestion pathway in the activity and resistance mechanisms for this important class of antimalarials.

# Thesis including published works declaration

I hereby declare that this thesis contains no material which has been accepted for the award of any other degree or diploma at any university or equivalent institution and that, to the best of my knowledge and belief, this thesis contains no material previously published or written by another person, except where due reference is made in the text of the thesis.

This thesis includes one original paper published in a peer reviewed journal. The core theme of the thesis is the mechanism of action ozonide antimalarials. The ideas, development and writing up of all the papers in the thesis were the principal responsibility of myself, the student, working within the Faculty of Pharmacy and Pharmaceutical Sciences under the supervision of Dr Darren Creek and Prof Susan Charman.

The inclusion of co-authors reflects the fact that the work came from active collaboration between researchers and acknowledges input into team-based research.

In the case of Chapter 2 my contribution to the work involved the following:

| **Publication Title** | **Status** | **Nature and extent (%) of student contribution** |
|---|---|---|
| Parasite-mediated degradation of synthetic ozonide antimalarials impacts *in vitro* antimalarial activity | Published | Study design, laboratory experiments, data analysis and interpretation, preparation of the initial draft and subsequent revisions and formulation of conclusions and hypothesis generation from the results of the study, 60% |

The following co-authors contributed to the work in Chapter 2:

| **Co-author names** | **Nature and extent (%) of Co-author's contribution** | **Monash student** |
|---|---|---|
| Lukas Stingelin | Laboratory experiments, data analysis and interpretation, review of manuscript, 10% | No |
| Tuo Yang | Advice on study design and review of the manuscript, 5% | No |
| Leann Tilley | Advice on study design and review of the manuscript, 5% | No |
| Susan Charman | Advice on study design, supervision, data analysis and interpretation, review of the manuscript drafts and revisions, formulation of conclusions and hypothesis generation from the results of the study, 10% | No |
| Darren Creek | Advice on study design, supervision, data analysis and interpretation, review of the manuscript drafts and revisions, formulation of conclusions and hypothesis generation from the results of the study, 10% | No |

I have not renumbered sections of submitted or published papers within the thesis.

**Student signature:** 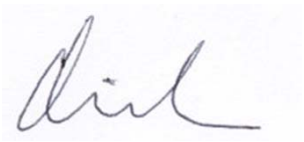 **Date:** 08/05/2018

The undersigned hereby certify that the above declaration correctly reflects the nature and extent of the student's and co-authors' contributions to this work. In instances where I am not the responsible author I have consulted with the responsible author to agree on the respective contributions of the authors.

**Main Supervisor signature:**  **Date:** 08/05/2018

# Acknowledgements

First and foremost, I would like to thank my supervisors, Dr Darren Creek and Professor Susan Charman for giving me the opportunity to pursue this challenging but highly rewarding PhD project. I have learnt a great deal from you both and I am sincerely grateful for the constant guidance and support that you have provided me during the course of this project. I would also like to thank my panel members, Professor Colin Pouton, Professor Ray Norton and Professor Leann Tilley for their invaluable advice throughout my candidature. I appreciate the contribution of Professor Jonathan Vennerstrom and his team (University of Nebraska Medical Centre) for the synthesis and provision of ozonide compounds and for their constructive advice. In addition, I would like to thank Dr Laura Edgington-Mitchell and Beth Anderson (both University of Melbourne) for the provision of compounds, assistance in the lab and advice with interpreting the protease activity work.

This research was supported by an Australian Postgraduate Award (APA). The Drug Delivery, Disposition and Dynamics (D4) Faculty is also gratefully acknowledged for their contribution to an international conference travel grant.

Further appreciation and thanks to all members of the Creek Lab, past and present. In particular, I would like to thank Dr Ghizal Siddiqui who made an invaluable contribution to this project. I am extremely grateful for your assistance with data analysis and experimental work, as well as the time you dedicated to critiquing my writing. On a personal level, I am sincerely appreciative of your constant advice, for pushing me towards the finishing line and for taking me out of the lab to play soccer. In addition, I would like to thank Amanda De Paoli and Dr Dovile Anderson for assistance with lab work and mass spectrometry, respectively.

For technical assistance with LC-MS instruments I would like to express my appreciation to the staff of the Helen Macpherson Smith Trust Lab and the Centre for Drug Candidate Optimisation. In particular, I am grateful to Dr Rahul Patil and Dr Francis Chiu for

their expert advice and for providing reagents. My fellow students and staff from the D4 Faculty are also appreciated for their support and friendship.

I would especially like to thank my friends and family, particularly my parents, Mauro and Chris, for their unconditional support and constant encouragement. Finally, from the bottom of my heart I wish to thank my partner, Amy Habgood. Without your unwavering patience, love and support this thesis would not have been possible. I love you.

# Publications

Publications to support this thesis:

1. **Giannangelo C**, Stingelin L, Yang T, Tilley L, Charman SA, Creek DJ. 2018. Parasite-mediated degradation of synthetic ozonide antimalarials impacts *in vitro* antimalarial activity. Antimicrob Agents Chemother 62:e01566-01517.

Manuscripts in preparation:

2. **Giannangelo C**, Siddiqui G, Anderson B, Edgington-Mitchell LE, Charman SA, Creek DJ. Revealing the biochemical pathways targeted by peroxide antimalarials in 3D7 and *K13*-mutant artemisinin resistant *Plasmodium falciparum* with metabolomics and proteomics.
3. **Giannangelo C**, Anderson D, Vennerstrom JL, Charman SA, Creek DJ. Ozonide antimalarials alkylate haem in the malaria parasite *Plasmodium falciparum*.

Other publications during enrolment:

1. **Giannangelo C**, Ellis KM, Sexton AE, Stoessel D, Creek DJ. 2016. The role of metabolomics in antiparasitic drug discovery, p 321-342, Comprehensive analysis of parasite biology: from metabolism to drug discovery, vol 7. Wiley-VCH, Weinheim, Germany.
2. Yang T, Xie SC, Cao P, **Giannangelo C**, McCaw J, Creek DJ, Charman SA, Klonis N, Tilley L. 2016. Comparison of the exposure time-dependence of the activities of synthetic ozonide antimalarials and dihydroartemisinin against K13 wild-type and mutant *Plasmodium falciparum* strains. Antimicrob Agents Chemother 60:4501-4510.

# Communications

The results of this thesis were presented at the following scientific conferences:

1. **Giannangelo C**, Charman SA, Creek DJ. Metabolomics analysis of ozonide-treated *Plasmodium falciparum* reveals disruption of haemoglobin catabolism. British Society of Parasitology Spring Meeting. 2017, Dundee, Scotland. Oral presentation.
2. **Giannangelo C**, Charman SA, Creek DJ. Ozonide antimalarials disrupt haemoglobin catabolism in *Plasmodium falciparum*. Victoria Infection and Immunity Network. 2017, Melbourne, Australia. Oral presentation.
3. **Giannangelo C**, Charman SA, Creek DJ. Ozonide antimalarials disrupt haemoglobin catabolism in *Plasmodium falciparum*. Malaria in Melbourne. 2017, Melbourne, Australia. Poster presentation.
4. **Giannangelo C**, Yang T, Tilley L, Charman SA, Creek DJ. Activation and degradation of synthetic ozonide antimalarials is driven by malaria parasite haemoglobin digestion. International Congress for Tropical Medicine and Malaria. 2016. Brisbane, Australia. Poster presentation.
5. **Giannangelo C**, Yang T, Tilley L, Charman SA, Creek DJ. Exploring the balance between parasite-dependent activation and degradation of second generation ozonide antimalarials. Molecular Approaches to Malaria. 2016. Lorne, Australia. Poster presentation.
6. **Giannangelo C**, Charman SA, Creek DJ. Metabolomics analysis reveals novel changes to *Plasmodium falciparum* parasites treated with the antimalarial OZ277. Australian and New Zealand Society for Mass Spectrometry Conference. 2015. Brisbane, Australia. Poster presentation.

# List of abbreviations

| | |
|---|---|
| ABPP | activity-based protease probe |
| ACN | acetonitrile |
| ACT | artemisinin-based combination therapy |
| ALLN | N-acetyl-Leu-Leu-Norleu-al |
| Ala | alanine (A) |
| amp | ampere |
| Arg | arginine (R) |
| Asn | asparagine (N) |
| Asp | aspartic acid (D) |
| BCA | bicinchoninic acid |
| BSA | bovine serum albumin |
| CAPS | 3-(cyclohexylamino)-1-propanesulfonic acid |
| CCT | choline-phosphate cytidyltransferase |
| CDP | cytidine diphosphate |
| CE | capillary electrophoresis |
| CEPT | choline/ethanolamine phosphotransferase |
| CHAPS | 3-[(3-cholamidopropyl)-dimethylammonio]-1-propanesulfonate |
| CK | choline kinase |
| cm | centimetre |
| CMP | cytidine monophosphate |
| $CO_2$ | carbon dioxide |
| CuAAC | copper catalysed azide-alkyne cycloaddition |
| Cu | copper |
| CYP450 | cytochrome P450 |

| | |
|---|---|
| Cys | cysteine (C) |
| Da | Daltons |
| DBCO | dibenzocyclooctyne |
| DFO | desferrioxamine |
| DFP | deferiprone |
| DG | diglyceride |
| DHA | dihydroartemisinin |
| DHFR | dihydrofolate reductase |
| DHOD | dihydroorotate dehydrogenase |
| DHPS | dihydropterate synthase |
| DMSO | dimethyl sulphoxide |
| DNA | deoxyribonucleic acid |
| DPAP1 | dipeptidyl aminopeptidase 1 |
| DTT | dithiothreitol |
| E64d | (2S,3S)-trans-Epoxysuccinyl-L-leucylamido-3-methylbutane ethyl ester |
| ECT | ethanolamine-phosphate cytidyltransferase |
| EDTA | ethylenediamine tetra-acetic acid |
| EK | ethanolamine kinase |
| Fe | iron |
| FP | falcipain |
| g | gram |
| $g$ | gravity (relative centrifugal force) |
| G6PD | glucose-6-phosphate dehydrogenase |
| Glu | glutamic acid (E) |
| Gln | glutamine (Q) |

| | |
|---|---|
| Gly | glycine (G) |
| GSH | glutathione |
| GST | glutathione-S-transferase |
| $H_2O$ | water |
| h | hours |
| HAP | histo-aspartic protease |
| Hb | haemoglobin |
| Hct | haematocrit |
| HDP | haem detoxification protein |
| HEPES | 4-(2-hydroxyethyl)-1-piperazineethanesulfonic acid |
| HILIC | hydrophilic interaction liquid chromatography |
| His | histidine (H) |
| HIV | human immunodeficiency virus |
| HO | haem oxygenase |
| HPLC | high performance liquid chromatography |
| HRP | histidine rich protein |
| $IC_{50}$ | 50% inhibitory concentration |
| IPT | intermittent preventative therapy |
| ITN | insecticide-treated bed net |
| kDa | kilo Dalton |
| LC | liquid chromatography |
| Leu | leucine (L) |
| LIP | labile iron pool |
| Lys | lysine (K) |
| M | molar |

| | |
|---|---|
| Met | methionine (M) |
| min | minutes |
| mg | milligram |
| mL | millilitres |
| mM | millimolar |
| mm | millimetre |
| MMV | Medicines for Malaria Venture |
| MS | mass spectrometry |
| MSI | Metabolomics Standards Initiative |
| MW | molecular weight |
| *m/z* | mass-to-charge-ratio |
| $N_2$ | nitrogen gas |
| $NaHCO_3$ | sodium bicarbonate |
| NaOH | sodium hydroxide |
| NBD | nitrobenzyldiazole |
| ng | nanogram |
| nM | nanomolar |
| nm | nanometres |
| $O_2$ | oxygen |
| PA | phosphatidic acid |
| PABA | para-aminobenzoic acid |
| PAGE | polyacrylamide gel electrophoresis |
| PBS | phosphate buffered saline |
| PBQC | pooled biological quality control |
| PC | photocleavable (Chapter 3) |

| | |
|---|---|
| PC | phosphatidylcholine (Chapter 4) |
| PE | phosphatidylethanolamine |
| *P. falciparum* | *Plasmodium falciparum* |
| *Pf*A-M1 | *P. falciparum* M1 alanyl aminopeptidase |
| *Pf*A-M17 | *P. falciparum* M17 leucyl aminopeptidase |
| *Pf*M18AAP | *P. falciparum* M18 aspartyl aminopeptidase |
| *Pf*APP | *P. falciparum* aminopeptidase P |
| Phe | phenylalanine (F) |
| PI3K | phosphatidylinositol-3-kinase |
| PIPES | 1,4-piperazinediethanesulfonic acid |
| PMT | phosphoethanolamine N-methyltransferase |
| Pro | proline (P) |
| PS | phosphatidylserine |
| QC | quality control |
| RBC | red blood cell |
| rpm | revolutions per minute |
| RSD | relative standard deviation |
| SD | standard deviation |
| SDC | sodium deoxycholate |
| SDS | sodium dodecyl sulphate |
| sec | second |
| SEM | standard error of the mean |
| SERCA | sarco-endoplasmic reticulum $Ca^{2+}$-ATPase |
| Ser | serine (S) |
| SP | sulphadoxine-pyrimethamine |

| | |
|---|---|
| SPAAC | strain promoted azide-alkyne cycloaddition |
| sPLS-DA | sparse partial least squares – discriminant analysis |
| TBS | Tris buffered saline |
| TCEP | tris(2-carboxyethyl)phosphine |
| TCTP | translationally controlled tumour protein |
| TG | triglyceride |
| Thr | threonine (T) |
| Tris | 2-amino-2-(hydroxymethyl)-1,3-propanediol |
| Trp | tryptophan (W) |
| Tyr | tyrosine (Y) |
| UHPLC | ultra-high performance liquid chromatography |
| UMP | uridine monophosphate |
| UV | ultraviolet |
| Val | valine (V) |
| v/v | volume per volume |
| WHO | World Health Organisation |
| XIC | extracted ion current |
| α | alpha |
| β | beta |
| °C | degrees Celsius |
| µg | microgram |
| µL | microlitres |
| µM | micromolar |

# Chapter 1

# Introduction

# 1.1 MALARIA

Malaria is an infectious disease caused by protozoan parasites of the genus *Plasmodium* and is responsible for significant health and socioeconomic burden in many low-income tropical and sub-tropical parts of the world (1, 2). Despite the steady decline in human malaria deaths over the past decade, mortality rates have stalled or increased in most malaria endemic regions since 2015. There were 216 million cases and 445 000 deaths attributable to malaria in 2016, and most of these were in sub-Saharan Africa. Fever is the most common clinical manifestation caused by infection, however, life-threating complications frequently arise, particularly in pregnant women and children under the age of five. There are five *Plasmodium* species that are capable of infecting and causing disease in humans, including *P. falciparum*, *P. vivax*, *P. ovale*, *P. malariae* and *P. knowlesi*. Infections caused by *P. falciparum* are responsible for the greatest morbidity and mortality, accounting for more than 90% of malaria deaths. The absence of a reliable and highly efficacious vaccine means treatment is heavily reliant on antimalarial drug therapy. However, the emergence and spread of drug resistant parasites is a major obstacle to control efforts and consequently there is an urgent need for the discovery and development of new drugs to treat malaria.

# 1.2 BURDEN OF DISEASE

## 1.2.1 Epidemiology

Malaria is most concentrated in sub-Saharan Africa (Figure 1), where 90% of reported cases occur. The Southeast Asia region and the Eastern Mediterranean report 7% and 2% of worldwide malaria cases, respectively (3). Malaria associated mortality follows the same pattern, with 92% of deaths occurring in sub-Saharan Africa (3), 6% in Southeast Asia and 2% in the Eastern Mediterranean. Deaths in children under the age of five account for 70% of

global malaria deaths. Other highly susceptible populations include non-immune adults, such as travellers to malaria endemic areas, and pregnant women. Malaria during pregnancy also causes indirect mortality through abortion and intrauterine growth retardation, which increases infant mortality rates (4).

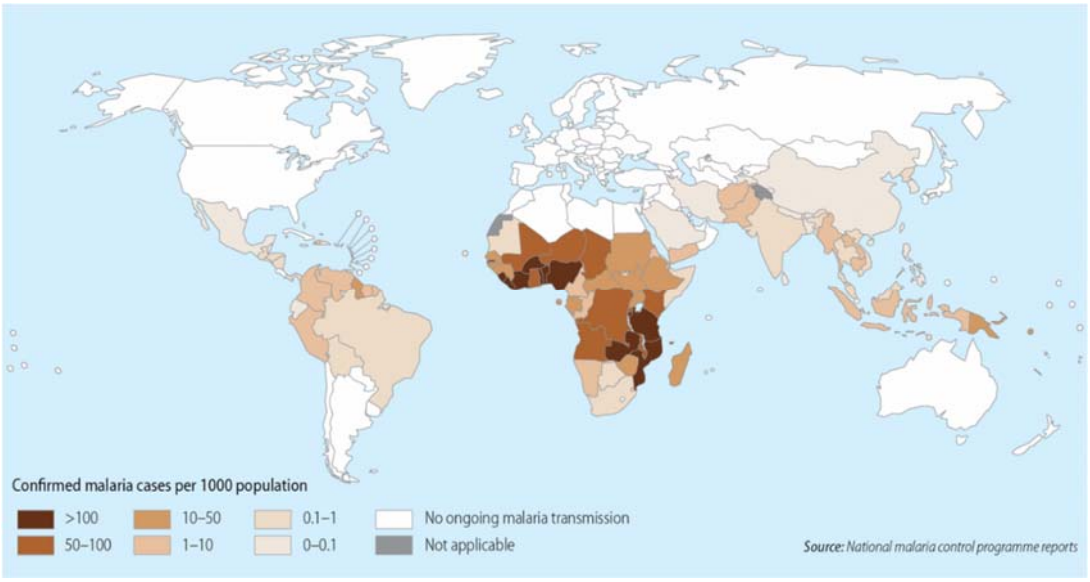


**Figure 1:** Geographical distribution of malaria in 2014. Adapted from (5).

In high transmission settings like Africa and parts of Oceania, *P. falciparum* is the major parasite species responsible for malaria. In these regions, naturally acquired immunity typically prevents fatal complications in many adults who mostly experience asymptomatic infections. Prior to acquiring immunity, young children suffer the most morbidity and mortality in settings of intense transmission. As well as age, genetic traits such as haemoglobinopathies and glucose-6-phosphate dehydrogenase (G6PD) deficiency are protective in these areas. Where transmission is low, such as in Asia and Central and South America, people do not acquire full protective immunity and symptoms occur anytime throughout a person's lifetime. In these regions, *P. falciparum* and *P. vivax* malaria are equally prevalent (6) and environmental, social or economic changes typically trigger epidemics in all age groups.

The co-existence of poverty worsens the burden of disease in malaria-affected areas. Wars, civil disturbances, poor education, rapid population increases, and underdevelopment are also common in poverty-stricken areas, which further complicates malaria control efforts (7). As malaria is highly sensitive to climate factors, global warming and increased frequency of extreme weather events, such as flooding, may facilitate the spread of infection by providing new habitats for the mosquito vector. In fact, climate suitability and the global population at risk of malaria is projected to increase in the near future (8). Despite these risks, malaria eradication is once again seen as an achievable goal (9). Its realisation will depend on increased financial investment in malaria programs and research and the widespread deployment of evidence-based malaria control interventions.

### 1.2.2 Clinical pathophysiology

Malaria infection begins with the bite of an infected mosquito, followed by a 1-2 week developmental stage in the liver before parasites enter the blood stream and invade host red blood cells (RBCs), as further detailed below (Section 1.3). The liver stage of *Plasmodium* infection is asymptomatic, creating a 1-2 week latency between the bite of an infected mosquito and the onset of the clinical syndrome of malaria (10). Clinical symptoms occur during the blood stage of infection due to the alteration and sequestration of parasite-infected RBCs and the release of toxins when RBCs rupture (11). The most common symptom of uncomplicated malaria is fever which fluctuates in severity throughout the course of the sickness. Other common symptoms may include headache, fatigue, muscle ache, diarrhoea, nausea and vomiting (1). Infected individuals may also present with splenic or hepatic enlargement (1). Many malaria symptoms are general in nature and common to a number of infectious diseases, making differential diagnosis difficult. Microscopic investigation of blood smears or other diagnostic tests may confirm *Plasmodium* infection, however, it is recommended that all febrile children in malaria-endemic regions be treated with antimalarials unless parasitaemia can be

excluded (7). The severity of symptoms depends on various host factors, such as age, immunity, pregnancy and comorbidities. Remarkably, people living in highly malaria-endemic areas can remain asymptomatic despite having detectable parasitaemia (7).

Uncomplicated malaria causes substantial morbidity and requires treatment with antimalarial drugs as soon as possible to prevent the development of serious complications. Following prompt and effective treatment, uncomplicated falciparum malaria has a mortality rate of only 0.1% (1). Most mortality and serious complications, including permanent damage, is associated with severe malaria. Severe malaria varies with age and regional parasite transmission levels and is most common in young children, non-immune adults and pregnant woman. It incorporates several complications, including cerebral malaria, severe anaemia, acidosis and hypoglycaemia, pulmonary oedema, acute kidney injury and jaundice (1). In Africa, where malaria transmission is stable, most malaria deaths occur in young children. In this population, severe disease most commonly presents as cerebral malaria or severe anaemia and causes convulsions and coma (12). Although these syndromes also form part of the clinical picture in adults, severe malaria in adults is more commonly a multisystem disorder, particularly disrupting liver and kidney function (12). Sequestration of infected cells in the patient microvasculature underlies the pathology of severe falciparum malaria (13). The rupture of RBCs at the end of the intraerythrocytic development cycle also contributes to malaria-related pathogenesis by releasing host and parasite toxins into the blood stream. This causes local and systemic reactions, such as endothelial damage and fever (14, 15).

## 1.3 THE PARASITE LIFECYCLE

The *Plasmodium* parasite has a complex life cycle (Figure 2) that involves multiple stages in both the mosquito vector and the vertebrate host (10). An infected female *Anopheles*

mosquito transmits infection during a blood meal by injecting the microscopic motile sporozoites residing in her salivary glands into the dermis of the mammalian host. The sporozoites slowly migrate away from the inoculation site over 1-3 h (16), exiting the dermis and entering the host circulation when they reach a blood vessel (10). Once in the bloodstream, sporozoites quickly access the liver and infiltrate the hepatocytes by exiting the sinusoids through Kupffer or endothelial cells in a process known as cell traversal (17). When they locate a suitable hepatocyte, the parasite forms a parasitophorous vacuole membrane and undergoes exoerythrocytic schizogony over a period of 9-16 days (12). *P. vivax* and *P. ovale* may also form dormant liver-resident hypnozoites that cause recurrent malaria attacks months to years after the initial infection. Fully developed exoerythrocytic schizonts release tens of thousands of daughter merozoites into the hepatic vasculature in packets called merosomes. These merosomes rupture and release free merozoites that invade the host RBCs and initiate the erythrocytic stage of infection.

RBC invasion is a complex molecular process initiated by low-affinity interactions between the surface proteins of the merozoite and receptors on the surface of the target RBC (18, 19). Initially, the parasite reorientates, bringing its apical end into direct contact with the erythrocyte surface, and specific ligand-receptor interactions of the apical organelle (micronemes, rhoptries and dense granules) form a tight junction that allows merozoite entry to the RBC. Invagination of the RBC membrane forms a parasitophorous vacuole around the invading merozoite and invasion is complete when the tight junction closes behind the parasite, leaving it enclosed within a parasitophorous vacuole in the RBC cytoplasm (20).

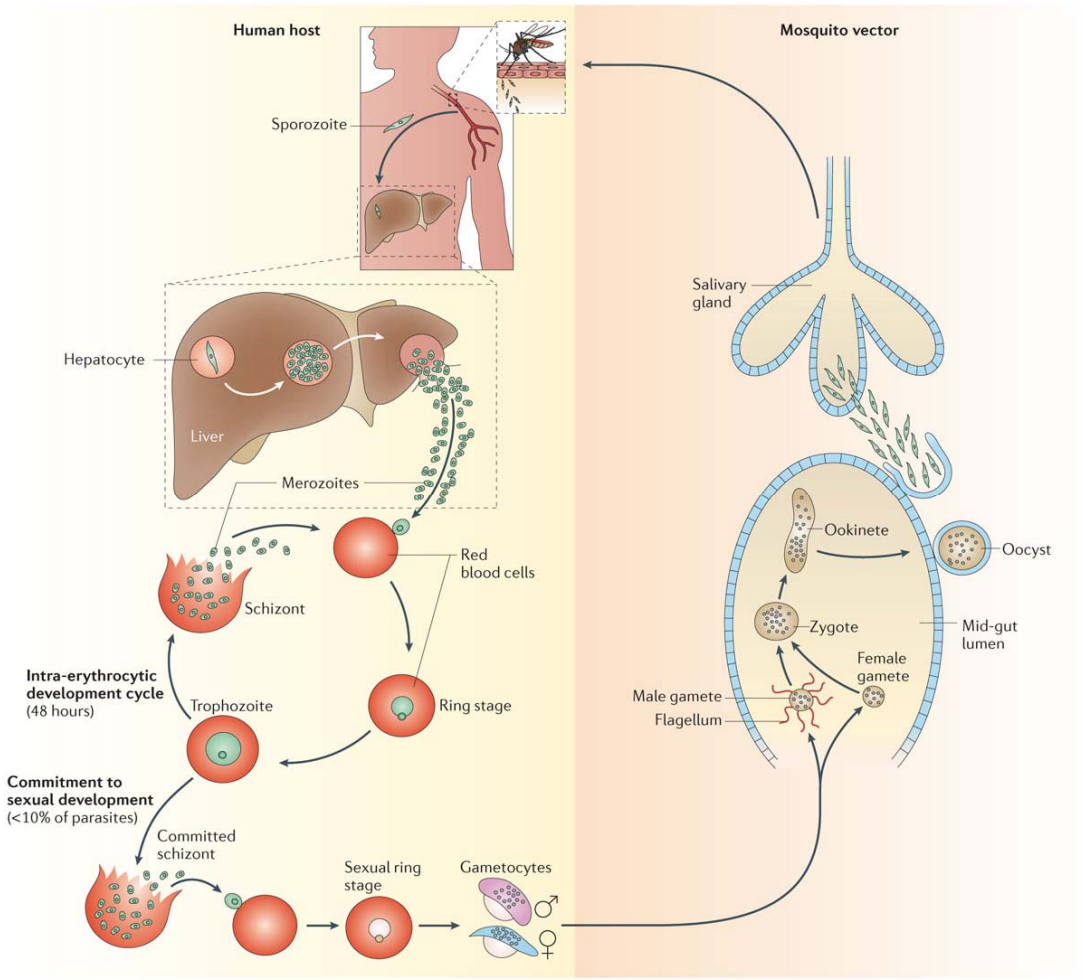


**Figure 2:** The lifecycle of *Plasmodium falciparum* in the human and mosquito hosts. Adapted from (21).

During the intraerythrocytic stage, the parasite matures over 24-72 hours, depending on the *Plasmodium* species, inducing extensive structural remodelling of the RBC by exporting hundreds of proteins into the host cell cytoplasm via a vesicle-mediated secretory system. This allows the parasite to import necessary nutrients, dispose of waste products and evade detection by the host immune system. During this intraerythrocytic phase of growth, the parasite develops from the early ring stage to form trophozoites and eventually erythrocytic schizonts. The trophozoite stage is the most metabolically active phase of intraerythrocytic development, whereby the parasite grows significantly in size and consumes vast amounts of host cell

haemoglobin. The developing parasite eventually undergoes asexual replication and cell division in the schizont stage, producing 16-32 merozoites that are released into the bloodstream when the host RBC ruptures (20). These daughter merozoites go on to invade new RBCs to continue the asexual intraerythrocytic cycle.

Prior to schizogony during asexual cycling, a subset of parasites will commit to sexual development and mature into the male and female sexual forms of the parasite known as gametocytes (22). When a female *Anopheles* mosquito ingests the mature male and female forms during a blood meal, fertilisation of the fully mature female macrogamete by the male microgamete occurs in the mosquito midgut. The resulting zygote differentiates into a motile ookinete that traverses the midgut wall to form an oocyst. Parasite asexual replication in the oocyst produces thousands of sporozoites, which, upon rupture of the oocyst, travel to the mosquito salivary glands. They reside here until the mosquito transmits the infective sporozoites to the next human host during a blood feed, thus, continuing the *Plasmodium* lifecycle (10).

### 1.3.1 Haemoglobin catabolism

Haemoglobin accounts for 95% of the soluble protein within RBCs. During its short intraerythrocytic residence, the parasite consumes up to 75% of the host haemoglobin, mostly during the mature trophozoite stage of infection (23). This massive catabolic process is essential for parasite survival and inhibiting haemoglobin degradation impedes parasite growth (24-26). Amino acids from radiolabelled haemoglobin have been shown to be incorporated into parasite proteins (27, 28), suggesting the *Plasmodium* parasite relies on haemoglobin-derived amino acids for the synthesis of new proteins (29). The parasite has a limited capacity to manufacture amino acids *de novo* but can also scavenge them from the host serum (29, 30). This allows the parasite to survive in medium containing only isoleucine (absent in

haemoglobin), which is the sole exogenously required amino acid needed for parasite growth (29). The supply of amino acids from haemoglobin degradation greatly exceeds the metabolic requirements of the parasite and it appears to expel vast quantities of globin-derived amino acids during its maturation within the RBC (31, 32). For this reason, it has been proposed that haemoglobin digestion also serves non-anabolic functions (33). This includes allowing the parasite to make room for itself in the host RBC to accommodate its increase in size (34) or maintaining the osmotic stability of the infected RBC (35).

#### 1.3.1.1 Parasite-mediated haemoglobin digestion

The parasite acquires haemoglobin by ingesting RBC cytosol through a specialised endocytotic structure known as the cytostome. The cytostome forms at the parasite surface by invagination of the parasitophorous vacuole and parasite plasma membranes (36-38). It is thought that the resulting double-membrane bound vesicles that pinch from the cytostome become acidified pre-digestive vacuole compartments as early as the mid-ring stage of parasite development (14 h post invasion) (37, 39). As the parasite matures into a trophozoite, multiple acidic compartments coalesce to produce a single digestive vacuole that is continually fed by haemoglobin containing vesicles (37, 40). Non-cytostomal structures may also play a role in haemoglobin uptake and endocytosis, however, the significance of their contribution is not fully known (38, 41).

The digestive vacuole is the major site of haemoglobin digestion in the parasite. Partial haemoglobin degradation likely begins prior to digestive vacuole maturation in pre-digestive vacuole compartments and transport vesicles at the mid-ring stage. During this stage, small haemozoin crystals are detectable in parasites (37, 42, 43) and haemoglobin digesting proteases have been found to be expressed (44), some of which are known to be transported to the plasma membrane and become part of the cytostome (45) and early acidic endocytotic structures (37).

The haemozoin forming catalysts, haem detoxification protein (HDP) (46) and lipids (47, 48), are also present at these early endocytotic structures, indicating ring stage parasites contain all of the necessary machinery to initiate haemoglobin degradation.

Within the digestive vacuole, haemoglobin degradation is a semi-ordered process carried out by a series of functionally redundant proteolytic enzymes (49) (Figure 3). The early steps have been well characterised and are driven by the plasmepsin and falcipain (FP) endopeptidases. The *P. falciparum* genome encodes 10 plasmepsins (50), four of which are localised and function within the digestive vacuole. These include plasmepsin I, II, IV and histo-aspartic protease (HAP) (51). Plasmepsins I and II are thought to promote the initial unravelling of the globin subunits by cleaving native haemoglobin at the hinge region of the alpha-globin chain, thereby allowing further proteolysis (52). Plasmepsin IV and HAP have less ability to degrade haemoglobin but show some proteolytic activity *in vitro* (51). Secondary cleavage is continued by the plasmepsins as well as FP 2A, 2B and 3. It was originally thought that the FPs were unable to cleave non-digested haemoglobin (53) but more recent evidence suggests FP 2 (54) and FP 3 (55) can cleave intact haemoglobin at multiple sites in the amino acid sequence and may participate in initial haemoglobin digestion within the digestive vacuole (56). Inhibiting plasmepsin and FP activity with pepstatin and E64, respectively, completely abrogates haemoglobin proteolysis, demonstrating that both protease groups are involved in haemoglobin degradation (52, 57). Interestingly, all digestive vacuole plasmepsins are dispensable for intracellular growth (58), highlighting the functional redundancy between the plasmepsin and FP enzymes. FP 2 knockout parasites also remain viable but accumulate undigested haemoglobin at the trophozoite stage (59). In contrast, FP 3 is refractory to genetic deletion. The FPs are also thought to be the primary activator of plasmepsins, further emphasising their key role in haemoglobin catabolism (60).

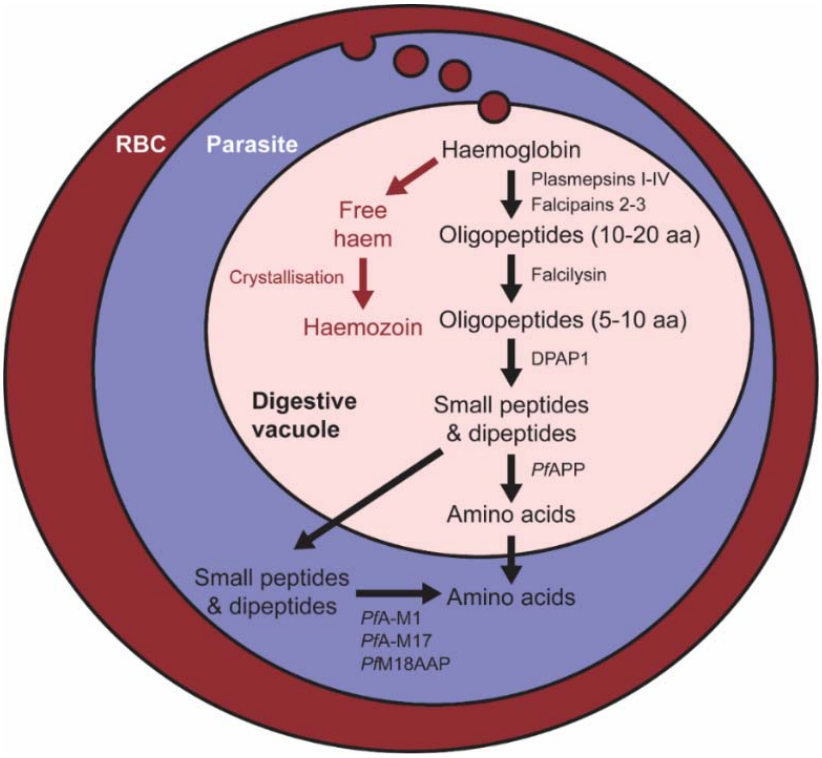


**Figure 3:** Haemoglobin digestion cascade within *Plasmodium falciparum* trophozoites. Haemoglobin is transported into the parasite digestive vacuole and degraded by a series of proteases into peptides and eventually amino acids. Toxic free haem released as a by-product of digestion is crystallised into non-toxic haemozoin. DPAP1, dipeptidyl aminopeptidase 1; *Pf*APP, *P. falciparum* aminopeptidase P; *Pf*A-M1, *P. falciparum* M1 alanyl aminopeptidase; *Pf*A-M17, *P. falciparum* M17 leucyl aminopeptidase; *Pf*M18AAP, *P. falciparum* M18 aspartyl aminopeptidase RBC, red blood cell.

The metalloprotease falcilysin is a digestive vacuole protease expressed in trophozoite stage parasites (61) that is unable to digest native haemoglobin or denatured globin. Falcilysin prefers to cleave polar residues of peptide fragments that are up to 20 amino acids long (62). The oligopeptides generated by plasmepsin and FP proteolysis are thought to be cleaved by falcilysin into short polypeptide chains 5-10 amino acids in length (62), which are then degraded by the cysteine exopeptidase dipeptidyl aminopeptidase 1 (DPAP1) (63). DPAP1 expression peaks during the trophozoite stage (61, 64) and the protein is localised to the digestive vacuole (63). Attempts to genetically disrupt DPAP1 have so far been unsuccessful

as it is thought to have an essential role in the final steps of haemoglobin catabolism. DPAP1 removes dipeptides from the polypeptides produced by upstream proteases, thereby facilitating the production of amino acids by downstream aminopeptidases (65).

*Plasmodium* aminopeptidases have varying degrees of substrate specificity and work synergistically to release amino acids from small peptides and dipeptides in both the parasite digestive vacuole and cytosol. Aminopeptidase P (*Pf*APP) is located in the digestive vacuole and cytosol (66), targeting oligopeptides with proline in the P1 position (67). In the digestive vacuole, *Pf*APP may lead to more efficient haemoglobin catabolism by cleaving N-terminal amino acids adjacent to proline, thereby providing good peptide substrates for DPAP1, which cannot accommodate P1 proline residues (67). The M1 alanyl aminopeptidase (*Pf*A-M1) is digestive vacuole-localised and has broad substrate specificity with a preference for cleaving at leucine and methionine residues (68). Inhibition of *Pf*A-M1 leads to a swollen digestive vacuole and an accumulation of haemoglobin oligopeptides (66, 69). However, optimal activity occurs at pH 7.4, so there is disagreement as to whether it has a primary role in haemoglobin catabolism in the acidic environment of the digestive vacuole (70). The high concentration of peptide substrates in the digestive vacuole may drive binding to the enzyme and promote peptidase activity, despite an unfavourable acidic environment (71).

Cytosolic metalloaminopeptidases, including *Pf*A-M1, M17 leucyl aminopeptidase (*Pf*A-M17) and M18 aspartyl aminopeptidase (*Pf*M18AAP), digest the small peptides delivered to the cytosol into their amino acid constituents. *Pf*A-M1 and *Pf*A-M17 prefer cleaving at leucine residues and are essential for the intracellular regulation of leucine and isoleucine (72). In contrast, *Pf*M18AAP is not essential for parasite survival, but preferentially cleaves at glutamate and aspartate residues (73, 74).

#### 1.3.1.2 Haem detoxification in the parasite

Each molecule of haemoglobin digested by the parasite releases four molecules of haem (ferriprotoporphyrin IX). The iron located at the centre of the haem porphyrin ring is a transition metal that exists in either the ferrous (+2) or ferric (+3) forms. Redox active free haem causes considerable damage to the parasite through the generation of free radicals, reactive oxygen species and lipid peroxidation (75-77). The lipophilic nature of haem may also induce cell injury by directly destabilising lipid membranes (78).

The main mechanism for haem detoxification is via a unique pathway that crystallises haem into an insoluble non-toxic and unreactive biopolymer called haemozoin (Figure 3). Haemozoin synthesis within *P. falciparum* is thought to involve proteins (that promote haem nucleation) and neutral lipids (that catalyse polymerisation) (79, 80). The main protein involved in catalysing haemozoin formation is HDP. Compared to histidine rich protein (HRP) 2 (81) and neutral lipids (82), HDP is the most potent haemozoin catalyst known in *Plasmodium* parasites (46, 83). Several antimalarial drugs target the haemozoin synthesis pathway as it is a parasite specific process that is essential for survival (84).

Alternative methods of haem detoxification also exist in the *Plasmodium* parasite. Reduced glutathione spontaneously degrades haem by disrupting the haem porphyrin ring (85) and the protein EXP1, which has glutathione-S-transferase (GST) activity, facilitates detoxification by conjugating glutathione to haem (86). These processes are optimal at neutral pH, suggesting they may be involved in haem detoxification within the parasite cytosol, rather than the digestive vacuole (85, 87). *P. falciparum* also contains a single haem oxygenase like protein (*Pf*HO) localised to the apicoplast organelle (88). In contrast to mammalian cells that detoxify haem using haem oxygenase, *Pf*HO plays a minor role (if any) in haem detoxification relative to the haemozoin synthesis pathway (89).

# 1.4 STRATEGIES FOR MALARIA CONTROL

Controlling malaria infection requires a multidimensional strategy that targets both the *Plasmodium* parasite and the mosquito vector. The first approach is malaria prevention, which includes vector control (stopping the *Anopheles* mosquito from biting humans), chemoprevention (suppressing infections using drugs) and potentially vaccination in the near future. The second approach for controlling malaria is treatment with antimalarial drugs.

## 1.4.1 Malaria prevention

Insecticide-treated bed nets (ITNs) and indoor residual spraying (IRS) are two of the most effective methods that targets the mosquito vector and prevent malaria transmission (3). Currently, pyrethroids are the only insecticide class recommended for use in ITNs (90), while IRS of homes also typically use pyrethroids and some other pesticide classes. Unfortunately, there are reports of resistance to all insecticides that are currently used for malaria vector control, highlighting the urgent need for development of new safe and effective insecticides to target malaria vectors. Effective environmental management strategies may also reduce vector populations that transmit the *Plasmodium* parasite. In particular, removal of vector breeding habitats by draining swamps and modifying aquatic environments are beneficial for reducing parasite transmission. Improving building design by applying screens to windows and doors can also impede transmission by reducing the number of bites for susceptible individuals.

Chemoprevention strategies employ antimalarial medicines for prophylaxis of infection by either inhibiting liver stage parasites (causal prophylaxis) or killing asexual blood stages (suppressive prophylaxis). The goal is to prevent illness by maintaining therapeutic levels of drug in the body during periods of high infection risk. This approach is commonly utilised by non-immune people travelling to malaria endemic countries, as well as individuals in special risk groups who live in malaria endemic areas, such as pregnant women (intermittent

preventative therapy in pregnancy, IPTp) and infants in the first year of life (IPTi). It is also recommended that children aged 3 to 59 months living in seasonal transmission zones receive IPT at set times during the transmission season. Preventative antimalarial treatment is highly successful when administered appropriately, but prolonged exposure of parasites to low drug concentrations could encourage the development of antimalarial resistance (91). In addition, routine chemoprevention may compromise the development of natural immunity (7).

The search for a highly effective malaria vaccine has been largely unsuccessful, mostly because the malaria parasite employs sophisticated mechanisms that allow it to evade the host immune system (92). There are currently a number of vaccine projects underway, but the only candidate to complete Phase III testing is RTS,S/AS01. This vaccine candidate targets the circumsporozoite protein of *P. falciparum* and displays good safety but only reduces the clinical incidence of malaria by 39%, and immunity progressively declines in the 12 months following the last dose (3). RTS,S is being implemented on a pilot scale in some African countries, with the aim of more wide scale deployment in the next 5 years as a complementary tool to other malaria control methods (93).

### 1.4.2 Malaria treatment

The treatment of *Plasmodium* infection with antimalarial drugs is a vital part of malaria control. Rapid treatment of uncomplicated malaria is crucial for preventing progression to severe disease and death. Prompt therapy impedes parasite transmission by reducing disease duration and the likelihood that sexual stage gametocytes will be transferred to mosquitos if an infected person is bitten. Most antimalarial drugs that are currently available act on the parasite erythrocytic stages, resulting in clearance of parasitaemia and abating of clinical symptoms. The WHO currently recommends artemisinin-based combination therapies (ACTs) as the first line treatment for uncomplicated falciparum malaria in all endemic areas (94). Utilising

appropriate antimalarial combinations reduces the likelihood of drug resistance developing, helping to protect current and future antimalarial medicines. In the case of ACTs, the fast-acting artemisinin component is combined with a long acting partner drug. ACTs are well tolerated and have contributed substantially to the reduction in malaria associated morbidity and mortality since their introduction. In cases of severe malaria, parenteral artesunate is the treatment of choice (95).

## 1.4.3 Antimalarial drugs

Rapid elimination of *Plasmodium* parasites from an infected individual is the ultimate goal of antimalarial treatment, thereby curing infection and preventing progression to severe disease. Antimalarial medicines achieve this by direct parasiticidal activity, with most currently available drugs exerting their activity on the erythrocytic stage of the parasite. This is particularly beneficial for resolving the clinical symptoms of malaria, but in the case of *P. vivax* or *P. ovale* infection, activity against the exoerythrocytic stages is also important to prevent relapse by liver forms of the parasite.

### 1.4.3.1 Currently available antimalarials

The most rapidly acting antimalarial drugs currently available are based on the natural product artemisinin. Artemisinin itself has poor pharmaceutical properties and only semisynthetic derivatives of artemisinin are used clinically. These include dihydroartemisinin (DHA), artesunate and artemether. ACTs are used in a 3-day treatment course and are the most effective antimalarial treatment options currently available. They rapidly reduce parasite burden in infected patients, are effective against multidrug resistant parasites (1) and are also active against gametocytes and thereby block parasite transmission (96). Artemisinin and its semisynthetic derivatives are described in more detail in section 1.5.

Another important class of antimalarials is the quinolines, derived originally from quinine, a naturally occurring alkaloid from the bark of the cinchona tree that was serendipitously discovered in the 17$^{th}$ century as an effective remedy for malaria and fever (97). Quinine continues to have a limited role in certain clinical situations today, but dose-dependent side effects and serious neurological and cardiac complications have impacted its widespread use (97). During the early 20$^{th}$ century, several synthetic quinine analogues were developed and one of the most important of these was the 4-aminoquinoline, chloroquine. The exact mechanism by which chloroquine exerts its activity is still a matter of debate, but it is generally thought to involve disruption of haem detoxification within the parasite digestive vacuole (98). Chloroquine is affordable, easy to manufacture, well tolerated at therapeutic doses and historically was highly effective for malaria prevention or treatment until resistance limited its effectiveness.

A number of 4-aminoquinoline derivatives were developed to combat chloroquine resistance and have varying degrees of activity against resistant parasites (98). Examples include amodiaquine and the dimeric 4-aminoquinoline piperaquine. Unfortunately, these drugs can cause toxic side effects, such as hepatotoxicity, agranulocytosis and cardiac complications and parasites resistant to these compounds have emerged in the field (98, 99). The new chloroquine derivative, ferroquine, has promising potential for malaria treatment as it is effective against various chloroquine sensitive and resistant *P. falciparum* strains as well as *P. vivax* parasites (100). Several arylamino alcohol derivatives based on quinine were also developed, these included mefloquine, halofantrine and lumefantrine. While these drugs exhibit good activity against multiple chloroquine resistant strains of *P. falciparum* (98, 101, 102), resistance and the risk of neuropsychiatric side effects (mefloquine), erratic absorption (halofantrine and lumefantrine) and a high risk of cardiac toxicity (halofantrine) limit their

therapeutic application (98). As a group, the arylamino alcohols are thought to act by a distinct mechanism to the 4-aminoquinolines (103, 104).

The 8-aminoquinoline, primaquine, is unique among antimalarials due to its potency against liver-stage parasites (hypnozoites) and it is the only medicine approved for the radical cure of relapsing malaria caused by *P. vivax* (98). Due to its short half-life, primaquine must be administered daily over 14 days to achieve a cure. The discovery of a long-acting anti-relapse medication, tafenoquine, is now in advanced stages of clinical development (105) and has the benefit of a shorter treatment duration compared to primaquine (106). Unfortunately, severe haemolytic toxicity in G6PD deficient patients is a risk with both of these drugs (107).

Antifolates target the essential folate biosynthesis pathway in bacteria and protozoa (108). Targeting folate metabolism occurs through the inhibition of two integral enzymes in the biosynthetic pathway, dihydropteroate synthase (DHPS) or dihydrofolate reductase (DHFR). Pyrimethamine and proguanil are two commonly used antifolate drugs that target the *Plasmodium* DHFR enzyme. Proguanil itself is a prodrug that is metabolised to the active compound, cycloguanil, *in vivo*. Inhibitors of DHPS are predominantly sulphonamides (sulphadoxine) or sulphones (dapsone) that indirectly perturb folate metabolism by way of their structural similarity with the natural DHPS substrate, para-aminobenzoic acid (PABA) (108). Typically, sulphadoxine with pyrimethamine (SP) is given as a combination as inhibition of DHPS and DHFR is synergistic (98). Unfortunately, extensive antifolate use caused the rapid development of antifolate resistant *Plasmodium* parasites, which are now widespread in the field (109).

The 2-hydroxynaphthoquinone, atovaquone, inhibits the *Plasmodium* mitochondrial electron transport chain through specific inhibition of the cytochrome *bc*1 complex (110), causing collapse of the mitochondrial membrane potential (111). The *Plasmodium* electron

transport chain maintains a constant pool of ubiquinone for the enzyme dihydroorotate dehydrogenase (DHODH), which catalyses the fourth step in *de novo* pyrimidine synthesis (112). Atovaquone-induced shutdown of DHODH-dependent pyrimidine synthesis is lethal to the parasite, which lacks the ability to scavenge pyrimidines from its environment (113). Monotherapy with atovaquone is not recommended as parasites rapidly develop atovaquone resistance (114). For this reason, the combination of atovaquone and proguanil, which shows strong antimalarial synergism (115), is typically used.

Antibacterial agents that target bacterial protein translation machinery are also effective for the treatment and prevention of malaria infection (116). Tetracyclines, macrolides and lincosamides display considerable antimalarial activity in apicomplexan protozoa, like *Plasmodium*, as these parasites contain a bacterially-derived translation apparatus within the apicoplast organelle, which can be targeted to kill the parasite (117). Inhibition of organellar translation causes a delayed death effect, whereby parasites transmit a defective apicoplast to their progeny, which eventually succumb to antibacterial drug treatment in the second infection cycle (118). Fluoroquinolone antibiotics also exhibit antimalarial activity and target the *Plasmodium* apicoplast causing a delayed death effect, but instead of translation, are thought to inhibit apicoplast DNA gyrase activity (119). These drugs are therefore too slow-acting to be used alone for malaria treatment and must be combined with a fast-acting partner drug. Alternatively, they are useful as malaria prophylactics. The antibacterial rifampicin is active against malaria parasites but has a primary target outside of the *Plasmodium* apicoplast and does not induce delayed death (119).

#### 1.4.3.2 Novel antimalarials in development

Malaria elimination and eradication requires the development of new antimalarial drugs that are affordable, safe, effective and that act by novel mechanisms. There has been a dramatic

increase in the number and diversity of novel molecules entering pre-clinical and early clinical development over the last decade (120). This is largely a result of increased collaboration between academia and industry in the drug discovery and development process (120). Product development partnerships, like the Medicines for Malaria Venture (MMV), have played a significant role in facilitating these relationships as well as allocating resources to promising projects. In addition, identification of specific quantitative criteria that a molecule must meet before being considered for development, known as a target candidate profile, has improved the quality of molecules entering clinical development with the potential to become viable medicines (121). Ideal candidate molecules should be able to rapidly clear parasites from the body, have broad parasite and lifecycle stage activity and be long-acting, safe and affordable.

Increased uptake of hit discovery programs that employ phenotypic screening and subsequent target identification has characterised a range of new chemotypes with novel molecular targets. Most of the antimalarials in clinical development with novel targets have been identified in this way. The spiroindolone, KAE609, is the most advanced compound identified through this approach. KAE609 targets the parasite plasma membrane ion channel, *Pf*ATP4, which regulates parasite osmotic homeostasis (122). Subsequently, several other chemical series were also found to target *Pf*ATP4 (123), including SJ733 (124), which has advanced to clinical trials. Phenotypic screening also led to the discovery of MMV048, which disrupts intracellular trafficking and signalling through inhibition of phosphatidylinositol 4-kinase (125) and KAF156, which inhibits the cyclic amine resistance locus protein, although it is uncertain whether this is the main mechanism of parasite killing (126). DDD498 is another example of a compound identified from a large-scale phenotypic screening programme and inhibits the *P. falciparum* translation elongation factor 2, a novel antimalarial target (127).

The development of DSM265 and OZ439 are examples of alternative discovery approaches that have led to promising drug candidates. DSM265 was specifically designed to

selectively inhibit *Pf*DHODH, a key enzyme involved in *de novo* pyrimidine synthesis (128), while the completely synthetic peroxide antimalarial, OZ439, was developed based on the peroxide bond of the artemisinins (129). OZ439, which is in advanced stages of clinical development, is discussed further in section 1.6.

# 1.5 ARTEMISININ AND SEMISYNTHETIC DERIVATIVES

## 1.5.1 Development and clinical applications

Artemisinin was discovered in 1971 by a group of Chinese scientists who extracted the active constituent of the *Artemisia annua* plant, a traditional Chinese medicine used for its antipyretic properties for over 1500 years. Artemisinin (Figure 4) was found to contain an endoperoxide group within a sesquiterpene lactone backbone (130), have potent *in vitro* activity against *P. falciparum*, and cure patients with uncomplicated and severe malaria (131). Artemisinin itself has limited pharmaceutical application as it is highly crystalline and poorly soluble in both oil and water. As a result, a series of highly potent semisynthetic artemisinin derivatives, with improved pharmaceutical properties, were developed. These included the artemisinin derivatives that are in use today, namely, DHA, artemether and artesunate (Figure 4). Both artemether and artesunate are converted to the active metabolite DHA *in vivo* (132, 133). While 50% of the clinical efficacy of artemether can be attributed to DHA (134), artesunate is intrinsically unstable (half-life of several minutes) and likely undergoes rapid non-enzymatic conversion to DHA, which contributes most of its antimalarial activity (135).

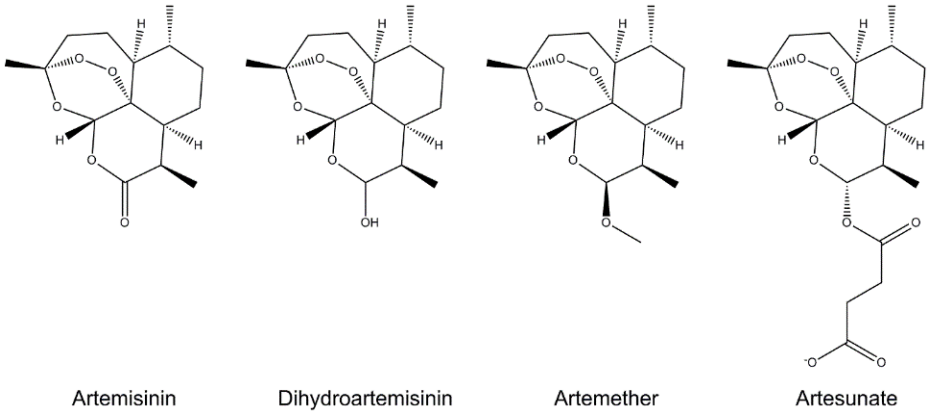


**Figure 4:** Chemical structures of artemisinin and the clinically used semisynthetic artemisinin derivatives, dihydroartemisinin, artemether and artesunate.

The artemisinins are rapid acting antimalarial drugs that kill all species of *Plasmodium* that infect humans (135). They are most potent against the asexual stage of infection, particularly trophozoites, but uniquely among currently available antimalarials, are also active against the early ring stages. Artemisinins have transmission blocking potential in areas of low transmission due to their gametocytocidal activity (96) but are ineffective against hepatic stages and therefore not useful for causal prophylaxis (135). Clinically, the artemisinins are relatively safe, providing a distinct advantage over other currently available antimalarials. They were initially deployed as monotherapy in a 7-day treatment course with multiple daily dosing more than 30 years ago. However, this was associated with poor compliance, as patients often discontinued treatment early, resulting in high rates of recrudescence. In 2006, the WHO began to phase out oral artemisinin-based monotherapy in an effort to improve efficacy and minimise the development of resistance (5). ACTs were introduced the following year, which are now the standard of care for the treatment of uncomplicated infection caused by *P. falciparum*.

The WHO recommends five ACTs, including artesunate/SP, artemether/lumefantrine, artesunate/amodiaquine, artesunate/mefloquine and DHA/piperaquine. A sixth ACT, artesunate/pyronaridine, is on the WHO list of prequalified medicines. All of these

combinations are administered either once or twice daily for three days, with the choice of ACT depending on regional parasite sensitivity. In severe malaria, patients are treated with parenteral artesunate (intravenous or intramuscular) for at least 24 h, or until they tolerate oral medication. A complete 3-day course of oral ACT follows cessation of parenteral treatment.

### 1.5.2 Limitations of ACTs

Economic and pharmacokinetic liabilities are the major limiting factors for the clinical application of artemisinins. While the cost of ACTs has become more affordable in recent years, the artemisinin component remains considerably more expensive than completely synthetic antimalarials, like chloroquine and SP (1, 136). Until recently, the only practical option for obtaining the artemisinin (or artemisinic acid) starting material needed for derivatisation into the clinically used artemisinin derivatives is isolation from the plant source. Cultivation of the *Artemisia annua* plant is time consuming and subject to seasonal variations, while extraction from the plant typically yields less than 1% artemisinin (137). These factors directly raise the inherent cost of these compounds and has led to a market for counterfeit artemisinins, which often contain sub-therapeutic doses of the active ingredient, increasing the likelihood of treatment failure and the development of resistance (138). Fortunately, cost-effective technologies aimed at enhancing artemisinin production are under development (137, 139).

All artemisinin derivatives suffer from poor biopharmaceutical properties, such as variable absorption (artemether) and hydrolytic instability (artesunate) (135, 140). The major limiting factor is their short *in vivo* half-life, which varies from $< 1$ h to up to 4 h, depending on the derivative, and often leads to parasite recrudescence when artemisinins are used as monotherapy (98, 141). Combining artemisinin with a longer-acting partner drug prevents recrudescence and achieves a shorter treatment course. However, due to the mismatch in

biological half-life, long-term exposure of parasites to low doses of the partner drug alone may result in partner drug resistance (142).

The biggest concern facing future use of ACTs is the emergence of artemisinin resistant parasites in the Greater Mekong Subregion (143). At the epicentre in Cambodia, artemisinin resistance compromises the therapeutic efficacy of all five WHO recommended ACTs (failure rate of more than 10%) (144). Although some ACTs still clear artemisinin resistant infections, if resistant parasites spread to Africa, where more than 90% of malaria deaths occur, it could have devastating consequences on human life. Artemisinin resistance is discussed in more detail in Section 1.5.4.

### 1.5.3 Mechanism of action

The precise mechanism that mediates artemisinin antimalarial activity is an active area of research. While artemisinins exhibit activity against all blood stages of the *Plasmodium* parasite, including the early ring stage, there are substantial stage-dependent differences in parasite susceptibility to artemisinins. Ring stage parasites (6-20 h post invasion) have been shown to be relatively resistant to short (4 h) pulses of either artemisinin or DHA, whereas trophozoites (> 20 h post invasion) exhibited a 10- to 100-fold higher sensitivity, depending on the artemisinin derivative (145). A subpopulation of early-ring stage parasites (2-4 h post invasion) that exhibit hypersensitivity to short-pulsed artemisinin exposure has also been reported (145). The hypersensitivity of early-ring stage parasites may also account for the variable potency of artemisinins reported in ring stage parasites (146, 147).

Recent reports have suggested that *in vitro* parasite susceptibility to artemisinins is not solely dependent on the drug concentration, as increasing the drug concentration did not result in enhanced parasite killing, especially if the treatment duration was reduced (145, 148). The relationship between artemisinin exposure time and the applied drug concentration was

observed as stage-dependent differences in the time required to induce a parasiticidal response (145). Ring stage parasites were virtually unaffected by short-pulsed treatment with artemisinins (< 4 h), exhibiting an extended delay in their onset of response, while trophozoites were highly sensitive to the parasiticidal effect of even a 2 h pulsed artemisinin treatment (145). Extending the duration of treatment was shown to overcome the differential sensitivity between relatively unresponsive ring stages and highly susceptible trophozoites.

#### 1.5.3.1 The peroxide bond and iron-mediated activation

The peroxide bond is essential for artemisinin activity. Derivatives that have the peroxide bond replaced by an ether linkage are completely devoid of *in vitro* activity (149, 150). Even simple peroxides, such as *t*-butyl hydroperoxide, exhibit antimalarial activity by way of their ability to generate reactive oxygen species that promote oxidative stress (151). Short-term treatment (2 h) with artemisinin or DHA has been shown to exert dose-dependent prooxidant activity in *P. falciparum* parasites (152) and coincubation with prooxidant drugs (153) enhanced antimalarial activity. In contrast, antioxidant and free radical scavenging drugs have been shown to antagonise artemisinin activity (153-155), providing clear evidence of a relationship between oxidative stress and the antimalarial activity of artemisinins.

Iron reactivity is a feature of all artemisinins that possess antimalarial activity (156). Under *in vitro* conditions, artemisinins are reported to be stable in the presence of ferric iron but undergo reductive scission of the peroxide bond by ferrous iron (157). Ferrous iron induces homolytic cleavage of the artemisinin peroxide bond, producing unstable oxygen-centred radicals that rearrange into carbon-centred radicals. These are thought to be the primary toxic species responsible for artemisinin activity (156, 158, 159), however, various minor artemisinin-derived intermediates may also be involved (160-163).

Within the parasite, iron is an essential nutrient required for growth and is involved in multiple cellular functions (164). Infected RBCs contain a bioavailable pool of free iron known as the labile iron pool (LIP), which exists at least partially in the reduced form (165). The importance of free iron to the biological activation of artemisinins has been investigated *in vitro* using iron chelators, which effectively depletes free intracellular iron available to the parasite. The iron chelator desferrioxamine (DFO) was shown to antagonise the activity of various artemisinins (166, 167) and also reduce artemisinin-induced membrane protein oxidation (168). However, it is also possible that DFO abrogates artemisinin activity via an iron chelation independent antioxidant effect (169, 170), which protects the parasite from downstream artemisinin-induced oxidative damage rather than preventing drug activation. More recent studies showed that the iron chelators bipyridyl and deferiprone (DFP) marginally antagonise artemisinin and DHA activity during the trophozoite stage and a maximum of 15% of artemisinin activity during this asexual growth period was attributable to iron from the LIP (44). In the early-ring and mid-ring stages, this figure was 35% and < 20%, respectively (44), suggesting other iron-based activators are crucial for the antimalarial activity of artemisinins.

Haem released through the process of parasite haemoglobin digestion is the most abundant form of iron within the parasite (164). Most intraparasitic haem is sequestered as inert haemozoin, however, some haem can escape this detoxification process (171) and is thought to be a biologically important activator of artemisinin antimalarials (172). Artemisinin potency has been shown to correlate with periods of active haemoglobin digestion and activity depends on a functioning haemoglobin uptake and digestion system (152). Reduced haem has also been shown to be a more efficient activator of artemisinins than inorganic iron, haemin and haemoglobin (173). Inhibiting the activity of cysteine proteases (FP 2 and FP 3) involved in parasite haemoglobin digestion using ALLN or E64d has been reported to completely abrogate artemisinin and DHA activity in trophozoite and hypersensitive early ring stage parasites (44,

152). Similarly, genetic deletion of FP 2 was shown to protect parasites from artemisinin-induced growth inhibition. In mid-ring stage parasites, haemoglobin-derived haem only contributed 25% of artemisinin activity, suggesting other activators or activation independent mechanisms are responsible for activity during this stage of asexual parasite growth.

A haemoglobin digestion product, most likely free haem, appears to be a more important mediator of artemisinin bioactivation than free ferrous iron. In addition, modulating the endogenous haem biosynthesis pathway within parasites has been reported to enhance or reduce artemisinin-mediated cytotoxicity (174-176). It is likely that this selective activation by haem within the parasite mediates the specific parasiticidal activity, and low human toxicity, of the artemisinin antimalarials (154).

Several alternative activation mechanisms have also been proposed that may contribute to artemisinin activity. Specific mitochondrial activation by haem-containing components of the electron transport chain (177) or iron independent activation by parasite cofactors involved in maintaining redox homeostasis have been suggested (178). Direct inhibition of parasite targets by non-activated artemisinins is another possibility. This has recently been proposed for the target *P. falciparum* phosphatidylinositol-3-kinase (*Pf*PI3K), which is potently inhibited by DHA (179). In this case, the peroxide bond is still a necessary structural feature for reversible inhibition of *Pf*PI3K.

#### 1.5.3.2 Intraparasitic targets

Artemisinin-derived radicals are proposed to alkylate or cause oxidative damage to numerous parasite components, including proteins, lipids and small molecules. Early *in vitro* investigations provided the first biological evidence that artemisinins alkylate malaria parasite proteins. Radiolabelled DHA specifically alkylated six proteins within *P. falciparum* infected RBCs (180). One of these proteins was later identified as being the *P. falciparum*

translationally controlled tumour protein (TCTP) homologue (181). The sarco-endoplasmic reticulum ATPase (SERCA) pump, *Pf*ATP6, also gained initial popularity as a possible target of artemisinins due to the structural similarity between the selective mammalian SERCA inhibitor thapsigargin and artemisinin, both of which are sesquiterpene lactones (166). The FP family of haemoglobin-digesting cysteine proteases were also proposed targets for artemisinins (182). Free sulfhydryl groups of cysteine residues in *Plasmodium* proteins were found to be susceptible to oxidation and alkylation by artemisinin-derived radicals (183, 184). Therefore, it is likely that cysteine residues represent an alkylation site within the FP proteases, and possibly other proteins containing free thiol groups.

More recently, chemical proteomics experiments identified over 100 protein targets of artemisinins after *in situ* treatment of trophozoite stage *P falciparum* cultures with alkyne and azide functionalised artemisinin probes (176, 185). The alkylated proteins were isolated using click chemistry-based reactions and identified using LC-MS/MS, revealing that artemisinins alkylate parasite proteins involved in many vital cellular processes. A high proportion of the labelled proteins possess free thiol groups that can be reversibly glutathionylated (186), further supporting the hypothesis that free thiol groups of cysteine residues may act as the target for protein alkylation by the artemisinins.

In these studies, proteins involved with haemoglobin digestion were one of the main targets of the artemisinin probes (176, 185), consistent with reports that artemisinins disrupt the haemoglobin digestion pathway (187-189). Artemisinin probes were also found to alkylate enzymes involved in pyrimidine and purine biosynthesis as well as purine salvage, the parasite antioxidant defence system and glycolysis (176, 185). Ribosomal, chaperone and transporter proteins as well as proteins involved with parasite-host cell invasion and the host immune response were also labelled by the artemisinin probes. The membrane-bound glutathione-S-transferase enzyme, EXP1, which is involved in glutathione-mediated haem detoxification (86)

and *Pf*PI3K, which may be associated with the mechanism of artemisinin resistance (179), are also proposed targets. These findings point to an indiscriminate targeting effect by artemisinin-derived radicals, consistent with studies showing artemisinins disrupt multiple cellular pathways within the parasite (187, 188) and that parasites engage a generalised cellular stress response in an attempt to overcome artemisinin induced damage (148, 190).

In addition to proteins, artemisinin alkylation of small molecule targets has also been demonstrated. *In vitro*, artemisinins alkylate haem analogues (191), haem itself (192-196), and haem in *P. falciparum* infected RBC cultures (172). The *in vitro* potency of a variety of artemisinin derivatives correlates with haem binding, suggesting a relationship exists between haem alkylation and artemisinin antimalarial activity (197). Haem alkylation also occurs within artemisinin treated *Plasmodium* infected mice and was found to positively correlate with *in vivo* parasite susceptibly to artemisinin (198, 199). However, the exact role of the alkylated haem adduct in the mechanism of artemisinin action is not yet known.

Artemisinin derivatives also react with thiol-containing small molecules, such as cysteine (184) and glutathione (200, 201). A reduction in the level of total glutathione (202) and alterations in the abundance of total thiols occurs following artemisinin treatment within *P. falciparum* infected RBCs (203, 204). Glutathione is vital for maintaining intracellular redox homeostasis (205) and has a role in cytoplasmic haem detoxification (85). Therefore, artemisinin-induced depletion of intracellular glutathione, mediated by glutathione alkylation, may disrupt haem detoxification and weaken the parasite antioxidant defence system.

Radiolabelled artemisinin also accumulates at parasite membrane structures (206), including at the digestive vacuole membrane. Disruption to digestive vacuole integrity is one of the earliest morphological changes following artemisinin treatment, while other intraparasitic compartments (such as the endoplasmic reticulum and mitochondria) remain

unaffected (207). Fluorescently labelled artemisinin derivatives were found to accumulate in digestive vacuole-associated neutral lipid bodies and promote oxidative damage to the vacuole membrane (208, 209). Artemisinin-induced membrane damage occurs through lipid peroxidation and the production of reactive oxygen species (210), which may be a direct effect of activated artemisinin or occur via the redox capabilities of alkylated haem adducts (211). Haem is commonly associated with membranes *in vivo* and may be responsible for initiating this peroxidation process (210). Reactivity with membrane associated proteins, such as transporters, may also contribute to artemisinin induced membrane damage (166).

The biological significance of other putative artemisinin targets remains controversial. The importance of the mitochondria as a target was initially described in a yeast model (212) and later confirmed in *P. berghei* (177). Mitochondrial dysfunction is thought to be caused by artemisinin-derived reactive oxygen species that induce mitochondrial membrane lipid peroxidation (177, 213). Artemisinin-mediated oxidative insult may also damage DNA (202, 214, 215), which reportedly induces a DNA damage response in artemisinin-treated parasites (216).

Compelling evidence exists supporting the theory that activated artemisinins exert their rapid and specific toxicity against the *Plasmodium* parasite through indiscriminate reactivity with an array of susceptible intracellular targets. Although direct inhibition of specific parasite targets has been proposed, it is generally accepted that iron-dependent activation is a prerequisite for antimalarial activity. The biological relevance and role of each of these targets in artemisinin-mediated parasite killing has not been determined. However, investigations into artemisinin-induced metabolic dysregulation in *P. falciparum* directly implicates a number of essential biochemical pathways (187, 188).

### 1.5.4 Artemisinin resistance

Artemisinin resistance in *P. falciparum* was first reported in 2008 in clinical isolates from the Pailin province of western Cambodia, a region synonymous with the emergence of multi-drug resistant parasites (143). Retrospective analysis showed that resistance likely emerged in Cambodia prior to 2001 and the widespread deployment of ACTs (144). Starting with the epicentre in western Cambodia, resistant parasites spread or emerged independently (217) throughout the Greater Mekong Subregion and are now firmly established in Vietnam (218, 219), Laos (218), Thailand (218, 220) and eastern and central Myanmar (218). Resistance is emerging in northwestern Myanmar along the border with India (221) and in China at the Myanmar-China border (222, 223). Work is currently under way as part of the Tracking Resistance to Artemisinin Collaboration to assess whether the resistance phenotype has travelled further westward into Bangladesh and India.

Clinical artemisinin resistance manifests as delayed parasite clearance (clearance half-life > 5 h) after ACT treatment (218). Although delayed parasite clearance following an ACT does not always lead to treatment failure, high failure rates are commonly observed in areas of the Greater Mekong Subregion where there is concomitant resistance to artemisinin and the partner drug (144). Periodic examination of blood smears shows that artemisinin resistant *P. falciparum* parasites persist in the blood of infected individuals even after a standard 3-day treatment with a usually curative ACT. Parasite clearance times were found to correlate with increased *in vitro* survival of early ring stage parasites (0-3 h post invasion) that are exposed to a 6 h pulse of DHA, mimicking the short *in vivo* half-life of artemisinins (224, 225). More recently, a genetic molecular marker for artemisinin resistance was mapped to the *P. falciparum Kelch13 (K13)* locus (226) and this gene has been associated with *in vitro* and *in vivo* resistance to artemisinins (217, 227).

Multiple single nucleotide polymorphisms have been found throughout *K13* (228-231). However, only a small proportion of the more than 200 known *K13* alleles are associated with resistance (218, 223, 224, 227) and only a handful of these are validated by *in vitro* data as having a causal role in artemisinin resistance in Southeast Asian field isolates. These include the Y493H, R539T, I543T and C580Y mutations (144, 224, 226, 227). Low frequency nonsynonymous *K13* mutations also exist in Africa but are not associated with clinical or *in vitro* artemisinin resistance (231-235). Further investigations are needed to confirm whether a newly identified African *K13* polymorphism (M579I) from *P. falciparum* parasites that exhibit a delayed *in vivo* clearance phenotype and increased *in vitro* ring stage survival, represents emergence of artemisinin resistance in Africa (236).

It is thought that *K13*-mutant parasites have enhanced cytoprotective capabilities (including enhanced antioxidant defence and stress response systems) that allow them to overcome short-term artemisinin-induced damage (148, 237). There is an upregulation of mRNA expression for genes involved in protein folding and repair, especially unfolded protein response pathways, as well as regulators of the cellular response to oxidative stress (238). Other proteins also show an association with resistance and may provide a genetic background in which *K13* mutations are more likely to emerge (230, 239). Reduced abundance of haemoglobin-derived peptides was also linked to artemisinin resistance (237).

Artemisinin resistance presents a major threat to malaria control efforts, even more so if it emerges in Africa. To prevent this from occurring, and to prevent the development of high-level artemisinin resistance, the WHO is now recommending malaria be eliminated from the Greater Mekong Subregion. This will require new antimalarial drugs that overcome the clinical limitations of currently used artemisinin-based therapies.

# 1.6 SYNTHETIC PEROXIDE ANTIMALARIALS

The peroxide bond of artemisinin provided a template for the design of new, synthetic peroxide-based antimalarials that are cheap, easy to manufacture and not limited by the physicochemical and pharmacokinetic liabilities of artemisinin derivatives. A major advance in the development of synthetic peroxide antimalarials was the discovery of simplified trioxanes, based on artemisinin, which lack a lactone ring but retain antimalarial potency (240-242). These simplified trioxanes revealed that extensive structural modifications are possible without compromising antimalarial activity and led to the development of a diverse group of synthetic peroxides that bear no structural resemblance to artemisinin or its semisynthetic derivatives (apart from the peroxide bond) but have equivalent antimalarial potency (241).

Structural modifications significantly influence the antimalarial activity of synthetic peroxides. There appears to be a positive correlation between antimalarial activity and lipophilicity, which can be problematic for developing compounds with the required drug-like physicochemical properties that allow good oral absorption and bioavailability (243). A breakthrough for synthetic peroxide antimalarials came with the development of novel dispiro-1,2,4-trioxolanes that have an optimal balance between potent antimalarial activity, appropriate biopharmaceutical properties and inexpensive synthesis (244).

## 1.6.1 1,2,4-trioxolane antimalarials

The discovery and development of highly potent, fully synthetic dispiro-1,2,4-trioxolane antimalarials, collectively known as ozonides, was made possible by the invention of a novel cross-ozonolysis reaction (Grisbaum coozonolysis) (245) that allowed economically feasible and scalable synthesis of tetra-substituted 1,2,4-trioxolanes (secondary ozonides) (246). Systematic examination of a range of 1,2,4-trioxolanes revealed many compounds with equivalent or superior *in vitro* activity to the semisynthetic artemisinin derivatives (243, 244,

246). The active trioxolanes are characterised by an ozonide ring flanked by one adamantane and a cyclohexane substituent, generally at the 4-position. The cyclohexane was substituted with various side chains at the 8' position to improve antimalarial and pharmaceutical properties (246).

The most promising trioxolane to emerge from the first-generation series of ozonides was the amino amide OZ277 (later known as RBx11160 or arterolane, Figure 5), which was selected as a developmental candidate primarily based on its attractive toxicological profile and good *in vitro* and *in vivo* efficacy (244). OZ277 was found to be fast acting, have comparable activity to clinically-used semisynthetic artemisinins in *in vitro* assays against various *P. falciparum* strains and be highly effective following *in vivo* oral dosing in *P. berghei*. A single 3 mg/kg oral dose of OZ277 was more active than DHA and artemether when measured 72 h post-dose and required a significantly lower effective dose to induce a 50%, 90% and 99% reduction in *P. berghei* parasitaemia. In addition, OZ277 treatment produced a much longer time to recrudescence relative to some artemisinin derivatives (244) and it had potent activity against a range of African field isolates (247).

OZ277 advanced to clinical trials based on an acceptable biopharmaceutical profile, potent antimalarial activity and low potential for toxicity. In clinical trials, OZ277 with piperaquine administered as a single daily dose for three days, had similar activity to that of standard artemether-lumefantrine combination therapy (248). However, in healthy volunteers, the OZ277 half-life was only 2- to 3-fold longer than that of DHA (249) and when administered as monotherapy, infected patients exhibited a higher clearance and reduced OZ277 exposure relative to non-infected volunteers (250, 251). The mechanistic basis for the *in vivo* clearance of OZ277 was thought to be due to CYP450-mediated metabolism that results in inactive adamantane-hydroxylated metabolites (252), however, this only partially contributes to OZ277 clearance (129).

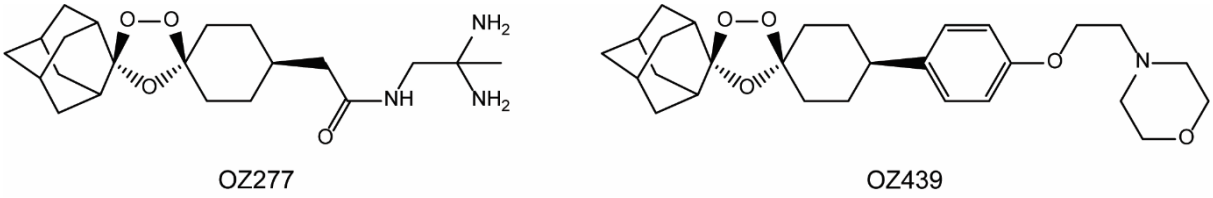


**Figure 5:** Chemical structures of the first- and second-generation ozonides, OZ277 and OZ439, respectively.

The reaction of ozonides with endogenous sources of reduced iron in blood and other tissues was proposed to represent a significant *in vivo* clearance pathway for OZ277 and other first-generation ozonides (129). The first-generation series of ozonides, like OZ277, are highly susceptible to chemical degradation by inorganic iron sources *in vitro* (253) and rapidly degrade when incubated with non-infected rat or human blood at 37°C, forming degradation products consistent with cleavage of the peroxide bond (129). The degradation rate increases approximately 5-fold in the presence of low levels of parasite infection and was proposed as a plausible basis for reduced OZ277 exposure in the plasma of malaria-infected patients relative to healthy volunteers (251, 254). A design strategy aimed at stabilising the peroxide bond to iron-mediated degradation, whilst maintaining the necessary reactivity required for antimalarial activity, was implemented to improve the *in vivo* exposure profile of the ozonides. This eventually led to the development and selection of the next-generation clinical candidate, OZ439 (Figure 5) (129).

Ozonide susceptibility to iron-mediated degradation depends on the chemical structure. Quantum mechanical studies with the second-generation ozonide precursor, OZ27, indicated that the *cis*-8'-phenyl group of the second-generation compounds reduced steric accessibility of the peroxide bond to iron by providing greater steric shielding than the *cis*-8'-alkyl group of first-generation ozonides (255). As a result, ozonides that contain a *cis*-8'-phenyl group, like OZ439, were reported to be up to 50-fold more stable to iron-mediated degradation compared

to the first-generation compounds (129). Consistent with these findings, OZ439 was found to be 15- to 20-fold more stable in non-infected rat and human blood, respectively, compared to OZ277 (129). OZ439 exhibited only a minor increase in degradation rate and was more than 20-fold more stable than OZ277 in the presence of *P. falciparum*-infected human RBCs (1% parasitaemia) suspended in plasma at 45% Hct (129).

An overall improvement in oral bioavailability, and enhanced stability of the OZ439 peroxide bond in blood, translated to a superior blood concentration versus time profile relative to OZ277 following a 3 mg/kg oral dose in rats (129). Reduced iron-mediated clearance also resulted in a prolonged half-life (more than 20 h) after oral dosing in rats (129), which was significantly longer than the semisynthetic artemisinins (approximately 30 min) and the first-generation ozonide, OZ277 (approximately 1 h) (244).

When tested in a *P. berghei* model of malaria, the *in vivo* efficacy of OZ439 was found to be superior to a range of drugs from different antimalarial classes. Oral treatment with OZ439 rapidly reduced parasite burden in infected mice, was curative following a single oral dose (30 mg/kg) and parasitaemia was undetectable up to 30 days post infection (single oral 100 mg/kg dose) (129). In contrast to other peroxide antimalarials (synthetic and semisynthetic), OZ439 was also found to display prophylactic activity superior to the benchmark chemoprophylactic drug, mefloquine (129). *In vitro*, OZ439 was active against all blood-stages of *Plasmodium* (129), including sexual stage gametocytes (96), displaying comparable levels of parasite growth inhibition to the clinically-used artemisinin derivatives.

Unlike its first-generation predecessor, the exposure profile of OZ439 is similar in both malaria infected patients and healthy volunteers and demonstrates an extended *in vivo* half-life of approximately 46-62 h (256, 257). OZ439 is also associated with minimal side effects (129, 257) making it an ideal candidate to be part of a single dose antimalarial treatment. Although

long half-life peroxides may be more likely to select for resistance than short-acting derivatives (258), this risk should be minimised by combining OZ439 with an appropriate partner drug. OZ439 was originally being developed in combination with piperaquine but is now in advanced stages of clinical development with ferroquine (ClinicalTrials.gov Identifier: NCT02497612).

#### 1.6.1.1 Clinical applications

The first-generation ozonide OZ277 became the first synthetic peroxide antimalarial to reach the market when it was approved for use as a fixed dose combination with piperaquine (Synriam$^{TM}$) in India. Despite having lower exposure levels in infected patients relative to healthy individuals, the pharmaceutical company Ranbaxy continued its development and showed that the OZ277-piperaquine combination is as safe and effective as artemether-lumefantrine when used as a 3-day treatment (248).

OZ439 is the first long half-life peroxide antimalarial and offers the potential for a single dose oral cure of uncomplicated malaria when combined with an effective partner drug (129). In clinical trials, OZ439 was found to be effective against *P. falciparum* and *P. vivax* infection and there was no correlation between *K13* genotype and rate of parasite killing, suggesting longer lived peroxides, such as OZ439, may be less affected by the mechanisms that mediate artemisinin resistance (256). In a subsequent multi-site study in Africa and Vietnam, efficacy of a single dose treatment with OZ439 and piperaquine was approximately 70% at day 28 post dose (259). Efficacy was considerably lower in Vietnamese patients, who also show a correlation between parasite clearance time and *K13* genotype (259). However, the sensitivity of *P. falciparum* parasites to the partner drug, piperaquine, was not reported in this study. Larger cohorts are required to assess whether clinical artemisinin cross-resistance with OZ439 is a potential problem in the field. Phase IIb clinical trials in combination with

ferroquine, which is active against chloroquine, mefloquine and piperaquine resistant *P. falciparum* (260-262), and has never been clinically deployed as single therapy, are ongoing.

## 1.6.2 Mechanism of action

The ozonide antimalarials display similar clinical efficacy to DHA, however their antimalarial mechanism of action has been less extensively studied and is currently only poorly defined. Given that OZ439 is in advanced stages of clinical development and artemisinin resistance is rapidly spreading, this compound represents a potential alternative for the artemisinin-based therapies. Like the artemisinins, selective activation of the peroxide bond within the parasite likely leads to specific parasite toxicity. The presence of the peroxide bond indicates the ozonides and artemisinins may act via similar mechanisms, and they have been found to be antagonistic *in vitro* (263). The antimalarial mechanism is generally thought to involve non-specific alkylation of intraparasitic targets following iron-mediated activation of the peroxide bond. Accordingly, significant work has gone into detailing the role of iron-mediated reactivity in the antimalarial mode of action of ozonides.

### 1.6.2.1 Peroxide bond activation

Ozonide antimalarial activity is peroxide bond dependent. Non-peroxide isosteres are inactive (246, 264), suggesting that, like the artemisinins, reductive cleavage of the peroxide bond by free iron or haem is a pre-requisite for activity. The importance of iron-mediated activation was demonstrated using the iron chelators DFO and DFP, which was found to moderately antagonise the activity of a simple *cis*-8'-alkyl ozonide (when ozonide and chelator pressure was maintained throughout the parasite lifecycle) and prevent ozonide accumulation within parasites (167). These studies indicated that chelatable sources of parasite iron may play a role in the activation and subsequent covalent modification of parasite targets. Inorganic Fe(II) iron has been shown to induce reductive cleavage of the peroxide bond of simple 1,2,4-

trioxolanes by preferential attack of the O1 oxygen atom adjacent to the cyclohexane ring, which is less sterically hindered than the O2 atom next to the adamantane substructure (265). The resulting oxygen-centred radicals rearrange by β-scission to form carbon-centred radicals that were captured using the radical trapping agent 4-oxo-TEMPO (253). *In vitro*, TEMPO analogues antagonise OZ277 activity (266), presumably by reacting with the toxic ozonide-derived radicals that are thought to damage intraparasitic molecules.

Examination of ozonide degradation rates in the presence of inorganic Fe(II) iron showed no direct correlation between biological activity and iron reactivity (253). While ozonides that are unreactive with iron are devoid of antimalarial activity, iron reactivity alone doesn't guarantee activity (253, 267), suggesting other factors are also important. Like the artemisinins, the abundance of haemoglobin-derived haem within the parasite is thought to play a role in activation of the ozonide peroxide bond. Ozonides are stable in the presence of undigested haemoglobin (268) but react rapidly with free haem in a simplified test system (269). Furthermore, the extent of haem alkylation was found to correlate with *in vitro* activity against *P. falciparum*. Within the parasite, chemical inhibition of haemoglobin digestion using the cysteine protease inhibitor E64d completely abrogated short-pulsed OZ277- and OZ439-mediated antimalarial activity, whereas chelation of free iron using the iron chelator bipyridyl had a negligible impact on short-pulsed ozonide activity (270). These studies indicated that, like the artemisinins, a haemoglobin digestion product, most likely free haem, is the biologically relevant iron source responsible for peroxide-bond activation within the parasite. The observation that ozonide activity correlates with parasite lifecycle stages when haemoglobin digestion is most active also supports this hypothesis (270).

#### 1.6.2.2 Stage- and time-dependent antimalarial activity

A complex relationship between parasite stage, drug concentration and exposure time appears to govern ozonide activity (270-272). Like the artemisinins, the exposure of tightly synchronised parasites to short-pulsed ozonide treatment was found to distinguish stage- and time-dependent differences in antimalarial activity (273). Although the ozonides display activity against all stages of the asexual lifecycle (270-272), parasites are most sensitive to short-pulsed treatment during the trophozoite stage when there is a higher level of readily available haemoglobin-derived haem for peroxide bond activation (270). Ozonide-mediated parasite killing was also found to be highly dependent on the duration of drug exposure similar to the artemisinins (145) and differences in stage-specific sensitivity could be overcome by extending the drug pulse duration. Mid-ring stage parasites were relatively insensitive to 1-3 h ozonide pulses but exhibited significantly improved sensitivity when the duration of exposure was increased to 6 h or longer (270-272). Extending the duration of ozonide treatment reduced the difference in sensitivity between relatively insensitive mid-ring stage parasites and highly susceptible trophozoite stage parasites (270-272).

The temporal response to ozonide treatment was found to vary depending on ozonide structure, such that the time required to render parasites 50% non-viable was extended for OZ439 compared to OZ277 (270). Consistent with differential blood stability between first- and second-generation ozonides (129), it is likely that the *cis*-8'-phenyl substituent of OZ439 restricts access to the peroxide bond to a greater extent than the less bulky *cis*-8'-alkyl group of OZ277, resulting in slower haem-mediated activation and lower levels of parasite death at short exposure times. It was also proposed that differences in toxicity of the activated form of the drug and drug physicochemical properties have a role in time-dependent variations in activity between ozonides (270).

*K13*-mediated artemisinin resistance was found to be associated with an enhanced cell stress response during the ring stage of the parasite asexual lifecycle (148). This allowed resistant parasites to overcome short-pulsed treatment with an artemisinin derivative and when tested *in vitro*, manifested as increased parasite survival in the next asexual lifecycle (224). For both OZ277 and OZ439, the duration of exposure necessary for effective *in vitro* killing of artemisinin resistant *K13*-mutant parasites was greater than in isogenic wildtype parasites, indicating a level of cross-resistance between the artemisinins and both first- and second-generation ozonide antimalarials (270). Interestingly, other studies have shown that *K13* mutations only confer *in vitro* cross-resistance to OZ277, and mutant parasites remain susceptible to short-pulsed OZ439 treatment (274-276). While it is possible that OZ439 is protected from *K13*-mediated cross-resistance, differential ozonide susceptibility may also reflect subtle variations in experimental protocols between the studies (270, 274-276). Extending the duration of *in vitro* ring stage exposure was found to render *K13* resistant parasites susceptible to ozonide treatment (270, 277) and simulations of *in vivo* response suggested the prolonged half-life of OZ439 will result in significantly improved efficacy against artemisinin resistant parasites (270).

The degree of *in vitro* susceptibility is dependent not just on the duration of drug exposure, but also on the type of *K13* mutation. When tested against a panel of artemisinin resistant and sensitive culture adapted isolates from Cambodia, as well as reference lines (C580Y, R539T, I543T), the level of cross-resistance with ozonides was found to be greatest in parasites with the I543T mutation (276). Interestingly, parasites with the C580Y and R539T mutations displayed no apparent cross-resistance to a 6 h pulse with OZ439, while I543T mutants displayed significantly increased ring stage survival.

### 1.6.2.3 Intraparasitic targets

It is generally accepted that haem-mediated reductive activation of the ozonide peroxide bond forms highly reactive radical species that are responsible for mediating antimalarial activity against the *Plasmodium* parasite. Like the artemisinins, ozonide-derived radicals are proposed to indiscriminately damage parasite components by inducing oxidative damage or covalently reacting with intracellular targets (266, 278). The promiscuous targeting effect of activated ozonides is thought to disrupt a variety of essential parasite functions, which leads to rapid death of the malaria parasite (278).

A variety of essential parasite proteins have been proposed as potential targets of the ozonide antimalarials. The parasite SERCA orthologue, *Pf*ATP6, was initially described as a potential target of the artemisinins (166) and was also tested for specific inhibition by the synthetic ozonide antimalarial OZ277 (263). OZ277 was found to be a poor inhibitor of *Pf*ATP6, indicating other protein targets may be more important mediators of activity. Parasite stage- and concentration-dependent alkylation of a range of *P. falciparum* proteins by ozonide-derived radicals was previously described using monoclonal antibodies for OZ277 and OZ439 (279). Protein alkylation, as detected by distinct bands on western blots, was found to be ozonide specific, indicating OZ439 and OZ277 may alkylate distinct protein targets within parasites. The identity of the protein targets detected and their relevance to ozonide antimalarial activity were not determined in this study. Although previous investigations have indicated that the ozonide mode of action involves an irreversible reaction with parasite components (167, 266), this study represented the first confirmation that the ozonides, like the artemisinins, can form adducts with parasite proteins.

An array of potential ozonide protein targets were recently identified in *P. falciparum* trophozoite stage parasites (278) by applying the same chemical proteomics methodology

previously utilised to identify artemisinin protein targets (176, 185). More than 60 protein targets were identified using a clickable ozonide probe based on the ozonide core structure. The identified alkylated proteins are involved in essential parasite processes, including glycolysis, haemoglobin digestion, antioxidant defence, protein synthesis and protein stress pathways and are localised to the parasite digestive vacuole and cytosol (278). The diverse alkylation profile suggested ozonide parasiticidal activity involves disruption to a number of critical biochemical pathways, however, untargeted metabolomic profiling of parasites treated with OZ277 and OZ439 revealed no major alterations in parasite metabolism (280). Like the artemisinins, approximately 70% of the detected ozonide protein targets have a glutathione binding motif and the alkylation profile was found to share more than 80% similarity with a corresponding artemisinin probe, suggesting a common, promiscuous targeting mechanism of action (278). It is important to note that this study used lethal drug concentrations for relatively long exposure times, which could promote non-specific alkylation of proteins unrelated to the toxic insult responsible for parasite killing. A significant proportion of the proteins identified are also commonly detected as the most abundant proteins in untargeted proteomic-based studies of trophozoite stage parasites (281-283). Further work is needed to determine the functional importance of the identified proteins to ozonide antimalarial activity.

Similar to the artemisinins, activated ozonides have been shown to alkylate small molecules *in vitro*, including radical trapping agents (253, 266) and reduced haem (269). Unlike the artemisinins (184, 200, 201), *in vitro* alkylation of thiol containing molecules, such as cysteine and glutathione, have not been reported. The reaction with biological haem within the parasite has been proposed to lead to ozonide activation (270). Given the high abundance of haem within the parasite and its likely close proximity with activated ozonide, haem represents a potential biologically relevant target. While the alkylated haem adduct has not been detected in parasites, in a simplified test system, ozonide alkylation of haem correlated

with antimalarial activity (269, 284). The haem alkylation efficiency of structurally similar 1,2,4-trioxolanes with varying levels of antimalarial activity was determined by measuring the extent of haem loss after 30 s under reducing conditions (269). Trioxolanes with a 50% inhibitory concentration ($IC_{50}$) less than 20 nM exhibited a haem alkylation efficiency greater than 60%, whereas less active 1,2,4-trioxolanes ($IC_{50}$ more than 100 nM) displayed a haem alkylation efficiency below 40% (269). Whether ozonide alkylation of biological haem or other small molecules, such as thiols, is an important process in the antimalarial mechanism of action of the ozonides within *P. falciparum* parasites has not been thoroughly explored.

The biological activity of ozonides may also involve damage to lipids and membrane structures within the parasite. Fluorescently labelled 1,2,4-trioxolane probes have been shown to accumulate within digestive vacuole-associated neutral lipid bodies, which are thought to be involved in haemozoin crystallisation (208). As haemoglobin-derived haem is the most likely iron source responsible for peroxide bond activation (270), it has been proposed that the ozonides are activated by haem associated with neutral lipid bodies or that ozonide-derived haem adducts accumulate within the neutral lipid bodies, promoting oxidative damage of membrane lipids (208). Ozonide-mediated peroxidation of phosphatidylcholine, one of the major constituents of the *P. falciparum* digestive vacuole membrane (48), occurred *in vitro* following reductive activation by iron (285). Trioxolane-dependent membrane lipid peroxidation occurred at all stages of parasite asexual development (208), indicating damage to vacuolar membrane integrity may contribute to the mechanism of ozonide action (207, 208).

The prevailing model for ozonide antimalarial activity (Figure 6) is that haemoglobin-derived free haem mediates reductive activation of the ozonide peroxide bond giving rise to toxic carbon-centred radicals that indiscriminately damage vital intraparasitic components, including lipids, haem and a range of proteins, by direct alkylation or oxidative insult. This promiscuous targeting effect likely corrupts multiple biochemical pathways that are important

for parasite survival, however, the functional changes to parasite metabolism and the hierarchy of drug-induced dysregulation are not well understood. Various methods can be used to help identify drug targets and molecular mechanisms of action, including systems biology-based approaches like proteomics and metabolomics, which may be particularly informative for drugs that have a multifaceted mode of action, such as the ozonides. A detailed review of metabolomics principals and the application of metabolomics to the investigation of antiparasitic drug mechanisms of action is provided in Giannangelo *et al*. 2016 (286) (Appendix 1).

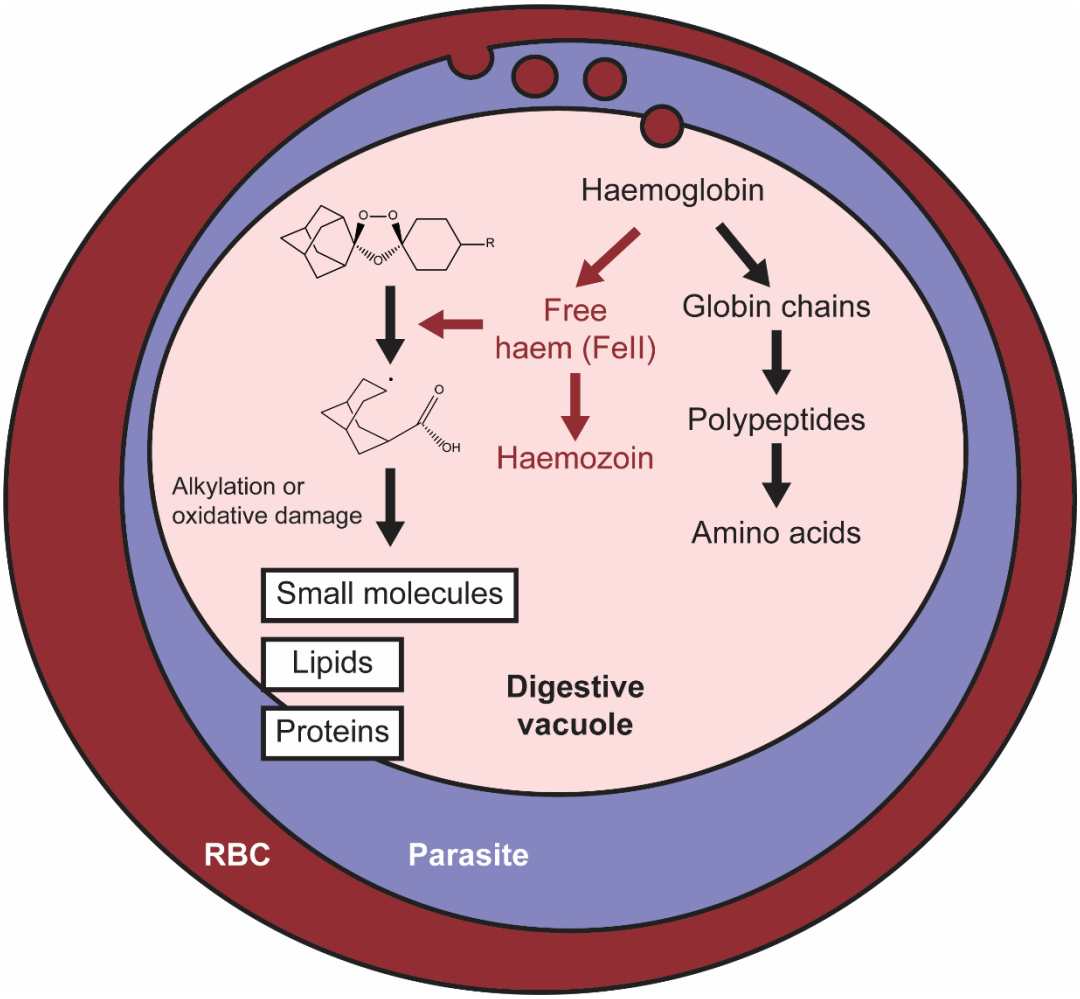


**Figure 6:** Prevailing model for ozonide action within *P. falciparum* trophozoite stage parasites. Haemoglobin-derived free haem activates the ozonides by cleavage of the peroxide bond, producing toxic radical species that rearrange to form carbon-centred radicals. These free radicals mediate antimalarial activity by indiscriminately reacting with a range of intracellular targets, including proteins, lipids and small molecules, ultimately leading to parasite death.

## 1.7 AIMS OF THIS THESIS

A fundamental hypothesis of the work presented in this thesis is that haem-mediated activation of ozonide antimalarials gives rise to toxic radical species and these highly reactive intermediates are responsible for activity in the malaria parasite. The ozonide-derived radicals generated following activation likely react with susceptible parasite components proximal to the site of activation, whether they be proteins, lipids or metabolites. The available evidence indicates alkylation of parasite proteins is involved in ozonide antimalarial activity (278, 279), while examination of the kinetics of parasite *in vitro* response to ozonide treatment confirmed the importance of drug exposure time on action (270-272). Other than proteins, ozonides are also capable of alkylating small molecules such as haem (269, 284) and radical trapping agents (253, 266). In a simplified system, haem alkylation was correlated with *in vitro* antimalarial activity. However, the biological importance of ozonide reactivity with haem, or other small molecule species within a complex parasite environment has not been thoroughly explored. It is also important to note that many mechanistic studies that aim to identify molecular targets and biochemical pathways of drug action (185, 187, 188, 278, 280) have used *in vitro* culture conditions (parasitaemia and haematocrit) that do not reflect the culture environment used to measure drug activity. Whether this impacts ozonide activity or behaviour in these artificial conditions has not been well studied.

For drugs that have a promiscuous targeting effect, such as the ozonides, characterisation of the temporal response to treatment may facilitate differentiation of the initial targets and biochemical pathways perturbed by drug treatment from downstream molecular events (187). Given the proposed non-specific molecular targets of activated ozonides, an untargeted, systems-based methodology is an ideal approach to interrogate their mode of action and dissect the drug-induced hierarchy of dysregulation that occurs within the parasite.

Therefore, the investigations in this thesis were designed with the primary goal of enabling a time-dependent and unbiased characterisation of the biologically important intraparasitic targets and parasite biochemical pathways involved in ozonide antimalarial activity.

The ozonides are a chemically diverse group of compounds with potent antimalarial activity, low toxicity and some have a superior pharmacokinetic profile compared to the semisynthetic artemisinins. OZ277 (arterolane) was the first synthetic peroxide antimalarial to make it to market and is currently approved for use in India as a fixed dose combination with piperaquine (Synriam$^{TM}$). OZ439 (artefenomel) is one of the most advanced antimalarial drug candidates currently in clinical development and the first long half-life peroxide antimalarial. Remarkably, OZ439 in combination with a suitable partner drug offers hope for a single-dose oral cure of malaria infection in humans (129). Given the rapid spread of artemisinin resistance and its advanced position in the clinical development pipeline, OZ439 is a potential alternative to the front-line artemisinin-based antimalarials that are currently in use. In this thesis, the first- and second-generation ozonides, OZ277 and OZ439, respectively, were selected for detailed biochemical analysis.

The first specific aim was to characterise the antimalarial activity and drug stability profiles of OZ277 and OZ439 under *in vitro* conditions used in mechanistic studies (Chapter 2). Haem-mediated activation of the ozonide peroxide bond leads to degradation of the parent compound, therefore, degradation and antimalarial activity are intimately related. Iron-mediated reactivity is also a mechanism for *in vivo* ozonide clearance and increased ozonide degradation occurs in the presence of parasitised cells compared to non-infected RBCs alone (129). Many biochemical and biomimetic approaches have been utilised to identify the molecular targets and biochemical pathways perturbed in response to peroxide treatment (176, 185, 187, 278). For optimal assay performance, many of these *in vitro* investigations require specific conditions, such as high parasitaemia (185, 278, 280), which differ considerably from

those used to measure *in vitro* activity. Given peroxide bond activation is mediated by a parasite driven process (haemoglobin digestion) and is essential for activity, accurate interpretation of the biological relevance of results from these *in vitro* experiments relies on a clear understanding of the interplay between parasite-mediated drug degradation and biological activity under varying experimental conditions. Therefore, a major goal was to accurately define a set of conditions for mechanistic-based studies with OZ277 and OZ439 by performing a quantitative assessment of parasite-mediated drug degradation and *in vitro* antimalarial activity at varying levels of parasitaemia, lifecycle stages and in the presence of selected inhibitors.

The second major aim was to investigate the molecular targets and sub-cellular localisation pattern of selected ozonide antimalarials using the previously defined mechanistic conditions (Chapter 3). Once activated, ozonides alkylate an array of *P. falciparum* proteins in an apparently indiscriminate manner (278, 279). The second-generation ozonide, OZ439 (*cis*-8'-phenyl substituted), and its first-generation predecessor, OZ277 (*cis*-8'-alkyl substituted), differentially impact protein alkylation profiles in parasites (279), indicating intraparasitic protein alkylation may be ozonide specific. Activated ozonides also have the potential to covalently modify small molecules *in vitro*, including radical trapping agents (253, 266) and reduced haem (269). The reaction with biological haem generates ozonide-derived radicals that likely react with susceptible parasite targets proximal to the site of activation, independent of their chemical class. Therefore, in Chapter 3, the alkylation profile of non-protein targets was assessed in *P. falciparum* parasites using untargeted methods and the sub-cellular localisation pattern of ozonide-derived protein adducts visualised in *P. falciparum* infected RBCs.

Following haem-mediated activation and subsequent alkylation of intraparasitic molecules, the biochemical pathways perturbed by ozonide treatment that lead to parasite death

are not well characterised. Therefore, the next specific aim was to investigate the temporal biochemical response of *P. falciparum* parasites treated with OZ277 and OZ439 (Chapter 4). The ozonide alkylation profile (278) indicates proteins in a number of essential parasite molecular pathways are affected in response to drug treatment, making systems-based approaches such as metabolomics and proteomics, attractive tools for studying the mechanism of action of ozonides. Untargeted metabolomics and proteomics techniques have been successfully used to study mechanisms of action of novel and existing drugs in parasites, including *P. falciparum* (187, 188, 280, 287-291). A comprehensive multi-omics-based approach allowed untargeted observation of drug-dependent changes in parasite biochemistry over time, enabling the identification of early ozonide-induced effects to be distinguished from a non-specific death phenotype.

In the final chapter, the methods used in previous chapters were applied to the investigation of ozonide activity in selected *K13*-mutant, artemisinin resistant, and *K13*-wildtype, artemisinin sensitive, parasite lines. Emerging resistance to artemisinin-based therapies in the Greater Mekong Subregion is a threat to worldwide malaria control efforts. Resistant parasites with a *K13* mutation are thought to temporarily overcome artemisinin-induced insult during the ring stage of the asexual developmental cycle by mounting an enhanced stress response (148). The resistance phenotype was shown to be associated with functional changes in proteostasis and oxidative stress pathways (237, 238) that are thought to make the parasite more resilient to drug-induced oxidative damage. Resistant parasites have been shown to have reduced abundance of haemoglobin-derived peptides, indicating these parasites may have impaired haemoglobin uptake or digestion (237), potentially producing less haemoglobin-derived haem that is necessary for peroxide bond activation. Given ozonides (in particular OZ439) are potential alternatives for the artemisinins, the final aim was to investigate the biochemical response of paired *K13*-mutant resistant and *K13*-wildtype sensitive parasites

to ozonide treatment, and to assess ozonide stability, as a marker of peroxide bond activation, in the same parasite lines (Chapter 5).

The research detailed in this thesis works towards the ultimate goal of understanding the mechanism of action of ozonide antimalarials in *P. falciparum*. Knowledge of the biologically important molecular targets and biochemical pathways vital for ozonide action will help inform the appropriateness of ozonides to treat artemisinin resistant *P. falciparum* infections, aid in the selection of appropriate partner drugs for combination therapy, monitor for efficacy and resistance, as well as benefit the development of antimalarial drugs in the future.

## 1.8 REFERENCES


1. White NJ, Pukrittayakamee S, Hien TT, Faiz MA, Mokuolu OA, Dondorp AM. 2014. Malaria. Lancet 383:723-735.
2. WHO. 2017. World Malaria Report 2017. World Health Organisation, Geneva.
3. WHO. 2016. World Malaria Report 2016. World Health Organisation, Geneva.
4. Guyatt HL, Snow RW. 2001. Malaria in pregnancy as an indirect cause of infant mortality in sub-Saharan Africa. Trans R Soc Trop Med Hyg 95:569-576.
5. WHO. 2014. World Malaria Report 2014. World Health Organisation, Geneva.
6. Gething PW, Smith DL, Patil AP, Tatem AJ, Snow RW, Hay SI. 2010. Climate change and the global malaria recession. Nature 465:342-345.
7. Greenwood BM, Bojang K, Whitty CJ, Targett GA. 2005. Malaria. Lancet 365:1487-1498.
8. Caminade C, Kovats S, Rocklov J, Tompkins AM, Morse AP, Colón-González FJ, Stenlund H, Martens P, Lloyd SJ. 2014. Impact of climate change on global malaria distribution. Proc Natl Acad Sci U S A 111:3286-3291.
9. Roberts L, Enserink M. 2007. Malaria. Did they really say ... eradication? Science 318:1544-1545.
10. Tuteja R. 2007. Malaria− an overview. FEBS J 274:4670-4679.
11. Dondorp AM, Kager PA, Vreeken J, White NJ. 2000. Abnormal blood flow and red blood cell deformability in severe malaria. Parasitol Today 16:228-232.
12. Cowman AF, Healer J, Marapana D, Marsh K. 2016. Malaria: biology and disease. Cell 167:610-624.
13. Pongponratn E, Turner GD, Day NP, Phu NH, Simpson JA, Stepniewska K, Mai NT, Viriyavejakul P, Looareesuwan S, Hien TT, Ferguson DJ, White NJ. 2003. An ultrastructural study of the brain in fatal *Plasmodium falciparum* malaria. Am J Trop Med Hyg 69:345-359.
14. Cunnington AJ, Walther M, Riley EM. 2013. Piecing together the puzzle of severe malaria. Sci Transl Med 5:211-218.
15. Karunaweera ND, Grau GE, Gamage P, Carter R, Mendis KN. 1992. Dynamics of fever and serum levels of tumor necrosis factor are closely associated during clinical paroxysms in *Plasmodium vivax* malaria. Proc Natl Acad Sci U S A 89:3200-3203.
16. Yamauchi LM, Coppi A, Snounou G, Sinnis P. 2007. *Plasmodium* sporozoites trickle out of the injection site. Cell Microbiol 9:1215-1222.

17. Tavares J, Formaglio P, Thiberge S, Mordelet E, Van Rooijen N, Medvinsky A, Ménard R, Amino R. 2013. Role of host cell traversal by the malaria sporozoite during liver infection. J Exp Med 210:905-915.
18. Bannister L, Dluzewski A. 1990. The ultrastructure of red cell invasion in malaria infections: a review. Blood Cells 16:257-292.
19. Lin CS, Uboldi AD, Epp C, Bujard H, Tsuboi T, Czabotar PE, Cowman AF. 2016. Multiple *Plasmodium falciparum* merozoite surface protein 1 complexes mediate merozoite binding to human erythrocytes. J Biol Chem 291:7703-7715.
20. Cowman AF, Crabb BS. 2006. Invasion of red blood cells by malaria parasites. Cell 124:755-766.
21. Josling GA, Llinas M. 2015. Sexual development in *Plasmodium* parasites: knowing when it's time to commit. Nat Rev Micro 13:573-587.
22. Bruce M, Alano P, Duthie S, Carter R. 1990. Commitment of the malaria parasite *Plasmodium falciparum* to sexual and asexual development. Parasitology 100:191-200.
23. Loria P, Miller S, Foley M, Tilley L. 1999. Inhibition of the peroxidative degradation of haem as the basis of action of chloroquine and other quinoline antimalarials. Biochem J 339 363-370.
24. Francis SE, Gluzman I, Oksman A, Knickerbocker A, Mueller R, Bryant M, Sherman D, Russell D, Goldberg D. 1994. Molecular characterization and inhibition of a *Plasmodium falciparum* aspartic hemoglobinase. EMBO J 13:306-317.
25. Rosenthal PJ. 1995. *Plasmodium falciparum*: effects of proteinase inhibitors on globin hydrolysis by cultured malaria parasites. Exp Parasitol 80:272-281.
26. Rosenthal PJ, McKerrow JH, Rasnick D, Leech JH. 1989. *Plasmodium falciparum*: inhibitors of lysosomal cysteine proteinases inhibit a trophozoite proteinase and block parasite development. Mol Biochem Parasitol 35:177-183.
27. McCormick GJ. 1970. Amino acid transport and incorporation in red blood cells of normal and *Plasmodium knowlesi*-infected rhesus monkeys. Exp Parasitol 27:143-149.
28. Sherman IW, Tanigoshi L. 1970. Incorporation of 14 C-amino-acids by malaria (*Plasmodium lophurae*) IV. *In vivo* utilization of host cell haemoglobin. Int J Biochem 1:635-637.
29. Liu J, Istvan ES, Gluzman IY, Gross J, Goldberg DE. 2006. *Plasmodium falciparum* ensures its amino acid supply with multiple acquisition pathways and redundant proteolytic enzyme systems. Proc Natl Acad Sci U S A 103:8840-8845.

30. Babbitt SE, Altenhofen L, Cobbold SA, Istvan ES, Fennell C, Doerig C, Llinás M, Goldberg DE. 2012. *Plasmodium falciparum* responds to amino acid starvation by entering into a hibernatory state. Proc Natl Acad Sci U S A 109:E3278-E3287.
31. Zarchin S, Krugliak M, Ginsburg H. 1986. Digestion of the host erythrocyte by malaria parasites is the primary target for quinoline containing antimalarials. Biochem Pharmacol 35:2435-2442.
32. Cenedella RJ, Rosen H, Angel CR, Saxe LH. 1968. Free amino-acid production *in vitro* by *Plasmodium berghei*. Am J Trop Med Hyg 17:800-803.
33. Dalal S, Klemba M. 2015. Amino acid efflux by asexual blood-stage *Plasmodium falciparum* and its utility in interrogating the kinetics of hemoglobin endocytosis and catabolism *in vivo*. Mol Biochem Parasitol 201:116-122.
34. Krugliak M, Zhang J, Ginsburg H. 2002. Intraerythrocytic *Plasmodium falciparum* utilizes only a fraction of the amino acids derived from the digestion of host cell cytosol for the biosynthesis of its proteins. Mol Biochem Parasitol 119:249-256.
35. Lew VL, Tiffert T, Ginsburg H. 2003. Excess hemoglobin digestion and the osmotic stability of *Plasmodium falciparum*–infected red blood cells. Blood 101:4189-4194.
36. Aikawa M, Hepler PK, Huff CG, Sprinz H. 1966. The feeding mechanism of avian malarial parasites. J Cell Biol 28:355-373.
37. Abu Bakar N, Klonis N, Hanssen E, Chan C, Tilley L. 2010. Digestive-vacuole genesis and endocytic processes in the early intraerythrocytic stages of *Plasmodium falciparum*. J Cell Sci 123:441-450.
38. Elliott DA, McIntosh MT, Hosgood HD, Chen S, Zhang G, Baevova P, Joiner KA. 2008. Four distinct pathways of hemoglobin uptake in the malaria parasite *Plasmodium falciparum*. Proc Natl Acad Sci U S A 105:2463-2468.
39. Gruring C, Spielmann T. 2012. Imaging of live malaria blood stage parasites. Methods Enzymol 506:81-92.
40. Dluzewski AR, Ling IT, Hopkins JM, Grainger M, Margos G, Mitchell GH, Holder AA, Bannister LH. 2008. Formation of the food vacuole in *Plasmodium falciparum*: a potential role for the 19 kDa fragment of merozoite surface protein 1 (MSP1(19)). PloS One 3:e3085.
41. Milani KJ, Schneider TG, Taraschi TF. 2015. Defining the morphology and mechanism of the hemoglobin transport pathway in *Plasmodium falciparum*-infected erythrocytes. Eukaryot cell 14:415-426.

42. Asawamabasakda W, Ittarat I, Chang C-C, McElroy P, Meshnick SR. 1994. Effects of antimalarials and protease inhibitors on plasmodial hemozoin production. Mol Biochem Parasitol 67:183-191.
43. Orjih AU, Fitch CD. 1993. Hemozoin production by *Plasmodium falciparum*: variation with strain and exposure to chloroquine. BBA-Gen Subjects 1157:270-274.
44. Xie SC, Dogovski C, Hanssen E, Chiu F, Yang T, Crespo MP, Stafford C, Batinovic S, Teguh S, Charman S, Klonis N, Tilley L. 2016. Haemoglobin degradation underpins the sensitivity of early ring stage *Plasmodium falciparum* to artemisinins. J Cell Sci 129:406-416.
45. Klemba M, Beatty W, Gluzman I, Goldberg DE. 2004. Trafficking of plasmepsin II to the food vacuole of the malaria parasite *Plasmodium falciparum*. J Cell Biol 164:47-56.
46. Jani D, Nagarkatti R, Beatty W, Angel R, Slebodnick C, Andersen J, Kumar S, Rathore D. 2008. HDP-a novel heme detoxification protein from the malaria parasite. PLoS Pathog 4:e1000053.
47. Bendrat K, Berger BJ, Cerami A. 1995. Haem polymerization in malaria. Nature 378:138-139.
48. Jackson KE, Klonis N, Ferguson DJ, Adisa A, Dogovski C, Tilley L. 2004. Food vacuole-associated lipid bodies and heterogeneous lipid environments in the malaria parasite, *Plasmodium falciparum*. Mol Microbiol 54:109-122.
49. Goldberg DE. 2005. Hemoglobin degradation, p 275-291. *In* Compans RW, Cooper MD, Honjo T, Koprowski H, Melchers F, Oldstone MBA, Olsnes S, Potter M, Vogt PK, Wagner H, Sullivan D, Krishna S (ed), Malaria: Drugs, disease and post-genomic biology, vol 295. Springer Berlin Heidelberg.
50. Coombs GH, Goldberg DE, Klemba M, Berry C, Kay J, Mottram JC. 2001. Aspartic proteases of Plasmodium falciparum and other parasitic protozoa as drug targets. Trends Parasitol 17:532-537.
51. Banerjee R, Liu J, Beatty W, Pelosof L, Klemba M, Goldberg DE. 2002. Four plasmepsins are active in the *Plasmodium falciparum* food vacuole, including a protease with an active-site histidine. Proc Natl Acad Sci U S A 99:990-995.
52. Gluzman IY, Francis SE, Oksman A, Smith CE, Duffin KL, Goldberg DE. 1994. Order and specificity of the *Plasmodium falciparum* hemoglobin degradation pathway. J Clin Invest 93:1602-1608.

53. Francis SE, Gluzman IY, Oksman A, Banerjee D, Goldberg DE. 1996. Characterization of native falcipain, an enzyme involved in *Plasmodium falciparum* hemoglobin degradation. Mol Biochem Parasitol 83:189-200.

54. Shenai BR, Sijwali PS, Singh A, Rosenthal PJ. 2000. Characterization of native and recombinant falcipain-2, a principal trophozoite cysteine protease and essential hemoglobinase of *Plasmodium falciparum*. J Biol Chem 275:29000-29010.

55. Sijwali PS, Shenai BR, Jiri G, Singh A, Rosenthal PJ. 2001. Expression and characterization of the *Plasmodium falciparum* haemoglobinase falcipain-3. Biochem J 360:481-489.

56. Subramanian S, Hardt M, Choe Y, Niles RK, Johansen EB, Legac J, Gut J, Kerr ID, Craik CS, Rosenthal PJ. 2009. Hemoglobin cleavage site-specificity of the *Plasmodium falciparum* cysteine proteases falcipain-2 and falcipain-3. PloS One 4:e5156.

57. Goldberg DE, Slater AF, Cerami A, Henderson GB. 1990. Hemoglobin degradation in the malaria parasite *Plasmodium falciparum*: an ordered process in a unique organelle. Proc Natl Acad Sci U S A 87:2931-2935.

58. Omara-Opyene AL, Moura PA, Sulsona CR, Bonilla JA, Yowell CA, Fujioka H, Fidock DA, Dame JB. 2004. Genetic disruption of the *Plasmodium falciparum* digestive vacuole plasmepsins demonstrates their functional redundancy. J Biol Chem 279:54088-54096.

59. Sijwali PS, Rosenthal PJ. 2004. Gene disruption confirms a critical role for the cysteine protease falcipain-2 in hemoglobin hydrolysis by *Plasmodium falciparum*. Proc Natl Acad Sci U S A 101:4384-4389.

60. Drew ME, Banerjee R, Uffman EW, Gilbertson S, Rosenthal PJ, Goldberg DE. 2008. *Plasmodium* food vacuole plasmepsins are activated by falcipains. J Biol Chem 283:12870-12876.

61. Bozdech Z, Llinas M, Pulliam BL, Wong ED, Zhu J, DeRisi JL. 2003. The transcriptome of the intraerythrocytic developmental cycle of *Plasmodium falciparum*. PLoS Biol 1:E5.

62. Eggleson KK, Duffin KL, Goldberg DE. 1999. Identification and characterization of falcilysin, a metallopeptidase involved in hemoglobin catabolism within the malaria parasite *Plasmodium falciparum*. J Biol Chem 274:32411-32417.

63. Klemba M, Gluzman I, Goldberg DE. 2004. A *Plasmodium falciparum* dipeptidyl aminopeptidase I participates in vacuolar hemoglobin degradation. J Biol Chem 279:43000-43007.

64. Llinas M, Bozdech Z, Wong ED, Adai AT, DeRisi JL. 2006. Comparative whole genome transcriptome analysis of three *Plasmodium falciparum* strains. Nucleic Acids Res 34:1166-1173.

65. Wang F, Krai P, Deu E, Bibb B, Lauritzen C, Pedersen J, Bogyo M, Klemba M. 2011. Biochemical characterization of *Plasmodium falciparum* dipeptidyl aminopeptidase 1. Mol Biochem Parasitol 175:10-20.

66. Ragheb D, Bompiani K, Dalal S, Klemba M. 2009. Evidence for catalytic roles for *Plasmodium falciparum* aminopeptidase P in the food vacuole and cytosol. J Biol Chem 284:24806-24815.

67. Dalal S, Klemba M. 2007. Roles for two aminopeptidases in vacuolar hemoglobin catabolism in *Plasmodium falciparum*. J Biol Chem 282:35978-35987.

68. Poreba M, McGowan S, Skinner-Adams TS, Trenholme KR, Gardiner DL, Whisstock JC, To J, Salvesen GS, Dalton JP, Drag M. 2012. Fingerprinting the substrate specificity of M1 and M17 aminopeptidases of human malaria, *Plasmodium falciparum*. PloS One 7:e31938.

69. Harbut MB, Velmourougane G, Dalal S, Reiss G, Whisstock JC, Onder O, Brisson D, McGowan S, Klemba M, Greenbaum DC. 2011. Bestatin-based chemical biology strategy reveals distinct roles for malaria M1- and M17-family aminopeptidases. Proc Natl Acad Sci U S A 108:E526-534.

70. Skinner-Adams TS, Stack CM, Trenholme KR, Brown CL, Grembecka J, Lowther J, Mucha A, Drag M, Kafarski P, McGowan S. 2010. *Plasmodium falciparum* neutral aminopeptidases: new targets for anti-malarials. Trends Biochem Sci 35:53-61.

71. Ragheb D, Dalal S, Bompiani KM, Ray WK, Klemba M. 2011. Distribution and biochemical properties of an M1-family aminopeptidase in *Plasmodium falciparum* indicate a role in vacuolar hemoglobin catabolism. J Biol Chem 286:27255-27265.

72. Martin RE, Kirk K. 2007. Transport of the essential nutrient isoleucine in human erythrocytes infected with the malaria parasite *Plasmodium falciparum*. Blood 109:2217-2224.

73. Sivaraman KK, Oellig CA, Huynh K, Atkinson SC, Poreba M, Perugini MA, Trenholme KR, Gardiner DL, Salvesen G, Drag M. 2012. X-ray crystal structure and specificity of the *Plasmodium falciparum* malaria aminopeptidase PfM18AAP. J Mol Biol 422:495-507.

74. Teuscher F, Gatton ML, Chen N, Peters J, Kyle DE, Cheng Q. 2010. Artemisinin-induced dormancy in *Plasmodium falciparum*: duration, recovery rates, and implications in treatment failure. J Infect Dis 202:1362-1368.
75. Aft RL, Mueller G. 1983. Hemin-mediated DNA strand scission. J Biol Chem 258:12069-12072.
76. Aft RL, Mueller GC. 1984. Hemin-mediated oxidative degradation of proteins. J Biol Chem 259:301-305.
77. Klouche K, Morena M, Canaud B, Descomps B, Beraud JJ, Cristol JP. 2004. Mechanism of in vitro heme-induced LDL oxidation: effects of antioxidants. Eur J Clin Invest 34:619-625.
78. Kumar S, Bandyopadhyay U. 2005. Free heme toxicity and its detoxification systems in human. Toxicol Lett 157:175-188.
79. Egan TJ. 2008. Recent advances in understanding the mechanism of hemozoin (malaria pigment) formation. J Inorg Biochem 102:1288-1299.
80. Toh SQ, Glanfield A, Gobert GN, Jones MK. 2010. Heme and blood-feeding parasites: friends or foes? Parasit Vectors 3:108.
81. Sullivan DJ, Jr., Gluzman IY, Goldberg DE. 1996. *Plasmodium* hemozoin formation mediated by histidine-rich proteins. Science 271:219-222.
82. Fitch CD, Cai GZ, Chen YF, Shoemaker JD. 1999. Involvement of lipids in ferriprotoporphyrin IX polymerization in malaria. Biochim Biophys Acta 1454:31-37.
83. Chugh M, Sundararaman V, Kumar S, Reddy VS, Siddiqui WA, Stuart KD, Malhotra P. 2013. Protein complex directs hemoglobin-to-hemozoin formation in *Plasmodium falciparum*. Proc Natl Acad Sci U S A 110:5392-5397.
84. Fong KY, Wright DW. 2013. Hemozoin and antimalarial drug discovery. Future Med Chem 5:1437-1450.
85. Atamna H, Ginsburg H. 1995. Heme degradation in the presence of glutathione. A proposed mechanism to account for the high levels of non-heme iron found in the membranes of hemoglobinopathic red blood cells. J Biol Chem 270:24876-24883.
86. Lisewski Andreas M, Quiros Joel P, Ng Caroline L, Adikesavan Anbu K, Miura K, Putluri N, Eastman Richard T, Scanfeld D, Regenbogen Sam J, Altenhofen L, Llinás M, Sreekumar A, Long C, Fidock David A, Lichtarge O. 2014. Supergenomic network compression and the discovery of EXP1 as a glutathione transferase inhibited by artesunate. Cell 158:916-928.

87. Harwaldt P, Rahlfs S, Becker K. 2002. Glutathione S-transferase of the malarial parasite *Plasmodium falciparum*: characterization of a potential drug target. Biol Chem 383:821-830.

88. Okada K. 2009. The novel heme oxygenase-like protein from *Plasmodium falciparum* converts heme to bilirubin IXα in the apicoplast. FEBS Lett 583:313-319.

89. van Dooren GG, Kennedy AT, McFadden GI. 2012. The use and abuse of heme in apicomplexan parasites. Antioxid Redox Signal 17:634-656.

90. Lindblade KA, Mwandama D, Mzilahowa T, Steinhardt L, Gimnig J, Shah M, Bauleni A, Wong J, Wiegand R, Howell P, Zoya J, Chiphwanya J, Mathanga DP. 2015. A cohort study of the effectiveness of insecticide-treated bed nets to prevent malaria in an area of moderate pyrethroid resistance, Malawi. Malar J 14:31.

91. O'Meara WP, Smith DL, McKenzie FE. 2006. Potential impact of intermittent preventive treatment (IPT) on spread of drug-resistant malaria. PLoS Med 3:e141.

92. Daily Já, Scanfeld D, Pochet N, Le Roch K, Plouffe D, Kamal M, Sarr O, Mboup S, Ndir O, Wypij D. 2007. Distinct physiological states of *Plasmodium falciparum* in malaria-infected patients. Nature 450:1091-1095.

93. WHO. 2016. Malaria vaccine: WHO position paper–January 2016. Weekly epidemiological record.

94. WHO. 2015. Guidelines for the treatment of malaria. Third edition. World Health Organisation, Geneva.

95. group SEAQAMTS. 2005. Artesunate versus quinine for treatment of severe falciparum malaria: a randomised trial. Lancet 366:717-725.

96. Delves M, Plouffe D, Scheurer C, Meister S, Wittlin S, Winzeler EA, Sinden RE, Leroy D. 2012. The activities of current antimalarial drugs on the life cycle stages of *Plasmodium*: a comparative study with human and rodent parasites. PLoS Med 9:e1001169.

97. Achan J, Talisuna AO, Erhart A, Yeka A, Tibenderana JK, Baliraine FN, Rosenthal PJ, D'Alessandro U. 2011. Quinine, an old anti-malarial drug in a modern world: role in the treatment of malaria. Malar J 10:144.

98. Schlitzer M. 2007. Malaria chemotherapeutics part I: History of antimalarial drug development, currently used therapeutics, and drugs in clinical development. ChemMedChem 2:944-986.

99. Davis TM, Hung T-Y, Sim K, Karunajeewa HA, Ilett KF. 2005. Piperaquine. Drugs 65:75-87.

100. Biot C, Nosten F, Fraisse L, Ter-Minassian D, Khalife J, Dive D. 2011. The antimalarial ferroquine: from bench to clinic. Parasite 18:207-214.

101. Bhattacharjee AK, Karle JM. 1998. Functional correlation of molecular electronic properties with potency of synthetic carbinolamine antimalarial agents. Bioorg Med Chem 6:1927-1933.

102. Ringwald P, Eboumbou ECM, Bickii J, Basco LK. 1999. *In vitro* activities of pyronaridine, alone and in combination with other antimalarial drugs, against *Plasmodium falciparum*. Antimicrob Agents Chemother 43:1525-1527.

103. Woodrow C, Krishna S. 2006. Antimalarial drugs: recent advances in molecular determinants of resistance and their clinical significance. Cell Mol Life Sci 63:1586-1596.

104. Uhlemann A-C, Ramharter M, Lell B, Kremsner PG, Krishna S. 2005. Amplification of *Plasmodium falciparum* multidrug resistance gene 1 in isolates from Gabon. J Infect Dis 192:1830-1835.

105. Llanos-Cuentas A, Lacerda MV, Rueangweerayut R, Krudsood S, Gupta SK, Kochar SK, Arthur P, Chuenchom N, Möhrle JJ, Duparc S, Uqwueqbulam C, Kleim J, Carter N, Green J, Kellam L. 2014. Tafenoquine plus chloroquine for the treatment and relapse prevention of *Plasmodium vivax* malaria (DETECTIVE): a multicentre, double-blind, randomised, phase 2b dose-selection study. Lancet 383:1049-1058.

106. Ebstie YA, Abay SM, Tadesse WT, Ejigu DA. 2016. Tafenoquine and its potential in the treatment and relapse prevention of *Plasmodium vivax* malaria: the evidence to date. Drug Des Devel Ther 10:2387-2399.

107. Shanks GD, Oloo AJ, Aleman GM, Ohrt C, Klotz FW, Braitman D, Horton J, Brueckner R. 2001. A new primaquine analogue, tafenoquine (WR 238605), for prophylaxis against *Plasmodium falciparum* malaria. Clin Infect Dis 33:1968-1974.

108. Nzila A. 2006. The past, present and future of antifolates in the treatment of *Plasmodium falciparum* infection. J Antimicrob Chemother 57:1043-1054.

109. Plowe CV, Cortese JF, Djimde A, Nwanyanwu OC, Watkins WM, Winstanley PA, Franco JGE, Mollinedo RE, Avila JC, Cespedes JL. 1997. Mutations in *Plasmodium falciparum* dihydrofolate reductase and dihydropteroate synthase and epidemiologic patterns of pyrimethamine-sulfadoxine use and resistance. J Infect Dis 176:1590-1596.

110. Fry M, Pudney M. 1992. Site of action of the antimalarial hydroxynaphthoquinone, 2-[trans-4-(4'-chlorophenyl) cyclohexyl]-3-hydroxy-1,4-naphthoquinone (566C80). Biochem Pharmacol 43:1545-1553.

111. Srivastava IK, Rottenberg H, Vaidya AB. 1997. Atovaquone, a broad spectrum antiparasitic drug, collapses mitochondrial membrane potential in a malarial parasite. J Biol Chem 272:3961-3966.

112. Rodrigues T, Lopes F, Moreira R. 2010. Inhibitors of the mitochondrial electron transport chain and de novo pyrimidine biosynthesis as antimalarials: the present status. Curr Med Chem 17:929-956.

113. Belen Cassera M, Zhang Y, Z Hazleton K, L Schramm V. 2011. Purine and pyrimidine pathways as targets in *Plasmodium falciparum*. Curr Top Med Chem 11:2103-2115.

114. Srivastava IK, Morrisey JM, Darrouzet E, Daldal F, Vaidya AB. 1999. Resistance mutations reveal the atovaquone-binding domain of cytochrome b in malaria parasites. Mol Microbiol 33:704-711.

115. Srivastava IK, Vaidya AB. 1999. A mechanism for the synergistic antimalarial action of atovaquone and proguanil. Antimicrob Agents Chemother 43:1334-1339.

116. Coatney GR, Greenberg J. 1952. The use of antibiotics in the treatment of malaria. Ann N Y Acad Sci 55:1075-1081.

117. McFadden GI, Reith ME, Munhalland J, Lan-Unnasch N. 1996. Plastid in human parasites. Nature 381:482.

118. Goodman CD, Pasaje CFA, Kennedy K, McFadden GI, Ralph SA. 2016. Targeting protein translation in organelles of the apicomplexa. Trends Parasitol 32:953-965.

119. Uddin T, McFadden GI, Goodman CD. 2018. Validation of putative apicoplast-targeting drugs using a chemical supplementation assay in cultured human malaria parasites. Antimicrob Agents Chemother 62:ACC-01161.

120. Wells TNC, van Huijsduijnen RH, Van Voorhis WC. 2015. Malaria medicines: a glass half full? Nat Rev Drug Discov 14:424-442.

121. Burrows JN, van Huijsduijnen RH, Möhrle JJ, Oeuvray C, Wells TN. 2013. Designing the next generation of medicines for malaria control and eradication. Malar J 12:1.

122. Spillman NJ, Allen RJ, McNamara CW, Yeung BK, Winzeler EA, Diagana TT, Kirk K. 2013. Na+ regulation in the malaria parasite *Plasmodium falciparum* involves the cation ATPase PfATP4 and is a target of the spiroindolone antimalarials. Cell Host Microbe 13:227-237.

123. Lehane AM, Ridgway MC, Baker E, Kirk K. 2014. Diverse chemotypes disrupt ion homeostasis in the malaria parasite. Mol Microbiol 94:327-339.

124. Jiménez-Díaz MB, Ebert D, Salinas Y, Pradhan A, Lehane AM, Myrand-Lapierre M-E, O'Loughlin KG, Shackleford DM, Justino de Almeida M, Carrillo AK, Clark JA,

Dennis ASM, Diep J, Deng X, Duffy S, Endsley AN, Fedewa G, Guiguemde WA, Gómez MG, Holbrook G, Horst J, Kim CC, Liu J, Lee MCS, Matheny A, Martínez MS, Miller G, Rodríguez-Alejandre A, Sanz L, Sigal M, Spillman NJ, Stein PD, Wang Z, Zhu F, Waterson D, Knapp S, Shelat A, Avery VM, Fidock DA, Gamo F-J, Charman SA, Mirsalis JC, Ma H, Ferrer S, Kirk K, Angulo-Barturen I, Kyle DE, DeRisi JL, Floyd DM, Guy RK. 2014. (+)-SJ733, a clinical candidate for malaria that acts through ATP4 to induce rapid host-mediated clearance of *Plasmodium*. Proc Natl Acad Sci U S A 111:E5455-E5462.

125. Ghidelli-Disse S, Lafuente-Monasterio MJ, Waterson D, Witty M, Younis Y, Paquet T, Street LJ, Chibale K, Gamo-Benito FJ, Bantscheff M. 2014. Identification of *Plasmodium* PI4 kinase as target of MMV390048 by chemoproteomics. Malar J 13:P38.

126. Kuhen KL, Chatterjee AK, Rottmann M, Gagaring K, Borboa R, Buenviaje J, Chen Z, Francek C, Wu T, Nagle A, Barnes SW, Plouffe D, Lee MCS, Fidock DA, Graumans W, van de Vegte-Bolmer M, van Gemert GJ, Wirjanata G, Sebayang B, Marfurt J, Russell B, Suwanarusk R, Price RN, Nosten F, Tungtaeng A, Gettayacamin M, Sattabongkot J, Taylor J, Walker JR, Tully D, Patra KP, Flannery EL, Vinetz JM, Renia L, Sauerwein RW, Winzeler EA, Glynne RJ, Diagana TT. 2014. KAF156 is an antimalarial clinical candidate with potential for use in prophylaxis, treatment, and prevention of disease transmission. Antimicrob Agents Chemother 58:5060-5067.

127. Baragana B, Hallyburton I, Lee MCS, Norcross NR, Grimaldi R, Otto TD, Proto WR, Blagborough AM, Meister S, Wirjanata G, Ruecker A, Upton LM, Abraham TS, Almeida MJ, Pradhan A, Porzelle A, Martinez MS, Bolscher JM, Woodland A, Norval S, Zuccotto F, Thomas J, Simeons F, Stojanovski L, Osuna-Cabello M, Brock PM, Churcher TS, Sala KA, Zakutansky SE, Jimenez-Diaz MB, Sanz LM, Riley J, Basak R, Campbell M, Avery VM, Sauerwein RW, Dechering KJ, Noviyanti R, Campo B, Frearson JA, Angulo-Barturen I, Ferrer-Bazaga S, Gamo FJ, Wyatt PG, Leroy D, Siegl P, Delves MJ, Kyle DE, Wittlin S, Marfurt J, et al. 2015. A novel multiple-stage antimalarial agent that inhibits protein synthesis. Nature 522:315-320.

128. Phillips MA, Lotharius J, Marsh K, White J, Dayan A, White KL, Njoroge JW, El Mazouni F, Lao Y, Kokkonda S, Tomchick DR, Deng X, Laird T, Bhatia SN, March S, Ng CL, Fidock DA, Wittlin S, Lafuente-Monasterio M, Benito FJ, Alonso LM, Martinez MS, Jimenez-Diaz MB, Bazaga SF, Angulo-Barturen I, Haselden JN, Louttit J, Cui Y, Sridhar A, Zeeman AM, Kocken C, Sauerwein R, Dechering K, Avery VM,

Duffy S, Delves M, Sinden R, Ruecker A, Wickham KS, Rochford R, Gahagen J, Iyer L, Riccio E, Mirsalis J, Bathhurst I, Rueckle T, Ding X, Campo B, Leroy D, Rogers MJ, et al. 2015. A long-duration dihydroorotate dehydrogenase inhibitor (DSM265) for prevention and treatment of malaria. Sci Transl Med 7:296ra111.

129. Charman SA, Arbe-Barnes S, Bathurst IC, Brun R, Campbell M, Charman WN, Chiu FC, Chollet J, Craft JC, Creek DJ, Dong Y, Matile H, Maurer M, Morizzi J, Nguyen T, Papastogiannidis P, Scheurer C, Shackleford DM, Sriraghavan K, Stingelin L, Tang Y, Urwyler H, Wang X, White KL, Wittlin S, Zhou L, Vennerstrom JL. 2011. Synthetic ozonide drug candidate OZ439 offers new hope for a single-dose cure of uncomplicated malaria. Proc Natl Acad Sci U S A 108:4400-4405.
130. Qinghaosu. CRG. 1977. A new sesquiterpene lactone—Qinghaosu. Chin Sci Bull 3:142.
131. Klayman DL. 1985. Qinghaosu (artemisinin): an antimalarial drug from China. Science 228:1049-1055.
132. Barradell LB, Fitton A. 1995. Artesunate. A review of its pharmacology and therapeutic efficacy in the treatment of malaria. Drugs 50:714-741.
133. Lee IS, Hufford CD. 1990. Metabolism of antimalarial sesquiterpene lactones. Pharmacol Ther 48:345-355.
134. Meshnick SR, Taylor T, Kamchonwongpaisan S. 1996. Artemisinin and the antimalarial endoperoxides: from herbal remedy to targeted chemotherapy. Microbiol Rev 60:301-315.
135. Woodrow CJ, Haynes RK, Krishna S. 2005. Artemisinins. Postgrad Med J 81:71-78.
136. Watsierah CA, Ouma C. 2014. Access to artemisinin-based combination therapy (ACT) and quinine in malaria holoendemic regions of western Kenya. Malar J 13:290.
137. Muangphrom P, Seki H, Fukushima EO, Muranaka T. 2016. Artemisinin-based antimalarial research: application of biotechnology to the production of artemisinin, its mode of action, and the mechanism of resistance of *Plasmodium* parasites. J Nat Med 70:318-334.
138. Newton PN, McGready R, Fernandez F, Green MD, Sunjio M, Bruneton C, Phanouvong S, Millet P, Whitty CJ, Talisuna AO, Proux S, Christophel EM, Malenga G, Singhasivanon P, Bojang K, Kaur H, Palmer K, Day NP, Greenwood BM, Nosten F, White NJ. 2006. Manslaughter by fake artesunate in Asia--will Africa be next? PLoS Med 3:e197.

139. Ro DK, Paradise EM, Ouellet M, Fisher KJ, Newman KL, Ndungu JM, Ho KA, Eachus RA, Ham TS, Kirby J, Chang MC, Withers ST, Shiba Y, Sarpong R, Keasling JD. 2006. Production of the antimalarial drug precursor artemisinic acid in engineered yeast. Nature 440:940-943.

140. Sriram D, Rao VS, Chandrasekhar KVG, Yogeeswari P. 2004. Progress in the research of artemisinin and its analogues as antimalarials: an update. Nat Prod Res 18:503-527.

141. Woodrow CJ, White NJ. 2016. The clinical impact of artemisinin resistance in Southeast Asia and the potential for future spread. FEMS Microbiol Rev 41:34-48.

142. Kremsner PG, Krishna S. 2004. Antimalarial combinations. Lancet 364:285-294.

143. Dondorp AM, Nosten F, Yi P, Das D, Phyo AP, Tarning J, Lwin KM, Ariey F, Hanpithakpong W, Lee SJ, Ringwald P, Silamut K, Imwong M, Chotivanich K, Lim P, Herdman T, An SS, Yeung S, Singhasivanon P, Day NP, Lindegardh N, Socheat D, White NJ. 2009. Artemisinin resistance in *Plasmodium falciparum* malaria. N Engl J Med 361:455-467.

144. WHO. 2017. Status report on artemisinin and ACT resistance (April 2017).

145. Klonis N, Xie SC, McCaw JM, Crespo-Ortiz MP, Zaloumis SG, Simpson JA, Tilley L. 2013. Altered temporal response of malaria parasites determines differential sensitivity to artemisinin. Proc Natl Acad Sci U S A 110:5157-5162.

146. ter Kuile F, White NJ, Holloway P, Pasvol G, Krishna S. 1993. *Plasmodium falciparum*: *in vitro* studies of the pharmacodynamic properties of drugs used for the treatment of severe malaria. Exp Parasitol 76:85-95.

147. Skinner TS, Manning LS, Johnston WA, Davis TM. 1996. *In vitro* stage-specific sensitivity of *Plasmodium falciparum* to quinine and artemisinin drugs. Int J Parasitol 26:519-525.

148. Dogovski C, Xie SC, Burgio G, Bridgford J, Mok S, McCaw JM, Chotivanich K, Kenny S, Gnädig N, Straimer J, Bozdech Z, Fidock DA, Simpson JA, Dondorp AM, Foote S, Klonis N, Tilley L. 2015. Targeting the cell stress response of *Plasmodium falciparum* to overcome artemisinin resistance. PLoS Biol 13:e1002132.

149. Avery MA, Gao F, Chong WK, Mehrotra S, Milhous WK. 1993. Structure-activity relationships of the antimalarial agent artemisinin. 1. Synthesis and comparative molecular field analysis of C-9 analogs of artemisinin and 10-deoxoartemisinin. J Med Chem 36:4264-4275.

150. Cumming JN, Ploypradith P, Posner GH. 1996. Antimalarial activity of artemisinin (qinghaosu) and related trioxanes: mechanism (s) of action. Adv Pharmacol 37:253-297.

151. Clark I, Hunt N, Cowden W, Maxwell LE, Mackie E. 1984. Radical-mediated damage to parasites and erythrocytes in *Plasmodium vinckei* infected mice after injection of t-butyl hydroperoxide. Clin Exp Immunol 56:524-530.

152. Klonis N, Crespo-Ortiz MP, Bottova I, Abu-Bakar N, Kenny S, Rosenthal PJ, Tilley L. 2011. Artemisinin activity against *Plasmodium falciparum* requires hemoglobin uptake and digestion. Proc Natl Acad Sci U S A 108:11405-11410.

153. Krungkrai SR, Yuthavong Y. 1987. The antimalarial action on *Plasmodium falciparum* of qinghaosu and artesunate in combination with agents which modulate oxidant stress. Trans R Soc Trop Med Hyg 81:710-714.

154. Meshnick SR. 2002. Artemisinin: mechanisms of action, resistance and toxicity. Int J Parasitol 32:1655-1660.

155. Levander OA, Ager A, Morris VC, May RG. 1989. Qinghaosu, dietary vitamin E, selenium, and cod-liver oil: effect on the susceptibility of mice to the malarial parasite *Plasmodium yoelii*. Am J Clin Nutr 50:346-352.

156. O'Neill PM, Barton VE, Ward SA. 2010. The molecular mechanism of action of artemisinin--the debate continues. Molecules 15:1705-1721.

157. Creek DJ, Chiu FC, Prankerd RJ, Charman SA, Charman WN. 2005. Kinetics of iron-mediated artemisinin degradation: effect of solvent composition and iron salt. J Pharm Sci 94:1820-1829.

158. Posner GH, Wang D, Cumming JN, Oh CH, French AN, Bodley AL, Shapiro TA. 1995. Further evidence supporting the importance of and the restrictions on a carbon-centered radical for high antimalarial activity of 1, 2, 4-trioxanes like artemisinin. J Med Chem 38:2273-2275.

159. Wang D-Y, Wu Y, Wu Y-L, Li Y, Shan F. 1999. Synthesis, iron (II)-induced cleavage and in vivo antimalarial efficacy of 10-(2-hydroxy-1-naphthyl)-deoxoqinghaosu (-deoxoartemisinin). J Chem Soc Perkin Trans 1:1827-1832.

160. Wu W-M, Wu Y, Wu Y-L, Yao Z-J, Zhou C-M, Li Y, Shan F. 1998. Unified mechanistic framework for the Fe (II)-induced cleavage of qinghaosu and derivatives/analogues. The first spin-trapping evidence for the previously postulated secondary C-4 radical. J Am Chem Soc 120:3316-3325.

161. Posner GH, Oh CH, Wang D, Gerena L, Milhous WK, Meshnick SR, Asawamahasadka W. 1994. Mechanism-based design, synthesis, and *in vitro* antimalarial testing of new 4-methylated trioxanes structurally related to artemisinin: the importance of a carbon-centered radical for antimalarial activity. J Med Chem 37:1256-1258.

162. Posner GH, Park SB, González L, Wang D, Cumming JN, Klinedinst D, Shapiro TA, Bachi MD. 1996. Evidence for the importance of high-valent Fe O and of a diketone in the molecular mechanism of action of antimalarial trioxane analogs of artemisinin. J Am Chem Soc 118:3537-3538.

163. Szpilman AM, Korshin EE, Hoos R, Posner GH, Bachi MD. 2001. Iron (II)-induced degradation of antimalarial β-sulfonyl endoperoxides. Evidence for the generation of potentially cytotoxic carbocations. J Org Chem 66:6531-6540.

164. Scholl PF, Tripathi AK, Sullivan DJ. 2005. Bioavailable iron and heme metabolism in *Plasmodium falciparum*. Curr Top Microbiol Immunol 295:293-324.

165. Breuer W, Epsztejn S, Cabantchik ZI. 1995. Iron acquired from transferrin by K562 cells is delivered into a cytoplasmic pool of chelatable iron (II). J Biol Chem 270:24209-24215.

166. Eckstein-Ludwig U, Webb RJ, Van Goethem ID, East JM, Lee AG, Kimura M, O'Neill PM, Bray PG, Ward SA, Krishna S. 2003. Artemisinins target the SERCA of *Plasmodium falciparum*. Nature 424:957-961.

167. Stocks PA, Bray PG, Barton VE, Al-Helal M, Jones M, Araujo NC, Gibbons P, Ward SA, Hughes RH, Biagini GA, Davies J, Amewu R, Mercer AE, Ellis G, O'Neill PM. 2007. Evidence for a common non-heme chelatable-iron-dependent activation mechanism for semisynthetic and synthetic endoperoxide antimalarial drugs. Angew Chem Int Ed Engl 46:6278-6283.

168. Meshnick SR, Yang YZ, Lima V, Kuypers F, Kamchonwongpaisan S, Yuthavong Y. 1993. Iron-dependent free radical generation from the antimalarial agent artemisinin (qinghaosu). Antimicrob Agents Chemother 37:1108-1114.

169. Reeder BJ, Hider RC, Wilson MT. 2008. Iron chelators can protect against oxidative stress through ferryl heme reduction. Free Radic Biol Med 44:264-273.

170. Reeder BJ, Wilson MT. 2005. Desferrioxamine inhibits production of cytotoxic heme to protein cross-linked myoglobin: a mechanism to protect against oxidative stress without iron chelation. Chem Res Toxicol 18:1004-1011.

171. Ginsburg H, Famin O, Zhang J, Krugliak M. 1998. Inhibition of glutathione-dependent degradation of heme by chloroquine and amodiaquine as a possible basis for their antimalarial mode of action. Biochem Pharmacol 56:1305-1313.

172. Meshnick SR, Thomas A, Ranz A, Xu CM, Pan HZ. 1991. Artemisinin (qinghaosu): the role of intracellular hemin in its mechanism of antimalarial action. Mol Biochem Parasitol 49:181-189.

173. Zhang S, Gerhard GS. 2008. Heme activates artemisinin more efficiently than hemin, inorganic iron, or hemoglobin. Bioorg Med Chem 16:7853-7861.

174. Zhang S, Gerhard GS. 2009. Heme mediates cytotoxicity from artemisinin and serves as a general anti-proliferation target. PloS One 4:e7472.

175. Zhang C-J, Wang J, Zhang J, Lee YM, Feng G, Lim TK, Shen H-M, Lin Q, Liu B. 2016. Mechanism-guided design and synthesis of a mitochondria-targeting artemisinin analogue with enhanced anticancer activity. Angew Chem Int Ed Engl 128:13974-13978.

176. Wang J, Zhang C-J, Chia WN, Loh CC, Li Z, Lee YM, He Y, Yuan L-X, Lim TK, Liu M, Liew CX, Lee YQ, Zhang J, Lu N, Lim CT, Hua Z-C, Liu B, Shen H-M, Tan KSW, Lin Q. 2015. Haem-activated promiscuous targeting of artemisinin in *Plasmodium falciparum*. Nat Commun 6:10111.

177. Wang J, Huang L, Li J, Fan Q, Long Y, Li Y, Zhou B. 2010. Artemisinin directly targets malarial mitochondria through its specific mitochondrial activation. PloS One 5:e9582.

178. Haynes RK, Chan WC, Wong HN, Li KY, Wu WK, Fan KM, Sung HH, Williams ID, Prosperi D, Melato S, Coghi P, Monti D. 2010. Facile oxidation of leucomethylene blue and dihydroflavins by artemisinins: relationship with flavoenzyme function and antimalarial mechanism of action. ChemMedChem 5:1282-1299.

179. Mbengue A, Bhattacharjee S, Pandharkar T, Liu HN, Estiu G, Stahelin RV, Rizk SS, Njimoh DL, Ryan Y, Chotivanich K, Nguon C, Ghorbal M, Lopez-Rubio JJ, Pfrender M, Emrich S, Mohandas N, Dondorp AM, Wiest O, Haldar K. 2015. A molecular mechanism of artemisinin resistance in *Plasmodium falciparum* malaria. Nature 520:683-687.

180. Asawamahasakda W, Ittarat I, Pu Y-M, Ziffer H, Meshnick SR. 1994. Reaction of antimalarial endoperoxides with specific parasite proteins. Antimicrob Agents Chemother 38:1854-1858.

181. Bhisutthibhan J, Pan XQ, Hossler PA, Walker DJ, Yowell CA, Carlton J, Dame JB, Meshnick SR. 1998. The *Plasmodium falciparum* translationally controlled tumor

protein homolog and its reaction with the antimalarial drug artemisinin. J Biol Chem 273:16192-16198.

182. Pandey AV, Tekwani BL, Singh RL, Chauhan VS. 1999. Artemisinin, an endoperoxide antimalarial, disrupts the hemoglobin catabolism and heme detoxification systems in malarial parasite. J Biol Chem 274:19383-19388.

183. Wu W-M, Chen Y-L, Zhai Z, Xiao S-H, Wu Y-L. 2003. Study on the mechanism of action of artemether against schistosomes: the identification of cysteine adducts of both carbon-centred free radicals derived from artemether. Bioorg Med Chem Lett 13:1645-1647.

184. Wu Y, Yue ZY, Wu YL. 1999. Interaction of qinghaosu (artemisinin) with cysteine sulfhydryl mediated by traces of non-heme iron. Angew Chem Int Ed Engl 38:2580-2582.

185. Ismail HM, Barton V, Phanchana M, Charoensutthivarakul S, Wong MHL, Hemingway J, Biagini GA, O'Neill PM, Ward SA. 2016. Artemisinin activity-based probes identify multiple molecular targets within the asexual stage of the malaria parasites *Plasmodium falciparum* 3D7. Proc Natl Acad Sci U S A 113:2080-2085.

186. Kehr S, Jortzik E, Delahunty C, Yates III JR, Rahlfs S, Becker K. 2011. Protein S-glutathionylation in malaria parasites. Antioxid Redox Signal 15:2855-2865.

187. Cobbold SA, Chua HH, Nijagal B, Creek DJ, Ralph SA, McConville MJ. 2015. Metabolic dysregulation induced in *Plasmodium falciparum* by dihydroartemisinin and other front line antimalarial drugs. J Infect Dis 213:276-286.

188. Creek DJ, Chua HH, Cobbold SA, Nijagal B, MacRae JI, Dickerman BK, Gilson PR, Ralph SA, McConville MJ. 2016. Metabolomics-based screening of the malaria box reveals both novel and established mechanisms of action. Antimicrob Agents Chemother 60:6650-6663.

189. Hoppe HC, van Schalkwyk DA, Wiehart UI, Meredith SA, Egan J, Weber BW. 2004. Antimalarial quinolines and artemisinin inhibit endocytosis in *Plasmodium falciparum*. Antimicrob Agents Chemother 48:2370-2378.

190. Chen N, LaCrue AN, Teuscher F, Waters NC, Gatton ML, Kyle DE, Cheng Q. 2014. Fatty acid synthesis and pyruvate metabolism pathways remain active in dihydroartemisinin-induced dormant ring stages of *Plasmodium falciparum*. Antimicrob Agents Chemother 58:4773-4781.

191. Robert A, Meunier B. 1997. Characterization of the first covalent adduct between artemisinin and a heme model. J Am Chem Soc 119:5968-5969.

192. Hong Y-L, Yang Y-Z, Meshnick SR. 1994. The interaction of artemisinin with malarial hemozoin. Mol Biochem Parasitol 63:121-128.

193. Benoit-Vical F, Robert A, Meunier B. 2000. *In vitro* and *in vivo* potentiation of artemisinin and synthetic endoperoxide antimalarial drugs by metalloporphyrins. Antimicrob Agents Chemother 44:2836-2841.

194. Robert A, Cazelles J, Meunier B. 2001. Characterization of the alkylation product of heme by the antimalarial drug artemisinin. Angew Chem Int Ed Engl 40:1954-1957.

195. Laurent S, Robert A, Meunier B. 2005. C10-modified artemisinin derivatives: efficient heme-alkylating agents. Angew Chem Int Ed Engl 44:2060-2063.

196. Loup C, Lelievre J, Benoit-Vical F, Meunier B. 2007. Trioxaquines and heme-artemisinin adducts inhibit the *in vitro* formation of hemozoin better than chloroquine. Antimicrob Agents Chemother 51:3768-3770.

197. Paitayatat S, Tarnchompoo B, Thebtaranonth Y, Yuthavong Y. 1997. Correlation of antimalarial activity of artemisinin derivatives with binding affinity with ferroprotoporphyrin IX. J Med Chem 40:633-638.

198. Robert A, Benoit-Vical F, Claparols C, Meunier B. 2005. The antimalarial drug artemisinin alkylates heme in infected mice. Proc Natl Acad Sci U S A 102:13676-13680.

199. Robert A, Claparols C, Witkowski B, Benoit-Vical F. 2013. Correlation between *Plasmodium yoelii nigeriensis* susceptibility to artemisinin and alkylation of heme by the drug. Antimicrob Agents Chemother 57:3998-4000.

200. Wang D-Y, Wu Y-L. 2000. A possible antimalarial action mode of qinghaosu (artemisinin) series compounds. Alkylation of reduced glutathione by C-centered primary radicals produced from antimalarial compound qinghaosu and 12-(2,4-dimethoxyphenyl)-12-deoxoqinghaosu. Chem Commun 22:2193-2194.

201. Mukanganyama S, Naik YS, Widersten M, Mannervik B, Hasler JA. 2001. Proposed reductive metabolism of artemisinin by glutathione transferases in vitro. Free Radic Res 35:427-434.

202. Gopalakrishnan AM, Kumar N. 2015. Antimalarial action of artesunate involves DNA damage mediated by reactive oxygen species. Antimicrob Agents Chemother 59:317-325.

203. Kasozi D, Mohring F, Rahlfs S, Meyer AJ, Becker K. 2013. Real-time imaging of the intracellular glutathione redox potential in the malaria parasite *Plasmodium falciparum*. PLoS Pathog 9:e1003782.

204. Mohring F, Jortzik E, Becker K. 2016. Comparison of methods probing the intracellular redox milieu in *Plasmodium falciparum*. Mol Biochem Parasitol 206:75-83.
205. Becker K, Tilley L, Vennerstrom JL, Roberts D, Rogerson S, Ginsburg H. 2004. Oxidative stress in malaria parasite-infected erythrocytes: host-parasite interactions. Int J Parasitol 34:163-189.
206. Maeno Y, Toyoshima T, Fujioka H, Ito Y, Meshnick SR, Benakis A, Milhous WK, Aikawa M. 1993. Morphologic effects of artemisinin in *Plasmodium falciparum*. Am J Trop Med Hyg 49:485-491.
207. del Pilar Crespo M, Avery TD, Hanssen E, Fox E, Robinson TV, Valente P, Taylor DK, Tilley L. 2008. Artemisinin and a series of novel endoperoxide antimalarials exert early effects on digestive vacuole morphology. Antimicrob Agents Chemother 52:98-109.
208. Hartwig CL, Lauterwasser EMW, Mahajan SS, Hoke JM, Cooper RA, Renslo AR. 2011. Investigating the antimalarial action of 1,2,4-trioxolanes with fluorescent chemical probes. J Med Chem 54:8207-8213.
209. Hartwig CL, Rosenthal AS, D'Angelo J, Griffin CE, Posner GH, Cooper RA. 2009. Accumulation of artemisinin trioxane derivatives within neutral lipids of *Plasmodium falciparum* malaria parasites is endoperoxide-dependent. Biochem Pharmacol 77:322-336.
210. O'Neill PM, Posner GH. 2004. A medicinal chemistry perspective on artemisinin and related endoperoxides. J Med Chem 47:2945-2964.
211. Berman PA, Adams PA. 1997. Artemisinin enhances heme-catalysed oxidation of lipid membranes. Free Radic Biol Med 22:1283-1288.
212. Li W, Mo W, Shen D, Sun L, Wang J, Lu S, Gitschier JM, Zhou B. 2005. Yeast model uncovers dual roles of mitochondria in action of artemisinin. PLoS Genet 1:e36.
213. Antoine T, Fisher N, Amewu R, O'Neill PM, Ward SA, Biagini GA. 2014. Rapid kill of malaria parasites by artemisinin and semi-synthetic endoperoxides involves ROS-dependent depolarization of the membrane potential. J Antimicrob Chemother 69:1005-1016.
214. Wu W-M, Yao Z-J, Wu Y-L, Jiang K, Wang Y-F, Cehn H-B, Shan F, Li Y. 1996. Ferrous ion induced cleavage of the peroxy bond in qinghaosu and its derivatives and the DNA damage associated with this process. Chem Commun 18:2213-2214.
215. Yang YZ, Little B, Meshnick SR. 1994. Alkylation of proteins by artemisinin. Effects of heme, pH, and drug structure. Biochem Pharmacol 48:569-573.

216. Gupta DK, Patra AT, Zhu L, Gupta AP, Bozdech Z. 2016. DNA damage regulation and its role in drug-related phenotypes in the malaria parasites. Sci Rep 6:23603.

217. Takala-Harrison S, Jacob CG, Arze C, Cummings MP, Silva JC, Dondorp AM, Fukuda MM, Hien TT, Mayxay M, Noedl H, Nosten F, Kyaw MP, Nhien NTT, Imwong M, Bethell D, Se Y, Lon C, Tyner SD, Saunders DL, Ariey F, Mercereau-Puijalon O, Menard D, Newton PN, Khanthavong M, Hongvanthong B, Starzengruber P, Fuehrer H-P, Swoboda P, Khan WA, Phyo AP, Nyunt MM, Nyunt MH, Brown TS, Adams M, Pepin CS, Bailey J, Tan JC, Ferdig MT, Clark TG, Miotto O, MacInnis B, Kwiatkowski DP, White NJ, Ringwald P, Plowe CV. 2015. Independent emergence of artemisinin resistance mutations among *Plasmodium falciparum* in southeast Asia. J Infect Dis 211:670-679.

218. Ashley EA, Dhorda M, Fairhurst RM, Amaratunga C, Lim P, Suon S, Sreng S, Anderson JM, Mao S, Sam B, Sopha C, Chuor CM, Nguon C, Sovannaroth S, Pukrittayakamee S, Jittamala P, Chotivanich K, Chutasmit K, Suchatsoonthorn C, Runcharoen R, Hien TT, Thuy-Nhien NT, Thanh NV, Phu NH, Htut Y, Han KT, Aye KH, Mokuolu OA, Olaosebikan RR, Folaranmi OO, Mayxay M, Khanthavong M, Hongvanthong B, Newton PN, Onyamboko MA, Fanello CI, Tshefu AK, Mishra N, Valecha N, Phyo AP, Nosten F, Yi P, Tripura R, Borrmann S, Bashraheil M, Peshu J, Faiz MA, Ghose A, Hossain MA, Samad R, et al. 2014. Spread of artemisinin resistance in *Plasmodium falciparum* malaria. N Engl J Med 371:411-423.

219. Hien TT, Thuy-Nhien NT, Phu NH, Boni MF, Thanh NV, Nha-Ca NT, Thai CQ, Van Toi P, Thuan PD, Merson L. 2012. *In vivo* susceptibility of *Plasmodium falciparum* to artesunate in Binh Phuoc Province, Vietnam. Malar J 11:355.

220. Phyo AP, Nkhoma S, Stepniewska K, Ashley EA, Nair S, McGready R, ler Moo C, Al-Saai S, Dondorp AM, Lwin KM, Singhasivanon P, Day NP, White NJ, Anderson TJ, Nosten F. 2012. Emergence of artemisinin-resistant malaria on the western border of Thailand: a longitudinal study. Lancet 379:1960-1966.

221. Tun KM, Imwong M, Lwin KM, Win AA, Hlaing TM, Hlaing T, Lin K, Kyaw MP, Plewes K, Faiz MA. 2015. Spread of artemisinin-resistant *Plasmodium falciparum* in Myanmar: a cross-sectional survey of the K13 molecular marker. Lancet Infect Dis 15:415-421.

222. Wang Z, Wang Y, Cabrera M, Zhang Y, Gupta B, Wu Y, Kemirembe K, Hu Y, Liang X, Brashear A, Shrestha S, Li X, Miao J, Sun X, Yang Z, Cui L. 2015. Artemisinin

resistance at the China-Myanmar border and association with mutations in the K13-propeller gene. Antimicrob Agents Chemother 59:6952-6959.

223. Huang F, Takala-Harrison S, Jacob CG, Liu H, Sun X, Yang H, Nyunt MM, Adams M, Zhou S, Xia Z, Ringwald P, Bustos MD, Tang L, Plowe CV. 2015. A single mutation in K13 predominates in Southern China and is associated with delayed clearance of *Plasmodium falciparum* following artemisinin treatment. J Infect Dis 212:1629-1635.

224. Straimer J, Gnadig NF, Witkowski B, Amaratunga C, Duru V, Ramadani AP, Dacheux M, Khim N, Zhang L, Lam S, Gregory PD, Urnov FD, Mercereau-Puijalon O, Benoit-Vical F, Fairhurst RM, Menard D, Fidock DA. 2015. Drug resistance. K13-propeller mutations confer artemisinin resistance in *Plasmodium falciparum* clinical isolates. Science 347:428-431.

225. Witkowski B, Amaratunga C, Khim N, Sreng S, Chim P, Kim S, Lim P, Mao S, Sopha C, Sam B, Anderson JM, Duong S, Chuor CM, Taylor WR, Suon S, Mercereau-Puijalon O, Fairhurst RM, Menard D. 2013. Novel phenotypic assays for the detection of artemisinin-resistant *Plasmodium falciparum* malaria in Cambodia: *in-vitro* and *ex-vivo* drug-response studies. Lancet Infect Dis 13:1043-1049.

226. Ariey F, Witkowski B, Amaratunga C, Beghain J, Langlois A-C, Khim N, Kim S, Duru V, Bouchier C, Ma L, Lim P, Leang R, Duong S, Sreng S, Suon S, Chuor CM, Bout DM, Menard S, Rogers WO, Genton B, Fandeur T, Miotto O, Ringwald P, Le Bras J, Berry A, Barale J-C, Fairhurst RM, Benoit-Vical F, Mercereau-Puijalon O, Menard D. 2014. A molecular marker of artemisinin-resistant *Plasmodium falciparum* malaria. Nature 505:50-55.

227. Amaratunga C, Witkowski B, Dek D, Try V, Khim N, Miotto O, Menard D, Fairhurst RM. 2014. *Plasmodium falciparum* founder populations in western Cambodia have reduced artemisinin sensitivity *in vitro*. Antimicrob Agents Chemother 58:4935-4937.

228. Takala-Harrison S, Clark TG, Jacob CG, Cummings MP, Miotto O, Dondorp AM, Fukuda MM, Nosten F, Noedl H, Imwong M. 2013. Genetic loci associated with delayed clearance of *Plasmodium falciparum* following artemisinin treatment in Southeast Asia. Proc Natl Acad Sci U S A 110:240-245.

229. Takala-Harrison S, Jacob CG, Arze C, Cummings MP, Silva JC, Dondorp AM, Fukuda MM, Hien TT, Mayxay M, Noedl H. 2014. Independent emergence of *Plasmodium falciparum* artemisinin resistance mutations in Southeast Asia. J Infect Dis 211:670-679.

230. Miotto O, Amato R, Ashley EA, MacInnis B, Almagro-Garcia J, Amaratunga C, Lim P, Mead D, Oyola SO, Dhorda M, Imwong M, Woodrow C, Manske M, Stalker J, Drury E, Campino S, Amenga-Etego L, Thanh TN, Tran HT, Ringwald P, Bethell D, Nosten F, Phyo AP, Pukrittayakamee S, Chotivanich K, Chuor CM, Nguon C, Suon S, Sreng S, Newton PN, Mayxay M, Khanthavong M, Hongvanthong B, Htut Y, Han KT, Kyaw MP, Faiz MA, Fanello CI, Onyamboko M, Mokuolu OA, Jacob CG, Takala-Harrison S, Plowe CV, Day NP, Dondorp AM, Spencer CC, McVean G, Fairhurst RM, White NJ, Kwiatkowski DP. 2015. Genetic architecture of artemisinin-resistant *Plasmodium falciparum*. Nat Genet 47:226-234.

231. Ménard D, Khim N, Beghain J, Adegnika AA, Shafiul-Alam M, Amodu O, Rahim-Awab G, Barnadas C, Berry A, Boum Y, Bustos MD, Cao J, Chen J-H, Collet L, Cui L, Thakur G-D, Dieye A, Djallé D, Dorkenoo MA, Eboumbou-Moukoko CE, Espino F-E-CJ, Fandeur T, Ferreira-da-Cruz M-F, Fola AA, Fuehrer H-P, Hassan AM, Herrera S, Hongvanthong B, Houzé S, Ibrahim ML, Jahirul-Karim M, Jiang L, Kano S, Ali-Khan W, Khanthavong M, Kremsner PG, Lacerda M, Leang R, Leelawong M, Li M, Lin K, Mazarati J-B, Ménard S, Morlais I, Muhindo-Mavoko H, Musset L, Na-Bangchang K, Nambozi M, Niaré K, Noedl H, et al. 2016. A worldwide map of *Plasmodium falciparum* K13-propeller polymorphisms. N Engl J Med 374:2453-2464.

232. Fairhurst RM. 2015. Understanding artemisinin-resistant malaria: what a difference a year makes. Curr Opin Infect Dis 28:417-425.

233. Taylor S, Parobek C, DeConti D, Kayentao K, Coulibaly S, Greenwood B, Tagbor H, Williams J, Bojang K, Njie F. 2015. Absence of putative *Plasmodium falciparum* artemisinin resistance mutations in sub-Saharan Africa: A molecular epidemiologic study. J Infect Dis 211:680-688.

234. Torrentino-Madamet M, Fall B, Benoit N, Camara C, Amalvict R, Fall M, Dionne P, Fall KB, Nakoulima A, Diatta B. 2014. Limited polymorphisms in k13 gene in *Plasmodium falciparum* isolates from Dakar, Senegal in 2012–2013. Malar J 13:472.

235. Boussaroque A, Fall B, Madamet M, Wade KA, Fall M, Nakoulima A, Fall KB, Dionne P, Benoit N, Diatta B. 2016. Prevalence of anti-malarial resistance genes in Dakar, Senegal from 2013 to 2014. Malar J 15:347.

236. Lu F, Culleton R, Zhang M, Ramaprasad A, von Seidlein L, Zhou H, Zhu G, Tang J, Liu Y, Wang W, Cao Y, Xu S, Gu Y, Li J, Zhang C, Gao Q, Menard D, Pain A, Yang H, Zhang Q, Cao J. 2017. Emergence of indigenous artemisinin-resistant *Plasmodium falciparum* in Africa. N Engl J Med 376:991-993.

237. Siddiqui G, Srivastava A, Russell AS, Creek DJ. 2017. Multi-omics based identification of specific biochemical changes associated with PfKelch13-mutant artemisinin resistant *Plasmodium falciparum*. J Infect Dis 215:1435-1444.

238. Mok S, Ashley EA, Ferreira PE, Zhu L, Lin Z, Yeo T, Chotivanich K, Imwong M, Pukrittayakamee S, Dhorda M, Nguon C, Lim P, Amaratunga C, Suon S, Hien TT, Htut Y, Faiz MA, Onyamboko MA, Mayxay M, Newton PN, Tripura R, Woodrow CJ, Miotto O, Kwiatkowski DP, Nosten F, Day NP, Preiser PR, White NJ, Dondorp AM, Fairhurst RM, Bozdech Z. 2015. Drug resistance. Population transcriptomics of human malaria parasites reveals the mechanism of artemisinin resistance. Science 347:431-435.

239. Hott A, Casandra D, Sparks KN, Morton LC, Castanares G-G, Rutter A, Kyle DE. 2015. Artemisinin-resistant *Plasmodium falciparum* exhibit altered patterns of development in infected erythrocytes. Antimicrob Agents Chemother 59:3156-3167.

240. Ploypradith P. 2004. Development of artemisinin and its structurally simplified trioxane derivatives as antimalarial drugs. Acta tropica 89:329-342.

241. Jefford CW. 2007. New developments in synthetic peroxidic drugs as artemisinin mimics. Drug Discov Today 12:487-495.

242. Cumming JN, Wang D, Park SB, Shapiro TA, Posner GH. 1998. Design, synthesis, derivatization, and structure− activity relationships of simplified, tricyclic, 1, 2, 4-trioxane alcohol analogues of the antimalarial artemisinin. J Med Chem 41:952-964.

243. Tang Y, Dong Y, Vennerstrom JL. 2004. Synthetic peroxides as antimalarials. Med Res Rev 24:425-448.

244. Vennerstrom JL, Arbe-Barnes S, Brun R, Charman SA, Chiu FC, Chollet J, Dong Y, Dorn A, Hunziker D, Matile H, McIntosh K, Padmanilayam M, Santo Tomas J, Scheurer C, Scorneaux B, Tang Y, Urwyler H, Wittlin S, Charman WN. 2004. Identification of an antimalarial synthetic trioxolane drug development candidate. Nature 430:900-904.

245. Griesbaum K, Liu X, Kassiaris A, Scherer M. 1997. Ozonolyses of O-alkylated ketoximes in the presence of carbonyl groups: a facile access to ozonides. Liebigs Annalen 1997:1381-1390.

246. Dong Y, Chollet J, Matile H, Charman SA, Chiu FC, Charman WN, Scorneaux B, Urwyler H, Santo Tomas J, Scheurer C. 2005. Spiro and dispiro-1, 2, 4-trioxolanes as antimalarial peroxides: charting a workable structure-activity relationship using simple prototypes. J Med Chem 48:4953-4961.

247. Kreidenweiss A, Mordmüller B, Krishna S, Kremsner PG. 2006. Antimalarial activity of a synthetic endoperoxide (RBx-11160/OZ277) against *Plasmodium falciparum* isolates from Gabon. Antimicrob Agents Chemother 50:1535-1537.

248. Valecha N, Krudsood S, Tangpukdee N, Mohanty S, Sharma S, Tyagi P, Anvikar A, Mohanty R, Rao B, Jha A. 2012. Arterolane maleate plus piperaquine phosphate for treatment of uncomplicated *Plasmodium falciparum* malaria: a comparative, multicenter, randomized clinical trial. Clin Infect Dis 55:663-671.

249. Orrell C, Little F, Smith P, Folb P, Taylor W, Olliaro P, Barnes KI. 2008. Pharmacokinetics and tolerability of artesunate and amodiaquine alone and in combination in healthy volunteers. Eur J Clin Pharmacol 64:683-690.

250. Valecha N, Looareesuwan S, Martensson A, Abdulla SM, Krudsood S, Tangpukdee N, Mohanty S, Mishra SK, Tyagi P, Sharma S. 2010. Arterolane, a new synthetic trioxolane for treatment of uncomplicated *Plasmodium falciparum* malaria: a phase II, multicenter, randomized, dose-finding clinical trial. Clin Infect Dis 51:684-691.

251. Saha N, Moehrle JJ, Zutshi A, Sharma P, Kaur P, Iyer SS. 2014. Safety, tolerability and pharmacokinetic profile of single and multiple oral doses of arterolane (RBx11160) maleate in healthy subjects. J Clin Pharmacol 54:386-393.

252. Zhou L, Alker A, Ruf A, Wang X, Chiu FC, Morizzi J, Charman SA, Charman WN, Scheurer C, Wittlin S. 2008. Characterization of the two major CYP450 metabolites of ozonide (1, 2, 4-trioxolane) OZ277. Bioorg Med Chem Lett 18:1555-1558.

253. Creek DJ, Charman WN, Chiu FC, Prankerd RJ, McCullough KJ, Dong Y, Vennerstrom JL, Charman SA. 2007. Iron-mediated degradation kinetics of substituted dispiro-1,2,4-trioxolane antimalarials. J Pharm Sci 96:2945-2956.

254. Gautam A, Ahmed T, Sharma P, Varshney B, Kothari M, Saha N, Roy A, Moehrle JJ, Paliwal J. 2011. Pharmacokinetics and pharmacodynamics of arterolane maleate following multiple oral doses in adult patients with *P. falciparum* malaria. J Clin Pharmacol 51:1519-1528.

255. Creek DJ, Chalmers DK, Charman WN, Duke BJ. 2008. Quantum chemical study of the intermediate complex required for iron-mediated reactivity and antimalarial activity of dispiro-1, 2, 4-trioxolanes. J Mol Graph Model 27:394-400.

256. Phyo AP, Jittamala P, Nosten FH, Pukrittayakamee S, Imwong M, White NJ, Duparc S, Macintyre F, Baker M, Möhrle JJ. 2015. Antimalarial activity of artefenomel (OZ439), a novel synthetic antimalarial endoperoxide, in patients with *Plasmodium*

*falciparum* and *Plasmodium vivax* malaria: an open-label phase 2 trial. Lancet Infect Dis 16:61-69.

257. Moehrle JJ, Duparc S, Siethoff C, van Giersbergen PL, Craft JC, Arbe-Barnes S, Charman SA, Gutierrez M, Wittlin S, Vennerstrom JL. 2013. First-in-man safety and pharmacokinetics of synthetic ozonide OZ439 demonstrates an improved exposure profile relative to other peroxide antimalarials. Br J Clin Pharmacol 75:524-537.
258. Stepniewska K, White NJ. 2008. Pharmacokinetic determinants of the window of selection for antimalarial drug resistance. Antimicrob Agents Chemother 52:1589-1596.
259. Macintyre F, Adoke Y, Tiono AB, Duong TT, Mombo-Ngoma G, Bouyou-Akotet M, Tinto H, Bassat Q, Issifou S, Adamy M. 2017. A randomised, double-blind clinical phase II trial of the efficacy, safety, tolerability and pharmacokinetics of a single dose combination treatment with artefenomel and piperaquine in adults and children with uncomplicated *Plasmodium falciparum* malaria. BMC Med 15:181.
260. Barends M, Jaidee A, Khaohirun N, Singhasivanon P, Nosten F. 2007. *In vitro* activity of ferroquine (SSR 97193) against *Plasmodium falciparum* isolates from the Thai-Burmese border. Malar J 6:81.
261. Henry M, Briolant S, Fontaine A, Mosnier J, Baret E, Amalvict R, Fusaï T, Fraisse L, Rogier C, Pradines B. 2008. *In vitro* activity of ferroquine is independent of polymorphisms in transport protein genes implicated in quinoline resistance in *Plasmodium falciparum*. Antimicrob Agents Chemother 52:2755-2759.
262. Kreidenweiss A, Kremsner PG, Dietz K, Mordmueller B. 2006. *In vitro* activity of ferroquine (SAR97193) is independent of chloroquine resistance in *Plasmodium falciparum*. Am J Trop Med Hyg 75:1178-1181.
263. Uhlemann AC, Wittlin S, Matile H, Bustamante LY, Krishna S. 2007. Mechanism of antimalarial action of the synthetic trioxolane RBX11160 (OZ277). Antimicrob Agents Chemother 51:667-672.
264. Kaiser M, Wittlin S, Nehrbass-Stuedli A, Dong Y, Wang X, Hemphill A, Matile H, Brun R, Vennerstrom JL. 2007. Peroxide bond-dependent antiplasmodial specificity of artemisinin and OZ277 (RBx11160). Antimicrob Agents Chemother 51:2991-2993.
265. Tang Y, Dong Y, Wang X, Sriraghavan K, Wood JK, Vennerstrom JL. 2005. Dispiro-1,2,4-trioxane analogues of a prototype dispiro-1,2,4-trioxolane: mechanistic comparators for artemisinin in the context of reaction pathways with iron(II). J Org Chem 70:5103-5110.

266. Fügi MA, Wittlin S, Dong Y, Vennerstrom JL. 2010. Probing the antimalarial mechanism of artemisinin and OZ277 (arterolane) with nonperoxidic isosteres and nitroxyl radicals. Antimicrob Agents Chemother 54:1042-1046.

267. Wang X, Dong Y, Wittlin S, Creek D, Chollet J, Charman SA, Tomas JS, Scheurer C, Snyder C, Vennerstrom JL. 2007. Spiro- and dispiro-1,2-dioxolanes: contribution of iron(II)-mediated one-electron vs two-electron reduction to the activity of antimalarial peroxides. J Med Chem 50:5840-5847.

268. Creek DJ, Ryan E, Charman WN, Chiu FC, Prankerd RJ, Vennerstrom JL, Charman SA. 2009. Stability of peroxide antimalarials in the presence of human hemoglobin. Antimicrob Agents Chemother 53:3496-3500.

269. Creek DJ, Charman WN, Chiu FC, Prankerd RJ, Dong Y, Vennerstrom JL, Charman SA. 2008. Relationship between antimalarial activity and heme alkylation for spiro- and dispiro-1,2,4-trioxolane antimalarials. Antimicrob Agents Chemother 52:1291-1296.

270. Yang T, Xie SC, Cao P, Giannangelo C, McCaw J, Creek DJ, Charman SA, Klonis N, Tilley L. 2016. Comparison of the exposure time-dependence of the activities of synthetic ozonide antimalarials and dihydroartemisinin against K13 wild-type and mutant *Plasmodium falciparum* strains. Antimicrob Agents Chemother 60:4501-4510.

271. Hofer S, Brun R, Maerki S, Matile H, Scheurer C, Wittlin S. 2008. *In vitro* assessment of the pharmacodynamic properties of DB75, piperaquine, OZ277 and OZ401 in cultures of *Plasmodium falciparum*. J Antimicrob Chemother 62:1061-1064.

272. Maerki S, Brun R, Charman SA, Dorn A, Matile H, Wittlin S. 2006. *In vitro* assessment of the pharmacodynamic properties and the partitioning of OZ277/RBx-11160 in cultures of *Plasmodium falciparum*. J Antimicrob Chemother 58:52-58.

273. Xie SC, Dogovski C, Kenny S, Tilley L, Klonis N. 2014. Optimal assay design for determining the *in vitro* sensitivity of ring stage *Plasmodium falciparum* to artemisinins. Int J Parasitol 44:893-899.

274. Siriwardana A, Iyengar K, Roepe PD. 2016. Endoperoxide drug cross-resistance patterns for *Plasmodium falciparum* exhibiting an artemisinin delayed-clearance phenotype. Antimicrob Agents Chemother 60:6952-6956.

275. Baumgärtner F, Jourdan J, Scheurer C, Blasco B, Campo B, Mäser P, Wittlin S. 2017. *In vitro* activity of anti-malarial ozonides against an artemisinin-resistant isolate. Malar J 16:45.

276. Straimer J, Gnädig NF, Stokes BH, Ehrenberger M, Crane AA, Fidock DA. 2017. *Plasmodium falciparum* K13 mutations differentially impact ozonide susceptibility and parasite fitness *in vitro*. mBio 8:e00172-00117.

277. Lanteri CA, Chaorattanakawee S, Lon C, Saunders DL, Rutvisuttinunt W, Yingyuen K, Bathurst I, Ding XC, Tyner SD. 2014. *Ex vivo* activity of endoperoxide antimalarials, including artemisone and arterolane, against multidrug-resistant *Plasmodium falciparum* isolates from Cambodia. Antimicrob Agents Chemother 58:5831-5840.

278. Ismail HM, Barton VE, Panchana M, Charoensutthivarakul S, Biagini GA, Ward SA, O'Neill PM. 2016. A click chemistry-based proteomic approach reveals that 1, 2, 4-trioxolane and artemisinin antimalarials share a common protein alkylation profile. Angew Chem Int Ed Engl 55:6401-6405.

279. Jourdan J, Matile H, Reift E, Biehlmaier O, Dong Y, Wang X, Mäser P, Vennerstrom JL, Wittlin S. 2015. Monoclonal antibodies that recognize the alkylation signature of antimalarial ozonides OZ277 (arterolane) and OZ439 (artefenomel). ACS Infect Dis 2:54-61.

280. Allman EL, Painter HJ, Samra J, Carrasquilla M, Llinás M. 2016. Metabolomic profiling of the malaria box reveals antimalarial target pathways. Antimicrob Agents Chemother 60:6635-6649.

281. Florens L, Washburn MP, Raine JD, Anthony RM, Grainger M, Haynes JD, Moch JK, Muster N, Sacci JB, Tabb DL, Witney AA, Wolters D, Wu Y, Gardner MJ, Holder AA, Sinden RE, Yates JR, Carucci DJ. 2002. A proteomic view of the *Plasmodium falciparum* life cycle. Nature 419:520.

282. Silvestrini F, Lasonder E, Olivieri A, Camarda G, van Schaijk B, Sanchez M, Younis Younis S, Sauerwein R, Alano P. 2010. Protein export marks the early phase of gametocytogenesis of the human malaria parasite *Plasmodium falciparum*. Mol Cell Proteomics 9:1437-1448.

283. Treeck M, Sanders John L, Elias Joshua E, Boothroyd John C. 2011. The phosphoproteomes of *Plasmodium falciparum* and *Toxoplasma gondii* reveal unusual adaptations within and beyond the parasites' boundaries. Cell Host Microbe 10:410-419.

284. Wang X, Creek DJ, Schiaffo CE, Dong Y, Chollet J, Scheurer C, Wittlin S, Charman SA, Dussault PH, Wood JK, Vennerstrom JL. 2009. Spiroadamantyl 1,2,4-trioxolane, 1,2,4-trioxane, and 1,2,4-trioxepane pairs: relationship between peroxide bond iron(II)

reactivity, heme alkylation efficiency, and antimalarial activity. Bioorg Med Chem Lett 19:4542-4545.

285. Bousejra-El Garah F, Wong MH-L, Amewu RK, Muangnoicharoen S, Maggs JL, Stigliani J-L, Park BK, Chadwick J, Ward SA, O'Neill PM. 2011. Comparison of the reactivity of antimalarial 1, 2, 4, 5-tetraoxanes with 1, 2, 4-trioxolanes in the presence of ferrous iron salts, heme, and ferrous iron salts/phosphatidylcholine. J Med Chem 54:6443-6455.

286. Giannangelo CR, Ellis KM, Sexton AE, Stoessel D, Creek DJ. 2016. The role of metabolomics in antiparasitic drug discovery, p 321-342, Comprehensive analysis of parasite biology: from metabolism to drug discovery, vol 7. Wiley-VCH, Weinheim, Germany.

287. Cowell AN, Istvan ES, Lukens AK, Gomez-Lorenzo MG, Vanaerschot M, Sakata-Kato T, Flannery EL, Magistrado P, Owen E, Abraham M, LaMonte G, Painter HJ, Williams RM, Franco V, Linares M, Arriaga I, Bopp S, Corey VC, Gnädig NF, Coburn-Flynn O, Reimer C, Gupta P, Murithi JM, Moura PA, Fuchs O, Sasaki E, Kim SW, Teng CH, Wang LT, Akidil A, Adjalley S, Willis PA, Siegel D, Tanaseichuk O, Zhong Y, Zhou Y, Llinás M, Ottilie S, Gamo F-J, Lee MCS, Goldberg DE, Fidock DA, Wirth DF, Winzeler EA. 2018. Mapping the malaria parasite druggable genome by using *in vitro* evolution and chemogenomics. Science 359:191-199.

288. Prieto JH, Koncarevic S, Park SK, Yates J, III, Becker K. 2009. Large-scale differential proteome analysis in *Plasmodium falciparum* under drug treatment. PloS One 3:e4098.

289. Briolant S, Almeras L, Belghazi M, Boucomont-Chapeaublanc E, Wurtz N, Fontaine A, Granjeaud S, Fusaï T, Rogier C, Pradines B. 2010. *Plasmodium falciparum* proteome changes in response to doxycycline treatment. Malar J 9:141.

290. Bullard KM, Broccardo C, Keenan SM. 2015. Effects of cyclin-dependent kinase inhibitor Purvalanol B application on protein expression and developmental progression in intra-erythrocytic *Plasmodium falciparum* parasites. Malar J 14:147.

291. Le Roch KG, Johnson JR, Ahiboh H, Chung D-WD, Prudhomme J, Plouffe D, Henson K, Zhou Y, Witola W, Yates JR, Mamoun CB, Winzeler EA, Vial H. 2008. A systematic approach to understand the mechanism of action of the bisthiazolium compound T4 on the human malaria parasite, *Plasmodium falciparum*. BMC genomics 9:513.

# Chapter 2

# Parasite-mediated degradation of synthetic ozonide antimalarials impacts *in vitro* antimalarial activity

Giannangelo C, Stingelin L, Yang T, Tilley L, Charman SA, Creek DJ. 2018. Parasite-mediated degradation of synthetic ozonide antimalarials impacts *in vitro* antimalarial activity. Antimicrob Agents Chemother 62:e01566-01517.

AMERICAN SOCIETY FOR MICROBIOLOGY | Antimicrobial Agents and Chemotherapy®





# Parasite-Mediated Degradation of Synthetic Ozonide Antimalarials Impacts *In Vitro* Antimalarial Activity

**Carlo Giannangelo,[a] Lukas Stingelin,[a]* Tuo Yang,[b] Leann Tilley,[b] Susan A. Charman,[a] Darren J. Creek[a]**

[a]Monash Institute of Pharmaceutical Sciences, Faculty of Pharmacy and Pharmaceutical Sciences, Monash University, Parkville, Victoria, Australia

[b]Department of Biochemistry and Molecular Biology, Bio21 Molecular Science and Biotechnology Institute, The University of Melbourne, Parkville, Victoria, Australia

**ABSTRACT** The peroxide bond of the artemisinins inspired the development of a class of fully synthetic 1,2,4-trioxolane-based antimalarials, collectively known as the ozonides. Similar to the artemisinins, heme-mediated degradation of the ozonides generates highly reactive radical species that are thought to mediate parasite killing by damaging critical parasite biomolecules. We examined the relationship between parasite dependent degradation and antimalarial activity for two ozonides, OZ277 (arterolane) and OZ439 (artefenomel), using a combination of *in vitro* drug stability and pulsed-exposure activity assays. Our results showed that drug degradation is parasite stage dependent and positively correlates with parasite load. Increasing trophozoite-stage parasitemia leads to substantially higher rates of degradation for both OZ277 and OZ439, and this is associated with a reduction in *in vitro* antimalarial activity. Under conditions of very high parasitemia (~90%), OZ277 and OZ439 were rapidly degraded and completely devoid of activity in trophozoite-stage parasite cultures exposed to a 3-h drug pulse. This study highlights the impact of increasing parasite load on ozonide stability and *in vitro* antimalarial activity and should be considered when investigating the antimalarial mode of action of the ozonide antimalarials under conditions of high parasitemia.

**KEYWORDS** *Plasmodium falciparum*, antimalarial activity, artefenomel, arterolane, ozonide, peroxide antimalarial, stability

Malaria remains a significant threat to human health in many parts of the developing world and was responsible for approximately 429,000 deaths in 2015 (1). The greatest morbidity and mortality in humans is caused by the parasite species *Plasmodium falciparum* and, in the absence of a reliable vaccine, management is heavily reliant on effective chemotherapeutic intervention. Rapid acting semisynthetic peroxide antimalarials based on artemisinin are the cornerstone of the current drug treatment strategy and are recommended in combination with a suitable long acting partner drug (artemisinin combination therapy [ACT]) as the first-line option for uncomplicated malaria. In the case of severe malaria, parenteral artesunate followed by ACT is the recommended course of treatment (2). Unfortunately, the artemisinins have short *in vivo* half-lives (1 to 2 h) that dictate the need for multiple doses over a 3-day treatment course, and this prevents their use in malaria prophylaxis. Of major concern is the emergence and spread of artemisinin resistant malaria in the Greater Mekong Subregion (3, 4), highlighting the urgent need for new and effective therapies.

OZ439 (artefenomel) is one of the most advanced antimalarial drug candidates currently in clinical development (5–8), and its first-generation predecessor, OZ277 (arterolane), is approved for use in India as a fixed-dose combination with piperaquine (9–12). Both of these ozonides are fully synthetic, and like the artemisinins (13), contain a peroxide bond that is required for activity (14–16). The artemisinins (17,

**Received** 3 August 2017 **Returned for modification** 22 September 2017 **Accepted** 16 December 2017

**Accepted manuscript posted online** 20 December 2017

**Citation** Giannangelo C, Stingelin L, Yang T, Tilley L, Charman SA, Creek DJ. 2018. Parasite-mediated degradation of synthetic ozonide antimalarials impacts *in vitro* antimalarial activity. Antimicrob Agents Chemother 62:e01566-17. https://doi.org/10.1128/AAC.01566-17.



Address correspondence to Susan A. Charman, susan.charman@monash.edu, or Darren J. Creek, darren.creek@monash.edu.

* Present address: Lukas Stingelin, College of Biology, Hunan University, Changsha, China.

S.A.C. and D.J.C. contributed equally to this article.

18) and the ozonides (19, 20) act on all blood stages of the parasite, including sexual-stage gametocytes (21). Similar to the artemisinins, OZ277 has a relatively short *in vivo* half-life that is only two to three times longer than that for dihydroartemisinin (DHA). In contrast, OZ439 has a greatly extended *in vivo* half-life and exposure profile and is currently undergoing phase II clinical trials in combination with ferroquine (ClinicalTrials.gov registration no. NCT02497612).

Although the mechanism of artemisinin action has not been completely resolved, it is widely accepted that artemisinins must be activated by iron-mediated reduction of the peroxide bond for antimalarial activity (22–25). Iron-mediated activation gives rise to highly reactive radical species that are thought to modify crucial parasite biomolecules resulting in cellular damage and parasite death (26). Recent work has confirmed that the most likely source of the iron-based activator is heme released through the process of parasite hemoglobin digestion (27–29). Blocking hemoglobin digestion with falcipain hemoglobinase inhibitors antagonized artemisinin activity up to 100-fold in trophozoite-stage parasites when a short pulse of drug exposure was used (28). Consistent with this hypothesis, the potency of artemisinin antimalarials is significantly lower during the mid-ring stage when hemoglobin digestion is less active (27, 30). Other potential mechanisms for artemisinin activity, including mitochondrial activation (31) and iron-independent pathways, such as direct inhibition of *P. falciparum* phosphatidylinositol-3-kinase (32) and the cofactor model (33), have also been proposed.

Recent *in vitro* studies have used drug pulse activity assays to examine the exposure time dependence of parasite response to selected peroxide antimalarials (34–36) across the asexual parasite life cycle. The extent of parasite killing was found to be dependent on parasite strain and life cycle stage, drug concentration, and drug exposure time. Similar to the artemisinins (30), short pulse treatment with the ozonides was less effective against mid-ring-stage parasites than against trophozoites, an observation consistent with enhanced hemoglobin degradation during the trophozoite stage. Accordingly, the iron chelator bipyridyl (BiPy) had little effect on ozonide potency, whereas inhibition of hemoglobin digestion using the falcipain inhibitor E64d significantly antagonized ozonide action. These results indicate that, like the artemisinins, the ozonides require active hemoglobin digestion for potent antimalarial activity. Moreover, extending the ozonide exposure time to mimic *in vivo* exposure led to enhanced activity and more effective killing than for the clinically used artemisinin derivative DHA (34).

Previous studies have also demonstrated that the ozonides are susceptible to chemical degradation in noninfected red blood cells (RBCs) and degrade at a higher rate in parasitized RBCs (5). The rate of degradation depends on the chemical structure; first-generation ozonides such as OZ277 have a more exposed peroxide bond and degrade more quickly than next-generation compounds such as OZ439 that contain a more sterically hindered peroxide bond (16, 37, 38). The increased rate of degradation of OZ277 in infected RBCs has been linked to the reduced plasma exposure seen with OZ277 in malaria-infected patients (9) relative to healthy volunteers (12). Notably, a similar decreased exposure was not evident when malaria patients were treated with OZ439 (7).

Understanding the mechanism of action of both the artemisinins and the ozonides is an active area of research. Various biochemical and biomimetic approaches have been utilized to identify both the molecular targets of peroxide antimalarials and parasite biochemical pathways perturbed in response to drug treatment (29, 39–42). Many of these *in vitro* techniques require the use of specific conditions such as high parasitemia (39, 40, 42, 43) for optimal assay performance, and these conditions differ considerably from those used in typical *in vitro* drug activity measurements. Given that the reactivity of the peroxide bond is essential for antimalarial activity, accurate interpretation of the biological relevance of results from *in vitro* experiments relies on a clear understanding of the interplay between parasite-mediated drug degradation

and biological activity under various experimental conditions, such as varying hematocrit (Hct), parasitemia, or both.

The aim of the present study was to quantitatively assess both parasite-mediated drug degradation and the *in vitro* antimalarial activity of the ozonides at various levels of parasitemia, at various life cycle stages, and in the presence of selected inhibitors. We show that reduced ozonide potency at high parasitemia correlates with a significantly enhanced rate of drug degradation *in vitro*. Our results indicate that parasite load and drug degradation are important variables to consider when investigating the antimalarial mode of action of peroxides *in vitro*.

## RESULTS

**Assessment of ozonide washing procedure for drug pulse assays.** Removal of the ozonides from *in vitro* culture in the pulse activity assay format was recently shown to be insufficient if a standard washing method (three washes with culture medium) was used (34). Under the conditions tested by Yang et al. (200 $\mu$l, 0.2% Hct), effective removal of drug was achieved by washing cells with complete RPMI medium (containing 5% serum and 0.25% Albumax II) and incorporating a plate change as part of the washing method. In light of this, the suitability of different washing procedures was assessed for our specific *in vitro* conditions using 2% Hct and 0.5% Albumax II in RPMI. Using a method similar to that described previously (34), noninfected RBCs were exposed to drug, the drug was washed out, infected RBCs were added to the culture, and parasite growth was assessed after 48 h relative to an untreated control. DHA was effectively removed from RBCs according to the standard wash procedure, and parasite growth was equivalent to that of the untreated controls (data not shown). In comparison, when RBCs were incubated with either ozonide and washing was performed using the standard drug washout procedure, residual antimalarial activity was detected (see Fig. S1 in the supplemental material), and significant residual drug concentrations were measured by liquid chromatography-mass spectrometry (LC-MS) (Fig. 1, blue bars). When a plate transfer was incorporated into the standard wash method, OZ277 was effectively removed up to the maximum concentration tested (4.8 $\mu$M; see Fig. S2A in the supplemental material); however, a concentration-dependent reduction in parasite growth was still evident with OZ439-treated RBCs (see Fig. S2B in the supplemental material). Incorporating both the plate transfer and a modified washing medium containing 5% Albumax II led to efficient removal of OZ439 at concentrations up to 2.4 $\mu$M (see Fig. S2B, gray, in the supplemental material). At an intermediate Albumax II concentration of 2%, removal of OZ439 was effective up to a concentration of 1.2 $\mu$M (see Fig. S2B, red, in the supplemental material). Quantitative analysis confirmed that the optimized washing procedure (four washes containing 2% Albumax II and a plate change) reduced residual drug levels to below their limit of quantitation (Fig. 1, red bars).

**Ozonide stability in noninfected RBCs.** The extent of ozonide degradation under our standard *in vitro* culture conditions (2% Hct in RPMI containing 0.5% Albumax II)

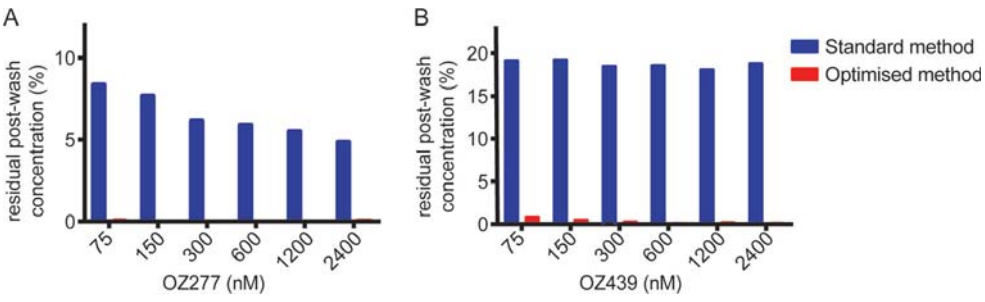


**FIG 1** Assessment of drug washout protocol for pulse activity assays with OZ277 and OZ439. LC-MS quantification of the amount of OZ277 (A) and OZ439 (B) remaining in RBC cultures (2% Hct) after washing using either the standard (blue) or the optimized (red) washing protocol, as defined in Materials and Methods. Values represent the means of two independent experiments (one experiment for 2,400 nM).

**TABLE 1** Activity, degradation half-lives, and rate constants of OZ277 and OZ439 in noninfected and *P. falciparum*-infected RBCs[a]

| | | OZ277 | | | OZ439 | | |
|---|---|---|---|---|---|---|---|
| Parasite stage | Condition(s) | $IC_{50\_3h}$ (nM) | Half-life (h) | $k$ ($h^{-1}$) | $IC_{50\_3h}$ (nM) | Half-life (h) | $k$ ($h^{-1}$) |
| Noninfected | 2% Hct | | 8.9 ± 2.1 | 0.078 ± 0.018 | | 41 ± 17 | 0.017 ± 0.007 |
| | 2% Hct + DFP | | 27 ± 4.1 | 0.026 ± 0.004 | | 63 ± 34 | 0.011 ± 0.006 |
| Mid-rings | 1% P | NA | 7.5 ± 0.9 | 0.092 ± 0.011 | NA | 25 ± 3.5 | 0.028 ± 0.004 |
| | 10% P | NA | 4.1 ± 0.5 | 0.17 ± 0.022 | NA | 18 ± 6.7 | 0.038 ± 0.014 |
| | 10% P + DFP | NA | 4.8 ± 0.7 | 0.15 ± 0.022 | NA | 22 ± 4.3 | 0.031 ± 0.006 |
| | 10% P + E64d | NA | 5.8 ± 0.6 | 0.12 ± 0.012 | NA | 20 ± 6.6 | 0.034 ± 0.011 |
| Trophozoites | 1% P | 31 ± 23 | 3.5 ± 0.8 | 0.20 ± 0.047 | 31 ± 11 | 19 ± 2.5 | 0.037 ± 0.005 |
| | 10% P | 295 ± 119 | 1.3 ± 0.2 | 0.51 ± 0.089 | 398 ± 272 | 3.7 ± 0.5 | 0.19 ± 0.024 |
| | 10% P + DFP | 377 ± 223 | 1.2 ± 0.2 | 0.57 ± 0.11 | 469 ± 271 | 3.7 ± 0.2 | 0.19 ± 0.011 |
| | 10% P + E64d | NA | 1.8 ± 0.4 | 0.39 ± 0.080 | NA | 6.4 ± 3.70 | 0.11 ± 0.063 |
| | >90% P | NA | 0.060, 0.10 | 12, 6.9 | NA | 0.30, 0.20 | 2.3, 3.5 |

[a]Values represent the means ± the standard deviations of three to five independent experiments (individual values from two independent experiments for >90% P condition). $IC_{50\_3h}$, 50% inhibitory concentration to a 3-h drug pulse; P, parasitemia; NA, not active. For the $IC_{50\_3h}$ determinations, parasites were exposed to drug for 3-h pulse, washed using an optimized washing method to remove drug, diluted to 0.5% parasitemia, and incubated for 48 to 72 h before parasite growth was assessed. For the half-life and $k$ determinations, the starting concentration of drug was 100 nM.

was examined following a 6 h incubation with noninfected RBCs. For OZ277, there was approximately 40% loss over this time period, which was reduced to <20% loss in the presence of the iron chelator deferiprone (DFP). Under the same conditions, minimal loss of OZ439 was observed over the incubation period (>85% remaining after 6 h), either in the absence or in the presence of DFP. Degradation rate constants for OZ277 and OZ439 in noninfected RBCs in the presence and absence of DFP are presented in Table 1. The stability of both compounds was confirmed in complete culture medium without RBCs (no significant degradation observed).

**Parasite-dependent drug degradation and ozonide antimalarial activity at high parasitemia.** The effect of increasing parasitemia on the apparent rate of ozonide degradation was examined at different parasite stages. For OZ277, there was a significant increase in the apparent rate of drug degradation in 1% trophozoite-infected cells compared to noninfected RBCs, both at 2% Hct (Fig. 2A). In comparison, OZ439 stability was not significantly affected by the presence of trophozoites at 1% parasitemia (Fig. 2B). When the parasitemia was increased from 1 to 10% trophozoites, a marked increase in the apparent rate of degradation of both OZ277 and OZ439 was observed (Fig. 2A and B). When mid-trophozoite-stage cultures were substantially enriched to >90% parasitemia, there was a further increase in the apparent rate of degradation for both compounds, displaying an almost 100-fold higher degradation rate constant compared to that for a 1% trophozoite culture. At low parasitemia (1%), mid-ring-stage degradation of both ozonides was not significantly different from the noninfected RBC controls over the 6 h incubation period (see Fig. S3A and B in the supplemental material). Increasing the parasitemia from 1 to 10% mid-rings had only a moderate effect on the rate of degradation of OZ277 and no detectable effect on the degradation of OZ439 (see Fig. S3A and B in the supplemental material). At 10% ring-stage parasitemia, the rate of ozonide degradation was significantly lower than that for trophozoite-stage cultures at the same parasitemia, and rate constants were comparable to those for trophozoites at 1% parasitemia (Table 1).

The parasite-dependent degradation of OZ277 was also assessed under more physiologically relevant conditions using asynchronous parasite cultures. Human RBCs were suspended in human plasma at a physiological Hct of 45%, and the parasitemia was varied between 0.2 and 3.8%. A similar progressive increase in the rate of degradation was apparent under these conditions (see Table S1 in the supplemental material). Increasing parasite load by altering the Hct between 15 and 45%, while maintaining a constant 1% parasitemia also resulted in increased degradation of OZ277 (see Table S2 in the supplemental material).

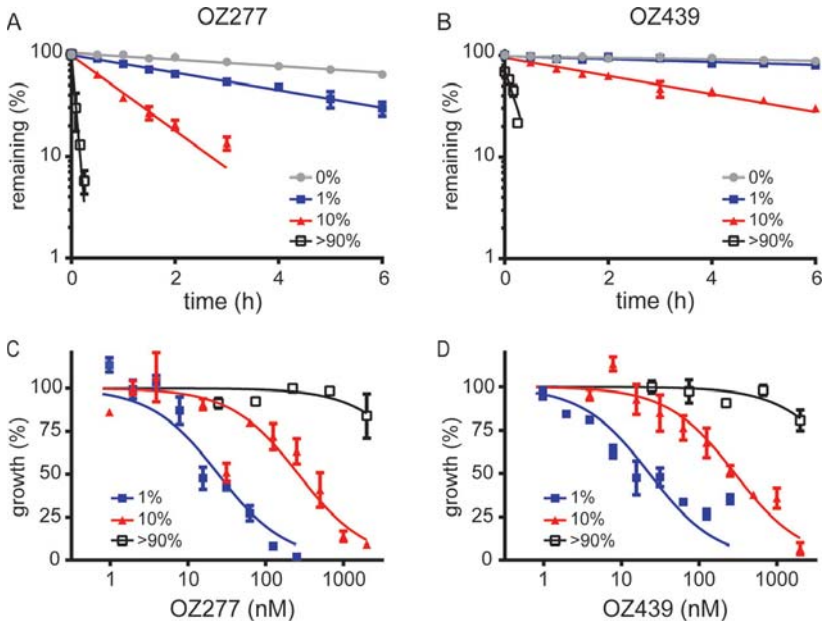


**FIG 2** Parasite-dependent increase in ozonide degradation rate at increasing levels of trophozoite-stage parasitemia and the corresponding loss of *in vitro* activity. (A and B) Degradation profiles of OZ277 (A) and OZ439 (B) in noninfected RBCs (gray) and synchronized trophozoite-stage parasites at 1% (blue), 10% (red), and >90% (black) parasitemia. The starting concentration of both drugs was 100 nM. Values represent the means of two independent experiments or the means ± the standard errors of the mean (SEM) of three to five independent experiments. (C and D) Representative growth inhibition profiles of 3-h pulse treatment with OZ277 (C) and OZ439 (D) in 1% (blue), 10% (red), and >90% (black) trophozoite-stage cultures. Values represent the means of two technical replicates or the means ± the SEM of three technical replicates.

To determine whether a relationship existed between the number of parasites in a culture and the degradation rate constant ($k$), the number of parasites per $\mu$l of culture was plotted against the respective degradation rate constant under each condition (Fig. 3). A positive correlation was apparent for both OZ277 and OZ439 at standard *in vitro* conditions of 2% Hct. The same trend was also apparent for OZ277 when incubated under the more physiologically relevant conditions, although we acknowledge that these conditions are not directly comparable due to differences in parasite strain, medium, and drug concentration.

The dependence of the apparent ozonide degradation rate on parasitemia and asexual parasite stage led us to assess how the differences in stability affected the *in*

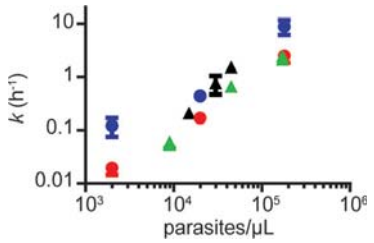


**FIG 3** Relationship between degradation rate constant ($k$) and parasite load for OZ277 and OZ439. The degradation rate constants for 100 nM OZ277 (blue circles) and OZ439 (red circles) were determined when incubated with 3D7 strain *P. falciparum* parasites at different parasite loads achieved by increasing parasitemia and maintaining 2% Hct. To represent conditions comparable to human blood, degradation rate constants were also determined for 360 nM OZ277 when incubated with K1 strain-infected human RBCs suspended in human plasma. Different parasite loads were achieved by either altering parasitemia and maintaining 45% Hct (green triangles) or altering Hct (15, 30, and 45%) and maintaining constant 1% parasitemia (black triangles). Rate constants represent the means of two independent experiments or the means ± the SEM of three or more independent experiments minus the average degradation rate constant observed in noninfected RBCs.

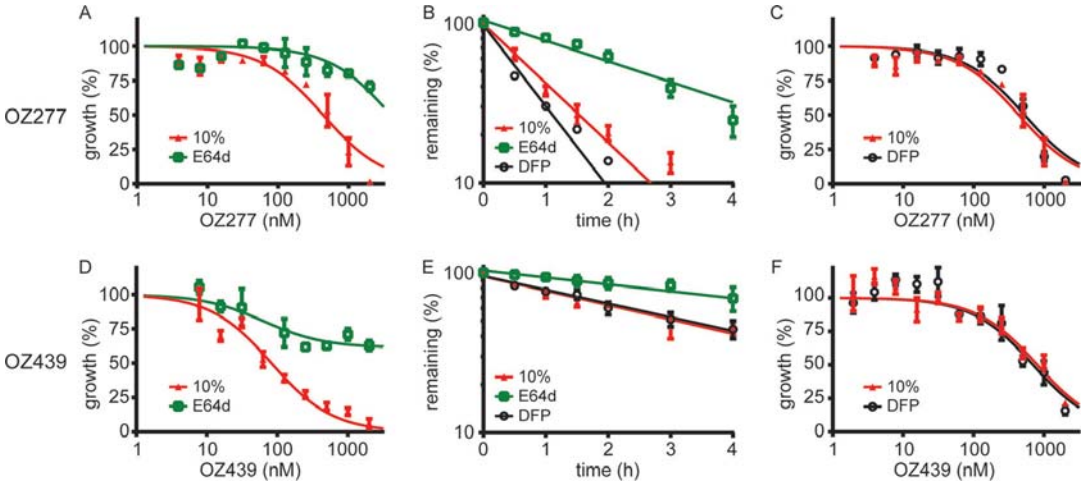


**FIG 4** Activity and degradation profiles of OZ277 and OZ439 in the presence or absence of sublethal concentrations of DFP and E64d. (A) Representative 3-h activity profile of OZ277 in trophozoite-stage parasites in the absence (red) or presence (green) of 10 $\mu$M E64d. Values represent the means ± the SEM of three technical replicates. (B) Stability profile of OZ277 (100 nM) in trophozoite-infected RBCs at 10% parasitemia in the absence (red) or presence (green) of 10 $\mu$M E64d or 250 $\mu$M DFP (black). Values represent the means of two independent experiments or the means ± the SEM of three to four independent experiments. (C) Representative 3-h activity profile of OZ277 in trophozoite-stage parasites in the absence (red) or presence (black) of 250 $\mu$M DFP. Values represent the means ± the SEM of three technical replicates. (D) Representative 3-h activity profile of OZ439 in trophozoite-stage parasites in the absence (red) or presence (green) of 10 $\mu$M E64d. Values represent the means ± the SEM of three technical replicates. (E) Stability profile of OZ439 (100 nM) in trophozoite-infected RBCs at 10% parasitemia in the absence (red) or presence (green) of 10 $\mu$M E64d or 250 $\mu$M DFP (black). Values represent the means of two independent experiments or the means ± the SEM of three to four independent experiments. (F) Representative 3-h activity profile of OZ439 in trophozoite-stage parasites in the absence (red) or presence of 250 $\mu$M DFP (black). Values represent the means ± the SEM of three technical replicates.

*vitro* potency (i.e., the 50% inhibitory concentration [$IC_{50}$]). The sensitivity of synchronized mid-ring- and mid-trophozoite-stage cultures to a 3-h pulse with OZ277 or OZ439 was determined under low (1%)- and high (10%)-parasitemia conditions. In mid-ring-stage parasites, both ozonides showed poor activity and no significant change in the *in vitro* potency of either drug was apparent when parasitemia was increased to 10% (see Fig. S3C and D in the supplemental material). Incubation with a culture of high trophozoite parasitemia (10%) was associated with an ~10-fold reduction in antimalarial activity compared to a low (1%) trophozoite infected culture in response to a 3-h pulse with either OZ277 or OZ439 (Fig. 2C and D). Enriched mid-trophozoite-stage cultures (>90% parasitemia) displayed a further significant reduction in potency (Fig. 2C and D), such that parasite growth was unaffected by a 3-h ozonide pulse up to a concentration of 2 $\mu$M.

**Iron source responsible for increased ozonide degradation at high parasitemia.** The roles of chelatable iron and hemoglobin-derived heme in ozonide degradation and antimalarial activity at high parasitemia (10%) were assessed using sublethal concentrations of the iron chelator DFP and the falcipain inhibitor E64d, respectively. In mid-ring-stage parasites, the addition of either E64d or DFP had a negligible effect on the apparent rate of drug degradation of OZ277 and OZ439 (see Fig. S4A and B in the supplemental material). Under these conditions E64D, but not DFP, reduced OZ277 activity in mid-rings (see Fig. S4C in the supplemental material), but no effect was observed on the limited ring-stage activity of OZ439 under these conditions (see Fig. S4D in the supplemental material).

In trophozoites (10% parasitemia), E64d substantially reduced both OZ277 activity in the 3-h pulse assay (Fig. 4A) and the apparent rate of degradation (Fig. 4B). When OZ277 was coincubated with DFP, activity was unaffected (Fig. 4C), and there was minimal impact on the rate of degradation (Fig. 4B). Similarly, at 10% parasitemia, the addition of E64d also caused a marked reduction in OZ439 activity (Fig. 4D) and rate of degradation (Fig. 4E), whereas DFP had minimal effect on either activity or the rate of degradation (Fig. 4E and F).

## DISCUSSION

The existing literature strongly supports the hypothesis that, like the artemisinins, ozonide antimalarial activity requires activation of the peroxide bond by a reduced iron source (16, 38, 44, 45), inextricably linking compound degradation and antimalarial activity. The requirement for hemoglobin digestion as a prerequisite for antimalarial activity has previously been demonstrated for DHA (27, 28, 30) and has recently also been reported for selected ozonides (34). These studies showed that OZ277 and OZ439 display stage-specific differences in antimalarial activity that correlate with periods of active hemoglobin digestion. The relative lack of sensitivity to a 3-h pulse with an ozonide during the mid-ring stage is also in agreement with previous reports that show ozonides exhibit increased activity at longer exposure times (19, 20, 34). Although the exact molecular target(s) responsible for parasite death after ozonide treatment is incompletely understood, activated peroxides are likely capable of covalently modifying parasite proteins (42), which is thought to ultimately result in parasite death. In the current investigations, we quantified the apparent rate of ozonide degradation in parallel to measuring ozonide activity under conditions of increased parasitemia as commonly used in mechanistic biochemical investigations. Understanding the relationship between degradation, activity, and stage specificity is essential to enable the informed interpretation of mechanistic data generated under these *in vitro* incubation conditions.

Consistent with previous results in noninfected blood (5), OZ277 degraded in the presence of noninfected RBCs under our standard culture conditions using 2% Hct, whereas OZ439 demonstrated minimal degradation. Most of the iron in noninfected RBCs is bound in the form of hemoglobin and concentrations of free heme are low (46). Noninfected erythrocytes also contain a pool of free iron known as the labile iron pool (LIP) (47) in which iron exists in a chelatable form (48) that is at least partially reduced (49). DFP, a membrane-permeable iron chelator, selectively chelates ferric iron, which in turn shifts the equilibrium of iron species from the ferrous to the ferric form. In the presence of DFP, the rate of OZ277 degradation was significantly reduced (Table 1) consistent with the hypothesis that free, chelatable iron, most likely as part of the LIP, is responsible for the degradation of OZ277 in noninfected RBCs. Previous studies have shown that ferric iron has no impact on the degradation of OZ277 (38). Unlike OZ277, OZ439 displays limited reactivity toward free $Fe^{2+}$ (5), likely explaining the relative stability observed for OZ439 in noninfected RBCs.

Both OZ277 and OZ439 displayed a higher rate of degradation when incubated with trophozoite-stage parasites compared to either ring stages or noninfected RBCs (Fig. 2A and B; see also Fig. S2A and B in the supplemental material). Although OZ439 was generally more stable than OZ277, the apparent rate of degradation of both compounds was significantly higher under conditions of high parasitemia (10 and $>$90%) for trophozoite-stage parasites, but less so for the mid-ring stage (see Fig. S2A and B in the supplemental material). Parasitic hemoglobin digestion is most active during the trophozoite stage of the parasite asexual life cycle (50) and liberates a large amount of redox-active free heme. The cell-permeable falcipain inhibitor E64d can be used to block hemoglobin degradation (leading to an accumulation of undigested hemoglobin) and subsequent heme release in *P. falciparum* (27, 51), while DFP is capable of depleting free $Fe^{2+}$ in the parasite LIP (52). Prolonged exposure to either compound alone may be detrimental to the parasite. However, under the conditions tested, short incubations of E64d or DFP alone had no detectable effect on parasite growth, a finding consistent with previous reports (27, 34). Stabilization of both ozonides in parasitized RBCs (10% parasitemia) by E64d, but not by DFP (Fig. 4), is consistent with a parasite-mediated hemoglobin degradation product, most likely free heme, contributing to the parasitemia-dependent degradation of the parent ozonides in trophozoites. Previous *in vitro* studies have shown that the ozonides are stable in the presence of intact hemoglobin (53) but susceptible to heme-catalyzed degradation (37), further demonstrating the role of hemoglobin digestion in promoting ozonide degradation. The lack

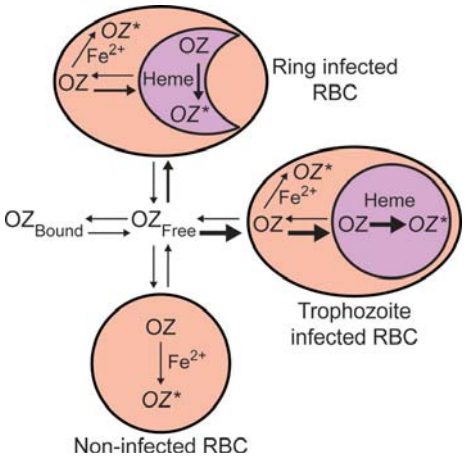


**FIG 5** Proposed pathways for ozonide degradation in an asynchronous *P. falciparum* culture. In an *in vitro* system, an equilibrium exists between ozonide (OZ) that is bound to proteins or lipids ($OZ_{Bound}$) and free (unbound) drug ($OZ_{Free}$) that is available to permeate into an infected or noninfected RBC. The parasite stage (ring or trophozoite) and the relative proportion of each cell population (ring infected, trophozoite infected, and noninfected cells) differentially contribute to ozonide degradation. Hemoglobin-derived free heme (shown as heme) is the most significant catalyst, leading to degraded ozonide (*OZ**) and is most abundant in trophozoite-infected RBC when hemoglobin digestion is most active. Trophozoite-mediated degradation is therefore the dominant ozonide degradation pathway (dark bold arrows), whereas the relative contribution of ring-stage parasites is less substantial (bold arrows) since hemoglobin digestion is not as active. In all cell populations, free ferrous iron as part of the labile iron pool ($Fe^{2+}$) likely plays a minor role in degradation. Paired and single arrows represent reversible and irreversible processes, respectively, and bolder arrows represent more dominant pathways.

of a measurable effect of DFP on ozonide stability indicates free ferrous iron does not have a significant role in ozonide degradation under high parasitemia conditions (Fig. 4 and Table 1). For OZ439, the rate of degradation in the presence of E64d returned to levels similar to that seen in noninfected RBCs. Although the rate of OZ277 degradation was significantly reduced after the addition of E64d, it did not return to the noninfected control level, suggesting other factors may be contributing to *in vitro* degradation of OZ277 that are unrelated to antimalarial activity. This could potentially include aqueous mediated degradation pathways, common to first generation ozonides like OZ277 (54) or interaction with intraparasitic flavin cofactors, similar to that described for the artemisinins (55).

The measured rate of ozonide degradation in this experimental system reflects the contributions from each of the individual degradation processes that occur simultaneously in the different cell populations (i.e., noninfected and infected RBCs; Fig. 5). Ozonides within a *P. falciparum* infected RBC culture environment are in equilibrium between protein- (or lipid)-bound and free (unbound) drug, the latter of which can diffuse across membranes and enter infected and noninfected RBCs. The apparent rate of ozonide degradation in infected RBCs is substantially greater than that in noninfected RBCs (Table 1). Therefore, parasite load (the number of infected RBCs per $\mu$l), which is dependent on both parasitemia and Hct, is the primary determinant of the overall rate of degradation.

Similar to previous results that used the $Fe^{2+}$-specific iron chelator bipyridyl (34), iron chelation with DFP had no appreciable affect on ozonide antimalarial activity (Fig. 4 and Table 1). However, inhibition of *in vitro* antiparasitic activity by coincubation with E64d supports the prevailing hypothesis that heme-mediated activation of the parent ozonide, rather than free iron-mediated activation, is essential for antimalarial activity. In this context, it is uncertain how a higher rate of degradation (or activation) observed with increased parasite load, might affect antimalarial potency. Our results show that at high trophozoite-stage parasitemia, the increased apparent rate of ozonide degradation parallels a significant and progressive reduction in *in vitro* antimalarial activity. Indeed, at the extreme conditions of >90% parasitemia, a 3-h pulse with either ozonide

had no detectable effect on parasite growth (Fig. 2C and D). It is noted that the 3 h incubation at high parasitemia alone does not detrimentally affect parasite viability, since the enriched culture (>90% parasitemia) drug-free controls demonstrated the same growth as untreated 1% parasitemia culture when each condition was diluted to 0.5% parasitemia and incubated over 48 h. Interestingly, the rate of degradation of DHA also increases in the presence of *P. falciparum* infection (45% Hct) compared to noninfected RBCs (see Table S3 in the supplemental material) and antimalarial activity to a 3-h pulse is reduced when trophozoite-stage parasitemia increases from 1 to 10% (see Fig. S5 in the supplemental material). Together with the current data for OZ277 and OZ439, this indicates that parasite-mediated degradation and reduced activity under *in vitro* conditions of high trophozoite parasitemia could be a property of all peroxide antimalarials.

The activity of peroxide antimalarials is governed by parasite stage, drug concentration, and exposure time (34), while artemisinin resistance is associated with multiple mutations in the parasite protein K13 (56, 57). Recent evidence suggests that the duration of exposure necessary for effective killing is greater in artemisinin-resistant parasites compared to the wild type (34) and that the degree of K13 mutant susceptibility to OZ277 and OZ439 is dependent on the type of K13 mutation (35). Although the mechanism of artemisinin resistance remains elusive, some reports have suggested that it may involve an elevated stress response that enables the parasite to withstand the impact of short-term radical-mediated cellular damage (58). In our studies, the increase in trophozoite parasitemia results in a substantially reduced duration of parasite exposure to intact drug. Under conditions of very high parasitemia (>90%) where the duration of exposure and antimalarial activity are both limited, it is plausible that wild-type *P. falciparum* stress response mechanisms are able to overcome the short-lived radical-mediated damage until the drug is effectively depleted, resulting in an apparent loss of antimalarial activity.

Studies recently reported by Ismail et al. described a number of alkylated parasite proteins following treatment of high parasitemia, trophozoite-stage cultures with modified ozonide probes (42). Although the activity of the modified ozonide probes was not reported under the same conditions, our observations would suggest the possibility for limited antimalarial activity under these conditions used, assuming of course that the ozonide probes displayed similar stability properties to OZ277 and OZ439. Our results indicate that rapid peroxide activation is not sufficient to induce substantial antiparasitic activity when the duration of exposure to parent drug is limited. Therefore, the biochemical impact of peroxide antimalarials observed under *in vitro* conditions of high parasitemia should be interpreted with caution when investigating mechanisms of antimalarial activity.

The reduced activity of ozonide antimalarials at higher levels of *in vitro* parasitemia could also be related to the increased number of parasite targets that need to be engaged for growth inhibition to occur. This phenomenon is similar to the previously described inoculum effect, where increased concentrations of drug are required to inhibit growth as the concentration of microorganisms is increased. The inoculum effect has been described for various antimalarials, including chloroquine (59), quinine, mefloquine, halofantrine, and DHA (60). Antimalarials, such as chloroquine and mefloquine, that do not undergo parasite-mediated degradation, exhibit only a 2- to 3-fold reduction in activity in sensitive parasites for a 10-fold increase in parasitemia and the mechanism has been attributed to depletion of drug from the extracellular medium (60). For peroxides that mediate parasite killing by irreversible target modification, we hypothesize that the amount of activated drug per parasite, rather than the initial drug concentration in the culture system, may be the primary determinant of drug action. Therefore, increasing the parasite load effectively decreases the amount of drug available to inhibit each parasite, resulting in the observed decrease in antiparasitic activity. The pronounced decrease in potency of >10-fold in going from 1% parasitemia to 10% parasitemia or higher, and the corresponding progressive increase in the rate of drug degradation, may suggest that a combination of this modified

inoculum effect and limited duration of exposure due to rapid degradation of the parent drug could be the basis for reduced ozonide potency at high *in vitro* parasitemia.

All measurements of ozonide stability in the present study were determined using an initial ozonide concentration of 100 nM. Since we have not explored whether degradation rates are concentration dependent, these degradation rate constants are specific for this particular starting concentration. Although it is not possible to quantitatively extrapolate this *in vitro* data to what might be seen *in vivo*, the results do raise interesting questions regarding possible clinical implications under conditions of hyperparasitemia. In the case of arterolane (OZ277), reduced plasma concentrations are seen in malaria patients compared to healthy volunteers (9), which is consistent with the increased rate of peroxide degradation in the presence of parasites as detected *in vitro*, although this effect is somewhat attenuated when OZ277 is combined with piperaquine (9). It was also noted that as patient parasitemia levels were reduced there was a corresponding increase in plasma concentrations of arterolane after daily dosing (9), providing further support for the role of parasites in peroxide clearance. Additional clinical studies have also shown malaria-infected patients with a high parasite burden (either increased parasitemia, Hct, or both) have increased rates of recrudescence compared to patients with lower parasitemias, when treated with the peroxide antimalarial, artesunate (61), so it is interesting to speculate whether enhanced drug degradation at high parasite load could have impacted peroxide exposure and antimalarial efficacy. The undertreatment of hyperparasitemic malaria patients is a contributing factor to drug resistance in the field (62) and, as such, the potential influence of parasite load on heme-mediated clearance of peroxide antimalarials clearly warrants further investigation.

**Conclusion.** This study systematically demonstrates that parasite-mediated degradation of selected ozonide antimalarials is associated with a significant reduction in activity under *in vitro* conditions of high trophozoite parasitemia. In addition, ozonide degradation is more rapid when exposed to parasites in the trophozoite stage compared to the ring stage of the asexual life cycle, is positively correlated with parasite load, and can be stabilized in the presence of the falcipain inhibitor E64d. These results indicate a balance between heme-mediated activation and degradation appears to be critical for optimal *in vitro* activity of these drugs. This has implications for *in vitro* mechanistic studies that are conducted under conditions that substantially reduce ozonide stability and antimalarial activity and, as such, parasite load should be considered when making associations between peroxide antimalarial activity and biochemical perturbations *in vitro*.

## MATERIALS AND METHODS

**Reagents.** SYBR green I nucleic acid staining dye (10,000× in dimethyl sulfoxide [DMSO]) was purchased from Life Technologies. E64d and potassium dichromate ($K_2Cr_2O_7$) were from Sigma-Aldrich. Acetonitrile (ACN) was LC-MS grade (B&J Brand). OZ277 and OZ439 were provided by the Medicines for Malaria Venture (Geneva). Human RBCs and human plasma were obtained from the Australian Red Cross Blood Service in Melbourne (Victoria, Australia).

**Culturing of parasites and synchronization.** The 3D7 strain of *P. falciparum* was maintained in continuous culture in human RBCs suspended with RPMI 1640 medium (10.4 g/liter), HEPES (5.94 g/liter), hypoxanthine (50 mg/liter), $NaHCO_3$ (2.1 g/liter), and Albumax II (5 g/liter) at 37°C under a gas environment of 94% $N_2$, 5% $CO_2$, and 1% $O_2$, as previously described (63). To examine the effect of parasite stage on drug activity and rate of drug degradation, synchronized cultures were achieved using multiple treatments with 5% sorbitol (64). Synchronization and parasitemia were confirmed by light-microscopic evaluation of Giemsa-stained thin blood smears (>600 parasites counted per slide), and the Hct was determined by counting cells with a hemocytometer.

**Washing procedure and drug pulse activity assays.** Two different washing procedures were explored using *in vitro* culture conditions of 2% Hct and varying parasitemia in 200 μl of culture medium. The standard procedure involved four washes with 200 μl of complete RPMI culture medium supplemented with 0.5% Albumax II. The optimized method included four washes with 200 μl of complete RPMI culture medium supplemented with 2 to 5% Albumax II and involved transferring cultures to a fresh plate after the last wash. The effectiveness of each method was assessed by incubating various concentrations of OZ277 or OZ439 with noninfected RBCs for 3 h and then removing the drug using either the standard or optimized washing procedure and testing for residual drug activity by adding infected RBCs to the washed cells. Parasite growth was then determined after 48 h relative to an

untreated control. Quantification of the concentration of drug remaining in the wells after washing was performed by LC-MS as described below.

Parasite sensitivity to the ozonides was assessed using drug pulse activity assays as described previously (65). Briefly, parasites of a specific age were exposed to drug for a defined period of time and parasite viability determined in the next asexual cycle after the drug was removed by washing. Drug stock solutions in DMSO were first diluted with 50% ACN/$H_2O$ and then serially diluted with 50% ACN/$H_2O$ in V-bottom microplates to provide the desired concentration range for spiking into the infected RBC culture. Spiking solutions (5 $\mu$l) were then added to the appropriate wells of a flat-bottom microplate containing the synchronized mid-ring- or mid-trophozoite-stage parasites so that a final Hct of 2% and either 1 or 10% parasitemia was achieved. Experiments using enriched trophozoite cultures used a commercially available magnetic cell fractionation system (Miltenyi Biotec) to magnetically separate synchronized mid-trophozoite-stage parasites from noninfected RBCs (66). After the magnetic harvest, the mid-trophozoite-stage culture was incubated at 37°C for 1 h, and the Hct was adjusted to 2%. Spiking solutions of drug were prepared as described above and added to the appropriate wells of a flat-bottom microplate containing the enriched culture so that a final Hct of 2% and enriched trophozoite parasitemia was achieved.

Cultures were then incubated with drug for 3 h at 37°C under a gas environment of 94% $N_2$, 5% $CO_2$, and 1% $O_2$. At the end of the incubation period, the drug was removed by washing cultures in a V-bottom microplate using the optimized washing protocol described previously. For all levels of parasitemia tested (1%, 10%, and enriched), cultures were then adjusted to 0.5% parasitemia and 2% Hct (final volume, 200 $\mu$l) to support parasite reinvasion into the next asexual cycle and prevent collapse of high parasitemia cultures. This was achieved by resuspending a proportion of the infected culture from each well into a flat-bottom microplate containing complete RPMI medium and fresh noninfected RBCs so that the desired final culture conditions were obtained. Cultures were incubated under these conditions (2% final Hct; 0.5% final parasitemia) for 48 to 72 h at 37°C and a gas environment of 94% $N_2$, 5% $CO_2$, and 1% $O_2$. Unwashed samples matching the 48 h growth conditions (2% final Hct; 0.5% final parasitemia) that were maintained under lethal drug pressure for 48 to 72 h acted as controls for 100% parasite killing, and infected erythrocytes that were incubated in the absence of drug served as controls for parasite growth. Assays were performed in duplicate or triplicate in at least two independent experiments using RBCs from different donors.

After 48 to 72 h of growth, parasite drug susceptibility was assessed by measurement of SYBR green I fluorescence as previously described (67). Briefly, lysis buffer containing 0.1 $\mu$l/ml SYBR green I was added to each well, and the contents were mixed until no visible erythrocyte sediment remained. After 1 to 2 h of incubation in the dark at room temperature, fluorescence was measured using an Enspire plate reader (Perkin-Elmer) with excitation and emission wavelengths of 485 and 530 nm, respectively. The fluorescence values were plotted against the logarithm of the drug concentration, and the data analyzed using Prism (v6.05; GraphPad Software, San Diego, CA) by nonlinear regression [log(inhibitor) versus normalized response] to yield the drug concentration that produced 50% growth inhibition relative to the drug-free controls ($IC_{50}$).

**Parasite- and RBC-mediated drug degradation.** Samples for assessment of OZ277 and OZ439 degradation were prepared in parallel to the parasite sensitivity samples using the same batch of noninfected and *P. falciparum* (3D7 strain)-infected RBCs. Parasite cultures (1 and 10% parasitemia, 2% Hct) and noninfected RBCs (2% Hct) were spiked with test compound to a final concentration of 100 nM in a flat-bottom microplate. The plate was incubated at 37°C under a gas environment of 94% $N_2$, 5% $CO_2$, and 1% $O_2$. At each sampling point (between 0 and 6 h), 10 $\mu$l of 0.4 M $K_2Cr_2O_7$ was added to the appropriate culture well in the flat-bottom plate to immediately oxidize $Fe^{2+}$ to $Fe^{3+}$. Proteins were then precipitated by addition of 300 $\mu$l of ACN (containing 150 ng/ml of diazepam as the internal standard), and the samples were transferred to microcentrifuge tubes, vortex mixed, and allowed to extract on ice for 10 min. After centrifugation for 5 min at 4°C, 150 $\mu$l of supernatant was transferred to an analytical vial and stored at 4°C until analysis within 8 h.

For each LC-MS analytical run, calibration standards were freshly prepared in noninfected RBCs suspended in complete culture medium (2% Hct). Aliquots (100 $\mu$l) were first stabilized with 10 $\mu$l of 0.4 M $K_2CrO_7$ and then spiked with compound stock solution (prepared in 50% ACN/$H_2O$) to achieve concentrations typically between 3 and 250 nM. Calibration standards were then vortex mixed, extracted on ice for 10 min, and centrifuged at 4°C for 5 min. Supernatant (150 $\mu$l) was then transferred to analytical vials for analysis.

**LC-MS analysis.** Drug stability samples were analyzed using a Shimadzu 8050 triple quadrupole mass spectrometer coupled with a Shimadzu high-pressure liquid chromatography system. Analytical separation was performed on an Ascentis Express $C_{18}$ reversed-phase column (50 by 2.1 mm, 2.7 $\mu$m) with a guard column of the same material (Sigma-Aldrich). Compounds were eluted using a binary gradient solvent system consisting of Milli-Q water with 0.05% formic acid (solvent A) and ACN (solvent B). The gradient profile was as follows: 0 to 0.2 min, 2% B; 0.2 to 0.3 min, 2 to 10% B; 0.3 to 2.7 min, 10 to 70% B; 2.7 to 2.8 min, 70 to 95% B; 2.8 to 3.3 min, 95% B; 3.3 to 3.5 min, 95 to 2% B; and 3.5 to 4 min, 2% B. The peaks of interest eluted between 2 and 3 min at a flow rate of 0.4 ml/min. Mass spectrometry was performed at heat block and desolvation temperatures of 250°C and a heating and drying gas flow of 10 liters/min. Nebulizing gas flow was set at 3 liters/min. The interface voltage and interface temperature were 2 kV and 300°C, respectively. Compounds were monitored by multiple reaction monitoring (MRM) employing electrospray ionization in positive mode. The *m/z* fragmentation transitions for MRM of OZ277, OZ439, and diazepam were *m/z* 393.2 to 227.1, *m/z* 470.1 to 304.1, and *m/z* 285 to 154.1, respectively. The cone voltage for the different compounds was optimized by infusing individual working

stock solutions and ranged from 14 to 32 V. Data were acquired and processed using the Lab Solutions software.

Analyte concentrations were determined by comparison to calibration standards prepared in the same matrix. Quality control (QC) samples were also included in the analysis of the study samples. The validity of each analytical run was determined by ensuring the regression coefficient ($R^2$) for the calibration curve was >0.999 and the measured concentration of the QC samples was within ±15% of the nominal concentration. The limits of quantitation for OZ277 and OZ439 were determined to be 8 and 4 nM, respectively. Experimental degradation data were fit to a first-order exponential decay function, based on initial rates.

**Effect of iron chelation and cysteine protease inhibition on ozonide degradation and antimalarial activity.** A stock solution of the iron chelator DFP was prepared at 500 mM in water by dropwise addition of 1 M HCl until complete dissolution occurred. A stock solution of the cysteine protease inhibitor E64d (10 mM) was prepared in DMSO. Synchronized mid-ring- and mid-trophozoite-stage 3D7 parasites at 10% parasitemia were pretreated for 30 min with either DFP (250 μM) or E64d (10 μM), followed by incubation with OZ277 or OZ439 for an additional 3 h. Parasite sensitivity and the rate of drug degradation were determined using the SYBR green I and LC-MS assays, respectively, as described above.

## SUPPLEMENTAL MATERIAL

Supplemental material for this article may be found at https://doi.org/10.1128/AAC.01566-17.

**SUPPLEMENTAL FILE 1,** PDF file, 0.6 MB.

## ACKNOWLEDGMENTS

We thank the Australian Red Cross Blood Service for their donation of human RBCs and plasma, Phil Wright and Kim Deadman of the Helen Macpherson Smith Trust lab from Monash Institute for Pharmaceutical Sciences (MIPS) for advice and technical assistance with the LC-MS instruments, and Rahul Patil, Francis Chiu, and Jessica Saunders from the Centre for Drug Candidate Optimization at MIPS for reagents, LC-MS advice, and technical assistance.

Partial financial support was provided by the National Health and Medical Research Council (grants APP1128003 and APP1088855).

## REFERENCES

1. World Health Organization. 2016. World malaria report 2016. World Health Organization, Geneva, Switzerland.
2. World Health Organization. 2015. Guidelines for the treatment of malaria, 3rd ed. World Health Organization, Geneva, Switzerland.
3. Ashley EA, Dhorda M, Fairhurst RM, Amaratunga C, Lim P, Suon S, Sreng S, Anderson JM, Mao S, Sam B, Sopha C, Chuor CM, Nguon C, Sovannaroth S, Pukrittayakamee S, Jittamala P, Chotivanich K, Chutasmit K, et al. 2014. Spread of artemisinin resistance in *Plasmodium falciparum* malaria. N Engl J Med 371:411–423. https://doi.org/10.1056/NEJMoa1314981.
4. Dondorp AM, Nosten F, Yi P, Das D, Phyo AP, Tarning J, Lwin KM, Ariey F, Hanpithakpong W, Lee SJ, Ringwald P, Silamut K, Imwong M, Chotivanich K, Lim P, Herdman T, An SS, Yeung S, Singhasivanon P, Day NP, Lindegardh N, Socheat D, White NJ. 2009. Artemisinin resistance in *Plasmodium falciparum* malaria. N Engl J Med 361:455–467. https://doi.org/10.1056/NEJMoa0808859.
5. Charman SA, Arbe-Barnes S, Bathurst IC, Brun R, Campbell M, Charman WN, Chiu FC, Chollet J, Craft JC, Creek DJ, Dong Y, Matile H, Maurer M, Morizzi J, Nguyen T, Papastogiannidis P, Scheurer C, Shackleford DM, Sriraghavan K, Stingelin L, Tang Y, Urwyler H, Wang X, White KL, Wittlin S, Zhou L, Vennerstrom JL. 2011. Synthetic ozonide drug candidate OZ439 offers new hope for a single-dose cure of uncomplicated malaria. Proc Natl Acad Sci U S A 108:4400–4405. https://doi.org/10.1073/pnas.1015762108.
6. Moehrle JJ, Duparc S, Siethoff C, van Giersbergen PL, Craft JC, Arbe-Barnes S, Charman SA, Gutierrez M, Wittlin S, Vennerstrom JL. 2013. First-in-man safety and pharmacokinetics of synthetic ozonide OZ439 demonstrates an improved exposure profile relative to other peroxide antimalarials. Br J Clin Pharmacol 75:524–537. https://doi.org/10.1111/j.1365-2125.2012.04368.x.
7. Phyo AP, Jittamala P, Nosten FH, Pukrittayakamee S, Imwong M, White NJ, Duparc S, Macintyre F, Baker M, Möhrle JJ. 2015. Antimalarial activity of artefenomel (OZ439), a novel synthetic antimalarial endoperoxide, in patients with *Plasmodium falciparum* and *Plasmodium vivax* malaria: an open-label phase 2 trial. Lancet Infect Dis 16:61–69. https://doi.org/10.1016/S1473-3099(15)00320-5.
8. McCarthy JS, Baker M, O'Rourke P, Marquart L, Griffin P, van Huijsduijnen RH, Möhrle JJ. 2016. Efficacy of OZ439 (artefenomel) against early *Plasmodium falciparum* blood-stage malaria infection in healthy volunteers. J Antimicrob Chemother 71:2620–2627. https://doi.org/10.1093/jac/dkw174.
9. Gautam A, Ahmed T, Sharma P, Varshney B, Kothari M, Saha N, Roy A, Moehrle JJ, Paliwal J. 2011. Pharmacokinetics and pharmacodynamics of arterolane maleate following multiple oral doses in adult patients with *Plasmodium falciparum* malaria. J Clin Pharmacol 51:1519–1528. https://doi.org/10.1177/0091270010385578.
10. Valecha N, Krudsood S, Tangpukdee N, Mohanty S, Sharma S, Tyagi P, Anvikar A, Mohanty R, Rao B, Jha A. 2012. Arterolane maleate plus piperaquine phosphate for treatment of uncomplicated *Plasmodium falciparum* malaria: a comparative, multicenter, randomized clinical trial. Clin Infect Dis 55:663–671. https://doi.org/10.1093/cid/cis475.
11. Valecha N, Looareesuwan S, Martensson A, Abdulla SM, Krudsood S, Tangpukdee N, Mohanty S, Mishra SK, Tyagi P, Sharma S. 2010. Arterolane, a new synthetic trioxolane for treatment of uncomplicated *Plasmodium falciparum* malaria: a phase II, multicenter, randomized, dose-finding clinical trial. Clin Infect Dis 51:684–691. https://doi.org/10.1086/655831.
12. Saha N, Moehrle JJ, Zutshi A, Sharma P, Kaur P, Iyer SS. 2014. Safety, tolerability and pharmacokinetic profile of single and multiple oral doses of arterolane (RBx11160) maleate in healthy subjects. J Clin Pharmacol 54:386–393. https://doi.org/10.1002/jcph.232.
13. Posner GH, Oh CH, Wang D, Gerena L, Milhous WK, Meshnick SR, Asawamahasadka W. 1994. Mechanism-based design, synthesis, and *in vitro* antimalarial testing of new 4-methylated trioxanes structurally related to artemisinin: the importance of a carbon-centered radical for

antimalarial activity. J Med Chem 37:1256–1258. https://doi.org/10.1021/jm00035a003.
14. Dong Y, Chollet J, Matile H, Charman SA, Chiu FC, Charman WN, Scorneaux B, Urwyler H, Santo Tomas J, Scheurer C. 2005. Spiro- and dispiro-1,2,4-trioxolanes as antimalarial peroxides: charting a workable structure-activity relationship using simple prototypes. J Med Chem 48:4953–4961. https://doi.org/10.1021/jm049040u.
15. Kaiser M, Wittlin S, Nehrbass-Stuedli A, Dong Y, Wang X, Hemphill A, Matile H, Brun R, Vennerstrom JL. 2007. Peroxide bond-dependent antiplasmodial specificity of artemisinin and OZ277 (RBx11160). Antimicrob Agents Chemother 51:2991–2993. https://doi.org/10.1128/AAC.00225-07.
16. Tang Y, Dong Y, Wang X, Sriraghavan K, Wood JK, Vennerstrom JL. 2005. Dispiro-1,2,4-trioxane analogues of a prototype dispiro-1,2,4-trioxolane: mechanistic comparators for artemisinin in the context of reaction pathways with iron(II). J Org Chem 70:5103–5110. https://doi.org/10.1021/jo050385+.
17. Skinner TS, Manning LS, Johnston WA, Davis TM. 1996. *In vitro* stage-specific sensitivity of *Plasmodium falciparum* to quinine and artemisinin drugs. Int J Parasitol 26:519–525. https://doi.org/10.1016/0020-7519(96)89380-5.
18. Geary TG, Divo AA, Jensen JB. 1989. Stage-specific actions of antimalarial drugs on *Plasmodium falciparum* in culture. Am J Trop Med Hyg 40:240–244. https://doi.org/10.4269/ajtmh.1989.40.240.
19. Hofer S, Brun R, Maerki S, Matile H, Scheurer C, Wittlin S. 2008. *In vitro* assessment of the pharmacodynamic properties of DB75, piperaquine, OZ277, and OZ401 in cultures of *Plasmodium falciparum*. J Antimicrob Chemother 62:1061–1064. https://doi.org/10.1093/jac/dkn315.
20. Maerki S, Brun R, Charman SA, Dorn A, Matile H, Wittlin S. 2006. *In vitro* assessment of the pharmacodynamic properties and the partitioning of OZ277/RBx-11160 in cultures of *Plasmodium falciparum*. J Antimicrob Chemother 58:52–58. https://doi.org/10.1093/jac/dkl209.
21. Delves M, Plouffe D, Scheurer C, Meister S, Wittlin S, Winzeler EA, Sinden RE, Leroy D. 2012. The activities of current antimalarial drugs on the life cycle stages of *Plasmodium*: a comparative study with human and rodent parasites. PLoS Med 9:e1001169. https://doi.org/10.1371/journal.pmed.1001169.
22. Meshnick SR, Thomas A, Ranz A, Xu CM, Pan HZ. 1991. Artemisinin (qinghaosu): the role of intracellular hemin in its mechanism of antimalarial action. Mol Biochem Parasitol 49:181–189. https://doi.org/10.1016/0166-6851(91)90062-B.
23. Meshnick SR, Yang YZ, Lima V, Kuypers F, Kamchonwongpaisan S, Yuthavong Y. 1993. Iron-dependent free radical generation from the antimalarial agent artemisinin (qinghaosu). Antimicrob Agents Chemother 37:1108–1114. https://doi.org/10.1128/AAC.37.5.1108.
24. Posner GH, Oh CH. 1992. Regiospecifically oxygen-18 labeled 1,2,4-trioxane: a simple chemical model system to probe the mechanism (s) for the antimalarial activity of artemisinin (qinghaosu). J Am Chem Soc 114:8328–8329. https://doi.org/10.1021/ja00047a076.
25. Zhang F, Gosser DK, Meshnick SR. 1992. Hemin-catalyzed decomposition of artemisinin (qinghaosu). Biochem Pharmacol 43:1805–1809. https://doi.org/10.1016/0006-2952(92)90713-S.
26. Li J, Zhou B. 2010. Biological actions of artemisinin: insights from medicinal chemistry studies. Molecules 15:1378–1397. https://doi.org/10.3390/molecules15031378.
27. Xie SC, Dogovski C, Hanssen E, Chiu F, Yang T, Crespo MP, Stafford C, Batinovic S, Teguh S, Charman S. 2016. Haemoglobin degradation underpins the sensitivity of early ring stage *Plasmodium falciparum* to artemisinins. J Cell Sci 129:406–416. https://doi.org/10.1242/jcs.178830.
28. Klonis N, Crespo-Ortiz MP, Bottova I, Abu-Bakar N, Kenny S, Rosenthal PJ, Tilley L. 2011. Artemisinin activity against *Plasmodium falciparum* requires hemoglobin uptake and digestion. Proc Natl Acad Sci U S A 108:11405–11410. https://doi.org/10.1073/pnas.1104063108.
29. Wang J, Zhang C-J, Chia WN, Loh CC, Li Z, Lee YM, He Y, Yuan L-X, Lim TK, Liu M, Liew CX, Lee YQ, Zhang J, Lu N, Lim CT, Hua Z-C, Liu B, Shen H-M, Tan KSW, Lin Q. 2015. Haem-activated promiscuous targeting of artemisinin in *Plasmodium falciparum*. Nat Commun 6:10111. https://doi.org/10.1038/ncomms10111.
30. Klonis N, Xie SC, McCaw JM, Crespo-Ortiz MP, Zaloumis SG, Simpson JA, Tilley L. 2013. Altered temporal response of malaria parasites determines differential sensitivity to artemisinin. Proc Natl Acad Sci U S A 110:5157–5162. https://doi.org/10.1073/pnas.1217452110.
31. Wang J, Huang L, Li J, Fan Q, Long Y, Li Y, Zhou B. 2010. Artemisinin directly targets malarial mitochondria through its specific mitochondrial activation. PLoS One 5:e9582. https://doi.org/10.1371/journal.pone.0009582.
32. Mbengue A, Bhattacharjee S, Pandharkar T, Liu HN, Estiu G, Stahelin RV, Rizk SS, Njimoh DL, Ryan Y, Chotivanich K, Nguon C, Ghorbal M, Lopez-Rubio JJ, Pfrender M, Emrich S, Mohandas N, Dondorp AM, Wiest O, Haldar K. 2015. A molecular mechanism of artemisinin resistance in *Plasmodium falciparum* malaria. Nature 520:683–687. https://doi.org/10.1038/nature14412.
33. Haynes RK, Cheu KW, Chan HW, Wong HN, Li KY, Tang MM, Chen MJ, Guo ZF, Guo ZH, Sinniah K, Witte AB, Coghi P, Monti D. 2012. Interactions between artemisinins and other antimalarial drugs in relation to the cofactor model-a unifying proposal for drug action. ChemMedChem 7:2204–2226. https://doi.org/10.1002/cmdc.201200383.
34. Yang T, Xie SC, Cao P, Giannangelo C, McCaw J, Creek DJ, Charman SA, Klonis N, Tilley L. 2016. A comparison of the exposure time-dependence of the activities of synthetic ozonide antimalarials and dihydroartemisinin against K13 wild-type and mutant *Plasmodium falciparum*. Antimicrob Agents Chemother 60:4501–4510. https://doi.org/10.1128/AAC.00574-16.
35. Straimer J, Gnädig NF, Stokes BH, Ehrenberger M, Crane AA, Fidock DA. 2017. *Plasmodium falciparum* K13 mutations differentially impact ozonide susceptibility and parasite fitness *in vitro*. mBio 8:e00172-17. https://doi.org/10.1128/mBio.00172-17.
36. Baumgärtner F, Jourdan J, Scheurer C, Blasco B, Campo B, Mäser P, Wittlin S. 2017. *In vitro* activity of antimalarial ozonides against an artemisinin-resistant isolate. Malar J 16:45. https://doi.org/10.1186/s12936-017-1696-0.
37. Creek DJ, Charman WN, Chiu FC, Prankerd RJ, Dong Y, Vennerstrom JL, Charman SA. 2008. Relationship between antimalarial activity and heme alkylation for spiro- and dispiro-1,2,4-trioxolane antimalarials. Antimicrob Agents Chemother 52:1291–1296. https://doi.org/10.1128/AAC.01033-07.
38. Creek DJ, Charman WN, Chiu FC, Prankerd RJ, McCullough KJ, Dong Y, Vennerstrom JL, Charman SA. 2007. Iron-mediated degradation kinetics of substituted dispiro-1,2,4-trioxolane antimalarials. J Pharm Sci 96:2945–2956. https://doi.org/10.1002/jps.20958.
39. Ismail HM, Barton V, Phanchana M, Charoensutthivarakul S, Wong MHL, Hemingway J, Biagini GA, O'Neill PM, Ward SA. 2016. Artemisinin activity-based probes identify multiple molecular targets within the asexual stage of the malaria parasites *Plasmodium falciparum* 3D7. Proc Natl Acad Sci U S A 113:2080–2085. https://doi.org/10.1073/pnas.1600459113.
40. Cobbold SA, Chua HH, Nijagal B, Creek DJ, Ralph SA, McConville MJ. 2015. Metabolic dysregulation induced in *Plasmodium falciparum* by dihydroartemisinin and other front line antimalarial drugs. J Infect Dis 213:276–286. https://doi.org/10.1093/infdis/jiv372.
41. O'Neill PM, Barton VE, Ward SA. 2010. The molecular mechanism of action of artemisinin: the debate continues. Molecules 15:1705–1721. https://doi.org/10.3390/molecules15031705.
42. Ismail HM, Barton VE, Panchana M, Charoensutthivarakul S, Biagini GA, Ward SA, O'Neill PM. 2016. A click chemistry-based proteomic approach reveals that 1,2,4-trioxolane and artemisinin antimalarials share a common protein alkylation profile. Angew Chem Int Ed Engl 55:6401–6405. https://doi.org/10.1002/anie.201512062.
43. Allman EL, Painter HJ, Samra J, Carrasquilla M, Llinás M. 2016. Metabolomic profiling of the malaria box reveals antimalarial target pathways. Antimicrob Agents Chemother 60:6635–6649. https://doi.org/10.1128/AAC.01224-16.
44. Wang X, Dong Y, Wittlin S, Creek D, Chollet J, Charman SA, Tomas JS, Scheurer C, Snyder C, Vennerstrom JL. 2007. Spiro- and dispiro-1,2-dioxolanes: contribution of iron(II)-mediated one-electron versus two-electron reduction to the activity of antimalarial peroxides. J Med Chem 50:5840–5847. https://doi.org/10.1021/jm0707673.
45. Fügi MA, Wittlin S, Dong Y, Vennerstrom JL. 2010. Probing the antimalarial mechanism of artemisinin and OZ277 (arterolane) with nonperoxidic isosteres and nitroxyl radicals. Antimicrob Agents Chemother 54:1042–1046. https://doi.org/10.1128/AAC.01305-09.
46. Scholl PF, Tripathi AK, Sullivan DJ. 2005. Bioavailable iron and heme metabolism in *Plasmodium falciparum*. Curr Top Microbiol Immunol 295:293–324.
47. Prus E, Fibach E. 2008. The labile iron pool in human erythroid cells. Br J Haematol 142:301–307. https://doi.org/10.1111/j.1365-2141.2008.07192.x.
48. Petrat F, Groot Hd, Sustmann R, Rauen U. 2002. The chelatable iron pool

in living cells: a methodically defined quantity. Biol Chem 383:489–502. https://doi.org/10.1515/BC.2002.051.
49. Breuer W, Epsztejn S, Cabantchik ZI. 1995. Iron acquired from transferrin by K562 cells is delivered into a cytoplasmic pool of chelatable iron (II). J Biol Chem 270:24209–24215. https://doi.org/10.1074/jbc.270.41.24209.
50. Francis SE, Sullivan DJ, Jr, Goldberg ED. 1997. Hemoglobin metabolism in the malaria parasite *Plasmodium falciparum*. Annu Rev Microbiol 51:97–123. https://doi.org/10.1146/annurev.micro.51.1.97.
51. Rosenthal PJ. 2004. Cysteine proteases of malaria parasites. Int J Parasitol 34:1489–1499. https://doi.org/10.1016/j.ijpara.2004.10.003.
52. Clark M, Fisher NC, Kasthuri R, Cerami Hand C. 2013. Parasite maturation and host serum iron influence the labile iron pool of erythrocyte-stage *Plasmodium falciparum*. Br J Haematol 161:262–269. https://doi.org/10.1111/bjh.12234.
53. Creek DJ, Ryan E, Charman WN, Chiu FC, Prankerd RJ, Vennerstrom JL, Charman SA. 2009. Stability of peroxide antimalarials in the presence of human hemoglobin. Antimicrob Agents Chemother 53:3496–3500. https://doi.org/10.1128/AAC.00363-09.
54. Perry CS, Charman SA, Prankerd RJ, Chiu FCK, Dong Y, Vennerstrom JL, Charman WN. 2006. Chemical kinetics and aqueous degradation pathways of a new class of synthetic ozonide antimalarials. J Pharm Sci 95:737–747. https://doi.org/10.1002/jps.20568.
55. Haynes RK, Chan WC, Wong HN, Li KY, Wu WK, Fan KM, Sung HH, Williams ID, Prosperi D, Melato S, Coghi P, Monti D. 2010. Facile oxidation of leucomethylene blue and dihydroflavins by artemisinins: relationship with flavoenzyme function and antimalarial mechanism of action. ChemMedChem 5:1282–1299. https://doi.org/10.1002/cmdc.201000225.
56. Straimer J, Gnadig NF, Witkowski B, Amaratunga C, Duru V, Ramadani AP, Dacheux M, Khim N, Zhang L, Lam S, Gregory PD, Urnov FD, Mercereau-Puijalon O, Benoit-Vical F, Fairhurst RM, Menard D, Fidock DA. 2015. Drug resistance: K13-propeller mutations confer artemisinin resistance in *Plasmodium falciparum* clinical isolates. Science 347:428–431. https://doi.org/10.1126/science.1260867.
57. Ariey F, Witkowski B, Amaratunga C, Beghain J, Langlois A-C, Khim N, Kim S, Duru V, Bouchier C, Ma L, Lim P, Leang R, Duong S, Sreng S, Suon S, Chuor CM, Bout DM, Menard S, Rogers WO, Genton B, Fandeur T, Miotto O, Ringwald P, Le Bras J, Berry A, Barale J-C, Fairhurst RM, Benoit-Vical F, Mercereau-Puijalon O, Menard D. 2014. A molecular marker of artemisinin-resistant *Plasmodium falciparum* malaria. Nature 505:50–55. https://doi.org/10.1038/nature12876.
58. Dogovski C, Xie SC, Burgio G, Bridgford J, Mok S, McCaw JM, Chotivanich K, Kenny S, Gnädig N, Straimer J, Bozdech Z, Fidock DA, Simpson JA, Dondorp AM, Foote S, Klonis N, Tilley L. 2015. Targeting the cell stress response of *Plasmodium falciparum* to overcome artemisinin resistance. PLoS Biol 13:e1002132. https://doi.org/10.1371/journal.pbio.1002132.
59. Gluzman IY, Schlesinger PH, Krogstad DJ. 1987. Inoculum effect with chloroquine and *Plasmodium falciparum*. Antimicrob Agents Chemother 31:32–36. https://doi.org/10.1128/AAC.31.1.32.
60. Duraisingh MT, Jones P, Sambou I, Von Seidlein L, Pinder M, Warhurst DC. 1999. Inoculum effect leads to overestimation of *in vitro* resistance for artemisinin derivatives and standard antimalarials: a Gambian field study. Parasitology 119:435–440. https://doi.org/10.1017/S0031182099004953.
61. Ittarat W, Pickard AL, Rattanasinganchan P, Wilairatana P, Looareesuwan S, Emery K, Low J, Udomsangpetch R, Meshnick SR. 2003. Recrudescence in artesunate-treated patients with falciparum malaria is dependent on parasite burden not on parasite factors. Am J Trop Med Hyg 68:147–152.
62. White NJ, Pongtavornpinyo W, Maude RJ, Saralamba S, Aguas R, Stepniewska K, Lee SJ, Dondorp AM, White LJ, Day NP. 2009. Hyperparasitaemia and low dosing are an important source of anti-malarial drug resistance. Malar J 8:253. https://doi.org/10.1186/1475-2875-8-253.
63. Trager W, Jensen JB. 1976. Human malaria parasites in continuous culture. Science 193:673–675. https://doi.org/10.1126/science.781840.
64. Lambros C, Vanderberg JP. 1979. Synchronization of *Plasmodium falciparum* erythrocytic stages in culture. J Parasitol 65:418–420. https://doi.org/10.2307/3280287.
65. Xie SC, Dogovski C, Kenny S, Tilley L, Klonis N. 2014. Optimal assay design for determining the *in vitro* sensitivity of ring stage *Plasmodium falciparum* to artemisinins. Int J Parasitol 44:893–899. https://doi.org/10.1016/j.ijpara.2014.07.008.
66. Mata-Cantero L, Lafuente M, Sanz L, Rodriguez M. 2014. Magnetic isolation of *Plasmodium falciparum* schizonts iRBCs to generate a high parasitaemia and synchronized *in vitro* culture. Malar J 13:112–120. https://doi.org/10.1186/1475-2875-13-112.
67. Smilkstein M, Sriwilaijaroen N, Kelly JX, Wilairat P, Riscoe M. 2004. Simple and inexpensive fluorescence-based technique for high-throughput antimalarial drug screening. Antimicrob Agents Chemother 48:1803–1806. https://doi.org/10.1128/AAC.48.5.1803-1806.2004.

**Supplementary material**

# Parasite-mediated degradation of synthetic ozonide antimalarials impacts *in vitro* antimalarial activity

Carlo Giannangelo[a], Lukas Stingelin[a*] , Tuo Yang[b], Leann Tilley[b], Susan A. Charman[a†] and Darren J. Creek[a†#]

Monash Institute of Pharmaceutical Sciences, Faculty of Pharmacy and Pharmaceutical Sciences, Melbourne, VIC, Australia[a]; Department of Biochemistry and Molecular Biology, Bio21 Molecular Science and Biotechnology Institute, The University of Melbourne, Melbourne, VIC, Australia[b]

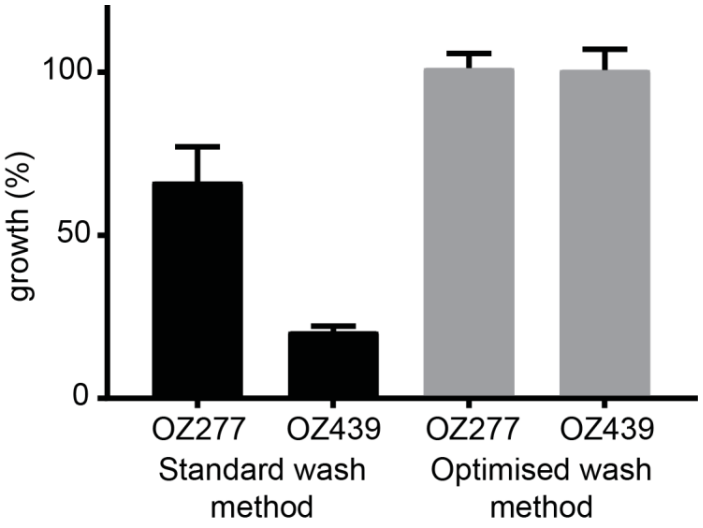


**FIG S1** Residual activity of OZ277 and OZ439 following the standard and optimised washing methods. 600 nM OZ277 and OZ439 were incubated with non-infected RBCs (2% Hct) for 3 h at 37°C and then removed using either the standard (0.5% Albumax II washing medium and no plate transfer) (black) or optimised (2% Albumax washing medium and plate transfer) (grey) washing method. Infected RBCs were added (2% Hct and 1% parasitemia final) and growth assessed after 48 h. Values are expressed relative to untreated controls and represent the mean (± SEM) of three technical replicates.

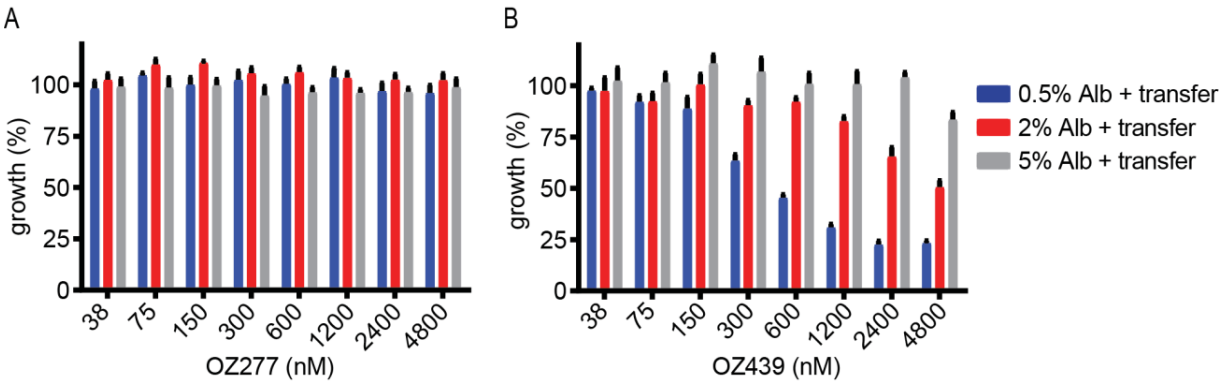


**FIG S2** Assessment of drug washout protocol for pulse activity assays with OZ277 and OZ439. Relative *P. falciparum* growth observed after 48 hours when first incubated with non-infected RBCs (2% Hct) that were exposed to OZ277 (A) or OZ439 (B) for 3 h at 37°C at the concentrations indicated. After the 3 h exposure, RBCs were washed four times with medium containing either 0.5% (blue), 2% (red) or 5% (grey) Albumax II and in each case transferred to a new plate prior to testing residual drug activity 48 h later. Values are expressed relative to untreated controls and represent the mean (± SEM) of three technical replicates.

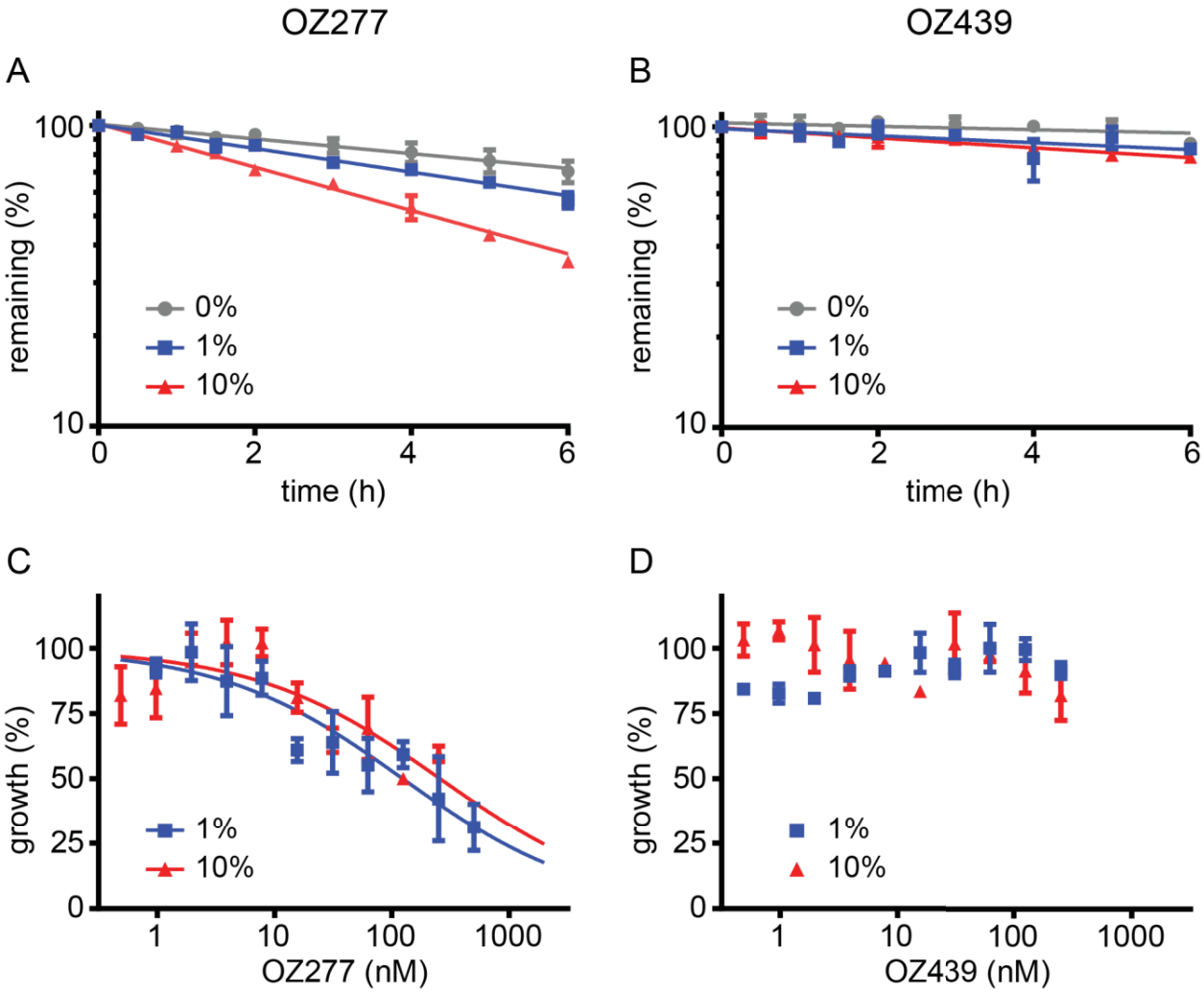


**FIG S3** Stability and representative activity profiles of synchronised mid-ring stage parasites exposed to 3 h OZ277 and OZ439 pulse treatment. Degradation profiles of (A) OZ277 and (B) OZ439 in non-infected RBCs (grey) and synchronised mid-ring stage parasites at 1% (blue) and 10% (red) parasitemia. Values represent the mean of two or mean (± SEM) of three to four independent experiments. Representative activity profiles for a 3 h pulse treatment with (C) OZ277 and (D) OZ439 in 1% (blue) and 10% (red) mid-ring stage cultures. Values represent the mean of two or mean (±SEM) of three technical replicates.

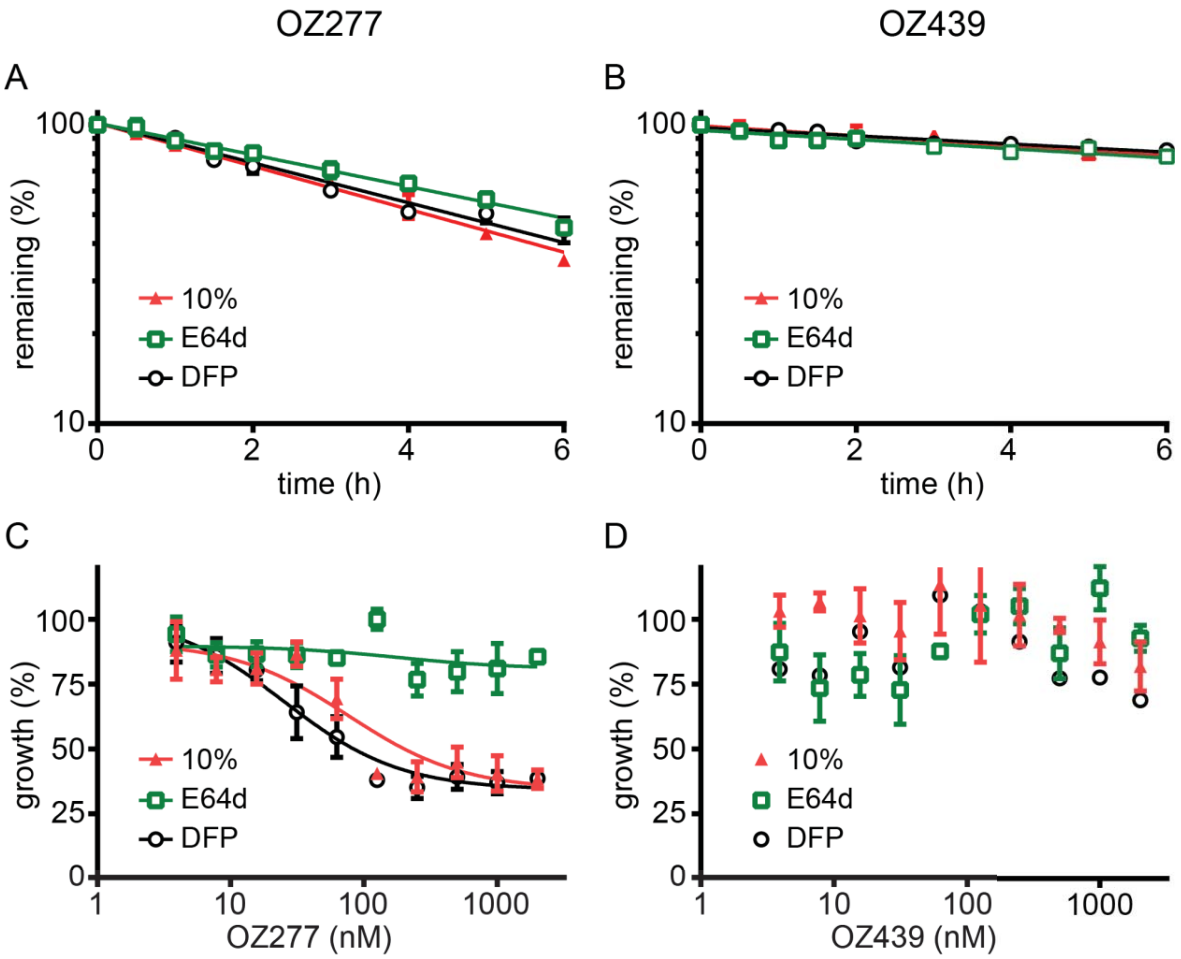


**FIG S4** Inhibition of hemoglobin digestion and iron chelation on ozonide activity and stability in mid-ring stage parasites. Stability profiles of (A) OZ277 and (B) OZ439 in 10% mid-ring stage cultures in the absence (red) or presence (green) of 10 µM E64d or 250 µM DFP (black). Values represent the mean of two or mean (± SD) of three to four independent experiments. Representative mid-ring stage (10% parasitemia) 3 h activity profiles for (C) OZ277 and (D) OZ439 in the absence (red) and presence (green) of 10 µM E64d or 250 µM DFP (black). Values represent the mean (± SEM) of three technical replicates.

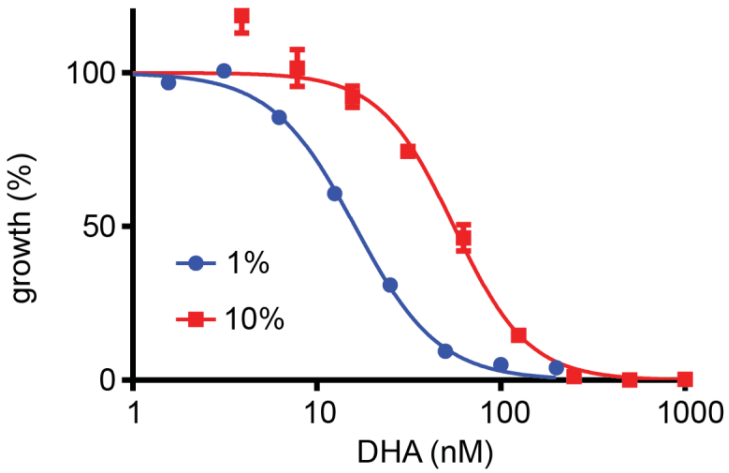


**FIG S5** Representative activity profile of synchronised trophozoite stage parasites exposed to 3 h DHA pulse treatment in 1% (blue) and 10% (red) parasitemia cultures (2% Hct). Values represent the mean (±SEM) of three technical replicates.

**TABLE S1** Degradation half-lives (h) and rate constants ($h^{-1}$) of OZ277 at increasing parasitemia in a physiologically relevant blood-like environment.

| Parasitemia | 45% hematocrit | |
|---|---|---|
| | Half-life (h)* | *k* ($h^{-1}$) |
| 0% | 3.9 ± 0.2 | 0.18 ± 0.0094 |
| 0.2% | 2.9 ± 0.2 | 0.24 ± 0.015 |
| 1% | 0.8 ± 0.06 | 0.84 ± 0.060 |
| 3.8% | 0.3, 0.3 | 2.3, 2.6 |

* OZ277 (starting concentration 360 nM) was incubated in a physiologically-relevant environment consisting of non-infected or *P. falciparum*-infected (K1 strain) human RBCs resuspended in human plasma at defined parasitemia and 45% hematocrit. Remaining drug concentrations were determined using the LCMS method described by Charman *et al* (1). Half-lives represent the mean (± SD) of three independent experiments, with the exception of the 3.8% parasitemia condition where the individual values from two experiments are shown.

**TABLE S2** Degradation half-lives (h) and rate constants ($h^{-1}$) of OZ277 at increasing haematocrit and constant parasitemia

| Hematocrit | 0% parasitemia | | 1% parasitemia | |
|---|---|---|---|---|
| | Half-life (h)* | *k* ($h^{-1}$) | Half-life (h)* | *k* ($h^{-1}$) |
| 15% | 12.8 ± 15.7 | 0.054 ± 0.066 | 1.8 ± 0.1 | 0.39 ± 0.030 |
| 30% | 3.9 ± 0.6 | 0.18 ± 0.030 | 0.7 ± 0.2 | 0.94 ± 0.29 |
| 45% | 3.2 ± 0.3 | 0.22 ± 0.024 | 0.4 ± 0.03 | 1.7 ± 0.13 |

* OZ277 (starting concentration 360 nM) was incubated in a physiologically-relevant environment consisting of non-infected or *P. falciparum*-infected (K1 strain) human RBCs resuspended in human plasma at 1% parasitemia and increasing hematocrit. Remaining drug concentrations were determined using the LCMS method described by Charman *et al* (1). Half-lives represent the mean (± SD) of three independent experiments.

**TABLE S3** Degradation rate constant ($h^{-1}$) for DHA in non-infected and infected (1% parasitemia) red blood cells at 45% Hct

| *k* ($h^{-1}$) * | |
|---|---|
| 0% parasitemia | 1% parasitemia |
| 0.25 ± 0.096 | 0.91 ± 0.25 |

*DHA (starting concentration 360 nM) was incubated in a physiologically-relevant environment consisting of non-infected or *P. falciparum*-infected (K1 strain) human RBCs resuspended in human plasma. Rate constants represent the mean (± SD) of four or five independent experiments for 0% and 1% parasitemia respectively.

## References

1. **Charman SA, Arbe-Barnes S, Bathurst IC, Brun R, Campbell M, Charman WN, Chiu FC, Chollet J, Craft JC, Creek DJ, Dong Y, Matile H, Maurer M, Morizzi J, Nguyen T, Papastogiannidis P, Scheurer C, Shackleford DM, Sriraghavan K, Stingelin L, Tang Y, Urwyler H, Wang X, White KL, Wittlin S, Zhou L, Vennerstrom JL.** 2011. Synthetic ozonide drug candidate OZ439 offers new hope for a single-dose cure of uncomplicated malaria. Proc Natl Acad Sci U S A **108:**4400-4405.

# Chapter 3

# Molecular targets and sub-cellular localisation of ozonide antimalarials in *P. falciparum*

## 3.1 ABSTRACT

The antimalarial mechanism of action of the ozonides is generally thought to involve non-specific alkylation of intraparasitic proteins by highly reactive drug-derived radicals. Considering the promiscuous nature of the radicals, it is possible that modifications of intraparasitic targets other than proteins are also involved in their mode of action. In this study, the *in situ* reaction of selected ozonides with *P. falciparum* small molecule targets was examined to provide further insight into the molecular targets involved in ozonide drug action. In addition, the covalent reaction between ozonides and proteins was exploited to visually explore the time-dependent distribution of ozonide-derived protein alkylation products within *P. falciparum* parasites. A novel click chemistry-based enrichment method was developed to isolate ozonide-derived small molecule adducts, however no ozonide-alkylated metabolites were detected using a generic polar metabolomics extraction procedure. Using an extraction method optimised for solubilisation of free haem, untargeted LC-MS analysis of ozonide-treated parasites identified several regioisomers of the ozonide-alkylated haem adduct, suggesting haem alkylation may be involved in the ozonide mechanism of action. Confocal microscopic analysis revealed widespread ozonide-derived protein alkylation that did not co-localise with a specific parasite compartment and was substantially diminished in the presence of E64d, consistent with haem-mediated drug activation and indiscriminate alkylation of parasite proteins. This study directly demonstrates the ozonide modification of parasite proteins and haem within the parasite and supports the proposal that this process may have a role in their antimalarial mode of action. These data are consistent with the "cluster bomb" hypothesis of activity, whereby haem-mediated activation of ozonides leads to direct alkylation of haem, as well as widespread alkylation of proteins throughout the cell.

## 3.2 INTRODUCTION

Peroxide-based antimalarial drugs, like the artemisinins and the ozonides, are potent antimalarials, but mediate parasiticidal activity by a poorly understood mechanism. A defining feature of these drugs is the peroxide pharmacophore, which is an essential structural component for artemisinin- (1) and ozonide- (2, 3) induced parasite killing. Analogues lacking the peroxide bond are completely devoid of *in vitro* activity (2-5). The proposed mode of action involves peroxide bond cleavage by an intraparasitic reduced iron source, most likely free haem, generating artemisinin- or ozonide-derived oxygen-centred radicals that rearrange to form carbon-centred radicals (2, 3, 6-8). These highly reactive intermediates are thought to cause the toxic drug effect by covalently reacting with proteins and other intraparasitic biomolecules.

Radicals formed by haem-mediated activation of the artemisinin peroxide bond have been reported to alkylate a variety of essential protein targets within the parasite (9-13). The alkylation of small molecule intraparasitic targets may also be involved in the antimalarial mode of action of the artemisinins, as covalent interactions with glutathione (14), cysteine (15) and haem (16-25) have all been reported for the artemisinins. In addition, artemisinin-induced membrane damage (26-28) indicates intraparasitic lipids are also possible alkylation targets. The biological significance of adduct formation with these molecules and their importance to the mechanism of artemisinin action are unknown, but these studies demonstrate that peroxide antimalarials as a class are capable of forming adducts with small molecule targets, as well as proteins.

Covalent modification of parasite proteins has also been reported to be central to the activity of ozonide antimalarials. Stage-specific alkylation of *P. falciparum* proteins by ozonide-derived radicals was previously described using monoclonal antibodies for OZ277 and OZ439 (29). In this study, protein alkylation was ozonide-specific, indicating the *cis*-8'-phenyl

substituent of the next generation ozonides, like OZ439, and the *cis*-8'-alkyl group of their first-generation predecessors, such as OZ277, may differentially impact the ozonide protein alkylation profile. Although the identity of the protein targets and their relevance to the parasiticidal mechanism were not determined, this study represents the first confirmation that ozonides, like artemisinins, covalently react with parasite proteins.

Simple alkyne- and azide-modified ozonide probes based on the OZ03 core structure (the 1,2,4-trioxolane core flanked by a cyclohexane moiety on one side and an adamantane group containing the alkyne or azide 'click-handle' on the other) were used to isolate more than 60 ozonide-alkylated proteins in trophozoite infected cultures by copper-mediated or copper free click chemistry reactions, respectively (30). The alkylation profile shared a 90% similarity with a corresponding clickable artemisinin-based probe, suggesting a common promiscuous targeting effect is involved in the mechanism of action of both drugs.

Like the artemisinins, activated ozonides also have the potential to alkylate small molecule targets *in vitro*, as has been demonstrated in biomimetic experiments with radical trapping agents (6, 31) and reduced haem (32, 33). The reductive reaction of the ozonide peroxide bond with biological haem within the parasite is generally accepted to lead to ozonide activation and, given the likely close proximity of haem and the activated ozonide, haem could represent a biologically relevant target. The alkylated haem adduct may disrupt haem detoxification processes within the parasite (34, 35) and in a simplified *in vitro* system, the extent of ozonide alkylation of haem was found to be correlated with antimalarial activity for a series of ozonide analogues (32).

The prevailing evidence suggests that the ozonides act by a "cluster bomb" mechanism, whereby haem-activated drug alkylates multiple susceptible intraparasitic targets. To date, the identification of ozonide molecular targets has primarily focused on intraparasitic proteins. Whether ozonide alkylation of biological haem or other small molecule targets within the

parasite also plays a role in the mechanism of ozonide action has not been thoroughly explored. Given the promiscuous nature of ozonide-derived radicals, it is possible that activated ozonides directly react with susceptible groups of intraparasitic targets other than proteins. In this study, a novel untargeted click chemistry-based metabolomics strategy was developed for the global identification of alkylated small molecules within *P. falciparum* parasites, with the aim of characterising the intraparasitic small molecule targets of the ozonides. In addition, the ozonide-protein covalent interaction was used as a tool for determining the sub-cellular distribution of selected azide-modified ozonide adducts within *P. falciparum* parasites.

# 3.3 MATERIALS AND METHODS

## 3.3.1 Reagents

SYBR green I nucleic acid staining dye (10,000x in DMSO), LysoTracker Red DND-99, NucBlue Ready Probes and Pierce streptavidin agarose were purchased from Life Technologies. Triton X-100, formic acid, dimethyl sulfoxide, E64d, hemin (≥ 80%), sodium hydrosulfite (sodium dithionite) (~85%), bovine serum albumin (≥ 98%), acetone Emplura grade and glacial acetic acid were from Sigma Aldrich. Photocleavable (PC) biotin-dibenzocyclooctyne (DBCO) and DBCO-Sulfo-Cy5 were from Jena Bioscience. Methanol (Merck) and acetonitrile (B&J Brand) were LC-MS grade. Human RBCs were obtained from the Australian Red Cross Blood Service in Melbourne (VIC, Australia). OZ277 and OZ439 were provided by the Medicines for Malaria Venture (Geneva). All azide and alkyne functionalised ozonide probes were generously provided by Professor Jonathan Vennerstrom (University of Nebraska).

## 3.3.2 Culturing of parasites and synchronisation

*P. falciparum* parasites (3D7 strain) were maintained in continuous culture in human RBCs suspended with RPMI 1640 medium (10.4 g/L), HEPES (5.94 g/L), hypoxanthine (50 mg/L), $NaHCO_3$ (2.1 g/L) and Albumax II (5 g/L) at 37 °C under a gas environment of 94% $N_2$, 5% $CO_2$ and 1% $O_2$, as previously described (36). For all experiments, parasites were tightly synchronised to the desired lifecycle stage using multiple treatments with 5% sorbitol (37). Synchronisation and parasitaemia were assessed by light microscopic evaluation of Giemsa-stained thin blood smears (> 500 parasites counted per slide) and the haematocrit (Hct) determined by counting cells with a hemocytometer.

### 3.3.3 Antimalarial activity of azide and alkyne functionalised ozonide probes

The antimalarial activity of the alkyne (OZ727, OZ747 and carbaOZ727) and azide (OZ754, OZ758, OZ759 and carba OZ758) modified ozonide probes (Figure 1) were assessed using the standard drug sensitivity assay (38) by exposing *P. falciparum* parasites to a drug dilution series for 48 h (1% parasitaemia and 2% Hct) in a 96-well plate format. Samples maintained under lethal DHA drug pressure (≥ 200 nM) for 48 h acted as controls for 100% parasite killing and infected RBCs incubated in the absence of drug acted as controls for parasite growth. After 48 h of drug pressure, lysis buffer containing 0.1 μL/mL SYBR Green I was added to each well and the contents mixed until no visible erythrocyte sediment remained. After 1-2 h of incubation in the dark at room temperature, fluorescence was measured using an Enspire Plate Reader (Perkin Elmer) with excitation and emission wavelengths of 485 and 530 nm, respectively. Fluorescence values were plotted against the logarithm of the drug concentration and the data analysed in GraphPad Prism (version 6.05, GraphPad Software, San Diego, CA) by nonlinear regression (log(inhibitor) vs normalised response) to yield the drug concentration that produced 50% growth inhibition relative to the drug-free controls ($IC_{50}$). Experiments were performed with duplicate or triplicate technical replicates in at least two independent experiments.

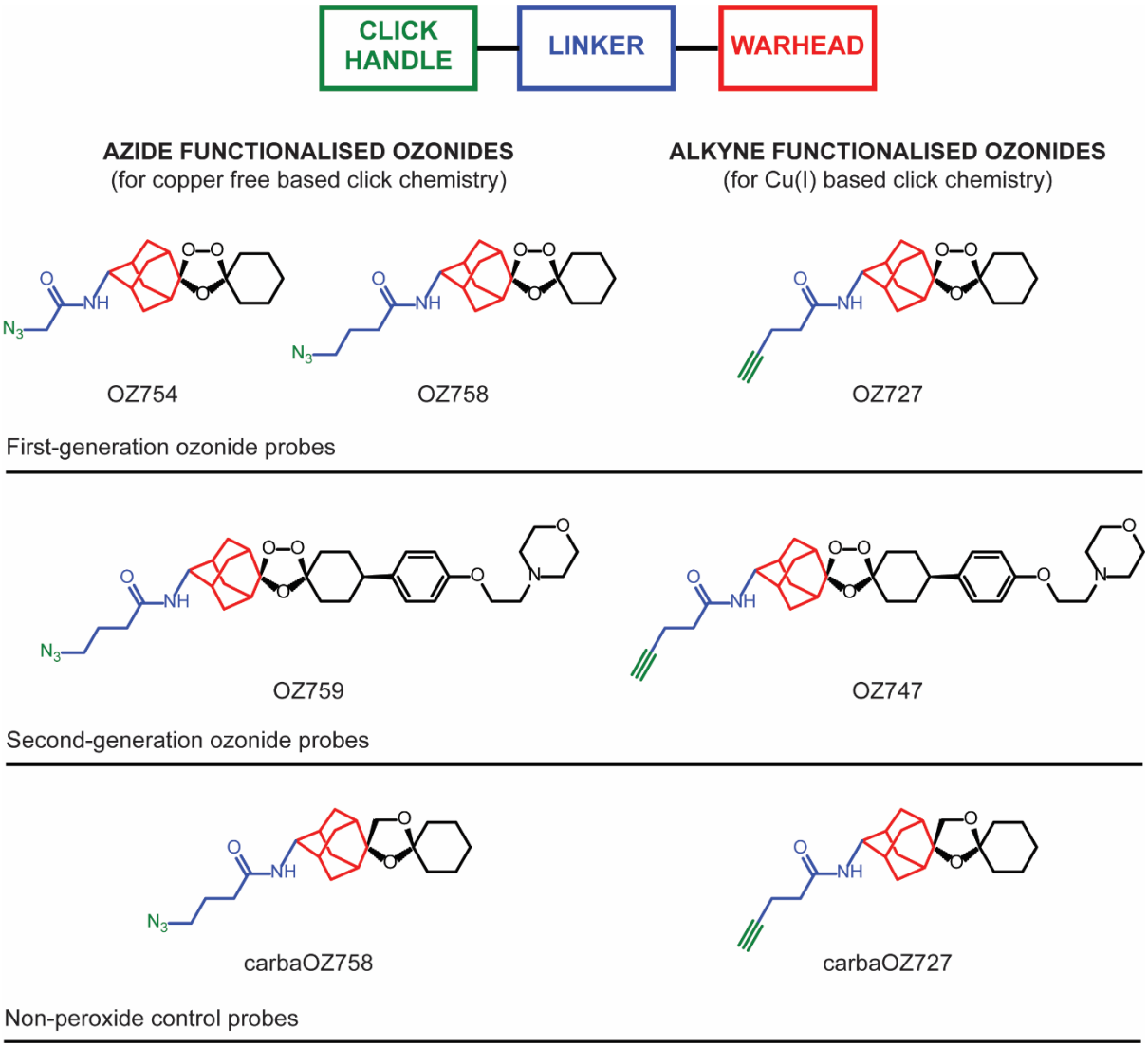


**Figure 1:** Chemical structures of alkyne and azide functionalised ozonide probes and non-peroxide control probes.

### 3.3.4 Sample preparation for click chemistry-mediated isolation of ozonide modified metabolites in *P. falciparum*

For the pull-down of ozonide-metabolite adducts, synchronised *P. falciparum* trophozoite stage cultures (10% parasitaemia and 2% Hct) were treated with 1 µM of OZ754 or an equivalent volume of DMSO for 5 h. Intracellular parasites were harvested from a 30 mL infected RBC culture using 0.1% saponin and the metabolites extracted from the resulting cell lysate using cold methanol (200 µL).

To isolate OZ754 labelled metabolites PC biotin-DBCO was added to the methanol mixture to react with the azide tagged metabolites in the copper free-strain promoted azide-alkyne cycloaddition (SPAAC) reaction. The reaction was allowed to proceed for 1 h. Probe-labelled metabolites were then enriched by affinity-purification with streptavidin agarose beads for 1 h and washed ten times with 50% methanol to minimise non-specific binding. The resultant purified metabolites were isolated from the agarose support by UV irradiation (345 nm) for 1 h, followed by agitation at room temperature for a further 1 h. Beads were pelleted at 1000 x *g* for 5 min and the supernatant collected and stored at -80°C until LC-MS analysis.

### 3.3.5 Sample preparation for identification of ozonide-alkylated haem adducts in *P. falciparum*

Infected RBC cultures (30 mL) synchronised to the trophozoite stage (10% parasitaemia and 2% Hct) were treated with 1 μM of OZ277 or OZ754 or an equivalent volume of DMSO for 3 h and the parasites harvested using 0.1% saponin. The resulting parasite lysates were stored at -80°C until sample preparation. The *P. falciparum* lysates were vortexed and diluted with acetic acid (200 μL) and extracted by the addition of acetone (750 μL). The mixture was vortexed and then centrifuged at 4,000 rpm for 30 min and the supernatant collected, dried and resuspended in methanol/$H_2O$/formic acid (60/40/1) (18). Samples were analysed by LC-MS within 12 h of sample preparation.

### 3.3.6 Spectrophotometric monitoring of alkylated haem adduct degradation

Freshly prepared haemin (final concentration, 10 μM) and degassed 50% ACN/$H_2O$ were added to a sealed spectrophotometer cell containing 5 mg sodium dithionite. Rapid addition of OZ277 (final concentration, 10 μM) to the spectrophotometer cell (final volume, 2 mL) initiated the reaction with reduced haem. Haem absorbance was measured at 0.1 s

intervals between 350 to 550 nm at 1 nm resolution using a Shimadzu UV-3600 spectrophotometer. Absorbance was assessed at regular intervals up to 60 min after addition of drug to the spectrophotometer cell to monitor degradation of the ozonide-alkylated haem adduct. Absorbance of the haem adduct (472 nm) was normalised to the initial haem absorbance (418 nm). After the last time point, samples of the reaction mixture were collected and stored at -20°C prior to LC-MS analysis.

### 3.3.7 Untargeted LC-MS analysis for identification of ozonide modified metabolites

All metabolite extracts were analysed using high resolution MS (Q Exactive, ThermoFisher) coupled with a Dionex Ultimate 3000 UHPLC system (ThermoFisher). Analytical separation was performed on a 50 x 2.1 mm, 2.7 µM Ascentis Express C18 reversed phase column with a guard column of the same material (Sigma Aldrich) and water with 0.1% formic acid (A) and ACN with 0.1% formic acid (B) as the mobile phases. The gradient profile was as follows: 0-20 min, 25-60% B; 20-23 min, 60-100% B; 23-25min, 100% B; 25-26 min, 100-20% B and 26-30 min 20% B.

For LC-MS analysis, initial identification and relative quantification of putative metabolites was performed using the IDEOM workflow (39). Metabolites of interest were confirmed by manual integration of raw LC-MS peak areas using TraceFinder (ThermoFisher). The molecular formulae of the putative ozonide-derived adducts were determined based on accurate mass and the identity of the alkylated metabolites manually derived by subtracting the chemical formula for the adamantane-derived radical ($C_{10}H_{14}O_2$), which is known to form during Fe(II)-mediated ozonide degradation (40). The ozonide-alkylated haem adduct was considered present when the *m/z* was detected (782.3 for OZ277 and 880.3 for OZ754) with

the expected isotopic pattern (M-2 due to $Fe^{54}$) and the extracted ion current (XIC) exhibited a signal to noise ratio > 3 (18).

### 3.3.8 Sub-cellular localisation experiments

Synchronised trophozoite stage parasites (10% parasitaemia and 2% Hct) were treated with an azido-ozonide probe (OZ754, OZ758, OZ759 or carbaOZ758) or DMSO for up to 3 h. In experiments assessing the impact of cysteine protease inhibition on probe localisation, parasites were pre-treated with 10 μM of E64d for 30 min prior to probe addition. Following incubation with drug, the cells were washed with complete RPMI medium and phosphate buffered saline (PBS), then LysoTracker Red (150 nM for 30 min) was used to stain the parasite digestive vacuole. Cells were then washed with PBS before fixation with 4% paraformaldehyde containing 0.0075% glutaraldehyde (30 min), as previously described (41). After fixing, the cells were washed with tris buffered saline (TBS), permeabilised using 0.1% Triton X-100 for 10 min and then washed again in TBS. The cells were then blocked with 1-3% BSA for 60 min and washed with TBS. The SPAAC reaction was initiated by the addition of DBCO-tagged Cy5 (up to 20 μM) for 1 to 16 h, depending on the experiment. After the SPAAC reaction, the cells were washed in TBS, then incubated with Hoechst 33342 for 20 min to stain the nucleus. Cells were mounted onto a glass slide with Vectashield Hardset Antifade Mounting Medium (Vector Laboratories), and the coverslips inverted onto the slide and sealed. Images were taken on an inverted Leica SP8 confocal microscope using a 63x objective and processed in either ImageJ 1.51f or Adobe Photoshop Creative Cloud 2017.

# 3.4 RESULTS

## 3.4.1 Antimalarial activity of alkyne and azide functionalised ozonide probes

The azide and alkyne functionalised probes (Figure 1) retained potent *in vitro* activity against *P. falciparum* (1% parasitaemia and 2% Hct) in the standard 48 h $IC_{50}$ assay (38) (Table 1). Values were consistent with previously reported literature values (30) and with OZ277 and OZ439 activity, indicating alkyne/azide modification does not significantly affect antimalarial activity. As expected, the non-peroxide control probes were inactive (Table 1), confirming essentiality of the peroxide bond for antimalarial activity.

**Table 1:** Antimalarial activity of alkyne and azide functionalised ozonide probes and non-peroxide control probes [a].

| Functionality | Compound | $IC_{50}$ (nM) |
|---|---|---|
| Alkyne [b] | OZ727 | 12, 12 |
| | OZ747 | 48, 67 |
| | carbaOZ727 | Not active |
| Azide [c] | OZ754 | 16 ± 11 |
| | OZ758 | 15 ± 10 |
| | OZ759 | 38 ± 19 |
| | carbaOZ758 | Not active |

[a] Parasites were exposed to drug for 48 h under standard *in vitro* conditions (1% parasitaemia and 2% Hct)

[b] Individual values from two independent experiments, each with three technical replicates are shown.

[c] Values represent the mean (± SD) of at least 3 independent experiments, each with two or three technical replicates.

### 3.4.2 Development of a method to identify ozonide alkylated small molecule targets in *P. falciparum*

A novel click chemistry-based enrichment approach, combined with an untargeted metabolomics platform, was developed to identify ozonide metabolite targets after *in situ* treatment of trophozoite stage *P. falciparum* parasites. A similar click chemistry-based proteomics method has been employed for affinity purification and MS-based identification of drug protein targets (12, 13, 30, 42), however, the trypsin-mediated release mechanism for proteomics is not suitable for release of drug-alkylated metabolites. Therefore, a photoreactive biotin reporter was utilised, which enables affinity purification with streptavidin-agarose beads and release of the captured metabolites by UV irradiation followed by high-resolution MS analysis.

The stability of the ozonide probes was measured under copper catalysed click chemistry conditions to investigate the potential for unwanted Cu(I)-mediated cleavage of the peroxide bond during the pull-down procedure (43). Cu(I) caused rapid reductive cleavage of the OZ727 and OZ747 peroxide bond (≤ 20% of the parent compound remaining after 1 h) (Figure 2, blue and green lines), whereas the non-peroxide control probe, carbaOZ727, was relatively stable over the 16 h incubation period (Figure 2, red line). For this reason, a copper free approach with the PC biotin-DBCO and azide-modified ozonide probes was used for purification and isolation of ozonide labelled small molecules (Figure 3A).

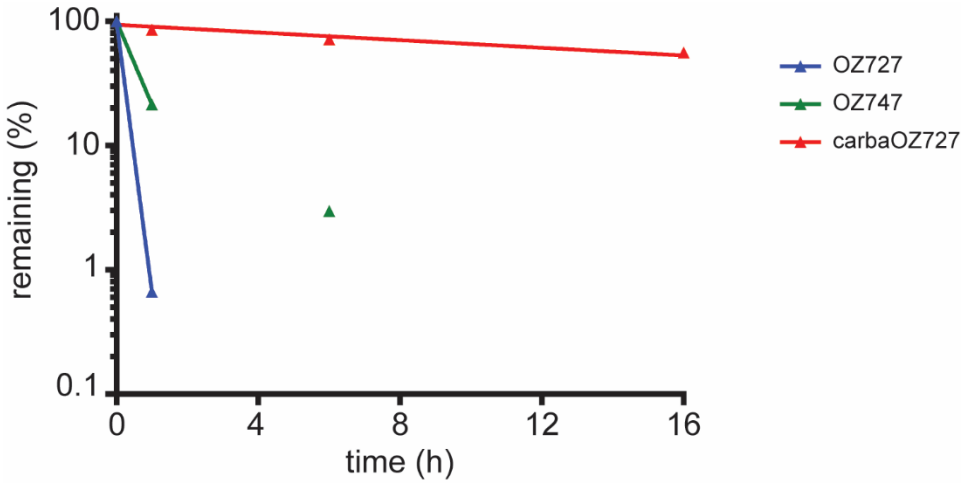


**Figure 2:** Stability profile of OZ727 (blue), OZ754 (green) and carbaOZ727 (red) under copper catalysed click reaction conditions (2 mM copper sulphate, 10 mM tris(3-hydroxypropyltriazolylmethyl)amine, 12.5 mM sodium ascorbate). The starting concentration of each probe was 1 µM.

As a proof of concept, OZ754 (1 µM) was pulled-down from a methanol solution replicating the copper free click chemistry conditions of a methanol metabolite extract. To determine the different products forming throughout the experiment protocol, samples were taken at various points in the workflow and subjected to untargeted LC-MS analysis. The click-reacted OZ754-DBCO compound was only detected in the drug-treated samples and was significantly more abundant in the post-UV release fraction (Figure 3B), demonstrating this method can successfully isolate click reacted OZ754 from a methanol extract. Intact OZ754 was only detected in the drug-treated post-streptavidin fraction (Figure 3C), indicating that not all of the OZ754 reacted with the PC biotin-DBCO. Features corresponding to the DBCO linker (Figure 3D) were detected in the post-streptavidin fraction of both the OZ754 and DMSO samples, suggesting some spontaneous photo-cleavage of the PC biotin-DBCO molecule occurred prior to the UV-induced release step, most likely due to UV exposure during sample preparation. Nevertheless, significantly elevated levels of the DBCO linker were observed after

UV-induced release in both the DMSO and OZ754 samples, indicating successful capture of the biotin containing components by streptavidin and UV irradiation-triggered release from the agarose support. The features corresponding to the non-streptavidin bound PC biotin-DBCO (1001.4205 Da) (Figure 3E) and the non-streptavidin bound OZ754 PC biotin-DBCO (1363.6159 Da) (Figure 3F) were not detected in this study. The duration of the click reaction (0.5, 1 or 3 h) did not affect the relative amounts of any of the products formed. Taken together, these findings validate this approach for pulling down and identifying molecules containing the ozonide-derived adamantane moiety, which is anticipated for ozonide-modified metabolites (6, 7, 32, 40).

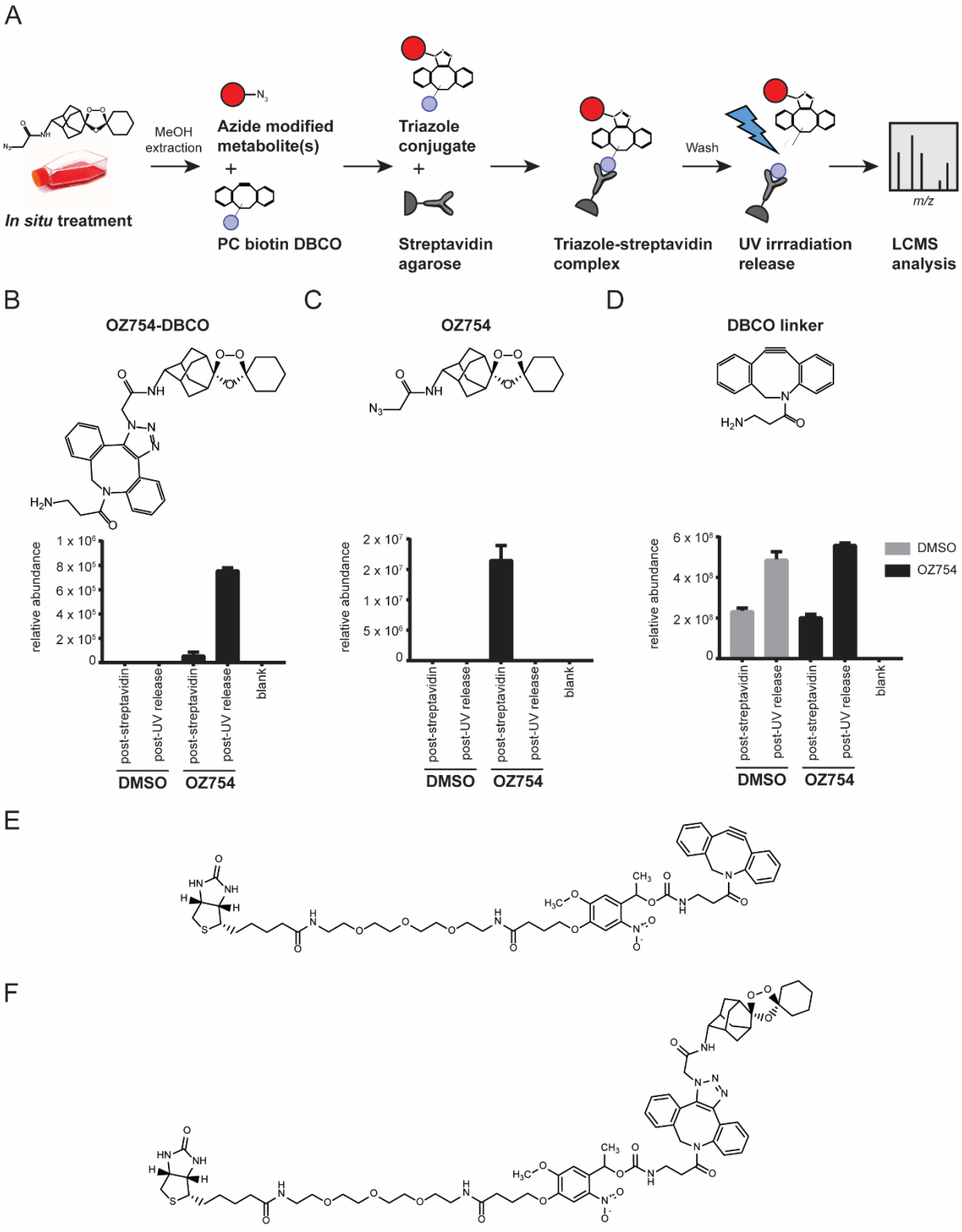


**Figure 3:** Workflow for the copper free click chemistry-mediated identification of ozonide-modified metabolites and the predicted chemical species formed at various points in the experimental workflow. (A) General workflow for copper free click chemistry-mediated identification of ozonide-modified metabolites after *in situ* treatment of *P. falciparum* parasites with an azido ozonide. The azide-modified metabolites were extracted and tagged with a

photocleavable biotin-dibenzocyclooctyne (PC biotin-DBCO) via the strain promoted azide–alkyne cycloaddition click reaction, followed by affinity purification with streptavidin agarose beads. The captured molecules were released from the agarose support via UV irradiation before untargeted LC-MS analysis for metabolite identification. (B-D) Chemical structures (based on accurate mass) and relative abundance of products formed following copper free click chemistry-based pull-down of OZ754 (black). DMSO treatment was used as a negative control (grey). Samples were collected after incubation of the triazole conjugate with streptavidin agarose beads (post-streptavidin) and following UV irradiation release of the triazole conjugate from the agarose support (post-UV release). (E) Proposed structure of non-streptavidin bound PC biotin-DBCO (exact mass 1001.4205 Da) expected in the DMSO and OZ754 post-streptavidin samples that was not detected. (F) Proposed structure of non-streptavidin bound OZ754 PC biotin-DBCO (exact mass 1363.6159 Da) expected in the OZ754 post-streptavidin sample that was not detected.

When the corresponding reaction was performed under copper catalysed reaction conditions with the appropriate alkyne-modified probe and PC biotin-azide, a product with a mass that corresponds to the click-reacted OZ727-derived keto acid degradation product was identified in the post-photorelease sample (Figures 4A-C). Under these conditions the OZ727 triazole complex with the peroxide bond still intact (459.2846 Da) (Figure 4D) was not detected. While the copper-mediated approach may be applicable for non-peroxide-based drugs, this finding further indicates that the copper catalysed reaction conditions are unsuitable for click chemistry-mediated pull-down of ozonide-alkylated metabolites.

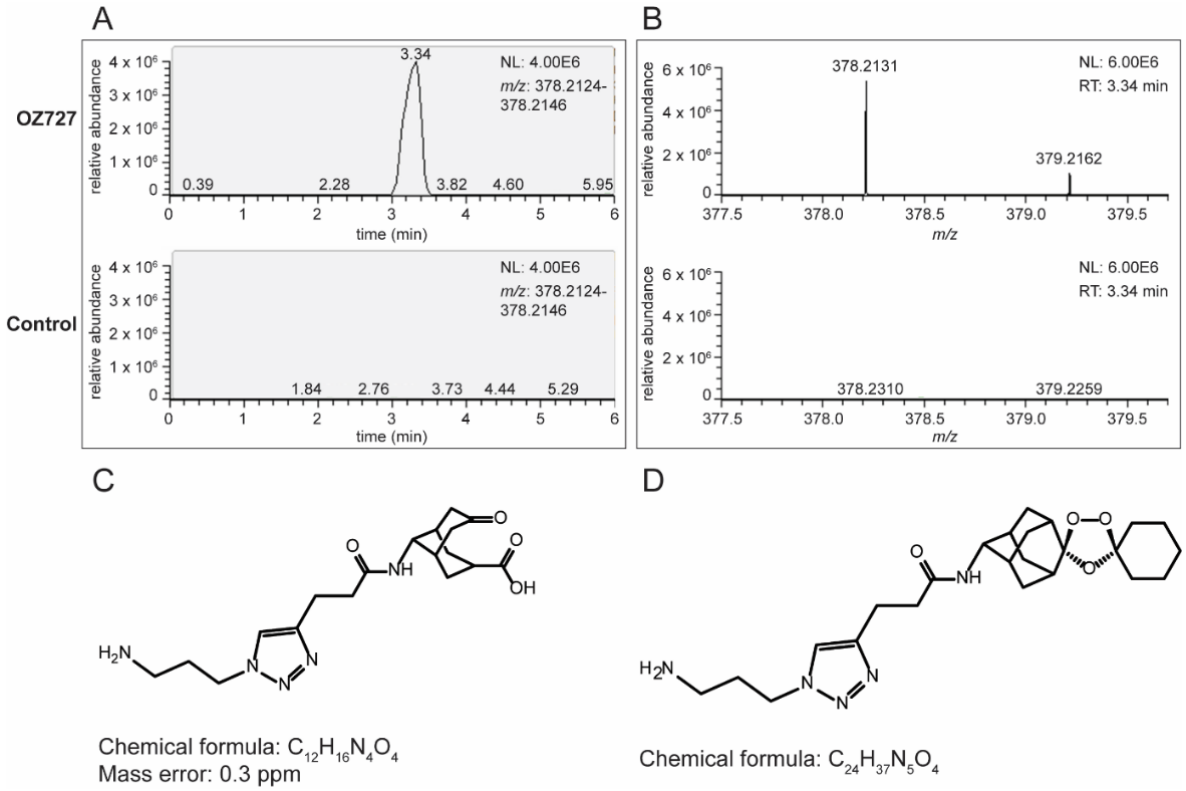


**Figure 4:** Identification of the putative OZ727-derived metabolite under copper catalysed click reaction conditions. (A) Chromatogram of the putative OZ727-derived keto acid degradation product (*m/z*: 378.2131, positive ionisation mode) that was detected following UV irradiation release in the OZ727 treatment samples. (B) Raw mass spectra of the putative OZ727-derived keto acid degradation product at a retention time (RT) of 3.34 min. (C) Proposed chemical structure, formula (based on accurate mass) and calculated mass error relative to the experimentally observed mass (377.2062 Da) for the putative OZ727-derived metabolite. (D) Expected chemical structure for the intact OZ727 triazole complex. NL, normalised level.

The copper free click chemistry approach with the azide-modified OZ754 probe was applied to investigate ozonide small molecule targets within the *P. falciparum* parasite. A polar metabolomics extraction procedure with 100% methanol as the extraction solvent was used, which routinely extracts around 700 putative metabolites from *P. falciparum* infected RBCs, including amino acids, carbohydrates, nucleotides, peptides and some lipids. Although similar ozonide probes label a substantial number of parasite proteins (30), under the conditions tested

here, no unique drug-metabolite adducts were detected in parasite cultures exposed to 1 µM of OZ754 for 5 h. However, the OZ754 triazole complex was detected in drug treated parasite cultures, confirming that this approach is capable of pulling-down small molecules from a complex parasite metabolite extract (Figures 5A-D).

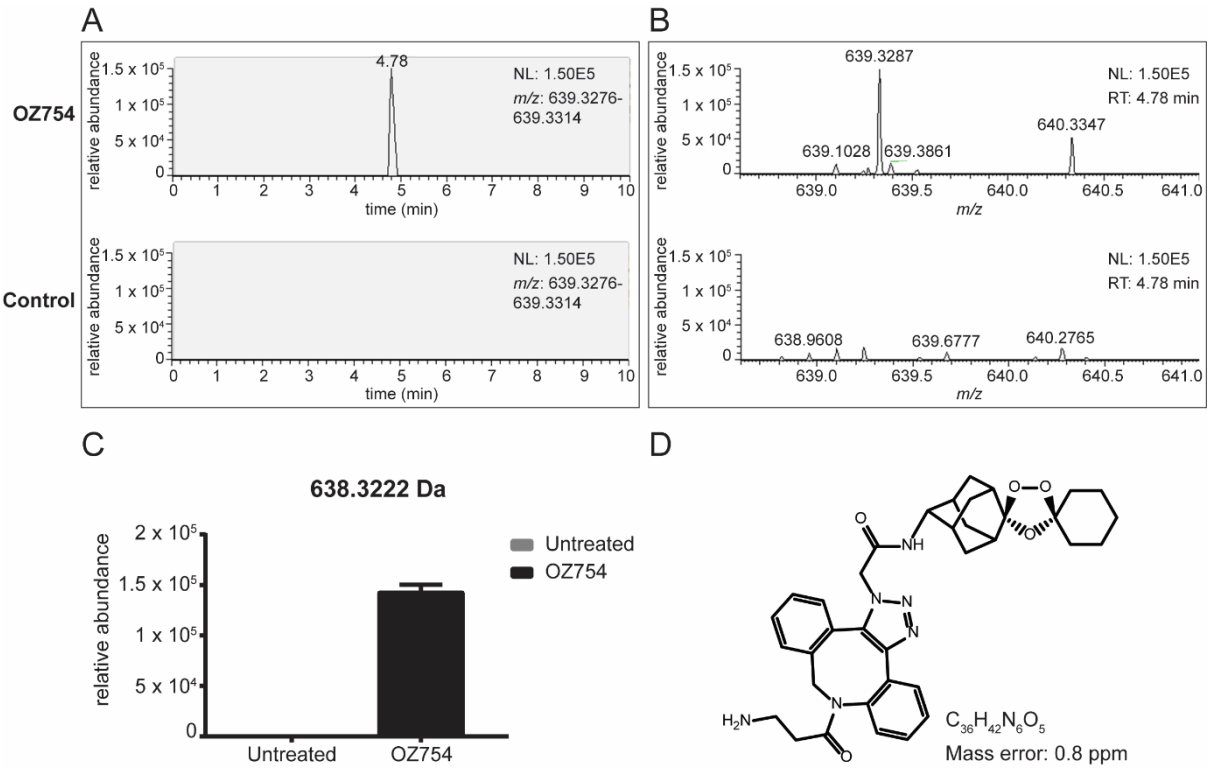


**Figure 5:** Identification of the putative OZ754 triazole complex in drug-treated trophozoite infected RBCs. (A) Representative chromatogram of the putative OZ754 triazole complex (*m/z*: 639.3295, positive ionisation mode) that was detected in drug treated parasite cultures. (B) Representative raw mass spectra of the putative OZ754 triazole complex at a retention time (RT) of 4.78 min. (C) Relative abundance (mean ± SD of four biological replicates) of the putative OZ754 triazole complex (638.3222 Da) detected in drug treated parasite cultures (black) and untreated control cultures (grey). (D) Expected chemical structure of the intact OZ754 triazole complex and calculated mass error relative to the experimentally observed mass. NL, normalised level.

### 3.4.3 Haem as an *in vitro* target for the ozonides

As the *in vitro* activity of the ozonides has previously been found to be directly correlated with extent of haem alkylation *in vitro* (32), haem was investigated as a potential intraparasitic target of the ozonides. Haem was not detected in LC-MS-based metabolomics analysis of a standard methanol extract of *P. falciparum* infected RBCs (Figure 6), indicating intraparasitic haem adducts are unlikely to be detected using this extraction method. Instead, an acidic acetone extraction (18), optimised for solubilisation of free haem, was employed, which allowed the identification of haem from parasite lysates (Figure 6).

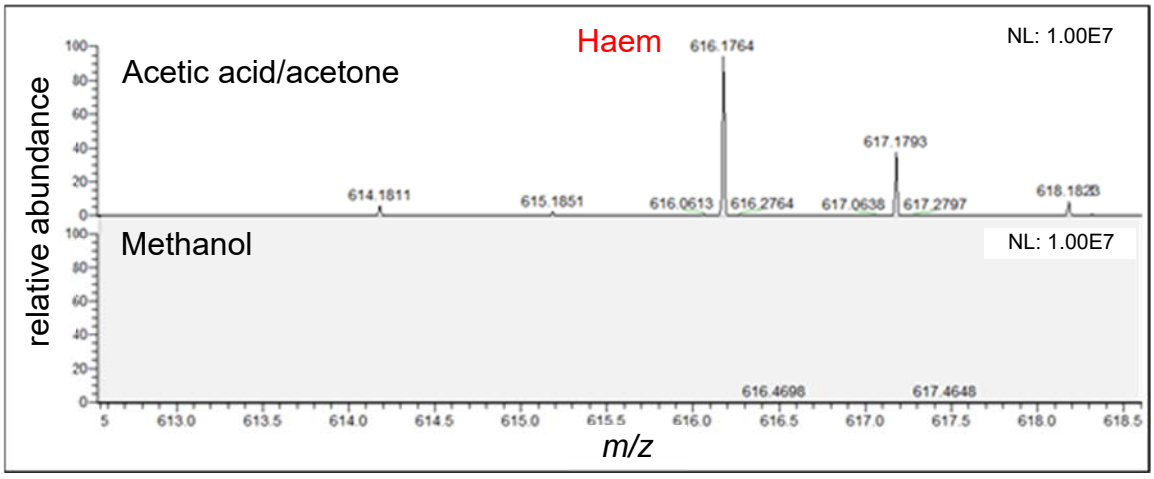


**Figure 6:** Haem mass spectra from acetic acid/acetone (top) and methanol (bottom) extracts of *P. falciparum* trophozoite lysates. NL, normalised level.

To assess ozonide haem alkylation, trophozoite stage parasites were exposed to 1 µM of OZ277 (non-azide tagged) for 3 h and saponin-lysed pellets subjected to direct acetic acid/acetone extraction before untargeted LC-MS analysis. Several unique molecular features in the OZ277 treated samples were absent or of very low abundance in the control samples, indicating they may be ozonide-derived adducts (Figure 7). The alkylated haem adduct (Figure 8A) was detected (*m/z*: 782.3) with the expected isotopic pattern (M-2 due to $Fe^{54}$) and the

extracted ion chromatogram exhibited peaks with signal/noise ratio > 3 (18). Two potential regioisomers of the alkylated haem adduct were detected, with retention times ranging from 10-13 min (Figures 8B-D). The OZ277-derived 4-substituted cyclohexanone (Figure 9A) and adamantane lactone (Figure 9B), by-products of the iron-mediated degradation of ozonides (31), were also detected.

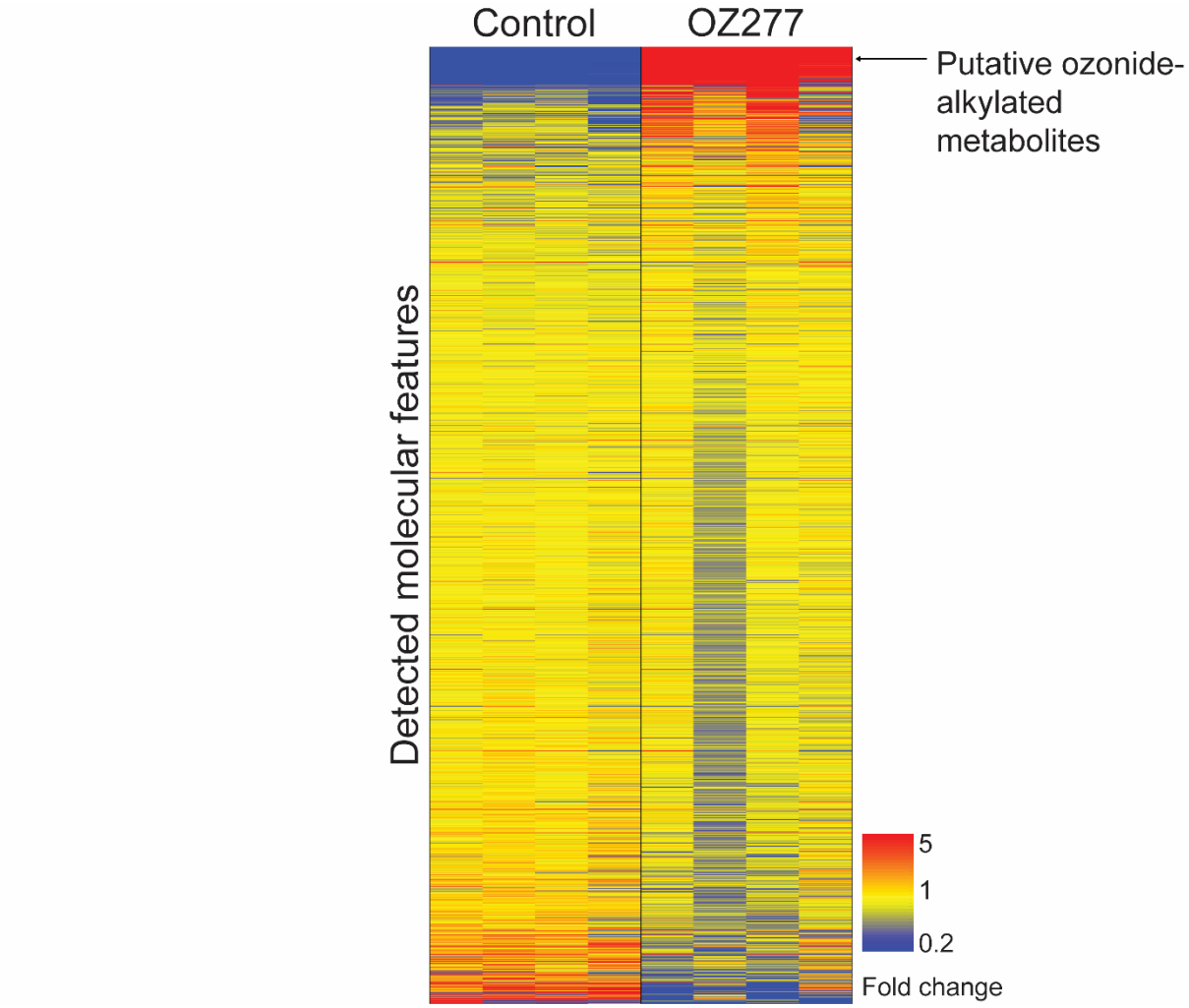


**Figure 7:** Heatmap depicting the relative abundance of all molecular features that were detected after acetic acid/acetone extraction of OZ277-treated trophozoite infected RBCs. Trophozoite infected RBCs were treated with 1 μM of OZ277 (four biological replicates) or an equal volume of DMSO (control, four biological replicates) for 3 h and the parasites were isolated with 0.1% saponin prior to acetic acid/acetone extraction and LC-MS analysis.

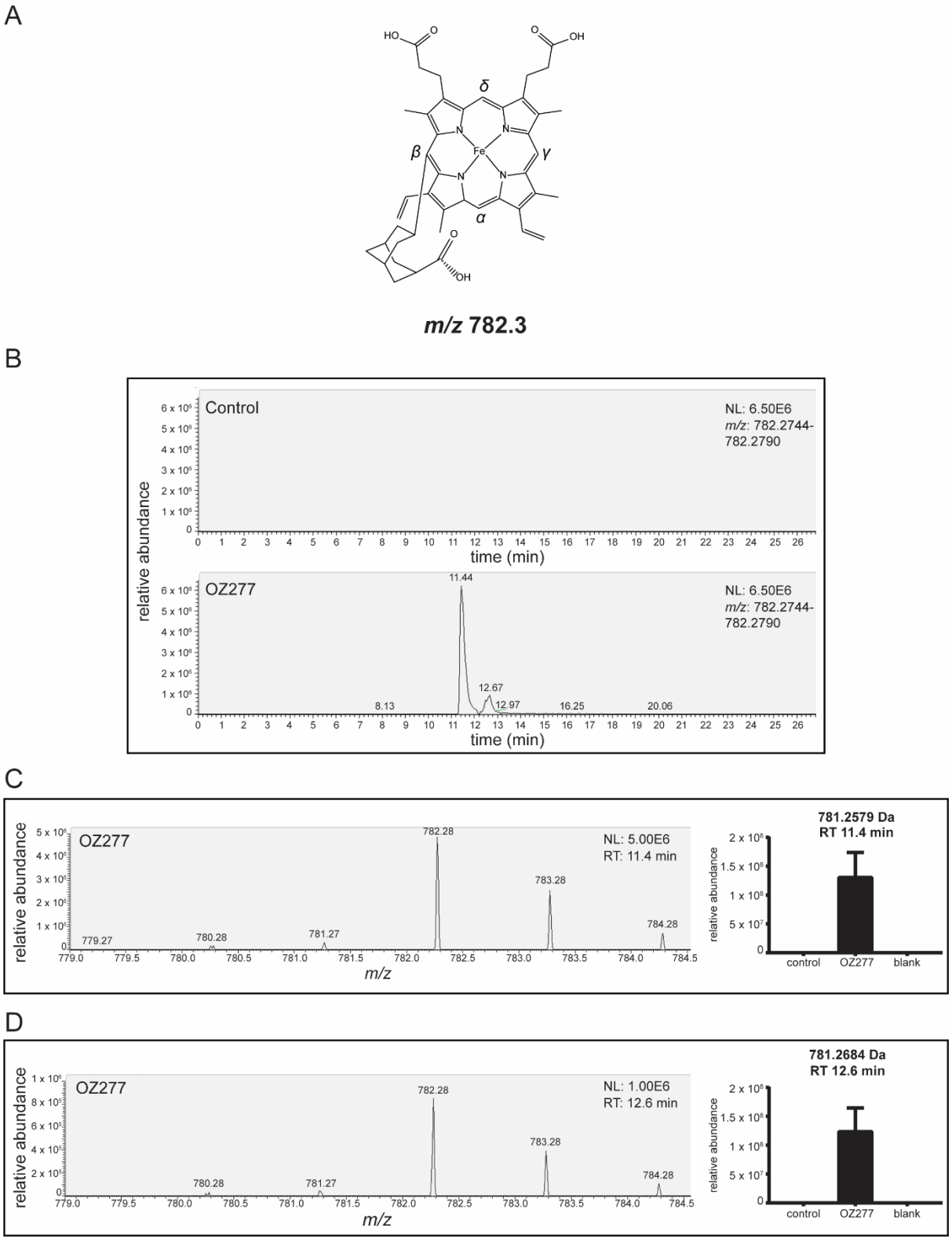


**Figure 8:** Identification of putative ozonide-alkylated haem adducts in OZ277-treated trophozoite infected RBCs. (A) Chemical structure of the OZ277-alkylated haem adduct (*m/z* 782.3). Only alkylation at the β *meso* position is shown, but the product is likely to be a mixture of isomeric adducts. (B) Representative chromatogram of the putative OZ277-

alkylated haem adducts (positive ionisation mode) that were identified in drug-treated trophozoite cultures. (C-D) Representative raw mass spectra (left) and relative abundance (right) for the features corresponding to the alkylated haem adduct at a retention time (RT) of 11.4 min (C) and 12.6 min (D) detected in extracts from OZ277-treated *P. falciparum* parasites. For B-D above, trophozoite infected cultures were treated for 3 h with OZ277 (1 μM) or an equivalent volume of DMSO (control). Relative abundance is expressed as the mean peak area ± SEM of four biological replicates. NL, normalised level.

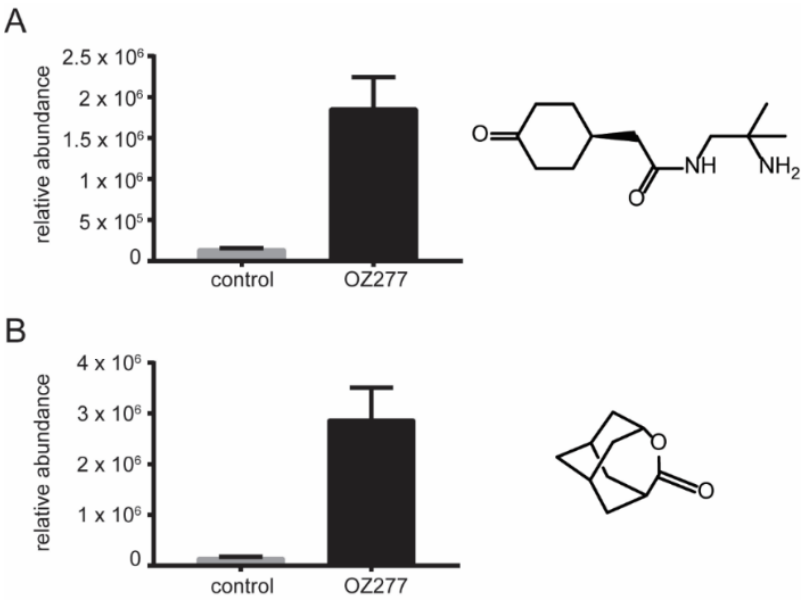


**Figure 9:** Identification of OZ277-derived degradation products in acetic acid/acetone extracts from drug-treated trophozite infected RBCs. (A) Relative abundance (mean peak height ± SEM of four biological replicates) and chemical structure of the OZ277-derived 4-substituted cyclohexanone known to form upon iron mediated degradation of OZ277 (31). (B) Relative abundance (mean peak height ± SEM of four biological replicates) and chemical structure of the OZ277-derived adamantane lactone known to form upon iron mediated degradation of OZ277 (31).

The molecular formulae of the other unique metabolites detected after OZ277 treatment were determined based on accurate mass (mass error less than 2 ppm) (Table 2) and the formulae of most of the metabolites in Table 2 suggest they are all close structural analogues. The haem molecule itself is composed of four pyrrole rings and, interestingly, most of the remaining covalently modified metabolites corresponded to either mono-, di- or tri-pyrrolic species. The relative abundance and proposed chemical structures (based on exact mass) for the putative haem-derived alkylation products 1-3 (mono-pyrrole), 15 and 16 (di-pyrrole) and 21 (tri-pyrrole) in Table 2 are shown in Figures 10A-C. Haem can undergo non-enzymatic, oxidative degradation into its individual pyrrolic components (44) and a proposed scheme for this is presented (Figure 10D). The corresponding non-alkylated haem oxidation end products were not identified in the control samples and there was no significant difference in the relative abundance of haem itself between the treatment and control groups (Figure 11).

**Table 2:** Putative ozonide-alkylated haem degradation products identified in *P. falciparum* parasites after treatment with OZ277.

| | Identified mass | RT (min) | Formula[a] | Mass error (ppm) | Mean peak intensity | | Formula (non-modified metabolite)[b] |
|---|---|---|---|---|---|---|---|
| | | | | | OZ277 | DMSO | |
| 1* | 301.1678 | 4.04 | $C_{18}H_{23}NO_3$ | 0.00 | 1081851 | 0 | $C_8H_9NO$ |
| 2* | 301.1678 | 6.96 | $C_{18}H_{23}NO_3$ | 0.00 | 568640 | 0 | $C_8H_9NO$ |
| 3* | 301.1679 | 4.54 | $C_{18}H_{23}NO_3$ | 0.40 | 982031 | 0 | $C_8H_9NO$ |
| 4 | 313.1677 | 5.38 | $C_{19}H_{23}NO_3$ | 0.30 | 95220 | 0 | $C_9H_9NO$ |
| 5 | 315.1833 | 7.98 | $C_{19}H_{25}NO_3$ | 0.50 | 139106 | 0 | $C_9H_{11}NO$ |
| 6 | 317.1626 | 3.70 | $C_{18}H_{23}NO_4$ | 0.20 | 838533 | 0 | $C_8H_9NO_2$ |
| 7 | 317.1628 | 3.40 | $C_{18}H_{23}NO_4$ | 0.30 | 537351 | 0 | $C_8H_9NO_2$ |
| 8 | 331.1782 | 7.18 | $C_{19}H_{25}NO_4$ | 0.30 | 1085531 | 0 | $C_9H_{11}NO_2$ |
| 9 | 331.1784 | 3.95 | $C_{19}H_{25}NO_4$ | 0.10 | 1042339 | 0 | $C_9H_{11}NO_2$ |
| 10 | 331.1784 | 4.10 | $C_{19}H_{25}NO_4$ | 0.10 | 449934 | 0 | $C_9H_{11}NO_2$ |
| 11 | 333.1938 | 2.58 | $C_{19}H_{27}NO_4$ | 0.60 | 579851 | 0 | $C_9H_{13}NO_2$ |
| 12 | 345.1938 | 7.72 | $C_{20}H_{27}NO_4$ | 0.50 | 1977769 | 0 | $C_{10}H_{14}O_2$ |
| 13 | 375.1683 | 2.73 | $C_{20}H_{25}NO_6$ | 0.30 | 86344 | 0 | $C_{10}H_{11}NO_4$ |
| 14 | 377.2203 | 5.32 | $C_{21}H_{31}NO_5$ | 0.20 | 401947 | 0 | $C_{11}H_{17}NO_3$ |
| 15 | 480.2264 | 5.08 | $C_{27}H_{32}N_2O_6$ | 0.70 | 2982342 | 0 | $C_{17}H_{18}N_2O_4$ |
| 16 | 480.2264 | 4.87 | $C_{27}H_{32}N_2O_6$ | 0.80 | 1701435 | 0 | $C_{17}H_{18}N_2O_4$ |
| 17 | 484.2215 | 1.10 | $C_{26}H_{32}N_2O_7$ | 1.10 | 220386 | 0 | $C_{16}H_{18}N_2O_5$ |
| 18 | 494.2422 | 6.13 | $C_{28}H_{34}N_2O_6$ | 1.00 | 161586 | 0 | $C_{18}H_{20}N_2O_4$ |
| 19 | 512.2528 | 3.32 | $C_{28}H_{36}N_2O_7$ | 1.10 | 426493 | 0 | $C_{18}H_{22}N_2O_5$ |
| 20 | 512.2529 | 4.84 | $C_{28}H_{36}N_2O_7$ | 1.30 | 88603 | 0 | $C_{18}H_{22}N_2O_5$ |
| 21 | 631.2896 | 5.81 | $C_{35}H_{41}N_3O_8$ | 0.40 | 714529 | 0 | $C_{25}H_{27}N_3O_6$ |

[a] Determined from the accurate mass of the identified metabolite.

[b] Calculated by subtracting the adamantane derived radical ($C_{10}H_{14}O_2$) from the formula of the identified metabolite.

* Also detected after the reaction of haem and OZ277 in 50%ACN/$H_2O$ under reducing conditions.

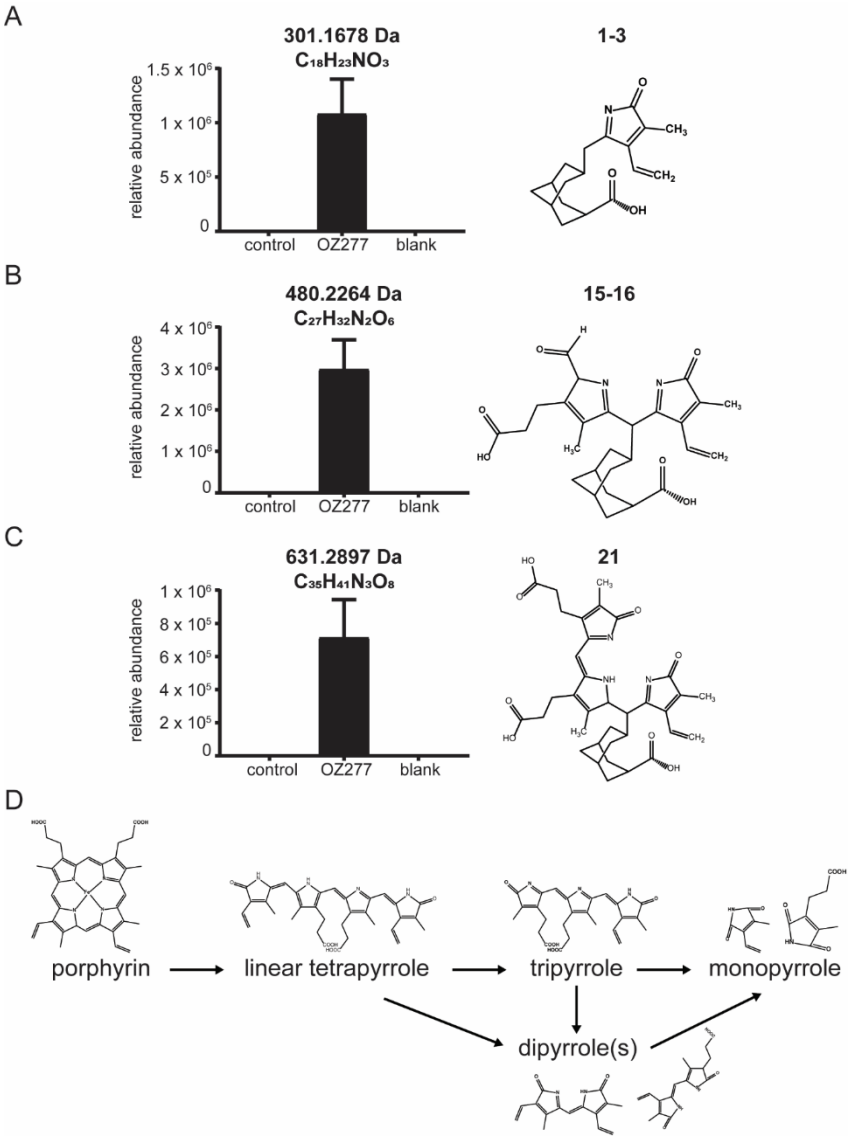


**Figure 10:** Identification of putative ozonide-derived alkylated haem degradation products. (A) Relative abundance (mean peak height ± SEM of four biological replicates) for the putative mono-pyrrole alkylated haem degradation product (301.1678 Da, adducts 1-3 in Table 2) detected in OZ277-treated *P. falciparum* parasites and the proposed chemical structure (based on exact mass). (B) Relative abundance (mean peak height ± SEM of four biological replicates) for the putative di-pyrrole alkylated haem degradation product (480.2264 Da, adducts 15 and 16 in Table 2) detected in OZ277-treated *P. falciparum* parasites and the proposed chemical structure (based on exact mass). (C) Relative abundance (mean peak height ± SEM of four biological replicates) for the putative tri-pyrrole alkylated haem degradation product (631.2897 Da, adduct 21 in Table 2) detected in OZ277-treated *P. falciparum* parasites and the proposed chemical structure (based on exact mass). (E) Proposed scheme for the non-enzymatic oxidative degradation of haem (adapted from Schaefer *et al*. 1985(44)).

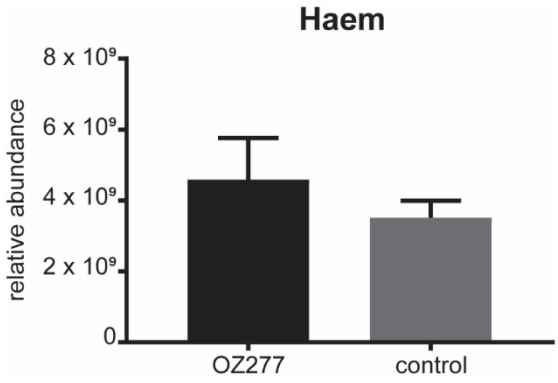


**Figure 11:** Relative abundance (mean peak height ± SD of four biological replicates) of haem in *P. falciparum* parasites following treatment with 1 μM of OZ277 (black) or an equivalent volume of DMSO (control, grey) (p-value = 0.14, Student's *t* test).

To confirm that the putative haem adduct resulted from covalent modification of the haem porphyrin ring by the ozonide-derived adamantane radical, the same experiments were performed with OZ754 (Figure 1). OZ754 consists of the 1,2,4-trioxolane core flanked by a cyclohexane moiety on one side and an adamantane group containing an azide tag on the other. Alkylation of haem by the modified adamantane-derived radical of OZ754 resulted in an alkylated haem adduct with a mass shift of 98.0229 Da (consistent with the mass of the azide tag), corresponding to an *m/z* of 880.3 (Figure 12). Five putative regioisomers of the OZ754-alkyklated haem adduct were identified, with retention times between 8 and 23 min (Figures 13A-F), which have the expected mass and meet the criteria for an alkylated haem adduct. In addition to the intact alkylated product, several of the same putative alkylated haem degradation products detected in the OZ277 study were also identified, but with the expected mass shift corresponding to azide modification on the adamantane ring (Table 3). The corresponding OZ754-derived adamantane lactone (Figure 14) was also detected, however the cyclohexanone portion of OZ754 (98.07317 Da) was not identified as the MS settings for this analysis did not allow detection of features below 150 Da.

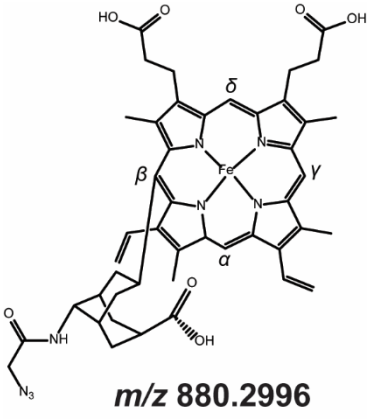


**Figure 12:** Chemical structure for the OZ754-alkylated haem adduct (*m/z* 880.3). Only alkylation at the β *meso* position is shown, but the product is likely to be a mixture of isomeric adducts.

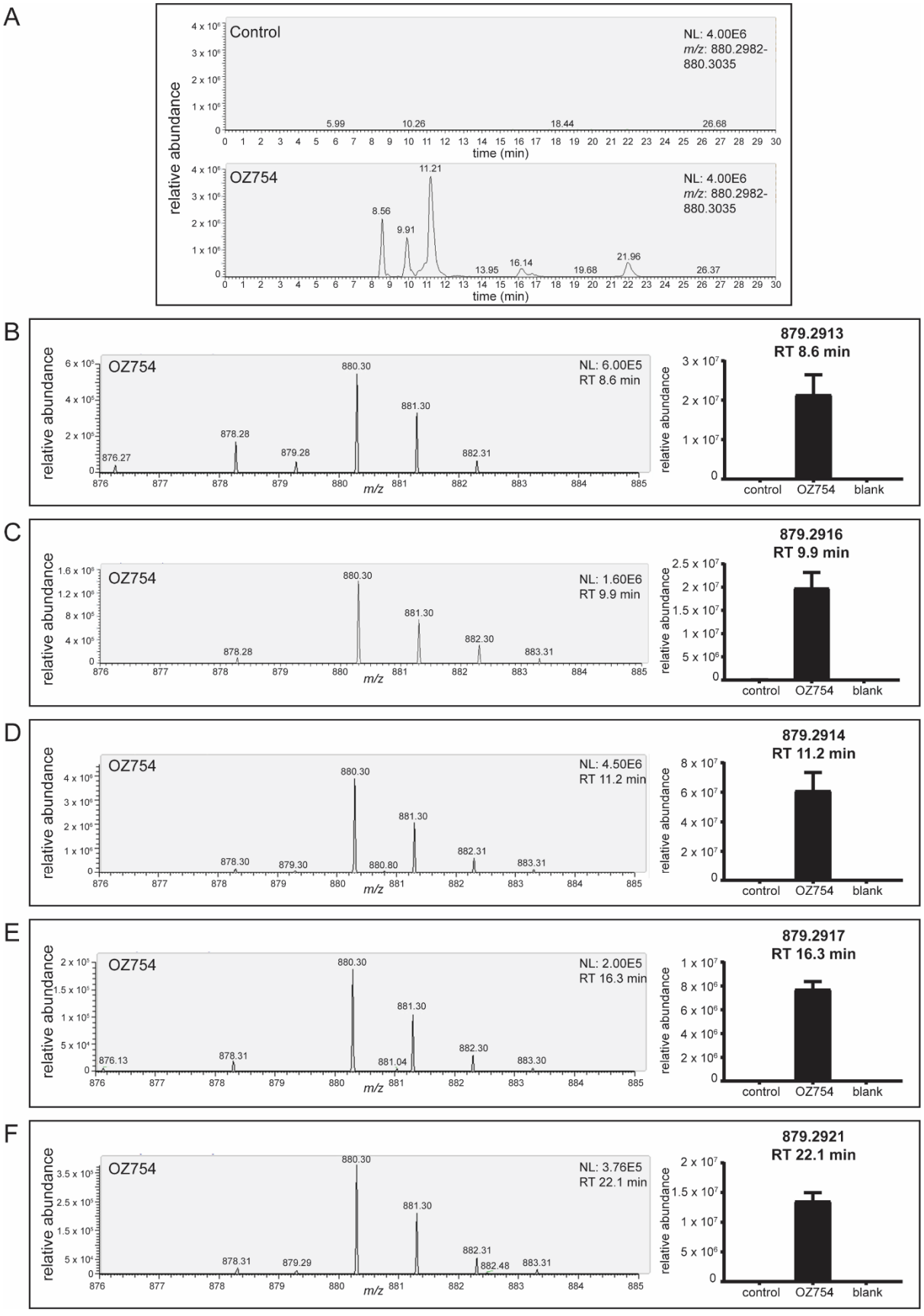


**Figure 13:** Identification of putative ozonide-alkylated haem adducts in OZ754-treated trophozoite infected RBCs. (A) Representative chromatogram of the putative OZ754-alkylated

haem adducts (*m/z*: 880.3, positive ionisation mode) that were identified in drug-treated trophozoite cultures. (B-F) Representative raw mass spectra (left) and relative abundance (right) for the features corresponding to the alkylated haem adduct at a retention time (RT) of 8.6 min (B), 9.9 min (C), 11.2 min (D), 16.3 min (E) and 21.1 min (F) detected in extracts from OZ754-treated *P. falciparum* parasites. In A-F above, parasites were treated with OZ754 (1 μM) or an equal volume of DMSO (control) for 3 h. The relative abundance is expressed as the mean peak area ± SEM of four biological replicates. NL, normalised level; RT, retention time.

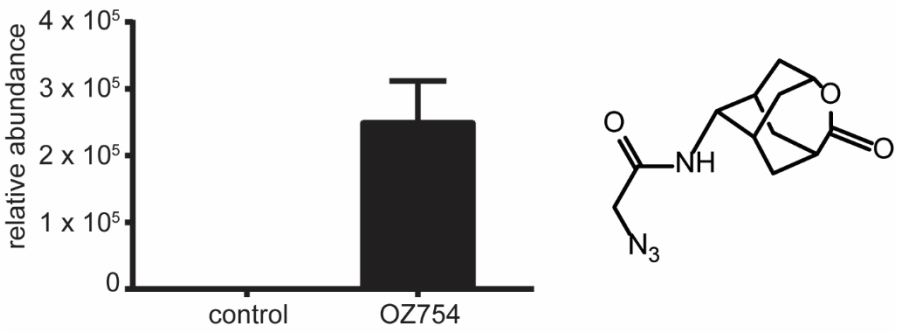


**Figure 14:** Relative abundance and chemical structure of the OZ754-derived adamantane lactone. Relative abundance is expressed as the mean peak height ± SEM of four biological replicates.

**Table 3:** Putative alkylated haem degradation products detected in OZ754-treated *P. falciparum* infected RBCs.

| Identified mass | Retention time (min) | Mean peak area | | Corresponding feature in OZ277 study (Table 2) |
|---|---|---|---|---|
| | | OZ754 | DMSO | |
| 399.1907 | 2.13 | 100029 | 0 | 1-3 |
| 411.1906 | 3.41 | 219759 | 8968 | 4 |
| 429.2011 | 1.60 | 54524 | 0 | 8-10 |
| 443.2164 | 3.61 | 108324 | 0 | 12 |
| 473.1909 | 1.20 | 3737914 | 0 | 13 |

### 3.4.4 Confirmation of alkylated haem adduct degradation

To determine whether the putative alkylated haem degradation products were ozonide derived, the break-down of the alkylated haem adduct was monitored by visible spectrophotometric analysis of the Fe(II) haem and OZ277 reaction under reducing conditions in ACN/$H_2O$ (32). Addition of OZ277 caused an instantaneous disappearance of the haem $A_{415}$ peak. The major reaction product formed had an absorption peak at 472 nm (Figure 15A), which likely results from the alkylation of the haem porphyrin ring by the ozonide-derived adamantane radical (32, 34, 45). A progressive decline in the peak absorbance at 472 nm was then observed over the following 1 h period (Figure 15A), indicative of deterioration of the alkylated haem adduct over time. More than 90% of the original haem-ozonide reaction product remained after 15 min, but this substantially declined to approximately 5% within 1 h (Figure 15B). LC-MS analysis of the final reaction mixture detected a metabolite with a mass (301.1678 Da) and retention time (4.04, 4.53 and 6.96 min) corresponding to the OZ277-derived adamantane-alkylated mono-pyrrolic compounds that were also detected in OZ277-treated *P. falciparum* parasites (adducts 1-3 in Table 2 and Figure 10A). These features correspond to the simplest alkylated-haem degradation end products. The same metabolite was absent in control samples containing either OZ277 or haem alone (Figure 15C). As expected, the intact alkylated haem adduct was not detected by LC-MS in this study and haem itself was only identified in control samples that contained haem without drug (haem alone, Figure 15D).

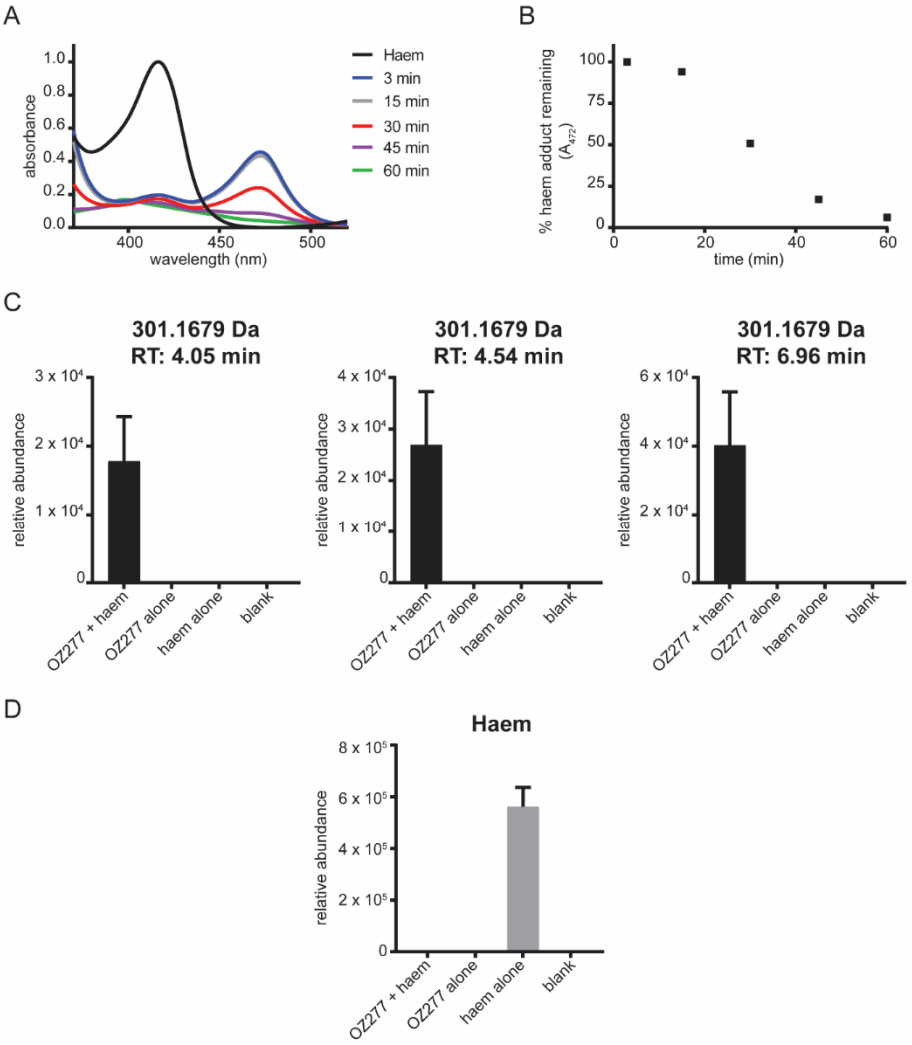


**Figure 15:** Confirmation of alkylated haem adduct degradation. (A) Visible spectra of unreacted Fe(II) haem (black line) and the reaction product between haem (10 µM) and OZ277 (10 µM), 3, 15, 30, 45 and 60 min (blue, grey, red, purple and green lines respectively) after drug addition in 50% ACN/$H_2O$ with excess dithionite. (B) Percentage of reaction product (haem adduct) remaining versus time. For each time point, the absorption peak at 472 nm (reaction product) was normalised to the 3 min absorbance value. (C) Relative abundance (mean peak area ± SEM of at least three biological replicates) of the putative alkylated haem oxidation end product (301.1679 Da) detected after the reaction between haem and OZ277 (black). The same feature was absent in samples without haem (OZ277 alone), without OZ277 (haem alone) and in the solvent blank. (D) Relative abundance (mean peak area ± SEM of at least three biological replicates) of haem detected in samples containing both haem and OZ277 (OZ277 + haem), and in samples without haem (OZ277 alone), without OZ277 (haem alone, grey) and in the solvent blank.

### 3.4.5 Ozonide sub-cellular localisation in *P. falciparum* parasites

The ozonide antimalarials have been reported to covalently react with a range of intraparasitic proteins (29, 30). This covalent interaction was exploited to assess ozonide sub-cellular distribution by confocal microscopic analysis of azido-ozonide treated *P. falciparum* parasites that were fixed and incubated with a DBCO-tagged fluorophore (Cy5). Titration of the copper free click reaction time (Figure 16A) and DBCO dye concentration (Figure 16B) for parasites treated with OZ754 (1 μM) indicated that optimal signal intensity and minimal background fluorescence was achieved with a click reaction time of 1 h and DBCO-Cy5 concentration of 5-10 μM. A concentration-dependent increase in fluorescence intensity was observed when parasites were incubated with increasing concentrations of OZ754 for 3 h (0, 0.1 or 1 μM) (Figure 17). Independent of the drug concentration, under the conditions tested, OZ754 did not appear to co-localise with a specific sub-cellular compartment and was distributed throughout the parasite within 3 h of treatment.

Ozonide antimalarial activity has also been reported to be highly dependent on exposure time (8, 46, 47), which necessitates a time-dependent assessment of the intraparasitic distribution pattern of OZ754 at varying durations of exposure up to 3 h (Figure 18). Negligible intracellular staining was observed at the shortest time points tested (5 min and 30 min), suggesting there is minimal protein alkylation after these short durations of exposure. By 1 h, OZ754 was distributed throughout the parasite and the signal intensity was strongest after 3 h of drug exposure, indicative of a time-dependent increase in protein alkylation. Co-localisation with a specific parasite compartment was not evident at any of the time points. Interestingly, strong intracellular staining did not appear to co-localise with the digestive vacuole marker, Lysotracker. At all of the time points tested there was no signal from the DMSO control treated cells, confirming the observed parasite staining was OZ754 specific.

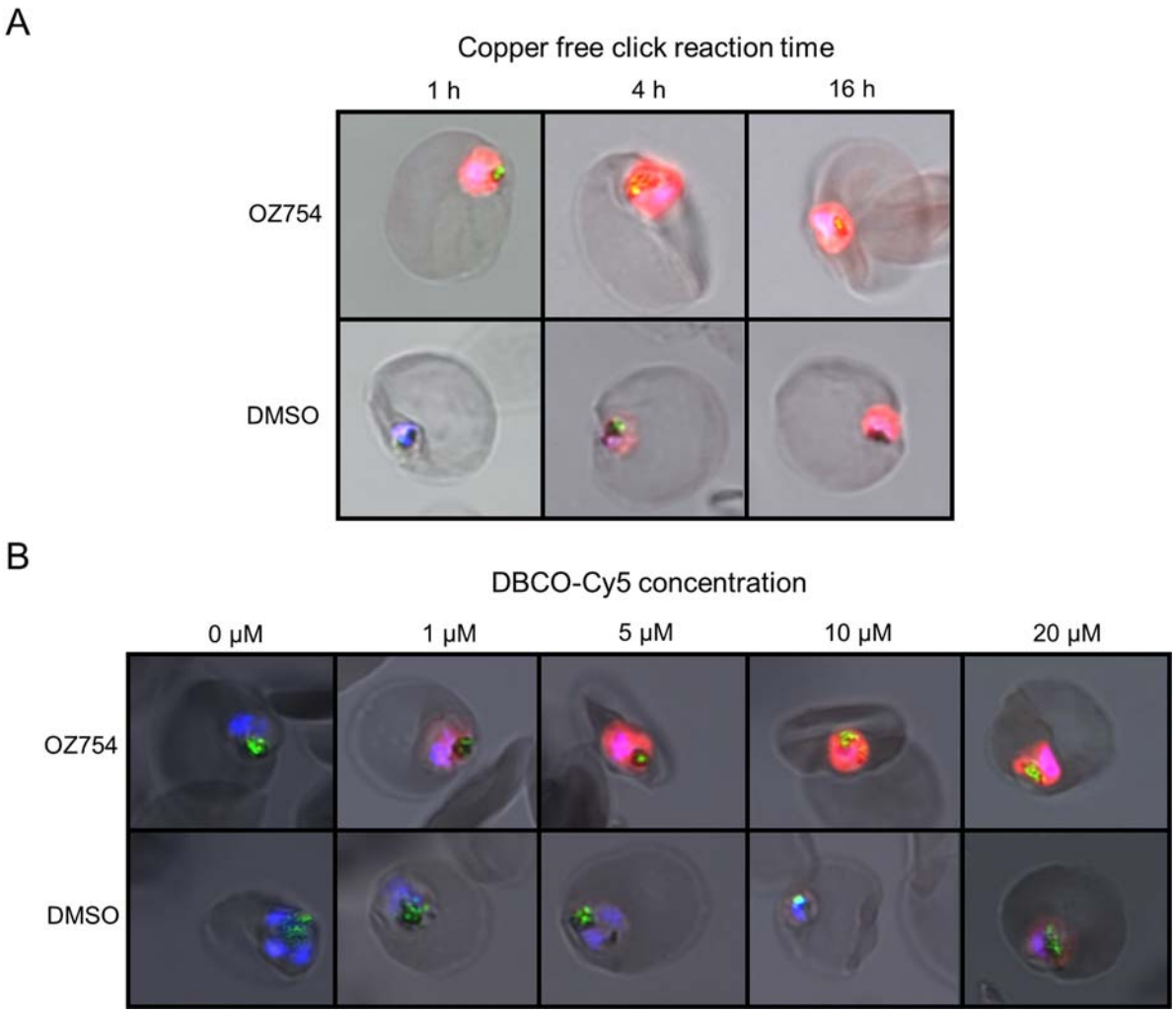


**Figure 16:** Optimisation of the copper free click chemistry reaction conditions for confocal microscopic analysis of azido ozonide sub-cellular localisation in *P. falciparum* infected RBCs. (A) Fluorescence signal with increasing duration of the copper free click reaction time (1, 4 and 16 h with 20 µM DBCO-Cy5) for parasites treated with OZ754 (1 µM) or an equivalent volume of DMSO for 3 h. (B) Titration of the DBCO-Cy5 dye at escalating concentrations up to 20 µM (copper free click reaction time 1 h) for parasites treated with OZ754 (1 µM) or an equivalent volume of DMSO for 3 h. In A and B, the nucleus was stained with Hoechst (blue) and the digestive vacuole was stained with LysoTracker Red (green). Drug localisation was determined by the copper free click reaction between the azido ozonide-modified proteins and DBCO-Cy5 (red).

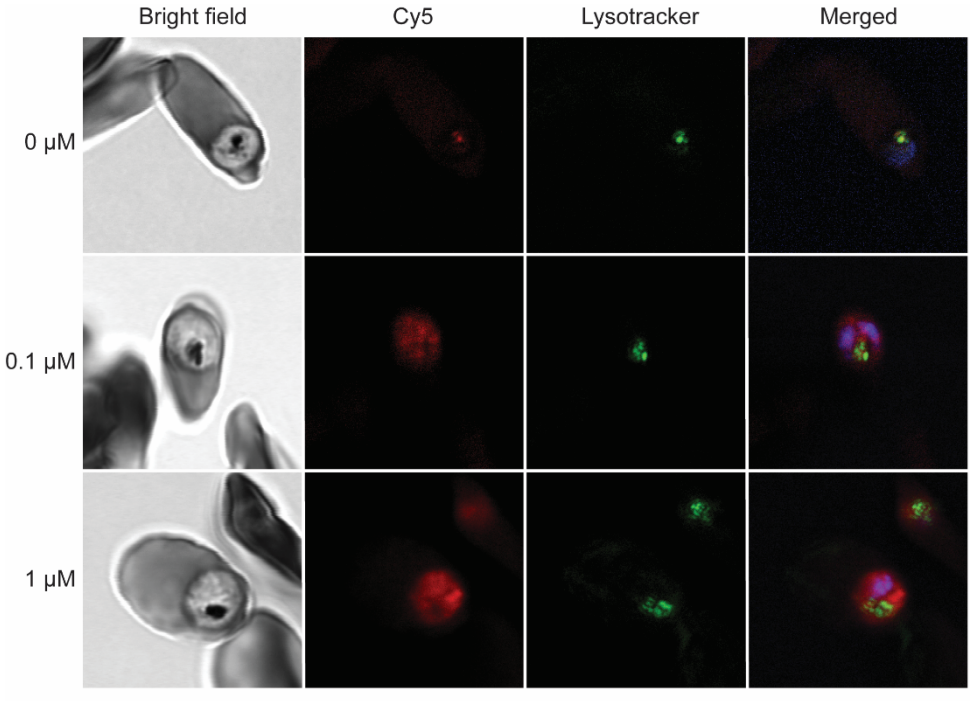


**Figure 17:** Concentration-dependent increase in fluorescence with escalating concentrations of OZ754 (0, 0.1 and 1 µM). Parasites were incubated with OZ754 for 3 h. The nucleus was stained with Hoechst (blue) and the digestive vacuole was stained with LysoTracker Red (green). Drug localisation was determined by the copper free click reaction between the azido ozonide-modified proteins and DBCO-Cy5 (red).

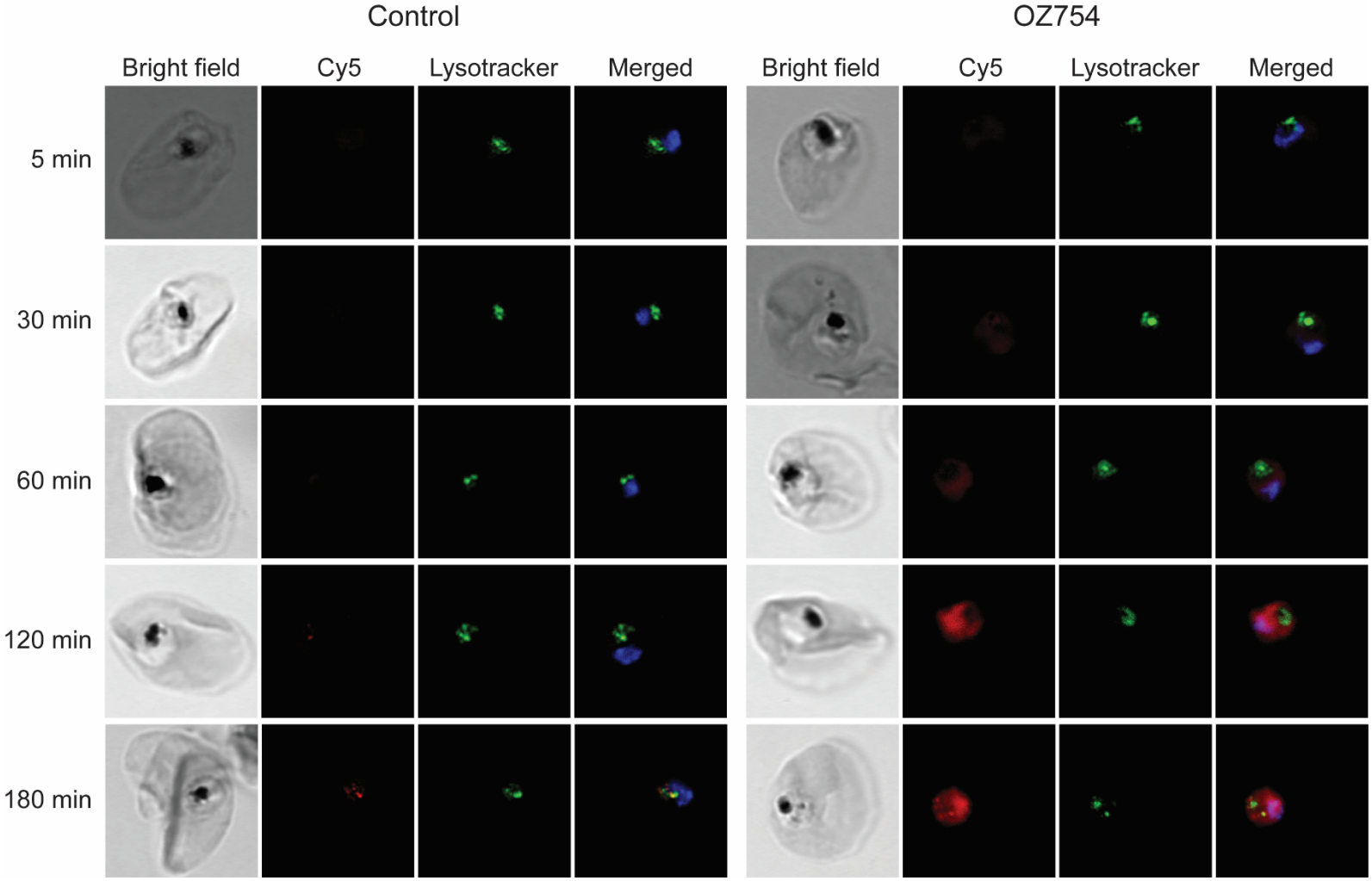


**Figure 18:** Time-dependent distribution of OZ754 in *P. falciparum* trophozoite stage parasites. Parasites were exposed to OZ754 (1 μM) for 5, 30, 60 120 or 180 min. The nucleus was stained with Hoechst (blue) and the digestive vacuole was stained with LysoTracker Red (green). Drug localisation was determined by the copper free click reaction between the azido ozonide-modified proteins and DBCO-Cy5 (red).

The same methodology was applied to directly compare the sub-cellular distributions of the azido ozonide probes, OZ758 and OZ759 (Figure 19), which are structurally similar to the first- and second-generation ozonides OZ03 and OZ439, respectively. OZ758 was distributed throughout the entire parasite within 3 h and exhibited a similar localisation pattern to the structurally similar compound OZ754. Less pronounced intracellular staining was apparent with OZ759, indicating there was reduced protein labelling after a 3 h exposure compared to OZ758. OZ759 was also less widely distributed throughout the parasite, appearing to localise more closely with the parasite digestive vacuole. Incubation with the non-peroxide control probe, carbaOZ758, produced some background fluorescence, likely related to non-covalent binding of these somewhat lipophilic probes, whereas there was no signal in the DMSO treated samples.

To confirm that the localisation pattern is associated with activity, parasites were pre-incubated with the falcipain inhibitor E64d, which is known to antagonise ozonide activity (8). Parasites that were treated with a combination of E64d and either OZ758 or OZ759 (Figure 19, + E64d), compared to either ozonide probe alone (Figure 19, - E64d), showed substantially diminished intracellular staining.

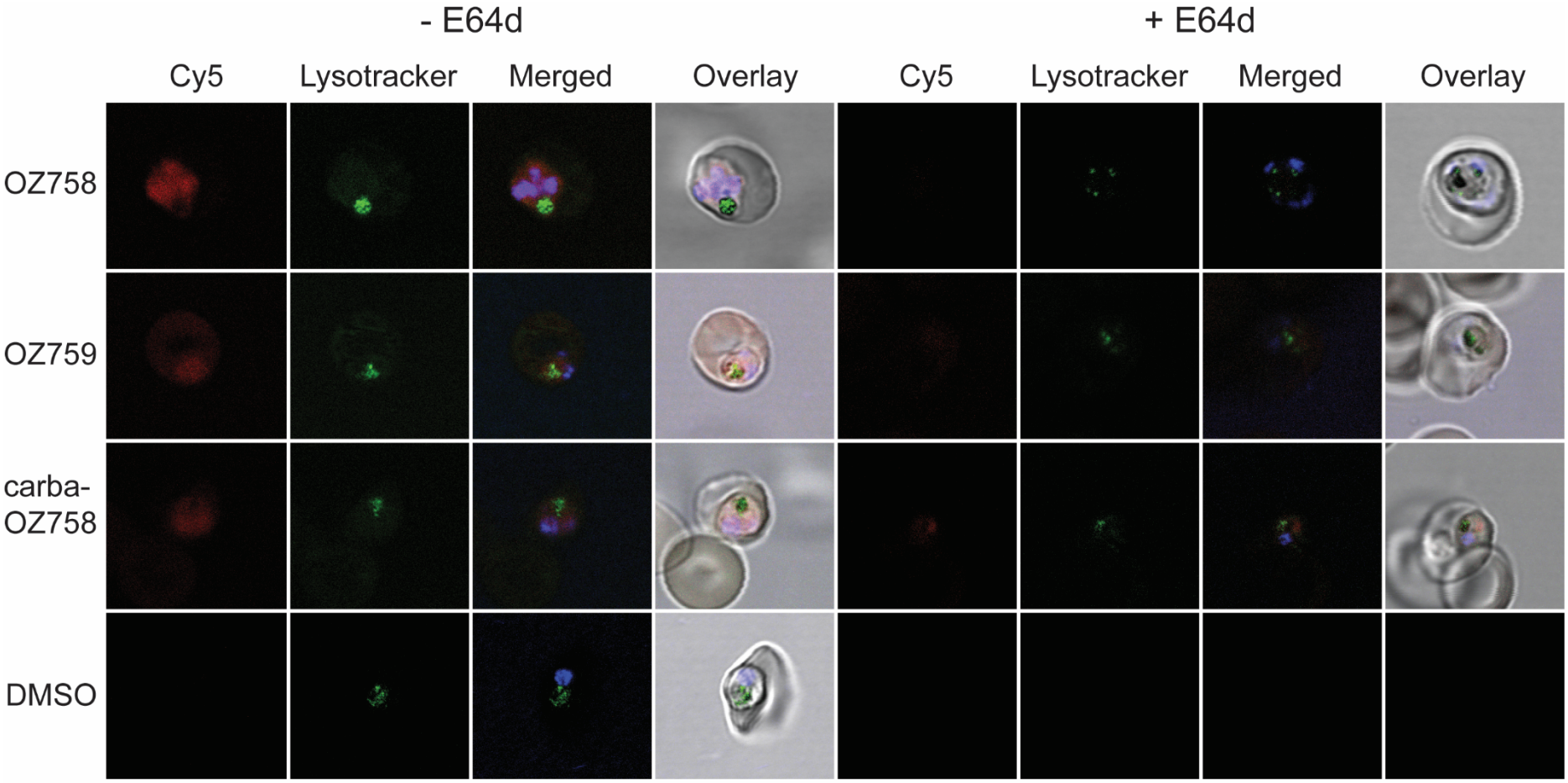


**Figure 19:** Sub-cellular distribution of OZ758, OZ759 and carbaOZ758 in the absence (-E64d) and presence (+E64d) of the falcipain inhibitor E64d. The concentration of all probes was 1 µM and the concentration of E64d was 10 µM. The nucleus was stained with Hoechst (blue) and the digestive vacuole was stained with LysoTracker Red (green). Drug localisation was determined by the copper free click reaction between the azido ozonide-modified proteins and DBCO-Cy5 (red).

## 3.5 DISCUSSION

The ozonide antimalarials are thought to act via a "cluster bomb" mechanism involving reductive cleavage of the peroxide bond, which produces toxic radical species that indiscriminately alkylate parasite proteins, eventually leading to parasite death (6, 29, 30, 48). Given the reported promiscuous targeting of ozonide-derived radicals towards parasite proteins (30), this study explored the possibility that intraparasitic targets other than proteins are involved in the ozonide antimalarial mode of action. In addition to causing widespread alkylation of parasite proteins, it was shown that ozonide-derived radicals form covalent adducts with intraparasitic haem following *in vitro* treatment of *P. falciparum* parasites.

Reactivity with biological haem is generally thought to be responsible for activation of the ozonide peroxide bond (3, 8, 32, 49) and haem is hypothesised to be a biological target given its high concentration in the malaria parasite (up to 400 mM) (50) and its close proximity to activated drug. Closely related artemisinin-based peroxides have also been reported to form covalent adducts with haem both *in vitro* and *in vivo* (16, 17, 19, 20, 22-25, 32, 45), and ozonide *in vitro* activity has been shown to directly correlate with extent of haem alkylation in a simplified test system (32, 33).

The haem molecule consists of four pyrrole rings connected by carbon methene bridges and a central iron coordinated to the four pyrrole nitrogens. Each pyrrole ring contains a methyl group and either a vinyl or propionic acid side chain. The alkylated haem adduct has been proposed to form by covalent modification of the *meso* carbons of the haem porphyrin ring (Figure 8A) by an ozonide-derived secondary carbon-centred radical (32, 33). As reported by Robert *et al*. (45), this reaction produces a mixture of isomeric haem adducts, similar to those seen with the artemisinins. Radical trapping agents have captured the ozonide-derived secondary carbon-centred radical following peroxide bond cleavage by inorganic iron (31, 40) and the same radicals have been suggested to form near the haem macrocycle following the

reaction with Fe(II) haem within the parasite, triggering haem alkylation (32). To date however, the ozonide-alkylated haem adduct has not been detected in *P. falciparum* parasites.

Using an acetic acid/acetone extraction (18) to solubilise free haem and untargeted LC-MS analysis, the results reported here identified ozonide-alkylated haem adducts from drug-treated *P. falciparum* infected RBCs. Based on the *in vitro* reaction between ozonides and haem (32, 51), analysis of OZ277-treated parasites identified two peaks (11.4 and 12.4 min) with the expected *m/z* (782.3) and isotopic pattern that is consistent with alkylation of the haem macrocycle by ozonide-derived adamantane radicals and the formation of regioisomeric haem adducts (Figures 8B-D). Although more detailed structural characterisation of the alkylated adduct was not performed, using OZ754 (modified on the adamantane ring), it was confirmed that the identified features were drug-derived and the result of modification by the adamantane portion of the ozonide molecule. Five isomeric peaks were detected (8.7, 9.9, 16.3 and 22.1 min) with the expected isotopic pattern and mass shift (98.0229 Da) corresponding to haem alkylation by an OZ754-derived adamantane radical (*m/z* 880.3) (Figures 13A-F).

It is unclear why five isomeric peaks were detected for the OZ754 haem adduct (likely representing at least the four possible regioisomers produced by alkylation at the α, β, γ and δ *meso* carbons of haem) and only two were detected in OZ277 treated parasites. Previously, Bousejra-El Garah *et al*. reported the detection of four isomeric peaks for the reaction of a series of tetraoxanes with haem under *in vitro* conditions (51), similar to that described for the artemisinins (45). It is possible that the azide tail of OZ754 allowed better separation of the isomeric haem adducts with the chromatographic method used in this study, while the OZ277 haem adducts co-eluted, or the formation of low abundant OZ277-haem adducts could have been below the limit of detection. In addition to the four regioisomeric adducts that are generally thought to be produced by alkylation of the haem *meso* carbons, modifications of the porphyrin ring at other sites (52), such as at the vinyl side chains, could potentially result in

additional low abundant regioisomeric adducts. Further structural elucidation is needed to determine the precise alkylation sites on the haem porphyrin ring by the azide-tagged ozonide-derived adamantane radical.

Under the conditions tested, there was no significant change in the level of haem itself after drug treatment. It is expected that the high intraparasitic concentration of haem (50) mostly exists in the ferric form, which has been reported to be unreactive with peroxides (32). The relatively small proportion existing in the ferrous state that is capable of alkylating intraparasitic peroxides would likely result in only a minor change in absolute haem levels that is not detectable by MS.

In these studies, a series of putative ozonide-alkylated haem degradation products were also identified. The proposed formulae for these species (Table 2) were calculated based on MS-derived accurate mass (mass error less than 2 ppm) and the modified metabolites deduced by subtracting the chemical formula for the adamantane-derived radical ($C_{10}H_{14}O_2$) that has been reported to form during Fe(II)-mediated ozonide degradation (40). While it is possible that the modified chemical species are metabolites other than haem oxidation end products, none of the calculated formulae, apart from $C_9H_{11}NO_2$ (phenylalanine), corresponded to a biologically relevant metabolite. Unfortunately, high confidence identification and absolute quantitation of the putatively identified alkylated haem degradation products were not possible in the current study due to the absence of authentic standards for comparison of orthogonal metabolite properties (mass and retention times or MS/MS fragmentation pattern) and calibration, respectively.

Unlike mammalian cells that detoxify haem using haem oxygenase (HO), *Pf*HO is thought to play a very minor role in haem detoxification within the parasite (53). Therefore, it is unlikely that *Pf*HO-mediated degradation was responsible for the formation of alkylated oxidation end products in this study. Haem is susceptible to non-enzymatic oxidative

degradation by random attack at the tetra-pyrrole carbon methene bridges, producing a combination of pyrrolic-based cleavage products (44). It is possible that oxidative destruction of the ozonide modified haem molecule led to the formation of alkylated oxidative end products within the parasite, or in solution following extraction. Notably, corresponding non-alkylated haem oxidation end products were not identified in the untreated control samples, raising the possibility that ozonide alkylation of the haem macrocycle destabilises the porphyrin ring, inducing degradation.

Spectrophotometric analysis revealed that the reaction of ozonide-derived radicals with Fe(II) haem caused rapid disappearance of the haem Soret band (415 nm) and resulted in the appearance of an unstable absorption peak at 472 nm, which corresponds to the alkylated haem adduct (32). The absorbance of the haem-ozonide complex almost completely disappeared by 60 min, and the initial lag-phase in reaction kinetics is consistent with an oxidative mechanism inducing decomposition of the haem porphyrin ring. Instability of the alkylated haem adduct has also been demonstrated for the artemisinin-modified haem adduct under similar conditions (54, 55). Notably, the same three isomeric metabolites were detected in this simplified test system as in OZ277-treated *P. falciparum* cultures (adducts 1-3 in Table 2 and Figure 10A) and the corresponding feature was also identified in infected cultures treated with OZ754. This putative metabolite corresponds to an ozonide-derived adamantane-alkylated mono-pyrrolic compound, the most rudimentary of the alkylated-haem degradation end products. While this was the only common haem degradation product between the three sets of experiments, there was overlap in the ozonide-derived degradation products detected in OZ277- and OZ754-treated parasites. Substantially different reaction conditions between the physiological environment of the parasite (aqueous environment with glutathione as the main intracellular reducing agent) and the tightly controlled chemical environment within a simplified experimental system (partially organic with excess dithionite as the reducing agent) could

affect the nature of the degradation products formed. It has been noted previously that reaction conditions can affect reaction rates and distribution of products formed in these types of experiments (19, 32, 56). Taken together, these data indicate that the putative alkylated haem degradation products identified in parasite extracts most likely result from destruction of the ozonide-alkylated haem adduct, possibly via non-enzymatic oxidative degradation (44).

In addition to haem, ozonides might also be expected to form adducts with susceptible groups of other small molecule targets, such as thiol-containing compounds like glutathione, given the proposed promiscuous nature of ozonide-derived radicals. As haem is highly abundant within the parasite (50), a click chemistry-based enrichment method, combined with an untargeted metabolomics platform, was developed to isolate and enrich for the non-haem small molecule targets of the ozonides. However, under the conditions tested here, no other ozonide-alkylated small molecule adducts were detected. The ability to successfully pull-down OZ754 from a complex parasite extract and detect the clicked compound by LC-MS analysis, indicates that it may be possible to isolate and detect very low abundant adducts using increased volumes of parasite culture.

Little is known about the functional importance of the alkylated haem adduct to the biological activity of the ozonides. Like the artemisinins, it has been suggested that haem adducts compromise haem detoxification by preventing crystal growth (35) or inhibit enzymes that catalyse haemozoin formation, such as *P. falciparum* HRP 2 (34). It is also possible that the haem adducts themselves (or their breakdown products) are toxic to the parasite, potentially by causing direct oxidative damage to parasite membranes (27). Alternatively, the covalent reaction between ozonides and haem may compete with the "true" intraparasitic ozonide targets and therefore be detrimental for antimalarial activity, as has been suggested for the artemisinins (57), or represent an inert by-product that arises due to the close proximity of the haem activator and the resultant ozonide-derived radical.

It is interesting to note that reduced susceptibility of *P. yoelii* to artemisinin was correlated with a significant reduction in haem-artemisinin adducts (18), suggesting perturbations to haem metabolism may reduce parasite sensitivity to peroxides. In artemisinin resistant *P. falciparum*, susceptibility was found to be linked to mutations in the parasite protein K13 (58) and cross-resistance has been demonstrated with the ozonides (8, 59). While there is currently no evidence that altered haem metabolism is involved in *K13*-mediated artemisinin resistance, there is evidence that reduced haemoglobin degradation is involved (60), potentially providing less haemoglobin-derived haem for drug activation, and that other genetic factors may enhance *K13*-mediated resistance (61, 62). It would be interesting to compare levels of the alkylated haem adduct within artemisinin sensitive and resistant parasites to determine if altered haem metabolism is a contributing factor in the resistance mechanism. In this respect, there is potential for the alkylated haem adduct (or its degradation product) to be developed as a biomarker of ozonide activation and therefore provide a simple, quantitative indicator of parasite susceptibility to peroxide treatment. More work will be needed to determine whether the alkylated haem adduct is a sensitive marker of parasite susceptibility to ozonides.

In this study, the clickable probes based on OZ03 (OZ754 and OZ758) did not co-localise with a specific subcellular compartment and were widely distributed throughout the parasite within 1 h of treatment (Figures 18 and 19). The interaction of peroxide antimalarials with an array of intraparasitic proteins has been widely reported (12, 13, 29, 30) and these findings are consistent with widespread and indiscriminate alkylation of proteins within the parasite. The non-specific localisation pattern also agrees with earlier confocal microscopy work that used fluorescent ozonide conjugates (63, 64) and fluorescent antibodies against OZ277 and OZ439 (29) to demonstrate diffuse drug localisation within *Plasmodium* parasites. However, some of these earlier studies (63, 64) used the fluorescence signal derived from the intact ozonide and not its alkylation signature. It was confirmed that the cellular distribution

observed in this study was related to activity, as the fluorescence signal was substantially reduced by pre-incubation with the cell-permeable falcipain inhibitor, E64d, which has previously been shown to inhibit ozonide activity (8). This finding is indicative of impaired drug activation by a haemoglobin-derived breakdown product, most likely free haem, and reduced protein alkylation.

The OZ759 probe, based on the second-generation ozonide OZ439, was less widely distributed throughout the parasite and appeared more closely localised with the parasite digestive vacuole, when compared to the probes based on the first-generation OZ03 scaffold (Figure 19). Co-localisation of OZ759 with the parasite digestive vacuole is consistent with second-generation ozonides only being activated by haemoglobin-derived free haem (8, 65), which is located in or around the digestive vacuole. In comparison, the first-generation ozonides have been reported to be reactive with both haem and iron (31, 32, 66, 67), the latter being located throughout the parasite and possibly explaining the diffuse localisation pattern for OZ754- and OZ758-derived protein adducts observed in these studies. Therefore, the distinctive localisation pattern between first- and second-generation ozonides is likely due to differences in iron-mediated reactivity within the parasite, which results in an altered protein alkylation profile. In addition, it has previously been shown that the second-generation ozonides require a longer exposure time to achieve the same level of parasite killing as the first-generation compounds, like OZ277 (8). The proposed basis for this is that the peroxide bond is more sterically restricted in the second-generation ozonides because of the *cis*-8'-phenyl substituent (32). This may lead to lower levels of haem-mediated activation and subsequent protein alkylation at shorter incubation times. Therefore, extending the duration of exposure may result in a more widespread pattern of distribution, similar to that seen with OZ754 and OZ758. An alternative hypothesis is that the different physicochemical properties of the second-generation compounds lead to differences in intraparasitic accumulation or

interaction with different parasite proteins. A direct comparison of the time-dependent alkylation profile between the first- and second-generation ozonides, either by SDS-PAGE or by pulling-down and identifying the interacting proteins by MS, similar to that previously described (12, 13, 30), could be performed to interrogate this further.

Given that haem was identified as an intraparasitic ozonide target, that the reaction with haem was found to be central for activation (68) and that the ozonides have been shown to alkylate digestive vacuole proteins (30), it is surprising that there was not a clearer co-localisation of ozonide compounds with the parasite digestive vacuole by confocal microscopy. One possible explanation for this is that haemozoin in the parasite digestive vacuole quenched the fluorescence signal. Haemozoin is a good acceptor for energy-transfer (69) and is known to readily quench the fluorescence signal of acridine-based fluorophores (64). An alternative approach to assess digestive vacuole localisation could be to utilise a fluorescent probe that is poorly quenched by haemozoin, such as one based on the nitrobenzyldiazole (NBD) fluorochrome (64). Unfortunately, DBCO-tagged NBD probes are not readily available.

## 3.6 CONCLUSIONS

This study shows, for the first time, that ozonides covalently react with haem within the *Plasmodium* parasite, forming ozonide-haem adducts and alkylated haem degradation products that can be detected by MS. These data, along with the ozonide subcellular distribution in *P. falciparum* parasites, is consistent with the "cluster bomb" hypothesis of activity, whereby activated ozonides lead to widespread alkylation of intraparasitic targets, including proteins and haem. Surprisingly though, no additional small molecule targets were identified. The protein adducts formed from second-generation ozonides (which are reactive primarily with reduced haem), have a different sub-cellular distribution compared to first-generation ozonides (which are reactive with both free iron and haem), suggesting distinct protein targets may be involved in their antimalarial activity. Furthermore, it is proposed that the alkylated haem adduct (or its degradation products) could be a potentially valuable biomarker of ozonide activity. Additional validation would be needed to define the functional relevance of ozonide-alkylated haem to drug action and to determine whether haem alkylation correlates with *in vitro* and *in vivo* activity.

## 3.7 REFERENCES


1. O'Neill PM, Barton VE, Ward SA. 2010. The molecular mechanism of action of artemisinin--the debate continues. Molecules 15:1705-1721.
2. Dong Y, Chollet J, Matile H, Charman SA, Chiu FC, Charman WN, Scorneaux B, Urwyler H, Santo Tomas J, Scheurer C. 2005. Spiro and dispiro-1, 2, 4-trioxolanes as antimalarial peroxides: charting a workable structure-activity relationship using simple prototypes. J Med Chem 48:4953-4961.
3. Kaiser M, Wittlin S, Nehrbass-Stuedli A, Dong Y, Wang X, Hemphill A, Matile H, Brun R, Vennerstrom JL. 2007. Peroxide bond-dependent antiplasmodial specificity of artemisinin and OZ277 (RBx11160). Antimicrob Agents Chemother 51:2991-2993.
4. Avery MA, Gao F, Chong WK, Mehrotra S, Milhous WK. 1993. Structure-activity relationships of the antimalarial agent artemisinin. 1. Synthesis and comparative molecular field analysis of C-9 analogs of artemisinin and 10-deoxoartemisinin. J Med Chem 36:4264-4275.
5. Cumming JN, Ploypradith P, Posner GH. 1996. Antimalarial activity of artemisinin (qinghaosu) and related trioxanes: mechanism (s) of action. Adv Pharmacol 37:253-297.
6. Fügi MA, Wittlin S, Dong Y, Vennerstrom JL. 2010. Probing the antimalarial mechanism of artemisinin and OZ277 (arterolane) with nonperoxidic isosteres and nitroxyl radicals. Antimicrob Agents Chemother 54:1042-1046.
7. Wang X, Dong Y, Wittlin S, Creek D, Chollet J, Charman SA, Tomas JS, Scheurer C, Snyder C, Vennerstrom JL. 2007. Spiro- and dispiro-1,2-dioxolanes: contribution of iron(II)-mediated one-electron vs two-electron reduction to the activity of antimalarial peroxides. J Med Chem 50:5840-5847.
8. Yang T, Xie SC, Cao P, Giannangelo C, McCaw J, Creek DJ, Charman SA, Klonis N, Tilley L. 2016. Comparison of the exposure time-dependence of the activities of synthetic ozonide antimalarials and dihydroartemisinin against K13 wild-type and mutant *Plasmodium falciparum* strains. Antimicrob Agents Chemother 60:4501-4510.
9. Asawamahasakda W, Ittarat I, Pu Y-M, Ziffer H, Meshnick SR. 1994. Reaction of antimalarial endoperoxides with specific parasite proteins. Antimicrob Agents Chemother 38:1854-1858.

10. Bhisutthibhan J, Pan XQ, Hossler PA, Walker DJ, Yowell CA, Carlton J, Dame JB, Meshnick SR. 1998. The *Plasmodium falciparum* translationally controlled tumor protein homolog and its reaction with the antimalarial drug artemisinin. J Biol Chem 273:16192-16198.
11. Eckstein-Ludwig U, Webb RJ, Van Goethem ID, East JM, Lee AG, Kimura M, O'Neill PM, Bray PG, Ward SA, Krishna S. 2003. Artemisinins target the SERCA of *Plasmodium falciparum*. Nature 424:957-961.
12. Wang J, Zhang C-J, Chia WN, Loh CC, Li Z, Lee YM, He Y, Yuan L-X, Lim TK, Liu M, Liew CX, Lee YQ, Zhang J, Lu N, Lim CT, Hua Z-C, Liu B, Shen H-M, Tan KSW, Lin Q. 2015. Haem-activated promiscuous targeting of artemisinin in *Plasmodium falciparum*. Nat Commun 6:10111.
13. Ismail HM, Barton V, Phanchana M, Charoensutthivarakul S, Wong MHL, Hemingway J, Biagini GA, O'Neill PM, Ward SA. 2016. Artemisinin activity-based probes identify multiple molecular targets within the asexual stage of the malaria parasites *Plasmodium falciparum* 3D7. Proc Natl Acad Sci U S A 113:2080-2085.
14. Wang D-Y, Wu Y-L. 2000. A possible antimalarial action mode of qinghaosu (artemisinin) series compounds. Alkylation of reduced glutathione by C-centered primary radicals produced from antimalarial compound qinghaosu and 12-(2,4-dimethoxyphenyl)-12-deoxoqinghaosu. Chem Commun 22:2193-2194.
15. Wu Y, Yue ZY, Wu YL. 1999. Interaction of qinghaosu (artemisinin) with cysteine sulfhydryl mediated by traces of non-heme iron. Angew Chem Int Ed Engl 38:2580-2582.
16. Meshnick SR, Thomas A, Ranz A, Xu CM, Pan HZ. 1991. Artemisinin (qinghaosu): the role of intracellular hemin in its mechanism of antimalarial action. Mol Biochem Parasitol 49:181-189.
17. Robert A, Benoit-Vical F, Claparols C, Meunier B. 2005. The antimalarial drug artemisinin alkylates heme in infected mice. Proc Natl Acad Sci U S A 102:13676-13680.
18. Robert A, Claparols C, Witkowski B, Benoit-Vical F. 2013. Correlation between *Plasmodium yoelii nigeriensis* susceptibility to artemisinin and alkylation of heme by the drug. Antimicrob Agents Chemother 57:3998-4000.
19. Robert A, Coppel Y, Meunier B. 2002. Alkylation of heme by the antimalarial drug artemisinin. Chem Commun 5:414-415.

20. Hong Y-L, Yang Y-Z, Meshnick SR. 1994. The interaction of artemisinin with malarial hemozoin. Mol Biochem Parasitol 63:121-128.
21. Meshnick SR, Dobson MJ. 2001. The history of antimalarial drugs. Antimalarial chemotherapy:15-25.
22. Benoit-Vical F, Robert A, Meunier B. 2000. *In vitro* and *in vivo* potentiation of artemisinin and synthetic endoperoxide antimalarial drugs by metalloporphyrins. Antimicrob Agents Chemother 44:2836-2841.
23. Robert A, Cazelles J, Meunier B. 2001. Characterization of the alkylation product of heme by the antimalarial drug artemisinin. Angew Chem Int Ed Engl 40:1954-1957.
24. Laurent S, Robert A, Meunier B. 2005. C10-modified artemisinin derivatives: efficient heme-alkylating agents. Angew Chem Int Ed Engl 44:2060-2063.
25. Loup C, Lelievre J, Benoit-Vical F, Meunier B. 2007. Trioxaquines and heme-artemisinin adducts inhibit the *in vitro* formation of hemozoin better than chloroquine. Antimicrob Agents Chemother 51:3768-3770.
26. Hartwig CL, Rosenthal AS, D'Angelo J, Griffin CE, Posner GH, Cooper RA. 2009. Accumulation of artemisinin trioxane derivatives within neutral lipids of *Plasmodium falciparum* malaria parasites is endoperoxide-dependent. Biochem Pharmacol 77:322-336.
27. Berman PA, Adams PA. 1997. Artemisinin enhances heme-catalysed oxidation of lipid membranes. Free Radic Biol Med 22:1283-1288.
28. del Pilar Crespo M, Avery TD, Hanssen E, Fox E, Robinson TV, Valente P, Taylor DK, Tilley L. 2008. Artemisinin and a series of novel endoperoxide antimalarials exert early effects on digestive vacuole morphology. Antimicrob Agents Chemother 52:98-109.
29. Jourdan J, Matile H, Reift E, Biehlmaier O, Dong Y, Wang X, Mäser P, Vennerstrom JL, Wittlin S. 2015. Monoclonal antibodies that recognize the alkylation signature of antimalarial ozonides OZ277 (arterolane) and OZ439 (artefenomel). ACS Infect Dis 2:54-61.
30. Ismail HM, Barton VE, Panchana M, Charoensutthivarakul S, Biagini GA, Ward SA, O'Neill PM. 2016. A click chemistry-based proteomic approach reveals that 1, 2, 4-trioxolane and artemisinin antimalarials share a common protein alkylation profile. Angew Chem Int Ed Engl 55:6401-6405.
31. Creek DJ, Charman WN, Chiu FC, Prankerd RJ, McCullough KJ, Dong Y, Vennerstrom JL, Charman SA. 2007. Iron-mediated degradation kinetics of substituted dispiro-1,2,4-trioxolane antimalarials. J Pharm Sci 96:2945-2956.

32. Creek DJ, Charman WN, Chiu FC, Prankerd RJ, Dong Y, Vennerstrom JL, Charman SA. 2008. Relationship between antimalarial activity and heme alkylation for spiro- and dispiro-1,2,4-trioxolane antimalarials. Antimicrob Agents Chemother 52:1291-1296.

33. Wang X, Creek DJ, Schiaffo CE, Dong Y, Chollet J, Scheurer C, Wittlin S, Charman SA, Dussault PH, Wood JK, Vennerstrom JL. 2009. Spiroadamantyl 1,2,4-trioxolane, 1,2,4-trioxane, and 1,2,4-trioxepane pairs: relationship between peroxide bond iron(II) reactivity, heme alkylation efficiency, and antimalarial activity. Bioorg Med Chem Lett 19:4542-4545.

34. Kannan R, Sahal D, Chauhan VS. 2002. Heme-artemisinin adducts are crucial mediators of the ability of artemisinin to inhibit heme polymerization. Chem Biol 9:321-332.

35. Solomonov I, Osipova M, Feldman Y, Baehtz C, Kjaer K, Robinson IK, Webster GT, McNaughton D, Wood BR, Weissbuch I. 2007. Crystal nucleation, growth, and morphology of the synthetic malaria pigment β-hematin and the effect thereon by quinoline additives: the malaria pigment as a target of various antimalarial drugs. J Am Chem Soc 129:2615-2627.

36. Trager W, Jensen JB. 1976. Human malaria parasites in continuous culture. Science 193:673-675.

37. Lambros C, Vanderberg JP. 1979. Synchronization of *Plasmodium falciparum* erythrocytic stages in culture. J Parasitol 65:418-420.

38. Smilkstein M, Sriwilaijaroen N, Kelly JX, Wilairat P, Riscoe M. 2004. Simple and inexpensive fluorescence-based technique for high-throughput antimalarial drug screening. Antimicrob Agents Chemother 48:1803-1806.

39. Creek DJ, Jankevics A, Burgess KE, Breitling R, Barrett MP. 2012. IDEOM: an Excel interface for analysis of LC-MS-based metabolomics data. Bioinformatics (Oxford, England) 28:1048-1049.

40. Tang Y, Dong Y, Wang X, Sriraghavan K, Wood JK, Vennerstrom JL. 2005. Dispiro-1,2,4-trioxane analogues of a prototype dispiro-1,2,4-trioxolane: mechanistic comparators for artemisinin in the context of reaction pathways with iron(II). J Org Chem 70:5103-5110.

41. Tonkin CJ, van Dooren GG, Spurck TP, Struck NS, Good RT, Handman E, Cowman AF, McFadden GI. 2004. Localization of organellar proteins in *Plasmodium falciparum*

using a novel set of transfection vectors and a new immunofluorescence fixation method. Mol Biochem Parasitol 137:13-21.

42. Penarete-Vargas DM, Boisson A, Urbach S, Chantelauze H, Peyrottes S, Fraisse L, Vial HJ. 2014. A chemical proteomics approach for the search of pharmacological targets of the antimalarial clinical candidate albitiazolium in *Plasmodium falciparum* using photocrosslinking and click chemistry. PloS One 9:e113918.
43. Bousejra-El Garah F, Pitié M, Vendier L, Meunier B, Robert A. 2009. Alkylating ability of artemisinin after Cu (I)-induced activation. JBIC J Biol Inorg Chem 14:601-610.
44. Schaefer WH, Harris TM, Guengerich FP. 1985. Characterization of the enzymic and nonenzymic peroxidative degradation of iron porphyrins and cytochrome P-450 heme. Biochemistry 24:3254-3263.
45. Robert A, Coppel Y, Meunier B. 2002. NMR characterization of covalent adducts obtained by alkylation of heme with the antimalarial drug artemisinin. Inorganica chimica acta 339:488-496.
46. Hofer S, Brun R, Maerki S, Matile H, Scheurer C, Wittlin S. 2008. *In vitro* assessment of the pharmacodynamic properties of DB75, piperaquine, OZ277 and OZ401 in cultures of *Plasmodium falciparum*. J Antimicrob Chemother 62:1061-1064.
47. Maerki S, Brun R, Charman SA, Dorn A, Matile H, Wittlin S. 2006. *In vitro* assessment of the pharmacodynamic properties and the partitioning of OZ277/RBx-11160 in cultures of *Plasmodium falciparum*. J Antimicrob Chemother 58:52-58.
48. Tang Y, Dong Y, Vennerstrom JL. 2004. Synthetic peroxides as antimalarials. Med Res Rev 24:425-448.
49. Dong Y, Vennerstrom JL. 2003. Mechanisms of *in situ* activation for peroxidic antimalarials. Redox Rep 8:284-288.
50. Scholl PF, Tripathi AK, Sullivan DJ. 2005. Bioavailable iron and heme metabolism in *Plasmodium falciparum*. Curr Top Microbiol Immunol 295:293-324.
51. Bousejra-El Garah F, Wong MH-L, Amewu RK, Muangnoicharoen S, Maggs JL, Stigliani J-L, Park BK, Chadwick J, Ward SA, O'Neill PM. 2011. Comparison of the reactivity of antimalarial 1, 2, 4, 5-tetraoxanes with 1, 2, 4-trioxolanes in the presence of ferrous iron salts, heme, and ferrous iron salts/phosphatidylcholine. J Med Chem 54:6443-6455.
52. Robert A, Meunier B. 1997. Characterization of the first covalent adduct between artemisinin and a heme model. J Am Chem Soc 119:5968-5969.

53. van Dooren GG, Kennedy AT, McFadden GI. 2012. The use and abuse of heme in apicomplexan parasites. Antioxid Redox Signal 17:634-656.
54. Zhang S, Gerhard GS. 2008. Heme activates artemisinin more efficiently than hemin, inorganic iron, or hemoglobin. Bioorg Med Chem 16:7853-7861.
55. Zhang S, Gerhard GS. 2009. Heme mediates cytotoxicity from artemisinin and serves as a general anti-proliferation target. PloS One 4:e7472.
56. Creek DJ, Chiu FC, Prankerd RJ, Charman SA, Charman WN. 2005. Kinetics of iron-mediated artemisinin degradation: effect of solvent composition and iron salt. J Pharm Sci 94:1820-1829.
57. Vattanaviboon P, Siritanaratkul N, Ketpirune J, Wilairat P, Yuthavong Y. 2002. Membrane heme as a host factor in reducing effectiveness of dihydroartemisinin. Biochem Pharmacol 64:91-98.
58. Ariey F, Witkowski B, Amaratunga C, Beghain J, Langlois A-C, Khim N, Kim S, Duru V, Bouchier C, Ma L, Lim P, Leang R, Duong S, Sreng S, Suon S, Chuor CM, Bout DM, Menard S, Rogers WO, Genton B, Fandeur T, Miotto O, Ringwald P, Le Bras J, Berry A, Barale J-C, Fairhurst RM, Benoit-Vical F, Mercereau-Puijalon O, Menard D. 2014. A molecular marker of artemisinin-resistant *Plasmodium falciparum* malaria. Nature 505:50-55.
59. Straimer J, Gnädig NF, Stokes BH, Ehrenberger M, Crane AA, Fidock DA. 2017. *Plasmodium falciparum* K13 mutations differentially impact ozonide susceptibility and parasite fitness *in vitro*. mBio 8:e00172-00117.
60. Siddiqui G, Srivastava A, Russell AS, Creek DJ. 2017. Multi-omics based identification of specific biochemical changes associated with PfKelch13-mutant artemisinin resistant *Plasmodium falciparum*. J Infect Dis 215:1435-1444.
61. Straimer J, Gnadig NF, Witkowski B, Amaratunga C, Duru V, Ramadani AP, Dacheux M, Khim N, Zhang L, Lam S, Gregory PD, Urnov FD, Mercereau-Puijalon O, Benoit-Vical F, Fairhurst RM, Menard D, Fidock DA. 2015. Drug resistance. K13-propeller mutations confer artemisinin resistance in *Plasmodium falciparum* clinical isolates. Science 347:428-431.
62. Miotto O, Amato R, Ashley EA, MacInnis B, Almagro-Garcia J, Amaratunga C, Lim P, Mead D, Oyola SO, Dhorda M, Imwong M, Woodrow C, Manske M, Stalker J, Drury E, Campino S, Amenga-Etego L, Thanh TN, Tran HT, Ringwald P, Bethell D, Nosten F, Phyo AP, Pukrittayakamee S, Chotivanich K, Chuor CM, Nguon C, Suon S, Sreng S, Newton PN, Mayxay M, Khanthavong M, Hongvanthong B, Htut Y, Han KT, Kyaw

MP, Faiz MA, Fanello CI, Onyamboko M, Mokuolu OA, Jacob CG, Takala-Harrison S, Plowe CV, Day NP, Dondorp AM, Spencer CC, McVean G, Fairhurst RM, White NJ, Kwiatkowski DP. 2015. Genetic architecture of artemisinin-resistant *Plasmodium falciparum*. Nat Genet 47:226-234.

63. Uhlemann AC, Wittlin S, Matile H, Bustamante LY, Krishna S. 2007. Mechanism of antimalarial action of the synthetic trioxolane RBX11160 (OZ277). Antimicrob Agents Chemother 51:667-672.
64. Stocks PA, Bray PG, Barton VE, Al-Helal M, Jones M, Araujo NC, Gibbons P, Ward SA, Hughes RH, Biagini GA, Davies J, Amewu R, Mercer AE, Ellis G, O'Neill PM. 2007. Evidence for a common non-heme chelatable-iron-dependent activation mechanism for semisynthetic and synthetic endoperoxide antimalarial drugs. Angew Chem Int Ed Engl 46:6278-6283.
65. Giannangelo C, Stingelin L, Yang T, Tilley L, Charman SA, Creek DJ. 2018. Parasite-mediated degradation of synthetic ozonide antimalarials impacts *in vitro* antimalarial activity. Antimicrob Agents Chemother 62:e01566-01517.
66. Charman SA, Arbe-Barnes S, Bathurst IC, Brun R, Campbell M, Charman WN, Chiu FC, Chollet J, Craft JC, Creek DJ, Dong Y, Matile H, Maurer M, Morizzi J, Nguyen T, Papastogiannidis P, Scheurer C, Shackleford DM, Sriraghavan K, Stingelin L, Tang Y, Urwyler H, Wang X, White KL, Wittlin S, Zhou L, Vennerstrom JL. 2011. Synthetic ozonide drug candidate OZ439 offers new hope for a single-dose cure of uncomplicated malaria. Proc Natl Acad Sci U S A 108:4400-4405.
67. Wang X, Dong Y, Wittlin S, Charman SA, Chiu FC, Chollet J, Katneni K, Mannila J, Morizzi J, Ryan E, Scheurer C, Steuten J, Santo Tomas J, Snyder C, Vennerstrom JL. 2013. Comparative antimalarial activities and ADME profiles of ozonides (1,2,4-trioxolanes) OZ277, OZ439, and their 1,2-dioxolane, 1,2,4-trioxane, and 1,2,4,5-tetraoxane isosteres. J Med Chem 56:2547-2555.
68. Xie SC, Dogovski C, Hanssen E, Chiu F, Yang T, Crespo MP, Stafford C, Batinovic S, Teguh S, Charman S, Klonis N, Tilley L. 2016. Haemoglobin degradation underpins the sensitivity of early ring stage *Plasmodium falciparum* to artemisinins. J Cell Sci 129:406-416.
69. Pato C, Célier C, Rezaei H, Grosclaude J, Marden MC. 2004. Heme as an optical probe of a conformational transition of ovine recPrP. Protein Sci 13:1100-1107.

# Chapter 4

# Peroxide-induced perturbations of *P. falciparum* biochemical pathways

## 4.1 ABSTRACT

The peroxides are an important class of antimalarial that are active against all blood-stages of the malaria parasite *P. falciparum*. However, detailed information on the biochemical mechanisms underlying their activity are lacking. The existing literature indicates that they require reductive activation within the parasite and that the resulting radicals alkylate and cause oxidative damage to various intraparasitic components. This study aimed to identify the biochemical pathways affected by the ozonides, OZ277 and OZ439, and the clinically used artemisinin derivative, DHA, within *P. falciparum*-infected RBCs by combining untargeted metabolomic, peptidomic and proteomic analyses. Infected RBCs were exposed to the peroxides for up to 3 h, and drug-induced disruption to haemoglobin catabolism was the major pathway affected. Metabolomics analysis revealed a depletion of short chain haemoglobin-derived peptides within 3 h of drug exposure. Further untargeted peptidomic studies confirmed haemoglobin-derived peptides were perturbed. Using various activity-based protease probes, changes in haemoglobin protease activity were observed within 1 h of peroxide treatment. When the duration of treatment was extended beyond 3 h, additional biochemical pathways were impacted, namely lipid, pyrimidine and amino acid metabolism. The major finding from the proteomic analysis was that proteins involved in translation and the ubiquitin-proteasome system were increased in abundance after treatment, which is suggestive of the parasite engaging a stress response. Taken together, these data point to a mechanism of action involving initial impairment of haemoglobin catabolism, consistent with drug activation within the parasite food vacuole, and subsequent engagement of a stress response to manage peroxide-induced damage.

## 4.2 INTRODUCTION

For artemisinin and ozonide antimalarials, the prevailing evidence indicates that they act via a promiscuous targeting effect, involving haem-mediated peroxide bond activation, and damage of multiple intraparasitic targets (1-3). Previous untargeted (4) and semi-targeted (5) metabolomics studies exploring the biochemical impact of artemisinins on parasite function support this hypothesis, revealing a pleiotropic effect on parasite metabolism. Consistent with activation within the parasite digestive vacuole and drug-dependent damage of vacuolar membrane integrity, artemisinin exposure induces disruption of parasite haemoglobin catabolism, manifesting as a depletion of haemoglobin-derived peptides (4, 5). Decreased abundance of haemoglobin-derived peptides and the accumulation of undigested haemoglobin (6) suggests artemisinin action involves disruption of the haemoglobin degradation pathway, either through inhibition of haemoglobin uptake (6, 7), impaired haemoglobin proteolysis (8) or a combination of both.

In addition, artemisinins appear to perturb parasite pyrimidine biosynthesis by way of depleting key metabolic intermediates, such as carbamoyl-aspartate, and redirecting carbon into malate production (5). The impact of treatment on intracellular levels of other metabolite classes, including nucleotides, lipids and sugars, and disruption of the mitochondrial membrane potential (9), points to non-specific inhibition of a number of biochemical pathways (2, 4, 5).

Similar to the artemisinins, ozonide antimalarials are also thought to disrupt multiple pathways within the parasite. They have been reported to target proteins in the glycolytic, haemoglobin degradation, antioxidant defence, protein synthesis and protein stress pathways (3). Approximately 80% of proteins alkylated as a result of treatment with the ozonides were also found to be alkylated by artemisinins, suggesting a common mode of action. Surprisingly, untargeted metabolomic profiling of *P. falciparum* parasites treated with OZ277 and OZ439

previously revealed no major alterations in parasite metabolism (10). In this study, magnetically purified trophozoite stage parasites were incubated with drug for 2.5 h, conditions that, according to the activity and stability data previously characterised for OZ277 and OZ439, results in rapid drug degradation and no measurable antimalarial activity (11).

The aim of the current study was to investigate the time-dependent biochemical impact of selected peroxide antimalarials on *P. falciparum* biochemistry at different stages of the parasite asexual lifecycle. Untargeted metabolomic profiling allowed monitoring of drug-dependent changes in metabolite abundance over time, enabling the identification of early effects on parasite metabolism to be distinguished from a non-specific death phenotype. This was combined with peptidomic and proteomic analysis to provide a comprehensive multi-omics-based evaluation of peroxide-induced perturbations on *P. falciparum* biochemistry, and helped to understand the mechanistic basis for activity of these important antimalarials.

# 4.3 MATERIALS AND METHODS

## 4.3.1 Reagents

Ethyl acetate, sodium deoxycholate (SDC), ammonium acetate, ammonium hydroxide, ammonium carbonate, dithiothreitol (DTT), tris(2-carboxyethyl)phosphine (TCEP), iodoacetamide, formaldehyde, formaldehyde-D2, 13C-formaldehyde-D2, sodium cyanoborohydride, cyanoborodeuteride and ammonia were purchased from Sigma Aldrich. The phosphatase inhibitors sodium fluoride, sodium orthovanadate and beta glycerophosphate were also from Sigma Aldrich and complete EDTA-free protease inhibitor cocktail from Roche. Sequencing grade modified trypsin was from Promega. Chloroform (LiChrosolv) and N-acetyl-Leu-Leu-Norleu-al (ALLN) were from Merck. Activity-based protease probes (ABPPs) were provided by Doctor Laura Edgington-Mitchell (University of Melbourne).

## 4.3.2 *P. falciparum* cell culture and parasite drug treatment for metabolomics, peptidomics and proteomics experiments

An integrated multi-omics-based approach (metabolomics, peptidomics and proteomics) was employed to comprehensively assess the time-dependent impact of peroxide antimalarial treatment on *P. falciparum* parasites (Figure 1). *P. falciparum* parasites (3D7 strain) were cultured as described in Chapter 3 (Section 3.3.2). All experiments used mid-trophozoite (28-34 h post invasion) or mid-ring (6-12 h post invasion) stage parasite cultures that were adjusted to 10% parasitaemia and 2% Hct prior to initiating drug incubations. Trophozoite stage parasites were treated with 300 nM of OZ277 or OZ439 and 100 nM of DHA. Ring stage parasites were incubated with 1 μM of OZ277 or OZ439 and 300 nM of DHA. Infected RBCs that were incubated with an equivalent volume of DMSO (final concentration ≤ 0.03%) were used as the untreated controls. Metabolomics studies also

included treatment of non-infected RBCs as a control. All experiments were performed on at least four independent occasions.

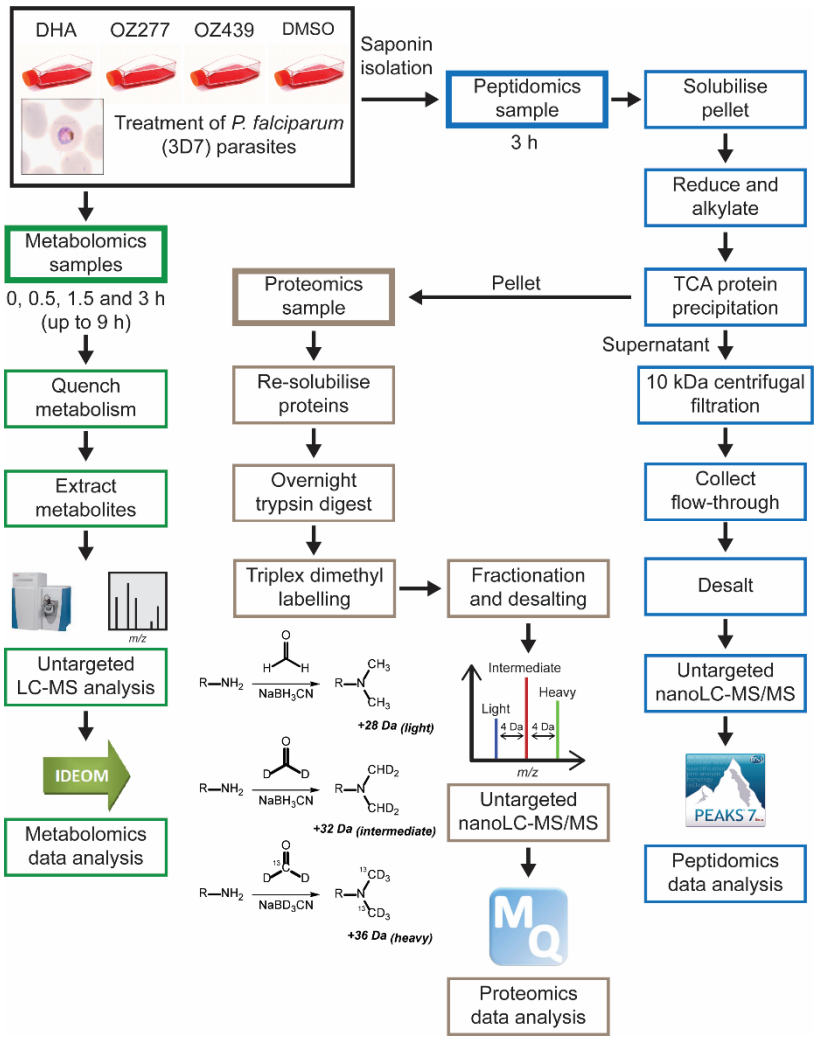


**Figure 1:** Integrative multi-omics-based workflow for the comprehensive analysis of peroxide antimalarial action in *P. falciparum* infected RBCs. Metabolomics (green boxes) samples were extracted from infected RBCs at regular intervals (up to 9 h after drug addition) using organic solvent and the extracted samples were analysed by LC-MS and processed using IDEOM. For peptidomics (blue boxes), endogenous peptides were extracted from saponin lysed parasites, samples were subjected to 10 kDa cut-off centrifugal filtration and then an equal amount of peptides were used for analysis by nanoLC-MS/MS before data was processed using PEAKS software. Protein pellets following trichloracetic acid (TCA) precipitation were collected for proteomic sample preparation (brown boxes). Equal amount of proteins were digested using trypsin, labelled using dimethyl labelling to allow differential quantitative proteomic analysis and examined using nanoLC-MS/MS followed by data processing using MaxQuant.

## 4.3.3 Untargeted metabolomics experiments

### 4.3.3.1 Metabolomics sample preparation

Comprehensive time-course analysis was performed to determine the peroxide-induced metabolic profile in ring and trophozoite stage parasites. Ring stage parasite cultures were exposed to OZ277 and OZ439 for 0, 3, 6 and 9 h prior to metabolite extraction, while the treatment durations for DHA were 0, 1.5, 3 and 6 h. As artemisinins have been shown to act more rapidly than ozonides (12) the earlier 1.5 h time point was added, and the later 9 h time point omitted, for the DHA ring stage experiments. Trophozoite stage parasite cultures were exposed to drug for much shorter durations of 0, 0.5, 1.5 and 3 h. The change in the duration of drug treatment between the parasite asexual lifecycle stages was conducted in order to measure the early effects of peroxide treatment on the more sensitive trophozoite stage parasites. Long-term peroxide treatment was also assessed in trophozoite stage cultures by exposing parasites to drug for up to 9 h. All subsequent steps were performed on ice or at 4°C.

Post drug incubation, the desired number of cells were pelleted by centrifugation at 1,000 x *g* for 3 min and the culture medium was removed. Parasite metabolism was quenched by the addition of ice-cold PBS, pelleted again and the supernatant discarded prior to metabolite extraction. For ring stage experiments, metabolites were extracted from 2 x $10^8$ cells using 200 µL of cold chloroform/methanol/water (1:3:1). For trophozoite stage experiments where parasites were exposed to drug for up to 3 h, metabolites were extracted from 1 x $10^8$ cells using 150 µL of cold chloroform/methanol/water (1:3:1). For trophozoite stage experiments where long-term peroxide treatment was used (up to 9 h), metabolites were extracted from 1 x $10^8$ cells using 150 µL of cold methanol. The extraction solvent containing the internal standard compounds CHAPS (3-[(3-cholamidopropyl)-dimethylammonio]-1-propanesulfonate), CAPS (3-(cyclohexylamino)-1-propanesulfonic acid), PIPES (1,4-

piperazinediethanesulfonic acid) and TRIS (2-amino-2-(hydroxymethyl)-1,3-propanediol) was directly added to the cell pellet, mixed by pipetting and subjected to automatic vortex mixing for 1 h at 4°C. Following the 1 h incubation, samples were pelleted by centrifugation at 21,100 x *g* for 10 min, 110 µL of particle free supernatant was transferred to glass LC-MS vials and stored at -80°C until analysis. A 15 µL aliquot of each sample was combined to generate a pooled biological quality control (PBQC) sample for analytical quality control and metabolite identification procedures.

#### 4.3.3.2 Metabolomics LC-MS analysis and data processing

Untargeted LC-MS analysis was performed as previously described (4, 13). Briefly, metabolite samples were separated on a ZIC-pHILIC column, (5 µm, 150 x 4.6 mm, Merck) with a Dionex Ultimate 3000 UHPLC system (ThermoFisher) using 20 mM ammonium carbonate (solvent A) and 100% ACN (solvent B) as the mobile phases. The 32 min gradient HPLC run was from 80% B to 50% B over 15 min, then to 5% B at 18 min, followed by a wash with 5% B for 3 min and re-equilibrated with 80% B at a flow rate of 0.3 mL/min. Metabolite detection was performed using a high-resolution Q Exactive MS (ThermoFisher) in both positive and negative ionisation modes. The PBQC sample was run periodically throughout each LC-MS batch to monitor signal reproducibility and support downstream metabolite identification. Extraction solvent blank samples were also analysed to identify possible contaminating chemical species. To aid in metabolite identification, approximately 250 authentic metabolite standards were analysed prior to each LC-MS batch and their peaks and retention time manually checked using the ToxID software (ThermoFisher).

Metabolomics data were analysed using the IDEOM workflow (14). Briefly, the IDEOM processing pipeline uses msconvert for conversion of raw files to mzXML files and split polarity, XCMS to extract raw peak intensities and mzMatch to align samples, filter noise,

fill missing peaks and annotate related peaks. Manual assessment of spiked internal standards, total ion chromatograms and median peak heights ensured signal reproducibility and allowed exclusion of outlier samples. High confidence metabolite identification (MSI level 1) was made by matching accurate mass and retention time to authentic metabolite standards (15). Putative identifications (MSI level 2) for metabolites lacking standards were based on exact mass and predicted retention times (16). Specifically, the identification of peptides were based on either accurate mass or a combination of accurate mass and MS/MS analysis, which allowed definitive confirmation of the amino acid sequence in selected peptides. Due to variability in the ring study sample groups (relative standard deviation (RSD) of the median peak intensities > 20%), LC-MS peak heights representing metabolite abundances were normalised by median peak height. The metabolite abundances for each sample group in the trophozoite studies exhibited an RSD < 15% and were not normalised. Univariate statistical analysis was performed using IDEOM and Welch's *t* test (14). Multivariate statistical analysis was performed on the mean centred and auto-scaled data using the web-based tools in Metaboanalyst (17). Sparse partial least squares – discriminant analysis (sPLS-DA) algorithms were run with increasing numbers of metabolites in each component (up to 150 metabolites), with minor changes to the model when more than 10 metabolites were used. The final sPLS-DA plots shown were developed using 10 metabolites in each component. Significant metabolites (p-value ≤ 0.05) were confirmed by manual integration of raw LC-MS peak areas in TraceFinder (ThermoFisher).

## 4.3.4 Untargeted peptidomics experiments

### 4.3.4.1 Peptidomics sample preparation

Intracellular parasites were harvested from infected RBCs after 3 h of drug treatment, using 0.1% saponin. Parasite proteins were solubilised in lysis buffer (100 mM HEPES buffer,

1% SDC, pH 8.1) containing protease and phosphatase inhibitor (20mM sodium fluoride, 0.1mM sodium orthovanadate and 10mM beta-glycelrophosphate) using pulse sonication (3 x 45 sec cycles of 10 amp) on ice. Solubilised proteins were reduced and alkylated with 10 mM TCEP and 40 mM iodoacetamide at 95°C for 5 min, then precipitated using trichloroacetic acid (TCA) at a 1:4 (v/v) ratio on ice for 10 min. Samples were then centrifuged at 21,100 x *g* for 10 min and the pellets collected for proteomic sample preparation. The supernatants, which consisted of acid soluble proteins and endogenous peptides, were subjected to centrifugal filtration (10 kDa cut-off filters, Amicon Ultra) and the flow-through containing endogenous peptides was collected. Residual SDC was removed by the addition of an equal amount of ethyl acetate to the combined sample, spun at 2000 x *g* for 5 min and the top layer (containing SDC) was discarded (18). Peptide concentration in drug-treated and control samples were measured by a bicinchoninic acid (BCA) protein assay (Thermo Scientific Pierce) and equal concentration of peptides (53-75 µg) were used for peptidomic analysis. Peptide samples were then subjected to desalting using in-house generated C18 StageTips (19). The elutes were then dried and resuspended in 20 µL of 2% (v/v) ACN and 0.1% (v/v) formic acid for LC-MS/MS analysis.

#### 4.3.4.2 Peptidomics nanoLC-MS/MS analysis and data processing

LC-MS/MS was performed using an Ultimate U3000 Nano LC system (Dionex) and Q Exactive Orbitrap MS (ThermoFisher) as previously described (13).

Peptide identification was performed using PEAKS DB software (20). Maximum mass deviation and false discovery rates were set at 0.5 Da and 0.01, respectively. No post translational modification or digestion were selected and identified peptide sequences were matched to *Homo sapiens* and *P. falciparum* databases. Further analysis and statistics

(Student's *t* test) were performed using TraceFinder (ThermoFisher) and Microsoft Excel, respectively.

## 4.3.5 Untargeted proteomics experiments

### 4.3.5.1 Triplex stable isotope dimethyl labelling and ion-exchange fractionation for proteomic samples

Pellets collected after TCA precipitation (Section 4.3.4.1) were washed twice with 1 mL of ice-cold acetone and dried at 95°C for 30 sec. Proteins were re-solubilised in lysis buffer using the probe sonicator (3 x 45 sec). Total protein concentration was accurately determined by a BCA protein assay and 1000 µg of protein from each sample was incubated overnight with trypsin (1:50) at 37°C. Quantitative triplex stable isotope dimethyl labelling was initiated on the following day using light, intermediate or heavy dimethyl labelling reagents (21). This triplex labelling approach allowed differential labelling of three different samples and downstream simultaneous quantitative LC-MS/MS analysis. Light labelling reagent consisted of 40 mM formaldehyde with 20 mM cyanoborohydride and produced a 28 Da mass increase per primary amine. Intermediate labelling consisted of formaldehyde-D2 with 20 mM cyanoborohydride (32 Da mass increase). Heavy labelling was achieved with 40 mM 13C-formaldehyde-D2 with 20 mM cyanoborodeuteride (36 Da mass increase). The labelling reactions were allowed to proceed for 1 h at room temperature while rotating end-over-end, after which the reactions were quenched by the addition of 1% ammonia and 5% formic acid and the samples were mixed together. Residual SDC was removed by the addition of an equal volume of ethyl acetate to the combined sample, spun at 2000 x *g* for 5 min and the top layer (containing SDC) discarded (18).

The bottom phase containing peptides was subjected to ion-exchange fractionation using a disposable Strong Cationic Exchange Solid Phase Extraction cartridge (Agilent Bond

Elut) (22). The cartridge was activated with 100% methanol and equilibrated with 0.1% (v/v) formic acid, before the sample was loaded at a flow rate of 1 drop/sec. The flow through was collected and the cartridge was washed three times with 50% (v/v) ethyl acetate and 0.5% (v/v) formic acid, then three times with 0.1% formic acid. Bound peptides were eluted at 1 drop/sec using 500 µL of elution buffers containing an increasing amount of ammonium acetate (100 mM, 150 mM, 200 mM, 250 mM and 300 mM) with 20% (v/v) ACN and 0.5% (v/v) formic acid. The final elution buffer consisted of 80% ACN and 5% ammonium hydroxide. The elutes were then desalted using in-house generated StageTips as described in Section 4.3.4.1 (19), dried and resuspended in 20 µL of 2% (v/v) ACN and 0.1% (v/v) formic acid for LC-MS/MS analysis.

#### 4.3.5.2 Proteomics nanoLC-MS/MS analysis and data processing

LC-MS/MS analysis was performed according to the same methodology as described in Section 4.3.4.2, but +1 to +8 mass identification was not enabled.

Protein identification and quantification was performed using the proteomics software, MaxQuant (23). The data analysis parameters in MaxQuant were set as previously described (13) with minor modifications. Dimethylation settings were adjusted to triplets, and DimetNterm0 with DimetLys0, DimetNterm4 with DimetLys4 and DimetNterm8 with DimetLys8 selected as light, intermediate and heavy label, respectively. To correct for differences in protein amount between groups, the protein ratios were normalised in MaxQuant at the peptide level so that the log2 ratios is zero (23). Known contaminants such as trypsin, keratin and reverse sequences were removed from the MaxQuant output. Fold-changes for the drug treated samples relative to the DMSO control samples were calculated in Microsoft Excel. One sample t-test was used to test the mean of combined experiment groups against the known mean ($\mu = 0$) (24). The bioinformatics interaction network analysis tool STRINGdb (25) was

used to build a protein-protein interaction network using the significantly perturbed proteins. Connectivity was based on experimental, database and co-expression evidence and a strict minimum required interaction score (> 0.7) was applied to limit false positive associations in the predicted network. The STRINGdb protein connectivity output was exported to Cytoscape 3.6 (26) and the ClusterONE algorithm was used to integrate and visualise relationships between proteins that were significantly perturbed by drug treatment.

### 4.3.6 Temporal profiling of protease activity using activity-based protease probes

A range of ABPPs (Table 1) were used to measure protease activity within *P. falciparum* parasites following ozonide exposure. In these assays, tightly synchronised trophozoite stage parasites (28-34 h post invasion, 10% parasitaemia and 2% Hct) were treated with OZ277 (300 or 1000 nM) or OZ439 (300 nM) for up to 5 h. Untreated parasite controls contained an equivalent volume of DMSO. Following ozonide treatment, parasite lysates were prepared on ice using 0.1% saponin. Lysates were resuspended in citrate buffer (pH 5.5, 0.1% Triton X-100, 4 mM DTT) or PBS (pH 7.2), then pulse sonicated three times, centrifuged, and the supernatant transferred to fresh tubes. Protein content in each sample was determined by BCA protein assay and an equal amount of each sample was incubated with the desired ABPP (0.1-4 μM) for 30 min at 37°C to label residual active proteases. In experiments including the reversible cysteine protease inhibitor ALLN, parasite lysates were pre-incubated with 10 μM of the inhibitor for 30 min prior to addition of the ABPP for a further 15 min. In all cases, the reaction was quenched by the addition of 5x reducing buffer, boiled and separated by SDS-PAGE on 15% polyacrylamide gels. ABPPs with a biotin handle were subjected to SDS-PAGE and probed with streptavidin-Cy5 via western blotting.

Protein bands were visualised using an Amersham Typhoon 5 Biomolecular Imager (GE Healthcare Life Sciences), scanning at the Cy5 wavelength (excitation/emission: 649/670 nm). Coomassie staining was used to confirm equal protein loading. Images were processed in either ImageJ 1.51f or Adobe Photoshop Creative Cloud 2017.

**Table 1:** Activity-based protease probes used for determining protease activity in ozonide treated *P. falciparum* parasites.

| **Activity-based protease probes** | | | |
|---|---|---|---|
| **Cy5 handle** | **Target protease family** | **Biotin handle** | **Target protease family** |
| FY01 | Cysteine | DCG04 | Cysteine |
| BMV109 | Cysteine | | |
| MS-3-19 | Cysteine | | |
| PK101 | Serine | | |

# 4.4 RESULTS

## 4.4.1 Untargeted metabolomics analysis of peroxide-treated ring stage parasites

Untargeted metabolomics was applied to profile the metabolic changes in *P. falciparum* ring stage parasites treated with the ozonides, OZ277 and OZ439 (both 1 μM), and the clinically relevant artemisinin derivative, DHA (0.3 μM), over a time course of up to 9 h. Four biological replicates were independently prepared from different cultures on separate days, and all samples were analysed in a single LC-MS batch. Analytical reproducibility was monitored by periodic analysis of PBQC samples throughout the batch. The relative standard deviation (RSD) of the median peak intensities for the PBQC was below 12% in both positive and negative ionisation modes, which is within the acceptable limits for metabolomics experiments (27). The RSD value for each sample group was between 6-21%.

A total of 659 putative metabolites were identified in peroxide-treated ring stage parasite cultures (supplementary material: Appendix 2), including amino acids (14%), carbohydrates (10%), lipids (30%), nucleotides (4%), peptides (12%) and other metabolites (30%). Univariate analysis of all detected features in the untargeted metabolomics data set from ring stage infected RBCs showed less than 2% of the metabolome to be significantly altered by peroxide treatment ($p$-value $< 0.05$ and fold-change $\geq 1.5$) and a clear temporal increase in the percentage of drug-induced metabolic perturbations (Figure 2A). All peroxides induced significant metabolic changes within 3 h of drug exposure, with DHA having the most pronounced impact on the cellular metabolome compared to OZ277 and OZ439. Although only a small number of drug-induced changes were evident in the metabolome, there was considerable overlap in the metabolites that were significantly affected by peroxide treatment. (Figure 2B).

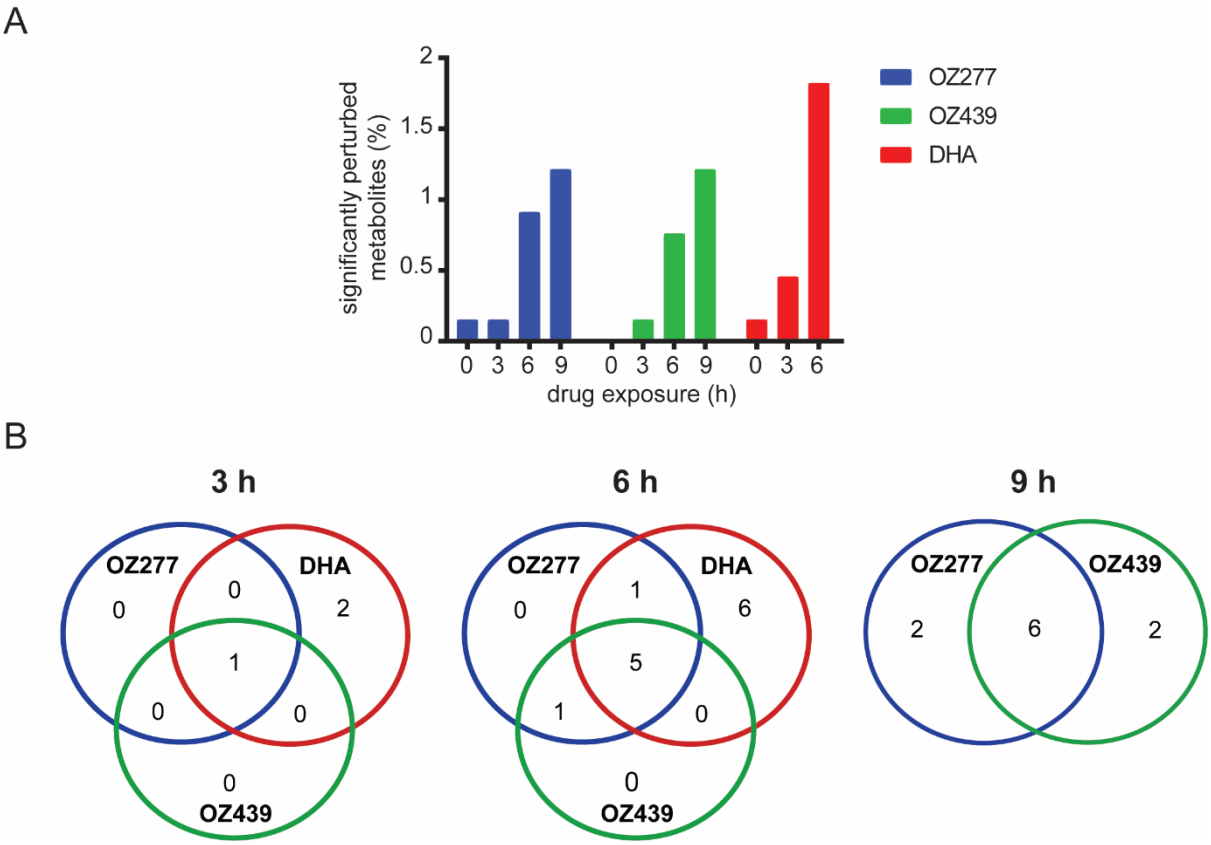


**Figure 2:** Peroxide-induced metabolic perturbations in ring infected RBCs. (A) Percentage of significantly perturbed metabolites (Welch's *t* test; p-value < 0.05 and fold-change > 1.5) at each time point (0, 3, 6 and 9 h) of OZ277- (blue), OZ439- (green) and DHA- (red) treated ring stage infected cultures. (B) Venn diagrams representing the number of metabolites significantly affected by each treatment (DHA, OZ277, OZ439) after 3, 6 and 9 h of drug exposure.

Metabolomics analysis revealed that the putative haemoglobin-derived peptides Pro-Pro-Val-Gln (altered in DHA treated cells), Pro-Asp (altered in DHA treated cells) and Pro-Ala (altered in all drug treated cells) were the first detectable metabolites to be significantly perturbed by peroxide treatment in ring infected RBCs. The abundance of these peptides was depleted by 3 h of drug treatment relative to the levels in the untreated controls. The dipeptides Pro-Glu, Pro-Ala and Pro-Asp and the tetrapeptide Pro-Pro-Val-Gln were the only peptides consistently perturbed after treatment with all three peroxides tested (Figure 3A). These differentially abundant peptides could all be mapped to haemoglobin and showed a clear time-

dependent depletion in abundance in the peroxide treated parasite cultures compared to the untreated controls (Figure 3B). Consistent with the known time-dependence of activity for peroxide antimalarials (12), DHA had a more rapid impact on peptide abundance compared to OZ277 and OZ439. The non-haemoglobin-derived peptide, putatively identified as Glu-Ser-Thr, was also significantly depleted in all drug treated cells at the 6 h time point.

Peroxide treatment of ring stage infected RBCs (> 3 h) was also found to disrupt metabolites involved in the *de novo* synthesis of phosphatidylcholine (PC) and phosphatidylethanolamine (PE). Analysis of all metabolites in these biosynthetic pathways (also known as the Kennedy Pathways, Figure 4) revealed a time-dependent increase in the abundance of choline phosphate, ethanolamine phosphate and CDP-ethanolamine, while no changes in the abundance of choline, CDP-choline, PC or PE levels were detected. Ethanolamine was not identified in this metabolomics analysis. CMP, which is released as a by-product in the last step of PC and PE synthesis, also exhibited a time-dependent increase in abundance with drug treatment.

In addition to peptide and lipid metabolism, 6 h of DHA treatment was also found to perturb metabolites involved in carbohydrate metabolism and various miscellaneous pathways. While OZ277 and OZ439 also induced significant depletion of succinate by 9 h of exposure (supplementary material: Appendix 2). DHA treatment was not analysed at the 9 h time point.

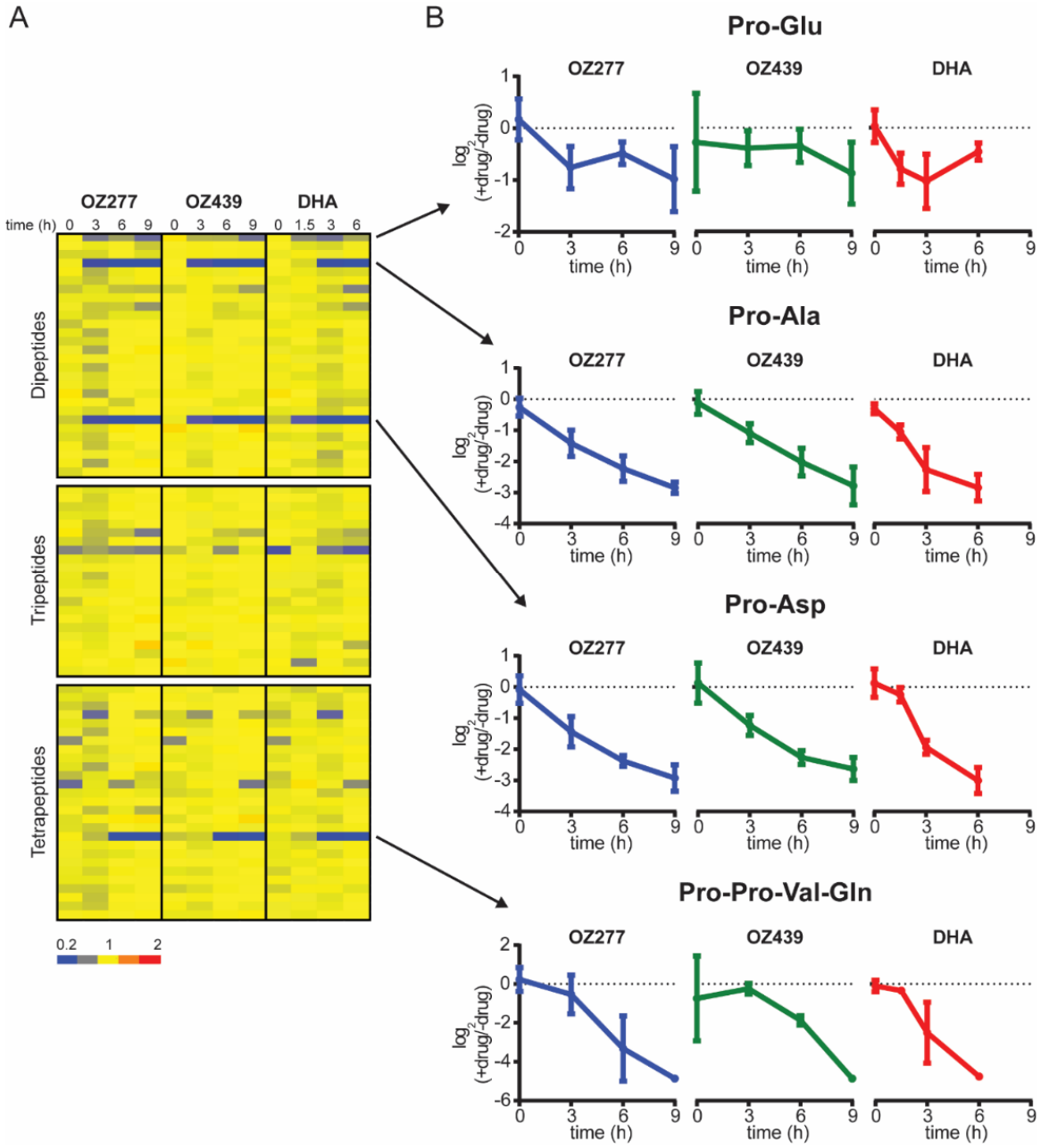


**Figure 3:** Peroxide-induced perturbations to peptide metabolism in ring infected RBCs. (A) Heatmap showing the average fold-change for all identified peptides at each time point after OZ277, OZ439 and DHA treatment of ring stage parasites. For each time point, values represent the average of four biological replicates, expressed relative to the average untreated control value (four biological replicates) for that respective time point. (B) Time-dependent decrease in the abundance of the four peptides consistently disrupted after peroxide treatment. Values are the average fold-change (± SD) relative to the untreated control of four biological replicates.

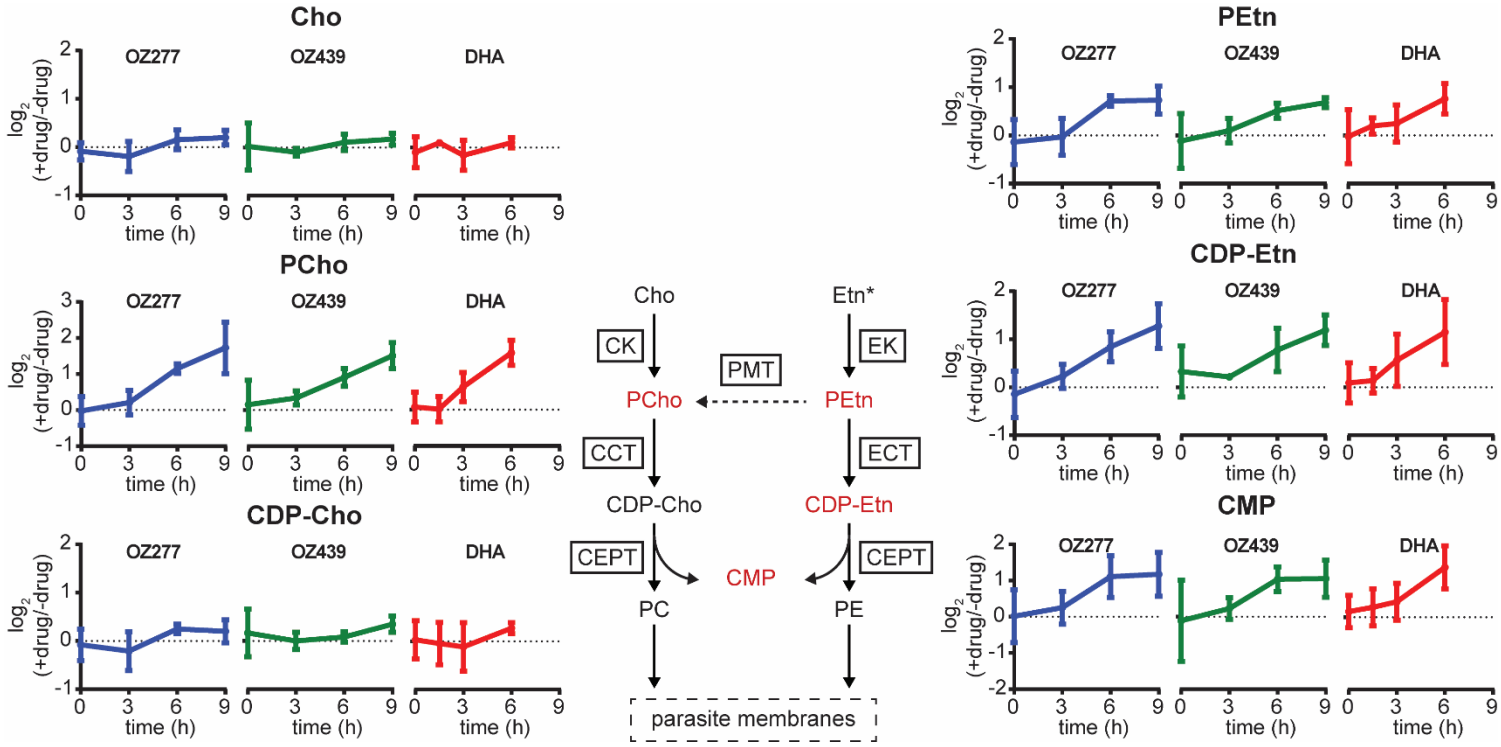


**Figure 4:** Time-dependent perturbations of metabolites involved in the phosphatidylcholine and phosphatidylethanolamine *de novo* synthesis pathways. The abundances of each of the metabolites after treatment with OZ277 (blue), OZ439 (green) and DHA (red) are the average fold-change (± SD) relative to the untreated control of four biological replicates. Metabolites in red were increased in abundance after drug treatment. Enzyme are shown in solid boxes. The dashed arrow represents an alternative route for the synthesis of PC from Etn in *P. falciparum* parasites. CCT, choline-phosphate cytidyltransferase; CDP-, cytidine-diphospho-; CEPT, choline/ethanolamine phosphotransferase; Cho, choline; CK, choline kinase; CMP, cytidine monophosphate; ECT, ethanolamine-phosphate cytidyltransferase; EK, ethanolamine kinase; Etn, ethanolamine; PC, phosphatidylcholine; PE, phosphatidylethanolamine; PCho, choline phosphate; PEtn, ethanolamine phosphate; PMT, phosphoethanolamine N-methyltransferase; *not detected.

Multivariate analysis of the drug-treated ring stage metabolomics dataset further emphasised a role for haemoglobin catabolism and PC and PE synthesis in the mode of action of peroxide antimalarials. After 3, 6 and 9 h of drug incubation, sparse partial least squares – discriminant analysis (sPLS-DA) revealed that haemoglobin-derived peptides (Pro-Ala, Pro-Asp and Pro-Pro-Val-Gln) were responsible for the greatest difference between the peroxide-treated samples and the controls (Figures 5A, 5B and 5C), while disruption of metabolites involved in PC and PE biosynthesis (choline phosphate and CDP-ethanolamine) became apparent after 6 h (Figures 5B and 5C).

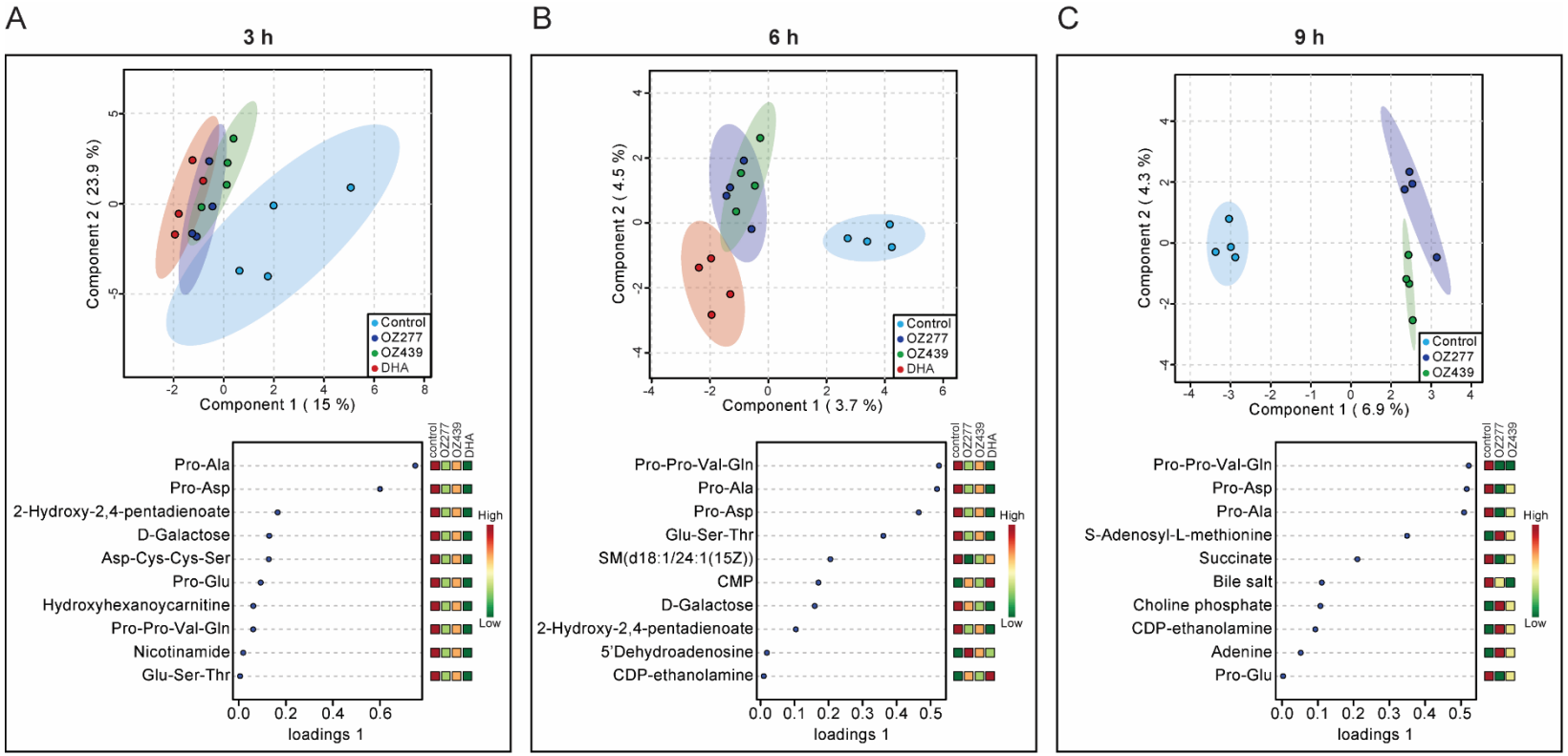


**Figure 5:** Sparse partial least squares – discriminant analysis (sPLS-DA) of the metabolomics data for peroxide-treated ring infected RBCs. (A) sPLS-DA plot (top) for metabolite levels from samples treated with OZ277 (blue), OZ439 (green), DHA (red) or DMSO (control, light blue) for 3 h and the variable importance in projection plot (bottom) for the metabolites selected by the sPLS-DA model in component one. (B) sPLS-DA plot for metabolite levels from samples treated with OZ277 (blue), OZ439 (green), DHA (red) or DMSO (control, light blue) for 6 h and the variable importance in projection plot (bottom) for the metabolites selected by the sPLS-DA model in component one. (C) sPLS-DA plot for metabolite levels from samples treated with OZ277 (blue), OZ439 (green), or DMSO (control, light blue) for 9 h and the variable importance in projection plot (bottom) for the metabolites selected by the sPLS-DA model in component one.

### 4.4.2 Untargeted metabolomics analysis of trophozoite stage parasites exposed to pulsed peroxide treatment

Untargeted metabolomics was also applied to profile the peroxide-induced metabolic changes in RBC cultures infected with *P. falciparum* trophozoites, the most susceptible RBC stage of the parasite to peroxide treatment. Trophozoite infected RBCs were treated for up to 3 h with 300 nM of OZ277 and OZ439 and 100 nM of DHA, concentrations that correspond to the $IC_{50}$ for a 3 h pulse of each drug under the same *in vitro* conditions used in this metabolomics study (10% parasitaemia and 2% Hct) (11). A time course analysis allowed direct observation of drug-dependent changes in metabolite abundance over time and enabled the identification of early effects on parasite metabolism to be distinguished from a non-specific death phenotype. The RSD of the median peak intensities for the PBQC samples (21 technical replicates) was 13% and 8% for positive and negative ionisation modes, respectively, demonstrating acceptable reproducibility of the analytical run. The RSD for each sample group, consisting of a minimum of three biological replicates, was below 13%.

Metabolomics analysis of trophozoite infected cultures treated with OZ277, OZ439 and DHA identified 650 putative metabolites that were distributed across a range of metabolite classes (supplementary material: Appendix 2). Compared to RBCs infected with ring stage parasites, there were almost twice as many peptides identified in trophozoite infected cultures (20% versus 12% of all putative metabolites), consistent with a general increase in proteolytic activity during the trophozoite stage (28). Univariate analysis of all putatively identified metabolites revealed that between 3% and 9% (depending on the drug) of the metabolome was significantly altered by peroxide treatment (p-value $< 0.05$ and fold-change $\geq 1.5$) within 3 h of drug exposure (Figure 6A). There was a time-dependent increase in the number of metabolites significantly perturbed by drug treatment, with DHA having the greatest impact on

the trophozoite infected RBC metabolome over the 3 h time course. Pathway enrichment analysis showed that under the conditions used in this metabolomics study, all three peroxide antimalarials disproportionately affected peptide metabolism, with 20-35% of putatively identified peptides significantly perturbed by drug treatment after 3 h (p-value < 0.05) (Figure 6B). DHA had a more rapid impact on peptide metabolism, with 30% of identified peptides significantly altered after 1.5 h, compared to 2% and 9% for OZ277 and OZ439, respectively (Figure 6B).

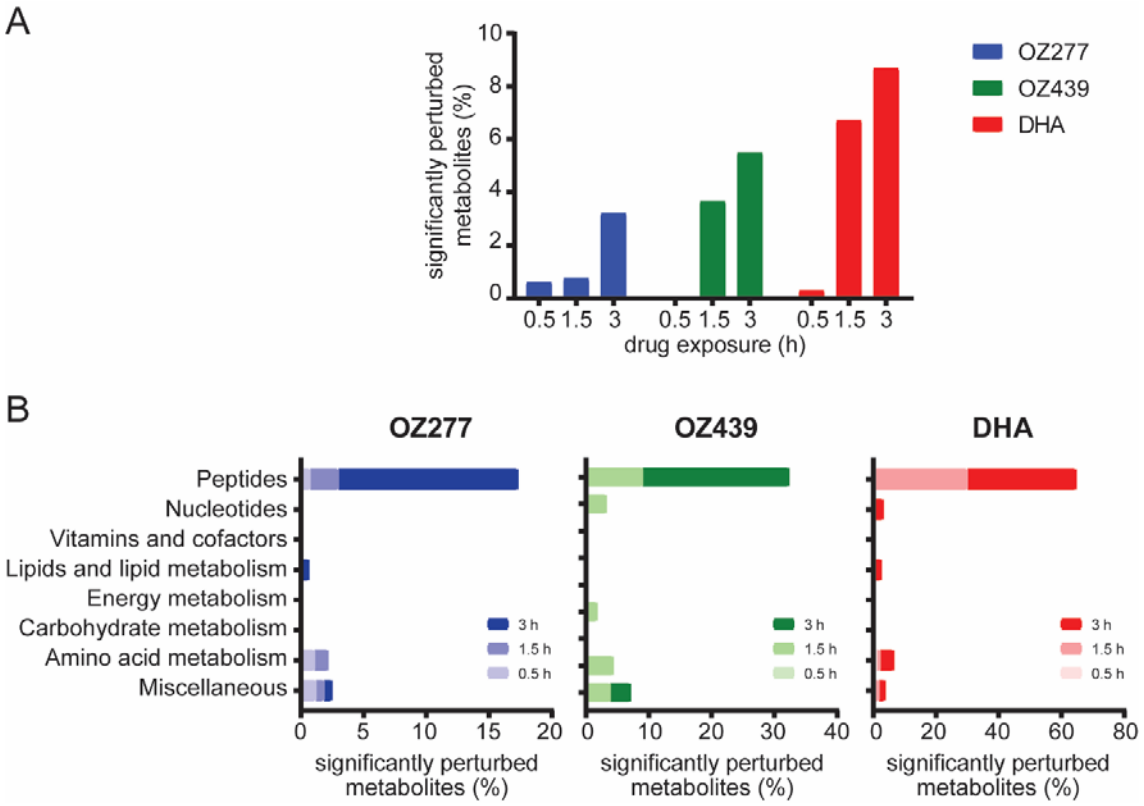


**Figure 6:** Peroxide-induced metabolic perturbations in trophozoite infected RBCs. (A) Percentage of significantly perturbed metabolites (Welch's *t* test; p-value < 0.05 and fold-change ≥ 1.5) following increasing durations of OZ277 (blue), OZ439 (green) and DHA (red) exposure (0.5, 1.5 and 3 h) in trophozoite infected RBCs. (B) Pathway enrichment analysis showing the percentage of significantly perturbed metabolites (Welch's *t* test; p-value < 0.05 and fold-change > 1.5) as a function of metabolite class for increasing durations of OZ277 (blue), OZ439 (green) and DHA (red) treatment.

The temporal abundance profile for all identified peptides showed that both ozonides and DHA caused a depletion in the abundance of a selection of peptides within 3 h of drug exposure (Figures 7A and 7B). Whilst the amino acid sequence of only a subset of these differentially regulated peptides could be confirmed by MS/MS, the majority of peptides that were decreased in abundance by at least 1.5-fold could be mapped to either the alpha or beta chains of haemoglobin (Figure 7C).

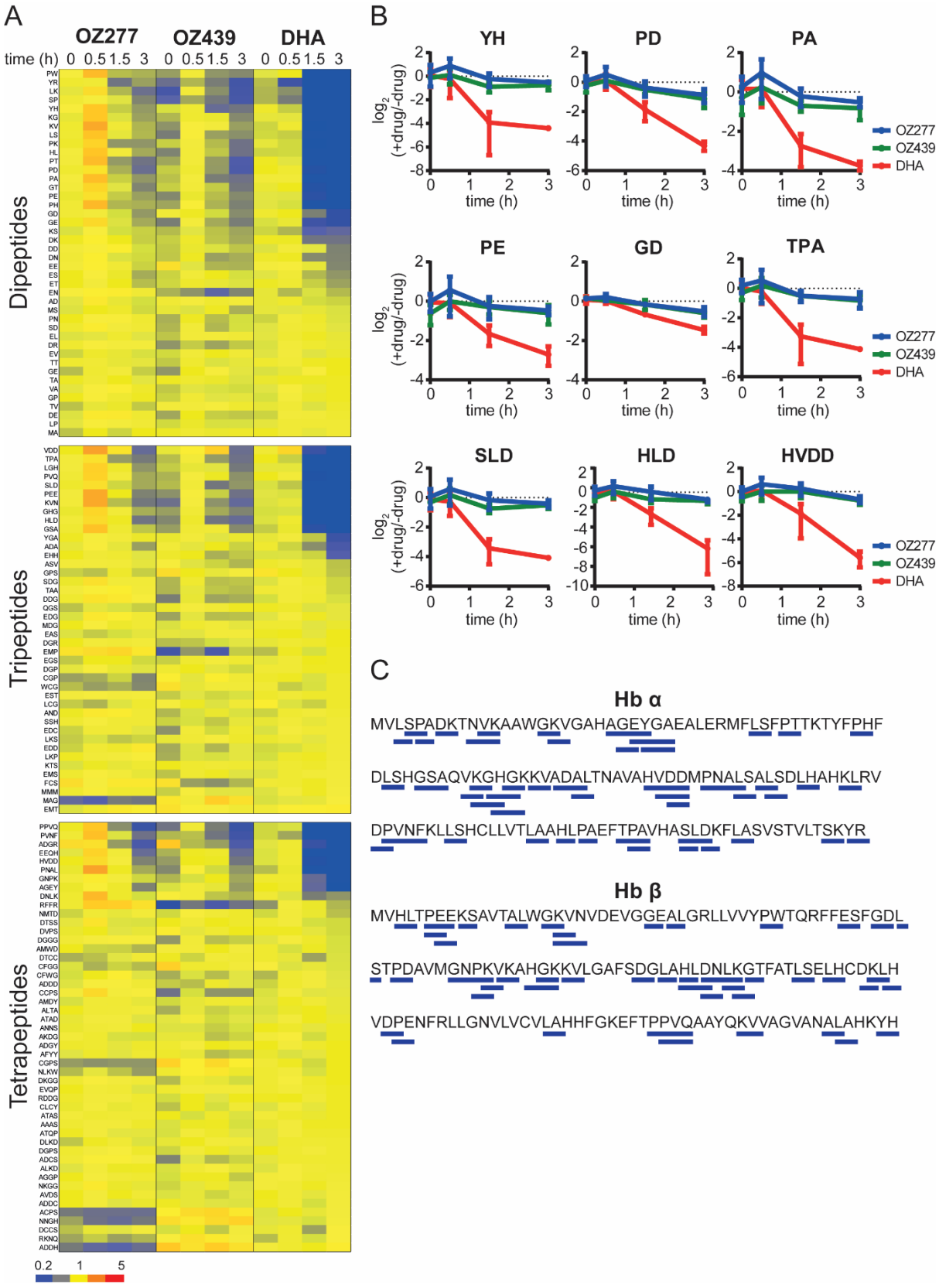


**Figure 7:** Peroxide-induced perturbations to peptide metabolism in trophozoite infected RBCs. (A) Heatmap showing the average fold-change for all identified peptides at each time point in trophozoite infected cultures after treatment with OZ277, OZ439 and DHA. Values represent

the average of at least three biological replicates, expressed relative to the average untreated control value (at least seven biological replicates) for that respective time point. (B) Representative time profiles showing the progressive depletion in abundance of a selection of putative haemoglobin-derived peptides after peroxide treatment. Values are the average fold-change (± SD) relative to the untreated control of at least three biological replicates. (C) Haemoglobin alpha (Hb α) and haemoglobin beta (Hb β) sequence coverage for putative haemoglobin (Hb)-derived peptides that were differentially abundant (≥ 1.5-fold) following peroxide antimalarial treatment relative to the untreated control. The peptide sequences PA, PT, PE, PEE, HLD, SLD, PPVQ, PVNF and HVDD have been confirmed by MS/MS analysis. For all other putative peptide sequences, all potential isomers have been mapped.

### 4.4.3 Untargeted metabolomics analysis of long-term peroxide-treated trophozoite stage parasites

In a separate untargeted metabolomics study aimed at assessing the biochemical impact of long term peroxide exposure, trophozoite infected cultures were treated with OZ277, OZ439 and DHA for up to 9 h. Prolonged peroxide exposure (> 3 h) induced metabolic perturbations to biochemical pathways beyond peptide metabolism, including amino acid, lipid, cofactor and vitamin, and nucleotide metabolism (Figure 8), which may represent secondary pathways involved in peroxide antimalarial activity. Unsurprisingly, drug-induced disruption of peptide metabolism was still the most significantly affected pathway after 9 h.

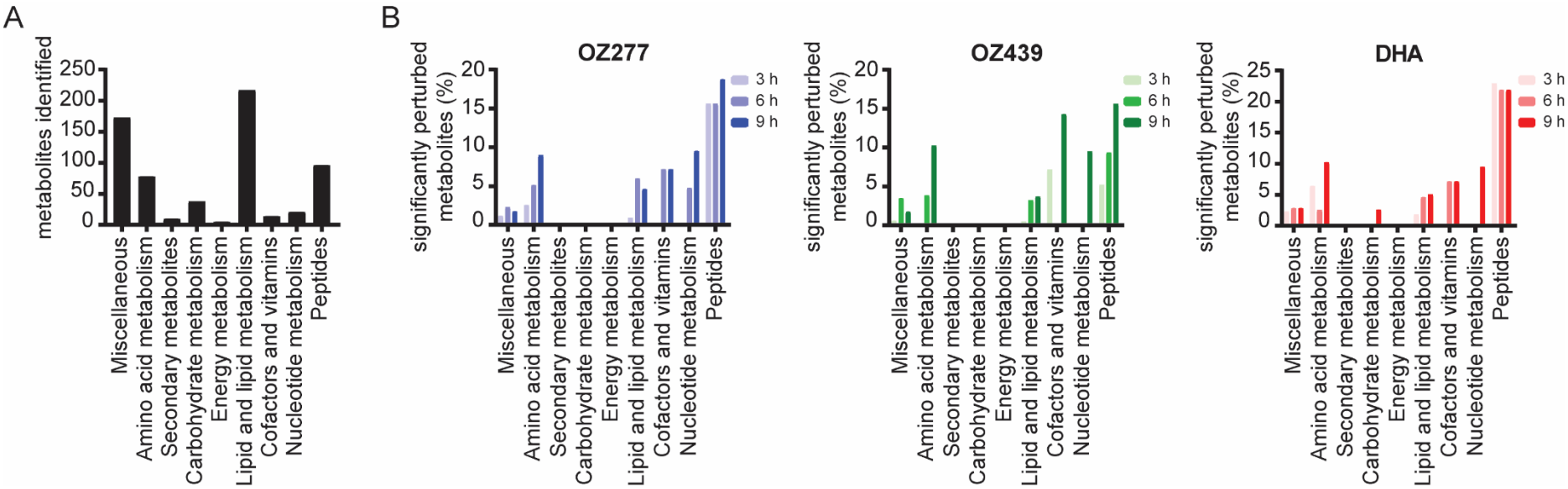


**Figure 8:** Metabolic perturbations in trophozoite infected RBCs after extended peroxide treatment (A) The number of metabolites identified in each metabolite class after extended treatment of trophozoite infected RBCs with OZ277, OZ439 and DHA. (B) Pathway enrichment analysis showing the percentage of significantly perturbed metabolites (Welch's *t* test; p-value < 0.05 and fold-change > 1.5) as a function of metabolite class for increasing treatment durations (3, 6 and 9h) with OZ277, OZ439 (both 300 nM) and DHA (100 nM).

Approximately 5% of the 217 putatively identified lipid metabolites were significantly affected by peroxide treatment after 9 h of exposure (p-value ≤ 0.05 and fold-change ≥ 1.5) (Figure 9A). Similar to what was seen in the ring stage, metabolites involved in *de novo* synthesis of PC and PE lipids accumulated in a time-dependent manner (Figure 9B). Interestingly, depletion of some species of PC and PE lipids became apparent after only 9 h of drug exposure. The other main structural glycerophospholipids within the parasite, phosphatidylserine (PS), phosphatidylinositol (PI) and phosphatidylglycerol (PG), were also depleted with prolonged exposure to peroxide antimalarials (Figures 9A and 9B). Di- (DG) and triglycerides (TG) are the two main neutral glycerolipid species within the parasite and both showed a temporal depletion in abundance (Figure 9A). Phosphatic acids (no significant change detected) and DGs are the direct metabolic precursors in the *de novo* synthesis of PC and PE lipids and are used to synthesise TGs (Figure 9 C).

In addition to the effect on peptide and lipid metabolism, prolonged peroxide treatment also induced disruption to pyrimidine biosynthesis (Figure 10). Metabolites of the *de novo* pyrimidine biosynthesis pathway, L-aspartate, N-carbamoyl-L-aspartate and UMP were depleted in abundance after drug treatment. The relative abundance of all putatively identified metabolites following peroxide exposure is provided in the supplementary material (Appendix 2).

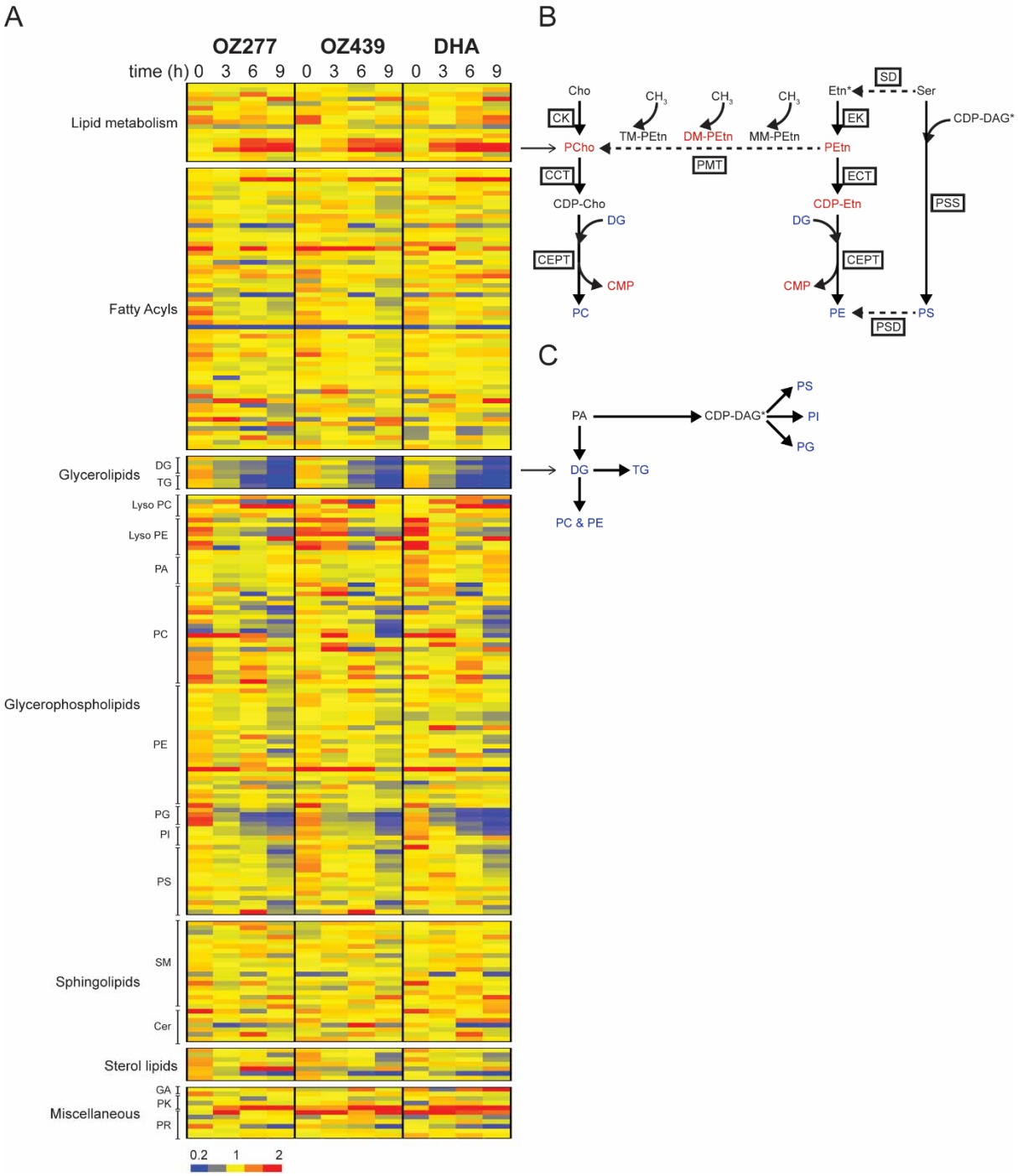


**Figure 9:** Peroxide-induced perturbations to lipid metabolism in trophozoite infected RBCs. (A) Heatmap showing the average fold-change for all identified lipids at each time point after prolonged exposure with OZ277, OZ439 and DHA in trophozoite stage *P. falciparum* parasites. Values represent the average of three biological replicates, expressed relative to the average untreated control value for that respective time point. (B) *De novo* synthesis pathways for PC and PE in *P. falciparum*. Enzymes are shown in solid boxes. The dashed arrows represent alternative routes for the synthesis of PC and PE lipids in *P. falciparum*. (C) Pathways for the synthesis of phospholipids and triglycerides from phosphatidic acid precursors. For B and C

above, metabolites in red and blue were increased and decreased in abundance after drug treatment, respectively. CCT, choline-phosphate cytidyltransferase; CDP-, cytidine-diphospho-; CEPT, choline/ethanolamine phosphotransferase; Cer, ceramide; Cho, choline; CK, choline kinase; CMP, cytidine monophosphate; DAG/DG, diglyceride; DM-, dimethyl-; ECT, ethanolamine-phosphate cyitidyltransferase; EK, ethanolamine kinase; Etn, ethanolamine; GA, gangliosides; MM-, monomethyl; PA, phosphatidic acid, PC, phosphatidylcholine; PCho, choline phosphate; PE, phosphatidylethanolamine; PEtn, ethanolamine phosphate; PG, phosphatidylglycerol; PI, phosphatidylinositol; PMT, phosphoethanolamine N-methyltransferase; PK, polyketides; PR, prenols; PS, phosphatidylserine; PSD, phosphatidylserine decarboxylase; PSS, phosphatidylserine synthase; SD, serine decarboxylase; SM, sphingomyelin; TG, triglyceride; TM-,trimethyl; *not detected.

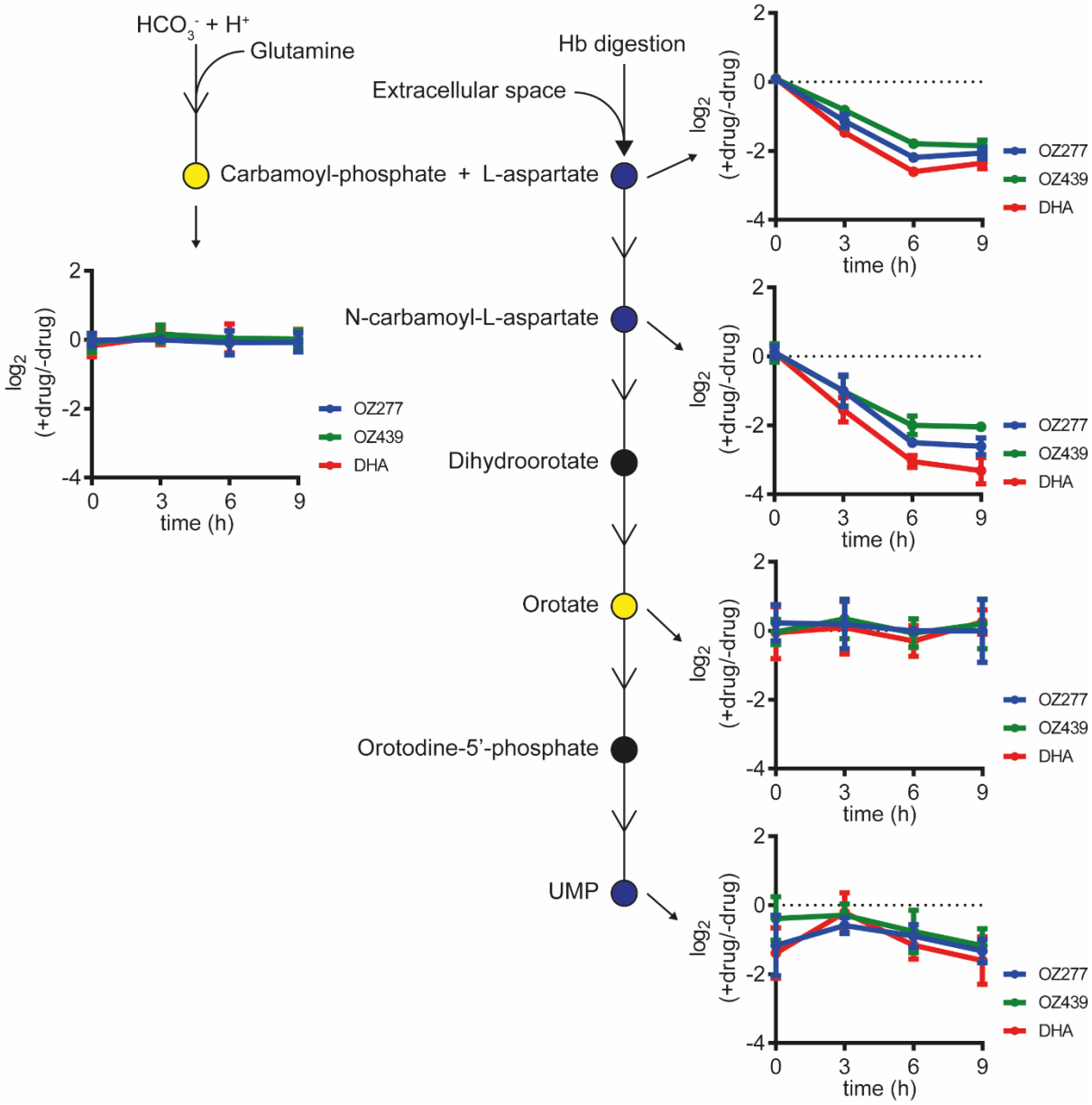


**Figure 10:** Peroxide-induced perturbation of pyrimidine biosynthesis in trophozoite infected RBCs. Values are the average fold-change (± SD) relative to the untreated control of three biological replicates. For the pyrimidine biosynthesis pathway, blue circles represent decreased abundance, yellow circles represent no change and black circles represent metabolites that were not detected. Hb, haemoglobin; UMP, uridine monophosphate.

### 4.4.4 Peptidomic analysis of peroxide-treated *P. falciparum* parasites

A limitation of the metabolomics workflow is that only peptides up to four amino acids in length are identified. To assay the relative abundance of longer endogenous peptides (< 10 kDa), a MS/MS-based peptidomics approach was employed. Peptidomic samples were prepared from whole parasite extracts that were generated from trophozoite stage parasites treated with OZ277, OZ439 (both 300 nM), DHA (100 nM) or an equivalent volume of DMSO for 3 h. Peptides were enriched by an acid extraction method, followed by filtration through a 10 kDa filtration column and the resulting peptide extracts were subjected to nanoLC-MS/MS analysis.

Peptidomics analysis of peroxide-treated parasites identified a total of 59 endogenous *P. falciparum* peptides and 59 endogenous human peptides. Parasites treated with OZ277 had significantly altered abundance of 30 peptides compared to the untreated controls (p-value < 0.05) (supplementary material: Appendix 3). Of these, 17 peptides originating from *H. sapiens* were elevated, all of which were from haemoglobin alpha and beta chains (Figure 11). Treatment with OZ439 resulted in five significant changes to the abundance of *P. falciparum*-derived peptides (supplementary material: Appendix 3) and induced accumulation of six peptides originating from haemoglobin (Figure 11). Similar to the ozonides, DHA treatment also disrupted the levels of parasite and haemoglobin-derived peptides within the parasite (supplementary material: Appendix 3), however, 26 haemoglobin peptides were significantly reduced and four peptides were significantly increased in abundance relative to the untreated control (Figure 11).


**Figure 11:** Sequence coverage and relative abundance of endogenous peptides originating from haemoglobin alpha (Hb α) and haemoglobin beta (Hb β) in OZ277-, OZ439- and DHA-treated parasites. Peptide abundances are the average fold-change following drug treatment, expressed relative to the untreated control (DMSO) from at least three biological replicates. Solid lines represent significant changes in peptide abundance relative to the untreated control (p-value < 0.05). Dashed lines represent non-significant (NS) changes.

### 4.4.5 Proteomic analysis of ozonide-treated *P. falciparum* parasites

Global proteomic analysis was performed using reductive dimethyl labelling (13) to identify quantitative differences in protein levels between peroxide treated and untreated trophozoite stage *P. falciparum* parasites. In these experiments, infected RBC cultures (10% parasitaemia and 2% Hct) were exposed to OZ277, OZ439 (both 300 nM), DHA (100 nM) or an equivalent volume of DMSO for 3 h. A total of 1294, 1284 and 1613 proteins were identified with at least two unique peptides in a minimum of three independent experiments in OZ277, OZ439 and DHA treated parasites, respectively (a full list of identified proteins is available in the supplementary material, Appendix 4). DHA caused the most significant changes to the parasite proteome, with 20% of proteins significantly increased in abundance and 5% significantly decreased compared to the control. OZ277 and OZ439 induced significant increases in approximately 10% of the proteome and significant decreases in < 1% compared to the control (Figures 12A and 12B). There was considerable overlap of the perturbed proteins between the three antimalarial peroxides (Figure 12C and Appendix 5), consistent with these drugs impacting similar biochemical pathways within the parasite. Approximately 25% of the proteins significantly perturbed following OZ277 or OZ439 treatment were also reported alkylation targets of peroxide antimalarials in *P. falciparum* (Appendix 5) (1-3). Of the proteins significantly perturbed following DHA treatment, almost 40% were previously identified peroxide alkylation targets (Appendix 5) (1-3).

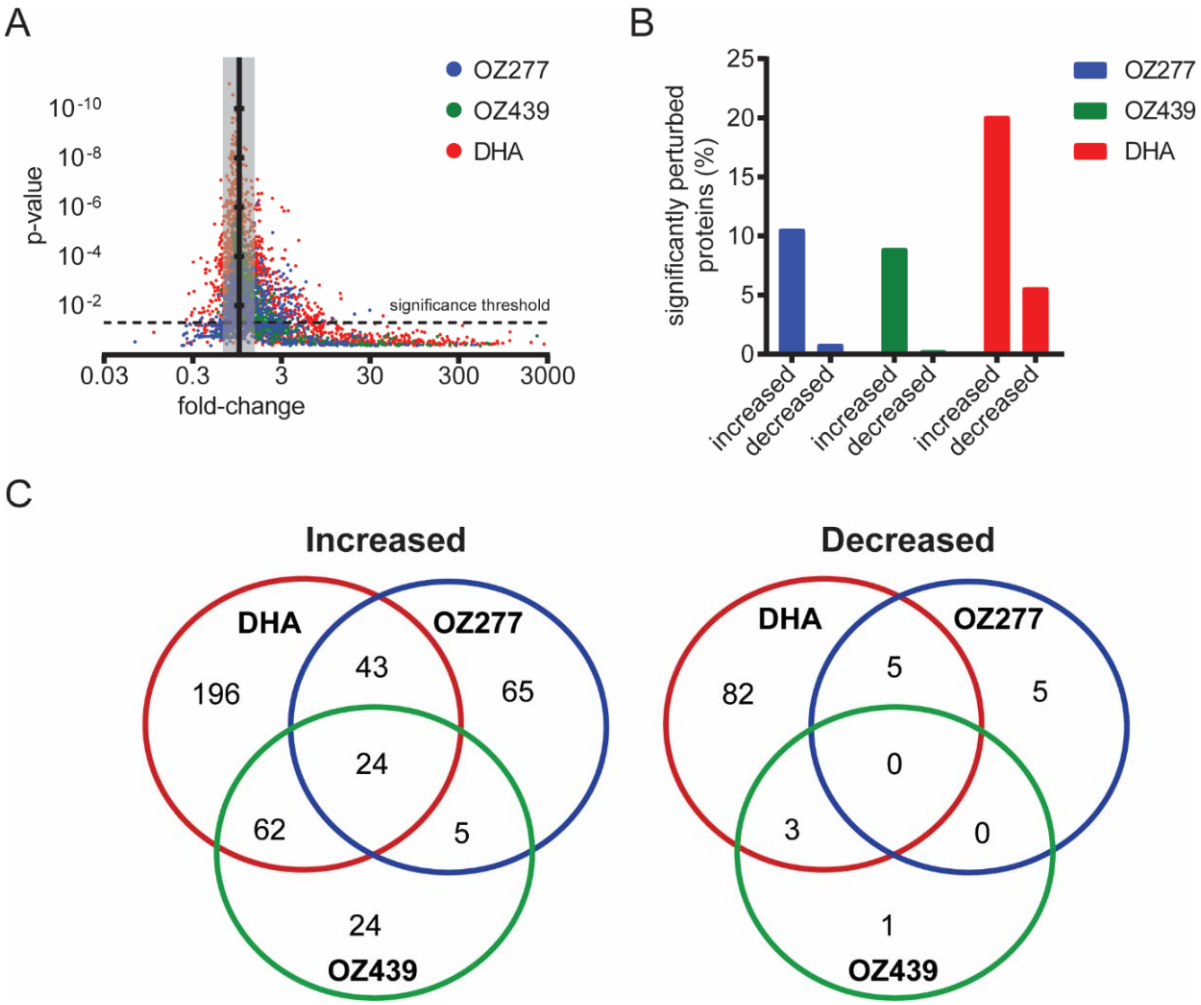


**Figure 12:** Overview of peroxide-induced disruption to the *P. falciparum* proteome. (A) Volcano plot of proteins identified in at least three independent experiments following treatment of trophozoite stage parasites with OZ277 (1294 proteins, indicated by blue colour dots), OZ439 (1284 proteins, green dots) and DHA (1613 proteins, red dots). Proteins above the significance threshold (p-value $\leq 0.05$) and outside the grey shaded area (fold-change $\geq 1.5$) were considered significant. (B) Percentage of parasite and human proteins that were significantly increased and decreased in abundance following treatment with OZ277, OZ439 and DHA. (C) Venn diagrams represent the overlap in parasite and human proteins that were significantly increased and decreased in abundance by peroxide treatment (DHA – red circle, OZ277 – blue circle, OZ439 – green circle).

Functional enrichment analysis with STRINGdb (25) revealed that proteins from 14 pathways were significantly enriched in the parasites treated with OZ277, compared to two pathways for OZ439 treatment and 19 pathways for DHA (Figures 13A and 13B). The proteasomal pathway was significantly enriched following treatment of trophozoite stage parasites with all three peroxides, consistent with reports that peroxides induce a stress response that engages the parasite proteasomal system (29). Approximately 80% of significantly enriched pathways were common between the DHA and OZ277 treated parasite proteomes, with proteins from proteasomal, transcription, translation and metabolic processes all functionally enriched (Figure 13).

Clustering analysis of proteins perturbed by OZ277 revealed that translation regulation (p-value = 5.494E-9) and proteasome system (p-value = 3.444E-6) related proteins were the two major protein interaction networks (Figure 14). Parasite proteins in these two networks (translation regulation and proteasome system) were significantly upregulated by OZ277. Similar protein clustering was also observed for parasite proteins dysregulated by DHA and OZ439 treatment, with upregulated proteins involved in the proteasome system (p-values 0 and 4.277E-9, respectively) and translational regulation (p-values 0 and 4.948E-4, respectively) the two dominant pathways perturbed.

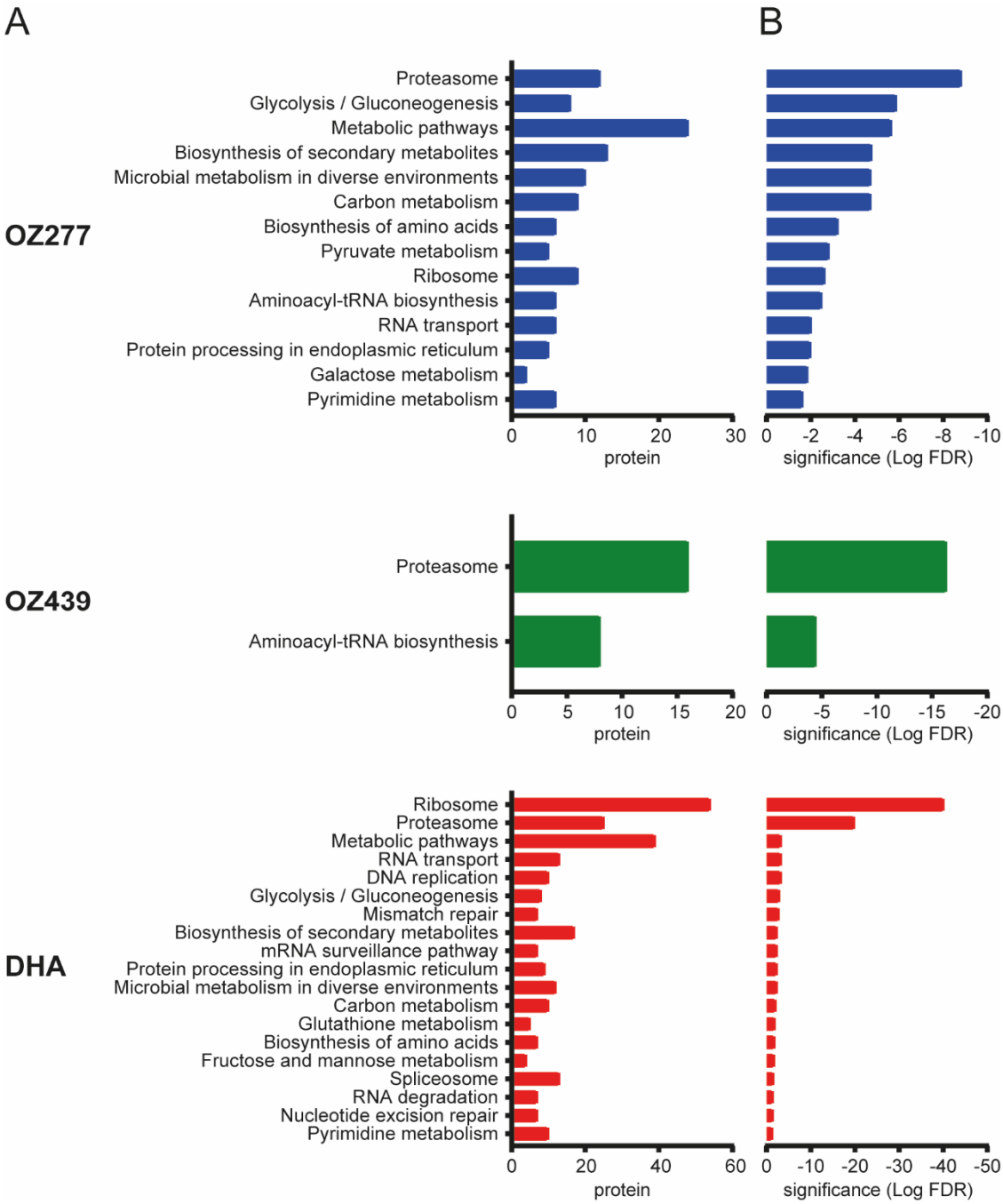


**Figure 13:** Significantly enriched parasite pathways based on dysregulated protein abundances following peroxide antimalarial treatment of trophozoite stage parasites. (A) The number of proteins identified within each functionally enriched pathway following treatment of trophozoite stage parasites with OZ277 (blue bars), OZ439 (green bars) and DHA (red bars). (B) False discovery rate (FDR) for each enriched category. Enriched pathways and FDRs were determined using the web-based tool STRINGdb.

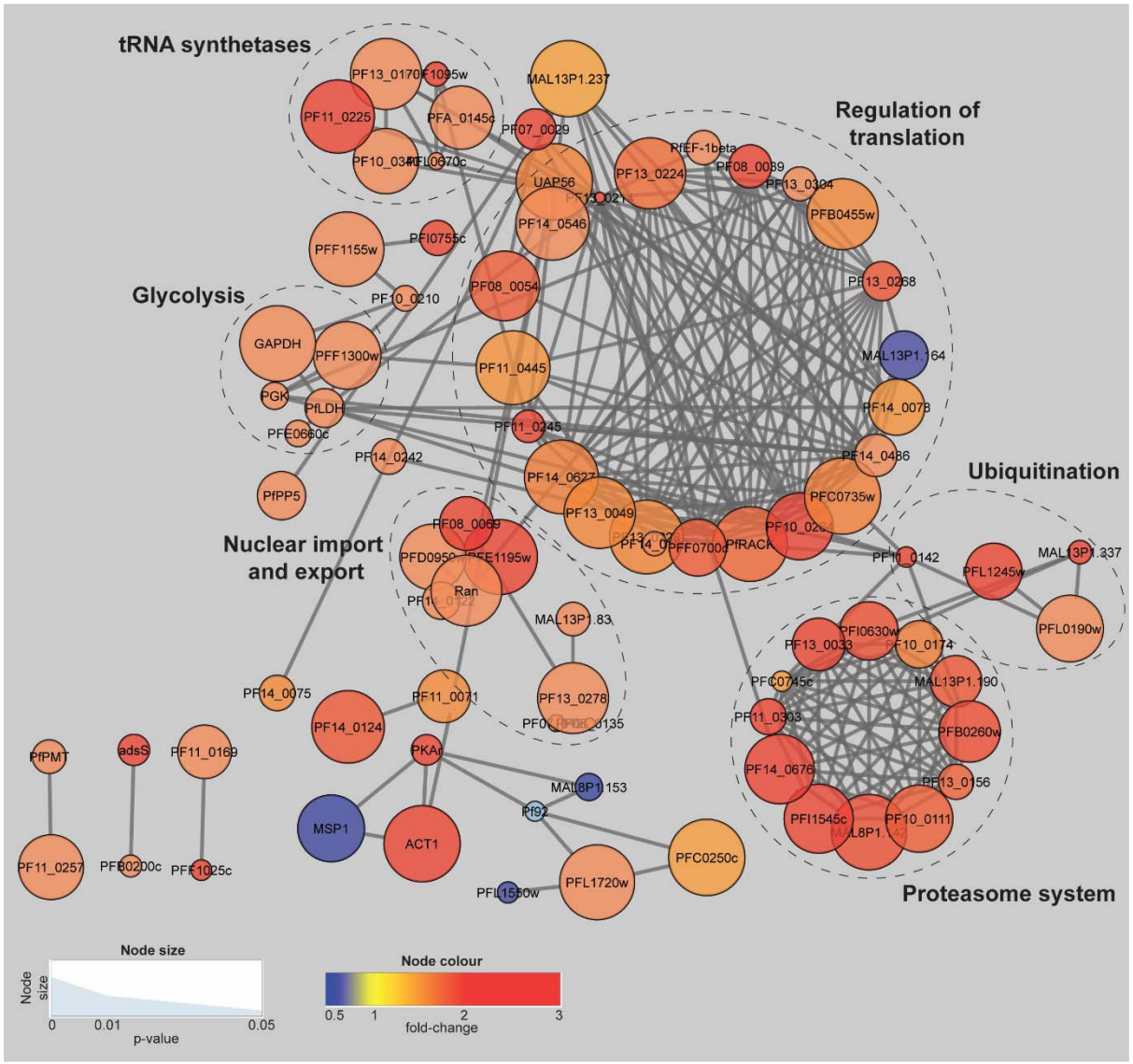


**Figure 14:** Network analysis of parasite proteins perturbed following treatment with OZ277. The network analysis was built using the STRINGdb interaction network analysis output (connectivity was based on experimental, database and co-expression evidence with a minimum required interaction score of 0.7) in Cytoscape 3.6 with the ClusterONE algorithm. Node size represents p-value and node colour represents fold-change from at least three independent replicates.

Haemoglobin catabolism, lipid metabolism and pyrimidine biosynthesis were the significantly affected pathways identified with metabolomics. Targeted analysis of the proteins involved in haemoglobin digestion revealed that peroxide treatment also affected the abundance of haemoglobin digesting proteases (Figure 15). Although no significant change (p-value $\leq 0.05$ and fold-change $\geq 1.5$) in the abundance of haemoglobin itself was detected within the parasite after peroxide treatment (see supplementary material: Appendix 4), falcipains 2 and 3 (FP 2 and FP 3) and the plasmepsins (PM I, PM II, PM IV and HAP) which are all involved in the initial stages of the haemoglobin degradation pathway were increased in abundance in treated samples compared to the controls (Figure 15). There was no significant change in the abundance of falcilysin, which is hypothesised to be involved in the middle stages of the haemoglobin digestion cascade, however, dipeptidyl aminopeptidase 1 (DPAP1), which removes dipeptides from the polypeptides produced by upstream proteases, was significantly increased in abundance in treated samples compared to the control (Figure 15). The alanyl aminopeptidase (*Pf*A-M1), leucyl aminopeptidase (*Pf*A-M17) and aspartyl aminopeptidase (*Pf*M18AAP) metalloproteases that catalyse the final step in haemoglobin digestion were all increased in abundance after peroxide treatment.

Analysis of the proteins involved in *de novo* PC and PE synthesis (Figure 16) revealed that the initial enzymes in each of the pathways, choline kinase (CK) and ethanolamine kinase (EK), respectively, were increased in abundance following drug treatment. Ethanolamine-phosphate cytidyltransferase (ECT) and phosphoethanolamine N-methyltransferase (PMT), which connects the PE and PC biosynthetic pathways via ethanolamine phosphate and choline phosphate, were also elevated in abundance compared to the control levels. No detectable change in the abundance of the other enzymes involved in PC and PE biosynthesis were observed after drug treatment. In the pyrimidine biosynthetic pathway, four out of the six enzymes were elevated in abundance compared to the control levels (Figure 17).

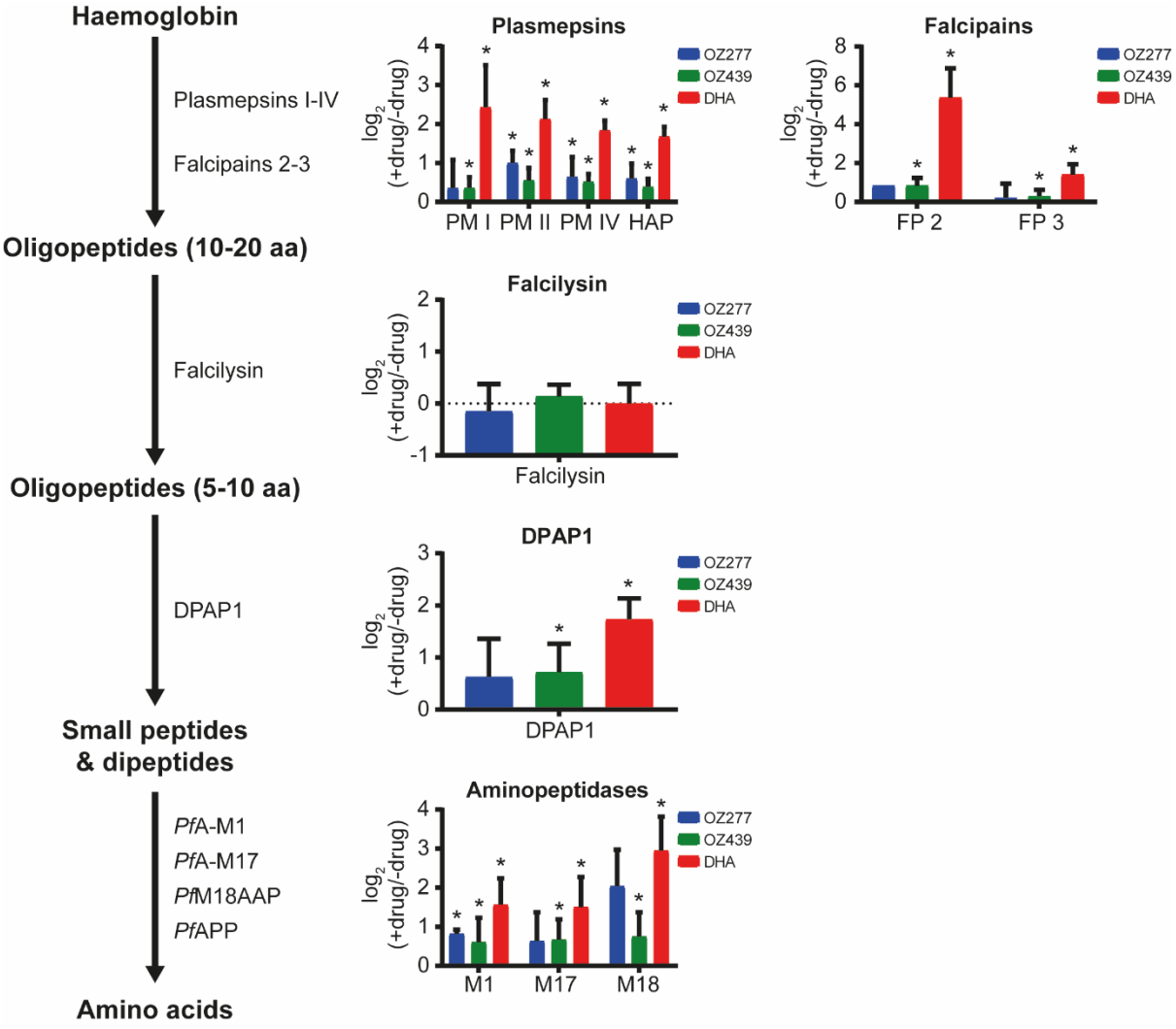


**Figure 15:** Peroxide-induced changes in the abundance of proteases involved in haemoglobin digestion. Values are the average fold-change (± SD) relative to the untreated control of at least three biological replicates. Falcipain 2 (FP 2) was identified in only two OZ277 treatment experiments, therefore the mean alone is shown. *Pf*APP was not identified in any of the proteomic experiments. DPAP1, dipeptidyl aminopeptidase 1; FP, falcipain; *Pf*APP, aminopeptidase P; *Pf*A-M1, alanyl aminopeptidase; *Pf*A-M17, leucyl aminopeptidase; *Pf*M18APP, aspartyl aminopeptidase; PM, plasmepsin; * p-value < 0.05.

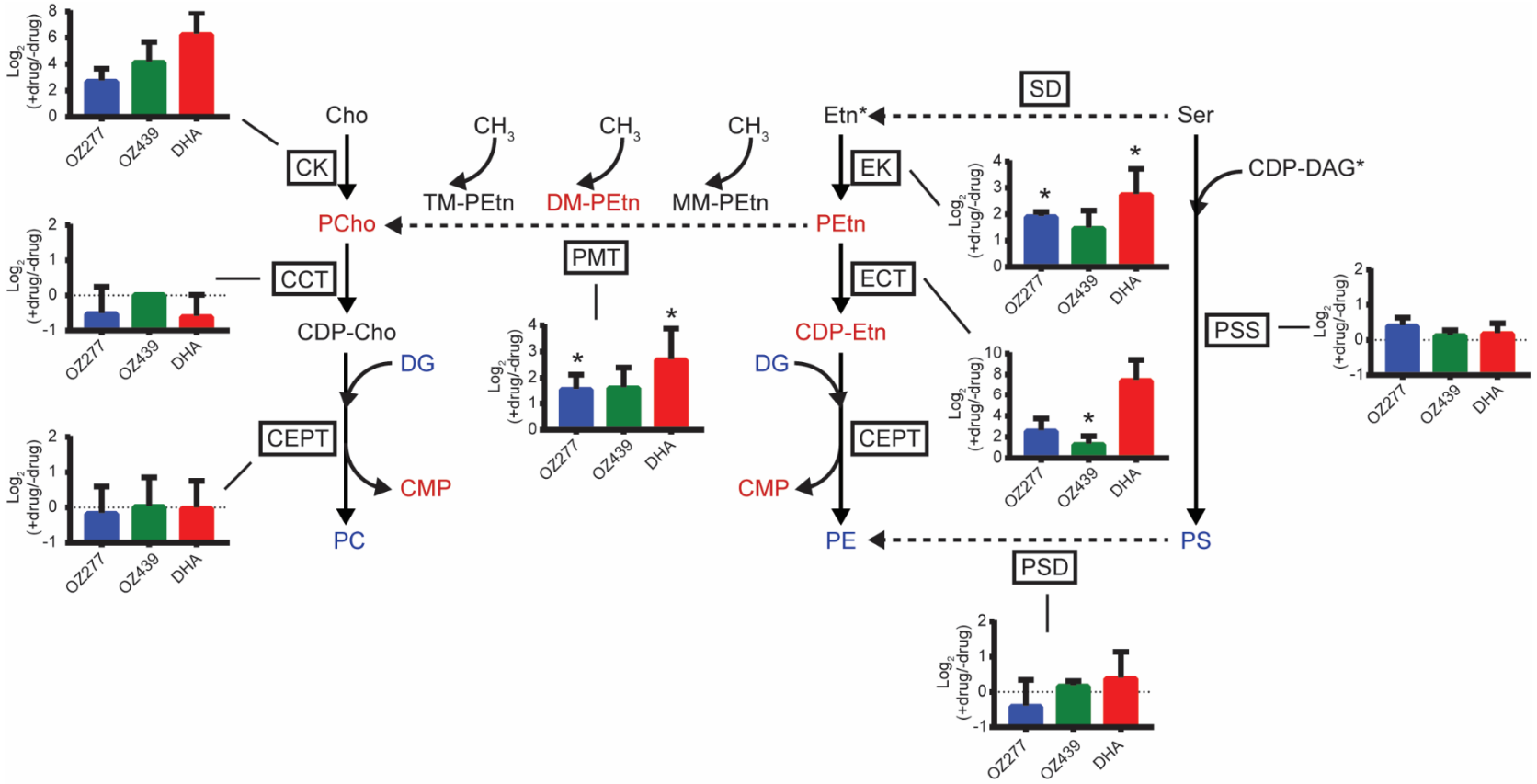


**Figure 16:** Peroxide-induced changes in protein abundance for enzymes involved in the synthesis of phosphatidylcholine and phosphatidylethanolamine lipids within *P. falciparum* parasites. Values are the average fold-change (± SD) relative to the untreated control of at least three biological replicates. CCT was only identified in one OZ439 experiment, therefore the mean from one experiment is shown. The last step in both the PC and PE branches of the Kennedy Pathways are catalysed by the enzyme CEPT. For ease of representation, the abundance of CEPT is only shown for the PC branch of the pathway. * p-value < 0.05

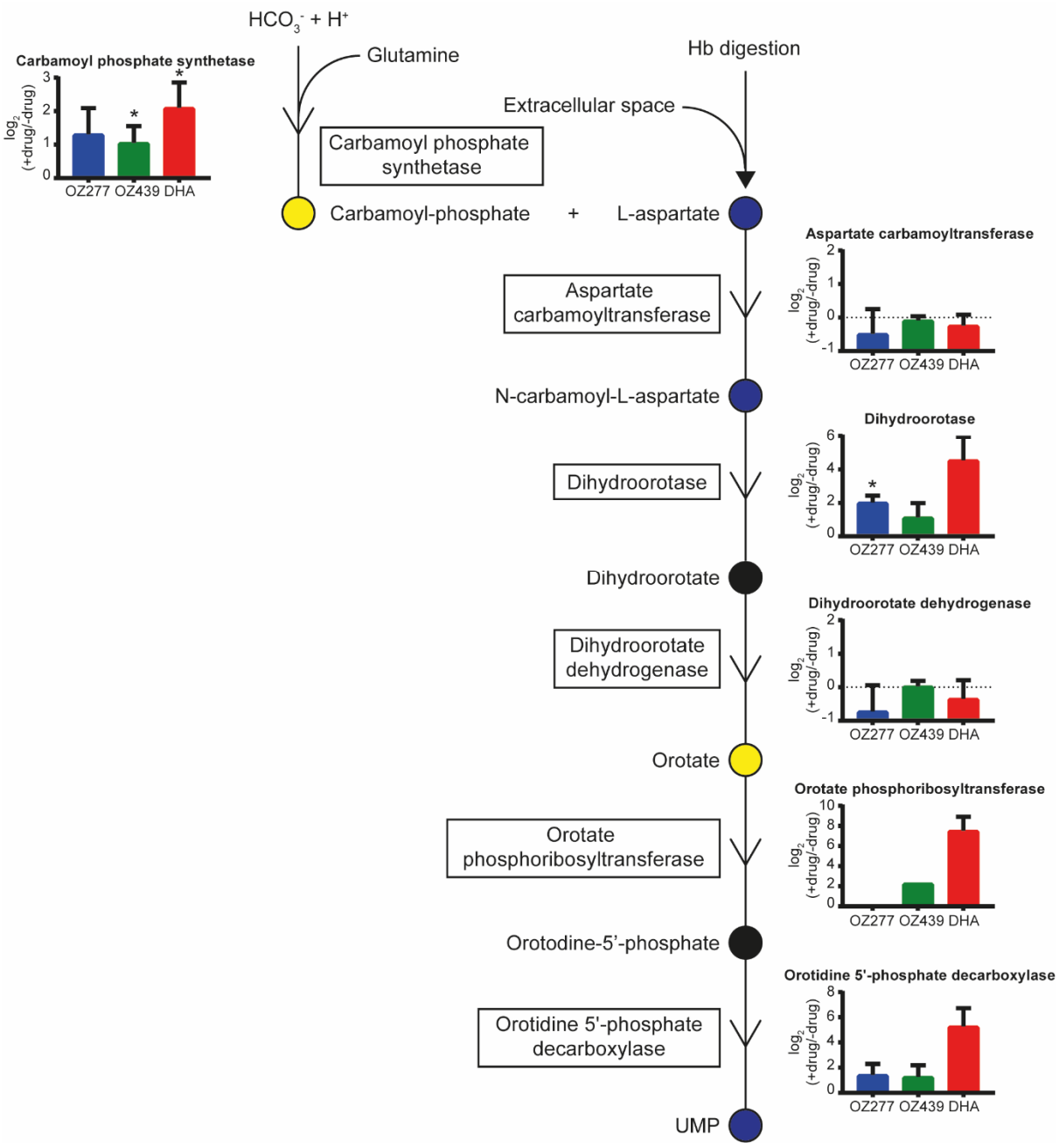


**Figure 17:** Peroxide-induced changes in protein abundance for enzymes involved in the *P. falciparum* pyrimidine biosynthesis pathway. Values are the average fold-change (± SD) relative to the untreated control of at least three biological replicates. Orotate phosphoribosyltransferase was not detected in OZ277 treated parasites and was only identified in one OZ439 experiment. * p-value < 0.05

### 4.4.6 Ozonide-induced disruption of haemoglobin protease activity

To determine whether the activity of proteases involved in haemoglobin digestion were also altered by ozonide treatment, a detailed analysis of cysteine protease activity was performed using a range of activity-based protease probes (ABPPs) (30). ABPPs are small molecules designed to covalently modify the active site of enzymes in an activity-dependent manner (Figure 18) (31). The ABPP approach has previously been applied in *P. falciparum* to identify active protease expression (32, 33) and to monitor drug-induced changes to protease activity (34-36).

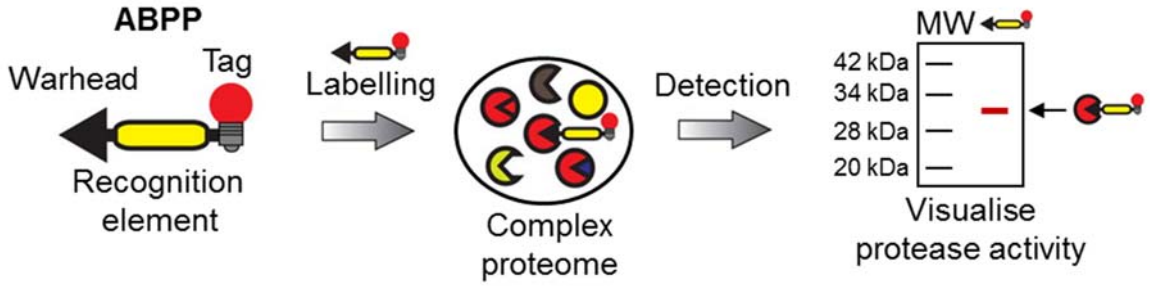


**Figure 18:** Workflow for activity-based protease probe (ABPP) experiments. ABPPs consists of an electrophilic warhead that reacts with the enzyme active site, a recognition site that drives selectivity for the protease of interest and a tag (such as a fluorescent dye or biotin) for visualisation or affinity purification. This approach allows treatment of a complex proteome, such as a cell lysate, and selective labelling of the active form of the protease of interest. Protease activity can then be visualised in a gel-based format. Adapted from Deu *et al*. 2012 (37).

In the ABPP experiments, trophozoite stage parasites were exposed to OZ277 or OZ439 (300 or 1000 nM) for up to 5 h and protease activity determined by labelling residual active protease in the parasite lysate with different ABPPs. The biotinylated epoxide ABPP, DCG04 (33), was used to label the haemoglobin digesting cysteine proteases, DPAP1, FP 2, and FP 3 under acidic (pH 5.5) and neutral (pH 7.2) pH conditions, then probed with streptavidin-Cy5

via western blot analysis to allow visualisation of protease activity. FP 2 and FP 3 are known to migrate at 28 kDa in an SDS-PAGE, while DPAP1 migrates at approximately 20 kDa (36). For both OZ277 and OZ439 treated samples, there was a time-dependent increase in the activity of proteases with molecular weights consistent with that of the FPs and DPAP1 under both acidic (Figures 19A and 19B) and neutral (Figures 19C and 19D) conditions, which could be inhibited by pre-treatment of the lysate with the cysteine protease inhibitor, ALLN (Figure 19E). In general, FP and DPAP1 activity were increased within 1 h of OZ277 treatment, when compared with the DMSO controls, and showed a trend towards returning to the untreated level of activity as the duration of OZ277 exposure increased. In contrast, OZ439 induced a peak in FP 2/3 and DPAP1 activity after 3-5h of drug exposure, consistent with it having a slower onset of action within the parasite (12). Notably, both ozonides caused an increase in activity of FP 1, the only falcipain not localised to the digestive vacuole and thought to have a role in RBC invasion (33). Increased FP 1 activity was only apparent at the 1 h drug treatment time point and only under acidic conditions.

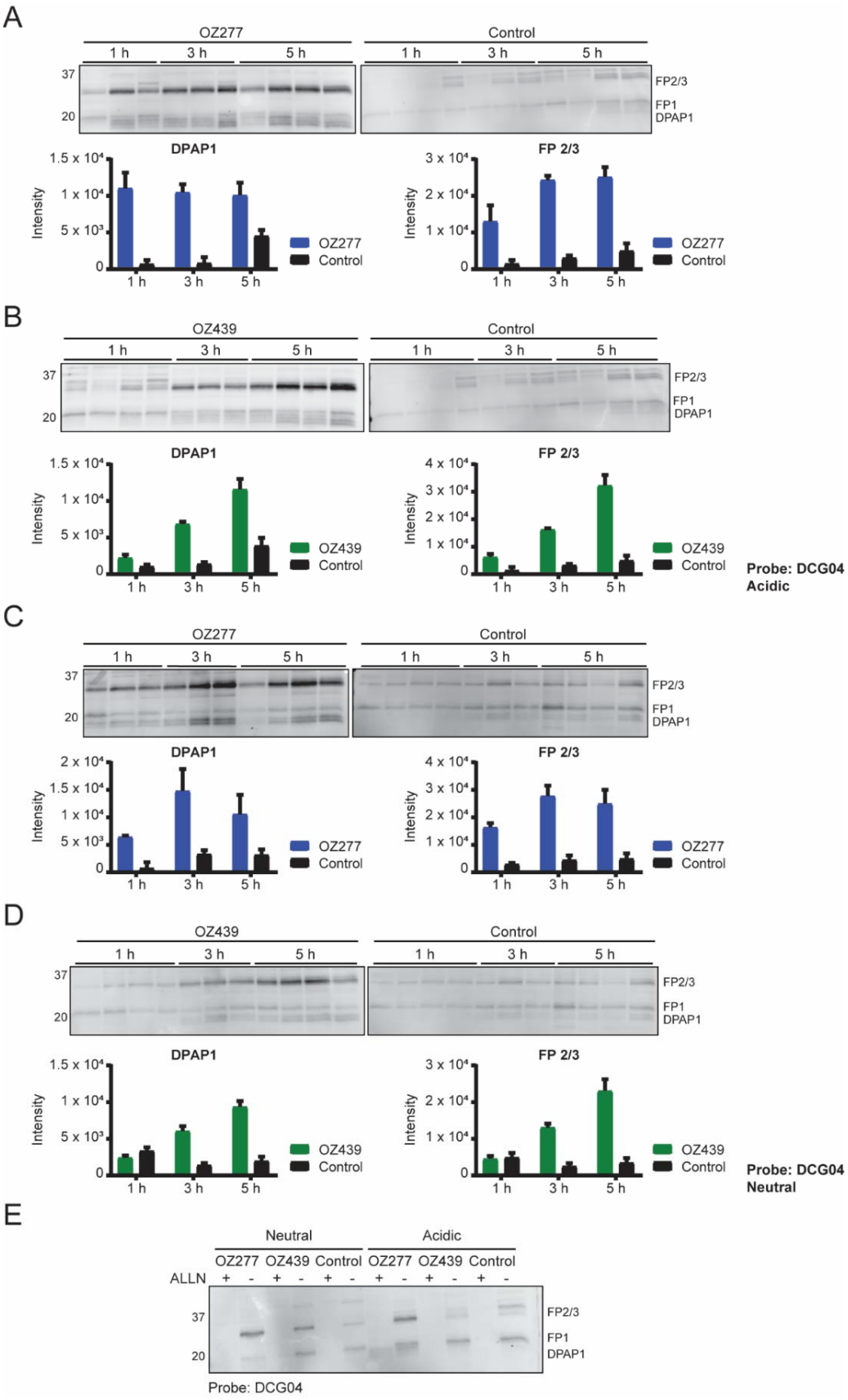


**Figure 19:** Parasite cysteine protease activity after peroxide treatment using the activity-based protease probe (ABPP) DCG04. (A-B) Cysteine protease activity and densitometric analysis

of the dipeptidyl aminopeptidase 1 (DPAP1) and falcipain (FP) 2/3 signal after OZ277 (A) and OZ439 (B) treatment of *P. falciparum* trophozoite stage parasites using DCG04 at pH 5.5 (acidic). (C-D) Cysteine protease activity and densitometric analysis of the DPAP1 and FP 2/3 signal after OZ277 (C) and OZ439 (D) treatment of *P. falciparum* trophozoite stage parasites using DCG04 at pH 7.2 (neutral). In A-D, live parasites were treated for 1, 3 or 5 h with OZ277, OZ439 or DMSO (control) in 3-4 independent experiments and the saponin lysates were labelled with DCG04 to determine residual cysteine protease activity. (E) Identification of ALLN inhibition of cysteine protease activity under neutral and acidic pH conditions. Live parasites were treated for 3 h with OZ277, OZ439 or DMSO (control) and the saponin lysates were pre-incubated with (+) or without (-) the cysteine protease inhibitor ALLN (10 μM for 30 min) prior to labelling with DCG04.

The ozonide-induced increases in activity of FPs and DPAP1 were confirmed by another cysteine protease targeting probe, FY01 (36) in acidic (Figure 20) and neutral (Figure 21) conditions. Drug treatment also caused decreased activity of an unidentified parasite protease at 75 kDa (pH 7.2) and similar to the FPs and DPAP1, OZ277 treatment had a more rapid effect than OZ439 (Figure 21). Additional parasite cysteine proteases (~37 and 50 kDa) that had increased activity following drug treatment were also identified under acidic conditions (Figure 20), although their identity and role in haemoglobin catabolism could not be confirmed.

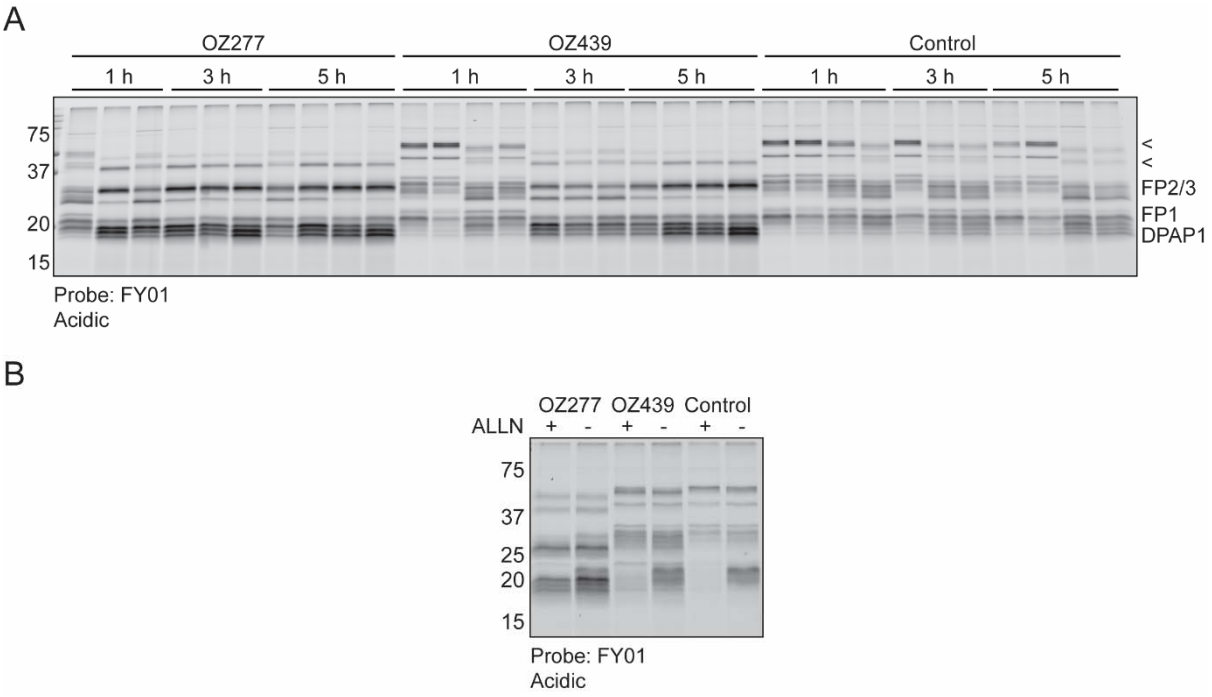


**Figure 20:** Parasite cysteine protease activity after peroxide treatment using the activity-based protease probe (ABPP) FY01 at acidic pH. (A) SDS-PAGE gel showing parasite cysteine protease activity after OZ277, OZ439 and DMSO (control) treatment of trophozoite stage parasites using the FY01 probe, at pH 5.5. Live parasites were treated for 1, 3 or 5 h in 3-4 independent experiments. Treated parasites were saponin lysed and labelled with FY01 to determine residual cysteine protease activity. (B) Identification of ALLN inhibition of cysteine protease activity at pH 5.5. Live parasites were treated for 3 h with OZ277, OZ439 or DMSO (control) and the saponin lysates were pre-incubated with (+) or without (-) the cysteine protease inhibitor ALLN (10 μM for 30 min) prior to labelling with FY01. <, unidentified protease.

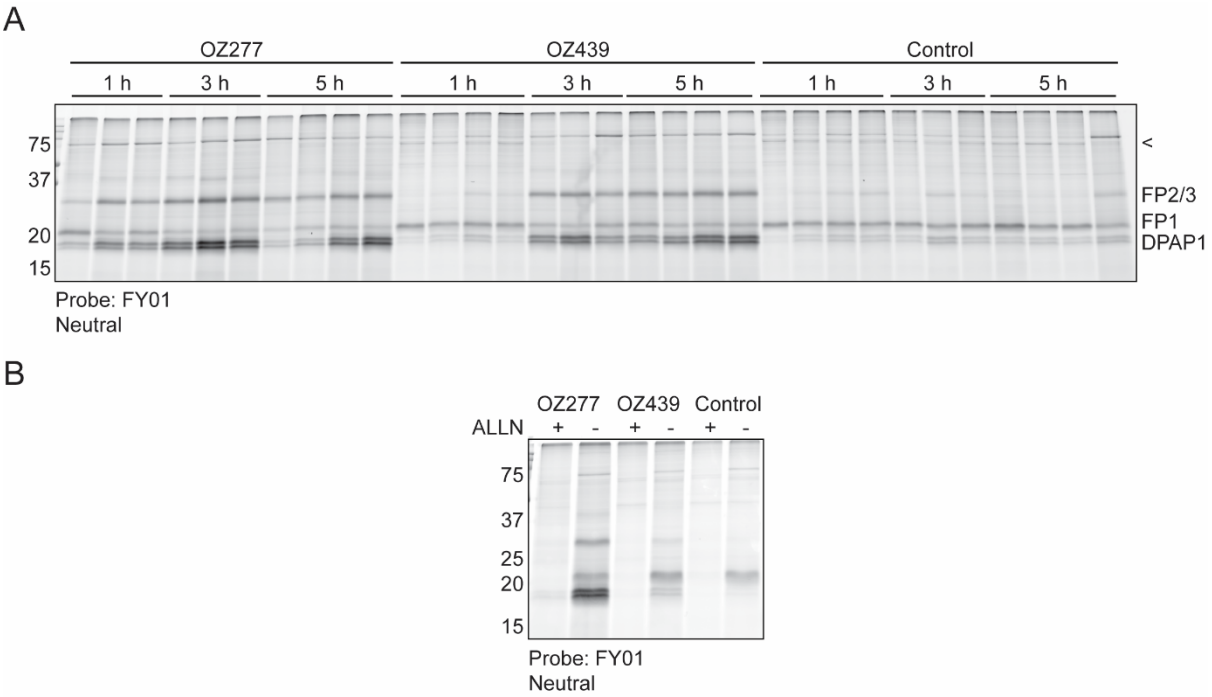


**Figure 21:** Parasite cysteine protease activity after peroxide treatment using the activity-based protease probe (ABPP) FY01 at neutral pH. (A) SDS-PAGE gel showing parasite cysteine protease activity after OZ277, OZ439 and DMSO (control) treatment of trophozoite stage parasites using the FY01 probe, at pH 7.2. Live parasites were treated for 1, 3 or 5 h in 3-4 independent experiments. Treated parasites were saponin lysed and labelled with FY01 to determine residual cysteine protease activity. (B) Identification of ALLN inhibition of cysteine protease activity at pH 7.2. Live parasites were treated for 3 h with OZ277, OZ439 or DMSO (control) and the saponin lysates were pre-incubated with (+) or without (-) the cysteine protease inhibitor ALLN (10 μM for 30 min) prior to labelling with FY01. <, unidentified protease.

In addition to DCG04 and FY01, the Cy5-labelled cysteine protease targeting probes BMV109 (38) and MS-3-19 (39) revealed that drug treatment induced an increase in the activity of parasite proteases that migrated at 28 kDa, consistent with the molecular weight of FP 2 and FP 3 (Figures 22A and 22B), however, DPAP1 was not labelled by these probes. The serine protease targeting probe, PK101, revealed drug-induced alterations in activity of several serine proteases that migrated at 12, 25 and 37 kDa at neutral pH (Figure 23). The identity of

these serine proteases was not probed any further in this study. No drug-induced changes to serine protease activity were identified at acidic pH using the ABPP, PK101.

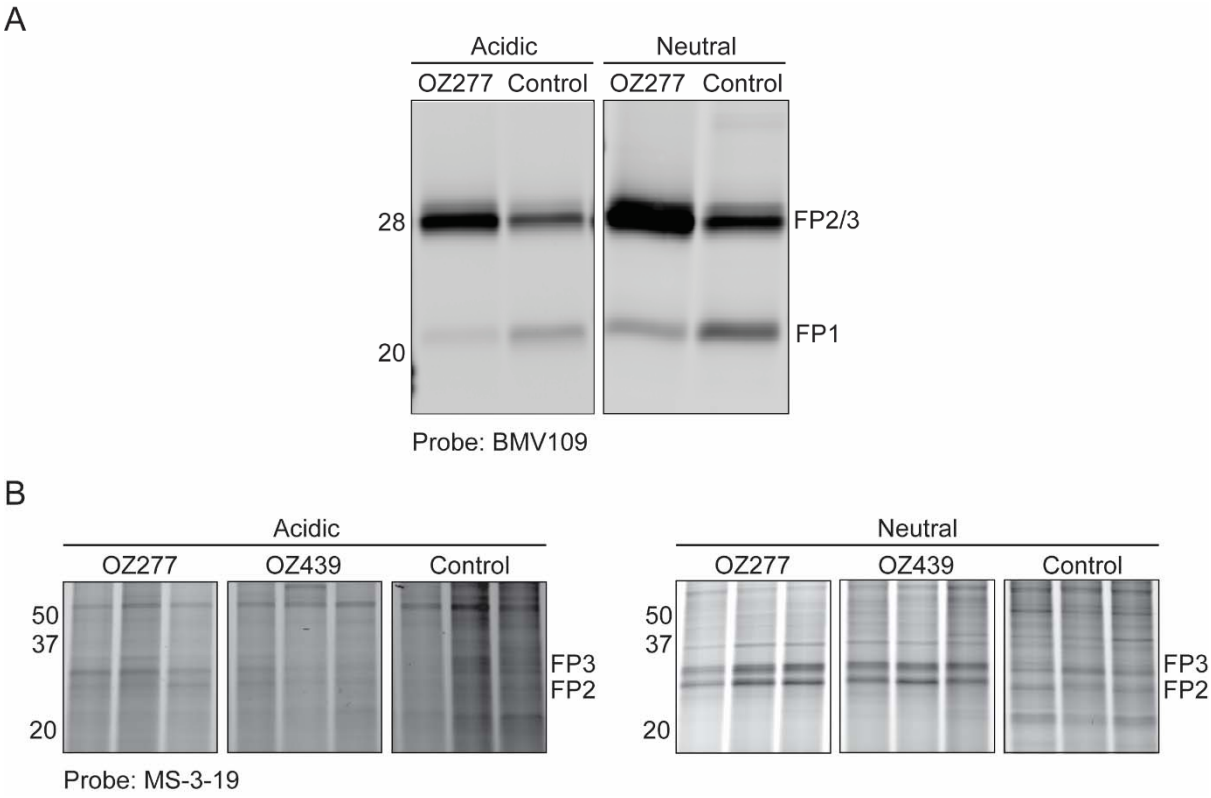


**Figure 22:** Parasite cysteine protease activity after peroxide treatment using the activity-based protease probes (ABPPs) BMV109 and MS-3-19. (A) SDS-PAGE gels showing parasite cysteine protease activity after OZ277 and DMSO (control) treatment of trophozoite stage parasites using BMV109, at pH 5.5 (acidic) and pH 7.2 (neutral). Live parasites were treated for 3 h and the saponin lysates were labelled with BMV109 to determine residual cysteine protease activity. (B) SDS-PAGE gels showing parasite cysteine protease activity after OZ277, OZ439 and DMSO (control) treatment of trophozoite stage parasites using the MS-3-19 probe at pH 5.5 (acidic) and pH 7.2 (neutral). Live parasites were treated for 3 h in three independent experiments and the saponin lysates were labelled with MS-3-19 to determine residual cysteine protease activity.

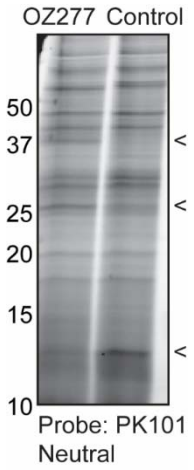


**Figure 23:** SDS-PAGE gel showing parasite serine protease activity after OZ277 treatment using the activity-based protease probe (ABPP) PK101 at pH 7.2. Live parasites were treated for 3 h with OZ277 (1 μM) or DMSO (control) and the saponin lysates were labelled with PK101 to determine residual serine protease activity.

## 4.5 DISCUSSION

In the current study, the parasite biochemical pathways that are perturbed in response to peroxide antimalarials were assessed using untargeted metabolomic, peptidomic and proteomic profiling of ozonide and DHA treated *P. falciparum*. The comprehensive multi-omics analysis revealed that peroxide antimalarials rapidly disrupt haemoglobin catabolism prior to affecting other biochemical pathways and that parasites engage a stress response to manage peroxide-induced damage.

Promiscuous artemisinin- and ozonide-derived radicals reportedly alkylate parasite proteins involved in various biochemical functions (1-3), pointing to a multi-modal mechanism of action. The time-resolved metabolomics approach employed in this study allowed the mapping of primary and secondary peroxide-induced effects on parasite metabolism and revealed that peroxide exposure of 3 h or less primarily induced depletion of short chain haemoglobin-derived peptides, which was the first detectable metabolic disturbance following drug treatment. In peroxide-treated trophozoite cultures, pronounced peptide depletion occurred within 1.5 h of DHA exposure and within 3 h of OZ277 and OZ439 exposure (Figure 7). In ring stage cultures significantly fewer haemoglobin-derived peptides were altered in abundance following drug treatment, however, similar to trophozoite cultures, DHA induced a more rapid depletion of haemoglobin-derived peptides compared to the ozonides (Figure 3). These findings are consistent with the reported exposure time-dependence of activity for these three peroxide antimalarials (12).

Previous metabolomics studies of trophozoite infected RBCs have also demonstrated drug-induced depletion of haemoglobin-derived peptides following treatment with DHA and artemisinin (4, 5). However, this is the first study reported in ring stage parasites. Digestion of host cell haemoglobin is essential for parasite survival, as it provides amino acids for protein

synthesis and serves additional non-anabolic functions, such as maintaining osmotic stability of the infected RBC (40-42). Haemoglobin digestion is most active during the trophozoite stage of the RBC infection (43) and provides the iron-based activator (most likely free haem) necessary for peroxide bond activation and potent antimalarial activity (7, 12, 44), explaining the profound impact of peroxide antimalarials on haemoglobin-derived small peptides during the trophozoite stage of parasite development. Although it is generally assumed that little haemoglobin digestion occurs during the earlier ring stage parasite, active haemoglobin proteases are expressed (32) and small haemozoin crystals, by-products of haemoglobin digestion, have been detected in these parasites (45-47). This indicates that active haemoglobin degradation does occur in ring stage parasites and supports the observation of peroxide antimalarials also inducing depletion of haemoglobin-derived small peptides during this stage of asexual growth.

Peroxide-induced depletion of haemoglobin-derived small peptides could be the result of either an impaired haemoglobin uptake mechanism or a blockage in the haemoglobin degradation pathway, or a combination of the two. Artemisinins reportedly inhibit haemoglobin uptake in *P. falciparum* infected RBCs (6, 7), and it is plausible that this is also a feature of the antimalarial mechanism of action of ozonides. However, the results presented in this study pointed to a mechanism for disruption of haemoglobin catabolism involving a specific ozonide effect on the proteases involved in haemoglobin digestion. Along with the drug-dependent depletion of haemoglobin-derived small peptides identified by metabolomics, peptidomics analysis of peptide peaks originating from the alpha and beta chains of haemoglobin showed that there is a drug-induced accumulation of longer chain haemoglobin-derived peptides, which was most pronounced after OZ277 treatment (Figure 11). The accumulation of larger peptides and depletion of shorter haemoglobin-derived di, tri and tetrapeptides suggests haemoglobin digesting proteases involved in the conversion of large to

small peptides were affected by ozonide treatment. In contrast, the depletion of both long and short chain haemoglobin peptides following DHA treatment suggests the DHA-induced disruption of haemoglobin catabolism may involve mechanisms that occur upstream of the haemoglobin proteases, possibly through inhibition of haemoglobin uptake (6, 7).

Furthermore, proteomics analysis showed that all of the proteases involved in the haemoglobin digestion pathway, with the exception of falcilysin, were increased in abundance following drug treatment when compared to control levels (Figure 15). Ozonides and artemisinins are known to alkylate proteins localised to the parasite digestive vacuole, including proteases involved in the haemoglobin digestion pathway (Appendix 5) (1-3). Unlike previous reports suggesting that FPs are the likely intraparasitic targets of artemisinins that induce disruption of haemoglobin catabolism (8), recent studies indicated that the plasmepsins, DPAP1 and *Pf*A-M1, are haemoglobin digesting proteases targeted by peroxide antimalarials (not FPs) (1-3). Rapid disruption of haemoglobin catabolism by the peroxide antimalarials agrees with the hypothesis that peroxide-based drugs are activated by Fe(II) to produce reactive intermediates in the parasite digestive vacuole. It is plausible that the resulting radicals alkylate and inactive digestive vacuole proteins, including haemoglobin digesting proteases (1-3), which could represent the initial intraparasitic targets of peroxide antimalarials. In addition, the elevated abundance of proteins in the haemoglobin digestion cascade may signify a parasite response to peroxide-induced impairment of haemoglobin digestion.

A series of ABPPs demonstrated that ozonide treatment resulted in a time-dependent increase in the activity of parasite cysteine proteases involved in haemoglobin digestion (FP 2/3 and DPAP1) (Figures 19-22) and the change in protease activity correlated with the known relative rates of OZ277 and OZ439 action (12). In general, parasite FP and DPAP1 activity increased within 1 h of exposure to OZ277 and 3 h to OZ439. These experiments indicated that ozonides may not act as inhibitors of the cysteine proteases

involved in haemoglobin digestion, but rather, it appears that the parasite responds to ozonide-induced disruption of haemoglobin digestion by increasing FP and DPAP1 activity, possibly as a compensatory mechanism for ozonide-mediated inhibition of other haemoglobin digesting proteases, such as the plasmepsins (3). While total protein levels between the treatment and control groups were normalised prior to incubation with the ABPP, it is highly likely that increased FP and DPAP1 abundance in response to peroxide treatment (as determined by quantitative proteomics) is the major contributing factor to the increase in protease activity observed in these experiments.

Unlike cysteine proteases (and serine and threonine proteases) that have nucleophilic active site residues that can be directly targeted by the electrophilic functional group of ABPPs, aspartic proteases (and metalloproteases), such as the plasmepsins, use active site residues to activate water molecules that serve as the nucleophile for peptide bond hydrolysis (30). For this reason, ABPPs are unable to directly alkylate aspartic proteases and therefore ABPPs could not be used to measure parasite plasmepsin activity following peroxide treatment. In future work this could be overcome by appending the ABPP to a photocrosslinking group that, when activated by UV light, can form a covalent bond with nearby groups on the protease. Unfortunately, these ABPPs are more difficult to synthesise, are less specific and are able to bind to inactive proteases (30).

Notably, there was evidence for increased activity of cysteine proteases other than FP and DPAP1 when ozonide treated parasites were labelled with the FY01 probe under acidic (Figure 20) and neutral (Figure 21) conditions. These proteases migrated at approximately 37, 50 and 75 kDa on a SDS-PAGE gel, but further characterisation was not performed, and their identity could not be confirmed. One possibility is that they represent active pro-forms of DPAP1. Parasite DPAP1, similar to its mammalian homologue, cathepsin C (48), is expressed as a 77 kDa pro-enzyme that is proteolytically processed upon maturation (49). The 37 and

50 kDa protein bands that were observed on the SDS-PAGE gel potentially correspond to the predicted molecular masses of DPAP1 pro-forms (38 and 56 kDa) in *P. falciparum* (49).

Using the multi-omics-based techniques and direct evaluation of cysteine protease activity, haemoglobin digestion was found to be a primary pathway affected by peroxide antimalarial treatment within *P. falciparum* infected RBCs. One caveat is that the precise origin of the depleted di, tri and tetrapeptides identified by untargeted metabolomic screening cannot be definitively determined based on such short sequences. MS/MS confirmation of the amino acid sequence was obtained for a subset of these depleted peptides and all could be mapped to haemoglobin. Most of the remaining putative peptides (or their isomers) that were depleted by peroxide treatment but whose sequence could not be confirmed by MS/MS are also present in the sequence of haemoglobin. Combined with additional lines of evidence pointing to a mechanism involving peroxide-induced disruption to haemoglobin digestion, it is strongly suggestive that these small peptides originate from haemoglobin. An alternative hypothesis is that they are derived from parasite-mediated proteasomal turnover of damaged and misfolded proteins (29), although this is more likely to result in an accumulation of small peptides, not a depletion. To definitively establish the source of these peptides, future experiments where parasites are grown in medium containing isotope-labelled amino acids prior to drug treatment could differentiate haemoglobin- from parasite-derived peptides, as isotope-labelled amino acids should only be incorporated into parasite proteins and therefore be absent in peptides originating from haemoglobin.

While altered peptide metabolism was the primary metabolic phenotype following short durations of peroxide exposure, extending treatment beyond 3 h induced disruption of additional biochemical pathways, including lipid and nucleotide metabolism (Figure 8). In both ring and trophozoite infected RBCs, peroxide treatment induced accumulation of several metabolic intermediates in the *de novo* synthesis pathways for PC and PE lipids (known as the

Kennedy Pathways) (Figures 4 and 9), which are the major lipid components of parasite membranes (50). The *de novo* Kennedy Pathways are crucial for asexual parasite growth and consist of three enzymatic reactions that synthesise PC and PE from host-scavenged choline and ethanolamine, respectively. A transversal pathway also exists in *P. falciparum*, whereby phosphoethanolamine N-methyltransferase (PMT) catalyses the triple methylation of ethanolamine phosphate to choline phosphate, linking the PC and PE branches of the Kennedy Pathways (51, 52). To a lesser extent, decarboxylation of PS also contributes to the PE pool within *P. falciparum* infected RBCs (53).

The products of the first reactions in the Kennedy Pathways, choline phosphate and ethanolamine phosphate were increased in abundance after extended peroxide treatment (> 3 h of drug exposure) in both ring and trophozoite infected RBCs (Figures 4 and 9), while the dimethyl-ethanolamine phosphate intermediate in the *Pf*PMT-mediated transversal pathway was also elevated (Figure 9). In the PE branch, CDP-ethanolamine was found to be increased in abundance after extended peroxide treatment (evident in both ring and trophozoite treated cultures), but there was no significant change in abundance of the corresponding metabolite in the PC branch, CDP-choline (Figures 4 and 9). It is plausible that accumulation of these metabolites is due to drug-induced inhibition of one or more of the enzymes in the Kennedy Pathways. Artemisinins (but not ozonides) reportedly alkylate *Pf*PMT (1), however, no other enzymes in the Kennedy Pathways are known to be alkylation targets for the artemisinins or the ozonides (Appendix 5). Interestingly, the proteomic analysis revealed that all enzymes directly upstream of the elevated metabolites in the Kennedy Pathways were upregulated after peroxide treatment. Therefore, rather than a blockage in the pathway, a more likely explanation for the observed metabolic phenotype is that increased levels of CK, EK, PMT and ECT (Figure 16), led to the accumulation of their metabolite products, possibly to increase the synthesis of PC and PE as a biochemical response to peroxide-induced membrane damage.

This is consistent with reports that the biological activity of peroxides involves non-specific damage to parasite membranes through lipid peroxidation and the production of reactive oxygen species (54-58). Peroxide-dependent membrane lipid peroxidation has been shown to occur at all stages of parasite intraerythrocytic development and when monitored using an oxidation sensitive lipid probe, only became apparent after extended durations of drug exposure (> 3 h) (56). These findings agree with the time-scale for peroxide-induced disruption of lipid metabolism in this study when measured by metabolomics. Furthermore, ozonide-mediated peroxidation of phosphatidylcholine has been demonstrated *in vitro* following reductive drug activation by iron (59).

Parasite PC and PE synthesis is thought to be regulated by the intracellular pool of choline phosphate and ethanolamine phosphate, which are the substrates for the rate-limiting enzymes in the PC and PE branches of the Kennedy pathways, CCT and ECT, respectively (60, 61). Elevated concentrations of these two metabolites (choline phosphate and ethanolamine phosphate) has been found to increase the rate of CCT- and ECT-mediated catalysis in *Plasmodium* infected RBCs (60, 61). Therefore, specific accumulation of choline phosphate and ethanolamine phosphate by upregulating CK and EK abundance (as evidenced by quantitative proteomics analysis, Figure 16) in response to peroxide-mediated membrane damage may represent a means to increase the metabolic flux through the Kennedy Pathways, thereby increasing PC and PE that can be incorporated into membranes. Elevated levels of the downstream by-product released at the final catalytic step in PC and PE synthesis, CMP (Figure 9B), also supports this hypothesis.

In addition to PC and PE biosynthesis, prolonged peroxide exposure in trophozoite infected RBCs led to a temporal depletion in the abundance of DGs and TGs (Figure 9), which are the two main glycerolipid species in *P. falciparum* parasites (50). Within the parasite, DGs and TGs are packaged into lipid droplets called neutral lipid bodies, which are closely

associated with the parasite digestive vacuole, residing internally or on the periphery of the digestive vacuole membrane (62-64). Neutral lipid bodies are thought to concentrate free haem released as a by-product of haemoglobin digestion and catalyse its biocrystallisation into non-toxic haemozoin (63-65). The digestive vacuole localisation and role in haem detoxification places neutral lipid bodies in the same environment as where peroxide antimalarials are generally thought to be activated by haemoglobin-derived haem (12, 44, 66). Furthermore, confocal microscopic analysis showed that fluorescently-tagged artemisinin and ozonide derivatives appear to accumulate in neutral lipid bodies within live *P. falciparum*-infected RBCs (55, 56). In this context, it is predicted that activated drug itself, or alkylated haem adducts, promote oxidative damage of nearby targets, including DGs and TGs within neutral lipid bodies, altering the lipid composition of peroxide-treated infected RBCs. Interestingly, all of the depleted DGs and TGs detected in this study were composed of unsaturated fatty acid chains, which are more susceptible to oxidative damage than saturated lipids (67).

Disruption of the parasite pyrimidine biosynthetic pathway at both the metabolite (Figure 10) and protein levels (Figure 17) were also apparent in peroxide-treated trophozoite infected cultures. This finding is consistent with previous studies demonstrating DHA-induced alterations in parasite pyrimidine metabolism (5). *P. falciparum* parasites lack the ability to scavenge pyrimidines from the environment and are therefore completely reliant on the *de novo* synthesis pathway (68). Carbamoyl phosphate synthetase and aspartate carbamoyltransferase, which catalyse the initial steps of parasite pyrimidine biosynthesis, are both reported to be alkylation targets of artemisinins, although this has not yet been shown for the ozonides (Appendix 5) (1). Peroxide-induced inhibition of one or both of these initial pyrimidine biosynthetic enzymes may be responsible for the reduced abundance of N-carbamoyl-L-aspartate observed in this study, while reduced amino acid acquisition through impaired haemoglobin digestion may explain the profound reduction in L-aspartate levels. A depletion

in these initial biosynthetic intermediates may lead to disruption of downstream metabolite levels and a corresponding increase in the protein levels of some pyrimidine biosynthetic enzymes as a compensatory response, as was demonstrated in this study.

The prevailing evidence indicates that peroxide antimalarials affect multiple aspects of parasite biochemistry, which is consistent with previous reports (4, 5) and a mechanism of resistance involving enhanced cytoprotective capabilities (13, 29, 69). Global proteome analysis of peroxide-treated *P. falciparum* infected RBCs revealed a pronounced upregulation of proteins involved in protein translation and the ubiquitin-proteasome system (Figure 14), indicative of the parasite engaging a generalised response to stress (70). To mitigate peroxide-mediated cellular damage, the parasite is thought to elicit a stress response reminiscent of the unfolded protein response in other organisms (71), which engages the ubiquitin-proteasome system (29). Peroxide-induced oxidative insult and widespread protein alkylation is thought to induce accumulation of damaged and misfolded proteins (29, 72, 73) and in the absence of robust unfolded protein response machinery, the *Plasmodium* parasite relies on translational regulation, mediated by eIF2-α phosphorylation, (74) and a functional ubiquitin-proteasome system to restore proteostasis (75, 76). Unsurprisingly, specifically targeting the parasite proteasome with proteasome inhibitors has been found to be synergistic with DHA against *P. falciparum* and the combination has been shown to overcome *K13*-mediated artemisinin resistance *in vitro* and *in vivo* (29).

Ozonide and artemisinin antimalarials appear to impact the same biochemical pathways in *P. falciparum* infected RBCs pointing to a common mechanism of action. A model for peroxide antimalarial activity is proposed (Figure 24), whereby haemoglobin-derived free haem activates ozonides (and artemisinins) within the parasite digestive vacuole and the resulting drug-derived radicals initially target the machinery involved in haemoglobin digestion, leading to rapid disruption of haemoglobin catabolism, an essential parasite process.

Time-dependent profiling revealed that drug-induced impairment of the pyrimidine biosynthetic pathway and damage to lipids, including parasite membranes and digestive vacuole-associated neutral lipid bodies, may be secondary effects mediated by peroxide antimalarials. Targeting multiple essential biochemical pathways may contribute to the toxicity of peroxide antimalarials towards all asexual stages of the parasite, including early ring stages which are notoriously insensitive to antimalarial treatment (77). Although these were the main metabolic pathways affected by peroxide exposure in this study, other parasite functions may also be impacted given the promiscuous nature of peroxide-derived radicals towards intraparasitic components (1-3). In response to widespread peroxide-induced cellular damage, the parasite appears to defend itself by engaging a stress response that involves regulating translation and overexpressing proteins involved in the ubiquitin-proteasome system. It is likely that once peroxide-mediated damage overwhelms these defensive mechanisms that death of the parasite rapidly ensues.

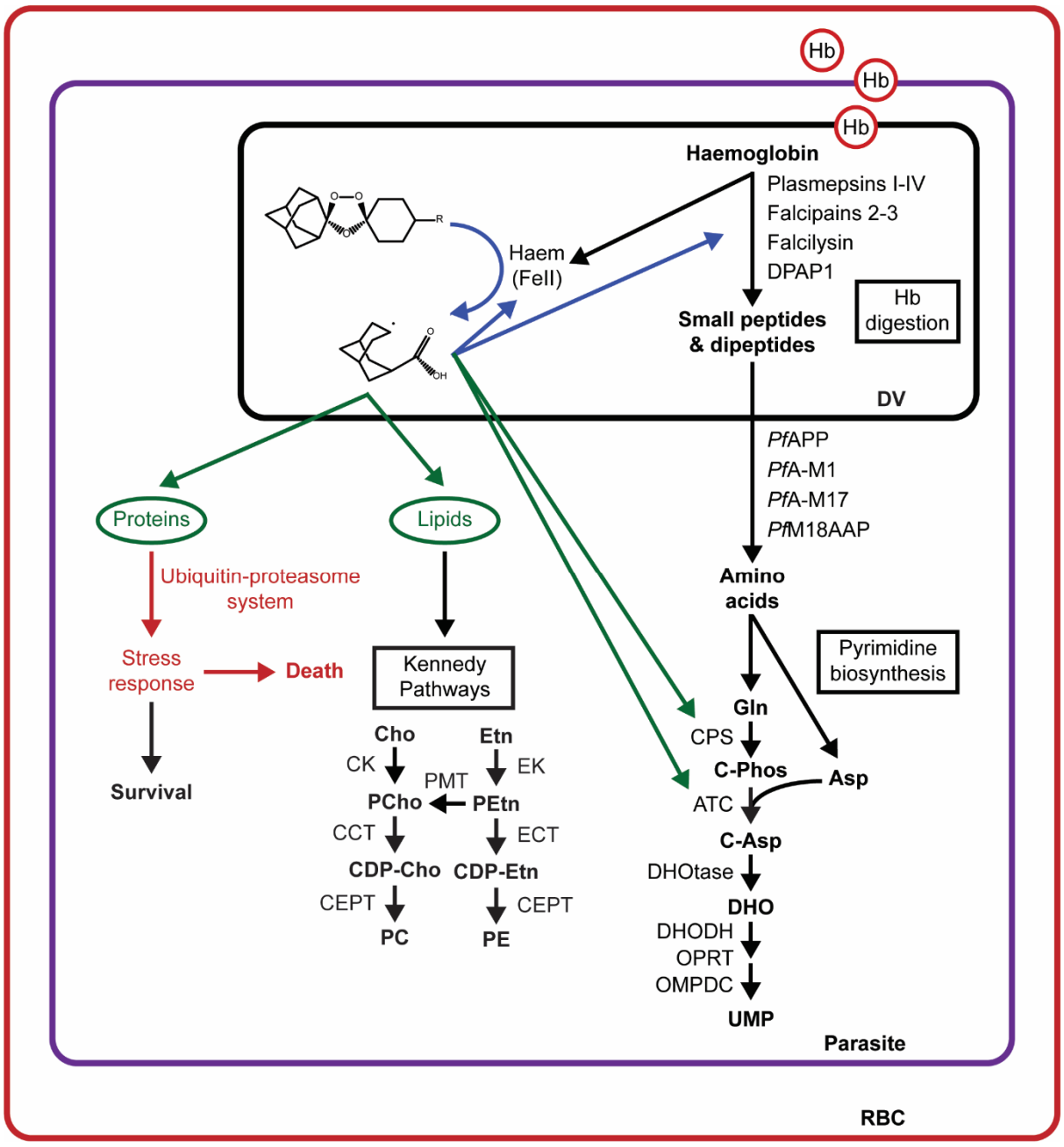


**Figure 24:** Proposed model for peroxide antimalarial activity in *P. falciparum* infected RBCs. Haemoglobin-derived haem activates peroxide antimalarials within the parasite digestive vacuole. The resulting drug-derived radicals initially damage components proximal to the activation site, including haem and proteases involved in haemoglobin digestion (arrows shown in blue). This leads to disruption of the haemoglobin degradation pathway. To correct the peroxide-induced impairment, parasites may respond by increasing the abundance and activity of proteases involved in haemoglobin catabolism. Peroxide radicals induce further oxidative insult and cause widespread alkylation of parasite components as the duration of drug exposure is increased (arrows shown in green). This may include damage to lipids, inducing upregulation

of the Kennedy Pathways, and proteins involved in other vital parasite functions, such as pyrimidine biosynthesis. To mitigate peroxide-induced cellular damage, the parasite engages a stress response involving translational regulation and the ubiquitin-proteasome system, and death occurs when peroxide-mediated damage overwhelms the parasite's defensive mechanisms (arrows shown in red). Asp, aspartic acid; ATC, aspartate carbamoyltransferase; C-Asp, carbamoyl-aspartate, C-Phos, carbamoyl-phosphate; CCT, choline-phosphate cytidyltransferase; CDP-, cytidine-diphospho-; CEPT, choline/ethanolamine phosphotransferase; Cho, choline; CK, choline kinase; CMP, cytidine monophosphate; CPS, carbamoyl phosphate synthetase; DHO, dihydroorotate; DHODH, dihydroorotate dehydrogenase; DHOtase, dihydroorotase; DV, digestive vacuole; ECT, ethanolamine-phosphate cytidyltransferase; EK, ethanolamine kinase; Etn, ethanolamine; Gln, glutamine; Hb, haemoglobin; OMPDC, orotodine 5'-phosphate decarboxylase; OPRT, orotate phosphoribosyltransferase; PC, phosphatidylcholine; PE, phosphatidylethanolamine; PCho, choline phosphate; PEtn, ethanolamine phosphate; PMT, phosphoethanolamine N-methyltransferase; RBC, red blood cell; UMP, uridine monophosphate.

## 4.6 CONCLUSIONS

In this study the temporal biochemical response of OZ277-, OZ439- and DHA-treated *P. falciparum* infected RBCs was investigated using an untargeted multi-omics-based approach. All three peroxides affected the same biochemical pathways, suggesting they mediate activity by similar mechanisms. However, in general, DHA had a more rapid and pronounced effect compared to the ozonides. Haemoglobin digestion was found to be the primary pathway affected, with metabolomics and peptidomics analysis identifying rapid drug-induced disruption of haemoglobin catabolism, while ABPP studies revealed drug-dependent alterations in haemoglobin protease activity within 1 h of drug exposure. Together, these data show that haemoglobin catabolism appears to be the most significant initial metabolic disturbance following peroxide treatment in *P. falciparum* parasites, consistent with a mechanism of action that involves iron-mediated activation to produce peroxide-derived radicals in the parasite digestive vacuole. Extending the duration of peroxide treatment beyond 3 h induced disruption of additional biochemical pathways, including lipid and nucleotide metabolism, which may represent secondary biochemical pathways affected by this important class of antimalarials. Proteomics analysis also confirmed that proteins involved in these vital pathways are altered in response to peroxide antimalarial exposure. The most striking finding in the proteome of peroxide-treated parasites was an upregulation of proteins involved in translation and the ubiquitin-proteasome system, which is indicative of a cellular response to stress. Taken together, these data indicated that peroxides initially disrupt haemoglobin catabolism prior to affecting other biochemical pathways, and that the parasite engages a stress response to manage peroxide-induced damage.

The malaria field is facing growing concerns with the spread of multi-drug resistant parasites that are causing widespread treatment failures. Understanding the biochemical

mechanisms underpinning peroxide activity, and the parasite's response to treatment, offers a potential route for targeting the malaria parasite with novel drug combinations that may have improved antimalarial efficacy, and limit the impact of drug resistance.

# 4.7 REFERENCES


1. Wang J, Zhang C-J, Chia WN, Loh CC, Li Z, Lee YM, He Y, Yuan L-X, Lim TK, Liu M, Liew CX, Lee YQ, Zhang J, Lu N, Lim CT, Hua Z-C, Liu B, Shen H-M, Tan KSW, Lin Q. 2015. Haem-activated promiscuous targeting of artemisinin in *Plasmodium falciparum*. Nat Commun 6:10111.
2. Ismail HM, Barton V, Phanchana M, Charoensutthivarakul S, Wong MHL, Hemingway J, Biagini GA, O'Neill PM, Ward SA. 2016. Artemisinin activity-based probes identify multiple molecular targets within the asexual stage of the malaria parasites *Plasmodium falciparum* 3D7. Proc Natl Acad Sci U S A 113:2080-2085.
3. Ismail HM, Barton VE, Panchana M, Charoensutthivarakul S, Biagini GA, Ward SA, O'Neill PM. 2016. A click chemistry-based proteomic approach reveals that 1, 2, 4-trioxolane and artemisinin antimalarials share a common protein alkylation profile. Angew Chem Int Ed Engl 55:6401-6405.
4. Creek DJ, Chua HH, Cobbold SA, Nijagal B, MacRae JI, Dickerman BK, Gilson PR, Ralph SA, McConville MJ. 2016. Metabolomics-based screening of the malaria box reveals both novel and established mechanisms of action. Antimicrob Agents Chemother 60:6650-6663.
5. Cobbold SA, Chua HH, Nijagal B, Creek DJ, Ralph SA, McConville MJ. 2015. Metabolic dysregulation induced in *Plasmodium falciparum* by dihydroartemisinin and other front line antimalarial drugs. J Infect Dis 213:276-286.
6. Hoppe HC, van Schalkwyk DA, Wiehart UI, Meredith SA, Egan J, Weber BW. 2004. Antimalarial quinolines and artemisinin inhibit endocytosis in *Plasmodium falciparum*. Antimicrob Agents Chemother 48:2370-2378.
7. Klonis N, Crespo-Ortiz MP, Bottova I, Abu-Bakar N, Kenny S, Rosenthal PJ, Tilley L. 2011. Artemisinin activity against *Plasmodium falciparum* requires hemoglobin uptake and digestion. Proc Natl Acad Sci U S A 108:11405-11410.
8. Pandey AV, Tekwani BL, Singh RL, Chauhan VS. 1999. Artemisinin, an endoperoxide antimalarial, disrupts the hemoglobin catabolism and heme detoxification systems in malarial parasite. J Biol Chem 274:19383-19388.
9. Antoine T, Fisher N, Amewu R, O'Neill PM, Ward SA, Biagini GA. 2014. Rapid kill of malaria parasites by artemisinin and semi-synthetic endoperoxides involves ROS-

dependent depolarization of the membrane potential. J Antimicrob Chemother 69:1005-1016.

10. Allman EL, Painter HJ, Samra J, Carrasquilla M, Llinás M. 2016. Metabolomic profiling of the malaria box reveals antimalarial target pathways. Antimicrob Agents Chemother 60:6635-6649.
11. Giannangelo C, Stingelin L, Yang T, Tilley L, Charman SA, Creek DJ. 2018. Parasite-mediated degradation of synthetic ozonide antimalarials impacts *in vitro* antimalarial activity. Antimicrob Agents Chemother 62:e01566-01517.
12. Yang T, Xie SC, Cao P, Giannangelo C, McCaw J, Creek DJ, Charman SA, Klonis N, Tilley L. 2016. Comparison of the exposure time-dependence of the activities of synthetic ozonide antimalarials and dihydroartemisinin against K13 wild-type and mutant *Plasmodium falciparum* strains. Antimicrob Agents Chemother 60:4501-4510.
13. Siddiqui G, Srivastava A, Russell AS, Creek DJ. 2017. Multi-omics based identification of specific biochemical changes associated with PfKelch13-mutant artemisinin resistant *Plasmodium falciparum*. J Infect Dis 215:1435-1444.
14. Creek DJ, Jankevics A, Burgess KE, Breitling R, Barrett MP. 2012. IDEOM: an Excel interface for analysis of LC-MS-based metabolomics data. Bioinformatics (Oxford, England) 28:1048-1049.
15. Sumner LW, Amberg A, Barrett D, Beale MH, Beger R, Daykin CA, Fan TW-M, Fiehn O, Goodacre R, Griffin JL. 2007. Proposed minimum reporting standards for chemical analysis. Metabolomics 3:211-221.
16. Creek DJ, Jankevics A, Breitling R, Watson DG, Barrett MP, Burgess KE. 2011. Toward global metabolomics analysis with hydrophilic interaction liquid chromatography-mass spectrometry: improved metabolite identification by retention time prediction. Anal Chem 83:8703-8710.
17. Xia J, Sinelnikov IV, Han B, Wishart DS. 2015. MetaboAnalyst 3.0—making metabolomics more meaningful. Nucleic Acids Res 43:W251-W257.
18. Yeung YG, Stanley ER. 2010. Rapid detergent removal from peptide samples with ethyl acetate for mass spectrometry analysis. Curr Protoc Protein Sci 59:16.12.11-16.12.15.
19. Rappsilber J, Ishihama Y, Mann M. 2003. Stop and go extraction tips for matrix-assisted laser desorption/ionization, nanoelectrospray, and LC/MS sample pretreatment in proteomics. Anal Chem 75:663-670.

20. Zhang J, Xin L, Shan B, Chen W, Xie M, Yuen D, Zhang W, Zhang Z, Lajoie GA, Ma B. 2012. PEAKS DB: de novo sequencing assisted database search for sensitive and accurate peptide identification. Mol Cell Proteomics 11:M111. 010587.
21. Boersema PJ, Raijmakers R, Lemeer S, Mohammed S, Heck AJ. 2009. Multiplex peptide stable isotope dimethyl labeling for quantitative proteomics. Nat Protoc 4:484-494.
22. Lin Y, Liu Y, Li J, Zhao Y, He Q, Han W, Chen P, Wang X, Liang S. 2010. Evaluation and optimization of removal of an acid-insoluble surfactant for shotgun analysis of membrane proteome. Electrophoresis 31:2705-2713.
23. Cox J, Mann M. 2008. MaxQuant enables high peptide identification rates, individualized ppb-range mass accuracies and proteome-wide protein quantification. Nat Biotechnol 26:1367-1372.
24. Dallas DC, Guerrero A, Parker EA, Robinson RC, Gan J, German JB, Barile D, Lebrilla CB. 2015. Current peptidomics: Applications, purification, identification, quantification, and functional analysis. Proteomics 15:1026-1038.
25. Szklarczyk D, Morris JH, Cook H, Kuhn M, Wyder S, Simonovic M, Santos A, Doncheva NT, Roth A, Bork P. 2016. The STRING database in 2017: quality-controlled protein–protein association networks, made broadly accessible. Nucleic Acids Res 45:D362-D368.
26. Shannon P, Markiel A, Ozier O, Baliga NS, Wang JT, Ramage D, Amin N, Schwikowski B, Ideker T. 2003. Cytoscape: A software environment for integrated models of biomolecular interaction networks. Genome Res 13:2498-2504.
27. Kirwan JA, Weber RJ, Broadhurst DI, Viant MR. 2014. Direct infusion mass spectrometry metabolomics dataset: a benchmark for data processing and quality control. Sci Data 1:140012.
28. Pattanaik P, Jain B, Ravindra G, Gopi HN, Pal PP, Balaram H, Balaram P. 2003. Stage-specific profiling of *Plasmodium falciparum* proteases using an internally quenched multispecificity protease substrate. Biochem Biophys Res Commun 309:974-979.
29. Dogovski C, Xie SC, Burgio G, Bridgford J, Mok S, McCaw JM, Chotivanich K, Kenny S, Gnädig N, Straimer J, Bozdech Z, Fidock DA, Simpson JA, Dondorp AM, Foote S, Klonis N, Tilley L. 2015. Targeting the cell stress response of *Plasmodium falciparum* to overcome artemisinin resistance. PLoS Biol 13:e1002132.
30. Sanman LE, Bogyo M. 2014. Activity-based profiling of proteases. Annu Rev Biochem 83:249-273.

31. Edgington LE, Verdoes M, Bogyo M. 2011. Functional imaging of proteases: recent advances in the design and application of substrate-based and activity-based probes. Curr Opin Chem Biol 15:798-805.
32. Xie SC, Dogovski C, Hanssen E, Chiu F, Yang T, Crespo MP, Stafford C, Batinovic S, Teguh S, Charman S, Klonis N, Tilley L. 2016. Haemoglobin degradation underpins the sensitivity of early ring stage *Plasmodium falciparum* to artemisinins. J Cell Sci 129:406-416.
33. Greenbaum DC, Baruch A, Grainger M, Bozdech Z, Medzihradszky KF, Engel J, DeRisi J, Holder AA, Bogyo M. 2002. A role for the protease falcipain 1 in host cell invasion by the human malaria parasite. Science 298:2002-2006.
34. Stolze SC, Deu E, Kaschani F, Li N, Florea BI, Richau KH, Colby T, van der Hoorn RA, Overkleeft HS, Bogyo M. 2012. The antimalarial natural product symplostatin 4 is a nanomolar inhibitor of the food vacuole falcipains. Chem Biol 19:1546-1555.
35. Deu E, Chen IT, Lauterwasser EM, Valderramos J, Li H, Edgington LE, Renslo AR, Bogyo M. 2013. Ferrous iron-dependent drug delivery enables controlled and selective release of therapeutic agents *in vivo*. Proc Natl Acad Sci U S A 110:18244-18249.
36. Deu E, Leyva MJ, Albrow VE, Rice MJ, Ellman JA, Bogyo M. 2010. Functional studies of *Plasmodium falciparum* dipeptidyl aminopeptidase I using small molecule inhibitors and active site probes. Chem Biol 17:808-819.
37. Deu E, Verdoes M, Bogyo M. 2012. New approaches for dissecting protease functions to improve probe development and drug discovery. Nat Struct Mol Biol 19:9-16.
38. Segal E, Prestwood TR, van der Linden WA, Carmi Y, Bhattacharya N, Withana N, Verdoes M, Habtezion A, Engleman EG, Bogyo M. 2015. Detection of intestinal cancer by local, topical application of a quenched fluorescence probe for cysteine cathepsins. Chem Biol 22:148-158.
39. Kasperkiewicz P, Poreba M, Snipas SJ, Parker H, Winterbourn CC, Salvesen GS, Drag M. 2014. Design of ultrasensitive probes for human neutrophil elastase through hybrid combinatorial substrate library profiling. Proc Natl Acad Sci U S A 111:2518-2523.
40. Sherman IW, Tanigoshi L. 1970. Incorporation of 14 C-amino-acids by malaria (*Plasmodium lophurae*) IV. *In vivo* utilization of host cell haemoglobin. Int J Biochem 1:635-637.
41. Lew VL, Tiffert T, Ginsburg H. 2003. Excess hemoglobin digestion and the osmotic stability of *Plasmodium falciparum*–infected red blood cells. Blood 101:4189-4194.

42. Krugliak M, Zhang J, Ginsburg H. 2002. Intraerythrocytic *Plasmodium falciparum* utilizes only a fraction of the amino acids derived from the digestion of host cell cytosol for the biosynthesis of its proteins. Mol Biochem Parasitol 119:249-256.
43. Francis SE, Sullivan Jr DJ, Goldberg, E D. 1997. Hemoglobin metabolism in the malaria parasite *Plasmodium falciparum*. Annu Rev Microbiol 51:97-123.
44. Meshnick SR, Thomas A, Ranz A, Xu CM, Pan HZ. 1991. Artemisinin (qinghaosu): the role of intracellular hemin in its mechanism of antimalarial action. Mol Biochem Parasitol 49:181-189.
45. Gruring C, Spielmann T. 2012. Imaging of live malaria blood stage parasites. Methods Enzymol 506:81-92.
46. Orjih AU, Fitch CD. 1993. Hemozoin production by *Plasmodium falciparum*: variation with strain and exposure to chloroquine. BBA-Gen Subjects 1157:270-274.
47. Abu Bakar N, Klonis N, Hanssen E, Chan C, Tilley L. 2010. Digestive-vacuole genesis and endocytic processes in the early intraerythrocytic stages of *Plasmodium falciparum*. J Cell Sci 123:441-450.
48. Cigić B, Križaj I, Kralj B, Turk V, Pain RH. 1998. Stoichiometry and heterogeneity of the pro-region chain in tetrameric human cathepsin C. Biochim Biophys Acta Protein Struct Mol Enzymol 1382:143-150.
49. Klemba M, Gluzman I, Goldberg DE. 2004. A *Plasmodium falciparum* dipeptidyl aminopeptidase I participates in vacuolar hemoglobin degradation. J Biol Chem 279:43000-43007.
50. Gulati S, Ekland EH, Ruggles KV, Chan RB, Jayabalasingham B, Zhou B, Mantel P-Y, Lee MC, Spottiswoode N, Coburn-Flynn O. 2015. Profiling the essential nature of lipid metabolism in asexual blood and gametocyte stages of *Plasmodium falciparum*. Cell Host Microbe 18:371-381.
51. Pessi G, Choi J-Y, Reynolds JM, Voelker DR, Mamoun CB. 2005. *In vivo* evidence for the specificity of *Plasmodium falciparum* phosphoethanolamine methyltransferase and its coupling to the Kennedy pathway. J Biol Chem 280:12461-12466.
52. Pessi G, Kociubinski G, Mamoun CB. 2004. A pathway for phosphatidylcholine biosynthesis in *Plasmodium falciparum* involving phosphoethanolamine methylation. Proc Natl Acad Sci U S A 101:6206-6211.
53. Elabbadi N, Ancelin ML, Vial H. 1997. Phospholipid metabolism of serine in *Plasmodium*-infected erythrocytes involves phosphatidylserine and direct serine decarboxylation. Biochem J 324:435.

54. O'Neill PM, Posner GH. 2004. A medicinal chemistry perspective on artemisinin and related endoperoxides. J Med Chem 47:2945-2964.
55. Hartwig CL, Lauterwasser EMW, Mahajan SS, Hoke JM, Cooper RA, Renslo AR. 2011. Investigating the antimalarial action of 1,2,4-trioxolanes with fluorescent chemical probes. J Med Chem 54:8207-8213.
56. Hartwig CL, Rosenthal AS, D'Angelo J, Griffin CE, Posner GH, Cooper RA. 2009. Accumulation of artemisinin trioxane derivatives within neutral lipids of *Plasmodium falciparum* malaria parasites is endoperoxide-dependent. Biochem Pharmacol 77:322-336.
57. del Pilar Crespo M, Avery TD, Hanssen E, Fox E, Robinson TV, Valente P, Taylor DK, Tilley L. 2008. Artemisinin and a series of novel endoperoxide antimalarials exert early effects on digestive vacuole morphology. Antimicrob Agents Chemother 52:98-109.
58. Berman PA, Adams PA. 1997. Artemisinin enhances heme-catalysed oxidation of lipid membranes. Free Radic Biol Med 22:1283-1288.
59. Bousejra-El Garah F, Wong MH-L, Amewu RK, Muangnoicharoen S, Maggs JL, Stigliani J-L, Park BK, Chadwick J, Ward SA, O'Neill PM. 2011. Comparison of the reactivity of antimalarial 1, 2, 4, 5-tetraoxanes with 1, 2, 4-trioxolanes in the presence of ferrous iron salts, heme, and ferrous iron salts/phosphatidylcholine. J Med Chem 54:6443-6455.
60. Ancelin ML, Vial HJ. 1989. Regulation of phosphatidylcholine biosynthesis in *Plasmodium*-infected erythrocytes. Biochim Biophys Acta Lipids Lipid Metab 1001:82-89.
61. Maheshwari S, Lavigne M, Contet A, Alberge B, Pihan E, Kocken C, Wengelnik K, Douguet D, Vial H, Cerdan R. 2013. Biochemical characterization of *Plasmodium falciparum* CTP: phosphoethanolamine cytidylyltransferase shows that only one of the two cytidylyltransferase domains is active. Biochem J 450:159-167.
62. Vielemeyer O, McIntosh MT, Joiner KA, Coppens I. 2004. Neutral lipid synthesis and storage in the intraerythrocytic stages of *Plasmodium falciparum*. Mol Biochem Parasitol 135:197-209.
63. Hoang AN, Sandlin RD, Omar A, Egan TJ, Wright DW. 2010. The neutral lipid composition present in the digestive vacuole of *Plasmodium falciparum* concentrates heme and mediates β-hematin formation with an unusually low activation energy. Biochemistry 49:10107-10116.

64. Jackson KE, Klonis N, Ferguson DJ, Adisa A, Dogovski C, Tilley L. 2004. Food vacuole-associated lipid bodies and heterogeneous lipid environments in the malaria parasite, *Plasmodium falciparum*. Mol Microbiol 54:109-122.

65. Pisciotta JM, Coppens I, Tripathi AK, Scholl PF, Shuman J, Bajad S, Shulaev V, Sullivan DJ, Jr. 2007. The role of neutral lipid nanospheres in *Plasmodium falciparum* haem crystallization. Biochem J 402:197-204.

66. Meshnick SR, Yang YZ, Lima V, Kuypers F, Kamchonwongpaisan S, Yuthavong Y. 1993. Iron-dependent free radical generation from the antimalarial agent artemisinin (qinghaosu). Antimicrob Agents Chemother 37:1108-1114.

67. Cheng Z, Li Y. 2007. What is responsible for the initiating chemistry of iron-mediated lipid peroxidation: an update. Chem Rev 107:748-766.

68. Belen Cassera M, Zhang Y, Z Hazleton K, L Schramm V. 2011. Purine and pyrimidine pathways as targets in *Plasmodium falciparum*. Curr Top Med Chem 11:2103-2115.

69. Mok S, Ashley EA, Ferreira PE, Zhu L, Lin Z, Yeo T, Chotivanich K, Imwong M, Pukrittayakamee S, Dhorda M, Nguon C, Lim P, Amaratunga C, Suon S, Hien TT, Htut Y, Faiz MA, Onyamboko MA, Mayxay M, Newton PN, Tripura R, Woodrow CJ, Miotto O, Kwiatkowski DP, Nosten F, Day NP, Preiser PR, White NJ, Dondorp AM, Fairhurst RM, Bozdech Z. 2015. Drug resistance. Population transcriptomics of human malaria parasites reveals the mechanism of artemisinin resistance. Science 347:431-435.

70. Wek RC, Jiang H-Y, Anthony TG. 2006. Coping with stress: eIF2 kinases and translational control. Biochem Soc Trans 34:7-11.

71. Gosline SJ, Nascimento M, McCall L-I, Zilberstein D, Thomas DY, Matlashewski G, Hallett M. 2011. Intracellular eukaryotic parasites have a distinct unfolded protein response. PloS One 6:e19118.

72. Tilley L, Straimer J, Gnädig NF, Ralph SA, Fidock DA. 2016. Artemisinin action and resistance in *Plasmodium falciparum*. Trends Parasitol 32:682-696.

73. Paloque L, Ramadani AP, Mercereau-Puijalon O, Augereau J-M, Benoit-Vical F. 2016. *Plasmodium falciparum*: multifaceted resistance to artemisinins. Malar J 15:149.

74. Chaubey S, Grover M, Tatu U. 2014. Endoplasmic reticulum stress triggers gametocytogenesis in the malaria parasite. J Biol Chem 289:16662-16674.

75. Ponts N, Saraf A, Chung D-WD, Harris A, Prudhomme J, Washburn MP, Florens L, Le Roch KG. 2011. Unraveling the ubiquitome of the human malaria parasite. J Biol Chem 286:40320-40330.

76. Aminake MN, Arndt H-D, Pradel G. 2012. The proteasome of malaria parasites: A multi-stage drug target for chemotherapeutic intervention? Int J Parasitol Drugs Drug Resist 2:1-10.

77. Wilson DW, Langer C, Goodman CD, McFadden GI, Beeson JG. 2013. Defining the timing of action of antimalarial drugs against *Plasmodium falciparum*. Antimicrob Agents Chemother 57:1455-1467.

# Chapter 5

# Biochemical impact of peroxide antimalarials on *K13*-mutant artemisinin resistant and sensitive *P. falciparum* parasites

## 5.1 ABSTRACT

The emergence and spread of *P. falciparum* parasites that are resistant to first-line artemisinin-based combination therapies threatens worldwide malaria control efforts. Closely related ozonide antimalarials also display cross-resistance *in vitro* and OZ439, an ozonide in advanced stages of clinical development, has shown reduced efficacy in combination with piperaquine when deployed in areas where artemisinin resistant parasites are endemic. This study investigated the biochemical response of paired *K13*-mutant artemisinin resistant (Cam3.II$^{R539T}$) and sensitive (Cam3.II$^{rev}$) parasites to the clinically-used artemisinin derivative, DHA, and the ozonide antimalarials, OZ277 and OZ439, using an untargeted metabolomics approach. In both the resistant and sensitive lines, all three peroxides caused disruption to peptide metabolism manifested as a reduction in the abundance of peptides derived from haemoglobin. Drug-induced depletion of haemoglobin-derived peptides was more pronounced in the sensitive line than resistant. Elevated gamma–glutamylcysteine suggests enhanced antioxidant capacity in resistant parasites, and several non-haemoglobin-derived peptides were also perturbed in response to peroxide exposure in resistant parasites but were unchanged in the sensitive line. This work highlights the differential biochemical response of artemisinin resistant and sensitive parasites to pulsed *in vitro* peroxide exposure and emphasises the role of altered peptide metabolism in the mechanism of action and resistance for this important class of antimalarials.

## 5.2 INTRODUCTION

Artemisinin-based combination therapies (ACTs) are the first line treatment for *P. falciparum* malaria and have contributed significantly to the reduction in malaria incidence and mortality since the start of this century (1). A decade after the implementation of artemisinin-based treatments for clinical use, resistance emerged in a malaria endemic area on the Thailand/Cambodia border (2) and has rapidly spread throughout the Greater Mekong Sub-region (3). The spread of artemisinin resistant *P. falciparum* parasites is leading to increasing rates of ACT failure in South East Asia and is threatening ongoing efforts to eradicate malaria.

Clinically, artemisinin resistance manifests as a delay in parasite clearance time following ACT treatment (2) and is associated with increased survival of ring stage parasites after short term exposure to artemisinins *in vitro* (4). A molecular marker for artemisinin resistance has been mapped to the *P. falciparum K13* locus (5) and is associated with *in vitro* and *in vivo* resistance to artemisinins (6, 7). Several different single nucleotide polymorphisms have been found in *K13* (6, 8-10), however, only a small proportion of the 186 known *K13* alleles in Asia are associated with resistance (3, 11-13). The most prevalent *K13* polymorphisms that are validated artemisinin resistance mutations in South East Asia are C580Y, R539T and Y493H (10).

*P. falciparum* parasites that harbor a resistance-causing *K13* mutation are generally thought to overcome artemisinin-induced insult by mounting an enhanced stress response (14). Population transcriptomic analysis implicated genes responsible for protein folding and repair, and oxidative stress in the artemisinin resistance mechanism (15). Furthermore, global metabolomic analysis supports the hypothesis that resistant parasites are more resilient to drug induced oxidative damage, revealing an increased abundance of the main parasite antioxidant, glutathione, and its precursor, gamma-glutamylcysteine (16). A reduction in the abundance of haemoglobin-derived peptides also accompanied artemisinin resistance, indicating that these

parasites may have impaired haemoglobin uptake or digestion (16), potentially producing lower levels of haemoglobin-derived haem, which is necessary for peroxide bond activation.

In *K13*-mutant resistant parasites, the duration of ozonide exposure necessary for effective killing was reported to be greater than in *K13*-wildtype lines (17), indicating *K13* mutations also confer cross-resistance to the ozonides (18-20). The degree of *in vitro* parasite susceptibility may also depend on the type of *K13* mutation, with the level of cross resistance appearing to be greatest in parasites with the I543T mutation relative to other *K13* alleles (C580Y, R539T) (20). Longer lived peroxides, such as OZ439, may be less affected by the mechanisms that mediate artemisinin resistance (17, 19-21). However, recent clinical data suggests that OZ439 with piperaquine is less effective at curing patients infected with artemisinin resistant parasites (22), although a role for piperaquine resistance in these results cannot be ruled out.

The aim of the current study was to investigate the comparative degradation rates of peroxide antimalarials in paired *K13*-mutant artemisinin resistant and sensitive parasites as an indicator of peroxide bond activation, and to assess the global parasite metabolic response to pulsed *in vitro* ozonide and DHA exposure.

# 5.3 MATERIALS AND METHODS

## 5.3.1 Culturing of parasites and synchronisation

Asexual *P. falciparum* parasites were cultured as described in Chapter 3 (Section 3.3.2). The artemisinin resistant and sensitive *P. falciparum* isolates used in this study were kindly provided by Professor David Fidock, Columbia University and included the common *K13*-mutant, Cam3.II$^{R539T}$, and the *K13*-wildtype on an isogenic background (Cam3.II$^{rev}$) (13).

## 5.3.2 Parasite-mediated drug degradation

### 5.3.2.1 Sample preparation

To assess ozonide stability, *P. falciparum* infected and non-infected RBCs were prepared as previously described (23), with minor modifications. The apparent rate of OZ277, OZ439 and DHA degradation was quantified in tightly synchronised ring (8-12 h post invasion), early-trophozoite (18-24 h post invasion) and mid-trophozoite (30-34 h post invasion) parasite cultures adjusted to 4% parasitaemia. Parasite incubations with drug were performed at 10% and 35% Hct in trophozoite and ring stage studies, respectively. Non-infected RBC control cultures at the same Hct were also analysed. In all experiments, the starting concentration of drug was 100 nM. For each asexual *P. falciparum* stage tested (ring, early trophozoite and late trophozoite) biological replicates were independently prepared using different cultures on separate days.

### 5.3.2.2 LC-MS analysis

Samples were assayed for intact drug concentrations on a Shimadzu 8050 triple quadrupole MS, coupled with a Shimadzu HPLC system, as previously described (23), with minor modification to the solvent composition. Solvent A consisted of Milli-Q water with 0.1%

formic acid and solvent B was acetonitrile with 0.1% formic acid. Analytical separation and MS parameters were unchanged (23).

Data were acquired and processed using the Lab solutions software with analyte concentrations determined by comparison with freshly prepared calibration standards (23). Experimental degradation data were fit to a first-order exponential decay function, based on initial rates, and degradation half-lives were calculated in Microsoft Excel. Statistical comparisons between artemisinin sensitive and resistant lines utilised Student's *t*-test ($\alpha = 0.05$).

## 5.3.3 Metabolomics experiments

### 5.3.3.1 Parasite treatment and sample preparation

Prior to incubation with drug, the age of paired artemisinin sensitive and resistant parasites was confirmed by analysis of Giemsa stained thin blood smears and the parasitaemia and Hct were adjusted to 4% and 2%, respectively. In Chapter 4, DHA, OZ277 and OZ439 were shown to cause a temporal biochemical response in parasites, whereby DHA induced the most rapid impact, followed by OZ277 and OZ439. For the metabolomics experiments conducted in this study, a concentration of 100 nM was used for each drug and exposure times of 1, 3 and 5 h were selected for DHA, OZ277 and OZ439, respectively. Under the conditions used in this metabolomics study (4% parasitaemia and 2% Hct), these concentrations and exposure times were previously found to be sub-lethal in both the Cam3.II$^{R539T}$ and Cam3.II$^{rev}$ parasite lines (unpublished data).

Early trophozoite stage parasite cultures were incubated under the aforementioned conditions at 37 °C and after the designated drug incubation time, metabolites were extracted from the washed cell pellets (1 x $10^8$ cells) as described in Chapter 4 (Section 4.3.3.1), with ice cold methanol (containing 1 μM of the internal standards CAPS, CHAPS, PIPES and TRIS) as

the extraction solvent. Infected parasite cultures that were incubated with an equivalent volume of DMSO acted as the untreated control. Non-infected RBC control cultures (2% Hct) incubated with drug or DMSO were also prepared and metabolites were extracted in the same way as the infected cultures. A pooled biological quality control (PBQC) sample was also prepared as previously described (Chapter 4, Section 4.3.3.1). All samples were stored in glass LC-MS vials at -80°C until LC-MS analysis.

### 5.3.3.2 LC-MS analysis and data processing

Metabolomics samples were analysed by LC coupled with high resolution MS and the resulting data analysed according to the methods described in Chapter 4 (Section 4.3.3.2), with minor modifications. Metabolite abundances were normalised to the median peak intensity and univariate statistical analysis performed (Welch's *t* test), both using IDEOM. The peak areas for metabolites of interest were confirmed by manual integration of raw LC-MS data using TraceFinder (ThermoFisher). For peptides that were found to be altered by ≥ 1.5-fold following peroxide treatment and the previously identified artemisinin resistance-associated metabolites (16), one-way analysis of variance (ANOVA) ($\alpha = 0.05$) for multiple comparison and post hoc analysis using the Tukey test was applied to identify significant changes between the treated and untreated control samples in the Cam3.II$^{R539T}$ and Cam3.II$^{rev}$ parasite lines.

# 5.4 RESULTS

## 5.4.1 Peroxide degradation in artemisinin resistant and sensitive parasites

To investigate whether the rate of peroxide activation is different in artemisinin resistant (Cam3.II$^{R539T}$) compared to sensitive (Cam3.II$^{rev}$) parasites, degradation rates for DHA, OZ277 and OZ439 were quantified at different parasite stages. No notable differences in degradation rate were observed between artemisinin resistant and sensitive isolates at the ring stage, which is the stage associated with the greatest level of *in vitro* resistance (14, 17, 24). Likewise, no significant difference in the degradation rates between sensitive and resistant parasites were observed for OZ277, OZ439 or DHA in either early or mid-trophozoite stage parasites (Table 1).

**Table 1:** Degradation half-lives of OZ277, OZ439 and DHA in ring, early trophozoite and mid trophozoite stage Cam3.II$^{R539T}$ and Cam3.II$^{rev}$ parasite lines [a].

| | **Half-life (h)** | | | | | |
|---|---|---|---|---|---|---|
| | **Ring [b]** | | **Early trophozoite [c]** | | **Mid trophozoite [b]** | |
| | Cam3.II$^{R539T}$ | Cam3.II$^{rev}$ | Cam3.II$^{R539T}$ | Cam3.II$^{rev}$ | Cam3.II$^{R539T}$ | Cam3.II$^{rev}$ |
| OZ277 | 0.7, 0.9 | 0.7, 1.0 | 1.1 ± 0.2 | 0.8 ± 0.3 | 0.9, 1.0 | 0.9, 1.0 |
| OZ439 | 9.5, 12.8 | 10.8, 13.8 | 8.8 ± 9.1 | 6.9 ± 6.7 | 2.0, 1.9 | 2.5, 3.0 |
| DHA | 1.2, 1.3 | 1.0, 1.6 | 2.3 ± 1.4 | 1.4 ± 0.7 | 0.9, 1.1 | 1.0, 1.3 |

[a] For the half-life determinations, the starting concertation of drug was 100 nM and experiments were performed at 4% parasitaemia and 35% (ring stage) or 10% (trophozoite stage) Hct.

[b] Values represent the half-lives from two independent experiments.

[c] Values represent the mean half-life ± standard deviations of three independent experiments and, for each drug, statistical comparisons between Cam3.II$^{R539T}$ and Cam3.II$^{rev}$ lines utilised Student's *t*-test ($\alpha = 0.05$).

## 5.4.2 Metabolic response of artemisinin resistant and sensitive parasites to peroxide treatment

An untargeted metabolomics study was employed to determine the metabolic response of paired artemisinin resistant (Cam3.II$^{R539T}$) and sensitive (Cam3.II$^{rev}$) *P. falciparum* parasites to *in vitro* treatment with the ozonide antimalarials, OZ277 and OZ439, as well as the clinically-used artemisinin derivative, DHA. Although differential parasite susceptibility is greatest at the early ring stage (14, 17, 24), difficulties were encountered in reproducibly detecting parasite-associated metabolite features above the host RBC background in the ring stages. Therefore, this study focused on early trophozoites, which still exhibit a measurable difference in *in vitro* susceptibility to pulsed peroxide exposure (14, 17, 24). Overall, more than 750 metabolites from a range of metabolite classes were reproducibly detected and putatively identified (supplementary material: Appendix 6).

### 5.4.2.1 Alterations to basal peptide levels in artemisinin resistant parasites

In Chapter 4 (Sections 4.4.1 and 4.4.2) it was found that substantial depletion of short-chain peptides was the first metabolic disturbance following peroxide antimalarial treatment in the 3D7 *P. falciparum* parasite strain. In the current study, the resistance-causing *K13* mutation R539T was found to be associated with altered peptide metabolism even in the absence of drug treatment. Manual integration of LC-MS data for all putatively identified peptide features confirmed that 20% of peptides were significantly lower in abundance in the resistant line compared to the sensitive (Figure 1A), while 16% of peptides were found to be significantly increased (Figure 1B).

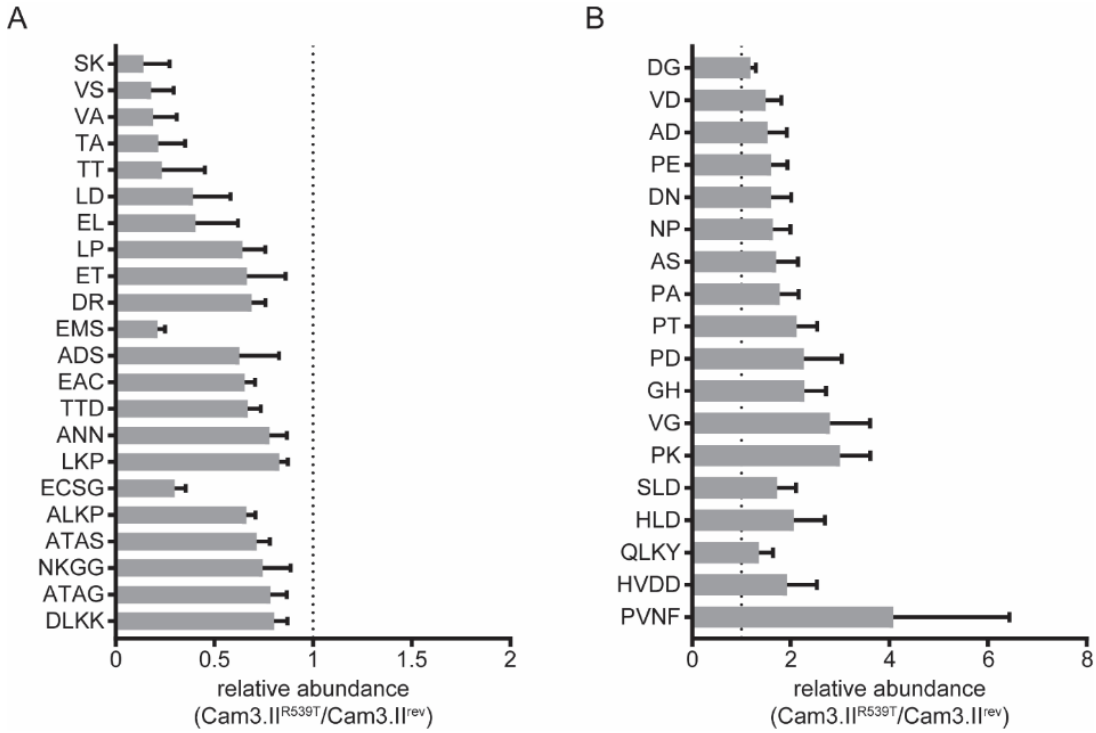


**Figure 1:** Differentially abundant peptides in artemisinin resistant (Cam3.II$^{R539T}$) versus artemisinin sensitive (Cam3.II$^{rev}$) parasite infected RBCs. Relative abundance (mean peak area ± SD of five biological replicates) of peptides that were significantly depleted (A) and significantly elevated (B) (p-value < 0.05) in the *K13*-mutant artemisinin resistant parasite line (Cam3.II$^{R539T}$) expressed relative to the *K13*-wildtype artemisinin sensitive parasite line (Cam3.II$^{rev}$).

### 5.4.2.2 Peroxide-induced alterations in peptide metabolism

Metabolomics analysis revealed that incubation with 100 nM of each peroxide antimalarial (OZ277, OZ439 and DHA) only had a modest impact on *P. falciparum* metabolism under the conditions tested. In both the resistant and sensitive parasite lines, only around 2.5% of all putative metabolites identified were significantly perturbed by peroxide exposure (p-value < 0.05). Out of the metabolic pathways where more than 20 metabolites were putatively identified, the peptide class showed the greatest proportion of significant drug-induced changes (Figure 2). Approximately 4.5%, of the 109 detected peptides were

significantly altered by drug treatment in the resistant and sensitive lines relative to the respective untreated controls. In both lines, DHA and OZ277 were responsible for the greatest proportion of significant peptide changes, followed by OZ439 (Figure 2). The apparent disproportionate change to nucleotide metabolism (16 metabolites identified) in the sensitive line following OZ277 treatment was due to one metabolite, ADP, which was only 25% lower in OZ277-treated sensitive parasites. Given that peroxide exposure predominantly disrupted peptide metabolism in the 3D7 *P. falciparum* parasite strain (Chapter 4), and that the metabolite pathway enrichment analysis suggested that the major impact of drug treatment involved peptide metabolism, detailed analysis in the current study focused primarily on the peptide class.

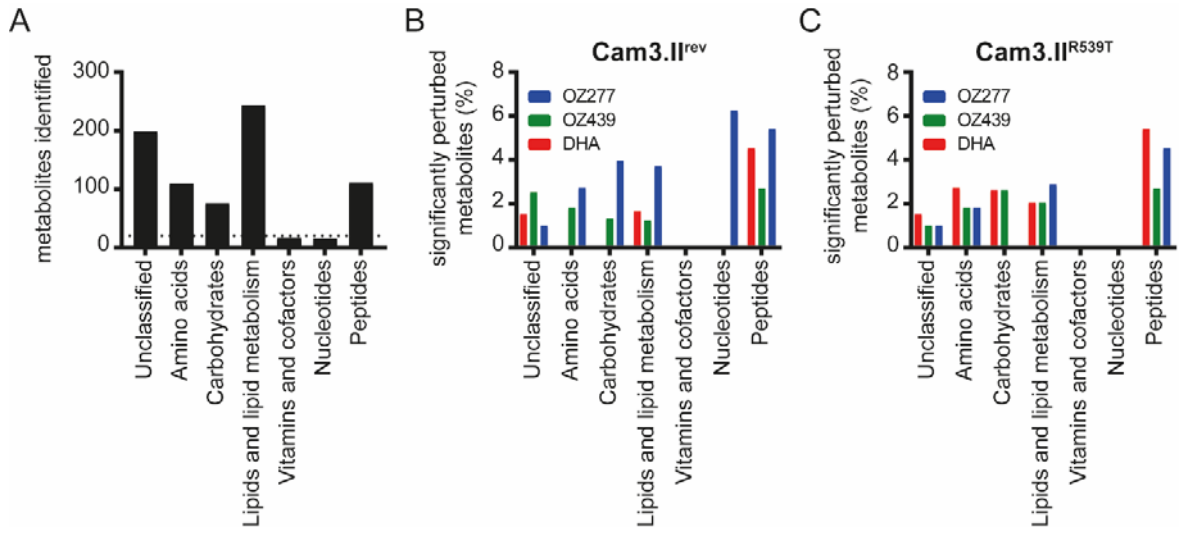


**Figure 2:** Enrichment analysis of the Cam3.II$^{rev}$ and Cam3.II$^{R539T}$ metabolic pathways affected by peroxide antimalarial treatment. (A) The number of metabolites identified in each metabolite class after treatment of early trophozoite stage *P. falciparum* parasites with OZ277, OZ439 and DHA. The dotted line is the 20 metabolite threshold. (B) Pathway enrichment analysis showing the percentage of significantly perturbed metabolites (Welch's *t* test; p-value < 0.05) as a function of metabolite class in the *K13*-wildtype artemisinin sensitive line (Cam3.II$^{rev}$). (C) Pathway enrichment analysis showing the percentage of significantly perturbed metabolites (Welch's *t* test; p-value < 0.05) as a function of metabolite class in the *K13*-mutant artemisinin resistant line (Cam3.II$^{R539T}$).

A targeted analysis of the LC-MS raw data identified 26 peptides for which abundance differed by more than 1.5-fold in drug-exposed parasites compared to control in either the resistant or sensitive parasite lines (Figure 3). Although not all differentially abundant peptides reached statistical significance (testing for significance at $\alpha = 0.05$, one-way ANOVA with Tukey's post-hoc), in the sensitive line, a drug-induced increase in the abundance of only two peptides was apparent, while the majority (> 70%) of differentially abundant peptides were depleted compared to the DMSO control (Figure 3A). The same trend was also apparent following peroxide treatment in the resistant line (Figure 3B). Interestingly, the extent of peptide depletion was greater in the sensitive parasite cultures than in the resistant. This was apparent for 17 out of the 20 peptides that were decreased in abundance following peroxide treatment in the sensitive line (Figure 3) and was not seen with any other metabolite class.

Notably, all except two of the peptides showing a decreased abundance after treatment of the sensitive line could be mapped to either the alpha or beta chains of haemoglobin (Figure 4). The two peptides that did not map to haemoglobin were putatively identified as Ala-Gly-Pro (AGP) and Asp-Ser-Ser (DSS). It is possible that these LC-MS features represent isomeric peptides, but no isomers of AGP and DSS were able to be mapped to haemoglobin. The peptides Glu-Ser (ES, MS/MS confirmed), which was depleted to the same extent in both parasite lines after peroxide treatment, and Glu-Lys (EK, putative identification), which was only depleted following treatment with OZ277, were also mapped to haemoglobin. The peptide putatively identified as Phe-Cys-Arg (FCR), which was unique in that it was depleted by peroxide treatment in the resistant line but unchanged in the sensitive line, was not haemoglobin-derived (potential isomers of FCR are also not haemoglobin-derived). Out of the peptides that were increased in abundance following peroxide treatment in the resistant (SK, TT, EMS and AMDY) and sensitive lines (CMFT and QFQH), only Thr-Thr (TT) and Ser-Lys

(SK, or its isomer) could be mapped to haemoglobin. The masses of these increased peptides did not correspond to any other metabolites known to be present in *P. falciparum*.

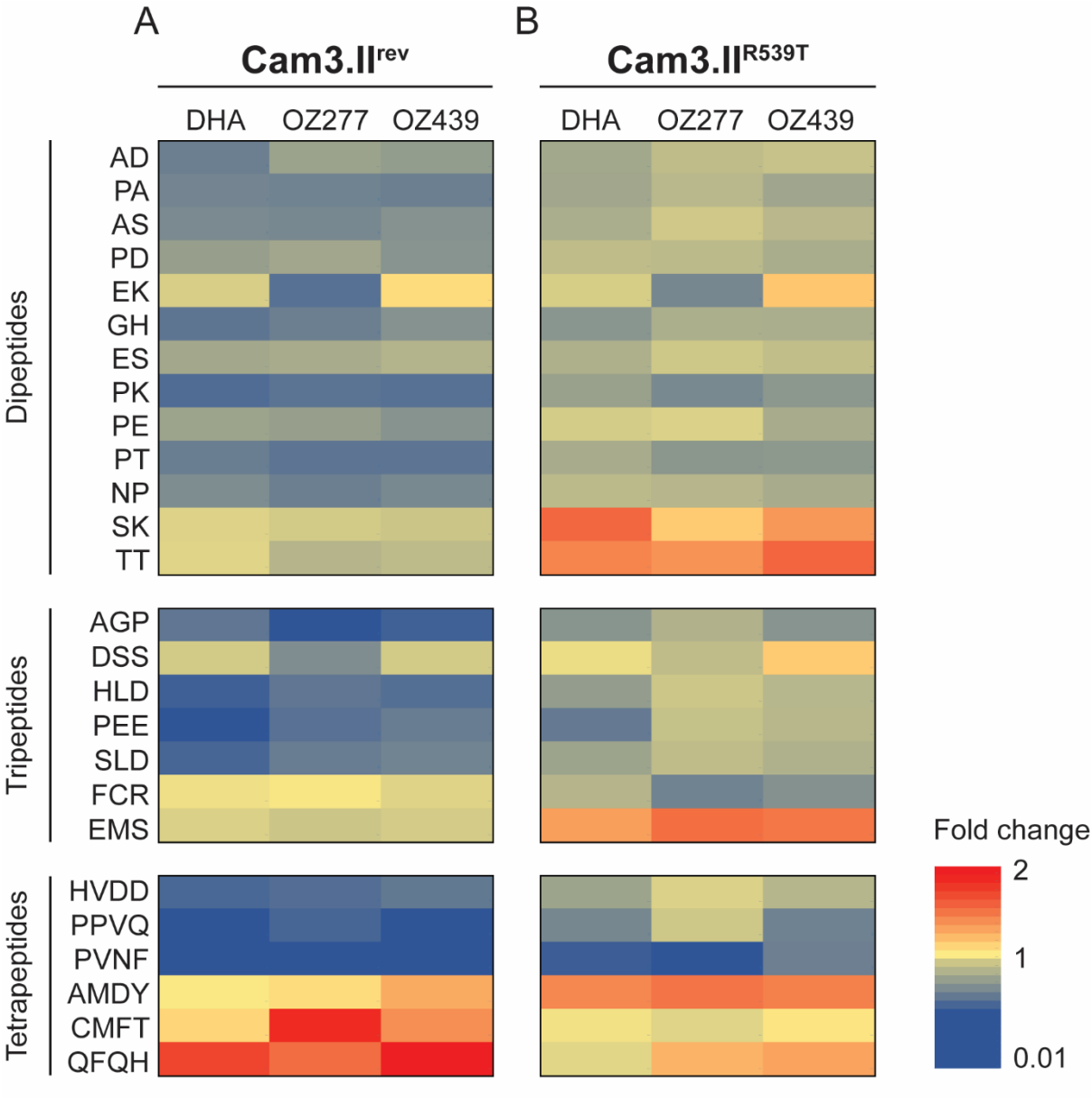


**Figure 3:** Peroxide-induced alterations in peptide abundance. Heatmap of the peptides that were altered in abundance (≥ 1.5-fold relative to the untreated control) following peroxide treatment in the *K13*-wildtype artemisinin sensitive (Cam3.II$^{rev}$) (A) and *K13*-mutant artemisinin resistant (Cam3.II$^{R539T}$) (B) parasite lines. Data shown are the average for three or five biological replicates expressed relative to the average for the untreated control from the same parasite line.

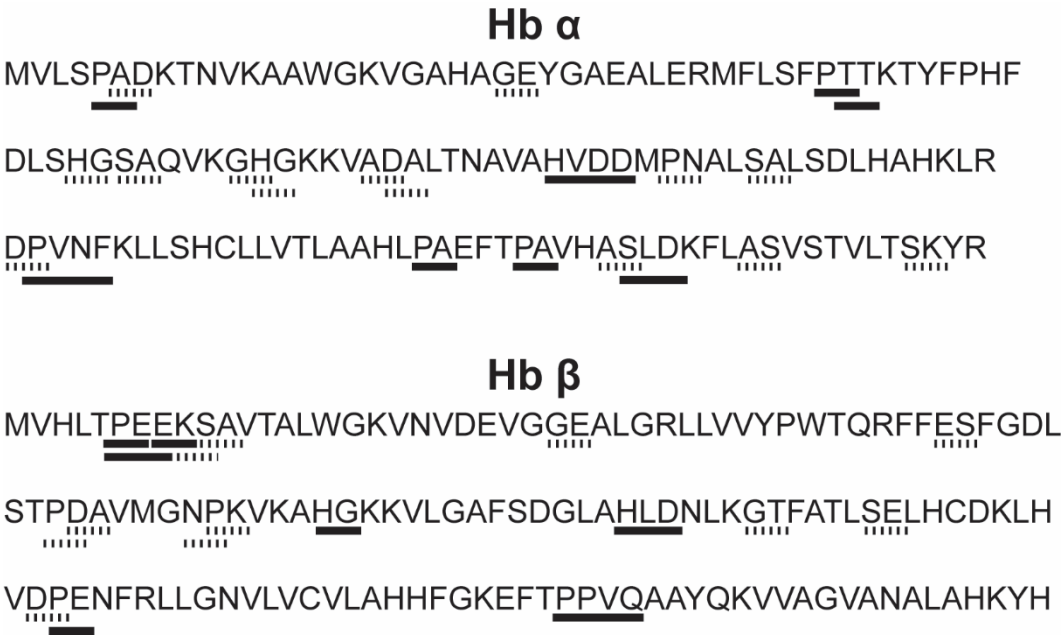


**Figure 4:** Sequence coverage for putative haemoglobin (Hb)-derived peptides that were altered in abundance following peroxide antimalarial treatment relative to the untreated control. All peptides, except TT and SK (or its isomer) were reduced in abundance compared to control levels. The solid black bars represent peptide sequences that were confirmed by MS/MS analysis of *P. falciparum* metabolite extracts and the dashed bars represent putative peptide sequences. For putative peptide sequences, all potential isomers have been mapped.

Interestingly, most (75%) of the peptides showing greater depletion in sensitive relative to resistant parasites after peroxide exposure were also found to have significantly (p-value < 0.05) higher basal levels in the *K13*-resistant line (Figures 1 and 5). The remaining 25% of peptides that were depleted to a greater extent in sensitive parasites also appeared to be present at higher base-line levels in resistant parasites (Figure 5), although the difference was not statistically significant. In general, following treatment of the resistant line, the abundance of these same peptides remained higher than the basal level that was detected in untreated (DMSO) sensitive parasites (Figure 5).

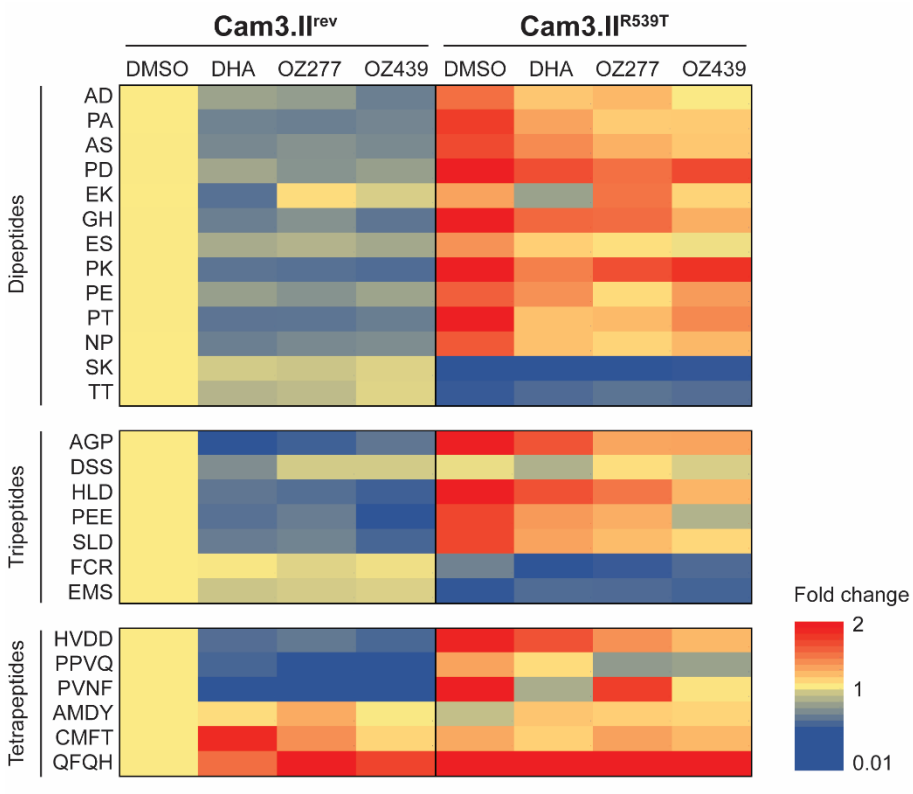


**Figure 5:** Elevated levels of differentially abundant peptides in the Cam3.II$^{R539T}$ parasite line. Heatmap of the peptides that were altered in abundance (≥ 1.5-fold relative to the untreated control) following peroxide or DMSO treatment in the *K13*-mutant artemisinin resistant (Cam3.II$^{R539T}$) and *K13*-wildtype artemisinin sensitive (Cam3.II$^{rev}$) parasite lines. Data shown are the average for three or five biological replicates expressed relative to the average for the untreated control from the sensitive parasite line (DMSO, Cam3.II$^{rev}$).

### 5.4.2.3 Peroxide-induced alterations of known resistance-associated metabolites

*K13*-mediated artemisinin resistance was previously shown to be associated with an accumulation of the metabolites, glutathione, gamma-glutamylcysteine and NAD+ and a depletion of L-proline amide (16). A targeted analysis of these specific metabolites confirmed a 4-fold increase in basal levels of gamma-glutamylcysteine (Figure 6A) and a 50% reduction in basal L-proline amide abundance (Figure 6B) in the resistant parasites compared to the isogenic sensitive control line. However, no significant differences in basal glutathione (Figure

6C) or NAD+ (Figure 6D) abundance were detected under the conditions used in this study. Following drug exposure, average gamma-glutamylcysteine levels showed a trend towards increased abundance (1.3-2.8-fold) relative to the DMSO control parasites in the sensitive line (Figure 6A), but these differences were not statistically significant (testing for significance at $\alpha = 0.05$, one-way ANOVA with Tukey's post-hoc). These trends were less than 1.4-fold in drug treated resistant parasites (Figure 6A). The gamma-glutamylcysteine abundance in drug-treated sensitive parasites was still below the basal level detected in resistant parasites. Apart from L-proline amide, which was depleted by approximately 50% in the sensitive line after DHA exposure (p-value < 0.05) (Figure 6B), no other drug-induced changes in abundance were detected in the sensitive or resistant lines for this previously reported set of resistance-associated metabolites (Figures 6C and 6D).

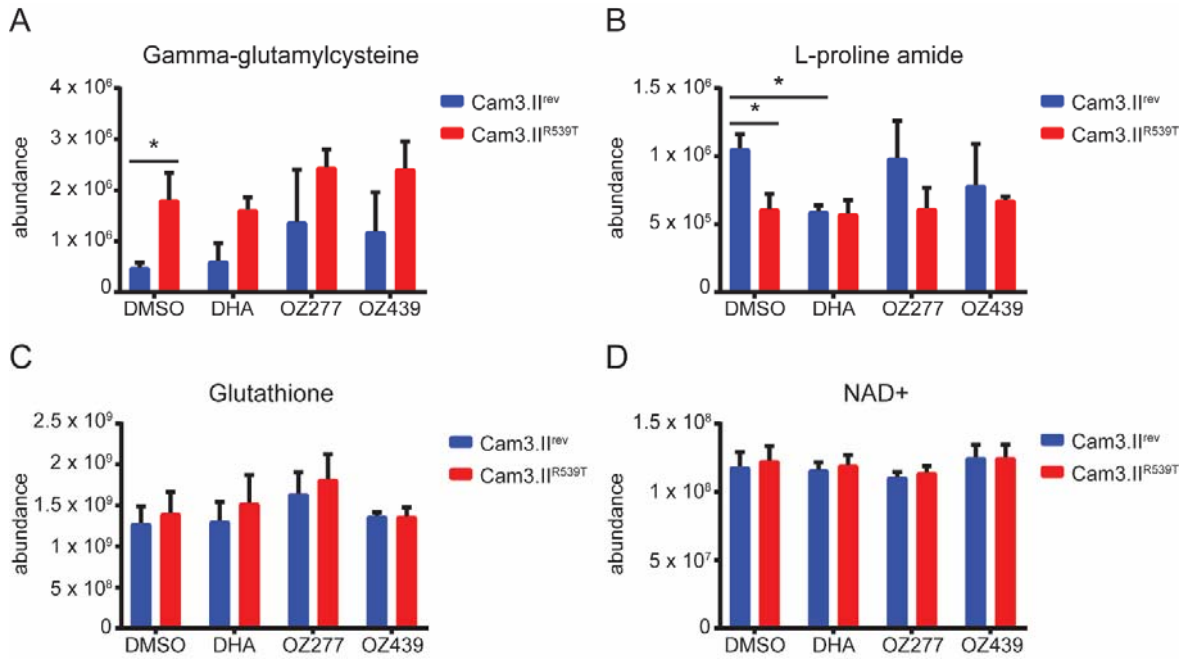


**Figure 6:** Peroxide-induced alterations of known *K13*-artemisinin resistance associated metabolites. Absolute abundance (mean peak area ± SEM of three to five biological replicates) of gamma-glutamylcysteine (A), L-proline amide (B), glutathione (C) and NAD+ (D) in the Cam3.II$^{rev}$ (blue) and Cam3.II$^{R539T}$ (red) parasite lines in the absence (DMSO) and presence of DHA, OZ277 and OZ439 drug pressure. * p-value < 0.05.

## 5.5 DISCUSSION

Artemisinin resistance is associated with point mutations in the *K13* gene (5) and the spread of resistant parasites in Southeast Asia is leading to high rates of treatment failure with current front-line artemisinin-based combination therapies (11, 25-27). This study investigated the differential biochemical response of paired *K13*-mutant artemisinin-resistant (Cam3.II$^{R539T}$) and *K13*-wildtype artemisinin-sensitive (Cam3.II$^{rev}$) parasites to pulsed exposure with selected peroxide antimalarials using an untargeted metabolomics approach. Global metabolomics analysis revealed ozonide (OZ277 and OZ439) and DHA exposure primarily disrupted parasite peptide metabolism in both the sensitive and resistant lines, similar to that seen in the 3D7 strain of *P. falciparum* (Chapter 4). However, drug treatment induced a more pronounced decrease in putative haemoglobin-derived peptides in the artemisinin-sensitive line than in the artemisinin-resistant strain and this was further associated with increased antioxidant capacity in resistant parasites.

A depletion in the abundance of haemoglobin-derived peptides following exposure to peroxides is consistent with the idea that the ozonides and DHA undergo haem-mediated activation within the parasite digestive vacuole (28, 29) and that drug-derived radicals alkylate and inactivate digestive vacuole proteins (30, 31), rapidly disrupting haemoglobin catabolism. Impaired haemoglobin metabolism is detrimental to parasite survival (32) and most likely contributes to the toxic pleiotropic insult of peroxides on the *P. falciparum* parasite. It should be noted many of the peptides that were differentially abundant in the sensitive and resistant lines after peroxide exposure did not reach statistical significance. A distinguishing feature between the response of the Cam3.II$^{rev}$ and Cam3.II$^{R539T}$ lines to pulsed peroxide exposure was the relative level of drug-induced haemoglobin peptide depletion. Overall, drug treatment caused a less pronounced reduction in peptide abundance in the resistant line compared with

the sensitive line (Figure 3). This is suggestive of a diminished impact on haemoglobin catabolism in resistant parasites, which could be a contributing factor to the increased survival of *K13*-mutants that are subjected to pulsed treatment with peroxide antimalarials.

Resistance could arise due to decreased drug activation or the alleviation of downstream damage. Despite altered haemoglobin degradation in resistant parasites potentially providing less haemoglobin-derived haem for drug activation (16), mathematical modelling of *in vitro* drug response kinetics suggested that altered drug activation does not play a role in *K13*-mediated DHA resistance (14). A direct assessment of peroxide bond activation was performed by comparing the rates of degradation (expressed as half-life, Table 1) of DHA, OZ277 and OZ439 in the Cam3.II$^{rev}$ and Cam3.II$^{R539T}$ lines across the parasite RBC lifecycle. No detectable difference in comparative peroxide degradation rate was observed at the ring, early trophozoite or mid-trophozoite stages under the conditions tested in this study, indicating decreased formation of drug-derived radicals may not be involved in *K13*-mediated resistance. Other mechanisms, such as an enhanced stress response (14) and augmented antioxidant defence pathways (16, 33, 34), likely have a more important role in the resistance mechanism.

Targeted analysis of previously identified metabolite resistance markers (16) confirmed a significant increase in the metabolite gamma-glutamylcysteine in resistant parasites (Figure 6A). In response to drug exposure, gamma-glutamylcysteine levels increased to a greater extent in the sensitive line but remained below the basal levels detected in resistant parasites (Figure 6A). Gamma-glutamylcysteine is the precursor to glutathione, the main intracellular antioxidant in *P. falciparum* (35). Unlike the previous study (16), which was performed on magnet-purified parasite cultures, a significant accumulation of glutathione itself was not detected in resistant parasites, and no change was detected in response to drug treatment (Figure 6C). This is most likely due to an inability to detect a significant difference in intraparasitic glutathione above the high levels of glutathione in the RBC background (36).

A specific LC-MS-based thiol derivatisation assay (37) of magnet-purified parasites will most likely be required to accurately quantify glutathione levels in peroxide-treated parasites. Another proposed resistance-associated metabolite, phosphatidylinositol-3-phosphate, identified in parasites with a different genetic background (*K13*$^{C580Y}$-mutant parasites on a NF54 background) (38), was not detected in this untargeted metabolomics analysis.

An augmented antioxidant defence is consistent with artemisinin resistant parasites having enhanced cytoprotective capabilities (14) and is in line with the presumed role of K13 in regulating parasite response to stress (39, 40). It is plausible that increased antioxidant capacity enables resistant parasites to mop up peroxide-derived radicals, repair alkylated proteins and better manage short-term peroxide-induced stress. This may limit disruption to haemoglobin metabolism and the depletion of haemoglobin-derived peptides in *K13*-mutant parasites. Interestingly, increased glutathione levels have been implicated in rodent models of artemisinin resistance (41), adaptive responses against oxidative stress were found to be important in a *K13*-wildtype model of artemisinin resistance (34) and altered glutathione metabolism was recently linked to the *K13*-mediated artemisinin resistance mechanism (33).

Based on the studies described in this chapter, increased glutathione-mediated detoxification is the most likely explanation for peroxide antimalarials causing less extensive depletion of haemoglobin-derived peptides in artemisinin resistant parasites when compared to the sensitive line. However, increased survival of inherently peroxide-resistant parasites contributing to the peptide phenotype observed in this study cannot be definitively ruled out. This seems a less likely explanation as, under the conditions used in this study (100 nM of DHA, OZ277 or OZ439 for 1, 3 or 5 h respectively at 4% parasitaemia and 2% Hct) the drug doses and exposure durations induced no detectable decrease in Cam3.II$^{rev}$ and Cam3.II$^{R539T}$ parasite growth when viability was assessed 48 h after drug removal from the cultures (viability was determined by analysis of Giemsa stained blood smears in the next parasite lifecycle

relative to untreated controls, unpublished data). In addition, these results do not eliminate the possibility for differential drug uptake between resistant and sensitive parasites contributing to the difference in peptide depletion, although the measured degradation half-lives (Table 1) suggest no difference in levels of drug activation over time. Future studies investigating differential drug accumulation between the resistant and sensitive lines could be conducted by directly measuring the drug concentration ratio between the infected RBC and the external medium.

Interestingly, a differential baseline abundance of selected haemoglobin-derived peptides was detected between the paired Cam3.II$^{R539T}$ and Cam3.II$^{rev}$ parasite lines (Figures 1 and 5). The basal levels of short-chain peptides were generally higher in resistant, than in sensitive, parasites and after treatment of resistant parasites the abundances of these same peptides remained above the basal level detected in the sensitive line (Figure 5). As a result, resistant parasites may be less affected by the downstream consequences of peroxide-mediated disruption to haemoglobin catabolism. Although alterations in baseline abundance of short-chain haemoglobin-derived peptides (tetrapeptides and smaller) were not previously shown in resistant parasites (16), the previous study was performed using magnet-purified parasites, a procedure that likely induces parasite stress and significant alterations to peptide levels (Giannangelo and Creek, unpublished data). In addition, the previous metabolomics study by Siddiqui *et al*. only reported the differentially abundant metabolites that were common between multiple *K13*-mutant resistant lines and their isogenic controls. It is likely that these variations in experimental design explain the differential findings between the two studies.

Peroxide-induced increases in the abundance of three unique non-haemoglobin-derived peptides were also detected in *K13*-mutant parasites after drug exposure. Notably, these peptides were unchanged by drug treatment in the sensitive line. It is anticipated that these unusual findings are related to resistance-associated alterations in parasite proteostasis and

elevated unfolded protein response pathways (13, 15). However, further work is needed to determine the origin of these unique peptides, possibly in experiments using isotope-labelled amino acids (as described in Chapter 4, Section 4.5), and to determine how altered peptide metabolism is involved in the mechanism of action and resistance of the peroxide antimalarials in *P. falciparum*.

The proposed model for peroxide antimalarial action presented in Chapter 4, has now been expanded to include potential pathways for *K13*-associated resistance (Figure 7). These findings are consistent with elevated stress response pathways, including enhanced antioxidant capacity and altered protein regulation in *K13*-resistant parasites. This may culminate in less radical-mediated parasite damage and increased survival to short pulses of peroxide exposure. While this study shows the impact of the *K13* mutation, R539T, on the parasite response to the peroxide antimalarials DHA, OZ277 and OZ439, further studies on diverse *K13* genotypes are needed to confirm these findings and determine their relationship with clinical peroxide antimalarial resistance.

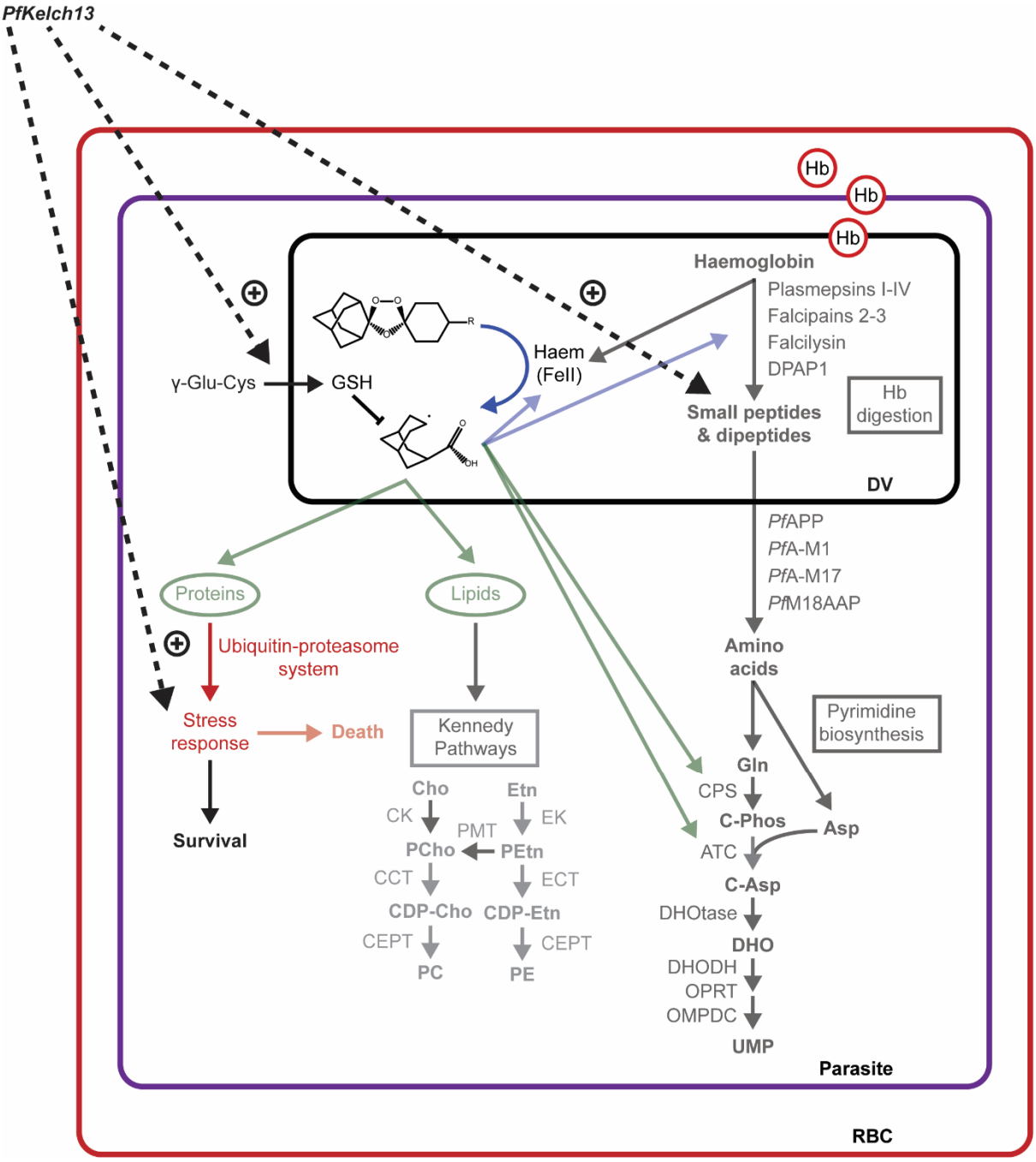


**Figure 7:** Proposed model for the mechanisms contributing to the action and *K13*-mediated resistance of peroxide antimalarials in *P. falciparum*. Peroxides are activated by an iron source, most likely haemoglobin-derived haem, within the parasite digestive vacuole. The resulting drug-derived radicals alkylate haem and disrupt haemoglobin catabolism (arrows shown in blue) as well damage other parasite components (arrows shown in green). An elevated antioxidant defence system in the form of increased glutathione levels may limit radical-mediated parasite damage. This may lead to peroxide antimalarials having a less pronounced impact on the abundance of haemoglobin-derived peptides in the resistant line, compared to

the sensitive. Death of the parasite occurs when the radical-mediated damage overwhelms the parasite's own stress response (arrows shown in red). Enhanced cellular stress pathways (14) may also allow *K13*-mutatnt parasites to overcome short-term peroxide-induced damage leading to increased parasite survival (shown in black). Positive (+) symbols indicate processes and pathways that may be increased in *K13*-mutant parasites. Asp, aspartic acid; ATC, aspartate carbamoyltransferase; C-Asp, carbamoyl-aspartate, C-Phos, carbamoyl-phosphate; CCT, choline-phosphate cytidyltransferase; CDP-, cytidine-diphospho-; CEPT, choline/ethanolamine phosphotransferase; Cho, choline; CK, choline kinase; CMP, cytidine monophosphate; CPS, carbamoyl phosphate synthetase; DHO, dihydroorotate; DHODH, dihydroorotate dehydrogenase; DHOtase, dihydroorotase; DV, digestive vacuole; ECT, ethanolamine-phosphate cytidyltransferase; EK, ethanolamine kinase; Etn, ethanolamine; Gln, glutamine; GSH, glutathione; Hb, haemoglobin; OMPDC, orotodine 5'-phosphate decarboxylase; OPRT, orotate phosphoribosyltransferase; PC, phosphatidylcholine; PE, phosphatidylethanolamine; PCho, choline phosphate; PEtn, ethanolamine phosphate; PMT, phosphoethanolamine N-methyltransferase; RBC, red blood cell; UMP, uridine monophosphate; γ-Glu-Cys, gamma-glutamylcysteine.

## 5.6 CONCLUSIONS

These studies demonstrated that pulsed peroxide exposure perturbed peptide metabolism in both *K13*-mutant artemisinin-resistant and *K13*-wildtype artemisinin-sensitive parasites. The basal levels of haemoglobin-derived peptides were significantly elevated in resistant parasites and drug exposure caused a more dramatic depletion of these same peptides in the sensitive line. Diminished intraparasitic drug activation does not appear to play a role in *K13*-mediated artemisinin resistance as the three drugs displayed a similar rate of degradation in resistant and sensitive parasite lines. The differential response of resistant and sensitive parasites may be associated with enhanced antioxidant capacity, as evidenced by elevated levels of the glutathione precursor gamma-glutamylcysteine in Cam3.II$^{R539T}$ parasite cultures. This may lead to diminished intracellular radical damage in artemisinin resistant parasites compared to the sensitive strains, which was ultimately detected as a less pronounced effect on haemoglobin catabolism. Moreover, the drug-induced response of resistant parasites was associated with unique alterations in the abundance of selected non-haemoglobin derived peptides, further emphasising the importance of protease and peptide metabolism in the mechanisms of action and resistance of the peroxide antimalarials.

## 5.7 REFERENCES


1. WHO. 2016. World Malaria Report 2016. World Health Organisation, Geneva.
2. Dondorp AM, Nosten F, Yi P, Das D, Phyo AP, Tarning J, Lwin KM, Ariey F, Hanpithakpong W, Lee SJ, Ringwald P, Silamut K, Imwong M, Chotivanich K, Lim P, Herdman T, An SS, Yeung S, Singhasivanon P, Day NP, Lindegardh N, Socheat D, White NJ. 2009. Artemisinin resistance in *Plasmodium falciparum* malaria. N Engl J Med 361:455-467.
3. Ashley EA, Dhorda M, Fairhurst RM, Amaratunga C, Lim P, Suon S, Sreng S, Anderson JM, Mao S, Sam B, Sopha C, Chuor CM, Nguon C, Sovannaroth S, Pukrittayakamee S, Jittamala P, Chotivanich K, Chutasmit K, Suchatsoonthorn C, Runcharoen R, Hien TT, Thuy-Nhien NT, Thanh NV, Phu NH, Htut Y, Han KT, Aye KH, Mokuolu OA, Olaosebikan RR, Folaranmi OO, Mayxay M, Khanthavong M, Hongvanthong B, Newton PN, Onyamboko MA, Fanello CI, Tshefu AK, Mishra N, Valecha N, Phyo AP, Nosten F, Yi P, Tripura R, Borrmann S, Bashraheil M, Peshu J, Faiz MA, Ghose A, Hossain MA, Samad R, et al. 2014. Spread of artemisinin resistance in *Plasmodium falciparum* malaria. N Engl J Med 371:411-423.
4. Witkowski B, Khim N, Chim P, Kim S, Ke S, Kloeung N, Chy S, Duong S, Leang R, Ringwald P, Dondorp AM, Tripura R, Benoit-Vical F, Berry A, Gorgette O, Ariey F, Barale JC, Mercereau-Puijalon O, Menard D. 2013. Reduced artemisinin susceptibility of *Plasmodium falciparum* ring stages in western Cambodia. Antimicrob Agents Chemother 57:914-923.
5. Ariey F, Witkowski B, Amaratunga C, Beghain J, Langlois A-C, Khim N, Kim S, Duru V, Bouchier C, Ma L, Lim P, Leang R, Duong S, Sreng S, Suon S, Chuor CM, Bout DM, Menard S, Rogers WO, Genton B, Fandeur T, Miotto O, Ringwald P, Le Bras J, Berry A, Barale J-C, Fairhurst RM, Benoit-Vical F, Mercereau-Puijalon O, Menard D. 2014. A molecular marker of artemisinin-resistant *Plasmodium falciparum* malaria. Nature 505:50-55.
6. Takala-Harrison S, Jacob CG, Arze C, Cummings MP, Silva JC, Dondorp AM, Fukuda MM, Hien TT, Mayxay M, Noedl H. 2014. Independent emergence of *Plasmodium falciparum* artemisinin resistance mutations in Southeast Asia. J Infect Dis 211:670-679.

7. Amaratunga C, Witkowski B, Dek D, Try V, Khim N, Miotto O, Menard D, Fairhurst RM. 2014. *Plasmodium falciparum* founder populations in western Cambodia have reduced artemisinin sensitivity *in vitro*. Antimicrob Agents Chemother 58:4935-4937.
8. Takala-Harrison S, Clark TG, Jacob CG, Cummings MP, Miotto O, Dondorp AM, Fukuda MM, Nosten F, Noedl H, Imwong M. 2013. Genetic loci associated with delayed clearance of *Plasmodium falciparum* following artemisinin treatment in Southeast Asia. Proc Natl Acad Sci U S A 110:240-245.
9. Miotto O, Amato R, Ashley EA, MacInnis B, Almagro-Garcia J, Amaratunga C, Lim P, Mead D, Oyola SO, Dhorda M, Imwong M, Woodrow C, Manske M, Stalker J, Drury E, Campino S, Amenga-Etego L, Thanh TN, Tran HT, Ringwald P, Bethell D, Nosten F, Phyo AP, Pukrittayakamee S, Chotivanich K, Chuor CM, Nguon C, Suon S, Sreng S, Newton PN, Mayxay M, Khanthavong M, Hongvanthong B, Htut Y, Han KT, Kyaw MP, Faiz MA, Fanello CI, Onyamboko M, Mokuolu OA, Jacob CG, Takala-Harrison S, Plowe CV, Day NP, Dondorp AM, Spencer CC, McVean G, Fairhurst RM, White NJ, Kwiatkowski DP. 2015. Genetic architecture of artemisinin-resistant *Plasmodium falciparum*. Nat Genet 47:226-234.
10. Ménard D, Khim N, Beghain J, Adegnika AA, Shafiul-Alam M, Amodu O, Rahim-Awab G, Barnadas C, Berry A, Boum Y, Bustos MD, Cao J, Chen J-H, Collet L, Cui L, Thakur G-D, Dieye A, Djallé D, Dorkenoo MA, Eboumbou-Moukoko CE, Espino F-E-CJ, Fandeur T, Ferreira-da-Cruz M-F, Fola AA, Fuehrer H-P, Hassan AM, Herrera S, Hongvanthong B, Houzé S, Ibrahim ML, Jahirul-Karim M, Jiang L, Kano S, Ali-Khan W, Khanthavong M, Kremsner PG, Lacerda M, Leang R, Leelawong M, Li M, Lin K, Mazarati J-B, Ménard S, Morlais I, Muhindo-Mavoko H, Musset L, Na-Bangchang K, Nambozi M, Niaré K, Noedl H, et al. 2016. A worldwide map of *Plasmodium falciparum* K13-propeller polymorphisms. N Engl J Med 374:2453-2464.
11. Amaratunga C, Lim P, Suon S, Sreng S, Mao S, Sopha C, Sam B, Dek D, Try V, Amato R, Blessborn D, Song L, Tullo GS, Fay MP, Anderson JM, Tarning J, Fairhurst RM. 2016. Dihydroartemisinin-piperaquine resistance in *Plasmodium falciparum* malaria in Cambodia: a multisite prospective cohort study. Lancet Infect Dis 16:357-365.
12. Huang F, Takala-Harrison S, Jacob CG, Liu H, Sun X, Yang H, Nyunt MM, Adams M, Zhou S, Xia Z, Ringwald P, Bustos MD, Tang L, Plowe CV. 2015. A single mutation in K13 predominates in Southern China and is associated with delayed clearance of *Plasmodium falciparum* following artemisinin treatment. J Infect Dis 212:1629-1635.

13. Straimer J, Gnadig NF, Witkowski B, Amaratunga C, Duru V, Ramadani AP, Dacheux M, Khim N, Zhang L, Lam S, Gregory PD, Urnov FD, Mercereau-Puijalon O, Benoit-Vical F, Fairhurst RM, Menard D, Fidock DA. 2015. Drug resistance. K13-propeller mutations confer artemisinin resistance in *Plasmodium falciparum* clinical isolates. Science 347:428-431.
14. Dogovski C, Xie SC, Burgio G, Bridgford J, Mok S, McCaw JM, Chotivanich K, Kenny S, Gnädig N, Straimer J, Bozdech Z, Fidock DA, Simpson JA, Dondorp AM, Foote S, Klonis N, Tilley L. 2015. Targeting the cell stress response of *Plasmodium falciparum* to overcome artemisinin resistance. PLoS Biol 13:e1002132.
15. Mok S, Ashley EA, Ferreira PE, Zhu L, Lin Z, Yeo T, Chotivanich K, Imwong M, Pukrittayakamee S, Dhorda M, Nguon C, Lim P, Amaratunga C, Suon S, Hien TT, Htut Y, Faiz MA, Onyamboko MA, Mayxay M, Newton PN, Tripura R, Woodrow CJ, Miotto O, Kwiatkowski DP, Nosten F, Day NP, Preiser PR, White NJ, Dondorp AM, Fairhurst RM, Bozdech Z. 2015. Drug resistance. Population transcriptomics of human malaria parasites reveals the mechanism of artemisinin resistance. Science 347:431-435.
16. Siddiqui G, Srivastava A, Russell AS, Creek DJ. 2017. Multi-omics based identification of specific biochemical changes associated with PfKelch13-mutant artemisinin resistant *Plasmodium falciparum*. J Infect Dis 215:1435-1444.
17. Yang T, Xie SC, Cao P, Giannangelo C, McCaw J, Creek DJ, Charman SA, Klonis N, Tilley L. 2016. Comparison of the exposure time-dependence of the activities of synthetic ozonide antimalarials and dihydroartemisinin against K13 wild-type and mutant *Plasmodium falciparum* strains. Antimicrob Agents Chemother 60:4501-4510.
18. Siriwardana A, Iyengar K, Roepe PD. 2016. Endoperoxide drug cross-resistance patterns for *Plasmodium falciparum* exhibiting an artemisinin delayed-clearance phenotype. Antimicrob Agents Chemother 60:6952-6956.
19. Baumgärtner F, Jourdan J, Scheurer C, Blasco B, Campo B, Mäser P, Wittlin S. 2017. *In vitro* activity of anti-malarial ozonides against an artemisinin-resistant isolate. Malar J 16:45.
20. Straimer J, Gnädig NF, Stokes BH, Ehrenberger M, Crane AA, Fidock DA. 2017. *Plasmodium falciparum* K13 mutations differentially impact ozonide susceptibility and parasite fitness *in vitro*. mBio 8:e00172-00117.
21. Phyo AP, Jittamala P, Nosten FH, Pukrittayakamee S, Imwong M, White NJ, Duparc S, Macintyre F, Baker M, Möhrle JJ. 2015. Antimalarial activity of artefenomel

(OZ439), a novel synthetic antimalarial endoperoxide, in patients with *Plasmodium falciparum* and *Plasmodium vivax* malaria: an open-label phase 2 trial. Lancet Infect Dis 16:61-69.

22. Macintyre F, Adoke Y, Tiono AB, Duong TT, Mombo-Ngoma G, Bouyou-Akotet M, Tinto H, Bassat Q, Issifou S, Adamy M. 2017. A randomised, double-blind clinical phase II trial of the efficacy, safety, tolerability and pharmacokinetics of a single dose combination treatment with artefenomel and piperaquine in adults and children with uncomplicated *Plasmodium falciparum* malaria. BMC Med 15:181.
23. Giannangelo C, Stingelin L, Yang T, Tilley L, Charman SA, Creek DJ. 2018. Parasite-mediated degradation of synthetic ozonide antimalarials impacts *in vitro* antimalarial activity. Antimicrob Agents Chemother 62:e01566-01517.
24. Witkowski B, Amaratunga C, Khim N, Sreng S, Chim P, Kim S, Lim P, Mao S, Sopha C, Sam B, Anderson JM, Duong S, Chuor CM, Taylor WR, Suon S, Mercereau-Puijalon O, Fairhurst RM, Menard D. 2013. Novel phenotypic assays for the detection of artemisinin-resistant *Plasmodium falciparum* malaria in Cambodia: *in-vitro* and *ex-vivo* drug-response studies. Lancet Infect Dis 13:1043-1049.
25. Rogers WO, Sem R, Tero T, Chim P, Lim P, Muth S, Socheat D, Ariey F, Wongsrichanalai C. 2009. Failure of artesunate-mefloquine combination therapy for uncomplicated *Plasmodium falciparum* malaria in southern Cambodia. Malar J 8:10.
26. Saunders DL, Vanachayangkul P, Lon C. 2014. Dihydroartemisinin–piperaquine failure in Cambodia. N Engl J Med 371:484-485.
27. Spring MD, Lin JT, Manning JE, Vanachayangkul P, Somethy S, Bun R, Se Y, Chann S, Ittiverakul M, Sia-ngam P, Kuntawunginn W, Arsanok M, Buathong N, Chaorattanakawee S, Gosi P, Ta-aksorn W, Chanarat N, Sundrakes S, Kong N, Heng TK, Nou S, Teja-isavadharm P, Pichyangkul S, Phann ST, Balasubramanian S, Juliano JJ, Meshnick SR, Chour CM, Prom S, Lanteri CA, Lon C, Saunders DL. 2015. Dihydroartemisinin-piperaquine failure associated with a triple mutant including kelch13 C580Y in Cambodia: an observational cohort study. Lancet Infect Dis 15:683-691.
28. Meshnick SR, Thomas A, Ranz A, Xu CM, Pan HZ. 1991. Artemisinin (qinghaosu): the role of intracellular hemin in its mechanism of antimalarial action. Mol Biochem Parasitol 49:181-189.
29. Dong Y, Vennerstrom JL. 2003. Mechanisms of *in situ* activation for peroxidic antimalarials. Redox Rep 8:284-288.

30. Ismail HM, Barton V, Phanchana M, Charoensutthivarakul S, Wong MHL, Hemingway J, Biagini GA, O'Neill PM, Ward SA. 2016. Artemisinin activity-based probes identify multiple molecular targets within the asexual stage of the malaria parasites *Plasmodium falciparum* 3D7. Proc Natl Acad Sci U S A 113:2080-2085.
31. Ismail HM, Barton VE, Panchana M, Charoensutthivarakul S, Biagini GA, Ward SA, O'Neill PM. 2016. A click chemistry-based proteomic approach reveals that 1, 2, 4-trioxolane and artemisinin antimalarials share a common protein alkylation profile. Angew Chem Int Ed Engl 55:6401-6405.
32. Goldberg DE. 2005. Hemoglobin degradation, p 275-291. *In* Compans RW, Cooper MD, Honjo T, Koprowski H, Melchers F, Oldstone MBA, Olsnes S, Potter M, Vogt PK, Wagner H, Sullivan D, Krishna S (ed), Malaria: Drugs, disease and post-genomic biology, vol 295. Springer Berlin Heidelberg.
33. Phompradit P, Chaijaroenkul W, Na-Bangchang K. 2017. Cellular mechanisms of action and resistance of *Plasmodium falciparum* to artemisinin. Parasitol Res 116:3331-3339.
34. Rocamora F, Zhu L, Liong KY, Dondorp A, Miotto O, Mok S, Bozdech Z. 2018. Oxidative stress and protein damage responses mediate artemisinin resistance in malaria parasites. PLoS Pathog 14:e1006930.
35. Muller S. 2004. Redox and antioxidant systems of the malaria parasite *Plasmodium falciparum*. Mol Microbiol 53:1291-1305.
36. Barrand MA, Winterberg M, Ng F, Nguyen M, Kirk K, Hladky SB. 2012. Glutathione export from human erythrocytes and *Plasmodium falciparum* malaria parasites. Biochem J 448:389-400.
37. Patzewitz EM, Wong EH, Müller S. 2012. Dissecting the role of glutathione biosynthesis in *Plasmodium falciparum*. Mol Microbiol 83:304-318.
38. Mbengue A, Bhattacharjee S, Pandharkar T, Liu HN, Estiu G, Stahelin RV, Rizk SS, Njimoh DL, Ryan Y, Chotivanich K, Nguon C, Ghorbal M, Lopez-Rubio JJ, Pfrender M, Emrich S, Mohandas N, Dondorp AM, Wiest O, Haldar K. 2015. A molecular mechanism of artemisinin resistance in *Plasmodium falciparum* malaria. Nature 520:683-687.
39. Tilley L, Straimer J, Gnädig NF, Ralph SA, Fidock DA. 2016. Artemisinin action and resistance in *Plasmodium falciparum*. Trends Parasitol 32:682-696.
40. Paloque L, Ramadani AP, Mercereau-Puijalon O, Augereau J-M, Benoit-Vical F. 2016. *Plasmodium falciparum*: multifaceted resistance to artemisinins. Malar J 15:149.

41. Chandra R, Tripathi LM, Saxena JK, Puri SK. 2011. Implication of intracellular glutathione and its related enzymes on resistance of malaria parasites to the antimalarial drug artemether. Parasitol Int 60:97-100.

# Chapter 6

# Conclusions and perspectives

## 6.1 RESEARCH SUMMARY

Malaria continues to cause significant morbidity, mortality and socioeconomic hardship in many developing countries. New antimalarials are vital for effective malaria control and for minimising the burden of disease caused by *Plasmodium* infection in the future. Fully synthetic peroxide antimalarials, known as ozonides, offer low manufacturing costs and some possess superior pharmacokinetic properties when compared to currently used artemisinins. They are one of the most advanced drug classes currently in clinical development and include OZ277 (arterolane) (1), which is already on the market, and OZ439 (artefenomel) (2), the first long half-life peroxide, which is undergoing Phase IIb clinical trials (ClinicalTrials.gov Identifier: NCT02497612).

The mode of action of the ozonides, like the artemisinins, is an active area of research, but detailed information on the biochemical mechanisms underlying the activity of these compounds is lacking. The peroxide bond is known to be essential for both artemisinin- and ozonide-induced toxicity (3-5), pointing to a common mode of action against the *Plasmodium* parasite. It is widely accepted that ozonide antimalarial activity requires activation of the peroxide bond by a reduced iron source (6-9) and recent work has confirmed that the most likely source of the iron-based activator is free haem released through the process of parasite haemoglobin digestion (10). The activation process gives rise to highly reactive radicals that indiscriminately alkylate a range of intraparasitic proteins involved in essential processes within the cell (11, 12). This thesis examined the non-protein targets of ozonide antimalarials and the biochemical pathways impacted by ozonides in artemisinin-sensitive and resistant *P. falciparum* parasites.

## 6.2 PARASITE-MEDIATED DEGRADATION OF SYNTHETIC OZONIDE ANTIMALARIALS IMPACTS *IN VITRO* ANTIMALARIAL ACTIVITY

Iron-mediated reactivity is essential for ozonide activity. Within the parasite, drug activation is dependent on parasite-mediated haemoglobin digestion, which leads to degradation of the parent compound. Therefore, antimalarial activity and drug degradation are linked by a parasite-driven process. Often, studies investigating the biochemical pathways and molecular targets involved in peroxide antimalarial activity use specific *in vitro* conditions, such as high parasitaemia, for optimal assay performance. These conditions differ significantly from those used to measure *in vitro* drug activity. For peroxide antimalarials, which rely on parasite-mediated degradation for activity, it is unclear how these artificial *in vitro* conditions affect ozonide activity and stability. Therefore, a clear understanding of the relationship between parasite-mediated drug degradation and biological activity under these experimental conditions are needed for accurate interpretation of results from these *in vitro* mechanistic experiments.

A quantitative assessment of ozonide stability and antimalarial activity at varying levels of parasitaemia, different parasite lifecycle stages and in the presence of selected inhibitors, determined the relationship between parasite-mediated drug degradation and *in vitro* activity for OZ277 and OZ439. Both ozonides were relatively stable in non-infected RBCs at 2% Hct and drug degradation was stabilised with the iron chelator DFP, consistent with reports suggesting free, chelatable iron that is part of the labile iron pool (LIP) is responsible for ozonide degradation in non-infected cells (2). In infected cultures, drug degradation was parasite lifecycle stage-dependent and positively correlated with parasitaemia in trophozoites. Increasing parasitaemia from 1% to 10% trophozoites was associated with a substantial

increase in the rate of degradation for both ozonides tested, and the rate of degradation increased almost 100-fold when the parasitaemia was enriched to > 90% trophozoites (relative to a 1% trophozoite culture). This trend paralleled a significant and progressive reduction in *in vitro* antimalarial activity, to the extent that both ozonides were devoid of activity in enriched (> 90%) trophozoite cultures. In ring stage cultures, increasing the parasitaemia had a modest impact on the rate of OZ277 degradation, while OZ439 stability was unaffected. Increasing the ring stage parasite load had no measurable effect on *in vitro* antimalarial activity.

Ozonide activity is known to depend on the parasite stage being treated, the drug concentration applied to the culture and the duration of drug exposure (10, 13, 14). It was hypothesised that under conditions of high trophozoite parasitaemia (10% to > 90%), where both the duration of parasite exposure to intact drug and antimalarial activity are limited, that the parasite stress response mechanisms can cope with the short term ozonide-induced insult until the drug is effectively depleted. This leads to an apparent loss of antimalarial activity. While an alternative theory was that an increased number of parasite targets need to be inhibited to result in the same level of drug-induced growth inhibition as in a low parasitaemia culture, it is likely that a combination of these mechanisms are responsible for the observed reduction in ozonide activity at high trophozoite parasitaemia.

Ozonide degradation was stabilised in high trophozoite parasitaemia cultures (10%) with the addition of the falcipain inhibitor E64d, but not with DFP, consistent with a haemoglobin digestion product, most likely free haem, contributing to the parasitaemia-dependent degradation of ozonides under these conditions. E64d also ablated antimalarial activity under these conditions, supporting the prevailing hypothesis that haemoglobin-derived haem induces peroxide bond activation within the parasite (10). DFP had no apparent impact on the activity of short (3 h) durations of ozonide exposure under the conditions used in this study, consistent with a previous report using a different iron chelator, bipyridyl (10). Notably,

iron chelators, including DFP, have been shown to antagonise the activity of simple ozonide esters when the duration of co-incubation is prolonged to 48 h and higher concentrations of DFP (500 μM vs 250 μM) are used (15). As has been shown with artemisinins, the antagonism of peroxide antimalarial activity by iron chelators appears to depend on both the concentration and type of iron chelator that is used, the peroxide antimalarial being tested, the chelator and peroxide exposure duration and the *in vitro* culture conditions, including the parasite asexual lifecycle stage being tested (10, 15, 16).

Moreover, the data presented in this chapter showed that a balance between haem-mediated activation and degradation processes are essential for optimal ozonide activity *in vitro*. These data highlight the impact of parasite load on ozonide stability and *in vitro* antimalarial activity and show that ozonide potency will be limited under very high trophozoite parasitaemia conditions that substantially reduce ozonide stability. The results of *in vitro* mechanistic studies performed under the same conditions should, therefore, be interpreted with caution. In this context, careful consideration of incubation conditions and peroxide stability is paramount when investigating the ozonide antimalarial mode of action and when making associations between activity and biochemical perturbations *in vitro*.

## 6.3 MOLECULAR TARGETS AND SUB-CELLULAR LOCALISATION OF OZONIDE ANTIMALARIALS IN *P. FALCIPARUM*

Alkylation of intraparasitic targets is thought to be an important step in the mode of action of ozonides, and peroxide-based antimalarials in general. Following activation by an intracellular iron source, ozonide-derived radicals react indiscriminately with parasite proteins (11). The promiscuous nature of ozonide-derived radicals suggests other intraparasitic targets may also contribute to the parasiticidal activity of ozonides. The development of a standardised set of high parasitaemia culture conditions (10% parasitaemia), whereby ozonides still exhibit appreciable *in vitro* activity (Chapter 2), allowed an untargeted investigation of the intraparasitic small molecule targets of selected ozonide antimalarials, as well as examination of the sub-cellular distribution of ozonide-derived protein adducts within the *P. falciparum* parasite.

Using OZ277 as a model ozonide, incubation with trophozoite stage cultures produced ozonide-alkylated haem adducts (*m/z* 782.3) that were detected by LC-MS. The reaction with intraparasitic haem is thought to promote ozonide peroxide bond activation (10), and the extent of haem alkylation is known to be correlated with *in vitro* antimalarial activity in a simplified experimental system (17). This study extends those findings, showing that haem is also a biological target for the ozonides within the parasite and may contribute to their antimalarial mode of action. Alkylation of the haem porphyrin ring by the ozonide-derived adamantane radical was confirmed using OZ754, which has a chemically-modified adamantane group and resulted in formation of an alkylated haem adduct with the expected mass shift. The functional importance of ozonide haem alkylation and whether intraparasitic haem adduct formation correlates with ozonide activity remains unknown but could be the subject of future studies.

One possible application is that the haem alkylation product could be developed as a surrogate biomarker for ozonide activation. *K13*-mediated artemisinin resistance has recently been linked to impaired haemoglobin catabolism (18), therefore it would also be interesting to determine whether there is any correlation between the level of haem alkylation and antiparasitic activity of ozonides in *K13*-mutant resistant parasites, similar to the approach described with artemisinin in an artemisinin-resistant *P. yoelii* mouse infection model (19).

In addition to the haem adduct, untargeted LC-MS analysis identified various oxidative degradation products from alkylated haem in *P. falciparum* parasites incubated with either OZ277 or OZ754. Haem can undergo non-enzymatic, oxidative degradation (20) and it is likely that oxidative destruction of the ozonide-modified haem molecule led to formation of these end products. The smallest alkylated haem degradation product detected in infected cultures (an alkylated mono-pyrrole), was also detected after the *in vitro* reaction between OZ277 and haem under reducing conditions in ACN/$H_2O$ (17), confirming that these novel metabolites are derived from the ozonide alkylated haem molecule.

A novel click chemistry-based enrichment method was also developed to isolate and identify other low abundant small molecule targets, such as glutathione, lipids or other metabolites. However, no ozonide-alkylated metabolites were detected using a generic polar metabolomics extraction procedure followed by untargeted LC-MS analysis. Surprisingly, this suggests that apart from haem, ozonide-derived radicals may not alkylate small molecule targets within *P. falciparum* parasites.

The sub-cellular distribution of ozonide-derived protein adducts was also analysed. Protein adducts were found to be widespread throughout the parasite within 1 h of ozonide exposure, consistent with activation and indiscriminate alkylation of parasite proteins (11, 12). Interestingly, there was no clear co-localisation with the parasite digestive vacuole by confocal

microscopy. This is surprising given that ozonides are known to react and form covalent adducts with haem and digestive vacuole-associated proteins (11). One potential explanation for this is that haemozoin in the digestive vacuole quenched the fluorescence signal of Cy5. An alternative approach for future experiments could use a nitrobenzyldiazole-based fluorochrome instead, which is poorly quenched by haemozoin (15).

A direct comparison of the second-generation ozonide, OZ759, and the first-generation compound, OZ758, revealed a distinct sub-cellular localisation pattern. OZ759 was more closely localised to the digestive vacuole and less widely distributed throughout the cell, suggesting these drugs may alkylate unique proteins within the parasite. This could be explained by differences in iron reactivity, whereby second-generation ozonides are reactive only with haem, which is primarily located in or around the digestive vacuole, and first-generation compounds, which are reactive with both haem and iron, the latter being located widely throughout the cell. It is also possible that differences in intraparasitic accumulation between ozonides lead to an altered protein alkylation pattern within parasites. Future studies could explore these questions further by directly comparing the time-dependent protein alkylation profiles of first- and second-generation ozonides by pulling-down interacting proteins and performing MS-based identification (11, 21, 22).

This series of studies revealed that as well as proteins, ozonides form covalent adducts with intraparasitic haem. These data, along with the sub-cellular distribution of ozonide alkylated proteins, are consistent with the “cluster bomb” hypothesis of activity, whereby activated ozonides lead to widespread alkylation of intraparasitic targets, including proteins and haem.

## 6.4 PEROXIDE-INDUCED PERTURBATIONS OF *P. FALCIPARUM* BIOCHEMICAL PATHWAYS

Following iron-mediated activation and subsequent alkylation of intraparasitic molecules, the biochemical pathways perturbed by peroxide treatment that lead to parasite death are not well characterised. The temporal biochemical response of peroxide-treated *P. falciparum* parasites was investigated using an untargeted multi-omics-based approach, incorporating metabolomic, peptidomic and proteomic analyses.

A time-resolved metabolomics-based approach allowed temporal observation of drug-dependent changes in metabolite abundance and the mapping of primary and secondary peroxide-induced effects on parasite metabolism. Untargeted metabolomic profiling showed that altered haemoglobin catabolism was the most significant initial metabolic disturbance following peroxide treatment in *P. falciparum* infected RBCs, consistent with the hypothesis that these peroxide-based drugs are activated by Fe(II) to produce reactive intermediates in the parasite digestive vacuole. Short durations of peroxide exposure (< 3 h) specifically disrupted parasite peptide metabolism, inducing a pronounced depletion of short peptides most likely originating from haemoglobin. Additional pathways were affected when the duration of peroxide exposure was extended beyond 3 h, including lipid, nucleotide and amino acid metabolism. These processes could represent secondary biochemical pathways involved in peroxide antimalarial toxicity.

Further untargeted peptidomic studies confirmed haemoglobin-derived peptides were perturbed after peroxide treatment and pointed to the disruption of proteases involved in the conversion of large to small peptides being affected by drug treatment. Using activity-based protease probes, the activity of cysteine proteases involved in haemoglobin digestion were found to increase within 1 h of ozonide exposure and proteomic analysis revealed elevated

abundance of haemoglobin-digesting proteases after drug treatment, possibly representing a parasite response to impaired haemoglobin digestion. In this context, the functional relevance of impaired haemoglobin digestion to the mechanism of peroxide antimalarial activity could be explored further in studies that force parasites to rely solely on haemoglobin digestion for amino acids. *P. falciparum* parasites can survive in medium containing only isoleucine (the only amino acid absent in haemoglobin) as haemoglobin can provide all of their amino acid requirements (23). Peroxide-treated parasites that are grown in a minimal medium may be more sensitive to the effects of peroxide antimalarials as they are unable to scavenge exogenous amino acids. Alternatively, supplementing parasites with excess amino acids may overcome peroxide-mediated effects on haemoglobin digestion and at least prolong parasite survival. It is unlikely that amino acid supplementation alone would completely rescue peroxide-treated parasites as disruption of multiple biochemical pathways are known to be involved in the peroxide antimalarial mode of action.

While the depletion of short chain haemoglobin-derived peptides in this study is strongly suggestive of an impact on parasite haemoglobin digestion, it is interesting to consider how this metabolic phenotype could be exploited further as a potential biomarker for peroxide antimalarial activity. Although peptide depletion is unlikely to be a sensitive biomarker in the context of clinical activity, it could prove useful for screening of both peroxide activity and rate of drug action *in vitro*. Current *in vitro* methods employ drug sensitivity assays that only provide an assessment of parasite viability between 48-72 h after drug treatment, in the next asexual cycle (24, 25). A method based on the monitoring of one or several key peptides (a peptide signature) could provide a potentially sensitive readout of peroxide activity and rate of action within the same parasite lifecycle. This could be the subject of further investigations utilising peroxides with wide-ranging antimalarial activities.

Untargeted proteome analysis revealed drug-induced disruption to the same pathways that were found to be affected in the metabolomics studies, however the major finding at the protein level was the elevated abundance of translation regulation machinery and components of the ubiquitin-proteasome system. Peroxide-induced oxidative stress (26) and widespread protein alkylation (11, 21, 22) are thought to lead to an accumulation of damaged and misfolded proteins within the parasite that are subsequently tagged with ubiquitin for proteasomal degradation (27). Specific upregulation of these proteins suggests that the parasite initiates a stress response to mitigate the peroxide-mediated toxic insult and that parasite death likely occurs when cellular damage overwhelms this defensive system (27).

This multi-omics-based approach has provided a better understanding of the biochemical mechanisms underpinning peroxide antimalarial activity, and the *P. falciparum* response to treatment. It has shown that peroxides initially disrupt haemoglobin catabolism prior to affecting other biochemical pathways, and that parasites engage a stress response to manage peroxide-induced damage. Modulating the activity of these pathways, either chemically or via genetic manipulation, could provide additional functional insight into their relevance to peroxide-induced toxicity. Furthermore, targeting these pathways may be synergistic with peroxide treatment, as has been shown for proteasome inhibition and DHA (27), and provide additional avenues for improving peroxide antimalarial efficacy.

## 6.5 BIOCHEMICAL IMPACT OF PEROXIDE ANTIMALARIALS ON *K13*-MUTANT ARTEMISININ RESISTANT AND SENSITIVE *P. FALCIPARUM* PARASITES

The emergence and spread of artemisinin resistant parasites is leading to increased rates of ACT failure in Southeast Asia, threatening ongoing efforts to eradicate malaria. Resistance is associated with mutations in the *K13* gene (28) and parasites expressing mutant *K13* are also cross-resistant to the ozonides, OZ277 and OZ439 (10, 29).

Untargeted metabolomics analysis revealed peroxide exposure primarily disrupted peptide metabolism in both the sensitive (Cam3.II$^{rev}$, *K13*-wildtype) and resistant (Cam3.II$^{R539T}$, *K13*-mutant) lines. All drugs caused a depletion in haemoglobin-derived peptides, with more pronounced peptide depletion occurring in the sensitive line. In general, the haemoglobin-derived peptides that were reduced following peroxide exposure were initially elevated in abundance in untreated resistant parasites compared with the sensitive controls. Several differentially abundant non-haemoglobin-derived peptides were also identified in response to peroxide treatment in resistant parasites, which may be associated with altered proteostasis and elevated unfolded protein response pathways in *K13*-mutant resistant parasites (27, 30, 31). Given that proteins involved in parasite stress response pathways were elevated in abundance after peroxide treatment in the *P. falciparum* 3D7 parasite strain, it would also be beneficial to compare the proteome and peptidome of peroxide-treated *K13*-mutant artemisinin resistant and *K13*-wildtype artemisinin sensitive parasite lines.

This study also showed that *K13*-mediated resistance is associated with enhanced antioxidant capacity. Elevated levels of the glutathione precursor, gamma-glutamylcysteine, were detected in resistant parasites, which is consistent with previous reports (18). Elevated

levels of glutathione itself were not detected, most likely due to an inability to detect glutathione levels above that in the RBC background. A specific LC-MS-based thiol derivatisation method (32) will most likely be required to accurately quantify glutathione levels in peroxide-treated infected cultures. Direct assessment of peroxide bond activation was also assessed by comparing the relative degradation of DHA, OZ277 and OZ439 in the resistant and sensitive parasite lines. No detectable difference in comparative peroxide degradation rate was observed, showing that diminished intraparasitic drug activation was not involved in the resistance mechanism. Therefore, enhanced glutathione-mediated detoxification of peroxide radicals may explain why depletion of haemoglobin peptides after peroxide treatment is less dramatic in resistant parasites.

Taken together, these studies further emphasise the importance of haemoglobin catabolism and peptide metabolism in ozonide activity and *K13*-mediated peroxide resistance. They also point to a role for enhanced antioxidant capacity in the *K13*-mediated resistance mechanism.

## 6.6 CONCLUDING REMARKS

The studies described in this thesis expand our current understanding of the modes of action and resistance of peroxide antimalarials in *P. falciparum*, demonstrating a central role for the parasite haemoglobin digestion pathway in the activity and resistance mechanisms for this important class of antimalarials. A model for peroxide antimalarial activity (Figure 1) is proposed whereby haemoglobin-derived free haem activates the peroxide drug within the parasite digestive vacuole. The resulting drug-derived oxygen-centred radicals rearrange to form carbon-centred radicals that initially alkylate proteins and molecules in their immediate vicinity, including haem and proteases involved in haemoglobin digestion. Disruption of the haemoglobin digestion pathway is therefore the first detectable metabolic disturbance in peroxide-treated parasites, and in response to impaired haemoglobin catabolism the parasite upregulates the abundance and activity of proteins involved in the haemoglobin degradation pathway. Peroxide radicals then induce further oxidative insult and cause widespread alkylation of additional parasite components, which all contribute to peroxide-mediated toxicity towards the *Plasmodium* parasite. This toxic insult may include damage to lipids in cellular membranes and proteins involved in essential biochemical functions, such as pyrimidine biosynthesis. A potentially useful study would be to accurately quantify the proportion of drug that alkylates different molecular species within the parasite.

To mitigate widespread peroxide-induced cellular damage, the parasite defends itself by engaging a stress response. This involves regulating translation and overexpressing proteins in the ubiquitin-proteasome system to remove damaged and misfolded proteins and restore proteostasis. Death of the parasite occurs when peroxide-mediated damage overwhelms these defensive mechanisms.

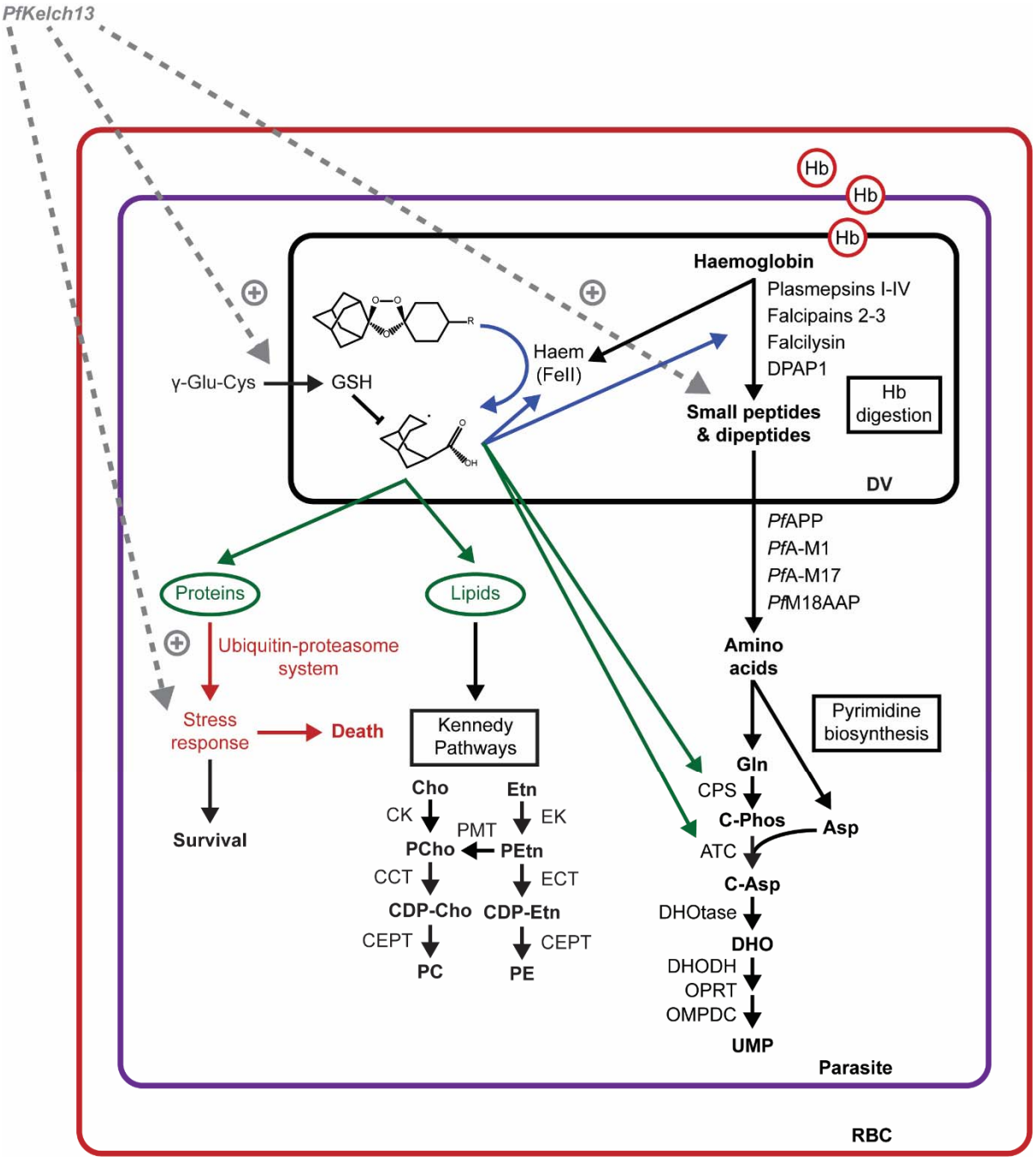


**Figure 1:** Proposed model for peroxide antimalarial killing and mechanisms contributing to *K13*-mediated resistance. Peroxides are activated by an iron source, most likely haemoglobin-derived haem, within the parasite digestive vacuole. The resulting drug-derived radicals initially alkylate proteins and molecules proximal to the activation site, including haem and proteases involved in haemoglobin digestion (shown in blue), disrupting the haemoglobin degradation pathway. Peroxide radicals induce further oxidative insult and cause widespread alkylation of parasite components as the duration of drug exposure is increased (shown in green). To mitigate peroxide-induced cellular damage, the parasite engages a stress response

involving translational regulation and the ubiquitin-proteasome system, and death occurs when the radical-mediated damage overwhelms these parasite defensive mechanisms (shown in red). In resistant parasites, the *K13* (*PfKelch13*) mutation may lead to enhanced cellular stress pathways, altered haemoglobin catabolism and increased antioxidant capacity (shown as grey dashed arrows). These mechanisms may enable *K13*-mutatnt parasites to survive short-term peroxide-induced damage. Asp, aspartic acid; ATC, aspartate carbamoyltransferase; C-Asp, carbamoyl-aspartate, C-Phos, carbamoyl-phosphate; CCT, choline-phosphate cytidyltransferase; CDP-, cytidine-diphospho-; CEPT, choline/ethanolamine phosphotransferase; Cho, choline; CK, choline kinase; CMP, cytidine monophosphate; CPS, carbamoyl phosphate synthetase; DHO, dihydroorotate; DHODH, dihydroorotate dehydrogenase; DHOtase, dihydroorotase; DV, digestive vacuole; ECT, ethanolamine-phosphate cytidyltransferase; EK, ethanolamine kinase; Etn, ethanolamine; Gln, glutamine; GSH, glutathione; Hb, haemoglobin; OMPDC, orotodine 5'-phosphate decarboxylase; OPRT, orotate phosphoribosyltransferase; PC, phosphatidylcholine; PE, phosphatidylethanolamine; PCho, choline phosphate; PEtn, ethanolamine phosphate; PMT, phosphoethanolamine N-methyltransferase; RBC, red blood cell; UMP, uridine monophosphate; γ-Glu-Cys, gamma-glutamylcysteine.

In the context of *K13*-mediated artemisinin resistance, *K13* mutations may affect several factors that contribute to enhanced survival when parasites are exposed to short-term peroxide-induced damage. Resistance could potentially arise due to decreased drug activation, the alleviation of downstream damage, or a combination of both. Peroxide exposure causes a more dramatic depletion of haemoglobin-derived small peptides in the sensitive line and the basal level of these same peptides are significantly elevated in resistant parasites. The prevailing evidence indicates that enhanced antioxidant capacity minimises the damage of drug-derived radicals within *K13*-resistant parasites. It is also thought that these parasites engage an enhanced stress response involving the ubiquitin-proteasome system, thereby promoting parasite survival (27).

The information described in this thesis provides a better understanding of the mechanisms that underpin the activity and resistance of peroxide antimalarials in *P. falciparum*. It is hoped that these contributions will aid in the fight against malaria and guide further development and understanding of not only peroxides but other antimalarials, which will one day help to eradicate this devastating disease.

## 6.7 REFERENCES


1. Vennerstrom JL, Arbe-Barnes S, Brun R, Charman SA, Chiu FC, Chollet J, Dong Y, Dorn A, Hunziker D, Matile H, McIntosh K, Padmanilayam M, Santo Tomas J, Scheurer C, Scorneaux B, Tang Y, Urwyler H, Wittlin S, Charman WN. 2004. Identification of an antimalarial synthetic trioxolane drug development candidate. Nature 430:900-904.
2. Charman SA, Arbe-Barnes S, Bathurst IC, Brun R, Campbell M, Charman WN, Chiu FC, Chollet J, Craft JC, Creek DJ, Dong Y, Matile H, Maurer M, Morizzi J, Nguyen T, Papastogiannidis P, Scheurer C, Shackleford DM, Sriraghavan K, Stingelin L, Tang Y, Urwyler H, Wang X, White KL, Wittlin S, Zhou L, Vennerstrom JL. 2011. Synthetic ozonide drug candidate OZ439 offers new hope for a single-dose cure of uncomplicated malaria. Proc Natl Acad Sci U S A 108:4400-4405.
3. Avery MA, Gao F, Chong WK, Mehrotra S, Milhous WK. 1993. Structure-activity relationships of the antimalarial agent artemisinin. 1. Synthesis and comparative molecular field analysis of C-9 analogs of artemisinin and 10-deoxoartemisinin. J Med Chem 36:4264-4275.
4. Kaiser M, Wittlin S, Nehrbass-Stuedli A, Dong Y, Wang X, Hemphill A, Matile H, Brun R, Vennerstrom JL. 2007. Peroxide bond-dependent antiplasmodial specificity of artemisinin and OZ277 (RBx11160). Antimicrob Agents Chemother 51:2991-2993.
5. Dong Y, Chollet J, Matile H, Charman SA, Chiu FC, Charman WN, Scorneaux B, Urwyler H, Santo Tomas J, Scheurer C. 2005. Spiro and dispiro-1, 2, 4-trioxolanes as antimalarial peroxides: charting a workable structure-activity relationship using simple prototypes. J Med Chem 48:4953-4961.
6. Creek DJ, Charman WN, Chiu FC, Prankerd RJ, McCullough KJ, Dong Y, Vennerstrom JL, Charman SA. 2007. Iron-mediated degradation kinetics of substituted dispiro-1,2,4-trioxolane antimalarials. J Pharm Sci 96:2945-2956.
7. Fügi MA, Wittlin S, Dong Y, Vennerstrom JL. 2010. Probing the antimalarial mechanism of artemisinin and OZ277 (arterolane) with nonperoxidic isosteres and nitroxyl radicals. Antimicrob Agents Chemother 54:1042-1046.
8. Tang Y, Dong Y, Wang X, Sriraghavan K, Wood JK, Vennerstrom JL. 2005. Dispiro-1,2,4-trioxane analogues of a prototype dispiro-1,2,4-trioxolane: mechanistic

comparators for artemisinin in the context of reaction pathways with iron(II). J Org Chem 70:5103-5110.

9. Wang X, Dong Y, Wittlin S, Creek D, Chollet J, Charman SA, Tomas JS, Scheurer C, Snyder C, Vennerstrom JL. 2007. Spiro- and dispiro-1,2-dioxolanes: contribution of iron(II)-mediated one-electron vs two-electron reduction to the activity of antimalarial peroxides. J Med Chem 50:5840-5847.
10. Yang T, Xie SC, Cao P, Giannangelo C, McCaw J, Creek DJ, Charman SA, Klonis N, Tilley L. 2016. Comparison of the exposure time-dependence of the activities of synthetic ozonide antimalarials and dihydroartemisinin against K13 wild-type and mutant *Plasmodium falciparum* strains. Antimicrob Agents Chemother 60:4501-4510.
11. Ismail HM, Barton VE, Panchana M, Charoensutthivarakul S, Biagini GA, Ward SA, O'Neill PM. 2016. A click chemistry-based proteomic approach reveals that 1, 2, 4-trioxolane and artemisinin antimalarials share a common protein alkylation profile. Angew Chem Int Ed Engl 55:6401-6405.
12. Jourdan J, Matile H, Reift E, Biehlmaier O, Dong Y, Wang X, Mäser P, Vennerstrom JL, Wittlin S. 2015. Monoclonal antibodies that recognize the alkylation signature of antimalarial ozonides OZ277 (arterolane) and OZ439 (artefenomel). ACS Infect Dis 2:54-61.
13. Hofer S, Brun R, Maerki S, Matile H, Scheurer C, Wittlin S. 2008. *In vitro* assessment of the pharmacodynamic properties of DB75, piperaquine, OZ277 and OZ401 in cultures of *Plasmodium falciparum*. J Antimicrob Chemother 62:1061-1064.
14. Maerki S, Brun R, Charman SA, Dorn A, Matile H, Wittlin S. 2006. *In vitro* assessment of the pharmacodynamic properties and the partitioning of OZ277/RBx-11160 in cultures of *Plasmodium falciparum*. J Antimicrob Chemother 58:52-58.
15. Stocks PA, Bray PG, Barton VE, Al-Helal M, Jones M, Araujo NC, Gibbons P, Ward SA, Hughes RH, Biagini GA, Davies J, Amewu R, Mercer AE, Ellis G, O'Neill PM. 2007. Evidence for a common non-heme chelatable-iron-dependent activation mechanism for semisynthetic and synthetic endoperoxide antimalarial drugs. Angew Chem Int Ed Engl 46:6278-6283.
16. Xie SC, Dogovski C, Hanssen E, Chiu F, Yang T, Crespo MP, Stafford C, Batinovic S, Teguh S, Charman S, Klonis N, Tilley L. 2016. Haemoglobin degradation underpins the sensitivity of early ring stage *Plasmodium falciparum* to artemisinins. J Cell Sci 129:406-416.

17. Creek DJ, Charman WN, Chiu FC, Prankerd RJ, Dong Y, Vennerstrom JL, Charman SA. 2008. Relationship between antimalarial activity and heme alkylation for spiro- and dispiro-1,2,4-trioxolane antimalarials. Antimicrob Agents Chemother 52:1291-1296.
18. Siddiqui G, Srivastava A, Russell AS, Creek DJ. 2017. Multi-omics based identification of specific biochemical changes associated with PfKelch13-mutant artemisinin resistant *Plasmodium falciparum*. J Infect Dis 215:1435-1444.
19. Robert A, Claparols C, Witkowski B, Benoit-Vical F. 2013. Correlation between *Plasmodium yoelii nigeriensis* susceptibility to artemisinin and alkylation of heme by the drug. Antimicrob Agents Chemother 57:3998-4000.
20. Schaefer WH, Harris TM, Guengerich FP. 1985. Characterization of the enzymic and nonenzymic peroxidative degradation of iron porphyrins and cytochrome P-450 heme. Biochemistry 24:3254-3263.
21. Ismail HM, Barton V, Phanchana M, Charoensutthivarakul S, Wong MHL, Hemingway J, Biagini GA, O'Neill PM, Ward SA. 2016. Artemisinin activity-based probes identify multiple molecular targets within the asexual stage of the malaria parasites *Plasmodium falciparum* 3D7. Proc Natl Acad Sci U S A 113:2080-2085.
22. Wang J, Zhang C-J, Chia WN, Loh CC, Li Z, Lee YM, He Y, Yuan L-X, Lim TK, Liu M, Liew CX, Lee YQ, Zhang J, Lu N, Lim CT, Hua Z-C, Liu B, Shen H-M, Tan KSW, Lin Q. 2015. Haem-activated promiscuous targeting of artemisinin in *Plasmodium falciparum*. Nat Commun 6:10111.
23. Liu J, Istvan ES, Gluzman IY, Gross J, Goldberg DE. 2006. *Plasmodium falciparum* ensures its amino acid supply with multiple acquisition pathways and redundant proteolytic enzyme systems. Proc Natl Acad Sci U S A 103:8840-8845.
24. Smilkstein M, Sriwilaijaroen N, Kelly JX, Wilairat P, Riscoe M. 2004. Simple and inexpensive fluorescence-based technique for high-throughput antimalarial drug screening. Antimicrob Agents Chemother 48:1803-1806.
25. Xie SC, Dogovski C, Kenny S, Tilley L, Klonis N. 2014. Optimal assay design for determining the *in vitro* sensitivity of ring stage *Plasmodium falciparum* to artemisinins. Int J Parasitol 44:893-899.
26. O'Neill PM, Barton VE, Ward SA. 2010. The molecular mechanism of action of artemisinin--the debate continues. Molecules 15:1705-1721.
27. Dogovski C, Xie SC, Burgio G, Bridgford J, Mok S, McCaw JM, Chotivanich K, Kenny S, Gnädig N, Straimer J, Bozdech Z, Fidock DA, Simpson JA, Dondorp AM, Foote S,

Klonis N, Tilley L. 2015. Targeting the cell stress response of *Plasmodium falciparum* to overcome artemisinin resistance. PLoS Biol 13:e1002132.

28. Ariey F, Witkowski B, Amaratunga C, Beghain J, Langlois A-C, Khim N, Kim S, Duru V, Bouchier C, Ma L, Lim P, Leang R, Duong S, Sreng S, Suon S, Chuor CM, Bout DM, Menard S, Rogers WO, Genton B, Fandeur T, Miotto O, Ringwald P, Le Bras J, Berry A, Barale J-C, Fairhurst RM, Benoit-Vical F, Mercereau-Puijalon O, Menard D. 2014. A molecular marker of artemisinin-resistant *Plasmodium falciparum* malaria. Nature 505:50-55.
29. Straimer J, Gnädig NF, Stokes BH, Ehrenberger M, Crane AA, Fidock DA. 2017. *Plasmodium falciparum* K13 mutations differentially impact ozonide susceptibility and parasite fitness *in vitro*. mBio 8:e00172-00117.
30. Mok S, Ashley EA, Ferreira PE, Zhu L, Lin Z, Yeo T, Chotivanich K, Imwong M, Pukrittayakamee S, Dhorda M, Nguon C, Lim P, Amaratunga C, Suon S, Hien TT, Htut Y, Faiz MA, Onyamboko MA, Mayxay M, Newton PN, Tripura R, Woodrow CJ, Miotto O, Kwiatkowski DP, Nosten F, Day NP, Preiser PR, White NJ, Dondorp AM, Fairhurst RM, Bozdech Z. 2015. Drug resistance. Population transcriptomics of human malaria parasites reveals the mechanism of artemisinin resistance. Science 347:431-435.
31. Straimer J, Gnadig NF, Witkowski B, Amaratunga C, Duru V, Ramadani AP, Dacheux M, Khim N, Zhang L, Lam S, Gregory PD, Urnov FD, Mercereau-Puijalon O, Benoit-Vical F, Fairhurst RM, Menard D, Fidock DA. 2015. Drug resistance. K13-propeller mutations confer artemisinin resistance in *Plasmodium falciparum* clinical isolates. Science 347:428-431.
32. Patzewitz EM, Wong EH, Müller S. 2012. Dissecting the role of glutathione biosynthesis in *Plasmodium falciparum*. Mol Microbiol 83:304-318.

# Appendix 1

# The role of metabolomics in antiparasitic drug discovery

Giannangelo C, Ellis KM, Sexton AE, Stoessel D, Creek DJ. 2016. The role of metabolomics in antiparasitic drug discovery, p 321-342, Comprehensive analysis of parasite biology: from metabolism to drug discovery, vol 7. Wiley-VCH, Weinheim, Germany.

# 14
# The Role of Metabolomics in Antiparasitic Drug Discovery

*Carlo R. Giannangelo, Katherine M. Ellis, Anna E. Sexton, Daniel Stoessel, and Darren J. Creek**

## Abstract

Metabolomics involves the global measurement of small molecule metabolites in a biological system and allows the comprehensive investigation of metabolic pathways in pathogenic parasites. Metabolomics studies have enabled the discovery of novel aspects of parasite metabolism that constitute attractive drug targets, and have elucidated metabolic targets of antiparasitic compounds. This chapter provides an introduction to parasite metabolomics and describes metabolomics methods suitable for kinetoplastid and apicomplexan parasites. Several examples are provided describing applications of metabolomics to understand the mechanisms of action and resistance for a range of antiprotozoal compounds. This unbiased elucidation of drug mechanisms with metabolomics will facilitate the discovery and development of new drugs for parasitic diseases of global importance.

## Introduction

Protozoan parasites are a diverse group of eukaryotic pathogens that are responsible for a variety of life-threatening infections in humans, including malaria (*Plasmodium* spp.), African Trypanosomiasis (*Trypanosoma brucei*), Chagas disease (*Trypanosoma cruzi*), and Leishmaniasis (*Leishmania* spp.). These diseases primarily affect tropical and subtropical regions of the world and cause significant morbidity and mortality as well as exacerbate poverty and economic hardship in developing countries. More than 1 million deaths occur annually as a result of protozoan-related diseases [1], and approximately 3.8 billion people are threatened by the risk of infection each year [2].

Control and prevention of these parasitic diseases are heavily reliant on antiprotozoal drug therapy, as there are currently no safe and highly effective vaccines. Unfortunately, the currently used antiprotozoals are severely limited

*Corresponding author.

*Comprehensive Analysis of Parasite Biology: From Metabolism to Drug Discovery,*
First Edition. Edited by Sylke Müller, Rachel Cerdan, and Ovidiu Radulescu.

by liabilities including poor efficacy, drug resistance, toxicity, high cost, and inadequate pharmacokinetic properties. Exacerbating this problem, the majority of antiprotozoal drugs currently in clinical use act by as-yet-unknown modes of action. This impacts our ability to optimize treatment strategies, understand parasite resistance mechanisms, and monitor drug efficacy and toxicity. In the context of these liabilities and the unlikely prospect of effective vaccines for human protozoan parasites in the near future, there is an urgent need for the discovery of new drugs that are safe, effective, and act by novel mechanisms. Despite this necessity, there has been an ongoing failure to invest into basic research and development for these diseases [3, 4]. Consequently, there are significant gaps in our fundamental understanding of the biology of these pathogens [4] and a paucity of new therapeutic products and new chemical entities being approved for the treatment of these tropical diseases [5].

The successful development of tropical medicines faces unique challenges. The ideal drug should be cheap to manufacture and distribute, be orally active, and require only once daily administration or result in a single dose cure. Furthermore, complexities in parasite biology must also be considered, such as latent parasite forms, the location of parasites within host cells, drug efflux mechanisms, and the existence of multiple life-cycle stages. Unfortunately, there is a dearth of validated molecular targets for parasitic diseases due to the lack of detailed information concerning the targets of currently used antiprotozoal drugs. These issues represent major obstacles for the success of drug discovery efforts in parasitic diseases [6].

Thousands of antiparasitic hit compounds have been identified in recent years, following the application of phenotypic screening of large compound libraries against whole organism systems [7–9]. Lead compounds that emerge from these screening programs inherently possess favorable drug-like characteristics, including cell permeability and inhibition of essential targets, which contribute to the success of this approach. The trypanocidal compounds fexinidazole and SCYX-7158 [3] and the antimalarial compounds KAE609 [10], KAF156 [11], and MMV390048 [12] have all advanced to preclinical and clinical trials after emerging from phenotypic screening programs. The phenotypic screening approach, however, forgoes mechanistic information relating to drug mode of action. As such, the elucidation of drug targets and mechanistic information from hits derived from these screens is now a primary goal [13]. An untargeted approach aimed at discerning drug modes of action, which does not rely on *a priori* knowledge of a drug's mechanism of action, will greatly improve the drug discovery process for parasitic diseases by informing rational drug design, and improve our existing understanding of the medicines currently in clinical use [14]. Untargeted metabolomics is an emerging discipline that offers a rapid, unbiased, and system-wide approach for the investigation of parasite metabolic pathways, the elucidation of drug modes of action, and the discovery of likely drug targets.

## Principles of Metabolomics

The field of metabolomics is the branch of omics technology concerned with the high-throughput identification and quantification of low-molecular-weight molecules (<1500 Da) in a biological system [14–16]. The complement of small molecules in a system, known as the *metabolome*, includes a range of chemically diverse species, of varying abundance, that are produced through the interactions of larger macromolecules, including DNA, RNA, and proteins. Its close relationship with the phenotype makes metabolomics ideal for assessing the physiological state of an organism or system at a snapshot in time. Consequently, metabolomics has found applications in a diverse range of fields, such as the nutritional sciences [17], personalized medicine [18], toxicology [19], and biomarker discovery for disease diagnosis and monitoring in a variety of cancers [20–22], cardiovascular diseases [23–25], and neurological conditions [26, 27]. Metabolomics is a promising tool for antiparasitic drug discovery, and it has already demonstrated utility in the validation of known targets and the discovery of new drug targets for a range of diseases.

## Metabolomics in Drug Discovery

Perturbations to metabolic pathways underpin many disease-state processes, and the identification of enzyme targets within these pathways may represent novel sites for therapeutic intervention. The application of metabolomics to cancer has provided further insight into potential drug targets in energy production pathways within cancer cells, which rely on aerobic glycolysis in a process known as the *Warburg effect* [28].

As untargeted metabolomics provides a global measurement of metabolic alterations within a system, this unbiased methodology can reveal changes to novel or unexplored biochemical pathways, offering a distinct advantage over traditional enzyme inhibition assays. This approach has been applied to neuropathic pain models in rats, which revealed dysregulation of sphingomyelin–ceramide metabolism [29], with the metabolite *N*,*N*-dimethylsphingosine (DMS) highly abundant in rats with neuropathic pain. In this case, metabolomics has revealed a previously unexplored target for therapeutic intervention, as inhibition of DMS production could serve as a potentially attractive therapeutic option for neuropathic pain [29].

In response to viral infection, metabolomics has been used to identify the change in abundance of a number of key metabolites *in vitro.* Human fibroblasts infected with influenza A virus (IVA), herpes simplex virus type-1 (HSV-1), and human cytomegalovirus (HCMV) revealed significant metabolic perturbations that were consistent with the pharmacology of known antivirals and provided insight into possible new antiviral targets [30]. IVA-infected fibroblasts showed a significant upregulation of acetylneuraminic acid, consistent with the mechanism

of action of the anti-influenza drugs such as oseltamivir, which selectively inhibit viral neuraminidase. In the case of HSV-1, changes in the 2′-deoxynucleotides, dTTP and dTMP, were seen, which is consistent with the mechanism of action of HSV-1 treatments such as acyclovir that inhibit viral thymidine kinase. Combined with metabolic flux analysis, metabolomics on HCMV-infected cells revealed changes to tricarboxylic acid (TCA) cycle intermediates and flux through fatty acid biosynthesis, via the enzyme acetyl-coenzyme A carboxylase, as the most significant perturbations [30]. This enzyme is not a current antiviral target but may represent a useful target for future intervention for the treatment of HCMV [30].

Understanding the targets of anti-infective drugs currently in use and those in the developmental pipeline is invaluable for informing rational drug design and overcoming resistance. The antimicrobial triphenylbismuthdichloride was found to inhibit the bacterial pyruvate dehydrogenase complex in a metabolomics investigation in *Staphylococcus aureus* [31]. The identification of this enzyme as an effective drug target now offers new hope in the potential treatment of multidrug-resistant bacterial pathogens [31].

In the field of antiprotozoal drug discovery, metabolomic analysis of sensitive and resistant parasites that have been treated with antiprotozoal compounds can detect drug-induced perturbations to specific parasite metabolites and pathways, offering a global, unbiased approach to discovery of potential drug targets as well as mechanisms of drug action and resistance [14, 28]. It also offers a system-wide approach to analyze parasite biochemistry and host–parasite interactions, leading to the identification of essential parasite pathways and novel enzymes that can be targeted for therapeutic intervention. This review discusses current metabolomics methodology, the application of metabolomics to antiparasitic drug discovery and summarizes the impact of antiprotozoals on kinetoplastid and apicomplexan parasite metabolism.

## Metabolomics Methodology

Protozoan parasites contain complex mixtures of thousands of small molecules that vary greatly in their chemical properties and abundance. The nature of the metabolome is highly dependent on both the genome and the environment and is unique for different stages of the parasite life cycle. Therefore, metabolomics analysis requires a validated and highly robust methodology (Figure 14.1) to reproducibly measure the most comprehensive range of metabolites from each sample, in order to obtain the most reliable approximation of the organism's physiology under defined conditions [32, 33].

### Study Design

The design of metabolomics experiments can vary widely depending on the aim of the study. A truly untargeted metabolomics approach is suitable for

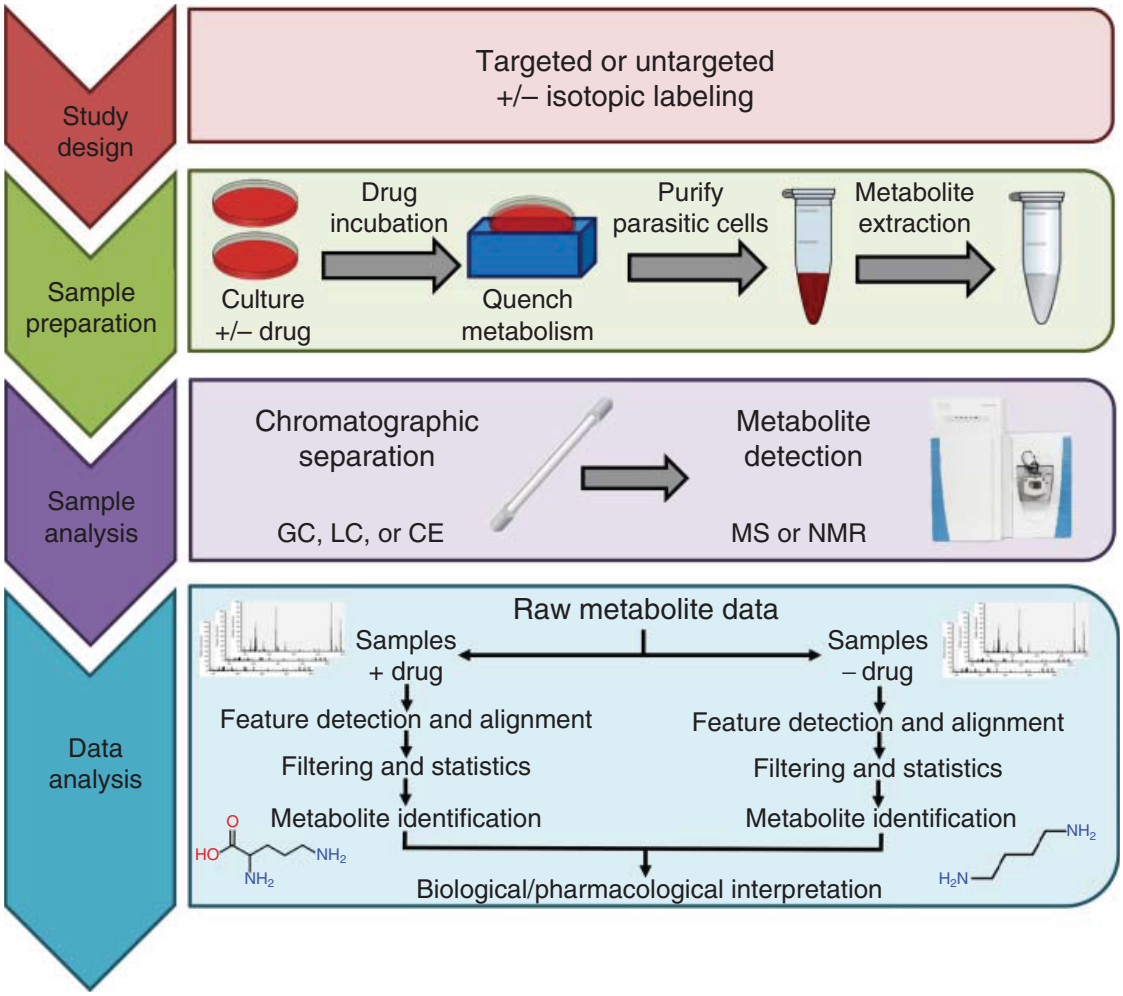


**Figure 14.1** General metabolomics workflow for *in vitro* drug mechanism of action studies using protozoan parasites. Parasites are grown in culture and incubated with the test compound for the desired duration. Metabolism is then quenched by rapid cooling, and the parasitic cells may be isolated before metabolite extraction using organic solvent. Metabolite extracts are then analyzed using an appropriate detection method such as mass spectrometry (MS) or nuclear magnetic resonance (NMR) after chromatographic separation with either gas chromatography (GC). liquid chromatography (LC) or capillary electrophoresis (CE) after chromatographic separation. The raw metabolite data must then be processed to determine specific drug-induced metabolic perturbations responsible for parasite death.

hypothesis-free studies, such as the unbiased discovery of drug targets for novel compounds or clinical biomarker discovery. While it is not possible to measure every metabolite in a single experiment, the extraction and analytical conditions can be optimized to detect a wide range of metabolites with diverse chemical properties, and this often involves a combination of analytical techniques and data processing approaches [28, 34]. An alternative approach is to apply targeted metabolomics, whereby a predefined range of metabolites or pathways are analyzed. This approach is suitable for hypothesis-testing experiments, allows

improved sensitivity and quantification accuracy, and may be combined with stable isotope labeling to perform flux calculations [14, 35, 36].

The metabolic response of parasites to drug treatment can be measured in *in vitro* or *in vivo* systems, although host factors may complicate biochemical interpretation in the latter. *In vitro* cell culture systems allow metabolism to be studied in a controlled environment, which is important to delineate pharmacological effects from background variations in parasite metabolism. The choice of growth media is an important consideration, as nutrient availability can interfere with drug action or metabolic response, as demonstrated for the trypanocidal activity of antifolate drugs [37]. Drug incubation times and concentrations can be tuned to investigate primary and secondary effects of drugs on metabolism, and it is generally desirable to obtain samples before a generalized death phenotype is apparent. For optimal statistical power, it is important to have a minimum of four separate biological replicates, and the inclusion of time-series analysis can add further confidence and insight into temporal responses [38].

#### Sample Preparation

Accurate analysis of intracellular metabolism requires rapid quenching of cell metabolism to minimize the introduction of unwanted variance during sample preparation. Lowering the sample temperature to 0 °C is the most common quenching method for protozoa. Alternative quenching procedures developed in other microbes, such as filtration or freezing in cold methanol, are generally unsuitable for protozoan parasites due to metabolite leakage (DJ Creek and MP Barrett).

Once metabolism has been quenched, parasites may be washed and/or isolated from host cells, followed by extraction of metabolites and removal of macromolecules. Organic solvent extractions are generally effective and compatible with downstream mass spectrometry analysis (Table 14.1).

#### Sample Analysis

The combination of chromatographic separation paired to mass spectrometry (MS) allows for the most comprehensive analysis of highly complex metabolomics samples. Other techniques including Nuclear Magnetic Resonance (NMR), Fourier Transform Infra-red (FTIR), and Raman spectroscopy may also be applied, albeit with lower metabolite coverage.

Mass spectrometry provides sensitive detection of a wide range of metabolites, and the simultaneous identification of hundreds of metabolites has been facilitated by advances in high-resolution mass spectrometry (Time-of-Flight, Orbitrap, and FT-ICR). Sensitive detection and identification of metabolites are further improved by coupling MS to chromatographic separation techniques, such as gas chromatography (GC), liquid chromatography (LC), or capillary electrophoresis (CE). GC produces high-resolution and reproducible separation

**Table 14.1** Metabolomic quenching and extraction techniques for *Plasmodium* and *Trypanosomatid* parasites.

| Parasite | Life-cycle stage | Quenching method | Extraction method |
|---|---|---|---|
| *Plasmodium* spp. | Blood stage | Not quenched | 90% methanol [39] |
| | Blood stage | 4 volumes of 100% methanol at −70 °C | 80% MeOH on dry ice [40] |
| | Blood stage | Not quenched | 100% MeOH then MeOH:$H_2O$ 8 : 2 plus sonication [41] |
| | Saponin extracted | Frozen −80 °C | Chloroform:MeOH:ACN 2 : 1 : 1 plus steel beads, then TissueLyser [42] |
| | Various blood stages | Not quenched | 100% MeOH on dry ice, then 80% EtOH with sonication [43] |
| | Blood stage | Methanol/water/ chloroform 4 : 3 : 1 | Biphasic liquid–liquid extraction at pH-adjusted solvents [38] |
| | Blood stage | Rapid cooling in dry ice ethanol bath | Chloroform:methanol:water 1 : 3 : 1 shaking 1 h [44] |
| | Blood stage | Ice-cold PBS | 80% ACN [45] |
| *Trypanosomatids* | Blood stage | Rapid cooling in dry-ice ethanol bath | Chloroform:methanol:water 1 : 3 : 1 shaking 1 h [46, 47] |
| | Blood stage | Not quenched | 80 °C ethanol 2 min [48, 49] |

and is ideal for volatile compounds, and has been applied to the sensitive detection of *Plasmodium*-infected blood [50]. However, nonvolatile compounds require derivatization, resulting in low throughput, sensitivity, and reproducibility [51].

LC methods are readily coupled to high-resolution MS and are ideal for the analysis of a wide range of soluble metabolites. The availability of diverse LC column chemistries allows the analytical method to be optimized for certain metabolite classes [14, 51].

Reversed-phase chromatography is the most common form of chromatography applied to global metabolite profiling studies. This method is highly robust and provides extensive coverage of lipids and nonpolar secondary metabolites, but is not appropriate for the analysis of polar compounds, which constitute the majority of metabolic intermediates in the essential central metabolic pathways.

The addition of ion-pairing reagents can improve retention and resolution of polar metabolites; however, these are often not compatible with MS detection. Hydrophilic interaction chromatography (HILIC), ion chromatography (IC), and CE are well suited for the profiling of primary metabolites, and HILIC has been extensively applied to parasite metabolomics [14].

Method validation is a key consideration when selecting the ideal method or combination of methods for a metabolomics study. While metabolite coverage is of primary concern, method reproducibility is of critical importance to allow label-free semiquantitative comparisons of treated and untreated samples in a statistically robust manner. The inclusion of multiple internal standards, and periodic analysis of matched quality control samples, is essential to monitor analytical performance and potentially correct for signal drift.

#### Metabolite Identification

The identification of metabolites in untargeted metabolomics studies is a key bottleneck that must be overcome to infer biological or pharmacological meaning. The Metabolomics Standards Initiative has defined four different confidence levels by which a metabolite is identified [52]. The highest level of identification confidence (level 1) requires the comparison of two or more orthogonal properties with authentic chemical standards, which have been analyzed under identical analytical conditions. In practice, this is achieved by the combination of MSMS or retention time data with high-resolution mass spectrometry. However, it is important to note that successful dereplication of isomeric species often requires optimization of the chromatographic or fragmentation parameters. In the absence of authentic chemical standards for every parasite-derived metabolite, external databases or predictive algorithms for mass, MSMS, and/or retention time may be used to provide putative identification (level 2). Unidentified metabolite features from known (level 3) or unknown (level 4) metabolite classes should also be reported, as these may represent novel endogenous or drug-derived metabolites [53, 54].

#### Data Analysis

Any metabolomics analysis will produce large datasets; therefore, it is essential that the data are analyzed in an efficient and meaningful way to measure the relative abundance of hundreds of metabolites [28]. Several commercial and open-source software packages are available for the detection and alignment of metabolite features (peaks) and downstream artifact filtering, metabolite identification, statistical comparison, and pathway or network modeling [55].

### Metabolomics for Drug Discovery in Kinetoplastid Parasites

Kinetoplastida comprise a phylogenetically ancient group of protozoa, many of which can cause significant diseases in humans and animals. They are responsible for extensive morbidity and mortality in the developing world and also place a substantial economic burden on the countries that are affected [56, 57]. These protozoa include the South American trypanosome, *T. cruzi*, which causes

Chagas disease; the *T. brucei* subspecies, which causes human African trypanosomiasis (HAT); and multiple *Leishmania* species, which cause various forms of Leishmaniasis.

### Human African Trypanosomiasis

HAT, also known as *sleeping sickness*, is caused by infection of the host with *Trypanosoma brucei rhodesiense* or *Trypanosoma brucei gambiense* [58, 59] following a bite by the tsetse fly vector. In the first stage of the disease, known as the hemolymphatic phase, nonspecific symptoms such as headache and fever are most common. Stage 2 is considered the neurological phase and occurs when the parasite crosses the blood–brain barrier, inevitably resulting in death in the absence of effective treatment [60]. Although reported HAT mortality has significantly declined in recent years [2], there are serious concerns regarding drug resistance [49], cost, and toxicity for the currently available arsenal of trypanocidal medicines. Treatment options for stage 1 of the disease include suramin and pentamidine, both of which must be administered by injection [61, 62], while stage 2 treatment utilizes melarsoprol or eflornithine, either as monotherapy or in combination with nifurtimox [63–65].

A metabolomics approach has been used to explore the mechanisms of action of several trypanocidal compounds in *T. b. brucei* [66, 67]. Untargeted metabolomic analysis of eflornithine has confirmed its mode of action. Eflornithine treatment induced predictable changes in the levels of polyamine pathway intermediates, resulting in significant accumulation of ornithine and depletion of putrescine, mediated by the inhibition of ornithine decarboxylase. Due to the untargeted nature of the method, the analysis also revealed the absence of arginase activity as well as drug-induced changes in N-acetylated ornithine and putrescine and depletion of the downstream polyamine pathway product spermidine [67]. Polyamines serve an important role in trypanosomes, combining with glutathione to form trypanothione, the major intracellular antioxidant molecule [68–70]. Oxidative stress was also thought to be involved in nifurtimox action [65, 71]. However, metabolomic analysis revealed additive, but not synergistic, metabolic perturbations for eflornithine and nifurtimox, which supports the lack of trypanocidal synergism observed *in vitro* [67]. The untargeted metabolomics analysis of nifurtimox treatment confirmed metabolic activation by nitroreductase to form a reactive nitrile intermediate [72, 73] and revealed changes in endogenous metabolites involved in nucleotide and carbohydrate metabolism [67].

Untargeted metabolomics applied to pentamidine-treated parasites showed nonspecific changes in metabolite levels that could not be directly related to a specific metabolic pathway [37]. Rather, the drug may impact nonmetabolic parasite targets, by interacting with nucleic acids or may even disrupt the mitochondrial membrane potential [74, 75].

Metabolomics has also been utilized for drug target discovery for novel antitrypanosomal compounds. Halogenated pyrimidines have demonstrated high affinity for the trypanosomal uracil uptake transporter, leading to incorporation of 5-fluorouracil into pyrimidine nucleotides and RNA [46]. The analogs 5-fluoro-2′-deoxyuridine and 5-fluoro-2′-deoxycytidine demonstrated prodrug activity, with the active metabolite 5F-dUMP inhibiting thymidylate synthase activity. Overall, these studies showed that halogenated pyrimidines interfere with pyrimidine salvage in *T. b. brucei* by distinct mechanisms [46]. Curcumin analogs bearing a monoenone linker motif show highly potent trypanocidal activity. Untargeted metabolomics revealed significant depletion of intracellular thiols, such as trypanothione and glutathione. This was most likely mediated through the rapid formation of drug-thiol adducts and was not apparent in drug-resistant parasites, confirming the link between thiol depletion and trypanocidal activity [53].

### Chagas Disease

Chagas disease, or American trypanosomiasis, is caused by infection with the parasite *T. cruzi*, following the bite of an infected triatomine bug. Up to 10 million people are infected [2] with the disease manifested by low-grade fever, lymphocytosis, and hyperthermia [76]. Although the acute phase may remain asymptomatic, it can progress to a chronic phase and cause death by cardiac failure [76]. Benznidazole and nifurtimox are the only licensed medicines with proven efficacy against Chagas disease; however, drug resistance has been identified [77, 78].

Multiple drug-specific metabolomic perturbations were observed in *T. cruzi* following benznidazole treatment [54]. Benznidazole is believed to be activated by an unusual type I nitroreductase, leading to the formation of a dihydroxy-dihydroimidazole derivative, which decomposes to give toxic glyoxal [73, 79]. A metabolomics study identified depletion of low-molecular-weight thiols by covalent binding of activated benznidazole, which is believed to be responsible for the drug's toxicity [54]. This is consistent with the drug's proposed mechanism, involving covalent modification of lipids, DNA, and proteins [80, 81]. However, key oxidation products of nucleotides could not be detected [54].

### Leishmaniasis

Infection with *Leishmania* spp. can cause a complex disease state that may manifest as visceral, cutaneous, or mucocutaneous clinical forms. The parasite is transmitted by the bite of a sandfly and, once inside the host, largely resides in macrophages [82]. Drugs currently available for the treatment of Leishmaniasis include miltefosine, amphotericin B [83], and pentavalent antimonials ($Sb^V$) [84]. Unfortunately, they are restricted by less than ideal pharmacokinetics, toxicity, and poor efficacy. The mode of action for miltefosine has been proposed to involve inhibition of protein kinase B [85], influencing lipid metabolism, GPI anchor

synthesis, and signal transduction [86]. It has also been suggested to interact with lipid monolayers [87], membrane phospholipids [88], and choline transport [89] and induce apoptotic responses including DNA fragmentation and chromatin condensation [90]. Untargeted metabolomic analysis identified increased alkene fragment release, which is proposed to be synchronized with the production of reactive oxygen species [91]. This study also identified signs of DNA damage by detecting changes in thiols and polyamines, loss of cell membrane integrity, and intact native membrane phospholipids [91]. Amphotericin B is believed to inhibit glucose uptake and compromises the permeability barrier to small metabolites in *L. donovani* promastigotes by affecting membrane sterols [92]. $Sb^V$ is believed to inhibit trypanothione reductase activity in the parasite [93] and stimulate macrophages to kill their intracellular invaders [94]. An untargeted metabolomic approach has also been used to investigate the mechanisms of resistance to antimonial drug combinations in *L. donovani.* Experimentally generated resistant lines demonstrate metabolic adaptations that protect against drug-induced and external oxidative stress, in addition to changes in membrane fluidity and drug uptake [84].

## Metabolomics for Drug Discovery in Apicomplexan Parasites

The *Apicomplexa* phylum contains several human pathogens that are responsible for significant morbidity and mortality worldwide, including five species of *Plasmodium* that cause human malaria. The *Plasmodium* parasite has a complex life cycle and is transmitted by the bite of the female *Anopheles* mosquito during a blood feed. Patients experience symptoms during the parasite's asexual replication within host red blood cells, and current treatments act on this stage. However, resistance has now emerged to the first- and last-line therapeutic agents, the artemisinins, which threatens to make the disease untreatable [95]. Use of other antimalarials, such as quinolines and antifolates, is already limited by widespread resistance, highlighting the urgent need for new antimalarials with novel modes of action.

### Antimalarial Drug Mechanisms

Several approved antimalarial medicines act by perturbing parasite metabolism. Metabolomics, as an approach to detect drug-induced changes in parasite metabolism, has been validated with studies of the antimalarial atovaquone [96]. Atovaquone acts by inhibiting the cytochrome $bc_1$ complex in the mitochondrial electron transport chain, consequently leading to the dysfunction of dihydroorotate dehydrogenase (DHODH). DHODH dysfunction perturbs pyrimidine synthesis, which is ultimately fatal to the parasite [97, 98]. As expected, metabolomics analysis of atovaquone-treated *Plasmodium falciparum*–infected red blood cells (iRBCs) showed an accumulation of the substrate of DHODH,

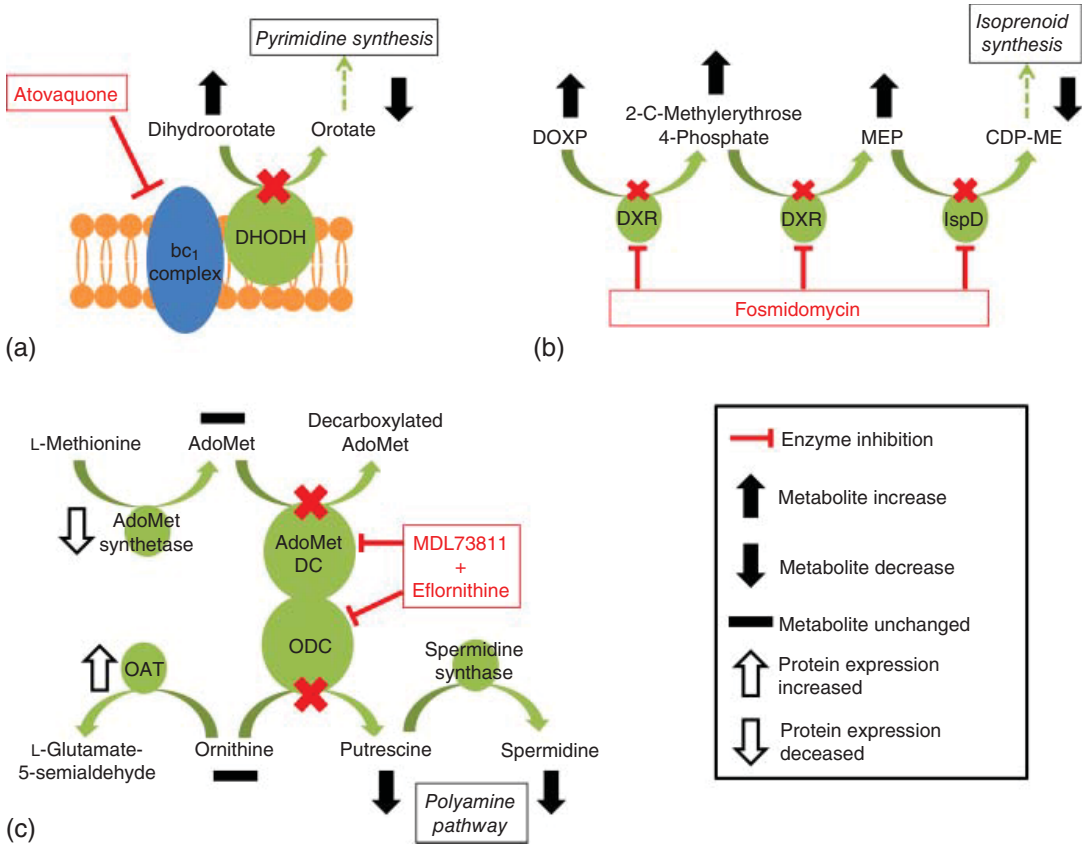


**Figure 14.2** Schematic of metabolic mechanisms of action of three anti-apicomplexan compounds. (a) Atovaquone inhibits the cyctochrome bc1 complex in the mitochondria. This inhibits oxidation of the ubiquinone cofactor resulting in dysfunction of dihydroorotate dehydrogenase (DHODH) such that dihydroorotate accumulates and pyrimidine synthesis is disrupted [96]. (b) Fosmidomycin inhibits deoxyxylulose phosphate reductoisomerase (DXR) causing accumulation of 1-D-deoxyxylulose 5-phosphate (DOXP). It also inhibits methylerythritol phosphate cytidylyltransferase (IspD) causing the accumulation of 2-*C*-methylerythrose and methylerythritol phosphate (MEP) and the depletion of cytidine diphosphate methylerythritol (CDP-ME). This disrupts isoprenoid biosynthesis [42]. (c) Together, eflornithine and MDL73811 inhibit the bifunctional enzyme, *S*-adenosylmethionine decarboxylase/ornithine decarboxylase (AdoMetDC/ODC), which leads to the depletion of polyamines and is ultimately fatal to the parasite. The substrate of AdoMetDC, AdoMet, does not accumulate as expected upon AdoMetDC inhibition. This is due to the decreased expression of AdoMet synthetase, as revealed by transcriptomics and proteomics, such that less AdoMet is synthesized. Similarly, the substrate of ODC, ornithine, does not accumulate as expected upon ODC inhibition. This is due to the increase in ornithine aminotransferase (OAT) expression, which degrades ornithine [41].

dihydroorotate, and its precursor, carbamoyl-L-aspartate (Figure 14.2a). Complementarily, the products of DHODH activity, downstream pyrimidine nucleotides, were depleted [45, 96]. Antifolate drugs kill malaria parasites by inhibition of either dihydrofolate reductase (DHFR) or dihydropteroate synthase (DHPS), perturbing folate metabolism and consequently depriving the pyrimidine synthesis pathway of essential intermediates [99]. This depletion of thymidine nucleotides

by cycloguanil has been confirmed using metabolomics methodology [45]. Another antifolate, proguanil, mediated dysregulation of arginine metabolism, suggesting that a novel mechanism may be involved in the antimalarial mechanism of this drug. Other antimalarials including dihydroartemisinin and chloroquine induced perturbations in hemoglobin-derived peptides, consistent with their proposed mechanisms of action involving the parasite digestive vacuole [45].

### *Plasmodium* Drug-Resistance Mechanisms

Resistance has emerged to all available antimalarial drugs, and resistance mechanisms must be considered during the development of new antimalarials. Genomic sequencing is effective at detecting the genetic mutations associated with drug resistance, but does not always elucidate the mechanisms responsible for resistance. Chloroquine (CQ) resistance is primarily associated with mutations in *P. falciparum* CQ-resistance transporter (*pfcrt*) [100]. However, the molecular mechanisms by which point mutations in PfCRT facilitate CQ resistance remain unclear. Metabolomics revealed an accumulation of many hemoglobin-derived peptides in lines of *P. falciparum* expressing the CQ-resistant form of PfCRT compared to lines expressing the CQ-sensitive form [39]. This suggests impaired hemoglobin digestion in CQ-resistant parasites. Indeed, there was a fitness cost attributed to the expression of the CQ-resistant form of PfCRT [39], which could explain the reemergence of CQ-sensitive parasites in the field following cessation of widespread CQ use.

### Novel Anti-Apicomplexan Compounds

Based on the success of atovaquone, differences in human and parasite electron transport chains have been investigated as potential drug targets for malaria. It was found that *P. falciparum* lacks a canonical NADH dehydrogenase and instead possesses a bacterial-like type II NADH:ubiquinone reductase (PfNDH2) situated upstream of the $bc_1$ complex in the electron transport chain [101]. Biagini *et al.* [96] led a drug discovery initiative to find drugs with activity against PfNDH2 that could kill atovaquone-resistant parasites. Upon treatment of iRBCs with the novel quinolone compound, CK-2-68, metabolomics detected perturbations consistent with DHODH dysfunction. This confirmed that the mechanism of action of CK-2-68 was via disruption of the electron transport chain [96].

Investigation of host and parasite metabolism led to the discovery that, unlike humans, malaria parasites possess a nonmevalonate isoprenoid biosynthesis pathway [102]. Several antibiotics target this pathway in bacteria, and when tested, it was found that these antibiotics had antimalarial activity [103]. Fosmidomycin was one such drug, which blocks isoprenoid synthesis in *Escherichia coli* via inhibiting deoxyxylulose phosphate reductoisomerase (DXR) [104]. Targeted metabolomics of fosmidomycin-treated *P. falciparum* showed the anticipated

accumulation of DXR's substrate, 1-D-deoxyxylulose 5-phosphate (DOXP), but did not detect the expected depletion of its product, methylerythritol phosphate (MEP). In fact, MEP levels increased. There was depletion in metabolites further downstream in the isoprenoid pathway, including cytidine diphosphate methylerythritol (CDP-ME), the product of the enzyme methylerythritol phosphate cytidylyltransferase (IspD) (Figure 14.2b). This suggests that fosmidomycin may also target IspD, which was supported by *in vitro* inhibition of recombinant IspD. Supplementation of fosmidomycin-treated parasites with a downstream isoprenoid was able to rescue *P. falciparum*, suggesting that fosmidomycin exclusively targets the isoprenoid pathway [42]. Fosmidomycin is currently in clinical trials in combination with clindamycin [105, 106] for uncomplicated malaria.

Eflornithine, when coadministered with a bis(benzyl)polyamine analog, can cure mice of the rodent malaria strain, *Plasmodium berghei* [107]. Together, eflornithine and the bis(benzyl)polyamine analog, MDL73811, inhibit the bifunctional *S*-adenosylmethionine decarboxylase/ornithine decarboxylase (AdoMetDC/ODC) enzyme, blocking polyamine synthesis [108, 109]. To investigate polyamine depletion as an antimalarial strategy, a combined transcriptomics, proteomics, and metabolomics study was performed [41]. Metabolomics confirmed that polyamine depletion is induced by eflornithine-MDL73811 (Figure 14.2c). Surprisingly, the substrate of AdoMetDC AdoMet (*S*-adenosylmethionine), did not accumulate as expected, upon inhibition of the enzyme. Proteomics and transcriptomics detected a decrease in AdoMet synthetase such that less AdoMet would be synthesized, revealing a compensatory feedback mechanism in *P. falciparum.* Furthermore, the substrate of ornithine decarboxylase (ODC), ornithine, did not accumulate upon drug treatment as occurs in trypanosomes. This can be explained by the increase in ornithine aminotransferase (OAT) expression, which degrades ornithine.

## Summary

Due to the lack of information on the mechanisms of action of current drugs, there are very few well-defined clinically relevant drug targets for protozoan parasites. Therefore, recent high-throughput screens of large compound libraries belonging to pharmaceutical companies [7, 110] have been invaluable for identifying novel antiparasitic compounds from a diverse range of chemical classes. However, there is a significant bottleneck in the development of these compounds for clinical use due to a lack of information regarding their mechanism of action [13]. Metabolomics represents a novel approach for understanding parasite biology and provides a valuable way to capture a global, untargeted perspective on drug-induced changes to parasite metabolism, which can then generate hypotheses regarding mechanisms of drug action. This will support the rational design of novel antiparasitic compounds that overcome issues relating to drug toxicity, resistance, and poor pharmacokinetic properties. It will also aid in the optimal utilization of the current repertoire of drugs by better guiding combination

therapies and the monitoring of efficacy and resistance. Metabolomics has already revealed the modes of action of multiple antiparasitic drugs [53, 67, 91, 96] and has uncovered many fundamental aspects of parasite biology such as isoprenoid synthesis in *P. falciparum* [42] and pyrimidine metabolism in *T. brucei* [46] that could be targeted for therapeutic intervention.

Metabolomics has been driven forward by the recent advances in analytical technologies that allow for greater metabolite coverage from complex biological matrices with increased sensitivity and resolution [111]. This will continue to improve in coming years, and the ability to efficiently analyze and biochemically interpret omics scale data will likely be the limiting steps in the progression of metabolomics in the drug discovery field. However, the improvement and accessibility of a variety of freely available data analysis packages are beginning to overcome this hurdle. The interpretation of metabolomics data, and the ability to link changes in metabolite levels with drug mechanisms, largely relies on our knowledge of parasite biochemical pathways and their interactions with host cell metabolism, which is unfortunately not completely understood [14]. Metabolomics can facilitate traditional biochemical approaches to more comprehensively annotate and characterize parasite metabolites and pathways, thus enhancing our ability to interpret drug-induced metabolic perturbations.

The integration of metabolomics data across multiple levels of systems biology, including the proteome, transcriptome, and genome, also offers huge potential for drug discovery. It will allow mechanisms of drug action to be discerned in more detail and allow researchers to better understand modes of resistance from a system-wide perspective, across multiple molecular levels. The advent of metabolomic $^{13}$C-flux analysis also provides further in-depth investigations of drug mechanisms and potential biochemical targets by identifying choke points in parasite metabolism [112]. When combined with computational approaches, network analysis can help explain therapeutic effects and aid in the development of predictive *in silico* models for drug action, which may offer extensive financial savings during the drug discovery process [113, 114].

Metabolomics is not only limited to the investigation of drug mechanisms of action and the identification of drug targets, but also has applications across the entire drug discovery pipeline, including identification of biomarkers and the analysis of off-target actions that could explain toxicity and adverse effects. Metabolomics has already demonstrated utility in drug discovery for parasitic diseases and will play an important role in its future, fostering the development of novel drugs to combat these life-threatening infections.

## References

1. Lozano, R., Naghavi, M., Foreman, K., Lim, S., Shibuya, K., Aboyans, V., Abraham, J. *et al.* (2012) Global and regional mortality from 235 causes of death for 20 age groups in 1990 and 2010: a systematic analysis for the Global Burden of Disease Study 2010. *Lancet*, **380** (9859), 2095–2128.
2. Andrews, K.T., Fisher, G., and Skinner-Adams, T.S. (2014) Drug

repurposing and human parasitic protozoan diseases. *Int. J. Parasitol.: Drugs Drug Resist*, **4** (2), 95–111.

3. Burrows, J.N., Elliott, R.L., Kaneko, T., Mowbray, C.E., and Waterson, D. (2014) The role of modern drug discovery in the fight against neglected and tropical diseases. *Med. Chem. Commun*, **5** (6), 688–700.
4. Renslo, A.R. and McKerrow, J.H. (2006) Drug discovery and development for neglected parasitic diseases. *Nat. Chem. Biol*, **2** (12), 701–710.
5. Pedrique, B., Strub-Wourgaft, N., Some, C., Olliaro, P., Trouiller, P., Ford, N., Pécoul, B. *et al.* (2013) The drug and vaccine landscape for neglected diseases (2000-11): a systematic assessment. *Lancet Global Health*, **1** (6), e371–e379.
6. Gilbert, I.H. (2013) Drug discovery for neglected diseases: molecular target-based and phenotypic approaches: miniperspectives series on phenotypic screening for antiinfective targets. *J. Med. Chem*, **56** (20), 7719–7726.
7. Gamo, F.J., Sanz, L.M., Vidal, J., de Cozar, C., Alvarez, E., Lavandera, J.L., Vanderwall, D.E. *et al.* (2010) Thousands of chemical starting points for antimalarial lead identification. *Nature*, **465** (7296), 305–310.
8. Sanz, L.M., Jimenez-Diaz, M.B., Crespo, B., De-Cozar, C., Almela, M.J., Angulo-Barturen, I., Castaneda, P. *et al.* (2011) Cyclopropyl carboxamides, a chemically novel class of antimalarial agents identified in a phenotypic screen. *Antimicrob. Agents Chemother*, **55** (12), 5740–5745.
9. Sykes, M.L., Baell, J.B., Kaiser, M., Chatelain, E., Moawad, S.R., Ganame, D., Ioset, J.R. *et al.* (2012) Identification of compounds with anti-proliferative activity against *Trypanosoma brucei brucei* strain 427 by a whole cell viability based HTS campaign. *PLoS Negl. Trop. Dis*, **6** (11), e1896.
10. Rottmann, M., McNamara, C., Yeung, B.K., Lee, M.C., Zou, B., Russell, B., Seitz, P. *et al.* (2010) Spiroindolones, a potent compound class for the treatment of malaria. *Science*, **329** (5996), 1175–1180.
11. Leong, F.J., Zhao, R., Zeng, S., Magnusson, B., Diagana, T.T., and Pertel, P. (2014) A first-in-human randomized, double-blind, placebo-controlled, single-and multiple-ascending oral dose study of novel imidazolopiperazine KAF156 to assess its safety, tolerability, and pharmacokinetics in healthy adult volunteers. *Antimicrob. Agents Chemother*, **58** (11), 6437–6443.
12. Younis, Y., Douelle, F., Feng, T.-S., Cabrera, D.G., Manach, C.L., Nchinda, A.T., Duffy, S. *et al.* (2012) 3,5-Diaryl-2-aminopyridines as a novel class of orally active antimalarials demonstrating single dose cure in mice and clinical candidate potential. *J. Med. Chem*, **55** (7), 3479–3487.
13. Guiguemde, W.A., Shelat, A.A., Garcia-Bustos, J.F., Diagana, T.T., Gamo, F.J., and Guy, R.K. (2012) Global phenotypic screening for antimalarials. *Chem. Biol.*, **19** (1), 116–129.
14. Creek, D.J. and Barret, M.P. (2014) Determination of antiprotozoal drug mechanisms by metabolomics approaches. *Parasitology*, **141**(Special Issue 01), 83–92.
15. Roessner, U. and Bowne, J. (2009) What is metabolomics all about? *Biotechniques*, **46** (5), 363.
16. Wishart, D.S. (2008) Applications of metabolomics in drug discovery and development. *Drugs R D*, **9** (5), 307–322.
17. Gibney, M.J., Walsh, M., Brennan, L., Roche, H.M., German, B., and Van Ommen, B. (2005) Metabolomics in human nutrition: opportunities and challenges. *Am. J. Clin. Nutr.*, **82** (3), 497–503.
18. Baraldi, E., Carraro, S., Giordano, G., Reniero, F., Perilongo, G., and Zacchello, F. (2009) Metabolomics: moving towards personalized medicine. *Ital. J. Pediatr*, **35** (1), 30.
19. Robertson, D.G. (2010) Muscling mussels: metabolomic evaluation of toxicity. *Toxicol. Sci*, **115** (2), 305–306.

20. Fan, X., Bai, J., and Shen, P. (2005) Diagnosis of breast cancer using HPLC metabonomics fingerprints coupled with computational methods. *Conf. Proc. IEEE Eng. Med. Biol. Soc*, **6**, 6081–6084.
21. Odunsi, K., Wollman, R.M., Ambrosone, C.B., Hutson, A., McCann, S.E., Tammela, J., Geisler, J.P. *et al.* (2005) Detection of epithelial ovarian cancer using 1H-NMR-based metabonomics. *Int. J. Cancer*, **113** (5), 782–788.
22. Serkova, N.J., Gamito, E.J., Jones, R.H., O'Donnell, C., Brown, J.L., Green, S., Sullivan, H. *et al.* (2008) The metabolites citrate, myo-inositol, and spermine are potential age-independent markers of prostate cancer in human expressed prostatic secretions. *Prostate*, **68** (6), 620–628.
23. Brindle, J.T., Antti, H., Holmes, E., Tranter, G., Nicholson, J.K., Bethell, H.W., Clarke, S. *et al.* (2002) Rapid and noninvasive diagnosis of the presence and severity of coronary heart disease using 1H-NMR-based metabonomics. *Nat. Med*, **8** (12), 1439–1445.
24. Brindle, J.T., Nicholson, J.K., Schofield, P.M., Grainger, D.J., and Holmes, E. (2003) Application of chemometrics to 1H NMR spectroscopic data to investigate a relationship between human serum metabolic profiles and hypertension. *Analyst*, **128** (1), 32–36.
25. Dunn, W.B., Broadhurst, D.I., Deepak, S.M., Buch, M.H., McDowell, G., Spasic, I., Ellis, D.I. *et al.* (2007) Serum metabolomics reveals many novel metabolic markers of heart failure, including pseudouridine and 2-oxoglutarate. *Metabolomics*, **3** (4), 413–426.
26. Bogdanov, M., Matson, W.R., Wang, L., Matson, T., Saunders-Pullman, R., Bressman, S.S., and Beal, M.F. (2008) Metabolomic profiling to develop blood biomarkers for Parkinson's disease. *Brain*, **131** (2), 389–396.
27. Han, X., Holtzman, D.M., McKeel, D.W., Kelley, J., and Morris, J.C. (2002) Substantial sulfatide deficiency and ceramide elevation in very early Alzheimer's disease: potential role in disease pathogenesis. *J. Neurochem*, **82** (4), 809–818.
28. Beyoğlu, D. and Idle, J.R. (2013) Metabolomics and its potential in drug development. *Biochem. Pharmacol*, **85** (1), 12–20.
29. Patti, G.J., Yanes, O., Shriver, L.P., Courade, J.P., Tautenhahn, R., Manchester, M., and Siuzdak, G. (2012) Metabolomics implicates altered sphingolipids in chronic pain of neuropathic origin. *Nat. Chem. Biol*, **8** (3), 232–234.
30. Rabinowitz, J.D., Purdy, J.G., Vastag, L., Shenk, T., and Koyuncu, E. (2011) Metabolomics in drug target discovery. *Cold Spring Harbor Symp. Quant. Biol.*, **76**, 235–246.
31. Birkenstock, T., Liebeke, M., Winstel, V., Krismer, B., Gekeler, C., Niemiec, M.J., Bisswanger, H. *et al.* (2012) Exometabolome analysis identifies pyruvate dehydrogenase as a target for the antibiotic triphenylbismuthdichloride in multiresistant bacterial pathogens. *J. Biol. Chem.*, **287** (4), 2887–2895.
32. Lakshmanan, V., Rhee, K.Y., and Daily, J.P. (2011) Metabolomics and malaria biology. *Mol. Biochem. Parasitol.*, **175** (2), 104–111.
33. Lakshmanan, V., Rhee, K.Y., Wang, W., Yu, Y., Khafizov, K., Fiser, A., Wu, P. *et al.* (2012) Metabolomic analysis of patient plasma yields evidence of plant-like α-linolenic acid metabolism in *Plasmodium falciparum*. *J. Infect. Dis.*, **206** (2), 238–248.
34. Park, Y.H., Shi, Y.P., Liang, B., Medriano, C.A.D., Jeon, Y.H., Torres, E., Uppal, K. *et al.* (2015) High-resolution metabolomics to discover potential parasite-specific biomarkers in a *Plasmodium falciparum* erythrocytic stage culture system. *Malar. J*, **14**, 122.
35. Dunn, W., Erban, A., Weber, R.M., Creek, D., Brown, M., Breitling, R., Hankemeier, T. *et al.* (2013) Mass appeal: metabolite identification in mass spectrometry-focused untargeted metabolomics. *Metabolomics*, **9** (1), 44–66.

36. Kwon, Y.K., Lu, W., Melamud, E., Khanam, N., Bognar, A., and Rabinowitz, J.D. (2008) A domino effect in antifolate drug action in *Escherichia coli*. *Nat. Chem. Biol*, **4** (10), 602–608.
37. Creek, D.J., Nijagal, B., Kim, D.-H., Rojas, F., Matthews, K.R., and Barrett, M.P. (2013) Metabolomics guides rational development of a simplified cell culture medium for drug screening against *Trypanosoma brucei*. *Antimicrob. Agents Chemother*, **57** (6), 2768–2779.
38. Sana, T.R., Gordon, D.B., Fischer, S.M., Tichy, S.E., Kitagawa, N., Lai, C., Gosnell, W.L. *et al.* (2013) Global mass spectrometry based metabolomics profiling of erythrocytes infected with *Plasmodium falciparum*. *PLoS One*, **8** (4), e60840.
39. Lewis, I.A., Wacker, M., Olszewski, K.L., Cobbold, S.A., Baska, K.S., Tan, A., Ferdig, M.T. *et al.* (2014) Metabolic QTL analysis links chloroquine resistance in *Plasmodium falciparum* to impaired hemoglobin catabolism. *PLos Genet*, **10** (1), e1004085.
40. Olszewski, K.L. and Llinas, M. (2013) Extraction of hydrophilic metabolites from *Plasmodium falciparum*-infected erythrocytes for metabolomic analysis. *Methods Mol. Biol*, **923**, 259–266.
41. van Brummelen, A.C., Olszewski, K.L., Wilinski, D., Llinas, M., Louw, A.I., and Birkholtz, L.M. (2009) Co-inhibition of *Plasmodium falciparum* S-adenosylmethionine decarboxylase/ornithine decarboxylase reveals perturbation-specific compensatory mechanisms by transcriptome, proteome, and metabolome analyses. *J. Biol. Chem.*, **284** (7), 4635–4646.
42. Zhang, B., Watts, K.M., Hodge, D., Kemp, L.M., Hunstad, D.A., Hicks, L.M., and Odom, A.R. (2011) A second target of the antimalarial and antibacterial agent fosmidomycin revealed by cellular metabolic profiling. *Biochemistry*, **50** (17), 3570–3577.
43. O'Hara, J.K., Kerwin, L.J., Cobbold, S.A., Tai, J., Bedell, T.A., Reider, P.J., and Llinás, M. (2014) Targeting NAD+ metabolism in the human malaria parasite *Plasmodium falciparum*. *PLoS One*, **9** (4), e94061.
44. Storm, J., Sethia, S., Blackburn, G.J., Chokkathukalam, A., Watson, D.G., Beitling, R., Coombs, G.H., and Müller, S. (2014) Phospho*enol*pyruvate carboxylase identified as a key enzyme in erythroocytic *plasmodium falciparum carbon metabolism*. *PLoS Pathog.*, **10** (1), e1003876.
45. Cobbold, S.A., Chua, H.H., Nijagal, B., Creek, D.J., Ralph, S.A., and McConville, M.J. (2015) Metabolic dysregulation induced in *Plasmodium falciparum* by dihydroartemisinin and other front line antimalarial drugs. *J. Infect. Dis.*, **13** (2), 276–86.
46. Ali, J.A.M., Creek, D.J., Burgess, K., Allison, H.C., Field, M.C., Mäser, P., and De Koning, H.P. (2013) Pyrimidine salvage in *Trypanosoma brucei* bloodstream forms and the trypanocidal action of halogenated pyrimidines. *Mol. Pharmacol*, **83** (2), 439–453.
47. t'Kindt, R., Jankevics, A., Scheltema, R.A., Zheng, L., Watson, D.G., Dujardin, J.-C., Breitling, R. *et al.* (2010) Towards an unbiased metabolic profiling of protozoan parasites: optimisation of a *Leishmania* sampling protocol for HILIC-orbitrap analysis. *Anal. Bioanal. Chem*, **398** (5), 2059–2069.
48. Kamleh, A., Barrett, M., Wildridge, D., Burchmore, R., Scheltema, R., and Watson, D. (2008) Metabolomic profiling using Orbitrap Fourier transform mass spectrometry with hydrophilic interaction chromatography: a method with wide applicability to analysis of biomolecules. *Rapid Commun. Mass Spectrom*, **22** (12), 1912–1918.
49. Vincent, I.M., Creek, D., Watson, D.G., Kamleh, M.A., Woods, D.J., Wong, P.E., Burchmore, R.J.S. *et al.* (2010) A molecular mechanism for eflornithine resistance in African trypanosomes. *PLoS Pathog*, **6** (11), e1001204.
50. Berna, A.Z., McCarthy, J.S., Wang, X.R., Saliba, K.J., Bravo, F.G., Cassells, J., Padovan, B. *et al.* (2015) Biomarkers of infection with *Plasmodium falciparum* detected in human breath. *J. Infect. Dis.*http://jid.oxfordjournals.org/

content/early/2015/03/25/infdis.jiv176.short.

51. Zhang, T., Creek, D.J., Barrett, M.P., Blackburn, G., and Watson, D.G. (2012) Evaluation of coupling reversed phase, aqueous normal phase, and hydrophilic interaction liquid chromatography with orbitrap mass spectrometry for metabolomic studies of human urine. *Anal. Chem*, **84** (4), 1994–2001.
52. Sumner, L.W., Amberg, A., Barrett, D., Beale, M.H., Beger, R., Daykin, C.A., Fan, T.W.-M. *et al.* (2007) Proposed minimum reporting standards for chemical analysis. *Metabolomics*, **3** (3), 211–221.
53. Alkhaldi, A.A., Creek, D.J., Ibrahim, H., Kim, D.H., Quashie, N.B., Burgess, K.E., Changtam, C. *et al.* (2015) Potent trypanocidal curcumin analogs bearing a monoenone linker motif act on *Trypanosoma brucei* by forming an adduct with trypanothione. *Mol. Pharmacol*, **87** (3), 451–464.
54. Trochine, A., Creek, D.J., Faral-Tello, P., Barrett, M.P., and Robello, C. (2014) Benznidazole biotransformation and multiple targets in *Trypanosoma cruzi* revealed by metabolomics. *PLoS Negl. Trop. Dis*, **8** (5), e2844.
55. Moco, S., Vervoort, J., Bino, R.J., De Vos, R.C., and Bino, R. (2007) Metabolomics technologies and metabolite identification. *TrAC, Trends Anal. Chem*, **26** (9), 855–866.
56. Conteh, L., Engels, T., and Molyneux, D.H. (2010) Socioeconomic aspects of neglected tropical diseases. *Lancet*, **375** (9710), 239–247.
57. Mathers, C.D., Ezzati, M., and Lopez, A.D. (2007) Measuring the burden of neglected tropical diseases: the global burden of disease framework. *PLoS Negl. Trop. Dis*, **1** (2), e114.
58. Brun, R., Blum, J., Chappuis, F., and Burri, C. (2010) Human african trypanosomiasis. *Lancet*, **375** (9709), 148–159.
59. Ferrins, L., Rahmani, R., Sykes, M.L., Jones, A.J., Avery, V.M., Teston, E., Almohaywi, B. *et al.* (2013) 3-(Oxazolo[4,5-*b*]pyridin-2-yl)anilides as a novel class of potent inhibitors for the kinetoplastid *Trypanosoma brucei*, the causative agent for human African trypanosomiasis. *Eur. J. Med. Chem*, **66**, 450–465.
60. Barrett, M.P., Boykin, D.W., Brun, R., and Tidwell, R.R. (2007) Human African trypanosomiasis: pharmacological re-engagement with a neglected disease. *Br. J. Pharmacol*, **152** (8), 1155–1171.
61. Brun, R., Don, R., Jacobs, R.T., Wang, M.Z., and Barrett, M.P. (2011) Development of novel drugs for human African trypanosomiasis. *Future Microbiol*, **6** (6), 677–691.
62. Simarro, P.P., Diarra, A., Ruiz Postigo, J.A., Franco, J.R., and Jannin, J.G. (2011) The human African trypanosomiasis control and surveillance programme of the World Health Organization 2000-2009: the way forward. *PLoS Negl. Trop. Dis*, **5** (2), e1007.
63. de Koning, H.P. (2001) Transporters in African trypanosomes: role in drug action and resistance. *Int. J. Parasitol.*, **31** (5–6), 512–522.
64. Nok, A.J. (2003) Arsenicals (melarsoprol), pentamidine and suramin in the treatment of human African trypanosomiasis. *Parasitol. Res.*, **90** (1), 71–79.
65. Priotto, G., Kasparian, S., Mutombo, W., Ngouama, D., Ghorashian, S., Arnold, U., Ghabri, S. *et al.* (2009) Nifurtimox-eflornithine combination therapy for second-stage African *Trypanosoma brucei gambiense* trypanosomiasis: a multicentre, randomised, phase III, non-inferiority trial. *Lancet*, **374** (9683), 56–64.
66. Drexler, D.M., Reily, M.D., and Shipkova, P.A. (2011) Advances in mass spectrometry applied to pharmaceutical metabolomics. *Anal. Bioanal. Chem*, **399** (8), 2645–2653.
67. Vincent, I.M., Creek, D.J., Burgess, K., Woods, D.J., Burchmore, R.J., and Barrett, M.P. (2012) Untargeted metabolomics reveals a lack of synergy between nifurtimox and eflornithine against *Trypanosoma brucei*. *PLoS Negl. Trop. Dis*, **6** (5), e1618.
68. Bacchi, C.J., Garofalo, J., Mockenhaupt, D., McCann, P.P., Diekema, K.A., Pegg,

A.E., Nathan, H.C. *et al.* (1983) In vivo effects of α-dl-Difluoromethylornithine on the metabolism and morphology of *Trypanosoma brucei brucei*. *Mol. Biochem. Parasitol.*, **7** (3), 209–225.

**69.** Fairlamb, A.H., Blackburn, P., Ulrich, P., Chait, B.T., and Cerami, A. (1985) Trypanothione: a novel bis(glutathionyl)spermidine cofactor for glutathione reductase in trypanosomatids. *Science*, **227** (4693), 1485–1487.

**70.** Fairlamb, A.H., Henderson, G.B., Bacchi, C.J., and Cerami, A. (1987) In vivo effects of difluoromethylornithine on trypanothione and polyamine levels in bloodstream forms of *Trypanosoma brucei*. *Mol. Biochem. Parasitol.*, **24** (2), 185–191.

**71.** Boiani, M., Piacenza, L., Hernandez, P., Boiani, L., Cerecetto, H., Gonzalez, M., and Denicola, A. (2010) Mode of action of nifurtimox and N-oxide-containing heterocycles against *Trypanosoma cruzi*: is oxidative stress involved? *Biochem. Pharmacol*, **79** (12), 1736–1745.

**72.** Hall, B.S., Bot, C., and Wilkinson, S.R. (2011) Nifurtimox activation by trypanosomal type I nitroreductases generates cytotoxic nitrile metabolites. *J. Biol. Chem.*, **286** (15), 13088–13095.

**73.** Wilkinson, S.R., Taylor, M.C., Horn, D., Kelly, J.M., and Cheeseman, I. (2008) A mechanism for cross-resistance to nifurtimox and benznidazole in trypanosomes. *Proc. Natl. Acad. Sci. U.S.A.*, **105** (13), 5022–5027.

**74.** Lanteri, C.A., Tidwell, R.R., and Meshnick, S.R. (2008) The mitochondrion is a site of trypanocidal action of the aromatic diamidine DB75 in bloodstream forms of *Trypanosoma brucei*. *Antimicrob. Agents Chemother*, **52** (3), 875–882.

**75.** Wilson, W.D., Tanious, F.A., Mathis, A., Tevis, D., Hall, J.E., and Boykin, D.W. (2008) Antiparasitic compounds that target DNA. *Biochimie*, **90** (7), 999–1014.

**76.** Prata, A. (2001) Clinical and epidemiological aspects of Chagas disease. *Lancet Infect. Dis.*, **1** (2), 92–100.

**77.** Murta, S.M., Gazzinelli, R.T., Brener, Z., and Romanha, A.J. (1998) Molecular characterization of susceptible and naturally resistant strains of *Trypanosoma cruzi* to benznidazole and nifurtimox. *Mol. Biochem. Parasitol.*, **93** (2), 203–214.

**78.** Rodriques Coura, J. and de Castro, S.L. (2002) A critical review on Chagas disease chemotherapy. *Mem. Inst. Oswaldo Cruz*, **97** (1), 3–24.

**79.** Hall, B.S. and Wilkinson, S.R. (2012) Activation of benznidazole by trypanosomal type I nitroreductases results in glyoxal formation. *Antimicrob. Agents Chemother*, **56** (1), 115–123.

**80.** Castro, J.A. and Diaz de Toranzo, E.G. (1988) Toxic effects of nifurtimox and benznidazole, two drugs used against American trypanosomiasis (Chagas' disease). *Biomed. Environ. Sci.*, **1** (1), 19–33.

**81.** Maya, J.D., Cassels, B.K., Iturriaga-Vasquez, P., Ferreira, J., Faundez, M., Galanti, N., Ferreira, A. *et al.* (2007) Mode of action of natural and synthetic drugs against *Trypanosoma cruzi* and their interaction with the mammalian host. *Comp. Biochem. Physiol., Part A Mol. Integr. Physiol.*, **146** (4), 601–620.

**82.** Desjeux, P. (1996) Leishmaniasis: public health aspects and control. *Clin. Dermatol.*, **14** (5), 417–423.

**83.** Singh, N., Kumar, M., and Singh, R.K. (2012) Leishmaniasis: current status of available drugs and new potential drug targets. *Asian Pac. J. Trop. Med*, **5** (6), 485–497.

**84.** Berg, M., García-Hernández, R., Cuypers, B., Vanaerschot, M., Manzano, J.I., Poveda, J.A., Ferragut, J.A. *et al.* (2015) Experimental resistance to drug combinations in *Leishmania donovani*: metabolic and phenotypic adaptations. *Antimicrob. Agents Chemother*, **59** (4), 2242–2255.

**85.** Ruiter, G.A., Zerp, S.F., Bartelink, H., Van Blitterswijk, W.J., and Verheij, M. (2003) Anti-cancer alkyl-lysophospholipids inhibit the phosphatidylinositol 3-kinase-Akt/PKB

survival pathway. *Anticancer Drugs*, **14** (2), 167–173.
**86.** Lux, H., Hart, D.T., Parker, P.J., and Klenner, T. (1996) in *Platelet-Activating Factor and Related Lipid Mediators 2*, vol. **416** (eds S. Nigam, G. Kunkel, and S. Prescott), Springer, pp. 201–211.
**87.** Rakotomanga, M., Loiseau, P.M., and Saint-Pierre-Chazalet, M. (2004) Hexadecylphosphocholine interaction with lipid monolayers. *Biochim. Biophys. Acta, Biomembr.*, **1661** (2), 212–218.
**88.** Imbert, L., Ramos, R.G., Libong, D., Abreu, S., Loiseau, P.M., and Chaminade, P. (2012) Identification of phospholipid species affected by miltefosine action in *Leishmania donovani* cultures using LC-ELSD, LC-ESI/MS, and multivariate data analysis. *Anal. Bioanal. Chem*, **402** (3), 1169–1182.
**89.** Zufferey, R. and Mamoun, C.B. (2002) Choline transport in *Leishmania major* promastigotes and its inhibition by choline and phosphocholine analogs. *Mol. Biochem. Parasitol.*, **125** (1-2), 127–134.
**90.** Moreira, W., Leprohon, P., and Ouellette, M. (2011) Tolerance to drug-induced cell death favours the acquisition of multidrug resistance in *Leishmania*. *Cell Death Dis.*, **2** (9), e201.
**91.** Vincent, I.M., Weidt, S., Rivas, L., Burgess, K., Smith, T.K., and Ouellette, M. (2014) Untargeted metabolomic analysis of miltefosine action in *Leishmania infantum* reveals changes to the internal lipid metabolism. *Int. J. Parasitol.: Drugs Drug Resist*, **4** (1), 20–27.
**92.** Saha, A.K., Mukherjee, T., and Bhaduri, A. (1986) Mechanism of action of amphotericin B on *Leishmania donovani* promastigotes. *Mol. Biochem. Parasitol.*, **19** (3), 195–200.
**93.** Ashutosh, S.S. and Goyal, N. (2007) Molecular mechanisms of antimony resistance in *Leishmania*. *J. Med. Microbiol*, **56**(Pt. 2), 143–153.
**94.** Mookerjee Basu, J., Mookerjee, A., Sen, P., Bhaumik, S., Banerjee, S., Naskar, K., Choudhuri, S.K. *et al.* (2006) Sodium antimony gluconate induces generation of reactive oxygen species and nitric oxide via phosphoinositide 3-kinase and mitogen-activated protein kinase activation in *Leishmania donovani*-infected macrophages. *Antimicrob. Agents Chemother*, **50** (5), 1788–1797.
**95.** Dondorp, A.M., Nosten, F., Yi, P., Das, D., Phyo, A.P., Tarning, J., Lwin, K.M. *et al.* (2009) Artemisinin resistance in *Plasmodium falciparum* malaria. *N. Engl. J. Med*, **361** (5), 455–467.
**96.** Biagini, G.A., Fisher, N., Shone, A.E., Mubaraki, M.A., Srivastava, A., Hill, A., Antoine, T. *et al.* (2012) Generation of quinolone antimalarials targeting the *Plasmodium falciparum* mitochondrial respiratory chain for the treatment and prophylaxis of malaria. *Proc. Natl. Acad. Sci. U.S.A.*, **109** (21), 8298–8303.
**97.** Fry, M. and Pudney, M. (1992) Site of action of the antimalarial hydroxynaphthoquinone, 2-[trans-4-(4'-chlorophenyl) cyclohexyl]-3-hydroxy-1,4-naphthoquinone (566C80). *Biochem. Pharmacol*, **43** (7), 1545–1553.
**98.** Srivastava, I.K., Rottenberg, H., and Vaidya, A.B. (1997) Atovaquone, a broad spectrum antiparasitic drug, collapses mitochondrial membrane potential in a malarial parasite. *J. Biol. Chem.*, **272** (7), 3961–3966.
**99.** Ferone, R. (1977) Folate metabolism in malaria. *Bull. World Health Org*, **55** (2-3), 291–298.
**100.** Fidock, D.A., Nomura, T., Talley, A.K., Cooper, R.A., Dzekunov, S.M., Ferdig, M.T., Ursos, L.M. *et al.* (2000) Mutations in the *P. falciparum* digestive vacuole transmembrane protein PfCRT and evidence for their role in chloroquine resistance. *Mol. Cell*, **6** (4), 861–871.
**101.** Fisher, N., Bray, P.G., Ward, S.A., and Biagini, G.A. (2007) The malaria parasite type II NADH:quinone oxidoreductase: an alternative enzyme for an alternative lifestyle. *Trends Parasitol.*, **23** (7), 305–310.
**102.** Cassera, M.B., Gozzo, F.C., D'Alexandri, F.L., Merino, E.F., del Portillo, H.A., Peres, V.J., Almeida,

I.C. *et al.* (2004) The methylerythritol phosphate pathway is functionally active in all intraerythrocytic stages of *Plasmodium falciparum*. *J. Biol. Chem.*, **279** (50), 51749–51759.

**103.** Jomaa, H., Wiesner, J., Sanderbrand, S., Altincicek, B., Weidemeyer, C., Hintz, M., Turbachova, I. *et al.* (1999) Inhibitors of the nonmevalonate pathway of isoprenoid biosynthesis as antimalarial drugs. *Science*, **285** (5433), 1573–1576.

**104.** Koppisch, A.T., Fox, D.T., Blagg, B.S., and Poulter, C.D. (2002) *E. coli* MEP synthase: steady-state kinetic analysis and substrate binding. *Biochemistry*, **41** (1), 236–243.

**105.** Borrmann, S., Lundgren, I., Oyakhirome, S., Impouma, B., Matsiegui, P.B., Adegnika, A.A., Issifou, S. *et al.* (2006) Fosmidomycin plus clindamycin for treatment of pediatric patients aged 1 to 14 years with *Plasmodium falciparum* malaria. *Antimicrob. Agents Chemother*, **50** (8), 2713–2718.

**106.** Na-Bangchang, K., Ruengweerayut, R., Karbwang, J., Chauemung, A., and Hutchinson, D. (2007) Pharmacokinetics and pharmacodynamics of fosmidomycin monotherapy and combination therapy with clindamycin in the treatment of multidrug resistant *falciparum* malaria. *Malar. J*, **6**, 70.

**107.** Bitonti, A.J., Dumont, J.A., Bush, T.L., Edwards, M.L., Stemerick, D.M., McCann, P.P., and Sjoerdsma, A. (1989) Bis(benzyl)polyamine analogs inhibit the growth of chloroquine-resistant human malaria parasites (*Plasmodium falciparum*) *in vitro* and in combination with alpha-difluoromethylornithine cure murine malaria. *Proc. Natl. Acad. Sci. U.S.A.*, **86** (2), 651–655.

**108.** Assaraf, Y.G., Golenser, J., Spira, D.T., Messer, G., and Bachrach, U. (1987) Cytostatic effect of DL-alpha-difluoromethylornithine against *Plasmodium falciparum* and its reversal by diamines and spermidine. *Parasitol. Res.*, **73** (4), 313–318.

**109.** Wright, P.S., Byers, T.L., Cross-Doersen, D.E., McCann, P.P., and Bitonti, A.J. (1991) Irreversible inhibition of S-adenosylmethionine decarboxylase in *Plasmodium falciparum*-infected erythrocytes: growth inhibition in vitro. *Biochem. Pharmacol*, **41** (11), 1713–1718.

**110.** Guiguemde, W.A., Shelat, A.A., Bouck, D., Duffy, S., Crowther, G.J., Davis, P.H., Smithson, D.C. *et al.* (2010) Chemical genetics of *Plasmodium falciparum*. *Nature*, **465** (7296), 311–315.

**111.** Scheltema, R.A., Decuypere, S., T'Kindt, R., Dujardin, J.-C., Coombs, G.H., and Breitling, R. (2010) The potential of metabolomics for *Leishmania* research in the post-genomics era. *Parasitology*, **137** (9), 1291–1302.

**112.** Saunders, E.C., De Souza, D.P., Naderer, T., Sernee, M.F., Ralton, J.E., Doyle, M.A., Macrae, J.I. *et al.* (2010) Central carbon metabolism of *Leishmania* parasites. *Parasitology*, **137** (9), 1303–1313.

**113.** Kim, D.H. and Creek, D.J. (2015) What role can metabolomics play in the discovery and development of new medicines for infectious diseases? *Bioanalysis*, **7** (6), 629–631.

**114.** Zhao, S. and Iyengar, R. (2012) Systems pharmacology: network analysis to identify multiscale mechanisms of drug action. *Annu. Rev. Pharmacol. Toxicol.*, **52**, 505–521.

# Appendix 2

# Chapter 4 – metabolomics supplementary material

| Ring stage metabolomics experiment | | | | | | | | | | | | | | | | | | | | | | | | | | | | |
|---|---|---|---|---|---|---|---|---|---|---|---|---|---|---|---|---|---|---|---|---|---|---|---|---|---|---|---|---|
| | | | | | 0 h | | | | | | 1.5 h | | 3 h | | | | | | 6 h | | | | | | 9 h | | | |
| | | | | | Fold change (vs DMSO) | | | ttest: | ttest: | ttest: | Fold change (vs DMSO) | ttest: | Fold change (vs DMSO) | | | ttest: | ttest: | ttest: | Fold change (vs DMSO) | | | ttest: | ttest: | ttest: | Fold change (vs DMSO) | | ttest: | ttest: |
| Mass | RT | FORMULA | Putative metabolite | Map | OZ277 | OZ439 | DHA | OZ277 | OZ439 | DHA | DHA | DHA | OZ277 | OZ439 | DHA | OZ277 | OZ439 | DHA | OZ277 | OZ439 | DHA | OZ277 | OZ439 | DHA | OZ277 | OZ439 | OZ277 | OZ439 |
| 383.1085 | 14.3 | C14H17N5O8 | Succinyladenosine | Miscellaneous | 1.60 | 4.03 | 1.70 | NA | 0.3813 | 0.6352 | 1.23 | 0.6284 | 0.61 | 1.32 | 0.73 | 0.5630 | 0.6468 | 0.6337 | 0.93 | 0.91 | 0.65 | 0.8940 | 0.8586 | 0.5127 | 0.94 | 1.00 | 0.9554 | 0.9998 |
| 234.1619 | 4.3 | C15H22O2 | Bakkenolide A | Miscellaneous | 1.47 | 3.96 | 1.56 | 0.5819 | 0.4476 | 0.5791 | 1.65 | 0.6146 | 0.90 | 1.03 | 1.97 | 0.8757 | 0.9702 | 0.5743 | 0.81 | 1.17 | 0.93 | 0.7515 | 0.8297 | 0.9204 | 0.79 | 0.90 | 0.6386 | 0.8478 |
| 330.0124 | 15.5 | C14H6N2O8 | PQQ | Miscellaneous | 1.49 | 1.72 | 1.61 | 0.7596 | 0.6665 | 0.7182 | 0.85 | 0.7555 | 0.81 | 0.88 | 0.90 | 0.7108 | 0.8212 | 0.8490 | 1.04 | 1.31 | 0.99 | 0.9355 | 0.5482 | 0.9807 | 0.95 | 1.08 | 0.9566 | 0.9357 |
| 259.1785 | 7.7 | C13H25NO4 | Hexanoylcarnitine | Miscellaneous | 1.42 | 1.07 | 1.40 | 0.7121 | 0.9315 | 0.7228 | 0.98 | 0.9670 | 0.62 | 1.05 | 0.83 | 0.4820 | 0.9356 | 0.7155 | 0.88 | 1.11 | 0.83 | 0.8524 | 0.8388 | 0.7723 | 2.06 | 0.96 | 0.4689 | 0.9526 |
| 138.0430 | 7.7 | C6H6N2O2 | 4-Nitroaniline | Miscellaneous | 1.43 | 1.32 | 1.92 | 0.0631 | 0.4471 | 0.2184 | 0.93 | 0.8683 | 0.40 | 0.81 | 0.56 | 0.0953 | 0.5979 | 0.1817 | 1.06 | 1.20 | 1.55 | 0.9085 | 0.5609 | 0.2656 | 0.74 | 1.17 | 0.4474 | 0.7717 |
| 189.1114 | 15.1 | C7H15N3O3 | L-Homocitrulline | Miscellaneous | 1.38 | 1.17 | 1.29 | 0.6183 | 0.8594 | 0.7454 | 1.14 | 0.8820 | 0.83 | 1.07 | 0.90 | 0.8053 | 0.9283 | 0.8973 | 1.29 | 0.97 | 1.16 | 0.7388 | 0.9566 | 0.8172 | 0.99 | 0.94 | 0.9742 | 0.8538 |
| 213.0095 | 7.6 | C8H7NO4S | Indoxylsulfate | Miscellaneous | 1.30 | 1.39 | 1.39 | 0.5248 | 0.4239 | 0.4289 | 0.96 | 0.8125 | 1.04 | 1.09 | 0.80 | 0.8788 | 0.7014 | 0.3550 | 1.10 | 1.13 | 1.20 | 0.6420 | 0.6276 | 0.3587 | 1.20 | 1.09 | 0.4740 | 0.6561 |
| 293.1993 | 4.2 | C17H27NO3 | (+/-)-5-[(tert-Butylamino)-2'-hydroxypropoxy]-1,2,3,4-tetrahydro-1-naphthol | Miscellaneous | 1.35 | 6.52 | 1.50 | 0.6655 | 0.4142 | 0.6484 | 1.17 | 0.8506 | 0.91 | 0.69 | 1.46 | 0.9037 | 0.6161 | 0.7023 | 0.92 | 1.19 | 0.79 | 0.9287 | 0.8380 | 0.7964 | 0.91 | 0.83 | 0.9052 | 0.8449 |
| 206.1670 | 4.3 | C14H22O | alpha-Irone | Miscellaneous | 1.24 | 2.13 | 1.12 | 0.5119 | 0.5194 | 0.7784 | 1.59 | 0.4622 | 1.23 | 1.08 | 1.72 | 0.5569 | 0.8666 | 0.5228 | 0.90 | 1.08 | 0.94 | 0.7286 | 0.8529 | 0.8490 | 0.74 | 0.78 | 0.3664 | 0.4347 |
| 326.1214 | 16.0 | C12H22O10 | 2-O-alpha-L-Rhamnopyranosyl-D-glucopyranose | Miscellaneous | 1.29 | 1.30 | 1.05 | 0.5202 | 0.6365 | 0.9238 | 1.18 | 0.3867 | 0.83 | 1.16 | 0.95 | 0.5027 | 0.5135 | 0.8193 | 1.09 | 1.29 | 1.13 | 0.7032 | 0.3526 | 0.5636 | 1.36 | 1.24 | 0.0629 | 0.1585 |
| 425.3505 | 4.7 | C25H47NO4 | Oleoylcarnitine | Miscellaneous | 1.25 | 1.00 | 0.74 | 0.7660 | 0.9946 | 0.6215 | 1.23 | 0.4445 | 1.20 | 0.88 | 0.99 | 0.7191 | 0.6999 | 0.9839 | 1.04 | 1.06 | 0.86 | 0.8961 | 0.8443 | 0.5906 | 0.62 | 0.66 | 0.5762 | 0.6144 |
| 473.3507 | 4.6 | C29H47NO4 | Docosa-4-7-10-13-16-pentaenoylcarnitine | Miscellaneous | 1.19 | 0.48 | 0.83 | 0.8626 | NA | 0.8136 | 1.21 | 0.7594 | 1.28 | 0.70 | 0.96 | 0.7053 | 0.5486 | 0.9526 | 0.98 | 1.23 | 0.87 | 0.9706 | 0.7410 | 0.8466 | 0.45 | 0.79 | NA | 0.8340 |
| 712.3664 | 15.0 | C36H56O14 | Digitalin | Miscellaneous | 1.23 | 1.02 | 1.09 | 0.6719 | 0.9783 | 0.8792 | 0.84 | 0.2853 | 1.00 | 1.07 | 1.01 | 0.9658 | 0.6539 | 0.9360 | 0.92 | 0.94 | 0.97 | 0.7277 | 0.7691 | 0.8505 | 0.94 | 1.04 | 0.5573 | 0.8282 |
| 166.0841 | 12.3 | C6H14O5 | 3-deoxy-D-galactose | Miscellaneous | 1.35 | 1.30 | 1.17 | 0.3572 | 0.4724 | 0.6183 | 0.77 | 0.4038 | 0.97 | 1.09 | 1.03 | 0.9364 | 0.8451 | 0.9387 | 0.95 | 0.89 | 0.99 | 0.8796 | 0.6914 | 0.9741 | 0.96 | 1.04 | 0.9145 | 0.9100 |
| 397.3193 | 4.8 | C23H43NO4 | trans-Hexadec-2-enoylcarnitine | Miscellaneous | 1.19 | 0.94 | 0.80 | 0.8149 | 0.9298 | 0.7106 | 0.93 | 0.8074 | 1.36 | 0.78 | 0.89 | 0.6172 | 0.5728 | 0.8027 | 1.08 | 1.19 | 0.92 | 0.8567 | 0.6117 | 0.8162 | 0.55 | 0.63 | 0.4915 | 0.5747 |
| 223.0842 | 4.5 | C11H13NO4 | Bendiocarb | Miscellaneous | 1.18 | 0.48 | 0.99 | 0.7471 | 0.1783 | 0.9873 | 1.37 | 0.2023 | 1.38 | 0.98 | 1.07 | 0.3788 | 0.8827 | 0.7147 | 0.75 | 0.91 | 0.91 | 0.2884 | 0.7553 | 0.7299 | 0.65 | 0.82 | 0.5192 | 0.7520 |
| 268.1210 | 4.9 | C16H16N2O2 | N-Butyl-beta-carboline-3-carboxylate | Miscellaneous | 1.20 | 0.97 | 1.06 | 0.4402 | 0.8677 | 0.7498 | 1.22 | 0.1158 | 1.22 | 0.89 | 1.12 | 0.4982 | 0.6684 | 0.6877 | 0.76 | 0.96 | 0.91 | 0.1122 | 0.8227 | 0.4679 | 0.86 | 0.92 | 0.6899 | 0.8411 |
| 136.0373 | 16.1 | C4H8O5 | Erythronicacid | Miscellaneous | 1.23 | 1.92 | 2.64 | 0.8155 | 0.6101 | 0.4000 | 1.02 | 0.9820 | 0.64 | 0.76 | 0.73 | 0.6910 | 0.8128 | 0.7902 | 0.93 | 1.27 | 1.03 | 0.9487 | 0.8174 | 0.9766 | 1.30 | 1.25 | 0.7577 | 0.8198 |
| 302.1732 | 4.3 | C15H26O6 | Tributyrin | Miscellaneous | 1.11 | 0.38 | 0.88 | 0.8808 | 0.3476 | 0.8466 | 1.23 | 0.8023 | 2.90 | 1.50 | 1.74 | 0.3328 | 0.6838 | 0.5364 | 0.72 | 0.64 | 0.89 | 0.7227 | 0.6492 | 0.9010 | 0.54 | 0.55 | 0.4751 | 0.4865 |
| 186.0531 | 14.1 | C8H10O5 | 2-hydroxy-3-carboxy-4,5-cyclopropylhex-5-enoate | Miscellaneous | 1.23 | 1.06 | 1.09 | 0.1624 | 0.6929 | 0.3629 | 1.23 | 0.0323 | 0.92 | 0.85 | 0.83 | 0.5800 | 0.2933 | 0.2533 | 0.98 | 1.07 | 1.08 | 0.7186 | 0.3413 | 0.4042 | 1.12 | 1.03 | 0.4273 | 0.8032 |
| 241.2769 | 7.7 | C16H35N | Hexadeceylamin | Miscellaneous | 1.16 | 0.79 | 1.05 | 0.7638 | 0.5734 | 0.9092 | 1.05 | 0.8612 | 1.04 | 0.85 | 0.94 | 0.8888 | 0.5278 | 0.8364 | 0.74 | 0.79 | 0.81 | 0.2275 | 0.3711 | 0.4044 | 0.61 | 0.66 | 0.2808 | 0.3779 |
| 278.1519 | 4.2 | C16H22O4 | 2-Ethylhexyl phthalate | Miscellaneous | 1.15 | 1.24 | 0.80 | 0.6863 | 0.7650 | 0.5329 | 0.89 | 0.2390 | 1.20 | 0.78 | 1.10 | 0.5801 | 0.5370 | 0.8699 | 1.49 | 1.06 | 0.89 | 0.3909 | 0.8904 | 0.7046 | 0.82 | 0.74 | 0.6094 | 0.4515 |
| 149.1052 | 9.4 | C6H15NO3 | Triethanolamine | Miscellaneous | 1.21 | 1.27 | 1.45 | 0.5978 | 0.5603 | 0.3937 | 1.35 | 0.3361 | 0.72 | 0.81 | 7.39 | 0.1026 | 0.3519 | 0.4006 | 1.10 | 1.80 | 0.95 | 0.8086 | 0.2329 | 0.8672 | 0.33 | 0.42 | 0.2039 | 0.2539 |
| 390.2770 | 4.0 | C24H38O4 | Bis(2-ethylhexyl)phthalate | Miscellaneous | 1.14 | 1.77 | 1.11 | 0.5720 | 0.4306 | 0.6325 | 1.18 | 0.3987 | 0.94 | 1.01 | 1.19 | 0.7430 | 0.9743 | 0.6443 | 1.01 | 1.14 | 1.00 | 0.9380 | 0.4047 | 0.9902 | 0.93 | 1.02 | 0.5077 | 0.8882 |
| 413.3505 | 4.7 | C24H47NO4 | Heptadecanoylcarnitine | Miscellaneous | 1.11 | 0.98 | 0.72 | 0.8809 | 0.9758 | 0.5579 | 1.14 | 0.5680 | 1.43 | 0.94 | 0.96 | 0.5108 | 0.8051 | 0.8781 | 1.20 | 1.11 | 1.03 | 0.4790 | 0.7188 | 0.9119 | 0.62 | 0.60 | 0.5917 | 0.5741 |
| 283.3239 | 8.2 | C19H41N | CTAB | Miscellaneous | 1.12 | 0.89 | 2.01 | 0.7092 | 0.7427 | 0.4001 | 0.96 | 0.9282 | 1.28 | 1.42 | 1.83 | 0.4422 | 0.4765 | 0.3701 | 0.78 | 0.65 | 1.02 | 0.5833 | 0.3690 | 0.9693 | 1.03 | 0.81 | 0.9253 | 0.5450 |
| 271.2512 | 4.5 | C16H33NO2 | Undecanoylcholine | Miscellaneous | 1.11 | 0.86 | 0.95 | 0.7699 | 0.7007 | 0.8777 | 1.08 | 0.6730 | 1.07 | 0.85 | 1.04 | 0.8278 | 0.5758 | 0.9126 | 0.94 | 0.96 | 0.92 | 0.7569 | 0.8671 | 0.7308 | 0.92 | 0.98 | 0.8451 | 0.9587 |
| 428.3657 | 4.0 | C29H48O2 | (24R,24'R)-Fucosterol epoxide | Miscellaneous | 1.08 | 0.55 | 0.87 | 0.8290 | 0.2832 | 0.7221 | 1.01 | 0.9800 | 1.51 | 1.21 | 1.45 | 0.3514 | 0.7032 | 0.3236 | 0.81 | 0.99 | 0.86 | 0.6745 | 0.9853 | 0.7626 | 1.00 | 0.99 | 0.9991 | 0.9738 |
| 381.0226 | 16.6 | C8H17NO12P2 | N-Acetyl-D-glucosamine 1,6-bisphosphate | Miscellaneous | 1.15 | 1.24 | 1.05 | 0.7352 | 0.5436 | 0.9082 | 0.93 | 0.8540 | 0.79 | 0.90 | 0.83 | 0.5427 | 0.7839 | 0.6684 | 1.04 | 1.02 | 1.04 | 0.9201 | 0.9601 | 0.9200 | 1.08 | 1.19 | 0.8222 | 0.5967 |
| 244.0409 | 13.8 | C10H12O5S | 2-(4-sulfophenyl)butyrate | Miscellaneous | 1.08 | 0.95 | 0.91 | 0.9152 | 0.9491 | 0.9007 | 1.09 | 0.8740 | 0.80 | 1.14 | 1.00 | 0.6775 | 0.8031 | 0.9931 | 0.82 | 0.95 | 1.07 | 0.7184 | 0.9317 | 0.9043 | 0.93 | 1.08 | 0.7754 | 0.6864 |
| 371.3035 | 4.9 | C21H41NO4 | Tetradecanoylcarnitine | Miscellaneous | 1.07 | 0.90 | 0.83 | 0.9110 | 0.8381 | 0.6870 | 1.10 | 0.6889 | 1.13 | 0.73 | 0.88 | 0.7898 | 0.3645 | 0.7356 | 1.27 | 1.21 | 1.10 | 0.4467 | 0.5574 | 0.7165 | 0.71 | 0.86 | 0.6175 | 0.8149 |
| 171.0645 | 14.9 | C6H9N3O3 | 6-diazo-5-oxonorleucine | Miscellaneous | 1.11 | 1.67 | 1.24 | 0.7375 | 0.1373 | 0.5216 | 1.13 | 0.6888 | 0.92 | 0.97 | 1.02 | 0.7992 | 0.9245 | 0.9464 | 0.88 | 1.19 | 1.01 | 0.6581 | 0.5583 | 0.9660 | 1.35 | 1.14 | 0.4422 | 0.4981 |
| 96.0211 | 17.3 | C5H4O2 | Furfural | Miscellaneous | 1.11 | 1.23 | 1.06 | 0.7384 | 0.5520 | 0.8322 | 0.87 | 0.7137 | 0.72 | 1.09 | 1.00 | 0.4024 | 0.8481 | 0.9986 | 1.23 | 1.34 | 1.31 | 0.6411 | 0.5511 | 0.5408 | 1.36 | 1.39 | 0.4616 | 0.4067 |
| 614.1726 | 8.7 | C23H31N6O12P | 7,8-H2pterin-6-ylmethyl-l-(4-aminophenyl)-1-deoxy-5-[1-α -D-ribofuranosyl 5-phosphate]-D-ribitol | Miscellaneous | 1.05 | 0.89 | 0.97 | 0.8231 | 0.7406 | 0.8983 | 1.06 | 0.8495 | 1.26 | 1.13 | 1.06 | 0.4635 | 0.7525 | 0.8918 | 0.93 | 1.01 | 0.96 | 0.8645 | 0.9791 | 0.9154 | 0.93 | 0.92 | 0.7763 | 0.7311 |
| 170.1307 | 4.3 | C10H18O2 | (E)-3,7-Dimethylocta-1,6-diene-3,8-diol | Miscellaneous | 1.03 | 0.57 | 0.65 | 0.9505 | 0.2852 | 0.3732 | 1.06 | 0.8876 | 1.66 | 0.92 | 0.98 | 0.2791 | 0.7961 | 0.9472 | 0.94 | 1.08 | 0.96 | 0.7783 | 0.7523 | 0.8614 | 0.89 | 0.94 | 0.8167 | 0.9154 |
| 427.3663 | 4.6 | C25H49NO4 | Stearoylcarnitine | Miscellaneous | 1.03 | 0.99 | 0.79 | 0.9636 | 0.9875 | 0.6518 | 1.03 | 0.8711 | 1.39 | 0.91 | 1.03 | 0.5226 | 0.6767 | 0.9073 | 1.03 | 1.03 | 0.95 | 0.8987 | 0.8942 | 0.8069 | 0.66 | 0.68 | 0.6046 | 0.6268 |
| 177.9975 | 11.2 | C5H11AsO2 | Arsenobetaine | Miscellaneous | 1.06 | 1.11 | 0.99 | 0.9440 | 0.9083 | 0.9923 | 1.15 | 0.8356 | 0.96 | 0.87 | 0.86 | 0.9496 | 0.8321 | 0.8261 | 1.10 | 1.02 | 1.05 | 0.8914 | 0.9728 | 0.9435 | 1.24 | 1.20 | 0.7793 | 0.7893 |
| 290.0038 | 18.7 | C6H11O11P | 3-phosphoglucarate | Miscellaneous | 1.11 | 1.20 | 1.17 | 0.7646 | 0.5170 | 0.6429 | 0.89 | 0.8159 | 0.61 | 0.84 | 0.73 | 0.3264 | 0.7553 | 0.5728 | 1.04 | 1.06 | 0.98 | 0.9383 | 0.9168 | 0.9693 | 1.10 | 1.22 | 0.6707 | 0.3548 |

| | | | | | | | | | | | | | | | | | | | | | | | | | | | | |
|---|---|---|---|---|---|---|---|---|---|---|---|---|---|---|---|---|---|---|---|---|---|---|---|---|---|---|---|---|
| 193.0409 | 14.5 | C6H11NO4S | γ-thiomethyl glutamate | Miscellaneous | 1.09 | 1.19 | 0.98 | 0.7588 | 0.5377 | 0.9273 | 0.94 | 0.7423 | 0.92 | 0.98 | 0.89 | 0.6468 | 0.8779 | 0.5795 | 1.17 | 1.08 | 1.02 | 0.3122 | 0.7168 | 0.9173 | 1.07 | 1.16 | 0.6969 | 0.5259 |
| 185.0090 | 17.2 | C3H8NO6P | D-O-Phosphoserine | Miscellaneous | 1.06 | 1.21 | 0.97 | 0.7298 | 0.3062 | 0.8088 | 0.96 | 0.9242 | 0.76 | 0.83 | 0.84 | 0.4504 | 0.6297 | 0.6558 | 1.02 | 1.06 | 1.01 | 0.9655 | 0.8909 | 0.9819 | 1.31 | 1.27 | 0.2989 | 0.0796 |
| 241.0950 | 5.0 | C11H15NO5 | Methocarbamol | Miscellaneous | 1.05 | 1.08 | 1.08 | 0.8585 | 0.6725 | 0.6228 | 1.04 | 0.8989 | 0.84 | 0.84 | 0.76 | 0.4666 | 0.3129 | 0.1822 | 0.89 | 0.90 | 1.06 | 0.6549 | 0.6854 | 0.7973 | 1.37 | 1.11 | 0.2698 | 0.5938 |
| 324.1534 | 16.6 | C12H24N2O8 | Procollagen 5-(D-galactosyloxy)-L-lysine | Miscellaneous | 1.07 | 1.07 | 0.88 | 0.8614 | 0.8446 | 0.6883 | 1.06 | 0.8413 | 0.87 | 1.11 | 1.05 | 0.6279 | 0.7390 | 0.8993 | 1.03 | 1.14 | 1.09 | 0.9074 | 0.6772 | 0.7859 | 1.16 | 1.14 | 0.6602 | 0.6421 |
| 174.1367 | 20.9 | C8H18N2O2 | Ne,Ne dimethyllysine | Miscellaneous | 1.06 | 1.14 | 1.05 | 0.8318 | 0.7264 | 0.8772 | 0.98 | 0.9537 | 0.84 | 0.96 | 0.90 | 0.5549 | 0.8853 | 0.7569 | 1.07 | 1.05 | 1.01 | 0.8102 | 0.8567 | 0.9617 | 1.08 | 0.98 | 0.7094 | 0.9095 |
| 160.0921 | 5.0 | C8H16OS | 2-Methyl-4-propyl-1,3-oxathiane | Miscellaneous | 1.06 | 1.07 | 1.09 | 0.8598 | 0.8665 | 0.7523 | 0.93 | 0.8693 | 1.16 | 1.27 | 1.37 | 0.6753 | 0.6574 | 0.3545 | 0.75 | 0.75 | 0.59 | 0.4610 | 0.4702 | 0.2560 | 0.76 | 0.62 | 0.5874 | 0.3769 |
| 257.1123 | 14.1 | C9H15N5O4 | 4a-Hydroxytetrahydrobiopterin | Miscellaneous | 1.03 | 1.02 | 1.10 | 0.8554 | 0.7881 | 0.2801 | 1.11 | 0.1911 | 0.98 | 0.96 | 0.91 | 0.9123 | 0.7634 | 0.5233 | 1.04 | 1.09 | 1.03 | 0.6731 | 0.2617 | 0.6877 | 0.95 | 0.81 | 0.7534 | 0.2975 |
| 369.1934 | 10.7 | C22H27NO4 | Corydaline | Miscellaneous | 1.03 | 0.98 | 0.92 | 0.9381 | 0.9523 | 0.8423 | 1.04 | 0.9414 | 0.86 | 0.87 | 0.88 | 0.7422 | 0.7656 | 0.7882 | 1.01 | 1.07 | 0.95 | 0.9812 | 0.8718 | 0.8981 | 1.02 | 1.01 | 0.9750 | 0.9767 |
| 358.1411 | 14.5 | C20H22O6 | Miroestrol | Miscellaneous | 1.06 | 1.12 | 1.08 | 0.7354 | 0.4885 | 0.5070 | 1.15 | 0.5329 | 1.11 | 1.09 | 1.03 | 0.3341 | 0.4860 | 0.8776 | 1.08 | 1.15 | 1.06 | 0.5715 | 0.2945 | 0.6709 | 0.97 | 1.14 | 0.8097 | 0.4273 |
| 177.0282 | 7.6 | C6H11NOS2 | Sulforaphane | Miscellaneous | 1.05 | 0.89 | 0.98 | 0.9242 | 0.8081 | 0.9599 | 1.20 | 0.4545 | 0.89 | 1.16 | 0.74 | 0.7925 | 0.7346 | 0.4512 | 1.33 | 1.25 | 1.19 | 0.2939 | 0.4348 | 0.4858 | 1.05 | 1.13 | 0.9046 | 0.7535 |
| 188.0143 | 4.5 | C7H8O4S | Benzyl sulfate | Miscellaneous | 1.01 | 1.12 | 1.07 | 0.9173 | 0.3159 | 0.1763 | 1.10 | 0.4875 | 0.90 | 0.98 | 1.01 | 0.4025 | 0.8765 | 0.9346 | 0.93 | 0.97 | 0.93 | 0.5082 | 0.7971 | 0.5017 | 1.03 | 1.05 | 0.7660 | 0.4415 |
| 171.0895 | 13.7 | C8H13NO3 | Crotanecine | Miscellaneous | 1.03 | 1.05 | 0.92 | 0.8533 | 0.7694 | 0.6709 | 1.03 | 0.8865 | 0.95 | 0.92 | 0.79 | 0.8422 | 0.7070 | 0.2038 | 1.08 | 1.09 | 1.02 | 0.6621 | 0.7403 | 0.9323 | 1.18 | 1.05 | 0.6070 | 0.8784 |
| 205.0948 | 11.2 | C8H15NO5 | N-Acetyl-D-fucosamine | Miscellaneous | 1.03 | 1.04 | 1.01 | 0.9096 | 0.9177 | 0.9775 | 0.97 | 0.9150 | 0.97 | 1.05 | 1.07 | 0.8724 | 0.7840 | 0.7947 | 0.99 | 0.65 | 0.57 | 0.9752 | 0.0728 | 0.0376 | 1.10 | 1.10 | 0.5615 | 0.6654 |
| 321.0997 | 13.0 | C11H19N3O6S | gamma-L-Glutamyl-L-cysteinyl-beta-alanine | Miscellaneous | 1.03 | 1.08 | 0.93 | 0.8357 | 0.7457 | 0.6995 | 0.98 | 0.9410 | 0.80 | 1.04 | 0.95 | 0.5025 | 0.9138 | 0.8892 | 1.04 | 1.03 | 1.08 | 0.8954 | 0.8952 | 0.7882 | 1.18 | 1.23 | 0.3629 | 0.1530 |
| 275.1736 | 9.2 | C13H25NO5 | Hydroxyhexanoylcarnitine | Miscellaneous | 1.01 | 0.94 | 1.00 | 0.9476 | 0.5424 | 0.9844 | 1.11 | 0.2573 | 0.80 | 0.93 | 0.77 | 0.1549 | 0.6022 | 0.1036 | 1.02 | 0.91 | 1.11 | 0.8528 | 0.2088 | 0.1907 | 1.12 | 1.08 | 0.3752 | 0.4586 |
| 320.0509 | 16.3 | C8H17O11P | octulose 8-phosphate | Miscellaneous | 1.03 | 1.12 | 0.97 | 0.8980 | 0.6501 | 0.8870 | 0.95 | 0.8911 | 0.89 | 1.01 | 0.95 | 0.6721 | 0.9710 | 0.8896 | 1.13 | 1.11 | 1.14 | 0.6138 | 0.6734 | 0.6037 | 1.18 | 1.19 | 0.5526 | 0.5169 |
| 515.0450 | 16.2 | C13H19N5O13P2 | 3-(ADP)-glycerate | Miscellaneous | 1.00 | 1.24 | 1.05 | 0.9988 | 0.6192 | 0.9008 | 0.84 | 0.6788 | 0.97 | 1.17 | 0.89 | 0.9420 | 0.6624 | 0.7400 | 1.12 | 1.15 | 1.12 | 0.6839 | 0.6377 | 0.6861 | 1.37 | 1.55 | 0.4411 | 0.2052 |
| 159.1260 | 13.4 | C8H17NO2 | Methacholine | Miscellaneous | 1.00 | 1.20 | 0.98 | 0.9903 | 0.6635 | 0.9377 | 1.07 | 0.8749 | 0.84 | 0.98 | 0.93 | 0.6627 | 0.9557 | 0.8848 | 1.08 | 1.06 | 1.07 | 0.8618 | 0.8932 | 0.8663 | 1.14 | 1.09 | 0.6232 | 0.7067 |
| 155.1310 | 5.0 | C9H17NO | 3-(1-Pyrrolidinyl)-2-pentanone | Miscellaneous | 0.98 | 1.19 | 0.96 | 0.9472 | 0.6579 | 0.9169 | 0.85 | 0.6676 | 1.14 | 1.33 | 1.16 | 0.7351 | 0.5879 | 0.6841 | 0.73 | 0.96 | 0.81 | 0.4219 | 0.8995 | 0.5768 | 0.86 | 0.73 | 0.7183 | 0.4243 |
| 173.1052 | 11.8 | C8H15NO3 | N-Acetyl-L-leucine | Miscellaneous | 0.98 | 1.13 | 1.00 | 0.9723 | 0.8383 | 0.9940 | 1.04 | 0.9500 | 0.84 | 0.96 | 0.91 | 0.7648 | 0.9505 | 0.8833 | 1.06 | 1.01 | 1.04 | 0.9276 | 0.9806 | 0.9425 | 1.16 | 1.12 | 0.7960 | 0.8331 |
| 350.0614 | 16.6 | C9H19O12P | nonulose 9-phosphate | Miscellaneous | 1.01 | 1.15 | 1.03 | 0.9416 | 0.6007 | 0.8726 | 0.93 | 0.7421 | 0.90 | 1.03 | 0.97 | 0.6401 | 0.9178 | 0.9311 | 1.07 | 1.10 | 1.13 | 0.7244 | 0.6727 | 0.5918 | 1.13 | 1.13 | 0.4546 | 0.4628 |
| 278.1882 | 4.1 | C17H26O3 | [6]-Paradol | Miscellaneous | 0.94 | 1.35 | 0.98 | 0.8724 | 0.7032 | 0.9631 | 1.01 | 0.9736 | 1.18 | 1.04 | 1.20 | 0.6210 | 0.9323 | 0.6542 | 0.81 | 0.88 | 0.77 | 0.4954 | 0.6476 | 0.3715 | 0.59 | 0.66 | 0.3513 | 0.4326 |
| 237.0849 | 12.9 | C8H15NO7 | N-Glycolyl-D-glucosamine | Miscellaneous | 0.99 | 1.16 | 1.06 | 0.9751 | 0.7474 | 0.9054 | 0.93 | 0.8275 | 0.89 | 0.94 | 1.01 | 0.7529 | 0.8836 | 0.9781 | 1.09 | 1.16 | 1.06 | 0.7970 | 0.6878 | 0.8803 | 1.22 | 1.16 | 0.5927 | 0.7051 |
| 195.0895 | 4.9 | C10H13NO3 | Damascenine | Miscellaneous | 0.96 | 0.85 | 0.84 | 0.9084 | 0.6470 | 0.5696 | 1.15 | 0.6742 | 1.08 | 1.00 | 0.99 | 0.7486 | 0.9985 | 0.9540 | 0.80 | 0.87 | 0.89 | 0.3315 | 0.5638 | 0.6101 | 0.79 | 1.03 | 0.5894 | 0.9468 |
| 383.1429 | 13.7 | C14H25NO11 | N-Acetyllactosamine | Miscellaneous | 0.99 | 1.09 | 0.96 | 0.9688 | 0.7180 | 0.8602 | 1.01 | 0.9626 | 0.89 | 1.00 | 0.91 | 0.5859 | 0.9915 | 0.6919 | 1.08 | 1.08 | 1.06 | 0.6616 | 0.6358 | 0.6884 | 1.17 | 1.17 | 0.4785 | 0.5266 |
| 143.0947 | 10.8 | C7H13NO2 | 4-(Trimethylammonio)but-2-enoate | Miscellaneous | 0.95 | 1.21 | 1.03 | 0.9369 | 0.7985 | 0.9587 | 1.00 | 0.9995 | 0.81 | 0.91 | 0.95 | 0.7925 | 0.9135 | 0.9572 | 1.00 | 1.04 | 1.01 | 0.9976 | 0.9638 | 0.9905 | 1.18 | 1.15 | 0.7928 | 0.8161 |
| 486.2062 | 21.7 | C18H34N2O13 | Glucosylgalactosylhydroxylysine | Miscellaneous | 1.00 | 1.15 | 1.05 | 0.9841 | 0.6368 | 0.7590 | 0.93 | 0.7510 | 0.84 | 0.91 | 0.88 | 0.4691 | 0.7179 | 0.6658 | 1.03 | 0.93 | 0.95 | 0.8907 | 0.7457 | 0.8120 | 1.29 | 1.16 | 0.1508 | 0.4102 |
| 321.0696 | 19.5 | C11H15NO10 | beta-Citryl-L-glutamic acid | Miscellaneous | 1.00 | 1.40 | 0.95 | 0.9959 | 0.4641 | 0.7646 | 0.93 | 0.9203 | 0.66 | 0.97 | 0.88 | 0.5438 | 0.9653 | 0.8653 | 1.03 | 1.05 | 0.97 | 0.9710 | 0.9443 | 0.9716 | 1.25 | 1.22 | 0.4806 | 0.2977 |
| 256.1211 | 4.9 | C15H16N2O2 | ancymidol | Miscellaneous | 0.97 | 0.81 | 0.95 | 0.8774 | 0.2320 | 0.7936 | 1.00 | 0.9901 | 0.95 | 0.96 | 0.97 | 0.7571 | 0.7609 | 0.8845 | 1.17 | 1.12 | 1.05 | 0.4110 | 0.5262 | 0.7022 | 1.02 | 1.06 | 0.9146 | 0.8193 |
| 251.1005 | 14.4 | C9H17NO7 | Muramic acid | Miscellaneous | 0.99 | 1.09 | 0.99 | 0.9687 | 0.7994 | 0.9742 | 0.88 | 0.5554 | 0.90 | 1.04 | 0.98 | 0.6348 | 0.8659 | 0.9393 | 1.07 | 0.97 | 0.99 | 0.7651 | 0.8885 | 0.9614 | 1.14 | 1.13 | 0.6456 | 0.6533 |
| 186.0641 | 14.2 | C7H10N2O4 | (S)-AMPA | Miscellaneous | 0.99 | 1.07 | 1.00 | 0.9599 | 0.7508 | 0.9991 | 1.14 | 0.4256 | 0.83 | 0.89 | 0.87 | 0.2767 | 0.4536 | 0.5008 | 1.00 | 1.08 | 1.09 | 0.9928 | 0.6849 | 0.5926 | 1.10 | 1.19 | 0.4649 | 0.2381 |
| 202.0591 | 15.4 | C7H10N2O5 | N3-fumaramoyl-L-2,3-diaminopropanoate | Miscellaneous | 0.98 | 1.06 | 0.96 | 0.9431 | 0.8758 | 0.9085 | 1.01 | 0.9754 | 0.87 | 1.01 | 0.85 | 0.6549 | 0.9733 | 0.6591 | 1.10 | 1.03 | 1.09 | 0.7745 | 0.9294 | 0.7816 | 1.16 | 1.06 | 0.5535 | 0.8151 |
| 270.0964 | 14.6 | C10H14N4O5 | 6-Hydroxyl-1,6-dihydropurine ribonucleoside | Miscellaneous | 0.93 | 1.14 | 0.80 | 0.8681 | 0.8055 | 0.6984 | 1.01 | 0.9652 | 0.70 | 0.88 | 0.89 | 0.2088 | 0.6865 | 0.6957 | 1.04 | 0.98 | 0.94 | 0.8841 | 0.9214 | 0.8192 | 1.24 | 1.25 | 0.2392 | 0.3549 |
| 126.0252 | 14.7 | C5H6N2S | Pyrazinemethanethiol | Miscellaneous | 0.97 | 1.00 | 0.96 | 0.9381 | 0.9988 | 0.9207 | 1.01 | 0.9825 | 0.88 | 0.94 | 0.97 | 0.7332 | 0.8773 | 0.9397 | 1.04 | 1.02 | 1.06 | 0.9076 | 0.9653 | 0.8689 | 1.08 | 1.08 | 0.8519 | 0.8511 |
| 621.0278 | 17.8 | C15H22N5O16P3 | ADP ribose 1",2"-phosphate | Miscellaneous | 0.99 | 1.39 | 0.97 | 0.9683 | 0.4108 | 0.9240 | 0.80 | 0.3879 | 0.88 | 0.82 | 0.79 | 0.4905 | 0.4116 | 0.3584 | 0.98 | 1.06 | 0.86 | 0.9254 | 0.8082 | 0.5871 | 1.15 | 1.10 | 0.6963 | 0.7849 |
| 131.0736 | 11.6 | C9H9N | Tolylacetonitrile | Miscellaneous | 0.96 | 1.07 | 1.03 | 0.6241 | 0.6368 | 0.7157 | 1.02 | 0.8896 | 0.91 | 0.93 | 0.78 | 0.6118 | 0.7137 | 0.2576 | 1.18 | 1.08 | 0.95 | 0.2372 | 0.6745 | 0.6965 | 0.97 | 1.07 | 0.7395 | 0.3710 |
| 163.0845 | 15.7 | C6H13NO4 | Deoxymannojirimycin | Miscellaneous | 0.97 | 0.86 | 1.05 | 0.9067 | 0.6327 | 0.8358 | 0.72 | 0.2646 | 0.69 | 0.90 | 0.76 | 0.2829 | 0.6898 | 0.5541 | 1.05 | 1.29 | 0.95 | 0.8813 | 0.3712 | 0.9259 | 1.07 | 1.23 | 0.8050 | 0.5244 |
| 246.1368 | 8.8 | C14H18N2O2 | Hypaphorine | Miscellaneous | 0.97 | 0.98 | 0.97 | 0.9478 | 0.9637 | 0.9439 | 1.07 | 0.8788 | 1.00 | 1.03 | 0.90 | 0.9973 | 0.9555 | 0.8168 | 1.07 | 1.03 | 1.04 | 0.8802 | 0.9547 | 0.9238 | 1.07 | 1.09 | 0.8881 | 0.8498 |
| 150.0542 | 9.3 | C6H6N4O | 1-Methylhypoxanthine | Miscellaneous | 0.95 | 1.04 | 0.88 | 0.5579 | 0.7198 | 0.2175 | 1.13 | 0.2833 | 0.84 | 0.91 | 0.85 | 0.2145 | 0.4078 | 0.2362 | 0.95 | 0.98 | 0.96 | 0.6252 | 0.8634 | 0.7374 | 1.26 | 1.14 | 0.2144 | 0.3353 |
| 145.0527 | 8.8 | C9H7NO | 3-Methyleneoxindole | Miscellaneous | 0.98 | 1.14 | 1.06 | 0.9639 | 0.7988 | 0.9142 | 1.12 | 0.8154 | 0.92 | 0.90 | 0.83 | 0.8639 | 0.8141 | 0.6837 | 1.14 | 1.09 | 1.17 | 0.7752 | 0.8451 | 0.7392 | 1.11 | 1.15 | 0.8372 | 0.7912 |
| 245.1629 | 8.1 | C12H23NO4 | 2-Methylbutyroylcarnitine | Miscellaneous | 0.94 | 1.10 | 0.94 | 0.7541 | 0.6288 | 0.8087 | 1.19 | 0.5462 | 0.88 | 0.95 | 0.93 | 0.5975 | 0.8322 | 0.7848 | 1.08 | 1.13 | 1.08 | 0.7036 | 0.5598 | 0.7211 | 1.08 | 1.04 | 0.6554 | 0.8312 |
| 199.1212 | 10.5 | C10H17NO3 | Tussilagine | Miscellaneous | 0.96 | 1.01 | 1.08 | 0.7832 | 0.9791 | 0.5905 | 1.06 | 0.8085 | 0.92 | 0.95 | 0.90 | 0.7410 | 0.8616 | 0.7374 | 0.87 | 1.01 | 0.95 | 0.6545 | 0.9806 | 0.8624 | 1.78 | 1.31 | 0.0303 | 0.3218 |
| 220.1062 | 13.1 | C8H16N2O5 | N-Acetyl-beta-D-glucosaminylamine | Miscellaneous | 0.94 | 1.07 | 0.89 | 0.7770 | 0.7961 | 0.5961 | 0.95 | 0.7148 | 0.88 | 0.93 | 0.89 | 0.4404 | 0.6535 | 0.4351 | 1.05 | 1.06 | 1.00 | 0.6171 | 0.5184 | 0.9950 | 1.17 | 1.08 | 0.4363 | 0.6301 |
| 374.1371 | 10.2 | C20H22O7 | Kievitone hydrate | Miscellaneous | 0.94 | 1.11 | 1.03 | 0.6072 | 0.5569 | 0.8496 | 1.05 | 0.7983 | 1.03 | 1.07 | 1.02 | 0.9295 | 0.8190 | 0.9595 | 1.07 | 1.15 | 1.17 | 0.8328 | 0.6203 | 0.6600 | 1.21 | 1.08 | 0.2175 | 0.5621 |

| | | | | | | | | | | | | | | | | | | | | | | | | | | | |
|---|---|---|---|---|---|---|---|---|---|---|---|---|---|---|---|---|---|---|---|---|---|---|---|---|---|---|---|
| 214.0412 | 9.0 | C8H10N2O3S | Sulfacetamide | Miscellaneous | 0.96 | 0.97 | 1.02 | 0.9325 | 0.9426 | 0.9666 | 1.14 | 0.7657 | 0.98 | 0.99 | 0.84 | 0.9678 | 0.9758 | 0.7156 | 1.09 | 1.07 | 1.04 | 0.8499 | 0.8882 | 0.9339 | 1.12 | 1.13 | 0.7495 | 0.7658 |
| 187.0633 | 8.8 | C11H9NO2 | Indoleacrylicacid | Miscellaneous | 0.95 | 1.04 | 0.93 | 0.8679 | 0.8777 | 0.7523 | 1.12 | 0.6138 | 0.79 | 0.84 | 0.85 | 0.3878 | 0.5029 | 0.5188 | 0.93 | 1.05 | 0.99 | 0.5225 | 0.7351 | 0.9280 | 1.10 | 1.17 | 0.8379 | 0.7459 |
| 98.0845 | 10.5 | C5H10N2 | xi-4,5-Dihydro-2,4(5)-dimethyl-1H-imidazole | Miscellaneous | 0.93 | 0.92 | 0.94 | 0.4863 | 0.5024 | 0.5877 | 0.98 | 0.8536 | 0.93 | 0.98 | 0.96 | 0.6894 | 0.8922 | 0.8282 | 1.15 | 1.14 | 1.07 | 0.1461 | 0.3651 | 0.5174 | 1.00 | 1.06 | 0.9827 | 0.7677 |
| 129.0578 | 11.6 | C9H7N | Quinoline | Miscellaneous | 0.98 | 1.08 | 1.07 | 0.9674 | 0.8317 | 0.8985 | 0.96 | 0.9126 | 0.92 | 0.96 | 0.95 | 0.8154 | 0.9095 | 0.8983 | 1.01 | 1.05 | 1.07 | 0.9730 | 0.8855 | 0.8554 | 1.13 | 1.09 | 0.2488 | 0.5849 |
| 272.0298 | 15.9 | C7H13O9P | α-(2,6-anhydro-3-deoxy-D-arabino-heptulopyranosid)onate 7-phosphate | Miscellaneous | 0.93 | 0.83 | 0.95 | 0.5443 | 0.2695 | 0.7176 | 1.11 | 0.7323 | 0.81 | 0.86 | 0.86 | 0.2076 | 0.3718 | 0.4290 | 1.29 | 1.14 | 1.17 | 0.1075 | 0.1961 | 0.0949 | 1.19 | 1.22 | 0.6234 | 0.5401 |
| 300.1111 | 4.9 | C16H16N2O4 | 5-Nitro-2-(3-phenylpropylamino)benzoic acid | Miscellaneous | 0.98 | 1.07 | 0.92 | 0.9786 | 0.9274 | 0.9210 | 0.77 | 0.6629 | 0.93 | 1.00 | 0.72 | 0.9223 | 0.9973 | 0.6136 | 0.93 | 1.02 | 0.90 | 0.9227 | 0.9835 | 0.8897 | 1.08 | 1.13 | 0.7292 | 0.5382 |
| 249.0309 | 18.5 | C8H11NO6S | Norepinephrinesulfate | Miscellaneous | 0.95 | 1.32 | 0.92 | 0.8499 | 0.2954 | 0.7444 | 0.86 | 0.7727 | 0.65 | 0.83 | 0.79 | 0.4095 | 0.7410 | 0.6839 | 1.00 | 1.07 | 0.98 | 0.9982 | 0.9117 | 0.9749 | 1.27 | 1.40 | 0.8013 | 0.7173 |
| 595.0117 | 17.3 | C13H20N5O16P3 | 3-(ADP)-2-phosphoglycerate | Miscellaneous | 0.91 | 1.12 | 0.97 | 0.7426 | 0.7990 | 0.9146 | 0.97 | 0.9421 | 0.77 | 0.96 | 0.87 | 0.5636 | 0.9302 | 0.7862 | 1.04 | 1.01 | 1.01 | 0.9352 | 0.9829 | 0.9836 | 1.08 | 1.20 | 0.7532 | 0.3055 |
| 125.0478 | 12.2 | C6H7NO2 | N-Ethylmaleimide | Miscellaneous | 0.93 | 1.09 | 0.97 | 0.8502 | 0.8378 | 0.9472 | 0.98 | 0.9308 | 0.89 | 0.96 | 0.87 | 0.7098 | 0.8893 | 0.6973 | 1.05 | 1.07 | 1.06 | 0.8619 | 0.8098 | 0.8392 | 1.09 | 1.11 | 0.7220 | 0.5859 |
| 261.1212 | 12.9 | C11H19NO6 | Lotaustralin | Miscellaneous | 0.89 | 1.20 | 1.03 | 0.8610 | 0.7910 | 0.9655 | 1.01 | 0.9923 | 0.77 | 0.99 | 1.09 | 0.7488 | 0.9886 | 0.9209 | 1.04 | 1.17 | 1.06 | 0.9637 | 0.8557 | 0.9450 | 1.09 | 1.07 | 0.7987 | 0.8510 |
| 127.9122 | 9.9 | HI | hydrogen iodide | Miscellaneous | 0.88 | 0.77 | 0.99 | 0.7329 | 0.4984 | 0.9829 | 1.09 | 0.7424 | 1.15 | 1.17 | 1.01 | 0.6980 | 0.6751 | 0.9537 | 0.75 | 0.91 | 0.78 | 0.5282 | 0.8231 | 0.5687 | 1.11 | 0.97 | 0.8824 | 0.9658 |
| 294.1833 | 4.1 | C17H26O4 | Phytuberin | Miscellaneous | 0.94 | 1.08 | 0.62 | 0.7243 | 0.7480 | 0.0806 | 0.88 | 0.6345 | 0.85 | 0.90 | 0.75 | 0.5588 | 0.6781 | 0.2641 | 0.99 | 0.97 | 0.96 | 0.9627 | 0.9043 | 0.8658 | 0.82 | 0.77 | 0.6014 | 0.4746 |
| 268.0795 | 14.7 | C9H16O9 | 2(alpha-D-Mannosyl)-D-glycerate | Miscellaneous | 0.94 | 0.96 | 0.97 | 0.7252 | 0.8302 | 0.8990 | 1.01 | 0.9360 | 0.79 | 0.94 | 0.76 | 0.1933 | 0.7147 | 0.1662 | 0.95 | 1.06 | 0.97 | 0.7561 | 0.7793 | 0.8600 | 1.10 | 1.20 | 0.8080 | 0.6180 |
| 198.0639 | 14.2 | C8H10N2O4 | (S)-2-Amino-3-(3-hydroxy-4-oxo-4H-pyridin-1-yl)propanoate | Miscellaneous | 0.94 | 1.24 | 0.99 | 0.8888 | 0.6011 | 0.9764 | 0.95 | 0.8531 | 1.04 | 0.99 | 1.16 | 0.8682 | 0.9819 | 0.6575 | 1.04 | 1.03 | 1.04 | 0.8773 | 0.9302 | 0.9035 | 1.11 | 1.08 | 0.5245 | 0.6672 |
| 291.0954 | 12.4 | C11H17NO8 | 2-Deoxy-2,3-dehydro-N-acetylneuraminic acid | Miscellaneous | 0.95 | 0.87 | 0.96 | 0.8392 | 0.5997 | 0.8565 | 0.91 | 0.3618 | 0.90 | 1.07 | 1.02 | 0.6315 | 0.6858 | 0.9229 | 1.05 | 1.08 | 1.09 | 0.6591 | 0.5948 | 0.5021 | 1.08 | 1.11 | 0.8376 | 0.7903 |
| 210.0740 | 13.7 | C7H14O7 | alpha-D-Mannoheptulopyranose | Miscellaneous | 0.93 | 0.98 | 0.97 | 0.9134 | 0.9799 | 0.9666 | 0.97 | 0.9637 | 0.90 | 0.97 | 0.85 | 0.8576 | 0.9635 | 0.8032 | 1.07 | 1.05 | 1.09 | 0.9174 | 0.9361 | 0.8948 | 1.16 | 1.14 | 0.5755 | 0.5972 |
| 147.0896 | 12.2 | C6H13NO3 | N-hydroxyisoleucine | Miscellaneous | 0.93 | 1.09 | 0.95 | 0.6292 | 0.7568 | 0.7577 | 0.91 | 0.6762 | 0.80 | 0.90 | 0.85 | 0.4626 | 0.7487 | 0.6093 | 1.04 | 1.11 | 1.13 | 0.8793 | 0.6800 | 0.6325 | 1.18 | 1.21 | 0.8221 | 0.7848 |
| 218.0403 | 13.3 | C12H10O2S | cis-1,2-Dihydroxy-1,2-dihydrodibenzothiophene | Miscellaneous | 0.91 | 1.13 | 0.95 | 0.7148 | 0.7499 | 0.8547 | 0.88 | 0.7591 | 0.77 | 0.94 | 0.88 | 0.5245 | 0.8832 | 0.7780 | 1.05 | 1.09 | 1.09 | 0.8906 | 0.8338 | 0.8256 | 1.07 | 1.16 | 0.6632 | 0.3318 |
| 143.0583 | 12.2 | C6H9NO3 | Vinylacetylglycine | Miscellaneous | 0.94 | 1.74 | 1.41 | 0.8602 | 0.3066 | 0.2816 | 1.05 | 0.7045 | 0.95 | 0.95 | 0.81 | 0.7233 | 0.7259 | 0.4427 | 0.92 | 1.07 | 0.91 | 0.6938 | 0.7675 | 0.5600 | 1.19 | 1.09 | 0.5655 | 0.6653 |
| 220.0848 | 10.8 | C11H12N2O3 | 5-Hydroxytryptophan | Miscellaneous | 1.02 | 0.55 | 0.27 | 0.9868 | 0.5901 | NA | 1.04 | 0.9441 | 0.94 | 0.94 | 0.99 | 0.9007 | 0.9396 | 0.9863 | 1.91 | 1.32 | 0.82 | 0.5402 | 0.7643 | NA | 1.18 | 1.15 | 0.3420 | 0.3209 |
| 181.0409 | 11.8 | C5H11NO4S | DL-Methionine sulfone | Miscellaneous | 0.90 | 0.97 | 1.02 | 0.2246 | 0.7629 | 0.7845 | 0.83 | 0.1291 | 0.97 | 0.89 | 0.98 | 0.8935 | 0.6766 | 0.9508 | 1.11 | 1.11 | 1.06 | 0.4232 | 0.3713 | 0.6730 | 0.00 | 0.00 | NA | NA |
| 408.2873 | 5.0 | C24H40O5 | Bile salt | Miscellaneous | 0.92 | 1.05 | 0.98 | 0.6662 | 0.7841 | 0.9096 | 0.94 | 0.4491 | 0.99 | 0.99 | 0.90 | 0.9227 | 0.9406 | 0.5753 | 1.14 | 1.04 | 1.02 | 0.1166 | 0.7096 | 0.8204 | 0.81 | 0.80 | 0.0355 | 0.0393 |
| 541.0604 | 14.1 | C15H21N5O13P2 | Cyclic ADP-ribose | Miscellaneous | 0.92 | 0.89 | 0.67 | 0.6326 | 0.5639 | 0.2615 | 0.99 | 0.9626 | 1.04 | 1.13 | 0.93 | 0.9230 | 0.7836 | 0.8776 | 1.29 | 1.22 | 1.15 | 0.3887 | 0.4986 | 0.5951 | 1.10 | 1.08 | 0.4077 | 0.5239 |
| 139.0633 | 7.7 | C7H9NO2 | 5-Acetyl-2,4-dimethyloxazole | Miscellaneous | 0.91 | 1.08 | 1.04 | 0.9028 | 0.9241 | 0.9589 | 0.98 | 0.9706 | 0.93 | 0.96 | 0.92 | 0.9155 | 0.9495 | 0.9089 | 1.16 | 1.21 | 1.11 | 0.8356 | 0.7933 | 0.8818 | 1.24 | 1.24 | 0.5584 | 0.5349 |
| 456.1613 | 15.8 | C18H28N6O4S2 | Ovothiol disulfide | Miscellaneous | 0.88 | 1.21 | 0.76 | 0.8309 | 0.8010 | 0.6958 | 0.75 | 0.6769 | 0.74 | 0.82 | 0.99 | 0.6943 | 0.7884 | 0.9920 | 1.25 | 0.97 | 1.01 | 0.8109 | 0.9714 | 0.9938 | 1.00 | 0.94 | 0.9990 | 0.9327 |
| 89.0841 | 16.6 | C4H11NO | N-dimethylethanolamine | Miscellaneous | 0.89 | 1.12 | 0.94 | 0.7595 | 0.8039 | 0.8835 | 1.04 | 0.9494 | 0.81 | 0.90 | 0.88 | 0.6614 | 0.8397 | 0.8149 | 1.16 | 1.10 | 1.03 | 0.7897 | 0.8543 | 0.9557 | 1.60 | 1.24 | 0.5812 | 0.7721 |
| 231.1471 | 8.9 | C11H21NO4 | Isobutyryl-L-carnitine | Miscellaneous | 0.92 | 1.05 | 1.00 | 0.8111 | 0.9002 | 0.9972 | 0.99 | 0.9675 | 0.90 | 0.99 | 0.90 | 0.7731 | 0.9883 | 0.7594 | 1.12 | 1.11 | 1.09 | 0.7551 | 0.7591 | 0.8088 | 1.07 | 1.03 | 0.8542 | 0.9263 |
| 190.0953 | 11.9 | C7H14N2O4 | N5-acetyl-N5-hydroxy-L-ornithine | Miscellaneous | 0.91 | 1.14 | 0.86 | 0.7501 | 0.7371 | 0.6128 | 1.01 | 0.9837 | 0.93 | 1.14 | 1.15 | 0.8289 | 0.7281 | 0.7510 | 1.18 | 1.04 | 1.05 | 0.7402 | 0.9174 | 0.9113 | 1.09 | 1.11 | 0.8171 | 0.7969 |
| 114.0794 | 10.7 | C5H10N2O | 3-Amino-2-piperidone | Miscellaneous | 0.93 | 0.80 | 0.81 | 0.8309 | 0.5000 | 0.5401 | 1.03 | 0.9531 | 0.65 | 0.93 | 0.83 | 0.4292 | 0.8532 | 0.6667 | 0.84 | 0.72 | 0.85 | 0.6844 | 0.4347 | 0.6917 | 1.44 | 1.08 | 0.4716 | 0.8757 |
| 265.0810 | 10.2 | C10H11N5O4 | 5'-Dehydroadenosine | Miscellaneous | 0.91 | 0.88 | 0.65 | 0.7992 | 0.7416 | 0.3996 | 1.10 | 0.8657 | 1.62 | 1.14 | 1.45 | 0.2523 | 0.8198 | 0.4251 | 2.63 | 2.62 | 2.45 | 0.0396 | 0.1170 | 0.0432 | 0.54 | 0.73 | 0.2304 | 0.3914 |
| 267.0956 | 16.7 | C9H17NO8 | Neuraminic acid | Miscellaneous | 0.91 | 1.05 | 0.99 | 0.6887 | 0.8468 | 0.9591 | 0.92 | 0.6080 | 0.89 | 0.92 | 0.90 | 0.5869 | 0.6663 | 0.6620 | 1.15 | 1.08 | 1.09 | 0.2652 | 0.5482 | 0.4754 | 1.24 | 1.25 | 0.3174 | 0.3477 |
| 348.1104 | 13.0 | C20H16N2O4 | Camptothecin | Miscellaneous | 0.91 | 0.98 | 1.02 | 0.7421 | 0.9547 | 0.9442 | 1.01 | 0.9334 | 0.89 | 0.97 | 0.90 | 0.5618 | 0.8230 | 0.5373 | 1.08 | 1.06 | 0.99 | 0.3556 | 0.6151 | 0.9306 | 1.11 | 1.13 | 0.6647 | 0.6225 |
| 246.0855 | 10.5 | C9H14N2O6 | 5-6-Dihydrouridine | Miscellaneous | 0.85 | 0.83 | 0.66 | 0.6174 | 0.3819 | 0.1416 | 0.82 | 0.5156 | 1.10 | 0.83 | 1.23 | 0.8206 | 0.5507 | 0.3517 | 1.02 | 0.72 | 1.17 | 0.8710 | 0.2642 | 0.4809 | 0.76 | 0.78 | 0.4291 | 0.4599 |
| 288.0594 | 12.1 | C10H12N2O8 | Orotidine | Miscellaneous | 0.90 | 1.08 | 0.96 | 0.4982 | 0.8163 | 0.8185 | 0.96 | 0.9048 | 0.80 | 0.92 | 0.89 | 0.4906 | 0.8163 | 0.7570 | 1.03 | 1.06 | 1.00 | 0.9190 | 0.8672 | 0.9912 | 1.22 | 1.20 | 0.2062 | 0.1227 |
| 304.1020 | 15.8 | C10H16N4O7 | Vicine | Miscellaneous | 0.89 | 1.14 | 1.09 | 0.8295 | 0.8242 | 0.8804 | 1.04 | 0.9291 | 0.93 | 0.95 | 0.75 | 0.8918 | 0.9246 | 0.5882 | 0.94 | 0.93 | 0.92 | 0.8873 | 0.8820 | 0.8505 | 1.18 | 0.96 | 0.7753 | 0.9318 |
| 213.1113 | 14.2 | C9H15N3O3 | Methyl 2-diazoacetamidohexonate | Miscellaneous | 0.90 | 1.02 | 0.90 | 0.9193 | 0.9849 | 0.9165 | 1.14 | 0.8890 | 0.91 | 0.89 | 0.90 | 0.9194 | 0.8976 | 0.9135 | 1.11 | 1.13 | 1.07 | 0.9124 | 0.8902 | 0.9358 | 1.18 | 1.08 | 0.8602 | 0.9318 |
| 289.1274 | 13.3 | C11H19N3O6 | Ophthalmicacid | Miscellaneous | 0.91 | 0.99 | 0.94 | 0.7562 | 0.9823 | 0.8434 | 0.87 | 0.6786 | 0.82 | 0.96 | 0.90 | 0.6414 | 0.9249 | 0.8388 | 0.95 | 0.97 | 1.01 | 0.8835 | 0.9189 | 0.9725 | 1.14 | 1.17 | 0.6772 | 0.6356 |
| 334.0665 | 15.9 | C9H19O11P | sn-glycero-3-Phospho-1-inositol | Miscellaneous | 0.90 | 1.07 | 1.00 | 0.5571 | 0.7404 | 0.9900 | 0.91 | 0.4935 | 0.92 | 1.01 | 1.00 | 0.7142 | 0.9638 | 0.9876 | 0.99 | 1.05 | 0.88 | 0.9624 | 0.8184 | 0.4732 | 1.03 | 1.04 | 0.8403 | 0.7918 |
| 112.0160 | 12.0 | C5H4O3 | 2-Furoate | Miscellaneous | 0.88 | 1.02 | 0.89 | 0.5136 | 0.9476 | 0.4659 | 0.96 | 0.8712 | 1.08 | 1.14 | 1.13 | 0.6505 | 0.5596 | 0.6197 | 1.04 | 0.97 | 1.07 | 0.8540 | 0.9026 | 0.8176 | 0.88 | 0.91 | 0.5543 | 0.6421 |
| 243.1471 | 8.4 | C12H21NO4 | Tiglylcarnitine | Miscellaneous | 0.88 | 1.02 | 0.99 | 0.4785 | 0.9284 | 0.9497 | 1.07 | 0.7672 | 0.97 | 0.99 | 1.04 | 0.8539 | 0.9481 | 0.8612 | 1.03 | 1.19 | 1.07 | 0.8384 | 0.1627 | 0.6024 | 0.92 | 0.93 | 0.4251 | 0.3925 |
| 246.0505 | 12.6 | C6H15O8P | Glycerophosphoglycerol | Miscellaneous | 0.90 | 1.11 | 0.96 | 0.7291 | 0.7048 | 0.8957 | 0.96 | 0.8497 | 0.82 | 0.96 | 0.86 | 0.4491 | 0.8887 | 0.6105 | 1.09 | 1.10 | 0.98 | 0.6782 | 0.7231 | 0.9355 | 1.10 | 1.16 | 0.7404 | 0.6284 |

| | | | | | | | | | | | | | | | | | | | | | | | | | | | | |
|---|---|---|---|---|---|---|---|---|---|---|---|---|---|---|---|---|---|---|---|---|---|---|---|---|---|---|---|---|
| 200.0297 | 11.8 | C12H8OS | dibenzothiophene-5-oxide | Miscellaneous | 0.90 | 1.12 | 0.93 | 0.5141 | 0.6078 | 0.6818 | 0.96 | 0.8728 | 0.82 | 1.00 | 0.82 | 0.3933 | 0.9860 | 0.4557 | 0.99 | 1.06 | 1.05 | 0.9649 | 0.7981 | 0.8492 | 1.12 | 1.20 | 0.3258 | 0.1545 |
| 212.0086 | 12.5 | C5H9O7P | P-DPD | Miscellaneous | 0.91 | 1.00 | 0.97 | 0.8076 | 0.9898 | 0.9251 | 0.99 | 0.9859 | 0.97 | 0.95 | 0.85 | 0.9305 | 0.8827 | 0.5851 | 1.06 | 1.07 | 1.01 | 0.8421 | 0.8394 | 0.9823 | 1.09 | 1.15 | 0.8388 | 0.7548 |
| 183.0568 | 11.0 | C5H13NO4S | Choline sulfate | Miscellaneous | 0.89 | 0.83 | 0.99 | 0.2949 | 0.6637 | 0.9660 | 1.03 | 0.9034 | 0.88 | 0.95 | 0.90 | 0.6694 | 0.8625 | 0.7211 | 1.07 | 0.97 | 1.11 | 0.7829 | 0.9072 | 0.7353 | 1.24 | 1.24 | 0.4096 | 0.2895 |
| 309.1058 | 14.7 | C11H19NO9 | O-Acetylneuraminic acid | Miscellaneous | 0.89 | 1.04 | 0.94 | 0.7993 | 0.9283 | 0.8915 | 0.83 | 0.5758 | 1.01 | 1.03 | 0.90 | 0.9706 | 0.9341 | 0.7792 | 0.94 | 1.02 | 0.94 | 0.8523 | 0.9631 | 0.8203 | 1.11 | 1.11 | 0.8045 | 0.7920 |
| 222.0740 | 14.1 | C8H14O7 | 6-Acetyl-D-glucose | Miscellaneous | 0.89 | 1.01 | 0.98 | 0.3954 | 0.9213 | 0.8731 | 1.13 | 0.0689 | 1.09 | 1.22 | 1.22 | 0.8046 | 0.2643 | 0.3112 | 1.13 | 1.13 | 1.05 | 0.1616 | 0.1744 | 0.5388 | 1.08 | 1.05 | 0.6750 | 0.7657 |
| 259.0365 | 17.0 | C6H13NO8S | N-Sulfo-D-glucosamine | Miscellaneous | 0.87 | 0.94 | 0.90 | 0.7614 | 0.8895 | 0.8060 | 1.08 | 0.8338 | 0.93 | 0.97 | 0.97 | 0.8551 | 0.9366 | 0.9315 | 1.02 | 1.04 | 1.05 | 0.9727 | 0.9362 | 0.9213 | 1.10 | 1.10 | 0.8377 | 0.8117 |
| 287.1117 | 15.3 | C11H17N3O6 | N-Ribosylhistidine | Miscellaneous | 0.88 | 1.07 | 0.95 | 0.6419 | 0.8210 | 0.8454 | 0.92 | 0.6250 | 0.98 | 1.00 | 0.96 | 0.9117 | 0.9927 | 0.8828 | 1.10 | 1.15 | 1.06 | 0.7109 | 0.4974 | 0.7422 | 1.22 | 1.27 | 0.2846 | 0.1857 |
| 358.1112 | 15.0 | C12H22O12 | melibionate | Miscellaneous | 0.87 | 1.02 | 0.98 | 0.3764 | 0.9244 | 0.9005 | 0.91 | 0.3342 | 0.89 | 1.00 | 0.97 | 0.4792 | 0.9975 | 0.8705 | 1.05 | 1.04 | 1.06 | 0.6862 | 0.7719 | 0.6876 | 1.12 | 1.09 | 0.4395 | 0.6763 |
| 377.1258 | 11.5 | C22H19NO5 | Chelilutine | Miscellaneous | 0.87 | 0.93 | 0.96 | 0.7341 | 0.8644 | 0.9284 | 0.70 | 0.3060 | 0.80 | 0.86 | 0.85 | 0.5148 | 0.6558 | 0.5582 | 2.12 | 1.77 | 1.29 | 0.1783 | 0.1458 | 0.5175 | 1.03 | 1.18 | 0.9476 | 0.6851 |
| 468.0047 | 16.6 | C16H12N4O9S2 | tartrazine | Miscellaneous | 0.87 | 1.17 | 0.90 | 0.4399 | 0.6888 | 0.5377 | 0.92 | 0.7545 | 0.92 | 1.02 | 0.95 | 0.7968 | 0.9630 | 0.8843 | 0.97 | 0.93 | 0.98 | 0.9308 | 0.8146 | 0.9499 | 1.08 | 1.10 | 0.6853 | 0.4565 |
| 247.1421 | 11.4 | C11H21NO5 | Hydroxybutyrylcarnitine | Miscellaneous | 0.86 | 0.98 | 0.85 | 0.4557 | 0.9204 | 0.4445 | 1.00 | 0.9728 | 0.96 | 1.08 | 1.03 | 0.8048 | 0.6256 | 0.8776 | 0.98 | 1.03 | 0.99 | 0.8884 | 0.8441 | 0.9311 | 1.11 | 1.12 | 0.3897 | 0.3379 |
| 223.1055 | 13.3 | C8H17NO6 | N-acetyl -D-glucosaminitol | Miscellaneous | 0.86 | 1.07 | 1.03 | 0.1749 | 0.7021 | 0.7846 | 0.88 | 0.6316 | 0.89 | 1.01 | 0.96 | 0.5595 | 0.9637 | 0.8983 | 1.09 | 1.04 | 1.02 | 0.7222 | 0.8719 | 0.9098 | 1.15 | 1.21 | 0.3744 | 0.0940 |
| 151.0302 | 10.5 | C4H9NO3S | methiin | Miscellaneous | 0.84 | 0.92 | 0.97 | 0.5017 | 0.7672 | 0.9143 | 0.93 | 0.7245 | 0.87 | 0.85 | 0.81 | 0.4989 | 0.3698 | 0.3242 | 0.98 | 0.89 | 0.91 | 0.8556 | 0.4857 | 0.3957 | 1.17 | 1.12 | 0.4069 | 0.5943 |
| 181.0963 | 10.2 | C7H11N5O | 6-methyltetrahydropterin | Miscellaneous | 0.83 | 1.02 | 0.76 | 0.3325 | 0.9253 | 0.1243 | 1.20 | 0.4613 | 0.90 | 0.73 | 0.71 | 0.6663 | 0.2599 | 0.2906 | 1.12 | 0.99 | 0.79 | 0.6774 | 0.9801 | 0.2863 | 0.94 | 1.10 | 0.7470 | 0.7187 |
| 191.0794 | 12.8 | C7H13NO5 | 2-amino-3,7-dideoxy-D-threo-hept-6-ulosonate | Miscellaneous | 0.86 | 1.05 | 1.07 | 0.7573 | 0.9237 | 0.8808 | 0.98 | 0.9669 | 0.85 | 0.91 | 0.98 | 0.6563 | 0.7776 | 0.9357 | 0.89 | 0.87 | 0.94 | 0.7087 | 0.6703 | 0.8528 | 1.09 | 1.19 | 0.8091 | 0.6694 |
| 265.1311 | 8.4 | C14H19NO4 | N(alpha)-Benzyloxycarbonyl-L-leucine | Miscellaneous | 0.86 | 0.91 | 0.89 | 0.4367 | 0.6046 | 0.5869 | 1.04 | 0.7542 | 0.90 | 0.96 | 0.85 | 0.4951 | 0.8445 | 0.3095 | 1.12 | 1.18 | 1.01 | 0.5032 | 0.3854 | 0.9621 | 1.05 | 1.17 | 0.7817 | 0.4038 |
| 212.0470 | 11.6 | C13H8O3 | Urolithin B | Miscellaneous | 0.85 | 0.89 | 0.75 | 0.7189 | 0.7793 | 0.5074 | 0.88 | 0.8318 | 0.91 | 0.96 | 0.81 | 0.8623 | 0.9383 | 0.7094 | 1.05 | 1.05 | 1.05 | 0.9209 | 0.9254 | 0.9309 | 1.07 | 1.01 | 0.6936 | 0.9671 |
| 223.1208 | 10.4 | C12H17NO3 | Cerulenin | Miscellaneous | 0.84 | 0.93 | 0.86 | 0.8613 | 0.9375 | 0.8830 | 1.15 | 0.8835 | 0.97 | 0.95 | 0.82 | 0.9722 | 0.9534 | 0.8340 | 1.09 | 1.06 | 1.18 | 0.9193 | 0.9439 | 0.8568 | 1.02 | 1.03 | 0.9795 | 0.9759 |
| 242.0192 | 15.6 | C6H11O8P | D-myo-Inositol 1,2-cyclic phosphate | Miscellaneous | 0.84 | 1.29 | 1.07 | 0.6817 | 0.5198 | 0.8030 | 1.01 | 0.9856 | 0.80 | 1.19 | 0.94 | 0.6655 | 0.7263 | 0.9258 | 1.55 | 1.15 | 1.22 | 0.1774 | 0.7581 | 0.6668 | 1.12 | 0.91 | 0.5714 | 0.6476 |
| 185.1053 | 11.2 | C9H15NO3 | Otonecine | Miscellaneous | 0.83 | 1.00 | 0.92 | 0.4138 | 0.9861 | 0.7177 | 1.06 | 0.8145 | 0.85 | 0.96 | 0.94 | 0.4195 | 0.8895 | 0.8328 | 1.18 | 1.17 | 1.11 | 0.5203 | 0.5817 | 0.6759 | 1.14 | 1.11 | 0.3971 | 0.4290 |
| 183.0896 | 5.0 | C9H13NO3 | Ginkgotoxin | Miscellaneous | 0.85 | 1.06 | 0.88 | 0.7638 | 0.8715 | 0.8120 | 1.04 | 0.8713 | 0.84 | 1.10 | 1.04 | 0.4103 | 0.6479 | 0.8902 | 1.00 | 0.89 | 0.94 | 0.9987 | 0.6106 | 0.7212 | 1.39 | 0.98 | 0.1010 | 0.9389 |
| 243.1042 | 10.6 | C10H17N3O2S | Biotin amide | Miscellaneous | 0.83 | 0.96 | 0.87 | 0.6137 | 0.9054 | 0.7054 | 1.01 | 0.9813 | 0.94 | 1.10 | 0.97 | 0.7598 | 0.7562 | 0.9197 | 1.35 | 1.26 | 1.14 | 0.3528 | 0.4250 | 0.6609 | 1.03 | 1.07 | 0.9226 | 0.8243 |
| 277.0913 | 15.6 | C9H15N3O7 | Lycomarasmine B | Miscellaneous | 0.81 | 1.13 | 0.97 | 0.5899 | 0.7691 | 0.9383 | 1.00 | 0.9959 | 0.83 | 0.87 | 0.89 | 0.6485 | 0.7316 | 0.7944 | 1.03 | 0.97 | 1.00 | 0.9320 | 0.9326 | 0.9984 | 1.19 | 1.09 | 0.7097 | 0.8044 |
| 86.0367 | 13.9 | C4H6O2 | 1,4-Lactone | Miscellaneous | 0.82 | 0.89 | 0.94 | 0.2992 | 0.5280 | 0.7221 | 0.95 | 0.7368 | 0.95 | 0.95 | 0.94 | 0.8044 | 0.7250 | 0.7292 | 1.17 | 1.17 | 1.16 | 0.3607 | 0.3404 | 0.3600 | 1.25 | 1.26 | 0.3253 | 0.3714 |
| 297.3396 | 7.7 | C20H43N | Tetrapentylammonium | Miscellaneous | 0.71 | 0.71 | 0.89 | 0.6049 | 0.6073 | 0.8578 | 2.61 | 0.4104 | 0.96 | 0.57 | 0.57 | 0.9589 | 0.5862 | 0.5849 | 0.88 | 0.43 | 0.66 | 0.7928 | 0.1864 | 0.4287 | 0.78 | 0.72 | 0.6236 | 0.5292 |
| 207.1107 | 13.4 | C8H17NO5 | N-Ethylglycocyamine | Miscellaneous | 0.78 | 0.86 | 0.98 | 0.4388 | 0.7663 | 0.9451 | 1.02 | 0.9360 | 0.78 | 0.90 | 0.89 | 0.4534 | 0.7481 | 0.7340 | 1.09 | 1.06 | 1.08 | 0.7608 | 0.8358 | 0.7828 | 1.02 | 0.93 | 0.9369 | 0.6437 |
| 649.6361 | 5.2 | C42H83NO3 | N-Lignoceroylsphingosine | Miscellaneous | 0.79 | 0.85 | 0.97 | 0.5798 | 0.7421 | 0.9404 | 0.84 | 0.8145 | 1.05 | 1.21 | 1.19 | 0.9570 | 0.8061 | 0.8315 | 1.07 | 0.83 | 1.08 | 0.9299 | 0.8295 | 0.9227 | 1.06 | 0.88 | 0.9327 | 0.8462 |
| 149.0689 | 15.6 | C5H11NO4 | 4-amino-4-deoxy-L-arabinose | Miscellaneous | 0.72 | 0.93 | 0.98 | 0.6636 | 0.9271 | 0.9701 | 0.87 | 0.8799 | 0.83 | 0.96 | 1.00 | 0.8073 | 0.9628 | 0.9990 | 0.92 | 1.16 | 1.06 | 0.9225 | 0.8537 | 0.9347 | 0.88 | 0.99 | 0.8478 | 0.9873 |
| 326.1917 | 3.8 | C18H30O3S | 2-Dodecylbenzenesulfonic acid | Miscellaneous | 0.71 | 0.48 | 0.69 | 0.5228 | 0.2716 | 0.5089 | 1.54 | 0.3699 | 0.91 | 1.14 | 1.30 | 0.8243 | 0.7619 | 0.5699 | 1.09 | 1.30 | 0.91 | 0.8459 | 0.6141 | 0.8113 | 0.78 | 0.97 | 0.4005 | 0.9254 |
| 157.1101 | 10.1 | C8H15NO2 | Homostachydrine | Miscellaneous | 0.70 | 0.94 | 0.82 | 0.0649 | 0.7275 | 0.3882 | 1.00 | 0.9949 | 0.81 | 0.99 | 0.85 | 0.3617 | 0.9480 | 0.6308 | 0.92 | 0.86 | 1.03 | 0.7554 | 0.5487 | 0.9279 | 1.34 | 0.89 | 0.2543 | 0.6871 |
| 856.2626 | 20.7 | C38H48O22 | Sesaminol glucosyl-(1->2)-[glucosyl-(1->6)]-glucoside | Miscellaneous | 0.69 | 0.57 | 1.04 | 0.3804 | 0.2413 | 0.9233 | 0.90 | 0.8543 | 0.96 | 1.12 | 1.09 | 0.9333 | 0.7969 | 0.8597 | 0.84 | 0.83 | 0.92 | 0.7420 | 0.7299 | 0.8810 | 1.03 | 1.05 | 0.9597 | 0.9292 |
| 144.1263 | 10.5 | C7H16N2O | N-Acetylcadaverine | Miscellaneous | 0.65 | 1.36 | 0.34 | 0.4493 | 0.4684 | NA | 1.19 | 0.7791 | 1.03 | 1.70 | 1.02 | 0.9638 | 0.2562 | 0.9712 | 0.67 | 0.60 | 0.53 | 0.3194 | 0.1717 | 0.0231 | 0.88 | 1.10 | 0.7985 | 0.7745 |
| 116.1314 | 13.3 | C6H16N2 | 1,6-diaminohexane | Miscellaneous | 0.71 | 0.51 | 0.74 | 0.6178 | 0.3674 | 0.7347 | 1.04 | NA | 0.00 | 0.66 | 7.62 | NA | NA | 0.4031 | 0.00 | 2.45 | 2.16 | NA | NA | NA | 0.00 | 3.33 | NA | NA |
| 312.1761 | 3.8 | C17H28O3S | N-Undecylbenzenesulfonic acid | Miscellaneous | 0.57 | 0.41 | 0.59 | 0.4554 | 0.3208 | 0.4809 | 1.34 | 0.4546 | 0.96 | 1.10 | 1.26 | 0.9195 | 0.8094 | 0.5702 | 1.17 | 1.44 | 0.98 | 0.7207 | 0.5117 | 0.9610 | 0.87 | 1.11 | 0.5694 | 0.7856 |
| 133.0739 | 8.7 | C5H11NO3 | 3-nitro-2-pentanol | Miscellaneous | 0.38 | 0.69 | 0.41 | 0.2316 | 0.5101 | 0.2473 | 0.82 | 0.4960 | 1.02 | 0.91 | 0.83 | 0.9434 | 0.7024 | 0.4104 | 1.14 | 1.26 | 0.95 | 0.6517 | 0.3505 | 0.8784 | 1.26 | 1.37 | 0.5336 | 0.4402 |
| 370.3083 | 4.0 | C22H42O4 | Di(2-ethylhexyl) adipate | Miscellaneous | 0.32 | 0.00 | 0.72 | NA | NA | 0.7240 | 0.28 | 0.3219 | 8.14 | 4.69 | 6.91 | 0.3567 | 0.2824 | NA | 0.18 | 2.11 | 1.14 | NA | 0.4118 | 0.8536 | 0.51 | 0.57 | 0.5922 | 0.6382 |
| 679.1041 | 13.0 | C21H27N7O15P2 | nicotinamide guanine dinucleotide | Miscellaneous | 0.00 | 0.00 | 0.00 | NA | NA | NA | 0.98 | 0.9593 | 0.54 | 0.73 | 0.86 | NA | 0.6946 | 0.8034 | 3.91 | 4.38 | 1.15 | 0.2148 | 0.1502 | NA | 0.74 | 1.10 | 0.7668 | 0.9218 |
| 146.0579 | 14.3 | C6H10O4 | (S)-2-Aceto-2-hydroxybutanoate | Amino Acid Metabolism | 1.55 | 0.74 | 1.74 | 0.5922 | 0.4079 | 0.2574 | 0.71 | 0.5813 | 1.02 | 0.62 | 0.80 | 0.9758 | 0.4995 | 0.6994 | 1.07 | 1.16 | 1.02 | 0.9030 | 0.7848 | 0.9675 | 0.59 | 1.33 | 0.3725 | 0.2879 |
| 201.1364 | 10.5 | C10H19NO3 | N-(5-Methyl-3-oxohexyl)alanine | Amino Acid Metabolism | 1.49 | 1.42 | 1.30 | 0.3918 | 0.5535 | 0.6713 | 0.95 | 0.9236 | 1.11 | 1.80 | 1.05 | 0.8510 | 0.1104 | 0.9302 | 0.94 | 0.88 | 0.56 | 0.9222 | 0.8428 | 0.4269 | 0.87 | 1.07 | 0.8313 | 0.9134 |
| 209.0688 | 7.6 | C10H11NO4 | 4-Hydroxyphenylacetylglycine | Amino Acid Metabolism | 1.24 | 1.42 | 1.42 | 0.5732 | 0.3445 | 0.3682 | 1.04 | 0.8330 | 0.85 | 0.93 | 0.84 | 0.1331 | 0.4619 | 0.0582 | 0.93 | 0.94 | 1.03 | 0.5639 | 0.6695 | 0.7734 | 1.18 | 1.03 | 0.3469 | 0.8542 |
| 204.0899 | 11.6 | C11H12N2O2 | L-Tryptophan | Amino Acid Metabolism | 1.24 | 1.35 | 1.23 | 0.5071 | 0.3692 | 0.5417 | 1.03 | 0.8088 | 0.87 | 0.91 | 0.88 | 0.3666 | 0.5467 | 0.4815 | 1.09 | 1.09 | 1.05 | 0.4170 | 0.5339 | 0.6995 | 1.05 | 1.06 | 0.5243 | 0.3637 |

| | | | | | | | | | | | | | | | | | | | | | | | | | | | | |
|---|---|---|---|---|---|---|---|---|---|---|---|---|---|---|---|---|---|---|---|---|---|---|---|---|---|---|---|---|
| 174.1004 | 13.5 | C7H14N2O3 | N-Acetylornithine | Amino Acid Metabolism | 1.29 | 0.99 | 1.31 | 0.4637 | 0.9882 | 0.5646 | 0.87 | 0.8167 | 0.70 | 1.12 | 1.11 | 0.4201 | 0.8388 | 0.8068 | 1.19 | 1.27 | 1.06 | 0.7073 | 0.4777 | 0.9033 | 1.19 | 1.12 | 0.6530 | 0.7606 |
| 149.0511 | 11.5 | C5H11NO2S | L-Methionine | Amino Acid Metabolism | 1.20 | 1.40 | 1.25 | 0.5896 | 0.3311 | 0.5264 | 0.95 | 0.6076 | 0.89 | 0.93 | 0.89 | 0.4310 | 0.6329 | 0.4778 | 1.11 | 1.07 | 1.13 | 0.2545 | 0.4803 | 0.2900 | 1.11 | 1.09 | 0.2098 | 0.3545 |
| 111.9926 | 14.3 | CH5O4P | Hydroxymethylphosphonate | Amino Acid Metabolism | 1.12 | 1.58 | 1.05 | 0.7701 | 0.5468 | 0.9163 | 0.99 | 0.9810 | 0.93 | 0.99 | 0.85 | 0.7467 | 0.9534 | 0.5333 | 0.80 | 0.87 | 0.85 | 0.4897 | 0.6151 | 0.5217 | 0.69 | 0.81 | 0.0742 | 0.3226 |
| 179.0582 | 8.2 | C9H9NO3 | Hippurate | Amino Acid Metabolism | 1.14 | 1.25 | 1.05 | 0.6091 | 0.4146 | 0.9104 | 0.84 | 0.6371 | 0.80 | 0.86 | 0.72 | 0.5524 | 0.7019 | 0.4798 | 1.06 | 1.12 | 1.02 | 0.9130 | 0.8071 | 0.9715 | 1.15 | 1.16 | 0.6420 | 0.5483 |
| 307.0835 | 14.1 | C10H17N3O6S | Glutathione | Amino Acid Metabolism | 1.16 | 0.99 | 1.17 | 0.6832 | 0.9799 | 0.6748 | 0.99 | 0.8975 | 0.92 | 1.01 | 0.94 | 0.4995 | 0.9479 | 0.6191 | 1.05 | 1.06 | 1.04 | 0.7153 | 0.6232 | 0.6811 | 1.09 | 1.07 | 0.5687 | 0.6657 |
| 149.0476 | 5.8 | C8H7NO2 | 2,3-Dihydroxyindole | Amino Acid Metabolism | 1.12 | 1.00 | 1.26 | 0.6173 | 0.9990 | 0.3358 | 1.02 | 0.9435 | 1.01 | 1.03 | 0.90 | 0.9843 | 0.9025 | 0.6826 | 1.03 | 1.11 | 0.98 | 0.9247 | 0.7610 | 0.9483 | 1.02 | 0.99 | 0.9446 | 0.9808 |
| 148.0372 | 14.9 | C5H8O5 | (R)-2-Hydroxyglutarate | Amino Acid Metabolism | 1.16 | 1.28 | 1.14 | 0.7043 | 0.5290 | 0.7382 | 1.03 | 0.8723 | 0.97 | 1.02 | 0.92 | 0.8580 | 0.9378 | 0.7054 | 1.03 | 0.99 | 1.07 | 0.8789 | 0.9559 | 0.7178 | 1.12 | 1.15 | 0.5885 | 0.5019 |
| 172.0483 | 15.2 | C6H8N2O4 | Hydantoin-5-propionate | Amino Acid Metabolism | 1.06 | 1.25 | 1.11 | 0.8578 | 0.5549 | 0.7938 | 1.00 | 0.9912 | 0.93 | 1.02 | 0.91 | 0.8032 | 0.9548 | 0.7774 | 1.00 | 1.00 | 0.97 | 0.9893 | 0.9897 | 0.9212 | 1.04 | 1.03 | 0.9081 | 0.9353 |
| 211.0359 | 15.0 | C4H10N3O5P | Phosphocreatine | Amino Acid Metabolism | 1.03 | 1.04 | 0.99 | 0.9148 | 0.9393 | 0.9698 | 1.12 | 0.7822 | 0.88 | 1.03 | 0.94 | 0.7453 | 0.9437 | 0.9147 | 1.05 | 1.00 | 0.95 | 0.8909 | 0.9959 | 0.9041 | 0.99 | 1.06 | 0.9602 | 0.7749 |
| 283.0458 | 16.6 | C8H14NO8P | N2-Acetyl-L-aminoadipyl-delta-phosphate | Amino Acid Metabolism | 1.06 | 1.15 | 1.05 | 0.8961 | 0.7159 | 0.9117 | 1.00 | 0.9999 | 0.89 | 0.98 | 0.95 | 0.7425 | 0.9588 | 0.9038 | 1.01 | 1.06 | 1.03 | 0.9736 | 0.8745 | 0.9445 | 0.99 | 1.08 | 0.9827 | 0.8354 |
| 312.0223 | 16.0 | C9H16N2O5Se | gamma-Glutamyl-Se-methylselenocysteine | Amino Acid Metabolism | 1.07 | 1.08 | 1.13 | 0.9130 | 0.8840 | 0.8494 | 1.05 | 0.9237 | 0.95 | 0.99 | 1.15 | 0.8868 | 0.9706 | 0.7109 | 0.87 | 0.92 | 0.92 | 0.6038 | 0.7637 | 0.7628 | 1.08 | 1.08 | 0.8028 | 0.7859 |
| 197.0688 | 10.3 | C9H11NO4 | N-Hydroxy-L-tyrosine | Amino Acid Metabolism | 1.07 | 2.04 | 1.73 | 0.8564 | 0.2867 | 0.2414 | 1.28 | 0.4765 | 0.83 | 0.34 | 0.59 | 0.7143 | NA | 0.3833 | 1.25 | 1.03 | 0.52 | 0.4566 | 0.9299 | 0.2212 | 0.49 | 0.31 | 0.0882 | 0.0545 |
| 146.1055 | 22.5 | C6H14N2O2 | L-Lysine | Amino Acid Metabolism | 1.05 | 1.17 | 1.04 | 0.9055 | 0.6870 | 0.9085 | 1.05 | 0.8735 | 0.82 | 0.95 | 0.87 | 0.4933 | 0.8617 | 0.6713 | 0.97 | 0.99 | 0.93 | 0.9054 | 0.9656 | 0.7695 | 0.96 | 0.95 | 0.8645 | 0.8489 |
| 117.0790 | 11.3 | C5H11NO2 | Betaine | Amino Acid Metabolism | 1.01 | 1.21 | 1.03 | 0.9759 | 0.7203 | 0.9502 | 0.89 | 0.8477 | 0.85 | 0.97 | 0.92 | 0.7693 | 0.9644 | 0.9049 | 1.06 | 1.13 | 1.08 | 0.9188 | 0.8335 | 0.8950 | 1.32 | 1.23 | 0.5322 | 0.5477 |
| 175.0481 | 14.4 | C6H9NO5 | N-Acetyl-L-aspartate | Amino Acid Metabolism | 1.06 | 1.24 | 0.72 | 0.8496 | 0.7124 | 0.4528 | 0.76 | 0.5500 | 0.94 | 1.03 | 0.93 | 0.8355 | 0.9312 | 0.8483 | 0.86 | 1.09 | 1.08 | 0.7018 | 0.8041 | 0.7840 | 1.45 | 1.41 | 0.3522 | 0.2066 |
| 145.0739 | 12.4 | C6H11NO3 | [FA oxo,amino(6:0)] 3-oxo-5S-amino-hexanoic acid | Amino Acid Metabolism | 1.05 | 0.98 | 0.99 | 0.9156 | 0.9706 | 0.9911 | 1.16 | 0.7232 | 0.87 | 0.87 | 0.79 | 0.7584 | 0.7449 | 0.5333 | 1.11 | 1.11 | 1.06 | 0.8339 | 0.8340 | 0.8967 | 1.13 | 1.18 | 0.8226 | 0.7502 |
| 237.0308 | 16.9 | C7H11NO6S | S-Cysteinosuccinic acid | Amino Acid Metabolism | 1.05 | 1.20 | 0.97 | 0.8972 | 0.6798 | 0.9397 | 0.95 | 0.8526 | 0.86 | 0.92 | 0.85 | 0.6106 | 0.7672 | 0.6039 | 1.10 | 1.10 | 1.00 | 0.6883 | 0.7267 | 0.9860 | 1.12 | 1.14 | 0.7568 | 0.7302 |
| 126.0429 | 11.4 | C5H6N2O2 | Imidazole-4-acetate | Amino Acid Metabolism | 1.02 | 1.15 | 1.08 | 0.9279 | 0.5592 | 0.6931 | 0.79 | 0.3676 | 1.10 | 1.92 | 0.97 | 0.8634 | 0.3297 | 0.9540 | 0.00 | 0.57 | 0.00 | NA | NA | NA | 3.37 | 0.00 | NA | NA |
| 139.9873 | 15.4 | C2H5O5P | Phosphonoacetate | Amino Acid Metabolism | 1.02 | 1.21 | 1.19 | 0.8857 | 0.4825 | 0.2136 | 1.01 | 0.9789 | 0.84 | 1.04 | 0.89 | 0.3103 | 0.8791 | 0.5765 | 0.99 | 1.09 | 1.01 | 0.9706 | 0.6135 | 0.9466 | 1.28 | 1.30 | 0.2666 | 0.2931 |
| 119.0583 | 14.3 | C4H9NO3 | L-Threonine | Amino Acid Metabolism | 1.00 | 1.15 | 1.06 | 0.9524 | 0.4044 | 0.6191 | 1.00 | 0.9810 | 0.88 | 0.99 | 0.88 | 0.4541 | 0.9476 | 0.5179 | 1.01 | 0.96 | 0.90 | 0.9570 | 0.7696 | 0.4441 | 0.90 | 0.95 | 0.1809 | 0.4404 |
| 145.1103 | 13.4 | C7H15NO2 | 4-Trimethylammoniobutanoate | Amino Acid Metabolism | 1.00 | 1.19 | 0.98 | 0.9876 | 0.5839 | 0.8943 | 1.07 | 0.8481 | 0.85 | 0.96 | 0.90 | 0.6219 | 0.9229 | 0.7977 | 1.08 | 1.07 | 1.07 | 0.8196 | 0.8447 | 0.8425 | 1.17 | 1.12 | 0.4359 | 0.4937 |
| 430.0653 | 15.2 | C11H20N4O10P2 | CMP-2-aminoethylphosphonate | Amino Acid Metabolism | 1.02 | 1.20 | 1.06 | 0.9270 | 0.4580 | 0.7942 | 0.94 | 0.7590 | 0.89 | 0.93 | 0.90 | 0.5827 | 0.7597 | 0.6843 | 1.01 | 1.01 | 0.99 | 0.9730 | 0.9520 | 0.9624 | 1.12 | 1.11 | 0.6111 | 0.6091 |
| 167.9824 | 12.7 | C3H5O6P | 3-Phosphonopyruvate | Amino Acid Metabolism | 1.00 | 1.17 | 1.04 | 0.9847 | 0.6418 | 0.8582 | 0.97 | 0.9415 | 0.88 | 1.02 | 0.99 | 0.6292 | 0.9492 | 0.9706 | 1.25 | 1.24 | 1.28 | 0.3834 | 0.4305 | 0.3460 | 1.32 | 1.38 | 0.5422 | 0.4246 |
| 132.0898 | 21.7 | C5H12N2O2 | L-Ornithine | Amino Acid Metabolism | 1.01 | 1.07 | 1.18 | 0.9787 | 0.8686 | 0.5473 | 0.92 | 0.8086 | 0.89 | 0.93 | 0.95 | 0.5019 | 0.6662 | 0.8295 | 1.05 | 1.05 | 1.12 | 0.8756 | 0.8558 | 0.6845 | 1.13 | 1.09 | 0.6396 | 0.7438 |
| 175.0957 | 15.8 | C6H13N3O3 | L-Citrulline | Amino Acid Metabolism | 1.01 | 1.14 | 1.03 | 0.9810 | 0.7223 | 0.9350 | 1.00 | 0.9930 | 0.84 | 0.95 | 0.86 | 0.5398 | 0.8526 | 0.6062 | 1.02 | 1.04 | 1.01 | 0.9308 | 0.8633 | 0.9598 | 1.17 | 1.09 | 0.5900 | 0.7340 |
| 165.0461 | 13.3 | C5H11NO3S | L-Methionine S-oxide | Amino Acid Metabolism | 0.98 | 1.14 | 1.01 | 0.9369 | 0.6867 | 0.9816 | 1.02 | 0.9519 | 0.87 | 1.00 | 0.91 | 0.6883 | 0.9982 | 0.8057 | 1.11 | 1.11 | 1.02 | 0.7998 | 0.8065 | 0.9569 | 0.98 | 0.96 | 0.9261 | 0.8725 |
| 117.0790 | 12.5 | C5H11NO2 | L-Valine | Amino Acid Metabolism | 0.99 | 1.34 | 1.00 | 0.9679 | 0.4939 | 0.9882 | 0.87 | 0.5695 | 0.75 | 0.90 | 0.86 | 0.3559 | 0.7242 | 0.6012 | 1.04 | 1.05 | 1.06 | 0.8112 | 0.7990 | 0.7567 | 0.99 | 1.06 | 0.9656 | 0.6117 |
| 105.0426 | 15.6 | C3H7NO3 | L-Serine | Amino Acid Metabolism | 0.99 | 1.53 | 1.04 | 0.8788 | 0.3092 | 0.6299 | 0.97 | 0.7870 | 0.86 | 0.90 | 0.82 | 0.2180 | 0.3974 | 0.1522 | 1.10 | 1.12 | 1.03 | 0.3997 | 0.3517 | 0.8209 | 1.04 | 1.01 | 0.7136 | 0.9312 |
| 156.0534 | 11.0 | C6H8N2O3 | 4-Imidazolone-5-propanoate | Amino Acid Metabolism | 0.99 | 1.11 | 0.75 | 0.8883 | 0.4407 | 0.4169 | 0.95 | 0.7774 | 0.95 | 1.01 | 0.99 | 0.7521 | 0.9462 | 0.9401 | 0.99 | 0.99 | 0.95 | 0.9747 | 0.9573 | 0.7162 | 1.24 | 1.13 | 0.1894 | 0.5492 |
| 398.1373 | 16.3 | C15H22N6O5S | S-Adenosyl-L-methionine | Amino Acid Metabolism | 0.97 | 1.11 | 1.07 | 0.8854 | 0.6012 | 0.6919 | 0.95 | 0.6379 | 0.93 | 1.00 | 0.93 | 0.6641 | 0.9832 | 0.5990 | 1.07 | 0.90 | 0.94 | 0.7280 | 0.5974 | 0.6979 | 1.37 | 1.36 | 0.0089 | 0.0005 |
| 159.0896 | 12.3 | C7H13NO3 | 5-Acetamidopentanoate | Amino Acid Metabolism | 0.96 | 1.15 | 1.01 | 0.9372 | 0.7897 | 0.9847 | 0.99 | 0.9812 | 0.75 | 0.92 | 0.91 | 0.5615 | 0.8643 | 0.8562 | 1.05 | 1.01 | 1.04 | 0.9178 | 0.9853 | 0.9382 | 1.25 | 1.13 | 0.6284 | 0.7647 |

| | | | | | | | | | | | | | | | | | | | | | | | | | | | | | |
|---|---|---|---|---|---|---|---|---|---|---|---|---|---|---|---|---|---|---|---|---|---|---|---|---|---|---|---|---|---|
| 174.1116 | 23.4 | C6H14N4O2 | L-Arginine | Amino Acid Metabolism | 0.98 | 1.09 | 1.06 | 0.8997 | 0.6984 | 0.7714 | 1.04 | 0.8611 | 0.82 | 0.93 | 0.89 | 0.3571 | 0.7425 | 0.6573 | 1.08 | 1.08 | 1.05 | 0.6204 | 0.6486 | 0.7423 | 1.11 | 1.09 | 0.5193 | 0.5924 |
| 155.0695 | 14.6 | C6H9N3O2 | L-Histidine | Amino Acid Metabolism | 0.98 | 1.09 | 0.92 | 0.8851 | 0.6637 | 0.6507 | 1.01 | 0.9555 | 0.91 | 0.92 | 0.81 | 0.4727 | 0.5560 | 0.1734 | 0.89 | 0.93 | 0.77 | 0.3973 | 0.6772 | 0.1258 | 0.95 | 0.97 | 0.7332 | 0.8456 |
| 131.0946 | 11.2 | C6H13NO2 | L-Leucine | Amino Acid Metabolism | 0.97 | 1.08 | 0.97 | 0.4613 | 0.5259 | 0.5076 | 1.08 | 0.4223 | 0.83 | 0.91 | 0.87 | 0.3823 | 0.6680 | 0.5530 | 1.14 | 1.04 | 1.06 | 0.4136 | 0.7699 | 0.6064 | 1.10 | 1.13 | 0.3499 | 0.2027 |
| 117.0539 | 15.7 | C3H7N3O2 | Guanidinoacetate | Amino Acid Metabolism | 1.00 | 0.48 | 0.98 | 0.9964 | 0.4962 | 0.9842 | 1.03 | 0.9670 | 1.02 | 1.22 | 0.88 | 0.9793 | 0.7390 | 0.8444 | 0.92 | 1.07 | 0.88 | 0.9277 | 0.9433 | 0.8813 | 1.16 | 0.94 | 0.8808 | 0.9477 |
| 131.0946 | 10.9 | C6H13NO2 | L-Isoleucine | Amino Acid Metabolism | 0.96 | 1.05 | 0.95 | 0.5302 | 0.6695 | 0.4646 | 1.07 | 0.6249 | 0.91 | 1.00 | 0.93 | 0.4293 | 0.9899 | 0.7057 | 1.08 | 1.07 | 1.04 | 0.6069 | 0.6623 | 0.8114 | 1.05 | 1.09 | 0.5155 | 0.2422 |
| 181.0739 | 12.9 | C9H11NO3 | L-Tyrosine | Amino Acid Metabolism | 0.96 | 1.06 | 1.06 | 0.5194 | 0.7021 | 0.4351 | 1.01 | 0.9336 | 0.92 | 0.95 | 0.93 | 0.4966 | 0.7317 | 0.6589 | 1.10 | 1.08 | 1.03 | 0.5823 | 0.6259 | 0.8504 | 1.05 | 1.08 | 0.5408 | 0.2979 |
| 161.1052 | 13.3 | C7H15NO3 | L-Carnitine | Amino Acid Metabolism | 0.95 | 1.13 | 0.96 | 0.7828 | 0.7256 | 0.8312 | 1.05 | 0.9009 | 0.82 | 0.98 | 0.93 | 0.5858 | 0.9610 | 0.8627 | 1.11 | 1.05 | 1.09 | 0.7615 | 0.8862 | 0.8125 | 1.18 | 1.10 | 0.3950 | 0.5640 |
| 203.1158 | 11.0 | C9H17NO4 | O-Acetylcarnitine | Amino Acid Metabolism | 0.95 | 1.13 | 0.98 | 0.7850 | 0.6912 | 0.9179 | 1.10 | 0.8085 | 0.87 | 0.95 | 0.91 | 0.6967 | 0.8855 | 0.8184 | 1.00 | 1.01 | 1.03 | 0.9934 | 0.9751 | 0.9274 | 1.18 | 1.14 | 0.4869 | 0.4739 |
| 132.0535 | 15.2 | C4H8N2O3 | L-Asparagine | Amino Acid Metabolism | 0.96 | 1.07 | 0.99 | 0.7367 | 0.7051 | 0.9192 | 1.04 | 0.8369 | 0.91 | 0.94 | 0.95 | 0.5865 | 0.7548 | 0.8163 | 1.13 | 1.13 | 1.09 | 0.5184 | 0.4901 | 0.6055 | 1.18 | 1.19 | 0.1330 | 0.0814 |
| 117.0578 | 11.6 | C8H7N | Indole | Amino Acid Metabolism | 0.94 | 0.97 | 0.87 | 0.2411 | 0.7539 | 0.0844 | 0.96 | 0.7464 | 0.82 | 0.98 | 0.86 | 0.2568 | 0.9229 | 0.4524 | 1.06 | 1.01 | 0.92 | 0.5501 | 0.9354 | 0.5621 | 1.03 | 1.09 | 0.7768 | 0.4315 |
| 204.1108 | 11.9 | C8H16N2O4 | N6-Acetyl-N6-hydroxy-L-lysine | Amino Acid Metabolism | 0.97 | 1.07 | 1.00 | 0.9515 | 0.8750 | 0.9948 | 0.98 | 0.9532 | 0.94 | 1.05 | 0.90 | 0.8978 | 0.9088 | 0.7942 | 1.07 | 1.07 | 1.09 | 0.8731 | 0.8740 | 0.8290 | 1.21 | 1.14 | 0.6871 | 0.7793 |
| 147.0532 | 14.5 | C5H9NO4 | L-Glutamate | Amino Acid Metabolism | 0.97 | 1.06 | 0.97 | 0.8463 | 0.6922 | 0.8693 | 1.02 | 0.9088 | 0.95 | 1.02 | 0.93 | 0.7280 | 0.8431 | 0.6466 | 1.08 | 1.11 | 1.04 | 0.4928 | 0.4219 | 0.7252 | 1.18 | 1.17 | 0.3518 | 0.3915 |
| 131.0694 | 14.6 | C4H9N3O2 | Creatine | Amino Acid Metabolism | 0.95 | 1.10 | 0.75 | 0.6916 | 0.7147 | 0.4285 | 0.92 | 0.7882 | 0.96 | 0.93 | 0.90 | 0.8653 | 0.7812 | 0.7245 | 1.11 | 1.12 | 1.02 | 0.6903 | 0.7281 | 0.9419 | 1.20 | 1.17 | 0.1661 | 0.2036 |
| 102.0318 | 13.6 | C4H6O3 | Succinate semialdehyde | Amino Acid Metabolism | 0.96 | 0.99 | 1.04 | 0.8596 | 0.9670 | 0.8675 | 0.96 | 0.7645 | 0.93 | 1.02 | 0.86 | 0.4179 | 0.8270 | 0.1965 | 1.13 | 1.20 | 1.10 | 0.1093 | 0.1171 | 0.2234 | 1.09 | 1.11 | 0.5848 | 0.5216 |
| 290.1227 | 16.6 | C10H18N4O6 | N-(L-Arginino)succinate | Amino Acid Metabolism | 0.98 | 1.10 | 0.98 | 0.9199 | 0.7522 | 0.9263 | 0.95 | 0.8503 | 0.87 | 1.00 | 0.94 | 0.5818 | 0.9977 | 0.8518 | 1.02 | 1.00 | 1.01 | 0.9621 | 0.9874 | 0.9660 | 1.06 | 1.02 | 0.7836 | 0.9008 |
| 129.0426 | 10.2 | C5H7NO3 | 5-Oxoproline | Amino Acid Metabolism | 0.95 | 1.05 | 0.96 | 0.8179 | 0.8437 | 0.8614 | 1.00 | 0.9904 | 0.88 | 0.97 | 0.90 | 0.5118 | 0.8778 | 0.6290 | 1.06 | 1.07 | 1.07 | 0.7064 | 0.6985 | 0.7088 | 1.05 | 1.07 | 0.8009 | 0.6998 |
| 165.0790 | 10.2 | C9H11NO2 | L-Phenylalanine | Amino Acid Metabolism | 0.94 | 1.04 | 0.95 | 0.2465 | 0.6225 | 0.4264 | 1.05 | 0.6951 | 0.93 | 0.96 | 0.95 | 0.4642 | 0.7102 | 0.6294 | 1.03 | 1.02 | 0.98 | 0.7727 | 0.8032 | 0.7827 | 1.04 | 1.01 | 0.7015 | 0.9415 |
| 190.0590 | 15.3 | C6H10N2O5 | N-Carbamyl-L-glutamate | Amino Acid Metabolism | 0.94 | 1.07 | 0.98 | 0.8807 | 0.8632 | 0.9571 | 0.95 | 0.8716 | 0.94 | 0.97 | 0.90 | 0.8835 | 0.9459 | 0.7935 | 1.05 | 1.03 | 1.09 | 0.8893 | 0.9335 | 0.8113 | 1.08 | 1.12 | 0.8484 | 0.7926 |
| 146.0691 | 15.0 | C5H10N2O3 | L-Glutamine | Amino Acid Metabolism | 0.94 | 1.03 | 0.88 | 0.4585 | 0.8199 | 0.2995 | 1.03 | 0.8239 | 0.94 | 1.03 | 0.95 | 0.5157 | 0.7861 | 0.7349 | 1.06 | 1.21 | 1.11 | 0.5287 | 0.0853 | 0.3130 | 1.14 | 1.11 | 0.1943 | 0.3430 |
| 103.0997 | 19.7 | C5H13NO | Choline | Amino Acid Metabolism | 0.94 | 1.06 | 0.95 | 0.6031 | 0.7822 | 0.7650 | 1.07 | 0.6881 | 0.86 | 0.94 | 0.90 | 0.3576 | 0.7485 | 0.6234 | 1.11 | 1.08 | 1.08 | 0.5710 | 0.6833 | 0.6922 | 1.14 | 1.12 | 0.3045 | 0.3418 |
| 188.1525 | 21.3 | C9H20N2O2 | N6,N6,N6-Trimethyl-L-lysine | Amino Acid Metabolism | 0.94 | 1.08 | 0.99 | 0.9011 | 0.8842 | 0.9896 | 1.03 | 0.9419 | 0.86 | 0.96 | 0.90 | 0.6878 | 0.9102 | 0.7952 | 1.09 | 1.11 | 1.09 | 0.7755 | 0.7467 | 0.7968 | 1.20 | 1.15 | 0.6786 | 0.7488 |
| 115.0633 | 12.8 | C5H9NO2 | L-Proline | Amino Acid Metabolism | 0.94 | 1.07 | 0.96 | 0.5827 | 0.6352 | 0.6750 | 1.01 | 0.9262 | 0.87 | 1.00 | 0.83 | 0.3723 | 0.9959 | 0.3468 | 0.98 | 1.00 | 0.93 | 0.8871 | 0.9839 | 0.5959 | 1.00 | 1.02 | 0.9861 | 0.8700 |
| 177.0459 | 8.2 | C6H11NO3S | N-Formyl-L-methionine | Amino Acid Metabolism | 0.94 | 1.05 | 0.98 | 0.8528 | 0.9043 | 0.9571 | 1.59 | 0.4479 | 1.09 | 1.80 | 1.08 | 0.9199 | 0.3848 | 0.9265 | 1.14 | 0.96 | 1.77 | 0.8815 | 0.9647 | 0.4123 | 1.31 | 1.46 | 0.7605 | 0.5997 |
| 113.0589 | 9.8 | C4H7N3O | Creatinine | Amino Acid Metabolism | 0.93 | 1.01 | 0.93 | 0.8954 | 0.9883 | 0.8837 | 1.03 | 0.9201 | 0.86 | 1.13 | 0.88 | 0.4855 | 0.6872 | 0.5797 | 1.05 | 0.99 | 0.85 | 0.7510 | 0.9569 | 0.3268 | 1.20 | 1.08 | 0.4170 | 0.7003 |
| 384.1217 | 13.6 | C14H20N6O5S | S-Adenosyl-L-homocysteine | Amino Acid Metabolism | 0.94 | 1.07 | 1.01 | 0.7892 | 0.7607 | 0.9625 | 0.99 | 0.9564 | 0.85 | 0.90 | 0.89 | 0.2489 | 0.5110 | 0.5320 | 1.18 | 1.31 | 1.17 | 0.2078 | 0.1658 | 0.2365 | 1.17 | 1.15 | 0.3578 | 0.4018 |
| 246.1329 | 17.1 | C9H18N4O4 | N2-(D-1-Carboxyethyl)-L-arginine | Amino Acid Metabolism | 0.94 | 1.17 | 1.02 | 0.8330 | 0.6256 | 0.9381 | 0.92 | 0.6213 | 0.87 | 1.00 | 0.89 | 0.4268 | 0.9922 | 0.5372 | 1.10 | 1.21 | 1.10 | 0.4350 | 0.3022 | 0.5326 | 1.19 | 1.08 | 0.3656 | 0.6772 |
| 229.0884 | 14.7 | C9H15N3O2S | Ergothioneine | Amino Acid Metabolism | 0.93 | 1.02 | 0.98 | 0.8784 | 0.9615 | 0.9655 | 0.96 | 0.8989 | 0.83 | 0.93 | 0.85 | 0.6309 | 0.8536 | 0.6774 | 1.06 | 1.07 | 1.11 | 0.8704 | 0.8518 | 0.7489 | 1.03 | 1.03 | 0.9459 | 0.9439 |
| 89.0477 | 14.7 | C3H7NO2 | L-Alanine | Amino Acid Metabolism | 0.92 | 1.11 | 0.93 | 0.7529 | 0.7953 | 0.7875 | 0.95 | 0.9061 | 0.82 | 0.89 | 0.78 | 0.5503 | 0.7672 | 0.5420 | 0.78 | 0.81 | 0.73 | 0.5160 | 0.5855 | 0.3837 | 0.83 | 0.92 | 0.4195 | 0.7498 |
| 130.1107 | 18.4 | C6H14N2O | N-Acetylputrescine | Amino Acid Metabolism | 0.91 | 1.01 | 0.98 | 0.5161 | 0.9443 | 0.9045 | 1.14 | 0.2451 | 0.91 | 1.00 | 0.95 | 0.4495 | 0.9950 | 0.6907 | 1.05 | 1.10 | 1.04 | 0.6079 | 0.5390 | 0.7415 | 1.21 | 1.16 | 0.2301 | 0.3626 |
| 204.1474 | 19.8 | C9H20N2O3 | 3-Hydroxy-N6,N6,N6-trimethyl-L-lysine | Amino Acid Metabolism | 0.94 | 0.95 | 0.96 | 0.8301 | 0.8367 | 0.8669 | 0.96 | 0.7650 | 0.92 | 0.92 | 0.82 | 0.7618 | 0.6934 | 0.3626 | 1.16 | 1.06 | 1.00 | 0.4277 | 0.7766 | 0.9821 | 1.22 | 1.16 | 0.5510 | 0.6718 |
| 141.0192 | 15.8 | C2H8NO4P | Ethanolamine phosphate | Amino Acid Metabolism | 0.95 | 0.95 | 1.02 | 0.8207 | 0.8096 | 0.9408 | 1.16 | 0.5402 | 0.96 | 1.07 | 1.26 | 0.8111 | 0.7493 | 0.4305 | 1.67 | 1.47 | 1.79 | 0.1435 | 0.2577 | 0.1888 | 1.70 | 1.60 | 0.1733 | 0.1639 |
| 612.1522 | 17.2 | C20H32N6O12S2 | Glutathione disulfide | Amino Acid Metabolism | 0.95 | 1.59 | 1.13 | 0.8958 | 0.2804 | 0.7153 | 0.92 | 0.6613 | 0.92 | 0.97 | 0.86 | 0.7470 | 0.8745 | 0.4919 | 1.19 | 1.14 | 1.08 | 0.3311 | 0.4675 | 0.7495 | 1.01 | 1.05 | 0.9767 | 0.9086 |

| | | | | | | | | | | | | | | | | | | | | | | | | | | | | | |
|---|---|---|---|---|---|---|---|---|---|---|---|---|---|---|---|---|---|---|---|---|---|---|---|---|---|---|---|---|---|
| 203.0795 | 12.2 | C8H13NO5 | N2-Acetyl-L-aminoadipate | Amino Acid Metabolism | 0.89 | 1.13 | 0.95 | 0.6977 | 0.7919 | 0.8702 | 0.99 | 0.9884 | 0.77 | 0.93 | 0.86 | 0.5816 | 0.8822 | 0.7803 | 1.04 | 1.06 | 1.04 | 0.9381 | 0.8965 | 0.9256 | 1.20 | 1.18 | 0.5244 | 0.5131 |
| 243.0856 | 13.7 | C9H13N3O5 | gamma-Glutamyl-beta-cyanoalanine | Amino Acid Metabolism | 0.92 | 1.03 | 1.03 | 0.7686 | 0.8992 | 0.9065 | 0.99 | 0.9249 | 0.93 | 0.99 | 0.91 | 0.6588 | 0.9293 | 0.5902 | 1.06 | 1.06 | 1.08 | 0.5935 | 0.6445 | 0.4847 | 1.06 | 1.10 | 0.7621 | 0.6598 |
| 161.0688 | 11.1 | C6H11NO4 | O-Acetyl-L-homoserine | Amino Acid Metabolism | 0.89 | 1.13 | 1.01 | 0.5517 | 0.5089 | 0.9562 | 1.12 | 0.5568 | 0.92 | 0.82 | 0.83 | 0.6700 | 0.2713 | 0.3173 | 1.29 | 1.40 | 1.03 | 0.2624 | 0.0920 | 0.8705 | 1.06 | 1.10 | 0.7697 | 0.6724 |
| 218.1267 | 17.1 | C9H18N2O4 | N2-(D-1-Carboxyethyl)-L-lysine | Amino Acid Metabolism | 0.92 | 1.10 | 1.05 | 0.8057 | 0.7722 | 0.8832 | 1.07 | 0.6603 | 0.94 | 1.02 | 0.87 | 0.7606 | 0.9371 | 0.4438 | 0.99 | 0.98 | 0.96 | 0.9639 | 0.9182 | 0.7979 | 1.08 | 1.15 | 0.7546 | 0.6203 |
| 133.0376 | 14.8 | C4H7NO4 | L-Aspartate | Amino Acid Metabolism | 0.91 | 0.98 | 0.89 | 0.7535 | 0.9462 | 0.7225 | 1.05 | 0.8967 | 0.92 | 0.96 | 0.88 | 0.8128 | 0.9028 | 0.6929 | 0.98 | 0.96 | 0.93 | 0.9438 | 0.9097 | 0.8387 | 1.16 | 1.18 | 0.6856 | 0.6726 |
| 232.1059 | 13.7 | C9H16N2O5 | N2-Succinyl-L-ornithine | Amino Acid Metabolism | 0.87 | 0.99 | 0.91 | 0.6236 | 0.9789 | 0.6810 | 0.89 | 0.7879 | 0.81 | 1.05 | 0.88 | 0.6068 | 0.9111 | 0.7850 | 1.17 | 1.20 | 1.09 | 0.7127 | 0.6355 | 0.8182 | 1.00 | 0.99 | 0.9869 | 0.9726 |
| 103.0633 | 15.4 | C4H9NO2 | 4-Aminobutanoate | Amino Acid Metabolism | 0.88 | 1.18 | 1.00 | 0.3522 | 0.4750 | 0.9774 | 1.00 | 0.9894 | 0.95 | 1.04 | 0.88 | 0.7087 | 0.8482 | 0.4570 | 1.16 | 1.09 | 1.14 | 0.2227 | 0.6223 | 0.3657 | 1.07 | 1.14 | 0.6912 | 0.4955 |
| 219.1107 | 8.7 | C9H17NO5 | Pantothenate | Amino Acid Metabolism | 0.89 | 0.99 | 0.89 | 0.5642 | 0.9771 | 0.5560 | 1.01 | 0.9640 | 0.97 | 1.03 | 0.86 | 0.9129 | 0.9129 | 0.5889 | 1.11 | 1.15 | 1.09 | 0.6869 | 0.6546 | 0.7405 | 1.00 | 1.04 | 0.9969 | 0.8968 |
| 197.1165 | 12.3 | C9H15N3O2 | Hercynine | Amino Acid Metabolism | 0.91 | 1.26 | 1.43 | 0.8349 | 0.6427 | 0.4083 | 0.96 | 0.9294 | 0.93 | 1.11 | 0.99 | 0.8381 | 0.8244 | 0.9745 | 0.84 | 0.85 | 1.00 | 0.6099 | 0.6294 | 0.9935 | 1.05 | 0.93 | 0.9196 | 0.8783 |
| 129.0790 | 12.4 | C6H11NO2 | L-Pipecolate | Amino Acid Metabolism | 0.88 | 0.99 | 0.91 | 0.6334 | 0.9681 | 0.7253 | 1.06 | 0.8040 | 0.91 | 0.93 | 0.89 | 0.7470 | 0.8030 | 0.7419 | 0.88 | 0.86 | 0.81 | 0.7116 | 0.6584 | 0.5656 | 0.39 | 0.40 | 0.3378 | 0.3398 |
| 103.0633 | 14.0 | C4H9NO2 | N,N-Dimethylglycine | Amino Acid Metabolism | 0.86 | 1.05 | 0.88 | 0.1840 | 0.4804 | 0.2680 | 1.02 | 0.8594 | 0.90 | 0.91 | 0.85 | 0.4358 | 0.4162 | 0.2555 | 1.18 | 1.13 | 1.03 | 0.1618 | 0.2111 | 0.7083 | 1.12 | 1.10 | 0.3363 | 0.4857 |
| 182.0578 | 8.8 | C9H10O4 | 3-(4-Hydroxyphenyl)lactate | Amino Acid Metabolism | 0.86 | 1.03 | 0.85 | 0.5421 | 0.8689 | 0.4437 | 1.02 | 0.9315 | 0.92 | 0.97 | 0.86 | 0.7442 | 0.9103 | 0.5884 | 1.01 | 0.94 | 0.82 | 0.9818 | 0.9020 | 0.6804 | 0.90 | 0.95 | 0.7897 | 0.8615 |
| 87.0684 | 10.4 | C4H9NO | 4-Aminobutanal | Amino Acid Metabolism | 0.83 | 0.99 | 0.55 | 0.3161 | 0.9514 | 0.0308 | 1.04 | 0.8346 | 0.76 | 0.86 | 0.82 | 0.1861 | 0.4893 | 0.3854 | 1.18 | 1.07 | 1.08 | 0.3198 | 0.5830 | 0.5721 | 0.98 | 0.91 | 0.9331 | 0.6407 |
| 125.9988 | 10.5 | C2H6O4S | 2-Hydroxyethanesulfonate | Amino Acid Metabolism | 0.82 | 0.90 | 0.88 | 0.3277 | 0.8093 | 0.6262 | 0.98 | 0.8874 | 0.83 | 0.87 | 0.75 | 0.5934 | 0.6416 | 0.3293 | 1.03 | 1.12 | 0.99 | 0.9331 | 0.6529 | 0.9671 | 1.43 | 1.26 | 0.4217 | 0.5975 |
| 297.0897 | 7.7 | C11H15N5O3S | 5'-Methylthioadenosine | Amino Acid Metabolism | 0.84 | 1.17 | 0.81 | 0.5740 | 0.6270 | 0.4583 | 0.96 | 0.8555 | 0.96 | 0.98 | 0.86 | 0.8585 | 0.8530 | 0.3677 | 1.17 | 1.34 | 1.02 | 0.3599 | 0.0907 | 0.8683 | 1.15 | 1.25 | 0.4086 | 0.2217 |
| 192.0634 | 12.6 | C7H12O6 | Quinate | Amino Acid Metabolism | 0.85 | 0.88 | 0.96 | 0.7755 | 0.8186 | 0.9343 | 0.93 | 0.8882 | 1.08 | 0.99 | 0.84 | 0.8930 | 0.9805 | 0.7465 | 1.02 | 1.00 | 1.04 | 0.9733 | 0.9998 | 0.9443 | 1.17 | 1.26 | 0.7970 | 0.7065 |
| 113.0478 | 14.7 | C5H7NO2 | (S)-1-Pyrroline-5-carboxylate | Amino Acid Metabolism | 0.83 | 0.91 | 0.70 | 0.8404 | 0.9162 | 0.7021 | 0.89 | 0.8821 | 0.94 | 0.97 | 0.66 | 0.9471 | 0.9715 | 0.6124 | 0.92 | 0.87 | 0.93 | 0.9024 | 0.8399 | 0.9213 | 1.01 | 1.02 | 0.9844 | 0.9727 |
| 322.1376 | 15.4 | C12H22N2O8 | Avenic acid A | Amino Acid Metabolism | 0.81 | 0.90 | 0.91 | 0.7104 | 0.8391 | 0.8617 | 0.98 | 0.9155 | 0.92 | 0.96 | 1.02 | 0.4946 | 0.7758 | 0.9185 | 1.05 | 1.06 | 1.07 | 0.8052 | 0.7751 | 0.7328 | 1.31 | 1.16 | 0.1047 | 0.3135 |
| 264.1111 | 5.0 | C13H16N2O4 | Formyl-N-acetyl-5-methoxykynurenamine | Amino Acid Metabolism | 0.85 | 0.65 | 0.77 | 0.8560 | 0.6481 | 0.7821 | 1.12 | 0.8733 | 0.66 | 0.95 | 0.63 | 0.6089 | 0.9331 | 0.5338 | 1.32 | 1.18 | 1.15 | 0.6866 | 0.8156 | 0.8386 | 0.43 | 0.99 | NA | 0.9953 |
| 129.0790 | 7.8 | C6H11NO2 | N4-Acetylaminobutanal | Amino Acid Metabolism | 0.78 | 1.09 | 0.73 | 0.2130 | 0.7635 | 0.1574 | 1.25 | 0.4399 | 0.66 | 0.65 | 0.86 | 0.1548 | 0.2128 | 0.6297 | 0.74 | 0.84 | 0.53 | 0.5106 | 0.7206 | 0.2631 | 1.41 | 1.09 | 0.1387 | 0.6842 |
| 301.0563 | 14.7 | C8H16NO9P | N-Acetyl-D-glucosamine 6-phosphate | Amino Acid Metabolism | 0.79 | 1.13 | 0.99 | 0.3740 | 0.3288 | 0.9261 | 0.89 | 0.3490 | 0.90 | 1.00 | 0.92 | 0.4237 | 0.9771 | 0.5466 | 1.01 | 1.06 | 0.99 | 0.8984 | 0.5795 | 0.9484 | 1.11 | 1.13 | 0.6428 | 0.5827 |
| 131.0583 | 14.4 | C5H9NO3 | L-Glutamate 5-semialdehyde | Amino Acid Metabolism | 0.75 | 1.09 | 1.00 | 0.3832 | 0.6498 | 0.9854 | 0.95 | 0.8122 | 0.84 | 0.96 | 0.88 | 0.4145 | 0.8593 | 0.5845 | 1.08 | 0.97 | 0.97 | 0.6440 | 0.8587 | 0.8484 | 1.06 | 1.07 | 0.5765 | 0.5882 |
| 114.0316 | 14.7 | C5H6O3 | 2-Hydroxy-2,4-pentadienoate | Amino Acid Metabolism | 0.71 | 0.93 | 0.48 | 0.3417 | 0.8827 | 0.1031 | 1.09 | 0.8476 | 0.66 | 0.91 | 0.60 | 0.1317 | 0.6712 | 0.0933 | 0.73 | 0.79 | 0.61 | 0.1214 | 0.2165 | 0.0487 | 0.82 | 1.03 | 0.6428 | 0.9285 |
| 183.1260 | 11.1 | C10H17NO2 | Acetylpseudotropine | Biosynthesis of Secondary Metabolites | 1.15 | 1.23 | 1.26 | 0.7559 | 0.6702 | 0.6135 | 1.05 | 0.9334 | 0.78 | 1.06 | 0.91 | 0.5814 | 0.9025 | 0.8444 | 1.20 | 1.30 | 1.28 | 0.7272 | 0.5961 | 0.5971 | 1.14 | 1.17 | 0.7037 | 0.5873 |
| 88.0636 | 14.2 | C3H8N2O | N,N'-Dimethylurea | Biosynthesis of Secondary Metabolites | 1.15 | 1.18 | 1.08 | 0.5036 | 0.4232 | 0.7656 | 1.06 | 0.5767 | 0.88 | 0.82 | 0.93 | 0.1154 | 0.1015 | 0.5543 | 1.02 | 1.02 | 1.05 | 0.8424 | 0.8745 | 0.6623 | 1.19 | 1.30 | 0.3696 | 0.1900 |
| 220.1825 | 4.4 | C15H24O | 2-trans,6-trans-Farnesal | Biosynthesis of Secondary Metabolites | 1.06 | 1.52 | 0.87 | 0.8417 | 0.6171 | 0.5747 | 1.34 | 0.4202 | 1.29 | 1.10 | 1.85 | 0.3587 | 0.7650 | 0.4789 | 1.00 | 1.00 | 1.07 | 0.9851 | 0.9872 | 0.8175 | 0.69 | 0.78 | 0.2217 | 0.3759 |
| 202.0950 | 9.8 | C8H14N2O4 | Proclavaminic acid | Biosynthesis of Secondary Metabolites | 0.98 | 1.08 | 1.01 | NA | NA | NA | 1.27 | 0.8111 | 0.68 | 0.83 | 0.80 | 0.7221 | 0.8623 | 0.8408 | 1.48 | 0.51 | 1.71 | 0.6678 | NA | 0.4504 | 1.23 | 1.06 | 0.7457 | 0.9389 |
| 357.1571 | 15.0 | C20H23NO5 | deacetylcolchicine | Biosynthesis of Secondary Metabolites | 1.05 | 0.86 | 1.08 | 0.5588 | 0.6894 | 0.3350 | 1.04 | 0.7929 | 1.07 | 0.99 | 0.95 | 0.7008 | 0.9725 | 0.8247 | 1.09 | 1.16 | 1.11 | 0.4253 | 0.0867 | 0.3861 | 1.11 | 1.00 | 0.5292 | 0.9982 |
| 240.1473 | 10.1 | C12H20N2O3 | Slaframine | Biosynthesis of Secondary Metabolites | 0.96 | 1.03 | 0.97 | 0.7137 | 0.8706 | 0.8256 | 1.09 | 0.5141 | 0.86 | 0.98 | 0.92 | 0.2670 | 0.8859 | 0.6005 | 1.06 | 1.08 | 1.03 | 0.6662 | 0.6042 | 0.8554 | 1.08 | 1.00 | 0.4998 | 0.9647 |

| | | | | | | | | | | | | | | | | | | | | | | | | | | | | |
|---|---|---|---|---|---|---|---|---|---|---|---|---|---|---|---|---|---|---|---|---|---|---|---|---|---|---|---|---|
| 331.0845 | 13.2 | C20H13NO4 | Sanguinarine | Biosynthesis of Secondary Metabolites | 0.84 | 1.08 | 0.89 | 0.6715 | 0.8574 | 0.7733 | 0.90 | 0.6793 | 1.00 | 1.12 | 0.96 | 0.9901 | 0.6773 | 0.8654 | 1.11 | 1.15 | 1.10 | 0.5769 | 0.5475 | 0.7224 | 1.17 | 1.02 | 0.6091 | 0.9556 |
| 153.0789 | 7.6 | C8H11NO2 | vanillylamine | Biosynthesis of Secondary Metabolites | 0.84 | 0.86 | 0.86 | 0.3192 | 0.3583 | 0.4416 | 1.01 | 0.9267 | 0.73 | 0.88 | 0.85 | 0.1214 | 0.4505 | 0.3420 | 1.06 | 1.05 | 1.03 | 0.4634 | 0.7265 | 0.6552 | 1.19 | 1.12 | 0.2126 | 0.4616 |
| 361.0944 | 12.5 | C21H15NO5 | Chelirubine | Biosynthesis of Secondary Metabolites | 0.67 | 1.02 | 1.23 | 0.4274 | 0.9776 | 0.5763 | 1.09 | 0.7373 | 0.91 | 0.87 | 0.81 | 0.6809 | 0.3346 | 0.2257 | 1.32 | 0.93 | 0.94 | 0.1134 | 0.5838 | 0.6685 | 1.07 | 1.33 | 0.7802 | 0.3415 |
| 179.0794 | 14.0 | C6H13NO5 | D-Glucosamine | Carbohydrate Metabolism | 1.97 | 2.11 | 2.10 | 0.0527 | 0.0345 | 0.0454 | 1.06 | 0.7468 | 0.86 | 0.86 | 0.88 | 0.4169 | 0.4394 | 0.6151 | 0.84 | 0.88 | 0.83 | 0.3593 | 0.4227 | 0.3376 | 0.94 | 1.02 | 0.8003 | 0.9303 |
| 260.0296 | 15.6 | C6H13O9P | D-Fructose 6-phosphate | Carbohydrate Metabolism | 1.47 | 1.96 | 1.08 | 0.6099 | 0.2912 | 0.8855 | 0.98 | 0.9821 | 0.83 | 0.95 | 0.46 | 0.5638 | 0.8853 | 0.2780 | 1.10 | 1.15 | 4.66 | 0.8326 | 0.7553 | 0.0275 | 1.33 | 2.05 | 0.2958 | 0.2708 |
| 180.0634 | 17.0 | C6H12O6 | D-Fructose | Carbohydrate Metabolism | 1.36 | 1.54 | 1.37 | 0.3622 | 0.2797 | 0.3648 | 1.02 | 0.9408 | 0.85 | 0.93 | 0.93 | 0.4821 | 0.7645 | 0.8017 | 1.06 | 1.09 | 1.09 | 0.7942 | 0.7159 | 0.7358 | 1.19 | 1.15 | 0.1035 | 0.0599 |
| 424.0370 | 14.5 | C12H18N4O7P2S | Thiamin diphosphate | Carbohydrate Metabolism | 1.20 | 1.40 | 1.02 | 0.6789 | 0.5953 | 0.9682 | 0.86 | 0.6783 | 0.70 | 0.92 | 0.83 | 0.3215 | 0.7974 | 0.5445 | 1.00 | 1.00 | 1.00 | 0.9910 | 0.9981 | 0.9953 | 1.01 | 1.04 | 0.9099 | 0.7409 |
| 260.0296 | 16.5 | C6H13O9P | D-Glucose 6-phosphate | Carbohydrate Metabolism | 1.23 | 1.27 | 1.30 | 0.5340 | 0.6175 | 0.4087 | 1.06 | 0.8407 | 0.91 | 0.98 | 0.93 | 0.6976 | 0.9488 | 0.8102 | 1.05 | 1.00 | 0.99 | 0.8339 | 0.9878 | 0.9495 | 1.07 | 1.02 | 0.8168 | 0.9528 |
| 134.0216 | 15.7 | C4H6O5 | (S)-Malate | Carbohydrate Metabolism | 1.29 | 1.33 | 0.96 | 0.4759 | 0.4325 | 0.9306 | 0.98 | 0.9104 | 0.89 | 0.95 | 0.89 | 0.6812 | 0.8550 | 0.7489 | 1.06 | 1.01 | 0.97 | 0.8518 | 0.9748 | 0.9234 | 1.08 | 1.08 | 0.6529 | 0.4638 |
| 309.9856 | 17.3 | C5H12O11P2 | D-Ribose 1,5-bisphosphate | Carbohydrate Metabolism | 1.18 | 1.44 | 0.81 | 0.6704 | 0.3854 | 0.5773 | 0.89 | 0.7839 | 0.72 | 0.98 | 0.97 | 0.4846 | 0.9651 | 0.9634 | 1.17 | 1.26 | 1.22 | 0.7576 | 0.6879 | 0.7194 | 1.39 | 1.42 | 0.5368 | 0.4713 |
| 84.0212 | 11.1 | C4H4O2 | 3-Butynoate | Carbohydrate Metabolism | 1.12 | 1.17 | 1.07 | 0.6189 | 0.6214 | 0.6703 | 1.16 | 0.6857 | 0.86 | 0.99 | 0.86 | 0.6811 | 0.9741 | 0.7219 | 1.27 | 1.19 | 1.20 | 0.4865 | 0.6255 | 0.6818 | 1.02 | 1.08 | 0.9471 | 0.5170 |
| 214.0243 | 14.6 | C5H11O7P | 2-Deoxy-D-ribose 5-phosphate | Carbohydrate Metabolism | 1.17 | 0.61 | 0.85 | 0.8152 | 0.5429 | 0.8447 | 0.93 | 0.9233 | 0.92 | 0.93 | 0.94 | 0.9162 | 0.9317 | 0.9292 | 1.15 | 1.19 | 1.04 | 0.8642 | 0.8400 | 0.9618 | 1.24 | 1.49 | 0.8095 | 0.6279 |
| 132.0423 | 12.7 | C5H8O4 | 2-Acetolactate | Carbohydrate Metabolism | 1.08 | 1.07 | 1.08 | 0.4841 | 0.7388 | 0.5107 | 0.98 | 0.8512 | 1.06 | 1.11 | 0.95 | 0.7942 | 0.4391 | 0.7535 | 1.24 | 1.23 | 1.18 | 0.2107 | 0.2356 | 0.3137 | 1.16 | 1.30 | 0.5193 | 0.2208 |
| 106.0266 | 11.7 | C3H6O4 | D-Glycerate | Carbohydrate Metabolism | 1.03 | 1.34 | 1.03 | 0.9214 | 0.5588 | 0.9283 | 1.09 | 0.7034 | 0.88 | 1.23 | 0.92 | 0.6500 | 0.6642 | 0.8261 | 1.01 | 1.06 | 1.03 | 0.9846 | 0.8373 | 0.9319 | 1.31 | 1.18 | 0.3513 | 0.3681 |
| 342.1163 | 16.2 | C12H22O11 | Lactose | Carbohydrate Metabolism | 1.06 | 1.23 | 1.14 | 0.5719 | 0.1767 | 0.3567 | 1.04 | 0.7107 | 0.86 | 0.89 | 0.87 | 0.4182 | 0.4209 | 0.3918 | 1.04 | 1.03 | 1.00 | 0.7637 | 0.8218 | 0.9728 | 1.08 | 1.15 | 0.5166 | 0.3169 |
| 260.0296 | 15.0 | C6H13O9P | D-Glucose 1-phosphate | Carbohydrate Metabolism | 1.05 | 1.18 | 0.79 | 0.7990 | 0.6061 | 0.4572 | 0.91 | 0.7891 | 0.83 | 0.95 | 0.90 | 0.5658 | 0.8825 | 0.7768 | 1.07 | 1.00 | 1.00 | 0.8302 | 0.9934 | 0.9882 | 1.23 | 1.25 | 0.4133 | 0.3253 |
| 169.9980 | 15.1 | C3H7O6P | Glycerone phosphate | Carbohydrate Metabolism | 1.02 | 1.24 | 1.08 | 0.9511 | 0.6430 | 0.8126 | 1.01 | 0.9694 | 0.88 | 1.00 | 1.06 | 0.6000 | 0.9888 | 0.8420 | 1.17 | 1.34 | 1.37 | 0.5903 | 0.4277 | 0.3883 | 1.58 | 1.54 | 0.4195 | 0.4306 |
| 344.1321 | 15.5 | C12H24O11 | Melibiitol | Carbohydrate Metabolism | 1.03 | 1.09 | 1.03 | 0.9510 | 0.8815 | 0.9659 | 1.05 | 0.9094 | 0.96 | 0.97 | 1.00 | 0.9369 | 0.9378 | 0.9928 | 1.13 | 1.14 | 1.16 | 0.7633 | 0.7744 | 0.7552 | 1.09 | 1.08 | 0.8735 | 0.8819 |
| 276.0247 | 17.3 | C6H13O10P | 6-Phospho-D-gluconate | Carbohydrate Metabolism | 1.04 | 1.13 | 0.95 | 0.8248 | 0.7462 | 0.8548 | 0.97 | 0.9399 | 0.82 | 0.98 | 0.92 | 0.5425 | 0.9649 | 0.8276 | 1.09 | 1.09 | 1.03 | 0.7920 | 0.8330 | 0.9351 | 1.15 | 1.18 | 0.3871 | 0.2802 |
| 194.0426 | 14.3 | C6H10O7 | D-Galacturonate | Carbohydrate Metabolism | 1.02 | 1.20 | 0.91 | 0.9436 | 0.6893 | 0.6910 | 0.96 | 0.9315 | 0.83 | 1.10 | 0.92 | 0.5883 | 0.8193 | 0.8483 | 0.98 | 1.02 | 0.98 | 0.9311 | 0.9487 | 0.9520 | 1.20 | 1.32 | 0.3437 | 0.1765 |
| 196.0583 | 13.3 | C6H12O7 | D-Gluconic acid | Carbohydrate Metabolism | 1.02 | 0.69 | 1.02 | 0.8958 | 0.1324 | 0.9137 | 0.91 | 0.7924 | 0.86 | 1.00 | 0.97 | 0.6413 | 0.9970 | 0.9358 | 1.13 | 1.09 | 1.08 | 0.7264 | 0.8067 | 0.8159 | 1.24 | 1.22 | 0.3351 | 0.2297 |
| 580.0342 | 18.6 | C15H22N2O18P2 | UDP-glucuronate | Carbohydrate Metabolism | 1.03 | 1.34 | 1.04 | 0.9296 | 0.4786 | 0.8970 | 0.95 | 0.9186 | 0.73 | 0.96 | 0.90 | 0.4796 | 0.9391 | 0.8358 | 1.11 | 1.05 | 1.05 | 0.7956 | 0.9073 | 0.9013 | 1.04 | 1.12 | 0.8828 | 0.6787 |
| 419.9623 | 18.5 | C6H15O15P3 | D-myo-Inositol 1,4,5-trisphosphate | Carbohydrate Metabolism | 1.01 | 1.31 | 0.98 | 0.9650 | 0.2783 | 0.9539 | 0.86 | 0.7827 | 0.75 | 1.04 | 0.95 | 0.5945 | 0.9557 | 0.9330 | 1.15 | 1.22 | 1.07 | 0.8110 | 0.7670 | 0.9101 | 1.00 | 1.11 | 0.9997 | 0.5317 |
| 178.0477 | 11.8 | C6H10O6 | D-Glucono-1,5-lactone | Carbohydrate Metabolism | 0.99 | 1.15 | 0.78 | 0.9371 | 0.6597 | 0.4253 | 1.03 | 0.9103 | 0.80 | 0.91 | 0.88 | 0.4815 | 0.7882 | 0.7362 | 1.07 | 1.07 | 1.05 | 0.8387 | 0.8538 | 0.8776 | 1.22 | 1.15 | 0.2521 | 0.2309 |
| 589.0822 | 17.2 | C16H25N5O15P2 | GDP-L-fucose | Carbohydrate Metabolism | 1.00 | 1.08 | 1.01 | 0.9882 | 0.6616 | 0.9700 | 0.97 | 0.9301 | 0.82 | 0.98 | 0.91 | 0.5006 | 0.9544 | 0.8085 | 1.04 | 1.10 | 1.12 | 0.8874 | 0.7976 | 0.7288 | 1.19 | 1.31 | 0.3450 | 0.0785 |
| 566.0549 | 16.0 | C15H24N2O17P2 | UDP-glucose | Carbohydrate Metabolism | 1.01 | 1.11 | 1.00 | 0.9707 | 0.7338 | 0.9892 | 0.98 | 0.9135 | 0.85 | 0.92 | 0.87 | 0.5339 | 0.7445 | 0.6024 | 1.10 | 1.08 | 1.12 | 0.5378 | 0.6519 | 0.4558 | 1.10 | 1.08 | 0.6431 | 0.7259 |
| 195.0744 | 16.9 | C6H13NO6 | 2-Amino-2-deoxy-D-gluconate | Carbohydrate Metabolism | 0.98 | 0.97 | 0.99 | 0.8783 | 0.8668 | 0.9250 | 1.10 | 0.7411 | 0.78 | 1.05 | 0.77 | 0.2741 | 0.9051 | 0.2796 | 0.76 | 0.61 | 0.67 | 0.3363 | 0.1444 | 0.1887 | 1.18 | 1.10 | 0.8063 | 0.8858 |
| 265.9592 | 17.6 | C3H8O10P2 | 3-Phospho-D-glyceroyl phosphate | Carbohydrate Metabolism | 0.97 | 1.28 | 0.94 | 0.9606 | 0.7183 | 0.9252 | 1.05 | 0.9409 | 0.76 | 1.01 | 0.99 | 0.6673 | 0.9873 | 0.9872 | 1.16 | 1.12 | 1.06 | 0.8218 | 0.8556 | 0.9339 | 1.03 | 1.10 | 0.9224 | 0.7093 |
| 230.0191 | 15.4 | C5H11O8P | D-Ribose 5-phosphate | Carbohydrate Metabolism | 0.99 | 1.37 | 0.93 | 0.9805 | 0.4293 | 0.8801 | 0.91 | 0.8543 | 0.72 | 0.88 | 0.82 | 0.4585 | 0.7932 | 0.7020 | 1.05 | 1.14 | 1.02 | 0.9097 | 0.8122 | 0.9708 | 1.34 | 1.29 | 0.2867 | 0.3514 |
| 605.0772 | 17.9 | C16H25N5O16P2 | GDP-mannose | Carbohydrate Metabolism | 0.99 | 1.19 | 1.05 | 0.9378 | 0.5953 | 0.7175 | 0.91 | 0.7303 | 0.82 | 0.97 | 0.94 | 0.3421 | 0.9026 | 0.8200 | 1.10 | 1.14 | 1.15 | 0.6597 | 0.5865 | 0.5752 | 1.27 | 1.16 | 0.5292 | 0.5240 |
| 259.0458 | 15.4 | C6H14NO8P | alpha-D-Glucosamine 1-phosphate | Carbohydrate Metabolism | 0.98 | 1.32 | 1.06 | 0.9231 | 0.5767 | 0.8052 | 0.96 | 0.9477 | 0.72 | 0.89 | 0.91 | 0.6015 | 0.8650 | 0.8868 | 1.11 | 1.17 | 1.00 | 0.8627 | 0.8064 | 0.9994 | 1.05 | 1.01 | 0.8093 | 0.9469 |

| | | | | | | | | | | | | | | | | | | | | | | | | | | | | |
|---|---|---|---|---|---|---|---|---|---|---|---|---|---|---|---|---|---|---|---|---|---|---|---|---|---|---|---|---|
| 118.0266 | 14.9 | C4H6O4 | Succinate | Carbohydrate Metabolism | 0.98 | 1.36 | 1.22 | 0.9120 | 0.3097 | 0.3117 | 1.00 | 0.9935 | 0.87 | 1.04 | 0.94 | 0.6685 | 0.9298 | 0.8802 | 0.99 | 1.02 | 1.03 | 0.9772 | 0.9689 | 0.9485 | 0.53 | 0.58 | 0.0154 | 0.0181 |
| 185.9929 | 16.7 | C3H7O7P | 3-Phospho-D-glycerate | Carbohydrate Metabolism | 0.98 | 1.23 | 0.99 | 0.8782 | 0.4134 | 0.9492 | 0.94 | 0.8484 | 0.81 | 0.96 | 0.88 | 0.5400 | 0.9297 | 0.7741 | 1.03 | 1.07 | 1.01 | 0.9386 | 0.8563 | 0.9707 | 1.12 | 1.15 | 0.6506 | 0.5280 |
| 319.0670 | 14.7 | C8H18NO10P | N-Gluconyl ethanolamine phosphate | Carbohydrate Metabolism | 0.95 | 1.36 | 0.88 | 0.9027 | 0.6788 | 0.7823 | 1.01 | 0.9859 | 0.86 | 1.05 | 0.99 | 0.7345 | 0.9315 | 0.9790 | 1.10 | 1.16 | 1.18 | 0.8042 | 0.7160 | 0.7192 | 1.40 | 1.30 | 0.2709 | 0.3627 |
| 342.1162 | 15.1 | C12H22O11 | Sucrose | Carbohydrate Metabolism | 0.95 | 1.07 | 1.01 | 0.7621 | 0.6129 | 0.9350 | 1.08 | 0.6095 | 0.79 | 0.85 | 0.83 | 0.4516 | 0.5315 | 0.4593 | 1.12 | 0.91 | 0.99 | 0.5087 | 0.5544 | 0.9489 | 1.01 | 1.06 | 0.9471 | 0.7452 |
| 262.0454 | 15.0 | C6H15O9P | D-Mannitol 1-phosphate | Carbohydrate Metabolism | 0.97 | 1.09 | 1.01 | 0.8590 | 0.6484 | 0.9603 | 0.98 | 0.8825 | 0.88 | 0.99 | 0.90 | 0.4444 | 0.9259 | 0.5694 | 1.05 | 1.00 | 1.02 | 0.6820 | 0.9838 | 0.8540 | 1.20 | 1.22 | 0.3727 | 0.3471 |
| 254.1001 | 13.7 | C9H18O8 | 3-beta-D-Galactosyl-sn-glycerol | Carbohydrate Metabolism | 0.95 | 1.05 | 0.98 | 0.7624 | 0.8243 | 0.9117 | 1.07 | 0.7334 | 0.90 | 1.00 | 0.94 | 0.6063 | 0.9846 | 0.7861 | 1.05 | 1.09 | 1.09 | 0.8291 | 0.6942 | 0.7182 | 1.06 | 1.05 | 0.8075 | 0.8256 |
| 130.0265 | 11.8 | C5H6O4 | Mesaconate | Carbohydrate Metabolism | 0.95 | 1.07 | 1.42 | 0.7221 | 0.7973 | 0.3941 | 0.97 | 0.9112 | 0.90 | 0.95 | 0.94 | 0.7212 | 0.8623 | 0.8506 | 1.15 | 1.05 | 1.13 | 0.6039 | 0.8474 | 0.6493 | 1.15 | 1.17 | 0.3433 | 0.1732 |
| 232.0347 | 15.5 | C5H13O8P | D-Ribitol 5-phosphate | Carbohydrate Metabolism | 0.95 | 1.12 | 0.95 | 0.9393 | 0.8536 | 0.9316 | 0.96 | 0.9401 | 0.96 | 0.99 | 0.93 | 0.9351 | 0.9887 | 0.8878 | 1.07 | 1.04 | 1.03 | 0.8569 | 0.9141 | 0.9418 | 1.05 | 1.10 | 0.9087 | 0.8494 |
| 240.0844 | 14.2 | C8H16O8 | D-glycero-L-galacto-Octulose | Carbohydrate Metabolism | 0.94 | 1.02 | 0.97 | 0.4714 | 0.8159 | 0.6843 | 1.01 | 0.9373 | 0.98 | 0.95 | 0.87 | 0.9085 | 0.7386 | 0.4136 | 1.01 | 1.04 | 1.04 | 0.9569 | 0.8411 | 0.8458 | 1.15 | 1.31 | 0.5183 | 0.3338 |
| 537.0764 | 16.3 | C14H25N3O15P2 | CDP-ribitol | Carbohydrate Metabolism | 0.95 | 1.18 | 0.95 | 0.8315 | 0.6008 | 0.8289 | 0.95 | 0.8677 | 0.80 | 0.94 | 1.03 | 0.3769 | 0.8310 | 0.9373 | 1.05 | 1.02 | 1.10 | 0.8589 | 0.9553 | 0.7384 | 1.01 | 0.99 | 0.9771 | 0.9475 |
| 182.0790 | 13.9 | C6H14O6 | Mannitol | Carbohydrate Metabolism | 0.94 | 1.04 | 0.97 | 0.6672 | 0.8306 | 0.8375 | 1.03 | 0.7773 | 0.93 | 1.02 | 0.94 | 0.6492 | 0.9141 | 0.6371 | 1.09 | 1.16 | 1.15 | 0.5833 | 0.3051 | 0.3365 | 1.20 | 1.20 | 0.5456 | 0.5244 |
| 290.0403 | 15.9 | C7H15O10P | D-Sedoheptulose 7-phosphate | Carbohydrate Metabolism | 0.97 | 1.09 | 1.06 | 0.9473 | 0.8272 | 0.8921 | 1.10 | 0.8303 | 0.91 | 1.03 | 0.94 | 0.7679 | 0.9098 | 0.8519 | 1.04 | 1.07 | 1.07 | 0.9153 | 0.8422 | 0.8317 | 1.22 | 1.18 | 0.5267 | 0.5438 |
| 270.0951 | 16.6 | C9H18O9 | D-erythro-L-galacto-Nonulose | Carbohydrate Metabolism | 0.93 | 1.00 | 0.97 | 0.5800 | 0.9820 | 0.7197 | 1.05 | 0.7217 | 0.85 | 0.99 | 0.97 | 0.3008 | 0.9659 | 0.8342 | 1.12 | 0.99 | 1.12 | 0.1933 | 0.9373 | 0.4463 | 1.25 | 1.19 | 0.1368 | 0.2735 |
| 180.0634 | 12.6 | C6H12O6 | D-Glucose | Carbohydrate Metabolism | 0.90 | 1.02 | 1.00 | 0.7292 | 0.9289 | 0.9905 | 0.92 | 0.5504 | 0.87 | 0.97 | 0.81 | 0.5754 | 0.8681 | 0.2181 | 1.23 | 1.08 | 1.10 | 0.2587 | 0.7033 | 0.6184 | 1.12 | 1.13 | 0.7354 | 0.7252 |
| 244.0348 | 15.2 | C6H13O8P | L-Fuculose 1-phosphate | Carbohydrate Metabolism | 0.92 | 0.89 | 0.98 | 0.7227 | 0.6255 | 0.9110 | 0.94 | 0.5079 | 0.93 | 1.05 | 0.81 | 0.7708 | 0.6764 | 0.2858 | 1.08 | 1.03 | 0.87 | 0.7535 | 0.9145 | 0.6538 | 1.05 | 1.00 | 0.8693 | 0.9945 |
| 607.0816 | 14.9 | C17H27N3O17P2 | UDP-N-acetyl-D-galactosamine | Carbohydrate Metabolism | 0.92 | 0.92 | 0.94 | 0.8958 | 0.8887 | 0.9185 | 0.94 | 0.8837 | 0.93 | 0.95 | 0.92 | 0.8641 | 0.8889 | 0.8661 | 1.10 | 1.01 | 1.07 | 0.8207 | 0.9838 | 0.8704 | 1.11 | 1.17 | 0.8340 | 0.7689 |
| 177.0637 | 12.8 | C6H11NO5 | 4-Hydroxy-4-methylglutamate | Carbohydrate Metabolism | 0.91 | 0.93 | 0.89 | 0.6060 | 0.7599 | 0.5740 | 0.96 | 0.8127 | 0.90 | 0.99 | 0.93 | 0.5610 | 0.9492 | 0.7666 | 0.99 | 0.98 | 0.95 | 0.9786 | 0.9143 | 0.8052 | 1.14 | 1.14 | 0.3477 | 0.3061 |
| 809.1261 | 12.2 | C23H38N7O17P3S | Acetyl-CoA | Carbohydrate Metabolism | 0.91 | 0.95 | 0.95 | 0.6585 | 0.8181 | 0.8189 | 0.97 | 0.8925 | 0.83 | 0.94 | 0.91 | 0.3519 | 0.8015 | 0.7412 | 1.07 | 1.02 | 0.94 | 0.7654 | 0.9204 | 0.7531 | 0.99 | 1.03 | 0.9250 | 0.7904 |
| 174.0164 | 17.5 | C6H6O6 | cis-Aconitate | Carbohydrate Metabolism | 0.93 | 1.12 | 0.89 | 0.8621 | 0.7768 | 0.8021 | 0.91 | 0.7155 | 0.96 | 1.12 | 0.91 | 0.9138 | 0.7206 | 0.7222 | 1.11 | 0.90 | 1.07 | 0.7230 | 0.7397 | 0.8427 | 1.25 | 1.46 | 0.5416 | 0.3642 |
| 150.0164 | 16.9 | C4H6O6 | (R,R)-Tartaric acid | Carbohydrate Metabolism | 0.90 | 1.02 | 0.85 | 0.3544 | 0.8250 | 0.3181 | 0.89 | 0.1709 | 1.00 | 0.94 | 0.86 | 0.9975 | 0.5657 | 0.0714 | 1.16 | 1.10 | 1.06 | 0.3318 | 0.4023 | 0.6210 | 1.00 | 1.04 | 0.9974 | 0.7597 |
| 152.0685 | 12.9 | C5H12O5 | Ribitol | Carbohydrate Metabolism | 0.89 | 1.05 | 1.05 | 0.5256 | 0.7918 | 0.7473 | 1.03 | 0.8439 | 1.01 | 1.03 | 0.94 | 0.9797 | 0.7858 | 0.6549 | 1.29 | 1.16 | 1.13 | 0.3052 | 0.4666 | 0.4903 | 1.42 | 1.41 | 0.3433 | 0.3143 |
| 192.0270 | 17.7 | C6H8O7 | Citrate | Carbohydrate Metabolism | 0.90 | 1.04 | 0.95 | 0.8231 | 0.9233 | 0.9122 | 1.01 | 0.9843 | 0.92 | 0.99 | 0.87 | 0.8368 | 0.9863 | 0.6644 | 1.10 | 1.07 | 1.08 | 0.7777 | 0.8540 | 0.8338 | 1.17 | 1.13 | 0.6888 | 0.7511 |
| 162.0529 | 13.9 | C6H10O5 | (R)-2-Ethylmalate | Carbohydrate Metabolism | 0.93 | 1.99 | 1.38 | 0.8218 | 0.3078 | 0.3225 | 1.07 | 0.7916 | 0.88 | 0.91 | 0.89 | 0.5049 | 0.6372 | 0.6425 | 0.86 | 0.85 | 0.75 | 0.3685 | 0.2735 | 0.1821 | 0.93 | 1.04 | 0.7985 | 0.8531 |
| 120.0422 | 10.5 | C4H8O4 | D-Erythrose | Carbohydrate Metabolism | 0.88 | 1.18 | 0.92 | 0.4483 | 0.5880 | 0.6427 | 1.04 | 0.9265 | 1.03 | 1.17 | 0.96 | 0.9191 | 0.7029 | 0.9031 | 0.95 | 1.09 | 1.19 | 0.8681 | 0.7768 | 0.6056 | 1.50 | 1.40 | 0.1884 | 0.2431 |
| 164.0685 | 11.6 | C6H12O5 | L-Rhamnose | Carbohydrate Metabolism | 0.87 | 1.00 | 0.97 | 0.1910 | 0.9918 | 0.7895 | 1.06 | 0.6581 | 0.91 | 1.02 | 0.92 | 0.4018 | 0.8711 | 0.6669 | 1.04 | 0.97 | 0.97 | 0.7348 | 0.8416 | 0.8265 | 1.10 | 1.10 | 0.4867 | 0.4172 |
| 247.9486 | 19.7 | C3H6O9P2 | Cyclic 2,3-bisphospho-D-glycerate | Carbohydrate Metabolism | 0.89 | 1.18 | 0.89 | 0.6267 | 0.5318 | 0.6572 | 0.90 | 0.7129 | 0.80 | 0.93 | 0.85 | 0.4638 | 0.8303 | 0.6704 | 1.02 | 1.00 | 0.99 | 0.9384 | 0.9981 | 0.9758 | 1.21 | 1.21 | 0.4422 | 0.4618 |
| 166.0478 | 13.4 | C5H10O6 | D-Arabinonate | Carbohydrate Metabolism | 0.88 | 0.78 | 0.96 | 0.6714 | 0.5080 | 0.8724 | 0.95 | 0.7994 | 1.03 | 1.09 | 0.86 | 0.9401 | 0.8397 | 0.7151 | 0.91 | 0.92 | 0.92 | 0.7929 | 0.8016 | 0.8121 | 1.10 | 1.12 | 0.7778 | 0.7425 |
| 146.0216 | 15.3 | C5H6O5 | 2-Oxoglutarate | Carbohydrate Metabolism | 0.89 | 0.95 | 1.01 | 0.7914 | 0.9054 | 0.9741 | 0.93 | 0.8440 | 1.02 | 0.93 | 0.81 | 0.9368 | 0.7525 | 0.2477 | 0.77 | 0.70 | 0.56 | 0.6286 | 0.5360 | 0.3233 | 0.70 | 0.66 | 0.4073 | 0.3097 |
| 221.0900 | 12.3 | C8H15NO6 | N-Acetyl-D-mannosamine | Carbohydrate Metabolism | 0.84 | 1.02 | 0.84 | 0.5449 | 0.9682 | 0.5434 | 1.04 | 0.9351 | 0.75 | 0.91 | 0.89 | 0.5413 | 0.8555 | 0.8369 | 1.14 | 1.14 | 1.11 | 0.7809 | 0.7940 | 0.8201 | 1.15 | 1.15 | 0.5496 | 0.5221 |
| 90.0317 | 13.9 | C3H6O3 | (S)-Lactate | Carbohydrate Metabolism | 0.86 | 0.95 | 0.90 | 0.5696 | 0.8416 | 0.6985 | 0.89 | 0.5708 | 0.85 | 1.00 | 0.97 | 0.4871 | 0.9825 | 0.9001 | 1.20 | 1.05 | 1.13 | 0.3830 | 0.8002 | 0.5528 | 1.29 | 1.83 | 0.4691 | 0.1045 |
| 200.0086 | 12.7 | C4H9O7P | D-Erythrose 4-phosphate | Carbohydrate Metabolism | 0.82 | 0.99 | 1.03 | 0.5878 | 0.9758 | 0.9221 | 0.99 | 0.9659 | 0.87 | 1.04 | 1.08 | 0.3628 | 0.8336 | 0.6551 | 1.05 | 1.09 | 1.19 | 0.8473 | 0.7335 | 0.4756 | 1.31 | 1.34 | 0.5361 | 0.4671 |
| 210.0376 | 16.7 | C6H10O8 | D-Glucarate | Carbohydrate Metabolism | 0.85 | 0.93 | 0.95 | 0.6880 | 0.8538 | 0.9043 | 0.87 | 0.7021 | 0.91 | 0.91 | 0.77 | 0.8253 | 0.7876 | 0.3613 | 1.19 | 1.08 | 1.09 | 0.6452 | 0.8237 | 0.8144 | 1.12 | 1.14 | 0.8442 | 0.8078 |

| | | | | | | | | | | | | | | | | | | | | | | | | | | | | |
|---|---|---|---|---|---|---|---|---|---|---|---|---|---|---|---|---|---|---|---|---|---|---|---|---|---|---|---|---|
| 265.1160 | 11.1 | C10H19NO7 | D-1-[(3-Carboxypropyl)amino]-1-deoxyfructose | Carbohydrate Metabolism | 0.83 | 0.44 | 1.24 | 0.7264 | NA | 0.5432 | 0.92 | 0.8024 | 0.51 | 1.11 | 1.05 | 0.3883 | 0.8840 | 0.9300 | 1.53 | 1.57 | 1.79 | 0.4519 | 0.5682 | 0.4378 | 2.33 | 2.18 | 0.1531 | 0.3068 |
| 499.9285 | 19.3 | C6H16O18P4 | 1D-myo-Inositol 3,4,5,6-tetrakisphosphate | Carbohydrate Metabolism | 0.83 | 2.37 | 0.92 | NA | 0.5087 | 0.9484 | 0.77 | 0.7287 | 0.51 | 0.94 | 0.74 | 0.3869 | 0.9399 | 0.6872 | 1.33 | 1.46 | 1.31 | 0.7245 | 0.6894 | 0.7660 | 0.92 | 1.42 | 0.8429 | 0.2783 |
| 196.0583 | 13.9 | C6H12O7 | D-Mannonate | Carbohydrate Metabolism | 0.70 | 0.42 | 0.71 | 0.3616 | 0.0952 | 0.3283 | 0.96 | 0.9182 | 0.70 | 1.04 | 0.95 | 0.4130 | 0.9337 | 0.9073 | 1.06 | 1.09 | 1.04 | 0.8657 | 0.8247 | 0.9201 | 1.24 | 1.23 | 0.3064 | 0.2677 |
| 180.0633 | 14.7 | C6H12O6 | D-Galactose | Carbohydrate Metabolism | 0.63 | 1.15 | 0.39 | 0.3214 | 0.7793 | 0.1347 | 1.08 | 0.8733 | 0.66 | 0.91 | 0.60 | 0.1484 | 0.6749 | 0.0969 | 0.73 | 0.71 | 0.54 | 0.1746 | 0.1440 | 0.0457 | 0.73 | 1.03 | 0.5204 | 0.9465 |
| 379.1050 | 13.2 | C13H21N3O8S | (R)-S-Lactoylglutathione | Carbohydrate Metabolism | 0.68 | 0.88 | 0.62 | 0.5491 | 0.8284 | 0.4783 | 0.67 | 0.4387 | 1.03 | 1.02 | 0.85 | 0.9415 | 0.9669 | 0.5002 | 1.46 | 1.35 | 1.42 | 0.4321 | 0.5432 | 0.5835 | 1.43 | 1.50 | 0.7173 | 0.6687 |
| 370.0065 | 17.9 | C7H16O13P2 | D-Sedoheptulose 1,7-bisphosphate | Energy Metabolism | 1.30 | 1.82 | 1.03 | 0.6942 | 0.4794 | 0.9419 | 0.87 | 0.8634 | 0.75 | 1.00 | 1.04 | 0.5647 | 0.9984 | 0.9464 | 1.28 | 1.65 | 1.65 | 0.5595 | 0.3262 | 0.3565 | 1.59 | 1.51 | 0.5415 | 0.5311 |
| 427.0293 | 14.9 | C10H15N5O10P2 | ADP | Energy Metabolism | 1.12 | 1.23 | 1.12 | 0.7626 | 0.5566 | 0.7724 | 0.95 | 0.8214 | 0.88 | 0.98 | 0.93 | 0.5215 | 0.9397 | 0.7818 | 1.04 | 1.02 | 0.99 | 0.8555 | 0.9474 | 0.9685 | 1.16 | 1.18 | 0.3273 | 0.2237 |
| 506.9954 | 16.0 | C10H16N5O13P3 | ATP | Energy Metabolism | 1.10 | 1.23 | 1.00 | 0.6322 | 0.3294 | 0.9707 | 1.00 | 0.9904 | 0.87 | 0.96 | 0.94 | 0.6574 | 0.9223 | 0.8617 | 1.07 | 1.03 | 0.99 | 0.8461 | 0.9381 | 0.9701 | 1.05 | 1.08 | 0.7700 | 0.5295 |
| 339.9959 | 17.6 | C6H14O12P2 | D-Fructose 1,6-bisphosphate | Energy Metabolism | 1.05 | 1.37 | 0.96 | 0.8971 | 0.5273 | 0.8806 | 0.91 | 0.7868 | 0.87 | 1.00 | 1.03 | 0.5572 | 0.9978 | 0.9234 | 1.14 | 1.21 | 1.21 | 0.6353 | 0.5506 | 0.5248 | 1.32 | 1.29 | 0.4832 | 0.4193 |
| 743.0759 | 16.5 | C21H28N7O17P3 | NADP+ | Energy Metabolism | 1.02 | 1.14 | 1.01 | 0.9478 | 0.6326 | 0.9566 | 0.99 | 0.9735 | 0.89 | 0.98 | 0.94 | 0.6577 | 0.9474 | 0.8373 | 1.06 | 1.00 | 1.03 | 0.8091 | 0.9958 | 0.8964 | 1.15 | 1.19 | 0.5404 | 0.4642 |
| 663.1093 | 14.0 | C21H27N7O14P2 | NAD+ | Energy Metabolism | 0.99 | 1.21 | 0.87 | 0.9388 | 0.1421 | 0.6877 | 1.03 | 0.8171 | 0.93 | 0.99 | 0.99 | 0.5299 | 0.9479 | 0.9378 | 1.05 | 1.05 | 1.04 | 0.6518 | 0.7153 | 0.7859 | 1.03 | 1.04 | 0.5943 | 0.6195 |
| 97.9768 | 15.7 | H3O4P | Orthophosphate | Energy Metabolism | 0.93 | 0.82 | 0.96 | 0.7855 | 0.6191 | 0.8795 | 1.01 | 0.9568 | 0.87 | 0.95 | 0.81 | 0.2851 | 0.7765 | 0.1930 | 1.07 | 1.12 | 1.04 | 0.5357 | 0.5503 | 0.8024 | 1.01 | 1.09 | 0.9358 | 0.6778 |
| 665.1251 | 13.2 | C21H29N7O14P2 | NADH | Energy Metabolism | 0.89 | 1.15 | 0.89 | 0.6748 | 0.6189 | 0.6825 | 0.85 | 0.5455 | 0.85 | 0.96 | 0.99 | 0.3467 | 0.8552 | 0.9747 | 1.00 | 1.12 | 1.24 | 0.9880 | 0.6999 | 0.4662 | 1.31 | 1.48 | 0.5808 | 0.3902 |
| 745.0914 | 16.8 | C21H30N7O17P3 | NADPH | Energy Metabolism | 0.87 | 1.08 | 0.75 | 0.6726 | 0.7930 | 0.4294 | 0.74 | 0.4726 | 0.71 | 0.90 | 0.85 | 0.2671 | 0.7660 | 0.6994 | 0.93 | 0.96 | 1.06 | 0.8308 | 0.9133 | 0.8914 | 1.05 | 1.19 | 0.8201 | 0.3027 |
| 318.0351 | 15.1 | C8H15O11P | 3-Deoxy-D-manno-octulosonate 8-phosphate | Glycan Biosynthesis and Metabolism | 1.07 | 1.21 | 1.32 | 0.9292 | NA | 0.7405 | 1.01 | 0.9814 | 1.06 | 1.27 | 1.54 | 0.9241 | 0.7491 | 0.5381 | 1.90 | 2.20 | 3.32 | 0.4187 | 0.4723 | 0.2662 | 2.52 | 1.83 | 0.5510 | 0.6385 |
| 835.1423 | 14.9 | C25H40N7O17P3S | Crotonoyl-CoA | Lipid Metabolism | 1.31 | 1.79 | 1.02 | 0.7075 | 0.4180 | 0.9786 | 0.86 | 0.5759 | 0.97 | 1.22 | 0.88 | 0.8460 | 0.4058 | 0.6296 | 1.19 | 1.20 | 1.04 | 0.3361 | 0.4663 | 0.8454 | 1.18 | 1.05 | 0.3960 | 0.8161 |
| 384.3392 | 5.0 | C27H44O | Cholesta-5,7-dien-3beta-ol | Lipid Metabolism | 1.37 | 0.91 | 0.84 | 0.5201 | 0.8691 | 0.7509 | 0.68 | 0.2576 | 0.58 | 0.75 | 0.38 | 0.3712 | 0.5508 | 0.1540 | 1.28 | 1.75 | 1.11 | 0.3233 | 0.2812 | 0.7676 | 1.03 | 1.14 | 0.9582 | 0.8153 |
| 172.0137 | 14.8 | C3H9O6P | sn-Glycerol 3-phosphate | Lipid Metabolism | 1.04 | 1.27 | 1.09 | 0.8912 | 0.5736 | 0.7347 | 1.06 | 0.9028 | 1.08 | 1.26 | 1.69 | 0.8127 | 0.5706 | 0.3297 | 2.24 | 1.97 | 3.14 | 0.0891 | 0.1707 | 0.0924 | 1.26 | 1.28 | 0.5177 | 0.4756 |
| 472.1126 | 14.3 | C14H26N4O10P2 | CMP-N-trimethyl-2-aminoethylphosphonate | Lipid Metabolism | 1.00 | 1.19 | 0.97 | 0.9931 | 0.7744 | 0.9593 | 1.05 | 0.9315 | 0.84 | 0.99 | 0.96 | 0.7306 | 0.9780 | 0.9480 | 1.07 | 1.14 | 1.11 | 0.8831 | 0.7814 | 0.8259 | 1.11 | 1.09 | 0.5723 | 0.4915 |
| 488.1077 | 15.2 | C14H26N4O11P2 | CDP-choline | Lipid Metabolism | 0.98 | 1.15 | 1.04 | 0.9130 | 0.6234 | 0.8277 | 1.04 | 0.9039 | 0.82 | 0.94 | 0.91 | 0.5441 | 0.8758 | 0.8064 | 1.04 | 1.04 | 0.99 | 0.8848 | 0.9069 | 0.9695 | 1.16 | 1.26 | 0.4459 | 0.1476 |
| 257.1027 | 14.4 | C8H20NO6P | sn-glycero-3-Phosphocholine | Lipid Metabolism | 0.98 | 1.24 | 1.05 | 0.9268 | 0.5963 | 0.8314 | 1.04 | 0.9255 | 0.78 | 0.97 | 0.96 | 0.5694 | 0.9384 | 0.9396 | 1.17 | 1.09 | 1.22 | 0.6881 | 0.8471 | 0.6370 | 1.18 | 1.09 | 0.6397 | 0.8071 |
| 125.0146 | 14.7 | C2H7NO3S | Taurine | Lipid Metabolism | 0.98 | 1.06 | 1.02 | 0.9517 | 0.8867 | 0.9609 | 1.01 | 0.9505 | 0.94 | 1.09 | 0.92 | 0.8327 | 0.7346 | 0.7551 | 0.98 | 1.04 | 0.92 | 0.9275 | 0.8704 | 0.6983 | 1.04 | 1.15 | 0.9218 | 0.7070 |
| 921.2516 | 14.2 | C31H54N7O17P3S | Decanoyl-CoA | Lipid Metabolism | 0.96 | 1.12 | 0.92 | 0.9157 | 0.7989 | 0.8283 | 1.09 | 0.8296 | 0.86 | 0.92 | 0.85 | 0.7231 | 0.8461 | 0.6938 | 0.97 | 1.02 | 0.94 | 0.9440 | 0.9546 | 0.8696 | 1.16 | 1.21 | 0.2959 | 0.2129 |
| 215.0560 | 15.5 | C5H14NO6P | sn-glycero-3-Phosphoethanolamine | Lipid Metabolism | 0.94 | 1.05 | 0.94 | 0.7418 | 0.7665 | 0.7519 | 0.91 | 0.5202 | 0.96 | 1.03 | 1.05 | 0.6999 | 0.7539 | 0.7817 | 1.02 | 1.05 | 0.99 | 0.8669 | 0.7283 | 0.9205 | 1.12 | 1.16 | 0.5950 | 0.4775 |
| 446.0601 | 16.2 | C11H20N4O11P2 | CDP-ethanolamine | Lipid Metabolism | 0.91 | 0.99 | 0.96 | 0.4602 | 0.9651 | 0.7485 | 1.08 | 0.6487 | 0.94 | 0.99 | 1.09 | 0.7399 | 0.9436 | 0.6808 | 1.12 | 1.08 | 1.05 | 0.5376 | 0.6885 | 0.7899 | 2.38 | 2.21 | 0.0383 | 0.0292 |
| 183.0661 | 14.9 | C5H14NO4P | Choline phosphate | Lipid Metabolism | 0.90 | 1.26 | 1.05 | 0.6752 | 0.3779 | 0.8164 | 1.16 | 0.6722 | 1.14 | 1.16 | 1.63 | 0.5182 | 0.5541 | 0.3102 | 1.82 | 1.78 | 2.41 | 0.0538 | 0.1054 | 0.1139 | 3.35 | 2.73 | 0.0484 | 0.0091 |
| 216.0401 | 14.0 | C5H13O7P | 2-C-Methyl-D-erythritol 4-phosphate | Lipid Metabolism | 0.83 | 1.16 | 0.98 | 0.4210 | 0.3903 | 0.9355 | 0.73 | 0.1734 | 0.76 | 0.85 | 0.71 | 0.3531 | 0.5312 | 0.2500 | 0.88 | 0.90 | 0.92 | 0.5298 | 0.6422 | 0.6759 | 1.61 | 1.96 | 0.2466 | 0.1186 |
| 280.2403 | 4.0 | C18H32O2 | Linoleate | Lipids: Fatty Acyls | 3.42 | 1.50 | 2.58 | 0.3025 | 0.5127 | 0.2316 | 1.39 | 0.2914 | 1.31 | 1.55 | 1.47 | 0.4870 | 0.3687 | 0.5993 | 0.96 | 1.02 | 0.96 | 0.8981 | 0.9507 | 0.9057 | 0.62 | 0.70 | 0.4720 | 0.5362 |
| 200.1776 | 4.1 | C12H24O2 | Dodecanoic acid | Lipids: Fatty Acyls | 3.00 | 1.80 | 3.14 | 0.3195 | 0.4787 | 0.2740 | 1.37 | 0.4476 | 1.54 | 1.25 | 1.53 | 0.4676 | 0.5754 | 0.5989 | 0.71 | 0.80 | 0.79 | 0.4969 | 0.5998 | 0.6150 | 0.84 | 0.59 | 0.8375 | 0.5027 |
| 296.2349 | 4.1 | C18H32O3 | [FA (18:1)] 9R,10S-epoxy-12Z-octadecenoic acid | Lipids: Fatty Acyls | 2.55 | 0.69 | 2.30 | 0.1240 | 0.6394 | 0.1694 | 1.73 | 0.1965 | 1.58 | 2.26 | 1.51 | 0.2807 | 0.4453 | 0.3740 | 0.74 | 1.23 | 0.71 | 0.6384 | 0.6712 | 0.5973 | 0.57 | 0.51 | 0.5555 | 0.4945 |
| 248.1774 | 4.3 | C16H24O2 | [FA (16:4)] hexadecatetraenoic acid | Lipids: Fatty Acyls | 1.83 | 6.86 | 2.01 | 0.5456 | 0.4381 | 0.5702 | 2.19 | 0.5791 | 1.08 | 0.99 | 2.55 | 0.9354 | 0.9923 | 0.5514 | 0.82 | 1.05 | 0.95 | 0.8447 | 0.9612 | 0.9602 | 0.95 | 1.07 | 0.9380 | 0.9277 |
| 300.2664 | 4.1 | C18H36O3 | FA hydroxy(18:0) | Lipids: Fatty Acyls | 1.71 | 2.41 | 1.52 | 0.3846 | 0.4945 | 0.4288 | 1.10 | 0.8347 | 1.24 | 1.04 | 3.08 | 0.6600 | 0.9403 | 0.2434 | 0.78 | 0.98 | 0.80 | 0.4848 | 0.9580 | 0.5462 | 0.58 | 0.54 | 0.2943 | 0.2586 |
| 298.2511 | 4.0 | C18H34O3 | FA oxo(18:0) | Lipids: Fatty Acyls | 1.66 | 2.73 | 1.37 | 0.2754 | 0.4664 | 0.4935 | 1.37 | 0.4820 | 1.03 | 0.90 | 1.71 | 0.9356 | 0.8025 | 0.5518 | 0.90 | 0.99 | 0.84 | 0.7819 | 0.9887 | 0.6693 | 0.70 | 0.67 | 0.4300 | 0.3897 |
| 228.2089 | 4.1 | C14H28O2 | Tetradecanoic acid | Lipids: Fatty Acyls | 1.66 | 2.62 | 1.58 | 0.3336 | 0.4891 | 0.4644 | 1.36 | 0.5792 | 1.13 | 0.99 | 1.53 | 0.8049 | 0.9785 | 0.5982 | 0.94 | 1.01 | 0.91 | 0.9007 | 0.9885 | 0.8587 | 0.71 | 0.81 | 0.3994 | 0.6026 |
| 310.2872 | 3.9 | C20H38O2 | [FA (20:1)] 11Z-eicosenoic acid | Lipids: Fatty Acyls | 1.63 | 0.85 | 1.31 | 0.2282 | 0.7210 | 0.5184 | 1.17 | 0.5640 | 1.28 | 1.38 | 1.13 | 0.5549 | 0.3382 | 0.7246 | 0.88 | 1.19 | 0.78 | 0.6808 | 0.6977 | 0.5937 | 0.76 | 0.66 | 0.4772 | 0.3282 |
| 254.2249 | 4.0 | C16H30O2 | FA(16:1) | Lipids: Fatty Acyls | 1.65 | 0.97 | 1.04 | 0.2836 | 0.9523 | 0.9327 | 1.02 | 0.9286 | 1.12 | 1.26 | 1.24 | 0.7448 | 0.2856 | 0.6059 | 1.06 | 1.24 | 1.12 | 0.8081 | 0.5212 | 0.8040 | 0.67 | 0.72 | 0.3619 | 0.4270 |
| 278.2248 | 4.0 | C18H30O2 | [FA (18:3)] 9Z,12Z,15Z-octadecatrienoic acid | Lipids: Fatty Acyls | 1.54 | 0.98 | 1.29 | 0.4324 | 0.9725 | 0.5229 | 1.12 | 0.6131 | 1.12 | 1.12 | 1.19 | 0.6744 | 0.6548 | 0.7054 | 0.92 | 1.01 | 0.87 | 0.7311 | 0.9610 | 0.6034 | 0.64 | 0.69 | 0.3508 | 0.3878 |
| 256.2402 | 4.0 | C16H32O2 | FA(16:0) | Lipids: Fatty Acyls | 1.52 | 3.23 | 1.72 | 0.5025 | 0.4696 | 0.4250 | 1.08 | 0.9159 | 1.08 | 0.97 | 1.71 | 0.9069 | 0.9690 | 0.6052 | 0.92 | 1.10 | 0.90 | 0.9108 | 0.8940 | 0.8826 | 0.87 | 0.79 | 0.7918 | 0.6760 |
| 270.2195 | 4.1 | C16H30O3 | FA oxo(16:0) | Lipids: Fatty Acyls | 1.44 | 2.45 | 1.27 | 0.4412 | 0.5027 | 0.5916 | 1.28 | 0.6548 | 1.12 | 0.89 | 1.49 | 0.7923 | 0.7859 | 0.6005 | 0.89 | 0.95 | 0.81 | 0.7696 | 0.9101 | 0.5985 | 0.69 | 0.73 | 0.4144 | 0.4793 |
| 445.3192 | 4.7 | C27H43NO4 | N-oleoyl tyrosine | Lipids: Fatty Acyls | 1.41 | 1.35 | 1.11 | NA | NA | 0.9319 | 1.79 | NA | 1.32 | 0.67 | 0.91 | 0.6733 | 0.5947 | 0.8784 | 1.13 | 1.22 | 1.05 | 0.8925 | NA | 0.9582 | 0.33 | 0.68 | NA | NA |
| 282.2559 | 3.9 | C18H34O2 | [FA (18:1)] 9Z-octadecenoic acid | Lipids: Fatty Acyls | 1.36 | 1.17 | 1.20 | 0.4115 | 0.7683 | 0.6135 | 1.07 | 0.7470 | 1.15 | 1.02 | 1.09 | 0.6802 | 0.9399 | 0.8438 | 1.05 | 1.21 | 0.96 | 0.8724 | 0.6337 | 0.8917 | 0.70 | 0.77 | 0.3452 | 0.4493 |

| | | | | | | | | | | | | | | | | | | | | | | | | | | | | |
|---|---|---|---|---|---|---|---|---|---|---|---|---|---|---|---|---|---|---|---|---|---|---|---|---|---|---|---|---|
| 312.3031 | 3.9 | C25H40O2 | FA (20:0) | Lipids: Fatty Acyls | 1.41 | 1.98 | 1.55 | 0.4512 | 0.4960 | 0.3685 | 1.15 | 0.7481 | 1.06 | 0.99 | 1.51 | 0.8721 | 0.9826 | 0.5222 | 1.00 | 1.02 | 0.94 | 0.9953 | 0.9680 | 0.8775 | 0.92 | 0.81 | 0.7754 | 0.4858 |
| 574.4955 | 3.8 | C37H66O4 | Montecristin | Lipids: Fatty Acyls | 1.37 | 1.15 | 1.40 | 0.1834 | 0.6172 | 0.1566 | 1.01 | 0.9746 | 1.17 | 1.12 | 1.12 | 0.5568 | 0.7430 | 0.6697 | 0.69 | 0.74 | 0.89 | 0.4013 | 0.4991 | 0.7708 | 0.75 | 0.79 | 0.5326 | 0.5973 |
| 447.3351 | 4.6 | C27H45NO4 | N-stearoyl tyrosine | Lipids: Fatty Acyls | 1.33 | 1.04 | 0.83 | 0.7275 | 0.9599 | 0.7579 | 1.11 | 0.8259 | 1.21 | 0.89 | 1.08 | 0.7368 | 0.8432 | 0.8908 | 0.98 | 1.09 | 0.89 | 0.9716 | 0.8776 | 0.8269 | 0.56 | 0.70 | 0.4725 | 0.6161 |
| 272.2350 | 4.1 | C16H32O3 | FA hydroxy(16:0)] hexadecanoic acid | Lipids: Fatty Acyls | 1.33 | 2.27 | 1.56 | 0.4804 | 0.4996 | 0.4853 | 1.18 | 0.7175 | 1.44 | 1.02 | 1.57 | 0.4296 | 0.9514 | 0.5478 | 0.84 | 1.04 | 1.02 | 0.6013 | 0.9174 | 0.9625 | 0.82 | 0.74 | 0.6339 | 0.4763 |
| 242.2247 | 4.0 | C15H30O2 | FA methyl(14:0) | Lipids: Fatty Acyls | 1.32 | 1.21 | 1.26 | 0.4889 | 0.7507 | 0.5596 | 1.15 | 0.5150 | 1.35 | 1.06 | 1.57 | 0.4627 | 0.8459 | 0.3039 | 1.09 | 1.15 | 1.25 | 0.7828 | 0.6812 | 0.6158 | 0.73 | 0.79 | 0.4812 | 0.5907 |
| 342.2766 | 3.9 | C20H38O4 | 1,9S,11R,15S-tetrahydroxy-13E-prostaene | Lipids: Fatty Acyls | 1.28 | 1.69 | 1.23 | 0.6334 | 0.5907 | 0.6119 | 1.15 | 0.6443 | 1.01 | 0.74 | 1.23 | 0.9890 | 0.4542 | 0.7101 | 1.09 | 1.27 | 0.90 | 0.8105 | 0.5332 | 0.7697 | 0.78 | 0.83 | 0.4362 | 0.5333 |
| 172.1463 | 4.3 | C10H20O2 | Decanoic acid | Lipids: Fatty Acyls | 1.26 | 1.48 | 1.37 | 0.5724 | 0.6154 | 0.4519 | 1.11 | 0.6412 | 1.33 | 1.11 | 1.35 | 0.4586 | 0.6757 | 0.5518 | 1.02 | 1.03 | 0.98 | 0.9415 | 0.9257 | 0.9368 | 0.78 | 0.77 | 0.5438 | 0.5255 |
| 296.2712 | 3.9 | C19H36O2 | FA (19:1) | Lipids: Fatty Acyls | 1.24 | 0.50 | 1.26 | 0.5625 | 0.1047 | 0.5868 | 1.36 | 0.4590 | 1.39 | 1.03 | 1.10 | 0.2114 | 0.9200 | 0.8455 | 0.95 | 1.18 | 1.25 | 0.8832 | 0.6730 | 0.5717 | 0.94 | 1.03 | 0.8695 | 0.9382 |
| 423.3349 | 4.7 | C25H45NO4 | O-9Z,12Z-Hexadecadienoyl-R-carnitine | Lipids: Fatty Acyls | 1.23 | 0.87 | 0.63 | 0.7966 | 0.8402 | 0.5283 | 1.25 | 0.4878 | 1.36 | 0.91 | 1.06 | 0.6082 | 0.7974 | 0.8787 | 1.08 | 1.07 | 0.92 | 0.8134 | 0.8454 | 0.7833 | 0.63 | 0.66 | 0.6059 | 0.6394 |
| 284.2715 | 4.0 | C18H36O2 | Octadecanoic acid | Lipids: Fatty Acyls | 1.23 | 2.51 | 1.42 | 0.6907 | 0.4982 | 0.5228 | 0.91 | 0.8829 | 1.10 | 0.95 | 1.51 | 0.8620 | 0.9422 | 0.6381 | 1.02 | 1.13 | 0.99 | 0.9792 | 0.8353 | 0.9813 | 0.84 | 0.78 | 0.6984 | 0.5967 |
| 172.1100 | 4.9 | C9H16O3 | 9-Oxononanoic acid | Lipids: Fatty Acyls | 1.22 | 1.14 | 1.37 | 0.1660 | 0.3407 | 0.0337 | 1.03 | 0.7914 | 0.92 | 0.96 | 0.82 | 0.7211 | 0.8663 | 0.1778 | 0.99 | 1.03 | 0.93 | 0.9695 | 0.8740 | 0.6558 | 1.02 | 1.04 | 0.9199 | 0.8761 |
| 399.3349 | 4.7 | C23H45NO4 | O-Palmitoyl-R-carnitine | Lipids: Fatty Acyls | 1.15 | 1.00 | 0.73 | 0.8508 | 0.9959 | 0.6146 | 1.18 | 0.5652 | 1.46 | 0.88 | 1.01 | 0.5519 | 0.7311 | 0.9734 | 1.27 | 1.32 | 1.14 | 0.4676 | 0.5070 | 0.6744 | 0.64 | 0.64 | 0.5944 | 0.6019 |
| 158.1307 | 4.4 | C9H18O2 | FA methyl(8:0) | Lipids: Fatty Acyls | 1.18 | 1.24 | 1.69 | 0.6697 | 0.6660 | 0.3588 | 1.20 | 0.5832 | 1.06 | 0.99 | 1.09 | 0.8783 | 0.9791 | 0.8601 | 1.00 | 1.07 | 0.99 | 0.9860 | 0.8189 | 0.9719 | 0.90 | 0.89 | 0.8182 | 0.8010 |
| 270.2559 | 4.0 | C17H34O2 | FA (17:0) | Lipids: Fatty Acyls | 1.16 | 1.06 | 1.12 | 0.6619 | 0.9004 | 0.7348 | 1.06 | 0.8170 | 1.35 | 1.07 | 1.29 | 0.4198 | 0.8336 | 0.5041 | 1.11 | 1.24 | 1.09 | 0.7317 | 0.5691 | 0.8069 | 0.87 | 0.86 | 0.6972 | 0.6732 |
| 340.3340 | 3.9 | C22H44O2 | Docosanoic acid | Lipids: Fatty Acyls | 1.19 | 1.23 | 1.25 | 0.6158 | 0.6875 | 0.4506 | 1.06 | 0.8630 | 1.05 | 1.07 | 1.45 | 0.8371 | 0.8580 | 0.3715 | 0.95 | 0.93 | 1.15 | 0.8964 | 0.8697 | 0.7512 | 1.20 | 1.01 | 0.4685 | 0.9600 |
| 368.3654 | 3.8 | C24H48O2 | FA(24:0) | Lipids: Fatty Acyls | 1.18 | 1.26 | 1.32 | 0.5283 | 0.6398 | 0.4585 | 1.22 | 0.5760 | 1.06 | 1.12 | 2.62 | 0.8794 | 0.8266 | 0.2784 | 0.66 | 0.67 | 0.88 | 0.4121 | 0.3398 | 0.7230 | 1.04 | 0.80 | 0.9015 | 0.4733 |
| 214.1933 | 4.1 | C13H26O2 | FA methyl(12:0) dodecanoic acid | Lipids: Fatty Acyls | 1.09 | 0.94 | 1.17 | 0.7850 | 0.8900 | 0.6620 | 0.96 | 0.9000 | 1.30 | 1.21 | 1.31 | 0.5498 | 0.5329 | 0.4960 | 0.84 | 1.08 | 1.36 | 0.4687 | 0.7294 | 0.4239 | 0.73 | 0.76 | 0.4796 | 0.5417 |
| 224.1414 | 4.4 | C13H20O3 | [FA] Methyl jasmonate | Lipids: Fatty Acyls | 1.09 | 1.46 | 1.17 | 0.8732 | 0.6583 | 0.7908 | 1.32 | 0.6833 | 0.97 | 1.04 | 1.62 | 0.9459 | 0.9379 | 0.5790 | 0.87 | 0.96 | 0.85 | 0.7858 | 0.9415 | 0.7648 | 0.88 | 0.97 | 0.6849 | 0.9360 |
| 268.2404 | 4.0 | C17H32O2 | FA methyl(16:1) | Lipids: Fatty Acyls | 1.10 | 0.93 | 0.91 | 0.8031 | 0.9020 | 0.7922 | 1.19 | 0.5058 | 1.28 | 1.08 | 1.33 | 0.4943 | 0.7801 | 0.5225 | 1.01 | 1.18 | 1.07 | 0.9608 | 0.6164 | 0.8549 | 0.79 | 0.84 | 0.5464 | 0.6605 |
| 188.1411 | 4.6 | C10H20O3 | FA hydroxy(10:0) | Lipids: Fatty Acyls | 1.11 | 1.30 | 1.24 | 0.6550 | 0.3328 | 0.3732 | 0.92 | 0.7462 | 0.96 | 1.12 | 0.97 | 0.8722 | 0.6330 | 0.9043 | 1.13 | 0.96 | 1.09 | 0.6736 | 0.8940 | 0.7847 | 1.01 | 1.12 | 0.9657 | 0.6546 |
| 576.5109 | 3.8 | C37H68O4 | Cohibin C | Lipids: Fatty Acyls | 1.06 | 0.82 | 1.03 | 0.7039 | 0.2917 | 0.8628 | 1.05 | 0.8278 | 1.12 | 0.96 | 1.10 | 0.7333 | 0.9339 | 0.7818 | 0.64 | 0.60 | 0.82 | 0.3049 | 0.2661 | 0.6107 | 0.77 | 0.73 | 0.4726 | 0.4143 |
| 330.2564 | 3.9 | C22H34O2 | [FA (22:5)] 7Z,10Z,13Z,16Z,19Z-docosapentaenoic acid | Lipids: Fatty Acyls | 1.02 | 0.77 | 0.99 | 0.9341 | 0.4249 | 0.9823 | 1.19 | 0.5149 | 1.01 | 0.82 | 1.01 | 0.9783 | 0.5972 | 0.9836 | 1.14 | 1.20 | 1.07 | 0.7442 | 0.6780 | 0.8671 | 0.92 | 0.92 | 0.7720 | 0.8002 |
| 144.1150 | 4.6 | C8H16O2 | FA (8:0) octanoic acid | Lipids: Fatty Acyls | 1.01 | 1.62 | 1.08 | 0.9580 | 0.4803 | 0.7905 | 1.22 | 0.3279 | 0.90 | 0.98 | 0.98 | 0.7152 | 0.9445 | 0.9470 | 1.06 | 1.12 | 0.95 | 0.7731 | 0.6305 | 0.8094 | 0.82 | 0.87 | 0.3271 | 0.5216 |
| 186.1620 | 4.2 | C11H22O2 | [FA (11:0)] undecanoic acid | Lipids: Fatty Acyls | 0.97 | 1.50 | 1.11 | 0.9033 | 0.6216 | 0.7725 | 1.42 | 0.2638 | 1.07 | 0.91 | 1.10 | 0.8410 | 0.7382 | 0.8466 | 0.96 | 0.89 | 0.82 | 0.8579 | 0.6001 | 0.3345 | 0.74 | 0.71 | 0.3578 | 0.3032 |
| 130.0994 | 4.8 | C7H14O2 | FA methyl(6:0) | Lipids: Fatty Acyls | 1.01 | 1.41 | 1.08 | 0.9588 | 0.4608 | 0.6675 | 1.09 | 0.4813 | 0.95 | 1.06 | 0.91 | 0.8124 | 0.7636 | 0.6024 | 1.07 | 1.14 | 1.07 | 0.6537 | 0.3865 | 0.6522 | 1.00 | 1.00 | 0.9875 | 0.9866 |
| 298.2872 | 3.9 | C19H38O2 | FA methyl(18:0) | Lipids: Fatty Acyls | 0.99 | 0.95 | 1.17 | 0.9839 | 0.8935 | 0.5945 | 1.06 | 0.8766 | 1.17 | 1.07 | 1.34 | 0.6133 | 0.8452 | 0.4138 | 1.08 | 1.12 | 1.08 | 0.8291 | 0.7827 | 0.8468 | 0.98 | 0.89 | 0.9321 | 0.6494 |
| 116.0837 | 5.0 | C6H12O2 | Hexanoic acid | Lipids: Fatty Acyls | 0.99 | 1.32 | 1.10 | 0.9538 | 0.3739 | 0.5726 | 1.14 | 0.3596 | 0.91 | 0.98 | 0.93 | 0.5893 | 0.9060 | 0.6476 | 1.11 | 1.04 | 0.96 | 0.2440 | 0.6467 | 0.7621 | 1.10 | 1.11 | 0.5815 | 0.5304 |
| 222.1621 | 4.3 | C14H22O2 | 7E,9E,11-Dodecatrienyl acetate | Lipids: Fatty Acyls | 0.93 | 1.12 | 1.04 | 0.8287 | 0.8217 | 0.9013 | 1.22 | 0.5343 | 0.98 | 1.27 | 1.32 | 0.9318 | 0.5081 | 0.6082 | 0.87 | 0.80 | 0.64 | 0.6881 | 0.5244 | 0.2394 | 0.87 | 0.93 | 0.6107 | 0.7924 |
| 217.1314 | 9.9 | C10H19NO4 | O-Propanoylcarnitine | Lipids: Fatty Acyls | 0.98 | 1.11 | 1.00 | 0.9415 | 0.7794 | 0.9908 | 1.06 | 0.8845 | 0.89 | 1.00 | 0.95 | 0.7897 | 0.9969 | 0.9143 | 1.21 | 1.24 | 1.10 | 0.6955 | 0.6212 | 0.8435 | 1.10 | 1.11 | 0.8023 | 0.7821 |
| 156.1150 | 4.5 | C9H16O2 | FA methyl (8:1) | Lipids: Fatty Acyls | 0.93 | 1.16 | 1.04 | 0.7324 | 0.7069 | 0.8487 | 1.19 | 0.5039 | 1.12 | 1.05 | 1.28 | 0.5850 | 0.8077 | 0.3969 | 1.24 | 1.08 | 1.06 | 0.1768 | 0.7065 | 0.6780 | 0.86 | 0.97 | 0.5065 | 0.8740 |
| 130.0630 | 5.0 | C6H10O3 | [FA oxo(6:0)] 2-oxo-hexanoic acid | Lipids: Fatty Acyls | 0.97 | 1.12 | 1.03 | 0.8890 | 0.5797 | 0.9070 | 0.98 | 0.9112 | 0.81 | 0.89 | 0.83 | 0.5373 | 0.6898 | 0.5040 | 1.07 | 1.01 | 0.88 | 0.8697 | 0.9855 | 0.7339 | 0.98 | 0.96 | 0.9425 | 0.8817 |
| 178.0300 | 7.7 | C6H10O4S | 3,3'-Thiobispropanoic acid | Lipids: Fatty Acyls | 0.91 | 1.04 | 0.95 | 0.6311 | 0.8956 | 0.7740 | 0.95 | 0.8979 | 0.68 | 1.06 | 0.93 | 0.3366 | 0.8887 | 0.8576 | 1.32 | 1.43 | 1.25 | 0.4477 | 0.3358 | 0.5460 | 1.34 | 1.35 | 0.2271 | 0.2436 |
| 242.1002 | 15.5 | C8H18O8 | D-erythro-D-galacto-octitol | Lipids: Fatty Acyls | 0.85 | 0.96 | 0.90 | 0.4082 | 0.8526 | 0.6114 | 0.98 | 0.9000 | 0.89 | 0.97 | 0.99 | 0.6077 | 0.9094 | 0.9657 | 1.08 | 1.05 | 1.03 | 0.7307 | 0.8360 | 0.9089 | 1.13 | 1.06 | 0.6320 | 0.8298 |
| 215.1157 | 12.8 | C10H17NO4 | 2-Amino-9,10-epoxy-8-oxodecanoic acid | Lipids: Fatty Acyls | 0.84 | 1.10 | 1.03 | 0.7366 | 0.8657 | 0.9546 | 1.03 | 0.9493 | 0.82 | 0.95 | 0.94 | 0.6472 | 0.9058 | 0.8947 | 1.21 | 1.22 | 1.05 | 0.7050 | 0.6856 | 0.9261 | 0.93 | 0.96 | 0.8836 | 0.9474 |
| 239.1002 | 14.4 | C8H17NO7 | N-Gluconyl ethanolamine | Lipids: Fatty Acyls | 0.82 | 1.01 | 1.08 | 0.1246 | 0.9220 | 0.5281 | 1.01 | 0.9573 | 0.96 | 0.85 | 1.01 | 0.8383 | 0.4098 | 0.9168 | 0.99 | 1.03 | 0.94 | 0.9293 | 0.9063 | 0.7938 | 1.17 | 1.02 | 0.3207 | 0.9376 |
| 98.0367 | 13.8 | C5H6O2 | [FA (5:2)] 2,4-pentadienoic acid | Lipids: Fatty Acyls | 0.74 | 0.76 | 1.01 | 0.1940 | 0.4328 | 0.9794 | 0.85 | 0.2490 | 0.87 | 0.89 | 0.90 | 0.4724 | 0.4243 | 0.4251 | 1.09 | 1.16 | 1.08 | 0.5563 | 0.4400 | 0.5424 | 1.10 | 1.14 | 0.7004 | 0.6593 |
| 402.2255 | 4.0 | C20H34O8 | 5S-HETE di-endoperoxide | Lipids: Fatty Acyls | 0.35 | 0.12 | 0.49 | 0.1832 | NA | NA | 0.38 | 0.2815 | 1.11 | 1.14 | 1.51 | 0.9001 | 0.8700 | NA | 0.83 | 1.38 | 1.81 | 0.7406 | 0.6042 | 0.2038 | 0.53 | 0.47 | 0.4867 | 0.4295 |
| 669.4368 | 7.8 | C68H126N2O23 | Ganglioside GA1 (d18:1/24:0) | Lipids: Gangliosides | 1.14 | 1.05 | 1.14 | 0.4656 | 0.7412 | 0.4168 | 1.09 | 0.8483 | 1.06 | 2.22 | 1.79 | 0.8973 | 0.2766 | 0.2714 | 0.79 | 0.57 | 0.44 | 0.6464 | 0.3793 | 0.1550 | 0.59 | 0.55 | 0.4042 | 0.3765 |
| 602.5267 | 3.8 | C39H70O4 | 1-(14-methyl-pentadecanoyl)-2-(8-[3]-ladderane-octanyl)-sn-glycerol | Lipids: Glycerolipids | 0.98 | 0.72 | 0.92 | 0.9124 | 0.2110 | 0.6731 | 1.13 | 0.6225 | 1.17 | 1.05 | 1.17 | 0.6277 | 0.9098 | 0.6703 | 0.71 | 0.73 | 0.98 | 0.3946 | 0.4618 | 0.9667 | 0.91 | 0.90 | 0.7466 | 0.7324 |
| 266.0642 | 11.6 | C9H14O9 | Monoglyceride citrate | Lipids: Glycerolipids | 0.91 | 1.08 | 0.92 | 0.5701 | 0.5090 | 0.5712 | 1.07 | 0.5074 | 0.83 | 0.90 | 0.87 | 0.1652 | 0.4473 | 0.3610 | 0.99 | 1.15 | 1.05 | 0.9308 | 0.1095 | 0.4780 | 0.85 | 0.93 | 0.0904 | 0.3680 |

| | | | | | | | | | | | | | | | | | | | | | | | | | | | | | | |
|---|---|---|---|---|---|---|---|---|---|---|---|---|---|---|---|---|---|---|---|---|---|---|---|---|---|---|---|---|---|---|
| 725.5352 | 4.0 | C41H76NO7P | PE(P-36:3) | Lipids: Glycerophospholipids | 1.32 | 1.10 | 1.17 | 0.0698 | 0.5993 | 0.2547 | 1.07 | 0.7519 | 1.06 | 1.10 | 1.21 | 0.7932 | 0.7404 | 0.3985 | 0.92 | 0.84 | 0.98 | 0.7097 | 0.4947 | 0.9367 | 1.02 | 0.94 | 0.9108 | 0.7917 |
| 831.5059 | 3.8 | C46H74NO10P | PS(40:8) | Lipids: Glycerophospholipids | 1.26 | 0.79 | 1.10 | 0.6571 | 0.6515 | 0.8485 | 1.16 | 0.7930 | 0.88 | 0.85 | 1.24 | 0.8390 | 0.7961 | 0.7447 | 0.69 | 0.98 | 0.98 | 0.6134 | 0.9774 | 0.9783 | 0.87 | 0.89 | 0.8283 | 0.8455 |
| 713.4990 | 3.9 | C39H72NO8P | PE(34:3) | Lipids: Glycerophospholipids | 1.32 | 1.12 | 1.09 | 0.0893 | 0.7098 | 0.6127 | 1.19 | 0.2874 | 1.12 | 0.96 | 0.88 | 0.4197 | 0.7503 | 0.3738 | 0.78 | 0.80 | 0.76 | 0.1795 | 0.1745 | 0.1377 | 1.01 | 0.90 | 0.9699 | 0.6262 |
| 757.5625 | 4.1 | C42H80NO8P | PC(34:2) | Lipids: Glycerophospholipids | 1.30 | 0.89 | 1.25 | 0.1711 | 0.6088 | 0.2848 | 1.00 | 0.9995 | 1.10 | 1.12 | 1.33 | 0.7314 | 0.7255 | 0.3591 | 0.75 | 0.76 | 0.82 | 0.3625 | 0.4029 | 0.5699 | 1.13 | 1.00 | 0.7267 | 0.9926 |
| 809.5930 | 4.0 | C46H84NO8P | PC(38:4) | Lipids: Glycerophospholipids | 1.23 | 0.78 | 1.19 | 0.2869 | 0.4975 | 0.4197 | 1.05 | 0.8635 | 1.30 | 1.26 | 1.46 | 0.4022 | 0.5584 | 0.3075 | 0.74 | 0.68 | 0.79 | 0.3296 | 0.2597 | 0.4323 | 1.08 | 0.99 | 0.8142 | 0.9818 |
| 805.5625 | 4.0 | C46H80NO8P | PC(38:6) | Lipids: Glycerophospholipids | 1.21 | 0.77 | 1.20 | 0.3695 | 0.4317 | 0.4525 | 1.20 | 0.4270 | 1.23 | 1.07 | 1.21 | 0.4850 | 0.7911 | 0.4430 | 0.74 | 0.82 | 0.85 | 0.3043 | 0.5163 | 0.5494 | 1.13 | 1.06 | 0.7070 | 0.8578 |
| 785.5929 | 4.1 | C44H84NO8P | PC(36:2) | Lipids: Glycerophospholipids | 1.20 | 0.83 | 1.10 | 0.3404 | 0.5235 | 0.6498 | 1.21 | 0.5962 | 1.29 | 1.28 | 1.44 | 0.3408 | 0.5143 | 0.2493 | 0.75 | 0.66 | 0.84 | 0.3466 | 0.2515 | 0.5446 | 1.20 | 1.05 | 0.5749 | 0.8622 |
| 835.6078 | 4.0 | C48H86NO8P | PC(40:5) | Lipids: Glycerophospholipids | 1.21 | 0.76 | 1.15 | 0.3121 | 0.4708 | 0.4758 | 1.05 | 0.8669 | 1.32 | 1.21 | 1.49 | 0.4038 | 0.6241 | 0.2026 | 0.72 | 0.68 | 0.81 | 0.3458 | 0.3075 | 0.5154 | 1.07 | 0.99 | 0.8165 | 0.9634 |
| 749.5361 | 4.0 | C43H76NO7P | PE(P-38:5) | Lipids: Glycerophospholipids | 1.22 | 0.89 | 0.94 | 0.3381 | 0.7047 | 0.7824 | 1.05 | 0.8212 | 1.08 | 1.08 | 1.31 | 0.7207 | 0.7507 | 0.2487 | 0.82 | 0.82 | 0.83 | 0.5981 | 0.5977 | 0.5804 | 1.14 | 1.11 | 0.7392 | 0.7896 |
| 807.5055 | 3.8 | C44H74NO10P | PS(38:6) | Lipids: Glycerophospholipids | 1.18 | 0.90 | 1.10 | 0.5461 | 0.7046 | 0.7260 | 1.11 | 0.7719 | 1.03 | 1.00 | 1.31 | 0.9444 | 0.9992 | 0.5598 | 0.69 | 0.85 | 0.93 | 0.4734 | 0.7383 | 0.8875 | 0.96 | 0.84 | 0.9212 | 0.6833 |
| 507.3329 | 4.9 | C25H50NO7P | LysoPE(20:1) | Lipids: Glycerophospholipids | 1.20 | 1.27 | 1.03 | 0.4431 | 0.6598 | 0.8967 | 0.98 | 0.9145 | 0.88 | 0.69 | 0.90 | 0.5696 | 0.1387 | 0.5619 | 1.40 | 1.31 | 1.10 | 0.2659 | 0.3622 | 0.6348 | 0.91 | 1.07 | 0.6635 | 0.7570 |
| 785.5202 | 3.8 | C42H76NO10P | PS(36:3) | Lipids: Glycerophospholipids | 1.18 | 0.92 | 1.16 | 0.6400 | 0.7870 | 0.6231 | 1.16 | 0.6841 | 1.24 | 1.08 | 1.40 | 0.6376 | 0.8769 | 0.5035 | 0.63 | 0.73 | 0.82 | 0.4674 | 0.6082 | 0.7511 | 0.92 | 0.91 | 0.8685 | 0.8449 |
| 746.5103 | 3.7 | C40H75O10P | PG(34:2) | Lipids: Glycerophospholipids | 1.18 | 0.81 | 1.16 | 0.4274 | 0.4612 | 0.5489 | 1.08 | 0.7871 | 1.05 | 0.98 | 1.02 | 0.8950 | 0.9706 | 0.9681 | 0.58 | 0.82 | 0.70 | 0.3820 | 0.7102 | 0.5475 | 0.78 | 0.76 | 0.5632 | 0.5397 |
| 781.5622 | 4.1 | C44H80NO8P | PC(36:4) | Lipids: Glycerophospholipids | 1.16 | 0.76 | 1.11 | 0.6169 | 0.4791 | 0.7383 | 1.13 | 0.7499 | 1.18 | 1.11 | 1.27 | 0.6178 | 0.7883 | 0.5136 | 0.77 | 0.78 | 0.87 | 0.4656 | 0.5092 | 0.7118 | 1.08 | 0.98 | 0.8380 | 0.9538 |
| 543.3319 | 4.7 | C28H50NO7P | LysoPC(20:4) | Lipids: Glycerophospholipids | 1.15 | 0.56 | 0.96 | 0.6518 | 0.1467 | 0.8350 | 1.19 | 0.5137 | 0.92 | 0.84 | 0.89 | 0.8181 | 0.6162 | 0.7614 | 1.39 | 1.53 | 1.16 | 0.3670 | 0.3918 | 0.7002 | 0.73 | 0.79 | 0.3404 | 0.4866 |
| 467.3018 | 4.9 | C22H46NO7P | [LysoPC(14:0)] 1-tetradecanoyl-sn-glycero-3-phosphocholine | Lipids: Glycerophospholipids | 1.17 | 0.96 | 1.00 | 0.3426 | 0.8615 | 0.9884 | 1.13 | 0.4310 | 0.97 | 0.77 | 0.92 | 0.8943 | 0.1394 | 0.6724 | 1.13 | 1.20 | 1.01 | 0.6204 | 0.4565 | 0.9758 | 0.80 | 0.92 | 0.3161 | 0.7008 |
| 479.3378 | 4.8 | C24H50NO6P | LysoPC(O-16:1) | Lipids: Glycerophospholipids | 1.15 | 1.37 | 0.90 | 0.6289 | 0.6280 | 0.6819 | 1.15 | 0.2131 | 1.04 | 0.82 | 0.86 | 0.8862 | 0.3748 | 0.5164 | 1.32 | 1.33 | 1.06 | 0.2346 | 0.2674 | 0.7284 | 0.73 | 0.74 | 0.4386 | 0.4692 |
| 858.5259 | 3.8 | C45H79O13P | PI(36:4) | Lipids: Glycerophospholipids | 1.15 | 0.89 | 1.09 | 0.4909 | 0.6145 | 0.7207 | 1.02 | 0.9472 | 1.20 | 1.15 | 1.31 | 0.5591 | 0.7287 | 0.4298 | 0.76 | 0.86 | 0.97 | 0.5020 | 0.7230 | 0.9431 | 0.90 | 0.82 | 0.7564 | 0.5296 |
| 884.5419 | 3.8 | C47H81O13P | PI(38:5) | Lipids: Glycerophospholipids | 1.14 | 0.93 | 1.15 | 0.5579 | 0.7589 | 0.5285 | 1.08 | 0.6801 | 1.14 | 1.08 | 1.24 | 0.6949 | 0.8375 | 0.4656 | 0.67 | 0.70 | 0.80 | 0.3925 | 0.4468 | 0.6217 | 0.95 | 0.95 | 0.8685 | 0.8586 |
| 672.4734 | 3.8 | C37H69O8P | PA(34:2) | Lipids: Glycerophospholipids | 1.16 | 0.86 | 1.18 | 0.4301 | 0.5247 | 0.3358 | 1.09 | 0.7939 | 1.24 | 1.18 | 1.38 | 0.6155 | 0.7416 | 0.4253 | 0.59 | 0.67 | 0.85 | 0.3827 | 0.4862 | 0.7641 | 1.05 | 0.94 | 0.8976 | 0.8807 |
| 831.5777 | 4.0 | C48H82NO8P | PC(40:7) | Lipids: Glycerophospholipids | 1.15 | 0.60 | 1.19 | 0.5051 | 0.2281 | 0.4261 | 1.09 | 0.6872 | 1.16 | 1.00 | 1.45 | 0.6628 | 0.9914 | 0.2446 | 0.85 | 0.74 | 0.85 | 0.6095 | 0.3862 | 0.6147 | 1.16 | 1.07 | 0.6651 | 0.8416 |
| 783.5055 | 3.8 | C42H74NO10P | PS(36:4) | Lipids: Glycerophospholipids | 1.14 | 0.86 | 1.13 | 0.4473 | 0.4480 | 0.5898 | 1.18 | 0.5380 | 1.24 | 1.14 | 1.33 | 0.5824 | 0.7609 | 0.4522 | 0.67 | 0.75 | 0.91 | 0.4799 | 0.6047 | 0.8641 | 0.92 | 0.89 | 0.8194 | 0.7334 |
| 759.5773 | 4.1 | C42H82NO8P | PC(34:1) | Lipids: Glycerophospholipids | 1.13 | 0.81 | 1.14 | 0.5513 | 0.4279 | 0.5535 | 0.98 | 0.9402 | 1.17 | 1.17 | 1.39 | 0.5140 | 0.6246 | 0.2865 | 0.74 | 0.70 | 0.87 | 0.2861 | 0.2509 | 0.6012 | 1.11 | 0.98 | 0.7376 | 0.9407 |
| 493.3173 | 4.9 | C24H48NO7P | LysoPC(16:1) | Lipids: Glycerophospholipids | 1.12 | 1.08 | 0.99 | 0.6036 | 0.8756 | 0.9415 | 1.04 | 0.7937 | 1.01 | 0.81 | 0.84 | 0.9494 | 0.3994 | 0.4629 | 1.20 | 1.20 | 0.89 | 0.4877 | 0.5403 | 0.5999 | 0.85 | 0.89 | 0.5352 | 0.6713 |
| 773.5921 | 4.1 | C43H84NO8P | PE(38:1) | Lipids: Glycerophospholipids | 1.12 | 0.77 | 0.86 | 0.4884 | 0.2913 | 0.5010 | 1.01 | 0.9343 | 1.25 | 1.18 | 1.16 | 0.4106 | 0.5719 | 0.5562 | 0.77 | 0.70 | 0.98 | 0.3238 | 0.2672 | 0.9250 | 1.15 | 0.85 | 0.6353 | 0.6229 |
| 763.5151 | 4.0 | C43H74NO8P | PE(38:6) | Lipids: Glycerophospholipids | 1.12 | 0.88 | 1.13 | 0.7153 | 0.7533 | 0.6799 | 1.07 | 0.8130 | 0.97 | 0.98 | 1.22 | 0.9030 | 0.9575 | 0.5195 | 0.83 | 0.88 | 0.86 | 0.6556 | 0.7576 | 0.7034 | 1.02 | 1.03 | 0.9427 | 0.9259 |
| 787.5366 | 3.8 | C42H78NO10P | PS(36:2) | Lipids: Glycerophospholipids | 1.13 | 0.82 | 1.04 | 0.8166 | 0.6740 | 0.9332 | 0.98 | 0.9712 | 1.18 | 1.23 | 1.45 | 0.7855 | 0.7489 | 0.5590 | 0.58 | 0.57 | 0.90 | 0.4457 | 0.4388 | 0.8759 | 0.91 | 0.82 | 0.8793 | 0.7250 |
| 501.2852 | 4.7 | C25H44NO7P | LysoPE(20:4) | Lipids: Glycerophospholipids | 1.11 | 1.16 | 1.00 | 0.7906 | 0.6876 | 0.9914 | 1.23 | 0.4620 | 1.04 | 0.77 | 0.97 | 0.9021 | 0.4460 | 0.9374 | 1.16 | 1.18 | 0.99 | 0.6578 | 0.6680 | 0.9743 | 0.87 | 0.96 | 0.6626 | 0.9053 |
| 814.4797 | 7.6 | C46H71O10P | PG(18:4(6Z,9Z,12Z,15Z)/22:6(4Z,7Z,10Z,13Z,16Z,19Z)) | Lipids: Glycerophospholipids | 1.16 | 1.09 | 1.27 | 0.7162 | 0.8550 | 0.5993 | 1.11 | 0.8228 | 1.51 | 1.52 | 2.01 | 0.3096 | 0.5330 | 0.1830 | 0.50 | 0.37 | 0.77 | 0.2560 | 0.1740 | 0.5914 | 1.14 | 0.92 | 0.7698 | 0.8423 |
| 833.5936 | 4.0 | C48H84NO8P | PC(40:6) | Lipids: Glycerophospholipids | 1.10 | 0.77 | 1.07 | 0.6572 | 0.5089 | 0.7507 | 1.15 | 0.4757 | 1.44 | 1.19 | 1.44 | 0.2963 | 0.6372 | 0.2013 | 0.76 | 0.69 | 0.84 | 0.4456 | 0.3572 | 0.5870 | 1.13 | 1.08 | 0.7090 | 0.8130 |
| 723.5206 | 4.0 | C41H74NO7P | PE(P-36:4) | Lipids: Glycerophospholipids | 1.11 | 0.93 | 0.92 | 0.5450 | 0.7492 | 0.6824 | 1.05 | 0.7419 | 1.16 | 1.05 | 1.25 | 0.3429 | 0.8124 | 0.1760 | 0.82 | 0.86 | 0.82 | 0.4053 | 0.5496 | 0.4091 | 0.97 | 0.98 | 0.9098 | 0.9476 |

| | | | | | | | | | | | | | | | | | | | | | | | | | | | | | | |
|---|---|---|---|---|---|---|---|---|---|---|---|---|---|---|---|---|---|---|---|---|---|---|---|---|---|---|---|---|---|---|
| 521.3483 | 4.8 | C26H52NO7P | LysoPC(18:1) | Lipids: Glycerophospholipids | 1.10 | 1.36 | 0.86 | 0.7622 | 0.6488 | 0.5442 | 1.06 | 0.8151 | 1.04 | 0.83 | 0.89 | 0.8898 | 0.5039 | 0.6472 | 1.18 | 1.23 | 1.02 | 0.5536 | 0.5487 | 0.9438 | 0.78 | 0.76 | 0.5741 | 0.5541 |
| 772.5253 | 3.7 | C42H77O10P | PG(36:3) | Lipids: Glycerophospholipids | 1.10 | 0.78 | 1.10 | 0.7144 | 0.4083 | 0.7248 | 1.18 | 0.5730 | 1.04 | 0.87 | 1.07 | 0.9126 | 0.7549 | 0.8463 | 0.64 | 0.74 | 0.66 | 0.4653 | 0.6017 | 0.5083 | 0.98 | 0.94 | 0.9621 | 0.8906 |
| 809.5211 | 3.8 | C44H76NO10P | PS(38:5) | Lipids: Glycerophospholipids | 1.07 | 0.78 | 0.99 | 0.7127 | 0.3307 | 0.9777 | 1.02 | 0.9273 | 1.17 | 1.09 | 1.31 | 0.6286 | 0.8265 | 0.3987 | 0.66 | 0.74 | 0.87 | 0.4008 | 0.5139 | 0.7665 | 0.87 | 0.84 | 0.6796 | 0.5982 |
| 731.5460 | 4.1 | C40H78NO8P | PC(32:1) | Lipids: Glycerophospholipids | 1.07 | 0.73 | 1.08 | 0.7908 | 0.3028 | 0.7685 | 1.08 | 0.7481 | 1.10 | 1.08 | 1.26 | 0.7295 | 0.8008 | 0.4907 | 0.73 | 0.72 | 0.82 | 0.3020 | 0.2811 | 0.4971 | 0.96 | 0.92 | 0.8867 | 0.7679 |
| 537.3795 | 4.7 | C27H56NO7P | LysoPE(22:0) | Lipids: Glycerophospholipids | 1.10 | 1.24 | 0.77 | 0.7835 | 0.6919 | 0.3209 | 0.80 | 0.3036 | 1.07 | 1.15 | 0.88 | 0.8117 | 0.6652 | 0.5885 | 1.17 | 1.16 | 0.95 | 0.5260 | 0.5913 | 0.8681 | 0.69 | 0.83 | 0.3419 | 0.6013 |
| 811.5367 | 3.8 | C44H78NO10P | PS(38:4) | Lipids: Glycerophospholipids | 1.06 | 0.76 | 1.02 | 0.7714 | 0.1671 | 0.9415 | 0.95 | 0.8715 | 1.30 | 1.23 | 1.42 | 0.4482 | 0.6640 | 0.3573 | 0.64 | 0.60 | 0.90 | 0.3628 | 0.3195 | 0.8223 | 0.91 | 0.84 | 0.7849 | 0.6065 |
| 509.3487 | 4.8 | C25H52NO7P | LysoPE(20:0) | Lipids: Glycerophospholipids | 1.06 | 1.38 | 0.88 | 0.8315 | 0.6438 | 0.6281 | 1.07 | 0.6261 | 1.10 | 0.85 | 0.89 | 0.6547 | 0.4718 | 0.5660 | 1.54 | 1.51 | 1.27 | 0.1915 | 0.2750 | 0.4679 | 0.66 | 0.73 | 0.3623 | 0.4774 |
| 781.4905 | 3.8 | C42H72NO10P | PS(36:5) | Lipids: Glycerophospholipids | 1.05 | 0.74 | 0.96 | 0.8205 | 0.3279 | 0.8687 | 1.06 | 0.8050 | 0.88 | 0.75 | 0.88 | 0.5880 | 0.3397 | 0.6158 | 0.88 | 1.05 | 0.83 | 0.5648 | 0.8501 | 0.4343 | 1.00 | 0.97 | 0.9878 | 0.9117 |
| 410.2429 | 4.8 | C19H39O7P | LysoPA(16:0) | Lipids: Glycerophospholipids | 1.06 | 1.60 | 0.92 | 0.7008 | 0.5443 | 0.6850 | 1.05 | 0.8456 | 1.02 | 0.89 | 0.82 | 0.9126 | 0.6330 | 0.4198 | 1.14 | 1.25 | 1.07 | 0.6078 | 0.4045 | 0.7640 | 0.83 | 0.92 | 0.4599 | 0.7397 |
| 551.3950 | 4.6 | C28H58NO7P | LysoPC(20:0) | Lipids: Glycerophospholipids | 1.06 | 1.30 | 0.83 | 0.8314 | 0.6736 | 0.4194 | 1.06 | 0.6949 | 0.95 | 0.73 | 0.85 | 0.8203 | 0.2660 | 0.4934 | 1.03 | 1.06 | 0.93 | 0.8857 | 0.8403 | 0.7510 | 0.73 | 0.74 | 0.3476 | 0.3520 |
| 436.2586 | 4.8 | C21H41O7P | PA(18:1(9Z)/0:0) | Lipids: Glycerophospholipids | 1.05 | 1.52 | 0.88 | 0.7243 | 0.6052 | 0.4544 | 1.00 | 0.9983 | 0.99 | 0.90 | 0.80 | 0.9314 | 0.6375 | 0.3056 | 1.19 | 1.39 | 1.02 | 0.5436 | 0.3101 | 0.9482 | 0.74 | 0.85 | 0.3086 | 0.5310 |
| 751.5522 | 4.0 | C43H78NO7P | PE(O-38:5) | Lipids: Glycerophospholipids | 1.07 | 0.87 | 1.01 | 0.5296 | 0.4967 | 0.9071 | 0.95 | 0.6238 | 1.05 | 1.08 | 1.12 | 0.7514 | 0.6904 | 0.6631 | 0.82 | 0.76 | 0.88 | 0.3836 | 0.3284 | 0.5053 | 1.01 | 0.95 | 0.9666 | 0.7958 |
| 696.4733 | 3.8 | C39H69O8P | PA(36:4) | Lipids: Glycerophospholipids | 1.06 | 0.73 | 1.08 | 0.6813 | 0.2532 | 0.6061 | 1.08 | 0.8056 | 1.14 | 1.17 | 1.24 | 0.7117 | 0.7550 | 0.5796 | 0.69 | 0.71 | 0.95 | 0.4674 | 0.5207 | 0.9250 | 0.95 | 0.89 | 0.9051 | 0.7918 |
| 747.5191 | 3.9 | C43H74NO7P | PE(P-38:6) | Lipids: Glycerophospholipids | 1.05 | 0.86 | 1.03 | 0.8350 | 0.6408 | 0.9071 | 1.14 | 0.6970 | 0.97 | 1.03 | 1.24 | 0.9202 | 0.9253 | 0.4351 | 0.81 | 0.88 | 0.83 | 0.6513 | 0.7724 | 0.6683 | 0.95 | 0.85 | 0.8799 | 0.6725 |
| 465.3219 | 4.9 | C23H48NO6P | LysoPE(18:1) | Lipids: Glycerophospholipids | 1.04 | 1.35 | 0.89 | 0.8614 | 0.5484 | 0.4891 | 1.07 | 0.6114 | 1.01 | 0.84 | 0.94 | 0.9490 | 0.3297 | 0.7370 | 1.06 | 1.07 | 0.90 | 0.7247 | 0.7076 | 0.5331 | 0.82 | 0.90 | 0.4010 | 0.6643 |
| 739.5138 | 4.0 | C41H74NO8P | PE(36:4) | Lipids: Glycerophospholipids | 1.06 | 0.94 | 1.09 | 0.7114 | 0.7574 | 0.4792 | 1.06 | 0.7188 | 1.05 | 1.07 | 1.26 | 0.7526 | 0.7487 | 0.1567 | 0.87 | 0.88 | 0.95 | 0.5136 | 0.5698 | 0.7998 | 0.94 | 0.99 | 0.7766 | 0.9597 |
| 495.3327 | 4.8 | C24H50NO7P | LysoPC(16:0) | Lipids: Glycerophospholipids | 1.04 | 1.34 | 0.88 | 0.8776 | 0.6132 | 0.4920 | 1.03 | 0.8551 | 1.05 | 0.89 | 0.86 | 0.7804 | 0.5469 | 0.4950 | 1.12 | 1.20 | 0.94 | 0.5233 | 0.4009 | 0.7428 | 0.76 | 0.83 | 0.3784 | 0.5377 |
| 674.4885 | 3.8 | C37H71O8P | PA(34:1) | Lipids: Glycerophospholipids | 1.06 | 0.81 | 1.05 | 0.5191 | 0.2338 | 0.6790 | 0.90 | 0.7244 | 1.31 | 1.23 | 1.39 | 0.5051 | 0.6677 | 0.3798 | 0.61 | 0.65 | 0.94 | 0.3022 | 0.3772 | 0.8751 | 0.98 | 0.90 | 0.9662 | 0.7523 |
| 525.2850 | 4.6 | C27H44NO7P | LysoPE(22:6) | Lipids: Glycerophospholipids | 1.02 | 0.74 | 1.02 | 0.9489 | 0.4115 | 0.9201 | 1.33 | 0.0842 | 0.99 | 0.81 | 0.93 | 0.9687 | 0.4666 | 0.8139 | 1.16 | 1.30 | 1.02 | 0.4980 | 0.4678 | 0.9263 | 0.84 | 1.10 | 0.6370 | 0.7778 |
| 743.5463 | 4.0 | C41H78NO8P | PE(36:2) | Lipids: Glycerophospholipids | 1.04 | 0.77 | 1.11 | 0.8466 | 0.4492 | 0.5831 | 1.03 | 0.9006 | 1.16 | 1.31 | 1.27 | 0.6314 | 0.4511 | 0.4609 | 1.02 | 0.94 | 1.01 | 0.9317 | 0.7996 | 0.9541 | 0.97 | 1.05 | 0.9150 | 0.8626 |
| 774.5406 | 3.8 | C42H79O10P | PG(36:2) | Lipids: Glycerophospholipids | 1.01 | 0.73 | 1.05 | 0.9568 | 0.3760 | 0.8527 | 1.19 | 0.5027 | 1.13 | 0.95 | 1.12 | 0.7530 | 0.9157 | 0.7616 | 0.63 | 0.69 | 0.79 | 0.4111 | 0.5045 | 0.6529 | 0.93 | 0.86 | 0.8805 | 0.7413 |
| 493.3532 | 4.7 | C25H52NO6P | LysoPE(P-20:0) | Lipids: Glycerophospholipids | 1.03 | 1.36 | 0.80 | 0.9201 | 0.6554 | 0.4774 | 1.17 | 0.0854 | 1.11 | 0.92 | 1.08 | 0.6288 | 0.6741 | 0.6461 | 1.03 | 1.16 | 0.94 | 0.8795 | 0.5979 | 0.7440 | 0.74 | 0.73 | 0.4778 | 0.4593 |
| 481.3533 | 4.9 | C24H52NO6P | [LysoPC(16:2)] 1-hexadecyl-sn-glycero-3-phosphocholine | Lipids: Glycerophospholipids | 1.02 | 1.29 | 0.90 | 0.9490 | 0.6738 | 0.5902 | 1.01 | 0.9606 | 0.94 | 0.82 | 0.91 | 0.7278 | 0.2375 | 0.6170 | 1.31 | 1.20 | 0.99 | 0.1802 | 0.4776 | 0.9470 | 0.78 | 0.83 | 0.3592 | 0.4687 |
| 855.5046 | 3.8 | C48H74NO10P | PS(42:10) | Lipids: Glycerophospholipids | 0.99 | 0.67 | 0.91 | 0.9651 | 0.2191 | 0.7227 | 1.01 | 0.9885 | 1.13 | 0.99 | 1.15 | 0.7384 | 0.9828 | 0.6819 | 0.78 | 1.02 | 1.09 | 0.5375 | 0.9633 | 0.8626 | 0.81 | 0.85 | 0.6471 | 0.7252 |
| 698.4884 | 3.8 | C39H71O8P | PA(36:3) | Lipids: Glycerophospholipids | 1.02 | 0.83 | 1.24 | 0.8922 | 0.3962 | 0.1936 | 1.15 | 0.6155 | 1.19 | 1.16 | 1.27 | 0.6303 | 0.7920 | 0.4931 | 0.66 | 0.73 | 0.90 | 0.4451 | 0.5712 | 0.8401 | 0.95 | 0.85 | 0.9066 | 0.6661 |
| 777.5679 | 3.9 | C45H80NO7P | PE(P-40:5) | Lipids: Glycerophospholipids | 1.03 | 0.89 | 1.06 | 0.8894 | 0.6988 | 0.7889 | 0.95 | 0.8369 | 1.15 | 1.24 | 1.43 | 0.6262 | 0.5046 | 0.2925 | 0.74 | 0.69 | 0.80 | 0.3696 | 0.3759 | 0.4816 | 1.11 | 1.01 | 0.6212 | 0.9661 |
| 789.5510 | 3.8 | C42H80NO10P | PS(36:1) | Lipids: Glycerophospholipids | 1.02 | 0.81 | 0.98 | 0.9048 | 0.1135 | 0.8820 | 0.90 | 0.6946 | 1.26 | 1.16 | 1.31 | 0.4949 | 0.6885 | 0.4364 | 0.62 | 0.55 | 0.81 | 0.2750 | 0.2172 | 0.6069 | 0.90 | 0.86 | 0.7134 | 0.5403 |
| 825.5523 | 3.8 | C45H80NO10P | PS(39:4) | Lipids: Glycerophospholipids | 1.00 | 0.76 | 0.98 | 0.9895 | 0.4384 | 0.9631 | 0.97 | 0.9544 | 1.21 | 1.15 | 1.41 | 0.6922 | 0.8209 | 0.5330 | 0.66 | 0.64 | 0.94 | 0.4851 | 0.4588 | 0.9173 | 0.82 | 0.71 | 0.7119 | 0.5351 |
| 886.5571 | 3.8 | C47H83O13P | PI(38:4) | Lipids: Glycerophospholipids | 1.01 | 0.78 | 0.93 | 0.9733 | 0.1982 | 0.6994 | 0.97 | 0.8927 | 1.33 | 1.23 | 1.46 | 0.3379 | 0.5867 | 0.2116 | 0.65 | 0.60 | 0.89 | 0.2637 | 0.2127 | 0.7407 | 0.95 | 0.94 | 0.8420 | 0.8166 |
| 509.3848 | 4.8 | C26H56NO6P | LysoPC(O-18:0) | Lipids: Glycerophospholipids | 1.01 | 1.14 | 0.84 | 0.9700 | 0.8411 | 0.4547 | 0.87 | 0.5303 | 1.35 | 1.02 | 1.08 | 0.3183 | 0.9392 | 0.7664 | 1.13 | 1.12 | 1.10 | 0.6069 | 0.6514 | 0.7248 | 0.67 | 0.70 | 0.3550 | 0.4134 |
| 779.5833 | 4.0 | C45H82NO7P | PE(P-40:4) | Lipids: Glycerophospholipids | 1.03 | 0.89 | 1.08 | 0.8445 | 0.5753 | 0.4818 | 0.79 | 0.0717 | 1.25 | 0.95 | 1.26 | 0.3397 | 0.8769 | 0.3562 | 1.05 | 0.81 | 0.98 | 0.8314 | 0.3805 | 0.9493 | 1.07 | 1.01 | 0.7632 | 0.9667 |
| 700.5038 | 3.8 | C39H73O8P | PA(36:2) | Lipids: Glycerophospholipids | 0.99 | 0.91 | 1.17 | 0.9776 | 0.6849 | 0.4034 | 0.92 | 0.8072 | 1.22 | 1.26 | 1.43 | 0.5634 | 0.6647 | 0.3646 | 0.67 | 0.65 | 0.97 | 0.4330 | 0.4191 | 0.9538 | 0.93 | 0.85 | 0.8480 | 0.6620 |

| | | | | | | | | | | | | | | | | | | | | | | | | | | | | | |
|---|---|---|---|---|---|---|---|---|---|---|---|---|---|---|---|---|---|---|---|---|---|---|---|---|---|---|---|---|---|
| 481.3169 | 4.9 | C23H48NO7P | LysoPE(18:0) | Lipids: Glycerophospholipids | 0.98 | 1.20 | 0.92 | 0.9268 | 0.7275 | 0.6785 | 1.00 | 0.9831 | 1.00 | 0.85 | 0.90 | 0.9897 | 0.4444 | 0.6106 | 1.22 | 1.22 | 1.04 | 0.3815 | 0.4618 | 0.8724 | 0.90 | 0.82 | 0.7411 | 0.6190 |
| 519.3323 | 4.8 | C26H50NO7P | PC(18:2) | Lipids: Glycerophospholipids | 0.98 | 1.03 | 0.88 | 0.9421 | 0.9456 | 0.6386 | 1.13 | 0.4727 | 0.98 | 0.97 | 0.86 | 0.9570 | 0.9262 | 0.5763 | 1.21 | 1.21 | 0.96 | 0.5797 | 0.6152 | 0.8722 | 0.63 | 0.75 | 0.2400 | 0.4354 |
| 773.5350 | 3.9 | C45H76NO7P | PE(P-40:7) | Lipids: Glycerophospholipids | 0.99 | 0.80 | 1.00 | 0.9851 | 0.6755 | 0.9954 | 1.12 | 0.6989 | 0.97 | 1.11 | 1.20 | 0.9303 | 0.7872 | 0.5581 | 1.01 | 0.97 | 0.89 | 0.9924 | 0.9489 | 0.8170 | 1.10 | 1.05 | 0.7296 | 0.9089 |
| 862.5565 | 3.8 | C45H83O13P | PI(36:2) | Lipids: Glycerophospholipids | 0.98 | 0.90 | 1.02 | 0.8116 | 0.3957 | 0.8663 | 1.00 | 0.9907 | 1.27 | 1.19 | 1.50 | 0.4233 | 0.6675 | 0.2448 | 0.71 | 0.73 | 0.95 | 0.3034 | 0.3590 | 0.8927 | 0.98 | 0.86 | 0.9475 | 0.5622 |
| 864.5714 | 3.8 | C45H85O13P | PI(36:1) | Lipids: Glycerophospholipids | 0.99 | 0.85 | 0.88 | 0.9146 | 0.1542 | 0.3018 | 0.95 | 0.7790 | 1.34 | 1.15 | 1.38 | 0.3405 | 0.6870 | 0.3300 | 0.65 | 0.56 | 0.75 | 0.2163 | 0.1368 | 0.4017 | 0.89 | 0.87 | 0.6177 | 0.5032 |
| 523.3639 | 4.7 | C26H54NO7P | LysoPC(18:0) | Lipids: Glycerophospholipids | 0.99 | 1.35 | 0.73 | 0.9731 | 0.6722 | 0.2512 | 0.92 | 0.7416 | 1.14 | 0.90 | 0.85 | 0.6365 | 0.6917 | 0.4999 | 1.19 | 1.09 | 1.03 | 0.5387 | 0.7655 | 0.9183 | 0.69 | 0.68 | 0.3571 | 0.3550 |
| 761.5215 | 3.8 | C40H76NO10P | PS(34:1) | Lipids: Glycerophospholipids | 0.98 | 0.83 | 1.11 | 0.8101 | 0.0446 | 0.4347 | 0.97 | 0.7975 | 1.11 | 1.11 | 1.22 | 0.6835 | 0.7404 | 0.4608 | 0.67 | 0.70 | 0.89 | 0.1990 | 0.2719 | 0.6642 | 0.90 | 0.92 | 0.6768 | 0.7586 |
| 689.4995 | 3.8 | C37H72NO8P | PE(32:1) | Lipids: Glycerophospholipids | 0.98 | 0.94 | 1.08 | 0.9268 | 0.7776 | 0.6907 | 1.15 | 0.6672 | 1.04 | 1.04 | 1.03 | 0.8955 | 0.9143 | 0.9120 | 0.86 | 0.84 | 0.96 | 0.6591 | 0.6529 | 0.9263 | 1.00 | 0.88 | 0.9907 | 0.7071 |
| 727.5529 | 4.1 | C41H78NO7P | PE(P-36:2) | Lipids: Glycerophospholipids | 0.96 | 0.89 | 1.12 | 0.8750 | 0.6644 | 0.5920 | 0.88 | 0.6588 | 1.17 | 1.32 | 1.38 | 0.5748 | 0.4552 | 0.2956 | 0.86 | 1.03 | 1.10 | 0.5793 | 0.9458 | 0.7776 | 1.15 | 1.00 | 0.7113 | 0.9980 |
| 702.5196 | 3.8 | C39H75O8P | PA(36:1) | Lipids: Glycerophospholipids | 0.96 | 0.79 | 0.97 | 0.8383 | 0.1532 | 0.8265 | 0.90 | 0.7453 | 1.19 | 1.02 | 1.27 | 0.6276 | 0.9673 | 0.5490 | 0.56 | 0.55 | 0.84 | 0.1854 | 0.2140 | 0.6727 | 0.89 | 0.84 | 0.7464 | 0.6133 |
| 438.2740 | 4.7 | C21H43O7P | LysoPA(18:0) | Lipids: Glycerophospholipids | 0.95 | 1.61 | 0.74 | 0.8339 | 0.6004 | 0.2032 | 0.84 | 0.6153 | 1.18 | 0.97 | 0.88 | 0.5269 | 0.9069 | 0.6237 | 1.09 | 1.13 | 1.04 | 0.7887 | 0.7325 | 0.9170 | 0.72 | 0.73 | 0.3610 | 0.3787 |
| 837.5507 | 3.8 | C46H80NO10P | PS(40:5) | Lipids: Glycerophospholipids | 0.93 | 0.86 | 1.04 | 0.5298 | 0.2273 | 0.6646 | 0.98 | 0.9301 | 1.26 | 1.13 | 1.22 | 0.2888 | 0.6693 | 0.3679 | 0.83 | 0.75 | 0.97 | 0.4867 | 0.3431 | 0.9002 | 1.00 | 0.91 | 0.9953 | 0.6379 |
| 691.5149 | 3.8 | C37H74NO8P | PE(32:0) | Lipids: Glycerophospholipids | 0.95 | 0.92 | 0.96 | 0.7559 | 0.6035 | 0.7370 | 1.08 | 0.7686 | 1.18 | 1.09 | 1.10 | 0.5886 | 0.8214 | 0.7932 | 0.74 | 0.75 | 0.91 | 0.3646 | 0.4469 | 0.7682 | 1.06 | 1.00 | 0.8485 | 0.9999 |
| 775.5505 | 3.9 | C45H78NO7P | PE(P-40:6) | Lipids: Glycerophospholipids | 0.93 | 0.88 | 1.06 | 0.7695 | 0.7013 | 0.8131 | 0.92 | 0.7567 | 1.08 | 1.20 | 1.26 | 0.8198 | 0.6282 | 0.5941 | 0.85 | 0.73 | 0.92 | 0.6877 | 0.4941 | 0.7931 | 1.18 | 1.03 | 0.5288 | 0.9165 |
| 747.5769 | 4.1 | C41H82NO8P | PE(36:0) | Lipids: Glycerophospholipids | 0.92 | 0.87 | 1.05 | 0.5893 | 0.6627 | 0.7659 | 1.03 | 0.8421 | 1.30 | 1.04 | 1.27 | 0.2365 | 0.8293 | 0.2213 | 0.75 | 0.61 | 0.75 | 0.2153 | 0.0841 | 0.3413 | 1.01 | 1.14 | 0.9713 | 0.4606 |
| 715.5155 | 4.0 | C39H74NO8P | PE(34:2) | Lipids: Glycerophospholipids | 0.93 | 0.97 | 1.17 | 0.6756 | 0.8948 | 0.3508 | 0.98 | 0.9060 | 1.06 | 1.06 | 1.08 | 0.7698 | 0.8347 | 0.7571 | 0.87 | 0.80 | 0.85 | 0.6286 | 0.4337 | 0.5420 | 0.86 | 0.91 | 0.6110 | 0.7601 |
| 748.5246 | 3.8 | C40H77O10P | PG(34:1) | Lipids: Glycerophospholipids | 0.87 | 0.70 | 0.99 | 0.6331 | 0.3141 | 0.9692 | 1.09 | 0.7571 | 1.04 | 0.90 | 1.07 | 0.9181 | 0.8059 | 0.8595 | 0.60 | 0.75 | 0.79 | 0.3489 | 0.5657 | 0.6233 | 0.84 | 0.72 | 0.6733 | 0.4444 |
| 701.5372 | 4.1 | C39H76NO7P | PE(P-34:1) | Lipids: Glycerophospholipids | 0.88 | 0.84 | 0.93 | 0.3429 | 0.2966 | 0.5625 | 0.92 | 0.6461 | 1.32 | 1.18 | 1.57 | 0.0875 | 0.3986 | 0.1607 | 0.93 | 0.82 | 0.98 | 0.7366 | 0.3028 | 0.9156 | 1.05 | 1.15 | 0.7903 | 0.2629 |
| 717.5310 | 4.0 | C39H76NO8P | PE(34:1) | Lipids: Glycerophospholipids | 0.90 | 0.86 | 0.95 | 0.6326 | 0.5777 | 0.8149 | 0.79 | 0.3593 | 1.14 | 1.22 | 1.23 | 0.5964 | 0.5107 | 0.4802 | 0.95 | 0.81 | 0.94 | 0.8330 | 0.4275 | 0.8041 | 0.95 | 0.95 | 0.8209 | 0.8646 |
| 733.5622 | 4.1 | C40H80NO8P | PC(32:0) | Lipids: Glycerophospholipids | 0.89 | 0.79 | 0.97 | 0.6127 | 0.4075 | 0.8765 | 0.82 | 0.4500 | 1.32 | 1.23 | 1.32 | 0.1175 | 0.2053 | 0.1835 | 0.81 | 0.62 | 0.91 | 0.5638 | 0.2314 | 0.7670 | 1.19 | 1.03 | 0.4496 | 0.8938 |
| 451.3066 | 4.9 | C22H46NO6P | PC(14:1) | Lipids: Glycerophospholipids | 0.87 | 1.08 | 0.77 | 0.4882 | 0.8511 | 0.2898 | 1.01 | 0.9524 | 0.91 | 0.77 | 0.88 | 0.5165 | 0.1463 | 0.5084 | 1.29 | 1.30 | 1.03 | 0.1644 | 0.1292 | 0.7564 | 0.88 | 0.93 | 0.5708 | 0.7394 |
| 705.5302 | 4.2 | C38H76NO8P | PC(30:0) | Lipids: Glycerophospholipids | 0.87 | 0.72 | 0.92 | 0.5430 | 0.3174 | 0.6907 | 0.83 | 0.6040 | 1.16 | 1.09 | 1.26 | 0.5378 | 0.6557 | 0.3376 | 0.94 | 0.76 | 0.91 | 0.8499 | 0.2648 | 0.7454 | 1.15 | 1.14 | 0.5548 | 0.5217 |
| 669.4364 | 7.7 | C36H64NO8P | PE(31:4) | Lipids: Glycerophospholipids | 0.84 | 0.97 | 0.96 | 0.1719 | 0.7939 | 0.6571 | 0.97 | 0.7942 | 1.10 | 1.35 | 1.31 | 0.7269 | 0.3356 | 0.3216 | 0.78 | 0.64 | 0.89 | 0.5040 | 0.3222 | 0.6537 | 0.97 | 0.83 | 0.9182 | 0.5577 |
| 745.5611 | 4.0 | C41H80NO8P | PE(36:1) | Lipids: Glycerophospholipids | 0.80 | 0.86 | 0.83 | 0.2616 | 0.3834 | 0.3387 | 0.76 | 0.1988 | 1.23 | 1.18 | 1.12 | 0.4003 | 0.5777 | 0.6598 | 0.99 | 0.76 | 0.91 | 0.9822 | 0.3598 | 0.7810 | 0.94 | 1.04 | 0.7793 | 0.8869 |
| 763.5358 | 3.8 | C40H78NO10P | PS(34:0) | Lipids: Glycerophospholipids | 0.75 | 0.78 | 0.91 | 0.4940 | 0.5983 | 0.8400 | 0.88 | 0.6454 | 0.98 | 0.98 | 0.95 | 0.9197 | 0.9566 | 0.8835 | 0.94 | 0.93 | 1.11 | 0.7827 | 0.7971 | 0.6623 | 1.02 | 0.95 | 0.9156 | 0.8487 |
| 783.5770 | 4.6 | C44H82NO8P | PC(36:3) | Lipids: Glycerophospholipids | 0.67 | 0.63 | 0.97 | 0.3561 | 0.3274 | 0.9358 | 1.27 | 0.3361 | 1.30 | 1.14 | 1.46 | 0.5046 | 0.7777 | 0.1952 | 0.70 | 0.74 | 0.87 | 0.3204 | 0.3819 | 0.6938 | 0.85 | 0.78 | 0.7366 | 0.6397 |
| 655.4213 | 5.0 | C35H62NO8P | PE(12:0/18:4(6Z,9Z,12Z, 15Z)) | Lipids: Glycerophospholipids | 0.65 | 1.37 | 0.63 | 0.5289 | 0.5883 | 0.5338 | 0.73 | 0.6320 | 1.07 | 1.10 | 0.92 | 0.9151 | 0.8825 | 0.9039 | 0.96 | 1.12 | 1.24 | 0.9537 | 0.8613 | 0.6734 | 0.88 | 0.97 | 0.8475 | 0.9551 |
| 483.2613 | 7.7 | C47H84O16P2 | PIP(38:4) | Lipids: Glycerophospholipids | 0.64 | 0.62 | 0.69 | 0.3744 | 0.3340 | 0.4474 | 0.74 | 0.4183 | 1.40 | 1.33 | 1.19 | 0.2662 | 0.4566 | 0.5844 | 0.77 | 0.62 | 0.87 | 0.4471 | 0.2102 | 0.6359 | 1.23 | 1.08 | 0.7110 | 0.8451 |
| 525.3069 | 4.3 | C24H48NO9P | PS(18:0) | Lipids: Glycerophospholipids | 0.63 | 0.80 | 0.71 | 0.1127 | 0.3241 | 0.1691 | 0.69 | 0.4378 | 0.96 | 0.97 | 0.70 | 0.8733 | 0.9215 | 0.0855 | 1.16 | 1.20 | 0.96 | 0.6359 | 0.6154 | 0.9092 | 0.94 | 0.94 | 0.8682 | 0.8568 |
| 268.1679 | 4.2 | C15H24O4 | Bisacurone epoxide | Lipids: Prenols | 1.02 | 0.75 | 1.11 | 0.9027 | 0.4988 | 0.5359 | 0.72 | 0.3773 | 1.85 | 0.88 | 1.23 | 0.4589 | 0.7305 | 0.6221 | 1.05 | 1.13 | 1.10 | 0.8381 | 0.7238 | 0.8283 | 1.09 | 0.86 | 0.7820 | 0.6840 |
| 861.6181 | 7.6 | C46H87NO13 | Lactosylceramide(d18 | Lipids: Sphingolipids | 2.50 | 3.32 | 4.71 | 0.4674 | 0.2538 | 0.1146 | 1.27 | 0.6092 | 0.74 | 1.04 | 1.42 | 0.7280 | 0.9395 | 0.5640 | 0.99 | 0.76 | 1.14 | 0.9843 | 0.6587 | 0.7894 | 2.29 | 1.60 | 0.0700 | 0.3756 |
| 828.7092 | 7.6 | C48H97N2O6P | SM(d43:1) | Lipids: Sphingolipids | 1.48 | 0.63 | 1.50 | 0.4573 | 0.4905 | 0.4263 | 0.89 | 0.8244 | 4.02 | 3.16 | 4.52 | 0.3374 | 0.3342 | 0.2683 | 0.92 | 0.34 | 0.98 | 0.8788 | 0.1065 | 0.9721 | 0.85 | 0.69 | 0.8059 | 0.6489 |
| 229.2405 | 4.9 | C14H31NO | [SP (14:0)] 1-deoxy-tetradecasphinganine | Lipids: Sphingolipids | 1.27 | 1.05 | 0.95 | 0.3588 | 0.8918 | 0.8811 | 1.26 | 0.0208 | 0.72 | 0.69 | 0.71 | 0.3705 | 0.3218 | 0.3489 | 1.07 | 1.10 | 1.12 | 0.7049 | 0.6740 | 0.5860 | 0.86 | 1.17 | 0.6680 | 0.6579 |
| 786.6618 | 6.4 | C45H91N2O6P | SM(d40:1) | Lipids: Sphingolipids | 1.21 | 0.77 | 1.37 | 0.6835 | 0.6045 | 0.4813 | 1.01 | 0.9768 | 2.14 | 1.69 | 3.06 | 0.2793 | 0.4916 | 0.2206 | 0.67 | 0.38 | 0.82 | 0.4198 | 0.1438 | 0.6318 | 0.93 | 0.68 | 0.8999 | 0.5398 |
| 812.6775 | 4.8 | C47H93N2O6P | SM(d18:1/24:1(15Z)) | Lipids: Sphingolipids | 1.19 | 0.93 | 1.02 | 0.6238 | 0.8455 | 0.9493 | 0.86 | 0.5110 | 1.59 | 0.98 | 1.74 | 0.2199 | 0.9576 | 0.1402 | 0.49 | 0.53 | 0.53 | 0.0550 | 0.0696 | 0.0705 | 1.08 | 1.10 | 0.8353 | 0.7918 |

| | | | | | | | | | | | | | | | | | | | | | | | | | | | | | |
|---|---|---|---|---|---|---|---|---|---|---|---|---|---|---|---|---|---|---|---|---|---|---|---|---|---|---|---|---|---|
| 840.7087 | 5.0 | C49H97N2O6P | SM(d44:2) | Lipids: Sphingolipids | 1.16 | 0.71 | 1.02 | 0.6706 | 0.4286 | 0.9549 | 0.87 | 0.6281 | 1.81 | 1.60 | 2.01 | 0.2059 | 0.3572 | 0.1316 | 0.63 | 0.47 | 0.75 | 0.2492 | 0.0860 | 0.3177 | 0.96 | 0.80 | 0.8970 | 0.6076 |
| 299.2826 | 4.5 | C18H37NO2 | [SP] Sphing-4-enine | Lipids: Sphingolipids | 1.13 | 1.29 | 1.09 | 0.7551 | 0.5914 | 0.8146 | 0.99 | 0.9824 | 1.22 | 1.06 | 1.12 | 0.5104 | 0.8306 | 0.6792 | 0.95 | 0.95 | 0.85 | 0.8854 | 0.8929 | 0.7214 | 0.96 | 0.98 | 0.9074 | 0.9523 |
| 461.3353 | 4.7 | C24H47NO7 | Psychosine | Lipids: Sphingolipids | 1.09 | 1.20 | 0.91 | 0.8730 | 0.7724 | 0.8320 | 1.06 | 0.8105 | 1.38 | 1.12 | 1.05 | 0.4235 | 0.7072 | 0.8464 | 1.37 | 1.52 | 1.25 | 0.3593 | 0.2601 | 0.5240 | 0.76 | 0.86 | 0.6161 | 0.7689 |
| 800.6773 | 4.8 | C46H93N2O6P | SM(d41:1) | Lipids: Sphingolipids | 1.09 | 0.76 | 1.08 | 0.7462 | 0.3773 | 0.8177 | 0.94 | 0.8277 | 1.42 | 1.19 | 1.45 | 0.3541 | 0.6151 | 0.2558 | 0.78 | 0.57 | 0.88 | 0.4803 | 0.2178 | 0.6837 | 0.90 | 0.78 | 0.7597 | 0.5416 |
| 273.2668 | 5.3 | C16H35NO2 | Hexadecasphinganine | Lipids: Sphingolipids | 1.00 | 0.76 | 0.60 | 0.9971 | 0.6900 | 0.4344 | 1.29 | 0.1400 | 2.57 | 1.19 | 1.51 | 0.3971 | 0.4217 | 0.2310 | 0.91 | 0.96 | 0.79 | 0.4723 | 0.7773 | 0.1808 | 0.50 | 0.56 | 0.5433 | 0.5993 |
| 758.6305 | 4.7 | C43H87N2O6P | SM(d38:1) | Lipids: Sphingolipids | 1.06 | 0.90 | 0.99 | 0.5651 | 0.4133 | 0.9537 | 0.98 | 0.9263 | 1.50 | 1.23 | 1.66 | 0.2189 | 0.5456 | 0.1492 | 0.78 | 0.64 | 0.97 | 0.4551 | 0.2402 | 0.9168 | 1.04 | 0.94 | 0.8214 | 0.8012 |
| 798.6625 | 4.5 | C46H91N2O6P | SM(d41:2) | Lipids: Sphingolipids | 1.05 | 0.88 | 1.03 | 0.8040 | 0.3968 | 0.8292 | 1.02 | 0.9128 | 1.45 | 1.48 | 1.49 | 0.2293 | 0.2133 | 0.1288 | 0.81 | 0.72 | 0.93 | 0.2552 | 0.1885 | 0.6851 | 0.97 | 0.86 | 0.9067 | 0.5597 |
| 842.7229 | 5.1 | C49H99N2O6P | SM(d44:1) | Lipids: Sphingolipids | 1.04 | 0.84 | 1.08 | 0.8329 | 0.5249 | 0.7158 | 0.85 | 0.6711 | 1.37 | 1.42 | 1.93 | 0.5055 | 0.5307 | 0.1811 | 0.74 | 0.56 | 0.85 | 0.5568 | 0.3563 | 0.7300 | 0.82 | 0.68 | 0.5430 | 0.3473 |
| 672.5212 | 4.4 | C37H73N2O6P | SM(d32:2) | Lipids: Sphingolipids | 1.02 | 1.19 | 0.90 | 0.9344 | 0.6773 | 0.6158 | 1.00 | 0.9734 | 1.05 | 0.91 | 0.94 | 0.8090 | 0.6321 | 0.7968 | 1.02 | 1.29 | 1.02 | 0.8331 | 0.2835 | 0.8212 | 0.71 | 0.80 | 0.4238 | 0.5608 |
| 810.6625 | 4.3 | C47H91N2O6P | SM(d42:3) | Lipids: Sphingolipids | 1.04 | 0.92 | 1.01 | 0.8186 | 0.6308 | 0.9448 | 1.00 | 0.9869 | 1.25 | 1.23 | 1.46 | 0.2966 | 0.3687 | 0.0495 | 0.81 | 0.71 | 0.98 | 0.1970 | 0.1084 | 0.9008 | 0.95 | 0.99 | 0.8137 | 0.9587 |
| 756.6150 | 4.4 | C43H85N2O6P | SM(d38:2) | Lipids: Sphingolipids | 1.01 | 1.02 | 0.90 | 0.9557 | 0.9493 | 0.6184 | 1.04 | 0.8279 | 1.06 | 1.03 | 1.20 | 0.7326 | 0.8976 | 0.2921 | 0.81 | 0.81 | 1.02 | 0.4072 | 0.4391 | 0.9295 | 0.79 | 0.89 | 0.2652 | 0.5728 |
| 814.6921 | 5.1 | C47H95N2O6P | SM(d18:0/24:1(15Z)) | Lipids: Sphingolipids | 1.02 | 0.77 | 1.18 | 0.9420 | 0.3823 | 0.4705 | 1.05 | 0.8778 | 1.59 | 1.49 | 2.22 | 0.3201 | 0.4227 | 0.1809 | 0.87 | 0.66 | 0.94 | 0.7258 | 0.3905 | 0.8634 | 0.87 | 0.70 | 0.6849 | 0.3817 |
| 646.5053 | 4.5 | C35H71N2O6P | EPC(d33:1) | Lipids: Sphingolipids | 0.96 | 1.59 | 0.88 | 0.8658 | 0.5195 | 0.4577 | 0.94 | 0.7225 | 0.95 | 0.72 | 0.73 | 0.8183 | 0.1031 | 0.1111 | 1.19 | 1.25 | 1.01 | 0.2423 | 0.2949 | 0.9436 | 0.71 | 0.75 | 0.3685 | 0.4598 |
| 287.2824 | 4.6 | C17H37NO2 | [SP (17:0)] heptadecasphinganine | Lipids: Sphingolipids | 0.93 | 0.85 | 0.86 | 0.8696 | 0.7172 | 0.7297 | 0.97 | 0.8840 | 1.43 | 0.81 | 1.21 | 0.4072 | 0.4928 | 0.5544 | 0.97 | 0.88 | 0.85 | 0.8270 | 0.5255 | 0.3258 | 0.59 | 0.64 | 0.3966 | 0.4959 |
| 700.5524 | 4.4 | C39H77N2O6P | SM(d34:2) | Lipids: Sphingolipids | 0.95 | 1.20 | 0.91 | 0.7289 | 0.6134 | 0.4653 | 1.11 | 0.4507 | 0.88 | 0.82 | 0.92 | 0.3363 | 0.1560 | 0.5581 | 1.03 | 1.23 | 1.03 | 0.8005 | 0.2238 | 0.7884 | 0.74 | 0.81 | 0.3781 | 0.5190 |
| 379.2486 | 5.0 | C18H38NO5P | [SP] Sphing-4-enine-1-phosphate | Lipids: Sphingolipids | 0.95 | 0.94 | 0.91 | 0.7787 | 0.7959 | 0.5254 | 0.89 | 0.5624 | 1.00 | 0.86 | 0.92 | 0.9842 | 0.3765 | 0.6918 | 1.27 | 1.40 | 1.20 | 0.2557 | 0.2007 | 0.2735 | 1.01 | 0.99 | 0.9189 | 0.9567 |
| 784.6471 | 4.4 | C45H89N2O6P | SM(d40:2) | Lipids: Sphingolipids | 0.93 | 0.95 | 0.94 | 0.5958 | 0.6363 | 0.5194 | 0.96 | 0.8126 | 1.07 | 1.03 | 1.12 | 0.7106 | 0.8697 | 0.4716 | 0.79 | 0.73 | 0.87 | 0.2281 | 0.1655 | 0.3650 | 0.89 | 0.89 | 0.6142 | 0.6085 |
| 619.5907 | 3.9 | C40H77NO3 | Cer(d40:2) | Lipids: Sphingolipids | 0.92 | 0.63 | 0.73 | 0.6572 | 0.3471 | 0.2363 | 0.90 | 0.8438 | 1.49 | 1.31 | 1.49 | 0.4450 | 0.6690 | 0.5541 | 0.84 | 0.64 | 1.02 | 0.7773 | 0.5413 | 0.9726 | 1.01 | 0.90 | 0.9724 | 0.7544 |
| 674.5366 | 4.5 | C37H75N2O6P | SM(d32:1) | Lipids: Sphingolipids | 0.88 | 1.27 | 0.78 | 0.3450 | 0.5859 | 0.0666 | 0.92 | 0.5924 | 0.97 | 0.86 | 0.84 | 0.8123 | 0.2180 | 0.1494 | 1.11 | 1.11 | 1.08 | 0.5660 | 0.6064 | 0.7368 | 0.80 | 0.85 | 0.5031 | 0.6073 |
| 647.6213 | 3.9 | C42H81NO3 | [SP (24:0)] N-(15Z-tetracosenoyl)-sphing-4-enine | Lipids: Sphingolipids | 0.87 | 0.58 | 0.66 | 0.7271 | 0.3386 | 0.3893 | 0.80 | 0.7923 | 1.25 | 1.12 | 1.19 | 0.7557 | 0.8885 | 0.8572 | 0.95 | 0.92 | 0.94 | 0.9444 | 0.9152 | 0.9374 | 0.86 | 0.80 | 0.7405 | 0.6059 |
| 537.5122 | 3.9 | C34H67NO3 | [SP (16:0)] N-(hexadecanoyl)-sphing-4-enine | Lipids: Sphingolipids | 0.85 | 0.56 | 0.82 | 0.5809 | 0.1638 | 0.5268 | 1.03 | 0.9127 | 1.18 | 0.94 | 1.06 | 0.6009 | 0.8560 | 0.8836 | 0.84 | 0.81 | 0.98 | 0.6440 | 0.6544 | 0.9509 | 1.00 | 0.85 | 0.9867 | 0.6056 |
| 730.5997 | 4.5 | C41H83N2O6P | SM(d36:1) | Lipids: Sphingolipids | 0.83 | 0.97 | 0.81 | 0.2141 | 0.8986 | 0.1841 | 0.87 | 0.5877 | 1.25 | 1.10 | 1.13 | 0.1392 | 0.3393 | 0.3118 | 0.92 | 0.83 | 1.04 | 0.7544 | 0.4305 | 0.8989 | 0.95 | 0.90 | 0.8375 | 0.6293 |
| 688.5524 | 4.5 | C38H77N2O6P | SM(d33:1) | Lipids: Sphingolipids | 0.82 | 1.14 | 0.80 | 0.2444 | 0.6843 | 0.1691 | 0.87 | 0.5256 | 1.06 | 0.91 | 0.91 | 0.6132 | 0.2719 | 0.1790 | 1.09 | 1.11 | 1.09 | 0.6049 | 0.5071 | 0.6968 | 0.81 | 0.83 | 0.4918 | 0.5381 |
| 381.2647 | 5.0 | C18H40NO5P | [SP] Sphinganine-1-phosphate | Lipids: Sphingolipids | 0.81 | 0.67 | 0.88 | 0.6252 | 0.4454 | 0.7230 | 1.03 | 0.9447 | 1.57 | 1.08 | 1.14 | 0.3323 | 0.8833 | 0.7590 | 1.19 | 1.10 | 1.12 | 0.6229 | 0.7920 | 0.7060 | 0.89 | 1.01 | 0.8108 | 0.9818 |
| 668.4296 | 5.0 | C68H124N2O23 | GalNAcbeta1-3Galalpha1-4Galbeta1-4Glcbeta-Cer(d18:1/24:1(15Z)) | Lipids: Sphingolipids | 0.78 | 1.45 | 0.74 | 0.5367 | 0.5470 | 0.4511 | 0.74 | 0.4943 | 1.23 | 1.25 | 1.00 | 0.6600 | 0.6603 | 0.9995 | 0.85 | 0.80 | 1.03 | 0.6738 | 0.6128 | 0.9214 | 0.75 | 0.88 | 0.5197 | 0.7307 |
| 702.5679 | 4.4 | C39H79N2O6P | SM(d34:1) | Lipids: Sphingolipids | 0.72 | 1.10 | 0.75 | 0.1449 | 0.7900 | 0.1815 | 0.80 | 0.4649 | 1.10 | 0.99 | 0.92 | 0.5133 | 0.9109 | 0.2666 | 1.00 | 0.99 | 1.08 | 0.9873 | 0.9692 | 0.7998 | 0.89 | 0.91 | 0.7340 | 0.7643 |
| 716.5837 | 4.5 | C40H81N2O6P | SM(d35:1) | Lipids: Sphingolipids | 0.66 | 0.96 | 0.74 | 0.1195 | 0.8898 | 0.1225 | 0.90 | 0.6770 | 1.07 | 0.80 | 0.88 | 0.6418 | 0.3237 | 0.2355 | 0.98 | 0.96 | 1.08 | 0.9070 | 0.8226 | 0.7265 | 0.88 | 0.90 | 0.6416 | 0.6755 |
| 446.3761 | 4.0 | C29H50O3 | Nebrosteroid M | Lipids: Sterol lipids | 1.13 | 0.67 | 1.10 | 0.6686 | 0.3543 | 0.7856 | 1.28 | 0.4809 | 1.19 | 1.09 | 1.54 | 0.5793 | 0.8369 | 0.3493 | 0.88 | 0.98 | 0.93 | 0.7311 | 0.9625 | 0.8535 | 0.90 | 0.92 | 0.7176 | 0.7943 |
| 462.3712 | 4.0 | C29H50O4 | [ST hydroxy(3:2/3:0/3:0)] (5Z,7E)-(1R,2R,3R)-3-(hydroxy-propyl)-19-nor-9,10-seco-5,7-cholestadien-1,3,25-triol | Lipids: Sterol lipids | 1.11 | 0.63 | 0.95 | 0.7562 | 0.4040 | 0.8903 | 1.20 | 0.7407 | 1.11 | 1.04 | 0.95 | 0.7890 | 0.9407 | 0.9241 | 0.89 | 1.10 | 0.96 | 0.7823 | 0.8713 | 0.9306 | 0.95 | 1.13 | 0.8593 | 0.4428 |
| 878.7004 | 6.6 | C56H94O7 | 3-O-(6'-O-(13Z,16Z,19Z-docosatrienoyl)-beta-D-glucopyranosyl)-campest-5-en-3beta-ol | Lipids: Sterol lipids | 1.08 | 0.80 | 1.17 | 0.7318 | 0.4520 | 0.4343 | 0.99 | 0.9800 | 1.35 | 1.30 | 1.64 | 0.1336 | 0.3640 | 0.1275 | 0.91 | 0.52 | 0.97 | 0.8051 | 0.0954 | 0.9250 | 1.05 | 0.78 | 0.8443 | 0.4571 |
| 368.3444 | 3.8 | C27H44 | [ST] (5Z,7E)-9,10-seco-5,7,10(19)-cholestatriene | Lipids: Sterol lipids | 1.05 | 0.66 | 1.10 | 0.8441 | 0.2600 | 0.6793 | 1.12 | 0.7718 | 1.20 | 1.18 | 1.06 | 0.6387 | 0.6661 | 0.8731 | 0.70 | 0.72 | 0.99 | 0.5230 | 0.5429 | 0.9841 | 1.12 | 0.92 | 0.7988 | 0.8259 |
| 466.3116 | 3.7 | C27H46O4S | Cholesterolsulfate | Lipids: Sterol lipids | 1.00 | 1.00 | 1.00 | 0.9848 | 0.9931 | 0.9861 | 1.14 | 0.6874 | 1.09 | 1.05 | 1.23 | 0.8137 | 0.9202 | 0.5964 | 0.71 | 0.83 | 1.00 | 0.4897 | 0.6997 | 0.9996 | 0.82 | 0.81 | 0.6599 | 0.6472 |
| 195.0563 | 12.5 | C6H13NO4S | MES | Medium Component | 1.11 | 1.14 | 1.06 | 0.5533 | 0.5279 | 0.7291 | 1.09 | 0.7717 | 0.76 | 0.79 | 0.80 | 0.3915 | 0.4395 | 0.5150 | 0.98 | 1.07 | 0.95 | 0.9348 | 0.8023 | 0.8589 | 1.02 | 0.94 | 0.9412 | 0.8044 |
| 209.0721 | 11.2 | C7H15NO4S | MOPS | Medium Component | 1.08 | 1.07 | 1.02 | 0.5359 | 0.6030 | 0.8254 | 0.90 | 0.5707 | 0.93 | 0.95 | 0.93 | 0.7956 | 0.8562 | 0.7653 | 0.95 | 1.00 | 1.03 | 0.8259 | 0.9823 | 0.8836 | 1.03 | 0.99 | 0.9051 | 0.9619 |
| 354.0562 | 5.1 | C19H14O5S | Phenolsulfonphthalein | Medium Component | 1.01 | 0.94 | 1.03 | 0.9722 | 0.8538 | 0.9342 | 0.99 | 0.9392 | 0.84 | 1.17 | 1.08 | 0.3706 | 0.4322 | 0.6995 | 0.97 | 1.05 | 0.94 | 0.7759 | 0.4250 | 0.5102 | 1.10 | 1.01 | 0.7232 | 0.9732 |
| 238.0985 | 10.5 | C8H18N2O4S | HEPES | Medium Component | 0.93 | 0.97 | 0.79 | 0.8110 | 0.8938 | 0.5642 | 1.00 | 0.9918 | 0.83 | 0.92 | 0.82 | 0.4466 | 0.7129 | 0.3938 | 1.02 | 1.05 | 0.97 | 0.8526 | 0.7359 | 0.8263 | 1.03 | 1.03 | 0.8819 | 0.8479 |
| 151.0304 | 14.1 | C8H18N2O6S2 | PIPES | Medium Component | 0.61 | 0.97 | 0.74 | 0.1866 | 0.9339 | 0.3963 | 1.01 | 0.9722 | 0.88 | 1.05 | 0.86 | 0.4481 | 0.8175 | 0.5667 | 1.05 | 1.06 | 0.99 | 0.7305 | 0.7441 | 0.9708 | 1.13 | 1.15 | 0.5323 | 0.5351 |
| 191.0252 | 14.8 | C6H9NO4S | a Cysteine adduct | Medium Contaminant | 0.82 | 0.96 | 0.83 | 0.8398 | 0.9643 | 0.8442 | 0.74 | 0.7494 | 0.89 | 0.96 | 0.72 | 0.9105 | 0.9652 | 0.7332 | 0.80 | 0.94 | 0.90 | 0.8425 | 0.9605 | 0.9288 | 1.28 | 1.33 | 0.8453 | 0.8193 |
| 299.0769 | 14.9 | C9H18NO8P | D-4'-Phosphopantothenate | Metabolism of Cofactors and Vitamins | 1.80 | 1.45 | 1.22 | 0.1969 | 0.5472 | 0.7251 | 0.86 | 0.7058 | 0.87 | 1.05 | 0.81 | 0.6687 | 0.8809 | 0.6100 | 0.97 | 0.86 | 0.77 | 0.9236 | 0.6512 | 0.4847 | 0.77 | 0.88 | 0.3735 | 0.4971 |

| | | | | | | | | | | | | | | | | | | | | | | | | | | | | | |
|---|---|---|---|---|---|---|---|---|---|---|---|---|---|---|---|---|---|---|---|---|---|---|---|---|---|---|---|---|---|
| 225.0636 | 13.0 | C10H11NO5 | 4-Amino-4-deoxychorismate | Metabolism of Cofactors and Vitamins | 1.15 | 1.03 | 1.11 | 0.6547 | 0.9492 | 0.7748 | 0.85 | 0.6229 | 0.86 | 0.99 | 0.95 | 0.5012 | 0.9805 | 0.8557 | 1.03 | 1.02 | 1.07 | 0.8872 | 0.9089 | 0.7472 | 1.10 | 1.07 | 0.6826 | 0.7887 |
| 785.1577 | 11.4 | C27H33N9O15P2 | FAD | Metabolism of Cofactors and Vitamins | 1.03 | 1.27 | 0.94 | 0.8932 | 0.4052 | 0.8197 | 0.86 | 0.4905 | 0.93 | 0.95 | 0.96 | 0.7749 | 0.8464 | 0.8798 | 1.03 | 1.01 | 0.90 | 0.8887 | 0.9741 | 0.6521 | 1.07 | 1.08 | 0.7517 | 0.7198 |
| 144.0423 | 13.7 | C6H8O4 | 2,3-Dimethylmaleate | Metabolism of Cofactors and Vitamins | 0.97 | 1.05 | 1.03 | 0.8612 | 0.7914 | 0.8999 | 1.08 | 0.6913 | 0.86 | 0.88 | 0.86 | 0.3860 | 0.4929 | 0.4837 | 0.97 | 1.00 | 0.98 | 0.9119 | 0.9933 | 0.9580 | 1.11 | 1.12 | 0.5755 | 0.4441 |
| 239.1022 | 10.5 | C9H13N5O3 | Dihydrobiopterin | Metabolism of Cofactors and Vitamins | 0.95 | 0.97 | 0.90 | 0.8564 | 0.9133 | 0.7260 | 1.05 | 0.8312 | 0.93 | 0.95 | 0.86 | 0.7112 | 0.7747 | 0.4070 | 0.99 | 1.03 | 0.99 | 0.9533 | 0.8088 | 0.9480 | 0.97 | 1.06 | 0.8840 | 0.7187 |
| 334.0567 | 15.2 | C11H15N2O8P | Nicotinamide D-ribonucleotide | Metabolism of Cofactors and Vitamins | 0.97 | 1.08 | 0.98 | 0.7260 | 0.5754 | 0.8636 | 0.98 | 0.8767 | 0.91 | 1.02 | 0.98 | 0.5092 | 0.8835 | 0.9363 | 1.06 | 1.08 | 1.07 | 0.7576 | 0.6802 | 0.7273 | 1.10 | 1.10 | 0.4197 | 0.3492 |
| 249.0405 | 13.7 | C8H12NO6P | Pyridoxine phosphate | Metabolism of Cofactors and Vitamins | 0.96 | 1.08 | 0.98 | 0.8763 | 0.7557 | 0.9255 | 0.98 | 0.9247 | 0.95 | 0.98 | 0.96 | 0.8112 | 0.9352 | 0.8484 | 0.99 | 1.02 | 1.02 | 0.9869 | 0.9542 | 0.9569 | 1.06 | 1.07 | 0.9125 | 0.9002 |
| 115.0270 | 14.9 | C4H5NO3 | Maleamate | Metabolism of Cofactors and Vitamins | 0.95 | 1.08 | 1.02 | 0.7603 | 0.6964 | 0.9384 | 0.72 | 0.2424 | 0.95 | 1.01 | 0.79 | 0.7248 | 0.9663 | 0.4561 | 0.85 | 1.07 | 0.86 | 0.5297 | 0.6961 | 0.5172 | 0.96 | 1.16 | 0.8996 | 0.4512 |
| 244.0880 | 8.9 | C10H16N2O3S | Biotin | Metabolism of Cofactors and Vitamins | 0.92 | 0.99 | 0.86 | 0.5932 | 0.9463 | 0.3093 | 1.19 | 0.1435 | 0.85 | 0.89 | 0.76 | 0.3901 | 0.4011 | 0.0636 | 1.07 | 0.96 | 0.97 | 0.6383 | 0.7506 | 0.8198 | 0.90 | 0.93 | 0.4153 | 0.5208 |
| 180.0536 | 14.2 | C8H8N2O3 | Nicotinurate | Metabolism of Cofactors and Vitamins | 0.94 | 0.99 | 0.90 | 0.7470 | 0.9515 | 0.6099 | 0.93 | 0.5787 | 0.92 | 1.06 | 0.96 | 0.6128 | 0.7190 | 0.8202 | 1.01 | 1.05 | 1.07 | 0.9071 | 0.8300 | 0.5813 | 1.27 | 1.22 | 0.1631 | 0.3732 |
| 169.0739 | 8.2 | C8H11NO3 | Pyridoxine | Metabolism of Cofactors and Vitamins | 0.91 | 0.94 | 0.68 | 0.5083 | 0.6992 | 0.2644 | 1.09 | 0.1509 | 0.89 | 0.91 | 0.83 | 0.4691 | 0.3925 | 0.0598 | 1.08 | 1.08 | 1.06 | 0.5448 | 0.4962 | 0.7027 | 1.14 | 1.13 | 0.6971 | 0.7183 |
| 187.1210 | 11.8 | C9H17NO3 | 8-Amino-7-oxononanoate | Metabolism of Cofactors and Vitamins | 0.94 | 0.83 | 0.90 | 0.7927 | 0.5305 | 0.6725 | 1.04 | 0.8121 | 0.98 | 0.99 | 0.91 | 0.9440 | 0.9662 | 0.6257 | 1.01 | 1.00 | 1.01 | 0.9675 | 0.9993 | 0.9458 | 1.14 | 1.15 | 0.6718 | 0.6556 |
| 264.1046 | 20.0 | C12H16N4OS | Thiamin | Metabolism of Cofactors and Vitamins | 0.90 | 0.97 | 0.97 | 0.5884 | 0.9015 | 0.8929 | 1.00 | 0.9972 | 0.95 | 0.96 | 0.95 | 0.7491 | 0.7981 | 0.8173 | 1.12 | 1.11 | 1.02 | 0.5147 | 0.4804 | 0.8551 | 1.05 | 1.07 | 0.8093 | 0.7403 |
| 167.0582 | 8.2 | C8H9NO3 | Pyridoxal | Metabolism of Cofactors and Vitamins | 0.86 | 0.83 | 1.03 | 0.5763 | 0.6600 | 0.9360 | 1.15 | 0.6416 | 0.97 | 1.05 | 0.95 | 0.9162 | 0.8731 | 0.8699 | 1.09 | 1.13 | 1.15 | 0.8029 | 0.7249 | 0.6299 | 1.20 | 1.18 | 0.6036 | 0.6470 |
| 122.0480 | 7.7 | C6H6N2O | Nicotinamide | Metabolism of Cofactors and Vitamins | 0.78 | 1.38 | 0.83 | 0.3119 | 0.3463 | 0.4575 | 1.06 | 0.8178 | 0.72 | 0.88 | 0.71 | 0.0639 | 0.4592 | 0.1179 | 1.16 | 1.27 | 0.92 | 0.3314 | 0.2083 | 0.6068 | 0.97 | 1.14 | 0.8673 | 0.5813 |
| 443.0246 | 17.5 | C10H15N5O11P2 | GDP | Nucleotide Metabolism | 1.37 | 1.55 | 1.46 | 0.3781 | 0.1927 | 0.2886 | 0.98 | 0.9204 | 1.00 | 1.05 | 0.99 | 1.0000 | 0.8201 | 0.9529 | 1.13 | 1.03 | 1.11 | 0.5321 | 0.8642 | 0.5873 | 1.04 | 1.10 | 0.8794 | 0.6818 |
| 176.0433 | 16.4 | C5H8N2O5 | N-Carbamoyl-L-aspartate | Nucleotide Metabolism | 1.22 | 1.50 | 1.17 | 0.6657 | 0.5779 | 0.7189 | 0.92 | 0.9057 | 0.69 | 0.90 | 0.86 | 0.6102 | 0.8917 | 0.8510 | 0.90 | 0.91 | 0.92 | 0.8670 | 0.8910 | 0.8929 | 0.82 | 0.77 | 0.5138 | 0.3288 |
| 228.0859 | 13.3 | C8H12N4O4 | Decitabine | Nucleotide Metabolism | 1.13 | 0.83 | 0.87 | 0.4742 | 0.6084 | 0.6437 | 1.08 | 0.6894 | 0.79 | 0.95 | 0.89 | 0.2591 | 0.7031 | 0.3423 | 1.16 | 1.02 | 1.11 | 0.3197 | 0.9103 | 0.4415 | 1.06 | 1.18 | 0.8206 | 0.5161 |
| 463.0741 | 17.9 | C14H18N5O11P | N6-(1,2-Dicarboxyethyl)-AMP | Nucleotide Metabolism | 1.17 | 1.33 | 0.85 | 0.7218 | 0.4941 | 0.7780 | 0.75 | 0.3838 | 0.68 | 0.84 | 0.58 | 0.3838 | 0.7080 | 0.3485 | 0.59 | 0.71 | 0.78 | 0.2579 | 0.5593 | 0.5667 | 1.50 | 1.78 | 0.5314 | 0.1399 |
| 427.0294 | 16.0 | C10H15N5O10P2 | dGDP | Nucleotide Metabolism | 1.05 | 1.25 | 0.96 | 0.8341 | 0.3778 | 0.8449 | 0.97 | 0.9548 | 0.80 | 0.97 | 0.87 | 0.5930 | 0.9551 | 0.7925 | 1.08 | 1.12 | 1.04 | 0.8666 | 0.8177 | 0.9382 | 1.11 | 1.14 | 0.5926 | 0.3253 |
| 507.9789 | 17.4 | C10H15N4O14P3 | ITP | Nucleotide Metabolism | 1.04 | 1.47 | 1.01 | 0.9513 | 0.5659 | 0.9876 | 0.86 | 0.8684 | 0.74 | 1.00 | 0.91 | 0.7115 | 0.9999 | 0.9171 | 1.21 | 1.23 | 1.15 | 0.7804 | 0.7719 | 0.8433 | 1.17 | 1.19 | 0.7873 | 0.7528 |
| 482.9845 | 17.5 | C9H16N3O14P3 | CTP | Nucleotide Metabolism | 1.05 | 1.25 | 0.99 | 0.8493 | 0.3566 | 0.9782 | 0.92 | 0.6022 | 0.90 | 1.12 | 0.97 | 0.4908 | 0.7232 | 0.9073 | 1.33 | 1.46 | 1.17 | 0.4223 | 0.4517 | 0.6820 | 1.55 | 1.52 | 0.1504 | 0.0432 |
| 97.9673 | 17.5 | H2O4S | Sulfate | Nucleotide Metabolism | 1.03 | 1.04 | 1.00 | 0.8112 | 0.7542 | 0.9801 | 1.01 | 0.9461 | 0.95 | 1.01 | 0.87 | 0.7755 | 0.9670 | 0.4684 | 1.03 | 1.05 | 1.00 | 0.8422 | 0.7703 | 0.9757 | 1.06 | 1.05 | 0.7693 | 0.8155 |
| 491.0004 | 15.2 | C10H16N5O12P3 | dATP | Nucleotide Metabolism | 1.00 | 1.37 | 0.94 | 0.9891 | 0.4736 | 0.7169 | 0.96 | 0.9437 | 0.88 | 0.97 | 1.03 | 0.7849 | 0.9498 | 0.9580 | 0.94 | 0.91 | 0.94 | 0.9187 | 0.8737 | 0.9106 | 1.08 | 1.07 | 0.7064 | 0.6809 |
| 522.9908 | 18.6 | C10H16N5O14P3 | GTP | Nucleotide Metabolism | 1.02 | 1.28 | 0.93 | 0.9518 | 0.4041 | 0.8075 | 0.94 | 0.8516 | 0.75 | 0.91 | 0.82 | 0.4189 | 0.8374 | 0.6236 | 1.08 | 1.07 | 0.96 | 0.8451 | 0.8733 | 0.9242 | 0.93 | 1.06 | 0.7577 | 0.7880 |
| 347.0628 | 15.5 | C10H14N5O7P | dGMP | Nucleotide Metabolism | 1.00 | 2.19 | 0.89 | 0.9760 | 0.3334 | 0.4694 | 0.95 | 0.8254 | 0.97 | 0.98 | 0.93 | 0.8669 | 0.9354 | 0.7971 | 1.16 | 1.00 | 1.00 | 0.5555 | 0.9849 | 0.9871 | 1.15 | 1.15 | 0.3497 | 0.3354 |

| | | | | | | | | | | | | | | | | | | | | | | | | | | | | |
|---|---|---|---|---|---|---|---|---|---|---|---|---|---|---|---|---|---|---|---|---|---|---|---|---|---|---|---|---|
| 404.0023 | 16.1 | C9H14N2O12P2 | UDP | Nucleotide Metabolism | 0.97 | 1.13 | 1.04 | 0.8156 | 0.6323 | 0.7662 | 0.96 | 0.8195 | 0.92 | 1.03 | 0.97 | 0.6681 | 0.8574 | 0.9158 | 1.02 | 1.02 | 0.99 | 0.8015 | 0.8690 | 0.9609 | 1.07 | 1.09 | 0.7469 | 0.6817 |
| 128.0586 | 14.7 | C5H8N2O2 | 5,6-Dihydrothymine | Nucleotide Metabolism | 0.96 | 1.11 | 0.92 | 0.8935 | 0.7960 | 0.8303 | 0.93 | 0.8443 | 0.78 | 0.87 | 0.86 | 0.5667 | 0.7461 | 0.7226 | 1.09 | 1.09 | 1.10 | 0.8227 | 0.7994 | 0.8061 | 1.17 | 1.17 | 0.6061 | 0.6222 |
| 483.9686 | 17.3 | C9H15N2O15P3 | UTP | Nucleotide Metabolism | 0.97 | 1.05 | 0.97 | 0.8817 | 0.7788 | 0.8295 | 0.87 | 0.7225 | 0.76 | 0.97 | 0.93 | 0.4573 | 0.9445 | 0.8795 | 1.40 | 1.52 | 1.31 | 0.5131 | 0.5089 | 0.6475 | 1.40 | 1.53 | 0.1869 | 0.0211 |
| 428.0129 | 16.4 | C10H14N4O11P2 | IDP | Nucleotide Metabolism | 0.96 | 1.26 | 0.91 | 0.9346 | 0.6544 | 0.8294 | 0.83 | 0.7841 | 0.83 | 1.02 | 1.00 | 0.7592 | 0.9721 | 0.9954 | 1.08 | 1.11 | 1.10 | 0.8928 | 0.8614 | 0.8693 | 1.22 | 1.17 | 0.6190 | 0.6258 |
| 136.0385 | 10.2 | C5H4N4O | Hypoxanthine | Nucleotide Metabolism | 0.93 | 1.03 | 0.88 | 0.4106 | 0.7369 | 0.1290 | 1.07 | 0.5017 | 0.92 | 0.93 | 0.93 | 0.4470 | 0.5219 | 0.5452 | 1.06 | 1.10 | 1.01 | 0.3798 | 0.3560 | 0.9184 | 1.05 | 1.06 | 0.5841 | 0.4681 |
| 348.0470 | 15.3 | C10H13N4O8P | IMP | Nucleotide Metabolism | 0.96 | 1.07 | 1.00 | 0.8590 | 0.7401 | 0.9977 | 0.96 | 0.8682 | 0.94 | 1.03 | 0.89 | 0.8593 | 0.9370 | 0.7446 | 1.02 | 1.01 | 0.95 | 0.9325 | 0.9608 | 0.8060 | 1.02 | 1.05 | 0.9064 | 0.8022 |
| 323.0520 | 16.4 | C9H14N3O8P | CMP | Nucleotide Metabolism | 0.95 | 1.09 | 1.08 | 0.8444 | 0.8560 | 0.7862 | 1.23 | 0.4207 | 1.19 | 1.16 | 1.44 | 0.4198 | 0.4652 | 0.3355 | 2.08 | 1.96 | 2.53 | 0.0418 | 0.0443 | 0.0265 | 2.09 | 1.92 | 0.0780 | 0.0992 |
| 151.0495 | 12.3 | C5H5N5O | Guanine | Nucleotide Metabolism | 0.92 | 0.98 | 0.88 | 0.2834 | 0.9137 | 0.3469 | 0.93 | 0.6577 | 0.77 | 0.83 | 0.75 | 0.1892 | 0.3223 | 0.1788 | 0.93 | 0.98 | 0.90 | 0.7422 | 0.9234 | 0.6305 | 0.90 | 0.89 | 0.4780 | 0.2053 |
| 135.0545 | 9.7 | C5H5N5 | Adenine | Nucleotide Metabolism | 0.90 | 1.00 | 0.86 | 0.4819 | 0.9953 | 0.3523 | 0.96 | 0.7558 | 0.89 | 0.85 | 0.90 | 0.3814 | 0.2490 | 0.5038 | 1.24 | 1.24 | 1.20 | 0.0814 | 0.0576 | 0.2544 | 1.20 | 1.19 | 0.0562 | 0.0294 |
| 112.0273 | 12.1 | C4H4N2O2 | Orotate(Fragment) | Nucleotide Metabolism | 0.91 | 1.12 | 1.02 | 0.5556 | 0.7428 | 0.8867 | 0.90 | 0.7099 | 0.83 | 0.98 | 0.98 | 0.5927 | 0.9604 | 0.9628 | 1.10 | 1.14 | 1.09 | 0.7729 | 0.7307 | 0.7850 | 1.10 | 1.11 | 0.4906 | 0.2658 |
| 267.0967 | 9.2 | C10H13N5O4 | Adenosine | Nucleotide Metabolism | 0.89 | 1.14 | 0.99 | 0.2260 | 0.1272 | 0.9489 | 1.02 | 0.8823 | 0.88 | 0.99 | 0.91 | 0.4483 | 0.9588 | 0.5360 | 1.04 | 1.11 | 1.04 | 0.7852 | 0.4520 | 0.7921 | 1.19 | 1.28 | 0.1402 | 0.0757 |
| 363.0580 | 16.5 | C10H14N5O8P | GMP | Nucleotide Metabolism | 0.92 | 0.96 | 0.95 | 0.7151 | 0.8406 | 0.8360 | 0.84 | 0.1926 | 0.89 | 1.02 | 0.90 | 0.4477 | 0.8796 | 0.6210 | 1.02 | 1.00 | 1.04 | 0.9285 | 0.9995 | 0.7998 | 1.10 | 1.10 | 0.6832 | 0.6153 |
| 347.0630 | 13.6 | C10H14N5O7P | AMP | Nucleotide Metabolism | 0.91 | 1.00 | 0.93 | 0.6963 | 0.9843 | 0.7820 | 0.88 | 0.5572 | 0.89 | 0.98 | 0.95 | 0.6305 | 0.9353 | 0.8632 | 1.03 | 1.14 | 1.08 | 0.9013 | 0.5814 | 0.7413 | 1.19 | 1.21 | 0.3395 | 0.2768 |
| 338.0628 | 15.2 | C9H15N4O8P | 1-(5'-Phosphoribosyl)-5-amino-4-imidazolecarboxamide | Nucleotide Metabolism | 0.88 | 1.18 | 0.94 | 0.4415 | 0.5856 | 0.6769 | 1.09 | 0.7449 | 0.85 | 0.86 | 0.89 | 0.5637 | 0.6286 | 0.7685 | 1.05 | 1.18 | 1.10 | 0.8459 | 0.5743 | 0.7543 | 1.05 | 1.21 | 0.7744 | 0.2352 |
| 168.0284 | 12.4 | C5H4N4O3 | Urate | Nucleotide Metabolism | 0.84 | 0.64 | 0.80 | 0.8313 | 0.6014 | 0.7895 | 0.93 | 0.9256 | 1.00 | 1.21 | 0.63 | 0.9972 | 0.7891 | 0.5643 | 0.97 | 1.00 | 1.13 | 0.9648 | 0.9953 | 0.8686 | 1.28 | 1.24 | 0.8047 | 0.8206 |
| 268.0809 | 10.9 | C10H12N4O5 | Inosine | Nucleotide Metabolism | 0.76 | 0.97 | 0.78 | 0.2551 | 0.9300 | 0.2969 | 0.81 | 0.5121 | 0.72 | 0.84 | 0.79 | 0.2417 | 0.5317 | 0.4164 | 1.03 | 1.14 | 0.90 | 0.7489 | 0.4187 | 0.2842 | 1.03 | 1.07 | 0.7705 | 0.5909 |
| 244.1059 | 14.9 | C10H16N2O5 | Glu-Pro | Peptide(di-) | 1.42 | 1.03 | 1.46 | 0.4472 | 0.9659 | 0.4228 | 1.16 | 0.7854 | 0.73 | 1.02 | 0.89 | 0.5837 | 0.9744 | 0.8203 | 1.10 | 1.07 | 0.90 | 0.8497 | 0.8688 | 0.8385 | 0.53 | 0.55 | 0.0900 | 0.1010 |
| 204.0747 | 15.3 | C7H12N2O5 | Ala-Asp | Peptide(di-) | 1.27 | 1.20 | 1.18 | 0.2573 | 0.5325 | 0.6218 | 1.03 | 0.9466 | 1.07 | 1.20 | 0.82 | 0.7777 | 0.4018 | 0.4268 | 0.85 | 0.93 | 0.85 | 0.3848 | 0.6227 | 0.3891 | 0.83 | 1.06 | 0.4862 | 0.8476 |
| 247.0804 | 15.5 | C8H13N3O6 | Asn-Asp | Peptide(di-) | 1.10 | 1.22 | 1.02 | 0.9194 | 0.8319 | 0.9798 | 1.03 | 0.9441 | 0.97 | 0.91 | 0.76 | 0.9411 | 0.8119 | 0.4982 | 1.23 | 1.11 | 1.19 | 0.5492 | 0.7650 | 0.6422 | 0.90 | 0.99 | 0.7569 | 0.9780 |
| 230.0901 | 15.3 | C9H14N2O5 | Aspartyl-L-proline | Peptide(di-) | 1.15 | 1.10 | 1.22 | 0.4920 | 0.5998 | 0.3771 | 0.90 | 0.6476 | 0.95 | 1.03 | 0.87 | 0.8066 | 0.9099 | 0.6485 | 1.09 | 1.09 | 0.98 | 0.7617 | 0.7435 | 0.9609 | 0.13 | 0.16 | 0.0004 | 0.0004 |
| 248.0645 | 17.1 | C8H12N2O7 | Asp-Asp | Peptide(di-) | 1.07 | 1.40 | 1.04 | 0.8050 | 0.5430 | 0.9151 | 0.62 | 0.1935 | 0.57 | 0.76 | 0.55 | 0.1031 | 0.3648 | 0.1260 | 0.70 | 0.76 | 0.72 | 0.1620 | 0.2234 | 0.2028 | 1.03 | 1.02 | 0.9261 | 0.9524 |
| 220.0692 | 15.4 | C7H12N2O6 | Asp-Ser | Peptide(di-) | 1.02 | 1.15 | 1.03 | 0.9210 | 0.4667 | 0.8703 | 0.97 | 0.8096 | 0.97 | 1.02 | 0.97 | 0.8274 | 0.9067 | 0.8457 | 1.01 | 1.06 | 1.03 | 0.9221 | 0.7287 | 0.8212 | 1.02 | 1.09 | 0.9592 | 0.7960 |
| 262.0804 | 13.9 | C9H14N2O7 | Glu-Asp | Peptide(di-) | 1.04 | 0.99 | 1.06 | 0.9163 | 0.9892 | 0.8666 | 0.97 | 0.9169 | 0.82 | 0.98 | 0.95 | 0.4645 | 0.9390 | 0.8541 | 0.95 | 1.02 | 0.91 | 0.8575 | 0.9556 | 0.7436 | 0.79 | 0.70 | 0.1556 | 0.0948 |
| 248.1008 | 14.6 | C9H16N2O6 | Glu-Thr | Peptide(di-) | 1.03 | 1.22 | 1.08 | 0.9555 | 0.6503 | 0.8529 | 0.95 | 0.8830 | 0.77 | 0.95 | 0.87 | 0.4494 | 0.8788 | 0.7235 | 0.95 | 0.96 | 0.89 | 0.8539 | 0.9119 | 0.7020 | 1.06 | 0.98 | 0.5323 | 0.7333 |
| 218.0901 | 10.1 | C8H14N2O5 | L-Ala-L-Glu | Peptide(di-) | 0.97 | 1.28 | 0.97 | 0.9256 | 0.6558 | 0.9081 | 0.94 | 0.9010 | 0.74 | 1.01 | 0.87 | 0.5739 | 0.9923 | 0.8229 | 1.19 | 1.10 | 1.11 | 0.7325 | 0.8600 | 0.8550 | 0.67 | 0.96 | 0.0416 | 0.7535 |
| 234.0852 | 15.5 | C8H14N2O6 | Thr-Asp | Peptide(di-) | 0.99 | 1.10 | 0.99 | 0.8645 | 0.5341 | 0.8680 | 1.00 | 0.9943 | 0.89 | 0.96 | 0.92 | 0.6041 | 0.8654 | 0.7468 | 1.13 | 1.12 | 1.05 | 0.5677 | 0.6513 | 0.8366 | 0.93 | 0.90 | 0.7074 | 0.6298 |
| 289.1387 | 18.1 | C10H19N5O5 | Asp-Arg | Peptide(di-) | 0.99 | 1.19 | 1.14 | 0.9473 | 0.5277 | 0.5161 | 0.88 | 0.6938 | 0.35 | 0.42 | 0.26 | 0.0653 | 0.0802 | 0.0452 | 0.19 | 0.21 | 0.13 | 0.0104 | 0.0091 | 0.0085 | 1.21 | 1.20 | 0.5751 | 0.5870 |
| 261.1326 | 18.0 | C10H19N3O5 | Lys-Asp | Peptide(di-) | 0.94 | 1.13 | 0.95 | 0.8998 | 0.8395 | 0.9286 | 1.03 | 0.9649 | 0.76 | 0.97 | 0.86 | 0.6816 | 0.9632 | 0.8398 | 1.13 | 1.12 | 1.11 | 0.8571 | 0.8667 | 0.8756 | 1.18 | 1.18 | 0.7163 | 0.7181 |
| 233.1376 | 16.4 | C9H19N3O4 | Lys-Ser | Peptide(di-) | 0.98 | 1.09 | 1.13 | 0.9252 | 0.7545 | 0.7380 | 0.98 | 0.9356 | 0.83 | 1.01 | 0.84 | 0.5490 | 0.9695 | 0.6600 | 0.84 | 0.87 | 0.70 | 0.5841 | 0.6596 | 0.2394 | 1.08 | 0.97 | 0.7668 | 0.8884 |
| 245.1739 | 21.8 | C11H23N3O3 | Lys-Val | Peptide(di-) | 0.97 | 1.17 | 0.99 | 0.8849 | 0.5030 | 0.9667 | 0.91 | 0.4607 | 0.87 | 0.91 | 0.88 | 0.4329 | 0.5725 | 0.5126 | 1.07 | 1.07 | 1.06 | 0.6446 | 0.7109 | 0.7187 | 1.32 | 1.23 | 0.3154 | 0.3140 |
| 260.1373 | 11.0 | C11H20N2O5 | Glu-Leu | Peptide(di-) | 0.95 | 1.11 | 0.96 | 0.7399 | 0.6406 | 0.7784 | 0.93 | 0.7388 | 0.95 | 1.02 | 0.95 | 0.7176 | 0.9130 | 0.8200 | 0.95 | 0.99 | 0.98 | 0.8116 | 0.9709 | 0.9419 | 1.09 | 1.10 | 0.4597 | 0.3688 |
| 202.1318 | 12.8 | C9H18N2O3 | Leu-Ala | Peptide(di-) | 0.95 | 1.05 | 0.92 | 0.8787 | 0.8961 | 0.8188 | 0.96 | 0.8711 | 0.87 | 0.97 | 0.85 | 0.4934 | 0.8947 | 0.5017 | 1.05 | 1.03 | 1.06 | 0.7979 | 0.8463 | 0.7222 | 1.11 | 1.08 | 0.8452 | 0.8770 |
| 246.1217 | 12.3 | C10H18N2O5 | Leu-Asp | Peptide(di-) | 0.94 | 1.13 | 1.00 | 0.9068 | 0.8203 | 0.9983 | 1.02 | 0.9679 | 0.76 | 0.89 | 0.85 | 0.4982 | 0.7573 | 0.6962 | 1.08 | 1.12 | 1.07 | 0.8265 | 0.7707 | 0.8706 | 1.09 | 1.10 | 0.4606 | 0.4417 |
| 228.1474 | 13.1 | C11H20N2O3 | Leu-Pro | Peptide(di-) | 0.94 | 1.58 | 1.04 | NA | 0.6942 | NA | 1.18 | 0.7820 | 0.87 | 1.00 | 0.94 | 0.8167 | 0.9998 | 0.9259 | 1.33 | 1.20 | 1.24 | 0.5581 | 0.7098 | 0.6589 | 1.15 | 1.13 | 0.4469 | 0.4530 |
| 218.1267 | 13.0 | C9H18N2O4 | Leu-Ser | Peptide(di-) | 0.93 | 1.16 | 1.04 | 0.7692 | 0.5478 | 0.8791 | 0.94 | 0.7793 | 0.83 | 1.04 | 0.92 | 0.4948 | 0.8942 | 0.8072 | 0.92 | 0.88 | 0.92 | 0.7302 | 0.6408 | 0.7225 | 0.95 | 0.94 | 0.9165 | 0.8993 |
| 236.0833 | 10.5 | C8H16N2O4S | Met-Ser | Peptide(di-) | 0.90 | 1.10 | 0.93 | 0.7690 | 0.7976 | 0.8299 | 1.01 | 0.9857 | 0.81 | 1.00 | 0.96 | 0.5594 | 0.9897 | 0.9118 | 0.96 | 1.09 | 1.01 | 0.9106 | 0.8130 | 0.9710 | 1.21 | 0.95 | 0.3591 | 0.8107 |
| 188.1160 | 12.2 | C8H16N2O3 | Val-Ala | Peptide(di-) | 0.90 | 1.01 | 0.91 | 0.6445 | 0.9695 | 0.6985 | 0.93 | 0.7034 | 0.83 | 0.96 | 0.83 | 0.4178 | 0.8277 | 0.3950 | 1.13 | 1.04 | 1.06 | 0.3295 | 0.7929 | 0.5947 | 1.19 | 1.16 | 0.4687 | 0.5259 |
| 186.1007 | 11.4 | C8H14N2O3 | Ala-Pro | Peptide(di-) | 0.87 | 1.00 | 0.91 | 0.6303 | 0.9957 | 0.7692 | 1.11 | 0.6013 | 0.88 | 0.96 | 0.91 | 0.5262 | 0.8583 | 0.6821 | 1.09 | 1.13 | 1.00 | 0.7050 | 0.6188 | 0.9956 | 0.14 | 0.15 | 0.0010 | 0.0004 |
| 176.0796 | 21.7 | C6H12N2O4 | Ala-Ser | Peptide(di-) | 0.87 | 1.06 | 0.96 | 0.6540 | 0.8638 | 0.8956 | 1.03 | 0.9266 | 0.88 | 1.01 | 0.97 | 0.6439 | 0.9647 | 0.9253 | 1.08 | 1.04 | 1.02 | 0.7835 | 0.9002 | 0.9515 | 1.25 | 1.61 | 0.7800 | 0.4948 |
| 229.1063 | 13.7 | C9H15N3O4 | Asn-Pro | Peptide(di-) | 0.84 | 0.96 | 0.81 | 0.2812 | 0.8591 | 0.1741 | 0.48 | 0.0288 | 0.36 | 0.47 | 0.22 | 0.0335 | 0.0484 | 0.0159 | 0.22 | 0.26 | 0.14 | 0.0005 | 0.0002 | 0.0007 | 1.24 | 1.27 | 0.2580 | 0.3118 |
| 162.0639 | 12.8 | C5H10N2O4 | Gly-Ser | Peptide(di-) | 0.82 | 1.10 | 0.93 | 0.6617 | 0.8476 | 0.8750 | 1.03 | 0.9292 | 0.98 | 0.99 | 1.03 | 0.9503 | 0.9815 | 0.9388 | 1.10 | 1.10 | 1.14 | 0.7660 | 0.7528 | 0.6790 | 1.18 | 1.14 | 0.5994 | 0.6719 |
| 190.0954 | 17.2 | C7H14N2O4 | Thr-Ala | Peptide(di-) | 0.82 | 0.87 | 0.98 | 0.5370 | 0.7651 | 0.9467 | 1.02 | 0.9278 | 0.91 | 1.01 | 0.85 | 0.6955 | 0.9841 | 0.5818 | 0.81 | 0.87 | 0.60 | 0.2595 | 0.5097 | 0.0387 | 0.97 | 1.11 | 0.9375 | 0.8409 |
| 422.1108 | 15.8 | C14H22N4O9S | Ala-Asp-Asp-Cys | Peptide(tetra-) | 1.08 | 1.16 | 1.03 | 0.7221 | 0.4051 | 0.8951 | 0.91 | 0.6290 | 0.80 | 0.94 | 0.94 | 0.0653 | 0.4862 | 0.6534 | 0.95 | 1.14 | 1.12 | 0.7229 | 0.1705 | 0.1321 | 1.18 | 1.10 | 0.5648 | 0.7235 |
| 394.1161 | 17.1 | C13H22N4O8S | Ala-Asp-Cys-Ser | Peptide(tetra-) | 1.09 | 0.98 | 0.96 | 0.8776 | 0.9599 | 0.9225 | 0.96 | 0.9081 | 0.86 | 0.95 | 0.98 | 0.6850 | 0.8830 | 0.9654 | 1.05 | 1.26 | 1.24 | 0.9093 | 0.5608 | 0.6057 | 1.22 | 1.18 | 0.5867 | 0.6819 |
| 376.1594 | 17.1 | C14H24N4O8 | Ala-Thr-Ala-Asp | Peptide(tetra-) | 1.03 | 0.82 | 0.91 | 0.9404 | 0.7119 | 0.8458 | 0.78 | 0.1776 | 0.79 | 0.86 | 0.25 | 0.4628 | 0.4634 | 0.0078 | 0.14 | 0.28 | 0.00 | 0.0004 | 0.0000 | NA | 1.21 | 1.19 | 0.6115 | 0.6439 |

| | | | | | | | | | | | | | | | | | | | | | | | | | | | | |
|---|---|---|---|---|---|---|---|---|---|---|---|---|---|---|---|---|---|---|---|---|---|---|---|---|---|---|---|---|
| 426.0880 | 16.8 | C13H22N4O8S2 | Asp-Cys-Cys-Ser | Peptide(tetra-) | 1.06 | 0.94 | 0.97 | 0.8544 | 0.8526 | 0.9377 | 0.94 | 0.8390 | 1.02 | 0.94 | 1.08 | 0.9459 | 0.7248 | 0.7577 | 1.13 | 1.01 | 1.07 | 0.5400 | 0.9684 | 0.7057 | 0.82 | 0.78 | 0.5619 | 0.4463 |
| 445.2541 | 13.4 | C19H35N5O7 | Ala-Leu-Lys-Asp | Peptide(tetra-) | 0.97 | 0.88 | 0.79 | 0.9490 | 0.7413 | 0.6050 | 0.98 | 0.9156 | 0.53 | 0.68 | 0.51 | 0.1750 | 0.3232 | 0.1602 | 1.12 | 1.13 | 0.99 | 0.4818 | 0.3450 | 0.9421 | 1.17 | 1.28 | 0.5471 | 0.3557 |
| 461.1870 | 16.9 | C16H27N7O9 | Arg-Asp-Asp-Gly | Peptide(tetra-) | 1.02 | 1.08 | 1.06 | 0.9096 | 0.7913 | 0.7614 | 0.97 | 0.9022 | 0.81 | 1.00 | 0.91 | 0.3804 | 0.9912 | 0.7253 | 1.22 | 1.14 | 1.07 | 0.2869 | 0.5519 | 0.7088 | 1.27 | 1.24 | 0.4403 | 0.3527 |
| 624.3495 | 14.8 | C30H44N10O5 | Arg-Phe-Phe-Arg | Peptide(tetra-) | 0.98 | 1.14 | 0.94 | 0.9504 | 0.7548 | 0.8685 | 0.90 | 0.7440 | 0.94 | 0.90 | 0.97 | 0.8347 | 0.7271 | 0.9281 | 1.03 | 0.98 | 1.02 | 0.9183 | 0.9520 | 0.9394 | 0.98 | 1.21 | 0.9750 | 0.7441 |
| 440.1764 | 14.7 | C16H24N8O7 | Asn-Asn-Gly-His | Peptide(tetra-) | 0.95 | 0.92 | 0.87 | 0.8665 | 0.7207 | 0.6222 | 1.07 | 0.6966 | 0.87 | 0.89 | 0.94 | 0.4654 | 0.5644 | 0.7234 | 1.00 | 0.99 | 1.04 | 0.9946 | 0.9352 | 0.7893 | 1.21 | 1.20 | 0.6086 | 0.6036 |
| 489.2436 | 13.9 | C20H35N5O9 | Asp-Leu-Lys-Asp | Peptide(tetra-) | 0.97 | 1.28 | 1.01 | 0.9330 | 0.6082 | 0.9782 | 1.01 | 0.9865 | 0.77 | 0.97 | 0.95 | 0.5918 | 0.9602 | 0.9248 | 1.08 | 1.11 | 1.04 | 0.8752 | 0.8416 | 0.9460 | 1.10 | 1.22 | 0.7072 | 0.4877 |
| 251.1560 | 22.0 | C22H42N6O7 | Asp-Leu-Lys-Lys | Peptide(tetra-) | 0.98 | 1.00 | 0.93 | 0.9450 | 0.9947 | 0.8535 | 1.01 | 0.9723 | 0.89 | 0.97 | 0.89 | 0.6228 | 0.9048 | 0.7059 | 0.92 | 0.99 | 1.02 | 0.7271 | 0.9535 | 0.9594 | 1.40 | 1.22 | 0.3946 | 0.4090 |
| 550.3123 | 15.6 | C26H42N6O7 | Gln-Leu-Lys-Tyr | Peptide(tetra-) | 0.96 | 1.06 | 0.95 | 0.8822 | 0.8421 | 0.8792 | 0.99 | 0.9633 | 1.00 | 1.01 | 1.00 | 0.9829 | 0.9696 | 0.9843 | 1.09 | 1.04 | 1.05 | 0.6426 | 0.8413 | 0.7975 | 0.86 | 0.98 | 0.7432 | 0.9610 |
| 550.3112 | 15.9 | C26H42N6O7 | Glu-Lys-Lys-Phe | Peptide(tetra-) | 0.96 | 1.11 | 0.95 | 0.8191 | 0.4545 | 0.7891 | 0.95 | 0.6568 | 0.93 | 1.07 | 1.02 | 0.6516 | 0.5777 | 0.9156 | 1.11 | 1.08 | 1.16 | 0.3551 | 0.5765 | 0.0870 | 0.88 | 0.57 | 0.7897 | 0.3377 |
| 424.1595 | 11.4 | C18H24N4O8 | Ala-Asp-Gly-Tyr | Peptide(tetra-) | 0.95 | 0.92 | 0.90 | 0.8971 | 0.8676 | 0.7835 | 1.08 | 0.6793 | 0.90 | 0.96 | 0.90 | 0.5922 | 0.8302 | 0.5907 | 0.97 | 1.07 | 1.01 | 0.8999 | 0.7834 | 0.9747 | 0.95 | 0.96 | 0.8668 | 0.8931 |
| 374.2164 | 14.5 | C16H30N4O6 | Ala-Leu-Thr-Ala | Peptide(tetra-) | 0.94 | 1.06 | 1.01 | 0.8301 | 0.8657 | 0.9750 | 0.96 | 0.8590 | 0.93 | 0.99 | 0.98 | 0.7935 | 0.9596 | 0.9365 | 1.12 | 1.07 | 1.04 | 0.6329 | 0.7747 | 0.8842 | 1.16 | 1.15 | 0.5333 | 0.5622 |
| 498.1793 | 10.3 | C21H30N4O8S | Ala-Met-Asp-Tyr | Peptide(tetra-) | 0.91 | 1.22 | 0.98 | 0.7844 | 0.6957 | 0.9593 | 1.00 | 0.9954 | 0.74 | 0.93 | 0.89 | 0.5964 | 0.9068 | 0.8617 | 1.11 | 1.08 | 1.12 | 0.8595 | 0.9038 | 0.8530 | 0.76 | 0.96 | 0.2509 | 0.6536 |
| 389.1706 | 13.9 | C18H23N5O5 | Ala-Trp-Gly-Gly | Peptide(tetra-) | 0.94 | 0.88 | 0.89 | 0.8059 | 0.7687 | 0.7162 | 0.94 | 0.6339 | 0.88 | 0.89 | 0.89 | 0.5261 | 0.6189 | 0.5614 | 1.10 | 1.06 | 1.14 | 0.5536 | 0.7427 | 0.4476 | 1.46 | 1.58 | 0.5970 | 0.5133 |
| 390.1754 | 16.9 | C15H26N4O8 | Ala-Val-Asp-Ser | Peptide(tetra-) | 0.90 | 0.91 | 0.91 | 0.8100 | 0.8208 | 0.8443 | 0.96 | 0.8457 | 1.01 | 1.10 | 0.86 | 0.9789 | 0.6431 | 0.4446 | 1.36 | 1.27 | 1.16 | 0.3970 | 0.4807 | 0.5734 | 0.99 | 0.97 | 0.9807 | 0.9253 |
| 439.2427 | 10.9 | C20H33N5O6 | Asn-Leu-Pro-Pro | Peptide(tetra-) | 0.92 | 1.04 | 0.97 | 0.8007 | 0.9013 | 0.9201 | 0.93 | 0.7083 | 0.88 | 0.96 | 0.87 | 0.6751 | 0.9030 | 0.5759 | 1.21 | 1.15 | 1.09 | 0.4075 | 0.6309 | 0.7291 | 0.00 | 0.00 | NA | NA |
| 471.2332 | 12.4 | C20H33N5O8 | Asp-Leu-Gln-Pro | Peptide(tetra-) | 0.91 | 1.14 | 1.00 | 0.7796 | 0.7320 | 0.9940 | 1.08 | 0.7958 | 0.84 | 0.95 | 0.95 | 0.5502 | 0.8709 | 0.8816 | 1.11 | 1.02 | 1.00 | 0.6786 | 0.9392 | 0.9885 | 1.18 | 1.08 | 0.6277 | 0.7943 |
| 376.1594 | 16.7 | C14H24N4O8 | Asp-Val-Gly-Ser | Peptide(tetra-) | 0.91 | 0.87 | 0.96 | 0.7448 | 0.7371 | 0.8643 | 1.06 | 0.6277 | 0.94 | 0.90 | 0.84 | 0.7661 | 0.4983 | 0.3316 | 1.03 | 1.01 | 0.97 | 0.8465 | 0.9555 | 0.8562 | 0.98 | 1.10 | 0.9493 | 0.7345 |
| 500.1767 | 10.3 | C21H32N4O6S2 | Cys-Leu-Cys-Tyr | Peptide(tetra-) | 0.87 | 1.02 | 0.97 | 0.7798 | 0.9766 | 0.9474 | 0.98 | 0.9644 | 0.83 | 0.89 | 0.94 | 0.6709 | 0.7869 | 0.8997 | 1.05 | 1.09 | 1.11 | 0.8977 | 0.8301 | 0.7991 | 1.04 | 1.01 | 0.6490 | 0.9051 |
| 716.2952 | 10.5 | C40H40N6O7 | Trp-Trp-Tyr-Tyr | Peptide(tetra-) | 0.86 | 1.17 | 0.89 | 0.7621 | 0.7337 | 0.8231 | 0.98 | 0.9376 | 0.77 | 0.99 | 0.86 | 0.4738 | 0.9765 | 0.6955 | 1.14 | 1.12 | 0.99 | 0.6052 | 0.6781 | 0.9715 | 1.08 | 1.13 | 0.6432 | 0.3759 |
| 318.1541 | 17.8 | C12H22N4O6 | Ala-Ala-Ala-Ser | Peptide(tetra-) | 0.86 | 0.98 | 0.93 | 0.8084 | 0.9703 | 0.9007 | 0.84 | 0.3930 | 0.92 | 1.10 | 1.04 | 0.6390 | 0.7314 | 0.8995 | 0.93 | 0.89 | 0.90 | 0.7661 | 0.6804 | 0.6789 | 1.09 | 1.09 | 0.7910 | 0.7867 |
| 376.1416 | 14.6 | C14H24N4O6S | Ala-Cys-Pro-Ser | Peptide(tetra-) | 0.84 | 0.85 | 0.86 | 0.6374 | 0.6611 | 0.6802 | 1.03 | 0.9601 | 0.84 | 0.90 | 1.00 | 0.7430 | 0.8273 | 0.9958 | 0.95 | 0.99 | 0.91 | 0.9206 | 0.9919 | 0.8657 | 1.09 | 1.12 | 0.8851 | 0.8628 |
| 348.1645 | 16.4 | C13H24N4O7 | Ala-Thr-Ala-Ser | Peptide(tetra-) | 0.79 | 0.89 | 0.83 | 0.3079 | 0.5054 | 0.3573 | 1.00 | 0.9924 | 0.91 | 0.98 | 0.93 | 0.8242 | 0.9637 | 0.8747 | 1.02 | 1.06 | 1.06 | 0.9727 | 0.8958 | 0.8821 | 1.22 | 1.13 | 0.4484 | 0.5918 |
| 461.1870 | 17.8 | C16H27N7O9 | Asn-Thr-Asn-Asn | Peptide(tetra-) | 0.64 | 0.63 | 0.66 | 0.5268 | 0.5313 | 0.5571 | 0.94 | 0.9218 | 0.97 | 1.04 | 1.00 | 0.9625 | 0.9552 | 0.9976 | 1.10 | 1.07 | 0.98 | 0.8686 | 0.9071 | 0.9681 | 1.08 | 0.96 | 0.8693 | 0.9252 |
| 362.1264 | 14.8 | C13H22N4O6S | Cys-Gly-Pro-Ser | Peptide(tetra-) | 0.53 | 0.89 | 0.86 | 0.0451 | 0.5054 | 0.4084 | 1.47 | 0.3702 | 0.93 | 1.03 | 0.98 | 0.8753 | 0.9473 | 0.9621 | 0.67 | 1.07 | 0.64 | 0.4464 | 0.8887 | 0.3713 | 1.27 | 1.29 | 0.3407 | 0.3806 |
| 318.1177 | 15.3 | C11H18N4O7 | Ala-Asn-Asp | Peptide(tri-) | 1.33 | 1.16 | 1.12 | 0.4132 | 0.7793 | 0.8327 | 1.06 | 0.7863 | 0.79 | 1.06 | 0.84 | 0.3368 | 0.8104 | 0.5124 | 0.80 | 0.83 | 0.75 | 0.5950 | 0.6465 | 0.5498 | 1.16 | 1.11 | 0.7027 | 0.7692 |
| 319.1018 | 16.5 | C11H17N3O8 | Ala-Asp-Asp | Peptide(tri-) | 1.22 | 1.16 | 1.11 | 0.7424 | 0.8693 | 0.8686 | 0.94 | 0.9086 | 0.93 | 1.43 | 1.18 | 0.9011 | 0.5541 | 0.7773 | 1.14 | 1.10 | 0.78 | 0.8124 | 0.8552 | 0.6337 | 1.05 | 1.12 | 0.9297 | 0.8237 |
| 261.0961 | 15.2 | C9H15N3O6 | Ala-Asp-Gly | Peptide(tri-) | 1.01 | 1.51 | 1.27 | 0.9852 | 0.5957 | 0.7511 | 0.62 | 0.4971 | 1.20 | 0.96 | 1.05 | 0.6036 | 0.9475 | 0.9015 | 1.01 | 1.00 | 0.87 | 0.9907 | 0.9988 | 0.7959 | 1.11 | 1.19 | 0.7169 | 0.4927 |
| 291.1069 | 15.5 | C10H17N3O7 | Ala-Asp-Ser | Peptide(tri-) | 1.09 | 1.23 | 1.17 | 0.8714 | 0.6887 | 0.7757 | 1.09 | 0.8217 | 0.86 | 0.94 | 0.90 | 0.7145 | 0.8698 | 0.7999 | 1.05 | 1.07 | 1.03 | 0.9052 | 0.8517 | 0.9421 | 1.06 | 1.05 | 0.7020 | 0.7720 |
| 305.0859 | 16.8 | C10H15N3O8 | Asp-Asp-Gly | Peptide(tri-) | 1.07 | 1.02 | 1.20 | 0.8028 | 0.9522 | 0.5011 | 1.01 | 0.9668 | 0.92 | 1.09 | 1.18 | 0.8109 | 0.8313 | 0.7245 | 1.22 | 1.13 | 1.21 | 0.3875 | 0.6239 | 0.5115 | 1.17 | 1.16 | 0.7484 | 0.7631 |
| 275.1116 | 14.3 | C10H17N3O6 | Glu-Ala-Gly | Peptide(tri-) | 1.03 | 1.18 | 1.05 | 0.9456 | 0.7568 | 0.9288 | 0.96 | 0.9004 | 0.81 | 0.97 | 0.95 | 0.5763 | 0.9304 | 0.9082 | 0.96 | 0.99 | 0.93 | 0.9012 | 0.9779 | 0.8329 | 0.58 | 0.77 | 0.0981 | 0.1845 |
| 305.1225 | 14.6 | C11H19N3O7 | Glu-Ala-Ser | Peptide(tri-) | 1.03 | 1.09 | 1.04 | 0.8823 | 0.6150 | 0.7942 | 0.92 | 0.7823 | 0.99 | 1.05 | 1.02 | 0.9736 | 0.8446 | 0.9425 | 1.13 | 1.24 | 1.09 | 0.6067 | 0.4424 | 0.7026 | 1.19 | 1.10 | 0.3165 | 0.4070 |
| 335.1329 | 14.7 | C12H21N3O8 | Glu-Ser-Thr | Peptide(tri-) | 0.98 | 1.14 | 0.97 | 0.9679 | 0.7632 | 0.9386 | 0.90 | 0.7376 | 0.91 | 0.93 | 0.96 | 0.7845 | 0.8511 | 0.9189 | 0.95 | 1.06 | 1.00 | 0.8918 | 0.8688 | 0.9937 | 0.60 | 0.93 | 0.1565 | 0.8574 |
| 335.1329 | 15.8 | C12H21N3O8 | Thr-Thr-Asp | Peptide(tri-) | 0.97 | 1.07 | 1.04 | 0.9334 | 0.8609 | 0.9065 | 0.98 | 0.9332 | 0.98 | 1.04 | 0.96 | 0.9485 | 0.8950 | 0.8973 | 1.08 | 1.18 | 1.09 | 0.8179 | 0.6538 | 0.7849 | 1.11 | 1.08 | 0.4496 | 0.3932 |
| 346.1603 | 17.7 | C12H22N6O6 | Asp-Gly-Arg | Peptide(tri-) | 0.98 | 1.06 | 1.04 | 0.9409 | 0.8239 | 0.8816 | 0.90 | 0.5720 | 0.97 | 0.90 | 0.95 | 0.9032 | 0.6378 | 0.8200 | 1.04 | 0.96 | 0.98 | 0.8679 | 0.8405 | 0.9373 | 1.14 | 1.10 | 0.7250 | 0.7996 |
| 356.2423 | 21.1 | C17H32N4O4 | Leu-Lys-Pro | Peptide(tri-) | 0.95 | 1.08 | 1.03 | 0.7403 | 0.7811 | 0.8663 | 0.99 | 0.9638 | 0.98 | 0.98 | 1.03 | 0.8832 | 0.9000 | 0.8901 | 0.99 | 1.01 | 0.99 | 0.9623 | 0.9549 | 0.9476 | 1.13 | 1.09 | 0.5168 | 0.6475 |
| 334.1853 | 15.4 | C13H26N4O6 | Lys-Thr-Ser | Peptide(tri-) | 0.96 | 0.92 | 1.16 | 0.9610 | 0.9113 | 0.8370 | 0.90 | 0.8601 | 0.92 | 0.97 | 0.92 | 0.8856 | 0.9592 | 0.8914 | 1.10 | 1.07 | 1.04 | 0.8777 | 0.9141 | 0.9454 | 1.13 | 1.08 | 0.6945 | 0.7919 |
| 348.2008 | 15.3 | C14H28N4O6 | Lys-Thr-Thr | Peptide(tri-) | 0.95 | 1.11 | 0.97 | 0.7590 | 0.6700 | 0.8933 | 0.97 | 0.8752 | 0.81 | 0.93 | 0.91 | 0.3474 | 0.7842 | 0.7392 | 1.05 | 1.05 | 1.04 | 0.8160 | 0.8504 | 0.8572 | 1.14 | 1.14 | 0.6037 | 0.6386 |
| 346.2218 | 17.4 | C15H30N4O5 | Lys-Thr-Val | Peptide(tri-) | 0.94 | 1.04 | 1.00 | 0.6155 | 0.8603 | 0.9922 | 0.99 | 0.9387 | 0.88 | 0.96 | 0.94 | 0.5087 | 0.8674 | 0.8104 | 0.95 | 1.02 | 0.94 | 0.8610 | 0.9407 | 0.8041 | 1.00 | 1.00 | 0.9959 | 0.9921 |
| 365.1257 | 11.9 | C13H23N3O7S | Glu-Met-Ser | Peptide(tri-) | 0.94 | 0.99 | 0.97 | 0.8727 | 0.9795 | 0.9368 | 0.97 | 0.8737 | 0.90 | 1.01 | 0.86 | 0.6110 | 0.9765 | 0.4879 | 1.02 | 1.05 | 1.07 | 0.9241 | 0.7959 | 0.7181 | 1.14 | 1.11 | 0.6740 | 0.7644 |
| 379.1412 | 12.1 | C14H25N3O7S | Glu-Met-Thr | Peptide(tri-) | 0.94 | 1.01 | 0.92 | 0.8214 | 0.9563 | 0.7767 | 0.92 | 0.7289 | 0.96 | 1.03 | 0.93 | 0.8817 | 0.8734 | 0.6734 | 1.04 | 1.01 | 1.05 | 0.8763 | 0.9606 | 0.8240 | 1.39 | 1.29 | 0.0833 | 0.2313 |
| 277.1097 | 12.6 | C10H19N3O4S | Met-Ala-Gly | Peptide(tri-) | 0.93 | 1.11 | 0.96 | 0.7098 | 0.7114 | 0.8376 | 1.01 | 0.9442 | 0.92 | 0.97 | 0.93 | 0.6412 | 0.9040 | 0.7814 | 1.13 | 1.06 | 1.01 | 0.4693 | 0.7651 | 0.9679 | 1.13 | 1.07 | 0.8253 | 0.9043 |
| 408.1468 | 15.4 | C18H24N4O5S | Thr-Trp-Cys | Peptide(tri-) | 0.90 | 1.11 | 0.97 | 0.8509 | 0.8492 | 0.9512 | 0.99 | 0.9886 | 0.89 | 1.01 | 0.96 | 0.8107 | 0.9864 | 0.9383 | 1.01 | 1.07 | 1.03 | 0.9881 | 0.8827 | 0.9607 | 1.15 | 1.17 | 0.8238 | 0.8147 |
| 263.1118 | 15.1 | C9H17N3O6 | Ala-Ser-Ser | Peptide(tri-) | 0.88 | 1.04 | 0.97 | 0.6732 | 0.9096 | 0.9310 | 0.93 | 0.7964 | 0.88 | 1.02 | 0.91 | 0.6638 | 0.9319 | 0.7470 | 1.00 | 0.95 | 0.98 | 0.9863 | 0.8462 | 0.9357 | 1.80 | 1.19 | 0.3236 | 0.7828 |
| 338.0714 | 14.5 | C10H18N4O5S2 | Asn-Cys-Cys | Peptide(tri-) | 0.88 | 1.16 | 0.99 | 0.4223 | 0.5931 | 0.9631 | 0.89 | 0.5772 | 0.77 | 0.91 | 0.85 | 0.2445 | 0.6402 | 0.5762 | 1.02 | 0.90 | 0.82 | 0.9386 | 0.7292 | 0.4275 | 0.88 | 0.95 | 0.5155 | 0.7938 |
| 275.0937 | 10.6 | C10H17N3O4S | Cys-Gly-Pro | Peptide(tri-) | 0.84 | 0.91 | 0.88 | 0.5126 | 0.7210 | 0.6237 | 1.09 | 0.5229 | 1.02 | 0.94 | 0.89 | 0.9284 | 0.7639 | 0.6123 | 1.16 | 1.15 | 1.01 | 0.4811 | 0.4597 | 0.9749 | 1.10 | 1.07 | 0.8694 | 0.9112 |
| 318.1540 | 16.1 | C10H19N3O6 | Thr-Ala-Ser | Peptide(tri-) | 0.61 | 0.82 | 0.41 | 0.3710 | 0.7368 | 0.1970 | 0.98 | 0.9596 | 0.71 | 0.97 | 0.57 | 0.2850 | 0.9058 | 0.1319 | 0.64 | 0.65 | 0.47 | 0.0081 | 0.0079 | 0.0025 | 1.17 | 1.09 | 0.3844 | 0.6124 |
| 245.1012 | 12.5 | C9H15N3O5 | Asparaginyl-Hydroxyproline | Peptides | 1.00 | 1.22 | 1.15 | 0.9799 | 0.5288 | 0.4873 | 0.89 | 0.7426 | 0.73 | 0.89 | 0.83 | 0.2537 | 0.7192 | 0.5544 | 1.04 | 1.10 | 0.98 | 0.8912 | 0.6910 | 0.9553 | 1.28 | 1.10 | 0.0578 | 0.5599 |
| 234.0673 | 8.0 | C8H14N2O4S | Cysteinyl-Hydroxyproline | Peptides | 0.88 | 1.03 | 0.93 | 0.8129 | 0.9493 | 0.8985 | 1.10 | 0.8142 | 1.09 | 1.00 | 0.92 | 0.8596 | 0.9989 | 0.8631 | 1.16 | 1.15 | 1.19 | 0.7416 | 0.7550 | 0.6773 | 1.16 | 1.31 | 0.6526 | 0.4587 |
| 126.0317 | 16.8 | C6H6O3 | Benzene-1,2,4-triol | Xenobiotics Biodegradation and Metabolism | 1.06 | 1.15 | 1.05 | 0.8167 | 0.6450 | 0.8173 | 1.07 | 0.7996 | 0.98 | 1.04 | 0.95 | 0.9504 | 0.8821 | 0.8601 | 1.04 | 1.00 | 0.95 | 0.8836 | 0.9958 | 0.8375 | 1.01 | 0.95 | 0.9730 | 0.8809 |
| 137.0477 | 11.9 | C7H7NO2 | Anthranilate | Xenobiotics Biodegradation and Metabolism | 0.98 | 1.10 | 0.90 | 0.9153 | 0.8098 | 0.6864 | 1.00 | 0.9947 | 0.77 | 0.58 | 0.88 | 0.5696 | 0.3305 | 0.8006 | 1.00 | 1.07 | 1.29 | 0.9978 | 0.8985 | 0.6330 | 1.26 | 1.10 | 0.4906 | 0.6527 |
| 351.1101 | 12.9 | C12H21N3O7S | S-(2-Hydroxyethyl)glutathione | Xenobiotics Biodegradation and Metabolism | 0.91 | 0.96 | 1.00 | 0.8424 | 0.9226 | 0.9997 | 0.89 | 0.6903 | 1.00 | 1.01 | 0.96 | 0.9954 | 0.9810 | 0.9196 | 1.00 | 1.05 | 1.09 | 0.9902 | 0.8948 | 0.7911 | 1.14 | 1.12 | 0.7552 | 0.7841 |

| | | | | | | | | | | | | | | | | | | | | | | | | | | | | |
|---|---|---|---|---|---|---|---|---|---|---|---|---|---|---|---|---|---|---|---|---|---|---|---|---|---|---|---|---|
| 128.0473 | 13.8 | C6H8O3 | 2-Hydroxy-cis-hex-2,4-dienoate | Xenobiotics Biodegradation and Metabolism | 0.86 | 1.02 | 0.92 | 0.4449 | 0.9140 | 0.6639 | 0.87 | 0.3363 | 0.99 | 0.98 | 0.98 | 0.9466 | 0.9210 | 0.9217 | 1.09 | 1.22 | 1.13 | 0.6614 | 0.2697 | 0.5191 | 1.22 | 1.25 | 0.5062 | 0.4367 |

| Trophozoite stage metabolomics experiment | | | | | | | | | | | | | | | | | | | | | | | | | | | | | |
|---|---|---|---|---|---|---|---|---|---|---|---|---|---|---|---|---|---|---|---|---|---|---|---|---|---|---|---|---|---|
| | | | | | 0 h | | | | | | 0.5 h | | | | | | 1.5 h | | | | | | 3 h | | | | | | |
| | | | | | Fold change (vs DMSO) | | | ttest: | ttest: | ttest: | Fold change (vs DMSO) | | | ttest: | ttest: | ttest: | Fold change (vs DMSO) | | | ttest: | ttest: | ttest: | Fold change (vs DMSO) | | | ttest: | ttest: | ttest: |
| Mass | RT | FORMULA | Putative metabolite | Map | OZ277 | OZ439 | DHA | OZ277 | OZ439 | DHA | OZ277 | OZ439 | DHA | OZ277 | OZ439 | DHA | OZ277 | OZ439 | DHA | OZ277 | OZ439 | DHA | OZ277 | OZ439 | DHA | OZ277 | OZ439 | DHA |
| 204.0998 | 7.0 | C9H16O5 | Diethyl (2R,3R)-2-methyl-3-hydroxysuccinate | Miscellaneous | 0.96 | 0.80 | 1.05 | 0.8795 | 0.3748 | 0.8344 | 1.46 | 1.26 | 1.47 | 0.1319 | 0.3683 | 0.2267 | 0.82 | 0.86 | 0.86 | 0.5254 | 0.5022 | 0.6164 | 1.46 | 1.56 | 1.61 | 0.3087 | 0.3513 | 0.0414 |
| 112.0160 | 11.8 | C5H4O3 | 2-Furoate | Miscellaneous | 0.90 | 1.02 | 1.12 | 0.7610 | 0.9425 | 0.6349 | 1.19 | 1.09 | 1.36 | 0.6530 | 0.8265 | 0.2989 | 1.18 | 1.26 | 1.04 | 0.6637 | 0.4788 | 0.8515 | 0.88 | 0.95 | 1.07 | 0.6326 | 0.8894 | 0.8012 |
| 166.0840 | 12.2 | C6H14O5 | 3-deoxy-D-galactose | Miscellaneous | 0.59 | 0.56 | 0.72 | 0.1800 | 0.1796 | 0.3507 | 1.04 | 1.08 | 1.33 | 0.8224 | 0.6702 | 0.4525 | 0.63 | 1.61 | 0.99 | 0.2785 | 0.5074 | 0.9755 | 1.32 | 1.28 | 0.98 | 0.6605 | 0.4347 | 0.9743 |
| 163.0843 | 15.7 | C6H13NO4 | Deoxymannojirimycin | Miscellaneous | 1.00 | 1.66 | 1.11 | 0.9984 | 0.0422 | 0.7247 | 0.79 | 1.16 | 1.32 | 0.4415 | 0.7100 | 0.2472 | 0.90 | 1.52 | 1.02 | 0.7723 | 0.1933 | 0.9330 | 0.62 | 1.34 | 0.98 | 0.1921 | 0.4161 | 0.9402 |
| 146.0149 | 13.5 | C4H6N2O2S | ZAPA | Miscellaneous | 1.41 | 1.08 | 1.49 | 0.2488 | 0.8928 | 0.1782 | 0.96 | 0.94 | 1.31 | 0.9066 | 0.7078 | 0.2736 | 1.06 | 0.92 | 1.12 | 0.8068 | 0.5757 | 0.5052 | 1.31 | 1.04 | 1.07 | 0.4059 | 0.7909 | 0.6852 |
| 157.1101 | 9.9 | C8H15NO2 | Homostachydrine | Miscellaneous | 1.07 | 0.55 | 0.97 | 0.8211 | 0.0277 | 0.9026 | 1.40 | 0.95 | 1.30 | 0.1939 | 0.7697 | 0.3335 | 1.24 | 0.74 | 1.00 | 0.5078 | 0.3697 | 0.9942 | 1.49 | 0.83 | 1.11 | 0.3698 | 0.3738 | 0.7309 |
| 205.0950 | 10.8 | C8H15NO5 | N-Acetyl-D-fucosamine | Miscellaneous | 1.00 | 0.67 | 0.84 | 0.9719 | 0.0521 | 0.3603 | 1.45 | 1.09 | 1.29 | 0.0454 | 0.7751 | 0.3176 | 1.28 | 0.57 | 0.95 | 0.1340 | 0.0215 | 0.7659 | 1.34 | 0.72 | 0.91 | 0.0738 | 0.2143 | 0.6515 |
| 191.0795 | 12.6 | C7H13NO5 | 2-amino-3,7-dideoxy-D-threo-hept-6-ulosonate | Miscellaneous | 0.90 | 0.80 | 1.09 | 0.5300 | 0.2441 | 0.5795 | 1.23 | 0.98 | 1.29 | 0.1086 | 0.8972 | 0.1464 | 1.11 | 0.98 | 1.02 | 0.3823 | 0.8952 | 0.7861 | 1.16 | 0.95 | 1.09 | 0.3436 | 0.7147 | 0.5756 |
| 193.0739 | 5.0 | C10H11NO3 | Cichorine | Miscellaneous | 0.88 | 1.20 | 0.81 | 0.4631 | 0.2213 | 0.3145 | 1.02 | 1.00 | 1.29 | 0.8778 | 0.9920 | 0.1259 | 0.91 | 1.09 | 1.03 | 0.6961 | 0.6881 | 0.8553 | 1.10 | 1.25 | 1.29 | 0.4120 | 0.3167 | 0.1734 |
| 85.0892 | 14.5 | C5H11N | Piperidine | Miscellaneous | 0.80 | 0.84 | 0.85 | 0.1823 | 0.2006 | 0.2819 | 0.89 | 1.19 | 1.27 | 0.3646 | 0.1114 | 0.0454 | 0.84 | 1.32 | 1.12 | 0.4673 | 0.2205 | 0.3333 | 1.26 | 1.23 | 2.10 | 0.3972 | 0.2869 | 0.0001 |
| 408.2877 | 5.1 | C24H40O5 | Bile salt | Miscellaneous | 1.11 | 1.00 | 1.16 | 0.5029 | 0.9664 | 0.2511 | 1.03 | 1.06 | 1.25 | 0.7661 | 0.5660 | 0.1672 | 1.00 | 1.16 | 0.99 | 0.9692 | 0.4813 | 0.9030 | 1.17 | 0.95 | 0.98 | 0.2888 | 0.7879 | 0.9075 |
| 246.0506 | 12.5 | C6H15O8P | Glycerophosphoglycerol | Miscellaneous | 1.11 | 0.87 | 1.03 | 0.5761 | 0.3368 | 0.8522 | 1.26 | 1.02 | 1.22 | 0.0839 | 0.8920 | 0.2176 | 1.14 | 0.92 | 1.04 | 0.3757 | 0.4287 | 0.6684 | 1.14 | 0.97 | 1.13 | 0.2303 | 0.8448 | 0.3675 |
| 313.1315 | 12.4 | C18H19NO4 | Acetylcaranine | Miscellaneous | 1.10 | 1.08 | 1.01 | 0.7525 | 0.7106 | 0.9452 | 1.08 | 1.19 | 1.21 | 0.6132 | 0.3277 | 0.3152 | 1.02 | 1.11 | 0.96 | 0.9393 | 0.6863 | 0.8104 | 1.02 | 1.10 | 0.99 | 0.9044 | 0.6774 | 0.9538 |
| 179.0582 | 8.1 | C9H9NO3 | N-Acetylanthranilate | Miscellaneous | 1.07 | 0.65 | 0.98 | 0.7362 | 0.0668 | 0.9130 | 1.44 | 0.91 | 1.20 | 0.1143 | 0.4805 | 0.2552 | 1.27 | 0.87 | 1.05 | 0.0775 | 0.3263 | 0.6891 | 1.14 | 0.81 | 1.01 | 0.2774 | 0.1383 | 0.9189 |
| 212.0086 | 12.5 | C5H9O7P | P-DPD | Miscellaneous | 1.33 | 0.35 | 0.92 | 0.5689 | 0.0564 | 0.8484 | 1.74 | 0.86 | 1.19 | 0.3097 | 0.7788 | 0.7276 | 1.58 | 0.42 | 1.13 | 0.4068 | 0.1252 | 0.7767 | 1.40 | 0.65 | 0.73 | 0.5217 | 0.4188 | 0.5249 |
| 213.0096 | 7.4 | C8H7NO4S | Indoxylsulfate | Miscellaneous | 1.22 | 0.97 | 1.14 | 0.5399 | 0.8562 | 0.6249 | 0.96 | 1.07 | 1.19 | 0.8904 | 0.8240 | 0.4616 | 0.88 | 1.05 | 1.12 | 0.6903 | 0.7872 | 0.6406 | 0.93 | 1.26 | 1.02 | 0.7532 | 0.2608 | 0.9386 |
| 383.1075 | 14.3 | C14H17N5O8 | Succinyladenosine | Miscellaneous | 1.00 | 1.07 | 1.00 | 0.9807 | 0.4005 | 0.9936 | 1.07 | 1.00 | 1.18 | 0.7283 | 0.9896 | 0.3489 | 1.19 | 1.07 | 1.10 | 0.5477 | 0.6166 | 0.4849 | 1.01 | 1.00 | 0.97 | 0.9320 | 0.9842 | 0.7957 |
| 246.0853 | 10.4 | C9H14N2O6 | L-alpha-Aspartyl-L-hydroxyproline | Miscellaneous | 1.01 | 0.42 | 0.90 | 0.9684 | 0.1795 | 0.6927 | 0.94 | 0.73 | 1.18 | 0.8306 | 0.3135 | 0.4709 | 1.00 | 0.73 | 0.79 | 0.9974 | 0.2894 | 0.3271 | 1.02 | 0.64 | 1.01 | 0.9474 | 0.2219 | 0.9559 |
| 96.0213 | 17.6 | C5H4O2 | Furfural | Miscellaneous | 0.87 | 1.16 | 1.10 | 0.1802 | 0.6507 | 0.4514 | 0.94 | 1.02 | 1.18 | 0.5988 | 0.8885 | 0.2451 | 1.19 | 0.86 | 1.08 | 0.2489 | 0.5487 | 0.6032 | 1.05 | 1.59 | 1.16 | 0.8979 | 0.0498 | 0.4025 |
| 186.0641 | 14.1 | C7H10N2O4 | (S)-AMPA | Miscellaneous | 1.12 | 0.99 | 1.04 | 0.1967 | 0.9259 | 0.7087 | 1.11 | 0.93 | 1.18 | 0.4015 | 0.7865 | 0.0150 | 1.04 | 1.02 | 1.02 | 0.5971 | 0.8586 | 0.7741 | 0.99 | 0.89 | 1.08 | 0.9190 | 0.2303 | 0.3645 |
| 237.0849 | 15.7 | C8H15NO7 | N-Glycolyl-D-mannosamine | Miscellaneous | 1.05 | 1.12 | 1.04 | 0.8069 | 0.6768 | 0.8006 | 0.89 | 1.03 | 1.17 | 0.3868 | 0.8847 | 0.3486 | 0.95 | 1.27 | 1.16 | 0.7860 | 0.1166 | 0.2568 | 1.03 | 1.05 | 1.25 | 0.8539 | 0.8043 | 0.1160 |
| 270.0963 | 14.6 | C10H14N4O5 | 6-Hydroxyl-1,6-dihydropurine ribonucleoside | Miscellaneous | 1.14 | 0.69 | 1.02 | 0.5555 | 0.0049 | 0.9150 | 1.50 | 0.91 | 1.17 | 0.0977 | 0.6404 | 0.3863 | 1.16 | 0.78 | 0.91 | 0.3758 | 0.2117 | 0.6116 | 1.09 | 0.65 | 0.87 | 0.6384 | 0.0809 | 0.3326 |
| 259.0365 | 16.9 | C6H13NO8S | N-Sulfo-D-glucosamine | Miscellaneous | 0.91 | 1.14 | 1.00 | 0.6981 | 0.7457 | 0.9952 | 1.01 | 1.10 | 1.16 | 0.9617 | 0.6695 | 0.4556 | 1.00 | 1.30 | 1.04 | 0.9944 | 0.2451 | 0.8459 | 0.98 | 1.08 | 1.09 | 0.9453 | 0.7566 | 0.6663 |
| 348.1105 | 12.9 | C20H16N2O4 | Camptothecin | Miscellaneous | 1.08 | 1.03 | 1.03 | 0.1100 | 0.4229 | 0.7658 | 1.21 | 1.05 | 1.16 | 0.0822 | 0.6481 | 0.1234 | 1.08 | 1.03 | 1.02 | 0.3039 | 0.7307 | 0.7048 | 1.07 | 0.97 | 1.06 | 0.3846 | 0.7690 | 0.5757 |
| 204.1109 | 17.7 | C8H16N2O4 | N5-(L-1-Carboxyethyl)-L-ornithine | Miscellaneous | 1.09 | 1.09 | 1.09 | 0.4365 | 0.3892 | 0.4502 | 1.06 | 1.00 | 1.16 | 0.5701 | 0.9896 | 0.2192 | 1.05 | 1.07 | 0.99 | 0.4938 | 0.6249 | 0.9516 | 1.04 | 0.96 | 1.10 | 0.7748 | 0.8675 | 0.4680 |
| 541.0603 | 14.0 | C15H21N5O13P2 | Cyclic ADP-ribose | Miscellaneous | 1.09 | 0.95 | 1.04 | 0.5300 | 0.5301 | 0.6456 | 1.23 | 1.00 | 1.16 | 0.1133 | 0.9517 | 0.0872 | 1.04 | 0.87 | 0.99 | 0.7468 | 0.0641 | 0.9065 | 1.09 | 0.92 | 1.06 | 0.4818 | 0.3268 | 0.5437 |
| 679.1041 | 13.0 | C21H27N7O15P2 | nicotinamide guanine dinucleotide | Miscellaneous | 1.07 | 0.87 | 0.98 | 0.3981 | 0.1122 | 0.8523 | 1.35 | 1.03 | 1.16 | 0.0514 | 0.8050 | 0.2578 | 1.08 | 0.90 | 0.96 | 0.4586 | 0.3461 | 0.6144 | 1.20 | 0.89 | 1.05 | 0.0537 | 0.4622 | 0.5914 |
| 334.0670 | 15.9 | C9H19O11P | sn-glycero-3-Phospho-1-inositol | Miscellaneous | 1.13 | 0.95 | 1.00 | 0.5475 | 0.6482 | 0.9784 | 1.18 | 0.97 | 1.16 | 0.1437 | 0.7072 | 0.1829 | 1.01 | 0.85 | 0.96 | 0.9037 | 0.1208 | 0.6296 | 0.99 | 0.84 | 0.88 | 0.9443 | 0.0462 | 0.2142 |
| 205.9981 | 17.3 | C7H7ClO5 | 2-chloro-3-methyl-maleylacetate | Miscellaneous | 1.03 | 0.86 | 1.02 | 0.6635 | 0.0890 | 0.8254 | 1.16 | 1.09 | 1.15 | 0.0729 | 0.2609 | 0.0868 | 1.03 | 1.04 | 1.00 | 0.7810 | 0.7607 | 0.9560 | 1.16 | 1.01 | 1.09 | 0.1505 | 0.9264 | 0.3951 |
| 387.0409 | 18.9 | C10H17N3O9S2 | glutathione-sulfite | Miscellaneous | 0.65 | 0.85 | 1.28 | 0.3932 | 0.7423 | 0.6627 | 0.80 | 0.92 | 1.15 | 0.2405 | 0.6873 | 0.7462 | 0.67 | 0.87 | 0.79 | 0.1688 | 0.5644 | 0.3847 | 0.91 | 1.19 | 1.05 | 0.3625 | 0.2692 | 0.7300 |
| 247.1420 | 11.3 | C11H21NO5 | Hydroxybutyrylcarnitine | Miscellaneous | 0.73 | 1.33 | 1.16 | 0.3291 | 0.1671 | 0.5970 | 0.77 | 0.99 | 1.15 | 0.3908 | 0.9715 | 0.5723 | 0.78 | 1.11 | 0.91 | 0.4002 | 0.6224 | 0.6795 | 0.87 | 1.09 | 1.17 | 0.6510 | 0.7432 | 0.4816 |
| 137.0477 | 11.8 | C7H7NO2 | 1-carboxymethylpyridinium | Miscellaneous | 1.04 | 1.08 | 1.04 | 0.9369 | 0.7817 | 0.9113 | 1.08 | 0.86 | 1.15 | 0.8616 | 0.5794 | 0.6153 | 0.72 | 0.94 | 0.95 | 0.3757 | 0.8263 | 0.8791 | 1.14 | 0.99 | 1.24 | 0.7728 | 0.9629 | 0.4842 |
| 324.1531 | 16.5 | C12H24N2O8 | Procollagen 5-(D-galactosyloxy)-L-lysine | Miscellaneous | 0.82 | 1.06 | 1.03 | 0.2507 | 0.6765 | 0.8163 | 1.01 | 1.17 | 1.14 | 0.9796 | 0.3747 | 0.5379 | 0.98 | 1.24 | 1.01 | 0.9312 | 0.1064 | 0.9670 | 0.96 | 1.03 | 1.06 | 0.7362 | 0.8689 | 0.6819 |
| 444.3604 | 3.9 | C29H48O3 | 3beta-Hydroxy-4beta-methyl-5alpha-cholest-7-ene-4alpha-carboxylate | Miscellaneous | 0.91 | 1.20 | 0.97 | 0.5485 | 0.5757 | 0.8444 | 0.82 | 1.22 | 1.14 | 0.3316 | 0.3866 | 0.4880 | 0.92 | 1.23 | 1.14 | 0.7663 | 0.4414 | 0.5416 | 0.83 | 1.12 | 0.92 | 0.3399 | 0.6728 | 0.5751 |
| 143.0946 | 10.7 | C7H13NO2 | 4-(Trimethylammonio)but-2-enoate | Miscellaneous | 1.26 | 0.44 | 0.98 | 0.1003 | 0.0049 | 0.9129 | 1.49 | 0.77 | 1.13 | 0.0834 | 0.3833 | 0.6520 | 1.68 | 0.56 | 1.18 | 0.0791 | 0.0280 | 0.4970 | 1.37 | 0.59 | 0.90 | 0.0289 | 0.0782 | 0.6178 |
| 707.2490 | 16.3 | C26H45NO21 | Lacto-N-tetraose | Miscellaneous | 0.65 | 1.04 | 0.95 | 0.1960 | 0.8916 | 0.8494 | 0.86 | 1.22 | 1.13 | 0.6316 | 0.5139 | 0.6297 | 0.86 | 1.37 | 1.14 | 0.5577 | 0.1545 | 0.5107 | 0.79 | 1.21 | 1.05 | 0.4148 | 0.6225 | 0.8576 |
| 218.0402 | 13.3 | C12H10O2S | cis-1,2-Dihydroxy-1,2-dihydrodibenzothiophene | Miscellaneous | 0.91 | 0.92 | 0.96 | 0.5805 | 0.5176 | 0.7627 | 1.11 | 1.17 | 1.13 | 0.5143 | 0.3188 | 0.4051 | 0.99 | 0.97 | 0.98 | 0.9704 | 0.8079 | 0.8351 | 0.96 | 1.15 | 0.96 | 0.7709 | 0.2715 | 0.7207 |

| | | | | | | | | | | | | | | | | | | | | | | | | | | | | | |
|---|---|---|---|---|---|---|---|---|---|---|---|---|---|---|---|---|---|---|---|---|---|---|---|---|---|---|---|---|---|
| 321.0694 | 19.9 | C11H15NO10 | beta-Citryl-L-glutamic acid | Miscellaneous | 1.10 | 0.61 | 0.88 | 0.8059 | 0.0662 | 0.6250 | 1.41 | 1.06 | 1.13 | 0.3892 | 0.8396 | 0.7102 | 1.13 | 0.68 | 1.05 | 0.7228 | 0.1733 | 0.8518 | 1.07 | 0.84 | 0.82 | 0.8227 | 0.5304 | 0.4618 |
| 189.1114 | 15.0 | C7H15N3O3 | L-Homocitrulline | Miscellaneous | 1.43 | 1.16 | 1.30 | 0.1765 | 0.3891 | 0.1849 | 1.23 | 1.18 | 1.13 | 0.2593 | 0.3398 | 0.3744 | 1.16 | 0.88 | 1.00 | 0.2787 | 0.4451 | 0.9940 | 1.06 | 0.91 | 0.97 | 0.7941 | 0.7128 | 0.7844 |
| 374.1368 | 10.2 | C20H22O7 | Kievitone hydrate | Miscellaneous | 0.96 | 0.74 | 1.06 | 0.8179 | 0.1103 | 0.7022 | 1.23 | 1.10 | 1.13 | 0.1197 | 0.4898 | 0.4386 | 1.09 | 0.93 | 1.02 | 0.3299 | 0.5107 | 0.8145 | 1.15 | 1.00 | 1.11 | 0.2306 | 0.9921 | 0.3742 |
| 138.0316 | 16.0 | C7H6O3 | protocatechualdehyde | Miscellaneous | 1.08 | 1.01 | 1.04 | 0.5595 | 0.9824 | 0.7767 | 1.03 | 1.17 | 1.13 | 0.8740 | 0.4843 | 0.4720 | 1.08 | 1.26 | 1.01 | 0.6586 | 0.2084 | 0.9308 | 1.12 | 0.98 | 1.13 | 0.5995 | 0.9073 | 0.4943 |
| 291.0956 | 12.3 | C11H17NO8 | 2-Deoxy-2,3-dehydro-N-acetylneuraminic acid | Miscellaneous | 0.93 | 1.03 | 1.02 | 0.6722 | 0.7598 | 0.8701 | 1.06 | 1.17 | 1.12 | 0.6167 | 0.2240 | 0.4040 | 1.02 | 1.10 | 1.03 | 0.9181 | 0.4265 | 0.7631 | 0.94 | 1.07 | 1.03 | 0.6059 | 0.5752 | 0.8039 |
| 202.0590 | 15.4 | C7H10N2O5 | N3-fumaramoyl-L-2,3-diaminopropanoate | Miscellaneous | 1.10 | 0.66 | 0.96 | 0.6211 | 0.0089 | 0.7539 | 1.30 | 0.97 | 1.12 | 0.1085 | 0.8670 | 0.4682 | 1.21 | 0.78 | 1.02 | 0.2731 | 0.1098 | 0.8995 | 1.11 | 0.85 | 0.93 | 0.5281 | 0.3565 | 0.6285 |
| 559.1343 | 15.2 | C18H31N3O13P2 | dTDP-alpha-D-desosamine | Miscellaneous | 1.05 | 1.19 | 1.10 | 0.6644 | 0.1445 | 0.4320 | 1.11 | 1.09 | 1.12 | 0.3208 | 0.6935 | 0.3079 | 0.98 | 1.09 | 0.92 | 0.7994 | 0.1765 | 0.3789 | 1.00 | 1.26 | 1.17 | 0.9974 | 0.3900 | 0.2850 |
| 206.1671 | 4.2 | C14H22O | alpha-Irone | Miscellaneous | 1.18 | 1.21 | 1.22 | 0.4983 | 0.2007 | 0.4520 | 1.05 | 1.04 | 1.12 | 0.6742 | 0.7069 | 0.3912 | 0.97 | 1.01 | 1.05 | 0.7696 | 0.9569 | 0.5835 | 1.00 | 0.95 | 0.99 | 0.9674 | 0.6549 | 0.9037 |
| 261.1211 | 12.8 | C11H19NO6 | Lotaustralin | Miscellaneous | 0.89 | 1.04 | 0.94 | 0.4800 | 0.7041 | 0.5580 | 1.03 | 1.07 | 1.12 | 0.8878 | 0.6147 | 0.5156 | 1.02 | 1.18 | 1.05 | 0.8839 | 0.1900 | 0.6565 | 0.91 | 1.06 | 1.07 | 0.3591 | 0.5224 | 0.5381 |
| 125.0477 | 12.1 | C6H7NO2 | N-Ethylmaleimide | Miscellaneous | 0.65 | 1.04 | 0.98 | 0.1183 | 0.8495 | 0.9140 | 0.91 | 1.18 | 1.12 | 0.6366 | 0.4774 | 0.6273 | 0.94 | 1.19 | 0.98 | 0.7723 | 0.3204 | 0.9105 | 0.85 | 1.14 | 1.11 | 0.2648 | 0.5063 | 0.5767 |
| 136.0373 | 16.2 | C4H8O5 | Erythronicacid | Miscellaneous | 1.24 | 1.52 | 1.22 | 0.2645 | 0.5885 | 0.3162 | 1.03 | 0.99 | 1.11 | 0.8812 | 0.9713 | 0.6579 | 0.97 | 0.94 | 0.91 | 0.8823 | 0.8673 | 0.6819 | 0.98 | 0.96 | 1.08 | 0.9154 | 0.9146 | 0.7124 |
| 358.1412 | 14.4 | C20H22O6 | Miroestrol | Miscellaneous | 0.92 | 1.02 | 1.03 | 0.6665 | 0.9043 | 0.8610 | 1.10 | 1.12 | 1.11 | 0.5310 | 0.3519 | 0.4243 | 0.98 | 1.11 | 1.01 | 0.9027 | 0.5275 | 0.9511 | 0.95 | 1.10 | 1.03 | 0.7350 | 0.3628 | 0.8096 |
| 161.0324 | 8.0 | C5H7NO5 | A-Ketoglutaricacidoxime | Miscellaneous | 0.96 | 0.87 | 0.95 | 0.8982 | 0.5802 | 0.8050 | 1.26 | 0.98 | 1.11 | 0.3457 | 0.9057 | 0.4606 | 1.16 | 0.70 | 0.89 | 0.3495 | 0.1280 | 0.4300 | 1.14 | 0.88 | 0.94 | 0.2032 | 0.5378 | 0.6859 |
| 621.0274 | 17.9 | C15H22N5O16P3 | ADP ribose 1",2"-phosphate | Miscellaneous | 0.82 | 0.96 | 1.00 | 0.4669 | 0.8623 | 0.9882 | 0.96 | 1.20 | 1.11 | 0.7800 | 0.4224 | 0.6492 | 0.90 | 1.17 | 1.09 | 0.5571 | 0.4695 | 0.6959 | 1.06 | 1.17 | 1.24 | 0.7504 | 0.6003 | 0.0942 |
| 272.0297 | 21.8 | C7H13O9P | β-(2,6-anhydro-3-deoxy-D-arabino-heptulopyranosid)onate 7-phosphate | Miscellaneous | 0.86 | 0.91 | 0.97 | 0.2840 | 0.5458 | 0.8145 | 1.04 | 1.07 | 1.11 | 0.7801 | 0.6805 | 0.3765 | 0.95 | 1.09 | 1.00 | 0.5875 | 0.5989 | 0.9789 | 0.96 | 1.03 | 1.02 | 0.6930 | 0.8599 | 0.7983 |
| 202.0264 | 14.9 | C11H6O4 | Bergaptol | Miscellaneous | 0.99 | 1.20 | 1.04 | 0.9473 | 0.4824 | 0.8217 | 0.88 | 1.10 | 1.11 | 0.5211 | 0.5867 | 0.5580 | 0.92 | 1.10 | 0.89 | 0.7523 | 0.5766 | 0.5085 | 0.90 | 1.07 | 1.09 | 0.6254 | 0.6720 | 0.6410 |
| 318.2044 | 4.7 | C16H30O6 | (-)-Menthyl O-beta-D-glucoside | Miscellaneous | 1.15 | 0.98 | 1.07 | 0.2251 | 0.7836 | 0.5322 | 1.22 | 0.92 | 1.11 | 0.1808 | 0.5723 | 0.4119 | 1.15 | 0.82 | 1.05 | 0.4107 | 0.2081 | 0.7041 | 1.24 | 0.81 | 1.01 | 0.1185 | 0.1269 | 0.9551 |
| 242.0192 | 17.3 | C6H11O8P | D-myo-Inositol 1,2-cyclic phosphate | Miscellaneous | 1.08 | 3.13 | 1.01 | 0.7379 | 0.0081 | 0.9408 | 1.21 | 1.01 | 1.11 | 0.2598 | 0.9277 | 0.4092 | 1.10 | 0.86 | 1.01 | 0.6057 | 0.1818 | 0.9542 | 1.13 | 0.82 | 1.05 | 0.5093 | 0.1351 | 0.7266 |
| 869.3022 | 17.2 | C32H55NO26 | 1,3-alpha-D-Mannosyl-(1,2-N-acetyl-alpha-D-glucosaminyl)-1,2-alpha-D-mannosyl-1,2-alpha-D-mannosyl-D-mannose | Miscellaneous | 0.78 | 1.66 | 1.16 | 0.1809 | 0.0613 | 0.4180 | 0.82 | 1.42 | 1.10 | 0.4338 | 0.1512 | 0.7165 | 0.71 | 1.41 | 1.04 | 0.1576 | 0.3138 | 0.8700 | 0.61 | 1.24 | 1.10 | 0.0520 | 0.4079 | 0.7348 |
| 193.0409 | 11.0 | C6H11NO4S | γ-thiomethyl glutamate | Miscellaneous | 1.00 | 0.64 | 0.91 | 0.9863 | 0.0752 | 0.6219 | 1.08 | 1.17 | 1.09 | 0.5995 | 0.5491 | 0.6258 | 1.05 | 0.96 | 1.08 | 0.7508 | 0.9301 | 0.6880 | 1.04 | 1.07 | 1.06 | 0.7969 | 0.7397 | 0.7166 |
| 427.3660 | 4.5 | C25H49NO4 | Stearoylcarnitine | Miscellaneous | 0.81 | 0.72 | 0.87 | 0.6350 | 0.3554 | 0.7055 | 0.76 | 0.94 | 1.09 | 0.3301 | 0.7699 | 0.7495 | 0.77 | 1.22 | 1.02 | 0.3350 | 0.5412 | 0.9502 | 0.75 | 0.94 | 1.00 | 0.3593 | 0.8226 | 0.9970 |
| 289.1273 | 13.2 | C11H19N3O6 | Ophthalmicacid | Miscellaneous | 0.80 | 1.14 | 0.89 | 0.1051 | 0.1684 | 0.3339 | 0.96 | 1.05 | 1.09 | 0.7565 | 0.7887 | 0.6071 | 0.93 | 1.13 | 1.05 | 0.5953 | 0.1714 | 0.7053 | 0.99 | 1.25 | 1.32 | 0.9387 | 0.3416 | 0.1512 |
| 186.0531 | 14.0 | C8H10O5 | 2-hydroxy-3-carboxy-4,5-cyclopropylhex-5-enoate | Miscellaneous | 1.02 | 0.72 | 0.96 | 0.9036 | 0.0636 | 0.7697 | 1.17 | 0.94 | 1.09 | 0.3629 | 0.6913 | 0.5571 | 1.15 | 0.85 | 1.03 | 0.5270 | 0.4748 | 0.8529 | 1.12 | 0.84 | 1.09 | 0.3269 | 0.3815 | 0.5555 |
| 275.1735 | 9.1 | C13H25NO5 | Hydroxyhexanoycarnitine | Miscellaneous | 0.99 | 0.97 | 1.01 | 0.9751 | 0.8506 | 0.9618 | 0.98 | 0.90 | 1.09 | 0.9480 | 0.5213 | 0.6027 | 1.04 | 1.05 | 0.98 | 0.8668 | 0.7652 | 0.8981 | 0.88 | 0.97 | 1.13 | 0.6891 | 0.8967 | 0.5001 |
| 288.0596 | 12.1 | C10H12N2O8 | Orotidine | Miscellaneous | 1.00 | 0.98 | 1.06 | 0.9920 | 0.7946 | 0.5623 | 1.10 | 1.03 | 1.08 | 0.5501 | 0.8070 | 0.5960 | 1.13 | 1.05 | 1.08 | 0.5248 | 0.7017 | 0.3801 | 0.98 | 1.00 | 0.97 | 0.8976 | 0.9723 | 0.7858 |
| 115.0998 | 11.8 | C6H13NO | Trimethylaminoacetone | Miscellaneous | 1.09 | 0.81 | 0.98 | 0.8252 | 0.3997 | 0.9560 | 1.19 | 0.93 | 1.08 | 0.6856 | 0.7626 | 0.7757 | 1.13 | 0.85 | 0.93 | 0.7591 | 0.4932 | 0.7978 | 1.13 | 0.85 | 1.20 | 0.7709 | 0.5414 | 0.5269 |
| 251.1004 | 14.3 | C9H17NO7 | Muramic acid | Miscellaneous | 1.03 | 0.83 | 0.93 | 0.7655 | 0.1109 | 0.2980 | 1.15 | 1.02 | 1.08 | 0.2298 | 0.8975 | 0.5112 | 1.15 | 0.96 | 1.05 | 0.2035 | 0.7793 | 0.5016 | 1.14 | 0.94 | 1.07 | 0.1484 | 0.6377 | 0.4384 |
| 269.0928 | 16.1 | C10H12FN5O3 | 5'-deoxy-5'-fluoroadenosine | Miscellaneous | 0.84 | 1.14 | 1.02 | 0.6417 | 0.4843 | 0.9253 | 0.86 | 0.94 | 1.08 | 0.5770 | 0.7764 | 0.7291 | 0.97 | 1.14 | 0.99 | 0.9276 | 0.5356 | 0.9747 | 1.04 | 1.06 | 1.17 | 0.8604 | 0.7461 | 0.3618 |
| 175.0846 | 13.1 | C7H13NO4 | N-Carboxyethyl-g-aminobutyricacid | Miscellaneous | 0.97 | 0.89 | 0.94 | 0.7927 | 0.0379 | 0.3583 | 1.13 | 0.85 | 1.07 | 0.4932 | 0.2721 | 0.6931 | 1.07 | 1.09 | 0.96 | 0.7542 | 0.4057 | 0.7344 | 0.99 | 0.90 | 0.97 | 0.9407 | 0.3302 | 0.7878 |
| 384.1214 | 13.5 | C21H20O7 | Anthocyanin 3'-O-beta-D-glucoside | Miscellaneous | 1.01 | 1.18 | 1.09 | 0.9090 | 0.1366 | 0.3224 | 1.09 | 0.93 | 1.07 | 0.6599 | 0.6426 | 0.6233 | 1.11 | 1.00 | 0.98 | 0.7076 | 0.9994 | 0.8929 | 0.99 | 0.89 | 0.94 | 0.9519 | 0.4816 | 0.5769 |
| 278.0642 | 22.6 | C10H14O9 | hexane-6-ol-1,3,4,6-tetracarboxylate | Miscellaneous | 0.94 | 1.29 | 1.05 | 0.7314 | 0.3670 | 0.7167 | 1.06 | 1.06 | 1.07 | 0.7896 | 0.7743 | 0.6832 | 1.09 | 1.19 | 0.93 | 0.7827 | 0.1991 | 0.6997 | 0.93 | 0.99 | 0.83 | 0.7592 | 0.9312 | 0.3211 |
| 234.1216 | 17.6 | C9H18N2O5 | 2,6-Diamino-7-hydroxy-azelaic acid | Miscellaneous | 0.95 | 1.06 | 1.05 | 0.6662 | 0.6330 | 0.6048 | 0.99 | 1.02 | 1.07 | 0.9449 | 0.8937 | 0.6020 | 0.90 | 1.02 | 1.02 | 0.3105 | 0.8761 | 0.8878 | 0.94 | 1.03 | 1.06 | 0.6505 | 0.8708 | 0.7494 |
| 257.1121 | 14.0 | C9H15N5O4 | 4a-Hydroxytetrahydrobiopterin | Miscellaneous | 0.96 | 0.85 | 1.12 | 0.7834 | 0.0992 | 0.1287 | 1.08 | 0.98 | 1.07 | 0.6316 | 0.9118 | 0.5758 | 1.07 | 0.92 | 1.06 | 0.6676 | 0.4188 | 0.6206 | 1.07 | 0.93 | 1.01 | 0.6041 | 0.5446 | 0.9067 |
| 326.1216 | 15.9 | C12H22O10 | 2-O-alpha-L-Rhamnopyranosyl-D-glucopyranose | Miscellaneous | 1.03 | 1.02 | 0.98 | 0.6038 | 0.6626 | 0.7246 | 1.06 | 0.97 | 1.07 | 0.6573 | 0.7621 | 0.5821 | 1.00 | 0.93 | 1.03 | 0.9707 | 0.3288 | 0.6981 | 0.95 | 0.90 | 1.01 | 0.4888 | 0.2153 | 0.9296 |
| 222.0739 | 14.0 | C8H14O7 | 6-Acetyl-D-glucose | Miscellaneous | 0.98 | 0.82 | 1.02 | 0.8386 | 0.1903 | 0.7837 | 1.06 | 0.95 | 1.06 | 0.5954 | 0.7096 | 0.5205 | 1.13 | 0.99 | 1.00 | 0.4479 | 0.9467 | 0.9964 | 1.00 | 0.99 | 1.09 | 0.9768 | 0.9682 | 0.3493 |
| 159.1259 | 13.3 | C8H17NO2 | Methacholine | Miscellaneous | 1.14 | 0.87 | 1.07 | 0.6345 | 0.5164 | 0.7736 | 1.09 | 0.82 | 1.06 | 0.7904 | 0.2458 | 0.7643 | 1.17 | 0.86 | 1.02 | 0.5509 | 0.4075 | 0.9349 | 1.09 | 0.91 | 1.16 | 0.7778 | 0.6478 | 0.5326 |

| | | | | | | | | | | | | | | | | | | | | | | | | | | | | |
|---|---|---|---|---|---|---|---|---|---|---|---|---|---|---|---|---|---|---|---|---|---|---|---|---|---|---|---|---|
| 630.1908 | 14.7 | C26H34N2O16 | oxindole-3-acetyl-aspartate-N-beta-glucosyl-beta-1,4-glucose | Miscellaneous | 0.49 | 1.66 | 1.00 | 0.2831 | 0.1743 | 0.9991 | 0.54 | 1.47 | 1.06 | 0.3877 | 0.3701 | 0.8995 | 0.49 | 1.69 | 0.84 | 0.2499 | 0.0633 | 0.6833 | 0.47 | 1.22 | 0.70 | 0.2587 | 0.6558 | 0.4875 |
| 282.0953 | 13.6 | C10H18O9 | Xylobiose | Miscellaneous | 1.35 | 0.39 | 1.00 | 0.1785 | 0.0172 | 0.9860 | 1.53 | 0.67 | 1.06 | 0.1639 | 0.2004 | 0.8340 | 1.39 | 0.44 | 0.97 | 0.1348 | 0.0405 | 0.9204 | 1.50 | 0.57 | 1.00 | 0.0640 | 0.0711 | 0.9889 |
| 213.1111 | 14.0 | C9H15N3O3 | Methyl 2-diazoacetamidohexonate | Miscellaneous | 0.68 | 1.57 | 1.04 | 0.2622 | 0.0688 | 0.9026 | 0.74 | 1.46 | 1.06 | 0.2919 | 0.3986 | 0.8432 | 0.61 | 1.44 | 0.93 | 0.0875 | 0.1127 | 0.7827 | 0.59 | 1.24 | 1.13 | 0.1264 | 0.5353 | 0.6959 |
| 112.0272 | 12.0 | C4H6N2O3 | 3-ureidoacrylate | Miscellaneous | 0.98 | 0.95 | 1.04 | 0.8955 | 0.5308 | 0.7122 | 1.13 | 1.04 | 1.06 | 0.4275 | 0.7537 | 0.6586 | 1.10 | 0.99 | 1.05 | 0.5255 | 0.9636 | 0.6136 | 1.01 | 0.99 | 0.99 | 0.9389 | 0.9122 | 0.8971 |
| 424.0372 | 14.5 | C14H18NO10S2 | Sinalbin | Miscellaneous | 1.06 | 1.29 | 1.05 | 0.6789 | 0.0157 | 0.6715 | 1.07 | 1.07 | 1.06 | 0.5226 | 0.5584 | 0.6439 | 1.06 | 1.11 | 0.99 | 0.6962 | 0.6723 | 0.9425 | 1.03 | 0.99 | 0.96 | 0.8369 | 0.9674 | 0.5957 |
| 147.0896 | 13.1 | C6H13NO3 | Fagomine | Miscellaneous | 0.37 | 0.82 | 0.77 | 0.1149 | 0.6357 | 0.5338 | 0.46 | 1.17 | 1.06 | 0.1178 | 0.6859 | 0.8633 | 0.92 | 1.33 | 0.88 | 0.8643 | 0.3165 | 0.6746 | 0.99 | 1.06 | 1.38 | 0.9807 | 0.8820 | 0.3207 |
| 308.1583 | 20.9 | C12H24N2O7 | psicoselysine | Miscellaneous | 0.97 | 1.29 | 1.01 | 0.7982 | 0.1566 | 0.9483 | 1.09 | 0.97 | 1.06 | 0.6440 | 0.8658 | 0.6886 | 1.02 | 1.15 | 0.99 | 0.9112 | 0.3376 | 0.9313 | 0.93 | 0.97 | 0.84 | 0.5372 | 0.8774 | 0.1969 |
| 486.2062 | 21.7 | C18H34N2O13 | Glucosylgalactosylhydroxylysine | Miscellaneous | 0.93 | 0.87 | 0.99 | 0.5210 | 0.1064 | 0.8804 | 1.08 | 1.03 | 1.06 | 0.4992 | 0.8391 | 0.6467 | 1.01 | 1.03 | 0.99 | 0.9141 | 0.8178 | 0.9357 | 0.98 | 0.94 | 1.04 | 0.7938 | 0.7070 | 0.7475 |
| 363.1434 | 11.6 | C17H21N3O6 | phe-FMDP | Miscellaneous | 0.98 | 0.99 | 0.88 | 0.8643 | 0.9414 | 0.2875 | 1.05 | 1.06 | 1.06 | 0.7263 | 0.5892 | 0.7377 | 1.03 | 1.06 | 1.02 | 0.6845 | 0.6546 | 0.8303 | 0.89 | 1.01 | 1.07 | 0.3100 | 0.9151 | 0.4986 |
| 350.0616 | 16.6 | C9H19O12P | nonulose 9-phosphate | Miscellaneous | 0.99 | 1.03 | 1.04 | 0.8822 | 0.7057 | 0.6427 | 1.04 | 1.13 | 1.06 | 0.7690 | 0.4065 | 0.6812 | 0.91 | 1.11 | 0.98 | 0.2124 | 0.4063 | 0.8216 | 0.96 | 1.07 | 1.17 | 0.6178 | 0.6067 | 0.1117 |
| 300.1114 | 4.9 | C16H16N2O4 | 5-Nitro-2-(3-phenylpropylamino)benzoic acid | Miscellaneous | 0.77 | 0.77 | 0.93 | 0.0268 | 0.0052 | 0.4089 | 1.20 | 1.07 | 1.05 | 0.3442 | 0.6758 | 0.6883 | 1.08 | 1.10 | 1.02 | 0.7316 | 0.5673 | 0.8632 | 0.90 | 0.99 | 1.14 | 0.4446 | 0.9434 | 0.4094 |
| 324.1059 | 14.6 | C12H20O10 | Bis-D-fructose 2',1:2,1'-dianhydride | Miscellaneous | 0.96 | 0.64 | 0.87 | 0.8878 | 0.0743 | 0.5311 | 1.23 | 1.08 | 1.05 | 0.3749 | 0.6152 | 0.7810 | 1.11 | 0.92 | 0.92 | 0.5396 | 0.6984 | 0.5547 | 1.04 | 0.96 | 0.87 | 0.7222 | 0.8036 | 0.3399 |
| 199.1210 | 10.4 | C10H17NO3 | Tussilagine | Miscellaneous | 1.16 | 0.67 | 1.00 | 0.6070 | 0.1341 | 0.9988 | 1.46 | 0.83 | 1.05 | 0.2186 | 0.3666 | 0.8109 | 0.95 | 0.57 | 0.82 | 0.8130 | 0.0550 | 0.4436 | 0.97 | 0.64 | 0.99 | 0.8923 | 0.0327 | 0.9731 |
| 383.1426 | 13.6 | C14H25NO11 | N-Acetyllactosamine | Miscellaneous | 1.24 | 0.38 | 0.97 | 0.2630 | 0.0118 | 0.9081 | 1.50 | 0.55 | 1.05 | 0.1320 | 0.0988 | 0.8668 | 1.54 | 0.48 | 1.05 | 0.0489 | 0.0511 | 0.8811 | 1.42 | 0.54 | 1.03 | 0.0824 | 0.0472 | 0.9335 |
| 305.0412 | 13.4 | C9H12N3O7P | 3',5'-Cyclic CMP | Miscellaneous | 0.53 | 0.97 | 1.11 | 0.2572 | 0.9472 | 0.8346 | 0.62 | 1.06 | 1.05 | 0.2540 | 0.8525 | 0.9145 | 0.59 | 1.38 | 0.94 | 0.2233 | 0.3975 | 0.8612 | 0.71 | 1.35 | 1.22 | 0.3734 | 0.3373 | 0.4862 |
| 358.1113 | 15.0 | C12H22O12 | melibionate | Miscellaneous | 0.90 | 1.07 | 1.04 | 0.3434 | 0.5075 | 0.7400 | 0.98 | 1.07 | 1.05 | 0.8350 | 0.5316 | 0.5749 | 1.01 | 1.08 | 1.00 | 0.8917 | 0.3310 | 0.9956 | 0.93 | 1.07 | 1.09 | 0.4944 | 0.5458 | 0.3697 |
| 241.0586 | 19.9 | C10H11NO6 | N-23-dihydroxybenzoyl-L-serine | Miscellaneous | 1.05 | 0.67 | 0.86 | 0.8822 | 0.1207 | 0.5684 | 1.35 | 1.04 | 1.04 | 0.4354 | 0.8783 | 0.8994 | 1.19 | 0.74 | 1.05 | 0.5737 | 0.2517 | 0.8564 | 1.10 | 0.88 | 0.86 | 0.7320 | 0.6712 | 0.5400 |
| 185.1054 | 11.2 | C9H15NO3 | Otonecine | Miscellaneous | 1.15 | 0.79 | 1.00 | 0.6149 | 0.2146 | 0.9954 | 1.16 | 0.78 | 1.04 | 0.6387 | 0.1338 | 0.8437 | 1.20 | 0.75 | 1.03 | 0.5533 | 0.2178 | 0.9015 | 1.31 | 0.76 | 1.13 | 0.4272 | 0.1470 | 0.6273 |
| 380.1628 | 8.1 | C23H24O5 | 2,2-Dimethyl-3-[4-(acetyloxy)phenyl]-4-ethyl-2H-1-benzopyran-7-ol acetate | Miscellaneous | 0.87 | 0.77 | 0.90 | 0.6285 | 0.2311 | 0.6341 | 1.04 | 1.33 | 1.03 | 0.8459 | 0.3628 | 0.8913 | 1.26 | 1.18 | 1.20 | 0.5382 | 0.5176 | 0.2656 | 1.12 | 1.61 | 1.04 | 0.7050 | 0.2123 | 0.8687 |
| 397.3190 | 4.8 | C23H43NO4 | trans-Hexadec-2-enoylcarnitine | Miscellaneous | 0.94 | 1.12 | 1.32 | 0.9091 | 0.5094 | 0.4676 | 0.76 | 1.12 | 1.03 | 0.3780 | 0.6713 | 0.8771 | 0.79 | 1.21 | 0.96 | 0.4462 | 0.2336 | 0.8751 | 0.85 | 1.08 | 1.03 | 0.6211 | 0.7841 | 0.9011 |
| 172.0484 | 15.2 | C6H8N2O4 | (R)-AMAA | Miscellaneous | 1.11 | 0.66 | 0.99 | 0.6232 | 0.0192 | 0.9718 | 1.37 | 1.00 | 1.03 | 0.2573 | 0.9896 | 0.8808 | 1.04 | 0.68 | 0.55 | 0.8626 | 0.0297 | 0.0067 | 0.86 | 0.65 | 0.44 | 0.2417 | 0.0032 | 0.0000 |
| 111.9831 | 12.7 | CH4O4S | Monomethyl sulfate | Miscellaneous | 0.76 | 1.01 | 0.87 | 0.5297 | 0.9719 | 0.7377 | 1.01 | 1.20 | 1.03 | 0.9792 | 0.4683 | 0.9226 | 0.84 | 1.32 | 0.94 | 0.2080 | 0.1586 | 0.7171 | 0.84 | 1.37 | 1.18 | 0.3200 | 0.2453 | 0.4511 |
| 198.0639 | 14.1 | C8H10N2O4 | (S)-2-Amino-3-(3-hydroxy-4-oxo-4H-pyridin-1-yl)propanoate | Miscellaneous | 1.13 | 1.02 | 1.01 | 0.1340 | 0.8266 | 0.9177 | 1.21 | 0.99 | 1.03 | 0.0863 | 0.8520 | 0.6819 | 1.13 | 1.06 | 1.05 | 0.2965 | 0.2026 | 0.3599 | 1.15 | 0.92 | 1.07 | 0.1953 | 0.3145 | 0.4649 |
| 173.1051 | 11.8 | C8H15NO3 | N-Acetyl-L-leucine | Miscellaneous | 0.56 | 1.63 | 1.15 | 0.3088 | 0.0958 | 0.7319 | 0.55 | 1.14 | 1.03 | 0.2524 | 0.7295 | 0.9410 | 0.49 | 1.52 | 0.95 | 0.1615 | 0.0834 | 0.8806 | 0.66 | 1.51 | 1.37 | 0.3930 | 0.3124 | 0.4006 |
| 366.1574 | 14.6 | C21H22N2O4 | Apodine | Miscellaneous | 1.12 | 0.91 | 0.98 | 0.6819 | 0.4986 | 0.9239 | 1.17 | 1.04 | 1.03 | 0.5940 | 0.7494 | 0.8768 | 1.05 | 0.84 | 0.87 | 0.8274 | 0.3706 | 0.4903 | 1.07 | 0.85 | 0.77 | 0.8274 | 0.2903 | 0.2543 |
| 190.0952 | 11.9 | C7H14N2O4 | N5-acetyl-N5-hydroxy-L-ornithine | Miscellaneous | 0.84 | 0.70 | 0.88 | 0.5365 | 0.1987 | 0.6247 | 1.04 | 1.13 | 1.02 | 0.8809 | 0.7388 | 0.9193 | 1.07 | 1.18 | 1.14 | 0.7289 | 0.7391 | 0.5144 | 0.85 | 1.03 | 1.11 | 0.4813 | 0.9294 | 0.6836 |
| 267.0956 | 16.7 | C9H17NO8 | Neuraminic acid | Miscellaneous | 0.90 | 1.07 | 1.07 | 0.4677 | 0.5953 | 0.5897 | 1.03 | 1.12 | 1.02 | 0.7717 | 0.4176 | 0.8563 | 1.17 | 1.17 | 1.15 | 0.4147 | 0.4440 | 0.1702 | 1.01 | 1.02 | 1.16 | 0.9364 | 0.8920 | 0.1755 |
| 223.1055 | 12.0 | C8H17NO6 | N-acetyl -D-glucosaminitol | Miscellaneous | 0.84 | 0.93 | 0.92 | 0.5598 | 0.6852 | 0.6859 | 0.94 | 1.11 | 1.02 | 0.8332 | 0.6103 | 0.9269 | 0.90 | 1.08 | 1.01 | 0.7090 | 0.6750 | 0.9452 | 0.84 | 1.06 | 1.12 | 0.4539 | 0.7520 | 0.6082 |
| 209.0688 | 5.2 | C10H11NO4 | N-Benzyloxycarbonylglycine | Miscellaneous | 1.14 | 1.59 | 1.22 | 0.4994 | 0.2208 | 0.2244 | 0.93 | 1.04 | 1.02 | 0.7363 | 0.8882 | 0.9247 | 0.97 | 1.09 | 0.93 | 0.7566 | 0.4571 | 0.5696 | 1.22 | 1.16 | 1.23 | 0.1910 | 0.3977 | 0.0354 |
| 149.0688 | 15.6 | C5H11NO4 | 4-amino-4-deoxy-L-arabinose | Miscellaneous | 1.21 | 0.96 | 1.09 | 0.4225 | 0.8149 | 0.5653 | 1.19 | 0.89 | 1.02 | 0.5748 | 0.5245 | 0.9236 | 1.11 | 1.02 | 1.12 | 0.7291 | 0.8767 | 0.5353 | 1.14 | 0.94 | 0.91 | 0.5740 | 0.5653 | 0.4688 |
| 86.0366 | 14.0 | C4H6O2 | 1,4-Lactone | Miscellaneous | 1.08 | 0.83 | 0.95 | 0.6172 | 0.3906 | 0.6842 | 1.04 | 0.90 | 1.02 | 0.7419 | 0.4627 | 0.9182 | 0.97 | 0.92 | 0.90 | 0.8416 | 0.4479 | 0.3558 | 0.98 | 1.03 | 0.96 | 0.7747 | 0.8206 | 0.5743 |
| 245.1626 | 8.0 | C12H23NO4 | 2-Methylbutyroylcarnitine | Miscellaneous | 0.79 | 1.66 | 1.21 | 0.4170 | 0.0364 | 0.4953 | 0.67 | 1.14 | 1.02 | 0.1325 | 0.5899 | 0.9471 | 0.78 | 1.52 | 0.99 | 0.2771 | 0.0349 | 0.9617 | 0.71 | 1.19 | 1.19 | 0.1871 | 0.5442 | 0.4806 |
| 100.0524 | 4.7 | C5H8O2 | 5-Valerolactone | Miscellaneous | 1.13 | 1.07 | 1.06 | 0.1408 | 0.4037 | 0.5364 | 1.11 | 0.91 | 1.01 | 0.2003 | 0.3813 | 0.8801 | 1.09 | 0.90 | 0.99 | 0.2507 | 0.4374 | 0.8923 | 1.10 | 0.87 | 0.99 | 0.2864 | 0.1748 | 0.8709 |
| 174.1367 | 21.0 | C8H18N2O2 | Ne,Ne dimethyllysine | Miscellaneous | 0.91 | 1.23 | 1.13 | 0.4887 | 0.4776 | 0.4692 | 0.87 | 1.23 | 1.01 | 0.4877 | 0.3012 | 0.9553 | 1.16 | 1.27 | 1.07 | 0.6092 | 0.2531 | 0.6602 | 0.84 | 1.19 | 0.93 | 0.2318 | 0.4600 | 0.7311 |
| 151.0633 | 5.2 | C8H9NO2 | N-Acetoxyarylamine | Miscellaneous | 1.28 | 1.00 | 1.03 | 0.3457 | 0.9984 | 0.8938 | 1.22 | 0.84 | 1.00 | 0.3442 | 0.5740 | 0.9949 | 1.35 | 0.83 | 1.09 | 0.1042 | 0.5781 | 0.6337 | 1.21 | 0.87 | 0.95 | 0.1720 | 0.4948 | 0.7749 |
| 515.0452 | 16.4 | C13H19N5O13P2 | 3-(ADP)-glycerate | Miscellaneous | 0.96 | 0.87 | 0.98 | 0.7371 | 0.4157 | 0.8666 | 1.07 | 1.10 | 1.00 | 0.6378 | 0.5136 | 0.9917 | 0.99 | 1.05 | 1.02 | 0.9635 | 0.6713 | 0.8711 | 1.09 | 1.21 | 1.11 | 0.2652 | 0.1593 | 0.2918 |
| 390.2768 | 4.0 | C24H38O4 | Bis(2-ethylhexyl)phthalate | Miscellaneous | 0.89 | 1.12 | 1.00 | 0.5067 | 0.4444 | 0.9852 | 0.85 | 1.04 | 0.99 | 0.3452 | 0.6196 | 0.9590 | 0.98 | 1.22 | 1.08 | 0.9038 | 0.0888 | 0.5554 | 0.84 | 1.43 | 0.93 | 0.2944 | 0.0654 | 0.4862 |
| 381.0228 | 16.8 | C8H17NO12P2 | N-Acetyl-D-glucosamine 1,6-bisphosphate | Miscellaneous | 1.01 | 1.07 | 1.05 | 0.9411 | 0.7793 | 0.6626 | 1.15 | 1.05 | 0.99 | 0.3159 | 0.6375 | 0.9215 | 0.98 | 0.90 | 0.96 | 0.9138 | 0.5845 | 0.7730 | 1.09 | 0.92 | 1.11 | 0.5359 | 0.5530 | 0.3290 |
| 294.1832 | 4.3 | C17H26O4 | Phytuberin | Miscellaneous | 1.11 | 0.98 | 1.00 | 0.2747 | 0.6732 | 0.9693 | 1.00 | 0.79 | 0.99 | 0.9937 | 0.0932 | 0.9296 | 1.10 | 0.82 | 1.14 | 0.4848 | 0.0636 | 0.2622 | 1.05 | 0.84 | 0.94 | 0.7230 | 0.2646 | 0.5872 |

| | | | | | | | | | | | | | | | | | | | | | | | | | | | | |
|---|---|---|---|---|---|---|---|---|---|---|---|---|---|---|---|---|---|---|---|---|---|---|---|---|---|---|---|---|
| 187.0633 | 8.7 | C11H9NO2 | Indoleacrylicacid | Miscellaneous | 0.93 | 1.17 | 1.08 | 0.8165 | 0.3694 | 0.7395 | 0.87 | 1.03 | 0.99 | 0.6811 | 0.9101 | 0.9432 | 0.91 | 1.20 | 0.99 | 0.7252 | 0.3274 | 0.9422 | 0.93 | 1.10 | 1.14 | 0.8064 | 0.7140 | 0.5475 |
| 320.0510 | 16.3 | C8H17O11P | octulose 8-phosphate | Miscellaneous | 0.87 | 0.62 | 0.95 | 0.4381 | 0.0129 | 0.7370 | 1.05 | 1.13 | 0.98 | 0.8168 | 0.6365 | 0.9288 | 0.99 | 0.95 | 1.04 | 0.9677 | 0.8732 | 0.8198 | 0.96 | 1.06 | 1.08 | 0.8223 | 0.8223 | 0.6651 |
| 428.3654 | 4.0 | C29H48O2 | (24R,24'R)-Fucosterol epoxide | Miscellaneous | 0.93 | 1.08 | 0.93 | 0.5818 | 0.4183 | 0.4879 | 0.81 | 1.07 | 0.98 | 0.1259 | 0.6253 | 0.8845 | 1.00 | 1.23 | 1.13 | 0.9913 | 0.2804 | 0.3238 | 0.84 | 1.13 | 0.93 | 0.1343 | 0.5065 | 0.4540 |
| 413.3502 | 4.6 | C24H47NO4 | Heptadecanoylcarnitine | Miscellaneous | 0.90 | 0.88 | 0.78 | 0.8133 | 0.7011 | 0.3352 | 0.72 | 0.91 | 0.98 | 0.1018 | 0.6578 | 0.8855 | 0.82 | 1.03 | 0.98 | 0.3437 | 0.9011 | 0.9204 | 0.92 | 1.02 | 1.04 | 0.7752 | 0.9043 | 0.8288 |
| 161.0688 | 11.1 | C6H11NO4 | O-Acetylhomoserine | Miscellaneous | 0.96 | 0.80 | 1.12 | 0.9081 | 0.4574 | 0.6942 | 1.08 | 0.86 | 0.97 | 0.7271 | 0.4106 | 0.8475 | 1.16 | 0.74 | 0.81 | 0.3548 | 0.0179 | 0.1110 | 0.96 | 0.86 | 1.02 | 0.8221 | 0.3864 | 0.9222 |
| 292.1526 | 5.1 | C13H24O7 | Heptopyranosides | Miscellaneous | 1.17 | 1.15 | 1.06 | 0.4646 | 0.6080 | 0.7026 | 1.07 | 0.93 | 0.96 | 0.6184 | 0.7046 | 0.8046 | 1.24 | 0.91 | 1.00 | 0.0206 | 0.5816 | 0.9745 | 1.37 | 0.92 | 1.07 | 0.0042 | 0.6261 | 0.6704 |
| 377.1259 | 11.4 | C22H19NO5 | Chelilutine | Miscellaneous | 1.18 | 0.79 | 0.94 | 0.5062 | 0.2318 | 0.7411 | 1.50 | 0.83 | 0.96 | 0.0305 | 0.4637 | 0.8493 | 1.28 | 0.68 | 0.91 | 0.0654 | 0.2107 | 0.5494 | 1.32 | 0.83 | 0.98 | 0.0592 | 0.3817 | 0.9302 |
| 246.1367 | 8.7 | C14H18N2O2 | Hypaphorine | Miscellaneous | 0.92 | 1.19 | 1.05 | 0.7968 | 0.4290 | 0.8434 | 0.90 | 0.93 | 0.96 | 0.7190 | 0.7828 | 0.8254 | 1.01 | 1.26 | 1.00 | 0.9785 | 0.3173 | 0.9977 | 0.98 | 1.11 | 1.28 | 0.9598 | 0.7424 | 0.2978 |
| 259.0459 | 12.1 | C6H14NO8P | glycerophosphoserine | Miscellaneous | 1.03 | 1.66 | 1.46 | 0.9285 | 0.0103 | 0.0875 | 0.77 | 0.65 | 0.96 | 0.3783 | 0.2620 | 0.8103 | 0.88 | 1.22 | 1.00 | 0.5728 | 0.2011 | 0.9897 | 0.80 | 0.81 | 1.30 | 0.3655 | 0.5888 | 0.0759 |
| 290.0042 | 19.0 | C6H11O11P | 3-phosphoglucarate | Miscellaneous | 0.91 | 1.06 | 0.88 | 0.5758 | 0.5744 | 0.1958 | 1.17 | 1.10 | 0.95 | 0.2146 | 0.5537 | 0.6944 | 0.92 | 0.91 | 0.94 | 0.4386 | 0.3607 | 0.5992 | 1.01 | 1.02 | 1.06 | 0.9487 | 0.8265 | 0.4992 |
| 371.3033 | 4.9 | C21H41NO4 | Tetradecanoylcarnitine | Miscellaneous | 0.83 | 1.15 | 1.15 | 0.6012 | 0.4720 | 0.6783 | 0.84 | 1.01 | 0.94 | 0.5120 | 0.9568 | 0.7371 | 0.66 | 1.10 | 0.86 | 0.1510 | 0.6456 | 0.4584 | 0.74 | 1.20 | 1.02 | 0.3458 | 0.5143 | 0.9384 |
| 223.1207 | 10.3 | C12H17NO3 | Cerulenin | Miscellaneous | 0.50 | 1.67 | 1.20 | 0.0701 | 0.0767 | 0.6071 | 0.60 | 1.13 | 0.94 | 0.1299 | 0.6843 | 0.8441 | 0.58 | 1.47 | 1.16 | 0.1684 | 0.1493 | 0.6789 | 0.57 | 1.27 | 1.29 | 0.0605 | 0.4378 | 0.4639 |
| 113.9447 | 21.3 | H2O3S2 | H2S2O3 | Miscellaneous | 0.82 | 0.87 | 0.84 | 0.2305 | 0.2631 | 0.1818 | 1.10 | 1.06 | 0.94 | 0.4295 | 0.6043 | 0.4295 | 1.02 | 1.00 | 1.07 | 0.8495 | 0.9778 | 0.5060 | 0.99 | 1.13 | 1.00 | 0.9294 | 0.1364 | 0.9599 |
| 278.1883 | 4.0 | C17H26O3 | [6]-Paradol | Miscellaneous | 0.99 | 1.19 | 0.94 | 0.9464 | 0.1181 | 0.7018 | 0.89 | 1.35 | 0.94 | 0.5580 | 0.1952 | 0.7033 | 0.86 | 1.31 | 1.09 | 0.2521 | 0.2337 | 0.4420 | 0.89 | 1.30 | 1.10 | 0.4381 | 0.1983 | 0.6641 |
| 425.3502 | 4.6 | C25H47NO4 | Oleoylcarnitine | Miscellaneous | 0.92 | 0.89 | 0.87 | 0.8523 | 0.5834 | 0.5494 | 0.70 | 0.90 | 0.93 | 0.2027 | 0.6356 | 0.7113 | 0.78 | 1.17 | 0.93 | 0.3621 | 0.4221 | 0.7579 | 0.92 | 1.03 | 1.02 | 0.8002 | 0.8663 | 0.9084 |
| 265.0809 | 10.1 | C10H11N5O4 | 5'-Dehydroadenosine | Miscellaneous | 0.95 | 1.21 | 0.86 | 0.7941 | 0.7799 | 0.5220 | 1.21 | 0.72 | 0.92 | 0.6059 | 0.4454 | 0.8094 | 0.99 | 1.11 | 1.08 | 0.9731 | 0.6638 | 0.7378 | 0.87 | 1.02 | 1.09 | 0.5885 | 0.8616 | 0.4890 |
| 534.1742 | 16.4 | C26H30O12 | Dalpanin | Miscellaneous | 0.82 | 1.36 | 1.21 | 0.7241 | 0.6358 | 0.6580 | 0.89 | 0.92 | 0.92 | 0.6869 | 0.6442 | 0.6661 | 0.95 | 0.85 | 0.87 | 0.6856 | 0.3712 | 0.2752 | 0.87 | 0.86 | 0.91 | 0.5681 | 0.4384 | 0.6175 |
| 595.0115 | 17.5 | C13H20N5O16P3 | 3-(ADP)-2-phosphoglycerate | Miscellaneous | 0.75 | 1.17 | 0.92 | 0.1067 | 0.1421 | 0.5462 | 0.87 | 1.14 | 0.92 | 0.2739 | 0.3603 | 0.5688 | 0.78 | 1.07 | 0.90 | 0.0756 | 0.4301 | 0.3551 | 0.88 | 1.17 | 1.09 | 0.3519 | 0.1311 | 0.5915 |
| 220.0850 | 10.0 | C11H12N2O3 | 5-Hydroxytryptophan | Miscellaneous | 1.03 | 0.77 | 0.97 | 0.9259 | 0.1302 | 0.8636 | 1.10 | 0.81 | 0.91 | 0.6273 | 0.1448 | 0.5659 | 1.03 | 0.76 | 0.89 | 0.8636 | 0.0656 | 0.3526 | 0.98 | 0.82 | 0.85 | 0.9231 | 0.2183 | 0.4239 |
| 259.1784 | 7.4 | C13H25NO4 | Hexanoylcarnitine | Miscellaneous | 1.14 | 1.85 | 1.35 | 0.8507 | 0.1935 | 0.4833 | 0.48 | 0.67 | 0.90 | 0.1290 | 0.3534 | 0.7332 | 0.75 | 1.40 | 1.04 | 0.5803 | 0.2341 | 0.9124 | 0.71 | 1.49 | 1.29 | 0.4750 | 0.4336 | 0.4534 |
| 423.3347 | 4.7 | C25H45NO4 | Linoelaidylcarnitine | Miscellaneous | 1.02 | 1.02 | 0.89 | 0.9664 | 0.9189 | 0.6217 | 0.65 | 1.00 | 0.89 | 0.0980 | 0.9976 | 0.5175 | 0.83 | 1.08 | 0.93 | 0.4759 | 0.6765 | 0.7504 | 0.83 | 1.15 | 1.05 | 0.5909 | 0.6096 | 0.8102 |
| 224.0911 | 9.7 | C9H12N4O3 | Temurin | Miscellaneous | 1.04 | 0.82 | 0.93 | 0.8791 | 0.1809 | 0.7329 | 1.63 | 0.93 | 0.88 | 0.2907 | 0.7899 | 0.6729 | 0.97 | 0.67 | 0.15 | 0.9104 | 0.1663 | 0.0001 | 0.68 | 0.66 | 0.03 | 0.0246 | 0.0440 | NA |
| 249.0307 | 18.7 | C8H11NO6S | Norepinephrinesulfate | Miscellaneous | 0.94 | 1.02 | 1.06 | 0.9311 | 0.9645 | 0.9032 | 1.05 | 0.82 | 0.88 | 0.9547 | 0.7301 | 0.8542 | 1.19 | 0.96 | 1.16 | 0.8307 | 0.9222 | 0.7689 | 1.13 | 1.04 | 0.80 | 0.8794 | 0.9259 | 0.6683 |
| 143.0582 | 9.4 | C6H9NO3 | Vinylacetylglycine | Miscellaneous | 1.08 | 0.78 | 0.80 | 0.8992 | 0.6700 | 0.5902 | 1.12 | 0.54 | 0.87 | 0.8972 | 0.4309 | 0.8489 | 1.24 | 0.66 | 0.92 | 0.7783 | 0.4257 | 0.8662 | 1.04 | 0.77 | 0.80 | 0.9362 | 0.5506 | 0.5382 |
| 146.0479 | 7.5 | C8H6N2O | 1(2H)-Phthalazinone | Miscellaneous | 0.89 | 1.33 | 0.90 | 0.5024 | 0.2325 | 0.5713 | 1.01 | 0.64 | 0.86 | 0.9641 | 0.1577 | 0.6011 | 1.06 | 0.73 | 1.00 | 0.7595 | 0.3067 | 0.9791 | 1.13 | 0.76 | 1.01 | 0.3989 | 0.2891 | 0.9589 |
| 293.1990 | 4.1 | C17H27NO3 | (+/-)-5-[(tert-Butylamino)-2'-hydroxypropoxy]-1,2,3,4-tetrahydro-1-naphthol | Miscellaneous | 0.79 | 1.18 | 0.73 | 0.4028 | 0.3551 | 0.2240 | 0.89 | 0.94 | 0.85 | 0.6273 | 0.6917 | 0.4053 | 0.74 | 1.04 | 0.86 | 0.3197 | 0.8194 | 0.5345 | 0.83 | 1.13 | 0.90 | 0.5043 | 0.4081 | 0.5820 |
| 340.1305 | 10.1 | C20H20O5 | Glepidotin B | Miscellaneous | 0.85 | 0.83 | 0.74 | 0.5813 | 0.6497 | 0.1819 | 0.95 | 0.96 | 0.84 | 0.8557 | 0.8588 | 0.3406 | 0.94 | 1.28 | 1.19 | 0.8841 | 0.2200 | 0.4393 | 0.98 | 1.21 | 1.20 | 0.9458 | 0.1651 | 0.3965 |
| 473.3504 | 4.5 | C29H47NO4 | Docosa-4-7-10-13-16-pentaenoylcarnitine | Miscellaneous | 0.89 | 1.04 | 1.12 | 0.8889 | 0.9321 | 0.8284 | 0.44 | 1.14 | 0.79 | 0.2441 | 0.8239 | 0.6513 | 0.82 | 2.05 | 1.16 | 0.7933 | 0.2175 | 0.7871 | 0.96 | 1.68 | 1.33 | 0.9495 | 0.4471 | 0.4639 |
| 202.0741 | 9.9 | C11H10N2O2 | alpha,beta-Didehydrotryptophan | Miscellaneous | 0.99 | 1.03 | 0.95 | 0.9875 | 0.8250 | 0.8236 | 1.04 | 0.72 | 0.79 | 0.8869 | 0.1510 | 0.3163 | 1.27 | 0.67 | 1.13 | 0.3239 | 0.1991 | 0.4973 | 1.10 | 0.82 | 0.90 | 0.7889 | 0.5971 | 0.7467 |
| 214.0956 | 7.8 | C9H14N2O4 | Pyrimidine nucleoside | Miscellaneous | 1.13 | 1.04 | 1.00 | 0.7548 | 0.9223 | 0.9996 | 0.90 | 0.71 | 0.77 | 0.8501 | 0.5347 | 0.6116 | 1.14 | 0.74 | 0.97 | 0.7232 | 0.3831 | 0.8705 | 1.23 | 0.76 | 1.01 | 0.6110 | 0.3870 | 0.9707 |
| 162.0317 | 5.1 | C9H6O3 | Umbelliferone | Miscellaneous | 1.15 | 1.44 | 1.04 | 0.7373 | 0.0408 | 0.9002 | 1.08 | 0.67 | 0.76 | 0.8471 | 0.3761 | 0.4657 | 1.32 | 0.99 | 0.79 | 0.3177 | 0.9720 | 0.3002 | 1.61 | 0.80 | 1.20 | 0.2849 | 0.4756 | 0.4086 |
| 145.0527 | 7.5 | C9H7NO | 3-Methyleneoxindole | Miscellaneous | 0.71 | 1.07 | 1.04 | 0.5155 | 0.9222 | 0.9244 | 0.92 | 0.55 | 0.71 | 0.8071 | 0.0877 | 0.3121 | 1.14 | 0.48 | 0.87 | 0.5861 | 0.0271 | 0.5696 | 0.79 | 0.78 | 0.66 | 0.5578 | 0.5168 | 0.3543 |
| 228.1110 | 7.5 | C10H16N2O4 | (S)-ATPA | Miscellaneous | 1.05 | 0.96 | 0.88 | 0.8739 | 0.9163 | 0.6732 | 0.80 | 0.40 | 0.69 | 0.6567 | 0.1557 | 0.4412 | 1.51 | 0.62 | 0.95 | 0.3272 | 0.1943 | 0.8311 | 1.33 | 0.72 | 1.17 | 0.3703 | 0.2281 | 0.5883 |
| 133.0739 | 8.6 | C5H11NO3 | N-hydroxyvaline | Miscellaneous | 1.11 | 1.17 | 1.10 | 0.7091 | 0.7797 | 0.6748 | 0.79 | 0.62 | 0.69 | 0.4547 | 0.1601 | 0.2178 | 1.16 | 1.12 | 1.41 | 0.4639 | 0.5168 | 0.3161 | 1.09 | 0.98 | 1.02 | 0.6675 | 0.8722 | 0.8643 |
| 173.0476 | 7.1 | C10H7NO2 | 2-Quinolinecarboxylic acid | Miscellaneous | 0.67 | 0.44 | 0.92 | 0.4128 | 0.1934 | 0.8453 | 0.63 | 0.48 | 0.55 | 0.5011 | 0.3285 | 0.3910 | 1.13 | 0.59 | 0.75 | 0.6894 | 0.0318 | 0.1588 | 0.70 | 0.59 | 0.67 | 0.4037 | 0.2182 | 0.3772 |
| 150.0680 | 4.9 | C9H10O2 | Phenylpropanoate | Amino Acid Metabolism | 0.68 | 1.66 | 0.98 | 0.3304 | 0.0940 | 0.9554 | 0.67 | 1.34 | 3.40 | 0.4392 | 0.2849 | 0.3581 | 0.59 | 1.54 | 0.82 | 0.2881 | 0.0797 | 0.5780 | 0.72 | 1.39 | 1.23 | 0.5312 | 0.3270 | 0.5562 |
| 140.9829 | 28.0 | CH4NO5P | Carbamoyl phosphate | Amino Acid Metabolism | 0.63 | 0.95 | 1.05 | 0.2831 | 0.8701 | 0.8229 | 3.38 | 2.86 | 3.04 | 0.0039 | 0.0593 | 0.0010 | 1.31 | 2.03 | 0.74 | 0.6206 | 0.1589 | 0.3263 | 1.06 | 0.83 | 0.95 | 0.7426 | 0.3351 | 0.7417 |
| 197.1164 | 12.2 | C9H15N3O2 | Hercynine | Amino Acid Metabolism | 0.35 | 1.15 | 1.02 | 0.2709 | 0.8211 | 0.9803 | 0.39 | 1.50 | 1.35 | 0.1351 | 0.4089 | 0.6282 | 0.44 | 1.58 | 0.87 | 0.2015 | 0.2812 | 0.7831 | 0.58 | 1.68 | 1.21 | 0.1781 | 0.3381 | 0.5831 |
| 160.0371 | 11.8 | C6H8O5 | 2-Oxoadipate | Amino Acid Metabolism | 0.80 | 0.88 | 0.96 | 0.4511 | 0.5558 | 0.8498 | 1.10 | 1.21 | 1.30 | 0.6974 | 0.5689 | 0.3195 | 1.21 | 1.22 | 1.01 | 0.4405 | 0.5009 | 0.9396 | 0.96 | 1.19 | 0.86 | 0.8643 | 0.5424 | 0.4859 |
| 110.0481 | 12.2 | C5H6N2O | Imidazole-4-acetaldehyde | Amino Acid Metabolism | 0.61 | 1.28 | 1.16 | 0.2746 | 0.5596 | 0.7129 | 0.55 | 1.45 | 1.21 | 0.1310 | 0.2605 | 0.6896 | 0.57 | 1.43 | 0.92 | 0.1708 | 0.2434 | 0.8267 | 0.73 | 1.41 | 1.16 | 0.1721 | 0.3564 | 0.4865 |
| 182.0579 | 8.7 | C9H10O4 | 3-(4-Hydroxyphenyl)lactate | Amino Acid Metabolism | 1.09 | 0.98 | 1.13 | 0.3251 | 0.7833 | 0.2727 | 1.29 | 1.12 | 1.20 | 0.0413 | 0.4168 | 0.0486 | 1.03 | 0.96 | 0.98 | 0.7064 | 0.6742 | 0.6810 | 1.10 | 1.04 | 1.03 | 0.3097 | 0.7829 | 0.7614 |
| 187.0844 | 7.1 | C8H13NO4 | N2-Acetyl-L-aminoadipate semialdehyde | Amino Acid Metabolism | 0.59 | 0.44 | 0.73 | 0.2921 | 0.1623 | 0.5460 | 1.43 | 0.92 | 1.20 | 0.4989 | 0.8769 | 0.7570 | 1.94 | 0.32 | 1.34 | 0.3808 | 0.1005 | 0.5885 | 0.65 | 0.59 | 0.73 | 0.4347 | 0.3115 | 0.5888 |
| 219.1105 | 8.6 | C9H17NO5 | Pantothenate | Amino Acid Metabolism | 1.07 | 0.72 | 0.95 | 0.6403 | 0.2419 | 0.7323 | 1.30 | 0.95 | 1.19 | 0.1906 | 0.7586 | 0.1952 | 1.28 | 0.96 | 1.07 | 0.1138 | 0.7095 | 0.5915 | 1.16 | 1.01 | 1.11 | 0.5260 | 0.9737 | 0.4905 |
| 115.0633 | 12.7 | C5H9NO2 | L-Proline | Amino Acid Metabolism | 0.69 | 1.15 | 1.09 | 0.2881 | 0.4241 | 0.4470 | 1.06 | 0.99 | 1.18 | 0.6653 | 0.9311 | 0.2058 | 1.10 | 1.03 | 1.11 | 0.5551 | 0.8088 | 0.3834 | 1.05 | 0.86 | 1.00 | 0.7524 | 0.4073 | 0.9758 |

| | | | | | | | | | | | | | | | | | | | | | | | | | | | | | |
|---|---|---|---|---|---|---|---|---|---|---|---|---|---|---|---|---|---|---|---|---|---|---|---|---|---|---|---|---|---|
| 211.0360 | 15.0 | C4H10N3O5P | Phosphocreatine | Amino Acid Metabolism | 1.07 | 0.79 | 1.03 | 0.6654 | 0.0803 | 0.8164 | 1.21 | 0.95 | 1.17 | 0.4375 | 0.7337 | 0.3509 | 1.10 | 0.82 | 1.00 | 0.6501 | 0.2137 | 0.9759 | 1.14 | 0.95 | 1.05 | 0.6063 | 0.7617 | 0.7939 |
| 250.0622 | 13.9 | C8H14N2O5S | gamma-L-Glutamyl-L-cysteine | Amino Acid Metabolism | 0.90 | 1.03 | 1.00 | 0.5040 | 0.6898 | 0.9752 | 1.14 | 1.09 | 1.17 | 0.4943 | 0.5720 | 0.3898 | 1.31 | 1.03 | 1.24 | 0.3308 | 0.8131 | 0.1021 | 1.06 | 1.26 | 1.22 | 0.5412 | 0.1317 | 0.2095 |
| 87.0684 | 10.6 | C4H9NO | 4-Aminobutanal | Amino Acid Metabolism | 0.98 | 0.87 | 1.13 | 0.9127 | 0.2375 | 0.2521 | 1.09 | 0.92 | 1.17 | 0.6182 | 0.7001 | 0.3719 | 1.17 | 1.02 | 0.96 | 0.4469 | 0.8552 | 0.6796 | 0.89 | 1.01 | 0.85 | 0.3271 | 0.9247 | 0.3048 |
| 148.0372 | 14.9 | C5H8O5 | (R)-2-Hydroxyglutarate | Amino Acid Metabolism | 0.97 | 1.04 | 1.03 | 0.8345 | 0.7565 | 0.7654 | 1.17 | 1.12 | 1.17 | 0.3079 | 0.4814 | 0.2257 | 0.96 | 1.04 | 0.98 | 0.7823 | 0.6576 | 0.7996 | 1.01 | 1.01 | 1.06 | 0.9697 | 0.9146 | 0.5301 |
| 174.0529 | 15.9 | C7H10O5 | (2S)-2-Isopropyl-3-oxosuccinate | Amino Acid Metabolism | 0.72 | 0.54 | 0.84 | 0.4229 | 0.1434 | 0.6142 | 0.95 | 1.45 | 1.16 | 0.8757 | 0.3188 | 0.6717 | 0.84 | 1.18 | 1.10 | 0.5993 | 0.7356 | 0.7815 | 0.86 | 1.34 | 1.24 | 0.6425 | 0.4367 | 0.4957 |
| 113.0477 | 14.7 | C5H7NO2 | (S)-1-Pyrroline-5-carboxylate | Amino Acid Metabolism | 1.06 | 1.05 | 1.02 | 0.9288 | 0.8604 | 0.9658 | 1.26 | 0.77 | 1.16 | 0.7161 | 0.4580 | 0.7180 | 1.31 | 0.86 | 0.98 | 0.6015 | 0.5523 | 0.9549 | 1.03 | 0.76 | 0.72 | 0.9156 | 0.3341 | 0.1917 |
| 125.9987 | 10.6 | C2H6O4S | 2-Hydroxyethanesulfonate | Amino Acid Metabolism | 0.90 | 0.94 | 1.02 | 0.4283 | 0.6676 | 0.8325 | 1.11 | 1.23 | 1.16 | 0.5359 | 0.3663 | 0.4240 | 1.21 | 1.19 | 1.09 | 0.4904 | 0.5112 | 0.5489 | 1.06 | 1.02 | 0.97 | 0.8422 | 0.9281 | 0.8662 |
| 116.0473 | 13.8 | C5H8O3 | 3-Methyl-2-oxobutanoic acid | Amino Acid Metabolism | 0.67 | 1.39 | 1.01 | 0.3615 | 0.3650 | 0.9694 | 1.20 | 1.10 | 1.15 | 0.7229 | 0.7356 | 0.6808 | 0.86 | 1.12 | 1.02 | 0.7169 | 0.3727 | 0.9183 | 0.80 | 1.11 | 1.22 | 0.4241 | 0.7262 | 0.5746 |
| 111.9926 | 14.3 | CH5O4P | Hydroxymethylphosphonate | Amino Acid Metabolism | 0.91 | 1.15 | 0.99 | 0.5167 | 0.2558 | 0.9501 | 1.02 | 1.24 | 1.15 | 0.9211 | 0.1885 | 0.4066 | 0.94 | 1.06 | 1.12 | 0.6754 | 0.6132 | 0.3284 | 0.86 | 1.06 | 0.91 | 0.2456 | 0.7506 | 0.5250 |
| 129.0427 | 10.1 | C5H7NO3 | 5-Oxoproline | Amino Acid Metabolism | 0.93 | 1.09 | 1.04 | 0.7638 | 0.7096 | 0.8324 | 1.12 | 1.10 | 1.15 | 0.4352 | 0.3498 | 0.2111 | 0.95 | 1.10 | 1.00 | 0.6873 | 0.3977 | 0.9710 | 1.01 | 1.03 | 1.04 | 0.9000 | 0.7796 | 0.6989 |
| 243.0856 | 13.6 | C9H13N3O5 | gamma-Glutamyl-beta-cyanoalanine | Amino Acid Metabolism | 1.01 | 0.81 | 0.95 | 0.9484 | 0.2871 | 0.6728 | 1.25 | 1.06 | 1.15 | 0.0239 | 0.6548 | 0.2476 | 1.06 | 0.94 | 1.02 | 0.7273 | 0.7360 | 0.8679 | 1.00 | 0.93 | 0.99 | 0.9789 | 0.6554 | 0.9441 |
| 146.0579 | 11.0 | C6H10O4 | (S)-2-Aceto-2-hydroxybutanoate | Amino Acid Metabolism | 0.78 | 0.69 | 1.01 | 0.2272 | 0.0462 | 0.9482 | 0.93 | 1.13 | 1.15 | 0.8235 | 0.6856 | 0.6356 | 1.27 | 1.34 | 1.10 | 0.5213 | 0.5143 | 0.6922 | 1.23 | 1.26 | 1.33 | 0.3737 | 0.5897 | 0.2877 |
| 174.1116 | 23.6 | C6H14N4O2 | L-Arginine | Amino Acid Metabolism | 0.86 | 1.10 | 1.02 | 0.2400 | 0.6844 | 0.8328 | 0.94 | 1.06 | 1.14 | 0.4113 | 0.5913 | 0.1919 | 0.93 | 1.13 | 1.02 | 0.4600 | 0.2096 | 0.8298 | 0.93 | 1.13 | 1.08 | 0.4000 | 0.2299 | 0.4594 |
| 398.1373 | 16.3 | C15H22N6O5S | S-Adenosyl-L-methionine | Amino Acid Metabolism | 1.13 | 1.23 | 1.12 | 0.4733 | 0.0901 | 0.1350 | 1.17 | 0.99 | 1.14 | 0.2602 | 0.9326 | 0.1839 | 0.99 | 0.99 | 1.08 | 0.9447 | 0.9488 | 0.2290 | 1.03 | 1.02 | 1.22 | 0.6910 | 0.8713 | 0.0201 |
| 117.0790 | 12.4 | C5H11NO2 | L-Valine | Amino Acid Metabolism | 0.91 | 0.93 | 1.01 | 0.3729 | 0.6482 | 0.9099 | 1.22 | 1.08 | 1.14 | 0.3451 | 0.6461 | 0.3934 | 0.98 | 1.05 | 0.92 | 0.8876 | 0.6873 | 0.4531 | 1.00 | 1.02 | 0.83 | 0.9900 | 0.8470 | 0.0458 |
| 89.0477 | 14.6 | C3H7NO2 | L-Alanine | Amino Acid Metabolism | 0.98 | 0.98 | 1.01 | 0.8886 | 0.8365 | 0.8531 | 1.03 | 0.95 | 1.14 | 0.7288 | 0.6863 | 0.2263 | 1.05 | 0.99 | 1.03 | 0.6311 | 0.8396 | 0.7017 | 1.06 | 1.02 | 1.00 | 0.4999 | 0.6538 | 0.9493 |
| 229.0883 | 14.7 | C9H15N3O2S | Ergothioneine | Amino Acid Metabolism | 0.64 | 1.66 | 1.00 | 0.3314 | 0.1494 | 0.9921 | 0.60 | 1.51 | 1.14 | 0.2382 | 0.3352 | 0.7089 | 0.64 | 1.61 | 1.03 | 0.2528 | 0.1292 | 0.9336 | 0.59 | 1.38 | 1.19 | 0.2555 | 0.4681 | 0.6556 |
| 141.0192 | 15.7 | C2H8NO4P | Ethanolamine phosphate | Amino Acid Metabolism | 1.03 | 1.15 | 1.07 | 0.8291 | 0.0512 | 0.5382 | 1.14 | 1.06 | 1.14 | 0.4651 | 0.6659 | 0.3434 | 1.00 | 0.96 | 1.02 | 0.9975 | 0.7782 | 0.9108 | 1.04 | 0.89 | 1.43 | 0.8781 | 0.5080 | 0.0772 |
| 276.1322 | 15.5 | C11H20N2O6 | N6-(L-1,3-Dicarboxypropyl)-L-lysine | Amino Acid Metabolism | 1.06 | 0.69 | 1.03 | 0.7958 | 0.0890 | 0.8800 | 1.49 | 0.94 | 1.13 | 0.1325 | 0.7433 | 0.5632 | 1.26 | 0.78 | 1.08 | 0.2311 | 0.2326 | 0.6742 | 1.13 | 0.87 | 0.91 | 0.6040 | 0.3137 | 0.5609 |
| 192.0634 | 12.5 | C7H12O6 | Quinate | Amino Acid Metabolism | 1.07 | 1.08 | 1.14 | 0.8594 | 0.7472 | 0.6199 | 1.17 | 0.96 | 1.13 | 0.6526 | 0.8504 | 0.5558 | 1.00 | 1.04 | 0.95 | 0.9944 | 0.8467 | 0.8353 | 1.18 | 1.00 | 1.27 | 0.6895 | 0.9918 | 0.3384 |
| 129.0790 | 12.4 | C6H11NO2 | L-Pipecolate | Amino Acid Metabolism | 1.04 | 1.16 | 1.07 | 0.8154 | 0.2709 | 0.6766 | 1.11 | 0.93 | 1.13 | 0.6740 | 0.6437 | 0.5243 | 1.13 | 0.91 | 0.78 | 0.6866 | 0.3844 | 0.1516 | 0.77 | 0.70 | 0.48 | 0.1394 | 0.0577 | 0.0015 |
| 155.0695 | 14.6 | C6H9N3O2 | L-Histidine | Amino Acid Metabolism | 1.03 | 0.80 | 1.04 | 0.8297 | 0.0744 | 0.6861 | 1.20 | 0.97 | 1.13 | 0.1082 | 0.7050 | 0.2918 | 1.06 | 0.99 | 0.89 | 0.5058 | 0.9341 | 0.2296 | 1.00 | 0.91 | 0.96 | 0.9820 | 0.4092 | 0.6449 |
| 167.9824 | 12.6 | C3H5O6P | 3-Phosphonopyruvate | Amino Acid Metabolism | 0.85 | 0.97 | 1.01 | 0.3642 | 0.8103 | 0.9647 | 1.01 | 1.12 | 1.13 | 0.9670 | 0.5692 | 0.6407 | 0.94 | 0.93 | 1.07 | 0.6044 | 0.6397 | 0.4963 | 1.00 | 1.15 | 1.03 | 0.9870 | 0.3137 | 0.7699 |
| 301.0565 | 14.6 | C8H16NO9P | N-Acetyl-D-glucosamine 6-phosphate | Amino Acid Metabolism | 1.10 | 0.66 | 1.00 | 0.5295 | 0.0312 | 0.9895 | 1.36 | 0.94 | 1.12 | 0.1415 | 0.5220 | 0.3767 | 1.13 | 0.72 | 0.94 | 0.4422 | 0.0502 | 0.6248 | 1.17 | 0.76 | 1.06 | 0.2600 | 0.0326 | 0.7242 |
| 247.0691 | 13.9 | C9H13NO7 | N-Succinyl-L-glutamate | Amino Acid Metabolism | 1.04 | 0.96 | 1.06 | 0.8035 | 0.8902 | 0.6437 | 1.22 | 1.02 | 1.12 | 0.2286 | 0.9058 | 0.5023 | 1.21 | 0.96 | 1.16 | 0.1091 | 0.6763 | 0.2616 | 1.04 | 0.89 | 1.08 | 0.5791 | 0.3293 | 0.3538 |
| 226.1064 | 15.5 | C9H14N4O3 | Carnosine | Amino Acid Metabolism | 1.28 | 0.36 | 0.93 | 0.5865 | 0.0427 | 0.8483 | 1.71 | 0.81 | 1.12 | 0.2500 | 0.6322 | 0.7711 | 1.34 | 0.47 | 1.11 | 0.5099 | 0.1501 | 0.7853 | 1.16 | 0.62 | 0.81 | 0.7187 | 0.2662 | 0.6454 |
| 123.9927 | 14.8 | C2H5O4P | Phosphonoacetaldehyde | Amino Acid Metabolism | 1.10 | 1.02 | 1.02 | 0.1758 | 0.8764 | 0.8761 | 1.09 | 1.15 | 1.12 | 0.5005 | 0.3628 | 0.5215 | 0.92 | 0.89 | 1.66 | 0.3844 | 0.3684 | 0.0006 | 1.09 | 1.01 | 1.80 | 0.2448 | 0.9165 | 0.0002 |
| 213.0641 | 12.7 | C9H11NO5 | N,N-Dihydroxy-L-tyrosine | Amino Acid Metabolism | 1.02 | 0.98 | 1.00 | 0.8528 | 0.7314 | 0.9588 | 1.07 | 1.06 | 1.12 | 0.7363 | 0.6830 | 0.4816 | 1.19 | 0.97 | 1.08 | 0.3053 | 0.6484 | 0.3900 | 1.02 | 0.97 | 1.09 | 0.7875 | 0.8222 | 0.3197 |
| 430.0653 | 15.1 | C11H20N4O10P2 | CMP-2-aminoethylphosphonate | Amino Acid Metabolism | 1.14 | 0.61 | 0.95 | 0.6560 | 0.0419 | 0.8235 | 1.34 | 0.95 | 1.11 | 0.2473 | 0.8481 | 0.6374 | 1.28 | 0.69 | 1.04 | 0.4283 | 0.0912 | 0.8416 | 1.20 | 0.82 | 0.89 | 0.5457 | 0.4073 | 0.5795 |
| 203.1157 | 11.0 | C9H17NO4 | O-Acetylcarnitine | Amino Acid Metabolism | 0.92 | 1.18 | 1.12 | 0.8326 | 0.4758 | 0.6543 | 0.94 | 1.02 | 1.11 | 0.8669 | 0.9284 | 0.6395 | 0.95 | 1.15 | 0.93 | 0.8768 | 0.5011 | 0.7576 | 0.94 | 1.05 | 1.28 | 0.8672 | 0.8388 | 0.3096 |

| | | | | | | | | | | | | | | | | | | | | | | | | | | | | | |
|---|---|---|---|---|---|---|---|---|---|---|---|---|---|---|---|---|---|---|---|---|---|---|---|---|---|---|---|---|---|
| 171.0532 | 7.4 | C7H9NO4 | 2,3,4,5-Tetrahydrodipicolinate | Amino Acid Metabolism | 0.73 | 0.79 | 1.18 | 0.3964 | 0.6337 | 0.6282 | 1.06 | 1.10 | 1.11 | 0.8547 | 0.6221 | 0.4915 | 1.10 | 1.04 | 0.92 | 0.5927 | 0.6603 | 0.5396 | 0.88 | 0.89 | 0.89 | 0.3985 | 0.5310 | 0.5739 |
| 146.1054 | 22.6 | C6H14N2O2 | L-Lysine | Amino Acid Metabolism | 0.93 | 0.92 | 1.02 | 0.4235 | 0.3493 | 0.8258 | 1.19 | 1.12 | 1.10 | 0.1835 | 0.2487 | 0.3409 | 1.03 | 1.12 | 0.79 | 0.7062 | 0.1079 | 0.0040 | 0.83 | 0.88 | 0.69 | 0.0767 | 0.3040 | 0.0037 |
| 119.0582 | 14.3 | C4H9NO3 | L-Threonine | Amino Acid Metabolism | 0.99 | 1.06 | 0.96 | 0.9192 | 0.6822 | 0.5550 | 1.08 | 1.02 | 1.10 | 0.5545 | 0.8678 | 0.3632 | 1.00 | 1.02 | 0.92 | 0.9955 | 0.6565 | 0.3473 | 1.07 | 1.05 | 1.11 | 0.4231 | 0.7872 | 0.2179 |
| 307.0836 | 14.0 | C10H17N3O6S | Glutathione | Amino Acid Metabolism | 1.05 | 0.98 | 0.99 | 0.2325 | 0.5293 | 0.8906 | 1.14 | 1.05 | 1.10 | 0.1068 | 0.4125 | 0.1256 | 1.02 | 0.98 | 1.01 | 0.5838 | 0.8421 | 0.8349 | 1.04 | 0.96 | 1.05 | 0.5238 | 0.6285 | 0.4982 |
| 149.0510 | 11.5 | C5H11NO2S | L-Methionine | Amino Acid Metabolism | 1.01 | 0.95 | 0.99 | 0.9633 | 0.6019 | 0.9461 | 1.07 | 1.08 | 1.09 | 0.5575 | 0.4861 | 0.4252 | 1.09 | 1.04 | 1.03 | 0.5194 | 0.7540 | 0.7945 | 1.09 | 1.01 | 1.05 | 0.4110 | 0.9624 | 0.7406 |
| 204.0899 | 11.6 | C11H12N2O2 | L-Tryptophan | Amino Acid Metabolism | 0.96 | 0.93 | 1.04 | 0.5901 | 0.5897 | 0.6539 | 1.10 | 1.11 | 1.09 | 0.4983 | 0.3967 | 0.5085 | 1.05 | 1.08 | 1.02 | 0.7716 | 0.4808 | 0.8363 | 0.97 | 1.04 | 0.94 | 0.7838 | 0.7945 | 0.6093 |
| 131.0583 | 14.3 | C5H9NO3 | 5-Aminolevulinate | Amino Acid Metabolism | 0.94 | 0.99 | 0.96 | 0.6479 | 0.9154 | 0.6465 | 0.96 | 0.99 | 1.09 | 0.7603 | 0.9325 | 0.4997 | 0.95 | 1.11 | 1.02 | 0.6405 | 0.3984 | 0.8258 | 1.04 | 1.08 | 1.17 | 0.5847 | 0.7007 | 0.0779 |
| 159.0896 | 12.4 | C7H13NO3 | 5-Acetamidopentanoate | Amino Acid Metabolism | 0.23 | 0.64 | 0.37 | 0.0013 | 0.0779 | 0.0038 | 0.74 | 1.41 | 1.08 | 0.3094 | 0.1018 | 0.7494 | 0.26 | 0.51 | 0.54 | 0.0065 | 0.0385 | 0.0620 | 1.63 | 0.86 | 2.42 | 0.6001 | 0.6243 | 0.0375 |
| 197.0689 | 10.2 | C9H11NO4 | N-Hydroxy-L-tyrosine | Amino Acid Metabolism | 0.98 | 1.04 | 0.96 | 0.9113 | 0.8553 | 0.8466 | 1.04 | 1.01 | 1.08 | 0.8584 | 0.9558 | 0.6112 | 0.88 | 1.12 | 0.97 | 0.6357 | 0.6689 | 0.8640 | 0.95 | 1.06 | 1.07 | 0.8627 | 0.6546 | 0.5544 |
| 219.0742 | 13.7 | C8H13NO6 | O-Succinyl-L-homoserine | Amino Acid Metabolism | 0.97 | 0.92 | 1.01 | 0.8856 | 0.6196 | 0.9716 | 1.29 | 0.99 | 1.08 | 0.2144 | 0.9278 | 0.5812 | 1.10 | 0.97 | 0.91 | 0.4702 | 0.8391 | 0.2290 | 1.01 | 0.94 | 1.01 | 0.9307 | 0.7031 | 0.9533 |
| 240.1224 | 14.2 | C10H16N4O3 | beta-Alanyl-N(pi)-methyl-L-histidine | Amino Acid Metabolism | 1.28 | 0.16 | 0.81 | 0.3724 | NA | 0.5847 | 1.80 | 0.71 | 1.08 | 0.1150 | 0.5784 | 0.8671 | 1.75 | 0.25 | 1.24 | 0.1405 | 0.0405 | 0.6085 | 1.50 | 0.52 | 0.94 | 0.1822 | 0.2159 | 0.8864 |
| 312.0221 | 15.9 | C9H16N2O5Se | gamma-Glutamyl-Se-methylselenocysteine | Amino Acid Metabolism | 0.82 | 0.67 | 0.90 | 0.4670 | 0.2948 | 0.6505 | 0.97 | 1.29 | 1.07 | 0.9037 | 0.4946 | 0.8157 | 0.88 | 1.11 | 1.01 | 0.5923 | 0.8277 | 0.9684 | 0.85 | 1.11 | 1.12 | 0.4736 | 0.7414 | 0.6667 |
| 259.0457 | 15.6 | C5H10NO7P | L-Glutamyl 5-phosphate | Amino Acid Metabolism | 1.18 | 0.43 | 0.87 | 0.4737 | 0.0083 | 0.5661 | 1.40 | 0.80 | 1.07 | 0.1581 | 0.5266 | 0.8147 | 1.37 | 0.55 | 1.10 | 0.2428 | 0.0503 | 0.7046 | 1.31 | 0.68 | 0.80 | 0.2832 | 0.2462 | 0.4010 |
| 146.0690 | 14.9 | C5H10N2O3 | L-Glutamine | Amino Acid Metabolism | 0.98 | 0.95 | 1.03 | 0.8179 | 0.5715 | 0.7331 | 1.03 | 0.91 | 1.07 | 0.7747 | 0.3050 | 0.4755 | 1.12 | 1.06 | 1.12 | 0.1573 | 0.5834 | 0.1338 | 1.05 | 0.98 | 1.04 | 0.5664 | 0.8304 | 0.5524 |
| 133.0375 | 14.7 | C4H7NO4 | L-Aspartate | Amino Acid Metabolism | 1.00 | 1.00 | 0.98 | 0.9922 | 0.9982 | 0.8559 | 1.05 | 1.03 | 1.07 | 0.5662 | 0.7061 | 0.4330 | 0.98 | 1.05 | 0.94 | 0.8985 | 0.4407 | 0.3674 | 0.99 | 0.99 | 1.09 | 0.9029 | 0.9663 | 0.3669 |
| 117.0789 | 11.3 | C5H11NO2 | Betaine | Amino Acid Metabolism | 1.10 | 0.98 | 1.06 | 0.5796 | 0.9051 | 0.7511 | 1.14 | 0.83 | 1.07 | 0.5343 | 0.1778 | 0.6942 | 1.35 | 0.98 | 1.04 | 0.1057 | 0.8918 | 0.7829 | 0.93 | 0.86 | 0.96 | 0.6709 | 0.4237 | 0.8209 |
| 131.0694 | 14.5 | C4H9N3O2 | Creatine | Amino Acid Metabolism | 0.98 | 0.94 | 1.10 | 0.8837 | 0.7032 | 0.5509 | 1.01 | 0.92 | 1.07 | 0.9535 | 0.3405 | 0.5752 | 1.20 | 1.15 | 1.07 | 0.2251 | 0.2761 | 0.5820 | 0.83 | 0.94 | 1.05 | 0.1317 | 0.7350 | 0.7222 |
| 132.0898 | 21.8 | C5H12N2O2 | L-Ornithine | Amino Acid Metabolism | 0.78 | 1.04 | 0.93 | 0.0332 | 0.7583 | 0.3851 | 1.01 | 1.13 | 1.06 | 0.9202 | 0.4423 | 0.6127 | 1.03 | 1.13 | 1.11 | 0.7958 | 0.1751 | 0.3067 | 0.93 | 1.07 | 1.15 | 0.3682 | 0.5390 | 0.1684 |
| 145.1103 | 13.3 | C7H15NO2 | 4-Trimethylammoniobutanoate | Amino Acid Metabolism | 1.02 | 0.97 | 1.04 | 0.8040 | 0.8322 | 0.7063 | 0.93 | 0.98 | 1.06 | 0.4925 | 0.8463 | 0.5553 | 1.08 | 1.01 | 1.06 | 0.4903 | 0.9145 | 0.4801 | 0.95 | 1.05 | 1.08 | 0.5362 | 0.7373 | 0.4031 |
| 147.0531 | 14.5 | C5H9NO4 | L-Glutamate | Amino Acid Metabolism | 0.91 | 0.96 | 0.94 | 0.3821 | 0.6702 | 0.5719 | 1.03 | 1.05 | 1.06 | 0.7510 | 0.6657 | 0.5496 | 1.01 | 1.03 | 0.98 | 0.8582 | 0.7699 | 0.7935 | 0.86 | 1.08 | 1.00 | 0.0910 | 0.5819 | 0.9704 |
| 161.1051 | 13.2 | C7H15NO3 | L-Carnitine | Amino Acid Metabolism | 1.00 | 1.36 | 1.21 | 0.9963 | 0.4203 | 0.6246 | 0.80 | 0.98 | 1.06 | 0.6634 | 0.9562 | 0.8651 | 0.93 | 1.15 | 0.90 | 0.8968 | 0.5714 | 0.7672 | 0.97 | 1.05 | 1.42 | 0.9645 | 0.8995 | 0.2905 |
| 103.0633 | 14.3 | C4H9NO2 | N,N-Dimethylglycine | Amino Acid Metabolism | 0.89 | 0.90 | 0.95 | 0.3723 | 0.5448 | 0.6851 | 1.06 | 1.17 | 1.05 | 0.6051 | 0.3163 | 0.6864 | 0.94 | 1.01 | 0.97 | 0.6194 | 0.9709 | 0.7915 | 0.93 | 1.09 | 1.00 | 0.5017 | 0.5821 | 0.9651 |
| 203.0795 | 12.1 | C8H13NO5 | N2-Acetyl-L-aminoadipate | Amino Acid Metabolism | 0.74 | 1.05 | 0.94 | 0.2526 | 0.8069 | 0.7926 | 0.88 | 1.16 | 1.05 | 0.5087 | 0.4452 | 0.8307 | 0.98 | 1.17 | 1.00 | 0.9219 | 0.3469 | 0.9797 | 0.83 | 1.16 | 1.07 | 0.3095 | 0.4775 | 0.7161 |
| 189.0639 | 13.9 | C7H11NO5 | N-Acetyl-L-glutamate | Amino Acid Metabolism | 1.06 | 0.82 | 0.90 | 0.7602 | 0.2016 | 0.2583 | 1.14 | 0.99 | 1.05 | 0.5895 | 0.9343 | 0.7843 | 1.16 | 0.84 | 1.13 | 0.5730 | 0.1168 | 0.3391 | 1.10 | 0.95 | 1.14 | 0.3760 | 0.6860 | 0.2121 |
| 131.0946 | 11.3 | C6H13NO2 | L-Leucine | Amino Acid Metabolism | 0.98 | 1.18 | 1.02 | 0.7782 | 0.0681 | 0.8618 | 1.07 | 0.97 | 1.04 | 0.6199 | 0.7808 | 0.6884 | 1.03 | 1.04 | 0.98 | 0.7500 | 0.7264 | 0.8641 | 0.96 | 1.02 | 0.95 | 0.6547 | 0.8554 | 0.5728 |
| 246.1329 | 17.0 | C9H18N4O4 | N2-(D-1-Carboxyethyl)-L-arginine | Amino Acid Metabolism | 1.03 | 0.82 | 0.97 | 0.8722 | 0.0661 | 0.8106 | 1.23 | 0.95 | 1.04 | 0.1487 | 0.7281 | 0.8101 | 1.19 | 1.00 | 0.98 | 0.1743 | 0.9966 | 0.8512 | 1.01 | 0.90 | 1.03 | 0.8906 | 0.2579 | 0.7656 |
| 175.0957 | 15.7 | C6H13N3O3 | L-Citrulline | Amino Acid Metabolism | 1.00 | 0.91 | 1.03 | 0.9645 | 0.2421 | 0.7367 | 1.11 | 0.99 | 1.04 | 0.4702 | 0.9406 | 0.6934 | 1.13 | 0.96 | 1.04 | 0.4589 | 0.7458 | 0.6281 | 1.12 | 0.91 | 1.12 | 0.1668 | 0.2505 | 0.0751 |
| 181.0739 | 12.9 | C9H11NO3 | L-Tyrosine | Amino Acid Metabolism | 1.03 | 1.04 | 1.08 | 0.7895 | 0.7812 | 0.4101 | 0.99 | 0.95 | 1.03 | 0.8886 | 0.7385 | 0.7644 | 0.98 | 0.98 | 1.00 | 0.8555 | 0.9206 | 0.9651 | 0.97 | 0.94 | 0.97 | 0.7101 | 0.7153 | 0.7827 |
| 129.0790 | 7.7 | C6H11NO2 | N4-Acetylaminobutanal | Amino Acid Metabolism | 1.12 | 0.90 | 1.02 | 0.3731 | 0.5256 | 0.9002 | 0.90 | 0.79 | 1.03 | 0.4684 | 0.1451 | 0.8014 | 1.25 | 0.80 | 0.94 | 0.2295 | 0.1428 | 0.6822 | 1.22 | 0.88 | 0.95 | 0.0570 | 0.3723 | 0.7096 |
| 103.0997 | 20.1 | C5H13NO | Choline | Amino Acid Metabolism | 0.71 | 1.27 | 1.05 | 0.1957 | 0.2137 | 0.8393 | 0.84 | 1.24 | 1.03 | 0.2510 | 0.1957 | 0.8667 | 0.77 | 1.51 | 1.06 | 0.1813 | 0.1146 | 0.7683 | 0.76 | 1.27 | 1.13 | 0.1237 | 0.2553 | 0.5366 |
| 130.1106 | 18.9 | C6H14N2O | N-Acetylputrescine | Amino Acid Metabolism | 1.03 | 1.07 | 1.01 | 0.8210 | 0.6537 | 0.9487 | 1.13 | 1.07 | 1.03 | 0.4487 | 0.6964 | 0.8615 | 1.18 | 1.13 | 1.20 | 0.0978 | 0.2754 | 0.0835 | 0.94 | 0.90 | 0.93 | 0.3475 | 0.3400 | 0.5213 |

| | | | | | | | | | | | | | | | | | | | | | | | | | | | | |
|---|---|---|---|---|---|---|---|---|---|---|---|---|---|---|---|---|---|---|---|---|---|---|---|---|---|---|---|---|
| 105.0426 | 15.6 | C3H7NO3 | L-Serine | Amino Acid Metabolism | 0.91 | 1.07 | 1.03 | 0.5607 | 0.6263 | 0.8002 | 1.00 | 1.00 | 1.03 | 0.9933 | 0.9934 | 0.8413 | 0.90 | 1.01 | 0.93 | 0.3679 | 0.9570 | 0.4800 | 1.11 | 0.97 | 1.03 | 0.5232 | 0.8352 | 0.8104 |
| 283.0455 | 16.5 | C8H14NO8P | N2-Acetyl-L-aminoadipyl-delta-phosphate | Amino Acid Metabolism | 1.14 | 1.04 | 1.05 | 0.2029 | 0.8431 | 0.6277 | 1.16 | 0.95 | 1.02 | 0.2997 | 0.5316 | 0.7898 | 1.17 | 0.92 | 1.05 | 0.3520 | 0.4371 | 0.6163 | 1.01 | 0.92 | 1.03 | 0.9599 | 0.4880 | 0.8172 |
| 174.1005 | 13.4 | C7H14N2O3 | N-Acetylornithine | Amino Acid Metabolism | 0.97 | 1.46 | 1.14 | 0.8345 | 0.0083 | 0.4120 | 0.87 | 1.06 | 1.02 | 0.3325 | 0.7192 | 0.8676 | 0.94 | 1.25 | 1.10 | 0.6486 | 0.1983 | 0.5205 | 0.93 | 1.07 | 1.07 | 0.6616 | 0.7029 | 0.5740 |
| 232.1058 | 13.2 | C9H16N2O5 | N2-Succinyl-L-ornithine | Amino Acid Metabolism | 0.95 | 0.77 | 0.95 | 0.8633 | 0.3910 | 0.7908 | 1.46 | 1.20 | 1.02 | 0.3349 | 0.3700 | 0.9229 | 0.88 | 0.96 | 0.79 | 0.5893 | 0.7308 | 0.1573 | 0.76 | 0.74 | 0.69 | 0.1629 | 0.0785 | 0.1363 |
| 131.0946 | 10.8 | C6H13NO2 | L-Isoleucine | Amino Acid Metabolism | 0.92 | 1.11 | 1.07 | 0.4088 | 0.2557 | 0.4946 | 1.08 | 1.01 | 1.02 | 0.4461 | 0.9605 | 0.8853 | 1.01 | 1.06 | 0.94 | 0.9187 | 0.6806 | 0.4015 | 0.94 | 1.02 | 0.91 | 0.4303 | 0.9091 | 0.3930 |
| 190.0477 | 10.7 | C7H10O6 | 3-Dehydroquinate | Amino Acid Metabolism | 0.96 | 1.22 | 1.11 | 0.7717 | 0.4002 | 0.3961 | 0.93 | 1.16 | 1.01 | 0.6470 | 0.4431 | 0.9190 | 0.93 | 1.34 | 1.12 | 0.7546 | 0.1729 | 0.5504 | 0.84 | 1.23 | 1.13 | 0.3188 | 0.4477 | 0.4586 |
| 132.0534 | 15.1 | C4H8N2O3 | L-Asparagine | Amino Acid Metabolism | 0.98 | 1.02 | 1.03 | 0.8260 | 0.8161 | 0.8043 | 1.05 | 1.07 | 1.01 | 0.6019 | 0.6326 | 0.9293 | 1.00 | 1.08 | 1.05 | 0.9720 | 0.4007 | 0.5543 | 1.06 | 0.98 | 1.07 | 0.5341 | 0.8758 | 0.5259 |
| 138.0428 | 10.3 | C6H6N2O2 | Urocanate | Amino Acid Metabolism | 0.70 | 0.90 | 1.28 | 0.2146 | 0.6674 | 0.3228 | 1.07 | 0.93 | 1.00 | 0.5236 | 0.6430 | 0.9669 | 0.97 | 0.93 | 1.05 | 0.7480 | 0.5836 | 0.6331 | 0.44 | 0.96 | 1.07 | 0.0872 | 0.6413 | 0.4452 |
| 165.0790 | 10.2 | C9H11NO2 | L-Phenylalanine | Amino Acid Metabolism | 0.94 | 0.85 | 0.91 | 0.1839 | 0.1287 | 0.0495 | 0.98 | 0.93 | 0.99 | 0.8743 | 0.2968 | 0.9348 | 1.02 | 1.00 | 1.03 | 0.8887 | 0.9502 | 0.6385 | 1.02 | 0.95 | 0.96 | 0.6736 | 0.6329 | 0.5093 |
| 170.0150 | 14.7 | C6H6N2O2S | Thiourocanic acid | Amino Acid Metabolism | 0.75 | 1.77 | 1.09 | 0.4702 | 0.0162 | 0.7757 | 0.59 | 1.38 | 0.99 | 0.2235 | 0.3812 | 0.9804 | 0.61 | 1.70 | 1.02 | 0.1956 | 0.0292 | 0.9585 | 0.64 | 1.44 | 1.28 | 0.2974 | 0.3508 | 0.4988 |
| 612.1518 | 17.2 | C20H32N6O12S2 | Glutathione disulfide | Amino Acid Metabolism | 0.81 | 0.99 | 1.09 | 0.4134 | 0.9766 | 0.7419 | 0.91 | 0.98 | 0.99 | 0.4085 | 0.8693 | 0.9457 | 0.91 | 0.98 | 0.92 | 0.3799 | 0.8412 | 0.3481 | 0.96 | 0.97 | 1.01 | 0.5495 | 0.7039 | 0.8825 |
| 145.0739 | 12.4 | C6H11NO3 | [FA oxo,amino(6:0)] 3-oxo-5S-amino-hexanoic acid | Amino Acid Metabolism | 1.24 | 0.93 | 1.19 | 0.6249 | 0.7952 | 0.6157 | 1.02 | 0.71 | 0.99 | 0.9490 | 0.1773 | 0.9534 | 1.12 | 0.88 | 0.96 | 0.7341 | 0.6063 | 0.8657 | 1.11 | 0.69 | 1.07 | 0.8059 | 0.2111 | 0.8188 |
| 204.1474 | 19.9 | C9H20N2O3 | 3-Hydroxy-N6,N6,N6-trimethyl-L-lysine | Amino Acid Metabolism | 0.76 | 1.44 | 0.99 | 0.3912 | 0.1928 | 0.9740 | 0.75 | 1.10 | 0.98 | 0.1935 | 0.7132 | 0.9345 | 0.90 | 1.39 | 1.10 | 0.6645 | 0.0481 | 0.6832 | 0.71 | 1.18 | 1.08 | 0.1681 | 0.4983 | 0.7037 |
| 188.1525 | 21.4 | C9H20N2O2 | N6,N6,N6-Trimethyl-L-lysine | Amino Acid Metabolism | 0.81 | 0.80 | 0.94 | 0.1695 | 0.1342 | 0.6622 | 1.01 | 1.03 | 0.98 | 0.9670 | 0.8713 | 0.9062 | 1.04 | 0.95 | 1.13 | 0.7557 | 0.5903 | 0.2718 | 1.06 | 1.01 | 1.00 | 0.4654 | 0.9100 | 0.9983 |
| 260.0121 | 12.8 | C6H13O7PS | S-Methyl-5-thio-D-ribose 1-phosphate | Amino Acid Metabolism | 0.96 | 0.93 | 0.94 | 0.8974 | 0.8068 | 0.7866 | 1.10 | 0.96 | 0.98 | 0.6592 | 0.7452 | 0.8761 | 1.08 | 0.99 | 0.99 | 0.6110 | 0.9203 | 0.9500 | 0.99 | 0.98 | 0.94 | 0.9598 | 0.9163 | 0.6547 |
| 113.0589 | 9.7 | C4H7N3O | Creatinine | Amino Acid Metabolism | 0.94 | 0.84 | 1.06 | 0.6727 | 0.5377 | 0.6602 | 1.01 | 0.95 | 0.95 | 0.9647 | 0.8007 | 0.7063 | 1.22 | 1.27 | 1.17 | 0.3154 | 0.2441 | 0.1482 | 0.99 | 1.01 | 1.09 | 0.9146 | 0.9484 | 0.4972 |
| 162.0351 | 7.8 | C6H10O3S | 1,2-Dihydroxy-5-(methylthio)pent-1-en-3-one | Amino Acid Metabolism | 0.90 | 1.12 | 0.95 | 0.4906 | 0.3101 | 0.6594 | 1.05 | 0.92 | 0.94 | 0.7809 | 0.5178 | 0.6218 | 0.96 | 1.04 | 1.08 | 0.8380 | 0.5832 | 0.3918 | 0.83 | 1.07 | 0.76 | 0.2937 | 0.6757 | 0.0515 |
| 297.0894 | 7.4 | C11H15N5O3S | 5'-Methylthioadenosine | Amino Acid Metabolism | 0.91 | 1.17 | 0.96 | 0.6866 | 0.5931 | 0.8214 | 0.91 | 0.83 | 0.83 | 0.7710 | 0.5145 | 0.4258 | 1.02 | 0.92 | 1.10 | 0.9001 | 0.6098 | 0.5788 | 0.97 | 0.87 | 1.09 | 0.9217 | 0.5356 | 0.4339 |
| 117.0578 | 8.9 | C8H7N | Indole | Amino Acid Metabolism | 0.72 | 0.97 | 1.01 | 0.1518 | 0.7549 | 0.9205 | 0.69 | 0.84 | 0.82 | 0.1097 | 0.3019 | 0.1497 | 0.72 | 0.92 | 0.82 | 0.1796 | 0.5747 | 0.3002 | 1.04 | 0.92 | 1.00 | 0.7826 | 0.7078 | 0.9796 |
| 139.9873 | 17.9 | C2H5O5P | Acetyl phosphate | Amino Acid Metabolism | 0.73 | 0.95 | 0.83 | 0.0420 | 0.7724 | 0.1670 | 0.90 | 1.08 | 0.81 | 0.3561 | 0.5963 | 0.1085 | 0.84 | 0.96 | 0.96 | 0.2712 | 0.6390 | 0.7216 | 0.89 | 1.15 | 1.03 | 0.5150 | 0.2269 | 0.8170 |
| 114.0317 | 15.6 | C5H6O3 | 2-Hydroxy-2,4-pentadienoate | Amino Acid Metabolism | 0.45 | 0.54 | 1.03 | 0.1769 | NA | 0.9139 | 0.64 | 1.62 | 0.62 | 0.4344 | 0.4159 | 0.4203 | 0.84 | 1.75 | 1.13 | 0.7221 | 0.1102 | 0.7907 | 1.23 | 1.62 | 1.17 | 0.4195 | 0.1065 | 0.5532 |
| 174.0793 | 7.4 | C10H10N2O | Indole-3-acetamide | Amino Acid Metabolism | 0.77 | 0.57 | 1.02 | 0.6456 | NA | 0.9675 | 0.86 | 0.51 | 0.57 | 0.6590 | 0.1450 | 0.2117 | 1.28 | 0.56 | 0.90 | 0.3283 | 0.0168 | 0.6037 | 0.95 | 0.68 | 0.60 | 0.8918 | 0.3020 | 0.1838 |
| 156.0422 | 13.8 | C7H8O4 | 2,3-Dihydro-2,3-dihydroxybenzoate | Biosynthesis of Polyketides and Nonribosomal Peptides | 0.79 | 1.42 | 1.13 | 0.7231 | 0.2348 | 0.7718 | 0.94 | 1.25 | 1.25 | 0.9079 | 0.5227 | 0.5871 | 0.72 | 1.40 | 0.97 | 0.6307 | 0.2394 | 0.9341 | 0.78 | 1.19 | 1.33 | 0.6896 | 0.5762 | 0.5018 |
| 307.0840 | 15.2 | C18H13NO4 | Stealthin C | Biosynthesis of Polyketides and Nonribosomal Peptides | 1.04 | 1.04 | 1.01 | 0.4423 | 0.3220 | 0.8788 | 0.85 | 1.06 | 1.09 | 0.4096 | 0.4358 | 0.1960 | 1.02 | 1.05 | 1.02 | 0.4759 | 0.4403 | 0.5020 | 1.04 | 1.00 | 1.08 | 0.5209 | 0.9898 | 0.3242 |
| 306.0522 | 12.2 | C18H10O5 | Kinobscurinone | Biosynthesis of Polyketides and Nonribosomal Peptides | 0.98 | 1.12 | 1.13 | 0.9463 | 0.6875 | 0.5396 | 0.93 | 0.96 | 0.88 | 0.7214 | 0.7974 | 0.5707 | 1.15 | 1.00 | 0.95 | 0.4176 | 0.9790 | 0.6005 | 1.08 | 0.95 | 0.90 | 0.6764 | 0.7290 | 0.4214 |
| 341.1626 | 10.9 | C20H23NO4 | 5,8,13,13a-Tetrahydrocolumbamine | Biosynthesis of Secondary Metabolites | 0.99 | 0.92 | 0.87 | 0.9499 | 0.8614 | 0.3926 | 1.91 | 1.10 | 1.93 | 0.0356 | 0.8232 | 0.0316 | 1.13 | 1.04 | 1.03 | 0.6849 | 0.7793 | 0.8575 | 1.22 | 1.22 | 1.33 | 0.3032 | 0.4099 | 0.0845 |

| | | | | | | | | | | | | | | | | | | | | | | | | | | | | | |
|---|---|---|---|---|---|---|---|---|---|---|---|---|---|---|---|---|---|---|---|---|---|---|---|---|---|---|---|---|---|
| 331.0844 | 13.2 | C20H13NO4 | Sanguinarine | Biosynthesis of Secondary Metabolites | 1.13 | 0.61 | 1.04 | 0.6928 | 0.0600 | 0.8636 | 1.34 | 0.83 | 1.28 | 0.2860 | 0.3098 | 0.3563 | 0.58 | 0.68 | 0.77 | 0.1648 | 0.2568 | 0.4248 | 1.49 | 0.69 | 1.39 | 0.4036 | 0.2036 | 0.4061 |
| 199.0481 | 7.4 | C8H9NO5 | Clavulanic acid | Biosynthesis of Secondary Metabolites | 0.84 | 0.78 | 0.88 | 0.5728 | 0.4207 | 0.5570 | 1.05 | 1.07 | 1.14 | 0.8144 | 0.3886 | 0.1840 | 0.95 | 0.86 | 1.12 | 0.8953 | 0.4764 | 0.5401 | 1.34 | 1.27 | 1.17 | 0.2524 | 0.3236 | 0.5127 |
| 240.1471 | 10.1 | C12H20N2O3 | Slaframine | Biosynthesis of Secondary Metabolites | 0.97 | 0.83 | 0.94 | 0.7944 | 0.0244 | 0.3991 | 1.14 | 0.91 | 1.12 | 0.3485 | 0.3206 | 0.2724 | 1.09 | 0.95 | 0.99 | 0.5121 | 0.2696 | 0.9000 | 1.03 | 0.87 | 1.04 | 0.7072 | 0.0416 | 0.5720 |
| 155.0946 | 13.4 | C8H13NO2 | Retronecine | Biosynthesis of Secondary Metabolites | 0.96 | 1.28 | 0.95 | 0.7133 | 0.0741 | 0.6487 | 1.15 | 0.99 | 1.11 | 0.4752 | 0.9544 | 0.4086 | 1.13 | 1.05 | 1.04 | 0.6257 | 0.7181 | 0.7877 | 1.09 | 1.08 | 1.00 | 0.3662 | 0.6755 | 0.9836 |
| 88.0637 | 14.1 | C3H8N2O | N,N'-Dimethylurea | Biosynthesis of Secondary Metabolites | 1.19 | 1.28 | 1.06 | 0.0091 | 0.4884 | 0.4155 | 1.12 | 1.02 | 1.08 | 0.1465 | 0.8113 | 0.2047 | 1.13 | 1.00 | 1.02 | 0.1702 | 0.9738 | 0.8013 | 1.08 | 0.97 | 1.11 | 0.2483 | 0.7544 | 0.1651 |
| 357.1573 | 14.9 | C20H23NO5 | deacetylcolchicine | Biosynthesis of Secondary Metabolites | 0.97 | 1.02 | 1.05 | 0.8893 | 0.9344 | 0.7767 | 0.93 | 1.04 | 1.08 | 0.6912 | 0.7922 | 0.5936 | 0.88 | 1.11 | 0.94 | 0.5144 | 0.4609 | 0.6088 | 0.90 | 1.09 | 0.98 | 0.5010 | 0.5995 | 0.8908 |
| 155.0582 | 11.6 | C7H9NO3 | (3S,5S)-carbapenam | Biosynthesis of Secondary Metabolites | 1.19 | 1.22 | 1.19 | 0.6950 | 0.6047 | 0.5349 | 1.01 | 0.93 | 1.05 | 0.9743 | 0.7490 | 0.8329 | 0.96 | 0.97 | 0.84 | 0.9197 | 0.8835 | 0.4645 | 1.11 | 1.02 | 1.29 | 0.8137 | 0.9482 | 0.3161 |
| 365.0898 | 11.4 | C20H15NO6 | 6-Methylpretetramide | Biosynthesis of Secondary Metabolites | 1.30 | 0.71 | 0.96 | 0.7733 | 0.7177 | 0.9566 | 1.40 | 0.46 | 1.04 | 0.7662 | 0.4945 | 0.9664 | 1.26 | 0.42 | 0.73 | 0.8243 | 0.4165 | 0.7151 | 1.64 | 0.50 | 0.51 | 0.6560 | 0.4247 | 0.4206 |
| 153.0790 | 7.4 | C8H11NO2 | vanillylamine | Biosynthesis of Secondary Metabolites | 0.94 | 0.88 | 0.84 | 0.7879 | 0.6222 | 0.3481 | 0.92 | 0.85 | 0.88 | 0.6985 | 0.2124 | 0.4358 | 1.22 | 0.86 | 1.15 | 0.3937 | 0.3175 | 0.3761 | 0.95 | 0.97 | 0.93 | 0.8543 | 0.9066 | 0.7179 |
| 202.0953 | 9.8 | C8H14N2O4 | Proclavaminic acid | Biosynthesis of Secondary Metabolites | 0.92 | 0.88 | 0.66 | 0.8670 | 0.6665 | 0.2893 | 0.96 | 1.42 | 0.69 | 0.9230 | 0.4046 | 0.5004 | 1.00 | 0.93 | 1.04 | 0.9921 | 0.9112 | 0.9249 | 0.93 | 0.83 | 0.85 | 0.8967 | 0.7840 | 0.7444 |
| 309.1059 | 13.1 | C11H19NO9 | N-Acetylneuraminate | Carbohydrate Metabolism | 1.41 | 0.13 | 0.98 | 0.6730 | 0.1671 | 0.9847 | 2.40 | 0.23 | 1.24 | 0.3939 | 0.2111 | 0.7857 | 1.73 | 0.18 | 0.81 | 0.5277 | 0.1894 | 0.7890 | 2.02 | 0.15 | 1.26 | 0.4793 | 0.1822 | 0.7793 |
| 195.0743 | 16.8 | C6H13NO6 | 2-Amino-2-deoxy-D-gluconate | Carbohydrate Metabolism | 1.25 | 0.57 | 1.01 | 0.5628 | 0.1347 | 0.9770 | 1.60 | 0.63 | 1.22 | 0.3373 | 0.1497 | 0.5932 | 1.30 | 0.55 | 0.89 | 0.5459 | 0.1642 | 0.7759 | 1.47 | 0.58 | 1.26 | 0.4495 | 0.1451 | 0.5837 |
| 194.0427 | 15.5 | C6H10O7 | D-Glucuronate | Carbohydrate Metabolism | 0.91 | 0.99 | 1.05 | 0.3345 | 0.9438 | 0.5706 | 1.13 | 1.08 | 1.21 | 0.3588 | 0.6905 | 0.1998 | 1.12 | 1.18 | 1.02 | 0.1313 | 0.3761 | 0.8271 | 0.96 | 1.02 | 0.97 | 0.6154 | 0.8830 | 0.6864 |
| 180.0633 | 14.7 | C6H12O6 | D-Mannose | Carbohydrate Metabolism | 0.95 | 0.58 | 0.72 | 0.8583 | 0.3687 | 0.2990 | 1.07 | 0.93 | 1.21 | 0.7957 | 0.8699 | 0.7153 | 0.89 | 0.68 | 0.63 | 0.6917 | 0.2751 | 0.0749 | 0.85 | 0.92 | 0.82 | 0.3471 | 0.7112 | 0.2808 |
| 162.0528 | 12.6 | C6H10O5 | 3-Ethylmalate | Carbohydrate Metabolism | 0.83 | 0.99 | 0.99 | 0.4953 | 0.9514 | 0.9525 | 1.03 | 1.14 | 1.20 | 0.9003 | 0.6240 | 0.4032 | 1.01 | 1.23 | 1.10 | 0.9742 | 0.3616 | 0.5548 | 0.93 | 1.22 | 1.20 | 0.7453 | 0.4385 | 0.4208 |
| 424.1694 | 20.0 | C16H28N2O11 | Chitobiose | Carbohydrate Metabolism | 0.88 | 0.46 | 0.90 | 0.8382 | 0.1170 | 0.8066 | 1.00 | 1.39 | 1.17 | 0.9939 | 0.5180 | 0.7545 | 0.85 | 1.08 | 1.06 | 0.6911 | 0.9003 | 0.8619 | 0.84 | 1.12 | 1.11 | 0.6511 | 0.8190 | 0.8137 |
| 537.0761 | 16.4 | C14H25N3O15P2 | CDP-ribitol | Carbohydrate Metabolism | 1.06 | 0.83 | 0.86 | 0.6983 | 0.2473 | 0.1658 | 1.44 | 0.97 | 1.16 | 0.0300 | 0.8111 | 0.2050 | 1.17 | 0.76 | 0.97 | 0.0678 | 0.0115 | 0.7458 | 1.14 | 0.90 | 1.04 | 0.2528 | 0.4358 | 0.7824 |
| 262.0454 | 15.0 | C6H15O9P | D-Mannitol 1-phosphate | Carbohydrate Metabolism | 1.15 | 0.56 | 0.95 | 0.3319 | 0.0026 | 0.7280 | 1.41 | 0.90 | 1.14 | 0.0037 | 0.5591 | 0.4072 | 1.20 | 0.69 | 1.01 | 0.2439 | 0.1329 | 0.9375 | 1.24 | 0.81 | 1.06 | 0.1280 | 0.3433 | 0.7747 |
| 152.0685 | 12.8 | C5H12O5 | Ribitol | Carbohydrate Metabolism | 0.70 | 0.88 | 1.06 | 0.2019 | 0.6520 | 0.8255 | 1.02 | 1.48 | 1.14 | 0.9404 | 0.3508 | 0.6681 | 0.77 | 1.10 | 1.07 | 0.3043 | 0.8004 | 0.8110 | 0.68 | 1.24 | 1.04 | 0.3303 | 0.6330 | 0.9109 |
| 221.0900 | 12.1 | C8H15NO6 | N-Acetyl-D-mannosamine | Carbohydrate Metabolism | 0.74 | 1.15 | 0.92 | 0.2309 | 0.5283 | 0.7154 | 0.93 | 1.31 | 1.14 | 0.6819 | 0.1794 | 0.5229 | 0.99 | 1.25 | 1.10 | 0.9751 | 0.1763 | 0.6253 | 0.82 | 1.15 | 1.06 | 0.2208 | 0.4568 | 0.7656 |
| 150.0528 | 14.2 | C5H10O5 | D-Xylose | Carbohydrate Metabolism | 0.95 | 1.01 | 0.99 | 0.7646 | 0.9330 | 0.9355 | 1.19 | 0.88 | 1.13 | 0.2390 | 0.4585 | 0.4158 | 0.72 | 0.88 | 0.76 | 0.0317 | 0.0256 | 0.0030 | 0.90 | 0.89 | 1.07 | 0.4051 | 0.4915 | 0.4227 |
| 607.0817 | 14.9 | C17H27N3O17P2 | UDP-N-acetyl-D-galactosamine | Carbohydrate Metabolism | 1.22 | 0.75 | 1.03 | 0.1304 | 0.0730 | 0.8487 | 1.38 | 0.81 | 1.12 | 0.0431 | 0.1149 | 0.4270 | 1.19 | 0.73 | 0.99 | 0.1743 | 0.0516 | 0.9523 | 1.24 | 0.72 | 1.03 | 0.1481 | 0.0584 | 0.8659 |
| 146.0216 | 15.3 | C5H6O5 | 2-Oxoglutarate | Carbohydrate Metabolism | 0.88 | 1.25 | 1.03 | 0.3867 | 0.1739 | 0.8144 | 1.00 | 1.22 | 1.12 | 0.9900 | 0.3262 | 0.4903 | 0.82 | 1.18 | 0.99 | 0.2128 | 0.1603 | 0.9643 | 0.82 | 1.13 | 1.08 | 0.1996 | 0.5069 | 0.6899 |
| 605.0773 | 18.0 | C16H25N5O16P2 | GDP-mannose | Carbohydrate Metabolism | 1.01 | 1.08 | 1.07 | 0.9797 | 0.5986 | 0.7185 | 1.05 | 1.02 | 1.11 | 0.8381 | 0.9485 | 0.5469 | 0.94 | 1.01 | 0.94 | 0.8068 | 0.9173 | 0.7315 | 1.04 | 0.97 | 1.16 | 0.8868 | 0.8839 | 0.3478 |
| 134.0216 | 15.8 | C4H6O5 | (S)-Malate | Carbohydrate Metabolism | 1.00 | 0.99 | 1.07 | 0.9611 | 0.9318 | 0.4548 | 1.13 | 1.04 | 1.11 | 0.2626 | 0.8111 | 0.3249 | 0.98 | 1.04 | 0.92 | 0.8251 | 0.7453 | 0.2045 | 0.95 | 0.94 | 0.97 | 0.6221 | 0.7315 | 0.7287 |
| 244.0349 | 15.2 | C6H13O8P | L-Fuculose 1-phosphate | Carbohydrate Metabolism | 0.93 | 0.65 | 0.83 | 0.7929 | 0.0331 | 0.3108 | 1.23 | 1.12 | 1.11 | 0.4100 | 0.5737 | 0.6253 | 1.19 | 0.76 | 1.11 | 0.3702 | 0.1314 | 0.5598 | 1.21 | 0.96 | 0.95 | 0.5014 | 0.8378 | 0.7251 |
| 200.0086 | 12.6 | C4H9O7P | D-Erythrose 4-phosphate | Carbohydrate Metabolism | 0.76 | 0.87 | 0.87 | 0.3275 | 0.5325 | 0.5718 | 0.92 | 1.07 | 1.10 | 0.6674 | 0.7427 | 0.7209 | 0.92 | 1.02 | 1.04 | 0.4964 | 0.9369 | 0.7533 | 0.97 | 1.10 | 1.01 | 0.8000 | 0.5668 | 0.9624 |

| | | | | | | | | | | | | | | | | | | | | | | | | | | | | | |
|---|---|---|---|---|---|---|---|---|---|---|---|---|---|---|---|---|---|---|---|---|---|---|---|---|---|---|---|---|---|
| 196.0582 | 13.3 | C6H12O7 | D-Gluconic acid | Carbohydrate Metabolism | 0.98 | 1.09 | 1.07 | 0.7988 | 0.5832 | 0.4767 | 1.06 | 1.08 | 1.10 | 0.5369 | 0.5239 | 0.3787 | 1.01 | 1.05 | 1.05 | 0.8948 | 0.6126 | 0.5684 | 1.01 | 1.00 | 1.03 | 0.9008 | 0.9667 | 0.6383 |
| 260.0297 | 16.6 | C6H13O9P | D-Glucose 6-phosphate | Carbohydrate Metabolism | 1.08 | 0.87 | 1.00 | 0.1947 | 0.0717 | 0.9883 | 1.12 | 1.08 | 1.10 | 0.0217 | 0.1205 | 0.0997 | 1.04 | 1.06 | 1.04 | 0.2341 | 0.4458 | 0.4815 | 1.11 | 0.95 | 1.09 | 0.1292 | 0.6352 | 0.2317 |
| 106.0266 | 11.7 | C3H6O4 | D-Glycerate | Carbohydrate Metabolism | 0.88 | 1.23 | 1.04 | 0.4872 | 0.0782 | 0.8242 | 1.02 | 1.16 | 1.10 | 0.8670 | 0.1991 | 0.4671 | 0.97 | 1.14 | 1.04 | 0.7463 | 0.0905 | 0.6669 | 0.91 | 1.07 | 1.01 | 0.3037 | 0.5421 | 0.9210 |
| 150.0529 | 11.8 | C5H10O5 | D-Ribose | Carbohydrate Metabolism | 0.94 | 0.87 | 0.99 | 0.6947 | 0.2846 | 0.9690 | 1.10 | 1.10 | 1.10 | 0.3560 | 0.5440 | 0.4837 | 0.99 | 1.07 | 1.07 | 0.8618 | 0.6780 | 0.5200 | 0.98 | 1.07 | 1.06 | 0.8745 | 0.6961 | 0.6219 |
| 566.0550 | 16.1 | C15H24N2O17P2 | UDP-glucose | Carbohydrate Metabolism | 1.07 | 0.92 | 1.03 | 0.3533 | 0.4894 | 0.6395 | 1.15 | 0.98 | 1.09 | 0.1868 | 0.8189 | 0.4260 | 1.07 | 0.86 | 1.01 | 0.4549 | 0.0814 | 0.8740 | 1.06 | 0.98 | 1.07 | 0.5025 | 0.7958 | 0.4296 |
| 254.1002 | 13.6 | C9H18O8 | 3-beta-D-Galactosyl-sn-glycerol | Carbohydrate Metabolism | 1.08 | 0.77 | 1.00 | 0.2803 | 0.0098 | 0.9736 | 1.27 | 0.91 | 1.09 | 0.0417 | 0.3380 | 0.3494 | 1.09 | 0.83 | 0.99 | 0.3012 | 0.1103 | 0.9425 | 1.16 | 0.84 | 1.01 | 0.0628 | 0.0934 | 0.9046 |
| 90.0316 | 9.5 | C3H6O3 | (S)-Lactate | Carbohydrate Metabolism | 0.98 | 1.02 | 1.01 | 0.9212 | 0.8632 | 0.9722 | 1.00 | 1.06 | 1.08 | 0.9811 | 0.7104 | 0.5541 | 0.91 | 1.11 | 0.93 | 0.4179 | 0.2600 | 0.4805 | 0.98 | 1.01 | 0.95 | 0.8630 | 0.9055 | 0.5933 |
| 177.0636 | 12.9 | C6H11NO5 | 4-Hydroxy-4-methylglutamate | Carbohydrate Metabolism | 1.00 | 1.10 | 1.11 | 0.9811 | 0.4624 | 0.4436 | 1.10 | 1.08 | 1.08 | 0.5088 | 0.6778 | 0.6321 | 1.00 | 1.08 | 1.04 | 0.9780 | 0.4776 | 0.7450 | 0.96 | 0.97 | 1.00 | 0.7770 | 0.8446 | 0.9841 |
| 178.0478 | 11.9 | C6H10O6 | D-Glucono-1,5-lactone | Carbohydrate Metabolism | 0.99 | 1.04 | 1.03 | 0.9383 | 0.7489 | 0.7516 | 1.12 | 1.05 | 1.08 | 0.4227 | 0.7217 | 0.5414 | 1.08 | 1.06 | 1.07 | 0.5748 | 0.4492 | 0.3645 | 1.05 | 1.02 | 1.07 | 0.4710 | 0.8535 | 0.3925 |
| 589.0825 | 17.3 | C16H25N5O15P2 | GDP-L-fucose | Carbohydrate Metabolism | 1.09 | 0.94 | 1.05 | 0.5478 | 0.4999 | 0.4748 | 1.08 | 1.05 | 1.07 | 0.4983 | 0.7062 | 0.5676 | 1.01 | 1.00 | 1.01 | 0.9121 | 0.9682 | 0.8599 | 1.05 | 0.96 | 1.10 | 0.6658 | 0.7395 | 0.4038 |
| 180.0634 | 12.7 | C6H12O6 | D-Glucose | Carbohydrate Metabolism | 0.96 | 1.05 | 1.02 | 0.7874 | 0.7173 | 0.8560 | 1.00 | 1.00 | 1.07 | 0.9879 | 0.9831 | 0.5828 | 1.01 | 1.03 | 1.01 | 0.9497 | 0.7789 | 0.9512 | 0.97 | 1.11 | 1.19 | 0.7884 | 0.5942 | 0.1567 |
| 580.0344 | 18.8 | C15H22N2O18P2 | UDP-glucuronate | Carbohydrate Metabolism | 1.04 | 0.68 | 0.94 | 0.7992 | 0.0101 | 0.6409 | 1.36 | 0.98 | 1.07 | 0.0777 | 0.9047 | 0.7033 | 1.12 | 0.82 | 1.00 | 0.3607 | 0.1997 | 0.9823 | 1.14 | 0.88 | 1.00 | 0.2785 | 0.2964 | 0.9983 |
| 192.0270 | 17.9 | C6H8O7 | Citrate | Carbohydrate Metabolism | 0.88 | 1.63 | 1.28 | 0.7416 | 0.2678 | 0.3776 | 1.11 | 1.22 | 1.07 | 0.8299 | 0.5693 | 0.8456 | 0.91 | 1.27 | 1.08 | 0.8492 | 0.3744 | 0.7917 | 0.81 | 1.17 | 0.97 | 0.5693 | 0.6257 | 0.9161 |
| 180.0634 | 16.9 | C6H12O6 | D-Fructose | Carbohydrate Metabolism | 1.00 | 0.98 | 1.03 | 0.9542 | 0.7146 | 0.5679 | 1.06 | 1.01 | 1.06 | 0.4398 | 0.9146 | 0.3334 | 1.03 | 0.99 | 1.01 | 0.6576 | 0.9134 | 0.8405 | 1.01 | 0.94 | 1.08 | 0.9489 | 0.4623 | 0.2036 |
| 210.0376 | 16.8 | C6H10O8 | D-Glucarate | Carbohydrate Metabolism | 0.61 | 1.54 | 1.06 | 0.1834 | 0.1215 | 0.8555 | 0.67 | 1.43 | 1.06 | 0.2779 | 0.2563 | 0.8651 | 0.61 | 1.57 | 1.00 | 0.1489 | 0.1174 | 0.9971 | 0.59 | 1.32 | 1.18 | 0.1362 | 0.3983 | 0.6548 |
| 179.0794 | 16.2 | C6H13NO5 | D-Glucosamine | Carbohydrate Metabolism | 1.10 | 0.52 | 0.98 | 0.6741 | 0.0043 | 0.9123 | 1.36 | 0.82 | 1.06 | 0.2857 | 0.5192 | 0.8443 | 1.44 | 0.63 | 1.20 | 0.2603 | 0.0484 | 0.4448 | 1.40 | 0.84 | 0.95 | 0.1713 | 0.4195 | 0.8054 |
| 230.0192 | 15.4 | C5H11O8P | D-Ribose 5-phosphate | Carbohydrate Metabolism | 0.89 | 1.01 | 0.97 | 0.2960 | 0.9554 | 0.7257 | 0.98 | 1.15 | 1.06 | 0.9109 | 0.5163 | 0.7733 | 0.94 | 1.09 | 0.97 | 0.3896 | 0.4964 | 0.6777 | 0.93 | 1.13 | 1.00 | 0.4302 | 0.3858 | 0.9936 |
| 174.0163 | 17.7 | C6H6O6 | cis-Aconitate | Carbohydrate Metabolism | 1.11 | 0.97 | 0.86 | 0.6031 | 0.8452 | 0.4099 | 1.22 | 0.93 | 1.05 | 0.6366 | 0.8044 | 0.8836 | 1.29 | 1.11 | 1.05 | 0.5445 | 0.5059 | 0.8553 | 0.91 | 0.99 | 1.03 | 0.6531 | 0.9512 | 0.8504 |
| 84.0212 | 11.0 | C4H4O2 | 3-Butynoate | Carbohydrate Metabolism | 0.82 | 1.06 | 1.03 | 0.5970 | 0.8042 | 0.9143 | 0.95 | 0.99 | 1.05 | 0.8862 | 0.9558 | 0.8392 | 1.00 | 1.24 | 0.94 | 0.9901 | 0.4009 | 0.7969 | 0.91 | 0.94 | 1.40 | 0.7473 | 0.7934 | 0.1289 |
| 166.0477 | 13.3 | C5H10O6 | D-Arabinonate | Carbohydrate Metabolism | 0.67 | 1.62 | 1.13 | 0.2300 | 0.2406 | 0.6702 | 0.77 | 1.33 | 1.05 | 0.4384 | 0.2402 | 0.8708 | 0.68 | 1.41 | 1.12 | 0.2374 | 0.0928 | 0.6550 | 0.67 | 1.39 | 1.42 | 0.1765 | 0.3073 | 0.0780 |
| 88.0159 | 14.5 | C3H4O3 | Pyruvate | Carbohydrate Metabolism | 1.08 | 0.66 | 0.91 | 0.7360 | 0.2207 | 0.6341 | 1.37 | 0.72 | 1.05 | 0.2810 | 0.1404 | 0.8378 | 1.19 | 0.69 | 0.84 | 0.5258 | 0.1193 | 0.4447 | 1.34 | 0.78 | 1.00 | 0.3101 | 0.1662 | 0.9997 |
| 424.0366 | 14.5 | C12H18N4O7P2S | Thiamin diphosphate | Carbohydrate Metabolism | 1.16 | 1.10 | 1.03 | 0.1891 | 0.1725 | 0.7903 | 0.98 | 1.09 | 1.04 | 0.9120 | 0.4041 | 0.7717 | 0.98 | 0.92 | 0.91 | 0.8937 | 0.6291 | 0.3110 | 1.12 | 1.04 | 0.98 | 0.3879 | 0.8058 | 0.8657 |
| 182.0790 | 13.8 | C6H14O6 | Mannitol | Carbohydrate Metabolism | 0.92 | 1.24 | 1.03 | 0.5131 | 0.1619 | 0.7449 | 0.93 | 1.08 | 1.04 | 0.6632 | 0.5850 | 0.7634 | 0.90 | 1.10 | 1.00 | 0.5288 | 0.5283 | 0.9818 | 0.96 | 1.06 | 0.99 | 0.7570 | 0.6642 | 0.9452 |
| 260.0296 | 15.1 | C6H13O9P | D-Glucose 1-phosphate | Carbohydrate Metabolism | 1.08 | 0.91 | 1.02 | 0.5089 | 0.5238 | 0.8547 | 1.14 | 0.97 | 1.03 | 0.2968 | 0.7576 | 0.7740 | 1.09 | 0.89 | 1.03 | 0.4303 | 0.2521 | 0.7296 | 1.11 | 0.89 | 0.99 | 0.4665 | 0.2420 | 0.8489 |
| 120.0423 | 10.5 | C4H8O4 | L-Erythrulose | Carbohydrate Metabolism | 0.91 | 0.97 | 0.98 | 0.2984 | 0.8224 | 0.8176 | 1.08 | 1.13 | 1.03 | 0.4001 | 0.2977 | 0.7628 | 0.98 | 1.12 | 1.12 | 0.8759 | 0.3777 | 0.3073 | 1.01 | 1.05 | 1.10 | 0.8782 | 0.4988 | 0.1421 |
| 276.0248 | 17.5 | C6H13O10P | 6-Phospho-D-gluconate | Carbohydrate Metabolism | 1.01 | 0.90 | 0.97 | 0.9495 | 0.0067 | 0.4606 | 1.14 | 1.09 | 1.02 | 0.0739 | 0.2936 | 0.7854 | 1.00 | 0.94 | 0.97 | 0.8909 | 0.2844 | 0.4849 | 1.07 | 0.99 | 1.04 | 0.2628 | 0.8600 | 0.4469 |
| 290.0405 | 15.9 | C7H15O10P | D-Sedoheptulose 7-phosphate | Carbohydrate Metabolism | 0.90 | 0.70 | 0.92 | 0.4936 | 0.2264 | 0.6306 | 0.93 | 1.21 | 1.02 | 0.7278 | 0.5327 | 0.9376 | 0.97 | 1.16 | 1.10 | 0.8318 | 0.6934 | 0.6237 | 0.93 | 1.12 | 1.05 | 0.7021 | 0.7016 | 0.8098 |
| 185.9929 | 16.7 | C3H7O7P | 3-Phospho-D-glycerate | Carbohydrate Metabolism | 0.91 | 1.13 | 1.02 | 0.5134 | 0.3187 | 0.8588 | 1.03 | 1.09 | 1.01 | 0.7952 | 0.5172 | 0.9151 | 0.93 | 0.97 | 0.99 | 0.5275 | 0.7383 | 0.8532 | 0.93 | 1.00 | 1.05 | 0.3676 | 0.9767 | 0.5658 |
| 260.0298 | 17.8 | C6H13O9P | D-Mannose 1-phosphate | Carbohydrate Metabolism | 0.89 | 1.09 | 0.99 | 0.2409 | 0.5371 | 0.9432 | 1.01 | 1.12 | 1.00 | 0.9352 | 0.4192 | 0.9902 | 0.91 | 1.01 | 0.93 | 0.6418 | 0.9460 | 0.5053 | 0.97 | 1.04 | 1.16 | 0.8427 | 0.7209 | 0.2550 |
| 150.0165 | 17.0 | C4H6O6 | (R,R)-Tartaric acid | Carbohydrate Metabolism | 0.77 | 1.12 | 0.93 | 0.0936 | 0.5044 | 0.5884 | 1.01 | 1.11 | 0.99 | 0.9731 | 0.3998 | 0.9258 | 0.96 | 1.21 | 1.11 | 0.8799 | 0.1892 | 0.5590 | 0.81 | 1.18 | 1.02 | 0.0688 | 0.2529 | 0.8880 |
| 255.7053 | 5.2 | C21H36N7O16P3S | CoA | Carbohydrate Metabolism | 1.01 | 0.83 | 0.94 | 0.9184 | 0.3740 | 0.5235 | 1.04 | 0.72 | 0.97 | 0.7911 | 0.4151 | 0.8415 | 1.09 | 0.71 | 1.08 | 0.6674 | 0.0417 | 0.6206 | 0.94 | 0.74 | 0.85 | 0.6405 | 0.1363 | 0.1334 |
| 150.0529 | 12.3 | C5H10O5 | L-Arabinose | Carbohydrate Metabolism | 0.82 | 0.66 | 0.64 | 0.1805 | 0.3043 | 0.0152 | 1.16 | 0.86 | 0.95 | 0.4628 | 0.4131 | 0.8160 | 1.24 | 0.90 | 1.05 | 0.3390 | 0.5132 | 0.7512 | 1.05 | 0.83 | 0.99 | 0.8062 | 0.3821 | 0.9673 |

| | | | | | | | | | | | | | | | | | | | | | | | | | | | | |
|---|---|---|---|---|---|---|---|---|---|---|---|---|---|---|---|---|---|---|---|---|---|---|---|---|---|---|---|---|
| 809.1253 | 12.3 | C23H38N7O17P3S | Acetyl-CoA | Carbohydrate Metabolism | 1.03 | 0.89 | 0.93 | 0.8378 | 0.3024 | 0.5243 | 0.99 | 1.18 | 0.95 | 0.9242 | 0.1636 | 0.7170 | 1.14 | 1.01 | 1.05 | 0.4807 | 0.9412 | 0.6382 | 0.91 | 1.02 | 1.00 | 0.5792 | 0.8069 | 0.9696 |
| 260.0297 | 15.7 | C6H13O9P | D-Mannose 6-phosphate | Carbohydrate Metabolism | 0.84 | 3.76 | 0.86 | 0.3263 | 0.0689 | 0.3986 | 0.97 | 1.24 | 0.95 | 0.8693 | 0.5261 | 0.8135 | 1.01 | 0.99 | 1.16 | 0.9061 | 0.9139 | 0.3429 | 2.58 | 1.07 | 1.00 | 0.3969 | 0.8118 | 0.9787 |
| 309.9858 | 17.6 | C5H12O11P2 | D-Ribose 1,5-bisphosphate | Carbohydrate Metabolism | 0.77 | 1.24 | 1.04 | 0.1268 | 0.0671 | 0.8170 | 0.86 | 1.07 | 0.92 | 0.4313 | 0.7606 | 0.6695 | 0.83 | 1.04 | 0.94 | 0.4420 | 0.8223 | 0.7272 | 0.87 | 1.07 | 1.14 | 0.5418 | 0.7230 | 0.5046 |
| 379.1047 | 13.1 | C13H21N3O8S | (R)-S-Lactoylglutathione | Carbohydrate Metabolism | 1.22 | 0.96 | 1.03 | 0.6059 | 0.8957 | 0.9375 | 1.08 | 0.79 | 0.90 | 0.7125 | 0.4417 | 0.6220 | 1.22 | 0.67 | 0.86 | 0.2172 | 0.1901 | 0.4288 | 1.11 | 0.78 | 1.05 | 0.5624 | 0.2722 | 0.7518 |
| 169.9980 | 15.1 | C3H7O6P | Glycerone phosphate | Carbohydrate Metabolism | 0.85 | 0.98 | 1.01 | 0.4357 | 0.9334 | 0.9474 | 0.92 | 1.03 | 0.88 | 0.7049 | 0.9228 | 0.5455 | 0.96 | 0.90 | 1.06 | 0.8368 | 0.6829 | 0.7540 | 0.95 | 0.94 | 0.85 | 0.7814 | 0.6425 | 0.1781 |
| 265.9591 | 17.9 | C3H8O10P2 | 3-Phospho-D-glyceroyl phosphate | Carbohydrate Metabolism | 0.75 | 0.97 | 0.83 | 0.0744 | 0.8200 | 0.1445 | 0.93 | 1.15 | 0.85 | 0.4542 | 0.4302 | 0.1708 | 0.87 | 0.96 | 0.99 | 0.3491 | 0.5732 | 0.9172 | 0.90 | 1.15 | 1.06 | 0.5348 | 0.3811 | 0.6238 |
| 167.9823 | 17.8 | C3H5O6P | Phosphoenolpyruvate | Carbohydrate Metabolism | 0.72 | 1.03 | 0.84 | 0.0547 | 0.7692 | 0.2152 | 0.90 | 1.12 | 0.84 | 0.4133 | 0.4947 | 0.2004 | 0.87 | 0.97 | 0.96 | 0.2976 | 0.7069 | 0.6551 | 0.91 | 1.13 | 1.03 | 0.5719 | 0.3490 | 0.8166 |
| 663.1088 | 13.9 | C21H27N7O14P2 | NAD+ | Energy Metabolism | 1.06 | 0.94 | 1.01 | 0.6363 | 0.4056 | 0.9033 | 1.15 | 1.00 | 1.13 | 0.1549 | 0.9672 | 0.0673 | 1.03 | 0.90 | 0.96 | 0.7371 | 0.1022 | 0.5666 | 1.06 | 0.93 | 1.05 | 0.5589 | 0.2625 | 0.5275 |
| 743.0754 | 16.6 | C21H28N7O17P3 | NADP+ | Energy Metabolism | 1.01 | 1.08 | 1.04 | 0.8518 | 0.4029 | 0.4534 | 1.07 | 1.09 | 1.01 | 0.3631 | 0.3175 | 0.8654 | 0.98 | 0.97 | 0.98 | 0.5714 | 0.4757 | 0.5226 | 1.01 | 1.01 | 1.06 | 0.8164 | 0.9288 | 0.3757 |
| 210.0740 | 13.7 | C7H14O7 | Sedoheptulose | Energy Metabolism | 0.76 | 1.55 | 1.07 | 0.2446 | 0.0222 | 0.7795 | 0.74 | 1.22 | 1.01 | 0.1374 | 0.3756 | 0.9618 | 0.74 | 1.36 | 1.03 | 0.1052 | 0.0712 | 0.8693 | 0.80 | 1.25 | 1.19 | 0.2551 | 0.4089 | 0.4543 |
| 339.9960 | 17.8 | C6H14O12P2 | D-Fructose 1,6-bisphosphate | Energy Metabolism | 0.91 | 1.18 | 1.02 | 0.2558 | 0.1766 | 0.8139 | 1.00 | 1.08 | 1.01 | 0.9882 | 0.5621 | 0.9254 | 0.88 | 1.06 | 0.97 | 0.2517 | 0.3802 | 0.6932 | 0.95 | 1.07 | 1.10 | 0.6071 | 0.5884 | 0.3291 |
| 506.9956 | 16.2 | C10H16N5O13P3 | ATP | Energy Metabolism | 0.99 | 0.96 | 1.00 | 0.9260 | 0.5293 | 0.9587 | 1.06 | 1.04 | 1.01 | 0.3643 | 0.6585 | 0.8935 | 0.97 | 0.97 | 0.98 | 0.5510 | 0.7050 | 0.4634 | 1.01 | 1.03 | 1.08 | 0.9067 | 0.7057 | 0.2370 |
| 427.0291 | 14.9 | C10H15N5O10P2 | ADP | Energy Metabolism | 1.02 | 1.06 | 1.01 | 0.7384 | 0.6425 | 0.7174 | 1.03 | 1.08 | 0.99 | 0.6364 | 0.0698 | 0.8803 | 0.92 | 1.04 | 0.97 | 0.0499 | 0.5569 | 0.4709 | 1.01 | 0.95 | 1.00 | 0.7288 | 0.4468 | 0.9344 |
| 370.0068 | 18.1 | C7H16O13P2 | D-Sedoheptulose 1,7-bisphosphate | Energy Metabolism | 0.94 | 0.88 | 0.99 | 0.6978 | 0.1822 | 0.9544 | 1.00 | 1.18 | 0.97 | 0.9876 | 0.3911 | 0.8861 | 0.91 | 0.91 | 1.03 | 0.4839 | 0.5234 | 0.7177 | 1.06 | 1.04 | 1.12 | 0.6777 | 0.8004 | 0.2044 |
| 97.9768 | 15.7 | H3O4P | Orthophosphate | Energy Metabolism | 0.97 | 0.94 | 0.94 | 0.5994 | 0.6505 | 0.4069 | 1.01 | 1.01 | 0.97 | 0.8277 | 0.7940 | 0.4696 | 0.98 | 1.00 | 0.92 | 0.6904 | 0.9204 | 0.1406 | 1.09 | 1.03 | 1.09 | 0.1765 | 0.6820 | 0.1826 |
| 318.0353 | 15.0 | C8H15O11P | 3-Deoxy-D-manno-octulosonate 8-phosphate | Glycan Biosynthesis and Metabolism | 0.91 | 1.06 | 0.95 | 0.7376 | 0.6992 | 0.8040 | 0.96 | 1.11 | 0.89 | 0.8837 | 0.7804 | 0.7212 | 0.81 | 0.97 | 0.96 | 0.2788 | 0.8710 | 0.7946 | 1.20 | 1.39 | 0.84 | 0.2929 | 0.2888 | 0.6035 |
| 472.1123 | 14.2 | C14H26N4O10P2 | CMP-N-trimethyl-2-aminoethylphosphonate | Lipid Metabolism | 1.28 | 0.24 | 0.86 | 0.6061 | 0.0447 | 0.7579 | 1.77 | 0.75 | 1.19 | 0.2888 | 0.6622 | 0.7387 | 1.52 | 0.28 | 1.13 | 0.4446 | 0.0983 | 0.8005 | 1.41 | 0.60 | 0.72 | 0.4757 | 0.3918 | 0.5460 |
| 340.3341 | 3.8 | C22H44O2 | Docosanoic acid | Lipid Metabolism | 0.78 | 0.82 | 1.02 | 0.2801 | 0.3304 | 0.9190 | 1.01 | 1.71 | 1.14 | 0.9755 | 0.1062 | 0.4635 | 0.93 | 0.95 | 1.62 | 0.5598 | 0.7926 | 0.1065 | 1.05 | 0.94 | 0.88 | 0.8762 | 0.7513 | 0.4772 |
| 183.0660 | 14.8 | C5H14NO4P | Choline phosphate | Lipid Metabolism | 1.07 | 1.14 | 1.00 | 0.5766 | 0.4209 | 0.9966 | 1.13 | 0.90 | 1.14 | 0.5657 | 0.5877 | 0.4627 | 1.15 | 1.07 | 1.98 | 0.4148 | 0.6121 | 0.0057 | 1.12 | 1.10 | 1.99 | 0.1793 | 0.4365 | 0.0000 |
| 368.3656 | 3.8 | C24H48O2 | Tetracosanoic acid | Lipid Metabolism | 0.90 | 0.80 | 1.35 | 0.6264 | 0.2724 | 0.2432 | 0.93 | 1.09 | 1.12 | 0.4862 | 0.5076 | 0.5302 | 0.83 | 0.94 | 1.38 | 0.2429 | 0.6818 | 0.1127 | 0.83 | 1.08 | 0.84 | 0.2253 | 0.5789 | 0.2400 |
| 446.0605 | 16.1 | C11H20N4O11P2 | CDP-ethanolamine | Lipid Metabolism | 1.03 | 1.08 | 1.09 | 0.7709 | 0.5066 | 0.3537 | 1.11 | 1.02 | 1.09 | 0.1269 | 0.8337 | 0.2628 | 1.08 | 0.90 | 1.06 | 0.2948 | 0.0539 | 0.3930 | 1.04 | 0.96 | 1.59 | 0.7128 | 0.4880 | 0.0001 |
| 215.0560 | 15.5 | C5H14NO6P | sn-glycero-3-Phosphoethanolamine | Lipid Metabolism | 0.82 | 1.15 | 1.05 | 0.3328 | 0.3467 | 0.7982 | 0.86 | 1.25 | 1.09 | 0.3905 | 0.2873 | 0.6843 | 0.83 | 1.26 | 1.03 | 0.2314 | 0.2865 | 0.8590 | 0.84 | 1.21 | 1.04 | 0.2151 | 0.2998 | 0.7940 |
| 102.0317 | 13.4 | C4H6O3 | Acetoacetate | Lipid Metabolism | 1.09 | 1.65 | 1.33 | 0.7050 | 0.3273 | 0.2077 | 1.02 | 1.02 | 1.09 | 0.9429 | 0.9225 | 0.6926 | 0.89 | 1.14 | 0.97 | 0.7190 | 0.4356 | 0.9075 | 0.92 | 1.06 | 1.21 | 0.7710 | 0.8359 | 0.3514 |
| 438.2740 | 4.7 | C21H43O7P | LPA(18:0) | Lipid Metabolism | 0.95 | 0.81 | 0.89 | 0.8446 | 0.3940 | 0.4383 | 0.93 | 0.89 | 1.07 | 0.5478 | 0.5271 | 0.7012 | 0.92 | 1.04 | 1.09 | 0.6058 | 0.8767 | 0.6741 | 0.75 | 0.88 | 0.92 | 0.1869 | 0.5513 | 0.7391 |
| 488.1072 | 15.1 | C14H26N4O11P2 | CDP-choline | Lipid Metabolism | 1.14 | 0.79 | 0.99 | 0.6178 | 0.2550 | 0.9525 | 1.29 | 0.98 | 1.06 | 0.2164 | 0.9394 | 0.7879 | 1.21 | 0.74 | 0.89 | 0.3999 | 0.1039 | 0.5308 | 1.22 | 0.83 | 0.82 | 0.3608 | 0.3460 | 0.3350 |
| 172.0136 | 14.7 | C3H9O6P | sn-Glycerol 3-phosphate | Lipid Metabolism | 1.11 | 0.59 | 0.90 | 0.4646 | 0.0028 | 0.4833 | 1.34 | 0.92 | 1.05 | 0.0321 | 0.7000 | 0.7135 | 1.20 | 0.68 | 0.95 | 0.2006 | 0.0534 | 0.7396 | 1.09 | 0.73 | 0.86 | 0.5012 | 0.0999 | 0.3860 |
| 449.3146 | 4.9 | C26H43NO5 | Chenodeoxyglycocholate | Lipid Metabolism | 1.04 | 0.98 | 1.51 | 0.6687 | 0.9218 | 0.3770 | 0.96 | 0.87 | 1.04 | 0.7502 | 0.5014 | 0.8311 | 0.98 | 1.00 | 0.91 | 0.8712 | 0.9970 | 0.3760 | 1.00 | 1.06 | 1.00 | 0.9609 | 0.6493 | 0.9956 |
| 216.0402 | 13.1 | C5H13O7P | 2-C-Methyl-D-erythritol 4-phosphate | Lipid Metabolism | 0.88 | 0.51 | 0.62 | 0.6561 | 0.2387 | 0.0865 | 1.45 | 1.20 | 1.03 | 0.3461 | 0.4074 | 0.8918 | 1.15 | 0.81 | 0.86 | 0.4702 | 0.3504 | 0.4862 | 1.35 | 0.98 | 1.26 | 0.1961 | 0.8864 | 0.2673 |
| 257.1026 | 14.3 | C8H20NO6P | sn-glycero-3-Phosphocholine | Lipid Metabolism | 0.64 | 1.24 | 0.98 | 0.1935 | 0.3616 | 0.9413 | 0.58 | 1.27 | 1.03 | 0.0720 | 0.3562 | 0.9058 | 0.66 | 1.42 | 0.97 | 0.1110 | 0.0759 | 0.9062 | 0.68 | 1.38 | 1.10 | 0.1518 | 0.2645 | 0.7120 |
| 125.0147 | 14.7 | C2H7NO3S | Taurine | Lipid Metabolism | 1.00 | 1.02 | 1.04 | 0.9908 | 0.9155 | 0.6547 | 0.97 | 1.00 | 1.02 | 0.7327 | 0.9686 | 0.8300 | 0.97 | 1.05 | 0.95 | 0.7406 | 0.6060 | 0.5076 | 1.00 | 1.00 | 0.96 | 0.9827 | 0.9919 | 0.5777 |
| 169.0501 | 14.9 | C4H12NO4P | Phosphodimethylethanolamine | Lipid Metabolism | 1.01 | 1.07 | 0.98 | 0.9226 | 0.3695 | 0.7809 | 0.94 | 1.07 | 1.01 | 0.4732 | 0.6392 | 0.8851 | 0.94 | 1.05 | 1.07 | 0.5144 | 0.5804 | 0.4825 | 0.95 | 1.02 | 1.00 | 0.5836 | 0.7205 | 0.9887 |
| 921.2511 | 14.1 | C31H54N7O17P3S | Decanoyl-CoA | Lipid Metabolism | 1.06 | 1.04 | 0.95 | 0.5258 | 0.6985 | 0.3560 | 1.15 | 1.11 | 1.00 | 0.1213 | 0.1995 | 0.9503 | 1.04 | 1.07 | 1.03 | 0.4968 | 0.2076 | 0.6012 | 1.04 | 1.10 | 1.10 | 0.6745 | 0.3043 | 0.4117 |
| 284.2715 | 3.9 | C18H36O2 | Octadecanoic acid | Lipid Metabolism | 0.78 | 0.80 | 0.98 | 0.2757 | 0.3126 | 0.9272 | 0.82 | 1.20 | 0.95 | 0.1238 | 0.1348 | 0.7057 | 0.83 | 0.89 | 1.16 | 0.2178 | 0.5373 | 0.3267 | 0.83 | 0.81 | 0.74 | 0.3227 | 0.2369 | 0.1204 |
| 256.2402 | 3.9 | C16H32O2 | Hexadecanoic acid | Lipid Metabolism | 0.79 | 0.86 | 1.02 | 0.1965 | 0.3836 | 0.9344 | 0.82 | 1.17 | 0.91 | 0.1392 | 0.1764 | 0.5432 | 0.87 | 0.91 | 1.19 | 0.2804 | 0.5623 | 0.1749 | 0.85 | 0.85 | 0.75 | 0.3995 | 0.2715 | 0.0897 |
| 340.2978 | 3.9 | C21H40O3 | FA oxo(21:0) | Lipids: Fatty Acyls | 0.96 | 1.16 | 0.93 | 0.7898 | 0.5005 | 0.6028 | 0.98 | 1.21 | 1.24 | 0.8270 | 0.2254 | 0.0824 | 1.00 | 0.90 | 1.05 | 0.9892 | 0.3558 | 0.5982 | 0.75 | 0.86 | 0.71 | 0.0193 | 0.1979 | 0.0182 |
| 312.2662 | 4.0 | C19H36O3 | FA oxo(19:0) | Lipids: Fatty Acyls | 0.95 | 1.18 | 1.06 | 0.8200 | 0.2896 | 0.7542 | 0.94 | 1.30 | 1.18 | 0.7021 | 0.1333 | 0.2542 | 0.85 | 0.86 | 0.92 | 0.5327 | 0.4357 | 0.6884 | 0.76 | 0.90 | 0.59 | 0.0626 | 0.3767 | 0.0047 |
| 447.3346 | 4.6 | C27H45NO4 | N-stearoyl tyrosine | Lipids: Fatty Acyls | 0.98 | 1.34 | 1.00 | 0.9748 | 0.3378 | 0.9966 | 0.67 | 1.07 | 1.15 | 0.5015 | 0.8567 | 0.6762 | 0.87 | 1.40 | 0.88 | 0.7901 | 0.2297 | 0.7344 | 0.70 | 1.21 | 1.14 | 0.5548 | 0.6548 | 0.6817 |
| 399.3346 | 4.7 | C23H45NO4 | O-Palmitoyl-R-carnitine | Lipids: Fatty Acyls | 1.07 | 0.95 | 0.88 | 0.8845 | 0.7672 | 0.5177 | 0.80 | 1.10 | 1.07 | 0.2419 | 0.6061 | 0.6628 | 0.91 | 1.17 | 1.09 | 0.5951 | 0.3803 | 0.6291 | 0.75 | 0.90 | 0.86 | 0.1931 | 0.5934 | 0.4471 |
| 224.1413 | 4.3 | C13H20O3 | [FA] Methyl jasmonate | Lipids: Fatty Acyls | 1.06 | 1.07 | 0.94 | 0.7760 | 0.5314 | 0.7220 | 1.05 | 1.03 | 1.05 | 0.7287 | 0.8905 | 0.7525 | 1.07 | 0.90 | 0.98 | 0.6257 | 0.7362 | 0.8744 | 1.15 | 1.00 | 0.98 | 0.2423 | 0.9983 | 0.8941 |
| 231.1472 | 8.9 | C11H21NO4 | O-Butanoylcarnitine | Lipids: Fatty Acyls | 0.83 | 1.52 | 1.07 | 0.5574 | 0.0629 | 0.8134 | 0.81 | 1.22 | 1.04 | 0.3831 | 0.3886 | 0.8418 | 0.80 | 1.47 | 1.07 | 0.4155 | 0.0462 | 0.8009 | 0.75 | 1.28 | 1.17 | 0.2946 | 0.3873 | 0.5107 |
| 346.2352 | 4.3 | C18H34O6 | [FA hydroxy(18:0)] 9-hydroperoxy-12,13-dihydroxy-10-octadecenoic acid | Lipids: Fatty Acyls | 1.23 | 0.88 | 0.96 | 0.1264 | 0.1211 | 0.7121 | 1.05 | 0.83 | 1.03 | 0.6406 | 0.2264 | 0.7523 | 1.17 | 0.90 | 1.05 | 0.1758 | 0.6048 | 0.6828 | 1.12 | 0.88 | 1.03 | 0.1662 | 0.3815 | 0.8753 |
| 298.2869 | 3.8 | C19H38O2 | FA methyl(18:0) | Lipids: Fatty Acyls | 0.84 | 0.81 | 1.04 | 0.3422 | 0.1933 | 0.8206 | 0.88 | 1.00 | 1.03 | 0.2798 | 0.9913 | 0.8977 | 0.82 | 0.99 | 1.12 | 0.2882 | 0.9631 | 0.5049 | 0.84 | 0.93 | 0.90 | 0.1548 | 0.6607 | 0.4073 |
| 270.2559 | 3.9 | C17H34O2 | FA (17:0) | Lipids: Fatty Acyls | 0.94 | 0.90 | 1.39 | 0.7306 | 0.4956 | 0.4203 | 0.87 | 1.14 | 1.02 | 0.2841 | 0.4806 | 0.9184 | 0.92 | 1.03 | 1.33 | 0.5163 | 0.9023 | 0.0477 | 0.82 | 1.01 | 0.90 | 0.1403 | 0.9606 | 0.4950 |

| | | | | | | | | | | | | | | | | | | | | | | | | | | | | | |
|---|---|---|---|---|---|---|---|---|---|---|---|---|---|---|---|---|---|---|---|---|---|---|---|---|---|---|---|---|---|
| 354.3501 | 3.8 | C23H46O2 | [FA (23:0)] tricosanoic acid | Lipids: Fatty Acyls | 0.98 | 0.48 | 1.09 | 0.9289 | 0.1342 | 0.6680 | 0.74 | 0.96 | 1.02 | 0.0653 | 0.7848 | 0.9293 | 0.77 | 1.01 | 1.47 | 0.1754 | 0.9601 | 0.0328 | 0.79 | 1.12 | 0.91 | 0.3009 | 0.6656 | 0.6829 |
| 312.3031 | 3.8 | C20H40O2 | FA (20:0) | Lipids: Fatty Acyls | 0.85 | 0.83 | 0.98 | 0.4400 | 0.3563 | 0.9075 | 0.78 | 1.20 | 1.00 | 0.0508 | 0.1834 | 0.9799 | 0.86 | 0.92 | 1.14 | 0.1543 | 0.6015 | 0.2602 | 0.83 | 0.89 | 0.77 | 0.2464 | 0.4597 | 0.1372 |
| 217.1314 | 9.8 | C10H19NO4 | O-Propanoylcarnitine | Lipids: Fatty Acyls | 0.90 | 1.03 | 1.00 | 0.7264 | 0.8788 | 0.9993 | 0.94 | 0.95 | 0.98 | 0.8044 | 0.7158 | 0.8901 | 0.93 | 1.15 | 0.93 | 0.7527 | 0.5041 | 0.6803 | 0.92 | 1.05 | 1.22 | 0.7446 | 0.8278 | 0.2901 |
| 248.1776 | 4.2 | C16H24O2 | [FA (16:4)] hexadecatetraenoic acid | Lipids: Fatty Acyls | 1.09 | 0.99 | 0.93 | 0.4928 | 0.9753 | 0.5873 | 1.01 | 1.07 | 0.98 | 0.8939 | 0.2013 | 0.6980 | 1.13 | 1.05 | 1.06 | 0.3677 | 0.2713 | 0.4204 | 0.90 | 0.99 | 0.95 | 0.4000 | 0.8721 | 0.4996 |
| 330.2565 | 3.8 | C22H34O2 | [FA (22:5)] 7Z,10Z,13Z,16Z,19Z-docosapentaenoic acid | Lipids: Fatty Acyls | 1.00 | 0.87 | 0.87 | 0.9674 | 0.2141 | 0.1052 | 0.97 | 1.09 | 0.97 | 0.7624 | 0.4728 | 0.7356 | 0.81 | 0.82 | 1.00 | 0.2389 | 0.3110 | 0.9592 | 0.86 | 0.80 | 0.91 | 0.0834 | 0.0542 | 0.3866 |
| 156.0787 | 4.7 | C8H12O3 | [FA oxo(8:1)] 5-oxo-7-octenoic acid | Lipids: Fatty Acyls | 1.10 | 1.05 | 1.04 | 0.1417 | 0.6676 | 0.6104 | 1.05 | 0.89 | 0.96 | 0.5995 | 0.2085 | 0.6666 | 1.08 | 0.87 | 0.96 | 0.2848 | 0.3235 | 0.5313 | 1.07 | 0.89 | 0.97 | 0.4042 | 0.1647 | 0.6819 |
| 215.1157 | 12.8 | C10H17NO4 | 2-Amino-9,10-epoxy-8-oxodecanoic acid | Lipids: Fatty Acyls | 0.98 | 0.97 | 0.99 | 0.9307 | 0.8790 | 0.9650 | 0.94 | 0.97 | 0.95 | 0.8129 | 0.8738 | 0.8140 | 0.99 | 1.01 | 0.96 | 0.9742 | 0.9301 | 0.7156 | 1.08 | 1.00 | 1.24 | 0.6808 | 0.9793 | 0.1299 |
| 306.2563 | 3.9 | C20H34O2 | Icosatrienoic acid | Lipids: Fatty Acyls | 1.42 | 1.30 | 1.64 | 0.0831 | 0.3260 | 0.1500 | 0.87 | 0.98 | 0.94 | 0.5693 | 0.9386 | 0.7611 | 1.01 | 0.98 | 1.00 | 0.9083 | 0.8960 | 0.9776 | 0.90 | 0.89 | 0.83 | 0.5355 | 0.5224 | 0.2109 |
| 282.2560 | 3.9 | C18H34O2 | [FA (18:1)] 9Z-octadecenoic acid | Lipids: Fatty Acyls | 0.92 | 1.00 | 1.33 | 0.4947 | 0.9770 | 0.3699 | 0.84 | 1.00 | 0.94 | 0.1787 | 0.9729 | 0.5977 | 0.94 | 0.94 | 1.12 | 0.4761 | 0.5711 | 0.2443 | 0.85 | 0.90 | 0.80 | 0.1511 | 0.2486 | 0.0282 |
| 304.2406 | 3.9 | C20H32O2 | FA (20:4) | Lipids: Fatty Acyls | 1.10 | 0.96 | 0.98 | 0.3616 | 0.6506 | 0.8427 | 0.89 | 0.91 | 0.91 | 0.1179 | 0.2624 | 0.4832 | 0.79 | 0.94 | 0.92 | 0.0600 | 0.5687 | 0.5106 | 0.73 | 0.93 | 0.84 | 0.1351 | 0.4306 | 0.0201 |
| 268.2405 | 3.9 | C17H32O2 | FA methyl(16:1) | Lipids: Fatty Acyls | 1.01 | 0.83 | 5.09 | 0.9538 | 0.1034 | 0.3584 | 0.86 | 0.90 | 0.91 | 0.4260 | 0.6347 | 0.5675 | 0.91 | 1.00 | 1.70 | 0.4726 | 0.9993 | 0.1975 | 0.76 | 0.95 | 0.78 | 0.0838 | 0.7576 | 0.1180 |
| 213.1364 | 4.4 | C11H19NO3 | N-Heptanoylhomoserine lactone | Lipids: Fatty Acyls | 1.33 | 1.26 | 1.37 | 0.7329 | NA | 0.6640 | 0.95 | 0.85 | 0.89 | 0.9492 | 0.8126 | 0.8451 | 0.85 | 0.96 | 1.39 | 0.8090 | 0.9255 | 0.2793 | 1.13 | 0.66 | 0.85 | 0.5523 | 0.0811 | 0.5732 |
| 278.2249 | 3.9 | C18H30O2 | [FA (18:3)] 9Z,12Z,15Z-octadecatrienoic acid | Lipids: Fatty Acyls | 1.08 | 1.18 | 1.18 | 0.1891 | 0.0022 | 0.2459 | 0.90 | 0.84 | 0.86 | 0.4940 | 0.2944 | 0.4017 | 0.93 | 0.92 | 1.05 | 0.3858 | 0.5492 | 0.5587 | 0.96 | 0.96 | 0.80 | 0.7396 | 0.6987 | 0.0276 |
| 310.2873 | 3.8 | C20H38O2 | [FA (20:1)] 11Z-eicosenoic acid | Lipids: Fatty Acyls | 0.86 | 0.71 | 2.21 | 0.5458 | 0.2501 | 0.3606 | 0.87 | 1.05 | 0.73 | 0.4167 | 0.8313 | 0.0488 | 0.74 | 0.89 | 1.63 | 0.2985 | 0.7258 | 0.0587 | 0.96 | 1.23 | 0.90 | 0.8327 | 0.3683 | 0.4419 |
| 813.9780 | 5.1 | C79H141N3O31 | Ganglioside GM1 (d18:1/24:1(15Z)) | Lipids: Gangliosides | 1.11 | 1.00 | 1.05 | 0.5958 | 0.9941 | 0.7410 | 1.27 | 1.09 | 1.26 | 0.3689 | 0.5651 | 0.1588 | 1.03 | 0.82 | 1.04 | 0.8605 | 0.1897 | 0.8009 | 1.14 | 0.91 | 1.04 | 0.5625 | 0.4259 | 0.8541 |
| 380.2924 | 4.0 | C23H40O4 | MG(20:3) | Lipids: Glycerolipids | 0.91 | 0.86 | 0.88 | 0.6787 | 0.5249 | 0.6180 | 0.95 | 1.06 | 0.90 | 0.8322 | 0.7771 | 0.6993 | 1.06 | 0.69 | 0.80 | 0.8036 | 0.2050 | 0.2757 | 1.01 | 0.80 | 0.84 | 0.9559 | 0.5875 | 0.3213 |
| 655.4217 | 5.2 | C35H62NO8P | PE(12:0/18:4(6Z,9Z,12Z,15Z)) | Lipids: Glycerophospholipids | 1.13 | 1.30 | 1.11 | 0.1753 | 0.2344 | 0.2699 | 1.08 | 1.13 | 1.31 | 0.6703 | 0.5368 | 0.1366 | 0.94 | 1.05 | 1.01 | 0.6650 | 0.6368 | 0.9343 | 1.12 | 0.97 | 1.14 | 0.5809 | 0.8484 | 0.2554 |
| 824.5566 | 3.7 | C46H81O10P | PG(40:5) | Lipids: Glycerophospholipids | 1.11 | 0.92 | 1.02 | 0.3854 | 0.3223 | 0.8753 | 1.09 | 1.09 | 1.29 | 0.3338 | 0.4058 | 0.0440 | 1.03 | 0.99 | 1.08 | 0.8169 | 0.9375 | 0.2851 | 0.91 | 0.84 | 0.74 | 0.5137 | 0.1143 | 0.0008 |
| 733.5617 | 4.2 | C40H80NO8P | PC(32:0) | Lipids: Glycerophospholipids | 0.83 | 0.84 | 0.97 | 0.3772 | 0.3965 | 0.8867 | 0.97 | 1.13 | 1.25 | 0.6887 | 0.4194 | 0.3154 | 0.91 | 0.98 | 1.05 | 0.3245 | 0.8517 | 0.7088 | 0.84 | 0.95 | 1.00 | 0.1838 | 0.7062 | 0.9945 |
| 525.3072 | 4.3 | C24H48NO9P | PS(18:0) | Lipids: Glycerophospholipids | 0.78 | 0.92 | 1.01 | 0.4687 | 0.7874 | 0.9695 | 0.81 | 1.13 | 1.21 | 0.2503 | 0.5055 | 0.5718 | 0.89 | 1.23 | 1.19 | 0.3096 | 0.2755 | 0.3994 | 0.82 | 0.96 | 0.93 | 0.2863 | 0.8154 | 0.7531 |
| 467.3371 | 5.0 | C23H50NO6P | [PE(O-18:2)] 1-octadecyl-sn-glycero-3-phosphoethanolamine | Lipids: Glycerophospholipids | 0.89 | 0.82 | 0.94 | 0.4219 | 0.0894 | 0.5615 | 1.06 | 1.13 | 1.21 | 0.4100 | 0.1857 | 0.1430 | 1.04 | 0.91 | 1.06 | 0.8285 | 0.4487 | 0.6371 | 0.93 | 1.10 | 1.00 | 0.3925 | 0.6522 | 0.9611 |
| 691.5148 | 3.8 | C37H74NO8P | PE(32:0) | Lipids: Glycerophospholipids | 0.79 | 1.14 | 0.94 | 0.2407 | 0.4140 | 0.7761 | 0.87 | 1.34 | 1.21 | 0.3489 | 0.2209 | 0.3498 | 0.92 | 1.19 | 1.16 | 0.6474 | 0.4431 | 0.4040 | 0.76 | 1.11 | 0.99 | 0.0804 | 0.5195 | 0.9702 |
| 512.3111 | 3.9 | C24H49O9P | [PG (18:0)] 1-octadecanoyl-sn-glycero-3-phospho-(1'-sn-glycerol) | Lipids: Glycerophospholipids | 1.00 | 1.23 | 0.94 | 0.9749 | 0.1022 | 0.6855 | 0.98 | 1.00 | 1.20 | 0.9039 | 0.9964 | 0.2977 | 0.99 | 1.00 | 1.17 | 0.9691 | 0.9926 | 0.2527 | 0.86 | 0.82 | 0.90 | 0.2484 | 0.1834 | 0.4408 |
| 748.5251 | 3.8 | C40H77O10P | PG(34:1) | Lipids: Glycerophospholipids | 0.94 | 0.99 | 0.99 | 0.6236 | 0.9041 | 0.9377 | 0.98 | 1.07 | 1.19 | 0.8930 | 0.5923 | 0.1022 | 0.96 | 1.07 | 1.07 | 0.8407 | 0.4686 | 0.4873 | 0.87 | 0.90 | 0.76 | 0.3412 | 0.3726 | 0.0285 |
| 879.5844 | 3.8 | C45H86NO13P | [PI(36:0) | Lipids: Glycerophospholipids | 0.90 | 0.98 | 0.93 | 0.2527 | 0.6718 | 0.2441 | 1.01 | 1.14 | 1.17 | 0.9483 | 0.3211 | 0.2621 | 0.99 | 1.08 | 1.08 | 0.9566 | 0.4370 | 0.4578 | 0.93 | 1.04 | 1.01 | 0.6391 | 0.5947 | 0.9113 |
| 669.4362 | 5.2 | C36H64NO8P | PE(13:0/18:4(6Z,9Z,12Z,15Z)) | Lipids: Glycerophospholipids | 1.06 | 1.44 | 1.17 | 0.6083 | 0.0015 | 0.1151 | 1.02 | 1.14 | 1.16 | 0.9218 | 0.5209 | 0.4426 | 0.97 | 1.19 | 1.03 | 0.7924 | 0.1335 | 0.7500 | 1.05 | 1.02 | 1.09 | 0.7453 | 0.9023 | 0.3906 |
| 600.3273 | 4.3 | C27H53O12P | [PI(18:0)] 1-octadecanoyl-sn-glycero-3-phospho-(1'-myo-inositol) | Lipids: Glycerophospholipids | 0.86 | 1.03 | 0.95 | 0.4603 | 0.8774 | 0.7973 | 0.97 | 1.04 | 1.16 | 0.7671 | 0.7978 | 0.5085 | 0.96 | 1.05 | 1.09 | 0.4106 | 0.3488 | 0.3650 | 0.87 | 0.91 | 0.88 | 0.3288 | 0.5013 | 0.4809 |
| 713.4997 | 4.0 | C39H72NO8P | PE(34:3) | Lipids: Glycerophospholipids | 0.94 | 1.16 | 1.03 | 0.4770 | 0.1262 | 0.7758 | 0.98 | 1.04 | 1.16 | 0.8680 | 0.7502 | 0.2425 | 0.98 | 1.10 | 0.96 | 0.8416 | 0.3207 | 0.6143 | 0.95 | 1.00 | 0.86 | 0.6020 | 0.9653 | 0.1994 |
| 674.4886 | 3.8 | C37H71O8P | PA(34:1) | Lipids: Glycerophospholipids | 0.83 | 1.06 | 0.98 | 0.3445 | 0.7527 | 0.8993 | 0.88 | 1.25 | 1.16 | 0.2092 | 0.2265 | 0.4365 | 0.87 | 1.20 | 1.18 | 0.2715 | 0.3569 | 0.3589 | 0.81 | 1.08 | 0.93 | 0.0835 | 0.4662 | 0.5961 |
| 776.5555 | 3.8 | C42H81O10P | PG(36:1) | Lipids: Glycerophospholipids | 0.96 | 1.00 | 1.05 | 0.7691 | 0.9682 | 0.6282 | 0.93 | 1.09 | 1.15 | 0.4554 | 0.3617 | 0.1960 | 0.95 | 1.02 | 1.04 | 0.6763 | 0.8327 | 0.5336 | 0.80 | 0.87 | 0.71 | 0.0499 | 0.1420 | 0.0045 |
| 763.5357 | 3.8 | C40H78NO10P | PS(34:0) | Lipids: Glycerophospholipids | 1.11 | 0.91 | 0.94 | 0.4128 | 0.2947 | 0.4420 | 1.22 | 1.06 | 1.14 | 0.1452 | 0.5775 | 0.2124 | 1.16 | 0.96 | 1.05 | 0.4658 | 0.5893 | 0.6321 | 0.96 | 0.89 | 0.85 | 0.7364 | 0.0461 | 0.0370 |

| | | | | | | | | | | | | | | | | | | | | | | | | | | | | |
|---|---|---|---|---|---|---|---|---|---|---|---|---|---|---|---|---|---|---|---|---|---|---|---|---|---|---|---|---|
| 672.4735 | 3.8 | C37H69O8P | PA(34:2) | Lipids: Glycerophospholipids | 0.88 | 1.08 | 0.96 | 0.4234 | 0.6047 | 0.8105 | 0.85 | 1.30 | 1.13 | 0.1750 | 0.2703 | 0.4236 | 0.82 | 1.21 | 1.11 | 0.2160 | 0.5353 | 0.5201 | 0.76 | 1.11 | 0.93 | 0.0573 | 0.2927 | 0.6360 |
| 689.4996 | 3.8 | C37H72NO8P | PE(32:1) | Lipids: Glycerophospholipids | 0.85 | 1.27 | 1.00 | 0.3956 | 0.1312 | 0.9942 | 0.83 | 1.25 | 1.13 | 0.2526 | 0.2877 | 0.5118 | 0.93 | 1.18 | 1.14 | 0.6959 | 0.4542 | 0.4346 | 0.82 | 1.19 | 1.00 | 0.1338 | 0.2429 | 0.9838 |
| 884.5417 | 3.8 | C47H81O13P | PI(38:5) | Lipids: Glycerophospholipids | 0.92 | 0.64 | 0.79 | 0.4941 | 0.0010 | 0.0672 | 1.17 | 0.95 | 1.13 | 0.3338 | 0.7068 | 0.3059 | 1.17 | 0.87 | 1.26 | 0.3990 | 0.4105 | 0.0824 | 1.08 | 0.96 | 0.90 | 0.6141 | 0.8392 | 0.3673 |
| 862.5561 | 3.8 | C45H83O13P | PI(36:2) | Lipids: Glycerophospholipids | 0.92 | 0.93 | 0.93 | 0.5394 | 0.5331 | 0.5470 | 1.03 | 1.09 | 1.12 | 0.8356 | 0.3869 | 0.3305 | 1.13 | 1.19 | 1.22 | 0.3624 | 0.2643 | 0.0471 | 0.91 | 0.98 | 0.94 | 0.5327 | 0.8536 | 0.6047 |
| 774.5410 | 3.8 | C42H79O10P | PG(36:2) | Lipids: Glycerophospholipids | 0.95 | 1.02 | 0.97 | 0.5747 | 0.8627 | 0.7478 | 0.98 | 1.09 | 1.12 | 0.8469 | 0.4088 | 0.2167 | 1.00 | 1.04 | 1.09 | 0.9936 | 0.7429 | 0.2666 | 0.90 | 0.95 | 0.79 | 0.4680 | 0.5828 | 0.0289 |
| 772.5253 | 3.7 | C42H77O10P | PG(36:3) | Lipids: Glycerophospholipids | 1.02 | 1.13 | 1.05 | 0.7466 | 0.0277 | 0.6162 | 0.94 | 1.05 | 1.12 | 0.5788 | 0.5677 | 0.2498 | 1.05 | 1.15 | 1.06 | 0.7924 | 0.3648 | 0.4561 | 0.90 | 0.91 | 0.81 | 0.5085 | 0.4442 | 0.0531 |
| 702.5197 | 3.8 | C39H75O8P | PA(36:1) | Lipids: Glycerophospholipids | 0.80 | 1.01 | 0.97 | 0.3150 | 0.9496 | 0.9064 | 0.85 | 1.25 | 1.12 | 0.2217 | 0.1136 | 0.4635 | 0.93 | 1.13 | 1.12 | 0.5782 | 0.4259 | 0.5321 | 0.76 | 1.05 | 0.90 | 0.0642 | 0.6430 | 0.5127 |
| 509.3845 | 4.8 | C26H56NO6P | LysoPC(O-18:2) | Lipids: Glycerophospholipids | 0.91 | 0.76 | 0.78 | 0.5490 | 0.0737 | 0.1082 | 1.04 | 1.11 | 1.12 | 0.8160 | 0.6767 | 0.5780 | 1.01 | 0.96 | 1.13 | 0.9579 | 0.8084 | 0.4978 | 0.88 | 1.00 | 0.98 | 0.4536 | 0.9910 | 0.8798 |
| 751.5516 | 4.0 | C43H78NO7P | PE(O-38:5) | Lipids: Glycerophospholipids | 0.96 | 0.92 | 0.97 | 0.7167 | 0.4737 | 0.8060 | 1.10 | 1.13 | 1.12 | 0.4249 | 0.4675 | 0.4000 | 0.98 | 1.07 | 1.07 | 0.9143 | 0.7079 | 0.5356 | 0.95 | 1.02 | 1.01 | 0.6795 | 0.8356 | 0.9205 |
| 523.3635 | 4.7 | C26H54NO7P | LysoPC(18:0) | Lipids: Glycerophospholipids | 0.99 | 0.69 | 0.79 | 0.9694 | 0.1907 | 0.2089 | 0.88 | 1.05 | 1.11 | 0.2189 | 0.7940 | 0.5484 | 0.97 | 0.97 | 1.11 | 0.8407 | 0.9123 | 0.6363 | 0.77 | 0.95 | 0.87 | 0.2891 | 0.8404 | 0.5700 |
| 811.5369 | 3.8 | C44H78NO10P | PS(38:4) | Lipids: Glycerophospholipids | 0.88 | 0.82 | 0.93 | 0.4394 | 0.2296 | 0.6677 | 0.93 | 1.08 | 1.11 | 0.4551 | 0.5678 | 0.4377 | 0.95 | 1.15 | 1.17 | 0.6406 | 0.6279 | 0.2589 | 0.89 | 1.00 | 0.96 | 0.2756 | 0.9723 | 0.7033 |
| 701.5367 | 4.0 | C39H76NO7P | PE(P-34:1) | Lipids: Glycerophospholipids | 0.91 | 0.94 | 1.03 | 0.5616 | 0.6921 | 0.8722 | 1.04 | 1.18 | 1.11 | 0.7102 | 0.2553 | 0.4617 | 0.98 | 1.03 | 1.01 | 0.9032 | 0.8249 | 0.9375 | 0.88 | 0.96 | 0.99 | 0.3773 | 0.8090 | 0.9490 |
| 837.5506 | 3.8 | C46H80NO10P | PS(40:5) | Lipids: Glycerophospholipids | 0.91 | 0.79 | 0.92 | 0.4571 | 0.0980 | 0.5278 | 0.96 | 1.08 | 1.10 | 0.7664 | 0.5512 | 0.4569 | 1.02 | 1.04 | 1.18 | 0.8713 | 0.8649 | 0.1726 | 0.93 | 0.95 | 0.90 | 0.6165 | 0.5964 | 0.3946 |
| 807.5056 | 3.8 | C44H74NO10P | PS(38:6) | Lipids: Glycerophospholipids | 1.03 | 1.05 | 1.01 | 0.8125 | 0.7259 | 0.9385 | 0.89 | 1.03 | 1.10 | 0.3464 | 0.8555 | 0.4493 | 0.91 | 1.13 | 1.02 | 0.4420 | 0.5481 | 0.8772 | 0.85 | 1.05 | 0.95 | 0.1485 | 0.5433 | 0.6374 |
| 789.5522 | 3.8 | C42H80NO10P | PS(36:1) | Lipids: Glycerophospholipids | 0.88 | 0.94 | 0.96 | 0.3833 | 0.6147 | 0.7669 | 1.00 | 1.14 | 1.10 | 0.9989 | 0.1376 | 0.3976 | 0.96 | 1.11 | 1.13 | 0.6367 | 0.4698 | 0.2013 | 0.89 | 1.02 | 0.96 | 0.2154 | 0.7906 | 0.6847 |
| 777.5671 | 4.0 | C45H80NO7P | PE(P-40:5) | Lipids: Glycerophospholipids | 0.90 | 1.01 | 1.02 | 0.4239 | 0.9262 | 0.8488 | 0.97 | 1.15 | 1.10 | 0.8604 | 0.4409 | 0.5134 | 0.97 | 1.13 | 1.08 | 0.8590 | 0.6026 | 0.5855 | 0.90 | 1.03 | 0.96 | 0.3811 | 0.8182 | 0.7065 |
| 864.5716 | 3.8 | C45H85O13P | PI(36:1) | Lipids: Glycerophospholipids | 0.92 | 0.96 | 0.98 | 0.5626 | 0.7667 | 0.8712 | 1.06 | 1.09 | 1.10 | 0.6819 | 0.5185 | 0.4121 | 0.94 | 1.03 | 1.11 | 0.6727 | 0.6682 | 0.1725 | 0.98 | 1.05 | 0.91 | 0.8608 | 0.4864 | 0.2922 |
| 886.5566 | 3.8 | C47H83O13P | PI(38:4) | Lipids: Glycerophospholipids | 0.91 | 0.70 | 0.92 | 0.6249 | 0.0480 | 0.6166 | 1.02 | 1.01 | 1.09 | 0.9473 | 0.9620 | 0.6426 | 1.06 | 1.06 | 1.21 | 0.7886 | 0.8409 | 0.2226 | 0.96 | 0.96 | 0.90 | 0.8628 | 0.8159 | 0.5281 |
| 768.4951 | 3.7 | C42H73O10P | PG(36:5) | Lipids: Glycerophospholipids | 1.19 | 1.22 | 1.22 | 0.0987 | 0.4784 | 0.3452 | 0.93 | 1.04 | 1.09 | 0.6270 | 0.7515 | 0.5613 | 0.99 | 1.01 | 1.05 | 0.9503 | 0.8955 | 0.5917 | 0.99 | 0.96 | 0.73 | 0.9416 | 0.7596 | 0.0052 |
| 759.5770 | 4.1 | C42H82NO8P | PC(34:1) | Lipids: Glycerophospholipids | 0.84 | 0.90 | 0.91 | 0.3276 | 0.5460 | 0.6164 | 0.87 | 1.14 | 1.08 | 0.3095 | 0.4624 | 0.6713 | 0.89 | 1.05 | 1.04 | 0.4234 | 0.8013 | 0.8245 | 0.87 | 1.00 | 0.94 | 0.2103 | 0.9789 | 0.6692 |
| 858.5262 | 3.8 | C45H79O13P | PI(36:4) | Lipids: Glycerophospholipids | 0.89 | 0.78 | 0.86 | 0.3521 | 0.0315 | 0.1787 | 0.98 | 0.99 | 1.08 | 0.8541 | 0.9498 | 0.5046 | 0.96 | 1.10 | 1.20 | 0.7512 | 0.7654 | 0.1468 | 0.94 | 0.99 | 0.97 | 0.6415 | 0.9011 | 0.8282 |
| 761.5217 | 3.8 | C40H76NO10P | PS(34:1) | Lipids: Glycerophospholipids | 0.95 | 0.88 | 0.93 | 0.6725 | 0.3816 | 0.4416 | 1.05 | 1.03 | 1.08 | 0.6520 | 0.6621 | 0.5015 | 1.01 | 0.98 | 1.11 | 0.9131 | 0.8954 | 0.1648 | 0.91 | 0.91 | 0.87 | 0.1872 | 0.3022 | 0.1390 |
| 779.5834 | 3.9 | C45H82NO7P | PE(P-40:4) | Lipids: Glycerophospholipids | 0.99 | 0.96 | 0.98 | 0.9111 | 0.7878 | 0.8685 | 1.15 | 1.17 | 1.08 | 0.3544 | 0.3179 | 0.6279 | 1.06 | 0.95 | 1.13 | 0.7386 | 0.7217 | 0.3018 | 1.04 | 0.95 | 1.05 | 0.7662 | 0.7066 | 0.7065 |
| 833.5931 | 4.0 | C48H84NO8P | PC(40:6) | Lipids: Glycerophospholipids | 0.84 | 1.04 | 0.94 | 0.3762 | 0.8408 | 0.7479 | 0.81 | 1.08 | 1.07 | 0.1166 | 0.6939 | 0.7203 | 0.86 | 1.22 | 1.01 | 0.3862 | 0.2670 | 0.9576 | 0.72 | 1.03 | 0.89 | 0.0487 | 0.8971 | 0.4585 |
| 787.5368 | 3.8 | C42H78NO10P | PS(36:2) | Lipids: Glycerophospholipids | 0.89 | 0.88 | 0.94 | 0.3944 | 0.2838 | 0.5930 | 1.01 | 1.11 | 1.07 | 0.8862 | 0.2314 | 0.4973 | 0.96 | 1.17 | 1.11 | 0.7278 | 0.3983 | 0.2025 | 0.90 | 1.02 | 0.93 | 0.2217 | 0.7246 | 0.4187 |
| 745.5613 | 4.0 | C41H80NO8P | PE(36:1) | Lipids: Glycerophospholipids | 0.90 | 1.08 | 0.97 | 0.3846 | 0.4429 | 0.8097 | 0.94 | 1.04 | 1.07 | 0.4729 | 0.6773 | 0.4809 | 0.97 | 1.03 | 1.04 | 0.7782 | 0.6198 | 0.6126 | 1.00 | 1.15 | 1.16 | 0.9898 | 0.3355 | 0.1594 |
| 825.5526 | 3.8 | C45H80NO10P | PS(39:4) | Lipids: Glycerophospholipids | 0.68 | 1.18 | 0.91 | 0.1683 | 0.4166 | 0.7026 | 0.75 | 1.24 | 1.07 | 0.0918 | 0.2303 | 0.7643 | 0.78 | 1.33 | 1.17 | 0.2313 | 0.3674 | 0.5182 | 0.68 | 1.11 | 0.97 | 0.0503 | 0.5367 | 0.8946 |
| 809.5926 | 4.1 | C46H84NO8P | PC(38:4) | Lipids: Glycerophospholipids | 0.93 | 0.81 | 0.88 | 0.4886 | 0.0659 | 0.2491 | 0.95 | 1.06 | 1.06 | 0.6263 | 0.6997 | 0.6797 | 1.01 | 1.01 | 1.08 | 0.9521 | 0.9644 | 0.5915 | 0.93 | 0.96 | 0.93 | 0.4821 | 0.7664 | 0.4702 |
| 696.4733 | 3.8 | C39H69O8P | PA(36:4) | Lipids: Glycerophospholipids | 1.00 | 1.01 | 0.99 | 0.9617 | 0.9151 | 0.8808 | 1.00 | 1.11 | 1.05 | 0.9857 | 0.4860 | 0.7139 | 1.00 | 1.01 | 1.14 | 0.9951 | 0.9806 | 0.3293 | 0.84 | 1.03 | 0.89 | 0.0848 | 0.7918 | 0.1699 |
| 700.5038 | 3.8 | C39H73O8P | PA(36:2) | Lipids: Glycerophospholipids | 0.86 | 1.22 | 0.99 | 0.3727 | 0.1590 | 0.9671 | 0.81 | 1.22 | 1.05 | 0.0760 | 0.2481 | 0.7545 | 0.90 | 1.10 | 1.15 | 0.4293 | 0.5092 | 0.3850 | 0.75 | 1.02 | 0.87 | 0.0545 | 0.8482 | 0.2559 |
| 717.5311 | 4.0 | C39H76NO8P | PE(34:1) | Lipids: Glycerophospholipids | 0.83 | 1.01 | 1.04 | 0.2060 | 0.9531 | 0.8293 | 0.92 | 1.12 | 1.05 | 0.4054 | 0.4424 | 0.7170 | 0.92 | 1.10 | 1.01 | 0.3527 | 0.4684 | 0.9052 | 0.90 | 1.10 | 1.10 | 0.2667 | 0.3993 | 0.4721 |
| 809.5214 | 3.8 | C44H76NO10P | PS(38:5) | Lipids: Glycerophospholipids | 1.05 | 0.89 | 0.97 | 0.6293 | 0.1134 | 0.6912 | 1.02 | 0.98 | 1.05 | 0.8316 | 0.8842 | 0.6067 | 1.04 | 1.04 | 1.11 | 0.6287 | 0.8524 | 0.1572 | 0.95 | 0.97 | 0.90 | 0.6405 | 0.7570 | 0.2174 |

| | | | | | | | | | | | | | | | | | | | | | | | | | | | | | |
|---|---|---|---|---|---|---|---|---|---|---|---|---|---|---|---|---|---|---|---|---|---|---|---|---|---|---|---|---|---|
| 479.3373 | 4.8 | C24H50NO6P | LysoPC(O-16:1) | Lipids: Glycerophospholipids | 0.98 | 0.99 | 0.92 | 0.8790 | 0.9434 | 0.3582 | 1.02 | 1.14 | 1.03 | 0.8916 | 0.5562 | 0.7642 | 1.04 | 0.94 | 1.13 | 0.8162 | 0.6599 | 0.2403 | 0.89 | 0.99 | 0.98 | 0.4057 | 0.8777 | 0.8892 |
| 509.3482 | 4.8 | C25H52NO7P | LysoPE(20:0) | Lipids: Glycerophospholipids | 0.90 | 0.75 | 0.82 | 0.4630 | 0.0812 | 0.0922 | 0.95 | 1.01 | 1.03 | 0.6689 | 0.9655 | 0.8049 | 1.00 | 0.91 | 1.04 | 0.9793 | 0.6310 | 0.8001 | 0.85 | 0.85 | 0.94 | 0.4500 | 0.3675 | 0.6896 |
| 757.5621 | 4.1 | C42H80NO8P | PC(34:2) | Lipids: Glycerophospholipids | 0.89 | 0.94 | 0.92 | 0.3291 | 0.5322 | 0.4586 | 0.90 | 1.13 | 1.03 | 0.4448 | 0.4976 | 0.8420 | 0.90 | 1.07 | 1.00 | 0.4678 | 0.7304 | 0.9776 | 0.89 | 1.06 | 0.95 | 0.2221 | 0.6130 | 0.5988 |
| 493.3528 | 4.7 | C25H52NO6P | PE(P-20:0) | Lipids: Glycerophospholipids | 0.90 | 0.93 | 0.86 | 0.6275 | 0.8354 | 0.2857 | 0.84 | 0.97 | 1.03 | 0.1681 | 0.8608 | 0.7816 | 1.13 | 1.14 | 1.11 | 0.5778 | 0.4867 | 0.3045 | 0.83 | 0.99 | 0.92 | 0.1690 | 0.9667 | 0.5352 |
| 723.5201 | 4.0 | C41H74NO7P | PE(P-36:4) | Lipids: Glycerophospholipids | 1.02 | 0.92 | 1.01 | 0.8882 | 0.3470 | 0.9275 | 1.01 | 1.03 | 1.03 | 0.9147 | 0.8566 | 0.8500 | 0.98 | 1.08 | 1.04 | 0.8993 | 0.6952 | 0.6974 | 0.95 | 1.05 | 1.03 | 0.6266 | 0.7326 | 0.7358 |
| 698.4887 | 3.8 | C39H71O8P | PA(36:3) | Lipids: Glycerophospholipids | 0.88 | 1.04 | 0.96 | 0.1849 | 0.7564 | 0.6606 | 0.92 | 1.16 | 1.03 | 0.3409 | 0.3007 | 0.8242 | 0.93 | 1.02 | 1.13 | 0.5559 | 0.9056 | 0.2836 | 0.79 | 1.05 | 0.88 | 0.0259 | 0.5206 | 0.1271 |
| 451.3062 | 4.9 | C22H46NO6P | PC(14:1) | Lipids: Glycerophospholipids | 0.79 | 0.91 | 0.96 | 0.1340 | 0.2940 | 0.6964 | 1.00 | 0.98 | 1.02 | 0.9795 | 0.8165 | 0.7993 | 0.91 | 0.99 | 1.01 | 0.5433 | 0.8082 | 0.8840 | 0.81 | 1.01 | 0.96 | 0.0994 | 0.9617 | 0.7143 |
| 727.5519 | 4.1 | C41H78NO7P | PE(P-36:2) | Lipids: Glycerophospholipids | 0.97 | 0.94 | 0.94 | 0.7957 | 0.5329 | 0.5710 | 0.99 | 1.05 | 1.02 | 0.9252 | 0.7353 | 0.8780 | 0.98 | 1.16 | 1.12 | 0.8681 | 0.5302 | 0.3886 | 0.97 | 0.97 | 0.95 | 0.8622 | 0.8867 | 0.7022 |
| 517.3166 | 4.9 | C26H48NO7P | [PC(18:3)] | Lipids: Glycerophospholipids | 0.72 | 0.59 | 0.66 | 0.0998 | 0.0374 | 0.0336 | 1.12 | 1.04 | 1.02 | 0.4040 | 0.8294 | 0.8859 | 1.00 | 1.06 | 1.00 | 0.9929 | 0.8092 | 0.9805 | 0.92 | 1.14 | 1.00 | 0.4907 | 0.4423 | 0.9758 |
| 855.5057 | 3.8 | C48H74NO10P | PS(42:10) | Lipids: Glycerophospholipids | 0.89 | 1.40 | 1.05 | 0.3924 | 0.0088 | 0.6952 | 0.79 | 1.15 | 1.02 | 0.2340 | 0.5313 | 0.9293 | 0.80 | 1.23 | 1.02 | 0.2750 | 0.3251 | 0.9100 | 0.86 | 1.19 | 1.01 | 0.3703 | 0.2412 | 0.9193 |
| 749.5358 | 4.0 | C43H76NO7P | PE(P-38:5) | Lipids: Glycerophospholipids | 0.95 | 0.94 | 1.01 | 0.7139 | 0.4985 | 0.8778 | 0.98 | 1.04 | 1.02 | 0.9012 | 0.7982 | 0.9022 | 0.99 | 1.18 | 1.08 | 0.9237 | 0.3326 | 0.4794 | 1.00 | 1.10 | 1.04 | 0.9883 | 0.4160 | 0.6754 |
| 808.5106 | 3.8 | C41H77O13P | PI(32:1) | Lipids: Glycerophospholipids | 0.88 | 0.85 | 0.90 | 0.3512 | 0.2353 | 0.4612 | 0.98 | 1.06 | 1.01 | 0.8321 | 0.7027 | 0.9377 | 0.90 | 1.05 | 1.06 | 0.4375 | 0.7886 | 0.7567 | 0.80 | 1.06 | 0.90 | 0.0540 | 0.6857 | 0.3779 |
| 814.4797 | 7.4 | C46H71O10P | PG(18:4(6Z,9Z,12Z,15Z)/ 22:6(4Z,7Z,10Z,13Z,16Z, 19Z)) | Lipids: Glycerophospholipids | 0.95 | 0.72 | 0.81 | 0.7561 | 0.1231 | 0.1977 | 0.96 | 1.01 | 1.01 | 0.7876 | 0.9733 | 0.9633 | 1.13 | 0.82 | 1.21 | 0.6431 | 0.0664 | 0.1931 | 0.77 | 0.86 | 0.83 | 0.0173 | 0.2969 | 0.1126 |
| 410.2430 | 4.9 | C19H39O7P | [PA(16:0/0:0)] 1-hexadecanoyl-2-sn-glycero-3-phosphate | Lipids: Glycerophospholipids | 0.98 | 0.92 | 0.84 | 0.8928 | 0.4672 | 0.0079 | 0.91 | 0.86 | 1.01 | 0.2073 | 0.1644 | 0.9312 | 1.05 | 0.95 | 1.04 | 0.6068 | 0.6600 | 0.6205 | 0.87 | 0.88 | 1.07 | 0.5379 | 0.2358 | 0.6383 |
| 739.5155 | 4.0 | C41H74NO8P | PE(36:4) | Lipids: Glycerophospholipids | 0.92 | 0.97 | 0.97 | 0.4338 | 0.7686 | 0.7955 | 0.93 | 1.03 | 1.01 | 0.4379 | 0.8769 | 0.9424 | 0.96 | 1.10 | 1.08 | 0.6912 | 0.6344 | 0.4228 | 0.99 | 1.11 | 1.08 | 0.9065 | 0.4591 | 0.3178 |
| 785.5203 | 3.8 | C42H76NO10P | PS(36:3) | Lipids: Glycerophospholipids | 0.94 | 1.02 | 1.01 | 0.6872 | 0.8694 | 0.9179 | 0.94 | 1.04 | 1.01 | 0.5711 | 0.5540 | 0.9118 | 1.02 | 1.11 | 1.05 | 0.8374 | 0.4767 | 0.4723 | 0.94 | 1.06 | 0.87 | 0.1987 | 0.4073 | 0.0225 |
| 831.5063 | 3.8 | C46H74NO10P | PS(40:8) | Lipids: Glycerophospholipids | 1.02 | 0.78 | 0.99 | 0.8296 | 0.1822 | 0.9372 | 0.92 | 0.86 | 1.01 | 0.3913 | 0.2254 | 0.9440 | 1.19 | 1.20 | 1.10 | 0.2099 | 0.6156 | 0.4439 | 1.01 | 0.89 | 0.97 | 0.9498 | 0.2823 | 0.6793 |
| 767.5457 | 4.0 | C43H78NO8P | PE(38:4) | Lipids: Glycerophospholipids | 0.95 | 1.00 | 0.97 | 0.6493 | 0.9724 | 0.7585 | 1.02 | 1.02 | 1.01 | 0.8540 | 0.9118 | 0.9569 | 0.98 | 1.00 | 1.10 | 0.8481 | 0.9803 | 0.1590 | 1.03 | 1.05 | 1.04 | 0.7319 | 0.4857 | 0.6010 |
| 781.5616 | 4.1 | C44H80NO8P | PC(36:4) | Lipids: Glycerophospholipids | 0.93 | 0.87 | 0.90 | 0.4072 | 0.1238 | 0.1690 | 0.99 | 1.04 | 1.00 | 0.9283 | 0.7855 | 0.9696 | 1.02 | 0.94 | 1.03 | 0.8770 | 0.6867 | 0.7805 | 0.95 | 0.95 | 0.88 | 0.5407 | 0.6431 | 0.1066 |
| 483.2618 | 7.5 | C47H84O16P2 | PIP(38:4) | Lipids: Glycerophospholipids | 0.84 | 1.36 | 1.04 | 0.5307 | 0.4541 | 0.8504 | 0.75 | 1.09 | 1.00 | 0.0799 | 0.5816 | 0.9813 | 0.73 | 0.92 | 1.03 | 0.2368 | 0.7828 | 0.8945 | 0.64 | 0.98 | 0.86 | 0.1341 | 0.9591 | 0.5853 |
| 715.5154 | 4.0 | C39H74NO8P | PE(34:2) | Lipids: Glycerophospholipids | 0.86 | 1.09 | 1.03 | 0.3317 | 0.5270 | 0.8308 | 0.85 | 1.14 | 1.00 | 0.2381 | 0.5040 | 0.9990 | 0.84 | 1.16 | 1.01 | 0.1490 | 0.3811 | 0.9693 | 0.86 | 1.16 | 1.02 | 0.2040 | 0.3412 | 0.8669 |
| 465.3216 | 4.9 | C23H48NO6P | LysoPE(18:1) | Lipids: Glycerophospholipids | 0.81 | 0.93 | 0.83 | 0.0039 | 0.0559 | 0.0043 | 0.91 | 0.95 | 1.00 | 0.4688 | 0.6038 | 0.9833 | 0.92 | 0.93 | 1.03 | 0.6212 | 0.3799 | 0.7512 | 0.83 | 1.10 | 1.02 | 0.1803 | 0.5965 | 0.8327 |
| 741.5300 | 4.0 | C41H76NO8P | PE(36:3) | Lipids: Glycerophospholipids | 0.92 | 1.06 | 1.02 | 0.3700 | 0.4917 | 0.8584 | 0.93 | 1.01 | 0.99 | 0.4364 | 0.9272 | 0.9371 | 0.97 | 1.13 | 1.05 | 0.7443 | 0.3070 | 0.4653 | 0.96 | 1.10 | 1.07 | 0.6333 | 0.4213 | 0.4851 |
| 783.5057 | 3.8 | C42H74NO10P | PS(36:4) | Lipids: Glycerophospholipids | 0.94 | 0.96 | 0.91 | 0.7034 | 0.7271 | 0.3951 | 0.88 | 0.99 | 0.99 | 0.1625 | 0.9207 | 0.9025 | 1.00 | 1.19 | 1.07 | 0.9585 | 0.5715 | 0.4249 | 0.90 | 1.05 | 0.92 | 0.2613 | 0.6197 | 0.2659 |
| 793.5611 | 4.0 | C45H80NO8P | PE(40:5) | Lipids: Glycerophospholipids | 1.00 | 0.91 | 0.96 | 0.9511 | 0.1631 | 0.6128 | 1.09 | 1.00 | 0.98 | 0.5639 | 0.9691 | 0.8437 | 1.03 | 0.92 | 1.09 | 0.8184 | 0.4271 | 0.2988 | 0.99 | 1.03 | 0.96 | 0.9585 | 0.6072 | 0.5651 |
| 805.5618 | 4.1 | C46H80NO8P | PC(38:6) | Lipids: Glycerophospholipids | 0.83 | 0.90 | 0.87 | 0.0965 | 0.2895 | 0.1895 | 0.85 | 1.04 | 0.98 | 0.2652 | 0.7903 | 0.8931 | 0.92 | 1.09 | 1.01 | 0.5923 | 0.5826 | 0.9664 | 0.85 | 1.07 | 0.90 | 0.0994 | 0.5982 | 0.3275 |
| 481.3533 | 4.9 | C24H52NO6P | [LysoPC(16:2)] 1-hexadecyl-sn-glycero-3-phosphocholine | Lipids: Glycerophospholipids | 0.83 | 0.68 | 0.89 | 0.1925 | 0.0367 | 0.0771 | 0.97 | 0.89 | 0.97 | 0.6976 | 0.1903 | 0.7181 | 0.94 | 0.94 | 0.94 | 0.6776 | 0.4758 | 0.5813 | 0.93 | 0.93 | 0.97 | 0.6418 | 0.5526 | 0.8238 |
| 765.5302 | 4.0 | C43H76NO8P | PE(38:5) | Lipids: Glycerophospholipids | 1.04 | 1.03 | 1.00 | 0.4303 | 0.6469 | 0.9875 | 1.00 | 1.03 | 0.97 | 0.9755 | 0.8268 | 0.6929 | 1.03 | 1.02 | 1.04 | 0.7778 | 0.8593 | 0.4658 | 1.06 | 1.05 | 1.06 | 0.4236 | 0.5668 | 0.2589 |
| 521.3479 | 4.8 | C26H52NO7P | LysoPC(18:1) | Lipids: Glycerophospholipids | 0.96 | 0.77 | 0.87 | 0.8202 | 0.1587 | 0.1963 | 0.86 | 0.95 | 0.97 | 0.2501 | 0.7879 | 0.8220 | 1.05 | 0.98 | 1.14 | 0.7865 | 0.9199 | 0.3016 | 0.87 | 0.96 | 0.86 | 0.5522 | 0.8659 | 0.3560 |
| 743.5465 | 4.0 | C41H78NO8P | PE(36:2) | Lipids: Glycerophospholipids | 1.02 | 1.11 | 1.02 | 0.7979 | 0.1799 | 0.8120 | 0.93 | 0.99 | 0.96 | 0.5309 | 0.9220 | 0.6883 | 0.95 | 1.13 | 1.08 | 0.5282 | 0.2969 | 0.2748 | 1.01 | 1.09 | 1.08 | 0.7932 | 0.4443 | 0.3290 |

| | | | | | | | | | | | | | | | | | | | | | | | | | | | | | |
|---|---|---|---|---|---|---|---|---|---|---|---|---|---|---|---|---|---|---|---|---|---|---|---|---|---|---|---|---|---|
| 551.3947 | 4.6 | C28H58NO7P | LysoPC(20:0) | Lipids: Glycerophospholipids | 0.86 | 0.67 | 0.77 | 0.5279 | 0.0852 | 0.2299 | 0.77 | 0.98 | 0.96 | 0.1570 | 0.9383 | 0.8499 | 0.92 | 1.20 | 1.11 | 0.6387 | 0.3839 | 0.5982 | 0.90 | 1.07 | 0.87 | 0.5539 | 0.6985 | 0.3879 |
| 495.3322 | 4.9 | C24H50NO7P | LysoPC(16:0) | Lipids: Glycerophospholipids | 0.87 | 0.82 | 0.81 | 0.3635 | 0.0427 | 0.0399 | 0.91 | 0.90 | 0.96 | 0.2227 | 0.2271 | 0.6574 | 1.03 | 0.93 | 1.13 | 0.8675 | 0.6285 | 0.2129 | 0.81 | 1.00 | 1.00 | 0.3249 | 0.9991 | 0.9817 |
| 763.5149 | 4.0 | C43H74NO8P | PE(38:6) | Lipids: Glycerophospholipids | 0.85 | 1.15 | 1.01 | 0.3991 | 0.4175 | 0.9582 | 0.81 | 1.12 | 0.95 | 0.1282 | 0.6183 | 0.7593 | 0.87 | 1.30 | 1.12 | 0.2935 | 0.1444 | 0.4122 | 0.85 | 1.16 | 1.08 | 0.2424 | 0.4244 | 0.5662 |
| 453.2862 | 4.9 | C21H44NO7P | LysoPE(16:0) | Lipids: Glycerophospholipids | 0.74 | 1.01 | 0.79 | 0.0960 | 0.9770 | 0.1591 | 0.84 | 0.96 | 0.95 | 0.1960 | 0.7785 | 0.7566 | 0.86 | 0.93 | 0.95 | 0.3509 | 0.6289 | 0.6873 | 0.85 | 1.03 | 0.98 | 0.2814 | 0.8068 | 0.8363 |
| 501.2850 | 4.7 | C25H44NO7P | LysoPE(20:4) | Lipids: Glycerophospholipids | 0.86 | 0.65 | 0.81 | 0.5753 | 0.1266 | 0.3935 | 0.75 | 0.86 | 0.94 | 0.0703 | 0.3179 | 0.7139 | 0.95 | 0.92 | 0.92 | 0.8266 | 0.7404 | 0.6102 | 0.86 | 0.94 | 0.85 | 0.3146 | 0.7445 | 0.1458 |
| 737.4999 | 4.0 | C41H72NO8P | PE(36:5) | Lipids: Glycerophospholipids | 0.90 | 1.18 | 1.07 | 0.4412 | 0.1111 | 0.6341 | 0.98 | 1.04 | 0.93 | 0.8927 | 0.8541 | 0.6647 | 0.99 | 1.09 | 0.97 | 0.9164 | 0.5620 | 0.7546 | 0.83 | 1.25 | 0.89 | 0.0420 | 0.1484 | 0.2969 |
| 481.3166 | 4.9 | C23H48NO7P | LysoPE(18:0) | Lipids: Glycerophospholipids | 0.92 | 0.76 | 0.86 | 0.6151 | 0.0171 | 0.1474 | 0.96 | 0.96 | 0.92 | 0.4761 | 0.6931 | 0.4869 | 1.05 | 0.98 | 1.03 | 0.7649 | 0.8827 | 0.8001 | 0.86 | 0.94 | 0.99 | 0.4736 | 0.7469 | 0.9598 |
| 479.3020 | 4.8 | C23H46NO7P | PE(18:1) | Lipids: Glycerophospholipids | 0.87 | 0.86 | 0.95 | 0.5435 | 0.3710 | 0.7826 | 0.78 | 1.01 | 0.91 | 0.1411 | 0.9824 | 0.5422 | 0.84 | 1.11 | 0.98 | 0.3984 | 0.6220 | 0.8800 | 0.75 | 1.01 | 0.85 | 0.1735 | 0.9549 | 0.2926 |
| 527.3012 | 4.6 | C27H46NO7P | LysoPE(22:5) | Lipids: Glycerophospholipids | 0.85 | 0.76 | 0.91 | 0.5435 | 0.2981 | 0.7457 | 0.68 | 0.74 | 0.88 | 0.0801 | 0.1712 | 0.6167 | 0.76 | 1.05 | 0.92 | 0.3057 | 0.8634 | 0.7427 | 1.03 | 1.04 | 1.00 | 0.8547 | 0.7906 | 0.9918 |
| 529.3169 | 4.5 | C27H48NO7P | LysoPE(22:4) | Lipids: Glycerophospholipids | 0.87 | 0.67 | 0.92 | 0.5709 | 0.2494 | 0.7332 | 0.84 | 0.76 | 0.88 | 0.3168 | 0.1670 | 0.5813 | 0.95 | 0.95 | 0.92 | 0.7897 | 0.8336 | 0.6678 | 1.01 | 0.84 | 1.05 | 0.9187 | 0.2893 | 0.7583 |
| 310.1779 | 4.2 | C17H26O5 | Botrydial | Lipids: Prenols | 1.21 | 1.04 | 0.96 | 0.0180 | 0.5271 | 0.7429 | 1.11 | 0.81 | 0.99 | 0.5485 | 0.1838 | 0.9458 | 1.17 | 0.69 | 1.04 | 0.3971 | 0.1199 | 0.7835 | 1.02 | 0.84 | 0.86 | 0.8376 | 0.1214 | 0.2311 |
| 382.1308 | 10.7 | C15H28O7P2 | [PR] Farnesyl pyrophosphate | Lipids: Prenols | 0.79 | 1.51 | 1.20 | 0.5552 | 0.5203 | 0.5568 | 0.79 | 1.12 | 0.97 | 0.3051 | 0.5492 | 0.8653 | 0.98 | 1.01 | 0.95 | 0.9374 | 0.9620 | 0.7669 | 0.77 | 0.93 | 0.94 | 0.1656 | 0.6174 | 0.7231 |
| 299.2824 | 4.4 | C18H37NO2 | [SP] Sphing-4-enine | Lipids: Sphingolipids | 0.96 | 0.71 | 1.01 | 0.8532 | 0.2774 | 0.9725 | 1.15 | 1.18 | 1.28 | 0.5979 | 0.4553 | 0.3101 | 1.04 | 0.92 | 0.98 | 0.8560 | 0.7433 | 0.9291 | 1.04 | 0.98 | 1.05 | 0.8522 | 0.9089 | 0.7908 |
| 381.2646 | 5.2 | C18H40NO5P | [SP] Sphinganine-1-phosphate | Lipids: Sphingolipids | 1.04 | 0.72 | 0.96 | 0.8990 | 0.1560 | 0.8613 | 1.13 | 0.91 | 1.23 | 0.6307 | 0.5829 | 0.3156 | 1.09 | 0.91 | 1.13 | 0.6797 | 0.7574 | 0.5756 | 1.07 | 0.78 | 1.03 | 0.7370 | 0.3011 | 0.9000 |
| 716.5833 | 4.4 | C40H81N2O6P | SM(d35:1) | Lipids: Sphingolipids | 0.95 | 0.81 | 0.93 | 0.8135 | 0.2721 | 0.6256 | 0.95 | 0.96 | 1.21 | 0.8430 | 0.7141 | 0.2422 | 1.20 | 0.98 | 1.14 | 0.3076 | 0.9028 | 0.3113 | 0.99 | 0.92 | 1.02 | 0.9314 | 0.5431 | 0.8903 |
| 730.5988 | 4.4 | C41H83N2O6P | SM(d36:1) | Lipids: Sphingolipids | 0.84 | 1.04 | 0.98 | 0.4032 | 0.8565 | 0.9086 | 0.94 | 1.13 | 1.18 | 0.5920 | 0.2923 | 0.3421 | 0.92 | 1.21 | 1.10 | 0.5307 | 0.1935 | 0.5300 | 0.86 | 1.06 | 1.06 | 0.3374 | 0.6615 | 0.7326 |
| 702.5674 | 4.4 | C39H79N2O6P | SM(d34:1) | Lipids: Sphingolipids | 0.90 | 0.87 | 0.95 | 0.6032 | 0.4848 | 0.7913 | 1.02 | 1.06 | 1.18 | 0.8765 | 0.5072 | 0.3803 | 1.06 | 1.10 | 1.16 | 0.6997 | 0.5036 | 0.2947 | 0.92 | 1.00 | 1.04 | 0.6149 | 1.0000 | 0.8124 |
| 668.4298 | 5.2 | C68H124N2O23 | GalNAcbeta1-3Galalpha1-4Galbeta1-4Glcbeta-Cer(d18:1/24:1(15Z)) | Lipids: Sphingolipids | 0.94 | 1.31 | 1.06 | 0.5494 | 0.0183 | 0.5997 | 0.98 | 1.27 | 1.17 | 0.9117 | 0.2239 | 0.3967 | 0.88 | 1.08 | 1.07 | 0.2829 | 0.4949 | 0.5811 | 0.91 | 0.99 | 1.06 | 0.5365 | 0.9452 | 0.6778 |
| 784.6464 | 4.4 | C45H89N2O6P | SM(d40:2) | Lipids: Sphingolipids | 0.84 | 0.97 | 0.86 | 0.3763 | 0.8801 | 0.4142 | 0.91 | 1.06 | 1.17 | 0.4662 | 0.6737 | 0.3600 | 0.99 | 1.29 | 1.12 | 0.9236 | 0.0596 | 0.4797 | 0.80 | 1.15 | 1.09 | 0.1687 | 0.3495 | 0.6186 |
| 674.5362 | 4.4 | C37H75N2O6P | SM(d32:1) | Lipids: Sphingolipids | 0.82 | 0.77 | 0.89 | 0.2999 | 0.2815 | 0.5126 | 1.02 | 1.04 | 1.16 | 0.7981 | 0.6638 | 0.4449 | 1.02 | 1.05 | 1.09 | 0.9197 | 0.8238 | 0.5382 | 0.95 | 1.00 | 1.07 | 0.7488 | 0.9840 | 0.7315 |
| 810.6617 | 4.3 | C47H91N2O6P | SM(d42:3) | Lipids: Sphingolipids | 0.84 | 1.05 | 0.96 | 0.2863 | 0.7487 | 0.7859 | 0.90 | 1.16 | 1.13 | 0.4098 | 0.3463 | 0.4451 | 0.86 | 1.18 | 1.01 | 0.2638 | 0.2144 | 0.9485 | 0.82 | 1.16 | 1.07 | 0.1988 | 0.3655 | 0.6849 |
| 688.5518 | 4.4 | C38H77N2O6P | SM(d33:1) | Lipids: Sphingolipids | 0.93 | 0.77 | 0.95 | 0.6713 | 0.2527 | 0.7383 | 1.04 | 1.01 | 1.13 | 0.7239 | 0.8635 | 0.4934 | 1.10 | 0.97 | 1.10 | 0.5865 | 0.8522 | 0.4936 | 1.03 | 0.96 | 1.04 | 0.8713 | 0.7220 | 0.8104 |
| 301.2980 | 7.4 | C18H39NO2 | Sphinganine | Lipids: Sphingolipids | 1.07 | 0.65 | 0.92 | 0.8794 | 0.0922 | 0.7300 | 1.02 | 0.82 | 1.11 | 0.9187 | 0.4259 | 0.6656 | 1.19 | 0.80 | 1.11 | 0.5244 | 0.4343 | 0.5662 | 1.15 | 0.77 | 0.98 | 0.5961 | 0.3156 | 0.9499 |
| 728.5838 | 4.4 | C41H81N2O6P | SM(d36:2) | Lipids: Sphingolipids | 0.77 | 1.16 | 0.91 | 0.2487 | 0.4146 | 0.6627 | 0.77 | 1.22 | 1.08 | 0.1419 | 0.3153 | 0.7108 | 0.73 | 1.33 | 1.00 | 0.0827 | 0.2157 | 0.9791 | 0.77 | 1.25 | 1.10 | 0.1393 | 0.3038 | 0.6930 |
| 700.5519 | 4.4 | C39H77N2O6P | SM(d34:2) | Lipids: Sphingolipids | 0.88 | 1.07 | 0.96 | 0.3631 | 0.7541 | 0.7636 | 0.88 | 1.11 | 1.08 | 0.2283 | 0.4386 | 0.5859 | 0.96 | 1.16 | 1.05 | 0.7420 | 0.3210 | 0.6914 | 0.90 | 1.17 | 1.06 | 0.4232 | 0.3135 | 0.6515 |
| 379.2490 | 5.2 | C18H38NO5P | [SP] Sphing-4-enine-1-phosphate | Lipids: Sphingolipids | 1.01 | 1.07 | 1.04 | 0.9749 | 0.6472 | 0.7800 | 1.02 | 1.01 | 1.07 | 0.9219 | 0.9663 | 0.7260 | 0.97 | 1.14 | 1.14 | 0.8404 | 0.6677 | 0.3915 | 1.07 | 0.93 | 1.05 | 0.5212 | 0.7470 | 0.7489 |
| 756.6145 | 4.4 | C43H85N2O6P | SM(d38:2) | Lipids: Sphingolipids | 0.85 | 1.05 | 0.89 | 0.3337 | 0.7862 | 0.4876 | 0.91 | 1.09 | 1.06 | 0.3831 | 0.5745 | 0.7473 | 0.95 | 1.10 | 1.02 | 0.7192 | 0.6533 | 0.8814 | 0.93 | 1.26 | 1.16 | 0.6520 | 0.1508 | 0.3704 |
| 619.5906 | 3.9 | C40H77NO3 | Cer(d40:2) | Lipids: Sphingolipids | 0.73 | 1.27 | 0.99 | 0.3084 | 0.2969 | 0.9802 | 0.62 | 1.34 | 1.05 | 0.0964 | 0.2498 | 0.8512 | 0.68 | 1.56 | 1.14 | 0.1743 | 0.1438 | 0.6384 | 0.61 | 1.16 | 1.12 | 0.0871 | 0.5037 | 0.7088 |
| 647.6213 | 3.9 | C42H81NO3 | [SP (24:0)] N-(15Z-tetracosenoyl)-sphing-4-enine | Lipids: Sphingolipids | 0.84 | 1.53 | 1.00 | 0.3313 | 0.2767 | 0.9879 | 0.78 | 1.23 | 1.02 | 0.1894 | 0.2613 | 0.9262 | 0.88 | 1.45 | 1.15 | 0.5509 | 0.0470 | 0.4118 | 0.66 | 1.10 | 0.92 | 0.0246 | 0.4166 | 0.6315 |
| 537.5115 | 4.0 | C34H67NO3 | [SP (16:0)] N-(hexadecanoyl)-sphing-4-enine | Lipids: Sphingolipids | 0.93 | 0.96 | 0.88 | 0.7140 | 0.8415 | 0.5593 | 1.00 | 1.05 | 1.00 | 0.9909 | 0.7625 | 0.9802 | 1.08 | 1.05 | 1.17 | 0.6232 | 0.7078 | 0.1359 | 0.92 | 1.05 | 0.92 | 0.6352 | 0.6679 | 0.5160 |
| 461.3356 | 4.8 | C24H47NO7 | Psychosine | Lipids: Sphingolipids | 0.98 | 1.06 | 0.96 | 0.9407 | 0.6365 | 0.8269 | 0.77 | 1.03 | 0.98 | 0.1528 | 0.8698 | 0.8755 | 0.92 | 1.22 | 1.07 | 0.5894 | 0.3841 | 0.6945 | 0.70 | 1.03 | 0.97 | 0.1073 | 0.8983 | 0.8662 |
| 368.3444 | 3.8 | C27H44 | [ST] (5Z,7E)-9,10-seco-5,7,10(19)-cholestatriene | Lipids: Sterol lipids | 0.88 | 0.81 | 0.83 | 0.4522 | 0.0973 | 0.1679 | 0.89 | 1.18 | 1.21 | 0.5036 | 0.3472 | 0.1467 | 0.94 | 1.06 | 1.06 | 0.7660 | 0.8337 | 0.7112 | 0.89 | 0.94 | 0.86 | 0.6161 | 0.6391 | 0.2952 |
| 466.3119 | 3.7 | C27H46O4S | Cholesterolsulfate | Lipids: Sterol lipids | 1.02 | 0.89 | 1.01 | 0.8892 | 0.4288 | 0.9386 | 1.04 | 1.07 | 1.06 | 0.8498 | 0.6717 | 0.6528 | 1.05 | 0.98 | 1.11 | 0.7900 | 0.8807 | 0.4476 | 0.94 | 0.95 | 0.88 | 0.7348 | 0.7001 | 0.2550 |
| 446.3758 | 4.0 | C29H50O3 | Nebrosteroid M | Lipids: Sterol Lipids | 0.95 | 0.86 | 0.92 | 0.7033 | 0.1078 | 0.4303 | 0.84 | 1.00 | 0.96 | 0.1896 | 0.9849 | 0.7015 | 0.93 | 1.18 | 1.10 | 0.4605 | 0.1053 | 0.2246 | 0.81 | 1.08 | 0.93 | 0.0455 | 0.6263 | 0.3551 |
| 238.0985 | 10.4 | C8H18N2O4S | HEPES | Medium Component | 1.02 | 0.93 | 1.00 | 0.7353 | 0.5981 | 0.9787 | 1.15 | 1.05 | 1.15 | 0.0551 | 0.5376 | 0.1948 | 1.03 | 0.96 | 0.94 | 0.7268 | 0.4185 | 0.3393 | 1.08 | 1.00 | 1.11 | 0.2337 | 0.9577 | 0.1019 |
| 195.0564 | 7.7 | C6H13NO4S | MES | Medium Component | 1.08 | 0.97 | 1.10 | 0.5729 | 0.7879 | 0.3994 | 1.17 | 1.08 | 1.15 | 0.3155 | 0.4634 | 0.1730 | 1.09 | 1.04 | 1.01 | 0.3599 | 0.7352 | 0.9166 | 1.15 | 1.01 | 1.04 | 0.1342 | 0.9576 | 0.5972 |
| 151.0303 | 14.2 | C8H18N2O6S2 | PIPES | Medium Component | 1.10 | 1.05 | 1.05 | 0.4306 | 0.4760 | 0.4616 | 1.19 | 1.07 | 1.07 | 0.0614 | 0.4641 | 0.3980 | 1.03 | 0.95 | 0.94 | 0.6966 | 0.3395 | 0.2754 | 1.11 | 0.93 | 1.07 | 0.1796 | 0.3123 | 0.3380 |
| 354.0564 | 5.2 | C19H14O5S | Phenolsulfonphthalein | Medium Component | 1.18 | 1.30 | 1.14 | 0.2399 | 0.1165 | 0.3660 | 0.96 | 1.02 | 1.04 | 0.8709 | 0.9547 | 0.8578 | 1.00 | 1.20 | 0.91 | 0.9946 | 0.4717 | 0.5578 | 1.34 | 1.13 | 1.15 | 0.2586 | 0.7263 | 0.5286 |
| 785.1571 | 11.3 | C27H33N9O15P2 | FAD | Metabolism of Cofactors and Vitamins | 1.06 | 0.87 | 0.92 | 0.7431 | 0.4519 | 0.1848 | 1.12 | 1.16 | 1.23 | 0.1730 | 0.0840 | 0.0807 | 1.07 | 0.99 | 1.03 | 0.5490 | 0.9420 | 0.6332 | 1.06 | 1.04 | 1.01 | 0.6750 | 0.7282 | 0.8978 |

| | | | | | | | | | | | | | | | | | | | | | | | | | | | | | |
|---|---|---|---|---|---|---|---|---|---|---|---|---|---|---|---|---|---|---|---|---|---|---|---|---|---|---|---|---|---|
| 225.0637 | 13.1 | C10H11NO5 | 4-Amino-4-deoxychorismate | Metabolism of Cofactors and Vitamins | 0.92 | 1.12 | 1.13 | 0.4363 | 0.2366 | 0.1875 | 1.10 | 1.15 | 1.19 | 0.4824 | 0.2876 | 0.2076 | 0.99 | 0.93 | 0.94 | 0.9698 | 0.3188 | 0.4430 | 0.95 | 1.04 | 1.09 | 0.4096 | 0.5665 | 0.1102 |
| 334.0565 | 15.1 | C11H15N2O8P | Nicotinamide D-ribonucleotide | Metabolism of Cofactors and Vitamins | 1.02 | 0.80 | 0.97 | 0.8545 | 0.3038 | 0.7427 | 1.21 | 1.03 | 1.14 | 0.0654 | 0.8729 | 0.2159 | 1.11 | 0.96 | 1.00 | 0.1661 | 0.6835 | 0.9515 | 1.10 | 0.90 | 1.09 | 0.2481 | 0.5448 | 0.4309 |
| 249.0403 | 13.6 | C8H12NO6P | Pyridoxine phosphate | Metabolism of Cofactors and Vitamins | 0.99 | 1.23 | 1.06 | 0.9694 | 0.1216 | 0.6967 | 1.17 | 1.03 | 1.11 | 0.4569 | 0.8572 | 0.3299 | 0.99 | 1.00 | 0.95 | 0.9353 | 0.9785 | 0.6504 | 1.00 | 1.05 | 1.15 | 0.9996 | 0.7759 | 0.2825 |
| 441.1400 | 16.5 | C19H19N7O6 | Folate | Metabolism of Cofactors and Vitamins | 1.02 | 1.35 | 1.01 | 0.8580 | 0.3347 | 0.9465 | 1.16 | 1.08 | 1.09 | 0.1561 | 0.4523 | 0.4195 | 1.01 | 0.90 | 0.97 | 0.9430 | 0.4604 | 0.7937 | 1.08 | 1.18 | 1.08 | 0.3795 | 0.1065 | 0.2938 |
| 244.0880 | 8.8 | C10H16N2O3S | Biotin | Metabolism of Cofactors and Vitamins | 1.06 | 0.99 | 0.91 | 0.4622 | 0.9484 | 0.3627 | 1.35 | 0.94 | 1.08 | 0.0056 | 0.6804 | 0.5005 | 1.38 | 1.00 | 1.06 | 0.1539 | 0.9936 | 0.6275 | 1.21 | 1.06 | 1.01 | 0.2282 | 0.7305 | 0.9429 |
| 217.0586 | 19.9 | C8H11NO6 | 2-(Hydroxymethyl)-3-(acetamidomethylene)succinate | Metabolism of Cofactors and Vitamins | 1.05 | 0.65 | 0.88 | 0.8696 | 0.1313 | 0.6447 | 1.39 | 1.06 | 1.08 | 0.2322 | 0.8445 | 0.7714 | 1.16 | 0.77 | 1.04 | 0.6065 | 0.3562 | 0.8950 | 1.06 | 0.84 | 0.81 | 0.8358 | 0.5113 | 0.3727 |
| 255.0740 | 12.4 | C11H13NO6 | Nicotinate D-ribonucleoside | Metabolism of Cofactors and Vitamins | 0.81 | 1.00 | 0.98 | 0.3392 | 0.9799 | 0.8992 | 1.00 | 1.19 | 1.07 | 0.9998 | 0.2621 | 0.7093 | 0.91 | 1.00 | 1.02 | 0.6395 | 0.9756 | 0.8896 | 0.99 | 1.11 | 1.12 | 0.9655 | 0.5396 | 0.5170 |
| 187.1210 | 11.7 | C9H17NO3 | 8-Amino-7-oxononanoate | Metabolism of Cofactors and Vitamins | 1.13 | 0.87 | 1.13 | 0.8032 | 0.6127 | 0.7384 | 1.27 | 0.71 | 1.07 | 0.6304 | 0.2058 | 0.8226 | 1.16 | 0.76 | 0.94 | 0.7515 | 0.4042 | 0.8704 | 1.31 | 0.83 | 1.31 | 0.5934 | 0.5171 | 0.4252 |
| 299.0770 | 14.9 | C9H18NO8P | D-4'-Phosphopantothenate | Metabolism of Cofactors and Vitamins | 1.09 | 1.50 | 1.16 | 0.6745 | 0.0888 | 0.4334 | 1.04 | 0.96 | 1.05 | 0.8734 | 0.8892 | 0.7954 | 0.87 | 1.01 | 0.75 | 0.4964 | 0.9539 | 0.1215 | 0.89 | 0.85 | 0.75 | 0.5386 | 0.5165 | 0.0819 |
| 326.1226 | 12.9 | C13H18N4O6 | 6,7-Dimethyl-8-(1-D-ribityl)lumazine | Metabolism of Cofactors and Vitamins | 1.10 | 1.37 | 1.17 | 0.6150 | 0.0737 | 0.1911 | 1.04 | 1.03 | 1.04 | 0.8700 | 0.8667 | 0.8438 | 1.02 | 0.92 | 1.00 | 0.9317 | 0.6174 | 0.9988 | 0.88 | 0.89 | 0.84 | 0.2965 | 0.4817 | 0.1710 |
| 264.1045 | 20.7 | C12H16N4OS | Thiamin | Metabolism of Cofactors and Vitamins | 0.93 | 0.93 | 0.93 | 0.5825 | 0.3706 | 0.5074 | 1.06 | 1.06 | 1.01 | 0.5195 | 0.6902 | 0.9266 | 1.04 | 0.95 | 1.10 | 0.7151 | 0.8177 | 0.2305 | 0.93 | 0.92 | 1.06 | 0.3903 | 0.5785 | 0.6113 |
| 169.0738 | 8.1 | C8H11NO3 | Pyridoxine | Metabolism of Cofactors and Vitamins | 0.88 | 0.98 | 1.01 | 0.4541 | 0.8997 | 0.9337 | 1.04 | 1.00 | 0.99 | 0.7034 | 0.9924 | 0.9581 | 1.09 | 1.13 | 0.98 | 0.4099 | 0.3860 | 0.8507 | 0.99 | 1.17 | 1.19 | 0.9425 | 0.4168 | 0.2707 |
| 144.0422 | 15.7 | C6H8O4 | 2,3-Dimethylmaleate | Metabolism of Cofactors and Vitamins | 0.64 | 0.42 | 0.76 | 0.2551 | 0.0824 | 0.4784 | 0.77 | 1.35 | 0.88 | 0.4997 | 0.5829 | 0.7715 | 0.84 | 1.09 | 1.30 | 0.6173 | 0.8938 | 0.4947 | 0.80 | 1.31 | 0.96 | 0.5188 | 0.6074 | 0.9156 |
| 122.0480 | 7.5 | C6H6N2O | Nicotinamide | Metabolism of Cofactors and Vitamins | 0.76 | 0.78 | 1.29 | 0.4729 | 0.5090 | 0.6920 | 0.65 | 0.66 | 0.86 | 0.1583 | 0.1990 | 0.6401 | 1.01 | 1.09 | 0.95 | 0.9447 | 0.6836 | 0.7218 | 0.99 | 0.99 | 0.94 | 0.9663 | 0.9579 | 0.7231 |
| 507.9789 | 17.7 | C10H15N4O14P3 | ITP | Nucleotide Metabolism | 1.37 | 0.31 | 0.89 | 0.5272 | 0.0562 | 0.8066 | 2.05 | 0.73 | 1.33 | 0.2083 | 0.4601 | 0.5542 | 1.32 | 0.33 | 0.97 | 0.5126 | 0.0834 | 0.9509 | 1.50 | 0.56 | 0.92 | 0.3303 | 0.1690 | 0.8535 |
| 176.0432 | 16.5 | C5H8N2O5 | N-Carbamoyl-L-aspartate | Nucleotide Metabolism | 0.71 | 0.97 | 0.94 | 0.2950 | 0.9693 | 0.8434 | 1.02 | 1.29 | 1.32 | 0.9527 | 0.6617 | 0.4402 | 0.85 | 1.41 | 0.90 | 0.5330 | 0.5383 | 0.7360 | 0.84 | 1.00 | 0.93 | 0.5263 | 0.9959 | 0.8170 |
| 168.0283 | 12.4 | C5H4N4O3 | Urate | Nucleotide Metabolism | 1.72 | 2.18 | 1.55 | 0.5141 | 0.2326 | 0.3733 | 0.80 | 1.39 | 1.29 | 0.7991 | 0.6885 | 0.7227 | 0.65 | 1.69 | 1.14 | 0.5562 | 0.5192 | 0.8055 | 0.69 | 1.63 | 1.12 | 0.5625 | 0.3730 | 0.8316 |
| 158.0328 | 10.9 | C5H6N2O4 | (S)-Dihydroorotate | Nucleotide Metabolism | 0.82 | 0.90 | 1.03 | 0.4949 | 0.8833 | 0.9297 | 0.99 | 1.11 | 1.27 | 0.9637 | 0.8202 | 0.4641 | 0.97 | 1.21 | 0.91 | 0.8637 | 0.6737 | 0.7300 | 0.96 | 0.88 | 0.93 | 0.8562 | 0.7220 | 0.7630 |
| 156.0172 | 10.0 | C5H4N2O4 | Orotate | Nucleotide Metabolism | 0.99 | 1.04 | 1.05 | 0.9370 | 0.9142 | 0.7936 | 1.06 | 1.06 | 1.20 | 0.7840 | 0.8247 | 0.2975 | 0.84 | 1.06 | 0.81 | 0.2821 | 0.7062 | 0.2554 | 0.85 | 0.84 | 0.75 | 0.3197 | 0.2928 | 0.0759 |
| 128.0585 | 14.6 | C5H8N2O2 | 5,6-Dihydrothymine | Nucleotide Metabolism | 1.06 | 0.66 | 0.95 | 0.6915 | 0.0182 | 0.6646 | 1.35 | 0.87 | 1.15 | 0.1613 | 0.4735 | 0.5009 | 1.48 | 0.64 | 1.07 | 0.0636 | 0.0050 | 0.6930 | 1.14 | 0.81 | 0.93 | 0.3214 | 0.2656 | 0.6024 |
| 338.0633 | 14.9 | C9H15N4O8P | 1-(5'-Phosphoribosyl)-5-amino-4-imidazolecarboxamide | Nucleotide Metabolism | 0.83 | 1.10 | 1.17 | 0.5227 | 0.6457 | 0.4628 | 0.78 | 1.04 | 1.13 | 0.5561 | 0.9365 | 0.6149 | 0.76 | 0.96 | 0.82 | 0.4463 | 0.7953 | 0.3864 | 1.00 | 1.17 | 1.18 | 0.9877 | 0.7362 | 0.2902 |
| 348.0471 | 15.2 | C10H13N4O8P | IMP | Nucleotide Metabolism | 1.03 | 1.21 | 1.12 | 0.8557 | 0.1638 | 0.4703 | 1.08 | 1.02 | 1.11 | 0.7058 | 0.9434 | 0.4580 | 0.89 | 1.11 | 0.92 | 0.2453 | 0.1367 | 0.4625 | 1.05 | 1.06 | 1.17 | 0.7276 | 0.8477 | 0.3149 |
| 323.0516 | 16.4 | C9H14N3O8P | CMP | Nucleotide Metabolism | 1.00 | 0.94 | 0.94 | 0.9939 | 0.7933 | 0.6851 | 1.11 | 1.03 | 1.10 | 0.4263 | 0.7393 | 0.4199 | 1.03 | 0.95 | 1.15 | 0.9091 | 0.6775 | 0.1001 | 1.16 | 1.05 | 1.53 | 0.3479 | 0.3944 | 0.0169 |
| 347.0629 | 13.5 | C10H14N5O7P | dGMP | Nucleotide Metabolism | 0.96 | 1.02 | 1.03 | 0.7070 | 0.6806 | 0.6727 | 1.10 | 1.06 | 1.10 | 0.3757 | 0.4937 | 0.4039 | 1.04 | 1.06 | 1.02 | 0.7108 | 0.4784 | 0.7920 | 1.02 | 0.94 | 1.02 | 0.8660 | 0.5286 | 0.8214 |

| | | | | | | | | | | | | | | | | | | | | | | | | | | | | |
|---|---|---|---|---|---|---|---|---|---|---|---|---|---|---|---|---|---|---|---|---|---|---|---|---|---|---|---|---|
| 268.0809 | 10.9 | C10H12N4O5 | Inosine | Nucleotide Metabolism | 0.74 | 0.96 | 0.83 | 0.1563 | 0.8424 | 0.3732 | 1.06 | 0.96 | 1.07 | 0.6967 | 0.8509 | 0.6319 | 0.98 | 1.04 | 0.93 | 0.8962 | 0.8116 | 0.5235 | 1.09 | 0.89 | 0.89 | 0.5558 | 0.4099 | 0.3332 |
| 106.0266 | 16.8 | C2H2O3 | Glyoxylate | Nucleotide Metabolism | 0.97 | 1.24 | 1.05 | 0.8119 | 0.2596 | 0.6033 | 1.03 | 1.10 | 1.06 | 0.8381 | 0.4367 | 0.6738 | 0.92 | 0.93 | 0.98 | 0.7311 | 0.6236 | 0.9028 | 0.92 | 1.02 | 1.03 | 0.5424 | 0.8446 | 0.7473 |
| 463.0737 | 18.1 | C14H18N5O11P | N6-(1,2-Dicarboxyethyl)-AMP | Nucleotide Metabolism | 0.84 | 1.41 | 0.94 | 0.3143 | 0.0082 | 0.6571 | 0.90 | 1.08 | 1.06 | 0.4171 | 0.7464 | 0.6928 | 1.12 | 0.96 | 0.97 | 0.4831 | 0.8103 | 0.6813 | 0.91 | 0.76 | 0.91 | 0.5267 | 0.0960 | 0.4888 |
| 112.0273 | 15.1 | C4H4N2O2 | Orotate(Fragment) | Nucleotide Metabolism | 0.92 | 0.92 | 0.92 | 0.3299 | 0.3151 | 0.3460 | 0.95 | 1.03 | 1.05 | 0.2796 | 0.6772 | 0.4026 | 0.99 | 1.11 | 1.00 | 0.8998 | 0.3499 | 0.9968 | 1.06 | 1.05 | 1.06 | 0.5940 | 0.7060 | 0.4474 |
| 267.0967 | 9.1 | C10H13N5O4 | Adenosine | Nucleotide Metabolism | 0.99 | 0.85 | 0.98 | 0.9443 | 0.3221 | 0.8781 | 1.04 | 1.05 | 1.05 | 0.8522 | 0.7691 | 0.8074 | 0.98 | 0.95 | 1.00 | 0.9247 | 0.7888 | 0.9722 | 0.96 | 0.98 | 1.12 | 0.8121 | 0.8289 | 0.4131 |
| 332.0527 | 14.5 | C10H13N4O7P | dIMP | Nucleotide Metabolism | 0.88 | 0.89 | 0.93 | 0.6276 | 0.7123 | 0.7484 | 0.99 | 1.16 | 1.04 | 0.9713 | 0.4823 | 0.8390 | 0.87 | 1.04 | 0.97 | 0.6073 | 0.8988 | 0.8775 | 0.93 | 1.01 | 0.95 | 0.7284 | 0.9497 | 0.7993 |
| 363.0578 | 16.5 | C10H14N5O8P | GMP | Nucleotide Metabolism | 0.85 | 1.57 | 1.21 | 0.3189 | 0.2689 | 0.4123 | 0.94 | 1.14 | 1.04 | 0.7007 | 0.6394 | 0.8446 | 0.90 | 1.09 | 0.81 | 0.2852 | 0.3981 | 0.0415 | 0.81 | 1.01 | 0.97 | 0.1042 | 0.9705 | 0.8197 |
| 404.0028 | 15.9 | C9H14N2O12P2 | UDP | Nucleotide Metabolism | 1.03 | 1.52 | 1.22 | 0.7273 | 0.5513 | 0.2955 | 1.04 | 1.00 | 1.04 | 0.8018 | 0.9918 | 0.8140 | 0.99 | 0.91 | 0.86 | 0.9568 | 0.6280 | 0.4377 | 0.98 | 0.77 | 1.10 | 0.9098 | 0.1625 | 0.5059 |
| 104.0110 | 14.8 | C3H4O4 | Malonate | Nucleotide Metabolism | 1.03 | 0.70 | 0.88 | 0.8756 | 0.3005 | 0.5133 | 0.71 | 0.84 | 1.03 | 0.3921 | 0.2693 | 0.8792 | 1.21 | 0.94 | 1.06 | 0.5385 | 0.7932 | 0.7573 | 1.05 | 0.96 | 0.98 | 0.8357 | 0.8170 | 0.9380 |
| 482.9841 | 18.0 | C9H16N3O14P3 | CTP | Nucleotide Metabolism | 1.03 | 1.20 | 1.07 | 0.7689 | 0.1558 | 0.4779 | 1.08 | 1.07 | 1.02 | 0.3498 | 0.6367 | 0.8567 | 1.02 | 0.90 | 0.92 | 0.8003 | 0.2947 | 0.3188 | 1.05 | 0.99 | 1.03 | 0.3910 | 0.8862 | 0.6665 |
| 443.0243 | 17.6 | C10H15N5O11P2 | GDP | Nucleotide Metabolism | 0.90 | 1.37 | 1.03 | 0.2988 | 0.1142 | 0.7870 | 0.84 | 1.09 | 1.01 | 0.1990 | 0.6183 | 0.9362 | 0.91 | 1.15 | 1.00 | 0.5975 | 0.0809 | 0.9716 | 0.97 | 0.99 | 1.16 | 0.6497 | 0.9586 | 0.0696 |
| 136.0384 | 10.2 | C5H4N4O | Hypoxanthine | Nucleotide Metabolism | 0.98 | 0.85 | 0.94 | 0.7713 | 0.0447 | 0.4707 | 1.12 | 0.91 | 0.98 | 0.4788 | 0.4812 | 0.8842 | 1.13 | 0.94 | 1.05 | 0.3250 | 0.2592 | 0.4960 | 1.00 | 0.91 | 1.05 | 0.9727 | 0.3555 | 0.5607 |
| 427.0296 | 16.2 | C10H15N5O10P2 | dGDP | Nucleotide Metabolism | 0.98 | 0.97 | 0.97 | 0.7581 | 0.8336 | 0.6208 | 1.08 | 1.02 | 0.98 | 0.5193 | 0.8114 | 0.8167 | 0.98 | 0.97 | 0.96 | 0.9116 | 0.8147 | 0.6354 | 1.07 | 0.97 | 1.09 | 0.6462 | 0.6626 | 0.3204 |
| 483.9686 | 17.6 | C9H15N2O15P3 | UTP | Nucleotide Metabolism | 1.05 | 1.16 | 1.03 | 0.6581 | 0.1645 | 0.7970 | 1.07 | 1.00 | 0.98 | 0.5741 | 0.9861 | 0.8221 | 0.94 | 0.93 | 0.84 | 0.6447 | 0.5712 | 0.1189 | 1.06 | 0.97 | 1.04 | 0.6218 | 0.8459 | 0.6927 |
| 491.0005 | 15.4 | C10H16N5O12P3 | dATP | Nucleotide Metabolism | 1.10 | 1.16 | 1.01 | 0.6631 | 0.1114 | 0.9659 | 1.11 | 1.04 | 0.97 | 0.5575 | 0.8047 | 0.8320 | 0.93 | 0.88 | 0.79 | 0.5178 | 0.3596 | 0.0204 | 1.02 | 0.98 | 0.69 | 0.8728 | 0.9004 | 0.0039 |
| 347.0631 | 14.9 | C10H14N5O7P | AMP | Nucleotide Metabolism | 1.04 | 0.99 | 1.02 | 0.5795 | 0.9711 | 0.8652 | 1.12 | 1.01 | 0.97 | 0.4061 | 0.9268 | 0.7656 | 0.99 | 0.89 | 0.97 | 0.9391 | 0.3971 | 0.7094 | 1.07 | 0.89 | 1.01 | 0.5145 | 0.1315 | 0.8818 |
| 151.0494 | 12.3 | C5H5N5O | Guanine | Nucleotide Metabolism | 0.82 | 1.11 | 0.91 | 0.3513 | 0.4065 | 0.5330 | 0.96 | 0.83 | 0.96 | 0.8428 | 0.2347 | 0.8283 | 1.01 | 0.91 | 0.93 | 0.9684 | 0.2932 | 0.5117 | 0.94 | 1.03 | 0.85 | 0.7703 | 0.8539 | 0.1823 |
| 522.9904 | 18.9 | C10H16N5O14P3 | GTP | Nucleotide Metabolism | 0.93 | 1.25 | 0.99 | 0.5365 | 0.1216 | 0.9465 | 0.99 | 1.08 | 0.95 | 0.9377 | 0.6224 | 0.6657 | 0.87 | 1.03 | 0.90 | 0.3586 | 0.8129 | 0.3040 | 0.99 | 1.04 | 1.10 | 0.9351 | 0.8038 | 0.4375 |
| 466.9891 | 17.1 | C9H16N3O13P3 | dCTP | Nucleotide Metabolism | 1.22 | 1.19 | 1.12 | 0.5328 | 0.4154 | 0.7162 | 1.44 | 0.86 | 0.95 | 0.1805 | 0.7254 | 0.8621 | 1.05 | 0.83 | 0.90 | 0.8383 | 0.6470 | 0.6805 | 1.11 | 0.92 | 0.96 | 0.6000 | 0.6978 | 0.8332 |
| 135.0545 | 9.6 | C5H5N5 | Adenine | Nucleotide Metabolism | 1.11 | 0.92 | 1.01 | 0.5159 | 0.4148 | 0.9167 | 1.08 | 0.81 | 0.94 | 0.7035 | 0.2707 | 0.6901 | 1.14 | 0.96 | 1.01 | 0.6096 | 0.7800 | 0.9234 | 0.95 | 0.90 | 0.97 | 0.7062 | 0.4118 | 0.7970 |
| 481.9892 | 15.8 | C10H17N2O14P3 | dTTP | Nucleotide Metabolism | 1.11 | 1.70 | 1.09 | 0.6928 | 0.2264 | 0.6988 | 1.06 | 0.83 | 0.88 | 0.8190 | 0.4912 | 0.5623 | 0.92 | 0.93 | 0.63 | 0.7579 | 0.7868 | 0.0615 | 1.20 | 0.95 | 0.74 | 0.4590 | 0.8264 | 0.1542 |
| 188.1159 | 12.1 | C8H16N2O3 | Val-Ala | Peptide(di-) | 0.96 | 0.83 | 0.95 | 0.8433 | 0.2467 | 0.7335 | 1.25 | 0.95 | 1.22 | 0.1397 | 0.7060 | 0.1776 | 1.30 | 0.91 | 0.99 | 0.1160 | 0.1905 | 0.8400 | 1.04 | 0.89 | 1.03 | 0.7180 | 0.3808 | 0.7583 |
| 276.0962 | 13.8 | C10H16N2O7 | Glu-Glu | Peptide(di-) | 1.14 | 1.49 | 1.19 | 0.3927 | 0.0577 | 0.2804 | 1.30 | 0.95 | 1.22 | 0.3961 | 0.8549 | 0.4126 | 1.09 | 0.78 | 0.98 | 0.7596 | 0.3156 | 0.9257 | 0.86 | 0.77 | 0.65 | 0.5992 | 0.1488 | 0.0276 |
| 172.0847 | 14.1 | C7H12N2O3 | Glycylproline | Peptide(di-) | 1.00 | 0.87 | 0.90 | 0.9764 | 0.0982 | 0.3123 | 1.27 | 1.10 | 1.18 | 0.2946 | 0.3480 | 0.0479 | 1.07 | 0.95 | 0.99 | 0.4768 | 0.5518 | 0.9269 | 1.02 | 0.96 | 1.03 | 0.8061 | 0.6809 | 0.7316 |
| 246.1215 | 12.3 | C10H18N2O5 | Glu-Val | Peptide(di-) | 0.88 | 0.89 | 0.94 | 0.4329 | 0.5901 | 0.6890 | 1.03 | 1.12 | 1.16 | 0.7960 | 0.4815 | 0.4070 | 0.98 | 1.01 | 0.94 | 0.8803 | 0.9770 | 0.6391 | 0.91 | 1.11 | 0.99 | 0.5361 | 0.5382 | 0.9627 |
| 262.0801 | 16.7 | C9H14N2O7 | Glu-Asp | Peptide(di-) | 0.93 | 0.74 | 0.87 | 0.7884 | 0.0205 | 0.3761 | 1.36 | 1.00 | 1.15 | 0.1706 | 0.9806 | 0.5141 | 1.36 | 0.85 | 1.11 | 0.3049 | 0.2625 | 0.4787 | 1.08 | 0.83 | 1.06 | 0.6672 | 0.1089 | 0.6854 |
| 261.1327 | 18.0 | C10H19N3O5 | Lys-Asp | Peptide(di-) | 1.17 | 0.78 | 1.11 | 0.4700 | 0.1288 | 0.5690 | 1.28 | 0.97 | 1.14 | 0.3066 | 0.8766 | 0.5445 | 1.33 | 0.83 | 1.08 | 0.3545 | 0.2790 | 0.6794 | 1.14 | 0.80 | 0.88 | 0.5867 | 0.2225 | 0.5308 |
| 248.0644 | 17.2 | C8H12N2O7 | Asp-Asp | Peptide(di-) | 1.14 | 0.84 | 0.93 | 0.5024 | 0.1271 | 0.6558 | 1.25 | 0.99 | 1.13 | 0.2860 | 0.9709 | 0.5723 | 1.32 | 0.93 | 0.95 | 0.2138 | 0.6655 | 0.7519 | 0.89 | 0.83 | 0.64 | 0.5041 | 0.1919 | 0.0127 |
| 289.1386 | 16.4 | C10H19N5O5 | Asp-Arg | Peptide(di-) | 1.06 | 0.69 | 0.92 | 0.6295 | 0.0769 | 0.3924 | 1.25 | 0.84 | 1.13 | 0.0620 | 0.1735 | 0.3162 | 1.18 | 0.73 | 1.05 | 0.1641 | 0.0068 | 0.7334 | 1.18 | 0.84 | 0.98 | 0.2068 | 0.1990 | 0.9174 |
| 186.1004 | 11.3 | C8H14N2O3 | Ala-Pro | Peptide(di-) | 1.19 | 0.82 | 1.12 | 0.5287 | 0.6089 | 0.5742 | 1.96 | 1.19 | 1.12 | 0.2039 | 0.5967 | 0.6868 | 0.86 | 0.61 | 0.15 | 0.4106 | 0.0080 | 0.0000 | 0.69 | 0.56 | 0.07 | 0.0102 | 0.0105 | 0.0000 |
| 220.1059 | 13.0 | C8H16N2O5 | Thr-Thr | Peptide(di-) | 1.05 | 0.84 | 1.05 | 0.7857 | 0.2028 | 0.7345 | 1.09 | 1.06 | 1.12 | 0.4847 | 0.6872 | 0.4769 | 0.98 | 0.93 | 1.03 | 0.8861 | 0.5185 | 0.8405 | 0.96 | 0.97 | 1.01 | 0.8009 | 0.8615 | 0.9615 |
| 229.1063 | 13.7 | C9H15N3O4 | Asn-Pro | Peptide(di-) | 1.01 | 0.77 | 0.87 | 0.9435 | 0.0408 | 0.2990 | 1.25 | 1.03 | 1.12 | 0.2391 | 0.8717 | 0.5391 | 1.26 | 0.81 | 1.04 | 0.3680 | 0.1096 | 0.7662 | 1.07 | 0.90 | 0.93 | 0.6631 | 0.4505 | 0.6148 |
| 218.1266 | 16.9 | C9H18N2O4 | Thr-Val | Peptide(di-) | 0.82 | 1.15 | 0.98 | 0.1786 | 0.3441 | 0.8721 | 0.98 | 1.15 | 1.11 | 0.8733 | 0.4098 | 0.5614 | 1.00 | 1.21 | 0.94 | 0.9768 | 0.2259 | 0.5856 | 0.84 | 1.06 | 1.04 | 0.1272 | 0.7157 | 0.7554 |
| 220.0882 | 10.4 | C8H16N2O3S | Met-Ala | Peptide(di-) | 0.82 | 1.00 | 1.03 | 0.2745 | 0.9998 | 0.4611 | 1.01 | 1.08 | 1.11 | 0.9391 | 0.4691 | 0.2990 | 0.87 | 0.99 | 0.97 | 0.4098 | 0.9255 | 0.6543 | 1.00 | 1.04 | 1.09 | 0.9599 | 0.6591 | 0.3728 |
| 234.0850 | 15.4 | C8H14N2O6 | Glu-Ser | Peptide(di-) | 1.00 | 0.87 | 0.94 | 0.9862 | 0.5209 | 0.6387 | 1.24 | 1.11 | 1.11 | 0.1974 | 0.5368 | 0.5590 | 0.99 | 1.01 | 0.79 | 0.9585 | 0.9553 | 0.0079 | 0.75 | 0.91 | 0.69 | 0.0438 | 0.4740 | 0.0200 |
| 220.0695 | 15.4 | C7H12N2O6 | Asp-Ser | Peptide(di-) | 1.05 | 0.79 | 0.95 | 0.8426 | 0.0855 | 0.6864 | 1.34 | 1.12 | 1.10 | 0.1539 | 0.3810 | 0.5133 | 1.17 | 0.79 | 1.05 | 0.4960 | 0.1137 | 0.7009 | 1.09 | 0.90 | 0.95 | 0.6428 | 0.5261 | 0.7606 |
| 228.1473 | 10.1 | C11H20N2O3 | Leu-Pro | Peptide(di-) | 0.96 | 0.89 | 0.96 | 0.6052 | 0.3545 | 0.5583 | 1.26 | 1.00 | 1.10 | 0.2106 | 0.9692 | 0.3762 | 1.18 | 0.91 | 1.08 | 0.2352 | 0.2017 | 0.3399 | 1.11 | 0.91 | 1.08 | 0.0357 | 0.2532 | 0.2659 |
| 248.1007 | 14.5 | C9H16N2O6 | Glu-Thr | Peptide(di-) | 1.01 | 0.88 | 1.00 | 0.9408 | 0.2186 | 0.9742 | 1.16 | 1.04 | 1.07 | 0.0794 | 0.6436 | 0.4569 | 1.01 | 0.98 | 0.86 | 0.8404 | 0.8091 | 0.0414 | 0.80 | 0.93 | 0.73 | 0.0123 | 0.2826 | 0.0004 |
| 260.1373 | 10.9 | C11H20N2O5 | Glu-Leu | Peptide(di-) | 0.93 | 0.82 | 0.95 | 0.6715 | 0.2889 | 0.7371 | 0.96 | 1.14 | 1.07 | 0.8509 | 0.3699 | 0.6618 | 1.05 | 1.13 | 1.03 | 0.5885 | 0.5706 | 0.8087 | 0.95 | 1.10 | 0.98 | 0.6380 | 0.5438 | 0.8607 |
| 230.0903 | 15.2 | C9H14N2O5 | Asp-Pro | Peptide(di-) | 1.05 | 0.85 | 1.00 | 0.7194 | 0.5136 | 0.9956 | 1.42 | 1.07 | 1.06 | 0.2760 | 0.7206 | 0.7530 | 0.77 | 0.70 | 0.28 | 0.1894 | 0.0344 | 0.0000 | 0.55 | 0.46 | 0.05 | 0.0047 | 0.0011 | 0.0000 |
| 245.1739 | 13.7 | C11H23N3O3 | Lys-Val | Peptide(di-) | 1.06 | 0.68 | 0.88 | 0.7969 | 0.3951 | 0.4212 | 2.30 | 1.24 | 1.06 | 0.1659 | 0.5720 | 0.8595 | 1.11 | 1.16 | 0.21 | 0.7306 | 0.3924 | 0.0001 | 0.78 | 0.72 | 0.02 | 0.2921 | 0.1031 | NA |
| 204.0746 | 15.9 | C7H12N2O5 | Ala-Asp | Peptide(di-) | 0.95 | 1.09 | 0.98 | 0.8392 | 0.6462 | 0.9169 | 1.37 | 1.20 | 1.05 | 0.2614 | 0.2762 | 0.8185 | 0.98 | 1.06 | 0.89 | 0.9454 | 0.7946 | 0.4356 | 0.89 | 1.13 | 0.87 | 0.5820 | 0.2073 | 0.4524 |
| 190.0952 | 14.1 | C7H14N2O4 | Thr-Ala | Peptide(di-) | 1.00 | 1.02 | 0.99 | 0.9862 | 0.8567 | 0.9410 | 1.10 | 1.05 | 1.02 | 0.5311 | 0.7567 | 0.8233 | 1.01 | 0.99 | 1.00 | 0.9630 | 0.9651 | 0.9934 | 0.95 | 0.93 | 1.03 | 0.5957 | 0.6394 | 0.8378 |

| | | | | | | | | | | | | | | | | | | | | | | | | | | | | |
|---|---|---|---|---|---|---|---|---|---|---|---|---|---|---|---|---|---|---|---|---|---|---|---|---|---|---|---|---|
| 247.0803 | 15.6 | C8H13N3O6 | Asn-Asp | Peptide(di-) | 1.10 | 0.83 | 1.04 | 0.6219 | 0.1376 | 0.8120 | 1.31 | 1.03 | 1.02 | 0.2518 | 0.8760 | 0.9264 | 0.93 | 0.72 | 0.66 | 0.6158 | 0.0320 | 0.0106 | 0.88 | 0.76 | 0.64 | 0.3440 | 0.0280 | 0.0075 |
| 190.0589 | 16.1 | C6H10N2O5 | Asp-Gly | Peptide(di-) | 1.10 | 1.11 | 1.05 | 0.1197 | 0.0059 | 0.3902 | 1.15 | 1.03 | 1.01 | 0.2142 | 0.7844 | 0.9363 | 0.89 | 0.89 | 0.62 | 0.0387 | 0.3357 | 0.0000 | 0.70 | 0.66 | 0.36 | 0.0043 | 0.0012 | 0.0000 |
| 301.1425 | 8.6 | C16H19N3O3 | Trp-Pro | Peptide(di-) | 1.21 | 0.71 | 0.95 | 0.4437 | 0.3185 | 0.7473 | 2.03 | 1.12 | 1.01 | 0.1651 | 0.7033 | 0.9818 | 0.81 | 0.69 | 0.11 | 0.2706 | 0.0051 | 0.0000 | 0.77 | 0.65 | 0.00 | 0.0609 | 0.0627 | NA |
| 176.0796 | 13.1 | C6H12N2O4 | Thr-Gly | Peptide(di-) | 1.16 | 0.85 | 0.99 | 0.4099 | 0.5897 | 0.9170 | 1.61 | 1.13 | 1.00 | 0.2429 | 0.6092 | 0.9934 | 0.95 | 0.85 | 0.28 | 0.8586 | 0.2064 | 0.0000 | 0.64 | 0.59 | 0.14 | 0.0177 | 0.0068 | 0.0000 |
| 204.0745 | 14.7 | C7H12N2O5 | Glu-Gly | Peptide(di-) | 1.03 | 0.62 | 0.91 | 0.9061 | 0.0383 | 0.6190 | 1.59 | 1.18 | 0.99 | 0.1940 | 0.4471 | 0.9395 | 0.93 | 0.75 | 0.41 | 0.6327 | 0.1508 | 0.0019 | 0.75 | 0.62 | 0.36 | 0.0159 | 0.0014 | 0.0000 |
| 204.1108 | 11.8 | C8H16N2O4 | Val-Ser | Peptide(di-) | 0.80 | 0.69 | 0.92 | 0.3729 | 0.1632 | 0.7588 | 1.07 | 1.00 | 0.98 | 0.7122 | 0.9882 | 0.9205 | 1.14 | 1.22 | 1.24 | 0.4610 | 0.7147 | 0.2842 | 0.85 | 0.96 | 1.02 | 0.4307 | 0.8967 | 0.9447 |
| 203.1269 | 16.6 | C8H17N3O3 | Lys-Gly | Peptide(di-) | 0.98 | 0.79 | 0.97 | 0.8633 | 0.5541 | 0.8188 | 1.84 | 1.06 | 0.96 | 0.1679 | 0.8253 | 0.8625 | 0.93 | 0.99 | 0.19 | 0.6359 | 0.9574 | 0.0000 | 0.72 | 0.65 | 0.01 | 0.1054 | 0.0533 | NA |
| 236.0831 | 10.4 | C8H16N2O4S | Met-Ser | Peptide(di-) | 0.94 | 0.98 | 0.97 | 0.5111 | 0.8291 | 0.7038 | 1.01 | 0.94 | 0.95 | 0.9473 | 0.5433 | 0.4898 | 1.04 | 1.02 | 0.98 | 0.6892 | 0.8565 | 0.8158 | 0.88 | 0.77 | 0.92 | 0.2976 | 0.0506 | 0.3847 |
| 216.1108 | 11.5 | C9H16N2O4 | Thr-Pro | Peptide(di-) | 1.14 | 0.74 | 1.02 | 0.5915 | 0.4449 | 0.9226 | 2.02 | 1.13 | 0.95 | 0.2318 | 0.7058 | 0.8588 | 0.70 | 0.71 | 0.16 | 0.1625 | 0.1930 | 0.0000 | 0.57 | 0.46 | 0.05 | 0.0068 | 0.0023 | 0.0000 |
| 244.1058 | 14.9 | C10H16N2O5 | Glu-Pro | Peptide(di-) | 0.99 | 0.65 | 0.96 | 0.9501 | 0.2079 | 0.7705 | 1.48 | 0.99 | 0.94 | 0.3851 | 0.9772 | 0.8221 | 0.84 | 0.81 | 0.32 | 0.3885 | 0.2060 | 0.0000 | 0.72 | 0.65 | 0.15 | 0.0056 | 0.0381 | 0.0000 |
| 252.1219 | 12.1 | C11H16N4O3 | Pro-His | Peptide(di-) | 1.09 | 0.73 | 0.95 | 0.7333 | 0.2277 | 0.7708 | 2.05 | 1.28 | 0.90 | 0.1668 | 0.3837 | 0.6596 | 0.78 | 0.78 | 0.18 | 0.1610 | 0.0543 | 0.0001 | 0.77 | 0.63 | 0.19 | 0.1374 | 0.0056 | 0.0000 |
| 243.1584 | 15.2 | C11H21N3O3 | Lys-Pro | Peptide(di-) | 1.04 | 0.85 | 0.97 | 0.8212 | 0.7621 | 0.8468 | 1.67 | 1.16 | 0.88 | 0.2802 | 0.5937 | 0.6090 | 0.69 | 0.80 | 0.21 | 0.0702 | 0.3882 | 0.0001 | 0.68 | 0.57 | 0.03 | 0.0342 | 0.0314 | 0.0000 |
| 268.1536 | 8.2 | C12H20N4O3 | His-Leu | Peptide(di-) | 1.19 | 0.63 | 0.88 | 0.4237 | 0.3201 | 0.4674 | 1.87 | 1.13 | 0.88 | 0.1886 | 0.7220 | 0.7220 | 1.15 | 0.83 | 0.15 | 0.6878 | 0.4787 | 0.0009 | 0.75 | 0.57 | 0.04 | 0.1002 | 0.0058 | 0.0000 |
| 275.1117 | 15.1 | C10H17N3O6 | Glu-Gln | Peptide(di-) | 0.97 | 1.11 | 1.05 | 0.8396 | 0.7333 | 0.5587 | 1.24 | 0.96 | 0.87 | 0.3353 | 0.8026 | 0.3765 | 0.97 | 1.00 | 0.67 | 0.7734 | 0.9890 | 0.0047 | 0.72 | 0.86 | 0.45 | 0.0031 | 0.3012 | 0.0000 |
| 218.1266 | 8.2 | C9H18N2O4 | Leu-Ser | Peptide(di-) | 1.07 | 0.61 | 0.88 | 0.7599 | 0.1866 | 0.5230 | 1.89 | 1.25 | 0.85 | 0.1531 | 0.4644 | 0.6063 | 0.97 | 0.72 | 0.17 | 0.9332 | 0.1270 | 0.0009 | 0.79 | 0.67 | 0.02 | 0.2982 | 0.0121 | 0.0000 |
| 318.1329 | 9.9 | C15H18N4O4 | Tyr-His | Peptide(di-) | 1.24 | 0.91 | 1.04 | 0.5621 | 0.7902 | 0.8562 | 1.84 | 1.07 | 0.85 | 0.1869 | 0.8301 | 0.6544 | 0.85 | 0.54 | 0.07 | 0.4280 | 0.0099 | 0.0000 | 0.70 | 0.58 | 0.05 | 0.0145 | 0.0053 | 0.0000 |
| 261.0962 | 17.1 | C9H15N3O6 | Asp-Gln | Peptide(di-) | 1.22 | 0.77 | 0.98 | 0.7271 | 0.6188 | 0.9523 | 1.31 | 0.68 | 0.79 | 0.4824 | 0.3010 | 0.5128 | 1.34 | 0.50 | 0.92 | 0.3695 | 0.0946 | 0.7604 | 1.09 | 0.64 | 0.80 | 0.8045 | 0.2449 | 0.5359 |
| 233.1374 | 16.4 | C9H19N3O4 | Lys-Ser | Peptide(di-) | 0.92 | 0.80 | 0.87 | 0.6896 | 0.1502 | 0.3442 | 1.24 | 0.94 | 0.78 | 0.4551 | 0.7330 | 0.2366 | 0.89 | 0.82 | 0.48 | 0.5085 | 0.1960 | 0.0000 | 0.86 | 0.74 | 0.51 | 0.2191 | 0.0274 | 0.0001 |
| 259.1896 | 12.4 | C12H25N3O3 | Leu-Lys | Peptide(di-) | 0.96 | 0.44 | 0.78 | 0.8992 | NA | 0.3936 | 1.52 | 1.13 | 0.67 | 0.4269 | 0.7690 | 0.3854 | 0.79 | 0.67 | 0.00 | 0.5269 | 0.0919 | NA | 0.55 | 0.43 | 0.00 | 0.0185 | 0.0020 | NA |
| 202.1317 | 7.4 | C9H18N2O3 | Leu-Ala | Peptide(di-) | 1.09 | 0.49 | 0.78 | 0.8185 | 0.1380 | 0.3428 | 1.21 | 0.75 | 0.61 | 0.6240 | 0.3821 | 0.2194 | 0.94 | 0.60 | 0.04 | 0.8561 | 0.1694 | NA | 0.64 | 0.44 | 0.00 | 0.0782 | 0.0018 | NA |
| 337.1746 | 14.1 | C15H23N5O4 | L-Tyrosyl-L-arginine | Peptide(di-) | 1.05 | 0.55 | 0.81 | 0.9001 | 0.3273 | 0.4789 | 1.09 | 0.78 | 0.42 | 0.8239 | 0.5615 | 0.0893 | 0.58 | 0.62 | 0.00 | 0.0566 | 0.0777 | NA | 0.72 | 0.43 | 0.00 | 0.0235 | 0.0051 | NA |
| 389.1906 | 16.0 | C15H27N5O7 | Ala-Lys-Asp-Gly | Peptide(tetra-) | 1.13 | 0.97 | 1.14 | 0.1611 | 0.7078 | 0.1349 | 1.05 | 0.98 | 1.24 | 0.8091 | 0.8865 | 0.1756 | 0.91 | 0.82 | 0.89 | 0.6379 | 0.0216 | 0.3468 | 0.90 | 0.87 | 1.00 | 0.1473 | 0.0964 | 0.9922 |
| 375.1749 | 17.5 | C14H25N5O7 | Asp-Lys-Gly-Gly | Peptide(tetra-) | 1.07 | 0.80 | 1.08 | 0.6096 | 0.0262 | 0.4267 | 1.25 | 1.08 | 1.21 | 0.1343 | 0.7004 | 0.2109 | 1.17 | 0.98 | 1.04 | 0.2142 | 0.8422 | 0.6263 | 1.10 | 0.89 | 1.01 | 0.6025 | 0.3607 | 0.9018 |
| 445.2535 | 13.3 | C19H35N5O7 | Ala-Leu-Lys-Asp | Peptide(tetra-) | 0.94 | 0.91 | 0.93 | 0.7499 | 0.6417 | 0.4548 | 1.15 | 1.09 | 1.20 | 0.0942 | 0.3106 | 0.0763 | 1.00 | 1.21 | 1.08 | 0.9926 | 0.0680 | 0.3164 | 1.02 | 0.98 | 1.08 | 0.8894 | 0.8556 | 0.4153 |
| 300.1435 | 16.5 | C12H20N4O5 | Ala-Gly-Gly-Pro | Peptide(tetra-) | 1.00 | 0.89 | 1.15 | 0.9640 | 0.4370 | 0.3047 | 1.20 | 1.02 | 1.20 | 0.1750 | 0.8766 | 0.1972 | 1.10 | 1.02 | 1.06 | 0.3115 | 0.7189 | 0.4473 | 1.08 | 0.84 | 1.10 | 0.5583 | 0.2301 | 0.4657 |
| 304.1019 | 15.8 | C10H16N4O7 | Asp-Gly-Gly-Gly | Peptide(tetra-) | 1.10 | 0.69 | 0.95 | 0.7165 | 0.0700 | 0.7958 | 1.20 | 1.11 | 1.19 | 0.4744 | 0.5515 | 0.4563 | 1.23 | 0.81 | 1.05 | 0.3776 | 0.2448 | 0.8145 | 1.21 | 0.85 | 0.90 | 0.3923 | 0.4579 | 0.5786 |
| 624.3496 | 14.8 | C30H44N10O5 | Arg-Phe-Phe-Arg | Peptide(tetra-) | 1.07 | 0.34 | 0.68 | 0.7813 | NA | 0.3333 | 1.78 | 0.60 | 1.18 | 0.2638 | 0.4469 | 0.6981 | 1.74 | 0.45 | 1.00 | 0.0684 | 0.1643 | 0.9919 | 1.46 | 0.58 | 0.79 | 0.4401 | 0.3481 | 0.6460 |
| 376.1591 | 17.1 | C14H24N4O8 | Ala-Thr-Ala-Asp | Peptide(tetra-) | 0.98 | 0.96 | 0.96 | 0.9020 | 0.7108 | 0.6959 | 1.17 | 1.13 | 1.17 | 0.2233 | 0.2655 | 0.2465 | 1.16 | 0.88 | 1.01 | 0.1270 | 0.2884 | 0.8825 | 0.94 | 0.95 | 0.99 | 0.5600 | 0.5959 | 0.9125 |
| 204.0746 | 15.5 | C14H24N4O10 | Asp-Thr-Ser-Ser | Peptide(tetra-) | 0.97 | 1.00 | 1.07 | 0.8890 | 0.9939 | 0.7257 | 1.41 | 1.11 | 1.17 | 0.1683 | 0.5798 | 0.4257 | 0.94 | 1.01 | 0.90 | 0.7970 | 0.9459 | 0.5117 | 0.92 | 1.03 | 0.88 | 0.7917 | 0.8781 | 0.5828 |
| 318.1538 | 16.0 | C12H22N4O6 | Ala-Ala-Ala-Ser | Peptide(tetra-) | 1.06 | 0.91 | 0.99 | 0.7654 | 0.5158 | 0.9227 | 1.15 | 1.00 | 1.16 | 0.5094 | 0.9858 | 0.3453 | 1.13 | 1.03 | 1.02 | 0.5271 | 0.8658 | 0.8719 | 1.03 | 0.90 | 1.03 | 0.8591 | 0.5884 | 0.8531 |
| 408.1144 | 15.0 | C14H24N4O6S2 | Cys-Cys-Pro-Ser | Peptide(tetra-) | 1.15 | 0.57 | 0.92 | 0.3469 | 0.0020 | 0.6098 | 1.59 | 0.90 | 1.16 | 0.0030 | 0.5256 | 0.3974 | 1.18 | 0.69 | 0.95 | 0.3823 | 0.1022 | 0.8007 | 1.22 | 0.69 | 0.96 | 0.2766 | 0.0849 | 0.8581 |
| 415.2067 | 16.7 | C17H29N5O7 | Ala-Thr-Gln-Pro | Peptide(tetra-) | 1.02 | 0.91 | 0.96 | 0.8542 | 0.2359 | 0.6088 | 1.17 | 1.14 | 1.16 | 0.2084 | 0.2457 | 0.1486 | 0.96 | 1.05 | 1.04 | 0.4828 | 0.7844 | 0.5398 | 0.96 | 0.95 | 1.05 | 0.7286 | 0.5473 | 0.6543 |
| 559.3113 | 23.6 | C27H41N7O6 | Asn-Leu-Lys-Trp | Peptide(tetra-) | 0.80 | 1.06 | 1.07 | 0.3670 | 0.7660 | 0.7521 | 0.96 | 1.30 | 1.15 | 0.8530 | 0.3579 | 0.5479 | 0.82 | 1.38 | 0.91 | 0.2677 | 0.1653 | 0.6396 | 0.70 | 1.04 | 1.01 | 0.1020 | 0.8942 | 0.9632 |
| 479.1683 | 10.8 | C17H29N5O9S | Asn-Met-Thr-Asp | Peptide(tetra-) | 0.87 | 0.88 | 0.88 | 0.5782 | 0.6051 | 0.5642 | 1.08 | 1.22 | 1.15 | 0.6935 | 0.4033 | 0.5540 | 0.97 | 1.09 | 0.99 | 0.8938 | 0.6052 | 0.9219 | 1.13 | 1.04 | 0.81 | 0.6312 | 0.8160 | 0.1926 |
| 424.1592 | 11.4 | C18H24N4O8 | Ala-Asp-Gly-Tyr | Peptide(tetra-) | 1.04 | 1.06 | 1.01 | 0.8506 | 0.5745 | 0.9152 | 1.05 | 1.20 | 1.15 | 0.6979 | 0.2728 | 0.2985 | 0.97 | 1.01 | 1.04 | 0.8269 | 0.9456 | 0.7621 | 1.03 | 1.04 | 1.00 | 0.8523 | 0.6989 | 0.9650 |
| 471.2329 | 12.3 | C20H33N5O8 | Glu-Val-Gln-Pro | Peptide(tetra-) | 1.01 | 1.05 | 1.05 | 0.9230 | 0.7277 | 0.5893 | 1.11 | 1.16 | 1.14 | 0.2977 | 0.2077 | 0.3166 | 1.09 | 1.14 | 1.05 | 0.6017 | 0.4412 | 0.5379 | 0.94 | 1.13 | 1.02 | 0.6699 | 0.3317 | 0.8935 |
| 500.1769 | 10.3 | C21H32N4O6S2 | Cys-Leu-Cys-Tyr | Peptide(tetra-) | 0.99 | 0.82 | 0.93 | 0.9303 | 0.0235 | 0.4464 | 1.17 | 1.00 | 1.13 | 0.1937 | 0.9605 | 0.2084 | 0.99 | 0.90 | 0.97 | 0.8519 | 0.3301 | 0.6372 | 1.07 | 1.09 | 1.02 | 0.4832 | 0.3555 | 0.7707 |
| 390.1749 | 16.9 | C15H26N4O8 | Ala-Val-Asp-Ser | Peptide(tetra-) | 1.01 | 0.93 | 1.01 | 0.9631 | 0.5968 | 0.8850 | 1.14 | 0.97 | 1.11 | 0.3788 | 0.8737 | 0.5051 | 1.02 | 0.87 | 0.96 | 0.8730 | 0.1335 | 0.6405 | 1.08 | 0.95 | 1.13 | 0.3516 | 0.6922 | 0.2144 |
| 374.1912 | 15.5 | C14H26N6O6 | Asn-Lys-Gly-Gly | Peptide(tetra-) | 1.06 | 0.88 | 1.15 | 0.3773 | 0.0596 | 0.0480 | 1.36 | 0.97 | 1.10 | 0.1237 | 0.8292 | 0.5045 | 1.00 | 1.04 | 1.03 | 0.9632 | 0.7382 | 0.8208 | 0.98 | 0.94 | 1.12 | 0.8214 | 0.6778 | 0.3058 |
| 422.1105 | 16.0 | C14H22N4O9S | Ala-Asp-Asp-Cys | Peptide(tetra-) | 1.01 | 1.02 | 1.02 | 0.9366 | 0.9176 | 0.8742 | 1.15 | 0.98 | 1.08 | 0.2749 | 0.9147 | 0.5888 | 0.94 | 0.94 | 0.90 | 0.4634 | 0.7250 | 0.3745 | 0.99 | 0.94 | 1.14 | 0.9400 | 0.7207 | 0.3054 |
| 511.1895 | 7.5 | C25H29N5O5S | Cys-Phe-Trp-Gly | Peptide(tetra-) | 0.89 | 0.76 | 0.79 | 0.3564 | 0.0407 | 0.0884 | 1.01 | 0.92 | 1.08 | 0.9703 | 0.7222 | 0.6939 | 1.31 | 0.80 | 1.16 | 0.4288 | 0.1333 | 0.3319 | 0.94 | 0.95 | 0.94 | 0.6737 | 0.6682 | 0.6979 |
| 374.1435 | 13.8 | C14H22N4O8 | Asp-Gly-Pro-Ser | Peptide(tetra-) | 1.05 | 0.88 | 1.00 | 0.7101 | 0.4310 | 0.9917 | 1.16 | 1.11 | 1.07 | 0.4362 | 0.5575 | 0.6420 | 1.23 | 1.02 | 1.13 | 0.3358 | 0.9092 | 0.3618 | 1.04 | 0.97 | 1.06 | 0.8264 | 0.8387 | 0.6573 |
| 544.3085 | 23.6 | C21H40N10O7 | Arg-Lys-Asn-Gln | Peptide(tetra-) | 0.74 | 1.25 | 0.80 | 0.1361 | 0.2812 | 0.3779 | 0.84 | 1.47 | 1.07 | 0.5079 | 0.1224 | 0.8307 | 0.72 | 1.35 | 0.90 | 0.4171 | 0.3058 | 0.6933 | 0.78 | 1.20 | 1.25 | 0.5624 | 0.7202 | 0.5396 |
| 417.1968 | 15.7 | C15H27N7O7 | Ala-Asp-Gly-Arg | Peptide(tetra-) | 1.52 | 1.82 | 0.95 | 0.2863 | 0.3192 | 0.9146 | 1.48 | 0.80 | 1.06 | 0.3488 | 0.6904 | 0.8942 | 0.71 | 0.72 | 0.39 | 0.2844 | 0.5385 | 0.0336 | 0.45 | 0.46 | 0.00 | 0.0301 | 0.0115 | NA |
| 484.1916 | 15.3 | C19H28N6O9 | Asp-Val-Asp-His | Peptide(tetra-) | 1.00 | 0.70 | 0.93 | 0.9765 | 0.1096 | 0.5555 | 1.55 | 1.00 | 1.06 | 0.2362 | 0.9948 | 0.8106 | 1.20 | 1.00 | 0.27 | 0.4336 | 0.9972 | 0.0001 | 0.63 | 0.59 | 0.02 | 0.0066 | 0.0036 | 0.0000 |
| 414.2226 | 15.4 | C17H30N6O6 | Asn-Lys-Gly-Pro | Peptide(tetra-) | 1.15 | 0.78 | 1.05 | 0.3324 | 0.4852 | 0.7071 | 1.34 | 0.91 | 1.06 | 0.3054 | 0.7512 | 0.7978 | 1.18 | 1.00 | 0.53 | 0.5171 | 0.9929 | 0.0023 | 0.88 | 0.74 | 0.18 | 0.3346 | 0.1940 | 0.0001 |
| 434.1284 | 18.0 | C15H22N4O11 | Ala-Asp-Asp-Asp | Peptide(tetra-) | 0.94 | 0.84 | 0.87 | 0.6439 | 0.1948 | 0.2940 | 1.22 | 0.81 | 1.06 | 0.3062 | 0.1136 | 0.7020 | 1.23 | 1.04 | 1.16 | 0.2804 | 0.7871 | 0.2903 | 1.08 | 0.95 | 0.95 | 0.6312 | 0.7228 | 0.7848 |
| 456.1611 | 15.7 | C17H24N6O9 | Ala-Asp-Asp-His | Peptide(tetra-) | 0.61 | 1.82 | 1.15 | 0.3351 | 0.0354 | 0.7281 | 0.52 | 1.44 | 1.06 | 0.2350 | 0.4512 | 0.8947 | 0.49 | 1.80 | 1.01 | 0.1695 | 0.1453 | 0.9890 | 0.55 | 1.47 | 1.34 | 0.2343 | 0.4162 | 0.4773 |
| 489.2430 | 13.9 | C20H35N5O9 | Asp-Leu-Lys-Asp | Peptide(tetra-) | 0.83 | 0.98 | 0.96 | 0.1357 | 0.7814 | 0.5927 | 1.02 | 1.01 | 1.05 | 0.9259 | 0.9095 | 0.7417 | 1.09 | 1.13 | 1.07 | 0.5152 | 0.1822 | 0.4771 | 0.93 | 1.12 | 1.05 | 0.3383 | 0.3110 | 0.5795 |
| 394.1159 | 17.1 | C13H22N4O8S | Ala-Asp-Cys-Ser | Peptide(tetra-) | 1.09 | 0.63 | 0.97 | 0.6808 | 0.0362 | 0.8469 | 1.27 | 0.94 | 1.05 | 0.1962 | 0.7416 | 0.8069 | 1.27 | 0.80 | 1.06 | 0.1875 | 0.3034 | 0.7355 | 1.19 | 0.87 | 1.06 | 0.3476 | 0.4958 | 0.7772 |
| 426.0877 | 16.8 | C13H22N4O8S2 | Asp-Cys-Cys-Ser | Peptide(tetra-) | 0.82 | 0.90 | 0.98 | 0.4350 | 0.5805 | 0.9150 | 0.98 | 1.00 | 1.05 | 0.9486 | 0.9812 | 0.8709 | 0.95 | 0.84 | 0.72 | 0.8011 | 0.2214 | 0.0641 | 1.17 | 1.16 | 1.24 | 0.3061 | 0.4355 | 0.4405 |
| 541.2131 | 15.9 | C21H31N7O10 | Glu-Glu-Gln-His | Peptide(tetra-) | 0.95 | 0.77 | 0.92 | 0.8296 | 0.4938 | 0.6678 | 1.67 | 1.02 | 1.05 | 0.2529 | 0.9593 | 0.8815 | 1.12 | 1.04 | 0.13 | 0.7095 | 0.8869 | 0.0003 | 0.53 | 0.53 | 0.00 | 0.0263 | 0.0144 | NA |
| 438.1752 | 11.2 | C19H26N4O8 | Glu-Ala-Gly-Tyr | Peptide(tetra-) | 1.00 | 0.91 | 1.01 | 0.9657 | 0.7239 | 0.9519 | 1.27 | 1.12 | 1.04 | 0.2021 | 0.5927 | 0.7632 | 1.03 | 0.98 | 0.52 | 0.8720 | 0.8640 | 0.0003 | 0.63 | 0.71 | 0.21 | 0.0051 | 0.0210 | 0.0000 |
| 348.1642 | 16.4 | C13H24N4O7 | Ala-Thr-Ala-Ser | Peptide(tetra-) | 1.14 | 1.00 | 1.12 | 0.1476 | 0.9779 | 0.1961 | 1.07 | 0.90 | 1.04 | 0.4740 | 0.1756 | 0.6418 | 1.09 | 1.03 | 0.99 | 0.3472 | 0.7382 | 0.8863 | 1.08 | 0.93 | 1.03 | 0.4410 | 0.6074 | 0.7499 |
| 404.1654 | 16.8 | C14H24N6O8 | Ala-Asn-Asn-Ser | Peptide(tetra-) | 0.99 | 0.94 | 1.01 | 0.9695 | 0.5667 | 0.9026 | 1.10 | 0.93 | 1.04 | 0.5493 | 0.6451 | 0.7922 | 1.12 | 0.85 | 0.97 | 0.3932 | 0.4040 | 0.7037 | 1.00 | 0.90 | 1.00 | 0.9956 | 0.4354 | 0.9917 |
| 416.1908 | 10.0 | C17H28N4O8 | Asp-Val-Pro-Ser | Peptide(tetra-) | 0.99 | 1.33 | 1.02 | 0.9514 | 0.4649 | 0.9045 | 1.00 | 0.97 | 1.03 | 0.9781 | 0.8919 | 0.8680 | 0.95 | 1.07 | 0.96 | 0.7522 | 0.7329 | 0.8034 | 0.98 | 1.01 | 0.89 | 0.7845 | 0.9495 | 0.2526 |
| 498.1790 | 10.5 | C21H30N4O8S | Ala-Met-Asp-Tyr | Peptide(tetra-) | 0.91 | 0.88 | 0.94 | 0.2807 | 0.5977 | 0.4516 | 1.10 | 0.98 | 1.02 | 0.5234 | 0.7775 | 0.8190 | 1.09 | 1.07 | 1.08 | 0.1564 | 0.6449 | 0.3872 | 0.97 | 1.06 | 0.98 | 0.7571 | 0.6373 | 0.7587 |
| 362.1263 | 14.7 | C13H22N4O6S | Cys-Gly-Pro-Ser | Peptide(tetra-) | 0.71 | 1.69 | 1.10 | 0.3366 | 0.0350 | 0.7452 | 0.68 | 1.31 | 1.02 | 0.3139 | 0.4049 | 0.9589 | 0.69 | 1.58 | 0.88 | 0.2829 | 0.0305 | 0.6690 | 0.69 | 1.32 | 1.00 | 0.3017 | 0.3974 | 0.9873 |
| 376.1417 | 14.6 | C14H24N4O6S | Ala-Cys-Pro-Ser | Peptide(tetra-) | 0.60 | 1.32 | 0.94 | 0.2609 | 0.5851 | 0.8693 | 0.56 | 1.54 | 1.01 | 0.2518 | 0.4083 | 0.9771 | 0.56 | 1.63 | 0.98 | 0.1773 | 0.3422 | 0.9518 | 0.55 | 1.38 | 1.16 | 0.2506 | 0.5402 | 0.7569 |
| 461.1866 | 17.0 | C16H27N7O9 | Arg-Asp-Asp-Gly | Peptide(tetra-) | 1.04 | 0.89 | 1.03 | 0.7935 | 0.3975 | 0.7639 | 1.14 | 1.02 | 1.01 | 0.4155 | 0.9127 | 0.9470 | 1.17 | 0.94 | 1.11 | 0.3556 | 0.5493 | 0.4132 | 1.05 | 1.00 | 1.02 | 0.7245 | 0.9860 | 0.8680 |
| 374.2162 | 14.4 | C16H30N4O6 | Ala-Leu-Thr-Ala | Peptide(tetra-) | 1.01 | 0.76 | 0.92 | 0.9482 | 0.2624 | 0.3784 | 1.08 | 0.97 | 0.99 | 0.4533 | 0.8385 | 0.9627 | 1.11 | 0.86 | 1.01 | 0.5569 | 0.2090 | 0.9491 | 1.11 | 0.90 | 0.98 | 0.4377 | 0.4885 | 0.8486 |
| 413.2273 | 9.5 | C18H31N5O6 | Ala-Leu-Asn-Pro | Peptide(tetra-) | 0.99 | 0.65 | 0.80 | 0.9623 | 0.1699 | 0.2548 | 2.38 | 1.27 | 0.99 | 0.1397 | 0.4816 | 0.9738 | 1.02 | 0.88 | 0.18 | 0.9412 | 0.4551 | 0.0001 | 0.75 | 0.69 | 0.12 | 0.0447 | 0.0274 | 0.0000 |
| 440.1034 | 16.5 | C14H24N4O8S2 | Asp-Thr-Cys-Cys | Peptide(tetra-) | 0.77 | 1.03 | 1.05 | 0.0217 | 0.8991 | 0.6874 | 0.81 | 0.87 | 0.97 | 0.0745 | 0.2441 | 0.8426 | 0.95 | 1.11 | 0.73 | 0.6750 | 0.6655 | 0.0246 | 1.10 | 1.10 | 0.92 | 0.5158 | 0.5757 | 0.5342 |
| 359.2170 | 13.8 | C15H29N5O5 | Ala-Lys-Ala-Ala | Peptide(tetra-) | 1.13 | 0.56 | 0.93 | 0.5636 | 0.2931 | 0.7347 | 2.29 | 1.19 | 0.97 | 0.1037 | 0.6738 | 0.9371 | 0.81 | 0.68 | 0.00 | 0.2185 | 0.2148 | NA | 0.60 | 0.52 | 0.00 | 0.0678 | 0.0031 | NA |

| | | | | | | | | | | | | | | | | | | | | | | | | | | | | |
|---|---|---|---|---|---|---|---|---|---|---|---|---|---|---|---|---|---|---|---|---|---|---|---|---|---|---|---|---|
| 440.1766 | 14.7 | C16H24N8O7 | Asn-Asn-Gly-His | Peptide(tetra-) | 0.73 | 1.52 | 0.94 | 0.3375 | 0.2242 | 0.8594 | 0.57 | 1.37 | 0.96 | 0.1221 | 0.3797 | 0.9052 | 0.53 | 1.56 | 0.90 | 0.0455 | 0.0441 | 0.7073 | 0.60 | 1.70 | 1.18 | 0.0825 | 0.1973 | 0.5875 |
| 382.1312 | 10.7 | C16H22N4O5S | Cys-Phe-Gly-Gly | Peptide(tetra-) | 0.93 | 1.71 | 1.24 | 0.8308 | 0.4207 | 0.4568 | 0.77 | 1.06 | 0.93 | 0.3196 | 0.7113 | 0.7470 | 0.87 | 1.05 | 0.97 | 0.3261 | 0.7424 | 0.8520 | 0.80 | 1.15 | 0.93 | 0.1595 | 0.4739 | 0.6585 |
| 488.2590 | 13.3 | C20H36N6O8 | Asn-Leu-Lys-Asp | Peptide(tetra-) | 1.06 | 1.26 | 1.09 | 0.6307 | 0.0318 | 0.4586 | 2.04 | 1.13 | 0.93 | 0.1321 | 0.6747 | 0.7558 | 1.04 | 0.83 | 0.62 | 0.7984 | 0.1640 | 0.0095 | 0.89 | 0.78 | 0.69 | 0.2605 | 0.1246 | 0.0067 |
| 562.2432 | 14.5 | C30H34N4O7 | Ala-Phe-Tyr-Tyr | Peptide(tetra-) | 0.94 | 1.04 | 0.99 | 0.4375 | 0.8601 | 0.9243 | 1.04 | 0.98 | 0.92 | 0.7419 | 0.8473 | 0.4005 | 0.95 | 0.80 | 0.97 | 0.4944 | 0.0684 | 0.6650 | 1.07 | 0.85 | 1.00 | 0.6419 | 0.2090 | 0.9635 |
| 439.2428 | 10.8 | C20H33N5O6 | Asn-Leu-Pro-Pro | Peptide(tetra-) | 1.02 | 0.57 | 0.88 | 0.9201 | 0.4128 | 0.5322 | 1.83 | 1.08 | 0.91 | 0.2232 | 0.8430 | 0.7754 | 0.67 | 0.62 | 0.07 | 0.1178 | 0.1004 | 0.0002 | 0.40 | 0.40 | 0.00 | 0.0007 | 0.0006 | NA |
| 521.1952 | 16.7 | C23H31N5O7S | Ala-Met-Trp-Asp | Peptide(tetra-) | 1.02 | 1.17 | 1.06 | 0.9380 | 0.0793 | 0.6166 | 0.87 | 1.13 | 0.90 | 0.4362 | 0.3459 | 0.5786 | 0.86 | 1.01 | 1.00 | 0.3913 | 0.8955 | 0.9922 | 0.78 | 1.16 | 0.91 | 0.1614 | 0.3813 | 0.6086 |
| 475.2425 | 7.5 | C23H33N5O6 | Asn-Phe-Val-Pro | Peptide(tetra-) | 1.09 | 0.79 | 0.88 | 0.7430 | 0.4074 | 0.5183 | 1.95 | 0.81 | 0.74 | 0.2477 | 0.5307 | 0.4421 | 0.93 | 0.59 | 0.10 | 0.8202 | 0.1087 | 0.0006 | 0.56 | 0.42 | 0.00 | 0.0453 | 0.0001 | NA |
| 347.1330 | 16.0 | C13H21N3O8 | Glu-Ala-Glu | Peptide(tri-) | 1.02 | 0.98 | 1.08 | 0.9515 | 0.9663 | 0.5953 | 2.44 | 1.28 | 1.64 | 0.1472 | 0.3908 | 0.1005 | 1.44 | 1.72 | 0.39 | 0.2144 | 0.0170 | 0.0038 | 0.53 | 0.55 | 0.00 | 0.0801 | 0.0658 | NA |
| 379.1412 | 12.0 | C14H25N3O7S | Glu-Met-Thr | Peptide(tri-) | 0.94 | 1.45 | 1.11 | 0.7079 | 0.4559 | 0.4752 | 1.07 | 1.28 | 1.28 | 0.6741 | 0.0952 | 0.1333 | 1.35 | 1.23 | 1.30 | 0.1826 | 0.0428 | 0.0346 | 1.31 | 1.09 | 1.33 | 0.1001 | 0.2224 | 0.0585 |
| 365.0889 | 16.2 | C12H19N3O8S | Glu-Asp-Cys | Peptide(tri-) | 0.86 | 0.68 | 0.91 | 0.5454 | 0.0414 | 0.6118 | 1.10 | 1.12 | 1.20 | 0.6194 | 0.4778 | 0.2413 | 1.09 | 0.88 | 1.08 | 0.4762 | 0.4153 | 0.4603 | 0.96 | 1.05 | 1.09 | 0.8176 | 0.7488 | 0.5358 |
| 319.1017 | 16.6 | C11H17N3O8 | Glu-Asp-Gly | Peptide(tri-) | 0.91 | 0.73 | 0.95 | 0.6868 | 0.0398 | 0.7646 | 1.36 | 0.96 | 1.20 | 0.2051 | 0.8274 | 0.4378 | 1.30 | 0.81 | 1.03 | 0.3196 | 0.2090 | 0.8719 | 1.09 | 0.82 | 0.97 | 0.6746 | 0.1247 | 0.8627 |
| 277.0911 | 15.6 | C9H15N3O7 | Asp-Gly-Ser | Peptide(tri-) | 0.99 | 0.78 | 0.94 | 0.9783 | 0.0927 | 0.6956 | 1.47 | 1.06 | 1.19 | 0.1782 | 0.7628 | 0.4138 | 1.11 | 0.81 | 1.06 | 0.6509 | 0.2260 | 0.7391 | 1.11 | 0.83 | 0.88 | 0.6406 | 0.2706 | 0.4785 |
| 411.1312 | 13.9 | C15H29N3O4S3 | Met-Met-Met | Peptide(tri-) | 1.06 | 0.85 | 0.94 | 0.3109 | 0.1373 | 0.4257 | 1.26 | 1.22 | 1.16 | 0.0402 | 0.0373 | 0.0587 | 1.06 | 0.95 | 1.03 | 0.4339 | 0.6503 | 0.6208 | 1.06 | 0.95 | 1.17 | 0.6026 | 0.7076 | 0.0924 |
| 309.1327 | 8.1 | C14H19N3O5 | Ala-Gly-Tyr | Peptide(tri-) | 1.02 | 0.99 | 0.98 | 0.8379 | 0.9482 | 0.8249 | 1.23 | 1.15 | 1.16 | 0.1008 | 0.5174 | 0.1455 | 1.13 | 0.95 | 0.83 | 0.6693 | 0.6893 | 0.1291 | 0.99 | 0.99 | 0.40 | 0.9748 | 0.9321 | 0.0000 |
| 342.1899 | 9.7 | C15H26N4O5 | Leu-Asn-Pro | Peptide(tri-) | 1.11 | 0.78 | 1.01 | 0.3280 | 0.5217 | 0.9594 | 1.68 | 1.20 | 1.14 | 0.2471 | 0.5275 | 0.6145 | 1.15 | 1.00 | 0.25 | 0.6395 | 0.9939 | 0.0002 | 0.75 | 0.67 | 0.00 | 0.0708 | 0.0410 | NA |
| 305.0857 | 18.1 | C10H15N3O8 | Asp-Asp-Gly | Peptide(tri-) | 1.06 | 0.62 | 0.90 | 0.7991 | 0.0122 | 0.6006 | 1.43 | 0.98 | 1.14 | 0.2126 | 0.9419 | 0.6507 | 1.37 | 0.73 | 1.08 | 0.1904 | 0.1616 | 0.7179 | 1.23 | 0.76 | 0.91 | 0.3217 | 0.2883 | 0.6908 |
| 346.1600 | 17.6 | C12H19N5O6 | Ser-Ser-His | Peptide(tri-) | 1.07 | 0.87 | 0.98 | 0.6846 | 0.2218 | 0.8903 | 1.22 | 0.91 | 1.12 | 0.1777 | 0.4446 | 0.4495 | 1.09 | 0.84 | 0.97 | 0.4641 | 0.2964 | 0.7384 | 1.09 | 0.97 | 1.08 | 0.3173 | 0.8517 | 0.4456 |
| 335.1326 | 15.8 | C12H21N3O8 | Glu-Ser-Thr | Peptide(tri-) | 1.17 | 0.84 | 1.04 | 0.4476 | 0.0926 | 0.7498 | 1.20 | 0.95 | 1.11 | 0.1996 | 0.6227 | 0.4244 | 1.17 | 0.88 | 1.04 | 0.3566 | 0.2504 | 0.7034 | 1.18 | 0.91 | 1.04 | 0.3057 | 0.4963 | 0.7197 |
| 346.2215 | 17.4 | C15H30N4O5 | Leu-Lys-Ser | Peptide(tri-) | 0.84 | 0.98 | 0.99 | 0.5201 | 0.9236 | 0.9716 | 0.92 | 1.10 | 1.10 | 0.6628 | 0.6673 | 0.6485 | 0.83 | 1.20 | 0.96 | 0.1883 | 0.3605 | 0.7878 | 0.87 | 1.04 | 1.09 | 0.3777 | 0.8664 | 0.6031 |
| 275.1482 | 15.1 | C11H21N3O5 | Val-Ala-Ser | Peptide(tri-) | 1.14 | 1.23 | 1.04 | 0.3558 | 0.3100 | 0.7507 | 1.14 | 0.94 | 1.10 | 0.5116 | 0.7759 | 0.5759 | 1.12 | 0.87 | 0.97 | 0.4806 | 0.4494 | 0.8454 | 0.96 | 0.79 | 0.82 | 0.7326 | 0.0357 | 0.0458 |
| 291.1067 | 15.5 | C10H17N3O7 | Glu-Gly-Ser | Peptide(tri-) | 0.84 | 0.85 | 0.97 | 0.3780 | 0.4278 | 0.8646 | 1.01 | 1.05 | 1.10 | 0.9447 | 0.7898 | 0.6636 | 1.02 | 1.19 | 1.00 | 0.8839 | 0.3333 | 0.9797 | 0.88 | 1.07 | 1.02 | 0.2561 | 0.6652 | 0.9000 |
| 287.1116 | 15.2 | C11H17N3O6 | Asp-Gly-Pro | Peptide(tri-) | 0.96 | 1.07 | 1.09 | 0.7486 | 0.3911 | 0.3894 | 1.23 | 1.00 | 1.09 | 0.2135 | 0.9978 | 0.4535 | 0.98 | 0.96 | 1.03 | 0.9019 | 0.7502 | 0.7762 | 0.94 | 0.88 | 1.03 | 0.4938 | 0.3228 | 0.7806 |
| 355.1200 | 11.6 | C15H21N3O5S | Phe-Cys-Ser | Peptide(tri-) | 1.52 | 1.45 | 1.09 | 0.0611 | 0.1690 | 0.7739 | 1.21 | 0.71 | 1.07 | 0.3746 | 0.3919 | 0.7873 | 1.38 | 0.67 | 1.02 | 0.1844 | 0.4568 | 0.9495 | 1.37 | 0.78 | 1.15 | 0.1106 | 0.5574 | 0.6381 |
| 365.1255 | 11.9 | C13H23N3O7S | Glu-Met-Ser | Peptide(tri-) | 1.06 | 0.82 | 0.93 | 0.7749 | 0.3898 | 0.6347 | 1.24 | 1.06 | 1.07 | 0.3036 | 0.8024 | 0.6829 | 1.13 | 1.03 | 1.12 | 0.3982 | 0.9369 | 0.4269 | 0.98 | 0.94 | 1.14 | 0.9151 | 0.8130 | 0.5657 |
| 321.0995 | 12.8 | C11H19N3O6S | Met-Asp-Gly | Peptide(tri-) | 1.00 | 0.92 | 1.08 | 0.9980 | 0.4282 | 0.3857 | 1.25 | 1.05 | 1.07 | 0.1132 | 0.7565 | 0.7024 | 1.04 | 1.11 | 0.95 | 0.8184 | 0.3952 | 0.6311 | 1.09 | 0.96 | 0.99 | 0.2789 | 0.7920 | 0.9302 |
| 334.1851 | 15.3 | C13H26N4O6 | Lys-Thr-Ser | Peptide(tri-) | 0.92 | 1.00 | 0.97 | 0.3533 | 0.9685 | 0.7445 | 1.00 | 1.05 | 1.07 | 0.9933 | 0.6365 | 0.4616 | 0.98 | 1.08 | 1.04 | 0.7427 | 0.6224 | 0.6122 | 1.07 | 1.08 | 1.12 | 0.3692 | 0.5686 | 0.2072 |
| 346.1600 | 15.6 | C12H22N6O6 | Asp-Gly-Arg | Peptide(tri-) | 1.01 | 0.80 | 0.98 | 0.9739 | 0.0657 | 0.8508 | 1.14 | 0.83 | 1.07 | 0.3969 | 0.2139 | 0.6126 | 1.10 | 0.89 | 1.04 | 0.4970 | 0.3950 | 0.7159 | 1.13 | 0.95 | 1.01 | 0.4006 | 0.7186 | 0.9574 |
| 318.1174 | 15.3 | C11H18N4O7 | Ala-Asn-Asp | Peptide(tri-) | 1.00 | 0.79 | 0.87 | 0.9918 | 0.1115 | 0.4173 | 1.37 | 0.91 | 1.07 | 0.2042 | 0.6169 | 0.7134 | 1.33 | 0.99 | 1.11 | 0.3416 | 0.9632 | 0.4899 | 1.09 | 0.92 | 1.06 | 0.6764 | 0.6473 | 0.7323 |
| 383.1801 | 11.0 | C16H25N5O6 | Leu-Asp-His | Peptide(tri-) | 1.12 | 0.65 | 0.93 | 0.5759 | 0.0564 | 0.6846 | 1.55 | 1.04 | 1.05 | 0.2292 | 0.8907 | 0.8514 | 1.02 | 0.59 | 0.20 | 0.9310 | 0.0175 | 0.0001 | 0.58 | 0.53 | 0.02 | 0.0006 | 0.0004 | 0.0000 |
| 356.2421 | 21.1 | C17H32N4O4 | Leu-Lys-Pro | Peptide(tri-) | 1.03 | 0.76 | 0.89 | 0.7210 | 0.0109 | 0.1782 | 1.12 | 0.93 | 1.04 | 0.2270 | 0.4925 | 0.6767 | 1.17 | 0.91 | 1.02 | 0.1984 | 0.5290 | 0.8350 | 1.27 | 0.96 | 1.10 | 0.0159 | 0.5911 | 0.3007 |
| 290.1226 | 16.6 | C10H18N4O6 | Gln-Gly-Ser | Peptide(tri-) | 0.82 | 1.00 | 1.03 | 0.2281 | 0.9829 | 0.8365 | 0.96 | 1.19 | 1.04 | 0.7475 | 0.3909 | 0.7944 | 0.91 | 1.09 | 0.94 | 0.2716 | 0.5015 | 0.5197 | 0.85 | 1.02 | 0.97 | 0.1456 | 0.9336 | 0.7693 |
| 275.0937 | 10.5 | C10H17N3O4S | Cys-Gly-Pro | Peptide(tri-) | 0.72 | 1.31 | 1.05 | 0.3840 | 0.3277 | 0.9007 | 0.75 | 0.97 | 1.02 | 0.2957 | 0.8824 | 0.9371 | 0.87 | 1.32 | 0.92 | 0.5850 | 0.2343 | 0.7552 | 0.64 | 1.08 | 1.03 | 0.0741 | 0.7738 | 0.8770 |
| 375.1460 | 9.0 | C15H25N3O6S | Glu-Met-Pro | Peptide(tri-) | 1.43 | 0.43 | 0.81 | 0.4379 | 0.0771 | 0.6065 | 1.52 | 0.69 | 1.02 | 0.0993 | 0.4076 | 0.9580 | 1.64 | 0.45 | 0.90 | 0.0373 | 0.1978 | 0.7498 | 1.38 | 0.84 | 1.02 | 0.1203 | 0.5525 | 0.9282 |
| 259.1172 | 11.2 | C10H17N3O5 | Gly-Pro-Ser | Peptide(tri-) | 0.86 | 1.52 | 1.41 | 0.6773 | 0.5557 | 0.3438 | 0.82 | 1.01 | 1.01 | 0.4456 | 0.9466 | 0.9480 | 1.04 | 0.97 | 0.98 | 0.8485 | 0.8831 | 0.8929 | 0.85 | 1.18 | 0.83 | 0.4739 | 0.4642 | 0.4664 |
| 305.1223 | 14.5 | C11H19N3O7 | Glu-Ala-Ser | Peptide(tri-) | 0.94 | 0.97 | 1.00 | 0.6792 | 0.8742 | 0.9848 | 0.84 | 0.95 | 1.01 | 0.1860 | 0.8047 | 0.9611 | 0.89 | 1.14 | 0.96 | 0.3745 | 0.4640 | 0.7555 | 0.97 | 1.15 | 1.00 | 0.7457 | 0.4257 | 0.9972 |
| 261.1325 | 16.4 | C10H19N3O5 | Thr-Ala-Ala | Peptide(tri-) | 1.02 | 0.85 | 1.03 | 0.8573 | 0.1636 | 0.7493 | 1.32 | 1.03 | 1.00 | 0.2470 | 0.8619 | 0.9916 | 1.01 | 0.83 | 0.58 | 0.9564 | 0.0556 | 0.0001 | 0.85 | 0.75 | 0.58 | 0.0633 | 0.0022 | 0.0000 |
| 233.1011 | 12.8 | C8H15N3O5 | Ala-Gly-Ser | Peptide(tri-) | 1.07 | 0.71 | 0.85 | 0.7333 | 0.5031 | 0.2629 | 1.92 | 1.09 | 0.99 | 0.1757 | 0.7874 | 0.9767 | 1.07 | 1.11 | 0.32 | 0.7664 | 0.4978 | 0.0002 | 0.83 | 0.65 | 0.20 | 0.2896 | 0.0423 | 0.0002 |
| 340.1860 | 15.8 | C14H24N6O4 | Lys-Gly-His | Peptide(tri-) | 1.17 | 0.84 | 0.97 | 0.2112 | 0.7218 | 0.8396 | 1.71 | 0.98 | 0.97 | 0.2125 | 0.9440 | 0.9101 | 1.04 | 0.95 | 0.09 | 0.8384 | 0.8533 | 0.0000 | 0.69 | 0.60 | 0.00 | 0.0367 | 0.0261 | NA |
| 277.1095 | 12.6 | C10H19N3O4S | Met-Ala-Gly | Peptide(tri-) | 0.52 | 1.40 | 0.91 | 0.2402 | 0.3079 | 0.8333 | 0.47 | 1.11 | 0.96 | 0.0563 | 0.7428 | 0.9080 | 0.61 | 1.74 | 0.97 | 0.1547 | 0.0214 | 0.9373 | 0.59 | 1.46 | 1.23 | 0.1027 | 0.3225 | 0.4537 |
| 421.1714 | 10.8 | C17H23N7O6 | Glu-His-His | Peptide(tri-) | 1.01 | 1.04 | 0.92 | 0.9406 | 0.6431 | 0.5637 | 1.11 | 1.01 | 0.94 | 0.6903 | 0.9605 | 0.6853 | 1.07 | 0.77 | 0.87 | 0.6797 | 0.0829 | 0.2545 | 0.95 | 0.83 | 0.47 | 0.7291 | 0.0861 | 0.0000 |
| 291.1249 | 10.9 | C11H21N3O4S | Leu-Cys-Gly | Peptide(tri-) | 0.84 | 1.21 | 1.32 | 0.6393 | 0.6782 | 0.4871 | 0.78 | 1.00 | 0.93 | 0.2819 | 0.9954 | 0.7239 | 0.94 | 0.93 | 0.86 | 0.7139 | 0.6731 | 0.4287 | 1.06 | 1.11 | 1.05 | 0.8176 | 0.4925 | 0.7714 |
| 373.1483 | 16.7 | C15H23N3O8 | Glu-Glu-Pro | Peptide(tri-) | 1.16 | 0.67 | 0.94 | 0.6170 | 0.1382 | 0.7998 | 2.30 | 1.23 | 0.92 | 0.1852 | 0.5579 | 0.7960 | 1.01 | 0.85 | 0.12 | 0.9632 | 0.3328 | 0.0001 | 0.63 | 0.57 | 0.02 | 0.0148 | 0.0099 | 0.0000 |
| 269.1124 | 13.2 | C10H15N5O4 | Gly-Gly-His | Peptide(tri-) | 0.99 | 0.72 | 0.90 | 0.9614 | 0.4197 | 0.5338 | 1.63 | 1.10 | 0.91 | 0.2612 | 0.7935 | 0.7605 | 1.12 | 0.75 | 0.11 | 0.6945 | 0.2458 | 0.0000 | 0.76 | 0.64 | 0.00 | 0.0576 | 0.0285 | NA |
| 377.1065 | 18.1 | C13H19N3O10 | Glu-Asp-Asp | Peptide(tri-) | 0.86 | 0.75 | 0.88 | 0.4300 | 0.0364 | 0.2570 | 1.09 | 0.94 | 0.91 | 0.7318 | 0.7626 | 0.6490 | 1.04 | 0.79 | 0.98 | 0.7761 | 0.1320 | 0.9161 | 1.37 | 0.96 | 1.09 | 0.0519 | 0.7181 | 0.4425 |
| 287.1480 | 15.2 | C12H21N3O5 | Thr-Ala-Pro | Peptide(tri-) | 1.14 | 0.81 | 1.01 | 0.5124 | 0.4276 | 0.9193 | 1.44 | 1.13 | 0.86 | 0.4383 | 0.6846 | 0.5676 | 0.70 | 0.70 | 0.11 | 0.0353 | 0.0485 | 0.0000 | 0.61 | 0.56 | 0.06 | 0.0257 | 0.0046 | 0.0000 |
| 364.1203 | 9.2 | C16H20N4O4S | Trp-Cys-Gly | Peptide(tri-) | 0.81 | 1.46 | 1.11 | 0.5627 | 0.5009 | 0.7527 | 0.71 | 0.98 | 0.85 | 0.2191 | 0.9161 | 0.4368 | 0.76 | 1.12 | 0.91 | 0.1367 | 0.4774 | 0.5869 | 0.65 | 1.13 | 1.04 | 0.0175 | 0.5477 | 0.8272 |
| 333.1536 | 11.4 | C13H23N3O7 | Glu-Ser-Val | Peptide(tri-) | 1.04 | 0.80 | 0.91 | 0.8755 | 0.1487 | 0.6485 | 1.49 | 1.12 | 0.83 | 0.3344 | 0.6813 | 0.5321 | 0.88 | 0.60 | 0.09 | 0.5477 | 0.0062 | 0.0000 | 0.75 | 0.69 | 0.06 | 0.0204 | 0.0031 | 0.0000 |
| 589.4469 | 4.4 | C32H64NO6P | N-(tetradecanoyl)-sphing-4-enine-1-phosphate | Sphingolipids [SP] | 0.82 | 0.84 | 0.94 | 0.2328 | 0.2604 | 0.7181 | 1.16 | 0.94 | 1.27 | 0.3084 | 0.4901 | 0.1914 | 1.18 | 0.91 | 1.13 | 0.0942 | 0.2895 | 0.1771 | 1.09 | 0.93 | 1.02 | 0.6366 | 0.4936 | 0.9074 |

| Trophozoite stage metabolomics experiment (extended treatment) | | | | | | | | | | | | | | | | | | | | | | | | | | | | | | |
|---|---|---|---|---|---|---|---|---|---|---|---|---|---|---|---|---|---|---|---|---|---|---|---|---|---|---|---|---|---|---|
| | | | | | 0 h | | | | | | 3 h | | | | | | 6 h | | | | | | 9 h | | | | | | | |
| | | | | | Fold change (vs DMSO) | | | ttest: | ttest: | ttest: | Fold change (vs DMSO) | | | ttest: | ttest: | ttest: | Fold change (vs DMSO) | | | ttest: | ttest: | ttest: | Fold change (vs DMSO) | | | ttest: | ttest: | ttest: |
| Mass | RT | FORMULA | Putative metabolite | Map | OZ277 | OZ439 | DHA | OZ277 | OZ439 | DHA | OZ277 | OZ439 | DHA | OZ277 | OZ439 | DHA | OZ277 | OZ439 | DHA | OZ277 | OZ439 | DHA | OZ277 | OZ439 | DHA | OZ277 | OZ439 | DHA |
| 193.0410 | 14.6 | C6H11NO4S | γ-thiomethyl glutamate | Miscellaneous | 0.87 | 0.91 | 0.92 | 0.6585 | 0.7389 | 0.7674 | 1.07 | 1.03 | 1.05 | 0.6995 | 0.7808 | 0.8248 | 1.03 | 0.89 | 0.89 | 0.9221 | 0.7486 | 0.7271 | 0.91 | 0.96 | 0.99 | 0.5758 | 0.7452 | 0.9577 |
| 143.1310 | 28.5 | C8H17NO | (-)-Hygroline | Miscellaneous | 1.34 | 1.48 | 1.29 | 0.3582 | 0.1464 | 0.3193 | 0.98 | 0.80 | 0.90 | 0.9698 | 0.6693 | 0.8329 | 1.19 | 1.43 | 1.43 | 0.3491 | 0.0797 | 0.0909 | 1.80 | 2.59 | 2.41 | 0.3228 | 0.1610 | 0.1475 |
| 293.1990 | 28.1 | C17H27NO3 | (+/-)-5-[(tert-Butylamino)-2'-hydroxypropoxy]-1,2,3,4-tetrahydro-1-naphthol | Miscellaneous | 1.23 | 1.08 | 0.92 | 0.4621 | 0.7849 | 0.7483 | 0.77 | 0.92 | 0.86 | 0.1063 | 0.6908 | 0.1976 | 0.84 | 1.22 | 1.10 | 0.1916 | 0.0884 | 0.3108 | 0.89 | 1.04 | 1.15 | 0.7097 | 0.8791 | 0.5923 |
| 428.3657 | 4.1 | C29H48O2 | (24R,24'R)-Fucosterol epoxide | Miscellaneous | 0.75 | 0.81 | 0.86 | 0.4359 | 0.5522 | 0.7089 | 0.89 | 1.02 | 0.86 | 0.6638 | 0.9613 | 0.6346 | 1.06 | 1.27 | 1.32 | 0.8642 | 0.5213 | 0.3911 | 0.91 | 1.08 | 0.85 | 0.7612 | 0.8564 | 0.6651 |
| 198.0639 | 14.1 | C8H10N2O4 | (S)-2-Amino-3-(3-hydroxy-4-oxo-4H-pyridin-1-yl)propanoate | Miscellaneous | 0.99 | 1.05 | 1.06 | 0.9252 | 0.8411 | 0.7635 | 0.90 | 1.08 | 0.88 | 0.5804 | 0.6691 | 0.5480 | 0.96 | 0.91 | 0.91 | 0.6328 | 0.3136 | 0.7912 | 0.78 | 1.02 | 0.85 | 0.0617 | 0.8106 | 0.0218 |
| 186.0641 | 14.2 | C7H10N2O4 | (S)-AMPA | Miscellaneous | 0.97 | 1.04 | 0.94 | 0.8163 | 0.7578 | 0.6832 | 0.84 | 0.94 | 0.92 | 0.1644 | 0.5781 | 0.6357 | 1.02 | 0.94 | 0.83 | 0.8216 | 0.4642 | 0.4660 | 0.87 | 0.92 | 0.92 | 0.1377 | 0.2489 | 0.2840 |
| 891.2838 | 17.4 | C32H55NO26 | 1,3-alpha-D-Mannosyl-(1,2-N-acetyl-alpha-D-glucosaminyl)-1,2-alpha-D-mannosyl-1,2-alpha-D-mannosyl-D-mannose | Miscellaneous | 1.03 | 0.94 | 1.08 | 0.9560 | 0.8949 | 0.8763 | 1.07 | 1.08 | 1.08 | 0.8820 | 0.8448 | 0.8601 | 1.18 | 0.88 | 0.94 | 0.7730 | 0.7927 | 0.8904 | 0.93 | 0.96 | 0.91 | 0.8783 | 0.9352 | 0.8514 |
| 226.1681 | 7.8 | C12H22N2O2 | 1,8-Diazacyclotetradecane-2,9-dione | Miscellaneous | 1.34 | 1.05 | 1.22 | 0.1384 | 0.8070 | 0.3139 | 0.88 | 0.92 | 1.03 | 0.4891 | 0.6692 | 0.8830 | 0.95 | 1.00 | 1.08 | 0.8022 | 0.9811 | 0.6265 | 0.85 | 0.80 | 1.05 | 0.2650 | 0.3829 | 0.7453 |
| 375.2985 | 4.2 | C20H38O5 | 13-14-DihydroPGF-1a | Miscellaneous | 0.09 | 0.41 | 0.21 | 0.2208 | 0.3786 | 0.2641 | 0.30 | 0.32 | 0.61 | 0.5394 | 0.5469 | 0.7278 | 0.44 | 0.39 | 0.28 | 0.4182 | 0.3494 | 0.2875 | 0.11 | 0.32 | 0.15 | 0.1861 | 0.2681 | 0.1959 |
| 196.0405 | 8.3 | C6H12O5S | 1-thio-β-D-glucose | Miscellaneous | 1.20 | 1.17 | 1.24 | 0.7083 | 0.7711 | 0.6577 | 0.73 | 0.78 | 0.80 | 0.5620 | 0.6530 | 0.6845 | 0.61 | 0.60 | 0.52 | 0.3845 | 0.3886 | 0.3022 | 0.31 | 0.34 | 0.28 | 0.1975 | 0.2080 | 0.1825 |
| 365.1321 | 14.8 | C14H23NO10 | 2-(acetylamino)-1-5-anhydro-2-deoxy-3-O-b-D-galactopyranosyl-D-arabino-Hex-1-enitol | Miscellaneous | 1.02 | 1.08 | 0.98 | 0.9554 | 0.8220 | 0.9321 | 1.17 | 0.88 | 1.00 | 0.6599 | 0.6604 | 0.9987 | 1.10 | 0.96 | 1.15 | 0.8121 | 0.9048 | 0.7146 | 1.11 | 1.04 | 1.07 | 0.7988 | 0.9186 | 0.8330 |
| 290.0615 | 14.7 | C9H16O9 | 2(alpha-D-Mannosyl)-D-glycerate | Miscellaneous | 0.87 | 0.96 | 0.80 | 0.6948 | 0.9216 | 0.5176 | 0.83 | 0.97 | 0.93 | 0.6741 | 0.9448 | 0.8774 | 1.12 | 1.11 | 1.46 | 0.7966 | 0.8309 | 0.4769 | 0.89 | 0.81 | 0.90 | 0.8269 | 0.6798 | 0.8358 |
| 381.0936 | 16.5 | C15H17F3N4O2 | 2,4-diamino-6-methyl-5,3'-(2-trifluoromethylphenoxy)prop-1'-yloxypyrimidine | Miscellaneous | 1.01 | 1.15 | 1.07 | 0.9622 | 0.4409 | 0.6940 | 1.05 | 1.04 | 1.14 | 0.6175 | 0.7572 | 0.5250 | 1.04 | 0.97 | 1.00 | 0.7630 | 0.8383 | 0.9838 | 0.93 | 0.93 | 0.90 | 0.3486 | 0.3553 | 0.3286 |
| 291.0954 | 11.8 | C11H17NO8 | 2,7-Anhydro-alpha-N-acetylneuraminic acid | Miscellaneous | 1.27 | 0.38 | 0.81 | 0.2630 | 0.0276 | 0.7244 | 3.17 | 2.04 | 3.34 | 0.0609 | 0.4389 | 0.0171 | 0.68 | 0.42 | 0.82 | 0.2689 | 0.0002 | 0.6559 | 0.55 | 1.36 | 1.65 | 0.3918 | 0.5240 | 0.2589 |
| 261.0613 | 14.7 | C6H16NO8P | 2-amino-2-deoxyglucitol-6-phosphate | Miscellaneous | 1.31 | 1.08 | 1.00 | 0.7705 | 0.9239 | 0.9983 | 0.93 | 1.00 | 0.72 | 0.9379 | 0.9967 | 0.7317 | 0.79 | 0.75 | 0.94 | 0.7734 | 0.7250 | 0.9448 | 0.82 | 0.87 | 0.94 | 0.7630 | 0.8387 | 0.9390 |
| 191.0795 | 12.0 | C7H13NO5 | 2-amino-3,7-dideoxy-D-threo-hept-6-ulosonate | Miscellaneous | 1.23 | 1.00 | 0.99 | 0.4137 | 0.9921 | 0.9727 | 0.90 | 1.18 | 1.19 | 0.6545 | 0.4996 | 0.4324 | 1.09 | 1.21 | 1.11 | 0.6670 | 0.3530 | 0.5429 | 0.91 | 0.91 | 0.90 | 0.6955 | 0.7664 | 0.7036 |
| 205.9981 | 17.6 | C7H7ClO5 | 2-chloro-3-methyl-maleylacetate | Miscellaneous | 0.73 | 1.36 | 1.28 | 0.5191 | 0.5132 | 0.5505 | 0.66 | 0.97 | 0.73 | 0.5265 | 0.9239 | 0.6334 | 1.01 | 1.10 | 0.70 | 0.9825 | 0.8220 | 0.5717 | 0.94 | 0.86 | 0.57 | 0.9404 | NA | 0.2625 |
| 278.1517 | 28.2 | C16H22O4 | 2-Ethylhexyl phthalate | Miscellaneous | 0.99 | 0.95 | 1.01 | 0.9760 | 0.8542 | 0.9623 | 1.00 | 1.12 | 1.08 | 0.9966 | 0.6463 | 0.7473 | 1.00 | 1.16 | 1.17 | 0.9991 | 0.4129 | 0.3048 | 0.97 | 1.12 | 1.09 | 0.7067 | 0.6089 | 0.4799 |
| 242.1518 | 7.9 | C13H22O4 | 2-isocapryloyl-3R-hydroxymethyl-γ-butyrolactone | Miscellaneous | 1.38 | 1.16 | 1.55 | 0.1349 | 0.5189 | 0.0595 | 1.01 | 0.95 | 0.89 | 0.9703 | 0.8058 | 0.6883 | 1.20 | 1.18 | 1.22 | 0.5708 | 0.4454 | 0.4065 | 0.69 | 0.80 | 0.91 | 0.0488 | 0.2531 | 0.2652 |
| 245.1628 | 8.2 | C12H23NO4 | 2-Methylbutyroylcarnitine | Miscellaneous | 0.97 | 0.91 | 0.95 | 0.9556 | 0.8624 | 0.9240 | 0.99 | 1.08 | 1.03 | 0.9778 | 0.8763 | 0.9389 | 0.99 | 1.03 | 1.13 | 0.9855 | 0.9395 | 0.7649 | 1.01 | 0.94 | 1.01 | 0.9903 | 0.8805 | 0.9876 |
| 372.1270 | 12.4 | C12H22O10 | 2-O-alpha-L-Rhamnopyranosyl-D-glucopyranose | Miscellaneous | 1.29 | 0.87 | 1.11 | 0.7519 | 0.8603 | 0.9235 | 0.91 | 0.67 | 1.25 | 0.9064 | NA | 0.7842 | 1.59 | 1.73 | 1.34 | 0.6257 | 0.6439 | 0.6266 | 1.16 | 1.03 | 1.24 | 0.8556 | 0.9664 | 0.7396 |
| 311.2096 | 27.9 | C17H29NO4 | 2-trans,4-cis-Decadienoylcarnitine | Miscellaneous | 0.74 | 0.92 | 0.92 | 0.0883 | 0.4773 | 0.4694 | 1.09 | 1.15 | 1.31 | 0.6129 | 0.2822 | 0.0927 | 1.13 | 1.16 | 1.12 | 0.1241 | 0.0767 | 0.0388 | 0.97 | 1.03 | 1.09 | 0.6913 | 0.8106 | 0.0945 |
| 332.0531 | 14.5 | C16H12O8 | 3,3',4',5,7-Pentahydroxy-8-methoxyflavone | Miscellaneous | 0.98 | 1.03 | 1.28 | 0.9563 | 0.9255 | 0.5018 | 0.70 | 0.76 | 0.60 | 0.1445 | 0.0727 | 0.0205 | 0.75 | 0.58 | 0.60 | 0.3155 | 0.1450 | 0.1709 | 0.79 | 0.95 | 0.76 | 0.4619 | 0.8761 | 0.4398 |
| 114.0793 | 27.9 | C5H10N2O | 3-Amino-2-piperidone | Miscellaneous | 0.96 | 1.23 | 0.98 | 0.8308 | 0.3331 | 0.9170 | 1.09 | 1.20 | 1.17 | 0.6863 | 0.3793 | 0.4439 | 0.87 | 0.83 | 0.73 | 0.0678 | 0.1166 | 0.0250 | 1.04 | 1.09 | 1.06 | 0.7637 | 0.4944 | 0.6901 |
| 204.0787 | 28.2 | C12H12O3 | 3-Butylidene-7-hydroxyphthalide | Miscellaneous | 0.97 | 0.73 | 0.69 | 0.9120 | 0.2165 | 0.2284 | 0.95 | 0.97 | 1.01 | 0.6935 | 0.8122 | 0.9278 | 1.34 | 1.52 | 1.42 | 0.3240 | 0.1487 | 0.1541 | 1.21 | 1.41 | 1.10 | 0.3955 | 0.2868 | 0.6254 |
| 166.0842 | 12.2 | C6H14O5 | 3-deoxy-D-galactose | Miscellaneous | 1.12 | 1.20 | 1.20 | 0.8799 | 0.8074 | 0.7760 | 0.82 | 1.06 | 1.05 | 0.7514 | 0.9068 | 0.9425 | 1.18 | 1.13 | 1.25 | 0.8293 | 0.8420 | 0.7742 | 0.92 | 1.43 | 1.23 | 0.9156 | 0.6925 | 0.7917 |

| | | | | | | | | | | | | | | | | | | | | | | | | | | | | | |
|---|---|---|---|---|---|---|---|---|---|---|---|---|---|---|---|---|---|---|---|---|---|---|---|---|---|---|---|---|---|
| 134.0943 | 27.9 | C5H12O | 3-Methylbutanol | Miscellaneous | 0.90 | 1.21 | 0.89 | 0.4257 | 0.1668 | 0.4945 | 1.22 | 1.28 | 1.28 | 0.3211 | 0.2454 | 0.2064 | 0.99 | 0.88 | 0.86 | 0.9530 | 0.1530 | 0.1399 | 0.97 | 0.98 | 1.01 | 0.8668 | 0.9058 | 0.9675 |
| 145.0527 | 11.6 | C9H7NO | 3-Methyleneoxindole | Miscellaneous | 0.98 | 1.03 | 0.97 | 0.7882 | 0.7665 | 0.8852 | 0.85 | 0.96 | 0.93 | 0.1954 | 0.8314 | 0.4598 | 0.79 | 0.76 | 0.92 | 0.1145 | 0.0454 | 0.3626 | 0.73 | 0.75 | 0.86 | 0.0526 | 0.0794 | 0.4380 |
| 135.0433 | 28.1 | C6H5N3O | 3-N4-ethenocytosine | Miscellaneous | 0.87 | 1.21 | 0.87 | 0.7595 | 0.7142 | 0.6955 | 1.13 | 1.00 | 0.94 | 0.8018 | 0.9979 | 0.8866 | 1.16 | 1.06 | 0.68 | 0.6536 | 0.8551 | 0.3042 | 1.22 | 1.19 | 1.10 | 0.4097 | 0.6385 | 0.7025 |
| 225.1730 | 7.8 | C13H20O2 | 4-Heptyloxyphenol | Miscellaneous | 0.92 | 0.89 | 1.00 | 0.8411 | 0.7216 | 0.9979 | 0.68 | 0.41 | 0.32 | 0.5432 | 0.2962 | 0.2433 | 1.70 | 0.93 | 1.49 | 0.2291 | 0.8596 | 0.3038 | 1.36 | 1.08 | 1.55 | 0.4531 | 0.8636 | 0.0395 |
| 212.0433 | 7.3 | C7H6N2O3 | 4-Hydroxy-3-nitrosobenzamide | Miscellaneous | 1.15 | 1.05 | 1.07 | 0.4299 | 0.7558 | 0.6596 | 0.94 | 1.02 | 1.05 | 0.7493 | 0.9265 | 0.7578 | 0.99 | 1.02 | 1.06 | 0.9721 | 0.9143 | 0.6843 | 0.86 | 0.82 | 0.96 | 0.3165 | 0.2505 | 0.7306 |
| 142.0630 | 28.2 | C7H10O3 | 4-Oxocyclohexanecarboxylate | Miscellaneous | 1.11 | 1.06 | 0.98 | 0.4478 | 0.6330 | 0.8854 | 0.90 | 0.69 | 1.02 | 0.6658 | 0.2277 | 0.9142 | 0.86 | 0.94 | 0.91 | 0.2087 | 0.5542 | 0.4110 | 1.08 | 0.89 | 0.95 | 0.7152 | 0.4159 | 0.4694 |
| 265.0810 | 10.2 | C10H11N5O4 | 5'-Dehydroadenosine | Miscellaneous | 0.78 | 0.43 | 0.91 | 0.7151 | NA | 0.9158 | 0.76 | 0.38 | 0.61 | NA | NA | NA | 0.83 | 1.64 | 1.79 | 0.8171 | 0.3415 | 0.2546 | 0.46 | 0.82 | 0.71 | 0.1898 | 0.5658 | 0.4619 |
| 184.1099 | 7.9 | C10H16O3 | 5-exo-Hydroxy-1,2-campholide | Miscellaneous | 1.43 | 0.86 | 0.68 | 0.2877 | 0.6797 | 0.4211 | 0.90 | 0.78 | 1.11 | 0.7276 | 0.5290 | 0.7386 | 1.08 | 0.93 | 1.22 | 0.8508 | 0.8596 | 0.4073 | 0.67 | 0.58 | 1.00 | 0.2743 | 0.1060 | 0.9900 |
| 300.1109 | 4.7 | C16H16N2O4 | 5-Nitro-2-(3-phenylpropylamino)benzoic acid | Miscellaneous | 0.96 | 0.87 | 1.01 | 0.8953 | 0.6678 | 0.9619 | 0.96 | 1.03 | 1.30 | 0.7333 | 0.7878 | 0.0556 | 1.30 | 1.40 | 1.41 | 0.4428 | 0.1059 | 0.0881 | 1.21 | 1.26 | 1.16 | 0.4780 | 0.3955 | 0.6357 |
| 222.0740 | 14.1 | C8H14O7 | 6-Acetyl-D-glucose | Miscellaneous | 0.97 | 0.98 | 1.02 | 0.8975 | 0.9509 | 0.9635 | 0.89 | 1.01 | 1.06 | 0.5466 | 0.9598 | 0.7976 | 1.02 | 0.82 | 0.94 | 0.9282 | 0.4263 | 0.7391 | 0.82 | 0.86 | 0.86 | 0.3053 | 0.4634 | 0.4851 |
| 270.0963 | 14.7 | C10H14N4O5 | 6-Hydroxyl-1,6-dihydropurine ribonucleoside | Miscellaneous | 0.95 | 0.86 | 1.06 | 0.8893 | 0.6881 | 0.8780 | 0.89 | 1.01 | 0.95 | 0.6820 | 0.9873 | 0.8861 | 0.93 | 0.83 | 1.08 | 0.8280 | 0.5808 | 0.8452 | 0.92 | 0.86 | 0.89 | 0.7719 | 0.6649 | 0.7613 |
| 173.0090 | 15.6 | C7H5NO3 | 6-Imino-5-oxocyclohexa-1,3-dienecarboxylate | Miscellaneous | 0.88 | 1.21 | 0.89 | 0.7536 | 0.6064 | 0.7386 | 1.23 | 1.53 | 1.44 | 0.5225 | 0.5183 | 0.4213 | 0.86 | 1.07 | 1.10 | 0.6377 | 0.7816 | 0.7000 | 0.66 | 1.09 | 1.21 | 0.1445 | 0.7586 | 0.5970 |
| 181.0964 | 10.2 | C7H11N5O | 6-methyltetrahydropterin | Miscellaneous | 0.64 | 0.84 | 0.70 | 0.1697 | 0.5008 | 0.2525 | 1.17 | 1.31 | 1.23 | 0.5454 | 0.4861 | 0.3043 | 0.95 | 0.83 | 0.74 | 0.8436 | 0.4691 | 0.4141 | 1.56 | 1.41 | 1.11 | 0.3449 | 0.3865 | 0.8280 |
| 343.0839 | 12.5 | C12H15N3O4S | Albendazole sulfone | Miscellaneous | 1.03 | 0.86 | 1.02 | 0.8844 | 0.5371 | 0.9236 | 1.00 | 1.13 | 1.16 | 0.9891 | 0.6929 | 0.6087 | 1.13 | 1.01 | 1.06 | 0.6829 | 0.9803 | 0.8464 | 0.96 | 1.04 | 1.04 | 0.8574 | 0.8738 | 0.8981 |
| 206.1670 | 4.4 | C14H22O | alpha-Irone | Miscellaneous | 0.99 | 0.93 | 0.96 | 0.9822 | 0.9149 | 0.9533 | 0.99 | 1.09 | 1.08 | 0.9929 | 0.8743 | 0.8907 | 1.07 | 1.11 | 1.25 | 0.9043 | 0.8502 | 0.7006 | 0.93 | 0.74 | 0.95 | 0.8770 | 0.5148 | 0.9034 |
| 208.1576 | 4.9 | C12H20N2O | Ammodendrine | Miscellaneous | 1.05 | 0.97 | 0.99 | 0.7862 | 0.8592 | 0.9778 | 0.91 | 0.89 | 0.83 | 0.6364 | 0.5478 | 0.3955 | 1.14 | 1.04 | 1.13 | 0.1730 | 0.7508 | 0.1743 | 0.84 | 1.09 | 0.83 | 0.1022 | 0.6799 | 0.1012 |
| 256.1212 | 7.8 | C15H16N2O2 | ancymidol | Miscellaneous | 1.20 | 0.99 | 1.23 | 0.5117 | 0.9728 | 0.5332 | 1.10 | 0.92 | 1.00 | 0.5940 | 0.6530 | 0.9995 | 0.95 | 0.94 | 1.32 | 0.8527 | 0.6861 | 0.3847 | 1.22 | 1.20 | 1.14 | 0.3506 | 0.5983 | 0.5019 |
| 349.0985 | 14.4 | C20H15N3O | Angustine | Miscellaneous | 0.88 | 1.14 | 0.76 | 0.5943 | 0.5682 | 0.3390 | 1.01 | 1.10 | 0.98 | 0.9590 | 0.6777 | 0.9449 | 1.09 | 1.10 | 1.03 | 0.6832 | 0.7173 | 0.8794 | 0.94 | 0.96 | 1.05 | 0.7676 | 0.8876 | 0.7817 |
| 360.1578 | 14.6 | C20H24O6 | Antheridiogen-An | Miscellaneous | 0.53 | 0.58 | 0.84 | NA | NA | 0.9046 | 0.49 | 0.76 | 0.70 | NA | NA | 0.7645 | 0.74 | 0.32 | 0.38 | 0.8034 | NA | NA | 0.83 | 0.45 | 0.67 | 0.8400 | NA | NA |
| 518.1070 | 15.1 | C24H22O13 | Apigenin 7-(6''-malonylglucoside) | Miscellaneous | 0.81 | 1.10 | 1.32 | 0.7380 | 0.6262 | 0.1936 | 1.40 | 1.79 | 1.80 | 0.0845 | 0.1848 | 0.0186 | 2.97 | 2.57 | 3.93 | 0.0765 | 0.0015 | 0.0002 | 5.89 | 5.35 | 7.55 | 0.0637 | 0.0071 | 0.0339 |
| 222.0892 | 7.7 | C12H14O4 | Apiole | Miscellaneous | 0.96 | 0.92 | 0.91 | 0.8889 | 0.7833 | 0.7690 | 1.15 | 1.01 | 1.15 | 0.6713 | 0.9648 | 0.4052 | 0.95 | 1.00 | 1.21 | 0.7788 | 0.9799 | 0.3078 | 1.06 | 0.97 | 1.33 | 0.5238 | 0.8710 | 0.3000 |
| 223.0844 | 28.5 | C11H13NO4 | Bendiocarb | Miscellaneous | 1.11 | 1.43 | 1.30 | 0.7248 | 0.2439 | 0.4258 | 1.05 | 1.01 | 1.16 | 0.7804 | 0.9474 | 0.4409 | 0.99 | 1.29 | 1.11 | 0.9526 | 0.3247 | 0.6454 | 1.14 | 1.12 | 1.00 | 0.4029 | 0.4974 | 0.9847 |
| 202.0268 | 15.0 | C11H6O4 | Bergaptol | Miscellaneous | 0.87 | 0.86 | 1.05 | 0.4535 | 0.4453 | 0.7081 | 0.87 | 0.91 | 0.80 | 0.3129 | 0.1820 | 0.2150 | 0.66 | 0.67 | 0.62 | 0.1289 | 0.1406 | 0.1376 | 0.79 | 0.99 | 0.80 | 0.3995 | 0.9646 | 0.4742 |
| 321.0697 | 19.5 | C11H15NO10 | beta-Citryl-L-glutamic acid | Miscellaneous | 1.01 | 1.27 | 1.13 | 0.9673 | 0.5122 | 0.6645 | 0.93 | 1.04 | 0.93 | 0.7811 | 0.8744 | 0.7827 | 0.96 | 0.97 | 0.94 | 0.9152 | 0.9255 | 0.8632 | 1.24 | 1.23 | 0.97 | 0.3566 | 0.4182 | 0.9105 |
| 243.1039 | 10.6 | C10H17N3O2S | Biotin amide | Miscellaneous | 1.31 | 1.14 | 1.19 | 0.3803 | 0.6601 | 0.6793 | 0.84 | 0.83 | 1.06 | 0.6125 | 0.6779 | 0.8876 | 0.88 | 1.13 | 1.17 | 0.7788 | 0.7248 | 0.6755 | 0.91 | 1.05 | 0.92 | 0.7209 | 0.8942 | 0.8412 |
| 223.1209 | 14.5 | C12H17NO3 | Cerulenin | Miscellaneous | 1.05 | 1.04 | 1.15 | 0.7343 | 0.7550 | 0.2991 | 1.12 | 1.04 | 1.18 | 0.2166 | 0.5463 | 0.1415 | 1.13 | 1.17 | 1.03 | 0.1107 | 0.3409 | 0.6715 | 0.90 | 1.00 | 1.01 | 0.0770 | 0.9982 | 0.9318 |
| 614.3961 | 9.2 | C32H58N2O7S | CHAPS | Miscellaneous | 0.99 | 1.08 | 1.08 | 0.9422 | 0.6152 | 0.6185 | 0.96 | 1.07 | 1.21 | 0.5923 | 0.5074 | 0.0191 | 1.12 | 1.19 | 1.00 | 0.3643 | 0.4108 | 0.9729 | 1.08 | 0.99 | 1.07 | 0.3876 | 0.9159 | 0.6327 |
| 183.0168 | 28.4 | C7H5NO5 | chelidamate | Miscellaneous | 1.32 | 1.19 | 1.10 | 0.0865 | 0.3309 | 0.6666 | 1.14 | 1.15 | 1.19 | 0.7602 | 0.6899 | 0.5216 | 1.01 | 0.95 | 1.02 | 0.9832 | 0.8292 | 0.9265 | 0.87 | 0.89 | 0.98 | 0.5411 | 0.5908 | 0.8927 |
| 229.1327 | 4.8 | C12H12N4 | Chrysoidine free base | Miscellaneous | 1.12 | 1.12 | 1.07 | 0.5293 | 0.4800 | 0.6004 | 1.07 | 1.17 | 1.24 | 0.6470 | 0.2927 | 0.0714 | 1.27 | 1.10 | 1.01 | 0.3831 | 0.2090 | 0.8721 | 1.52 | 1.43 | 1.08 | 0.0813 | 0.0814 | 0.7554 |
| 469.1367 | 14.3 | C24H20O9 | Cinchonain 1a | Miscellaneous | 0.91 | 1.02 | 0.92 | 0.6950 | 0.9579 | 0.7321 | 0.81 | 0.90 | 0.90 | 0.6045 | 0.8003 | 0.7912 | 1.02 | 0.93 | 0.88 | 0.6934 | 0.4233 | 0.6964 | 0.96 | 0.95 | 0.76 | 0.8591 | 0.8033 | 0.2597 |
| 305.0859 | 17.9 | C10H15N3O8 | Convicine | Miscellaneous | 1.03 | 1.26 | 1.00 | 0.9399 | 0.5054 | 0.9959 | 1.06 | 1.05 | 1.02 | 0.8818 | 0.9019 | 0.9563 | 0.98 | 0.96 | 0.94 | 0.9520 | 0.9183 | 0.8826 | 1.06 | 1.24 | 1.08 | 0.7967 | 0.4648 | 0.7238 |
| 171.0896 | 7.9 | C8H13NO3 | Crotanecine | Miscellaneous | 1.13 | 0.92 | 1.16 | 0.5834 | 0.7918 | 0.6111 | 0.96 | 1.15 | 1.24 | 0.8597 | 0.6675 | 0.3377 | 1.16 | 1.13 | 1.31 | 0.5475 | 0.5822 | 0.3551 | 1.10 | 0.94 | 1.12 | 0.5812 | 0.7238 | 0.4010 |
| 120.0938 | 4.2 | C9H12 | Cumene | Miscellaneous | 0.74 | 1.14 | 0.63 | 0.7407 | 0.8658 | 0.6614 | 0.99 | 1.58 | 1.72 | 0.9911 | 0.5975 | 0.5365 | 0.42 | 0.41 | 0.43 | 0.1669 | 0.1244 | 0.1554 | 0.54 | 0.95 | 0.64 | 0.3645 | 0.8785 | 0.4330 |
| 541.0614 | 14.1 | C15H21N5O13P2 | Cyclic ADP-ribose | Miscellaneous | 1.10 | 0.84 | 1.11 | 0.5666 | 0.4188 | 0.6454 | 0.87 | 1.17 | 0.99 | 0.3922 | 0.4182 | 0.9692 | 0.80 | 0.84 | 0.92 | 0.1796 | 0.2586 | 0.5437 | 0.88 | 1.16 | 0.91 | 0.4700 | 0.6429 | 0.5684 |
| 97.0640 | 7.7 | C4H7N3 | Deoxycytosine | Miscellaneous | 0.82 | 1.13 | 0.95 | 0.6565 | 0.7616 | 0.9134 | 0.95 | 1.00 | 1.04 | 0.8200 | 0.9870 | 0.7526 | 0.91 | 0.95 | 0.83 | 0.8044 | 0.9237 | 0.6851 | 1.06 | 1.44 | 0.33 | 0.7878 | 0.4763 | 0.0599 |
| 236.0087 | 16.1 | C12H6O4 | Dibenzo[1,4]dioxin-2,3-dione | Miscellaneous | 0.97 | 1.12 | 1.16 | 0.8728 | 0.4869 | 0.4770 | 0.74 | 0.79 | 0.90 | 0.2112 | 0.2777 | 0.5807 | 0.90 | 1.02 | 0.96 | 0.6290 | 0.9277 | 0.8416 | 0.61 | 0.85 | 0.53 | 0.2194 | 0.6112 | 0.1653 |
| 200.0298 | 11.7 | C12H8OS | dibenzothiophene-5-oxide | Miscellaneous | 0.93 | 0.86 | 0.81 | 0.8484 | 0.7042 | 0.6352 | 1.34 | 1.21 | 1.19 | 0.6067 | 0.5620 | 0.5536 | 1.09 | 1.00 | 0.63 | 0.8462 | 0.9993 | 0.4188 | 1.06 | 1.21 | 0.94 | 0.8412 | 0.7339 | 0.8160 |
| 373.0960 | 13.9 | C15H19N3OCl2 | Diclobutrazol | Miscellaneous | 1.09 | 0.90 | 0.88 | 0.5134 | 0.5644 | 0.4650 | 0.90 | 0.84 | 1.02 | 0.3890 | 0.1868 | 0.8565 | 1.00 | 0.93 | 1.11 | 0.9901 | 0.3771 | 0.4379 | 0.70 | 0.80 | 0.98 | 0.0712 | 0.2597 | 0.9047 |
| 227.1885 | 4.5 | C12H23N | Dicyclohexylamine | Miscellaneous | 1.01 | 0.96 | 1.11 | 0.9742 | 0.9364 | 0.8224 | 0.89 | 1.29 | 1.25 | 0.7362 | 0.6669 | 0.6100 | 1.07 | 0.86 | 0.92 | 0.8651 | 0.6708 | 0.8346 | 0.92 | 0.95 | 0.95 | 0.7609 | 0.8544 | 0.8346 |
| 712.3664 | 15.0 | C36H56O14 | Digitalin | Miscellaneous | 0.96 | 1.09 | 1.06 | 0.7930 | 0.7126 | 0.7086 | 0.75 | 0.88 | 0.84 | 0.0030 | 0.4967 | 0.1489 | 0.45 | 0.57 | 0.56 | 0.0065 | 0.0078 | 0.0589 | 0.66 | 0.74 | 0.52 | 0.2083 | 0.3020 | 0.1046 |
| 96.9690 | 15.0 | [H2PO4]- | Dihydrogenphosphate | Miscellaneous | 1.12 | 1.08 | 0.95 | 0.5872 | 0.8175 | 0.8507 | 1.53 | 1.58 | 2.06 | 0.0473 | 0.0629 | 0.0113 | 2.44 | 2.32 | 2.63 | 0.0096 | 0.0130 | 0.0286 | 3.38 | 2.81 | 2.98 | 0.0090 | 0.0019 | 0.0160 |
| 141.9855 | 16.0 | C2H7O3PS | dimethylthiophosphate | Miscellaneous | 1.61 | 1.48 | 1.49 | 0.1278 | 0.1817 | 0.1742 | 1.30 | 0.88 | 1.03 | 0.2594 | 0.7740 | 0.9132 | 0.82 | 1.14 | 1.14 | 0.4788 | 0.4693 | 0.4777 | 0.97 | 0.69 | 0.67 | 0.7951 | 0.0775 | 0.0530 |
| 240.0747 | 28.5 | C10H12N2O5 | Dinoseb | Miscellaneous | 1.30 | 1.16 | 1.18 | 0.1580 | 0.3904 | 0.3289 | 1.16 | 1.02 | 1.06 | 0.4653 | 0.9141 | 0.7459 | 0.91 | 1.01 | 0.97 | 0.5507 | 0.9675 | 0.8650 | 1.07 | 0.97 | 1.08 | 0.5398 | 0.8635 | 0.4672 |
| 242.0193 | 16.8 | C6H11O8P | D-myo-Inositol 1,2-cyclic phosphate | Miscellaneous | 1.07 | 1.03 | 1.07 | 0.4454 | 0.7336 | 0.3941 | 1.01 | 1.02 | 1.12 | 0.9209 | 0.7994 | 0.1209 | 1.11 | 1.01 | 1.25 | 0.3350 | 0.8953 | 0.1859 | 1.30 | 1.11 | 1.58 | 0.3218 | 0.5869 | 0.0931 |
| 473.3507 | 4.5 | C29H47NO4 | Docosa-4-7-10-13-16-pentaenoylcarnitine | Miscellaneous | 0.96 | 0.93 | 1.17 | 0.9643 | NA | NA | 0.75 | 2.00 | 1.22 | NA | NA | NA | 1.01 | 1.34 | 1.63 | NA | NA | NA | 1.79 | 2.18 | 2.97 | NA | NA | NA |
| 211.1573 | 4.8 | C12H21NO2 | Elaeokanine C | Miscellaneous | 0.76 | 0.77 | 0.80 | 0.4929 | 0.5484 | 0.5720 | 1.03 | 1.31 | 1.25 | 0.9505 | 0.4440 | 0.6676 | 1.13 | 0.93 | 0.63 | 0.8643 | 0.8881 | 0.4834 | 1.21 | 1.00 | 1.06 | 0.5051 | 0.9977 | 0.8821 |
| 244.0535 | 13.9 | C11H13N2Cl | Epibatidine | Miscellaneous | 1.10 | 1.08 | 1.03 | 0.5335 | 0.6114 | 0.8796 | 0.97 | 0.98 | 1.10 | 0.6656 | 0.8350 | 0.2836 | 1.22 | 1.13 | 1.20 | 0.1683 | 0.2841 | 0.1203 | 1.00 | 1.00 | 1.11 | 0.9688 | 0.9685 | 0.2420 |
| 275.1481 | 15.2 | C11H21N3O5 | Epsilon-(gamma-Glutamyl)-lysine | Miscellaneous | 1.37 | 1.30 | 1.45 | 0.4001 | 0.2818 | 0.0172 | 0.63 | 0.92 | 0.61 | 0.1858 | 0.7935 | 0.1676 | 0.43 | 0.55 | 0.28 | 0.2009 | 0.2944 | 0.1371 | 0.34 | 0.44 | 0.09 | 0.1549 | 0.1893 | NA |

| | | | | | | | | | | | | | | | | | | | | | | | | | | | |
|---|---|---|---|---|---|---|---|---|---|---|---|---|---|---|---|---|---|---|---|---|---|---|---|---|---|---|---|
| 291.0507 | 15.0 | C15H11NO4 | Evoxanthidine | Miscellaneous | 1.43 | 1.36 | 1.17 | 0.5487 | 0.6417 | 0.7907 | 1.52 | 1.12 | 1.17 | 0.5645 | 0.8864 | 0.8223 | 1.44 | 1.38 | 1.32 | 0.6608 | 0.6018 | 0.7065 | 1.31 | 0.96 | 1.18 | 0.7028 | 0.9579 | 0.8120 |
| 292.0769 | 16.5 | C13H19NO2S | Fenothiocarb | Miscellaneous | 1.15 | 1.05 | 1.03 | 0.3942 | 0.7881 | 0.8429 | 0.94 | 1.11 | 1.24 | 0.6804 | 0.4053 | 0.3407 | 1.10 | 1.01 | 1.03 | 0.2196 | 0.8419 | 0.6354 | 1.04 | 0.91 | 0.99 | 0.8344 | 0.5429 | 0.9484 |
| 388.1247 | 16.3 | C12H25N2O10P | Fructoselysine 6-phosphate | Miscellaneous | 1.07 | 1.12 | 1.11 | 0.6684 | 0.2492 | 0.3929 | 0.99 | 0.98 | 1.05 | 0.9645 | 0.9234 | 0.7839 | 0.85 | 0.79 | 0.78 | 0.4621 | 0.3965 | 0.3294 | 0.71 | 0.73 | 0.66 | 0.2172 | 0.2320 | 0.1562 |
| 321.0995 | 12.8 | C11H19N3O6S | gamma-L-Glutamyl-L-cysteinyl-beta-alanine | Miscellaneous | 0.95 | 1.06 | 0.85 | 0.9025 | 0.8835 | 0.6729 | 1.11 | 1.15 | 1.09 | 0.7527 | 0.7153 | 0.8273 | 1.05 | 0.95 | 0.95 | 0.8592 | 0.8588 | 0.8649 | 1.00 | 0.99 | 0.90 | 0.9924 | 0.9702 | 0.7396 |
| 573.0874 | 12.5 | C16H25N5O14P2 | GDP-3,6-dideoxy-D-galactose | Miscellaneous | 1.40 | 1.02 | 1.88 | 0.3509 | 0.9659 | 0.4792 | 0.86 | 1.84 | 1.13 | 0.5446 | 0.0292 | 0.5056 | 1.66 | 1.28 | 1.20 | 0.1000 | 0.5694 | 0.4514 | 0.69 | 0.81 | 0.63 | 0.3121 | 0.5759 | 0.2513 |
| 246.0504 | 12.5 | C6H15O8P | Glycerophosphoglycerol | Miscellaneous | 1.06 | 1.06 | 1.14 | 0.4559 | 0.5662 | 0.3969 | 0.94 | 1.09 | 0.91 | 0.6949 | 0.6262 | 0.5864 | 1.03 | 1.05 | 0.93 | 0.8229 | 0.7310 | 0.5992 | 0.81 | 0.88 | 0.63 | 0.2879 | 0.3817 | 0.0604 |
| 615.1691 | 13.2 | C34H32N4O4Fe | Heme | Miscellaneous | 1.05 | 1.01 | 1.14 | 0.8595 | 0.9839 | 0.6819 | 0.81 | 0.93 | 0.97 | 0.2597 | 0.6372 | 0.8564 | 1.09 | 1.13 | 1.07 | 0.3816 | 0.1976 | 0.4988 | 0.94 | 1.03 | 0.96 | 0.5603 | 0.7693 | 0.6729 |
| 413.3506 | 4.6 | C24H47NO4 | Heptadecanoylcarnitine | Miscellaneous | 1.33 | 1.12 | 1.01 | 0.1905 | 0.6966 | 0.9510 | 1.21 | 1.16 | 1.25 | 0.6264 | 0.7592 | 0.6075 | 0.98 | 1.08 | 1.02 | 0.9591 | 0.8962 | 0.9599 | 0.82 | 0.77 | 0.94 | 0.6935 | 0.6345 | 0.9093 |
| 261.1212 | 12.1 | C11H19NO6 | Heterodendrin | Miscellaneous | 1.07 | 1.08 | 1.17 | 0.7670 | 0.7058 | 0.3941 | 0.95 | 1.03 | 0.84 | 0.7842 | 0.8353 | 0.4115 | 1.19 | 1.28 | 1.12 | 0.6760 | 0.5488 | 0.7961 | 0.93 | 0.79 | 0.96 | 0.7732 | 0.3749 | 0.8909 |
| 157.1102 | 10.1 | C8H15NO2 | Homostachydrine | Miscellaneous | 0.83 | 1.10 | 1.10 | 0.8080 | 0.8874 | 0.9041 | 1.38 | 1.02 | 1.39 | 0.7005 | 0.9778 | 0.7296 | 0.81 | 0.83 | 0.81 | 0.7039 | 0.7640 | 0.7328 | 0.86 | 1.03 | 1.00 | 0.8379 | 0.9702 | 0.9955 |
| 550.3021 | 17.6 | C28H38N8O4 | Hordatine A | Miscellaneous | 1.06 | 1.06 | 1.03 | 0.6676 | 0.6728 | 0.8507 | 0.92 | 1.05 | 1.14 | 0.5427 | 0.5628 | 0.0917 | 1.12 | 0.94 | 1.05 | 0.2656 | 0.4930 | 0.5571 | 1.03 | 1.02 | 0.94 | 0.7644 | 0.8822 | 0.6597 |
| 247.1420 | 11.4 | C11H21NO5 | Hydroxybutyrylcarnitine | Miscellaneous | 1.18 | 1.18 | 1.00 | 0.6765 | 0.6995 | 0.9965 | 1.04 | 1.12 | 0.96 | 0.9380 | 0.7322 | 0.9243 | 1.01 | 0.95 | 1.03 | 0.9713 | 0.8831 | 0.9443 | 0.91 | 0.76 | 0.85 | 0.7844 | 0.5285 | 0.6801 |
| 275.1731 | 9.2 | C13H25NO5 | Hydroxyhexanoylcarnitine | Miscellaneous | 0.79 | 0.85 | 0.92 | 0.7452 | 0.8193 | 0.9070 | 1.32 | 1.24 | 1.00 | 0.6918 | 0.7551 | 0.9983 | 1.01 | 0.98 | 1.21 | 0.9912 | 0.9670 | 0.7589 | 1.36 | 1.18 | 1.34 | 0.6223 | 0.8248 | 0.7226 |
| 233.1263 | 28.3 | C10H19NO5 | Hydroxypropionylcarnitine | Miscellaneous | 1.06 | 0.97 | 0.88 | 0.4794 | 0.7556 | 0.3020 | 1.10 | 1.00 | 1.24 | 0.6250 | 0.9900 | 0.2152 | 0.87 | 1.02 | 0.95 | 0.1750 | 0.8799 | 0.6462 | 0.80 | 0.85 | 0.93 | 0.1353 | 0.0065 | 0.4167 |
| 246.1368 | 8.8 | C14H18N2O2 | Hypaphorine | Miscellaneous | 1.01 | 1.01 | 1.03 | 0.9593 | 0.9824 | 0.9172 | 0.93 | 1.05 | 1.05 | 0.7184 | 0.8507 | 0.8261 | 1.05 | 0.99 | 1.03 | 0.8136 | 0.9500 | 0.8946 | 0.93 | 0.91 | 0.92 | 0.7060 | 0.6702 | 0.7451 |
| 98.0480 | 7.7 | C4H6N2O | Imidazole-4-methanol | Miscellaneous | 1.15 | 1.55 | 1.39 | 0.7024 | 0.2434 | 0.3978 | 0.95 | 0.84 | 1.01 | 0.8158 | 0.5333 | 0.9395 | 1.34 | 1.42 | 1.40 | 0.3832 | 0.4861 | 0.4309 | 1.07 | 1.26 | 1.21 | 0.7657 | 0.6110 | 0.6382 |
| 187.0634 | 8.8 | C11H9NO2 | Indoleacrylicacid | Miscellaneous | 1.21 | 1.12 | 1.06 | 0.5489 | 0.6113 | 0.8074 | 0.93 | 1.00 | 1.10 | 0.7947 | 0.9927 | 0.7557 | 1.14 | 1.12 | 1.20 | 0.6041 | 0.6592 | 0.5824 | 0.95 | 0.86 | 1.04 | 0.8153 | 0.4742 | 0.8902 |
| 221.8945 | 27.1 | C2H3O2I | iodoacetate | Miscellaneous | 1.05 | 1.07 | 1.09 | 0.6758 | 0.5308 | 0.5279 | 0.95 | 0.95 | 1.04 | 0.7686 | 0.7907 | 0.8409 | 0.32 | 1.10 | 0.90 | 0.0066 | 0.4646 | 0.5929 | 0.45 | 1.06 | 1.02 | 0.1286 | 0.6418 | 0.8634 |
| 231.1107 | 4.8 | C10H17NO5 | Isovalerylglutamicacid | Miscellaneous | 1.94 | 1.31 | 1.08 | 0.1016 | 0.3954 | 0.7928 | 0.86 | 1.11 | 1.27 | 0.7953 | 0.8824 | 0.5383 | 2.89 | 2.54 | 2.72 | 0.2131 | 0.0710 | 0.2233 | 1.40 | 1.92 | 1.43 | 0.4242 | 0.1822 | 0.2028 |
| 724.2751 | 16.5 | C26H45NO21 | Lacto-N-tetraose | Miscellaneous | 0.97 | 1.06 | 1.01 | 0.9466 | 0.8906 | 0.9846 | 1.03 | 1.06 | 1.04 | 0.9504 | 0.9067 | 0.9329 | 1.04 | 1.05 | 1.04 | 0.9347 | 0.9206 | 0.9336 | 1.08 | 1.00 | 0.96 | 0.8851 | 0.9944 | 0.9363 |
| 206.0580 | 21.7 | C11H10O4 | Lathodoratin | Miscellaneous | 0.92 | 1.04 | 1.17 | 0.7075 | 0.8562 | 0.2575 | 0.91 | 0.99 | 0.95 | 0.7187 | 0.9625 | 0.8338 | 0.99 | 0.82 | 0.86 | 0.9661 | 0.3513 | 0.5819 | 1.13 | 1.15 | 1.12 | 0.7542 | 0.6852 | 0.7605 |
| 189.1114 | 15.1 | C7H15N3O3 | L-Homocitrulline | Miscellaneous | 0.80 | 0.85 | 0.81 | 0.7028 | 0.7221 | 0.7238 | 0.87 | 1.15 | 0.89 | 0.8378 | 0.8645 | 0.8519 | 0.93 | 0.55 | 1.10 | 0.8943 | 0.3877 | 0.8478 | 1.14 | 0.86 | 1.06 | 0.8402 | 0.8441 | 0.9352 |
| 228.1474 | 11.9 | C11H20N2O3 | L-isoleucyl-L-proline | Miscellaneous | 1.09 | 0.94 | 1.11 | 0.7323 | 0.7969 | 0.7326 | 1.04 | 1.25 | 1.06 | 0.8684 | 0.3811 | 0.6800 | 1.12 | 1.02 | 1.14 | 0.6099 | 0.9194 | 0.5683 | 0.96 | 0.88 | 0.89 | 0.8396 | 0.4219 | 0.5133 |
| 194.0725 | 14.6 | C5H12N2OS | L-methioninamide | Miscellaneous | 0.93 | 0.97 | 0.85 | 0.7695 | 0.9119 | 0.5573 | 1.15 | 1.13 | 1.15 | 0.2098 | 0.1908 | 0.1158 | 1.19 | 1.18 | 1.16 | 0.3855 | 0.2464 | 0.4422 | 0.80 | 0.82 | 0.95 | 0.2748 | 0.3057 | 0.7569 |
| 314.1266 | 7.8 | C17H15NO4 | Longifolonine | Miscellaneous | 1.02 | 0.82 | 1.14 | 0.9669 | 0.6341 | 0.7273 | 1.14 | 1.10 | 1.11 | 0.4691 | 0.7635 | 0.6491 | 0.96 | 0.83 | 1.26 | 0.5080 | 0.3429 | 0.2472 | 1.22 | 1.03 | 1.08 | 0.4064 | 0.8839 | 0.6235 |
| 207.1624 | 28.4 | C13H21NO | Luciduline | Miscellaneous | 0.97 | 1.00 | 0.80 | 0.8773 | 0.9833 | 0.3930 | 0.89 | 1.25 | 1.26 | 0.5721 | 0.3592 | 0.2390 | 0.69 | 0.66 | 0.60 | 0.0841 | 0.0677 | 0.0516 | 1.61 | 1.61 | 2.20 | 0.1820 | 0.1550 | 0.0464 |
| 275.1884 | 28.2 | C17H25NO2 | Lycoflexine | Miscellaneous | 0.93 | 1.02 | 0.99 | 0.7789 | 0.9448 | 0.9637 | 0.86 | 1.09 | 1.01 | 0.5723 | 0.6967 | 0.9743 | 0.95 | 1.22 | 1.05 | 0.8167 | 0.3485 | 0.8250 | 1.22 | 1.26 | 1.22 | 0.1826 | 0.1748 | 0.2773 |
| 431.2308 | 11.2 | C24H30O6 | Magnoshinin | Miscellaneous | 1.15 | 1.21 | 1.29 | 0.6353 | 0.5083 | 0.3922 | 0.88 | 0.92 | 0.82 | 0.6628 | 0.8033 | 0.5034 | 0.84 | 0.75 | 0.66 | 0.5435 | 0.0311 | 0.1980 | 0.77 | 0.75 | 0.70 | 0.5096 | 0.4594 | 0.3663 |
| 358.1112 | 15.0 | C12H22O12 | melibionate | Miscellaneous | 0.98 | 1.10 | 1.10 | 0.8698 | 0.5233 | 0.5053 | 1.01 | 0.98 | 0.91 | 0.9417 | 0.8944 | 0.5313 | 0.86 | 0.91 | 0.89 | 0.4649 | 0.5852 | 0.5833 | 0.89 | 0.92 | 0.92 | 0.4885 | 0.5894 | 0.5813 |
| 231.1622 | 28.5 | C15H21NO | Metazocine | Miscellaneous | 1.17 | 1.30 | 1.55 | 0.5650 | 0.3317 | 0.2915 | 1.09 | 1.08 | 1.08 | 0.7667 | 0.7907 | 0.7687 | 0.91 | 0.99 | 1.14 | 0.6864 | 0.9631 | 0.5807 | 0.97 | 0.98 | 1.16 | 0.9221 | 0.9527 | 0.5960 |
| 159.1260 | 13.3 | C8H17NO2 | Methacholine | Miscellaneous | 1.18 | 1.17 | 1.11 | 0.7120 | 0.7472 | 0.8299 | 1.01 | 0.98 | 1.03 | 0.9875 | 0.9745 | 0.9410 | 1.09 | 1.08 | 1.05 | 0.8511 | 0.8777 | 0.9250 | 1.00 | 0.97 | 0.95 | 0.9983 | 0.9384 | 0.8904 |
| 111.9830 | 8.0 | CH4O4S | Monomethyl sulfate | Miscellaneous | 1.16 | 1.12 | 1.11 | 0.3392 | 0.4803 | 0.5228 | 0.90 | 0.98 | 1.06 | 0.2708 | 0.7428 | 0.2651 | 1.10 | 1.10 | 1.19 | 0.2466 | 0.2491 | 0.1442 | 0.96 | 0.91 | 0.99 | 0.7698 | 0.5823 | 0.9687 |
| 312.1360 | 28.4 | C19H20O4 | Montanin A | Miscellaneous | 1.37 | 1.11 | 0.98 | 0.2793 | 0.6975 | 0.9254 | 0.97 | 1.15 | 1.22 | 0.8945 | 0.4042 | 0.4724 | 1.12 | 1.12 | 1.15 | 0.3865 | 0.4206 | 0.3483 | 0.75 | 0.94 | 0.89 | 0.0492 | 0.6812 | 0.2806 |
| 251.1005 | 14.4 | C9H17NO7 | Muramic acid | Miscellaneous | 1.03 | 1.09 | 1.01 | 0.8231 | 0.5670 | 0.9569 | 0.98 | 1.06 | 1.03 | 0.8457 | 0.6233 | 0.8327 | 1.08 | 1.04 | 1.09 | 0.4268 | 0.6968 | 0.5528 | 0.99 | 0.98 | 0.90 | 0.9454 | 0.8659 | 0.4830 |
| 773.2739 | 3.9 | C34H44O19 | Myricoside | Miscellaneous | 0.95 | 0.87 | 0.81 | 0.9045 | 0.7473 | 0.6547 | 0.99 | 1.27 | 1.13 | 0.9659 | 0.5288 | 0.7137 | 1.39 | 1.20 | 1.29 | 0.3596 | 0.6599 | 0.4816 | 0.68 | 0.82 | 0.78 | 0.0406 | 0.3728 | 0.1024 |
| 390.2884 | 28.3 | C23H35NO3 | Myxalamid D | Miscellaneous | 1.28 | 1.29 | 1.15 | 0.1050 | 0.1314 | 0.2871 | 0.83 | 1.11 | 0.94 | 0.1342 | 0.6912 | 0.5858 | 1.41 | 1.09 | 1.29 | 0.3731 | 0.7188 | 0.3733 | 1.44 | 1.02 | 1.40 | 0.0287 | 0.9343 | 0.0389 |
| 223.1057 | 12.1 | C8H17NO6 | N-acetyl -D-glucosaminitol | Miscellaneous | 0.92 | 1.09 | 1.03 | 0.8677 | 0.8721 | 0.9581 | 1.15 | 1.51 | 1.26 | 0.7776 | 0.4791 | 0.6330 | 1.12 | 1.01 | 1.08 | 0.7705 | 0.9895 | 0.8518 | 1.10 | 0.90 | 1.26 | 0.8156 | 0.8404 | 0.7179 |
| 205.0950 | 10.8 | C8H15NO5 | N-Acetyl-D-fucosamine | Miscellaneous | 1.02 | 0.97 | 1.14 | 0.9881 | 0.9781 | 0.9137 | 1.01 | 1.09 | 1.04 | 0.9929 | 0.9453 | 0.9722 | 5.24 | 5.29 | 5.81 | 0.4077 | 0.4191 | 0.4138 | 0.95 | 0.98 | 1.02 | 0.9627 | 0.9866 | 0.9884 |
| 237.0849 | 12.5 | C8H15NO7 | N-Acetyl-D-glucosaminate | Miscellaneous | 0.98 | 0.90 | 0.64 | 0.9538 | 0.7841 | 0.2920 | 0.97 | 1.81 | 1.27 | 0.9222 | 0.2473 | 0.3656 | 1.45 | 0.76 | 1.33 | 0.1627 | 0.3407 | 0.4613 | 0.51 | 0.59 | 0.52 | 0.2011 | 0.2633 | 0.2030 |
| 383.1430 | 13.7 | C14H25NO11 | N-Acetyllactosamine | Miscellaneous | 0.97 | 1.01 | 1.01 | 0.9125 | 0.9698 | 0.9775 | 1.05 | 1.14 | 1.08 | 0.8852 | 0.7455 | 0.8237 | 0.98 | 0.94 | 1.04 | 0.9564 | 0.8675 | 0.9048 | 0.96 | 0.89 | 0.81 | 0.9167 | 0.7760 | 0.5946 |
| 173.1052 | 11.8 | C8H15NO3 | N-Acetyl-L-leucine | Miscellaneous | 1.12 | 1.03 | 1.15 | 0.9011 | 0.9723 | 0.8882 | 1.01 | 1.10 | 0.97 | 0.9921 | 0.9223 | 0.9680 | 0.90 | 0.96 | 1.04 | 0.9154 | 0.9635 | 0.9640 | 1.04 | 1.14 | 1.03 | 0.9606 | 0.8853 | 0.9705 |
| 351.1169 | 15.0 | C13H21NO10 | N-Acetyl-O-acetylneuraminate | Miscellaneous | 1.16 | 1.20 | 1.16 | 0.3137 | 0.4798 | 0.2166 | 1.74 | 1.25 | 1.76 | 0.0410 | 0.4181 | 0.0518 | 2.31 | 2.21 | 2.28 | 0.0120 | 0.0546 | 0.0179 | 3.44 | 2.85 | 2.90 | 0.0132 | 0.0116 | 0.0196 |
| 253.0950 | 4.6 | C12H15NO5 | N-Acetylvanilalanine | Miscellaneous | 1.64 | 1.21 | 1.21 | 0.4011 | 0.6242 | 0.6494 | 1.45 | 1.24 | 1.03 | 0.2176 | 0.3295 | 0.8965 | 1.12 | 1.15 | 1.29 | 0.7183 | 0.5744 | 0.4219 | 0.94 | 0.72 | 0.92 | 0.8692 | 0.4551 | 0.8259 |
| 229.1678 | 7.8 | C12H23NO3 | N-Decanoylglycine | Miscellaneous | 1.30 | 1.03 | 1.44 | 0.4429 | 0.8615 | 0.0873 | 0.77 | 0.86 | 1.13 | 0.5255 | 0.6521 | 0.6878 | 0.95 | 1.03 | 1.04 | 0.8957 | 0.9295 | 0.8960 | 0.94 | 0.85 | 1.10 | 0.5437 | 0.4137 | 0.3362 |
| 255.1106 | 4.8 | C12H17NO5 | N-D-Glucosylarylamine | Miscellaneous | 1.26 | 0.92 | 0.94 | 0.5290 | 0.6438 | 0.7971 | 0.84 | 0.90 | 1.08 | 0.4920 | 0.5950 | 0.8021 | 1.74 | 1.13 | 1.28 | 0.4780 | 0.6727 | 0.4007 | 0.87 | 0.94 | 1.00 | 0.6723 | 0.8627 | 0.9888 |
| 207.1107 | 13.3 | C8H17NO5 | N-Ethylglycocyamine | Miscellaneous | 1.12 | 1.12 | 1.10 | 0.5108 | 0.5838 | 0.6430 | 0.90 | 0.97 | 0.95 | 0.6229 | 0.8510 | 0.7464 | 1.12 | 1.02 | 1.08 | 0.4571 | 0.9266 | 0.6409 | 1.01 | 0.94 | 0.96 | 0.9731 | 0.7714 | 0.7767 |
| 125.0476 | 12.3 | C6H7NO2 | N-Ethylmaleimide | Miscellaneous | 1.03 | 1.08 | 1.12 | 0.9365 | 0.8998 | 0.8335 | 0.99 | 1.04 | 0.89 | 0.9915 | 0.9485 | 0.8294 | 1.10 | 1.01 | 1.05 | 0.8504 | 0.9924 | 0.9302 | 0.64 | 0.93 | 1.12 | 0.3852 | 0.8887 | 0.8581 |
| 267.0954 | 16.7 | C9H17NO8 | Neuraminic acid | Miscellaneous | 0.89 | 0.85 | 0.77 | 0.6839 | 0.6349 | 0.4290 | 1.03 | 1.12 | 1.18 | 0.9308 | 0.6718 | 0.5302 | 1.08 | 0.84 | 0.95 | 0.8093 | 0.6181 | 0.8968 | 1.07 | 0.98 | 1.03 | 0.8436 | 0.9452 | 0.9284 |
| 143.0331 | 6.2 | C4H5N3O3 | N-methylisocyanurate | Miscellaneous | 1.53 | 0.68 | 1.43 | 0.3459 | 0.3448 | 0.6192 | 1.00 | 0.97 | 0.99 | 0.9940 | 0.9604 | 0.9758 | 0.98 | 0.95 | 1.18 | 0.9734 | 0.9304 | 0.7841 | 0.85 | 0.86 | 0.46 | 0.7056 | 0.7936 | 0.2073 |
| 215.1521 | 7.8 | C11H21NO3 | N-Nonanoylglycine | Miscellaneous | 1.20 | 1.21 | 1.66 | 0.1935 | 0.6308 | 0.2869 | 0.75 | 0.72 | 0.91 | 0.4297 | 0.3292 | 0.8017 | 0.69 | 0.93 | 1.12 | 0.2203 | 0.7194 | 0.7073 | 0.97 | 0.79 | 0.96 | 0.8561 | 0.3990 | 0.8687 |
| 350.0616 | 16.6 | C9H19O12P | nonulose 9-phosphate | Miscellaneous | 0.99 | 1.10 | 0.94 | 0.9643 | 0.4616 | 0.6903 | 0.91 | 1.07 | 1.04 | 0.5091 | 0.5705 | 0.8217 | 1.01 | 1.04 | 1.09 | 0.9686 | 0.8747 | 0.7143 | 1.10 | 1.10 | 1.06 | 0.6027 | 0.6041 | 0.7833 |
| 243.1835 | 4.7 | C13H25NO3 | N-Undecanoylglycine | Miscellaneous | 0.86 | 0.85 | 1.19 | 0.6571 | 0.6658 | 0.7316 | 0.88 | 1.24 | 1.22 | 0.7314 | 0.6449 | 0.6852 | 1.26 | 0.87 | 0.99 | 0.6377 | 0.6822 | 0.9896 | 0.96 | 1.16 | 0.90 | 0.8514 | 0.6892 | 0.6725 |
| 320.0508 | 16.2 | C8H17O11P | octulose 8-phosphate | Miscellaneous | 2.04 | 1.22 | 2.08 | 0.0661 | 0.5380 | 0.0416 | 0.84 | 0.98 | 0.89 | 0.6579 | 0.9470 | 0.7426 | 1.04 | 1.01 | 1.00 | 0.9327 | 0.9708 | 0.9919 | 1.00 | 1.02 | 0.94 | 0.9940 | 0.9534 | 0.8600 |
| 129.1518 | 6.4 | C8H19N | Octylamine | Miscellaneous | 1.11 | 1.11 | 1.08 | 0.4288 | 0.4660 | 0.5578 | 1.02 | 0.99 | 0.98 | 0.8956 | 0.9310 | 0.8598 | 0.99 | 1.06 | 1.03 | 0.9360 | 0.7277 | 0.8473 | 0.88 | 0.96 | 0.96 | 0.2847 | 0.7611 | 0.6901 |
| 613.3754 | 7.8 | C33H55NO7 | O-glucosyl-tomatidine | Miscellaneous | 1.43 | 0.87 | 0.78 | 0.3827 | 0.7296 | 0.5362 | 0.81 | 0.66 | 0.82 | 0.6298 | 0.4451 | 0.6971 | 1.18 | 1.07 | 1.35 | 0.6243 | 0.8511 | 0.3606 | 1.04 | 0.70 | 0.82 | 0.8980 | 0.3206 | 0.2541 |

| | | | | | | | | | | | | | | | | | | | | | | | | | | | | |
|---|---|---|---|---|---|---|---|---|---|---|---|---|---|---|---|---|---|---|---|---|---|---|---|---|---|---|---|---|
| 289.1274 | 13.3 | C11H19N3O6 | Ophthalmicacid | Miscellaneous | 1.01 | 0.98 | 0.92 | 0.9635 | 0.9421 | 0.7780 | 0.95 | 1.02 | 0.91 | 0.8953 | 0.9694 | 0.8553 | 1.14 | 1.01 | 0.82 | 0.6320 | 0.9654 | 0.5568 | 0.96 | 0.87 | 0.82 | 0.8304 | 0.5721 | 0.5634 |
| 185.1053 | 11.2 | C9H15NO3 | Otonecine | Miscellaneous | 1.02 | 1.03 | 1.20 | 0.9525 | 0.9103 | 0.5695 | 0.98 | 1.15 | 1.25 | 0.9333 | 0.6489 | 0.4179 | 1.01 | 1.01 | 1.07 | 0.9575 | 0.9578 | 0.7168 | 0.92 | 0.89 | 0.91 | 0.6572 | 0.6043 | 0.6699 |
| 261.0782 | 13.4 | C8H13N3O2S | Ovothiol B | Miscellaneous | 1.00 | 0.97 | 1.71 | 0.9931 | 0.8778 | 0.5247 | 1.21 | 2.66 | 1.04 | 0.5960 | 0.3330 | 0.8767 | 0.57 | 0.26 | 0.78 | 0.6253 | 0.4016 | 0.8206 | 0.85 | 2.17 | 0.77 | 0.3779 | 0.5056 | 0.2358 |
| 456.1613 | 15.7 | C18H28N6O4S2 | Ovothiol disulfide | Miscellaneous | 0.91 | 0.84 | 0.81 | 0.8631 | 0.7690 | 0.6783 | 0.86 | 0.87 | 0.89 | 0.8268 | 0.8411 | 0.8833 | 1.06 | 0.95 | 0.79 | 0.8985 | 0.9226 | 0.6831 | 0.80 | 0.86 | 0.84 | 0.6557 | 0.7742 | 0.7530 |
| 114.0066 | 19.2 | C3H2N2O3 | parabanate | Miscellaneous | 0.64 | 0.49 | 0.93 | 0.4271 | 0.2922 | 0.8767 | 0.83 | 0.60 | 0.78 | 0.7680 | 0.5280 | 0.7679 | 0.73 | 1.20 | 0.61 | 0.6567 | 0.7978 | 0.5027 | 0.97 | 1.51 | 0.71 | 0.9689 | 0.6330 | 0.6892 |
| 717.5313 | 5.4 | C39H76NO8P | PC(17:0/14:1) | Miscellaneous | 1.29 | 1.16 | 1.20 | 0.0361 | 0.3510 | 0.0421 | 0.84 | 0.99 | 0.95 | 0.0552 | 0.8717 | 0.5113 | 1.15 | 1.22 | 1.27 | 0.0285 | 0.2791 | 0.0729 | 0.79 | 0.91 | 0.78 | 0.1910 | 0.5302 | 0.1791 |
| 212.0086 | 12.3 | C5H9O7P | P-DPD | Miscellaneous | 1.08 | 1.02 | 1.01 | 0.2561 | 0.6846 | 0.8604 | 0.95 | 0.96 | 0.98 | 0.0929 | 0.5384 | 0.5372 | 1.11 | 1.08 | 1.13 | 0.4037 | 0.5146 | 0.1808 | 0.93 | 0.92 | 0.94 | 0.2005 | 0.1631 | 0.3713 |
| 261.0783 | 13.8 | C9H12N2O4S | penem CGP31608 | Miscellaneous | 1.17 | 0.81 | 1.11 | 0.7692 | 0.6598 | 0.8661 | 0.83 | 0.75 | 0.85 | 0.5973 | 0.2973 | 0.5471 | 0.88 | 1.10 | 0.91 | 0.6885 | 0.7420 | 0.7169 | 0.95 | 0.96 | 1.05 | 0.8488 | 0.8776 | 0.8655 |
| 243.1988 | 5.2 | C17H25N | Phencyclidine | Miscellaneous | 0.54 | 1.05 | 2.02 | 0.6043 | 0.9603 | 0.5148 | 0.81 | 1.13 | 0.52 | 0.7616 | 0.8318 | 0.4642 | 2.55 | 2.73 | 1.09 | 0.2581 | 0.0344 | 0.9100 | 1.18 | 0.56 | 0.64 | 0.6887 | 0.2158 | 0.2870 |
| 294.1831 | 27.9 | C17H26O4 | Phytuberin | Miscellaneous | 0.99 | 0.97 | 0.99 | 0.9581 | 0.8264 | 0.9295 | 1.00 | 1.05 | 1.08 | 0.9892 | 0.6278 | 0.4838 | 1.07 | 1.08 | 1.13 | 0.4515 | 0.3676 | 0.2093 | 0.98 | 0.94 | 1.00 | 0.5659 | 0.3682 | 0.9079 |
| 512.1169 | 14.6 | C20H27NO12 | Proteacin | Miscellaneous | 0.64 | 1.03 | 0.58 | 0.2528 | 0.8832 | 0.2842 | 1.06 | 0.96 | 0.73 | 0.8380 | 0.8738 | 0.4254 | 1.18 | 0.96 | 0.95 | 0.1279 | 0.9088 | 0.8809 | 0.60 | 0.89 | 0.78 | NA | 0.8457 | 0.7055 |
| 308.1582 | 20.8 | C12H24N2O7 | psicoselysine | Miscellaneous | 0.89 | 1.11 | 0.97 | 0.5557 | 0.7131 | 0.8941 | 0.99 | 1.06 | 0.88 | 0.9783 | 0.8415 | 0.6682 | 0.62 | 0.78 | 0.50 | 0.1441 | 0.4579 | 0.0783 | 0.50 | 0.56 | 0.31 | 0.0996 | 0.1382 | 0.0507 |
| 464.2667 | 10.5 | C28H36N2O4 | Psychotrine | Miscellaneous | 1.02 | 0.95 | 1.06 | 0.9277 | 0.7975 | 0.7883 | 1.23 | 0.90 | 1.14 | 0.3077 | 0.5917 | 0.4676 | 1.01 | 1.00 | 0.96 | 0.9299 | 0.9722 | 0.7597 | 1.21 | 1.00 | 1.27 | 0.1275 | 0.9767 | 0.1602 |
| 123.0433 | 7.7 | C5H5N3O | Pyrazinamide | Miscellaneous | 1.14 | 0.49 | 0.76 | 0.8387 | 0.4807 | 0.7410 | 0.44 | 0.54 | 1.13 | 0.2583 | 0.3294 | 0.8477 | 1.17 | 0.89 | 1.48 | 0.3020 | 0.6899 | 0.4281 | 0.61 | 0.90 | 1.28 | 0.0292 | 0.4005 | 0.6126 |
| 298.0544 | 4.1 | C12H15N2O3PS | Quinalphos | Miscellaneous | 1.24 | 1.44 | 2.36 | 0.6042 | 0.4775 | 0.3699 | 0.97 | 1.15 | 1.23 | 0.8631 | 0.4903 | 0.5835 | 2.21 | 1.38 | 1.52 | 0.2925 | 0.3734 | 0.0395 | 1.74 | 0.76 | 1.02 | 0.3969 | 0.1448 | 0.9145 |
| 222.1620 | 27.9 | C14H22O2 | Rishitin | Miscellaneous | 0.98 | 1.10 | 1.06 | 0.9029 | 0.4991 | 0.7543 | 0.93 | 1.00 | 1.03 | 0.7149 | 0.9761 | 0.8543 | 1.05 | 1.02 | 1.09 | 0.7394 | 0.9095 | 0.5672 | 0.98 | 0.92 | 1.01 | 0.7793 | 0.4927 | 0.8618 |
| 353.0894 | 13.3 | C19H15NO6 | Rugosinone | Miscellaneous | 1.33 | 1.17 | 1.19 | 0.4068 | 0.5394 | 0.4684 | 1.42 | 1.23 | 1.30 | 0.1222 | 0.2959 | 0.2473 | 1.07 | 1.08 | 1.20 | 0.8479 | 0.7473 | 0.5089 | 1.18 | 1.03 | 1.10 | 0.4337 | 0.8691 | 0.6608 |
| 321.0631 | 15.0 | C16H14N2O3 | Saphenic acid methyl ester | Miscellaneous | 1.31 | 1.29 | 1.12 | 0.4823 | 0.0369 | 0.4186 | 1.18 | 0.86 | 1.00 | 0.5443 | 0.5299 | 0.9964 | 1.19 | 1.01 | 1.27 | 0.6292 | 0.9662 | 0.4229 | 1.29 | 1.17 | 1.36 | 0.2333 | 0.4229 | 0.0613 |
| 334.0664 | 15.9 | C9H19O11P | sn-glycero-3-Phospho-1-inositol | Miscellaneous | 1.12 | 1.01 | 1.19 | 0.6172 | 0.9490 | 0.6191 | 0.97 | 1.16 | 0.96 | 0.5414 | 0.3308 | 0.7441 | 0.76 | 0.73 | 0.64 | 0.1502 | 0.0889 | 0.0451 | 0.86 | 0.78 | 0.64 | 0.4872 | 0.2732 | 0.1261 |
| 266.1551 | 3.8 | C12H26O4S | sodium dodecyl sulfate | Miscellaneous | 1.78 | 1.44 | 1.62 | 0.0559 | 0.3175 | 0.0915 | 1.40 | 2.00 | 1.15 | 0.4966 | 0.4582 | 0.5611 | 1.45 | 2.93 | 1.17 | 0.3208 | 0.4130 | 0.4477 | 1.22 | 1.15 | 2.29 | 0.2640 | 0.4987 | 0.4216 |
| 319.0839 | 12.7 | C13H12ClN5 | tetcyclacis | Miscellaneous | 0.88 | 0.77 | 1.20 | 0.6395 | 0.3389 | 0.6631 | 0.46 | 0.54 | 0.53 | 0.0834 | 0.0995 | 0.1000 | 1.24 | 1.69 | 1.28 | 0.3279 | 0.0417 | 0.2311 | 0.84 | 0.92 | 0.96 | 0.3612 | 0.6500 | 0.8067 |
| 886.5591 | 3.8 | C55H74N4O6 | tetrahydrogeranylgeranyl-bacteriopheophytin | Miscellaneous | 0.94 | 1.16 | 1.28 | 0.7657 | 0.3348 | 0.3699 | 1.28 | 1.02 | 1.44 | 0.4679 | 0.9460 | 0.2187 | 0.84 | 0.90 | 0.82 | 0.6023 | 0.7421 | 0.5359 | 1.30 | 1.10 | 1.41 | 0.1263 | 0.7022 | 0.0934 |
| 136.0749 | 7.7 | C6H8N4 | Tetrahydropteridine | Miscellaneous | 1.04 | 1.34 | 0.93 | 0.8975 | 0.4035 | 0.7574 | 1.05 | 0.96 | 0.85 | 0.8640 | 0.8858 | 0.5648 | 0.76 | 0.92 | 0.86 | 0.3755 | 0.8305 | 0.5721 | 0.82 | 1.04 | 0.96 | 0.4628 | 0.8926 | 0.8785 |
| 178.0300 | 7.8 | C5H8O2S | THTC | Miscellaneous | 1.10 | 1.25 | 1.39 | NA | 0.8600 | 0.7386 | 0.97 | 1.31 | 1.17 | 0.9707 | 0.7496 | 0.8955 | 1.12 | 1.06 | 1.48 | 0.8094 | 0.9028 | 0.4267 | 1.07 | 1.28 | 1.43 | 0.8985 | 0.7012 | 0.4532 |
| 397.3192 | 4.7 | C23H43NO4 | trans-Hexadec-2-enoylcarnitine | Miscellaneous | 0.99 | 1.21 | 1.41 | 0.9869 | 0.7082 | 0.5922 | 0.80 | 1.12 | 0.98 | 0.7162 | 0.8369 | 0.9782 | 0.79 | 0.97 | 1.03 | 0.7077 | 0.9460 | 0.9553 | 0.77 | 0.91 | 0.86 | 0.4269 | 0.8245 | 0.5631 |
| 266.1646 | 4.2 | C12H27O4P | Tributyl phosphate | Miscellaneous | 2.29 | 1.82 | 1.77 | 0.1528 | 0.1771 | 0.2492 | 0.71 | 0.69 | 0.82 | 0.3869 | 0.3016 | 0.6808 | 1.81 | 1.95 | 2.18 | 0.2923 | 0.3091 | 0.3511 | 0.93 | 0.73 | 0.73 | 0.8504 | 0.4882 | 0.4997 |
| 1133.7796 | 7.9 | C60H111NO18 | Trihexosylceramide (d18:1/24:1(15Z)) | Miscellaneous | 1.68 | 1.09 | 1.33 | 0.0166 | 0.7519 | 0.2603 | 1.16 | 1.16 | 1.23 | 0.7520 | 0.5446 | 0.1622 | 1.32 | 1.41 | 1.16 | 0.4514 | 0.2112 | 0.6293 | 0.97 | 0.78 | 1.37 | 0.8913 | 0.1303 | 0.4912 |
| 199.1210 | 10.3 | C10H17NO3 | Tussilagine | Miscellaneous | 0.99 | 0.95 | 1.06 | 0.9768 | 0.8756 | 0.8817 | 0.91 | 1.11 | 1.16 | 0.5967 | 0.6415 | 0.5565 | 1.12 | 0.69 | 0.98 | 0.6199 | 0.2860 | 0.9461 | 1.07 | 1.10 | 0.85 | 0.8304 | 0.7910 | 0.7496 |
| 258.1943 | 6.2 | C13H23NO3 | Valeroidine | Miscellaneous | 1.11 | 1.11 | 1.02 | 0.1748 | 0.1775 | 0.7781 | 1.11 | 1.00 | 1.08 | 0.3892 | 0.9745 | 0.4556 | 1.01 | 0.93 | 0.99 | 0.8900 | 0.4155 | 0.9268 | 0.91 | 0.97 | 1.05 | 0.1647 | 0.5735 | 0.6918 |
| 304.1018 | 15.9 | C10H16N4O7 | Vicine | Miscellaneous | 1.05 | 1.05 | 1.20 | 0.8762 | 0.8667 | 0.5535 | 1.15 | 1.25 | 1.13 | 0.6936 | 0.5281 | 0.7348 | 1.07 | 1.10 | 1.03 | 0.8132 | 0.7831 | 0.9379 | 1.32 | 0.90 | 1.22 | 0.4943 | 0.7788 | 0.6397 |
| 282.0951 | 13.7 | C10H18O9 | Xylobiose | Miscellaneous | 1.17 | 1.09 | 1.06 | 0.5929 | 0.8011 | 0.8334 | 0.91 | 1.08 | 1.05 | 0.7450 | 0.8140 | 0.8730 | 1.08 | 0.95 | 1.05 | 0.8326 | 0.8732 | 0.8896 | 0.96 | 0.98 | 0.89 | 0.9048 | 0.9635 | 0.7238 |
| 146.0580 | 14.2 | C6H10O4 | (S)-2-Aceto-2-hydroxybutanoate | Amino Acid Metabolism | 1.06 | 0.96 | 1.03 | 0.7275 | 0.8081 | 0.8651 | 0.94 | 1.09 | 1.02 | 0.4918 | 0.3932 | 0.8910 | 1.01 | 0.95 | 1.39 | 0.8552 | 0.5914 | 0.2819 | 0.94 | 0.72 | 0.73 | 0.8252 | 0.0480 | 0.0494 |
| 132.0423 | 14.9 | C5H8O4 | (S)-2-Acetolactate | Amino Acid Metabolism | 0.94 | 1.08 | 0.85 | 0.4668 | 0.4308 | 0.2321 | 1.16 | 1.04 | 0.78 | 0.2840 | 0.7420 | 0.2954 | 0.64 | 1.01 | 0.86 | 0.0699 | 0.9697 | 0.4822 | 1.00 | 1.13 | 0.96 | 0.9814 | 0.5197 | 0.8719 |
| 145.0739 | 12.4 | C6H11NO3 | [FA oxo,amino(6:0)] 3-oxo-5S-amino-hexanoic acid | Amino Acid Metabolism | 0.96 | 1.02 | 1.17 | 0.9478 | 0.9694 | 0.8188 | 1.26 | 1.17 | 1.20 | 0.7132 | 0.7990 | 0.7628 | 0.92 | 0.77 | 1.01 | 0.9033 | 0.7065 | 0.9942 | 1.34 | 1.01 | 1.07 | 0.7033 | 0.9842 | 0.9140 |
| 162.0350 | 8.0 | C6H10O3S | 1,2-Dihydroxy-5-(methylthio)pent-1-en-3-one | Amino Acid Metabolism | 0.87 | 1.34 | 1.33 | 0.8252 | 0.4653 | 0.5380 | 0.49 | 0.58 | 0.30 | 0.1486 | 0.2021 | 0.0879 | 0.30 | 0.41 | 0.25 | 0.0829 | 0.1081 | 0.0724 | 0.22 | 0.33 | 0.23 | 0.0028 | 0.0042 | 0.0024 |
| 171.0532 | 7.9 | C7H9NO4 | 2,3,4,5-Tetrahydrodipicolinate | Amino Acid Metabolism | 1.69 | 1.17 | 1.74 | 0.0610 | 0.5247 | 0.0526 | 1.18 | 1.05 | 1.21 | 0.3269 | 0.7399 | 0.2190 | 0.94 | 1.14 | 1.22 | 0.7484 | 0.3534 | 0.2280 | 1.08 | 1.11 | 1.24 | 0.6365 | 0.5690 | 0.0546 |
| 87.0320 | 15.6 | C3H5NO2 | 2-Aminoacrylate | Amino Acid Metabolism | 0.98 | 1.10 | 1.23 | 0.9229 | 0.4679 | 0.1506 | 1.10 | 1.47 | 1.55 | 0.6040 | 0.3727 | 0.2747 | 1.10 | 1.33 | 1.14 | 0.4365 | 0.3418 | 0.2986 | 0.91 | 1.02 | 1.06 | 0.5414 | 0.7403 | 0.6712 |
| 148.0160 | 27.8 | C6H7NO | 2-Aminophenol | Amino Acid Metabolism | 0.59 | 0.67 | 0.76 | 0.2948 | 0.4393 | 0.2544 | 0.78 | 0.97 | 0.51 | 0.1352 | 0.7908 | 0.2193 | 0.81 | 0.68 | 1.05 | 0.6930 | 0.4514 | 0.4966 | 0.95 | 1.20 | 1.50 | 0.9468 | 0.7440 | 0.4275 |
| 158.0579 | 7.8 | C7H10O4 | 2-Isopropylmaleate | Amino Acid Metabolism | 1.22 | 1.06 | 1.37 | 0.2925 | 0.6744 | 0.1654 | 1.10 | 1.26 | 1.37 | 0.6551 | 0.0540 | 0.1103 | 0.98 | 1.33 | 0.98 | 0.9080 | 0.0848 | 0.8617 | 0.89 | 0.69 | 0.96 | 0.2278 | 0.0628 | 0.6804 |
| 102.0317 | 13.3 | C4H6O3 | 2-Oxobutanoate | Amino Acid Metabolism | 1.00 | 1.03 | 1.00 | 0.9994 | 0.8690 | 0.9927 | 1.07 | 1.11 | 1.07 | 0.7118 | 0.5950 | 0.6890 | 0.69 | 1.00 | 1.08 | 0.4764 | 0.9960 | 0.6780 | 0.95 | 0.84 | 0.99 | 0.6244 | 0.4202 | 0.9527 |
| 182.0580 | 27.9 | C9H10O4 | 3-(4-Hydroxyphenyl)lactate | Amino Acid Metabolism | 0.76 | 0.90 | 0.84 | 0.2075 | 0.5199 | 0.3520 | 0.98 | 1.00 | 1.05 | 0.8939 | 0.9971 | 0.7632 | 1.15 | 1.10 | 1.11 | 0.0465 | 0.1148 | 0.1462 | 0.87 | 1.02 | 1.07 | 0.1841 | 0.8444 | 0.3870 |
| 197.0689 | 5.0 | C9H11NO4 | 3,4-Dihydroxy-L-phenylalanine | Amino Acid Metabolism | 0.91 | 1.70 | 0.58 | 0.9104 | 0.2237 | 0.3720 | 1.15 | 0.70 | 1.28 | 0.5755 | 0.6073 | 0.4386 | 6.69 | 5.75 | 8.32 | 0.0059 | 0.0424 | 0.1305 | 0.60 | 1.32 | 1.19 | 0.1626 | 0.5905 | 0.3193 |
| 153.0426 | 7.8 | C7H7NO3 | 3-Hydroxyanthranilate | Amino Acid Metabolism | 1.57 | 1.50 | 1.69 | 0.0501 | 0.1437 | 0.0414 | 0.72 | 0.93 | 0.69 | 0.3664 | 0.7161 | 0.1287 | 1.27 | 1.09 | 1.20 | 0.4999 | 0.8680 | 0.6392 | 0.83 | 0.57 | 0.89 | 0.4353 | 0.0494 | 0.4475 |
| 116.0473 | 12.7 | C5H8O3 | 3-Methyl-2-oxobutanoic acid | Amino Acid Metabolism | 0.94 | 1.04 | 0.92 | 0.5764 | 0.7247 | 0.4859 | 1.06 | 1.34 | 1.23 | 0.7136 | 0.2172 | 0.2833 | 1.04 | 1.01 | 1.19 | 0.8069 | 0.9655 | 0.7003 | 0.93 | 1.22 | 1.01 | 0.8635 | 0.6259 | 0.9551 |

| | | | | | | | | | | | | | | | | | | | | | | | | | | | | | |
|---|---|---|---|---|---|---|---|---|---|---|---|---|---|---|---|---|---|---|---|---|---|---|---|---|---|---|---|---|---|
| 87.0683 | 10.5 | C4H9NO | 4-Aminobutanal | Amino Acid Metabolism | 0.94 | 1.43 | 0.89 | 0.7473 | 0.0206 | 0.2999 | 1.06 | 1.08 | 1.06 | 0.7845 | 0.6778 | 0.7255 | 0.81 | 1.06 | 1.29 | 0.2002 | 0.7222 | 0.0841 | 0.89 | 1.03 | 0.88 | 0.4547 | 0.8791 | 0.3923 |
| 103.0633 | 12.4 | C4H9NO2 | 4-Aminobutanoate | Amino Acid Metabolism | 1.07 | 1.05 | 1.00 | 0.7421 | 0.8167 | 0.9723 | 1.37 | 1.17 | 1.35 | 0.4601 | 0.6759 | 0.0787 | 0.92 | 1.23 | 1.05 | 0.4826 | 0.2145 | 0.7459 | 1.08 | 1.29 | 1.08 | 0.5494 | 0.2739 | 0.6214 |
| 152.0473 | 28.7 | C8H8O3 | 4-Hydroxyphenylacetate | Amino Acid Metabolism | 1.15 | 1.07 | 1.13 | 0.3254 | 0.6331 | 0.4021 | 0.89 | 0.96 | 0.98 | 0.4969 | 0.7570 | 0.9049 | 0.98 | 1.07 | 1.09 | 0.8717 | 0.5725 | 0.4493 | 0.95 | 0.97 | 0.94 | 0.3346 | 0.7977 | 0.5473 |
| 209.0688 | 7.8 | C10H11NO4 | 4-Hydroxyphenylacetylglycine | Amino Acid Metabolism | 1.43 | 1.34 | 1.64 | 0.1333 | 0.2115 | 0.0560 | 1.05 | 1.18 | 1.18 | 0.8163 | 0.4270 | 0.4449 | 1.03 | 1.02 | 1.08 | 0.8926 | 0.9307 | 0.7357 | 1.16 | 1.00 | 1.10 | 0.5103 | 0.9906 | 0.6115 |
| 130.0630 | 8.2 | C6H10O3 | 4-Methyl-2-oxopentanoate | Amino Acid Metabolism | 0.90 | 1.00 | 0.97 | 0.3330 | 0.9862 | 0.7535 | 1.07 | 1.09 | 1.04 | 0.4677 | 0.4568 | 0.6696 | 0.91 | 0.93 | 0.99 | 0.3394 | 0.3380 | 0.9141 | 1.02 | 1.12 | 1.09 | 0.5498 | 0.1623 | 0.0293 |
| 159.0896 | 12.6 | C7H13NO3 | 5-Acetamidopentanoate | Amino Acid Metabolism | 2.57 | 1.76 | 2.15 | 0.4119 | 0.5687 | 0.5021 | 2.55 | 1.22 | 1.03 | 0.4561 | 0.7322 | 0.9395 | 0.50 | 0.43 | 1.44 | 0.5546 | 0.4993 | 0.7395 | 1.05 | 0.49 | 0.51 | 0.9637 | 0.5532 | 0.5655 |
| 173.0801 | 14.1 | C6H11N3O3 | 5-Guanidino-2-oxopentanoate | Amino Acid Metabolism | 1.21 | 1.73 | 1.38 | 0.0848 | 0.3400 | 0.3761 | 1.12 | 1.65 | 1.10 | 0.7320 | 0.1099 | 0.7664 | 0.89 | 0.73 | 0.85 | 0.5003 | 0.1705 | 0.4040 | 0.95 | 1.01 | 0.90 | 0.8385 | 0.9647 | 0.7158 |
| 220.0847 | 10.8 | C11H12N2O3 | 5-Hydroxy-L-tryptophan | Amino Acid Metabolism | 1.10 | 1.09 | 1.04 | 0.6868 | 0.7048 | 0.8646 | 0.90 | 1.04 | 0.91 | 0.5773 | 0.8322 | 0.1543 | 0.99 | 1.16 | 0.92 | 0.9624 | 0.4667 | 0.5453 | 0.85 | 0.94 | 0.81 | 0.3220 | 0.7789 | 0.1745 |
| 187.0846 | 7.8 | C8H13NO4 | 6-Acetamido-2-oxohexanoate | Amino Acid Metabolism | 0.98 | 0.82 | 0.94 | 0.9541 | 0.6522 | 0.8670 | 0.89 | 1.16 | 1.21 | 0.6726 | 0.6962 | 0.2786 | 0.97 | 1.13 | 0.98 | 0.9151 | 0.6619 | 0.9509 | 0.87 | 0.71 | 0.85 | 0.4727 | 0.1794 | 0.5192 |
| 139.9875 | 15.4 | C2H5O5P | Acetyl phosphate | Amino Acid Metabolism | 1.20 | 1.07 | 1.12 | 0.6396 | 0.8486 | 0.7865 | 0.88 | 1.01 | 1.01 | 0.7621 | 0.9810 | 0.9865 | 1.08 | 1.21 | 1.05 | 0.8431 | 0.6548 | 0.9256 | 1.29 | 1.03 | 1.38 | 0.4867 | 0.9620 | 0.3914 |
| 122.0368 | 27.8 | C7H6O2 | Benzoate | Amino Acid Metabolism | 1.11 | 1.05 | 1.05 | 0.2956 | 0.5787 | 0.5384 | 0.96 | 1.03 | 0.99 | 0.7595 | 0.8101 | 0.9561 | 1.12 | 1.08 | 1.13 | 0.1196 | 0.5925 | 0.1044 | 0.93 | 0.91 | 0.95 | 0.3140 | 0.3700 | 0.4568 |
| 101.0841 | 28.0 | C5H11NO | Betaine aldehyde | Amino Acid Metabolism | 0.84 | 1.10 | 1.04 | 0.2307 | 0.4683 | 0.7358 | 1.10 | 1.08 | 1.07 | 0.4409 | 0.2684 | 0.5435 | 1.12 | 1.11 | 1.12 | 0.2963 | 0.3528 | 0.3605 | 1.02 | 1.01 | 1.01 | 0.8563 | 0.9590 | 0.9053 |
| 113.0589 | 9.8 | C4H7N3O | Creatinine | Amino Acid Metabolism | 1.73 | 1.29 | 1.08 | 0.6621 | 0.8209 | 0.9393 | 0.98 | 1.18 | 1.23 | 0.9721 | 0.7719 | 0.6943 | 1.09 | 1.01 | 1.45 | 0.7671 | 0.9859 | 0.4104 | 0.59 | 0.97 | 0.53 | 0.3079 | 0.9555 | 0.2705 |
| 178.0412 | 14.2 | C5H10N2O3S | Cys-Gly | Amino Acid Metabolism | 0.93 | 0.91 | 0.94 | 0.6750 | 0.6739 | 0.7245 | 0.95 | 1.03 | 0.86 | 0.8232 | 0.8833 | 0.5108 | 1.02 | 0.98 | 0.85 | 0.8939 | 0.9285 | 0.5765 | 0.94 | 0.93 | 1.00 | 0.6235 | 0.4459 | 0.9871 |
| 259.0457 | 15.6 | C6H14NO8P | D-Glucosamine 6-phosphate | Amino Acid Metabolism | 0.91 | 0.96 | 0.97 | 0.5819 | 0.7950 | 0.8715 | 1.10 | 1.06 | 1.01 | 0.0801 | 0.4174 | 0.8873 | 0.98 | 1.03 | 1.02 | 0.8376 | 0.7669 | 0.9215 | 0.99 | 1.03 | 0.96 | 0.9456 | 0.7824 | 0.7630 |
| 153.0790 | 4.8 | C8H11NO2 | Dopamine | Amino Acid Metabolism | 1.24 | 1.23 | 1.16 | 0.3178 | 0.4283 | 0.5127 | 1.05 | 1.06 | 1.18 | 0.7675 | 0.7425 | 0.3586 | 1.08 | 1.10 | 1.31 | 0.4175 | 0.2544 | 0.1718 | 1.16 | 1.02 | 1.22 | 0.2866 | 0.9010 | 0.2597 |
| 142.0742 | 12.9 | C6H10N2O2 | Ectoine | Amino Acid Metabolism | 1.31 | 1.31 | 1.68 | 0.5294 | 0.5602 | 0.4138 | 0.74 | 1.09 | 1.00 | 0.4100 | 0.7549 | 0.9936 | 0.73 | 0.86 | 0.95 | 0.3389 | 0.6215 | 0.8689 | 0.95 | 0.85 | 0.96 | 0.8285 | 0.6581 | 0.9060 |
| 141.0191 | 15.9 | C2H8NO4P | Ethanolamine phosphate | Amino Acid Metabolism | 0.93 | 1.01 | 1.11 | 0.7789 | 0.9752 | 0.7214 | 1.17 | 1.25 | 1.34 | 0.4644 | 0.3728 | 0.3566 | 1.75 | 1.70 | 1.47 | 0.1106 | 0.1843 | 0.3361 | 1.50 | 1.60 | 1.09 | 0.3092 | 0.2448 | 0.7824 |
| 312.0221 | 16.0 | C9H16N2O5Se | gamma-Glutamyl-Se-methylselenocysteine | Amino Acid Metabolism | 1.20 | 1.18 | 1.12 | 0.1852 | 0.5001 | 0.3903 | 0.76 | 0.80 | 0.93 | 0.1495 | 0.2460 | 0.5650 | 0.85 | 0.95 | 0.84 | 0.4818 | 0.7360 | 0.3427 | 0.73 | 0.77 | 0.65 | 0.3334 | 0.4078 | 0.2179 |
| 250.0623 | 8.4 | C8H14N2O5S | gamma-L-Glutamyl-L-cysteine | Amino Acid Metabolism | 1.00 | 1.05 | 0.84 | 0.9893 | 0.8547 | 0.6233 | 1.08 | 1.03 | 1.23 | 0.6549 | 0.7881 | 0.1426 | 1.21 | 1.14 | 1.22 | 0.3292 | 0.3499 | 0.4856 | 0.97 | 0.90 | 0.98 | 0.7766 | 0.4483 | 0.8876 |
| 179.0582 | 8.0 | C9H9NO3 | Hippurate | Amino Acid Metabolism | 1.48 | 0.93 | 0.93 | 0.1995 | 0.8771 | 0.8836 | 1.22 | 1.59 | 1.00 | 0.5364 | 0.1400 | 0.9962 | 1.12 | 1.12 | 1.22 | 0.5740 | 0.7652 | 0.0544 | 0.57 | 0.59 | 0.49 | 0.0523 | 0.1130 | 0.1008 |
| 240.1223 | 14.2 | C10H16N4O3 | Homocarnosine | Amino Acid Metabolism | 1.20 | 1.16 | 1.13 | 0.5127 | 0.6257 | 0.4629 | 0.85 | 1.10 | 1.12 | 0.5662 | 0.6981 | 0.6279 | 0.87 | 0.77 | 0.93 | 0.7096 | 0.4635 | 0.8301 | 0.98 | 0.85 | 0.98 | 0.9559 | 0.5584 | 0.9360 |
| 168.0425 | 15.0 | C8H8O4 | Homogentisate | Amino Acid Metabolism | 1.17 | 1.46 | 1.68 | 0.8359 | 0.5121 | 0.3078 | 1.67 | 1.38 | 2.08 | 0.0510 | 0.1776 | 0.0115 | 2.30 | 1.84 | 2.35 | 0.0413 | 0.1459 | 0.0742 | 5.69 | 5.40 | 5.68 | 0.0037 | 0.0036 | 0.0157 |
| 172.0484 | 15.2 | C6H8N2O4 | Hydantoin-5-propionate | Amino Acid Metabolism | 1.11 | 1.08 | 1.01 | 0.5941 | 0.6935 | 0.9604 | 0.56 | 0.74 | 0.55 | 0.0624 | 0.2412 | 0.0596 | 0.56 | 0.60 | 0.54 | 0.0748 | 0.0906 | 0.0679 | 0.52 | 0.50 | 0.44 | 0.0182 | 0.0022 | 0.0075 |
| 111.9925 | 14.3 | CH5O4P | Hydroxymethylphosphonate | Amino Acid Metabolism | 1.22 | 1.15 | 1.05 | 0.1366 | 0.2565 | 0.6331 | 1.09 | 1.13 | 1.12 | 0.3048 | 0.2029 | 0.2817 | 1.07 | 1.06 | 1.18 | 0.7138 | 0.7229 | 0.3174 | 1.12 | 1.08 | 1.05 | 0.5541 | 0.6569 | 0.7659 |
| 110.0480 | 14.8 | C5H6N2O | Imidazole-4-acetaldehyde | Amino Acid Metabolism | 0.95 | 1.02 | 0.96 | 0.6454 | 0.8547 | 0.7171 | 1.06 | 1.02 | 1.22 | 0.4315 | 0.8177 | 0.0327 | 1.09 | 0.95 | 1.08 | 0.3475 | 0.4062 | 0.2070 | 0.93 | 0.87 | 0.83 | 0.5925 | 0.1773 | 0.0754 |
| 161.0688 | 11.2 | C6H11NO4 | L-2-Aminoadipate | Amino Acid Metabolism | 1.11 | 1.00 | 1.15 | 0.6873 | 0.9996 | 0.5861 | 0.94 | 1.11 | 1.14 | 0.6536 | 0.6198 | 0.4957 | 1.04 | 0.87 | 1.14 | 0.9199 | 0.6649 | 0.6926 | 1.04 | 0.99 | 0.72 | 0.8876 | 0.9694 | 0.4395 |
| 89.0477 | 15.0 | C3H7NO2 | L-Alanine | Amino Acid Metabolism | 1.43 | 3.78 | 0.55 | 0.7239 | 0.1795 | 0.4087 | 4.34 | 7.56 | 3.69 | 0.0463 | 0.1980 | 0.0327 | 0.15 | 0.92 | 0.70 | 0.1344 | 0.9016 | 0.5370 | 0.80 | 0.10 | 0.10 | 0.7167 | 0.1920 | 0.1943 |
| 133.0375 | 16.1 | C4H7NO4 | L-Aspartate | Amino Acid Metabolism | 1.05 | 1.06 | 1.07 | 0.7494 | 0.7209 | 0.6945 | 0.46 | 0.56 | 0.37 | 0.0367 | 0.0641 | 0.0276 | 0.22 | 0.29 | 0.16 | 0.0379 | 0.0446 | 0.0347 | 0.24 | 0.28 | 0.19 | 0.0301 | 0.0250 | 0.0290 |
| 117.0426 | 12.8 | C4H7NO3 | L-Aspartate 4-semialdehyde | Amino Acid Metabolism | 0.66 | 0.61 | 0.92 | 0.4074 | 0.3320 | 0.4219 | 0.95 | 0.94 | 0.64 | 0.6125 | 0.5812 | 0.3812 | 0.79 | 0.76 | 1.19 | 0.6508 | 0.5997 | 0.1029 | 1.08 | 1.45 | 1.43 | 0.9226 | 0.4666 | 0.4806 |
| 161.1052 | 11.9 | C7H15NO3 | L-Carnitine | Amino Acid Metabolism | 1.09 | 0.94 | 0.98 | 0.9133 | 0.9408 | 0.9770 | 0.86 | 1.24 | 0.91 | 0.8163 | 0.7849 | 0.8910 | 0.88 | 0.87 | 1.05 | 0.8555 | 0.8378 | 0.9401 | 0.83 | 0.85 | 0.80 | 0.7734 | 0.8125 | 0.7428 |
| 240.0239 | 16.1 | C6H12N2O4S2 | L-Cystine | Amino Acid Metabolism | 0.72 | 0.98 | 0.89 | 0.6131 | 0.9685 | 0.8621 | 1.91 | 1.58 | 1.80 | 0.1197 | 0.3402 | 0.1980 | 1.60 | 1.46 | 1.67 | 0.4984 | 0.1660 | 0.2297 | 0.69 | 0.71 | 1.02 | 0.4271 | 0.4589 | 0.9803 |

| | | | | | | | | | | | | | | | | | | | | | | | | | | | | | |
|---|---|---|---|---|---|---|---|---|---|---|---|---|---|---|---|---|---|---|---|---|---|---|---|---|---|---|---|---|---|
| 155.0695 | 13.9 | C6H9N3O2 | L-Histidine | Amino Acid Metabolism | 29.36 | 1.29 | 1.38 | 0.0157 | 0.3801 | 0.3425 | 0.79 | 1.02 | 18.38 | 0.1342 | 0.8676 | 0.0677 | 1.02 | 4.90 | 1.09 | 0.9846 | 0.0687 | 0.9407 | 0.08 | 0.37 | 0.85 | 0.4214 | 0.5650 | 0.9030 |
| 190.0954 | 14.1 | C7H14N2O4 | LL-2,6-Diaminoheptanedioate | Amino Acid Metabolism | 1.19 | 1.15 | 1.10 | 0.7887 | 0.8336 | 0.8873 | 0.96 | 0.95 | 1.03 | 0.9561 | 0.9436 | 0.9633 | 1.08 | 0.96 | 1.04 | 0.8950 | 0.9498 | 0.9450 | 1.06 | 0.97 | 1.07 | 0.9246 | 0.9654 | 0.9094 |
| 146.1055 | 22.4 | C6H14N2O2 | L-Lysine | Amino Acid Metabolism | 0.97 | 1.03 | 0.97 | 0.7871 | 0.8026 | 0.8189 | 0.82 | 1.08 | 0.75 | 0.2093 | 0.6125 | 0.1224 | 0.79 | 0.82 | 0.69 | 0.1694 | 0.1887 | 0.0427 | 0.57 | 0.63 | 0.54 | 0.1096 | 0.1472 | 0.1057 |
| 165.0460 | 13.2 | C5H11NO3S | L-Methionine S-oxide | Amino Acid Metabolism | 0.95 | 0.96 | 1.12 | 0.8090 | 0.7773 | 0.7296 | 1.27 | 1.36 | 1.22 | 0.1529 | 0.1121 | 0.2932 | 1.11 | 1.24 | 1.30 | 0.6689 | 0.4494 | 0.2371 | 1.13 | 1.10 | 1.16 | 0.5113 | 0.6443 | 0.5627 |
| 165.0790 | 5.0 | C9H11NO2 | L-Phenylalanine | Amino Acid Metabolism | 0.95 | 0.82 | 0.71 | 0.7877 | 0.3556 | 0.2283 | 1.10 | 1.05 | 1.23 | 0.3664 | 0.5979 | 0.1230 | 1.07 | 0.91 | 1.10 | 0.7969 | 0.5562 | 0.6357 | 1.30 | 1.21 | 1.11 | 0.3287 | 0.2172 | 0.6848 |
| 129.0790 | 12.4 | C6H11NO2 | L-Pipecolate | Amino Acid Metabolism | 1.02 | 1.02 | 1.10 | 0.9650 | 0.9465 | 0.8535 | 0.57 | 0.94 | 0.30 | 0.1545 | 0.8646 | 0.0394 | 0.33 | 0.40 | 0.09 | 0.1593 | 0.1885 | 0.1027 | 0.43 | 0.49 | 0.08 | 0.1943 | 0.1505 | 0.0566 |
| 240.0669 | 4.2 | C11H12N2O2 | L-Tryptophan | Amino Acid Metabolism | 1.55 | 1.34 | 5.75 | 0.1137 | 0.2617 | 0.4170 | 0.97 | 1.01 | 0.98 | 0.8962 | 0.9527 | 0.9378 | 3.45 | 1.17 | 1.26 | 0.3836 | 0.5017 | 0.3421 | 3.29 | 0.80 | 1.29 | 0.2739 | 0.1158 | 0.2388 |
| 181.0739 | 7.9 | C9H11NO3 | L-Tyrosine | Amino Acid Metabolism | 1.13 | 1.01 | 0.96 | 0.5593 | 0.9677 | 0.8370 | 0.93 | 0.99 | 1.01 | 0.6704 | 0.9378 | 0.9449 | 1.14 | 0.98 | 1.28 | 0.6828 | 0.9137 | 0.3429 | 0.98 | 0.83 | 0.94 | 0.9075 | 0.4491 | 0.5065 |
| 195.0897 | 4.9 | C10H13NO3 | L-Tyrosine methyl ester | Amino Acid Metabolism | 1.89 | 0.95 | 0.72 | 0.3372 | 0.8283 | 0.1610 | 1.04 | 1.15 | 1.15 | 0.9422 | 0.6749 | 0.7505 | 0.80 | 0.81 | 1.33 | 0.5577 | 0.4235 | 0.3703 | 0.70 | 1.50 | 0.99 | 0.3532 | 0.4852 | 0.9843 |
| 117.0790 | 14.3 | C5H11NO2 | L-Valine | Amino Acid Metabolism | 0.72 | 0.97 | 0.89 | 0.2816 | 0.9060 | 0.6300 | 1.26 | 1.21 | 1.43 | 0.2091 | 0.2597 | 0.1680 | 0.94 | 1.05 | 1.00 | 0.6793 | 0.7094 | 0.9703 | 0.99 | 0.71 | 0.97 | 0.9188 | 0.0895 | 0.8291 |
| 290.1226 | 16.7 | C10H18N4O6 | N-(L-Arginino)succinate | Amino Acid Metabolism | 1.09 | 0.93 | 0.98 | 0.6477 | 0.6466 | 0.9127 | 0.78 | 0.97 | 0.84 | 0.6002 | 0.9567 | 0.7266 | 1.09 | 0.95 | 1.03 | 0.7965 | 0.8751 | 0.9334 | 0.80 | 0.87 | 0.87 | 0.2939 | 0.6078 | 0.6605 |
| 169.0853 | 12.5 | C7H11N3O2 | N(pi)-Methyl-L-histidine | Amino Acid Metabolism | 0.85 | 0.95 | 1.02 | 0.8893 | 0.9687 | 0.9853 | 1.31 | 1.27 | 1.15 | 0.8222 | 0.8341 | 0.8982 | 0.96 | 0.91 | 0.99 | 0.9667 | 0.9267 | 0.9886 | 0.97 | 1.18 | 1.34 | 0.9751 | 0.8732 | 0.7850 |
| 246.1328 | 14.1 | C9H18N4O4 | N2-(D-1-Carboxyethyl)-L-arginine | Amino Acid Metabolism | 0.91 | 0.98 | 1.19 | 0.9035 | 0.9667 | 0.8168 | 0.61 | 0.90 | 0.57 | 0.3109 | 0.8094 | 0.3824 | 0.65 | 0.66 | 0.38 | 0.3229 | 0.3215 | 0.1229 | 0.50 | 0.59 | 0.34 | 0.1291 | 0.1869 | 0.0730 |
| 218.1267 | 17.0 | C9H18N2O4 | N2-(D-1-Carboxyethyl)-L-lysine | Amino Acid Metabolism | 0.95 | 0.90 | 1.05 | 0.8073 | 0.6767 | 0.8614 | 0.91 | 1.06 | 1.00 | 0.7292 | 0.8115 | 0.9900 | 1.03 | 1.00 | 1.02 | 0.8788 | 0.9978 | 0.9509 | 0.86 | 0.67 | 0.65 | 0.6520 | 0.3012 | 0.2773 |
| 203.0793 | 14.8 | C8H13NO5 | N2-Acetyl-L-aminoadipate | Amino Acid Metabolism | 1.03 | 1.09 | 0.93 | 0.7316 | 0.4587 | 0.6404 | 1.19 | 1.19 | 1.25 | 0.3193 | 0.3559 | 0.2140 | 1.10 | 1.06 | 1.00 | 0.5085 | 0.4936 | 0.9654 | 0.98 | 0.93 | 0.98 | 0.8991 | 0.5490 | 0.8601 |
| 204.1111 | 17.8 | C8H16N2O4 | N6-Acetyl-N6-hydroxy-L-lysine | Amino Acid Metabolism | 0.91 | 0.97 | 0.97 | 0.5531 | 0.8396 | 0.8597 | 0.78 | 0.96 | 1.07 | 0.1908 | 0.7275 | 0.5253 | 1.03 | 0.94 | 1.02 | 0.3768 | 0.2174 | 0.8925 | 0.95 | 0.91 | 0.97 | 0.6860 | 0.5181 | 0.8491 |
| 301.0563 | 14.7 | C8H16NO9P | N-Acetyl-D-glucosamine 6-phosphate | Amino Acid Metabolism | 0.98 | 0.95 | 0.93 | 0.8116 | 0.6199 | 0.3015 | 0.94 | 1.06 | 1.09 | 0.4200 | 0.5023 | 0.4970 | 1.01 | 0.99 | 1.04 | 0.9372 | 0.9364 | 0.7572 | 0.91 | 0.93 | 0.91 | 0.2643 | 0.3445 | 0.1894 |
| 174.1005 | 13.5 | C7H14N2O3 | N-Acetylornithine | Amino Acid Metabolism | 1.06 | 1.15 | 1.00 | 0.8641 | 0.6617 | 0.9970 | 0.89 | 0.97 | 0.93 | 0.7314 | 0.9477 | 0.8202 | 1.31 | 1.05 | 1.16 | 0.4126 | 0.7748 | 0.5759 | 0.76 | 0.93 | 0.83 | 0.3334 | 0.8140 | 0.5833 |
| 130.1106 | 18.2 | C6H14N2O | N-Acetylputrescine | Amino Acid Metabolism | 1.13 | 1.15 | 1.05 | 0.0528 | 0.1837 | 0.6983 | 1.12 | 1.13 | 1.06 | 0.4193 | 0.4227 | 0.6884 | 1.20 | 1.03 | 1.20 | 0.3977 | 0.8606 | 0.1332 | 1.04 | 1.06 | 0.92 | 0.8012 | 0.6512 | 0.6303 |
| 190.0590 | 15.3 | C6H10N2O5 | N-Carbamyl-L-glutamate | Amino Acid Metabolism | 1.10 | 1.14 | 1.09 | 0.6710 | 0.4132 | 0.6108 | 0.61 | 0.72 | 0.58 | 0.1239 | 0.1991 | 0.0824 | 0.58 | 0.60 | 0.55 | 0.1305 | 0.1415 | 0.1109 | 0.51 | 0.52 | 0.54 | 0.0070 | 0.0104 | 0.0298 |
| 153.0557 | 12.5 | C4H12NO3P | N-Dimethyl-2-aminoethylphosphonate | Amino Acid Metabolism | 1.10 | 1.05 | 1.16 | 0.3409 | 0.7079 | 0.4887 | 1.01 | 1.28 | 1.10 | 0.9660 | 0.2464 | 0.5944 | 0.88 | 0.75 | 0.90 | 0.6100 | 0.3355 | 0.6577 | 0.95 | 0.90 | 0.90 | 0.7958 | 0.3539 | 0.4030 |
| 203.1158 | 4.8 | C9H17NO4 | O-Acetylcarnitine | Amino Acid Metabolism | 1.09 | 1.30 | 0.98 | 0.8567 | 0.5655 | 0.9535 | 1.25 | 1.32 | 0.85 | 0.7101 | 0.6394 | 0.8260 | 0.64 | 0.86 | 0.57 | 0.2039 | 0.5956 | 0.1212 | 0.44 | 0.45 | 0.41 | 0.1920 | 0.1977 | 0.1761 |
| 185.0089 | 16.2 | C3H8NO6P | O-Phospho-L-serine | Amino Acid Metabolism | 0.97 | 1.06 | 0.98 | 0.9317 | 0.8598 | 0.9407 | 0.67 | 0.68 | 0.55 | 0.2551 | 0.2907 | 0.1523 | 0.32 | 0.47 | 0.21 | 0.0862 | 0.1523 | 0.0599 | 0.21 | 0.24 | 0.08 | 0.0587 | 0.0649 | 0.0551 |
| 219.1107 | 8.6 | C9H17NO5 | Pantothenate | Amino Acid Metabolism | 0.99 | 1.18 | 1.08 | 0.9134 | 0.3613 | 0.1679 | 1.03 | 1.16 | 1.08 | 0.8578 | 0.3915 | 0.7282 | 1.48 | 1.22 | 1.29 | 0.1264 | 0.4063 | 0.4542 | 0.87 | 0.95 | 0.83 | 0.2238 | 0.7772 | 0.0377 |
| 121.0891 | 28.7 | C8H11N | Phenethylamine | Amino Acid Metabolism | 1.12 | 1.01 | 1.00 | 0.6410 | 0.9617 | 0.9977 | 0.93 | 0.99 | 1.11 | 0.3276 | 0.9103 | 0.3828 | 0.95 | 0.92 | 0.95 | 0.7586 | 0.5634 | 0.7350 | 0.96 | 0.95 | 0.97 | 0.6477 | 0.6547 | 0.5745 |
| 211.0359 | 15.0 | C4H10N3O5P | Phosphocreatine | Amino Acid Metabolism | 0.92 | 1.09 | 0.97 | 0.8895 | 0.8744 | 0.9599 | 0.99 | 1.09 | 0.94 | 0.9890 | 0.8679 | 0.9050 | 0.99 | 0.73 | 1.00 | 0.9799 | 0.6479 | 0.9994 | 1.01 | 1.02 | 0.91 | 0.9793 | 0.9691 | 0.8740 |
| 123.9926 | 14.9 | C2H5O4P | Phosphonoacetaldehyde | Amino Acid Metabolism | 1.11 | 1.07 | 1.09 | 0.0807 | 0.4272 | 0.3526 | 1.44 | 1.44 | 1.78 | 0.1350 | 0.0630 | 0.0015 | 2.76 | 2.34 | 2.81 | 0.0065 | 0.0149 | 0.0273 | 3.83 | 3.60 | 3.55 | 0.0275 | 0.0139 | 0.0154 |
| 384.1217 | 13.6 | C14H20N6O5S | S-Adenosyl-L-homocysteine | Amino Acid Metabolism | 0.95 | 1.08 | 1.23 | 0.8018 | 0.7201 | 0.3013 | 1.13 | 1.19 | 1.00 | 0.6382 | 0.4333 | 0.9903 | 0.77 | 0.90 | 0.61 | 0.3918 | 0.7524 | 0.1777 | 0.63 | 0.68 | 0.40 | 0.1866 | 0.1800 | 0.0355 |
| 398.1373 | 16.2 | C15H22N6O5S | S-Adenosyl-L-methionine | Amino Acid Metabolism | 0.81 | 0.98 | 0.82 | 0.6798 | 0.9767 | 0.7008 | 1.39 | 1.42 | 1.47 | 0.3387 | 0.3672 | 0.3305 | 1.20 | 1.23 | 1.26 | 0.5647 | 0.5310 | 0.5518 | 1.53 | 1.49 | 1.33 | 0.2123 | 0.2005 | 0.2656 |
| 426.0880 | 16.8 | C13H22N4O8S2 | S-glutathionyl-L-cysteine | Amino Acid Metabolism | 0.93 | 1.49 | 0.87 | 0.8415 | 0.1915 | 0.7148 | 1.18 | 2.09 | 1.52 | 0.7248 | 0.0798 | 0.5195 | 0.99 | 0.83 | 1.08 | 0.9886 | 0.5590 | 0.8697 | 0.43 | 0.55 | 0.68 | 0.2677 | 0.3489 | 0.5094 |
| 260.0118 | 12.7 | C6H13O7PS | S-Methyl-5-thio-D-ribose 1-phosphate | Amino Acid Metabolism | 0.89 | 0.98 | 0.92 | 0.8688 | 0.9802 | 0.9031 | 0.48 | 0.66 | 0.46 | 0.0945 | 0.3337 | 0.1612 | 0.34 | 0.36 | 0.27 | 0.0968 | 0.1050 | 0.0803 | 0.25 | 0.39 | 0.17 | 0.0309 | 0.0355 | 0.0189 |
| 170.0150 | 14.7 | C6H6N2O2S | Thiourocanic acid | Amino Acid Metabolism | 0.79 | 0.93 | 0.89 | 0.6206 | 0.8772 | 0.7588 | 0.73 | 0.87 | 0.71 | 0.5991 | 0.8026 | 0.5861 | 0.88 | 0.85 | 0.87 | 0.7286 | 0.6237 | 0.7591 | 0.71 | 0.78 | 0.81 | 0.3224 | 0.4933 | 0.6216 |

| | | | | | | | | | | | | | | | | | | | | | | | | | | | | |
|---|---|---|---|---|---|---|---|---|---|---|---|---|---|---|---|---|---|---|---|---|---|---|---|---|---|---|---|---|
| 138.0429 | 7.9 | C6H6N2O2 | Urocanate | Amino Acid Metabolism | 1.73 | 1.54 | 1.45 | 0.1809 | 0.4473 | 0.2035 | 1.16 | 2.47 | 0.97 | 0.8041 | 0.4531 | 0.9382 | 1.00 | 1.12 | 1.05 | 0.9997 | 0.5932 | 0.7996 | 0.92 | 0.69 | 0.81 | 0.7789 | 0.2807 | 0.5711 |
| 156.0423 | 7.8 | C7H8O4 | 2,3-Dihydro-2,3-dihydroxybenzoate | Biosynthesis of Polyketides and Nonribosomal Peptides | 1.19 | 1.20 | 1.29 | 0.2834 | 0.0761 | 0.1088 | 0.89 | 1.05 | 0.96 | 0.6075 | 0.8275 | 0.8884 | 0.97 | 0.82 | 0.81 | 0.7447 | 0.3349 | 0.1533 | 0.74 | 0.73 | 0.93 | 0.2117 | 0.1505 | 0.6113 |
| 454.3427 | 17.3 | C28H48O3 | Cathasterone | Biosynthesis of Secondary Metabolites | 1.08 | 0.95 | 1.01 | 0.3435 | 0.5458 | 0.8804 | 1.01 | 1.22 | 1.21 | 0.8396 | 0.0544 | 0.0028 | 0.93 | 0.91 | 0.98 | 0.2901 | 0.1924 | 0.7530 | 0.82 | 0.95 | 0.93 | 0.0334 | 0.5497 | 0.2578 |
| 199.0480 | 7.9 | C8H9NO5 | Clavulanic acid | Biosynthesis of Secondary Metabolites | 1.38 | 0.93 | 1.37 | 0.2740 | 0.7000 | 0.3452 | 1.27 | 0.78 | 1.20 | 0.5464 | 0.1959 | 0.1398 | 1.12 | 1.18 | 1.78 | 0.7203 | 0.5711 | 0.2217 | 1.44 | 0.98 | 1.26 | 0.2893 | 0.9241 | 0.3135 |
| 363.1101 | 14.0 | C21H17NO5 | Dihydrochelirubine | Biosynthesis of Secondary Metabolites | 1.22 | 1.27 | 1.35 | 0.4796 | 0.4324 | 0.2370 | 0.92 | 1.06 | 1.03 | 0.8206 | 0.8382 | 0.9063 | 0.79 | 0.93 | 0.95 | 0.3278 | 0.7411 | 0.8574 | 0.94 | 0.99 | 0.92 | 0.6236 | 0.9639 | 0.7916 |
| 194.0579 | 7.8 | C10H10O4 | Ferulate | Biosynthesis of Secondary Metabolites | 1.22 | 1.06 | 1.31 | 0.2362 | 0.7079 | 0.2259 | 0.95 | 1.06 | 1.05 | 0.7917 | 0.8179 | 0.8046 | 1.13 | 1.10 | 1.07 | 0.6233 | 0.6820 | 0.7739 | 0.90 | 0.77 | 1.09 | 0.5539 | 0.3620 | 0.7329 |
| 346.1528 | 4.4 | C18H19NO5 | Melicopicine | Biosynthesis of Secondary Metabolites | 1.30 | 1.14 | 1.07 | 0.2731 | 0.5869 | 0.7670 | 1.14 | 1.47 | 1.27 | 0.3358 | 0.0806 | 0.2246 | 1.33 | 1.29 | 1.18 | 0.3088 | 0.3356 | 0.4659 | 1.08 | 0.95 | 0.89 | 0.8153 | 0.8998 | 0.7332 |
| 155.1310 | 28.3 | C9H17NO | N-Methylpelletierine | Biosynthesis of Secondary Metabolites | 0.81 | 0.96 | 1.28 | 0.4092 | 0.8707 | 0.4325 | 0.74 | 0.98 | 0.91 | 0.4190 | 0.9624 | 0.7230 | 1.14 | 1.05 | 1.07 | 0.5800 | 0.9103 | 0.6389 | 0.94 | 0.92 | 0.88 | 0.8206 | 0.7826 | 0.6808 |
| 155.0946 | 7.8 | C8H13NO2 | Retronecine | Biosynthesis of Secondary Metabolites | 1.26 | 1.11 | 1.19 | 0.1961 | 0.5325 | 0.3224 | 0.90 | 1.08 | 0.99 | 0.6159 | 0.6707 | 0.9638 | 1.24 | 1.24 | 1.24 | 0.3415 | 0.2451 | 0.2277 | 0.98 | 0.92 | 1.34 | 0.8743 | 0.7647 | 0.2401 |
| 331.0838 | 12.9 | C20H13NO4 | Sanguinarine | Biosynthesis of Secondary Metabolites | 1.01 | 1.07 | 1.15 | 0.9369 | 0.6163 | 0.2872 | 1.21 | 1.26 | 1.26 | 0.2783 | 0.3341 | 0.2559 | 1.03 | 0.96 | 0.92 | 0.8768 | 0.7747 | 0.3490 | 1.01 | 1.20 | 1.01 | 0.9187 | 0.1448 | 0.9173 |
| 240.1474 | 12.0 | C12H20N2O3 | Slaframine | Biosynthesis of Secondary Metabolites | 1.09 | 1.04 | 1.07 | 0.7958 | 0.9033 | 0.8509 | 1.03 | 1.19 | 1.05 | 0.9264 | 0.6508 | 0.8416 | 1.02 | 0.84 | 0.93 | 0.9451 | 0.5350 | 0.7842 | 0.89 | 1.01 | 0.94 | 0.6945 | 0.9845 | 0.8657 |
| 141.1153 | 28.4 | C8H15NO | tropine | Biosynthesis of Secondary Metabolites | 1.09 | 0.91 | 1.21 | 0.7677 | 0.8405 | 0.5188 | 0.76 | 0.78 | 1.02 | 0.3347 | 0.4166 | 0.9234 | 0.73 | 1.03 | 1.06 | 0.2338 | 0.9275 | 0.8034 | 1.28 | 0.79 | 1.05 | 0.2561 | 0.5499 | 0.8662 |
| 150.0165 | 17.1 | C4H6O6 | (R,R)-Tartaric acid | Carbohydrate Metabolism | 1.14 | 1.08 | 1.05 | 0.0783 | 0.1557 | 0.5317 | 0.94 | 0.98 | 1.07 | 0.3778 | 0.7550 | 0.2808 | 1.02 | 1.02 | 1.04 | 0.7390 | 0.7764 | 0.6245 | 0.90 | 0.89 | 0.95 | 0.0993 | 0.1613 | 0.3201 |
| 136.0372 | 16.1 | C4H8O5 | [FA trihydroxy(4:0)] 2,3,4-trihydroxy-butanoic acid | Carbohydrate Metabolism | 1.24 | 1.22 | 1.24 | 0.8719 | 0.8827 | 0.8725 | 0.90 | 1.01 | 0.90 | 0.9367 | 0.9935 | 0.9363 | 1.34 | 0.96 | 1.25 | 0.8306 | 0.9723 | 0.8645 | 0.89 | 1.07 | 0.84 | 0.9250 | 0.9586 | 0.8949 |
| 536.1591 | 3.9 | C18H32O18 | 1-4-beta-D-Glucan | Carbohydrate Metabolism | 1.92 | 1.84 | 2.45 | 0.1588 | 0.2547 | 0.4377 | 1.34 | 2.05 | 1.25 | 0.5625 | 0.2448 | 0.4779 | 2.35 | 0.64 | 1.42 | 0.4350 | 0.5877 | 0.6472 | 2.33 | 0.50 | 1.57 | 0.3146 | 0.4525 | 0.6629 |
| 194.0791 | 12.8 | C7H14O6 | 1-O-Methyl-myo-inositol | Carbohydrate Metabolism | 0.84 | 0.83 | 0.84 | 0.4447 | 0.4451 | 0.6737 | 1.39 | 1.35 | 1.18 | 0.3422 | 0.3771 | 0.6628 | 0.97 | 0.81 | 1.12 | 0.8958 | 0.5004 | 0.7418 | 0.92 | 0.97 | 0.89 | 0.8219 | 0.8874 | 0.7674 |
| 195.0744 | 12.4 | C6H13NO6 | 2-Amino-2-deoxy-D-gluconate | Carbohydrate Metabolism | 0.83 | 1.09 | 1.08 | 0.6635 | 0.8411 | 0.8603 | 1.40 | 1.26 | 0.97 | 0.4399 | 0.5888 | 0.9044 | 0.59 | 0.76 | 0.88 | 0.3299 | 0.5348 | 0.7902 | 1.34 | 1.29 | 1.53 | 0.3728 | 0.6099 | 0.4572 |
| 146.0216 | 15.2 | C5H6O5 | 2-Oxoglutarate | Carbohydrate Metabolism | 1.13 | 1.15 | 0.99 | 0.8196 | 0.8071 | 0.9826 | 0.57 | 0.84 | 0.53 | 0.1736 | 0.7088 | 0.1655 | 0.67 | 0.69 | 0.59 | 0.1971 | 0.3104 | 0.1620 | 0.72 | 0.63 | 0.53 | 0.2854 | 0.1799 | 0.1148 |
| 276.0820 | 13.7 | C9H18O8 | 3-beta-D-Galactosyl-sn-glycerol | Carbohydrate Metabolism | 1.03 | 0.85 | 0.93 | 0.9409 | 0.7004 | 0.8756 | 1.04 | 1.09 | 1.30 | 0.8879 | 0.7656 | 0.3658 | 0.96 | 0.93 | 1.13 | 0.8905 | 0.7621 | 0.6561 | 0.96 | 1.25 | 1.00 | 0.9058 | 0.5294 | 0.9894 |
| 265.9592 | 17.8 | C3H8O10P2 | 3-Phospho-D-glyceroyl phosphate | Carbohydrate Metabolism | 1.17 | 1.55 | 1.26 | 0.8172 | 0.5678 | 0.6759 | 1.03 | 1.17 | 1.05 | 0.9116 | 0.6515 | 0.8617 | 1.19 | 1.19 | 1.20 | 0.4689 | 0.3946 | 0.6884 | 1.68 | 1.89 | 1.27 | 0.0511 | 0.1003 | 0.2042 |
| 177.0638 | 12.6 | C6H11NO5 | 4-Hydroxy-4-methylglutamate | Carbohydrate Metabolism | 1.05 | 1.21 | 1.40 | 0.7398 | 0.3177 | 0.0542 | 0.96 | 1.13 | 1.06 | 0.8964 | 0.6749 | 0.7927 | 0.75 | 0.79 | 0.80 | 0.1492 | 0.1945 | 0.2764 | 0.72 | 0.96 | 0.50 | 0.3493 | 0.8749 | 0.1494 |
| 104.0474 | 7.8 | C4H8O3 | 4-Hydroxybutanoic acid | Carbohydrate Metabolism | 1.10 | 0.99 | 0.97 | 0.2729 | 0.9296 | 0.6844 | 0.87 | 0.98 | 1.00 | 0.3229 | 0.8167 | 0.9867 | 0.99 | 1.01 | 1.07 | 0.8962 | 0.8780 | 0.4841 | 0.94 | 0.90 | 0.96 | 0.5297 | 0.5075 | 0.8048 |
| 276.0246 | 17.3 | C6H13O10P | 6-Phospho-D-gluconate | Carbohydrate Metabolism | 0.95 | 1.35 | 1.06 | 0.8100 | 0.3992 | 0.8292 | 0.93 | 1.02 | 0.88 | 0.6688 | 0.8929 | 0.4945 | 1.05 | 0.99 | 0.98 | 0.7461 | 0.9440 | 0.9546 | 1.02 | 1.12 | 0.87 | 0.4770 | 0.2607 | 0.1189 |
| 88.0523 | 7.9 | C4H8O2 | Butanoic acid | Carbohydrate Metabolism | 1.02 | 0.85 | 0.90 | 0.8733 | 0.3432 | 0.5265 | 0.83 | 0.93 | 0.87 | 0.2469 | 0.5707 | 0.4151 | 0.98 | 1.03 | 1.13 | 0.8861 | 0.7951 | 0.2790 | 0.85 | 0.99 | 1.02 | 0.4596 | 0.9129 | 0.9113 |
| 174.0165 | 17.4 | C6H6O6 | cis-Aconitate | Carbohydrate Metabolism | 0.99 | 1.04 | 0.99 | 0.9889 | 0.9367 | 0.9883 | 1.00 | 1.11 | 1.16 | 0.9977 | 0.8196 | 0.7471 | 1.31 | 1.20 | 1.04 | 0.5617 | 0.5780 | 0.9291 | 0.81 | 0.84 | 0.98 | 0.5754 | 0.6289 | 0.9640 |
| 209.0536 | 17.7 | C6H8O7 | Citrate | Carbohydrate Metabolism | 1.01 | 1.17 | 0.93 | 0.9872 | 0.7940 | 0.9019 | 0.86 | 0.90 | 0.95 | 0.7398 | 0.8171 | 0.9146 | 0.93 | 0.82 | 1.00 | 0.9108 | 0.7079 | 0.9971 | 0.92 | 0.82 | 0.87 | 0.8686 | 0.6642 | 0.8066 |

| | | | | | | | | | | | | | | | | | | | | | | | | | | | | | |
|---|---|---|---|---|---|---|---|---|---|---|---|---|---|---|---|---|---|---|---|---|---|---|---|---|---|---|---|---|---|
| 166.0479 | 12.7 | C5H10O6 | D-Arabinonate | Carbohydrate Metabolism | 0.91 | 0.93 | 1.06 | 0.7554 | 0.8279 | 0.8888 | 0.98 | 1.03 | 0.98 | 0.9604 | 0.9312 | 0.9461 | 1.09 | 0.93 | 1.00 | 0.7592 | 0.8188 | 0.9964 | 0.82 | 0.83 | 0.82 | 0.6867 | 0.7009 | 0.6962 |
| 120.0422 | 10.4 | C4H8O4 | D-Erythrose | Carbohydrate Metabolism | 1.18 | 1.47 | 1.16 | 0.5534 | 0.2872 | 0.6460 | 0.86 | 1.02 | 0.93 | 0.6640 | 0.9655 | 0.8346 | 0.81 | 0.84 | 0.84 | 0.4742 | 0.5203 | 0.6213 | 1.16 | 0.96 | 1.37 | 0.4782 | 0.8386 | 0.1066 |
| 200.0086 | 12.6 | C4H9O7P | D-Erythrose 4-phosphate | Carbohydrate Metabolism | 0.98 | 1.36 | 1.17 | 0.9690 | 0.5668 | 0.7654 | 1.14 | 1.16 | 1.10 | 0.7999 | 0.7792 | 0.8524 | 1.14 | 0.96 | 1.42 | 0.8084 | 0.9527 | 0.6331 | 1.23 | 1.36 | 1.02 | 0.6276 | 0.3904 | 0.9690 |
| 178.0478 | 13.2 | C6H10O6 | D-Glucono-1,5-lactone | Carbohydrate Metabolism | 1.43 | 1.04 | 1.38 | 0.6143 | 0.8569 | 0.6225 | 1.07 | 1.07 | 1.16 | 0.8028 | 0.8310 | 0.6684 | 1.93 | 1.93 | 2.76 | 0.2484 | 0.1737 | 0.2326 | 1.09 | 1.01 | 0.79 | 0.7084 | 0.9831 | 0.4059 |
| 179.0794 | 16.3 | C6H13NO5 | D-Glucosamine | Carbohydrate Metabolism | 1.16 | 1.16 | 1.12 | 0.8419 | 0.8537 | 0.8838 | 1.30 | 1.01 | 1.10 | 0.7800 | 0.9931 | 0.9033 | 1.02 | 0.90 | 0.92 | 0.9802 | 0.9029 | 0.9265 | 0.92 | 0.90 | 0.95 | 0.9128 | 0.9042 | 0.9511 |
| 226.0688 | 14.2 | C6H12O6 | D-Glucose | Carbohydrate Metabolism | 1.52 | 1.04 | 1.32 | 0.2747 | 0.8790 | 0.4917 | 1.17 | 1.16 | 1.11 | 0.6323 | 0.6780 | 0.6372 | 0.85 | 0.88 | 0.95 | 0.3408 | 0.4712 | 0.7606 | 0.91 | 1.16 | 1.04 | 0.7338 | 0.7490 | 0.9085 |
| 282.0116 | 16.5 | C6H13O9P | D-Glucose 6-phosphate | Carbohydrate Metabolism | 1.08 | 0.91 | 0.88 | 0.8420 | 0.8113 | 0.7667 | 0.91 | 1.06 | 1.03 | 0.7697 | 0.8508 | 0.9132 | 1.24 | 1.16 | 1.27 | 0.5130 | 0.5877 | 0.4991 | 0.80 | 0.94 | 0.83 | 0.5373 | 0.8541 | 0.6137 |
| 194.0427 | 14.3 | C6H10O7 | D-Glucuronate | Carbohydrate Metabolism | 1.16 | 1.27 | 1.16 | 0.4991 | 0.3267 | 0.4699 | 1.13 | 1.03 | 0.99 | 0.5565 | 0.8740 | 0.9734 | 1.21 | 1.23 | 1.21 | 0.2232 | 0.2346 | 0.3542 | 0.96 | 0.94 | 1.00 | 0.8366 | 0.7718 | 0.9996 |
| 150.0528 | 14.2 | C5H10O5 | D-Ribose | Carbohydrate Metabolism | 0.87 | 1.02 | 0.70 | 0.7265 | 0.9655 | 0.4166 | 1.11 | 1.15 | 1.09 | 0.6619 | 0.5794 | 0.8136 | 1.10 | 1.21 | 1.09 | 0.5489 | 0.4274 | 0.6669 | 0.99 | 1.02 | 1.23 | 0.9497 | 0.9104 | 0.3465 |
| 309.9855 | 17.4 | C5H12O11P2 | D-Ribose 1,5-bisphosphate | Carbohydrate Metabolism | 1.19 | 1.29 | 1.26 | 0.4409 | 0.4740 | 0.3927 | 0.93 | 0.98 | 1.02 | 0.8649 | 0.9510 | 0.9678 | 0.94 | 0.97 | 0.94 | 0.8879 | 0.9375 | 0.9007 | 1.06 | 1.20 | 1.02 | 0.8662 | 0.6070 | 0.9589 |
| 290.0402 | 16.0 | C7H15O10P | D-Sedoheptulose 7-phosphate | Carbohydrate Metabolism | 1.09 | 1.10 | 1.13 | 0.6330 | 0.7083 | 0.2142 | 0.80 | 0.87 | 0.91 | 0.3216 | 0.5207 | 0.6169 | 0.96 | 0.98 | 0.93 | 0.8738 | 0.9270 | 0.7893 | 0.78 | 0.88 | 0.65 | 0.2992 | 0.6531 | 0.1547 |
| 589.0818 | 17.2 | C16H25N5O15P2 | GDP-L-fucose | Carbohydrate Metabolism | 0.98 | 1.23 | 1.14 | 0.9335 | 0.4232 | 0.5438 | 0.96 | 1.00 | 0.96 | 0.8585 | 0.9835 | 0.8484 | 0.97 | 1.03 | 1.10 | 0.9005 | 0.9241 | 0.7531 | 0.93 | 0.97 | 0.85 | 0.6890 | 0.9019 | 0.3894 |
| 605.0775 | 17.9 | C16H25N5O16P2 | GDP-mannose | Carbohydrate Metabolism | 1.11 | 1.32 | 1.24 | 0.5259 | 0.3710 | 0.3429 | 0.98 | 1.21 | 1.07 | 0.9121 | 0.5237 | 0.7869 | 1.02 | 1.04 | 1.12 | 0.8926 | 0.8612 | 0.7383 | 1.01 | 1.19 | 0.98 | 0.9726 | 0.4653 | 0.9227 |
| 291.9749 | 17.5 | C6H9O9P | L-Ascorbate 6-phosphate | Carbohydrate Metabolism | 1.13 | 1.20 | 1.15 | 0.3966 | 0.3441 | 0.2750 | 0.94 | 1.03 | 0.99 | 0.5632 | 0.7756 | 0.9126 | 1.16 | 1.12 | 1.14 | 0.3545 | 0.3106 | 0.3322 | 1.12 | 1.14 | 1.17 | 0.3003 | 0.3057 | 0.3561 |
| 244.0349 | 15.2 | C6H13O8P | L-Fuculose 1-phosphate | Carbohydrate Metabolism | 0.90 | 1.04 | 1.04 | 0.8407 | 0.9410 | 0.9381 | 0.95 | 0.96 | 0.79 | 0.8667 | 0.9161 | 0.5948 | 1.02 | 0.99 | 1.17 | 0.9610 | 0.9883 | 0.6893 | 1.10 | 1.21 | 1.06 | 0.8504 | 0.7239 | 0.9111 |
| 221.0900 | 13.6 | C8H15NO6 | N-Acetyl-D-mannosamine | Carbohydrate Metabolism | 0.94 | 0.87 | 0.88 | 0.8293 | 0.5843 | 0.5319 | 0.93 | 0.99 | 1.15 | 0.8168 | 0.9683 | 0.7048 | 0.91 | 1.10 | 1.07 | 0.6695 | 0.7700 | 0.7752 | 0.99 | 1.24 | 0.99 | 0.9755 | 0.5450 | 0.9798 |
| 309.1058 | 14.7 | C11H19NO9 | N-Acetylneuraminate | Carbohydrate Metabolism | 1.11 | 0.86 | 0.95 | 0.8396 | 0.5535 | 0.8952 | 0.97 | 1.12 | 0.90 | 0.9393 | 0.6992 | 0.7029 | 0.92 | 1.02 | 1.23 | 0.6624 | 0.9184 | 0.5346 | 0.83 | 0.96 | 0.94 | 0.2099 | 0.8809 | 0.8196 |
| 89.9953 | 17.4 | C2H2O4 | Oxalate | Carbohydrate Metabolism | 1.16 | 1.17 | 1.16 | 0.0374 | 0.0510 | 0.0818 | 1.04 | 1.05 | 1.11 | 0.8076 | 0.7125 | 0.4107 | 1.10 | 1.11 | 1.04 | 0.5920 | 0.2538 | 0.7942 | 0.91 | 0.83 | 0.92 | 0.1797 | 0.0875 | 0.2609 |
| 167.9824 | 17.2 | C3H5O6P | Phosphoenolpyruvate | Carbohydrate Metabolism | 1.13 | 1.24 | 1.13 | 0.6088 | 0.4696 | 0.5600 | 0.87 | 1.02 | 0.94 | 0.4857 | 0.9044 | 0.7503 | 1.06 | 1.01 | 0.97 | 0.7264 | 0.9415 | 0.9084 | 1.22 | 1.25 | 1.13 | 0.0909 | 0.0227 | 0.1629 |
| 88.0160 | 14.7 | C3H4O3 | Pyruvate | Carbohydrate Metabolism | 0.79 | 0.99 | 0.76 | 0.1856 | 0.9258 | 0.1596 | 1.07 | 0.96 | 0.95 | 0.6242 | 0.7955 | 0.7766 | 0.97 | 0.94 | 0.89 | 0.8028 | 0.5518 | 0.2983 | 0.96 | 1.04 | 1.05 | 0.5240 | 0.7392 | 0.5774 |
| 152.0685 | 12.9 | C5H12O5 | Ribitol | Carbohydrate Metabolism | 1.06 | 0.95 | 1.32 | 0.9069 | 0.9505 | 0.5515 | 0.84 | 1.06 | 1.94 | 0.9002 | 0.9616 | 0.6354 | 0.30 | 0.79 | 0.47 | NA | 0.7376 | NA | 0.58 | 0.58 | 0.60 | 0.4990 | 0.5258 | NA |
| 364.0981 | 16.0 | C12H22O11 | Sucrose | Carbohydrate Metabolism | 0.98 | 1.03 | 1.00 | 0.9493 | 0.9233 | 0.9966 | 1.15 | 1.21 | 1.14 | 0.7051 | 0.5598 | 0.5696 | 0.83 | 0.85 | 0.92 | 0.6663 | 0.6969 | 0.8353 | 0.98 | 0.99 | 0.88 | 0.9618 | 0.9802 | 0.6435 |
| 424.0372 | 14.6 | C12H18N4O7P2S | Thiamin diphosphate | Carbohydrate Metabolism | 0.96 | 1.19 | 0.99 | 0.8642 | 0.6193 | 0.9531 | 0.89 | 1.15 | 0.95 | 0.6858 | 0.5543 | 0.8554 | 0.69 | 0.89 | 0.62 | 0.3380 | 0.7076 | 0.2422 | 0.69 | 0.76 | 0.44 | 0.1646 | 0.2145 | 0.0207 |
| 580.0340 | 18.6 | C15H22N2O18P2 | UDP-glucuronate | Carbohydrate Metabolism | 0.90 | 1.21 | 1.07 | 0.7054 | 0.5734 | 0.8133 | 1.04 | 1.11 | 1.00 | 0.8119 | 0.4888 | 0.9934 | 0.94 | 0.93 | 0.95 | 0.6983 | 0.6768 | 0.8648 | 1.02 | 1.07 | 0.80 | 0.9245 | 0.7430 | 0.3541 |
| 339.9960 | 18.7 | C6H14O12P2 | D-Fructose 1,6-bisphosphate | Energy Metabolism | 1.13 | 1.48 | 1.37 | 0.6589 | 0.0606 | 0.1051 | 0.69 | 0.83 | 0.88 | 0.1625 | 0.3840 | 0.6765 | 0.91 | 1.08 | 0.91 | 0.6516 | 0.6428 | 0.6769 | 0.88 | 0.91 | 0.86 | 0.5864 | 0.5409 | 0.4553 |
| 370.0069 | 17.9 | C7H16O13P2 | D-Sedoheptulose 1,7-bisphosphate | Energy Metabolism | 0.74 | 1.14 | 1.08 | 0.5163 | 0.7500 | 0.8103 | 0.96 | 0.79 | 0.92 | 0.9201 | 0.5895 | 0.9014 | 0.92 | 0.84 | 0.69 | 0.5022 | 0.5544 | 0.4702 | 1.42 | 0.90 | 0.55 | 0.4153 | 0.7734 | 0.3296 |
| 665.1249 | 13.1 | C21H29N7O14P2 | NADH | Energy Metabolism | 0.99 | 0.98 | 0.91 | 0.9840 | 0.9632 | 0.8506 | 0.73 | 0.88 | 0.88 | 0.4057 | 0.7638 | 0.7306 | 1.01 | 0.82 | 1.00 | 0.9869 | 0.6596 | 0.9961 | 0.85 | 1.02 | 0.80 | 0.5097 | 0.9321 | 0.4818 |
| 743.0757 | 16.5 | C21H28N7O17P3 | NADP+ | Energy Metabolism | 1.09 | 1.30 | 1.23 | 0.5154 | 0.2205 | 0.1923 | 0.89 | 1.06 | 1.04 | 0.1519 | 0.6959 | 0.8215 | 0.97 | 1.03 | 1.00 | 0.8519 | 0.8660 | 0.9929 | 1.03 | 1.06 | 0.93 | 0.7069 | 0.4688 | 0.3574 |
| 97.9769 | 18.0 | H3O4P | Orthophosphate | Energy Metabolism | 1.04 | 1.44 | 1.08 | 0.7305 | 0.0036 | 0.3218 | 0.97 | 1.10 | 1.36 | 0.6909 | 0.1270 | 0.0053 | 0.82 | 1.01 | 0.76 | 0.0576 | 0.8760 | 0.0259 | 0.72 | 0.97 | 0.96 | 0.0012 | 0.3438 | 0.0705 |
| 423.3347 | 7.8 | C25H45NO4 | O-9Z,12Z-Hexadecadienoyl-R-carnitine | Fatty Acyls [FA] | 0.66 | 0.64 | 0.73 | 0.5876 | 0.6115 | 0.6980 | 0.98 | 0.83 | 0.89 | 0.9767 | 0.8161 | 0.8875 | 1.10 | 1.46 | 1.82 | 0.9010 | 0.5103 | 0.3248 | 1.58 | 1.18 | 0.86 | 0.4810 | 0.8417 | 0.7428 |
| 335.0616 | 15.6 | C8H15O11P | 3-Deoxy-D-manno-octulosonate 8-phosphate | Glycan Biosynthesis and Metabolism | 0.90 | 0.90 | 0.98 | 0.8012 | 0.8092 | 0.9583 | 0.77 | 1.11 | 1.03 | 0.6633 | 0.8648 | 0.9593 | 1.04 | 1.05 | 1.02 | 0.9331 | 0.9215 | 0.9707 | 0.79 | 1.06 | 1.08 | 0.6028 | 0.9011 | 0.8852 |
| 507.3693 | 4.7 | C26H54NO6P | 1-(11Z-octadecenyl)-sn-glycero-3-phosphocholine | Glycerophospholipids [GP] | 0.99 | 1.06 | 0.94 | 0.9588 | 0.7767 | 0.8111 | 0.99 | 1.00 | 0.98 | 0.9657 | 0.9879 | 0.8917 | 1.01 | 0.83 | 0.97 | 0.9690 | 0.5493 | 0.8993 | 1.00 | 1.01 | 0.92 | 0.9853 | 0.9736 | 0.7690 |
| 145.1103 | 13.3 | C7H15NO2 | Acetylcholine | Lipid Metabolism | 1.12 | 1.08 | 1.07 | 0.5020 | 0.7315 | 0.7780 | 1.03 | 1.08 | 1.15 | 0.8790 | 0.7186 | 0.4584 | 1.17 | 1.06 | 1.17 | 0.3195 | 0.7532 | 0.3473 | 0.97 | 0.94 | 0.94 | 0.8865 | 0.7912 | 0.7488 |

| | | | | | | | | | | | | | | | | | | | | | | | | | | | | |
|---|---|---|---|---|---|---|---|---|---|---|---|---|---|---|---|---|---|---|---|---|---|---|---|---|---|---|---|---|
| 488.1069 | 15.3 | C14H26N4O11P2 | CDP-choline | Lipid Metabolism | 1.01 | 1.06 | 0.93 | 0.9870 | 0.8708 | 0.8503 | 0.95 | 1.01 | 0.99 | 0.8855 | 0.9833 | 0.9732 | 0.94 | 0.89 | 1.06 | 0.8474 | 0.7299 | 0.8512 | 1.06 | 1.04 | 1.32 | 0.8439 | 0.9013 | 0.4000 |
| 446.0603 | 16.2 | C11H20N4O11P2 | CDP-ethanolamine | Lipid Metabolism | 1.02 | 1.04 | 0.97 | 0.9188 | 0.8441 | 0.8713 | 1.21 | 1.22 | 1.74 | 0.2833 | 0.2865 | 0.0959 | 1.74 | 1.62 | 2.04 | 0.0548 | 0.1064 | 0.1180 | 1.91 | 1.76 | 1.93 | 0.0809 | 0.0206 | 0.1578 |
| 384.3393 | 5.1 | C27H44O | Cholesta-5,7-dien-3beta-ol | Lipid Metabolism | 1.23 | 1.21 | 1.02 | 0.4871 | 0.4350 | 0.9496 | 0.88 | 1.10 | 1.18 | 0.3575 | 0.3771 | 0.1920 | 1.59 | 1.10 | 1.25 | 0.0672 | 0.5530 | 0.4187 | 0.94 | 1.16 | 0.75 | 0.6045 | 0.2780 | 0.0917 |
| 229.0715 | 14.4 | C5H14NO4P | Choline phosphate | Lipid Metabolism | 1.05 | 1.03 | 1.01 | 0.9552 | 0.9787 | 0.9955 | 1.06 | 1.08 | 1.18 | 0.9453 | 0.9259 | 0.8318 | 1.19 | 1.25 | 1.34 | 0.8133 | 0.7619 | 0.6950 | 0.82 | 1.22 | 1.21 | 0.8116 | 0.7876 | 0.7983 |
| 172.1464 | 4.3 | C10H20O2 | Decanoic acid | Lipid Metabolism | 1.36 | 1.19 | 1.23 | 0.2761 | 0.5637 | 0.4712 | 1.36 | 0.86 | 1.07 | 0.5851 | 0.8532 | 0.9315 | 1.03 | 0.58 | 1.21 | 0.9718 | NA | 0.8205 | 1.75 | 1.60 | 2.10 | 0.6188 | 0.6785 | 0.5005 |
| 921.2525 | 14.2 | C31H54N7O17P3S | Decanoyl-CoA | Lipid Metabolism | 0.81 | 0.91 | 0.81 | 0.5975 | 0.8181 | 0.5878 | 0.68 | 1.17 | 0.70 | 0.2828 | 0.6707 | 0.2914 | 0.73 | 0.82 | 0.78 | 0.1686 | 0.3819 | 0.6439 | 0.67 | 0.75 | 0.59 | 0.0591 | 0.0628 | 0.0711 |
| 200.1776 | 4.1 | C12H24O2 | Dodecanoic acid | Lipid Metabolism | 0.86 | 0.72 | 0.82 | 0.7538 | 0.5467 | 0.6833 | 0.93 | 1.13 | 1.10 | 0.7016 | 0.5096 | 0.5905 | 1.15 | 1.03 | 1.09 | 0.5683 | 0.9151 | 0.5400 | 0.72 | 0.85 | 0.80 | 0.2522 | 0.5293 | 0.3700 |
| 254.2246 | 4.0 | C16H30O2 | FA(16:1) | Lipid Metabolism | 1.54 | 1.19 | 1.35 | 0.1288 | 0.4635 | 0.1726 | 1.09 | 1.20 | 0.94 | 0.6773 | 0.6526 | 0.7154 | 1.23 | 1.27 | 1.33 | 0.2226 | 0.4237 | 0.1154 | 0.97 | 0.97 | 0.85 | 0.8061 | 0.8369 | 0.2950 |
| 256.2401 | 4.0 | C16H32O2 | Hexadecanoic acid | Lipid Metabolism | 1.53 | 1.69 | 1.26 | 0.2784 | 0.3209 | 0.4551 | 1.35 | 1.07 | 1.03 | 0.5069 | 0.9032 | 0.9416 | 1.29 | 0.80 | 1.31 | 0.6066 | 0.2267 | 0.3617 | 1.14 | 1.20 | 1.55 | 0.6229 | 0.2484 | 0.1056 |
| 284.2714 | 3.9 | C18H36O2 | Octadecanoic acid | Lipid Metabolism | 1.47 | 1.70 | 1.18 | 0.2374 | 0.2790 | 0.5304 | 1.12 | 0.99 | 1.04 | 0.7603 | 0.9766 | 0.8895 | 1.35 | 0.98 | 1.27 | 0.5329 | 0.9203 | 0.3722 | 1.16 | 1.18 | 1.63 | 0.5727 | 0.4984 | 0.0440 |
| 169.0505 | 14.9 | C4H12NO4P | Phosphodimethylethanolamine | Lipid Metabolism | 1.05 | 0.82 | 0.91 | 0.8208 | 0.2828 | 0.5275 | 1.61 | 1.38 | 1.62 | 0.0639 | 0.2602 | 0.1267 | 2.20 | 2.26 | 2.69 | 0.0170 | 0.0593 | 0.0072 | 3.91 | 3.49 | 3.18 | 0.0540 | 0.0405 | 0.0560 |
| 257.1028 | 14.4 | C8H20NO6P | sn-glycero-3-Phosphocholine | Lipid Metabolism | 1.11 | 1.14 | 1.20 | 0.7599 | 0.6802 | 0.6258 | 0.95 | 1.06 | 1.03 | 0.8710 | 0.8668 | 0.9292 | 1.25 | 1.09 | 1.09 | 0.5984 | 0.8170 | 0.8150 | 0.90 | 0.80 | 0.77 | 0.7286 | 0.4829 | 0.4628 |
| 125.0147 | 14.7 | C2H7NO3S | Taurine | Lipid Metabolism | 1.06 | 1.01 | 0.94 | 0.9180 | 0.9872 | 0.9038 | 0.96 | 1.14 | 0.97 | 0.9445 | 0.7985 | 0.9528 | 0.86 | 0.86 | 1.05 | 0.7732 | 0.7902 | 0.9366 | 1.06 | 0.97 | 1.29 | 0.8999 | 0.9418 | 0.7098 |
| 228.2089 | 4.0 | C14H28O2 | Tetradecanoic acid | Lipid Metabolism | 0.94 | 1.20 | 1.10 | 0.8329 | 0.4356 | 0.6490 | 1.13 | 1.15 | 1.03 | 0.6254 | 0.6960 | 0.8511 | 1.17 | 1.04 | 1.27 | 0.5183 | 0.8389 | 0.2458 | 1.06 | 0.97 | 1.18 | 0.7860 | 0.7817 | 0.1219 |
| 186.1620 | 28.4 | C11H22O2 | [FA (11:0)] undecanoic acid | Lipids: Fatty Acyls | 1.08 | 1.06 | 1.05 | 0.1697 | 0.2706 | 0.4068 | 0.93 | 0.98 | 0.96 | 0.7441 | 0.9278 | 0.8467 | 1.09 | 1.13 | 1.15 | 0.7089 | 0.6331 | 0.5858 | 1.00 | 0.97 | 0.99 | 0.9924 | 0.8220 | 0.9727 |
| 282.2559 | 8.0 | C18H34O2 | [FA (18:1)] 9Z-octadecenoic acid | Lipids: Fatty Acyls | 0.94 | 0.85 | 1.05 | 0.7978 | 0.5269 | 0.8640 | 1.05 | 1.21 | 1.20 | 0.8408 | 0.4671 | 0.4748 | 1.00 | 0.94 | 1.18 | 0.9904 | 0.7790 | 0.5790 | 0.76 | 0.75 | 0.96 | 0.0766 | 0.2129 | 0.8304 |
| 278.2245 | 4.0 | C18H30O2 | [FA (18:3)] 9Z,12Z,15Z-octadecatrienoic acid | Lipids: Fatty Acyls | 1.32 | 1.22 | 1.33 | 0.3423 | 0.3572 | 0.1825 | 0.84 | 0.96 | 1.52 | 0.4252 | 0.8536 | 0.4597 | 1.21 | 1.02 | 1.15 | 0.1944 | 0.8725 | 0.3845 | 0.85 | 0.75 | 1.01 | 0.5429 | 0.3272 | 0.9559 |
| 330.2560 | 3.9 | C22H34O2 | [FA (22:5)] 7Z,10Z,13Z,16Z,19Z-docosapentaenoic acid | Lipids: Fatty Acyls | 1.09 | 0.99 | 0.91 | 0.7958 | 0.9781 | 0.8072 | 1.01 | 1.14 | 0.95 | 0.9681 | 0.6627 | 0.8602 | 1.84 | 1.66 | 2.10 | 0.0646 | 0.1577 | 0.0280 | 0.91 | 1.05 | 1.08 | 0.2761 | 0.6386 | 0.5603 |
| 98.0368 | 15.7 | C5H6O2 | [FA (5:2)] 2,4-pentadienoic acid | Lipids: Fatty Acyls | 1.10 | 1.35 | 1.06 | 0.7347 | 0.3064 | 0.8304 | 1.10 | 1.20 | 1.33 | 0.7736 | 0.5836 | 0.2421 | 0.91 | 0.91 | 0.82 | 0.4433 | 0.4522 | 0.1844 | 2.25 | 1.71 | 3.21 | 0.1501 | 0.2978 | 0.0154 |
| 160.0736 | 4.8 | C7H12O4 | [FA (7:0/2:0)] Heptanedioic acid | Lipids: Fatty Acyls | 0.88 | 0.98 | 0.90 | 0.5717 | 0.9504 | 0.6167 | 1.05 | 1.28 | 0.90 | 0.8886 | 0.4456 | 0.7507 | 1.09 | 1.15 | 1.18 | 0.6493 | 0.1958 | 0.2003 | 1.07 | 0.76 | 1.00 | 0.8980 | 0.3129 | 0.9867 |
| 240.2089 | 28.5 | C15H28O2 | [FA dimethyl(13:0)] 2,5-dimethyl-2E-tridecenoic acid | Lipids: Fatty Acyls | 1.16 | 1.13 | 1.03 | 0.0666 | 0.3153 | 0.6889 | 0.90 | 0.97 | 0.95 | 0.4537 | 0.7978 | 0.7226 | 0.97 | 1.07 | 1.04 | 0.8725 | 0.7917 | 0.7928 | 1.08 | 1.02 | 1.16 | 0.5896 | 0.6576 | 0.1370 |
| 365.2775 | 28.2 | C18H36O6 | [FA hydroxy(18:0)] 9,10,12,13-tetrahydroxy-octadecanoic acid | Lipids: Fatty Acyls | 1.13 | 1.07 | 1.20 | 0.5345 | 0.6914 | 0.3578 | 1.04 | 0.99 | 0.98 | 0.8694 | 0.9696 | 0.9079 | 0.93 | 1.16 | 1.35 | 0.7712 | 0.5355 | 0.1610 | 0.91 | 0.83 | 0.79 | 0.4181 | 0.2418 | 0.0654 |
| 311.2460 | 4.4 | C18H30O3 | [FA oxo(5:1/5:0/8:0)] (1S,2S)-3-oxo-2-(2'Z-pentenyl)-cyclopentaneoctanoic acid | Lipids: Fatty Acyls | 1.15 | 1.32 | 1.01 | 0.6646 | 0.3962 | 0.9767 | 1.16 | 1.33 | 1.01 | 0.6929 | 0.4048 | 0.9813 | 0.92 | 1.21 | 0.81 | 0.9146 | 0.8269 | 0.7956 | 1.23 | 1.29 | 1.23 | 0.3463 | 0.3060 | 0.3512 |
| 618.4712 | 28.4 | C34H66O9 | 1-(O-alpha-D-glucopyranosyl)-3-keto-(25R,27R)-octacosanediol | Lipids: Fatty Acyls | 1.13 | 1.33 | 1.03 | 0.9097 | 0.8116 | 0.9754 | 0.75 | 0.91 | 0.91 | 0.7993 | 0.9287 | 0.9277 | 0.91 | 1.06 | 1.00 | 0.7670 | 0.8614 | 0.9891 | 1.25 | 0.87 | 0.99 | 0.7915 | 0.8785 | 0.9925 |
| 215.1158 | 12.7 | C10H17NO4 | 2-Amino-9,10-epoxy-8-oxodecanoic acid | Lipids: Fatty Acyls | 1.32 | 1.04 | 1.18 | 0.2517 | 0.8053 | 0.3623 | 1.07 | 1.33 | 1.09 | 0.6305 | 0.0941 | 0.7120 | 1.07 | 0.91 | 0.82 | 0.8260 | 0.7446 | 0.5508 | 1.03 | 0.97 | 0.84 | 0.9201 | 0.9142 | 0.5577 |
| 190.1722 | 4.2 | C14H22 | 3,5,7-Trimethyl-2E,4E,6E,8E-undecatetraene | Lipids: Fatty Acyls | 1.34 | 1.29 | 1.17 | 0.2657 | 0.2258 | 0.6257 | 0.93 | 1.21 | 0.91 | 0.8507 | 0.6800 | 0.8142 | 0.33 | 0.59 | 0.57 | 0.0352 | 0.1255 | 0.1044 | 0.88 | 0.94 | 0.90 | 0.5073 | 0.7241 | 0.5749 |
| 309.3031 | 4.9 | C20H36O | 3,7,11,15-Tetramethyl-6,10,14-hexadecatrien-1-ol | Lipids: Fatty Acyls | 0.70 | 0.90 | 0.65 | 0.5350 | 0.8509 | 0.5244 | 0.70 | 0.92 | 1.22 | 0.6420 | 0.9082 | 0.7700 | 0.88 | 0.73 | 0.88 | 0.8255 | 0.5692 | 0.8091 | 0.54 | 0.92 | 0.76 | 0.2141 | 0.8373 | 0.5422 |
| 214.1569 | 4.2 | C12H22O3 | 3-Oxododecanoic acid | Lipids: Fatty Acyls | 0.77 | 0.67 | 0.66 | 0.5373 | 0.3757 | 0.3807 | 0.97 | 1.69 | 1.14 | 0.9573 | 0.5214 | 0.5660 | 0.25 | 0.46 | 0.57 | 0.0143 | 0.0332 | 0.0702 | 1.06 | 1.20 | 0.98 | 0.8980 | 0.7906 | 0.9704 |
| 118.0630 | 7.9 | C5H10O3 | 5-Hydroxypentanoate | Lipids: Fatty Acyls | 0.57 | 1.00 | 0.62 | 0.4881 | 0.9982 | 0.5909 | 0.85 | 1.20 | 1.51 | 0.8505 | 0.8131 | 0.6101 | 0.84 | 0.81 | 0.88 | 0.4658 | 0.4363 | 0.5785 | 0.50 | 0.88 | 0.70 | 0.2989 | 0.7678 | 0.5262 |
| 311.3187 | 4.8 | C20H38O | 6Z,9Z-Eicosadien-11-ol | Lipids: Fatty Acyls | 1.23 | 1.14 | 1.17 | 0.1203 | 0.3979 | 0.2431 | 1.01 | 1.24 | 1.14 | 0.8672 | 0.3681 | 0.2455 | 1.09 | 0.93 | 1.19 | 0.7661 | 0.8481 | 0.7622 | 0.81 | 0.72 | 0.92 | 0.3835 | 0.1920 | 0.6685 |
| 213.2457 | 7.9 | C14H28 | 6Z-Tetradecene | Lipids: Fatty Acyls | 1.67 | 0.95 | 1.16 | 0.4131 | 0.9263 | 0.7344 | 0.91 | 1.27 | 1.53 | 0.8576 | 0.6549 | 0.4725 | 0.96 | 0.82 | 0.58 | 0.8648 | 0.4653 | 0.2795 | 0.79 | 0.86 | 0.90 | 0.6783 | 0.7760 | 0.8560 |
| 440.0931 | 15.4 | C18H34Br2O2 | 9,10-dibromo-stearic acid | Lipids: Fatty Acyls | 1.32 | 0.87 | 0.66 | 0.5159 | 0.5697 | 0.1518 | 1.13 | 1.06 | 1.05 | 0.7807 | 0.8323 | 0.8788 | 1.00 | 0.96 | 0.96 | 0.9983 | 0.8140 | 0.8085 | 0.64 | 0.91 | 0.79 | 0.3334 | 0.8272 | 0.5156 |
| 399.2986 | 5.4 | C22H38O5 | 9-oxo-11R,15S-dihydroxy-16,16-dimethyl-13E-prostaenoic acid | Lipids: Fatty Acyls | 1.09 | 0.99 | 1.10 | 0.6139 | 0.9567 | 0.6346 | 0.99 | 0.99 | 1.06 | 0.9682 | 0.9663 | 0.7526 | 0.97 | 1.13 | 1.18 | 0.9748 | 0.8898 | 0.8590 | 0.97 | 0.90 | 0.94 | 0.8896 | 0.5885 | 0.7409 |
| 172.1100 | 4.7 | C9H16O3 | 9-Oxononanoic acid | Lipids: Fatty Acyls | 1.18 | 0.93 | 0.99 | 0.8820 | 0.9457 | 0.9920 | 0.85 | 0.89 | 1.07 | 0.8882 | 0.9124 | 0.9512 | 1.16 | 1.04 | 1.10 | 0.6067 | 0.6696 | 0.5282 | 0.99 | 0.82 | 0.99 | 0.9900 | 0.8076 | 0.9876 |

| | | | | | | | | | | | | | | | | | | | | | | | | | | | | |
|---|---|---|---|---|---|---|---|---|---|---|---|---|---|---|---|---|---|---|---|---|---|---|---|---|---|---|---|---|
| 171.1623 | 28.6 | C10H21NO | decanamide | Lipids: Fatty Acyls | 1.13 | 1.20 | 1.19 | 0.3847 | 0.4863 | 0.5864 | 1.04 | 1.08 | 1.07 | 0.8484 | 0.6930 | 0.7339 | 1.14 | 1.22 | 1.16 | 0.5987 | 0.5521 | 0.5913 | 1.02 | 0.97 | 1.01 | 0.8628 | 0.8367 | 0.9505 |
| 199.1936 | 28.6 | C12H25NO | Dodecanamide | Lipids: Fatty Acyls | 1.34 | 1.31 | 1.17 | 0.3529 | 0.1584 | 0.2972 | 1.17 | 1.21 | 1.27 | 0.6773 | 0.3684 | 0.3678 | 1.05 | 1.01 | 0.84 | 0.8876 | 0.9780 | 0.6587 | 0.69 | 0.89 | 0.87 | 0.3631 | 0.7068 | 0.6360 |
| 198.1621 | 28.2 | C12H22O2 | FA (12:1) dodecenoic acid | Lipids: Fatty Acyls | 1.10 | 0.92 | 0.91 | 0.7785 | 0.8219 | 0.7822 | 0.99 | 1.14 | 1.11 | 0.9657 | 0.5454 | 0.6080 | 1.00 | 1.18 | 1.35 | 0.9878 | 0.5331 | 0.1487 | 0.74 | 0.87 | 0.68 | 0.4746 | 0.7170 | 0.3711 |
| 213.1729 | 28.2 | C12H20O2 | FA (12:2) | Lipids: Fatty Acyls | 0.92 | 1.01 | 1.10 | 0.7855 | 0.9676 | 0.7450 | 1.02 | 0.87 | 0.98 | 0.9631 | 0.7570 | 0.9589 | 0.86 | 1.14 | 0.88 | 0.4047 | 0.4488 | 0.4879 | 1.04 | 1.25 | 1.10 | 0.8037 | 0.3052 | 0.7027 |
| 227.1885 | 4.8 | C13H22O2 | FA (13:2) tridecadienoic acid | Lipids: Fatty Acyls | 1.35 | 1.30 | 1.55 | 0.4534 | 0.4012 | 0.1876 | 1.11 | 1.09 | 1.37 | 0.6339 | 0.5788 | 0.0615 | 2.18 | 2.70 | 0.89 | 0.3194 | 0.0145 | 0.8072 | 1.13 | 0.84 | 0.90 | 0.6997 | 0.2716 | 0.6420 |
| 226.1928 | 28.5 | C14H26O2 | FA (14:1) tetradecenoic acid | Lipids: Fatty Acyls | 3.31 | 2.06 | 1.14 | 0.0080 | 0.1772 | 0.7639 | 1.13 | 3.29 | 3.59 | 0.7955 | 0.2204 | 0.2143 | 1.10 | 1.09 | 1.21 | 0.5784 | 0.4736 | 0.1909 | 1.21 | 1.58 | 1.63 | 0.3394 | 0.1111 | 0.4319 |
| 246.1594 | 10.1 | C14H24O2 | FA (14:1)nonanoic acid | Lipids: Fatty Acyls | 1.42 | 1.40 | 1.48 | 0.0076 | 0.2399 | 0.1372 | 0.94 | 1.14 | 1.04 | 0.7348 | 0.4894 | 0.8511 | 0.83 | 0.86 | 1.04 | 0.0876 | 0.3904 | 0.3885 | 1.12 | 0.96 | 0.97 | 0.5756 | 0.7340 | 0.7852 |
| 208.1828 | 4.6 | C14H24O | FA (14:2) tetradecadienal | Lipids: Fatty Acyls | 1.08 | 1.14 | 0.97 | 0.6109 | 0.2841 | 0.8216 | 1.16 | 1.14 | 1.00 | 0.2886 | 0.1910 | 0.9748 | 1.80 | 0.77 | 1.17 | 0.1121 | 0.0532 | 0.1908 | 1.06 | 1.01 | 0.94 | 0.5689 | 0.9290 | 0.6188 |
| 252.2089 | 4.2 | C16H28O2 | FA (16:2) | Lipids: Fatty Acyls | 0.67 | 1.13 | 0.63 | 0.3738 | 0.7729 | 0.3813 | 1.85 | 0.93 | 0.86 | 0.0578 | 0.8340 | 0.6498 | 0.46 | 0.70 | 0.64 | 0.0355 | 0.0867 | 0.0514 | 1.25 | 1.03 | 2.11 | 0.5311 | 0.8418 | 0.0967 |
| 270.2558 | 28.5 | C17H34O2 | FA (17:0) | Lipids: Fatty Acyls | 0.94 | 0.86 | 0.81 | 0.8663 | 0.6858 | 0.5715 | 0.64 | 0.85 | 1.06 | 0.4623 | 0.7532 | 0.9041 | 0.99 | 1.07 | 0.99 | 0.9434 | 0.7564 | 0.9645 | 0.67 | 0.95 | 1.10 | 0.0809 | 0.7612 | 0.7193 |
| 312.3028 | 3.9 | C20H40O2 | FA (20:0) | Lipids: Fatty Acyls | 1.23 | 1.15 | 1.09 | 0.2341 | 0.1008 | 0.3906 | 1.37 | 1.06 | 1.24 | 0.1155 | 0.7842 | 0.1239 | 1.28 | 1.01 | 1.16 | 0.5198 | 0.9753 | 0.4853 | 0.89 | 0.98 | 0.90 | 0.3057 | 0.9239 | 0.3556 |
| 304.2402 | 3.9 | C20H32O2 | FA (20:4) | Lipids: Fatty Acyls | 1.35 | 1.51 | 1.20 | 0.1940 | 0.1516 | 0.4390 | 1.18 | 1.12 | 1.12 | 0.5874 | 0.7864 | 0.6062 | 1.42 | 1.22 | 1.54 | 0.2355 | 0.4921 | 0.1488 | 1.02 | 0.96 | 1.37 | 0.9141 | 0.7985 | 0.0559 |
| 144.1150 | 4.5 | C8H16O2 | FA (8:0) octanoic acid | Lipids: Fatty Acyls | 1.17 | 1.40 | 1.15 | 0.5329 | 0.2561 | 0.6044 | 0.98 | 1.13 | 1.25 | 0.9356 | 0.4609 | 0.2750 | 1.09 | 1.03 | 1.11 | 0.7676 | 0.9196 | 0.7358 | 1.29 | 1.20 | 1.67 | 0.4568 | 0.6235 | 0.0251 |
| 126.1045 | 4.3 | C8H14O | FA (8:1) octenal | Lipids: Fatty Acyls | 1.11 | 1.17 | 1.17 | 0.6824 | 0.5296 | 0.5815 | 0.90 | 0.92 | 0.99 | 0.6959 | 0.7352 | 0.9634 | 0.51 | 0.84 | 1.00 | 0.0537 | 0.4439 | 0.9956 | 1.22 | 1.17 | 1.36 | 0.6706 | 0.7290 | 0.5002 |
| 188.1412 | 7.8 | C10H20O3 | FA hydroxy(10:0) | Lipids: Fatty Acyls | 1.33 | 1.22 | 0.97 | 0.4134 | 0.5968 | 0.9411 | 1.09 | 1.27 | 1.39 | 0.7606 | 0.5395 | 0.3455 | 0.85 | 1.16 | 1.29 | 0.4044 | 0.4007 | 0.2975 | 0.69 | 1.02 | 1.06 | 0.2265 | 0.9195 | 0.8361 |
| 272.2351 | 28.5 | C16H32O3 | FA hydroxy(16:0)] hexadecanoic acid | Lipids: Fatty Acyls | 1.07 | 0.72 | 0.90 | 0.8189 | 0.3393 | 0.6949 | 0.88 | 1.09 | 0.95 | 0.5001 | 0.7741 | 0.7667 | 0.94 | 0.95 | 0.87 | 0.7268 | 0.7890 | 0.4557 | 0.91 | 0.75 | 1.05 | 0.4577 | 0.3837 | 0.8069 |
| 300.2664 | 4.0 | C18H36O3 | FA hydroxy(18:0) | Lipids: Fatty Acyls | 1.31 | 1.30 | 1.33 | 0.0398 | 0.0432 | 0.0503 | 1.10 | 1.14 | 1.17 | 0.5497 | 0.5189 | 0.2878 | 1.16 | 1.02 | 1.07 | 0.6820 | 0.9576 | 0.8323 | 0.92 | 0.77 | 0.76 | 0.5718 | 0.0424 | 0.0302 |
| 331.2721 | 4.2 | C18H34O4 | FA hydroxy(18:1)] | Lipids: Fatty Acyls | 1.11 | 1.41 | 1.04 | 0.6625 | 0.4030 | 0.9080 | 0.76 | 0.81 | 0.91 | 0.5846 | 0.6636 | 0.8278 | 0.25 | 0.44 | 0.52 | 0.0184 | 0.0427 | 0.0625 | 0.95 | 0.90 | 1.14 | 0.8372 | 0.6503 | 0.5678 |
| 132.0787 | 7.8 | C6H12O3 | FA hydroxy(6:0) | Lipids: Fatty Acyls | 0.58 | 0.97 | 0.53 | 0.4547 | 0.9641 | 0.4591 | 0.80 | 1.17 | 1.45 | 0.7783 | 0.8356 | 0.6356 | 1.01 | 0.98 | 1.05 | 0.9363 | 0.8782 | 0.6802 | 0.45 | 0.91 | 0.72 | 0.2346 | 0.8353 | 0.5442 |
| 146.0943 | 7.8 | C7H14O3 | FA hydroxy(7:0) | Lipids: Fatty Acyls | 1.46 | 1.28 | 1.27 | 0.0202 | 0.2110 | 0.1578 | 0.95 | 0.94 | 0.91 | 0.7764 | 0.7576 | 0.4779 | 0.95 | 1.12 | 1.12 | 0.7534 | 0.5065 | 0.6273 | 0.84 | 0.72 | 1.02 | 0.4801 | 0.1209 | 0.8999 |
| 160.1100 | 7.8 | C8H16O3 | FA hydroxy(8:0) hydroxy-octanoic acid | Lipids: Fatty Acyls | 0.98 | 1.16 | 0.99 | 0.9261 | 0.6926 | 0.9715 | 0.81 | 1.23 | 1.13 | 0.2828 | 0.2554 | 0.5063 | 0.96 | 1.08 | 1.09 | 0.8564 | 0.7886 | 0.7274 | 0.74 | 0.68 | 1.06 | 0.1243 | 0.1083 | 0.6387 |
| 174.1256 | 7.8 | C9H18O3 | FA hydroxy(9:0) hydroxy-nonanoic acid | Lipids: Fatty Acyls | 1.48 | 1.09 | 1.28 | 0.1140 | 0.7677 | 0.3012 | 0.90 | 0.98 | 0.91 | 0.6738 | 0.9134 | 0.6470 | 0.98 | 1.10 | 1.18 | 0.9405 | 0.6795 | 0.4670 | 0.78 | 0.84 | 0.84 | 0.3409 | 0.4512 | 0.2677 |
| 214.1933 | 28.5 | C13H26O2 | FA methyl(12:0) dodecanoic acid | Lipids: Fatty Acyls | 1.66 | 1.38 | 1.39 | 0.0160 | 0.1987 | 0.1293 | 0.85 | 1.08 | 0.96 | 0.5725 | 0.7206 | 0.8250 | 0.87 | 0.99 | 0.96 | 0.4806 | 0.9195 | 0.7379 | 0.86 | 0.92 | 1.31 | 0.5496 | 0.7343 | 0.2484 |
| 242.2246 | 4.0 | C15H30O2 | FA methyl(14:0) | Lipids: Fatty Acyls | 1.23 | 1.23 | 1.31 | 0.3087 | 0.1140 | 0.1790 | 0.98 | 1.06 | 1.05 | 0.9066 | 0.7528 | 0.7937 | 1.16 | 1.04 | 1.24 | 0.2763 | 0.7820 | 0.1559 | 0.93 | 0.86 | 0.85 | 0.6361 | 0.4095 | 0.3218 |
| 258.1830 | 4.2 | C14H26O4 | FA methyl(15:0) tridecanedioic acid | Lipids: Fatty Acyls | 1.53 | 1.33 | 1.27 | 0.0732 | 0.3590 | 0.3579 | 1.21 | 1.30 | 0.94 | 0.5290 | 0.6418 | 0.7757 | 0.34 | 0.39 | 0.36 | 0.3192 | 0.3473 | 0.3291 | 1.19 | 1.00 | 1.07 | 0.4977 | 0.9991 | 0.6258 |
| 268.2401 | 28.5 | C17H32O2 | FA methyl(16:1) | Lipids: Fatty Acyls | 0.09 | 0.40 | 0.20 | 0.2434 | 0.4006 | 0.2844 | 0.39 | 0.36 | 0.66 | 0.5838 | 0.5623 | 0.7613 | 1.04 | 1.01 | 1.01 | 0.8720 | 0.9692 | 0.9161 | 0.13 | 0.34 | 0.19 | 0.1879 | 0.2714 | 0.2084 |
| 298.2872 | 3.9 | C19H38O2 | FA methyl(18:0) | Lipids: Fatty Acyls | 1.20 | 1.24 | 1.26 | 0.2238 | 0.1643 | 0.1251 | 1.18 | 0.97 | 1.05 | 0.5491 | 0.7642 | 0.7218 | 1.46 | 1.35 | 1.35 | 0.2102 | 0.1197 | 0.1691 | 0.92 | 0.89 | 0.97 | 0.5770 | 0.4074 | 0.7348 |
| 130.0994 | 4.7 | C7H14O2 | FA methyl(6:0) | Lipids: Fatty Acyls | 1.17 | 1.22 | 1.05 | 0.5166 | 0.4373 | 0.8525 | 1.05 | 1.02 | 1.22 | 0.8769 | 0.9347 | 0.1609 | 1.06 | 1.05 | 1.05 | 0.8025 | 0.8459 | 0.8433 | 1.30 | 1.12 | 1.26 | 0.4633 | 0.6984 | 0.3071 |
| 158.1307 | 4.4 | C9H18O2 | FA methyl(8:0) | Lipids: Fatty Acyls | 1.12 | 1.13 | 1.15 | 0.5268 | 0.4512 | 0.2657 | 1.00 | 1.08 | 1.11 | 0.9941 | 0.7288 | 0.5958 | 1.01 | 0.99 | 0.92 | 0.9807 | 0.9588 | 0.7631 | 0.95 | 0.87 | 0.91 | 0.7845 | 0.4789 | 0.6720 |
| 270.2194 | 4.0 | C16H30O3 | FA oxo(16:0) | Lipids: Fatty Acyls | 1.37 | 1.18 | 1.12 | 0.3217 | 0.5941 | 0.7281 | 0.84 | 0.97 | 1.02 | 0.5988 | 0.9330 | 0.9594 | 1.16 | 0.98 | 1.17 | 0.5933 | 0.9258 | 0.5378 | 0.90 | 0.86 | 0.90 | 0.6940 | 0.6072 | 0.6980 |
| 298.2508 | 4.0 | C18H34O3 | FA oxo(18:0) | Lipids: Fatty Acyls | 1.30 | 1.33 | 1.14 | 0.2234 | 0.5196 | 0.6212 | 0.96 | 1.09 | 0.93 | 0.9151 | 0.8401 | 0.8195 | 1.37 | 0.99 | 1.19 | 0.4257 | 0.9515 | 0.4851 | 1.09 | 0.90 | 1.20 | 0.7232 | 0.6619 | 0.2819 |
| 144.0787 | 7.8 | C7H12O3 | FA oxo(7:0) | Lipids: Fatty Acyls | 1.52 | 1.69 | 1.33 | 0.1025 | 0.2948 | 0.3476 | 1.16 | 1.19 | 0.99 | 0.7300 | 0.7035 | 0.9768 | 0.86 | 1.10 | 1.02 | 0.2825 | 0.4027 | 0.8774 | 1.04 | 1.08 | 1.21 | 0.8404 | 0.7189 | 0.1180 |
| 158.0943 | 4.8 | C8H14O3 | FA oxo(8:0) oxo-octanoic acid | Lipids: Fatty Acyls | 1.33 | 1.00 | 1.00 | 0.1272 | 0.9857 | 0.9905 | 1.07 | 1.12 | 1.06 | 0.7034 | 0.3055 | 0.5291 | 0.96 | 1.02 | 1.01 | 0.7068 | 0.8558 | 0.8756 | 0.88 | 0.86 | 0.97 | 0.5035 | 0.4486 | 0.7905 |
| 116.0837 | 4.8 | C6H12O2 | Hexanoic acid | Lipids: Fatty Acyls | 1.13 | 1.23 | 1.06 | 0.1877 | 0.3848 | 0.4241 | 0.91 | 1.07 | 0.97 | 0.5416 | 0.5374 | 0.7822 | 1.09 | 1.06 | 1.13 | 0.7519 | 0.8229 | 0.6112 | 0.91 | 0.96 | 1.10 | 0.4236 | 0.6535 | 0.3340 |
| 280.2402 | 3.9 | C18H32O2 | Linoleate | Lipids: Fatty Acyls | 1.18 | 1.14 | 1.28 | 0.4884 | 0.5742 | 0.2207 | 0.92 | 1.04 | 0.99 | 0.7582 | 0.8753 | 0.9827 | 1.65 | 1.08 | 1.26 | 0.0655 | 0.6914 | 0.2865 | 0.98 | 0.97 | 1.02 | 0.9199 | 0.9011 | 0.9271 |
| 313.2981 | 4.4 | C19H39NO2 | Margaroyl-EA | Lipids: Fatty Acyls | 1.06 | 0.80 | 0.67 | 0.9096 | 0.6958 | 0.5289 | 0.96 | 1.07 | 1.02 | 0.8943 | 0.7336 | 0.9187 | 0.66 | 0.55 | 0.85 | 0.5383 | 0.4268 | 0.7984 | 0.87 | 1.37 | 0.98 | 0.5822 | 0.3060 | 0.9271 |
| 447.3350 | 4.6 | C27H45NO4 | N-stearoyl tyrosine | Lipids: Fatty Acyls | 1.61 | 0.59 | 0.60 | 0.5479 | 0.4827 | 0.4931 | 3.78 | 1.04 | 1.09 | 0.0133 | 0.9284 | 0.8062 | 1.14 | 1.22 | 1.14 | 0.9031 | 0.8645 | 0.9043 | 0.89 | 1.60 | 1.41 | 0.4917 | 0.5097 | 0.1658 |
| 231.1471 | 8.9 | C11H21NO4 | O-Butanoylcarnitine | Lipids: Fatty Acyls | 1.05 | 1.18 | 1.10 | 0.9577 | 0.8590 | 0.9105 | 1.17 | 1.37 | 1.05 | 0.8733 | 0.7522 | 0.9567 | 1.05 | 0.96 | 1.03 | 0.8801 | 0.9119 | 0.9239 | 1.63 | 1.54 | 1.13 | 0.6363 | 0.6919 | 0.9102 |
| 399.3349 | 5.9 | C23H45NO4 | O-Palmitoyl-R-carnitine | Lipids: Fatty Acyls | 1.03 | 1.11 | 1.09 | 0.9204 | 0.7862 | 0.8111 | 0.49 | 0.95 | 0.98 | 0.1425 | 0.8702 | 0.9376 | 1.05 | 1.06 | 1.11 | 0.9310 | 0.9308 | 0.8511 | 1.03 | 0.97 | 1.00 | 0.9234 | 0.9234 | 0.9967 |
| 102.0681 | 7.8 | C5H10O2 | Pentanoate | Lipids: Fatty Acyls | 1.10 | 1.06 | 1.08 | 0.8745 | 0.9245 | 0.9107 | 0.95 | 1.00 | 1.06 | 0.9287 | 0.9988 | 0.9302 | 1.00 | 1.07 | 1.08 | 0.9785 | 0.7130 | 0.5783 | 0.99 | 1.02 | 1.04 | 0.9854 | 0.9725 | 0.9415 |
| 174.0892 | 28.2 | C8H14O4 | Suberic acid | Lipids: Fatty Acyls | 1.16 | 0.94 | 1.08 | 0.4100 | 0.7401 | 0.6624 | 0.86 | 0.99 | 0.98 | 0.5548 | 0.9594 | 0.9443 | 0.88 | 1.03 | 1.01 | 0.1234 | 0.7164 | 0.9217 | 0.85 | 0.80 | 0.90 | 0.4250 | 0.3354 | 0.5674 |
| 668.4300 | 7.9 | C68H124N2O23 | Ganglioside GA1 (d18:1/24:1(15Z)) | Lipids: Gangliosides | 1.06 | 1.17 | 1.27 | 0.5710 | 0.1999 | 0.1553 | 1.10 | 1.10 | 1.18 | 0.4960 | 0.5971 | 0.3623 | 1.15 | 1.58 | 1.59 | 0.7945 | 0.3983 | 0.5673 | 1.00 | 1.17 | 0.98 | 0.9977 | 0.4241 | 0.7355 |
| 602.5270 | 3.7 | C39H70O4 | 1-(14-methyl-pentadecanoyl)-2-(8-[3]-ladderane-octanyl)-sn-glycerol | Lipids: Glycerolipids | 1.06 | 0.81 | 1.46 | 0.7490 | 0.4710 | 0.4433 | 1.05 | 0.83 | 0.55 | 0.9393 | 0.7176 | 0.3945 | 0.86 | 0.82 | 0.67 | 0.4459 | 0.5470 | 0.0035 | 1.28 | 0.96 | 2.70 | 0.6662 | 0.8650 | 0.2794 |
| 611.5488 | 3.9 | C37H70O5 | DG(34:1) | Lipids: Glycerolipids | 1.25 | 1.36 | 1.10 | 0.1804 | 0.0881 | 0.5003 | 0.87 | 0.83 | 0.97 | 0.1959 | 0.3283 | 0.6915 | 0.56 | 0.52 | 0.34 | 0.0846 | 0.0091 | 0.0017 | 0.47 | 0.47 | 0.42 | 0.0863 | 0.0882 | 0.0582 |
| 639.5803 | 4.7 | C39H74O5 | DG(36:1) | Lipids: Glycerolipids | 0.80 | 0.93 | 0.72 | 0.5413 | 0.8640 | 0.4188 | 0.67 | 1.09 | 0.76 | 0.1482 | 0.6871 | 0.4793 | 0.59 | 0.62 | 0.68 | 0.0788 | 0.0992 | 0.2343 | 0.20 | 0.26 | 0.23 | 0.0721 | 0.0825 | 0.0702 |
| 637.5646 | 5.0 | C39H72O5 | DG(36:2) | Lipids: Glycerolipids | 1.25 | 1.26 | 1.11 | 0.3525 | 0.4936 | 0.5682 | 0.68 | 0.75 | 0.78 | 0.1176 | 0.1903 | 0.2423 | 0.65 | 0.69 | 0.53 | 0.1634 | 0.1602 | 0.0552 | 0.32 | 0.56 | 0.45 | 0.0335 | 0.0642 | 0.0677 |
| 849.7782 | 5.7 | C53H100O6 | TG(50:1) | Lipids: Glycerolipids | 1.38 | 1.25 | 1.13 | 0.3342 | 0.0387 | 0.5541 | 0.74 | 0.87 | 0.83 | 0.0760 | 0.3212 | 0.1620 | 0.34 | 0.47 | 0.28 | 0.0549 | 0.0887 | 0.0526 | 0.36 | 0.45 | 0.23 | 0.0623 | 0.0844 | 0.0561 |
| 875.7942 | 6.1 | C55H102O6 | TG(52:2) | Lipids: Glycerolipids | 1.39 | 1.25 | 1.20 | 0.1379 | 0.1715 | 0.4698 | 0.70 | 0.80 | 0.65 | 0.1930 | 0.3454 | 0.1459 | 0.38 | 0.54 | 0.34 | 0.0851 | 0.2054 | 0.0915 | 0.17 | 0.21 | 0.11 | 0.0254 | 0.0236 | 0.0275 |
| 901.8098 | 6.2 | C57H104O6 | TG(54:3) | Lipids: Glycerolipids | 1.23 | 0.95 | 1.24 | 0.4110 | 0.8121 | 0.3893 | 0.83 | 0.94 | 0.69 | 0.3861 | 0.7923 | 0.1475 | 0.51 | 0.66 | 0.34 | 0.1526 | 0.3251 | 0.0988 | 0.20 | 0.28 | 0.13 | 0.0832 | 0.1022 | 0.0781 |

| | | | | | | | | | | | | | | | | | | | | | | | | | | | | | |
|---|---|---|---|---|---|---|---|---|---|---|---|---|---|---|---|---|---|---|---|---|---|---|---|---|---|---|---|---|---|
| 481.3536 | 4.7 | C24H52NO6P | [LysoPC(16:2)] 1-hexadecyl-sn-glycero-3-phosphocholine | Lipids: Glycerophospholipids | 1.20 | 1.24 | 1.26 | 0.2295 | 0.2805 | 0.1063 | 0.81 | 0.83 | 0.67 | 0.5038 | 0.5476 | 0.2957 | 1.41 | 1.20 | 1.51 | 0.1895 | 0.4638 | 0.1284 | 0.27 | 0.38 | 0.15 | 0.0219 | 0.0359 | 0.0293 |
| 517.3166 | 4.7 | C26H48NO7P | [PC(18:3)] | Lipids: Glycerophospholipids | 1.00 | 1.00 | 1.05 | 0.9912 | 0.9909 | 0.8360 | 1.09 | 1.10 | 0.91 | 0.5305 | 0.4521 | 0.6364 | 0.90 | 0.30 | 0.37 | 0.8836 | NA | NA | 1.19 | 0.99 | 1.33 | 0.2059 | 0.9198 | 0.1324 |
| 519.3696 | 28.4 | C27H54NO6P | [PC(19:2)] 1-(1Z,12Z-nonadecadienyl)-sn-glycero-3-phosphocholine | Lipids: Glycerophospholipids | 1.18 | 1.48 | 1.55 | 0.3209 | 0.0631 | 0.1276 | 0.77 | 1.21 | 1.27 | 0.5331 | 0.6337 | 0.4523 | 0.82 | 0.81 | 0.70 | 0.6391 | 0.6518 | 0.4165 | 0.00 | 0.00 | 0.00 | NA | NA | NA |
| 512.3109 | 3.9 | C24H49O9P | [PG (18:0)] 1-octadecanoyl-sn-glycero-3-phospho-(1'-sn-glycerol) | Lipids: Glycerophospholipids | 0.88 | 0.99 | 0.90 | 0.6634 | 0.9601 | 0.7247 | 1.43 | 1.56 | 1.38 | 0.4490 | 0.4040 | 0.4915 | 0.81 | 0.93 | 0.48 | 0.3498 | 0.8183 | 0.0377 | 0.89 | 1.14 | 1.11 | 0.7393 | 0.6673 | 0.6965 |
| 521.3488 | 7.8 | C26H52NO7P | LysoPC(18:1) | Lipids: Glycerophospholipids | 1.32 | 1.14 | 0.87 | 0.4772 | 0.4458 | 0.4589 | 0.60 | 0.81 | 0.55 | 0.1216 | 0.3843 | 0.0951 | 0.54 | 0.25 | 1.49 | 0.3300 | NA | 0.4634 | 0.65 | 0.67 | 0.42 | 0.0849 | 0.0601 | 0.0116 |
| 551.3957 | 4.5 | C28H58NO7P | LysoPC(20:0) | Lipids: Glycerophospholipids | 0.74 | 0.91 | 1.05 | 0.4378 | 0.7628 | 0.9114 | 1.52 | 1.74 | 1.63 | 0.5550 | 0.1507 | 0.2695 | 1.96 | 1.85 | 2.13 | 0.2952 | 0.4286 | 0.1625 | 0.00 | 1.27 | 0.45 | NA | NA | NA |
| 479.3377 | 4.7 | C24H50NO6P | LysoPC(O-16:1) | Lipids: Glycerophospholipids | 1.27 | 1.31 | 1.08 | 0.3356 | 0.2934 | 0.7816 | 1.05 | 0.97 | 0.97 | 0.8740 | 0.9326 | 0.8480 | 1.12 | 0.92 | 1.09 | 0.6045 | 0.7423 | 0.7208 | 14.44 | 0.00 | 27.23 | NA | NA | 0.2401 |
| 509.3849 | 4.7 | C26H56NO6P | LysoPC(O-18:2) | Lipids: Glycerophospholipids | 1.08 | 1.16 | 1.02 | 0.6294 | 0.4006 | 0.9087 | 1.22 | 1.35 | 1.40 | 0.3163 | 0.0687 | 0.1284 | 1.36 | 1.10 | 1.32 | 0.2201 | 0.6624 | 0.3387 | 1.10 | 1.09 | 1.16 | 0.4218 | 0.7503 | 0.5298 |
| 453.2857 | 4.7 | C21H44NO7P | LysoPE(16:0) | Lipids: Glycerophospholipids | 1.24 | 1.30 | 1.14 | 0.1185 | 0.1053 | 0.4251 | 0.82 | 1.06 | 0.97 | 0.3783 | 0.8098 | 0.8510 | 0.89 | 0.72 | 0.82 | 0.7933 | 0.5114 | 0.7205 | 0.98 | 0.94 | 1.22 | 0.8724 | 0.8140 | 0.2672 |
| 481.3173 | 4.7 | C23H48NO7P | LysoPE(18:0) | Lipids: Glycerophospholipids | 1.62 | 1.68 | 2.23 | 0.5268 | 0.3325 | 0.4690 | 0.70 | 1.71 | 0.96 | 0.3759 | 0.2107 | 0.8967 | 1.04 | 1.02 | 1.32 | 0.9109 | 0.9575 | 0.4586 | 0.62 | 0.96 | 0.77 | 0.1484 | 0.9208 | 0.3110 |
| 479.3015 | 4.6 | C23H46NO7P | LysoPE(18:1) | Lipids: Glycerophospholipids | 1.16 | 1.11 | 1.53 | 0.5530 | 0.6206 | 0.3018 | 1.09 | 1.39 | 1.28 | 0.7475 | 0.1722 | 0.2822 | 0.76 | 0.61 | 0.76 | 0.5550 | 0.3070 | 0.5266 | 1.01 | 0.97 | 0.99 | 0.9555 | 0.9315 | 0.9504 |
| 477.2859 | 4.7 | C23H44NO7P | LysoPE(18:2) | Lipids: Glycerophospholipids | 1.70 | 1.68 | 2.15 | 0.3373 | 0.2271 | 0.4424 | 0.85 | 1.47 | 0.93 | 0.6360 | 0.2637 | 0.7424 | 0.61 | 0.51 | 0.63 | 0.4428 | 0.3501 | 0.4675 | 0.55 | 0.72 | 0.59 | 0.1103 | 0.4368 | 0.1264 |
| 509.3485 | 4.7 | C25H52NO7P | LysoPE(20:0) | Lipids: Glycerophospholipids | 1.52 | 1.75 | 1.88 | 0.2417 | 0.3186 | 0.3961 | 0.83 | 1.84 | 1.12 | 0.4898 | 0.2779 | 0.3980 | 1.03 | 0.94 | 1.11 | 0.9448 | 0.8679 | 0.7311 | 0.54 | 0.63 | 0.67 | 0.1561 | 0.2953 | 0.2556 |
| 501.2858 | 4.6 | C25H44NO7P | LysoPE(20:4) | Lipids: Glycerophospholipids | 1.15 | 1.14 | 1.16 | 0.3165 | 0.3821 | 0.3568 | 0.94 | 1.10 | 1.23 | 0.8072 | 0.5763 | 0.1802 | 0.92 | 0.70 | 0.82 | 0.8528 | 0.4431 | 0.6608 | 2.56 | 2.39 | 3.90 | 0.3232 | 0.4389 | 0.0919 |
| 525.2860 | 4.5 | C27H44NO7P | LysoPE(22:6) | Lipids: Glycerophospholipids | 1.74 | 1.67 | 2.23 | 0.3310 | 0.1857 | 0.4824 | 0.86 | 1.48 | 0.92 | 0.6642 | 0.2470 | 0.7381 | 0.89 | 0.55 | 0.67 | 0.8276 | 0.4071 | 0.5324 | 0.75 | 0.98 | 0.97 | 0.1608 | 0.9450 | 0.8733 |
| 563.3955 | 28.4 | C29H58NO7P | LysoPE(24:1) | Lipids: Glycerophospholipids | 1.52 | 2.87 | 3.44 | NA | 0.3828 | 0.5017 | 0.27 | 1.47 | 1.13 | NA | 0.5195 | 0.8641 | 0.95 | 1.14 | 1.19 | 0.9217 | 0.7537 | 0.6371 | 1.14 | 1.36 | 1.03 | 0.8512 | 0.7520 | NA |
| 674.4896 | 3.8 | C37H71O8P | PA(34:1) | Lipids: Glycerophospholipids | 1.03 | 0.88 | 0.91 | 0.8990 | 0.6257 | 0.7540 | 1.16 | 1.18 | 1.29 | 0.5796 | 0.6682 | 0.3961 | 0.96 | 1.10 | 1.04 | 0.8767 | 0.6785 | 0.8404 | 1.07 | 1.12 | 1.21 | 0.8267 | 0.6007 | 0.4466 |
| 672.4726 | 3.8 | C37H69O8P | PA(34:2) | Lipids: Glycerophospholipids | 1.07 | 1.14 | 1.39 | 0.7309 | 0.4992 | 0.3660 | 0.96 | 0.92 | 1.11 | 0.8719 | 0.7181 | 0.4792 | 0.96 | 1.00 | 1.01 | 0.8684 | 0.9959 | 0.9756 | 1.18 | 1.11 | 1.32 | 0.4921 | 0.7303 | 0.1070 |
| 702.5199 | 3.8 | C39H75O8P | PA(36:1) | Lipids: Glycerophospholipids | 1.13 | 1.34 | 1.49 | 0.4853 | 0.1454 | 0.1739 | 0.96 | 0.94 | 1.14 | 0.8501 | 0.7052 | 0.2745 | 0.94 | 0.99 | 0.86 | 0.7949 | 0.9421 | 0.5115 | 1.18 | 1.06 | 1.29 | 0.3552 | 0.8010 | 0.1905 |
| 700.5048 | 3.8 | C39H73O8P | PA(36:2) | Lipids: Glycerophospholipids | 0.97 | 1.06 | 1.27 | 0.9019 | 0.7875 | 0.4512 | 0.90 | 0.83 | 1.05 | 0.6248 | 0.3468 | 0.8064 | 0.93 | 0.92 | 0.92 | 0.7403 | 0.6899 | 0.7031 | 1.03 | 0.89 | 1.20 | 0.8720 | 0.6922 | 0.3708 |
| 698.4890 | 3.8 | C39H71O8P | PA(36:3) | Lipids: Glycerophospholipids | 1.01 | 1.09 | 1.31 | 0.9373 | 0.5123 | 0.3329 | 0.92 | 0.91 | 1.26 | 0.6832 | 0.5854 | 0.1534 | 0.88 | 0.86 | 0.95 | 0.6168 | 0.5746 | 0.8196 | 1.04 | 0.96 | 1.31 | 0.4138 | 0.8316 | 0.0641 |
| 696.4736 | 3.8 | C39H69O8P | PA(36:4) | Lipids: Glycerophospholipids | 1.07 | 1.14 | 1.26 | 0.7663 | 0.5453 | 0.4250 | 0.81 | 0.92 | 1.06 | 0.4714 | 0.7902 | 0.7664 | 0.94 | 0.96 | 0.92 | 0.8572 | 0.9009 | 0.7634 | 1.11 | 0.95 | 1.17 | 0.5769 | 0.8336 | 0.2494 |
| 519.3322 | 4.7 | C26H50NO7P | PC(18:2) | Lipids: Glycerophospholipids | 1.02 | 1.22 | 1.45 | 0.9252 | 0.5857 | 0.3997 | 0.89 | 0.83 | 1.03 | 0.7593 | 0.6207 | 0.9251 | 0.41 | 0.23 | 0.33 | NA | NA | NA | 1.16 | 1.19 | 1.23 | 0.7111 | 0.7309 | 0.4915 |
| 705.5311 | 4.2 | C38H76NO8P | PC(30:0) | Lipids: Glycerophospholipids | 1.29 | 1.44 | 1.43 | 0.3597 | 0.2558 | 0.5760 | 0.97 | 3.46 | 1.33 | NA | 0.1452 | 0.8213 | 1.09 | 1.01 | 1.18 | 0.6307 | 0.9575 | 0.2274 | 0.00 | 0.00 | 0.00 | NA | NA | NA |
| 733.5623 | 6.3 | C40H80NO8P | PC(32:0) | Lipids: Glycerophospholipids | 1.03 | 0.92 | 0.94 | 0.8527 | 0.6383 | 0.7526 | 0.82 | 0.88 | 0.91 | 0.6005 | 0.7052 | 0.7926 | 0.70 | 1.16 | 1.07 | 0.3266 | 0.7239 | 0.8673 | 0.61 | 0.65 | 0.78 | 0.2705 | 0.3477 | 0.5017 |
| 731.5476 | 4.9 | C40H78NO8P | PC(32:1) | Lipids: Glycerophospholipids | 1.12 | 0.93 | 0.93 | 0.8136 | 0.8740 | 0.8545 | 0.76 | 0.62 | 0.70 | 0.4299 | 0.1447 | 0.2226 | 0.58 | 0.65 | 0.88 | 0.1041 | 0.1492 | 0.5938 | 1.18 | 1.20 | 1.22 | 0.4816 | 0.4847 | 0.4424 |
| 729.5309 | 4.1 | C40H76NO8P | PC(32:2) | Lipids: Glycerophospholipids | 1.40 | 1.10 | 0.52 | 0.0987 | 0.5905 | 0.0395 | 1.08 | 1.14 | 1.18 | 0.8143 | 0.6206 | 0.5127 | 0.86 | 1.03 | 1.02 | 0.3610 | 0.9279 | 0.9430 | 0.43 | 0.60 | 0.59 | 0.0412 | 0.0958 | 0.0858 |
| 787.6094 | 6.9 | C44H86NO8P | PC(36:1) | Lipids: Glycerophospholipids | 1.63 | 1.28 | 1.37 | 0.2148 | 0.4005 | 0.3956 | 0.80 | 0.85 | 0.86 | 0.2995 | 0.4597 | 0.3558 | 0.80 | 0.93 | 0.87 | 0.1614 | 0.6748 | 0.4172 | 0.50 | 0.51 | 0.44 | 0.0764 | 0.0819 | 0.0601 |
| 785.5935 | 6.3 | C44H84NO8P | PC(36:2) | Lipids: Glycerophospholipids | 0.60 | 0.96 | 1.03 | 0.0887 | 0.5965 | 0.7132 | 0.91 | 1.04 | 0.87 | 0.3890 | 0.7394 | 0.5219 | 0.37 | 0.90 | 0.96 | 0.0345 | 0.4661 | 0.7950 | 0.70 | 0.45 | 0.54 | 0.2643 | 0.0552 | 0.0482 |
| 783.5774 | 6.1 | C44H82NO8P | PC(36:3) | Lipids: Glycerophospholipids | 0.49 | 1.16 | 0.82 | 0.3007 | 0.2389 | 0.3988 | 0.81 | 1.40 | 1.50 | 0.6841 | 0.1543 | 0.1009 | 1.56 | 1.16 | 0.92 | 0.3823 | 0.7838 | 0.9143 | 0.66 | 0.34 | 0.66 | 0.1772 | 0.0407 | 0.1733 |

| | | | | | | | | | | | | | | | | | | | | | | | | | | | | | |
|---|---|---|---|---|---|---|---|---|---|---|---|---|---|---|---|---|---|---|---|---|---|---|---|---|---|---|---|---|---|
| 811.6076 | 4.6 | C46H86NO8P | PC(38:3) | Lipids: Glycerophospholipids | 2.52 | 0.96 | 1.94 | 0.2842 | 0.9239 | 0.1380 | 2.07 | 3.15 | 2.61 | 0.0696 | 0.0021 | 0.0573 | 1.44 | 1.14 | 1.19 | 0.4048 | 0.5817 | 0.4319 | 0.58 | 0.46 | 0.49 | 0.2071 | 0.1346 | 0.1519 |
| 809.5934 | 5.3 | C46H84NO8P | PC(38:4) | Lipids: Glycerophospholipids | 1.15 | 1.07 | 1.03 | 0.7072 | 0.8625 | 0.9405 | 1.02 | 1.05 | 1.24 | 0.8973 | 0.7744 | 0.4594 | 1.01 | 0.79 | 1.27 | 0.9836 | 0.5400 | 0.4502 | 0.91 | 0.92 | 0.90 | 0.6277 | 0.7076 | 0.6987 |
| 809.5933 | 6.1 | C46H84NO8P | PE(41:4) | Lipids: Glycerophospholipids | 1.26 | 0.91 | 1.01 | 0.6866 | 0.7561 | 0.9700 | 1.04 | 1.60 | 1.78 | 0.8250 | 0.1347 | 0.1228 | 1.34 | 2.09 | 0.61 | 0.4176 | 0.0349 | 0.3509 | 0.89 | 0.96 | 0.61 | 0.7020 | 0.9153 | 0.2200 |
| 805.5624 | 5.4 | C46H80NO8P | PC(38:6) | Lipids: Glycerophospholipids | 3.46 | 2.97 | 1.96 | 0.0138 | 0.0048 | 0.3820 | 2.30 | 2.00 | 3.05 | 0.0375 | 0.2216 | 0.0022 | 0.59 | 0.40 | 0.82 | 0.3436 | 0.1989 | 0.6443 | 1.55 | 0.69 | 0.38 | 0.0451 | 0.2864 | 0.0334 |
| 831.5781 | 4.0 | C48H82NO8P | PC(40:7) | Lipids: Glycerophospholipids | 0.65 | 0.94 | 0.74 | 0.3068 | 0.8404 | 0.4245 | 0.84 | 2.01 | 0.90 | 0.6314 | 0.1946 | 0.7571 | 1.25 | 1.34 | 1.13 | 0.3766 | 0.4045 | 0.6185 | 1.55 | 1.68 | 1.62 | 0.2206 | 0.2326 | 0.2365 |
| 719.5821 | 4.2 | C40H82NO7P | PC(O-32:0) | Lipids: Glycerophospholipids | 1.43 | 1.04 | 0.99 | 0.1369 | 0.8915 | 0.9777 | 1.01 | 0.97 | 0.89 | 0.9586 | 0.8960 | 0.6676 | 1.16 | 1.11 | 1.26 | 0.6126 | 0.7119 | 0.3870 | 0.90 | 0.85 | 0.80 | 0.5854 | 0.4683 | 0.0592 |
| 745.5979 | 4.1 | C42H84NO7P | PC(P-34:0) | Lipids: Glycerophospholipids | 1.47 | 1.05 | 0.93 | 0.2197 | 0.8632 | 0.8038 | 0.85 | 0.92 | 0.96 | 0.4842 | 0.7163 | 0.8485 | 1.20 | 1.09 | 1.47 | 0.6027 | 0.7385 | 0.1494 | 1.02 | 0.88 | 1.15 | 0.9425 | 0.7487 | 0.6519 |
| 771.6130 | 4.1 | C44H86NO7P | PC(P-36:1) | Lipids: Glycerophospholipids | 1.36 | 1.11 | 1.03 | 0.0989 | 0.6383 | 0.8928 | 0.99 | 0.94 | 0.99 | 0.9594 | 0.8727 | 0.9767 | 1.56 | 1.62 | 1.49 | 0.1649 | 0.1823 | 0.1300 | 0.98 | 0.75 | 0.98 | 0.9051 | 0.3254 | 0.9121 |
| 765.5665 | 4.6 | C44H80NO7P | PC(P-36:4) | Lipids: Glycerophospholipids | 1.36 | 0.89 | 1.31 | 0.1965 | 0.6284 | 0.3615 | 0.99 | 0.98 | 1.08 | 0.9762 | 0.9348 | 0.7704 | 1.33 | 1.30 | 1.15 | 0.3583 | 0.2834 | 0.5232 | 0.86 | 0.91 | 0.97 | 0.5765 | 0.7305 | 0.8236 |
| 795.6129 | 4.1 | C46H86NO7P | PC(P-38:3) | Lipids: Glycerophospholipids | 1.36 | 1.33 | 1.06 | 0.1113 | 0.1878 | 0.7677 | 0.81 | 0.88 | 1.23 | 0.0940 | 0.1782 | 0.1237 | 1.30 | 1.59 | 1.68 | 0.3056 | 0.1668 | 0.0731 | 0.99 | 1.03 | 0.88 | 0.9739 | 0.8329 | 0.1713 |
| 819.6138 | 4.0 | C48H86NO7P | PC(P-40:5) | Lipids: Glycerophospholipids | 1.74 | 1.44 | 1.63 | 0.0322 | 0.1136 | 0.0767 | 0.88 | 1.06 | 0.98 | 0.5504 | 0.8449 | 0.9263 | 2.09 | 1.09 | 1.51 | 0.0373 | 0.8035 | 0.2281 | 0.86 | 0.66 | 0.54 | 0.3907 | 0.1251 | 0.0260 |
| 680.5101 | 20.5 | C35H70NO8P | PE(30:0) | Lipids: Glycerophospholipids | 1.57 | 1.22 | 0.98 | 0.1260 | 0.5415 | 0.9535 | 0.82 | 1.19 | 0.93 | 0.7259 | 0.5639 | 0.8283 | 1.00 | 1.06 | 1.07 | 0.9879 | 0.3462 | 0.2706 | 0.74 | 1.03 | 0.96 | 0.6550 | 0.9573 | 0.9128 |
| 655.4215 | 7.8 | C35H62NO8P | PE(30:4) | Lipids: Glycerophospholipids | 1.04 | 1.00 | 1.05 | 0.5101 | 0.9769 | 0.4437 | 1.02 | 1.06 | 0.97 | 0.7854 | 0.3840 | 0.7252 | 1.46 | 1.49 | 1.15 | 0.1905 | 0.1560 | 0.5656 | 0.79 | 0.94 | 0.99 | 0.0732 | 0.3992 | 0.9394 |
| 691.5149 | 3.8 | C37H74NO8P | PE(32:0) | Lipids: Glycerophospholipids | 1.25 | 0.94 | 1.11 | 0.5104 | 0.8667 | 0.7084 | 1.20 | 0.87 | 1.25 | 0.4404 | 0.5899 | 0.5904 | 1.10 | 1.16 | 1.28 | 0.7436 | 0.5349 | 0.3098 | 0.85 | 0.68 | 0.91 | 0.6040 | 0.3478 | 0.7521 |
| 689.4992 | 3.8 | C37H72NO8P | PE(32:1) | Lipids: Glycerophospholipids | 1.03 | 1.24 | 1.01 | 0.9292 | 0.4024 | 0.9786 | 0.90 | 0.97 | 1.17 | 0.6388 | 0.8646 | 0.4062 | 1.14 | 1.19 | 1.22 | 0.5143 | 0.3168 | 0.2584 | 0.92 | 0.97 | 1.06 | 0.7738 | 0.9140 | 0.8476 |
| 715.5154 | 4.8 | C39H74NO8P | PE(34:2) | Lipids: Glycerophospholipids | 1.10 | 1.27 | 1.08 | 0.6858 | 0.2988 | 0.7028 | 0.90 | 1.04 | 1.10 | 0.6451 | 0.8049 | 0.5022 | 1.04 | 1.03 | 0.93 | 0.6883 | 0.8823 | 0.6442 | 0.86 | 0.82 | 1.00 | 0.2546 | 0.1793 | 0.9925 |
| 745.5625 | 5.2 | C41H80NO8P | PE(36:1) | Lipids: Glycerophospholipids | 1.18 | 1.24 | 1.28 | 0.5407 | 0.3368 | 0.2511 | 0.91 | 1.02 | 0.92 | 0.5373 | 0.9166 | 0.7563 | 1.01 | 0.98 | 0.97 | 0.9717 | 0.9184 | 0.8412 | 0.87 | 1.04 | 0.88 | 0.5820 | 0.8630 | 0.5702 |
| 745.5626 | 6.1 | C41H80NO8P | PC(33:1) | Lipids: Glycerophospholipids | 1.06 | 1.06 | 1.05 | 0.4913 | 0.4175 | 0.4744 | 0.86 | 1.02 | 0.88 | 0.0819 | 0.7976 | 0.0859 | 0.96 | 0.94 | 0.94 | 0.5679 | 0.6494 | 0.2384 | 0.70 | 0.86 | 0.89 | 0.1061 | 0.3749 | 0.4187 |
| 743.5469 | 5.5 | C41H78NO8P | PE(36:2) | Lipids: Glycerophospholipids | 1.08 | 1.03 | 0.94 | 0.6123 | 0.7711 | 0.6133 | 0.93 | 1.02 | 0.87 | 0.6855 | 0.8268 | 0.3784 | 1.03 | 1.11 | 0.80 | 0.7412 | 0.3879 | 0.2009 | 0.73 | 0.54 | 0.65 | 0.1546 | 0.0482 | 0.1011 |
| 741.5317 | 5.0 | C41H76NO8P | PE(36:3) | Lipids: Glycerophospholipids | 1.14 | 1.04 | 0.75 | 0.3602 | 0.7728 | 0.2514 | 0.89 | 0.94 | 0.88 | 0.0779 | 0.2986 | 0.0499 | 1.04 | 1.09 | 1.00 | 0.8690 | 0.7389 | 0.9995 | 0.79 | 0.84 | 0.67 | 0.1682 | 0.2915 | 0.0648 |
| 741.5311 | 5.9 | C41H76NO8P | PC(33:3) | Lipids: Glycerophospholipids | 1.12 | 0.98 | 0.94 | 0.6423 | 0.9389 | 0.7866 | 1.06 | 1.01 | 1.11 | 0.7632 | 0.9627 | 0.5972 | 1.09 | 1.00 | 1.19 | 0.6177 | 0.9820 | 0.2455 | 0.75 | 0.69 | 0.80 | 0.2912 | 0.2127 | 0.3889 |
| 739.5152 | 6.1 | C41H74NO8P | PE(36:4) | Lipids: Glycerophospholipids | 1.05 | 1.03 | 1.03 | 0.7507 | 0.8235 | 0.8148 | 0.94 | 1.03 | 1.01 | 0.6657 | 0.8561 | 0.9802 | 0.87 | 0.69 | 0.64 | 0.4535 | 0.0888 | 0.0764 | 0.84 | 0.81 | 0.66 | 0.3122 | 0.1175 | 0.0408 |
| 737.4997 | 4.0 | C41H72NO8P | PE(36:5) | Lipids: Glycerophospholipids | 0.92 | 0.88 | 0.93 | 0.5642 | 0.5359 | 0.5779 | 1.12 | 1.22 | 1.91 | 0.5667 | 0.5322 | 0.0082 | 1.05 | 1.04 | 0.87 | 0.8440 | 0.8206 | 0.5223 | 0.79 | 1.10 | 1.46 | 0.1111 | 0.3468 | 0.0811 |
| 773.5930 | 4.8 | C43H84NO8P | PE(38:1) | Lipids: Glycerophospholipids | 1.25 | 1.05 | 0.95 | 0.1433 | 0.6801 | 0.7371 | 0.86 | 0.96 | 0.80 | 0.1527 | 0.8079 | 0.0766 | 1.56 | 1.13 | 1.04 | 0.3622 | 0.5337 | 0.8255 | 1.03 | 1.04 | 0.99 | 0.8029 | 0.8174 | 0.9549 |
| 773.5933 | 5.6 | C43H84NO8P | PC(35:1) | Lipids: Glycerophospholipids | 1.28 | 1.24 | 1.17 | 0.0695 | 0.2800 | 0.4275 | 1.04 | 1.01 | 1.02 | 0.6518 | 0.9559 | 0.8797 | 0.68 | 0.70 | 0.75 | 0.1863 | 0.2011 | 0.2665 | 0.75 | 0.78 | 0.71 | 0.3297 | 0.3727 | 0.2734 |
| 771.5773 | 4.8 | C43H82NO8P | PE(38:2) | Lipids: Glycerophospholipids | 1.35 | 1.18 | 1.14 | 0.0980 | 0.3353 | 0.3632 | 0.98 | 0.96 | 0.99 | 0.8995 | 0.5677 | 0.9499 | 1.01 | 0.91 | 0.92 | 0.9525 | 0.4796 | 0.5483 | 0.49 | 0.49 | 0.43 | 0.1187 | 0.1187 | 0.0992 |
| 767.5464 | 5.8 | C43H78NO8P | PE(38:4) | Lipids: Glycerophospholipids | 1.19 | 1.18 | 0.99 | 0.4412 | 0.4340 | 0.9705 | 0.85 | 0.77 | 1.06 | 0.2649 | 0.1375 | 0.7554 | 0.87 | 1.03 | 0.98 | 0.3598 | 0.7783 | 0.8655 | 0.62 | 0.82 | 0.66 | 0.0068 | 0.0461 | 0.0002 |
| 765.5308 | 5.9 | C43H76NO8P | PE(38:5) | Lipids: Glycerophospholipids | 1.20 | 1.19 | 1.14 | 0.3939 | 0.3669 | 0.5478 | 0.93 | 0.98 | 1.05 | 0.6539 | 0.9217 | 0.6982 | 0.97 | 1.06 | 1.03 | 0.7137 | 0.5667 | 0.8569 | 0.98 | 1.00 | 1.09 | 0.8783 | 0.9905 | 0.5657 |
| 763.5147 | 4.0 | C43H74NO8P | PE(38:6) | Lipids: Glycerophospholipids | 1.21 | 1.07 | 1.06 | 0.2989 | 0.7101 | 0.7587 | 0.91 | 1.43 | 1.50 | 0.7510 | 0.2163 | 0.0319 | 1.35 | 0.98 | 1.42 | 0.4281 | 0.9430 | 0.1878 | 0.50 | 0.85 | 0.50 | 0.0082 | 0.2771 | 0.0529 |
| 793.5609 | 4.0 | C45H80NO8P | PE(40:5) | Lipids: Glycerophospholipids | 1.32 | 1.25 | 1.21 | 0.4191 | 0.5199 | 0.6330 | 0.80 | 0.84 | 0.74 | 0.7030 | 0.7519 | 0.6039 | 1.25 | 1.04 | 1.17 | 0.3961 | 0.8345 | 0.3624 | 0.69 | 0.86 | 0.75 | 0.3859 | 0.7603 | 0.4474 |
| 791.5458 | 3.9 | C45H78NO8P | PE(40:6) | Lipids: Glycerophospholipids | 1.28 | 1.14 | 0.97 | 0.1668 | 0.4775 | 0.8915 | 0.89 | 0.87 | 1.01 | 0.3032 | 0.3560 | 0.9194 | 1.41 | 1.16 | 1.13 | 0.1221 | 0.5709 | 0.5688 | 0.95 | 0.82 | 1.03 | 0.7376 | 0.1875 | 0.6492 |
| 751.5512 | 6.7 | C43H78NO7P | PE(O-38:5) | Lipids: Glycerophospholipids | 1.16 | 1.29 | 1.05 | 0.6338 | 0.5859 | 0.8822 | 0.80 | 1.04 | 0.96 | 0.3371 | 0.8996 | 0.8435 | 0.92 | 1.10 | 0.98 | 0.7557 | 0.6875 | 0.9222 | 1.05 | 1.00 | 1.07 | 0.8766 | 0.9930 | 0.5371 |

| | | | | | | | | | | | | | | | | | | | | | | | | | | | | | |
|---|---|---|---|---|---|---|---|---|---|---|---|---|---|---|---|---|---|---|---|---|---|---|---|---|---|---|---|---|---|
| 701.5350 | 4.0 | C39H76NO7P | PE(P-34:1) | Lipids: Glycerophospholipids | 1.13 | 0.92 | 0.99 | 0.6014 | 0.7006 | 0.9548 | 1.06 | 1.07 | 1.17 | 0.7357 | 0.8048 | 0.5558 | 1.28 | 1.23 | 1.28 | 0.4490 | 0.6068 | 0.4392 | 0.90 | 0.91 | 0.95 | 0.4244 | 0.6763 | 0.7755 |
| 723.5202 | 5.0 | C41H74NO7P | PE(P-36:4) | Lipids: Glycerophospholipids | 1.23 | 1.05 | 0.91 | 0.3213 | 0.7995 | 0.6898 | 0.86 | 0.90 | 1.03 | 0.3768 | 0.6458 | 0.8886 | 0.64 | 0.73 | 0.81 | 0.1205 | 0.2497 | 0.3717 | 1.24 | 1.10 | 1.23 | 0.2478 | 0.6515 | 0.2664 |
| 749.5355 | 5.3 | C43H76NO7P | PE(P-38:5) | Lipids: Glycerophospholipids | 0.83 | 0.71 | 0.45 | 0.6366 | 0.4403 | 0.2008 | 0.94 | 0.94 | 0.79 | 0.8088 | 0.7837 | 0.3337 | 1.40 | 1.05 | 0.85 | 0.1464 | 0.8380 | 0.5156 | 0.71 | 0.67 | 0.82 | 0.0942 | 0.1252 | 0.2060 |
| 779.5820 | 4.9 | C45H82NO7P | PE(P-40:4) | Lipids: Glycerophospholipids | 1.05 | 0.83 | 0.78 | 0.5477 | 0.0262 | 0.1002 | 0.76 | 1.38 | 1.31 | 0.0828 | 0.0511 | 0.1016 | 1.03 | 0.98 | 1.07 | 0.6715 | 0.8190 | 0.7868 | 0.63 | 0.66 | 0.89 | 0.0172 | 0.0186 | 0.5572 |
| 777.5680 | 3.9 | C45H80NO7P | PE(P-40:5) | Lipids: Glycerophospholipids | 1.24 | 1.01 | 0.91 | 0.2382 | 0.9519 | 0.5387 | 0.98 | 1.11 | 1.11 | 0.7898 | 0.2154 | 0.3149 | 1.11 | 0.98 | 1.19 | 0.5565 | 0.9016 | 0.2570 | 0.92 | 0.84 | 1.01 | 0.2211 | 0.0719 | 0.9212 |
| 775.5510 | 4.8 | C45H78NO7P | PE(P-40:6) | Lipids: Glycerophospholipids | 1.35 | 1.31 | 1.17 | 0.2480 | 0.2936 | 0.5333 | 0.80 | 0.77 | 0.78 | 0.4049 | 0.3087 | 0.4277 | 1.09 | 1.02 | 1.09 | 0.7870 | 0.9413 | 0.7384 | 0.74 | 0.82 | 0.93 | 0.2764 | 0.5148 | 0.7270 |
| 773.5368 | 3.9 | C45H76NO7P | PE(P-40:7) | Lipids: Glycerophospholipids | 1.14 | 1.15 | 1.10 | 0.6024 | 0.6153 | 0.6782 | 0.94 | 1.09 | 1.02 | 0.8384 | 0.8007 | 0.9363 | 1.11 | 1.03 | 1.16 | 0.8354 | 0.9008 | 0.6312 | 0.99 | 1.02 | 1.14 | 0.9660 | 0.9468 | 0.6136 |
| 748.5261 | 3.8 | C40H77O10P | PG(34:1) | Lipids: Glycerophospholipids | 1.77 | 1.91 | 1.65 | 0.2362 | 0.2006 | 0.3308 | 0.80 | 0.78 | 0.78 | 0.5425 | 0.5036 | 0.4693 | 0.46 | 0.61 | 0.43 | 0.0095 | 0.1664 | 0.0072 | 0.76 | 0.93 | 0.97 | 0.5151 | 0.8822 | 0.9297 |
| 776.5571 | 3.8 | C42H81O10P | PG(36:1) | Lipids: Glycerophospholipids | 1.58 | 1.38 | 1.28 | 0.0377 | 0.3061 | 0.2330 | 0.79 | 0.74 | 0.68 | 0.5217 | 0.4486 | 0.3565 | 0.50 | 0.64 | 0.48 | 0.0313 | 0.1099 | 0.0408 | 0.31 | 0.32 | 0.26 | 0.1465 | 0.1519 | 0.1349 |
| 774.5416 | 3.8 | C42H79O10P | PG(36:2) | Lipids: Glycerophospholipids | 1.83 | 1.49 | 1.37 | 0.0734 | 0.1822 | 0.2112 | 0.74 | 0.72 | 0.59 | 0.4085 | 0.3785 | 0.2330 | 0.63 | 0.80 | 0.59 | 0.0576 | 0.2931 | 0.0267 | 0.48 | 0.49 | 0.45 | 0.1874 | 0.1877 | 0.1713 |
| 864.5738 | 3.8 | C45H85O13P | PI(36:1) | Lipids: Glycerophospholipids | 1.76 | 1.48 | 1.27 | 0.0353 | 0.2237 | 0.1633 | 0.96 | 0.81 | 0.71 | 0.8884 | 0.5439 | 0.3681 | 0.71 | 0.83 | 0.54 | 0.1959 | 0.4426 | 0.0780 | 0.50 | 0.48 | 0.35 | 0.3045 | 0.2910 | 0.2208 |
| 862.5589 | 3.8 | C45H83O13P | PI(36:2) | Lipids: Glycerophospholipids | 0.98 | 1.25 | 1.28 | 0.9419 | 0.4780 | 0.4607 | 0.84 | 0.86 | 1.15 | 0.3279 | 0.3697 | 0.4877 | 0.68 | 0.87 | 0.65 | 0.2656 | 0.6381 | 0.2270 | 0.61 | 0.53 | 0.47 | 0.1923 | 0.1354 | 0.1192 |
| 858.5274 | 3.8 | C45H79O13P | PI(36:4) | Lipids: Glycerophospholipids | 1.05 | 1.38 | 1.34 | 0.7606 | 0.0773 | 0.2368 | 0.83 | 0.79 | 1.02 | 0.3747 | 0.2247 | 0.9279 | 0.86 | 0.89 | 0.95 | 0.6335 | 0.6849 | 0.8486 | 0.65 | 0.58 | 0.50 | 0.2429 | 0.1782 | 0.1380 |
| 916.6049 | 9.8 | C49H89O13P | PI(40:3) | Lipids: Glycerophospholipids | 1.11 | 1.26 | 1.53 | 0.6204 | 0.1786 | 0.3388 | 0.97 | 0.96 | 1.15 | 0.9100 | 0.8440 | 0.4127 | 0.91 | 1.14 | 1.03 | 0.6100 | 0.2088 | 0.5882 | 1.35 | 1.09 | 1.37 | 0.2083 | 0.6511 | 0.1656 |
| 525.3060 | 4.3 | C24H48NO9P | PS(18:0) | Lipids: Glycerophospholipids | 1.04 | 1.03 | 0.98 | 0.8062 | 0.8461 | 0.9201 | 1.07 | 1.13 | 1.06 | 0.5889 | 0.2318 | 0.5030 | 0.89 | 0.73 | 0.75 | 0.7236 | 0.2557 | 0.3539 | 0.82 | 0.74 | 0.87 | 0.1635 | 0.0752 | 0.3149 |
| 763.5377 | 3.7 | C40H78NO10P | PS(34:0) | Lipids: Glycerophospholipids | 1.30 | 1.37 | 2.02 | 0.4386 | 0.3134 | 0.4141 | 0.77 | 1.20 | 1.01 | 0.2745 | 0.4092 | 0.9626 | 0.89 | 0.94 | 0.76 | 0.2286 | 0.7721 | 0.0260 | 0.61 | 0.84 | 0.72 | 0.0473 | 0.5325 | 0.1042 |
| 761.5208 | 3.8 | C40H76NO10P | PS(34:1) | Lipids: Glycerophospholipids | 1.14 | 1.21 | 1.08 | 0.3764 | 0.3939 | 0.5716 | 1.01 | 0.89 | 0.97 | 0.9650 | 0.4112 | 0.7725 | 1.01 | 1.07 | 1.04 | 0.9420 | 0.7006 | 0.7894 | 0.45 | 0.47 | 0.52 | 0.0581 | 0.0412 | 0.0578 |
| 759.5054 | 3.8 | C40H74NO10P | PS(34:2) | Lipids: Glycerophospholipids | 1.10 | 1.33 | 1.11 | 0.5912 | 0.1555 | 0.4565 | 0.91 | 1.08 | 1.18 | 0.5891 | 0.6931 | 0.3188 | 1.00 | 0.99 | 0.99 | 0.9922 | 0.9474 | 0.9686 | 0.67 | 0.72 | 0.71 | 0.0897 | 0.1173 | 0.1099 |
| 785.5209 | 3.8 | C42H76NO10P | PS(36:3) | Lipids: Glycerophospholipids | 1.20 | 1.38 | 1.14 | 0.3435 | 0.3293 | 0.6412 | 0.82 | 0.95 | 0.88 | 0.3097 | 0.7590 | 0.5008 | 0.90 | 1.13 | 1.05 | 0.4653 | 0.5850 | 0.8425 | 0.76 | 0.78 | 0.76 | 0.1691 | 0.2268 | 0.2225 |
| 783.5062 | 3.8 | C42H74NO10P | PS(36:4) | Lipids: Glycerophospholipids | 1.12 | 1.47 | 1.15 | 0.5254 | 0.2010 | 0.5353 | 0.96 | 1.04 | 1.09 | 0.8623 | 0.8435 | 0.6629 | 1.06 | 1.08 | 1.06 | 0.6309 | 0.7098 | 0.6151 | 0.67 | 0.64 | 0.64 | 0.0934 | 0.0779 | 0.0769 |
| 811.5373 | 6.1 | C44H78NO10P | PS(38:4) | Lipids: Glycerophospholipids | 1.13 | 1.47 | 1.12 | 0.3489 | 0.0080 | 0.2492 | 0.92 | 1.02 | 1.11 | 0.5653 | 0.7830 | 0.2611 | 0.96 | 1.07 | 0.98 | 0.8478 | 0.7084 | 0.9334 | 0.82 | 0.73 | 0.78 | 0.1136 | 0.0484 | 0.0642 |
| 807.5056 | 3.8 | C44H74NO10P | PS(38:6) | Lipids: Glycerophospholipids | 1.03 | 1.10 | 0.94 | 0.7924 | 0.5628 | 0.6945 | 1.11 | 1.31 | 1.47 | 0.5334 | 0.0864 | 0.1315 | 1.09 | 1.15 | 1.09 | 0.4986 | 0.6162 | 0.6766 | 0.82 | 0.89 | 0.83 | 0.2392 | 0.5592 | 0.2785 |
| 825.5524 | 3.7 | C45H80NO10P | PS(39:4) | Lipids: Glycerophospholipids | 1.01 | 1.27 | 0.99 | 0.9494 | 0.2266 | 0.9192 | 0.96 | 0.96 | 1.18 | 0.8214 | 0.7483 | 0.2160 | 0.99 | 1.07 | 1.07 | 0.9848 | 0.9132 | 0.9151 | 0.89 | 0.88 | 0.91 | 0.3512 | 0.4990 | 0.4808 |
| 839.5684 | 3.8 | C46H82NO10P | PS(40:4) | Lipids: Glycerophospholipids | 1.08 | 1.17 | 1.12 | 0.9026 | 0.7754 | 0.8440 | 0.98 | 0.92 | 1.14 | 0.9668 | 0.8889 | 0.8172 | 0.78 | 0.84 | 0.84 | 0.5904 | 0.6830 | 0.6852 | 0.90 | 0.84 | 0.94 | 0.8496 | 0.7435 | 0.9056 |
| 831.5056 | 3.8 | C46H74NO10P | PS(40:8) | Lipids: Glycerophospholipids | 1.29 | 1.22 | 1.40 | 0.4295 | 0.0374 | 0.2426 | 1.17 | 0.84 | 1.21 | 0.5465 | 0.0974 | 0.0965 | 1.11 | 1.19 | 1.16 | 0.7958 | 0.7168 | 0.7160 | 1.17 | 1.02 | 1.26 | 0.1358 | 0.9293 | 0.1316 |
| 849.6104 | 4.1 | C44H86NO9P | PS(O-16:0/22:1(11Z)) | Lipids: Glycerophospholipids | 1.11 | 1.37 | 1.06 | 0.8035 | 0.5573 | 0.8898 | 1.02 | 0.97 | 1.12 | 0.9672 | 0.9387 | 0.7903 | 0.75 | 0.91 | 0.88 | 0.0846 | 0.4865 | 0.3068 | 1.00 | 0.88 | 0.94 | 0.9933 | 0.7364 | 0.8892 |
| 585.3638 | 7.8 | C26H54NO8P | PS(O-20:0/0:0) | Lipids: Glycerophospholipids | 0.88 | 0.91 | 1.03 | 0.6498 | 0.7156 | 0.9192 | 1.03 | 1.10 | 1.01 | 0.7733 | 0.4356 | 0.9338 | 0.95 | 1.06 | 1.40 | 0.9094 | 0.8405 | 0.3965 | 0.83 | 0.83 | 0.79 | 0.2930 | 0.3060 | 0.2085 |
| 821.5788 | 5.5 | C42H82NO9P | PS(O-36:1) | Lipids: Glycerophospholipids | 1.38 | 1.25 | 1.37 | 0.0737 | 0.5858 | 0.1446 | 0.77 | 0.66 | 0.92 | 0.4066 | 0.2633 | 0.8509 | 0.99 | 1.13 | 0.94 | 0.9547 | 0.3359 | 0.5591 | 0.52 | 0.47 | 1.14 | 0.3683 | 0.3252 | 0.8854 |
| 819.5635 | 4.6 | C42H80NO9P | PS(O-36:2) | Lipids: Glycerophospholipids | 1.11 | 1.04 | 0.96 | 0.5129 | 0.8020 | 0.7864 | 0.94 | 0.99 | 0.96 | 0.3243 | 0.8286 | 0.6650 | 1.97 | 2.06 | 1.10 | 0.0213 | 0.0184 | 0.6112 | 0.64 | 0.68 | 0.61 | 0.0775 | 0.1081 | 0.0789 |

| | | | | | | | | | | | | | | | | | | | | | | | | | | | | |
|---|---|---|---|---|---|---|---|---|---|---|---|---|---|---|---|---|---|---|---|---|---|---|---|---|---|---|---|---|
| 668.1729 | 12.7 | C33H32O15 | [Fv hydroxy,methoxy,methyl,acetyl(5:0)] 3,4,2',3',4'-Pentahydroxy-4-methoxychalcone 4-methyl ether 4'-O-(2''-O-caffeoyl-6''-O-acetylglucoside) | Lipids: Polyketides | 0.75 | 0.74 | 0.72 | 0.2383 | 0.1940 | 0.1815 | 1.11 | 1.24 | 1.10 | 0.5094 | 0.2069 | 0.5033 | 0.94 | 0.98 | 0.97 | 0.6906 | 0.8754 | 0.8580 | 0.71 | 1.11 | 0.82 | 0.1959 | 0.7619 | 0.3665 |
| 537.1119 | 10.4 | C23H20O14 | 5,3',4'-Trihydroxy-3-methoxy-6,7-methylenedioxyflavone 4'-glucuronide | Lipids: Polyketides | 1.50 | 1.13 | 1.17 | 0.2686 | 0.6963 | 0.5795 | 0.85 | 1.02 | 0.97 | 0.1673 | 0.8583 | 0.7837 | 0.59 | 0.76 | 0.78 | 0.2711 | 0.4710 | 0.4970 | 1.03 | 1.21 | 0.90 | 0.7868 | 0.1866 | 0.4544 |
| 336.1363 | 14.7 | C21H20O4 | Durlettone | Lipids: Polyketides | 0.99 | 1.03 | 1.05 | 0.9515 | 0.8626 | 0.7090 | 1.01 | 1.02 | 1.28 | 0.9614 | 0.9206 | 0.4496 | 1.17 | 1.32 | 1.27 | 0.7358 | 0.6614 | 0.6108 | 0.98 | 0.80 | 0.87 | 0.8326 | 0.0726 | 0.3268 |
| 610.0948 | 14.9 | C29H22O15 | Epigallocatechin 3,5,-di-O-gallate | Lipids: Polyketides | 0.72 | 1.00 | 0.53 | 0.5825 | 0.9959 | 0.3068 | 1.10 | 1.17 | 1.23 | 0.8834 | 0.8164 | 0.7894 | 1.94 | 2.08 | 2.56 | 0.0103 | 0.0074 | 0.0593 | 0.91 | 0.92 | 0.95 | 0.8556 | 0.8446 | 0.8937 |
| 484.2665 | 7.8 | C24H38O7 | [PR trihydroxy(2:0)] (-)-8alpha,15-diacetoxy-4beta,9alpha,14beta-trihydroxy-3(16)-fusicoccene | Lipids: Prenols | 1.03 | 1.40 | 1.20 | 0.8265 | 0.2913 | 0.2354 | 1.54 | 1.37 | 1.91 | 0.0109 | 0.1305 | 0.0030 | 1.04 | 1.28 | 0.83 | 0.9421 | 0.4883 | 0.7883 | 2.88 | 2.69 | 2.62 | 0.0003 | 0.0011 | 0.0149 |
| 239.2248 | 28.2 | C15H26O | [PR] (-)-alpha-Bisabolol | Lipids: Prenols | 0.58 | 0.67 | 0.56 | 0.0627 | 0.2899 | 0.0521 | 0.75 | 1.04 | 1.19 | 0.6564 | 0.8419 | 0.3777 | 1.13 | 1.25 | 1.28 | 0.6396 | 0.3405 | 0.4545 | 1.09 | 0.75 | 0.59 | 0.9220 | 0.7429 | 0.5737 |
| 746.5109 | 3.7 | C47H70O7 | [PR] 1'-Hydroxy-4-keto-gamma-carotene glucoside/ 1'-OH-4-Keto-gamma-carotene glucoside/ (Carotenoid K-G) | Lipids: Prenols | 0.94 | 1.04 | 0.97 | 0.8197 | 0.8768 | 0.8949 | 1.15 | 1.23 | 0.91 | 0.5240 | 0.3299 | 0.6848 | 0.63 | 0.76 | 0.55 | 0.0208 | 0.2597 | 0.0267 | 1.00 | 1.10 | 0.89 | 0.9985 | 0.6020 | 0.2816 |
| 614.3967 | 9.2 | C40H54O5 | [PR] 4-Hydroxymytiloxanthin | Lipids: Prenols | 1.57 | 1.25 | 1.03 | 0.1313 | 0.3224 | 0.8842 | 0.99 | 0.83 | 0.76 | 0.9617 | 0.5130 | 0.3683 | 1.11 | 1.17 | 1.05 | 0.4772 | 0.3099 | 0.7818 | 0.43 | 0.38 | 0.36 | 0.2189 | 0.1954 | 0.1847 |
| 302.2246 | 4.1 | C20H30O2 | [PR] Abietic acid | Lipids: Prenols | 1.06 | 1.02 | 1.05 | 0.7976 | 0.9267 | 0.8293 | 0.93 | 1.15 | 1.11 | 0.3966 | 0.1324 | 0.2210 | 1.00 | 1.34 | 1.73 | 0.9993 | 0.3731 | 0.0992 | 1.09 | 0.93 | 1.05 | 0.3877 | 0.7073 | 0.8214 |
| 382.1310 | 10.7 | C15H28O7P2 | [PR] Farnesyl pyrophosphate | Lipids: Prenols | 0.93 | 2.03 | 1.95 | 0.8087 | 0.4065 | 0.4904 | 2.57 | 3.51 | 2.20 | 0.3231 | 0.2330 | 0.3987 | 1.14 | 1.10 | 1.26 | 0.7228 | 0.8074 | 0.6010 | 1.16 | 1.92 | 1.58 | 0.5300 | 0.2077 | 0.1688 |
| 182.0943 | 7.9 | C10H14O3 | [PR] Iridotrial | Lipids: Prenols | 0.96 | 0.97 | 1.32 | 0.9418 | 0.9409 | 0.6601 | 0.99 | 1.07 | 1.10 | 0.9683 | 0.8514 | 0.8159 | 1.66 | 1.41 | 0.69 | 0.3691 | 0.2649 | 0.3572 | 1.12 | 1.14 | 1.11 | 0.6384 | 0.7497 | 0.7665 |
| 229.2405 | 7.8 | C14H31NO | [SP (14:0)] 1-deoxy-tetradecasphinganine | Lipids: Sphingolipids | 12.57 | 1.65 | 0.56 | 0.0151 | 0.3781 | 0.1265 | 1.75 | 3.26 | 1.11 | 0.0558 | 0.1655 | 0.8024 | 0.89 | 0.84 | 1.11 | 0.6137 | 0.4526 | 0.6207 | 1.88 | 1.32 | 1.68 | 0.1934 | 0.3885 | 0.3032 |
| 695.5306 | 10.9 | C38H75NO8 | [SP (14:0)] N-(tetradecanoyl)-1-beta-glucosyl-sphinganine | Lipids: Sphingolipids | 0.89 | 0.83 | 0.91 | 0.6144 | 0.5243 | 0.7094 | 0.99 | 1.14 | 1.00 | 0.9782 | 0.6280 | 0.9827 | 0.96 | 0.86 | 1.21 | 0.5228 | 0.2136 | 0.3479 | 1.52 | 1.04 | 1.32 | 0.1771 | 0.9081 | 0.3532 |
| 537.5126 | 4.8 | C34H67NO3 | [SP (16:0)] N-(hexadecanoyl)-sphing-4-enine | Lipids: Sphingolipids | 1.11 | 0.98 | 0.93 | 0.3930 | 0.8092 | 0.3885 | 0.95 | 1.23 | 1.23 | 0.6563 | 0.1360 | 0.1297 | 1.20 | 1.02 | 1.00 | 0.7705 | 0.9748 | 0.9942 | 1.14 | 0.98 | 1.01 | 0.2755 | 0.7870 | 0.8108 |
| 647.6216 | 4.1 | C42H81NO3 | [SP (24:0)] N-(15Z-tetracosenoyl)-sphing-4-enine | Lipids: Sphingolipids | 1.11 | 1.11 | 1.02 | 0.8381 | 0.8617 | 0.9740 | 1.06 | 1.18 | 1.15 | 0.9295 | 0.8159 | 0.8366 | 1.28 | 1.27 | 1.34 | 0.6041 | 0.5872 | 0.4811 | 1.19 | 0.99 | 1.09 | 0.7277 | 0.9886 | 0.8788 |
| 840.7079 | 4.7 | C49H97N2O6P | [SP (26:0)] N-(17Z-hexacosenoyl)-sphing-4-enine-1-phosphocholine | Lipids: Sphingolipids | 1.13 | 1.04 | 0.98 | 0.7482 | 0.9170 | 0.9643 | 0.87 | 0.83 | 0.89 | 0.7690 | 0.6958 | 0.7922 | 1.52 | 1.07 | 1.02 | 0.2575 | 0.7377 | 0.9072 | 0.66 | 0.64 | 0.76 | 0.5460 | 0.5501 | 0.6709 |
| 287.2460 | 4.3 | C16H33NO3 | [SP hydroxy,hydroxy,methyl(10:2/2:0)] 6R-(8-hydroxydecyl)-2R-(hydroxymethyl)-piperidin-3R-ol | Lipids: Sphingolipids | 0.78 | 0.85 | 1.04 | 0.5082 | 0.6644 | 0.9233 | 1.00 | 1.00 | 1.08 | 0.9779 | 0.9942 | 0.6880 | 0.63 | 1.18 | 1.00 | 0.0843 | 0.5224 | 0.9851 | 1.22 | 1.14 | 1.08 | 0.3896 | 0.6016 | 0.7369 |
| 386.2418 | 22.4 | C19H31NO6 | [SP] Pramanicin | Lipids: Sphingolipids | 2.73 | 1.42 | 1.81 | 0.0573 | 0.5106 | 0.2370 | 1.24 | 1.19 | 1.32 | 0.6506 | 0.6967 | 0.4983 | 1.02 | 1.09 | 0.98 | 0.8290 | 0.3309 | 0.7778 | 1.06 | 1.15 | 1.38 | 0.8020 | 0.5467 | 0.2425 |
| 299.2823 | 4.9 | C18H37NO2 | [SP] Sphing-4-enine | Lipids: Sphingolipids | 1.03 | 1.02 | 0.97 | 0.2887 | 0.7790 | 0.4038 | 1.12 | 1.15 | 1.22 | 0.1152 | 0.2467 | 0.0617 | 1.29 | 1.05 | 1.56 | 0.7802 | 0.9604 | 0.6398 | 1.03 | 1.00 | 1.09 | 0.3585 | 0.8757 | 0.0951 |
| 379.2487 | 7.9 | C18H38NO5P | [SP] Sphing-4-enine-1-phosphate | Lipids: Sphingolipids | 1.35 | 1.37 | 1.04 | 0.6803 | 0.7071 | 0.9627 | 0.97 | 0.97 | 1.07 | 0.9629 | 0.9682 | 0.9252 | 0.57 | 2.43 | 0.00 | NA | 0.3627 | NA | 1.23 | 1.27 | 1.57 | 0.7987 | 0.7843 | 0.6324 |
| 381.2642 | 7.9 | C18H40NO5P | [SP] Sphinganine-1-phosphate | Lipids: Sphingolipids | 0.81 | 1.19 | 1.24 | 0.4738 | 0.8198 | 0.6885 | 0.44 | 0.63 | 0.93 | NA | 0.6021 | 0.9403 | 0.94 | 0.94 | 1.19 | 0.9532 | 0.9485 | 0.8664 | 0.70 | 0.61 | 0.40 | 0.6973 | 0.5497 | NA |
| 621.6058 | 5.0 | C40H79NO3 | Cer(d40:1) | Lipids: Sphingolipids | 1.29 | 0.89 | 1.03 | 0.7812 | 0.8977 | 0.9803 | 0.86 | 0.97 | 0.86 | 0.8855 | 0.9748 | 0.8926 | 1.32 | 1.23 | 1.24 | 0.2894 | 0.4406 | 0.4051 | 0.84 | 1.27 | 0.85 | 0.8793 | 0.8301 | 0.8793 |
| 315.2772 | 28.3 | C18H37NO3 | Dehydrophytosphingosine | Lipids: Sphingolipids | 1.20 | 0.85 | 1.04 | 0.6447 | 0.5616 | 0.9132 | 1.37 | 1.27 | 1.31 | 0.3736 | 0.5023 | 0.3955 | 1.76 | 1.41 | 1.69 | 0.2302 | 0.4705 | 0.0793 | 0.78 | 0.95 | 1.09 | 0.3261 | 0.8083 | 0.6314 |
| 461.3352 | 4.7 | C24H47NO7 | Psychosine | Lipids: Sphingolipids | 0.68 | 0.96 | 0.88 | 0.4715 | 0.9161 | 0.7997 | 1.16 | 0.76 | 0.99 | 0.5583 | 0.3132 | 0.9654 | 1.11 | 0.97 | 1.27 | 0.8813 | 0.9615 | 0.7029 | 0.92 | 0.89 | 0.86 | 0.8423 | 0.7608 | 0.7021 |
| 798.6616 | 4.6 | C46H91N2O6P | SM(d17:1/24:1(15Z)) | Lipids: Sphingolipids | 1.19 | 1.31 | 1.18 | 0.7788 | 0.6883 | 0.7926 | 0.99 | 1.29 | 1.02 | 0.9900 | 0.7243 | 0.9778 | 1.18 | 1.20 | 1.10 | 0.4142 | 0.5939 | 0.4976 | 0.98 | 1.04 | 1.09 | 0.9609 | 0.9518 | 0.8704 |

| | | | | | | | | | | | | | | | | | | | | | | | | | | | | | |
|---|---|---|---|---|---|---|---|---|---|---|---|---|---|---|---|---|---|---|---|---|---|---|---|---|---|---|---|---|---|
| 674.5360 | 5.5 | C37H75N2O6P | SM(d32:1) | Lipids: Sphingolipids | 0.67 | 0.78 | 1.00 | 0.3461 | 0.4972 | 0.9933 | 0.92 | 1.11 | 0.82 | 0.6562 | 0.5735 | 0.3873 | 0.87 | 0.89 | 1.16 | 0.6571 | 0.6924 | 0.6383 | 0.81 | 0.87 | 0.93 | 0.3248 | 0.4941 | 0.7148 |
| 688.5516 | 7.8 | C38H77N2O6P | SM(d33:1) | Lipids: Sphingolipids | 1.17 | 0.97 | 1.00 | 0.6261 | 0.9205 | 0.9929 | 1.04 | 1.06 | 1.12 | 0.8937 | 0.8535 | 0.6492 | 1.06 | 1.07 | 1.44 | 0.7556 | 0.8453 | 0.1884 | 0.87 | 0.83 | 0.98 | 0.3839 | 0.4979 | 0.9420 |
| 702.5673 | 6.5 | C39H79N2O6P | SM(d34:1) | Lipids: Sphingolipids | 1.22 | 1.04 | 0.87 | 0.6185 | 0.9146 | 0.7543 | 0.95 | 0.91 | 1.15 | 0.9057 | 0.8126 | 0.7000 | 0.63 | 1.04 | 1.08 | 0.3061 | 0.8697 | 0.7876 | 1.08 | 1.10 | 0.81 | 0.8317 | 0.8664 | 0.5373 |
| 700.5515 | 5.6 | C39H77N2O6P | SM(d34:2) | Lipids: Sphingolipids | 0.67 | 0.50 | 1.25 | 0.2140 | 0.0688 | 0.5174 | 0.93 | 0.57 | 0.47 | 0.7377 | 0.1992 | 0.0287 | 1.02 | 0.92 | 1.08 | 0.9144 | 0.3650 | 0.4561 | 1.07 | 1.03 | 0.44 | 0.6165 | 0.8909 | 0.0042 |
| 716.5831 | 4.3 | C40H81N2O6P | SM(d35:1) | Lipids: Sphingolipids | 1.20 | 1.05 | 1.13 | 0.3438 | 0.8089 | 0.5859 | 0.94 | 1.01 | 1.01 | 0.7392 | 0.9517 | 0.9445 | 1.42 | 1.35 | 1.15 | 0.2927 | 0.3631 | 0.3896 | 0.86 | 0.87 | 0.91 | 0.1928 | 0.4851 | 0.4992 |
| 730.5990 | 7.8 | C41H83N2O6P | SM(d36:1) | Lipids: Sphingolipids | 1.58 | 1.16 | 1.85 | 0.2575 | 0.7194 | 0.2944 | 0.79 | 0.87 | 1.15 | 0.2501 | 0.5112 | 0.6060 | 0.85 | 1.20 | 1.07 | 0.6645 | 0.5905 | 0.8760 | 0.92 | 0.92 | 1.06 | 0.8203 | 0.8467 | 0.8662 |
| 728.5833 | 7.8 | C41H81N2O6P | SM(d36:2) | Lipids: Sphingolipids | 0.97 | 0.84 | 0.91 | 0.9591 | 0.7300 | 0.8565 | 0.91 | 0.96 | 1.19 | 0.8645 | 0.9322 | 0.7050 | 0.97 | 1.11 | 1.34 | 0.9292 | 0.7343 | 0.6021 | 1.51 | 1.26 | 1.41 | 0.2322 | 0.7010 | 0.4736 |
| 758.6297 | 7.8 | C43H87N2O6P | SM(d38:1) | Lipids: Sphingolipids | 1.20 | 0.80 | 0.91 | 0.7939 | 0.7189 | 0.8694 | 0.86 | 0.68 | 1.12 | 0.8189 | 0.5540 | 0.8477 | 0.98 | 1.07 | 1.10 | 0.9140 | 0.8074 | 0.7848 | 0.84 | 0.78 | 0.93 | 0.7723 | 0.7267 | 0.9073 |
| 784.6458 | 7.7 | C45H89N2O6P | SM(d40:2) | Lipids: Sphingolipids | 1.17 | 1.02 | 1.20 | 0.5773 | 0.9126 | 0.4178 | 1.10 | 1.12 | 1.24 | 0.6529 | 0.6441 | 0.4158 | 1.03 | 1.13 | 1.29 | 0.8511 | 0.5771 | 0.4784 | 1.16 | 0.71 | 0.92 | 0.7197 | 0.4598 | 0.8428 |
| 810.6617 | 5.7 | C47H91N2O6P | SM(d42:3) | Lipids: Sphingolipids | 1.06 | 1.09 | 1.32 | 0.8624 | 0.7184 | 0.2409 | 1.07 | 1.04 | 1.11 | 0.3973 | 0.8581 | 0.6201 | 0.76 | 0.91 | 1.00 | 0.0117 | 0.1157 | 0.9596 | 0.93 | 0.87 | 1.05 | 0.6758 | 0.6602 | 0.8859 |
| 826.6932 | 4.7 | C48H95N2O6P | SM(d43:2) | Lipids: Sphingolipids | 1.27 | 0.87 | 1.06 | 0.1057 | 0.4768 | 0.7313 | 1.08 | 1.15 | 1.27 | 0.4321 | 0.1498 | 0.0413 | 1.25 | 1.30 | 1.21 | 0.5890 | 0.2817 | 0.3293 | 1.60 | 1.64 | 1.74 | 0.0645 | 0.1082 | 0.0669 |
| 842.7226 | 4.8 | C49H99N2O6P | SM(d44:1) | Lipids: Sphingolipids | 1.08 | 1.05 | 1.07 | 0.7838 | 0.8503 | 0.8343 | 1.17 | 1.07 | 1.13 | 0.6132 | 0.4985 | 0.3740 | 1.23 | 1.37 | 1.14 | 0.4456 | 0.2207 | 0.5983 | 1.11 | 1.17 | 1.28 | 0.5048 | 0.5093 | 0.3845 |
| 392.2926 | 28.5 | C24H40O4 | [ST hydrox] 3alpha,7alpha-Dihydroxy-5beta-cholan-24-oic Acid | Lipids: Sterol lipids | 1.01 | 1.23 | 1.06 | 0.9526 | 0.3147 | 0.7043 | 1.21 | 1.15 | 1.09 | 0.2087 | 0.5035 | 0.6866 | 0.96 | 0.95 | 1.04 | 0.8390 | 0.8369 | 0.8411 | 0.96 | 0.86 | 1.05 | 0.7235 | 0.3948 | 0.6484 |
| 482.1712 | 15.0 | C24H30O8 | [ST hydroxy(3:0)] 3-hydroxy-estra-1,3,5(10)-trien-17-one 3-D-glucuronide | Lipids: Sterol lipids | 1.36 | 1.36 | 1.38 | 0.1489 | 0.1770 | 0.1795 | 0.85 | 0.88 | 0.93 | 0.4628 | 0.3515 | 0.4844 | 0.51 | 0.45 | 0.46 | 0.0122 | 0.0060 | 0.0038 | 0.96 | 0.60 | 0.71 | 0.7824 | 0.0633 | 0.1225 |
| 422.2676 | 28.5 | C24H38O6 | [ST Trihydroxy,ox] 3alpha,7beta,12alpha-Trihydroxy-6-oxo-5alpha-cholan-24-oic Acid | Lipids: Sterol lipids | 1.25 | 1.34 | 1.04 | 0.1851 | 0.1272 | 0.7921 | 0.79 | 0.80 | 0.70 | 0.1970 | 0.0769 | 0.0478 | 1.30 | 1.09 | 1.16 | 0.2797 | 0.7215 | 0.5259 | 0.30 | 0.29 | 0.27 | 0.0472 | 0.0468 | 0.0521 |
| 368.3443 | 5.1 | C27H44 | [ST] (5Z,7E)-9,10-seco-5,7,10(19)-cholestatriene | Lipids: Sterol lipids | 1.40 | 1.24 | 1.09 | 0.0419 | 0.2453 | 0.5543 | 1.03 | 1.25 | 1.20 | 0.8658 | 0.1565 | 0.2482 | 2.31 | 0.77 | 0.86 | 0.2259 | 0.5304 | 0.6143 | 0.84 | 0.76 | 0.89 | 0.4430 | 0.2884 | 0.5918 |
| 408.2877 | 4.8 | C24H40O5 | Cholate | Lipids: Sterol lipids | 1.28 | 0.72 | 0.70 | 0.3728 | 0.2299 | 0.1301 | 0.83 | 0.69 | 0.90 | 0.8000 | 0.6494 | 0.8824 | 1.12 | 1.05 | 0.85 | 0.8316 | 0.9282 | 0.7660 | 2.04 | 1.38 | 1.39 | 0.1979 | 0.5053 | 0.1473 |
| 466.3115 | 3.7 | C27H46O4S | Cholesterolsulfate | Lipids: Sterol lipids | 0.82 | 1.40 | 0.97 | 0.2404 | 0.4090 | 0.8275 | 1.01 | 1.02 | 0.89 | 0.9656 | 0.8866 | 0.6039 | 0.97 | 1.03 | 0.98 | 0.8327 | 0.8915 | 0.9161 | 0.60 | 0.56 | 0.62 | 0.1962 | 0.1671 | 0.2128 |
| 624.3502 | 14.8 | C33H52O11 | Spongipregnoloside A | Lipids: Sterol Lipids | 1.37 | 1.20 | 1.41 | 0.2131 | 0.2480 | 0.1771 | 1.04 | 0.92 | 1.12 | 0.7450 | 0.6143 | 0.3365 | 1.03 | 0.88 | 1.12 | 0.8943 | 0.5012 | 0.7781 | 1.18 | 0.97 | 1.02 | 0.2305 | 0.8840 | 0.7981 |
| 221.1086 | 9.2 | C9H19NO3S | CAPS | Medium Component | 1.33 | 1.27 | 0.98 | 0.1362 | 0.1807 | 0.8855 | 0.99 | 1.06 | 0.97 | 0.9539 | 0.7766 | 0.9046 | 1.15 | 1.33 | 1.04 | 0.3457 | 0.4770 | 0.7979 | 0.90 | 0.90 | 0.85 | 0.5757 | 0.5602 | 0.4735 |
| 354.0563 | 5.0 | C19H14O5S | Phenolsulfonphthalein | Medium Component | 1.01 | 1.06 | 1.03 | 0.9454 | 0.7273 | 0.8278 | 0.99 | 1.03 | 1.06 | 0.9581 | 0.7450 | 0.4539 | 1.10 | 0.99 | 1.05 | 0.2588 | 0.9368 | 0.7504 | 1.02 | 0.95 | 1.16 | 0.9076 | 0.7869 | 0.5383 |
| 302.0606 | 14.0 | C8H18N2O6S2 | PIPES | Medium Component | 1.10 | 1.01 | 1.06 | 0.7542 | 0.9721 | 0.8573 | 0.88 | 1.04 | 1.04 | 0.3567 | 0.7455 | 0.7503 | 0.98 | 1.07 | 1.11 | 0.7044 | 0.4001 | 0.2841 | 0.73 | 0.83 | 0.81 | 0.1693 | 0.3385 | 0.3002 |
| 237.0308 | 16.9 | C6H9NO4S | a Cysteine adduct | Medium Contaminant | 1.11 | 1.07 | 1.08 | 0.4703 | 0.6200 | 0.5327 | 0.94 | 0.98 | 1.03 | 0.5020 | 0.8817 | 0.6842 | 1.00 | 1.03 | 1.03 | 0.9701 | 0.8162 | 0.8181 | 0.99 | 0.93 | 0.99 | 0.9443 | 0.5495 | 0.9600 |
| 144.0423 | 15.2 | C6H8O4 | 2,3-Dimethylmaleate | Metabolism of Cofactors and Vitamins | 1.03 | 1.17 | 1.11 | 0.8718 | 0.3676 | 0.5721 | 0.88 | 0.96 | 0.94 | 0.3578 | 0.7686 | 0.6765 | 1.15 | 1.24 | 1.23 | 0.4929 | 0.3440 | 0.3308 | 0.93 | 0.92 | 0.95 | 0.4184 | 0.3793 | 0.6309 |
| 225.0637 | 12.9 | C10H11NO5 | 4-Amino-4-deoxychorismate | Metabolism of Cofactors and Vitamins | 0.55 | 0.47 | 0.54 | 0.1263 | 0.2434 | 0.1256 | 1.01 | 0.98 | 0.83 | 0.9898 | 0.9526 | 0.6818 | 1.15 | 1.31 | 1.40 | 0.5559 | 0.3217 | 0.2093 | 0.68 | 0.62 | 0.77 | 0.0878 | 0.0498 | 0.2764 |
| 139.0745 | 7.6 | C6H9N3O | 4-Amino-5-hydroxymethyl-2-methylpyrimidine | Metabolism of Cofactors and Vitamins | 1.06 | 1.13 | 1.11 | 0.6159 | 0.3189 | 0.4819 | 1.33 | 1.21 | 1.22 | 0.3841 | 0.3499 | 0.0464 | 1.16 | 1.25 | 1.23 | 0.5837 | 0.6010 | 0.4768 | 1.24 | 1.16 | 1.00 | 0.1760 | 0.2338 | 0.9930 |
| 165.0426 | 5.2 | C8H7NO3 | 4-Pyridoxolactone | Metabolism of Cofactors and Vitamins | 1.33 | 1.57 | 1.43 | 0.4272 | 0.1288 | 0.4014 | 0.90 | 0.34 | 1.04 | 0.6979 | 0.0340 | 0.8405 | 1.06 | 0.81 | 1.04 | 0.5788 | 0.5621 | 0.6898 | 0.88 | 1.06 | 1.33 | 0.5422 | 0.8377 | 0.3725 |
| 326.1226 | 12.8 | C13H18N4O6 | 6,7-Dimethyl-8-(1-D-ribityl)lumazine | Metabolism of Cofactors and Vitamins | 0.78 | 0.78 | 1.04 | 0.5205 | 0.4875 | 0.7699 | 0.95 | 0.98 | 0.79 | 0.6737 | 0.8252 | 0.5135 | 0.70 | 0.81 | 0.61 | 0.2302 | 0.5181 | 0.1423 | 1.11 | 1.29 | 1.36 | 0.8625 | 0.6283 | 0.5500 |
| 187.1211 | 7.8 | C9H17NO3 | 8-Amino-7-oxononanoate | Metabolism of Cofactors and Vitamins | 0.85 | 1.16 | 0.88 | 0.6807 | 0.6224 | 0.7401 | 0.91 | 1.09 | 1.02 | 0.8168 | 0.8520 | 0.9702 | 0.94 | 0.58 | 0.58 | 0.9164 | 0.4318 | 0.4266 | 0.55 | 0.67 | 0.38 | 0.3147 | 0.4566 | 0.1973 |
| 299.0769 | 14.9 | C9H18NO8P | D-4'-Phosphopantothenate | Metabolism of Cofactors and Vitamins | 1.13 | 0.83 | 1.26 | 0.6508 | 0.1872 | 0.6295 | 0.85 | 1.29 | 0.75 | 0.3868 | 0.5676 | 0.1926 | 0.00 | 0.14 | 0.00 | NA | NA | NA | 0.79 | 0.82 | 1.16 | 0.5468 | 0.6062 | 0.4713 |
| 122.0480 | 7.9 | C6H6N2O | Nicotinamide | Metabolism of Cofactors and Vitamins | 0.52 | 0.72 | 0.34 | NA | 0.6843 | NA | 0.15 | 0.41 | 0.20 | NA | 0.1822 | NA | 0.97 | 1.17 | 1.15 | 0.9504 | 0.7356 | 0.7985 | 0.00 | 0.11 | 0.00 | NA | NA | NA |
| 334.0565 | 13.9 | C11H15N2O8P | Nicotinamide D-ribonucleotide | Metabolism of Cofactors and Vitamins | 1.24 | 0.81 | 1.52 | 0.7102 | 0.7263 | 0.5255 | 1.27 | 1.78 | 1.66 | 0.5540 | 0.1589 | 0.2230 | 1.15 | 1.17 | 1.23 | 0.2519 | 0.2428 | 0.1271 | 0.95 | 1.24 | 1.34 | 0.8383 | 0.7185 | 0.2637 |
| 277.0562 | 16.6 | C11H13NO6 | Nicotinate D-ribonucleoside | Metabolism of Cofactors and Vitamins | 1.06 | 1.04 | 1.12 | 0.6280 | 0.6911 | 0.1627 | 1.22 | 1.03 | 1.28 | 0.1366 | 0.6913 | 0.0355 | 1.14 | 1.09 | 1.15 | 0.6099 | 0.6722 | 0.6008 | 0.94 | 1.02 | 1.13 | 0.4550 | 0.8495 | 0.1612 |

| | | | | | | | | | | | | | | | | | | | | | | | | | | | | | |
|---|---|---|---|---|---|---|---|---|---|---|---|---|---|---|---|---|---|---|---|---|---|---|---|---|---|---|---|---|---|
| 335.0407 | 15.2 | C11H14NO9P | Nicotinate D-ribonucleotide | Metabolism of Cofactors and Vitamins | 1.03 | 1.06 | 1.03 | 0.9340 | 0.8459 | 0.9242 | 1.00 | 1.10 | 1.11 | 0.9875 | 0.7524 | 0.7215 | 1.55 | 1.39 | 1.74 | 0.0040 | 0.0042 | 0.0300 | 0.83 | 0.82 | 0.76 | 0.5164 | 0.5162 | 0.4013 |
| 167.0583 | 8.2 | C8H9NO3 | Pyridoxal | Metabolism of Cofactors and Vitamins | 1.04 | 1.08 | 1.01 | 0.8036 | 0.5786 | 0.9519 | 1.05 | 1.14 | 1.23 | 0.5659 | 0.1205 | 0.0200 | 1.11 | 1.09 | 1.20 | 0.8661 | 0.8934 | 0.7700 | 1.83 | 1.59 | 2.05 | 0.0003 | 0.0259 | 0.0085 |
| 249.0399 | 13.7 | C8H12NO6P | Pyridoxine phosphate | Metabolism of Cofactors and Vitamins | 1.05 | 0.99 | 1.02 | 0.8870 | 0.9735 | 0.9609 | 1.11 | 0.94 | 1.16 | 0.8609 | 0.9120 | 0.8072 | 0.99 | 1.03 | 1.07 | 0.9893 | 0.9441 | 0.8708 | 0.94 | 1.04 | 1.01 | 0.9062 | 0.9416 | 0.9932 |
| 264.1044 | 19.7 | C12H16N4OS | Thiamin | Metabolism of Cofactors and Vitamins | 0.94 | 0.94 | 0.95 | 0.8238 | 0.8108 | 0.8435 | 1.02 | 1.06 | 1.25 | 0.9230 | 0.7910 | 0.5407 | 1.43 | 1.17 | 1.22 | 0.3407 | 0.5764 | 0.3378 | 0.89 | 1.06 | 0.80 | 0.8351 | 0.9162 | 0.6613 |
| 135.0545 | 9.7 | C5H5N5 | Adenine | Nucleotide Metabolism | 0.95 | 1.19 | 1.19 | 0.8417 | 0.4928 | 0.2754 | 1.46 | 1.34 | 1.40 | 0.0974 | 0.1555 | 0.0669 | 0.88 | 1.00 | 1.17 | 0.5456 | 0.9819 | 0.4451 | 0.96 | 0.84 | 0.91 | 0.8932 | 0.5755 | 0.7258 |
| 267.0967 | 9.2 | C10H13N5O4 | Adenosine | Nucleotide Metabolism | 1.25 | 1.33 | 1.32 | 0.6097 | 0.5185 | 0.5850 | 1.08 | 1.14 | 1.20 | 0.6606 | 0.6360 | 0.3346 | 0.96 | 1.50 | 0.97 | 0.9205 | 0.4010 | 0.9096 | 1.15 | 1.19 | 1.38 | 0.4722 | 0.5286 | 0.1855 |
| 347.0631 | 14.8 | C10H14N5O7P | AMP | Nucleotide Metabolism | 1.08 | 1.11 | 0.90 | 0.7418 | 0.6491 | 0.6757 | 0.85 | 1.00 | 1.04 | 0.3158 | 0.9827 | 0.7827 | 1.16 | 1.03 | 1.10 | 0.1605 | 0.7009 | 0.6173 | 0.85 | 0.86 | 0.96 | 0.4923 | 0.4962 | 0.8541 |
| 128.0222 | 29.7 | C4H4N2O3 | Barbiturate | Nucleotide Metabolism | 1.05 | 1.14 | 1.06 | 0.7322 | 0.5349 | 0.6728 | 0.93 | 1.01 | 0.98 | 0.6065 | 0.9319 | 0.9065 | 0.59 | 0.61 | 0.93 | 0.4515 | 0.5606 | 0.8961 | 1.09 | 1.07 | 1.13 | 0.4398 | 0.4445 | 0.3239 |
| 323.0518 | 16.2 | C9H14N3O8P | CMP | Nucleotide Metabolism | 0.33 | 0.26 | 1.15 | 0.1039 | 0.0823 | 0.7686 | 1.13 | 0.92 | 0.63 | 0.8017 | 0.8659 | 0.4953 | 1.81 | 1.66 | 2.08 | 0.0394 | 0.1643 | 0.1464 | 0.67 | 2.06 | 1.36 | 0.6260 | 0.2034 | 0.5548 |
| 243.0855 | 13.7 | C9H13N3O5 | Cytidine | Nucleotide Metabolism | 1.14 | 1.06 | 1.03 | 0.4913 | 0.7281 | 0.8353 | 1.20 | 1.23 | 1.76 | 0.2075 | 0.1340 | 0.0679 | 0.92 | 0.96 | 1.04 | 0.7056 | 0.8325 | 0.8402 | 1.78 | 1.65 | 1.80 | 0.0940 | 0.0179 | 0.1483 |
| 111.0432 | 7.9 | C4H5N3O | Cytosine | Nucleotide Metabolism | 1.06 | 0.99 | 1.00 | 0.7383 | 0.9343 | 0.9925 | 0.93 | 0.99 | 1.13 | 0.7895 | 0.9509 | 0.4533 | 1.07 | 0.97 | 1.19 | 0.7067 | 0.8919 | 0.2204 | 0.86 | 0.97 | 0.85 | 0.5695 | 0.9003 | 0.5112 |
| 307.0569 | 15.2 | C9H14N3O7P | dCMP | Nucleotide Metabolism | 1.21 | 0.91 | 1.05 | 0.4023 | 0.4749 | 0.7326 | 0.94 | 0.91 | 0.80 | 0.7411 | 0.6164 | 0.2007 | 0.86 | 0.90 | 0.82 | 0.6638 | 0.7655 | 0.5858 | 0.86 | 0.86 | 0.95 | 0.3527 | 0.5347 | 0.6308 |
| 273.0960 | 14.7 | C9H13N3O4 | Deoxycytidine | Nucleotide Metabolism | 1.24 | 1.12 | 1.10 | 0.5650 | 0.7361 | 0.7647 | 0.91 | 0.98 | 1.23 | 0.7840 | 0.9579 | 0.5503 | 2.30 | 1.18 | 1.19 | 0.0999 | 0.1233 | 0.1256 | 1.00 | 0.89 | 0.94 | 0.9996 | 0.7148 | 0.8412 |
| 427.0295 | 16.0 | C10H15N5O10P2 | dGDP | Nucleotide Metabolism | 0.61 | 0.57 | 0.54 | 0.3467 | 0.3090 | 0.2810 | 0.73 | 1.27 | 0.61 | 0.6065 | 0.6165 | 0.4594 | 0.99 | 0.95 | 0.94 | 0.9058 | 0.3984 | 0.7885 | 1.77 | 1.02 | 0.99 | 0.3132 | 0.8111 | 0.9106 |
| 443.0243 | 17.7 | C10H15N5O11P2 | GDP | Nucleotide Metabolism | 0.82 | 1.09 | 1.06 | 0.3663 | 0.7443 | 0.7874 | 1.17 | 1.11 | 0.94 | 0.2255 | 0.5904 | 0.6253 | 1.33 | 1.34 | 1.37 | 0.0970 | 0.2401 | 0.2732 | 1.05 | 1.22 | 0.87 | 0.5384 | 0.1489 | 0.0808 |
| 151.0494 | 12.3 | C5H5N5O | Guanine | Nucleotide Metabolism | 0.97 | 1.22 | 1.16 | 0.8263 | 0.4452 | 0.4614 | 0.98 | 1.20 | 1.23 | 0.8703 | 0.4844 | 0.3028 | 0.62 | 0.71 | 0.73 | 0.1379 | 0.3250 | 0.2737 | 0.97 | 1.07 | 0.97 | 0.9204 | 0.8115 | 0.9186 |
| 428.0134 | 16.4 | C10H14N4O11P2 | IDP | Nucleotide Metabolism | 1.01 | 1.17 | 0.90 | 0.9342 | 0.3908 | 0.5474 | 1.05 | 0.84 | 0.86 | 0.8443 | 0.4848 | 0.5364 | 0.95 | 1.01 | 1.01 | 0.9667 | 0.9951 | 0.9951 | 0.43 | 0.52 | 0.47 | 0.0351 | 0.0627 | 0.0423 |
| 268.0807 | 10.9 | C10H12N4O5 | Inosine | Nucleotide Metabolism | 0.83 | 0.92 | 0.92 | 0.8848 | 0.9484 | 0.9461 | 0.95 | 1.01 | 1.08 | 0.9669 | 0.9915 | 0.9520 | 0.96 | 0.94 | 1.03 | 0.9539 | 0.9092 | 0.9628 | 1.17 | 1.19 | 1.17 | 0.8985 | 0.8847 | 0.8995 |
| 176.0434 | 16.4 | C5H8N2O5 | N-Carbamoyl-L-aspartate | Nucleotide Metabolism | 1.09 | 0.96 | 0.90 | 0.8965 | 0.9440 | 0.8568 | 0.91 | 1.14 | 0.79 | 0.8850 | 0.8421 | 0.7145 | 0.17 | 0.24 | 0.12 | 0.0765 | 0.0889 | 0.0693 | 0.80 | 1.00 | 0.74 | 0.7197 | 0.9965 | 0.5743 |
| 102.0429 | 7.9 | C3H6N2O2 | N-Formiminoglycine | Nucleotide Metabolism | 1.11 | 1.04 | 1.08 | 0.7428 | 0.8153 | 0.7546 | 0.49 | 0.49 | 0.35 | 0.1037 | 0.1027 | 0.0602 | 1.07 | 1.08 | 0.99 | 0.6581 | 0.4948 | 0.9354 | 0.17 | 0.24 | 0.10 | 0.0098 | 0.0127 | 0.0110 |
| 156.0171 | 12.0 | C5H4N2O4 | Orotate | Nucleotide Metabolism | 1.08 | 0.96 | 0.97 | 0.3527 | 0.6496 | 0.6233 | 0.88 | 0.98 | 0.96 | 0.5146 | 0.9275 | 0.8248 | 0.99 | 0.96 | 0.82 | 0.9239 | 0.7673 | 0.2248 | 0.87 | 0.82 | 0.98 | 0.2797 | 0.3185 | 0.8993 |
| 97.9674 | 17.6 | H2O4S | Sulfate | Nucleotide Metabolism | 1.09 | 0.92 | 0.90 | 0.7933 | 0.8139 | 0.7706 | 1.07 | 1.17 | 0.99 | 0.8685 | 0.6685 | 0.9893 | 1.03 | 0.99 | 1.02 | 0.5918 | 0.8650 | 0.8492 | 0.98 | 1.07 | 1.19 | 0.9470 | 0.7802 | 0.6466 |
| 404.0022 | 16.1 | C9H14N2O12P2 | UDP | Nucleotide Metabolism | 1.04 | 1.09 | 1.07 | 0.7271 | 0.5326 | 0.6063 | 1.01 | 1.11 | 1.01 | 0.8364 | 0.2247 | 0.7951 | 0.94 | 1.05 | 1.06 | 0.5500 | 0.7330 | 0.7809 | 0.95 | 0.95 | 0.98 | 0.3321 | 0.6288 | 0.7933 |
| 324.0352 | 15.0 | C9H13N2O9P | UMP | Nucleotide Metabolism | 1.06 | 1.03 | 1.09 | 0.7197 | 0.8604 | 0.5788 | 0.87 | 0.93 | 0.95 | 0.1103 | 0.4123 | 0.6976 | 0.53 | 0.67 | 0.44 | 0.1268 | 0.4086 | 0.0934 | 0.88 | 0.95 | 0.80 | 0.1717 | 0.5791 | 0.0258 |
| 112.0272 | 11.8 | C4H4N2O2 | Uracil | Nucleotide Metabolism | 0.44 | 0.87 | 0.37 | 0.1236 | 0.7725 | 0.1061 | 0.65 | 0.82 | 0.87 | 0.1410 | 0.4624 | 0.5507 | 1.01 | 0.99 | 1.07 | 0.9302 | 0.9401 | 0.7418 | 0.37 | 0.51 | 0.31 | 0.1919 | 0.3145 | 0.1661 |
| 168.0283 | 12.2 | C5H4N4O3 | Urate | Nucleotide Metabolism | 1.21 | 1.08 | 1.12 | 0.3996 | 0.6907 | 0.4560 | 1.04 | 0.98 | 0.97 | 0.8491 | 0.9064 | 0.8984 | 0.84 | 1.01 | 0.64 | 0.8019 | 0.9921 | 0.6087 | 0.94 | 0.93 | 0.89 | 0.7204 | 0.6797 | 0.4960 |
| 246.1216 | 12.3 | C10H18N2O5 | L-beta-aspartyl-L-leucine | Peptide | 1.01 | 0.93 | 0.88 | 0.9920 | 0.9553 | 0.9257 | 1.59 | 4.44 | 1.46 | 0.5590 | 0.2950 | 0.6084 | 0.86 | 0.75 | 0.80 | 0.3025 | 0.1842 | 0.1213 | 0.70 | 0.51 | 0.27 | 0.5169 | 0.3749 | 0.1569 |
| 260.1371 | 10.9 | C11H20N2O5 | L-gamma-glutamyl-L-isoleucine | Peptide | 1.11 | 1.27 | 1.08 | 0.6486 | 0.2182 | 0.7011 | 0.88 | 0.96 | 0.78 | 0.2978 | 0.8257 | 0.0689 | 0.77 | 0.89 | 0.81 | 0.1441 | 0.6100 | 0.1458 | 0.65 | 0.80 | 0.70 | 0.0509 | 0.3518 | 0.0394 |
| 176.0798 | 12.2 | C6H12N2O4 | Ala-Ser | Peptide(di-) | 1.11 | 1.00 | 1.12 | 0.4465 | 0.9698 | 0.4234 | 0.91 | 0.99 | 0.86 | 0.6845 | 0.9632 | 0.4379 | 0.26 | 0.35 | 0.16 | 0.1049 | 0.1264 | 0.0924 | 0.72 | 0.82 | 0.73 | 0.4457 | 0.6033 | 0.4662 |
| 176.0798 | 21.7 | C6H12N2O4 | Thr-Gly | Peptide(di-) | 1.12 | 1.06 | 1.02 | 0.7820 | 0.8512 | 0.9434 | 0.75 | 0.76 | 0.74 | 0.1751 | 0.2252 | 0.2998 | 1.11 | 0.96 | 1.06 | 0.5116 | 0.7702 | 0.7505 | 0.51 | 0.62 | 0.56 | 0.2120 | 0.3074 | 0.2515 |
| 186.1005 | 11.4 | C8H14N2O3 | Ala-Pro | Peptide(di-) | 1.13 | 1.07 | 0.95 | 0.2116 | 0.7068 | 0.5770 | 1.01 | 1.03 | 1.12 | 0.9425 | 0.8390 | 0.4321 | 0.20 | 0.26 | 0.02 | 0.0083 | 0.0147 | 0.0157 | 0.92 | 0.98 | 0.97 | 0.6485 | 0.9173 | 0.8404 |
| 188.1160 | 13.7 | C8H16N2O3 | Gly-Leu | Peptide(di-) | 1.28 | 0.98 | 1.17 | 0.4930 | 0.9015 | 0.6479 | 0.23 | 0.39 | 0.03 | 0.0183 | 0.0356 | 0.0237 | 1.03 | 0.97 | 1.16 | 0.9684 | 0.9679 | 0.8214 | 0.11 | 0.16 | 0.01 | 0.0732 | 0.0818 | 0.0659 |
| 188.1161 | 12.1 | C8H16N2O3 | Val-Ala | Peptide(di-) | 0.97 | 0.93 | 0.93 | 0.8812 | 0.7714 | 0.7980 | 0.34 | 0.49 | 0.19 | 0.0170 | 0.0423 | 0.0233 | 1.11 | 0.99 | 1.00 | 0.5701 | 0.9734 | 0.9820 | 0.18 | 0.26 | 0.14 | 0.0569 | 0.0618 | 0.0568 |

| | | | | | | | | | | | | | | | | | | | | | | | | | | | | |
|---|---|---|---|---|---|---|---|---|---|---|---|---|---|---|---|---|---|---|---|---|---|---|---|---|---|---|---|---|
| 190.0590 | 16.3 | C6H10N2O5 | Asp-Gly | Peptide(di-) | 1.09 | 0.94 | 1.16 | 0.7399 | 0.7398 | 0.5570 | 0.62 | 0.75 | 0.60 | 0.0747 | 0.1774 | 0.0687 | 0.43 | 0.48 | 0.25 | 0.0599 | 0.0894 | 0.0427 | 0.60 | 0.63 | 0.57 | 0.0985 | 0.1249 | 0.0799 |
| 202.1317 | 12.8 | C9H18N2O3 | Leu-Ala | Peptide(di-) | 1.01 | 1.05 | 0.97 | 0.9661 | 0.8357 | 0.7496 | 1.01 | 0.98 | 1.30 | 0.9436 | 0.8842 | 0.3621 | 0.95 | 0.80 | 0.87 | 0.9033 | 0.6584 | 0.7815 | 0.90 | 0.99 | 0.93 | 0.6331 | 0.9456 | 0.7202 |
| 203.1271 | 16.6 | C8H17N3O3 | Lys-Gly | Peptide(di-) | 1.08 | 1.05 | 1.05 | 0.7159 | 0.8533 | 0.8561 | 1.02 | 0.84 | 0.93 | 0.9468 | 0.5808 | 0.7749 | 0.25 | 0.38 | 0.00 | 0.0342 | 0.0501 | NA | 1.11 | 1.03 | 1.02 | 0.6522 | 0.9302 | 0.9409 |
| 204.0746 | 15.7 | C7H12N2O5 | Ala-Asp | Peptide(di-) | 1.35 | 1.38 | 1.24 | 0.5312 | 0.4438 | 0.4311 | 0.17 | 0.39 | 0.03 | 0.0449 | 0.0845 | 0.0420 | 0.66 | 0.78 | 0.63 | 0.3119 | 0.5176 | 0.2638 | 0.19 | 0.29 | 0.01 | 0.0987 | 0.1170 | 0.0709 |
| 204.0746 | 15.2 | C7H12N2O5 | Glu-Gly | Peptide(di-) | 1.07 | 1.20 | 1.10 | 0.6959 | 0.4264 | 0.5972 | 0.73 | 0.88 | 0.63 | 0.0717 | 0.4570 | 0.0349 | 0.52 | 0.95 | 0.78 | 0.0638 | 0.8785 | 0.3627 | 0.49 | 0.51 | 0.46 | 0.0160 | 0.0076 | 0.0059 |
| 212.0912 | 11.8 | C8H12N4O3 | Gly-His | Peptide(di-) | 1.06 | 1.03 | 1.11 | 0.8542 | 0.9220 | 0.7303 | 0.47 | 0.62 | 0.33 | 0.1205 | 0.2182 | 0.0854 | 0.72 | 0.75 | 0.75 | 0.0997 | 0.1049 | 0.0840 | 0.28 | 0.33 | 0.16 | 0.0484 | 0.0578 | 0.0514 |
| 216.1110 | 11.4 | C9H16N2O4 | Thr-Pro | Peptide(di-) | 1.06 | 1.00 | 0.96 | 0.7830 | 0.9722 | 0.8044 | 0.63 | 0.80 | 0.60 | 0.0780 | 0.2769 | 0.0636 | 0.19 | 0.23 | 0.00 | 0.0314 | 0.0336 | NA | 0.54 | 0.58 | 0.50 | 0.0611 | 0.0806 | 0.0492 |
| 220.0696 | 15.4 | C7H12N2O6 | Asp-Ser | Peptide(di-) | 1.14 | 1.14 | 1.05 | 0.6168 | 0.6299 | 0.8537 | 0.69 | 0.88 | 0.65 | 0.3318 | 0.6615 | 0.2951 | 0.62 | 0.63 | 0.57 | 0.1829 | 0.1782 | 0.1353 | 0.37 | 0.42 | 0.14 | 0.1290 | 0.1500 | 0.0837 |
| 220.0883 | 10.4 | C8H16N2O3S | Met-Ala | Peptide(di-) | 1.30 | 1.26 | 1.20 | 0.3925 | 0.5049 | 0.5134 | 0.54 | 0.76 | 0.42 | 0.0028 | 0.1007 | 0.0020 | 1.04 | 1.01 | 1.20 | 0.4922 | 0.8759 | 0.2917 | 0.27 | 0.31 | 0.22 | 0.0025 | 0.0032 | 0.0032 |
| 226.1067 | 14.8 | C9H14N4O3 | Ala-His | Peptide(di-) | 1.09 | 1.21 | 1.09 | 0.6630 | 0.2875 | 0.4902 | 0.56 | 0.81 | 0.63 | 0.0076 | 0.1236 | 0.0160 | 0.89 | 0.68 | 0.88 | 0.5986 | 0.1946 | 0.5590 | 0.56 | 0.58 | 0.87 | 0.1822 | 0.2028 | 0.6361 |
| 229.1063 | 13.7 | C9H15N3O4 | Asn-Pro | Peptide(di-) | 1.04 | 0.93 | 1.03 | 0.8210 | 0.7913 | 0.9278 | 0.43 | 0.59 | 0.06 | 0.0754 | 0.2153 | 0.0332 | 1.00 | 0.94 | 1.18 | 0.9863 | 0.8200 | 0.5113 | 0.15 | 0.21 | 0.05 | 0.0200 | 0.0229 | 0.0252 |
| 230.0907 | 15.1 | C9H14N2O5 | Asp-Pro | Peptide(di-) | 0.93 | 0.91 | 0.86 | 0.5548 | 0.5249 | 0.3160 | 0.60 | 0.74 | 0.47 | 0.0853 | 0.2389 | 0.0420 | 0.23 | 0.22 | 0.02 | 0.1230 | 0.1157 | 0.0825 | 0.36 | 0.44 | 0.33 | 0.0199 | 0.0240 | 0.0248 |
| 234.0852 | 15.5 | C8H14N2O6 | Thr-Asp | Peptide(di-) | 1.05 | 0.95 | 1.28 | 0.9501 | 0.9476 | 0.7598 | 0.96 | 1.29 | 1.06 | 0.9470 | 0.7378 | 0.9245 | 0.44 | 0.47 | 0.39 | 0.0106 | 0.0145 | 0.0099 | 0.82 | 1.12 | 1.15 | 0.7804 | 0.8664 | 0.8658 |
| 236.0833 | 10.5 | C8H16N2O4S | Met-Ser | Peptide(di-) | 1.22 | 0.97 | 1.01 | 0.2081 | 0.7524 | 0.9470 | 0.88 | 0.96 | 0.78 | 0.6686 | 0.8792 | 0.3721 | 0.74 | 0.78 | 0.88 | 0.2600 | 0.3006 | 0.4970 | 0.64 | 0.72 | 0.62 | 0.0551 | 0.1086 | 0.0528 |
| 243.1583 | 15.1 | C11H21N3O3 | Lys-Pro | Peptide(di-) | 1.11 | 1.18 | 1.21 | 0.5186 | 0.3377 | 0.0758 | 0.96 | 1.08 | 0.99 | 0.7424 | 0.5810 | 0.9208 | 0.22 | 0.26 | 0.00 | 0.0500 | 0.0502 | NA | 0.97 | 1.09 | 0.93 | 0.8455 | 0.6847 | 0.6478 |
| 244.1059 | 14.9 | C10H16N2O5 | Glu-Pro | Peptide(di-) | 0.92 | 1.13 | 0.93 | 0.8491 | 0.8099 | 0.8737 | 1.08 | 1.19 | 1.18 | 0.8531 | 0.6886 | 0.7249 | 0.30 | 0.40 | 0.02 | 0.0518 | 0.0739 | NA | 1.01 | 1.03 | 0.94 | 0.9831 | 0.9397 | 0.9104 |
| 244.1787 | 13.3 | C12H24N2O3 | Ile-Leu | Peptide(di-) | 1.07 | 1.03 | 1.12 | 0.7904 | 0.9183 | 0.7481 | 1.06 | 1.10 | 1.08 | 0.8294 | 0.7889 | 0.7430 | 0.97 | 1.14 | 1.28 | 0.7792 | 0.5417 | 0.2293 | 0.94 | 0.86 | 0.89 | 0.7946 | 0.5504 | 0.6931 |
| 245.1740 | 13.7 | C11H23N3O3 | Lys-Val | Peptide(di-) | 1.28 | 1.13 | 1.19 | 0.4292 | 0.6453 | 0.5691 | 0.39 | 0.72 | 0.00 | 0.0612 | 0.4106 | NA | 0.22 | 0.32 | 0.00 | 0.0474 | 0.0678 | NA | 0.15 | 0.27 | 0.00 | 0.0355 | 0.0521 | NA |
| 247.0804 | 15.6 | C8H13N3O6 | Asn-Asp | Peptide(di-) | 1.15 | 1.12 | 1.44 | 0.5644 | 0.6021 | 0.3448 | 0.30 | 0.51 | 0.00 | 0.0242 | 0.0988 | NA | 0.66 | 0.68 | 0.63 | 0.1557 | 0.1744 | 0.1493 | 0.09 | 0.18 | 0.00 | NA | 0.0263 | NA |
| 248.0645 | 17.1 | C8H12N2O7 | Asp-Asp | Peptide(di-) | 0.97 | 0.96 | 0.85 | 0.9415 | 0.9238 | 0.6803 | 0.32 | 0.55 | 0.02 | 0.0324 | 0.1113 | NA | 0.63 | 0.67 | 0.58 | 0.0558 | 0.0805 | 0.0422 | 0.14 | 0.18 | 0.00 | 0.0409 | 0.0506 | NA |
| 248.1008 | 14.6 | C9H16N2O6 | Glu-Thr | Peptide(di-) | 1.02 | 0.98 | 0.86 | 0.9227 | 0.8860 | 0.4808 | 1.14 | 1.13 | 1.15 | 0.3725 | 0.2345 | 0.3987 | 0.46 | 0.50 | 0.39 | 0.0308 | 0.0399 | 0.0315 | 1.03 | 1.13 | 1.08 | 0.8265 | 0.5383 | 0.5413 |
| 261.1324 | 18.0 | C10H19N3O5 | Lys-Asp | Peptide(di-) | 1.03 | 1.17 | 1.10 | 0.8138 | 0.4422 | 0.7474 | 0.99 | 1.23 | 1.40 | 0.9564 | 0.5487 | 0.3783 | 1.30 | 1.11 | 1.17 | 0.4537 | 0.7057 | 0.6430 | 0.93 | 0.99 | 0.89 | 0.6853 | 0.9443 | 0.5552 |
| 262.0801 | 13.9 | C9H14N2O7 | Glu-Asp | Peptide(di-) | 1.19 | 1.11 | 1.21 | 0.2867 | 0.5869 | 0.1746 | 0.63 | 0.74 | 0.54 | 0.1360 | 0.2411 | 0.0843 | 0.54 | 0.62 | 0.28 | 0.1812 | 0.2460 | 0.0511 | 0.60 | 0.53 | 0.53 | 0.1317 | 0.0330 | 0.0071 |
| 276.0957 | 16.6 | C10H16N2O7 | Glu-Glu | Peptide(di-) | 0.87 | 1.01 | 0.92 | 0.1369 | 0.9349 | 0.3559 | 1.00 | 1.08 | 1.18 | 0.9979 | 0.6508 | 0.2462 | 0.26 | 0.31 | 0.17 | 0.0034 | 0.0037 | 0.0086 | 1.03 | 1.08 | 1.15 | 0.8533 | 0.7067 | 0.4913 |
| 289.1385 | 16.4 | C10H19N5O5 | Asp-Arg | Peptide(di-) | 1.30 | 1.19 | 1.26 | 0.4486 | 0.2764 | 0.2775 | 0.24 | 0.48 | 0.02 | 0.0066 | 0.0399 | 0.0115 | 1.21 | 1.16 | 1.25 | 0.4520 | 0.4744 | 0.3167 | 0.11 | 0.12 | 0.00 | 0.0364 | 0.0367 | NA |
| 344.1372 | 4.6 | C18H20N2O5 | Tyr-Tyr | Peptide(di-) | 1.37 | 1.18 | 1.27 | 0.2841 | 0.4329 | 0.2749 | 1.06 | 0.88 | 0.93 | 0.8329 | 0.5557 | 0.5701 | 1.04 | 1.16 | 1.14 | 0.7681 | 0.3632 | 0.4867 | 1.09 | 0.96 | 1.03 | 0.5292 | 0.7877 | 0.7904 |
| 179.0742 | 7.8 | C14H22N4O7 | Ala-Asp-Gly-Pro | Peptide(tetra-) | 0.88 | 0.96 | 1.11 | 0.6107 | 0.8440 | 0.6839 | 0.94 | 1.29 | 1.04 | 0.6179 | 0.3725 | 0.7534 | 1.02 | 1.02 | 1.02 | 0.9160 | 0.8885 | 0.8900 | 0.98 | 0.84 | 1.29 | 0.9381 | 0.5504 | 0.5130 |
| 186.0821 | 7.8 | C15H24N4O7 | Glu-Ala-Gly-Pro | Peptide(tetra-) | 1.06 | 1.13 | 1.11 | 0.6625 | 0.4800 | 0.5890 | 0.81 | 1.01 | 1.07 | 0.2957 | 0.9543 | 0.5470 | 1.05 | 1.06 | 1.03 | 0.7418 | 0.6615 | 0.8332 | 1.01 | 0.93 | 0.96 | 0.9765 | 0.7192 | 0.8317 |
| 186.0821 | 27.9 | C15H24N4O7 | Ala-Ala-Asp-Pro | Peptide(tetra-) | 1.05 | 1.01 | 1.00 | 0.4650 | 0.7598 | 0.9680 | 0.99 | 1.01 | 1.01 | 0.7515 | 0.7780 | 0.8607 | 0.96 | 1.03 | 1.03 | 0.4702 | 0.5046 | 0.2818 | 0.98 | 0.95 | 0.99 | 0.4097 | 0.0320 | 0.6253 |
| 193.0899 | 7.8 | C16H26N4O7 | Glu-Ala-Ala-Pro | Peptide(tetra-) | 1.05 | 1.00 | 1.15 | 0.8901 | 0.9934 | 0.6964 | 0.75 | 0.67 | 1.07 | 0.4379 | 0.2921 | 0.8322 | 1.11 | 1.07 | 1.09 | 0.5935 | 0.7275 | 0.6126 | 0.74 | 0.66 | 0.62 | 0.4027 | 0.4181 | 0.2607 |
| 193.0899 | 27.9 | C16H26N4O7 | Asp-Val-Gly-Pro | Peptide(tetra-) | 1.03 | 1.10 | 1.03 | 0.9045 | 0.6945 | 0.9140 | 1.11 | 1.49 | 1.46 | 0.5273 | 0.0212 | 0.0486 | 1.06 | 1.04 | 1.05 | 0.1185 | 0.2396 | 0.1999 | 0.92 | 0.96 | 1.03 | 0.3005 | 0.8731 | 0.9100 |
| 318.1538 | 17.8 | C12H22N4O6 | Ala-Ala-Ala-Ser | Peptide(tetra-) | 0.86 | 0.91 | 0.92 | 0.7975 | 0.8707 | 0.8842 | 1.13 | 1.22 | 1.29 | 0.7748 | 0.6823 | 0.6520 | 1.03 | 1.00 | 1.10 | 0.7196 | 0.9571 | 0.5256 | 1.13 | 1.04 | 1.03 | 0.8276 | 0.9403 | 0.9594 |
| 362.1258 | 14.8 | C13H22N4O6S | Cys-Gly-Pro-Ser | Peptide(tetra-) | 1.23 | 1.07 | 1.23 | 0.1835 | 0.6564 | 0.1855 | 0.97 | 1.12 | 1.11 | 0.8354 | 0.5419 | 0.5785 | 0.95 | 0.86 | 0.75 | 0.8982 | 0.7397 | 0.6121 | 0.85 | 0.71 | 0.95 | 0.2300 | 0.1326 | 0.6885 |
| 375.1748 | 7.8 | C14H25N5O7 | Ala-Ala-Gln-Ser | Peptide(tetra-) | 0.79 | 0.97 | 0.75 | 0.4565 | 0.9287 | 0.4636 | 0.71 | 0.99 | 0.77 | 0.3685 | 0.9675 | 0.4575 | 0.91 | 1.44 | 1.05 | 0.8159 | 0.4995 | 0.8956 | 0.69 | 0.73 | 0.66 | 0.0925 | 0.2171 | 0.0472 |
| 375.1750 | 27.9 | C14H25N5O7 | Asn-Val-Gly-Ser | Peptide(tetra-) | 1.06 | 1.45 | 1.13 | 0.8795 | 0.5202 | 0.6772 | 0.18 | 0.47 | 0.00 | 0.0309 | 0.1565 | NA | 1.00 | 1.02 | 1.08 | 0.9686 | 0.8325 | 0.4043 | 0.08 | 0.12 | 0.00 | 0.0290 | 0.0276 | NA |
| 376.1418 | 14.6 | C14H24N4O6S | Ala-Cys-Pro-Ser | Peptide(tetra-) | 0.92 | 0.98 | 0.98 | 0.3719 | 0.8272 | 0.8379 | 1.05 | 1.07 | 1.07 | 0.6378 | 0.4418 | 0.4692 | 0.85 | 0.78 | 0.86 | 0.5524 | 0.3889 | 0.7557 | 0.96 | 0.95 | 0.90 | 0.6075 | 0.6444 | 0.2959 |
| 389.1905 | 7.8 | C15H27N5O7 | Asn-Leu-Gly-Ser | Peptide(tetra-) | 0.99 | 1.02 | 1.02 | 0.9471 | 0.8620 | 0.8361 | 1.08 | 1.06 | 1.14 | 0.4904 | 0.5000 | 0.0254 | 0.71 | 1.12 | 1.34 | 0.3458 | 0.7739 | 0.2808 | 0.91 | 0.93 | 0.92 | 0.0957 | 0.3154 | 0.2862 |
| 389.1907 | 27.9 | C15H27N5O7 | Ala-Lys-Asp-Gly | Peptide(tetra-) | 1.40 | 1.26 | 1.07 | 0.2127 | 0.6179 | 0.7551 | 0.00 | 0.30 | 0.00 | NA | NA | NA | 1.01 | 1.03 | 1.01 | 0.8526 | 0.7078 | 0.7624 | 0.00 | 0.08 | 0.00 | NA | NA | NA |
| 394.1158 | 17.1 | C13H22N4O8S | Ala-Asp-Cys-Ser | Peptide(tetra-) | 1.13 | 1.08 | 0.82 | 0.8403 | 0.9004 | 0.7500 | 1.75 | 2.12 | 2.04 | 0.0212 | 0.1744 | 0.0104 | 1.16 | 1.06 | 1.31 | 0.7699 | 0.9060 | 0.6654 | 1.22 | 1.08 | 0.94 | 0.5519 | 0.8326 | 0.8907 |
| 403.2063 | 27.9 | C16H29N5O7 | Ala-Leu-Asn-Ser | Peptide(tetra-) | 0.95 | 0.94 | 0.95 | 0.6521 | 0.6050 | 0.6568 | 1.05 | 1.13 | 1.10 | 0.7471 | 0.3130 | 0.4271 | 1.09 | 1.14 | 1.07 | 0.3921 | 0.2349 | 0.0763 | 0.94 | 0.93 | 0.92 | 0.1525 | 0.1583 | 0.2119 |
| 414.2227 | 15.4 | C17H30N6O6 | Asn-Lys-Gly-Pro | Peptide(tetra-) | 1.04 | 1.17 | 1.00 | 0.8561 | 0.6226 | 0.9840 | 0.19 | 0.44 | 0.00 | NA | 0.0480 | NA | 0.31 | 0.49 | 0.09 | 0.0314 | 0.1395 | 0.0203 | 0.09 | 0.07 | 0.00 | NA | NA | NA |
| 416.1907 | 10.1 | C17H28N4O8 | Asp-Val-Pro-Ser | Peptide(tetra-) | 1.16 | 1.18 | 0.94 | 0.6878 | 0.6043 | 0.8595 | 0.17 | 0.63 | 0.00 | NA | 0.3333 | NA | 0.47 | 0.56 | 0.27 | 0.2680 | 0.3369 | 0.1689 | 0.08 | 0.08 | 0.00 | NA | NA | NA |
| 417.2220 | 27.9 | C17H31N5O7 | Ala-Leu-Gln-Ser | Peptide(tetra-) | 1.02 | 0.86 | 0.95 | 0.9728 | 0.6420 | 0.8710 | 0.84 | 1.03 | 0.85 | 0.4353 | 0.8529 | 0.2587 | 1.01 | 0.99 | 0.96 | 0.9159 | 0.8594 | 0.5695 | 0.38 | 0.48 | 0.35 | 0.1437 | 0.1972 | 0.1404 |
| 429.2224 | 14.7 | C18H31N5O7 | Ala-Lys-Asp-Pro | Peptide(tetra-) | 0.86 | 0.81 | 0.86 | 0.5627 | 0.4547 | 0.6151 | 1.10 | 1.15 | 1.15 | 0.7854 | 0.6442 | 0.6591 | 0.17 | 0.19 | 0.00 | NA | NA | NA | 1.03 | 1.06 | 1.06 | 0.9373 | 0.8560 | 0.8856 |
| 439.2431 | 10.8 | C20H33N5O6 | Asn-Leu-Pro-Pro | Peptide(tetra-) | 1.12 | 1.04 | 1.08 | 0.6894 | 0.8703 | 0.7447 | 1.05 | 1.22 | 1.23 | 0.8654 | 0.5651 | 0.4913 | 0.06 | 0.14 | 0.00 | NA | 0.0788 | NA | 1.04 | 1.00 | 0.90 | 0.8385 | 0.9822 | 0.5857 |
| 444.2810 | 7.8 | C18H36N8O5 | Ala-Lys-Ala-Arg | Peptide(tetra-) | 1.50 | 1.09 | 1.04 | 0.2696 | 0.6348 | 0.8496 | 1.16 | 1.16 | 1.11 | 0.3594 | 0.1501 | 0.5669 | 1.28 | 1.35 | 1.71 | 0.5419 | 0.5972 | 0.1844 | 1.08 | 0.72 | 0.99 | 0.7290 | 0.1604 | 0.9267 |
| 459.2070 | 9.2 | C17H29N7O8 | Ala-Asn-Gln-Gln | Peptide(tetra-) | 1.23 | 0.92 | 0.78 | 0.3900 | 0.7002 | 0.2269 | 0.78 | 0.78 | 0.99 | 0.0464 | 0.1266 | 0.9820 | 1.29 | 1.12 | 1.13 | 0.2338 | 0.5609 | 0.5628 | 1.15 | 1.12 | 1.26 | 0.3226 | 0.6000 | 0.0211 |
| 460.2648 | 14.2 | C19H36N6O7 | Asn-Lys-Thr-Val | Peptide(tetra-) | 1.00 | 1.15 | 1.04 | 0.9933 | 0.6379 | 0.9325 | 0.52 | 0.77 | 0.72 | 0.3494 | 0.6968 | 0.5642 | 0.08 | 0.18 | 0.00 | NA | 0.1201 | NA | 1.34 | 0.94 | 1.07 | 0.2769 | 0.8630 | 0.8823 |
| 461.1872 | 17.8 | C16H27N7O9 | Asn-Thr-Asn-Asn | Peptide(tetra-) | 0.94 | 0.90 | 1.00 | 0.8042 | 0.6852 | 0.9866 | 0.88 | 0.94 | 0.95 | 0.5324 | 0.7892 | 0.7811 | 1.06 | 1.08 | 1.13 | 0.7057 | 0.4621 | 0.4053 | 0.80 | 0.91 | 0.89 | 0.2332 | 0.6401 | 0.4860 |
| 461.1872 | 17.0 | C16H27N7O9 | Arg-Asp-Asp-Gly | Peptide(tetra-) | 3.35 | 2.06 | 5.26 | 0.3699 | 0.5002 | 0.2869 | 0.53 | 0.73 | 1.14 | NA | NA | 0.9032 | 1.09 | 1.05 | 1.07 | 0.7737 | 0.8593 | 0.8336 | 3.00 | 0.86 | 1.68 | 0.4184 | 0.8764 | 0.5765 |
| 469.1366 | 14.3 | C19H23N5O7 | Asp-Trp-Gly-Gly | Peptide(tetra-) | 1.07 | 1.01 | 1.13 | 0.8535 | 0.9565 | 0.6254 | 1.19 | 0.95 | 0.96 | 0.4347 | 0.8051 | 0.8527 | 1.06 | 1.03 | 1.05 | 0.7564 | 0.9003 | 0.8901 | 1.09 | 1.30 | 1.09 | 0.3609 | 0.1114 | 0.5837 |
| 470.3470 | 11.7 | C24H46N4O5 | Leu-Leu-Leu-Leu | Peptide(tetra-) | 1.19 | 0.97 | 1.31 | 0.6944 | 0.9236 | 0.5736 | 1.77 | 1.76 | 1.45 | 0.1866 | 0.3075 | 0.3577 | 0.94 | 1.10 | 1.15 | 0.6617 | 0.4827 | 0.3435 | 1.73 | 1.05 | 1.30 | 0.2958 | 0.9261 | 0.6330 |
| 475.2434 | 4.8 | C23H33N5O6 | Ala-Leu-Trp-Ser | Peptide(tetra-) | 1.15 | 0.98 | 1.12 | 0.7629 | 0.9431 | 0.6604 | 0.08 | 0.30 | 0.00 | 0.0165 | 0.0355 | NA | 0.00 | 0.11 | 0.00 | NA | NA | NA | 0.03 | 0.03 | 0.00 | NA | NA | NA |
| 477.1710 | 3.9 | C17H27N5O11 | Asn-Glu-Glu-Ser | Peptide(tetra-) | 1.07 | 1.06 | 0.93 | 0.8040 | 0.8622 | 0.8190 | 0.58 | 0.84 | 0.13 | 0.1802 | 0.6136 | 0.0338 | 3.13 | 1.31 | 1.27 | 0.0760 | 0.7793 | 0.7801 | 0.15 | 0.22 | 0.06 | 0.0873 | 0.0979 | 0.0792 |
| 484.1921 | 15.2 | C19H28N6O9 | Asp-Val-Asp-His | Peptide(tetra-) | 1.05 | 1.25 | 1.12 | 0.6545 | 0.1359 | 0.3311 | 1.01 | 1.06 | 1.09 | 0.9764 | 0.4236 | 0.4782 | 0.10 | 0.16 | 0.00 | 0.0536 | 0.0552 | NA | 1.08 | 1.08 | 1.06 | 0.5906 | 0.6296 | 0.6729 |
| 488.3075 | 7.8 | C20H40N8O6 | Arg-Lys-Val-Ser | Peptide(tetra-) | 0.82 | 0.88 | 0.87 | 0.0480 | 0.1514 | 0.1146 | 0.97 | 1.13 | 1.10 | 0.7728 | 0.0159 | 0.0122 | 0.77 | 0.92 | 1.78 | 0.3779 | 0.7748 | 0.1358 | 0.93 | 0.97 | 0.99 | 0.4343 | 0.6519 | 0.9335 |
| 489.2437 | 14.0 | C20H35N5O9 | Asp-Leu-Lys-Asp | Peptide(tetra-) | 1.01 | 1.09 | 0.79 | 0.9631 | 0.7507 | 0.3898 | 0.60 | 1.06 | 0.86 | 0.1857 | 0.8903 | 0.6544 | 0.60 | 0.74 | 0.40 | 0.3740 | 0.5810 | 0.2013 | 0.59 | 0.53 | 0.36 | 0.1707 | 0.0645 | 0.0451 |
| 515.2015 | 28.4 | C24H29N5O8 | Asn-Gly-Tyr-Tyr | Peptide(tetra-) | 1.02 | 0.94 | 0.97 | 0.9482 | 0.8762 | 0.9307 | 0.82 | 0.98 | 0.86 | 0.6370 | 0.9646 | 0.6590 | 1.10 | 1.14 | 1.04 | 0.6981 | 0.3603 | 0.8944 | 0.86 | 0.90 | 0.74 | 0.5869 | 0.6909 | 0.4559 |
| 518.3256 | 7.8 | C23H46N6O5S | Ile-Lys-Lys-Met | Peptide(tetra-) | 0.86 | 1.03 | 0.88 | 0.5865 | 0.9115 | 0.6003 | 0.85 | 0.94 | 0.99 | 0.5668 | 0.8232 | 0.9651 | 1.42 | 1.46 | 1.20 | 0.3015 | 0.0808 | 0.7781 | 0.81 | 0.98 | 0.79 | 0.1721 | 0.8786 | 0.1566 |
| 520.1956 | 14.1 | C19H32N6O9S | Asp-Met-Gln-Gln | Peptide(tetra-) | 0.97 | 0.99 | 0.96 | 0.5997 | 0.8975 | 0.4618 | 1.02 | 1.01 | 1.05 | 0.5021 | 0.5765 | 0.1349 | 0.93 | 0.87 | 1.06 | 0.7311 | 0.6013 | 0.8510 | 0.98 | 0.97 | 0.99 | 0.5205 | 0.3720 | 0.8706 |
| 529.2753 | 4.8 | C24H35N9O5 | Ala-Phe-Arg-His | Peptide(tetra-) | 1.09 | 1.16 | 1.19 | 0.7099 | 0.6815 | 0.4393 | 0.71 | 0.87 | 0.78 | 0.2385 | 0.6301 | 0.3700 | 0.98 | 0.88 | 0.62 | 0.9469 | 0.6279 | 0.0439 | 0.40 | 0.46 | 0.20 | 0.0901 | 0.1167 | 0.0619 |
| 532.2614 | 12.3 | C20H36N8O9 | Arg-Lys-Asp-Asp | Peptide(tetra-) | 0.88 | 1.02 | 0.96 | 0.7600 | 0.9679 | 0.9167 | 0.80 | 1.03 | 0.74 | 0.5707 | 0.9168 | 0.4499 | 0.92 | 0.88 | 1.16 | 0.6511 | 0.4053 | 0.6267 | 0.66 | 0.63 | 0.57 | 0.3861 | 0.3029 | 0.2405 |
| 532.3339 | 28.4 | C22H41N7O7 | Arg-Leu-Leu-Asp | Peptide(tetra-) | 1.72 | 1.49 | 2.16 | 0.2143 | 0.2856 | 0.4936 | 1.35 | 1.99 | 1.24 | 0.5784 | 0.2845 | 0.4816 | 1.15 | 1.74 | 1.43 | 0.6516 | 0.1890 | 0.0108 | 2.16 | 0.53 | 1.55 | 0.3346 | 0.4659 | 0.6838 |
| 535.1586 | 3.9 | C20H30N4O6S3 | Cys-Met-Cys-Tyr | Peptide(tetra-) | 0.94 | 0.95 | 0.82 | 0.5881 | 0.5371 | 0.1732 | 1.05 | 1.03 | 0.96 | 0.8330 | 0.8868 | 0.8128 | 2.25 | 0.68 | 1.46 | 0.4467 | 0.6452 | 0.6233 | 1.09 | 1.10 | 1.16 | 0.5488 | 0.5473 | 0.2856 |
| 550.3124 | 16.5 | C26H42N6O7 | Gln-Leu-Lys-Tyr | Peptide(tetra-) | 1.22 | 1.02 | 1.11 | 0.2648 | 0.9043 | 0.5835 | 1.00 | 1.12 | 1.11 | 0.9905 | 0.6052 | 0.6625 | 0.80 | 0.96 | 1.02 | 0.2256 | 0.5294 | 0.8875 | 0.94 | 0.77 | 1.01 | 0.5727 | 0.2500 | 0.9454 |

| | | | | | | | | | | | | | | | | | | | | | | | | | | | | |
|---|---|---|---|---|---|---|---|---|---|---|---|---|---|---|---|---|---|---|---|---|---|---|---|---|---|---|---|---|
| 557.3327 | 7.8 | C28H43N7O5 | Lys-Lys-Trp-Pro | Peptide(tetra-) | 1.16 | 0.98 | 1.18 | 0.3954 | 0.9163 | 0.3794 | 0.98 | 1.11 | 1.11 | 0.9242 | 0.6413 | 0.6443 | 0.79 | 0.72 | 1.41 | 0.7267 | 0.6438 | 0.5445 | 0.86 | 0.70 | 0.96 | 0.1595 | 0.0863 | 0.7659 |
| 562.2436 | 14.6 | C30H34N4O7 | Ala-Phe-Tyr-Tyr | Peptide(tetra-) | 0.40 | 0.80 | 1.26 | NA | 0.6375 | 0.6509 | 0.19 | 0.52 | 0.34 | NA | 0.3441 | 0.1637 | 1.14 | 1.20 | 1.32 | 0.6735 | 0.6106 | 0.4678 | 0.69 | 0.66 | 1.00 | 0.2518 | 0.2196 | 0.9968 |
| 578.2279 | 14.5 | C24H34N8O7S | Arg-Trp-Asp-Cys | Peptide(tetra-) | 1.12 | 1.12 | 1.10 | 0.2038 | 0.2387 | 0.2964 | 0.97 | 0.99 | 1.06 | 0.8917 | 0.9541 | 0.6699 | 1.02 | 0.78 | 0.86 | 0.9187 | 0.2819 | 0.3550 | 0.85 | 0.90 | 0.88 | 0.0974 | 0.4894 | 0.1156 |
| 229.1063 | 12.3 | C9H15N3O4 | Gly-Gly-Pro | Peptide(tri-) | 1.23 | 1.30 | 1.34 | 0.1722 | 0.4773 | 0.4430 | 0.79 | 0.76 | 1.08 | 0.5446 | 0.5062 | 0.8823 | 0.94 | 0.95 | 1.11 | 0.8418 | 0.8714 | 0.7914 | 0.90 | 2.28 | 6.97 | NA | 0.4473 | 0.1098 |
| 261.1324 | 16.4 | C10H19N3O5 | Thr-Ala-Ala | Peptide(tri-) | 1.27 | 1.07 | 1.30 | 0.4403 | 0.7832 | 0.1211 | 1.05 | 1.23 | 1.02 | 0.7961 | 0.4199 | 0.9282 | 0.57 | 0.58 | 0.50 | 0.1525 | 0.1573 | 0.1208 | 1.05 | 0.98 | 0.98 | 0.8628 | 0.9438 | 0.9392 |
| 287.1482 | 15.1 | C12H21N3O5 | Thr-Ala-Pro | Peptide(tri-) | 0.96 | 1.16 | 1.01 | 0.8430 | 0.5394 | 0.9760 | 1.11 | 1.14 | 1.15 | 0.5622 | 0.5027 | 0.4555 | 0.13 | 0.23 | 0.00 | NA | 0.0788 | NA | 1.06 | 0.96 | 1.04 | 0.7159 | 0.7680 | 0.8249 |
| 287.1845 | 28.3 | C13H25N3O4 | Leu-Val-Gly | Peptide(tri-) | 1.10 | 0.95 | 0.95 | 0.8018 | 0.8289 | 0.8610 | 0.99 | 1.16 | 0.96 | 0.9673 | 0.5229 | 0.8880 | 1.07 | 1.03 | 1.13 | 0.6750 | 0.8377 | 0.5870 | 0.64 | 0.72 | 0.57 | 0.3374 | 0.4575 | 0.2669 |
| 291.1066 | 15.6 | C10H17N3O7 | Ala-Asp-Ser | Peptide(tri-) | 1.06 | 0.95 | 1.11 | 0.7204 | 0.7517 | 0.3621 | 1.09 | 1.11 | 1.16 | 0.5723 | 0.1370 | 0.1911 | 0.98 | 0.99 | 0.89 | 0.9546 | 0.9648 | 0.5315 | 1.04 | 0.92 | 0.92 | 0.6934 | 0.3058 | 0.3503 |
| 291.1252 | 11.0 | C11H21N3O4S | Leu-Cys-Gly | Peptide(tri-) | 1.10 | 1.09 | 0.99 | 0.5203 | 0.7644 | 0.8985 | 0.18 | 0.33 | 0.00 | 0.0632 | 0.0899 | NA | 1.08 | 1.16 | 1.29 | 0.8376 | 0.6791 | 0.5562 | 0.05 | 0.11 | 0.00 | NA | 0.0274 | NA |
| 305.1221 | 14.6 | C11H19N3O7 | Glu-Ala-Ser | Peptide(tri-) | 1.09 | 1.04 | 1.02 | 0.7371 | 0.8813 | 0.9303 | 0.19 | 0.35 | 0.00 | 0.0558 | 0.0930 | NA | 0.97 | 0.86 | 0.70 | 0.9151 | 0.6077 | 0.2450 | 0.09 | 0.12 | 0.00 | 0.0018 | 0.0021 | NA |
| 318.1538 | 16.1 | C12H22N4O6 | Lys-Asp-Gly | Peptide(tri-) | 1.09 | 1.09 | 1.00 | 0.8557 | 0.8678 | 0.9981 | 0.85 | 0.95 | 0.93 | 0.8215 | 0.9351 | 0.9072 | 1.10 | 1.03 | 1.10 | 0.6337 | 0.8605 | 0.5508 | 0.85 | 0.80 | 0.76 | 0.7342 | 0.6462 | 0.6111 |
| 334.1851 | 15.4 | C13H26N4O6 | Lys-Thr-Ser | Peptide(tri-) | 0.84 | 1.01 | 0.46 | 0.7658 | 0.9853 | 0.3217 | 0.98 | 1.03 | 0.90 | 0.9583 | 0.9399 | 0.8461 | 1.07 | 1.07 | 1.20 | 0.8089 | 0.8231 | 0.5640 | 0.64 | 0.75 | 0.73 | 0.2891 | 0.3344 | 0.3189 |
| 335.1329 | 14.8 | C12H21N3O8 | Glu-Ser-Thr | Peptide(tri-) | 1.06 | 1.12 | 0.97 | 0.8396 | 0.7607 | 0.9043 | 1.03 | 0.97 | 1.02 | 0.9450 | 0.9072 | 0.8952 | 1.13 | 1.17 | 1.08 | 0.7291 | 0.7800 | 0.8597 | 0.87 | 0.91 | 1.02 | 0.7081 | 0.8112 | 0.9559 |
| 335.1330 | 15.7 | C12H21N3O8 | Thr-Thr-Asp | Peptide(tri-) | 1.18 | 1.18 | 0.96 | 0.6364 | 0.6287 | 0.8525 | 1.07 | 1.21 | 1.19 | 0.8252 | 0.6368 | 0.6290 | 0.99 | 1.18 | 1.02 | 0.9597 | 0.6959 | 0.9342 | 1.13 | 1.08 | 1.02 | 0.7839 | 0.8605 | 0.9497 |
| 346.1600 | 17.7 | C12H22N6O6 | Asp-Gly-Arg | Peptide(tri-) | 0.98 | 1.13 | 0.99 | 0.8939 | 0.4304 | 0.9263 | 1.05 | 1.10 | 1.00 | 0.7868 | 0.4028 | 0.9739 | 0.90 | 0.82 | 0.87 | 0.5744 | 0.3663 | 0.3884 | 0.77 | 0.84 | 0.86 | 0.0113 | 0.1065 | 0.1654 |
| 348.2008 | 15.3 | C14H28N4O6 | Lys-Thr-Thr | Peptide(tri-) | 1.17 | 1.08 | 1.16 | 0.5026 | 0.7474 | 0.3389 | 0.89 | 0.94 | 1.05 | 0.5957 | 0.7683 | 0.7676 | 1.14 | 0.90 | 0.91 | 0.4323 | 0.4058 | 0.5141 | 0.92 | 0.86 | 0.76 | 0.6271 | 0.4498 | 0.2465 |
| 351.1099 | 11.9 | C12H21N3O7S | Glu-Cys-Thr | Peptide(tri-) | 1.16 | 1.13 | 1.11 | 0.6210 | 0.7078 | 0.7383 | 0.99 | 1.09 | 1.08 | 0.9739 | 0.7782 | 0.8293 | 1.05 | 1.01 | 1.11 | 0.7526 | 0.9720 | 0.4627 | 1.03 | 0.93 | 0.98 | 0.9302 | 0.7957 | 0.9609 |
| 351.1101 | 13.4 | C12H21N3O7S | Met-Asp-Ser | Peptide(tri-) | 1.09 | 1.03 | 1.07 | 0.5770 | 0.8857 | 0.5354 | 0.96 | 0.99 | 1.11 | 0.6613 | 0.8607 | 0.5658 | 1.03 | 1.07 | 0.99 | 0.8790 | 0.5818 | 0.9267 | 1.06 | 1.04 | 1.14 | 0.8040 | 0.8468 | 0.4419 |
| 364.1205 | 9.2 | C16H20N4O4S | Trp-Cys-Gly | Peptide(tri-) | 0.88 | 0.94 | 0.87 | 0.3393 | 0.6734 | 0.6120 | 0.81 | 1.24 | 0.99 | 0.2853 | 0.1989 | 0.9694 | 1.11 | 0.94 | 1.13 | 0.6902 | 0.7943 | 0.6938 | 0.83 | 1.31 | 0.99 | 0.0806 | 0.2621 | 0.9785 |
| 365.1255 | 13.2 | C13H23N3O7S | Met-Thr-Asp | Peptide(tri-) | 0.93 | 0.97 | 0.90 | 0.8506 | 0.9349 | 0.6969 | 0.78 | 0.83 | 0.77 | 0.6176 | 0.6837 | 0.5817 | 0.92 | 0.75 | 1.11 | 0.7493 | 0.2670 | 0.6566 | 0.65 | 0.87 | 0.72 | 0.0294 | 0.5151 | 0.3191 |
| 365.1256 | 11.8 | C13H23N3O7S | Glu-Met-Ser | Peptide(tri-) | 0.83 | 1.06 | 0.84 | 0.3432 | 0.7838 | 0.2800 | 0.93 | 0.99 | 0.98 | 0.7219 | 0.9409 | 0.8360 | 1.00 | 0.85 | 0.95 | 0.9952 | 0.7273 | 0.9135 | 1.09 | 1.08 | 1.30 | 0.7717 | 0.8340 | 0.3503 |
| 373.1485 | 16.6 | C15H23N3O8 | Glu-Glu-Pro | Peptide(tri-) | 1.15 | 1.06 | 1.12 | 0.3306 | 0.6208 | 0.4085 | 0.56 | 0.62 | 0.55 | 0.1850 | 0.2263 | 0.1780 | 0.09 | 0.18 | 0.00 | 0.0031 | 0.0044 | NA | 0.44 | 0.45 | 0.39 | 0.0575 | 0.0597 | 0.0445 |
| 383.1805 | 11.0 | C16H25N5O6 | Leu-Asp-His | Peptide(tri-) | 1.04 | 1.12 | 1.18 | 0.9218 | 0.6188 | 0.5178 | 0.18 | 0.59 | 0.00 | 0.0404 | 0.2296 | NA | 0.13 | 0.26 | 0.00 | 0.0230 | 0.0308 | NA | 0.11 | 0.15 | 0.00 | NA | 0.0156 | NA |
| 411.1312 | 14.0 | C15H29N3O4S3 | Met-Met-Met | Peptide(tri-) | 1.04 | 0.98 | 1.11 | 0.8768 | 0.9505 | 0.7024 | 0.91 | 1.01 | 0.99 | 0.7364 | 0.9568 | 0.9846 | 0.96 | 0.97 | 0.86 | 0.8627 | 0.8938 | 0.6135 | 0.93 | 0.86 | 0.88 | 0.7839 | 0.5568 | 0.6359 |
| 152.1200 | 4.3 | C10H16O | (1R,4S)-fenchan-2-one | Prenol Lipids [PR] | 1.51 | 1.55 | 1.82 | 0.2344 | 0.1802 | 0.3631 | 1.04 | 1.31 | 1.36 | 0.9088 | 0.4730 | 0.1834 | 0.75 | 1.18 | 0.96 | 0.2674 | 0.4439 | 0.8686 | 1.29 | 1.15 | 1.17 | 0.4749 | 0.6861 | 0.6098 |
| 365.0894 | 16.2 | C12H19N3O8S | 2-S-Glutathionyl acetate | Xenobiotics Biodegradation and Metabolism | 1.58 | 1.19 | 0.97 | 0.1437 | 0.5760 | 0.9094 | 0.95 | 1.05 | 1.27 | 0.8627 | 0.8676 | 0.4485 | 1.07 | 1.14 | 0.93 | 0.5955 | 0.5435 | 0.6223 | 0.87 | 1.11 | 1.29 | 0.6695 | 0.5651 | 0.4410 |
| 137.0477 | 5.6 | C7H7NO2 | Anthranilate | Xenobiotics Biodegradation and Metabolism | 1.09 | 1.15 | 1.02 | 0.6359 | 0.4854 | 0.9342 | 1.06 | 1.16 | 1.25 | 0.6072 | 0.4241 | 0.2913 | 1.08 | 1.04 | 1.16 | 0.3563 | 0.6036 | 0.1914 | 1.11 | 1.10 | 0.78 | 0.6326 | 0.4280 | 0.1639 |
| 126.0317 | 15.3 | C6H6O3 | Benzene-1,2,4-triol | Xenobiotics Biodegradation and Metabolism | 1.10 | 1.04 | 1.08 | 0.4078 | 0.8396 | 0.4872 | 1.08 | 1.04 | 1.14 | 0.1855 | 0.4197 | 0.0792 | 1.07 | 0.98 | 0.98 | 0.6427 | 0.9043 | 0.9413 | 1.25 | 1.23 | 1.28 | 0.2144 | 0.2882 | 0.2046 |
| 162.0680 | 28.2 | C10H10O2 | cis-1,2-Dihydronaphthalene-1,2-diol | Xenobiotics Biodegradation and Metabolism | 1.27 | 1.13 | 1.38 | 0.3360 | 0.5746 | 0.1862 | 1.02 | 1.09 | 1.12 | 0.9046 | 0.5802 | 0.3910 | 1.02 | 1.08 | 1.06 | 0.9003 | 0.7000 | 0.7873 | 0.65 | 0.80 | 0.67 | 0.1911 | 0.3915 | 0.1984 |
| 113.0840 | 28.2 | C6H11NO | epsilon-Caprolactam | Xenobiotics Biodegradation and Metabolism | 1.05 | 1.02 | 1.23 | 0.7882 | 0.9147 | 0.3416 | 1.00 | 1.00 | 1.22 | 0.9928 | 0.9814 | 0.2141 | 0.97 | 1.51 | 1.11 | 0.9328 | 0.2854 | 0.7559 | 0.95 | 0.94 | 0.96 | 0.8320 | 0.7805 | 0.8551 |
| 166.0266 | 12.1 | C8H6O4 | Phthalate | Xenobiotics Biodegradation and Metabolism | 1.54 | 1.52 | 1.94 | 0.5817 | 0.1825 | 0.0765 | 1.23 | 1.05 | 1.11 | 0.4122 | 0.7746 | 0.5563 | 0.99 | 1.02 | 1.01 | 0.8957 | 0.8075 | 0.9196 | 0.70 | 0.87 | 0.79 | 0.3799 | 0.7330 | 0.5781 |
| 185.9753 | 20.8 | C4H6O4S | Thiodiacetic acid | Xenobiotics Biodegradation and Metabolism | 0.99 | 1.03 | 1.03 | 0.8788 | 0.7503 | 0.7254 | 0.99 | 0.96 | 0.90 | 0.9507 | 0.7680 | 0.4971 | 0.99 | 0.93 | 1.01 | 0.9231 | 0.5537 | 0.9665 | 1.01 | 0.98 | 0.94 | 0.9197 | 0.8594 | 0.4356 |

# Appendix 3

# Chapter 4 – peptidomics supplementary material

| Protein | Uniprot ID | Peptide sequence | OZ277 | | | OZ439 | | | DHA | | |
|---|---|---|---|---|---|---|---|---|---|---|---|
| | | | Fold-change | SD | P-value | Fold-change | SD | P-value | Fold-change | SD | P-value |
| ***Homo sapiens*** | | | | | | | | | | | |
| Beta-adducin | P35612 | VNVADEVQR | 6.04 | 3.79 | 0.0763 | 0.86 | 1.14 | 0.8513 | 26.27 | 35.91 | 0.1119 |
| E3 ubiquitin-protein ligase RNF6 | Q9Y252 | ITSEELQQRL | 2.36 | 1.69 | 0.2050 | 5412.69 | 7654.70 | 0.5001 | 7835.17 | 12435.13 | 0.1834 |
| Haemoglobin α | P69905 | SVSTVLTSKYR | 0.31 | 0.42 | 0.2596 | | | | 26.66 | 52.31 | 0.3989 |
| | | EFTPAVH | 0.43 | 0.39 | 0.1283 | 2.13 | 1.71 | 0.3724 | 0.22 | 0.28 | 0.0001 |
| | | RVDPVNF | 0.96 | | | 5.56 | 6.76 | 0.3627 | 6.36 | 13.91 | 0.3473 |
| | | DPVNF | 1.08 | 0.65 | 0.8177 | 1.38 | 1.06 | 0.6000 | 0.46 | 0.70 | 0.1616 |
| | | YGAEALER | 1.21 | 0.14 | 0.0532 | 1.22 | 0.89 | 0.6522 | 0.20 | 0.17 | 0.0000 |
| | | VLSPADKTNVKA | 1.25 | 0.40 | 0.2989 | 1.34 | 0.54 | 0.2986 | 1.16 | 0.94 | 0.6538 |
| | | LSFPTTKT | 1.47 | 0.75 | 0.3033 | 0.93 | 0.52 | 0.8033 | 0.27 | 0.18 | 0.0000 |
| | | LPAEFTPAVH | 1.79 | 1.12 | 0.2528 | 1.12 | 0.39 | 0.6425 | 0.43 | 0.40 | 0.0052 |
| | | AHVDDMPNALS | 1.80 | 0.89 | 0.1689 | 2.86 | | | 0.07 | 0.11 | 0.0000 |
| | | HAGEYGAEALER | 1.93 | 0.89 | 0.1303 | | | | 0.93 | 1.71 | 0.9337 |
| | | NAVAHVDDMPNALS | 2.24 | 1.07 | 0.1038 | 2.40 | 1.64 | 0.2785 | 0.53 | 0.78 | 0.1316 |
| | | KTYFP | 2.37 | 0.67 | 0.0265 | 1.79 | 0.33 | 0.0520 | 3.69 | 2.05 | 0.0076 |
| | | VDPVNF | 2.43 | 0.66 | 0.0224 | 1.74 | 0.40 | 0.0330 | 0.21 | 0.11 | 0.0000 |
| | | VAHVDDMPNALS | 2.61 | 1.32 | 0.0917 | | | | 0.07 | 0.05 | 0.0000 |
| | | AVAHVDDMPNALS | 2.65 | 1.27 | 0.0810 | 1.38 | | | 8.09 | 15.81 | 0.3726 |
| | | PAEFTPAVHA | 2.87 | 1.79 | 0.1277 | 1.82 | 1.40 | 0.3235 | 1.51 | 1.45 | 0.3515 |
| | | HVDDMPNALSA | 2.96 | 0.69 | 0.0110 | 3.62 | 5.13 | 0.3820 | 0.22 | 0.21 | 0.0000 |
| | | HAGEYGAEALE | 3.19 | 1.05 | 0.0247 | 2.76 | 0.35 | 0.0129 | 1.01 | 0.99 | 0.9724 |
| | | HVDDMPNAL | 3.78 | 1.48 | 0.0328 | | | | 0.12 | 0.10 | 0.0005 |
| | | PAEFTPAVH | 3.82 | 3.23 | 0.1801 | 2.05 | 1.00 | 0.1270 | 0.58 | 0.83 | 0.1995 |
| | | AHAGEYGAEALE | 4.56 | 2.45 | 0.0620 | | | | 10.06 | 21.32 | 0.3456 |
| | | VLSPAD | 4.84 | 2.83 | 0.0727 | 6.18 | 6.89 | 0.2297 | 5.15 | 2.17 | 0.0010 |
| | | HVDDMPNALS | 5.27 | 2.57 | 0.0450 | 4.12 | 4.30 | 0.4915 | 0.33 | 0.41 | 0.0105 |
| | | PAEFTPAVHASLD | 5.58 | 3.46 | 0.1485 | 2.26 | | | 0.20 | 0.19 | 0.0002 |
| | | MVLSPAD | 5.90 | 2.95 | 0.0448 | 38.70 | 70.64 | 0.3640 | 6.02 | 3.25 | 0.0065 |
| | | VDPVNFK | 6.94 | 4.35 | 0.0717 | 10.78 | 15.66 | 0.3002 | 1.49 | 1.06 | 0.2661 |
| | | VDPVNFKLLS | 7.03 | 4.64 | 0.1531 | | | | 0.41 | 0.53 | 0.3640 |
| | | TYFPH | 8.67 | 5.56 | 0.1395 | 1.85 | 0.91 | 0.2452 | 16.52 | 10.95 | 0.0095 |

| | | | | | | | | | | | |
|---|---|---|---|---|---|---|---|---|---|---|---|
| | | HLPAEFTPAVH | 0.53 | 0.46 | 0.1330 | | | | 0.72 | | |
| Haemoglobin β | P68871 | HVDPENFR | 0.78 | 0.87 | 0.7013 | 101.17 | | | 4.17 | 8.71 | 0.4611 |
| | | GKVNVDEVGGEALGR | 1.15 | 0.16 | 0.2560 | | | | 0.02 | 0.01 | 0.0034 |
| | | EFTPPVQ | 1.23 | 0.29 | 0.3041 | 1.88 | 1.22 | 0.3349 | 0.15 | 0.11 | 0.0001 |
| | | VNVDEVGGEALGR | 1.24 | 0.98 | 0.6529 | 1.25 | 1.04 | 0.7133 | 2.77 | 3.78 | 0.2272 |
| | | TPEEKSAVTAL | 1.58 | 0.61 | 0.1530 | 1.93 | 1.05 | 0.1734 | 1.15 | 2.33 | 0.8629 |
| | | EFTPPVQA | 1.95 | 1.45 | 0.2807 | 1.09 | 0.60 | 0.7891 | 0.15 | 0.16 | 0.0019 |
| | | HVDPENF | 2.03 | 0.60 | 0.0415 | 1.87 | 0.39 | 0.0219 | 0.24 | 0.18 | 0.0000 |
| | | FTPPVQ | 2.06 | 0.95 | 0.1124 | 4.80 | 5.44 | 0.2565 | 0.23 | 0.16 | 0.0000 |
| | | KEFTPPVQA | 2.16 | | | 1.05 | 0.85 | 0.9102 | 0.29 | 0.16 | 0.0000 |
| | | VHLTPEEKSAVT | 2.19 | 1.25 | 0.1531 | | | | 0.07 | | |
| | | KEFTPPVQ | 2.29 | 2.30 | 0.3419 | 1.34 | 0.68 | 0.3922 | 0.61 | 0.28 | 0.0055 |
| | | GKVNVDEVGGEALG | 2.51 | 0.26 | 0.0013 | 2.24 | 2.04 | 0.3112 | 0.35 | 0.09 | 0.0067 |
| | | GKVNVDEVGGEA | 3.10 | 0.88 | 0.0175 | 1.51 | 0.55 | 0.1611 | 0.11 | 0.07 | 0.0000 |
| | | KVNVDEVGGEALG | 3.32 | 0.78 | 0.0093 | | | | 0.11 | 0.07 | 0.0001 |
| | | VDPENF | 3.84 | 1.73 | 0.0462 | 4.51 | 4.76 | 0.2366 | 0.14 | 0.07 | 0.0000 |
| | | VDPENFR | 4.30 | 1.82 | 0.0362 | 1.77 | 0.25 | 0.0088 | 0.31 | 0.17 | 0.0000 |
| | | KVNVDEVGGEAL | 5.29 | 1.19 | 0.0055 | 422.07 | | | 5.74 | 12.65 | 0.4490 |
| | | VNVDEVGGEALG | 5.97 | 0.84 | 0.0013 | 3.29 | 2.66 | 0.1830 | 0.29 | 0.20 | 0.0000 |
| | | NVDEVGGEALG | 6.15 | 0.68 | 0.0006 | 3.12 | 1.07 | 0.0283 | 0.47 | 0.25 | 0.0005 |
| | | PEEKSAVTAL | 97.28 | 69.60 | 0.0698 | 3.29 | 1.21 | 0.0321 | 0.38 | 0.42 | 0.0041 |
| | | SDGLAHLDNLK | 575.07 | 36.13 | 0.0283 | 1.23 | 0.13 | 0.0924 | 118.17 | 248.08 | 0.2996 |
| | | DKLHVDPENF | | | | | | | 0.91 | 0.85 | 0.8670 |
| Oncostatin-M-specific receptor subunit beta | Q99650 | NKEVEEERIAG | 1.14 | 0.85 | 0.7569 | 0.46 | 0.45 | 0.1709 | 207.28 | 540.63 | 0.3517 |
| Spectrin beta chain, erythrocytic | P11277 | SSWESLQPEPSHPY | 7.05 | 9.66 | 0.3912 | 237.71 | 411.71 | 0.4243 | 8807.67 | 21563.87 | 0.3631 |
| ***Plasmodium falciparum*** | | | | | | | | | | | |
| 40S ribosomal protein S28e, putative | Q8IKL9 | GDSELAGRFL | 0.02 | 0.02 | 0.0000 | 15191.55 | 21484.02 | 0.5000 | 1587.78 | 3546.12 | 0.3737 |
| | | FMGDSELAGR | 0.98 | 1.11 | 0.9747 | 106.66 | 150.83 | 0.5030 | 24.10 | 49.57 | 0.3054 |
| Acyl-CoA synthetase | Q8I6Z1 | AKDMSQELELNK | 7076.63 | 8191.23 | 0.1825 | 0.10 | | | 6857.22 | 6280.62 | 0.0711 |
| Adenosylhomocysteinase | P50250 | GPFKSNEYRY | 50.31 | 65.78 | 0.4814 | 0.12 | | | 2076.55 | 3508.36 | 0.3220 |
| | | SGPFKSNEYRY | 16479.14 | 28497.22 | 0.4221 | | | | 4563.38 | 7043.59 | 0.2858 |

| | | | | | | | | | | | |
|---|---|---|---|---|---|---|---|---|---|---|---|
| Antigen 332, DBL-like protein | Q8IHN4 | TSIDLDKNLLR | 1369.95 | 1941.62 | 0.2533 | 0.08 | 0.02 | 0.0118 | 856.65 | 1899.66 | 0.3708 |
| Asparagine-rich antigen | Q8IJW6 | NVNSEIQTEHL | 181.30 | 251.56 | 0.2472 | 0.29 | 0.50 | 0.1330 | 69.05 | 114.06 | 0.1655 |
| ATP-dependent zinc metalloprotease FTSH 1 | Q8I526 | HDEEDEYINE | 13.14 | 25.38 | 0.4095 | 0.23 | 0.39 | 0.0747 | 0.79 | 0.88 | 0.5471 |
| Circumsporozoite-related antigen | Q8IIF0 | EEELVEVNK | 0.18 | 0.11 | 0.0007 | 0.24 | 0.33 | 0.0581 | 0.27 | 0.38 | 0.0024 |
| Conserved Plasmodium protein | C6S3C0 | DPNDLPPERHP | 1.07 | 0.13 | 0.3419 | 0.80 | 1.05 | 0.7786 | 0.83 | 0.92 | 0.6331 |
| Conserved Plasmodium protein | O96191 | EQKNTEVNLPESLNNATTKKN | 5487.42 | 6122.08 | 0.1710 | 0.00 | | | 7616.07 | 5335.13 | 0.0649 |
| Conserved Plasmodium protein | Q8IJ39 | LPKIGASSASNSLS | 630.76 | 1142.24 | 0.3507 | 0.00 | | | 10068.90 | 12602.15 | 0.2084 |
| Elongation factor 2 | Q8IKW5 | PQLDQYLDKL | 27321.28 | 15707.14 | 0.0948 | | | | 9531.84 | 16503.37 | 0.4225 |
| EMP1-trafficking protein | Q8IBF2 | DEENKVEKEM | 0.43 | 0.45 | 0.0866 | 2961.37 | 4187.57 | 0.5001 | 1967.96 | 4399.95 | 0.3741 |
| Erythrocyte membrane-associated antigen | Q8IC35 | NNNTLTNTNNLDNSLK | 41.02 | 59.48 | 0.3640 | 486.65 | 514.61 | 0.4094 | 572.62 | 716.01 | 0.0791 |
| Eukaryotic translation initiation factor 3 subunit E | Q8I3I5 | INNKIVAPDT | 28.99 | 55.47 | 0.3871 | 21.46 | 37.11 | 0.4404 | 3.11 | 3.65 | 0.1767 |
| | | YHINNKIVAPDT | 7876.10 | 11089.01 | 0.2506 | | | | 7237.20 | 12535.09 | 0.4227 |
| | | HINNKIVAPDT | 10021.54 | 17889.24 | 0.3442 | 0.02 | | | 65.78 | 74.20 | 0.1791 |
| Heat shock protein 70 | Q8IB24 | APAGSGPTVEEVD | 2.05 | 0.68 | 0.0536 | 0.69 | 0.66 | 0.4973 | 3.06 | 3.14 | 0.1325 |
| | | PGAGMPGNAPAGSGPTVEEVD | 2.26 | 2.65 | 0.4120 | 0.75 | 0.77 | 0.6348 | 1.31 | 1.21 | 0.5174 |
| | | PGNAPAGSGPTVEEVD | 2.87 | 1.82 | 0.1321 | 0.56 | 0.57 | 0.3172 | 2.37 | 1.00 | 0.0109 |
| Heat shock protein 70 | Q8II24 | EDLDSIKDATKQ | 47.62 | 54.21 | 0.1839 | 0.50 | 0.80 | 0.3908 | 5.11 | 7.87 | 0.2162 |
| Histone H2A | C6KT18 | SGGVLPNIHNV | 0.03 | 0.02 | 0.0001 | 71.08 | 79.74 | 0.2674 | 6061.91 | 14841.38 | 0.3631 |
| | | SQLKAGTANQDY | 0.53 | 0.33 | 0.0654 | 1.10 | 1.59 | 0.9233 | 0.91 | 0.84 | 0.7869 |
| | | GAGAPVYL | 36.10 | 69.53 | 0.3871 | 0.63 | 0.77 | 0.4961 | 5.39 | 13.00 | 0.4064 |
| | | VRNDEELNKF | 48.28 | 47.67 | 0.2279 | 0.00 | | | 1807.60 | 3117.16 | 0.4212 |
| | | ASGGVLPNIHNV | 2094.61 | 3513.61 | 0.4105 | 0.00 | | | 5592.87 | 8278.14 | 0.1589 |
| Mature parasite-infected erythrocyte surface antigen | Q8I492 | ETDDEEETLVVK | 2.79 | 5.01 | 0.5267 | 5.48 | 9.16 | 0.4863 | 0.39 | 0.48 | 0.0157 |
| | | NIETDDEEETLVVK | 19.23 | 38.43 | 0.4127 | 4588.54 | 7947.58 | 0.4227 | 3.12 | 7.44 | 0.4789 |
| Merozoite TRAP-like protein | Q8IJB7 | DEDLDNIEGDNITK | 0.32 | 0.35 | 0.0305 | 0.47 | 0.36 | 0.1231 | 0.03 | 0.04 | 0.0000 |
| | | SDEDLDNIEGDNITK | 0.45 | 0.34 | 0.0459 | 0.43 | 0.37 | 0.1169 | 0.31 | 0.38 | 0.0029 |

| | | | | | | | | | | | |
|---|---|---|---|---|---|---|---|---|---|---|---|
| Nucleoporin NUP100/NSP100, putative | Q8I398 | GNFQDSNNLLK | 221.62 | 385.74 | 0.3357 | 49.76 | 70.35 | 0.5064 | 258.98 | 309.11 | 0.0963 |
| Polyadenylate-binding protein | Q8I5H4 | NFNTNLRGQINQ | 3.34 | 2.37 | 0.1428 | 594.21 | 840.31 | 0.5005 | 2953.88 | 7806.28 | 0.3556 |
| | | NMNNQKQLPLN | 6.26 | 5.16 | 0.1342 | 17.33 | 28.09 | 0.4200 | 225.67 | 558.67 | 0.3283 |
| Probable cathepsin C | Q8IIJ9 | TYDTKLNNILN | 3351.83 | 4366.89 | 0.3152 | | | | 5185.43 | 8978.87 | 0.4226 |
| RNA-binding protein, putative | Q8I2R8 | IVTNPYERT | 2.44 | 2.42 | 0.3207 | 5.05 | 8.59 | 0.5003 | 2.96 | 4.24 | 0.2673 |
| RNA-binding protein, putative | Q8IB66 | YGGMDSPNQMR | 4.85 | 3.42 | 0.1097 | 10.84 | 18.75 | 0.4596 | 69.61 | 161.26 | 0.3033 |
| Sexual stage-specific protein | Q6ZMA7 | DANDKAKKPAGKGSPST LQTPGSSSGASLH | 6797.21 | 12577.98 | 0.3590 | 0.02 | | | 20252.03 | 28774.05 | 0.2540 |
| SNF2 helicase, putative | C6KT82 | AADRSNNDNLPEIN | 3.95 | 2.09 | 0.0667 | 1.99 | 1.45 | 0.5089 | 4.61 | 2.40 | 0.0143 |
| Thioredoxin peroxidase 1 | Q8IL80 | PSEEGVSEYLSKL | 5.38 | 4.87 | 0.4241 | 293.58 | 489.44 | 0.4093 | 276.39 | 583.22 | 0.2581 |
| | | KPSEEGVSEYLSKL | 1855.73 | 2437.72 | 0.2254 | 0.65 | 0.75 | 0.6309 | 15.69 | 30.79 | 0.4102 |
| Ubiquitin-60S ribosomal protein L40 | Q8ID50 | AIEPSLAQLAQKY | 0.04 | 0.05 | 0.0000 | 1852.72 | 3209.01 | 0.4229 | 0.58 | 0.81 | 0.3075 |
| Uncharacterized protein | Q8IBT7 | EIERLDDTSSSE | 0.13 | 0.23 | 0.0048 | 0.24 | 0.27 | 0.0396 | 0.04 | 0.11 | 0.0000 |
| | | DDVTNIQTGRETN | 0.26 | 0.09 | 0.0005 | 0.17 | 0.19 | 0.0168 | 0.07 | 0.12 | 0.0000 |
| | | DDVTNIQTGRET | 0.30 | 0.08 | 0.0004 | 0.25 | 0.28 | 0.0424 | 0.09 | 0.17 | 0.0000 |
| | | NIDDVTNIQTGRETN | 0.36 | 0.21 | 0.0091 | 0.29 | 0.26 | 0.0410 | 0.08 | 0.16 | 0.0000 |
| | | IDDVTNIQTGRETN | 0.54 | 0.28 | 0.0439 | 0.36 | 0.35 | 0.0855 | 0.09 | 0.12 | 0.0000 |
| | | NEDEIERDNF | 0.62 | 0.27 | 0.0702 | 0.42 | 0.37 | 0.1116 | 0.32 | 0.34 | 0.0019 |
| Uncharacterized protein | Q8IC42 | LASSSTTESSVSGLNTNE AHV | 2.56 | 2.50 | 0.3006 | 0.84 | 1.20 | 0.8395 | 2.98 | 3.08 | 0.1396 |
| | | SSSTTESSVSGLNTNEAH V | 3.34 | 2.71 | 0.1827 | 0.63 | 0.52 | 0.3494 | 65.41 | 158.68 | 0.3241 |
| | | STTESSVSGLNTNEAHV | 4.73 | 3.65 | 0.1332 | 1.55 | 2.65 | 0.7540 | 35.09 | 41.41 | 0.0723 |
| | | TESSVSGLNTNEAHV | 44.82 | 84.08 | 0.3738 | 20.09 | 33.84 | 0.4315 | 137.65 | 180.18 | 0.0916 |
| | | TSNLASSSTTESSVSGLN TNEAHV | 1301.40 | 2204.26 | 0.4143 | 0.01 | | | 3018.66 | 2933.92 | 0.2168 |
| Uncharacterized protein | Q8IL16 | INDVNENTYR | 6.11 | 3.20 | 0.0496 | 2.24 | 2.37 | 0.4606 | 12.74 | 9.09 | 0.0142 |
| | | PVTSINDVNENTYRS | 6.64 | 2.41 | 0.0184 | 1.06 | 0.91 | 0.9257 | 99.66 | 238.52 | 0.3158 |
| | | INDVNENTYRS | 10.05 | 8.67 | 0.1279 | 4.14 | 4.15 | 0.3211 | 33.34 | 32.79 | 0.0401 |
| | | SINDVNENTYR | 79.69 | 147.09 | 0.3631 | 3.86 | 6.55 | 0.5281 | 18.41 | 18.21 | 0.0447 |
| Uncharacterized protein | Q8IM76 | YDELRTLG | 42.54 | 71.87 | 0.4222 | 1.39 | 2.40 | 0.8055 | 14.94 | 32.07 | 0.3358 |
| Uncharacterized protein MAL13P1.336 | Q8ID39 | DIRNLNDPPKVNNNEA | 169.29 | 325.26 | 0.3769 | 29.56 | 41.81 | 0.5109 | 3888.48 | 7242.30 | 0.2963 |

# Appendix 4

# Chapter 4 – proteomics supplementary material

| OZ277 | | | | |
|---|---|---|---|---|
| **Fasta headers** | **N** | **Mean** | **SD** | **P-value** |
| tr\|Q8I3G6\|Q8I3G6_PLAF7 SNARE protein, putative OS=Plasmodium falciparum (isolate 3D7) GN=PfSyn6 PE=4 SV=1 | 4 | 0.38 | 0.20 | 0.0311 |
| sp\|Q8ID66\|PF92_PLAF7 Merozoite surface protein P92 OS=Plasmodium falciparum (isolate 3D7) GN=PF92 PE=1 SV=1 | 4 | 0.50 | 0.28 | 0.0367 |
| tr\|Q8I0U8\|Q8I0U8_PLAF7 Merozoite surface protein 1 OS=Plasmodium falciparum (isolate 3D7) GN=MSP1 PE=4 SV=1 | 4 | 0.58 | 0.14 | 0.0034 |
| tr\|Q8IDN2\|Q8IDN2_PLAF7 Uncharacterized protein OS=Plasmodium falciparum (isolate 3D7) GN=PF13_0245 PE=4 SV=1 | 4 | 0.61 | 0.35 | 0.0409 |
| tr\|Q8I531\|Q8I531_PLAF7 Transcription factor with AP2 domain(S), putative OS=Plasmodium falciparum (isolate 3D7) GN=ApiAP2 PE=4 SV=1 | 4 | 0.61 | 0.38 | 0.0497 |
| tr\|Q8I5A0\|Q8I5A0_PLAF7 Dihydrolipoyl dehydrogenase OS=Plasmodium falciparum (isolate 3D7) GN=PFL1550w PE=3 SV=2 | 4 | 0.62 | 0.34 | 0.0352 |
| tr\|O77388\|O77388_PLAF7 HVA22/TB2/DP1 family protein, putative OS=Plasmodium falciparum (isolate 3D7) GN=PFC0730w PE=4 SV=1 | 4 | 0.64 | 0.16 | 0.0039 |
| tr\|Q8IE20\|Q8IE20_PLAF7 Elongation factor Tu OS=Plasmodium falciparum (isolate 3D7) GN=MAL13P1.164 PE=3 SV=1 | 4 | 0.65 | 0.22 | 0.0099 |
| tr\|Q8IL71\|Q8IL71_PLAF7 Vesicle-associated membrane protein, putative OS=Plasmodium falciparum (isolate 3D7) GN=PF14_0377 PE=4 SV=1 | 4 | 0.65 | 0.39 | 0.0454 |
| tr\|Q8I527\|Q8I527_PLAF7 Hydroxyethylthiazole kinase, putative OS=Plasmodium falciparum (isolate 3D7) GN=PFL1920c PE=4 SV=1 | 4 | 0.67 | 0.28 | 0.0168 |
| tr\|Q8IJP9\|Q8IJP9_PLAF7 ADA2-like protein OS=Plasmodium falciparum (isolate 3D7) GN=PF10_0143 PE=4 SV=1 | 4 | 0.68 | 0.40 | 0.0423 |
| tr\|Q8IC37\|Q8IC37_PLAF7 Uncharacterized protein OS=Plasmodium falciparum (isolate 3D7) GN=MAL7P1.11 PE=4 SV=1 | 4 | 0.68 | 0.42 | 0.0477 |
| tr\|Q8I5B2\|Q8I5B2_PLAF7 Conserved Plasmodium protein OS=Plasmodium falciparum (isolate 3D7) GN=PFL1485w PE=4 SV=2 | 4 | 0.68 | 0.32 | 0.0232 |
| tr\|Q8IBP0\|Q8IBP0_PLAF7 Uncharacterized protein OS=Plasmodium falciparum (isolate 3D7) GN=PF07_0087 PE=4 SV=1 | 4 | 0.69 | 0.18 | 0.0049 |
| tr\|Q8ILC9\|Q8ILC9_PLAF7 Uncharacterized protein OS=Plasmodium falciparum (isolate 3D7) GN=PF14_0315 PE=4 SV=2 | 4 | 0.69 | 0.42 | 0.0449 |
| tr\|Q8IIV1\|Q8IIV1_PLAF7 Histone H2B OS=Plasmodium falciparum (isolate 3D7) GN=PF11_0062 PE=3 SV=1 | 4 | 0.70 | 0.09 | 0.0006 |
| tr\|Q8IBC3\|Q8IBC3_PLAF7 Prohibitin, putative OS=Plasmodium falciparum (isolate 3D7) GN=PF08_0006 PE=4 SV=1 | 4 | 0.70 | 0.44 | 0.0499 |
| tr\|Q8IL56\|Q8IL56_PLAF7 Structure specific recognition protein OS=Plasmodium falciparum (isolate 3D7) GN=PF14_0393 PE=4 SV=1 | 4 | 0.70 | 0.39 | 0.0375 |
| tr\|Q8I5L4\|Q8I5L4_PLAF7 Phospholipid-translocating ATPase OS=Plasmodium falciparum (isolate 3D7) GN=PFL0950c PE=4 SV=1 | 4 | 0.70 | 0.41 | 0.0431 |
| tr\|Q8II93\|Q8II93_PLAF7 Protein phosphatase, putative OS=Plasmodium falciparum (isolate 3D7) GN=PF11_0281 PE=4 SV=2 | 4 | 0.70 | 0.28 | 0.0161 |
| tr\|C0H5J5\|C0H5J5_PLAF7 Polyadenylate-binding protein, putative OS=Plasmodium falciparum (isolate 3D7) GN=MAL13P1.303 PE=4 SV=1 | 4 | 0.70 | 0.38 | 0.0341 |
| tr\|Q8I6T2\|Q8I6T2_PLAF7 Isocitrate dehydrogenase [NADP] OS=Plasmodium falciparum (isolate 3D7) GN=PF13_0242 PE=3 SV=1 | 4 | 0.71 | 0.28 | 0.0148 |
| tr\|Q8I445\|Q8I445_PLAF7 Uncharacterized protein OS=Plasmodium falciparum (isolate 3D7) GN=PFE0280c PE=4 SV=1 | 4 | 0.71 | 0.33 | 0.0228 |
| tr\|Q8I328\|Q8I328_PLAF7 Putative uncharacterized protein OS=Plasmodium falciparum (isolate 3D7) GN=PFI0605c PE=4 SV=1 | 4 | 0.72 | 0.25 | 0.0106 |
| tr\|O96275\|O96275_PLAF7 Liver stage antigen 3 OS=Plasmodium falciparum (isolate 3D7) GN=PFB0915w PE=4 SV=1 | 4 | 0.72 | 0.18 | 0.0039 |
| tr\|C6KSV9\|C6KSV9_PLAF7 SWI/SNF-related matrix-associated actin-dependent regulator of chromatin OS=Plasmodium falciparum (isolate 3D7) GN=PFF0560c PE=4 SV=1 | 4 | 0.72 | 0.44 | 0.0474 |
| tr\|Q8I5T2\|Q8I5T2_PLAF7 Glutathione peroxidase OS=Plasmodium falciparum (isolate 3D7) GN=PFL0595c PE=3 SV=1 | 4 | 0.73 | 0.24 | 0.0093 |
| tr\|Q8IBI5\|Q8IBI5_PLAF7 Cysteine desulfurase, putative OS=Plasmodium falciparum (isolate 3D7) GN=MAL7P1.150 PE=3 SV=1 | 4 | 0.73 | 0.20 | 0.0054 |
| tr\|Q8IIC0\|Q8IIC0_PLAF7 Uncharacterized protein OS=Plasmodium falciparum (isolate 3D7) GN=PF11_0254 PE=4 SV=1 | 4 | 0.73 | 0.41 | 0.0374 |
| tr\|C6KT11\|C6KT11_PLAF7 Mitochondrial import receptor subunit tom40 OS=Plasmodium falciparum (isolate 3D7) GN=PFF0825c PE=4 SV=1 | 4 | 0.74 | 0.44 | 0.0429 |
| tr\|Q8II36\|Q8II36_PLAF7 Aquaglyceroporin OS=Plasmodium falciparum (isolate 3D7) GN=PF11_0338 PE=3 SV=1 | 4 | 0.74 | 0.46 | 0.0479 |

| | | | | |
|---|---|---|---|---|
| tr\|Q8IIB6\|Q8IIB6_PLAF7 GrpE protein homolog OS=Plasmodium falciparum (isolate 3D7) GN=PF11_0258 PE=3 SV=2 | 4 | 0.74 | 0.36 | 0.0262 |
| tr\|Q8ILP3\|Q8ILP3_PLAF7 Surface protein, Pf113 OS=Plasmodium falciparum (isolate 3D7) GN=Pf113 PE=4 SV=1 | 4 | 0.75 | 0.32 | 0.0183 |
| tr\|Q8IIR7\|Q8IIR7_PLAF7 Endoplasmic reticulum-resident calcium binding protein OS=Plasmodium falciparum (isolate 3D7) GN=PF11_0098 PE=4 SV=1 | 4 | 0.75 | 0.36 | 0.0259 |
| tr\|Q8IIJ4\|Q8IIJ4_PLAF7 Uncharacterized protein OS=Plasmodium falciparum (isolate 3D7) GN=PF11_0179 PE=4 SV=1 | 4 | 0.75 | 0.21 | 0.0057 |
| tr\|Q8I489\|Q8I489_PLAF7 Heat shock protein, putative OS=Plasmodium falciparum (isolate 3D7) GN=PFE0055c PE=4 SV=2 | 4 | 0.75 | 0.13 | 0.0015 |
| tr\|Q8IKE8\|Q8IKE8_PLAF7 Uncharacterized protein OS=Plasmodium falciparum (isolate 3D7) GN=PF14_0657 PE=4 SV=1 | 4 | 0.76 | 0.46 | 0.0455 |
| tr\|Q8IIR6\|Q8IIR6_PLAF7 Heat shock protein DnaJ homologue Pfj2 OS=Plasmodium falciparum (isolate 3D7) GN=PF11_0099 PE=4 SV=1 | 4 | 0.76 | 0.19 | 0.0041 |
| tr\|O96236\|O96236_PLAF7 DNA-directed RNA polymerase OS=Plasmodium falciparum (isolate 3D7) GN=PFB0715w PE=3 SV=3 | 4 | 0.76 | 0.46 | 0.0467 |
| tr\|Q8IDH5\|Q8IDH5_PLAF7 Thioredoxin-related protein, putative OS=Plasmodium falciparum (isolate 3D7) GN=PF13_0272 PE=4 SV=1 | 4 | 0.76 | 0.21 | 0.0055 |
| tr\|C0H488\|C0H488_PLAF7 Uncharacterized protein OS=Plasmodium falciparum (isolate 3D7) GN=PFD0170c PE=4 SV=1 | 4 | 0.77 | 0.11 | 0.0008 |
| tr\|Q8I205\|Q8I205_PLAF7 Uncharacterized protein OS=Plasmodium falciparum (isolate 3D7) GN=PFD0095c PE=4 SV=1 | 4 | 0.77 | 0.42 | 0.0351 |
| tr\|Q8I2X4\|Q8I2X4_PLAF7 Heat shock protein 70 (HSP70) homologue OS=Plasmodium falciparum (isolate 3D7) GN=PFI0875w PE=3 SV=1 | 4 | 0.77 | 0.18 | 0.0034 |
| tr\|Q8I0V4\|Q8I0V4_PLAF7 Endoplasmin homolog, putative OS=Plasmodium falciparum (isolate 3D7) GN=PFL1070c PE=1 SV=1 | 4 | 0.78 | 0.14 | 0.0016 |
| tr\|Q8I4U7\|Q8I4U7_PLAF7 Uncharacterized protein OS=Plasmodium falciparum (isolate 3D7) GN=PFL2335w PE=4 SV=1 | 4 | 0.78 | 0.44 | 0.0378 |
| tr\|Q8IE18\|Q8IE18_PLAF7 Uncharacterized protein OS=Plasmodium falciparum (isolate 3D7) GN=PF13_0165 PE=4 SV=1 | 4 | 0.80 | 0.48 | 0.0452 |
| tr\|Q8IM32\|Q8IM32_PLAF7 Uncharacterized protein OS=Plasmodium falciparum (isolate 3D7) GN=PF14_0059 PE=4 SV=1 | 4 | 0.80 | 0.48 | 0.0443 |
| tr\|C6KTC7\|C6KTC7_PLAF7 DNAJ domain protein, putative OS=Plasmodium falciparum (isolate 3D7) GN=PFF1415c PE=4 SV=1 | 4 | 0.80 | 0.17 | 0.0025 |
| tr\|C0H5I5\|C0H5I5_PLAF7 Splicing factor 3b subunit, putative OS=Plasmodium falciparum (isolate 3D7) GN=PF13_0296 PE=4 SV=1 | 4 | 0.80 | 0.29 | 0.0113 |
| tr\|Q8IJD0\|Q8IJD0_PLAF7 Merozoite capping protein 1 OS=Plasmodium falciparum (isolate 3D7) GN=PF10_0268 PE=4 SV=1 | 4 | 0.80 | 0.38 | 0.0248 |
| tr\|Q8ILA9\|Q8ILA9_PLAF7 Uncharacterized protein OS=Plasmodium falciparum (isolate 3D7) GN=PF14_0336 PE=4 SV=1 | 4 | 0.80 | 0.18 | 0.0029 |
| tr\|Q8IK12\|Q8IK12_PLAF7 Uncharacterized protein OS=Plasmodium falciparum (isolate 3D7) GN=PF10_0028 PE=4 SV=1 | 4 | 0.80 | 0.22 | 0.0052 |
| tr\|O77375\|O77375_PLAF7 DNA-directed RNA polymerase OS=Plasmodium falciparum (isolate 3D7) GN=PFC0805w PE=3 SV=1 | 4 | 0.80 | 0.49 | 0.0454 |
| sp\|P69905\|HBA_HUMAN Hemoglobin subunit alpha OS=Homo sapiens GN=HBA1 PE=1 SV=2;tr\|G3V1N2\|G3V1N2_HUMAN HCG1745306, isoform CRA_a OS=Homo sapiens GN=HBA2 PE=1 SV=1 | 4 | 0.81 | 0.30 | 0.0129 |
| tr\|C0H571\|C0H571_PLAF7 High molecular weight rhoptry protein-2 OS=Plasmodium falciparum (isolate 3D7) GN=RhopH2 PE=4 SV=1 | 4 | 0.81 | 0.19 | 0.0037 |
| tr\|Q8IKC8\|Q8IKC8_PLAF7 Exported protein 2 OS=Plasmodium falciparum (isolate 3D7) GN=EXP-2 PE=4 SV=1 | 4 | 0.81 | 0.12 | 0.0010 |
| tr\|Q8IBF2\|Q8IBF2_PLAF7 Uncharacterized protein OS=Plasmodium falciparum (isolate 3D7) GN=MAL7P1.171 PE=4 SV=1 | 4 | 0.81 | 0.11 | 0.0006 |
| tr\|Q8IIS4\|Q8IIS4_PLAF7 Transcription factor with AP2 domain(S), putative OS=Plasmodium falciparum (isolate 3D7) GN=PF11_0091 PE=4 SV=1 | 4 | 0.81 | 0.51 | 0.0495 |
| tr\|Q8I5T3\|Q8I5T3_PLAF7 p-type ATPase, putative OS=Plasmodium falciparum (isolate 3D7) GN=PFL0590c PE=3 SV=1 | 4 | 0.81 | 0.14 | 0.0013 |
| tr\|Q8IL07\|Q8IL07_PLAF7 Centrin-2 OS=Plasmodium falciparum (isolate 3D7) GN=CEN2 PE=4 SV=1 | 4 | 0.81 | 0.29 | 0.0118 |
| tr\|Q8IJV6\|Q8IJV6_PLAF7 Adenylate kinase, putative OS=Plasmodium falciparum (isolate 3D7) GN=PF10_0086 PE=3 SV=1 | 4 | 0.81 | 0.08 | 0.0002 |
| tr\|Q8IJ72\|Q8IJ72_PLAF7 Bromodomain protein, putative OS=Plasmodium falciparum (isolate 3D7) GN=PF10_0328 PE=1 SV=1 | 4 | 0.81 | 0.26 | 0.0086 |
| tr\|Q7K6A5\|Q7K6A5_PLAF7 Multidrug resistance protein OS=Plasmodium falciparum (isolate 3D7) GN=PfMDR1 PE=3 SV=1 | 4 | 0.81 | 0.34 | 0.0179 |

| | | | | |
|---|---|---|---|---|
| tr\|Q76NM4\|Q76NM4_PLAF7 Rab11a, GTPase OS=Plasmodium falciparum (isolate 3D7) GN=Rab11a PE=1 SV=1 | 4 | 0.82 | 0.48 | 0.0424 |
| tr\|C0H5L7\|C0H5L7_PLAF7 Uncharacterized protein OS=Plasmodium falciparum (isolate 3D7) GN=MAL13P1.352 PE=4 SV=1 | 4 | 0.82 | 0.34 | 0.0172 |
| tr\|Q76NN8\|Q76NN8_PLAF7 Calcium-transporting ATPase, putative OS=Plasmodium falciparum (isolate 3D7) GN=PFA_0310c PE=3 SV=1 | 4 | 0.82 | 0.10 | 0.0005 |
| tr\|Q8II24\|Q8II24_PLAF7 Heat shock protein hsp70 homologue OS=Plasmodium falciparum (isolate 3D7) GN=PF11_0351 PE=3 SV=1 | 4 | 0.84 | 0.19 | 0.0031 |
| tr\|Q8IJ76\|Q8IJ76_PLAF7 Uncharacterized protein OS=Plasmodium falciparum (isolate 3D7) GN=PF10_0323 PE=4 SV=1 | 4 | 0.84 | 0.06 | 0.0001 |
| tr\|Q8I1X3\|Q8I1X3_PLAF7 Secy-independent transporter protein, putative OS=Plasmodium falciparum (isolate 3D7) GN=PFD0275w PE=4 SV=2 | 4 | 0.84 | 0.11 | 0.0006 |
| sp\|P28289\|TMOD1_HUMAN Tropomodulin-1 OS=Homo sapiens GN=TMOD1 PE=1 SV=1;sp\|P28289-2\|TMOD1_HUMAN Isoform 2 of Tropomodulin-1 OS=Homo sapiens GN=TMOD1 | 4 | 0.84 | 0.30 | 0.0112 |
| tr\|Q8IIV8\|Q8IIV8_PLAF7 Uncharacterized protein OS=Plasmodium falciparum (isolate 3D7) GN=PF11_0055 PE=4 SV=1 | 4 | 0.84 | 0.25 | 0.0067 |
| tr\|C0H4Y6\|C0H4Y6_PLAF7 Protein disulfide-isomerase OS=Plasmodium falciparum (isolate 3D7) GN=PfPDI-8 PE=3 SV=1 | 4 | 0.84 | 0.16 | 0.0018 |
| tr\|Q8I484\|Q8I484_PLAF7 Rhoptry-associated protein 2, RAP2 OS=Plasmodium falciparum (isolate 3D7) GN=RAP2 PE=4 SV=1 | 4 | 0.85 | 0.08 | 0.0003 |
| tr\|Q8I1Z8\|Q8I1Z8_PLAF7 Uncharacterized protein OS=Plasmodium falciparum (isolate 3D7) GN=PFD0150w PE=4 SV=1 | 4 | 0.85 | 0.14 | 0.0013 |
| tr\|Q8IJZ4\|Q8IJZ4_PLAF7 Uncharacterized protein OS=Plasmodium falciparum (isolate 3D7) GN=PF10_0046 PE=4 SV=1 | 4 | 0.87 | 0.52 | 0.0442 |
| sp\|P68871\|HBB_HUMAN Hemoglobin subunit beta OS=Homo sapiens GN=HBB PE=1 SV=2 | 4 | 0.88 | 0.29 | 0.0089 |
| tr\|Q8I1T2\|Q8I1T2_PLAF7 Nuclear cap-binding protein, putative OS=Plasmodium falciparum (isolate 3D7) GN=PFD0750w PE=4 SV=1 | 4 | 0.88 | 0.17 | 0.0018 |
| tr\|Q8IHN4\|Q8IHN4_PLAF7 Antigen 332, DBL-like protein OS=Plasmodium falciparum (isolate 3D7) GN=PF11_0506 PE=4 SV=2 | 4 | 0.88 | 0.13 | 0.0009 |
| tr\|C0H5H5\|C0H5H5_PLAF7 Uncharacterized protein OS=Plasmodium falciparum (isolate 3D7) GN=MAL13P1.229 PE=4 SV=1 | 4 | 0.88 | 0.36 | 0.0157 |
| tr\|Q8ILE3\|Q8ILE3_PLAF7 Uncharacterized protein OS=Plasmodium falciparum (isolate 3D7) GN=PF14_0301 PE=4 SV=1 | 4 | 0.89 | 0.17 | 0.0018 |
| tr\|Q7K6B0\|Q7K6B0_PLAF7 PfRab18, GTPase OS=Plasmodium falciparum (isolate 3D7) GN=rab18 PE=3 SV=1 | 4 | 0.89 | 0.19 | 0.0025 |
| tr\|Q8IJN9\|Q8IJN9_PLAF7 Hsp60 OS=Plasmodium falciparum (isolate 3D7) GN=PF10_0153 PE=3 SV=1 | 4 | 0.89 | 0.08 | 0.0002 |
| sp\|Q9H4G4\|GAPR1_HUMAN Golgi-associated plant pathogenesis-related protein 1 OS=Homo sapiens GN=GLIPR2 PE=1 SV=3;tr\|Q5VZR0\|Q5VZR0_HUMAN Golgi-associated plant pathogenesis-related protein 1 OS=Homo sapiens GN=GLIPR2 PE=1 SV=1 | 4 | 0.90 | 0.16 | 0.0015 |
| tr\|O96271\|O96271_PLAF7 Replication factor C subunit 1, putative OS=Plasmodium falciparum (isolate 3D7) GN=PFB0895c PE=4 SV=1 | 4 | 0.90 | 0.38 | 0.0175 |
| tr\|Q76NL8\|Q76NL8_PLAF7 Falcilysin OS=Plasmodium falciparum (isolate 3D7) GN=fln PE=1 SV=1 | 4 | 0.90 | 0.40 | 0.0198 |
| tr\|Q8I3F1\|Q8I3F1_PLAF7 Uncharacterized protein OS=Plasmodium falciparum (isolate 3D7) GN=PFE1600w PE=4 SV=1 | 4 | 0.90 | 0.14 | 0.0010 |
| tr\|Q8IKF6\|Q8IKF6_PLAF7 Uncharacterized protein OS=Plasmodium falciparum (isolate 3D7) GN=PF14_0649 PE=4 SV=1 | 4 | 0.90 | 0.20 | 0.0027 |
| tr\|Q8IIK8\|Q8IIK8_PLAF7 Peptidyl-prolyl cis-trans isomerase OS=Plasmodium falciparum (isolate 3D7) GN=PF11_0164 PE=3 SV=1 | 4 | 0.90 | 0.14 | 0.0010 |
| tr\|Q8IAN7\|Q8IAN7_PLAF7 Tubulin gamma chain OS=Plasmodium falciparum (isolate 3D7) GN=g-tub PE=3 SV=1 | 4 | 0.91 | 0.12 | 0.0007 |
| tr\|Q8I0U6\|Q8I0U6_PLAF7 DNAJ protein, putative OS=Plasmodium falciparum (isolate 3D7) GN=RESA PE=4 SV=1 | 4 | 0.92 | 0.20 | 0.0027 |
| tr\|Q8IB78\|Q8IB78_PLAF7 Nucleoside transporter, putative OS=Plasmodium falciparum (isolate 3D7) GN=MAL8P1.32 PE=4 SV=1 | 4 | 0.92 | 0.11 | 0.0004 |
| tr\|Q8IFM0\|Q8IFM0_PLAF7 Uncharacterized protein OS=Plasmodium falciparum (isolate 3D7) GN=PFD1170c PE=4 SV=1 | 4 | 0.93 | 0.14 | 0.0009 |
| tr\|O97238\|O97238_PLAF7 Putative uncharacterized protein OS=Plasmodium falciparum (isolate 3D7) GN=PFC0240c PE=4 SV=3 | 4 | 0.93 | 0.37 | 0.0148 |
| tr\|Q8IIH4\|Q8IIH4_PLAF7 U2 snRNP auxiliary factor, small subunit, putative OS=Plasmodium falciparum (isolate 3D7) GN=PF11_0200 PE=4 SV=1 | 4 | 0.93 | 0.13 | 0.0008 |
| tr\|Q8IAU7\|Q8IAU7_PLAF7 Uncharacterized protein OS=Plasmodium falciparum (isolate 3D7) GN=MAL8P1.105 PE=4 SV=1 | 4 | 0.93 | 0.10 | 0.0003 |

| | | | | |
|---|---|---|---|---|
| tr\|Q8I487\|Q8I487_PLAF7 Skeleton-binding protein 1 OS=Plasmodium falciparum (isolate 3D7) GN=PfSBP1 PE=4 SV=1 | 4 | 0.93 | 0.02 | 0.0000 |
| tr\|Q8I4R5\|Q8I4R5_PLAF7 Rhoptry neck protein 3, putative OS=Plasmodium falciparum (isolate 3D7) GN=PFL2505c PE=4 SV=1 | 4 | 0.93 | 0.08 | 0.0001 |
| sp\|P04921-2\|GLPC_HUMAN Isoform Glycophorin-D of Glycophorin-C OS=Homo sapiens GN=GYPC;sp\|P04921-3\|GLPC_HUMAN Isoform 3 of Glycophorin-C OS=Homo sapiens GN=GYPC;sp\|P04921\|GLPC_HUMAN Glycophorin-C OS=Homo sapiens GN=GYPC PE=1 SV=1 | 4 | 0.93 | 0.16 | 0.0013 |
| tr\|Q8IJW4\|Q8IJW4_PLAF7 Eukaryotic translation initiation factor 3 subunit D OS=Plasmodium falciparum (isolate 3D7) GN=PF10_0077 PE=3 SV=1 | 4 | 0.94 | 0.40 | 0.0185 |
| tr\|Q8IB03\|Q8IB03_PLAF7 ClpB protein, putative OS=Plasmodium falciparum (isolate 3D7) GN=PF08_0063 PE=1 SV=1 | 4 | 0.94 | 0.14 | 0.0009 |
| tr\|C0H4M6\|C0H4M6_PLAF7 Regulator of chromosome condensation, putative OS=Plasmodium falciparum (isolate 3D7) GN=MAL7P1.38 PE=4 SV=1 | 4 | 0.94 | 0.17 | 0.0015 |
| tr\|Q8IIF0\|Q8IIF0_PLAF7 Circumsporozoite-related antigen OS=Plasmodium falciparum (isolate 3D7) GN=PF11_0224 PE=4 SV=1 | 4 | 0.94 | 0.19 | 0.0020 |
| tr\|Q8IKJ0\|Q8IKJ0_PLAF7 ATP synthase (C/AC39) subunit, putative OS=Plasmodium falciparum (isolate 3D7) GN=PF14_0615 PE=4 SV=1 | 4 | 0.94 | 0.07 | 0.0001 |
| tr\|O96260\|O96260_PLAF7 Replication factor C, subunit 2 OS=Plasmodium falciparum (isolate 3D7) GN=PFB0840w PE=4 SV=1 | 4 | 0.95 | 0.50 | 0.0322 |
| tr\|Q8IKY7\|Q8IKY7_PLAF7 SNARE protein, putative OS=Plasmodium falciparum (isolate 3D7) GN=PfVti1 PE=4 SV=1 | 4 | 0.95 | 0.05 | 0.0000 |
| tr\|Q8IAZ3\|Q8IAZ3_PLAF7 Eukaryotic translation initiation factor 3 subunit G OS=Plasmodium falciparum (isolate 3D7) GN=MAL8P1.83 PE=3 SV=1 | 4 | 0.95 | 0.33 | 0.0104 |
| tr\|Q8I3N3\|Q8I3N3_PLAF7 Mitochondrial processing peptidase alpha subunit, putative OS=Plasmodium falciparum (isolate 3D7) GN=PFE1155c PE=3 SV=2 | 4 | 0.96 | 0.23 | 0.0038 |
| tr\|Q8IEE5\|Q8IEE5_PLAF7 DNA replication licensing factor MCM4-related OS=Plasmodium falciparum (isolate 3D7) GN=PF13_0095 PE=3 SV=1 | 4 | 0.96 | 0.56 | 0.0411 |
| tr\|Q8IL16\|Q8IL16_PLAF7 Uncharacterized protein OS=Plasmodium falciparum (isolate 3D7) GN=PF14_0434 PE=4 SV=1 | 4 | 0.97 | 0.16 | 0.0012 |
| tr\|C0H570\|C0H570_PLAF7 RNA binding protein, putative OS=Plasmodium falciparum (isolate 3D7) GN=PFI1435w PE=4 SV=1 | 4 | 0.97 | 0.03 | 0.0000 |
| tr\|Q8IE67\|Q8IE67_PLAF7 Phosphoribosylpyrophosphate synthetase OS=Plasmodium falciparum (isolate 3D7) GN=PF13_0143 PE=4 SV=1 | 4 | 0.98 | 0.15 | 0.0009 |
| tr\|Q8I3V8\|Q8I3V8_PLAF7 RNA recognition motif, putative OS=Plasmodium falciparum (isolate 3D7) GN=PFE0750c PE=4 SV=1 | 4 | 0.98 | 0.20 | 0.0024 |
| tr\|Q8IJX4\|Q8IJX4_PLAF7 Conserved Plasmodium protein OS=Plasmodium falciparum (isolate 3D7) GN=PF10_0067 PE=4 SV=2 | 4 | 0.98 | 0.55 | 0.0380 |
| tr\|Q8IJX8\|Q8IJX8_PLAF7 Uncharacterized protein OS=Plasmodium falciparum (isolate 3D7) GN=PF10_0063 PE=4 SV=1 | 4 | 0.99 | 0.32 | 0.0085 |
| tr\|Q8I5H4\|Q8I5H4_PLAF7 Polyadenylate-binding protein, putative OS=Plasmodium falciparum (isolate 3D7) GN=PFL1170w PE=4 SV=1 | 4 | 1.00 | 0.18 | 0.0015 |
| tr\|Q8IK24\|Q8IK24_PLAF7 Acyl CoA binding protein, putative OS=Plasmodium falciparum (isolate 3D7) GN=PF10_0016 PE=4 SV=1 | 4 | 1.01 | 0.55 | 0.0346 |
| tr\|O77310\|O77310_PLAF7 Cytoadherence linked asexual protein 3.1 OS=Plasmodium falciparum (isolate 3D7) GN=RhopH1(3.1) PE=4 SV=2;tr\|O77309\|O77309_PLAF7 Cytoadherence linked asexual protein 3.2 OS=Plasmodium falciparum (isolate 3D7) GN=RhopH1(3.2) PE=4 SV=3 | 4 | 1.03 | 0.06 | 0.0001 |
| tr\|Q8I2F2\|Q8I2F2_PLAF7 Putative uncharacterized protein OS=Plasmodium falciparum (isolate 3D7) GN=PFI1780w PE=1 SV=1 | 4 | 1.03 | 0.06 | 0.0001 |
| tr\|O96191\|O96191_PLAF7 Conserved Plasmodium protein OS=Plasmodium falciparum (isolate 3D7) GN=PFB0490c PE=4 SV=1 | 4 | 1.04 | 0.06 | 0.0000 |
| tr\|Q8I0V3\|Q8I0V3_PLAF7 Chaperonin, cpn60 OS=Plasmodium falciparum (isolate 3D7) GN=PFL1545c PE=3 SV=2 | 4 | 1.04 | 0.26 | 0.0042 |
| tr\|Q8I5V9\|Q8I5V9_PLAF7 Uncharacterized protein OS=Plasmodium falciparum (isolate 3D7) GN=PFL0445w PE=4 SV=1 | 4 | 1.05 | 0.33 | 0.0079 |
| tr\|Q8IBT2\|Q8IBT2_PLAF7 Eukaryotic translation initiation factor 3 subunit I OS=Plasmodium falciparum (isolate 3D7) GN=MAL7P1.81 PE=3 SV=1 | 4 | 1.05 | 0.18 | 0.0013 |
| tr\|Q8I206\|Q8I206_PLAF7 Uncharacterized protein OS=Plasmodium falciparum (isolate 3D7) GN=PFD0090c PE=4 SV=1 | 4 | 1.05 | 0.12 | 0.0004 |
| tr\|C0H4M1\|C0H4M1_PLAF7 AAA family ATPase, putative OS=Plasmodium falciparum (isolate 3D7) GN=MAL7P1.209 PE=4 SV=1 | 4 | 1.05 | 0.16 | 0.0009 |
| tr\|Q8IIQ7\|Q8IIQ7_PLAF7 Asparagine-rich antigen OS=Plasmodium falciparum (isolate 3D7) GN=PF11_0111 PE=4 SV=1 | 4 | 1.07 | 0.47 | 0.0203 |
| tr\|Q8IEC8\|Q8IEC8_PLAF7 DnaJ/SEC63 protein, putative OS=Plasmodium falciparum (isolate 3D7) GN=PF13_0102 PE=4 SV=1 | 4 | 1.07 | 0.37 | 0.0100 |
| tr\|Q8IE14\|Q8IE14_PLAF7 Signal peptidase I OS=Plasmodium falciparum (isolate 3D7) GN=SP21 PE=4 SV=1 | 4 | 0.24 | 0.25 | 0.1553 |

| | | | | |
|---|---|---|---|---|
| tr\|Q8I655\|Q8I655_PLAF7 Ribosome associated membrane protein RAMP4, putative OS=Plasmodium falciparum (isolate 3D7) GN=PFB0888w PE=4 SV=2 | 4 | 0.24 | 0.24 | 0.1394 |
| tr\|Q8ID59\|Q8ID59_PLAF7 DNA-directed RNA polymerase 2, putative OS=Plasmodium falciparum (isolate 3D7) GN=PF13_0341 PE=3 SV=1 | 4 | 0.25 | 0.18 | 0.0650 |
| tr\|Q8IKW1\|Q8IKW1_PLAF7 Uncharacterized protein OS=Plasmodium falciparum (isolate 3D7) GN=PF14_0490 PE=4 SV=1 | 4 | 0.26 | 0.24 | 0.1247 |
| tr\|Q8IDX8\|Q8IDX8_PLAF7 Merozoite Surface Protein 7, MSP7 OS=Plasmodium falciparum (isolate 3D7) GN=MSP7 PE=4 SV=1 | 4 | 0.26 | 0.33 | 0.2139 |
| tr\|Q8IAN8\|Q8IAN8_PLAF7 Uncharacterized protein OS=Plasmodium falciparum (isolate 3D7) GN=PF08_0124 PE=4 SV=1 | 4 | 0.32 | 0.37 | 0.1769 |
| sp\|P20073-2\|ANXA7_HUMAN Isoform 2 of Annexin A7 OS=Homo sapiens GN=ANXA7;sp\|P20073\|ANXA7_HUMAN Annexin A7 OS=Homo sapiens GN=ANXA7 PE=1 SV=3 | 4 | 0.33 | 0.22 | 0.0590 |
| tr\|Q9TY96\|Q9TY96_PLAF7 Serine repeat antigen 6 (SERA-6) OS=Plasmodium falciparum (isolate 3D7) GN=SERA-6 PE=1 SV=3 | 4 | 0.34 | 0.36 | 0.1542 |
| tr\|Q8I457\|Q8I457_PLAF7 ATP-dependent helicase, putative OS=Plasmodium falciparum (isolate 3D7) GN=PFE0215w PE=3 SV=1 | 4 | 0.34 | 0.30 | 0.1022 |
| tr\|Q8IK20\|Q8IK20_PLAF7 Uncharacterized protein OS=Plasmodium falciparum (isolate 3D7) GN=PF10_0020 PE=4 SV=1 | 4 | 0.38 | 0.26 | 0.0627 |
| tr\|Q8I492\|Q8I492_PLAF7 Mature parasite-infected erythrocyte surface antigen (MESA) or PfEMP2 OS=Plasmodium falciparum (isolate 3D7) GN=MESA PE=4 SV=1 | 4 | 1.07 | 0.11 | 0.0003 |
| tr\|Q8IDP9\|Q8IDP9_PLAF7 Uncharacterized protein OS=Plasmodium falciparum (isolate 3D7) GN=PF13_0239 PE=4 SV=1 | 4 | 0.39 | 0.45 | 0.1811 |
| tr\|Q8I1R5\|Q8I1R5_PLAF7 LETM1-like protein, putative OS=Plasmodium falciparum (isolate 3D7) GN=PFD0835c PE=4 SV=1 | 4 | 0.41 | 0.46 | 0.1736 |
| tr\|O97269\|O97269_PLAF7 Putative uncharacterized protein OS=Plasmodium falciparum (isolate 3D7) GN=PFC0670c PE=4 SV=1 | 4 | 0.41 | 0.27 | 0.0568 |
| tr\|Q8IBT7\|Q8IBT7_PLAF7 Uncharacterized protein OS=Plasmodium falciparum (isolate 3D7) GN=MAL7P1.77 PE=4 SV=1 | 4 | 0.46 | 0.31 | 0.0581 |
| tr\|Q8I3A0\|Q8I3A0_PLAF7 Cu2+-transporting ATPase, Cu2+ transporter OS=Plasmodium falciparum (isolate 3D7) GN=PFI0240c PE=3 SV=1 | 4 | 0.48 | 0.43 | 0.1119 |
| sp\|P26447\|S10A4_HUMAN Protein S100-A4 OS=Homo sapiens GN=S100A4 PE=1 SV=1 | 4 | 0.50 | 0.35 | 0.0668 |
| sp\|P02730\|B3AT_HUMAN Band 3 anion transport protein OS=Homo sapiens GN=SLC4A1 PE=1 SV=3;tr\|A0A0A0MS98\|A0A0A0MS98_HUMAN Band 3 anion transport protein OS=Homo sapiens GN=SLC4A1 PE=1 SV=1 | 4 | 1.07 | 0.19 | 0.0014 |
| sp\|Q9H1E5\|TMX4_HUMAN Thioredoxin-related transmembrane protein 4 OS=Homo sapiens GN=TMX4 PE=1 SV=1 | 4 | 0.52 | 0.35 | 0.0592 |
| tr\|Q8I2X3\|Q8I2X3_PLAF7 Glideosome-associated protein 50 OS=Plasmodium falciparum (isolate 3D7) GN=GAP50 PE=1 SV=1 | 4 | 0.52 | 0.33 | 0.0529 |
| sp\|O77374\|PF07_PLAF7 Uncharacterized protein PFC0810c OS=Plasmodium falciparum (isolate 3D7) GN=PFC0810c PE=3 SV=1 | 4 | 0.52 | 0.36 | 0.0638 |
| tr\|Q8II41\|Q8II41_PLAF7 Conserved Plasmodium membrane protein OS=Plasmodium falciparum (isolate 3D7) GN=PF11_0333 PE=4 SV=2 | 4 | 0.52 | 0.35 | 0.0566 |
| tr\|Q8IKC7\|Q8IKC7_PLAF7 Inorganic anion exchanger, inorganic anion antiporter OS=Plasmodium falciparum (isolate 3D7) GN=PF14_0679 PE=4 SV=1 | 4 | 0.53 | 0.36 | 0.0591 |
| tr\|Q7KWI7\|Q7KWI7_PLAF7 Plasmodium exported protein OS=Plasmodium falciparum (isolate 3D7) GN=PFB0921c PE=4 SV=1 | 4 | 0.53 | 0.37 | 0.0649 |
| sp\|O75695\|XRP2_HUMAN Protein XRP2 OS=Homo sapiens GN=RP2 PE=1 SV=4 | 4 | 0.54 | 0.51 | 0.1273 |
| tr\|Q8I5B6\|Q8I5B6_PLAF7 Heat shock protein hslv OS=Plasmodium falciparum (isolate 3D7) GN=HslV PE=4 SV=2 | 4 | 0.54 | 0.59 | 0.1641 |
| tr\|Q8I526\|Q8I526_PLAF7 Cell division protein FtsH, putative OS=Plasmodium falciparum (isolate 3D7) GN=PFL1925w PE=3 SV=1 | 4 | 0.54 | 0.35 | 0.0547 |
| tr\|Q8ID24\|Q8ID24_PLAF7 Mitochondrial import inner membrane translocase, putative OS=Plasmodium falciparum (isolate 3D7) GN=PF13_0358 PE=4 SV=1 | 4 | 0.54 | 0.62 | 0.1781 |
| tr\|Q8I0X2\|Q8I0X2_PLAF7 Acyl-CoA synthetase, PfACS3 OS=Plasmodium falciparum (isolate 3D7) GN=ACS3 PE=4 SV=1;tr\|C0H5N0\|C0H5N0_PLAF7 Acyl-CoA synthetase, PfACS4 OS=Plasmodium falciparum (isolate 3D7) GN=MAL13P1.485 PE=4 SV=1 | 4 | 0.54 | 0.38 | 0.0647 |
| tr\|Q8I2V9\|Q8I2V9_PLAF7 Protein disulfide isomerase OS=Plasmodium falciparum (isolate 3D7) GN=PfPDI-9 PE=4 SV=1 | 4 | 0.55 | 0.37 | 0.0587 |
| tr\|Q8IL75\|Q8IL75_PLAF7 Ubiquinol-cytochrome C reductase iron-sulfur subunit, putative OS=Plasmodium falciparum (isolate 3D7) GN=PF14_0373 PE=4 SV=1 | 4 | 0.55 | 0.37 | 0.0594 |
| tr\|O97246\|O97246_PLAF7 Putative uncharacterized protein OS=Plasmodium falciparum (isolate 3D7) GN=PFC0280c PE=4 SV=1 | 4 | 0.55 | 0.36 | 0.0578 |
| tr\|Q8II53\|Q8II53_PLAF7 Uncharacterized protein OS=Plasmodium falciparum (isolate 3D7) GN=PF11_0321 PE=4 SV=1 | 4 | 0.55 | 0.38 | 0.0617 |

| | | | | |
|---|---|---|---|---|
| tr\|Q8IET3\|Q8IET3_PLAF7 SNARE protein, putative OS=Plasmodium falciparum (isolate 3D7) GN=PfVAMP8 PE=4 SV=1 | 4 | 0.55 | 0.37 | 0.0584 |
| tr\|Q8IDI7\|Q8IDI7_PLAF7 Uncharacterized protein OS=Plasmodium falciparum (isolate 3D7) GN=MAL13P1.258 PE=4 SV=1 | 4 | 0.55 | 0.37 | 0.0575 |
| sp\|Q9TY95\|SERA_PLAF7 Serine-repeat antigen protein OS=Plasmodium falciparum (isolate 3D7) GN=SERA PE=1 SV=1 | 4 | 0.55 | 0.37 | 0.0607 |
| tr\|Q8I3A2\|Q8I3A2_PLAF7 Bacterial histone-like protein OS=Plasmodium falciparum (isolate 3D7) GN=PfHU PE=4 SV=1 | 4 | 0.55 | 0.38 | 0.0610 |
| tr\|C6KSR6\|C6KSR6_PLAF7 Uncharacterized protein OS=Plasmodium falciparum (isolate 3D7) GN=PFF0335c PE=4 SV=1 | 4 | 0.56 | 0.37 | 0.0569 |
| tr\|O97243\|O97243_PLAF7 Putative uncharacterized protein OS=Plasmodium falciparum (isolate 3D7) GN=PFC0265c PE=4 SV=2 | 4 | 0.56 | 0.46 | 0.0940 |
| tr\|O77361\|O77361_PLAF7 Putative uncharacterized protein OS=Plasmodium falciparum (isolate 3D7) GN=PFC0435w PE=4 SV=1 | 4 | 0.56 | 0.37 | 0.0564 |
| sp\|Q8I5G1\|YPF10_PLAF7 Uncharacterized protein PFL1235c OS=Plasmodium falciparum (isolate 3D7) GN=PFL1235c PE=3 SV=1 | 4 | 0.56 | 0.40 | 0.0660 |
| tr\|Q8IEJ6\|Q8IEJ6_PLAF7 Branched-chain alpha keto-acid dehydrogenase, putative OS=Plasmodium falciparum (isolate 3D7) GN=PF13_0070 PE=4 SV=1 | 4 | 0.56 | 0.39 | 0.0623 |
| tr\|Q8IDC4\|Q8IDC4_PLAF7 Preribosomal processosome UTP, putative OS=Plasmodium falciparum (isolate 3D7) GN=PF13_0310 PE=4 SV=1 | 4 | 0.56 | 0.47 | 0.0950 |
| tr\|Q8I3F0\|Q8I3F0_PLAF7 Uncharacterized protein OS=Plasmodium falciparum (isolate 3D7) GN=PFE1605w PE=4 SV=1 | 4 | 0.56 | 0.39 | 0.0624 |
| tr\|Q8ILN5\|Q8ILN5_PLAF7 Mitochondrial protein import protein TIM13, putative OS=Plasmodium falciparum (isolate 3D7) GN=PF14_0208 PE=4 SV=1 | 4 | 0.57 | 0.38 | 0.0579 |
| tr\|Q8I5S7\|Q8I5S7_PLAF7 Choline transporter OS=Plasmodium falciparum (isolate 3D7) GN=PFL0620c PE=4 SV=1 | 4 | 0.57 | 0.38 | 0.0601 |
| tr\|O96252\|O96252_PLAF7 ATP synthase subunit alpha OS=Plasmodium falciparum (isolate 3D7) GN=PFB0795w PE=3 SV=1 | 4 | 0.57 | 0.39 | 0.0598 |
| tr\|Q8IKL7\|Q8IKL7_PLAF7 Splicing factor 3B subunit 2-like protein OS=Plasmodium falciparum (isolate 3D7) GN=PF14_0587 PE=4 SV=1 | 4 | 0.58 | 0.41 | 0.0690 |
| tr\|Q8I0W9\|Q8I0W9_PLAF7 Stearoyl-CoA Delta 9 desaturase, putative OS=Plasmodium falciparum (isolate 3D7) GN=PFE0555w PE=3 SV=1 | 4 | 0.58 | 0.37 | 0.0540 |
| tr\|Q9NFA0\|Q9NFA0_PLAF7 Signal peptidase, putative OS=Plasmodium falciparum (isolate 3D7) GN=PFC0912w PE=4 SV=1 | 4 | 0.58 | 0.39 | 0.0609 |
| tr\|Q8IBL4\|Q8IBL4_PLAF7 Uncharacterized protein OS=Plasmodium falciparum (isolate 3D7) GN=MAL7P1.126 PE=4 SV=1 | 4 | 0.58 | 0.46 | 0.0884 |
| tr\|Q8IEQ3\|Q8IEQ3_PLAF7 Hydrolase, putative OS=Plasmodium falciparum (isolate 3D7) GN=PF13_0032 PE=4 SV=1 | 4 | 0.58 | 0.39 | 0.0581 |
| tr\|Q8IKY5\|Q8IKY5_PLAF7 Appr-1-p processing domain protein OS=Plasmodium falciparum (isolate 3D7) GN=PF14_0466 PE=4 SV=1 | 4 | 0.58 | 0.40 | 0.0622 |
| tr\|Q8IIX5\|Q8IIX5_PLAF7 Uncharacterized protein OS=Plasmodium falciparum (isolate 3D7) GN=PF11_0037 PE=4 SV=1 | 4 | 0.58 | 0.39 | 0.0580 |
| sp\|Q00577\|PURA_HUMAN Transcriptional activator protein Pur-alpha OS=Homo sapiens GN=PURA PE=1 SV=2 | 4 | 0.58 | 0.40 | 0.0622 |
| tr\|Q8IDY3\|Q8IDY3_PLAF7 Uncharacterized protein OS=Plasmodium falciparum (isolate 3D7) GN=PF13_0192 PE=4 SV=1 | 4 | 0.58 | 0.39 | 0.0591 |
| tr\|Q8IIC3\|Q8IIC3_PLAF7 Endoplasmic reticulum oxidoreductin, putative OS=Plasmodium falciparum (isolate 3D7) GN=PF11_0251 PE=4 SV=2 | 4 | 0.58 | 0.39 | 0.0585 |
| tr\|Q8I0V2\|Q8I0V2_PLAF7 ATP synthase subunit beta OS=Plasmodium falciparum (isolate 3D7) GN=PFL1725w PE=3 SV=1 | 4 | 0.59 | 0.39 | 0.0580 |
| tr\|Q8I298\|Q8I298_PLAF7 Putative uncharacterized protein OS=Plasmodium falciparum (isolate 3D7) GN=PFA_0210c PE=4 SV=1 | 4 | 0.59 | 0.39 | 0.0586 |
| tr\|Q8IIV2\|Q8IIV2_PLAF7 Histone H4 OS=Plasmodium falciparum (isolate 3D7) GN=PF11_0061 PE=3 SV=1 | 4 | 0.59 | 0.39 | 0.0575 |
| tr\|Q8I5A9\|Q8I5A9_PLAF7 Rab2, GTPase OS=Plasmodium falciparum (isolate 3D7) GN=Rab2 PE=3 SV=1 | 4 | 0.59 | 0.41 | 0.0654 |
| tr\|Q8I611\|Q8I611_PLAF7 Uncharacterized protein OS=Plasmodium falciparum (isolate 3D7) GN=PFL0170w PE=4 SV=1 | 4 | 0.59 | 0.39 | 0.0549 |
| tr\|Q8I2A1\|Q8I2A1_PLAF7 Putative uncharacterized protein OS=Plasmodium falciparum (isolate 3D7) GN=PFA_0195w PE=4 SV=1 | 4 | 0.59 | 0.39 | 0.0576 |
| tr\|Q8I377\|Q8I377_PLAF7 ATP-dependent heat shock protein, putative OS=Plasmodium falciparum (isolate 3D7) GN=PFI0355c PE=4 SV=1 | 4 | 0.59 | 0.40 | 0.0595 |
| sp\|P62344\|CDPK1_PLAF7 Calcium-dependent protein kinase 1 OS=Plasmodium falciparum (isolate 3D7) GN=CPK1 PE=3 SV=2 | 4 | 0.59 | 0.40 | 0.0611 |
| tr\|Q8IAV1\|Q8IAV1_PLAF7 Uncharacterized protein OS=Plasmodium falciparum (isolate 3D7) GN=PF08_0091 PE=4 SV=1 | 4 | 0.59 | 0.40 | 0.0586 |

| | | | | |
|---|---|---|---|---|
| tr\|Q8IJS2\|Q8IJS2_PLAF7 Uncharacterized protein OS=Plasmodium falciparum (isolate 3D7) GN=PF10_0120 PE=4 SV=1 | 4 | 0.59 | 0.42 | 0.0648 |
| tr\|Q8IKL1\|Q8IKL1_PLAF7 Uncharacterized protein OS=Plasmodium falciparum (isolate 3D7) GN=PF14_0593 PE=4 SV=1 | 4 | 0.60 | 0.40 | 0.0587 |
| tr\|Q8II23\|Q8II23_PLAF7 Protein disulfide isomerase related protein OS=Plasmodium falciparum (isolate 3D7) GN=PF11_0352 PE=4 SV=1 | 4 | 0.60 | 0.39 | 0.0548 |
| tr\|Q5MYR6\|Q5MYR6_PLAF7 1-cys peroxiredoxin OS=Plasmodium falciparum (isolate 3D7) GN=prx PE=1 SV=1 | 4 | 0.60 | 0.41 | 0.0612 |
| tr\|Q8IK07\|Q8IK07_PLAF7 Conserved Plasmodium protein OS=Plasmodium falciparum (isolate 3D7) GN=PF10_0033 PE=4 SV=2 | 4 | 0.60 | 0.40 | 0.0593 |
| tr\|Q8IIK1\|Q8IIK1_PLAF7 Uncharacterized protein OS=Plasmodium falciparum (isolate 3D7) GN=PF11_0172 PE=4 SV=1 | 4 | 0.60 | 0.40 | 0.0596 |
| tr\|Q8IKV8\|Q8IKV8_PLAF7 Sortilin, putative OS=Plasmodium falciparum (isolate 3D7) GN=PF14_0493 PE=4 SV=1 | 4 | 0.60 | 0.39 | 0.0552 |
| tr\|C6KSY4\|C6KSY4_PLAF7 Organic anion transporter OS=Plasmodium falciparum (isolate 3D7) GN=PFF0690c PE=4 SV=1 | 4 | 0.60 | 0.42 | 0.0645 |
| tr\|Q8IKS4\|Q8IKS4_PLAF7 Hemolysin, putative OS=Plasmodium falciparum (isolate 3D7) GN=PF14_0528 PE=4 SV=2 | 4 | 0.60 | 0.42 | 0.0640 |
| tr\|O96217\|O96217_PLAF7 Conserved Plasmodium protein OS=Plasmodium falciparum (isolate 3D7) GN=PFB0620w PE=4 SV=1 | 4 | 0.60 | 0.38 | 0.0510 |
| tr\|Q8IKG8\|Q8IKG8_PLAF7 Rhoptry protein, putative OS=Plasmodium falciparum (isolate 3D7) GN=PF14_0637 PE=4 SV=2 | 4 | 0.60 | 0.41 | 0.0597 |
| tr\|Q8IE43\|Q8IE43_PLAF7 Uncharacterized protein OS=Plasmodium falciparum (isolate 3D7) GN=PF13_0154 PE=4 SV=1 | 4 | 0.60 | 0.41 | 0.0590 |
| tr\|O97245\|O97245_PLAF7 Glycerol-3-phosphate dehydrogenase OS=Plasmodium falciparum (isolate 3D7) GN=PFC0275w PE=3 SV=1 | 4 | 0.61 | 0.41 | 0.0598 |
| tr\|Q8IL96\|Q8IL96_PLAF7 N-acetyltransferase, putative OS=Plasmodium falciparum (isolate 3D7) GN=PF14_0350 PE=4 SV=2 | 4 | 0.61 | 0.39 | 0.0530 |
| tr\|Q8IJF2\|Q8IJF2_PLAF7 Conserved Plasmodium protein OS=Plasmodium falciparum (isolate 3D7) GN=PF10_0246 PE=4 SV=2 | 4 | 0.61 | 0.41 | 0.0585 |
| sp\|Q08210\|PYRD_PLAF7 Dihydroorotate dehydrogenase (quinone), mitochondrial OS=Plasmodium falciparum (isolate 3D7) GN=PFF0160c PE=1 SV=1 | 4 | 0.61 | 0.43 | 0.0677 |
| tr\|Q8IB72\|Q8IB72_PLAF7 DNAJ protein, putative OS=Plasmodium falciparum (isolate 3D7) GN=PF08_0032 PE=4 SV=1 | 4 | 0.61 | 0.41 | 0.0585 |
| tr\|C0H5H0\|C0H5H0_PLAF7 Heat shock protein 70 (Hsp70), putative OS=Plasmodium falciparum (isolate 3D7) GN=MAL13P1.540 PE=3 SV=1 | 4 | 0.61 | 0.41 | 0.0586 |
| tr\|Q8IC43\|Q8IC43_PLAF7 Uncharacterized protein OS=Plasmodium falciparum (isolate 3D7) GN=PF07_0007 PE=4 SV=1 | 4 | 1.08 | 0.38 | 0.0112 |
| tr\|Q8IKN7\|Q8IKN7_PLAF7 Uncharacterized protein OS=Plasmodium falciparum (isolate 3D7) GN=PF14_0567 PE=4 SV=1 | 4 | 0.61 | 0.40 | 0.0547 |
| tr\|Q8I546\|Q8I546_PLAF7 Conserved Plasmodium membrane protein OS=Plasmodium falciparum (isolate 3D7) GN=PFL1825w PE=4 SV=1 | 4 | 0.61 | 0.40 | 0.0534 |
| sp\|Q8ILT5\|SEY1_PLAF7 Protein SEY1 homolog OS=Plasmodium falciparum (isolate 3D7) GN=PF14_0159 PE=3 SV=2 | 4 | 0.61 | 0.41 | 0.0578 |
| tr\|C0H564\|C0H564_PLAF7 Monocarboxylate transporter, putative OS=Plasmodium falciparum (isolate 3D7) GN=PFI1295c PE=4 SV=1 | 4 | 0.62 | 0.41 | 0.0584 |
| tr\|Q8IJW2\|Q8IJW2_PLAF7 Uncharacterized protein OS=Plasmodium falciparum (isolate 3D7) GN=PF10_0079 PE=4 SV=1 | 4 | 1.09 | 0.42 | 0.0139 |
| tr\|Q8ILY8\|Q8ILY8_PLAF7 Uncharacterized protein OS=Plasmodium falciparum (isolate 3D7) GN=PF14_0105 PE=4 SV=1 | 4 | 0.62 | 0.42 | 0.0598 |
| tr\|Q8IET1\|Q8IET1_PLAF7 Uncharacterized protein OS=Plasmodium falciparum (isolate 3D7) GN=PF13_0018 PE=4 SV=1 | 4 | 0.62 | 0.44 | 0.0682 |
| tr\|Q8IK82\|Q8IK82_PLAF7 Bromodomain protein, putative OS=Plasmodium falciparum (isolate 3D7) GN=PF14_0724 PE=1 SV=1 | 4 | 0.62 | 0.43 | 0.0638 |
| tr\|Q8ILL1\|Q8ILL1_PLAF7 Uncharacterized protein OS=Plasmodium falciparum (isolate 3D7) GN=PF14_0232 PE=4 SV=1 | 4 | 0.62 | 0.42 | 0.0602 |
| tr\|Q8I202\|Q8I202_PLAF7 Uncharacterized protein OS=Plasmodium falciparum (isolate 3D7) GN=PFD0115c PE=4 SV=1 | 4 | 0.62 | 0.50 | 0.0900 |
| tr\|Q8ILU2\|Q8ILU2_PLAF7 Uncharacterized protein OS=Plasmodium falciparum (isolate 3D7) GN=PF14_0152 PE=4 SV=1 | 4 | 0.62 | 0.43 | 0.0625 |
| tr\|Q8II85\|Q8II85_PLAF7 Uncharacterized protein OS=Plasmodium falciparum (isolate 3D7) GN=PF11_0289 PE=4 SV=1 | 4 | 0.62 | 0.62 | 0.1381 |
| tr\|Q8IDW0\|Q8IDW0_PLAF7 1-deoxy-D-xylulose 5-phosphate synthase OS=Plasmodium falciparum (isolate 3D7) GN=MAL13P1.186 PE=4 SV=1 | 4 | 0.62 | 0.41 | 0.0567 |
| tr\|C0H4P4\|C0H4P4_PLAF7 Uncharacterized protein OS=Plasmodium falciparum (isolate 3D7) GN=MAL7P1.146 PE=4 SV=1 | 4 | 0.62 | 0.59 | 0.1245 |

| | | | | |
|---|---|---|---|---|
| tr\|Q8IDN6\|Q8IDN6_PLAF7 Sec61 alpha subunit, PfSec61 OS=Plasmodium falciparum (isolate 3D7) GN=Sec61 PE=3 SV=1 | 4 | 0.62 | 0.42 | 0.0591 |
| tr\|C6KST1\|C6KST1_PLAF7 Uncharacterized protein OS=Plasmodium falciparum (isolate 3D7) GN=PFF0410w PE=4 SV=1 | 4 | 0.62 | 0.42 | 0.0599 |
| tr\|Q8ILZ1\|Q8ILZ1_PLAF7 Rhoptry-associated protein 1, RAP1 OS=Plasmodium falciparum (isolate 3D7) GN=PF14_0102 PE=4 SV=1 | 4 | 0.62 | 0.40 | 0.0539 |
| sp\|Q8I6U8\|GBP_PLAF7 Glycophorin-binding protein OS=Plasmodium falciparum (isolate 3D7) GN=GBP PE=3 SV=1 | 4 | 0.62 | 0.42 | 0.0590 |
| tr\|Q7KQM5\|Q7KQM5_PLAF7 Early transcribed membrane protein 14.1, etramp14.1 OS=Plasmodium falciparum (isolate 3D7) GN=etramp14.1 PE=4 SV=1 | 4 | 0.63 | 0.42 | 0.0588 |
| tr\|Q8IBV7\|Q8IBV7_PLAF7 Histone H2B OS=Plasmodium falciparum (isolate 3D7) GN=PF07_0054 PE=3 SV=1 | 4 | 0.63 | 0.42 | 0.0565 |
| tr\|Q8IE73\|Q8IE73_PLAF7 MSF1-like protein, putative OS=Plasmodium falciparum (isolate 3D7) GN=PF13_0138 PE=4 SV=1 | 4 | 0.63 | 0.40 | 0.0520 |
| tr\|Q8IAL4\|Q8IAL4_PLAF7 Uncharacterized protein OS=Plasmodium falciparum (isolate 3D7) GN=PF08_0134 PE=4 SV=1 | 4 | 0.63 | 0.43 | 0.0617 |
| tr\|Q8I415\|Q8I415_PLAF7 Single-strand binding protein, putative OS=Plasmodium falciparum (isolate 3D7) GN=PFE0435c PE=1 SV=1 | 4 | 0.63 | 0.42 | 0.0588 |
| tr\|Q8IEG8\|Q8IEG8_PLAF7 Uncharacterized protein OS=Plasmodium falciparum (isolate 3D7) GN=MAL13P1.75 PE=4 SV=1 | 4 | 0.63 | 0.42 | 0.0585 |
| tr\|Q6ZMA7\|Q6ZMA7_PLAF7 Sexual stage-specific protein OS=Plasmodium falciparum (isolate 3D7) GN=PFD0310w PE=4 SV=1 | 4 | 0.63 | 0.40 | 0.0506 |
| tr\|C6KT67\|C6KT67_PLAF7 Coronin binding protein OS=Plasmodium falciparum (isolate 3D7) GN=PFF1110c PE=4 SV=1 | 4 | 0.64 | 0.44 | 0.0623 |
| tr\|Q8I0W7\|Q8I0W7_PLAF7 Snrnp protein, putative OS=Plasmodium falciparum (isolate 3D7) GN=PFE0925c PE=3 SV=1 | 4 | 0.64 | 0.41 | 0.0533 |
| sp\|O97239\|DOP1_PLAF7 Protein dopey homolog PFC0245c OS=Plasmodium falciparum (isolate 3D7) GN=PFC0245c PE=2 SV=1 | 4 | 0.64 | 0.43 | 0.0596 |
| tr\|O97323\|O97323_PLAF7 SNARE protein OS=Plasmodium falciparum (isolate 3D7) GN=PfSec22 PE=4 SV=2 | 4 | 0.64 | 0.44 | 0.0640 |
| tr\|Q8I255\|Q8I255_PLAF7 Putative uncharacterized protein OS=Plasmodium falciparum (isolate 3D7) GN=PFA_0430c PE=4 SV=1 | 4 | 0.64 | 0.43 | 0.0576 |
| tr\|Q8IHZ6\|Q8IHZ6_PLAF7 DNAJ protein, putative OS=Plasmodium falciparum (isolate 3D7) GN=PF11_0380 PE=4 SV=2 | 4 | 0.64 | 0.43 | 0.0589 |
| tr\|Q8IJG6\|Q8IJG6_PLAF7 Uncharacterized protein OS=Plasmodium falciparum (isolate 3D7) GN=PF10_0232 PE=4 SV=1 | 4 | 0.64 | 0.43 | 0.0581 |
| tr\|Q8IKZ6\|Q8IKZ6_PLAF7 Multidrug resistance protein 2 (Heavy metal transport family) OS=Plasmodium falciparum (isolate 3D7) GN=PfMDR2 PE=3 SV=1 | 4 | 0.64 | 0.42 | 0.0566 |
| tr\|Q8IDB8\|Q8IDB8_PLAF7 Uncharacterized protein OS=Plasmodium falciparum (isolate 3D7) GN=MAL13P1.288 PE=4 SV=1 | 4 | 0.64 | 0.43 | 0.0586 |
| tr\|Q8I1T1\|Q8I1T1_PLAF7 Adenylate kinase 1 OS=Plasmodium falciparum (isolate 3D7) GN=GAK PE=3 SV=1 | 4 | 0.64 | 0.43 | 0.0597 |
| tr\|Q8II11\|Q8II11_PLAF7 Conserved Plasmodium protein OS=Plasmodium falciparum (isolate 3D7) GN=PF11_0364 PE=4 SV=1 | 4 | 0.64 | 0.44 | 0.0600 |
| tr\|Q8I472\|Q8I472_PLAF7 Zinc binding protein, putative OS=Plasmodium falciparum (isolate 3D7) GN=PFE0140c PE=4 SV=1 | 4 | 0.64 | 0.54 | 0.0959 |
| tr\|Q8ILB6\|Q8ILB6_PLAF7 Uncharacterized protein OS=Plasmodium falciparum (isolate 3D7) GN=PF14_0329 PE=4 SV=1 | 4 | 0.64 | 0.42 | 0.0543 |
| tr\|Q8I5Q6\|Q8I5Q6_PLAF7 Thioredoxin peroxidase OS=Plasmodium falciparum (isolate 3D7) GN=PFL0725w PE=1 SV=1 | 4 | 0.64 | 0.43 | 0.0587 |
| tr\|Q8IBH9\|Q8IBH9_PLAF7 Cation transporting ATPase, cation transporter OS=Plasmodium falciparum (isolate 3D7) GN=PF07_0115 PE=3 SV=1 | 4 | 0.65 | 0.43 | 0.0586 |
| tr\|C6KT71\|C6KT71_PLAF7 Superoxide dismutase OS=Plasmodium falciparum (isolate 3D7) GN=PfSOD2 PE=4 SV=1 | 4 | 0.65 | 0.43 | 0.0575 |
| tr\|Q8I517\|Q8I517_PLAF7 Uncharacterized protein OS=Plasmodium falciparum (isolate 3D7) GN=PFL1980c PE=4 SV=1 | 4 | 0.65 | 0.41 | 0.0528 |
| tr\|Q8I450\|Q8I450_PLAF7 Actin-like protein, putative OS=Plasmodium falciparum (isolate 3D7) GN=PFE0255w PE=3 SV=1 | 4 | 0.65 | 0.43 | 0.0579 |
| tr\|C0H4G7\|C0H4G7_PLAF7 Uncharacterized protein OS=Plasmodium falciparum (isolate 3D7) GN=PFE1465w PE=4 SV=1 | 4 | 0.65 | 0.45 | 0.0621 |
| tr\|C0H4W6\|C0H4W6_PLAF7 Sec61 beta subunit, putative OS=Plasmodium falciparum (isolate 3D7) GN=MAL8P1.51 PE=4 SV=1 | 4 | 0.65 | 0.44 | 0.0607 |
| sp\|C0H4W3\|HEPF1_PLAF7 Probable ATP-dependent helicase PF08_0048 OS=Plasmodium falciparum (isolate 3D7) GN=PF08_0048 PE=3 SV=1 | 4 | 0.65 | 0.44 | 0.0586 |
| sp\|O77384\|LRR4_PLAF7 Protein PFC0760c OS=Plasmodium falciparum (isolate 3D7) GN=PFC0760c PE=4 SV=1 | 4 | 0.65 | 0.45 | 0.0615 |

| | | | | |
|---|---|---|---|---|
| tr\|Q8I3Q6\|Q8I3Q6_PLAF7 Uncharacterized protein OS=Plasmodium falciparum (isolate 3D7) GN=PFE1025c PE=4 SV=1 | 4 | 0.65 | 0.44 | 0.0611 |
| tr\|Q8IBU1\|Q8IBU1_PLAF7 Zinc transporter, putative OS=Plasmodium falciparum (isolate 3D7) GN=PF07_0065 PE=4 SV=1 | 4 | 0.65 | 0.44 | 0.0610 |
| tr\|C6KST7\|C6KST7_PLAF7 Uncharacterized protein OS=Plasmodium falciparum (isolate 3D7) GN=PFF0445w PE=4 SV=1 | 4 | 0.65 | 0.44 | 0.0593 |
| tr\|C6KTB8\|C6KTB8_PLAF7 Protein kinase PK4 OS=Plasmodium falciparum (isolate 3D7) GN=PfPK4 PE=4 SV=1 | 4 | 0.65 | 0.44 | 0.0607 |
| tr\|Q8IL32\|Q8IL32_PLAF7 HSP90 OS=Plasmodium falciparum (isolate 3D7) GN=PF14_0417 PE=1 SV=1 | 4 | 0.65 | 0.44 | 0.0577 |
| tr\|Q8I3N0\|Q8I3N0_PLAF7 DNAJ protein, putative OS=Plasmodium falciparum (isolate 3D7) GN=PFE1170w PE=4 SV=1 | 4 | 0.65 | 0.44 | 0.0584 |
| tr\|Q8I665\|Q8I665_PLAF7 Conserved Plasmodium protein OS=Plasmodium falciparum (isolate 3D7) GN=PFB0194w PE=4 SV=1 | 4 | 0.66 | 0.44 | 0.0573 |
| tr\|Q8IAZ1\|Q8IAZ1_PLAF7 Uncharacterized protein OS=Plasmodium falciparum (isolate 3D7) GN=MAL8P1.85 PE=4 SV=1 | 4 | 0.66 | 0.43 | 0.0554 |
| tr\|O97336\|O97336_PLAF7 Putative uncharacterized protein OS=Plasmodium falciparum (isolate 3D7) GN=PFC0085c PE=4 SV=2 | 4 | 0.66 | 0.44 | 0.0577 |
| tr\|Q9U0N4\|Q9U0N4_PLAF7 ABC transporter, (CT family), putative OS=Plasmodium falciparum (isolate 3D7) GN=PfMRP PE=3 SV=1 | 4 | 0.66 | 0.42 | 0.0535 |
| tr\|Q8I305\|Q8I305_PLAF7 Transporter, putative OS=Plasmodium falciparum (isolate 3D7) GN=PFI0720w PE=4 SV=1 | 4 | 0.66 | 0.43 | 0.0549 |
| sp\|O94919\|ENDD1_HUMAN Endonuclease domain-containing 1 protein OS=Homo sapiens GN=ENDOD1 PE=1 SV=2 | 4 | 0.66 | 0.45 | 0.0622 |
| tr\|Q8I2A8\|Q8I2A8_PLAF7 Nucleoside transporter, putative OS=Plasmodium falciparum (isolate 3D7) GN=PFA_0160c PE=4 SV=1 | 4 | 0.66 | 0.43 | 0.0556 |
| tr\|Q8I6Z1\|Q8I6Z1_PLAF7 Acyl-coA synthetase, PfACS5 OS=Plasmodium falciparum (isolate 3D7) GN=PfACS5 PE=4 SV=1 | 4 | 0.66 | 0.44 | 0.0565 |
| tr\|Q8I2I2\|Q8I2I2_PLAF7 Organelle processing peptidase, putative OS=Plasmodium falciparum (isolate 3D7) GN=PFI1625c PE=3 SV=1 | 4 | 0.66 | 0.45 | 0.0595 |
| tr\|Q8IKM7\|Q8IKM7_PLAF7 Uncharacterized protein OS=Plasmodium falciparum (isolate 3D7) GN=PF14_0577 PE=4 SV=1 | 4 | 0.66 | 0.44 | 0.0588 |
| sp\|P46468\|CDAT_PLAF7 Putative cell division cycle ATPase OS=Plasmodium falciparum (isolate 3D7) GN=PF07_0047 PE=3 SV=2 | 4 | 0.66 | 0.44 | 0.0582 |
| tr\|Q8IJ37\|Q8IJ37_PLAF7 Pyruvate kinase OS=Plasmodium falciparum (isolate 3D7) GN=PF10_0363 PE=3 SV=1 | 4 | 0.66 | 0.42 | 0.0526 |
| tr\|Q8I5E9\|Q8I5E9_PLAF7 Uncharacterized protein OS=Plasmodium falciparum (isolate 3D7) GN=PFL1300c PE=4 SV=1 | 4 | 0.66 | 0.44 | 0.0579 |
| tr\|Q7KQL1\|Q7KQL1_PLAF7 Myb2 protein OS=Plasmodium falciparum (isolate 3D7) GN=PF10_0327 PE=4 SV=1 | 4 | 0.66 | 0.45 | 0.0591 |
| tr\|Q8I5I0\|Q8I5I0_PLAF7 Uncharacterized protein OS=Plasmodium falciparum (isolate 3D7) GN=PFL1140w PE=4 SV=1 | 4 | 0.66 | 0.45 | 0.0602 |
| tr\|Q8I5C6\|Q8I5C6_PLAF7 Uncharacterized protein OS=Plasmodium falciparum (isolate 3D7) GN=PFL1415w PE=4 SV=1 | 4 | 0.66 | 0.70 | 0.1558 |
| tr\|Q8I3T4\|Q8I3T4_PLAF7 Transcriptional regulator, putative OS=Plasmodium falciparum (isolate 3D7) GN=PFE0870w PE=4 SV=1 | 4 | 0.66 | 0.44 | 0.0583 |
| tr\|Q8IDI2\|Q8IDI2_PLAF7 Uncharacterized protein OS=Plasmodium falciparum (isolate 3D7) GN=PF13_0270 PE=4 SV=1 | 4 | 0.66 | 0.80 | 0.1965 |
| tr\|Q76NM7\|Q76NM7_PLAF7 Rab5b, GTPase OS=Plasmodium falciparum (isolate 3D7) GN=Rab5b PE=3 SV=1 | 4 | 0.67 | 0.45 | 0.0586 |
| tr\|Q8IL86\|Q8IL86_PLAF7 Sec62, putative OS=Plasmodium falciparum (isolate 3D7) GN=PF14_0361 PE=4 SV=2 | 4 | 0.67 | 0.44 | 0.0577 |
| tr\|O77389\|O77389_PLAF7 Formate-nitrate transporter, putative OS=Plasmodium falciparum (isolate 3D7) GN=PFC0725c PE=4 SV=2 | 4 | 0.67 | 0.43 | 0.0544 |
| tr\|O77376\|O77376_PLAF7 Band 7-related protein OS=Plasmodium falciparum (isolate 3D7) GN=PFC0800w PE=4 SV=1 | 4 | 0.67 | 0.45 | 0.0595 |
| sp\|Q6LFN2\|ZNRF1_PLAF7 RING finger protein PFF0165c OS=Plasmodium falciparum (isolate 3D7) GN=PFF0165c PE=2 SV=1 | 4 | 0.67 | 0.45 | 0.0588 |
| tr\|Q8IIH7\|Q8IIH7_PLAF7 Uncharacterized protein OS=Plasmodium falciparum (isolate 3D7) GN=PF11_0197 PE=4 SV=1 | 4 | 0.67 | 0.45 | 0.0580 |
| tr\|Q8IE22\|Q8IE22_PLAF7 ER lumen protein retaining receptor 1, putative OS=Plasmodium falciparum (isolate 3D7) GN=MAL13P1.163 PE=4 SV=1 | 4 | 0.67 | 0.45 | 0.0584 |
| tr\|Q8IJR2\|Q8IJR2_PLAF7 Uncharacterized protein OS=Plasmodium falciparum (isolate 3D7) GN=PF10_0130 PE=4 SV=1 | 4 | 0.67 | 0.45 | 0.0585 |
| tr\|Q8ILD4\|Q8ILD4_PLAF7 Uncharacterized protein OS=Plasmodium falciparum (isolate 3D7) GN=PF14_0310 PE=4 SV=1 | 4 | 0.67 | 0.45 | 0.0585 |

| | | | | |
|---|---|---|---|---|
| tr\|Q8IKZ7\|Q8IKZ7_PLAF7 Uncharacterized protein OS=Plasmodium falciparum (isolate 3D7) GN=PF14_0454 PE=4 SV=1 | 4 | 0.67 | 0.57 | 0.1012 |
| tr\|Q8IK92\|Q8IK92_PLAF7 Uncharacterized protein OS=Plasmodium falciparum (isolate 3D7) GN=PF14_0714 PE=4 SV=1 | 4 | 0.67 | 0.45 | 0.0586 |
| tr\|Q8II35\|Q8II35_PLAF7 Uncharacterized protein OS=Plasmodium falciparum (isolate 3D7) GN=PF11_0339 PE=4 SV=1 | 4 | 0.67 | 0.46 | 0.0611 |
| tr\|Q9U0H0\|Q9U0H0_PLAF7 Uncharacterized protein OS=Plasmodium falciparum (isolate 3D7) GN=PFD0595w PE=4 SV=1 | 4 | 0.67 | 0.49 | 0.0696 |
| tr\|Q8I5W2\|Q8I5W2_PLAF7 Tim10 homologue, putative OS=Plasmodium falciparum (isolate 3D7) GN=PFL0430w PE=4 SV=1 | 4 | 0.67 | 0.47 | 0.0655 |
| tr\|Q8IAK9\|Q8IAK9_PLAF7 Uncharacterized protein OS=Plasmodium falciparum (isolate 3D7) GN=PF08_0137 PE=4 SV=1 | 4 | 0.67 | 0.43 | 0.0520 |
| tr\|Q8IDZ5\|Q8IDZ5_PLAF7 Transmembrane protein Tmp21 homologue, putative OS=Plasmodium falciparum (isolate 3D7) GN=MAL13P1.171 PE=4 SV=1 | 4 | 0.67 | 0.45 | 0.0584 |
| tr\|C0H4K1\|C0H4K1_PLAF7 Centrin, putative OS=Plasmodium falciparum (isolate 3D7) GN=MAL7P1.10 PE=4 SV=1 | 4 | 0.68 | 0.46 | 0.0605 |
| tr\|Q8IB31\|Q8IB31_PLAF7 Uncharacterized protein OS=Plasmodium falciparum (isolate 3D7) GN=MAL8P1.62 PE=4 SV=1 | 4 | 0.68 | 0.45 | 0.0585 |
| sp\|P17066\|HSP76_HUMAN Heat shock 70 kDa protein 6 OS=Homo sapiens GN=HSPA6 PE=1 SV=2;sp\|P48741\|HSP77_HUMAN Putative heat shock 70 kDa protein 7 OS=Homo sapiens GN=HSPA7 PE=5 SV=2 | 4 | 0.68 | 0.46 | 0.0603 |
| tr\|C6KT04\|C6KT04_PLAF7 Uncharacterized protein OS=Plasmodium falciparum (isolate 3D7) GN=PFF0790c PE=4 SV=1 | 4 | 0.68 | 0.45 | 0.0578 |
| sp\|Q9UJC5\|SH3L2_HUMAN SH3 domain-binding glutamic acid-rich-like protein 2 OS=Homo sapiens GN=SH3BGRL2 PE=1 SV=2 | 4 | 0.68 | 0.49 | 0.0696 |
| tr\|Q8I476\|Q8I476_PLAF7 Merozoite Surface Protein 8, MSP8 OS=Plasmodium falciparum (isolate 3D7) GN=MSP8 PE=4 SV=1 | 4 | 0.68 | 0.45 | 0.0569 |
| tr\|C0H4Q1\|C0H4Q1_PLAF7 Uncharacterized protein OS=Plasmodium falciparum (isolate 3D7) GN=PF07_0120 PE=4 SV=1 | 4 | 0.68 | 0.46 | 0.0597 |
| tr\|Q8IIW1\|Q8IIW1_PLAF7 Qa-SNARE protein, putative OS=Plasmodium falciparum (isolate 3D7) GN=Syn13 PE=4 SV=2 | 4 | 0.68 | 0.45 | 0.0556 |
| tr\|Q8I510\|Q8I510_PLAF7 Uncharacterized protein OS=Plasmodium falciparum (isolate 3D7) GN=PFL2015w PE=4 SV=1 | 4 | 0.68 | 0.46 | 0.0588 |
| tr\|Q8IAQ8\|Q8IAQ8_PLAF7 Vacuolar proton translocating ATPase subunit A, putative OS=Plasmodium falciparum (isolate 3D7) GN=PF08_0113 PE=4 SV=1 | 4 | 0.68 | 0.45 | 0.0579 |
| tr\|Q8IE52\|Q8IE52_PLAF7 Chromatin assembly factor 1 subunit, putative OS=Plasmodium falciparum (isolate 3D7) GN=PF13_0149 PE=4 SV=1 | 4 | 0.68 | 0.45 | 0.0573 |
| tr\|X6R4N5\|X6R4N5_HUMAN Erythroid membrane-associated protein OS=Homo sapiens GN=ERMAP PE=1 SV=1;sp\|Q96PL5\|ERMAP_HUMAN Erythroid membrane-associated protein OS=Homo sapiens GN=ERMAP PE=1 SV=1 | 4 | 0.68 | 0.44 | 0.0533 |
| tr\|Q8I468\|Q8I468_PLAF7 Ser/Arg-rich splicing factor, putative OS=Plasmodium falciparum (isolate 3D7) GN=PFE0160c PE=4 SV=1 | 4 | 0.68 | 0.46 | 0.0580 |
| tr\|Q8I3R2\|Q8I3R2_PLAF7 Uncharacterized protein OS=Plasmodium falciparum (isolate 3D7) GN=PFE0995c PE=4 SV=1 | 4 | 0.68 | 0.46 | 0.0579 |
| tr\|Q8IEL0\|Q8IEL0_PLAF7 Uncharacterized protein OS=Plasmodium falciparum (isolate 3D7) GN=MAL13P1.50 PE=4 SV=1 | 4 | 0.68 | 0.46 | 0.0579 |
| tr\|Q8I5S4\|Q8I5S4_PLAF7 Bromodomain protein, putative OS=Plasmodium falciparum (isolate 3D7) GN=PFL0635c PE=4 SV=1 | 4 | 0.68 | 0.46 | 0.0603 |
| tr\|Q8I291\|Q8I291_PLAF7 Transporter, putative OS=Plasmodium falciparum (isolate 3D7) GN=PFA_0245w PE=4 SV=1 | 4 | 0.68 | 0.47 | 0.0633 |
| sp\|P06753-6\|TPM3_HUMAN Isoform 6 of Tropomyosin alpha-3 chain OS=Homo sapiens GN=TPM3;sp\|P06753\|TPM3_HUMAN Tropomyosin alpha-3 chain OS=Homo sapiens GN=TPM3 PE=1 SV=2 | 4 | 0.68 | 0.46 | 0.0593 |
| tr\|Q8IJ28\|Q8IJ28_PLAF7 Antigen UB05 OS=Plasmodium falciparum (isolate 3D7) GN=PF10_0372 PE=4 SV=2 | 4 | 0.68 | 0.46 | 0.0589 |
| tr\|O96205\|O96205_PLAF7 Conserved Plasmodium protein OS=Plasmodium falciparum (isolate 3D7) GN=PFB0560w PE=4 SV=2 | 4 | 0.68 | 0.46 | 0.0575 |
| tr\|Q8IL08\|Q8IL08_PLAF7 Uncharacterized protein OS=Plasmodium falciparum (isolate 3D7) GN=PF14_0442 PE=4 SV=1 | 4 | 0.68 | 0.46 | 0.0579 |
| tr\|Q8I6S5\|Q8I6S5_PLAF7 2-oxoglutarate dehydrogenase E1 component OS=Plasmodium falciparum (isolate 3D7) GN=PF08_0045 PE=4 SV=1 | 4 | 0.68 | 0.47 | 0.0625 |
| sp\|Q08211\|DHX9_HUMAN ATP-dependent RNA helicase A OS=Homo sapiens GN=DHX9 PE=1 SV=4 | 4 | 0.69 | 0.45 | 0.0565 |
| tr\|Q8I5Q3\|Q8I5Q3_PLAF7 10 kd chaperonin OS=Plasmodium falciparum (isolate 3D7) GN=Cpn10 PE=3 SV=2 | 4 | 0.69 | 0.46 | 0.0577 |

| | | | | |
|---|---|---|---|---|
| tr\|Q8I5K4\|Q8I5K4_PLAF7 Chromodomain protein OS=Plasmodium falciparum (isolate 3D7) GN=PFL1005c PE=4 SV=1 | 4 | 0.69 | 0.44 | 0.0511 |
| tr\|Q9U0N1\|Q9U0N1_PLAF7 Glutamic acid-rich protein (Garp) OS=Plasmodium falciparum (isolate 3D7) GN=PFA_0620c PE=4 SV=1 | 4 | 0.69 | 0.46 | 0.0586 |
| tr\|Q8I289\|Q8I289_PLAF7 Putative uncharacterized protein OS=Plasmodium falciparum (isolate 3D7) GN=PFA_0255c PE=4 SV=1 | 4 | 0.69 | 0.46 | 0.0580 |
| tr\|C0H4M7\|C0H4M7_PLAF7 Uncharacterized protein OS=Plasmodium falciparum (isolate 3D7) GN=MAL7P1.67 PE=4 SV=1 | 4 | 0.69 | 0.45 | 0.0543 |
| tr\|Q8IIU7\|Q8IIU7_PLAF7 Conserved Plasmodium protein OS=Plasmodium falciparum (isolate 3D7) GN=PF11_0067 PE=4 SV=2 | 4 | 1.11 | 0.19 | 0.0014 |
| tr\|Q8IJY4\|Q8IJY4_PLAF7 Regulator of nonsense transcripts, putative OS=Plasmodium falciparum (isolate 3D7) GN=PF10_0057 PE=4 SV=1 | 4 | 0.69 | 0.46 | 0.0581 |
| tr\|Q8IBY8\|Q8IBY8_PLAF7 Uncharacterized protein OS=Plasmodium falciparum (isolate 3D7) GN=PF07_0042 PE=4 SV=1 | 4 | 0.69 | 0.46 | 0.0581 |
| tr\|Q8IJN3\|Q8IJN3_PLAF7 Serine/Threonine protein kinase, FIKK family OS=Plasmodium falciparum (isolate 3D7) GN=FIKK-10.1 PE=4 SV=2 | 4 | 0.69 | 0.47 | 0.0593 |
| tr\|C6KT82\|C6KT82_PLAF7 Smarca-related protein OS=Plasmodium falciparum (isolate 3D7) GN=PFF1185w PE=4 SV=1 | 4 | 0.69 | 0.46 | 0.0572 |
| tr\|Q8III6\|Q8III6_PLAF7 Heat shock protein 90, putative OS=Plasmodium falciparum (isolate 3D7) GN=PF11_0188 PE=3 SV=1 | 4 | 0.69 | 0.46 | 0.0576 |
| tr\|Q8IAX8\|Q8IAX8_PLAF7 DNA/RNA-binding protein Alba, putative OS=Plasmodium falciparum (isolate 3D7) GN=PF08_0074 PE=4 SV=1 | 4 | 1.12 | 0.16 | 0.0009 |
| tr\|C6KT90\|C6KT90_PLAF7 Uncharacterized protein OS=Plasmodium falciparum (isolate 3D7) GN=PFF1230c PE=4 SV=1 | 4 | 0.70 | 0.53 | 0.0774 |
| tr\|Q8I333\|Q8I333_PLAF7 Falstatin, putative OS=Plasmodium falciparum (isolate 3D7) GN=PFI0580c PE=4 SV=1 | 4 | 0.70 | 0.48 | 0.0608 |
| tr\|Q8IBA2\|Q8IBA2_PLAF7 RNA helicase, putative OS=Plasmodium falciparum (isolate 3D7) GN=MAL8P1.19 PE=3 SV=1 | 4 | 0.70 | 0.56 | 0.0881 |
| tr\|Q8IJF4\|Q8IJF4_PLAF7 Formin 2, putative OS=Plasmodium falciparum (isolate 3D7) GN=PF10_0244 PE=4 SV=2 | 4 | 0.70 | 0.47 | 0.0588 |
| tr\|C0H4Z7\|C0H4Z7_PLAF7 Uncharacterized protein OS=Plasmodium falciparum (isolate 3D7) GN=MAL8P1.206 PE=4 SV=1 | 4 | 0.70 | 0.47 | 0.0590 |
| tr\|A0A087X0C8\|A0A087X0C8_HUMAN Calpain-5 OS=Homo sapiens GN=CAPN5 PE=1 SV=1;tr\|E7EV01\|E7EV01_HUMAN Calpain-5 OS=Homo sapiens GN=CAPN5 PE=1 SV=2;sp\|O15484\|CAN5_HUMAN Calpain-5 OS=Homo sapiens GN=CAPN5 PE=1 SV=2 | 4 | 0.70 | 0.45 | 0.0526 |
| tr\|Q8IKR4\|Q8IKR4_PLAF7 Uncharacterized protein OS=Plasmodium falciparum (isolate 3D7) GN=PF14_0538 PE=4 SV=1 | 4 | 0.70 | 0.49 | 0.0636 |
| tr\|Q8IL28\|Q8IL28_PLAF7 Apicoplast 1-acyl-sn-glycerol-3-phosphate acyltransferase, putative OS=Plasmodium falciparum (isolate 3D7) GN=PF14_0421 PE=4 SV=2 | 4 | 0.70 | 0.46 | 0.0564 |
| tr\|Q8IJ69\|Q8IJ69_PLAF7 Sec1 family protein, putative OS=Plasmodium falciparum (isolate 3D7) GN=PF10_0331 PE=4 SV=2 | 4 | 0.70 | 0.46 | 0.0563 |
| tr\|Q8IJL2\|Q8IJL2_PLAF7 Uncharacterized protein OS=Plasmodium falciparum (isolate 3D7) GN=PF10_0183 PE=4 SV=1 | 4 | 1.13 | 0.67 | 0.0436 |
| tr\|Q8IE81\|Q8IE81_PLAF7 Uncharacterized protein OS=Plasmodium falciparum (isolate 3D7) GN=PF13_0134 PE=4 SV=1 | 4 | 0.70 | 0.47 | 0.0586 |
| tr\|Q8IKB6\|Q8IKB6_PLAF7 Histone deacetylase, putative OS=Plasmodium falciparum (isolate 3D7) GN=PF14_0690 PE=4 SV=2 | 4 | 0.70 | 0.48 | 0.0605 |
| tr\|Q8I4W4\|Q8I4W4_PLAF7 Signal recognition particle, beta subunit, putative OS=Plasmodium falciparum (isolate 3D7) GN=PFL2245w PE=4 SV=1 | 4 | 0.70 | 0.48 | 0.0602 |
| tr\|Q8IKH2\|Q8IKH2_PLAF7 Transcription factor with AP2 domain(S), putative OS=Plasmodium falciparum (isolate 3D7) GN=ApiAP2 PE=1 SV=1 | 4 | 0.70 | 0.50 | 0.0660 |
| tr\|Q8I2W2\|Q8I2W2_PLAF7 DNAJ-like molecular chaperone protein, putative OS=Plasmodium falciparum (isolate 3D7) GN=PFI0935w PE=4 SV=1 | 4 | 0.70 | 0.48 | 0.0605 |
| tr\|Q8II32\|Q8II32_PLAF7 Uncharacterized protein OS=Plasmodium falciparum (isolate 3D7) GN=PF11_0342 PE=4 SV=1 | 4 | 0.70 | 0.47 | 0.0590 |
| tr\|Q8IBD0\|Q8IBD0_PLAF7 Uncharacterized protein OS=Plasmodium falciparum (isolate 3D7) GN=PF08_0004 PE=4 SV=1 | 4 | 0.70 | 0.48 | 0.0617 |
| tr\|Q8I669\|Q8I669_PLAF7 Plasmodium exported protein OS=Plasmodium falciparum (isolate 3D7) GN=PFB0106c PE=4 SV=1 | 4 | 0.71 | 0.47 | 0.0582 |
| tr\|Q8IBE9\|Q8IBE9_PLAF7 Uncharacterized protein OS=Plasmodium falciparum (isolate 3D7) GN=MAL7P1.174 PE=4 SV=1 | 4 | 0.71 | 0.46 | 0.0534 |
| tr\|C0H4E7\|C0H4E7_PLAF7 Uncharacterized protein OS=Plasmodium falciparum (isolate 3D7) GN=PFE0910w PE=4 SV=1 | 4 | 0.71 | 1.21 | 0.3276 |
| tr\|Q8I398\|Q8I398_PLAF7 Putative uncharacterized protein OS=Plasmodium falciparum (isolate 3D7) GN=PFI0250c PE=4 SV=1 | 4 | 0.71 | 0.47 | 0.0570 |

| | | | | |
|---|---|---|---|---|
| tr\|Q8IJR6\|Q8IJR6_PLAF7 Conserved Plasmodium protein OS=Plasmodium falciparum (isolate 3D7) GN=PF10_0126 PE=4 SV=1 | 4 | 0.71 | 0.47 | 0.0577 |
| tr\|Q8II64\|Q8II64_PLAF7 Uncharacterized protein OS=Plasmodium falciparum (isolate 3D7) GN=PF11_0310 PE=4 SV=1 | 4 | 0.71 | 0.46 | 0.0533 |
| tr\|Q8IIU5\|Q8IIU5_PLAF7 Conserved Plasmodium protein OS=Plasmodium falciparum (isolate 3D7) GN=PF11_0069 PE=4 SV=2 | 4 | 0.71 | 0.45 | 0.0505 |
| tr\|Q8ILB0\|Q8ILB0_PLAF7 Uncharacterized protein OS=Plasmodium falciparum (isolate 3D7) GN=PF14_0335 PE=4 SV=1 | 4 | 0.71 | 0.48 | 0.0586 |
| tr\|Q7K6A8\|Q7K6A8_PLAF7 Rab1b, GTPase OS=Plasmodium falciparum (isolate 3D7) GN=Rab1b PE=4 SV=1 | 4 | 0.71 | 0.48 | 0.0583 |
| tr\|Q8IDP8\|Q8IDP8_PLAF7 Aspartate carbamoyltransferase OS=Plasmodium falciparum (isolate 3D7) GN=atcasE PE=3 SV=1 | 4 | 0.71 | 0.48 | 0.0583 |
| tr\|C0H5I2\|C0H5I2_PLAF7 Uncharacterized protein OS=Plasmodium falciparum (isolate 3D7) GN=MAL13P1.266 PE=4 SV=1 | 4 | 0.71 | 0.47 | 0.0554 |
| tr\|Q8IDS0\|Q8IDS0_PLAF7 Vacuolar ATP synthase subunit D, putative OS=Plasmodium falciparum (isolate 3D7) GN=PF13_0227 PE=4 SV=1 | 4 | 1.14 | 0.50 | 0.0194 |
| tr\|O97227\|O97227_PLAF7 Dihydrolipoamide acyltransferase, putative OS=Plasmodium falciparum (isolate 3D7) GN=PFC0170c PE=3 SV=1 | 4 | 0.71 | 0.48 | 0.0599 |
| tr\|Q8I5Y3\|Q8I5Y3_PLAF7 Eukaryotic translation initiation factor 3 subunit C OS=Plasmodium falciparum (isolate 3D7) GN=PFL0310c PE=3 SV=1 | 4 | 1.14 | 0.12 | 0.0003 |
| tr\|Q8I3W9\|Q8I3W9_PLAF7 PfRab1a OS=Plasmodium falciparum (isolate 3D7) GN=Rab1a PE=3 SV=1 | 4 | 0.71 | 0.49 | 0.0607 |
| tr\|Q8ILQ8\|Q8ILQ8_PLAF7 Uncharacterized protein OS=Plasmodium falciparum (isolate 3D7) GN=PF14_0186 PE=4 SV=2 | 4 | 0.71 | 0.48 | 0.0595 |
| tr\|Q8ID84\|Q8ID84_PLAF7 Uncharacterized protein OS=Plasmodium falciparum (isolate 3D7) GN=PF13_0331 PE=4 SV=1 | 4 | 0.71 | 0.46 | 0.0538 |
| tr\|C6KSL9\|C6KSL9_PLAF7 Uncharacterized protein OS=Plasmodium falciparum (isolate 3D7) GN=PFF0090w PE=4 SV=1 | 4 | 0.72 | 0.47 | 0.0548 |
| sp\|P27105\|STOM_HUMAN Erythrocyte band 7 integral membrane protein OS=Homo sapiens GN=STOM PE=1 SV=3 | 4 | 0.72 | 0.47 | 0.0551 |
| tr\|Q8ILA1\|Q8ILA1_PLAF7 Uncharacterized protein OS=Plasmodium falciparum (isolate 3D7) GN=PF14_0344 PE=4 SV=1 | 4 | 0.72 | 0.47 | 0.0568 |
| tr\|Q8IJI9\|Q8IJI9_PLAF7 Uncharacterized protein OS=Plasmodium falciparum (isolate 3D7) GN=PF10_0208 PE=4 SV=1 | 4 | 0.72 | 0.50 | 0.0639 |
| tr\|Q8IBI8\|Q8IBI8_PLAF7 Protein phosphatase, putative OS=Plasmodium falciparum (isolate 3D7) GN=PF07_0110 PE=4 SV=1 | 4 | 0.72 | 0.49 | 0.0615 |
| tr\|C0H4J4\|C0H4J4_PLAF7 Uncharacterized protein OS=Plasmodium falciparum (isolate 3D7) GN=MAL7P1.225.2 PE=4 SV=1;tr\|C0H4J3\|C0H4J3_PLAF7 Uncharacterized protein OS=Plasmodium falciparum (isolate 3D7) GN=MAL7P1.225.1 PE=4 SV=1 | 4 | 0.72 | 0.49 | 0.0601 |
| tr\|Q8IM53\|Q8IM53_PLAF7 Cytochrome c, putative OS=Plasmodium falciparum (isolate 3D7) GN=PF14_0038 PE=3 SV=1 | 4 | 0.72 | 0.49 | 0.0598 |
| tr\|C6KSP9\|C6KSP9_PLAF7 RNA binding protein, putative OS=Plasmodium falciparum (isolate 3D7) GN=PFF0250w PE=4 SV=1 | 4 | 0.72 | 0.48 | 0.0580 |
| tr\|Q7KWJ5\|Q7KWJ5_PLAF7 Hexose transporter, PfHT1 OS=Plasmodium falciparum (isolate 3D7) GN=HT1 PE=3 SV=1 | 4 | 0.72 | 0.47 | 0.0541 |
| tr\|Q8IAM3\|Q8IAM3_PLAF7 WD-repeat protein, putative OS=Plasmodium falciparum (isolate 3D7) GN=PF08_0130 PE=4 SV=1 | 4 | 1.15 | 0.33 | 0.0058 |
| tr\|Q8IDE0\|Q8IDE0_PLAF7 Mitochondrial inner membrane translocase, putative OS=Plasmodium falciparum (isolate 3D7) GN=PF13_0300 PE=4 SV=1 | 4 | 0.72 | 1.31 | 0.3508 |
| tr\|Q8IE40\|Q8IE40_PLAF7 Ribose-phosphate pyrophosphokinase, putative OS=Plasmodium falciparum (isolate 3D7) GN=PF13_0157 PE=4 SV=1 | 4 | 0.72 | 0.50 | 0.0632 |
| tr\|Q8IK15\|Q8IK15_PLAF7 PF70 protein OS=Plasmodium falciparum (isolate 3D7) GN=PF10_0025 PE=4 SV=1 | 4 | 0.72 | 0.48 | 0.0576 |
| sp\|Q8I3H7\|TIP_PLAF7 T-cell immunomodulatory protein homolog OS=Plasmodium falciparum (isolate 3D7) GN=PFE1445c PE=3 SV=1 | 4 | 0.72 | 0.48 | 0.0574 |
| tr\|Q8ILC8\|Q8ILC8_PLAF7 DNA topoisomerase 2 OS=Plasmodium falciparum (isolate 3D7) GN=PF14_0316 PE=3 SV=1 | 4 | 0.72 | 0.48 | 0.0575 |
| tr\|Q8I310\|Q8I310_PLAF7 Phospholipid or glycerol acyltransferase, putative OS=Plasmodium falciparum (isolate 3D7) GN=PFI0695c PE=4 SV=1 | 4 | 0.72 | 0.48 | 0.0573 |
| tr\|Q7KQK4\|Q7KQK4_PLAF7 Zinc finger transcription factor (Krox1) OS=Plasmodium falciparum (isolate 3D7) GN=PFL0465c PE=4 SV=1 | 4 | 0.72 | 0.59 | 0.0927 |
| tr\|Q8IFP5\|Q8IFP5_PLAF7 Uncharacterized protein OS=Plasmodium falciparum (isolate 3D7) GN=PFD1037w PE=4 SV=1 | 4 | 0.72 | 0.49 | 0.0585 |
| sp\|Q86SG5\|S1A7A_HUMAN Protein S100-A7A OS=Homo sapiens GN=S100A7A PE=1 SV=3;sp\|P31151\|S10A7_HUMAN Protein S100-A7 OS=Homo sapiens GN=S100A7 PE=1 SV=4 | 4 | 0.73 | 0.63 | 0.1033 |

| | | | | |
|---|---|---|---|---|
| tr\|Q8IBP8\|Q8IBP8_PLAF7 Ferrodoxin reductase-like protein OS=Plasmodium falciparum (isolate 3D7) GN=PF07_0085 PE=4 SV=1 | 4 | 0.73 | 0.53 | 0.0711 |
| tr\|Q8IEE2\|Q8IEE2_PLAF7 Uncharacterized protein OS=Plasmodium falciparum (isolate 3D7) GN=PF13_0099 PE=4 SV=1 | 4 | 0.73 | 0.48 | 0.0579 |
| tr\|Q8IIA9\|Q8IIA9_PLAF7 Mitochondrial inner membrane translocase subunit TIM44, putative OS=Plasmodium falciparum (isolate 3D7) GN=PF11_0265 PE=4 SV=2 | 4 | 0.73 | 0.48 | 0.0569 |
| tr\|Q8IHN1\|Q8IHN1_PLAF7 Ring-infected erythrocyte surface antigen, putative OS=Plasmodium falciparum (isolate 3D7) GN=PF11_0509 PE=4 SV=1 | 4 | 0.73 | 0.47 | 0.0546 |
| tr\|O96128\|O96128_PLAF7 Early transcribed membrane protein 2, ETRAMP2 OS=Plasmodium falciparum (isolate 3D7) GN=SEP2 PE=4 SV=1 | 4 | 0.73 | 0.49 | 0.0583 |
| tr\|Q8IIY1\|Q8IIY1_PLAF7 Uncharacterized protein OS=Plasmodium falciparum (isolate 3D7) GN=PF11_0025 PE=4 SV=1;tr\|Q8IJ11\|Q8IJ11_PLAF7 Pfmc-2TM Maurers cleft two transmembrane protein OS=Plasmodium falciparum (isolate 3D7) GN=PF10_0390 PE=4 SV=2 | 4 | 0.73 | 0.49 | 0.0585 |
| tr\|C0H4S8\|C0H4S8_PLAF7 Uncharacterized protein OS=Plasmodium falciparum (isolate 3D7) GN=MAL8P1.127 PE=4 SV=1 | 4 | 0.73 | 0.49 | 0.0587 |
| tr\|Q8I395\|Q8I395_PLAF7 RhopH3 OS=Plasmodium falciparum (isolate 3D7) GN=PFI0265c PE=4 SV=1 | 4 | 0.73 | 0.49 | 0.0577 |
| sp\|P23276\|KELL_HUMAN Kell blood group glycoprotein OS=Homo sapiens GN=KEL PE=1 SV=2 | 4 | 0.73 | 0.49 | 0.0583 |
| tr\|Q8IJA5\|Q8IJA5_PLAF7 Transcription factor, putative OS=Plasmodium falciparum (isolate 3D7) GN=PF10_0293 PE=3 SV=1 | 4 | 0.73 | 0.52 | 0.0663 |
| tr\|Q8IIU8\|Q8IIU8_PLAF7 40S ribosomal protein S4 OS=Plasmodium falciparum (isolate 3D7) GN=PF11_0065 PE=3 SV=2 | 4 | 1.17 | 0.73 | 0.0483 |
| tr\|Q8I3I5\|Q8I3I5_PLAF7 Eukaryotic translation initiation factor 3 subunit E OS=Plasmodium falciparum (isolate 3D7) GN=PFE1405c PE=3 SV=1 | 4 | 0.73 | 0.49 | 0.0582 |
| tr\|Q8IHZ2\|Q8IHZ2_PLAF7 Uncharacterized protein OS=Plasmodium falciparum (isolate 3D7) GN=PF11_0384 PE=4 SV=1 | 4 | 0.73 | 0.49 | 0.0588 |
| tr\|Q8IIW0\|Q8IIW0_PLAF7 PfSNF2L OS=Plasmodium falciparum (isolate 3D7) GN=PF11_0053 PE=4 SV=1 | 4 | 0.74 | 0.49 | 0.0580 |
| tr\|Q8IJT8\|Q8IJT8_PLAF7 Conserved Plasmodium protein OS=Plasmodium falciparum (isolate 3D7) GN=PF10_0104 PE=4 SV=1 | 4 | 0.74 | 0.49 | 0.0585 |
| tr\|Q8IDZ8\|Q8IDZ8_PLAF7 Cochaperonin OS=Plasmodium falciparum (isolate 3D7) GN=PfCpn20 PE=3 SV=1 | 4 | 0.74 | 0.49 | 0.0578 |
| tr\|A0A087WY82\|A0A087WY82_HUMAN Junctional adhesion molecule A OS=Homo sapiens GN=F11R PE=1 SV=1;sp\|Q9Y624\|JAM1_HUMAN Junctional adhesion molecule A OS=Homo sapiens GN=F11R PE=1 SV=1 | 4 | 0.74 | 0.56 | 0.0770 |
| tr\|Q8IIK2\|Q8IIK2_PLAF7 Uncharacterized protein OS=Plasmodium falciparum (isolate 3D7) GN=PF11_0171 PE=4 SV=1 | 4 | 0.74 | 0.49 | 0.0580 |
| tr\|Q8ILD7\|Q8ILD7_PLAF7 Uncharacterized protein OS=Plasmodium falciparum (isolate 3D7) GN=PF14_0307 PE=4 SV=1 | 4 | 0.74 | 0.49 | 0.0574 |
| tr\|Q8I3F3\|Q8I3F3_PLAF7 Early transcribed membrane protein 5, ETRAMP5 OS=Plasmodium falciparum (isolate 3D7) GN=ETRAMP5 PE=4 SV=1 | 4 | 0.74 | 0.50 | 0.0596 |
| tr\|Q8ID37\|Q8ID37_PLAF7 U1 small nuclear ribonucleoprotein, putative OS=Plasmodium falciparum (isolate 3D7) GN=MAL13P1.338 PE=4 SV=1 | 4 | 0.74 | 0.49 | 0.0576 |
| tr\|O77313\|O77313_PLAF7 N-ethylmaleimide sensitive fusion protein, putative OS=Plasmodium falciparum (isolate 3D7) GN=PFC0140c PE=3 SV=1 | 4 | 0.74 | 0.49 | 0.0576 |
| tr\|Q8I2G1\|Q8I2G1_PLAF7 Ring-exported protein 1 OS=Plasmodium falciparum (isolate 3D7) GN=REX1 PE=4 SV=1 | 4 | 0.74 | 0.49 | 0.0565 |
| tr\|Q8IEB3\|Q8IEB3_PLAF7 Uncharacterized protein OS=Plasmodium falciparum (isolate 3D7) GN=PF13_0116 PE=4 SV=1 | 4 | 0.74 | 0.49 | 0.0578 |
| tr\|O77325\|O77325_PLAF7 PRP19-like protein, putative OS=Plasmodium falciparum (isolate 3D7) GN=PFC0365w PE=4 SV=1 | 4 | 0.74 | 0.49 | 0.0570 |
| tr\|Q8IK17\|Q8IK17_PLAF7 Uncharacterized protein OS=Plasmodium falciparum (isolate 3D7) GN=PF10_0023 PE=4 SV=1 | 4 | 0.74 | 0.50 | 0.0580 |
| tr\|Q8IB44\|Q8IB44_PLAF7 Uncharacterized protein OS=Plasmodium falciparum (isolate 3D7) GN=MAL8P1.53 PE=4 SV=1 | 4 | 0.74 | 0.51 | 0.0614 |
| tr\|Q8I5I3\|Q8I5I3_PLAF7 Phospholipid-transporting ATPase, putative OS=Plasmodium falciparum (isolate 3D7) GN=PFL1125w PE=4 SV=1 | 4 | 0.74 | 0.52 | 0.0643 |
| tr\|C6KSL5\|C6KSL5_PLAF7 Pfmc-2TM Maurers cleft two transmembrane protein OS=Plasmodium falciparum (isolate 3D7) GN=PfMC-2TM PE=4 SV=1 | 4 | 0.74 | 0.51 | 0.0609 |
| tr\|Q8IJZ3\|Q8IJZ3_PLAF7 Uncharacterized protein OS=Plasmodium falciparum (isolate 3D7) GN=PF10_0047 PE=4 SV=1 | 4 | 0.74 | 0.50 | 0.0578 |
| tr\|Q8IJ34\|Q8IJ34_PLAF7 ADP/ATP transporter on adenylate translocase OS=Plasmodium falciparum (isolate 3D7) GN=PF10_0366 PE=3 SV=1 | 4 | 0.74 | 0.48 | 0.0537 |

| | | | | |
|---|---|---|---|---|
| tr\|Q8I420\|Q8I420_PLAF7 Triose phosphate transporter OS=Plasmodium falciparum (isolate 3D7) GN=PfoTPT PE=4 SV=1 | 4 | 0.74 | 0.50 | 0.0594 |
| tr\|Q8IJC7\|Q8IJC7_PLAF7 Centrin-3 OS=Plasmodium falciparum (isolate 3D7) GN=PF10_0271 PE=4 SV=2 | 4 | 0.74 | 0.51 | 0.0603 |
| tr\|Q8IJW6\|Q8IJW6_PLAF7 Asparagine-rich antigen OS=Plasmodium falciparum (isolate 3D7) GN=PF10_0075 PE=4 SV=1 | 4 | 0.74 | 0.50 | 0.0577 |
| tr\|Q8I5S6\|Q8I5S6_PLAF7 Eukaryotic translation initiation factor 3 subunit A OS=Plasmodium falciparum (isolate 3D7) GN=PFL0625c PE=3 SV=1 | 4 | 1.18 | 0.26 | 0.0027 |
| tr\|Q8I5L6\|Q8I5L6_PLAF7 Clathrin heavy chain OS=Plasmodium falciparum (isolate 3D7) GN=PFL0930w PE=3 SV=1 | 4 | 0.74 | 0.50 | 0.0577 |
| tr\|Q8I3Z9\|Q8I3Z9_PLAF7 Topoisomerase I OS=Plasmodium falciparum (isolate 3D7) GN=PFE0520c PE=4 SV=1 | 4 | 0.75 | 0.50 | 0.0576 |
| tr\|Q8IJP8\|Q8IJP8_PLAF7 Prohibitin, putative OS=Plasmodium falciparum (isolate 3D7) GN=PF10_0144 PE=4 SV=1 | 4 | 0.75 | 0.50 | 0.0582 |
| sp\|Q8I4V5\|UTP11_PLAF7 Probable U3 small nucleolar RNA-associated protein 11 OS=Plasmodium falciparum (isolate 3D7) GN=PFL2295w PE=3 SV=1 | 4 | 0.75 | 0.53 | 0.0675 |
| tr\|Q8I3A5\|Q8I3A5_PLAF7 Signal peptidase, putative OS=Plasmodium falciparum (isolate 3D7) GN=PFI0215c PE=4 SV=1 | 4 | 0.75 | 0.50 | 0.0593 |
| tr\|O96127\|O96127_PLAF7 Conserved Plasmodium protein OS=Plasmodium falciparum (isolate 3D7) GN=PFB0115w PE=4 SV=1 | 4 | 0.75 | 0.50 | 0.0575 |
| sp\|P07384\|CAN1_HUMAN Calpain-1 catalytic subunit OS=Homo sapiens GN=CAPN1 PE=1 SV=1 | 4 | 1.19 | 0.44 | 0.0119 |
| tr\|Q8IIC8\|Q8IIC8_PLAF7 Uncharacterized protein OS=Plasmodium falciparum (isolate 3D7) GN=PF11_0246 PE=4 SV=1 | 4 | 1.20 | 0.36 | 0.0069 |
| tr\|Q8IBD1\|Q8IBD1_PLAF7 Tryptophan/threonine-rich antigen OS=Plasmodium falciparum (isolate 3D7) GN=PF08_0003 PE=4 SV=1 | 4 | 0.75 | 0.50 | 0.0585 |
| tr\|Q8IIC4\|Q8IIC4_PLAF7 High mobility group-like protein NHP2, putative OS=Plasmodium falciparum (isolate 3D7) GN=PF11_0250 PE=4 SV=1 | 4 | 0.75 | 0.50 | 0.0582 |
| tr\|Q8I5E7\|Q8I5E7_PLAF7 ATP-dependent RNA helicase, putative OS=Plasmodium falciparum (isolate 3D7) GN=PFL1310c PE=3 SV=1 | 4 | 0.75 | 0.51 | 0.0603 |
| tr\|Q8I5T8\|Q8I5T8_PLAF7 Uncharacterized protein OS=Plasmodium falciparum (isolate 3D7) GN=PFL0555c PE=4 SV=1 | 4 | 0.75 | 0.50 | 0.0580 |
| tr\|Q8I5H7\|Q8I5H7_PLAF7 GTP cyclohydrolase I OS=Plasmodium falciparum (isolate 3D7) GN=PFL1155w PE=4 SV=1 | 4 | 0.75 | 0.50 | 0.0579 |
| sp\|Q8I1U7\|SMC3_PLAF7 Structural maintenance of chromosomes protein 3 homolog OS=Plasmodium falciparum (isolate 3D7) GN=PFD0685c PE=3 SV=1 | 4 | 0.75 | 0.50 | 0.0578 |
| tr\|Q8IE99\|Q8IE99_PLAF7 Splicing factor, putative OS=Plasmodium falciparum (isolate 3D7) GN=MAL13P1.120 PE=4 SV=1 | 4 | 0.75 | 0.50 | 0.0582 |
| tr\|C0H5M6\|C0H5M6_PLAF7 Uncharacterized protein OS=Plasmodium falciparum (isolate 3D7) GN=MAL13P1.465 PE=4 SV=1 | 4 | 0.76 | 0.52 | 0.0624 |
| tr\|Q8IEQ6\|Q8IEQ6_PLAF7 Uncharacterized protein OS=Plasmodium falciparum (isolate 3D7) GN=PF13_0031 PE=4 SV=1 | 4 | 0.76 | 0.50 | 0.0574 |
| tr\|Q8IIJ8\|Q8IIJ8_PLAF7 Heat shock protein 101, putative OS=Plasmodium falciparum (isolate 3D7) GN=PF11_0175 PE=1 SV=1 | 4 | 0.76 | 0.50 | 0.0573 |
| tr\|Q8IAW0\|Q8IAW0_PLAF7 Importin subunit alpha OS=Plasmodium falciparum (isolate 3D7) GN=PF08_0087 PE=3 SV=1 | 4 | 1.20 | 0.71 | 0.0425 |
| tr\|Q8I5M3\|Q8I5M3_PLAF7 Uncharacterized protein OS=Plasmodium falciparum (isolate 3D7) GN=PFL0895c PE=4 SV=1 | 4 | 0.76 | 0.49 | 0.0540 |
| tr\|Q8I5M6\|Q8I5M6_PLAF7 Conserved Plasmodium protein OS=Plasmodium falciparum (isolate 3D7) GN=PFL0880c PE=4 SV=1 | 4 | 0.76 | 0.49 | 0.0539 |
| tr\|Q8IJU2\|Q8IJU2_PLAF7 Conserved Plasmodium protein OS=Plasmodium falciparum (isolate 3D7) GN=PF10_0100 PE=4 SV=1 | 4 | 0.76 | 0.51 | 0.0588 |
| tr\|Q8IEJ5\|Q8IEJ5_PLAF7 Uncharacterized protein OS=Plasmodium falciparum (isolate 3D7) GN=PF13_0071 PE=4 SV=1 | 4 | 0.76 | 0.52 | 0.0609 |
| sp\|P61225\|RAP2B_HUMAN Ras-related protein Rap-2b OS=Homo sapiens GN=RAP2B PE=1 SV=1 | 4 | 0.76 | 0.51 | 0.0595 |
| tr\|Q8ILQ3\|Q8ILQ3_PLAF7 Uncharacterized protein OS=Plasmodium falciparum (isolate 3D7) GN=PF14_0191 PE=4 SV=1 | 4 | 0.76 | 0.51 | 0.0581 |
| tr\|Q8IJI0\|Q8IJI0_PLAF7 Pre-mRNA splicing factor, putative OS=Plasmodium falciparum (isolate 3D7) GN=PF10_0217 PE=4 SV=1 | 4 | 0.76 | 0.52 | 0.0599 |
| tr\|C0H535\|C0H535_PLAF7 Putative uncharacterized protein OS=Plasmodium falciparum (isolate 3D7) GN=PFI0610w PE=4 SV=1 | 4 | 0.76 | 0.50 | 0.0548 |
| tr\|Q8ILS0\|Q8ILS0_PLAF7 Pseudouridine synthase, putative OS=Plasmodium falciparum (isolate 3D7) GN=PF14_0174 PE=4 SV=1 | 4 | 0.76 | 0.50 | 0.0548 |
| tr\|Q8IJI4\|Q8IJI4_PLAF7 10b antigen, putative OS=Plasmodium falciparum (isolate 3D7) GN=PF10_0213 PE=4 SV=1 | 4 | 0.76 | 0.49 | 0.0514 |

| | | | | |
|---|---|---|---|---|
| tr\|Q8I2N0\|Q8I2N0_PLAF7 Phosphatidylserine decarboxylase OS=Plasmodium falciparum (isolate 3D7) GN=PfPSD PE=4 SV=1 | 4 | 0.76 | 0.51 | 0.0566 |
| tr\|Q8ILU8\|Q8ILU8_PLAF7 Ribonucleoprotein, putative OS=Plasmodium falciparum (isolate 3D7) GN=PF14_0146 PE=4 SV=1 | 4 | 0.77 | 0.52 | 0.0609 |
| tr\|Q8IB66\|Q8IB66_PLAF7 RNA binding protein, putative OS=Plasmodium falciparum (isolate 3D7) GN=MAL8P1.40 PE=4 SV=1 | 4 | 0.77 | 0.52 | 0.0588 |
| tr\|Q8IDG4\|Q8IDG4_PLAF7 Uncharacterized protein OS=Plasmodium falciparum (isolate 3D7) GN=PF13_0281 PE=4 SV=1 | 4 | 0.77 | 0.52 | 0.0591 |
| tr\|Q8II73\|Q8II73_PLAF7 Spermidine synthase OS=Plasmodium falciparum (isolate 3D7) GN=PF11_0301 PE=1 SV=1 | 4 | 0.77 | 0.52 | 0.0583 |
| sp\|Q8ID39\|Y13P2_PLAF7 Uncharacterized protein MAL13P1.336 OS=Plasmodium falciparum (isolate 3D7) GN=MAL13P1.336 PE=4 SV=1 | 4 | 0.77 | 0.52 | 0.0587 |
| tr\|C6KSR8\|C6KSR8_PLAF7 Translation initiation factor IF-2, putative OS=Plasmodium falciparum (isolate 3D7) GN=PFF0345w PE=4 SV=1 | 4 | 1.24 | 0.14 | 0.0004 |
| tr\|Q8ILZ5\|Q8ILZ5_PLAF7 Tetratricopeptide repeat family protein, putative OS=Plasmodium falciparum (isolate 3D7) GN=PF14_0098 PE=4 SV=1 | 4 | 0.77 | 0.51 | 0.0572 |
| tr\|Q8IFP1\|Q8IFP1_PLAF7 U5 small nuclear ribonucleoprotein-specific protein, putative OS=Plasmodium falciparum (isolate 3D7) GN=PFD1060w PE=4 SV=1 | 4 | 0.78 | 0.52 | 0.0583 |
| tr\|Q8I1X5\|Q8I1X5_PLAF7 Pre-mRNA splicing factor, putative OS=Plasmodium falciparum (isolate 3D7) GN=PFD0265w PE=4 SV=1 | 4 | 0.78 | 0.52 | 0.0582 |
| sp\|Q9BVK6\|TMED9_HUMAN Transmembrane emp24 domain-containing protein 9 OS=Homo sapiens GN=TMED9 PE=1 SV=2 | 4 | 0.78 | 0.66 | 0.1005 |
| tr\|Q8IM35\|Q8IM35_PLAF7 RNA binding protein, putative OS=Plasmodium falciparum (isolate 3D7) GN=PF14_0056 PE=4 SV=1 | 4 | 0.78 | 0.53 | 0.0603 |
| tr\|Q8IM45\|Q8IM45_PLAF7 Uncharacterized protein OS=Plasmodium falciparum (isolate 3D7) GN=PF14_0046 PE=4 SV=1 | 4 | 1.25 | 0.64 | 0.0301 |
| tr\|C0H4F1\|C0H4F1_PLAF7 Uncharacterized protein OS=Plasmodium falciparum (isolate 3D7) GN=PFE0990w PE=4 SV=1 | 4 | 0.78 | 0.53 | 0.0597 |
| tr\|Q9NFE6\|Q9NFE6_PLAF7 Eukaryotic translation initiation factor 3 subunit K OS=Plasmodium falciparum (isolate 3D7) GN=PFC0441c PE=3 SV=1 | 4 | 0.78 | 0.54 | 0.0623 |
| tr\|Q8IKR1\|Q8IKR1_PLAF7 V-type H(+)-translocating pyrophosphatase, putative OS=Plasmodium falciparum (isolate 3D7) GN=PF14_0541 PE=3 SV=1 | 4 | 0.78 | 0.53 | 0.0595 |
| tr\|Q8I3K0\|Q8I3K0_PLAF7 Uncharacterized protein OS=Plasmodium falciparum (isolate 3D7) GN=PFE1320w PE=4 SV=1 | 4 | 0.78 | 0.54 | 0.0627 |
| tr\|Q8IB73\|Q8IB73_PLAF7 Oxoglutarate/malate translocator protein, putative OS=Plasmodium falciparum (isolate 3D7) GN=PF08_0031 PE=3 SV=1 | 4 | 0.78 | 0.59 | 0.0761 |
| tr\|Q8ILL3\|Q8ILL3_PLAF7 60S ribosomal protein L5, putative OS=Plasmodium falciparum (isolate 3D7) GN=PF14_0230 PE=3 SV=1 | 4 | 1.25 | 0.44 | 0.0111 |
| tr\|Q8I5E0\|Q8I5E0_PLAF7 Uncharacterized protein OS=Plasmodium falciparum (isolate 3D7) GN=PFL1345c PE=4 SV=1 | 4 | 0.78 | 0.52 | 0.0578 |
| tr\|Q8ILL5\|Q8ILL5_PLAF7 Uncharacterized protein OS=Plasmodium falciparum (isolate 3D7) GN=PF14_0228 PE=4 SV=1 | 4 | 0.78 | 0.52 | 0.0577 |
| tr\|C6KSY5\|C6KSY5_PLAF7 Uncharacterized protein OS=Plasmodium falciparum (isolate 3D7) GN=PFF0695w PE=4 SV=1 | 4 | 0.78 | 0.52 | 0.0576 |
| tr\|Q8I4R9\|Q8I4R9_PLAF7 DEAD/DEAH box helicase, putative OS=Plasmodium falciparum (isolate 3D7) GN=PFL2475w PE=3 SV=1 | 4 | 0.78 | 0.52 | 0.0568 |
| tr\|Q8IE00\|Q8IE00_PLAF7 Eukaryotic translation initiation factor 6 OS=Plasmodium falciparum (isolate 3D7) GN=EIF6 PE=3 SV=1 | 4 | 0.78 | 0.63 | 0.0902 |
| tr\|Q8IJD2\|Q8IJD2_PLAF7 Uncharacterized protein OS=Plasmodium falciparum (isolate 3D7) GN=PF10_0266 PE=4 SV=1 | 4 | 0.78 | 0.55 | 0.0647 |
| tr\|Q8IJZ2\|Q8IJZ2_PLAF7 Conserved Plasmodium protein OS=Plasmodium falciparum (isolate 3D7) GN=PF10_0048 PE=4 SV=1 | 4 | 0.78 | 0.52 | 0.0576 |
| tr\|Q8IBF1\|Q8IBF1_PLAF7 Uncharacterized protein OS=Plasmodium falciparum (isolate 3D7) GN=MAL7P1.172 PE=4 SV=1 | 4 | 0.78 | 0.53 | 0.0601 |
| tr\|Q8I3R7\|Q8I3R7_PLAF7 Vacuolar ATP synthetase OS=Plasmodium falciparum (isolate 3D7) GN=PFE0965c PE=3 SV=1 | 4 | 0.79 | 0.53 | 0.0603 |
| tr\|Q8IDT3\|Q8IDT3_PLAF7 Uncharacterized protein OS=Plasmodium falciparum (isolate 3D7) GN=PF13_0219 PE=4 SV=1 | 4 | 0.79 | 0.53 | 0.0591 |
| tr\|Q8IL69\|Q8IL69_PLAF7 Uncharacterized protein OS=Plasmodium falciparum (isolate 3D7) GN=PF14_0380 PE=4 SV=1 | 4 | 0.79 | 0.53 | 0.0583 |
| tr\|B9ZSI8\|B9ZSI8_PLAF7 Phosphatidate cytidylyltransferase, putative OS=Plasmodium falciparum (isolate 3D7) GN=PFA_0485w PE=4 SV=1 | 4 | 0.79 | 1.20 | 0.2794 |
| sp\|Q8IBZ9\|CRT_PLAF7 Putative chloroquine resistance transporter OS=Plasmodium falciparum (isolate 3D7) GN=CG10 PE=3 SV=1 | 4 | 0.79 | 0.54 | 0.0601 |
| tr\|Q8IBB4\|Q8IBB4_PLAF7 Uncharacterized protein OS=Plasmodium falciparum (isolate 3D7) GN=PF08_0010 PE=4 SV=1 | 4 | 0.79 | 0.53 | 0.0569 |

| | | | | |
|---|---|---|---|---|
| tr\|Q8I2H1\|Q8I2H1_PLAF7 UBX domain, putative OS=Plasmodium falciparum (isolate 3D7) GN=PFI1680w PE=4 SV=1 | 4 | 0.79 | 0.53 | 0.0577 |
| tr\|Q8II99\|Q8II99_PLAF7 Uncharacterized protein OS=Plasmodium falciparum (isolate 3D7) GN=PF11_0275 PE=4 SV=1 | 4 | 0.80 | 0.53 | 0.0579 |
| tr\|Q8I441\|Q8I441_PLAF7 60S ribosomal subunit protein L24-2, putative OS=Plasmodium falciparum (isolate 3D7) GN=PFE0300c PE=4 SV=1 | 4 | 0.80 | 0.55 | 0.0630 |
| tr\|C0H541\|C0H541_PLAF7 Putative uncharacterized protein OS=Plasmodium falciparum (isolate 3D7) GN=PFI0823w PE=4 SV=1 | 4 | 1.25 | 0.38 | 0.0070 |
| tr\|Q8IKL9\|Q8IKL9_PLAF7 40S ribosomal protein S28e, putative OS=Plasmodium falciparum (isolate 3D7) GN=PF14_0585 PE=3 SV=1 | 4 | 1.25 | 0.64 | 0.0297 |
| tr\|Q8I3V9\|Q8I3V9_PLAF7 Uncharacterized protein OS=Plasmodium falciparum (isolate 3D7) GN=PFE0745w PE=4 SV=1 | 4 | 0.80 | 0.98 | 0.2018 |
| tr\|C0H4L6\|C0H4L6_PLAF7 Uncharacterized protein OS=Plasmodium falciparum (isolate 3D7) GN=MAL7P1.204 PE=4 SV=1 | 4 | 0.80 | 0.51 | 0.0530 |
| tr\|Q8II57\|Q8II57_PLAF7 Structural maintenance of chromosome protein, putative OS=Plasmodium falciparum (isolate 3D7) GN=PF11_0317 PE=4 SV=1 | 4 | 0.80 | 0.57 | 0.0690 |
| tr\|Q8IHV7\|Q8IHV7_PLAF7 Conserved Plasmodium protein OS=Plasmodium falciparum (isolate 3D7) GN=PF11_0419 PE=4 SV=2 | 4 | 0.80 | 0.53 | 0.0576 |
| tr\|Q8I2T2\|Q8I2T2_PLAF7 Ubiquitin-like protein, putative OS=Plasmodium falciparum (isolate 3D7) GN=PFI1085w PE=4 SV=1 | 4 | 0.80 | 0.54 | 0.0599 |
| tr\|Q8IJ39\|Q8IJ39_PLAF7 Conserved Plasmodium protein OS=Plasmodium falciparum (isolate 3D7) GN=PF10_0361 PE=4 SV=1 | 4 | 0.80 | 0.54 | 0.0583 |
| tr\|Q8IAU1\|Q8IAU1_PLAF7 RNA helicase, putative OS=Plasmodium falciparum (isolate 3D7) GN=PF08_0096 PE=3 SV=1 | 4 | 0.80 | 0.53 | 0.0556 |
| tr\|Q8IJX3\|Q8IJX3_PLAF7 RNA binding protein, putative OS=Plasmodium falciparum (isolate 3D7) GN=PF10_0068 PE=4 SV=1 | 4 | 0.80 | 0.53 | 0.0565 |
| tr\|Q8IB67\|Q8IB67_PLAF7 Histone acetyltransferase GCN5, putative OS=Plasmodium falciparum (isolate 3D7) GN=gcn5 PE=1 SV=2 | 4 | 0.80 | 0.53 | 0.0557 |
| tr\|Q8I1V1\|Q8I1V1_PLAF7 26S proteasome AAA-ATPase subunit RPT3, putative OS=Plasmodium falciparum (isolate 3D7) GN=PFD0665c PE=3 SV=1 | 4 | 1.26 | 0.53 | 0.0177 |
| tr\|C6KSW5\|C6KSW5_PLAF7 Eukaryotic translation initiation factor 3 subunit L OS=Plasmodium falciparum (isolate 3D7) GN=PFF0590c PE=3 SV=1 | 4 | 0.80 | 0.54 | 0.0587 |
| tr\|O96264\|O96264_PLAF7 DEAD/DEAH box helicase, putative OS=Plasmodium falciparum (isolate 3D7) GN=PFB0860c PE=3 SV=1 | 4 | 0.81 | 0.63 | 0.0831 |
| tr\|Q8IKJ1\|Q8IKJ1_PLAF7 Phosphatase, putative OS=Plasmodium falciparum (isolate 3D7) GN=PF14_0614 PE=4 SV=2 | 4 | 1.27 | 0.69 | 0.0350 |
| tr\|Q8IKM5\|Q8IKM5_PLAF7 60S ribosomal protein L27, putative OS=Plasmodium falciparum (isolate 3D7) GN=PF14_0579 PE=1 SV=2 | 4 | 1.28 | 0.65 | 0.0289 |
| tr\|Q8I569\|Q8I569_PLAF7 Uncharacterized protein OS=Plasmodium falciparum (isolate 3D7) GN=PFL1705w PE=4 SV=1 | 4 | 0.81 | 0.54 | 0.0578 |
| tr\|C0H5C6\|C0H5C6_PLAF7 SNARE protein, putative OS=Plasmodium falciparum (isolate 3D7) GN=PfSNAP23 PE=4 SV=1 | 4 | 0.81 | 0.53 | 0.0555 |
| tr\|Q8I207\|Q8I207_PLAF7 Uncharacterized protein OS=Plasmodium falciparum (isolate 3D7) GN=PFD0080c PE=4 SV=1 | 4 | 1.28 | 0.58 | 0.0219 |
| tr\|Q8ILY9\|Q8ILY9_PLAF7 Eukaryotic translation initiation factor 2 gamma subunit, putative OS=Plasmodium falciparum (isolate 3D7) GN=PF14_0104 PE=4 SV=1 | 4 | 1.29 | 0.64 | 0.0277 |
| tr\|Q8I240\|Q8I240_PLAF7 Bromodomain protein, putative OS=Plasmodium falciparum (isolate 3D7) GN=PFA_0510w PE=1 SV=1 | 4 | 0.81 | 0.56 | 0.0618 |
| tr\|Q8I308\|Q8I308_PLAF7 Putative uncharacterized protein OS=Plasmodium falciparum (isolate 3D7) GN=PFI0705w PE=4 SV=1 | 4 | 0.81 | 0.54 | 0.0587 |
| sp\|O15770\|GSHR_PLAF7 Glutathione reductase OS=Plasmodium falciparum (isolate 3D7) GN=GR3 PE=2 SV=4 | 4 | 1.31 | 0.75 | 0.0406 |
| tr\|Q8I266\|Q8I266_PLAF7 Lipid/sterol:H+ symporter OS=Plasmodium falciparum (isolate 3D7) GN=PFA_0375c PE=4 SV=1 | 4 | 1.31 | 0.56 | 0.0183 |
| tr\|Q8IJC1\|Q8IJC1_PLAF7 Uncharacterized protein OS=Plasmodium falciparum (isolate 3D7) GN=PF10_0277 PE=4 SV=1 | 4 | 0.81 | 0.54 | 0.0574 |
| tr\|Q8IM23\|Q8IM23_PLAF7 Fibrillarin, putative OS=Plasmodium falciparum (isolate 3D7) GN=PF14_0068 PE=3 SV=1 | 4 | 0.81 | 0.54 | 0.0577 |
| tr\|Q8IIS2\|Q8IIS2_PLAF7 Uncharacterized protein OS=Plasmodium falciparum (isolate 3D7) GN=PF11_0093 PE=4 SV=1 | 4 | 0.81 | 0.54 | 0.0575 |
| tr\|O96150\|O96150_PLAF7 DNA-directed RNA polymerase II 16 kDa subunit, putative OS=Plasmodium falciparum (isolate 3D7) GN=PFB0245c PE=4 SV=1 | 4 | 0.82 | 0.55 | 0.0605 |
| sp\|O97313\|RS3A_PLAF7 40S ribosomal protein S3a OS=Plasmodium falciparum (isolate 3D7) GN=MAL3P7.35 PE=1 SV=1 | 4 | 1.32 | 0.40 | 0.0068 |
| tr\|Q8IHW7\|Q8IHW7_PLAF7 Conserved Plasmodium protein OS=Plasmodium falciparum (isolate 3D7) GN=PF11_0409 PE=4 SV=1 | 4 | 0.82 | 0.54 | 0.0559 |

| | | | | |
|---|---|---|---|---|
| tr\|Q8I635\|Q8I635_PLAF7 Uncharacterized protein OS=Plasmodium falciparum (isolate 3D7) GN=PFL0050c PE=4 SV=1 | 4 | 0.82 | 0.54 | 0.0569 |
| tr\|Q8IHM9\|Q8IHM9_PLAF7 Plasmodium exported protein OS=Plasmodium falciparum (isolate 3D7) GN=PF11_0511 PE=4 SV=2 | 4 | 0.82 | 0.53 | 0.0534 |
| tr\|Q8IM36\|Q8IM36_PLAF7 Ribosome biogenesis protein BOP1 homolog OS=Plasmodium falciparum (isolate 3D7) GN=PF14_0055 PE=3 SV=1 | 4 | 0.82 | 0.54 | 0.0560 |
| tr\|B9ZSJ0\|B9ZSJ0_PLAF7 Putative uncharacterized protein OS=Plasmodium falciparum (isolate 3D7) GN=PFA_0570w PE=4 SV=1 | 4 | 0.82 | 0.55 | 0.0574 |
| tr\|Q8IJV7\|Q8IJV7_PLAF7 Nucleolar protein NOP5, putative OS=Plasmodium falciparum (isolate 3D7) GN=PF10_0085 PE=4 SV=1 | 4 | 0.82 | 0.55 | 0.0586 |
| tr\|Q8IK93\|Q8IK93_PLAF7 Uncharacterized protein OS=Plasmodium falciparum (isolate 3D7) GN=PF14_0713 PE=4 SV=1 | 4 | 0.82 | 0.56 | 0.0604 |
| tr\|O77315\|O77315_PLAF7 DNA-directed RNA polymerase subunit I, putative OS=Plasmodium falciparum (isolate 3D7) GN=PFC0155c PE=4 SV=2 | 4 | 0.82 | 0.55 | 0.0584 |
| tr\|Q8IDB7\|Q8IDB7_PLAF7 RNA binding protein, putative OS=Plasmodium falciparum (isolate 3D7) GN=PF13_0315 PE=4 SV=1 | 4 | 0.83 | 0.55 | 0.0575 |
| tr\|Q8IL21\|Q8IL21_PLAF7 RNA helicase, putative OS=Plasmodium falciparum (isolate 3D7) GN=PF14_0429 PE=4 SV=1 | 4 | 0.83 | 0.55 | 0.0578 |
| tr\|Q8I3T1\|Q8I3T1_PLAF7 Eukaryotic translation initiation factor 3 subunit B OS=Plasmodium falciparum (isolate 3D7) GN=PFE0885w PE=3 SV=1 | 4 | 0.83 | 0.55 | 0.0575 |
| tr\|Q8IET8\|Q8IET8_PLAF7 ATP dependent DEAD-box helicase, putative OS=Plasmodium falciparum (isolate 3D7) GN=MAL13P1.14 PE=4 SV=1 | 4 | 0.83 | 0.62 | 0.0751 |
| tr\|Q8IHW3\|Q8IHW3_PLAF7 Conserved Plasmodium protein OS=Plasmodium falciparum (isolate 3D7) GN=PF11_0413 PE=4 SV=2 | 4 | 1.33 | 0.71 | 0.0334 |
| tr\|Q8IJF6\|Q8IJF6_PLAF7 Conserved Plasmodium protein OS=Plasmodium falciparum (isolate 3D7) GN=PF10_0242 PE=4 SV=2 | 4 | 0.84 | 0.56 | 0.0579 |
| tr\|C0H469\|C0H469_PLAF7 Putative uncharacterized protein OS=Plasmodium falciparum (isolate 3D7) GN=PFC0430w PE=4 SV=1 | 4 | 0.84 | 0.57 | 0.0609 |
| tr\|Q8IK89\|Q8IK89_PLAF7 Uncharacterized protein OS=Plasmodium falciparum (isolate 3D7) GN=PF14_0717 PE=4 SV=1 | 4 | 0.84 | 0.59 | 0.0655 |
| tr\|Q8I2R8\|Q8I2R8_PLAF7 RNA binding protein, putative OS=Plasmodium falciparum (isolate 3D7) GN=PFI1175c PE=4 SV=1 | 4 | 0.84 | 0.56 | 0.0577 |
| tr\|C0H4W2\|C0H4W2_PLAF7 Lsm3 homologue, putative OS=Plasmodium falciparum (isolate 3D7) GN=PF08_0049 PE=4 SV=1 | 4 | 1.34 | 0.74 | 0.0359 |
| tr\|Q8I488\|Q8I488_PLAF7 PIESP2 erythrocyte surface protein OS=Plasmodium falciparum (isolate 3D7) GN=PFE0060w PE=4 SV=1 | 4 | 0.84 | 0.57 | 0.0607 |
| tr\|Q8IHR4\|Q8IHR4_PLAF7 Dynamin-like protein OS=Plasmodium falciparum (isolate 3D7) GN=dyn1 PE=3 SV=1 | 4 | 0.84 | 0.57 | 0.0600 |
| tr\|Q8I490\|Q8I490_PLAF7 Uncharacterized protein OS=Plasmodium falciparum (isolate 3D7) GN=PFE0050w PE=4 SV=1 | 4 | 0.85 | 0.58 | 0.0597 |
| tr\|Q8IEN2\|Q8IEN2_PLAF7 40S ribosomal protein S27, putative OS=Plasmodium falciparum (isolate 3D7) GN=PF13_0045 PE=1 SV=1 | 4 | 1.38 | 0.43 | 0.0078 |
| tr\|Q8IJZ9\|Q8IJZ9_PLAF7 U5 small nuclear ribonuclear protein, putative OS=Plasmodium falciparum (isolate 3D7) GN=PF10_0041 PE=4 SV=1 | 4 | 0.85 | 0.57 | 0.0582 |
| tr\|C6KSR3\|C6KSR3_PLAF7 Polypyrimidine tract binding protein, putative OS=Plasmodium falciparum (isolate 3D7) GN=PFF0320c PE=4 SV=1 | 4 | 0.85 | 0.55 | 0.0525 |
| tr\|C0H5L9\|C0H5L9_PLAF7 Membrane associated histidine-rich protein, MAHRP-1 OS=Plasmodium falciparum (isolate 3D7) GN=MAHRP1 PE=4 SV=1 | 4 | 0.86 | 0.57 | 0.0577 |
| tr\|Q8IC16\|Q8IC16_PLAF7 DNA helicase OS=Plasmodium falciparum (isolate 3D7) GN=PF07_0023 PE=3 SV=1 | 4 | 0.86 | 0.56 | 0.0548 |
| tr\|Q8III3\|Q8III3_PLAF7 Uncharacterized protein OS=Plasmodium falciparum (isolate 3D7) GN=PF11_0191 PE=4 SV=1 | 4 | 0.86 | 0.56 | 0.0541 |
| tr\|Q8I0W8\|Q8I0W8_PLAF7 Deoxyribodipyrimidine photolyase (Photoreactivating enzyme, DNA photolyase), putative OS=Plasmodium falciparum (isolate 3D7) GN=PFE0675c PE=4 SV=1 | 4 | 0.86 | 0.57 | 0.0577 |
| tr\|Q8IIW6\|Q8IIW6_PLAF7 Actin-like protein, putative OS=Plasmodium falciparum (isolate 3D7) GN=PF11_0047 PE=3 SV=1 | 4 | 0.86 | 0.57 | 0.0568 |
| tr\|Q8ID32\|Q8ID32_PLAF7 Ribosome biogenesis protein MRT4, putative OS=Plasmodium falciparum (isolate 3D7) GN=MAL13P1.341 PE=3 SV=1 | 4 | 0.86 | 0.58 | 0.0591 |
| tr\|Q8IDQ2\|Q8IDQ2_PLAF7 Kelch protein, putative OS=Plasmodium falciparum (isolate 3D7) GN=PF13_0238 PE=4 SV=1 | 4 | 0.86 | 0.58 | 0.0599 |
| tr\|Q8IIS9\|Q8IIS9_PLAF7 Uncharacterized protein OS=Plasmodium falciparum (isolate 3D7) GN=PF11_0086 PE=4 SV=1 | 4 | 0.86 | 0.58 | 0.0588 |
| tr\|C6KSP3\|C6KSP3_PLAF7 Uncharacterized protein OS=Plasmodium falciparum (isolate 3D7) GN=PFF0220w PE=4 SV=1 | 4 | 0.86 | 0.58 | 0.0577 |
| tr\|Q8IKI9\|Q8IKI9_PLAF7 ATP-dependent protease la, putative OS=Plasmodium falciparum (isolate 3D7) GN=PF14_0616 PE=4 SV=1 | 4 | 0.86 | 0.69 | 0.0875 |

| | | | | |
|---|---|---|---|---|
| tr\|Q8ILZ7\|Q8ILZ7_PLAF7 RNA binding protein, putative OS=Plasmodium falciparum (isolate 3D7) GN=PF14_0096 PE=4 SV=1 | 4 | 0.86 | 0.59 | 0.0604 |
| tr\|Q8IJI8\|Q8IJI8_PLAF7 RNA helicase, putative OS=Plasmodium falciparum (isolate 3D7) GN=PF10_0209 PE=4 SV=1 | 4 | 0.87 | 0.59 | 0.0599 |
| tr\|Q8IJJ5\|Q8IJJ5_PLAF7 Conserved protein OS=Plasmodium falciparum (isolate 3D7) GN=PF10_0200 PE=4 SV=1 | 4 | 0.87 | 0.57 | 0.0566 |
| tr\|Q8I4T6\|Q8I4T6_PLAF7 Uncharacterized protein OS=Plasmodium falciparum (isolate 3D7) GN=PFL2390c PE=4 SV=1 | 4 | 0.87 | 0.58 | 0.0589 |
| tr\|Q8IJC0\|Q8IJC0_PLAF7 Nucleolar preribosomal assembly protein, putative OS=Plasmodium falciparum (isolate 3D7) GN=PF10_0278 PE=4 SV=1 | 4 | 0.87 | 0.57 | 0.0545 |
| sp\|P61074\|PCNA_PLAF7 Proliferating cell nuclear antigen OS=Plasmodium falciparum (isolate 3D7) GN=PCNA PE=3 SV=1 | 4 | 1.38 | 0.15 | 0.0004 |
| tr\|Q8IKY0\|Q8IKY0_PLAF7 Transcription factor with AP2 domain(S), putative OS=Plasmodium falciparum (isolate 3D7) GN=ApiAP2 PE=4 SV=1 | 4 | 0.87 | 0.60 | 0.0619 |
| tr\|O96169\|O96169_PLAF7 RNA binding protein, putative OS=Plasmodium falciparum (isolate 3D7) GN=PFB0370c PE=4 SV=1 | 4 | 0.88 | 0.59 | 0.0582 |
| tr\|Q8I0V5\|Q8I0V5_PLAF7 Acyl carrier protein OS=Plasmodium falciparum (isolate 3D7) GN=PFL0415w PE=4 SV=1 | 4 | 0.88 | 0.62 | 0.0658 |
| tr\|Q8I431\|Q8I431_PLAF7 60S ribosomal protein L4, putative OS=Plasmodium falciparum (isolate 3D7) GN=PFE0350c PE=1 SV=1 | 4 | 1.38 | 0.51 | 0.0124 |
| tr\|C0H592\|C0H592_PLAF7 REX2 protein OS=Plasmodium falciparum (isolate 3D7) GN=REX2 PE=4 SV=1;tr\|Q8I2G0\|Q8I2G0_PLAF7 Ring-exported protein 2 OS=Plasmodium falciparum (isolate 3D7) GN=REX2 PE=4 SV=1 | 4 | 0.88 | 0.60 | 0.0611 |
| tr\|Q8I2H3\|Q8I2H3_PLAF7 Vacuolar ATP synthase subunit E, putative OS=Plasmodium falciparum (isolate 3D7) GN=PFI1670c PE=3 SV=2 | 4 | 0.88 | 0.61 | 0.0629 |
| tr\|C6KSX2\|C6KSX2_PLAF7 Nucleolar GTP-binding protein 1, putative OS=Plasmodium falciparum (isolate 3D7) GN=PFF0625w PE=4 SV=1 | 4 | 0.88 | 0.57 | 0.0539 |
| tr\|Q8I562\|Q8I562_PLAF7 Clustered-asparagine-rich protein OS=Plasmodium falciparum (isolate 3D7) GN=PFL1745c PE=4 SV=2 | 4 | 0.88 | 0.58 | 0.0567 |
| tr\|Q8ILR7\|Q8ILR7_PLAF7 DNA helicase OS=Plasmodium falciparum (isolate 3D7) GN=PF14_0177 PE=3 SV=1 | 4 | 0.89 | 0.59 | 0.0583 |
| tr\|Q8IKS1\|Q8IKS1_PLAF7 Uncharacterized protein OS=Plasmodium falciparum (isolate 3D7) GN=PF14_0531 PE=4 SV=1 | 4 | 1.40 | 0.55 | 0.0146 |
| tr\|O77385\|O77385_PLAF7 Protein kinase, putative OS=Plasmodium falciparum (isolate 3D7) GN=Pfcrk-4 PE=4 SV=1 | 4 | 0.89 | 0.59 | 0.0574 |
| tr\|Q8ILQ6\|Q8ILQ6_PLAF7 Uncharacterized protein OS=Plasmodium falciparum (isolate 3D7) GN=PF14_0188 PE=4 SV=2 | 4 | 0.89 | 0.63 | 0.0659 |
| tr\|C0H4U4\|C0H4U4_PLAF7 Uncharacterized protein OS=Plasmodium falciparum (isolate 3D7) GN=MAL8P1.95 PE=4 SV=1 | 4 | 0.89 | 0.60 | 0.0580 |
| tr\|Q8IKQ9\|Q8IKQ9_PLAF7 Signal peptide peptidase OS=Plasmodium falciparum (isolate 3D7) GN=SPP PE=4 SV=2 | 4 | 0.89 | 0.61 | 0.0602 |
| tr\|Q8ID26\|Q8ID26_PLAF7 Uncharacterized protein OS=Plasmodium falciparum (isolate 3D7) GN=PF13_0356 PE=4 SV=1 | 4 | 0.90 | 0.60 | 0.0577 |
| tr\|Q8ILU3\|Q8ILU3_PLAF7 RNA-binding protein Nova-1, putative OS=Plasmodium falciparum (isolate 3D7) GN=PF14_0151 PE=4 SV=1 | 4 | 0.90 | 0.57 | 0.0509 |
| tr\|Q8I2S6\|Q8I2S6_PLAF7 DNA-directed RNA polymerase II, putative OS=Plasmodium falciparum (isolate 3D7) GN=PFI1130c PE=4 SV=1 | 4 | 0.90 | 0.61 | 0.0595 |
| tr\|C6KT34\|C6KT34_PLAF7 Cell division cycle protein 48 homologue, putative OS=Plasmodium falciparum (isolate 3D7) GN=PFF0940c PE=3 SV=1 | 4 | 1.41 | 0.08 | 0.0001 |
| tr\|C6KTB9\|C6KTB9_PLAF7 Ethanolaminephosphotransferase, putative OS=Plasmodium falciparum (isolate 3D7) GN=PFF1375c PE=3 SV=1 | 4 | 0.90 | 0.61 | 0.0598 |
| tr\|Q8IDF8\|Q8IDF8_PLAF7 Putative rRNA methyltransferase OS=Plasmodium falciparum (isolate 3D7) GN=PF13_0286 PE=3 SV=1 | 4 | 0.90 | 0.63 | 0.0642 |
| tr\|Q8IE31\|Q8IE31_PLAF7 Uncharacterized protein OS=Plasmodium falciparum (isolate 3D7) GN=PF13_0162 PE=4 SV=1 | 4 | 0.90 | 0.62 | 0.0610 |
| tr\|Q8I259\|Q8I259_PLAF7 Putative uncharacterized protein OS=Plasmodium falciparum (isolate 3D7) GN=PFA_0410w PE=4 SV=1 | 4 | 1.41 | 0.76 | 0.0336 |
| tr\|O97250\|O97250_PLAF7 60S ribosomal protein L7, putative OS=Plasmodium falciparum (isolate 3D7) GN=PFC0300c PE=1 SV=2 | 4 | 1.42 | 0.29 | 0.0023 |
| tr\|Q8I322\|Q8I322_PLAF7 Putative uncharacterized protein OS=Plasmodium falciparum (isolate 3D7) GN=PFI0635c PE=4 SV=1 | 4 | 0.91 | 0.62 | 0.0604 |
| tr\|Q8IC35\|Q8IC35_PLAF7 Erythrocyte membrane-associated antigen OS=Plasmodium falciparum (isolate 3D7) GN=MAL7P1.12 PE=4 SV=1 | 4 | 0.91 | 0.58 | 0.0517 |
| tr\|O77390\|O77390_PLAF7 Putative uncharacterized protein OS=Plasmodium falciparum (isolate 3D7) GN=PFC0720w PE=4 SV=2 | 4 | 0.91 | 0.65 | 0.0681 |

| | | | | |
|---|---|---|---|---|
| tr\|Q8I3T5\|Q8I3T5_PLAF7 Splicing factor, putative OS=Plasmodium falciparum (isolate 3D7) GN=PFE0865c PE=4 SV=2 | 4 | 0.91 | 0.61 | 0.0583 |
| tr\|O97266\|O97266_PLAF7 Translation initiation factor E4, putative OS=Plasmodium falciparum (isolate 3D7) GN=PFC0635c PE=3 SV=1 | 4 | 0.91 | 0.61 | 0.0577 |
| tr\|Q8IC42\|Q8IC42_PLAF7 Uncharacterized protein OS=Plasmodium falciparum (isolate 3D7) GN=PF07_0008 PE=4 SV=1 | 4 | 0.91 | 0.63 | 0.0628 |
| tr\|Q8IEI6\|Q8IEI6_PLAF7 Uncharacterized protein OS=Plasmodium falciparum (isolate 3D7) GN=PF13_0076 PE=4 SV=1 | 4 | 0.92 | 0.65 | 0.0676 |
| tr\|Q8IDB0\|Q8IDB0_PLAF7 40S ribosomal protein S13, putative OS=Plasmodium falciparum (isolate 3D7) GN=PF13_0316 PE=1 SV=1 | 4 | 1.44 | 0.25 | 0.0014 |
| tr\|Q8I551\|Q8I551_PLAF7 Uncharacterized protein OS=Plasmodium falciparum (isolate 3D7) GN=PFL1800w PE=4 SV=1 | 4 | 0.92 | 0.62 | 0.0599 |
| tr\|Q8IKW4\|Q8IKW4_PLAF7 Uncharacterized protein OS=Plasmodium falciparum (isolate 3D7) GN=PF14_0487 PE=4 SV=1 | 4 | 0.92 | 0.62 | 0.0595 |
| tr\|Q8II01\|Q8II01_PLAF7 Tudor staphylococcal nuclease OS=Plasmodium falciparum (isolate 3D7) GN=TSN PE=4 SV=1 | 4 | 0.92 | 0.63 | 0.0607 |
| tr\|Q8IBZ2\|Q8IBZ2_PLAF7 Lysophospholipase, putative OS=Plasmodium falciparum (isolate 3D7) GN=PF07_0040 PE=4 SV=1 | 4 | 1.44 | 0.90 | 0.0490 |
| tr\|Q8I3H9\|Q8I3H9_PLAF7 Nucleolar preribosomal GTPase, putative OS=Plasmodium falciparum (isolate 3D7) GN=PFE1435c PE=4 SV=1 | 4 | 0.93 | 0.63 | 0.0595 |
| tr\|Q6ZMA8\|Q6ZMA8_PLAF7 Vacuolar ATP synthase subunit b OS=Plasmodium falciparum (isolate 3D7) GN=PFD0305c PE=3 SV=1 | 4 | 1.45 | 0.15 | 0.0003 |
| tr\|Q8IDM3\|Q8IDM3_PLAF7 Uncharacterized protein OS=Plasmodium falciparum (isolate 3D7) GN=MAL13P1.237 PE=4 SV=1 | 4 | 1.45 | 0.11 | 0.0001 |
| tr\|Q8I618\|Q8I618_PLAF7 Conserved Plasmodium protein OS=Plasmodium falciparum (isolate 3D7) GN=PFL0135w PE=4 SV=2 | 4 | 0.93 | 0.61 | 0.0562 |
| tr\|O77396\|O77396_PLAF7 Proteasome component C8, putative OS=Plasmodium falciparum (isolate 3D7) GN=PFC0745c PE=4 SV=1 | 4 | 1.48 | 0.81 | 0.0362 |
| tr\|Q8IM15\|Q8IM15_PLAF7 HAP protein OS=Plasmodium falciparum (isolate 3D7) GN=PF14_0078 PE=1 SV=1 | 4 | 1.51 | 0.46 | 0.0073 |
| tr\|Q8IAW1\|Q8IAW1_PLAF7 RNA binding protein, putative OS=Plasmodium falciparum (isolate 3D7) GN=PF08_0086 PE=4 SV=1 | 4 | 0.94 | 0.78 | 0.0958 |
| tr\|Q8IIR9\|Q8IIR9_PLAF7 Casein kinase II, alpha subunit, putative OS=Plasmodium falciparum (isolate 3D7) GN=PF11_0096 PE=4 SV=1 | 4 | 1.53 | 0.17 | 0.0004 |
| tr\|Q8IHU0\|Q8IHU0_PLAF7 Uncharacterized protein OS=Plasmodium falciparum (isolate 3D7) GN=PF11_0437 PE=1 SV=1 | 4 | 0.94 | 0.63 | 0.0591 |
| tr\|Q8I358\|Q8I358_PLAF7 Exoribonuclease, putative OS=Plasmodium falciparum (isolate 3D7) GN=PFI0455w PE=4 SV=1 | 4 | 0.94 | 0.63 | 0.0576 |
| tr\|Q8IAL3\|Q8IAL3_PLAF7 Uncharacterized protein OS=Plasmodium falciparum (isolate 3D7) GN=PF08_0135 PE=4 SV=1 | 4 | 1.55 | 0.95 | 0.0479 |
| tr\|Q8IM16\|Q8IM16_PLAF7 Plasmepsin IV OS=Plasmodium falciparum (isolate 3D7) GN=PF14_0075 PE=1 SV=1 | 4 | 1.56 | 0.66 | 0.0181 |
| tr\|Q8IIU3\|Q8IIU3_PLAF7 RuvB DNA helicase, putative OS=Plasmodium falciparum (isolate 3D7) GN=PF11_0071 PE=4 SV=1 | 4 | 1.57 | 0.51 | 0.0085 |
| tr\|C0H523\|C0H523_PLAF7 Putative uncharacterized protein OS=Plasmodium falciparum (isolate 3D7) GN=PFI0336w PE=4 SV=1 | 4 | 0.95 | 0.60 | 0.0502 |
| tr\|Q8ILG6\|Q8ILG6_PLAF7 Coatamer protein, beta subunit, putative OS=Plasmodium falciparum (isolate 3D7) GN=PF14_0277 PE=4 SV=2 | 4 | 0.95 | 0.64 | 0.0583 |
| tr\|Q8IKT7\|Q8IKT7_PLAF7 Uncharacterized protein OS=Plasmodium falciparum (isolate 3D7) GN=PF14_0515 PE=4 SV=1 | 4 | 0.95 | 0.66 | 0.0627 |
| tr\|Q8IBJ1\|Q8IBJ1_PLAF7 Ubiquitin carboxyl-terminal hydrolase OS=Plasmodium falciparum (isolate 3D7) GN=MAL7P1.147 PE=3 SV=1 | 4 | 0.95 | 0.65 | 0.0601 |
| tr\|Q8ID85\|Q8ID85_PLAF7 ATP-dependent DNA helicase, putative OS=Plasmodium falciparum (isolate 3D7) GN=PF13_0330 PE=4 SV=1 | 4 | 0.95 | 0.64 | 0.0581 |
| tr\|Q8I511\|Q8I511_PLAF7 DEAD/DEAH box helicase, putative OS=Plasmodium falciparum (isolate 3D7) GN=PFL2010c PE=4 SV=2 | 4 | 0.96 | 0.65 | 0.0615 |
| tr\|Q8I3I6\|Q8I3I6_PLAF7 Beta adaptin protein, putative OS=Plasmodium falciparum (isolate 3D7) GN=PFE1400c PE=4 SV=2 | 4 | 0.96 | 0.64 | 0.0589 |
| tr\|Q8IDR9\|Q8IDR9_PLAF7 40S ribosomal protein S6, putative OS=Plasmodium falciparum (isolate 3D7) GN=PF13_0228 PE=1 SV=1 | 4 | 1.59 | 0.24 | 0.0009 |
| tr\|Q8IDF0\|Q8IDF0_PLAF7 DNA helicase OS=Plasmodium falciparum (isolate 3D7) GN=PF13_0291 PE=3 SV=1 | 4 | 0.97 | 0.65 | 0.0579 |
| tr\|Q8I547\|Q8I547_PLAF7 Uncharacterized protein OS=Plasmodium falciparum (isolate 3D7) GN=PFL1820w PE=4 SV=1 | 4 | 0.97 | 0.65 | 0.0587 |
| tr\|Q8ILV2\|Q8ILV2_PLAF7 60S ribosomal protein L10, putative OS=Plasmodium falciparum (isolate 3D7) GN=PF14_0141 PE=1 SV=1 | 4 | 0.97 | 0.71 | 0.0710 |

| | | | | |
|---|---|---|---|---|
| tr\|Q8IC08\|Q8IC08_PLAF7 DNA-directed RNA polymerase 2 8.2 kDa polypeptide, putative OS=Plasmodium falciparum (isolate 3D7) GN=PF07_0027 PE=3 SV=1 | 4 | 0.98 | 0.70 | 0.0677 |
| tr\|Q9TY94\|Q9TY94_PLAF7 DEAD box helicase, UAP56 OS=Plasmodium falciparum (isolate 3D7) GN=UAP56 PE=4 SV=1 | 4 | 1.61 | 0.02 | 0.0000 |
| tr\|Q8IIT1\|Q8IIT1_PLAF7 Conserved Plasmodium protein OS=Plasmodium falciparum (isolate 3D7) GN=PF11_0084 PE=4 SV=2 | 4 | 0.98 | 0.98 | 0.1397 |
| tr\|O77395\|O77395_PLAF7 40S ribosomal protein S15A, putative OS=Plasmodium falciparum (isolate 3D7) GN=PFC0735w PE=1 SV=1 | 4 | 1.62 | 0.09 | 0.0000 |
| tr\|Q8IHQ8\|Q8IHQ8_PLAF7 Uncharacterized protein OS=Plasmodium falciparum (isolate 3D7) GN=PF11_0471 PE=4 SV=1 | 4 | 0.98 | 0.65 | 0.0571 |
| tr\|Q8IB09\|Q8IB09_PLAF7 Asparagine-rich antigen OS=Plasmodium falciparum (isolate 3D7) GN=PF08_0060 PE=4 SV=1 | 4 | 0.99 | 0.67 | 0.0608 |
| tr\|Q8IBJ9\|Q8IBJ9_PLAF7 Mago nashi protein homolog, putative OS=Plasmodium falciparum (isolate 3D7) GN=MAL7P1.139 PE=4 SV=2 | 4 | 0.99 | 0.63 | 0.0513 |
| tr\|Q8I1Q5\|Q8I1Q5_PLAF7 Eukaryotic translation initiation factor 3 subunit M OS=Plasmodium falciparum (isolate 3D7) GN=PFD0880w PE=3 SV=1 | 4 | 1.00 | 0.70 | 0.0659 |
| tr\|Q8IL83\|Q8IL83_PLAF7 Cleavage and polyadenylation specificity factor protein, putative OS=Plasmodium falciparum (isolate 3D7) GN=PF14_0364 PE=4 SV=1 | 4 | 1.00 | 0.64 | 0.0534 |
| tr\|Q8IKH8\|Q8IKH8_PLAF7 40S ribosomal protein S3, putative OS=Plasmodium falciparum (isolate 3D7) GN=PF14_0627 PE=1 SV=1 | 4 | 1.63 | 0.25 | 0.0009 |
| tr\|Q8I573\|Q8I573_PLAF7 Uncharacterized protein OS=Plasmodium falciparum (isolate 3D7) GN=PFL1685w PE=4 SV=1 | 4 | 1.00 | 1.49 | 0.2716 |
| tr\|Q8I442\|Q8I442_PLAF7 Uncharacterized protein OS=Plasmodium falciparum (isolate 3D7) GN=PFE0295w PE=4 SV=1 | 4 | 1.01 | 1.45 | 0.2592 |
| tr\|Q8I5T4\|Q8I5T4_PLAF7 DNA helicase OS=Plasmodium falciparum (isolate 3D7) GN=PFL0580w PE=3 SV=1 | 4 | 1.02 | 0.68 | 0.0577 |
| tr\|C6KSR5\|C6KSR5_PLAF7 Coatomer alpha subunit, putative OS=Plasmodium falciparum (isolate 3D7) GN=PFF0330w PE=4 SV=1 | 4 | 1.02 | 0.69 | 0.0598 |
| tr\|O97248\|O97248_PLAF7 40S ribosomal protein S23, putative OS=Plasmodium falciparum (isolate 3D7) GN=PFC0290w PE=1 SV=1 | 4 | 1.03 | 0.69 | 0.0589 |
| tr\|Q8IL13\|Q8IL13_PLAF7 Helicase, putative OS=Plasmodium falciparum (isolate 3D7) GN=PF14_0437 PE=3 SV=2 | 4 | 1.03 | 0.70 | 0.0604 |
| tr\|C6KT09\|C6KT09_PLAF7 Malate:quinone oxidoreductase, putative OS=Plasmodium falciparum (isolate 3D7) GN=PFF0815w PE=4 SV=1 | 4 | 1.03 | 0.68 | 0.0560 |
| tr\|Q8ILM0\|Q8ILM0_PLAF7 Cyclophilin, putative OS=Plasmodium falciparum (isolate 3D7) GN=PF14_0223 PE=4 SV=2 | 4 | 1.03 | 0.66 | 0.0522 |
| tr\|Q8IDS6\|Q8IDS6_PLAF7 60S ribosomal protein L18a OS=Plasmodium falciparum (isolate 3D7) GN=PF13_0224 PE=1 SV=1 | 4 | 1.73 | 0.33 | 0.0019 |
| tr\|O96258\|O96258_PLAF7 40S ribosomal protein S26e, putative OS=Plasmodium falciparum (isolate 3D7) GN=PFB0830w PE=1 SV=1 | 4 | 1.03 | 0.70 | 0.0599 |
| tr\|Q8I280\|Q8I280_PLAF7 V-type ATPase, subunit C, putative OS=Plasmodium falciparum (isolate 3D7) GN=PFA_0300c PE=4 SV=1 | 4 | 1.04 | 0.69 | 0.0573 |
| tr\|Q8IE84\|Q8IE84_PLAF7 Vacuolar ATP synthase subunit G, putative OS=Plasmodium falciparum (isolate 3D7) GN=PF13_0130 PE=4 SV=1 | 4 | 1.04 | 0.69 | 0.0579 |
| tr\|Q8IBA0\|Q8IBA0_PLAF7 Receptor for activated C kinase homolog, PfRACK OS=Plasmodium falciparum (isolate 3D7) GN=PfRACK PE=4 SV=1 | 4 | 1.75 | 0.23 | 0.0006 |
| tr\|Q8I2X0\|Q8I2X0_PLAF7 Eukaryotic translation initiation factor 3 subunit 5, putative OS=Plasmodium falciparum (isolate 3D7) GN=PFI0895c PE=4 SV=1 | 4 | 1.05 | 0.69 | 0.0563 |
| tr\|Q8II72\|Q8II72_PLAF7 Uncharacterized protein OS=Plasmodium falciparum (isolate 3D7) GN=PF11_0302 PE=4 SV=1 | 4 | 1.75 | 0.15 | 0.0002 |
| tr\|Q8IEK1\|Q8IEK1_PLAF7 M1-family aminopeptidase OS=Plasmodium falciparum (isolate 3D7) GN=MAL13P1.56 PE=4 SV=1 | 4 | 1.76 | 0.13 | 0.0001 |
| tr\|C0H4T1\|C0H4T1_PLAF7 Coatomer epsilon subunit, putative OS=Plasmodium falciparum (isolate 3D7) GN=MAL8P1.121:exon:1 PE=4 SV=1 | 4 | 1.05 | 0.78 | 0.0728 |
| tr\|Q8IKA6\|Q8IKA6_PLAF7 DNAJ protein, putative OS=Plasmodium falciparum (isolate 3D7) GN=PF14_0700 PE=4 SV=1 | 4 | 1.05 | 0.70 | 0.0577 |
| tr\|Q8I5U3\|Q8I5U3_PLAF7 Uncharacterized protein OS=Plasmodium falciparum (isolate 3D7) GN=PFL0530c PE=4 SV=1 | 4 | 1.06 | 0.69 | 0.0551 |
| tr\|Q8IE82\|Q8IE82_PLAF7 60S ribosomal protein L23a, putative OS=Plasmodium falciparum (isolate 3D7) GN=PF13_0132 PE=1 SV=1 | 4 | 1.06 | 0.75 | 0.0673 |
| tr\|Q8IBX7\|Q8IBX7_PLAF7 Uncharacterized protein OS=Plasmodium falciparum (isolate 3D7) GN=MAL7P1.36 PE=4 SV=1 | 4 | 1.06 | 0.71 | 0.0592 |
| tr\|Q8I6S4\|Q8I6S4_PLAF7 Peptidyl-prolyl cis-trans isomerase OS=Plasmodium falciparum (isolate 3D7) GN=PfCyP24 PE=3 SV=1 | 4 | 1.06 | 0.72 | 0.0607 |
| tr\|Q8I3B0\|Q8I3B0_PLAF7 60S ribosomal protein L32, putative OS=Plasmodium falciparum (isolate 3D7) GN=PFI0190w PE=4 SV=1 | 4 | 1.06 | 0.71 | 0.0588 |

| | | | | |
|---|---|---|---|---|
| tr\|C0H553\|C0H553_PLAF7 Flavodoxin-like protein OS=Plasmodium falciparum (isolate 3D7) GN=PFI1140w PE=4 SV=1 | 4 | 1.07 | 0.95 | 0.1091 |
| tr\|Q7KQK6\|Q7KQK6_PLAF7 GTP-binding nuclear protein ran/tc4 OS=Plasmodium falciparum (isolate 3D7) GN=PF11_0183 PE=4 SV=1 | 4 | 1.80 | 0.45 | 0.0041 |
| tr\|Q8IB24\|Q8IB24_PLAF7 Heat shock 70 kDa protein OS=Plasmodium falciparum (isolate 3D7) GN=PF08_0054 PE=3 SV=1 | 4 | 1.81 | 0.38 | 0.0024 |
| tr\|Q8ILK4\|Q8ILK4_PLAF7 Uncharacterized protein OS=Plasmodium falciparum (isolate 3D7) GN=PF14_0239 PE=4 SV=2 | 4 | 1.07 | 0.72 | 0.0577 |
| tr\|Q8IJS7\|Q8IJS7_PLAF7 QF122 antigen OS=Plasmodium falciparum (isolate 3D7) GN=PF10_0115 PE=4 SV=1 | 4 | 1.82 | 0.66 | 0.0119 |
| tr\|Q8ILE8\|Q8ILE8_PLAF7 60S ribosomal protein L14, putative OS=Plasmodium falciparum (isolate 3D7) GN=PF14_0296 PE=1 SV=1 | 4 | 1.08 | 0.72 | 0.0577 |
| tr\|Q8I374\|Q8I374_PLAF7 Subunit of proteaseome activator complex, putative OS=Plasmodium falciparum (isolate 3D7) GN=PFI0370c PE=4 SV=1 | 4 | 1.08 | 0.73 | 0.0605 |
| tr\|C0H5J2\|C0H5J2_PLAF7 Uncharacterized protein OS=Plasmodium falciparum (isolate 3D7) GN=MAL13P1.295 PE=4 SV=1 | 4 | 1.08 | 0.73 | 0.0600 |
| tr\|C6KTC9\|C6KTC9_PLAF7 RNA binding protein, putative OS=Plasmodium falciparum (isolate 3D7) GN=PFF1425w PE=4 SV=1 | 4 | 1.08 | 1.13 | 0.1510 |
| tr\|Q8IB14\|Q8IB14_PLAF7 High mobility group protein OS=Plasmodium falciparum (isolate 3D7) GN=PfHMGB2 PE=1 SV=1 | 4 | 1.09 | 0.73 | 0.0582 |
| tr\|C6KSY6\|C6KSY6_PLAF7 60S ribosomal protein L19, putative OS=Plasmodium falciparum (isolate 3D7) GN=PFF0700c PE=1 SV=1 | 4 | 1.83 | 0.55 | 0.0070 |
| tr\|Q8I3T8\|Q8I3T8_PLAF7 60S ribosomal protein L12, putative OS=Plasmodium falciparum (isolate 3D7) GN=PFE0850c PE=3 SV=2 | 4 | 1.09 | 0.74 | 0.0602 |
| tr\|Q8I3U6\|Q8I3U6_PLAF7 40S ribosomal protein S14, putative OS=Plasmodium falciparum (isolate 3D7) GN=PFE0810c PE=1 SV=1 | 4 | 1.09 | 0.74 | 0.0601 |
| tr\|Q8I3J5\|Q8I3J5_PLAF7 DNA helicase OS=Plasmodium falciparum (isolate 3D7) GN=PFE1345c PE=3 SV=1 | 4 | 1.10 | 0.73 | 0.0576 |
| tr\|Q8II16\|Q8II16_PLAF7 Coatomer delta subunit, putative OS=Plasmodium falciparum (isolate 3D7) GN=PF11_0359 PE=4 SV=1 | 4 | 1.10 | 0.73 | 0.0568 |
| tr\|Q8IHT2\|Q8IHT2_PLAF7 Translation initiation factor eIF-1A, putative OS=Plasmodium falciparum (isolate 3D7) GN=PF11_0447 PE=3 SV=2 | 4 | 1.10 | 0.74 | 0.0590 |
| tr\|Q8IAR6\|Q8IAR6_PLAF7 Proteasome subunit alpha type 5, putative OS=Plasmodium falciparum (isolate 3D7) GN=PF08_0109 PE=4 SV=1 | 4 | 1.10 | 0.75 | 0.0605 |
| tr\|Q8I463\|Q8I463_PLAF7 60S ribosomal protein L31, putative OS=Plasmodium falciparum (isolate 3D7) GN=PFE0185c PE=1 SV=1 | 4 | 1.10 | 0.74 | 0.0578 |
| tr\|Q8IHT9\|Q8IHT9_PLAF7 60S ribosomal protein L35Ae, putative OS=Plasmodium falciparum (isolate 3D7) GN=PF11_0438 PE=1 SV=1 | 4 | 1.11 | 0.74 | 0.0583 |
| tr\|Q8I502\|Q8I502_PLAF7 40S ribosomal protein S17, putative OS=Plasmodium falciparum (isolate 3D7) GN=PFL2055w PE=1 SV=1 | 4 | 1.11 | 0.74 | 0.0576 |
| tr\|Q8IJZ7\|Q8IJZ7_PLAF7 60S ribosomal protein L13, putative OS=Plasmodium falciparum (isolate 3D7) GN=PF10_0043 PE=1 SV=1 | 4 | 1.11 | 0.74 | 0.0582 |
| tr\|Q8I3R0\|Q8I3R0_PLAF7 40S ribosomal protein S9, putative OS=Plasmodium falciparum (isolate 3D7) GN=PFE1005w PE=3 SV=1 | 4 | 1.11 | 0.74 | 0.0577 |
| tr\|Q8IIX0\|Q8IIX0_PLAF7 60S acidic ribosomal protein p1, putative OS=Plasmodium falciparum (isolate 3D7) GN=PF11_0043 PE=3 SV=1 | 4 | 1.12 | 0.75 | 0.0583 |
| tr\|Q8I2Q0\|Q8I2Q0_PLAF7 Putative uncharacterized protein OS=Plasmodium falciparum (isolate 3D7) GN=PFI1270w PE=4 SV=1 | 4 | 1.83 | 1.14 | 0.0486 |
| tr\|C6KSR4\|C6KSR4_PLAF7 Uncharacterized protein OS=Plasmodium falciparum (isolate 3D7) GN=PFF0325c PE=4 SV=1 | 4 | 1.12 | 0.73 | 0.0546 |
| sp\|Q76NM6\|VATA_PLAF7 V-type proton ATPase catalytic subunit A OS=Plasmodium falciparum (isolate 3D7) GN=vapA PE=3 SV=1 | 4 | 1.12 | 0.73 | 0.0552 |
| tr\|Q8IFP2\|Q8IFP2_PLAF7 40S ribosomal protein S19, putative OS=Plasmodium falciparum (isolate 3D7) GN=PFD1055w PE=1 SV=1 | 4 | 1.12 | 0.75 | 0.0587 |
| tr\|Q8II61\|Q8II61_PLAF7 60S ribosomal protein P0 OS=Plasmodium falciparum (isolate 3D7) GN=PF11_0313 PE=3 SV=1 | 4 | 1.13 | 0.77 | 0.0603 |
| tr\|Q8ILN8\|Q8ILN8_PLAF7 40S ribosomal protein S25, putative OS=Plasmodium falciparum (isolate 3D7) GN=PF14_0205 PE=1 SV=2 | 4 | 1.13 | 0.76 | 0.0581 |
| tr\|Q8IE85\|Q8IE85_PLAF7 60S ribosomal protein L6, putative OS=Plasmodium falciparum (isolate 3D7) GN=PF13_0129 PE=1 SV=1 | 4 | 1.13 | 0.75 | 0.0577 |
| tr\|Q8IDV1\|Q8IDV1_PLAF7 60S ribosomal protein L6-2, putative OS=Plasmodium falciparum (isolate 3D7) GN=PF13_0213 PE=1 SV=1 | 4 | 1.14 | 0.76 | 0.0588 |
| sp\|Q8ILW9\|ACT2_PLAF7 Actin-2 OS=Plasmodium falciparum (isolate 3D7) GN=PF14_0124 PE=3 SV=1 | 4 | 1.86 | 0.32 | 0.0014 |
| tr\|Q8I426\|Q8I426_PLAF7 Nuclear pore associated protein (NLP4), putative OS=Plasmodium falciparum (isolate 3D7) GN=PFE0380c PE=4 SV=1 | 4 | 1.14 | 0.77 | 0.0596 |

| | | | | |
|---|---|---|---|---|
| sp\|P04040\|CATA_HUMAN Catalase OS=Homo sapiens GN=CAT PE=1 SV=3 | 4 | 1.88 | 0.60 | 0.0082 |
| tr\|Q8IIL0\|Q8IIL0_PLAF7 Falcipain-3 OS=Plasmodium falciparum (isolate 3D7) GN=PF11_0162 PE=3 SV=1 | 4 | 1.15 | 0.78 | 0.0603 |
| tr\|Q8IDI5\|Q8IDI5_PLAF7 60S ribosomal protein L17, putative OS=Plasmodium falciparum (isolate 3D7) GN=PF13_0268 PE=1 SV=1 | 4 | 1.88 | 0.72 | 0.0137 |
| tr\|Q8IIA2\|Q8IIA2_PLAF7 Ribosomal protein S18, putative OS=Plasmodium falciparum (isolate 3D7) GN=PF11_0272 PE=1 SV=1 | 4 | 1.15 | 0.76 | 0.0570 |
| tr\|Q8IL02\|Q8IL02_PLAF7 40S ribosomal protein S2, putative OS=Plasmodium falciparum (isolate 3D7) GN=PF14_0448 PE=1 SV=1 | 4 | 1.15 | 0.77 | 0.0584 |
| sp\|Q7KQM1\|PRI1_PLAF7 DNA primase small subunit OS=Plasmodium falciparum (isolate 3D7) GN=PF14_0366 PE=3 SV=1 | 4 | 1.15 | 0.74 | 0.0517 |
| tr\|Q8I447\|Q8I447_PLAF7 DNA mismatch repair protein MSH6 OS=Plasmodium falciparum (isolate 3D7) GN=PFE0270c PE=3 SV=1 | 4 | 1.15 | 0.83 | 0.0679 |
| tr\|Q8IES0\|Q8IES0_PLAF7 Small heat shock protein, putative OS=Plasmodium falciparum (isolate 3D7) GN=PF13_0021 PE=3 SV=1 | 4 | 1.16 | 0.77 | 0.0573 |
| tr\|Q8I3T9\|Q8I3T9_PLAF7 60S ribosomal protein L8, putative OS=Plasmodium falciparum (isolate 3D7) GN=PFE0845c PE=1 SV=1 | 4 | 1.16 | 0.79 | 0.0607 |
| tr\|Q8IET7\|Q8IET7_PLAF7 40S ribosomal protein S7, putative OS=Plasmodium falciparum (isolate 3D7) GN=PF13_0014 PE=1 SV=1 | 4 | 1.16 | 0.77 | 0.0577 |
| tr\|Q8ILK3\|Q8ILK3_PLAF7 60S ribosomal protein L21e, putative OS=Plasmodium falciparum (isolate 3D7) GN=PF14_0240 PE=1 SV=1 | 4 | 1.16 | 0.81 | 0.0638 |
| tr\|Q8IAX5\|Q8IAX5_PLAF7 40S ribosomal protein S16, putative OS=Plasmodium falciparum (isolate 3D7) GN=PF08_0076 PE=1 SV=1 | 4 | 1.16 | 0.78 | 0.0587 |
| tr\|O77381\|O77381_PLAF7 40S ribosomal protein S11, putative OS=Plasmodium falciparum (isolate 3D7) GN=PFC0775w PE=1 SV=2 | 4 | 1.17 | 0.88 | 0.0775 |
| tr\|Q8IE09\|Q8IE09_PLAF7 60S ribosomal protein L23, putative OS=Plasmodium falciparum (isolate 3D7) GN=PF13_0171 PE=1 SV=1 | 4 | 1.17 | 0.78 | 0.0588 |
| tr\|Q8IIT3\|Q8IIT3_PLAF7 Lsm4 homologue, putative OS=Plasmodium falciparum (isolate 3D7) GN=PF11_0524 PE=4 SV=2 | 4 | 1.17 | 0.79 | 0.0588 |
| tr\|Q8IHW4\|Q8IHW4_PLAF7 V-type proton ATPase subunit F OS=Plasmodium falciparum (isolate 3D7) GN=PF11_0412 PE=3 SV=2 | 4 | 1.17 | 0.77 | 0.0557 |
| tr\|Q8IM10\|Q8IM10_PLAF7 40S ribosomal protein S8 OS=Plasmodium falciparum (isolate 3D7) GN=PF14_0083 PE=1 SV=1 | 4 | 1.17 | 0.78 | 0.0577 |
| tr\|Q8IEK3\|Q8IEK3_PLAF7 26S proteasome regulatory subunit 7, putative OS=Plasmodium falciparum (isolate 3D7) GN=PF13_0063 PE=3 SV=2 | 4 | 1.17 | 0.74 | 0.0512 |
| tr\|Q8IJK8\|Q8IJK8_PLAF7 Ribosomal protein L30e, putative OS=Plasmodium falciparum (isolate 3D7) GN=PF10_0187 PE=1 SV=1 | 4 | 1.17 | 0.82 | 0.0648 |
| tr\|Q8IL58\|Q8IL58_PLAF7 60S ribosomal protein L1, putative OS=Plasmodium falciparum (isolate 3D7) GN=PF14_0391 PE=4 SV=1 | 4 | 1.17 | 0.79 | 0.0586 |
| tr\|Q8IAX6\|Q8IAX6_PLAF7 60S ribosomal protein L13 OS=Plasmodium falciparum (isolate 3D7) GN=PF08_0075 PE=3 SV=1 | 4 | 1.18 | 0.78 | 0.0574 |
| tr\|Q8I3R6\|Q8I3R6_PLAF7 40S ribosomal protein S24 OS=Plasmodium falciparum (isolate 3D7) GN=PFE0975c PE=3 SV=1 | 4 | 1.18 | 0.79 | 0.0589 |
| tr\|Q8I574\|Q8I574_PLAF7 Splicing factor 3b, subunit 3, 130kD, putative OS=Plasmodium falciparum (isolate 3D7) GN=PFL1680w PE=4 SV=1 | 4 | 1.18 | 1.00 | 0.0994 |
| tr\|Q8II27\|Q8II27_PLAF7 RNA (Uracil-5-)methyltransferase, putative OS=Plasmodium falciparum (isolate 3D7) GN=PF11_0348 PE=4 SV=2 | 4 | 1.18 | 0.88 | 0.0750 |
| tr\|Q8IK02\|Q8IK02_PLAF7 Ribosomal protein S20e, putative OS=Plasmodium falciparum (isolate 3D7) GN=PF10_0038 PE=1 SV=1 | 4 | 1.19 | 0.81 | 0.0601 |
| tr\|C0H4T9\|C0H4T9_PLAF7 CAF1 family ribonuclease, putative OS=Plasmodium falciparum (isolate 3D7) GN=MAL8P1.104 PE=4 SV=1 | 4 | 1.19 | 0.89 | 0.0749 |
| tr\|Q8I4U5\|Q8I4U5_PLAF7 Tat-binding protein homolog OS=Plasmodium falciparum (isolate 3D7) GN=PFL2345c PE=3 SV=1 | 4 | 1.19 | 0.81 | 0.0600 |
| tr\|Q8ILL2\|Q8ILL2_PLAF7 60S ribosomal protein L7-3, putative OS=Plasmodium falciparum (isolate 3D7) GN=PF14_0231 PE=1 SV=2 | 4 | 1.19 | 0.80 | 0.0580 |
| tr\|O96153\|O96153_PLAF7 Proteasome 26S regulatory subunit, putative OS=Plasmodium falciparum (isolate 3D7) GN=PFB0260w PE=4 SV=3 | 4 | 1.94 | 0.53 | 0.0054 |
| tr\|Q8IJC6\|Q8IJC6_PLAF7 Ribosomal protein L3, putative OS=Plasmodium falciparum (isolate 3D7) GN=PF10_0272 PE=1 SV=1 | 4 | 1.19 | 0.79 | 0.0562 |
| tr\|O77343\|O77343_PLAF7 Transporter, putative OS=Plasmodium falciparum (isolate 3D7) GN=PFC0530w PE=4 SV=1 | 4 | 1.19 | 1.06 | 0.1086 |
| tr\|Q8I2W3\|Q8I2W3_PLAF7 Nucleosome assembly protein OS=Plasmodium falciparum (isolate 3D7) GN=PFI0930c PE=3 SV=1 | 4 | 1.20 | 0.80 | 0.0586 |
| tr\|Q8I2Z8\|Q8I2Z8_PLAF7 6-phosphofructokinase, putative OS=Plasmodium falciparum (isolate 3D7) GN=PFI0755c PE=4 SV=1 | 4 | 1.97 | 0.85 | 0.0185 |

| | | | | |
|---|---|---|---|---|
| tr\|Q8IHX2\|Q8IHX2_PLAF7 Malaria antigen OS=Plasmodium falciparum (isolate 3D7) GN=PF11_0404 PE=4 SV=1 | 4 | 1.20 | 1.14 | 0.1253 |
| tr\|Q8IES4\|Q8IES4_PLAF7 DNA ligase OS=Plasmodium falciparum (isolate 3D7) GN=PfLigI PE=3 SV=1 | 4 | 1.20 | 0.80 | 0.0572 |
| tr\|O77364\|O77364_PLAF7 60S ribosomal protein L26, putative OS=Plasmodium falciparum (isolate 3D7) GN=PFC0535w PE=1 SV=1 | 4 | 1.20 | 0.81 | 0.0590 |
| tr\|Q8II62\|Q8II62_PLAF7 60S ribosomal protein L38e, putative OS=Plasmodium falciparum (isolate 3D7) GN=PF11_0312 PE=1 SV=1 | 4 | 1.20 | 0.81 | 0.0593 |
| tr\|Q8ID28\|Q8ID28_PLAF7 Proteasome regulatory subunit, putative OS=Plasmodium falciparum (isolate 3D7) GN=MAL13P1.343 PE=4 SV=1 | 4 | 1.20 | 0.80 | 0.0579 |
| tr\|Q8IKH3\|Q8IKH3_PLAF7 26S proteasome subunit, putative OS=Plasmodium falciparum (isolate 3D7) GN=PF14_0632 PE=4 SV=1 | 4 | 1.20 | 0.82 | 0.0611 |
| tr\|C0H4A6\|C0H4A6_PLAF7 Ribosomal protein L15 OS=Plasmodium falciparum (isolate 3D7) GN=PFD0770c PE=1 SV=1 | 4 | 1.21 | 0.77 | 0.0506 |
| sp\|O97249\|RS12_PLAF7 40S ribosomal protein S12 OS=Plasmodium falciparum (isolate 3D7) GN=RPS12 PE=1 SV=1 | 4 | 1.21 | 0.81 | 0.0581 |
| tr\|Q8IHZ8\|Q8IHZ8_PLAF7 Uncharacterized protein OS=Plasmodium falciparum (isolate 3D7) GN=PF11_0378 PE=4 SV=1 | 4 | 1.22 | 0.84 | 0.0629 |
| tr\|C0H5B1\|C0H5B1_PLAF7 Asparagine-rich protein OS=Plasmodium falciparum (isolate 3D7) GN=MAL13P1.63 PE=4 SV=1 | 4 | 1.22 | 0.81 | 0.0576 |
| tr\|Q8IBN5\|Q8IBN5_PLAF7 40S ribosomal protein S5, putative OS=Plasmodium falciparum (isolate 3D7) GN=PF07_0088 PE=1 SV=1 | 4 | 1.22 | 0.82 | 0.0583 |
| tr\|Q8I713\|Q8I713_PLAF7 60S ribosomal protein L36 OS=Plasmodium falciparum (isolate 3D7) GN=PF11_0106 PE=1 SV=2 | 4 | 1.22 | 0.84 | 0.0617 |
| tr\|O97285\|O97285_PLAF7 ATP-dependent RNA Helicase, putative OS=Plasmodium falciparum (isolate 3D7) GN=PFC0915w PE=3 SV=1 | 4 | 1.23 | 0.84 | 0.0605 |
| tr\|Q8I444\|Q8I444_PLAF7 Small ubiquitin-related modifier, putative OS=Plasmodium falciparum (isolate 3D7) GN=PfSUMO PE=4 SV=1 | 4 | 1.23 | 0.82 | 0.0578 |
| tr\|Q8I6V3\|Q8I6V3_PLAF7 Plasmepsin II OS=Plasmodium falciparum (isolate 3D7) GN=PF14_0077 PE=3 SV=1 | 4 | 2.00 | 0.49 | 0.0039 |
| tr\|O96259\|O96259_PLAF7 Conserved Plasmodium protein OS=Plasmodium falciparum (isolate 3D7) GN=PFB0835c PE=4 SV=1 | 4 | 1.24 | 1.02 | 0.0942 |
| tr\|Q8IEQ1\|Q8IEQ1_PLAF7 26S proteasome regulatory subunit, putative OS=Plasmodium falciparum (isolate 3D7) GN=PF13_0033 PE=3 SV=1 | 4 | 2.00 | 0.65 | 0.0085 |
| tr\|Q8IHR8\|Q8IHR8_PLAF7 PfRab6, GTPase OS=Plasmodium falciparum (isolate 3D7) GN=Rab6 PE=3 SV=2 | 4 | 1.25 | 0.79 | 0.0504 |
| tr\|C0H5C2\|C0H5C2_PLAF7 40S ribosomal protein S15/S19, putative OS=Plasmodium falciparum (isolate 3D7) GN=MAL13P1.92 PE=1 SV=1 | 4 | 1.25 | 0.84 | 0.0590 |
| tr\|C6S3F0\|C6S3F0_PLAF7 Acylphosphatase, putative OS=Plasmodium falciparum (isolate 3D7) GN=PF11_0121 PE=3 SV=1 | 4 | 1.26 | 0.86 | 0.0612 |
| tr\|Q8IBQ6\|Q8IBQ6_PLAF7 60S ribosomal protein L11a, putative OS=Plasmodium falciparum (isolate 3D7) GN=PF07_0079 PE=1 SV=1 | 4 | 1.26 | 0.84 | 0.0571 |
| tr\|Q8IM66\|Q8IM66_PLAF7 Proteosome subunit, putative OS=Plasmodium falciparum (isolate 3D7) GN=PF14_0025 PE=4 SV=1 | 4 | 1.26 | 0.84 | 0.0578 |
| tr\|Q8IM31\|Q8IM31_PLAF7 Glycerophodiester phosphodiesterase, putative OS=Plasmodium falciparum (isolate 3D7) GN=PF14_0060 PE=4 SV=1 | 4 | 1.27 | 1.13 | 0.1109 |
| tr\|C6S3J6\|C6S3J6_PLAF7 Ribosomal protein L29, putative OS=Plasmodium falciparum (isolate 3D7) GN=PF14_0575a PE=1 SV=1 | 4 | 1.27 | 0.91 | 0.0689 |
| tr\|Q8IDN4\|Q8IDN4_PLAF7 Nucleic acid binding protein, putative OS=Plasmodium falciparum (isolate 3D7) GN=MAL13P1.233 PE=4 SV=1 | 4 | 1.28 | 0.87 | 0.0609 |
| sp\|Q7KQM4\|PLM1_PLAF7 Plasmepsin-1 OS=Plasmodium falciparum (isolate 3D7) GN=PF14_0076 PE=2 SV=1 | 4 | 1.28 | 0.84 | 0.0551 |
| tr\|A0A087WUQ6\|A0A087WUQ6_HUMAN Glutathione peroxidase OS=Homo sapiens GN=GPX1 PE=1 SV=1;sp\|P07203\|GPX1_HUMAN Glutathione peroxidase 1 OS=Homo sapiens GN=GPX1 PE=1 SV=4 | 4 | 1.28 | 0.89 | 0.0639 |
| tr\|Q8I2Y5\|Q8I2Y5_PLAF7 RNA binding protein, putative OS=Plasmodium falciparum (isolate 3D7) GN=PFI0820c PE=4 SV=1 | 4 | 1.28 | 0.86 | 0.0592 |
| tr\|Q8I3L4\|Q8I3L4_PLAF7 Acyl-CoA synthetase, PfACS10 OS=Plasmodium falciparum (isolate 3D7) GN=PfACS10 PE=4 SV=1 | 4 | 2.12 | 0.76 | 0.0116 |
| sp\|Q8IJD4\|RSSA_PLAF7 40S ribosomal protein SA OS=Plasmodium falciparum (isolate 3D7) GN=PF10_0264 PE=1 SV=1 | 4 | 2.13 | 0.50 | 0.0034 |
| tr\|Q8IHS5\|Q8IHS5_PLAF7 40S ribosomal protein S21 OS=Plasmodium falciparum (isolate 3D7) GN=PF11_0454 PE=1 SV=1 | 4 | 1.28 | 0.89 | 0.0640 |

| | | | | |
|---|---|---|---|---|
| tr\|Q8ID50\|Q8ID50_PLAF7 60S ribosomal protein L40/UBI, putative OS=Plasmodium falciparum (isolate 3D7) GN=PF13_0346 PE=1 SV=1;tr\|Q7KQK2\|Q7KQK2_PLAF7 PfpUB Plasmodium falciparum polyubiquitin OS=Plasmodium falciparum (isolate 3D7) GN=PFL0585w PE=4 SV=1 | 4 | 1.29 | 0.87 | 0.0597 |
| tr\|C0H4E8\|C0H4E8_PLAF7 Proteasome subunit beta type OS=Plasmodium falciparum (isolate 3D7) GN=PFE0915c PE=3 SV=1 | 4 | 1.29 | 0.87 | 0.0585 |
| tr\|Q8I5Q2\|Q8I5Q2_PLAF7 Uncharacterized protein OS=Plasmodium falciparum (isolate 3D7) GN=PFL0745c PE=4 SV=1 | 4 | 1.29 | 2.09 | 0.3035 |
| tr\|C0H4B1\|C0H4B1_PLAF7 Memo-like protein OS=Plasmodium falciparum (isolate 3D7) GN=PFD0850c PE=3 SV=1 | 4 | 1.29 | 0.86 | 0.0580 |
| sp\|O00806\|RLA2_PLAF7 60S acidic ribosomal protein P2 OS=Plasmodium falciparum (isolate 3D7) GN=MAL3P3.19 PE=3 SV=1 | 4 | 1.30 | 0.91 | 0.0643 |
| tr\|Q8IBH7\|Q8IBH7_PLAF7 Eukaryotic translation initiation factor 2 alpha subunit, putative OS=Plasmodium falciparum (isolate 3D7) GN=PF07_0117 PE=4 SV=1 | 4 | 1.30 | 0.90 | 0.0630 |
| sp\|P32119\|PRDX2_HUMAN Peroxiredoxin-2 OS=Homo sapiens GN=PRDX2 PE=1 SV=5;tr\|A6NIW5\|A6NIW5_HUMAN Peroxiredoxin 2, isoform CRA_a OS=Homo sapiens GN=PRDX2 PE=1 SV=2 | 4 | 2.21 | 1.17 | 0.0322 |
| tr\|Q8IIJ6\|Q8IIJ6_PLAF7 Ubiquitin C-terminal hydrolase, family 1, putative OS=Plasmodium falciparum (isolate 3D7) GN=PF11_0177 PE=4 SV=1 | 4 | 1.31 | 0.88 | 0.0582 |
| tr\|Q8IJW0\|Q8IJW0_PLAF7 26S proteasome regulatory subunit 4, putative OS=Plasmodium falciparum (isolate 3D7) GN=PF10_0081 PE=3 SV=2 | 4 | 1.32 | 0.93 | 0.0654 |
| tr\|Q8IIW5\|Q8IIW5_PLAF7 Casein kinase II subunit beta OS=Plasmodium falciparum (isolate 3D7) GN=PF11_0048 PE=3 SV=1 | 4 | 1.32 | 0.87 | 0.0560 |
| tr\|Q8I1S0\|Q8I1S0_PLAF7 Small GTP-binding protein sar1 OS=Plasmodium falciparum (isolate 3D7) GN=sar1 PE=3 SV=1 | 4 | 1.32 | 0.88 | 0.0582 |
| tr\|Q7KQK0\|Q7KQK0_PLAF7 CAMP-dependent protein kinase regulatory subunit, putative OS=Plasmodium falciparum (isolate 3D7) GN=PKAr PE=4 SV=1 | 4 | 2.21 | 1.04 | 0.0240 |
| tr\|Q8I5F9\|Q8I5F9_PLAF7 Ubiquitin-activating enzyme e1, putative OS=Plasmodium falciparum (isolate 3D7) GN=PFL1245w PE=4 SV=1 | 4 | 2.26 | 0.68 | 0.0071 |
| tr\|Q8IDR5\|Q8IDR5_PLAF7 Casein kinase II subunit beta OS=Plasmodium falciparum (isolate 3D7) GN=PfCK2beta2 PE=3 SV=1 | 4 | 1.34 | 0.89 | 0.0577 |
| tr\|C0H5G3\|C0H5G3_PLAF7 60S ribosomal protein L18 OS=Plasmodium falciparum (isolate 3D7) GN=MAL13P1.209 PE=1 SV=1 | 4 | 1.34 | 0.90 | 0.0586 |
| tr\|Q8I616\|Q8I616_PLAF7 High mobility group protein OS=Plasmodium falciparum (isolate 3D7) GN=PFL0145c PE=4 SV=1 | 4 | 1.35 | 0.93 | 0.0629 |
| tr\|Q8ILX3\|Q8ILX3_PLAF7 Uncharacterized protein OS=Plasmodium falciparum (isolate 3D7) GN=PF14_0120 PE=4 SV=1 | 4 | 1.35 | 0.89 | 0.0557 |
| tr\|Q9U0J0\|Q9U0J0_PLAF7 Replication factor a protein, putative OS=Plasmodium falciparum (isolate 3D7) GN=PFD0470c PE=4 SV=1 | 4 | 1.36 | 0.87 | 0.0521 |
| tr\|Q8IJT9\|Q8IJT9_PLAF7 Eukaryotic translation initiation factor 2, beta, putative OS=Plasmodium falciparum (isolate 3D7) GN=PF10_0103 PE=4 SV=1 | 4 | 1.36 | 0.92 | 0.0588 |
| tr\|C6KT23\|C6KT23_PLAF7 60S ribosomal protein L27a, putative OS=Plasmodium falciparum (isolate 3D7) GN=PFF0885w PE=1 SV=1 | 4 | 1.37 | 0.95 | 0.0627 |
| tr\|Q7KQJ9\|Q7KQJ9_PLAF7 Proliferating cell nuclear antigen OS=Plasmodium falciparum (isolate 3D7) GN=PFL1285c PE=3 SV=1 | 4 | 1.37 | 0.94 | 0.0609 |
| sp\|C6KT50\|PDX1_PLAF7 Pyridoxal 5-phosphate synthase subunit Pdx1 OS=Plasmodium falciparum (isolate 3D7) GN=pdx1 PE=1 SV=1 | 4 | 2.32 | 1.28 | 0.0359 |
| tr\|C6KST3\|C6KST3_PLAF7 Proteasome subunit alpha type 2, putative OS=Plasmodium falciparum (isolate 3D7) GN=PFF0420c PE=4 SV=1 | 4 | 1.39 | 0.93 | 0.0583 |
| tr\|Q8IK90\|Q8IK90_PLAF7 Proteosome subunit alpha type 1, putative OS=Plasmodium falciparum (isolate 3D7) GN=PF14_0716 PE=4 SV=1 | 4 | 1.40 | 0.93 | 0.0581 |
| tr\|Q8II60\|Q8II60_PLAF7 26S protease subunit regulatory subunit 6a, putative OS=Plasmodium falciparum (isolate 3D7) GN=PF11_0314 PE=3 SV=1 | 4 | 1.40 | 0.94 | 0.0592 |
| tr\|Q8IHY0\|Q8IHY0_PLAF7 Protein phosphatase 2C OS=Plasmodium falciparum (isolate 3D7) GN=PF11_0396 PE=3 SV=2 | 4 | 2.37 | 1.34 | 0.0384 |
| sp\|P63000\|RAC1_HUMAN Ras-related C3 botulinum toxin substrate 1 OS=Homo sapiens GN=RAC1 PE=1 SV=1;sp\|P63000-2\|RAC1_HUMAN Isoform B of Ras-related C3 botulinum toxin substrate 1 OS=Homo sapiens GN=RAC1 | 4 | 1.41 | 1.29 | 0.1158 |
| tr\|Q8IKX4\|Q8IKX4_PLAF7 Signal recognition particle SRP54, putative OS=Plasmodium falciparum (isolate 3D7) GN=PF14_0477 PE=3 SV=1 | 4 | 1.41 | 0.92 | 0.0551 |
| sp\|Q8I4X0\|ACT1_PLAF7 Actin-1 OS=Plasmodium falciparum (isolate 3D7) GN=PFL2215w PE=3 SV=1 | 4 | 2.39 | 0.08 | 0.0000 |
| tr\|Q8IC05\|Q8IC05_PLAF7 Heat shock protein 86 OS=Plasmodium falciparum (isolate 3D7) GN=PF07_0029 PE=1 SV=1 | 4 | 2.42 | 0.90 | 0.0126 |
| tr\|C0H4K6\|C0H4K6_PLAF7 Ubiquitin transferase, putative OS=Plasmodium falciparum (isolate 3D7) GN=MAL7P1.19 PE=4 SV=1 | 4 | 1.43 | 0.92 | 0.0529 |

| | | | | |
|---|---|---|---|---|
| tr\|Q8I3M5\|Q8I3M5_PLAF7 Karyopherin beta OS=Plasmodium falciparum (isolate 3D7) GN=PFE1195w PE=4 SV=1 | 4 | 2.43 | 0.30 | 0.0005 |
| sp\|P00441\|SODC_HUMAN Superoxide dismutase [Cu-Zn] OS=Homo sapiens GN=SOD1 PE=1 SV=2;tr\|H7BYH4\|H7BYH4_HUMAN Superoxide dismutase [Cu-Zn] OS=Homo sapiens GN=SOD1 PE=1 SV=1 | 4 | 2.49 | 0.72 | 0.0061 |
| tr\|Q8I5P5\|Q8I5P5_PLAF7 Glycerol-3-phosphate dehydrogenase [NAD(+)] OS=Plasmodium falciparum (isolate 3D7) GN=PFL0780w PE=1 SV=1 | 4 | 2.57 | 0.52 | 0.0022 |
| tr\|Q8IAR3\|Q8IAR3_PLAF7 Proteasome subunit alpha, putative OS=Plasmodium falciparum (isolate 3D7) GN=MAL8P1.128 PE=4 SV=2 | 4 | 1.46 | 0.94 | 0.0538 |
| tr\|Q8IBQ5\|Q8IBQ5_PLAF7 40S ribosomal protein S10, putative OS=Plasmodium falciparum (isolate 3D7) GN=PF07_0080 PE=1 SV=1 | 4 | 1.46 | 1.00 | 0.0607 |
| tr\|C0H4Q0\|C0H4Q0_PLAF7 Signal recognition particle SRP9, putative OS=Plasmodium falciparum (isolate 3D7) GN=MAL7P1.158 PE=4 SV=1 | 4 | 1.48 | 1.01 | 0.0611 |
| tr\|Q8I5N9\|Q8I5N9_PLAF7 DNA-binding chaperone, putative OS=Plasmodium falciparum (isolate 3D7) GN=PFL0815w PE=4 SV=1 | 4 | 1.48 | 1.01 | 0.0602 |
| tr\|Q8IDG2\|Q8IDG2_PLAF7 Proteasome subunit alpha type OS=Plasmodium falciparum (isolate 3D7) GN=MAL13P1.270 PE=3 SV=1 | 4 | 1.49 | 0.97 | 0.0550 |
| tr\|Q8I4U3\|Q8I4U3_PLAF7 Conserved Plasmodium protein OS=Plasmodium falciparum (isolate 3D7) GN=PFL2355w PE=4 SV=1 | 4 | 1.50 | 1.04 | 0.0636 |
| tr\|C0H4V6\|C0H4V6_PLAF7 14-3-3 protein, putative OS=Plasmodium falciparum (isolate 3D7) GN=MAL8P1.69 PE=3 SV=1 | 4 | 1.51 | 1.01 | 0.0583 |
| tr\|Q8I2G2\|Q8I2G2_PLAF7 Cytoadherence linked asexual protein 9(CLAG9) OS=Plasmodium falciparum (isolate 3D7) GN=CLAG9 PE=4 SV=1 | 4 | 1.52 | 1.78 | 0.1872 |
| sp\|Q8IAY6\|SODF_PLAF7 Superoxide dismutase [Fe] OS=Plasmodium falciparum (isolate 3D7) GN=SODB PE=1 SV=1 | 4 | 1.53 | 1.07 | 0.0638 |
| sp\|Q8IIJ9\|CATC_PLAF7 Probable cathepsin C OS=Plasmodium falciparum (isolate 3D7) GN=PF11_0174 PE=1 SV=1 | 4 | 1.54 | 1.02 | 0.0572 |
| tr\|Q8IIM8\|Q8IIM8_PLAF7 Uncharacterized protein OS=Plasmodium falciparum (isolate 3D7) GN=PF11_0142 PE=4 SV=1 | 4 | 2.63 | 1.45 | 0.0363 |
| tr\|Q8IL11\|Q8IL11_PLAF7 M17 leucyl aminopeptidase OS=Plasmodium falciparum (isolate 3D7) GN=LAP PE=1 SV=1 | 4 | 1.55 | 1.03 | 0.0578 |
| tr\|O96212\|O96212_PLAF7 Heat shock 40 kDa protein, putative OS=Plasmodium falciparum (isolate 3D7) GN=PFB0595w PE=4 SV=1 | 4 | 1.55 | 1.13 | 0.0712 |
| sp\|Q8IDF6\|PURA_PLAF7 Adenylosuccinate synthetase OS=Plasmodium falciparum (isolate 3D7) GN=Adss PE=3 SV=1 | 4 | 2.81 | 1.30 | 0.0231 |
| tr\|Q8I5Y9\|Q8I5Y9_PLAF7 Uncharacterized protein OS=Plasmodium falciparum (isolate 3D7) GN=PFL0280c PE=4 SV=1 | 4 | 2.82 | 0.32 | 0.0004 |
| tr\|Q8IBI3\|Q8IBI3_PLAF7 Proteasome subunit alpha type OS=Plasmodium falciparum (isolate 3D7) GN=PF07_0112 PE=3 SV=1 | 4 | 1.57 | 1.06 | 0.0597 |
| tr\|Q8IDF7\|Q8IDF7_PLAF7 V-type ATPase, putative OS=Plasmodium falciparum (isolate 3D7) GN=MAL13P1.271 PE=3 SV=1 | 4 | 1.60 | 1.27 | 0.0865 |
| sp\|Q7KQL3\|ARF1_PLAF7 ADP-ribosylation factor 1 OS=Plasmodium falciparum (isolate 3D7) GN=ARF1 PE=1 SV=1 | 4 | 1.61 | 1.06 | 0.0560 |
| tr\|Q8IIC9\|Q8IIC9_PLAF7 Translation elongation factor EF-1, subunit alpha, putative OS=Plasmodium falciparum (isolate 3D7) GN=PF11_0245 PE=4 SV=1 | 4 | 2.85 | 1.29 | 0.0217 |
| tr\|Q8IDG3\|Q8IDG3_PLAF7 Proteasome subunit alpha type OS=Plasmodium falciparum (isolate 3D7) GN=PF13_0282 PE=3 SV=1 | 4 | 1.61 | 1.08 | 0.0589 |
| tr\|Q8ILT0\|Q8ILT0_PLAF7 Glutamate dehydrogenase OS=Plasmodium falciparum (isolate 3D7) GN=PF14_0164 PE=3 SV=1 | 4 | 1.62 | 1.08 | 0.0574 |
| tr\|Q8I608\|Q8I608_PLAF7 Nucleosome assembly protein 1, putative OS=Plasmodium falciparum (isolate 3D7) GN=PFL0185c PE=1 SV=2 | 4 | 1.62 | 1.09 | 0.0586 |
| tr\|Q8I3B4\|Q8I3B4_PLAF7 DEAD/DEAH box helicase, putative OS=Plasmodium falciparum (isolate 3D7) GN=PFI0165c PE=4 SV=1 | 4 | 1.65 | 1.13 | 0.0611 |
| tr\|Q8IIB9\|Q8IIB9_PLAF7 Conserved Plasmodium protein OS=Plasmodium falciparum (isolate 3D7) GN=PF11_0255 PE=4 SV=2 | 4 | 1.66 | 1.08 | 0.0543 |
| tr\|C0H551\|C0H551_PLAF7 Glutamine synthetase, putative OS=Plasmodium falciparum (isolate 3D7) GN=PFI1110w PE=3 SV=1 | 4 | 1.68 | 1.12 | 0.0578 |
| tr\|Q7KQK3\|Q7KQK3_PLAF7 Heat shock protein DNAJ homologue Pfj4 OS=Plasmodium falciparum (isolate 3D7) GN=PFL0565w PE=4 SV=1 | 4 | 1.69 | 1.17 | 0.0629 |
| tr\|C6KTC6\|C6KTC6_PLAF7 Uncharacterized protein OS=Plasmodium falciparum (isolate 3D7) GN=PFF1410c PE=4 SV=1 | 4 | 1.70 | 1.44 | 0.0999 |
| tr\|C0H5J6\|C0H5J6_PLAF7 Sec24 subunit, putative OS=Plasmodium falciparum (isolate 3D7) GN=PF13_0324 PE=4 SV=1 | 4 | 1.70 | 1.21 | 0.0675 |
| tr\|Q8I535\|Q8I535_PLAF7 Long-chain-fatty-acid--CoA ligase, putative OS=Plasmodium falciparum (isolate 3D7) GN=PFL1880w PE=4 SV=1 | 4 | 1.71 | 1.11 | 0.0546 |

| | | | | |
|---|---|---|---|---|
| tr\|Q8IK74\|Q8IK74_PLAF7 Uncharacterized protein OS=Plasmodium falciparum (isolate 3D7) GN=PF14_0732 PE=4 SV=1 | 4 | 1.72 | 2.32 | 0.2345 |
| sp\|P00492\|HPRT_HUMAN Hypoxanthine-guanine phosphoribosyltransferase OS=Homo sapiens GN=HPRT1 PE=1 SV=2 | 4 | 1.73 | 1.19 | 0.0617 |
| sp\|Q7KQL5\|TBB_PLAF7 Tubulin beta chain OS=Plasmodium falciparum (isolate 3D7) GN=PF10_0084 PE=3 SV=1 | 4 | 2.94 | 0.58 | 0.0021 |
| tr\|Q8IDV0\|Q8IDV0_PLAF7 Elongation factor 1-gamma, putative OS=Plasmodium falciparum (isolate 3D7) GN=PF13_0214 PE=4 SV=2 | 4 | 2.97 | 1.84 | 0.0478 |
| tr\|Q8I5F4\|Q8I5F4_PLAF7 Uncharacterized protein OS=Plasmodium falciparum (isolate 3D7) GN=PFL1270w PE=4 SV=1 | 4 | 2.99 | 0.71 | 0.0035 |
| tr\|Q8ILB9\|Q8ILB9_PLAF7 Dynein-related AAA-type ATPase OS=Plasmodium falciparum (isolate 3D7) GN=PF14_0326 PE=4 SV=2 | 4 | 1.77 | 1.31 | 0.0730 |
| tr\|Q8IB60\|Q8IB60_PLAF7 PfSec23 protein OS=Plasmodium falciparum (isolate 3D7) GN=Pfsec23 PE=2 SV=1 | 4 | 1.78 | 1.22 | 0.0614 |
| tr\|Q8II42\|Q8II42_PLAF7 Conserved Plasmodium protein OS=Plasmodium falciparum (isolate 3D7) GN=PF11_0332 PE=4 SV=1 | 4 | 1.80 | 1.22 | 0.0598 |
| tr\|C6KT76\|C6KT76_PLAF7 Hexokinase OS=Plasmodium falciparum (isolate 3D7) GN=PFF1155w PE=3 SV=1 | 4 | 3.01 | 0.40 | 0.0007 |
| tr\|Q8IDQ9\|Q8IDQ9_PLAF7 Phosphoethanolamine N-methyltransferase OS=Plasmodium falciparum (isolate 3D7) GN=PfPMT PE=4 SV=1 | 4 | 3.02 | 1.33 | 0.0202 |
| tr\|Q8IJ60\|Q8IJ60_PLAF7 Methionine--tRNA ligase, putative OS=Plasmodium falciparum (isolate 3D7) GN=PF10_0340 PE=4 SV=1 | 4 | 3.04 | 0.75 | 0.0040 |
| tr\|O77355\|O77355_PLAF7 Pre-mRNA splicing factor, putative OS=Plasmodium falciparum (isolate 3D7) GN=PFC0465c PE=4 SV=2 | 4 | 1.83 | 2.98 | 0.3067 |
| tr\|Q76NM3\|Q76NM3_PLAF7 L-lactate dehydrogenase OS=Plasmodium falciparum (isolate 3D7) GN=PfLDH PE=1 SV=1 | 4 | 3.05 | 1.18 | 0.0140 |
| tr\|Q8I542\|Q8I542_PLAF7 Calcyclin binding protein, putative OS=Plasmodium falciparum (isolate 3D7) GN=PFL1845c PE=4 SV=2 | 4 | 1.87 | 1.36 | 0.0704 |
| tr\|C6KT13\|C6KT13_PLAF7 Uncharacterized protein OS=Plasmodium falciparum (isolate 3D7) GN=PFF0835w PE=4 SV=1 | 4 | 1.87 | 1.30 | 0.0636 |
| tr\|Q8I0P6\|Q8I0P6_PLAF7 Elongation factor 1-alpha OS=Plasmodium falciparum (isolate 3D7) GN=PF13_0304 PE=3 SV=1 | 4 | 3.11 | 1.37 | 0.0200 |
| tr\|Q8I3J0\|Q8I3J0_PLAF7 Hsp70 interacting protein, putative OS=Plasmodium falciparum (isolate 3D7) GN=PFE1370w PE=4 SV=1 | 4 | 1.88 | 1.26 | 0.0578 |
| tr\|Q8I566\|Q8I566_PLAF7 Serine hydroxymethyltransferase OS=Plasmodium falciparum (isolate 3D7) GN=PFL1720w PE=1 SV=1 | 4 | 3.15 | 0.39 | 0.0005 |
| tr\|Q8IKT5\|Q8IKT5_PLAF7 Peptidase, putative OS=Plasmodium falciparum (isolate 3D7) GN=PF14_0517 PE=3 SV=1 | 4 | 1.91 | 1.25 | 0.0556 |
| sp\|P27362\|PGK_PLAF7 Phosphoglycerate kinase OS=Plasmodium falciparum (isolate 3D7) GN=PGK PE=1 SV=1 | 4 | 3.19 | 1.60 | 0.0281 |
| tr\|C0H4L1\|C0H4L1_PLAF7 Uncharacterized protein OS=Plasmodium falciparum (isolate 3D7) GN=MAL7P1.202 PE=4 SV=1 | 4 | 1.94 | 1.34 | 0.0626 |
| tr\|Q8IL80\|Q8IL80_PLAF7 Thioredoxin peroxidase 1 OS=Plasmodium falciparum (isolate 3D7) GN=TPx1 PE=4 SV=1 | 4 | 1.94 | 1.31 | 0.0590 |
| tr\|Q8I5A3\|Q8I5A3_PLAF7 Asparagine-rich protein, putative OS=Plasmodium falciparum (isolate 3D7) GN=PFL1530w PE=4 SV=1 | 4 | 1.95 | 1.29 | 0.0566 |
| sp\|Q8I5R7\|SYP_PLAF7 Proline--tRNA ligase OS=Plasmodium falciparum (isolate 3D7) GN=proRS PE=1 SV=1 | 4 | 3.19 | 1.84 | 0.0406 |
| tr\|Q8IL88\|Q8IL88_PLAF7 HSP40, subfamily A, putative OS=Plasmodium falciparum (isolate 3D7) GN=PF14_0359 PE=4 SV=1 | 4 | 1.99 | 1.33 | 0.0576 |
| tr\|Q8I3X4\|Q8I3X4_PLAF7 Purine nucleotide phosphorylase, putative OS=Plasmodium falciparum (isolate 3D7) GN=PFE0660c PE=1 SV=1 | 4 | 3.33 | 1.69 | 0.0289 |
| sp\|Q8IKU0\|GLUPH_PLAF7 Bifunctional glucose-6-phosphate 1-dehydrogenase/6-phosphogluconolactonase OS=Plasmodium falciparum (isolate 3D7) GN=PF14_0511 PE=1 SV=1 | 4 | 2.01 | 1.34 | 0.0579 |
| tr\|Q8I261\|Q8I261_PLAF7 Beta3 proteasome subunit, putative OS=Plasmodium falciparum (isolate 3D7) GN=PFA_0400c PE=4 SV=1 | 4 | 2.03 | 1.42 | 0.0649 |
| tr\|Q8I2U5\|Q8I2U5_PLAF7 Inosine-5-monophosphate dehydrogenase OS=Plasmodium falciparum (isolate 3D7) GN=PFI1020c PE=3 SV=1 | 4 | 2.03 | 1.36 | 0.0576 |
| tr\|Q8I3M1\|Q8I3M1_PLAF7 Cytosolic preribosomal GTP-binding protein, putative OS=Plasmodium falciparum (isolate 3D7) GN=PFE1215c PE=4 SV=1 | 4 | 2.04 | 1.36 | 0.0580 |
| tr\|C0H4U5\|C0H4U5_PLAF7 Uncharacterized protein OS=Plasmodium falciparum (isolate 3D7) GN=PF08_0081 PE=4 SV=1 | 4 | 2.04 | 1.38 | 0.0590 |
| tr\|Q8IHY3\|Q8IHY3_PLAF7 Ubiquitin-related modifier 1 homolog OS=Plasmodium falciparum (isolate 3D7) GN=PF11_0393 PE=3 SV=1 | 4 | 2.11 | 1.44 | 0.0608 |
| tr\|O77330\|O77330_PLAF7 Asparagine synthetase OS=Plasmodium falciparum (isolate 3D7) GN=PFC0395w PE=4 SV=1 | 4 | 2.11 | 1.40 | 0.0574 |

| | | | | |
|---|---|---|---|---|
| tr\|C6KTA4\|C6KTA4_PLAF7 Pyruvate kinase OS=Plasmodium falciparum (isolate 3D7) GN=PFF1300w PE=1 SV=1 | 4 | 3.34 | 0.77 | 0.0032 |
| tr\|C0H5F2\|C0H5F2_PLAF7 Uncharacterized protein OS=Plasmodium falciparum (isolate 3D7) GN=MAL13P1.172 PE=4 SV=1 | 4 | 2.12 | 1.40 | 0.0564 |
| sp\|Q8I2J4\|PROF_PLAF7 Profilin OS=Plasmodium falciparum (isolate 3D7) GN=Pfn PE=3 SV=1 | 4 | 2.12 | 1.52 | 0.0678 |
| sp\|Q8ILC1\|STI1L_PLAF7 STI1-like protein OS=Plasmodium falciparum (isolate 3D7) GN=PF14_0324 PE=3 SV=1 | 4 | 2.12 | 1.35 | 0.0510 |
| tr\|Q8II82\|Q8II82_PLAF7 Uncharacterized protein OS=Plasmodium falciparum (isolate 3D7) GN=PF11_0292 PE=4 SV=1 | 4 | 2.13 | 1.38 | 0.0543 |
| tr\|Q8IC01\|Q8IC01_PLAF7 Cg4 protein OS=Plasmodium falciparum (isolate 3D7) GN=PF07_0033 PE=3 SV=1 | 4 | 2.13 | 1.38 | 0.0539 |
| tr\|Q8I5G5\|Q8I5G5_PLAF7 Uncharacterized protein OS=Plasmodium falciparum (isolate 3D7) GN=PFL1215c PE=4 SV=1 | 4 | 2.14 | 3.77 | 0.3387 |
| sp\|Q8IIG7\|YPF05_PLAF7 Uncharacterized protein PF11_0207 OS=Plasmodium falciparum (isolate 3D7) GN=PF11_0207 PE=4 SV=2 | 4 | 2.15 | 1.48 | 0.0626 |
| tr\|Q8II81\|Q8II81_PLAF7 Multiprotein bridging factor type 1, putative OS=Plasmodium falciparum (isolate 3D7) GN=PF11_0293 PE=4 SV=1 | 4 | 2.18 | 1.56 | 0.0679 |
| tr\|Q8IDC6\|Q8IDC6_PLAF7 Pyrroline carboxylate reductase OS=Plasmodium falciparum (isolate 3D7) GN=MAL13P1.284 PE=1 SV=1 | 4 | 2.18 | 1.48 | 0.0599 |
| tr\|Q8I1R6\|Q8I1R6_PLAF7 Bifunctional dihydrofolate reductase-thymidylate synthase OS=Plasmodium falciparum (isolate 3D7) GN=DHFR-TS PE=3 SV=1 | 4 | 2.19 | 1.52 | 0.0628 |
| tr\|C0H530\|C0H530_PLAF7 Ran-binding protein, putative OS=Plasmodium falciparum (isolate 3D7) GN=PFI0490c PE=4 SV=1 | 4 | 2.21 | 1.53 | 0.0633 |
| tr\|Q8IKP1\|Q8IKP1_PLAF7 DEAD box helicase, putative OS=Plasmodium falciparum (isolate 3D7) GN=PF14_0563 PE=4 SV=1 | 4 | 2.21 | 1.61 | 0.0710 |
| tr\|Q8I320\|Q8I320_PLAF7 Elongation factor 1-beta OS=Plasmodium falciparum (isolate 3D7) GN=PfEF-1beta PE=4 SV=1 | 4 | 3.42 | 1.50 | 0.0196 |
| tr\|Q8I3Y8\|Q8I3Y8_PLAF7 Myo-inositol 1-phosphate synthase, putative OS=Plasmodium falciparum (isolate 3D7) GN=PFE0585c PE=4 SV=1 | 4 | 2.22 | 1.48 | 0.0581 |
| tr\|Q8IJP3\|Q8IJP3_PLAF7 Cysteinyl-tRNA synthetase, putative OS=Plasmodium falciparum (isolate 3D7) GN=PF10_0149 PE=3 SV=2 | 4 | 2.25 | 1.63 | 0.0697 |
| tr\|Q8I238\|Q8I238_PLAF7 Chromatin assembly factor 1 protein WD40 domain, putative OS=Plasmodium falciparum (isolate 3D7) GN=PFA_0520c PE=4 SV=1 | 4 | 2.26 | 1.48 | 0.0548 |
| tr\|Q8ID43\|Q8ID43_PLAF7 Nucleoside diphosphate kinase OS=Plasmodium falciparum (isolate 3D7) GN=PF13_0349 PE=1 SV=1 | 4 | 2.27 | 1.54 | 0.0599 |
| tr\|Q8I4V8\|Q8I4V8_PLAF7 FK506-binding protein (FKBP)-type peptidyl-propyl isomerase OS=Plasmodium falciparum (isolate 3D7) GN=FKBP35 PE=1 SV=1 | 4 | 2.28 | 1.55 | 0.0599 |
| sp\|Q8ILI6\|AN32_PLAF7 Acidic leucine-rich nuclear phosphoprotein 32-related protein OS=Plasmodium falciparum (isolate 3D7) GN=PF14_0257 PE=3 SV=1 | 4 | 2.29 | 1.51 | 0.0562 |
| tr\|Q8I2W4\|Q8I2W4_PLAF7 Gamma-glutamylcysteine synthetase OS=Plasmodium falciparum (isolate 3D7) GN=PFI0925w PE=4 SV=1 | 4 | 2.31 | 1.52 | 0.0559 |
| tr\|Q8ILP6\|Q8ILP6_PLAF7 Glycine-tRNA ligase, putative OS=Plasmodium falciparum (isolate 3D7) GN=PF14_0198 PE=3 SV=2 | 4 | 2.31 | 1.57 | 0.0600 |
| tr\|Q8IJA0\|Q8IJA0_PLAF7 26S proteasome subunit, putative OS=Plasmodium falciparum (isolate 3D7) GN=PF10_0298 PE=4 SV=1 | 4 | 2.35 | 2.03 | 0.1039 |
| tr\|Q8IKK7\|Q8IKK7_PLAF7 Glyceraldehyde-3-phosphate dehydrogenase OS=Plasmodium falciparum (isolate 3D7) GN=GAPDH PE=3 SV=1 | 4 | 3.55 | 0.33 | 0.0002 |
| tr\|Q8IBM9\|Q8IBM9_PLAF7 Obg-like ATPase 1 OS=Plasmodium falciparum (isolate 3D7) GN=MAL7P1.122 PE=3 SV=1 | 4 | 2.42 | 1.60 | 0.0564 |
| tr\|Q8III5\|Q8III5_PLAF7 Uncharacterized protein OS=Plasmodium falciparum (isolate 3D7) GN=PF11_0189 PE=3 SV=1 | 4 | 2.43 | 1.58 | 0.0545 |
| tr\|C6KTA3\|C6KTA3_PLAF7 Uncharacterized protein OS=Plasmodium falciparum (isolate 3D7) GN=PFF1295w PE=4 SV=1 | 4 | 2.44 | 1.67 | 0.0612 |
| sp\|P50250\|SAHH_PLAF7 Adenosylhomocysteinase OS=Plasmodium falciparum (isolate 3D7) GN=PFE1050w PE=1 SV=2 | 4 | 2.46 | 1.65 | 0.0581 |
| tr\|Q8IBF6\|Q8IBF6_PLAF7 Transcription factor with AP2 domain(S), putative OS=Plasmodium falciparum (isolate 3D7) GN=ApiAP2 PE=4 SV=1 | 4 | 2.46 | 2.97 | 0.1961 |
| tr\|O77312\|O77312_PLAF7 Exportin 1, putative OS=Plasmodium falciparum (isolate 3D7) GN=PFC0135c PE=4 SV=2 | 4 | 2.47 | 1.65 | 0.0577 |
| tr\|Q8IEN3\|Q8IEN3_PLAF7 Carbamoyl phosphate synthetase OS=Plasmodium falciparum (isolate 3D7) GN=cpsSII PE=4 SV=1 | 4 | 2.48 | 1.77 | 0.0680 |
| tr\|Q8I2P2\|Q8I2P2_PLAF7 NAD synthase, putative OS=Plasmodium falciparum (isolate 3D7) GN=PFI1310w PE=4 SV=1 | 4 | 2.50 | 1.74 | 0.0642 |
| tr\|Q8IDK7\|Q8IDK7_PLAF7 Glutamate--tRNA ligase, putative OS=Plasmodium falciparum (isolate 3D7) GN=PF13_0257 PE=3 SV=1 | 4 | 2.52 | 1.61 | 0.0522 |

| | | | | |
|---|---|---|---|---|
| tr\|Q8IJR9\|Q8IJR9_PLAF7 GMP synthetase OS=Plasmodium falciparum (isolate 3D7) GN=PF10_0123 PE=1 SV=1 | 4 | 2.53 | 1.69 | 0.0580 |
| sp\|Q7KQL9\|ALF_PLAF7 Fructose-bisphosphate aldolase OS=Plasmodium falciparum (isolate 3D7) GN=PF14_0425 PE=3 SV=1 | 4 | 2.54 | 1.75 | 0.0617 |
| sp\|Q7KQL8\|THIO_PLAF7 Thioredoxin OS=Plasmodium falciparum (isolate 3D7) GN=PF14_0545 PE=1 SV=1 | 4 | 2.54 | 1.97 | 0.0812 |
| tr\|C6KSM2\|C6KSM2_PLAF7 MYND finger protein, putative OS=Plasmodium falciparum (isolate 3D7) GN=PFF0105w PE=4 SV=1 | 4 | 2.56 | 1.76 | 0.0620 |
| tr\|Q8IL94\|Q8IL94_PLAF7 Ribonucleoside-diphosphate reductase OS=Plasmodium falciparum (isolate 3D7) GN=PF14_0352 PE=3 SV=1 | 4 | 2.57 | 1.75 | 0.0606 |
| sp\|Q8I3Z5\|TCTP_PLAF7 Translationally-controlled tumor protein homolog OS=Plasmodium falciparum (isolate 3D7) GN=TCTP PE=1 SV=1 | 4 | 2.59 | 1.85 | 0.0675 |
| tr\|Q8I4Y9\|Q8I4Y9_PLAF7 Uncharacterized protein OS=Plasmodium falciparum (isolate 3D7) GN=PFL2120w PE=4 SV=1 | 4 | 2.59 | 1.73 | 0.0580 |
| tr\|Q76NN7\|Q76NN7_PLAF7 Peptidyl-prolyl cis-trans isomerase OS=Plasmodium falciparum (isolate 3D7) GN=PfCyP19 PE=3 SV=1 | 4 | 2.59 | 1.78 | 0.0622 |
| tr\|Q8IM38\|Q8IM38_PLAF7 Ribonucleotide reductase small subunit OS=Plasmodium falciparum (isolate 3D7) GN=PF14_0053 PE=4 SV=1 | 4 | 2.59 | 1.88 | 0.0704 |
| tr\|Q8ILK2\|Q8ILK2_PLAF7 Nascent polypeptide-associated complex subunit beta OS=Plasmodium falciparum (isolate 3D7) GN=PF14_0241 PE=3 SV=1 | 4 | 2.61 | 1.81 | 0.0632 |
| tr\|Q8I6Z4\|Q8I6Z4_PLAF7 RNAse L inhibitor protein, putative OS=Plasmodium falciparum (isolate 3D7) GN=MAL13P1.344 PE=3 SV=1 | 4 | 2.63 | 1.74 | 0.0564 |
| sp\|Q8ILQ7\|GST_PLAF7 Glutathione S-transferase OS=Plasmodium falciparum (isolate 3D7) GN=GST PE=3 SV=1 | 4 | 2.65 | 1.75 | 0.0562 |
| tr\|Q8IJN8\|Q8IJN8_PLAF7 Ribonucleotide reductase small subunit, putative OS=Plasmodium falciparum (isolate 3D7) GN=PF10_0154 PE=4 SV=2 | 4 | 2.66 | 1.94 | 0.0712 |
| tr\|O96203\|O96203_PLAF7 Peptide chain release factor subunit 1, putative OS=Plasmodium falciparum (isolate 3D7) GN=PFB0550w PE=4 SV=1 | 4 | 2.66 | 1.88 | 0.0662 |
| tr\|Q8IJH3\|Q8IJH3_PLAF7 Orotidine 5-phosphate decarboxylase OS=Plasmodium falciparum (isolate 3D7) GN=PF10_0225 PE=1 SV=1 | 4 | 2.68 | 2.24 | 0.0962 |
| tr\|Q8II43\|Q8II43_PLAF7 T-complex protein 1 subunit alpha OS=Plasmodium falciparum (isolate 3D7) GN=PF11_0331 PE=3 SV=1 | 4 | 2.68 | 1.85 | 0.0626 |
| tr\|Q8IAU3\|Q8IAU3_PLAF7 Dihydropteroate synthetase OS=Plasmodium falciparum (isolate 3D7) GN=DHPS PE=4 SV=1 | 4 | 2.68 | 1.76 | 0.0555 |
| tr\|C0H5I7\|C0H5I7_PLAF7 T-complex protein 1 subunit delta OS=Plasmodium falciparum (isolate 3D7) GN=MAL13P1.283 PE=3 SV=1 | 4 | 2.69 | 1.77 | 0.0560 |
| tr\|Q8IDZ9\|Q8IDZ9_PLAF7 Isoleucine-tRNA ligase, putative OS=Plasmodium falciparum (isolate 3D7) GN=PF13_0179 PE=3 SV=1 | 4 | 2.69 | 1.79 | 0.0570 |
| tr\|Q8I5C4\|Q8I5C4_PLAF7 T-complex protein 1 subunit gamma OS=Plasmodium falciparum (isolate 3D7) GN=PFL1425w PE=3 SV=1 | 4 | 2.70 | 1.89 | 0.0645 |
| tr\|Q8ID31\|Q8ID31_PLAF7 Alanine--tRNA ligase OS=Plasmodium falciparum (isolate 3D7) GN=PF13_0354 PE=3 SV=1 | 4 | 2.74 | 1.86 | 0.0599 |
| tr\|C6KT55\|C6KT55_PLAF7 Nascent polypeptide associated complex alpha chain, putative OS=Plasmodium falciparum (isolate 3D7) GN=PFF1050w PE=4 SV=1 | 4 | 2.74 | 1.90 | 0.0633 |
| tr\|Q8IKF0\|Q8IKF0_PLAF7 Helicase 45 OS=Plasmodium falciparum (isolate 3D7) GN=H45 PE=3 SV=1 | 4 | 2.74 | 1.86 | 0.0597 |
| tr\|Q9NLB2\|Q9NLB2_PLAF7 Glutaredoxin OS=Plasmodium falciparum (isolate 3D7) GN=GRX1 PE=1 SV=1 | 4 | 2.75 | 1.88 | 0.0614 |
| tr\|O97247\|O97247_PLAF7 T-complex protein beta subunit, putative OS=Plasmodium falciparum (isolate 3D7) GN=PFC0285c PE=3 SV=3 | 4 | 2.76 | 1.86 | 0.0590 |
| tr\|Q8IJS1\|Q8IJS1_PLAF7 Hypoxanthine phosphoribosyltransferase OS=Plasmodium falciparum (isolate 3D7) GN=PF10_0121 PE=4 SV=1 | 4 | 2.77 | 1.96 | 0.0662 |
| tr\|C6KSV3\|C6KSV3_PLAF7 Transketolase OS=Plasmodium falciparum (isolate 3D7) GN=PfTK PE=4 SV=1 | 4 | 2.78 | 1.86 | 0.0578 |
| tr\|Q8ILA4\|Q8ILA4_PLAF7 Glucose-6-phosphate isomerase OS=Plasmodium falciparum (isolate 3D7) GN=PF14_0341 PE=1 SV=1 | 4 | 2.81 | 1.85 | 0.0555 |
| tr\|Q7K6A4\|Q7K6A4_PLAF7 S-adenosylmethionine synthase OS=Plasmodium falciparum (isolate 3D7) GN=PfSAMS PE=3 SV=1 | 4 | 2.82 | 1.85 | 0.0552 |
| tr\|Q8IBS3\|Q8IBS3_PLAF7 Seryl-tRNA synthetase, putative OS=Plasmodium falciparum (isolate 3D7) GN=PF07_0073 PE=3 SV=1 | 4 | 2.82 | 1.90 | 0.0592 |
| sp\|Q8IJN7\|ENO_PLAF7 Enolase OS=Plasmodium falciparum (isolate 3D7) GN=ENO PE=3 SV=1 | 4 | 2.83 | 1.91 | 0.0594 |
| tr\|O96198\|O96198_PLAF7 Asparagine-tRNA ligase, putative OS=Plasmodium falciparum (isolate 3D7) GN=PFB0525w PE=3 SV=1 | 4 | 2.86 | 2.02 | 0.0660 |
| tr\|Q8IIG6\|Q8IIG6_PLAF7 Phosphoglycerate mutase, putative OS=Plasmodium falciparum (isolate 3D7) GN=PF11_0208 PE=1 SV=1 | 4 | 2.88 | 1.94 | 0.0589 |

| | | | | |
|---|---|---|---|---|
| tr\|Q8I603\|Q8I603_PLAF7 Eukaryotic initiation factor 5a, putative OS=Plasmodium falciparum (isolate 3D7) GN=PFL0210c PE=4 SV=1 | 4 | 2.88 | 1.98 | 0.0622 |
| tr\|C6KTB1\|C6KTB1_PLAF7 4-methyl-5(B-hydroxyethyl)-thiazol monophosphate biosynthesis enzyme OS=Plasmodium falciparum (isolate 3D7) GN=PFF1335c PE=4 SV=1 | 4 | 2.89 | 2.01 | 0.0638 |
| tr\|Q8ILI2\|Q8ILI2_PLAF7 Proliferation-associated protein 2g4, putative OS=Plasmodium falciparum (isolate 3D7) GN=PF14_0261 PE=4 SV=1 | 4 | 2.89 | 1.98 | 0.0619 |
| tr\|Q8IDJ8\|Q8IDJ8_PLAF7 Lysine--tRNA ligase OS=Plasmodium falciparum (isolate 3D7) GN=PF13_0262 PE=1 SV=1 | 4 | 2.89 | 1.94 | 0.0583 |
| tr\|C6KST5\|C6KST5_PLAF7 Chaperone, putative OS=Plasmodium falciparum (isolate 3D7) GN=PFF0430w PE=3 SV=1 | 4 | 2.91 | 1.92 | 0.0557 |
| tr\|Q8IKL5\|Q8IKL5_PLAF7 Valine-tRNA ligase, putative OS=Plasmodium falciparum (isolate 3D7) GN=PF14_0589 PE=3 SV=1 | 4 | 2.92 | 1.96 | 0.0588 |
| sp\|Q7KQM0\|TPIS_PLAF7 Triosephosphate isomerase OS=Plasmodium falciparum (isolate 3D7) GN=TPI PE=3 SV=1 | 4 | 2.93 | 2.06 | 0.0651 |
| tr\|O97282\|O97282_PLAF7 T-complex protein 1 epsilon subunit, putative OS=Plasmodium falciparum (isolate 3D7) GN=PFC0900w PE=3 SV=1 | 4 | 2.93 | 1.92 | 0.0555 |
| tr\|O97244\|O97244_PLAF7 Activator of Hsp90 ATPase, putative OS=Plasmodium falciparum (isolate 3D7) GN=PFC0270w PE=4 SV=3 | 4 | 2.93 | 1.96 | 0.0579 |
| tr\|Q8I5C5\|Q8I5C5_PLAF7 Macrophage migration inhibitory factor homologue OS=Plasmodium falciparum (isolate 3D7) GN=MIF PE=1 SV=1 | 4 | 2.98 | 2.13 | 0.0679 |
| tr\|Q76NN6\|Q76NN6_PLAF7 Ran binding protein 1, putative OS=Plasmodium falciparum (isolate 3D7) GN=PFD0950w PE=4 SV=1 | 4 | 3.98 | 0.96 | 0.0037 |
| tr\|O96220\|O96220_PLAF7 T-complex protein 1, putative OS=Plasmodium falciparum (isolate 3D7) GN=PFB0635w PE=3 SV=3 | 4 | 3.01 | 2.05 | 0.0606 |
| tr\|O97319\|O97319_PLAF7 Elongation factor 1 (EF-1), putative OS=Plasmodium falciparum (isolate 3D7) GN=PFC0870w PE=4 SV=2 | 4 | 3.04 | 2.08 | 0.0611 |
| tr\|O77379\|O77379_PLAF7 Proteasome regulatory protein, putative OS=Plasmodium falciparum (isolate 3D7) GN=PFC0785c PE=4 SV=1 | 4 | 3.04 | 2.71 | 0.1104 |
| tr\|Q8IJA9\|Q8IJA9_PLAF7 Adenosine deaminase, putative OS=Plasmodium falciparum (isolate 3D7) GN=PF10_0289 PE=4 SV=1 | 4 | 3.07 | 2.13 | 0.0634 |
| tr\|Q8IL48\|Q8IL48_PLAF7 tRNA binding protein, putative OS=Plasmodium falciparum (isolate 3D7) GN=PF14_0401 PE=4 SV=1 | 4 | 3.08 | 2.16 | 0.0649 |
| tr\|Q8IAM2\|Q8IAM2_PLAF7 1-cys peroxiredoxin OS=Plasmodium falciparum (isolate 3D7) GN=1-cyspxn PE=4 SV=1 | 4 | 3.11 | 2.16 | 0.0632 |
| tr\|Q8IKW5\|Q8IKW5_PLAF7 Elongation factor 2 OS=Plasmodium falciparum (isolate 3D7) GN=PF14_0486 PE=4 SV=1 | 4 | 4.68 | 1.72 | 0.0122 |
| tr\|Q8I3Y4\|Q8I3Y4_PLAF7 Glutathione synthetase OS=Plasmodium falciparum (isolate 3D7) GN=gS PE=3 SV=1 | 4 | 3.18 | 2.12 | 0.0578 |
| tr\|Q8IKU1\|Q8IKU1_PLAF7 p23 co-chaperone, putative OS=Plasmodium falciparum (isolate 3D7) GN=SBA1 PE=4 SV=2 | 4 | 3.18 | 2.36 | 0.0742 |
| tr\|Q8ILS7\|Q8ILS7_PLAF7 Prefoldin subunit 2, putative OS=Plasmodium falciparum (isolate 3D7) GN=PF14_0167 PE=4 SV=1 | 4 | 4.88 | 1.00 | 0.0023 |
| sp\|Q8I3Z1\|MLRR1_PLAF7 MATH and LRR domain-containing protein PFE0570w OS=Plasmodium falciparum (isolate 3D7) GN=PFE0570w PE=2 SV=1 | 4 | 3.21 | 4.02 | 0.2078 |
| tr\|Q7KWJ1\|Q7KWJ1_PLAF7 Acyl carrier protein OS=Plasmodium falciparum (isolate 3D7) GN=PFB0385w PE=3 SV=1 | 4 | 3.23 | 5.88 | 0.3520 |
| tr\|Q8IIW2\|Q8IIW2_PLAF7 Phenylalanine--tRNA ligase, putative OS=Plasmodium falciparum (isolate 3D7) GN=PF11_0051 PE=4 SV=1 | 4 | 3.30 | 2.27 | 0.0622 |
| tr\|Q8IJ74\|Q8IJ74_PLAF7 Uncharacterized protein OS=Plasmodium falciparum (isolate 3D7) GN=PF10_0325 PE=1 SV=1 | 4 | 3.33 | 2.25 | 0.0595 |
| sp\|Q6LFH8\|OAT_PLAF7 Ornithine aminotransferase OS=Plasmodium falciparum (isolate 3D7) GN=OAT PE=1 SV=1 | 4 | 4.97 | 1.68 | 0.0096 |
| sp\|Q8IL06\|YPF07_PLAF7 Uncharacterized protein PF14_0444 OS=Plasmodium falciparum (isolate 3D7) GN=PF14_0444 PE=4 SV=2 | 4 | 3.44 | 5.33 | 0.2877 |
| tr\|Q8IAM0\|Q8IAM0_PLAF7 Glutamate dehydrogenase, putative OS=Plasmodium falciparum (isolate 3D7) GN=PF08_0132 PE=4 SV=1 | 4 | 3.51 | 2.43 | 0.0632 |
| tr\|Q8IE68\|Q8IE68_PLAF7 Lsm6 homologue, putative OS=Plasmodium falciparum (isolate 3D7) GN=PF13_0142 PE=4 SV=1 | 4 | 3.65 | 4.73 | 0.2211 |
| tr\|Q8IBR6\|Q8IBR6_PLAF7 Prefoldin subunit 3, putative OS=Plasmodium falciparum (isolate 3D7) GN=MAL7P1.94 PE=4 SV=1 | 4 | 3.71 | 4.49 | 0.1975 |
| tr\|C6KTA9\|C6KTA9_PLAF7 C3h4-type ring finger protein, putative OS=Plasmodium falciparum (isolate 3D7) GN=PFF1325c PE=4 SV=1 | 4 | 3.89 | 7.20 | 0.3597 |
| tr\|Q8IDW4\|Q8IDW4_PLAF7 Nuclear movement protein, putative OS=Plasmodium falciparum (isolate 3D7) GN=PF13_0204 PE=4 SV=1 | 4 | 3.89 | 3.69 | 0.1256 |
| tr\|Q8IJ85\|Q8IJ85_PLAF7 Asparagine-rich antigen OS=Plasmodium falciparum (isolate 3D7) GN=PF10_0314 PE=4 SV=1 | 4 | 3.95 | 7.13 | 0.3488 |

| | | | | |
|---|---|---|---|---|
| tr\|Q8I2J3\|Q8I2J3_PLAF7 M18 aspartyl aminopeptidase OS=Plasmodium falciparum (isolate 3D7) GN=PfM18AAP PE=1 SV=1 | 4 | 4.11 | 3.75 | 0.1160 |
| tr\|Q8IM19\|Q8IM19_PLAF7 Nucleolar preribosomal GTPase, putative OS=Plasmodium falciparum (isolate 3D7) GN=PF14_0072 PE=4 SV=2 | 4 | 4.12 | 5.85 | 0.2538 |
| tr\|Q8I5D0\|Q8I5D0_PLAF7 Uncharacterized protein OS=Plasmodium falciparum (isolate 3D7) GN=PFL1395c PE=4 SV=1 | 4 | 4.23 | 7.13 | 0.3214 |
| tr\|Q8IJE1\|Q8IJE1_PLAF7 Conserved Plasmodium protein OS=Plasmodium falciparum (isolate 3D7) GN=PF10_0257 PE=4 SV=2 | 4 | 4.29 | 5.82 | 0.2371 |
| tr\|Q8II17\|Q8II17_PLAF7 DNA-directed RNA polymerase OS=Plasmodium falciparum (isolate 3D7) GN=PF11_0358 PE=3 SV=1 | 4 | 4.44 | 7.30 | 0.3106 |
| tr\|Q8IDM2\|Q8IDM2_PLAF7 Ethanolamine-phosphate cytidylyltransferase, putative OS=Plasmodium falciparum (isolate 3D7) GN=PF13_0253 PE=4 SV=1 | 4 | 6.24 | 7.28 | 0.1852 |
| tr\|Q8I425\|Q8I425_PLAF7 Uncharacterized protein OS=Plasmodium falciparum (isolate 3D7) GN=PFE0385w PE=4 SV=1 | 4 | 6.37 | 7.39 | 0.1831 |
| tr\|Q8I3N5\|Q8I3N5_PLAF7 G10 protein, putative OS=Plasmodium falciparum (isolate 3D7) GN=PFE1140c PE=4 SV=1 | 4 | 6.39 | 11.31 | 0.3408 |
| tr\|Q8IBL9\|Q8IBL9_PLAF7 Uncharacterized protein OS=Plasmodium falciparum (isolate 3D7) GN=PF07_0097 PE=4 SV=1 | 4 | 6.50 | 12.89 | 0.3874 |
| tr\|Q8IJ77\|Q8IJ77_PLAF7 S-adenosylmethionine decarboxylase-ornithine decarboxylase OS=Plasmodium falciparum (isolate 3D7) GN=PF10_0322 PE=3 SV=1 | 4 | 6.72 | 8.54 | 0.2134 |
| sp\|P62203\|CALM_PLAF7 Calmodulin OS=Plasmodium falciparum (isolate 3D7) GN=PF14_0323 PE=3 SV=2 | 4 | 7.33 | 9.74 | 0.2293 |
| tr\|Q8IBK8\|Q8IBK8_PLAF7 Mitochondrial import inner membrane translocase subunit tim14, putative OS=Plasmodium falciparum (isolate 3D7) GN=PF07_0103 PE=4 SV=1 | 4 | 9.06 | 17.25 | 0.3705 |
| tr\|Q8I500\|Q8I500_PLAF7 Mitochondrial import inner membrane translocase subunit, putative OS=Plasmodium falciparum (isolate 3D7) GN=PFL2065c PE=4 SV=2 | 4 | 10.25 | 20.00 | 0.3808 |
| tr\|O77327\|O77327_PLAF7 U2 snRNP spliceosome subunit, putative OS=Plasmodium falciparum (isolate 3D7) GN=PFC0375c PE=4 SV=1 | 4 | 10.40 | 20.08 | 0.3765 |
| tr\|Q8I3J6\|Q8I3J6_PLAF7 Uncharacterized protein OS=Plasmodium falciparum (isolate 3D7) GN=PFE1340w PE=3 SV=1 | 4 | 12.32 | 24.17 | 0.3830 |
| tr\|Q8IKT2\|Q8IKT2_PLAF7 6-phosphogluconate dehydrogenase, decarboxylating OS=Plasmodium falciparum (isolate 3D7) GN=PF14_0520 PE=3 SV=1 | 4 | 12.60 | 18.48 | 0.2660 |
| sp\|O77323\|TCPH_PLAF7 T-complex protein 1 subunit eta OS=Plasmodium falciparum (isolate 3D7) GN=MAL3P3.6 PE=3 SV=1 | 4 | 16.39 | 25.67 | 0.2913 |
| tr\|Q8I4Y5\|Q8I4Y5_PLAF7 ADP-ribosylation factor GTPase-activating protein OS=Plasmodium falciparum (isolate 3D7) GN=PFL2140c PE=1 SV=1 | 4 | 18.86 | 18.55 | 0.1350 |
| tr\|Q8IDP4\|Q8IDP4_PLAF7 Thioredoxin OS=Plasmodium falciparum (isolate 3D7) GN=trx2 PE=1 SV=1 | 4 | 20.43 | 40.38 | 0.3861 |
| tr\|O96221\|O96221_PLAF7 Sec31p putative OS=Plasmodium falciparum (isolate 3D7) GN=Sec31p PE=4 SV=3 | 4 | 23.03 | 27.20 | 0.1889 |
| tr\|C0H512\|C0H512_PLAF7 Putative uncharacterized protein OS=Plasmodium falciparum (isolate 3D7) GN=PFI0086w PE=4 SV=1 | 4 | 31.47 | 62.45 | 0.3879 |
| tr\|Q8IDG8\|Q8IDG8_PLAF7 Membrane-associated histidine rich protein 2 OS=Plasmodium falciparum (isolate 3D7) GN=PF13_0276 PE=4 SV=1 | 4 | 79.93 | 159.28 | 0.3895 |
| tr\|Q8I3L8\|Q8I3L8_PLAF7 Mitochondrial import receptor subunit, putative (TOM22) OS=Plasmodium falciparum (isolate 3D7) GN=PFE1230c PE=4 SV=1 | 4 | 101.42 | 202.37 | 0.3901 |
| tr\|Q8IBY4\|Q8IBY4_PLAF7 60S ribosomal protein L34-A, putative OS=Plasmodium falciparum (isolate 3D7) GN=PF07_0043 PE=1 SV=1 | 4 | 107.72 | 213.16 | 0.3866 |
| tr\|Q8IIB4\|Q8IIB4_PLAF7 60S ribosomal protein L35, putative OS=Plasmodium falciparum (isolate 3D7) GN=PF11_0260 PE=1 SV=2 | 4 | 283.24 | 512.24 | 0.3495 |
| tr\|Q8IL22\|Q8IL22_PLAF7 Histidine--tRNA ligase, putative OS=Plasmodium falciparum (isolate 3D7) GN=PF14_0428 PE=3 SV=1 | 4 | 420.29 | 836.42 | 0.3889 |
| tr\|C6KT18\|C6KT18_PLAF7 Histone H2A OS=Plasmodium falciparum (isolate 3D7) GN=PFF0860c PE=3 SV=1 | 4 | 459.81 | 919.15 | 0.3908 |
| tr\|Q9U0J2\|Q9U0J2_PLAF7 DNAJ protein OS=Plasmodium falciparum (isolate 3D7) GN=Pfj1 PE=3 SV=1 | 3 | 0.07 | 0.08 | 0.2930 |
| tr\|Q8ID90\|Q8ID90_PLAF7 Uncharacterized protein OS=Plasmodium falciparum (isolate 3D7) GN=MAL13P1.307 PE=4 SV=1 | 3 | 0.23 | 0.38 | 0.4092 |
| sp\|Q8I5D2\|ABRA_PLAF7 101 kDa malaria antigen OS=Plasmodium falciparum (isolate 3D7) GN=ABRA PE=3 SV=1 | 3 | 0.24 | 0.40 | 0.4105 |
| tr\|Q8I3L9\|Q8I3L9_PLAF7 Organelle ribosomal protein L7/L12, putative OS=Plasmodium falciparum (isolate 3D7) GN=PFE1225w PE=3 SV=1 | 3 | 0.27 | 0.36 | 0.3201 |
| tr\|Q8I5R4\|Q8I5R4_PLAF7 Phosphatidylinositol-glycan biosynthesis class O protein, putative OS=Plasmodium falciparum (isolate 3D7) GN=PFL0685w PE=4 SV=2 | 3 | 0.28 | 0.12 | 0.0545 |
| tr\|Q8I563\|Q8I563_PLAF7 Uncharacterized protein OS=Plasmodium falciparum (isolate 3D7) GN=PFL1740w PE=4 SV=1 | 3 | 0.29 | 0.43 | 0.3664 |

| | | | | |
|---|---|---|---|---|
| tr\|Q8ILQ4\|Q8ILQ4_PLAF7 Uncharacterized protein OS=Plasmodium falciparum (isolate 3D7) GN=PF14_0190 PE=4 SV=1 | 3 | 0.31 | 0.35 | 0.2620 |
| tr\|Q8ILE9\|Q8ILE9_PLAF7 ATP-specific succinyl-CoA synthetase beta subunit, putative OS=Plasmodium falciparum (isolate 3D7) GN=PF14_0295 PE=4 SV=1 | 3 | 0.36 | 0.32 | 0.1943 |
| sp\|P50498\|MSA2_PLAF7 Merozoite surface antigen 2 OS=Plasmodium falciparum (isolate 3D7) GN=MSA2 PE=1 SV=2 | 3 | 0.36 | 0.29 | 0.1660 |
| tr\|C0H4W0\|C0H4W0_PLAF7 Uncharacterized protein OS=Plasmodium falciparum (isolate 3D7) GN=MAL8P1.63 PE=4 SV=1 | 3 | 0.37 | 0.13 | 0.0384 |
| tr\|Q8IDY0\|Q8IDY0_PLAF7 MSP7-like protein OS=Plasmodium falciparum (isolate 3D7) GN=MAL13P1.174 PE=4 SV=1 | 3 | 0.37 | 0.32 | 0.1830 |
| tr\|Q8IEC2\|Q8IEC2_PLAF7 Uncharacterized protein OS=Plasmodium falciparum (isolate 3D7) GN=MAL13P1.103 PE=4 SV=1 | 3 | 0.38 | 0.27 | 0.1342 |
| tr\|Q8IE08\|Q8IE08_PLAF7 Qa-SNARE protein, putative OS=Plasmodium falciparum (isolate 3D7) GN=PfSyn5 PE=4 SV=1 | 3 | 0.45 | 0.38 | 0.1769 |
| sp\|O75531\|BAF_HUMAN Barrier-to-autointegration factor OS=Homo sapiens GN=BANF1 PE=1 SV=1 | 3 | 0.48 | 0.82 | 0.4187 |
| tr\|Q8IKP8\|Q8IKP8_PLAF7 Uncharacterized protein OS=Plasmodium falciparum (isolate 3D7) GN=PF14_0556 PE=4 SV=2 | 3 | 0.49 | 0.39 | 0.1609 |
| tr\|Q8IHV2\|Q8IHV2_PLAF7 Uncharacterized protein OS=Plasmodium falciparum (isolate 3D7) GN=PF11_0424 PE=4 SV=1 | 3 | 0.49 | 0.41 | 0.1758 |
| tr\|Q8ILG8\|Q8ILG8_PLAF7 Uncharacterized protein OS=Plasmodium falciparum (isolate 3D7) GN=PF14_0275 PE=4 SV=1 | 3 | 0.51 | 0.33 | 0.1122 |
| tr\|Q8IIR8\|Q8IIR8_PLAF7 Succinyl-CoA synthetase alpha subunit, putative OS=Plasmodium falciparum (isolate 3D7) GN=PF11_0097 PE=3 SV=2 | 3 | 0.51 | 0.49 | 0.2079 |
| tr\|Q8IEA6\|Q8IEA6_PLAF7 Dihydrolipamide succinyltransferase component of 2-oxoglutarate dehydrogenase complex OS=Plasmodium falciparum (isolate 3D7) GN=PF13_0121 PE=3 SV=1 | 3 | 0.54 | 0.34 | 0.1067 |
| tr\|Q8I544\|Q8I544_PLAF7 Uncharacterized protein OS=Plasmodium falciparum (isolate 3D7) GN=PFL1835w PE=4 SV=1 | 3 | 0.55 | 0.31 | 0.0905 |
| tr\|C0H561\|C0H561_PLAF7 Thioredoxin OS=Plasmodium falciparum (isolate 3D7) GN=Tlp2 PE=3 SV=1 | 3 | 0.56 | 0.48 | 0.1830 |
| tr\|C0H4A3\|C0H4A3_PLAF7 Uncharacterized protein OS=Plasmodium falciparum (isolate 3D7) GN=PFD0669c PE=4 SV=1 | 3 | 0.60 | 0.49 | 0.1653 |
| SV=1;sp\|Q00610-2\|CLH1_HUMAN Isoform 2 of Clathrin heavy chain 1 OS=Homo sapiens GN=CLTC;sp\|Q00610\|CLH1_HUMAN Clathrin heavy chain 1 OS=Homo sapiens GN=CLTC PE=1 SV=5 | 3 | 0.60 | 0.52 | 0.1830 |
| tr\|O96254\|O96254_PLAF7 Clathrin coat assembly protein, putative OS=Plasmodium falciparum (isolate 3D7) GN=PFB0805c PE=4 SV=1 | 3 | 0.61 | 0.48 | 0.1581 |
| tr\|C6KSS2\|C6KSS2_PLAF7 G-protein associated signal transduction protein, putative OS=Plasmodium falciparum (isolate 3D7) GN=PFF0365c PE=4 SV=1 | 3 | 0.64 | 0.56 | 0.1874 |
| tr\|Q8ILR0\|Q8ILR0_PLAF7 Uncharacterized protein OS=Plasmodium falciparum (isolate 3D7) GN=PF14_0184 PE=4 SV=1 | 3 | 0.64 | 0.32 | 0.0740 |
| tr\|C6KSV0\|C6KSV0_PLAF7 Histone H3 OS=Plasmodium falciparum (isolate 3D7) GN=PFF0510w PE=3 SV=1;tr\|C6KT19\|C6KT19_PLAF7 Histone H3 OS=Plasmodium falciparum (isolate 3D7) GN=PFF0865w PE=3 SV=1 | 3 | 0.66 | 0.31 | 0.0675 |
| tr\|Q8ILT8\|Q8ILT8_PLAF7 Dimethyladenosine transferase, putative OS=Plasmodium falciparum (isolate 3D7) GN=PF14_0156 PE=1 SV=1 | 3 | 0.67 | 0.71 | 0.2464 |
| tr\|C0H516\|C0H516_PLAF7 PfRab7, GTPase OS=Plasmodium falciparum (isolate 3D7) GN=Rab7 PE=3 SV=1 | 3 | 0.67 | 0.58 | 0.1832 |
| tr\|Q8I1Z2\|Q8I1Z2_PLAF7 CGI-201 protein, short form OS=Plasmodium falciparum (isolate 3D7) GN=PFD0180c PE=4 SV=1 | 3 | 0.67 | 0.32 | 0.0672 |
| tr\|Q8IEE9\|Q8IEE9_PLAF7 Cholinephosphate cytidylyltransferase OS=Plasmodium falciparum (isolate 3D7) GN=ctP PE=1 SV=1 | 3 | 0.71 | 0.48 | 0.1241 |
| tr\|C6KSY0\|C6KSY0_PLAF7 Transcription factor with AP2 domain(S), putative OS=Plasmodium falciparum (isolate 3D7) GN=ApiAP2 PE=4 SV=1 | 3 | 0.56 | 0.16 | 0.0280 |
| tr\|Q8IHS1\|Q8IHS1_PLAF7 Uncharacterized protein OS=Plasmodium falciparum (isolate 3D7) GN=PF11_0458 PE=4 SV=1 | 3 | 0.76 | 0.65 | 0.1820 |
| tr\|Q8ID42\|Q8ID42_PLAF7 Signal recognition particle receptor alpha subunit, putative OS=Plasmodium falciparum (isolate 3D7) GN=PF13_0350 PE=4 SV=1 | 3 | 0.77 | 0.51 | 0.1191 |
| tr\|Q8I2I3\|Q8I2I3_PLAF7 Putative uncharacterized protein OS=Plasmodium falciparum (isolate 3D7) GN=PFI1620c PE=4 SV=1 | 3 | 0.77 | 0.36 | 0.0654 |
| tr\|Q8IIH2\|Q8IIH2_PLAF7 Clathrin coat assembly protein, putative OS=Plasmodium falciparum (isolate 3D7) GN=PF11_0202 PE=4 SV=1 | 3 | 0.81 | 0.67 | 0.1740 |
| tr\|Q8IBM7\|Q8IBM7_PLAF7 BING4 (NUC141) WD-40 repeat protein, putative OS=Plasmodium falciparum (isolate 3D7) GN=PF07_0092 PE=4 SV=1 | 3 | 0.82 | 0.37 | 0.0635 |
| tr\|C6KT93\|C6KT93_PLAF7 Uncharacterized protein OS=Plasmodium falciparum (isolate 3D7) GN=PFF1245c PE=4 SV=1 | 3 | 0.70 | 0.04 | 0.0011 |

| | | | | |
|---|---|---|---|---|
| tr\|Q9U0I0\|Q9U0I0_PLAF7 Uncharacterized protein OS=Plasmodium falciparum (isolate 3D7) GN=PFD0535w PE=4 SV=1 | 3 | 0.85 | 0.75 | 0.1886 |
| tr\|Q8I1Y6\|Q8I1Y6_PLAF7 Uncharacterized protein OS=Plasmodium falciparum (isolate 3D7) GN=PFD0207c PE=4 SV=1 | 3 | 0.86 | 0.48 | 0.0893 |
| tr\|Q8IE02\|Q8IE02_PLAF7 Apurinic/apyrimidinic endonuclease Apn1 OS=Plasmodium falciparum (isolate 3D7) GN=apn1 PE=3 SV=1 | 3 | 0.86 | 0.75 | 0.1840 |
| tr\|Q8IHU4\|Q8IHU4_PLAF7 Uncharacterized protein OS=Plasmodium falciparum (isolate 3D7) GN=PF11_0433 PE=4 SV=1 | 3 | 0.89 | 0.61 | 0.1282 |
| tr\|Q8I283\|Q8I283_PLAF7 Cyclin-dependent kinases regulatory subunit OS=Plasmodium falciparum (isolate 3D7) GN=PFA_0285c PE=3 SV=1 | 3 | 0.90 | 0.70 | 0.1584 |
| tr\|Q8IHP7\|Q8IHP7_PLAF7 Uncharacterized protein OS=Plasmodium falciparum (isolate 3D7) GN=PF11_0482 PE=4 SV=1 | 3 | 0.92 | 0.42 | 0.0641 |
| tr\|Q8IKZ8\|Q8IKZ8_PLAF7 Uncharacterized protein OS=Plasmodium falciparum (isolate 3D7) GN=PF14_0453 PE=4 SV=1 | 3 | 0.75 | 0.14 | 0.0120 |
| tr\|Q8I6V0\|Q8I6V0_PLAF7 Cysteine proteinase falcipain-1 OS=Plasmodium falciparum (isolate 3D7) GN=PF14_0553 PE=3 SV=1 | 3 | 0.76 | 0.12 | 0.0081 |
| tr\|B9ZSI9\|B9ZSI9_PLAF7 Putative uncharacterized protein OS=Plasmodium falciparum (isolate 3D7) GN=PFA_0550w PE=4 SV=1 | 3 | 0.76 | 0.25 | 0.0336 |
| tr\|O97232\|O97232_PLAF7 1-cys-glutaredoxin-like protein-1 OS=Plasmodium falciparum (isolate 3D7) GN=PfGLP-1 PE=4 SV=1 | 3 | 0.94 | 0.91 | 0.2132 |
| tr\|Q8ILF7\|Q8ILF7_PLAF7 Glutamate dehydrogenase OS=Plasmodium falciparum (isolate 3D7) GN=PF14_0286 PE=1 SV=1 | 3 | 0.78 | 0.08 | 0.0031 |
| tr\|Q8I2T9\|Q8I2T9_PLAF7 Fe-S-cluster redox enzyme, putative OS=Plasmodium falciparum (isolate 3D7) GN=PFI1050c PE=4 SV=1 | 3 | 0.78 | 0.22 | 0.0251 |
| tr\|C0H4N9\|C0H4N9_PLAF7 Uncharacterized protein OS=Plasmodium falciparum (isolate 3D7) GN=MAL7P1.106 PE=4 SV=1 | 3 | 0.78 | 0.03 | 0.0006 |
| tr\|Q8ILN2\|Q8ILN2_PLAF7 Ctr copper transporter domain containing protein, putative OS=Plasmodium falciparum (isolate 3D7) GN=PF14_0211 PE=4 SV=1 | 3 | 0.79 | 0.19 | 0.0189 |
| tr\|C0H574\|C0H574_PLAF7 Putative uncharacterized protein OS=Plasmodium falciparum (isolate 3D7) GN=PFI1463w PE=4 SV=1 | 3 | 0.79 | 0.15 | 0.0121 |
| tr\|Q8IE96\|Q8IE96_PLAF7 Adenosine-diphosphatase OS=Plasmodium falciparum (isolate 3D7) GN=MAL13P1.121 PE=4 SV=1 | 3 | 0.79 | 0.02 | 0.0003 |
| tr\|Q8IJ92\|Q8IJ92_PLAF7 Uncharacterized protein OS=Plasmodium falciparum (isolate 3D7) GN=PF10_0307 PE=4 SV=1 | 3 | 0.80 | 0.10 | 0.0053 |
| tr\|C0H5E0\|C0H5E0_PLAF7 Uncharacterized protein OS=Plasmodium falciparum (isolate 3D7) GN=MAL13P1.360 PE=4 SV=1 | 3 | 0.99 | 0.53 | 0.0845 |
| tr\|Q8II05\|Q8II05_PLAF7 3-oxo-5-alpha-steroid 4-dehydrogenase, putative OS=Plasmodium falciparum (isolate 3D7) GN=PF11_0370 PE=4 SV=2 | 3 | 1.00 | 0.58 | 0.0953 |
| tr\|Q8I1T4\|Q8I1T4_PLAF7 Cyclin-dependent kinase, putative OS=Plasmodium falciparum (isolate 3D7) GN=Pfcrk-3 PE=4 SV=1 | 3 | 1.00 | 0.56 | 0.0893 |
| tr\|Q8ID44\|Q8ID44_PLAF7 Rhoptry protein OS=Plasmodium falciparum (isolate 3D7) GN=PfRhop148 PE=4 SV=1 | 3 | 1.02 | 0.51 | 0.0751 |
| tr\|Q8I5Y7\|Q8I5Y7_PLAF7 Uncharacterized protein OS=Plasmodium falciparum (isolate 3D7) GN=PFL0290w PE=4 SV=1 | 3 | 0.81 | 0.10 | 0.0048 |
| tr\|O96189\|O96189_PLAF7 Qa-SNARE protein OS=Plasmodium falciparum (isolate 3D7) GN=Syn17 PE=4 SV=1 | 3 | 0.81 | 0.13 | 0.0084 |
| tr\|Q8ILS4\|Q8ILS4_PLAF7 NOT family protein, putative OS=Plasmodium falciparum (isolate 3D7) GN=PF14_0170 PE=4 SV=1 | 3 | 1.07 | 0.94 | 0.1868 |
| tr\|Q8IBU0\|Q8IBU0_PLAF7 Uncharacterized protein OS=Plasmodium falciparum (isolate 3D7) GN=PF07_0066 PE=4 SV=1 | 3 | 1.10 | 1.15 | 0.2380 |
| tr\|Q8I564\|Q8I564_PLAF7 Uncharacterized protein OS=Plasmodium falciparum (isolate 3D7) GN=PFL1735c PE=4 SV=1 | 3 | 0.83 | 0.27 | 0.0336 |
| tr\|Q8IM28\|Q8IM28_PLAF7 ATP-dependent CLP protease, putative OS=Plasmodium falciparum (isolate 3D7) GN=PF14_0063 PE=4 SV=1 | 3 | 0.83 | 0.18 | 0.0145 |
| tr\|Q8I348\|Q8I348_PLAF7 Selenide water dikinase, putative OS=Plasmodium falciparum (isolate 3D7) GN=PFI0505c PE=4 SV=1 | 3 | 0.84 | 0.25 | 0.0278 |
| tr\|Q8IKQ3\|Q8IKQ3_PLAF7 Uncharacterized protein OS=Plasmodium falciparum (isolate 3D7) GN=PF14_0550 PE=4 SV=1 | 3 | 1.12 | 1.09 | 0.2170 |
| tr\|Q8ILZ9\|Q8ILZ9_PLAF7 Uncharacterized protein OS=Plasmodium falciparum (isolate 3D7) GN=PF14_0094 PE=4 SV=1 | 3 | 0.84 | 0.14 | 0.0093 |
| sp\|Q76NM1\|ERD2_PLAF7 ER lumen protein-retaining receptor OS=Plasmodium falciparum (isolate 3D7) GN=ERD2 PE=3 SV=1 | 3 | 0.84 | 0.05 | 0.0010 |
| tr\|Q8I2X8\|Q8I2X8_PLAF7 Putative uncharacterized protein OS=Plasmodium falciparum (isolate 3D7) GN=PFI0855w PE=4 SV=1 | 3 | 1.15 | 0.66 | 0.0953 |
| tr\|C6KSV8\|C6KSV8_PLAF7 Uncharacterized protein OS=Plasmodium falciparum (isolate 3D7) GN=PFF0555w PE=4 SV=1 | 3 | 1.16 | 0.90 | 0.1550 |

| | | | | |
|---|---|---|---|---|
| tr\|Q8I461\|Q8I461_PLAF7 Cation transporting P-ATPase OS=Plasmodium falciparum (isolate 3D7) GN=PfATPase3 PE=3 SV=1 | 3 | 0.84 | 0.09 | 0.0034 |
| tr\|Q8I2V7\|Q8I2V7_PLAF7 Dolichyl-diphosphooligosaccharide--protein glycosyltransferase 48 kDa subunit OS=Plasmodium falciparum (isolate 3D7) GN=PFI0960w PE=3 SV=1 | 3 | 1.16 | 1.14 | 0.2203 |
| sp\|P02042\|HBD_HUMAN Hemoglobin subunit delta OS=Homo sapiens GN=HBD PE=1 SV=2;tr\|E9PFT6\|E9PFT6_HUMAN Hemoglobin subunit delta OS=Homo sapiens GN=HBD PE=1 SV=1;tr\|E9PEW8\|E9PEW8_HUMAN Hemoglobin subunit delta (Fragment) OS=Homo sapiens GN=HBD PE=1 SV=1 | 3 | 0.85 | 0.28 | 0.0355 |
| tr\|Q8IL89\|Q8IL89_PLAF7 Succinyl CoA ligase, putative OS=Plasmodium falciparum (isolate 3D7) GN=PF14_0357 PE=4 SV=1 | 3 | 0.85 | 0.32 | 0.0433 |
| tr\|Q9U0L4\|Q9U0L4_PLAF7 Peptidyl-tRNA hydrolase PTH2, putative OS=Plasmodium falciparum (isolate 3D7) GN=PFD0355c PE=4 SV=2 | 3 | 0.85 | 0.27 | 0.0329 |
| tr\|Q8IDI0\|Q8IDI0_PLAF7 Uncharacterized protein OS=Plasmodium falciparum (isolate 3D7) GN=MAL13P1.262 PE=4 SV=1 | 3 | 0.85 | 0.12 | 0.0060 |
| tr\|Q8IKZ0\|Q8IKZ0_PLAF7 Uncharacterized protein OS=Plasmodium falciparum (isolate 3D7) GN=PF14_0461 PE=4 SV=1 | 3 | 0.86 | 0.17 | 0.0121 |
| tr\|Q8IIE5\|Q8IIE5_PLAF7 Conserved Plasmodium protein OS=Plasmodium falciparum (isolate 3D7) GN=PF11_0229 PE=4 SV=2 | 3 | 0.87 | 0.05 | 0.0011 |
| tr\|Q8I2T7\|Q8I2T7_PLAF7 Tetratricopeptide repeat family protein, putative OS=Plasmodium falciparum (isolate 3D7) GN=PFI1060w PE=4 SV=1 | 3 | 0.87 | 0.19 | 0.0157 |
| tr\|C6KTD8\|C6KTD8_PLAF7 DNA polymerase epsilon, catalytic subunit a, putative OS=Plasmodium falciparum (isolate 3D7) GN=PFF1470c PE=4 SV=1 | 3 | 0.88 | 0.35 | 0.0487 |
| tr\|Q8I3V1\|Q8I3V1_PLAF7 Metabolite/drug transporter, putative OS=Plasmodium falciparum (isolate 3D7) GN=PFE0785c PE=4 SV=1 | 3 | 1.26 | 1.55 | 0.2951 |
| tr\|Q8IIG3\|Q8IIG3_PLAF7 Uncharacterized protein OS=Plasmodium falciparum (isolate 3D7) GN=PF11_0211 PE=4 SV=1 | 3 | 1.29 | 0.63 | 0.0704 |
| tr\|C6KSZ5\|C6KSZ5_PLAF7 Ribonuclease, putative OS=Plasmodium falciparum (isolate 3D7) GN=PFF0745c PE=4 SV=1 | 3 | 0.88 | 0.07 | 0.0023 |
| tr\|O77349\|O77349_PLAF7 Putative uncharacterized protein OS=Plasmodium falciparum (isolate 3D7) GN=PFC0500w PE=4 SV=2 | 3 | 0.89 | 0.05 | 0.0011 |
| tr\|Q8IDJ7\|Q8IDJ7_PLAF7 Small nuclear ribonucleoprotein, putative OS=Plasmodium falciparum (isolate 3D7) GN=MAL13P1.253 PE=4 SV=1 | 3 | 0.89 | 0.19 | 0.0144 |
| tr\|Q8I285\|Q8I285_PLAF7 Putative uncharacterized protein OS=Plasmodium falciparum (isolate 3D7) GN=PFA_0275c PE=4 SV=1 | 3 | 0.90 | 0.25 | 0.0242 |
| tr\|Q8IBT8\|Q8IBT8_PLAF7 Uncharacterized protein OS=Plasmodium falciparum (isolate 3D7) GN=MAL7P1.76 PE=4 SV=1 | 3 | 1.39 | 1.15 | 0.1719 |
| tr\|O97278\|O97278_PLAF7 ABC transporter, putative OS=Plasmodium falciparum (isolate 3D7) GN=PFC0875w PE=4 SV=3 | 3 | 0.90 | 0.10 | 0.0045 |
| tr\|Q8ILM6\|Q8ILM6_PLAF7 Uncharacterized protein OS=Plasmodium falciparum (isolate 3D7) GN=PF14_0217 PE=4 SV=1 | 3 | 0.90 | 0.08 | 0.0023 |
| tr\|O96237\|O96237_PLAF7 Origin recognition complex subunit 5 OS=Plasmodium falciparum (isolate 3D7) GN=ORC5 PE=4 SV=1 | 3 | 0.91 | 0.18 | 0.0130 |
| tr\|C0H4S6\|C0H4S6_PLAF7 Uncharacterized protein OS=Plasmodium falciparum (isolate 3D7) GN=MAL8P1.130 PE=4 SV=1 | 3 | 1.44 | 0.61 | 0.0550 |
| tr\|Q8I3B3\|Q8I3B3_PLAF7 Putative uncharacterized protein OS=Plasmodium falciparum (isolate 3D7) GN=PFI0170w PE=4 SV=1 | 3 | 0.91 | 0.17 | 0.0116 |
| sp\|P30043\|BLVRB_HUMAN Flavin reductase (NADPH) OS=Homo sapiens GN=BLVRB PE=1 SV=3;tr\|M0QZL1\|M0QZL1_HUMAN Flavin reductase (NADPH) OS=Homo sapiens GN=BLVRB PE=1 SV=1;tr\|M0R192\|M0R192_HUMAN Flavin reductase (NADPH) OS=Homo sapiens GN=BLVRB PE=1 SV=1 | 3 | 1.47 | 1.27 | 0.1848 |
| tr\|Q8ILJ1\|Q8ILJ1_PLAF7 Uncharacterized protein OS=Plasmodium falciparum (isolate 3D7) GN=PF14_0252 PE=4 SV=1 | 3 | 0.91 | 0.16 | 0.0097 |
| tr\|O96168\|O96168_PLAF7 Conserved Plasmodium protein OS=Plasmodium falciparum (isolate 3D7) GN=PFB0365w PE=4 SV=3 | 3 | 0.91 | 0.04 | 0.0007 |
| tr\|Q8I482\|Q8I482_PLAF7 Chromosome assembly factor 1, CAF-1 OS=Plasmodium falciparum (isolate 3D7) GN=PFE0090w PE=4 SV=1 | 3 | 0.92 | 0.16 | 0.0095 |
| tr\|Q8I1P0\|Q8I1P0_PLAF7 60S ribosomal protein L7Ae/L30e, putative OS=Plasmodium falciparum (isolate 3D7) GN=PFD0960c PE=4 SV=1 | 3 | 0.92 | 0.12 | 0.0051 |
| tr\|Q8IDA3\|Q8IDA3_PLAF7 Uncharacterized protein OS=Plasmodium falciparum (isolate 3D7) GN=MAL13P1.299 PE=4 SV=1 | 3 | 0.93 | 0.19 | 0.0131 |
| tr\|Q8I274\|Q8I274_PLAF7 Rab5c, GTPase OS=Plasmodium falciparum (isolate 3D7) GN=Rab5c PE=3 SV=1 | 3 | 0.93 | 0.11 | 0.0048 |
| tr\|C0H5J0\|C0H5J0_PLAF7 Uncharacterized protein OS=Plasmodium falciparum (isolate 3D7) GN=MAL13P1.293 PE=4 SV=1 | 3 | 1.62 | 0.89 | 0.0885 |
| tr\|C0H5D0\|C0H5D0_PLAF7 Uncharacterized protein OS=Plasmodium falciparum (isolate 3D7) GN=MAL13P1.124 PE=4 SV=1 | 3 | 0.93 | 0.14 | 0.0074 |

| | | | | |
|---|---|---|---|---|
| tr\|Q8IBK1\|Q8IBK1_PLAF7 Exonuclease I, putative OS=Plasmodium falciparum (isolate 3D7) GN=PF07_0105 PE=4 SV=1 | 3 | 0.93 | 0.08 | 0.0022 |
| tr\|Q8IB40\|Q8IB40_PLAF7 C-13 antigen OS=Plasmodium falciparum (isolate 3D7) GN=MAL8P1.57 PE=4 SV=1 | 3 | 0.93 | 0.37 | 0.0489 |
| tr\|Q8I5P4\|Q8I5P4_PLAF7 Signal recognition particle SRP19, putative OS=Plasmodium falciparum (isolate 3D7) GN=PFL0785c PE=4 SV=1 | 3 | 1.85 | 1.44 | 0.1565 |
| tr\|Q8IKE6\|Q8IKE6_PLAF7 Uncharacterized protein OS=Plasmodium falciparum (isolate 3D7) GN=PF14_0659 PE=4 SV=1 | 3 | 1.89 | 2.28 | 0.2880 |
| tr\|Q8I3M7\|Q8I3M7_PLAF7 Transporter, putative OS=Plasmodium falciparum (isolate 3D7) GN=PFE1185w PE=4 SV=1 | 3 | 0.94 | 0.08 | 0.0022 |
| tr\|Q8I226\|Q8I226_PLAF7 TatD-like deoxyribonuclease, putative OS=Plasmodium falciparum (isolate 3D7) GN=PFA_0580c PE=4 SV=1 | 3 | 1.92 | 0.87 | 0.0625 |
| tr\|Q8IJQ9\|Q8IJQ9_PLAF7 Uncharacterized protein OS=Plasmodium falciparum (isolate 3D7) GN=PF10_0133 PE=4 SV=1 | 3 | 0.94 | 0.29 | 0.0302 |
| tr\|Q8IIG9\|Q8IIG9_PLAF7 Uncharacterized protein OS=Plasmodium falciparum (isolate 3D7) GN=PF11_0205 PE=4 SV=1 | 3 | 1.98 | 1.33 | 0.1237 |
| tr\|Q8I5L1\|Q8I5L1_PLAF7 Pre-mRNA splicing factor, putative OS=Plasmodium falciparum (isolate 3D7) GN=PFL0970w PE=4 SV=1 | 3 | 1.98 | 2.37 | 0.2838 |
| tr\|Q7K6B1\|Q7K6B1_PLAF7 Protein kinase c inhibitor-like protein, putative OS=Plasmodium falciparum (isolate 3D7) GN=PF08_0059 PE=4 SV=2 | 3 | 0.94 | 0.30 | 0.0312 |
| tr\|Q8I332\|Q8I332_PLAF7 Putative uncharacterized protein OS=Plasmodium falciparum (isolate 3D7) GN=PFI0585c PE=4 SV=1 | 3 | 2.05 | 1.77 | 0.1823 |
| tr\|Q8IBK0\|Q8IBK0_PLAF7 Uncharacterized protein OS=Plasmodium falciparum (isolate 3D7) GN=MAL7P1.138 PE=4 SV=1 | 3 | 2.08 | 1.01 | 0.0698 |
| tr\|Q8I344\|Q8I344_PLAF7 Nucleotide binding protein, putative OS=Plasmodium falciparum (isolate 3D7) GN=PFI0525w PE=4 SV=1 | 3 | 0.95 | 0.21 | 0.0160 |
| tr\|Q8IBL5\|Q8IBL5_PLAF7 Uncharacterized protein OS=Plasmodium falciparum (isolate 3D7) GN=PF07_0101 PE=4 SV=1 | 3 | 2.14 | 1.50 | 0.1322 |
| tr\|Q6ZLZ9\|Q6ZLZ9_PLAF7 Alpha tubulin OS=Plasmodium falciparum (isolate 3D7) GN=PFI0180w PE=3 SV=1 | 3 | 2.18 | 2.08 | 0.2116 |
| tr\|Q8I2K4\|Q8I2K4_PLAF7 Nucleolar protein Nop52, putative OS=Plasmodium falciparum (isolate 3D7) GN=PFI1510w PE=4 SV=1 | 3 | 2.21 | 3.15 | 0.3486 |
| tr\|Q8IDC8\|Q8IDC8_PLAF7 Uncharacterized protein OS=Plasmodium falciparum (isolate 3D7) GN=PF13_0309 PE=4 SV=1 | 3 | 2.22 | 1.64 | 0.1433 |
| tr\|Q8IIP3\|Q8IIP3_PLAF7 Conserved Plasmodium protein OS=Plasmodium falciparum (isolate 3D7) GN=PF11_0126 PE=4 SV=2 | 3 | 2.28 | 1.61 | 0.1338 |
| tr\|Q8I411\|Q8I411_PLAF7 Uncharacterized protein OS=Plasmodium falciparum (isolate 3D7) GN=PFE0460c PE=4 SV=1 | 3 | 0.97 | 0.02 | 0.0001 |
| tr\|C6KT22\|C6KT22_PLAF7 Uncharacterized protein OS=Plasmodium falciparum (isolate 3D7) GN=PFF0880c PE=4 SV=1 | 3 | 2.34 | 1.06 | 0.0621 |
| tr\|Q8IIW4\|Q8IIW4_PLAF7 Uncharacterized protein OS=Plasmodium falciparum (isolate 3D7) GN=PF11_0049 PE=4 SV=1 | 3 | 2.46 | 1.41 | 0.0946 |
| tr\|C0H524\|C0H524_PLAF7 P1 nuclease, putative OS=Plasmodium falciparum (isolate 3D7) GN=PFI0385c PE=4 SV=1 | 3 | 0.97 | 0.13 | 0.0064 |
| tr\|Q8IIG2\|Q8IIG2_PLAF7 Uncharacterized protein OS=Plasmodium falciparum (isolate 3D7) GN=PF11_0212 PE=3 SV=1 | 3 | 2.48 | 2.29 | 0.2008 |
| tr\|C0H5F1\|C0H5F1_PLAF7 Protein tyrosine phosphatase, putative OS=Plasmodium falciparum (isolate 3D7) GN=MAL13P1.168 PE=4 SV=1 | 3 | 0.97 | 0.10 | 0.0034 |
| tr\|Q8I6T0\|Q8I6T0_PLAF7 Aminomethyltransferase, mitochondrial OS=Plasmodium falciparum (isolate 3D7) GN=PF13_0345 PE=3 SV=1 | 3 | 0.97 | 0.20 | 0.0134 |
| tr\|Q8I2M1\|Q8I2M1_PLAF7 Guanylate kinase OS=Plasmodium falciparum (isolate 3D7) GN=PfGK PE=1 SV=1 | 3 | 2.64 | 1.72 | 0.1173 |
| tr\|C6KT35\|C6KT35_PLAF7 Acyl-CoA synthetase, PfACS12 OS=Plasmodium falciparum (isolate 3D7) GN=PfACS12 PE=4 SV=1 | 3 | 2.66 | 1.68 | 0.1112 |
| tr\|Q8I2D9\|Q8I2D9_PLAF7 Putative uncharacterized protein OS=Plasmodium falciparum (isolate 3D7) GN=PFA_0670c PE=4 SV=1 | 3 | 0.98 | 0.20 | 0.0132 |
| tr\|Q8I3Q3\|Q8I3Q3_PLAF7 Uncharacterized protein OS=Plasmodium falciparum (isolate 3D7) GN=PFE1045c PE=4 SV=1 | 3 | 0.98 | 0.12 | 0.0052 |
| tr\|Q8I2I8\|Q8I2I8_PLAF7 Putative uncharacterized protein OS=Plasmodium falciparum (isolate 3D7) GN=PFI1590c PE=4 SV=1 | 3 | 2.92 | 1.81 | 0.1076 |
| tr\|Q8IBN8\|Q8IBN8_PLAF7 DEAD box helicase, putative OS=Plasmodium falciparum (isolate 3D7) GN=MAL7P1.113 PE=3 SV=1 | 3 | 2.94 | 2.89 | 0.2196 |
| tr\|Q8I1U8\|Q8I1U8_PLAF7 Ubiquitinyl hydrolase 1 OS=Plasmodium falciparum (isolate 3D7) GN=PFD0680c PE=4 SV=1 | 3 | 2.98 | 2.06 | 0.1290 |
| tr\|Q8I3A9\|Q8I3A9_PLAF7 GTPase activating protein, GAP OS=Plasmodium falciparum (isolate 3D7) GN=PFI0195c PE=4 SV=1 | 3 | 2.99 | 1.53 | 0.0767 |

| | | | | |
|---|---|---|---|---|
| tr\|Q8IL42\|Q8IL42_PLAF7 Guanine nucleotide exchange factor, putative OS=Plasmodium falciparum (isolate 3D7) GN=PF14_0407 PE=4 SV=1 | 3 | 3.03 | 2.10 | 0.1296 |
| tr\|O97256\|O97256_PLAF7 Activator of Hsp90 ATPase homolog 1-like protein, putative OS=Plasmodium falciparum (isolate 3D7) GN=PFC0360w PE=4 SV=2 | 3 | 3.06 | 4.66 | 0.3732 |
| tr\|Q8I6Z8\|Q8I6Z8_PLAF7 Ubiquitin Carboxyl-terminal Hydrolase-like zinc finger protein OS=Plasmodium falciparum (isolate 3D7) GN=PF13_0096 PE=4 SV=1 | 3 | 0.99 | 0.27 | 0.0244 |
| tr\|Q8I296\|Q8I296_PLAF7 Ubiquitin carboxyl-terminal hydrolase, putative OS=Plasmodium falciparum (isolate 3D7) GN=PFA_0220w PE=4 SV=2 | 3 | 3.18 | 3.62 | 0.2674 |
| tr\|Q8IIA8\|Q8IIA8_PLAF7 Small nuclear ribonucleoprotein D1, putative OS=Plasmodium falciparum (isolate 3D7) GN=PF11_0266 PE=4 SV=1 | 3 | 0.99 | 0.36 | 0.0409 |
| tr\|O96174\|O96174_PLAF7 Conserved Plasmodium protein OS=Plasmodium falciparum (isolate 3D7) GN=PFB0395w PE=4 SV=1 | 3 | 3.41 | 5.16 | 0.3713 |
| tr\|J3QLD9\|J3QLD9_HUMAN Flotillin-2 OS=Homo sapiens GN=FLOT2 PE=1 SV=1;tr\|E7EMK3\|E7EMK3_HUMAN Flotillin-2 OS=Homo sapiens GN=FLOT2 PE=1 SV=1;sp\|Q14254\|FLOT2_HUMAN Flotillin-2 OS=Homo sapiens GN=FLOT2 PE=1 SV=2 | 3 | 0.99 | 0.03 | 0.0003 |
| tr\|Q8IKA0\|Q8IKA0_PLAF7 Uncharacterized protein OS=Plasmodium falciparum (isolate 3D7) GN=PF14_0706 PE=4 SV=1 | 3 | 0.99 | 0.03 | 0.0002 |
| tr\|O97273\|O97273_PLAF7 Putative uncharacterized protein OS=Plasmodium falciparum (isolate 3D7) GN=PFC0690c PE=4 SV=1 | 3 | 3.43 | 4.36 | 0.3070 |
| tr\|Q8I2X7\|Q8I2X7_PLAF7 ATP-dependent RNA Helicase, putative OS=Plasmodium falciparum (isolate 3D7) GN=PFI0860c PE=4 SV=1 | 3 | 0.99 | 0.25 | 0.0211 |
| tr\|Q8IB26\|Q8IB26_PLAF7 BRIX domain, putative OS=Plasmodium falciparum (isolate 3D7) GN=PF08_0053 PE=4 SV=1 | 3 | 1.00 | 0.18 | 0.0110 |
| tr\|O97225\|O97225_PLAF7 Spindle pole body protein, putative OS=Plasmodium falciparum (isolate 3D7) GN=PFC0165w PE=4 SV=3 | 3 | 1.00 | 0.15 | 0.0069 |
| tr\|Q8IB23\|Q8IB23_PLAF7 U3 small nucleolar ribonucleoprotein protein, putative OS=Plasmodium falciparum (isolate 3D7) GN=PF08_0055 PE=4 SV=1 | 3 | 3.71 | 5.17 | 0.3403 |
| sp\|O77392\|IPYR_PLAF7 Probable inorganic pyrophosphatase OS=Plasmodium falciparum (isolate 3D7) GN=MAL3P6.3 PE=3 SV=1;tr\|C0H477\|C0H477_PLAF7 Inorganic pyrophosphatase, putative OS=Plasmodium falciparum (isolate 3D7) GN=PFC0710w.1 PE=4 SV=1 | 3 | 1.00 | 0.27 | 0.0238 |
| sp\|P61076\|TRXR2_PLAF7 Thioredoxin reductase 2 OS=Plasmodium falciparum (isolate 3D7) GN=trxr2 PE=1 SV=2 | 3 | 3.74 | 2.64 | 0.1335 |
| tr\|O96204\|O96204_PLAF7 Conserved Plasmodium membrane protein OS=Plasmodium falciparum (isolate 3D7) GN=PFB0555c PE=4 SV=2 | 3 | 1.00 | 0.16 | 0.0083 |
| sp\|Q12931-2\|TRAP1_HUMAN Isoform 2 of Heat shock protein 75 kDa, mitochondrial OS=Homo sapiens GN=TRAP1;sp\|Q12931\|TRAP1_HUMAN Heat shock protein 75 kDa, mitochondrial OS=Homo sapiens GN=TRAP1 PE=1 SV=3 | 3 | 1.01 | 0.01 | 0.0001 |
| tr\|Q8I246\|Q8I246_PLAF7 Phenylalanyl-tRNA synthetase beta chain, putative OS=Plasmodium falciparum (isolate 3D7) GN=PFA_0480w PE=3 SV=1 | 3 | 3.84 | 2.72 | 0.1347 |
| tr\|Q8IJB1\|Q8IJB1_PLAF7 Uncharacterized protein OS=Plasmodium falciparum (isolate 3D7) GN=PF10_0287 PE=4 SV=1 | 3 | 1.01 | 0.15 | 0.0070 |
| sp\|Q8ILW6\|NMT_PLAF7 Glycylpeptide N-tetradecanoyltransferase OS=Plasmodium falciparum (isolate 3D7) GN=PF14_0127 PE=3 SV=1 | 3 | 3.86 | 2.41 | 0.1090 |
| tr\|Q8IC10\|Q8IC10_PLAF7 Cdk105, putative OS=Plasmodium falciparum (isolate 3D7) GN=MAL7P1.24 PE=4 SV=1 | 3 | 1.02 | 0.13 | 0.0052 |
| tr\|C6KSV4\|C6KSV4_PLAF7 Transcription elongation factor SPT5 OS=Plasmodium falciparum (isolate 3D7) GN=PFF0535c PE=3 SV=1 | 3 | 1.02 | 0.16 | 0.0078 |
| tr\|Q8I610\|Q8I610_PLAF7 Uncharacterized protein OS=Plasmodium falciparum (isolate 3D7) GN=PFL0175c PE=4 SV=1 | 3 | 4.34 | 5.15 | 0.2823 |
| tr\|C0H5B6\|C0H5B6_PLAF7 Uncharacterized protein OS=Plasmodium falciparum (isolate 3D7) GN=MAL13P1.79 PE=4 SV=1 | 3 | 1.05 | 0.10 | 0.0031 |
| tr\|Q8I388\|Q8I388_PLAF7 Developmental protein, putative OS=Plasmodium falciparum (isolate 3D7) GN=PFI0300w PE=4 SV=1 | 3 | 4.56 | 1.94 | 0.0552 |
| tr\|Q8IJU4\|Q8IJU4_PLAF7 Uncharacterized protein OS=Plasmodium falciparum (isolate 3D7) GN=PF10_0098 PE=4 SV=1 | 3 | 4.71 | 2.78 | 0.0994 |
| tr\|C0H4U0\|C0H4U0_PLAF7 Uncharacterized protein OS=Plasmodium falciparum (isolate 3D7) GN=MAL8P1.103 PE=4 SV=1 | 3 | 4.83 | 2.27 | 0.0663 |
| tr\|Q8IJS8\|Q8IJS8_PLAF7 DNA repair protein RAD23, putative OS=Plasmodium falciparum (isolate 3D7) GN=PF10_0114 PE=4 SV=1 | 3 | 5.12 | 2.43 | 0.0676 |
| tr\|Q8IDG9\|Q8IDG9_PLAF7 Uncharacterized protein OS=Plasmodium falciparum (isolate 3D7) GN=PF13_0275 PE=4 SV=1 | 3 | 5.27 | 7.82 | 0.3636 |
| tr\|Q8I378\|Q8I378_PLAF7 Putative uncharacterized protein OS=Plasmodium falciparum (isolate 3D7) GN=PFI0350c PE=4 SV=1 | 3 | 5.43 | 3.57 | 0.1187 |
| tr\|Q8ID72\|Q8ID72_PLAF7 Uncharacterized protein OS=Plasmodium falciparum (isolate 3D7) GN=PF13_0335 PE=4 SV=1 | 3 | 5.84 | 3.03 | 0.0791 |

| | | | | |
|---|---|---|---|---|
| tr\|Q8I2T4\|Q8I2T4_PLAF7 Putative uncharacterized protein OS=Plasmodium falciparum (isolate 3D7) GN=PFI1075w PE=4 SV=1 | 3 | 6.00 | 5.51 | 0.1997 |
| sp\|Q8IED2\|SMC2_PLAF7 Structural maintenance of chromosomes protein 2 OS=Plasmodium falciparum (isolate 3D7) GN=MAL13P1.96 PE=3 SV=1 | 3 | 6.08 | 8.90 | 0.3585 |
| tr\|Q8IIM5\|Q8IIM5_PLAF7 Glyoxalase I, putative OS=Plasmodium falciparum (isolate 3D7) GN=PF11_0145 PE=4 SV=1 | 3 | 6.24 | 5.54 | 0.1905 |
| tr\|Q8IDS7\|Q8IDS7_PLAF7 Na+-dependent Pi transporter, sodium-dependent phosphate transporter OS=Plasmodium falciparum (isolate 3D7) GN=MAL13P1.206 PE=4 SV=1 | 3 | 6.25 | 10.20 | 0.3998 |
| tr\|Q8IKS6\|Q8IKS6_PLAF7 Uncharacterized protein OS=Plasmodium falciparum (isolate 3D7) GN=PF14_0526 PE=4 SV=2 | 3 | 6.28 | 7.47 | 0.2827 |
| tr\|Q8IHZ1\|Q8IHZ1_PLAF7 UVB-resistance protein UVR8 homologue OS=Plasmodium falciparum (isolate 3D7) GN=PF11_0385 PE=4 SV=1 | 3 | 6.36 | 10.50 | 0.4042 |
| tr\|Q8IM71\|Q8IM71_PLAF7 Choline kinase OS=Plasmodium falciparum (isolate 3D7) GN=PF14_0020 PE=1 SV=1 | 3 | 6.76 | 5.82 | 0.1819 |
| tr\|Q8I5R6\|Q8I5R6_PLAF7 Uncharacterized protein OS=Plasmodium falciparum (isolate 3D7) GN=PFL0675c PE=4 SV=1 | 3 | 7.62 | 8.83 | 0.2737 |
| tr\|C0H5D3\|C0H5D3_PLAF7 SNARE protein, putative OS=Plasmodium falciparum (isolate 3D7) GN=PfYkt6.2 PE=4 SV=1 | 3 | 8.00 | 11.12 | 0.3390 |
| tr\|Q8I5S8\|Q8I5S8_PLAF7 Uncharacterized protein OS=Plasmodium falciparum (isolate 3D7) GN=PFL0615w PE=4 SV=1 | 3 | 8.31 | 13.61 | 0.4014 |
| tr\|Q8I3A1\|Q8I3A1_PLAF7 Replication factor A-related protein, putative OS=Plasmodium falciparum (isolate 3D7) GN=PFI0235w PE=4 SV=1 | 3 | 8.33 | 7.34 | 0.1883 |
| tr\|Q8IDH3\|Q8IDH3_PLAF7 Uncharacterized protein OS=Plasmodium falciparum (isolate 3D7) GN=PF13_0273 PE=4 SV=1 | 3 | 1.06 | 0.20 | 0.0119 |
| tr\|Q8IDD9\|Q8IDD9_PLAF7 Ubiquitin conjugating enzyme, putative OS=Plasmodium falciparum (isolate 3D7) GN=PF13_0301 PE=3 SV=1 | 3 | 9.53 | 13.65 | 0.3503 |
| tr\|Q8I624\|Q8I624_PLAF7 Uncharacterized protein OS=Plasmodium falciparum (isolate 3D7) GN=PFL0105w PE=4 SV=1 | 3 | 9.79 | 12.73 | 0.3142 |
| tr\|Q8IIF6\|Q8IIF6_PLAF7 Conserved Plasmodium protein OS=Plasmodium falciparum (isolate 3D7) GN=PF11_0218 PE=4 SV=2 | 3 | 9.81 | 11.37 | 0.2738 |
| sp\|Q8I236\|KAD6_PLAF7 Adenylate kinase isoenzyme 6 homolog OS=Plasmodium falciparum (isolate 3D7) GN=PFA_0530c PE=1 SV=1 | 3 | 9.98 | 4.09 | 0.0516 |
| tr\|Q8I5J2\|Q8I5J2_PLAF7 Uncharacterized protein OS=Plasmodium falciparum (isolate 3D7) GN=PFL1065c PE=4 SV=1 | 3 | 10.93 | 17.18 | 0.3853 |
| tr\|Q9NLB8\|Q9NLB8_PLAF7 EH (Eps15 homology) protein OS=Plasmodium falciparum (isolate 3D7) GN=PfPast-1 PE=4 SV=1 | 3 | 11.15 | 14.05 | 0.3030 |
| tr\|Q8I3J3\|Q8I3J3_PLAF7 Ubiquitin carboxyl-terminal hydrolase OS=Plasmodium falciparum (isolate 3D7) GN=PFE1355c PE=3 SV=1 | 3 | 11.17 | 13.01 | 0.2753 |
| sp\|Q8I3Y6\|PFD6_PLAF7 Probable prefoldin subunit 6 OS=Plasmodium falciparum (isolate 3D7) GN=PFE0595w PE=3 SV=2 | 3 | 13.07 | 17.28 | 0.3205 |
| tr\|Q8IEK8\|Q8IEK8_PLAF7 Uncharacterized protein OS=Plasmodium falciparum (isolate 3D7) GN=MAL13P1.52 PE=4 SV=1 | 3 | 13.83 | 18.50 | 0.3247 |
| tr\|Q8I1V0\|Q8I1V0_PLAF7 Lysine decarboxylase-like protein, putative OS=Plasmodium falciparum (isolate 3D7) GN=PFD0670c PE=4 SV=1 | 3 | 14.32 | 20.50 | 0.3500 |
| tr\|C0H586\|C0H586_PLAF7 Calcyclin binding protein, putative OS=Plasmodium falciparum (isolate 3D7) GN=PFI1610c PE=4 SV=1 | 3 | 14.87 | 16.17 | 0.2521 |
| tr\|Q8I5M2\|Q8I5M2_PLAF7 Arginyl-tRNA synthetase, putative OS=Plasmodium falciparum (isolate 3D7) GN=PFL0900c PE=3 SV=1 | 3 | 14.92 | 17.64 | 0.2805 |
| tr\|Q8IDZ0\|Q8IDZ0_PLAF7 Uncharacterized protein OS=Plasmodium falciparum (isolate 3D7) GN=PF13_0186 PE=4 SV=1 | 3 | 15.35 | 24.74 | 0.3950 |
| tr\|Q7KWJ4\|Q7KWJ4_PLAF7 Adenylosuccinate lyase OS=Plasmodium falciparum (isolate 3D7) GN=ASL PE=3 SV=1 | 3 | 16.43 | 26.69 | 0.3978 |
| tr\|Q8I272\|Q8I272_PLAF7 Centrin-1 OS=Plasmodium falciparum (isolate 3D7) GN=PfCEN1 PE=4 SV=1 | 3 | 18.49 | 31.77 | 0.4195 |
| tr\|O97284\|O97284_PLAF7 Putative uncharacterized protein OS=Plasmodium falciparum (isolate 3D7) GN=PFC0910w PE=4 SV=1 | 3 | 18.97 | 16.05 | 0.1772 |
| tr\|Q8I548\|Q8I548_PLAF7 Uncharacterized protein OS=Plasmodium falciparum (isolate 3D7) GN=PFL1815c PE=4 SV=1 | 3 | 1.07 | 0.11 | 0.0033 |
| tr\|O97314\|O97314_PLAF7 Putative uncharacterized protein OS=Plasmodium falciparum (isolate 3D7) GN=PFC1025w PE=4 SV=1 | 3 | 23.10 | 15.32 | 0.1206 |
| sp\|Q8IBP3\|ITPA_PLAF7 Inosine triphosphate pyrophosphatase OS=Plasmodium falciparum (isolate 3D7) GN=MAL7P1.110 PE=3 SV=1 | 3 | 26.84 | 23.85 | 0.1906 |
| tr\|Q8I538\|Q8I538_PLAF7 Uncharacterized protein OS=Plasmodium falciparum (isolate 3D7) GN=PFL1865w PE=4 SV=1 | 3 | 1.07 | 0.16 | 0.0069 |
| tr\|Q8I3V0\|Q8I3V0_PLAF7 BolA-like protein, putative OS=Plasmodium falciparum (isolate 3D7) GN=PFE0790c PE=1 SV=1 | 3 | 34.48 | 59.08 | 0.4185 |

| | | | | |
|---|---|---|---|---|
| tr\|Q8IAR7\|Q8IAR7_PLAF7 Tyrosyl-tRNA synthetase, putative OS=Plasmodium falciparum (isolate 3D7) GN=MAL8P1.125 PE=1 SV=1 | 3 | 50.53 | 70.23 | 0.3389 |
| tr\|Q8II92\|Q8II92_PLAF7 Deoxyuridine 5-triphosphate nucleotidohydrolase, putative OS=Plasmodium falciparum (isolate 3D7) GN=PF11_0282 PE=1 SV=1 | 3 | 73.62 | 108.21 | 0.3599 |
| tr\|Q8I2U4\|Q8I2U4_PLAF7 RNA binding protein, putative OS=Plasmodium falciparum (isolate 3D7) GN=PFI1025w PE=4 SV=1 | 3 | 1.07 | 0.06 | 0.0011 |
| tr\|Q8I4Y0\|Q8I4Y0_PLAF7 Kinesin-like protein OS=Plasmodium falciparum (isolate 3D7) GN=PFL2165w PE=1 SV=2 | 3 | 1.08 | 0.22 | 0.0134 |
| tr\|Q8ILM2\|Q8ILM2_PLAF7 GTPase, putative OS=Plasmodium falciparum (isolate 3D7) GN=PF14_0221 PE=4 SV=1 | 3 | 1.09 | 0.20 | 0.0107 |
| tr\|Q8IIM4\|Q8IIM4_PLAF7 Uncharacterized protein OS=Plasmodium falciparum (isolate 3D7) GN=PF11_0146 PE=4 SV=1 | 3 | 1.09 | 0.19 | 0.0098 |
| tr\|O96243\|O96243_PLAF7 Vacuolar protein-sorting protein VPS45, putative OS=Plasmodium falciparum (isolate 3D7) GN=PFB0750w PE=4 SV=1 | 3 | 1.09 | 0.25 | 0.0175 |
| sp\|Q99808\|S29A1_HUMAN Equilibrative nucleoside transporter 1 OS=Homo sapiens GN=SLC29A1 PE=1 SV=3;sp\|Q99808-2\|S29A1_HUMAN Isoform 2 of Equilibrative nucleoside transporter 1 OS=Homo sapiens GN=SLC29A1 | 3 | 1.10 | 0.13 | 0.0049 |
| tr\|Q8IFN9\|Q8IFN9_PLAF7 Eukaryotic initiation factor, putative OS=Plasmodium falciparum (isolate 3D7) GN=PFD1070w PE=3 SV=1 | 3 | 1.10 | 0.24 | 0.0155 |
| tr\|Q8IKC5\|Q8IKC5_PLAF7 Diacylglycerol kinase, putative OS=Plasmodium falciparum (isolate 3D7) GN=PF14_0681 PE=4 SV=2 | 3 | 1.10 | 0.22 | 0.0126 |
| tr\|O96265\|O96265_PLAF7 Small nuclear ribonucleoprotein, putative OS=Plasmodium falciparum (isolate 3D7) GN=PFB0865w PE=4 SV=1 | 3 | 1.11 | 0.13 | 0.0047 |
| tr\|C0H5I8\|C0H5I8_PLAF7 Uncharacterized protein OS=Plasmodium falciparum (isolate 3D7) GN=MAL13P1.286 PE=4 SV=1 | 3 | 1.12 | 0.22 | 0.0125 |
| tr\|Q8I3M0\|Q8I3M0_PLAF7 Uncharacterized protein OS=Plasmodium falciparum (isolate 3D7) GN=PFE1220w PE=4 SV=1 | 3 | 1.12 | 0.14 | 0.0049 |
| tr\|Q8IJR8\|Q8IJR8_PLAF7 Uncharacterized protein OS=Plasmodium falciparum (isolate 3D7) GN=PF10_0124 PE=4 SV=1 | 3 | 1.12 | 0.28 | 0.0201 |
| tr\|Q8I5Z0\|Q8I5Z0_PLAF7 Uncharacterized protein OS=Plasmodium falciparum (isolate 3D7) GN=PFL0275w PE=4 SV=1 | 3 | 1.13 | 0.16 | 0.0068 |
| tr\|Q8IL82\|Q8IL82_PLAF7 Uncharacterized protein OS=Plasmodium falciparum (isolate 3D7) GN=PF14_0365 PE=4 SV=1 | 3 | 1.13 | 0.25 | 0.0153 |
| sp\|Q8IIS5\|PESC_PLAF7 Pescadillo homolog OS=Plasmodium falciparum (isolate 3D7) GN=PF11_0090 PE=3 SV=1 | 3 | 1.14 | 0.18 | 0.0082 |
| tr\|Q8IIQ1\|Q8IIQ1_PLAF7 Replication factor C subunit 5, putative OS=Plasmodium falciparum (isolate 3D7) GN=PF11_0117 PE=4 SV=1 | 3 | 1.15 | 0.04 | 0.0003 |
| tr\|Q8I6Z5\|Q8I6Z5_PLAF7 Plasmepsin V OS=Plasmodium falciparum (isolate 3D7) GN=PF13_0133 PE=3 SV=1 | 3 | 1.16 | 0.17 | 0.0073 |
| tr\|C6KT59\|C6KT59_PLAF7 Radical SAM protein, putative OS=Plasmodium falciparum (isolate 3D7) GN=PFF1070c PE=4 SV=1 | 3 | 1.17 | 0.17 | 0.0071 |
| tr\|Q8IKK3\|Q8IKK3_PLAF7 DNA polymerase alpha subunit, putative OS=Plasmodium falciparum (isolate 3D7) GN=PF14_0602 PE=4 SV=1 | 3 | 1.18 | 0.01 | 0.0000 |
| tr\|Q8IE57\|Q8IE57_PLAF7 Uncharacterized protein OS=Plasmodium falciparum (isolate 3D7) GN=PF13_0147 PE=4 SV=1 | 3 | 1.18 | 0.24 | 0.0134 |
| tr\|Q8ID46\|Q8ID46_PLAF7 Uncharacterized protein OS=Plasmodium falciparum (isolate 3D7) GN=MAL13P1.333 PE=4 SV=1 | 3 | 1.19 | 0.09 | 0.0019 |
| tr\|C6KTE1\|C6KTE1_PLAF7 Uncharacterized protein OS=Plasmodium falciparum (isolate 3D7) GN=PFF1485w PE=4 SV=1 | 3 | 1.20 | 0.14 | 0.0044 |
| tr\|Q8I700\|Q8I700_PLAF7 Snornp protein gar1 homologue, putative OS=Plasmodium falciparum (isolate 3D7) GN=PF13_0051 PE=4 SV=1 | 3 | 1.21 | 0.16 | 0.0055 |
| tr\|Q8IKK4\|Q8IKK4_PLAF7 Replication factor C3 OS=Plasmodium falciparum (isolate 3D7) GN=PF14_0601 PE=4 SV=1 | 3 | 1.21 | 0.08 | 0.0014 |
| tr\|Q8IKH0\|Q8IKH0_PLAF7 60S ribosome subunit biogenesis protein NIP7 homolog OS=Plasmodium falciparum (isolate 3D7) GN=PF14_0635 PE=3 SV=2 | 3 | 1.22 | 0.14 | 0.0042 |
| tr\|C0H4G4\|C0H4G4_PLAF7 Uncharacterized protein OS=Plasmodium falciparum (isolate 3D7) GN=PFE1375c PE=4 SV=1 | 3 | 1.22 | 0.40 | 0.0335 |
| tr\|Q8I512\|Q8I512_PLAF7 Replication factor C subunit 4 OS=Plasmodium falciparum (isolate 3D7) GN=PFL2005w PE=4 SV=1 | 3 | 1.23 | 0.40 | 0.0341 |
| tr\|Q8IEM5\|Q8IEM5_PLAF7 NUDIX hydrolase, putative OS=Plasmodium falciparum (isolate 3D7) GN=PF13_0048 PE=4 SV=1 | 3 | 1.25 | 0.08 | 0.0014 |
| tr\|Q8IB94\|Q8IB94_PLAF7 Ubiquitin-protein ligase 1, putative OS=Plasmodium falciparum (isolate 3D7) GN=MAL8P1.23 PE=4 SV=1 | 3 | 1.26 | 0.29 | 0.0171 |
| tr\|Q8IEK4\|Q8IEK4_PLAF7 Clathrin-adaptor medium chain, putative OS=Plasmodium falciparum (isolate 3D7) GN=PF13_0062 PE=4 SV=1 | 3 | 1.26 | 0.13 | 0.0035 |

| | | | | |
|---|---|---|---|---|
| tr\|C0H549\|C0H549_PLAF7 Nucleolar preribosomal assembly protein, putative OS=Plasmodium falciparum (isolate 3D7) GN=PFI1070c PE=4 SV=1 | 3 | 1.26 | 0.04 | 0.0003 |
| tr\|Q8I410\|Q8I410_PLAF7 DNA-directed RNA polymerase OS=Plasmodium falciparum (isolate 3D7) GN=PFE0465c PE=3 SV=1 | 3 | 1.26 | 0.08 | 0.0012 |
| tr\|Q8II94\|Q8II94_PLAF7 Small nuclear ribonucleoprotein F OS=Plasmodium falciparum (isolate 3D7) GN=PF11_0280 PE=3 SV=2 | 3 | 1.28 | 0.17 | 0.0055 |
| tr\|O77369\|O77369_PLAF7 Putative uncharacterized protein OS=Plasmodium falciparum (isolate 3D7) GN=PFC0835c PE=4 SV=2 | 3 | 1.30 | 0.47 | 0.0409 |
| tr\|Q8IAZ7\|Q8IAZ7_PLAF7 Nucleolar preribosomal assembly protein, putative OS=Plasmodium falciparum (isolate 3D7) GN=PF08_0065 PE=4 SV=1 | 3 | 1.30 | 0.11 | 0.0025 |
| tr\|Q8IJA4\|Q8IJA4_PLAF7 RNA helicase, putative OS=Plasmodium falciparum (isolate 3D7) GN=PF10_0294 PE=4 SV=1 | 3 | 1.31 | 0.41 | 0.0310 |
| tr\|Q8IDM6\|Q8IDM6_PLAF7 Nucleoside transporter 1 OS=Plasmodium falciparum (isolate 3D7) GN=nt1 PE=4 SV=1 | 3 | 1.33 | 0.27 | 0.0135 |
| tr\|Q8IES2\|Q8IES2_PLAF7 Uncharacterized protein OS=Plasmodium falciparum (isolate 3D7) GN=MAL13P1.24 PE=4 SV=1 | 3 | 1.33 | 0.37 | 0.0247 |
| tr\|O96201\|O96201_PLAF7 Conserved Plasmodium protein OS=Plasmodium falciparum (isolate 3D7) GN=PFB0540w PE=4 SV=1 | 3 | 1.34 | 0.43 | 0.0325 |
| tr\|Q8IEI4\|Q8IEI4_PLAF7 Ubiquitin-like protein nedd8 homologue, putative OS=Plasmodium falciparum (isolate 3D7) GN=MAL13P1.64 PE=4 SV=1 | 3 | 1.34 | 0.30 | 0.0159 |
| tr\|C0H5K9\|C0H5K9_PLAF7 Phosphatidylserine synthase I, putative OS=Plasmodium falciparum (isolate 3D7) GN=MAL13P1.335 PE=4 SV=1 | 3 | 1.34 | 0.21 | 0.0081 |
| tr\|Q8IJC9\|Q8IJC9_PLAF7 DNA-directed RNA polymerase II, putative OS=Plasmodium falciparum (isolate 3D7) GN=PF10_0269 PE=4 SV=1 | 3 | 1.34 | 0.18 | 0.0060 |
| tr\|Q8IKN5\|Q8IKN5_PLAF7 Uncharacterized protein OS=Plasmodium falciparum (isolate 3D7) GN=PF14_0569 PE=4 SV=1 | 3 | 1.36 | 0.18 | 0.0056 |
| tr\|Q8IEC3\|Q8IEC3_PLAF7 N2,N2-dimethylguanosine tRNA methyltransferase, putative OS=Plasmodium falciparum (isolate 3D7) GN=PF13_0109 PE=4 SV=1 | 3 | 1.38 | 0.36 | 0.0224 |
| tr\|Q8ILV5\|Q8ILV5_PLAF7 Uncharacterized protein OS=Plasmodium falciparum (isolate 3D7) GN=PF14_0138 PE=4 SV=2 | 3 | 1.39 | 0.40 | 0.0264 |
| tr\|Q8I3Q8\|Q8I3Q8_PLAF7 Uncharacterized protein OS=Plasmodium falciparum (isolate 3D7) GN=PFE1015c PE=4 SV=1 | 3 | 1.39 | 0.09 | 0.0013 |
| tr\|Q8IHR6\|Q8IHR6_PLAF7 Coatomer subunit gamma OS=Plasmodium falciparum (isolate 3D7) GN=PF11_0463 PE=3 SV=1 | 3 | 1.39 | 0.28 | 0.0128 |
| sp\|Q8IHZ9\|KC1_PLAF7 Casein kinase I OS=Plasmodium falciparum (isolate 3D7) GN=CK1 PE=3 SV=1;tr\|C6S3F7\|C6S3F7_PLAF7 Casein kinase 1, PfCK1 OS=Plasmodium falciparum (isolate 3D7) GN=PfCK1 PE=3 SV=1 | 3 | 1.40 | 0.24 | 0.0094 |
| tr\|Q8I2M0\|Q8I2M0_PLAF7 Putative uncharacterized protein OS=Plasmodium falciparum (isolate 3D7) GN=PFI1425w PE=4 SV=1 | 3 | 1.40 | 0.10 | 0.0016 |
| tr\|Q8IE50\|Q8IE50_PLAF7 Myosin OS=Plasmodium falciparum (isolate 3D7) GN=MAL13P1.148 PE=4 SV=1 | 3 | 1.41 | 0.32 | 0.0167 |
| tr\|Q8ILI9\|Q8ILI9_PLAF7 DNA mismatch repair protein Msh2p, putative OS=Plasmodium falciparum (isolate 3D7) GN=PF14_0254 PE=3 SV=1 | 3 | 1.44 | 0.25 | 0.0103 |
| tr\|Q8I275\|Q8I275_PLAF7 PfAARP2 protein OS=Plasmodium falciparum (isolate 3D7) GN=AARP2 PE=4 SV=1 | 3 | 1.44 | 0.39 | 0.0239 |
| tr\|Q8IM64\|Q8IM64_PLAF7 40S ribosomal protein S31/UBI, putative OS=Plasmodium falciparum (isolate 3D7) GN=PF14_0027 PE=4 SV=1 | 3 | 1.46 | 0.19 | 0.0056 |
| tr\|Q8I586\|Q8I586_PLAF7 Asparagine/aspartate rich protein, putative OS=Plasmodium falciparum (isolate 3D7) GN=PFL1620w PE=4 SV=1 | 3 | 1.47 | 0.09 | 0.0013 |
| tr\|O97240\|O97240_PLAF7 AP endonuclease (DNA-[apurinic or apyrimidinic site] lyase), putative OS=Plasmodium falciparum (isolate 3D7) GN=PFC0250c PE=4 SV=2 | 3 | 1.48 | 0.01 | 0.0000 |
| tr\|Q8IHT3\|Q8IHT3_PLAF7 DNA-directed RNA polymerase I, putative OS=Plasmodium falciparum (isolate 3D7) GN=PF11_0445 PE=4 SV=1 | 3 | 1.52 | 0.08 | 0.0009 |
| tr\|Q8IE45\|Q8IE45_PLAF7 Uncharacterized protein OS=Plasmodium falciparum (isolate 3D7) GN=PF13_0153 PE=4 SV=1 | 3 | 1.53 | 0.14 | 0.0029 |
| sp\|O96184\|RL37A_PLAF7 60S ribosomal protein L37a OS=Plasmodium falciparum (isolate 3D7) GN=RPL37A PE=1 SV=1 | 3 | 1.57 | 0.12 | 0.0019 |
| tr\|Q8IEM3\|Q8IEM3_PLAF7 60S ribosomal protein L24, putative OS=Plasmodium falciparum (isolate 3D7) GN=PF13_0049 PE=1 SV=1 | 3 | 1.58 | 0.12 | 0.0018 |
| tr\|Q8IL92\|Q8IL92_PLAF7 Pantothenate kinase, putative OS=Plasmodium falciparum (isolate 3D7) GN=PF14_0354 PE=4 SV=1 | 3 | 1.60 | 0.21 | 0.0058 |
| tr\|C6KTB4\|C6KTB4_PLAF7 Acetyl-CoA synthetase OS=Plasmodium falciparum (isolate 3D7) GN=PFF1350c PE=4 SV=1 | 3 | 1.61 | 0.20 | 0.0049 |
| tr\|Q8IHU1\|Q8IHU1_PLAF7 Coproporphyrinogen oxidase, putative OS=Plasmodium falciparum (isolate 3D7) GN=PF11_0436 PE=4 SV=1 | 3 | 1.61 | 0.12 | 0.0019 |

| | | | | |
|---|---|---|---|---|
| tr\|Q8IDN9\|Q8IDN9_PLAF7 Uncharacterized protein OS=Plasmodium falciparum (isolate 3D7) GN=PF13_0243 PE=4 SV=1 | 3 | 1.62 | 0.21 | 0.0054 |
| tr\|Q8IJM0\|Q8IJM0_PLAF7 26s proteasome subunit p55, putative OS=Plasmodium falciparum (isolate 3D7) GN=PF10_0174 PE=4 SV=1 | 3 | 1.63 | 0.29 | 0.0104 |
| tr\|Q8I390\|Q8I390_PLAF7 Beta subunit of coatomer complex, putative OS=Plasmodium falciparum (isolate 3D7) GN=PFI0290c PE=4 SV=1 | 3 | 1.64 | 0.35 | 0.0148 |
| tr\|Q8IKG9\|Q8IKG9_PLAF7 Uncharacterized protein OS=Plasmodium falciparum (isolate 3D7) GN=PF14_0636 PE=4 SV=1 | 3 | 1.71 | 0.38 | 0.0164 |
| tr\|Q8I5S3\|Q8I5S3_PLAF7 Conserved Plasmodium protein OS=Plasmodium falciparum (isolate 3D7) GN=PFL0640w PE=4 SV=1 | 3 | 1.74 | 0.12 | 0.0016 |
| tr\|Q8IIG8\|Q8IIG8_PLAF7 Uncharacterized protein OS=Plasmodium falciparum (isolate 3D7) GN=PF11_0206 PE=4 SV=1 | 3 | 1.75 | 0.49 | 0.0249 |
| tr\|Q8IDT0\|Q8IDT0_PLAF7 Phosphatase, putative OS=Plasmodium falciparum (isolate 3D7) GN=PF13_0222 PE=4 SV=1 | 3 | 1.77 | 0.39 | 0.0160 |
| tr\|Q8I6T3\|Q8I6T3_PLAF7 Proteasome subunit beta type OS=Plasmodium falciparum (isolate 3D7) GN=PF13_0156 PE=3 SV=1 | 3 | 1.78 | 0.43 | 0.0187 |
| tr\|Q8IJT1\|Q8IJT1_PLAF7 Proteasome subunit beta type OS=Plasmodium falciparum (isolate 3D7) GN=PF10_0111 PE=3 SV=1 | 3 | 1.82 | 0.18 | 0.0033 |
| tr\|Q8IIA5\|Q8IIA5_PLAF7 Conserved Plasmodium protein OS=Plasmodium falciparum (isolate 3D7) GN=PF11_0269 PE=4 SV=1 | 3 | 1.83 | 0.04 | 0.0001 |
| tr\|Q8IDV2\|Q8IDV2_PLAF7 Proteasome regulatory component, putative OS=Plasmodium falciparum (isolate 3D7) GN=MAL13P1.190 PE=4 SV=1 | 3 | 1.85 | 0.31 | 0.0089 |
| tr\|Q7K6A9\|Q7K6A9_PLAF7 Proteasome subunit beta type OS=Plasmodium falciparum (isolate 3D7) GN=MAL8P1.142 PE=3 SV=1 | 3 | 1.91 | 0.06 | 0.0003 |
| tr\|Q8I323\|Q8I323_PLAF7 26S proteasome regulatory subunit, putative OS=Plasmodium falciparum (isolate 3D7) GN=PFI0630w PE=4 SV=1 | 3 | 1.92 | 0.27 | 0.0065 |
| tr\|Q8I0U7\|Q8I0U7_PLAF7 Proteasome, putative OS=Plasmodium falciparum (isolate 3D7) GN=PFI1545c PE=4 SV=1 | 3 | 1.98 | 0.18 | 0.0026 |
| tr\|Q8I403\|Q8I403_PLAF7 Uncharacterized protein OS=Plasmodium falciparum (isolate 3D7) GN=PFE0500c PE=4 SV=1 | 3 | 2.00 | 0.08 | 0.0005 |
| tr\|Q8II71\|Q8II71_PLAF7 26S proteasome regulatory complex subunit, putative OS=Plasmodium falciparum (isolate 3D7) GN=PF11_0303 PE=4 SV=2 | 3 | 2.03 | 0.47 | 0.0175 |
| tr\|Q8IB51\|Q8IB51_PLAF7 60S ribosomal protein L22, putative OS=Plasmodium falciparum (isolate 3D7) GN=PF08_0039 PE=1 SV=1 | 3 | 2.07 | 0.40 | 0.0120 |
| tr\|Q8IIE9\|Q8IIE9_PLAF7 PfGCN20 OS=Plasmodium falciparum (isolate 3D7) GN=PF11_0225 PE=3 SV=1 | 3 | 2.09 | 0.12 | 0.0011 |
| tr\|Q8IKC9\|Q8IKC9_PLAF7 Proteasome subunit beta type OS=Plasmodium falciparum (isolate 3D7) GN=PF14_0676 PE=3 SV=2 | 3 | 2.11 | 0.18 | 0.0024 |
| tr\|Q8IIQ6\|Q8IIQ6_PLAF7 Vacuolar protein sorting-associated protein 35 OS=Plasmodium falciparum (isolate 3D7) GN=PF11_0112 PE=3 SV=1 | 3 | 2.18 | 0.43 | 0.0129 |
| tr\|C6KT56\|C6KT56_PLAF7 Uncharacterized protein OS=Plasmodium falciparum (isolate 3D7) GN=PFF1055c PE=4 SV=1 | 3 | 2.21 | 0.15 | 0.0016 |
| sp\|Q8I1T8\|ASNA_PLAF7 ATPase ASNA1 homolog OS=Plasmodium falciparum (isolate 3D7) GN=PFD0725c PE=3 SV=1 | 3 | 2.30 | 0.82 | 0.0399 |
| tr\|Q8I294\|Q8I294_PLAF7 Putative uncharacterized protein OS=Plasmodium falciparum (isolate 3D7) GN=PFA_0230c PE=4 SV=1 | 3 | 2.32 | 0.63 | 0.0240 |
| tr\|Q8IJB8\|Q8IJB8_PLAF7 Uncharacterized protein OS=Plasmodium falciparum (isolate 3D7) GN=PF10_0280 PE=4 SV=1 | 3 | 2.33 | 0.92 | 0.0485 |
| tr\|Q8ID38\|Q8ID38_PLAF7 Skp1 family protein, putative OS=Plasmodium falciparum (isolate 3D7) GN=MAL13P1.337 PE=4 SV=2 | 3 | 2.33 | 0.75 | 0.0324 |
| tr\|Q8IJI3\|Q8IJI3_PLAF7 RNA binding protein, putative OS=Plasmodium falciparum (isolate 3D7) GN=PF10_0214 PE=4 SV=2 | 3 | 2.46 | 0.99 | 0.0493 |
| tr\|Q8IAL6\|Q8IAL6_PLAF7 Mannose-6-phosphate isomerase, putative OS=Plasmodium falciparum (isolate 3D7) GN=MAL8P1.156 PE=4 SV=1 | 3 | 2.59 | 0.15 | 0.0012 |
| tr\|Q8ILP4\|Q8ILP4_PLAF7 Pantothenate kinase, putative OS=Plasmodium falciparum (isolate 3D7) GN=PF14_0200 PE=4 SV=2 | 3 | 2.61 | 0.87 | 0.0350 |
| tr\|Q8I4T9\|Q8I4T9_PLAF7 CutA, putative OS=Plasmodium falciparum (isolate 3D7) GN=PFL2375c PE=4 SV=1 | 3 | 2.63 | 0.73 | 0.0245 |
| tr\|Q8IDI8\|Q8IDI8_PLAF7 Uncharacterized protein OS=Plasmodium falciparum (isolate 3D7) GN=MAL13P1.257 PE=1 SV=1 | 3 | 2.84 | 0.41 | 0.0069 |
| tr\|C6KT64\|C6KT64_PLAF7 Leucyl tRNA synthase OS=Plasmodium falciparum (isolate 3D7) GN=PFF1095w PE=3 SV=1 | 3 | 2.85 | 0.90 | 0.0317 |
| tr\|Q8IAY9\|Q8IAY9_PLAF7 Importin beta, putative OS=Plasmodium falciparum (isolate 3D7) GN=PF08_0069 PE=4 SV=1 | 3 | 2.85 | 0.45 | 0.0081 |
| tr\|Q8IM55\|Q8IM55_PLAF7 Phosphatase, putative OS=Plasmodium falciparum (isolate 3D7) GN=PF14_0036 PE=4 SV=2 | 3 | 2.91 | 0.56 | 0.0122 |

| | | | | |
|---|---|---|---|---|
| tr\|O77344\|O77344_PLAF7 Glycogen synthase kinase 3 OS=Plasmodium falciparum (isolate 3D7) GN=PfGSK-3 PE=4 SV=2 | 3 | 3.00 | 0.59 | 0.0128 |
| tr\|Q8IDE7\|Q8IDE7_PLAF7 Serine/threonine protein phosphatase OS=Plasmodium falciparum (isolate 3D7) GN=PfPP5 PE=4 SV=1 | 3 | 3.10 | 0.54 | 0.0101 |
| tr\|Q8I231\|Q8I231_PLAF7 UMP-CMP kinase, putative OS=Plasmodium falciparum (isolate 3D7) GN=PFA_0555c PE=3 SV=1 | 3 | 3.23 | 0.53 | 0.0087 |
| tr\|Q8IJI7\|Q8IJI7_PLAF7 Deoxyribose-phosphate aldolase, putative OS=Plasmodium falciparum (isolate 3D7) GN=PF10_0210 PE=4 SV=1 | 3 | 3.42 | 1.04 | 0.0298 |
| tr\|Q8IE10\|Q8IE10_PLAF7 Glutaminyl-tRNA synthetase, putative OS=Plasmodium falciparum (isolate 3D7) GN=PF13_0170 PE=3 SV=1 | 3 | 3.42 | 0.26 | 0.0019 |
| tr\|Q8I375\|Q8I375_PLAF7 Translation initiation factor SUI1, putative OS=Plasmodium falciparum (isolate 3D7) GN=PFI0365w PE=4 SV=1 | 3 | 3.44 | 1.38 | 0.0499 |
| tr\|Q8I3A4\|Q8I3A4_PLAF7 Prefoldin subunit 4 OS=Plasmodium falciparum (isolate 3D7) GN=PFI0220w PE=3 SV=1 | 3 | 3.46 | 0.17 | 0.0008 |
| tr\|Q8II79\|Q8II79_PLAF7 Farnesyl pyrophosphate synthase, putative OS=Plasmodium falciparum (isolate 3D7) GN=PF11_0295 PE=3 SV=2 | 3 | 3.55 | 0.34 | 0.0030 |
| tr\|Q8I4S1\|Q8I4S1_PLAF7 Thymidylate kinase, putative OS=Plasmodium falciparum (isolate 3D7) GN=PFL2465c PE=1 SV=1 | 3 | 3.62 | 0.53 | 0.0071 |
| tr\|Q8I501\|Q8I501_PLAF7 RabGDI protein OS=Plasmodium falciparum (isolate 3D7) GN=PFL2060c PE=1 SV=1 | 3 | 3.68 | 0.29 | 0.0021 |
| tr\|C0H4C7\|C0H4C7_PLAF7 Uncharacterized protein OS=Plasmodium falciparum (isolate 3D7) GN=PFE0290c PE=4 SV=1 | 3 | 3.71 | 0.32 | 0.0024 |
| tr\|C0H490\|C0H490_PLAF7 Cytosolic glyoxalase II OS=Plasmodium falciparum (isolate 3D7) GN=cGloII PE=3 SV=1 | 3 | 3.78 | 1.00 | 0.0225 |
| tr\|Q8IIB7\|Q8IIB7_PLAF7 Ethanolamine kinase, putative OS=Plasmodium falciparum (isolate 3D7) GN=PF11_0257 PE=4 SV=1 | 3 | 3.82 | 0.43 | 0.0042 |
| tr\|Q8IIA4\|Q8IIA4_PLAF7 Threonine--tRNA ligase, putative OS=Plasmodium falciparum (isolate 3D7) GN=PF11_0270 PE=3 SV=1 | 3 | 3.83 | 0.13 | 0.0004 |
| tr\|Q8ILX1\|Q8ILX1_PLAF7 Nuclear transport factor 2, putative OS=Plasmodium falciparum (isolate 3D7) GN=PF14_0122 PE=4 SV=2 | 3 | 3.84 | 0.85 | 0.0158 |
| sp\|Q8IIK4\|PDX2_PLAF7 Pyridoxal 5-phosphate synthase subunit Pdx2 OS=Plasmodium falciparum (isolate 3D7) GN=pdx2 PE=1 SV=2 | 3 | 3.87 | 0.61 | 0.0081 |
| tr\|Q8ILK1\|Q8ILK1_PLAF7 Arginine-N-methyltransferase, putative OS=Plasmodium falciparum (isolate 3D7) GN=PF14_0242 PE=4 SV=1 | 3 | 3.88 | 0.92 | 0.0182 |
| tr\|Q8I2B1\|Q8I2B1_PLAF7 Aspartyl-tRNA synthetase, putative OS=Plasmodium falciparum (isolate 3D7) GN=PFA_0145c PE=3 SV=1 | 3 | 3.93 | 0.47 | 0.0047 |
| tr\|Q8IDG6\|Q8IDG6_PLAF7 Ran-binding protein, putative OS=Plasmodium falciparum (isolate 3D7) GN=PF13_0278 PE=4 SV=1 | 3 | 3.96 | 0.31 | 0.0020 |
| tr\|Q8IKA9\|Q8IKA9_PLAF7 Dihydroorotase, putative OS=Plasmodium falciparum (isolate 3D7) GN=PF14_0697 PE=4 SV=1 | 3 | 4.03 | 1.32 | 0.0341 |
| tr\|Q8IEF5\|Q8IEF5_PLAF7 Exportin 1-like protein, putative OS=Plasmodium falciparum (isolate 3D7) GN=MAL13P1.83 PE=4 SV=1 | 3 | 4.30 | 1.08 | 0.0204 |
| tr\|Q8I250\|Q8I250_PLAF7 Tubulin-specific chaperone a, putative OS=Plasmodium falciparum (isolate 3D7) GN=PFA_0460c PE=4 SV=1 | 3 | 4.35 | 0.77 | 0.0102 |
| tr\|Q8ILZ3\|Q8ILZ3_PLAF7 CTP synthase OS=Plasmodium falciparum (isolate 3D7) GN=PF14_0100 PE=3 SV=1 | 3 | 4.58 | 1.45 | 0.0318 |
| tr\|Q8I607\|Q8I607_PLAF7 Ubiquitin conjugating enzyme E2, putative OS=Plasmodium falciparum (isolate 3D7) GN=PFL0190w PE=3 SV=1 | 3 | 4.81 | 0.49 | 0.0035 |
| tr\|Q8II87\|Q8II87_PLAF7 Conserved protein OS=Plasmodium falciparum (isolate 3D7) GN=PF11_0287 PE=4 SV=2 | 3 | 5.59 | 2.02 | 0.0409 |
| tr\|Q8IKQ7\|Q8IKQ7_PLAF7 Uncharacterized protein OS=Plasmodium falciparum (isolate 3D7) GN=PF14_0546 PE=4 SV=1 | 3 | 5.68 | 0.32 | 0.0011 |
| tr\|Q8IBG6\|Q8IBG6_PLAF7 60S ribosomal subunit export protein, putative OS=Plasmodium falciparum (isolate 3D7) GN=PF07_0121 PE=4 SV=1 | 3 | 8.73 | 3.14 | 0.0405 |
| tr\|O96142\|O96142_PLAF7 Aspartate aminotransferase OS=Plasmodium falciparum (isolate 3D7) GN=PFB0200c PE=1 SV=1 | 3 | 11.45 | 3.77 | 0.0343 |
| tr\|C0H579\|C0H579_PLAF7 Putative uncharacterized protein OS=Plasmodium falciparum (isolate 3D7) GN=PFI1525w PE=4 SV=1 | 3 | 18.39 | 7.37 | 0.0496 |
| tr\|Q8IKR2\|Q8IKR2_PLAF7 Uncharacterized protein OS=Plasmodium falciparum (isolate 3D7) GN=PF14_0540 PE=4 SV=1 | 3 | 19.97 | 5.22 | 0.0220 |
| tr\|Q8IDY6\|Q8IDY6_PLAF7 Uncharacterized protein OS=Plasmodium falciparum (isolate 3D7) GN=PF13_0190 PE=4 SV=1 | 3 | 29.76 | 6.36 | 0.0149 |
| sp\|O15439-2\|MRP4_HUMAN Isoform 2 of Multidrug resistance-associated protein 4 OS=Homo sapiens GN=ABCC4;sp\|O15439\|MRP4_HUMAN Multidrug resistance-associated protein 4 OS=Homo sapiens GN=ABCC4 PE=1 SV=3 | 2 | 1.15 | 0.30 | 0.1165 |

| | | | | |
|---|---|---|---|---|
| tr\|O96230\|O96230_PLAF7 Acyl-CoA synthetase, PfACS9 OS=Plasmodium falciparum (isolate 3D7) GN=ACS9 PE=4 SV=1 | 2 | 0.91 | 0.21 | 0.1016 |
| tr\|Q8IHS2\|Q8IHS2_PLAF7 Ubiquitin activating enzyme (E1) subunit Aos1, putative OS=Plasmodium falciparum (isolate 3D7) GN=Aos1 PE=4 SV=1 | 2 | 3.10 | 1.01 | 0.1442 |
| tr\|A0A087WXM8\|A0A087WXM8_HUMAN Basal cell adhesion molecule OS=Homo sapiens GN=BCAM PE=1 SV=1;sp\|P50895\|BCAM_HUMAN Basal cell adhesion molecule OS=Homo sapiens GN=BCAM PE=1 SV=2 | 2 | 0.46 | 0.60 | 0.4751 |
| tr\|Q8ILZ6\|Q8ILZ6_PLAF7 Phosphatidate cytidylyltransferase OS=Plasmodium falciparum (isolate 3D7) GN=CDS PE=3 SV=1 | 2 | 0.36 | 0.47 | 0.4709 |
| SV=1;sp\|P30085-2\|KCY_HUMAN Isoform 2 of UMP-CMP kinase OS=Homo sapiens GN=CMPK1;sp\|P30085\|KCY_HUMAN UMP-CMP kinase OS=Homo sapiens GN=CMPK1 PE=1 SV=3 | 2 | 3.51 | 0.37 | 0.0478 |
| tr\|Q8IE69\|Q8IE69_PLAF7 Dihydrofolate synthase/folylpolyglutamate synthase OS=Plasmodium falciparum (isolate 3D7) GN=DHFS-FPGS PE=4 SV=1 | 2 | 6.90 | 4.30 | 0.2642 |
| 2\|FLOT1_HUMAN Isoform 2 of Flotillin-1 OS=Homo sapiens GN=FLOT1;tr\|A2AB10\|A2AB10_HUMAN Flotillin-1 (Fragment) OS=Homo sapiens GN=FLOT1 PE=1 SV=1 | 2 | 0.99 | 0.03 | 0.0116 |
| tr\|E9PK54\|E9PK54_HUMAN Heat shock cognate 71 kDa protein (Fragment) OS=Homo sapiens GN=HSPA8 PE=1 SV=4 | 2 | 1.62 | 0.31 | 0.0847 |
| tr\|Q8IE65\|Q8IE65_PLAF7 Uncharacterized protein OS=Plasmodium falciparum (isolate 3D7) GN=m26-32-10 PE=4 SV=1 | 2 | 0.26 | 0.13 | 0.2249 |
| tr\|Q8IE80\|Q8IE80_PLAF7 Uncharacterized protein OS=Plasmodium falciparum (isolate 3D7) GN=MAL13P1.130 PE=4 SV=1 | 2 | 0.37 | 0.51 | 0.4955 |
| tr\|Q8IDI9\|Q8IDI9_PLAF7 Phosphatidylinositol transfer protein, putative OS=Plasmodium falciparum (isolate 3D7) GN=MAL13P1.256 PE=4 SV=2 | 2 | 1.01 | 0.05 | 0.0233 |
| tr\|C0H5A0\|C0H5A0_PLAF7 Uncharacterized protein OS=Plasmodium falciparum (isolate 3D7) GN=MAL13P1.26 PE=4 SV=1 | 2 | 2.82 | 2.07 | 0.3043 |
| tr\|Q8IDE5\|Q8IDE5_PLAF7 Protein phosphatase, putative OS=Plasmodium falciparum (isolate 3D7) GN=MAL13P1.275 PE=4 SV=1 | 2 | 1.24 | 0.50 | 0.1780 |
| tr\|Q8IEJ0\|Q8IEJ0_PLAF7 Uncharacterized protein OS=Plasmodium falciparum (isolate 3D7) GN=MAL13P1.61 PE=4 SV=1 | 2 | 1.39 | 0.29 | 0.0929 |
| tr\|C0H5B7\|C0H5B7_PLAF7 Phosphatidylinositol synthase OS=Plasmodium falciparum (isolate 3D7) GN=MAL13P1.82 PE=3 SV=1 | 2 | 0.78 | 0.30 | 0.1687 |
| tr\|C0H5C0\|C0H5C0_PLAF7 Enhancer of polycomb-like protein OS=Plasmodium falciparum (isolate 3D7) GN=MAL13P1.88 PE=3 SV=1 | 2 | 0.86 | 0.46 | 0.2279 |
| tr\|Q8IAS1\|Q8IAS1_PLAF7 Ubiquitin regulatory protein, putative OS=Plasmodium falciparum (isolate 3D7) GN=MAL8P1.122 PE=4 SV=1 | 2 | 22.55 | 11.85 | 0.2266 |
| tr\|Q8IB25\|Q8IB25_PLAF7 Uncharacterized protein OS=Plasmodium falciparum (isolate 3D7) GN=MAL8P1.64 PE=4 SV=1 | 2 | 1.17 | 0.23 | 0.0880 |
| tr\|C0H4V8\|C0H4V8_PLAF7 DNA helicase, putative OS=Plasmodium falciparum (isolate 3D7) GN=MAL8P1.65 PE=4 SV=1 | 2 | 2.01 | 1.13 | 0.2396 |
| tr\|C6KT25\|C6KT25_PLAF7 Malate dehydrogenase OS=Plasmodium falciparum (isolate 3D7) GN=MDH PE=3 SV=1 | 2 | 4.51 | 2.25 | 0.2156 |
| tr\|Q8IDR1\|Q8IDR1_PLAF7 Phosphoenolpyruvate carboxykinase OS=Plasmodium falciparum (isolate 3D7) GN=PEPCK PE=3 SV=1 | 2 | 5.21 | 2.16 | 0.1819 |
| tr\|Q8IC27\|Q8IC27_PLAF7 Uncharacterized protein OS=Plasmodium falciparum (isolate 3D7) GN=PF07_0016 PE=4 SV=1 | 2 | 0.70 | 0.04 | 0.0282 |
| tr\|Q8IBZ6\|Q8IBZ6_PLAF7 Cg2 protein OS=Plasmodium falciparum (isolate 3D7) GN=PF07_0037 PE=4 SV=1 | 2 | 0.62 | 0.77 | 0.4565 |
| tr\|Q8IBM6\|Q8IBM6_PLAF7 Uncharacterized protein OS=Plasmodium falciparum (isolate 3D7) GN=PF07_0093 PE=4 SV=1 | 2 | 0.59 | 0.03 | 0.0233 |
| tr\|Q8I6Z2\|Q8I6Z2_PLAF7 mRNA (N6-adenosine)-methyltransferase, putative OS=Plasmodium falciparum (isolate 3D7) GN=PF07_0123 PE=4 SV=1 | 2 | 1.39 | 0.99 | 0.2956 |
| tr\|C0H4U7\|C0H4U7_PLAF7 Uncharacterized protein OS=Plasmodium falciparum (isolate 3D7) GN=PF08_0067 PE=4 SV=1 | 2 | 0.43 | 0.37 | 0.3515 |
| sp\|Q8IAW3\|RU1C_PLAF7 U1 small nuclear ribonucleoprotein C OS=Plasmodium falciparum (isolate 3D7) GN=PF08_0084 PE=3 SV=1 | 2 | 1.00 | 0.11 | 0.0502 |
| tr\|Q8IAT5\|Q8IAT5_PLAF7 Acyl CoA binding protein, putative OS=Plasmodium falciparum (isolate 3D7) GN=PF08_0099 PE=4 SV=1 | 2 | 2.41 | 1.48 | 0.2608 |
| tr\|Q8IK01\|Q8IK01_PLAF7 Uncharacterized protein OS=Plasmodium falciparum (isolate 3D7) GN=PF10_0039 PE=4 SV=1 | 2 | 0.30 | 0.40 | 0.4765 |
| tr\|Q8IJQ1\|Q8IJQ1_PLAF7 Cdk7, putative OS=Plasmodium falciparum (isolate 3D7) GN=PF10_0141 PE=4 SV=1 | 2 | 1.71 | 0.11 | 0.0298 |
| tr\|Q7KQL4\|Q7KQL4_PLAF7 DNA polymerase OS=Plasmodium falciparum (isolate 3D7) GN=PF10_0165 PE=3 SV=1 | 2 | 1.44 | 0.06 | 0.0196 |

| | | | | |
|---|---|---|---|---|
| tr\|Q8IJG2\|Q8IJG2_PLAF7 Conserved Plasmodium protein OS=Plasmodium falciparum (isolate 3D7) GN=PF10_0236 PE=4 SV=1 | 2 | 0.66 | 0.34 | 0.2217 |
| tr\|Q8IJ90\|Q8IJ90_PLAF7 Uncharacterized protein OS=Plasmodium falciparum (isolate 3D7) GN=PF10_0309 PE=3 SV=1 | 2 | 1.20 | 0.45 | 0.1664 |
| tr\|Q8IIR0\|Q8IIR0_PLAF7 Uncharacterized protein OS=Plasmodium falciparum (isolate 3D7) GN=PF11_0108 PE=4 SV=1 | 2 | 0.66 | 0.24 | 0.1617 |
| tr\|Q8I6U5\|Q8I6U5_PLAF7 Falcipain-2, putative OS=Plasmodium falciparum (isolate 3D7) GN=PF11_0161 PE=3 SV=1;tr\|Q8I6U4\|Q8I6U4_PLAF7 Falcipain 2 OS=Plasmodium falciparum (isolate 3D7) GN=PF11_0165 PE=1 SV=1 | 2 | 1.78 | 2.51 | 0.4989 |
| tr\|Q8IIE1\|Q8IIE1_PLAF7 Uncharacterized protein OS=Plasmodium falciparum (isolate 3D7) GN=PF11_0233 PE=4 SV=1 | 2 | 1.03 | 0.05 | 0.0239 |
| tr\|Q8IIB5\|Q8IIB5_PLAF7 Nuclear preribosomal assembly protein, putative OS=Plasmodium falciparum (isolate 3D7) GN=PF11_0259 PE=4 SV=1 | 2 | 1.24 | 1.68 | 0.4851 |
| tr\|Q8II88\|Q8II88_PLAF7 Uncharacterized protein OS=Plasmodium falciparum (isolate 3D7) GN=PF11_0286 PE=4 SV=1 | 2 | 11.36 | 15.54 | 0.4894 |
| tr\|Q8II83\|Q8II83_PLAF7 Uncharacterized protein OS=Plasmodium falciparum (isolate 3D7) GN=PF11_0291 PE=4 SV=1 | 2 | 0.74 | 0.03 | 0.0199 |
| tr\|Q8II69\|Q8II69_PLAF7 Uncharacterized protein OS=Plasmodium falciparum (isolate 3D7) GN=PF11_0305 PE=4 SV=1 | 2 | 0.48 | 0.23 | 0.2081 |
| tr\|Q8II22\|Q8II22_PLAF7 Uncharacterized protein OS=Plasmodium falciparum (isolate 3D7) GN=PF11_0353 PE=4 SV=1 | 2 | 1.47 | 0.38 | 0.1140 |
| tr\|Q8IHP1\|Q8IHP1_PLAF7 Uncharacterized protein OS=Plasmodium falciparum (isolate 3D7) GN=PF11_0488 PE=4 SV=1 | 2 | 1.00 | 0.04 | 0.0161 |
| tr\|Q8I6T5\|Q8I6T5_PLAF7 Cop-coated vesicle membrane protein p24, putative OS=Plasmodium falciparum (isolate 3D7) GN=PF13_0082 PE=4 SV=1 | 2 | 1.02 | 0.69 | 0.2851 |
| tr\|Q8IEF7\|Q8IEF7_PLAF7 Methyltransferase, putative OS=Plasmodium falciparum (isolate 3D7) GN=PF13_0087 PE=4 SV=1 | 2 | 0.84 | 0.21 | 0.1110 |
| tr\|Q8IE30\|Q8IE30_PLAF7 Uncharacterized protein OS=Plasmodium falciparum (isolate 3D7) GN=PF13_0163 PE=4 SV=1 | 2 | 0.87 | 0.13 | 0.0668 |
| tr\|Q8IDZ6\|Q8IDZ6_PLAF7 Ubiquitin-activating enzyme, putative OS=Plasmodium falciparum (isolate 3D7) GN=PF13_0182 PE=4 SV=1 | 2 | 0.87 | 0.79 | 0.3625 |
| tr\|Q8IDV9\|Q8IDV9_PLAF7 Exoribonuclease, putative OS=Plasmodium falciparum (isolate 3D7) GN=PF13_0208 PE=4 SV=1 | 2 | 0.99 | 0.05 | 0.0248 |
| tr\|Q8IDQ6\|Q8IDQ6_PLAF7 Uncharacterized protein OS=Plasmodium falciparum (isolate 3D7) GN=PF13_0237 PE=4 SV=1 | 2 | 1.12 | 0.27 | 0.1060 |
| tr\|Q8IDH2\|Q8IDH2_PLAF7 MON1 protein OS=Plasmodium falciparum (isolate 3D7) GN=PF13_0274 PE=4 SV=1 | 2 | 1.15 | 0.45 | 0.1708 |
| tr\|Q8ID87\|Q8ID87_PLAF7 Uncharacterized protein OS=Plasmodium falciparum (isolate 3D7) GN=PF13_0329 PE=4 SV=1 | 2 | 0.88 | 0.10 | 0.0518 |
| tr\|Q8IM44\|Q8IM44_PLAF7 Uncharacterized protein OS=Plasmodium falciparum (isolate 3D7) GN=PF14_0047 PE=4 SV=1 | 2 | 1.18 | 0.01 | 0.0048 |
| tr\|Q8IM03\|Q8IM03_PLAF7 DNA-damage inducible protein, putative OS=Plasmodium falciparum (isolate 3D7) GN=PF14_0090 PE=4 SV=1 | 2 | 24.47 | 33.63 | 0.4908 |
| tr\|Q8ILW7\|Q8ILW7_PLAF7 AAA family ATPase, putative OS=Plasmodium falciparum (isolate 3D7) GN=PF14_0126 PE=3 SV=1 | 2 | 0.19 | 0.09 | 0.2021 |
| tr\|Q8ILR8\|Q8ILR8_PLAF7 Uncharacterized protein OS=Plasmodium falciparum (isolate 3D7) GN=PF14_0176 PE=4 SV=1 | 2 | 3.20 | 2.10 | 0.2770 |
| tr\|Q8ILJ7\|Q8ILJ7_PLAF7 Phosphoenolpyruvate carboxylase, putative OS=Plasmodium falciparum (isolate 3D7) GN=PF14_0246 PE=4 SV=1 | 2 | 2.14 | 0.56 | 0.1159 |
| tr\|Q8ILB8\|Q8ILB8_PLAF7 Methionine aminopeptidase 2 OS=Plasmodium falciparum (isolate 3D7) GN=PF14_0327 PE=3 SV=1 | 2 | 13.51 | 11.15 | 0.3364 |
| tr\|Q8IKV7\|Q8IKV7_PLAF7 Ribosome biogenesis protein tsr1, putative OS=Plasmodium falciparum (isolate 3D7) GN=PF14_0494 PE=4 SV=1 | 2 | 2.74 | 0.23 | 0.0375 |
| tr\|Q8IKP7\|Q8IKP7_PLAF7 Uncharacterized protein OS=Plasmodium falciparum (isolate 3D7) GN=PF14_0557 PE=3 SV=1 | 2 | 21.15 | 5.77 | 0.1214 |
| tr\|Q8IKI8\|Q8IKI8_PLAF7 Uncharacterized protein OS=Plasmodium falciparum (isolate 3D7) GN=PF14_0617 PE=4 SV=1 | 2 | 0.72 | 0.19 | 0.1184 |
| tr\|Q8IK65\|Q8IK65_PLAF7 Uncharacterized protein OS=Plasmodium falciparum (isolate 3D7) GN=PF14_0741 PE=4 SV=1;tr\|Q8IK49\|Q8IK49_PLAF7 Uncharacterized protein OS=Plasmodium falciparum (isolate 3D7) GN=PF14_0758 PE=4 SV=1 | 2 | 0.81 | 0.18 | 0.0997 |
| tr\|Q8ILY4\|Q8ILY4_PLAF7 Uncharacterized protein OS=Plasmodium falciparum (isolate 3D7) GN=PF14_0778 PE=4 SV=2 | 2 | 0.63 | 0.19 | 0.1330 |
| sp\|Q8I1Y0\|PF41_PLAF7 Merozoite surface protein P41 OS=Plasmodium falciparum (isolate 3D7) GN=PF41 PE=1 SV=1 | 2 | 0.40 | 0.49 | 0.4572 |
| tr\|Q8I278\|Q8I278_PLAF7 Putative uncharacterized protein OS=Plasmodium falciparum (isolate 3D7) GN=PFA_0315w PE=4 SV=1 | 2 | 8.16 | 6.64 | 0.3323 |

| | | | | |
|---|---|---|---|---|
| tr\|B9ZSJ1\|B9ZSJ1_PLAF7 Putative uncharacterized protein OS=Plasmodium falciparum (isolate 3D7) GN=PFA_0630c PE=4 SV=1 | 2 | 0.90 | 0.03 | 0.0145 |
| tr\|C6S3B4\|C6S3B4_PLAF7 Conserved protein OS=Plasmodium falciparum (isolate 3D7) GN=PFB0423c PE=4 SV=1 | 2 | 10.95 | 10.87 | 0.3897 |
| tr\|O96278\|O96278_PLAF7 Plasmodium exported protein (Hyp9) OS=Plasmodium falciparum (isolate 3D7) GN=PFB0930w PE=4 SV=2 | 2 | 1.04 | 0.34 | 0.1456 |
| tr\|O96279\|O96279_PLAF7 Cytoadherence linked asexual protein 2 OS=Plasmodium falciparum (isolate 3D7) GN=PFB0935w PE=4 SV=2 | 2 | 0.82 | 0.01 | 0.0072 |
| tr\|C0H468\|C0H468_PLAF7 Putative uncharacterized protein OS=Plasmodium falciparum (isolate 3D7) GN=PFC0080c PE=4 SV=1 | 2 | 2.47 | 2.10 | 0.3456 |
| tr\|O97252\|O97252_PLAF7 ATP-dependent Clp protease proteolytic subunit OS=Plasmodium falciparum (isolate 3D7) GN=PFC0310c PE=1 SV=1 | 2 | 0.53 | 0.51 | 0.3819 |
| tr\|C0H4A1\|C0H4A1_PLAF7 Uncharacterized protein OS=Plasmodium falciparum (isolate 3D7) GN=PFD0465c PE=4 SV=1 | 2 | 0.81 | 0.09 | 0.0503 |
| tr\|Q9U0I2\|Q9U0I2_PLAF7 Uncharacterized protein OS=Plasmodium falciparum (isolate 3D7) GN=PFD0525w PE=4 SV=2 | 2 | 7.62 | 7.71 | 0.3952 |
| tr\|Q8I1T0\|Q8I1T0_PLAF7 Uncharacterized protein OS=Plasmodium falciparum (isolate 3D7) GN=PFD0760c PE=4 SV=1 | 2 | 0.79 | 0.06 | 0.0331 |
| tr\|C0H4A8\|C0H4A8_PLAF7 PfMNL-2 CISD1-like iron-sulfur protein, putative OS=Plasmodium falciparum (isolate 3D7) GN=PFD0807c PE=4 SV=1 | 2 | 0.49 | 0.22 | 0.1963 |
| tr\|C0H4B9\|C0H4B9_PLAF7 Steroid dehydrogenase, putative OS=Plasmodium falciparum (isolate 3D7) GN=PFD1035w PE=4 SV=1 | 2 | 4.43 | 6.09 | 0.4906 |
| tr\|Q8IFP3\|Q8IFP3_PLAF7 Alpha-tubulin ii OS=Plasmodium falciparum (isolate 3D7) GN=PFD1050w PE=3 SV=1 | 2 | 4.00 | 0.26 | 0.0290 |
| tr\|Q8I469\|Q8I469_PLAF7 Uncharacterized protein OS=Plasmodium falciparum (isolate 3D7) GN=PFE0155w PE=4 SV=1 | 2 | 0.73 | 0.05 | 0.0311 |
| sp\|Q8I467\|CADF1_PLAF7 Cofilin/actin-depolymerizing factor homolog 1 OS=Plasmodium falciparum (isolate 3D7) GN=PFE0165w PE=1 SV=1 | 2 | 13.76 | 18.34 | 0.4812 |
| tr\|Q8I0X1\|Q8I0X1_PLAF7 3-methyl-2-oxobutanoate dehydrogenase (Lipoamide), putative OS=Plasmodium falciparum (isolate 3D7) GN=PFE0225w PE=4 SV=1 | 2 | 0.62 | 0.50 | 0.3309 |
| tr\|Q8I0X0\|Q8I0X0_PLAF7 SNAP protein (Soluble N-ethylmaleimide-sensitive factor Attachment Protein), putative OS=Plasmodium falciparum (isolate 3D7) GN=PFE0445c PE=4 SV=1 | 2 | 0.81 | 0.37 | 0.2015 |
| tr\|Q8I3U9\|Q8I3U9_PLAF7 Protein phosphatase, putative OS=Plasmodium falciparum (isolate 3D7) GN=PFE0795c PE=4 SV=1 | 2 | 0.93 | 0.42 | 0.1952 |
| tr\|Q8I3R4\|Q8I3R4_PLAF7 Uncharacterized protein OS=Plasmodium falciparum (isolate 3D7) GN=PFE0985w PE=4 SV=1 | 2 | 1.85 | 0.78 | 0.1833 |
| tr\|Q8I3J8\|Q8I3J8_PLAF7 Uncharacterized protein OS=Plasmodium falciparum (isolate 3D7) GN=PFE1330c PE=4 SV=1 | 2 | 1.17 | 1.03 | 0.3553 |
| tr\|Q8I3I7\|Q8I3I7_PLAF7 Uncharacterized protein OS=Plasmodium falciparum (isolate 3D7) GN=PFE1395c PE=4 SV=1 | 2 | 2.77 | 0.78 | 0.1253 |
| tr\|C6KSQ7\|C6KSQ7_PLAF7 Elongation of fatty acids protein OS=Plasmodium falciparum (isolate 3D7) GN=PFF0290w PE=3 SV=1 | 2 | 3.34 | 4.67 | 0.4962 |
| tr\|C6KSR7\|C6KSR7_PLAF7 Glutaredoxin-like protein, putative OS=Plasmodium falciparum (isolate 3D7) GN=PFF0340c PE=4 SV=1 | 2 | 3.83 | 4.43 | 0.4366 |
| tr\|C6KSU9\|C6KSU9_PLAF7 Uncharacterized protein OS=Plasmodium falciparum (isolate 3D7) GN=PFF0505c PE=4 SV=1 | 2 | 1.20 | 0.04 | 0.0165 |
| tr\|C6KT03\|C6KT03_PLAF7 Ndc80 homologue, putative OS=Plasmodium falciparum (isolate 3D7) GN=PFF0785w PE=4 SV=1 | 2 | 0.70 | 0.59 | 0.3431 |
| tr\|C6KT51\|C6KT51_PLAF7 Uncharacterized protein OS=Plasmodium falciparum (isolate 3D7) GN=PFF1030w PE=4 SV=1 | 2 | 0.48 | 0.67 | 0.4924 |
| tr\|C6KT72\|C6KT72_PLAF7 Transcription or splicing factor-like protein, putative OS=Plasmodium falciparum (isolate 3D7) GN=PFF1135w PE=4 SV=1 | 2 | 0.77 | 0.09 | 0.0534 |
| tr\|C6KTB3\|C6KTB3_PLAF7 Transportin OS=Plasmodium falciparum (isolate 3D7) GN=PFF1345w PE=4 SV=1 | 2 | 7.97 | 5.90 | 0.3070 |
| tr\|Q8IEU2\|Q8IEU2_PLAF7 Plasmodium falciparum gamete antigen 27/25 OS=Plasmodium falciparum (isolate 3D7) GN=pfg27-25 PE=1 SV=1 | 2 | 1.57 | 0.78 | 0.2159 |
| tr\|Q8I367\|Q8I367_PLAF7 Putative uncharacterized protein OS=Plasmodium falciparum (isolate 3D7) GN=PFI0405w PE=4 SV=1 | 2 | 0.80 | 0.24 | 0.1332 |
| tr\|C0H529\|C0H529_PLAF7 Small nuclear ribonucleoprotein (SnRNP), putative OS=Plasmodium falciparum (isolate 3D7) GN=PFI0475w PE=4 SV=1 | 2 | 1.01 | 1.04 | 0.4026 |
| sp\|C0H537\|TRM5_PLAF7 tRNA (guanine(37)-N1)-methyltransferase OS=Plasmodium falciparum (isolate 3D7) GN=PFI0700c PE=3 SV=1 | 2 | 3.31 | 0.85 | 0.1145 |
| tr\|Q8I301\|Q8I301_PLAF7 Ubiquitin conjugating enzyme, putative OS=Plasmodium falciparum (isolate 3D7) GN=PFI0740c PE=1 SV=1 | 2 | 16.21 | 3.15 | 0.0871 |

| | | | | |
|---|---|---|---|---|
| tr\|Q8I2V6\|Q8I2V6_PLAF7 Pyridoxal 5-phosphate dependent enzyme class III, putative OS=Plasmodium falciparum (isolate 3D7) GN=PFI0965w PE=3 SV=1 | 2 | 8.37 | 8.78 | 0.4065 |
| tr\|Q8I2U3\|Q8I2U3_PLAF7 Ubiquitin conjugating enzyme, putative OS=Plasmodium falciparum (isolate 3D7) GN=PFI1030c PE=3 SV=1 | 2 | 4.69 | 4.88 | 0.4043 |
| tr\|Q8I0U9\|Q8I0U9_PLAF7 Triose phosphate transporter OS=Plasmodium falciparum (isolate 3D7) GN=PfiTPT PE=4 SV=1 | 2 | 0.70 | 0.92 | 0.4732 |
| tr\|Q8I5U8\|Q8I5U8_PLAF7 Uncharacterized protein OS=Plasmodium falciparum (isolate 3D7) GN=PFL0505c PE=4 SV=1 | 2 | 0.73 | 0.05 | 0.0316 |
| tr\|Q8I5L3\|Q8I5L3_PLAF7 Ribulose-phosphate 3-epimerase OS=Plasmodium falciparum (isolate 3D7) GN=PFL0960w PE=1 SV=1 | 2 | 11.23 | 14.71 | 0.4754 |
| tr\|Q8I5H2\|Q8I5H2_PLAF7 Chromatin assembly protein (ASF1), putative OS=Plasmodium falciparum (isolate 3D7) GN=PFL1180w PE=4 SV=1 | 2 | 3.40 | 1.32 | 0.1712 |
| tr\|Q8I5G8\|Q8I5G8_PLAF7 Splicing factor 3b subunit, putative OS=Plasmodium falciparum (isolate 3D7) GN=PFL1200c PE=4 SV=1 | 2 | 0.33 | 0.44 | 0.4793 |
| tr\|Q8I5G0\|Q8I5G0_PLAF7 Uncharacterized protein OS=Plasmodium falciparum (isolate 3D7) GN=PFL1240c PE=4 SV=1 | 2 | 1.16 | 0.19 | 0.0727 |
| tr\|Q8I5E2\|Q8I5E2_PLAF7 Cyclin related protein, putative OS=Plasmodium falciparum (isolate 3D7) GN=PFL1335w PE=4 SV=2 | 2 | 0.82 | 0.27 | 0.1483 |
| tr\|Q8I5A4\|Q8I5A4_PLAF7 Pre-mRNA splicing factor RNA helicase, putative OS=Plasmodium falciparum (isolate 3D7) GN=PFL1525c PE=4 SV=1 | 2 | 0.85 | 0.10 | 0.0546 |
| tr\|Q8I553\|Q8I553_PLAF7 Ubiquitin activating enzyme, putative OS=Plasmodium falciparum (isolate 3D7) GN=PFL1790w PE=4 SV=1 | 2 | 1.22 | 0.74 | 0.2586 |
| tr\|Q8I528\|Q8I528_PLAF7 Dna gyrase subunit b, putative OS=Plasmodium falciparum (isolate 3D7) GN=PFL1915w PE=3 SV=1 | 2 | 4.14 | 4.69 | 0.4300 |
| tr\|C6S3L1\|C6S3L1_PLAF7 Erythrocyte membrane protein 1, PfEMP1 OS=Plasmodium falciparum (isolate 3D7) GN=PFL1970w PE=4 SV=1 | 2 | 0.63 | 0.54 | 0.3452 |
| tr\|Q8I506\|Q8I506_PLAF7 Uncharacterized protein OS=Plasmodium falciparum (isolate 3D7) GN=PFL2035c PE=4 SV=1 | 2 | 0.82 | 0.26 | 0.1388 |
| tr\|Q8I4Y3\|Q8I4Y3_PLAF7 Uncharacterized protein OS=Plasmodium falciparum (isolate 3D7) GN=PFL2150c PE=4 SV=1 | 2 | 7.33 | 6.32 | 0.3484 |
| tr\|Q8I4V1\|Q8I4V1_PLAF7 Conserved Plasmodium membrane protein OS=Plasmodium falciparum (isolate 3D7) GN=PFL2315c PE=4 SV=1 | 2 | 0.40 | 0.49 | 0.4558 |
| tr\|Q8I4S6\|Q8I4S6_PLAF7 DNA repair protein rhp16, putative OS=Plasmodium falciparum (isolate 3D7) GN=PFL2440w PE=4 SV=1 | 2 | 1.12 | 0.16 | 0.0652 |
| tr\|B9ZSJ3\|B9ZSJ3_PLAF7 Pfmc-2TM Maurers cleft two transmembrane protein OS=Plasmodium falciparum (isolate 3D7) GN=PfMC-2TM PE=4 SV=1;tr\|O96287\|O96287_PLAF7 Pfmc-2TM Maurers cleft two transmembrane protein OS=Plasmodium falciparum (isolate 3D7) GN=MC-2TM | 2 | 1.08 | 0.13 | 0.0533 |
| tr\|Q8IC17\|Q8IC17_PLAF7 Origin recognition complex subunit 2, putative OS=Plasmodium falciparum (isolate 3D7) GN=PfORC2 PE=4 SV=1 | 2 | 1.56 | 0.10 | 0.0278 |
| tr\|C0H4R8\|C0H4R8_PLAF7 Serine/Threonine protein kinase, FIKK family OS=Plasmodium falciparum (isolate 3D7) GN=PfTSTK0 PE=4 SV=1 | 2 | 1.48 | 0.49 | 0.1458 |
| tr\|E9PHR9\|E9PHR9_HUMAN Phospholipid scramblase 4 OS=Homo sapiens GN=PLSCR4 PE=1 SV=1;sp\|Q9NRQ2-2\|PLS4_HUMAN Isoform 2 of Phospholipid scramblase 4 OS=Homo sapiens GN=PLSCR4;sp\|Q9NRQ2\|PLS4_HUMAN Phospholipid scramblase 4 OS=Homo sapiens GN=PLSCR4 PE=1 SV=2 | 2 | 0.89 | 0.03 | 0.0148 |
| tr\|Q8ILV1\|Q8ILV1_PLAF7 Serine/threonine-protein phosphatase OS=Plasmodium falciparum (isolate 3D7) GN=PP1 PE=1 SV=1 | 2 | 1.48 | 0.28 | 0.0852 |
| tr\|C0H5G2\|C0H5G2_PLAF7 Rab11b, GTPase (Fragment) OS=Plasmodium falciparum (isolate 3D7) GN=Rab11b PE=3 SV=1 | 2 | 0.75 | 0.86 | 0.4354 |
| tr\|Q8I485\|Q8I485_PLAF7 Rhoptry-associated protein 3, RAP3 OS=Plasmodium falciparum (isolate 3D7) GN=RAP3 PE=4 SV=1 | 2 | 0.35 | 0.49 | 0.4910 |
| tr\|C6KT26\|C6KT26_PLAF7 Rhomboid protease ROM10 OS=Plasmodium falciparum (isolate 3D7) GN=ROM10 PE=4 SV=1 | 2 | 1.33 | 1.08 | 0.3317 |
| tr\|O96164\|O96164_PLAF7 Serine repeat antigen 4 (SERA-4) OS=Plasmodium falciparum (isolate 3D7) GN=SERA-4 PE=1 SV=1 | 2 | 0.06 | 0.06 | 0.3874 |
| tr\|O96163\|O96163_PLAF7 Serine repeat antigen 7 (SERA-7) OS=Plasmodium falciparum (isolate 3D7) GN=SERA-7 PE=3 SV=1 | 2 | 0.77 | 0.27 | 0.1578 |
| sp\|P27797\|CALR_HUMAN Calreticulin OS=Homo sapiens GN=CALR PE=1 SV=1 | 1 | 1.21 | | |
| sp\|P09543-2\|CN37_HUMAN Isoform CNPI of 2,3-cyclic-nucleotide 3-phosphodiesterase OS=Homo sapiens GN=CNP;sp\|P09543\|CN37_HUMAN 2,3-cyclic-nucleotide 3-phosphodiesterase OS=Homo sapiens GN=CNP PE=1 SV=2 | 1 | 0.83 | | |
| sp\|Q7K734\|FEN1_PLAF7 Flap endonuclease 1 OS=Plasmodium falciparum (isolate 3D7) GN=FEN1 PE=3 SV=1 | 1 | 1.02 | | |

| | | | | |
|---|---|---|---|---|
| tr\|G3V1D1\|G3V1D1_HUMAN Ferritin OS=Homo sapiens GN=FTH1 PE=1 SV=1;tr\|G3V192\|G3V192_HUMAN Ferritin OS=Homo sapiens GN=FTH1 PE=1 SV=1;sp\|P02794\|FRIH_HUMAN Ferritin heavy chain OS=Homo sapiens GN=FTH1 PE=1 SV=2 | 1 | 1.35 | | |
| tr\|Q8I5I8\|Q8I5I8_PLAF7 Glideosome-associated protein 45 OS=Plasmodium falciparum (isolate 3D7) GN=GAP45 PE=4 SV=1 | 1 | 0.85 | | |
| sp\|P62805\|H4_HUMAN Histone H4 OS=Homo sapiens GN=HIST1H4A PE=1 SV=2 | 1 | 4.18 | | |
| sp\|P34931\|HS71L_HUMAN Heat shock 70 kDa protein 1-like OS=Homo sapiens GN=HSPA1L PE=1 SV=2 | 1 | 0.05 | | |
| tr\|Q8IE63\|Q8IE63_PLAF7 Tetratricopeptide repeat family protein, putative OS=Plasmodium falciparum (isolate 3D7) GN=MAL13P1.139 PE=4 SV=1 | 1 | 0.37 | | |
| tr\|C0H5D7\|C0H5D7_PLAF7 Translation initiation factor EIF-2B gamma subunit, putative OS=Plasmodium falciparum (isolate 3D7) GN=MAL13P1.144 PE=4 SV=1 | 1 | 1.11 | | |
| tr\|C0H598\|C0H598_PLAF7 Uncharacterized protein OS=Plasmodium falciparum (isolate 3D7) GN=MAL13P1.21 PE=4 SV=1 | 1 | 0.86 | | |
| tr\|Q8IDP0\|Q8IDP0_PLAF7 Uncharacterized protein OS=Plasmodium falciparum (isolate 3D7) GN=MAL13P1.228 PE=4 SV=1 | 1 | 0.70 | | |
| tr\|C0H5H6\|C0H5H6_PLAF7 Uncharacterized protein OS=Plasmodium falciparum (isolate 3D7) GN=MAL13P1.234 PE=4 SV=1 | 1 | 1.18 | | |
| tr\|Q8IDK3\|Q8IDK3_PLAF7 Uncharacterized protein OS=Plasmodium falciparum (isolate 3D7) GN=MAL13P1.250 PE=4 SV=1 | 1 | 0.88 | | |
| tr\|Q8IEP7\|Q8IEP7_PLAF7 RED-like protein, putative OS=Plasmodium falciparum (isolate 3D7) GN=MAL13P1.34 PE=4 SV=1 | 1 | 0.90 | | |
| tr\|C0H5G7\|C0H5G7_PLAF7 RNA binding protein, putative OS=Plasmodium falciparum (isolate 3D7) GN=MAL13P1.385 PE=4 SV=1 | 1 | 0.89 | | |
| tr\|C0H5A6\|C0H5A6_PLAF7 Uncharacterized protein OS=Plasmodium falciparum (isolate 3D7) GN=MAL13P1.39 PE=4 SV=1 | 1 | 0.47 | | |
| tr\|Q8IEH3\|Q8IEH3_PLAF7 Uncharacterized protein OS=Plasmodium falciparum (isolate 3D7) GN=MAL13P1.73 PE=4 SV=1 | 1 | 27.11 | | |
| tr\|C0H5C1\|C0H5C1_PLAF7 Uncharacterized protein OS=Plasmodium falciparum (isolate 3D7) GN=MAL13P1.90 PE=4 SV=1 | 1 | 1.68 | | |
| tr\|Q8IBN7\|Q8IBN7_PLAF7 P36-like protein homologue, putative OS=Plasmodium falciparum (isolate 3D7) GN=MAL7P1.114 PE=4 SV=2 | 1 | 2.31 | | |
| tr\|Q8IBN1\|Q8IBN1_PLAF7 Uncharacterized protein OS=Plasmodium falciparum (isolate 3D7) GN=MAL7P1.119 PE=4 SV=1 | 1 | 0.70 | | |
| tr\|Q8IC31\|Q8IC31_PLAF7 Uncharacterized protein OS=Plasmodium falciparum (isolate 3D7) GN=MAL7P1.15 PE=4 SV=1 | 1 | 1.36 | | |
| tr\|C0H4K4\|C0H4K4_PLAF7 Uncharacterized protein OS=Plasmodium falciparum (isolate 3D7) GN=MAL7P1.17 PE=4 SV=1 | 1 | 0.98 | | |
| tr\|Q8IAN2\|Q8IAN2_PLAF7 Filament assembling protein, putative OS=Plasmodium falciparum (isolate 3D7) GN=MAL8P1.146 PE=4 SV=1 | 1 | 1.46 | | |
| tr\|C0H4V4\|C0H4V4_PLAF7 Uncharacterized protein OS=Plasmodium falciparum (isolate 3D7) GN=MAL8P1.73 PE=4 SV=1 | 1 | 0.33 | | |
| tr\|H3BRV9\|H3BRV9_HUMAN Nuclear transport factor 2 (Fragment) OS=Homo sapiens GN=NUTF2 PE=1 SV=1;sp\|P61970\|NTF2_HUMAN Nuclear transport factor 2 OS=Homo sapiens GN=NUTF2 PE=1 SV=1 | 1 | 4.21 | | |
| tr\|Q8IC44\|Q8IC44_PLAF7 STARP antigen OS=Plasmodium falciparum (isolate 3D7) GN=PF07_0006 PE=4 SV=1 | 1 | 1.12 | | |
| tr\|Q8IBV2\|Q8IBV2_PLAF7 Transcription elongation factor s-II, putative OS=Plasmodium falciparum (isolate 3D7) GN=PF07_0057 PE=4 SV=1 | 1 | 44.74 | | |
| tr\|Q8IBU8\|Q8IBU8_PLAF7 Uncharacterized protein OS=Plasmodium falciparum (isolate 3D7) GN=PF07_0061 PE=4 SV=1 | 1 | 0.92 | | |
| tr\|Q8IBH8\|Q8IBH8_PLAF7 Uncharacterized protein OS=Plasmodium falciparum (isolate 3D7) GN=PF07_0116 PE=4 SV=1 | 1 | 1.48 | | |
| tr\|Q8IBG5\|Q8IBG5_PLAF7 Nucleolus BRIX protein, putative OS=Plasmodium falciparum (isolate 3D7) GN=PF07_0122 PE=4 SV=1 | 1 | 0.41 | | |
| tr\|Q8IBF5\|Q8IBF5_PLAF7 Uncharacterized protein OS=Plasmodium falciparum (isolate 3D7) GN=PF07_0127 PE=4 SV=1 | 1 | 1.01 | | |
| tr\|Q8IB63\|Q8IB63_PLAF7 Uncharacterized protein OS=Plasmodium falciparum (isolate 3D7) GN=PF08_0035 PE=4 SV=1 | 1 | 0.29 | | |
| tr\|Q8IB11\|Q8IB11_PLAF7 MAC/Perforin, putative OS=Plasmodium falciparum (isolate 3D7) GN=PF08_0058 PE=4 SV=1 | 1 | 0.61 | | |
| tr\|Q8IAV6\|Q8IAV6_PLAF7 Uncharacterized protein OS=Plasmodium falciparum (isolate 3D7) GN=PF08_0089 PE=4 SV=1 | 1 | 3.83 | | |

| | | | | |
|---|---|---|---|---|
| tr\|C0H4S0\|C0H4S0_PLAF7 AAA family ATPase, putative OS=Plasmodium falciparum (isolate 3D7) GN=PF08_0117 PE=4 SV=1 | 1 | 0.93 | | |
| tr\|Q8IAP4\|Q8IAP4_PLAF7 GTPase activator, putative OS=Plasmodium falciparum (isolate 3D7) GN=PF08_0120 PE=4 SV=1 | 1 | 5.69 | | |
| tr\|C6S3D0\|C6S3D0_PLAF7 Conserved Plasmodium protein OS=Plasmodium falciparum (isolate 3D7) GN=PF10_0177b PE=4 SV=1 | 1 | 0.09 | | |
| tr\|Q8I6U7\|Q8I6U7_PLAF7 Citrate synthase OS=Plasmodium falciparum (isolate 3D7) GN=PF10_0218 PE=3 SV=1 | 1 | 0.81 | | |
| sp\|Q8IIU6\|RTCB_PLAF7 tRNA-splicing ligase RtcB homolog OS=Plasmodium falciparum (isolate 3D7) GN=PF11_0068 PE=3 SV=1 | 1 | 14.63 | | |
| tr\|Q8IIE2\|Q8IIE2_PLAF7 Uncharacterized protein OS=Plasmodium falciparum (isolate 3D7) GN=PF11_0232 PE=4 SV=1 | 1 | 0.81 | | |
| tr\|Q8IHU8\|Q8IHU8_PLAF7 Uncharacterized protein OS=Plasmodium falciparum (isolate 3D7) GN=PF11_0428 PE=4 SV=1 | 1 | 1.36 | | |
| tr\|Q8IHT4\|Q8IHT4_PLAF7 Uncharacterized protein OS=Plasmodium falciparum (isolate 3D7) GN=PF11_0443 PE=4 SV=1 | 1 | 1.00 | | |
| sp\|C6KSX0\|PF12_PLAF7 Merozoite surface protein P12 OS=Plasmodium falciparum (isolate 3D7) GN=PF12 PE=1 SV=1 | 1 | 2.92 | | |
| tr\|Q8IET0\|Q8IET0_PLAF7 Sodium/hydrogen exchanger, Na+, H+ antiporter OS=Plasmodium falciparum (isolate 3D7) GN=PF13_0019 PE=4 SV=1 | 1 | 0.55 | | |
| tr\|Q8IER6\|Q8IER6_PLAF7 Uncharacterized protein OS=Plasmodium falciparum (isolate 3D7) GN=PF13_0024 PE=4 SV=1 | 1 | 1.05 | | |
| tr\|Q8IEP9\|Q8IEP9_PLAF7 Vacuolar ATP synthase subunit h, putative OS=Plasmodium falciparum (isolate 3D7) GN=PF13_0034 PE=4 SV=2 | 1 | 1.25 | | |
| tr\|Q8I6T7\|Q8I6T7_PLAF7 ATP synthase subunit gamma OS=Plasmodium falciparum (isolate 3D7) GN=PF13_0061 PE=3 SV=1 | 1 | 4.67 | | |
| tr\|Q8IEE3\|Q8IEE3_PLAF7 Uncharacterized protein OS=Plasmodium falciparum (isolate 3D7) GN=PF13_0098 PE=4 SV=1 | 1 | 0.92 | | |
| tr\|Q8IDW3\|Q8IDW3_PLAF7 Tryptophan--tRNA ligase, putative OS=Plasmodium falciparum (isolate 3D7) GN=PF13_0205 PE=1 SV=1 | 1 | 17.00 | | |
| sp\|Q8IDG7\|YPF01_PLAF7 Uncharacterized protein PF13_0277 OS=Plasmodium falciparum (isolate 3D7) GN=PF13_0277 PE=3 SV=1 | 1 | 1.29 | | |
| tr\|Q8ID89\|Q8ID89_PLAF7 Cytochrome c oxidase subunit 2, putative OS=Plasmodium falciparum (isolate 3D7) GN=PF13_0327 PE=4 SV=1 | 1 | 0.81 | | |
| tr\|Q8ID62\|Q8ID62_PLAF7 Exosome complex exonuclease, putative OS=Plasmodium falciparum (isolate 3D7) GN=PF13_0340 PE=4 SV=1 | 1 | 1.37 | | |
| tr\|Q8ID49\|Q8ID49_PLAF7 Uncharacterized protein OS=Plasmodium falciparum (isolate 3D7) GN=PF13_0347 PE=4 SV=1 | 1 | 17.26 | | |
| tr\|Q8IM73\|Q8IM73_PLAF7 Uncharacterized protein OS=Plasmodium falciparum (isolate 3D7) GN=PF14_0018 PE=4 SV=2 | 1 | 0.73 | | |
| tr\|Q8IM43\|Q8IM43_PLAF7 Uncharacterized protein OS=Plasmodium falciparum (isolate 3D7) GN=PF14_0048 PE=4 SV=2 | 1 | 1.60 | | |
| tr\|Q8IM34\|Q8IM34_PLAF7 RNA binding protein, putative OS=Plasmodium falciparum (isolate 3D7) GN=PF14_0057 PE=4 SV=1 | 1 | 1.45 | | |
| tr\|Q8IM26\|Q8IM26_PLAF7 Uncharacterized protein OS=Plasmodium falciparum (isolate 3D7) GN=PF14_0065 PE=4 SV=1 | 1 | 0.62 | | |
| tr\|Q8IM09\|Q8IM09_PLAF7 Uncharacterized protein OS=Plasmodium falciparum (isolate 3D7) GN=PF14_0084 PE=4 SV=2 | 1 | 0.92 | | |
| tr\|Q8IM01\|Q8IM01_PLAF7 Uncharacterized protein OS=Plasmodium falciparum (isolate 3D7) GN=PF14_0092 PE=4 SV=2 | 1 | 0.86 | | |
| tr\|Q8ILW0\|Q8ILW0_PLAF7 SufC ATPase, putative OS=Plasmodium falciparum (isolate 3D7) GN=PF14_0133 PE=3 SV=1 | 1 | 0.30 | | |
| tr\|Q8ILV6\|Q8ILV6_PLAF7 DNAJ protein, putative OS=Plasmodium falciparum (isolate 3D7) GN=PF14_0137 PE=4 SV=1 | 1 | 0.24 | | |
| tr\|Q8ILM5\|Q8ILM5_PLAF7 Actin-related protein homolog, arp4 homolog OS=Plasmodium falciparum (isolate 3D7) GN=PF14_0218 PE=3 SV=1 | 1 | 0.17 | | |
| tr\|Q8ILD6\|Q8ILD6_PLAF7 Uncharacterized protein OS=Plasmodium falciparum (isolate 3D7) GN=PF14_0308 PE=4 SV=1 | 1 | 0.31 | | |
| tr\|Q8ILB4\|Q8ILB4_PLAF7 Cytochrome c oxidase assembly protein, putative OS=Plasmodium falciparum (isolate 3D7) GN=PF14_0331 PE=4 SV=1 | 1 | 0.86 | | |
| tr\|Q8IKZ5\|Q8IKZ5_PLAF7 Uncharacterized protein OS=Plasmodium falciparum (isolate 3D7) GN=PF14_0456 PE=4 SV=1 | 1 | 1.36 | | |
| tr\|Q8IKX8\|Q8IKX8_PLAF7 Rrp6 homologue, putative OS=Plasmodium falciparum (isolate 3D7) GN=PF14_0473 PE=4 SV=1 | 1 | 0.88 | | |
| tr\|Q8IKT9\|Q8IKT9_PLAF7 Uncharacterized protein OS=Plasmodium falciparum (isolate 3D7) GN=PF14_0512 PE=4 SV=1 | 1 | 1.07 | | |

| | | | | |
|---|---|---|---|---|
| tr\|Q8IKS5\|Q8IKS5_PLAF7 Uncharacterized protein OS=Plasmodium falciparum (isolate 3D7) GN=PF14_0527 PE=4 SV=1 | 1 | 0.23 | | |
| tr\|Q8IKS3\|Q8IKS3_PLAF7 Gamma-adaptin, putative OS=Plasmodium falciparum (isolate 3D7) GN=PF14_0529 PE=4 SV=1 | 1 | 1.42 | | |
| tr\|Q8IKQ5\|Q8IKQ5_PLAF7 ATPase, putative OS=Plasmodium falciparum (isolate 3D7) GN=PF14_0548 PE=4 SV=1 | 1 | 1.36 | | |
| tr\|Q8IKP6\|Q8IKP6_PLAF7 Uncharacterized protein OS=Plasmodium falciparum (isolate 3D7) GN=PF14_0558 PE=4 SV=1 | 1 | 0.82 | | |
| tr\|Q8I6U9\|Q8I6U9_PLAF7 Cytochrome c1, putative OS=Plasmodium falciparum (isolate 3D7) GN=PF14_0597 PE=4 SV=1 | 1 | 0.67 | | |
| tr\|Q8IKJ5\|Q8IKJ5_PLAF7 Zinc finger protein, putative OS=Plasmodium falciparum (isolate 3D7) GN=PF14_0610 PE=4 SV=1 | 1 | 1.19 | | |
| tr\|Q8IK86\|Q8IK86_PLAF7 Uncharacterized protein OS=Plasmodium falciparum (isolate 3D7) GN=PF14_0720 PE=4 SV=1 | 1 | 0.68 | | |
| tr\|Q8I257\|Q8I257_PLAF7 Putative uncharacterized protein OS=Plasmodium falciparum (isolate 3D7) GN=PFA_0420w PE=4 SV=1 | 1 | 2.77 | | |
| tr\|Q8I254\|Q8I254_PLAF7 Putative uncharacterized protein OS=Plasmodium falciparum (isolate 3D7) GN=PFA_0435w PE=3 SV=1 | 1 | 1.13 | | |
| tr\|Q8I0V9\|Q8I0V9_PLAF7 mRNA cleavage factor-like protein, putative OS=Plasmodium falciparum (isolate 3D7) GN=PFA_0450c PE=4 SV=1 | 1 | 1.23 | | |
| sp\|O96185\|YPF08_PLAF7 Uncharacterized protein PFB0460c OS=Plasmodium falciparum (isolate 3D7) GN=PFB0460c PE=3 SV=1 | 1 | 1.20 | | |
| tr\|O97334\|O97334_PLAF7 Regulatory protein, putative OS=Plasmodium falciparum (isolate 3D7) GN=PFC0100c PE=4 SV=2 | 1 | 0.64 | | |
| tr\|O77321\|O77321_PLAF7 DNA polymerase epsilon subunit B, putative OS=Plasmodium falciparum (isolate 3D7) GN=PFC0340w PE=4 SV=1 | 1 | 1.68 | | |
| tr\|O77363\|O77363_PLAF7 Putative uncharacterized protein OS=Plasmodium falciparum (isolate 3D7) GN=PFC0545c PE=4 SV=2 | 1 | 8.94 | | |
| tr\|C0H473\|C0H473_PLAF7 Co-chaperone p23, putative OS=Plasmodium falciparum (isolate 3D7) GN=PFC0581w PE=4 SV=1 | 1 | 0.94 | | |
| tr\|C0H474\|C0H474_PLAF7 Vesicle transport v-SNARE protein, putative OS=Plasmodium falciparum (isolate 3D7) GN=PFC0582c PE=4 SV=1 | 1 | 0.19 | | |
| tr\|O97320\|O97320_PLAF7 Histone H2A OS=Plasmodium falciparum (isolate 3D7) GN=PFC0920w PE=3 SV=1;sp\|Q71UI9\|H2AV_HUMAN Histone H2A.V OS=Homo sapiens GN=H2AFV PE=1 SV=3;sp\|P0C0S5\|H2AZ_HUMAN Histone H2A.Z OS=Homo sapiens GN=H2AFZ PE=1 SV=2 | 1 | 0.91 | | |
| tr\|O97303\|O97303_PLAF7 Putative uncharacterized protein OS=Plasmodium falciparum (isolate 3D7) GN=PFC1060c PE=4 SV=1 | 1 | 0.87 | | |
| tr\|Q9U0I8\|Q9U0I8_PLAF7 Uncharacterized protein OS=Plasmodium falciparum (isolate 3D7) GN=PFD0485w PE=4 SV=1 | 1 | 1.59 | | |
| tr\|Q9U0H1\|Q9U0H1_PLAF7 DNA polymerase OS=Plasmodium falciparum (isolate 3D7) GN=PFD0590c PE=3 SV=2 | 1 | 0.86 | | |
| tr\|Q8I1V2\|Q8I1V2_PLAF7 Phosphoglycerate mutase, putative OS=Plasmodium falciparum (isolate 3D7) GN=PFD0660w PE=1 SV=1 | 1 | 1.20 | | |
| tr\|C0H4A9\|C0H4A9_PLAF7 Uncharacterized protein OS=Plasmodium falciparum (isolate 3D7) GN=PFD0815c:exon:2 PE=4 SV=1 | 1 | 2.75 | | |
| tr\|Q8IFN1\|Q8IFN1_PLAF7 Uncharacterized protein OS=Plasmodium falciparum (isolate 3D7) GN=PFD1110w PE=4 SV=1 | 1 | 0.79 | | |
| sp\|Q8IFN0\|YD115_PLAF7 Uncharacterized protein PFD1115c OS=Plasmodium falciparum (isolate 3D7) GN=PFD1115c PE=2 SV=1 | 1 | 0.83 | | |
| tr\|Q8I3U1\|Q8I3U1_PLAF7 Ubiquitin carboxyl-terminal hydrolase OS=Plasmodium falciparum (isolate 3D7) GN=PFE0835w PE=3 SV=1 | 1 | 3.23 | | |
| tr\|Q8I3K7\|Q8I3K7_PLAF7 Membrane skeletal protein IMC1-related OS=Plasmodium falciparum (isolate 3D7) GN=PFE1285w PE=4 SV=1 | 1 | 0.79 | | |
| tr\|Q8I3I8\|Q8I3I8_PLAF7 RNA helicase-1 OS=Plasmodium falciparum (isolate 3D7) GN=PFE1390w PE=4 SV=1 | 1 | 2.28 | | |
| tr\|Q8I3H0\|Q8I3H0_PLAF7 Uncharacterized protein OS=Plasmodium falciparum (isolate 3D7) GN=PFE1485w PE=4 SV=1 | 1 | 0.45 | | |
| tr\|Q8I3G9\|Q8I3G9_PLAF7 RING zinc finger protein, putative OS=Plasmodium falciparum (isolate 3D7) GN=PFE1490c PE=4 SV=1 | 1 | 0.84 | | |
| tr\|C6KSW1\|C6KSW1_PLAF7 Uncharacterized protein OS=Plasmodium falciparum (isolate 3D7) GN=PFF0570c PE=4 SV=1 | 1 | 0.75 | | |
| tr\|C6KSX9\|C6KSX9_PLAF7 Syntaxin binding protein, putative OS=Plasmodium falciparum (isolate 3D7) GN=PFF0665c PE=4 SV=1 | 1 | 4.87 | | |
| tr\|C6KSZ7\|C6KSZ7_PLAF7 Uncharacterized protein OS=Plasmodium falciparum (isolate 3D7) GN=PFF0755c PE=4 SV=1 | 1 | 2.00 | | |

| | | | | |
|---|---|---|---|---|
| tr\|C6KT20\|C6KT20_PLAF7 Uncharacterized protein OS=Plasmodium falciparum (isolate 3D7) GN=PFF0870w PE=4 SV=1 | 1 | 0.68 | | |
| tr\|C6KT32\|C6KT32_PLAF7 Uncharacterized protein OS=Plasmodium falciparum (isolate 3D7) GN=PFF0930w PE=4 SV=1 | 1 | 0.74 | | |
| tr\|C0H531\|C0H531_PLAF7 DNA primase large subunit, putative OS=Plasmodium falciparum (isolate 3D7) GN=PFI0530c PE=4 SV=1 | 1 | 1.28 | | |
| tr\|Q8I324\|Q8I324_PLAF7 Putative uncharacterized protein OS=Plasmodium falciparum (isolate 3D7) GN=PFI0625c PE=4 SV=1 | 1 | 1.38 | | |
| tr\|Q8I302\|Q8I302_PLAF7 NADH dehydrogenase, putative OS=Plasmodium falciparum (isolate 3D7) GN=PFI0735c PE=4 SV=1 | 1 | 0.83 | | |
| tr\|C0H540\|C0H540_PLAF7 Apicoplast Ufd1 OS=Plasmodium falciparum (isolate 3D7) GN=PFI0810c PE=4 SV=1 | 1 | 1.27 | | |
| tr\|Q8I612\|Q8I612_PLAF7 Uncharacterized protein OS=Plasmodium falciparum (isolate 3D7) GN=PFL0165c PE=4 SV=1 | 1 | 1.36 | | |
| tr\|Q8I5Y8\|Q8I5Y8_PLAF7 Targeted glyoxalase II OS=Plasmodium falciparum (isolate 3D7) GN=PFL0285w PE=4 SV=1 | 1 | 0.39 | | |
| tr\|Q8I5X5\|Q8I5X5_PLAF7 Uncharacterized protein OS=Plasmodium falciparum (isolate 3D7) GN=PFL0350c PE=4 SV=1 | 1 | 1.24 | | |
| tr\|Q8I5M9\|Q8I5M9_PLAF7 Uncharacterized protein OS=Plasmodium falciparum (isolate 3D7) GN=PFL0865w PE=4 SV=1 | 1 | 2.29 | | |
| tr\|Q8I5E1\|Q8I5E1_PLAF7 Uncharacterized protein OS=Plasmodium falciparum (isolate 3D7) GN=PFL1340c PE=4 SV=1 | 1 | 0.81 | | |
| tr\|Q8I5B3\|Q8I5B3_PLAF7 Uncharacterized protein OS=Plasmodium falciparum (isolate 3D7) GN=PFL1480w PE=4 SV=1 | 1 | 1.36 | | |
| tr\|Q8I4T3\|Q8I4T3_PLAF7 PFG377 protein OS=Plasmodium falciparum (isolate 3D7) GN=PFL2405c PE=4 SV=1 | 1 | 1.77 | | |
| sp\|Q8I4T1\|VPS26_PLAF7 Vacuolar protein sorting-associated protein 26 OS=Plasmodium falciparum (isolate 3D7) GN=PFL2415w PE=3 SV=1 | 1 | 10.66 | | |
| tr\|O97307\|O97307_PLAF7 Pfmc-2TM Maurers cleft two transmembrane protein OS=Plasmodium falciparum (isolate 3D7) GN=PfMC-2TM PE=4 SV=1 | 1 | 0.87 | | |
| tr\|Q8I239\|Q8I239_PLAF7 Phosphatidylinositol-4-phosphate-5-kinase OS=Plasmodium falciparum (isolate 3D7) GN=PfPIP5K/NCS PE=4 SV=1 | 1 | 1.16 | | |
| tr\|Q7K6A0\|Q7K6A0_PLAF7 cAMP-dependent protein kinase catalytic subunit OS=Plasmodium falciparum (isolate 3D7) GN=PfPKAc PE=4 SV=1 | 1 | 2.65 | | |
| tr\|Q8IKV6\|Q8IKV6_PLAF7 Rhoptry neck protein 2 OS=Plasmodium falciparum (isolate 3D7) GN=PfRON2 PE=1 SV=1 | 1 | 0.79 | | |
| sp\|Q8I423\|PF38_PLAF7 Merozoite surface protein P38 OS=Plasmodium falciparum (isolate 3D7) GN=PFS38 PE=1 SV=1 | 1 | 0.63 | | |
| tr\|C0H4M0\|C0H4M0_PLAF7 Rifin-like protein OS=Plasmodium falciparum (isolate 3D7) GN=RAMA PE=4 SV=1 | 1 | 0.66 | | |
| tr\|Q8IIK5\|Q8IIK5_PLAF7 Moving junction protein OS=Plasmodium falciparum (isolate 3D7) GN=RON4 PE=4 SV=2 | 1 | 0.69 | | |
| sp\|Q5T1C6\|THEM4_HUMAN Acyl-coenzyme A thioesterase THEM4 OS=Homo sapiens GN=THEM4 PE=1 SV=1 | 1 | 0.35 | | |
| tr\|F5H1T6\|F5H1T6_HUMAN V-type proton ATPase subunit a OS=Homo sapiens GN=ATP6V0A1 PE=1 SV=1;tr\|B7Z641\|B7Z641_HUMAN V-type proton ATPase subunit a OS=Homo sapiens GN=ATP6V0A1 PE=1 SV=1;tr\|B7Z2A9\|B7Z2A9_HUMAN V-type proton ATPase subunit a OS=Homo sapiens GN | 1 | 1.00 | | |
| tr\|F8WDN7\|F8WDN7_HUMAN Phosphatidylinositide phosphatase SAC1 OS=Homo sapiens GN=SACM1L PE=1 SV=1;tr\|E9PGZ4\|E9PGZ4_HUMAN Phosphatidylinositide phosphatase SAC1 OS=Homo sapiens GN=SACM1L PE=1 SV=1;sp\|Q9NTJ5-2\|SAC1_HUMAN Isoform 2 of Phosphatidylinositide ph | 1 | 0.18 | | |
| sp\|P00390-5\|GSHR_HUMAN Isoform 4 of Glutathione reductase, mitochondrial OS=Homo sapiens GN=GSR;sp\|P00390-4\|GSHR_HUMAN Isoform 3 of Glutathione reductase, mitochondrial OS=Homo sapiens GN=GSR;sp\|P00390-2\|GSHR_HUMAN Isoform Cytoplasmic of Glutathione reduct | 1 | 0.99 | | |
| sp\|P04406-2\|G3P_HUMAN Isoform 2 of Glyceraldehyde-3-phosphate dehydrogenase OS=Homo sapiens GN=GAPDH;sp\|P04406\|G3P_HUMAN Glyceraldehyde-3-phosphate dehydrogenase OS=Homo sapiens GN=GAPDH PE=1 SV=3;tr\|E7EUT5\|E7EUT5_HUMAN Glyceraldehyde-3-phosphate dehydroge | 1 | 3.18 | | |
| tr\|C9JIF9\|C9JIF9_HUMAN Acylamino-acid-releasing enzyme OS=Homo sapiens GN=APEH PE=1 SV=1;sp\|P13798\|ACPH_HUMAN Acylamino-acid-releasing enzyme OS=Homo sapiens GN=APEH PE=1 SV=4;tr\|H7C393\|H7C393_HUMAN Acylamino-acid-releasing enzyme (Fragment) OS=Homo sapien | 1 | 2.67 | | |

| | | | | |
|---|---|---|---|---|
| sp\|Q13228\|SBP1_HUMAN Selenium-binding protein 1 OS=Homo sapiens GN=SELENBP1 PE=1 SV=2;sp\|Q13228-4\|SBP1_HUMAN Isoform 4 of Selenium-binding protein 1 OS=Homo sapiens GN=SELENBP1;sp\|Q13228-3\|SBP1_HUMAN Isoform 3 of Selenium-binding protein 1 OS=Homo sapiens | 1 | 3.16 | | |
| sp\|P08107\|HSP71_HUMAN Heat shock 70 kDa protein 1A/1B OS=Homo sapiens GN=HSPA1A PE=1 SV=5;sp\|P08107-2\|HSP71_HUMAN Isoform 2 of Heat shock 70 kDa protein 1A/1B OS=Homo sapiens GN=HSPA1A;tr\|V9GZ37\|V9GZ37_HUMAN Heat shock 70 kDa protein 1A/1B OS=Homo sapiens | 1 | 1.00 | | |
| tr\|A0A087WXH3\|A0A087WXH3_HUMAN Folate receptor gamma OS=Homo sapiens GN=FOLR3 PE=1 SV=1;sp\|P41439-3\|FOLR3_HUMAN Isoform 3 of Folate receptor gamma OS=Homo sapiens GN=FOLR3;tr\|F5H2G8\|F5H2G8_HUMAN Folate receptor gamma (Fragment) OS=Homo sapiens GN=FOLR3 PE= | 1 | 0.98 | | |
| sp\|P11142\|HSP7C_HUMAN Heat shock cognate 71 kDa protein OS=Homo sapiens GN=HSPA8 PE=1 SV=1;tr\|E9PKE3\|E9PKE3_HUMAN Heat shock cognate 71 kDa protein OS=Homo sapiens GN=HSPA8 PE=1 SV=1;sp\|P11142-2\|HSP7C_HUMAN Isoform 2 of Heat shock cognate 71 kDa protein OS | 1 | 1.09 | | |
| sp\|P63092-3\|GNAS2_HUMAN Isoform 3 of Guanine nucleotide-binding protein G(s) subunit alpha isoforms short OS=Homo sapiens GN=GNAS;sp\|P63092-2\|GNAS2_HUMAN Isoform Gnas-2 of Guanine nucleotide-binding protein G(s) subunit alpha isoforms short OS=Homo sapiens | 1 | 0.97 | | |
| tr\|A0A0A0MQS8\|A0A0A0MQS8_HUMAN Ammonium transporter Rh type A OS=Homo sapiens GN=RHAG PE=1 SV=1;sp\|Q02094\|RHAG_HUMAN Ammonium transporter Rh type A OS=Homo sapiens GN=RHAG PE=1 SV=2;tr\|A0A087WZZ4\|A0A087WZZ4_HUMAN Ammonium transporter Rh type A OS=Homo sapi | 1 | 1.15 | | |
| sp\|P68133\|ACTS_HUMAN Actin, alpha skeletal muscle OS=Homo sapiens GN=ACTA1 PE=1 SV=1;sp\|P68032\|ACTC_HUMAN Actin, alpha cardiac muscle 1 OS=Homo sapiens GN=ACTC1 PE=1 SV=1;sp\|P63267\|ACTH_HUMAN Actin, gamma-enteric smooth muscle OS=Homo sapiens GN=ACTG2 PE=1 | 1 | 1.16 | | |
| tr\|C9JZN1\|C9JZN1_HUMAN Guanine nucleotide-binding protein G(I)/G(S)/G(T) subunit beta-2 (Fragment) OS=Homo sapiens GN=GNB2 PE=1 SV=1;tr\|C9JIS1\|C9JIS1_HUMAN Guanine nucleotide-binding protein G(I)/G(S)/G(T) subunit beta-2 (Fragment) OS=Homo sapiens GN=GNB2 | 1 | 0.87 | | |
| tr\|D6RF44\|D6RF44_HUMAN Heterogeneous nuclear ribonucleoprotein D0 (Fragment) OS=Homo sapiens GN=HNRNPD PE=1 SV=4;tr\|D6RBQ9\|D6RBQ9_HUMAN Heterogeneous nuclear ribonucleoprotein D0 (Fragment) OS=Homo sapiens GN=HNRNPD PE=1 SV=1;tr\|H0YA96\|H0YA96_HUMAN Heterog | 1 | 0.88 | | |
| tr\|F8VV61\|F8VV61_HUMAN TBC1 domain family member 15 (Fragment) OS=Homo sapiens GN=TBC1D15 PE=1 SV=1;tr\|C9JA93\|C9JA93_HUMAN TBC1 domain family member 15 (Fragment) OS=Homo sapiens GN=TBC1D15 PE=1 SV=1;sp\|Q8TC07-2\|TBC15_HUMAN Isoform 2 of TBC1 domain family | 1 | 0.97 | | |
| sp\|Q00013\|EM55_HUMAN 55 kDa erythrocyte membrane protein OS=Homo sapiens GN=MPP1 PE=1 SV=2;sp\|Q00013-2\|EM55_HUMAN Isoform 2 of 55 kDa erythrocyte membrane protein OS=Homo sapiens GN=MPP1;sp\|Q00013-3\|EM55_HUMAN Isoform 3 of 55 kDa erythrocyte membrane prote | 1 | 1.04 | | |
| tr\|K7EPB2\|K7EPB2_HUMAN cAMP-dependent protein kinase type I-alpha regulatory subunit (Fragment) OS=Homo sapiens GN=PRKAR1A PE=1 SV=1;sp\|P10644-2\|KAP0_HUMAN Isoform 2 of cAMP-dependent protein kinase type I-alpha regulatory subunit OS=Homo sapiens GN=PRKAR1 | 1 | 1.04 | | |
| sp\|P48729-3\|KC1A_HUMAN Isoform 3 of Casein kinase I isoform alpha OS=Homo sapiens GN=CSNK1A1;sp\|P48729\|KC1A_HUMAN Casein kinase I isoform alpha OS=Homo sapiens GN=CSNK1A1 PE=1 SV=2;tr\|D6REM4\|D6REM4_HUMAN Casein kinase I isoform alpha OS=Homo sapiens GN=CSN | 1 | 0.91 | | |
| sp\|P48426-2\|PI42A_HUMAN Isoform 2 of Phosphatidylinositol 5-phosphate 4-kinase type-2 alpha OS=Homo sapiens GN=PIP4K2A;sp\|P48426\|PI42A_HUMAN Phosphatidylinositol 5-phosphate 4-kinase type-2 alpha OS=Homo sapiens GN=PIP4K2A PE=1 SV=2;tr\|H7BXS3\|H7BXS3_HUMAN | 1 | 0.89 | | |
| tr\|E9PLD0\|E9PLD0_HUMAN Ras-related protein Rab-1B OS=Homo sapiens GN=RAB1B PE=1 SV=1;sp\|Q9H0U4\|RAB1B_HUMAN Ras-related protein Rab-1B OS=Homo sapiens GN=RAB1B PE=1 SV=1;tr\|E7END7\|E7END7_HUMAN Ras-related protein Rab-1A OS=Homo sapiens GN=RAB1A PE=1 SV=1;sp | 1 | 1.14 | | |
| tr\|E7EV99\|E7EV99_HUMAN Alpha-adducin OS=Homo sapiens GN=ADD1 PE=1 SV=1;tr\|E7ENY0\|E7ENY0_HUMAN Alpha-adducin OS=Homo sapiens GN=ADD1 PE=1 SV=1;sp\|P35611-2\|ADDA_HUMAN Isoform 2 of Alpha-adducin OS=Homo sapiens GN=ADD1;sp\|P35611-6\|ADDA_HUMAN Isoform 6 of Alph | 1 | 1.02 | | |

| | | | | |
|---|---|---|---|---|
| tr\|C9JEN3\|C9JEN3_HUMAN Protein lifeguard 3 (Fragment) OS=Homo sapiens GN=TMBIM1 PE=1 SV=1;tr\|C9IYT2\|C9IYT2_HUMAN Protein lifeguard 3 (Fragment) OS=Homo sapiens GN=TMBIM1 PE=1 SV=1;tr\|F8WDY4\|F8WDY4_HUMAN Protein lifeguard 3 OS=Homo sapiens GN=TMBIM1 PE=1 SV | 1 | 0.94 | | |
| sp\|P11166\|GTR1_HUMAN Solute carrier family 2, facilitated glucose transporter member 1 OS=Homo sapiens GN=SLC2A1 PE=1 SV=2;tr\|C9JIM8\|C9JIM8_HUMAN Solute carrier family 2, facilitated glucose transporter member 1 (Fragment) OS=Homo sapiens GN=SLC2A1 PE=1 SV | 1 | 1.05 | | |
| tr\|Q13030\|Q13030_HUMAN Glycophorin Erik I-IV OS=Homo sapiens GN=GPErik PE=1 SV=1;tr\|E9PH25\|E9PH25_HUMAN Glycophorin-A OS=Homo sapiens GN=GYPA PE=1 SV=1;tr\|E7EQF3\|E7EQF3_HUMAN Glycophorin-A OS=Homo sapiens GN=GYPA PE=1 SV=1;tr\|E9PD10\|E9PD10_HUMAN Glycophori | 1 | 1.17 | | |
| tr\|J3QS39\|J3QS39_HUMAN Polyubiquitin-B (Fragment) OS=Homo sapiens GN=UBB PE=1 SV=1;tr\|J3QTR3\|J3QTR3_HUMAN Ubiquitin-40S ribosomal protein S27a (Fragment) OS=Homo sapiens GN=RPS27A PE=1 SV=1;tr\|F5H6Q2\|F5H6Q2_HUMAN Polyubiquitin-C (Fragment) OS=Homo sapiens | 1 | 0.87 | | |
| sp\|P16452-2\|EPB42_HUMAN Isoform Long of Erythrocyte membrane protein band 4.2 OS=Homo sapiens GN=EPB42;sp\|P16452-3\|EPB42_HUMAN Isoform 3 of Erythrocyte membrane protein band 4.2 OS=Homo sapiens GN=EPB42;sp\|P16452\|EPB42_HUMAN Erythrocyte membrane protein ba | 1 | 1.05 | | |
| tr\|Q4VB86\|Q4VB86_HUMAN EPB41 protein OS=Homo sapiens GN=EPB41 PE=1 SV=2;sp\|P11171-4\|41_HUMAN Isoform 4 of Protein 4.1 OS=Homo sapiens GN=EPB41;sp\|P11171-2\|41_HUMAN Isoform 2 of Protein 4.1 OS=Homo sapiens GN=EPB41;sp\|P11171-3\|41_HUMAN Isoform 3 of Protein | 1 | 1.07 | | |
| sp\|Q08495-2\|DEMA_HUMAN Isoform 2 of Dematin OS=Homo sapiens GN=DMTN;sp\|Q08495\|DEMA_HUMAN Dematin OS=Homo sapiens GN=DMTN PE=1 SV=3;sp\|Q08495-3\|DEMA_HUMAN Isoform 3 of Dematin OS=Homo sapiens GN=DMTN;tr\|E5RGQ0\|E5RGQ0_HUMAN Dematin (Fragment) OS=Homo sapiens | 1 | 1.01 | | |
| sp\|P35612\|ADDB_HUMAN Beta-adducin OS=Homo sapiens GN=ADD2 PE=1 SV=3;sp\|P35612-4\|ADDB_HUMAN Isoform 4 of Beta-adducin OS=Homo sapiens GN=ADD2;sp\|P35612-3\|ADDB_HUMAN Isoform 3 of Beta-adducin OS=Homo sapiens GN=ADD2;sp\|P35612-2\|ADDB_HUMAN Isoform 2 of Beta-a | 1 | 1.04 | | |
| sp\|P11277\|SPTB1_HUMAN Spectrin beta chain, erythrocytic OS=Homo sapiens GN=SPTB PE=1 SV=5;sp\|P11277-2\|SPTB1_HUMAN Isoform 2 of Spectrin beta chain, erythrocytic OS=Homo sapiens GN=SPTB;sp\|P11277-3\|SPTB1_HUMAN Isoform 3 of Spectrin beta chain, erythrocytic | 1 | 1.03 | | |
| sp\|P63261\|ACTG_HUMAN Actin, cytoplasmic 2 OS=Homo sapiens GN=ACTG1 PE=1 SV=1;sp\|P60709\|ACTB_HUMAN Actin, cytoplasmic 1 OS=Homo sapiens GN=ACTB PE=1 SV=1;tr\|I3L4N8\|I3L4N8_HUMAN Actin, cytoplasmic 2 (Fragment) OS=Homo sapiens GN=ACTG1 PE=1 SV=4;tr\|I3L3I0\|I3L | 1 | 1.04 | | |
| sp\|P02549-2\|SPTA1_HUMAN Isoform 2 of Spectrin alpha chain, erythrocytic 1 OS=Homo sapiens GN=SPTA1;sp\|P02549\|SPTA1_HUMAN Spectrin alpha chain, erythrocytic 1 OS=Homo sapiens GN=SPTA1 PE=1 SV=5;tr\|A0A087WZE4\|A0A087WZE4_HUMAN Spectrin alpha chain, erythrocyt | 1 | 1.02 | | |
| tr\|Q5SRQ6\|Q5SRQ6_HUMAN Casein kinase II subunit beta OS=Homo sapiens GN=CSNK2B PE=1 SV=2;sp\|P67870\|CSK2B_HUMAN Casein kinase II subunit beta OS=Homo sapiens GN=CSNK2B PE=1 SV=1;tr\|N0E644\|N0E644_HUMAN Casein kinase II subunit beta OS=Homo sapiens GN=CSNK2B- | 1 | 1.06 | | |
| sp\|P16157-10\|ANK1_HUMAN Isoform Er9 of Ankyrin-1 OS=Homo sapiens GN=ANK1;sp\|P16157-8\|ANK1_HUMAN Isoform Er7 of Ankyrin-1 OS=Homo sapiens GN=ANK1;sp\|P16157-5\|ANK1_HUMAN Isoform Er3 of Ankyrin-1 OS=Homo sapiens GN=ANK1;sp\|P16157-16\|ANK1_HUMAN Isoform Er15 of | 1 | 1.03 | | |
| tr\|K7N7A8\|K7N7A8_HUMAN Uncharacterized protein (Fragment) OS=Homo sapiens PE=3 SV=2;sp\|P29972-4\|AQP1_HUMAN Isoform 4 of Aquaporin-1 OS=Homo sapiens GN=AQP1;sp\|P29972-2\|AQP1_HUMAN Isoform 2 of Aquaporin-1 OS=Homo sapiens GN=AQP1;sp\|P29972-3\|AQP1_HUMAN Isofo | 1 | 1.10 | | |
| tr\|E7EU96\|E7EU96_HUMAN Casein kinase II subunit alpha OS=Homo sapiens GN=CSNK2A1 PE=1 SV=1;tr\|Q5U5J2\|Q5U5J2_HUMAN CSNK2A1 protein OS=Homo sapiens GN=CSNK2A1 PE=1 SV=1;sp\|P68400-2\|CSK21_HUMAN Isoform 2 of Casein kinase II subunit alpha OS=Homo sapiens GN=CS | 1 | 1.05 | | |
| tr\|E7EQ47\|E7EQ47_HUMAN Blood group Rh(CE) polypeptide OS=Homo sapiens GN=RHCE PE=4 SV=1;tr\|F6XSS0\|F6XSS0_HUMAN Blood group Rh(CE) polypeptide OS=Homo sapiens GN=RHCE PE=4 SV=1;sp\|P18577-9\|RHCE_HUMAN Isoform 4g of Blood group Rh(CE) polypeptide OS=Homo sapi | 1 | 1.04 | | |

| | | | | |
|---|---|---|---|---|
| sp\|P04632\|CPNS1_HUMAN Calpain small subunit 1 OS=Homo sapiens GN=CAPNS1 PE=1 SV=1;tr\|K7EIV0\|K7EIV0_HUMAN Calpain small subunit 1 (Fragment) OS=Homo sapiens GN=CAPNS1 PE=1 SV=2;tr\|A0A075B7C0\|A0A075B7C0_HUMAN Calpain small subunit 1 (Fragment) OS=Homo sapien | 1 | 0.96 | | |
| sp\|Q08722-2\|CD47_HUMAN Isoform OA3-293 of Leukocyte surface antigen CD47 OS=Homo sapiens GN=CD47;sp\|Q08722-3\|CD47_HUMAN Isoform OA3-305 of Leukocyte surface antigen CD47 OS=Homo sapiens GN=CD47;sp\|Q08722-4\|CD47_HUMAN Isoform OA3-312 of Leukocyte surface an | 1 | 0.95 | | |
| sp\|P61586\|RHOA_HUMAN Transforming protein RhoA OS=Homo sapiens GN=RHOA PE=1 SV=1;tr\|Q5JR07\|Q5JR07_HUMAN Rho-related GTP-binding protein RhoC (Fragment) OS=Homo sapiens GN=RHOC PE=1 SV=1;tr\|C9JNR4\|C9JNR4_HUMAN Transforming protein RhoA (Fragment) OS=Homo sa | 1 | 1.03 | | |
| sp\|P06753-5\|TPM3_HUMAN Isoform 5 of Tropomyosin alpha-3 chain OS=Homo sapiens GN=TPM3;sp\|P06753-2\|TPM3_HUMAN Isoform 2 of Tropomyosin alpha-3 chain OS=Homo sapiens GN=TPM3;tr\|A0A087WWU8\|A0A087WWU8_HUMAN Tropomyosin alpha-3 chain OS=Homo sapiens GN=TPM3 PE= | 1 | 0.93 | | |
| tr\|F8WCJ1\|F8WCJ1_HUMAN Eukaryotic translation initiation factor 5A OS=Homo sapiens GN=EIF5A2 PE=1 SV=1;tr\|C9J7B5\|C9J7B5_HUMAN Eukaryotic translation initiation factor 5A OS=Homo sapiens GN=EIF5A2 PE=1 SV=1;tr\|C9J4W5\|C9J4W5_HUMAN Eukaryotic translation init | 1 | 0.85 | | |
| tr\|F8WAR7\|F8WAR7_HUMAN Acetylcholinesterase OS=Homo sapiens GN=ACHE PE=1 SV=1;tr\|C9J2S3\|C9J2S3_HUMAN Acetylcholinesterase (Fragment) OS=Homo sapiens GN=ACHE PE=1 SV=4;tr\|F8WD68\|F8WD68_HUMAN Acetylcholinesterase OS=Homo sapiens GN=ACHE PE=1 SV=1;tr\|C9JZL6\|C | 1 | 0.84 | | |
| tr\|H0YID2\|H0YID2_HUMAN Adenylate kinase isoenzyme 1 (Fragment) OS=Homo sapiens GN=AK1 PE=1 SV=1;tr\|H0Y4J6\|H0Y4J6_HUMAN Adenylate kinase isoenzyme 1 (Fragment) OS=Homo sapiens GN=AK1 PE=1 SV=1;tr\|Q5T9B7\|Q5T9B7_HUMAN Adenylate kinase isoenzyme 1 OS=Homo sapi | 1 | 0.86 | | |
| sp\|Q9NP58-4\|ABCB6_HUMAN Isoform 2 of ATP-binding cassette sub-family B member 6, mitochondrial OS=Homo sapiens GN=ABCB6;sp\|Q9NP58\|ABCB6_HUMAN ATP-binding cassette sub-family B member 6, mitochondrial OS=Homo sapiens GN=ABCB6 PE=1 SV=1;tr\|H7BXK9\|H7BXK9_HUMA | 1 | 1.09 | | |
| tr\|F5H7S3\|F5H7S3_HUMAN Tropomyosin alpha-1 chain OS=Homo sapiens GN=TPM1 PE=1 SV=2;tr\|H7BYY1\|H7BYY1_HUMAN Tropomyosin 1 (Alpha), isoform CRA_m OS=Homo sapiens GN=TPM1 PE=1 SV=1;tr\|H0YK48\|H0YK48_HUMAN Tropomyosin alpha-1 chain OS=Homo sapiens GN=TPM1 PE=1 S | 1 | 1.01 | | |
| sp\|O75340-2\|PDCD6_HUMAN Isoform 2 of Programmed cell death protein 6 OS=Homo sapiens GN=PDCD6;sp\|O75340\|PDCD6_HUMAN Programmed cell death protein 6 OS=Homo sapiens GN=PDCD6 PE=1 SV=1;tr\|A0A024QZ42\|A0A024QZ42_HUMAN HCG1985580, isoform CRA_c OS=Homo sapiens | 1 | 0.71 | | |
| tr\|H0YDX6\|H0YDX6_HUMAN CD44 antigen (Fragment) OS=Homo sapiens GN=CD44 PE=1 SV=1;tr\|H0YD13\|H0YD13_HUMAN CD44 antigen OS=Homo sapiens GN=CD44 PE=1 SV=2;tr\|H0YD17\|H0YD17_HUMAN CD44 antigen (Fragment) OS=Homo sapiens GN=CD44 PE=1 SV=4;tr\|H0YDW7\|H0YDW7_HUMAN C | 1 | 0.99 | | |
| tr\|A0A087WUV8\|A0A087WUV8_HUMAN Basigin OS=Homo sapiens GN=BSG PE=1 SV=1;sp\|P35613-3\|BASI_HUMAN Isoform 3 of Basigin OS=Homo sapiens GN=BSG;sp\|P35613-4\|BASI_HUMAN Isoform 4 of Basigin OS=Homo sapiens GN=BSG;sp\|P35613-2\|BASI_HUMAN Isoform 2 of Basigin OS=Hom | 1 | 1.10 | | |
| tr\|H0YH81\|H0YH81_HUMAN ATP synthase subunit beta (Fragment) OS=Homo sapiens GN=ATP5B PE=1 SV=1;sp\|P06576\|ATPB_HUMAN ATP synthase subunit beta, mitochondrial OS=Homo sapiens GN=ATP5B PE=1 SV=3;tr\|F8W079\|F8W079_HUMAN ATP synthase subunit beta, mitochondrial | 1 | 0.89 | | |
| tr\|Q8I3J4\|Q8I3J4_PLAF7 Ubiquitin conjugating enzyme, putative OS=Plasmodium falciparum (isolate 3D7) GN=PFE1350c PE=1 SV=1;tr\|F8VQQ8\|F8VQQ8_HUMAN Ubiquitin-conjugating enzyme E2 N OS=Homo sapiens GN=UBE2N PE=1 SV=1;sp\|P61088\|UBE2N_HUMAN Ubiquitin-conjugati | 1 | 4.10 | | |
| sp\|P23634-7\|AT2B4_HUMAN Isoform ZB of Plasma membrane calcium-transporting ATPase 4 OS=Homo sapiens GN=ATP2B4;sp\|P23634-6\|AT2B4_HUMAN Isoform XB of Plasma membrane calcium-transporting ATPase 4 OS=Homo sapiens GN=ATP2B4;sp\|P23634-8\|AT2B4_HUMAN Isoform ZD o | 1 | 1.43 | | |
| tr\|A0A087X0H7\|A0A087X0H7_HUMAN Phospholipase DDHD1 OS=Homo sapiens GN=DDHD1 PE=1 SV=1;sp\|Q8NEL9-2\|DDHD1_HUMAN Isoform 2 of Phospholipase DDHD1 OS=Homo sapiens GN=DDHD1;sp\|Q8NEL9\|DDHD1_HUMAN Phospholipase DDHD1 OS=Homo sapiens GN=DDHD1 PE=1 SV=2;tr\|G3V2P6\|G | 1 | 8.21 | | |

| | | | | |
|---|---|---|---|---|
| tr\|E9PS74\|E9PS74_HUMAN Solute carrier family 43 member 3 (Fragment) OS=Homo sapiens GN=SLC43A3 PE=1 SV=1;sp\|Q8NBI5\|S43A3_HUMAN Solute carrier family 43 member 3 OS=Homo sapiens GN=SLC43A3 PE=1 SV=2;sp\|Q8NBI5-2\|S43A3_HUMAN Isoform 2 of Solute carrier family | 1 | 0.96 | | |
| sp\|P00387-2\|NB5R3_HUMAN Isoform 2 of NADH-cytochrome b5 reductase 3 OS=Homo sapiens GN=CYB5R3;sp\|P00387\|NB5R3_HUMAN NADH-cytochrome b5 reductase 3 OS=Homo sapiens GN=CYB5R3 PE=1 SV=3;sp\|P00387-3\|NB5R3_HUMAN Isoform 3 of NADH-cytochrome b5 reductase 3 OS=Ho | 1 | 0.78 | | |
| tr\|E9PNW4\|E9PNW4_HUMAN CD59 glycoprotein OS=Homo sapiens GN=CD59 PE=1 SV=1;tr\|E9PR17\|E9PR17_HUMAN CD59 glycoprotein OS=Homo sapiens GN=CD59 PE=1 SV=1;sp\|P13987\|CD59_HUMAN CD59 glycoprotein OS=Homo sapiens GN=CD59 PE=1 SV=1;tr\|H0YET2\|H0YET2_HUMAN CD59 glyco | 1 | 0.84 | | |
| tr\|Q8I427\|Q8I427_PLAF7 Cell differentiation protein rcd1, putative OS=Plasmodium falciparum (isolate 3D7) GN=PFE0375w PE=4 SV=1;sp\|Q92600-3\|RCD1_HUMAN Isoform 3 of Cell differentiation protein RCD1 homolog OS=Homo sapiens GN=RQCD1;sp\|Q92600\|RCD1_HUMAN Cell | 1 | 2.88 | | |
| tr\|A0A087X0E3\|A0A087X0E3_HUMAN Helicase SRCAP (Fragment) OS=Homo sapiens GN=SRCAP PE=1 SV=1;tr\|A0A0A0MS59\|A0A0A0MS59_HUMAN Helicase SRCAP OS=Homo sapiens GN=SRCAP PE=1 SV=1;sp\|Q6ZRS2-3\|SRCAP_HUMAN Isoform 3 of Helicase SRCAP OS=Homo sapiens GN=SRCAP;sp\|Q6Z | 1 | 0.92 | | |
| sp\|P00915\|CAH1_HUMAN Carbonic anhydrase 1 OS=Homo sapiens GN=CA1 PE=1 SV=2;tr\|E5RH81\|E5RH81_HUMAN Carbonic anhydrase 1 (Fragment) OS=Homo sapiens GN=CA1 PE=1 SV=4;tr\|E5RHP7\|E5RHP7_HUMAN Carbonic anhydrase 1 (Fragment) OS=Homo sapiens GN=CA1 PE=1 SV=1;tr\|E5 | 1 | 1.64 | | |
| tr\|O77351\|O77351_PLAF7 Putative uncharacterized protein OS=Plasmodium falciparum (isolate 3D7) GN=PFC0490w PE=4 SV=2;tr\|C9JSE3\|C9JSE3_HUMAN Fanconi anemia group G protein (Fragment) OS=Homo sapiens GN=FANCG PE=1 SV=1;sp\|O15287\|FANCG_HUMAN Fanconi anemia gr | 1 | 0.81 | | |
| tr\|F8VQX6\|F8VQX6_HUMAN Methyltransferase-like protein 7A (Fragment) OS=Homo sapiens GN=METTL7A PE=1 SV=1;tr\|H0YI09\|H0YI09_HUMAN Methyltransferase-like protein 7A (Fragment) OS=Homo sapiens GN=METTL7A PE=1 SV=1;sp\|Q9H8H3\|MET7A_HUMAN Methyltransferase-like p | 1 | 0.39 | | |
| tr\|X6R6Z1\|X6R6Z1_HUMAN Interleukin enhancer-binding factor 2 (Fragment) OS=Homo sapiens GN=ILF2 PE=1 SV=1;tr\|A0A0A0MRL0\|A0A0A0MRL0_HUMAN Interleukin enhancer-binding factor 2 OS=Homo sapiens GN=ILF2 PE=1 SV=1;tr\|B4DY09\|B4DY09_HUMAN Interleukin enhancer-bin | 1 | 0.35 | | |
| tr\|A4QPE4\|A4QPE4_HUMAN SPTBN2 protein OS=Homo sapiens GN=SPTBN2 PE=1 SV=1;sp\|O15020-2\|SPTN2_HUMAN Isoform 2 of Spectrin beta chain, non-erythrocytic 2 OS=Homo sapiens GN=SPTBN2;sp\|O15020\|SPTN2_HUMAN Spectrin beta chain, non-erythrocytic 2 OS=Homo sapiens G | 1 | 0.31 | | |
| tr\|D6RDX1\|D6RDX1_HUMAN Vesicular integral-membrane protein VIP36 (Fragment) OS=Homo sapiens GN=LMAN2 PE=1 SV=1;tr\|D6RBV2\|D6RBV2_HUMAN Vesicular integral-membrane protein VIP36 OS=Homo sapiens GN=LMAN2 PE=1 SV=1;sp\|Q12907\|LMAN2_HUMAN Vesicular integral-memb | 1 | 0.24 | | |
| tr\|F8W810\|F8W810_HUMAN Uncharacterized protein OS=Homo sapiens PE=4 SV=1;sp\|Q2VIR3-2\|IF2GL_HUMAN Isoform 2 of Putative eukaryotic translation initiation factor 2 subunit 3-like protein OS=Homo sapiens GN=EIF2S3L;sp\|Q2VIR3\|IF2GL_HUMAN Putative eukaryotic tr | 1 | 0.18 | | |

| **OZ439** | | | | |
|---|---|---|---|---|
| **Fasta headers** | **N** | **Mean** | **SD** | **P-value** |
| tr\|Q8I563\|Q8I563_PLAF7 Uncharacterized protein OS=Plasmodium falciparum (isolate 3D7) GN=PFL1740w PE=4 SV=1 | 4 | 0.58 | 0.25 | 0.0181 |
| tr\|Q8IAW1\|Q8IAW1_PLAF7 RNA binding protein, putative OS=Plasmodium falciparum (isolate 3D7) GN=PF08_0086 PE=4 SV=1 | 4 | 0.62 | 0.21 | 0.0095 |
| tr\|C6KSV8\|C6KSV8_PLAF7 Uncharacterized protein OS=Plasmodium falciparum (isolate 3D7) GN=PFF0555w PE=4 SV=1 | 4 | 0.62 | 0.13 | 0.0023 |
| tr\|Q8I0U9\|Q8I0U9_PLAF7 Triose phosphate transporter OS=Plasmodium falciparum (isolate 3D7) GN=PfiTPT PE=4 SV=1 | 4 | 0.66 | 0.31 | 0.0236 |
| tr\|Q8IEJ6\|Q8IEJ6_PLAF7 Branched-chain alpha keto-acid dehydrogenase, putative OS=Plasmodium falciparum (isolate 3D7) GN=PF13_0070 PE=4 SV=1 | 4 | 0.69 | 0.39 | 0.0374 |
| tr\|Q8I5W2\|Q8I5W2_PLAF7 Tim10 homologue, putative OS=Plasmodium falciparum (isolate 3D7) GN=PFL0430w PE=4 SV=1 | 4 | 0.71 | 0.44 | 0.0474 |
| tr\|Q8IK82\|Q8IK82_PLAF7 Bromodomain protein, putative OS=Plasmodium falciparum (isolate 3D7) GN=PF14_0724 PE=1 SV=1 | 4 | 0.72 | 0.31 | 0.0181 |

| | | | | |
|---|---|---|---|---|
| tr\|Q8I291\|Q8I291_PLAF7 Transporter, putative OS=Plasmodium falciparum (isolate 3D7) GN=PFA_0245w PE=4 SV=1 | 4 | 0.72 | 0.25 | 0.0100 |
| tr\|Q8IJ69\|Q8IJ69_PLAF7 Sec1 family protein, putative OS=Plasmodium falciparum (isolate 3D7) GN=PF10_0331 PE=4 SV=2 | 4 | 0.73 | 0.46 | 0.0493 |
| tr\|Q8IJX4\|Q8IJX4_PLAF7 Conserved Plasmodium protein OS=Plasmodium falciparum (isolate 3D7) GN=PF10_0067 PE=4 SV=2 | 4 | 0.73 | 0.18 | 0.0037 |
| tr\|O96217\|O96217_PLAF7 Conserved Plasmodium protein OS=Plasmodium falciparum (isolate 3D7) GN=PFB0620w PE=4 SV=1 | 4 | 0.74 | 0.25 | 0.0094 |
| sp\|P50498\|MSA2_PLAF7 Merozoite surface antigen 2 OS=Plasmodium falciparum (isolate 3D7) GN=MSA2 PE=1 SV=2 | 4 | 0.75 | 0.15 | 0.0021 |
| tr\|Q8I3B3\|Q8I3B3_PLAF7 Putative uncharacterized protein OS=Plasmodium falciparum (isolate 3D7) GN=PFI0170w PE=4 SV=1 | 4 | 0.75 | 0.25 | 0.0093 |
| tr\|Q8IBL4\|Q8IBL4_PLAF7 Uncharacterized protein OS=Plasmodium falciparum (isolate 3D7) GN=MAL7P1.126 PE=4 SV=1 | 4 | 0.76 | 0.22 | 0.0066 |
| tr\|Q8IKW1\|Q8IKW1_PLAF7 Uncharacterized protein OS=Plasmodium falciparum (isolate 3D7) GN=PF14_0490 PE=4 SV=1 | 4 | 0.77 | 0.46 | 0.0444 |
| tr\|Q8I573\|Q8I573_PLAF7 Uncharacterized protein OS=Plasmodium falciparum (isolate 3D7) GN=PFL1685w PE=4 SV=1 | 4 | 0.78 | 0.21 | 0.0049 |
| tr\|O96204\|O96204_PLAF7 Conserved Plasmodium membrane protein OS=Plasmodium falciparum (isolate 3D7) GN=PFB0555c PE=4 SV=2 | 4 | 0.78 | 0.36 | 0.0227 |
| tr\|Q8I5Y7\|Q8I5Y7_PLAF7 Uncharacterized protein OS=Plasmodium falciparum (isolate 3D7) GN=PFL0290w PE=4 SV=1 | 4 | 0.80 | 0.49 | 0.0463 |
| tr\|Q8IIW6\|Q8IIW6_PLAF7 Actin-like protein, putative OS=Plasmodium falciparum (isolate 3D7) GN=PF11_0047 PE=3 SV=1 | 4 | 0.80 | 0.45 | 0.0381 |
| tr\|Q8I489\|Q8I489_PLAF7 Heat shock protein, putative OS=Plasmodium falciparum (isolate 3D7) GN=PFE0055c PE=4 SV=2 | 4 | 0.81 | 0.13 | 0.0011 |
| tr\|O77388\|O77388_PLAF7 HVA22/TB2/DP1 family protein, putative OS=Plasmodium falciparum (isolate 3D7) GN=PFC0730w PE=4 SV=1 | 4 | 0.81 | 0.14 | 0.0013 |
| tr\|Q8IBT7\|Q8IBT7_PLAF7 Uncharacterized protein OS=Plasmodium falciparum (isolate 3D7) GN=MAL7P1.77 PE=4 SV=1 | 4 | 0.82 | 0.13 | 0.0011 |
| sp\|P20073-2\|ANXA7_HUMAN Isoform 2 of Annexin A7 OS=Homo sapiens GN=ANXA7;sp\|P20073\|ANXA7_HUMAN Annexin A7 OS=Homo sapiens GN=ANXA7 PE=1 SV=3 | 4 | 0.82 | 0.29 | 0.0107 |
| tr\|Q8IJV6\|Q8IJV6_PLAF7 Adenylate kinase, putative OS=Plasmodium falciparum (isolate 3D7) GN=PF10_0086 PE=3 SV=1 | 4 | 0.82 | 0.24 | 0.0067 |
| tr\|O97245\|O97245_PLAF7 Glycerol-3-phosphate dehydrogenase OS=Plasmodium falciparum (isolate 3D7) GN=PFC0275w PE=3 SV=1 | 4 | 0.82 | 0.15 | 0.0016 |
| sp\|P63000\|RAC1_HUMAN Ras-related C3 botulinum toxin substrate 1 OS=Homo sapiens GN=RAC1 PE=1 SV=1;sp\|P63000-2\|RAC1_HUMAN Isoform B of Ras-related C3 botulinum toxin substrate 1 OS=Homo sapiens GN=RAC1 | 4 | 0.82 | 0.33 | 0.0159 |
| tr\|Q8I461\|Q8I461_PLAF7 Cation transporting P-ATPase OS=Plasmodium falciparum (isolate 3D7) GN=PfATPase3 PE=3 SV=1 | 4 | 0.83 | 0.07 | 0.0002 |
| sp\|P26447\|S10A4_HUMAN Protein S100-A4 OS=Homo sapiens GN=S100A4 PE=1 SV=1 | 4 | 0.83 | 0.17 | 0.0021 |
| tr\|O96264\|O96264_PLAF7 DEAD/DEAH box helicase, putative OS=Plasmodium falciparum (isolate 3D7) GN=PFB0860c PE=3 SV=1 | 4 | 0.83 | 0.20 | 0.0034 |
| sp\|C0H4W3\|HEPF1_PLAF7 Probable ATP-dependent helicase PF08_0048 OS=Plasmodium falciparum (isolate 3D7) GN=PF08_0048 PE=3 SV=1 | 4 | 0.84 | 0.17 | 0.0021 |
| tr\|Q7KQK4\|Q7KQK4_PLAF7 Zinc finger transcription factor (Krox1) OS=Plasmodium falciparum (isolate 3D7) GN=PFL0465c PE=4 SV=1 | 4 | 0.84 | 0.03 | 0.0000 |
| tr\|Q8I298\|Q8I298_PLAF7 Putative uncharacterized protein OS=Plasmodium falciparum (isolate 3D7) GN=PFA_0210c PE=4 SV=1 | 4 | 0.84 | 0.02 | 0.0000 |
| tr\|Q8IBA2\|Q8IBA2_PLAF7 RNA helicase, putative OS=Plasmodium falciparum (isolate 3D7) GN=MAL8P1.19 PE=3 SV=1 | 4 | 0.85 | 0.39 | 0.0234 |
| tr\|Q8IE20\|Q8IE20_PLAF7 Elongation factor Tu OS=Plasmodium falciparum (isolate 3D7) GN=MAL13P1.164 PE=3 SV=1 | 4 | 0.85 | 0.03 | 0.0000 |
| tr\|Q8ILN5\|Q8ILN5_PLAF7 Mitochondrial protein import protein TIM13, putative OS=Plasmodium falciparum (isolate 3D7) GN=PF14_0208 PE=4 SV=1 | 4 | 0.85 | 0.15 | 0.0013 |
| tr\|Q8I5B2\|Q8I5B2_PLAF7 Conserved Plasmodium protein OS=Plasmodium falciparum (isolate 3D7) GN=PFL1485w PE=4 SV=2 | 4 | 0.85 | 0.12 | 0.0008 |
| tr\|Q8I5L4\|Q8I5L4_PLAF7 Phospholipid-translocating ATPase OS=Plasmodium falciparum (isolate 3D7) GN=PFL0950c PE=4 SV=1 | 4 | 0.85 | 0.16 | 0.0018 |
| tr\|Q8IC51\|Q8IC51_PLAF7 Pfmc-2TM Maurers cleft two transmembrane protein OS=Plasmodium falciparum (isolate 3D7) GN=PfMC-2TM PE=4 SV=1 | 4 | 0.86 | 0.16 | 0.0016 |
| tr\|Q8I4W4\|Q8I4W4_PLAF7 Signal recognition particle, beta subunit, putative OS=Plasmodium falciparum (isolate 3D7) GN=PFL2245w PE=4 SV=1 | 4 | 0.86 | 0.29 | 0.0091 |

| | | | | |
|---|---|---|---|---|
| tr\|Q8I611\|Q8I611_PLAF7 Uncharacterized protein OS=Plasmodium falciparum (isolate 3D7) GN=PFL0170w PE=4 SV=1 | 4 | 0.87 | 0.05 | 0.0000 |
| tr\|Q8IL75\|Q8IL75_PLAF7 Ubiquinol-cytochrome C reductase iron-sulfur subunit, putative OS=Plasmodium falciparum (isolate 3D7) GN=PF14_0373 PE=4 SV=1 | 4 | 0.87 | 0.08 | 0.0002 |
| tr\|Q8I0V2\|Q8I0V2_PLAF7 ATP synthase subunit beta OS=Plasmodium falciparum (isolate 3D7) GN=PFL1725w PE=3 SV=1 | 4 | 0.87 | 0.07 | 0.0002 |
| tr\|Q8I202\|Q8I202_PLAF7 Uncharacterized protein OS=Plasmodium falciparum (isolate 3D7) GN=PFD0115c PE=4 SV=1 | 4 | 0.87 | 0.13 | 0.0008 |
| tr\|Q8I5A0\|Q8I5A0_PLAF7 Dihydrolipoyl dehydrogenase OS=Plasmodium falciparum (isolate 3D7) GN=PFL1550w PE=3 SV=2 | 4 | 0.87 | 0.10 | 0.0004 |
| tr\|C0H4K1\|C0H4K1_PLAF7 Centrin, putative OS=Plasmodium falciparum (isolate 3D7) GN=MAL7P1.10 PE=4 SV=1 | 4 | 0.87 | 0.14 | 0.0010 |
| tr\|Q8I2I2\|Q8I2I2_PLAF7 Organelle processing peptidase, putative OS=Plasmodium falciparum (isolate 3D7) GN=PFI1625c PE=3 SV=1 | 4 | 0.87 | 0.08 | 0.0002 |
| tr\|Q5SRQ6\|Q5SRQ6_HUMAN Casein kinase II subunit beta OS=Homo sapiens GN=CSNK2B PE=1 SV=2;sp\|P67870\|CSK2B_HUMAN Casein kinase II subunit beta OS=Homo sapiens GN=CSNK2B PE=1 SV=1 | 4 | 0.87 | 0.33 | 0.0127 |
| tr\|Q8IET3\|Q8IET3_PLAF7 SNARE protein, putative OS=Plasmodium falciparum (isolate 3D7) GN=PfVAMP8 PE=4 SV=1 | 4 | 0.88 | 0.02 | 0.0000 |
| tr\|Q8I5S7\|Q8I5S7_PLAF7 Choline transporter OS=Plasmodium falciparum (isolate 3D7) GN=PFL0620c PE=4 SV=1 | 4 | 0.88 | 0.14 | 0.0012 |
| tr\|Q8I3F0\|Q8I3F0_PLAF7 Uncharacterized protein OS=Plasmodium falciparum (isolate 3D7) GN=PFE1605w PE=4 SV=1 | 4 | 0.88 | 0.09 | 0.0003 |
| tr\|Q8I526\|Q8I526_PLAF7 Cell division protein FtsH, putative OS=Plasmodium falciparum (isolate 3D7) GN=PFL1925w PE=3 SV=1 | 4 | 0.88 | 0.05 | 0.0001 |
| tr\|Q8IIV1\|Q8IIV1_PLAF7 Histone H2B OS=Plasmodium falciparum (isolate 3D7) GN=PF11_0062 PE=3 SV=1 | 4 | 0.88 | 0.10 | 0.0004 |
| tr\|Q8II53\|Q8II53_PLAF7 Uncharacterized protein OS=Plasmodium falciparum (isolate 3D7) GN=PF11_0321 PE=4 SV=1 | 4 | 0.88 | 0.13 | 0.0009 |
| tr\|Q8IHT2\|Q8IHT2_PLAF7 Translation initiation factor eIF-1A, putative OS=Plasmodium falciparum (isolate 3D7) GN=PF11_0447 PE=3 SV=2 | 4 | 0.88 | 0.20 | 0.0032 |
| tr\|Q8II93\|Q8II93_PLAF7 Protein phosphatase, putative OS=Plasmodium falciparum (isolate 3D7) GN=PF11_0281 PE=4 SV=2 | 4 | 0.88 | 0.09 | 0.0003 |
| sp\|Q9UJC5\|SH3L2_HUMAN SH3 domain-binding glutamic acid-rich-like protein 2 OS=Homo sapiens GN=SH3BGRL2 PE=1 SV=2 | 4 | 0.88 | 0.07 | 0.0001 |
| tr\|Q8IL16\|Q8IL16_PLAF7 Uncharacterized protein OS=Plasmodium falciparum (isolate 3D7) GN=PF14_0434 PE=4 SV=1 | 4 | 0.88 | 0.12 | 0.0006 |
| tr\|Q8ILY8\|Q8ILY8_PLAF7 Uncharacterized protein OS=Plasmodium falciparum (isolate 3D7) GN=PF14_0105 PE=4 SV=1 | 4 | 0.88 | 0.14 | 0.0010 |
| tr\|Q8IBP0\|Q8IBP0_PLAF7 Uncharacterized protein OS=Plasmodium falciparum (isolate 3D7) GN=PF07_0087 PE=4 SV=1 | 4 | 0.88 | 0.07 | 0.0001 |
| tr\|O96252\|O96252_PLAF7 ATP synthase subunit alpha OS=Plasmodium falciparum (isolate 3D7) GN=PFB0795w PE=3 SV=1 | 4 | 0.88 | 0.03 | 0.0000 |
| sp\|Q6LFN2\|ZNRF1_PLAF7 RING finger protein PFF0165c OS=Plasmodium falciparum (isolate 3D7) GN=PFF0165c PE=2 SV=1 | 4 | 0.89 | 0.15 | 0.0012 |
| tr\|Q7KWI7\|Q7KWI7_PLAF7 Plasmodium exported protein OS=Plasmodium falciparum (isolate 3D7) GN=PFB0921c PE=4 SV=1 | 4 | 0.89 | 0.21 | 0.0035 |
| tr\|Q8I546\|Q8I546_PLAF7 Conserved Plasmodium membrane protein OS=Plasmodium falciparum (isolate 3D7) GN=PFL1825w PE=4 SV=1 | 4 | 0.89 | 0.07 | 0.0001 |
| tr\|O77369\|O77369_PLAF7 Putative uncharacterized protein OS=Plasmodium falciparum (isolate 3D7) GN=PFC0835c PE=4 SV=2 | 4 | 0.89 | 0.48 | 0.0348 |
| tr\|Q8I527\|Q8I527_PLAF7 Hydroxyethylthiazole kinase, putative OS=Plasmodium falciparum (isolate 3D7) GN=PFL1920c PE=4 SV=1 | 4 | 0.89 | 0.04 | 0.0000 |
| tr\|Q8I5Q3\|Q8I5Q3_PLAF7 10 kd chaperonin OS=Plasmodium falciparum (isolate 3D7) GN=Cpn10 PE=3 SV=2 | 4 | 0.89 | 0.07 | 0.0001 |
| tr\|O96230\|O96230_PLAF7 Acyl-CoA synthetase, PfACS9 OS=Plasmodium falciparum (isolate 3D7) GN=ACS9 PE=4 SV=1 | 4 | 0.89 | 0.28 | 0.0078 |
| tr\|Q8IE67\|Q8IE67_PLAF7 Phosphoribosylpyrophosphate synthetase OS=Plasmodium falciparum (isolate 3D7) GN=PF13_0143 PE=4 SV=1 | 4 | 0.89 | 0.05 | 0.0001 |
| tr\|C6KSR6\|C6KSR6_PLAF7 Uncharacterized protein OS=Plasmodium falciparum (isolate 3D7) GN=PFF0335c PE=4 SV=1 | 4 | 0.90 | 0.06 | 0.0001 |
| tr\|Q8IIK1\|Q8IIK1_PLAF7 Uncharacterized protein OS=Plasmodium falciparum (isolate 3D7) GN=PF11_0172 PE=4 SV=1 | 4 | 0.90 | 0.04 | 0.0000 |
| tr\|Q8IEQ3\|Q8IEQ3_PLAF7 Hydrolase, putative OS=Plasmodium falciparum (isolate 3D7) GN=PF13_0032 PE=4 SV=1 | 4 | 0.90 | 0.06 | 0.0001 |

| | | | | |
|---|---|---|---|---|
| sp\|O94919\|ENDD1_HUMAN Endonuclease domain-containing 1 protein OS=Homo sapiens GN=ENDOD1 PE=1 SV=2 | 4 | 0.90 | 0.10 | 0.0004 |
| tr\|Q8IL96\|Q8IL96_PLAF7 N-acetyltransferase, putative OS=Plasmodium falciparum (isolate 3D7) GN=PF14_0350 PE=4 SV=2 | 4 | 0.90 | 0.10 | 0.0004 |
| tr\|Q8I2A1\|Q8I2A1_PLAF7 Putative uncharacterized protein OS=Plasmodium falciparum (isolate 3D7) GN=PFA_0195w PE=4 SV=1 | 4 | 0.90 | 0.10 | 0.0004 |
| tr\|O77325\|O77325_PLAF7 PRP19-like protein, putative OS=Plasmodium falciparum (isolate 3D7) GN=PFC0365w PE=4 SV=1 | 4 | 0.90 | 0.09 | 0.0003 |
| tr\|Q8I5E7\|Q8I5E7_PLAF7 ATP-dependent RNA helicase, putative OS=Plasmodium falciparum (isolate 3D7) GN=PFL1310c PE=3 SV=1 | 4 | 0.90 | 0.07 | 0.0001 |
| tr\|Q8I5Q6\|Q8I5Q6_PLAF7 Thioredoxin peroxidase OS=Plasmodium falciparum (isolate 3D7) GN=PFL0725w PE=1 SV=1 | 4 | 0.90 | 0.16 | 0.0015 |
| tr\|Q8IAL3\|Q8IAL3_PLAF7 Uncharacterized protein OS=Plasmodium falciparum (isolate 3D7) GN=PF08_0135 PE=4 SV=1 | 4 | 0.90 | 0.38 | 0.0185 |
| tr\|Q8I2R8\|Q8I2R8_PLAF7 RNA binding protein, putative OS=Plasmodium falciparum (isolate 3D7) GN=PFI1175c PE=4 SV=1 | 4 | 0.90 | 0.16 | 0.0015 |
| tr\|C6KSY4\|C6KSY4_PLAF7 Organic anion transporter OS=Plasmodium falciparum (isolate 3D7) GN=PFF0690c PE=4 SV=1 | 4 | 0.90 | 0.13 | 0.0008 |
| tr\|Q8IIJ4\|Q8IIJ4_PLAF7 Uncharacterized protein OS=Plasmodium falciparum (isolate 3D7) GN=PF11_0179 PE=4 SV=1 | 4 | 0.90 | 0.06 | 0.0001 |
| sp\|Q08211\|DHX9_HUMAN ATP-dependent RNA helicase A OS=Homo sapiens GN=DHX9 PE=1 SV=4 | 4 | 0.90 | 0.14 | 0.0011 |
| tr\|Q8I5B6\|Q8I5B6_PLAF7 Heat shock protein hslv OS=Plasmodium falciparum (isolate 3D7) GN=HslV PE=4 SV=2 | 4 | 0.54 | 0.54 | 0.1361 |
| tr\|Q8I531\|Q8I531_PLAF7 Transcription factor with AP2 domain(S), putative OS=Plasmodium falciparum (isolate 3D7) GN=ApiAP2 PE=4 SV=1 | 4 | 0.90 | 0.16 | 0.0014 |
| tr\|Q8IB31\|Q8IB31_PLAF7 Uncharacterized protein OS=Plasmodium falciparum (isolate 3D7) GN=MAL8P1.62 PE=4 SV=1 | 4 | 0.91 | 0.06 | 0.0001 |
| tr\|Q8I0U8\|Q8I0U8_PLAF7 Merozoite surface protein 1 OS=Plasmodium falciparum (isolate 3D7) GN=MSP1 PE=4 SV=1 | 4 | 0.91 | 0.05 | 0.0000 |
| tr\|Q8IDE0\|Q8IDE0_PLAF7 Mitochondrial inner membrane translocase, putative OS=Plasmodium falciparum (isolate 3D7) GN=PF13_0300 PE=4 SV=1 | 4 | 0.65 | 0.44 | 0.0605 |
| tr\|O97269\|O97269_PLAF7 Putative uncharacterized protein OS=Plasmodium falciparum (isolate 3D7) GN=PFC0670c PE=4 SV=1 | 4 | 0.65 | 0.44 | 0.0596 |
| tr\|Q8IBD3\|Q8IBD3_PLAF7 Uncharacterized protein OS=Plasmodium falciparum (isolate 3D7) GN=MAL8P1.3 PE=4 SV=1 | 4 | 0.91 | 0.23 | 0.0045 |
| tr\|Q8I344\|Q8I344_PLAF7 Nucleotide binding protein, putative OS=Plasmodium falciparum (isolate 3D7) GN=PFI0525w PE=4 SV=1 | 4 | 0.68 | 0.45 | 0.0563 |
| tr\|Q8I3Q3\|Q8I3Q3_PLAF7 Uncharacterized protein OS=Plasmodium falciparum (isolate 3D7) GN=PFE1045c PE=4 SV=1 | 4 | 0.68 | 0.48 | 0.0660 |
| tr\|Q8IJC7\|Q8IJC7_PLAF7 Centrin-3 OS=Plasmodium falciparum (isolate 3D7) GN=PF10_0271 PE=4 SV=2 | 4 | 0.91 | 0.25 | 0.0052 |
| tr\|C6KSY5\|C6KSY5_PLAF7 Uncharacterized protein OS=Plasmodium falciparum (isolate 3D7) GN=PFF0695w PE=4 SV=1 | 4 | 0.69 | 0.47 | 0.0595 |
| tr\|Q8IEG8\|Q8IEG8_PLAF7 Uncharacterized protein OS=Plasmodium falciparum (isolate 3D7) GN=MAL13P1.75 PE=4 SV=1 | 4 | 0.91 | 0.05 | 0.0001 |
| sp\|O97239\|DOP1_PLAF7 Protein dopey homolog PFC0245c OS=Plasmodium falciparum (isolate 3D7) GN=PFC0245c PE=2 SV=1 | 4 | 0.91 | 0.08 | 0.0002 |
| tr\|Q8I3W9\|Q8I3W9_PLAF7 PfRab1a OS=Plasmodium falciparum (isolate 3D7) GN=Rab1a PE=3 SV=1 | 4 | 0.91 | 0.13 | 0.0007 |
| tr\|Q8IM53\|Q8IM53_PLAF7 Cytochrome c, putative OS=Plasmodium falciparum (isolate 3D7) GN=PF14_0038 PE=3 SV=1 | 4 | 0.73 | 0.75 | 0.1470 |
| tr\|Q8I377\|Q8I377_PLAF7 ATP-dependent heat shock protein, putative OS=Plasmodium falciparum (isolate 3D7) GN=PFI0355c PE=4 SV=1 | 4 | 0.91 | 0.07 | 0.0001 |
| tr\|Q8I2X3\|Q8I2X3_PLAF7 Glideosome-associated protein 50 OS=Plasmodium falciparum (isolate 3D7) GN=GAP50 PE=1 SV=1 | 4 | 0.91 | 0.09 | 0.0002 |
| sp\|Q99808\|S29A1_HUMAN Equilibrative nucleoside transporter 1 OS=Homo sapiens GN=SLC29A1 PE=1 SV=3;sp\|Q99808-2\|S29A1_HUMAN Isoform 2 of Equilibrative nucleoside transporter 1 OS=Homo sapiens GN=SLC29A1 | 4 | 0.74 | 0.69 | 0.1230 |
| tr\|C6KT04\|C6KT04_PLAF7 Uncharacterized protein OS=Plasmodium falciparum (isolate 3D7) GN=PFF0790c PE=4 SV=1 | 4 | 0.91 | 0.06 | 0.0001 |
| tr\|Q8IFP5\|Q8IFP5_PLAF7 Uncharacterized protein OS=Plasmodium falciparum (isolate 3D7) GN=PFD1037w PE=4 SV=1 | 4 | 0.91 | 0.09 | 0.0003 |
| tr\|Q8I5S8\|Q8I5S8_PLAF7 Uncharacterized protein OS=Plasmodium falciparum (isolate 3D7) GN=PFL0615w PE=4 SV=1 | 4 | 0.75 | 0.77 | 0.1487 |

| | | | | |
|---|---|---|---|---|
| tr\|Q8IBI5\|Q8IBI5_PLAF7 Cysteine desulfurase, putative OS=Plasmodium falciparum (isolate 3D7) GN=MAL7P1.150 PE=3 SV=1 | 4 | 0.91 | 0.08 | 0.0002 |
| tr\|Q8I2W2\|Q8I2W2_PLAF7 DNAJ-like molecular chaperone protein, putative OS=Plasmodium falciparum (isolate 3D7) GN=PFI0935w PE=4 SV=1 | 4 | 0.91 | 0.10 | 0.0004 |
| tr\|Q8I564\|Q8I564_PLAF7 Uncharacterized protein OS=Plasmodium falciparum (isolate 3D7) GN=PFL1735c PE=4 SV=1 | 4 | 0.91 | 0.13 | 0.0008 |
| tr\|Q8I6T2\|Q8I6T2_PLAF7 Isocitrate dehydrogenase [NADP] OS=Plasmodium falciparum (isolate 3D7) GN=PF13_0242 PE=3 SV=1 | 4 | 0.91 | 0.03 | 0.0000 |
| tr\|Q8ILL1\|Q8ILL1_PLAF7 Uncharacterized protein OS=Plasmodium falciparum (isolate 3D7) GN=PF14_0232 PE=4 SV=1 | 4 | 0.91 | 0.05 | 0.0000 |
| tr\|Q8IK07\|Q8IK07_PLAF7 Conserved Plasmodium protein OS=Plasmodium falciparum (isolate 3D7) GN=PF10_0033 PE=4 SV=2 | 4 | 0.91 | 0.10 | 0.0004 |
| tr\|Q8IKZ6\|Q8IKZ6_PLAF7 Multidrug resistance protein 2 (Heavy metal transport family) OS=Plasmodium falciparum (isolate 3D7) GN=PfMDR2 PE=3 SV=1 | 4 | 0.91 | 0.08 | 0.0002 |
| tr\|Q8I517\|Q8I517_PLAF7 Uncharacterized protein OS=Plasmodium falciparum (isolate 3D7) GN=PFL1980c PE=4 SV=1 | 4 | 0.91 | 0.08 | 0.0002 |
| tr\|Q8IDB8\|Q8IDB8_PLAF7 Uncharacterized protein OS=Plasmodium falciparum (isolate 3D7) GN=MAL13P1.288 PE=4 SV=1 | 4 | 0.91 | 0.07 | 0.0001 |
| tr\|C0H4Q1\|C0H4Q1_PLAF7 Uncharacterized protein OS=Plasmodium falciparum (isolate 3D7) GN=PF07_0120 PE=4 SV=1 | 4 | 0.92 | 0.08 | 0.0002 |
| sp\|O77384\|LRR4_PLAF7 Protein PFC0760c OS=Plasmodium falciparum (isolate 3D7) GN=PFC0760c PE=4 SV=1 | 4 | 0.92 | 0.02 | 0.0000 |
| tr\|Q8IBP8\|Q8IBP8_PLAF7 Ferrodoxin reductase-like protein OS=Plasmodium falciparum (isolate 3D7) GN=PF07_0085 PE=4 SV=1 | 4 | 0.92 | 0.47 | 0.0305 |
| tr\|Q9U0N4\|Q9U0N4_PLAF7 ABC transporter, (CT family), putative OS=Plasmodium falciparum (isolate 3D7) GN=PfMRP PE=3 SV=1 | 4 | 0.92 | 0.08 | 0.0002 |
| tr\|Q8I0V5\|Q8I0V5_PLAF7 Acyl carrier protein OS=Plasmodium falciparum (isolate 3D7) GN=PFL0415w PE=4 SV=1 | 4 | 0.83 | 0.59 | 0.0671 |
| tr\|O97227\|O97227_PLAF7 Dihydrolipoamide acyltransferase, putative OS=Plasmodium falciparum (isolate 3D7) GN=PFC0170c PE=3 SV=1 | 4 | 0.92 | 0.02 | 0.0000 |
| tr\|Q8IIA9\|Q8IIA9_PLAF7 Mitochondrial inner membrane translocase subunit TIM44, putative OS=Plasmodium falciparum (isolate 3D7) GN=PF11_0265 PE=4 SV=2 | 4 | 0.92 | 0.10 | 0.0004 |
| tr\|Q8IKV8\|Q8IKV8_PLAF7 Sortilin, putative OS=Plasmodium falciparum (isolate 3D7) GN=PF14_0493 PE=4 SV=1 | 4 | 0.92 | 0.04 | 0.0000 |
| sp\|Q8I3H7\|TIP_PLAF7 T-cell immunomodulatory protein homolog OS=Plasmodium falciparum (isolate 3D7) GN=PFE1445c PE=3 SV=1 | 4 | 0.92 | 0.08 | 0.0002 |
| tr\|Q8I328\|Q8I328_PLAF7 Putative uncharacterized protein OS=Plasmodium falciparum (isolate 3D7) GN=PFI0605c PE=4 SV=1 | 4 | 0.92 | 0.07 | 0.0001 |
| tr\|Q76NM4\|Q76NM4_PLAF7 Rab11a, GTPase OS=Plasmodium falciparum (isolate 3D7) GN=Rab11a PE=1 SV=1 | 4 | 0.92 | 0.21 | 0.0030 |
| tr\|Q8IB72\|Q8IB72_PLAF7 DNAJ protein, putative OS=Plasmodium falciparum (isolate 3D7) GN=PF08_0032 PE=4 SV=1 | 4 | 0.92 | 0.03 | 0.0000 |
| tr\|Q8IET5\|Q8IET5_PLAF7 Uncharacterized protein OS=Plasmodium falciparum (isolate 3D7) GN=MAL13P1.15 PE=4 SV=1 | 4 | 0.85 | 0.61 | 0.0678 |
| tr\|Q9NFA0\|Q9NFA0_PLAF7 Signal peptidase, putative OS=Plasmodium falciparum (isolate 3D7) GN=PFC0912w PE=4 SV=1 | 4 | 0.92 | 0.07 | 0.0001 |
| tr\|Q8IBF1\|Q8IBF1_PLAF7 Uncharacterized protein OS=Plasmodium falciparum (isolate 3D7) GN=MAL7P1.172 PE=4 SV=1 | 4 | 0.92 | 0.05 | 0.0000 |
| tr\|Q8IEJ5\|Q8IEJ5_PLAF7 Uncharacterized protein OS=Plasmodium falciparum (isolate 3D7) GN=PF13_0071 PE=4 SV=1 | 4 | 0.92 | 0.03 | 0.0000 |
| tr\|Q8IAN7\|Q8IAN7_PLAF7 Tubulin gamma chain OS=Plasmodium falciparum (isolate 3D7) GN=g-tub PE=3 SV=1 | 4 | 0.92 | 0.08 | 0.0002 |
| tr\|Q8IAK9\|Q8IAK9_PLAF7 Uncharacterized protein OS=Plasmodium falciparum (isolate 3D7) GN=PF08_0137 PE=4 SV=1 | 4 | 0.92 | 0.08 | 0.0002 |
| tr\|Q8II24\|Q8II24_PLAF7 Heat shock protein hsp70 homologue OS=Plasmodium falciparum (isolate 3D7) GN=PF11_0351 PE=3 SV=1 | 4 | 0.92 | 0.04 | 0.0000 |
| tr\|Q8IK02\|Q8IK02_PLAF7 Ribosomal protein S20e, putative OS=Plasmodium falciparum (isolate 3D7) GN=PF10_0038 PE=1 SV=1 | 4 | 0.92 | 0.52 | 0.0377 |
| tr\|Q8IJD0\|Q8IJD0_PLAF7 Merozoite capping protein 1 OS=Plasmodium falciparum (isolate 3D7) GN=PF10_0268 PE=4 SV=1 | 4 | 0.93 | 0.06 | 0.0001 |
| tr\|C0H488\|C0H488_PLAF7 Uncharacterized protein OS=Plasmodium falciparum (isolate 3D7) GN=PFD0170c PE=4 SV=1 | 4 | 0.93 | 0.06 | 0.0001 |
| tr\|Q8II94\|Q8II94_PLAF7 Small nuclear ribonucleoprotein F OS=Plasmodium falciparum (isolate 3D7) GN=PF11_0280 PE=3 SV=2 | 4 | 0.87 | 0.58 | 0.0563 |
| tr\|Q8I1X3\|Q8I1X3_PLAF7 Secy-independent transporter protein, putative OS=Plasmodium falciparum (isolate 3D7) GN=PFD0275w PE=4 SV=2 | 4 | 0.93 | 0.03 | 0.0000 |

| | | | | |
|---|---|---|---|---|
| tr\|Q8IE43\|Q8IE43_PLAF7 Uncharacterized protein OS=Plasmodium falciparum (isolate 3D7) GN=PF13_0154 PE=4 SV=1 | 4 | 0.93 | 0.10 | 0.0003 |
| tr\|Q8IHR8\|Q8IHR8_PLAF7 PfRab6, GTPase OS=Plasmodium falciparum (isolate 3D7) GN=Rab6 PE=3 SV=2 | 4 | 0.93 | 0.06 | 0.0001 |
| sp\|Q8ILT5\|SEY1_PLAF7 Protein SEY1 homolog OS=Plasmodium falciparum (isolate 3D7) GN=PF14_0159 PE=3 SV=2 | 4 | 0.93 | 0.08 | 0.0002 |
| tr\|Q8IKZ8\|Q8IKZ8_PLAF7 Uncharacterized protein OS=Plasmodium falciparum (isolate 3D7) GN=PF14_0453 PE=4 SV=1 | 4 | 0.93 | 0.05 | 0.0001 |
| tr\|Q8I510\|Q8I510_PLAF7 Uncharacterized protein OS=Plasmodium falciparum (isolate 3D7) GN=PFL2015w PE=4 SV=1 | 4 | 0.93 | 0.08 | 0.0002 |
| tr\|Q8IBU1\|Q8IBU1_PLAF7 Zinc transporter, putative OS=Plasmodium falciparum (isolate 3D7) GN=PF07_0065 PE=4 SV=1 | 4 | 0.93 | 0.13 | 0.0007 |
| tr\|Q8IBV7\|Q8IBV7_PLAF7 Histone H2B OS=Plasmodium falciparum (isolate 3D7) GN=PF07_0054 PE=3 SV=1 | 4 | 0.93 | 0.11 | 0.0005 |
| tr\|Q8IJF2\|Q8IJF2_PLAF7 Conserved Plasmodium protein OS=Plasmodium falciparum (isolate 3D7) GN=PF10_0246 PE=4 SV=2 | 4 | 0.93 | 0.06 | 0.0001 |
| tr\|O96145\|O96145_PLAF7 UbiE/COQ5 methyltransferase family, putative OS=Plasmodium falciparum (isolate 3D7) GN=PFB0220w PE=3 SV=1 | 4 | 0.93 | 0.13 | 0.0008 |
| tr\|C6KSL9\|C6KSL9_PLAF7 Uncharacterized protein OS=Plasmodium falciparum (isolate 3D7) GN=PFF0090w PE=4 SV=1 | 4 | 0.93 | 0.10 | 0.0003 |
| tr\|Q8ILB6\|Q8ILB6_PLAF7 Uncharacterized protein OS=Plasmodium falciparum (isolate 3D7) GN=PF14_0329 PE=4 SV=1 | 4 | 0.93 | 0.06 | 0.0001 |
| tr\|Q8I3N3\|Q8I3N3_PLAF7 Mitochondrial processing peptidase alpha subunit, putative OS=Plasmodium falciparum (isolate 3D7) GN=PFE1155c PE=3 SV=2 | 4 | 0.93 | 0.05 | 0.0001 |
| tr\|C0H4M6\|C0H4M6_PLAF7 Regulator of chromosome condensation, putative OS=Plasmodium falciparum (isolate 3D7) GN=MAL7P1.38 PE=4 SV=1 | 4 | 0.93 | 0.06 | 0.0001 |
| tr\|Q8IDH5\|Q8IDH5_PLAF7 Thioredoxin-related protein, putative OS=Plasmodium falciparum (isolate 3D7) GN=PF13_0272 PE=4 SV=1 | 4 | 0.94 | 0.08 | 0.0002 |
| sp\|P62344\|CDPK1_PLAF7 Calcium-dependent protein kinase 1 OS=Plasmodium falciparum (isolate 3D7) GN=CPK1 PE=3 SV=2 | 4 | 0.94 | 0.13 | 0.0007 |
| tr\|Q8IKL1\|Q8IKL1_PLAF7 Uncharacterized protein OS=Plasmodium falciparum (isolate 3D7) GN=PF14_0593 PE=4 SV=1 | 4 | 0.94 | 0.09 | 0.0002 |
| tr\|Q8IEE2\|Q8IEE2_PLAF7 Uncharacterized protein OS=Plasmodium falciparum (isolate 3D7) GN=PF13_0099 PE=4 SV=1 | 4 | 0.94 | 0.11 | 0.0005 |
| tr\|Q8IIB6\|Q8IIB6_PLAF7 GrpE protein homolog OS=Plasmodium falciparum (isolate 3D7) GN=PF11_0258 PE=3 SV=2 | 4 | 0.94 | 0.04 | 0.0000 |
| tr\|O97320\|O97320_PLAF7 Histone H2A OS=Plasmodium falciparum (isolate 3D7) GN=PFC0920w PE=3 SV=1 | 4 | 0.94 | 0.04 | 0.0000 |
| tr\|C6KSR8\|C6KSR8_PLAF7 Translation initiation factor IF-2, putative OS=Plasmodium falciparum (isolate 3D7) GN=PFF0345w PE=4 SV=1 | 4 | 0.94 | 0.34 | 0.0114 |
| tr\|Q8I5S4\|Q8I5S4_PLAF7 Bromodomain protein, putative OS=Plasmodium falciparum (isolate 3D7) GN=PFL0635c PE=4 SV=1 | 4 | 0.94 | 0.11 | 0.0005 |
| tr\|Q8I3A2\|Q8I3A2_PLAF7 Bacterial histone-like protein OS=Plasmodium falciparum (isolate 3D7) GN=PfHU PE=4 SV=1 | 4 | 0.94 | 0.06 | 0.0001 |
| tr\|Q8IC42\|Q8IC42_PLAF7 Uncharacterized protein OS=Plasmodium falciparum (isolate 3D7) GN=PF07_0008 PE=4 SV=1 | 4 | 0.94 | 0.13 | 0.0008 |
| tr\|Q8II26\|Q8II26_PLAF7 Conserved Plasmodium protein OS=Plasmodium falciparum (isolate 3D7) GN=PF11_0349 PE=4 SV=2 | 4 | 0.94 | 0.35 | 0.0125 |
| tr\|Q8I415\|Q8I415_PLAF7 Single-strand binding protein, putative OS=Plasmodium falciparum (isolate 3D7) GN=PFE0435c PE=1 SV=1 | 4 | 0.94 | 0.12 | 0.0006 |
| sp\|Q8I6U8\|GBP_PLAF7 Glycophorin-binding protein OS=Plasmodium falciparum (isolate 3D7) GN=GBP PE=3 SV=1 | 4 | 0.94 | 0.20 | 0.0026 |
| tr\|Q8IL71\|Q8IL71_PLAF7 Vesicle-associated membrane protein, putative OS=Plasmodium falciparum (isolate 3D7) GN=PF14_0377 PE=4 SV=1 | 4 | 0.94 | 0.04 | 0.0000 |
| tr\|Q8I3F1\|Q8I3F1_PLAF7 Uncharacterized protein OS=Plasmodium falciparum (isolate 3D7) GN=PFE1600w PE=4 SV=1 | 4 | 0.94 | 0.09 | 0.0002 |
| tr\|Q8IIV2\|Q8IIV2_PLAF7 Histone H4 OS=Plasmodium falciparum (isolate 3D7) GN=PF11_0061 PE=3 SV=1 | 4 | 0.94 | 0.23 | 0.0038 |
| tr\|Q8I420\|Q8I420_PLAF7 Triose phosphate transporter OS=Plasmodium falciparum (isolate 3D7) GN=PfoTPT PE=4 SV=1 | 4 | 0.94 | 0.12 | 0.0005 |
| tr\|Q8II83\|Q8II83_PLAF7 Uncharacterized protein OS=Plasmodium falciparum (isolate 3D7) GN=PF11_0291 PE=4 SV=1 | 4 | 0.94 | 0.06 | 0.0001 |
| tr\|C6KT82\|C6KT82_PLAF7 Smarca-related protein OS=Plasmodium falciparum (isolate 3D7) GN=PFF1185w PE=4 SV=1 | 4 | 0.94 | 0.07 | 0.0001 |
| tr\|Q8IDP8\|Q8IDP8_PLAF7 Aspartate carbamoyltransferase OS=Plasmodium falciparum (isolate 3D7) GN=atcasE PE=3 SV=1 | 4 | 0.94 | 0.08 | 0.0002 |

| | | | | |
|---|---|---|---|---|
| tr\|C0H4W6\|C0H4W6_PLAF7 Sec61 beta subunit, putative OS=Plasmodium falciparum (isolate 3D7) GN=MAL8P1.51 PE=4 SV=1 | 4 | 0.94 | 0.10 | 0.0003 |
| tr\|Q8IBC3\|Q8IBC3_PLAF7 Prohibitin, putative OS=Plasmodium falciparum (isolate 3D7) GN=PF08_0006 PE=4 SV=1 | 4 | 0.94 | 0.08 | 0.0002 |
| tr\|Q8IIH4\|Q8IIH4_PLAF7 U2 snRNP auxiliary factor, small subunit, putative OS=Plasmodium falciparum (isolate 3D7) GN=PF11_0200 PE=4 SV=1 | 4 | 0.94 | 0.21 | 0.0027 |
| tr\|Q8IL32\|Q8IL32_PLAF7 HSP90 OS=Plasmodium falciparum (isolate 3D7) GN=PF14_0417 PE=1 SV=1 | 4 | 0.94 | 0.04 | 0.0000 |
| tr\|Q8IJN9\|Q8IJN9_PLAF7 Hsp60 OS=Plasmodium falciparum (isolate 3D7) GN=PF10_0153 PE=3 SV=1 | 4 | 0.94 | 0.07 | 0.0001 |
| tr\|Q8IKY7\|Q8IKY7_PLAF7 SNARE protein, putative OS=Plasmodium falciparum (isolate 3D7) GN=PfVti1 PE=4 SV=1 | 4 | 0.95 | 0.12 | 0.0006 |
| tr\|C0H5M6\|C0H5M6_PLAF7 Uncharacterized protein OS=Plasmodium falciparum (isolate 3D7) GN=MAL13P1.465 PE=4 SV=1 | 4 | 0.95 | 0.10 | 0.0003 |
| tr\|Q8IE52\|Q8IE52_PLAF7 Chromatin assembly factor 1 subunit, putative OS=Plasmodium falciparum (isolate 3D7) GN=PF13_0149 PE=4 SV=1 | 4 | 0.95 | 0.10 | 0.0003 |
| tr\|Q8I0V3\|Q8I0V3_PLAF7 Chaperonin, cpn60 OS=Plasmodium falciparum (isolate 3D7) GN=PFL1545c PE=3 SV=2 | 4 | 0.95 | 0.08 | 0.0002 |
| tr\|O97336\|O97336_PLAF7 Putative uncharacterized protein OS=Plasmodium falciparum (isolate 3D7) GN=PFC0085c PE=4 SV=2 | 4 | 0.95 | 0.09 | 0.0002 |
| tr\|O96191\|O96191_PLAF7 Conserved Plasmodium protein OS=Plasmodium falciparum (isolate 3D7) GN=PFB0490c PE=4 SV=1 | 4 | 0.95 | 0.07 | 0.0001 |
| tr\|Q8IM36\|Q8IM36_PLAF7 Ribosome biogenesis protein BOP1 homolog OS=Plasmodium falciparum (isolate 3D7) GN=PF14_0055 PE=3 SV=1 | 4 | 0.95 | 0.10 | 0.0003 |
| sp\|P46468\|CDAT_PLAF7 Putative cell division cycle ATPase OS=Plasmodium falciparum (isolate 3D7) GN=PF07_0047 PE=3 SV=2 | 4 | 0.95 | 0.02 | 0.0000 |
| tr\|Q8IKD1\|Q8IKD1_PLAF7 Uncharacterized protein OS=Plasmodium falciparum (isolate 3D7) GN=PF14_0674 PE=4 SV=1 | 4 | 0.95 | 0.12 | 0.0005 |
| tr\|Q8ILD4\|Q8ILD4_PLAF7 Uncharacterized protein OS=Plasmodium falciparum (isolate 3D7) GN=PF14_0310 PE=4 SV=1 | 4 | 0.95 | 0.07 | 0.0001 |
| tr\|Q8IJ37\|Q8IJ37_PLAF7 Pyruvate kinase OS=Plasmodium falciparum (isolate 3D7) GN=PF10_0363 PE=3 SV=1 | 4 | 0.95 | 0.04 | 0.0000 |
| tr\|O96275\|O96275_PLAF7 Liver stage antigen 3 OS=Plasmodium falciparum (isolate 3D7) GN=PFB0915w PE=4 SV=1 | 4 | 0.95 | 0.14 | 0.0009 |
| tr\|Q8IJG6\|Q8IJG6_PLAF7 Uncharacterized protein OS=Plasmodium falciparum (isolate 3D7) GN=PF10_0232 PE=4 SV=1 | 4 | 0.95 | 0.03 | 0.0000 |
| tr\|Q8IDZ5\|Q8IDZ5_PLAF7 Transmembrane protein Tmp21 homologue, putative OS=Plasmodium falciparum (isolate 3D7) GN=MAL13P1.171 PE=4 SV=1 | 4 | 0.95 | 0.05 | 0.0000 |
| tr\|Q8IDZ8\|Q8IDZ8_PLAF7 Cochaperonin OS=Plasmodium falciparum (isolate 3D7) GN=PfCpn20 PE=3 SV=1 | 4 | 0.95 | 0.07 | 0.0001 |
| tr\|Q8IL56\|Q8IL56_PLAF7 Structure specific recognition protein OS=Plasmodium falciparum (isolate 3D7) GN=PF14_0393 PE=4 SV=1 | 4 | 0.95 | 0.03 | 0.0000 |
| tr\|Q8IBD0\|Q8IBD0_PLAF7 Uncharacterized protein OS=Plasmodium falciparum (isolate 3D7) GN=PF08_0004 PE=4 SV=1 | 4 | 0.95 | 0.11 | 0.0005 |
| tr\|Q76NM7\|Q76NM7_PLAF7 Rab5b, GTPase OS=Plasmodium falciparum (isolate 3D7) GN=Rab5b PE=3 SV=1 | 4 | 0.95 | 0.07 | 0.0001 |
| tr\|Q8IK20\|Q8IK20_PLAF7 Uncharacterized protein OS=Plasmodium falciparum (isolate 3D7) GN=PF10_0020 PE=4 SV=1 | 4 | 0.95 | 0.48 | 0.0284 |
| tr\|Q8IHN4\|Q8IHN4_PLAF7 Antigen 332, DBL-like protein OS=Plasmodium falciparum (isolate 3D7) GN=PF11_0506 PE=4 SV=2 | 4 | 0.95 | 0.04 | 0.0000 |
| tr\|Q8I0W7\|Q8I0W7_PLAF7 Snrnp protein, putative OS=Plasmodium falciparum (isolate 3D7) GN=PFE0925c PE=3 SV=1 | 4 | 0.95 | 0.27 | 0.0058 |
| tr\|Q8IJ76\|Q8IJ76_PLAF7 Uncharacterized protein OS=Plasmodium falciparum (isolate 3D7) GN=PF10_0323 PE=4 SV=1 | 4 | 0.95 | 0.07 | 0.0001 |
| tr\|Q8I240\|Q8I240_PLAF7 Bromodomain protein, putative OS=Plasmodium falciparum (isolate 3D7) GN=PFA_0510w PE=1 SV=1 | 4 | 0.92 | 0.66 | 0.0682 |
| tr\|Q9U0N1\|Q9U0N1_PLAF7 Glutamic acid-rich protein (Garp) OS=Plasmodium falciparum (isolate 3D7) GN=PFA_0620c PE=4 SV=1 | 4 | 0.96 | 0.07 | 0.0001 |
| tr\|Q8I289\|Q8I289_PLAF7 Putative uncharacterized protein OS=Plasmodium falciparum (isolate 3D7) GN=PFA_0255c PE=4 SV=1 | 4 | 0.96 | 0.13 | 0.0007 |
| tr\|Q8ID46\|Q8ID46_PLAF7 Uncharacterized protein OS=Plasmodium falciparum (isolate 3D7) GN=MAL13P1.333 PE=4 SV=1 | 4 | 0.96 | 0.37 | 0.0137 |
| tr\|Q8I206\|Q8I206_PLAF7 Uncharacterized protein OS=Plasmodium falciparum (isolate 3D7) GN=PFD0090c PE=4 SV=1 | 4 | 0.96 | 0.07 | 0.0001 |
| tr\|Q8IEC8\|Q8IEC8_PLAF7 DnaJ/SEC63 protein, putative OS=Plasmodium falciparum (isolate 3D7) GN=PF13_0102 PE=4 SV=1 | 4 | 0.96 | 0.05 | 0.0000 |

| | | | | |
|---|---|---|---|---|
| tr\|Q8IKC8\|Q8IKC8_PLAF7 Exported protein 2 OS=Plasmodium falciparum (isolate 3D7) GN=EXP-2 PE=4 SV=1 | 4 | 0.96 | 0.06 | 0.0001 |
| tr\|Q8ILE3\|Q8ILE3_PLAF7 Uncharacterized protein OS=Plasmodium falciparum (isolate 3D7) GN=PF14_0301 PE=4 SV=1 | 4 | 0.96 | 0.10 | 0.0003 |
| tr\|C0H5J5\|C0H5J5_PLAF7 Polyadenylate-binding protein, putative OS=Plasmodium falciparum (isolate 3D7) GN=MAL13P1.303 PE=4 SV=1 | 4 | 0.96 | 0.07 | 0.0001 |
| tr\|Q8IFM0\|Q8IFM0_PLAF7 Uncharacterized protein OS=Plasmodium falciparum (isolate 3D7) GN=PFD1170c PE=4 SV=1 | 4 | 0.96 | 0.05 | 0.0000 |
| tr\|Q8I5K4\|Q8I5K4_PLAF7 Chromodomain protein OS=Plasmodium falciparum (isolate 3D7) GN=PFL1005c PE=4 SV=1 | 4 | 0.96 | 0.08 | 0.0001 |
| tr\|Q8I0U6\|Q8I0U6_PLAF7 DNAJ protein, putative OS=Plasmodium falciparum (isolate 3D7) GN=RESA PE=4 SV=1 | 4 | 0.96 | 0.05 | 0.0001 |
| tr\|Q8IIC8\|Q8IIC8_PLAF7 Uncharacterized protein OS=Plasmodium falciparum (isolate 3D7) GN=PF11_0246 PE=4 SV=1 | 4 | 0.96 | 0.07 | 0.0001 |
| tr\|Q8I487\|Q8I487_PLAF7 Skeleton-binding protein 1 OS=Plasmodium falciparum (isolate 3D7) GN=PfSBP1 PE=4 SV=1 | 4 | 0.96 | 0.11 | 0.0004 |
| tr\|Q8IL07\|Q8IL07_PLAF7 Centrin-2 OS=Plasmodium falciparum (isolate 3D7) GN=CEN2 PE=4 SV=1 | 4 | 0.96 | 0.10 | 0.0003 |
| tr\|Q8IEQ6\|Q8IEQ6_PLAF7 Uncharacterized protein OS=Plasmodium falciparum (isolate 3D7) GN=PF13_0031 PE=4 SV=1 | 4 | 0.96 | 0.06 | 0.0001 |
| tr\|Q8ILZ1\|Q8ILZ1_PLAF7 Rhoptry-associated protein 1, RAP1 OS=Plasmodium falciparum (isolate 3D7) GN=PF14_0102 PE=4 SV=1 | 4 | 0.96 | 0.06 | 0.0001 |
| tr\|Q8I5Q2\|Q8I5Q2_PLAF7 Uncharacterized protein OS=Plasmodium falciparum (isolate 3D7) GN=PFL0745c PE=4 SV=1 | 4 | 0.96 | 0.11 | 0.0004 |
| tr\|Q8IK17\|Q8IK17_PLAF7 Uncharacterized protein OS=Plasmodium falciparum (isolate 3D7) GN=PF10_0023 PE=4 SV=1 | 4 | 0.96 | 0.10 | 0.0003 |
| tr\|Q8I5T3\|Q8I5T3_PLAF7 p-type ATPase, putative OS=Plasmodium falciparum (isolate 3D7) GN=PFL0590c PE=3 SV=1 | 4 | 0.96 | 0.08 | 0.0002 |
| tr\|Q8IBY8\|Q8IBY8_PLAF7 Uncharacterized protein OS=Plasmodium falciparum (isolate 3D7) GN=PF07_0042 PE=4 SV=1 | 4 | 0.96 | 0.09 | 0.0002 |
| tr\|Q8ILB0\|Q8ILB0_PLAF7 Uncharacterized protein OS=Plasmodium falciparum (isolate 3D7) GN=PF14_0335 PE=4 SV=1 | 4 | 0.96 | 0.07 | 0.0001 |
| tr\|Q8III6\|Q8III6_PLAF7 Heat shock protein 90, putative OS=Plasmodium falciparum (isolate 3D7) GN=PF11_0188 PE=3 SV=1 | 4 | 0.96 | 0.02 | 0.0000 |
| tr\|Q8II41\|Q8II41_PLAF7 Conserved Plasmodium membrane protein OS=Plasmodium falciparum (isolate 3D7) GN=PF11_0333 PE=4 SV=2 | 4 | 0.96 | 0.54 | 0.0382 |
| tr\|Q8IIB5\|Q8IIB5_PLAF7 Nuclear preribosomal assembly protein, putative OS=Plasmodium falciparum (isolate 3D7) GN=PF11_0259 PE=4 SV=1 | 4 | 0.96 | 0.25 | 0.0045 |
| tr\|Q8I2G1\|Q8I2G1_PLAF7 Ring-exported protein 1 OS=Plasmodium falciparum (isolate 3D7) GN=REX1 PE=4 SV=1 | 4 | 0.96 | 0.06 | 0.0001 |
| tr\|Q8IIX5\|Q8IIX5_PLAF7 Uncharacterized protein OS=Plasmodium falciparum (isolate 3D7) GN=PF11_0037 PE=4 SV=1 | 4 | 0.96 | 0.12 | 0.0005 |
| tr\|O97278\|O97278_PLAF7 ABC transporter, putative OS=Plasmodium falciparum (isolate 3D7) GN=PFC0875w PE=4 SV=3 | 4 | 0.96 | 0.15 | 0.0009 |
| tr\|Q8IIU5\|Q8IIU5_PLAF7 Conserved Plasmodium protein OS=Plasmodium falciparum (isolate 3D7) GN=PF11_0069 PE=4 SV=2 | 4 | 0.96 | 0.07 | 0.0001 |
| tr\|Q8I266\|Q8I266_PLAF7 Lipid/sterol:H+ symporter OS=Plasmodium falciparum (isolate 3D7) GN=PFA_0375c PE=4 SV=1 | 4 | 0.96 | 0.08 | 0.0002 |
| tr\|Q8IDC4\|Q8IDC4_PLAF7 Preribosomal processosome UTP, putative OS=Plasmodium falciparum (isolate 3D7) GN=PF13_0310 PE=4 SV=1 | 4 | 0.97 | 0.12 | 0.0006 |
| tr\|Q8IK15\|Q8IK15_PLAF7 PF70 protein OS=Plasmodium falciparum (isolate 3D7) GN=PF10_0025 PE=4 SV=1 | 4 | 0.97 | 0.11 | 0.0004 |
| tr\|Q8IAV1\|Q8IAV1_PLAF7 Uncharacterized protein OS=Plasmodium falciparum (isolate 3D7) GN=PF08_0091 PE=4 SV=1 | 4 | 0.97 | 0.10 | 0.0003 |
| tr\|Q8IJC9\|Q8IJC9_PLAF7 DNA-directed RNA polymerase II, putative OS=Plasmodium falciparum (isolate 3D7) GN=PF10_0269 PE=4 SV=1 | 4 | 0.94 | 0.62 | 0.0563 |
| tr\|Q8I4R5\|Q8I4R5_PLAF7 Rhoptry neck protein 3, putative OS=Plasmodium falciparum (isolate 3D7) GN=PFL2505c PE=4 SV=1 | 4 | 0.97 | 0.05 | 0.0000 |
| tr\|Q8IHZ6\|Q8IHZ6_PLAF7 DNAJ protein, putative OS=Plasmodium falciparum (isolate 3D7) GN=PF11_0380 PE=4 SV=2 | 4 | 0.97 | 0.06 | 0.0001 |
| tr\|Q8ID37\|Q8ID37_PLAF7 U1 small nuclear ribonucleoprotein, putative OS=Plasmodium falciparum (isolate 3D7) GN=MAL13P1.338 PE=4 SV=1 | 4 | 0.97 | 0.10 | 0.0003 |
| tr\|Q7KWJ5\|Q7KWJ5_PLAF7 Hexose transporter, PfHT1 OS=Plasmodium falciparum (isolate 3D7) GN=HT1 PE=3 SV=1 | 4 | 0.97 | 0.05 | 0.0000 |
| tr\|C6KT67\|C6KT67_PLAF7 Coronin binding protein OS=Plasmodium falciparum (isolate 3D7) GN=PFF1110c PE=4 SV=1 | 4 | 0.97 | 0.08 | 0.0002 |

| | | | | |
|---|---|---|---|---|
| tr\|Q8I6Z1\|Q8I6Z1_PLAF7 Acyl-coA synthetase, PfACS5 OS=Plasmodium falciparum (isolate 3D7) GN=PfACS5 PE=4 SV=1 | 4 | 0.97 | 0.07 | 0.0001 |
| tr\|Q8ILZ9\|Q8ILZ9_PLAF7 Uncharacterized protein OS=Plasmodium falciparum (isolate 3D7) GN=PF14_0094 PE=4 SV=1 | 4 | 0.97 | 0.16 | 0.0013 |
| tr\|C0H5I2\|C0H5I2_PLAF7 Uncharacterized protein OS=Plasmodium falciparum (isolate 3D7) GN=MAL13P1.266 PE=4 SV=1 | 4 | 0.97 | 0.09 | 0.0002 |
| tr\|Q8ILM6\|Q8ILM6_PLAF7 Uncharacterized protein OS=Plasmodium falciparum (isolate 3D7) GN=PF14_0217 PE=4 SV=1 | 4 | 0.97 | 0.15 | 0.0011 |
| tr\|Q8IKJ0\|Q8IKJ0_PLAF7 ATP synthase (C/AC39) subunit, putative OS=Plasmodium falciparum (isolate 3D7) GN=PF14_0615 PE=4 SV=1 | 4 | 0.97 | 0.06 | 0.0001 |
| tr\|Q8I207\|Q8I207_PLAF7 Uncharacterized protein OS=Plasmodium falciparum (isolate 3D7) GN=PFD0080c PE=4 SV=1 | 4 | 0.97 | 0.03 | 0.0000 |
| sp\|Q8I4V5\|UTP11_PLAF7 Probable U3 small nucleolar RNA-associated protein 11 OS=Plasmodium falciparum (isolate 3D7) GN=PFL2295w PE=3 SV=1 | 4 | 0.97 | 0.06 | 0.0001 |
| sp\|P04921-2\|GLPC_HUMAN Isoform Glycophorin-D of Glycophorin-C OS=Homo sapiens GN=GYPC;sp\|P04921-3\|GLPC_HUMAN Isoform 3 of Glycophorin-C OS=Homo sapiens GN=GYPC;sp\|P04921\|GLPC_HUMAN Glycophorin-C OS=Homo sapiens GN=GYPC PE=1 SV=1 | 4 | 0.97 | 0.05 | 0.0000 |
| tr\|Q8IK12\|Q8IK12_PLAF7 Uncharacterized protein OS=Plasmodium falciparum (isolate 3D7) GN=PF10_0028 PE=4 SV=1 | 4 | 0.97 | 0.08 | 0.0002 |
| tr\|Q8IE22\|Q8IE22_PLAF7 ER lumen protein retaining receptor 1, putative OS=Plasmodium falciparum (isolate 3D7) GN=MAL13P1.163 PE=4 SV=1 | 4 | 0.97 | 0.02 | 0.0000 |
| tr\|Q9U0L4\|Q9U0L4_PLAF7 Peptidyl-tRNA hydrolase PTH2, putative OS=Plasmodium falciparum (isolate 3D7) GN=PFD0355c PE=4 SV=2 | 4 | 0.97 | 0.11 | 0.0004 |
| tr\|Q8IKL7\|Q8IKL7_PLAF7 Splicing factor 3B subunit 2-like protein OS=Plasmodium falciparum (isolate 3D7) GN=PF14_0587 PE=4 SV=1 | 4 | 0.97 | 0.53 | 0.0356 |
| tr\|Q8IHN1\|Q8IHN1_PLAF7 Ring-infected erythrocyte surface antigen, putative OS=Plasmodium falciparum (isolate 3D7) GN=PF11_0509 PE=4 SV=1 | 4 | 0.97 | 0.11 | 0.0004 |
| tr\|Q7KQM5\|Q7KQM5_PLAF7 Early transcribed membrane protein 14.1, etramp14.1 OS=Plasmodium falciparum (isolate 3D7) GN=etramp14.1 PE=4 SV=1 | 4 | 0.97 | 0.23 | 0.0036 |
| tr\|C0H541\|C0H541_PLAF7 Putative uncharacterized protein OS=Plasmodium falciparum (isolate 3D7) GN=PFI0823w PE=4 SV=1 | 4 | 0.97 | 0.54 | 0.0363 |
| tr\|O77376\|O77376_PLAF7 Band 7-related protein OS=Plasmodium falciparum (isolate 3D7) GN=PFC0800w PE=4 SV=1 | 4 | 0.97 | 0.08 | 0.0001 |
| tr\|Q8I3T4\|Q8I3T4_PLAF7 Transcriptional regulator, putative OS=Plasmodium falciparum (isolate 3D7) GN=PFE0870w PE=4 SV=1 | 4 | 0.97 | 0.02 | 0.0000 |
| tr\|Q8IK92\|Q8IK92_PLAF7 Uncharacterized protein OS=Plasmodium falciparum (isolate 3D7) GN=PF14_0714 PE=4 SV=1 | 4 | 0.97 | 0.09 | 0.0002 |
| tr\|C6KSP9\|C6KSP9_PLAF7 RNA binding protein, putative OS=Plasmodium falciparum (isolate 3D7) GN=PFF0250w PE=4 SV=1 | 4 | 0.97 | 0.05 | 0.0000 |
| tr\|Q6ZMA7\|Q6ZMA7_PLAF7 Sexual stage-specific protein OS=Plasmodium falciparum (isolate 3D7) GN=PFD0310w PE=4 SV=1 | 4 | 0.98 | 0.12 | 0.0005 |
| tr\|Q8I5E9\|Q8I5E9_PLAF7 Uncharacterized protein OS=Plasmodium falciparum (isolate 3D7) GN=PFL1300c PE=4 SV=1 | 4 | 0.98 | 0.04 | 0.0000 |
| tr\|Q8IIC4\|Q8IIC4_PLAF7 High mobility group-like protein NHP2, putative OS=Plasmodium falciparum (isolate 3D7) GN=PF11_0250 PE=4 SV=1 | 4 | 0.98 | 0.07 | 0.0001 |
| tr\|C6KTB8\|C6KTB8_PLAF7 Protein kinase PK4 OS=Plasmodium falciparum (isolate 3D7) GN=PfPK4 PE=4 SV=1 | 4 | 0.98 | 0.05 | 0.0000 |
| tr\|O77389\|O77389_PLAF7 Formate-nitrate transporter, putative OS=Plasmodium falciparum (isolate 3D7) GN=PFC0725c PE=4 SV=2 | 4 | 0.98 | 0.05 | 0.0000 |
| tr\|Q8IJ72\|Q8IJ72_PLAF7 Bromodomain protein, putative OS=Plasmodium falciparum (isolate 3D7) GN=PF10_0328 PE=1 SV=1 | 4 | 0.98 | 0.07 | 0.0001 |
| tr\|Q8IBF2\|Q8IBF2_PLAF7 Uncharacterized protein OS=Plasmodium falciparum (isolate 3D7) GN=MAL7P1.171 PE=4 SV=1 | 4 | 0.98 | 0.11 | 0.0004 |
| tr\|Q8IAU7\|Q8IAU7_PLAF7 Uncharacterized protein OS=Plasmodium falciparum (isolate 3D7) GN=MAL8P1.105 PE=4 SV=1 | 4 | 0.98 | 0.07 | 0.0001 |
| tr\|C6KST7\|C6KST7_PLAF7 Uncharacterized protein OS=Plasmodium falciparum (isolate 3D7) GN=PFF0445w PE=4 SV=1 | 4 | 0.98 | 0.08 | 0.0001 |
| tr\|Q8IIF0\|Q8IIF0_PLAF7 Circumsporozoite-related antigen OS=Plasmodium falciparum (isolate 3D7) GN=PF11_0224 PE=4 SV=1 | 4 | 0.98 | 0.05 | 0.0000 |
| tr\|Q8IJU2\|Q8IJU2_PLAF7 Conserved Plasmodium protein OS=Plasmodium falciparum (isolate 3D7) GN=PF10_0100 PE=4 SV=1 | 4 | 0.98 | 0.04 | 0.0000 |
| tr\|Q76NN8\|Q76NN8_PLAF7 Calcium-transporting ATPase, putative OS=Plasmodium falciparum (isolate 3D7) GN=PFA_0310c PE=3 SV=1 | 4 | 0.98 | 0.04 | 0.0000 |
| tr\|C6KSR3\|C6KSR3_PLAF7 Polypyrimidine tract binding protein, putative OS=Plasmodium falciparum (isolate 3D7) GN=PFF0320c PE=4 SV=1 | 4 | 0.98 | 0.06 | 0.0001 |

| | | | | |
|---|---|---|---|---|
| tr\|O77315\|O77315_PLAF7 DNA-directed RNA polymerase subunit I, putative OS=Plasmodium falciparum (isolate 3D7) GN=PFC0155c PE=4 SV=2 | 4 | 0.98 | 0.07 | 0.0001 |
| tr\|Q8I5P8\|Q8I5P8_PLAF7 Conserved Plasmodium membrane protein OS=Plasmodium falciparum (isolate 3D7) GN=SR10 PE=4 SV=1 | 4 | 0.98 | 0.22 | 0.0030 |
| tr\|Q8IL08\|Q8IL08_PLAF7 Uncharacterized protein OS=Plasmodium falciparum (isolate 3D7) GN=PF14_0442 PE=4 SV=1 | 4 | 0.98 | 0.13 | 0.0006 |
| tr\|C0H4M7\|C0H4M7_PLAF7 Uncharacterized protein OS=Plasmodium falciparum (isolate 3D7) GN=MAL7P1.67 PE=4 SV=1 | 4 | 0.98 | 0.09 | 0.0002 |
| tr\|Q8IE81\|Q8IE81_PLAF7 Uncharacterized protein OS=Plasmodium falciparum (isolate 3D7) GN=PF13_0134 PE=4 SV=1 | 4 | 0.98 | 0.18 | 0.0016 |
| tr\|C6S3J6\|C6S3J6_PLAF7 Ribosomal protein L29, putative OS=Plasmodium falciparum (isolate 3D7) GN=PF14_0575a PE=1 SV=1 | 4 | 0.98 | 0.38 | 0.0144 |
| tr\|Q8I669\|Q8I669_PLAF7 Plasmodium exported protein OS=Plasmodium falciparum (isolate 3D7) GN=PFB0106c PE=4 SV=1 | 4 | 0.98 | 0.14 | 0.0008 |
| tr\|Q8I665\|Q8I665_PLAF7 Conserved Plasmodium protein OS=Plasmodium falciparum (isolate 3D7) GN=PFB0194w PE=4 SV=1 | 4 | 0.98 | 0.17 | 0.0013 |
| tr\|Q8IB03\|Q8IB03_PLAF7 ClpB protein, putative OS=Plasmodium falciparum (isolate 3D7) GN=PF08_0063 PE=1 SV=1 | 4 | 0.99 | 0.05 | 0.0000 |
| tr\|Q8I551\|Q8I551_PLAF7 Uncharacterized protein OS=Plasmodium falciparum (isolate 3D7) GN=PFL1800w PE=4 SV=1 | 4 | 0.99 | 0.08 | 0.0001 |
| tr\|Q8ILP3\|Q8ILP3_PLAF7 Surface protein, Pf113 OS=Plasmodium falciparum (isolate 3D7) GN=Pf113 PE=4 SV=1 | 4 | 0.99 | 0.07 | 0.0001 |
| tr\|Q8IKJ1\|Q8IKJ1_PLAF7 Phosphatase, putative OS=Plasmodium falciparum (isolate 3D7) GN=PF14_0614 PE=4 SV=2 | 4 | 0.99 | 0.02 | 0.0000 |
| tr\|Q8IIJ8\|Q8IIJ8_PLAF7 Heat shock protein 101, putative OS=Plasmodium falciparum (isolate 3D7) GN=PF11_0175 PE=1 SV=1 | 4 | 0.99 | 0.05 | 0.0000 |
| tr\|C0H469\|C0H469_PLAF7 Putative uncharacterized protein OS=Plasmodium falciparum (isolate 3D7) GN=PFC0430w PE=4 SV=1 | 4 | 0.99 | 0.09 | 0.0002 |
| tr\|Q8IAQ8\|Q8IAQ8_PLAF7 Vacuolar proton translocating ATPase subunit A, putative OS=Plasmodium falciparum (isolate 3D7) GN=PF08_0113 PE=4 SV=1 | 4 | 0.99 | 0.08 | 0.0001 |
| tr\|Q8ILC9\|Q8ILC9_PLAF7 Uncharacterized protein OS=Plasmodium falciparum (isolate 3D7) GN=PF14_0315 PE=4 SV=2 | 4 | 0.99 | 0.08 | 0.0002 |
| tr\|Q8IKG8\|Q8IKG8_PLAF7 Rhoptry protein, putative OS=Plasmodium falciparum (isolate 3D7) GN=PF14_0637 PE=4 SV=2 | 4 | 0.99 | 0.07 | 0.0001 |
| tr\|Q8I569\|Q8I569_PLAF7 Uncharacterized protein OS=Plasmodium falciparum (isolate 3D7) GN=PFL1705w PE=4 SV=1 | 4 | 0.99 | 0.15 | 0.0009 |
| tr\|Q8IK89\|Q8IK89_PLAF7 Uncharacterized protein OS=Plasmodium falciparum (isolate 3D7) GN=PF14_0717 PE=4 SV=1 | 4 | 0.99 | 0.11 | 0.0004 |
| tr\|Q8IL89\|Q8IL89_PLAF7 Succinyl CoA ligase, putative OS=Plasmodium falciparum (isolate 3D7) GN=PF14_0357 PE=4 SV=1 | 4 | 0.99 | 0.35 | 0.0110 |
| tr\|Q8IJV7\|Q8IJV7_PLAF7 Nucleolar protein NOP5, putative OS=Plasmodium falciparum (isolate 3D7) GN=PF10_0085 PE=4 SV=1 | 4 | 0.99 | 0.09 | 0.0002 |
| tr\|Q8I305\|Q8I305_PLAF7 Transporter, putative OS=Plasmodium falciparum (isolate 3D7) GN=PFI0720w PE=4 SV=1 | 4 | 0.99 | 0.07 | 0.0001 |
| sp\|P07384\|CAN1_HUMAN Calpain-1 catalytic subunit OS=Homo sapiens GN=CAPN1 PE=1 SV=1 | 4 | 0.99 | 0.05 | 0.0000 |
| tr\|Q8IIH7\|Q8IIH7_PLAF7 Uncharacterized protein OS=Plasmodium falciparum (isolate 3D7) GN=PF11_0197 PE=4 SV=1 | 4 | 0.99 | 0.06 | 0.0001 |
| tr\|O96127\|O96127_PLAF7 Conserved Plasmodium protein OS=Plasmodium falciparum (isolate 3D7) GN=PFB0115w PE=4 SV=1 | 4 | 0.99 | 0.13 | 0.0006 |
| tr\|Q8IJ39\|Q8IJ39_PLAF7 Conserved Plasmodium protein OS=Plasmodium falciparum (isolate 3D7) GN=PF10_0361 PE=4 SV=1 | 4 | 0.99 | 0.12 | 0.0005 |
| tr\|Q8IDY3\|Q8IDY3_PLAF7 Uncharacterized protein OS=Plasmodium falciparum (isolate 3D7) GN=PF13_0192 PE=4 SV=1 | 4 | 0.99 | 0.04 | 0.0000 |
| tr\|Q8IJR2\|Q8IJR2_PLAF7 Uncharacterized protein OS=Plasmodium falciparum (isolate 3D7) GN=PF10_0130 PE=4 SV=1 | 4 | 0.99 | 0.09 | 0.0002 |
| tr\|Q8IJ92\|Q8IJ92_PLAF7 Uncharacterized protein OS=Plasmodium falciparum (isolate 3D7) GN=PF10_0307 PE=4 SV=1 | 4 | 0.99 | 0.07 | 0.0001 |
| sp\|P23276\|KELL_HUMAN Kell blood group glycoprotein OS=Homo sapiens GN=KEL PE=1 SV=2 | 4 | 0.99 | 0.06 | 0.0000 |
| tr\|Q8I205\|Q8I205_PLAF7 Uncharacterized protein OS=Plasmodium falciparum (isolate 3D7) GN=PFD0095c PE=4 SV=1 | 4 | 0.99 | 0.10 | 0.0003 |
| tr\|Q8IHP7\|Q8IHP7_PLAF7 Uncharacterized protein OS=Plasmodium falciparum (isolate 3D7) GN=PF11_0482 PE=4 SV=1 | 4 | 0.99 | 0.31 | 0.0079 |
| tr\|Q8IEI6\|Q8IEI6_PLAF7 Uncharacterized protein OS=Plasmodium falciparum (isolate 3D7) GN=PF13_0076 PE=4 SV=1 | 4 | 0.99 | 0.15 | 0.0009 |

| | | | | |
|---|---|---|---|---|
| tr\|Q8IJW6\|Q8IJW6_PLAF7 Asparagine-rich antigen OS=Plasmodium falciparum (isolate 3D7) GN=PF10_0075 PE=4 SV=1 | 4 | 0.99 | 0.02 | 0.0000 |
| tr\|Q8IL28\|Q8IL28_PLAF7 Apicoplast 1-acyl-sn-glycerol-3-phosphate acyltransferase, putative OS=Plasmodium falciparum (isolate 3D7) GN=PF14_0421 PE=4 SV=2 | 4 | 0.99 | 0.11 | 0.0004 |
| sp\|P28289\|TMOD1_HUMAN Tropomodulin-1 OS=Homo sapiens GN=TMOD1 PE=1 SV=1;sp\|P28289-2\|TMOD1_HUMAN Isoform 2 of Tropomodulin-1 OS=Homo sapiens GN=TMOD1 | 4 | 0.99 | 0.09 | 0.0002 |
| tr\|Q8I484\|Q8I484_PLAF7 Rhoptry-associated protein 2, RAP2 OS=Plasmodium falciparum (isolate 3D7) GN=RAP2 PE=4 SV=1 | 4 | 0.99 | 0.08 | 0.0002 |
| tr\|Q8IJA5\|Q8IJA5_PLAF7 Transcription factor, putative OS=Plasmodium falciparum (isolate 3D7) GN=PF10_0293 PE=3 SV=1 | 4 | 0.99 | 0.22 | 0.0030 |
| tr\|O77364\|O77364_PLAF7 60S ribosomal protein L26, putative OS=Plasmodium falciparum (isolate 3D7) GN=PFC0535w PE=1 SV=1 | 4 | 0.99 | 0.20 | 0.0020 |
| tr\|Q8IEK7\|Q8IEK7_PLAF7 Uncharacterized protein OS=Plasmodium falciparum (isolate 3D7) GN=MAL13P1.53 PE=4 SV=1 | 4 | 1.00 | 0.53 | 0.0333 |
| tr\|Q7K6A5\|Q7K6A5_PLAF7 Multidrug resistance protein OS=Plasmodium falciparum (isolate 3D7) GN=PfMDR1 PE=3 SV=1 | 4 | 1.00 | 0.08 | 0.0002 |
| sp\|P27105\|STOM_HUMAN Erythrocyte band 7 integral membrane protein OS=Homo sapiens GN=STOM PE=1 SV=3 | 4 | 1.00 | 0.05 | 0.0000 |
| tr\|Q8I5E0\|Q8I5E0_PLAF7 Uncharacterized protein OS=Plasmodium falciparum (isolate 3D7) GN=PFL1345c PE=4 SV=1 | 4 | 1.00 | 0.10 | 0.0003 |
| tr\|Q8I5T2\|Q8I5T2_PLAF7 Glutathione peroxidase OS=Plasmodium falciparum (isolate 3D7) GN=PFL0595c PE=3 SV=1 | 4 | 1.00 | 0.08 | 0.0001 |
| tr\|Q8IB66\|Q8IB66_PLAF7 RNA binding protein, putative OS=Plasmodium falciparum (isolate 3D7) GN=MAL8P1.40 PE=4 SV=1 | 4 | 1.00 | 0.06 | 0.0001 |
| sp\|P02730\|B3AT_HUMAN Band 3 anion transport protein OS=Homo sapiens GN=SLC4A1 PE=1 SV=3;tr\|A0A0A0MS98\|A0A0A0MS98_HUMAN Band 3 anion transport protein OS=Homo sapiens GN=SLC4A1 PE=1 SV=1 | 4 | 1.00 | 0.06 | 0.0001 |
| tr\|Q8IIR0\|Q8IIR0_PLAF7 Uncharacterized protein OS=Plasmodium falciparum (isolate 3D7) GN=PF11_0108 PE=4 SV=1 | 4 | 1.00 | 0.09 | 0.0002 |
| tr\|Q8IJZ9\|Q8IJZ9_PLAF7 U5 small nuclear ribonuclear protein, putative OS=Plasmodium falciparum (isolate 3D7) GN=PF10_0041 PE=4 SV=1 | 4 | 1.00 | 0.04 | 0.0000 |
| tr\|Q8IBE9\|Q8IBE9_PLAF7 Uncharacterized protein OS=Plasmodium falciparum (isolate 3D7) GN=MAL7P1.174 PE=4 SV=1 | 4 | 1.00 | 0.06 | 0.0001 |
| tr\|C6KT11\|C6KT11_PLAF7 Mitochondrial import receptor subunit tom40 OS=Plasmodium falciparum (isolate 3D7) GN=PFF0825c PE=4 SV=1 | 4 | 1.00 | 0.05 | 0.0000 |
| tr\|O77375\|O77375_PLAF7 DNA-directed RNA polymerase OS=Plasmodium falciparum (isolate 3D7) GN=PFC0805w PE=3 SV=1 | 4 | 1.00 | 0.06 | 0.0000 |
| tr\|Q8I488\|Q8I488_PLAF7 PIESP2 erythrocyte surface protein OS=Plasmodium falciparum (isolate 3D7) GN=PFE0060w PE=4 SV=1 | 4 | 1.00 | 0.09 | 0.0002 |
| tr\|Q8IFP1\|Q8IFP1_PLAF7 U5 small nuclear ribonucleoprotein-specific protein, putative OS=Plasmodium falciparum (isolate 3D7) GN=PFD1060w PE=4 SV=1 | 4 | 1.00 | 0.18 | 0.0016 |
| tr\|Q8IEL0\|Q8IEL0_PLAF7 Uncharacterized protein OS=Plasmodium falciparum (isolate 3D7) GN=MAL13P1.50 PE=4 SV=1 | 4 | 1.00 | 0.12 | 0.0005 |
| sp\|Q8I1U7\|SMC3_PLAF7 Structural maintenance of chromosomes protein 3 homolog OS=Plasmodium falciparum (isolate 3D7) GN=PFD0685c PE=3 SV=1 | 4 | 1.00 | 0.04 | 0.0000 |
| tr\|Q8ILA1\|Q8ILA1_PLAF7 Uncharacterized protein OS=Plasmodium falciparum (isolate 3D7) GN=PF14_0344 PE=4 SV=1 | 4 | 1.00 | 0.05 | 0.0000 |
| tr\|Q8IKF6\|Q8IKF6_PLAF7 Uncharacterized protein OS=Plasmodium falciparum (isolate 3D7) GN=PF14_0649 PE=4 SV=1 | 4 | 1.00 | 0.05 | 0.0000 |
| tr\|Q8I492\|Q8I492_PLAF7 Mature parasite-infected erythrocyte surface antigen (MESA) or PfEMP2 OS=Plasmodium falciparum (isolate 3D7) GN=MESA PE=4 SV=1 | 4 | 1.00 | 0.12 | 0.0004 |
| tr\|C0H4Z7\|C0H4Z7_PLAF7 Uncharacterized protein OS=Plasmodium falciparum (isolate 3D7) GN=MAL8P1.206 PE=4 SV=1 | 4 | 1.00 | 0.03 | 0.0000 |
| tr\|Q8I3F3\|Q8I3F3_PLAF7 Early transcribed membrane protein 5, ETRAMP5 OS=Plasmodium falciparum (isolate 3D7) GN=ETRAMP5 PE=4 SV=1 | 4 | 1.00 | 0.09 | 0.0002 |
| tr\|Q8IIC0\|Q8IIC0_PLAF7 Uncharacterized protein OS=Plasmodium falciparum (isolate 3D7) GN=PF11_0254 PE=4 SV=1 | 4 | 1.00 | 0.05 | 0.0000 |
| tr\|Q8IJW2\|Q8IJW2_PLAF7 Uncharacterized protein OS=Plasmodium falciparum (isolate 3D7) GN=PF10_0079 PE=4 SV=1 | 4 | 1.00 | 0.13 | 0.0007 |
| tr\|Q8ILQ8\|Q8ILQ8_PLAF7 Uncharacterized protein OS=Plasmodium falciparum (isolate 3D7) GN=PF14_0186 PE=4 SV=2 | 4 | 1.00 | 0.12 | 0.0004 |
| tr\|Q8IJR6\|Q8IJR6_PLAF7 Conserved Plasmodium protein OS=Plasmodium falciparum (isolate 3D7) GN=PF10_0126 PE=4 SV=1 | 4 | 1.01 | 0.07 | 0.0001 |
| tr\|Q8IHM9\|Q8IHM9_PLAF7 Plasmodium exported protein OS=Plasmodium falciparum (isolate 3D7) GN=PF11_0511 PE=4 SV=2 | 4 | 1.01 | 0.18 | 0.0014 |

| | | | | |
|---|---|---|---|---|
| tr\|O77310\|O77310_PLAF7 Cytoadherence linked asexual protein 3.1 OS=Plasmodium falciparum (isolate 3D7) GN=RhopH1(3.1) PE=4 SV=2;tr\|O77309\|O77309_PLAF7 Cytoadherence linked asexual protein 3.2 OS=Plasmodium falciparum (isolate 3D7) GN=RhopH1(3.2) PE=4 SV=3 | 4 | 1.01 | 0.04 | 0.0000 |
| tr\|O77313\|O77313_PLAF7 N-ethylmaleimide sensitive fusion protein, putative OS=Plasmodium falciparum (isolate 3D7) GN=PFC0140c PE=3 SV=1 | 4 | 1.01 | 0.06 | 0.0001 |
| tr\|Q8ILC8\|Q8ILC8_PLAF7 DNA topoisomerase 2 OS=Plasmodium falciparum (isolate 3D7) GN=PF14_0316 PE=3 SV=1 | 4 | 1.01 | 0.13 | 0.0006 |
| tr\|Q8I476\|Q8I476_PLAF7 Merozoite Surface Protein 8, MSP8 OS=Plasmodium falciparum (isolate 3D7) GN=MSP8 PE=4 SV=1 | 4 | 1.01 | 0.19 | 0.0018 |
| tr\|X6R4N5\|X6R4N5_HUMAN Erythroid membrane-associated protein OS=Homo sapiens GN=ERMAP PE=1 SV=1;sp\|Q96PL5\|ERMAP_HUMAN Erythroid membrane-associated protein OS=Homo sapiens GN=ERMAP PE=1 SV=1 | 4 | 1.01 | 0.06 | 0.0001 |
| tr\|Q8IM32\|Q8IM32_PLAF7 Uncharacterized protein OS=Plasmodium falciparum (isolate 3D7) GN=PF14_0059 PE=4 SV=1 | 4 | 1.01 | 0.29 | 0.0061 |
| tr\|Q8IKR1\|Q8IKR1_PLAF7 V-type H(+)-translocating pyrophosphatase, putative OS=Plasmodium falciparum (isolate 3D7) GN=PF14_0541 PE=3 SV=1 | 4 | 1.01 | 0.07 | 0.0001 |
| tr\|Q8IDN6\|Q8IDN6_PLAF7 Sec61 alpha subunit, PfSec61 OS=Plasmodium falciparum (isolate 3D7) GN=Sec61 PE=3 SV=1 | 4 | 1.01 | 0.06 | 0.0000 |
| tr\|Q8I395\|Q8I395_PLAF7 RhopH3 OS=Plasmodium falciparum (isolate 3D7) GN=PFI0265c PE=4 SV=1 | 4 | 1.01 | 0.08 | 0.0001 |
| tr\|Q8IK93\|Q8IK93_PLAF7 Uncharacterized protein OS=Plasmodium falciparum (isolate 3D7) GN=PF14_0713 PE=4 SV=1 | 4 | 1.01 | 0.10 | 0.0002 |
| tr\|O97225\|O97225_PLAF7 Spindle pole body protein, putative OS=Plasmodium falciparum (isolate 3D7) GN=PFC0165w PE=4 SV=3 | 4 | 1.01 | 0.05 | 0.0000 |
| tr\|Q8II73\|Q8II73_PLAF7 Spermidine synthase OS=Plasmodium falciparum (isolate 3D7) GN=PF11_0301 PE=1 SV=1 | 4 | 1.01 | 0.06 | 0.0001 |
| tr\|Q8ILS0\|Q8ILS0_PLAF7 Pseudouridine synthase, putative OS=Plasmodium falciparum (isolate 3D7) GN=PF14_0174 PE=4 SV=1 | 4 | 1.01 | 0.04 | 0.0000 |
| tr\|Q8IJ34\|Q8IJ34_PLAF7 ADP/ATP transporter on adenylate translocase OS=Plasmodium falciparum (isolate 3D7) GN=PF10_0366 PE=3 SV=1 | 4 | 1.01 | 0.05 | 0.0000 |
| tr\|Q8IJF4\|Q8IJF4_PLAF7 Formin 2, putative OS=Plasmodium falciparum (isolate 3D7) GN=PF10_0244 PE=4 SV=2 | 4 | 1.01 | 0.07 | 0.0001 |
| tr\|Q8I5I0\|Q8I5I0_PLAF7 Uncharacterized protein OS=Plasmodium falciparum (isolate 3D7) GN=PFL1140w PE=4 SV=1 | 4 | 1.01 | 0.23 | 0.0033 |
| tr\|C6KST1\|C6KST1_PLAF7 Uncharacterized protein OS=Plasmodium falciparum (isolate 3D7) GN=PFF0410w PE=4 SV=1 | 4 | 1.01 | 0.13 | 0.0006 |
| tr\|Q8IAU1\|Q8IAU1_PLAF7 RNA helicase, putative OS=Plasmodium falciparum (isolate 3D7) GN=PF08_0096 PE=3 SV=1 | 4 | 1.01 | 0.04 | 0.0000 |
| tr\|Q8IBJ9\|Q8IBJ9_PLAF7 Mago nashi protein homolog, putative OS=Plasmodium falciparum (isolate 3D7) GN=MAL7P1.139 PE=4 SV=2 | 4 | 1.01 | 0.05 | 0.0000 |
| tr\|C0H4M1\|C0H4M1_PLAF7 AAA family ATPase, putative OS=Plasmodium falciparum (isolate 3D7) GN=MAL7P1.209 PE=4 SV=1 | 4 | 1.01 | 0.09 | 0.0002 |
| tr\|Q8I1T2\|Q8I1T2_PLAF7 Nuclear cap-binding protein, putative OS=Plasmodium falciparum (isolate 3D7) GN=PFD0750w PE=4 SV=1 | 4 | 1.01 | 0.06 | 0.0001 |
| tr\|Q8IJI0\|Q8IJI0_PLAF7 Pre-mRNA splicing factor, putative OS=Plasmodium falciparum (isolate 3D7) GN=PF10_0217 PE=4 SV=1 | 4 | 1.01 | 0.28 | 0.0052 |
| tr\|C0H4J4\|C0H4J4_PLAF7 Uncharacterized protein OS=Plasmodium falciparum (isolate 3D7) GN=MAL7P1.225.2 PE=4 SV=1;tr\|C0H4J3\|C0H4J3_PLAF7 Uncharacterized protein OS=Plasmodium falciparum (isolate 3D7) GN=MAL7P1.225.1 PE=4 SV=1 | 4 | 1.01 | 0.32 | 0.0083 |
| tr\|Q8I5L6\|Q8I5L6_PLAF7 Clathrin heavy chain OS=Plasmodium falciparum (isolate 3D7) GN=PFL0930w PE=3 SV=1 | 4 | 1.01 | 0.08 | 0.0001 |
| tr\|Q8IKR4\|Q8IKR4_PLAF7 Uncharacterized protein OS=Plasmodium falciparum (isolate 3D7) GN=PF14_0538 PE=4 SV=1 | 4 | 1.01 | 0.06 | 0.0001 |
| tr\|Q8IHW7\|Q8IHW7_PLAF7 Conserved Plasmodium protein OS=Plasmodium falciparum (isolate 3D7) GN=PF11_0409 PE=4 SV=1 | 4 | 1.01 | 0.14 | 0.0007 |
| tr\|Q8III3\|Q8III3_PLAF7 Uncharacterized protein OS=Plasmodium falciparum (isolate 3D7) GN=PF11_0191 PE=4 SV=1 | 4 | 1.01 | 0.08 | 0.0001 |
| tr\|O96236\|O96236_PLAF7 DNA-directed RNA polymerase OS=Plasmodium falciparum (isolate 3D7) GN=PFB0715w PE=3 SV=3 | 4 | 1.01 | 0.10 | 0.0002 |
| tr\|Q8IJZ2\|Q8IJZ2_PLAF7 Conserved Plasmodium protein OS=Plasmodium falciparum (isolate 3D7) GN=PF10_0048 PE=4 SV=1 | 4 | 1.01 | 0.07 | 0.0001 |
| tr\|Q8IJZ3\|Q8IJZ3_PLAF7 Uncharacterized protein OS=Plasmodium falciparum (isolate 3D7) GN=PF10_0047 PE=4 SV=1 | 4 | 1.01 | 0.03 | 0.0000 |
| tr\|Q8ILU2\|Q8ILU2_PLAF7 Uncharacterized protein OS=Plasmodium falciparum (isolate 3D7) GN=PF14_0152 PE=4 SV=1 | 4 | 1.01 | 0.07 | 0.0001 |

| | | | | |
|---|---|---|---|---|
| tr\|Q8IJP9\|Q8IJP9_PLAF7 ADA2-like protein OS=Plasmodium falciparum (isolate 3D7) GN=PF10_0143 PE=4 SV=1 | 4 | 1.02 | 0.10 | 0.0003 |
| tr\|Q8I548\|Q8I548_PLAF7 Uncharacterized protein OS=Plasmodium falciparum (isolate 3D7) GN=PFL1815c PE=4 SV=1 | 4 | 1.02 | 0.16 | 0.0011 |
| tr\|Q8I4U7\|Q8I4U7_PLAF7 Uncharacterized protein OS=Plasmodium falciparum (isolate 3D7) GN=PFL2335w PE=4 SV=1 | 4 | 1.02 | 0.03 | 0.0000 |
| tr\|Q8IDF8\|Q8IDF8_PLAF7 Putative rRNA methyltransferase OS=Plasmodium falciparum (isolate 3D7) GN=PF13_0286 PE=3 SV=1 | 4 | 1.02 | 0.07 | 0.0001 |
| tr\|Q8IB78\|Q8IB78_PLAF7 Nucleoside transporter, putative OS=Plasmodium falciparum (isolate 3D7) GN=MAL8P1.32 PE=4 SV=1 | 4 | 1.02 | 0.07 | 0.0001 |
| sp\|Q08210\|PYRD_PLAF7 Dihydroorotate dehydrogenase (quinone), mitochondrial OS=Plasmodium falciparum (isolate 3D7) GN=PFF0160c PE=1 SV=1 | 4 | 1.02 | 0.12 | 0.0005 |
| tr\|Q8I468\|Q8I468_PLAF7 Ser/Arg-rich splicing factor, putative OS=Plasmodium falciparum (isolate 3D7) GN=PFE0160c PE=4 SV=1 | 4 | 1.02 | 0.06 | 0.0000 |
| tr\|Q8ILL5\|Q8ILL5_PLAF7 Uncharacterized protein OS=Plasmodium falciparum (isolate 3D7) GN=PF14_0228 PE=4 SV=1 | 4 | 1.02 | 0.09 | 0.0002 |
| tr\|C0H570\|C0H570_PLAF7 RNA binding protein, putative OS=Plasmodium falciparum (isolate 3D7) GN=PFI1435w PE=4 SV=1 | 4 | 1.02 | 0.03 | 0.0000 |
| tr\|Q8I6Z8\|Q8I6Z8_PLAF7 Ubiquitin Carboxyl-terminal Hydrolase-like zinc finger protein OS=Plasmodium falciparum (isolate 3D7) GN=PF13_0096 PE=4 SV=1 | 4 | 1.02 | 0.24 | 0.0034 |
| tr\|O96205\|O96205_PLAF7 Conserved Plasmodium protein OS=Plasmodium falciparum (isolate 3D7) GN=PFB0560w PE=4 SV=2 | 4 | 1.02 | 0.17 | 0.0012 |
| tr\|Q8I5K3\|Q8I5K3_PLAF7 Uncharacterized protein OS=Plasmodium falciparum (isolate 3D7) GN=PFL1010c PE=4 SV=1 | 4 | 1.02 | 0.18 | 0.0014 |
| sp\|O77374\|PF07_PLAF7 Uncharacterized protein PFC0810c OS=Plasmodium falciparum (isolate 3D7) GN=PFC0810c PE=3 SV=1 | 4 | 1.02 | 0.19 | 0.0016 |
| tr\|Q8IB44\|Q8IB44_PLAF7 Uncharacterized protein OS=Plasmodium falciparum (isolate 3D7) GN=MAL8P1.53 PE=4 SV=1 | 4 | 1.02 | 0.13 | 0.0005 |
| tr\|Q8IJ28\|Q8IJ28_PLAF7 Antigen UB05 OS=Plasmodium falciparum (isolate 3D7) GN=PF10_0372 PE=4 SV=2 | 4 | 1.02 | 0.04 | 0.0000 |
| tr\|Q8IDB7\|Q8IDB7_PLAF7 RNA binding protein, putative OS=Plasmodium falciparum (isolate 3D7) GN=PF13_0315 PE=4 SV=1 | 4 | 1.02 | 0.10 | 0.0002 |
| tr\|C0H5L9\|C0H5L9_PLAF7 Membrane associated histidine-rich protein, MAHRP-1 OS=Plasmodium falciparum (isolate 3D7) GN=MAHRP1 PE=4 SV=1 | 4 | 1.02 | 0.11 | 0.0003 |
| tr\|C0H4S8\|C0H4S8_PLAF7 Uncharacterized protein OS=Plasmodium falciparum (isolate 3D7) GN=MAL8P1.127 PE=4 SV=1 | 4 | 1.02 | 0.09 | 0.0002 |
| tr\|Q8IE40\|Q8IE40_PLAF7 Ribose-phosphate pyrophosphokinase, putative OS=Plasmodium falciparum (isolate 3D7) GN=PF13_0157 PE=4 SV=1 | 4 | 1.02 | 0.15 | 0.0009 |
| tr\|Q8IBI8\|Q8IBI8_PLAF7 Protein phosphatase, putative OS=Plasmodium falciparum (isolate 3D7) GN=PF07_0110 PE=4 SV=1 | 4 | 1.02 | 0.14 | 0.0007 |
| tr\|C0H4F1\|C0H4F1_PLAF7 Uncharacterized protein OS=Plasmodium falciparum (isolate 3D7) GN=PFE0990w PE=4 SV=1 | 4 | 1.02 | 0.09 | 0.0002 |
| tr\|Q8II64\|Q8II64_PLAF7 Uncharacterized protein OS=Plasmodium falciparum (isolate 3D7) GN=PF11_0310 PE=4 SV=1 | 4 | 1.03 | 0.11 | 0.0003 |
| tr\|Q8IE14\|Q8IE14_PLAF7 Signal peptidase I OS=Plasmodium falciparum (isolate 3D7) GN=SP21 PE=4 SV=1 | 4 | 1.03 | 0.22 | 0.0026 |
| tr\|C0H571\|C0H571_PLAF7 High molecular weight rhoptry protein-2 OS=Plasmodium falciparum (isolate 3D7) GN=RhopH2 PE=4 SV=1 | 4 | 1.03 | 0.11 | 0.0004 |
| tr\|Q8IJW0\|Q8IJW0_PLAF7 26S proteasome regulatory subunit 4, putative OS=Plasmodium falciparum (isolate 3D7) GN=PF10_0081 PE=3 SV=2 | 4 | 1.03 | 0.17 | 0.0012 |
| tr\|Q8IKS4\|Q8IKS4_PLAF7 Hemolysin, putative OS=Plasmodium falciparum (isolate 3D7) GN=PF14_0528 PE=4 SV=2 | 4 | 1.03 | 0.19 | 0.0016 |
| tr\|Q8I490\|Q8I490_PLAF7 Uncharacterized protein OS=Plasmodium falciparum (isolate 3D7) GN=PFE0050w PE=4 SV=1 | 4 | 1.03 | 0.07 | 0.0001 |
| tr\|Q8IBD1\|Q8IBD1_PLAF7 Tryptophan/threonine-rich antigen OS=Plasmodium falciparum (isolate 3D7) GN=PF08_0003 PE=4 SV=1 | 4 | 1.03 | 0.20 | 0.0020 |
| tr\|Q8II62\|Q8II62_PLAF7 60S ribosomal protein L38e, putative OS=Plasmodium falciparum (isolate 3D7) GN=PF11_0312 PE=1 SV=1 | 4 | 1.03 | 0.39 | 0.0136 |
| tr\|C6KT71\|C6KT71_PLAF7 Superoxide dismutase OS=Plasmodium falciparum (isolate 3D7) GN=PfSOD2 PE=4 SV=1 | 4 | 1.03 | 0.21 | 0.0021 |
| tr\|Q8IHZ2\|Q8IHZ2_PLAF7 Uncharacterized protein OS=Plasmodium falciparum (isolate 3D7) GN=PF11_0384 PE=4 SV=1 | 4 | 1.03 | 0.08 | 0.0001 |
| tr\|Q8IBH9\|Q8IBH9_PLAF7 Cation transporting ATPase, cation transporter OS=Plasmodium falciparum (isolate 3D7) GN=PF07_0115 PE=3 SV=1 | 4 | 1.03 | 0.10 | 0.0003 |
| tr\|C0H523\|C0H523_PLAF7 Putative uncharacterized protein OS=Plasmodium falciparum (isolate 3D7) GN=PFI0336w PE=4 SV=1 | 4 | 1.03 | 0.11 | 0.0003 |

| | | | | |
|---|---|---|---|---|
| tr\|O96150\|O96150_PLAF7 DNA-directed RNA polymerase II 16 kDa subunit, putative OS=Plasmodium falciparum (isolate 3D7) GN=PFB0245c PE=4 SV=1 | 4 | 1.03 | 0.14 | 0.0006 |
| sp\|P02042\|HBD_HUMAN Hemoglobin subunit delta OS=Homo sapiens GN=HBD PE=1 SV=2;tr\|E9PFT6\|E9PFT6_HUMAN Hemoglobin subunit delta OS=Homo sapiens GN=HBD PE=1 SV=1;tr\|E9PEW8\|E9PEW8_HUMAN Hemoglobin subunit delta (Fragment) OS=Homo sapiens GN=HBD PE=1 SV=1 | 4 | 1.03 | 0.27 | 0.0045 |
| tr\|Q8IJN3\|Q8IJN3_PLAF7 Serine/Threonine protein kinase, FIKK family OS=Plasmodium falciparum (isolate 3D7) GN=FIKK-10.1 PE=4 SV=2 | 4 | 1.03 | 0.13 | 0.0006 |
| tr\|Q8IJC1\|Q8IJC1_PLAF7 Uncharacterized protein OS=Plasmodium falciparum (isolate 3D7) GN=PF10_0277 PE=4 SV=1 | 4 | 1.03 | 0.08 | 0.0001 |
| sp\|P61074\|PCNA_PLAF7 Proliferating cell nuclear antigen OS=Plasmodium falciparum (isolate 3D7) GN=PCNA PE=3 SV=1 | 4 | 1.03 | 0.19 | 0.0015 |
| sp\|Q8IBZ9\|CRT_PLAF7 Putative chloroquine resistance transporter OS=Plasmodium falciparum (isolate 3D7) GN=CG10 PE=3 SV=1 | 4 | 1.04 | 0.12 | 0.0004 |
| sp\|O00806\|RLA2_PLAF7 60S acidic ribosomal protein P2 OS=Plasmodium falciparum (isolate 3D7) GN=MAL3P3.19 PE=3 SV=1 | 4 | 1.04 | 0.18 | 0.0014 |
| tr\|C6KT09\|C6KT09_PLAF7 Malate:quinone oxidoreductase, putative OS=Plasmodium falciparum (isolate 3D7) GN=PFF0815w PE=4 SV=1 | 4 | 1.04 | 0.29 | 0.0058 |
| tr\|Q8IM34\|Q8IM34_PLAF7 RNA binding protein, putative OS=Plasmodium falciparum (isolate 3D7) GN=PF14_0057 PE=4 SV=1 | 4 | 1.04 | 0.22 | 0.0025 |
| tr\|Q8IDG4\|Q8IDG4_PLAF7 Uncharacterized protein OS=Plasmodium falciparum (isolate 3D7) GN=PF13_0281 PE=4 SV=1 | 4 | 1.04 | 0.09 | 0.0002 |
| tr\|Q8IAX8\|Q8IAX8_PLAF7 DNA/RNA-binding protein Alba, putative OS=Plasmodium falciparum (isolate 3D7) GN=PF08_0074 PE=4 SV=1 | 4 | 1.04 | 0.06 | 0.0000 |
| tr\|Q8IL86\|Q8IL86_PLAF7 Sec62, putative OS=Plasmodium falciparum (isolate 3D7) GN=PF14_0361 PE=4 SV=2 | 4 | 1.04 | 0.07 | 0.0001 |
| tr\|Q8I3A5\|Q8I3A5_PLAF7 Signal peptidase, putative OS=Plasmodium falciparum (isolate 3D7) GN=PFI0215c PE=4 SV=1 | 4 | 1.04 | 0.20 | 0.0019 |
| tr\|Q8IEB3\|Q8IEB3_PLAF7 Uncharacterized protein OS=Plasmodium falciparum (isolate 3D7) GN=PF13_0116 PE=4 SV=1 | 4 | 1.04 | 0.08 | 0.0001 |
| tr\|Q8I255\|Q8I255_PLAF7 Putative uncharacterized protein OS=Plasmodium falciparum (isolate 3D7) GN=PFA_0430c PE=4 SV=1 | 4 | 1.04 | 0.06 | 0.0001 |
| tr\|Q7K6A8\|Q7K6A8_PLAF7 Rab1b, GTPase OS=Plasmodium falciparum (isolate 3D7) GN=Rab1b PE=4 SV=1 | 4 | 1.04 | 0.11 | 0.0003 |
| tr\|Q8IAW5\|Q8IAW5_PLAF7 Uncharacterized protein OS=Plasmodium falciparum (isolate 3D7) GN=PF08_0083 PE=4 SV=1 | 4 | 1.04 | 0.06 | 0.0001 |
| tr\|Q8I562\|Q8I562_PLAF7 Clustered-asparagine-rich protein OS=Plasmodium falciparum (isolate 3D7) GN=PFL1745c PE=4 SV=2 | 4 | 1.04 | 0.09 | 0.0002 |
| tr\|Q8II36\|Q8II36_PLAF7 Aquaglyceroporin OS=Plasmodium falciparum (isolate 3D7) GN=PF11_0338 PE=3 SV=1 | 4 | 1.04 | 0.13 | 0.0006 |
| sp\|P68871\|HBB_HUMAN Hemoglobin subunit beta OS=Homo sapiens GN=HBB PE=1 SV=2 | 4 | 1.04 | 0.27 | 0.0043 |
| tr\|C6KSX2\|C6KSX2_PLAF7 Nucleolar GTP-binding protein 1, putative OS=Plasmodium falciparum (isolate 3D7) GN=PFF0625w PE=4 SV=1 | 4 | 1.04 | 0.16 | 0.0009 |
| tr\|Q8ID32\|Q8ID32_PLAF7 Ribosome biogenesis protein MRT4, putative OS=Plasmodium falciparum (isolate 3D7) GN=MAL13P1.341 PE=3 SV=1 | 4 | 1.04 | 0.11 | 0.0003 |
| tr\|Q8ILU3\|Q8ILU3_PLAF7 RNA-binding protein Nova-1, putative OS=Plasmodium falciparum (isolate 3D7) GN=PF14_0151 PE=4 SV=1 | 4 | 1.04 | 0.12 | 0.0004 |
| tr\|Q8I5H7\|Q8I5H7_PLAF7 GTP cyclohydrolase I OS=Plasmodium falciparum (isolate 3D7) GN=PFL1155w PE=4 SV=1 | 4 | 1.04 | 0.06 | 0.0001 |
| tr\|Q8I450\|Q8I450_PLAF7 Actin-like protein, putative OS=Plasmodium falciparum (isolate 3D7) GN=PFE0255w PE=3 SV=1 | 4 | 1.04 | 0.06 | 0.0000 |
| tr\|Q8IJX3\|Q8IJX3_PLAF7 RNA binding protein, putative OS=Plasmodium falciparum (isolate 3D7) GN=PF10_0068 PE=4 SV=1 | 4 | 1.04 | 0.09 | 0.0002 |
| sp\|P61225\|RAP2B_HUMAN Ras-related protein Rap-2b OS=Homo sapiens GN=RAP2B PE=1 SV=1 | 4 | 1.04 | 0.13 | 0.0005 |
| tr\|Q8I3N0\|Q8I3N0_PLAF7 DNAJ protein, putative OS=Plasmodium falciparum (isolate 3D7) GN=PFE1170w PE=4 SV=1 | 4 | 1.04 | 0.09 | 0.0002 |
| tr\|Q7K6B0\|Q7K6B0_PLAF7 PfRab18, GTPase OS=Plasmodium falciparum (isolate 3D7) GN=rab18 PE=3 SV=1 | 4 | 1.04 | 0.14 | 0.0007 |
| tr\|Q8I3U6\|Q8I3U6_PLAF7 40S ribosomal protein S14, putative OS=Plasmodium falciparum (isolate 3D7) GN=PFE0810c PE=1 SV=1 | 4 | 1.04 | 0.16 | 0.0010 |
| tr\|Q8I4R9\|Q8I4R9_PLAF7 DEAD/DEAH box helicase, putative OS=Plasmodium falciparum (isolate 3D7) GN=PFL2475w PE=3 SV=1 | 4 | 1.04 | 0.17 | 0.0012 |
| sp\|Q8I5G1\|YPF10_PLAF7 Uncharacterized protein PFL1235c OS=Plasmodium falciparum (isolate 3D7) GN=PFL1235c PE=3 SV=1 | 4 | 1.04 | 0.44 | 0.0182 |

| | | | | |
|---|---|---|---|---|
| tr\|C0H5L7\|C0H5L7_PLAF7 Uncharacterized protein OS=Plasmodium falciparum (isolate 3D7) GN=MAL13P1.352 PE=4 SV=1 | 4 | 1.04 | 0.09 | 0.0002 |
| tr\|Q8ILZ5\|Q8ILZ5_PLAF7 Tetratricopeptide repeat family protein, putative OS=Plasmodium falciparum (isolate 3D7) GN=PF14_0098 PE=4 SV=1 | 4 | 1.05 | 0.17 | 0.0012 |
| tr\|Q8IJI4\|Q8IJI4_PLAF7 10b antigen, putative OS=Plasmodium falciparum (isolate 3D7) GN=PF10_0213 PE=4 SV=1 | 4 | 1.05 | 0.02 | 0.0000 |
| tr\|Q8IJZ4\|Q8IJZ4_PLAF7 Uncharacterized protein OS=Plasmodium falciparum (isolate 3D7) GN=PF10_0046 PE=4 SV=1 | 4 | 1.05 | 0.11 | 0.0003 |
| tr\|Q8IB26\|Q8IB26_PLAF7 BRIX domain, putative OS=Plasmodium falciparum (isolate 3D7) GN=PF08_0053 PE=4 SV=1 | 4 | 1.05 | 0.16 | 0.0009 |
| tr\|Q8IKH5\|Q8IKH5_PLAF7 Serine/threonine-protein phosphatase OS=Plasmodium falciparum (isolate 3D7) GN=PF14_0630 PE=3 SV=1 | 4 | 1.05 | 0.13 | 0.0006 |
| tr\|Q8I655\|Q8I655_PLAF7 Ribosome associated membrane protein RAMP4, putative OS=Plasmodium falciparum (isolate 3D7) GN=PFB0888w PE=4 SV=2 | 4 | 1.03 | 0.76 | 0.0737 |
| tr\|Q8IKE8\|Q8IKE8_PLAF7 Uncharacterized protein OS=Plasmodium falciparum (isolate 3D7) GN=PF14_0657 PE=4 SV=1 | 4 | 1.05 | 0.21 | 0.0022 |
| tr\|Q8IIU7\|Q8IIU7_PLAF7 Conserved Plasmodium protein OS=Plasmodium falciparum (isolate 3D7) GN=PF11_0067 PE=4 SV=2 | 4 | 1.05 | 0.08 | 0.0001 |
| tr\|Q8IIA2\|Q8IIA2_PLAF7 Ribosomal protein S18, putative OS=Plasmodium falciparum (isolate 3D7) GN=PF11_0272 PE=1 SV=1 | 4 | 1.05 | 0.21 | 0.0022 |
| tr\|Q8I2S6\|Q8I2S6_PLAF7 DNA-directed RNA polymerase II, putative OS=Plasmodium falciparum (isolate 3D7) GN=PFI1130c PE=4 SV=1 | 4 | 1.05 | 0.22 | 0.0025 |
| tr\|Q8ILN8\|Q8ILN8_PLAF7 40S ribosomal protein S25, putative OS=Plasmodium falciparum (isolate 3D7) GN=PF14_0205 PE=1 SV=2 | 4 | 1.05 | 0.21 | 0.0020 |
| tr\|Q8IKH8\|Q8IKH8_PLAF7 40S ribosomal protein S3, putative OS=Plasmodium falciparum (isolate 3D7) GN=PF14_0627 PE=1 SV=1 | 4 | 1.05 | 0.17 | 0.0012 |
| tr\|Q8IKY0\|Q8IKY0_PLAF7 Transcription factor with AP2 domain(S), putative OS=Plasmodium falciparum (isolate 3D7) GN=ApiAP2 PE=4 SV=1 | 4 | 1.05 | 0.48 | 0.0220 |
| tr\|Q8I398\|Q8I398_PLAF7 Putative uncharacterized protein OS=Plasmodium falciparum (isolate 3D7) GN=PFI0250c PE=4 SV=1 | 4 | 1.05 | 0.21 | 0.0021 |
| tr\|Q8I635\|Q8I635_PLAF7 Uncharacterized protein OS=Plasmodium falciparum (isolate 3D7) GN=PFL0050c PE=4 SV=1 | 4 | 1.05 | 0.11 | 0.0003 |
| tr\|Q8IFP2\|Q8IFP2_PLAF7 40S ribosomal protein S19, putative OS=Plasmodium falciparum (isolate 3D7) GN=PFD1055w PE=1 SV=1 | 4 | 1.05 | 0.18 | 0.0013 |
| tr\|Q8IJX8\|Q8IJX8_PLAF7 Uncharacterized protein OS=Plasmodium falciparum (isolate 3D7) GN=PF10_0063 PE=4 SV=1 | 4 | 1.05 | 0.05 | 0.0000 |
| tr\|C6KTB9\|C6KTB9_PLAF7 Ethanolaminephosphotransferase, putative OS=Plasmodium falciparum (isolate 3D7) GN=PFF1375c PE=3 SV=1 | 4 | 1.03 | 0.77 | 0.0749 |
| tr\|Q8I1T1\|Q8I1T1_PLAF7 Adenylate kinase 1 OS=Plasmodium falciparum (isolate 3D7) GN=GAK PE=3 SV=1 | 4 | 1.05 | 0.49 | 0.0234 |
| tr\|Q8ILL3\|Q8ILL3_PLAF7 60S ribosomal protein L5, putative OS=Plasmodium falciparum (isolate 3D7) GN=PF14_0230 PE=3 SV=1 | 4 | 1.05 | 0.22 | 0.0023 |
| tr\|Q8IDS0\|Q8IDS0_PLAF7 Vacuolar ATP synthase subunit D, putative OS=Plasmodium falciparum (isolate 3D7) GN=PF13_0227 PE=4 SV=1 | 4 | 1.06 | 0.11 | 0.0003 |
| tr\|Q9NFE6\|Q9NFE6_PLAF7 Eukaryotic translation initiation factor 3 subunit K OS=Plasmodium falciparum (isolate 3D7) GN=PFC0441c PE=3 SV=1 | 4 | 1.06 | 0.15 | 0.0008 |
| tr\|Q8IAX5\|Q8IAX5_PLAF7 40S ribosomal protein S16, putative OS=Plasmodium falciparum (isolate 3D7) GN=PF08_0076 PE=1 SV=1 | 4 | 1.06 | 0.13 | 0.0005 |
| tr\|Q7K6B1\|Q7K6B1_PLAF7 Protein kinase c inhibitor-like protein, putative OS=Plasmodium falciparum (isolate 3D7) GN=PF08_0059 PE=4 SV=2 | 4 | 1.06 | 0.21 | 0.0021 |
| sp\|Q8ID39\|Y13P2_PLAF7 Uncharacterized protein MAL13P1.336 OS=Plasmodium falciparum (isolate 3D7) GN=MAL13P1.336 PE=4 SV=1 | 4 | 1.06 | 0.05 | 0.0000 |
| tr\|C6KTC7\|C6KTC7_PLAF7 DNAJ domain protein, putative OS=Plasmodium falciparum (isolate 3D7) GN=PFF1415c PE=4 SV=1 | 4 | 1.06 | 0.16 | 0.0010 |
| tr\|Q8IDJ7\|Q8IDJ7_PLAF7 Small nuclear ribonucleoprotein, putative OS=Plasmodium falciparum (isolate 3D7) GN=MAL13P1.253 PE=4 SV=1 | 4 | 1.06 | 0.17 | 0.0010 |
| tr\|Q8IKH2\|Q8IKH2_PLAF7 Transcription factor with AP2 domain(S), putative OS=Plasmodium falciparum (isolate 3D7) GN=ApiAP2 PE=1 SV=1 | 4 | 1.06 | 0.12 | 0.0004 |
| tr\|Q8I3R2\|Q8I3R2_PLAF7 Uncharacterized protein OS=Plasmodium falciparum (isolate 3D7) GN=PFE0995c PE=4 SV=1 | 4 | 1.06 | 0.09 | 0.0002 |
| tr\|Q8IAZ7\|Q8IAZ7_PLAF7 Nucleolar preribosomal assembly protein, putative OS=Plasmodium falciparum (isolate 3D7) GN=PF08_0065 PE=4 SV=1 | 4 | 1.06 | 0.32 | 0.0067 |
| sp\|P69905\|HBA_HUMAN Hemoglobin subunit alpha OS=Homo sapiens GN=HBA1 PE=1 SV=2;tr\|G3V1N2\|G3V1N2_HUMAN HCG1745306, isoform CRA_a OS=Homo sapiens GN=HBA2 PE=1 SV=1 | 4 | 1.06 | 0.28 | 0.0047 |

| | | | | |
|---|---|---|---|---|
| sp\|Q76NM6\|VATA_PLAF7 V-type proton ATPase catalytic subunit A OS=Plasmodium falciparum (isolate 3D7) GN=vapA PE=3 SV=1 | 4 | 1.06 | 0.11 | 0.0003 |
| tr\|Q8IE09\|Q8IE09_PLAF7 60S ribosomal protein L23, putative OS=Plasmodium falciparum (isolate 3D7) GN=PF13_0171 PE=1 SV=1 | 4 | 1.06 | 0.34 | 0.0085 |
| tr\|Q8I3T8\|Q8I3T8_PLAF7 60S ribosomal protein L12, putative OS=Plasmodium falciparum (isolate 3D7) GN=PFE0850c PE=3 SV=2 | 4 | 1.07 | 0.25 | 0.0033 |
| tr\|Q8IC35\|Q8IC35_PLAF7 Erythrocyte membrane-associated antigen OS=Plasmodium falciparum (isolate 3D7) GN=MAL7P1.12 PE=4 SV=1 | 4 | 1.07 | 0.05 | 0.0000 |
| tr\|Q8IDB0\|Q8IDB0_PLAF7 40S ribosomal protein S13, putative OS=Plasmodium falciparum (isolate 3D7) GN=PF13_0316 PE=1 SV=1 | 4 | 1.07 | 0.18 | 0.0012 |
| tr\|Q8IBK1\|Q8IBK1_PLAF7 Exonuclease I, putative OS=Plasmodium falciparum (isolate 3D7) GN=PF07_0105 PE=4 SV=1 | 4 | 1.07 | 0.31 | 0.0061 |
| tr\|Q8IJY4\|Q8IJY4_PLAF7 Regulator of nonsense transcripts, putative OS=Plasmodium falciparum (isolate 3D7) GN=PF10_0057 PE=4 SV=1 | 4 | 1.07 | 0.15 | 0.0007 |
| tr\|Q8I544\|Q8I544_PLAF7 Uncharacterized protein OS=Plasmodium falciparum (isolate 3D7) GN=PFL1835w PE=4 SV=1 | 4 | 1.07 | 0.24 | 0.0030 |
| tr\|Q8IDF7\|Q8IDF7_PLAF7 V-type ATPase, putative OS=Plasmodium falciparum (isolate 3D7) GN=MAL13P1.271 PE=3 SV=1 | 4 | 1.07 | 0.08 | 0.0001 |
| tr\|Q8IKL9\|Q8IKL9_PLAF7 40S ribosomal protein S28e, putative OS=Plasmodium falciparum (isolate 3D7) GN=PF14_0585 PE=3 SV=1 | 4 | 1.07 | 0.31 | 0.0063 |
| tr\|Q8IC43\|Q8IC43_PLAF7 Uncharacterized protein OS=Plasmodium falciparum (isolate 3D7) GN=PF07_0007 PE=4 SV=1 | 4 | 1.07 | 0.13 | 0.0005 |
| tr\|Q8IKA0\|Q8IKA0_PLAF7 Uncharacterized protein OS=Plasmodium falciparum (isolate 3D7) GN=PF14_0706 PE=4 SV=1 | 4 | 1.07 | 0.12 | 0.0004 |
| tr\|C0H4L6\|C0H4L6_PLAF7 Uncharacterized protein OS=Plasmodium falciparum (isolate 3D7) GN=MAL7P1.204 PE=4 SV=1 | 4 | 1.07 | 0.07 | 0.0001 |
| tr\|Q8ID85\|Q8ID85_PLAF7 ATP-dependent DNA helicase, putative OS=Plasmodium falciparum (isolate 3D7) GN=PF13_0330 PE=4 SV=1 | 4 | 1.07 | 0.10 | 0.0002 |
| tr\|Q8IDQ2\|Q8IDQ2_PLAF7 Kelch protein, putative OS=Plasmodium falciparum (isolate 3D7) GN=PF13_0238 PE=4 SV=1 | 4 | 1.07 | 0.23 | 0.0028 |
| tr\|Q8ILU8\|Q8ILU8_PLAF7 Ribonucleoprotein, putative OS=Plasmodium falciparum (isolate 3D7) GN=PF14_0146 PE=4 SV=1 | 4 | 1.07 | 0.15 | 0.0008 |
| tr\|Q8IHZ8\|Q8IHZ8_PLAF7 Uncharacterized protein OS=Plasmodium falciparum (isolate 3D7) GN=PF11_0378 PE=4 SV=1 | 4 | 1.07 | 0.18 | 0.0014 |
| tr\|Q8IBB4\|Q8IBB4_PLAF7 Uncharacterized protein OS=Plasmodium falciparum (isolate 3D7) GN=PF08_0010 PE=4 SV=1 | 4 | 1.07 | 0.27 | 0.0043 |
| tr\|Q8I5H4\|Q8I5H4_PLAF7 Polyadenylate-binding protein, putative OS=Plasmodium falciparum (isolate 3D7) GN=PFL1170w PE=4 SV=1 | 4 | 1.07 | 0.03 | 0.0000 |
| tr\|Q8II11\|Q8II11_PLAF7 Conserved Plasmodium protein OS=Plasmodium falciparum (isolate 3D7) GN=PF11_0364 PE=4 SV=1 | 4 | 1.07 | 0.23 | 0.0027 |
| tr\|Q8ILV2\|Q8ILV2_PLAF7 60S ribosomal protein L10, putative OS=Plasmodium falciparum (isolate 3D7) GN=PF14_0141 PE=1 SV=1 | 4 | 1.08 | 0.29 | 0.0050 |
| tr\|Q8I3R7\|Q8I3R7_PLAF7 Vacuolar ATP synthetase OS=Plasmodium falciparum (isolate 3D7) GN=PFE0965c PE=3 SV=1 | 4 | 1.08 | 0.22 | 0.0024 |
| tr\|Q8I2F2\|Q8I2F2_PLAF7 Putative uncharacterized protein OS=Plasmodium falciparum (isolate 3D7) GN=PFI1780w PE=1 SV=1 | 4 | 1.08 | 0.10 | 0.0002 |
| tr\|O96128\|O96128_PLAF7 Early transcribed membrane protein 2, ETRAMP2 OS=Plasmodium falciparum (isolate 3D7) GN=SEP2 PE=4 SV=1 | 4 | 1.08 | 0.10 | 0.0002 |
| tr\|Q8ILL2\|Q8ILL2_PLAF7 60S ribosomal protein L7-3, putative OS=Plasmodium falciparum (isolate 3D7) GN=PF14_0231 PE=1 SV=2 | 4 | 1.08 | 0.20 | 0.0018 |
| tr\|O96201\|O96201_PLAF7 Conserved Plasmodium protein OS=Plasmodium falciparum (isolate 3D7) GN=PFB0540w PE=4 SV=1 | 4 | 1.08 | 0.14 | 0.0006 |
| tr\|Q8I2X4\|Q8I2X4_PLAF7 Heat shock protein 70 (HSP70) homologue OS=Plasmodium falciparum (isolate 3D7) GN=PFI0875w PE=3 SV=1 | 4 | 1.08 | 0.36 | 0.0090 |
| tr\|Q8ILY9\|Q8ILY9_PLAF7 Eukaryotic translation initiation factor 2 gamma subunit, putative OS=Plasmodium falciparum (isolate 3D7) GN=PF14_0104 PE=4 SV=1 | 4 | 1.08 | 0.24 | 0.0028 |
| tr\|Q8ILE8\|Q8ILE8_PLAF7 60S ribosomal protein L14, putative OS=Plasmodium falciparum (isolate 3D7) GN=PF14_0296 PE=1 SV=1 | 4 | 1.08 | 0.15 | 0.0007 |
| tr\|C0H535\|C0H535_PLAF7 Putative uncharacterized protein OS=Plasmodium falciparum (isolate 3D7) GN=PFI0610w PE=4 SV=1 | 4 | 1.08 | 0.12 | 0.0004 |
| tr\|Q8IIK2\|Q8IIK2_PLAF7 Uncharacterized protein OS=Plasmodium falciparum (isolate 3D7) GN=PF11_0171 PE=4 SV=1 | 4 | 1.08 | 0.21 | 0.0021 |
| tr\|Q8IBZ2\|Q8IBZ2_PLAF7 Lysophospholipase, putative OS=Plasmodium falciparum (isolate 3D7) GN=PF07_0040 PE=4 SV=1 | 4 | 1.08 | 0.19 | 0.0015 |
| tr\|B9ZSJ0\|B9ZSJ0_PLAF7 Putative uncharacterized protein OS=Plasmodium falciparum (isolate 3D7) GN=PFA_0570w PE=4 SV=1 | 4 | 1.08 | 0.15 | 0.0008 |

| | | | | |
|---|---|---|---|---|
| tr\|Q8IIU8\|Q8IIU8_PLAF7 40S ribosomal protein S4 OS=Plasmodium falciparum (isolate 3D7) GN=PF11_0065 PE=3 SV=2 | 4 | 1.08 | 0.16 | 0.0008 |
| tr\|Q8IJJ5\|Q8IJJ5_PLAF7 Conserved protein OS=Plasmodium falciparum (isolate 3D7) GN=PF10_0200 PE=4 SV=1 | 4 | 1.08 | 0.12 | 0.0004 |
| tr\|Q8IAZ3\|Q8IAZ3_PLAF7 Eukaryotic translation initiation factor 3 subunit G OS=Plasmodium falciparum (isolate 3D7) GN=MAL8P1.83 PE=3 SV=1 | 4 | 1.08 | 0.10 | 0.0002 |
| tr\|Q8IKH0\|Q8IKH0_PLAF7 60S ribosome subunit biogenesis protein NIP7 homolog OS=Plasmodium falciparum (isolate 3D7) GN=PF14_0635 PE=3 SV=2 | 4 | 1.08 | 0.34 | 0.0081 |
| tr\|C6KSP3\|C6KSP3_PLAF7 Uncharacterized protein OS=Plasmodium falciparum (isolate 3D7) GN=PFF0220w PE=4 SV=1 | 4 | 1.09 | 0.04 | 0.0000 |
| tr\|Q8IHR4\|Q8IHR4_PLAF7 Dynamin-like protein OS=Plasmodium falciparum (isolate 3D7) GN=dyn1 PE=3 SV=1 | 4 | 1.09 | 0.16 | 0.0009 |
| tr\|Q8ILG6\|Q8ILG6_PLAF7 Coatamer protein, beta subunit, putative OS=Plasmodium falciparum (isolate 3D7) GN=PF14_0277 PE=4 SV=2 | 4 | 1.09 | 0.18 | 0.0011 |
| tr\|Q8II85\|Q8II85_PLAF7 Uncharacterized protein OS=Plasmodium falciparum (isolate 3D7) GN=PF11_0289 PE=4 SV=1 | 4 | 1.09 | 0.51 | 0.0235 |
| tr\|Q8II61\|Q8II61_PLAF7 60S ribosomal protein P0 OS=Plasmodium falciparum (isolate 3D7) GN=PF11_0313 PE=3 SV=1 | 4 | 1.09 | 0.25 | 0.0031 |
| tr\|C0H5C2\|C0H5C2_PLAF7 40S ribosomal protein S15/S19, putative OS=Plasmodium falciparum (isolate 3D7) GN=MAL13P1.92 PE=1 SV=1 | 4 | 1.09 | 0.20 | 0.0016 |
| tr\|Q8II32\|Q8II32_PLAF7 Uncharacterized protein OS=Plasmodium falciparum (isolate 3D7) GN=PF11_0342 PE=4 SV=1 | 4 | 1.09 | 0.07 | 0.0001 |
| tr\|Q8I3T5\|Q8I3T5_PLAF7 Splicing factor, putative OS=Plasmodium falciparum (isolate 3D7) GN=PFE0865c PE=4 SV=2 | 4 | 1.09 | 0.16 | 0.0008 |
| tr\|Q8I2H3\|Q8I2H3_PLAF7 Vacuolar ATP synthase subunit E, putative OS=Plasmodium falciparum (isolate 3D7) GN=PFI1670c PE=3 SV=2 | 4 | 1.09 | 0.16 | 0.0008 |
| tr\|Q8IE82\|Q8IE82_PLAF7 60S ribosomal protein L23a, putative OS=Plasmodium falciparum (isolate 3D7) GN=PF13_0132 PE=1 SV=1 | 4 | 1.09 | 0.27 | 0.0040 |
| tr\|Q8IJZ7\|Q8IJZ7_PLAF7 60S ribosomal protein L13, putative OS=Plasmodium falciparum (isolate 3D7) GN=PF10_0043 PE=1 SV=1 | 4 | 1.09 | 0.25 | 0.0030 |
| tr\|Q8II57\|Q8II57_PLAF7 Structural maintenance of chromosome protein, putative OS=Plasmodium falciparum (isolate 3D7) GN=PF11_0317 PE=4 SV=1 | 4 | 1.09 | 0.14 | 0.0005 |
| tr\|Q8IE84\|Q8IE84_PLAF7 Vacuolar ATP synthase subunit G, putative OS=Plasmodium falciparum (isolate 3D7) GN=PF13_0130 PE=4 SV=1 | 4 | 1.09 | 0.17 | 0.0010 |
| tr\|Q8IDV1\|Q8IDV1_PLAF7 60S ribosomal protein L6-2, putative OS=Plasmodium falciparum (isolate 3D7) GN=PF13_0213 PE=1 SV=1 | 4 | 1.09 | 0.28 | 0.0046 |
| tr\|Q8ILK4\|Q8ILK4_PLAF7 Uncharacterized protein OS=Plasmodium falciparum (isolate 3D7) GN=PF14_0239 PE=4 SV=2 | 4 | 1.09 | 0.49 | 0.0211 |
| tr\|O97243\|O97243_PLAF7 Putative uncharacterized protein OS=Plasmodium falciparum (isolate 3D7) GN=PFC0265c PE=4 SV=2 | 4 | 1.09 | 0.26 | 0.0036 |
| tr\|Q8I2T2\|Q8I2T2_PLAF7 Ubiquitin-like protein, putative OS=Plasmodium falciparum (isolate 3D7) GN=PFI1085w PE=4 SV=1 | 4 | 1.10 | 0.04 | 0.0000 |
| tr\|Q8IE18\|Q8IE18_PLAF7 Uncharacterized protein OS=Plasmodium falciparum (isolate 3D7) GN=PF13_0165 PE=4 SV=1 | 4 | 1.10 | 0.07 | 0.0001 |
| tr\|C6KSW5\|C6KSW5_PLAF7 Eukaryotic translation initiation factor 3 subunit L OS=Plasmodium falciparum (isolate 3D7) GN=PFF0590c PE=3 SV=1 | 4 | 1.10 | 0.12 | 0.0003 |
| tr\|O97250\|O97250_PLAF7 60S ribosomal protein L7, putative OS=Plasmodium falciparum (isolate 3D7) GN=PFC0300c PE=1 SV=2 | 4 | 1.10 | 0.18 | 0.0012 |
| tr\|Q8I463\|Q8I463_PLAF7 60S ribosomal protein L31, putative OS=Plasmodium falciparum (isolate 3D7) GN=PFE0185c PE=1 SV=1 | 4 | 1.10 | 0.19 | 0.0014 |
| tr\|Q8I502\|Q8I502_PLAF7 40S ribosomal protein S17, putative OS=Plasmodium falciparum (isolate 3D7) GN=PFL2055w PE=1 SV=1 | 4 | 1.10 | 0.23 | 0.0025 |
| tr\|Q8ID24\|Q8ID24_PLAF7 Mitochondrial import inner membrane translocase, putative OS=Plasmodium falciparum (isolate 3D7) GN=PF13_0358 PE=4 SV=1 | 4 | 1.10 | 0.42 | 0.0134 |
| sp\|O97249\|RS12_PLAF7 40S ribosomal protein S12 OS=Plasmodium falciparum (isolate 3D7) GN=RPS12 PE=1 SV=1 | 4 | 1.10 | 0.23 | 0.0026 |
| tr\|Q8IIS9\|Q8IIS9_PLAF7 Uncharacterized protein OS=Plasmodium falciparum (isolate 3D7) GN=PF11_0086 PE=4 SV=1 | 4 | 1.10 | 0.02 | 0.0000 |
| tr\|Q76NL8\|Q76NL8_PLAF7 Falcilysin OS=Plasmodium falciparum (isolate 3D7) GN=flN PE=1 SV=1 | 4 | 1.10 | 0.19 | 0.0013 |
| tr\|Q8IIW0\|Q8IIW0_PLAF7 PfSNF2L OS=Plasmodium falciparum (isolate 3D7) GN=PF11_0053 PE=4 SV=1 | 4 | 1.10 | 0.11 | 0.0003 |
| tr\|Q8IL02\|Q8IL02_PLAF7 40S ribosomal protein S2, putative OS=Plasmodium falciparum (isolate 3D7) GN=PF14_0448 PE=1 SV=1 | 4 | 1.10 | 0.20 | 0.0016 |
| tr\|Q8IL58\|Q8IL58_PLAF7 60S ribosomal protein L1, putative OS=Plasmodium falciparum (isolate 3D7) GN=PF14_0391 PE=4 SV=1 | 4 | 1.10 | 0.22 | 0.0022 |

| | | | | |
|---|---|---|---|---|
| tr\|Q8IM10\|Q8IM10_PLAF7 40S ribosomal protein S8 OS=Plasmodium falciparum (isolate 3D7) GN=PF14_0083 PE=1 SV=1 | 4 | 1.10 | 0.20 | 0.0016 |
| tr\|C6KT23\|C6KT23_PLAF7 60S ribosomal protein L27a, putative OS=Plasmodium falciparum (isolate 3D7) GN=PFF0885w PE=1 SV=1 | 4 | 1.10 | 0.23 | 0.0023 |
| tr\|O97248\|O97248_PLAF7 40S ribosomal protein S23, putative OS=Plasmodium falciparum (isolate 3D7) GN=PFC0290w PE=1 SV=1 | 4 | 1.11 | 0.07 | 0.0001 |
| tr\|Q8II01\|Q8II01_PLAF7 Tudor staphylococcal nuclease OS=Plasmodium falciparum (isolate 3D7) GN=TSN PE=4 SV=1 | 4 | 1.11 | 0.36 | 0.0088 |
| tr\|Q8I3R6\|Q8I3R6_PLAF7 40S ribosomal protein S24 OS=Plasmodium falciparum (isolate 3D7) GN=PFE0975c PE=3 SV=1 | 4 | 1.11 | 0.12 | 0.0004 |
| tr\|Q8IE99\|Q8IE99_PLAF7 Splicing factor, putative OS=Plasmodium falciparum (isolate 3D7) GN=MAL13P1.120 PE=4 SV=1 | 4 | 1.11 | 0.24 | 0.0028 |
| tr\|Q8I322\|Q8I322_PLAF7 Putative uncharacterized protein OS=Plasmodium falciparum (isolate 3D7) GN=PFI0635c PE=4 SV=1 | 4 | 1.11 | 0.15 | 0.0007 |
| tr\|C0H5K9\|C0H5K9_PLAF7 Phosphatidylserine synthase I, putative OS=Plasmodium falciparum (isolate 3D7) GN=MAL13P1.335 PE=4 SV=1 | 4 | 1.11 | 0.11 | 0.0002 |
| tr\|C6KSV9\|C6KSV9_PLAF7 SWI/SNF-related matrix-associated actin-dependent regulator of chromatin OS=Plasmodium falciparum (isolate 3D7) GN=PFF0560c PE=4 SV=1 | 4 | 1.11 | 0.17 | 0.0009 |
| tr\|Q8IKM5\|Q8IKM5_PLAF7 60S ribosomal protein L27, putative OS=Plasmodium falciparum (isolate 3D7) GN=PF14_0579 PE=1 SV=2 | 4 | 1.11 | 0.19 | 0.0013 |
| tr\|Q8IAX6\|Q8IAX6_PLAF7 60S ribosomal protein L13 OS=Plasmodium falciparum (isolate 3D7) GN=PF08_0075 PE=3 SV=1 | 4 | 1.11 | 0.24 | 0.0027 |
| sp\|P06753-6\|TPM3_HUMAN Isoform 6 of Tropomyosin alpha-3 chain OS=Homo sapiens GN=TPM3;sp\|P06753\|TPM3_HUMAN Tropomyosin alpha-3 chain OS=Homo sapiens GN=TPM3 PE=1 SV=2 | 4 | 1.11 | 0.31 | 0.0058 |
| tr\|Q8ILJ1\|Q8ILJ1_PLAF7 Uncharacterized protein OS=Plasmodium falciparum (isolate 3D7) GN=PF14_0252 PE=4 SV=1 | 4 | 1.11 | 0.11 | 0.0003 |
| tr\|C0H4K6\|C0H4K6_PLAF7 Ubiquitin transferase, putative OS=Plasmodium falciparum (isolate 3D7) GN=MAL7P1.19 PE=4 SV=1 | 4 | 1.11 | 0.39 | 0.0109 |
| tr\|Q8I3T9\|Q8I3T9_PLAF7 60S ribosomal protein L8, putative OS=Plasmodium falciparum (isolate 3D7) GN=PFE0845c PE=1 SV=1 | 4 | 1.11 | 0.13 | 0.0005 |
| tr\|Q8IJC6\|Q8IJC6_PLAF7 Ribosomal protein L3, putative OS=Plasmodium falciparum (isolate 3D7) GN=PF10_0272 PE=1 SV=1 | 4 | 1.11 | 0.20 | 0.0015 |
| tr\|Q8I3Z9\|Q8I3Z9_PLAF7 Topoisomerase I OS=Plasmodium falciparum (isolate 3D7) GN=PFE0520c PE=4 SV=1 | 4 | 1.11 | 0.29 | 0.0045 |
| tr\|Q8IDS6\|Q8IDS6_PLAF7 60S ribosomal protein L18a OS=Plasmodium falciparum (isolate 3D7) GN=PF13_0224 PE=1 SV=1 | 4 | 1.11 | 0.23 | 0.0024 |
| tr\|C6KSR4\|C6KSR4_PLAF7 Uncharacterized protein OS=Plasmodium falciparum (isolate 3D7) GN=PFF0325c PE=4 SV=1 | 4 | 1.11 | 0.25 | 0.0029 |
| tr\|Q8IDR9\|Q8IDR9_PLAF7 40S ribosomal protein S6, putative OS=Plasmodium falciparum (isolate 3D7) GN=PF13_0228 PE=1 SV=1 | 4 | 1.11 | 0.29 | 0.0047 |
| tr\|Q8IIU3\|Q8IIU3_PLAF7 RuvB DNA helicase, putative OS=Plasmodium falciparum (isolate 3D7) GN=PF11_0071 PE=4 SV=1 | 4 | 1.11 | 0.15 | 0.0006 |
| tr\|Q8I3K0\|Q8I3K0_PLAF7 Uncharacterized protein OS=Plasmodium falciparum (isolate 3D7) GN=PFE1320w PE=4 SV=1 | 4 | 1.11 | 0.33 | 0.0069 |
| tr\|Q8IEM3\|Q8IEM3_PLAF7 60S ribosomal protein L24, putative OS=Plasmodium falciparum (isolate 3D7) GN=PF13_0049 PE=1 SV=1 | 4 | 1.11 | 0.12 | 0.0003 |
| tr\|Q8II99\|Q8II99_PLAF7 Uncharacterized protein OS=Plasmodium falciparum (isolate 3D7) GN=PF11_0275 PE=4 SV=1 | 4 | 1.11 | 0.08 | 0.0001 |
| tr\|Q8IE85\|Q8IE85_PLAF7 60S ribosomal protein L6, putative OS=Plasmodium falciparum (isolate 3D7) GN=PF13_0129 PE=1 SV=1 | 4 | 1.11 | 0.23 | 0.0025 |
| tr\|C0H5B6\|C0H5B6_PLAF7 Uncharacterized protein OS=Plasmodium falciparum (isolate 3D7) GN=MAL13P1.79 PE=4 SV=1 | 4 | 1.11 | 0.12 | 0.0003 |
| tr\|Q8IHT9\|Q8IHT9_PLAF7 60S ribosomal protein L35Ae, putative OS=Plasmodium falciparum (isolate 3D7) GN=PF11_0438 PE=1 SV=1 | 4 | 1.11 | 0.20 | 0.0017 |
| tr\|Q8IDW0\|Q8IDW0_PLAF7 1-deoxy-D-xylulose 5-phosphate synthase OS=Plasmodium falciparum (isolate 3D7) GN=MAL13P1.186 PE=4 SV=1 | 4 | 1.11 | 0.24 | 0.0027 |
| tr\|Q8IHV7\|Q8IHV7_PLAF7 Conserved Plasmodium protein OS=Plasmodium falciparum (isolate 3D7) GN=PF11_0419 PE=4 SV=2 | 4 | 1.12 | 0.16 | 0.0007 |
| tr\|Q8I5I3\|Q8I5I3_PLAF7 Phospholipid-transporting ATPase, putative OS=Plasmodium falciparum (isolate 3D7) GN=PFL1125w PE=4 SV=1 | 4 | 1.12 | 0.09 | 0.0002 |
| tr\|Q8IJT9\|Q8IJT9_PLAF7 Eukaryotic translation initiation factor 2, beta, putative OS=Plasmodium falciparum (isolate 3D7) GN=PF10_0103 PE=4 SV=1 | 4 | 1.12 | 0.29 | 0.0043 |
| tr\|Q8ILQ3\|Q8ILQ3_PLAF7 Uncharacterized protein OS=Plasmodium falciparum (isolate 3D7) GN=PF14_0191 PE=4 SV=1 | 4 | 1.12 | 0.10 | 0.0002 |

| | | | | |
|---|---|---|---|---|
| tr\|Q8I3R0\|Q8I3R0_PLAF7 40S ribosomal protein S9, putative OS=Plasmodium falciparum (isolate 3D7) GN=PFE1005w PE=3 SV=1 | 4 | 1.12 | 0.15 | 0.0007 |
| tr\|Q8I431\|Q8I431_PLAF7 60S ribosomal protein L4, putative OS=Plasmodium falciparum (isolate 3D7) GN=PFE0350c PE=1 SV=1 | 4 | 1.12 | 0.20 | 0.0016 |
| tr\|Q8IM23\|Q8IM23_PLAF7 Fibrillarin, putative OS=Plasmodium falciparum (isolate 3D7) GN=PF14_0068 PE=3 SV=1 | 4 | 1.12 | 0.25 | 0.0029 |
| tr\|O77395\|O77395_PLAF7 40S ribosomal protein S15A, putative OS=Plasmodium falciparum (isolate 3D7) GN=PFC0735w PE=1 SV=1 | 4 | 1.12 | 0.14 | 0.0006 |
| sp\|O97313\|RS3A_PLAF7 40S ribosomal protein S3a OS=Plasmodium falciparum (isolate 3D7) GN=MAL3P7.35 PE=1 SV=1 | 4 | 1.13 | 0.24 | 0.0026 |
| tr\|C6KSY6\|C6KSY6_PLAF7 60S ribosomal protein L19, putative OS=Plasmodium falciparum (isolate 3D7) GN=PFF0700c PE=1 SV=1 | 4 | 1.13 | 0.24 | 0.0027 |
| tr\|O97238\|O97238_PLAF7 Putative uncharacterized protein OS=Plasmodium falciparum (isolate 3D7) GN=PFC0240c PE=4 SV=3 | 4 | 1.13 | 0.17 | 0.0009 |
| tr\|Q8IJK8\|Q8IJK8_PLAF7 Ribosomal protein L30e, putative OS=Plasmodium falciparum (isolate 3D7) GN=PF10_0187 PE=1 SV=1 | 4 | 1.13 | 0.10 | 0.0002 |
| tr\|Q8I5Y3\|Q8I5Y3_PLAF7 Eukaryotic translation initiation factor 3 subunit C OS=Plasmodium falciparum (isolate 3D7) GN=PFL0310c PE=3 SV=1 | 4 | 1.13 | 0.08 | 0.0001 |
| tr\|Q8ILK3\|Q8ILK3_PLAF7 60S ribosomal protein L21e, putative OS=Plasmodium falciparum (isolate 3D7) GN=PF14_0240 PE=1 SV=1 | 4 | 1.13 | 0.23 | 0.0023 |
| tr\|Q8I358\|Q8I358_PLAF7 Exoribonuclease, putative OS=Plasmodium falciparum (isolate 3D7) GN=PFI0455w PE=4 SV=1 | 4 | 1.13 | 0.11 | 0.0003 |
| tr\|Q8I0W9\|Q8I0W9_PLAF7 Stearoyl-CoA Delta 9 desaturase, putative OS=Plasmodium falciparum (isolate 3D7) GN=PFE0555w PE=3 SV=1 | 4 | 1.14 | 0.27 | 0.0036 |
| tr\|Q8IB94\|Q8IB94_PLAF7 Ubiquitin-protein ligase 1, putative OS=Plasmodium falciparum (isolate 3D7) GN=MAL8P1.23 PE=4 SV=1 | 4 | 1.14 | 0.29 | 0.0044 |
| tr\|Q8IET7\|Q8IET7_PLAF7 40S ribosomal protein S7, putative OS=Plasmodium falciparum (isolate 3D7) GN=PF13_0014 PE=1 SV=1 | 4 | 1.14 | 0.16 | 0.0007 |
| sp\|Q8IJD4\|RSSA_PLAF7 40S ribosomal protein SA OS=Plasmodium falciparum (isolate 3D7) GN=PF10_0264 PE=1 SV=1 | 4 | 1.14 | 0.36 | 0.0082 |
| tr\|Q8IBY4\|Q8IBY4_PLAF7 60S ribosomal protein L34-A, putative OS=Plasmodium falciparum (isolate 3D7) GN=PF07_0043 PE=1 SV=1 | 4 | 1.14 | 0.28 | 0.0037 |
| tr\|O96169\|O96169_PLAF7 RNA binding protein, putative OS=Plasmodium falciparum (isolate 3D7) GN=PFB0370c PE=4 SV=1 | 4 | 1.14 | 0.13 | 0.0004 |
| tr\|Q8IDI5\|Q8IDI5_PLAF7 60S ribosomal protein L17, putative OS=Plasmodium falciparum (isolate 3D7) GN=PF13_0268 PE=1 SV=1 | 4 | 1.14 | 0.21 | 0.0016 |
| tr\|Q8IBT2\|Q8IBT2_PLAF7 Eukaryotic translation initiation factor 3 subunit I OS=Plasmodium falciparum (isolate 3D7) GN=MAL7P1.81 PE=3 SV=1 | 4 | 1.14 | 0.05 | 0.0000 |
| tr\|Q8IL13\|Q8IL13_PLAF7 Helicase, putative OS=Plasmodium falciparum (isolate 3D7) GN=PF14_0437 PE=3 SV=2 | 4 | 1.14 | 0.06 | 0.0000 |
| tr\|Q8I2N0\|Q8I2N0_PLAF7 Phosphatidylserine decarboxylase OS=Plasmodium falciparum (isolate 3D7) GN=PfPSD PE=4 SV=1 | 4 | 1.14 | 0.10 | 0.0002 |
| tr\|Q8I3H9\|Q8I3H9_PLAF7 Nucleolar preribosomal GTPase, putative OS=Plasmodium falciparum (isolate 3D7) GN=PFE1435c PE=4 SV=1 | 4 | 1.14 | 0.28 | 0.0037 |
| tr\|Q8IHS5\|Q8IHS5_PLAF7 40S ribosomal protein S21 OS=Plasmodium falciparum (isolate 3D7) GN=PF11_0454 PE=1 SV=1 | 4 | 1.14 | 0.42 | 0.0120 |
| tr\|Q8IC08\|Q8IC08_PLAF7 DNA-directed RNA polymerase 2 8.2 kDa polypeptide, putative OS=Plasmodium falciparum (isolate 3D7) GN=PF07_0027 PE=3 SV=1 | 4 | 1.14 | 0.17 | 0.0008 |
| tr\|Q8I3Q6\|Q8I3Q6_PLAF7 Uncharacterized protein OS=Plasmodium falciparum (isolate 3D7) GN=PFE1025c PE=4 SV=1 | 4 | 1.15 | 0.16 | 0.0007 |
| tr\|Q8IB67\|Q8IB67_PLAF7 Histone acetyltransferase GCN5, putative OS=Plasmodium falciparum (isolate 3D7) GN=gcn5 PE=1 SV=2 | 4 | 1.15 | 0.24 | 0.0023 |
| tr\|Q8I5M3\|Q8I5M3_PLAF7 Uncharacterized protein OS=Plasmodium falciparum (isolate 3D7) GN=PFL0895c PE=4 SV=1 | 4 | 1.15 | 0.23 | 0.0020 |
| tr\|Q8IBA0\|Q8IBA0_PLAF7 Receptor for activated C kinase homolog, PfRACK OS=Plasmodium falciparum (isolate 3D7) GN=PfRACK PE=4 SV=1 | 4 | 1.15 | 0.25 | 0.0026 |
| tr\|Q8I3I5\|Q8I3I5_PLAF7 Eukaryotic translation initiation factor 3 subunit E OS=Plasmodium falciparum (isolate 3D7) GN=PFE1405c PE=3 SV=1 | 4 | 1.15 | 0.11 | 0.0002 |
| tr\|C0H4U4\|C0H4U4_PLAF7 Uncharacterized protein OS=Plasmodium falciparum (isolate 3D7) GN=MAL8P1.95 PE=4 SV=1 | 4 | 1.15 | 0.54 | 0.0234 |
| tr\|Q8I3B0\|Q8I3B0_PLAF7 60S ribosomal protein L32, putative OS=Plasmodium falciparum (isolate 3D7) GN=PFI0190w PE=4 SV=1 | 4 | 1.15 | 0.24 | 0.0023 |
| tr\|Q8IIW1\|Q8IIW1_PLAF7 Qa-SNARE protein, putative OS=Plasmodium falciparum (isolate 3D7) GN=Syn13 PE=4 SV=2 | 4 | 1.15 | 0.26 | 0.0031 |
| tr\|Q8IBN5\|Q8IBN5_PLAF7 40S ribosomal protein S5, putative OS=Plasmodium falciparum (isolate 3D7) GN=PF07_0088 PE=1 SV=1 | 4 | 1.15 | 0.26 | 0.0029 |

| | | | | |
|---|---|---|---|---|
| tr\|O97266\|O97266_PLAF7 Translation initiation factor E4, putative OS=Plasmodium falciparum (isolate 3D7) GN=PFC0635c PE=3 SV=1 | 4 | 1.15 | 0.07 | 0.0001 |
| tr\|Q8IJW4\|Q8IJW4_PLAF7 Eukaryotic translation initiation factor 3 subunit D OS=Plasmodium falciparum (isolate 3D7) GN=PF10_0077 PE=3 SV=1 | 4 | 1.16 | 0.06 | 0.0000 |
| tr\|Q6ZMA8\|Q6ZMA8_PLAF7 Vacuolar ATP synthase subunit b OS=Plasmodium falciparum (isolate 3D7) GN=PFD0305c PE=3 SV=1 | 4 | 1.16 | 0.17 | 0.0008 |
| tr\|Q8IIR6\|Q8IIR6_PLAF7 Heat shock protein DnaJ homologue Pfj2 OS=Plasmodium falciparum (isolate 3D7) GN=PF11_0099 PE=4 SV=1 | 4 | 1.16 | 0.44 | 0.0137 |
| tr\|C0H4A6\|C0H4A6_PLAF7 Ribosomal protein L15 OS=Plasmodium falciparum (isolate 3D7) GN=PFD0770c PE=1 SV=1 | 4 | 1.16 | 0.16 | 0.0007 |
| tr\|O77381\|O77381_PLAF7 40S ribosomal protein S11, putative OS=Plasmodium falciparum (isolate 3D7) GN=PFC0775w PE=1 SV=2 | 4 | 1.16 | 0.39 | 0.0093 |
| tr\|C6KSR5\|C6KSR5_PLAF7 Coatomer alpha subunit, putative OS=Plasmodium falciparum (isolate 3D7) GN=PFF0330w PE=4 SV=1 | 4 | 1.16 | 0.13 | 0.0004 |
| tr\|Q8IDN9\|Q8IDN9_PLAF7 Uncharacterized protein OS=Plasmodium falciparum (isolate 3D7) GN=PF13_0243 PE=4 SV=1 | 4 | 1.16 | 0.38 | 0.0086 |
| tr\|Q8ILA9\|Q8ILA9_PLAF7 Uncharacterized protein OS=Plasmodium falciparum (isolate 3D7) GN=PF14_0336 PE=4 SV=1 | 4 | 1.16 | 0.32 | 0.0054 |
| tr\|Q8IIS2\|Q8IIS2_PLAF7 Uncharacterized protein OS=Plasmodium falciparum (isolate 3D7) GN=PF11_0093 PE=4 SV=1 | 4 | 1.17 | 0.36 | 0.0073 |
| tr\|Q8I599\|Q8I599_PLAF7 Cytochrome b5, putative OS=Plasmodium falciparum (isolate 3D7) GN=PFL1555w PE=3 SV=1 | 4 | 1.17 | 0.49 | 0.0177 |
| tr\|Q8IJT8\|Q8IJT8_PLAF7 Conserved Plasmodium protein OS=Plasmodium falciparum (isolate 3D7) GN=PF10_0104 PE=4 SV=1 | 4 | 1.17 | 0.32 | 0.0053 |
| tr\|Q8IIX0\|Q8IIX0_PLAF7 60S acidic ribosomal protein p1, putative OS=Plasmodium falciparum (isolate 3D7) GN=PF11_0043 PE=3 SV=1 | 4 | 1.17 | 0.33 | 0.0057 |
| tr\|Q8IIQ7\|Q8IIQ7_PLAF7 Asparagine-rich antigen OS=Plasmodium falciparum (isolate 3D7) GN=PF11_0111 PE=4 SV=1 | 4 | 1.17 | 0.16 | 0.0007 |
| tr\|Q8I2H1\|Q8I2H1_PLAF7 UBX domain, putative OS=Plasmodium falciparum (isolate 3D7) GN=PFI1680w PE=4 SV=1 | 4 | 1.17 | 0.27 | 0.0034 |
| tr\|Q8IBQ5\|Q8IBQ5_PLAF7 40S ribosomal protein S10, putative OS=Plasmodium falciparum (isolate 3D7) GN=PF07_0080 PE=1 SV=1 | 4 | 1.18 | 0.19 | 0.0011 |
| tr\|C0H553\|C0H553_PLAF7 Flavodoxin-like protein OS=Plasmodium falciparum (isolate 3D7) GN=PFI1140w PE=4 SV=1 | 4 | 1.18 | 0.32 | 0.0053 |
| tr\|Q8IB14\|Q8IB14_PLAF7 High mobility group protein OS=Plasmodium falciparum (isolate 3D7) GN=PfHMGB2 PE=1 SV=1 | 4 | 1.18 | 0.17 | 0.0008 |
| tr\|Q8I3V8\|Q8I3V8_PLAF7 RNA recognition motif, putative OS=Plasmodium falciparum (isolate 3D7) GN=PFE0750c PE=4 SV=1 | 4 | 1.18 | 0.19 | 0.0010 |
| tr\|Q8I5S6\|Q8I5S6_PLAF7 Eukaryotic translation initiation factor 3 subunit A OS=Plasmodium falciparum (isolate 3D7) GN=PFL0625c PE=3 SV=1 | 4 | 1.18 | 0.13 | 0.0004 |
| tr\|Q8IIE2\|Q8IIE2_PLAF7 Uncharacterized protein OS=Plasmodium falciparum (isolate 3D7) GN=PF11_0232 PE=4 SV=1 | 4 | 1.18 | 0.38 | 0.0082 |
| tr\|Q8IHX2\|Q8IHX2_PLAF7 Malaria antigen OS=Plasmodium falciparum (isolate 3D7) GN=PF11_0404 PE=4 SV=1 | 4 | 1.18 | 0.08 | 0.0001 |
| tr\|Q8I3J5\|Q8I3J5_PLAF7 DNA helicase OS=Plasmodium falciparum (isolate 3D7) GN=PFE1345c PE=3 SV=1 | 4 | 1.15 | 0.98 | 0.0999 |
| tr\|Q8IL82\|Q8IL82_PLAF7 Uncharacterized protein OS=Plasmodium falciparum (isolate 3D7) GN=PF14_0365 PE=4 SV=1 | 4 | 1.18 | 0.15 | 0.0006 |
| tr\|Q8ID26\|Q8ID26_PLAF7 Uncharacterized protein OS=Plasmodium falciparum (isolate 3D7) GN=PF13_0356 PE=4 SV=1 | 4 | 1.18 | 0.13 | 0.0003 |
| tr\|Q8IE45\|Q8IE45_PLAF7 Uncharacterized protein OS=Plasmodium falciparum (isolate 3D7) GN=PF13_0153 PE=4 SV=1 | 4 | 1.18 | 0.29 | 0.0040 |
| tr\|Q8I5V9\|Q8I5V9_PLAF7 Uncharacterized protein OS=Plasmodium falciparum (isolate 3D7) GN=PFL0445w PE=4 SV=1 | 4 | 1.19 | 0.38 | 0.0083 |
| tr\|Q8IL83\|Q8IL83_PLAF7 Cleavage and polyadenylation specificity factor protein, putative OS=Plasmodium falciparum (isolate 3D7) GN=PF14_0364 PE=4 SV=1 | 4 | 1.19 | 0.14 | 0.0004 |
| tr\|Q8IBQ6\|Q8IBQ6_PLAF7 60S ribosomal protein L11a, putative OS=Plasmodium falciparum (isolate 3D7) GN=PF07_0079 PE=1 SV=1 | 4 | 1.19 | 0.22 | 0.0017 |
| sp\|O96184\|RL37A_PLAF7 60S ribosomal protein L37a OS=Plasmodium falciparum (isolate 3D7) GN=RPL37A PE=1 SV=1 | 4 | 1.19 | 0.19 | 0.0011 |
| tr\|Q8IHW4\|Q8IHW4_PLAF7 V-type proton ATPase subunit F OS=Plasmodium falciparum (isolate 3D7) GN=PF11_0412 PE=3 SV=2 | 4 | 1.19 | 0.13 | 0.0004 |
| sp\|Q8I3Z1\|MLRR1_PLAF7 MATH and LRR domain-containing protein PFE0570w OS=Plasmodium falciparum (isolate 3D7) GN=PFE0570w PE=2 SV=1 | 4 | 1.19 | 0.10 | 0.0002 |
| tr\|Q8IE57\|Q8IE57_PLAF7 Uncharacterized protein OS=Plasmodium falciparum (isolate 3D7) GN=PF13_0147 PE=4 SV=1 | 4 | 1.19 | 0.23 | 0.0020 |

| | | | | |
|---|---|---|---|---|
| tr\|Q8ILZ7\|Q8ILZ7_PLAF7 RNA binding protein, putative OS=Plasmodium falciparum (isolate 3D7) GN=PF14_0096 PE=4 SV=1 | 4 | 1.19 | 0.20 | 0.0012 |
| tr\|Q8IKQ9\|Q8IKQ9_PLAF7 Signal peptide peptidase OS=Plasmodium falciparum (isolate 3D7) GN=SPP PE=4 SV=2 | 4 | 1.19 | 0.31 | 0.0046 |
| tr\|Q8I5T4\|Q8I5T4_PLAF7 DNA helicase OS=Plasmodium falciparum (isolate 3D7) GN=PFL0580w PE=3 SV=1 | 4 | 1.19 | 0.74 | 0.0481 |
| tr\|Q8IC16\|Q8IC16_PLAF7 DNA helicase OS=Plasmodium falciparum (isolate 3D7) GN=PF07_0023 PE=3 SV=1 | 4 | 1.19 | 0.60 | 0.0289 |
| tr\|Q8I0W8\|Q8I0W8_PLAF7 Deoxyribodipyrimidine photolyase (Photoreactivating enzyme, DNA photolyase), putative OS=Plasmodium falciparum (isolate 3D7) GN=PFE0675c PE=4 SV=1 | 4 | 1.20 | 0.28 | 0.0033 |
| tr\|Q8I3T1\|Q8I3T1_PLAF7 Eukaryotic translation initiation factor 3 subunit B OS=Plasmodium falciparum (isolate 3D7) GN=PFE0885w PE=3 SV=1 | 4 | 1.20 | 0.10 | 0.0002 |
| tr\|Q8IE96\|Q8IE96_PLAF7 Adenosine-diphosphatase OS=Plasmodium falciparum (isolate 3D7) GN=MAL13P1.121 PE=4 SV=1 | 4 | 1.20 | 0.62 | 0.0310 |
| tr\|Q8IBH7\|Q8IBH7_PLAF7 Eukaryotic translation initiation factor 2 alpha subunit, putative OS=Plasmodium falciparum (isolate 3D7) GN=PF07_0117 PE=4 SV=1 | 4 | 1.20 | 0.32 | 0.0049 |
| tr\|Q8IEN2\|Q8IEN2_PLAF7 40S ribosomal protein S27, putative OS=Plasmodium falciparum (isolate 3D7) GN=PF13_0045 PE=1 SV=1 | 4 | 1.20 | 0.30 | 0.0039 |
| tr\|Q8IM35\|Q8IM35_PLAF7 RNA binding protein, putative OS=Plasmodium falciparum (isolate 3D7) GN=PF14_0056 PE=4 SV=1 | 4 | 1.17 | 1.00 | 0.1011 |
| tr\|O96258\|O96258_PLAF7 40S ribosomal protein S26e, putative OS=Plasmodium falciparum (isolate 3D7) GN=PFB0830w PE=1 SV=1 | 4 | 1.17 | 0.88 | 0.0758 |
| tr\|C0H5G3\|C0H5G3_PLAF7 60S ribosomal protein L18 OS=Plasmodium falciparum (isolate 3D7) GN=MAL13P1.209 PE=1 SV=1 | 4 | 1.20 | 0.29 | 0.0037 |
| tr\|C0H5B1\|C0H5B1_PLAF7 Asparagine-rich protein OS=Plasmodium falciparum (isolate 3D7) GN=MAL13P1.63 PE=4 SV=1 | 4 | 1.21 | 0.19 | 0.0010 |
| tr\|Q8I280\|Q8I280_PLAF7 V-type ATPase, subunit C, putative OS=Plasmodium falciparum (isolate 3D7) GN=PFA_0300c PE=4 SV=1 | 4 | 1.21 | 0.22 | 0.0017 |
| tr\|Q8IIS4\|Q8IIS4_PLAF7 Transcription factor with AP2 domain(S), putative OS=Plasmodium falciparum (isolate 3D7) GN=PF11_0091 PE=4 SV=1 | 4 | 1.21 | 0.10 | 0.0002 |
| tr\|Q8IJF6\|Q8IJF6_PLAF7 Conserved Plasmodium protein OS=Plasmodium falciparum (isolate 3D7) GN=PF10_0242 PE=4 SV=2 | 4 | 1.21 | 0.08 | 0.0001 |
| tr\|Q8IDM3\|Q8IDM3_PLAF7 Uncharacterized protein OS=Plasmodium falciparum (isolate 3D7) GN=MAL13P1.237 PE=4 SV=1 | 4 | 1.21 | 0.08 | 0.0001 |
| tr\|Q8ILR7\|Q8ILR7_PLAF7 DNA helicase OS=Plasmodium falciparum (isolate 3D7) GN=PF14_0177 PE=3 SV=1 | 4 | 1.21 | 0.61 | 0.0284 |
| sp\|Q9TY95\|SERA_PLAF7 Serine-repeat antigen protein OS=Plasmodium falciparum (isolate 3D7) GN=SERA PE=1 SV=1 | 4 | 1.22 | 0.55 | 0.0212 |
| tr\|O77385\|O77385_PLAF7 Protein kinase, putative OS=Plasmodium falciparum (isolate 3D7) GN=Pfcrk-4 PE=4 SV=1 | 4 | 1.22 | 0.11 | 0.0002 |
| tr\|Q8IIL0\|Q8IIL0_PLAF7 Falcipain-3 OS=Plasmodium falciparum (isolate 3D7) GN=PF11_0162 PE=3 SV=1 | 4 | 1.22 | 0.32 | 0.0046 |
| tr\|C0H4Q0\|C0H4Q0_PLAF7 Signal recognition particle SRP9, putative OS=Plasmodium falciparum (isolate 3D7) GN=MAL7P1.158 PE=4 SV=1 | 4 | 1.22 | 0.43 | 0.0111 |
| tr\|O96271\|O96271_PLAF7 Replication factor C subunit 1, putative OS=Plasmodium falciparum (isolate 3D7) GN=PFB0895c PE=4 SV=1 | 4 | 1.22 | 0.44 | 0.0113 |
| tr\|Q8IB09\|Q8IB09_PLAF7 Asparagine-rich antigen OS=Plasmodium falciparum (isolate 3D7) GN=PF08_0060 PE=4 SV=1 | 4 | 1.23 | 0.17 | 0.0007 |
| tr\|Q8II23\|Q8II23_PLAF7 Protein disulfide isomerase related protein OS=Plasmodium falciparum (isolate 3D7) GN=PF11_0352 PE=4 SV=1 | 4 | 1.23 | 0.67 | 0.0349 |
| tr\|Q8IJS7\|Q8IJS7_PLAF7 QF122 antigen OS=Plasmodium falciparum (isolate 3D7) GN=PF10_0115 PE=4 SV=1 | 4 | 1.23 | 0.20 | 0.0012 |
| tr\|Q8IKA6\|Q8IKA6_PLAF7 DNAJ protein, putative OS=Plasmodium falciparum (isolate 3D7) GN=PF14_0700 PE=4 SV=1 | 4 | 1.23 | 0.42 | 0.0099 |
| tr\|Q8IKT7\|Q8IKT7_PLAF7 Uncharacterized protein OS=Plasmodium falciparum (isolate 3D7) GN=PF14_0515 PE=4 SV=1 | 4 | 1.23 | 0.12 | 0.0003 |
| sp\|O15770\|GSHR_PLAF7 Glutathione reductase OS=Plasmodium falciparum (isolate 3D7) GN=GR3 PE=2 SV=4 | 4 | 1.24 | 0.33 | 0.0051 |
| tr\|Q8II72\|Q8II72_PLAF7 Uncharacterized protein OS=Plasmodium falciparum (isolate 3D7) GN=PF11_0302 PE=4 SV=1 | 4 | 1.24 | 0.13 | 0.0003 |
| tr\|O96260\|O96260_PLAF7 Replication factor C, subunit 2 OS=Plasmodium falciparum (isolate 3D7) GN=PFB0840w PE=4 SV=1 | 4 | 1.24 | 0.73 | 0.0423 |
| tr\|Q8IE50\|Q8IE50_PLAF7 Myosin OS=Plasmodium falciparum (isolate 3D7) GN=MAL13P1.148 PE=4 SV=1 | 4 | 1.24 | 0.11 | 0.0002 |
| tr\|Q8IES4\|Q8IES4_PLAF7 DNA ligase OS=Plasmodium falciparum (isolate 3D7) GN=PfLigI PE=3 SV=1 | 4 | 1.24 | 0.54 | 0.0191 |

| | | | | |
|---|---|---|---|---|
| sp\|P04040\|CATA_HUMAN Catalase OS=Homo sapiens GN=CAT PE=1 SV=3 | 4 | 1.25 | 0.06 | 0.0000 |
| tr\|Q8IEC3\|Q8IEC3_PLAF7 N2,N2-dimethylguanosine tRNA methyltransferase, putative OS=Plasmodium falciparum (isolate 3D7) GN=PF13_0109 PE=4 SV=1 | 4 | 1.26 | 0.38 | 0.0071 |
| tr\|Q8IIA8\|Q8IIA8_PLAF7 Small nuclear ribonucleoprotein D1, putative OS=Plasmodium falciparum (isolate 3D7) GN=PF11_0266 PE=4 SV=1 | 4 | 1.26 | 0.16 | 0.0005 |
| tr\|Q8I348\|Q8I348_PLAF7 Selenide water dikinase, putative OS=Plasmodium falciparum (isolate 3D7) GN=PFI0505c PE=4 SV=1 | 4 | 1.26 | 0.31 | 0.0038 |
| tr\|Q8IAW0\|Q8IAW0_PLAF7 Importin subunit alpha OS=Plasmodium falciparum (isolate 3D7) GN=PF08_0087 PE=3 SV=1 | 4 | 1.26 | 0.24 | 0.0020 |
| tr\|Q8IJT1\|Q8IJT1_PLAF7 Proteasome subunit beta type OS=Plasmodium falciparum (isolate 3D7) GN=PF10_0111 PE=3 SV=1 | 4 | 1.26 | 0.15 | 0.0005 |
| tr\|Q8I2W3\|Q8I2W3_PLAF7 Nucleosome assembly protein OS=Plasmodium falciparum (isolate 3D7) GN=PFI0930c PE=3 SV=1 | 4 | 1.26 | 0.37 | 0.0065 |
| tr\|Q8I574\|Q8I574_PLAF7 Splicing factor 3b, subunit 3, 130kD, putative OS=Plasmodium falciparum (isolate 3D7) GN=PFL1680w PE=4 SV=1 | 4 | 1.26 | 0.28 | 0.0030 |
| tr\|Q7KQJ9\|Q7KQJ9_PLAF7 Proliferating cell nuclear antigen OS=Plasmodium falciparum (isolate 3D7) GN=PFL1285c PE=3 SV=1 | 4 | 1.28 | 0.28 | 0.0028 |
| sp\|Q8ILW9\|ACT2_PLAF7 Actin-2 OS=Plasmodium falciparum (isolate 3D7) GN=PF14_0124 PE=3 SV=1 | 4 | 1.28 | 0.24 | 0.0018 |
| tr\|C6S3F0\|C6S3F0_PLAF7 Acylphosphatase, putative OS=Plasmodium falciparum (isolate 3D7) GN=PF11_0121 PE=3 SV=1 | 4 | 1.28 | 0.24 | 0.0018 |
| sp\|Q7KQM4\|PLM1_PLAF7 Plasmepsin-1 OS=Plasmodium falciparum (isolate 3D7) GN=PF14_0076 PE=2 SV=1 | 4 | 1.28 | 0.27 | 0.0025 |
| tr\|Q9TY94\|Q9TY94_PLAF7 DEAD box helicase, UAP56 OS=Plasmodium falciparum (isolate 3D7) GN=UAP56 PE=4 SV=1 | 4 | 1.28 | 0.20 | 0.0011 |
| tr\|Q8II16\|Q8II16_PLAF7 Coatomer delta subunit, putative OS=Plasmodium falciparum (isolate 3D7) GN=PF11_0359 PE=4 SV=1 | 4 | 1.29 | 0.24 | 0.0017 |
| tr\|Q8IJB1\|Q8IJB1_PLAF7 Uncharacterized protein OS=Plasmodium falciparum (isolate 3D7) GN=PF10_0287 PE=4 SV=1 | 4 | 1.29 | 0.57 | 0.0202 |
| tr\|C0H4W2\|C0H4W2_PLAF7 Lsm3 homologue, putative OS=Plasmodium falciparum (isolate 3D7) GN=PF08_0049 PE=4 SV=1 | 4 | 1.30 | 0.41 | 0.0082 |
| tr\|Q8IM15\|Q8IM15_PLAF7 HAP protein OS=Plasmodium falciparum (isolate 3D7) GN=PF14_0078 PE=1 SV=1 | 4 | 1.30 | 0.20 | 0.0010 |
| tr\|Q8IE68\|Q8IE68_PLAF7 Lsm6 homologue, putative OS=Plasmodium falciparum (isolate 3D7) GN=PF13_0142 PE=4 SV=1 | 4 | 1.31 | 0.26 | 0.0022 |
| tr\|Q8IJD2\|Q8IJD2_PLAF7 Uncharacterized protein OS=Plasmodium falciparum (isolate 3D7) GN=PF10_0266 PE=4 SV=1 | 4 | 1.32 | 0.34 | 0.0043 |
| tr\|Q8IEM5\|Q8IEM5_PLAF7 NUDIX hydrolase, putative OS=Plasmodium falciparum (isolate 3D7) GN=PF13_0048 PE=4 SV=1 | 4 | 1.32 | 0.18 | 0.0007 |
| tr\|O97285\|O97285_PLAF7 ATP-dependent RNA Helicase, putative OS=Plasmodium falciparum (isolate 3D7) GN=PFC0915w PE=3 SV=1 | 4 | 1.33 | 0.09 | 0.0001 |
| tr\|Q8IHQ8\|Q8IHQ8_PLAF7 Uncharacterized protein OS=Plasmodium falciparum (isolate 3D7) GN=PF11_0471 PE=4 SV=1 | 4 | 1.33 | 0.37 | 0.0053 |
| tr\|Q8ID50\|Q8ID50_PLAF7 60S ribosomal protein L40/UBI, putative OS=Plasmodium falciparum (isolate 3D7) GN=PF13_0346 PE=1 SV=1;tr\|Q7KQK2\|Q7KQK2_PLAF7 PfpUB Plasmodium falciparum polyubiquitin OS=Plasmodium falciparum (isolate 3D7) GN=PFL0585w PE=4 SV=1 | 4 | 1.34 | 0.04 | 0.0000 |
| tr\|Q8IDN4\|Q8IDN4_PLAF7 Nucleic acid binding protein, putative OS=Plasmodium falciparum (isolate 3D7) GN=MAL13P1.233 PE=4 SV=1 | 4 | 1.34 | 0.10 | 0.0001 |
| tr\|Q8I2Y5\|Q8I2Y5_PLAF7 RNA binding protein, putative OS=Plasmodium falciparum (isolate 3D7) GN=PFI0820c PE=4 SV=1 | 4 | 1.35 | 0.17 | 0.0005 |
| tr\|Q8I2X0\|Q8I2X0_PLAF7 Eukaryotic translation initiation factor 3 subunit 5, putative OS=Plasmodium falciparum (isolate 3D7) GN=PFI0895c PE=4 SV=1 | 4 | 1.35 | 0.37 | 0.0053 |
| tr\|Q8IIH2\|Q8IIH2_PLAF7 Clathrin coat assembly protein, putative OS=Plasmodium falciparum (isolate 3D7) GN=PF11_0202 PE=4 SV=1 | 4 | 1.35 | 0.35 | 0.0045 |
| tr\|Q8I2G2\|Q8I2G2_PLAF7 Cytoadherence linked asexual protein 9(CLAG9) OS=Plasmodium falciparum (isolate 3D7) GN=CLAG9 PE=4 SV=1 | 4 | 1.35 | 0.35 | 0.0046 |
| tr\|Q8IDF0\|Q8IDF0_PLAF7 DNA helicase OS=Plasmodium falciparum (isolate 3D7) GN=PF13_0291 PE=3 SV=1 | 4 | 1.35 | 0.72 | 0.0329 |
| tr\|C6KT34\|C6KT34_PLAF7 Cell division cycle protein 48 homologue, putative OS=Plasmodium falciparum (isolate 3D7) GN=PFF0940c PE=3 SV=1 | 4 | 1.36 | 0.22 | 0.0012 |
| tr\|Q8IM45\|Q8IM45_PLAF7 Uncharacterized protein OS=Plasmodium falciparum (isolate 3D7) GN=PF14_0046 PE=4 SV=1 | 4 | 1.36 | 0.75 | 0.0360 |
| tr\|Q8IEI4\|Q8IEI4_PLAF7 Ubiquitin-like protein nedd8 homologue, putative OS=Plasmodium falciparum (isolate 3D7) GN=MAL13P1.64 PE=4 SV=1 | 4 | 1.36 | 0.29 | 0.0026 |

| | | | | |
|---|---|---|---|---|
| tr\|O77361\|O77361_PLAF7 Putative uncharacterized protein OS=Plasmodium falciparum (isolate 3D7) GN=PFC0435w PE=4 SV=1 | 4 | 1.30 | 0.88 | 0.0603 |
| tr\|Q7KQK6\|Q7KQK6_PLAF7 GTP-binding nuclear protein ran/tc4 OS=Plasmodium falciparum (isolate 3D7) GN=PF11_0183 PE=4 SV=1 | 4 | 1.36 | 0.20 | 0.0008 |
| sp\|O75695\|XRP2_HUMAN Protein XRP2 OS=Homo sapiens GN=RP2 PE=1 SV=4 | 4 | 1.31 | 0.97 | 0.0744 |
| tr\|Q8I1Q5\|Q8I1Q5_PLAF7 Eukaryotic translation initiation factor 3 subunit M OS=Plasmodium falciparum (isolate 3D7) GN=PFD0880w PE=3 SV=1 | 4 | 1.36 | 0.42 | 0.0076 |
| tr\|Q8IIT3\|Q8IIT3_PLAF7 Lsm4 homologue, putative OS=Plasmodium falciparum (isolate 3D7) GN=PF11_0524 PE=4 SV=2 | 4 | 1.36 | 0.26 | 0.0018 |
| tr\|Q8IKW4\|Q8IKW4_PLAF7 Uncharacterized protein OS=Plasmodium falciparum (isolate 3D7) GN=PF14_0487 PE=4 SV=1 | 4 | 1.36 | 0.14 | 0.0003 |
| tr\|Q8IE31\|Q8IE31_PLAF7 Uncharacterized protein OS=Plasmodium falciparum (isolate 3D7) GN=PF13_0162 PE=4 SV=1 | 4 | 1.33 | 1.03 | 0.0817 |
| tr\|Q8ILM0\|Q8ILM0_PLAF7 Cyclophilin, putative OS=Plasmodium falciparum (isolate 3D7) GN=PF14_0223 PE=4 SV=2 | 4 | 1.37 | 0.37 | 0.0051 |
| tr\|Q8IES0\|Q8IES0_PLAF7 Small heat shock protein, putative OS=Plasmodium falciparum (isolate 3D7) GN=PF13_0021 PE=3 SV=1 | 4 | 1.38 | 0.78 | 0.0387 |
| tr\|Q8I441\|Q8I441_PLAF7 60S ribosomal subunit protein L24-2, putative OS=Plasmodium falciparum (isolate 3D7) GN=PFE0300c PE=4 SV=1 | 4 | 1.38 | 0.21 | 0.0010 |
| sp\|Q8IAY6\|SODF_PLAF7 Superoxide dismutase [Fe] OS=Plasmodium falciparum (isolate 3D7) GN=SODB PE=1 SV=1 | 4 | 1.38 | 0.45 | 0.0089 |
| tr\|Q8IIR9\|Q8IIR9_PLAF7 Casein kinase II, alpha subunit, putative OS=Plasmodium falciparum (isolate 3D7) GN=PF11_0096 PE=4 SV=1 | 4 | 1.39 | 0.63 | 0.0216 |
| tr\|Q8IAR6\|Q8IAR6_PLAF7 Proteasome subunit alpha type 5, putative OS=Plasmodium falciparum (isolate 3D7) GN=PF08_0109 PE=4 SV=1 | 4 | 1.40 | 0.58 | 0.0166 |
| tr\|Q8ILT0\|Q8ILT0_PLAF7 Glutamate dehydrogenase OS=Plasmodium falciparum (isolate 3D7) GN=PF14_0164 PE=3 SV=1 | 4 | 1.41 | 0.32 | 0.0031 |
| tr\|Q8IIW4\|Q8IIW4_PLAF7 Uncharacterized protein OS=Plasmodium falciparum (isolate 3D7) GN=PF11_0049 PE=4 SV=1 | 4 | 1.41 | 0.48 | 0.0100 |
| tr\|Q8I713\|Q8I713_PLAF7 60S ribosomal protein L36 OS=Plasmodium falciparum (isolate 3D7) GN=PF11_0106 PE=1 SV=2 | 4 | 1.42 | 0.68 | 0.0246 |
| tr\|Q8IEA6\|Q8IEA6_PLAF7 Dihydrolipamide succinyltransferase component of 2-oxoglutarate dehydrogenase complex OS=Plasmodium falciparum (isolate 3D7) GN=PF13_0121 PE=3 SV=1 | 4 | 1.42 | 0.85 | 0.0444 |
| tr\|Q8IM16\|Q8IM16_PLAF7 Plasmepsin IV OS=Plasmodium falciparum (isolate 3D7) GN=PF14_0075 PE=1 SV=1 | 4 | 1.43 | 0.22 | 0.0010 |
| tr\|Q8I1S0\|Q8I1S0_PLAF7 Small GTP-binding protein sar1 OS=Plasmodium falciparum (isolate 3D7) GN=sar1 PE=3 SV=1 | 4 | 1.43 | 0.24 | 0.0013 |
| tr\|C6KT13\|C6KT13_PLAF7 Uncharacterized protein OS=Plasmodium falciparum (isolate 3D7) GN=PFF0835w PE=4 SV=1 | 4 | 1.43 | 0.39 | 0.0054 |
| tr\|Q8I608\|Q8I608_PLAF7 Nucleosome assembly protein 1, putative OS=Plasmodium falciparum (isolate 3D7) GN=PFL0185c PE=1 SV=2 | 4 | 1.43 | 0.26 | 0.0015 |
| tr\|Q8ILM2\|Q8ILM2_PLAF7 GTPase, putative OS=Plasmodium falciparum (isolate 3D7) GN=PF14_0221 PE=4 SV=1 | 4 | 1.43 | 0.50 | 0.0105 |
| tr\|C0H5J2\|C0H5J2_PLAF7 Uncharacterized protein OS=Plasmodium falciparum (isolate 3D7) GN=MAL13P1.295 PE=4 SV=1 | 4 | 1.44 | 0.14 | 0.0003 |
| tr\|Q8I6Z5\|Q8I6Z5_PLAF7 Plasmepsin V OS=Plasmodium falciparum (isolate 3D7) GN=PF13_0133 PE=3 SV=1 | 4 | 1.44 | 0.48 | 0.0095 |
| tr\|C0H5H0\|C0H5H0_PLAF7 Heat shock protein 70 (Hsp70), putative OS=Plasmodium falciparum (isolate 3D7) GN=MAL13P1.540 PE=3 SV=1 | 4 | 1.38 | 0.99 | 0.0678 |
| tr\|O96259\|O96259_PLAF7 Conserved Plasmodium protein OS=Plasmodium falciparum (isolate 3D7) GN=PFB0835c PE=4 SV=1 | 4 | 1.44 | 0.31 | 0.0027 |
| sp\|Q8IHZ9\|KC1_PLAF7 Casein kinase I OS=Plasmodium falciparum (isolate 3D7) GN=CK1 PE=3 SV=1;tr\|C6S3F7\|C6S3F7_PLAF7 Casein kinase 1, PfCK1 OS=Plasmodium falciparum (isolate 3D7) GN=PfCK1 PE=3 SV=1 | 4 | 1.44 | 0.24 | 0.0013 |
| tr\|Q8IIR7\|Q8IIR7_PLAF7 Endoplasmic reticulum-resident calcium binding protein OS=Plasmodium falciparum (isolate 3D7) GN=PF11_0098 PE=4 SV=1 | 4 | 1.39 | 0.99 | 0.0665 |
| tr\|Q8ILQ6\|Q8ILQ6_PLAF7 Uncharacterized protein OS=Plasmodium falciparum (isolate 3D7) GN=PF14_0188 PE=4 SV=2 | 4 | 1.44 | 0.22 | 0.0010 |
| tr\|C0H4V6\|C0H4V6_PLAF7 14-3-3 protein, putative OS=Plasmodium falciparum (isolate 3D7) GN=MAL8P1.69 PE=3 SV=1 | 4 | 1.44 | 0.25 | 0.0014 |
| tr\|Q8I444\|Q8I444_PLAF7 Small ubiquitin-related modifier, putative OS=Plasmodium falciparum (isolate 3D7) GN=PfSUMO PE=4 SV=1 | 4 | 1.44 | 0.19 | 0.0007 |
| sp\|Q7KQL3\|ARF1_PLAF7 ADP-ribosylation factor 1 OS=Plasmodium falciparum (isolate 3D7) GN=ARF1 PE=1 SV=1 | 4 | 1.45 | 0.26 | 0.0016 |

| | | | | |
|---|---|---|---|---|
| tr\|Q8I6V3\|Q8I6V3_PLAF7 Plasmepsin II OS=Plasmodium falciparum (isolate 3D7) GN=PF14_0077 PE=3 SV=1 | 4 | 1.47 | 0.36 | 0.0039 |
| tr\|Q8II60\|Q8II60_PLAF7 26S protease subunit regulatory subunit 6a, putative OS=Plasmodium falciparum (isolate 3D7) GN=PF11_0314 PE=3 SV=1 | 4 | 1.47 | 0.60 | 0.0163 |
| tr\|Q8I426\|Q8I426_PLAF7 Nuclear pore associated protein (NLP4), putative OS=Plasmodium falciparum (isolate 3D7) GN=PFE0380c PE=4 SV=1 | 4 | 1.49 | 0.28 | 0.0018 |
| sp\|Q7KQM1\|PRI1_PLAF7 DNA primase small subunit OS=Plasmodium falciparum (isolate 3D7) GN=PF14_0366 PE=3 SV=1 | 4 | 1.49 | 0.65 | 0.0200 |
| tr\|Q8ID28\|Q8ID28_PLAF7 Proteasome regulatory subunit, putative OS=Plasmodium falciparum (isolate 3D7) GN=MAL13P1.343 PE=4 SV=1 | 4 | 1.44 | 0.93 | 0.0537 |
| tr\|Q8I2U4\|Q8I2U4_PLAF7 RNA binding protein, putative OS=Plasmodium falciparum (isolate 3D7) GN=PFI1025w PE=4 SV=1 | 4 | 1.44 | 1.11 | 0.0804 |
| tr\|Q8I5C4\|Q8I5C4_PLAF7 T-complex protein 1 subunit gamma OS=Plasmodium falciparum (isolate 3D7) GN=PFL1425w PE=3 SV=1 | 4 | 1.49 | 0.43 | 0.0063 |
| tr\|C0H4Y6\|C0H4Y6_PLAF7 Protein disulfide-isomerase OS=Plasmodium falciparum (isolate 3D7) GN=PfPDI-8 PE=3 SV=1 | 4 | 1.44 | 1.00 | 0.0635 |
| tr\|Q8I259\|Q8I259_PLAF7 Putative uncharacterized protein OS=Plasmodium falciparum (isolate 3D7) GN=PFA_0410w PE=4 SV=1 | 4 | 1.50 | 0.10 | 0.0001 |
| tr\|Q8I616\|Q8I616_PLAF7 High mobility group protein OS=Plasmodium falciparum (isolate 3D7) GN=PFL0145c PE=4 SV=1 | 4 | 1.50 | 0.35 | 0.0033 |
| tr\|Q8IDR5\|Q8IDR5_PLAF7 Casein kinase II subunit beta OS=Plasmodium falciparum (isolate 3D7) GN=PfCK2beta2 PE=3 SV=1 | 4 | 1.50 | 0.80 | 0.0328 |
| tr\|Q8II27\|Q8II27_PLAF7 RNA (Uracil-5-)methyltransferase, putative OS=Plasmodium falciparum (isolate 3D7) GN=PF11_0348 PE=4 SV=2 | 4 | 1.50 | 0.41 | 0.0053 |
| tr\|Q8IEK1\|Q8IEK1_PLAF7 M1-family aminopeptidase OS=Plasmodium falciparum (isolate 3D7) GN=MAL13P1.56 PE=4 SV=1 | 4 | 1.52 | 0.83 | 0.0349 |
| tr\|Q8I0V4\|Q8I0V4_PLAF7 Endoplasmin homolog, putative OS=Plasmodium falciparum (isolate 3D7) GN=PFL1070c PE=1 SV=1 | 4 | 1.45 | 1.09 | 0.0763 |
| sp\|P00492\|HPRT_HUMAN Hypoxanthine-guanine phosphoribosyltransferase OS=Homo sapiens GN=HPRT1 PE=1 SV=2 | 4 | 1.52 | 0.41 | 0.0051 |
| tr\|Q8IKH3\|Q8IKH3_PLAF7 26S proteasome subunit, putative OS=Plasmodium falciparum (isolate 3D7) GN=PF14_0632 PE=4 SV=1 | 4 | 1.52 | 0.79 | 0.0306 |
| tr\|Q8IB24\|Q8IB24_PLAF7 Heat shock 70 kDa protein OS=Plasmodium falciparum (isolate 3D7) GN=PF08_0054 PE=3 SV=1 | 4 | 1.53 | 0.29 | 0.0018 |
| tr\|Q8IEE5\|Q8IEE5_PLAF7 DNA replication licensing factor MCM4-related OS=Plasmodium falciparum (isolate 3D7) GN=PF13_0095 PE=3 SV=1 | 4 | 1.48 | 0.97 | 0.0554 |
| tr\|O96153\|O96153_PLAF7 Proteasome 26S regulatory subunit, putative OS=Plasmodium falciparum (isolate 3D7) GN=PFB0260w PE=4 SV=3 | 4 | 1.53 | 0.64 | 0.0173 |
| tr\|Q8ILP6\|Q8ILP6_PLAF7 Glycine-tRNA ligase, putative OS=Plasmodium falciparum (isolate 3D7) GN=PF14_0198 PE=3 SV=2 | 4 | 1.54 | 0.59 | 0.0140 |
| tr\|O96212\|O96212_PLAF7 Heat shock 40 kDa protein, putative OS=Plasmodium falciparum (isolate 3D7) GN=PFB0595w PE=4 SV=1 | 4 | 1.55 | 0.29 | 0.0017 |
| tr\|Q8IJI9\|Q8IJI9_PLAF7 Uncharacterized protein OS=Plasmodium falciparum (isolate 3D7) GN=PF10_0208 PE=4 SV=1 | 4 | 1.49 | 1.02 | 0.0604 |
| tr\|Q8IB73\|Q8IB73_PLAF7 Oxoglutarate/malate translocator protein, putative OS=Plasmodium falciparum (isolate 3D7) GN=PF08_0031 PE=3 SV=1 | 4 | 1.56 | 0.61 | 0.0148 |
| tr\|Q8IK24\|Q8IK24_PLAF7 Acyl CoA binding protein, putative OS=Plasmodium falciparum (isolate 3D7) GN=PF10_0016 PE=4 SV=1 | 4 | 1.56 | 0.79 | 0.0290 |
| tr\|C6KT90\|C6KT90_PLAF7 Uncharacterized protein OS=Plasmodium falciparum (isolate 3D7) GN=PFF1230c PE=4 SV=1 | 4 | 1.50 | 1.21 | 0.0884 |
| tr\|Q8IIT1\|Q8IIT1_PLAF7 Conserved Plasmodium protein OS=Plasmodium falciparum (isolate 3D7) GN=PF11_0084 PE=4 SV=2 | 4 | 1.56 | 0.41 | 0.0047 |
| tr\|Q8I5F9\|Q8I5F9_PLAF7 Ubiquitin-activating enzyme e1, putative OS=Plasmodium falciparum (isolate 3D7) GN=PFL1245w PE=4 SV=1 | 4 | 1.57 | 0.52 | 0.0092 |
| tr\|Q8IL11\|Q8IL11_PLAF7 M17 leucyl aminopeptidase OS=Plasmodium falciparum (isolate 3D7) GN=LAP PE=1 SV=1 | 4 | 1.59 | 0.69 | 0.0189 |
| tr\|Q8I2Q0\|Q8I2Q0_PLAF7 Putative uncharacterized protein OS=Plasmodium falciparum (isolate 3D7) GN=PFI1270w PE=4 SV=1 | 4 | 1.59 | 0.52 | 0.0088 |
| tr\|Q8IKX4\|Q8IKX4_PLAF7 Signal recognition particle SRP54, putative OS=Plasmodium falciparum (isolate 3D7) GN=PF14_0477 PE=3 SV=1 | 4 | 1.59 | 0.58 | 0.0119 |
| tr\|Q8IJL2\|Q8IJL2_PLAF7 Uncharacterized protein OS=Plasmodium falciparum (isolate 3D7) GN=PF10_0183 PE=4 SV=1 | 4 | 1.59 | 0.21 | 0.0006 |
| tr\|Q8IC10\|Q8IC10_PLAF7 Cdk105, putative OS=Plasmodium falciparum (isolate 3D7) GN=MAL7P1.24 PE=4 SV=1 | 4 | 1.54 | 1.41 | 0.1165 |
| tr\|Q8IKT5\|Q8IKT5_PLAF7 Peptidase, putative OS=Plasmodium falciparum (isolate 3D7) GN=PF14_0517 PE=3 SV=1 | 4 | 1.59 | 0.54 | 0.0098 |

| | | | | |
|---|---|---|---|---|
| tr\|Q8IL94\|Q8IL94_PLAF7 Ribonucleoside-diphosphate reductase OS=Plasmodium falciparum (isolate 3D7) GN=PF14_0352 PE=3 SV=1 | 4 | 1.60 | 0.45 | 0.0056 |
| tr\|Q7KQK3\|Q7KQK3_PLAF7 Heat shock protein DNAJ homologue Pfj4 OS=Plasmodium falciparum (isolate 3D7) GN=PFL0565w PE=4 SV=1 | 4 | 1.60 | 0.56 | 0.0107 |
| tr\|Q8I447\|Q8I447_PLAF7 DNA mismatch repair protein MSH6 OS=Plasmodium falciparum (isolate 3D7) GN=PFE0270c PE=3 SV=1 | 4 | 1.61 | 0.78 | 0.0256 |
| tr\|C6KSV4\|C6KSV4_PLAF7 Transcription elongation factor SPT5 OS=Plasmodium falciparum (isolate 3D7) GN=PFF0535c PE=3 SV=1 | 4 | 1.59 | 1.42 | 0.1114 |
| tr\|Q8IK90\|Q8IK90_PLAF7 Proteosome subunit alpha type 1, putative OS=Plasmodium falciparum (isolate 3D7) GN=PF14_0716 PE=4 SV=1 | 4 | 1.61 | 0.67 | 0.0171 |
| tr\|C0H4B1\|C0H4B1_PLAF7 Memo-like protein OS=Plasmodium falciparum (isolate 3D7) GN=PFD0850c PE=3 SV=1 | 4 | 1.61 | 0.37 | 0.0032 |
| tr\|Q8I3M5\|Q8I3M5_PLAF7 Karyopherin beta OS=Plasmodium falciparum (isolate 3D7) GN=PFE1195w PE=4 SV=1 | 4 | 1.61 | 0.28 | 0.0014 |
| tr\|Q8IEQ1\|Q8IEQ1_PLAF7 26S proteasome regulatory subunit, putative OS=Plasmodium falciparum (isolate 3D7) GN=PF13_0033 PE=3 SV=1 | 4 | 1.62 | 0.78 | 0.0257 |
| tr\|C0H4U5\|C0H4U5_PLAF7 Uncharacterized protein OS=Plasmodium falciparum (isolate 3D7) GN=PF08_0081 PE=4 SV=1 | 4 | 1.62 | 0.67 | 0.0166 |
| tr\|Q8IM66\|Q8IM66_PLAF7 Proteosome subunit, putative OS=Plasmodium falciparum (isolate 3D7) GN=PF14_0025 PE=4 SV=1 | 4 | 1.63 | 0.81 | 0.0273 |
| tr\|Q8IAL6\|Q8IAL6_PLAF7 Mannose-6-phosphate isomerase, putative OS=Plasmodium falciparum (isolate 3D7) GN=MAL8P1.156 PE=4 SV=1 | 4 | 1.64 | 0.34 | 0.0024 |
| tr\|C0H4E8\|C0H4E8_PLAF7 Proteasome subunit beta type OS=Plasmodium falciparum (isolate 3D7) GN=PFE0915c PE=3 SV=1 | 4 | 1.64 | 0.83 | 0.0291 |
| tr\|Q8IDA3\|Q8IDA3_PLAF7 Uncharacterized protein OS=Plasmodium falciparum (isolate 3D7) GN=MAL13P1.299 PE=4 SV=1 | 4 | 1.61 | 1.21 | 0.0757 |
| sp\|Q8IIJ9\|CATC_PLAF7 Probable cathepsin C OS=Plasmodium falciparum (isolate 3D7) GN=PF11_0174 PE=1 SV=1 | 4 | 1.64 | 0.76 | 0.0231 |
| tr\|A0A087WUQ6\|A0A087WUQ6_HUMAN Glutathione peroxidase OS=Homo sapiens GN=GPX1 PE=1 SV=1;sp\|P07203\|GPX1_HUMAN Glutathione peroxidase 1 OS=Homo sapiens GN=GPX1 PE=1 SV=4 | 4 | 1.64 | 0.61 | 0.0128 |
| tr\|Q8I1V1\|Q8I1V1_PLAF7 26S proteasome AAA-ATPase subunit RPT3, putative OS=Plasmodium falciparum (isolate 3D7) GN=PFD0665c PE=3 SV=1 | 4 | 1.64 | 0.87 | 0.0323 |
| tr\|Q8IDG2\|Q8IDG2_PLAF7 Proteasome subunit alpha type OS=Plasmodium falciparum (isolate 3D7) GN=MAL13P1.270 PE=3 SV=1 | 4 | 1.65 | 0.76 | 0.0226 |
| tr\|Q8IAR3\|Q8IAR3_PLAF7 Proteasome subunit alpha, putative OS=Plasmodium falciparum (isolate 3D7) GN=MAL8P1.128 PE=4 SV=2 | 4 | 1.65 | 0.93 | 0.0379 |
| tr\|Q8I2J3\|Q8I2J3_PLAF7 M18 aspartyl aminopeptidase OS=Plasmodium falciparum (isolate 3D7) GN=PfM18AAP PE=1 SV=1 | 4 | 1.68 | 0.90 | 0.0333 |
| tr\|C6KST3\|C6KST3_PLAF7 Proteasome subunit alpha type 2, putative OS=Plasmodium falciparum (isolate 3D7) GN=PFF0420c PE=4 SV=1 | 4 | 1.69 | 0.88 | 0.0313 |
| tr\|Q8IAY9\|Q8IAY9_PLAF7 Importin beta, putative OS=Plasmodium falciparum (isolate 3D7) GN=PF08_0069 PE=4 SV=1 | 4 | 1.69 | 0.54 | 0.0081 |
| tr\|Q8IKC9\|Q8IKC9_PLAF7 Proteasome subunit beta type OS=Plasmodium falciparum (isolate 3D7) GN=PF14_0676 PE=3 SV=2 | 4 | 1.73 | 0.92 | 0.0326 |
| tr\|Q8IEK3\|Q8IEK3_PLAF7 26S proteasome regulatory subunit 7, putative OS=Plasmodium falciparum (isolate 3D7) GN=PF13_0063 PE=3 SV=2 | 4 | 1.73 | 0.79 | 0.0223 |
| tr\|Q8IIV8\|Q8IIV8_PLAF7 Uncharacterized protein OS=Plasmodium falciparum (isolate 3D7) GN=PF11_0055 PE=4 SV=1 | 4 | 1.66 | 1.43 | 0.1036 |
| tr\|Q8I3J0\|Q8I3J0_PLAF7 Hsp70 interacting protein, putative OS=Plasmodium falciparum (isolate 3D7) GN=PFE1370w PE=4 SV=1 | 4 | 1.76 | 0.50 | 0.0058 |
| tr\|Q8I6U5\|Q8I6U5_PLAF7 Falcipain-2, putative OS=Plasmodium falciparum (isolate 3D7) GN=PF11_0161 PE=3 SV=1;tr\|Q8I6U4\|Q8I6U4_PLAF7 Falcipain 2 OS=Plasmodium falciparum (isolate 3D7) GN=PF11_0165 PE=1 SV=1 | 4 | 1.80 | 0.57 | 0.0080 |
| tr\|Q8IDC8\|Q8IDC8_PLAF7 Uncharacterized protein OS=Plasmodium falciparum (isolate 3D7) GN=PF13_0309 PE=4 SV=1 | 4 | 1.70 | 1.89 | 0.1708 |
| tr\|Q8I333\|Q8I333_PLAF7 Falstatin, putative OS=Plasmodium falciparum (isolate 3D7) GN=PFI0580c PE=4 SV=1 | 4 | 1.70 | 1.58 | 0.1199 |
| sp\|Q8I4X0\|ACT1_PLAF7 Actin-1 OS=Plasmodium falciparum (isolate 3D7) GN=PFL2215w PE=3 SV=1 | 4 | 1.80 | 0.52 | 0.0060 |
| tr\|C0H4L1\|C0H4L1_PLAF7 Uncharacterized protein OS=Plasmodium falciparum (isolate 3D7) GN=MAL7P1.202 PE=4 SV=1 | 4 | 1.81 | 0.37 | 0.0022 |
| tr\|Q8IE73\|Q8IE73_PLAF7 MSF1-like protein, putative OS=Plasmodium falciparum (isolate 3D7) GN=PF13_0138 PE=4 SV=1 | 4 | 1.74 | 2.07 | 0.1915 |
| tr\|C0H5F2\|C0H5F2_PLAF7 Uncharacterized protein OS=Plasmodium falciparum (isolate 3D7) GN=MAL13P1.172 PE=4 SV=1 | 4 | 1.82 | 0.45 | 0.0039 |

| | | | | |
|---|---|---|---|---|
| tr\|Q8IIK8\|Q8IIK8_PLAF7 Peptidyl-prolyl cis-trans isomerase OS=Plasmodium falciparum (isolate 3D7) GN=PF11_0164 PE=3 SV=1 | 4 | 1.77 | 1.64 | 0.1205 |
| tr\|Q8I538\|Q8I538_PLAF7 Uncharacterized protein OS=Plasmodium falciparum (isolate 3D7) GN=PFL1865w PE=4 SV=1 | 4 | 1.77 | 1.33 | 0.0764 |
| tr\|Q8I2U5\|Q8I2U5_PLAF7 Inosine-5-monophosphate dehydrogenase OS=Plasmodium falciparum (isolate 3D7) GN=PFI1020c PE=3 SV=1 | 4 | 1.82 | 1.05 | 0.0401 |
| tr\|Q8I5C6\|Q8I5C6_PLAF7 Uncharacterized protein OS=Plasmodium falciparum (isolate 3D7) GN=PFL1415w PE=4 SV=1 | 4 | 1.80 | 1.74 | 0.1299 |
| tr\|Q8I3L4\|Q8I3L4_PLAF7 Acyl-CoA synthetase, PfACS10 OS=Plasmodium falciparum (isolate 3D7) GN=PfACS10 PE=4 SV=1 | 4 | 1.85 | 0.83 | 0.0210 |
| tr\|Q8I542\|Q8I542_PLAF7 Calcyclin binding protein, putative OS=Plasmodium falciparum (isolate 3D7) GN=PFL1845c PE=4 SV=2 | 4 | 1.87 | 0.52 | 0.0056 |
| tr\|Q8IIF6\|Q8IIF6_PLAF7 Conserved Plasmodium protein OS=Plasmodium falciparum (isolate 3D7) GN=PF11_0218 PE=4 SV=2 | 4 | 1.87 | 0.42 | 0.0029 |
| tr\|C0H5C6\|C0H5C6_PLAF7 SNARE protein, putative OS=Plasmodium falciparum (isolate 3D7) GN=PfSNAP23 PE=4 SV=1 | 4 | 1.82 | 1.32 | 0.0702 |
| tr\|C6S3E1\|C6S3E1_PLAF7 Leucine-rich repeat protein 8, LRR8 OS=Plasmodium falciparum (isolate 3D7) GN=PF10_0320a PE=4 SV=1 | 4 | 1.84 | 2.06 | 0.1721 |
| tr\|Q8IBI3\|Q8IBI3_PLAF7 Proteasome subunit alpha type OS=Plasmodium falciparum (isolate 3D7) GN=PF07_0112 PE=3 SV=1 | 4 | 1.88 | 1.10 | 0.0423 |
| tr\|Q8IDG3\|Q8IDG3_PLAF7 Proteasome subunit alpha type OS=Plasmodium falciparum (isolate 3D7) GN=PF13_0282 PE=3 SV=1 | 4 | 1.86 | 1.52 | 0.0924 |
| tr\|Q8IAL4\|Q8IAL4_PLAF7 Uncharacterized protein OS=Plasmodium falciparum (isolate 3D7) GN=PF08_0134 PE=4 SV=1 | 4 | 1.86 | 2.05 | 0.1673 |
| tr\|Q8I5A3\|Q8I5A3_PLAF7 Asparagine-rich protein, putative OS=Plasmodium falciparum (isolate 3D7) GN=PFL1530w PE=4 SV=1 | 4 | 1.89 | 0.21 | 0.0004 |
| tr\|Q8IIJ6\|Q8IIJ6_PLAF7 Ubiquitin C-terminal hydrolase, family 1, putative OS=Plasmodium falciparum (isolate 3D7) GN=PF11_0177 PE=4 SV=1 | 4 | 1.90 | 0.98 | 0.0309 |
| tr\|Q8I3B4\|Q8I3B4_PLAF7 DEAD/DEAH box helicase, putative OS=Plasmodium falciparum (isolate 3D7) GN=PFI0165c PE=4 SV=1 | 4 | 1.96 | 0.50 | 0.0044 |
| tr\|Q7KQK0\|Q7KQK0_PLAF7 CAMP-dependent protein kinase regulatory subunit, putative OS=Plasmodium falciparum (isolate 3D7) GN=PKAr PE=4 SV=1 | 4 | 1.97 | 0.75 | 0.0137 |
| tr\|Q9U0J0\|Q9U0J0_PLAF7 Replication factor a protein, putative OS=Plasmodium falciparum (isolate 3D7) GN=PFD0470c PE=4 SV=1 | 4 | 1.97 | 1.18 | 0.0446 |
| tr\|Q8IJQ9\|Q8IJQ9_PLAF7 Uncharacterized protein OS=Plasmodium falciparum (isolate 3D7) GN=PF10_0133 PE=4 SV=1 | 4 | 1.90 | 1.48 | 0.0830 |
| tr\|O77396\|O77396_PLAF7 Proteasome component C8, putative OS=Plasmodium falciparum (isolate 3D7) GN=PFC0745c PE=4 SV=1 | 4 | 1.91 | 1.42 | 0.0740 |
| tr\|Q8I2Z8\|Q8I2Z8_PLAF7 6-phosphofructokinase, putative OS=Plasmodium falciparum (isolate 3D7) GN=PFI0755c PE=4 SV=1 | 4 | 1.93 | 1.26 | 0.0548 |
| tr\|Q7K6A9\|Q7K6A9_PLAF7 Proteasome subunit beta type OS=Plasmodium falciparum (isolate 3D7) GN=MAL8P1.142 PE=3 SV=1 | 4 | 1.95 | 1.24 | 0.0520 |
| tr\|Q8I535\|Q8I535_PLAF7 Long-chain-fatty-acid--CoA ligase, putative OS=Plasmodium falciparum (isolate 3D7) GN=PFL1880w PE=4 SV=1 | 4 | 1.98 | 1.00 | 0.0286 |
| tr\|Q8IL88\|Q8IL88_PLAF7 HSP40, subfamily A, putative OS=Plasmodium falciparum (isolate 3D7) GN=PF14_0359 PE=4 SV=1 | 4 | 1.98 | 0.77 | 0.0144 |
| tr\|Q8I3V9\|Q8I3V9_PLAF7 Uncharacterized protein OS=Plasmodium falciparum (isolate 3D7) GN=PFE0745w PE=4 SV=1 | 4 | 1.97 | 1.27 | 0.0532 |
| tr\|Q8IEN3\|Q8IEN3_PLAF7 Carbamoyl phosphate synthetase OS=Plasmodium falciparum (isolate 3D7) GN=cpsSII PE=4 SV=1 | 4 | 2.08 | 0.86 | 0.0168 |
| tr\|Q8IHS1\|Q8IHS1_PLAF7 Uncharacterized protein OS=Plasmodium falciparum (isolate 3D7) GN=PF11_0458 PE=4 SV=1 | 4 | 1.98 | 1.92 | 0.1312 |
| sp\|Q8I3Z5\|TCTP_PLAF7 Translationally-controlled tumor protein homolog OS=Plasmodium falciparum (isolate 3D7) GN=TCTP PE=1 SV=1 | 4 | 2.09 | 0.97 | 0.0230 |
| tr\|Q8IBX7\|Q8IBX7_PLAF7 Uncharacterized protein OS=Plasmodium falciparum (isolate 3D7) GN=MAL7P1.36 PE=4 SV=1 | 4 | 1.98 | 1.91 | 0.1297 |
| tr\|Q8ILX3\|Q8ILX3_PLAF7 Uncharacterized protein OS=Plasmodium falciparum (isolate 3D7) GN=PF14_0120 PE=4 SV=1 | 4 | 1.99 | 1.73 | 0.1049 |
| tr\|Q9U0H0\|Q9U0H0_PLAF7 Uncharacterized protein OS=Plasmodium falciparum (isolate 3D7) GN=PFD0595w PE=4 SV=1 | 4 | 1.99 | 1.80 | 0.1137 |
| tr\|Q8I3N5\|Q8I3N5_PLAF7 G10 protein, putative OS=Plasmodium falciparum (isolate 3D7) GN=PFE1140c PE=4 SV=1 | 4 | 2.00 | 1.79 | 0.1113 |
| tr\|Q8IHW3\|Q8IHW3_PLAF7 Conserved Plasmodium protein OS=Plasmodium falciparum (isolate 3D7) GN=PF11_0413 PE=4 SV=2 | 4 | 2.00 | 1.55 | 0.0814 |
| tr\|C0H551\|C0H551_PLAF7 Glutamine synthetase, putative OS=Plasmodium falciparum (isolate 3D7) GN=PFI1110w PE=3 SV=1 | 4 | 2.01 | 1.37 | 0.0610 |

| | | | | |
|---|---|---|---|---|
| tr\|Q8IC05\|Q8IC05_PLAF7 Heat shock protein 86 OS=Plasmodium falciparum (isolate 3D7) GN=PF07_0029 PE=1 SV=1 | 4 | 2.13 | 1.24 | 0.0412 |
| tr\|Q8IJP3\|Q8IJP3_PLAF7 Cysteinyl-tRNA synthetase, putative OS=Plasmodium falciparum (isolate 3D7) GN=PF10_0149 PE=3 SV=2 | 4 | 2.17 | 0.66 | 0.0071 |
| sp\|C6KT50\|PDX1_PLAF7 Pyridoxal 5-phosphate synthase subunit Pdx1 OS=Plasmodium falciparum (isolate 3D7) GN=pdx1 PE=1 SV=1 | 4 | 2.15 | 1.44 | 0.0585 |
| tr\|C0H4U0\|C0H4U0_PLAF7 Uncharacterized protein OS=Plasmodium falciparum (isolate 3D7) GN=MAL8P1.103 PE=4 SV=1 | 4 | 2.17 | 1.79 | 0.0947 |
| tr\|Q8I3M1\|Q8I3M1_PLAF7 Cytosolic preribosomal GTP-binding protein, putative OS=Plasmodium falciparum (isolate 3D7) GN=PFE1215c PE=4 SV=1 | 4 | 2.17 | 0.62 | 0.0059 |
| tr\|Q8I323\|Q8I323_PLAF7 26S proteasome regulatory subunit, putative OS=Plasmodium falciparum (isolate 3D7) GN=PFI0630w PE=4 SV=1 | 4 | 2.19 | 1.37 | 0.0494 |
| tr\|C6KTA9\|C6KTA9_PLAF7 C3h4-type ring finger protein, putative OS=Plasmodium falciparum (isolate 3D7) GN=PFF1325c PE=4 SV=1 | 4 | 2.17 | 2.09 | 0.1294 |
| tr\|Q8IKA9\|Q8IKA9_PLAF7 Dihydroorotase, putative OS=Plasmodium falciparum (isolate 3D7) GN=PF14_0697 PE=4 SV=1 | 4 | 2.18 | 1.77 | 0.0909 |
| tr\|O96221\|O96221_PLAF7 Sec31p putative OS=Plasmodium falciparum (isolate 3D7) GN=Sec31p PE=4 SV=3 | 4 | 2.20 | 1.33 | 0.0449 |
| tr\|Q8I5P5\|Q8I5P5_PLAF7 Glycerol-3-phosphate dehydrogenase [NAD(+)] OS=Plasmodium falciparum (isolate 3D7) GN=PFL0780w PE=1 SV=1 | 4 | 2.20 | 1.32 | 0.0447 |
| tr\|C6KTA3\|C6KTA3_PLAF7 Uncharacterized protein OS=Plasmodium falciparum (isolate 3D7) GN=PFF1295w PE=4 SV=1 | 4 | 2.24 | 0.90 | 0.0157 |
| tr\|O77379\|O77379_PLAF7 Proteasome regulatory protein, putative OS=Plasmodium falciparum (isolate 3D7) GN=PFC0785c PE=4 SV=1 | 4 | 2.22 | 1.64 | 0.0737 |
| tr\|Q8I2V9\|Q8I2V9_PLAF7 Protein disulfide isomerase OS=Plasmodium falciparum (isolate 3D7) GN=PfPDI-9 PE=4 SV=1 | 4 | 2.22 | 1.73 | 0.0822 |
| tr\|Q76NN7\|Q76NN7_PLAF7 Peptidyl-prolyl cis-trans isomerase OS=Plasmodium falciparum (isolate 3D7) GN=PfCyP19 PE=3 SV=1 | 4 | 2.27 | 1.18 | 0.0308 |
| tr\|Q8IHT8\|Q8IHT8_PLAF7 Uncharacterized protein OS=Plasmodium falciparum (isolate 3D7) GN=PF11_0439 PE=4 SV=1 | 4 | 2.25 | 1.73 | 0.0800 |
| tr\|C6KT55\|C6KT55_PLAF7 Nascent polypeptide associated complex alpha chain, putative OS=Plasmodium falciparum (isolate 3D7) GN=PFF1050w PE=4 SV=1 | 4 | 2.30 | 1.20 | 0.0313 |
| tr\|Q8IIG9\|Q8IIG9_PLAF7 Uncharacterized protein OS=Plasmodium falciparum (isolate 3D7) GN=PF11_0205 PE=4 SV=1 | 4 | 2.28 | 2.38 | 0.1523 |
| tr\|C0H490\|C0H490_PLAF7 Cytosolic glyoxalase II OS=Plasmodium falciparum (isolate 3D7) GN=cGloII PE=3 SV=1 | 4 | 2.28 | 1.72 | 0.0769 |
| tr\|Q8I4V8\|Q8I4V8_PLAF7 FK506-binding protein (FKBP)-type peptidyl-propyl isomerase OS=Plasmodium falciparum (isolate 3D7) GN=FKBP35 PE=1 SV=1 | 4 | 2.28 | 1.76 | 0.0807 |
| tr\|Q8I2B1\|Q8I2B1_PLAF7 Aspartyl-tRNA synthetase, putative OS=Plasmodium falciparum (isolate 3D7) GN=PFA_0145c PE=3 SV=1 | 4 | 2.30 | 0.58 | 0.0042 |
| tr\|Q8I303\|Q8I303_PLAF7 BSD domain, putative OS=Plasmodium falciparum (isolate 3D7) GN=PFI0730w PE=4 SV=1 | 4 | 2.30 | 1.71 | 0.0741 |
| tr\|Q8IJ60\|Q8IJ60_PLAF7 Methionine--tRNA ligase, putative OS=Plasmodium falciparum (isolate 3D7) GN=PF10_0340 PE=4 SV=1 | 4 | 2.34 | 1.03 | 0.0198 |
| tr\|O97244\|O97244_PLAF7 Activator of Hsp90 ATPase, putative OS=Plasmodium falciparum (isolate 3D7) GN=PFC0270w PE=4 SV=3 | 4 | 2.31 | 1.70 | 0.0732 |
| tr\|Q8IAU3\|Q8IAU3_PLAF7 Dihydropteroate synthetase OS=Plasmodium falciparum (isolate 3D7) GN=DHPS PE=4 SV=1 | 4 | 2.31 | 1.74 | 0.0763 |
| tr\|C6KST5\|C6KST5_PLAF7 Chaperone, putative OS=Plasmodium falciparum (isolate 3D7) GN=PFF0430w PE=3 SV=1 | 4 | 2.39 | 1.23 | 0.0300 |
| tr\|Q8II87\|Q8II87_PLAF7 Conserved protein OS=Plasmodium falciparum (isolate 3D7) GN=PF11_0287 PE=4 SV=2 | 4 | 2.34 | 1.69 | 0.0690 |
| tr\|Q8ID72\|Q8ID72_PLAF7 Uncharacterized protein OS=Plasmodium falciparum (isolate 3D7) GN=PF13_0335 PE=4 SV=1 | 4 | 2.35 | 1.78 | 0.0779 |
| tr\|Q8I4Y9\|Q8I4Y9_PLAF7 Uncharacterized protein OS=Plasmodium falciparum (isolate 3D7) GN=PFL2120w PE=4 SV=1 | 4 | 2.36 | 1.75 | 0.0744 |
| tr\|Q8ILA7\|Q8ILA7_PLAF7 Uncharacterized protein OS=Plasmodium falciparum (isolate 3D7) GN=PF14_0338 PE=4 SV=2 | 4 | 2.37 | 1.99 | 0.0974 |
| sp\|Q8IIK4\|PDX2_PLAF7 Pyridoxal 5-phosphate synthase subunit Pdx2 OS=Plasmodium falciparum (isolate 3D7) GN=pdx2 PE=1 SV=2 | 4 | 2.38 | 1.68 | 0.0656 |
| tr\|O97247\|O97247_PLAF7 T-complex protein beta subunit, putative OS=Plasmodium falciparum (isolate 3D7) GN=PFC0285c PE=3 SV=3 | 4 | 2.40 | 1.21 | 0.0286 |
| sp\|Q8ILC1\|STI1L_PLAF7 STI1-like protein OS=Plasmodium falciparum (isolate 3D7) GN=PF14_0324 PE=3 SV=1 | 4 | 2.39 | 1.82 | 0.0779 |
| tr\|Q8IIB4\|Q8IIB4_PLAF7 60S ribosomal protein L35, putative OS=Plasmodium falciparum (isolate 3D7) GN=PF11_0260 PE=1 SV=2 | 4 | 2.39 | 2.80 | 0.1857 |

| | | | | |
|---|---|---|---|---|
| tr\|Q8I3A4\|Q8I3A4_PLAF7 Prefoldin subunit 4 OS=Plasmodium falciparum (isolate 3D7) GN=PFI0220w PE=3 SV=1 | 4 | 2.42 | 1.09 | 0.0215 |
| tr\|Q8III5\|Q8III5_PLAF7 Uncharacterized protein OS=Plasmodium falciparum (isolate 3D7) GN=PF11_0189 PE=3 SV=1 | 4 | 2.43 | 1.15 | 0.0242 |
| tr\|C0H5I7\|C0H5I7_PLAF7 T-complex protein 1 subunit delta OS=Plasmodium falciparum (isolate 3D7) GN=MAL13P1.283 PE=3 SV=1 | 4 | 2.44 | 1.37 | 0.0379 |
| tr\|C6KSV3\|C6KSV3_PLAF7 Transketolase OS=Plasmodium falciparum (isolate 3D7) GN=PfTK PE=4 SV=1 | 4 | 2.43 | 1.89 | 0.0830 |
| tr\|Q8ID84\|Q8ID84_PLAF7 Uncharacterized protein OS=Plasmodium falciparum (isolate 3D7) GN=PF13_0331 PE=4 SV=1 | 4 | 2.43 | 2.96 | 0.1988 |
| tr\|O77330\|O77330_PLAF7 Asparagine synthetase OS=Plasmodium falciparum (isolate 3D7) GN=PFC0395w PE=4 SV=1 | 4 | 2.43 | 1.74 | 0.0684 |
| tr\|Q8IL80\|Q8IL80_PLAF7 Thioredoxin peroxidase 1 OS=Plasmodium falciparum (isolate 3D7) GN=TPx1 PE=4 SV=1 | 4 | 2.44 | 1.98 | 0.0906 |
| tr\|Q8IDJ8\|Q8IDJ8_PLAF7 Lysine--tRNA ligase OS=Plasmodium falciparum (isolate 3D7) GN=PF13_0262 PE=1 SV=1 | 4 | 2.48 | 1.16 | 0.0238 |
| tr\|Q8IDC6\|Q8IDC6_PLAF7 Pyrroline carboxylate reductase OS=Plasmodium falciparum (isolate 3D7) GN=MAL13P1.284 PE=1 SV=1 | 4 | 2.48 | 1.82 | 0.0722 |
| tr\|Q8IJN8\|Q8IJN8_PLAF7 Ribonucleotide reductase small subunit, putative OS=Plasmodium falciparum (isolate 3D7) GN=PF10_0154 PE=4 SV=2 | 4 | 2.49 | 0.57 | 0.0032 |
| tr\|Q8I403\|Q8I403_PLAF7 Uncharacterized protein OS=Plasmodium falciparum (isolate 3D7) GN=PFE0500c PE=4 SV=1 | 4 | 2.48 | 1.57 | 0.0509 |
| tr\|Q8I3Y8\|Q8I3Y8_PLAF7 Myo-inositol 1-phosphate synthase, putative OS=Plasmodium falciparum (isolate 3D7) GN=PFE0585c PE=4 SV=1 | 4 | 2.48 | 1.76 | 0.0667 |
| tr\|Q8ILK2\|Q8ILK2_PLAF7 Nascent polypeptide-associated complex subunit beta OS=Plasmodium falciparum (isolate 3D7) GN=PF14_0241 PE=3 SV=1 | 4 | 2.59 | 1.55 | 0.0443 |
| tr\|Q8I501\|Q8I501_PLAF7 RabGDI protein OS=Plasmodium falciparum (isolate 3D7) GN=PFL2060c PE=1 SV=1 | 4 | 2.51 | 1.66 | 0.0564 |
| tr\|Q8I2X7\|Q8I2X7_PLAF7 ATP-dependent RNA Helicase, putative OS=Plasmodium falciparum (isolate 3D7) GN=PFI0860c PE=4 SV=1 | 4 | 2.54 | 2.57 | 0.1418 |
| tr\|Q8IIA4\|Q8IIA4_PLAF7 Threonine--tRNA ligase, putative OS=Plasmodium falciparum (isolate 3D7) GN=PF11_0270 PE=3 SV=1 | 4 | 2.56 | 2.47 | 0.1294 |
| tr\|Q8IDM2\|Q8IDM2_PLAF7 Ethanolamine-phosphate cytidylyltransferase, putative OS=Plasmodium falciparum (isolate 3D7) GN=PF13_0253 PE=4 SV=1 | 4 | 2.58 | 1.63 | 0.0503 |
| tr\|Q8I0X0\|Q8I0X0_PLAF7 SNAP protein (Soluble N-ethylmaleimide-sensitive factor Attachment Protein), putative OS=Plasmodium falciparum (isolate 3D7) GN=PFE0445c PE=4 SV=1 | 4 | 2.60 | 3.31 | 0.2149 |
| tr\|Q8I3X4\|Q8I3X4_PLAF7 Purine nucleotide phosphorylase, putative OS=Plasmodium falciparum (isolate 3D7) GN=PFE0660c PE=1 SV=1 | 4 | 2.62 | 1.43 | 0.0354 |
| sp\|Q7KQL5\|TBB_PLAF7 Tubulin beta chain OS=Plasmodium falciparum (isolate 3D7) GN=PF10_0084 PE=3 SV=1 | 4 | 2.63 | 1.61 | 0.0469 |
| sp\|Q8IJN7\|ENO_PLAF7 Enolase OS=Plasmodium falciparum (isolate 3D7) GN=ENO PE=3 SV=1 | 4 | 2.64 | 1.59 | 0.0452 |
| tr\|Q8IL48\|Q8IL48_PLAF7 tRNA binding protein, putative OS=Plasmodium falciparum (isolate 3D7) GN=PF14_0401 PE=4 SV=1 | 4 | 2.64 | 1.57 | 0.0433 |
| tr\|Q8IIG6\|Q8IIG6_PLAF7 Phosphoglycerate mutase, putative OS=Plasmodium falciparum (isolate 3D7) GN=PF11_0208 PE=1 SV=1 | 4 | 2.66 | 1.70 | 0.0527 |
| sp\|Q7KQL9\|ALF_PLAF7 Fructose-bisphosphate aldolase OS=Plasmodium falciparum (isolate 3D7) GN=PF14_0425 PE=3 SV=1 | 4 | 2.67 | 1.96 | 0.0729 |
| tr\|Q8IC01\|Q8IC01_PLAF7 Cg4 protein OS=Plasmodium falciparum (isolate 3D7) GN=PF07_0033 PE=3 SV=1 | 4 | 2.68 | 2.16 | 0.0893 |
| tr\|Q8IBS3\|Q8IBS3_PLAF7 Seryl-tRNA synthetase, putative OS=Plasmodium falciparum (isolate 3D7) GN=PF07_0073 PE=3 SV=1 | 4 | 2.69 | 1.54 | 0.0399 |
| tr\|Q9NLB2\|Q9NLB2_PLAF7 Glutaredoxin OS=Plasmodium falciparum (isolate 3D7) GN=GRX1 PE=1 SV=1 | 4 | 2.69 | 1.57 | 0.0414 |
| tr\|Q8II43\|Q8II43_PLAF7 T-complex protein 1 subunit alpha OS=Plasmodium falciparum (isolate 3D7) GN=PF11_0331 PE=3 SV=1 | 4 | 2.70 | 1.55 | 0.0401 |
| tr\|O96220\|O96220_PLAF7 T-complex protein 1, putative OS=Plasmodium falciparum (isolate 3D7) GN=PFB0635w PE=3 SV=3 | 4 | 2.70 | 1.78 | 0.0559 |
| tr\|C0H4G7\|C0H4G7_PLAF7 Uncharacterized protein OS=Plasmodium falciparum (isolate 3D7) GN=PFE1465w PE=4 SV=1 | 4 | 2.70 | 2.81 | 0.1502 |
| tr\|Q8ILS7\|Q8ILS7_PLAF7 Prefoldin subunit 2, putative OS=Plasmodium falciparum (isolate 3D7) GN=PF14_0167 PE=4 SV=1 | 4 | 2.72 | 1.52 | 0.0373 |
| tr\|Q76NN6\|Q76NN6_PLAF7 Ran binding protein 1, putative OS=Plasmodium falciparum (isolate 3D7) GN=PFD0950w PE=4 SV=1 | 4 | 2.72 | 1.70 | 0.0497 |
| sp\|Q8I2J4\|PROF_PLAF7 Profilin OS=Plasmodium falciparum (isolate 3D7) GN=Pfn PE=3 SV=1 | 4 | 2.74 | 1.75 | 0.0519 |

| | | | | |
|---|---|---|---|---|
| tr\|Q8I283\|Q8I283_PLAF7 Cyclin-dependent kinases regulatory subunit OS=Plasmodium falciparum (isolate 3D7) GN=PFA_0285c PE=3 SV=1 | 4 | 2.78 | 3.16 | 0.1769 |
| tr\|Q8I700\|Q8I700_PLAF7 Snornp protein gar1 homologue, putative OS=Plasmodium falciparum (isolate 3D7) GN=PF13_0051 PE=4 SV=1 | 4 | 2.79 | 3.54 | 0.2124 |
| tr\|Q8ILI2\|Q8ILI2_PLAF7 Proliferation-associated protein 2g4, putative OS=Plasmodium falciparum (isolate 3D7) GN=PF14_0261 PE=4 SV=1 | 4 | 2.81 | 2.39 | 0.1005 |
| tr\|Q8IJI7\|Q8IJI7_PLAF7 Deoxyribose-phosphate aldolase, putative OS=Plasmodium falciparum (isolate 3D7) GN=PF10_0210 PE=4 SV=1 | 4 | 2.82 | 2.00 | 0.0667 |
| tr\|Q8IKF0\|Q8IKF0_PLAF7 Helicase 45 OS=Plasmodium falciparum (isolate 3D7) GN=H45 PE=3 SV=1 | 4 | 2.83 | 1.75 | 0.0484 |
| tr\|C6KSM2\|C6KSM2_PLAF7 MYND finger protein, putative OS=Plasmodium falciparum (isolate 3D7) GN=PFF0105w PE=4 SV=1 | 4 | 2.83 | 1.42 | 0.0283 |
| tr\|O77355\|O77355_PLAF7 Pre-mRNA splicing factor, putative OS=Plasmodium falciparum (isolate 3D7) GN=PFC0465c PE=4 SV=2 | 4 | 2.84 | 3.62 | 0.2150 |
| tr\|C6KT76\|C6KT76_PLAF7 Hexokinase OS=Plasmodium falciparum (isolate 3D7) GN=PFF1155w PE=3 SV=1 | 4 | 2.86 | 2.49 | 0.1056 |
| tr\|Q8I5Y9\|Q8I5Y9_PLAF7 Uncharacterized protein OS=Plasmodium falciparum (isolate 3D7) GN=PFL0280c PE=4 SV=1 | 4 | 2.87 | 2.21 | 0.0805 |
| tr\|Q8IHU4\|Q8IHU4_PLAF7 Uncharacterized protein OS=Plasmodium falciparum (isolate 3D7) GN=PF11_0433 PE=4 SV=1 | 4 | 2.91 | 3.80 | 0.2229 |
| tr\|C6KT59\|C6KT59_PLAF7 Radical SAM protein, putative OS=Plasmodium falciparum (isolate 3D7) GN=PFF1070c PE=4 SV=1 | 4 | 2.92 | 3.99 | 0.2398 |
| tr\|Q8IJS1\|Q8IJS1_PLAF7 Hypoxanthine phosphoribosyltransferase OS=Plasmodium falciparum (isolate 3D7) GN=PF10_0121 PE=4 SV=1 | 4 | 2.92 | 2.02 | 0.0631 |
| tr\|C0H5E9\|C0H5E9_PLAF7 DNAJ like protein, putative OS=Plasmodium falciparum (isolate 3D7) GN=MAL13P1.162 PE=4 SV=1 | 4 | 2.92 | 1.60 | 0.0352 |
| tr\|Q8IDZ9\|Q8IDZ9_PLAF7 Isoleucine-tRNA ligase, putative OS=Plasmodium falciparum (isolate 3D7) GN=PF13_0179 PE=3 SV=1 | 4 | 2.92 | 1.84 | 0.0503 |
| tr\|Q8I5T1\|Q8I5T1_PLAF7 Uncharacterized protein OS=Plasmodium falciparum (isolate 3D7) GN=PFL0600w PE=4 SV=1 | 4 | 2.93 | 4.03 | 0.2417 |
| tr\|Q8I0P6\|Q8I0P6_PLAF7 Elongation factor 1-alpha OS=Plasmodium falciparum (isolate 3D7) GN=PF13_0304 PE=3 SV=1 | 4 | 2.93 | 1.85 | 0.0502 |
| tr\|Q8IDP9\|Q8IDP9_PLAF7 Uncharacterized protein OS=Plasmodium falciparum (isolate 3D7) GN=PF13_0239 PE=4 SV=1 | 4 | 2.93 | 2.80 | 0.1274 |
| sp\|P50250\|SAHH_PLAF7 Adenosylhomocysteinase OS=Plasmodium falciparum (isolate 3D7) GN=PFE1050w PE=1 SV=2 | 4 | 2.94 | 2.15 | 0.0717 |
| tr\|Q8I1V0\|Q8I1V0_PLAF7 Lysine decarboxylase-like protein, putative OS=Plasmodium falciparum (isolate 3D7) GN=PFD0670c PE=4 SV=1 | 4 | 3.00 | 2.03 | 0.0596 |
| tr\|Q8I586\|Q8I586_PLAF7 Asparagine/aspartate rich protein, putative OS=Plasmodium falciparum (isolate 3D7) GN=PFL1620w PE=4 SV=1 | 4 | 3.03 | 2.79 | 0.1177 |
| tr\|Q8IKK7\|Q8IKK7_PLAF7 Glyceraldehyde-3-phosphate dehydrogenase OS=Plasmodium falciparum (isolate 3D7) GN=GAPDH PE=3 SV=1 | 4 | 3.07 | 2.54 | 0.0939 |
| tr\|Q76NM3\|Q76NM3_PLAF7 L-lactate dehydrogenase OS=Plasmodium falciparum (isolate 3D7) GN=PfLDH PE=1 SV=1 | 4 | 3.08 | 2.38 | 0.0811 |
| tr\|Q8IAM0\|Q8IAM0_PLAF7 Glutamate dehydrogenase, putative OS=Plasmodium falciparum (isolate 3D7) GN=PF08_0132 PE=4 SV=1 | 4 | 3.09 | 1.18 | 0.0137 |
| tr\|Q8IM38\|Q8IM38_PLAF7 Ribonucleotide reductase small subunit OS=Plasmodium falciparum (isolate 3D7) GN=PF14_0053 PE=4 SV=1 | 4 | 3.11 | 2.17 | 0.0637 |
| tr\|Q8I603\|Q8I603_PLAF7 Eukaryotic initiation factor 5a, putative OS=Plasmodium falciparum (isolate 3D7) GN=PFL0210c PE=4 SV=1 | 4 | 3.12 | 2.08 | 0.0574 |
| tr\|Q8IDV0\|Q8IDV0_PLAF7 Elongation factor 1-gamma, putative OS=Plasmodium falciparum (isolate 3D7) GN=PF13_0214 PE=4 SV=2 | 4 | 3.13 | 2.48 | 0.0859 |
| tr\|C6KTA4\|C6KTA4_PLAF7 Pyruvate kinase OS=Plasmodium falciparum (isolate 3D7) GN=PFF1300w PE=1 SV=1 | 4 | 3.14 | 2.49 | 0.0862 |
| tr\|Q8ILA4\|Q8ILA4_PLAF7 Glucose-6-phosphate isomerase OS=Plasmodium falciparum (isolate 3D7) GN=PF14_0341 PE=1 SV=1 | 4 | 3.15 | 2.18 | 0.0631 |
| tr\|Q8IDQ9\|Q8IDQ9_PLAF7 Phosphoethanolamine N-methyltransferase OS=Plasmodium falciparum (isolate 3D7) GN=PfPMT PE=4 SV=1 | 4 | 3.15 | 2.09 | 0.0568 |
| tr\|Q8IAM2\|Q8IAM2_PLAF7 1-cys peroxiredoxin OS=Plasmodium falciparum (isolate 3D7) GN=1-cyspxn PE=4 SV=1 | 4 | 3.16 | 2.82 | 0.1108 |
| sp\|Q7KQM0\|TPIS_PLAF7 Triosephosphate isomerase OS=Plasmodium falciparum (isolate 3D7) GN=TPI PE=3 SV=1 | 4 | 3.20 | 2.39 | 0.0754 |
| tr\|Q7K6A4\|Q7K6A4_PLAF7 S-adenosylmethionine synthase OS=Plasmodium falciparum (isolate 3D7) GN=PfSAMS PE=3 SV=1 | 4 | 3.20 | 2.19 | 0.0613 |
| sp\|Q8ILI6\|AN32_PLAF7 Acidic leucine-rich nuclear phosphoprotein 32-related protein OS=Plasmodium falciparum (isolate 3D7) GN=PF14_0257 PE=3 SV=1 | 4 | 3.22 | 3.12 | 0.1311 |

| | | | | |
|---|---|---|---|---|
| tr\|O97319\|O97319_PLAF7 Elongation factor 1 (EF-1), putative OS=Plasmodium falciparum (isolate 3D7) GN=PFC0870w PE=4 SV=2 | 4 | 3.25 | 1.82 | 0.0373 |
| tr\|Q8IKI9\|Q8IKI9_PLAF7 ATP-dependent protease Ia, putative OS=Plasmodium falciparum (isolate 3D7) GN=PF14_0616 PE=4 SV=1 | 4 | 3.27 | 3.21 | 0.1346 |
| tr\|Q8IKW5\|Q8IKW5_PLAF7 Elongation factor 2 OS=Plasmodium falciparum (isolate 3D7) GN=PF14_0486 PE=4 SV=1 | 4 | 3.28 | 2.47 | 0.0771 |
| tr\|Q8IKM7\|Q8IKM7_PLAF7 Uncharacterized protein OS=Plasmodium falciparum (isolate 3D7) GN=PF14_0577 PE=4 SV=1 | 4 | 3.32 | 4.68 | 0.2512 |
| tr\|Q8I5C5\|Q8I5C5_PLAF7 Macrophage migration inhibitory factor homologue OS=Plasmodium falciparum (isolate 3D7) GN=MIF PE=1 SV=1 | 4 | 3.33 | 2.40 | 0.0693 |
| tr\|Q8I5T5\|Q8I5T5_PLAF7 Uncharacterized protein OS=Plasmodium falciparum (isolate 3D7) GN=PFL0575w PE=4 SV=1 | 4 | 3.34 | 4.83 | 0.2599 |
| sp\|P27362\|PGK_PLAF7 Phosphoglycerate kinase OS=Plasmodium falciparum (isolate 3D7) GN=PGK PE=1 SV=1 | 4 | 3.35 | 2.48 | 0.0738 |
| tr\|C6KTB1\|C6KTB1_PLAF7 4-methyl-5(B-hydroxyethyl)-thiazol monophosphate biosynthesis enzyme OS=Plasmodium falciparum (isolate 3D7) GN=PFF1335c PE=4 SV=1 | 4 | 3.35 | 3.16 | 0.1242 |
| tr\|O97282\|O97282_PLAF7 T-complex protein 1 epsilon subunit, putative OS=Plasmodium falciparum (isolate 3D7) GN=PFC0900w PE=3 SV=1 | 4 | 3.37 | 2.11 | 0.0494 |
| tr\|O77327\|O77327_PLAF7 U2 snRNP spliceosome subunit, putative OS=Plasmodium falciparum (isolate 3D7) GN=PFC0375c PE=4 SV=1 | 4 | 3.44 | 5.53 | 0.3011 |
| tr\|Q8I320\|Q8I320_PLAF7 Elongation factor 1-beta OS=Plasmodium falciparum (isolate 3D7) GN=PfEF-1beta PE=4 SV=1 | 4 | 3.48 | 2.76 | 0.0855 |
| tr\|Q8I274\|Q8I274_PLAF7 Rab5c, GTPase OS=Plasmodium falciparum (isolate 3D7) GN=Rab5c PE=3 SV=1 | 4 | 3.50 | 4.99 | 0.2550 |
| tr\|Q8IHY0\|Q8IHY0_PLAF7 Protein phosphatase 2C OS=Plasmodium falciparum (isolate 3D7) GN=PF11_0396 PE=3 SV=2 | 4 | 3.58 | 5.37 | 0.2748 |
| tr\|Q8IJA9\|Q8IJA9_PLAF7 Adenosine deaminase, putative OS=Plasmodium falciparum (isolate 3D7) GN=PF10_0289 PE=4 SV=1 | 4 | 3.59 | 2.73 | 0.0785 |
| sp\|Q6LFH8\|OAT_PLAF7 Ornithine aminotransferase OS=Plasmodium falciparum (isolate 3D7) GN=OAT PE=1 SV=1 | 4 | 3.60 | 3.07 | 0.1007 |
| tr\|Q8I5U3\|Q8I5U3_PLAF7 Uncharacterized protein OS=Plasmodium falciparum (isolate 3D7) GN=PFL0530c PE=4 SV=1 | 4 | 3.60 | 2.87 | 0.0870 |
| tr\|Q8I5F4\|Q8I5F4_PLAF7 Uncharacterized protein OS=Plasmodium falciparum (isolate 3D7) GN=PFL1270w PE=4 SV=1 | 4 | 3.64 | 2.37 | 0.0547 |
| tr\|O97323\|O97323_PLAF7 SNARE protein OS=Plasmodium falciparum (isolate 3D7) GN=PfSec22 PE=4 SV=2 | 4 | 3.65 | 5.42 | 0.2706 |
| tr\|Q8IB40\|Q8IB40_PLAF7 C-13 antigen OS=Plasmodium falciparum (isolate 3D7) GN=MAL8P1.57 PE=4 SV=1 | 4 | 3.67 | 5.72 | 0.2895 |
| tr\|Q8I6Z4\|Q8I6Z4_PLAF7 RNAse L inhibitor protein, putative OS=Plasmodium falciparum (isolate 3D7) GN=MAL13P1.344 PE=3 SV=1 | 4 | 3.76 | 2.22 | 0.0426 |
| tr\|Q8IJ74\|Q8IJ74_PLAF7 Uncharacterized protein OS=Plasmodium falciparum (isolate 3D7) GN=PF10_0325 PE=1 SV=1 | 4 | 3.89 | 3.37 | 0.1042 |
| tr\|Q8IBM7\|Q8IBM7_PLAF7 BING4 (NUC141) WD-40 repeat protein, putative OS=Plasmodium falciparum (isolate 3D7) GN=PF07_0092 PE=4 SV=1 | 4 | 3.93 | 5.57 | 0.2533 |
| tr\|Q8IKP8\|Q8IKP8_PLAF7 Uncharacterized protein OS=Plasmodium falciparum (isolate 3D7) GN=PF14_0556 PE=4 SV=2 | 4 | 4.04 | 6.30 | 0.2897 |
| tr\|C6KT45\|C6KT45_PLAF7 Cleavage stimulation factor subunit 1-like protein, putative OS=Plasmodium falciparum (isolate 3D7) GN=PFF1000w PE=4 SV=1 | 4 | 4.10 | 5.45 | 0.2295 |
| tr\|Q8IKZ7\|Q8IKZ7_PLAF7 Uncharacterized protein OS=Plasmodium falciparum (isolate 3D7) GN=PF14_0454 PE=4 SV=1 | 4 | 4.19 | 5.44 | 0.2216 |
| tr\|Q8IDI9\|Q8IDI9_PLAF7 Phosphatidylinositol transfer protein, putative OS=Plasmodium falciparum (isolate 3D7) GN=MAL13P1.256 PE=4 SV=2 | 4 | 4.22 | 6.87 | 0.3068 |
| sp\|Q8I1T8\|ASNA_PLAF7 ATPase ASNA1 homolog OS=Plasmodium falciparum (isolate 3D7) GN=PFD0725c PE=3 SV=1 | 4 | 4.32 | 3.60 | 0.0962 |
| tr\|Q8IIM8\|Q8IIM8_PLAF7 Uncharacterized protein OS=Plasmodium falciparum (isolate 3D7) GN=PF11_0142 PE=4 SV=1 | 4 | 4.37 | 3.90 | 0.1106 |
| tr\|Q8I566\|Q8I566_PLAF7 Serine hydroxymethyltransferase OS=Plasmodium falciparum (isolate 3D7) GN=PFL1720w PE=1 SV=1 | 4 | 4.42 | 3.38 | 0.0791 |
| sp\|O77392\|IPYR_PLAF7 Probable inorganic pyrophosphatase OS=Plasmodium falciparum (isolate 3D7) GN=MAL3P6.3 PE=3 SV=1;tr\|C0H477\|C0H477_PLAF7 Inorganic pyrophosphatase, putative OS=Plasmodium falciparum (isolate 3D7) GN=PFC0710w.1 PE=4 SV=1 | 4 | 4.52 | 6.40 | 0.2526 |
| tr\|Q8IJR9\|Q8IJR9_PLAF7 GMP synthetase OS=Plasmodium falciparum (isolate 3D7) GN=PF10_0123 PE=1 SV=1 | 4 | 4.71 | 5.20 | 0.1680 |
| tr\|Q8I5G8\|Q8I5G8_PLAF7 Splicing factor 3b subunit, putative OS=Plasmodium falciparum (isolate 3D7) GN=PFL1200c PE=4 SV=1 | 4 | 4.98 | 6.38 | 0.2165 |

| | | | | |
|---|---|---|---|---|
| tr\|Q8IL69\|Q8IL69_PLAF7 Uncharacterized protein OS=Plasmodium falciparum (isolate 3D7) GN=PF14_0380 PE=4 SV=1 | 4 | 5.10 | 8.26 | 0.3045 |
| tr\|O77390\|O77390_PLAF7 Putative uncharacterized protein OS=Plasmodium falciparum (isolate 3D7) GN=PFC0720w PE=4 SV=2 | 4 | 5.36 | 8.40 | 0.2918 |
| sp\|Q8IIG7\|YPF05_PLAF7 Uncharacterized protein PF11_0207 OS=Plasmodium falciparum (isolate 3D7) GN=PF11_0207 PE=4 SV=2 | 4 | 5.60 | 6.27 | 0.1716 |
| tr\|Q8IBJ1\|Q8IBJ1_PLAF7 Ubiquitin carboxyl-terminal hydrolase OS=Plasmodium falciparum (isolate 3D7) GN=MAL7P1.147 PE=3 SV=1 | 4 | 6.08 | 10.05 | 0.3131 |
| tr\|Q8IE10\|Q8IE10_PLAF7 Glutaminyl-tRNA synthetase, putative OS=Plasmodium falciparum (isolate 3D7) GN=PF13_0170 PE=3 SV=1 | 4 | 6.17 | 7.35 | 0.1918 |
| tr\|Q8I1Y6\|Q8I1Y6_PLAF7 Uncharacterized protein OS=Plasmodium falciparum (isolate 3D7) GN=PFD0207c PE=4 SV=1 | 4 | 6.61 | 7.81 | 0.1889 |
| tr\|O96203\|O96203_PLAF7 Peptide chain release factor subunit 1, putative OS=Plasmodium falciparum (isolate 3D7) GN=PFB0550w PE=4 SV=1 | 4 | 6.64 | 9.25 | 0.2467 |
| tr\|C0H5J6\|C0H5J6_PLAF7 Sec24 subunit, putative OS=Plasmodium falciparum (isolate 3D7) GN=PF13_0324 PE=4 SV=1 | 4 | 6.71 | 10.61 | 0.2956 |
| tr\|O97246\|O97246_PLAF7 Putative uncharacterized protein OS=Plasmodium falciparum (isolate 3D7) GN=PFC0280c PE=4 SV=1 | 4 | 6.76 | 12.51 | 0.3588 |
| tr\|Q8IDX8\|Q8IDX8_PLAF7 Merozoite Surface Protein 7, MSP7 OS=Plasmodium falciparum (isolate 3D7) GN=MSP7 PE=4 SV=1 | 4 | 6.79 | 12.36 | 0.3520 |
| tr\|Q8IL03\|Q8IL03_PLAF7 Glutaminyl-peptide cyclotransferase, putative OS=Plasmodium falciparum (isolate 3D7) GN=PF14_0447 PE=4 SV=1 | 4 | 7.11 | 12.96 | 0.3529 |
| tr\|Q8IDF9\|Q8IDF9_PLAF7 Inositol-polyphosphate 5-phosphatase OS=Plasmodium falciparum (isolate 3D7) GN=PF13_0285 PE=4 SV=1 | 4 | 7.21 | 13.76 | 0.3715 |
| sp\|Q8I5R7\|SYP_PLAF7 Proline--tRNA ligase OS=Plasmodium falciparum (isolate 3D7) GN=proRS PE=1 SV=1 | 4 | 7.58 | 8.11 | 0.1583 |
| tr\|Q8I472\|Q8I472_PLAF7 Zinc binding protein, putative OS=Plasmodium falciparum (isolate 3D7) GN=PFE0140c PE=4 SV=1 | 4 | 8.45 | 15.14 | 0.3457 |
| tr\|O96198\|O96198_PLAF7 Asparagine-tRNA ligase, putative OS=Plasmodium falciparum (isolate 3D7) GN=PFB0525w PE=3 SV=1 | 4 | 8.67 | 13.65 | 0.2935 |
| sp\|Q8ID66\|PF92_PLAF7 Merozoite surface protein P92 OS=Plasmodium falciparum (isolate 3D7) GN=PF92 PE=1 SV=1 | 4 | 8.87 | 15.99 | 0.3482 |
| tr\|Q8I4U3\|Q8I4U3_PLAF7 Conserved Plasmodium protein OS=Plasmodium falciparum (isolate 3D7) GN=PFL2355w PE=4 SV=1 | 4 | 9.05 | 16.60 | 0.3554 |
| tr\|Q8I261\|Q8I261_PLAF7 Beta3 proteasome subunit, putative OS=Plasmodium falciparum (isolate 3D7) GN=PFA_0400c PE=4 SV=1 | 4 | 9.08 | 13.54 | 0.2723 |
| tr\|Q8I3B7\|Q8I3B7_PLAF7 Retrieval receptor for endoplasmic reticulum membrane proteins, putative OS=Plasmodium falciparum (isolate 3D7) GN=PFI0150c PE=4 SV=1 | 4 | 9.39 | 17.17 | 0.3542 |
| tr\|Q8IJ77\|Q8IJ77_PLAF7 S-adenosylmethionine decarboxylase-ornithine decarboxylase OS=Plasmodium falciparum (isolate 3D7) GN=PF10_0322 PE=3 SV=1 | 4 | 9.66 | 14.23 | 0.2679 |
| tr\|Q8IBM9\|Q8IBM9_PLAF7 Obg-like ATPase 1 OS=Plasmodium falciparum (isolate 3D7) GN=MAL7P1.122 PE=3 SV=1 | 4 | 9.95 | 15.98 | 0.3014 |
| tr\|Q8II71\|Q8II71_PLAF7 26S proteasome regulatory complex subunit, putative OS=Plasmodium falciparum (isolate 3D7) GN=PF11_0303 PE=4 SV=2 | 4 | 10.02 | 12.21 | 0.1994 |
| tr\|Q8IM31\|Q8IM31_PLAF7 Glycerophodiester phosphodiesterase, putative OS=Plasmodium falciparum (isolate 3D7) GN=PF14_0060 PE=4 SV=1 | 4 | 10.65 | 18.24 | 0.3273 |
| tr\|C0H4P4\|C0H4P4_PLAF7 Uncharacterized protein OS=Plasmodium falciparum (isolate 3D7) GN=MAL7P1.146 PE=4 SV=1 | 4 | 12.30 | 23.23 | 0.3675 |
| tr\|Q8IDK7\|Q8IDK7_PLAF7 Glutamate--tRNA ligase, putative OS=Plasmodium falciparum (isolate 3D7) GN=PF13_0257 PE=3 SV=1 | 4 | 12.37 | 7.40 | 0.0443 |
| tr\|Q8IJP8\|Q8IJP8_PLAF7 Prohibitin, putative OS=Plasmodium falciparum (isolate 3D7) GN=PF10_0144 PE=4 SV=1 | 4 | 15.05 | 27.85 | 0.3588 |
| tr\|O77312\|O77312_PLAF7 Exportin 1, putative OS=Plasmodium falciparum (isolate 3D7) GN=PFC0135c PE=4 SV=2 | 4 | 16.72 | 30.15 | 0.3484 |
| tr\|Q8IM71\|Q8IM71_PLAF7 Choline kinase OS=Plasmodium falciparum (isolate 3D7) GN=PF14_0020 PE=1 SV=1 | 4 | 18.37 | 32.82 | 0.3445 |
| tr\|Q8I1R6\|Q8I1R6_PLAF7 Bifunctional dihydrofolate reductase-thymidylate synthase OS=Plasmodium falciparum (isolate 3D7) GN=DHFR-TS PE=3 SV=1 | 4 | 20.24 | 37.22 | 0.3562 |
| tr\|O96174\|O96174_PLAF7 Conserved Plasmodium protein OS=Plasmodium falciparum (isolate 3D7) GN=PFB0395w PE=4 SV=1 | 4 | 20.33 | 23.43 | 0.1810 |
| tr\|Q8IKL5\|Q8IKL5_PLAF7 Valine-tRNA ligase, putative OS=Plasmodium falciparum (isolate 3D7) GN=PF14_0589 PE=3 SV=1 | 4 | 22.54 | 41.72 | 0.3589 |
| tr\|Q8ID31\|Q8ID31_PLAF7 Alanine--tRNA ligase OS=Plasmodium falciparum (isolate 3D7) GN=PF13_0354 PE=3 SV=1 | 4 | 22.79 | 41.58 | 0.3531 |
| tr\|Q8IDI2\|Q8IDI2_PLAF7 Uncharacterized protein OS=Plasmodium falciparum (isolate 3D7) GN=PF13_0270 PE=4 SV=1 | 4 | 22.97 | 43.64 | 0.3699 |

| | | | | |
|---|---|---|---|---|
| tr\|Q7KWJ1\|Q7KWJ1_PLAF7 Acyl carrier protein OS=Plasmodium falciparum (isolate 3D7) GN=PFB0385w PE=3 SV=1 | 4 | 23.41 | 44.36 | 0.3688 |
| tr\|C0H4E7\|C0H4E7_PLAF7 Uncharacterized protein OS=Plasmodium falciparum (isolate 3D7) GN=PFE0910w PE=4 SV=1 | 4 | 24.11 | 35.72 | 0.2698 |
| tr\|Q8I3J6\|Q8I3J6_PLAF7 Uncharacterized protein OS=Plasmodium falciparum (isolate 3D7) GN=PFE1340w PE=3 SV=1 | 4 | 24.73 | 47.46 | 0.3739 |
| tr\|Q8I3A0\|Q8I3A0_PLAF7 Cu2+-transporting ATPase, Cu2+ transporter OS=Plasmodium falciparum (isolate 3D7) GN=PFI0240c PE=3 SV=1 | 4 | 24.85 | 47.50 | 0.3723 |
| tr\|Q8I310\|Q8I310_PLAF7 Phospholipid or glycerol acyltransferase, putative OS=Plasmodium falciparum (isolate 3D7) GN=PFI0695c PE=4 SV=1 | 4 | 25.16 | 48.33 | 0.3744 |
| tr\|Q8IHZ1\|Q8IHZ1_PLAF7 UVB-resistance protein UVR8 homologue OS=Plasmodium falciparum (isolate 3D7) GN=PF11_0385 PE=4 SV=1 | 4 | 26.42 | 30.05 | 0.1769 |
| tr\|C6KTB4\|C6KTB4_PLAF7 Acetyl-CoA synthetase OS=Plasmodium falciparum (isolate 3D7) GN=PFF1350c PE=4 SV=1 | 4 | 26.99 | 51.65 | 0.3728 |
| sp\|Q8ILQ7\|GST_PLAF7 Glutathione S-transferase OS=Plasmodium falciparum (isolate 3D7) GN=GST PE=3 SV=1 | 4 | 27.14 | 51.48 | 0.3692 |
| tr\|Q8II42\|Q8II42_PLAF7 Conserved Plasmodium protein OS=Plasmodium falciparum (isolate 3D7) GN=PF11_0332 PE=4 SV=1 | 4 | 27.40 | 45.36 | 0.3135 |
| tr\|Q8ILS4\|Q8ILS4_PLAF7 NOT family protein, putative OS=Plasmodium falciparum (isolate 3D7) GN=PF14_0170 PE=4 SV=1 | 4 | 30.29 | 58.18 | 0.3743 |
| tr\|C0H512\|C0H512_PLAF7 Putative uncharacterized protein OS=Plasmodium falciparum (isolate 3D7) GN=PFI0086w PE=4 SV=1 | 4 | 30.68 | 56.57 | 0.3575 |
| tr\|C6KT64\|C6KT64_PLAF7 Leucyl tRNA synthase OS=Plasmodium falciparum (isolate 3D7) GN=PFF1095w PE=3 SV=1 | 4 | 41.10 | 79.02 | 0.3747 |
| tr\|Q8IJS8\|Q8IJS8_PLAF7 DNA repair protein RAD23, putative OS=Plasmodium falciparum (isolate 3D7) GN=PF10_0114 PE=4 SV=1 | 4 | 41.63 | 64.96 | 0.2900 |
| tr\|C6KTC9\|C6KTC9_PLAF7 RNA binding protein, putative OS=Plasmodium falciparum (isolate 3D7) GN=PFF1425w PE=4 SV=1 | 4 | 43.33 | 49.36 | 0.1774 |
| tr\|Q8IJA0\|Q8IJA0_PLAF7 26S proteasome subunit, putative OS=Plasmodium falciparum (isolate 3D7) GN=PF10_0298 PE=4 SV=1 | 4 | 47.76 | 49.21 | 0.1476 |
| tr\|Q8IHU0\|Q8IHU0_PLAF7 Uncharacterized protein OS=Plasmodium falciparum (isolate 3D7) GN=PF11_0437 PE=1 SV=1 | 4 | 49.18 | 91.35 | 0.3605 |
| tr\|Q8IBL9\|Q8IBL9_PLAF7 Uncharacterized protein OS=Plasmodium falciparum (isolate 3D7) GN=PF07_0097 PE=4 SV=1 | 4 | 50.94 | 65.70 | 0.2187 |
| tr\|Q8IB60\|Q8IB60_PLAF7 PfSec23 protein OS=Plasmodium falciparum (isolate 3D7) GN=Pfsec23 PE=2 SV=1 | 4 | 51.11 | 98.98 | 0.3777 |
| tr\|Q8IKU1\|Q8IKU1_PLAF7 p23 co-chaperone, putative OS=Plasmodium falciparum (isolate 3D7) GN=SBA1 PE=4 SV=2 | 4 | 55.65 | 68.71 | 0.2037 |
| tr\|Q8IJ85\|Q8IJ85_PLAF7 Asparagine-rich antigen OS=Plasmodium falciparum (isolate 3D7) GN=PF10_0314 PE=4 SV=1 | 4 | 68.11 | 128.73 | 0.3676 |
| sp\|Q8IDF6\|PURA_PLAF7 Adenylosuccinate synthetase OS=Plasmodium falciparum (isolate 3D7) GN=Adss PE=3 SV=1 | 4 | 81.39 | 154.90 | 0.3705 |
| tr\|C6KT03\|C6KT03_PLAF7 Ndc80 homologue, putative OS=Plasmodium falciparum (isolate 3D7) GN=PFF0785w PE=4 SV=1 | 4 | 101.58 | 200.14 | 0.3848 |
| tr\|Q8I3M0\|Q8I3M0_PLAF7 Uncharacterized protein OS=Plasmodium falciparum (isolate 3D7) GN=PFE1220w PE=4 SV=1 | 4 | 105.22 | 208.88 | 0.3879 |
| tr\|Q8I2W4\|Q8I2W4_PLAF7 Gamma-glutamylcysteine synthetase OS=Plasmodium falciparum (isolate 3D7) GN=PFI0925w PE=4 SV=1 | 4 | 105.28 | 207.32 | 0.3846 |
| sp\|O77323\|TCPH_PLAF7 T-complex protein 1 subunit eta OS=Plasmodium falciparum (isolate 3D7) GN=MAL3P3.6 PE=3 SV=1 | 4 | 117.33 | 231.90 | 0.3861 |
| tr\|Q8IDV2\|Q8IDV2_PLAF7 Proteasome regulatory component, putative OS=Plasmodium falciparum (isolate 3D7) GN=MAL13P1.190 PE=4 SV=1 | 4 | 132.03 | 258.80 | 0.3827 |
| sp\|Q7KQL8\|THIO_PLAF7 Thioredoxin OS=Plasmodium falciparum (isolate 3D7) GN=PF14_0545 PE=1 SV=1 | 4 | 141.02 | 274.14 | 0.3792 |
| tr\|Q8ID52\|Q8ID52_PLAF7 Uncharacterized protein OS=Plasmodium falciparum (isolate 3D7) GN=MAL13P1.329 PE=4 SV=1 | 4 | 141.50 | 281.25 | 0.3884 |
| tr\|Q8I500\|Q8I500_PLAF7 Mitochondrial import inner membrane translocase subunit, putative OS=Plasmodium falciparum (isolate 3D7) GN=PFL2065c PE=4 SV=2 | 4 | 172.19 | 197.75 | 0.1800 |
| tr\|Q8IIW2\|Q8IIW2_PLAF7 Phenylalanine--tRNA ligase, putative OS=Plasmodium falciparum (isolate 3D7) GN=PF11_0051 PE=4 SV=1 | 4 | 236.36 | 441.98 | 0.3632 |
| tr\|Q8I3L8\|Q8I3L8_PLAF7 Mitochondrial import receptor subunit, putative (TOM22) OS=Plasmodium falciparum (isolate 3D7) GN=PFE1230c PE=4 SV=1 | 4 | 271.15 | 537.49 | 0.3873 |
| tr\|Q8IKC7\|Q8IKC7_PLAF7 Inorganic anion exchanger, inorganic anion antiporter OS=Plasmodium falciparum (isolate 3D7) GN=PF14_0679 PE=4 SV=1 | 4 | 356.14 | 710.49 | 0.3900 |
| tr\|Q8IDP4\|Q8IDP4_PLAF7 Thioredoxin OS=Plasmodium falciparum (isolate 3D7) GN=trx2 PE=1 SV=1 | 4 | 625.70 | 1078.68 | 0.3299 |

| | | | | |
|---|---|---|---|---|
| sp\|O75531\|BAF_HUMAN Barrier-to-autointegration factor OS=Homo sapiens GN=BANF1 PE=1 SV=1 | 4 | 661.46 | 1200.64 | 0.3510 |
| tr\|Q8IDG8\|Q8IDG8_PLAF7 Membrane-associated histidine rich protein 2 OS=Plasmodium falciparum (isolate 3D7) GN=PF13_0276 PE=4 SV=1 | 4 | 2297.27 | 2519.27 | 0.1657 |
| tr\|Q8IHP1\|Q8IHP1_PLAF7 Uncharacterized protein OS=Plasmodium falciparum (isolate 3D7) GN=PF11_0488 PE=4 SV=1 | 3 | 0.50 | 0.39 | 0.1576 |
| tr\|Q8I5R4\|Q8I5R4_PLAF7 Phosphatidylinositol-glycan biosynthesis class O protein, putative OS=Plasmodium falciparum (isolate 3D7) GN=PFL0685w PE=4 SV=2 | 3 | 0.52 | 0.34 | 0.1169 |
| tr\|Q8I6S5\|Q8I6S5_PLAF7 2-oxoglutarate dehydrogenase E1 component OS=Plasmodium falciparum (isolate 3D7) GN=PF08_0045 PE=4 SV=1 | 3 | 0.57 | 0.40 | 0.1352 |
| tr\|Q8IIP3\|Q8IIP3_PLAF7 Conserved Plasmodium protein OS=Plasmodium falciparum (isolate 3D7) GN=PF11_0126 PE=4 SV=2 | 3 | 0.63 | 0.59 | 0.2034 |
| tr\|B9ZSI9\|B9ZSI9_PLAF7 Putative uncharacterized protein OS=Plasmodium falciparum (isolate 3D7) GN=PFA_0550w PE=4 SV=1 | 3 | 0.65 | 0.33 | 0.0758 |
| tr\|Q8I5D0\|Q8I5D0_PLAF7 Uncharacterized protein OS=Plasmodium falciparum (isolate 3D7) GN=PFL1395c PE=4 SV=1 | 3 | 0.67 | 0.45 | 0.1246 |
| tr\|Q8IDS7\|Q8IDS7_PLAF7 Na+-dependent Pi transporter, sodium-dependent phosphate transporter OS=Plasmodium falciparum (isolate 3D7) GN=MAL13P1.206 PE=4 SV=1 | 3 | 0.68 | 0.47 | 0.1299 |
| tr\|Q8IHT4\|Q8IHT4_PLAF7 Uncharacterized protein OS=Plasmodium falciparum (isolate 3D7) GN=PF11_0443 PE=4 SV=1 | 3 | 0.68 | 0.46 | 0.1240 |
| tr\|Q5MYR6\|Q5MYR6_PLAF7 1-cys peroxiredoxin OS=Plasmodium falciparum (isolate 3D7) GN=prx PE=1 SV=1 | 3 | 0.68 | 0.59 | 0.1815 |
| tr\|C0H5G2\|C0H5G2_PLAF7 Rab11b, GTPase (Fragment) OS=Plasmodium falciparum (isolate 3D7) GN=Rab11b PE=3 SV=1 | 3 | 0.69 | 0.53 | 0.1540 |
| tr\|Q8I623\|Q8I623_PLAF7 PfmpC OS=Plasmodium falciparum (isolate 3D7) GN=PFL0110c PE=3 SV=1 | 3 | 0.69 | 0.63 | 0.1989 |
| tr\|O77351\|O77351_PLAF7 Putative uncharacterized protein OS=Plasmodium falciparum (isolate 3D7) GN=PFC0490w PE=4 SV=2 | 3 | 0.71 | 0.63 | 0.1919 |
| tr\|Q8IAZ5\|Q8IAZ5_PLAF7 Vacuolar sorting protein VPS9, putative OS=Plasmodium falciparum (isolate 3D7) GN=MAL8P1.82 PE=4 SV=1 | 3 | 0.71 | 0.40 | 0.0931 |
| tr\|Q9TY96\|Q9TY96_PLAF7 Serine repeat antigen 6 (SERA-6) OS=Plasmodium falciparum (isolate 3D7) GN=SERA-6 PE=1 SV=3 | 3 | 0.71 | 0.41 | 0.0965 |
| tr\|C0H4A3\|C0H4A3_PLAF7 Uncharacterized protein OS=Plasmodium falciparum (isolate 3D7) GN=PFD0669c PE=4 SV=1 | 3 | 0.72 | 0.65 | 0.1952 |
| tr\|C0H4A8\|C0H4A8_PLAF7 PfMNL-2 CISD1-like iron-sulfur protein, putative OS=Plasmodium falciparum (isolate 3D7) GN=PFD0807c PE=4 SV=1 | 3 | 0.73 | 0.42 | 0.0947 |
| tr\|Q8I6T5\|Q8I6T5_PLAF7 Cop-coated vesicle membrane protein p24, putative OS=Plasmodium falciparum (isolate 3D7) GN=PF13_0082 PE=4 SV=1 | 3 | 0.76 | 0.43 | 0.0927 |
| tr\|A0A087WY82\|A0A087WY82_HUMAN Junctional adhesion molecule A OS=Homo sapiens GN=F11R PE=1 SV=1;sp\|Q9Y624\|JAM1_HUMAN Junctional adhesion molecule A OS=Homo sapiens GN=F11R PE=1 SV=1 | 3 | 0.68 | 0.11 | 0.0090 |
| tr\|Q8IIE1\|Q8IIE1_PLAF7 Uncharacterized protein OS=Plasmodium falciparum (isolate 3D7) GN=PF11_0233 PE=4 SV=1 | 3 | 0.78 | 0.33 | 0.0550 |
| tr\|Q8I2R6\|Q8I2R6_PLAF7 Putative uncharacterized protein OS=Plasmodium falciparum (isolate 3D7) GN=PFI1185c PE=4 SV=1 | 3 | 0.68 | 0.26 | 0.0473 |
| tr\|Q8I5J2\|Q8I5J2_PLAF7 Uncharacterized protein OS=Plasmodium falciparum (isolate 3D7) GN=PFL1065c PE=4 SV=1 | 3 | 0.78 | 0.35 | 0.0619 |
| tr\|Q8IDE5\|Q8IDE5_PLAF7 Protein phosphatase, putative OS=Plasmodium falciparum (isolate 3D7) GN=MAL13P1.275 PE=4 SV=1 | 3 | 0.69 | 0.26 | 0.0457 |
| tr\|Q8IJS2\|Q8IJS2_PLAF7 Uncharacterized protein OS=Plasmodium falciparum (isolate 3D7) GN=PF10_0120 PE=4 SV=1 | 3 | 0.70 | 0.09 | 0.0059 |
| tr\|O96163\|O96163_PLAF7 Serine repeat antigen 7 (SERA-7) OS=Plasmodium falciparum (isolate 3D7) GN=SERA-7 PE=3 SV=1 | 3 | 0.82 | 0.73 | 0.1916 |
| sp\|Q8IED2\|SMC2_PLAF7 Structural maintenance of chromosomes protein 2 OS=Plasmodium falciparum (isolate 3D7) GN=MAL13P1.96 PE=3 SV=1 | 3 | 0.84 | 0.39 | 0.0666 |
| tr\|Q8I5X5\|Q8I5X5_PLAF7 Uncharacterized protein OS=Plasmodium falciparum (isolate 3D7) GN=PFL0350c PE=4 SV=1 | 3 | 0.85 | 0.55 | 0.1163 |
| tr\|Q8I275\|Q8I275_PLAF7 PfAARP2 protein OS=Plasmodium falciparum (isolate 3D7) GN=AARP2 PE=4 SV=1 | 3 | 0.86 | 0.63 | 0.1390 |
| tr\|Q8IDY0\|Q8IDY0_PLAF7 MSP7-like protein OS=Plasmodium falciparum (isolate 3D7) GN=MAL13P1.174 PE=4 SV=1 | 3 | 0.76 | 0.06 | 0.0022 |
| tr\|Q8ID87\|Q8ID87_PLAF7 Uncharacterized protein OS=Plasmodium falciparum (isolate 3D7) GN=PF13_0329 PE=4 SV=1 | 3 | 0.88 | 0.80 | 0.1943 |
| sp\|O15173\|PGRC2_HUMAN Membrane-associated progesterone receptor component 2 OS=Homo sapiens GN=PGRMC2 PE=1 SV=1;sp\|O15173-2\|PGRC2_HUMAN Isoform 2 of Membrane-associated progesterone receptor component 2 OS=Homo sapiens GN=PGRMC2 | 3 | 0.78 | 0.28 | 0.0402 |

| | | | | |
|---|---|---|---|---|
| tr\|Q8I4U9\|Q8I4U9_PLAF7 Conserved protein OS=Plasmodium falciparum (isolate 3D7) GN=PFL2325c PE=4 SV=1 | 3 | 0.78 | 0.08 | 0.0038 |
| tr\|Q8I506\|Q8I506_PLAF7 Uncharacterized protein OS=Plasmodium falciparum (isolate 3D7) GN=PFL2035c PE=4 SV=1 | 3 | 0.79 | 0.17 | 0.0152 |
| tr\|Q8IKQ3\|Q8IKQ3_PLAF7 Uncharacterized protein OS=Plasmodium falciparum (isolate 3D7) GN=PF14_0550 PE=4 SV=1 | 3 | 0.95 | 0.81 | 0.1813 |
| tr\|Q8IHN5\|Q8IHN5_PLAF7 Probable protein OS=Plasmodium falciparum (isolate 3D7) GN=PF11_0505 PE=4 SV=1 | 3 | 0.95 | 0.56 | 0.0986 |
| tr\|Q8I411\|Q8I411_PLAF7 Uncharacterized protein OS=Plasmodium falciparum (isolate 3D7) GN=PFE0460c PE=4 SV=1 | 3 | 0.95 | 0.70 | 0.1431 |
| tr\|B9ZSI8\|B9ZSI8_PLAF7 Phosphatidate cytidylyltransferase, putative OS=Plasmodium falciparum (isolate 3D7) GN=PFA_0485w PE=4 SV=1 | 3 | 0.81 | 0.23 | 0.0263 |
| tr\|A0A087X0C8\|A0A087X0C8_HUMAN Calpain-5 OS=Homo sapiens GN=CAPN5 PE=1 SV=1;tr\|E7EV01\|E7EV01_HUMAN Calpain-5 OS=Homo sapiens GN=CAPN5 PE=1 SV=2;sp\|O15484\|CAN5_HUMAN Calpain-5 OS=Homo sapiens GN=CAPN5 PE=1 SV=2 | 3 | 0.96 | 0.53 | 0.0879 |
| tr\|Q8IKD2\|Q8IKD2_PLAF7 RAP protein, putative OS=Plasmodium falciparum (isolate 3D7) GN=PF14_0673 PE=4 SV=1 | 3 | 0.82 | 0.14 | 0.0095 |
| tr\|Q8IET8\|Q8IET8_PLAF7 ATP dependent DEAD-box helicase, putative OS=Plasmodium falciparum (isolate 3D7) GN=MAL13P1.14 PE=4 SV=1 | 3 | 0.98 | 0.66 | 0.1247 |
| sp\|O97231\|RL44_PLAF7 60S ribosomal protein L44 OS=Plasmodium falciparum (isolate 3D7) GN=RPL44 PE=1 SV=3 | 3 | 1.00 | 0.42 | 0.0531 |
| sp\|Q00577\|PURA_HUMAN Transcriptional activator protein Pur-alpha OS=Homo sapiens GN=PURA PE=1 SV=2 | 3 | 0.85 | 0.18 | 0.0144 |
| tr\|Q8IBK8\|Q8IBK8_PLAF7 Mitochondrial import inner membrane translocase subunit tim14, putative OS=Plasmodium falciparum (isolate 3D7) GN=PF07_0103 PE=4 SV=1 | 3 | 0.85 | 0.07 | 0.0021 |
| tr\|Q8IDI7\|Q8IDI7_PLAF7 Uncharacterized protein OS=Plasmodium falciparum (isolate 3D7) GN=MAL13P1.258 PE=4 SV=1 | 3 | 0.86 | 0.07 | 0.0020 |
| tr\|Q8ILF7\|Q8ILF7_PLAF7 Glutamate dehydrogenase OS=Plasmodium falciparum (isolate 3D7) GN=PF14_0286 PE=1 SV=1 | 3 | 0.86 | 0.06 | 0.0017 |
| tr\|Q8I2K4\|Q8I2K4_PLAF7 Nucleolar protein Nop52, putative OS=Plasmodium falciparum (isolate 3D7) GN=PFI1510w PE=4 SV=1 | 3 | 1.05 | 0.96 | 0.1999 |
| tr\|Q8ILR8\|Q8ILR8_PLAF7 Uncharacterized protein OS=Plasmodium falciparum (isolate 3D7) GN=PF14_0176 PE=4 SV=1 | 3 | 1.06 | 0.72 | 0.1250 |
| tr\|C0H4N9\|C0H4N9_PLAF7 Uncharacterized protein OS=Plasmodium falciparum (isolate 3D7) GN=MAL7P1.106 PE=4 SV=1 | 3 | 0.87 | 0.06 | 0.0018 |
| tr\|Q8IHV2\|Q8IHV2_PLAF7 Uncharacterized protein OS=Plasmodium falciparum (isolate 3D7) GN=PF11_0424 PE=4 SV=1 | 3 | 0.87 | 0.06 | 0.0016 |
| tr\|Q8I5M6\|Q8I5M6_PLAF7 Conserved Plasmodium protein OS=Plasmodium falciparum (isolate 3D7) GN=PFL0880c PE=4 SV=1 | 3 | 0.88 | 0.34 | 0.0479 |
| tr\|Q8IJR8\|Q8IJR8_PLAF7 Uncharacterized protein OS=Plasmodium falciparum (isolate 3D7) GN=PF10_0124 PE=4 SV=1 | 3 | 1.14 | 0.93 | 0.1686 |
| tr\|Q9U0J2\|Q9U0J2_PLAF7 DNAJ protein OS=Plasmodium falciparum (isolate 3D7) GN=Pfj1 PE=3 SV=1 | 3 | 1.16 | 0.77 | 0.1212 |
| tr\|Q8I349\|Q8I349_PLAF7 Putative uncharacterized protein OS=Plasmodium falciparum (isolate 3D7) GN=PFI0500w PE=4 SV=1 | 3 | 1.18 | 0.69 | 0.0990 |
| tr\|O96202\|O96202_PLAF7 Mitochondrial ribosomal protein L12, putative OS=Plasmodium falciparum (isolate 3D7) GN=PFB0545c PE=4 SV=2 | 3 | 0.88 | 0.06 | 0.0016 |
| tr\|O96237\|O96237_PLAF7 Origin recognition complex subunit 5 OS=Plasmodium falciparum (isolate 3D7) GN=ORC5 PE=4 SV=1 | 3 | 1.19 | 0.50 | 0.0537 |
| tr\|Q8IEC2\|Q8IEC2_PLAF7 Uncharacterized protein OS=Plasmodium falciparum (isolate 3D7) GN=MAL13P1.103 PE=4 SV=1 | 3 | 0.88 | 0.02 | 0.0003 |
| tr\|C0H587\|C0H587_PLAF7 Putative uncharacterized protein OS=Plasmodium falciparum (isolate 3D7) GN=PFI1615w PE=4 SV=1 | 3 | 1.24 | 0.65 | 0.0813 |
| tr\|Q8IDI0\|Q8IDI0_PLAF7 Uncharacterized protein OS=Plasmodium falciparum (isolate 3D7) GN=MAL13P1.262 PE=4 SV=1 | 3 | 1.32 | 0.77 | 0.0967 |
| tr\|C0H4X1\|C0H4X1_PLAF7 U5 snrnp-specific protein, putative OS=Plasmodium falciparum (isolate 3D7) GN=MAL8P1.43 PE=4 SV=1 | 3 | 1.33 | 0.59 | 0.0605 |
| tr\|Q8I3G6\|Q8I3G6_PLAF7 SNARE protein, putative OS=Plasmodium falciparum (isolate 3D7) GN=PfSyn6 PE=4 SV=1 | 3 | 1.33 | 0.78 | 0.0986 |
| tr\|Q8IKK3\|Q8IKK3_PLAF7 DNA polymerase alpha subunit, putative OS=Plasmodium falciparum (isolate 3D7) GN=PF14_0602 PE=4 SV=1 | 3 | 1.37 | 0.79 | 0.0953 |
| tr\|O77343\|O77343_PLAF7 Transporter, putative OS=Plasmodium falciparum (isolate 3D7) GN=PFC0530w PE=4 SV=1 | 3 | 0.90 | 0.15 | 0.0087 |
| tr\|C0H4T1\|C0H4T1_PLAF7 Coatomer epsilon subunit, putative OS=Plasmodium falciparum (isolate 3D7) GN=MAL8P1.121:exon:1 PE=4 SV=1 | 3 | 1.40 | 0.71 | 0.0765 |

| | | | | |
|---|---|---|---|---|
| sp\|Q8IIS5\|PESC_PLAF7 Pescadillo homolog OS=Plasmodium falciparum (isolate 3D7) GN=PF11_0090 PE=3 SV=1 | 3 | 1.40 | 0.64 | 0.0636 |
| tr\|Q8II92\|Q8II92_PLAF7 Deoxyuridine 5-triphosphate nucleotidohydrolase, putative OS=Plasmodium falciparum (isolate 3D7) GN=PF11_0282 PE=1 SV=1 | 3 | 1.45 | 0.60 | 0.0521 |
| tr\|Q8IIW5\|Q8IIW5_PLAF7 Casein kinase II subunit beta OS=Plasmodium falciparum (isolate 3D7) GN=PF11_0048 PE=3 SV=1 | 3 | 1.53 | 0.88 | 0.0957 |
| tr\|O97273\|O97273_PLAF7 Putative uncharacterized protein OS=Plasmodium falciparum (isolate 3D7) GN=PFC0690c PE=4 SV=1 | 3 | 1.53 | 1.08 | 0.1329 |
| tr\|Q8I547\|Q8I547_PLAF7 Uncharacterized protein OS=Plasmodium falciparum (isolate 3D7) GN=PFL1820w PE=4 SV=1 | 3 | 1.58 | 0.79 | 0.0741 |
| tr\|Q8ILT8\|Q8ILT8_PLAF7 Dimethyladenosine transferase, putative OS=Plasmodium falciparum (isolate 3D7) GN=PF14_0156 PE=1 SV=1 | 3 | 1.58 | 1.21 | 0.1526 |
| sp\|Q9H1E5\|TMX4_HUMAN Thioredoxin-related transmembrane protein 4 OS=Homo sapiens GN=TMX4 PE=1 SV=1 | 3 | 1.59 | 1.58 | 0.2237 |
| tr\|Q7KQL1\|Q7KQL1_PLAF7 Myb2 protein OS=Plasmodium falciparum (isolate 3D7) GN=PF10_0327 PE=4 SV=1 | 3 | 1.60 | 0.96 | 0.1023 |
| tr\|Q8I1R5\|Q8I1R5_PLAF7 LETM1-like protein, putative OS=Plasmodium falciparum (isolate 3D7) GN=PFD0835c PE=4 SV=1 | 3 | 1.61 | 0.91 | 0.0921 |
| tr\|Q8IJV1\|Q8IJV1_PLAF7 Uncharacterized protein OS=Plasmodium falciparum (isolate 3D7) GN=PF10_0091 PE=4 SV=1 | 3 | 1.61 | 1.48 | 0.1994 |
| tr\|C6KTE1\|C6KTE1_PLAF7 Uncharacterized protein OS=Plasmodium falciparum (isolate 3D7) GN=PFF1485w PE=4 SV=1 | 3 | 1.63 | 0.72 | 0.0587 |
| tr\|Q8IL21\|Q8IL21_PLAF7 RNA helicase, putative OS=Plasmodium falciparum (isolate 3D7) GN=PF14_0429 PE=4 SV=1 | 3 | 1.64 | 1.09 | 0.1202 |
| tr\|Q8IEJ0\|Q8IEJ0_PLAF7 Uncharacterized protein OS=Plasmodium falciparum (isolate 3D7) GN=MAL13P1.61 PE=4 SV=1 | 3 | 1.65 | 0.96 | 0.0968 |
| sp\|P61076\|TRXR2_PLAF7 Thioredoxin reductase 2 OS=Plasmodium falciparum (isolate 3D7) GN=trxr2 PE=1 SV=2 | 3 | 1.73 | 1.57 | 0.1951 |
| tr\|Q8I4T9\|Q8I4T9_PLAF7 CutA, putative OS=Plasmodium falciparum (isolate 3D7) GN=PFL2375c PE=4 SV=1 | 3 | 1.83 | 0.76 | 0.0535 |
| tr\|Q8ID42\|Q8ID42_PLAF7 Signal recognition particle receptor alpha subunit, putative OS=Plasmodium falciparum (isolate 3D7) GN=PF13_0350 PE=4 SV=1 | 3 | 1.86 | 1.99 | 0.2462 |
| tr\|Q8IL87\|Q8IL87_PLAF7 eIF2A OS=Plasmodium falciparum (isolate 3D7) GN=PF14_0360 PE=4 SV=1 | 3 | 1.86 | 1.19 | 0.1125 |
| tr\|Q8IE08\|Q8IE08_PLAF7 Qa-SNARE protein, putative OS=Plasmodium falciparum (isolate 3D7) GN=PfSyn5 PE=4 SV=1 | 3 | 1.90 | 0.87 | 0.0629 |
| tr\|Q8II81\|Q8II81_PLAF7 Multiprotein bridging factor type 1, putative OS=Plasmodium falciparum (isolate 3D7) GN=PF11_0293 PE=4 SV=1 | 3 | 1.91 | 0.80 | 0.0540 |
| tr\|Q8ILG8\|Q8ILG8_PLAF7 Uncharacterized protein OS=Plasmodium falciparum (isolate 3D7) GN=PF14_0275 PE=4 SV=1 | 3 | 2.11 | 2.06 | 0.2180 |
| tr\|Q8ILD7\|Q8ILD7_PLAF7 Uncharacterized protein OS=Plasmodium falciparum (isolate 3D7) GN=PF14_0307 PE=4 SV=1 | 3 | 2.13 | 2.05 | 0.2135 |
| tr\|Q8I374\|Q8I374_PLAF7 Subunit of proteaseome activator complex, putative OS=Plasmodium falciparum (isolate 3D7) GN=PFI0370c PE=4 SV=1 | 3 | 2.16 | 2.32 | 0.2488 |
| tr\|C0H4C4\|C0H4C4_PLAF7 Uncharacterized protein OS=Plasmodium falciparum (isolate 3D7) GN=PFE0235c PE=4 SV=1 | 3 | 2.19 | 2.05 | 0.2059 |
| tr\|Q8II05\|Q8II05_PLAF7 3-oxo-5-alpha-steroid 4-dehydrogenase, putative OS=Plasmodium falciparum (isolate 3D7) GN=PF11_0370 PE=4 SV=2 | 3 | 2.19 | 2.30 | 0.2410 |
| tr\|Q8IDW4\|Q8IDW4_PLAF7 Nuclear movement protein, putative OS=Plasmodium falciparum (isolate 3D7) GN=PF13_0204 PE=4 SV=1 | 3 | 2.28 | 2.28 | 0.2259 |
| tr\|Q8I5Z0\|Q8I5Z0_PLAF7 Uncharacterized protein OS=Plasmodium falciparum (isolate 3D7) GN=PFL0275w PE=4 SV=1 | 3 | 2.30 | 1.88 | 0.1688 |
| tr\|C6KSL5\|C6KSL5_PLAF7 Pfmc-2TM Maurers cleft two transmembrane protein OS=Plasmodium falciparum (isolate 3D7) GN=PfMC-2TM PE=4 SV=1 | 3 | 2.31 | 2.19 | 0.2090 |
| tr\|Q8I4U5\|Q8I4U5_PLAF7 Tat-binding protein homolog OS=Plasmodium falciparum (isolate 3D7) GN=PFL2345c PE=3 SV=1 | 3 | 2.39 | 1.78 | 0.1453 |
| tr\|Q8I375\|Q8I375_PLAF7 Translation initiation factor SUI1, putative OS=Plasmodium falciparum (isolate 3D7) GN=PFI0365w PE=4 SV=1 | 3 | 2.39 | 2.13 | 0.1907 |
| tr\|Q8ILE4\|Q8ILE4_PLAF7 Qa-SNARE protein, putative OS=Plasmodium falciparum (isolate 3D7) GN=Syn11 PE=4 SV=1 | 3 | 2.40 | 3.37 | 0.3433 |
| tr\|Q8IJH3\|Q8IJH3_PLAF7 Orotidine 5-phosphate decarboxylase OS=Plasmodium falciparum (isolate 3D7) GN=PF10_0225 PE=1 SV=1 | 3 | 2.41 | 2.12 | 0.1880 |
| tr\|Q8IDZ0\|Q8IDZ0_PLAF7 Uncharacterized protein OS=Plasmodium falciparum (isolate 3D7) GN=PF13_0186 PE=4 SV=1 | 3 | 2.41 | 2.12 | 0.1880 |
| tr\|Q8IM19\|Q8IM19_PLAF7 Nucleolar preribosomal GTPase, putative OS=Plasmodium falciparum (isolate 3D7) GN=PF14_0072 PE=4 SV=2 | 3 | 2.41 | 2.12 | 0.1880 |

| | | | | |
|---|---|---|---|---|
| tr\|O97253\|O97253_PLAF7 Putative uncharacterized protein OS=Plasmodium falciparum (isolate 3D7) GN=PFC0315c PE=4 SV=2 | 3 | 2.41 | 2.12 | 0.1880 |
| tr\|O77367\|O77367_PLAF7 Ubiquitin-protein ligase, putative OS=Plasmodium falciparum (isolate 3D7) GN=PFC0845c PE=4 SV=3 | 3 | 2.41 | 2.12 | 0.1880 |
| tr\|Q8I3H2\|Q8I3H2_PLAF7 Cell cycle regulator protein, putative OS=Plasmodium falciparum (isolate 3D7) GN=PFE1470w PE=4 SV=1 | 3 | 2.41 | 2.12 | 0.1880 |
| sp\|P35754\|GLRX1_HUMAN Glutaredoxin-1 OS=Homo sapiens GN=GLRX PE=1 SV=2 | 3 | 2.41 | 2.11 | 0.1868 |
| tr\|Q8I383\|Q8I383_PLAF7 Putative uncharacterized protein OS=Plasmodium falciparum (isolate 3D7) GN=PFI0325c PE=4 SV=1 | 3 | 2.41 | 2.13 | 0.1893 |
| tr\|Q8IET1\|Q8IET1_PLAF7 Uncharacterized protein OS=Plasmodium falciparum (isolate 3D7) GN=PF13_0018 PE=4 SV=1 | 3 | 2.43 | 2.88 | 0.2816 |
| tr\|Q8IDG6\|Q8IDG6_PLAF7 Ran-binding protein, putative OS=Plasmodium falciparum (isolate 3D7) GN=PF13_0278 PE=4 SV=1 | 3 | 2.43 | 1.39 | 0.0933 |
| tr\|Q8IAR7\|Q8IAR7_PLAF7 Tyrosyl-tRNA synthetase, putative OS=Plasmodium falciparum (isolate 3D7) GN=MAL8P1.125 PE=1 SV=1 | 3 | 2.45 | 2.21 | 0.1944 |
| tr\|Q8ILY4\|Q8ILY4_PLAF7 Uncharacterized protein OS=Plasmodium falciparum (isolate 3D7) GN=PF14_0778 PE=4 SV=2 | 3 | 2.46 | 2.08 | 0.1777 |
| tr\|Q8ILB9\|Q8ILB9_PLAF7 Dynein-related AAA-type ATPase OS=Plasmodium falciparum (isolate 3D7) GN=PF14_0326 PE=4 SV=2 | 3 | 2.48 | 2.05 | 0.1714 |
| tr\|C0H549\|C0H549_PLAF7 Nucleolar preribosomal assembly protein, putative OS=Plasmodium falciparum (isolate 3D7) GN=PFI1070c PE=4 SV=1 | 3 | 2.50 | 2.88 | 0.2718 |
| tr\|O77316\|O77316_PLAF7 Putative uncharacterized protein OS=Plasmodium falciparum (isolate 3D7) GN=PFC0130c PE=4 SV=1 | 3 | 2.50 | 1.63 | 0.1177 |
| tr\|Q8IJB8\|Q8IJB8_PLAF7 Uncharacterized protein OS=Plasmodium falciparum (isolate 3D7) GN=PF10_0280 PE=4 SV=1 | 3 | 2.58 | 1.34 | 0.0795 |
| tr\|Q8ID43\|Q8ID43_PLAF7 Nucleoside diphosphate kinase OS=Plasmodium falciparum (isolate 3D7) GN=PF13_0349 PE=1 SV=1 | 3 | 2.59 | 1.63 | 0.1108 |
| sp\|P00441\|SODC_HUMAN Superoxide dismutase [Cu-Zn] OS=Homo sapiens GN=SOD1 PE=1 SV=2;tr\|H7BYH4\|H7BYH4_HUMAN Superoxide dismutase [Cu-Zn] OS=Homo sapiens GN=SOD1 PE=1 SV=1 | 3 | 2.71 | 1.51 | 0.0891 |
| tr\|Q8I238\|Q8I238_PLAF7 Chromatin assembly factor 1 protein WD40 domain, putative OS=Plasmodium falciparum (isolate 3D7) GN=PFA_0520c PE=4 SV=1 | 3 | 2.76 | 1.81 | 0.1187 |
| tr\|Q8IIB7\|Q8IIB7_PLAF7 Ethanolamine kinase, putative OS=Plasmodium falciparum (isolate 3D7) GN=PF11_0257 PE=4 SV=1 | 3 | 2.81 | 1.58 | 0.0909 |
| tr\|Q8IE00\|Q8IE00_PLAF7 Eukaryotic translation initiation factor 6 OS=Plasmodium falciparum (isolate 3D7) GN=EIF6 PE=3 SV=1 | 3 | 2.84 | 2.86 | 0.2281 |
| tr\|Q8IKQ7\|Q8IKQ7_PLAF7 Uncharacterized protein OS=Plasmodium falciparum (isolate 3D7) GN=PF14_0546 PE=4 SV=1 | 3 | 2.87 | 1.79 | 0.1094 |
| tr\|Q8IIM5\|Q8IIM5_PLAF7 Glyoxalase I, putative OS=Plasmodium falciparum (isolate 3D7) GN=PF11_0145 PE=4 SV=1 | 3 | 2.87 | 1.80 | 0.1098 |
| tr\|Q7KWJ4\|Q7KWJ4_PLAF7 Adenylosuccinate lyase OS=Plasmodium falciparum (isolate 3D7) GN=ASL PE=3 SV=1 | 3 | 3.02 | 1.75 | 0.0965 |
| sp\|Q8IIU6\|RTCB_PLAF7 tRNA-splicing ligase RtcB homolog OS=Plasmodium falciparum (isolate 3D7) GN=PF11_0068 PE=3 SV=1 | 3 | 3.08 | 1.75 | 0.0928 |
| sp\|Q8I467\|CADF1_PLAF7 Cofilin/actin-depolymerizing factor homolog 1 OS=Plasmodium falciparum (isolate 3D7) GN=PFE0165w PE=1 SV=1 | 3 | 3.11 | 1.75 | 0.0913 |
| tr\|Q8I3L9\|Q8I3L9_PLAF7 Organelle ribosomal protein L7/L12, putative OS=Plasmodium falciparum (isolate 3D7) GN=PFE1225w PE=3 SV=1 | 3 | 3.14 | 3.35 | 0.2459 |
| tr\|Q8I3V1\|Q8I3V1_PLAF7 Metabolite/drug transporter, putative OS=Plasmodium falciparum (isolate 3D7) GN=PFE0785c PE=4 SV=1 | 3 | 3.14 | 4.63 | 0.3610 |
| tr\|Q8II22\|Q8II22_PLAF7 Uncharacterized protein OS=Plasmodium falciparum (isolate 3D7) GN=PF11_0353 PE=4 SV=1 | 3 | 3.16 | 1.92 | 0.1045 |
| tr\|Q8ILZ3\|Q8ILZ3_PLAF7 CTP synthase OS=Plasmodium falciparum (isolate 3D7) GN=PF14_0100 PE=3 SV=1 | 3 | 3.25 | 1.77 | 0.0861 |
| tr\|Q8I511\|Q8I511_PLAF7 DEAD/DEAH box helicase, putative OS=Plasmodium falciparum (isolate 3D7) GN=PFL2010c PE=4 SV=2 | 3 | 3.33 | 3.52 | 0.2430 |
| tr\|Q8IM09\|Q8IM09_PLAF7 Uncharacterized protein OS=Plasmodium falciparum (isolate 3D7) GN=PF14_0084 PE=4 SV=2 | 3 | 3.46 | 4.34 | 0.3009 |
| tr\|Q8I250\|Q8I250_PLAF7 Tubulin-specific chaperone a, putative OS=Plasmodium falciparum (isolate 3D7) GN=PFA_0460c PE=4 SV=1 | 3 | 3.50 | 1.88 | 0.0846 |
| tr\|Q8I1T0\|Q8I1T0_PLAF7 Uncharacterized protein OS=Plasmodium falciparum (isolate 3D7) GN=PFD0760c PE=4 SV=1 | 3 | 3.52 | 4.57 | 0.3132 |
| tr\|Q8I3J3\|Q8I3J3_PLAF7 Ubiquitin carboxyl-terminal hydrolase OS=Plasmodium falciparum (isolate 3D7) GN=PFE1355c PE=3 SV=1 | 3 | 3.53 | 2.51 | 0.1350 |

| | | | | |
|---|---|---|---|---|
| tr\|O77363\|O77363_PLAF7 Putative uncharacterized protein OS=Plasmodium falciparum (isolate 3D7) GN=PFC0545c PE=4 SV=2 | 3 | 3.57 | 4.19 | 0.2779 |
| tr\|Q8II33\|Q8II33_PLAF7 Conserved Plasmodium protein OS=Plasmodium falciparum (isolate 3D7) GN=PF11_0341 PE=4 SV=1 | 3 | 3.62 | 3.65 | 0.2278 |
| tr\|Q8I5L3\|Q8I5L3_PLAF7 Ribulose-phosphate 3-epimerase OS=Plasmodium falciparum (isolate 3D7) GN=PFL0960w PE=1 SV=1 | 3 | 3.62 | 1.98 | 0.0864 |
| tr\|C0H4A1\|C0H4A1_PLAF7 Uncharacterized protein OS=Plasmodium falciparum (isolate 3D7) GN=PFD0465c PE=4 SV=1 | 3 | 3.78 | 6.42 | 0.4149 |
| tr\|O77321\|O77321_PLAF7 DNA polymerase epsilon subunit B, putative OS=Plasmodium falciparum (isolate 3D7) GN=PFC0340w PE=4 SV=1 | 3 | 3.86 | 5.04 | 0.3157 |
| tr\|C0H4Y0\|C0H4Y0_PLAF7 Ubiquitination-mediated degradation component, putative OS=Plasmodium falciparum (isolate 3D7) GN=PF08_0020 PE=4 SV=1 | 3 | 4.05 | 4.59 | 0.2662 |
| tr\|Q8I0U7\|Q8I0U7_PLAF7 Proteasome, putative OS=Plasmodium falciparum (isolate 3D7) GN=PFI1545c PE=4 SV=1 | 3 | 4.32 | 2.79 | 0.1149 |
| tr\|Q8I4Z9\|Q8I4Z9_PLAF7 t-SNARE, putative OS=Plasmodium falciparum (isolate 3D7) GN=PFL2070w PE=4 SV=1 | 3 | 4.41 | 6.67 | 0.3712 |
| tr\|Q8IDT0\|Q8IDT0_PLAF7 Phosphatase, putative OS=Plasmodium falciparum (isolate 3D7) GN=PF13_0222 PE=4 SV=1 | 3 | 4.87 | 5.14 | 0.2427 |
| tr\|Q8I3P8\|Q8I3P8_PLAF7 Uncharacterized protein OS=Plasmodium falciparum (isolate 3D7) GN=PFE1075c PE=4 SV=1 | 3 | 4.90 | 4.75 | 0.2162 |
| tr\|Q8I624\|Q8I624_PLAF7 Uncharacterized protein OS=Plasmodium falciparum (isolate 3D7) GN=PFL0105w PE=4 SV=1 | 3 | 4.93 | 5.90 | 0.2851 |
| tr\|Q8IKC5\|Q8IKC5_PLAF7 Diacylglycerol kinase, putative OS=Plasmodium falciparum (isolate 3D7) GN=PF14_0681 PE=4 SV=2 | 3 | 5.06 | 6.63 | 0.3170 |
| tr\|Q8I4Y5\|Q8I4Y5_PLAF7 ADP-ribosylation factor GTPase-activating protein OS=Plasmodium falciparum (isolate 3D7) GN=PFL2140c PE=1 SV=1 | 3 | 5.34 | 6.20 | 0.2747 |
| tr\|Q8I3Y4\|Q8I3Y4_PLAF7 Glutathione synthetase OS=Plasmodium falciparum (isolate 3D7) GN=gS PE=3 SV=1 | 3 | 5.50 | 5.11 | 0.2034 |
| tr\|C6KTD8\|C6KTD8_PLAF7 DNA polymerase epsilon, catalytic subunit a, putative OS=Plasmodium falciparum (isolate 3D7) GN=PFF1470c PE=4 SV=1 | 3 | 6.03 | 3.32 | 0.0881 |
| tr\|Q8IKP1\|Q8IKP1_PLAF7 DEAD box helicase, putative OS=Plasmodium falciparum (isolate 3D7) GN=PF14_0563 PE=4 SV=1 | 3 | 6.95 | 8.77 | 0.3038 |
| tr\|O97284\|O97284_PLAF7 Putative uncharacterized protein OS=Plasmodium falciparum (isolate 3D7) GN=PFC0910w PE=4 SV=1 | 3 | 7.60 | 7.63 | 0.2266 |
| tr\|Q8I3I6\|Q8I3I6_PLAF7 Beta adaptin protein, putative OS=Plasmodium falciparum (isolate 3D7) GN=PFE1400c PE=4 SV=2 | 3 | 8.13 | 11.98 | 0.3606 |
| tr\|Q8IJI3\|Q8IJI3_PLAF7 RNA binding protein, putative OS=Plasmodium falciparum (isolate 3D7) GN=PF10_0214 PE=4 SV=2 | 3 | 8.72 | 12.67 | 0.3556 |
| tr\|Q8IHY3\|Q8IHY3_PLAF7 Ubiquitin-related modifier 1 homolog OS=Plasmodium falciparum (isolate 3D7) GN=PF11_0393 PE=3 SV=1 | 3 | 9.20 | 12.08 | 0.3182 |
| tr\|Q8II17\|Q8II17_PLAF7 DNA-directed RNA polymerase OS=Plasmodium falciparum (isolate 3D7) GN=PF11_0358 PE=3 SV=1 | 3 | 9.46 | 14.34 | 0.3716 |
| tr\|Q8II82\|Q8II82_PLAF7 Uncharacterized protein OS=Plasmodium falciparum (isolate 3D7) GN=PF11_0292 PE=4 SV=1 | 3 | 10.01 | 14.55 | 0.3554 |
| tr\|Q8I3V0\|Q8I3V0_PLAF7 BolA-like protein, putative OS=Plasmodium falciparum (isolate 3D7) GN=PFE0790c PE=1 SV=1 | 3 | 10.66 | 13.51 | 0.3052 |
| tr\|Q8I308\|Q8I308_PLAF7 Putative uncharacterized protein OS=Plasmodium falciparum (isolate 3D7) GN=PFI0705w PE=4 SV=1 | 3 | 11.00 | 14.81 | 0.3273 |
| sp\|Q8IKU0\|GLUPH_PLAF7 Bifunctional glucose-6-phosphate 1-dehydrogenase/6-phosphogluconolactonase OS=Plasmodium falciparum (isolate 3D7) GN=PF14_0511 PE=1 SV=1 | 3 | 11.11 | 16.81 | 0.3707 |
| tr\|Q8I3C0\|Q8I3C0_PLAF7 Serine repeat antigen 9 (SERA-9) OS=Plasmodium falciparum (isolate 3D7) GN=SERA9 PE=3 SV=1 | 3 | 11.41 | 18.00 | 0.3867 |
| tr\|Q8IIG3\|Q8IIG3_PLAF7 Uncharacterized protein OS=Plasmodium falciparum (isolate 3D7) GN=PF11_0211 PE=4 SV=1 | 3 | 11.49 | 12.52 | 0.2529 |
| tr\|Q8ID59\|Q8ID59_PLAF7 DNA-directed RNA polymerase 2, putative OS=Plasmodium falciparum (isolate 3D7) GN=PF13_0341 PE=3 SV=1 | 3 | 12.80 | 21.98 | 0.4194 |
| tr\|Q8IJ30\|Q8IJ30_PLAF7 Enhancer of rudimentary homolog OS=Plasmodium falciparum (isolate 3D7) GN=PF10_0370 PE=3 SV=1 | 3 | 14.92 | 20.84 | 0.3408 |
| tr\|Q8IIA5\|Q8IIA5_PLAF7 Conserved Plasmodium protein OS=Plasmodium falciparum (isolate 3D7) GN=PF11_0269 PE=4 SV=1 | 3 | 16.01 | 24.66 | 0.3777 |
| tr\|Q8IK74\|Q8IK74_PLAF7 Uncharacterized protein OS=Plasmodium falciparum (isolate 3D7) GN=PF14_0732 PE=4 SV=1 | 3 | 16.38 | 26.49 | 0.3963 |
| tr\|Q8IBG6\|Q8IBG6_PLAF7 60S ribosomal subunit export protein, putative OS=Plasmodium falciparum (isolate 3D7) GN=PF07_0121 PE=4 SV=1 | 3 | 18.14 | 29.40 | 0.3971 |
| tr\|C6KT92\|C6KT92_PLAF7 Poly(A) polymerase PAP, putative OS=Plasmodium falciparum (isolate 3D7) GN=PFF1240w PE=4 SV=1 | 3 | 18.85 | 30.72 | 0.3992 |

| | | | | |
|---|---|---|---|---|
| tr\|Q8I6Z2\|Q8I6Z2_PLAF7 mRNA (N6-adenosine)-methyltransferase, putative OS=Plasmodium falciparum (isolate 3D7) GN=PF07_0123 PE=4 SV=1 | 3 | 19.26 | 31.34 | 0.3986 |
| tr\|Q8I5G5\|Q8I5G5_PLAF7 Uncharacterized protein OS=Plasmodium falciparum (isolate 3D7) GN=PFL1215c PE=4 SV=1 | 3 | 20.86 | 19.18 | 0.2004 |
| tr\|Q8IKT2\|Q8IKT2_PLAF7 6-phosphogluconate dehydrogenase, decarboxylating OS=Plasmodium falciparum (isolate 3D7) GN=PF14_0520 PE=3 SV=1 | 3 | 21.40 | 32.95 | 0.3774 |
| tr\|Q8I3A1\|Q8I3A1_PLAF7 Replication factor A-related protein, putative OS=Plasmodium falciparum (isolate 3D7) GN=PFI0235w PE=4 SV=1 | 3 | 23.75 | 38.20 | 0.3942 |
| tr\|Q8I5S3\|Q8I5S3_PLAF7 Conserved Plasmodium protein OS=Plasmodium falciparum (isolate 3D7) GN=PFL0640w PE=4 SV=1 | 3 | 25.04 | 41.69 | 0.4074 |
| tr\|Q8I5H2\|Q8I5H2_PLAF7 Chromatin assembly protein (ASF1), putative OS=Plasmodium falciparum (isolate 3D7) GN=PFL1180w PE=4 SV=1 | 3 | 26.26 | 43.03 | 0.4013 |
| tr\|Q8IL92\|Q8IL92_PLAF7 Pantothenate kinase, putative OS=Plasmodium falciparum (isolate 3D7) GN=PF14_0354 PE=4 SV=1 | 3 | 27.44 | 45.44 | 0.4054 |
| tr\|Q8I4S1\|Q8I4S1_PLAF7 Thymidylate kinase, putative OS=Plasmodium falciparum (isolate 3D7) GN=PFL2465c PE=1 SV=1 | 3 | 28.39 | 45.72 | 0.3947 |
| tr\|C0H540\|C0H540_PLAF7 Apicoplast Ufd1 OS=Plasmodium falciparum (isolate 3D7) GN=PFI0810c PE=4 SV=1 | 3 | 30.30 | 50.95 | 0.4112 |
| tr\|Q8I1U8\|Q8I1U8_PLAF7 Ubiquitinyl hydrolase 1 OS=Plasmodium falciparum (isolate 3D7) GN=PFD0680c PE=4 SV=1 | 3 | 33.86 | 56.41 | 0.4078 |
| tr\|C0H5B7\|C0H5B7_PLAF7 Phosphatidylinositol synthase OS=Plasmodium falciparum (isolate 3D7) GN=MAL13P1.82 PE=3 SV=1 | 3 | 35.01 | 59.08 | 0.4126 |
| tr\|C6KT35\|C6KT35_PLAF7 Acyl-CoA synthetase, PfACS12 OS=Plasmodium falciparum (isolate 3D7) GN=PfACS12 PE=4 SV=1 | 3 | 36.13 | 59.78 | 0.4050 |
| tr\|C0H4G4\|C0H4G4_PLAF7 Uncharacterized protein OS=Plasmodium falciparum (isolate 3D7) GN=PFE1375c PE=4 SV=1 | 3 | 36.71 | 62.11 | 0.4136 |
| tr\|Q8I5R6\|Q8I5R6_PLAF7 Uncharacterized protein OS=Plasmodium falciparum (isolate 3D7) GN=PFL0675c PE=4 SV=1 | 3 | 37.68 | 43.22 | 0.2701 |
| tr\|Q8IJB9\|Q8IJB9_PLAF7 Uncharacterized protein OS=Plasmodium falciparum (isolate 3D7) GN=PF10_0279 PE=4 SV=1 | 3 | 38.30 | 51.55 | 0.3269 |
| tr\|C6KT18\|C6KT18_PLAF7 Histone H2A OS=Plasmodium falciparum (isolate 3D7) GN=PFF0860c PE=3 SV=1 | 3 | 44.17 | 71.44 | 0.3963 |
| tr\|Q8IBZ6\|Q8IBZ6_PLAF7 Cg2 protein OS=Plasmodium falciparum (isolate 3D7) GN=PF07_0037 PE=4 SV=1 | 3 | 58.88 | 95.06 | 0.3956 |
| tr\|Q8ILI9\|Q8ILI9_PLAF7 DNA mismatch repair protein Msh2p, putative OS=Plasmodium falciparum (isolate 3D7) GN=PF14_0254 PE=3 SV=1 | 3 | 62.51 | 106.70 | 0.4170 |
| tr\|Q8I448\|Q8I448_PLAF7 Uncharacterized protein OS=Plasmodium falciparum (isolate 3D7) GN=PFE0265c PE=4 SV=1 | 3 | 63.92 | 93.04 | 0.3562 |
| tr\|Q8IHP4\|Q8IHP4_PLAF7 Mitochondrial ATP synthase delta subunit, putative OS=Plasmodium falciparum (isolate 3D7) GN=PF11_0485 PE=4 SV=1 | 3 | 66.74 | 103.16 | 0.3790 |
| tr\|C0H530\|C0H530_PLAF7 Ran-binding protein, putative OS=Plasmodium falciparum (isolate 3D7) GN=PFI0490c PE=4 SV=1 | 3 | 93.12 | 112.38 | 0.2877 |
| tr\|Q8I2P2\|Q8I2P2_PLAF7 NAD synthase, putative OS=Plasmodium falciparum (isolate 3D7) GN=PFI1310w PE=4 SV=1 | 3 | 142.55 | 244.14 | 0.4183 |
| tr\|C0H4W0\|C0H4W0_PLAF7 Uncharacterized protein OS=Plasmodium falciparum (isolate 3D7) GN=MAL8P1.63 PE=4 SV=1 | 3 | 166.94 | 258.40 | 0.3795 |
| tr\|Q8ILX1\|Q8ILX1_PLAF7 Nuclear transport factor 2, putative OS=Plasmodium falciparum (isolate 3D7) GN=PF14_0122 PE=4 SV=2 | 3 | 522.18 | 901.20 | 0.4213 |
| sp\|Q9H4G4\|GAPR1_HUMAN Golgi-associated plant pathogenesis-related protein 1 OS=Homo sapiens GN=GLIPR2 PE=1 SV=3;tr\|Q5VZR0\|Q5VZR0_HUMAN Golgi-associated plant pathogenesis-related protein 1 OS=Homo sapiens GN=GLIPR2 PE=1 SV=1 | 3 | 0.91 | 0.11 | 0.0044 |
| tr\|C6KT26\|C6KT26_PLAF7 Rhomboid protease ROM10 OS=Plasmodium falciparum (isolate 3D7) GN=ROM10 PE=4 SV=1 | 3 | 0.92 | 0.09 | 0.0030 |
| tr\|C0H5H5\|C0H5H5_PLAF7 Uncharacterized protein OS=Plasmodium falciparum (isolate 3D7) GN=MAL13P1.229 PE=4 SV=1 | 3 | 0.92 | 0.16 | 0.0105 |
| tr\|Q8IIC3\|Q8IIC3_PLAF7 Endoplasmic reticulum oxidoreductin, putative OS=Plasmodium falciparum (isolate 3D7) GN=PF11_0251 PE=4 SV=2 | 3 | 0.92 | 0.21 | 0.0176 |
| tr\|Q8IC37\|Q8IC37_PLAF7 Uncharacterized protein OS=Plasmodium falciparum (isolate 3D7) GN=MAL7P1.11 PE=4 SV=1 | 3 | 0.94 | 0.11 | 0.0044 |
| tr\|C6KSV0\|C6KSV0_PLAF7 Histone H3 OS=Plasmodium falciparum (isolate 3D7) GN=PFF0510w PE=3 SV=1 | 3 | 0.94 | 0.05 | 0.0010 |
| tr\|C0H4K4\|C0H4K4_PLAF7 Uncharacterized protein OS=Plasmodium falciparum (isolate 3D7) GN=MAL7P1.17 PE=4 SV=1 | 3 | 0.95 | 0.11 | 0.0042 |
| tr\|A0A087WXM8\|A0A087WXM8_HUMAN Basal cell adhesion molecule OS=Homo sapiens GN=BCAM PE=1 SV=1;sp\|P50895\|BCAM_HUMAN Basal cell adhesion molecule OS=Homo sapiens GN=BCAM PE=1 SV=2 | 3 | 0.95 | 0.02 | 0.0002 |

| | | | | |
|---|---|---|---|---|
| tr\|Q8I296\|Q8I296_PLAF7 Ubiquitin carboxyl-terminal hydrolase, putative OS=Plasmodium falciparum (isolate 3D7) GN=PFA_0220w PE=4 SV=2 | 3 | 0.95 | 0.18 | 0.0114 |
| tr\|Q8I410\|Q8I410_PLAF7 DNA-directed RNA polymerase OS=Plasmodium falciparum (isolate 3D7) GN=PFE0465c PE=3 SV=1 | 3 | 0.95 | 0.04 | 0.0005 |
| sp\|Q92621\|NU205_HUMAN Nuclear pore complex protein Nup205 OS=Homo sapiens GN=NUP205 PE=1 SV=3 | 3 | 0.96 | 0.04 | 0.0007 |
| tr\|C6KSY0\|C6KSY0_PLAF7 Transcription factor with AP2 domain(S), putative OS=Plasmodium falciparum (isolate 3D7) GN=ApiAP2 PE=4 SV=1 | 3 | 0.97 | 0.18 | 0.0110 |
| tr\|Q8I2D9\|Q8I2D9_PLAF7 Putative uncharacterized protein OS=Plasmodium falciparum (isolate 3D7) GN=PFA_0670c PE=4 SV=1 | 3 | 0.97 | 0.21 | 0.0156 |
| tr\|Q8IC27\|Q8IC27_PLAF7 Uncharacterized protein OS=Plasmodium falciparum (isolate 3D7) GN=PF07_0016 PE=4 SV=1 | 3 | 0.98 | 0.18 | 0.0107 |
| sp\|Q8I5D2\|ABRA_PLAF7 101 kDa malaria antigen OS=Plasmodium falciparum (isolate 3D7) GN=ABRA PE=3 SV=1 | 3 | 0.98 | 0.02 | 0.0001 |
| tr\|C6KSQ7\|C6KSQ7_PLAF7 Elongation of fatty acids protein OS=Plasmodium falciparum (isolate 3D7) GN=PFF0290w PE=3 SV=1 | 3 | 0.98 | 0.09 | 0.0029 |
| tr\|J3QLD9\|J3QLD9_HUMAN Flotillin-2 OS=Homo sapiens GN=FLOT2 PE=1 SV=1;tr\|E7EMK3\|E7EMK3_HUMAN Flotillin-2 OS=Homo sapiens GN=FLOT2 PE=1 SV=1;sp\|Q14254\|FLOT2_HUMAN Flotillin-2 OS=Homo sapiens GN=FLOT2 PE=1 SV=2 | 3 | 0.98 | 0.03 | 0.0003 |
| tr\|Q8IED7\|Q8IED7_PLAF7 Uncharacterized protein OS=Plasmodium falciparum (isolate 3D7) GN=MAL13P1.93 PE=4 SV=1 | 3 | 0.98 | 0.20 | 0.0138 |
| tr\|Q8ILR0\|Q8ILR0_PLAF7 Uncharacterized protein OS=Plasmodium falciparum (isolate 3D7) GN=PF14_0184 PE=4 SV=1 | 3 | 0.99 | 0.22 | 0.0165 |
| tr\|C0H5I5\|C0H5I5_PLAF7 Splicing factor 3b subunit, putative OS=Plasmodium falciparum (isolate 3D7) GN=PF13_0296 PE=4 SV=1 | 3 | 1.00 | 0.12 | 0.0048 |
| tr\|Q8I6T0\|Q8I6T0_PLAF7 Aminomethyltransferase, mitochondrial OS=Plasmodium falciparum (isolate 3D7) GN=PF13_0345 PE=3 SV=1 | 3 | 1.00 | 0.22 | 0.0159 |
| tr\|Q8I482\|Q8I482_PLAF7 Chromosome assembly factor 1, CAF-1 OS=Plasmodium falciparum (isolate 3D7) GN=PFE0090w PE=4 SV=1 | 3 | 1.01 | 0.19 | 0.0121 |
| tr\|Q8I1X5\|Q8I1X5_PLAF7 Pre-mRNA splicing factor, putative OS=Plasmodium falciparum (isolate 3D7) GN=PFD0265w PE=4 SV=1 | 3 | 1.01 | 0.11 | 0.0042 |
| tr\|Q8IBH8\|Q8IBH8_PLAF7 Uncharacterized protein OS=Plasmodium falciparum (isolate 3D7) GN=PF07_0116 PE=4 SV=1 | 3 | 1.01 | 0.32 | 0.0309 |
| sp\|O15400-2\|STX7_HUMAN Isoform 2 of Syntaxin-7 OS=Homo sapiens GN=STX7;sp\|O15400\|STX7_HUMAN Syntaxin-7 OS=Homo sapiens GN=STX7 PE=1 SV=4 | 3 | 1.02 | 0.10 | 0.0031 |
| tr\|Q8IKN7\|Q8IKN7_PLAF7 Uncharacterized protein OS=Plasmodium falciparum (isolate 3D7) GN=PF14_0567 PE=4 SV=1 | 3 | 1.02 | 0.24 | 0.0180 |
| tr\|B9ZSI0\|B9ZSI0_PLAF7 Putative uncharacterized protein OS=Plasmodium falciparum (isolate 3D7) GN=PFA_0165c PE=4 SV=1 | 3 | 1.02 | 0.38 | 0.0424 |
| tr\|Q9U0I0\|Q9U0I0_PLAF7 Uncharacterized protein OS=Plasmodium falciparum (isolate 3D7) GN=PFD0535w PE=4 SV=1 | 3 | 1.02 | 0.14 | 0.0064 |
| sp\|Q9BVM4\|GGACT_HUMAN Gamma-glutamylaminecyclotransferase OS=Homo sapiens GN=GGACT PE=1 SV=2 | 3 | 1.02 | 0.12 | 0.0048 |
| tr\|Q8IKE6\|Q8IKE6_PLAF7 Uncharacterized protein OS=Plasmodium falciparum (isolate 3D7) GN=PF14_0659 PE=4 SV=1 | 3 | 1.02 | 0.26 | 0.0203 |
| tr\|Q9NLB0\|Q9NLB0_PLAF7 Putative uncharacterized protein OS=Plasmodium falciparum (isolate 3D7) GN=PFC0282w PE=4 SV=1 | 3 | 1.02 | 0.29 | 0.0253 |
| tr\|C0H564\|C0H564_PLAF7 Monocarboxylate transporter, putative OS=Plasmodium falciparum (isolate 3D7) GN=PFI1295c PE=4 SV=1 | 3 | 1.03 | 0.16 | 0.0082 |
| sp\|Q8I1Y0\|PF41_PLAF7 Merozoite surface protein P41 OS=Plasmodium falciparum (isolate 3D7) GN=PF41 PE=1 SV=1 | 3 | 1.03 | 0.41 | 0.0484 |
| tr\|C0H592\|C0H592_PLAF7 REX2 protein OS=Plasmodium falciparum (isolate 3D7) GN=REX2 PE=4 SV=1;tr\|Q8I2G0\|Q8I2G0_PLAF7 Ring-exported protein 2 OS=Plasmodium falciparum (isolate 3D7) GN=REX2 PE=4 SV=1 | 3 | 1.04 | 0.11 | 0.0040 |
| tr\|Q8I0X2\|Q8I0X2_PLAF7 Acyl-CoA synthetase, PfACS3 OS=Plasmodium falciparum (isolate 3D7) GN=ACS3 PE=4 SV=1;tr\|C0H5N0\|C0H5N0_PLAF7 Acyl-CoA synthetase, PfACS4 OS=Plasmodium falciparum (isolate 3D7) GN=MAL13P1.485 PE=4 SV=1 | 3 | 1.06 | 0.25 | 0.0176 |
| tr\|Q8I5E2\|Q8I5E2_PLAF7 Cyclin related protein, putative OS=Plasmodium falciparum (isolate 3D7) GN=PFL1335w PE=4 SV=2 | 3 | 1.06 | 0.28 | 0.0224 |
| tr\|C0H5F1\|C0H5F1_PLAF7 Protein tyrosine phosphatase, putative OS=Plasmodium falciparum (isolate 3D7) GN=MAL13P1.168 PE=4 SV=1 | 3 | 1.07 | 0.25 | 0.0170 |
| tr\|Q8IDN2\|Q8IDN2_PLAF7 Uncharacterized protein OS=Plasmodium falciparum (isolate 3D7) GN=PF13_0245 PE=4 SV=1 | 3 | 1.09 | 0.33 | 0.0286 |
| tr\|Q8IK65\|Q8IK65_PLAF7 Uncharacterized protein OS=Plasmodium falciparum (isolate 3D7) GN=PF14_0741 PE=4 SV=1;tr\|Q8IK49\|Q8IK49_PLAF7 Uncharacterized protein OS=Plasmodium falciparum (isolate 3D7) GN=PF14_0758 PE=4 SV=1 | 3 | 1.09 | 0.15 | 0.0063 |

| | | | | |
|---|---|---|---|---|
| tr\|C6KT93\|C6KT93_PLAF7 Uncharacterized protein OS=Plasmodium falciparum (isolate 3D7) GN=PFF1245c PE=4 SV=1 | 3 | 1.09 | 0.43 | 0.0475 |
| tr\|F5GWF8\|F5GWF8_HUMAN Atlastin-3 (Fragment) OS=Homo sapiens GN=ATL3 PE=1 SV=1;tr\|F5H6I7\|F5H6I7_HUMAN Atlastin-3 OS=Homo sapiens GN=ATL3 PE=1 SV=1;sp\|Q6DD88\|ATLA3_HUMAN Atlastin-3 OS=Homo sapiens GN=ATL3 PE=1 SV=1 | 3 | 1.10 | 0.22 | 0.0134 |
| tr\|O96287\|O96287_PLAF7 Pfmc-2TM Maurers cleft two transmembrane protein OS=Plasmodium falciparum (isolate 3D7) GN=MC-2TM PE=4 SV=2;tr\|B9ZSJ3\|B9ZSJ3_PLAF7 Pfmc-2TM Maurers cleft two transmembrane protein OS=Plasmodium falciparum (isolate 3D7) GN=PfMC-2TM | 3 | 1.11 | 0.10 | 0.0026 |
| tr\|Q8ILV5\|Q8ILV5_PLAF7 Uncharacterized protein OS=Plasmodium falciparum (isolate 3D7) GN=PF14_0138 PE=4 SV=2 | 3 | 1.11 | 0.43 | 0.0472 |
| tr\|Q8IKS1\|Q8IKS1_PLAF7 Uncharacterized protein OS=Plasmodium falciparum (isolate 3D7) GN=PF14_0531 PE=4 SV=1 | 3 | 1.11 | 0.12 | 0.0036 |
| tr\|Q8I2A8\|Q8I2A8_PLAF7 Nucleoside transporter, putative OS=Plasmodium falciparum (isolate 3D7) GN=PFA_0160c PE=4 SV=1 | 3 | 1.11 | 0.25 | 0.0170 |
| tr\|Q8I6S4\|Q8I6S4_PLAF7 Peptidyl-prolyl cis-trans isomerase OS=Plasmodium falciparum (isolate 3D7) GN=PfCyP24 PE=3 SV=1 | 3 | 1.12 | 0.24 | 0.0148 |
| tr\|O96168\|O96168_PLAF7 Conserved Plasmodium protein OS=Plasmodium falciparum (isolate 3D7) GN=PFB0365w PE=4 SV=3 | 3 | 1.12 | 0.38 | 0.0365 |
| tr\|C6KT72\|C6KT72_PLAF7 Transcription or splicing factor-like protein, putative OS=Plasmodium falciparum (isolate 3D7) GN=PFF1135w PE=4 SV=1 | 3 | 1.15 | 0.14 | 0.0051 |
| tr\|Q8I4T6\|Q8I4T6_PLAF7 Uncharacterized protein OS=Plasmodium falciparum (isolate 3D7) GN=PFL2390c PE=4 SV=1 | 3 | 1.16 | 0.17 | 0.0068 |
| tr\|Q8IAM3\|Q8IAM3_PLAF7 WD-repeat protein, putative OS=Plasmodium falciparum (isolate 3D7) GN=PF08_0130 PE=4 SV=1 | 3 | 1.16 | 0.21 | 0.0102 |
| tr\|Q8I3M7\|Q8I3M7_PLAF7 Transporter, putative OS=Plasmodium falciparum (isolate 3D7) GN=PFE1185w PE=4 SV=1 | 3 | 1.16 | 0.25 | 0.0147 |
| tr\|C0H4S6\|C0H4S6_PLAF7 Uncharacterized protein OS=Plasmodium falciparum (isolate 3D7) GN=MAL8P1.130 PE=4 SV=1 | 3 | 1.17 | 0.11 | 0.0029 |
| tr\|C0H531\|C0H531_PLAF7 DNA primase large subunit, putative OS=Plasmodium falciparum (isolate 3D7) GN=PFI0530c PE=4 SV=1 | 3 | 1.17 | 0.15 | 0.0051 |
| tr\|Q8IKN5\|Q8IKN5_PLAF7 Uncharacterized protein OS=Plasmodium falciparum (isolate 3D7) GN=PF14_0569 PE=4 SV=1 | 3 | 1.18 | 0.11 | 0.0031 |
| tr\|Q8IJI8\|Q8IJI8_PLAF7 RNA helicase, putative OS=Plasmodium falciparum (isolate 3D7) GN=PF10_0209 PE=4 SV=1 | 3 | 1.19 | 0.14 | 0.0049 |
| tr\|Q8IKK4\|Q8IKK4_PLAF7 Replication factor C3 OS=Plasmodium falciparum (isolate 3D7) GN=PF14_0601 PE=4 SV=1 | 3 | 1.21 | 0.22 | 0.0108 |
| tr\|Q8I1P0\|Q8I1P0_PLAF7 60S ribosomal protein L7Ae/L30e, putative OS=Plasmodium falciparum (isolate 3D7) GN=PFD0960c PE=4 SV=1 | 3 | 1.21 | 0.21 | 0.0097 |
| tr\|Q8I618\|Q8I618_PLAF7 Conserved Plasmodium protein OS=Plasmodium falciparum (isolate 3D7) GN=PFL0135w PE=4 SV=2 | 3 | 1.26 | 0.20 | 0.0083 |
| tr\|Q8I512\|Q8I512_PLAF7 Replication factor C subunit 4 OS=Plasmodium falciparum (isolate 3D7) GN=PFL2005w PE=4 SV=1 | 3 | 1.26 | 0.46 | 0.0418 |
| tr\|Q8IL01\|Q8IL01_PLAF7 Uncharacterized protein OS=Plasmodium falciparum (isolate 3D7) GN=PF14_0449 PE=4 SV=1 | 3 | 1.27 | 0.12 | 0.0028 |
| tr\|O96265\|O96265_PLAF7 Small nuclear ribonucleoprotein, putative OS=Plasmodium falciparum (isolate 3D7) GN=PFB0865w PE=4 SV=1 | 3 | 1.29 | 0.37 | 0.0269 |
| tr\|Q8IHR6\|Q8IHR6_PLAF7 Coatomer subunit gamma OS=Plasmodium falciparum (isolate 3D7) GN=PF11_0463 PE=3 SV=1 | 3 | 1.29 | 0.08 | 0.0014 |
| tr\|Q8IDM6\|Q8IDM6_PLAF7 Nucleoside transporter 1 OS=Plasmodium falciparum (isolate 3D7) GN=nt1 PE=4 SV=1 | 3 | 1.31 | 0.51 | 0.0472 |
| tr\|Q8IHS2\|Q8IHS2_PLAF7 Ubiquitin activating enzyme (E1) subunit Aos1, putative OS=Plasmodium falciparum (isolate 3D7) GN=Aos1 PE=4 SV=1 | 3 | 1.33 | 0.14 | 0.0035 |
| tr\|Q8I3Q8\|Q8I3Q8_PLAF7 Uncharacterized protein OS=Plasmodium falciparum (isolate 3D7) GN=PFE1015c PE=4 SV=1 | 3 | 1.33 | 0.38 | 0.0254 |
| sp\|Q9BVK6\|TMED9_HUMAN Transmembrane emp24 domain-containing protein 9 OS=Homo sapiens GN=TMED9 PE=1 SV=2 | 3 | 1.34 | 0.50 | 0.0438 |
| tr\|C0H5J0\|C0H5J0_PLAF7 Uncharacterized protein OS=Plasmodium falciparum (isolate 3D7) GN=MAL13P1.293 PE=4 SV=1 | 3 | 1.37 | 0.29 | 0.0150 |
| tr\|Q8I390\|Q8I390_PLAF7 Beta subunit of coatomer complex, putative OS=Plasmodium falciparum (isolate 3D7) GN=PFI0290c PE=4 SV=1 | 3 | 1.40 | 0.18 | 0.0053 |
| tr\|Q8IJC0\|Q8IJC0_PLAF7 Nucleolar preribosomal assembly protein, putative OS=Plasmodium falciparum (isolate 3D7) GN=PF10_0278 PE=4 SV=1 | 3 | 1.44 | 0.34 | 0.0181 |
| sp\|P62203\|CALM_PLAF7 Calmodulin OS=Plasmodium falciparum (isolate 3D7) GN=PF14_0323 PE=3 SV=2 | 3 | 1.45 | 0.33 | 0.0171 |

| | | | | |
|---|---|---|---|---|
| tr\|C6KT56\|C6KT56_PLAF7 Uncharacterized protein OS=Plasmodium falciparum (isolate 3D7) GN=PFF1055c PE=4 SV=1 | 3 | 1.50 | 0.35 | 0.0177 |
| tr\|C6KTC6\|C6KTC6_PLAF7 Uncharacterized protein OS=Plasmodium falciparum (isolate 3D7) GN=PFF1410c PE=4 SV=1 | 3 | 1.56 | 0.56 | 0.0406 |
| tr\|Q8IB51\|Q8IB51_PLAF7 60S ribosomal protein L22, putative OS=Plasmodium falciparum (isolate 3D7) GN=PF08_0039 PE=1 SV=1 | 3 | 1.59 | 0.51 | 0.0329 |
| tr\|Q8I5N9\|Q8I5N9_PLAF7 DNA-binding chaperone, putative OS=Plasmodium falciparum (isolate 3D7) GN=PFL0815w PE=4 SV=1 | 3 | 1.60 | 0.32 | 0.0132 |
| tr\|Q8IBR6\|Q8IBR6_PLAF7 Prefoldin subunit 3, putative OS=Plasmodium falciparum (isolate 3D7) GN=MAL7P1.94 PE=4 SV=1 | 3 | 1.62 | 0.55 | 0.0368 |
| tr\|Q8ILR6\|Q8ILR6_PLAF7 Ubiquitin fusion degradation protein UFD1, putative OS=Plasmodium falciparum (isolate 3D7) GN=UFD1 PE=4 SV=2 | 3 | 1.65 | 0.45 | 0.0241 |
| tr\|Q8IIC9\|Q8IIC9_PLAF7 Translation elongation factor EF-1, subunit alpha, putative OS=Plasmodium falciparum (isolate 3D7) GN=PF11_0245 PE=4 SV=1 | 3 | 1.70 | 0.51 | 0.0283 |
| tr\|Q8IL22\|Q8IL22_PLAF7 Histidine--tRNA ligase, putative OS=Plasmodium falciparum (isolate 3D7) GN=PF14_0428 PE=3 SV=1 | 3 | 1.77 | 0.37 | 0.0142 |
| tr\|Q8IIB9\|Q8IIB9_PLAF7 Conserved Plasmodium protein OS=Plasmodium falciparum (isolate 3D7) GN=PF11_0255 PE=4 SV=2 | 3 | 1.83 | 0.53 | 0.0264 |
| tr\|Q8I3I7\|Q8I3I7_PLAF7 Uncharacterized protein OS=Plasmodium falciparum (isolate 3D7) GN=PFE1395c PE=4 SV=1 | 3 | 2.08 | 0.66 | 0.0323 |
| sp\|P32119\|PRDX2_HUMAN Peroxiredoxin-2 OS=Homo sapiens GN=PRDX2 PE=1 SV=5;tr\|A6NIW5\|A6NIW5_HUMAN Peroxiredoxin 2, isoform CRA_a OS=Homo sapiens GN=PRDX2 PE=1 SV=2 | 3 | 2.16 | 0.45 | 0.0143 |
| tr\|Q8I6T3\|Q8I6T3_PLAF7 Proteasome subunit beta type OS=Plasmodium falciparum (isolate 3D7) GN=PF13_0156 PE=3 SV=1 | 3 | 2.60 | 1.03 | 0.0489 |
| sp\|O95573\|ACSL3_HUMAN Long-chain-fatty-acid--CoA ligase 3 OS=Homo sapiens GN=ACSL3 PE=1 SV=3 | 2 | 3.69 | 2.76 | 0.3096 |
| tr\|Q8IE02\|Q8IE02_PLAF7 Apurinic/apyrimidinic endonuclease Apn1 OS=Plasmodium falciparum (isolate 3D7) GN=apn1 PE=3 SV=1 | 2 | 2.88 | 2.77 | 0.3802 |
| sp\|P27797\|CALR_HUMAN Calreticulin OS=Homo sapiens GN=CALR PE=1 SV=1;tr\|K7EJB9\|K7EJB9_HUMAN Calreticulin (Fragment) OS=Homo sapiens GN=CALR PE=1 SV=1 | 2 | 1.08 | 0.07 | 0.0288 |
| tr\|A0A087X243\|A0A087X243_HUMAN Glutathione S-transferase P (Fragment) OS=Homo sapiens GN=GSTP1 PE=1 SV=1;sp\|P09211\|GSTP1_HUMAN Glutathione S-transferase P OS=Homo sapiens GN=GSTP1 PE=1 SV=2 | 2 | 2.94 | 2.70 | 0.3670 |
| tr\|E9PNW4\|E9PNW4_HUMAN CD59 glycoprotein OS=Homo sapiens GN=CD59 PE=1 SV=1;tr\|E9PR17\|E9PR17_HUMAN CD59 glycoprotein OS=Homo sapiens GN=CD59 PE=1 SV=1;sp\|P13987\|CD59_HUMAN CD59 glycoprotein OS=Homo sapiens GN=CD59 PE=1 SV=1 | 2 | 1.43 | 0.81 | 0.2413 |
| tr\|Q8ILZ6\|Q8ILZ6_PLAF7 Phosphatidate cytidylyltransferase OS=Plasmodium falciparum (isolate 3D7) GN=CDS PE=3 SV=1 | 2 | 30.80 | 42.50 | 0.4922 |
| tr\|Q5T0D2\|Q5T0D2_HUMAN UMP-CMP kinase OS=Homo sapiens GN=CMPK1 PE=1 SV=1;sp\|P30085-2\|KCY_HUMAN Isoform 2 of UMP-CMP kinase OS=Homo sapiens GN=CMPK1;sp\|P30085\|KCY_HUMAN UMP-CMP kinase OS=Homo sapiens GN=CMPK1 PE=1 SV=3 | 2 | 3.48 | 1.93 | 0.2379 |
| tr\|Q8IE69\|Q8IE69_PLAF7 Dihydrofolate synthase/folylpolyglutamate synthase OS=Plasmodium falciparum (isolate 3D7) GN=DHFS-FPGS PE=4 SV=1 | 2 | 3.38 | 2.06 | 0.2594 |
| tr\|Q8IBE8\|Q8IBE8_PLAF7 Erythrocyte binding antigen 175 OS=Plasmodium falciparum (isolate 3D7) GN=eba-175 PE=1 SV=2 | 2 | 1.38 | 0.79 | 0.2444 |
| tr\|Q8IFM9\|Q8IFM9_PLAF7 Early transcribed membrane protein 4, ETRAMP4 OS=Plasmodium falciparum (isolate 3D7) GN=ETRAMP4 PE=4 SV=1 | 2 | 1.55 | 0.59 | 0.1680 |
| sp\|P17066\|HSP76_HUMAN Heat shock 70 kDa protein 6 OS=Homo sapiens GN=HSPA6 PE=1 SV=2;sp\|P48741\|HSP77_HUMAN Putative heat shock 70 kDa protein 7 OS=Homo sapiens GN=HSPA7 PE=5 SV=2 | 2 | 0.95 | 0.07 | 0.0318 |
| sp\|P01116-2\|RASK_HUMAN Isoform 2B of GTPase KRas OS=Homo sapiens GN=KRAS;sp\|P01116\|RASK_HUMAN GTPase KRas OS=Homo sapiens GN=KRAS PE=1 SV=1;sp\|P01111\|RASN_HUMAN GTPase NRas OS=Homo sapiens GN=NRAS PE=1 SV=1 | 2 | 0.99 | 0.12 | 0.0559 |
| tr\|C0H5D0\|C0H5D0_PLAF7 Uncharacterized protein OS=Plasmodium falciparum (isolate 3D7) GN=MAL13P1.124 PE=4 SV=1 | 2 | 0.50 | 0.64 | 0.4687 |
| tr\|C0H5D7\|C0H5D7_PLAF7 Translation initiation factor EIF-2B gamma subunit, putative OS=Plasmodium falciparum (isolate 3D7) GN=MAL13P1.144 PE=4 SV=1 | 2 | 12.61 | 13.93 | 0.4222 |
| tr\|Q8IDI8\|Q8IDI8_PLAF7 Uncharacterized protein OS=Plasmodium falciparum (isolate 3D7) GN=MAL13P1.257 PE=1 SV=1 | 2 | 31.85 | 43.95 | 0.4922 |
| tr\|C0H5I8\|C0H5I8_PLAF7 Uncharacterized protein OS=Plasmodium falciparum (isolate 3D7) GN=MAL13P1.286 PE=4 SV=1 | 2 | 21.45 | 29.09 | 0.4866 |
| tr\|C0H5J9\|C0H5J9_PLAF7 Uncharacterized protein OS=Plasmodium falciparum (isolate 3D7) GN=MAL13P1.308 PE=4 SV=1 | 2 | 3.40 | 2.03 | 0.2546 |

| | | | | |
|---|---|---|---|---|
| tr\|Q8ID38\|Q8ID38_PLAF7 Skp1 family protein, putative OS=Plasmodium falciparum (isolate 3D7) GN=MAL13P1.337 PE=4 SV=2 | 2 | 1.92 | 0.05 | 0.0127 |
| tr\|C0H5L4\|C0H5L4_PLAF7 Uncharacterized protein OS=Plasmodium falciparum (isolate 3D7) GN=MAL13P1.348 PE=4 SV=1 | 2 | 1.18 | 0.41 | 0.1520 |
| tr\|C0H5A4\|C0H5A4_PLAF7 U1 small nuclear ribonucleoprotein a, putative OS=Plasmodium falciparum (isolate 3D7) GN=MAL13P1.35 PE=4 SV=1 | 2 | 0.61 | 0.41 | 0.2849 |
| tr\|Q8IEK5\|Q8IEK5_PLAF7 Uncharacterized protein OS=Plasmodium falciparum (isolate 3D7) GN=MAL13P1.54 PE=4 SV=1 | 2 | 1.06 | 0.20 | 0.0841 |
| tr\|Q8IEG5\|Q8IEG5_PLAF7 Uncharacterized protein OS=Plasmodium falciparum (isolate 3D7) GN=MAL13P1.77 PE=4 SV=1 | 2 | 0.94 | 0.04 | 0.0187 |
| tr\|Q8IEF5\|Q8IEF5_PLAF7 Exportin 1-like protein, putative OS=Plasmodium falciparum (isolate 3D7) GN=MAL13P1.83 PE=4 SV=1 | 2 | 1.67 | 0.06 | 0.0165 |
| sp\|Q8IBP3\|ITPA_PLAF7 Inosine triphosphate pyrophosphatase OS=Plasmodium falciparum (isolate 3D7) GN=MAL7P1.110 PE=3 SV=1 | 2 | 14.19 | 15.22 | 0.4132 |
| tr\|Q8IBN8\|Q8IBN8_PLAF7 DEAD box helicase, putative OS=Plasmodium falciparum (isolate 3D7) GN=MAL7P1.113 PE=3 SV=1 | 2 | 23.97 | 4.23 | 0.0790 |
| tr\|C0H4K8\|C0H4K8_PLAF7 40S ribosomal protein S29, putative OS=Plasmodium falciparum (isolate 3D7) GN=MAL7P1.300 PE=1 SV=1 | 2 | 1.39 | 0.02 | 0.0073 |
| tr\|C0H4M5\|C0H4M5_PLAF7 Uncharacterized protein OS=Plasmodium falciparum (isolate 3D7) GN=MAL7P1.31 PE=4 SV=1 | 2 | 1.92 | 1.09 | 0.2430 |
| tr\|Q8IBS1\|Q8IBS1_PLAF7 Thioredoxin-like protein OS=Plasmodium falciparum (isolate 3D7) GN=MAL7P1.88 PE=4 SV=1 | 2 | 0.80 | 0.09 | 0.0490 |
| tr\|C0H4T9\|C0H4T9_PLAF7 CAF1 family ribonuclease, putative OS=Plasmodium falciparum (isolate 3D7) GN=MAL8P1.104 PE=4 SV=1 | 2 | 1.11 | 0.04 | 0.0169 |
| tr\|Q8IAU0\|Q8IAU0_PLAF7 Protein phosphatase, putative OS=Plasmodium falciparum (isolate 3D7) GN=MAL8P1.108 PE=4 SV=1 | 2 | 2.94 | 2.70 | 0.3670 |
| tr\|Q8IAS1\|Q8IAS1_PLAF7 Ubiquitin regulatory protein, putative OS=Plasmodium falciparum (isolate 3D7) GN=MAL8P1.122 PE=4 SV=1 | 2 | 27.14 | 34.75 | 0.4685 |
| tr\|Q8IAN5\|Q8IAN5_PLAF7 AAA family ATPase, putative OS=Plasmodium falciparum (isolate 3D7) GN=MAL8P1.144 PE=4 SV=1 | 2 | 2.70 | 2.45 | 0.3638 |
| tr\|Q8IB25\|Q8IB25_PLAF7 Uncharacterized protein OS=Plasmodium falciparum (isolate 3D7) GN=MAL8P1.64 PE=4 SV=1 | 2 | 0.67 | 0.91 | 0.4890 |
| tr\|C0H4V8\|C0H4V8_PLAF7 DNA helicase, putative OS=Plasmodium falciparum (isolate 3D7) GN=MAL8P1.65 PE=4 SV=1 | 2 | 34.20 | 44.67 | 0.4747 |
| tr\|Q8IAZ1\|Q8IAZ1_PLAF7 Uncharacterized protein OS=Plasmodium falciparum (isolate 3D7) GN=MAL8P1.85 PE=4 SV=1 | 2 | 3.15 | 2.36 | 0.3107 |
| tr\|C6KT25\|C6KT25_PLAF7 Malate dehydrogenase OS=Plasmodium falciparum (isolate 3D7) GN=MDH PE=3 SV=1 | 2 | 3.85 | 1.41 | 0.1615 |
| sp\|Q8NH64\|O51A7_HUMAN Olfactory receptor 51A7 OS=Homo sapiens GN=OR51A7 PE=2 SV=1 | 2 | 0.89 | 0.00 | 0.0019 |
| tr\|Q8IBZ8\|Q8IBZ8_PLAF7 Cg1 protein OS=Plasmodium falciparum (isolate 3D7) GN=PF07_0035 PE=4 SV=1 | 2 | 1.23 | 0.34 | 0.1232 |
| tr\|Q8IBZ5\|Q8IBZ5_PLAF7 Cg7 protein OS=Plasmodium falciparum (isolate 3D7) GN=PF07_0038 PE=4 SV=1 | 2 | 1.08 | 0.27 | 0.1109 |
| tr\|Q8IBY3\|Q8IBY3_PLAF7 Uncharacterized protein OS=Plasmodium falciparum (isolate 3D7) GN=PF07_0044 PE=4 SV=1 | 2 | 6.46 | 2.29 | 0.1563 |
| tr\|Q8IBU8\|Q8IBU8_PLAF7 Uncharacterized protein OS=Plasmodium falciparum (isolate 3D7) GN=PF07_0061 PE=4 SV=1 | 2 | 39.63 | 55.94 | 0.4994 |
| tr\|Q8IBU0\|Q8IBU0_PLAF7 Uncharacterized protein OS=Plasmodium falciparum (isolate 3D7) GN=PF07_0066 PE=4 SV=1 | 2 | 0.72 | 0.35 | 0.2124 |
| tr\|Q8IBL5\|Q8IBL5_PLAF7 Uncharacterized protein OS=Plasmodium falciparum (isolate 3D7) GN=PF07_0101 PE=4 SV=1 | 2 | 1.56 | 0.38 | 0.1082 |
| tr\|Q8IB55\|Q8IB55_PLAF7 RNA polymerase II mediator complex protein MED7, putative OS=Plasmodium falciparum (isolate 3D7) GN=PF08_0037 PE=4 SV=1 | 2 | 2.93 | 2.71 | 0.3684 |
| tr\|Q8IB23\|Q8IB23_PLAF7 U3 small nucleolar ribonucleoprotein protein, putative OS=Plasmodium falciparum (isolate 3D7) GN=PF08_0055 PE=4 SV=1 | 2 | 1.22 | 0.31 | 0.1114 |
| tr\|Q8IAW2\|Q8IAW2_PLAF7 Ubiquitin conjugating enzyme, putative OS=Plasmodium falciparum (isolate 3D7) GN=PF08_0085 PE=3 SV=1 | 2 | 2.94 | 2.70 | 0.3670 |
| tr\|Q8IAV0\|Q8IAV0_PLAF7 Methyltransferase, putative OS=Plasmodium falciparum (isolate 3D7) GN=PF08_0092 PE=4 SV=1 | 2 | 14.06 | 13.04 | 0.3694 |
| tr\|Q8IAT5\|Q8IAT5_PLAF7 Acyl CoA binding protein, putative OS=Plasmodium falciparum (isolate 3D7) GN=PF08_0099 PE=4 SV=1 | 2 | 3.05 | 2.53 | 0.3378 |
| tr\|Q8IAP4\|Q8IAP4_PLAF7 GTPase activator, putative OS=Plasmodium falciparum (isolate 3D7) GN=PF08_0120 PE=4 SV=1 | 2 | 2.94 | 2.70 | 0.3670 |
| tr\|Q8IAN8\|Q8IAN8_PLAF7 Uncharacterized protein OS=Plasmodium falciparum (isolate 3D7) GN=PF08_0124 PE=4 SV=1 | 2 | 54.84 | 59.78 | 0.4180 |

| | | | | |
|---|---|---|---|---|
| tr\|Q8IK19\|Q8IK19_PLAF7 Uncharacterized protein OS=Plasmodium falciparum (isolate 3D7) GN=PF10_0021 PE=4 SV=1 | 2 | 2.61 | 3.65 | 0.4962 |
| tr\|Q8IJR3\|Q8IJR3_PLAF7 Conserved Plasmodium protein OS=Plasmodium falciparum (isolate 3D7) GN=PF10_0129 PE=4 SV=1 | 2 | 0.52 | 0.65 | 0.4599 |
| tr\|Q7KQL4\|Q7KQL4_PLAF7 DNA polymerase OS=Plasmodium falciparum (isolate 3D7) GN=PF10_0165 PE=3 SV=1 | 2 | 8.27 | 10.60 | 0.4687 |
| tr\|Q8IJM0\|Q8IJM0_PLAF7 26s proteasome subunit p55, putative OS=Plasmodium falciparum (isolate 3D7) GN=PF10_0174 PE=4 SV=1 | 2 | 6.60 | 7.79 | 0.4430 |
| tr\|Q8IJI5\|Q8IJI5_PLAF7 Conserved Plasmodium protein OS=Plasmodium falciparum (isolate 3D7) GN=PF10_0212a PE=4 SV=2 | 2 | 11.50 | 14.85 | 0.4712 |
| tr\|Q8IJE1\|Q8IJE1_PLAF7 Conserved Plasmodium protein OS=Plasmodium falciparum (isolate 3D7) GN=PF10_0257 PE=4 SV=2 | 2 | 1.52 | 0.11 | 0.0312 |
| tr\|Q8IJA4\|Q8IJA4_PLAF7 RNA helicase, putative OS=Plasmodium falciparum (isolate 3D7) GN=PF10_0294 PE=4 SV=1 | 2 | 1.27 | 0.49 | 0.1677 |
| tr\|Q8IJ70\|Q8IJ70_PLAF7 Ubiquitin-conjugating enzyme, putative OS=Plasmodium falciparum (isolate 3D7) GN=PF10_0330 PE=1 SV=1 | 2 | 18.16 | 18.82 | 0.4027 |
| tr\|Q8IIU9\|Q8IIU9_PLAF7 Conserved Plasmodium protein OS=Plasmodium falciparum (isolate 3D7) GN=PF11_0064 PE=4 SV=2 | 2 | 2.79 | 2.05 | 0.3052 |
| tr\|Q8IIR8\|Q8IIR8_PLAF7 Succinyl-CoA synthetase alpha subunit, putative OS=Plasmodium falciparum (isolate 3D7) GN=PF11_0097 PE=3 SV=2 | 2 | 0.82 | 0.26 | 0.1433 |
| tr\|Q8IIR2\|Q8IIR2_PLAF7 rRNA processing protein, putative OS=Plasmodium falciparum (isolate 3D7) GN=PF11_0105 PE=4 SV=2 | 2 | 2.94 | 2.70 | 0.3670 |
| tr\|Q8IIQ6\|Q8IIQ6_PLAF7 Vacuolar protein sorting-associated protein 35 OS=Plasmodium falciparum (isolate 3D7) GN=PF11_0112 PE=3 SV=1 | 2 | 3.15 | 2.40 | 0.3149 |
| tr\|Q8IIQ1\|Q8IIQ1_PLAF7 Replication factor C subunit 5, putative OS=Plasmodium falciparum (isolate 3D7) GN=PF11_0117 PE=4 SV=1 | 2 | 1.69 | 0.81 | 0.2090 |
| tr\|Q8IIM4\|Q8IIM4_PLAF7 Uncharacterized protein OS=Plasmodium falciparum (isolate 3D7) GN=PF11_0146 PE=4 SV=1 | 2 | 1.17 | 0.40 | 0.1518 |
| tr\|Q8IIK7\|Q8IIK7_PLAF7 Uncharacterized protein OS=Plasmodium falciparum (isolate 3D7) GN=PF11_0166 PE=4 SV=1 | 2 | 1.69 | 0.36 | 0.0958 |
| tr\|Q8IIG8\|Q8IIG8_PLAF7 Uncharacterized protein OS=Plasmodium falciparum (isolate 3D7) GN=PF11_0206 PE=4 SV=1 | 2 | 3.90 | 1.34 | 0.1518 |
| tr\|Q8IIG2\|Q8IIG2_PLAF7 Uncharacterized protein OS=Plasmodium falciparum (isolate 3D7) GN=PF11_0212 PE=3 SV=1 | 2 | 6.09 | 8.53 | 0.4969 |
| tr\|Q8IIE9\|Q8IIE9_PLAF7 PfGCN20 OS=Plasmodium falciparum (isolate 3D7) GN=PF11_0225 PE=3 SV=1 | 2 | 1.77 | 0.15 | 0.0393 |
| tr\|Q8IIE5\|Q8IIE5_PLAF7 Conserved Plasmodium protein OS=Plasmodium falciparum (isolate 3D7) GN=PF11_0229 PE=4 SV=2 | 2 | 75.59 | 106.30 | 0.4982 |
| tr\|Q8II79\|Q8II79_PLAF7 Farnesyl pyrophosphate synthase, putative OS=Plasmodium falciparum (isolate 3D7) GN=PF11_0295 PE=3 SV=2 | 2 | 12.37 | 14.96 | 0.4503 |
| tr\|Q8II69\|Q8II69_PLAF7 Uncharacterized protein OS=Plasmodium falciparum (isolate 3D7) GN=PF11_0305 PE=4 SV=1 | 2 | 30.84 | 36.77 | 0.4459 |
| tr\|Q8IHX8\|Q8IHX8_PLAF7 Conserved Plasmodium protein OS=Plasmodium falciparum (isolate 3D7) GN=PF11_0398 PE=4 SV=2 | 2 | 5.15 | 4.38 | 0.3448 |
| tr\|Q8IHX6\|Q8IHX6_PLAF7 Conserved Plasmodium protein OS=Plasmodium falciparum (isolate 3D7) GN=PF11_0400 PE=4 SV=2 | 2 | 40.00 | 28.07 | 0.2933 |
| tr\|Q8IHX4\|Q8IHX4_PLAF7 Uncharacterized protein OS=Plasmodium falciparum (isolate 3D7) GN=PF11_0402 PE=4 SV=1 | 2 | 1.35 | 0.44 | 0.1450 |
| tr\|Q8IHU8\|Q8IHU8_PLAF7 Uncharacterized protein OS=Plasmodium falciparum (isolate 3D7) GN=PF11_0428 PE=4 SV=1 | 2 | 2.71 | 3.01 | 0.4234 |
| tr\|Q8IHT7\|Q8IHT7_PLAF7 Conserved Plasmodium protein OS=Plasmodium falciparum (isolate 3D7) GN=PF11_0440 PE=4 SV=1 | 2 | 0.61 | 0.15 | 0.1101 |
| tr\|Q8IHT3\|Q8IHT3_PLAF7 DNA-directed RNA polymerase I, putative OS=Plasmodium falciparum (isolate 3D7) GN=PF11_0445 PE=4 SV=1 | 2 | 1.54 | 0.21 | 0.0620 |
| sp\|Q8IER7\|RPB11_PLAF7 Probable DNA-directed RNA polymerase II subunit RPB11 OS=Plasmodium falciparum (isolate 3D7) GN=PF13_0023 PE=3 SV=1 | 2 | 20.86 | 29.26 | 0.4973 |
| tr\|Q8IEP9\|Q8IEP9_PLAF7 Vacuolar ATP synthase subunit h, putative OS=Plasmodium falciparum (isolate 3D7) GN=PF13_0034 PE=4 SV=2 | 2 | 1.11 | 0.11 | 0.0462 |
| tr\|Q8IEP4\|Q8IEP4_PLAF7 U3 small nucleolar RNA-associated protein 6, putative OS=Plasmodium falciparum (isolate 3D7) GN=PF13_0035 PE=4 SV=1 | 2 | 1.06 | 0.10 | 0.0446 |
| tr\|C0H5C7\|C0H5C7_PLAF7 RRM containing cyclophilin OS=Plasmodium falciparum (isolate 3D7) GN=PF13_0122 PE=4 SV=1 | 2 | 29.56 | 26.78 | 0.3627 |
| tr\|Q8IE30\|Q8IE30_PLAF7 Uncharacterized protein OS=Plasmodium falciparum (isolate 3D7) GN=PF13_0163 PE=4 SV=1 | 2 | 0.95 | 0.03 | 0.0137 |
| tr\|Q8IDY6\|Q8IDY6_PLAF7 Uncharacterized protein OS=Plasmodium falciparum (isolate 3D7) GN=PF13_0190 PE=4 SV=1 | 2 | 3.51 | 1.89 | 0.2315 |

| | | | | |
|---|---|---|---|---|
| tr\|Q8IDW3\|Q8IDW3_PLAF7 Tryptophan--tRNA ligase, putative OS=Plasmodium falciparum (isolate 3D7) GN=PF13_0205 PE=1 SV=1 | 2 | 3.62 | 1.73 | 0.2076 |
| tr\|Q8IDR8\|Q8IDR8_PLAF7 Aconitate hydratase OS=Plasmodium falciparum (isolate 3D7) GN=PF13_0229 PE=3 SV=1 | 2 | 0.37 | 0.40 | 0.4137 |
| tr\|Q8IDQ6\|Q8IDQ6_PLAF7 Uncharacterized protein OS=Plasmodium falciparum (isolate 3D7) GN=PF13_0237 PE=4 SV=1 | 2 | 2.95 | 2.68 | 0.3642 |
| tr\|Q8IDH3\|Q8IDH3_PLAF7 Uncharacterized protein OS=Plasmodium falciparum (isolate 3D7) GN=PF13_0273 PE=4 SV=1 | 2 | 1.40 | 0.34 | 0.1070 |
| tr\|Q8IDH2\|Q8IDH2_PLAF7 MON1 protein OS=Plasmodium falciparum (isolate 3D7) GN=PF13_0274 PE=4 SV=1 | 2 | 1.57 | 0.13 | 0.0361 |
| tr\|Q8IDG9\|Q8IDG9_PLAF7 Uncharacterized protein OS=Plasmodium falciparum (isolate 3D7) GN=PF13_0275 PE=4 SV=1 | 2 | 3.36 | 0.26 | 0.0345 |
| tr\|Q8IDD9\|Q8IDD9_PLAF7 Ubiquitin conjugating enzyme, putative OS=Plasmodium falciparum (isolate 3D7) GN=PF13_0301 PE=3 SV=1 | 2 | 4.26 | 0.83 | 0.0868 |
| tr\|Q8ID65\|Q8ID65_PLAF7 Uncharacterized protein OS=Plasmodium falciparum (isolate 3D7) GN=PF13_0339 PE=4 SV=1 | 2 | 0.47 | 0.54 | 0.4339 |
| tr\|Q8ID49\|Q8ID49_PLAF7 Uncharacterized protein OS=Plasmodium falciparum (isolate 3D7) GN=PF13_0347 PE=4 SV=1 | 2 | 0.93 | 0.61 | 0.2760 |
| tr\|Q8ID33\|Q8ID33_PLAF7 NADH-cytochrome B5 reductase, putative OS=Plasmodium falciparum (isolate 3D7) GN=PF13_0353 PE=4 SV=1 | 2 | 1.98 | 1.81 | 0.3652 |
| tr\|Q8IM75\|Q8IM75_PLAF7 Aminopeptidase, putative OS=Plasmodium falciparum (isolate 3D7) GN=PF14_0015 PE=4 SV=1 | 2 | 1.38 | 0.52 | 0.1653 |
| tr\|Q8IM68\|Q8IM68_PLAF7 Uncharacterized protein OS=Plasmodium falciparum (isolate 3D7) GN=PF14_0023 PE=4 SV=1 | 2 | 2.80 | 2.90 | 0.4024 |
| tr\|Q8IM55\|Q8IM55_PLAF7 Phosphatase, putative OS=Plasmodium falciparum (isolate 3D7) GN=PF14_0036 PE=4 SV=2 | 2 | 8.27 | 9.85 | 0.4457 |
| tr\|Q8IM44\|Q8IM44_PLAF7 Uncharacterized protein OS=Plasmodium falciparum (isolate 3D7) GN=PF14_0047 PE=4 SV=1 | 2 | 2.94 | 2.69 | 0.3646 |
| tr\|Q8IM43\|Q8IM43_PLAF7 Uncharacterized protein OS=Plasmodium falciparum (isolate 3D7) GN=PF14_0048 PE=4 SV=2 | 2 | 0.71 | 0.51 | 0.3001 |
| tr\|Q8IM28\|Q8IM28_PLAF7 ATP-dependent CLP protease, putative OS=Plasmodium falciparum (isolate 3D7) GN=PF14_0063 PE=4 SV=1 | 2 | 0.95 | 0.06 | 0.0266 |
| tr\|Q8IM11\|Q8IM11_PLAF7 Uncharacterized protein OS=Plasmodium falciparum (isolate 3D7) GN=PF14_0082 PE=4 SV=1 | 2 | 1.05 | 0.23 | 0.0968 |
| tr\|Q8ILW7\|Q8ILW7_PLAF7 AAA family ATPase, putative OS=Plasmodium falciparum (isolate 3D7) GN=PF14_0126 PE=3 SV=1 | 2 | 15.15 | 19.98 | 0.4777 |
| tr\|Q8ILV6\|Q8ILV6_PLAF7 DNAJ protein, putative OS=Plasmodium falciparum (isolate 3D7) GN=PF14_0137 PE=4 SV=1 | 2 | 1.00 | 0.58 | 0.2489 |
| tr\|Q8ILU4\|Q8ILU4_PLAF7 RNA polymerase small subunit, putative OS=Plasmodium falciparum (isolate 3D7) GN=PF14_0150 PE=4 SV=1 | 2 | 2.85 | 2.82 | 0.3880 |
| tr\|Q8ILQ9\|Q8ILQ9_PLAF7 ATP-dependent RNA Helicase, putative OS=Plasmodium falciparum (isolate 3D7) GN=PF14_0185 PE=4 SV=1 | 2 | 0.22 | 0.21 | 0.3788 |
| tr\|Q8ILP4\|Q8ILP4_PLAF7 Pantothenate kinase, putative OS=Plasmodium falciparum (isolate 3D7) GN=PF14_0200 PE=4 SV=2 | 2 | 1.49 | 0.07 | 0.0220 |
| tr\|Q8ILK1\|Q8ILK1_PLAF7 Arginine-N-methyltransferase, putative OS=Plasmodium falciparum (isolate 3D7) GN=PF14_0242 PE=4 SV=1 | 2 | 4.53 | 0.44 | 0.0437 |
| tr\|Q8ILI8\|Q8ILI8_PLAF7 CorA-like Mg2+ transporter protein, putative OS=Plasmodium falciparum (isolate 3D7) GN=PF14_0255 PE=4 SV=1 | 2 | 0.28 | 0.32 | 0.4335 |
| tr\|Q8ILB8\|Q8ILB8_PLAF7 Methionine aminopeptidase 2 OS=Plasmodium falciparum (isolate 3D7) GN=PF14_0327 PE=3 SV=1 | 2 | 2.86 | 2.81 | 0.3869 |
| tr\|Q8ILB7\|Q8ILB7_PLAF7 Mitochondrial import inner membrane translocase subunit Tim17, putative OS=Plasmodium falciparum (isolate 3D7) GN=PF14_0328 PE=4 SV=1 | 2 | 0.75 | 0.24 | 0.1422 |
| tr\|Q8ILB4\|Q8ILB4_PLAF7 Cytochrome c oxidase assembly protein, putative OS=Plasmodium falciparum (isolate 3D7) GN=PF14_0331 PE=4 SV=1 | 2 | 28.34 | 33.90 | 0.4470 |
| tr\|Q8IL42\|Q8IL42_PLAF7 Guanine nucleotide exchange factor, putative OS=Plasmodium falciparum (isolate 3D7) GN=PF14_0407 PE=4 SV=1 | 2 | 1.72 | 0.03 | 0.0071 |
| tr\|Q8IL23\|Q8IL23_PLAF7 Uncharacterized protein OS=Plasmodium falciparum (isolate 3D7) GN=PF14_0427 PE=4 SV=1 | 2 | 26.63 | 22.79 | 0.3465 |
| sp\|Q8IL06\|YPF07_PLAF7 Uncharacterized protein PF14_0444 OS=Plasmodium falciparum (isolate 3D7) GN=PF14_0444 PE=4 SV=2 | 2 | 0.97 | 0.19 | 0.0897 |
| tr\|Q8IKZ0\|Q8IKZ0_PLAF7 Uncharacterized protein OS=Plasmodium falciparum (isolate 3D7) GN=PF14_0461 PE=4 SV=1 | 2 | 0.89 | 0.01 | 0.0026 |
| tr\|Q8IKY8\|Q8IKY8_PLAF7 Chloroquine resistance marker protein OS=Plasmodium falciparum (isolate 3D7) GN=PF14_0463 PE=4 SV=1 | 2 | 1.24 | 0.07 | 0.0258 |
| tr\|Q8IKY5\|Q8IKY5_PLAF7 Appr-1-p processing domain protein OS=Plasmodium falciparum (isolate 3D7) GN=PF14_0466 PE=4 SV=1 | 2 | 0.63 | 0.71 | 0.4267 |

| | | | | |
|---|---|---|---|---|
| tr\|Q8IKU9\|Q8IKU9_PLAF7 Uncharacterized protein OS=Plasmodium falciparum (isolate 3D7) GN=PF14_0502 PE=4 SV=2 | 2 | 3.58 | 3.96 | 0.4225 |
| tr\|Q8IKS6\|Q8IKS6_PLAF7 Uncharacterized protein OS=Plasmodium falciparum (isolate 3D7) GN=PF14_0526 PE=4 SV=2 | 2 | 1.41 | 0.10 | 0.0330 |
| tr\|Q8IKS3\|Q8IKS3_PLAF7 Gamma-adaptin, putative OS=Plasmodium falciparum (isolate 3D7) GN=PF14_0529 PE=4 SV=1 | 2 | 3.25 | 2.25 | 0.2892 |
| tr\|Q8IKR2\|Q8IKR2_PLAF7 Uncharacterized protein OS=Plasmodium falciparum (isolate 3D7) GN=PF14_0540 PE=4 SV=1 | 2 | 17.01 | 20.93 | 0.4559 |
| tr\|Q8IKP7\|Q8IKP7_PLAF7 Uncharacterized protein OS=Plasmodium falciparum (isolate 3D7) GN=PF14_0557 PE=3 SV=1 | 2 | 2.80 | 2.88 | 0.4002 |
| sp\|Q8IKN4\|NNRE_PLAF7 NAD(P)H-hydrate epimerase OS=Plasmodium falciparum (isolate 3D7) GN=PF14_0570 PE=3 SV=2 | 2 | 2.94 | 2.70 | 0.3670 |
| tr\|Q8IKM0\|Q8IKM0_PLAF7 Mitochondrial ribosomal protein S4/S9, putative OS=Plasmodium falciparum (isolate 3D7) GN=PF14_0584 PE=4 SV=1 | 2 | 1.96 | 1.60 | 0.3331 |
| tr\|Q8IKI8\|Q8IKI8_PLAF7 Uncharacterized protein OS=Plasmodium falciparum (isolate 3D7) GN=PF14_0617 PE=4 SV=1 | 2 | 0.86 | 0.13 | 0.0658 |
| tr\|Q8IKG9\|Q8IKG9_PLAF7 Uncharacterized protein OS=Plasmodium falciparum (isolate 3D7) GN=PF14_0636 PE=4 SV=1 | 2 | 1.32 | 0.01 | 0.0041 |
| tr\|Q8IKD6\|Q8IKD6_PLAF7 Uncharacterized protein OS=Plasmodium falciparum (isolate 3D7) GN=PF14_0669 PE=4 SV=2 | 2 | 2.28 | 1.37 | 0.2562 |
| tr\|Q8IKB6\|Q8IKB6_PLAF7 Histone deacetylase, putative OS=Plasmodium falciparum (isolate 3D7) GN=PF14_0690 PE=4 SV=2 | 2 | 1.13 | 0.44 | 0.1702 |
| tr\|Q8IKA7\|Q8IKA7_PLAF7 GTPase activator, putative OS=Plasmodium falciparum (isolate 3D7) GN=PF14_0699 PE=4 SV=1 | 2 | 21.73 | 29.28 | 0.4846 |
| tr\|Q8ILP0\|Q8ILP0_PLAF7 Uncharacterized protein OS=Plasmodium falciparum (isolate 3D7) GN=PF14_0775 PE=4 SV=1 | 2 | 1.98 | 0.60 | 0.1352 |
| tr\|Q8I294\|Q8I294_PLAF7 Putative uncharacterized protein OS=Plasmodium falciparum (isolate 3D7) GN=PFA_0230c PE=4 SV=1 | 2 | 34.14 | 46.37 | 0.4872 |
| tr\|Q8I278\|Q8I278_PLAF7 Putative uncharacterized protein OS=Plasmodium falciparum (isolate 3D7) GN=PFA_0315w PE=4 SV=1 | 2 | 4.46 | 0.54 | 0.0546 |
| tr\|Q8I267\|Q8I267_PLAF7 Putative uncharacterized protein OS=Plasmodium falciparum (isolate 3D7) GN=PFA_0370w PE=4 SV=1 | 2 | 0.73 | 0.98 | 0.4819 |
| tr\|Q8I257\|Q8I257_PLAF7 Putative uncharacterized protein OS=Plasmodium falciparum (isolate 3D7) GN=PFA_0420w PE=4 SV=1 | 2 | 3.10 | 2.47 | 0.3265 |
| tr\|Q8I0V9\|Q8I0V9_PLAF7 mRNA cleavage factor-like protein, putative OS=Plasmodium falciparum (isolate 3D7) GN=PFA_0450c PE=4 SV=1 | 2 | 1.41 | 0.64 | 0.1987 |
| tr\|Q8I246\|Q8I246_PLAF7 Phenylalanyl-tRNA synthetase beta chain, putative OS=Plasmodium falciparum (isolate 3D7) GN=PFA_0480w PE=3 SV=1 | 2 | 2.11 | 0.03 | 0.0073 |
| tr\|Q8I233\|Q8I233_PLAF7 Replication factor c protein, putative OS=Plasmodium falciparum (isolate 3D7) GN=PFA_0545c PE=4 SV=1 | 2 | 1.02 | 0.18 | 0.0795 |
| tr\|Q8I231\|Q8I231_PLAF7 UMP-CMP kinase, putative OS=Plasmodium falciparum (isolate 3D7) GN=PFA_0555c PE=3 SV=1 | 2 | 3.24 | 2.27 | 0.2937 |
| tr\|B9ZSJ1\|B9ZSJ1_PLAF7 Putative uncharacterized protein OS=Plasmodium falciparum (isolate 3D7) GN=PFA_0630c PE=4 SV=1 | 2 | 1.09 | 0.25 | 0.1024 |
| tr\|O96142\|O96142_PLAF7 Aspartate aminotransferase OS=Plasmodium falciparum (isolate 3D7) GN=PFB0200c PE=1 SV=1 | 2 | 9.50 | 6.58 | 0.2901 |
| sp\|O96185\|YPF08_PLAF7 Uncharacterized protein PFB0460c OS=Plasmodium falciparum (isolate 3D7) GN=PFB0460c PE=3 SV=1 | 2 | 16.96 | 22.56 | 0.4805 |
| tr\|O96224\|O96224_PLAF7 Conserved Plasmodium protein OS=Plasmodium falciparum (isolate 3D7) GN=PFB0655c PE=4 SV=2 | 2 | 3.78 | 1.51 | 0.1750 |
| tr\|O96234\|O96234_PLAF7 Conserved Plasmodium protein OS=Plasmodium falciparum (isolate 3D7) GN=PFB0705w PE=4 SV=1 | 2 | 1.03 | 0.09 | 0.0409 |
| tr\|O96243\|O96243_PLAF7 Vacuolar protein-sorting protein VPS45, putative OS=Plasmodium falciparum (isolate 3D7) GN=PFB0750w PE=4 SV=1 | 2 | 76.22 | 85.35 | 0.4264 |
| tr\|O96254\|O96254_PLAF7 Clathrin coat assembly protein, putative OS=Plasmodium falciparum (isolate 3D7) GN=PFB0805c PE=4 SV=1 | 2 | 2.31 | 1.81 | 0.3223 |
| tr\|C6S3B8\|C6S3B8_PLAF7 Conserved Plasmodium protein OS=Plasmodium falciparum (isolate 3D7) GN=PFB0850c PE=4 SV=1 | 2 | 1.37 | 0.37 | 0.1200 |
| tr\|O97334\|O97334_PLAF7 Regulatory protein, putative OS=Plasmodium falciparum (isolate 3D7) GN=PFC0100c PE=4 SV=2 | 2 | 8.84 | 10.96 | 0.4584 |
| tr\|O77306\|O77306_PLAF7 Serine/threonine protein kinase, putative OS=Plasmodium falciparum (isolate 3D7) GN=PFC0105w PE=4 SV=1 | 2 | 3.09 | 2.47 | 0.3275 |
| tr\|Q9NLB3\|Q9NLB3_PLAF7 Putative uncharacterized protein OS=Plasmodium falciparum (isolate 3D7) GN=PFC0262c PE=4 SV=2 | 2 | 0.16 | 0.03 | 0.0856 |
| tr\|O97252\|O97252_PLAF7 ATP-dependent Clp protease proteolytic subunit OS=Plasmodium falciparum (isolate 3D7) GN=PFC0310c PE=1 SV=1 | 2 | 10.66 | 15.00 | 0.4984 |

| | | | | |
|---|---|---|---|---|
| tr\|O97256\|O97256_PLAF7 Activator of Hsp90 ATPase homolog 1-like protein, putative OS=Plasmodium falciparum (isolate 3D7) GN=PFC0360w PE=4 SV=2 | 2 | 407.20 | 574.41 | 0.4992 |
| tr\|O77349\|O77349_PLAF7 Putative uncharacterized protein OS=Plasmodium falciparum (isolate 3D7) GN=PFC0500w PE=4 SV=2 | 2 | 62.79 | 87.75 | 0.4962 |
| tr\|C0H474\|C0H474_PLAF7 Vesicle transport v-SNARE protein, putative OS=Plasmodium falciparum (isolate 3D7) GN=PFC0582c PE=4 SV=1 | 2 | 6.03 | 7.17 | 0.4452 |
| tr\|O97289\|O97289_PLAF7 Peptidase, putative OS=Plasmodium falciparum (isolate 3D7) GN=PFC0950c PE=4 SV=2 | 2 | 1.38 | 0.41 | 0.1311 |
| tr\|O97314\|O97314_PLAF7 Putative uncharacterized protein OS=Plasmodium falciparum (isolate 3D7) GN=PFC1025w PE=4 SV=1 | 2 | 4.25 | 0.85 | 0.0891 |
| tr\|Q8I272\|Q8I272_PLAF7 Centrin-1 OS=Plasmodium falciparum (isolate 3D7) GN=PfCEN1 PE=4 SV=1;sp\|P41208\|CETN2_HUMAN Centrin-2 OS=Homo sapiens GN=CETN2 PE=1 SV=1 | 2 | 0.96 | 0.17 | 0.0776 |
| tr\|Q8I1X9\|Q8I1X9_PLAF7 ATP-dependent RNA Helicase, putative OS=Plasmodium falciparum (isolate 3D7) GN=PFD0245c PE=4 SV=1 | 2 | 1.04 | 0.14 | 0.0585 |
| tr\|Q9U0I2\|Q9U0I2_PLAF7 Uncharacterized protein OS=Plasmodium falciparum (isolate 3D7) GN=PFD0525w PE=4 SV=2 | 2 | 2.80 | 0.08 | 0.0133 |
| tr\|Q8I1V2\|Q8I1V2_PLAF7 Phosphoglycerate mutase, putative OS=Plasmodium falciparum (isolate 3D7) GN=PFD0660w PE=1 SV=1 | 2 | 0.25 | 0.13 | 0.2155 |
| tr\|C0H4A7\|C0H4A7_PLAF7 Uncharacterized protein OS=Plasmodium falciparum (isolate 3D7) GN=PFD0795w PE=4 SV=1 | 2 | 1.22 | 0.33 | 0.1196 |
| tr\|C0H4B9\|C0H4B9_PLAF7 Steroid dehydrogenase, putative OS=Plasmodium falciparum (isolate 3D7) GN=PFD1035w PE=4 SV=1 | 2 | 32.43 | 18.63 | 0.2456 |
| tr\|Q8IFP3\|Q8IFP3_PLAF7 Alpha-tubulin ii OS=Plasmodium falciparum (isolate 3D7) GN=PFD1050w PE=3 SV=1 | 2 | 17.54 | 22.61 | 0.4706 |
| tr\|Q8IFN9\|Q8IFN9_PLAF7 Eukaryotic initiation factor, putative OS=Plasmodium falciparum (isolate 3D7) GN=PFD1070w PE=3 SV=1 | 2 | 1.04 | 0.07 | 0.0309 |
| tr\|Q8IFN1\|Q8IFN1_PLAF7 Uncharacterized protein OS=Plasmodium falciparum (isolate 3D7) GN=PFD1110w PE=4 SV=1 | 2 | 0.89 | 0.03 | 0.0168 |
| sp\|Q8IFN0\|YD115_PLAF7 Uncharacterized protein PFD1115c OS=Plasmodium falciparum (isolate 3D7) GN=PFD1115c PE=2 SV=1 | 2 | 0.95 | 0.05 | 0.0223 |
| tr\|Q8I469\|Q8I469_PLAF7 Uncharacterized protein OS=Plasmodium falciparum (isolate 3D7) GN=PFE0155w PE=4 SV=1 | 2 | 1.78 | 1.19 | 0.2821 |
| tr\|Q8I445\|Q8I445_PLAF7 Uncharacterized protein OS=Plasmodium falciparum (isolate 3D7) GN=PFE0280c PE=4 SV=1 | 2 | 0.06 | 0.04 | 0.2665 |
| tr\|C0H4C7\|C0H4C7_PLAF7 Uncharacterized protein OS=Plasmodium falciparum (isolate 3D7) GN=PFE0290c PE=4 SV=1 | 2 | 16.96 | 17.13 | 0.3949 |
| tr\|Q8I425\|Q8I425_PLAF7 Uncharacterized protein OS=Plasmodium falciparum (isolate 3D7) GN=PFE0385w PE=4 SV=1 | 2 | 3.40 | 2.04 | 0.2558 |
| tr\|Q8I416\|Q8I416_PLAF7 ATP-dependent RNA Helicase, putative OS=Plasmodium falciparum (isolate 3D7) GN=PFE0430w PE=3 SV=1 | 2 | 0.98 | 0.60 | 0.2611 |
| tr\|Q8I408\|Q8I408_PLAF7 Asparagine-tRNA ligase, putative OS=Plasmodium falciparum (isolate 3D7) GN=PFE0475w PE=3 SV=1 | 2 | 8.79 | 5.59 | 0.2688 |
| sp\|Q8I3Y6\|PFD6_PLAF7 Probable prefoldin subunit 6 OS=Plasmodium falciparum (isolate 3D7) GN=PFE0595w PE=3 SV=2 | 2 | 102.23 | 141.76 | 0.4937 |
| tr\|C0H4D6\|C0H4D6_PLAF7 GTP binding protein, putative OS=Plasmodium falciparum (isolate 3D7) GN=PFE0665c PE=3 SV=1 | 2 | 1.51 | 0.26 | 0.0783 |
| tr\|Q8I3U9\|Q8I3U9_PLAF7 Protein phosphatase, putative OS=Plasmodium falciparum (isolate 3D7) GN=PFE0795c PE=4 SV=1 | 2 | 1.40 | 0.49 | 0.1539 |
| tr\|Q8I3U0\|Q8I3U0_PLAF7 Transcription factor with AP2 domain(S), putative OS=Plasmodium falciparum (isolate 3D7) GN=PFE0840c PE=4 SV=1 | 2 | 0.86 | 0.98 | 0.4311 |
| tr\|C0H4E6\|C0H4E6_PLAF7 Uncharacterized protein OS=Plasmodium falciparum (isolate 3D7) GN=PFE0900w PE=4 SV=1 | 2 | 3.08 | 2.50 | 0.3321 |
| tr\|Q8I3R4\|Q8I3R4_PLAF7 Uncharacterized protein OS=Plasmodium falciparum (isolate 3D7) GN=PFE0985w PE=4 SV=1 | 2 | 1.10 | 0.21 | 0.0854 |
| tr\|Q8I3P1\|Q8I3P1_PLAF7 Uncharacterized protein OS=Plasmodium falciparum (isolate 3D7) GN=PFE1110w PE=4 SV=1 | 2 | 142.65 | 19.13 | 0.0602 |
| tr\|Q8I3J8\|Q8I3J8_PLAF7 Uncharacterized protein OS=Plasmodium falciparum (isolate 3D7) GN=PFE1330c PE=4 SV=1 | 2 | 1.00 | 0.22 | 0.1003 |
| tr\|Q8I3I8\|Q8I3I8_PLAF7 RNA helicase-1 OS=Plasmodium falciparum (isolate 3D7) GN=PFE1390w PE=4 SV=1 | 2 | 3.28 | 3.36 | 0.3993 |
| tr\|C6KSN1\|C6KSN1_PLAF7 Uncharacterized protein OS=Plasmodium falciparum (isolate 3D7) GN=PFF0150c PE=4 SV=1 | 2 | 1.05 | 0.14 | 0.0611 |
| tr\|C6KSX9\|C6KSX9_PLAF7 Syntaxin binding protein, putative OS=Plasmodium falciparum (isolate 3D7) GN=PFF0665c PE=4 SV=1 | 2 | 1.69 | 0.43 | 0.1141 |
| tr\|C6KT19\|C6KT19_PLAF7 Histone H3 OS=Plasmodium falciparum (isolate 3D7) GN=PFF0865w PE=3 SV=1 | 2 | 218.21 | 146.00 | 0.2813 |

| | | | | |
|---|---|---|---|---|
| tr\|C6KT21\|C6KT21_PLAF7 Uncharacterized protein OS=Plasmodium falciparum (isolate 3D7) GN=PFF0875w PE=4 SV=1 | 2 | 5.99 | 6.91 | 0.4358 |
| tr\|C6KT22\|C6KT22_PLAF7 Uncharacterized protein OS=Plasmodium falciparum (isolate 3D7) GN=PFF0880c PE=4 SV=1 | 2 | 3.50 | 1.90 | 0.2341 |
| tr\|C6KT51\|C6KT51_PLAF7 Uncharacterized protein OS=Plasmodium falciparum (isolate 3D7) GN=PFF1030w PE=4 SV=1 | 2 | 1.45 | 0.19 | 0.0602 |
| tr\|C6KT80\|C6KT80_PLAF7 Uncharacterized protein OS=Plasmodium falciparum (isolate 3D7) GN=PFF1175c PE=4 SV=1 | 2 | 2.76 | 2.63 | 0.3767 |
| tr\|C6KT96\|C6KT96_PLAF7 Uncharacterized protein OS=Plasmodium falciparum (isolate 3D7) GN=PFF1260c PE=4 SV=1 | 2 | 3.11 | 2.46 | 0.3248 |
| tr\|C6KTB3\|C6KTB3_PLAF7 Transportin OS=Plasmodium falciparum (isolate 3D7) GN=PFF1345w PE=4 SV=1 | 2 | 3.62 | 1.74 | 0.2084 |
| tr\|C6KTD1\|C6KTD1_PLAF7 Uncharacterized protein OS=Plasmodium falciparum (isolate 3D7) GN=PFF1435w PE=4 SV=1 | 2 | 1.25 | 0.16 | 0.0574 |
| tr\|C6KTE0\|C6KTE0_PLAF7 Microtubule-associated protein ytm1 homologue, putative OS=Plasmodium falciparum (isolate 3D7) GN=PFF1480w PE=4 SV=1 | 2 | 1.01 | 0.48 | 0.2058 |
| tr\|C6KTE4\|C6KTE4_PLAF7 DEAD/DEAH box ATP-dependent RNA helicase, putative OS=Plasmodium falciparum (isolate 3D7) GN=PFF1500c PE=3 SV=1 | 2 | 1.69 | 0.53 | 0.1388 |
| tr\|C6KTE8\|C6KTE8_PLAF7 Pfmc-2TM Maurers cleft two transmembrane protein OS=Plasmodium falciparum (isolate 3D7) GN=PFF1525c PE=4 SV=1 | 2 | 131.22 | 6.98 | 0.0239 |
| tr\|Q8I2M1\|Q8I2M1_PLAF7 Guanylate kinase OS=Plasmodium falciparum (isolate 3D7) GN=PfGK PE=1 SV=1 | 2 | 3.13 | 2.42 | 0.3180 |
| tr\|O77344\|O77344_PLAF7 Glycogen synthase kinase 3 OS=Plasmodium falciparum (isolate 3D7) GN=PfGSK-3 PE=4 SV=2 | 2 | 3.36 | 2.09 | 0.2641 |
| tr\|Q6ZLZ9\|Q6ZLZ9_PLAF7 Alpha tubulin OS=Plasmodium falciparum (isolate 3D7) GN=PFI0180w PE=3 SV=1 | 2 | 3.53 | 2.03 | 0.2455 |
| tr\|Q8I3A9\|Q8I3A9_PLAF7 GTPase activating protein, GAP OS=Plasmodium falciparum (isolate 3D7) GN=PFI0195c PE=4 SV=1 | 2 | 16.05 | 3.28 | 0.0913 |
| tr\|Q8I388\|Q8I388_PLAF7 Developmental protein, putative OS=Plasmodium falciparum (isolate 3D7) GN=PFI0300w PE=4 SV=1 | 2 | 3.64 | 1.71 | 0.2040 |
| tr\|Q8I384\|Q8I384_PLAF7 Arginase, putative OS=Plasmodium falciparum (isolate 3D7) GN=PFI0320w PE=1 SV=1 | 2 | 4.90 | 0.08 | 0.0070 |
| tr\|Q8I378\|Q8I378_PLAF7 Putative uncharacterized protein OS=Plasmodium falciparum (isolate 3D7) GN=PFI0350c PE=4 SV=1 | 2 | 2.78 | 0.21 | 0.0340 |
| tr\|C0H524\|C0H524_PLAF7 P1 nuclease, putative OS=Plasmodium falciparum (isolate 3D7) GN=PFI0385c PE=4 SV=1 | 2 | 1.04 | 0.32 | 0.1352 |
| tr\|Q8I367\|Q8I367_PLAF7 Putative uncharacterized protein OS=Plasmodium falciparum (isolate 3D7) GN=PFI0405w PE=4 SV=1 | 2 | 1.06 | 0.13 | 0.0545 |
| tr\|Q8I356\|Q8I356_PLAF7 Putative uncharacterized protein OS=Plasmodium falciparum (isolate 3D7) GN=PFI0465c PE=4 SV=1 | 2 | 1.21 | 0.49 | 0.1774 |
| tr\|C0H529\|C0H529_PLAF7 Small nuclear ribonucleoprotein (SnRNP), putative OS=Plasmodium falciparum (isolate 3D7) GN=PFI0475w PE=4 SV=1 | 2 | 3.09 | 2.48 | 0.3285 |
| tr\|Q8I332\|Q8I332_PLAF7 Putative uncharacterized protein OS=Plasmodium falciparum (isolate 3D7) GN=PFI0585c PE=4 SV=1 | 2 | 2.04 | 1.15 | 0.2423 |
| tr\|Q8I324\|Q8I324_PLAF7 Putative uncharacterized protein OS=Plasmodium falciparum (isolate 3D7) GN=PFI0625c PE=4 SV=1 | 2 | 16.76 | 22.53 | 0.4840 |
| tr\|Q8I318\|Q8I318_PLAF7 Putative uncharacterized protein OS=Plasmodium falciparum (isolate 3D7) GN=PFI0655c PE=4 SV=1 | 2 | 0.94 | 0.18 | 0.0871 |
| tr\|Q8I301\|Q8I301_PLAF7 Ubiquitin conjugating enzyme, putative OS=Plasmodium falciparum (isolate 3D7) GN=PFI0740c PE=1 SV=1 | 2 | 3.15 | 2.39 | 0.3132 |
| tr\|Q8I300\|Q8I300_PLAF7 Putative uncharacterized protein OS=Plasmodium falciparum (isolate 3D7) GN=PFI0745w PE=4 SV=1 | 2 | 3.11 | 2.46 | 0.3243 |
| tr\|Q8I2X8\|Q8I2X8_PLAF7 Putative uncharacterized protein OS=Plasmodium falciparum (isolate 3D7) GN=PFI0855w PE=4 SV=1 | 2 | 1.51 | 0.64 | 0.1868 |
| tr\|Q8I2V6\|Q8I2V6_PLAF7 Pyridoxal 5-phosphate dependent enzyme class III, putative OS=Plasmodium falciparum (isolate 3D7) GN=PFI0965w PE=3 SV=1 | 2 | 13.76 | 18.01 | 0.4753 |
| tr\|C0H546\|C0H546_PLAF7 Chaperone protein, putative OS=Plasmodium falciparum (isolate 3D7) GN=PFI0985c PE=4 SV=1 | 2 | 25.99 | 36.66 | 0.4992 |
| tr\|Q8I2U3\|Q8I2U3_PLAF7 Ubiquitin conjugating enzyme, putative OS=Plasmodium falciparum (isolate 3D7) GN=PFI1030c PE=3 SV=1 | 2 | 19.59 | 20.85 | 0.4108 |
| tr\|Q8I2T4\|Q8I2T4_PLAF7 Putative uncharacterized protein OS=Plasmodium falciparum (isolate 3D7) GN=PFI1075w PE=4 SV=1 | 2 | 3.32 | 2.15 | 0.2738 |
| tr\|Q8I2R5\|Q8I2R5_PLAF7 Putative uncharacterized protein OS=Plasmodium falciparum (isolate 3D7) GN=PFI1190w PE=4 SV=1 | 2 | 4.65 | 1.00 | 0.0959 |
| tr\|Q8I2R0\|Q8I2R0_PLAF7 Splicing factor 3A OS=Plasmodium falciparum (isolate 3D7) GN=PFI1215w PE=4 SV=1 | 2 | 20.57 | 29.05 | 0.4996 |

| | | | | |
|---|---|---|---|---|
| tr\|Q8I2Q6\|Q8I2Q6_PLAF7 Methyltransferase, putative OS=Plasmodium falciparum (isolate 3D7) GN=PFI1235w PE=4 SV=1 | 2 | 2.38 | 1.85 | 0.3200 |
| tr\|Q8I2P8\|Q8I2P8_PLAF7 Protein kinase, putative OS=Plasmodium falciparum (isolate 3D7) GN=PFI1280c PE=4 SV=1 | 2 | 7.21 | 3.34 | 0.2017 |
| tr\|Q8I2N3\|Q8I2N3_PLAF7 Putative uncharacterized protein OS=Plasmodium falciparum (isolate 3D7) GN=PFI1355w PE=4 SV=1 | 2 | 2.99 | 2.62 | 0.3526 |
| tr\|Q8I2M7\|Q8I2M7_PLAF7 Putative uncharacterized protein OS=Plasmodium falciparum (isolate 3D7) GN=PFI1385c PE=4 SV=1 | 2 | 1.37 | 0.44 | 0.1418 |
| tr\|C0H574\|C0H574_PLAF7 Putative uncharacterized protein OS=Plasmodium falciparum (isolate 3D7) GN=PFI1463w PE=4 SV=1 | 2 | 9.83 | 13.28 | 0.4853 |
| tr\|C0H579\|C0H579_PLAF7 Putative uncharacterized protein OS=Plasmodium falciparum (isolate 3D7) GN=PFI1525w PE=4 SV=1 | 2 | 42.13 | 12.71 | 0.1338 |
| tr\|Q8I2I8\|Q8I2I8_PLAF7 Putative uncharacterized protein OS=Plasmodium falciparum (isolate 3D7) GN=PFI1590c PE=4 SV=1 | 2 | 3.38 | 2.08 | 0.2611 |
| tr\|C0H586\|C0H586_PLAF7 Calcyclin binding protein, putative OS=Plasmodium falciparum (isolate 3D7) GN=PFI1610c PE=4 SV=1 | 2 | 14.82 | 14.11 | 0.3772 |
| tr\|Q8I638\|Q8I638_PLAF7 Octapeptide-repeat antigen, putative OS=Plasmodium falciparum (isolate 3D7) GN=PFL0035c PE=4 SV=1 | 2 | 3.40 | 2.04 | 0.2558 |
| tr\|Q8I634\|Q8I634_PLAF7 Protein with DNAJ domain (Resa-like), putative OS=Plasmodium falciparum (isolate 3D7) GN=PFL0055c PE=4 SV=1 | 2 | 1.07 | 0.21 | 0.0871 |
| tr\|Q8I610\|Q8I610_PLAF7 Uncharacterized protein OS=Plasmodium falciparum (isolate 3D7) GN=PFL0175c PE=4 SV=1 | 2 | 2.94 | 2.70 | 0.3670 |
| tr\|Q8I607\|Q8I607_PLAF7 Ubiquitin conjugating enzyme E2, putative OS=Plasmodium falciparum (isolate 3D7) GN=PFL0190w PE=3 SV=1 | 2 | 29.29 | 38.84 | 0.4796 |
| tr\|Q8I5V6\|Q8I5V6_PLAF7 Lsm7 homologue, putative OS=Plasmodium falciparum (isolate 3D7) GN=PFL0460w PE=4 SV=1 | 2 | 2.56 | 3.23 | 0.4643 |
| tr\|Q8I5U8\|Q8I5U8_PLAF7 Uncharacterized protein OS=Plasmodium falciparum (isolate 3D7) GN=PFL0505c PE=4 SV=1 | 2 | 7.84 | 7.93 | 0.3951 |
| tr\|Q8I5T7\|Q8I5T7_PLAF7 Minichromosome maintenance protein, putative OS=Plasmodium falciparum (isolate 3D7) GN=PFL0560c PE=3 SV=2 | 2 | 0.74 | 0.79 | 0.4138 |
| tr\|Q8I5M9\|Q8I5M9_PLAF7 Uncharacterized protein OS=Plasmodium falciparum (isolate 3D7) GN=PFL0865w PE=4 SV=1 | 2 | 2.94 | 2.70 | 0.3670 |
| tr\|Q8I5M2\|Q8I5M2_PLAF7 Arginyl-tRNA synthetase, putative OS=Plasmodium falciparum (isolate 3D7) GN=PFL0900c PE=3 SV=1 | 2 | 3.28 | 2.21 | 0.2832 |
| tr\|Q8I5L7\|Q8I5L7_PLAF7 Formin 2, putative OS=Plasmodium falciparum (isolate 3D7) GN=PFL0925w PE=4 SV=1 | 2 | 2.99 | 2.62 | 0.3526 |
| tr\|Q8I5H9\|Q8I5H9_PLAF7 Mitochondrial carrier protein, putative OS=Plasmodium falciparum (isolate 3D7) GN=PFL1145w PE=3 SV=1 | 2 | 6.43 | 7.54 | 0.4406 |
| tr\|Q8I5E1\|Q8I5E1_PLAF7 Uncharacterized protein OS=Plasmodium falciparum (isolate 3D7) GN=PFL1340c PE=4 SV=1 | 2 | 2.85 | 2.82 | 0.3880 |
| tr\|Q8I5B5\|Q8I5B5_PLAF7 Uncharacterized protein OS=Plasmodium falciparum (isolate 3D7) GN=PFL1470c PE=4 SV=1 | 2 | 1.45 | 0.77 | 0.2292 |
| tr\|Q8I5B3\|Q8I5B3_PLAF7 Uncharacterized protein OS=Plasmodium falciparum (isolate 3D7) GN=PFL1480w PE=4 SV=1 | 2 | 8.73 | 10.90 | 0.4603 |
| tr\|Q8I525\|Q8I525_PLAF7 Conserved Plasmodium protein OS=Plasmodium falciparum (isolate 3D7) GN=PFL1930w PE=4 SV=1 | 2 | 1.05 | 0.04 | 0.0163 |
| tr\|Q8I4Z4\|Q8I4Z4_PLAF7 Translation initiation factor SUI1, putative OS=Plasmodium falciparum (isolate 3D7) GN=PFL2095w PE=4 SV=1 | 2 | 1.42 | 0.28 | 0.0868 |
| tr\|Q8I4Y0\|Q8I4Y0_PLAF7 Kinesin-like protein OS=Plasmodium falciparum (isolate 3D7) GN=PFL2165w PE=1 SV=2 | 2 | 1.05 | 0.36 | 0.1529 |
| sp\|Q8I4T1\|VPS26_PLAF7 Vacuolar protein sorting-associated protein 26 OS=Plasmodium falciparum (isolate 3D7) GN=PFL2415w PE=3 SV=1 | 2 | 1.84 | 0.08 | 0.0186 |
| tr\|Q8I4S6\|Q8I4S6_PLAF7 DNA repair protein rhp16, putative OS=Plasmodium falciparum (isolate 3D7) GN=PFL2440w PE=4 SV=1 | 2 | 2.89 | 2.76 | 0.3780 |
| tr\|Q8I4R0\|Q8I4R0_PLAF7 Uncharacterized protein OS=Plasmodium falciparum (isolate 3D7) GN=PFL2530w PE=4 SV=1 | 2 | 2.89 | 0.10 | 0.0153 |
| tr\|Q9NLB8\|Q9NLB8_PLAF7 EH (Eps15 homology) protein OS=Plasmodium falciparum (isolate 3D7) GN=PfPast-1 PE=4 SV=1 | 2 | 25.06 | 31.68 | 0.4644 |
| tr\|Q8IDE7\|Q8IDE7_PLAF7 Serine/threonine protein phosphatase OS=Plasmodium falciparum (isolate 3D7) GN=PfPP5 PE=4 SV=1 | 2 | 5.40 | 4.28 | 0.3255 |
| tr\|Q8ID44\|Q8ID44_PLAF7 Rhoptry protein OS=Plasmodium falciparum (isolate 3D7) GN=PfRhop148 PE=4 SV=1 | 2 | 1.52 | 0.56 | 0.1616 |
| tr\|C0H4R8\|C0H4R8_PLAF7 Serine/Threonine protein kinase, FIKK family OS=Plasmodium falciparum (isolate 3D7) GN=PfTSTK0 PE=4 SV=1 | 2 | 1.57 | 0.13 | 0.0382 |
| tr\|C0H5D3\|C0H5D3_PLAF7 SNARE protein, putative OS=Plasmodium falciparum (isolate 3D7) GN=PfYkt6.2 PE=4 SV=1 | 2 | 1.35 | 1.65 | 0.4541 |

| | | | | |
|---|---|---|---|---|
| sp\|Q92508\|PIEZ1_HUMAN Piezo-type mechanosensitive ion channel component 1 OS=Homo sapiens GN=PIEZO1 PE=1 SV=4 | 2 | 0.93 | 0.04 | 0.0208 |
| tr\|E9PHR9\|E9PHR9_HUMAN Phospholipid scramblase 4 OS=Homo sapiens GN=PLSCR4 PE=1 SV=1;sp\|Q9NRQ2-2\|PLS4_HUMAN Isoform 2 of Phospholipid scramblase 4 OS=Homo sapiens GN=PLSCR4;sp\|Q9NRQ2\|PLS4_HUMAN Phospholipid scramblase 4 OS=Homo sapiens GN=PLSCR4 PE=1 SV=2 | 2 | 1.96 | 0.07 | 0.0154 |
| tr\|Q8ILY1\|Q8ILY1_PLAF7 Pfprex OS=Plasmodium falciparum (isolate 3D7) GN=POM1 PE=4 SV=1 | 2 | 1.37 | 0.09 | 0.0308 |
| tr\|Q8ILV1\|Q8ILV1_PLAF7 Serine/threonine-protein phosphatase OS=Plasmodium falciparum (isolate 3D7) GN=PP1 PE=1 SV=1 | 2 | 1.46 | 0.40 | 0.1217 |
| tr\|C6KTB6\|C6KTB6_PLAF7 6-pyruvoyltetrahydropterin synthase OS=Plasmodium falciparum (isolate 3D7) GN=PTPS PE=1 SV=1 | 2 | 4.25 | 0.84 | 0.0887 |
| tr\|Q8I485\|Q8I485_PLAF7 Rhoptry-associated protein 3, RAP3 OS=Plasmodium falciparum (isolate 3D7) GN=RAP3 PE=4 SV=1 | 2 | 27.90 | 38.10 | 0.4889 |
| sp\|O60673-2\|DPOLZ_HUMAN Isoform 2 of DNA polymerase zeta catalytic subunit OS=Homo sapiens GN=REV3L;sp\|O60673\|DPOLZ_HUMAN DNA polymerase zeta catalytic subunit OS=Homo sapiens GN=REV3L PE=1 SV=2 | 2 | 1.77 | 1.32 | 0.3095 |
| tr\|Q8I433\|Q8I433_PLAF7 Rhomboid protease ROM4 OS=Plasmodium falciparum (isolate 3D7) GN=ROM4 PE=4 SV=1 | 2 | 0.82 | 0.04 | 0.0216 |
| tr\|Q8IIK5\|Q8IIK5_PLAF7 Moving junction protein OS=Plasmodium falciparum (isolate 3D7) GN=RON4 PE=4 SV=2 | 2 | 1.08 | 0.13 | 0.0548 |
| sp\|Q86SG5\|S1A7A_HUMAN Protein S100-A7A OS=Homo sapiens GN=S100A7A PE=1 SV=3;sp\|P31151\|S10A7_HUMAN Protein S100-A7 OS=Homo sapiens GN=S100A7 PE=1 SV=4 | 2 | 1.12 | 0.73 | 0.2735 |
| tr\|C0H4J5\|C0H4J5_PLAF7 Stevor OS=Plasmodium falciparum (isolate 3D7) GN=Stevor PE=4 SV=1 | 2 | 0.79 | 0.47 | 0.2561 |
| sp\|P60174-1\|TPIS_HUMAN Isoform 2 of Triosephosphate isomerase OS=Homo sapiens GN=TPI1;sp\|P60174\|TPIS_HUMAN Triosephosphate isomerase OS=Homo sapiens GN=TPI1 PE=1 SV=3 | 2 | 3.25 | 2.25 | 0.2896 |
| sp\|O14980\|XPO1_HUMAN Exportin-1 OS=Homo sapiens GN=XPO1 PE=1 SV=1 | 2 | 1.32 | 0.26 | 0.0882 |
| sp\|P30043\|BLVRB_HUMAN Flavin reductase (NADPH) OS=Homo sapiens GN=BLVRB PE=1 SV=3;tr\|M0R192\|M0R192_HUMAN Flavin reductase (NADPH) OS=Homo sapiens GN=BLVRB PE=1 SV=1;tr\|M0QZL1\|M0QZL1_HUMAN Flavin reductase (NADPH) OS=Homo sapiens GN=BLVRB PE=1 SV=1 | 1 | 1.94 | | |
| tr\|A0A087X1A9\|A0A087X1A9_HUMAN Vesicle-trafficking protein SEC22b (Fragment) OS=Homo sapiens GN=SEC22B PE=1 SV=1;sp\|O75396\|SC22B_HUMAN Vesicle-trafficking protein SEC22b OS=Homo sapiens GN=SEC22B PE=1 SV=4 | 1 | 0.01 | | |
| sp\|O75131\|CPNE3_HUMAN Copine-3 OS=Homo sapiens GN=CPNE3 PE=1 SV=1 | 1 | 0.62 | | |
| tr\|Q8IEE9\|Q8IEE9_PLAF7 Cholinephosphate cytidylyltransferase OS=Plasmodium falciparum (isolate 3D7) GN=ctP PE=1 SV=1 | 1 | 1.03 | | |
| tr\|E7EWB4\|E7EWB4_HUMAN Dihydropyrimidinase-related protein 5 (Fragment) OS=Homo sapiens GN=DPYSL5 PE=1 SV=4;sp\|Q9BPU6\|DPYL5_HUMAN Dihydropyrimidinase-related protein 5 OS=Homo sapiens GN=DPYSL5 PE=1 SV=1 | 1 | 0.00 | | |
| sp\|P35908\|K22E_HUMAN Keratin, type II cytoskeletal 2 epidermal OS=Homo sapiens GN=KRT2 PE=1 SV=2 | 1 | 0.41 | | |
| tr\|G3V3R6\|G3V3R6_HUMAN Galectin OS=Homo sapiens GN=LGALS3 PE=1 SV=1;sp\|P17931\|LEG3_HUMAN Galectin-3 OS=Homo sapiens GN=LGALS3 PE=1 SV=5 | 1 | 0.27 | | |
| tr\|Q8IEA1\|Q8IEA1_PLAF7 Uncharacterized protein OS=Plasmodium falciparum (isolate 3D7) GN=MAL13P1.116 PE=4 SV=1 | 1 | 4.84 | | |
| tr\|Q8IE87\|Q8IE87_PLAF7 Uncharacterized protein OS=Plasmodium falciparum (isolate 3D7) GN=MAL13P1.128 PE=4 SV=1 | 1 | 0.65 | | |
| tr\|Q8IE74\|Q8IE74_PLAF7 Uncharacterized protein OS=Plasmodium falciparum (isolate 3D7) GN=MAL13P1.133 PE=4 SV=1 | 1 | 1.19 | | |
| tr\|Q8IE72\|Q8IE72_PLAF7 DEAD box helicase, putative OS=Plasmodium falciparum (isolate 3D7) GN=MAL13P1.134 PE=4 SV=1 | 1 | 4.84 | | |
| tr\|Q8IE19\|Q8IE19_PLAF7 GPI transamidase subunit PIG-U, putative OS=Plasmodium falciparum (isolate 3D7) GN=MAL13P1.165 PE=4 SV=1 | 1 | 1.51 | | |
| tr\|Q8IDY4\|Q8IDY4_PLAF7 MSP7-like protein OS=Plasmodium falciparum (isolate 3D7) GN=MAL13P1.173 PE=4 SV=1 | 1 | 4.84 | | |
| tr\|Q8IDT8\|Q8IDT8_PLAF7 Uncharacterized protein OS=Plasmodium falciparum (isolate 3D7) GN=MAL13P1.202 PE=4 SV=1 | 1 | 34.50 | | |
| tr\|Q8IDQ4\|Q8IDQ4_PLAF7 Uncharacterized protein OS=Plasmodium falciparum (isolate 3D7) GN=MAL13P1.217 PE=4 SV=1 | 1 | 1.22 | | |
| tr\|C0H5H6\|C0H5H6_PLAF7 Uncharacterized protein OS=Plasmodium falciparum (isolate 3D7) GN=MAL13P1.234 PE=4 SV=1 | 1 | 4.26 | | |

| | | | | |
|---|---|---|---|---|
| tr\|Q8IDM0\|Q8IDM0_PLAF7 Uncharacterized protein OS=Plasmodium falciparum (isolate 3D7) GN=MAL13P1.239 PE=4 SV=1 | 1 | 1.05 | | |
| tr\|C0H5A0\|C0H5A0_PLAF7 Uncharacterized protein OS=Plasmodium falciparum (isolate 3D7) GN=MAL13P1.26 PE=4 SV=1 | 1 | 0.82 | | |
| tr\|C0H5I9\|C0H5I9_PLAF7 GTP binding protein, putative OS=Plasmodium falciparum (isolate 3D7) GN=MAL13P1.294 PE=4 SV=1 | 1 | 4.84 | | |
| tr\|Q8IEM1\|Q8IEM1_PLAF7 U4/U6 small nuclear ribonucleoprotein, putative OS=Plasmodium falciparum (isolate 3D7) GN=MAL13P1.45 PE=4 SV=1 | 1 | 4.16 | | |
| tr\|Q8IEL5\|Q8IEL5_PLAF7 Mitochondrial ATP synthase delta subunit, putative OS=Plasmodium falciparum (isolate 3D7) GN=MAL13P1.47 PE=3 SV=1 | 1 | 1.23 | | |
| tr\|Q8IEH6\|Q8IEH6_PLAF7 Septum formation protein MAF homologue, putative OS=Plasmodium falciparum (isolate 3D7) GN=MAL13P1.69 PE=3 SV=2 | 1 | 4.84 | | |
| tr\|C0H5B3\|C0H5B3_PLAF7 Uncharacterized protein OS=Plasmodium falciparum (isolate 3D7) GN=MAL13P1.70 PE=4 SV=1 | 1 | 1.22 | | |
| tr\|C0H5C1\|C0H5C1_PLAF7 Uncharacterized protein OS=Plasmodium falciparum (isolate 3D7) GN=MAL13P1.90 PE=4 SV=1 | 1 | 1.01 | | |
| tr\|Q8IBP4\|Q8IBP4_PLAF7 Phosphoinositide-binding protein, putative OS=Plasmodium falciparum (isolate 3D7) GN=MAL7P1.108 PE=4 SV=2 | 1 | 0.92 | | |
| tr\|Q8IBN7\|Q8IBN7_PLAF7 P36-like protein homologue, putative OS=Plasmodium falciparum (isolate 3D7) GN=MAL7P1.114 PE=4 SV=2 | 1 | 4.84 | | |
| tr\|Q8IBL1\|Q8IBL1_PLAF7 Uncharacterized protein OS=Plasmodium falciparum (isolate 3D7) GN=MAL7P1.129 PE=4 SV=1 | 1 | 1.06 | | |
| tr\|Q8IBK0\|Q8IBK0_PLAF7 Uncharacterized protein OS=Plasmodium falciparum (isolate 3D7) GN=MAL7P1.138 PE=4 SV=1 | 1 | 1.80 | | |
| tr\|Q8IC33\|Q8IC33_PLAF7 Uncharacterized protein OS=Plasmodium falciparum (isolate 3D7) GN=MAL7P1.14 PE=4 SV=1 | 1 | 4.84 | | |
| tr\|Q8IC31\|Q8IC31_PLAF7 Uncharacterized protein OS=Plasmodium falciparum (isolate 3D7) GN=MAL7P1.15 PE=4 SV=1 | 1 | 1.10 | | |
| tr\|Q8IBT8\|Q8IBT8_PLAF7 Uncharacterized protein OS=Plasmodium falciparum (isolate 3D7) GN=MAL7P1.76 PE=4 SV=1 | 1 | 1.52 | | |
| tr\|C0H4N1\|C0H4N1_PLAF7 Uncharacterized protein OS=Plasmodium falciparum (isolate 3D7) GN=MAL7P1.83 PE=4 SV=1 | 1 | 8.60 | | |
| tr\|Q8IAP1\|Q8IAP1_PLAF7 Uncharacterized protein OS=Plasmodium falciparum (isolate 3D7) GN=MAL8P1.139 PE=4 SV=1 | 1 | 4.84 | | |
| tr\|Q8IBA8\|Q8IBA8_PLAF7 Uncharacterized protein OS=Plasmodium falciparum (isolate 3D7) GN=MAL8P1.18 PE=4 SV=1 | 1 | 4.84 | | |
| tr\|C0H4U9\|C0H4U9_PLAF7 Uncharacterized protein OS=Plasmodium falciparum (isolate 3D7) GN=MAL8P1.79 PE=4 SV=1 | 1 | 0.08 | | |
| sp\|Q9NU22\|MDN1_HUMAN Midasin OS=Homo sapiens GN=MDN1 PE=1 SV=2;tr\|Q5T795\|Q5T795_HUMAN Midasin (Fragment) OS=Homo sapiens GN=MDN1 PE=1 SV=1 | 1 | 8.32 | | |
| tr\|H0YI09\|H0YI09_HUMAN Methyltransferase-like protein 7A (Fragment) OS=Homo sapiens GN=METTL7A PE=1 SV=1;sp\|Q9H8H3\|MET7A_HUMAN Methyltransferase-like protein 7A OS=Homo sapiens GN=METTL7A PE=1 SV=1 | 1 | 4.84 | | |
| sp\|P48681\|NEST_HUMAN Nestin OS=Homo sapiens GN=NES PE=1 SV=2 | 1 | 1.48 | | |
| tr\|I3L0N3\|I3L0N3_HUMAN Vesicle-fusing ATPase OS=Homo sapiens GN=NSF PE=1 SV=1;sp\|P46459\|NSF_HUMAN Vesicle-fusing ATPase OS=Homo sapiens GN=NSF PE=1 SV=3;tr\|I3L0L3\|I3L0L3_HUMAN Vesicle-fusing ATPase (Fragment) OS=Homo sapiens GN=NSF PE=1 SV=1 | 1 | 0.89 | | |
| tr\|H3BRV9\|H3BRV9_HUMAN Nuclear transport factor 2 (Fragment) OS=Homo sapiens GN=NUTF2 PE=1 SV=1;sp\|P61970\|NTF2_HUMAN Nuclear transport factor 2 OS=Homo sapiens GN=NUTF2 PE=1 SV=1 | 1 | 4.84 | | |
| tr\|H7C368\|H7C368_HUMAN Oxysterol-binding protein (Fragment) OS=Homo sapiens GN=OSBP2 PE=1 SV=1 | 1 | 605.12 | | |
| tr\|Q8IDR1\|Q8IDR1_PLAF7 Phosphoenolpyruvate carboxykinase OS=Plasmodium falciparum (isolate 3D7) GN=PEPCK PE=3 SV=1 | 1 | 4.84 | | |
| tr\|Q8IC28\|Q8IC28_PLAF7 Methyltransferase, putative OS=Plasmodium falciparum (isolate 3D7) GN=PF07_0015 PE=4 SV=1 | 1 | 4.84 | | |
| tr\|Q8IBY9\|Q8IBY9_PLAF7 Uncharacterized protein OS=Plasmodium falciparum (isolate 3D7) GN=PF07_0041 PE=4 SV=1 | 1 | 44.47 | | |
| tr\|Q8IBQ0\|Q8IBQ0_PLAF7 Uncharacterized protein OS=Plasmodium falciparum (isolate 3D7) GN=PF07_0084 PE=4 SV=1 | 1 | 4.84 | | |
| tr\|Q8IBM6\|Q8IBM6_PLAF7 Uncharacterized protein OS=Plasmodium falciparum (isolate 3D7) GN=PF07_0093 PE=4 SV=1 | 1 | 0.79 | | |
| tr\|Q8IBJ8\|Q8IBJ8_PLAF7 Uncharacterized protein OS=Plasmodium falciparum (isolate 3D7) GN=PF07_0106 PE=4 SV=1 | 1 | 4.84 | | |

| | | | | |
|---|---|---|---|---|
| tr\|Q8IAV6\|Q8IAV6_PLAF7 Uncharacterized protein OS=Plasmodium falciparum (isolate 3D7) GN=PF08_0089 PE=4 SV=1 | 1 | 4.84 | | |
| tr\|C0H4S0\|C0H4S0_PLAF7 AAA family ATPase, putative OS=Plasmodium falciparum (isolate 3D7) GN=PF08_0117 PE=4 SV=1 | 1 | 4.84 | | |
| tr\|Q8IAN1\|Q8IAN1_PLAF7 Uncharacterized protein OS=Plasmodium falciparum (isolate 3D7) GN=PF08_0127 PE=4 SV=1 | 1 | 2.70 | | |
| tr\|Q8IK09\|Q8IK09_PLAF7 Uncharacterized protein OS=Plasmodium falciparum (isolate 3D7) GN=PF10_0031 PE=4 SV=1 | 1 | 4.84 | | |
| tr\|Q8IJX5\|Q8IJX5_PLAF7 Uncharacterized protein OS=Plasmodium falciparum (isolate 3D7) GN=PF10_0066 PE=4 SV=1 | 1 | 4.84 | | |
| tr\|Q8IJX2\|Q8IJX2_PLAF7 PPPDE peptidase, putative OS=Plasmodium falciparum (isolate 3D7) GN=PF10_0069 PE=4 SV=2 | 1 | 4.84 | | |
| tr\|Q8IJV9\|Q8IJV9_PLAF7 Conserved Plasmodium membrane protein OS=Plasmodium falciparum (isolate 3D7) GN=PF10_0082 PE=4 SV=2 | 1 | 249.73 | | |
| tr\|Q8IJU4\|Q8IJU4_PLAF7 Uncharacterized protein OS=Plasmodium falciparum (isolate 3D7) GN=PF10_0098 PE=4 SV=1 | 1 | 0.72 | | |
| tr\|Q8IJS0\|Q8IJS0_PLAF7 Phosphoglucomutase, putative OS=Plasmodium falciparum (isolate 3D7) GN=PF10_0122 PE=3 SV=1 | 1 | 4.84 | | |
| tr\|Q8IJQ6\|Q8IJQ6_PLAF7 Initiation factor 2 subunit family, putative OS=Plasmodium falciparum (isolate 3D7) GN=PF10_0136 PE=3 SV=1 | 1 | 4.84 | | |
| tr\|Q8IJQ1\|Q8IJQ1_PLAF7 Cdk7, putative OS=Plasmodium falciparum (isolate 3D7) GN=PF10_0141 PE=4 SV=1 | 1 | 7.63 | | |
| tr\|Q8IJP2\|Q8IJP2_PLAF7 Methionine aminopeptidase 1 OS=Plasmodium falciparum (isolate 3D7) GN=PF10_0150 PE=1 SV=1 | 1 | 4.84 | | |
| tr\|Q8IJG5\|Q8IJG5_PLAF7 Conserved Plasmodium protein OS=Plasmodium falciparum (isolate 3D7) GN=PF10_0233 PE=4 SV=2 | 1 | 4.84 | | |
| tr\|C6S3D4\|C6S3D4_PLAF7 Conserved Plasmodium protein OS=Plasmodium falciparum (isolate 3D7) GN=PF10_0246a PE=4 SV=1 | 1 | 1.92 | | |
| tr\|Q8IJC4\|Q8IJC4_PLAF7 Methyltransferase, putative OS=Plasmodium falciparum (isolate 3D7) GN=PF10_0274 PE=4 SV=2 | 1 | 4.84 | | |
| tr\|Q8IJB7\|Q8IJB7_PLAF7 Uncharacterized protein OS=Plasmodium falciparum (isolate 3D7) GN=PF10_0281 PE=4 SV=1 | 1 | 1.16 | | |
| tr\|Q8IJ99\|Q8IJ99_PLAF7 Uncharacterized protein OS=Plasmodium falciparum (isolate 3D7) GN=PF10_0299 PE=4 SV=1 | 1 | 4.84 | | |
| tr\|Q8IJ90\|Q8IJ90_PLAF7 Uncharacterized protein OS=Plasmodium falciparum (isolate 3D7) GN=PF10_0309 PE=3 SV=1 | 1 | 1.86 | | |
| tr\|Q8IJ89\|Q8IJ89_PLAF7 Uncharacterized protein OS=Plasmodium falciparum (isolate 3D7) GN=PF10_0310 PE=4 SV=1 | 1 | 4.84 | | |
| tr\|Q8IJ82\|Q8IJ82_PLAF7 DER1-like protein, putative OS=Plasmodium falciparum (isolate 3D7) GN=PF10_0317 PE=4 SV=1 | 1 | 0.01 | | |
| tr\|Q8IJ80\|Q8IJ80_PLAF7 Uncharacterized protein OS=Plasmodium falciparum (isolate 3D7) GN=PF10_0319 PE=4 SV=1 | 1 | 0.14 | | |
| tr\|Q8IJ79\|Q8IJ79_PLAF7 Leucine-rich repeat protein 8, LRR8 OS=Plasmodium falciparum (isolate 3D7) GN=PF10_0320 PE=4 SV=2 | 1 | 4.84 | | |
| tr\|Q8IJ66\|Q8IJ66_PLAF7 Flavoprotein subunit of succinate dehydrogenase OS=Plasmodium falciparum (isolate 3D7) GN=PF10_0334 PE=4 SV=1 | 1 | 0.73 | | |
| tr\|Q8IJ11\|Q8IJ11_PLAF7 Pfmc-2TM Maurers cleft two transmembrane protein OS=Plasmodium falciparum (isolate 3D7) GN=PF10_0390 PE=4 SV=2;tr\|Q8IIY1\|Q8IIY1_PLAF7 Uncharacterized protein OS=Plasmodium falciparum (isolate 3D7) GN=PF11_0025 PE=4 SV=1 | 1 | 0.75 | | |
| tr\|Q8IIX6\|Q8IIX6_PLAF7 Uncharacterized protein OS=Plasmodium falciparum (isolate 3D7) GN=PF11_0036 PE=4 SV=1 | 1 | 4.84 | | |
| tr\|C6S3F2\|C6S3F2_PLAF7 Serine esterase, putative OS=Plasmodium falciparum (isolate 3D7) GN=PF11_0168a PE=4 SV=1 | 1 | 0.88 | | |
| tr\|Q8IID6\|Q8IID6_PLAF7 Uncharacterized protein OS=Plasmodium falciparum (isolate 3D7) GN=PF11_0238 PE=4 SV=1 | 1 | 1.66 | | |
| tr\|Q8IID0\|Q8IID0_PLAF7 Uncharacterized protein OS=Plasmodium falciparum (isolate 3D7) GN=PF11_0244 PE=4 SV=1 | 1 | 51.56 | | |
| tr\|Q8II90\|Q8II90_PLAF7 tRNA (guanine-N(7)-)-methyltransferase OS=Plasmodium falciparum (isolate 3D7) GN=PF11_0284 PE=3 SV=1 | 1 | 4.84 | | |
| tr\|Q8II88\|Q8II88_PLAF7 Uncharacterized protein OS=Plasmodium falciparum (isolate 3D7) GN=PF11_0286 PE=4 SV=1 | 1 | 1.13 | | |
| tr\|Q8II65\|Q8II65_PLAF7 Conserved Plasmodium protein OS=Plasmodium falciparum (isolate 3D7) GN=PF11_0309 PE=4 SV=1 | 1 | 1.86 | | |
| tr\|Q8II47\|Q8II47_PLAF7 Uncharacterized protein OS=Plasmodium falciparum (isolate 3D7) GN=PF11_0327 PE=4 SV=1 | 1 | 1.67 | | |

| | | | | |
|---|---|---|---|---|
| tr\|Q8II38\|Q8II38_PLAF7 Pre-mRNA splicing factor, putative OS=Plasmodium falciparum (isolate 3D7) GN=PF11_0336 PE=4 SV=1 | 1 | 0.77 | | |
| tr\|Q8II00\|Q8II00_PLAF7 Uncharacterized protein OS=Plasmodium falciparum (isolate 3D7) GN=PF11_0375 PE=4 SV=1 | 1 | 4.84 | | |
| tr\|Q8IHN7\|Q8IHN7_PLAF7 Plasmodium exported protein (PHISTc) OS=Plasmodium falciparum (isolate 3D7) GN=PF11_0503 PE=4 SV=1 | 1 | 1.36 | | |
| tr\|Q8I701\|Q8I701_PLAF7 Deoxyhypusine hydroxylase OS=Plasmodium falciparum (isolate 3D7) GN=PF13_0013 PE=3 SV=1 | 1 | 4.84 | | |
| tr\|Q8IET6\|Q8IET6_PLAF7 Uncharacterized protein OS=Plasmodium falciparum (isolate 3D7) GN=PF13_0015 PE=4 SV=1 | 1 | 0.29 | | |
| tr\|Q8IES1\|Q8IES1_PLAF7 Uncharacterized protein OS=Plasmodium falciparum (isolate 3D7) GN=PF13_0020 PE=4 SV=1 | 1 | 4.84 | | |
| tr\|Q8IEN8\|Q8IEN8_PLAF7 Uncharacterized protein OS=Plasmodium falciparum (isolate 3D7) GN=PF13_0041 PE=4 SV=1 | 1 | 1.03 | | |
| tr\|Q8IEM0\|Q8IEM0_PLAF7 HORMA domain protein, putative OS=Plasmodium falciparum (isolate 3D7) GN=PF13_0050 PE=4 SV=1 | 1 | 1.44 | | |
| tr\|Q8I6T7\|Q8I6T7_PLAF7 ATP synthase subunit gamma OS=Plasmodium falciparum (isolate 3D7) GN=PF13_0061 PE=3 SV=1 | 1 | 0.97 | | |
| tr\|Q8IE78\|Q8IE78_PLAF7 Uncharacterized protein OS=Plasmodium falciparum (isolate 3D7) GN=PF13_0136 PE=4 SV=1 | 1 | 4.84 | | |
| tr\|Q8IE38\|Q8IE38_PLAF7 Nicotinic acid mononucleotide adenyltransferase OS=Plasmodium falciparum (isolate 3D7) GN=PF13_0159 PE=4 SV=1 | 1 | 4.84 | | |
| tr\|Q8IDZ2\|Q8IDZ2_PLAF7 Uncharacterized protein OS=Plasmodium falciparum (isolate 3D7) GN=PF13_0184 PE=4 SV=1 | 1 | 27.45 | | |
| tr\|Q8IDV9\|Q8IDV9_PLAF7 Exoribonuclease, putative OS=Plasmodium falciparum (isolate 3D7) GN=PF13_0208 PE=4 SV=1 | 1 | 1.09 | | |
| tr\|Q8IDV4\|Q8IDV4_PLAF7 Uncharacterized protein OS=Plasmodium falciparum (isolate 3D7) GN=PF13_0212 PE=4 SV=1 | 1 | 2.91 | | |
| tr\|Q8IDT7\|Q8IDT7_PLAF7 Uncharacterized protein OS=Plasmodium falciparum (isolate 3D7) GN=PF13_0217 PE=4 SV=1 | 1 | 4.84 | | |
| sp\|Q8IDG7\|YPF01_PLAF7 Uncharacterized protein PF13_0277 OS=Plasmodium falciparum (isolate 3D7) GN=PF13_0277 PE=3 SV=1 | 1 | 0.32 | | |
| tr\|Q8ID99\|Q8ID99_PLAF7 Uncharacterized protein OS=Plasmodium falciparum (isolate 3D7) GN=PF13_0321 PE=4 SV=1 | 1 | 0.65 | | |
| tr\|Q8ID74\|Q8ID74_PLAF7 Polynucleotide kinase, putative OS=Plasmodium falciparum (isolate 3D7) GN=PF13_0334 PE=4 SV=1 | 1 | 0.26 | | |
| tr\|Q8ID23\|Q8ID23_PLAF7 Mitochondrial carrier protein, putative OS=Plasmodium falciparum (isolate 3D7) GN=PF13_0359 PE=3 SV=1 | 1 | 26.02 | | |
| tr\|Q8IM69\|Q8IM69_PLAF7 Exopolyphosphatase, putative OS=Plasmodium falciparum (isolate 3D7) GN=PF14_0022 PE=4 SV=2 | 1 | 4.84 | | |
| tr\|Q8IM40\|Q8IM40_PLAF7 DNA mismatch repair protein, putative OS=Plasmodium falciparum (isolate 3D7) GN=PF14_0051 PE=4 SV=1 | 1 | 18.69 | | |
| tr\|Q8ILX9\|Q8ILX9_PLAF7 GTP binding protein, putative OS=Plasmodium falciparum (isolate 3D7) GN=PF14_0114 PE=4 SV=1 | 1 | 1.23 | | |
| tr\|Q8ILW8\|Q8ILW8_PLAF7 Deoxyhypusine synthase OS=Plasmodium falciparum (isolate 3D7) GN=PF14_0125 PE=4 SV=1 | 1 | 4.84 | | |
| sp\|Q8ILW6\|NMT_PLAF7 Glycylpeptide N-tetradecanoyltransferase OS=Plasmodium falciparum (isolate 3D7) GN=PF14_0127 PE=3 SV=1 | 1 | 4.84 | | |
| tr\|Q8ILW5\|Q8ILW5_PLAF7 Ubiquitin conjugating enzyme, putative OS=Plasmodium falciparum (isolate 3D7) GN=PF14_0128 PE=4 SV=1 | 1 | 4.84 | | |
| sp\|Q8ILR9\|YPF17_PLAF7 Protein PF14_0175 OS=Plasmodium falciparum (isolate 3D7) GN=PF14_0175 PE=3 SV=1 | 1 | 1.62 | | |
| tr\|Q8ILQ4\|Q8ILQ4_PLAF7 Uncharacterized protein OS=Plasmodium falciparum (isolate 3D7) GN=PF14_0190 PE=4 SV=1 | 1 | 4.84 | | |
| tr\|Q8ILM5\|Q8ILM5_PLAF7 Actin-related protein homolog, arp4 homolog OS=Plasmodium falciparum (isolate 3D7) GN=PF14_0218 PE=3 SV=1 | 1 | 1.16 | | |
| tr\|Q8ILL8\|Q8ILL8_PLAF7 Uncharacterized protein OS=Plasmodium falciparum (isolate 3D7) GN=PF14_0225 PE=4 SV=1 | 1 | 1.28 | | |
| tr\|Q8ILJ6\|Q8ILJ6_PLAF7 Uncharacterized protein OS=Plasmodium falciparum (isolate 3D7) GN=PF14_0247 PE=4 SV=2 | 1 | 1.24 | | |
| tr\|Q8ILH5\|Q8ILH5_PLAF7 Uncharacterized protein OS=Plasmodium falciparum (isolate 3D7) GN=PF14_0268 PE=4 SV=2 | 1 | 0.91 | | |
| tr\|Q8ILH0\|Q8ILH0_PLAF7 rRNA (Adenosine-2-O-)-methyltransferase, putative OS=Plasmodium falciparum (isolate 3D7) GN=PF14_0273 PE=4 SV=1 | 1 | 4.84 | | |
| tr\|Q8ILG1\|Q8ILG1_PLAF7 Uncharacterized protein OS=Plasmodium falciparum (isolate 3D7) GN=PF14_0282 PE=4 SV=1 | 1 | 4.84 | | |

| | | | | |
|---|---|---|---|---|
| tr\|Q8ILD6\|Q8ILD6_PLAF7 Uncharacterized protein OS=Plasmodium falciparum (isolate 3D7) GN=PF14_0308 PE=4 SV=1 | 1 | 4.84 | | |
| tr\|Q8ILD5\|Q8ILD5_PLAF7 Protein-L-isoaspartate O-methyltransferase beta-aspartate methyltransferase, putative OS=Plasmodium falciparum (isolate 3D7) GN=PF14_0309 PE=1 SV=1 | 1 | 4.84 | | |
| sp\|Q8ILC2\|TGTL_PLAF7 Queuine tRNA-ribosyltransferase-like protein OS=Plasmodium falciparum (isolate 3D7) GN=PF14_0322 PE=3 SV=1 | 1 | 4.84 | | |
| tr\|Q8IL76\|Q8IL76_PLAF7 Uncharacterized protein OS=Plasmodium falciparum (isolate 3D7) GN=PF14_0372 PE=4 SV=2 | 1 | 2.58 | | |
| tr\|Q8IL63\|Q8IL63_PLAF7 Adaptor complexes medium subunit family OS=Plasmodium falciparum (isolate 3D7) GN=PF14_0386 PE=4 SV=1 | 1 | 1.82 | | |
| tr\|Q8IL59\|Q8IL59_PLAF7 Uncharacterized protein OS=Plasmodium falciparum (isolate 3D7) GN=PF14_0390 PE=4 SV=1 | 1 | 4.84 | | |
| tr\|Q8IL54\|Q8IL54_PLAF7 Acid cluster protein 33 homologue, putative OS=Plasmodium falciparum (isolate 3D7) GN=PF14_0395 PE=4 SV=1 | 1 | 4.84 | | |
| tr\|Q8IL46\|Q8IL46_PLAF7 Protein prenyltransferase alpha subunit, putative OS=Plasmodium falciparum (isolate 3D7) GN=PF14_0403 PE=4 SV=2 | 1 | 4.84 | | |
| tr\|Q8IKY9\|Q8IKY9_PLAF7 SEL-1 protein, putative OS=Plasmodium falciparum (isolate 3D7) GN=PF14_0462 PE=4 SV=1 | 1 | 0.87 | | |
| tr\|Q8IKX8\|Q8IKX8_PLAF7 Rrp6 homologue, putative OS=Plasmodium falciparum (isolate 3D7) GN=PF14_0473 PE=4 SV=1 | 1 | 4.84 | | |
| tr\|Q8IKW6\|Q8IKW6_PLAF7 Uncharacterized protein OS=Plasmodium falciparum (isolate 3D7) GN=PF14_0485 PE=4 SV=1 | 1 | 24.15 | | |
| tr\|Q8IKV4\|Q8IKV4_PLAF7 Aminomethyltransferase, putative OS=Plasmodium falciparum (isolate 3D7) GN=PF14_0497 PE=4 SV=1 | 1 | 1.28 | | |
| tr\|Q8IKQ4\|Q8IKQ4_PLAF7 Uncharacterized protein OS=Plasmodium falciparum (isolate 3D7) GN=PF14_0549 PE=4 SV=1 | 1 | 73.35 | | |
| tr\|Q8IKP6\|Q8IKP6_PLAF7 Uncharacterized protein OS=Plasmodium falciparum (isolate 3D7) GN=PF14_0558 PE=4 SV=1 | 1 | 1.17 | | |
| tr\|Q8IKM8\|Q8IKM8_PLAF7 Ubiquitin carboxyl-terminal hydrolase OS=Plasmodium falciparum (isolate 3D7) GN=PF14_0576 PE=1 SV=2 | 1 | 4.84 | | |
| tr\|Q8IKM6\|Q8IKM6_PLAF7 Uncharacterized protein OS=Plasmodium falciparum (isolate 3D7) GN=PF14_0578 PE=4 SV=1 | 1 | 0.94 | | |
| tr\|Q8IKG0\|Q8IKG0_PLAF7 Uncharacterized protein OS=Plasmodium falciparum (isolate 3D7) GN=PF14_0645 PE=4 SV=1 | 1 | 91.91 | | |
| tr\|Q8IKE9\|Q8IKE9_PLAF7 U2 snRNP auxiliary factor, putative OS=Plasmodium falciparum (isolate 3D7) GN=PF14_0656 PE=4 SV=1 | 1 | 4.84 | | |
| tr\|Q8IKE4\|Q8IKE4_PLAF7 Uncharacterized protein OS=Plasmodium falciparum (isolate 3D7) GN=PF14_0661 PE=4 SV=1 | 1 | 4.84 | | |
| tr\|Q8IKB7\|Q8IKB7_PLAF7 Protein YIPF OS=Plasmodium falciparum (isolate 3D7) GN=PF14_0689 PE=3 SV=2 | 1 | 0.10 | | |
| tr\|Q8IKB0\|Q8IKB0_PLAF7 Uncharacterized protein OS=Plasmodium falciparum (isolate 3D7) GN=PF14_0696 PE=4 SV=2 | 1 | 0.40 | | |
| tr\|Q8I254\|Q8I254_PLAF7 Putative uncharacterized protein OS=Plasmodium falciparum (isolate 3D7) GN=PFA_0435w PE=3 SV=1 | 1 | 1.36 | | |
| tr\|Q8I237\|Q8I237_PLAF7 Transcription initiation factor TFIIB, putative OS=Plasmodium falciparum (isolate 3D7) GN=PFA_0525w PE=4 SV=1 | 1 | 21.01 | | |
| tr\|O77314\|O77314_PLAF7 Putative uncharacterized protein OS=Plasmodium falciparum (isolate 3D7) GN=PFC0145c PE=4 SV=1 | 1 | 1.82 | | |
| tr\|O77317\|O77317_PLAF7 HAD superfamily protein, putative OS=Plasmodium falciparum (isolate 3D7) GN=PFC0150w PE=4 SV=3 | 1 | 14.34 | | |
| tr\|O97241\|O97241_PLAF7 Ubiquitin conjugating enzyme E2, putative OS=Plasmodium falciparum (isolate 3D7) GN=PFC0255c PE=1 SV=1 | 1 | 4.84 | | |
| tr\|O77335\|O77335_PLAF7 YT521-B-like family protein, putative OS=Plasmodium falciparum (isolate 3D7) GN=PFC0410w PE=4 SV=2 | 1 | 1.60 | | |
| tr\|C0H473\|C0H473_PLAF7 Co-chaperone p23, putative OS=Plasmodium falciparum (isolate 3D7) GN=PFC0581w PE=4 SV=1 | 1 | 49.14 | | |
| tr\|O77380\|O77380_PLAF7 CPSF (Cleavage and polyadenylation specific factor), subunit A, putative OS=Plasmodium falciparum (isolate 3D7) GN=PFC0780w PE=4 SV=2 | 1 | 1.20 | | |
| tr\|O77371\|O77371_PLAF7 Cleavage and polyadenylation specificity factor protein, putative OS=Plasmodium falciparum (isolate 3D7) GN=PFC0825c PE=4 SV=1 | 1 | 55.00 | | |
| tr\|O97279\|O97279_PLAF7 Putative uncharacterized protein OS=Plasmodium falciparum (isolate 3D7) GN=PFC0885c PE=4 SV=1 | 1 | 11.04 | | |
| tr\|O97295\|O97295_PLAF7 O-acyltransferase OS=Plasmodium falciparum (isolate 3D7) GN=PFC0995c PE=3 SV=1 | 1 | 0.77 | | |

| | | | | |
|---|---|---|---|---|
| tr\|O97299\|O97299_PLAF7 Putative uncharacterized protein OS=Plasmodium falciparum (isolate 3D7) GN=PFC1030w PE=4 SV=1 | 1 | 15.52 | | |
| tr\|C6KSZ6\|C6KSZ6_PLAF7 Cyclin-dependent protein kinase, predicted OS=Plasmodium falciparum (isolate 3D7) GN=Pfcrk-5 PE=4 SV=1 | 1 | 2.03 | | |
| tr\|Q8I1Z9\|Q8I1Z9_PLAF7 Regulator of chromosome condensation, putative OS=Plasmodium falciparum (isolate 3D7) GN=PFD0145c PE=4 SV=1 | 1 | 112.53 | | |
| tr\|Q8I1Z2\|Q8I1Z2_PLAF7 CGI-201 protein, short form OS=Plasmodium falciparum (isolate 3D7) GN=PFD0180c PE=4 SV=1 | 1 | 0.93 | | |
| tr\|Q8I1X0\|Q8I1X0_PLAF7 Uncharacterized protein OS=Plasmodium falciparum (isolate 3D7) GN=PFD0290w PE=4 SV=1 | 1 | 20.35 | | |
| tr\|C0H499\|C0H499_PLAF7 Uncharacterized protein OS=Plasmodium falciparum (isolate 3D7) GN=PFD0415c PE=4 SV=1 | 1 | 1.11 | | |
| tr\|Q9U0H9\|Q9U0H9_PLAF7 Uncharacterized protein OS=Plasmodium falciparum (isolate 3D7) GN=PFD0540c PE=4 SV=1 | 1 | 1.76 | | |
| tr\|C0H4A9\|C0H4A9_PLAF7 Uncharacterized protein OS=Plasmodium falciparum (isolate 3D7) GN=PFD0815c:exon:2 PE=4 SV=1 | 1 | 2.07 | | |
| tr\|Q8I1Q4\|Q8I1Q4_PLAF7 Uncharacterized protein OS=Plasmodium falciparum (isolate 3D7) GN=PFD0885c PE=4 SV=1 | 1 | 4.84 | | |
| tr\|Q8I1Q0\|Q8I1Q0_PLAF7 Uncharacterized protein OS=Plasmodium falciparum (isolate 3D7) GN=PFD0905w PE=4 SV=1 | 1 | 4.84 | | |
| sp\|Q8I1N6\|AP2A_PLAF7 AP2/ERF domain-containing protein PFD0985w OS=Plasmodium falciparum (isolate 3D7) GN=PFD0985w PE=3 SV=2 | 1 | 1.10 | | |
| tr\|Q8IFN5\|Q8IFN5_PLAF7 Clathrin assembly protein, putative OS=Plasmodium falciparum (isolate 3D7) GN=PFD1090c PE=4 SV=1 | 1 | 32.69 | | |
| tr\|Q8I0X1\|Q8I0X1_PLAF7 3-methyl-2-oxobutanoate dehydrogenase (Lipoamide), putative OS=Plasmodium falciparum (isolate 3D7) GN=PFE0225w PE=4 SV=1 | 1 | 0.87 | | |
| tr\|Q8I427\|Q8I427_PLAF7 Cell differentiation protein rcd1, putative OS=Plasmodium falciparum (isolate 3D7) GN=PFE0375w PE=4 SV=1 | 1 | 32.36 | | |
| tr\|Q8I3X5\|Q8I3X5_PLAF7 Uncharacterized protein OS=Plasmodium falciparum (isolate 3D7) GN=PFE0655w PE=4 SV=1 | 1 | 0.85 | | |
| tr\|Q8I3X2\|Q8I3X2_PLAF7 Uncharacterized protein OS=Plasmodium falciparum (isolate 3D7) GN=PFE0670w PE=4 SV=1 | 1 | 79.64 | | |
| tr\|Q8I3U1\|Q8I3U1_PLAF7 Ubiquitin carboxyl-terminal hydrolase OS=Plasmodium falciparum (isolate 3D7) GN=PFE0835w PE=3 SV=1 | 1 | 8.47 | | |
| tr\|C0H4F3\|C0H4F3_PLAF7 BIS(5-nucleosyl)-tetraphosphatase (Diadenosine tetraphosphatase), putative OS=Plasmodium falciparum (isolate 3D7) GN=PFE1035c PE=3 SV=1 | 1 | 2.59 | | |
| tr\|Q8I3M2\|Q8I3M2_PLAF7 Uncharacterized protein OS=Plasmodium falciparum (isolate 3D7) GN=PFE1210c PE=4 SV=1 | 1 | 4.84 | | |
| tr\|Q8I3J7\|Q8I3J7_PLAF7 Uncharacterized protein OS=Plasmodium falciparum (isolate 3D7) GN=PFE1335c PE=4 SV=1 | 1 | 1.91 | | |
| tr\|Q8I3H0\|Q8I3H0_PLAF7 Uncharacterized protein OS=Plasmodium falciparum (isolate 3D7) GN=PFE1485w PE=4 SV=1 | 1 | 67.21 | | |
| tr\|Q8I3F6\|Q8I3F6_PLAF7 Mitochondrial ribosomal protein S16, putative OS=Plasmodium falciparum (isolate 3D7) GN=PFE1560c PE=4 SV=1 | 1 | 0.81 | | |
| tr\|C6KSP5\|C6KSP5_PLAF7 Glyoxalase I, putative OS=Plasmodium falciparum (isolate 3D7) GN=PFF0230c PE=4 SV=1 | 1 | 2.50 | | |
| sp\|C6KSQ6\|RAD50_PLAF7 Probable DNA repair protein RAD50 OS=Plasmodium falciparum (isolate 3D7) GN=PFF0285c PE=3 SV=1 | 1 | 2.04 | | |
| tr\|C6KSQ9\|C6KSQ9_PLAF7 RNA binding protein, putative OS=Plasmodium falciparum (isolate 3D7) GN=PFF0300w PE=4 SV=1 | 1 | 4.84 | | |
| tr\|C6KSR7\|C6KSR7_PLAF7 Glutaredoxin-like protein, putative OS=Plasmodium falciparum (isolate 3D7) GN=PFF0340c PE=4 SV=1 | 1 | 28.84 | | |
| tr\|C6KSU9\|C6KSU9_PLAF7 Uncharacterized protein OS=Plasmodium falciparum (isolate 3D7) GN=PFF0505c PE=4 SV=1 | 1 | 1.96 | | |
| tr\|C6KSV2\|C6KSV2_PLAF7 Uncharacterized protein OS=Plasmodium falciparum (isolate 3D7) GN=PFF0525w PE=4 SV=1 | 1 | 4.84 | | |
| tr\|C6KSZ9\|C6KSZ9_PLAF7 Uncharacterized protein OS=Plasmodium falciparum (isolate 3D7) GN=PFF0765c PE=4 SV=1 | 1 | 7.65 | | |
| tr\|C6KT32\|C6KT32_PLAF7 Uncharacterized protein OS=Plasmodium falciparum (isolate 3D7) GN=PFF0930w PE=4 SV=1 | 1 | 0.90 | | |
| tr\|C6KT61\|C6KT61_PLAF7 Uncharacterized protein OS=Plasmodium falciparum (isolate 3D7) GN=PFF1080w PE=4 SV=1 | 1 | 1.03 | | |
| tr\|C6KT75\|C6KT75_PLAF7 Ribonuclease OS=Plasmodium falciparum (isolate 3D7) GN=PFF1150w PE=3 SV=1 | 1 | 4.84 | | |
| tr\|C6KT97\|C6KT97_PLAF7 Oxidoreductase, short-chain dehydrogenase family, putative OS=Plasmodium falciparum (isolate 3D7) GN=PFF1265w PE=4 SV=1 | 1 | 0.05 | | |

| | | | | |
|---|---|---|---|---|
| tr\|C6KTD0\|C6KTD0_PLAF7 Amino acid transporter, putative OS=Plasmodium falciparum (isolate 3D7) GN=PFF1430c PE=4 SV=1 | 1 | 0.82 | | |
| tr\|O97232\|O97232_PLAF7 1-cys-glutaredoxin-like protein-1 OS=Plasmodium falciparum (isolate 3D7) GN=PfGLP-1 PE=4 SV=1 | 1 | 0.75 | | |
| tr\|Q8I3A3\|Q8I3A3_PLAF7 Ubiquitin specific protease, putative OS=Plasmodium falciparum (isolate 3D7) GN=PFI0225w PE=4 SV=1 | 1 | 5.10 | | |
| tr\|Q8I365\|Q8I365_PLAF7 Putative tRNA (cytidine(32)/guanosine(34)-2-O)-methyltransferase OS=Plasmodium falciparum (isolate 3D7) GN=PFI0415c PE=3 SV=1 | 1 | 4.84 | | |
| tr\|Q8I350\|Q8I350_PLAF7 Putative uncharacterized protein OS=Plasmodium falciparum (isolate 3D7) GN=PFI0495w PE=4 SV=1 | 1 | 1.07 | | |
| sp\|C0H537\|TRM5_PLAF7 tRNA (guanine(37)-N1)-methyltransferase OS=Plasmodium falciparum (isolate 3D7) GN=PFI0700c PE=3 SV=1 | 1 | 2.75 | | |
| tr\|C0H539\|C0H539_PLAF7 Putative uncharacterized protein OS=Plasmodium falciparum (isolate 3D7) GN=PFI0805w PE=4 SV=1 | 1 | 5.92 | | |
| tr\|Q8I2Y2\|Q8I2Y2_PLAF7 N-glycosylase/DNA lyase, putative OS=Plasmodium falciparum (isolate 3D7) GN=PFI0835c PE=4 SV=1 | 1 | 0.94 | | |
| tr\|Q8I2V7\|Q8I2V7_PLAF7 Dolichyl-diphosphooligosaccharide--protein glycosyltransferase 48 kDa subunit OS=Plasmodium falciparum (isolate 3D7) GN=PFI0960w PE=3 SV=1 | 1 | 0.84 | | |
| tr\|C0H552\|C0H552_PLAF7 Putative uncharacterized protein OS=Plasmodium falciparum (isolate 3D7) GN=PFI1120c PE=4 SV=1 | 1 | 4.84 | | |
| tr\|Q8I2S2\|Q8I2S2_PLAF7 Putative uncharacterized protein OS=Plasmodium falciparum (isolate 3D7) GN=PFI1150w PE=4 SV=1 | 1 | 4.84 | | |
| tr\|Q8I2N8\|Q8I2N8_PLAF7 Putative uncharacterized protein OS=Plasmodium falciparum (isolate 3D7) GN=PFI1330c PE=4 SV=1 | 1 | 0.11 | | |
| tr\|Q8I0W1\|Q8I0W1_PLAF7 mRNA processing protein, putative OS=Plasmodium falciparum (isolate 3D7) GN=PFI1600w PE=4 SV=1 | 1 | 1.27 | | |
| tr\|Q8I2G6\|Q8I2G6_PLAF7 Cytoadherence-linked protein OS=Plasmodium falciparum (isolate 3D7) GN=PFI1710w PE=4 SV=1 | 1 | 29.92 | | |
| tr\|Q8I630\|Q8I630_PLAF7 XPA binding protein 1, putative OS=Plasmodium falciparum (isolate 3D7) GN=PFL0075w PE=4 SV=1 | 1 | 4.84 | | |
| tr\|Q8I5Y8\|Q8I5Y8_PLAF7 Targeted glyoxalase II OS=Plasmodium falciparum (isolate 3D7) GN=PFL0285w PE=4 SV=1 | 1 | 1.71 | | |
| tr\|Q8I5X7\|Q8I5X7_PLAF7 Uncharacterized protein OS=Plasmodium falciparum (isolate 3D7) GN=PFL0340w PE=4 SV=1 | 1 | 4.84 | | |
| tr\|Q8I5W3\|Q8I5W3_PLAF7 Uncharacterized protein OS=Plasmodium falciparum (isolate 3D7) GN=PFL0425c PE=4 SV=1 | 1 | 1.64 | | |
| tr\|Q8I5V0\|Q8I5V0_PLAF7 ABC transporter, putative OS=Plasmodium falciparum (isolate 3D7) GN=PFL0495c PE=4 SV=1 | 1 | 0.83 | | |
| tr\|Q8I5P4\|Q8I5P4_PLAF7 Signal recognition particle SRP19, putative OS=Plasmodium falciparum (isolate 3D7) GN=PFL0785c PE=4 SV=1 | 1 | 1.76 | | |
| tr\|Q8I5N6\|Q8I5N6_PLAF7 Uncharacterized protein OS=Plasmodium falciparum (isolate 3D7) GN=PFL0830w PE=4 SV=1 | 1 | 1.03 | | |
| tr\|Q8I5K7\|Q8I5K7_PLAF7 Uncharacterized protein OS=Plasmodium falciparum (isolate 3D7) GN=PFL0990w PE=4 SV=1 | 1 | 3.51 | | |
| tr\|Q8I5G0\|Q8I5G0_PLAF7 Uncharacterized protein OS=Plasmodium falciparum (isolate 3D7) GN=PFL1240c PE=4 SV=1 | 1 | 1.30 | | |
| tr\|Q8I577\|Q8I577_PLAF7 Conserved Plasmodium protein OS=Plasmodium falciparum (isolate 3D7) GN=PFL1665c PE=4 SV=1 | 1 | 4.84 | | |
| tr\|Q8I576\|Q8I576_PLAF7 Uncharacterized protein OS=Plasmodium falciparum (isolate 3D7) GN=PFL1670c PE=4 SV=1 | 1 | 1.45 | | |
| tr\|Q8I559\|Q8I559_PLAF7 Conserved Plasmodium protein OS=Plasmodium falciparum (isolate 3D7) GN=PFL1760w PE=4 SV=2 | 1 | 1.43 | | |
| tr\|Q8I523\|Q8I523_PLAF7 3-hydroxyisobutyryl-coenzyme A hydrolase, putative OS=Plasmodium falciparum (isolate 3D7) GN=PFL1940w PE=4 SV=1 | 1 | 0.97 | | |
| tr\|Q8I508\|Q8I508_PLAF7 Conserved Plasmodium protein OS=Plasmodium falciparum (isolate 3D7) GN=PFL2025w PE=4 SV=1 | 1 | 4.84 | | |
| tr\|Q8I4Y3\|Q8I4Y3_PLAF7 Uncharacterized protein OS=Plasmodium falciparum (isolate 3D7) GN=PFL2150c PE=4 SV=1 | 1 | 4.84 | | |
| tr\|Q8I4X3\|Q8I4X3_PLAF7 Conserved Plasmodium protein OS=Plasmodium falciparum (isolate 3D7) GN=PFL2200w PE=4 SV=1 | 1 | 4.84 | | |
| tr\|Q8I4U1\|Q8I4U1_PLAF7 Uncharacterized protein OS=Plasmodium falciparum (isolate 3D7) GN=PFL2365w PE=4 SV=1 | 1 | 1.00 | | |
| tr\|Q8I4T4\|Q8I4T4_PLAF7 rRNA processing protein, putative OS=Plasmodium falciparum (isolate 3D7) GN=PFL2400w PE=4 SV=1 | 1 | 26.66 | | |
| tr\|Q8I3Y0\|Q8I3Y0_PLAF7 Orotate phosphoribosyltransferase OS=Plasmodium falciparum (isolate 3D7) GN=PfOPRT PE=3 SV=1 | 1 | 4.84 | | |

| | | | | |
|---|---|---|---|---|
| tr\|Q8IJR0\|Q8IJR0_PLAF7 Phosphoinositide phospholipase C OS=Plasmodium falciparum (isolate 3D7) GN=PI PLC PE=4 SV=2 | 1 | 4.84 | | |
| tr\|Q8I224\|Q8I224_PLAF7 Plasmoredoxin OS=Plasmodium falciparum (isolate 3D7) GN=Plrx PE=4 SV=1 | 1 | 4.84 | | |
| sp\|Q9H1D9\|RPC6_HUMAN DNA-directed RNA polymerase III subunit RPC6 OS=Homo sapiens GN=POLR3F PE=1 SV=1 | 1 | 1.19 | | |
| tr\|C0H484\|C0H484_PLAF7 RNA triphosphatase OS=Plasmodium falciparum (isolate 3D7) GN=Prt1 PE=4 SV=1 | 1 | 1.46 | | |
| tr\|F5H157\|F5H157_HUMAN Ras-related protein Rab-35 (Fragment) OS=Homo sapiens GN=RAB35 PE=1 SV=1;sp\|Q15286\|RAB35_HUMAN Ras-related protein Rab-35 OS=Homo sapiens GN=RAB35 PE=1 SV=1 | 1 | 1.33 | | |
| tr\|R4GN98\|R4GN98_HUMAN Protein S100 (Fragment) OS=Homo sapiens GN=S100A6 PE=1 SV=1;sp\|P06703\|S10A6_HUMAN Protein S100-A6 OS=Homo sapiens GN=S100A6 PE=1 SV=1 | 1 | 0.76 | | |
| sp\|P06702\|S10A9_HUMAN Protein S100-A9 OS=Homo sapiens GN=S100A9 PE=1 SV=1 | 1 | 1.00 | | |
| tr\|O96164\|O96164_PLAF7 Serine repeat antigen 4 (SERA-4) OS=Plasmodium falciparum (isolate 3D7) GN=SERA-4 PE=1 SV=1;tr\|O96166\|O96166_PLAF7 Serine repeat antigen 2 (SERA-2) OS=Plasmodium falciparum (isolate 3D7) GN=SERA-2 PE=3 SV=3 | 1 | 215.72 | | |
| sp\|Q9Y6M5\|ZNT1_HUMAN Zinc transporter 1 OS=Homo sapiens GN=SLC30A1 PE=1 SV=3 | 1 | 110.75 | | |
| tr\|Q8I098\|Q8I098_PLAF7 Erythrocyte membrane protein 1, PfEMP1 OS=Plasmodium falciparum (isolate 3D7) GN=VAR PE=4 SV=1 | 1 | 0.17 | | |
| sp\|Q5THJ4-2\|VP13D_HUMAN Isoform 2 of Vacuolar protein sorting-associated protein 13D OS=Homo sapiens GN=VPS13D;sp\|Q5THJ4\|VP13D_HUMAN Vacuolar protein sorting-associated protein 13D OS=Homo sapiens GN=VPS13D PE=1 SV=2 | 1 | 5.46 | | |
| tr\|C9JIF9\|C9JIF9_HUMAN Acylamino-acid-releasing enzyme OS=Homo sapiens GN=APEH PE=1 SV=1;sp\|P13798\|ACPH_HUMAN Acylamino-acid-releasing enzyme OS=Homo sapiens GN=APEH PE=1 SV=4;tr\|H7C393\|H7C393_HUMAN Acylamino-acid-releasing enzyme (Fragment) OS=Homo sapien | 1 | 3.16 | | |
| sp\|P04406\|G3P_HUMAN Glyceraldehyde-3-phosphate dehydrogenase OS=Homo sapiens GN=GAPDH PE=1 SV=3;sp\|P04406-2\|G3P_HUMAN Isoform 2 of Glyceraldehyde-3-phosphate dehydrogenase OS=Homo sapiens GN=GAPDH;tr\|E7EUT5\|E7EUT5_HUMAN Glyceraldehyde-3-phosphate dehydroge | 1 | 3.07 | | |
| sp\|Q13228\|SBP1_HUMAN Selenium-binding protein 1 OS=Homo sapiens GN=SELENBP1 PE=1 SV=2;sp\|Q13228-4\|SBP1_HUMAN Isoform 4 of Selenium-binding protein 1 OS=Homo sapiens GN=SELENBP1;sp\|Q13228-2\|SBP1_HUMAN Isoform 2 of Selenium-binding protein 1 OS=Homo sapiens | 1 | 2.78 | | |
| sp\|P00390-5\|GSHR_HUMAN Isoform 4 of Glutathione reductase, mitochondrial OS=Homo sapiens GN=GSR;sp\|P00390-4\|GSHR_HUMAN Isoform 3 of Glutathione reductase, mitochondrial OS=Homo sapiens GN=GSR;sp\|P00390-2\|GSHR_HUMAN Isoform Cytoplasmic of Glutathione reduct | 1 | 2.61 | | |
| tr\|E9PK54\|E9PK54_HUMAN Heat shock cognate 71 kDa protein (Fragment) OS=Homo sapiens GN=HSPA8 PE=1 SV=4;tr\|E9PQQ4\|E9PQQ4_HUMAN Heat shock cognate 71 kDa protein (Fragment) OS=Homo sapiens GN=HSPA8 PE=1 SV=1;tr\|E9PQK7\|E9PQK7_HUMAN Heat shock cognate 71 kDa p | 1 | 1.89 | | |
| sp\|P00915\|CAH1_HUMAN Carbonic anhydrase 1 OS=Homo sapiens GN=CA1 PE=1 SV=2;tr\|E5RH81\|E5RH81_HUMAN Carbonic anhydrase 1 (Fragment) OS=Homo sapiens GN=CA1 PE=1 SV=4;tr\|E5RHP7\|E5RHP7_HUMAN Carbonic anhydrase 1 (Fragment) OS=Homo sapiens GN=CA1 PE=1 SV=1;tr\|E5 | 1 | 1.86 | | |
| sp\|Q8TC07-2\|TBC15_HUMAN Isoform 2 of TBC1 domain family member 15 OS=Homo sapiens GN=TBC1D15;sp\|Q8TC07-3\|TBC15_HUMAN Isoform 3 of TBC1 domain family member 15 OS=Homo sapiens GN=TBC1D15;sp\|Q8TC07\|TBC15_HUMAN TBC1 domain family member 15 OS=Homo sapiens GN= | 1 | 1.61 | | |
| tr\|F5H018\|F5H018_HUMAN GTP-binding nuclear protein Ran (Fragment) OS=Homo sapiens GN=RAN PE=1 SV=4;tr\|B5MDF5\|B5MDF5_HUMAN GTP-binding nuclear protein Ran OS=Homo sapiens GN=RAN PE=1 SV=1;tr\|J3KQE5\|J3KQE5_HUMAN GTP-binding nuclear protein Ran (Fragment) OS= | 1 | 1.27 | | |
| tr\|A0A0A0MQS8\|A0A0A0MQS8_HUMAN Ammonium transporter Rh type A OS=Homo sapiens GN=RHAG PE=1 SV=1;sp\|Q02094\|RHAG_HUMAN Ammonium transporter Rh type A OS=Homo sapiens GN=RHAG PE=1 SV=2;tr\|A0A087WZZ4\|A0A087WZZ4_HUMAN Ammonium transporter Rh type A OS=Homo sapi | 1 | 1.19 | | |
| tr\|Q5JYX0\|Q5JYX0_HUMAN Cell division control protein 42 homolog (Fragment) OS=Homo sapiens GN=CDC42 PE=1 SV=1;sp\|P60953-1\|CDC42_HUMAN Isoform 1 of Cell division control protein 42 homolog OS=Homo sapiens GN=CDC42;sp\|P60953\|CDC42_HUMAN Cell division control | 1 | 1.19 | | |

| | | | | |
|---|---|---|---|---|
| tr\|H7BXK9\|H7BXK9_HUMAN ATP-binding cassette sub-family B member 6, mitochondrial (Fragment) OS=Homo sapiens GN=ABCB6 PE=1 SV=1;sp\|Q9NP58-4\|ABCB6_HUMAN Isoform 2 of ATP-binding cassette sub-family B member 6, mitochondrial OS=Homo sapiens GN=ABCB6;sp\|Q9NP58 | 1 | 1.11 | | |
| sp\|P68133\|ACTS_HUMAN Actin, alpha skeletal muscle OS=Homo sapiens GN=ACTA1 PE=1 SV=1;sp\|P68032\|ACTC_HUMAN Actin, alpha cardiac muscle 1 OS=Homo sapiens GN=ACTC1 PE=1 SV=1;sp\|P63267\|ACTH_HUMAN Actin, gamma-enteric smooth muscle OS=Homo sapiens GN=ACTG2 PE=1 | 1 | 1.09 | | |
| tr\|Q8I6V0\|Q8I6V0_PLAF7 Cysteine proteinase falcipain-1 OS=Plasmodium falciparum (isolate 3D7) GN=PF14_0553 PE=3 SV=1;tr\|H0YE04\|H0YE04_HUMAN Signal peptidase complex subunit 2 (Fragment) OS=Homo sapiens GN=SPCS2 PE=1 SV=1;tr\|A0A087WUC6\|A0A087WUC6_HUMAN Sign | 1 | 1.08 | | |
| tr\|E9PS74\|E9PS74_HUMAN Solute carrier family 43 member 3 (Fragment) OS=Homo sapiens GN=SLC43A3 PE=1 SV=1;sp\|Q8NBI5\|S43A3_HUMAN Solute carrier family 43 member 3 OS=Homo sapiens GN=SLC43A3 PE=1 SV=2;sp\|Q8NBI5-2\|S43A3_HUMAN Isoform 2 of Solute carrier family | 1 | 1.07 | | |
| tr\|Q13030\|Q13030_HUMAN Glycophorin Erik I-IV OS=Homo sapiens GN=GPErik PE=1 SV=1;tr\|E9PH25\|E9PH25_HUMAN Glycophorin-A OS=Homo sapiens GN=GYPA PE=1 SV=1;tr\|E7EQF3\|E7EQF3_HUMAN Glycophorin-A OS=Homo sapiens GN=GYPA PE=1 SV=1;tr\|E9PD10\|E9PD10_HUMAN Glycophori | 1 | 1.07 | | |
| tr\|H0YID2\|H0YID2_HUMAN Adenylate kinase isoenzyme 1 (Fragment) OS=Homo sapiens GN=AK1 PE=1 SV=1;tr\|H0Y4J6\|H0Y4J6_HUMAN Adenylate kinase isoenzyme 1 (Fragment) OS=Homo sapiens GN=AK1 PE=1 SV=1;tr\|Q5T9B7\|Q5T9B7_HUMAN Adenylate kinase isoenzyme 1 OS=Homo sapi | 1 | 1.07 | | |
| sp\|P11166\|GTR1_HUMAN Solute carrier family 2, facilitated glucose transporter member 1 OS=Homo sapiens GN=SLC2A1 PE=1 SV=2;tr\|C9JIM8\|C9JIM8_HUMAN Solute carrier family 2, facilitated glucose transporter member 1 (Fragment) OS=Homo sapiens GN=SLC2A1 PE=1 SV | 1 | 1.05 | | |
| tr\|H0YIW2\|H0YIW2_HUMAN Anaphase-promoting complex subunit 7 (Fragment) OS=Homo sapiens GN=ANAPC7 PE=1 SV=1;sp\|Q9UJX3-2\|APC7_HUMAN Isoform 2 of Anaphase-promoting complex subunit 7 OS=Homo sapiens GN=ANAPC7;sp\|Q9UJX3\|APC7_HUMAN Anaphase-promoting complex su | 1 | 1.03 | | |
| tr\|E7EQ47\|E7EQ47_HUMAN Blood group Rh(CE) polypeptide OS=Homo sapiens GN=RHCE PE=4 SV=1;tr\|F6XSS0\|F6XSS0_HUMAN Blood group Rh(CE) polypeptide OS=Homo sapiens GN=RHCE PE=4 SV=1;sp\|P18577-9\|RHCE_HUMAN Isoform 4g of Blood group Rh(CE) polypeptide OS=Homo sapi | 1 | 1.02 | | |
| tr\|E9PLD0\|E9PLD0_HUMAN Ras-related protein Rab-1B OS=Homo sapiens GN=RAB1B PE=1 SV=1;sp\|Q9H0U4\|RAB1B_HUMAN Ras-related protein Rab-1B OS=Homo sapiens GN=RAB1B PE=1 SV=1;tr\|E7END7\|E7END7_HUMAN Ras-related protein Rab-1A OS=Homo sapiens GN=RAB1A PE=1 SV=1;sp | 1 | 1.02 | | |
| tr\|C0H516\|C0H516_PLAF7 PfRab7, GTPase OS=Plasmodium falciparum (isolate 3D7) GN=Rab7 PE=3 SV=1;tr\|C9IZZ0\|C9IZZ0_HUMAN Ras-related protein Rab-7a (Fragment) OS=Homo sapiens GN=RAB7A PE=1 SV=1;tr\|C9J592\|C9J592_HUMAN Ras-related protein Rab-7a (Fragment) OS=H | 1 | 1.02 | | |
| sp\|P23634-7\|AT2B4_HUMAN Isoform ZB of Plasma membrane calcium-transporting ATPase 4 OS=Homo sapiens GN=ATP2B4;sp\|P23634-6\|AT2B4_HUMAN Isoform XB of Plasma membrane calcium-transporting ATPase 4 OS=Homo sapiens GN=ATP2B4;sp\|P23634-8\|AT2B4_HUMAN Isoform ZD o | 1 | 1.01 | | |
| tr\|A0A087WUV8\|A0A087WUV8_HUMAN Basigin OS=Homo sapiens GN=BSG PE=1 SV=1;tr\|A0A087X2B5\|A0A087X2B5_HUMAN Basigin (Fragment) OS=Homo sapiens GN=BSG PE=1 SV=1;sp\|P35613-3\|BASI_HUMAN Isoform 3 of Basigin OS=Homo sapiens GN=BSG;sp\|P35613-4\|BASI_HUMAN Isoform 4 o | 1 | 1.00 | | |
| sp\|P06753-5\|TPM3_HUMAN Isoform 5 of Tropomyosin alpha-3 chain OS=Homo sapiens GN=TPM3;sp\|P06753-2\|TPM3_HUMAN Isoform 2 of Tropomyosin alpha-3 chain OS=Homo sapiens GN=TPM3;tr\|A0A087WWU8\|A0A087WWU8_HUMAN Tropomyosin alpha-3 chain OS=Homo sapiens GN=TPM3 PE= | 1 | 1.00 | | |
| tr\|D6RAQ8\|D6RAQ8_HUMAN Calnexin (Fragment) OS=Homo sapiens GN=CANX PE=1 SV=1;tr\|D6RAU8\|D6RAU8_HUMAN Calnexin (Fragment) OS=Homo sapiens GN=CANX PE=1 SV=1;tr\|D6RB85\|D6RB85_HUMAN Calnexin (Fragment) OS=Homo sapiens GN=CANX PE=1 SV=1;tr\|D6RDP7\|D6RDP7_HUMAN Ca | 1 | 0.99 | | |
| sp\|P04632\|CPNS1_HUMAN Calpain small subunit 1 OS=Homo sapiens GN=CAPNS1 PE=1 SV=1;tr\|K7EIV0\|K7EIV0_HUMAN Calpain small subunit 1 (Fragment) OS=Homo sapiens GN=CAPNS1 PE=1 SV=2;tr\|A0A075B7C0\|A0A075B7C0_HUMAN Calpain small subunit 1 (Fragment) OS=Homo sapien | 1 | 0.98 | | |
| sp\|O75955\|FLOT1_HUMAN Flotillin-1 OS=Homo sapiens GN=FLOT1 PE=1 SV=3;sp\|O75955-2\|FLOT1_HUMAN Isoform 2 of Flotillin-1 OS=Homo sapiens GN=FLOT1;tr\|A2AB10\|A2AB10_HUMAN Flotillin-1 (Fragment) OS=Homo sapiens GN=FLOT1 PE=1 SV=1;tr\|A2AB12\|A2AB12_HUMAN Flotillin | 1 | 0.98 | | |

| | | | | |
|---|---|---|---|---|
| sp\|P35612\|ADDB_HUMAN Beta-adducin OS=Homo sapiens GN=ADD2 PE=1 SV=3;sp\|P35612-4\|ADDB_HUMAN Isoform 4 of Beta-adducin OS=Homo sapiens GN=ADD2;sp\|P35612-3\|ADDB_HUMAN Isoform 3 of Beta-adducin OS=Homo sapiens GN=ADD2;sp\|P35612-2\|ADDB_HUMAN Isoform 2 of Beta-a | 1 | 0.98 | | |
| sp\|P61224-2\|RAP1B_HUMAN Isoform 2 of Ras-related protein Rap-1b OS=Homo sapiens GN=RAP1B;sp\|P61224-3\|RAP1B_HUMAN Isoform 3 of Ras-related protein Rap-1b OS=Homo sapiens GN=RAP1B;sp\|P62834\|RAP1A_HUMAN Ras-related protein Rap-1A OS=Homo sapiens GN=RAP1A PE=1 | 1 | 0.97 | | |
| sp\|P11171-2\|41_HUMAN Isoform 2 of Protein 4.1 OS=Homo sapiens GN=EPB41;sp\|P11171\|41_HUMAN Protein 4.1 OS=Homo sapiens GN=EPB41 PE=1 SV=4;tr\|Q4VB86\|Q4VB86_HUMAN EPB41 protein OS=Homo sapiens GN=EPB41 PE=1 SV=2;sp\|P11171-4\|41_HUMAN Isoform 4 of Protein 4.1 O | 1 | 0.96 | | |
| sp\|P63261\|ACTG_HUMAN Actin, cytoplasmic 2 OS=Homo sapiens GN=ACTG1 PE=1 SV=1;sp\|P60709\|ACTB_HUMAN Actin, cytoplasmic 1 OS=Homo sapiens GN=ACTB PE=1 SV=1;tr\|I3L3I0\|I3L3I0_HUMAN Actin, cytoplasmic 2 (Fragment) OS=Homo sapiens GN=ACTG1 PE=1 SV=1;tr\|I3L1U9\|I3L | 1 | 0.95 | | |
| tr\|E7ERD7\|E7ERD7_HUMAN Long-chain-fatty-acid--CoA ligase 6 OS=Homo sapiens GN=ACSL6 PE=1 SV=1;sp\|Q9UKU0-7\|ACSL6_HUMAN Isoform 7 of Long-chain-fatty-acid--CoA ligase 6 OS=Homo sapiens GN=ACSL6;sp\|Q9UKU0-5\|ACSL6_HUMAN Isoform 5 of Long-chain-fatty-acid--CoA | 1 | 0.95 | | |
| sp\|P16452-3\|EPB42_HUMAN Isoform 3 of Erythrocyte membrane protein band 4.2 OS=Homo sapiens GN=EPB42;sp\|P16452\|EPB42_HUMAN Erythrocyte membrane protein band 4.2 OS=Homo sapiens GN=EPB42 PE=1 SV=3;sp\|P16452-2\|EPB42_HUMAN Isoform Long of Erythrocyte membrane | 1 | 0.94 | | |
| tr\|E7EV99\|E7EV99_HUMAN Alpha-adducin OS=Homo sapiens GN=ADD1 PE=1 SV=1;tr\|E7ENY0\|E7ENY0_HUMAN Alpha-adducin OS=Homo sapiens GN=ADD1 PE=1 SV=1;sp\|P35611-2\|ADDA_HUMAN Isoform 2 of Alpha-adducin OS=Homo sapiens GN=ADD1;sp\|P35611-6\|ADDA_HUMAN Isoform 6 of Alph | 1 | 0.94 | | |
| sp\|P00387-2\|NB5R3_HUMAN Isoform 2 of NADH-cytochrome b5 reductase 3 OS=Homo sapiens GN=CYB5R3;sp\|P00387\|NB5R3_HUMAN NADH-cytochrome b5 reductase 3 OS=Homo sapiens GN=CYB5R3 PE=1 SV=3;sp\|P00387-3\|NB5R3_HUMAN Isoform 3 of NADH-cytochrome b5 reductase 3 OS=Ho | 1 | 0.94 | | |
| tr\|Q8I5A9\|Q8I5A9_PLAF7 Rab2, GTPase OS=Plasmodium falciparum (isolate 3D7) GN=Rab2 PE=3 SV=1;tr\|E9PKL7\|E9PKL7_HUMAN Ras-related protein Rab-2A OS=Homo sapiens GN=RAB2A PE=1 SV=1;tr\|Q5HYI5\|Q5HYI5_HUMAN Putative uncharacterized protein DKFZp313C1541 OS=Homo | 1 | 0.93 | | |
| tr\|F8VWZ8\|F8VWZ8_HUMAN Rho GTPase-activating protein 29 OS=Homo sapiens GN=ARHGAP29 PE=1 SV=1;sp\|Q52LW3-2\|RHG29_HUMAN Isoform 2 of Rho GTPase-activating protein 29 OS=Homo sapiens GN=ARHGAP29;sp\|Q52LW3\|RHG29_HUMAN Rho GTPase-activating protein 29 OS=Homo s | 1 | 0.92 | | |
| sp\|P11277\|SPTB1_HUMAN Spectrin beta chain, erythrocytic OS=Homo sapiens GN=SPTB PE=1 SV=5;sp\|P11277-2\|SPTB1_HUMAN Isoform 2 of Spectrin beta chain, erythrocytic OS=Homo sapiens GN=SPTB;sp\|P11277-3\|SPTB1_HUMAN Isoform 3 of Spectrin beta chain, erythrocytic | 1 | 0.91 | | |
| tr\|Q5JR07\|Q5JR07_HUMAN Rho-related GTP-binding protein RhoC (Fragment) OS=Homo sapiens GN=RHOC PE=1 SV=1;tr\|C9JNR4\|C9JNR4_HUMAN Transforming protein RhoA (Fragment) OS=Homo sapiens GN=RHOA PE=1 SV=1;tr\|E9PQH6\|E9PQH6_HUMAN Rho-related GTP-binding protein Rh | 1 | 0.91 | | |
| sp\|P16157-10\|ANK1_HUMAN Isoform Er9 of Ankyrin-1 OS=Homo sapiens GN=ANK1;sp\|P16157-8\|ANK1_HUMAN Isoform Er7 of Ankyrin-1 OS=Homo sapiens GN=ANK1;sp\|P16157-5\|ANK1_HUMAN Isoform Er3 of Ankyrin-1 OS=Homo sapiens GN=ANK1;sp\|P16157-16\|ANK1_HUMAN Isoform Er15 of | 1 | 0.90 | | |
| tr\|F5H081\|F5H081_HUMAN Solute carrier family 2, facilitated glucose transporter member 4 OS=Homo sapiens GN=SLC2A4 PE=1 SV=1;tr\|I3L2R4\|I3L2R4_HUMAN Solute carrier family 2 (Facilitated glucose transporter), member 4, isoform CRA_b OS=Homo sapiens GN=SLC2A4 | 1 | 0.90 | | |
| sp\|Q00013\|EM55_HUMAN 55 kDa erythrocyte membrane protein OS=Homo sapiens GN=MPP1 PE=1 SV=2;sp\|Q00013-3\|EM55_HUMAN Isoform 3 of 55 kDa erythrocyte membrane protein OS=Homo sapiens GN=MPP1;sp\|Q00013-2\|EM55_HUMAN Isoform 2 of 55 kDa erythrocyte membrane prote | 1 | 0.89 | | |
| sp\|P02549\|SPTA1_HUMAN Spectrin alpha chain, erythrocytic 1 OS=Homo sapiens GN=SPTA1 PE=1 SV=5;sp\|P02549-2\|SPTA1_HUMAN Isoform 2 of Spectrin alpha chain, erythrocytic 1 OS=Homo sapiens GN=SPTA1;tr\|A0A087WZE4\|A0A087WZE4_HUMAN Spectrin alpha chain, erythrocyt | 1 | 0.89 | | |

| | | | | |
|---|---|---|---|---|
| sp\|P48729\|KC1A_HUMAN Casein kinase I isoform alpha OS=Homo sapiens GN=CSNK1A1 PE=1 SV=2;sp\|P48729-3\|KC1A_HUMAN Isoform 3 of Casein kinase I isoform alpha OS=Homo sapiens GN=CSNK1A1;sp\|P48729-2\|KC1A_HUMAN Isoform 2 of Casein kinase I isoform alpha OS=Homo s | 1 | 0.88 | | |
| tr\|H0YH81\|H0YH81_HUMAN ATP synthase subunit beta (Fragment) OS=Homo sapiens GN=ATP5B PE=1 SV=1;sp\|P06576\|ATPB_HUMAN ATP synthase subunit beta, mitochondrial OS=Homo sapiens GN=ATP5B PE=1 SV=3;tr\|F8W079\|F8W079_HUMAN ATP synthase subunit beta, mitochondrial | 1 | 0.87 | | |
| sp\|Q08495-2\|DEMA_HUMAN Isoform 2 of Dematin OS=Homo sapiens GN=DMTN;sp\|Q08495\|DEMA_HUMAN Dematin OS=Homo sapiens GN=DMTN PE=1 SV=3;sp\|Q08495-3\|DEMA_HUMAN Isoform 3 of Dematin OS=Homo sapiens GN=DMTN;sp\|Q08495-4\|DEMA_HUMAN Isoform 4 of Dematin OS=Homo sapie | 1 | 0.86 | | |
| tr\|J3QQY2\|J3QQY2_HUMAN Transmembrane and coiled-coil domain-containing protein 1 OS=Homo sapiens GN=TMCO1 PE=1 SV=1;tr\|J3KS45\|J3KS45_HUMAN Transmembrane and coiled-coil domain-containing protein 1 (Fragment) OS=Homo sapiens GN=TMCO1 PE=1 SV=1;tr\|J9JIE6\|J9J | 1 | 0.85 | | |
| sp\|Q08722-2\|CD47_HUMAN Isoform OA3-293 of Leukocyte surface antigen CD47 OS=Homo sapiens GN=CD47;sp\|Q08722-3\|CD47_HUMAN Isoform OA3-305 of Leukocyte surface antigen CD47 OS=Homo sapiens GN=CD47;sp\|Q08722-4\|CD47_HUMAN Isoform OA3-312 of Leukocyte surface an | 1 | 0.85 | | |
| sp\|O60885\|BRD4_HUMAN Bromodomain-containing protein 4 OS=Homo sapiens GN=BRD4 PE=1 SV=2;tr\|M0R0H4\|M0R0H4_HUMAN Bromodomain-containing protein 4 (Fragment) OS=Homo sapiens GN=BRD4 PE=1 SV=1;tr\|M0QYW0\|M0QYW0_HUMAN Bromodomain containing 4, isoform CRA_c OS=H | 1 | 0.85 | | |
| tr\|K7N7A8\|K7N7A8_HUMAN Uncharacterized protein (Fragment) OS=Homo sapiens PE=3 SV=2;sp\|P29972-4\|AQP1_HUMAN Isoform 4 of Aquaporin-1 OS=Homo sapiens GN=AQP1;sp\|P29972-2\|AQP1_HUMAN Isoform 2 of Aquaporin-1 OS=Homo sapiens GN=AQP1;sp\|P29972-3\|AQP1_HUMAN Isofo | 1 | 0.84 | | |
| sp\|P11142\|HSP7C_HUMAN Heat shock cognate 71 kDa protein OS=Homo sapiens GN=HSPA8 PE=1 SV=1;tr\|E9PKE3\|E9PKE3_HUMAN Heat shock cognate 71 kDa protein OS=Homo sapiens GN=HSPA8 PE=1 SV=1;sp\|P11142-2\|HSP7C_HUMAN Isoform 2 of Heat shock cognate 71 kDa protein OS | 1 | 0.84 | | |
| tr\|K7EM13\|K7EM13_HUMAN cAMP-dependent protein kinase type I-alpha regulatory subunit (Fragment) OS=Homo sapiens GN=PRKAR1A PE=1 SV=1;tr\|K7EPB2\|K7EPB2_HUMAN cAMP-dependent protein kinase type I-alpha regulatory subunit (Fragment) OS=Homo sapiens GN=PRKAR1A | 1 | 0.82 | | |
| tr\|F8WCJ1\|F8WCJ1_HUMAN Eukaryotic translation initiation factor 5A OS=Homo sapiens GN=EIF5A2 PE=1 SV=1;tr\|C9J7B5\|C9J7B5_HUMAN Eukaryotic translation initiation factor 5A OS=Homo sapiens GN=EIF5A2 PE=1 SV=1;tr\|C9J4W5\|C9J4W5_HUMAN Eukaryotic translation init | 1 | 0.81 | | |
| sp\|Q9H9G7-2\|AGO3_HUMAN Isoform 2 of Protein argonaute-3 OS=Homo sapiens GN=AGO3;sp\|Q9UKV8-2\|AGO2_HUMAN Isoform 2 of Protein argonaute-2 OS=Homo sapiens GN=AGO2;sp\|Q9UKV8\|AGO2_HUMAN Protein argonaute-2 OS=Homo sapiens GN=AGO2 PE=1 SV=3;sp\|Q9H9G7\|AGO3_HUMAN | 1 | 0.81 | | |
| sp\|P08107\|HSP71_HUMAN Heat shock 70 kDa protein 1A/1B OS=Homo sapiens GN=HSPA1A PE=1 SV=5;sp\|P08107-2\|HSP71_HUMAN Isoform 2 of Heat shock 70 kDa protein 1A/1B OS=Homo sapiens GN=HSPA1A;tr\|V9GZ37\|V9GZ37_HUMAN Heat shock 70 kDa protein 1A/1B OS=Homo sapiens | 1 | 0.79 | | |
| tr\|J3QS39\|J3QS39_HUMAN Polyubiquitin-B (Fragment) OS=Homo sapiens GN=UBB PE=1 SV=1;tr\|J3QTR3\|J3QTR3_HUMAN Ubiquitin-40S ribosomal protein S27a (Fragment) OS=Homo sapiens GN=RPS27A PE=1 SV=1;tr\|F5H6Q2\|F5H6Q2_HUMAN Polyubiquitin-C (Fragment) OS=Homo sapiens | 1 | 0.78 | | |
| tr\|C9JEN3\|C9JEN3_HUMAN Protein lifeguard 3 (Fragment) OS=Homo sapiens GN=TMBIM1 PE=1 SV=1;tr\|C9IYT2\|C9IYT2_HUMAN Protein lifeguard 3 (Fragment) OS=Homo sapiens GN=TMBIM1 PE=1 SV=1;tr\|F8WDY4\|F8WDY4_HUMAN Protein lifeguard 3 OS=Homo sapiens GN=TMBIM1 PE=1 SV | 1 | 0.78 | | |
| sp\|O75340\|PDCD6_HUMAN Programmed cell death protein 6 OS=Homo sapiens GN=PDCD6 PE=1 SV=1;tr\|A0A024QZ42\|A0A024QZ42_HUMAN HCG1985580, isoform CRA_c OS=Homo sapiens GN=PDCD6 PE=1 SV=1;sp\|O75340-2\|PDCD6_HUMAN Isoform 2 of Programmed cell death protein 6 OS=Hom | 1 | 0.77 | | |
| sp\|O15439-2\|MRP4_HUMAN Isoform 2 of Multidrug resistance-associated protein 4 OS=Homo sapiens GN=ABCC4;sp\|O15439\|MRP4_HUMAN Multidrug resistance-associated protein 4 OS=Homo sapiens GN=ABCC4 PE=1 SV=3;sp\|O15439-4\|MRP4_HUMAN Isoform 4 of Multidrug resistanc | 1 | 0.76 | | |

| | | | | |
|---|---|---|---|---|
| sp\|P48426-2\|PI42A_HUMAN Isoform 2 of Phosphatidylinositol 5-phosphate 4-kinase type-2 alpha OS=Homo sapiens GN=PIP4K2A;sp\|P48426\|PI42A_HUMAN Phosphatidylinositol 5-phosphate 4-kinase type-2 alpha OS=Homo sapiens GN=PIP4K2A PE=1 SV=2;tr\|H7BXS3\|H7BXS3_HUMAN | 1 | 0.73 | | |
| tr\|D6R9P3\|D6R9P3_HUMAN Heterogeneous nuclear ribonucleoprotein A/B OS=Homo sapiens GN=HNRNPAB PE=1 SV=1;tr\|D6RD18\|D6RD18_HUMAN Heterogeneous nuclear ribonucleoprotein A/B OS=Homo sapiens GN=HNRNPAB PE=1 SV=1;tr\|D6RBZ0\|D6RBZ0_HUMAN Heterogeneous nuclear rib | 1 | 0.69 | | |
| tr\|D6RF44\|D6RF44_HUMAN Heterogeneous nuclear ribonucleoprotein D0 (Fragment) OS=Homo sapiens GN=HNRNPD PE=1 SV=4;tr\|D6RBQ9\|D6RBQ9_HUMAN Heterogeneous nuclear ribonucleoprotein D0 (Fragment) OS=Homo sapiens GN=HNRNPD PE=1 SV=1;tr\|H0YA96\|H0YA96_HUMAN Heterog | 1 | 0.66 | | |
| tr\|H0Y524\|H0Y524_HUMAN Copine-1 (Fragment) OS=Homo sapiens GN=CPNE1 PE=1 SV=1;tr\|Q5JX45\|Q5JX45_HUMAN Copine-1 (Fragment) OS=Homo sapiens GN=CPNE1 PE=1 SV=1;tr\|E7ENH5\|E7ENH5_HUMAN Copine-1 OS=Homo sapiens GN=CPNE1 PE=1 SV=1;tr\|A6PVH9\|A6PVH9_HUMAN Copine-1 O | 1 | 0.65 | | |
| sp\|Q9GZT8-2\|GTPC1_HUMAN Isoform 2 of Putative GTP cyclohydrolase 1 type 2 NIF3L1 OS=Homo sapiens GN=NIF3L1;sp\|Q9GZT8\|GTPC1_HUMAN Putative GTP cyclohydrolase 1 type 2 NIF3L1 OS=Homo sapiens GN=NIF3L1 PE=1 SV=2;tr\|C9JN42\|C9JN42_HUMAN Putative GTP cyclohydrol | 1 | 4.84 | | |
| tr\|H3BQW8\|H3BQW8_HUMAN Hydroxyacylglutathione hydrolase, mitochondrial (Fragment) OS=Homo sapiens GN=HAGH PE=1 SV=1;tr\|H3BPK3\|H3BPK3_HUMAN Hydroxyacylglutathione hydrolase, mitochondrial (Fragment) OS=Homo sapiens GN=HAGH PE=1 SV=1;tr\|H3BPQ4\|H3BPQ4_HUMAN H | 1 | 4.84 | | |
| tr\|E7EMZ9\|E7EMZ9_HUMAN Transforming acidic coiled-coil-containing protein 2 OS=Homo sapiens GN=TACC2 PE=1 SV=1;tr\|E9PBC6\|E9PBC6_HUMAN Transforming acidic coiled-coil-containing protein 2 OS=Homo sapiens GN=TACC2 PE=1 SV=1;sp\|O95359-3\|TACC2_HUMAN Isoform 3 | 1 | 4.84 | | |
| tr\|I3L4M2\|I3L4M2_HUMAN Protein disulfide-isomerase (Fragment) OS=Homo sapiens GN=P4HB PE=1 SV=1;tr\|I3L398\|I3L398_HUMAN Protein disulfide-isomerase (Fragment) OS=Homo sapiens GN=P4HB PE=1 SV=1;tr\|I3L312\|I3L312_HUMAN Protein disulfide-isomerase (Fragment) OS | 1 | 9.79 | | |
| tr\|E2QRB9\|E2QRB9_HUMAN Thioredoxin reductase 1, cytoplasmic OS=Homo sapiens GN=TXNRD1 PE=1 SV=2;tr\|E9PIR7\|E9PIR7_HUMAN Thioredoxin reductase 1, cytoplasmic OS=Homo sapiens GN=TXNRD1 PE=1 SV=1;tr\|F8W809\|F8W809_HUMAN Thioredoxin reductase 1, cytoplasmic OS=H | 1 | 36.93 | | |
| tr\|F8WAR7\|F8WAR7_HUMAN Acetylcholinesterase OS=Homo sapiens GN=ACHE PE=1 SV=1;tr\|C9J2S3\|C9J2S3_HUMAN Acetylcholinesterase (Fragment) OS=Homo sapiens GN=ACHE PE=1 SV=4;tr\|F8WD68\|F8WD68_HUMAN Acetylcholinesterase OS=Homo sapiens GN=ACHE PE=1 SV=1;tr\|C9JZL6\|C | 1 | 100.54 | | |
| tr\|E9PQN4\|E9PQN4_HUMAN Complement receptor type 1 OS=Homo sapiens GN=CR1 PE=1 SV=2;tr\|Q5SR44\|Q5SR44_HUMAN Complement receptor type 1 OS=Homo sapiens GN=CR1 PE=1 SV=1;tr\|E9PDY4\|E9PDY4_HUMAN Complement receptor type 1 OS=Homo sapiens GN=CR1 PE=1 SV=1;sp\|P179 | 1 | 237.37 | | |
| tr\|Q8I3J4\|Q8I3J4_PLAF7 Ubiquitin conjugating enzyme, putative OS=Plasmodium falciparum (isolate 3D7) GN=PFE1350c PE=1 SV=1;tr\|F8VQQ8\|F8VQQ8_HUMAN Ubiquitin-conjugating enzyme E2 N OS=Homo sapiens GN=UBE2N PE=1 SV=1;sp\|P61088\|UBE2N_HUMAN Ubiquitin-conjugati | 1 | 548.97 | | |
| tr\|H0YDK0\|H0YDK0_HUMAN Centrosomal protein of 295 kDa (Fragment) OS=Homo sapiens GN=CEP295 PE=1 SV=1;sp\|Q9C0D2\|CE295_HUMAN Centrosomal protein of 295 kDa OS=Homo sapiens GN=CEP295 PE=2 SV=4;sp\|Q9C0D2-3\|CE295_HUMAN Isoform 3 of Centrosomal protein of 295 kD | 1 | 1.98 | | |
| tr\|A0A087X0E3\|A0A087X0E3_HUMAN Helicase SRCAP (Fragment) OS=Homo sapiens GN=SRCAP PE=1 SV=1;tr\|A0A0A0MS59\|A0A0A0MS59_HUMAN Helicase SRCAP OS=Homo sapiens GN=SRCAP PE=1 SV=1;sp\|Q6ZRS2-3\|SRCAP_HUMAN Isoform 3 of Helicase SRCAP OS=Homo sapiens GN=SRCAP;sp\|Q6Z | 1 | 9.57 | | |
| tr\|F8W150\|F8W150_HUMAN Ankyrin repeat domain-containing protein 13A (Fragment) OS=Homo sapiens GN=ANKRD13A PE=1 SV=1;tr\|S4R3U2\|S4R3U2_HUMAN Ankyrin repeat domain-containing protein 13A (Fragment) OS=Homo sapiens GN=ANKRD13A PE=1 SV=1;tr\|H0YIN8\|H0YIN8_HUMAN | 1 | 0.70 | | |
| tr\|F5H1T6\|F5H1T6_HUMAN V-type proton ATPase subunit a OS=Homo sapiens GN=ATP6V0A1 PE=1 SV=1;tr\|B7Z641\|B7Z641_HUMAN V-type proton ATPase subunit a OS=Homo sapiens GN=ATP6V0A1 PE=1 SV=1;tr\|B7Z2A9\|B7Z2A9_HUMAN V-type proton ATPase subunit a OS=Homo sapiens GN | 1 | 1.27 | | |

| | | | | |
|---|---|---|---|---|
| tr\|F5H6X6\|F5H6X6_HUMAN Neutral alpha-glucosidase AB OS=Homo sapiens GN=GANAB PE=1 SV=1;tr\|E9PKU7\|E9PKU7_HUMAN Neutral alpha-glucosidase AB OS=Homo sapiens GN=GANAB PE=1 SV=1;sp\|Q14697\|GANAB_HUMAN Neutral alpha-glucosidase AB OS=Homo sapiens GN=GANAB PE=1 S | 1 | 0.95 | | |
| tr\|M0R2K2\|M0R2K2_HUMAN Neuropathy target esterase (Fragment) OS=Homo sapiens GN=PNPLA6 PE=1 SV=1;tr\|M0QYT1\|M0QYT1_HUMAN Neuropathy target esterase (Fragment) OS=Homo sapiens GN=PNPLA6 PE=1 SV=1;tr\|M0R2C2\|M0R2C2_HUMAN Neuropathy target esterase (Fragment) O | 1 | 1.23 | | |
| tr\|H0YDX6\|H0YDX6_HUMAN CD44 antigen (Fragment) OS=Homo sapiens GN=CD44 PE=1 SV=1;tr\|H0YD13\|H0YD13_HUMAN CD44 antigen OS=Homo sapiens GN=CD44 PE=1 SV=2;tr\|H0YD17\|H0YD17_HUMAN CD44 antigen (Fragment) OS=Homo sapiens GN=CD44 PE=1 SV=4;tr\|H0YDW7\|H0YDW7_HUMAN C | 1 | 0.65 | | |
| sp\|Q9UQ80-2\|PA2G4_HUMAN Isoform 2 of Proliferation-associated protein 2G4 OS=Homo sapiens GN=PA2G4;sp\|Q9UQ80\|PA2G4_HUMAN Proliferation-associated protein 2G4 OS=Homo sapiens GN=PA2G4 PE=1 SV=3;tr\|F8W0A3\|F8W0A3_HUMAN Proliferation-associated protein 2G4 (Fr | 1 | 0.03 | | |
| sp\|Q9NR96-3\|TLR9_HUMAN Isoform 3 of Toll-like receptor 9 OS=Homo sapiens GN=TLR9;tr\|H0Y858\|H0Y858_HUMAN Uncharacterized protein (Fragment) OS=Homo sapiens PE=4 SV=1;sp\|Q9NR96-2\|TLR9_HUMAN Isoform 2 of Toll-like receptor 9 OS=Homo sapiens GN=TLR9;sp\|Q9NR96- | 1 | 0.63 | | |
| tr\|F8WDN7\|F8WDN7_HUMAN Phosphatidylinositide phosphatase SAC1 OS=Homo sapiens GN=SACM1L PE=1 SV=1;tr\|E9PGZ4\|E9PGZ4_HUMAN Phosphatidylinositide phosphatase SAC1 OS=Homo sapiens GN=SACM1L PE=1 SV=1;sp\|Q9NTJ5-2\|SAC1_HUMAN Isoform 2 of Phosphatidylinositide ph | 1 | 0.65 | | |
| tr\|U3KQJ8\|U3KQJ8_HUMAN Dynein heavy chain 11, axonemal OS=Homo sapiens GN=DNAH11 PE=4 SV=1;tr\|A0A087WYC6\|A0A087WYC6_HUMAN Dynein heavy chain 11, axonemal OS=Homo sapiens GN=DNAH11 PE=4 SV=1;sp\|Q96DT5\|DYH11_HUMAN Dynein heavy chain 11, axonemal OS=Homo sapi | 1 | 1.03 | | |

| **DHA** | | | | |
|---|---|---|---|---|
| **Fasta headers** | **N** | **Mean** | **SD** | **P-value** |
| tr\|Q8I573\|Q8I573_PLAF7 Uncharacterized protein OS=Plasmodium falciparum (isolate 3D7) GN=PFL1685w PE=4 SV=1 | 8 | 0.27 | 0.17 | 0.0032 |
| tr\|Q8IDX8\|Q8IDX8_PLAF7 Merozoite Surface Protein 7, MSP7 OS=Plasmodium falciparum (isolate 3D7) GN=MSP7 PE=4 SV=1 | 8 | 0.29 | 0.29 | 0.0245 |
| tr\|Q8IBT7\|Q8IBT7_PLAF7 Uncharacterized protein OS=Plasmodium falciparum (isolate 3D7) GN=MAL7P1.77 PE=4 SV=1 | 8 | 0.31 | 0.12 | 0.0002 |
| sp\|Q9TY95\|SERA_PLAF7 Serine-repeat antigen protein OS=Plasmodium falciparum (isolate 3D7) GN=SERA PE=1 SV=1 | 8 | 0.31 | 0.19 | 0.0026 |
| tr\|Q8I0U8\|Q8I0U8_PLAF7 Merozoite surface protein 1 OS=Plasmodium falciparum (isolate 3D7) GN=MSP1 PE=4 SV=1 | 8 | 0.37 | 0.14 | 0.0001 |
| sp\|P20073-2\|ANXA7_HUMAN Isoform 2 of Annexin A7 OS=Homo sapiens GN=ANXA7;sp\|P20073\|ANXA7_HUMAN Annexin A7 OS=Homo sapiens GN=ANXA7 PE=1 SV=3 | 8 | 0.42 | 0.18 | 0.0003 |
| tr\|Q8I298\|Q8I298_PLAF7 Putative uncharacterized protein OS=Plasmodium falciparum (isolate 3D7) GN=PFA_0210c PE=4 SV=1 | 8 | 0.42 | 0.19 | 0.0005 |
| tr\|C6KSR6\|C6KSR6_PLAF7 Uncharacterized protein OS=Plasmodium falciparum (isolate 3D7) GN=PFF0335c PE=4 SV=1 | 8 | 0.42 | 0.18 | 0.0003 |
| sp\|Q8ID66\|PF92_PLAF7 Merozoite surface protein P92 OS=Plasmodium falciparum (isolate 3D7) GN=PF92 PE=1 SV=1 | 8 | 0.42 | 0.23 | 0.0013 |
| tr\|Q8I526\|Q8I526_PLAF7 Cell division protein FtsH, putative OS=Plasmodium falciparum (isolate 3D7) GN=PFL1925w PE=3 SV=1 | 8 | 0.44 | 0.17 | 0.0002 |
| tr\|O77361\|O77361_PLAF7 Putative uncharacterized protein OS=Plasmodium falciparum (isolate 3D7) GN=PFC0435w PE=4 SV=1 | 8 | 0.46 | 0.37 | 0.0102 |
| tr\|Q8II41\|Q8II41_PLAF7 Conserved Plasmodium membrane protein OS=Plasmodium falciparum (isolate 3D7) GN=PF11_0333 PE=4 SV=2 | 8 | 0.48 | 0.26 | 0.0011 |
| tr\|Q8I0W9\|Q8I0W9_PLAF7 Stearoyl-CoA Delta 9 desaturase, putative OS=Plasmodium falciparum (isolate 3D7) GN=PFE0555w PE=3 SV=1 | 8 | 0.50 | 0.28 | 0.0013 |
| tr\|Q8IE14\|Q8IE14_PLAF7 Signal peptidase I OS=Plasmodium falciparum (isolate 3D7) GN=SP21 PE=4 SV=1 | 8 | 0.50 | 0.46 | 0.0167 |
| tr\|Q8IBL4\|Q8IBL4_PLAF7 Uncharacterized protein OS=Plasmodium falciparum (isolate 3D7) GN=MAL7P1.126 PE=4 SV=1 | 8 | 0.51 | 0.28 | 0.0014 |
| tr\|Q8I5Q2\|Q8I5Q2_PLAF7 Uncharacterized protein OS=Plasmodium falciparum (isolate 3D7) GN=PFL0745c PE=4 SV=1 | 8 | 0.52 | 0.30 | 0.0018 |
| tr\|Q8IBP0\|Q8IBP0_PLAF7 Uncharacterized protein OS=Plasmodium falciparum (isolate 3D7) GN=PF07_0087 PE=4 SV=1 | 8 | 0.53 | 0.12 | 0.0000 |

| | | | | |
|---|---|---|---|---|
| tr\|Q8IBU1\|Q8IBU1_PLAF7 Zinc transporter, putative OS=Plasmodium falciparum (isolate 3D7) GN=PF07_0065 PE=4 SV=1 | 8 | 0.54 | 0.33 | 0.0025 |
| tr\|Q8I291\|Q8I291_PLAF7 Transporter, putative OS=Plasmodium falciparum (isolate 3D7) GN=PFA_0245w PE=4 SV=1 | 8 | 0.54 | 0.20 | 0.0001 |
| tr\|C6KSY4\|C6KSY4_PLAF7 Organic anion transporter OS=Plasmodium falciparum (isolate 3D7) GN=PFF0690c PE=4 SV=1 | 8 | 0.54 | 0.23 | 0.0003 |
| tr\|Q8IAL4\|Q8IAL4_PLAF7 Uncharacterized protein OS=Plasmodium falciparum (isolate 3D7) GN=PF08_0134 PE=4 SV=1 | 8 | 0.55 | 0.23 | 0.0003 |
| tr\|O96252\|O96252_PLAF7 ATP synthase subunit alpha OS=Plasmodium falciparum (isolate 3D7) GN=PFB0795w PE=3 SV=1 | 8 | 0.55 | 0.20 | 0.0001 |
| tr\|O97269\|O97269_PLAF7 Putative uncharacterized protein OS=Plasmodium falciparum (isolate 3D7) GN=PFC0670c PE=4 SV=1 | 8 | 0.56 | 0.48 | 0.0136 |
| tr\|Q8IEJ6\|Q8IEJ6_PLAF7 Branched-chain alpha keto-acid dehydrogenase, putative OS=Plasmodium falciparum (isolate 3D7) GN=PF13_0070 PE=4 SV=1 | 8 | 0.58 | 0.34 | 0.0017 |
| tr\|Q8I531\|Q8I531_PLAF7 Transcription factor with AP2 domain(S), putative OS=Plasmodium falciparum (isolate 3D7) GN=ApiAP2 PE=4 SV=1 | 8 | 0.59 | 0.23 | 0.0002 |
| tr\|Q8I3A2\|Q8I3A2_PLAF7 Bacterial histone-like protein OS=Plasmodium falciparum (isolate 3D7) GN=PfHU PE=4 SV=1 | 8 | 0.59 | 0.22 | 0.0001 |
| tr\|Q8I611\|Q8I611_PLAF7 Uncharacterized protein OS=Plasmodium falciparum (isolate 3D7) GN=PFL0170w PE=4 SV=1 | 8 | 0.60 | 0.18 | 0.0000 |
| tr\|Q8ILY8\|Q8ILY8_PLAF7 Uncharacterized protein OS=Plasmodium falciparum (isolate 3D7) GN=PF14_0105 PE=4 SV=1 | 8 | 0.60 | 0.27 | 0.0004 |
| tr\|Q8IE43\|Q8IE43_PLAF7 Uncharacterized protein OS=Plasmodium falciparum (isolate 3D7) GN=PF13_0154 PE=4 SV=1 | 8 | 0.61 | 0.18 | 0.0000 |
| tr\|Q8IEQ3\|Q8IEQ3_PLAF7 Hydrolase, putative OS=Plasmodium falciparum (isolate 3D7) GN=PF13_0032 PE=4 SV=1 | 8 | 0.61 | 0.25 | 0.0002 |
| tr\|Q8IET3\|Q8IET3_PLAF7 SNARE protein, putative OS=Plasmodium falciparum (isolate 3D7) GN=PfVAMP8 PE=4 SV=1 | 8 | 0.62 | 0.21 | 0.0001 |
| tr\|Q8IKV8\|Q8IKV8_PLAF7 Sortilin, putative OS=Plasmodium falciparum (isolate 3D7) GN=PF14_0493 PE=4 SV=1 | 8 | 0.62 | 0.17 | 0.0000 |
| tr\|Q8I202\|Q8I202_PLAF7 Uncharacterized protein OS=Plasmodium falciparum (isolate 3D7) GN=PFD0115c PE=4 SV=1 | 8 | 0.62 | 0.39 | 0.0030 |
| tr\|O77388\|O77388_PLAF7 HVA22/TB2/DP1 family protein, putative OS=Plasmodium falciparum (isolate 3D7) GN=PFC0730w PE=4 SV=1 | 8 | 0.62 | 0.10 | 0.0000 |
| tr\|Q8IIV2\|Q8IIV2_PLAF7 Histone H4 OS=Plasmodium falciparum (isolate 3D7) GN=PF11_0061 PE=3 SV=1 | 8 | 0.62 | 0.08 | 0.0000 |
| tr\|Q8ILN5\|Q8ILN5_PLAF7 Mitochondrial protein import protein TIM13, putative OS=Plasmodium falciparum (isolate 3D7) GN=PF14_0208 PE=4 SV=1 | 8 | 0.62 | 0.27 | 0.0003 |
| tr\|Q8IL75\|Q8IL75_PLAF7 Ubiquinol-cytochrome C reductase iron-sulfur subunit, putative OS=Plasmodium falciparum (isolate 3D7) GN=PF14_0373 PE=4 SV=1 | 8 | 0.63 | 0.18 | 0.0000 |
| tr\|Q8I2A1\|Q8I2A1_PLAF7 Putative uncharacterized protein OS=Plasmodium falciparum (isolate 3D7) GN=PFA_0195w PE=4 SV=1 | 8 | 0.63 | 0.24 | 0.0002 |
| tr\|Q8I415\|Q8I415_PLAF7 Single-strand binding protein, putative OS=Plasmodium falciparum (isolate 3D7) GN=PFE0435c PE=1 SV=1 | 8 | 0.63 | 0.23 | 0.0001 |
| tr\|Q8ILL1\|Q8ILL1_PLAF7 Uncharacterized protein OS=Plasmodium falciparum (isolate 3D7) GN=PF14_0232 PE=4 SV=1 | 8 | 0.63 | 0.25 | 0.0002 |
| tr\|O96217\|O96217_PLAF7 Conserved Plasmodium protein OS=Plasmodium falciparum (isolate 3D7) GN=PFB0620w PE=4 SV=1 | 8 | 0.64 | 0.26 | 0.0002 |
| sp\|P26447\|S10A4_HUMAN Protein S100-A4 OS=Homo sapiens GN=S100A4 PE=1 SV=1 | 8 | 0.64 | 0.17 | 0.0000 |
| tr\|Q8IDY3\|Q8IDY3_PLAF7 Uncharacterized protein OS=Plasmodium falciparum (isolate 3D7) GN=PF13_0192 PE=4 SV=1 | 8 | 0.64 | 0.18 | 0.0000 |
| tr\|Q8IE52\|Q8IE52_PLAF7 Chromatin assembly factor 1 subunit, putative OS=Plasmodium falciparum (isolate 3D7) GN=PF13_0149 PE=4 SV=1 | 8 | 0.64 | 0.26 | 0.0002 |
| tr\|Q8I5W2\|Q8I5W2_PLAF7 Tim10 homologue, putative OS=Plasmodium falciparum (isolate 3D7) GN=PFL0430w PE=4 SV=1 | 8 | 0.64 | 0.36 | 0.0015 |
| tr\|Q7KQK4\|Q7KQK4_PLAF7 Zinc finger transcription factor (Krox1) OS=Plasmodium falciparum (isolate 3D7) GN=PFL0465c PE=4 SV=1 | 8 | 0.64 | 0.42 | 0.0035 |
| tr\|Q8ILD4\|Q8ILD4_PLAF7 Uncharacterized protein OS=Plasmodium falciparum (isolate 3D7) GN=PF14_0310 PE=4 SV=1 | 8 | 0.64 | 0.20 | 0.0000 |
| tr\|Q8IKW1\|Q8IKW1_PLAF7 Uncharacterized protein OS=Plasmodium falciparum (isolate 3D7) GN=PF14_0490 PE=4 SV=1 | 8 | 0.65 | 0.39 | 0.0023 |
| tr\|Q8IJC7\|Q8IJC7_PLAF7 Centrin-3 OS=Plasmodium falciparum (isolate 3D7) GN=PF10_0271 PE=4 SV=2 | 8 | 0.65 | 0.32 | 0.0007 |
| tr\|Q8IK20\|Q8IK20_PLAF7 Uncharacterized protein OS=Plasmodium falciparum (isolate 3D7) GN=PF10_0020 PE=4 SV=1 | 8 | 0.65 | 0.42 | 0.0033 |

| | | | | |
|---|---|---|---|---|
| tr\|Q8I5A0\|Q8I5A0_PLAF7 Dihydrolipoyl dehydrogenase OS=Plasmodium falciparum (isolate 3D7) GN=PFL1550w PE=3 SV=2 | 8 | 0.65 | 0.24 | 0.0001 |
| tr\|Q8I3F0\|Q8I3F0_PLAF7 Uncharacterized protein OS=Plasmodium falciparum (isolate 3D7) GN=PFE1605w PE=4 SV=1 | 8 | 0.65 | 0.23 | 0.0001 |
| tr\|Q8I0V2\|Q8I0V2_PLAF7 ATP synthase subunit beta OS=Plasmodium falciparum (isolate 3D7) GN=PFL1725w PE=3 SV=1 | 8 | 0.65 | 0.15 | 0.0000 |
| tr\|Q8I472\|Q8I472_PLAF7 Zinc binding protein, putative OS=Plasmodium falciparum (isolate 3D7) GN=PFE0140c PE=4 SV=1 | 8 | 0.65 | 0.38 | 0.0020 |
| tr\|Q8IIK1\|Q8IIK1_PLAF7 Uncharacterized protein OS=Plasmodium falciparum (isolate 3D7) GN=PF11_0172 PE=4 SV=1 | 8 | 0.65 | 0.28 | 0.0003 |
| tr\|Q8IIV1\|Q8IIV1_PLAF7 Histone H2B OS=Plasmodium falciparum (isolate 3D7) GN=PF11_0062 PE=3 SV=1 | 8 | 0.66 | 0.21 | 0.0000 |
| tr\|Q8IAV1\|Q8IAV1_PLAF7 Uncharacterized protein OS=Plasmodium falciparum (isolate 3D7) GN=PF08_0091 PE=4 SV=1 | 8 | 0.66 | 0.28 | 0.0003 |
| tr\|C0H488\|C0H488_PLAF7 Uncharacterized protein OS=Plasmodium falciparum (isolate 3D7) GN=PFD0170c PE=4 SV=1 | 8 | 0.66 | 0.17 | 0.0000 |
| tr\|Q9NFA0\|Q9NFA0_PLAF7 Signal peptidase, putative OS=Plasmodium falciparum (isolate 3D7) GN=PFC0912w PE=4 SV=1 | 8 | 0.67 | 0.12 | 0.0000 |
| tr\|Q8IKL7\|Q8IKL7_PLAF7 Splicing factor 3B subunit 2-like protein OS=Plasmodium falciparum (isolate 3D7) GN=PF14_0587 PE=4 SV=1 | 8 | 0.68 | 0.46 | 0.0042 |
| tr\|O97245\|O97245_PLAF7 Glycerol-3-phosphate dehydrogenase OS=Plasmodium falciparum (isolate 3D7) GN=PFC0275w PE=3 SV=1 | 8 | 0.68 | 0.14 | 0.0000 |
| tr\|Q8IBY8\|Q8IBY8_PLAF7 Uncharacterized protein OS=Plasmodium falciparum (isolate 3D7) GN=PF07_0042 PE=4 SV=1 | 8 | 0.68 | 0.27 | 0.0002 |
| tr\|Q8I2V9\|Q8I2V9_PLAF7 Protein disulfide isomerase OS=Plasmodium falciparum (isolate 3D7) GN=PfPDI-9 PE=4 SV=1 | 8 | 0.68 | 0.76 | 0.0389 |
| tr\|Q8I0W7\|Q8I0W7_PLAF7 Snrnp protein, putative OS=Plasmodium falciparum (isolate 3D7) GN=PFE0925c PE=3 SV=1 | 8 | 0.69 | 0.20 | 0.0000 |
| tr\|Q8IL96\|Q8IL96_PLAF7 N-acetyltransferase, putative OS=Plasmodium falciparum (isolate 3D7) GN=PF14_0350 PE=4 SV=2 | 8 | 0.69 | 0.21 | 0.0000 |
| tr\|Q8IE20\|Q8IE20_PLAF7 Elongation factor Tu OS=Plasmodium falciparum (isolate 3D7) GN=MAL13P1.164 PE=3 SV=1 | 8 | 0.69 | 0.18 | 0.0000 |
| tr\|Q8I527\|Q8I527_PLAF7 Hydroxyethylthiazole kinase, putative OS=Plasmodium falciparum (isolate 3D7) GN=PFL1920c PE=4 SV=1 | 8 | 0.69 | 0.18 | 0.0000 |
| tr\|Q8I377\|Q8I377_PLAF7 ATP-dependent heat shock protein, putative OS=Plasmodium falciparum (isolate 3D7) GN=PFI0355c PE=4 SV=1 | 8 | 0.69 | 0.25 | 0.0001 |
| tr\|Q8II32\|Q8II32_PLAF7 Uncharacterized protein OS=Plasmodium falciparum (isolate 3D7) GN=PF11_0342 PE=4 SV=1 | 8 | 0.70 | 0.23 | 0.0001 |
| tr\|C0H4Q1\|C0H4Q1_PLAF7 Uncharacterized protein OS=Plasmodium falciparum (isolate 3D7) GN=PF07_0120 PE=4 SV=1 | 8 | 0.70 | 0.27 | 0.0002 |
| tr\|C6KSY5\|C6KSY5_PLAF7 Uncharacterized protein OS=Plasmodium falciparum (isolate 3D7) GN=PFF0695w PE=4 SV=1 | 8 | 0.70 | 0.42 | 0.0023 |
| tr\|Q8IJF2\|Q8IJF2_PLAF7 Conserved Plasmodium protein OS=Plasmodium falciparum (isolate 3D7) GN=PF10_0246 PE=4 SV=2 | 8 | 0.70 | 0.18 | 0.0000 |
| tr\|Q8I5S7\|Q8I5S7_PLAF7 Choline transporter OS=Plasmodium falciparum (isolate 3D7) GN=PFL0620c PE=4 SV=1 | 8 | 0.70 | 0.12 | 0.0000 |
| sp\|O77374\|PF07_PLAF7 Uncharacterized protein PFC0810c OS=Plasmodium falciparum (isolate 3D7) GN=PFC0810c PE=3 SV=1 | 8 | 0.70 | 0.29 | 0.0003 |
| tr\|Q8IFP5\|Q8IFP5_PLAF7 Uncharacterized protein OS=Plasmodium falciparum (isolate 3D7) GN=PFD1037w PE=4 SV=1 | 8 | 0.70 | 0.28 | 0.0002 |
| tr\|Q8IDE0\|Q8IDE0_PLAF7 Mitochondrial inner membrane translocase, putative OS=Plasmodium falciparum (isolate 3D7) GN=PF13_0300 PE=4 SV=1 | 8 | 0.70 | 0.67 | 0.0206 |
| tr\|Q8IKL1\|Q8IKL1_PLAF7 Uncharacterized protein OS=Plasmodium falciparum (isolate 3D7) GN=PF14_0593 PE=4 SV=1 | 8 | 0.70 | 0.22 | 0.0000 |
| tr\|C6KT71\|C6KT71_PLAF7 Superoxide dismutase OS=Plasmodium falciparum (isolate 3D7) GN=PfSOD2 PE=4 SV=1 | 8 | 0.71 | 0.30 | 0.0003 |
| sp\|Q8ILT5\|SEY1_PLAF7 Protein SEY1 homolog OS=Plasmodium falciparum (isolate 3D7) GN=PF14_0159 PE=3 SV=2 | 8 | 0.71 | 0.22 | 0.0000 |
| tr\|C0H4K1\|C0H4K1_PLAF7 Centrin, putative OS=Plasmodium falciparum (isolate 3D7) GN=MAL7P1.10 PE=4 SV=1 | 8 | 0.71 | 0.28 | 0.0002 |
| tr\|Q8I255\|Q8I255_PLAF7 Putative uncharacterized protein OS=Plasmodium falciparum (isolate 3D7) GN=PFA_0430c PE=4 SV=1 | 8 | 0.72 | 0.29 | 0.0002 |
| tr\|Q8IKZ6\|Q8IKZ6_PLAF7 Multidrug resistance protein 2 (Heavy metal transport family) OS=Plasmodium falciparum (isolate 3D7) GN=PfMDR2 PE=3 SV=1 | 8 | 0.72 | 0.21 | 0.0000 |
| tr\|Q8IJG6\|Q8IJG6_PLAF7 Uncharacterized protein OS=Plasmodium falciparum (isolate 3D7) GN=PF10_0232 PE=4 SV=1 | 8 | 0.72 | 0.23 | 0.0000 |

| | | | | |
|---|---|---|---|---|
| tr\|Q8I5K4\|Q8I5K4_PLAF7 Chromodomain protein OS=Plasmodium falciparum (isolate 3D7) GN=PFL1005c PE=4 SV=1 | 8 | 0.72 | 0.24 | 0.0001 |
| tr\|Q8IB72\|Q8IB72_PLAF7 DNAJ protein, putative OS=Plasmodium falciparum (isolate 3D7) GN=PF08_0032 PE=4 SV=1 | 8 | 0.72 | 0.12 | 0.0000 |
| tr\|C0H4W6\|C0H4W6_PLAF7 Sec61 beta subunit, putative OS=Plasmodium falciparum (isolate 3D7) GN=MAL8P1.51 PE=4 SV=1 | 8 | 0.73 | 0.09 | 0.0000 |
| tr\|Q8I489\|Q8I489_PLAF7 Heat shock protein, putative OS=Plasmodium falciparum (isolate 3D7) GN=PFE0055c PE=4 SV=2 | 8 | 0.73 | 0.09 | 0.0000 |
| tr\|Q8I546\|Q8I546_PLAF7 Conserved Plasmodium membrane protein OS=Plasmodium falciparum (isolate 3D7) GN=PFL1825w PE=4 SV=1 | 8 | 0.73 | 0.13 | 0.0000 |
| tr\|Q8II23\|Q8II23_PLAF7 Protein disulfide isomerase related protein OS=Plasmodium falciparum (isolate 3D7) GN=PF11_0352 PE=4 SV=1 | 8 | 0.73 | 0.45 | 0.0024 |
| tr\|Q8IBD0\|Q8IBD0_PLAF7 Uncharacterized protein OS=Plasmodium falciparum (isolate 3D7) GN=PF08_0004 PE=4 SV=1 | 8 | 0.73 | 0.34 | 0.0005 |
| tr\|Q8I5Q6\|Q8I5Q6_PLAF7 Thioredoxin peroxidase OS=Plasmodium falciparum (isolate 3D7) GN=PFL0725w PE=1 SV=1 | 8 | 0.73 | 0.31 | 0.0003 |
| tr\|Q8I3N0\|Q8I3N0_PLAF7 DNAJ protein, putative OS=Plasmodium falciparum (isolate 3D7) GN=PFE1170w PE=4 SV=1 | 8 | 0.73 | 0.34 | 0.0005 |
| sp\|Q8I1U7\|SMC3_PLAF7 Structural maintenance of chromosomes protein 3 homolog OS=Plasmodium falciparum (isolate 3D7) GN=PFD0685c PE=3 SV=1 | 8 | 0.73 | 0.28 | 0.0002 |
| tr\|Q8IJF6\|Q8IJF6_PLAF7 Conserved Plasmodium protein OS=Plasmodium falciparum (isolate 3D7) GN=PF10_0242 PE=4 SV=2 | 8 | 0.73 | 0.23 | 0.0000 |
| tr\|Q8I5I0\|Q8I5I0_PLAF7 Uncharacterized protein OS=Plasmodium falciparum (isolate 3D7) GN=PFL1140w PE=4 SV=1 | 8 | 0.73 | 0.24 | 0.0001 |
| tr\|Q9U0N4\|Q9U0N4_PLAF7 ABC transporter, (CT family), putative OS=Plasmodium falciparum (isolate 3D7) GN=PfMRP PE=3 SV=1 | 8 | 0.73 | 0.31 | 0.0003 |
| tr\|Q8IDH5\|Q8IDH5_PLAF7 Thioredoxin-related protein, putative OS=Plasmodium falciparum (isolate 3D7) GN=PF13_0272 PE=4 SV=1 | 8 | 0.73 | 0.12 | 0.0000 |
| tr\|Q8IIX5\|Q8IIX5_PLAF7 Uncharacterized protein OS=Plasmodium falciparum (isolate 3D7) GN=PF11_0037 PE=4 SV=1 | 8 | 0.73 | 0.33 | 0.0004 |
| tr\|Q8I420\|Q8I420_PLAF7 Triose phosphate transporter OS=Plasmodium falciparum (isolate 3D7) GN=PfoTPT PE=4 SV=1 | 8 | 0.73 | 0.31 | 0.0003 |
| tr\|Q8IKS4\|Q8IKS4_PLAF7 Hemolysin, putative OS=Plasmodium falciparum (isolate 3D7) GN=PF14_0528 PE=4 SV=2 | 8 | 0.73 | 0.15 | 0.0000 |
| tr\|Q8I517\|Q8I517_PLAF7 Uncharacterized protein OS=Plasmodium falciparum (isolate 3D7) GN=PFL1980c PE=4 SV=1 | 8 | 0.73 | 0.15 | 0.0000 |
| tr\|Q8IKG8\|Q8IKG8_PLAF7 Rhoptry protein, putative OS=Plasmodium falciparum (isolate 3D7) GN=PF14_0637 PE=4 SV=2 | 8 | 0.74 | 0.31 | 0.0003 |
| tr\|Q8II57\|Q8II57_PLAF7 Structural maintenance of chromosome protein, putative OS=Plasmodium falciparum (isolate 3D7) GN=PF11_0317 PE=4 SV=1 | 8 | 0.74 | 0.57 | 0.0081 |
| tr\|Q8I3W9\|Q8I3W9_PLAF7 PfRab1a OS=Plasmodium falciparum (isolate 3D7) GN=Rab1a PE=3 SV=1 | 8 | 0.74 | 0.35 | 0.0006 |
| tr\|Q8IDN6\|Q8IDN6_PLAF7 Sec61 alpha subunit, PfSec61 OS=Plasmodium falciparum (isolate 3D7) GN=Sec61 PE=3 SV=1 | 8 | 0.74 | 0.27 | 0.0001 |
| tr\|Q8IDB8\|Q8IDB8_PLAF7 Uncharacterized protein OS=Plasmodium falciparum (isolate 3D7) GN=MAL13P1.288 PE=4 SV=1 | 8 | 0.74 | 0.15 | 0.0000 |
| tr\|Q6ZMA7\|Q6ZMA7_PLAF7 Sexual stage-specific protein OS=Plasmodium falciparum (isolate 3D7) GN=PFD0310w PE=4 SV=1 | 8 | 0.74 | 0.19 | 0.0000 |
| tr\|Q8IL69\|Q8IL69_PLAF7 Uncharacterized protein OS=Plasmodium falciparum (isolate 3D7) GN=PF14_0380 PE=4 SV=1 | 8 | 0.74 | 0.28 | 0.0001 |
| tr\|Q8IDW0\|Q8IDW0_PLAF7 1-deoxy-D-xylulose 5-phosphate synthase OS=Plasmodium falciparum (isolate 3D7) GN=MAL13P1.186 PE=4 SV=1 | 8 | 0.74 | 0.23 | 0.0000 |
| tr\|Q8I5B2\|Q8I5B2_PLAF7 Conserved Plasmodium protein OS=Plasmodium falciparum (isolate 3D7) GN=PFL1485w PE=4 SV=2 | 8 | 0.74 | 0.21 | 0.0000 |
| sp\|P69905\|HBA_HUMAN Hemoglobin subunit alpha OS=Homo sapiens GN=HBA1 PE=1 SV=2;tr\|G3V1N2\|G3V1N2_HUMAN HCG1745306, isoform CRA_a OS=Homo sapiens GN=HBA2 PE=1 SV=1 | 8 | 0.75 | 0.43 | 0.0016 |
| tr\|Q8IHZ6\|Q8IHZ6_PLAF7 DNAJ protein, putative OS=Plasmodium falciparum (isolate 3D7) GN=PF11_0380 PE=4 SV=2 | 8 | 0.75 | 0.26 | 0.0001 |
| tr\|Q9U0H0\|Q9U0H0_PLAF7 Uncharacterized protein OS=Plasmodium falciparum (isolate 3D7) GN=PFD0595w PE=4 SV=1 | 8 | 0.75 | 0.44 | 0.0018 |
| tr\|Q8I3T4\|Q8I3T4_PLAF7 Transcriptional regulator, putative OS=Plasmodium falciparum (isolate 3D7) GN=PFE0870w PE=4 SV=1 | 8 | 0.75 | 0.22 | 0.0000 |
| sp\|O77384\|LRR4_PLAF7 Protein PFC0760c OS=Plasmodium falciparum (isolate 3D7) GN=PFC0760c PE=4 SV=1 | 8 | 0.75 | 0.23 | 0.0000 |

| | | | | |
|---|---|---|---|---|
| tr\|Q8IL32\|Q8IL32_PLAF7 HSP90 OS=Plasmodium falciparum (isolate 3D7) GN=PF14_0417 PE=1 SV=1 | 8 | 0.75 | 0.17 | 0.0000 |
| tr\|C6KTB8\|C6KTB8_PLAF7 Protein kinase PK4 OS=Plasmodium falciparum (isolate 3D7) GN=PfPK4 PE=4 SV=1 | 8 | 0.75 | 0.28 | 0.0001 |
| tr\|Q8I2I2\|Q8I2I2_PLAF7 Organelle processing peptidase, putative OS=Plasmodium falciparum (isolate 3D7) GN=PFI1625c PE=3 SV=1 | 8 | 0.76 | 0.21 | 0.0000 |
| tr\|Q8IE22\|Q8IE22_PLAF7 ER lumen protein retaining receptor 1, putative OS=Plasmodium falciparum (isolate 3D7) GN=MAL13P1.163 PE=4 SV=1 | 8 | 0.76 | 0.14 | 0.0000 |
| tr\|Q8IJV6\|Q8IJV6_PLAF7 Adenylate kinase, putative OS=Plasmodium falciparum (isolate 3D7) GN=PF10_0086 PE=3 SV=1 | 8 | 0.76 | 0.32 | 0.0003 |
| tr\|Q8IIH7\|Q8IIH7_PLAF7 Uncharacterized protein OS=Plasmodium falciparum (isolate 3D7) GN=PF11_0197 PE=4 SV=1 | 8 | 0.76 | 0.16 | 0.0000 |
| tr\|O96275\|O96275_PLAF7 Liver stage antigen 3 OS=Plasmodium falciparum (isolate 3D7) GN=PFB0915w PE=4 SV=1 | 8 | 0.76 | 0.17 | 0.0000 |
| sp\|Q8I5G1\|YPF10_PLAF7 Uncharacterized protein PFL1235c OS=Plasmodium falciparum (isolate 3D7) GN=PFL1235c PE=3 SV=1 | 8 | 0.76 | 0.21 | 0.0000 |
| tr\|C0H5I2\|C0H5I2_PLAF7 Uncharacterized protein OS=Plasmodium falciparum (isolate 3D7) GN=MAL13P1.266 PE=4 SV=1 | 8 | 0.76 | 0.15 | 0.0000 |
| tr\|Q8I328\|Q8I328_PLAF7 Putative uncharacterized protein OS=Plasmodium falciparum (isolate 3D7) GN=PFI0605c PE=4 SV=1 | 8 | 0.76 | 0.11 | 0.0000 |
| tr\|Q8ILU2\|Q8ILU2_PLAF7 Uncharacterized protein OS=Plasmodium falciparum (isolate 3D7) GN=PF14_0152 PE=4 SV=1 | 8 | 0.76 | 0.34 | 0.0004 |
| tr\|Q8I6T2\|Q8I6T2_PLAF7 Isocitrate dehydrogenase [NADP] OS=Plasmodium falciparum (isolate 3D7) GN=PF13_0242 PE=3 SV=1 | 8 | 0.77 | 0.09 | 0.0000 |
| tr\|O97227\|O97227_PLAF7 Dihydrolipoamide acyltransferase, putative OS=Plasmodium falciparum (isolate 3D7) GN=PFC0170c PE=3 SV=1 | 8 | 0.77 | 0.29 | 0.0001 |
| tr\|Q8ILQ8\|Q8ILQ8_PLAF7 Uncharacterized protein OS=Plasmodium falciparum (isolate 3D7) GN=PF14_0186 PE=4 SV=2 | 8 | 0.77 | 0.33 | 0.0003 |
| tr\|Q8IBV7\|Q8IBV7_PLAF7 Histone H2B OS=Plasmodium falciparum (isolate 3D7) GN=PF07_0054 PE=3 SV=1 | 8 | 0.77 | 0.15 | 0.0000 |
| tr\|Q8IJ69\|Q8IJ69_PLAF7 Sec1 family protein, putative OS=Plasmodium falciparum (isolate 3D7) GN=PF10_0331 PE=4 SV=2 | 8 | 0.77 | 0.37 | 0.0006 |
| tr\|C6KST1\|C6KST1_PLAF7 Uncharacterized protein OS=Plasmodium falciparum (isolate 3D7) GN=PFF0410w PE=4 SV=1 | 8 | 0.77 | 0.32 | 0.0003 |
| tr\|Q8II93\|Q8II93_PLAF7 Protein phosphatase, putative OS=Plasmodium falciparum (isolate 3D7) GN=PF11_0281 PE=4 SV=2 | 8 | 0.77 | 0.03 | 0.0000 |
| tr\|Q8IK82\|Q8IK82_PLAF7 Bromodomain protein, putative OS=Plasmodium falciparum (isolate 3D7) GN=PF14_0724 PE=1 SV=1 | 8 | 0.78 | 0.15 | 0.0000 |
| tr\|C6KT04\|C6KT04_PLAF7 Uncharacterized protein OS=Plasmodium falciparum (isolate 3D7) GN=PFF0790c PE=4 SV=1 | 8 | 0.78 | 0.31 | 0.0002 |
| tr\|Q8I305\|Q8I305_PLAF7 Transporter, putative OS=Plasmodium falciparum (isolate 3D7) GN=PFI0720w PE=4 SV=1 | 8 | 0.78 | 0.23 | 0.0000 |
| tr\|Q8II11\|Q8II11_PLAF7 Conserved Plasmodium protein OS=Plasmodium falciparum (isolate 3D7) GN=PF11_0364 PE=4 SV=1 | 8 | 0.78 | 0.18 | 0.0000 |
| sp\|P68871\|HBB_HUMAN Hemoglobin subunit beta OS=Homo sapiens GN=HBB PE=1 SV=2 | 8 | 0.78 | 0.46 | 0.0021 |
| tr\|Q8ILC9\|Q8ILC9_PLAF7 Uncharacterized protein OS=Plasmodium falciparum (isolate 3D7) GN=PF14_0315 PE=4 SV=2 | 8 | 0.78 | 0.31 | 0.0002 |
| tr\|C6KT82\|C6KT82_PLAF7 Smarca-related protein OS=Plasmodium falciparum (isolate 3D7) GN=PFF1185w PE=4 SV=1 | 8 | 0.78 | 0.28 | 0.0001 |
| tr\|Q8IB31\|Q8IB31_PLAF7 Uncharacterized protein OS=Plasmodium falciparum (isolate 3D7) GN=MAL8P1.62 PE=4 SV=1 | 8 | 0.78 | 0.07 | 0.0000 |
| tr\|Q8IBH9\|Q8IBH9_PLAF7 Cation transporting ATPase, cation transporter OS=Plasmodium falciparum (isolate 3D7) GN=PF07_0115 PE=3 SV=1 | 8 | 0.79 | 0.16 | 0.0000 |
| tr\|Q8I3N3\|Q8I3N3_PLAF7 Mitochondrial processing peptidase alpha subunit, putative OS=Plasmodium falciparum (isolate 3D7) GN=PFE1155c PE=3 SV=2 | 8 | 0.79 | 0.15 | 0.0000 |
| tr\|Q8IJ37\|Q8IJ37_PLAF7 Pyruvate kinase OS=Plasmodium falciparum (isolate 3D7) GN=PF10_0363 PE=3 SV=1 | 8 | 0.79 | 0.27 | 0.0001 |
| tr\|Q8I5S4\|Q8I5S4_PLAF7 Bromodomain protein, putative OS=Plasmodium falciparum (isolate 3D7) GN=PFL0635c PE=4 SV=1 | 8 | 0.79 | 0.13 | 0.0000 |
| tr\|Q8IL07\|Q8IL07_PLAF7 Centrin-2 OS=Plasmodium falciparum (isolate 3D7) GN=CEN2 PE=4 SV=1 | 8 | 0.79 | 0.17 | 0.0000 |
| sp\|Q08210\|PYRD_PLAF7 Dihydroorotate dehydrogenase (quinone), mitochondrial OS=Plasmodium falciparum (isolate 3D7) GN=PFF0160c PE=1 SV=1 | 8 | 0.79 | 0.36 | 0.0005 |
| tr\|Q8IL28\|Q8IL28_PLAF7 Apicoplast 1-acyl-sn-glycerol-3-phosphate acyltransferase, putative OS=Plasmodium falciparum (isolate 3D7) GN=PF14_0421 PE=4 SV=2 | 8 | 0.79 | 0.25 | 0.0000 |

| | | | | |
|---|---|---|---|---|
| sp\|P46468\|CDAT_PLAF7 Putative cell division cycle ATPase OS=Plasmodium falciparum (isolate 3D7) GN=PF07_0047 PE=3 SV=2 | 8 | 0.79 | 0.28 | 0.0001 |
| tr\|Q8I6Z1\|Q8I6Z1_PLAF7 Acyl-coA synthetase, PfACS5 OS=Plasmodium falciparum (isolate 3D7) GN=PfACS5 PE=4 SV=1 | 8 | 0.79 | 0.25 | 0.0000 |
| sp\|C0H4W3\|HEPF1_PLAF7 Probable ATP-dependent helicase PF08_0048 OS=Plasmodium falciparum (isolate 3D7) GN=PF08_0048 PE=3 SV=1 | 8 | 0.79 | 0.12 | 0.0000 |
| tr\|O77325\|O77325_PLAF7 PRP19-like protein, putative OS=Plasmodium falciparum (isolate 3D7) GN=PFC0365w PE=4 SV=1 | 8 | 0.79 | 0.27 | 0.0001 |
| tr\|Q8I398\|Q8I398_PLAF7 Putative uncharacterized protein OS=Plasmodium falciparum (isolate 3D7) GN=PFI0250c PE=4 SV=1 | 8 | 0.79 | 0.29 | 0.0001 |
| tr\|Q8IE81\|Q8IE81_PLAF7 Uncharacterized protein OS=Plasmodium falciparum (isolate 3D7) GN=PF13_0134 PE=4 SV=1 | 8 | 0.79 | 0.36 | 0.0004 |
| tr\|Q8IBF1\|Q8IBF1_PLAF7 Uncharacterized protein OS=Plasmodium falciparum (isolate 3D7) GN=MAL7P1.172 PE=4 SV=1 | 8 | 0.79 | 0.35 | 0.0003 |
| tr\|Q8II85\|Q8II85_PLAF7 Uncharacterized protein OS=Plasmodium falciparum (isolate 3D7) GN=PF11_0289 PE=4 SV=1 | 8 | 0.79 | 0.70 | 0.0150 |
| tr\|Q8IEG8\|Q8IEG8_PLAF7 Uncharacterized protein OS=Plasmodium falciparum (isolate 3D7) GN=MAL13P1.75 PE=4 SV=1 | 8 | 0.79 | 0.17 | 0.0000 |
| tr\|Q8I5T2\|Q8I5T2_PLAF7 Glutathione peroxidase OS=Plasmodium falciparum (isolate 3D7) GN=PFL0595c PE=3 SV=1 | 8 | 0.79 | 0.14 | 0.0000 |
| tr\|Q8I3Q6\|Q8I3Q6_PLAF7 Uncharacterized protein OS=Plasmodium falciparum (isolate 3D7) GN=PFE1025c PE=4 SV=1 | 8 | 0.80 | 0.25 | 0.0000 |
| tr\|Q8I1T1\|Q8I1T1_PLAF7 Adenylate kinase 1 OS=Plasmodium falciparum (isolate 3D7) GN=GAK PE=3 SV=1 | 8 | 0.80 | 0.30 | 0.0001 |
| tr\|Q8I665\|Q8I665_PLAF7 Conserved Plasmodium protein OS=Plasmodium falciparum (isolate 3D7) GN=PFB0194w PE=4 SV=1 | 8 | 0.80 | 0.12 | 0.0000 |
| tr\|Q8IE67\|Q8IE67_PLAF7 Phosphoribosylpyrophosphate synthetase OS=Plasmodium falciparum (isolate 3D7) GN=PF13_0143 PE=4 SV=1 | 8 | 0.81 | 0.08 | 0.0000 |
| tr\|Q8I2X4\|Q8I2X4_PLAF7 Heat shock protein 70 (HSP70) homologue OS=Plasmodium falciparum (isolate 3D7) GN=PFI0875w PE=3 SV=1 | 8 | 0.81 | 0.25 | 0.0000 |
| tr\|Q8IHV7\|Q8IHV7_PLAF7 Conserved Plasmodium protein OS=Plasmodium falciparum (isolate 3D7) GN=PF11_0419 PE=4 SV=2 | 8 | 0.81 | 0.21 | 0.0000 |
| tr\|C0H5J5\|C0H5J5_PLAF7 Polyadenylate-binding protein, putative OS=Plasmodium falciparum (isolate 3D7) GN=MAL13P1.303 PE=4 SV=1 | 8 | 0.81 | 0.13 | 0.0000 |
| tr\|O96205\|O96205_PLAF7 Conserved Plasmodium protein OS=Plasmodium falciparum (isolate 3D7) GN=PFB0560w PE=4 SV=2 | 8 | 0.81 | 0.26 | 0.0000 |
| tr\|Q8IHR8\|Q8IHR8_PLAF7 PfRab6, GTPase OS=Plasmodium falciparum (isolate 3D7) GN=Rab6 PE=3 SV=2 | 8 | 0.81 | 0.07 | 0.0000 |
| tr\|Q8IIJ4\|Q8IIJ4_PLAF7 Uncharacterized protein OS=Plasmodium falciparum (isolate 3D7) GN=PF11_0179 PE=4 SV=1 | 8 | 0.81 | 0.08 | 0.0000 |
| tr\|O77389\|O77389_PLAF7 Formate-nitrate transporter, putative OS=Plasmodium falciparum (isolate 3D7) GN=PFC0725c PE=4 SV=2 | 8 | 0.81 | 0.16 | 0.0000 |
| sp\|Q8I6U8\|GBP_PLAF7 Glycophorin-binding protein OS=Plasmodium falciparum (isolate 3D7) GN=GBP PE=3 SV=1 | 8 | 0.81 | 0.34 | 0.0003 |
| tr\|Q8IJP9\|Q8IJP9_PLAF7 ADA2-like protein OS=Plasmodium falciparum (isolate 3D7) GN=PF10_0143 PE=4 SV=1 | 8 | 0.82 | 0.07 | 0.0000 |
| tr\|Q8IDZ8\|Q8IDZ8_PLAF7 Cochaperonin OS=Plasmodium falciparum (isolate 3D7) GN=PfCpn20 PE=3 SV=1 | 8 | 0.82 | 0.19 | 0.0000 |
| tr\|O77375\|O77375_PLAF7 DNA-directed RNA polymerase OS=Plasmodium falciparum (isolate 3D7) GN=PFC0805w PE=3 SV=1 | 8 | 0.82 | 0.29 | 0.0001 |
| tr\|Q8IIR6\|Q8IIR6_PLAF7 Heat shock protein DnaJ homologue Pfj2 OS=Plasmodium falciparum (isolate 3D7) GN=PF11_0099 PE=4 SV=1 | 8 | 0.82 | 0.27 | 0.0001 |
| sp\|O97239\|DOP1_PLAF7 Protein dopey homolog PFC0245c OS=Plasmodium falciparum (isolate 3D7) GN=PFC0245c PE=2 SV=1 | 8 | 0.82 | 0.23 | 0.0000 |
| tr\|Q8IJN3\|Q8IJN3_PLAF7 Serine/Threonine protein kinase, FIKK family OS=Plasmodium falciparum (isolate 3D7) GN=FIKK-10.1 PE=4 SV=2 | 8 | 0.82 | 0.36 | 0.0004 |
| tr\|Q8IEJ5\|Q8IEJ5_PLAF7 Uncharacterized protein OS=Plasmodium falciparum (isolate 3D7) GN=PF13_0071 PE=4 SV=1 | 8 | 0.82 | 0.21 | 0.0000 |
| tr\|Q8II53\|Q8II53_PLAF7 Uncharacterized protein OS=Plasmodium falciparum (isolate 3D7) GN=PF11_0321 PE=4 SV=1 | 8 | 0.82 | 0.50 | 0.0024 |
| tr\|Q8I3R2\|Q8I3R2_PLAF7 Uncharacterized protein OS=Plasmodium falciparum (isolate 3D7) GN=PFE0995c PE=4 SV=1 | 8 | 0.82 | 0.36 | 0.0003 |
| tr\|O97243\|O97243_PLAF7 Putative uncharacterized protein OS=Plasmodium falciparum (isolate 3D7) GN=PFC0265c PE=4 SV=2 | 8 | 0.82 | 0.51 | 0.0026 |
| tr\|Q8I5L4\|Q8I5L4_PLAF7 Phospholipid-translocating ATPase OS=Plasmodium falciparum (isolate 3D7) GN=PFL0950c PE=4 SV=1 | 8 | 0.83 | 0.11 | 0.0000 |

| | | | | |
|---|---|---|---|---|
| tr\|Q8IAK9\|Q8IAK9_PLAF7 Uncharacterized protein OS=Plasmodium falciparum (isolate 3D7) GN=PF08_0137 PE=4 SV=1 | 8 | 0.83 | 0.17 | 0.0000 |
| tr\|Q8IL71\|Q8IL71_PLAF7 Vesicle-associated membrane protein, putative OS=Plasmodium falciparum (isolate 3D7) GN=PF14_0377 PE=4 SV=1 | 8 | 0.83 | 0.24 | 0.0000 |
| tr\|Q8IL86\|Q8IL86_PLAF7 Sec62, putative OS=Plasmodium falciparum (isolate 3D7) GN=PF14_0361 PE=4 SV=2 | 8 | 0.83 | 0.24 | 0.0000 |
| tr\|O97323\|O97323_PLAF7 SNARE protein OS=Plasmodium falciparum (isolate 3D7) GN=PfSec22 PE=4 SV=2 | 8 | 0.83 | 0.65 | 0.0087 |
| tr\|Q8ILB6\|Q8ILB6_PLAF7 Uncharacterized protein OS=Plasmodium falciparum (isolate 3D7) GN=PF14_0329 PE=4 SV=1 | 8 | 0.83 | 0.07 | 0.0000 |
| tr\|Q8IB44\|Q8IB44_PLAF7 Uncharacterized protein OS=Plasmodium falciparum (isolate 3D7) GN=MAL8P1.53 PE=4 SV=1 | 8 | 0.83 | 0.21 | 0.0000 |
| tr\|Q8I289\|Q8I289_PLAF7 Putative uncharacterized protein OS=Plasmodium falciparum (isolate 3D7) GN=PFA_0255c PE=4 SV=1 | 8 | 0.83 | 0.19 | 0.0000 |
| tr\|C0H4M7\|C0H4M7_PLAF7 Uncharacterized protein OS=Plasmodium falciparum (isolate 3D7) GN=MAL7P1.67 PE=4 SV=1 | 8 | 0.83 | 0.15 | 0.0000 |
| tr\|Q8II24\|Q8II24_PLAF7 Heat shock protein hsp70 homologue OS=Plasmodium falciparum (isolate 3D7) GN=PF11_0351 PE=3 SV=1 | 8 | 0.83 | 0.06 | 0.0000 |
| tr\|Q8ILB0\|Q8ILB0_PLAF7 Uncharacterized protein OS=Plasmodium falciparum (isolate 3D7) GN=PF14_0335 PE=4 SV=1 | 8 | 0.84 | 0.22 | 0.0000 |
| tr\|C0H535\|C0H535_PLAF7 Putative uncharacterized protein OS=Plasmodium falciparum (isolate 3D7) GN=PFI0610w PE=4 SV=1 | 8 | 0.84 | 0.19 | 0.0000 |
| tr\|Q8I510\|Q8I510_PLAF7 Uncharacterized protein OS=Plasmodium falciparum (isolate 3D7) GN=PFL2015w PE=4 SV=1 | 8 | 0.84 | 0.34 | 0.0002 |
| tr\|C0H5H0\|C0H5H0_PLAF7 Heat shock protein 70 (Hsp70), putative OS=Plasmodium falciparum (isolate 3D7) GN=MAL13P1.540 PE=3 SV=1 | 8 | 0.84 | 0.59 | 0.0052 |
| tr\|Q8IB78\|Q8IB78_PLAF7 Nucleoside transporter, putative OS=Plasmodium falciparum (isolate 3D7) GN=MAL8P1.32 PE=4 SV=1 | 8 | 0.84 | 0.22 | 0.0000 |
| tr\|Q8IJI9\|Q8IJI9_PLAF7 Uncharacterized protein OS=Plasmodium falciparum (isolate 3D7) GN=PF10_0208 PE=4 SV=1 | 8 | 0.84 | 0.41 | 0.0007 |
| tr\|Q8IJ76\|Q8IJ76_PLAF7 Uncharacterized protein OS=Plasmodium falciparum (isolate 3D7) GN=PF10_0323 PE=4 SV=1 | 8 | 0.84 | 0.09 | 0.0000 |
| tr\|Q76NN8\|Q76NN8_PLAF7 Calcium-transporting ATPase, putative OS=Plasmodium falciparum (isolate 3D7) GN=PFA_0310c PE=3 SV=1 | 8 | 0.84 | 0.05 | 0.0000 |
| tr\|Q8IK92\|Q8IK92_PLAF7 Uncharacterized protein OS=Plasmodium falciparum (isolate 3D7) GN=PF14_0714 PE=4 SV=1 | 8 | 0.84 | 0.11 | 0.0000 |
| tr\|Q8IDC4\|Q8IDC4_PLAF7 Preribosomal processosome UTP, putative OS=Plasmodium falciparum (isolate 3D7) GN=PF13_0310 PE=4 SV=1 | 8 | 0.84 | 0.52 | 0.0027 |
| tr\|Q8I484\|Q8I484_PLAF7 Rhoptry-associated protein 2, RAP2 OS=Plasmodium falciparum (isolate 3D7) GN=RAP2 PE=4 SV=1 | 8 | 0.84 | 0.20 | 0.0000 |
| tr\|Q8I1X3\|Q8I1X3_PLAF7 Secy-independent transporter protein, putative OS=Plasmodium falciparum (isolate 3D7) GN=PFD0275w PE=4 SV=2 | 8 | 0.84 | 0.06 | 0.0000 |
| tr\|Q8IEE2\|Q8IEE2_PLAF7 Uncharacterized protein OS=Plasmodium falciparum (isolate 3D7) GN=PF13_0099 PE=4 SV=1 | 8 | 0.84 | 0.23 | 0.0000 |
| tr\|Q8ILP3\|Q8ILP3_PLAF7 Surface protein, Pf113 OS=Plasmodium falciparum (isolate 3D7) GN=Pf113 PE=4 SV=1 | 8 | 0.84 | 0.12 | 0.0000 |
| tr\|Q8I2R8\|Q8I2R8_PLAF7 RNA binding protein, putative OS=Plasmodium falciparum (isolate 3D7) GN=PFI1175c PE=4 SV=1 | 8 | 0.84 | 0.21 | 0.0000 |
| tr\|Q8I5E7\|Q8I5E7_PLAF7 ATP-dependent RNA helicase, putative OS=Plasmodium falciparum (isolate 3D7) GN=PFL1310c PE=3 SV=1 | 8 | 0.84 | 0.09 | 0.0000 |
| tr\|Q8IEC8\|Q8IEC8_PLAF7 DnaJ/SEC63 protein, putative OS=Plasmodium falciparum (isolate 3D7) GN=PF13_0102 PE=4 SV=1 | 8 | 0.84 | 0.05 | 0.0000 |
| tr\|Q8IIU5\|Q8IIU5_PLAF7 Conserved Plasmodium protein OS=Plasmodium falciparum (isolate 3D7) GN=PF11_0069 PE=4 SV=2 | 8 | 0.84 | 0.08 | 0.0000 |
| tr\|Q8IAQ8\|Q8IAQ8_PLAF7 Vacuolar proton translocating ATPase subunit A, putative OS=Plasmodium falciparum (isolate 3D7) GN=PF08_0113 PE=4 SV=1 | 8 | 0.84 | 0.18 | 0.0000 |
| tr\|Q8IJR2\|Q8IJR2_PLAF7 Uncharacterized protein OS=Plasmodium falciparum (isolate 3D7) GN=PF10_0130 PE=4 SV=1 | 8 | 0.84 | 0.12 | 0.0000 |
| tr\|Q8IL56\|Q8IL56_PLAF7 Structure specific recognition protein OS=Plasmodium falciparum (isolate 3D7) GN=PF14_0393 PE=4 SV=1 | 8 | 0.84 | 0.12 | 0.0000 |
| tr\|Q8IL08\|Q8IL08_PLAF7 Uncharacterized protein OS=Plasmodium falciparum (isolate 3D7) GN=PF14_0442 PE=4 SV=1 | 8 | 0.84 | 0.32 | 0.0001 |
| tr\|Q8IBI5\|Q8IBI5_PLAF7 Cysteine desulfurase, putative OS=Plasmodium falciparum (isolate 3D7) GN=MAL7P1.150 PE=3 SV=1 | 8 | 0.85 | 0.14 | 0.0000 |
| tr\|Q8IDP8\|Q8IDP8_PLAF7 Aspartate carbamoyltransferase OS=Plasmodium falciparum (isolate 3D7) GN=atcasE PE=3 SV=1 | 8 | 0.85 | 0.21 | 0.0000 |

| | | | | |
|---|---|---|---|---|
| tr\|C6KST7\|C6KST7_PLAF7 Uncharacterized protein OS=Plasmodium falciparum (isolate 3D7) GN=PFF0445w PE=4 SV=1 | 8 | 0.85 | 0.30 | 0.0001 |
| tr\|Q8IE40\|Q8IE40_PLAF7 Ribose-phosphate pyrophosphokinase, putative OS=Plasmodium falciparum (isolate 3D7) GN=PF13_0157 PE=4 SV=1 | 8 | 0.85 | 0.34 | 0.0002 |
| tr\|Q8IIC8\|Q8IIC8_PLAF7 Uncharacterized protein OS=Plasmodium falciparum (isolate 3D7) GN=PF11_0246 PE=4 SV=1 | 8 | 0.85 | 0.19 | 0.0000 |
| tr\|O77313\|O77313_PLAF7 N-ethylmaleimide sensitive fusion protein, putative OS=Plasmodium falciparum (isolate 3D7) GN=PFC0140c PE=3 SV=1 | 8 | 0.85 | 0.22 | 0.0000 |
| tr\|Q8IAU7\|Q8IAU7_PLAF7 Uncharacterized protein OS=Plasmodium falciparum (isolate 3D7) GN=MAL8P1.105 PE=4 SV=1 | 8 | 0.85 | 0.03 | 0.0000 |
| tr\|C6KSL9\|C6KSL9_PLAF7 Uncharacterized protein OS=Plasmodium falciparum (isolate 3D7) GN=PFF0090w PE=4 SV=1 | 8 | 0.85 | 0.28 | 0.0001 |
| sp\|Q8I3H7\|TIP_PLAF7 T-cell immunomodulatory protein homolog OS=Plasmodium falciparum (isolate 3D7) GN=PFE1445c PE=3 SV=1 | 8 | 0.85 | 0.31 | 0.0001 |
| tr\|Q7KWJ5\|Q7KWJ5_PLAF7 Hexose transporter, PfHT1 OS=Plasmodium falciparum (isolate 3D7) GN=HT1 PE=3 SV=1 | 8 | 0.85 | 0.15 | 0.0000 |
| tr\|Q8I5L6\|Q8I5L6_PLAF7 Clathrin heavy chain OS=Plasmodium falciparum (isolate 3D7) GN=PFL0930w PE=3 SV=1 | 8 | 0.85 | 0.23 | 0.0000 |
| tr\|Q8I5Q3\|Q8I5Q3_PLAF7 10 kd chaperonin OS=Plasmodium falciparum (isolate 3D7) GN=Cpn10 PE=3 SV=2 | 8 | 0.85 | 0.07 | 0.0000 |
| tr\|Q8I0V3\|Q8I0V3_PLAF7 Chaperonin, cpn60 OS=Plasmodium falciparum (isolate 3D7) GN=PFL1545c PE=3 SV=2 | 8 | 0.85 | 0.12 | 0.0000 |
| tr\|Q8IEB3\|Q8IEB3_PLAF7 Uncharacterized protein OS=Plasmodium falciparum (isolate 3D7) GN=PF13_0116 PE=4 SV=1 | 8 | 0.85 | 0.26 | 0.0000 |
| tr\|Q8I468\|Q8I468_PLAF7 Ser/Arg-rich splicing factor, putative OS=Plasmodium falciparum (isolate 3D7) GN=PFE0160c PE=4 SV=1 | 8 | 0.85 | 0.15 | 0.0000 |
| tr\|Q8III6\|Q8III6_PLAF7 Heat shock protein 90, putative OS=Plasmodium falciparum (isolate 3D7) GN=PF11_0188 PE=3 SV=1 | 8 | 0.86 | 0.16 | 0.0000 |
| tr\|Q8IK15\|Q8IK15_PLAF7 PF70 protein OS=Plasmodium falciparum (isolate 3D7) GN=PF10_0025 PE=4 SV=1 | 8 | 0.86 | 0.20 | 0.0000 |
| tr\|C6KT09\|C6KT09_PLAF7 Malate:quinone oxidoreductase, putative OS=Plasmodium falciparum (isolate 3D7) GN=PFF0815w PE=4 SV=1 | 8 | 0.86 | 0.45 | 0.0010 |
| tr\|Q8IDZ5\|Q8IDZ5_PLAF7 Transmembrane protein Tmp21 homologue, putative OS=Plasmodium falciparum (isolate 3D7) GN=MAL13P1.171 PE=4 SV=1 | 8 | 0.86 | 0.13 | 0.0000 |
| tr\|C6KTC7\|C6KTC7_PLAF7 DNAJ domain protein, putative OS=Plasmodium falciparum (isolate 3D7) GN=PFF1415c PE=4 SV=1 | 8 | 0.86 | 0.11 | 0.0000 |
| tr\|Q8IJ72\|Q8IJ72_PLAF7 Bromodomain protein, putative OS=Plasmodium falciparum (isolate 3D7) GN=PF10_0328 PE=1 SV=1 | 8 | 0.86 | 0.10 | 0.0000 |
| tr\|Q8I5I3\|Q8I5I3_PLAF7 Phospholipid-transporting ATPase, putative OS=Plasmodium falciparum (isolate 3D7) GN=PFL1125w PE=4 SV=1 | 8 | 0.86 | 0.34 | 0.0002 |
| tr\|Q8IJI4\|Q8IJI4_PLAF7 10b antigen, putative OS=Plasmodium falciparum (isolate 3D7) GN=PF10_0213 PE=4 SV=1 | 8 | 0.86 | 0.26 | 0.0000 |
| tr\|Q8IB03\|Q8IB03_PLAF7 ClpB protein, putative OS=Plasmodium falciparum (isolate 3D7) GN=PF08_0063 PE=1 SV=1 | 8 | 0.86 | 0.06 | 0.0000 |
| tr\|O77376\|O77376_PLAF7 Band 7-related protein OS=Plasmodium falciparum (isolate 3D7) GN=PFC0800w PE=4 SV=1 | 8 | 0.87 | 0.19 | 0.0000 |
| tr\|Q8IIB6\|Q8IIB6_PLAF7 GrpE protein homolog OS=Plasmodium falciparum (isolate 3D7) GN=PF11_0258 PE=3 SV=2 | 8 | 0.87 | 0.07 | 0.0000 |
| tr\|Q8IKC8\|Q8IKC8_PLAF7 Exported protein 2 OS=Plasmodium falciparum (isolate 3D7) GN=EXP-2 PE=4 SV=1 | 8 | 0.87 | 0.07 | 0.0000 |
| tr\|C6KT11\|C6KT11_PLAF7 Mitochondrial import receptor subunit tom40 OS=Plasmodium falciparum (isolate 3D7) GN=PFF0825c PE=4 SV=1 | 8 | 0.87 | 0.24 | 0.0000 |
| tr\|Q8I4U7\|Q8I4U7_PLAF7 Uncharacterized protein OS=Plasmodium falciparum (isolate 3D7) GN=PFL2335w PE=4 SV=1 | 8 | 0.87 | 0.17 | 0.0000 |
| tr\|Q8IL16\|Q8IL16_PLAF7 Uncharacterized protein OS=Plasmodium falciparum (isolate 3D7) GN=PF14_0434 PE=4 SV=1 | 8 | 0.87 | 0.22 | 0.0000 |
| tr\|Q8I5H7\|Q8I5H7_PLAF7 GTP cyclohydrolase I OS=Plasmodium falciparum (isolate 3D7) GN=PFL1155w PE=4 SV=1 | 8 | 0.87 | 0.20 | 0.0000 |
| tr\|Q8IJD0\|Q8IJD0_PLAF7 Merozoite capping protein 1 OS=Plasmodium falciparum (isolate 3D7) GN=PF10_0268 PE=4 SV=1 | 8 | 0.87 | 0.11 | 0.0000 |
| tr\|Q8IJR6\|Q8IJR6_PLAF7 Conserved Plasmodium protein OS=Plasmodium falciparum (isolate 3D7) GN=PF10_0126 PE=4 SV=1 | 8 | 0.87 | 0.17 | 0.0000 |
| tr\|Q7KWI7\|Q7KWI7_PLAF7 Plasmodium exported protein OS=Plasmodium falciparum (isolate 3D7) GN=PFB0921c PE=4 SV=1 | 8 | 0.87 | 0.31 | 0.0001 |
| tr\|Q8IIW1\|Q8IIW1_PLAF7 Qa-SNARE protein, putative OS=Plasmodium falciparum (isolate 3D7) GN=Syn13 PE=4 SV=2 | 8 | 0.87 | 0.34 | 0.0002 |

| | | | | |
|---|---|---|---|---|
| tr\|Q8IB73\|Q8IB73_PLAF7 Oxoglutarate/malate translocator protein, putative OS=Plasmodium falciparum (isolate 3D7) GN=PF08_0031 PE=3 SV=1 | 8 | 0.87 | 0.29 | 0.0001 |
| sp\|O77323\|TCPH_PLAF7 T-complex protein 1 subunit eta OS=Plasmodium falciparum (isolate 3D7) GN=MAL3P3.6 PE=3 SV=1 | 8 | 1129.23 | 2602.48 | 0.2594 |
| tr\|Q8IIW2\|Q8IIW2_PLAF7 Phenylalanine--tRNA ligase, putative OS=Plasmodium falciparum (isolate 3D7) GN=PF11_0051 PE=4 SV=1 | 8 | 937.94 | 2550.99 | 0.3329 |
| sp\|Q8IDF6\|PURA_PLAF7 Adenylosuccinate synthetase OS=Plasmodium falciparum (isolate 3D7) GN=Adss PE=3 SV=1 | 8 | 549.61 | 1490.63 | 0.3317 |
| tr\|Q8IJ77\|Q8IJ77_PLAF7 S-adenosylmethionine decarboxylase-ornithine decarboxylase OS=Plasmodium falciparum (isolate 3D7) GN=PF10_0322 PE=3 SV=1 | 8 | 93.59 | 218.95 | 0.2659 |
| sp\|Q7KQL8\|THIO_PLAF7 Thioredoxin OS=Plasmodium falciparum (isolate 3D7) GN=PF14_0545 PE=1 SV=1 | 8 | 757.79 | 2098.65 | 0.3411 |
| tr\|Q8IDM2\|Q8IDM2_PLAF7 Ethanolamine-phosphate cytidylyltransferase, putative OS=Plasmodium falciparum (isolate 3D7) GN=PF13_0253 PE=4 SV=1 | 8 | 181.77 | 483.81 | 0.3232 |
| tr\|Q8IDK7\|Q8IDK7_PLAF7 Glutamate--tRNA ligase, putative OS=Plasmodium falciparum (isolate 3D7) GN=PF13_0257 PE=3 SV=1 | 8 | 63.51 | 88.62 | 0.0823 |
| tr\|O97244\|O97244_PLAF7 Activator of Hsp90 ATPase, putative OS=Plasmodium falciparum (isolate 3D7) GN=PFC0270w PE=4 SV=3 | 8 | 286.47 | 726.01 | 0.3012 |
| tr\|Q8ILS7\|Q8ILS7_PLAF7 Prefoldin subunit 2, putative OS=Plasmodium falciparum (isolate 3D7) GN=PF14_0167 PE=4 SV=1 | 8 | 81.80 | 189.78 | 0.2623 |
| tr\|Q8IAU3\|Q8IAU3_PLAF7 Dihydropteroate synthetase OS=Plasmodium falciparum (isolate 3D7) GN=DHPS PE=4 SV=1 | 8 | 369.78 | 1014.79 | 0.3370 |
| sp\|Q8ILQ7\|GST_PLAF7 Glutathione S-transferase OS=Plasmodium falciparum (isolate 3D7) GN=GST PE=3 SV=1 | 8 | 142.45 | 348.62 | 0.2857 |
| tr\|Q8IKU1\|Q8IKU1_PLAF7 p23 co-chaperone, putative OS=Plasmodium falciparum (isolate 3D7) GN=SBA1 PE=4 SV=2 | 8 | 202.86 | 465.92 | 0.2579 |
| tr\|Q8I6Z4\|Q8I6Z4_PLAF7 RNAse L inhibitor protein, putative OS=Plasmodium falciparum (isolate 3D7) GN=MAL13P1.344 PE=3 SV=1 | 8 | 62.34 | 142.18 | 0.2549 |
| tr\|Q8IIW0\|Q8IIW0_PLAF7 PfSNF2L OS=Plasmodium falciparum (isolate 3D7) GN=PF11_0053 PE=4 SV=1 | 8 | 0.87 | 0.20 | 0.0000 |
| tr\|Q8I2W4\|Q8I2W4_PLAF7 Gamma-glutamylcysteine synthetase OS=Plasmodium falciparum (isolate 3D7) GN=PFI0925w PE=4 SV=1 | 8 | 589.20 | 1642.61 | 0.3441 |
| tr\|Q8I4V8\|Q8I4V8_PLAF7 FK506-binding protein (FKBP)-type peptidyl-propyl isomerase OS=Plasmodium falciparum (isolate 3D7) GN=FKBP35 PE=1 SV=1 | 8 | 826.05 | 2279.49 | 0.3395 |
| sp\|Q8I5R7\|SYP_PLAF7 Proline--tRNA ligase OS=Plasmodium falciparum (isolate 3D7) GN=proRS PE=1 SV=1 | 8 | 67.91 | 121.90 | 0.1591 |
| tr\|O96203\|O96203_PLAF7 Peptide chain release factor subunit 1, putative OS=Plasmodium falciparum (isolate 3D7) GN=PFB0550w PE=4 SV=1 | 8 | 36.37 | 61.46 | 0.1381 |
| tr\|C0H5J6\|C0H5J6_PLAF7 Sec24 subunit, putative OS=Plasmodium falciparum (isolate 3D7) GN=PF13_0324 PE=4 SV=1 | 8 | 54.21 | 88.26 | 0.1259 |
| tr\|Q8ID31\|Q8ID31_PLAF7 Alanine--tRNA ligase OS=Plasmodium falciparum (isolate 3D7) GN=PF13_0354 PE=3 SV=1 | 8 | 95.12 | 240.00 | 0.2993 |
| sp\|Q8IIG7\|YPF05_PLAF7 Uncharacterized protein PF11_0207 OS=Plasmodium falciparum (isolate 3D7) GN=PF11_0207 PE=4 SV=2 | 8 | 118.77 | 309.61 | 0.3139 |
| tr\|Q8I4Y9\|Q8I4Y9_PLAF7 Uncharacterized protein OS=Plasmodium falciparum (isolate 3D7) GN=PFL2120w PE=4 SV=1 | 8 | 138.03 | 372.60 | 0.3296 |
| tr\|O97282\|O97282_PLAF7 T-complex protein 1 epsilon subunit, putative OS=Plasmodium falciparum (isolate 3D7) GN=PFC0900w PE=3 SV=1 | 8 | 21.62 | 38.91 | 0.1600 |
| tr\|Q8IKL5\|Q8IKL5_PLAF7 Valine-tRNA ligase, putative OS=Plasmodium falciparum (isolate 3D7) GN=PF14_0589 PE=3 SV=1 | 8 | 87.37 | 231.84 | 0.3218 |
| tr\|Q8IJR9\|Q8IJR9_PLAF7 GMP synthetase OS=Plasmodium falciparum (isolate 3D7) GN=PF10_0123 PE=1 SV=1 | 8 | 48.69 | 115.52 | 0.2720 |
| tr\|Q8I5C5\|Q8I5C5_PLAF7 Macrophage migration inhibitory factor homologue OS=Plasmodium falciparum (isolate 3D7) GN=MIF PE=1 SV=1 | 8 | 30.90 | 66.00 | 0.2271 |
| tr\|O96198\|O96198_PLAF7 Asparagine-tRNA ligase, putative OS=Plasmodium falciparum (isolate 3D7) GN=PFB0525w PE=3 SV=1 | 8 | 167.74 | 462.45 | 0.3391 |
| tr\|Q8IAM0\|Q8IAM0_PLAF7 Glutamate dehydrogenase, putative OS=Plasmodium falciparum (isolate 3D7) GN=PF08_0132 PE=4 SV=1 | 8 | 16.95 | 29.57 | 0.1490 |
| tr\|O97247\|O97247_PLAF7 T-complex protein beta subunit, putative OS=Plasmodium falciparum (isolate 3D7) GN=PFC0285c PE=3 SV=3 | 8 | 56.82 | 144.83 | 0.3038 |
| tr\|Q8IBM9\|Q8IBM9_PLAF7 Obg-like ATPase 1 OS=Plasmodium falciparum (isolate 3D7) GN=MAL7P1.122 PE=3 SV=1 | 8 | 70.44 | 185.51 | 0.3184 |
| tr\|A0A087WUQ6\|A0A087WUQ6_HUMAN Glutathione peroxidase OS=Homo sapiens GN=GPX1 PE=1 SV=1;sp\|P07203\|GPX1_HUMAN Glutathione peroxidase 1 OS=Homo sapiens GN=GPX1 PE=1 SV=4 | 8 | 15.85 | 27.52 | 0.1472 |

| | | | | |
|---|---|---|---|---|
| tr\|Q8I3L8\|Q8I3L8_PLAF7 Mitochondrial import receptor subunit, putative (TOM22) OS=Plasmodium falciparum (isolate 3D7) GN=PFE1230c PE=4 SV=1 | 8 | 1133.44 | 1783.99 | 0.1154 |
| tr\|O77379\|O77379_PLAF7 Proteasome regulatory protein, putative OS=Plasmodium falciparum (isolate 3D7) GN=PFC0785c PE=4 SV=1 | 8 | 15.25 | 18.42 | 0.0517 |
| tr\|C6KST5\|C6KST5_PLAF7 Chaperone, putative OS=Plasmodium falciparum (isolate 3D7) GN=PFF0430w PE=3 SV=1 | 8 | 12.56 | 17.55 | 0.0826 |
| tr\|C0H5I7\|C0H5I7_PLAF7 T-complex protein 1 subunit delta OS=Plasmodium falciparum (isolate 3D7) GN=MAL13P1.283 PE=3 SV=1 | 8 | 17.82 | 32.12 | 0.1606 |
| tr\|Q8I1R6\|Q8I1R6_PLAF7 Bifunctional dihydrofolate reductase-thymidylate synthase OS=Plasmodium falciparum (isolate 3D7) GN=DHFR-TS PE=3 SV=1 | 8 | 57.01 | 146.32 | 0.3069 |
| tr\|Q8IJW2\|Q8IJW2_PLAF7 Uncharacterized protein OS=Plasmodium falciparum (isolate 3D7) GN=PF10_0079 PE=4 SV=1 | 8 | 0.88 | 0.29 | 0.0001 |
| tr\|Q8I603\|Q8I603_PLAF7 Eukaryotic initiation factor 5a, putative OS=Plasmodium falciparum (isolate 3D7) GN=PFL0210c PE=4 SV=1 | 8 | 12.49 | 15.52 | 0.0570 |
| tr\|Q8I5F4\|Q8I5F4_PLAF7 Uncharacterized protein OS=Plasmodium falciparum (isolate 3D7) GN=PFL1270w PE=4 SV=1 | 8 | 13.08 | 17.22 | 0.0689 |
| tr\|Q8I566\|Q8I566_PLAF7 Serine hydroxymethyltransferase OS=Plasmodium falciparum (isolate 3D7) GN=PFL1720w PE=1 SV=1 | 8 | 14.53 | 20.79 | 0.0885 |
| tr\|Q8IBC3\|Q8IBC3_PLAF7 Prohibitin, putative OS=Plasmodium falciparum (isolate 3D7) GN=PF08_0006 PE=4 SV=1 | 8 | 0.88 | 0.30 | 0.0001 |
| tr\|Q8IIM8\|Q8IIM8_PLAF7 Uncharacterized protein OS=Plasmodium falciparum (isolate 3D7) GN=PF11_0142 PE=4 SV=1 | 8 | 30.74 | 75.42 | 0.2868 |
| tr\|O77312\|O77312_PLAF7 Exportin 1, putative OS=Plasmodium falciparum (isolate 3D7) GN=PFC0135c PE=4 SV=2 | 8 | 15.64 | 27.80 | 0.1555 |
| tr\|C6KSM2\|C6KSM2_PLAF7 MYND finger protein, putative OS=Plasmodium falciparum (isolate 3D7) GN=PFF0105w PE=4 SV=1 | 8 | 74.27 | 199.15 | 0.3266 |
| tr\|Q8IJA9\|Q8IJA9_PLAF7 Adenosine deaminase, putative OS=Plasmodium falciparum (isolate 3D7) GN=PF10_0289 PE=4 SV=1 | 8 | 8.90 | 10.85 | 0.0533 |
| tr\|Q7KQK3\|Q7KQK3_PLAF7 Heat shock protein DNAJ homologue Pfj4 OS=Plasmodium falciparum (isolate 3D7) GN=PFL0565w PE=4 SV=1 | 8 | 12.76 | 17.93 | 0.0839 |
| tr\|Q8IB60\|Q8IB60_PLAF7 PfSec23 protein OS=Plasmodium falciparum (isolate 3D7) GN=Pfsec23 PE=2 SV=1 | 8 | 166.81 | 462.96 | 0.3421 |
| tr\|Q8I3X4\|Q8I3X4_PLAF7 Purine nucleotide phosphorylase, putative OS=Plasmodium falciparum (isolate 3D7) GN=PFE0660c PE=1 SV=1 | 8 | 17.08 | 36.42 | 0.2262 |
| tr\|Q8IDV0\|Q8IDV0_PLAF7 Elongation factor 1-gamma, putative OS=Plasmodium falciparum (isolate 3D7) GN=PF13_0214 PE=4 SV=2 | 8 | 8.89 | 11.39 | 0.0630 |
| tr\|Q8IJU2\|Q8IJU2_PLAF7 Conserved Plasmodium protein OS=Plasmodium falciparum (isolate 3D7) GN=PF10_0100 PE=4 SV=1 | 8 | 0.88 | 0.09 | 0.0000 |
| tr\|Q8IDG8\|Q8IDG8_PLAF7 Membrane-associated histidine rich protein 2 OS=Plasmodium falciparum (isolate 3D7) GN=PF13_0276 PE=4 SV=1 | 8 | 329.22 | 424.63 | 0.0644 |
| tr\|C6KSV3\|C6KSV3_PLAF7 Transketolase OS=Plasmodium falciparum (isolate 3D7) GN=PfTK PE=4 SV=1 | 8 | 8.80 | 11.88 | 0.0746 |
| tr\|Q8IEL0\|Q8IEL0_PLAF7 Uncharacterized protein OS=Plasmodium falciparum (isolate 3D7) GN=MAL13P1.50 PE=4 SV=1 | 8 | 0.88 | 0.18 | 0.0000 |
| tr\|Q8IKW5\|Q8IKW5_PLAF7 Elongation factor 2 OS=Plasmodium falciparum (isolate 3D7) GN=PF14_0486 PE=4 SV=1 | 8 | 7.83 | 9.44 | 0.0515 |
| tr\|Q8IIC0\|Q8IIC0_PLAF7 Uncharacterized protein OS=Plasmodium falciparum (isolate 3D7) GN=PF11_0254 PE=4 SV=1 | 8 | 0.88 | 0.31 | 0.0001 |
| tr\|Q8IJA0\|Q8IJA0_PLAF7 26S proteasome subunit, putative OS=Plasmodium falciparum (isolate 3D7) GN=PF10_0298 PE=4 SV=1 | 8 | 23.11 | 51.75 | 0.2471 |
| tr\|Q8I3A5\|Q8I3A5_PLAF7 Signal peptidase, putative OS=Plasmodium falciparum (isolate 3D7) GN=PFI0215c PE=4 SV=1 | 8 | 0.88 | 0.32 | 0.0001 |
| tr\|Q8II42\|Q8II42_PLAF7 Conserved Plasmodium protein OS=Plasmodium falciparum (isolate 3D7) GN=PF11_0332 PE=4 SV=1 | 8 | 106.79 | 290.00 | 0.3323 |
| sp\|Q6LFH8\|OAT_PLAF7 Ornithine aminotransferase OS=Plasmodium falciparum (isolate 3D7) GN=OAT PE=1 SV=1 | 8 | 8.53 | 11.82 | 0.0807 |
| tr\|C0H4M1\|C0H4M1_PLAF7 AAA family ATPase, putative OS=Plasmodium falciparum (isolate 3D7) GN=MAL7P1.209 PE=4 SV=1 | 8 | 0.88 | 0.13 | 0.0000 |
| tr\|Q76NM7\|Q76NM7_PLAF7 Rab5b, GTPase OS=Plasmodium falciparum (isolate 3D7) GN=Rab5b PE=3 SV=1 | 8 | 0.88 | 0.07 | 0.0000 |
| tr\|Q8IJP3\|Q8IJP3_PLAF7 Cysteinyl-tRNA synthetase, putative OS=Plasmodium falciparum (isolate 3D7) GN=PF10_0149 PE=3 SV=2 | 8 | 7.98 | 10.86 | 0.0763 |
| tr\|Q8ILI2\|Q8ILI2_PLAF7 Proliferation-associated protein 2g4, putative OS=Plasmodium falciparum (isolate 3D7) GN=PF14_0261 PE=4 SV=1 | 8 | 6.97 | 8.89 | 0.0621 |
| tr\|Q8IAN7\|Q8IAN7_PLAF7 Tubulin gamma chain OS=Plasmodium falciparum (isolate 3D7) GN=g-tub PE=3 SV=1 | 8 | 0.88 | 0.08 | 0.0000 |

| | | | | |
|---|---|---|---|---|
| tr\|C0H512\|C0H512_PLAF7 Putative uncharacterized protein OS=Plasmodium falciparum (isolate 3D7) GN=PFI0086w PE=4 SV=1 | 8 | 184.50 | 321.97 | 0.1491 |
| tr\|Q8I0V5\|Q8I0V5_PLAF7 Acyl carrier protein OS=Plasmodium falciparum (isolate 3D7) GN=PFL0415w PE=4 SV=1 | 8 | 0.88 | 0.42 | 0.0006 |
| tr\|C6KTA4\|C6KTA4_PLAF7 Pyruvate kinase OS=Plasmodium falciparum (isolate 3D7) GN=PFF1300w PE=1 SV=1 | 8 | 7.29 | 9.86 | 0.0749 |
| tr\|Q8IKK7\|Q8IKK7_PLAF7 Glyceraldehyde-3-phosphate dehydrogenase OS=Plasmodium falciparum (isolate 3D7) GN=GAPDH PE=3 SV=1 | 8 | 7.19 | 9.72 | 0.0749 |
| tr\|Q8IDP4\|Q8IDP4_PLAF7 Thioredoxin OS=Plasmodium falciparum (isolate 3D7) GN=trx2 PE=1 SV=1 | 8 | 214.04 | 529.03 | 0.2901 |
| tr\|O77330\|O77330_PLAF7 Asparagine synthetase OS=Plasmodium falciparum (isolate 3D7) GN=PFC0395w PE=4 SV=1 | 8 | 8.16 | 10.41 | 0.0623 |
| tr\|Q7K6A8\|Q7K6A8_PLAF7 Rab1b, GTPase OS=Plasmodium falciparum (isolate 3D7) GN=Rab1b PE=4 SV=1 | 8 | 0.89 | 0.19 | 0.0000 |
| tr\|Q8I5C4\|Q8I5C4_PLAF7 T-complex protein 1 subunit gamma OS=Plasmodium falciparum (isolate 3D7) GN=PFL1425w PE=3 SV=1 | 8 | 7.73 | 11.89 | 0.1086 |
| tr\|Q8IDQ9\|Q8IDQ9_PLAF7 Phosphoethanolamine N-methyltransferase OS=Plasmodium falciparum (isolate 3D7) GN=PfPMT PE=4 SV=1 | 8 | 6.57 | 8.03 | 0.0539 |
| tr\|Q7K6A4\|Q7K6A4_PLAF7 S-adenosylmethionine synthase OS=Plasmodium falciparum (isolate 3D7) GN=PfSAMS PE=3 SV=1 | 8 | 6.64 | 8.35 | 0.0593 |
| tr\|Q8IJ34\|Q8IJ34_PLAF7 ADP/ATP transporter on adenylate translocase OS=Plasmodium falciparum (isolate 3D7) GN=PF10_0366 PE=3 SV=1 | 8 | 0.89 | 0.16 | 0.0000 |
| tr\|Q8IJ28\|Q8IJ28_PLAF7 Antigen UB05 OS=Plasmodium falciparum (isolate 3D7) GN=PF10_0372 PE=4 SV=2 | 8 | 0.89 | 0.12 | 0.0000 |
| tr\|Q8IAM2\|Q8IAM2_PLAF7 1-cys peroxiredoxin OS=Plasmodium falciparum (isolate 3D7) GN=1-cyspxn PE=4 SV=1 | 8 | 7.29 | 10.74 | 0.0963 |
| sp\|P27362\|PGK_PLAF7 Phosphoglycerate kinase OS=Plasmodium falciparum (isolate 3D7) GN=PGK PE=1 SV=1 | 8 | 7.55 | 10.30 | 0.0767 |
| tr\|Q8I320\|Q8I320_PLAF7 Elongation factor 1-beta OS=Plasmodium falciparum (isolate 3D7) GN=PfEF-1beta PE=4 SV=1 | 8 | 9.06 | 14.52 | 0.1212 |
| tr\|Q8I4U3\|Q8I4U3_PLAF7 Conserved Plasmodium protein OS=Plasmodium falciparum (isolate 3D7) GN=PFL2355w PE=4 SV=1 | 8 | 29.02 | 74.51 | 0.3070 |
| tr\|Q8IM32\|Q8IM32_PLAF7 Uncharacterized protein OS=Plasmodium falciparum (isolate 3D7) GN=PF14_0059 PE=4 SV=1 | 8 | 0.89 | 0.30 | 0.0001 |
| tr\|Q8IJN9\|Q8IJN9_PLAF7 Hsp60 OS=Plasmodium falciparum (isolate 3D7) GN=PF10_0153 PE=3 SV=1 | 8 | 0.89 | 0.08 | 0.0000 |
| tr\|Q8II36\|Q8II36_PLAF7 Aquaglyceroporin OS=Plasmodium falciparum (isolate 3D7) GN=PF11_0338 PE=3 SV=1 | 8 | 0.89 | 0.24 | 0.0000 |
| tr\|Q76NM3\|Q76NM3_PLAF7 L-lactate dehydrogenase OS=Plasmodium falciparum (isolate 3D7) GN=PfLDH PE=1 SV=1 | 8 | 7.04 | 10.06 | 0.0883 |
| tr\|Q8IHZ2\|Q8IHZ2_PLAF7 Uncharacterized protein OS=Plasmodium falciparum (isolate 3D7) GN=PF11_0384 PE=4 SV=1 | 8 | 0.90 | 0.30 | 0.0001 |
| tr\|C0H5M6\|C0H5M6_PLAF7 Uncharacterized protein OS=Plasmodium falciparum (isolate 3D7) GN=MAL13P1.465 PE=4 SV=1 | 8 | 0.90 | 0.20 | 0.0000 |
| tr\|Q8IK12\|Q8IK12_PLAF7 Uncharacterized protein OS=Plasmodium falciparum (isolate 3D7) GN=PF10_0028 PE=4 SV=1 | 8 | 0.90 | 0.09 | 0.0000 |
| sp\|P00492\|HPRT_HUMAN Hypoxanthine-guanine phosphoribosyltransferase OS=Homo sapiens GN=HPRT1 PE=1 SV=2 | 8 | 8.36 | 13.30 | 0.1186 |
| sp\|Q8ILI6\|AN32_PLAF7 Acidic leucine-rich nuclear phosphoprotein 32-related protein OS=Plasmodium falciparum (isolate 3D7) GN=PF14_0257 PE=3 SV=1 | 8 | 6.88 | 11.47 | 0.1337 |
| tr\|Q8IK07\|Q8IK07_PLAF7 Conserved Plasmodium protein OS=Plasmodium falciparum (isolate 3D7) GN=PF10_0033 PE=4 SV=2 | 8 | 0.90 | 0.56 | 0.0027 |
| tr\|Q8IJZ3\|Q8IJZ3_PLAF7 Uncharacterized protein OS=Plasmodium falciparum (isolate 3D7) GN=PF10_0047 PE=4 SV=1 | 8 | 0.90 | 0.20 | 0.0000 |
| sp\|Q7KQL3\|ARF1_PLAF7 ADP-ribosylation factor 1 OS=Plasmodium falciparum (isolate 3D7) GN=ARF1 PE=1 SV=1 | 8 | 7.73 | 14.65 | 0.1791 |
| tr\|Q8IKM7\|Q8IKM7_PLAF7 Uncharacterized protein OS=Plasmodium falciparum (isolate 3D7) GN=PF14_0577 PE=4 SV=1 | 8 | 0.90 | 0.44 | 0.0006 |
| tr\|C0H571\|C0H571_PLAF7 High molecular weight rhoptry protein-2 OS=Plasmodium falciparum (isolate 3D7) GN=RhopH2 PE=4 SV=1 | 8 | 0.90 | 0.12 | 0.0000 |
| tr\|Q8IHY0\|Q8IHY0_PLAF7 Protein phosphatase 2C OS=Plasmodium falciparum (isolate 3D7) GN=PF11_0396 PE=3 SV=2 | 8 | 6.90 | 11.87 | 0.1443 |
| tr\|Q8IKX4\|Q8IKX4_PLAF7 Signal recognition particle SRP54, putative OS=Plasmodium falciparum (isolate 3D7) GN=PF14_0477 PE=3 SV=1 | 8 | 6.61 | 10.31 | 0.1128 |
| tr\|Q8II64\|Q8II64_PLAF7 Uncharacterized protein OS=Plasmodium falciparum (isolate 3D7) GN=PF11_0310 PE=4 SV=1 | 8 | 0.91 | 0.17 | 0.0000 |

| | | | | |
|---|---|---|---|---|
| tr\|C6KT67\|C6KT67_PLAF7 Coronin binding protein OS=Plasmodium falciparum (isolate 3D7) GN=PFF1110c PE=4 SV=1 | 8 | 0.91 | 0.39 | 0.0003 |
| tr\|Q8IK17\|Q8IK17_PLAF7 Uncharacterized protein OS=Plasmodium falciparum (isolate 3D7) GN=PF10_0023 PE=4 SV=1 | 8 | 0.91 | 0.15 | 0.0000 |
| tr\|Q8I450\|Q8I450_PLAF7 Actin-like protein, putative OS=Plasmodium falciparum (isolate 3D7) GN=PFE0255w PE=3 SV=1 | 8 | 0.91 | 0.30 | 0.0001 |
| tr\|X6R4N5\|X6R4N5_HUMAN Erythroid membrane-associated protein OS=Homo sapiens GN=ERMAP PE=1 SV=1;sp\|Q96PL5\|ERMAP_HUMAN Erythroid membrane-associated protein OS=Homo sapiens GN=ERMAP PE=1 SV=1 | 8 | 0.91 | 0.21 | 0.0000 |
| tr\|Q8IC01\|Q8IC01_PLAF7 Cg4 protein OS=Plasmodium falciparum (isolate 3D7) GN=PF07_0033 PE=3 SV=1 | 8 | 4.61 | 5.92 | 0.0635 |
| sp\|Q9UJC5\|SH3L2_HUMAN SH3 domain-binding glutamic acid-rich-like protein 2 OS=Homo sapiens GN=SH3BGRL2 PE=1 SV=2 | 8 | 0.91 | 0.15 | 0.0000 |
| tr\|Q8ILE3\|Q8ILE3_PLAF7 Uncharacterized protein OS=Plasmodium falciparum (isolate 3D7) GN=PF14_0301 PE=4 SV=1 | 8 | 0.91 | 0.10 | 0.0000 |
| tr\|Q8IHU0\|Q8IHU0_PLAF7 Uncharacterized protein OS=Plasmodium falciparum (isolate 3D7) GN=PF11_0437 PE=1 SV=1 | 8 | 40.60 | 98.56 | 0.2822 |
| tr\|Q8I2H1\|Q8I2H1_PLAF7 UBX domain, putative OS=Plasmodium falciparum (isolate 3D7) GN=PFI1680w PE=4 SV=1 | 8 | 0.91 | 0.11 | 0.0000 |
| tr\|Q8ILU8\|Q8ILU8_PLAF7 Ribonucleoprotein, putative OS=Plasmodium falciparum (isolate 3D7) GN=PF14_0146 PE=4 SV=1 | 8 | 0.91 | 0.33 | 0.0001 |
| tr\|O96212\|O96212_PLAF7 Heat shock 40 kDa protein, putative OS=Plasmodium falciparum (isolate 3D7) GN=PFB0595w PE=4 SV=1 | 8 | 7.46 | 15.24 | 0.2086 |
| tr\|Q8IJT8\|Q8IJT8_PLAF7 Conserved Plasmodium protein OS=Plasmodium falciparum (isolate 3D7) GN=PF10_0104 PE=4 SV=1 | 8 | 0.91 | 0.48 | 0.0010 |
| tr\|Q8IKY7\|Q8IKY7_PLAF7 SNARE protein, putative OS=Plasmodium falciparum (isolate 3D7) GN=PfVti1 PE=4 SV=1 | 8 | 0.91 | 0.06 | 0.0000 |
| tr\|Q8I500\|Q8I500_PLAF7 Mitochondrial import inner membrane translocase subunit, putative OS=Plasmodium falciparum (isolate 3D7) GN=PFL2065c PE=4 SV=2 | 8 | 46.94 | 62.15 | 0.0700 |
| tr\|O97336\|O97336_PLAF7 Putative uncharacterized protein OS=Plasmodium falciparum (isolate 3D7) GN=PFC0085c PE=4 SV=2 | 8 | 0.91 | 0.13 | 0.0000 |
| tr\|Q8IJW6\|Q8IJW6_PLAF7 Asparagine-rich antigen OS=Plasmodium falciparum (isolate 3D7) GN=PF10_0075 PE=4 SV=1 | 8 | 0.91 | 0.12 | 0.0000 |
| tr\|Q8IHN4\|Q8IHN4_PLAF7 Antigen 332, DBL-like protein OS=Plasmodium falciparum (isolate 3D7) GN=PF11_0506 PE=4 SV=2 | 8 | 0.91 | 0.07 | 0.0000 |
| tr\|Q8IJY4\|Q8IJY4_PLAF7 Regulator of nonsense transcripts, putative OS=Plasmodium falciparum (isolate 3D7) GN=PF10_0057 PE=4 SV=1 | 8 | 0.91 | 0.31 | 0.0001 |
| tr\|Q8I3T9\|Q8I3T9_PLAF7 60S ribosomal protein L8, putative OS=Plasmodium falciparum (isolate 3D7) GN=PFE0845c PE=1 SV=1 | 8 | 8.08 | 18.18 | 0.2491 |
| tr\|Q8IJ85\|Q8IJ85_PLAF7 Asparagine-rich antigen OS=Plasmodium falciparum (isolate 3D7) GN=PF10_0314 PE=4 SV=1 | 8 | 20.80 | 46.98 | 0.2507 |
| tr\|Q8I5T3\|Q8I5T3_PLAF7 p-type ATPase, putative OS=Plasmodium falciparum (isolate 3D7) GN=PFL0590c PE=3 SV=1 | 8 | 0.91 | 0.12 | 0.0000 |
| tr\|Q7K6B0\|Q7K6B0_PLAF7 PfRab18, GTPase OS=Plasmodium falciparum (isolate 3D7) GN=rab18 PE=3 SV=1 | 8 | 0.92 | 0.20 | 0.0000 |
| tr\|Q8I5E9\|Q8I5E9_PLAF7 Uncharacterized protein OS=Plasmodium falciparum (isolate 3D7) GN=PFL1300c PE=4 SV=1 | 8 | 0.92 | 0.11 | 0.0000 |
| tr\|Q8I4W4\|Q8I4W4_PLAF7 Signal recognition particle, beta subunit, putative OS=Plasmodium falciparum (isolate 3D7) GN=PFL2245w PE=4 SV=1 | 8 | 0.92 | 0.39 | 0.0003 |
| tr\|Q8IBI8\|Q8IBI8_PLAF7 Protein phosphatase, putative OS=Plasmodium falciparum (isolate 3D7) GN=PF07_0110 PE=4 SV=1 | 8 | 0.92 | 0.45 | 0.0007 |
| tr\|Q8IBL9\|Q8IBL9_PLAF7 Uncharacterized protein OS=Plasmodium falciparum (isolate 3D7) GN=PF07_0097 PE=4 SV=1 | 8 | 31.36 | 64.14 | 0.2092 |
| tr\|Q8IIB4\|Q8IIB4_PLAF7 60S ribosomal protein L35, putative OS=Plasmodium falciparum (isolate 3D7) GN=PF11_0260 PE=1 SV=2 | 8 | 370.05 | 716.81 | 0.1876 |
| tr\|Q8IDI2\|Q8IDI2_PLAF7 Uncharacterized protein OS=Plasmodium falciparum (isolate 3D7) GN=PF13_0270 PE=4 SV=1 | 8 | 28.92 | 76.36 | 0.3196 |
| sp\|O75695\|XRP2_HUMAN Protein XRP2 OS=Homo sapiens GN=RP2 PE=1 SV=4 | 8 | 0.92 | 0.36 | 0.0002 |
| tr\|O77385\|O77385_PLAF7 Protein kinase, putative OS=Plasmodium falciparum (isolate 3D7) GN=Pfcrk-4 PE=4 SV=1 | 8 | 0.92 | 0.19 | 0.0000 |
| tr\|Q8ILQ6\|Q8ILQ6_PLAF7 Uncharacterized protein OS=Plasmodium falciparum (isolate 3D7) GN=PF14_0188 PE=4 SV=2 | 8 | 3.93 | 5.97 | 0.1048 |
| tr\|Q8IIK2\|Q8IIK2_PLAF7 Uncharacterized protein OS=Plasmodium falciparum (isolate 3D7) GN=PF11_0171 PE=4 SV=1 | 8 | 0.92 | 0.44 | 0.0006 |

| | | | | |
|---|---|---|---|---|
| sp\|P61225\|RAP2B_HUMAN Ras-related protein Rap-2b OS=Homo sapiens GN=RAP2B PE=1 SV=1 | 8 | 0.92 | 0.19 | 0.0000 |
| tr\|C0H4Z7\|C0H4Z7_PLAF7 Uncharacterized protein OS=Plasmodium falciparum (isolate 3D7) GN=MAL8P1.206 PE=4 SV=1 | 8 | 0.92 | 0.07 | 0.0000 |
| tr\|Q8IB67\|Q8IB67_PLAF7 Histone acetyltransferase GCN5, putative OS=Plasmodium falciparum (isolate 3D7) GN=gcn5 PE=1 SV=2 | 8 | 0.92 | 0.33 | 0.0001 |
| tr\|Q8IM31\|Q8IM31_PLAF7 Glycerophodiester phosphodiesterase, putative OS=Plasmodium falciparum (isolate 3D7) GN=PF14_0060 PE=4 SV=1 | 8 | 25.66 | 65.02 | 0.3011 |
| tr\|Q8IKY0\|Q8IKY0_PLAF7 Transcription factor with AP2 domain(S), putative OS=Plasmodium falciparum (isolate 3D7) GN=ApiAP2 PE=4 SV=1 | 8 | 0.92 | 0.47 | 0.0008 |
| tr\|C0H4B1\|C0H4B1_PLAF7 Memo-like protein OS=Plasmodium falciparum (isolate 3D7) GN=PFD0850c PE=3 SV=1 | 8 | 13.79 | 33.54 | 0.2830 |
| sp\|P07384\|CAN1_HUMAN Calpain-1 catalytic subunit OS=Homo sapiens GN=CAPN1 PE=1 SV=1 | 8 | 0.92 | 0.10 | 0.0000 |
| tr\|O96264\|O96264_PLAF7 DEAD/DEAH box helicase, putative OS=Plasmodium falciparum (isolate 3D7) GN=PFB0860c PE=3 SV=1 | 8 | 0.93 | 0.25 | 0.0000 |
| tr\|Q8I266\|Q8I266_PLAF7 Lipid/sterol:H+ symporter OS=Plasmodium falciparum (isolate 3D7) GN=PFA_0375c PE=4 SV=1 | 8 | 0.93 | 0.05 | 0.0000 |
| tr\|O96236\|O96236_PLAF7 DNA-directed RNA polymerase OS=Plasmodium falciparum (isolate 3D7) GN=PFB0715w PE=3 SV=3 | 8 | 0.93 | 0.23 | 0.0000 |
| sp\|Q6LFN2\|ZNRF1_PLAF7 RING finger protein PFF0165c OS=Plasmodium falciparum (isolate 3D7) GN=PFF0165c PE=2 SV=1 | 8 | 0.93 | 0.06 | 0.0000 |
| tr\|Q8I3F1\|Q8I3F1_PLAF7 Uncharacterized protein OS=Plasmodium falciparum (isolate 3D7) GN=PFE1600w PE=4 SV=1 | 8 | 0.93 | 0.07 | 0.0000 |
| tr\|Q7K6A5\|Q7K6A5_PLAF7 Multidrug resistance protein OS=Plasmodium falciparum (isolate 3D7) GN=PfMDR1 PE=3 SV=1 | 8 | 0.93 | 0.05 | 0.0000 |
| tr\|Q8IKR1\|Q8IKR1_PLAF7 V-type H(+)-translocating pyrophosphatase, putative OS=Plasmodium falciparum (isolate 3D7) GN=PF14_0541 PE=3 SV=1 | 8 | 0.93 | 0.30 | 0.0000 |
| tr\|C0H570\|C0H570_PLAF7 RNA binding protein, putative OS=Plasmodium falciparum (isolate 3D7) GN=PFI1435w PE=4 SV=1 | 8 | 0.93 | 0.08 | 0.0000 |
| tr\|Q8IKJ0\|Q8IKJ0_PLAF7 ATP synthase (C/AC39) subunit, putative OS=Plasmodium falciparum (isolate 3D7) GN=PF14_0615 PE=4 SV=1 | 8 | 0.93 | 0.08 | 0.0000 |
| tr\|Q8IBJ1\|Q8IBJ1_PLAF7 Ubiquitin carboxyl-terminal hydrolase OS=Plasmodium falciparum (isolate 3D7) GN=MAL7P1.147 PE=3 SV=1 | 8 | 0.93 | 0.38 | 0.0002 |
| tr\|C6KSP9\|C6KSP9_PLAF7 RNA binding protein, putative OS=Plasmodium falciparum (isolate 3D7) GN=PFF0250w PE=4 SV=1 | 8 | 0.93 | 0.28 | 0.0000 |
| tr\|C0H4S8\|C0H4S8_PLAF7 Uncharacterized protein OS=Plasmodium falciparum (isolate 3D7) GN=MAL8P1.127 PE=4 SV=1 | 8 | 0.94 | 0.24 | 0.0000 |
| tr\|Q9U0N1\|Q9U0N1_PLAF7 Glutamic acid-rich protein (Garp) OS=Plasmodium falciparum (isolate 3D7) GN=PFA_0620c PE=4 SV=1 | 8 | 0.94 | 0.10 | 0.0000 |
| sp\|Q8I4V5\|UTP11_PLAF7 Probable U3 small nucleolar RNA-associated protein 11 OS=Plasmodium falciparum (isolate 3D7) GN=PFL2295w PE=3 SV=1 | 8 | 0.94 | 0.36 | 0.0002 |
| tr\|Q8ILQ3\|Q8ILQ3_PLAF7 Uncharacterized protein OS=Plasmodium falciparum (isolate 3D7) GN=PF14_0191 PE=4 SV=1 | 8 | 0.94 | 0.27 | 0.0000 |
| tr\|Q8I206\|Q8I206_PLAF7 Uncharacterized protein OS=Plasmodium falciparum (isolate 3D7) GN=PFD0090c PE=4 SV=1 | 8 | 0.94 | 0.05 | 0.0000 |
| tr\|Q8IBE9\|Q8IBE9_PLAF7 Uncharacterized protein OS=Plasmodium falciparum (isolate 3D7) GN=MAL7P1.174 PE=4 SV=1 | 8 | 0.94 | 0.19 | 0.0000 |
| tr\|Q8IBY4\|Q8IBY4_PLAF7 60S ribosomal protein L34-A, putative OS=Plasmodium falciparum (isolate 3D7) GN=PF07_0043 PE=1 SV=1 | 8 | 17.07 | 44.59 | 0.3149 |
| tr\|Q8IBX7\|Q8IBX7_PLAF7 Uncharacterized protein OS=Plasmodium falciparum (isolate 3D7) GN=MAL7P1.36 PE=4 SV=1 | 8 | 65.67 | 182.57 | 0.3429 |
| tr\|Q8I669\|Q8I669_PLAF7 Plasmodium exported protein OS=Plasmodium falciparum (isolate 3D7) GN=PFB0106c PE=4 SV=1 | 8 | 0.94 | 0.09 | 0.0000 |
| tr\|C6KTC9\|C6KTC9_PLAF7 RNA binding protein, putative OS=Plasmodium falciparum (isolate 3D7) GN=PFF1425w PE=4 SV=1 | 8 | 24.87 | 50.92 | 0.2096 |
| tr\|Q8IJP8\|Q8IJP8_PLAF7 Prohibitin, putative OS=Plasmodium falciparum (isolate 3D7) GN=PF10_0144 PE=4 SV=1 | 8 | 19.01 | 50.85 | 0.3255 |
| tr\|Q8IKF6\|Q8IKF6_PLAF7 Uncharacterized protein OS=Plasmodium falciparum (isolate 3D7) GN=PF14_0649 PE=4 SV=1 | 8 | 0.94 | 0.12 | 0.0000 |
| tr\|Q8ILC8\|Q8ILC8_PLAF7 DNA topoisomerase 2 OS=Plasmodium falciparum (isolate 3D7) GN=PF14_0316 PE=3 SV=1 | 8 | 0.94 | 0.33 | 0.0001 |
| tr\|Q8II73\|Q8II73_PLAF7 Spermidine synthase OS=Plasmodium falciparum (isolate 3D7) GN=PF11_0301 PE=1 SV=1 | 8 | 0.95 | 0.09 | 0.0000 |
| tr\|Q8IBF2\|Q8IBF2_PLAF7 Uncharacterized protein OS=Plasmodium falciparum (isolate 3D7) GN=MAL7P1.171 PE=4 SV=1 | 8 | 0.95 | 0.17 | 0.0000 |

| | | | | |
|---|---|---|---|---|
| tr\|Q8IDF7\|Q8IDF7_PLAF7 V-type ATPase, putative OS=Plasmodium falciparum (isolate 3D7) GN=MAL13P1.271 PE=3 SV=1 | 8 | 0.95 | 0.10 | 0.0000 |
| tr\|Q8IKJ1\|Q8IKJ1_PLAF7 Phosphatase, putative OS=Plasmodium falciparum (isolate 3D7) GN=PF14_0614 PE=4 SV=2 | 8 | 0.95 | 0.11 | 0.0000 |
| sp\|P04921-2\|GLPC_HUMAN Isoform Glycophorin-D of Glycophorin-C OS=Homo sapiens GN=GYPC;sp\|P04921-3\|GLPC_HUMAN Isoform 3 of Glycophorin-C OS=Homo sapiens GN=GYPC;sp\|P04921\|GLPC_HUMAN Glycophorin-C OS=Homo sapiens GN=GYPC PE=1 SV=1 | 8 | 0.95 | 0.08 | 0.0000 |
| tr\|Q8IHR4\|Q8IHR4_PLAF7 Dynamin-like protein OS=Plasmodium falciparum (isolate 3D7) GN=dyn1 PE=3 SV=1 | 8 | 0.95 | 0.29 | 0.0000 |
| tr\|Q8I551\|Q8I551_PLAF7 Uncharacterized protein OS=Plasmodium falciparum (isolate 3D7) GN=PFL1800w PE=4 SV=1 | 8 | 0.95 | 0.40 | 0.0003 |
| tr\|Q8ILZ1\|Q8ILZ1_PLAF7 Rhoptry-associated protein 1, RAP1 OS=Plasmodium falciparum (isolate 3D7) GN=PF14_0102 PE=4 SV=1 | 8 | 0.95 | 0.46 | 0.0006 |
| tr\|Q8IIC4\|Q8IIC4_PLAF7 High mobility group-like protein NHP2, putative OS=Plasmodium falciparum (isolate 3D7) GN=PF11_0250 PE=4 SV=1 | 8 | 0.95 | 0.13 | 0.0000 |
| tr\|Q8I205\|Q8I205_PLAF7 Uncharacterized protein OS=Plasmodium falciparum (isolate 3D7) GN=PFD0095c PE=4 SV=1 | 8 | 0.96 | 0.22 | 0.0000 |
| tr\|Q8IKQ9\|Q8IKQ9_PLAF7 Signal peptide peptidase OS=Plasmodium falciparum (isolate 3D7) GN=SPP PE=4 SV=2 | 8 | 0.96 | 0.45 | 0.0005 |
| tr\|Q8I2T2\|Q8I2T2_PLAF7 Ubiquitin-like protein, putative OS=Plasmodium falciparum (isolate 3D7) GN=PFI1085w PE=4 SV=1 | 8 | 0.96 | 0.21 | 0.0000 |
| tr\|Q8IKW4\|Q8IKW4_PLAF7 Uncharacterized protein OS=Plasmodium falciparum (isolate 3D7) GN=PF14_0487 PE=4 SV=1 | 8 | 0.96 | 0.34 | 0.0001 |
| tr\|Q8IIR7\|Q8IIR7_PLAF7 Endoplasmic reticulum-resident calcium binding protein OS=Plasmodium falciparum (isolate 3D7) GN=PF11_0098 PE=4 SV=1 | 8 | 0.96 | 0.63 | 0.0035 |
| tr\|Q8I4R5\|Q8I4R5_PLAF7 Rhoptry neck protein 3, putative OS=Plasmodium falciparum (isolate 3D7) GN=PFL2505c PE=4 SV=1 | 8 | 0.96 | 0.09 | 0.0000 |
| sp\|Q8IBZ9\|CRT_PLAF7 Putative chloroquine resistance transporter OS=Plasmodium falciparum (isolate 3D7) GN=CG10 PE=3 SV=1 | 8 | 0.96 | 0.33 | 0.0001 |
| sp\|Q8ID39\|Y13P2_PLAF7 Uncharacterized protein MAL13P1.336 OS=Plasmodium falciparum (isolate 3D7) GN=MAL13P1.336 PE=4 SV=1 | 8 | 0.97 | 0.30 | 0.0000 |
| tr\|Q8ILA1\|Q8ILA1_PLAF7 Uncharacterized protein OS=Plasmodium falciparum (isolate 3D7) GN=PF14_0344 PE=4 SV=1 | 8 | 0.97 | 0.13 | 0.0000 |
| tr\|Q8I488\|Q8I488_PLAF7 PIESP2 erythrocyte surface protein OS=Plasmodium falciparum (isolate 3D7) GN=PFE0060w PE=4 SV=1 | 8 | 0.97 | 0.35 | 0.0001 |
| tr\|Q8IFP1\|Q8IFP1_PLAF7 U5 small nuclear ribonucleoprotein-specific protein, putative OS=Plasmodium falciparum (isolate 3D7) GN=PFD1060w PE=4 SV=1 | 8 | 0.97 | 0.53 | 0.0013 |
| tr\|Q8IFM0\|Q8IFM0_PLAF7 Uncharacterized protein OS=Plasmodium falciparum (isolate 3D7) GN=PFD1170c PE=4 SV=1 | 8 | 0.97 | 0.05 | 0.0000 |
| tr\|Q8ILZ5\|Q8ILZ5_PLAF7 Tetratricopeptide repeat family protein, putative OS=Plasmodium falciparum (isolate 3D7) GN=PF14_0098 PE=4 SV=1 | 8 | 0.97 | 0.31 | 0.0001 |
| tr\|Q8I4R9\|Q8I4R9_PLAF7 DEAD/DEAH box helicase, putative OS=Plasmodium falciparum (isolate 3D7) GN=PFL2475w PE=3 SV=1 | 8 | 0.97 | 0.22 | 0.0000 |
| tr\|Q8I310\|Q8I310_PLAF7 Phospholipid or glycerol acyltransferase, putative OS=Plasmodium falciparum (isolate 3D7) GN=PFI0695c PE=4 SV=1 | 8 | 12.50 | 32.84 | 0.3172 |
| tr\|Q8I2W2\|Q8I2W2_PLAF7 DNAJ-like molecular chaperone protein, putative OS=Plasmodium falciparum (isolate 3D7) GN=PFI0935w PE=4 SV=1 | 8 | 0.97 | 0.39 | 0.0002 |
| tr\|C0H523\|C0H523_PLAF7 Putative uncharacterized protein OS=Plasmodium falciparum (isolate 3D7) GN=PFI0336w PE=4 SV=1 | 8 | 3.66 | 7.26 | 0.1967 |
| tr\|Q8IIF0\|Q8IIF0_PLAF7 Circumsporozoite-related antigen OS=Plasmodium falciparum (isolate 3D7) GN=PF11_0224 PE=4 SV=1 | 8 | 0.97 | 0.13 | 0.0000 |
| tr\|Q8IB66\|Q8IB66_PLAF7 RNA binding protein, putative OS=Plasmodium falciparum (isolate 3D7) GN=MAL8P1.40 PE=4 SV=1 | 8 | 0.97 | 0.13 | 0.0000 |
| tr\|Q8IJZ2\|Q8IJZ2_PLAF7 Conserved Plasmodium protein OS=Plasmodium falciparum (isolate 3D7) GN=PF10_0048 PE=4 SV=1 | 8 | 0.98 | 0.14 | 0.0000 |
| tr\|Q8IJ39\|Q8IJ39_PLAF7 Conserved Plasmodium protein OS=Plasmodium falciparum (isolate 3D7) GN=PF10_0361 PE=4 SV=1 | 8 | 0.98 | 0.32 | 0.0001 |
| sp\|P27105\|STOM_HUMAN Erythrocyte band 7 integral membrane protein OS=Homo sapiens GN=STOM PE=1 SV=3 | 8 | 0.98 | 0.04 | 0.0000 |
| tr\|Q8I395\|Q8I395_PLAF7 RhopH3 OS=Plasmodium falciparum (isolate 3D7) GN=PFI0265c PE=4 SV=1 | 8 | 0.98 | 0.10 | 0.0000 |
| tr\|Q8IBD1\|Q8IBD1_PLAF7 Tryptophan/threonine-rich antigen OS=Plasmodium falciparum (isolate 3D7) GN=PF08_0003 PE=4 SV=1 | 8 | 0.98 | 0.24 | 0.0000 |
| tr\|Q8IM23\|Q8IM23_PLAF7 Fibrillarin, putative OS=Plasmodium falciparum (isolate 3D7) GN=PF14_0068 PE=3 SV=1 | 8 | 2.25 | 3.01 | 0.0725 |

| | | | | |
|---|---|---|---|---|
| tr\|Q8IKH2\|Q8IKH2_PLAF7 Transcription factor with AP2 domain(S), putative OS=Plasmodium falciparum (isolate 3D7) GN=ApiAP2 PE=1 SV=1 | 8 | 0.98 | 0.33 | 0.0001 |
| tr\|Q8I5M3\|Q8I5M3_PLAF7 Uncharacterized protein OS=Plasmodium falciparum (isolate 3D7) GN=PFL0895c PE=4 SV=1 | 8 | 0.98 | 0.25 | 0.0000 |
| tr\|Q8IBA2\|Q8IBA2_PLAF7 RNA helicase, putative OS=Plasmodium falciparum (isolate 3D7) GN=MAL8P1.19 PE=3 SV=1 | 8 | 3.18 | 4.92 | 0.1103 |
| tr\|Q8IBZ2\|Q8IBZ2_PLAF7 Lysophospholipase, putative OS=Plasmodium falciparum (isolate 3D7) GN=PF07_0040 PE=4 SV=1 | 8 | 0.98 | 0.24 | 0.0000 |
| tr\|Q8IIS4\|Q8IIS4_PLAF7 Transcription factor with AP2 domain(S), putative OS=Plasmodium falciparum (isolate 3D7) GN=PF11_0091 PE=4 SV=1 | 8 | 2.77 | 4.72 | 0.1407 |
| tr\|Q8IIA9\|Q8IIA9_PLAF7 Mitochondrial inner membrane translocase subunit TIM44, putative OS=Plasmodium falciparum (isolate 3D7) GN=PF11_0265 PE=4 SV=2 | 8 | 0.98 | 0.18 | 0.0000 |
| tr\|Q8I3Z9\|Q8I3Z9_PLAF7 Topoisomerase I OS=Plasmodium falciparum (isolate 3D7) GN=PFE0520c PE=4 SV=1 | 8 | 0.98 | 0.35 | 0.0001 |
| tr\|Q8IIJ8\|Q8IIJ8_PLAF7 Heat shock protein 101, putative OS=Plasmodium falciparum (isolate 3D7) GN=PF11_0175 PE=1 SV=1 | 8 | 0.99 | 0.13 | 0.0000 |
| tr\|Q8IDG4\|Q8IDG4_PLAF7 Uncharacterized protein OS=Plasmodium falciparum (isolate 3D7) GN=PF13_0281 PE=4 SV=1 | 8 | 0.99 | 0.33 | 0.0001 |
| sp\|O94919\|ENDD1_HUMAN Endonuclease domain-containing 1 protein OS=Homo sapiens GN=ENDOD1 PE=1 SV=2 | 8 | 0.99 | 0.15 | 0.0000 |
| sp\|P28289\|TMOD1_HUMAN Tropomodulin-1 OS=Homo sapiens GN=TMOD1 PE=1 SV=1;sp\|P28289-2\|TMOD1_HUMAN Isoform 2 of Tropomodulin-1 OS=Homo sapiens GN=TMOD1 | 8 | 0.99 | 0.07 | 0.0000 |
| tr\|O96191\|O96191_PLAF7 Conserved Plasmodium protein OS=Plasmodium falciparum (isolate 3D7) GN=PFB0490c PE=4 SV=1 | 8 | 0.99 | 0.23 | 0.0000 |
| tr\|C0H4G7\|C0H4G7_PLAF7 Uncharacterized protein OS=Plasmodium falciparum (isolate 3D7) GN=PFE1465w PE=4 SV=1 | 8 | 0.99 | 0.58 | 0.0019 |
| tr\|Q8I487\|Q8I487_PLAF7 Skeleton-binding protein 1 OS=Plasmodium falciparum (isolate 3D7) GN=PfSBP1 PE=4 SV=1 | 8 | 0.99 | 0.12 | 0.0000 |
| tr\|Q8IKE8\|Q8IKE8_PLAF7 Uncharacterized protein OS=Plasmodium falciparum (isolate 3D7) GN=PF14_0657 PE=4 SV=1 | 8 | 0.99 | 0.39 | 0.0002 |
| tr\|Q8ILA9\|Q8ILA9_PLAF7 Uncharacterized protein OS=Plasmodium falciparum (isolate 3D7) GN=PF14_0336 PE=4 SV=1 | 8 | 0.99 | 0.54 | 0.0013 |
| tr\|Q8IBB4\|Q8IBB4_PLAF7 Uncharacterized protein OS=Plasmodium falciparum (isolate 3D7) GN=PF08_0010 PE=4 SV=1 | 8 | 0.99 | 0.51 | 0.0009 |
| tr\|C0H4M6\|C0H4M6_PLAF7 Regulator of chromosome condensation, putative OS=Plasmodium falciparum (isolate 3D7) GN=MAL7P1.38 PE=4 SV=1 | 8 | 1.00 | 0.14 | 0.0000 |
| tr\|Q8ILS0\|Q8ILS0_PLAF7 Pseudouridine synthase, putative OS=Plasmodium falciparum (isolate 3D7) GN=PF14_0174 PE=4 SV=1 | 8 | 1.00 | 0.16 | 0.0000 |
| tr\|Q8I492\|Q8I492_PLAF7 Mature parasite-infected erythrocyte surface antigen (MESA) or PfEMP2 OS=Plasmodium falciparum (isolate 3D7) GN=MESA PE=4 SV=1 | 8 | 1.00 | 0.10 | 0.0000 |
| tr\|Q76NL8\|Q76NL8_PLAF7 Falcilysin OS=Plasmodium falciparum (isolate 3D7) GN=flN PE=1 SV=1 | 8 | 1.00 | 0.30 | 0.0000 |
| tr\|Q8IK89\|Q8IK89_PLAF7 Uncharacterized protein OS=Plasmodium falciparum (isolate 3D7) GN=PF14_0717 PE=4 SV=1 | 8 | 1.00 | 0.17 | 0.0000 |
| tr\|Q8IIK8\|Q8IIK8_PLAF7 Peptidyl-prolyl cis-trans isomerase OS=Plasmodium falciparum (isolate 3D7) GN=PF11_0164 PE=3 SV=1 | 8 | 1.00 | 0.94 | 0.0193 |
| tr\|C6KTB9\|C6KTB9_PLAF7 Ethanolaminephosphotransferase, putative OS=Plasmodium falciparum (isolate 3D7) GN=PFF1375c PE=3 SV=1 | 8 | 1.00 | 0.68 | 0.0044 |
| tr\|Q8IAU1\|Q8IAU1_PLAF7 RNA helicase, putative OS=Plasmodium falciparum (isolate 3D7) GN=PF08_0096 PE=3 SV=1 | 8 | 1.00 | 0.34 | 0.0001 |
| tr\|Q8I3R7\|Q8I3R7_PLAF7 Vacuolar ATP synthetase OS=Plasmodium falciparum (isolate 3D7) GN=PFE0965c PE=3 SV=1 | 8 | 1.00 | 0.31 | 0.0000 |
| tr\|Q8IE18\|Q8IE18_PLAF7 Uncharacterized protein OS=Plasmodium falciparum (isolate 3D7) GN=PF13_0165 PE=4 SV=1 | 8 | 1.00 | 0.36 | 0.0001 |
| tr\|Q8I0W8\|Q8I0W8_PLAF7 Deoxyribodipyrimidine photolyase (Photoreactivating enzyme, DNA photolyase), putative OS=Plasmodium falciparum (isolate 3D7) GN=PFE0675c PE=4 SV=1 | 8 | 1.01 | 0.58 | 0.0017 |
| tr\|O96127\|O96127_PLAF7 Conserved Plasmodium protein OS=Plasmodium falciparum (isolate 3D7) GN=PFB0115w PE=4 SV=1 | 8 | 1.01 | 0.13 | 0.0000 |
| tr\|C6KSV9\|C6KSV9_PLAF7 SWI/SNF-related matrix-associated actin-dependent regulator of chromatin OS=Plasmodium falciparum (isolate 3D7) GN=PFF0560c PE=4 SV=1 | 8 | 1.94 | 2.33 | 0.0506 |
| tr\|Q8IJA5\|Q8IJA5_PLAF7 Transcription factor, putative OS=Plasmodium falciparum (isolate 3D7) GN=PF10_0293 PE=3 SV=1 | 8 | 1.01 | 0.43 | 0.0003 |
| tr\|O96150\|O96150_PLAF7 DNA-directed RNA polymerase II 16 kDa subunit, putative OS=Plasmodium falciparum (isolate 3D7) GN=PFB0245c PE=4 SV=1 | 8 | 1.02 | 0.17 | 0.0000 |
| tr\|Q8I3F3\|Q8I3F3_PLAF7 Early transcribed membrane protein 5, ETRAMP5 OS=Plasmodium falciparum (isolate 3D7) GN=ETRAMP5 PE=4 SV=1 | 8 | 1.02 | 0.33 | 0.0000 |

| | | | | |
|---|---|---|---|---|
| sp\|P23276\|KELL_HUMAN Kell blood group glycoprotein OS=Homo sapiens GN=KEL PE=1 SV=2 | 8 | 1.02 | 0.10 | 0.0000 |
| tr\|Q8I3V9\|Q8I3V9_PLAF7 Uncharacterized protein OS=Plasmodium falciparum (isolate 3D7) GN=PFE0745w PE=4 SV=1 | 8 | 1.02 | 0.92 | 0.0165 |
| tr\|Q8I2G1\|Q8I2G1_PLAF7 Ring-exported protein 1 OS=Plasmodium falciparum (isolate 3D7) GN=REX1 PE=4 SV=1 | 8 | 1.02 | 0.16 | 0.0000 |
| tr\|Q8ILL5\|Q8ILL5_PLAF7 Uncharacterized protein OS=Plasmodium falciparum (isolate 3D7) GN=PF14_0228 PE=4 SV=1 | 8 | 1.02 | 0.24 | 0.0000 |
| tr\|Q8IIH4\|Q8IIH4_PLAF7 U2 snRNP auxiliary factor, small subunit, putative OS=Plasmodium falciparum (isolate 3D7) GN=PF11_0200 PE=4 SV=1 | 8 | 1.02 | 0.16 | 0.0000 |
| tr\|Q8ID37\|Q8ID37_PLAF7 U1 small nuclear ribonucleoprotein, putative OS=Plasmodium falciparum (isolate 3D7) GN=MAL13P1.338 PE=4 SV=1 | 8 | 1.02 | 0.18 | 0.0000 |
| tr\|C0H541\|C0H541_PLAF7 Putative uncharacterized protein OS=Plasmodium falciparum (isolate 3D7) GN=PFI0823w PE=4 SV=1 | 8 | 1.02 | 0.48 | 0.0005 |
| tr\|Q8I490\|Q8I490_PLAF7 Uncharacterized protein OS=Plasmodium falciparum (isolate 3D7) GN=PFE0050w PE=4 SV=1 | 8 | 1.02 | 0.19 | 0.0000 |
| tr\|Q8IJF4\|Q8IJF4_PLAF7 Formin 2, putative OS=Plasmodium falciparum (isolate 3D7) GN=PF10_0244 PE=4 SV=2 | 8 | 1.03 | 0.17 | 0.0000 |
| sp\|P02730\|B3AT_HUMAN Band 3 anion transport protein OS=Homo sapiens GN=SLC4A1 PE=1 SV=3;tr\|A0A0A0MS98\|A0A0A0MS98_HUMAN Band 3 anion transport protein OS=Homo sapiens GN=SLC4A1 PE=1 SV=1 | 8 | 1.03 | 0.03 | 0.0000 |
| tr\|Q9NFE6\|Q9NFE6_PLAF7 Eukaryotic translation initiation factor 3 subunit K OS=Plasmodium falciparum (isolate 3D7) GN=PFC0441c PE=3 SV=1 | 8 | 1.03 | 0.13 | 0.0000 |
| tr\|Q8I1T2\|Q8I1T2_PLAF7 Nuclear cap-binding protein, putative OS=Plasmodium falciparum (isolate 3D7) GN=PFD0750w PE=4 SV=1 | 8 | 1.03 | 0.08 | 0.0000 |
| tr\|Q8I207\|Q8I207_PLAF7 Uncharacterized protein OS=Plasmodium falciparum (isolate 3D7) GN=PFD0080c PE=4 SV=1 | 8 | 1.03 | 0.11 | 0.0000 |
| tr\|Q8IHN1\|Q8IHN1_PLAF7 Ring-infected erythrocyte surface antigen, putative OS=Plasmodium falciparum (isolate 3D7) GN=PF11_0509 PE=4 SV=1 | 8 | 1.03 | 0.13 | 0.0000 |
| tr\|O77315\|O77315_PLAF7 DNA-directed RNA polymerase subunit I, putative OS=Plasmodium falciparum (isolate 3D7) GN=PFC0155c PE=4 SV=2 | 8 | 1.04 | 0.18 | 0.0000 |
| tr\|Q8I0U6\|Q8I0U6_PLAF7 DNAJ protein, putative OS=Plasmodium falciparum (isolate 3D7) GN=RESA PE=4 SV=1 | 8 | 1.04 | 0.08 | 0.0000 |
| tr\|Q8IE99\|Q8IE99_PLAF7 Splicing factor, putative OS=Plasmodium falciparum (isolate 3D7) GN=MAL13P1.120 PE=4 SV=1 | 8 | 1.04 | 0.12 | 0.0000 |
| sp\|Q08211\|DHX9_HUMAN ATP-dependent RNA helicase A OS=Homo sapiens GN=DHX9 PE=1 SV=4 | 8 | 1.04 | 0.18 | 0.0000 |
| tr\|Q8IBP8\|Q8IBP8_PLAF7 Ferrodoxin reductase-like protein OS=Plasmodium falciparum (isolate 3D7) GN=PF07_0085 PE=4 SV=1 | 8 | 1.04 | 0.67 | 0.0032 |
| tr\|Q8IHT2\|Q8IHT2_PLAF7 Translation initiation factor eIF-1A, putative OS=Plasmodium falciparum (isolate 3D7) GN=PF11_0447 PE=3 SV=2 | 8 | 1.05 | 0.32 | 0.0000 |
| tr\|Q8I569\|Q8I569_PLAF7 Uncharacterized protein OS=Plasmodium falciparum (isolate 3D7) GN=PFL1705w PE=4 SV=1 | 8 | 1.05 | 0.24 | 0.0000 |
| tr\|Q8IC42\|Q8IC42_PLAF7 Uncharacterized protein OS=Plasmodium falciparum (isolate 3D7) GN=PF07_0008 PE=4 SV=1 | 8 | 1.05 | 0.38 | 0.0001 |
| tr\|Q8IAZ3\|Q8IAZ3_PLAF7 Eukaryotic translation initiation factor 3 subunit G OS=Plasmodium falciparum (isolate 3D7) GN=MAL8P1.83 PE=3 SV=1 | 8 | 1.05 | 0.16 | 0.0000 |
| tr\|Q8I3I5\|Q8I3I5_PLAF7 Eukaryotic translation initiation factor 3 subunit E OS=Plasmodium falciparum (isolate 3D7) GN=PFE1405c PE=3 SV=1 | 8 | 1.05 | 0.20 | 0.0000 |
| tr\|Q8ID24\|Q8ID24_PLAF7 Mitochondrial import inner membrane translocase, putative OS=Plasmodium falciparum (isolate 3D7) GN=PF13_0358 PE=4 SV=1 | 8 | 72.95 | 137.02 | 0.1759 |
| tr\|C0H4Y6\|C0H4Y6_PLAF7 Protein disulfide-isomerase OS=Plasmodium falciparum (isolate 3D7) GN=PfPDI-8 PE=3 SV=1 | 8 | 1.05 | 0.70 | 0.0038 |
| tr\|O77310\|O77310_PLAF7 Cytoadherence linked asexual protein 3.1 OS=Plasmodium falciparum (isolate 3D7) GN=RhopH1(3.1) PE=4 SV=2;tr\|O77309\|O77309_PLAF7 Cytoadherence linked asexual protein 3.2 OS=Plasmodium falciparum (isolate 3D7) GN=RhopH1(3.2) PE=4 SV=3 | 8 | 1.06 | 0.12 | 0.0000 |
| tr\|Q8I3T1\|Q8I3T1_PLAF7 Eukaryotic translation initiation factor 3 subunit B OS=Plasmodium falciparum (isolate 3D7) GN=PFE0885w PE=3 SV=1 | 8 | 1.06 | 0.35 | 0.0001 |
| tr\|Q8I476\|Q8I476_PLAF7 Merozoite Surface Protein 8, MSP8 OS=Plasmodium falciparum (isolate 3D7) GN=MSP8 PE=4 SV=1 | 8 | 1.06 | 0.15 | 0.0000 |
| tr\|C0H5L7\|C0H5L7_PLAF7 Uncharacterized protein OS=Plasmodium falciparum (isolate 3D7) GN=MAL13P1.352 PE=4 SV=1 | 8 | 1.06 | 0.20 | 0.0000 |
| tr\|Q8I0V4\|Q8I0V4_PLAF7 Endoplasmin homolog, putative OS=Plasmodium falciparum (isolate 3D7) GN=PFL1070c PE=1 SV=1 | 8 | 1.06 | 0.77 | 0.0061 |
| tr\|Q8IJZ9\|Q8IJZ9_PLAF7 U5 small nuclear ribonuclear protein, putative OS=Plasmodium falciparum (isolate 3D7) GN=PF10_0041 PE=4 SV=1 | 8 | 1.06 | 0.30 | 0.0000 |

| | | | | |
|---|---|---|---|---|
| tr\|Q8IKC7\|Q8IKC7_PLAF7 Inorganic anion exchanger, inorganic anion antiporter OS=Plasmodium falciparum (isolate 3D7) GN=PF14_0679 PE=4 SV=1 | 8 | 100.31 | 281.96 | 0.3478 |
| tr\|C0H4F1\|C0H4F1_PLAF7 Uncharacterized protein OS=Plasmodium falciparum (isolate 3D7) GN=PFE0990w PE=4 SV=1 | 8 | 1.07 | 0.19 | 0.0000 |
| tr\|Q8III3\|Q8III3_PLAF7 Uncharacterized protein OS=Plasmodium falciparum (isolate 3D7) GN=PF11_0191 PE=4 SV=1 | 8 | 1.07 | 0.23 | 0.0000 |
| tr\|C0H5L9\|C0H5L9_PLAF7 Membrane associated histidine-rich protein, MAHRP-1 OS=Plasmodium falciparum (isolate 3D7) GN=MAHRP1 PE=4 SV=1 | 8 | 1.07 | 0.19 | 0.0000 |
| tr\|Q8IE09\|Q8IE09_PLAF7 60S ribosomal protein L23, putative OS=Plasmodium falciparum (isolate 3D7) GN=PF13_0171 PE=1 SV=1 | 8 | 2.74 | 3.34 | 0.0536 |
| tr\|Q7KQM5\|Q7KQM5_PLAF7 Early transcribed membrane protein 14.1, etramp14.1 OS=Plasmodium falciparum (isolate 3D7) GN=etramp14.1 PE=4 SV=1 | 8 | 1.08 | 0.30 | 0.0000 |
| tr\|Q8IJV7\|Q8IJV7_PLAF7 Nucleolar protein NOP5, putative OS=Plasmodium falciparum (isolate 3D7) GN=PF10_0085 PE=4 SV=1 | 8 | 1.08 | 0.18 | 0.0000 |
| tr\|Q8I5Y3\|Q8I5Y3_PLAF7 Eukaryotic translation initiation factor 3 subunit C OS=Plasmodium falciparum (isolate 3D7) GN=PFL0310c PE=3 SV=1 | 8 | 1.08 | 0.13 | 0.0000 |
| tr\|Q8IJX3\|Q8IJX3_PLAF7 RNA binding protein, putative OS=Plasmodium falciparum (isolate 3D7) GN=PF10_0068 PE=4 SV=1 | 8 | 1.08 | 0.10 | 0.0000 |
| tr\|Q8IEQ6\|Q8IEQ6_PLAF7 Uncharacterized protein OS=Plasmodium falciparum (isolate 3D7) GN=PF13_0031 PE=4 SV=1 | 8 | 1.08 | 0.17 | 0.0000 |
| tr\|Q8I5S6\|Q8I5S6_PLAF7 Eukaryotic translation initiation factor 3 subunit A OS=Plasmodium falciparum (isolate 3D7) GN=PFL0625c PE=3 SV=1 | 8 | 1.08 | 0.14 | 0.0000 |
| tr\|Q8IBT2\|Q8IBT2_PLAF7 Eukaryotic translation initiation factor 3 subunit I OS=Plasmodium falciparum (isolate 3D7) GN=MAL7P1.81 PE=3 SV=1 | 8 | 1.08 | 0.21 | 0.0000 |
| tr\|Q8IJC1\|Q8IJC1_PLAF7 Uncharacterized protein OS=Plasmodium falciparum (isolate 3D7) GN=PF10_0277 PE=4 SV=1 | 8 | 1.08 | 0.26 | 0.0000 |
| sp\|P62344\|CDPK1_PLAF7 Calcium-dependent protein kinase 1 OS=Plasmodium falciparum (isolate 3D7) GN=CPK1 PE=3 SV=2 | 8 | 1.08 | 0.74 | 0.0045 |
| tr\|Q8IIS2\|Q8IIS2_PLAF7 Uncharacterized protein OS=Plasmodium falciparum (isolate 3D7) GN=PF11_0093 PE=4 SV=1 | 8 | 1.86 | 2.56 | 0.0795 |
| tr\|Q8IC16\|Q8IC16_PLAF7 DNA helicase OS=Plasmodium falciparum (isolate 3D7) GN=PF07_0023 PE=3 SV=1 | 8 | 1.09 | 0.75 | 0.0046 |
| tr\|Q8IAL3\|Q8IAL3_PLAF7 Uncharacterized protein OS=Plasmodium falciparum (isolate 3D7) GN=PF08_0135 PE=4 SV=1 | 8 | 1.09 | 0.61 | 0.0015 |
| tr\|Q8IJJ5\|Q8IJJ5_PLAF7 Conserved protein OS=Plasmodium falciparum (isolate 3D7) GN=PF10_0200 PE=4 SV=1 | 8 | 1.09 | 0.21 | 0.0000 |
| tr\|O77327\|O77327_PLAF7 U2 snRNP spliceosome subunit, putative OS=Plasmodium falciparum (isolate 3D7) GN=PFC0375c PE=4 SV=1 | 8 | 5.84 | 11.29 | 0.1872 |
| tr\|Q8IDQ2\|Q8IDQ2_PLAF7 Kelch protein, putative OS=Plasmodium falciparum (isolate 3D7) GN=PF13_0238 PE=4 SV=1 | 8 | 1.10 | 0.38 | 0.0001 |
| tr\|Q8IJI0\|Q8IJI0_PLAF7 Pre-mRNA splicing factor, putative OS=Plasmodium falciparum (isolate 3D7) GN=PF10_0217 PE=4 SV=1 | 8 | 1.10 | 0.27 | 0.0000 |
| tr\|Q8IIU7\|Q8IIU7_PLAF7 Conserved Plasmodium protein OS=Plasmodium falciparum (isolate 3D7) GN=PF11_0067 PE=4 SV=2 | 8 | 1.10 | 0.19 | 0.0000 |
| tr\|O96128\|O96128_PLAF7 Early transcribed membrane protein 2, ETRAMP2 OS=Plasmodium falciparum (isolate 3D7) GN=SEP2 PE=4 SV=1 | 8 | 1.11 | 0.26 | 0.0000 |
| tr\|Q8I562\|Q8I562_PLAF7 Clustered-asparagine-rich protein OS=Plasmodium falciparum (isolate 3D7) GN=PFL1745c PE=4 SV=2 | 8 | 1.11 | 0.44 | 0.0002 |
| tr\|Q8I2F2\|Q8I2F2_PLAF7 Putative uncharacterized protein OS=Plasmodium falciparum (isolate 3D7) GN=PFI1780w PE=1 SV=1 | 8 | 1.11 | 0.11 | 0.0000 |
| tr\|Q8I322\|Q8I322_PLAF7 Putative uncharacterized protein OS=Plasmodium falciparum (isolate 3D7) GN=PFI0635c PE=4 SV=1 | 8 | 1.12 | 0.23 | 0.0000 |
| tr\|Q8IAW1\|Q8IAW1_PLAF7 RNA binding protein, putative OS=Plasmodium falciparum (isolate 3D7) GN=PF08_0086 PE=4 SV=1 | 8 | 1.12 | 0.70 | 0.0026 |
| tr\|Q8IIV8\|Q8IIV8_PLAF7 Uncharacterized protein OS=Plasmodium falciparum (isolate 3D7) GN=PF11_0055 PE=4 SV=1 | 8 | 1.13 | 0.98 | 0.0142 |
| tr\|C6KSW5\|C6KSW5_PLAF7 Eukaryotic translation initiation factor 3 subunit L OS=Plasmodium falciparum (isolate 3D7) GN=PFF0590c PE=3 SV=1 | 8 | 1.13 | 0.22 | 0.0000 |
| tr\|Q8IJW4\|Q8IJW4_PLAF7 Eukaryotic translation initiation factor 3 subunit D OS=Plasmodium falciparum (isolate 3D7) GN=PF10_0077 PE=3 SV=1 | 8 | 1.13 | 0.23 | 0.0000 |
| tr\|Q8IDB7\|Q8IDB7_PLAF7 RNA binding protein, putative OS=Plasmodium falciparum (isolate 3D7) GN=PF13_0315 PE=4 SV=1 | 8 | 1.13 | 0.27 | 0.0000 |
| tr\|Q8I5H4\|Q8I5H4_PLAF7 Polyadenylate-binding protein, putative OS=Plasmodium falciparum (isolate 3D7) GN=PFL1170w PE=4 SV=1 | 8 | 1.13 | 0.09 | 0.0000 |
| tr\|Q8IL13\|Q8IL13_PLAF7 Helicase, putative OS=Plasmodium falciparum (isolate 3D7) GN=PF14_0437 PE=3 SV=2 | 8 | 1.14 | 0.33 | 0.0000 |

| | | | | |
|---|---|---|---|---|
| tr\|C0H553\|C0H553_PLAF7 Flavodoxin-like protein OS=Plasmodium falciparum (isolate 3D7) GN=PFI1140w PE=4 SV=1 | 8 | 1.14 | 0.70 | 0.0025 |
| tr\|O77355\|O77355_PLAF7 Pre-mRNA splicing factor, putative OS=Plasmodium falciparum (isolate 3D7) GN=PFC0465c PE=4 SV=2 | 8 | 3.53 | 6.40 | 0.1630 |
| tr\|Q8I2S6\|Q8I2S6_PLAF7 DNA-directed RNA polymerase II, putative OS=Plasmodium falciparum (isolate 3D7) GN=PFI1130c PE=4 SV=1 | 8 | 1.15 | 0.29 | 0.0000 |
| tr\|C0H469\|C0H469_PLAF7 Putative uncharacterized protein OS=Plasmodium falciparum (isolate 3D7) GN=PFC0430w PE=4 SV=1 | 8 | 1.15 | 0.25 | 0.0000 |
| tr\|Q8IM35\|Q8IM35_PLAF7 RNA binding protein, putative OS=Plasmodium falciparum (isolate 3D7) GN=PF14_0056 PE=4 SV=1 | 8 | 1.16 | 0.90 | 0.0081 |
| tr\|Q8IIS9\|Q8IIS9_PLAF7 Uncharacterized protein OS=Plasmodium falciparum (isolate 3D7) GN=PF11_0086 PE=4 SV=1 | 8 | 1.16 | 0.24 | 0.0000 |
| tr\|Q8IK93\|Q8IK93_PLAF7 Uncharacterized protein OS=Plasmodium falciparum (isolate 3D7) GN=PF14_0713 PE=4 SV=1 | 8 | 1.16 | 0.36 | 0.0000 |
| tr\|Q8I1Q5\|Q8I1Q5_PLAF7 Eukaryotic translation initiation factor 3 subunit M OS=Plasmodium falciparum (isolate 3D7) GN=PFD0880w PE=3 SV=1 | 8 | 1.16 | 0.33 | 0.0000 |
| tr\|Q8IDF8\|Q8IDF8_PLAF7 Putative rRNA methyltransferase OS=Plasmodium falciparum (isolate 3D7) GN=PF13_0286 PE=3 SV=1 | 8 | 1.17 | 0.37 | 0.0000 |
| tr\|Q8I447\|Q8I447_PLAF7 DNA mismatch repair protein MSH6 OS=Plasmodium falciparum (isolate 3D7) GN=PFE0270c PE=3 SV=1 | 8 | 1.17 | 0.59 | 0.0008 |
| tr\|Q8IHM9\|Q8IHM9_PLAF7 Plasmodium exported protein OS=Plasmodium falciparum (isolate 3D7) GN=PF11_0511 PE=4 SV=2 | 8 | 1.17 | 0.19 | 0.0000 |
| tr\|Q8ID32\|Q8ID32_PLAF7 Ribosome biogenesis protein MRT4, putative OS=Plasmodium falciparum (isolate 3D7) GN=MAL13P1.341 PE=3 SV=1 | 8 | 1.18 | 0.19 | 0.0000 |
| tr\|Q8IC43\|Q8IC43_PLAF7 Uncharacterized protein OS=Plasmodium falciparum (isolate 3D7) GN=PF07_0007 PE=4 SV=1 | 8 | 1.18 | 0.34 | 0.0000 |
| tr\|Q8IIW6\|Q8IIW6_PLAF7 Actin-like protein, putative OS=Plasmodium falciparum (isolate 3D7) GN=PF11_0047 PE=3 SV=1 | 8 | 1.18 | 0.45 | 0.0001 |
| tr\|C6KSP3\|C6KSP3_PLAF7 Uncharacterized protein OS=Plasmodium falciparum (isolate 3D7) GN=PFF0220w PE=4 SV=1 | 8 | 1.18 | 0.21 | 0.0000 |
| tr\|Q8I635\|Q8I635_PLAF7 Uncharacterized protein OS=Plasmodium falciparum (isolate 3D7) GN=PFL0050c PE=4 SV=1 | 8 | 1.18 | 0.18 | 0.0000 |
| tr\|Q8ID84\|Q8ID84_PLAF7 Uncharacterized protein OS=Plasmodium falciparum (isolate 3D7) GN=PF13_0331 PE=4 SV=1 | 8 | 1.18 | 0.63 | 0.0011 |
| tr\|Q8I3T5\|Q8I3T5_PLAF7 Splicing factor, putative OS=Plasmodium falciparum (isolate 3D7) GN=PFE0865c PE=4 SV=2 | 8 | 1.20 | 0.36 | 0.0000 |
| tr\|Q8IJX8\|Q8IJX8_PLAF7 Uncharacterized protein OS=Plasmodium falciparum (isolate 3D7) GN=PF10_0063 PE=4 SV=1 | 8 | 1.20 | 0.10 | 0.0000 |
| tr\|C0H4L6\|C0H4L6_PLAF7 Uncharacterized protein OS=Plasmodium falciparum (isolate 3D7) GN=MAL7P1.204 PE=4 SV=1 | 8 | 1.20 | 0.12 | 0.0000 |
| tr\|O77390\|O77390_PLAF7 Putative uncharacterized protein OS=Plasmodium falciparum (isolate 3D7) GN=PFC0720w PE=4 SV=2 | 8 | 1.73 | 2.36 | 0.0763 |
| tr\|Q8IIQ7\|Q8IIQ7_PLAF7 Asparagine-rich antigen OS=Plasmodium falciparum (isolate 3D7) GN=PF11_0111 PE=4 SV=1 | 8 | 1.20 | 0.15 | 0.0000 |
| tr\|Q8IE84\|Q8IE84_PLAF7 Vacuolar ATP synthase subunit G, putative OS=Plasmodium falciparum (isolate 3D7) GN=PF13_0130 PE=4 SV=1 | 8 | 1.21 | 0.53 | 0.0003 |
| sp\|P04040\|CATA_HUMAN Catalase OS=Homo sapiens GN=CAT PE=1 SV=3 | 8 | 1.22 | 0.31 | 0.0000 |
| tr\|Q8IKR4\|Q8IKR4_PLAF7 Uncharacterized protein OS=Plasmodium falciparum (isolate 3D7) GN=PF14_0538 PE=4 SV=1 | 8 | 1.22 | 0.97 | 0.0091 |
| tr\|Q8I240\|Q8I240_PLAF7 Bromodomain protein, putative OS=Plasmodium falciparum (isolate 3D7) GN=PFA_0510w PE=1 SV=1 | 8 | 1.23 | 0.98 | 0.0093 |
| tr\|Q8I3V8\|Q8I3V8_PLAF7 RNA recognition motif, putative OS=Plasmodium falciparum (isolate 3D7) GN=PFE0750c PE=4 SV=1 | 8 | 1.24 | 0.26 | 0.0000 |
| tr\|Q8IJD2\|Q8IJD2_PLAF7 Uncharacterized protein OS=Plasmodium falciparum (isolate 3D7) GN=PF10_0266 PE=4 SV=1 | 8 | 1.24 | 0.32 | 0.0000 |
| tr\|Q8IC35\|Q8IC35_PLAF7 Erythrocyte membrane-associated antigen OS=Plasmodium falciparum (isolate 3D7) GN=MAL7P1.12 PE=4 SV=1 | 8 | 1.25 | 0.39 | 0.0000 |
| tr\|Q8I5V9\|Q8I5V9_PLAF7 Uncharacterized protein OS=Plasmodium falciparum (isolate 3D7) GN=PFL0445w PE=4 SV=1 | 8 | 1.25 | 0.56 | 0.0004 |
| tr\|C0H5C6\|C0H5C6_PLAF7 SNARE protein, putative OS=Plasmodium falciparum (isolate 3D7) GN=PfSNAP23 PE=4 SV=1 | 8 | 1.25 | 0.67 | 0.0011 |
| tr\|Q8II99\|Q8II99_PLAF7 Uncharacterized protein OS=Plasmodium falciparum (isolate 3D7) GN=PF11_0275 PE=4 SV=1 | 8 | 1.25 | 0.18 | 0.0000 |
| tr\|C6KSR3\|C6KSR3_PLAF7 Polypyrimidine tract binding protein, putative OS=Plasmodium falciparum (isolate 3D7) GN=PFF0320c PE=4 SV=1 | 8 | 1.25 | 0.43 | 0.0001 |

| | | | | |
|---|---|---|---|---|
| tr\|Q8IAX8\|Q8IAX8_PLAF7 DNA/RNA-binding protein Alba, putative OS=Plasmodium falciparum (isolate 3D7) GN=PF08_0074 PE=4 SV=1 | 8 | 1.25 | 0.44 | 0.0001 |
| tr\|Q8IDS0\|Q8IDS0_PLAF7 Vacuolar ATP synthase subunit D, putative OS=Plasmodium falciparum (isolate 3D7) GN=PF13_0227 PE=4 SV=1 | 8 | 1.26 | 0.32 | 0.0000 |
| tr\|C6KT90\|C6KT90_PLAF7 Uncharacterized protein OS=Plasmodium falciparum (isolate 3D7) GN=PFF1230c PE=4 SV=1 | 8 | 1.27 | 0.95 | 0.0069 |
| tr\|C6KSX2\|C6KSX2_PLAF7 Nucleolar GTP-binding protein 1, putative OS=Plasmodium falciparum (isolate 3D7) GN=PFF0625w PE=4 SV=1 | 8 | 1.27 | 0.22 | 0.0000 |
| tr\|Q8ILU3\|Q8ILU3_PLAF7 RNA-binding protein Nova-1, putative OS=Plasmodium falciparum (isolate 3D7) GN=PF14_0151 PE=4 SV=1 | 8 | 1.28 | 0.48 | 0.0001 |
| tr\|Q8I2H3\|Q8I2H3_PLAF7 Vacuolar ATP synthase subunit E, putative OS=Plasmodium falciparum (isolate 3D7) GN=PFI1670c PE=3 SV=2 | 8 | 1.28 | 0.48 | 0.0001 |
| tr\|Q8ILR7\|Q8ILR7_PLAF7 DNA helicase OS=Plasmodium falciparum (isolate 3D7) GN=PF14_0177 PE=3 SV=1 | 8 | 1.28 | 0.93 | 0.0058 |
| tr\|O96271\|O96271_PLAF7 Replication factor C subunit 1, putative OS=Plasmodium falciparum (isolate 3D7) GN=PFB0895c PE=4 SV=1 | 8 | 1.29 | 0.46 | 0.0001 |
| tr\|O96258\|O96258_PLAF7 40S ribosomal protein S26e, putative OS=Plasmodium falciparum (isolate 3D7) GN=PFB0830w PE=1 SV=1 | 8 | 3.04 | 5.43 | 0.1577 |
| tr\|Q8IE82\|Q8IE82_PLAF7 60S ribosomal protein L23a, putative OS=Plasmodium falciparum (isolate 3D7) GN=PF13_0132 PE=1 SV=1 | 8 | 1.29 | 0.26 | 0.0000 |
| tr\|Q8IEE5\|Q8IEE5_PLAF7 DNA replication licensing factor MCM4-related OS=Plasmodium falciparum (isolate 3D7) GN=PF13_0095 PE=3 SV=1 | 8 | 1.30 | 1.23 | 0.0204 |
| tr\|Q8I358\|Q8I358_PLAF7 Exoribonuclease, putative OS=Plasmodium falciparum (isolate 3D7) GN=PFI0455w PE=4 SV=1 | 8 | 1.30 | 0.23 | 0.0000 |
| tr\|Q8ID26\|Q8ID26_PLAF7 Uncharacterized protein OS=Plasmodium falciparum (isolate 3D7) GN=PF13_0356 PE=4 SV=1 | 8 | 1.30 | 0.35 | 0.0000 |
| tr\|O97266\|O97266_PLAF7 Translation initiation factor E4, putative OS=Plasmodium falciparum (isolate 3D7) GN=PFC0635c PE=3 SV=1 | 8 | 1.32 | 0.28 | 0.0000 |
| tr\|Q8ILZ7\|Q8ILZ7_PLAF7 RNA binding protein, putative OS=Plasmodium falciparum (isolate 3D7) GN=PF14_0096 PE=4 SV=1 | 8 | 1.32 | 0.25 | 0.0000 |
| tr\|Q8IM45\|Q8IM45_PLAF7 Uncharacterized protein OS=Plasmodium falciparum (isolate 3D7) GN=PF14_0046 PE=4 SV=1 | 8 | 1.32 | 0.81 | 0.0024 |
| tr\|Q8IEI6\|Q8IEI6_PLAF7 Uncharacterized protein OS=Plasmodium falciparum (isolate 3D7) GN=PF13_0076 PE=4 SV=1 | 8 | 1.33 | 0.69 | 0.0009 |
| tr\|Q8I2N0\|Q8I2N0_PLAF7 Phosphatidylserine decarboxylase OS=Plasmodium falciparum (isolate 3D7) GN=PfPSD PE=4 SV=1 | 8 | 1.33 | 0.87 | 0.0036 |
| tr\|Q76NM4\|Q76NM4_PLAF7 Rab11a, GTPase OS=Plasmodium falciparum (isolate 3D7) GN=Rab11a PE=1 SV=1 | 8 | 1.34 | 0.84 | 0.0028 |
| tr\|Q8I333\|Q8I333_PLAF7 Falstatin, putative OS=Plasmodium falciparum (isolate 3D7) GN=PFI0580c PE=4 SV=1 | 8 | 1.35 | 1.44 | 0.0330 |
| tr\|Q8I3T8\|Q8I3T8_PLAF7 60S ribosomal protein L12, putative OS=Plasmodium falciparum (isolate 3D7) GN=PFE0850c PE=3 SV=2 | 8 | 1.35 | 0.41 | 0.0000 |
| tr\|Q8I574\|Q8I574_PLAF7 Splicing factor 3b, subunit 3, 130kD, putative OS=Plasmodium falciparum (isolate 3D7) GN=PFL1680w PE=4 SV=1 | 8 | 1.35 | 0.78 | 0.0017 |
| tr\|Q8IHX2\|Q8IHX2_PLAF7 Malaria antigen OS=Plasmodium falciparum (isolate 3D7) GN=PF11_0404 PE=4 SV=1 | 8 | 1.35 | 0.54 | 0.0002 |
| tr\|B9ZSJ0\|B9ZSJ0_PLAF7 Putative uncharacterized protein OS=Plasmodium falciparum (isolate 3D7) GN=PFA_0570w PE=4 SV=1 | 8 | 1.36 | 0.32 | 0.0000 |
| sp\|P61074\|PCNA_PLAF7 Proliferating cell nuclear antigen OS=Plasmodium falciparum (isolate 3D7) GN=PCNA PE=3 SV=1 | 8 | 1.36 | 0.42 | 0.0000 |
| tr\|Q8IDV1\|Q8IDV1_PLAF7 60S ribosomal protein L6-2, putative OS=Plasmodium falciparum (isolate 3D7) GN=PF13_0213 PE=1 SV=1 | 8 | 1.36 | 0.59 | 0.0003 |
| tr\|Q8IB09\|Q8IB09_PLAF7 Asparagine-rich antigen OS=Plasmodium falciparum (isolate 3D7) GN=PF08_0060 PE=4 SV=1 | 8 | 1.36 | 0.32 | 0.0000 |
| tr\|Q8IJZ4\|Q8IJZ4_PLAF7 Uncharacterized protein OS=Plasmodium falciparum (isolate 3D7) GN=PF10_0046 PE=4 SV=1 | 8 | 1.36 | 0.24 | 0.0000 |
| tr\|C0H5J2\|C0H5J2_PLAF7 Uncharacterized protein OS=Plasmodium falciparum (isolate 3D7) GN=MAL13P1.295 PE=4 SV=1 | 8 | 1.36 | 0.58 | 0.0003 |
| tr\|Q8I3U6\|Q8I3U6_PLAF7 40S ribosomal protein S14, putative OS=Plasmodium falciparum (isolate 3D7) GN=PFE0810c PE=1 SV=1 | 8 | 1.37 | 0.61 | 0.0004 |
| tr\|C0H4J4\|C0H4J4_PLAF7 Uncharacterized protein OS=Plasmodium falciparum (isolate 3D7) GN=MAL7P1.225.2 PE=4 SV=1;tr\|C0H4J3\|C0H4J3_PLAF7 Uncharacterized protein OS=Plasmodium falciparum (isolate 3D7) GN=MAL7P1.225.1 PE=4 SV=1 | 8 | 1.37 | 0.63 | 0.0005 |
| sp\|Q8I3Z1\|MLRR1_PLAF7 MATH and LRR domain-containing protein PFE0570w OS=Plasmodium falciparum (isolate 3D7) GN=PFE0570w PE=2 SV=1 | 8 | 1.38 | 0.17 | 0.0000 |

| | | | | |
|---|---|---|---|---|
| tr\|Q8I2X0\|Q8I2X0_PLAF7 Eukaryotic translation initiation factor 3 subunit 5, putative OS=Plasmodium falciparum (isolate 3D7) GN=PFI0895c PE=4 SV=1 | 8 | 1.38 | 0.73 | 0.0011 |
| tr\|O96169\|O96169_PLAF7 RNA binding protein, putative OS=Plasmodium falciparum (isolate 3D7) GN=PFB0370c PE=4 SV=1 | 8 | 1.39 | 0.57 | 0.0002 |
| tr\|Q8ID85\|Q8ID85_PLAF7 ATP-dependent DNA helicase, putative OS=Plasmodium falciparum (isolate 3D7) GN=PF13_0330 PE=4 SV=1 | 8 | 1.40 | 0.19 | 0.0000 |
| tr\|Q8ILE8\|Q8ILE8_PLAF7 60S ribosomal protein L14, putative OS=Plasmodium falciparum (isolate 3D7) GN=PF14_0296 PE=1 SV=1 | 8 | 1.40 | 0.63 | 0.0004 |
| tr\|Q8IC08\|Q8IC08_PLAF7 DNA-directed RNA polymerase 2 8.2 kDa polypeptide, putative OS=Plasmodium falciparum (isolate 3D7) GN=PF07_0027 PE=3 SV=1 | 8 | 1.40 | 0.43 | 0.0000 |
| tr\|C6KSR8\|C6KSR8_PLAF7 Translation initiation factor IF-2, putative OS=Plasmodium falciparum (isolate 3D7) GN=PFF0345w PE=4 SV=1 | 8 | 1.40 | 0.59 | 0.0003 |
| sp\|P06753-6\|TPM3_HUMAN Isoform 6 of Tropomyosin alpha-3 chain OS=Homo sapiens GN=TPM3;sp\|P06753\|TPM3_HUMAN Tropomyosin alpha-3 chain OS=Homo sapiens GN=TPM3 PE=1 SV=2 | 8 | 1.41 | 1.21 | 0.0132 |
| tr\|Q8II01\|Q8II01_PLAF7 Tudor staphylococcal nuclease OS=Plasmodium falciparum (isolate 3D7) GN=TSN PE=4 SV=1 | 8 | 1.41 | 0.78 | 0.0013 |
| sp\|Q76NM6\|VATA_PLAF7 V-type proton ATPase catalytic subunit A OS=Plasmodium falciparum (isolate 3D7) GN=vapA PE=3 SV=1 | 8 | 1.41 | 0.57 | 0.0002 |
| tr\|Q8IIA2\|Q8IIA2_PLAF7 Ribosomal protein S18, putative OS=Plasmodium falciparum (isolate 3D7) GN=PF11_0272 PE=1 SV=1 | 8 | 1.41 | 0.58 | 0.0002 |
| tr\|Q8I5T4\|Q8I5T4_PLAF7 DNA helicase OS=Plasmodium falciparum (isolate 3D7) GN=PFL0580w PE=3 SV=1 | 8 | 1.41 | 0.89 | 0.0029 |
| tr\|Q8ILL3\|Q8ILL3_PLAF7 60S ribosomal protein L5, putative OS=Plasmodium falciparum (isolate 3D7) GN=PF14_0230 PE=3 SV=1 | 8 | 1.42 | 0.54 | 0.0001 |
| tr\|Q8IB14\|Q8IB14_PLAF7 High mobility group protein OS=Plasmodium falciparum (isolate 3D7) GN=PfHMGB2 PE=1 SV=1 | 8 | 1.42 | 0.60 | 0.0003 |
| tr\|Q8I502\|Q8I502_PLAF7 40S ribosomal protein S17, putative OS=Plasmodium falciparum (isolate 3D7) GN=PFL2055w PE=1 SV=1 | 8 | 1.43 | 0.46 | 0.0001 |
| tr\|Q8IDF0\|Q8IDF0_PLAF7 DNA helicase OS=Plasmodium falciparum (isolate 3D7) GN=PF13_0291 PE=3 SV=1 | 8 | 1.43 | 1.02 | 0.0053 |
| sp\|P63000\|RAC1_HUMAN Ras-related C3 botulinum toxin substrate 1 OS=Homo sapiens GN=RAC1 PE=1 SV=1;sp\|P63000-2\|RAC1_HUMAN Isoform B of Ras-related C3 botulinum toxin substrate 1 OS=Homo sapiens GN=RAC1 | 8 | 1.44 | 0.88 | 0.0024 |
| tr\|C6KSR5\|C6KSR5_PLAF7 Coatomer alpha subunit, putative OS=Plasmodium falciparum (isolate 3D7) GN=PFF0330w PE=4 SV=1 | 8 | 1.44 | 0.22 | 0.0000 |
| tr\|Q8IK02\|Q8IK02_PLAF7 Ribosomal protein S20e, putative OS=Plasmodium falciparum (isolate 3D7) GN=PF10_0038 PE=1 SV=1 | 8 | 1.44 | 0.86 | 0.0022 |
| tr\|Q8IKI9\|Q8IKI9_PLAF7 ATP-dependent protease Ia, putative OS=Plasmodium falciparum (isolate 3D7) GN=PF14_0616 PE=4 SV=1 | 8 | 1.45 | 1.70 | 0.0464 |
| tr\|Q8IDB0\|Q8IDB0_PLAF7 40S ribosomal protein S13, putative OS=Plasmodium falciparum (isolate 3D7) GN=PF13_0316 PE=1 SV=1 | 8 | 1.45 | 0.56 | 0.0002 |
| tr\|Q8IFP2\|Q8IFP2_PLAF7 40S ribosomal protein S19, putative OS=Plasmodium falciparum (isolate 3D7) GN=PFD1055w PE=1 SV=1 | 8 | 1.45 | 0.45 | 0.0000 |
| tr\|O96260\|O96260_PLAF7 Replication factor C, subunit 2 OS=Plasmodium falciparum (isolate 3D7) GN=PFB0840w PE=4 SV=1 | 8 | 1.46 | 0.95 | 0.0033 |
| tr\|Q8IDR9\|Q8IDR9_PLAF7 40S ribosomal protein S6, putative OS=Plasmodium falciparum (isolate 3D7) GN=PF13_0228 PE=1 SV=1 | 8 | 1.46 | 0.51 | 0.0001 |
| tr\|O77381\|O77381_PLAF7 40S ribosomal protein S11, putative OS=Plasmodium falciparum (isolate 3D7) GN=PFC0775w PE=1 SV=2 | 8 | 1.47 | 0.68 | 0.0005 |
| tr\|Q8IE73\|Q8IE73_PLAF7 MSF1-like protein, putative OS=Plasmodium falciparum (isolate 3D7) GN=PF13_0138 PE=4 SV=1 | 8 | 2.46 | 5.22 | 0.2248 |
| tr\|C0H4U4\|C0H4U4_PLAF7 Uncharacterized protein OS=Plasmodium falciparum (isolate 3D7) GN=MAL8P1.95 PE=4 SV=1 | 8 | 1.47 | 0.99 | 0.0040 |
| tr\|Q8I3J5\|Q8I3J5_PLAF7 DNA helicase OS=Plasmodium falciparum (isolate 3D7) GN=PFE1345c PE=3 SV=1 | 8 | 1.47 | 1.19 | 0.0102 |
| tr\|Q8I280\|Q8I280_PLAF7 V-type ATPase, subunit C, putative OS=Plasmodium falciparum (isolate 3D7) GN=PFA_0300c PE=4 SV=1 | 8 | 1.47 | 0.58 | 0.0002 |
| tr\|Q8IIX0\|Q8IIX0_PLAF7 60S acidic ribosomal protein p1, putative OS=Plasmodium falciparum (isolate 3D7) GN=PF11_0043 PE=3 SV=1 | 8 | 1.47 | 0.41 | 0.0000 |
| tr\|Q8ILG6\|Q8ILG6_PLAF7 Coatamer protein, beta subunit, putative OS=Plasmodium falciparum (isolate 3D7) GN=PF14_0277 PE=4 SV=2 | 8 | 1.48 | 0.27 | 0.0000 |
| tr\|Q8IDM3\|Q8IDM3_PLAF7 Uncharacterized protein OS=Plasmodium falciparum (isolate 3D7) GN=MAL13P1.237 PE=4 SV=1 | 8 | 1.48 | 0.34 | 0.0000 |
| tr\|Q8I441\|Q8I441_PLAF7 60S ribosomal subunit protein L24-2, putative OS=Plasmodium falciparum (isolate 3D7) GN=PFE0300c PE=4 SV=1 | 8 | 1.48 | 0.78 | 0.0010 |

| | | | | |
|---|---|---|---|---|
| tr\|Q8IKT7\|Q8IKT7_PLAF7 Uncharacterized protein OS=Plasmodium falciparum (isolate 3D7) GN=PF14_0515 PE=4 SV=1 | 8 | 1.48 | 0.42 | 0.0000 |
| tr\|O97248\|O97248_PLAF7 40S ribosomal protein S23, putative OS=Plasmodium falciparum (isolate 3D7) GN=PFC0290w PE=1 SV=1 | 8 | 1.48 | 0.37 | 0.0000 |
| tr\|Q8I3H9\|Q8I3H9_PLAF7 Nucleolar preribosomal GTPase, putative OS=Plasmodium falciparum (isolate 3D7) GN=PFE1435c PE=4 SV=1 | 8 | 1.48 | 0.34 | 0.0000 |
| tr\|Q8IAX6\|Q8IAX6_PLAF7 60S ribosomal protein L13 OS=Plasmodium falciparum (isolate 3D7) GN=PF08_0075 PE=3 SV=1 | 8 | 1.48 | 0.58 | 0.0002 |
| tr\|C6KT34\|C6KT34_PLAF7 Cell division cycle protein 48 homologue, putative OS=Plasmodium falciparum (isolate 3D7) GN=PFF0940c PE=3 SV=1 | 8 | 1.48 | 0.48 | 0.0000 |
| tr\|C6S3J6\|C6S3J6_PLAF7 Ribosomal protein L29, putative OS=Plasmodium falciparum (isolate 3D7) GN=PF14_0575a PE=1 SV=1 | 8 | 1.49 | 0.48 | 0.0000 |
| tr\|Q8IHW4\|Q8IHW4_PLAF7 V-type proton ATPase subunit F OS=Plasmodium falciparum (isolate 3D7) GN=PF11_0412 PE=3 SV=2 | 8 | 1.49 | 0.54 | 0.0001 |
| tr\|Q8IIU8\|Q8IIU8_PLAF7 40S ribosomal protein S4 OS=Plasmodium falciparum (isolate 3D7) GN=PF11_0065 PE=3 SV=2 | 8 | 1.50 | 0.47 | 0.0000 |
| tr\|Q8IHW7\|Q8IHW7_PLAF7 Conserved Plasmodium protein OS=Plasmodium falciparum (isolate 3D7) GN=PF11_0409 PE=4 SV=1 | 8 | 1.50 | 1.11 | 0.0067 |
| tr\|Q6ZMA8\|Q6ZMA8_PLAF7 Vacuolar ATP synthase subunit b OS=Plasmodium falciparum (isolate 3D7) GN=PFD0305c PE=3 SV=1 | 8 | 1.50 | 0.43 | 0.0000 |
| tr\|Q8IKA6\|Q8IKA6_PLAF7 DNAJ protein, putative OS=Plasmodium falciparum (isolate 3D7) GN=PF14_0700 PE=4 SV=1 | 8 | 1.50 | 0.74 | 0.0007 |
| tr\|Q8IE31\|Q8IE31_PLAF7 Uncharacterized protein OS=Plasmodium falciparum (isolate 3D7) GN=PF13_0162 PE=4 SV=1 | 8 | 1.50 | 1.15 | 0.0079 |
| tr\|Q8IM36\|Q8IM36_PLAF7 Ribosome biogenesis protein BOP1 homolog OS=Plasmodium falciparum (isolate 3D7) GN=PF14_0055 PE=3 SV=1 | 8 | 1.50 | 1.18 | 0.0085 |
| tr\|Q8ILL2\|Q8ILL2_PLAF7 60S ribosomal protein L7-3, putative OS=Plasmodium falciparum (isolate 3D7) GN=PF14_0231 PE=1 SV=2 | 8 | 1.50 | 0.67 | 0.0004 |
| tr\|Q8IDP9\|Q8IDP9_PLAF7 Uncharacterized protein OS=Plasmodium falciparum (isolate 3D7) GN=PF13_0239 PE=4 SV=1 | 8 | 4.72 | 10.91 | 0.2607 |
| sp\|O00806\|RLA2_PLAF7 60S acidic ribosomal protein P2 OS=Plasmodium falciparum (isolate 3D7) GN=MAL3P3.19 PE=3 SV=1 | 8 | 1.52 | 0.62 | 0.0002 |
| tr\|C0H5B1\|C0H5B1_PLAF7 Asparagine-rich protein OS=Plasmodium falciparum (isolate 3D7) GN=MAL13P1.63 PE=4 SV=1 | 8 | 1.52 | 0.71 | 0.0005 |
| tr\|Q8IKM5\|Q8IKM5_PLAF7 60S ribosomal protein L27, putative OS=Plasmodium falciparum (isolate 3D7) GN=PF14_0579 PE=1 SV=2 | 8 | 1.53 | 0.64 | 0.0003 |
| sp\|O97249\|RS12_PLAF7 40S ribosomal protein S12 OS=Plasmodium falciparum (isolate 3D7) GN=RPS12 PE=1 SV=1 | 8 | 1.53 | 0.69 | 0.0004 |
| tr\|Q8IAX5\|Q8IAX5_PLAF7 40S ribosomal protein S16, putative OS=Plasmodium falciparum (isolate 3D7) GN=PF08_0076 PE=1 SV=1 | 8 | 1.54 | 0.45 | 0.0000 |
| tr\|Q8I3R0\|Q8I3R0_PLAF7 40S ribosomal protein S9, putative OS=Plasmodium falciparum (isolate 3D7) GN=PFE1005w PE=3 SV=1 | 8 | 1.54 | 0.62 | 0.0002 |
| tr\|Q8IL02\|Q8IL02_PLAF7 40S ribosomal protein S2, putative OS=Plasmodium falciparum (isolate 3D7) GN=PF14_0448 PE=1 SV=1 | 8 | 1.54 | 0.63 | 0.0002 |
| tr\|Q8I426\|Q8I426_PLAF7 Nuclear pore associated protein (NLP4), putative OS=Plasmodium falciparum (isolate 3D7) GN=PFE0380c PE=4 SV=1 | 8 | 1.54 | 0.53 | 0.0001 |
| tr\|Q8II61\|Q8II61_PLAF7 60S ribosomal protein P0 OS=Plasmodium falciparum (isolate 3D7) GN=PF11_0313 PE=3 SV=1 | 8 | 1.55 | 0.46 | 0.0000 |
| tr\|Q8IKL9\|Q8IKL9_PLAF7 40S ribosomal protein S28e, putative OS=Plasmodium falciparum (isolate 3D7) GN=PF14_0585 PE=3 SV=1 | 8 | 1.55 | 0.71 | 0.0004 |
| tr\|Q8IL58\|Q8IL58_PLAF7 60S ribosomal protein L1, putative OS=Plasmodium falciparum (isolate 3D7) GN=PF14_0391 PE=4 SV=1 | 8 | 1.55 | 0.67 | 0.0003 |
| tr\|Q8I713\|Q8I713_PLAF7 60S ribosomal protein L36 OS=Plasmodium falciparum (isolate 3D7) GN=PF11_0106 PE=1 SV=2 | 8 | 1.55 | 0.53 | 0.0001 |
| tr\|Q8IKH8\|Q8IKH8_PLAF7 40S ribosomal protein S3, putative OS=Plasmodium falciparum (isolate 3D7) GN=PF14_0627 PE=1 SV=1 | 8 | 1.55 | 0.50 | 0.0000 |
| tr\|Q8ILK4\|Q8ILK4_PLAF7 Uncharacterized protein OS=Plasmodium falciparum (isolate 3D7) GN=PF14_0239 PE=4 SV=2 | 8 | 1.56 | 0.27 | 0.0000 |
| tr\|C6KT23\|C6KT23_PLAF7 60S ribosomal protein L27a, putative OS=Plasmodium falciparum (isolate 3D7) GN=PFF0885w PE=1 SV=1 | 8 | 1.56 | 0.49 | 0.0000 |
| tr\|O97250\|O97250_PLAF7 60S ribosomal protein L7, putative OS=Plasmodium falciparum (isolate 3D7) GN=PFC0300c PE=1 SV=2 | 8 | 1.56 | 0.58 | 0.0001 |
| tr\|Q8ILY9\|Q8ILY9_PLAF7 Eukaryotic translation initiation factor 2 gamma subunit, putative OS=Plasmodium falciparum (isolate 3D7) GN=PF14_0104 PE=4 SV=1 | 8 | 1.57 | 0.84 | 0.0011 |
| tr\|Q8IM10\|Q8IM10_PLAF7 40S ribosomal protein S8 OS=Plasmodium falciparum (isolate 3D7) GN=PF14_0083 PE=1 SV=1 | 8 | 1.58 | 0.65 | 0.0002 |

| | | | | |
|---|---|---|---|---|
| tr\|Q8IDS6\|Q8IDS6_PLAF7 60S ribosomal protein L18a OS=Plasmodium falciparum (isolate 3D7) GN=PF13_0224 PE=1 SV=1 | 8 | 1.58 | 0.61 | 0.0002 |
| tr\|Q8I3B0\|Q8I3B0_PLAF7 60S ribosomal protein L32, putative OS=Plasmodium falciparum (isolate 3D7) GN=PFI0190w PE=4 SV=1 | 8 | 1.58 | 0.58 | 0.0001 |
| tr\|Q8IDI5\|Q8IDI5_PLAF7 60S ribosomal protein L17, putative OS=Plasmodium falciparum (isolate 3D7) GN=PF13_0268 PE=1 SV=1 | 8 | 1.58 | 0.60 | 0.0001 |
| sp\|O97313\|RS3A_PLAF7 40S ribosomal protein S3a OS=Plasmodium falciparum (isolate 3D7) GN=MAL3P7.35 PE=1 SV=1 | 8 | 1.58 | 0.67 | 0.0003 |
| tr\|Q8II27\|Q8II27_PLAF7 RNA (Uracil-5-)methyltransferase, putative OS=Plasmodium falciparum (isolate 3D7) GN=PF11_0348 PE=4 SV=2 | 8 | 1.58 | 0.85 | 0.0011 |
| tr\|Q8IIU3\|Q8IIU3_PLAF7 RuvB DNA helicase, putative OS=Plasmodium falciparum (isolate 3D7) GN=PF11_0071 PE=4 SV=1 | 8 | 1.59 | 0.29 | 0.0000 |
| tr\|Q8ILK3\|Q8ILK3_PLAF7 60S ribosomal protein L21e, putative OS=Plasmodium falciparum (isolate 3D7) GN=PF14_0240 PE=1 SV=1 | 8 | 1.59 | 0.66 | 0.0002 |
| tr\|O77395\|O77395_PLAF7 40S ribosomal protein S15A, putative OS=Plasmodium falciparum (isolate 3D7) GN=PFC0735w PE=1 SV=1 | 8 | 1.59 | 0.56 | 0.0001 |
| tr\|Q8IJX4\|Q8IJX4_PLAF7 Conserved Plasmodium protein OS=Plasmodium falciparum (isolate 3D7) GN=PF10_0067 PE=4 SV=2 | 8 | 1.60 | 0.74 | 0.0005 |
| tr\|Q8ID50\|Q8ID50_PLAF7 60S ribosomal protein L40/UBI, putative OS=Plasmodium falciparum (isolate 3D7) GN=PF13_0346 PE=1 SV=1;tr\|Q7KQK2\|Q7KQK2_PLAF7 PfpUB Plasmodium falciparum polyubiquitin OS=Plasmodium falciparum (isolate 3D7) GN=PFL0585w PE=4 SV=1 | 8 | 1.60 | 0.20 | 0.0000 |
| tr\|Q8IET7\|Q8IET7_PLAF7 40S ribosomal protein S7, putative OS=Plasmodium falciparum (isolate 3D7) GN=PF13_0014 PE=1 SV=1 | 8 | 1.60 | 0.64 | 0.0002 |
| tr\|C0H5C2\|C0H5C2_PLAF7 40S ribosomal protein S15/S19, putative OS=Plasmodium falciparum (isolate 3D7) GN=MAL13P1.92 PE=1 SV=1 | 8 | 1.61 | 0.82 | 0.0009 |
| tr\|C0H4K6\|C0H4K6_PLAF7 Ubiquitin transferase, putative OS=Plasmodium falciparum (isolate 3D7) GN=MAL7P1.19 PE=4 SV=1 | 8 | 1.62 | 0.71 | 0.0004 |
| tr\|Q8IHT9\|Q8IHT9_PLAF7 60S ribosomal protein L35Ae, putative OS=Plasmodium falciparum (isolate 3D7) GN=PF11_0438 PE=1 SV=1 | 8 | 1.63 | 0.57 | 0.0001 |
| tr\|Q8I444\|Q8I444_PLAF7 Small ubiquitin-related modifier, putative OS=Plasmodium falciparum (isolate 3D7) GN=PfSUMO PE=4 SV=1 | 8 | 1.64 | 0.24 | 0.0000 |
| tr\|C6KSY6\|C6KSY6_PLAF7 60S ribosomal protein L19, putative OS=Plasmodium falciparum (isolate 3D7) GN=PFF0700c PE=1 SV=1 | 8 | 1.64 | 0.63 | 0.0002 |
| tr\|Q8I463\|Q8I463_PLAF7 60S ribosomal protein L31, putative OS=Plasmodium falciparum (isolate 3D7) GN=PFE0185c PE=1 SV=1 | 8 | 1.64 | 0.47 | 0.0000 |
| tr\|C6KSR4\|C6KSR4_PLAF7 Uncharacterized protein OS=Plasmodium falciparum (isolate 3D7) GN=PFF0325c PE=4 SV=1 | 8 | 1.66 | 0.66 | 0.0002 |
| tr\|Q8IE85\|Q8IE85_PLAF7 60S ribosomal protein L6, putative OS=Plasmodium falciparum (isolate 3D7) GN=PF13_0129 PE=1 SV=1 | 8 | 1.66 | 0.48 | 0.0000 |
| tr\|O97238\|O97238_PLAF7 Putative uncharacterized protein OS=Plasmodium falciparum (isolate 3D7) GN=PFC0240c PE=4 SV=3 | 8 | 1.67 | 1.78 | 0.0328 |
| tr\|Q8I3K0\|Q8I3K0_PLAF7 Uncharacterized protein OS=Plasmodium falciparum (isolate 3D7) GN=PFE1320w PE=4 SV=1 | 8 | 1.49 | 2.22 | 0.0993 |
| tr\|Q8IJS7\|Q8IJS7_PLAF7 QF122 antigen OS=Plasmodium falciparum (isolate 3D7) GN=PF10_0115 PE=4 SV=1 | 8 | 1.67 | 0.29 | 0.0000 |
| tr\|Q8IBQ6\|Q8IBQ6_PLAF7 60S ribosomal protein L11a, putative OS=Plasmodium falciparum (isolate 3D7) GN=PF07_0079 PE=1 SV=1 | 8 | 1.67 | 0.72 | 0.0003 |
| tr\|Q8IES4\|Q8IES4_PLAF7 DNA ligase OS=Plasmodium falciparum (isolate 3D7) GN=PfLigI PE=3 SV=1 | 8 | 1.67 | 0.79 | 0.0005 |
| tr\|C6S3F0\|C6S3F0_PLAF7 Acylphosphatase, putative OS=Plasmodium falciparum (isolate 3D7) GN=PF11_0121 PE=3 SV=1 | 8 | 1.68 | 0.27 | 0.0000 |
| tr\|Q8IHQ8\|Q8IHQ8_PLAF7 Uncharacterized protein OS=Plasmodium falciparum (isolate 3D7) GN=PF11_0471 PE=4 SV=1 | 8 | 1.68 | 0.51 | 0.0000 |
| tr\|Q8II62\|Q8II62_PLAF7 60S ribosomal protein L38e, putative OS=Plasmodium falciparum (isolate 3D7) GN=PF11_0312 PE=1 SV=1 | 8 | 1.69 | 0.90 | 0.0011 |
| tr\|Q8ILV2\|Q8ILV2_PLAF7 60S ribosomal protein L10, putative OS=Plasmodium falciparum (isolate 3D7) GN=PF14_0141 PE=1 SV=1 | 8 | 1.69 | 0.59 | 0.0001 |
| tr\|C0H4A6\|C0H4A6_PLAF7 Ribosomal protein L15 OS=Plasmodium falciparum (isolate 3D7) GN=PFD0770c PE=1 SV=1 | 8 | 1.70 | 0.74 | 0.0003 |
| tr\|Q8I5E0\|Q8I5E0_PLAF7 Uncharacterized protein OS=Plasmodium falciparum (isolate 3D7) GN=PFL1345c PE=4 SV=1 | 8 | 1.72 | 1.89 | 0.0371 |
| tr\|Q8IJZ7\|Q8IJZ7_PLAF7 60S ribosomal protein L13, putative OS=Plasmodium falciparum (isolate 3D7) GN=PF10_0043 PE=1 SV=1 | 8 | 1.72 | 0.76 | 0.0004 |
| tr\|Q8II16\|Q8II16_PLAF7 Coatomer delta subunit, putative OS=Plasmodium falciparum (isolate 3D7) GN=PF11_0359 PE=4 SV=1 | 8 | 1.72 | 0.53 | 0.0000 |

| | | | | |
|---|---|---|---|---|
| tr\|Q8I431\|Q8I431_PLAF7 60S ribosomal protein L4, putative OS=Plasmodium falciparum (isolate 3D7) GN=PFE0350c PE=1 SV=1 | 8 | 1.73 | 0.91 | 0.0010 |
| tr\|Q8IAR6\|Q8IAR6_PLAF7 Proteasome subunit alpha type 5, putative OS=Plasmodium falciparum (isolate 3D7) GN=PF08_0109 PE=4 SV=1 | 8 | 1.73 | 0.72 | 0.0003 |
| tr\|Q8IK24\|Q8IK24_PLAF7 Acyl CoA binding protein, putative OS=Plasmodium falciparum (isolate 3D7) GN=PF10_0016 PE=4 SV=1 | 8 | 1.73 | 1.28 | 0.0065 |
| tr\|Q8IBJ9\|Q8IBJ9_PLAF7 Mago nashi protein homolog, putative OS=Plasmodium falciparum (isolate 3D7) GN=MAL7P1.139 PE=4 SV=2 | 8 | 1.74 | 1.50 | 0.0133 |
| tr\|Q8IJL2\|Q8IJL2_PLAF7 Uncharacterized protein OS=Plasmodium falciparum (isolate 3D7) GN=PF10_0183 PE=4 SV=1 | 8 | 1.75 | 0.74 | 0.0003 |
| tr\|Q9TY94\|Q9TY94_PLAF7 DEAD box helicase, UAP56 OS=Plasmodium falciparum (isolate 3D7) GN=UAP56 PE=4 SV=1 | 8 | 1.75 | 0.62 | 0.0001 |
| tr\|Q8IKZ7\|Q8IKZ7_PLAF7 Uncharacterized protein OS=Plasmodium falciparum (isolate 3D7) GN=PF14_0454 PE=4 SV=1 | 8 | 1.76 | 0.76 | 0.0003 |
| tr\|Q8ILM0\|Q8ILM0_PLAF7 Cyclophilin, putative OS=Plasmodium falciparum (isolate 3D7) GN=PF14_0223 PE=4 SV=2 | 8 | 1.77 | 0.61 | 0.0001 |
| tr\|Q8I2W3\|Q8I2W3_PLAF7 Nucleosome assembly protein OS=Plasmodium falciparum (isolate 3D7) GN=PFI0930c PE=3 SV=1 | 8 | 1.78 | 0.82 | 0.0005 |
| tr\|Q8IJT9\|Q8IJT9_PLAF7 Eukaryotic translation initiation factor 2, beta, putative OS=Plasmodium falciparum (isolate 3D7) GN=PF10_0103 PE=4 SV=1 | 8 | 1.78 | 1.21 | 0.0043 |
| tr\|Q8IDN4\|Q8IDN4_PLAF7 Nucleic acid binding protein, putative OS=Plasmodium falciparum (isolate 3D7) GN=MAL13P1.233 PE=4 SV=1 | 8 | 1.79 | 0.27 | 0.0000 |
| tr\|Q8I2X3\|Q8I2X3_PLAF7 Glideosome-associated protein 50 OS=Plasmodium falciparum (isolate 3D7) GN=GAP50 PE=1 SV=1 | 8 | 1.08 | 1.35 | 0.0569 |
| tr\|Q8IIT3\|Q8IIT3_PLAF7 Lsm4 homologue, putative OS=Plasmodium falciparum (isolate 3D7) GN=PF11_0524 PE=4 SV=2 | 8 | 1.80 | 0.65 | 0.0001 |
| tr\|Q8IAW0\|Q8IAW0_PLAF7 Importin subunit alpha OS=Plasmodium falciparum (isolate 3D7) GN=PF08_0087 PE=3 SV=1 | 8 | 1.80 | 0.52 | 0.0000 |
| tr\|C0H5G3\|C0H5G3_PLAF7 60S ribosomal protein L18 OS=Plasmodium falciparum (isolate 3D7) GN=MAL13P1.209 PE=1 SV=1 | 8 | 1.80 | 0.86 | 0.0006 |
| tr\|O96259\|O96259_PLAF7 Conserved Plasmodium protein OS=Plasmodium falciparum (isolate 3D7) GN=PFB0835c PE=4 SV=1 | 8 | 1.80 | 1.09 | 0.0023 |
| tr\|O97285\|O97285_PLAF7 ATP-dependent RNA Helicase, putative OS=Plasmodium falciparum (isolate 3D7) GN=PFC0915w PE=3 SV=1 | 8 | 1.80 | 0.58 | 0.0000 |
| tr\|Q8IJW0\|Q8IJW0_PLAF7 26S proteasome regulatory subunit 4, putative OS=Plasmodium falciparum (isolate 3D7) GN=PF10_0081 PE=3 SV=2 | 8 | 1.85 | 0.74 | 0.0002 |
| sp\|O15770\|GSHR_PLAF7 Glutathione reductase OS=Plasmodium falciparum (isolate 3D7) GN=GR3 PE=2 SV=4 | 8 | 1.85 | 0.84 | 0.0004 |
| tr\|C0H4W2\|C0H4W2_PLAF7 Lsm3 homologue, putative OS=Plasmodium falciparum (isolate 3D7) GN=PF08_0049 PE=4 SV=1 | 8 | 1.86 | 0.96 | 0.0009 |
| tr\|Q8IBA0\|Q8IBA0_PLAF7 Receptor for activated C kinase homolog, PfRACK OS=Plasmodium falciparum (isolate 3D7) GN=PfRACK PE=4 SV=1 | 8 | 1.89 | 0.67 | 0.0001 |
| tr\|Q8IEN2\|Q8IEN2_PLAF7 40S ribosomal protein S27, putative OS=Plasmodium falciparum (isolate 3D7) GN=PF13_0045 PE=1 SV=1 | 8 | 1.91 | 0.79 | 0.0003 |
| tr\|Q8I2G2\|Q8I2G2_PLAF7 Cytoadherence linked asexual protein 9(CLAG9) OS=Plasmodium falciparum (isolate 3D7) GN=CLAG9 PE=4 SV=1 | 8 | 1.91 | 1.54 | 0.0097 |
| tr\|Q7KQK6\|Q7KQK6_PLAF7 GTP-binding nuclear protein ran/tc4 OS=Plasmodium falciparum (isolate 3D7) GN=PF11_0183 PE=4 SV=1 | 8 | 1.92 | 0.86 | 0.0004 |
| tr\|Q8ILN8\|Q8ILN8_PLAF7 40S ribosomal protein S25, putative OS=Plasmodium falciparum (isolate 3D7) GN=PF14_0205 PE=1 SV=2 | 8 | 1.92 | 1.25 | 0.0034 |
| tr\|Q8IBN5\|Q8IBN5_PLAF7 40S ribosomal protein S5, putative OS=Plasmodium falciparum (isolate 3D7) GN=PF07_0088 PE=1 SV=1 | 8 | 1.92 | 1.20 | 0.0027 |
| tr\|Q8IIR9\|Q8IIR9_PLAF7 Casein kinase II, alpha subunit, putative OS=Plasmodium falciparum (isolate 3D7) GN=PF11_0096 PE=4 SV=1 | 8 | 1.95 | 1.30 | 0.0039 |
| tr\|Q8IJC6\|Q8IJC6_PLAF7 Ribosomal protein L3, putative OS=Plasmodium falciparum (isolate 3D7) GN=PF10_0272 PE=1 SV=1 | 8 | 1.95 | 1.02 | 0.0010 |
| tr\|Q8I616\|Q8I616_PLAF7 High mobility group protein OS=Plasmodium falciparum (isolate 3D7) GN=PFL0145c PE=4 SV=1 | 8 | 1.98 | 0.73 | 0.0001 |
| tr\|Q8I3A0\|Q8I3A0_PLAF7 Cu2+-transporting ATPase, Cu2+ transporter OS=Plasmodium falciparum (isolate 3D7) GN=PFI0240c PE=3 SV=1 | 8 | 7.93 | 20.76 | 0.3159 |
| tr\|Q8IJK8\|Q8IJK8_PLAF7 Ribosomal protein L30e, putative OS=Plasmodium falciparum (isolate 3D7) GN=PF10_0187 PE=1 SV=1 | 8 | 1.99 | 0.96 | 0.0006 |
| tr\|Q8I3N5\|Q8I3N5_PLAF7 G10 protein, putative OS=Plasmodium falciparum (isolate 3D7) GN=PFE1140c PE=4 SV=1 | 8 | 2.02 | 2.37 | 0.0470 |
| sp\|Q8IJD4\|RSSA_PLAF7 40S ribosomal protein SA OS=Plasmodium falciparum (isolate 3D7) GN=PF10_0264 PE=1 SV=1 | 8 | 2.03 | 1.12 | 0.0013 |

| | | | | |
|---|---|---|---|---|
| tr\|Q8I1S0\|Q8I1S0_PLAF7 Small GTP-binding protein sar1 OS=Plasmodium falciparum (isolate 3D7) GN=sar1 PE=3 SV=1 | 8 | 2.04 | 0.92 | 0.0004 |
| tr\|Q8IBH7\|Q8IBH7_PLAF7 Eukaryotic translation initiation factor 2 alpha subunit, putative OS=Plasmodium falciparum (isolate 3D7) GN=PF07_0117 PE=4 SV=1 | 8 | 2.05 | 0.88 | 0.0003 |
| tr\|O96153\|O96153_PLAF7 Proteasome 26S regulatory subunit, putative OS=Plasmodium falciparum (isolate 3D7) GN=PFB0260w PE=4 SV=3 | 8 | 2.06 | 0.97 | 0.0005 |
| tr\|C0H4V6\|C0H4V6_PLAF7 14-3-3 protein, putative OS=Plasmodium falciparum (isolate 3D7) GN=MAL8P1.69 PE=3 SV=1 | 8 | 2.08 | 0.94 | 0.0004 |
| tr\|Q8IHZ8\|Q8IHZ8_PLAF7 Uncharacterized protein OS=Plasmodium falciparum (isolate 3D7) GN=PF11_0378 PE=4 SV=1 | 8 | 2.09 | 2.00 | 0.0213 |
| tr\|Q8I3R6\|Q8I3R6_PLAF7 40S ribosomal protein S24 OS=Plasmodium falciparum (isolate 3D7) GN=PFE0975c PE=3 SV=1 | 8 | 2.12 | 1.58 | 0.0068 |
| tr\|C0H4E8\|C0H4E8_PLAF7 Proteasome subunit beta type OS=Plasmodium falciparum (isolate 3D7) GN=PFE0915c PE=3 SV=1 | 8 | 2.15 | 1.56 | 0.0058 |
| tr\|Q7KQJ9\|Q7KQJ9_PLAF7 Proliferating cell nuclear antigen OS=Plasmodium falciparum (isolate 3D7) GN=PFL1285c PE=3 SV=1 | 8 | 2.17 | 0.70 | 0.0001 |
| tr\|C0H4P4\|C0H4P4_PLAF7 Uncharacterized protein OS=Plasmodium falciparum (isolate 3D7) GN=MAL7P1.146 PE=4 SV=1 | 8 | 1.92 | 3.19 | 0.1322 |
| tr\|Q8I2Y5\|Q8I2Y5_PLAF7 RNA binding protein, putative OS=Plasmodium falciparum (isolate 3D7) GN=PFI0820c PE=4 SV=1 | 8 | 2.18 | 0.94 | 0.0003 |
| tr\|Q8IIJ6\|Q8IIJ6_PLAF7 Ubiquitin C-terminal hydrolase, family 1, putative OS=Plasmodium falciparum (isolate 3D7) GN=PF11_0177 PE=4 SV=1 | 8 | 2.19 | 1.33 | 0.0023 |
| tr\|Q8ID28\|Q8ID28_PLAF7 Proteasome regulatory subunit, putative OS=Plasmodium falciparum (isolate 3D7) GN=MAL13P1.343 PE=4 SV=1 | 8 | 2.22 | 1.43 | 0.0031 |
| sp\|Q8IAY6\|SODF_PLAF7 Superoxide dismutase [Fe] OS=Plasmodium falciparum (isolate 3D7) GN=SODB PE=1 SV=1 | 8 | 2.23 | 1.09 | 0.0007 |
| tr\|Q8IBQ5\|Q8IBQ5_PLAF7 40S ribosomal protein S10, putative OS=Plasmodium falciparum (isolate 3D7) GN=PF07_0080 PE=1 SV=1 | 8 | 2.23 | 1.06 | 0.0006 |
| tr\|O77396\|O77396_PLAF7 Proteasome component C8, putative OS=Plasmodium falciparum (isolate 3D7) GN=PFC0745c PE=4 SV=1 | 8 | 2.27 | 1.61 | 0.0053 |
| tr\|O77364\|O77364_PLAF7 60S ribosomal protein L26, putative OS=Plasmodium falciparum (isolate 3D7) GN=PFC0535w PE=1 SV=1 | 8 | 2.28 | 2.22 | 0.0225 |
| tr\|C6KST3\|C6KST3_PLAF7 Proteasome subunit alpha type 2, putative OS=Plasmodium falciparum (isolate 3D7) GN=PFF0420c PE=4 SV=1 | 8 | 2.29 | 1.20 | 0.0010 |
| tr\|Q8IB24\|Q8IB24_PLAF7 Heat shock 70 kDa protein OS=Plasmodium falciparum (isolate 3D7) GN=PF08_0054 PE=3 SV=1 | 8 | 2.29 | 0.87 | 0.0001 |
| tr\|Q8IL83\|Q8IL83_PLAF7 Cleavage and polyadenylation specificity factor protein, putative OS=Plasmodium falciparum (isolate 3D7) GN=PF14_0364 PE=4 SV=1 | 8 | 2.31 | 2.06 | 0.0157 |
| tr\|Q8I608\|Q8I608_PLAF7 Nucleosome assembly protein 1, putative OS=Plasmodium falciparum (isolate 3D7) GN=PFL0185c PE=1 SV=2 | 8 | 2.33 | 0.74 | 0.0000 |
| tr\|Q8IHW3\|Q8IHW3_PLAF7 Conserved Plasmodium protein OS=Plasmodium falciparum (isolate 3D7) GN=PF11_0413 PE=4 SV=2 | 8 | 2.34 | 2.22 | 0.0205 |
| tr\|Q8IK90\|Q8IK90_PLAF7 Proteosome subunit alpha type 1, putative OS=Plasmodium falciparum (isolate 3D7) GN=PF14_0716 PE=4 SV=1 | 8 | 2.35 | 1.40 | 0.0021 |
| tr\|Q8I1V1\|Q8I1V1_PLAF7 26S proteasome AAA-ATPase subunit RPT3, putative OS=Plasmodium falciparum (isolate 3D7) GN=PFD0665c PE=3 SV=1 | 8 | 2.36 | 1.34 | 0.0016 |
| tr\|Q8IEQ1\|Q8IEQ1_PLAF7 26S proteasome regulatory subunit, putative OS=Plasmodium falciparum (isolate 3D7) GN=PF13_0033 PE=3 SV=1 | 8 | 2.36 | 1.59 | 0.0041 |
| tr\|Q8I259\|Q8I259_PLAF7 Putative uncharacterized protein OS=Plasmodium falciparum (isolate 3D7) GN=PFA_0410w PE=4 SV=1 | 8 | 2.37 | 0.38 | 0.0000 |
| tr\|Q8ILX3\|Q8ILX3_PLAF7 Uncharacterized protein OS=Plasmodium falciparum (isolate 3D7) GN=PF14_0120 PE=4 SV=1 | 8 | 2.38 | 1.80 | 0.0072 |
| tr\|Q9U0J0\|Q9U0J0_PLAF7 Replication factor a protein, putative OS=Plasmodium falciparum (isolate 3D7) GN=PFD0470c PE=4 SV=1 | 8 | 2.39 | 0.89 | 0.0001 |
| tr\|Q8IIT1\|Q8IIT1_PLAF7 Conserved Plasmodium protein OS=Plasmodium falciparum (isolate 3D7) GN=PF11_0084 PE=4 SV=2 | 8 | 2.41 | 1.08 | 0.0004 |
| tr\|C6KT13\|C6KT13_PLAF7 Uncharacterized protein OS=Plasmodium falciparum (isolate 3D7) GN=PFF0835w PE=4 SV=1 | 8 | 2.43 | 1.11 | 0.0004 |
| tr\|Q8IEK3\|Q8IEK3_PLAF7 26S proteasome regulatory subunit 7, putative OS=Plasmodium falciparum (isolate 3D7) GN=PF13_0063 PE=3 SV=2 | 8 | 2.48 | 1.59 | 0.0031 |
| tr\|Q8IM53\|Q8IM53_PLAF7 Cytochrome c, putative OS=Plasmodium falciparum (isolate 3D7) GN=PF14_0038 PE=3 SV=1 | 8 | 1.07 | 1.42 | 0.0689 |
| tr\|Q8IDR5\|Q8IDR5_PLAF7 Casein kinase II subunit beta OS=Plasmodium falciparum (isolate 3D7) GN=PfCK2beta2 PE=3 SV=1 | 8 | 2.55 | 2.05 | 0.0097 |
| tr\|Q8I3B4\|Q8I3B4_PLAF7 DEAD/DEAH box helicase, putative OS=Plasmodium falciparum (isolate 3D7) GN=PFI0165c PE=4 SV=1 | 8 | 2.62 | 1.78 | 0.0043 |

| | | | | |
|---|---|---|---|---|
| tr\|Q8I3J6\|Q8I3J6_PLAF7 Uncharacterized protein OS=Plasmodium falciparum (isolate 3D7) GN=PFE1340w PE=3 SV=1 | 8 | 18.89 | 47.56 | 0.2983 |
| tr\|Q8IIL0\|Q8IIL0_PLAF7 Falcipain-3 OS=Plasmodium falciparum (isolate 3D7) GN=PF11_0162 PE=3 SV=1 | 8 | 2.64 | 1.20 | 0.0004 |
| tr\|Q8IM66\|Q8IM66_PLAF7 Proteosome subunit, putative OS=Plasmodium falciparum (isolate 3D7) GN=PF14_0025 PE=4 SV=1 | 8 | 2.65 | 1.82 | 0.0045 |
| sp\|Q8ILW9\|ACT2_PLAF7 Actin-2 OS=Plasmodium falciparum (isolate 3D7) GN=PF14_0124 PE=3 SV=1 | 8 | 2.65 | 1.33 | 0.0008 |
| tr\|Q8IKH3\|Q8IKH3_PLAF7 26S proteasome subunit, putative OS=Plasmodium falciparum (isolate 3D7) GN=PF14_0632 PE=4 SV=1 | 8 | 2.73 | 2.18 | 0.0093 |
| tr\|Q8I5F9\|Q8I5F9_PLAF7 Ubiquitin-activating enzyme e1, putative OS=Plasmodium falciparum (isolate 3D7) GN=PFL1245w PE=4 SV=1 | 8 | 2.75 | 1.65 | 0.0021 |
| tr\|Q8I5U3\|Q8I5U3_PLAF7 Uncharacterized protein OS=Plasmodium falciparum (isolate 3D7) GN=PFL0530c PE=4 SV=1 | 8 | 2.76 | 2.09 | 0.0073 |
| tr\|Q8II60\|Q8II60_PLAF7 26S protease subunit regulatory subunit 6a, putative OS=Plasmodium falciparum (isolate 3D7) GN=PF11_0314 PE=3 SV=1 | 8 | 2.76 | 1.51 | 0.0013 |
| tr\|Q8IL11\|Q8IL11_PLAF7 M17 leucyl aminopeptidase OS=Plasmodium falciparum (isolate 3D7) GN=LAP PE=1 SV=1 | 8 | 2.83 | 2.00 | 0.0052 |
| tr\|Q8IBI3\|Q8IBI3_PLAF7 Proteasome subunit alpha type OS=Plasmodium falciparum (isolate 3D7) GN=PF07_0112 PE=3 SV=1 | 8 | 2.85 | 1.98 | 0.0047 |
| tr\|Q8I3M5\|Q8I3M5_PLAF7 Karyopherin beta OS=Plasmodium falciparum (isolate 3D7) GN=PFE1195w PE=4 SV=1 | 8 | 2.90 | 1.41 | 0.0006 |
| tr\|Q8IEK1\|Q8IEK1_PLAF7 M1-family aminopeptidase OS=Plasmodium falciparum (isolate 3D7) GN=MAL13P1.56 PE=4 SV=1 | 8 | 2.95 | 1.77 | 0.0022 |
| tr\|Q8II72\|Q8II72_PLAF7 Uncharacterized protein OS=Plasmodium falciparum (isolate 3D7) GN=PF11_0302 PE=4 SV=1 | 8 | 3.05 | 0.55 | 0.0000 |
| tr\|C0H4U5\|C0H4U5_PLAF7 Uncharacterized protein OS=Plasmodium falciparum (isolate 3D7) GN=PF08_0081 PE=4 SV=1 | 8 | 3.07 | 1.13 | 0.0001 |
| tr\|Q8IDG3\|Q8IDG3_PLAF7 Proteasome subunit alpha type OS=Plasmodium falciparum (isolate 3D7) GN=PF13_0282 PE=3 SV=1 | 8 | 3.08 | 3.18 | 0.0289 |
| tr\|Q8IHS5\|Q8IHS5_PLAF7 40S ribosomal protein S21 OS=Plasmodium falciparum (isolate 3D7) GN=PF11_0454 PE=1 SV=1 | 8 | 3.09 | 3.31 | 0.0337 |
| tr\|C0H4Q0\|C0H4Q0_PLAF7 Signal recognition particle SRP9, putative OS=Plasmodium falciparum (isolate 3D7) GN=MAL7P1.158 PE=4 SV=1 | 8 | 3.09 | 2.68 | 0.0139 |
| tr\|Q8I3J0\|Q8I3J0_PLAF7 Hsp70 interacting protein, putative OS=Plasmodium falciparum (isolate 3D7) GN=PFE1370w PE=4 SV=1 | 8 | 3.15 | 2.07 | 0.0036 |
| tr\|Q8IM15\|Q8IM15_PLAF7 HAP protein OS=Plasmodium falciparum (isolate 3D7) GN=PF14_0078 PE=1 SV=1 | 8 | 3.20 | 0.60 | 0.0000 |
| sp\|Q8I4X0\|ACT1_PLAF7 Actin-1 OS=Plasmodium falciparum (isolate 3D7) GN=PFL2215w PE=3 SV=1 | 8 | 3.20 | 1.65 | 0.0009 |
| tr\|Q8I5A3\|Q8I5A3_PLAF7 Asparagine-rich protein, putative OS=Plasmodium falciparum (isolate 3D7) GN=PFL1530w PE=4 SV=1 | 8 | 3.23 | 1.19 | 0.0001 |
| sp\|Q7KQM1\|PRI1_PLAF7 DNA primase small subunit OS=Plasmodium falciparum (isolate 3D7) GN=PF14_0366 PE=3 SV=1 | 8 | 3.23 | 3.54 | 0.0364 |
| tr\|Q8I2Z8\|Q8I2Z8_PLAF7 6-phosphofructokinase, putative OS=Plasmodium falciparum (isolate 3D7) GN=PFI0755c PE=4 SV=1 | 8 | 3.26 | 3.01 | 0.0184 |
| tr\|C6KTA9\|C6KTA9_PLAF7 C3h4-type ring finger protein, putative OS=Plasmodium falciparum (isolate 3D7) GN=PFF1325c PE=4 SV=1 | 8 | 3.08 | 4.28 | 0.0812 |
| tr\|Q8IES0\|Q8IES0_PLAF7 Small heat shock protein, putative OS=Plasmodium falciparum (isolate 3D7) GN=PF13_0021 PE=3 SV=1 | 8 | 3.28 | 2.37 | 0.0058 |
| tr\|Q8I542\|Q8I542_PLAF7 Calcyclin binding protein, putative OS=Plasmodium falciparum (isolate 3D7) GN=PFL1845c PE=4 SV=2 | 8 | 3.28 | 1.93 | 0.0020 |
| sp\|Q8IIJ9\|CATC_PLAF7 Probable cathepsin C OS=Plasmodium falciparum (isolate 3D7) GN=PF11_0174 PE=1 SV=1 | 8 | 3.31 | 1.08 | 0.0001 |
| tr\|Q8IAR3\|Q8IAR3_PLAF7 Proteasome subunit alpha, putative OS=Plasmodium falciparum (isolate 3D7) GN=MAL8P1.128 PE=4 SV=2 | 8 | 3.33 | 2.91 | 0.0142 |
| tr\|Q8I5C6\|Q8I5C6_PLAF7 Uncharacterized protein OS=Plasmodium falciparum (isolate 3D7) GN=PFL1415w PE=4 SV=1 | 8 | 1.52 | 3.10 | 0.2084 |
| tr\|Q8I3L4\|Q8I3L4_PLAF7 Acyl-CoA synthetase, PfACS10 OS=Plasmodium falciparum (isolate 3D7) GN=PfACS10 PE=4 SV=1 | 8 | 3.40 | 2.90 | 0.0128 |
| tr\|Q7KWJ1\|Q7KWJ1_PLAF7 Acyl carrier protein OS=Plasmodium falciparum (isolate 3D7) GN=PFB0385w PE=3 SV=1 | 8 | 3.58 | 8.46 | 0.2700 |
| tr\|Q8IDG2\|Q8IDG2_PLAF7 Proteasome subunit alpha type OS=Plasmodium falciparum (isolate 3D7) GN=MAL13P1.270 PE=3 SV=1 | 8 | 3.50 | 3.16 | 0.0165 |
| tr\|Q8IM16\|Q8IM16_PLAF7 Plasmepsin IV OS=Plasmodium falciparum (isolate 3D7) GN=PF14_0075 PE=1 SV=1 | 8 | 3.58 | 0.67 | 0.0000 |

| | | | | |
|---|---|---|---|---|
| tr\|Q8IJN8\|Q8IJN8_PLAF7 Ribonucleotide reductase small subunit, putative OS=Plasmodium falciparum (isolate 3D7) GN=PF10_0154 PE=4 SV=2 | 8 | 3.59 | 2.19 | 0.0024 |
| tr\|Q8ILT0\|Q8ILT0_PLAF7 Glutamate dehydrogenase OS=Plasmodium falciparum (isolate 3D7) GN=PF14_0164 PE=3 SV=1 | 8 | 3.74 | 2.51 | 0.0040 |
| tr\|O97246\|O97246_PLAF7 Putative uncharacterized protein OS=Plasmodium falciparum (isolate 3D7) GN=PFC0280c PE=4 SV=1 | 8 | 2.13 | 4.54 | 0.2260 |
| tr\|Q8IC05\|Q8IC05_PLAF7 Heat shock protein 86 OS=Plasmodium falciparum (isolate 3D7) GN=PF07_0029 PE=1 SV=1 | 8 | 3.92 | 4.01 | 0.0280 |
| tr\|C0H551\|C0H551_PLAF7 Glutamine synthetase, putative OS=Plasmodium falciparum (isolate 3D7) GN=PFI1110w PE=3 SV=1 | 8 | 4.00 | 3.93 | 0.0238 |
| tr\|Q8I2U5\|Q8I2U5_PLAF7 Inosine-5-monophosphate dehydrogenase OS=Plasmodium falciparum (isolate 3D7) GN=PFI1020c PE=3 SV=1 | 8 | 4.26 | 3.77 | 0.0151 |
| tr\|C0H4L1\|C0H4L1_PLAF7 Uncharacterized protein OS=Plasmodium falciparum (isolate 3D7) GN=MAL7P1.202 PE=4 SV=1 | 8 | 4.27 | 2.47 | 0.0018 |
| tr\|Q8IEN3\|Q8IEN3_PLAF7 Carbamoyl phosphate synthetase OS=Plasmodium falciparum (isolate 3D7) GN=cpsSII PE=4 SV=1 | 8 | 4.28 | 2.94 | 0.0045 |
| tr\|Q8I6V3\|Q8I6V3_PLAF7 Plasmepsin II OS=Plasmodium falciparum (isolate 3D7) GN=PF14_0077 PE=3 SV=1 | 8 | 4.36 | 1.80 | 0.0002 |
| sp\|C6KT50\|PDX1_PLAF7 Pyridoxal 5-phosphate synthase subunit Pdx1 OS=Plasmodium falciparum (isolate 3D7) GN=pdx1 PE=1 SV=1 | 8 | 4.42 | 3.16 | 0.0055 |
| tr\|C0H4E7\|C0H4E7_PLAF7 Uncharacterized protein OS=Plasmodium falciparum (isolate 3D7) GN=PFE0910w PE=4 SV=1 | 8 | 4.97 | 8.12 | 0.1268 |
| sp\|Q8I3Z5\|TCTP_PLAF7 Translationally-controlled tumor protein homolog OS=Plasmodium falciparum (isolate 3D7) GN=TCTP PE=1 SV=1 | 8 | 4.54 | 3.54 | 0.0084 |
| tr\|Q8I3Y8\|Q8I3Y8_PLAF7 Myo-inositol 1-phosphate synthase, putative OS=Plasmodium falciparum (isolate 3D7) GN=PFE0585c PE=4 SV=1 | 8 | 4.62 | 5.09 | 0.0373 |
| tr\|Q8ILP6\|Q8ILP6_PLAF7 Glycine-tRNA ligase, putative OS=Plasmodium falciparum (isolate 3D7) GN=PF14_0198 PE=3 SV=2 | 8 | 4.68 | 4.49 | 0.0215 |
| tr\|C0H5F2\|C0H5F2_PLAF7 Uncharacterized protein OS=Plasmodium falciparum (isolate 3D7) GN=MAL13P1.172 PE=4 SV=1 | 8 | 4.68 | 3.19 | 0.0043 |
| tr\|Q8I2Q0\|Q8I2Q0_PLAF7 Putative uncharacterized protein OS=Plasmodium falciparum (isolate 3D7) GN=PFI1270w PE=4 SV=1 | 8 | 4.70 | 1.34 | 0.0000 |
| tr\|Q8I535\|Q8I535_PLAF7 Long-chain-fatty-acid--CoA ligase, putative OS=Plasmodium falciparum (isolate 3D7) GN=PFL1880w PE=4 SV=1 | 8 | 4.71 | 4.14 | 0.0146 |
| sp\|Q7KQL5\|TBB_PLAF7 Tubulin beta chain OS=Plasmodium falciparum (isolate 3D7) GN=PF10_0084 PE=3 SV=1 | 8 | 4.87 | 4.88 | 0.0256 |
| tr\|Q8IL88\|Q8IL88_PLAF7 HSP40, subfamily A, putative OS=Plasmodium falciparum (isolate 3D7) GN=PF14_0359 PE=4 SV=1 | 8 | 5.13 | 3.44 | 0.0039 |
| sp\|Q8I2J4\|PROF_PLAF7 Profilin OS=Plasmodium falciparum (isolate 3D7) GN=Pfn PE=3 SV=1 | 8 | 5.23 | 6.14 | 0.0467 |
| tr\|Q76NN7\|Q76NN7_PLAF7 Peptidyl-prolyl cis-trans isomerase OS=Plasmodium falciparum (isolate 3D7) GN=PfCyP19 PE=3 SV=1 | 8 | 5.27 | 4.63 | 0.0147 |
| tr\|Q8IL48\|Q8IL48_PLAF7 tRNA binding protein, putative OS=Plasmodium falciparum (isolate 3D7) GN=PF14_0401 PE=4 SV=1 | 8 | 5.30 | 3.13 | 0.0020 |
| sp\|Q7KQM4\|PLM1_PLAF7 Plasmepsin-1 OS=Plasmodium falciparum (isolate 3D7) GN=PF14_0076 PE=2 SV=1 | 8 | 5.37 | 6.02 | 0.0396 |
| tr\|Q8IL80\|Q8IL80_PLAF7 Thioredoxin peroxidase 1 OS=Plasmodium falciparum (isolate 3D7) GN=TPx1 PE=4 SV=1 | 8 | 5.41 | 5.23 | 0.0221 |
| tr\|Q8ILK2\|Q8ILK2_PLAF7 Nascent polypeptide-associated complex subunit beta OS=Plasmodium falciparum (isolate 3D7) GN=PF14_0241 PE=3 SV=1 | 8 | 5.54 | 5.17 | 0.0191 |
| tr\|Q8IJ60\|Q8IJ60_PLAF7 Methionine--tRNA ligase, putative OS=Plasmodium falciparum (isolate 3D7) GN=PF10_0340 PE=4 SV=1 | 8 | 5.68 | 4.02 | 0.0052 |
| tr\|Q8IM38\|Q8IM38_PLAF7 Ribonucleotide reductase small subunit OS=Plasmodium falciparum (isolate 3D7) GN=PF14_0053 PE=4 SV=1 | 8 | 5.71 | 5.91 | 0.0292 |
| tr\|Q8I5B6\|Q8I5B6_PLAF7 Heat shock protein hslv OS=Plasmodium falciparum (isolate 3D7) GN=HslV PE=4 SV=2 | 8 | 11.59 | 29.94 | 0.3097 |
| tr\|Q8IE68\|Q8IE68_PLAF7 Lsm6 homologue, putative OS=Plasmodium falciparum (isolate 3D7) GN=PF13_0142 PE=4 SV=1 | 8 | 5.85 | 5.80 | 0.0246 |
| tr\|Q8I5Y9\|Q8I5Y9_PLAF7 Uncharacterized protein OS=Plasmodium falciparum (isolate 3D7) GN=PFL0280c PE=4 SV=1 | 8 | 5.86 | 4.77 | 0.0104 |
| sp\|Q8IJN7\|ENO_PLAF7 Enolase OS=Plasmodium falciparum (isolate 3D7) GN=ENO PE=3 SV=1 | 8 | 5.91 | 5.85 | 0.0245 |
| tr\|Q8IIG6\|Q8IIG6_PLAF7 Phosphoglycerate mutase, putative OS=Plasmodium falciparum (isolate 3D7) GN=PF11_0208 PE=1 SV=1 | 8 | 5.98 | 6.36 | 0.0325 |
| tr\|Q8III5\|Q8III5_PLAF7 Uncharacterized protein OS=Plasmodium falciparum (isolate 3D7) GN=PF11_0189 PE=3 SV=1 | 8 | 6.02 | 4.60 | 0.0077 |

| | | | | |
|---|---|---|---|---|
| sp\|P50250\|SAHH_PLAF7 Adenosylhomocysteinase OS=Plasmodium falciparum (isolate 3D7) GN=PFE1050w PE=1 SV=2 | 8 | 6.04 | 7.04 | 0.0457 |
| tr\|C6KT55\|C6KT55_PLAF7 Nascent polypeptide associated complex alpha chain, putative OS=Plasmodium falciparum (isolate 3D7) GN=PFF1050w PE=4 SV=1 | 8 | 6.13 | 5.16 | 0.0122 |
| sp\|Q7KQL9\|ALF_PLAF7 Fructose-bisphosphate aldolase OS=Plasmodium falciparum (isolate 3D7) GN=PF14_0425 PE=3 SV=1 | 8 | 6.27 | 6.79 | 0.0347 |
| sp\|Q8ILC1\|STI1L_PLAF7 STI1-like protein OS=Plasmodium falciparum (isolate 3D7) GN=PF14_0324 PE=3 SV=1 | 8 | 6.43 | 6.69 | 0.0298 |
| tr\|Q8I0P6\|Q8I0P6_PLAF7 Elongation factor 1-alpha OS=Plasmodium falciparum (isolate 3D7) GN=PF13_0304 PE=3 SV=1 | 8 | 6.44 | 6.98 | 0.0349 |
| tr\|Q7KQK0\|Q7KQK0_PLAF7 CAMP-dependent protein kinase regulatory subunit, putative OS=Plasmodium falciparum (isolate 3D7) GN=PKAr PE=4 SV=1 | 8 | 6.45 | 6.98 | 0.0347 |
| tr\|Q8IDC6\|Q8IDC6_PLAF7 Pyrroline carboxylate reductase OS=Plasmodium falciparum (isolate 3D7) GN=MAL13P1.284 PE=1 SV=1 | 8 | 6.54 | 5.77 | 0.0149 |
| tr\|Q9NLB2\|Q9NLB2_PLAF7 Glutaredoxin OS=Plasmodium falciparum (isolate 3D7) GN=GRX1 PE=1 SV=1 | 8 | 6.63 | 7.33 | 0.0376 |
| tr\|C6KT76\|C6KT76_PLAF7 Hexokinase OS=Plasmodium falciparum (isolate 3D7) GN=PFF1155w PE=3 SV=1 | 8 | 6.67 | 7.84 | 0.0470 |
| tr\|Q8IKF0\|Q8IKF0_PLAF7 Helicase 45 OS=Plasmodium falciparum (isolate 3D7) GN=H45 PE=3 SV=1 | 8 | 7.07 | 7.10 | 0.0260 |
| tr\|Q8II43\|Q8II43_PLAF7 T-complex protein 1 subunit alpha OS=Plasmodium falciparum (isolate 3D7) GN=PF11_0331 PE=3 SV=1 | 8 | 7.16 | 7.76 | 0.0349 |
| tr\|Q8ILA4\|Q8ILA4_PLAF7 Glucose-6-phosphate isomerase OS=Plasmodium falciparum (isolate 3D7) GN=PF14_0341 PE=1 SV=1 | 8 | 7.17 | 5.49 | 0.0077 |
| tr\|Q8IL94\|Q8IL94_PLAF7 Ribonucleoside-diphosphate reductase OS=Plasmodium falciparum (isolate 3D7) GN=PF14_0352 PE=3 SV=1 | 8 | 7.19 | 7.30 | 0.0270 |
| tr\|Q8IJS1\|Q8IJS1_PLAF7 Hypoxanthine phosphoribosyltransferase OS=Plasmodium falciparum (isolate 3D7) GN=PF10_0121 PE=4 SV=1 | 8 | 7.20 | 7.56 | 0.0309 |
| sp\|Q7KQM0\|TPIS_PLAF7 Triosephosphate isomerase OS=Plasmodium falciparum (isolate 3D7) GN=TPI PE=3 SV=1 | 8 | 7.31 | 8.58 | 0.0469 |
| tr\|Q8I261\|Q8I261_PLAF7 Beta3 proteasome subunit, putative OS=Plasmodium falciparum (isolate 3D7) GN=PFA_0400c PE=4 SV=1 | 8 | 7.51 | 8.77 | 0.0458 |
| tr\|Q8I5P5\|Q8I5P5_PLAF7 Glycerol-3-phosphate dehydrogenase [NAD(+)] OS=Plasmodium falciparum (isolate 3D7) GN=PFL0780w PE=1 SV=1 | 8 | 7.52 | 8.10 | 0.0342 |
| tr\|O97319\|O97319_PLAF7 Elongation factor 1 (EF-1), putative OS=Plasmodium falciparum (isolate 3D7) GN=PFC0870w PE=4 SV=2 | 8 | 7.60 | 7.72 | 0.0271 |
| tr\|Q8I2J3\|Q8I2J3_PLAF7 M18 aspartyl aminopeptidase OS=Plasmodium falciparum (isolate 3D7) GN=PfM18AAP PE=1 SV=1 | 8 | 7.70 | 6.35 | 0.0110 |
| tr\|Q8IBS3\|Q8IBS3_PLAF7 Seryl-tRNA synthetase, putative OS=Plasmodium falciparum (isolate 3D7) GN=PF07_0073 PE=3 SV=1 | 8 | 7.76 | 7.72 | 0.0249 |
| tr\|Q8IDZ9\|Q8IDZ9_PLAF7 Isoleucine-tRNA ligase, putative OS=Plasmodium falciparum (isolate 3D7) GN=PF13_0179 PE=3 SV=1 | 8 | 7.99 | 7.39 | 0.0183 |
| tr\|Q8IKT5\|Q8IKT5_PLAF7 Peptidase, putative OS=Plasmodium falciparum (isolate 3D7) GN=PF14_0517 PE=3 SV=1 | 8 | 8.03 | 4.48 | 0.0014 |
| tr\|Q8IDJ8\|Q8IDJ8_PLAF7 Lysine--tRNA ligase OS=Plasmodium falciparum (isolate 3D7) GN=PF13_0262 PE=1 SV=1 | 8 | 8.37 | 7.23 | 0.0136 |
| tr\|Q8I3M1\|Q8I3M1_PLAF7 Cytosolic preribosomal GTP-binding protein, putative OS=Plasmodium falciparum (isolate 3D7) GN=PFE1215c PE=4 SV=1 | 8 | 8.57 | 8.22 | 0.0214 |
| tr\|O96220\|O96220_PLAF7 T-complex protein 1, putative OS=Plasmodium falciparum (isolate 3D7) GN=PFB0635w PE=3 SV=3 | 8 | 8.90 | 8.54 | 0.0215 |
| tr\|Q76NN6\|Q76NN6_PLAF7 Ran binding protein 1, putative OS=Plasmodium falciparum (isolate 3D7) GN=PFD0950w PE=4 SV=1 | 8 | 9.22 | 10.48 | 0.0418 |
| tr\|Q8IJ74\|Q8IJ74_PLAF7 Uncharacterized protein OS=Plasmodium falciparum (isolate 3D7) GN=PF10_0325 PE=1 SV=1 | 8 | 10.64 | 12.49 | 0.0467 |
| tr\|C6KTA3\|C6KTA3_PLAF7 Uncharacterized protein OS=Plasmodium falciparum (isolate 3D7) GN=PFF1295w PE=4 SV=1 | 8 | 10.86 | 12.62 | 0.0453 |
| tr\|C6KTB1\|C6KTB1_PLAF7 4-methyl-5(B-hydroxyethyl)-thiazol monophosphate biosynthesis enzyme OS=Plasmodium falciparum (isolate 3D7) GN=PFF1335c PE=4 SV=1 | 8 | 11.17 | 11.78 | 0.0314 |
| tr\|O96221\|O96221_PLAF7 Sec31p putative OS=Plasmodium falciparum (isolate 3D7) GN=Sec31p PE=4 SV=3 | 8 | 14.12 | 9.95 | 0.0051 |
| tr\|Q8I655\|Q8I655_PLAF7 Ribosome associated membrane protein RAMP4, putative OS=Plasmodium falciparum (isolate 3D7) GN=PFB0888w PE=4 SV=2 | 8 | 0.28 | 0.35 | 0.0577 |
| tr\|Q9TY96\|Q9TY96_PLAF7 Serine repeat antigen 6 (SERA-6) OS=Plasmodium falciparum (isolate 3D7) GN=SERA-6 PE=1 SV=3 | 7 | 0.26 | 0.25 | 0.0353 |
| tr\|Q8I563\|Q8I563_PLAF7 Uncharacterized protein OS=Plasmodium falciparum (isolate 3D7) GN=PFL1740w PE=4 SV=1 | 7 | 0.38 | 0.32 | 0.0194 |

| | | | | |
|---|---|---|---|---|
| tr\|C6KSV8\|C6KSV8_PLAF7 Uncharacterized protein OS=Plasmodium falciparum (isolate 3D7) GN=PFF0555w PE=4 SV=1 | 7 | 0.52 | 0.30 | 0.0037 |
| tr\|C0H564\|C0H564_PLAF7 Monocarboxylate transporter, putative OS=Plasmodium falciparum (isolate 3D7) GN=PFI1295c PE=4 SV=1 | 7 | 0.55 | 0.24 | 0.0010 |
| tr\|Q8I6S5\|Q8I6S5_PLAF7 2-oxoglutarate dehydrogenase E1 component OS=Plasmodium falciparum (isolate 3D7) GN=PF08_0045 PE=4 SV=1 | 7 | 0.57 | 0.28 | 0.0019 |
| tr\|Q8I461\|Q8I461_PLAF7 Cation transporting P-ATPase OS=Plasmodium falciparum (isolate 3D7) GN=PfATPase3 PE=3 SV=1 | 7 | 0.60 | 0.19 | 0.0001 |
| tr\|Q8IDI7\|Q8IDI7_PLAF7 Uncharacterized protein OS=Plasmodium falciparum (isolate 3D7) GN=MAL13P1.258 PE=4 SV=1 | 7 | 0.60 | 0.24 | 0.0005 |
| tr\|Q8IKP8\|Q8IKP8_PLAF7 Uncharacterized protein OS=Plasmodium falciparum (isolate 3D7) GN=PF14_0556 PE=4 SV=2 | 7 | 0.62 | 0.21 | 0.0003 |
| tr\|Q8IL89\|Q8IL89_PLAF7 Succinyl CoA ligase, putative OS=Plasmodium falciparum (isolate 3D7) GN=PF14_0357 PE=4 SV=1 | 7 | 0.63 | 0.33 | 0.0022 |
| tr\|Q8I599\|Q8I599_PLAF7 Cytochrome b5, putative OS=Plasmodium falciparum (isolate 3D7) GN=PFL1555w PE=3 SV=1 | 7 | 0.66 | 0.37 | 0.0032 |
| tr\|Q8IBK8\|Q8IBK8_PLAF7 Mitochondrial import inner membrane translocase subunit tim14, putative OS=Plasmodium falciparum (isolate 3D7) GN=PF07_0103 PE=4 SV=1 | 7 | 0.68 | 0.34 | 0.0019 |
| tr\|Q5MYR6\|Q5MYR6_PLAF7 1-cys peroxiredoxin OS=Plasmodium falciparum (isolate 3D7) GN=prx PE=1 SV=1 | 7 | 0.68 | 0.37 | 0.0028 |
| tr\|O97320\|O97320_PLAF7 Histone H2A OS=Plasmodium falciparum (isolate 3D7) GN=PFC0920w PE=3 SV=1 | 7 | 0.69 | 0.26 | 0.0004 |
| tr\|Q8IIC3\|Q8IIC3_PLAF7 Endoplasmic reticulum oxidoreductin, putative OS=Plasmodium falciparum (isolate 3D7) GN=PF11_0251 PE=4 SV=2 | 7 | 0.70 | 0.30 | 0.0008 |
| tr\|Q7KQL1\|Q7KQL1_PLAF7 Myb2 protein OS=Plasmodium falciparum (isolate 3D7) GN=PF10_0327 PE=4 SV=1 | 7 | 0.71 | 0.34 | 0.0014 |
| tr\|Q8I3Q3\|Q8I3Q3_PLAF7 Uncharacterized protein OS=Plasmodium falciparum (isolate 3D7) GN=PFE1045c PE=4 SV=1 | 7 | 0.71 | 0.34 | 0.0015 |
| tr\|A0A087WY82\|A0A087WY82_HUMAN Junctional adhesion molecule A OS=Homo sapiens GN=F11R PE=1 SV=1;sp\|Q9Y624\|JAM1_HUMAN Junctional adhesion molecule A OS=Homo sapiens GN=F11R PE=1 SV=1 | 7 | 0.71 | 0.37 | 0.0021 |
| tr\|Q8I5Y7\|Q8I5Y7_PLAF7 Uncharacterized protein OS=Plasmodium falciparum (isolate 3D7) GN=PFL0290w PE=4 SV=1 | 7 | 0.72 | 0.31 | 0.0009 |
| tr\|Q9U0L4\|Q9U0L4_PLAF7 Peptidyl-tRNA hydrolase PTH2, putative OS=Plasmodium falciparum (isolate 3D7) GN=PFD0355c PE=4 SV=2 | 7 | 0.73 | 0.30 | 0.0007 |
| tr\|O96204\|O96204_PLAF7 Conserved Plasmodium membrane protein OS=Plasmodium falciparum (isolate 3D7) GN=PFB0555c PE=4 SV=2 | 7 | 0.73 | 0.30 | 0.0006 |
| tr\|Q8IJS2\|Q8IJS2_PLAF7 Uncharacterized protein OS=Plasmodium falciparum (isolate 3D7) GN=PF10_0120 PE=4 SV=1 | 7 | 0.74 | 0.28 | 0.0004 |
| tr\|Q8IKN7\|Q8IKN7_PLAF7 Uncharacterized protein OS=Plasmodium falciparum (isolate 3D7) GN=PF14_0567 PE=4 SV=1 | 7 | 0.75 | 0.28 | 0.0004 |
| tr\|C0H5H5\|C0H5H5_PLAF7 Uncharacterized protein OS=Plasmodium falciparum (isolate 3D7) GN=MAL13P1.229 PE=4 SV=1 | 7 | 0.75 | 0.25 | 0.0002 |
| tr\|Q8IEA6\|Q8IEA6_PLAF7 Dihydrolipamide succinyltransferase component of 2-oxoglutarate dehydrogenase complex OS=Plasmodium falciparum (isolate 3D7) GN=PF13_0121 PE=3 SV=1 | 7 | 0.77 | 0.28 | 0.0003 |
| tr\|Q8I348\|Q8I348_PLAF7 Selenide water dikinase, putative OS=Plasmodium falciparum (isolate 3D7) GN=PFI0505c PE=4 SV=1 | 7 | 0.78 | 0.22 | 0.0001 |
| tr\|Q8ILM6\|Q8ILM6_PLAF7 Uncharacterized protein OS=Plasmodium falciparum (isolate 3D7) GN=PF14_0217 PE=4 SV=1 | 7 | 0.78 | 0.32 | 0.0007 |
| tr\|Q8IKZ8\|Q8IKZ8_PLAF7 Uncharacterized protein OS=Plasmodium falciparum (isolate 3D7) GN=PF14_0453 PE=4 SV=1 | 7 | 0.78 | 0.14 | 0.0000 |
| tr\|Q8ILZ9\|Q8ILZ9_PLAF7 Uncharacterized protein OS=Plasmodium falciparum (isolate 3D7) GN=PF14_0094 PE=4 SV=1 | 7 | 0.78 | 0.08 | 0.0000 |
| tr\|Q8I3G6\|Q8I3G6_PLAF7 SNARE protein, putative OS=Plasmodium falciparum (isolate 3D7) GN=PfSyn6 PE=4 SV=1 | 7 | 0.78 | 0.74 | 0.0307 |
| tr\|Q8IDT3\|Q8IDT3_PLAF7 Uncharacterized protein OS=Plasmodium falciparum (isolate 3D7) GN=PF13_0219 PE=4 SV=1 | 7 | 0.79 | 0.43 | 0.0028 |
| tr\|Q8IM19\|Q8IM19_PLAF7 Nucleolar preribosomal GTPase, putative OS=Plasmodium falciparum (isolate 3D7) GN=PF14_0072 PE=4 SV=2 | 7 | 221.97 | 386.64 | 0.1796 |
| tr\|Q8IJS8\|Q8IJS8_PLAF7 DNA repair protein RAD23, putative OS=Plasmodium falciparum (isolate 3D7) GN=PF10_0114 PE=4 SV=1 | 7 | 296.48 | 573.68 | 0.2205 |
| sp\|Q8IIK4\|PDX2_PLAF7 Pyridoxal 5-phosphate synthase subunit Pdx2 OS=Plasmodium falciparum (isolate 3D7) GN=pdx2 PE=1 SV=2 | 7 | 194.81 | 372.49 | 0.2157 |
| tr\|Q8II87\|Q8II87_PLAF7 Conserved protein OS=Plasmodium falciparum (isolate 3D7) GN=PF11_0287 PE=4 SV=2 | 7 | 140.67 | 303.52 | 0.2661 |

| | | | | |
|---|---|---|---|---|
| tr\|Q8I501\|Q8I501_PLAF7 RabGDI protein OS=Plasmodium falciparum (isolate 3D7) GN=PFL2060c PE=1 SV=1 | 7 | 546.48 | 1380.72 | 0.3354 |
| tr\|Q8I4Y5\|Q8I4Y5_PLAF7 ADP-ribosylation factor GTPase-activating protein OS=Plasmodium falciparum (isolate 3D7) GN=PFL2140c PE=1 SV=1 | 7 | 83.04 | 151.09 | 0.1961 |
| tr\|C0H490\|C0H490_PLAF7 Cytosolic glyoxalase II OS=Plasmodium falciparum (isolate 3D7) GN=cGloII PE=3 SV=1 | 7 | 252.83 | 600.64 | 0.3080 |
| tr\|C6KT64\|C6KT64_PLAF7 Leucyl tRNA synthase OS=Plasmodium falciparum (isolate 3D7) GN=PFF1095w PE=3 SV=1 | 7 | 422.19 | 980.96 | 0.2982 |
| tr\|C0H4U0\|C0H4U0_PLAF7 Uncharacterized protein OS=Plasmodium falciparum (isolate 3D7) GN=MAL8P1.103 PE=4 SV=1 | 7 | 91.54 | 135.70 | 0.1245 |
| tr\|Q8I2P2\|Q8I2P2_PLAF7 NAD synthase, putative OS=Plasmodium falciparum (isolate 3D7) GN=PFI1310w PE=4 SV=1 | 7 | 261.57 | 646.03 | 0.3253 |
| tr\|Q8IM71\|Q8IM71_PLAF7 Choline kinase OS=Plasmodium falciparum (isolate 3D7) GN=PF14_0020 PE=1 SV=1 | 7 | 79.48 | 166.19 | 0.2527 |
| tr\|Q8II82\|Q8II82_PLAF7 Uncharacterized protein OS=Plasmodium falciparum (isolate 3D7) GN=PF11_0292 PE=4 SV=1 | 7 | 76.53 | 119.17 | 0.1402 |
| tr\|C0H530\|C0H530_PLAF7 Ran-binding protein, putative OS=Plasmodium falciparum (isolate 3D7) GN=PFI0490c PE=4 SV=1 | 7 | 233.38 | 506.51 | 0.2686 |
| tr\|Q8IJI7\|Q8IJI7_PLAF7 Deoxyribose-phosphate aldolase, putative OS=Plasmodium falciparum (isolate 3D7) GN=PF10_0210 PE=4 SV=1 | 7 | 155.96 | 391.57 | 0.3326 |
| tr\|Q8IJH3\|Q8IJH3_PLAF7 Orotidine 5-phosphate decarboxylase OS=Plasmodium falciparum (isolate 3D7) GN=PF10_0225 PE=1 SV=1 | 7 | 38.58 | 66.67 | 0.1766 |
| tr\|Q8IDV2\|Q8IDV2_PLAF7 Proteasome regulatory component, putative OS=Plasmodium falciparum (isolate 3D7) GN=MAL13P1.190 PE=4 SV=1 | 7 | 331.44 | 840.80 | 0.3372 |
| tr\|Q8IKA9\|Q8IKA9_PLAF7 Dihydroorotase, putative OS=Plasmodium falciparum (isolate 3D7) GN=PF14_0697 PE=4 SV=1 | 7 | 23.42 | 38.46 | 0.1583 |
| tr\|Q8IIA4\|Q8IIA4_PLAF7 Threonine--tRNA ligase, putative OS=Plasmodium falciparum (isolate 3D7) GN=PF11_0270 PE=3 SV=1 | 7 | 20.33 | 28.00 | 0.1031 |
| tr\|Q8IDW4\|Q8IDW4_PLAF7 Nuclear movement protein, putative OS=Plasmodium falciparum (isolate 3D7) GN=PF13_0204 PE=4 SV=1 | 7 | 88.16 | 217.71 | 0.3252 |
| tr\|Q8IKP1\|Q8IKP1_PLAF7 DEAD box helicase, putative OS=Plasmodium falciparum (isolate 3D7) GN=PF14_0563 PE=4 SV=1 | 7 | 36.93 | 77.73 | 0.2555 |
| tr\|Q8I238\|Q8I238_PLAF7 Chromatin assembly factor 1 protein WD40 domain, putative OS=Plasmodium falciparum (isolate 3D7) GN=PFA_0520c PE=4 SV=1 | 7 | 135.52 | 347.00 | 0.3413 |
| tr\|Q8IE10\|Q8IE10_PLAF7 Glutaminyl-tRNA synthetase, putative OS=Plasmodium falciparum (isolate 3D7) GN=PF13_0170 PE=3 SV=1 | 7 | 13.81 | 17.44 | 0.0811 |
| tr\|Q8I3Y4\|Q8I3Y4_PLAF7 Glutathione synthetase OS=Plasmodium falciparum (isolate 3D7) GN=gS PE=3 SV=1 | 7 | 12.44 | 19.09 | 0.1353 |
| tr\|C6KSL5\|C6KSL5_PLAF7 Pfmc-2TM Maurers cleft two transmembrane protein OS=Plasmodium falciparum (isolate 3D7) GN=PfMC-2TM PE=4 SV=1 | 7 | 445.36 | 982.82 | 0.2758 |
| sp\|P00441\|SODC_HUMAN Superoxide dismutase [Cu-Zn] OS=Homo sapiens GN=SOD1 PE=1 SV=2;tr\|H7BYH4\|H7BYH4_HUMAN Superoxide dismutase [Cu-Zn] OS=Homo sapiens GN=SOD1 PE=1 SV=1 | 7 | 10.00 | 11.13 | 0.0550 |
| tr\|Q8II17\|Q8II17_PLAF7 DNA-directed RNA polymerase OS=Plasmodium falciparum (isolate 3D7) GN=PF11_0358 PE=3 SV=1 | 7 | 89.82 | 207.23 | 0.2951 |
| tr\|Q8IAL6\|Q8IAL6_PLAF7 Mannose-6-phosphate isomerase, putative OS=Plasmodium falciparum (isolate 3D7) GN=MAL8P1.156 PE=4 SV=1 | 7 | 22.97 | 51.11 | 0.2793 |
| tr\|Q8I3A4\|Q8I3A4_PLAF7 Prefoldin subunit 4 OS=Plasmodium falciparum (isolate 3D7) GN=PFI0220w PE=3 SV=1 | 7 | 11.31 | 20.02 | 0.1856 |
| tr\|Q8IKT2\|Q8IKT2_PLAF7 6-phosphogluconate dehydrogenase, decarboxylating OS=Plasmodium falciparum (isolate 3D7) GN=PF14_0520 PE=3 SV=1 | 7 | 12.68 | 17.58 | 0.1049 |
| tr\|C6KT18\|C6KT18_PLAF7 Histone H2A OS=Plasmodium falciparum (isolate 3D7) GN=PFF0860c PE=3 SV=1 | 7 | 1958.39 | 4622.68 | 0.3052 |
| tr\|Q8ID72\|Q8ID72_PLAF7 Uncharacterized protein OS=Plasmodium falciparum (isolate 3D7) GN=PF13_0335 PE=4 SV=1 | 7 | 25.45 | 58.53 | 0.2938 |
| tr\|C6KTB4\|C6KTB4_PLAF7 Acetyl-CoA synthetase OS=Plasmodium falciparum (isolate 3D7) GN=PFF1350c PE=4 SV=1 | 7 | 149.67 | 391.90 | 0.3513 |
| tr\|Q8II71\|Q8II71_PLAF7 26S proteasome regulatory complex subunit, putative OS=Plasmodium falciparum (isolate 3D7) GN=PF11_0303 PE=4 SV=2 | 7 | 12.20 | 23.78 | 0.2237 |
| tr\|Q8IL22\|Q8IL22_PLAF7 Histidine--tRNA ligase, putative OS=Plasmodium falciparum (isolate 3D7) GN=PF14_0428 PE=3 SV=1 | 7 | 9.90 | 18.64 | 0.2096 |
| sp\|Q8IKU0\|GLUPH_PLAF7 Bifunctional glucose-6-phosphate 1-dehydrogenase/6-phosphogluconolactonase OS=Plasmodium falciparum (isolate 3D7) GN=PF14_0511 PE=1 SV=1 | 7 | 37.29 | 92.93 | 0.3293 |
| tr\|Q8I6Z8\|Q8I6Z8_PLAF7 Ubiquitin Carboxyl-terminal Hydrolase-like zinc finger protein OS=Plasmodium falciparum (isolate 3D7) GN=PF13_0096 PE=4 SV=1 | 7 | 14.18 | 22.02 | 0.1394 |

| | | | | |
|---|---|---|---|---|
| tr\|Q8ILS4\|Q8ILS4_PLAF7 NOT family protein, putative OS=Plasmodium falciparum (isolate 3D7) GN=PF14_0170 PE=4 SV=1 | 7 | 14.05 | 30.85 | 0.2737 |
| tr\|Q8IIW5\|Q8IIW5_PLAF7 Casein kinase II subunit beta OS=Plasmodium falciparum (isolate 3D7) GN=PF11_0048 PE=3 SV=1 | 7 | 11.15 | 23.54 | 0.2566 |
| tr\|C0H4T1\|C0H4T1_PLAF7 Coatomer epsilon subunit, putative OS=Plasmodium falciparum (isolate 3D7) GN=MAL8P1.121:exon:1 PE=4 SV=1 | 7 | 6.01 | 7.15 | 0.0679 |
| tr\|Q8I374\|Q8I374_PLAF7 Subunit of proteaseome activator complex, putative OS=Plasmodium falciparum (isolate 3D7) GN=PFI0370c PE=4 SV=1 | 7 | 95.67 | 249.19 | 0.3489 |
| tr\|Q8I3M0\|Q8I3M0_PLAF7 Uncharacterized protein OS=Plasmodium falciparum (isolate 3D7) GN=PFE1220w PE=4 SV=1 | 7 | 24.05 | 59.34 | 0.3248 |
| tr\|Q8I403\|Q8I403_PLAF7 Uncharacterized protein OS=Plasmodium falciparum (isolate 3D7) GN=PFE0500c PE=4 SV=1 | 7 | 3.92 | 4.79 | 0.0736 |
| tr\|Q8IEC3\|Q8IEC3_PLAF7 N2,N2-dimethylguanosine tRNA methyltransferase, putative OS=Plasmodium falciparum (isolate 3D7) GN=PF13_0109 PE=4 SV=1 | 7 | 5.12 | 8.96 | 0.1814 |
| tr\|Q8IET1\|Q8IET1_PLAF7 Uncharacterized protein OS=Plasmodium falciparum (isolate 3D7) GN=PF13_0018 PE=4 SV=1 | 7 | 0.80 | 0.33 | 0.0007 |
| tr\|Q8IHS1\|Q8IHS1_PLAF7 Uncharacterized protein OS=Plasmodium falciparum (isolate 3D7) GN=PF11_0458 PE=4 SV=1 | 7 | 22.32 | 56.11 | 0.3331 |
| tr\|Q8IIF6\|Q8IIF6_PLAF7 Conserved Plasmodium protein OS=Plasmodium falciparum (isolate 3D7) GN=PF11_0218 PE=4 SV=2 | 7 | 3.18 | 3.97 | 0.0785 |
| tr\|Q8IL82\|Q8IL82_PLAF7 Uncharacterized protein OS=Plasmodium falciparum (isolate 3D7) GN=PF14_0365 PE=4 SV=1 | 7 | 6.01 | 12.15 | 0.2388 |
| sp\|P02042\|HBD_HUMAN Hemoglobin subunit delta OS=Homo sapiens GN=HBD PE=1 SV=2;tr\|E9PFT6\|E9PFT6_HUMAN Hemoglobin subunit delta OS=Homo sapiens GN=HBD PE=1 SV=1;tr\|E9PEW8\|E9PEW8_HUMAN Hemoglobin subunit delta (Fragment) OS=Homo sapiens GN=HBD PE=1 SV=1 | 7 | 0.80 | 0.43 | 0.0026 |
| tr\|Q8IJC0\|Q8IJC0_PLAF7 Nucleolar preribosomal assembly protein, putative OS=Plasmodium falciparum (isolate 3D7) GN=PF10_0278 PE=4 SV=1 | 7 | 3.20 | 4.73 | 0.1232 |
| tr\|Q8I6Z5\|Q8I6Z5_PLAF7 Plasmepsin V OS=Plasmodium falciparum (isolate 3D7) GN=PF13_0133 PE=3 SV=1 | 7 | 5.69 | 11.97 | 0.2552 |
| tr\|Q8I0X2\|Q8I0X2_PLAF7 Acyl-CoA synthetase, PfACS3 OS=Plasmodium falciparum (isolate 3D7) GN=ACS3 PE=4 SV=1;tr\|C0H5N0\|C0H5N0_PLAF7 Acyl-CoA synthetase, PfACS4 OS=Plasmodium falciparum (isolate 3D7) GN=MAL13P1.485 PE=4 SV=1 | 7 | 0.81 | 0.41 | 0.0021 |
| tr\|Q8IHZ1\|Q8IHZ1_PLAF7 UVB-resistance protein UVR8 homologue OS=Plasmodium falciparum (isolate 3D7) GN=PF11_0385 PE=4 SV=1 | 7 | 12.87 | 17.47 | 0.0992 |
| tr\|Q8ILB9\|Q8ILB9_PLAF7 Dynein-related AAA-type ATPase OS=Plasmodium falciparum (isolate 3D7) GN=PF14_0326 PE=4 SV=2 | 7 | 6.84 | 15.15 | 0.2773 |
| tr\|Q8I1Y6\|Q8I1Y6_PLAF7 Uncharacterized protein OS=Plasmodium falciparum (isolate 3D7) GN=PFD0207c PE=4 SV=1 | 7 | 15.08 | 25.52 | 0.1690 |
| sp\|O75531\|BAF_HUMAN Barrier-to-autointegration factor OS=Homo sapiens GN=BANF1 PE=1 SV=1 | 7 | 210.26 | 498.76 | 0.3074 |
| tr\|Q8IC37\|Q8IC37_PLAF7 Uncharacterized protein OS=Plasmodium falciparum (isolate 3D7) GN=MAL7P1.11 PE=4 SV=1 | 7 | 4.05 | 8.14 | 0.2359 |
| tr\|Q8IBM7\|Q8IBM7_PLAF7 BING4 (NUC141) WD-40 repeat protein, putative OS=Plasmodium falciparum (isolate 3D7) GN=PF07_0092 PE=4 SV=1 | 7 | 2.45 | 3.55 | 0.1179 |
| tr\|Q8I564\|Q8I564_PLAF7 Uncharacterized protein OS=Plasmodium falciparum (isolate 3D7) GN=PFL1735c PE=4 SV=1 | 7 | 0.82 | 0.36 | 0.0010 |
| tr\|Q8ILD7\|Q8ILD7_PLAF7 Uncharacterized protein OS=Plasmodium falciparum (isolate 3D7) GN=PF14_0307 PE=4 SV=1 | 7 | 2.50 | 2.76 | 0.0532 |
| tr\|C6KT59\|C6KT59_PLAF7 Radical SAM protein, putative OS=Plasmodium falciparum (isolate 3D7) GN=PFF1070c PE=4 SV=1 | 7 | 1.91 | 2.13 | 0.0550 |
| tr\|Q8IB40\|Q8IB40_PLAF7 C-13 antigen OS=Plasmodium falciparum (isolate 3D7) GN=MAL8P1.57 PE=4 SV=1 | 7 | 2.91 | 4.22 | 0.1180 |
| tr\|Q7K6B1\|Q7K6B1_PLAF7 Protein kinase c inhibitor-like protein, putative OS=Plasmodium falciparum (isolate 3D7) GN=PF08_0059 PE=4 SV=2 | 7 | 0.82 | 0.19 | 0.0000 |
| tr\|Q8I283\|Q8I283_PLAF7 Cyclin-dependent kinases regulatory subunit OS=Plasmodium falciparum (isolate 3D7) GN=PFA_0285c PE=3 SV=1 | 7 | 1.83 | 2.14 | 0.0644 |
| tr\|C6KSV4\|C6KSV4_PLAF7 Transcription elongation factor SPT5 OS=Plasmodium falciparum (isolate 3D7) GN=PFF0535c PE=3 SV=1 | 7 | 1.85 | 2.31 | 0.0781 |
| tr\|O77343\|O77343_PLAF7 Transporter, putative OS=Plasmodium falciparum (isolate 3D7) GN=PFC0530w PE=4 SV=1 | 7 | 3.36 | 6.69 | 0.2325 |
| tr\|Q8I5T5\|Q8I5T5_PLAF7 Uncharacterized protein OS=Plasmodium falciparum (isolate 3D7) GN=PFL0575w PE=4 SV=1 | 7 | 2.61 | 3.34 | 0.0838 |
| tr\|Q8IDA3\|Q8IDA3_PLAF7 Uncharacterized protein OS=Plasmodium falciparum (isolate 3D7) GN=MAL13P1.299 PE=4 SV=1 | 7 | 1.85 | 2.51 | 0.0988 |

| | | | | |
|---|---|---|---|---|
| tr\|A0A087X0C8\|A0A087X0C8_HUMAN Calpain-5 OS=Homo sapiens GN=CAPN5 PE=1 SV=1;tr\|E7EV01\|E7EV01_HUMAN Calpain-5 OS=Homo sapiens GN=CAPN5 PE=1 SV=2;sp\|O15484\|CAN5_HUMAN Calpain-5 OS=Homo sapiens GN=CAPN5 PE=1 SV=2 | 7 | 2.60 | 4.68 | 0.1912 |
| tr\|Q8I511\|Q8I511_PLAF7 DEAD/DEAH box helicase, putative OS=Plasmodium falciparum (isolate 3D7) GN=PFL2010c PE=4 SV=2 | 7 | 2.03 | 2.24 | 0.0534 |
| tr\|Q8IC10\|Q8IC10_PLAF7 Cdk105, putative OS=Plasmodium falciparum (isolate 3D7) GN=MAL7P1.24 PE=4 SV=1 | 7 | 2.09 | 3.33 | 0.1483 |
| tr\|Q8IK74\|Q8IK74_PLAF7 Uncharacterized protein OS=Plasmodium falciparum (isolate 3D7) GN=PF14_0732 PE=4 SV=1 | 7 | 1.67 | 2.12 | 0.0828 |
| tr\|Q8IJQ9\|Q8IJQ9_PLAF7 Uncharacterized protein OS=Plasmodium falciparum (isolate 3D7) GN=PF10_0133 PE=4 SV=1 | 7 | 3.85 | 8.35 | 0.2680 |
| tr\|Q8I2A8\|Q8I2A8_PLAF7 Nucleoside transporter, putative OS=Plasmodium falciparum (isolate 3D7) GN=PFA_0160c PE=4 SV=1 | 7 | 0.83 | 0.50 | 0.0047 |
| tr\|Q8IDC8\|Q8IDC8_PLAF7 Uncharacterized protein OS=Plasmodium falciparum (isolate 3D7) GN=PF13_0309 PE=4 SV=1 | 7 | 1.90 | 2.08 | 0.0516 |
| tr\|Q8IJ92\|Q8IJ92_PLAF7 Uncharacterized protein OS=Plasmodium falciparum (isolate 3D7) GN=PF10_0307 PE=4 SV=1 | 7 | 0.84 | 0.05 | 0.0000 |
| tr\|Q5SRQ6\|Q5SRQ6_HUMAN Casein kinase II subunit beta OS=Homo sapiens GN=CSNK2B PE=1 SV=2;sp\|P67870\|CSK2B_HUMAN Casein kinase II subunit beta OS=Homo sapiens GN=CSNK2B PE=1 SV=1 | 7 | 2.40 | 4.06 | 0.1698 |
| tr\|Q8I5G5\|Q8I5G5_PLAF7 Uncharacterized protein OS=Plasmodium falciparum (isolate 3D7) GN=PFL1215c PE=4 SV=1 | 7 | 17.55 | 31.16 | 0.1869 |
| tr\|Q8IDN2\|Q8IDN2_PLAF7 Uncharacterized protein OS=Plasmodium falciparum (isolate 3D7) GN=PF13_0245 PE=4 SV=1 | 7 | 0.85 | 0.75 | 0.0239 |
| sp\|P50498\|MSA2_PLAF7 Merozoite surface antigen 2 OS=Plasmodium falciparum (isolate 3D7) GN=MSA2 PE=1 SV=2 | 7 | 13.94 | 35.93 | 0.3443 |
| tr\|Q8ID59\|Q8ID59_PLAF7 DNA-directed RNA polymerase 2, putative OS=Plasmodium falciparum (isolate 3D7) GN=PF13_0341 PE=3 SV=1 | 7 | 5.14 | 8.77 | 0.1720 |
| tr\|Q8I344\|Q8I344_PLAF7 Nucleotide binding protein, putative OS=Plasmodium falciparum (isolate 3D7) GN=PFI0525w PE=4 SV=1 | 7 | 0.86 | 0.41 | 0.0015 |
| tr\|Q8I1X5\|Q8I1X5_PLAF7 Pre-mRNA splicing factor, putative OS=Plasmodium falciparum (isolate 3D7) GN=PFD0265w PE=4 SV=1 | 7 | 0.86 | 0.38 | 0.0009 |
| tr\|Q8IE96\|Q8IE96_PLAF7 Adenosine-diphosphatase OS=Plasmodium falciparum (isolate 3D7) GN=MAL13P1.121 PE=4 SV=1 | 7 | 0.86 | 0.59 | 0.0082 |
| tr\|O77369\|O77369_PLAF7 Putative uncharacterized protein OS=Plasmodium falciparum (isolate 3D7) GN=PFC0835c PE=4 SV=2 | 7 | 0.86 | 0.31 | 0.0003 |
| tr\|Q8I5S8\|Q8I5S8_PLAF7 Uncharacterized protein OS=Plasmodium falciparum (isolate 3D7) GN=PFL0615w PE=4 SV=1 | 7 | 3.36 | 7.72 | 0.2937 |
| tr\|B9ZSI8\|B9ZSI8_PLAF7 Phosphatidate cytidylyltransferase, putative OS=Plasmodium falciparum (isolate 3D7) GN=PFA_0485w PE=4 SV=1 | 7 | 0.56 | 0.66 | 0.0677 |
| tr\|Q8I5D0\|Q8I5D0_PLAF7 Uncharacterized protein OS=Plasmodium falciparum (isolate 3D7) GN=PFL1395c PE=4 SV=1 | 7 | 0.52 | 0.59 | 0.0587 |
| tr\|Q8I274\|Q8I274_PLAF7 Rab5c, GTPase OS=Plasmodium falciparum (isolate 3D7) GN=Rab5c PE=3 SV=1 | 7 | 0.88 | 0.12 | 0.0000 |
| sp\|Q9H4G4\|GAPR1_HUMAN Golgi-associated plant pathogenesis-related protein 1 OS=Homo sapiens GN=GLIPR2 PE=1 SV=3;tr\|Q5VZR0\|Q5VZR0_HUMAN Golgi-associated plant pathogenesis-related protein 1 OS=Homo sapiens GN=GLIPR2 PE=1 SV=1 | 7 | 0.89 | 0.13 | 0.0000 |
| tr\|Q8I1R5\|Q8I1R5_PLAF7 LETM1-like protein, putative OS=Plasmodium falciparum (isolate 3D7) GN=PFD0835c PE=4 SV=1 | 7 | 0.89 | 0.41 | 0.0011 |
| sp\|Q99808\|S29A1_HUMAN Equilibrative nucleoside transporter 1 OS=Homo sapiens GN=SLC29A1 PE=1 SV=3;sp\|Q99808-2\|S29A1_HUMAN Isoform 2 of Equilibrative nucleoside transporter 1 OS=Homo sapiens GN=SLC29A1 | 7 | 0.90 | 0.54 | 0.0045 |
| tr\|Q8IBD3\|Q8IBD3_PLAF7 Uncharacterized protein OS=Plasmodium falciparum (isolate 3D7) GN=MAL8P1.3 PE=4 SV=1 | 7 | 0.91 | 0.35 | 0.0004 |
| tr\|Q8ILJ1\|Q8ILJ1_PLAF7 Uncharacterized protein OS=Plasmodium falciparum (isolate 3D7) GN=PF14_0252 PE=4 SV=1 | 7 | 0.92 | 0.26 | 0.0001 |
| tr\|Q8IJB1\|Q8IJB1_PLAF7 Uncharacterized protein OS=Plasmodium falciparum (isolate 3D7) GN=PF10_0287 PE=4 SV=1 | 7 | 0.93 | 0.14 | 0.0000 |
| tr\|Q8I4T6\|Q8I4T6_PLAF7 Uncharacterized protein OS=Plasmodium falciparum (isolate 3D7) GN=PFL2390c PE=4 SV=1 | 7 | 0.93 | 0.42 | 0.0011 |
| tr\|Q8I700\|Q8I700_PLAF7 Snornp protein gar1 homologue, putative OS=Plasmodium falciparum (isolate 3D7) GN=PF13_0051 PE=4 SV=1 | 7 | 0.94 | 0.28 | 0.0001 |
| tr\|Q8ID46\|Q8ID46_PLAF7 Uncharacterized protein OS=Plasmodium falciparum (isolate 3D7) GN=MAL13P1.333 PE=4 SV=1 | 7 | 0.94 | 0.34 | 0.0003 |
| tr\|Q8IHP7\|Q8IHP7_PLAF7 Uncharacterized protein OS=Plasmodium falciparum (isolate 3D7) GN=PF11_0482 PE=4 SV=1 | 7 | 0.95 | 0.27 | 0.0001 |

| | | | | |
|---|---|---|---|---|
| tr\|Q8IBK1\|Q8IBK1_PLAF7 Exonuclease I, putative OS=Plasmodium falciparum (isolate 3D7) GN=PF07_0105 PE=4 SV=1 | 7 | 0.96 | 0.12 | 0.0000 |
| tr\|O96201\|O96201_PLAF7 Conserved Plasmodium protein OS=Plasmodium falciparum (isolate 3D7) GN=PFB0540w PE=4 SV=1 | 7 | 1.00 | 0.32 | 0.0002 |
| tr\|Q8I3B3\|Q8I3B3_PLAF7 Putative uncharacterized protein OS=Plasmodium falciparum (isolate 3D7) GN=PFI0170w PE=4 SV=1 | 7 | 1.01 | 0.44 | 0.0009 |
| tr\|Q8IHU4\|Q8IHU4_PLAF7 Uncharacterized protein OS=Plasmodium falciparum (isolate 3D7) GN=PF11_0433 PE=4 SV=1 | 7 | 1.02 | 0.46 | 0.0011 |
| tr\|C0H5I5\|C0H5I5_PLAF7 Splicing factor 3b subunit, putative OS=Plasmodium falciparum (isolate 3D7) GN=PF13_0296 PE=4 SV=1 | 7 | 1.02 | 0.23 | 0.0000 |
| tr\|C0H592\|C0H592_PLAF7 REX2 protein OS=Plasmodium falciparum (isolate 3D7) GN=REX2 PE=4 SV=1;tr\|Q8I2G0\|Q8I2G0_PLAF7 Ring-exported protein 2 OS=Plasmodium falciparum (isolate 3D7) GN=REX2 PE=4 SV=1 | 7 | 1.03 | 0.30 | 0.0001 |
| tr\|Q8IKA0\|Q8IKA0_PLAF7 Uncharacterized protein OS=Plasmodium falciparum (isolate 3D7) GN=PF14_0706 PE=4 SV=1 | 7 | 1.03 | 0.10 | 0.0000 |
| sp\|Q00577\|PURA_HUMAN Transcriptional activator protein Pur-alpha OS=Homo sapiens GN=PURA PE=1 SV=2 | 7 | 1.03 | 0.60 | 0.0039 |
| tr\|Q8IIY1\|Q8IIY1_PLAF7 Uncharacterized protein OS=Plasmodium falciparum (isolate 3D7) GN=PF11_0025 PE=4 SV=1;tr\|Q8IJ11\|Q8IJ11_PLAF7 Pfmc-2TM Maurers cleft two transmembrane protein OS=Plasmodium falciparum (isolate 3D7) GN=PF10_0390 PE=4 SV=2 | 7 | 1.05 | 0.18 | 0.0000 |
| tr\|O97278\|O97278_PLAF7 ABC transporter, putative OS=Plasmodium falciparum (isolate 3D7) GN=PFC0875w PE=4 SV=3 | 7 | 1.07 | 0.11 | 0.0000 |
| tr\|Q8IIA8\|Q8IIA8_PLAF7 Small nuclear ribonucleoprotein D1, putative OS=Plasmodium falciparum (isolate 3D7) GN=PF11_0266 PE=4 SV=1 | 7 | 1.07 | 0.48 | 0.0011 |
| tr\|Q8IKH5\|Q8IKH5_PLAF7 Serine/threonine-protein phosphatase OS=Plasmodium falciparum (isolate 3D7) GN=PF14_0630 PE=3 SV=1 | 7 | 1.07 | 0.18 | 0.0000 |
| tr\|Q8IJI8\|Q8IJI8_PLAF7 RNA helicase, putative OS=Plasmodium falciparum (isolate 3D7) GN=PF10_0209 PE=4 SV=1 | 7 | 1.08 | 0.48 | 0.0010 |
| tr\|Q8IAW5\|Q8IAW5_PLAF7 Uncharacterized protein OS=Plasmodium falciparum (isolate 3D7) GN=PF08_0083 PE=4 SV=1 | 7 | 1.09 | 0.21 | 0.0000 |
| tr\|O97225\|O97225_PLAF7 Spindle pole body protein, putative OS=Plasmodium falciparum (isolate 3D7) GN=PFC0165w PE=4 SV=3 | 7 | 1.09 | 0.38 | 0.0003 |
| tr\|Q8IE57\|Q8IE57_PLAF7 Uncharacterized protein OS=Plasmodium falciparum (isolate 3D7) GN=PF13_0147 PE=4 SV=1 | 7 | 1.09 | 0.37 | 0.0002 |
| sp\|O77392\|IPYR_PLAF7 Probable inorganic pyrophosphatase OS=Plasmodium falciparum (isolate 3D7) GN=MAL3P6.3 PE=3 SV=1;tr\|C0H477\|C0H477_PLAF7 Inorganic pyrophosphatase, putative OS=Plasmodium falciparum (isolate 3D7) GN=PFC0710w.1 PE=4 SV=1 | 7 | 1.10 | 0.77 | 0.0094 |
| tr\|Q8I3I6\|Q8I3I6_PLAF7 Beta adaptin protein, putative OS=Plasmodium falciparum (isolate 3D7) GN=PFE1400c PE=4 SV=2 | 7 | 1.11 | 0.57 | 0.0022 |
| tr\|Q8I548\|Q8I548_PLAF7 Uncharacterized protein OS=Plasmodium falciparum (isolate 3D7) GN=PFL1815c PE=4 SV=1 | 7 | 1.12 | 0.22 | 0.0000 |
| tr\|Q8IB26\|Q8IB26_PLAF7 BRIX domain, putative OS=Plasmodium falciparum (isolate 3D7) GN=PF08_0053 PE=4 SV=1 | 7 | 1.15 | 0.17 | 0.0000 |
| tr\|Q8IJC9\|Q8IJC9_PLAF7 DNA-directed RNA polymerase II, putative OS=Plasmodium falciparum (isolate 3D7) GN=PF10_0269 PE=4 SV=1 | 7 | 1.15 | 0.89 | 0.0143 |
| tr\|C0H5K9\|C0H5K9_PLAF7 Phosphatidylserine synthase I, putative OS=Plasmodium falciparum (isolate 3D7) GN=MAL13P1.335 PE=4 SV=1 | 7 | 1.15 | 0.24 | 0.0000 |
| tr\|Q8IDJ7\|Q8IDJ7_PLAF7 Small nuclear ribonucleoprotein, putative OS=Plasmodium falciparum (isolate 3D7) GN=MAL13P1.253 PE=4 SV=1 | 7 | 1.15 | 0.26 | 0.0000 |
| tr\|Q8II94\|Q8II94_PLAF7 Small nuclear ribonucleoprotein F OS=Plasmodium falciparum (isolate 3D7) GN=PF11_0280 PE=3 SV=2 | 7 | 1.16 | 0.62 | 0.0025 |
| tr\|Q8I538\|Q8I538_PLAF7 Uncharacterized protein OS=Plasmodium falciparum (isolate 3D7) GN=PFL1865w PE=4 SV=1 | 7 | 1.19 | 0.36 | 0.0001 |
| tr\|Q8IL21\|Q8IL21_PLAF7 RNA helicase, putative OS=Plasmodium falciparum (isolate 3D7) GN=PF14_0429 PE=4 SV=1 | 7 | 1.23 | 0.94 | 0.0135 |
| tr\|C0H5B6\|C0H5B6_PLAF7 Uncharacterized protein OS=Plasmodium falciparum (isolate 3D7) GN=MAL13P1.79 PE=4 SV=1 | 7 | 1.24 | 0.39 | 0.0002 |
| tr\|C0H5E9\|C0H5E9_PLAF7 DNAJ like protein, putative OS=Plasmodium falciparum (isolate 3D7) GN=MAL13P1.162 PE=4 SV=1 | 7 | 1.25 | 1.29 | 0.0424 |
| sp\|P32119\|PRDX2_HUMAN Peroxiredoxin-2 OS=Homo sapiens GN=PRDX2 PE=1 SV=5;tr\|A6NIW5\|A6NIW5_HUMAN Peroxiredoxin 2, isoform CRA_a OS=Homo sapiens GN=PRDX2 PE=1 SV=2 | 7 | 1.26 | 0.85 | 0.0076 |
| tr\|Q8I618\|Q8I618_PLAF7 Conserved Plasmodium protein OS=Plasmodium falciparum (isolate 3D7) GN=PFL0135w PE=4 SV=2 | 7 | 1.28 | 0.33 | 0.0001 |
| tr\|Q8I5M6\|Q8I5M6_PLAF7 Conserved Plasmodium protein OS=Plasmodium falciparum (isolate 3D7) GN=PFL0880c PE=4 SV=1 | 7 | 1.28 | 0.54 | 0.0007 |

| | | | | |
|---|---|---|---|---|
| tr\|Q8IAM3\|Q8IAM3_PLAF7 WD-repeat protein, putative OS=Plasmodium falciparum (isolate 3D7) GN=PF08_0130 PE=4 SV=1 | 7 | 1.28 | 0.31 | 0.0000 |
| tr\|Q8IKS1\|Q8IKS1_PLAF7 Uncharacterized protein OS=Plasmodium falciparum (isolate 3D7) GN=PF14_0531 PE=4 SV=1 | 7 | 1.35 | 1.14 | 0.0203 |
| tr\|Q8IB94\|Q8IB94_PLAF7 Ubiquitin-protein ligase 1, putative OS=Plasmodium falciparum (isolate 3D7) GN=MAL8P1.23 PE=4 SV=1 | 7 | 1.36 | 0.43 | 0.0002 |
| tr\|Q8I544\|Q8I544_PLAF7 Uncharacterized protein OS=Plasmodium falciparum (isolate 3D7) GN=PFL1835w PE=4 SV=1 | 7 | 1.36 | 0.86 | 0.0058 |
| tr\|Q8IKH0\|Q8IKH0_PLAF7 60S ribosome subunit biogenesis protein NIP7 homolog OS=Plasmodium falciparum (isolate 3D7) GN=PF14_0635 PE=3 SV=2 | 7 | 1.37 | 0.31 | 0.0000 |
| tr\|Q8I547\|Q8I547_PLAF7 Uncharacterized protein OS=Plasmodium falciparum (isolate 3D7) GN=PFL1820w PE=4 SV=1 | 7 | 1.45 | 1.11 | 0.0132 |
| tr\|Q8IIH2\|Q8IIH2_PLAF7 Clathrin coat assembly protein, putative OS=Plasmodium falciparum (isolate 3D7) GN=PF11_0202 PE=4 SV=1 | 7 | 1.46 | 0.26 | 0.0000 |
| tr\|Q8IIG9\|Q8IIG9_PLAF7 Uncharacterized protein OS=Plasmodium falciparum (isolate 3D7) GN=PF11_0205 PE=4 SV=1 | 7 | 1.49 | 1.22 | 0.0181 |
| tr\|Q8IDN9\|Q8IDN9_PLAF7 Uncharacterized protein OS=Plasmodium falciparum (isolate 3D7) GN=PF13_0243 PE=4 SV=1 | 7 | 1.52 | 0.65 | 0.0008 |
| tr\|Q8IE00\|Q8IE00_PLAF7 Eukaryotic translation initiation factor 6 OS=Plasmodium falciparum (isolate 3D7) GN=EIF6 PE=3 SV=1 | 7 | 1.53 | 1.02 | 0.0072 |
| tr\|Q8I2X7\|Q8I2X7_PLAF7 ATP-dependent RNA Helicase, putative OS=Plasmodium falciparum (isolate 3D7) GN=PFI0860c PE=4 SV=1 | 7 | 1.54 | 0.61 | 0.0005 |
| tr\|Q8I308\|Q8I308_PLAF7 Putative uncharacterized protein OS=Plasmodium falciparum (isolate 3D7) GN=PFI0705w PE=4 SV=1 | 7 | 1.56 | 1.05 | 0.0078 |
| tr\|Q8IET8\|Q8IET8_PLAF7 ATP dependent DEAD-box helicase, putative OS=Plasmodium falciparum (isolate 3D7) GN=MAL13P1.14 PE=4 SV=1 | 7 | 1.56 | 0.76 | 0.0016 |
| tr\|Q8IEM5\|Q8IEM5_PLAF7 NUDIX hydrolase, putative OS=Plasmodium falciparum (isolate 3D7) GN=PF13_0048 PE=4 SV=1 | 7 | 1.57 | 0.33 | 0.0000 |
| tr\|Q8ILM2\|Q8ILM2_PLAF7 GTPase, putative OS=Plasmodium falciparum (isolate 3D7) GN=PF14_0221 PE=4 SV=1 | 7 | 1.58 | 0.88 | 0.0031 |
| sp\|Q9H1E5\|TMX4_HUMAN Thioredoxin-related transmembrane protein 4 OS=Homo sapiens GN=TMX4 PE=1 SV=1 | 7 | 1.62 | 1.68 | 0.0435 |
| tr\|Q8I2U4\|Q8I2U4_PLAF7 RNA binding protein, putative OS=Plasmodium falciparum (isolate 3D7) GN=PFI1025w PE=4 SV=1 | 7 | 1.62 | 1.09 | 0.0075 |
| sp\|Q9BVK6\|TMED9_HUMAN Transmembrane emp24 domain-containing protein 9 OS=Homo sapiens GN=TMED9 PE=1 SV=2 | 7 | 1.62 | 1.13 | 0.0090 |
| tr\|Q8IE50\|Q8IE50_PLAF7 Myosin OS=Plasmodium falciparum (isolate 3D7) GN=MAL13P1.148 PE=4 SV=1 | 7 | 1.69 | 0.36 | 0.0000 |
| tr\|Q8I6S4\|Q8I6S4_PLAF7 Peptidyl-prolyl cis-trans isomerase OS=Plasmodium falciparum (isolate 3D7) GN=PfCyP24 PE=3 SV=1 | 7 | 1.69 | 0.28 | 0.0000 |
| tr\|Q8IEI4\|Q8IEI4_PLAF7 Ubiquitin-like protein nedd8 homologue, putative OS=Plasmodium falciparum (isolate 3D7) GN=MAL13P1.64 PE=4 SV=1 | 7 | 1.69 | 0.39 | 0.0000 |
| tr\|Q8IEM3\|Q8IEM3_PLAF7 60S ribosomal protein L24, putative OS=Plasmodium falciparum (isolate 3D7) GN=PF13_0049 PE=1 SV=1 | 7 | 1.70 | 0.63 | 0.0004 |
| tr\|Q8IJT1\|Q8IJT1_PLAF7 Proteasome subunit beta type OS=Plasmodium falciparum (isolate 3D7) GN=PF10_0111 PE=3 SV=1 | 7 | 1.71 | 0.23 | 0.0000 |
| sp\|Q8IHZ9\|KC1_PLAF7 Casein kinase I OS=Plasmodium falciparum (isolate 3D7) GN=CK1 PE=3 SV=1;tr\|C6S3F7\|C6S3F7_PLAF7 Casein kinase 1, PfCK1 OS=Plasmodium falciparum (isolate 3D7) GN=PfCK1 PE=3 SV=1 | 7 | 1.75 | 0.77 | 0.0010 |
| tr\|Q8IE45\|Q8IE45_PLAF7 Uncharacterized protein OS=Plasmodium falciparum (isolate 3D7) GN=PF13_0153 PE=4 SV=1 | 7 | 1.81 | 0.46 | 0.0000 |
| sp\|O96184\|RL37A_PLAF7 60S ribosomal protein L37a OS=Plasmodium falciparum (isolate 3D7) GN=RPL37A PE=1 SV=1 | 7 | 1.97 | 1.15 | 0.0040 |
| tr\|Q8I4U5\|Q8I4U5_PLAF7 Tat-binding protein homolog OS=Plasmodium falciparum (isolate 3D7) GN=PFL2345c PE=3 SV=1 | 7 | 2.05 | 1.67 | 0.0177 |
| tr\|Q8IAZ7\|Q8IAZ7_PLAF7 Nucleolar preribosomal assembly protein, putative OS=Plasmodium falciparum (isolate 3D7) GN=PF08_0065 PE=4 SV=1 | 7 | 2.16 | 1.59 | 0.0116 |
| sp\|P62203\|CALM_PLAF7 Calmodulin OS=Plasmodium falciparum (isolate 3D7) GN=PF14_0323 PE=3 SV=2 | 7 | 2.21 | 1.35 | 0.0050 |
| tr\|Q8I5N9\|Q8I5N9_PLAF7 DNA-binding chaperone, putative OS=Plasmodium falciparum (isolate 3D7) GN=PFL0815w PE=4 SV=1 | 7 | 2.43 | 1.46 | 0.0045 |
| tr\|Q8I323\|Q8I323_PLAF7 26S proteasome regulatory subunit, putative OS=Plasmodium falciparum (isolate 3D7) GN=PFI0630w PE=4 SV=1 | 7 | 2.47 | 1.69 | 0.0083 |
| tr\|Q8I586\|Q8I586_PLAF7 Asparagine/aspartate rich protein, putative OS=Plasmodium falciparum (isolate 3D7) GN=PFL1620w PE=4 SV=1 | 7 | 2.49 | 1.82 | 0.0109 |

| | | | | |
|---|---|---|---|---|
| tr\|Q7K6A9\|Q7K6A9_PLAF7 Proteasome subunit beta type OS=Plasmodium falciparum (isolate 3D7) GN=MAL8P1.142 PE=3 SV=1 | 7 | 2.55 | 2.21 | 0.0225 |
| tr\|Q8IKC9\|Q8IKC9_PLAF7 Proteasome subunit beta type OS=Plasmodium falciparum (isolate 3D7) GN=PF14_0676 PE=3 SV=2 | 7 | 3.02 | 2.48 | 0.0179 |
| tr\|Q8II81\|Q8II81_PLAF7 Multiprotein bridging factor type 1, putative OS=Plasmodium falciparum (isolate 3D7) GN=PF11_0293 PE=4 SV=1 | 7 | 3.41 | 2.87 | 0.0202 |
| tr\|Q8IIW4\|Q8IIW4_PLAF7 Uncharacterized protein OS=Plasmodium falciparum (isolate 3D7) GN=PF11_0049 PE=4 SV=1 | 7 | 3.57 | 3.16 | 0.0245 |
| tr\|Q8IIB9\|Q8IIB9_PLAF7 Conserved Plasmodium protein OS=Plasmodium falciparum (isolate 3D7) GN=PF11_0255 PE=4 SV=2 | 7 | 3.60 | 2.16 | 0.0045 |
| tr\|C6KTC6\|C6KTC6_PLAF7 Uncharacterized protein OS=Plasmodium falciparum (isolate 3D7) GN=PFF1410c PE=4 SV=1 | 7 | 3.72 | 3.39 | 0.0273 |
| tr\|Q8IIC9\|Q8IIC9_PLAF7 Translation elongation factor EF-1, subunit alpha, putative OS=Plasmodium falciparum (isolate 3D7) GN=PF11_0245 PE=4 SV=1 | 7 | 3.81 | 1.72 | 0.0011 |
| tr\|Q8IAY9\|Q8IAY9_PLAF7 Importin beta, putative OS=Plasmodium falciparum (isolate 3D7) GN=PF08_0069 PE=4 SV=1 | 7 | 4.61 | 3.15 | 0.0082 |
| tr\|Q8I2B1\|Q8I2B1_PLAF7 Aspartyl-tRNA synthetase, putative OS=Plasmodium falciparum (isolate 3D7) GN=PFA_0145c PE=3 SV=1 | 7 | 6.02 | 4.43 | 0.0114 |
| tr\|O96174\|O96174_PLAF7 Conserved Plasmodium protein OS=Plasmodium falciparum (isolate 3D7) GN=PFB0395w PE=4 SV=1 | 7 | 6.06 | 6.32 | 0.0442 |
| tr\|Q8IHY3\|Q8IHY3_PLAF7 Ubiquitin-related modifier 1 homolog OS=Plasmodium falciparum (isolate 3D7) GN=PF11_0393 PE=3 SV=1 | 7 | 6.22 | 6.69 | 0.0491 |
| tr\|Q8IBR6\|Q8IBR6_PLAF7 Prefoldin subunit 3, putative OS=Plasmodium falciparum (isolate 3D7) GN=MAL7P1.94 PE=4 SV=1 | 7 | 6.71 | 6.85 | 0.0413 |
| sp\|Q8I1T8\|ASNA_PLAF7 ATPase ASNA1 homolog OS=Plasmodium falciparum (isolate 3D7) GN=PFD0725c PE=3 SV=1 | 7 | 7.42 | 6.53 | 0.0238 |
| tr\|Q8ID43\|Q8ID43_PLAF7 Nucleoside diphosphate kinase OS=Plasmodium falciparum (isolate 3D7) GN=PF13_0349 PE=1 SV=1 | 7 | 7.49 | 6.58 | 0.0236 |
| tr\|Q8I1V0\|Q8I1V0_PLAF7 Lysine decarboxylase-like protein, putative OS=Plasmodium falciparum (isolate 3D7) GN=PFD0670c PE=4 SV=1 | 7 | 11.14 | 11.44 | 0.0419 |
| tr\|Q8IDY0\|Q8IDY0_PLAF7 MSP7-like protein OS=Plasmodium falciparum (isolate 3D7) GN=MAL13P1.174 PE=4 SV=1 | 6 | 0.29 | 0.21 | 0.0185 |
| sp\|Q8I5D2\|ABRA_PLAF7 101 kDa malaria antigen OS=Plasmodium falciparum (isolate 3D7) GN=ABRA PE=3 SV=1 | 6 | 0.31 | 0.20 | 0.0132 |
| tr\|Q8I3V1\|Q8I3V1_PLAF7 Metabolite/drug transporter, putative OS=Plasmodium falciparum (isolate 3D7) GN=PFE0785c PE=4 SV=1 | 6 | 0.44 | 0.31 | 0.0161 |
| tr\|C6KSY0\|C6KSY0_PLAF7 Transcription factor with AP2 domain(S), putative OS=Plasmodium falciparum (isolate 3D7) GN=ApiAP2 PE=4 SV=1 | 6 | 0.47 | 0.13 | 0.0004 |
| tr\|B9ZSI9\|B9ZSI9_PLAF7 Putative uncharacterized protein OS=Plasmodium falciparum (isolate 3D7) GN=PFA_0550w PE=4 SV=1 | 6 | 0.50 | 0.28 | 0.0070 |
| tr\|Q8IHV2\|Q8IHV2_PLAF7 Uncharacterized protein OS=Plasmodium falciparum (isolate 3D7) GN=PF11_0424 PE=4 SV=1 | 6 | 0.55 | 0.29 | 0.0059 |
| tr\|Q8IEC2\|Q8IEC2_PLAF7 Uncharacterized protein OS=Plasmodium falciparum (isolate 3D7) GN=MAL13P1.103 PE=4 SV=1 | 6 | 0.60 | 0.32 | 0.0058 |
| tr\|Q8I0U9\|Q8I0U9_PLAF7 Triose phosphate transporter OS=Plasmodium falciparum (isolate 3D7) GN=PfiTPT PE=4 SV=1 | 6 | 0.62 | 0.48 | 0.0253 |
| tr\|Q8ILG8\|Q8ILG8_PLAF7 Uncharacterized protein OS=Plasmodium falciparum (isolate 3D7) GN=PF14_0275 PE=4 SV=1 | 6 | 0.62 | 0.29 | 0.0031 |
| tr\|Q8ILR0\|Q8ILR0_PLAF7 Uncharacterized protein OS=Plasmodium falciparum (isolate 3D7) GN=PF14_0184 PE=4 SV=1 | 6 | 0.64 | 0.49 | 0.0230 |
| tr\|C0H4N9\|C0H4N9_PLAF7 Uncharacterized protein OS=Plasmodium falciparum (isolate 3D7) GN=MAL7P1.106 PE=4 SV=1 | 6 | 0.67 | 0.08 | 0.0000 |
| tr\|Q8IKY5\|Q8IKY5_PLAF7 Appr-1-p processing domain protein OS=Plasmodium falciparum (isolate 3D7) GN=PF14_0466 PE=4 SV=1 | 6 | 0.68 | 0.44 | 0.0132 |
| tr\|C0H4A3\|C0H4A3_PLAF7 Uncharacterized protein OS=Plasmodium falciparum (isolate 3D7) GN=PFD0669c PE=4 SV=1 | 6 | 0.71 | 0.34 | 0.0037 |
| tr\|Q7KWJ4\|Q7KWJ4_PLAF7 Adenylosuccinate lyase OS=Plasmodium falciparum (isolate 3D7) GN=ASL PE=3 SV=1 | 6 | 101.90 | 123.76 | 0.0998 |
| tr\|O97284\|O97284_PLAF7 Putative uncharacterized protein OS=Plasmodium falciparum (isolate 3D7) GN=PFC0910w PE=4 SV=1 | 6 | 123.85 | 161.73 | 0.1195 |
| tr\|Q8IKQ7\|Q8IKQ7_PLAF7 Uncharacterized protein OS=Plasmodium falciparum (isolate 3D7) GN=PF14_0546 PE=4 SV=1 | 6 | 813.56 | 1619.99 | 0.2734 |
| tr\|Q8I5R6\|Q8I5R6_PLAF7 Uncharacterized protein OS=Plasmodium falciparum (isolate 3D7) GN=PFL0675c PE=4 SV=1 | 6 | 154.89 | 298.90 | 0.2602 |
| tr\|Q8I250\|Q8I250_PLAF7 Tubulin-specific chaperone a, putative OS=Plasmodium falciparum (isolate 3D7) GN=PFA_0460c PE=4 SV=1 | 6 | 607.11 | 1408.63 | 0.3394 |

| | | | | |
|---|---|---|---|---|
| tr\|Q8ILZ3\|Q8ILZ3_PLAF7 CTP synthase OS=Plasmodium falciparum (isolate 3D7) GN=PF14_0100 PE=3 SV=1 | 6 | 344.59 | 743.75 | 0.3079 |
| tr\|Q8IDZ0\|Q8IDZ0_PLAF7 Uncharacterized protein OS=Plasmodium falciparum (isolate 3D7) GN=PF13_0186 PE=4 SV=1 | 6 | 80.90 | 121.40 | 0.1635 |
| tr\|C6S3E1\|C6S3E1_PLAF7 Leucine-rich repeat protein 8, LRR8 OS=Plasmodium falciparum (isolate 3D7) GN=PF10_0320a PE=4 SV=1 | 6 | 105.94 | 189.63 | 0.2295 |
| tr\|Q8IAR7\|Q8IAR7_PLAF7 Tyrosyl-tRNA synthetase, putative OS=Plasmodium falciparum (isolate 3D7) GN=MAL8P1.125 PE=1 SV=1 | 6 | 654.99 | 1589.55 | 0.3591 |
| tr\|Q8I6U5\|Q8I6U5_PLAF7 Falcipain-2, putative OS=Plasmodium falciparum (isolate 3D7) GN=PF11_0161 PE=3 SV=1;tr\|Q8I6U4\|Q8I6U4_PLAF7 Falcipain 2 OS=Plasmodium falciparum (isolate 3D7) GN=PF11_0165 PE=1 SV=1 | 6 | 41.06 | 75.65 | 0.2411 |
| tr\|Q8IHT8\|Q8IHT8_PLAF7 Uncharacterized protein OS=Plasmodium falciparum (isolate 3D7) GN=PF11_0439 PE=4 SV=1 | 6 | 73.56 | 134.15 | 0.2370 |
| tr\|Q8I3A1\|Q8I3A1_PLAF7 Replication factor A-related protein, putative OS=Plasmodium falciparum (isolate 3D7) GN=PFI0235w PE=4 SV=1 | 6 | 73.76 | 141.71 | 0.2584 |
| tr\|Q8ILX1\|Q8ILX1_PLAF7 Nuclear transport factor 2, putative OS=Plasmodium falciparum (isolate 3D7) GN=PF14_0122 PE=4 SV=2 | 6 | 2741.00 | 6705.45 | 0.3627 |
| tr\|Q8I425\|Q8I425_PLAF7 Uncharacterized protein OS=Plasmodium falciparum (isolate 3D7) GN=PFE0385w PE=4 SV=1 | 6 | 19.20 | 23.19 | 0.0983 |
| tr\|Q8I1U8\|Q8I1U8_PLAF7 Ubiquitinyl hydrolase 1 OS=Plasmodium falciparum (isolate 3D7) GN=PFD0680c PE=4 SV=1 | 6 | 83.33 | 167.70 | 0.2779 |
| tr\|Q8IIM5\|Q8IIM5_PLAF7 Glyoxalase I, putative OS=Plasmodium falciparum (isolate 3D7) GN=PF11_0145 PE=4 SV=1 | 6 | 161.40 | 383.01 | 0.3493 |
| tr\|Q8I3J3\|Q8I3J3_PLAF7 Ubiquitin carboxyl-terminal hydrolase OS=Plasmodium falciparum (isolate 3D7) GN=PFE1355c PE=3 SV=1 | 6 | 118.75 | 277.96 | 0.3433 |
| tr\|Q8I3V0\|Q8I3V0_PLAF7 BolA-like protein, putative OS=Plasmodium falciparum (isolate 3D7) GN=PFE0790c PE=1 SV=1 | 6 | 228.26 | 417.44 | 0.2381 |
| tr\|Q8I375\|Q8I375_PLAF7 Translation initiation factor SUI1, putative OS=Plasmodium falciparum (isolate 3D7) GN=PFI0365w PE=4 SV=1 | 6 | 28.18 | 54.56 | 0.2616 |
| tr\|Q8I4S1\|Q8I4S1_PLAF7 Thymidylate kinase, putative OS=Plasmodium falciparum (isolate 3D7) GN=PFL2465c PE=1 SV=1 | 6 | 78.07 | 183.41 | 0.3449 |
| tr\|C6KT35\|C6KT35_PLAF7 Acyl-CoA synthetase, PfACS12 OS=Plasmodium falciparum (isolate 3D7) GN=PfACS12 PE=4 SV=1 | 6 | 279.09 | 678.14 | 0.3597 |
| tr\|Q8I624\|Q8I624_PLAF7 Uncharacterized protein OS=Plasmodium falciparum (isolate 3D7) GN=PFL0105w PE=4 SV=1 | 6 | 44.50 | 99.35 | 0.3226 |
| tr\|Q8I0U7\|Q8I0U7_PLAF7 Proteasome, putative OS=Plasmodium falciparum (isolate 3D7) GN=PFI1545c PE=4 SV=1 | 6 | 81.40 | 191.71 | 0.3460 |
| tr\|Q8IL92\|Q8IL92_PLAF7 Pantothenate kinase, putative OS=Plasmodium falciparum (isolate 3D7) GN=PF14_0354 PE=4 SV=1 | 6 | 52.49 | 115.17 | 0.3150 |
| tr\|Q8ILI9\|Q8ILI9_PLAF7 DNA mismatch repair protein Msh2p, putative OS=Plasmodium falciparum (isolate 3D7) GN=PF14_0254 PE=3 SV=1 | 6 | 188.11 | 455.06 | 0.3577 |
| tr\|Q8IIA5\|Q8IIA5_PLAF7 Conserved Plasmodium protein OS=Plasmodium falciparum (isolate 3D7) GN=PF11_0269 PE=4 SV=1 | 6 | 68.04 | 157.34 | 0.3379 |
| tr\|Q8IJB8\|Q8IJB8_PLAF7 Uncharacterized protein OS=Plasmodium falciparum (isolate 3D7) GN=PF10_0280 PE=4 SV=1 | 6 | 15.66 | 29.38 | 0.2485 |
| tr\|Q8I5S3\|Q8I5S3_PLAF7 Conserved Plasmodium protein OS=Plasmodium falciparum (isolate 3D7) GN=PFL0640w PE=4 SV=1 | 6 | 38.29 | 87.31 | 0.3318 |
| tr\|C0H4G4\|C0H4G4_PLAF7 Uncharacterized protein OS=Plasmodium falciparum (isolate 3D7) GN=PFE1375c PE=4 SV=1 | 6 | 27.75 | 62.18 | 0.3241 |
| tr\|Q8ILA7\|Q8ILA7_PLAF7 Uncharacterized protein OS=Plasmodium falciparum (isolate 3D7) GN=PF14_0338 PE=4 SV=2 | 6 | 19.12 | 41.52 | 0.3104 |
| tr\|Q8IJI3\|Q8IJI3_PLAF7 RNA binding protein, putative OS=Plasmodium falciparum (isolate 3D7) GN=PF10_0214 PE=4 SV=2 | 6 | 5.24 | 5.09 | 0.0529 |
| tr\|Q8IDT0\|Q8IDT0_PLAF7 Phosphatase, putative OS=Plasmodium falciparum (isolate 3D7) GN=PF13_0222 PE=4 SV=1 | 6 | 7.40 | 13.15 | 0.2266 |
| tr\|Q8II83\|Q8II83_PLAF7 Uncharacterized protein OS=Plasmodium falciparum (isolate 3D7) GN=PF11_0291 PE=4 SV=1 | 6 | 0.74 | 0.09 | 0.0000 |
| tr\|Q8IIB5\|Q8IIB5_PLAF7 Nuclear preribosomal assembly protein, putative OS=Plasmodium falciparum (isolate 3D7) GN=PF11_0259 PE=4 SV=1 | 6 | 16.01 | 35.04 | 0.3140 |
| tr\|Q8IIG3\|Q8IIG3_PLAF7 Uncharacterized protein OS=Plasmodium falciparum (isolate 3D7) GN=PF11_0211 PE=4 SV=1 | 6 | 5.54 | 7.78 | 0.1413 |
| tr\|C0H4T9\|C0H4T9_PLAF7 CAF1 family ribonuclease, putative OS=Plasmodium falciparum (isolate 3D7) GN=MAL8P1.104 PE=4 SV=1 | 6 | 4.11 | 4.10 | 0.0575 |
| tr\|Q8I4T9\|Q8I4T9_PLAF7 CutA, putative OS=Plasmodium falciparum (isolate 3D7) GN=PFL2375c PE=4 SV=1 | 6 | 3.69 | 5.12 | 0.1372 |

| | | | | |
|---|---|---|---|---|
| tr\|O97273\|O97273_PLAF7 Putative uncharacterized protein OS=Plasmodium falciparum (isolate 3D7) GN=PFC0690c PE=4 SV=1 | 6 | 2.65 | 3.59 | 0.1300 |
| tr\|Q8IKK3\|Q8IKK3_PLAF7 DNA polymerase alpha subunit, putative OS=Plasmodium falciparum (isolate 3D7) GN=PF14_0602 PE=4 SV=1 | 6 | 2.05 | 2.18 | 0.0691 |
| tr\|C6KT03\|C6KT03_PLAF7 Ndc80 homologue, putative OS=Plasmodium falciparum (isolate 3D7) GN=PFF0785w PE=4 SV=1 | 6 | 45.64 | 110.26 | 0.3571 |
| tr\|Q8IDS7\|Q8IDS7_PLAF7 Na+-dependent Pi transporter, sodium-dependent phosphate transporter OS=Plasmodium falciparum (isolate 3D7) GN=MAL13P1.206 PE=4 SV=1 | 6 | 0.74 | 0.58 | 0.0258 |
| tr\|Q8IDI0\|Q8IDI0_PLAF7 Uncharacterized protein OS=Plasmodium falciparum (isolate 3D7) GN=MAL13P1.262 PE=4 SV=1 | 6 | 0.75 | 0.10 | 0.0000 |
| tr\|Q8I2K4\|Q8I2K4_PLAF7 Nucleolar protein Nop52, putative OS=Plasmodium falciparum (isolate 3D7) GN=PFI1510w PE=4 SV=1 | 6 | 18.21 | 27.68 | 0.1680 |
| tr\|Q8IJE1\|Q8IJE1_PLAF7 Conserved Plasmodium protein OS=Plasmodium falciparum (isolate 3D7) GN=PF10_0257 PE=4 SV=2 | 6 | 3.85 | 5.15 | 0.1263 |
| tr\|Q8II05\|Q8II05_PLAF7 3-oxo-5-alpha-steroid 4-dehydrogenase, putative OS=Plasmodium falciparum (isolate 3D7) GN=PF11_0370 PE=4 SV=2 | 6 | 2.46 | 3.47 | 0.1433 |
| tr\|Q8IAN8\|Q8IAN8_PLAF7 Uncharacterized protein OS=Plasmodium falciparum (isolate 3D7) GN=PF08_0124 PE=4 SV=1 | 6 | 15.54 | 35.73 | 0.3355 |
| tr\|Q8ILF7\|Q8ILF7_PLAF7 Glutamate dehydrogenase OS=Plasmodium falciparum (isolate 3D7) GN=PF14_0286 PE=1 SV=1 | 6 | 1.65 | 2.06 | 0.1080 |
| tr\|C6KT93\|C6KT93_PLAF7 Uncharacterized protein OS=Plasmodium falciparum (isolate 3D7) GN=PFF1245c PE=4 SV=1 | 6 | 0.76 | 0.19 | 0.0002 |
| sp\|Q8IL06\|YPF07_PLAF7 Uncharacterized protein PF14_0444 OS=Plasmodium falciparum (isolate 3D7) GN=PF14_0444 PE=4 SV=2 | 6 | 1.94 | 2.72 | 0.1399 |
| tr\|Q8ID52\|Q8ID52_PLAF7 Uncharacterized protein OS=Plasmodium falciparum (isolate 3D7) GN=MAL13P1.329 PE=4 SV=1 | 6 | 1.70 | 2.35 | 0.1372 |
| tr\|Q8IIR0\|Q8IIR0_PLAF7 Uncharacterized protein OS=Plasmodium falciparum (isolate 3D7) GN=PF11_0108 PE=4 SV=1 | 6 | 0.76 | 0.19 | 0.0002 |
| tr\|Q8ID42\|Q8ID42_PLAF7 Signal recognition particle receptor alpha subunit, putative OS=Plasmodium falciparum (isolate 3D7) GN=PF13_0350 PE=4 SV=1 | 6 | 0.77 | 0.45 | 0.0083 |
| tr\|Q8IAZ1\|Q8IAZ1_PLAF7 Uncharacterized protein OS=Plasmodium falciparum (isolate 3D7) GN=MAL8P1.85 PE=4 SV=1 | 6 | 0.77 | 0.14 | 0.0000 |
| tr\|O77351\|O77351_PLAF7 Putative uncharacterized protein OS=Plasmodium falciparum (isolate 3D7) GN=PFC0490w PE=4 SV=2 | 6 | 2.27 | 4.06 | 0.2286 |
| tr\|Q8I445\|Q8I445_PLAF7 Uncharacterized protein OS=Plasmodium falciparum (isolate 3D7) GN=PFE0280c PE=4 SV=1 | 6 | 2.16 | 3.99 | 0.2419 |
| tr\|Q8IL03\|Q8IL03_PLAF7 Glutaminyl-peptide cyclotransferase, putative OS=Plasmodium falciparum (isolate 3D7) GN=PF14_0447 PE=4 SV=1 | 6 | 1.42 | 2.18 | 0.1713 |
| tr\|C0H4W0\|C0H4W0_PLAF7 Uncharacterized protein OS=Plasmodium falciparum (isolate 3D7) GN=MAL8P1.63 PE=4 SV=1 | 6 | 3.00 | 4.46 | 0.1598 |
| tr\|Q8I411\|Q8I411_PLAF7 Uncharacterized protein OS=Plasmodium falciparum (isolate 3D7) GN=PFE0460c PE=4 SV=1 | 6 | 0.89 | 0.91 | 0.0637 |
| tr\|Q8I442\|Q8I442_PLAF7 Uncharacterized protein OS=Plasmodium falciparum (isolate 3D7) GN=PFE0295w PE=4 SV=1 | 6 | 0.81 | 0.99 | 0.1010 |
| tr\|Q8IE08\|Q8IE08_PLAF7 Qa-SNARE protein, putative OS=Plasmodium falciparum (isolate 3D7) GN=PfSyn5 PE=4 SV=1 | 6 | 1.02 | 1.69 | 0.2000 |
| tr\|Q8IET5\|Q8IET5_PLAF7 Uncharacterized protein OS=Plasmodium falciparum (isolate 3D7) GN=MAL13P1.15 PE=4 SV=1 | 6 | 0.92 | 1.39 | 0.1682 |
| tr\|Q8I5R4\|Q8I5R4_PLAF7 Phosphatidylinositol-glycan biosynthesis class O protein, putative OS=Plasmodium falciparum (isolate 3D7) GN=PFL0685w PE=4 SV=2 | 6 | 0.41 | 0.55 | 0.1270 |
| tr\|Q8I3B7\|Q8I3B7_PLAF7 Retrieval receptor for endoplasmic reticulum membrane proteins, putative OS=Plasmodium falciparum (isolate 3D7) GN=PFI0150c PE=4 SV=1 | 6 | 0.58 | 0.82 | 0.1426 |
| tr\|Q8I3L9\|Q8I3L9_PLAF7 Organelle ribosomal protein L7/L12, putative OS=Plasmodium falciparum (isolate 3D7) GN=PFE1225w PE=3 SV=1 | 6 | 0.44 | 0.92 | 0.2966 |
| tr\|Q8II26\|Q8II26_PLAF7 Conserved Plasmodium protein OS=Plasmodium falciparum (isolate 3D7) GN=PF11_0349 PE=4 SV=2 | 6 | 0.79 | 0.40 | 0.0044 |
| tr\|Q9U0J2\|Q9U0J2_PLAF7 DNAJ protein OS=Plasmodium falciparum (isolate 3D7) GN=Pfj1 PE=3 SV=1 | 6 | 0.80 | 0.67 | 0.0331 |
| tr\|Q8I482\|Q8I482_PLAF7 Chromosome assembly factor 1, CAF-1 OS=Plasmodium falciparum (isolate 3D7) GN=PFE0090w PE=4 SV=1 | 6 | 0.80 | 0.18 | 0.0001 |
| tr\|Q8IDI9\|Q8IDI9_PLAF7 Phosphatidylinositol transfer protein, putative OS=Plasmodium falciparum (isolate 3D7) GN=MAL13P1.256 PE=4 SV=2 | 6 | 0.81 | 0.40 | 0.0040 |
| tr\|Q9U0I0\|Q9U0I0_PLAF7 Uncharacterized protein OS=Plasmodium falciparum (isolate 3D7) GN=PFD0535w PE=4 SV=1 | 6 | 0.83 | 0.39 | 0.0035 |
| sp\|Q8IED2\|SMC2_PLAF7 Structural maintenance of chromosomes protein 2 OS=Plasmodium falciparum (isolate 3D7) GN=MAL13P1.96 PE=3 SV=1 | 6 | 0.84 | 0.46 | 0.0069 |

| | | | | |
|---|---|---|---|---|
| tr\|Q8I0X0\|Q8I0X0_PLAF7 SNAP protein (Soluble N-ethylmaleimide-sensitive factor Attachment Protein), putative OS=Plasmodium falciparum (isolate 3D7) GN=PFE0445c PE=4 SV=1 | 6 | 0.84 | 0.26 | 0.0005 |
| tr\|C0H561\|C0H561_PLAF7 Thioredoxin OS=Plasmodium falciparum (isolate 3D7) GN=Tlp2 PE=3 SV=1 | 6 | 0.86 | 0.48 | 0.0070 |
| tr\|O96168\|O96168_PLAF7 Conserved Plasmodium protein OS=Plasmodium falciparum (isolate 3D7) GN=PFB0365w PE=4 SV=3 | 6 | 0.87 | 0.18 | 0.0001 |
| tr\|Q8IC51\|Q8IC51_PLAF7 Pfmc-2TM Maurers cleft two transmembrane protein OS=Plasmodium falciparum (isolate 3D7) GN=PfMC-2TM PE=4 SV=1 | 6 | 0.88 | 0.10 | 0.0000 |
| tr\|O96230\|O96230_PLAF7 Acyl-CoA synthetase, PfACS9 OS=Plasmodium falciparum (isolate 3D7) GN=ACS9 PE=4 SV=1 | 6 | 0.88 | 0.35 | 0.0016 |
| sp\|P30043\|BLVRB_HUMAN Flavin reductase (NADPH) OS=Homo sapiens GN=BLVRB PE=1 SV=3;tr\|M0QZL1\|M0QZL1_HUMAN Flavin reductase (NADPH) OS=Homo sapiens GN=BLVRB PE=1 SV=1;tr\|M0R192\|M0R192_HUMAN Flavin reductase (NADPH) OS=Homo sapiens GN=BLVRB PE=1 SV=1 | 6 | 0.88 | 0.39 | 0.0027 |
| tr\|Q8I5J2\|Q8I5J2_PLAF7 Uncharacterized protein OS=Plasmodium falciparum (isolate 3D7) GN=PFL1065c PE=4 SV=1 | 6 | 0.89 | 0.44 | 0.0042 |
| tr\|O96237\|O96237_PLAF7 Origin recognition complex subunit 5 OS=Plasmodium falciparum (isolate 3D7) GN=ORC5 PE=4 SV=1 | 6 | 0.92 | 0.25 | 0.0003 |
| tr\|C0H5F1\|C0H5F1_PLAF7 Protein tyrosine phosphatase, putative OS=Plasmodium falciparum (isolate 3D7) GN=MAL13P1.168 PE=4 SV=1 | 6 | 0.93 | 0.37 | 0.0017 |
| sp\|Q76NM1\|ERD2_PLAF7 ER lumen protein-retaining receptor OS=Plasmodium falciparum (isolate 3D7) GN=ERD2 PE=3 SV=1 | 6 | 0.93 | 0.26 | 0.0003 |
| tr\|Q8I6T0\|Q8I6T0_PLAF7 Aminomethyltransferase, mitochondrial OS=Plasmodium falciparum (isolate 3D7) GN=PF13_0345 PE=3 SV=1 | 6 | 0.94 | 0.19 | 0.0001 |
| tr\|Q8I5G8\|Q8I5G8_PLAF7 Splicing factor 3b subunit, putative OS=Plasmodium falciparum (isolate 3D7) GN=PFL1200c PE=4 SV=1 | 6 | 0.96 | 0.66 | 0.0164 |
| tr\|Q8I3M7\|Q8I3M7_PLAF7 Transporter, putative OS=Plasmodium falciparum (isolate 3D7) GN=PFE1185w PE=4 SV=1 | 6 | 0.97 | 0.84 | 0.0372 |
| tr\|Q8II35\|Q8II35_PLAF7 Uncharacterized protein OS=Plasmodium falciparum (isolate 3D7) GN=PF11_0339 PE=4 SV=1 | 6 | 0.98 | 0.24 | 0.0002 |
| tr\|Q8I5Z0\|Q8I5Z0_PLAF7 Uncharacterized protein OS=Plasmodium falciparum (isolate 3D7) GN=PFL0275w PE=4 SV=1 | 6 | 0.99 | 0.47 | 0.0038 |
| tr\|Q8IEK7\|Q8IEK7_PLAF7 Uncharacterized protein OS=Plasmodium falciparum (isolate 3D7) GN=MAL13P1.53 PE=4 SV=1 | 6 | 1.02 | 0.36 | 0.0010 |
| tr\|Q8I1P0\|Q8I1P0_PLAF7 60S ribosomal protein L7Ae/L30e, putative OS=Plasmodium falciparum (isolate 3D7) GN=PFD0960c PE=4 SV=1 | 6 | 1.04 | 0.29 | 0.0003 |
| tr\|O96265\|O96265_PLAF7 Small nuclear ribonucleoprotein, putative OS=Plasmodium falciparum (isolate 3D7) GN=PFB0865w PE=4 SV=1 | 6 | 1.05 | 0.08 | 0.0000 |
| tr\|J3QLD9\|J3QLD9_HUMAN Flotillin-2 OS=Homo sapiens GN=FLOT2 PE=1 SV=1;tr\|E7EMK3\|E7EMK3_HUMAN Flotillin-2 OS=Homo sapiens GN=FLOT2 PE=1 SV=1;sp\|Q14254\|FLOT2_HUMAN Flotillin-2 OS=Homo sapiens GN=FLOT2 PE=1 SV=2 | 6 | 1.07 | 0.13 | 0.0000 |
| tr\|C0H4S6\|C0H4S6_PLAF7 Uncharacterized protein OS=Plasmodium falciparum (isolate 3D7) GN=MAL8P1.130 PE=4 SV=1 | 6 | 1.07 | 0.54 | 0.0045 |
| tr\|Q8I2D9\|Q8I2D9_PLAF7 Putative uncharacterized protein OS=Plasmodium falciparum (isolate 3D7) GN=PFA_0670c PE=4 SV=1 | 6 | 1.07 | 0.10 | 0.0000 |
| sp\|P17066\|HSP76_HUMAN Heat shock 70 kDa protein 6 OS=Homo sapiens GN=HSPA6 PE=1 SV=2;sp\|P48741\|HSP77_HUMAN Putative heat shock 70 kDa protein 7 OS=Homo sapiens GN=HSPA7 PE=5 SV=2 | 6 | 1.08 | 0.45 | 0.0021 |
| tr\|Q8I296\|Q8I296_PLAF7 Ubiquitin carboxyl-terminal hydrolase, putative OS=Plasmodium falciparum (isolate 3D7) GN=PFA_0220w PE=4 SV=2 | 6 | 1.11 | 0.40 | 0.0010 |
| tr\|Q8IKB6\|Q8IKB6_PLAF7 Histone deacetylase, putative OS=Plasmodium falciparum (isolate 3D7) GN=PF14_0690 PE=4 SV=2 | 6 | 1.15 | 0.61 | 0.0056 |
| tr\|Q8IKQ3\|Q8IKQ3_PLAF7 Uncharacterized protein OS=Plasmodium falciparum (isolate 3D7) GN=PF14_0550 PE=4 SV=1 | 6 | 1.16 | 0.93 | 0.0287 |
| tr\|Q8IJR8\|Q8IJR8_PLAF7 Uncharacterized protein OS=Plasmodium falciparum (isolate 3D7) GN=PF10_0124 PE=4 SV=1 | 6 | 1.20 | 0.62 | 0.0051 |
| tr\|C6KT45\|C6KT45_PLAF7 Cleavage stimulation factor subunit 1-like protein, putative OS=Plasmodium falciparum (isolate 3D7) GN=PFF1000w PE=4 SV=1 | 6 | 1.24 | 0.74 | 0.0093 |
| tr\|Q8I1Z8\|Q8I1Z8_PLAF7 Uncharacterized protein OS=Plasmodium falciparum (isolate 3D7) GN=PFD0150w PE=4 SV=1 | 6 | 1.28 | 0.79 | 0.0106 |
| tr\|Q8IKE6\|Q8IKE6_PLAF7 Uncharacterized protein OS=Plasmodium falciparum (isolate 3D7) GN=PF14_0659 PE=4 SV=1 | 6 | 1.28 | 1.20 | 0.0469 |
| sp\|Q8IIS5\|PESC_PLAF7 Pescadillo homolog OS=Plasmodium falciparum (isolate 3D7) GN=PF11_0090 PE=3 SV=1 | 6 | 1.28 | 0.33 | 0.0002 |
| tr\|Q8IKN5\|Q8IKN5_PLAF7 Uncharacterized protein OS=Plasmodium falciparum (isolate 3D7) GN=PF14_0569 PE=4 SV=1 | 6 | 1.35 | 0.30 | 0.0001 |

| | | | | |
|---|---|---|---|---|
| tr\|C0H5J0\|C0H5J0_PLAF7 Uncharacterized protein OS=Plasmodium falciparum (isolate 3D7) GN=MAL13P1.293 PE=4 SV=1 | 6 | 1.36 | 0.91 | 0.0149 |
| tr\|Q8I275\|Q8I275_PLAF7 PfAARP2 protein OS=Plasmodium falciparum (isolate 3D7) GN=AARP2 PE=4 SV=1 | 6 | 1.37 | 0.44 | 0.0006 |
| tr\|Q8I410\|Q8I410_PLAF7 DNA-directed RNA polymerase OS=Plasmodium falciparum (isolate 3D7) GN=PFE0465c PE=3 SV=1 | 6 | 1.38 | 0.16 | 0.0000 |
| tr\|Q8IHR6\|Q8IHR6_PLAF7 Coatomer subunit gamma OS=Plasmodium falciparum (isolate 3D7) GN=PF11_0463 PE=3 SV=1 | 6 | 1.46 | 0.25 | 0.0000 |
| tr\|Q8IKK4\|Q8IKK4_PLAF7 Replication factor C3 OS=Plasmodium falciparum (isolate 3D7) GN=PF14_0601 PE=4 SV=1 | 6 | 1.47 | 0.66 | 0.0028 |
| tr\|Q8IDM6\|Q8IDM6_PLAF7 Nucleoside transporter 1 OS=Plasmodium falciparum (isolate 3D7) GN=nt1 PE=4 SV=1 | 6 | 1.50 | 0.70 | 0.0033 |
| tr\|Q8I1T4\|Q8I1T4_PLAF7 Cyclin-dependent kinase, putative OS=Plasmodium falciparum (isolate 3D7) GN=Pfcrk-3 PE=4 SV=1 | 6 | 1.51 | 0.90 | 0.0094 |
| tr\|Q8I512\|Q8I512_PLAF7 Replication factor C subunit 4 OS=Plasmodium falciparum (isolate 3D7) GN=PFL2005w PE=4 SV=1 | 6 | 1.59 | 0.83 | 0.0054 |
| tr\|Q8IKC5\|Q8IKC5_PLAF7 Diacylglycerol kinase, putative OS=Plasmodium falciparum (isolate 3D7) GN=PF14_0681 PE=4 SV=2 | 6 | 1.64 | 1.11 | 0.0152 |
| tr\|Q8IIP3\|Q8IIP3_PLAF7 Conserved Plasmodium protein OS=Plasmodium falciparum (isolate 3D7) GN=PF11_0126 PE=4 SV=2 | 6 | 1.65 | 1.06 | 0.0123 |
| sp\|Q14964\|RB39A_HUMAN Ras-related protein Rab-39A OS=Homo sapiens GN=RAB39A PE=2 SV=2 | 6 | 1.68 | 0.72 | 0.0023 |
| tr\|Q8ILT8\|Q8ILT8_PLAF7 Dimethyladenosine transferase, putative OS=Plasmodium falciparum (isolate 3D7) GN=PF14_0156 PE=1 SV=1 | 6 | 1.70 | 0.62 | 0.0011 |
| tr\|Q8ILV5\|Q8ILV5_PLAF7 Uncharacterized protein OS=Plasmodium falciparum (isolate 3D7) GN=PF14_0138 PE=4 SV=2 | 6 | 1.72 | 0.80 | 0.0032 |
| tr\|Q8I3Q8\|Q8I3Q8_PLAF7 Uncharacterized protein OS=Plasmodium falciparum (isolate 3D7) GN=PFE1015c PE=4 SV=1 | 6 | 1.72 | 0.76 | 0.0026 |
| tr\|C0H549\|C0H549_PLAF7 Nucleolar preribosomal assembly protein, putative OS=Plasmodium falciparum (isolate 3D7) GN=PFI1070c PE=4 SV=1 | 6 | 1.78 | 1.54 | 0.0364 |
| tr\|Q8I390\|Q8I390_PLAF7 Beta subunit of coatomer complex, putative OS=Plasmodium falciparum (isolate 3D7) GN=PFI0290c PE=4 SV=1 | 6 | 1.81 | 0.28 | 0.0000 |
| tr\|C6KTD8\|C6KTD8_PLAF7 DNA polymerase epsilon, catalytic subunit a, putative OS=Plasmodium falciparum (isolate 3D7) GN=PFF1470c PE=4 SV=1 | 6 | 1.98 | 1.36 | 0.0160 |
| sp\|Q86SG5\|S1A7A_HUMAN Protein S100-A7A OS=Homo sapiens GN=S100A7A PE=1 SV=3;sp\|P31151\|S10A7_HUMAN Protein S100-A7 OS=Homo sapiens GN=S100A7 PE=1 SV=4 | 6 | 2.08 | 1.93 | 0.0463 |
| tr\|Q8IB51\|Q8IB51_PLAF7 60S ribosomal protein L22, putative OS=Plasmodium falciparum (isolate 3D7) GN=PF08_0039 PE=1 SV=1 | 6 | 2.40 | 1.40 | 0.0086 |
| tr\|C6KTE1\|C6KTE1_PLAF7 Uncharacterized protein OS=Plasmodium falciparum (isolate 3D7) GN=PFF1485w PE=4 SV=1 | 6 | 2.49 | 2.21 | 0.0396 |
| tr\|C6KT56\|C6KT56_PLAF7 Uncharacterized protein OS=Plasmodium falciparum (isolate 3D7) GN=PFF1055c PE=4 SV=1 | 6 | 2.54 | 1.64 | 0.0127 |
| tr\|Q8IDG6\|Q8IDG6_PLAF7 Ran-binding protein, putative OS=Plasmodium falciparum (isolate 3D7) GN=PF13_0278 PE=4 SV=1 | 6 | 2.55 | 1.82 | 0.0185 |
| tr\|Q8I6T3\|Q8I6T3_PLAF7 Proteasome subunit beta type OS=Plasmodium falciparum (isolate 3D7) GN=PF13_0156 PE=3 SV=1 | 6 | 2.57 | 1.57 | 0.0101 |
| tr\|Q8II92\|Q8II92_PLAF7 Deoxyuridine 5-triphosphate nucleotidohydrolase, putative OS=Plasmodium falciparum (isolate 3D7) GN=PF11_0282 PE=1 SV=1 | 6 | 3.69 | 2.50 | 0.0152 |
| sp\|P61076\|TRXR2_PLAF7 Thioredoxin reductase 2 OS=Plasmodium falciparum (isolate 3D7) GN=trxr2 PE=1 SV=2 | 6 | 4.13 | 1.96 | 0.0036 |
| tr\|Q8IIB7\|Q8IIB7_PLAF7 Ethanolamine kinase, putative OS=Plasmodium falciparum (isolate 3D7) GN=PF11_0257 PE=4 SV=1 | 6 | 6.81 | 6.37 | 0.0472 |
| tr\|Q8IBG6\|Q8IBG6_PLAF7 60S ribosomal subunit export protein, putative OS=Plasmodium falciparum (isolate 3D7) GN=PF07_0121 PE=4 SV=1 | 6 | 13.82 | 6.35 | 0.0031 |
| sp\|Q8I1Y0\|PF41_PLAF7 Merozoite surface protein P41 OS=Plasmodium falciparum (isolate 3D7) GN=PF41 PE=1 SV=1 | 5 | 0.36 | 0.21 | 0.0187 |
| tr\|O96163\|O96163_PLAF7 Serine repeat antigen 7 (SERA-7) OS=Plasmodium falciparum (isolate 3D7) GN=SERA-7 PE=3 SV=1 | 5 | 0.37 | 0.29 | 0.0442 |
| tr\|Q8IIR8\|Q8IIR8_PLAF7 Succinyl-CoA synthetase alpha subunit, putative OS=Plasmodium falciparum (isolate 3D7) GN=PF11_0097 PE=3 SV=2 | 5 | 0.39 | 0.20 | 0.0125 |
| tr\|Q8I506\|Q8I506_PLAF7 Uncharacterized protein OS=Plasmodium falciparum (isolate 3D7) GN=PFL2035c PE=4 SV=1 | 5 | 0.47 | 0.29 | 0.0223 |
| tr\|Q8I623\|Q8I623_PLAF7 PfmpC OS=Plasmodium falciparum (isolate 3D7) GN=PFL0110c PE=3 SV=1 | 5 | 0.48 | 0.20 | 0.0062 |
| tr\|C6KSZ5\|C6KSZ5_PLAF7 Ribonuclease, putative OS=Plasmodium falciparum (isolate 3D7) GN=PFF0745c PE=4 SV=1 | 5 | 0.51 | 0.37 | 0.0362 |

| | | | | |
|---|---|---|---|---|
| tr\|C0H4A8\|C0H4A8_PLAF7 PfMNL-2 CISD1-like iron-sulfur protein, putative OS=Plasmodium falciparum (isolate 3D7) GN=PFD0807c PE=4 SV=1 | 5 | 0.58 | 0.34 | 0.0200 |
| tr\|Q8IC27\|Q8IC27_PLAF7 Uncharacterized protein OS=Plasmodium falciparum (isolate 3D7) GN=PF07_0016 PE=4 SV=1 | 5 | 0.59 | 0.23 | 0.0045 |
| tr\|Q8I4Z9\|Q8I4Z9_PLAF7 t-SNARE, putative OS=Plasmodium falciparum (isolate 3D7) GN=PFL2070w PE=4 SV=1 | 5 | 0.61 | 0.39 | 0.0245 |
| tr\|O96145\|O96145_PLAF7 UbiE/COQ5 methyltransferase family, putative OS=Plasmodium falciparum (isolate 3D7) GN=PFB0220w PE=3 SV=1 | 5 | 0.66 | 0.30 | 0.0079 |
| sp\|Q8I467\|CADF1_PLAF7 Cofilin/actin-depolymerizing factor homolog 1 OS=Plasmodium falciparum (isolate 3D7) GN=PFE0165w PE=1 SV=1 | 5 | 432.96 | 698.80 | 0.2382 |
| tr\|O97256\|O97256_PLAF7 Activator of Hsp90 ATPase homolog 1-like protein, putative OS=Plasmodium falciparum (isolate 3D7) GN=PFC0360w PE=4 SV=2 | 5 | 490.49 | 1054.50 | 0.3570 |
| tr\|Q8IJ30\|Q8IJ30_PLAF7 Enhancer of rudimentary homolog OS=Plasmodium falciparum (isolate 3D7) GN=PF10_0370 PE=3 SV=1 | 5 | 114.83 | 126.43 | 0.1121 |
| tr\|Q8I607\|Q8I607_PLAF7 Ubiquitin conjugating enzyme E2, putative OS=Plasmodium falciparum (isolate 3D7) GN=PFL0190w PE=3 SV=1 | 5 | 715.05 | 1551.48 | 0.3610 |
| tr\|Q8IDD9\|Q8IDD9_PLAF7 Ubiquitin conjugating enzyme, putative OS=Plasmodium falciparum (isolate 3D7) GN=PF13_0301 PE=3 SV=1 | 5 | 98.32 | 165.11 | 0.2538 |
| tr\|C0H579\|C0H579_PLAF7 Putative uncharacterized protein OS=Plasmodium falciparum (isolate 3D7) GN=PFI1525w PE=4 SV=1 | 5 | 59.18 | 81.11 | 0.1781 |
| tr\|Q8I5M2\|Q8I5M2_PLAF7 Arginyl-tRNA synthetase, putative OS=Plasmodium falciparum (isolate 3D7) GN=PFL0900c PE=3 SV=1 | 5 | 348.27 | 728.51 | 0.3453 |
| tr\|Q8I5L3\|Q8I5L3_PLAF7 Ribulose-phosphate 3-epimerase OS=Plasmodium falciparum (isolate 3D7) GN=PFL0960w PE=1 SV=1 | 5 | 98.93 | 168.98 | 0.2606 |
| tr\|Q8I303\|Q8I303_PLAF7 BSD domain, putative OS=Plasmodium falciparum (isolate 3D7) GN=PFI0730w PE=4 SV=1 | 5 | 66.10 | 109.34 | 0.2478 |
| sp\|P35754\|GLRX1_HUMAN Glutaredoxin-1 OS=Homo sapiens GN=GLRX PE=1 SV=2 | 5 | 117.03 | 210.35 | 0.2814 |
| sp\|Q8IBP3\|ITPA_PLAF7 Inosine triphosphate pyrophosphatase OS=Plasmodium falciparum (isolate 3D7) GN=MAL7P1.110 PE=3 SV=1 | 5 | 118.66 | 244.67 | 0.3391 |
| tr\|O77367\|O77367_PLAF7 Ubiquitin-protein ligase, putative OS=Plasmodium falciparum (isolate 3D7) GN=PFC0845c PE=4 SV=3 | 5 | 48.31 | 58.02 | 0.1361 |
| sp\|Q8I3Y6\|PFD6_PLAF7 Probable prefoldin subunit 6 OS=Plasmodium falciparum (isolate 3D7) GN=PFE0595w PE=3 SV=2 | 5 | 687.52 | 1515.50 | 0.3678 |
| tr\|C0H4C7\|C0H4C7_PLAF7 Uncharacterized protein OS=Plasmodium falciparum (isolate 3D7) GN=PFE0290c PE=4 SV=1 | 5 | 58.53 | 92.10 | 0.2283 |
| tr\|Q8I2T4\|Q8I2T4_PLAF7 Putative uncharacterized protein OS=Plasmodium falciparum (isolate 3D7) GN=PFI1075w PE=4 SV=1 | 5 | 92.36 | 167.56 | 0.2852 |
| tr\|O97314\|O97314_PLAF7 Putative uncharacterized protein OS=Plasmodium falciparum (isolate 3D7) GN=PFC1025w PE=4 SV=1 | 5 | 47.83 | 67.32 | 0.1873 |
| tr\|Q8ILK1\|Q8ILK1_PLAF7 Arginine-N-methyltransferase, putative OS=Plasmodium falciparum (isolate 3D7) GN=PF14_0242 PE=4 SV=1 | 5 | 313.48 | 686.64 | 0.3650 |
| tr\|Q8IHS2\|Q8IHS2_PLAF7 Ubiquitin activating enzyme (E1) subunit Aos1, putative OS=Plasmodium falciparum (isolate 3D7) GN=Aos1 PE=4 SV=1 | 5 | 162.05 | 325.37 | 0.3278 |
| tr\|Q8IKR2\|Q8IKR2_PLAF7 Uncharacterized protein OS=Plasmodium falciparum (isolate 3D7) GN=PF14_0540 PE=4 SV=1 | 5 | 92.41 | 188.81 | 0.3353 |
| tr\|Q8I2I8\|Q8I2I8_PLAF7 Putative uncharacterized protein OS=Plasmodium falciparum (isolate 3D7) GN=PFI1590c PE=4 SV=1 | 5 | 52.70 | 103.63 | 0.3190 |
| tr\|O96142\|O96142_PLAF7 Aspartate aminotransferase OS=Plasmodium falciparum (isolate 3D7) GN=PFB0200c PE=1 SV=1 | 5 | 325.07 | 679.80 | 0.3452 |
| tr\|C0H586\|C0H586_PLAF7 Calcyclin binding protein, putative OS=Plasmodium falciparum (isolate 3D7) GN=PFI1610c PE=4 SV=1 | 5 | 109.61 | 200.33 | 0.2883 |
| tr\|Q8I294\|Q8I294_PLAF7 Putative uncharacterized protein OS=Plasmodium falciparum (isolate 3D7) GN=PFA_0230c PE=4 SV=1 | 5 | 74.86 | 138.20 | 0.2925 |
| tr\|Q8I246\|Q8I246_PLAF7 Phenylalanyl-tRNA synthetase beta chain, putative OS=Plasmodium falciparum (isolate 3D7) GN=PFA_0480w PE=3 SV=1 | 5 | 27.63 | 36.47 | 0.1654 |
| tr\|Q8I3A9\|Q8I3A9_PLAF7 GTPase activating protein, GAP OS=Plasmodium falciparum (isolate 3D7) GN=PFI0195c PE=4 SV=1 | 5 | 32.50 | 53.73 | 0.2476 |
| tr\|Q8I5H2\|Q8I5H2_PLAF7 Chromatin assembly protein (ASF1), putative OS=Plasmodium falciparum (isolate 3D7) GN=PFL1180w PE=4 SV=1 | 5 | 153.14 | 328.51 | 0.3561 |
| tr\|O77344\|O77344_PLAF7 Glycogen synthase kinase 3 OS=Plasmodium falciparum (isolate 3D7) GN=PfGSK-3 PE=4 SV=2 | 5 | 72.71 | 152.74 | 0.3471 |
| tr\|Q8I231\|Q8I231_PLAF7 UMP-CMP kinase, putative OS=Plasmodium falciparum (isolate 3D7) GN=PFA_0555c PE=3 SV=1 | 5 | 61.38 | 128.08 | 0.3443 |
| tr\|Q8I610\|Q8I610_PLAF7 Uncharacterized protein OS=Plasmodium falciparum (isolate 3D7) GN=PFL0175c PE=4 SV=1 | 5 | 32.96 | 57.41 | 0.2685 |

| | | | | |
|---|---|---|---|---|
| tr\|Q8I2M1\|Q8I2M1_PLAF7 Guanylate kinase OS=Plasmodium falciparum (isolate 3D7) GN=PfGK PE=1 SV=1 | 5 | 21.66 | 30.91 | 0.1922 |
| tr\|Q8II79\|Q8II79_PLAF7 Farnesyl pyrophosphate synthase, putative OS=Plasmodium falciparum (isolate 3D7) GN=PF11_0295 PE=3 SV=2 | 5 | 28.13 | 55.69 | 0.3219 |
| tr\|Q8I6Z2\|Q8I6Z2_PLAF7 mRNA (N6-adenosine)-methyltransferase, putative OS=Plasmodium falciparum (isolate 3D7) GN=PF07_0123 PE=4 SV=1 | 5 | 30.88 | 50.35 | 0.2422 |
| tr\|Q8I1T0\|Q8I1T0_PLAF7 Uncharacterized protein OS=Plasmodium falciparum (isolate 3D7) GN=PFD0760c PE=4 SV=1 | 5 | 0.67 | 0.15 | 0.0006 |
| tr\|Q8IJM0\|Q8IJM0_PLAF7 26s proteasome subunit p55, putative OS=Plasmodium falciparum (isolate 3D7) GN=PF10_0174 PE=4 SV=1 | 5 | 31.50 | 60.50 | 0.3090 |
| tr\|Q8IDI8\|Q8IDI8_PLAF7 Uncharacterized protein OS=Plasmodium falciparum (isolate 3D7) GN=MAL13P1.257 PE=1 SV=1 | 5 | 61.63 | 132.51 | 0.3571 |
| tr\|C0H4C4\|C0H4C4_PLAF7 Uncharacterized protein OS=Plasmodium falciparum (isolate 3D7) GN=PFE0235c PE=4 SV=1 | 5 | 37.60 | 66.58 | 0.2753 |
| tr\|Q8IM55\|Q8IM55_PLAF7 Phosphatase, putative OS=Plasmodium falciparum (isolate 3D7) GN=PF14_0036 PE=4 SV=2 | 5 | 27.33 | 54.94 | 0.3284 |
| tr\|Q8I388\|Q8I388_PLAF7 Developmental protein, putative OS=Plasmodium falciparum (isolate 3D7) GN=PFI0300w PE=4 SV=1 | 5 | 19.33 | 36.68 | 0.3040 |
| tr\|Q8IDE7\|Q8IDE7_PLAF7 Serine/threonine protein phosphatase OS=Plasmodium falciparum (isolate 3D7) GN=PfPP5 PE=4 SV=1 | 5 | 16.88 | 31.00 | 0.2903 |
| tr\|Q8I378\|Q8I378_PLAF7 Putative uncharacterized protein OS=Plasmodium falciparum (isolate 3D7) GN=PFI0350c PE=4 SV=1 | 5 | 8.28 | 8.78 | 0.1028 |
| tr\|Q8IM28\|Q8IM28_PLAF7 ATP-dependent CLP protease, putative OS=Plasmodium falciparum (isolate 3D7) GN=PF14_0063 PE=4 SV=1 | 5 | 0.67 | 0.18 | 0.0012 |
| tr\|Q8II22\|Q8II22_PLAF7 Uncharacterized protein OS=Plasmodium falciparum (isolate 3D7) GN=PF11_0353 PE=4 SV=1 | 5 | 33.11 | 66.39 | 0.3273 |
| tr\|Q8IIG2\|Q8IIG2_PLAF7 Uncharacterized protein OS=Plasmodium falciparum (isolate 3D7) GN=PF11_0212 PE=3 SV=1 | 5 | 26.56 | 53.82 | 0.3317 |
| tr\|Q8IIG8\|Q8IIG8_PLAF7 Uncharacterized protein OS=Plasmodium falciparum (isolate 3D7) GN=PF11_0206 PE=4 SV=1 | 5 | 71.26 | 154.87 | 0.3617 |
| tr\|Q8IIQ6\|Q8IIQ6_PLAF7 Vacuolar protein sorting-associated protein 35 OS=Plasmodium falciparum (isolate 3D7) GN=PF11_0112 PE=3 SV=1 | 5 | 20.02 | 39.09 | 0.3160 |
| tr\|C6KT22\|C6KT22_PLAF7 Uncharacterized protein OS=Plasmodium falciparum (isolate 3D7) GN=PFF0880c PE=4 SV=1 | 5 | 19.97 | 38.87 | 0.3148 |
| tr\|Q8I5L1\|Q8I5L1_PLAF7 Pre-mRNA splicing factor, putative OS=Plasmodium falciparum (isolate 3D7) GN=PFL0970w PE=4 SV=1 | 5 | 11.19 | 15.04 | 0.1716 |
| tr\|Q6ZLZ9\|Q6ZLZ9_PLAF7 Alpha tubulin OS=Plasmodium falciparum (isolate 3D7) GN=PFI0180w PE=3 SV=1 | 5 | 5.29 | 4.95 | 0.0749 |
| tr\|Q8I5T1\|Q8I5T1_PLAF7 Uncharacterized protein OS=Plasmodium falciparum (isolate 3D7) GN=PFL0600w PE=4 SV=1 | 5 | 0.68 | 0.15 | 0.0005 |
| tr\|Q8IBN8\|Q8IBN8_PLAF7 DEAD box helicase, putative OS=Plasmodium falciparum (isolate 3D7) GN=MAL7P1.113 PE=3 SV=1 | 5 | 22.27 | 40.21 | 0.2833 |
| tr\|Q8I3I7\|Q8I3I7_PLAF7 Uncharacterized protein OS=Plasmodium falciparum (isolate 3D7) GN=PFE1395c PE=4 SV=1 | 5 | 8.71 | 14.78 | 0.2578 |
| tr\|O96243\|O96243_PLAF7 Vacuolar protein-sorting protein VPS45, putative OS=Plasmodium falciparum (isolate 3D7) GN=PFB0750w PE=4 SV=1 | 5 | 18.89 | 33.79 | 0.2794 |
| tr\|C0H5D3\|C0H5D3_PLAF7 SNARE protein, putative OS=Plasmodium falciparum (isolate 3D7) GN=PfYkt6.2 PE=4 SV=1 | 5 | 6.60 | 9.81 | 0.2069 |
| tr\|O77316\|O77316_PLAF7 Putative uncharacterized protein OS=Plasmodium falciparum (isolate 3D7) GN=PFC0130c PE=4 SV=1 | 5 | 8.40 | 10.44 | 0.1465 |
| tr\|Q8IIE9\|Q8IIE9_PLAF7 PfGCN20 OS=Plasmodium falciparum (isolate 3D7) GN=PF11_0225 PE=3 SV=1 | 5 | 4.57 | 5.53 | 0.1385 |
| tr\|Q8IE02\|Q8IE02_PLAF7 Apurinic/apyrimidinic endonuclease Apn1 OS=Plasmodium falciparum (isolate 3D7) GN=apn1 PE=3 SV=1 | 5 | 29.66 | 59.50 | 0.3274 |
| tr\|C0H5D0\|C0H5D0_PLAF7 Uncharacterized protein OS=Plasmodium falciparum (isolate 3D7) GN=MAL13P1.124 PE=4 SV=1 | 5 | 0.68 | 0.35 | 0.0129 |
| tr\|Q8ILY4\|Q8ILY4_PLAF7 Uncharacterized protein OS=Plasmodium falciparum (isolate 3D7) GN=PF14_0778 PE=4 SV=2 | 5 | 8.64 | 10.98 | 0.1534 |
| tr\|C6KT72\|C6KT72_PLAF7 Transcription or splicing factor-like protein, putative OS=Plasmodium falciparum (isolate 3D7) GN=PFF1135w PE=4 SV=1 | 5 | 4.24 | 3.62 | 0.0590 |
| tr\|Q9NLB8\|Q9NLB8_PLAF7 EH (Eps15 homology) protein OS=Plasmodium falciparum (isolate 3D7) GN=PfPast-1 PE=4 SV=1 | 5 | 20.09 | 40.99 | 0.3346 |
| tr\|C0H5I8\|C0H5I8_PLAF7 Uncharacterized protein OS=Plasmodium falciparum (isolate 3D7) GN=MAL13P1.286 PE=4 SV=1 | 5 | 4.46 | 6.22 | 0.1840 |
| tr\|Q8IBZ6\|Q8IBZ6_PLAF7 Cg2 protein OS=Plasmodium falciparum (isolate 3D7) GN=PF07_0037 PE=4 SV=1 | 5 | 31.88 | 69.30 | 0.3618 |

| | | | | |
|---|---|---|---|---|
| tr\|Q8IHP1\|Q8IHP1_PLAF7 Uncharacterized protein OS=Plasmodium falciparum (isolate 3D7) GN=PF11_0488 PE=4 SV=1 | 5 | 2.83 | 2.74 | 0.0818 |
| tr\|Q8IJV1\|Q8IJV1_PLAF7 Uncharacterized protein OS=Plasmodium falciparum (isolate 3D7) GN=PF10_0091 PE=4 SV=1 | 5 | 0.69 | 0.37 | 0.0142 |
| tr\|O96189\|O96189_PLAF7 Qa-SNARE protein OS=Plasmodium falciparum (isolate 3D7) GN=Syn17 PE=4 SV=1 | 5 | 2.23 | 2.24 | 0.0901 |
| tr\|Q8IDG9\|Q8IDG9_PLAF7 Uncharacterized protein OS=Plasmodium falciparum (isolate 3D7) GN=PF13_0275 PE=4 SV=1 | 5 | 2.55 | 3.36 | 0.1648 |
| tr\|Q8IB23\|Q8IB23_PLAF7 U3 small nucleolar ribonucleoprotein protein, putative OS=Plasmodium falciparum (isolate 3D7) GN=PF08_0055 PE=4 SV=1 | 5 | 2.89 | 4.28 | 0.2057 |
| tr\|Q8IIQ1\|Q8IIQ1_PLAF7 Replication factor C subunit 5, putative OS=Plasmodium falciparum (isolate 3D7) GN=PF11_0117 PE=4 SV=1 | 5 | 1.81 | 1.65 | 0.0706 |
| tr\|A0A087WXM8\|A0A087WXM8_HUMAN Basal cell adhesion molecule OS=Homo sapiens GN=BCAM PE=1 SV=1;sp\|P50895\|BCAM_HUMAN Basal cell adhesion molecule OS=Homo sapiens GN=BCAM PE=1 SV=2 | 5 | 2.71 | 4.08 | 0.2108 |
| tr\|Q8IDH3\|Q8IDH3_PLAF7 Uncharacterized protein OS=Plasmodium falciparum (isolate 3D7) GN=PF13_0273 PE=4 SV=1 | 5 | 2.05 | 2.36 | 0.1247 |
| tr\|Q8I3P8\|Q8I3P8_PLAF7 Uncharacterized protein OS=Plasmodium falciparum (isolate 3D7) GN=PFE1075c PE=4 SV=1 | 5 | 36.39 | 80.24 | 0.3678 |
| sp\|P61970\|NTF2_HUMAN Nuclear transport factor 2 OS=Homo sapiens GN=NUTF2 PE=1 SV=1;tr\|H3BRV9\|H3BRV9_HUMAN Nuclear transport factor 2 (Fragment) OS=Homo sapiens GN=NUTF2 PE=1 SV=1 | 5 | 2.96 | 2.42 | 0.0521 |
| tr\|C6KSQ7\|C6KSQ7_PLAF7 Elongation of fatty acids protein OS=Plasmodium falciparum (isolate 3D7) GN=PFF0290w PE=3 SV=1 | 5 | 2.08 | 2.67 | 0.1567 |
| tr\|Q8IIE5\|Q8IIE5_PLAF7 Conserved Plasmodium protein OS=Plasmodium falciparum (isolate 3D7) GN=PF11_0229 PE=4 SV=2 | 5 | 1.95 | 2.50 | 0.1562 |
| tr\|Q8I332\|Q8I332_PLAF7 Putative uncharacterized protein OS=Plasmodium falciparum (isolate 3D7) GN=PFI0585c PE=4 SV=1 | 5 | 1.52 | 1.28 | 0.0560 |
| tr\|C0H574\|C0H574_PLAF7 Putative uncharacterized protein OS=Plasmodium falciparum (isolate 3D7) GN=PFI1463w PE=4 SV=1 | 5 | 3.25 | 5.91 | 0.2867 |
| tr\|O77349\|O77349_PLAF7 Putative uncharacterized protein OS=Plasmodium falciparum (isolate 3D7) GN=PFC0500w PE=4 SV=2 | 5 | 1.82 | 2.58 | 0.1888 |
| sp\|O15400-2\|STX7_HUMAN Isoform 2 of Syntaxin-7 OS=Homo sapiens GN=STX7;sp\|O15400\|STX7_HUMAN Syntaxin-7 OS=Homo sapiens GN=STX7 PE=1 SV=4 | 5 | 1.35 | 1.40 | 0.0975 |
| tr\|Q8ILR8\|Q8ILR8_PLAF7 Uncharacterized protein OS=Plasmodium falciparum (isolate 3D7) GN=PF14_0176 PE=4 SV=1 | 5 | 1.78 | 2.01 | 0.1193 |
| tr\|Q8IDF9\|Q8IDF9_PLAF7 Inositol-polyphosphate 5-phosphatase OS=Plasmodium falciparum (isolate 3D7) GN=PF13_0285 PE=4 SV=1 | 5 | 1.11 | 1.28 | 0.1241 |
| tr\|C0H5G2\|C0H5G2_PLAF7 Rab11b, GTPase (Fragment) OS=Plasmodium falciparum (isolate 3D7) GN=Rab11b PE=3 SV=1 | 5 | 1.05 | 1.23 | 0.1278 |
| tr\|Q8I457\|Q8I457_PLAF7 ATP-dependent helicase, putative OS=Plasmodium falciparum (isolate 3D7) GN=PFE0215w PE=3 SV=1 | 5 | 0.63 | 0.71 | 0.1146 |
| tr\|Q8ID90\|Q8ID90_PLAF7 Uncharacterized protein OS=Plasmodium falciparum (isolate 3D7) GN=MAL13P1.307 PE=4 SV=1 | 5 | 1.81 | 2.48 | 0.1773 |
| tr\|C0H4A1\|C0H4A1_PLAF7 Uncharacterized protein OS=Plasmodium falciparum (isolate 3D7) GN=PFD0465c PE=4 SV=1 | 5 | 0.35 | 0.31 | 0.0633 |
| tr\|Q8I349\|Q8I349_PLAF7 Putative uncharacterized protein OS=Plasmodium falciparum (isolate 3D7) GN=PFI0500w PE=4 SV=1 | 5 | 0.41 | 0.41 | 0.0916 |
| tr\|C6KSS2\|C6KSS2_PLAF7 G-protein associated signal transduction protein, putative OS=Plasmodium falciparum (isolate 3D7) GN=PFF0365c PE=4 SV=1 | 5 | 0.74 | 0.44 | 0.0206 |
| tr\|Q8IKD1\|Q8IKD1_PLAF7 Uncharacterized protein OS=Plasmodium falciparum (isolate 3D7) GN=PF14_0674 PE=4 SV=1 | 5 | 0.74 | 0.26 | 0.0033 |
| tr\|Q8ILE9\|Q8ILE9_PLAF7 ATP-specific succinyl-CoA synthetase beta subunit, putative OS=Plasmodium falciparum (isolate 3D7) GN=PF14_0295 PE=4 SV=1 | 5 | 0.75 | 0.57 | 0.0428 |
| tr\|C6KT26\|C6KT26_PLAF7 Rhomboid protease ROM10 OS=Plasmodium falciparum (isolate 3D7) GN=ROM10 PE=4 SV=1 | 5 | 0.76 | 0.44 | 0.0183 |
| tr\|Q8I5E2\|Q8I5E2_PLAF7 Cyclin related protein, putative OS=Plasmodium falciparum (isolate 3D7) GN=PFL1335w PE=4 SV=2 | 5 | 0.78 | 0.16 | 0.0004 |
| tr\|Q8I2I3\|Q8I2I3_PLAF7 Putative uncharacterized protein OS=Plasmodium falciparum (isolate 3D7) GN=PFI1620c PE=4 SV=1 | 5 | 0.78 | 0.37 | 0.0095 |
| tr\|Q8I5T8\|Q8I5T8_PLAF7 Uncharacterized protein OS=Plasmodium falciparum (isolate 3D7) GN=PFL0555c PE=4 SV=1 | 5 | 0.79 | 0.38 | 0.0092 |
| tr\|Q8I6T5\|Q8I6T5_PLAF7 Cop-coated vesicle membrane protein p24, putative OS=Plasmodium falciparum (isolate 3D7) GN=PF13_0082 PE=4 SV=1 | 5 | 0.80 | 0.52 | 0.0271 |
| tr\|Q8I5A9\|Q8I5A9_PLAF7 Rab2, GTPase OS=Plasmodium falciparum (isolate 3D7) GN=Rab2 PE=3 SV=1 | 5 | 0.83 | 0.18 | 0.0005 |

| | | | | |
|---|---|---|---|---|
| tr\|Q8I5K3\|Q8I5K3_PLAF7 Uncharacterized protein OS=Plasmodium falciparum (isolate 3D7) GN=PFL1010c PE=4 SV=1 | 5 | 0.84 | 0.17 | 0.0003 |
| sp\|O15173\|PGRC2_HUMAN Membrane-associated progesterone receptor component 2 OS=Homo sapiens GN=PGRMC2 PE=1 SV=1;sp\|O15173-2\|PGRC2_HUMAN Isoform 2 of Membrane-associated progesterone receptor component 2 OS=Homo sapiens GN=PGRMC2 | 5 | 0.85 | 0.55 | 0.0251 |
| tr\|Q8IBU0\|Q8IBU0_PLAF7 Uncharacterized protein OS=Plasmodium falciparum (isolate 3D7) GN=PF07_0066 PE=4 SV=1 | 5 | 0.85 | 0.50 | 0.0193 |
| tr\|Q9NLB0\|Q9NLB0_PLAF7 Putative uncharacterized protein OS=Plasmodium falciparum (isolate 3D7) GN=PFC0282w PE=4 SV=1 | 5 | 0.86 | 0.38 | 0.0071 |
| tr\|C0H5B7\|C0H5B7_PLAF7 Phosphatidylinositol synthase OS=Plasmodium falciparum (isolate 3D7) GN=MAL13P1.82 PE=3 SV=1 | 5 | 0.86 | 0.31 | 0.0033 |
| tr\|Q8IDE5\|Q8IDE5_PLAF7 Protein phosphatase, putative OS=Plasmodium falciparum (isolate 3D7) GN=MAL13P1.275 PE=4 SV=1 | 5 | 0.87 | 0.32 | 0.0037 |
| tr\|Q8I2R6\|Q8I2R6_PLAF7 Putative uncharacterized protein OS=Plasmodium falciparum (isolate 3D7) GN=PFI1185c PE=4 SV=1 | 5 | 0.90 | 0.20 | 0.0005 |
| tr\|Q8IKZ0\|Q8IKZ0_PLAF7 Uncharacterized protein OS=Plasmodium falciparum (isolate 3D7) GN=PF14_0461 PE=4 SV=1 | 5 | 0.90 | 0.12 | 0.0001 |
| sp\|P27797\|CALR_HUMAN Calreticulin OS=Homo sapiens GN=CALR PE=1 SV=1;tr\|K7EJB9\|K7EJB9_HUMAN Calreticulin (Fragment) OS=Homo sapiens GN=CALR PE=1 SV=1 | 5 | 0.90 | 0.41 | 0.0083 |
| tr\|Q8I5P8\|Q8I5P8_PLAF7 Conserved Plasmodium membrane protein OS=Plasmodium falciparum (isolate 3D7) GN=SR10 PE=4 SV=1 | 5 | 0.90 | 0.45 | 0.0110 |
| tr\|C0H516\|C0H516_PLAF7 PfRab7, GTPase OS=Plasmodium falciparum (isolate 3D7) GN=Rab7 PE=3 SV=1 | 5 | 0.90 | 0.27 | 0.0017 |
| tr\|Q8IK65\|Q8IK65_PLAF7 Uncharacterized protein OS=Plasmodium falciparum (isolate 3D7) GN=PF14_0741 PE=4 SV=1;tr\|Q8IK49\|Q8IK49_PLAF7 Uncharacterized protein OS=Plasmodium falciparum (isolate 3D7) GN=PF14_0758 PE=4 SV=1 | 5 | 0.93 | 0.14 | 0.0001 |
| tr\|Q8IIE1\|Q8IIE1_PLAF7 Uncharacterized protein OS=Plasmodium falciparum (isolate 3D7) GN=PF11_0233 PE=4 SV=1 | 5 | 0.94 | 0.19 | 0.0004 |
| sp\|Q9BVM4\|GGACT_HUMAN Gamma-glutamylaminecyclotransferase OS=Homo sapiens GN=GGACT PE=1 SV=2 | 5 | 1.01 | 0.23 | 0.0006 |
| tr\|Q8IIM4\|Q8IIM4_PLAF7 Uncharacterized protein OS=Plasmodium falciparum (isolate 3D7) GN=PF11_0146 PE=4 SV=1 | 5 | 1.01 | 0.27 | 0.0011 |
| tr\|C0H524\|C0H524_PLAF7 P1 nuclease, putative OS=Plasmodium falciparum (isolate 3D7) GN=PFI0385c PE=4 SV=1 | 5 | 1.03 | 0.34 | 0.0024 |
| tr\|Q8I4Y0\|Q8I4Y0_PLAF7 Kinesin-like protein OS=Plasmodium falciparum (isolate 3D7) GN=PFL2165w PE=1 SV=2 | 5 | 1.05 | 0.41 | 0.0047 |
| tr\|F5GWF8\|F5GWF8_HUMAN Atlastin-3 (Fragment) OS=Homo sapiens GN=ATL3 PE=1 SV=1;tr\|F5H6I7\|F5H6I7_HUMAN Atlastin-3 OS=Homo sapiens GN=ATL3 PE=1 SV=1;sp\|Q6DD88\|ATLA3_HUMAN Atlastin-3 OS=Homo sapiens GN=ATL3 PE=1 SV=1 | 5 | 1.06 | 0.12 | 0.0000 |
| tr\|B9ZSI0\|B9ZSI0_PLAF7 Putative uncharacterized protein OS=Plasmodium falciparum (isolate 3D7) GN=PFA_0165c PE=4 SV=1 | 5 | 1.10 | 0.27 | 0.0008 |
| tr\|O96287\|O96287_PLAF7 Pfmc-2TM Maurers cleft two transmembrane protein OS=Plasmodium falciparum (isolate 3D7) GN=MC-2TM PE=4 SV=2;tr\|B9ZSJ3\|B9ZSJ3_PLAF7 Pfmc-2TM Maurers cleft two transmembrane protein OS=Plasmodium falciparum (isolate 3D7) GN=PfMC-2TM | 5 | 1.18 | 0.30 | 0.0010 |
| tr\|Q8IIE2\|Q8IIE2_PLAF7 Uncharacterized protein OS=Plasmodium falciparum (isolate 3D7) GN=PF11_0232 PE=4 SV=1 | 5 | 1.24 | 0.31 | 0.0009 |
| tr\|Q8ID87\|Q8ID87_PLAF7 Uncharacterized protein OS=Plasmodium falciparum (isolate 3D7) GN=PF13_0329 PE=4 SV=1 | 5 | 1.27 | 0.76 | 0.0203 |
| tr\|Q8IM34\|Q8IM34_PLAF7 RNA binding protein, putative OS=Plasmodium falciparum (isolate 3D7) GN=PF14_0057 PE=4 SV=1 | 5 | 1.30 | 0.36 | 0.0012 |
| tr\|O96254\|O96254_PLAF7 Clathrin coat assembly protein, putative OS=Plasmodium falciparum (isolate 3D7) GN=PFB0805c PE=4 SV=1 | 5 | 1.43 | 0.62 | 0.0065 |
| tr\|Q8I2X8\|Q8I2X8_PLAF7 Putative uncharacterized protein OS=Plasmodium falciparum (isolate 3D7) GN=PFI0855w PE=4 SV=1 | 5 | 1.54 | 1.04 | 0.0294 |
| tr\|Q8IFN9\|Q8IFN9_PLAF7 Eukaryotic initiation factor, putative OS=Plasmodium falciparum (isolate 3D7) GN=PFD1070w PE=3 SV=1 | 5 | 1.55 | 0.44 | 0.0014 |
| tr\|Q8ID44\|Q8ID44_PLAF7 Rhoptry protein OS=Plasmodium falciparum (isolate 3D7) GN=PfRhop148 PE=4 SV=1 | 5 | 1.64 | 0.79 | 0.0097 |
| tr\|Q8IJA4\|Q8IJA4_PLAF7 RNA helicase, putative OS=Plasmodium falciparum (isolate 3D7) GN=PF10_0294 PE=4 SV=1 | 5 | 1.68 | 0.79 | 0.0090 |
| tr\|Q8IEJ0\|Q8IEJ0_PLAF7 Uncharacterized protein OS=Plasmodium falciparum (isolate 3D7) GN=MAL13P1.61 PE=4 SV=1 | 5 | 1.77 | 1.07 | 0.0210 |
| tr\|Q8IKG9\|Q8IKG9_PLAF7 Uncharacterized protein OS=Plasmodium falciparum (isolate 3D7) GN=PF14_0636 PE=4 SV=1 | 5 | 1.82 | 0.39 | 0.0005 |

| | | | | |
|---|---|---|---|---|
| tr\|Q8IKS6\|Q8IKS6_PLAF7 Uncharacterized protein OS=Plasmodium falciparum (isolate 3D7) GN=PF14_0526 PE=4 SV=2 | 5 | 1.99 | 0.66 | 0.0025 |
| tr\|Q8IL42\|Q8IL42_PLAF7 Guanine nucleotide exchange factor, putative OS=Plasmodium falciparum (isolate 3D7) GN=PF14_0407 PE=4 SV=1 | 5 | 2.06 | 0.86 | 0.0059 |
| tr\|Q8I3L5\|Q8I3L5_PLAF7 Uncharacterized protein OS=Plasmodium falciparum (isolate 3D7) GN=PFE1245w PE=4 SV=1 | 5 | 2.24 | 1.55 | 0.0320 |
| tr\|Q8IHT3\|Q8IHT3_PLAF7 DNA-directed RNA polymerase I, putative OS=Plasmodium falciparum (isolate 3D7) GN=PF11_0445 PE=4 SV=1 | 5 | 2.31 | 1.22 | 0.0132 |
| tr\|Q8ILP4\|Q8ILP4_PLAF7 Pantothenate kinase, putative OS=Plasmodium falciparum (isolate 3D7) GN=PF14_0200 PE=4 SV=2 | 5 | 2.47 | 1.01 | 0.0054 |
| tr\|Q8IBL5\|Q8IBL5_PLAF7 Uncharacterized protein OS=Plasmodium falciparum (isolate 3D7) GN=PF07_0101 PE=4 SV=1 | 5 | 2.93 | 1.90 | 0.0259 |
| tr\|Q8ID38\|Q8ID38_PLAF7 Skp1 family protein, putative OS=Plasmodium falciparum (isolate 3D7) GN=MAL13P1.337 PE=4 SV=2 | 5 | 2.94 | 1.51 | 0.0122 |
| tr\|Q8IEF5\|Q8IEF5_PLAF7 Exportin 1-like protein, putative OS=Plasmodium falciparum (isolate 3D7) GN=MAL13P1.83 PE=4 SV=1 | 5 | 3.34 | 1.27 | 0.0042 |
| tr\|Q8IBF6\|Q8IBF6_PLAF7 Transcription factor with AP2 domain(S), putative OS=Plasmodium falciparum (isolate 3D7) GN=ApiAP2 PE=4 SV=1 | 5 | 6.06 | 4.05 | 0.0286 |
| tr\|Q8IDY6\|Q8IDY6_PLAF7 Uncharacterized protein OS=Plasmodium falciparum (isolate 3D7) GN=PF13_0190 PE=4 SV=1 | 5 | 42.05 | 27.19 | 0.0259 |
| tr\|Q8I4U9\|Q8I4U9_PLAF7 Conserved protein OS=Plasmodium falciparum (isolate 3D7) GN=PFL2325c PE=4 SV=1 | 4 | 0.41 | 0.17 | 0.0174 |
| tr\|A0A087X243\|A0A087X243_HUMAN Glutathione S-transferase P (Fragment) OS=Homo sapiens GN=GSTP1 PE=1 SV=1;sp\|P09211\|GSTP1_HUMAN Glutathione S-transferase P OS=Homo sapiens GN=GSTP1 PE=1 SV=2 | 4 | 432.44 | 649.17 | 0.2749 |
| tr\|Q8I2V6\|Q8I2V6_PLAF7 Pyridoxal 5-phosphate dependent enzyme class III, putative OS=Plasmodium falciparum (isolate 3D7) GN=PFI0965w PE=3 SV=1 | 4 | 101.39 | 175.24 | 0.3310 |
| tr\|Q8I2U3\|Q8I2U3_PLAF7 Ubiquitin conjugating enzyme, putative OS=Plasmodium falciparum (isolate 3D7) GN=PFI1030c PE=3 SV=1 | 4 | 34.15 | 22.30 | 0.0549 |
| tr\|C6KTE8\|C6KTE8_PLAF7 Pfmc-2TM Maurers cleft two transmembrane protein OS=Plasmodium falciparum (isolate 3D7) GN=PFF1525c PE=4 SV=1 | 4 | 69.06 | 78.32 | 0.1760 |
| tr\|C6KTB3\|C6KTB3_PLAF7 Transportin OS=Plasmodium falciparum (isolate 3D7) GN=PFF1345w PE=4 SV=1 | 4 | 203.07 | 390.03 | 0.3743 |
| tr\|O77363\|O77363_PLAF7 Putative uncharacterized protein OS=Plasmodium falciparum (isolate 3D7) GN=PFC0545c PE=4 SV=2 | 4 | 26.54 | 27.28 | 0.1468 |
| tr\|C0H4Y0\|C0H4Y0_PLAF7 Ubiquitination-mediated degradation component, putative OS=Plasmodium falciparum (isolate 3D7) GN=PF08_0020 PE=4 SV=1 | 4 | 44.23 | 53.68 | 0.1980 |
| tr\|Q8IAT5\|Q8IAT5_PLAF7 Acyl CoA binding protein, putative OS=Plasmodium falciparum (isolate 3D7) GN=PF08_0099 PE=4 SV=1 | 4 | 45.83 | 49.79 | 0.1629 |
| tr\|Q8I278\|Q8I278_PLAF7 Putative uncharacterized protein OS=Plasmodium falciparum (isolate 3D7) GN=PFA_0315w PE=4 SV=1 | 4 | 94.22 | 175.25 | 0.3610 |
| sp\|Q8ILW6\|NMT_PLAF7 Glycylpeptide N-tetradecanoyltransferase OS=Plasmodium falciparum (isolate 3D7) GN=PF14_0127 PE=3 SV=1 | 4 | 72.24 | 131.16 | 0.3511 |
| tr\|Q8IE69\|Q8IE69_PLAF7 Dihydrofolate synthase/folylpolyglutamate synthase OS=Plasmodium falciparum (isolate 3D7) GN=DHFS-FPGS PE=4 SV=1 | 4 | 172.76 | 338.63 | 0.3827 |
| tr\|Q8ILB8\|Q8ILB8_PLAF7 Methionine aminopeptidase 2 OS=Plasmodium falciparum (isolate 3D7) GN=PF14_0327 PE=3 SV=1 | 4 | 164.46 | 317.24 | 0.3761 |
| tr\|Q8IAV0\|Q8IAV0_PLAF7 Methyltransferase, putative OS=Plasmodium falciparum (isolate 3D7) GN=PF08_0092 PE=4 SV=1 | 4 | 171.37 | 306.11 | 0.3444 |
| tr\|O96224\|O96224_PLAF7 Conserved Plasmodium protein OS=Plasmodium falciparum (isolate 3D7) GN=PFB0655c PE=4 SV=2 | 4 | 51.00 | 93.10 | 0.3534 |
| tr\|Q5T0D2\|Q5T0D2_HUMAN UMP-CMP kinase OS=Homo sapiens GN=CMPK1 PE=1 SV=1;sp\|P30085-2\|KCY_HUMAN Isoform 2 of UMP-CMP kinase OS=Homo sapiens GN=CMPK1;sp\|P30085\|KCY_HUMAN UMP-CMP kinase OS=Homo sapiens GN=CMPK1 PE=1 SV=3 | 4 | 139.15 | 272.15 | 0.3817 |
| tr\|Q8IAS1\|Q8IAS1_PLAF7 Ubiquitin regulatory protein, putative OS=Plasmodium falciparum (isolate 3D7) GN=MAL8P1.122 PE=4 SV=1 | 4 | 19.37 | 24.50 | 0.2121 |
| sp\|P60174-1\|TPIS_HUMAN Isoform 2 of Triosephosphate isomerase OS=Homo sapiens GN=TPI1;sp\|P60174\|TPIS_HUMAN Triosephosphate isomerase OS=Homo sapiens GN=TPI1 PE=1 SV=3 | 4 | 47.08 | 88.35 | 0.3647 |
| tr\|Q8IAU0\|Q8IAU0_PLAF7 Protein phosphatase, putative OS=Plasmodium falciparum (isolate 3D7) GN=MAL8P1.108 PE=4 SV=1 | 4 | 29.76 | 29.32 | 0.1354 |
| tr\|Q9U0I2\|Q9U0I2_PLAF7 Uncharacterized protein OS=Plasmodium falciparum (isolate 3D7) GN=PFD0525w PE=4 SV=2 | 4 | 10.39 | 10.00 | 0.1293 |
| sp\|Q8IIU6\|RTCB_PLAF7 tRNA-splicing ligase RtcB homolog OS=Plasmodium falciparum (isolate 3D7) GN=PF11_0068 PE=3 SV=1 | 4 | 44.58 | 80.54 | 0.3491 |

| | | | | |
|---|---|---|---|---|
| tr\|Q8IKP7\|Q8IKP7_PLAF7 Uncharacterized protein OS=Plasmodium falciparum (isolate 3D7) GN=PF14_0557 PE=3 SV=1 | 4 | 47.34 | 90.78 | 0.3736 |
| tr\|Q8I5U8\|Q8I5U8_PLAF7 Uncharacterized protein OS=Plasmodium falciparum (isolate 3D7) GN=PFL0505c PE=4 SV=1 | 4 | 16.21 | 22.22 | 0.2406 |
| sp\|Q8I236\|KAD6_PLAF7 Adenylate kinase isoenzyme 6 homolog OS=Plasmodium falciparum (isolate 3D7) GN=PFA_0530c PE=1 SV=1 | 4 | 17.13 | 17.19 | 0.1402 |
| tr\|Q8ILW7\|Q8ILW7_PLAF7 AAA family ATPase, putative OS=Plasmodium falciparum (isolate 3D7) GN=PF14_0126 PE=3 SV=1 | 4 | 73.58 | 128.78 | 0.3361 |
| tr\|Q8IDU2\|Q8IDU2_PLAF7 Uncharacterized protein OS=Plasmodium falciparum (isolate 3D7) GN=PF13_0215 PE=4 SV=1 | 4 | 8.00 | 6.12 | 0.0795 |
| tr\|Q8IDQ6\|Q8IDQ6_PLAF7 Uncharacterized protein OS=Plasmodium falciparum (isolate 3D7) GN=PF13_0237 PE=4 SV=1 | 4 | 16.64 | 26.40 | 0.2966 |
| tr\|Q8IFP3\|Q8IFP3_PLAF7 Alpha-tubulin ii OS=Plasmodium falciparum (isolate 3D7) GN=PFD1050w PE=3 SV=1 | 4 | 32.98 | 62.32 | 0.3676 |
| tr\|C6KTB6\|C6KTB6_PLAF7 6-pyruvoyltetrahydropterin synthase OS=Plasmodium falciparum (isolate 3D7) GN=PTPS PE=1 SV=1 | 4 | 14.81 | 23.70 | 0.3000 |
| tr\|Q8I4S6\|Q8I4S6_PLAF7 DNA repair protein rhp16, putative OS=Plasmodium falciparum (isolate 3D7) GN=PFL2440w PE=4 SV=1 | 4 | 65.06 | 127.93 | 0.3840 |
| tr\|C0H4V8\|C0H4V8_PLAF7 DNA helicase, putative OS=Plasmodium falciparum (isolate 3D7) GN=MAL8P1.65 PE=4 SV=1 | 4 | 20.01 | 36.54 | 0.3534 |
| tr\|C6KT25\|C6KT25_PLAF7 Malate dehydrogenase OS=Plasmodium falciparum (isolate 3D7) GN=MDH PE=3 SV=1 | 4 | 18.89 | 33.76 | 0.3446 |
| tr\|Q8I301\|Q8I301_PLAF7 Ubiquitin conjugating enzyme, putative OS=Plasmodium falciparum (isolate 3D7) GN=PFI0740c PE=1 SV=1 | 4 | 56.25 | 109.60 | 0.3802 |
| tr\|Q8IM44\|Q8IM44_PLAF7 Uncharacterized protein OS=Plasmodium falciparum (isolate 3D7) GN=PF14_0047 PE=4 SV=1 | 4 | 34.73 | 67.21 | 0.3774 |
| tr\|O77321\|O77321_PLAF7 DNA polymerase epsilon subunit B, putative OS=Plasmodium falciparum (isolate 3D7) GN=PFC0340w PE=4 SV=1 | 4 | 9.06 | 14.64 | 0.3037 |
| tr\|Q8II69\|Q8II69_PLAF7 Uncharacterized protein OS=Plasmodium falciparum (isolate 3D7) GN=PF11_0305 PE=4 SV=1 | 4 | 57.46 | 112.74 | 0.3831 |
| tr\|Q7KQL4\|Q7KQL4_PLAF7 DNA polymerase OS=Plasmodium falciparum (isolate 3D7) GN=PF10_0165 PE=3 SV=1 | 4 | 5.74 | 8.53 | 0.2712 |
| tr\|Q8I469\|Q8I469_PLAF7 Uncharacterized protein OS=Plasmodium falciparum (isolate 3D7) GN=PFE0155w PE=4 SV=1 | 4 | 3.55 | 2.52 | 0.0671 |
| tr\|Q8IBY3\|Q8IBY3_PLAF7 Uncharacterized protein OS=Plasmodium falciparum (isolate 3D7) GN=PF07_0044 PE=4 SV=1 | 4 | 8.40 | 12.13 | 0.2600 |
| tr\|Q8I383\|Q8I383_PLAF7 Putative uncharacterized protein OS=Plasmodium falciparum (isolate 3D7) GN=PFI0325c PE=4 SV=1 | 4 | 3.83 | 4.69 | 0.2009 |
| tr\|C0H4R8\|C0H4R8_PLAF7 Serine/Threonine protein kinase, FIKK family OS=Plasmodium falciparum (isolate 3D7) GN=PfTSTK0 PE=4 SV=1 | 4 | 2.93 | 2.88 | 0.1344 |
| tr\|O97240\|O97240_PLAF7 AP endonuclease (DNA-[apurinic or apyrimidinic site] lyase), putative OS=Plasmodium falciparum (isolate 3D7) GN=PFC0250c PE=4 SV=2 | 4 | 3.43 | 4.54 | 0.2275 |
| tr\|C0H540\|C0H540_PLAF7 Apicoplast Ufd1 OS=Plasmodium falciparum (isolate 3D7) GN=PFI0810c PE=4 SV=1 | 4 | 2.73 | 2.66 | 0.1328 |
| tr\|Q8I3H4\|Q8I3H4_PLAF7 Apicoplast TIC22, putative OS=Plasmodium falciparum (isolate 3D7) GN=PFE1460w PE=4 SV=1 | 4 | 2.79 | 3.08 | 0.1668 |
| tr\|C0H4B9\|C0H4B9_PLAF7 Steroid dehydrogenase, putative OS=Plasmodium falciparum (isolate 3D7) GN=PFD1035w PE=4 SV=1 | 4 | 12.93 | 21.32 | 0.3118 |
| tr\|Q8I4Z4\|Q8I4Z4_PLAF7 Translation initiation factor SUI1, putative OS=Plasmodium falciparum (isolate 3D7) GN=PFL2095w PE=4 SV=1 | 4 | 1.95 | 1.23 | 0.0510 |
| tr\|Q8IBK0\|Q8IBK0_PLAF7 Uncharacterized protein OS=Plasmodium falciparum (isolate 3D7) GN=MAL7P1.138 PE=4 SV=1 | 4 | 1.99 | 1.37 | 0.0626 |
| tr\|C0H529\|C0H529_PLAF7 Small nuclear ribonucleoprotein (SnRNP), putative OS=Plasmodium falciparum (isolate 3D7) GN=PFI0475w PE=4 SV=1 | 4 | 9.24 | 17.26 | 0.3630 |
| tr\|Q8ILQ4\|Q8ILQ4_PLAF7 Uncharacterized protein OS=Plasmodium falciparum (isolate 3D7) GN=PF14_0190 PE=4 SV=1 | 4 | 8.62 | 12.85 | 0.2719 |
| tr\|Q8I485\|Q8I485_PLAF7 Rhoptry-associated protein 3, RAP3 OS=Plasmodium falciparum (isolate 3D7) GN=RAP3 PE=4 SV=1 | 4 | 2.19 | 2.84 | 0.2202 |
| tr\|O97252\|O97252_PLAF7 ATP-dependent Clp protease proteolytic subunit OS=Plasmodium falciparum (isolate 3D7) GN=PFC0310c PE=1 SV=1 | 4 | 2.01 | 2.95 | 0.2664 |
| tr\|Q8I3C0\|Q8I3C0_PLAF7 Serine repeat antigen 9 (SERA-9) OS=Plasmodium falciparum (isolate 3D7) GN=SERA9 PE=3 SV=1 | 4 | 5.06 | 9.13 | 0.3481 |
| tr\|Q8IJG2\|Q8IJG2_PLAF7 Conserved Plasmodium protein OS=Plasmodium falciparum (isolate 3D7) GN=PF10_0236 PE=4 SV=1 | 4 | 1.00 | 0.64 | 0.0518 |
| tr\|O96164\|O96164_PLAF7 Serine repeat antigen 4 (SERA-4) OS=Plasmodium falciparum (isolate 3D7) GN=SERA-4 PE=1 SV=1 | 4 | 6.39 | 10.92 | 0.3269 |

| | | | | |
|---|---|---|---|---|
| tr\|Q8ILZ6\|Q8ILZ6_PLAF7 Phosphatidate cytidylyltransferase OS=Plasmodium falciparum (isolate 3D7) GN=CDS PE=3 SV=1 | 4 | 11.84 | 22.77 | 0.3747 |
| tr\|Q8IBH8\|Q8IBH8_PLAF7 Uncharacterized protein OS=Plasmodium falciparum (isolate 3D7) GN=PF07_0116 PE=4 SV=1 | 4 | 1.03 | 0.86 | 0.0966 |
| tr\|C6KT51\|C6KT51_PLAF7 Uncharacterized protein OS=Plasmodium falciparum (isolate 3D7) GN=PFF1030w PE=4 SV=1 | 4 | 0.99 | 0.67 | 0.0585 |
| tr\|A0A087WVQ6\|A0A087WVQ6_HUMAN Clathrin heavy chain OS=Homo sapiens GN=CLTC PE=1 SV=1;sp\|Q00610-2\|CLH1_HUMAN Isoform 2 of Clathrin heavy chain 1 OS=Homo sapiens GN=CLTC;sp\|Q00610\|CLH1_HUMAN Clathrin heavy chain 1 OS=Homo sapiens GN=CLTC PE=1 SV=5 | 4 | 0.85 | 0.55 | 0.0537 |
| tr\|C0H546\|C0H546_PLAF7 Chaperone protein, putative OS=Plasmodium falciparum (isolate 3D7) GN=PFI0985c PE=4 SV=1 | 4 | 1.89 | 3.03 | 0.3014 |
| tr\|Q8I272\|Q8I272_PLAF7 Centrin-1 OS=Plasmodium falciparum (isolate 3D7) GN=PfCEN1 PE=4 SV=1 | 4 | 2.88 | 4.79 | 0.3153 |
| tr\|Q8I2V7\|Q8I2V7_PLAF7 Dolichyl-diphosphooligosaccharide--protein glycosyltransferase 48 kDa subunit OS=Plasmodium falciparum (isolate 3D7) GN=PFI0960w PE=3 SV=1 | 4 | 1.54 | 2.49 | 0.3044 |
| tr\|G3V3R6\|G3V3R6_HUMAN Galectin OS=Homo sapiens GN=LGALS3 PE=1 SV=1;sp\|P17931\|LEG3_HUMAN Galectin-3 OS=Homo sapiens GN=LGALS3 PE=1 SV=5 | 4 | 0.75 | 0.49 | 0.0544 |
| tr\|Q8I5X5\|Q8I5X5_PLAF7 Uncharacterized protein OS=Plasmodium falciparum (isolate 3D7) GN=PFL0350c PE=4 SV=1 | 4 | 0.55 | 0.44 | 0.0899 |
| tr\|O97232\|O97232_PLAF7 1-cys-glutaredoxin-like protein-1 OS=Plasmodium falciparum (isolate 3D7) GN=PfGLP-1 PE=4 SV=1 | 4 | 0.67 | 0.77 | 0.1784 |
| tr\|Q8ILE4\|Q8ILE4_PLAF7 Qa-SNARE protein, putative OS=Plasmodium falciparum (isolate 3D7) GN=Syn11 PE=4 SV=1 | 4 | 0.41 | 0.30 | 0.0743 |
| tr\|Q8IHT4\|Q8IHT4_PLAF7 Uncharacterized protein OS=Plasmodium falciparum (isolate 3D7) GN=PF11_0443 PE=4 SV=1 | 4 | 0.44 | 0.30 | 0.0611 |
| tr\|C0H4T8\|C0H4T8_PLAF7 Uncharacterized protein OS=Plasmodium falciparum (isolate 3D7) GN=MAL8P1.107 PE=4 SV=1 | 4 | 0.11 | 0.10 | 0.1209 |
| tr\|Q8IEE9\|Q8IEE9_PLAF7 Cholinephosphate cytidylyltransferase OS=Plasmodium falciparum (isolate 3D7) GN=ctP PE=1 SV=1 | 4 | 0.67 | 0.34 | 0.0299 |
| tr\|Q8I1Z2\|Q8I1Z2_PLAF7 CGI-201 protein, short form OS=Plasmodium falciparum (isolate 3D7) GN=PFD0180c PE=4 SV=1 | 4 | 0.67 | 0.29 | 0.0189 |
| tr\|Q8I367\|Q8I367_PLAF7 Putative uncharacterized protein OS=Plasmodium falciparum (isolate 3D7) GN=PFI0405w PE=4 SV=1 | 4 | 0.70 | 0.26 | 0.0122 |
| tr\|C6KSV0\|C6KSV0_PLAF7 Histone H3 OS=Plasmodium falciparum (isolate 3D7) GN=PFF0510w PE=3 SV=1 | 4 | 0.71 | 0.03 | 0.0000 |
| tr\|Q8IAZ5\|Q8IAZ5_PLAF7 Vacuolar sorting protein VPS9, putative OS=Plasmodium falciparum (isolate 3D7) GN=MAL8P1.82 PE=4 SV=1 | 4 | 0.72 | 0.28 | 0.0140 |
| tr\|C0H4K4\|C0H4K4_PLAF7 Uncharacterized protein OS=Plasmodium falciparum (isolate 3D7) GN=MAL7P1.17 PE=4 SV=1 | 4 | 0.72 | 0.24 | 0.0089 |
| tr\|Q8I2T9\|Q8I2T9_PLAF7 Fe-S-cluster redox enzyme, putative OS=Plasmodium falciparum (isolate 3D7) GN=PFI1050c PE=4 SV=1 | 4 | 0.73 | 0.35 | 0.0245 |
| tr\|Q8IHT7\|Q8IHT7_PLAF7 Conserved Plasmodium protein OS=Plasmodium falciparum (isolate 3D7) GN=PF11_0440 PE=4 SV=1 | 4 | 0.77 | 0.36 | 0.0239 |
| tr\|Q8I3J8\|Q8I3J8_PLAF7 Uncharacterized protein OS=Plasmodium falciparum (isolate 3D7) GN=PFE1330c PE=4 SV=1 | 4 | 0.79 | 0.36 | 0.0214 |
| tr\|Q8IE30\|Q8IE30_PLAF7 Uncharacterized protein OS=Plasmodium falciparum (isolate 3D7) GN=PF13_0163 PE=4 SV=1 | 4 | 0.82 | 0.09 | 0.0003 |
| tr\|Q8I5Z2\|Q8I5Z2_PLAF7 Uncharacterized protein OS=Plasmodium falciparum (isolate 3D7) GN=PFL0265w PE=4 SV=1 | 4 | 0.87 | 0.24 | 0.0056 |
| tr\|Q8IHN5\|Q8IHN5_PLAF7 Probable protein OS=Plasmodium falciparum (isolate 3D7) GN=PF11_0505 PE=4 SV=1 | 4 | 0.89 | 0.42 | 0.0237 |
| tr\|Q8I3U9\|Q8I3U9_PLAF7 Protein phosphatase, putative OS=Plasmodium falciparum (isolate 3D7) GN=PFE0795c PE=4 SV=1 | 4 | 0.90 | 0.36 | 0.0158 |
| tr\|Q8ILN2\|Q8ILN2_PLAF7 Ctr copper transporter domain containing protein, putative OS=Plasmodium falciparum (isolate 3D7) GN=PF14_0211 PE=4 SV=1 | 4 | 0.90 | 0.23 | 0.0041 |
| tr\|Q8IKI8\|Q8IKI8_PLAF7 Uncharacterized protein OS=Plasmodium falciparum (isolate 3D7) GN=PF14_0617 PE=4 SV=1 | 4 | 0.91 | 0.32 | 0.0109 |
| tr\|Q8I1X9\|Q8I1X9_PLAF7 ATP-dependent RNA Helicase, putative OS=Plasmodium falciparum (isolate 3D7) GN=PFD0245c PE=4 SV=1 | 4 | 0.93 | 0.26 | 0.0059 |
| tr\|Q8IED7\|Q8IED7_PLAF7 Uncharacterized protein OS=Plasmodium falciparum (isolate 3D7) GN=MAL13P1.93 PE=4 SV=1 | 4 | 0.94 | 0.50 | 0.0324 |
| tr\|E9PHR9\|E9PHR9_HUMAN Phospholipid scramblase 4 OS=Homo sapiens GN=PLSCR4 PE=1 SV=1;sp\|Q9NRQ2-2\|PLS4_HUMAN Isoform 2 of Phospholipid scramblase 4 OS=Homo sapiens GN=PLSCR4;sp\|Q9NRQ2\|PLS4_HUMAN Phospholipid scramblase 4 OS=Homo sapiens GN=PLSCR4 PE=1 SV=2 | 4 | 0.97 | 0.15 | 0.0009 |

| | | | | |
|---|---|---|---|---|
| tr\|Q8IEK5\|Q8IEK5_PLAF7 Uncharacterized protein OS=Plasmodium falciparum (isolate 3D7) GN=MAL13P1.54 PE=4 SV=1 | 4 | 0.98 | 0.45 | 0.0223 |
| sp\|O75955\|FLOT1_HUMAN Flotillin-1 OS=Homo sapiens GN=FLOT1 PE=1 SV=3;sp\|O75955-2\|FLOT1_HUMAN Isoform 2 of Flotillin-1 OS=Homo sapiens GN=FLOT1 | 4 | 0.98 | 0.09 | 0.0002 |
| tr\|Q8I285\|Q8I285_PLAF7 Putative uncharacterized protein OS=Plasmodium falciparum (isolate 3D7) GN=PFA_0275c PE=4 SV=1 | 4 | 0.98 | 0.21 | 0.0027 |
| tr\|Q8I2T7\|Q8I2T7_PLAF7 Tetratricopeptide repeat family protein, putative OS=Plasmodium falciparum (isolate 3D7) GN=PFI1060w PE=4 SV=1 | 4 | 0.98 | 0.36 | 0.0117 |
| tr\|B9ZSJ1\|B9ZSJ1_PLAF7 Putative uncharacterized protein OS=Plasmodium falciparum (isolate 3D7) GN=PFA_0630c PE=4 SV=1 | 4 | 0.99 | 0.55 | 0.0378 |
| tr\|Q8IM09\|Q8IM09_PLAF7 Uncharacterized protein OS=Plasmodium falciparum (isolate 3D7) GN=PF14_0084 PE=4 SV=2 | 4 | 1.01 | 0.18 | 0.0016 |
| sp\|Q92621\|NU205_HUMAN Nuclear pore complex protein Nup205 OS=Homo sapiens GN=NUP205 PE=1 SV=3 | 4 | 1.02 | 0.13 | 0.0006 |
| tr\|Q8IB25\|Q8IB25_PLAF7 Uncharacterized protein OS=Plasmodium falciparum (isolate 3D7) GN=MAL8P1.64 PE=4 SV=1 | 4 | 1.05 | 0.06 | 0.0000 |
| tr\|Q8IM11\|Q8IM11_PLAF7 Uncharacterized protein OS=Plasmodium falciparum (isolate 3D7) GN=PF14_0082 PE=4 SV=1 | 4 | 1.08 | 0.20 | 0.0017 |
| tr\|Q8I6V0\|Q8I6V0_PLAF7 Cysteine proteinase falcipain-1 OS=Plasmodium falciparum (isolate 3D7) GN=PF14_0553 PE=3 SV=1 | 4 | 1.09 | 0.39 | 0.0117 |
| tr\|Q8IEK4\|Q8IEK4_PLAF7 Clathrin-adaptor medium chain, putative OS=Plasmodium falciparum (isolate 3D7) GN=PF13_0062 PE=4 SV=1 | 4 | 1.10 | 0.22 | 0.0021 |
| tr\|O97304\|O97304_PLAF7 SMN-like protein OS=Plasmodium falciparum (isolate 3D7) GN=PFC1050w PE=4 SV=1 | 4 | 1.15 | 0.10 | 0.0002 |
| sp\|Q12931-2\|TRAP1_HUMAN Isoform 2 of Heat shock protein 75 kDa, mitochondrial OS=Homo sapiens GN=TRAP1;sp\|Q12931\|TRAP1_HUMAN Heat shock protein 75 kDa, mitochondrial OS=Homo sapiens GN=TRAP1 PE=1 SV=3 | 4 | 1.20 | 0.08 | 0.0001 |
| tr\|C0H531\|C0H531_PLAF7 DNA primase large subunit, putative OS=Plasmodium falciparum (isolate 3D7) GN=PFI0530c PE=4 SV=1 | 4 | 1.29 | 0.37 | 0.0062 |
| tr\|Q8I3R4\|Q8I3R4_PLAF7 Uncharacterized protein OS=Plasmodium falciparum (isolate 3D7) GN=PFE0985w PE=4 SV=1 | 4 | 1.30 | 0.18 | 0.0007 |
| tr\|Q8IES2\|Q8IES2_PLAF7 Uncharacterized protein OS=Plasmodium falciparum (isolate 3D7) GN=MAL13P1.24 PE=4 SV=1 | 4 | 1.31 | 0.39 | 0.0070 |
| tr\|Q8IHU1\|Q8IHU1_PLAF7 Coproporphyrinogen oxidase, putative OS=Plasmodium falciparum (isolate 3D7) GN=PF11_0436 PE=4 SV=1 | 4 | 1.43 | 0.50 | 0.0109 |
| tr\|Q8I2M0\|Q8I2M0_PLAF7 Putative uncharacterized protein OS=Plasmodium falciparum (isolate 3D7) GN=PFI1425w PE=4 SV=1 | 4 | 1.47 | 0.52 | 0.0107 |
| tr\|Q8ILR6\|Q8ILR6_PLAF7 Ubiquitin fusion degradation protein UFD1, putative OS=Plasmodium falciparum (isolate 3D7) GN=UFD1 PE=4 SV=2 | 4 | 1.83 | 0.70 | 0.0135 |
| tr\|Q8IDH2\|Q8IDH2_PLAF7 MON1 protein OS=Plasmodium falciparum (isolate 3D7) GN=PF13_0274 PE=4 SV=1 | 4 | 1.92 | 0.61 | 0.0079 |
| tr\|Q8ILV1\|Q8ILV1_PLAF7 Serine/threonine-protein phosphatase OS=Plasmodium falciparum (isolate 3D7) GN=PP1 PE=1 SV=1 | 4 | 1.99 | 0.82 | 0.0165 |
| tr\|Q8IEK8\|Q8IEK8_PLAF7 Uncharacterized protein OS=Plasmodium falciparum (isolate 3D7) GN=MAL13P1.52 PE=4 SV=1 | 4 | 2.09 | 1.14 | 0.0349 |
| sp\|O97231\|RL44_PLAF7 60S ribosomal protein L44 OS=Plasmodium falciparum (isolate 3D7) GN=RPL44 PE=1 SV=3 | 4 | 2.27 | 0.98 | 0.0191 |
| tr\|Q8IBT8\|Q8IBT8_PLAF7 Uncharacterized protein OS=Plasmodium falciparum (isolate 3D7) GN=MAL7P1.76 PE=4 SV=1 | 4 | 2.33 | 1.14 | 0.0268 |
| tr\|Q8IJU4\|Q8IJU4_PLAF7 Uncharacterized protein OS=Plasmodium falciparum (isolate 3D7) GN=PF10_0098 PE=4 SV=1 | 4 | 2.50 | 1.52 | 0.0460 |
| tr\|Q8I5P4\|Q8I5P4_PLAF7 Signal recognition particle SRP19, putative OS=Plasmodium falciparum (isolate 3D7) GN=PFL0785c PE=4 SV=1 | 4 | 2.80 | 1.71 | 0.0464 |
| tr\|C6KT92\|C6KT92_PLAF7 Poly(A) polymerase PAP, putative OS=Plasmodium falciparum (isolate 3D7) GN=PFF1240w PE=4 SV=1 | 4 | 5.22 | 3.07 | 0.0424 |
| tr\|C6KSQ8\|C6KSQ8_PLAF7 Uncharacterized protein OS=Plasmodium falciparum (isolate 3D7) GN=PFF0295c PE=4 SV=1 | 4 | 5.51 | 3.29 | 0.0441 |
| tr\|O97253\|O97253_PLAF7 Putative uncharacterized protein OS=Plasmodium falciparum (isolate 3D7) GN=PFC0315c PE=4 SV=2 | 3 | 112.14 | 120.04 | 0.2471 |
| tr\|Q8I3H2\|Q8I3H2_PLAF7 Cell cycle regulator protein, putative OS=Plasmodium falciparum (isolate 3D7) GN=PFE1470w PE=4 SV=1 | 3 | 102.58 | 136.29 | 0.3222 |
| tr\|Q8I5B3\|Q8I5B3_PLAF7 Uncharacterized protein OS=Plasmodium falciparum (isolate 3D7) GN=PFL1480w PE=4 SV=1 | 3 | 68.55 | 95.93 | 0.3414 |
| tr\|Q8IL87\|Q8IL87_PLAF7 eIF2A OS=Plasmodium falciparum (isolate 3D7) GN=PF14_0360 PE=4 SV=1 | 3 | 45.65 | 36.53 | 0.1629 |

| | | | | |
|---|---|---|---|---|
| tr\|Q8I4Y3\|Q8I4Y3_PLAF7 Uncharacterized protein OS=Plasmodium falciparum (isolate 3D7) GN=PFL2150c PE=4 SV=1 | 3 | 147.43 | 240.88 | 0.4002 |
| tr\|Q8ILP0\|Q8ILP0_PLAF7 Uncharacterized protein OS=Plasmodium falciparum (isolate 3D7) GN=PF14_0775 PE=4 SV=1 | 3 | 31.17 | 25.12 | 0.1646 |
| tr\|Q8I3Y0\|Q8I3Y0_PLAF7 Orotate phosphoribosyltransferase OS=Plasmodium falciparum (isolate 3D7) GN=PfOPRT PE=3 SV=1 | 3 | 184.36 | 296.69 | 0.3944 |
| tr\|Q8I257\|Q8I257_PLAF7 Putative uncharacterized protein OS=Plasmodium falciparum (isolate 3D7) GN=PFA_0420w PE=4 SV=1 | 3 | 238.01 | 406.20 | 0.4170 |
| tr\|C6KT19\|C6KT19_PLAF7 Histone H3 OS=Plasmodium falciparum (isolate 3D7) GN=PFF0865w PE=3 SV=1 | 3 | 135.04 | 170.48 | 0.3037 |
| tr\|Q8IDW3\|Q8IDW3_PLAF7 Tryptophan--tRNA ligase, putative OS=Plasmodium falciparum (isolate 3D7) GN=PF13_0205 PE=1 SV=1 | 3 | 279.95 | 480.37 | 0.4191 |
| tr\|C0H5C7\|C0H5C7_PLAF7 RRM containing cyclophilin OS=Plasmodium falciparum (isolate 3D7) GN=PF13_0122 PE=4 SV=1 | 3 | 37.69 | 52.02 | 0.3363 |
| tr\|Q8IDR1\|Q8IDR1_PLAF7 Phosphoenolpyruvate carboxykinase OS=Plasmodium falciparum (isolate 3D7) GN=PEPCK PE=3 SV=1 | 3 | 65.39 | 104.17 | 0.3905 |
| tr\|Q8I384\|Q8I384_PLAF7 Arginase, putative OS=Plasmodium falciparum (isolate 3D7) GN=PFI0320w PE=1 SV=1 | 3 | 75.64 | 120.80 | 0.3915 |
| tr\|Q8IHU8\|Q8IHU8_PLAF7 Uncharacterized protein OS=Plasmodium falciparum (isolate 3D7) GN=PF11_0428 PE=4 SV=1 | 3 | 20.22 | 20.21 | 0.2251 |
| tr\|Q8I5M9\|Q8I5M9_PLAF7 Uncharacterized protein OS=Plasmodium falciparum (isolate 3D7) GN=PFL0865w PE=4 SV=1 | 3 | 54.53 | 60.21 | 0.2573 |
| tr\|C0H5D7\|C0H5D7_PLAF7 Translation initiation factor EIF-2B gamma subunit, putative OS=Plasmodium falciparum (isolate 3D7) GN=MAL13P1.144 PE=4 SV=1 | 3 | 93.20 | 153.30 | 0.4028 |
| tr\|C6KSR7\|C6KSR7_PLAF7 Glutaredoxin-like protein, putative OS=Plasmodium falciparum (isolate 3D7) GN=PFF0340c PE=4 SV=1 | 3 | 70.56 | 105.74 | 0.3672 |
| tr\|Q8I5L7\|Q8I5L7_PLAF7 Formin 2, putative OS=Plasmodium falciparum (isolate 3D7) GN=PFL0925w PE=4 SV=1 | 3 | 25.11 | 26.35 | 0.2406 |
| sp\|Q8IER7\|RPB11_PLAF7 Probable DNA-directed RNA polymerase II subunit RPB11 OS=Plasmodium falciparum (isolate 3D7) GN=PF13_0023 PE=3 SV=1 | 3 | 22.94 | 20.48 | 0.1919 |
| tr\|Q8IAP4\|Q8IAP4_PLAF7 GTPase activator, putative OS=Plasmodium falciparum (isolate 3D7) GN=PF08_0120 PE=4 SV=1 | 3 | 18.89 | 21.11 | 0.2613 |
| tr\|Q8IDC0\|Q8IDC0_PLAF7 Zinc finger protein, putative OS=Plasmodium falciparum (isolate 3D7) GN=PF13_0313 PE=4 SV=1 | 3 | 11.17 | 7.42 | 0.1208 |
| tr\|Q8I638\|Q8I638_PLAF7 Octapeptide-repeat antigen, putative OS=Plasmodium falciparum (isolate 3D7) GN=PFL0035c PE=4 SV=1 | 3 | 13.92 | 10.69 | 0.1528 |
| tr\|Q8IJ89\|Q8IJ89_PLAF7 Uncharacterized protein OS=Plasmodium falciparum (isolate 3D7) GN=PF10_0310 PE=4 SV=1 | 3 | 16.12 | 15.02 | 0.2042 |
| tr\|C0H4U7\|C0H4U7_PLAF7 Uncharacterized protein OS=Plasmodium falciparum (isolate 3D7) GN=PF08_0067 PE=4 SV=1 | 3 | 9.43 | 6.27 | 0.1209 |
| tr\|Q8I324\|Q8I324_PLAF7 Putative uncharacterized protein OS=Plasmodium falciparum (isolate 3D7) GN=PFI0625c PE=4 SV=1 | 3 | 101.09 | 172.60 | 0.4171 |
| tr\|Q8IJS0\|Q8IJS0_PLAF7 Phosphoglucomutase, putative OS=Plasmodium falciparum (isolate 3D7) GN=PF10_0122 PE=3 SV=1 | 3 | 14.33 | 13.16 | 0.2001 |
| tr\|Q8I300\|Q8I300_PLAF7 Putative uncharacterized protein OS=Plasmodium falciparum (isolate 3D7) GN=PFI0745w PE=4 SV=1 | 3 | 19.47 | 30.00 | 0.3779 |
| tr\|Q8I408\|Q8I408_PLAF7 Asparagine-tRNA ligase, putative OS=Plasmodium falciparum (isolate 3D7) GN=PFE0475w PE=3 SV=1 | 3 | 17.96 | 24.57 | 0.3329 |
| tr\|C6KSX9\|C6KSX9_PLAF7 Syntaxin binding protein, putative OS=Plasmodium falciparum (isolate 3D7) GN=PFF0665c PE=4 SV=1 | 3 | 7.46 | 7.98 | 0.2467 |
| tr\|Q8IM03\|Q8IM03_PLAF7 DNA-damage inducible protein, putative OS=Plasmodium falciparum (isolate 3D7) GN=PF14_0090 PE=4 SV=1 | 3 | 7.55 | 8.19 | 0.2512 |
| tr\|Q8ILU4\|Q8ILU4_PLAF7 RNA polymerase small subunit, putative OS=Plasmodium falciparum (isolate 3D7) GN=PF14_0150 PE=4 SV=1 | 3 | 21.03 | 34.10 | 0.3973 |
| sp\|C6KSX0\|PF12_PLAF7 Merozoite surface protein P12 OS=Plasmodium falciparum (isolate 3D7) GN=PF12 PE=1 SV=1 | 3 | 5.37 | 3.04 | 0.0922 |
| tr\|Q8IKS3\|Q8IKS3_PLAF7 Gamma-adaptin, putative OS=Plasmodium falciparum (isolate 3D7) GN=PF14_0529 PE=4 SV=1 | 3 | 9.53 | 12.99 | 0.3318 |
| tr\|Q8IE97\|Q8IE97_PLAF7 Uncharacterized protein OS=Plasmodium falciparum (isolate 3D7) GN=PF13_0125 PE=4 SV=1 | 3 | 5.25 | 4.53 | 0.1823 |
| tr\|Q8IBW5\|Q8IBW5_PLAF7 Pfmc-2TM Maurers cleft two transmembrane protein OS=Plasmodium falciparum (isolate 3D7) GN=PfMC-2TM PE=4 SV=1 | 3 | 10.45 | 15.53 | 0.3640 |
| tr\|Q8IEP9\|Q8IEP9_PLAF7 Vacuolar ATP synthase subunit h, putative OS=Plasmodium falciparum (isolate 3D7) GN=PF13_0034 PE=4 SV=2 | 3 | 6.69 | 8.31 | 0.2976 |
| tr\|Q8IEF7\|Q8IEF7_PLAF7 Methyltransferase, putative OS=Plasmodium falciparum (isolate 3D7) GN=PF13_0087 PE=4 SV=1 | 3 | 6.13 | 6.53 | 0.2454 |

| | | | | |
|---|---|---|---|---|
| tr\|Q8I0V9\|Q8I0V9_PLAF7 mRNA cleavage factor-like protein, putative OS=Plasmodium falciparum (isolate 3D7) GN=PFA_0450c PE=4 SV=1 | 3 | 4.49 | 2.88 | 0.1138 |
| tr\|Q8I448\|Q8I448_PLAF7 Uncharacterized protein OS=Plasmodium falciparum (isolate 3D7) GN=PFE0265c PE=4 SV=1 | 3 | 7.24 | 10.08 | 0.3395 |
| tr\|C6KTE0\|C6KTE0_PLAF7 Microtubule-associated protein ytm1 homologue, putative OS=Plasmodium falciparum (isolate 3D7) GN=PFF1480w PE=4 SV=1 | 3 | 6.14 | 8.41 | 0.3331 |
| sp\|C0H537\|TRM5_PLAF7 tRNA (guanine(37)-N1)-methyltransferase OS=Plasmodium falciparum (isolate 3D7) GN=PFI0700c PE=3 SV=1 | 3 | 5.80 | 7.52 | 0.3137 |
| tr\|Q8I418\|Q8I418_PLAF7 Guanidine nucleotide exchange factor OS=Plasmodium falciparum (isolate 3D7) GN=RCC1 PE=4 SV=1 | 3 | 3.05 | 1.53 | 0.0745 |
| tr\|Q8I3I8\|Q8I3I8_PLAF7 RNA helicase-1 OS=Plasmodium falciparum (isolate 3D7) GN=PFE1390w PE=4 SV=1 | 3 | 4.69 | 5.61 | 0.2845 |
| tr\|Q8IJB9\|Q8IJB9_PLAF7 Uncharacterized protein OS=Plasmodium falciparum (isolate 3D7) GN=PF10_0279 PE=4 SV=1 | 3 | 12.70 | 13.09 | 0.2348 |
| tr\|Q8IKV7\|Q8IKV7_PLAF7 Ribosome biogenesis protein tsr1, putative OS=Plasmodium falciparum (isolate 3D7) GN=PF14_0494 PE=4 SV=1 | 3 | 4.49 | 4.90 | 0.2534 |
| tr\|Q8IKD6\|Q8IKD6_PLAF7 Uncharacterized protein OS=Plasmodium falciparum (isolate 3D7) GN=PF14_0669 PE=4 SV=2 | 3 | 2.39 | 1.03 | 0.0568 |
| tr\|C0H5A6\|C0H5A6_PLAF7 Uncharacterized protein OS=Plasmodium falciparum (isolate 3D7) GN=MAL13P1.39 PE=4 SV=1 | 3 | 2.89 | 2.36 | 0.1688 |
| tr\|Q8ID49\|Q8ID49_PLAF7 Uncharacterized protein OS=Plasmodium falciparum (isolate 3D7) GN=PF13_0347 PE=4 SV=1 | 3 | 2.45 | 1.63 | 0.1212 |
| tr\|C6S3B4\|C6S3B4_PLAF7 Conserved protein OS=Plasmodium falciparum (isolate 3D7) GN=PFB0423c PE=4 SV=1 | 3 | 3.92 | 3.19 | 0.1676 |
| tr\|Q8I5E1\|Q8I5E1_PLAF7 Uncharacterized protein OS=Plasmodium falciparum (isolate 3D7) GN=PFL1340c PE=4 SV=1 | 3 | 9.36 | 14.95 | 0.3917 |
| sp\|O96185\|YPF08_PLAF7 Uncharacterized protein PFB0460c OS=Plasmodium falciparum (isolate 3D7) GN=PFB0460c PE=3 SV=1 | 3 | 2.88 | 3.07 | 0.2448 |
| tr\|Q8I634\|Q8I634_PLAF7 Protein with DNAJ domain (Resa-like), putative OS=Plasmodium falciparum (isolate 3D7) GN=PFL0055c PE=4 SV=1 | 3 | 2.53 | 2.26 | 0.1919 |
| tr\|Q8IBE8\|Q8IBE8_PLAF7 Erythrocyte binding antigen 175 OS=Plasmodium falciparum (isolate 3D7) GN=eba-175 PE=1 SV=2 | 3 | 2.00 | 0.98 | 0.0713 |
| tr\|Q8I241\|Q8I241_PLAF7 DNA-directed RNA polymerase 2, putative OS=Plasmodium falciparum (isolate 3D7) GN=PFA_0505c PE=4 SV=1 | 3 | 3.20 | 4.17 | 0.3153 |
| tr\|Q8IJQ1\|Q8IJQ1_PLAF7 Cdk7, putative OS=Plasmodium falciparum (isolate 3D7) GN=PF10_0141 PE=4 SV=1 | 3 | 6.19 | 8.62 | 0.3396 |
| tr\|C0H4X1\|C0H4X1_PLAF7 U5 snrnp-specific protein, putative OS=Plasmodium falciparum (isolate 3D7) GN=MAL8P1.43 PE=4 SV=1 | 3 | 1.75 | 0.72 | 0.0528 |
| tr\|Q8ILB4\|Q8ILB4_PLAF7 Cytochrome c oxidase assembly protein, putative OS=Plasmodium falciparum (isolate 3D7) GN=PF14_0331 PE=4 SV=1 | 3 | 2.70 | 3.22 | 0.2830 |
| tr\|O96278\|O96278_PLAF7 Plasmodium exported protein (Hyp9) OS=Plasmodium falciparum (isolate 3D7) GN=PFB0930w PE=4 SV=2 | 3 | 2.03 | 1.68 | 0.1717 |
| tr\|Q8IHX8\|Q8IHX8_PLAF7 Conserved Plasmodium protein OS=Plasmodium falciparum (isolate 3D7) GN=PF11_0398 PE=4 SV=2 | 3 | 8.94 | 14.72 | 0.4031 |
| tr\|Q8II33\|Q8II33_PLAF7 Conserved Plasmodium protein OS=Plasmodium falciparum (isolate 3D7) GN=PF11_0341 PE=4 SV=1 | 3 | 1.62 | 0.81 | 0.0741 |
| tr\|Q8ILJ7\|Q8ILJ7_PLAF7 Phosphoenolpyruvate carboxylase, putative OS=Plasmodium falciparum (isolate 3D7) GN=PF14_0246 PE=4 SV=1 | 3 | 2.08 | 1.79 | 0.1819 |
| tr\|Q8IKN0\|Q8IKN0_PLAF7 Uncharacterized protein OS=Plasmodium falciparum (isolate 3D7) GN=PF14_0574 PE=4 SV=1 | 3 | 2.22 | 2.39 | 0.2480 |
| tr\|C6KSU9\|C6KSU9_PLAF7 Uncharacterized protein OS=Plasmodium falciparum (isolate 3D7) GN=PFF0505c PE=4 SV=1 | 3 | 1.55 | 0.66 | 0.0562 |
| tr\|Q8I5H9\|Q8I5H9_PLAF7 Mitochondrial carrier protein, putative OS=Plasmodium falciparum (isolate 3D7) GN=PFL1145w PE=3 SV=1 | 3 | 2.27 | 2.66 | 0.2776 |
| tr\|C0H474\|C0H474_PLAF7 Vesicle transport v-SNARE protein, putative OS=Plasmodium falciparum (isolate 3D7) GN=PFC0582c PE=4 SV=1 | 3 | 3.00 | 3.17 | 0.2427 |
| tr\|Q8ILQ9\|Q8ILQ9_PLAF7 ATP-dependent RNA Helicase, putative OS=Plasmodium falciparum (isolate 3D7) GN=PF14_0185 PE=4 SV=1 | 3 | 3.12 | 4.41 | 0.3448 |
| tr\|Q8IC04\|Q8IC04_PLAF7 Heat shock protein 86 family protein OS=Plasmodium falciparum (isolate 3D7) GN=PF07_0030 PE=4 SV=1 | 3 | 1.70 | 1.60 | 0.2056 |
| tr\|Q8IJ90\|Q8IJ90_PLAF7 Uncharacterized protein OS=Plasmodium falciparum (isolate 3D7) GN=PF10_0309 PE=3 SV=1 | 3 | 1.74 | 1.60 | 0.2001 |
| tr\|Q8I226\|Q8I226_PLAF7 TatD-like deoxyribonuclease, putative OS=Plasmodium falciparum (isolate 3D7) GN=PFA_0580c PE=4 SV=1 | 3 | 1.45 | 0.98 | 0.1241 |
| tr\|Q8IE80\|Q8IE80_PLAF7 Uncharacterized protein OS=Plasmodium falciparum (isolate 3D7) GN=MAL13P1.130 PE=4 SV=1 | 3 | 1.21 | 0.85 | 0.1328 |

| | | | | |
|---|---|---|---|---|
| tr\|C0H4A7\|C0H4A7_PLAF7 Uncharacterized protein OS=Plasmodium falciparum (isolate 3D7) GN=PFD0795w PE=4 SV=1 | 3 | 1.03 | 0.45 | 0.0574 |
| tr\|Q8IEU2\|Q8IEU2_PLAF7 Plasmodium falciparum gamete antigen 27/25 OS=Plasmodium falciparum (isolate 3D7) GN=pfg27-25 PE=1 SV=1 | 3 | 1.10 | 0.78 | 0.1349 |
| tr\|C6KSV0\|C6KSV0_PLAF7 Histone H3 OS=Plasmodium falciparum (isolate 3D7) GN=PFF0510w PE=3 SV=1;tr\|C6KT19\|C6KT19_PLAF7 Histone H3 OS=Plasmodium falciparum (isolate 3D7) GN=PFF0865w PE=3 SV=1 | 3 | 0.99 | 0.45 | 0.0615 |
| tr\|Q8IBZ8\|Q8IBZ8_PLAF7 Cg1 protein OS=Plasmodium falciparum (isolate 3D7) GN=PF07_0035 PE=4 SV=1 | 3 | 0.48 | 0.16 | 0.0362 |
| tr\|C0H5E0\|C0H5E0_PLAF7 Uncharacterized protein OS=Plasmodium falciparum (isolate 3D7) GN=MAL13P1.360 PE=4 SV=1 | 3 | 1.18 | 0.94 | 0.1604 |
| tr\|Q8IHX4\|Q8IHX4_PLAF7 Uncharacterized protein OS=Plasmodium falciparum (isolate 3D7) GN=PF11_0402 PE=4 SV=1 | 3 | 1.62 | 1.76 | 0.2530 |
| tr\|Q6ZLZ9\|Q6ZLZ9_PLAF7 Alpha tubulin OS=Plasmodium falciparum (isolate 3D7) GN=PFI0180w PE=3 SV=1;tr\|Q8IFP3\|Q8IFP3_PLAF7 Alpha-tubulin ii OS=Plasmodium falciparum (isolate 3D7) GN=PFD1050w PE=3 SV=1 | 3 | 1.15 | 1.12 | 0.2179 |
| tr\|Q8I5T7\|Q8I5T7_PLAF7 Minichromosome maintenance protein, putative OS=Plasmodium falciparum (isolate 3D7) GN=PFL0560c PE=3 SV=2 | 3 | 0.98 | 0.61 | 0.1083 |
| tr\|Q8I2R0\|Q8I2R0_PLAF7 Splicing factor 3A OS=Plasmodium falciparum (isolate 3D7) GN=PFI1215w PE=4 SV=1 | 3 | 2.59 | 3.37 | 0.3145 |
| tr\|Q8IBU8\|Q8IBU8_PLAF7 Uncharacterized protein OS=Plasmodium falciparum (isolate 3D7) GN=PF07_0061 PE=4 SV=1 | 3 | 2.30 | 3.57 | 0.3805 |
| tr\|C0H5B4\|C0H5B4_PLAF7 Uncharacterized protein OS=Plasmodium falciparum (isolate 3D7) GN=MAL13P1.71 PE=4 SV=1 | 3 | 0.74 | 0.39 | 0.0809 |
| tr\|Q8I581\|Q8I581_PLAF7 Uncharacterized protein OS=Plasmodium falciparum (isolate 3D7) GN=PFL1645w PE=4 SV=1 | 3 | 2.39 | 3.83 | 0.3929 |
| tr\|Q8II88\|Q8II88_PLAF7 Uncharacterized protein OS=Plasmodium falciparum (isolate 3D7) GN=PF11_0286 PE=4 SV=1 | 3 | 0.70 | 0.46 | 0.1176 |
| tr\|Q8IHP4\|Q8IHP4_PLAF7 Mitochondrial ATP synthase delta subunit, putative OS=Plasmodium falciparum (isolate 3D7) GN=PF11_0485 PE=4 SV=1 | 3 | 2.40 | 3.50 | 0.3557 |
| tr\|Q8I0X1\|Q8I0X1_PLAF7 3-methyl-2-oxobutanoate dehydrogenase (Lipoamide), putative OS=Plasmodium falciparum (isolate 3D7) GN=PFE0225w PE=4 SV=1 | 3 | 0.61 | 0.33 | 0.0827 |
| tr\|Q8ILJ0\|Q8ILJ0_PLAF7 Uncharacterized protein OS=Plasmodium falciparum (isolate 3D7) GN=PF14_0253 PE=4 SV=2 | 3 | 1.00 | 1.14 | 0.2679 |
| tr\|Q8IE65\|Q8IE65_PLAF7 Uncharacterized protein OS=Plasmodium falciparum (isolate 3D7) GN=m26-32-10 PE=4 SV=1 | 3 | 1.84 | 2.91 | 0.3878 |
| tr\|Q8I2C5\|Q8I2C5_PLAF7 Rifin OS=Plasmodium falciparum (isolate 3D7) GN=RIF PE=4 SV=1 | 3 | 0.75 | 0.57 | 0.1508 |
| tr\|Q8IM43\|Q8IM43_PLAF7 Uncharacterized protein OS=Plasmodium falciparum (isolate 3D7) GN=PF14_0048 PE=4 SV=2 | 3 | 0.65 | 0.50 | 0.1542 |
| tr\|Q8I356\|Q8I356_PLAF7 Putative uncharacterized protein OS=Plasmodium falciparum (isolate 3D7) GN=PFI0465c PE=4 SV=1 | 3 | 0.73 | 0.58 | 0.1614 |
| tr\|Q8I528\|Q8I528_PLAF7 Dna gyrase subunit b, putative OS=Plasmodium falciparum (isolate 3D7) GN=PFL1915w PE=3 SV=1 | 3 | 0.73 | 0.69 | 0.2057 |
| tr\|Q8IFN1\|Q8IFN1_PLAF7 Uncharacterized protein OS=Plasmodium falciparum (isolate 3D7) GN=PFD1110w PE=4 SV=1 | 3 | 0.58 | 0.05 | 0.0023 |
| tr\|C6KSN1\|C6KSN1_PLAF7 Uncharacterized protein OS=Plasmodium falciparum (isolate 3D7) GN=PFF0150c PE=4 SV=1 | 3 | 0.72 | 0.57 | 0.1603 |
| tr\|Q8ILV6\|Q8ILV6_PLAF7 DNAJ protein, putative OS=Plasmodium falciparum (isolate 3D7) GN=PF14_0137 PE=4 SV=1 | 3 | 0.65 | 0.60 | 0.2013 |
| tr\|Q8I1V2\|Q8I1V2_PLAF7 Phosphoglycerate mutase, putative OS=Plasmodium falciparum (isolate 3D7) GN=PFD0660w PE=1 SV=1 | 3 | 0.61 | 0.69 | 0.2625 |
| tr\|Q8IJQ8\|Q8IJQ8_PLAF7 Uncharacterized protein OS=Plasmodium falciparum (isolate 3D7) GN=PF10_0134 PE=4 SV=1 | 3 | 0.86 | 1.15 | 0.3234 |
| tr\|Q8IBZ5\|Q8IBZ5_PLAF7 Cg7 protein OS=Plasmodium falciparum (isolate 3D7) GN=PF07_0038 PE=4 SV=1 | 3 | 0.43 | 0.26 | 0.0996 |
| tr\|Q8ID33\|Q8ID33_PLAF7 NADH-cytochrome B5 reductase, putative OS=Plasmodium falciparum (isolate 3D7) GN=PF13_0353 PE=4 SV=1 | 3 | 0.31 | 0.18 | 0.0951 |
| sp\|Q53TN4-3\|CYBR1_HUMAN Isoform 3 of Cytochrome b reductase 1 OS=Homo sapiens GN=CYBRD1;sp\|Q53TN4\|CYBR1_HUMAN Cytochrome b reductase 1 OS=Homo sapiens GN=CYBRD1 PE=1 SV=1 | 3 | 0.75 | 0.67 | 0.1951 |
| tr\|Q8IE87\|Q8IE87_PLAF7 Uncharacterized protein OS=Plasmodium falciparum (isolate 3D7) GN=MAL13P1.128 PE=4 SV=1 | 3 | 0.29 | 0.36 | 0.2979 |
| sp\|O14556\|G3PT_HUMAN Glyceraldehyde-3-phosphate dehydrogenase, testis-specific OS=Homo sapiens GN=GAPDHS PE=1 SV=2 | 3 | 0.48 | 0.41 | 0.1804 |

| | | | | |
|---|---|---|---|---|
| tr\|Q8I3U0\|Q8I3U0_PLAF7 Transcription factor with AP2 domain(S), putative OS=Plasmodium falciparum (isolate 3D7) GN=PFE0840c PE=4 SV=1 | 3 | 0.26 | 0.35 | 0.3228 |
| tr\|Q8IBM6\|Q8IBM6_PLAF7 Uncharacterized protein OS=Plasmodium falciparum (isolate 3D7) GN=PF07_0093 PE=4 SV=1 | 3 | 0.67 | 0.11 | 0.0088 |
| tr\|Q8IIK5\|Q8IIK5_PLAF7 Moving junction protein OS=Plasmodium falciparum (isolate 3D7) GN=RON4 PE=4 SV=2 | 3 | 0.70 | 0.12 | 0.0100 |
| sp\|Q8IFN0\|YD115_PLAF7 Uncharacterized protein PFD1115c OS=Plasmodium falciparum (isolate 3D7) GN=PFD1115c PE=2 SV=1 | 3 | 0.71 | 0.11 | 0.0083 |
| tr\|Q8IKD2\|Q8IKD2_PLAF7 RAP protein, putative OS=Plasmodium falciparum (isolate 3D7) GN=PF14_0673 PE=4 SV=1 | 3 | 0.77 | 0.11 | 0.0072 |
| tr\|C6S3L1\|C6S3L1_PLAF7 Erythrocyte membrane protein 1, PfEMP1 OS=Plasmodium falciparum (isolate 3D7) GN=PFL1970w PE=4 SV=1 | 3 | 0.79 | 0.23 | 0.0272 |
| tr\|R4GN98\|R4GN98_HUMAN Protein S100 (Fragment) OS=Homo sapiens GN=S100A6 PE=1 SV=1;sp\|P06703\|S10A6_HUMAN Protein S100-A6 OS=Homo sapiens GN=S100A6 PE=1 SV=1 | 3 | 0.79 | 0.15 | 0.0113 |
| tr\|O96202\|O96202_PLAF7 Mitochondrial ribosomal protein L12, putative OS=Plasmodium falciparum (isolate 3D7) GN=PFB0545c PE=4 SV=2 | 3 | 0.85 | 0.08 | 0.0028 |
| tr\|Q8IK58\|Q8IK58_PLAF7 Uncharacterized protein OS=Plasmodium falciparum (isolate 3D7) GN=PF14_0748 PE=4 SV=2 | 3 | 0.88 | 0.06 | 0.0017 |
| tr\|Q8IKY8\|Q8IKY8_PLAF7 Chloroquine resistance marker protein OS=Plasmodium falciparum (isolate 3D7) GN=PF14_0463 PE=4 SV=1 | 3 | 0.88 | 0.15 | 0.0093 |
| tr\|Q8I233\|Q8I233_PLAF7 Replication factor c protein, putative OS=Plasmodium falciparum (isolate 3D7) GN=PFA_0545c PE=4 SV=1 | 3 | 0.88 | 0.20 | 0.0172 |
| tr\|E9PK54\|E9PK54_HUMAN Heat shock cognate 71 kDa protein (Fragment) OS=Homo sapiens GN=HSPA8 PE=1 SV=4 | 3 | 0.89 | 0.30 | 0.0359 |
| sp\|O15439-2\|MRP4_HUMAN Isoform 2 of Multidrug resistance-associated protein 4 OS=Homo sapiens GN=ABCC4;sp\|O15439\|MRP4_HUMAN Multidrug resistance-associated protein 4 OS=Homo sapiens GN=ABCC4 PE=1 SV=3 | 3 | 0.90 | 0.12 | 0.0056 |
| sp\|Q8IAW3\|RU1C_PLAF7 U1 small nuclear ribonucleoprotein C OS=Plasmodium falciparum (isolate 3D7) GN=PF08_0084 PE=3 SV=1 | 3 | 0.90 | 0.11 | 0.0053 |
| tr\|Q8IB47\|Q8IB47_PLAF7 ATP-dependent RNA helicase prh1, putative OS=Plasmodium falciparum (isolate 3D7) GN=PF08_0042 PE=4 SV=1 | 3 | 0.94 | 0.21 | 0.0161 |
| tr\|Q8IC17\|Q8IC17_PLAF7 Origin recognition complex subunit 2, putative OS=Plasmodium falciparum (isolate 3D7) GN=PfORC2 PE=4 SV=1 | 3 | 1.00 | 0.11 | 0.0039 |
| tr\|Q8IDF2\|Q8IDF2_PLAF7 Uncharacterized protein OS=Plasmodium falciparum (isolate 3D7) GN=PF13_0290 PE=4 SV=1 | 3 | 1.01 | 0.20 | 0.0123 |
| tr\|Q8IIY8\|Q8IIY8_PLAF7 Plasmodium falciparum Maurers Cleft 2 transmembrane domain protein 11.1, PfMC-2TM_11.1 OS=Plasmodium falciparum (isolate 3D7) GN=MC-2TM PE=4 SV=2;tr\|C0H504\|C0H504_PLAF7 Pfmc-2TM Maurers cleft two transmembrane protein OS=Plasmodium | 3 | 1.01 | 0.17 | 0.0090 |
| tr\|C0H587\|C0H587_PLAF7 Putative uncharacterized protein OS=Plasmodium falciparum (isolate 3D7) GN=PFI1615w PE=4 SV=1 | 3 | 1.04 | 0.14 | 0.0061 |
| tr\|Q8ID65\|Q8ID65_PLAF7 Uncharacterized protein OS=Plasmodium falciparum (isolate 3D7) GN=PF13_0339 PE=4 SV=1 | 3 | 1.06 | 0.23 | 0.0153 |
| tr\|C0H5C0\|C0H5C0_PLAF7 Enhancer of polycomb-like protein OS=Plasmodium falciparum (isolate 3D7) GN=MAL13P1.88 PE=3 SV=1 | 3 | 1.06 | 0.32 | 0.0295 |
| tr\|O96234\|O96234_PLAF7 Conserved Plasmodium protein OS=Plasmodium falciparum (isolate 3D7) GN=PFB0705w PE=4 SV=1 | 3 | 1.07 | 0.06 | 0.0009 |
| tr\|O97289\|O97289_PLAF7 Peptidase, putative OS=Plasmodium falciparum (isolate 3D7) GN=PFC0950c PE=4 SV=2 | 3 | 1.11 | 0.14 | 0.0050 |
| tr\|Q8IM64\|Q8IM64_PLAF7 40S ribosomal protein S31/UBI, putative OS=Plasmodium falciparum (isolate 3D7) GN=PF14_0027 PE=4 SV=1 | 3 | 1.14 | 0.24 | 0.0142 |
| tr\|Q8IHP2\|Q8IHP2_PLAF7 Conserved Plasmodium protein OS=Plasmodium falciparum (isolate 3D7) GN=PF11_0487 PE=4 SV=1 | 3 | 1.14 | 0.30 | 0.0218 |
| tr\|H7C2G2\|H7C2G2_HUMAN NAD(P)(+)--arginine ADP-ribosyltransferase (Fragment) OS=Homo sapiens GN=ART4 PE=1 SV=1;sp\|Q93070\|NAR4_HUMAN Ecto-ADP-ribosyltransferase 4 OS=Homo sapiens GN=ART4 PE=2 SV=2 | 3 | 1.15 | 0.31 | 0.0232 |
| tr\|Q9U0H1\|Q9U0H1_PLAF7 DNA polymerase OS=Plasmodium falciparum (isolate 3D7) GN=PFD0590c PE=3 SV=2 | 3 | 1.17 | 0.32 | 0.0244 |
| tr\|B9ZSJ3\|B9ZSJ3_PLAF7 Pfmc-2TM Maurers cleft two transmembrane protein OS=Plasmodium falciparum (isolate 3D7) GN=PfMC-2TM PE=4 SV=1;tr\|O96287\|O96287_PLAF7 Pfmc-2TM Maurers cleft two transmembrane protein OS=Plasmodium falciparum (isolate 3D7) GN=MC-2TM | 3 | 1.18 | 0.15 | 0.0057 |
| tr\|Q8I5G0\|Q8I5G0_PLAF7 Uncharacterized protein OS=Plasmodium falciparum (isolate 3D7) GN=PFL1240c PE=4 SV=1 | 3 | 1.20 | 0.16 | 0.0056 |
| tr\|O96279\|O96279_PLAF7 Cytoadherence linked asexual protein 2 OS=Plasmodium falciparum (isolate 3D7) GN=PFB0935w PE=4 SV=2 | 3 | 1.22 | 0.20 | 0.0084 |

| | | | | |
|---|---|---|---|---|
| tr\|Q8IL01\|Q8IL01_PLAF7 Uncharacterized protein OS=Plasmodium falciparum (isolate 3D7) GN=PF14_0449 PE=4 SV=1 | 3 | 1.31 | 0.13 | 0.0032 |
| tr\|Q8IEP4\|Q8IEP4_PLAF7 U3 small nucleolar RNA-associated protein 6, putative OS=Plasmodium falciparum (isolate 3D7) GN=PF13_0035 PE=4 SV=1 | 3 | 1.33 | 0.05 | 0.0004 |
| tr\|Q8IDV9\|Q8IDV9_PLAF7 Exoribonuclease, putative OS=Plasmodium falciparum (isolate 3D7) GN=PF13_0208 PE=4 SV=1 | 3 | 1.34 | 0.40 | 0.0291 |
| tr\|C0H4M5\|C0H4M5_PLAF7 Uncharacterized protein OS=Plasmodium falciparum (isolate 3D7) GN=MAL7P1.31 PE=4 SV=1 | 3 | 1.37 | 0.27 | 0.0124 |
| tr\|Q8IB88\|Q8IB88_PLAF7 Uncharacterized protein OS=Plasmodium falciparum (isolate 3D7) GN=PF08_0026 PE=4 SV=1 | 3 | 1.42 | 0.56 | 0.0475 |
| tr\|Q8IEP7\|Q8IEP7_PLAF7 RED-like protein, putative OS=Plasmodium falciparum (isolate 3D7) GN=MAL13P1.34 PE=4 SV=1 | 3 | 1.43 | 0.37 | 0.0212 |
| sp\|Q8I1N6\|AP2A_PLAF7 AP2/ERF domain-containing protein PFD0985w OS=Plasmodium falciparum (isolate 3D7) GN=PFD0985w PE=3 SV=2 | 3 | 1.46 | 0.22 | 0.0076 |
| tr\|Q8IER6\|Q8IER6_PLAF7 Uncharacterized protein OS=Plasmodium falciparum (isolate 3D7) GN=PF13_0024 PE=4 SV=1 | 3 | 1.47 | 0.35 | 0.0187 |
| tr\|Q8I5B5\|Q8I5B5_PLAF7 Uncharacterized protein OS=Plasmodium falciparum (isolate 3D7) GN=PFL1470c PE=4 SV=1 | 3 | 1.49 | 0.48 | 0.0332 |
| tr\|O97334\|O97334_PLAF7 Regulatory protein, putative OS=Plasmodium falciparum (isolate 3D7) GN=PFC0100c PE=4 SV=2 | 3 | 2.13 | 0.16 | 0.0019 |
| tr\|Q8I4R0\|Q8I4R0_PLAF7 Uncharacterized protein OS=Plasmodium falciparum (isolate 3D7) GN=PFL2530w PE=4 SV=1 | 3 | 2.30 | 0.25 | 0.0038 |
| tr\|C0H5A0\|C0H5A0_PLAF7 Uncharacterized protein OS=Plasmodium falciparum (isolate 3D7) GN=MAL13P1.26 PE=4 SV=1 | 3 | 4.18 | 0.97 | 0.0173 |
| sp\|Q8I4T1\|VPS26_PLAF7 Vacuolar protein sorting-associated protein 26 OS=Plasmodium falciparum (isolate 3D7) GN=PFL2415w PE=3 SV=1 | 3 | 4.28 | 1.13 | 0.0225 |
| tr\|Q8IC33\|Q8IC33_PLAF7 Uncharacterized protein OS=Plasmodium falciparum (isolate 3D7) GN=MAL7P1.14 PE=4 SV=1 | 2 | 144.86 | 39.87 | 0.1224 |
| tr\|H3BRV9\|H3BRV9_HUMAN Nuclear transport factor 2 (Fragment) OS=Homo sapiens GN=NUTF2 PE=1 SV=1;sp\|P61970\|NTF2_HUMAN Nuclear transport factor 2 OS=Homo sapiens GN=NUTF2 PE=1 SV=1 | 2 | 765.32 | 1073.59 | 0.4974 |
| sp\|P34931\|HS71L_HUMAN Heat shock 70 kDa protein 1-like OS=Homo sapiens GN=HSPA1L PE=1 SV=2 | 2 | 104.97 | 72.23 | 0.2883 |
| tr\|Q8IKM8\|Q8IKM8_PLAF7 Ubiquitin carboxyl-terminal hydrolase OS=Plasmodium falciparum (isolate 3D7) GN=PF14_0576 PE=1 SV=2 | 2 | 198.92 | 257.39 | 0.4717 |
| tr\|Q8IIR2\|Q8IIR2_PLAF7 rRNA processing protein, putative OS=Plasmodium falciparum (isolate 3D7) GN=PF11_0105 PE=4 SV=2 | 2 | 96.04 | 74.62 | 0.3198 |
| sp\|Q8ILC2\|TGTL_PLAF7 Queuine tRNA-ribosyltransferase-like protein OS=Plasmodium falciparum (isolate 3D7) GN=PF14_0322 PE=3 SV=1 | 2 | 93.91 | 105.18 | 0.4264 |
| tr\|Q8IIX6\|Q8IIX6_PLAF7 Uncharacterized protein OS=Plasmodium falciparum (isolate 3D7) GN=PF11_0036 PE=4 SV=1 | 2 | 99.27 | 121.95 | 0.4553 |
| tr\|C0H5I9\|C0H5I9_PLAF7 GTP binding protein, putative OS=Plasmodium falciparum (isolate 3D7) GN=MAL13P1.294 PE=4 SV=1 | 2 | 177.59 | 244.57 | 0.4916 |
| tr\|O77306\|O77306_PLAF7 Serine/threonine protein kinase, putative OS=Plasmodium falciparum (isolate 3D7) GN=PFC0105w PE=4 SV=1 | 2 | 51.22 | 50.04 | 0.3848 |
| tr\|Q8I1Q0\|Q8I1Q0_PLAF7 Uncharacterized protein OS=Plasmodium falciparum (isolate 3D7) GN=PFD0905w PE=4 SV=1 | 2 | 86.75 | 112.29 | 0.4718 |
| tr\|Q8IAW2\|Q8IAW2_PLAF7 Ubiquitin conjugating enzyme, putative OS=Plasmodium falciparum (isolate 3D7) GN=PF08_0085 PE=3 SV=1 | 2 | 62.15 | 73.27 | 0.4424 |
| tr\|Q8IJX5\|Q8IJX5_PLAF7 Uncharacterized protein OS=Plasmodium falciparum (isolate 3D7) GN=PF10_0066 PE=4 SV=1 | 2 | 106.89 | 144.41 | 0.4855 |
| tr\|C6KT96\|C6KT96_PLAF7 Uncharacterized protein OS=Plasmodium falciparum (isolate 3D7) GN=PFF1260c PE=4 SV=1 | 2 | 151.72 | 209.96 | 0.4931 |
| tr\|Q8ILW8\|Q8ILW8_PLAF7 Deoxyhypusine synthase OS=Plasmodium falciparum (isolate 3D7) GN=PF14_0125 PE=4 SV=1 | 2 | 58.56 | 71.72 | 0.4544 |
| tr\|Q8I3U1\|Q8I3U1_PLAF7 Ubiquitin carboxyl-terminal hydrolase OS=Plasmodium falciparum (isolate 3D7) GN=PFE0835w PE=3 SV=1 | 2 | 78.83 | 103.91 | 0.4776 |
| tr\|Q8IM69\|Q8IM69_PLAF7 Exopolyphosphatase, putative OS=Plasmodium falciparum (isolate 3D7) GN=PF14_0022 PE=4 SV=2 | 2 | 51.86 | 62.22 | 0.4479 |
| tr\|C6KSZ9\|C6KSZ9_PLAF7 Uncharacterized protein OS=Plasmodium falciparum (isolate 3D7) GN=PFF0765c PE=4 SV=1 | 2 | 82.03 | 111.71 | 0.4880 |
| tr\|Q8IBN7\|Q8IBN7_PLAF7 P36-like protein homologue, putative OS=Plasmodium falciparum (isolate 3D7) GN=MAL7P1.114 PE=4 SV=2 | 2 | 98.12 | 135.98 | 0.4935 |
| tr\|Q8IJ70\|Q8IJ70_PLAF7 Ubiquitin-conjugating enzyme, putative OS=Plasmodium falciparum (isolate 3D7) GN=PF10_0330 PE=1 SV=1 | 2 | 53.01 | 69.89 | 0.4777 |

| | | | | |
|---|---|---|---|---|
| tr\|Q8I365\|Q8I365_PLAF7 Putative tRNA (cytidine(32)/guanosine(34)-2-O)-methyltransferase OS=Plasmodium falciparum (isolate 3D7) GN=PFI0415c PE=3 SV=1 | 2 | 28.70 | 30.19 | 0.4071 |
| tr\|Q8I2N3\|Q8I2N3_PLAF7 Putative uncharacterized protein OS=Plasmodium falciparum (isolate 3D7) GN=PFI1355w PE=4 SV=1 | 2 | 45.95 | 60.72 | 0.4784 |
| tr\|Q8I3M2\|Q8I3M2_PLAF7 Uncharacterized protein OS=Plasmodium falciparum (isolate 3D7) GN=PFE1210c PE=4 SV=1 | 2 | 21.67 | 20.33 | 0.3728 |
| tr\|Q8IKA7\|Q8IKA7_PLAF7 GTPase activator, putative OS=Plasmodium falciparum (isolate 3D7) GN=PF14_0699 PE=4 SV=1 | 2 | 20.40 | 19.77 | 0.3825 |
| tr\|C0H5J9\|C0H5J9_PLAF7 Uncharacterized protein OS=Plasmodium falciparum (isolate 3D7) GN=MAL13P1.308 PE=4 SV=1 | 2 | 39.91 | 52.40 | 0.4764 |
| tr\|C0H468\|C0H468_PLAF7 Putative uncharacterized protein OS=Plasmodium falciparum (isolate 3D7) GN=PFC0080c PE=4 SV=1 | 2 | 119.72 | 168.03 | 0.4976 |
| tr\|Q8I2Q6\|Q8I2Q6_PLAF7 Methyltransferase, putative OS=Plasmodium falciparum (isolate 3D7) GN=PFI1235w PE=4 SV=1 | 2 | 71.39 | 99.48 | 0.4953 |
| tr\|Q8IM68\|Q8IM68_PLAF7 Uncharacterized protein OS=Plasmodium falciparum (isolate 3D7) GN=PF14_0023 PE=4 SV=1 | 2 | 46.60 | 64.45 | 0.4929 |
| tr\|Q8IHX6\|Q8IHX6_PLAF7 Conserved Plasmodium protein OS=Plasmodium falciparum (isolate 3D7) GN=PF11_0400 PE=4 SV=2 | 2 | 10.50 | 5.78 | 0.2361 |
| tr\|Q8IL59\|Q8IL59_PLAF7 Uncharacterized protein OS=Plasmodium falciparum (isolate 3D7) GN=PF14_0390 PE=4 SV=1 | 2 | 42.22 | 58.15 | 0.4916 |
| tr\|Q8I668\|Q8I668_PLAF7 Conserved Plasmodium protein OS=Plasmodium falciparum (isolate 3D7) GN=PFB0161c PE=4 SV=2 | 2 | 11.38 | 8.97 | 0.3238 |
| tr\|C0H4E6\|C0H4E6_PLAF7 Uncharacterized protein OS=Plasmodium falciparum (isolate 3D7) GN=PFE0900w PE=4 SV=1 | 2 | 12.31 | 12.11 | 0.3870 |
| tr\|Q8IKX8\|Q8IKX8_PLAF7 Rrp6 homologue, putative OS=Plasmodium falciparum (isolate 3D7) GN=PF14_0473 PE=4 SV=1 | 2 | 38.20 | 52.62 | 0.4916 |
| sp\|Q8IKN4\|NNRE_PLAF7 NAD(P)H-hydrate epimerase OS=Plasmodium falciparum (isolate 3D7) GN=PF14_0570 PE=3 SV=2 | 2 | 10.32 | 8.71 | 0.3424 |
| tr\|Q8I2P8\|Q8I2P8_PLAF7 Protein kinase, putative OS=Plasmodium falciparum (isolate 3D7) GN=PFI1280c PE=4 SV=1 | 2 | 44.25 | 61.50 | 0.4945 |
| tr\|O96129\|O96129_PLAF7 Conserved Plasmodium protein OS=Plasmodium falciparum (isolate 3D7) GN=PFB0125c PE=4 SV=3 | 2 | 7.78 | 3.09 | 0.1743 |
| tr\|Q8II65\|Q8II65_PLAF7 Conserved Plasmodium protein OS=Plasmodium falciparum (isolate 3D7) GN=PF11_0309 PE=4 SV=1 | 2 | 12.26 | 13.79 | 0.4279 |
| tr\|Q8IB55\|Q8IB55_PLAF7 RNA polymerase II mediator complex protein MED7, putative OS=Plasmodium falciparum (isolate 3D7) GN=PF08_0037 PE=4 SV=1 | 2 | 18.95 | 24.68 | 0.4737 |
| tr\|Q8I5V6\|Q8I5V6_PLAF7 Lsm7 homologue, putative OS=Plasmodium falciparum (isolate 3D7) GN=PFL0460w PE=4 SV=1 | 2 | 56.04 | 78.59 | 0.4973 |
| PE=1 SV=1;tr\|Q8I6U5\|Q8I6U5_PLAF7 Falcipain-2, putative OS=Plasmodium falciparum (isolate 3D7) GN=PF11_0161 PE=3 SV=1 | 2 | 6.86 | 0.00 | 0.0002 |
| tr\|C0H4F3\|C0H4F3_PLAF7 BIS(5-nucleosyl)-tetraphosphatase (Diadenosine tetraphosphatase), putative OS=Plasmodium falciparum (isolate 3D7) GN=PFE1035c PE=3 SV=1 | 2 | 8.64 | 8.14 | 0.3738 |
| tr\|Q8IE78\|Q8IE78_PLAF7 Uncharacterized protein OS=Plasmodium falciparum (isolate 3D7) GN=PF13_0136 PE=4 SV=1 | 2 | 13.47 | 16.72 | 0.4587 |
| tr\|Q8ILJ6\|Q8ILJ6_PLAF7 Uncharacterized protein OS=Plasmodium falciparum (isolate 3D7) GN=PF14_0247 PE=4 SV=2 | 2 | 6.76 | 4.84 | 0.2982 |
| tr\|Q8IL23\|Q8IL23_PLAF7 Uncharacterized protein OS=Plasmodium falciparum (isolate 3D7) GN=PF14_0427 PE=4 SV=1 | 2 | 5.50 | 1.31 | 0.1060 |
| tr\|Q8IKU9\|Q8IKU9_PLAF7 Uncharacterized protein OS=Plasmodium falciparum (isolate 3D7) GN=PF14_0502 PE=4 SV=2 | 2 | 10.19 | 12.86 | 0.4636 |
| sp\|P68371\|TBB4B_HUMAN Tubulin beta-4B chain OS=Homo sapiens GN=TUBB4B PE=1 SV=1;sp\|P04350\|TBB4A_HUMAN Tubulin beta-4A chain OS=Homo sapiens GN=TUBB4A PE=1 SV=2 | 2 | 5.15 | 4.32 | 0.3408 |
| tr\|Q8ID21\|Q8ID21_PLAF7 Uncharacterized protein OS=Plasmodium falciparum (isolate 3D7) GN=MAL13P1.347 PE=4 SV=1 | 2 | 12.55 | 16.75 | 0.4817 |
| tr\|Q8I577\|Q8I577_PLAF7 Conserved Plasmodium protein OS=Plasmodium falciparum (isolate 3D7) GN=PFL1665c PE=4 SV=1 | 2 | 12.03 | 16.01 | 0.4809 |
| tr\|O97303\|O97303_PLAF7 Putative uncharacterized protein OS=Plasmodium falciparum (isolate 3D7) GN=PFC1060c PE=4 SV=1 | 2 | 7.12 | 8.36 | 0.4410 |
| tr\|Q8ILG1\|Q8ILG1_PLAF7 Uncharacterized protein OS=Plasmodium falciparum (isolate 3D7) GN=PF14_0282 PE=4 SV=1 | 2 | 4.71 | 3.76 | 0.3271 |
| tr\|O77335\|O77335_PLAF7 YT521-B-like family protein, putative OS=Plasmodium falciparum (isolate 3D7) GN=PFC0410w PE=4 SV=2 | 2 | 5.11 | 4.73 | 0.3691 |
| tr\|Q8I3P1\|Q8I3P1_PLAF7 Uncharacterized protein OS=Plasmodium falciparum (isolate 3D7) GN=PFE1110w PE=4 SV=1 | 2 | 4.37 | 2.90 | 0.2795 |

| | | | | |
|---|---|---|---|---|
| tr\|C0H4S0\|C0H4S0_PLAF7 AAA family ATPase, putative OS=Plasmodium falciparum (isolate 3D7) GN=PF08_0117 PE=4 SV=1 | 2 | 18.28 | 25.30 | 0.4931 |
| tr\|Q8IAV6\|Q8IAV6_PLAF7 Uncharacterized protein OS=Plasmodium falciparum (isolate 3D7) GN=PF08_0089 PE=4 SV=1 | 2 | 11.95 | 16.18 | 0.4864 |
| tr\|Q8I3H0\|Q8I3H0_PLAF7 Uncharacterized protein OS=Plasmodium falciparum (isolate 3D7) GN=PFE1485w PE=4 SV=1 | 2 | 13.08 | 17.86 | 0.4888 |
| tr\|Q8IIK7\|Q8IIK7_PLAF7 Uncharacterized protein OS=Plasmodium falciparum (isolate 3D7) GN=PF11_0166 PE=4 SV=1 | 2 | 3.53 | 2.39 | 0.2843 |
| tr\|C0H4K8\|C0H4K8_PLAF7 40S ribosomal protein S29, putative OS=Plasmodium falciparum (isolate 3D7) GN=MAL7P1.300 PE=1 SV=1 | 2 | 2.83 | 0.87 | 0.1357 |
| tr\|C0H473\|C0H473_PLAF7 Co-chaperone p23, putative OS=Plasmodium falciparum (isolate 3D7) GN=PFC0581w PE=4 SV=1 | 2 | 3.78 | 3.73 | 0.3874 |
| tr\|C6KT21\|C6KT21_PLAF7 Uncharacterized protein OS=Plasmodium falciparum (isolate 3D7) GN=PFF0875w PE=4 SV=1 | 2 | 3.09 | 2.11 | 0.2859 |
| tr\|Q8I553\|Q8I553_PLAF7 Ubiquitin activating enzyme, putative OS=Plasmodium falciparum (isolate 3D7) GN=PFL1790w PE=4 SV=1 | 2 | 3.75 | 3.80 | 0.3958 |
| tr\|Q8IDZ6\|Q8IDZ6_PLAF7 Ubiquitin-activating enzyme, putative OS=Plasmodium falciparum (isolate 3D7) GN=PF13_0182 PE=4 SV=1 | 2 | 4.71 | 5.56 | 0.4424 |
| tr\|Q8IDE8\|Q8IDE8_PLAF7 Histone-lysine N-methyltransferase, putative OS=Plasmodium falciparum (isolate 3D7) GN=PF13_0293 PE=4 SV=1 | 2 | 2.79 | 1.43 | 0.2214 |
| sp\|Q9Y6M5\|ZNT1_HUMAN Zinc transporter 1 OS=Homo sapiens GN=SLC30A1 PE=1 SV=3 | 2 | 3.70 | 3.84 | 0.4031 |
| tr\|Q8I3X2\|Q8I3X2_PLAF7 Uncharacterized protein OS=Plasmodium falciparum (isolate 3D7) GN=PFE0670w PE=4 SV=1 | 2 | 3.67 | 3.89 | 0.4096 |
| tr\|Q8IC31\|Q8IC31_PLAF7 Uncharacterized protein OS=Plasmodium falciparum (isolate 3D7) GN=MAL7P1.15 PE=4 SV=1 | 2 | 3.39 | 3.47 | 0.3993 |
| tr\|C6S3D0\|C6S3D0_PLAF7 Conserved Plasmodium protein OS=Plasmodium falciparum (isolate 3D7) GN=PF10_0177b PE=4 SV=1 | 2 | 3.90 | 4.44 | 0.4318 |
| sp\|P01116-2\|RASK_HUMAN Isoform 2B of GTPase KRas OS=Homo sapiens GN=KRAS;sp\|P01116\|RASK_HUMAN GTPase KRas OS=Homo sapiens GN=KRAS PE=1 SV=1;sp\|P01111\|RASN_HUMAN GTPase NRas OS=Homo sapiens GN=NRAS PE=1 SV=1 | 2 | 3.62 | 3.99 | 0.4210 |
| tr\|Q8IJI5\|Q8IJI5_PLAF7 Conserved Plasmodium protein OS=Plasmodium falciparum (isolate 3D7) GN=PF10_0212a PE=4 SV=2 | 2 | 3.60 | 3.99 | 0.4233 |
| tr\|C6KTE4\|C6KTE4_PLAF7 DEAD/DEAH box ATP-dependent RNA helicase, putative OS=Plasmodium falciparum (isolate 3D7) GN=PFF1500c PE=3 SV=1 | 2 | 2.10 | 0.48 | 0.1013 |
| tr\|Q8ILD6\|Q8ILD6_PLAF7 Uncharacterized protein OS=Plasmodium falciparum (isolate 3D7) GN=PF14_0308 PE=4 SV=1 | 2 | 18.03 | 25.33 | 0.4980 |
| tr\|Q8IB11\|Q8IB11_PLAF7 MAC/Perforin, putative OS=Plasmodium falciparum (isolate 3D7) GN=PF08_0058 PE=4 SV=1 | 2 | 2.64 | 2.54 | 0.3799 |
| tr\|Q8I2M7\|Q8I2M7_PLAF7 Putative uncharacterized protein OS=Plasmodium falciparum (isolate 3D7) GN=PFI1385c PE=4 SV=1 | 2 | 1.93 | 0.28 | 0.0659 |
| tr\|Q8IJK1\|Q8IJK1_PLAF7 Uncharacterized protein OS=Plasmodium falciparum (isolate 3D7) GN=PF10_0194 PE=4 SV=1 | 2 | 2.60 | 2.49 | 0.3788 |
| tr\|Q8II45\|Q8II45_PLAF7 Uncharacterized protein OS=Plasmodium falciparum (isolate 3D7) GN=PF11_0329 PE=4 SV=1 | 2 | 2.77 | 2.87 | 0.4021 |
| tr\|Q8IKB8\|Q8IKB8_PLAF7 Pre-mRNA-splicing factor ISY1 homolog, putative OS=Plasmodium falciparum (isolate 3D7) GN=PF14_0688 PE=4 SV=1 | 2 | 12.54 | 17.54 | 0.4964 |
| sp\|Q7K734\|FEN1_PLAF7 Flap endonuclease 1 OS=Plasmodium falciparum (isolate 3D7) GN=FEN1 PE=3 SV=1 | 2 | 3.19 | 3.74 | 0.4411 |
| tr\|C0H5C1\|C0H5C1_PLAF7 Uncharacterized protein OS=Plasmodium falciparum (isolate 3D7) GN=MAL13P1.90 PE=4 SV=1 | 2 | 1.78 | 0.15 | 0.0387 |
| tr\|Q8I224\|Q8I224_PLAF7 Plasmoredoxin OS=Plasmodium falciparum (isolate 3D7) GN=Plrx PE=4 SV=1 | 2 | 6.84 | 9.34 | 0.4892 |
| tr\|Q8I2R5\|Q8I2R5_PLAF7 Putative uncharacterized protein OS=Plasmodium falciparum (isolate 3D7) GN=PFI1190w PE=4 SV=1 | 2 | 1.91 | 1.16 | 0.2591 |
| tr\|Q8IM73\|Q8IM73_PLAF7 Uncharacterized protein OS=Plasmodium falciparum (isolate 3D7) GN=PF14_0018 PE=4 SV=2 | 2 | 1.69 | 0.09 | 0.0229 |
| tr\|Q8I6T7\|Q8I6T7_PLAF7 ATP synthase subunit gamma OS=Plasmodium falciparum (isolate 3D7) GN=PF13_0061 PE=3 SV=1 | 2 | 1.84 | 1.12 | 0.2585 |
| sp\|P27797\|CALR_HUMAN Calreticulin OS=Homo sapiens GN=CALR PE=1 SV=1 | 2 | 2.09 | 1.85 | 0.3555 |
| tr\|Q8IED9\|Q8IED9_PLAF7 Uncharacterized protein OS=Plasmodium falciparum (isolate 3D7) GN=MAL13P1.91 PE=4 SV=1 | 2 | 1.64 | 0.22 | 0.0600 |
| tr\|Q8IIK3\|Q8IIK3_PLAF7 Cyclophilin, putative OS=Plasmodium falciparum (isolate 3D7) GN=PF11_0170 PE=3 SV=1 | 2 | 1.67 | 0.48 | 0.1289 |

| | | | | |
|---|---|---|---|---|
| tr\|Q8ILB7\|Q8ILB7_PLAF7 Mitochondrial import inner membrane translocase subunit Tim17, putative OS=Plasmodium falciparum (isolate 3D7) GN=PF14_0328 PE=4 SV=1 | 2 | 2.09 | 1.94 | 0.3703 |
| tr\|H0Y564\|H0Y564_HUMAN Anaphase-promoting complex subunit 1 (Fragment) OS=Homo sapiens GN=ANAPC1 PE=1 SV=1;sp\|Q9H1A4\|APC1_HUMAN Anaphase-promoting complex subunit 1 OS=Homo sapiens GN=ANAPC1 PE=1 SV=1 | 2 | 1.56 | 0.30 | 0.0870 |
| tr\|C0H5B3\|C0H5B3_PLAF7 Uncharacterized protein OS=Plasmodium falciparum (isolate 3D7) GN=MAL13P1.70 PE=4 SV=1 | 2 | 1.59 | 0.58 | 0.1606 |
| tr\|E9PNW4\|E9PNW4_HUMAN CD59 glycoprotein OS=Homo sapiens GN=CD59 PE=1 SV=1;tr\|E9PR17\|E9PR17_HUMAN CD59 glycoprotein OS=Homo sapiens GN=CD59 PE=1 SV=1;sp\|P13987\|CD59_HUMAN CD59 glycoprotein OS=Homo sapiens GN=CD59 PE=1 SV=1 | 2 | 1.64 | 0.90 | 0.2360 |
| tr\|Q8I2Z9\|Q8I2Z9_PLAF7 Putative uncharacterized protein OS=Plasmodium falciparum (isolate 3D7) GN=PFI0750c PE=4 SV=1 | 2 | 1.51 | 0.14 | 0.0429 |
| tr\|Q8IFM9\|Q8IFM9_PLAF7 Early transcribed membrane protein 4, ETRAMP4 OS=Plasmodium falciparum (isolate 3D7) GN=ETRAMP4 PE=4 SV=1 | 2 | 1.53 | 0.35 | 0.1019 |
| tr\|Q8IEE3\|Q8IEE3_PLAF7 Uncharacterized protein OS=Plasmodium falciparum (isolate 3D7) GN=PF13_0098 PE=4 SV=1 | 2 | 1.53 | 0.43 | 0.1250 |
| tr\|C0H5H6\|C0H5H6_PLAF7 Uncharacterized protein OS=Plasmodium falciparum (isolate 3D7) GN=MAL13P1.234 PE=4 SV=1 | 2 | 1.59 | 0.82 | 0.2218 |
| sp\|P62805\|H4_HUMAN Histone H4 OS=Homo sapiens GN=HIST1H4A PE=1 SV=2 | 2 | 3.30 | 4.17 | 0.4650 |
| tr\|Q8IHW8\|Q8IHW8_PLAF7 Conserved Plasmodium protein OS=Plasmodium falciparum (isolate 3D7) GN=PF11_0408 PE=4 SV=1 | 2 | 1.49 | 0.52 | 0.1545 |
| tr\|C0H4A9\|C0H4A9_PLAF7 Uncharacterized protein OS=Plasmodium falciparum (isolate 3D7) GN=PFD0815c:exon:2 PE=4 SV=1 | 2 | 2.31 | 2.55 | 0.4227 |
| tr\|O96267\|O96267_PLAF7 Chromatin-binding protein, putative OS=Plasmodium falciparum (isolate 3D7) GN=PFB0875c PE=4 SV=3 | 2 | 1.46 | 0.68 | 0.2012 |
| tr\|C0H4V4\|C0H4V4_PLAF7 Uncharacterized protein OS=Plasmodium falciparum (isolate 3D7) GN=MAL8P1.73 PE=4 SV=1 | 2 | 2.53 | 3.01 | 0.4444 |
| tr\|Q8IC06\|Q8IC06_PLAF7 O-sialoglycoprotein endopeptidase, putative OS=Plasmodium falciparum (isolate 3D7) GN=MAL7P1.26 PE=4 SV=1 | 2 | 1.60 | 1.21 | 0.3127 |
| tr\|Q8I3G7\|Q8I3G7_PLAF7 Uncharacterized protein OS=Plasmodium falciparum (isolate 3D7) GN=PFE1500c PE=4 SV=1 | 2 | 1.58 | 1.18 | 0.3096 |
| tr\|Q8I5J4\|Q8I5J4_PLAF7 Uncharacterized protein OS=Plasmodium falciparum (isolate 3D7) GN=PFL1055c PE=4 SV=1 | 2 | 1.36 | 0.36 | 0.1178 |
| sp\|P30043\|BLVRB_HUMAN Flavin reductase (NADPH) OS=Homo sapiens GN=BLVRB PE=1 SV=3;tr\|M0R192\|M0R192_HUMAN Flavin reductase (NADPH) OS=Homo sapiens GN=BLVRB PE=1 SV=1;tr\|M0QZL1\|M0QZL1_HUMAN Flavin reductase (NADPH) OS=Homo sapiens GN=BLVRB PE=1 SV=1 | 2 | 1.52 | 1.08 | 0.2978 |
| tr\|Q8IKM0\|Q8IKM0_PLAF7 Mitochondrial ribosomal protein S4/S9, putative OS=Plasmodium falciparum (isolate 3D7) GN=PF14_0584 PE=4 SV=1 | 2 | 1.59 | 1.28 | 0.3296 |
| tr\|Q8IBN1\|Q8IBN1_PLAF7 Uncharacterized protein OS=Plasmodium falciparum (isolate 3D7) GN=MAL7P1.119 PE=4 SV=1 | 2 | 1.45 | 0.90 | 0.2635 |
| sp\|Q9UKV8-2\|AGO2_HUMAN Isoform 2 of Protein argonaute-2 OS=Homo sapiens GN=AGO2;sp\|Q9UKV8\|AGO2_HUMAN Protein argonaute-2 OS=Homo sapiens GN=AGO2 PE=1 SV=3 | 2 | 1.87 | 1.93 | 0.4021 |
| tr\|Q8IK01\|Q8IK01_PLAF7 Uncharacterized protein OS=Plasmodium falciparum (isolate 3D7) GN=PF10_0039 PE=4 SV=1 | 2 | 1.47 | 1.05 | 0.2987 |
| tr\|C0H4M0\|C0H4M0_PLAF7 Rifin-like protein OS=Plasmodium falciparum (isolate 3D7) GN=RAMA PE=4 SV=1 | 2 | 1.38 | 0.81 | 0.2504 |
| tr\|Q8IKQ5\|Q8IKQ5_PLAF7 ATPase, putative OS=Plasmodium falciparum (isolate 3D7) GN=PF14_0548 PE=4 SV=1 | 2 | 1.95 | 2.15 | 0.4228 |
| tr\|C6KSZ6\|C6KSZ6_PLAF7 Cyclin-dependent protein kinase, predicted OS=Plasmodium falciparum (isolate 3D7) GN=Pfcrk-5 PE=4 SV=1 | 2 | 1.23 | 0.43 | 0.1548 |
| tr\|Q8ILY1\|Q8ILY1_PLAF7 Pfprex OS=Plasmodium falciparum (isolate 3D7) GN=POM1 PE=4 SV=1 | 2 | 1.29 | 0.76 | 0.2493 |
| tr\|C6KTD4\|C6KTD4_PLAF7 Sec14-like cytosolic factor or phosphatidylinositol/phosphatidylcholine transfer protein, putative OS=Plasmodium falciparum (isolate 3D7) GN=PFF1450w PE=4 SV=1 | 2 | 16.56 | 23.36 | 0.4992 |
| tr\|Q8I5A4\|Q8I5A4_PLAF7 Pre-mRNA splicing factor RNA helicase, putative OS=Plasmodium falciparum (isolate 3D7) GN=PFL1525c PE=4 SV=1 | 2 | 1.15 | 0.31 | 0.1212 |
| tr\|Q8I416\|Q8I416_PLAF7 ATP-dependent RNA Helicase, putative OS=Plasmodium falciparum (isolate 3D7) GN=PFE0430w PE=3 SV=1 | 2 | 1.18 | 0.56 | 0.2050 |
| sp\|P61026\|RAB10_HUMAN Ras-related protein Rab-10 OS=Homo sapiens GN=RAB10 PE=1 SV=1 | 2 | 1.11 | 0.12 | 0.0475 |
| tr\|Q8IIU9\|Q8IIU9_PLAF7 Conserved Plasmodium protein OS=Plasmodium falciparum (isolate 3D7) GN=PF11_0064 PE=4 SV=2 | 2 | 1.16 | 0.57 | 0.2118 |

| | | | | |
|---|---|---|---|---|
| tr\|Q8IK49\|Q8IK49_PLAF7 Uncharacterized protein OS=Plasmodium falciparum (isolate 3D7) GN=PF14_0758 PE=4 SV=1;tr\|Q8IK65\|Q8IK65_PLAF7 Uncharacterized protein OS=Plasmodium falciparum (isolate 3D7) GN=PF14_0741 PE=4 SV=1 | 2 | 1.08 | 0.00 | 0.0015 |
| tr\|Q8I254\|Q8I254_PLAF7 Putative uncharacterized protein OS=Plasmodium falciparum (isolate 3D7) GN=PFA_0435w PE=3 SV=1 | 2 | 1.08 | 0.06 | 0.0264 |
| tr\|Q8I525\|Q8I525_PLAF7 Conserved Plasmodium protein OS=Plasmodium falciparum (isolate 3D7) GN=PFL1930w PE=4 SV=1 | 2 | 1.08 | 0.02 | 0.0096 |
| tr\|Q8I5I8\|Q8I5I8_PLAF7 Glideosome-associated protein 45 OS=Plasmodium falciparum (isolate 3D7) GN=GAP45 PE=4 SV=1 | 2 | 1.18 | 0.70 | 0.2517 |
| tr\|Q8IDK3\|Q8IDK3_PLAF7 Uncharacterized protein OS=Plasmodium falciparum (isolate 3D7) GN=MAL13P1.250 PE=4 SV=1 | 2 | 1.08 | 0.23 | 0.0961 |
| sp\|O75955\|FLOT1_HUMAN Flotillin-1 OS=Homo sapiens GN=FLOT1 PE=1 SV=3;sp\|O75955-2\|FLOT1_HUMAN Isoform 2 of Flotillin-1 OS=Homo sapiens GN=FLOT1;tr\|A2AB10\|A2AB10_HUMAN Flotillin-1 (Fragment) OS=Homo sapiens GN=FLOT1 PE=1 SV=1 | 2 | 1.05 | 0.01 | 0.0058 |
| sp\|Q8I423\|PF38_PLAF7 Merozoite surface protein P38 OS=Plasmodium falciparum (isolate 3D7) GN=PFS38 PE=1 SV=1 | 2 | 1.44 | 1.41 | 0.3853 |
| tr\|Q8IM01\|Q8IM01_PLAF7 Uncharacterized protein OS=Plasmodium falciparum (isolate 3D7) GN=PF14_0092 PE=4 SV=2 | 2 | 1.06 | 0.37 | 0.1554 |
| sp\|Q14254\|FLOT2_HUMAN Flotillin-2 OS=Homo sapiens GN=FLOT2 PE=1 SV=2;tr\|J3QLD9\|J3QLD9_HUMAN Flotillin-2 OS=Homo sapiens GN=FLOT2 PE=1 SV=1;tr\|E7EMK3\|E7EMK3_HUMAN Flotillin-2 OS=Homo sapiens GN=FLOT2 PE=1 SV=1 | 2 | 1.02 | 0.00 | 0.0020 |
| sp\|Q8NH64\|O51A7_HUMAN Olfactory receptor 51A7 OS=Homo sapiens GN=OR51A7 PE=2 SV=1 | 2 | 1.02 | 0.06 | 0.0248 |
| sp\|P35908\|K22E_HUMAN Keratin, type II cytoskeletal 2 epidermal OS=Homo sapiens GN=KRT2 PE=1 SV=2 | 2 | 2.28 | 2.89 | 0.4647 |
| tr\|Q7K6A0\|Q7K6A0_PLAF7 cAMP-dependent protein kinase catalytic subunit OS=Plasmodium falciparum (isolate 3D7) GN=PfPKAc PE=4 SV=1 | 2 | 1.37 | 1.30 | 0.3778 |
| sp\|Q5VU65-2\|P210L_HUMAN Isoform 2 of Nuclear pore membrane glycoprotein 210-like OS=Homo sapiens GN=NUP210L;sp\|Q5VU65\|P210L_HUMAN Nuclear pore membrane glycoprotein 210-like OS=Homo sapiens GN=NUP210L PE=2 SV=1 | 2 | 1.01 | 0.16 | 0.0694 |
| sp\|O14980\|XPO1_HUMAN Exportin-1 OS=Homo sapiens GN=XPO1 PE=1 SV=1 | 2 | 1.11 | 0.68 | 0.2604 |
| sp\|Q92508\|PIEZ1_HUMAN Piezo-type mechanosensitive ion channel component 1 OS=Homo sapiens GN=PIEZO1 PE=1 SV=4 | 2 | 1.00 | 0.06 | 0.0262 |
| sp\|Q9Y4E5-4\|ZN451_HUMAN Isoform 3 of Zinc finger protein 451 OS=Homo sapiens GN=ZNF451 | 2 | 1.03 | 0.35 | 0.1495 |
| tr\|C6KSW1\|C6KSW1_PLAF7 Uncharacterized protein OS=Plasmodium falciparum (isolate 3D7) GN=PFF0570c PE=4 SV=1 | 2 | 1.16 | 0.84 | 0.3015 |
| tr\|Q8IM75\|Q8IM75_PLAF7 Aminopeptidase, putative OS=Plasmodium falciparum (isolate 3D7) GN=PF14_0015 PE=4 SV=1 | 2 | 1.09 | 0.65 | 0.2544 |
| sp\|P61006\|RAB8A_HUMAN Ras-related protein Rab-8A OS=Homo sapiens GN=RAB8A PE=1 SV=1;sp\|P61006-2\|RAB8A_HUMAN Isoform 2 of Ras-related protein Rab-8A OS=Homo sapiens GN=RAB8A | 2 | 0.97 | 0.17 | 0.0796 |
| tr\|O96138\|O96138_PLAF7 Nucleolar preribosomal assembly protein, putative OS=Plasmodium falciparum (isolate 3D7) GN=PFB0175c PE=4 SV=2 | 2 | 0.97 | 0.20 | 0.0902 |
| sp\|P17066\|HSP76_HUMAN Heat shock 70 kDa protein 6 OS=Homo sapiens GN=HSPA6 PE=1 SV=2 | 2 | 0.96 | 0.01 | 0.0026 |
| tr\|C6KTD1\|C6KTD1_PLAF7 Uncharacterized protein OS=Plasmodium falciparum (isolate 3D7) GN=PFF1435w PE=4 SV=1 | 2 | 1.05 | 0.65 | 0.2622 |
| tr\|Q8I3G9\|Q8I3G9_PLAF7 RING zinc finger protein, putative OS=Plasmodium falciparum (isolate 3D7) GN=PFE1490c PE=4 SV=1 | 2 | 1.00 | 0.60 | 0.2528 |
| tr\|Q8IKV6\|Q8IKV6_PLAF7 Rhoptry neck protein 2 OS=Plasmodium falciparum (isolate 3D7) GN=PfRON2 PE=1 SV=1 | 2 | 1.01 | 0.60 | 0.2554 |
| tr\|C6S3B8\|C6S3B8_PLAF7 Conserved Plasmodium protein OS=Plasmodium falciparum (isolate 3D7) GN=PFB0850c PE=4 SV=1 | 2 | 0.94 | 0.36 | 0.1673 |
| sp\|O95573\|ACSL3_HUMAN Long-chain-fatty-acid--CoA ligase 3 OS=Homo sapiens GN=ACSL3 PE=1 SV=3 | 2 | 0.91 | 0.22 | 0.1063 |
| tr\|Q8I2K9\|Q8I2K9_PLAF7 Diacylglycerol kinase, putative OS=Plasmodium falciparum (isolate 3D7) GN=DGK1 PE=4 SV=2 | 2 | 0.91 | 0.31 | 0.1526 |
| sp\|P09543-2\|CN37_HUMAN Isoform CNPI of 2,3-cyclic-nucleotide 3-phosphodiesterase OS=Homo sapiens GN=CNP;sp\|P09543\|CN37_HUMAN 2,3-cyclic-nucleotide 3-phosphodiesterase OS=Homo sapiens GN=CNP PE=1 SV=2 | 2 | 0.94 | 0.49 | 0.2221 |
| sp\|O60673-2\|DPOLZ_HUMAN Isoform 2 of DNA polymerase zeta catalytic subunit OS=Homo sapiens GN=REV3L;sp\|O60673\|DPOLZ_HUMAN DNA polymerase zeta catalytic subunit OS=Homo sapiens GN=REV3L PE=1 SV=2 | 2 | 0.91 | 0.36 | 0.1739 |

| | | | | |
|---|---|---|---|---|
| tr\|Q8IKP6\|Q8IKP6_PLAF7 Uncharacterized protein OS=Plasmodium falciparum (isolate 3D7) GN=PF14_0558 PE=4 SV=1 | 2 | 0.88 | 0.16 | 0.0834 |
| tr\|Q8IAN2\|Q8IAN2_PLAF7 Filament assembling protein, putative OS=Plasmodium falciparum (isolate 3D7) GN=MAL8P1.146 PE=4 SV=1 | 2 | 0.82 | 0.12 | 0.0635 |
| tr\|Q8I272\|Q8I272_PLAF7 Centrin-1 OS=Plasmodium falciparum (isolate 3D7) GN=PfCEN1 PE=4 SV=1;sp\|P41208\|CETN2_HUMAN Centrin-2 OS=Homo sapiens GN=CETN2 PE=1 SV=1 | 2 | 0.80 | 0.12 | 0.0670 |
| tr\|Q8IAN5\|Q8IAN5_PLAF7 AAA family ATPase, putative OS=Plasmodium falciparum (isolate 3D7) GN=MAL8P1.144 PE=4 SV=1 | 2 | 0.78 | 0.03 | 0.0194 |
| tr\|Q8ID62\|Q8ID62_PLAF7 Exosome complex exonuclease, putative OS=Plasmodium falciparum (isolate 3D7) GN=PF13_0340 PE=4 SV=1 | 2 | 0.78 | 0.05 | 0.0283 |
| tr\|Q8I5V0\|Q8I5V0_PLAF7 ABC transporter, putative OS=Plasmodium falciparum (isolate 3D7) GN=PFL0495c PE=4 SV=1 | 2 | 0.75 | 0.01 | 0.0034 |
| tr\|Q8IBS1\|Q8IBS1_PLAF7 Thioredoxin-like protein OS=Plasmodium falciparum (isolate 3D7) GN=MAL7P1.88 PE=4 SV=1 | 2 | 0.75 | 0.16 | 0.0952 |
| tr\|C0H484\|C0H484_PLAF7 RNA triphosphatase OS=Plasmodium falciparum (isolate 3D7) GN=Prt1 PE=4 SV=1 | 2 | 0.80 | 0.53 | 0.2814 |
| tr\|Q8I302\|Q8I302_PLAF7 NADH dehydrogenase, putative OS=Plasmodium falciparum (isolate 3D7) GN=PFI0735c PE=4 SV=1 | 2 | 0.72 | 0.30 | 0.1793 |
| tr\|Q8I318\|Q8I318_PLAF7 Putative uncharacterized protein OS=Plasmodium falciparum (isolate 3D7) GN=PFI0655c PE=4 SV=1 | 2 | 0.73 | 0.34 | 0.2009 |
| tr\|C6KT32\|C6KT32_PLAF7 Uncharacterized protein OS=Plasmodium falciparum (isolate 3D7) GN=PFF0930w PE=4 SV=1 | 2 | 0.64 | 0.05 | 0.0365 |
| tr\|Q8IB57\|Q8IB57_PLAF7 Small nuclear ribonucleoprotein, putative OS=Plasmodium falciparum (isolate 3D7) GN=MAL8P1.48 PE=4 SV=1 | 2 | 0.67 | 0.34 | 0.2202 |
| tr\|C6S3D4\|C6S3D4_PLAF7 Conserved Plasmodium protein OS=Plasmodium falciparum (isolate 3D7) GN=PF10_0246a PE=4 SV=1 | 2 | 0.76 | 0.62 | 0.3347 |
| tr\|O96151\|O96151_PLAF7 Conserved Plasmodium protein OS=Plasmodium falciparum (isolate 3D7) GN=PFB0250w PE=4 SV=1 | 2 | 0.60 | 0.20 | 0.1519 |
| tr\|Q8IK62\|Q8IK62_PLAF7 Uncharacterized protein OS=Plasmodium falciparum (isolate 3D7) GN=PF14_0744 PE=4 SV=2 | 2 | 0.60 | 0.23 | 0.1671 |
| sp\|O75326-2\|SEM7A_HUMAN Isoform 2 of Semaphorin-7A OS=Homo sapiens GN=SEMA7A;sp\|O75326\|SEM7A_HUMAN Semaphorin-7A OS=Homo sapiens GN=SEMA7A PE=1 SV=1 | 2 | 0.65 | 0.48 | 0.3036 |
| tr\|C6KT80\|C6KT80_PLAF7 Uncharacterized protein OS=Plasmodium falciparum (isolate 3D7) GN=PFF1175c PE=4 SV=1 | 2 | 0.56 | 0.20 | 0.1552 |
| tr\|Q8IEG5\|Q8IEG5_PLAF7 Uncharacterized protein OS=Plasmodium falciparum (isolate 3D7) GN=MAL13P1.77 PE=4 SV=1 | 2 | 0.59 | 0.33 | 0.2383 |
| tr\|Q8I5I4\|Q8I5I4_PLAF7 Uncharacterized protein OS=Plasmodium falciparum (isolate 3D7) GN=PFL1115w PE=4 SV=1 | 2 | 0.62 | 0.43 | 0.2925 |
| tr\|Q8IL79\|Q8IL79_PLAF7 Copper transporter putative OS=Plasmodium falciparum (isolate 3D7) GN=PF14_0369 PE=4 SV=1 | 2 | 1.97 | 2.68 | 0.4885 |
| sp\|Q8IDG7\|YPF01_PLAF7 Uncharacterized protein PF13_0277 OS=Plasmodium falciparum (isolate 3D7) GN=PF13_0277 PE=3 SV=1 | 2 | 0.66 | 0.62 | 0.3725 |
| tr\|O77359\|O77359_PLAF7 Putative uncharacterized protein OS=Plasmodium falciparum (isolate 3D7) GN=PFC0450w PE=4 SV=1 | 2 | 0.48 | 0.00 | 0.0029 |
| tr\|F5H157\|F5H157_HUMAN Ras-related protein Rab-35 (Fragment) OS=Homo sapiens GN=RAB35 PE=1 SV=1;sp\|Q15286\|RAB35_HUMAN Ras-related protein Rab-35 OS=Homo sapiens GN=RAB35 PE=1 SV=1 | 2 | 0.62 | 0.57 | 0.3660 |
| tr\|Q8IJ66\|Q8IJ66_PLAF7 Flavoprotein subunit of succinate dehydrogenase OS=Plasmodium falciparum (isolate 3D7) GN=PF10_0334 PE=4 SV=1 | 2 | 0.50 | 0.24 | 0.2092 |
| tr\|Q8IAZ2\|Q8IAZ2_PLAF7 Uncharacterized protein OS=Plasmodium falciparum (isolate 3D7) GN=MAL8P1.84 PE=4 SV=1 | 2 | 0.51 | 0.30 | 0.2531 |
| tr\|Q8I350\|Q8I350_PLAF7 Putative uncharacterized protein OS=Plasmodium falciparum (isolate 3D7) GN=PFI0495w PE=4 SV=1 | 2 | 0.74 | 0.83 | 0.4266 |
| tr\|Q8IEN7\|Q8IEN7_PLAF7 Fork head domain protein, putative OS=Plasmodium falciparum (isolate 3D7) GN=PF13_0042 PE=4 SV=1 | 2 | 0.51 | 0.36 | 0.2941 |
| tr\|C0H5L4\|C0H5L4_PLAF7 Uncharacterized protein OS=Plasmodium falciparum (isolate 3D7) GN=MAL13P1.348 PE=4 SV=1 | 2 | 0.48 | 0.29 | 0.2599 |
| tr\|C0H4D6\|C0H4D6_PLAF7 GTP binding protein, putative OS=Plasmodium falciparum (isolate 3D7) GN=PFE0665c PE=3 SV=1 | 2 | 0.62 | 0.65 | 0.4093 |
| tr\|C0H5A4\|C0H5A4_PLAF7 U1 small nuclear ribonucleoprotein a, putative OS=Plasmodium falciparum (isolate 3D7) GN=MAL13P1.35 PE=4 SV=1 | 2 | 0.51 | 0.46 | 0.3596 |
| tr\|Q8I5Y8\|Q8I5Y8_PLAF7 Targeted glyoxalase II OS=Plasmodium falciparum (isolate 3D7) GN=PFL0285w PE=4 SV=1 | 2 | 1.10 | 1.45 | 0.4782 |
| tr\|Q8I4V1\|Q8I4V1_PLAF7 Conserved Plasmodium membrane protein OS=Plasmodium falciparum (isolate 3D7) GN=PFL2315c PE=4 SV=1 | 2 | 0.69 | 0.84 | 0.4510 |

| | | | | |
|---|---|---|---|---|
| tr\|C0H4J5\|C0H4J5_PLAF7 Stevor OS=Plasmodium falciparum (isolate 3D7) GN=Stevor PE=4 SV=1 | 2 | 0.56 | 0.62 | 0.4202 |
| tr\|Q8IJ80\|Q8IJ80_PLAF7 Uncharacterized protein OS=Plasmodium falciparum (isolate 3D7) GN=PF10_0319 PE=4 SV=1 | 2 | 0.38 | 0.29 | 0.3077 |
| tr\|Q8IDR8\|Q8IDR8_PLAF7 Aconitate hydratase OS=Plasmodium falciparum (isolate 3D7) GN=PF13_0229 PE=3 SV=1 | 2 | 0.38 | 0.29 | 0.3087 |
| tr\|Q8IJR3\|Q8IJR3_PLAF7 Conserved Plasmodium protein OS=Plasmodium falciparum (isolate 3D7) GN=PF10_0129 PE=4 SV=1 | 2 | 0.50 | 0.56 | 0.4243 |
| tr\|Q8IIF5\|Q8IIF5_PLAF7 Conserved Plasmodium protein OS=Plasmodium falciparum (isolate 3D7) GN=PF11_0219 PE=4 SV=2 | 2 | 0.36 | 0.30 | 0.3382 |
| tr\|Q8IM26\|Q8IM26_PLAF7 Uncharacterized protein OS=Plasmodium falciparum (isolate 3D7) GN=PF14_0065 PE=4 SV=1 | 2 | 0.83 | 1.11 | 0.4816 |
| tr\|Q9NLB3\|Q9NLB3_PLAF7 Putative uncharacterized protein OS=Plasmodium falciparum (isolate 3D7) GN=PFC0262c PE=4 SV=2 | 2 | 0.27 | 0.13 | 0.2091 |
| tr\|O77382\|O77382_PLAF7 Kinesin-like protein OS=Plasmodium falciparum (isolate 3D7) GN=PFC0770c PE=3 SV=1 | 2 | 0.23 | 0.12 | 0.2274 |
| tr\|Q8I433\|Q8I433_PLAF7 Rhomboid protease ROM4 OS=Plasmodium falciparum (isolate 3D7) GN=ROM4 PE=4 SV=1 | 2 | 0.47 | 0.61 | 0.4711 |
| tr\|Q8ILM5\|Q8ILM5_PLAF7 Actin-related protein homolog, arp4 homolog OS=Plasmodium falciparum (isolate 3D7) GN=PF14_0218 PE=3 SV=1 | 2 | 0.30 | 0.34 | 0.4274 |
| tr\|Q8IK19\|Q8IK19_PLAF7 Uncharacterized protein OS=Plasmodium falciparum (isolate 3D7) GN=PF10_0021 PE=4 SV=1 | 2 | 0.40 | 0.51 | 0.4655 |
| sp\|P06702\|S10A9_HUMAN Protein S100-A9 OS=Homo sapiens GN=S100A9 PE=1 SV=1 | 2 | 0.30 | 0.35 | 0.4399 |
| tr\|Q8I267\|Q8I267_PLAF7 Putative uncharacterized protein OS=Plasmodium falciparum (isolate 3D7) GN=PFA_0370w PE=4 SV=1 | 2 | 0.28 | 0.32 | 0.4322 |
| tr\|Q8IBU4\|Q8IBU4_PLAF7 GTP-binding translation elongation factor tu family protein, putative OS=Plasmodium falciparum (isolate 3D7) GN=PF07_0062 PE=4 SV=1 | 2 | 0.25 | 0.27 | 0.4180 |
| tr\|C6S3H2\|C6S3H2_PLAF7 Uncharacterized protein OS=Plasmodium falciparum (isolate 3D7) GN=PF14_0031a PE=4 SV=1 | 2 | 0.10 | 0.06 | 0.2612 |
| tr\|Q8ILI8\|Q8ILI8_PLAF7 CorA-like Mg2+ transporter protein, putative OS=Plasmodium falciparum (isolate 3D7) GN=PF14_0255 PE=4 SV=1 | 2 | 0.08 | 0.04 | 0.2398 |
| tr\|O96193\|O96193_PLAF7 Rab5a, GTPase OS=Plasmodium falciparum (isolate 3D7) GN=Rab5a PE=1 SV=1 | 2 | 0.07 | 0.06 | 0.3564 |
| tr\|Q8IJI1\|Q8IJI1_PLAF7 Conserved Plasmodium membrane protein OS=Plasmodium falciparum (isolate 3D7) GN=PF10_0216 PE=4 SV=2 | 2 | 0.04 | 0.01 | 0.0874 |
| tr\|H7BXK9\|H7BXK9_HUMAN ATP-binding cassette sub-family B member 6, mitochondrial (Fragment) OS=Homo sapiens GN=ABCB6 PE=1 SV=1;sp\|Q9NP58-4\|ABCB6_HUMAN Isoform 2 of ATP-binding cassette sub-family B member 6, mitochondrial OS=Homo sapiens GN=ABCB6;sp\|Q9NP58 | 1 | 1.16 | | |
| sp\|O15439-2\|MRP4_HUMAN Isoform 2 of Multidrug resistance-associated protein 4 OS=Homo sapiens GN=ABCC4;sp\|O15439\|MRP4_HUMAN Multidrug resistance-associated protein 4 OS=Homo sapiens GN=ABCC4 PE=1 SV=3;sp\|O15439-4\|MRP4_HUMAN Isoform 4 of Multidrug resistanc | 1 | 0.66 | | |
| tr\|F8WAR7\|F8WAR7_HUMAN Acetylcholinesterase OS=Homo sapiens GN=ACHE PE=1 SV=1;tr\|C9J2S3\|C9J2S3_HUMAN Acetylcholinesterase (Fragment) OS=Homo sapiens GN=ACHE PE=1 SV=4;tr\|F8WD68\|F8WD68_HUMAN Acetylcholinesterase OS=Homo sapiens GN=ACHE PE=1 SV=1;tr\|C9JZL6\|C | 1 | 53.02 | | |
| tr\|E7ERD7\|E7ERD7_HUMAN Long-chain-fatty-acid--CoA ligase 6 OS=Homo sapiens GN=ACSL6 PE=1 SV=1;sp\|Q9UKU0-7\|ACSL6_HUMAN Isoform 7 of Long-chain-fatty-acid--CoA ligase 6 OS=Homo sapiens GN=ACSL6;sp\|Q9UKU0-5\|ACSL6_HUMAN Isoform 5 of Long-chain-fatty-acid--CoA | 1 | 0.87 | | |
| sp\|P68133\|ACTS_HUMAN Actin, alpha skeletal muscle OS=Homo sapiens GN=ACTA1 PE=1 SV=1;sp\|P68032\|ACTC_HUMAN Actin, alpha cardiac muscle 1 OS=Homo sapiens GN=ACTC1 PE=1 SV=1;sp\|P63267\|ACTH_HUMAN Actin, gamma-enteric smooth muscle OS=Homo sapiens GN=ACTG2 PE=1 | 1 | 1.16 | | |
| sp\|P63261\|ACTG_HUMAN Actin, cytoplasmic 2 OS=Homo sapiens GN=ACTG1 PE=1 SV=1;sp\|P60709\|ACTB_HUMAN Actin, cytoplasmic 1 OS=Homo sapiens GN=ACTB PE=1 SV=1;tr\|I3L3I0\|I3L3I0_HUMAN Actin, cytoplasmic 2 (Fragment) OS=Homo sapiens GN=ACTG1 PE=1 SV=1;tr\|I3L1U9\|I3L | 1 | 0.88 | | |
| tr\|E7EV99\|E7EV99_HUMAN Alpha-adducin OS=Homo sapiens GN=ADD1 PE=1 SV=1;tr\|E7ENY0\|E7ENY0_HUMAN Alpha-adducin OS=Homo sapiens GN=ADD1 PE=1 SV=1;sp\|P35611-2\|ADDA_HUMAN Isoform 2 of Alpha-adducin OS=Homo sapiens GN=ADD1;sp\|P35611-6\|ADDA_HUMAN Isoform 6 of Alph | 1 | 0.84 | | |

| | | | | |
|---|---|---|---|---|
| sp\|P35612\|ADDB_HUMAN Beta-adducin OS=Homo sapiens GN=ADD2 PE=1 SV=3;sp\|P35612-4\|ADDB_HUMAN Isoform 4 of Beta-adducin OS=Homo sapiens GN=ADD2;sp\|P35612-3\|ADDB_HUMAN Isoform 3 of Beta-adducin OS=Homo sapiens GN=ADD2;sp\|P35612-2\|ADDB_HUMAN Isoform 2 of Beta-a | 1 | 1.01 | | |
| sp\|Q9H9G7-2\|AGO3_HUMAN Isoform 2 of Protein argonaute-3 OS=Homo sapiens GN=AGO3;sp\|Q9UKV8-2\|AGO2_HUMAN Isoform 2 of Protein argonaute-2 OS=Homo sapiens GN=AGO2;sp\|Q9UKV8\|AGO2_HUMAN Protein argonaute-2 OS=Homo sapiens GN=AGO2 PE=1 SV=3;sp\|Q9H9G7\|AGO3_HUMAN | 1 | 0.73 | | |
| tr\|H0YID2\|H0YID2_HUMAN Adenylate kinase isoenzyme 1 (Fragment) OS=Homo sapiens GN=AK1 PE=1 SV=1;tr\|H0Y4J6\|H0Y4J6_HUMAN Adenylate kinase isoenzyme 1 (Fragment) OS=Homo sapiens GN=AK1 PE=1 SV=1;tr\|Q5T9B7\|Q5T9B7_HUMAN Adenylate kinase isoenzyme 1 OS=Homo sapi | 1 | 1.56 | | |
| tr\|H0YIW2\|H0YIW2_HUMAN Anaphase-promoting complex subunit 7 (Fragment) OS=Homo sapiens GN=ANAPC7 PE=1 SV=1;sp\|Q9UJX3-2\|APC7_HUMAN Isoform 2 of Anaphase-promoting complex subunit 7 OS=Homo sapiens GN=ANAPC7;sp\|Q9UJX3\|APC7_HUMAN Anaphase-promoting complex su | 1 | 0.67 | | |
| sp\|P16157-10\|ANK1_HUMAN Isoform Er9 of Ankyrin-1 OS=Homo sapiens GN=ANK1;sp\|P16157-8\|ANK1_HUMAN Isoform Er7 of Ankyrin-1 OS=Homo sapiens GN=ANK1;sp\|P16157-5\|ANK1_HUMAN Isoform Er3 of Ankyrin-1 OS=Homo sapiens GN=ANK1;sp\|P16157-16\|ANK1_HUMAN Isoform Er15 of | 1 | 0.91 | | |
| tr\|F8W150\|F8W150_HUMAN Ankyrin repeat domain-containing protein 13A (Fragment) OS=Homo sapiens GN=ANKRD13A PE=1 SV=1;tr\|S4R3U2\|S4R3U2_HUMAN Ankyrin repeat domain-containing protein 13A (Fragment) OS=Homo sapiens GN=ANKRD13A PE=1 SV=1;tr\|H0YIN8\|H0YIN8_HUMAN | 1 | 0.69 | | |
| tr\|C9JIF9\|C9JIF9_HUMAN Acylamino-acid-releasing enzyme OS=Homo sapiens GN=APEH PE=1 SV=1;sp\|P13798\|ACPH_HUMAN Acylamino-acid-releasing enzyme OS=Homo sapiens GN=APEH PE=1 SV=4;tr\|H7C393\|H7C393_HUMAN Acylamino-acid-releasing enzyme (Fragment) OS=Homo sapien | 1 | 21.57 | | |
| tr\|K7N7A8\|K7N7A8_HUMAN Uncharacterized protein (Fragment) OS=Homo sapiens PE=3 SV=2;sp\|P29972-4\|AQP1_HUMAN Isoform 4 of Aquaporin-1 OS=Homo sapiens GN=AQP1;sp\|P29972-2\|AQP1_HUMAN Isoform 2 of Aquaporin-1 OS=Homo sapiens GN=AQP1;sp\|P29972-3\|AQP1_HUMAN Isofo | 1 | 0.82 | | |
| tr\|F8VWZ8\|F8VWZ8_HUMAN Rho GTPase-activating protein 29 OS=Homo sapiens GN=ARHGAP29 PE=1 SV=1;sp\|Q52LW3-2\|RHG29_HUMAN Isoform 2 of Rho GTPase-activating protein 29 OS=Homo sapiens GN=ARHGAP29;sp\|Q52LW3\|RHG29_HUMAN Rho GTPase-activating protein 29 OS=Homo s | 1 | 1.13 | | |
| sp\|P23634-7\|AT2B4_HUMAN Isoform ZB of Plasma membrane calcium-transporting ATPase 4 OS=Homo sapiens GN=ATP2B4;sp\|P23634-6\|AT2B4_HUMAN Isoform XB of Plasma membrane calcium-transporting ATPase 4 OS=Homo sapiens GN=ATP2B4;sp\|P23634-8\|AT2B4_HUMAN Isoform ZD o | 1 | 0.91 | | |
| tr\|H0YH81\|H0YH81_HUMAN ATP synthase subunit beta (Fragment) OS=Homo sapiens GN=ATP5B PE=1 SV=1;sp\|P06576\|ATPB_HUMAN ATP synthase subunit beta, mitochondrial OS=Homo sapiens GN=ATP5B PE=1 SV=3;tr\|F8W079\|F8W079_HUMAN ATP synthase subunit beta, mitochondrial | 1 | 0.65 | | |
| tr\|F5H1T6\|F5H1T6_HUMAN V-type proton ATPase subunit a OS=Homo sapiens GN=ATP6V0A1 PE=1 SV=1;tr\|B7Z641\|B7Z641_HUMAN V-type proton ATPase subunit a OS=Homo sapiens GN=ATP6V0A1 PE=1 SV=1;tr\|B7Z2A9\|B7Z2A9_HUMAN V-type proton ATPase subunit a OS=Homo sapiens GN | 1 | 1.03 | | |
| sp\|O60885\|BRD4_HUMAN Bromodomain-containing protein 4 OS=Homo sapiens GN=BRD4 PE=1 SV=2;tr\|M0R0H4\|M0R0H4_HUMAN Bromodomain-containing protein 4 (Fragment) OS=Homo sapiens GN=BRD4 PE=1 SV=1;tr\|M0QYW0\|M0QYW0_HUMAN Bromodomain containing 4, isoform CRA_c OS=H | 1 | 2.95 | | |
| sp\|P00915\|CAH1_HUMAN Carbonic anhydrase 1 OS=Homo sapiens GN=CA1 PE=1 SV=2;tr\|E5RH81\|E5RH81_HUMAN Carbonic anhydrase 1 (Fragment) OS=Homo sapiens GN=CA1 PE=1 SV=4;tr\|E5RHP7\|E5RHP7_HUMAN Carbonic anhydrase 1 (Fragment) OS=Homo sapiens GN=CA1 PE=1 SV=1;tr\|E5 | 1 | 1.44 | | |
| tr\|D6RAQ8\|D6RAQ8_HUMAN Calnexin (Fragment) OS=Homo sapiens GN=CANX PE=1 SV=1;tr\|D6RAU8\|D6RAU8_HUMAN Calnexin (Fragment) OS=Homo sapiens GN=CANX PE=1 SV=1;tr\|D6RB85\|D6RB85_HUMAN Calnexin (Fragment) OS=Homo sapiens GN=CANX PE=1 SV=1;tr\|D6RDP7\|D6RDP7_HUMAN Ca | 1 | 0.79 | | |
| tr\|A0A087WUV8\|A0A087WUV8_HUMAN Basigin OS=Homo sapiens GN=BSG PE=1 SV=1;tr\|A0A087X2B5\|A0A087X2B5_HUMAN Basigin (Fragment) OS=Homo sapiens GN=BSG PE=1 SV=1;sp\|P35613-3\|BASI_HUMAN Isoform 3 of Basigin OS=Homo sapiens GN=BSG;sp\|P35613-4\|BASI_HUMAN Isoform 4 o | 1 | 1.04 | | |

| | | | | |
|---|---|---|---|---|
| tr\|A0A087X0E3\|A0A087X0E3_HUMAN Helicase SRCAP (Fragment) OS=Homo sapiens GN=SRCAP PE=1 SV=1;tr\|A0A0A0MS59\|A0A0A0MS59_HUMAN Helicase SRCAP OS=Homo sapiens GN=SRCAP PE=1 SV=1;sp\|Q6ZRS2-3\|SRCAP_HUMAN Isoform 3 of Helicase SRCAP OS=Homo sapiens GN=SRCAP;sp\|Q6Z | 1 | 3.47 | | |
| sp\|P04632\|CPNS1_HUMAN Calpain small subunit 1 OS=Homo sapiens GN=CAPNS1 PE=1 SV=1;tr\|K7EIV0\|K7EIV0_HUMAN Calpain small subunit 1 (Fragment) OS=Homo sapiens GN=CAPNS1 PE=1 SV=2;tr\|A0A075B7C0\|A0A075B7C0_HUMAN Calpain small subunit 1 (Fragment) OS=Homo sapien | 1 | 0.74 | | |
| tr\|H0YDX6\|H0YDX6_HUMAN CD44 antigen (Fragment) OS=Homo sapiens GN=CD44 PE=1 SV=1;tr\|H0YD13\|H0YD13_HUMAN CD44 antigen OS=Homo sapiens GN=CD44 PE=1 SV=2;tr\|H0YD17\|H0YD17_HUMAN CD44 antigen (Fragment) OS=Homo sapiens GN=CD44 PE=1 SV=4;tr\|H0YDW7\|H0YDW7_HUMAN C | 1 | 0.33 | | |
| sp\|Q08722-2\|CD47_HUMAN Isoform OA3-293 of Leukocyte surface antigen CD47 OS=Homo sapiens GN=CD47;sp\|Q08722-3\|CD47_HUMAN Isoform OA3-305 of Leukocyte surface antigen CD47 OS=Homo sapiens GN=CD47;sp\|Q08722-4\|CD47_HUMAN Isoform OA3-312 of Leukocyte surface an | 1 | 0.86 | | |
| tr\|Q5JYX0\|Q5JYX0_HUMAN Cell division control protein 42 homolog (Fragment) OS=Homo sapiens GN=CDC42 PE=1 SV=1;sp\|P60953-1\|CDC42_HUMAN Isoform 1 of Cell division control protein 42 homolog OS=Homo sapiens GN=CDC42;sp\|P60953\|CDC42_HUMAN Cell division control | 1 | 1.31 | | |
| tr\|H0YDK0\|H0YDK0_HUMAN Centrosomal protein of 295 kDa (Fragment) OS=Homo sapiens GN=CEP295 PE=1 SV=1;sp\|Q9C0D2\|CE295_HUMAN Centrosomal protein of 295 kDa OS=Homo sapiens GN=CEP295 PE=2 SV=4;sp\|Q9C0D2-3\|CE295_HUMAN Isoform 3 of Centrosomal protein of 295 kD | 1 | 5.45 | | |
| tr\|H0Y524\|H0Y524_HUMAN Copine-1 (Fragment) OS=Homo sapiens GN=CPNE1 PE=1 SV=1;tr\|Q5JX45\|Q5JX45_HUMAN Copine-1 (Fragment) OS=Homo sapiens GN=CPNE1 PE=1 SV=1;tr\|E7ENH5\|E7ENH5_HUMAN Copine-1 OS=Homo sapiens GN=CPNE1 PE=1 SV=1;tr\|A6PVH9\|A6PVH9_HUMAN Copine-1 O | 1 | 0.64 | | |
| tr\|E9PQN4\|E9PQN4_HUMAN Complement receptor type 1 OS=Homo sapiens GN=CR1 PE=1 SV=2;tr\|Q5SR44\|Q5SR44_HUMAN Complement receptor type 1 OS=Homo sapiens GN=CR1 PE=1 SV=1;tr\|E9PDY4\|E9PDY4_HUMAN Complement receptor type 1 OS=Homo sapiens GN=CR1 PE=1 SV=1;sp\|P179 | 1 | 6.42 | | |
| sp\|P48729\|KC1A_HUMAN Casein kinase I isoform alpha OS=Homo sapiens GN=CSNK1A1 PE=1 SV=2;sp\|P48729-3\|KC1A_HUMAN Isoform 3 of Casein kinase I isoform alpha OS=Homo sapiens GN=CSNK1A1;sp\|P48729-2\|KC1A_HUMAN Isoform 2 of Casein kinase I isoform alpha OS=Homo s | 1 | 0.88 | | |
| sp\|P00387-2\|NB5R3_HUMAN Isoform 2 of NADH-cytochrome b5 reductase 3 OS=Homo sapiens GN=CYB5R3;sp\|P00387\|NB5R3_HUMAN NADH-cytochrome b5 reductase 3 OS=Homo sapiens GN=CYB5R3 PE=1 SV=3;sp\|P00387-3\|NB5R3_HUMAN Isoform 3 of NADH-cytochrome b5 reductase 3 OS=Ho | 1 | 0.82 | | |
| sp\|Q08495-2\|DEMA_HUMAN Isoform 2 of Dematin OS=Homo sapiens GN=DMTN;sp\|Q08495\|DEMA_HUMAN Dematin OS=Homo sapiens GN=DMTN PE=1 SV=3;sp\|Q08495-3\|DEMA_HUMAN Isoform 3 of Dematin OS=Homo sapiens GN=DMTN;sp\|Q08495-4\|DEMA_HUMAN Isoform 4 of Dematin OS=Homo sapie | 1 | 0.91 | | |
| tr\|U3KQJ8\|U3KQJ8_HUMAN Dynein heavy chain 11, axonemal OS=Homo sapiens GN=DNAH11 PE=4 SV=1;tr\|A0A087WYC6\|A0A087WYC6_HUMAN Dynein heavy chain 11, axonemal OS=Homo sapiens GN=DNAH11 PE=4 SV=1;sp\|Q96DT5\|DYH11_HUMAN Dynein heavy chain 11, axonemal OS=Homo sapi | 1 | 21.86 | | |
| tr\|F8WCJ1\|F8WCJ1_HUMAN Eukaryotic translation initiation factor 5A OS=Homo sapiens GN=EIF5A2 PE=1 SV=1;tr\|C9J7B5\|C9J7B5_HUMAN Eukaryotic translation initiation factor 5A OS=Homo sapiens GN=EIF5A2 PE=1 SV=1;tr\|C9J4W5\|C9J4W5_HUMAN Eukaryotic translation init | 1 | 0.89 | | |
| sp\|P11171-2\|41_HUMAN Isoform 2 of Protein 4.1 OS=Homo sapiens GN=EPB41;sp\|P11171\|41_HUMAN Protein 4.1 OS=Homo sapiens GN=EPB41 PE=1 SV=4;tr\|Q4VB86\|Q4VB86_HUMAN EPB41 protein OS=Homo sapiens GN=EPB41 PE=1 SV=2;sp\|P11171-4\|41_HUMAN Isoform 4 of Protein 4.1 O | 1 | 0.90 | | |
| sp\|P16452-3\|EPB42_HUMAN Isoform 3 of Erythrocyte membrane protein band 4.2 OS=Homo sapiens GN=EPB42;sp\|P16452\|EPB42_HUMAN Erythrocyte membrane protein band 4.2 OS=Homo sapiens GN=EPB42 PE=1 SV=3;sp\|P16452-2\|EPB42_HUMAN Isoform Long of Erythrocyte membrane | 1 | 0.98 | | |
| sp\|O75955\|FLOT1_HUMAN Flotillin-1 OS=Homo sapiens GN=FLOT1 PE=1 SV=3;sp\|O75955-2\|FLOT1_HUMAN Isoform 2 of Flotillin-1 OS=Homo sapiens GN=FLOT1;tr\|A2AB10\|A2AB10_HUMAN Flotillin-1 (Fragment) OS=Homo sapiens GN=FLOT1 PE=1 SV=1;tr\|A2AB12\|A2AB12_HUMAN Flotillin | 1 | 0.90 | | |

| | | | | |
|---|---|---|---|---|
| tr\|F5H6X6\|F5H6X6_HUMAN Neutral alpha-glucosidase AB OS=Homo sapiens GN=GANAB PE=1 SV=1;tr\|E9PKU7\|E9PKU7_HUMAN Neutral alpha-glucosidase AB OS=Homo sapiens GN=GANAB PE=1 SV=1;sp\|Q14697\|GANAB_HUMAN Neutral alpha-glucosidase AB OS=Homo sapiens GN=GANAB PE=1 S | 1 | 0.72 | | |
| sp\|P04406\|G3P_HUMAN Glyceraldehyde-3-phosphate dehydrogenase OS=Homo sapiens GN=GAPDH PE=1 SV=3;sp\|P04406-2\|G3P_HUMAN Isoform 2 of Glyceraldehyde-3-phosphate dehydrogenase OS=Homo sapiens GN=GAPDH;tr\|E7EUT5\|E7EUT5_HUMAN Glyceraldehyde-3-phosphate dehydroge | 1 | 18.18 | | |
| tr\|Q13030\|Q13030_HUMAN Glycophorin Erik I-IV OS=Homo sapiens GN=GPErik PE=1 SV=1;tr\|E9PH25\|E9PH25_HUMAN Glycophorin-A OS=Homo sapiens GN=GYPA PE=1 SV=1;tr\|E7EQF3\|E7EQF3_HUMAN Glycophorin-A OS=Homo sapiens GN=GYPA PE=1 SV=1;tr\|E9PD10\|E9PD10_HUMAN Glycophori | 1 | 0.54 | | |
| sp\|P00390-5\|GSHR_HUMAN Isoform 4 of Glutathione reductase, mitochondrial OS=Homo sapiens GN=GSR;sp\|P00390-4\|GSHR_HUMAN Isoform 3 of Glutathione reductase, mitochondrial OS=Homo sapiens GN=GSR;sp\|P00390-2\|GSHR_HUMAN Isoform Cytoplasmic of Glutathione reduct | 1 | 19.00 | | |
| tr\|H3BQW8\|H3BQW8_HUMAN Hydroxyacylglutathione hydrolase, mitochondrial (Fragment) OS=Homo sapiens GN=HAGH PE=1 SV=1;tr\|H3BPK3\|H3BPK3_HUMAN Hydroxyacylglutathione hydrolase, mitochondrial (Fragment) OS=Homo sapiens GN=HAGH PE=1 SV=1;tr\|H3BPQ4\|H3BPQ4_HUMAN H | 1 | 99.50 | | |
| tr\|D6R9P3\|D6R9P3_HUMAN Heterogeneous nuclear ribonucleoprotein A/B OS=Homo sapiens GN=HNRNPAB PE=1 SV=1;tr\|D6RD18\|D6RD18_HUMAN Heterogeneous nuclear ribonucleoprotein A/B OS=Homo sapiens GN=HNRNPAB PE=1 SV=1;tr\|D6RBZ0\|D6RBZ0_HUMAN Heterogeneous nuclear rib | 1 | 0.72 | | |
| tr\|D6RF44\|D6RF44_HUMAN Heterogeneous nuclear ribonucleoprotein D0 (Fragment) OS=Homo sapiens GN=HNRNPD PE=1 SV=4;tr\|D6RBQ9\|D6RBQ9_HUMAN Heterogeneous nuclear ribonucleoprotein D0 (Fragment) OS=Homo sapiens GN=HNRNPD PE=1 SV=1;tr\|H0YA96\|H0YA96_HUMAN Heterog | 1 | 0.49 | | |
| sp\|P08107\|HSP71_HUMAN Heat shock 70 kDa protein 1A/1B OS=Homo sapiens GN=HSPA1A PE=1 SV=5;sp\|P08107-2\|HSP71_HUMAN Isoform 2 of Heat shock 70 kDa protein 1A/1B OS=Homo sapiens GN=HSPA1A;tr\|V9GZ37\|V9GZ37_HUMAN Heat shock 70 kDa protein 1A/1B OS=Homo sapiens | 1 | 0.94 | | |
| tr\|E9PK54\|E9PK54_HUMAN Heat shock cognate 71 kDa protein (Fragment) OS=Homo sapiens GN=HSPA8 PE=1 SV=4;tr\|E9PQQ4\|E9PQQ4_HUMAN Heat shock cognate 71 kDa protein (Fragment) OS=Homo sapiens GN=HSPA8 PE=1 SV=1;tr\|E9PQK7\|E9PQK7_HUMAN Heat shock cognate 71 kDa p | 1 | 2.44 | | |
| sp\|P11142\|HSP7C_HUMAN Heat shock cognate 71 kDa protein OS=Homo sapiens GN=HSPA8 PE=1 SV=1;tr\|E9PKE3\|E9PKE3_HUMAN Heat shock cognate 71 kDa protein OS=Homo sapiens GN=HSPA8 PE=1 SV=1;sp\|P11142-2\|HSP7C_HUMAN Isoform 2 of Heat shock cognate 71 kDa protein OS | 1 | 0.97 | | |
| sp\|Q00013\|EM55_HUMAN 55 kDa erythrocyte membrane protein OS=Homo sapiens GN=MPP1 PE=1 SV=2;sp\|Q00013-3\|EM55_HUMAN Isoform 3 of 55 kDa erythrocyte membrane protein OS=Homo sapiens GN=MPP1;sp\|Q00013-2\|EM55_HUMAN Isoform 2 of 55 kDa erythrocyte membrane prote | 1 | 0.83 | | |
| tr\|A0A0A0MQS8\|A0A0A0MQS8_HUMAN Ammonium transporter Rh type A OS=Homo sapiens GN=RHAG PE=1 SV=1;sp\|Q02094\|RHAG_HUMAN Ammonium transporter Rh type A OS=Homo sapiens GN=RHAG PE=1 SV=2;tr\|A0A087WZZ4\|A0A087WZZ4_HUMAN Ammonium transporter Rh type A OS=Homo sapi | 1 | 1.76 | | |
| sp\|Q9GZT8-2\|GTPC1_HUMAN Isoform 2 of Putative GTP cyclohydrolase 1 type 2 NIF3L1 OS=Homo sapiens GN=NIF3L1;sp\|Q9GZT8\|GTPC1_HUMAN Putative GTP cyclohydrolase 1 type 2 NIF3L1 OS=Homo sapiens GN=NIF3L1 PE=1 SV=2;tr\|C9JN42\|C9JN42_HUMAN Putative GTP cyclohydrol | 1 | 40.91 | | |
| tr\|I3L4M2\|I3L4M2_HUMAN Protein disulfide-isomerase (Fragment) OS=Homo sapiens GN=P4HB PE=1 SV=1;tr\|I3L398\|I3L398_HUMAN Protein disulfide-isomerase (Fragment) OS=Homo sapiens GN=P4HB PE=1 SV=1;tr\|I3L312\|I3L312_HUMAN Protein disulfide-isomerase (Fragment) OS | 1 | 6.42 | | |
| sp\|Q9UQ80-2\|PA2G4_HUMAN Isoform 2 of Proliferation-associated protein 2G4 OS=Homo sapiens GN=PA2G4;sp\|Q9UQ80\|PA2G4_HUMAN Proliferation-associated protein 2G4 OS=Homo sapiens GN=PA2G4 PE=1 SV=3;tr\|F8W0A3\|F8W0A3_HUMAN Proliferation-associated protein 2G4 (Fr | 1 | 0.05 | | |
| sp\|O75340\|PDCD6_HUMAN Programmed cell death protein 6 OS=Homo sapiens GN=PDCD6 PE=1 SV=1;tr\|A0A024QZ42\|A0A024QZ42_HUMAN HCG1985580, isoform CRA_c OS=Homo sapiens GN=PDCD6 PE=1 SV=1;sp\|O75340-2\|PDCD6_HUMAN Isoform 2 of Programmed cell death protein 6 OS=Hom | 1 | 0.66 | | |

| | | | | |
|---|---|---|---|---|
| tr\|Q8I6V0\|Q8I6V0_PLAF7 Cysteine proteinase falcipain-1 OS=Plasmodium falciparum (isolate 3D7) GN=PF14_0553 PE=3 SV=1;tr\|H0YE04\|H0YE04_HUMAN Signal peptidase complex subunit 2 (Fragment) OS=Homo sapiens GN=SPCS2 PE=1 SV=1;tr\|A0A087WUC6\|A0A087WUC6_HUMAN Sign | 1 | 1.10 | | |
| tr\|Q8I3J4\|Q8I3J4_PLAF7 Ubiquitin conjugating enzyme, putative OS=Plasmodium falciparum (isolate 3D7) GN=PFE1350c PE=1 SV=1;tr\|F8VQQ8\|F8VQQ8_HUMAN Ubiquitin-conjugating enzyme E2 N OS=Homo sapiens GN=UBE2N PE=1 SV=1;sp\|P61088\|UBE2N_HUMAN Ubiquitin-conjugati | 1 | 3268.61 | | |
| sp\|P48426-2\|PI42A_HUMAN Isoform 2 of Phosphatidylinositol 5-phosphate 4-kinase type-2 alpha OS=Homo sapiens GN=PIP4K2A;sp\|P48426\|PI42A_HUMAN Phosphatidylinositol 5-phosphate 4-kinase type-2 alpha OS=Homo sapiens GN=PIP4K2A PE=1 SV=2;tr\|H7BXS3\|H7BXS3_HUMAN | 1 | 0.86 | | |
| tr\|M0R2K2\|M0R2K2_HUMAN Neuropathy target esterase (Fragment) OS=Homo sapiens GN=PNPLA6 PE=1 SV=1;tr\|M0QYT1\|M0QYT1_HUMAN Neuropathy target esterase (Fragment) OS=Homo sapiens GN=PNPLA6 PE=1 SV=1;tr\|M0R2C2\|M0R2C2_HUMAN Neuropathy target esterase (Fragment) O | 1 | 1.14 | | |
| tr\|K7EM13\|K7EM13_HUMAN cAMP-dependent protein kinase type I-alpha regulatory subunit (Fragment) OS=Homo sapiens GN=PRKAR1A PE=1 SV=1;tr\|K7EPB2\|K7EPB2_HUMAN cAMP-dependent protein kinase type I-alpha regulatory subunit (Fragment) OS=Homo sapiens GN=PRKAR1A | 1 | 0.66 | | |
| tr\|E9PLD0\|E9PLD0_HUMAN Ras-related protein Rab-1B OS=Homo sapiens GN=RAB1B PE=1 SV=1;sp\|Q9H0U4\|RAB1B_HUMAN Ras-related protein Rab-1B OS=Homo sapiens GN=RAB1B PE=1 SV=1;tr\|E7END7\|E7END7_HUMAN Ras-related protein Rab-1A OS=Homo sapiens GN=RAB1A PE=1 SV=1;sp | 1 | 0.95 | | |
| tr\|Q8I5A9\|Q8I5A9_PLAF7 Rab2, GTPase OS=Plasmodium falciparum (isolate 3D7) GN=Rab2 PE=3 SV=1;tr\|E9PKL7\|E9PKL7_HUMAN Ras-related protein Rab-2A OS=Homo sapiens GN=RAB2A PE=1 SV=1;tr\|Q5HYI5\|Q5HYI5_HUMAN Putative uncharacterized protein DKFZp313C1541 OS=Homo | 1 | 1.09 | | |
| tr\|C0H516\|C0H516_PLAF7 PfRab7, GTPase OS=Plasmodium falciparum (isolate 3D7) GN=Rab7 PE=3 SV=1;tr\|C9IZZ0\|C9IZZ0_HUMAN Ras-related protein Rab-7a (Fragment) OS=Homo sapiens GN=RAB7A PE=1 SV=1;tr\|C9J592\|C9J592_HUMAN Ras-related protein Rab-7a (Fragment) OS=H | 1 | 0.91 | | |
| tr\|F5H018\|F5H018_HUMAN GTP-binding nuclear protein Ran (Fragment) OS=Homo sapiens GN=RAN PE=1 SV=4;tr\|B5MDF5\|B5MDF5_HUMAN GTP-binding nuclear protein Ran OS=Homo sapiens GN=RAN PE=1 SV=1;tr\|J3KQE5\|J3KQE5_HUMAN GTP-binding nuclear protein Ran (Fragment) OS= | 1 | 1.18 | | |
| sp\|P61224-2\|RAP1B_HUMAN Isoform 2 of Ras-related protein Rap-1b OS=Homo sapiens GN=RAP1B;sp\|P61224-3\|RAP1B_HUMAN Isoform 3 of Ras-related protein Rap-1b OS=Homo sapiens GN=RAP1B;sp\|P62834\|RAP1A_HUMAN Ras-related protein Rap-1A OS=Homo sapiens GN=RAP1A PE=1 | 1 | 1.05 | | |
| tr\|E7EQ47\|E7EQ47_HUMAN Blood group Rh(CE) polypeptide OS=Homo sapiens GN=RHCE PE=4 SV=1;tr\|F6XSS0\|F6XSS0_HUMAN Blood group Rh(CE) polypeptide OS=Homo sapiens GN=RHCE PE=4 SV=1;sp\|P18577-9\|RHCE_HUMAN Isoform 4g of Blood group Rh(CE) polypeptide OS=Homo sapi | 1 | 1.16 | | |
| tr\|Q5JR07\|Q5JR07_HUMAN Rho-related GTP-binding protein RhoC (Fragment) OS=Homo sapiens GN=RHOC PE=1 SV=1;tr\|C9JNR4\|C9JNR4_HUMAN Transforming protein RhoA (Fragment) OS=Homo sapiens GN=RHOA PE=1 SV=1;tr\|E9PQH6\|E9PQH6_HUMAN Rho-related GTP-binding protein Rh | 1 | 0.86 | | |
| tr\|F8WDN7\|F8WDN7_HUMAN Phosphatidylinositide phosphatase SAC1 OS=Homo sapiens GN=SACM1L PE=1 SV=1;tr\|E9PGZ4\|E9PGZ4_HUMAN Phosphatidylinositide phosphatase SAC1 OS=Homo sapiens GN=SACM1L PE=1 SV=1;sp\|Q9NTJ5-2\|SAC1_HUMAN Isoform 2 of Phosphatidylinositide ph | 1 | 0.63 | | |
| sp\|Q13228\|SBP1_HUMAN Selenium-binding protein 1 OS=Homo sapiens GN=SELENBP1 PE=1 SV=2;sp\|Q13228-4\|SBP1_HUMAN Isoform 4 of Selenium-binding protein 1 OS=Homo sapiens GN=SELENBP1;sp\|Q13228-2\|SBP1_HUMAN Isoform 2 of Selenium-binding protein 1 OS=Homo sapiens | 1 | 14.78 | | |
| sp\|P11166\|GTR1_HUMAN Solute carrier family 2, facilitated glucose transporter member 1 OS=Homo sapiens GN=SLC2A1 PE=1 SV=2;tr\|C9JIM8\|C9JIM8_HUMAN Solute carrier family 2, facilitated glucose transporter member 1 (Fragment) OS=Homo sapiens GN=SLC2A1 PE=1 SV | 1 | 1.25 | | |
| tr\|F5H081\|F5H081_HUMAN Solute carrier family 2, facilitated glucose transporter member 4 OS=Homo sapiens GN=SLC2A4 PE=1 SV=1;tr\|I3L2R4\|I3L2R4_HUMAN Solute carrier family 2 (Facilitated glucose transporter), member 4, isoform CRA_b OS=Homo sapiens GN=SLC2A4 | 1 | 0.89 | | |
| tr\|E9PS74\|E9PS74_HUMAN Solute carrier family 43 member 3 (Fragment) OS=Homo sapiens GN=SLC43A3 PE=1 SV=1;sp\|Q8NBI5\|S43A3_HUMAN Solute carrier family 43 member 3 OS=Homo sapiens GN=SLC43A3 PE=1 SV=2;sp\|Q8NBI5-2\|S43A3_HUMAN Isoform 2 of Solute carrier family | 1 | 1.04 | | |

| | | | | |
|---|---|---|---|---|
| sp\|P02549\|SPTA1_HUMAN Spectrin alpha chain, erythrocytic 1 OS=Homo sapiens GN=SPTA1 PE=1 SV=5;sp\|P02549-2\|SPTA1_HUMAN Isoform 2 of Spectrin alpha chain, erythrocytic 1 OS=Homo sapiens GN=SPTA1;tr\|A0A087WZE4\|A0A087WZE4_HUMAN Spectrin alpha chain, erythrocyt | 1 | 0.94 | | |
| sp\|P11277\|SPTB1_HUMAN Spectrin beta chain, erythrocytic OS=Homo sapiens GN=SPTB PE=1 SV=5;sp\|P11277-2\|SPTB1_HUMAN Isoform 2 of Spectrin beta chain, erythrocytic OS=Homo sapiens GN=SPTB;sp\|P11277-3\|SPTB1_HUMAN Isoform 3 of Spectrin beta chain, erythrocytic | 1 | 0.96 | | |
| tr\|E7EMZ9\|E7EMZ9_HUMAN Transforming acidic coiled-coil-containing protein 2 OS=Homo sapiens GN=TACC2 PE=1 SV=1;tr\|E9PBC6\|E9PBC6_HUMAN Transforming acidic coiled-coil-containing protein 2 OS=Homo sapiens GN=TACC2 PE=1 SV=1;sp\|O95359-3\|TACC2_HUMAN Isoform 3 | 1 | 449.45 | | |
| sp\|Q8TC07-2\|TBC15_HUMAN Isoform 2 of TBC1 domain family member 15 OS=Homo sapiens GN=TBC1D15;sp\|Q8TC07-3\|TBC15_HUMAN Isoform 3 of TBC1 domain family member 15 OS=Homo sapiens GN=TBC1D15;sp\|Q8TC07\|TBC15_HUMAN TBC1 domain family member 15 OS=Homo sapiens GN= | 1 | 2.44 | | |
| sp\|Q9NR96-3\|TLR9_HUMAN Isoform 3 of Toll-like receptor 9 OS=Homo sapiens GN=TLR9;tr\|H0Y858\|H0Y858_HUMAN Uncharacterized protein (Fragment) OS=Homo sapiens PE=4 SV=1;sp\|Q9NR96-2\|TLR9_HUMAN Isoform 2 of Toll-like receptor 9 OS=Homo sapiens GN=TLR9;sp\|Q9NR96- | 1 | 0.04 | | |
| tr\|C9JEN3\|C9JEN3_HUMAN Protein lifeguard 3 (Fragment) OS=Homo sapiens GN=TMBIM1 PE=1 SV=1;tr\|C9IYT2\|C9IYT2_HUMAN Protein lifeguard 3 (Fragment) OS=Homo sapiens GN=TMBIM1 PE=1 SV=1;tr\|F8WDY4\|F8WDY4_HUMAN Protein lifeguard 3 OS=Homo sapiens GN=TMBIM1 PE=1 SV | 1 | 0.98 | | |
| tr\|J3QQY2\|J3QQY2_HUMAN Transmembrane and coiled-coil domain-containing protein 1 OS=Homo sapiens GN=TMCO1 PE=1 SV=1;tr\|J3KS45\|J3KS45_HUMAN Transmembrane and coiled-coil domain-containing protein 1 (Fragment) OS=Homo sapiens GN=TMCO1 PE=1 SV=1;tr\|J9JIE6\|J9J | 1 | 0.99 | | |
| sp\|P06753-5\|TPM3_HUMAN Isoform 5 of Tropomyosin alpha-3 chain OS=Homo sapiens GN=TPM3;sp\|P06753-2\|TPM3_HUMAN Isoform 2 of Tropomyosin alpha-3 chain OS=Homo sapiens GN=TPM3;tr\|A0A087WWU8\|A0A087WWU8_HUMAN Tropomyosin alpha-3 chain OS=Homo sapiens GN=TPM3 PE= | 1 | 1.24 | | |
| tr\|E2QRB9\|E2QRB9_HUMAN Thioredoxin reductase 1, cytoplasmic OS=Homo sapiens GN=TXNRD1 PE=1 SV=2;tr\|E9PIR7\|E9PIR7_HUMAN Thioredoxin reductase 1, cytoplasmic OS=Homo sapiens GN=TXNRD1 PE=1 SV=1;tr\|F8W809\|F8W809_HUMAN Thioredoxin reductase 1, cytoplasmic OS=H | 1 | 77.77 | | |
| tr\|J3QS39\|J3QS39_HUMAN Polyubiquitin-B (Fragment) OS=Homo sapiens GN=UBB PE=1 SV=1;tr\|J3QTR3\|J3QTR3_HUMAN Ubiquitin-40S ribosomal protein S27a (Fragment) OS=Homo sapiens GN=RPS27A PE=1 SV=1;tr\|F5H6Q2\|F5H6Q2_HUMAN Polyubiquitin-C (Fragment) OS=Homo sapiens | 1 | 0.83 | | |
| tr\|Q8ILD5\|Q8ILD5_PLAF7 Protein-L-isoaspartate O-methyltransferase beta-aspartate methyltransferase, putative OS=Plasmodium falciparum (isolate 3D7) GN=PF14_0309 PE=1 SV=1 | 1 | 1526.96 | | |
| tr\|Q8ILW5\|Q8ILW5_PLAF7 Ubiquitin conjugating enzyme, putative OS=Plasmodium falciparum (isolate 3D7) GN=PF14_0128 PE=4 SV=1 | 1 | 466.56 | | |
| sp\|Q9ULE4\|F184B_HUMAN Protein FAM184B OS=Homo sapiens GN=FAM184B PE=2 SV=3 | 1 | 428.83 | | |
| tr\|O97241\|O97241_PLAF7 Ubiquitin conjugating enzyme E2, putative OS=Plasmodium falciparum (isolate 3D7) GN=PFC0255c PE=1 SV=1 | 1 | 322.45 | | |
| tr\|Q8II00\|Q8II00_PLAF7 Uncharacterized protein OS=Plasmodium falciparum (isolate 3D7) GN=PF11_0375 PE=4 SV=1 | 1 | 281.33 | | |
| tr\|Q8IEA1\|Q8IEA1_PLAF7 Uncharacterized protein OS=Plasmodium falciparum (isolate 3D7) GN=MAL13P1.116 PE=4 SV=1 | 1 | 255.56 | | |
| tr\|Q8IJR0\|Q8IJR0_PLAF7 Phosphoinositide phospholipase C OS=Plasmodium falciparum (isolate 3D7) GN=PI PLC PE=4 SV=2 | 1 | 198.49 | | |
| tr\|Q8IKE4\|Q8IKE4_PLAF7 Uncharacterized protein OS=Plasmodium falciparum (isolate 3D7) GN=PF14_0661 PE=4 SV=1 | 1 | 158.55 | | |
| tr\|O77317\|O77317_PLAF7 HAD superfamily protein, putative OS=Plasmodium falciparum (isolate 3D7) GN=PFC0150w PE=4 SV=3 | 1 | 155.90 | | |
| tr\|Q8IDT7\|Q8IDT7_PLAF7 Uncharacterized protein OS=Plasmodium falciparum (isolate 3D7) GN=PF13_0217 PE=4 SV=1 | 1 | 145.20 | | |
| tr\|Q8II90\|Q8II90_PLAF7 tRNA (guanine-N(7)-)-methyltransferase OS=Plasmodium falciparum (isolate 3D7) GN=PF11_0284 PE=3 SV=1 | 1 | 130.47 | | |
| tr\|Q8IEH6\|Q8IEH6_PLAF7 Septum formation protein MAF homologue, putative OS=Plasmodium falciparum (isolate 3D7) GN=MAL13P1.69 PE=3 SV=2 | 1 | 129.30 | | |
| tr\|Q8IBQ0\|Q8IBQ0_PLAF7 Uncharacterized protein OS=Plasmodium falciparum (isolate 3D7) GN=PF07_0084 PE=4 SV=1 | 1 | 113.99 | | |

| | | | | |
|---|---|---|---|---|
| sp\|Q53H82\|LACB2_HUMAN Beta-lactamase-like protein 2 OS=Homo sapiens GN=LACTB2 PE=1 SV=2 | 1 | 112.49 | | |
| tr\|C6KSQ9\|C6KSQ9_PLAF7 RNA binding protein, putative OS=Plasmodium falciparum (isolate 3D7) GN=PFF0300w PE=4 SV=1 | 1 | 112.23 | | |
| tr\|Q8IJP2\|Q8IJP2_PLAF7 Methionine aminopeptidase 1 OS=Plasmodium falciparum (isolate 3D7) GN=PF10_0150 PE=1 SV=1 | 1 | 92.26 | | |
| sp\|Q9NU22\|MDN1_HUMAN Midasin OS=Homo sapiens GN=MDN1 PE=1 SV=2;tr\|Q5T795\|Q5T795_HUMAN Midasin (Fragment) OS=Homo sapiens GN=MDN1 PE=1 SV=1 | 1 | 89.95 | | |
| tr\|Q8IC28\|Q8IC28_PLAF7 Methyltransferase, putative OS=Plasmodium falciparum (isolate 3D7) GN=PF07_0015 PE=4 SV=1 | 1 | 84.46 | | |
| tr\|O97279\|O97279_PLAF7 Putative uncharacterized protein OS=Plasmodium falciparum (isolate 3D7) GN=PFC0885c PE=4 SV=1 | 1 | 83.78 | | |
| sp\|Q9UK32-2\|KS6A6_HUMAN Isoform 2 of Ribosomal protein S6 kinase alpha-6 OS=Homo sapiens GN=RPS6KA6;sp\|Q9UK32\|KS6A6_HUMAN Ribosomal protein S6 kinase alpha-6 OS=Homo sapiens GN=RPS6KA6 PE=1 SV=1 | 1 | 82.49 | | |
| tr\|Q8I4X3\|Q8I4X3_PLAF7 Conserved Plasmodium protein OS=Plasmodium falciparum (isolate 3D7) GN=PFL2200w PE=4 SV=1 | 1 | 82.26 | | |
| tr\|Q8I1Q4\|Q8I1Q4_PLAF7 Uncharacterized protein OS=Plasmodium falciparum (isolate 3D7) GN=PFD0885c PE=4 SV=1 | 1 | 82.15 | | |
| tr\|Q8ID23\|Q8ID23_PLAF7 Mitochondrial carrier protein, putative OS=Plasmodium falciparum (isolate 3D7) GN=PF13_0359 PE=3 SV=1 | 1 | 77.43 | | |
| tr\|Q8I630\|Q8I630_PLAF7 XPA binding protein 1, putative OS=Plasmodium falciparum (isolate 3D7) GN=PFL0075w PE=4 SV=1 | 1 | 70.66 | | |
| tr\|Q8I5X7\|Q8I5X7_PLAF7 Uncharacterized protein OS=Plasmodium falciparum (isolate 3D7) GN=PFL0340w PE=4 SV=1 | 1 | 68.31 | | |
| tr\|Q8IJ99\|Q8IJ99_PLAF7 Uncharacterized protein OS=Plasmodium falciparum (isolate 3D7) GN=PF10_0299 PE=4 SV=1 | 1 | 67.03 | | |
| tr\|Q8IFN5\|Q8IFN5_PLAF7 Clathrin assembly protein, putative OS=Plasmodium falciparum (isolate 3D7) GN=PFD1090c PE=4 SV=1 | 1 | 66.00 | | |
| tr\|Q8IBJ8\|Q8IBJ8_PLAF7 Uncharacterized protein OS=Plasmodium falciparum (isolate 3D7) GN=PF07_0106 PE=4 SV=1 | 1 | 60.72 | | |
| tr\|Q8IKE9\|Q8IKE9_PLAF7 U2 snRNP auxiliary factor, putative OS=Plasmodium falciparum (isolate 3D7) GN=PF14_0656 PE=4 SV=1 | 1 | 59.50 | | |
| tr\|Q8IL54\|Q8IL54_PLAF7 Acid cluster protein 33 homologue, putative OS=Plasmodium falciparum (isolate 3D7) GN=PF14_0395 PE=4 SV=1 | 1 | 57.52 | | |
| tr\|Q8IAP1\|Q8IAP1_PLAF7 Uncharacterized protein OS=Plasmodium falciparum (isolate 3D7) GN=MAL8P1.139 PE=4 SV=1 | 1 | 55.05 | | |
| tr\|Q8IE38\|Q8IE38_PLAF7 Nicotinic acid mononucleotide adenyltransferase OS=Plasmodium falciparum (isolate 3D7) GN=PF13_0159 PE=4 SV=1 | 1 | 53.14 | | |
| tr\|H0YI09\|H0YI09_HUMAN Methyltransferase-like protein 7A (Fragment) OS=Homo sapiens GN=METTL7A PE=1 SV=1;sp\|Q9H8H3\|MET7A_HUMAN Methyltransferase-like protein 7A OS=Homo sapiens GN=METTL7A PE=1 SV=1 | 1 | 52.84 | | |
| tr\|Q8IDY4\|Q8IDY4_PLAF7 MSP7-like protein OS=Plasmodium falciparum (isolate 3D7) GN=MAL13P1.173 PE=4 SV=1 | 1 | 52.65 | | |
| tr\|Q8IJG5\|Q8IJG5_PLAF7 Conserved Plasmodium protein OS=Plasmodium falciparum (isolate 3D7) GN=PF10_0233 PE=4 SV=2 | 1 | 51.69 | | |
| tr\|Q8IK09\|Q8IK09_PLAF7 Uncharacterized protein OS=Plasmodium falciparum (isolate 3D7) GN=PF10_0031 PE=4 SV=1 | 1 | 47.41 | | |
| tr\|Q8IKW6\|Q8IKW6_PLAF7 Uncharacterized protein OS=Plasmodium falciparum (isolate 3D7) GN=PF14_0485 PE=4 SV=1 | 1 | 44.86 | | |
| tr\|Q8I237\|Q8I237_PLAF7 Transcription initiation factor TFIIB, putative OS=Plasmodium falciparum (isolate 3D7) GN=PFA_0525w PE=4 SV=1 | 1 | 42.44 | | |
| tr\|Q8IJQ6\|Q8IJQ6_PLAF7 Initiation factor 2 subunit family, putative OS=Plasmodium falciparum (isolate 3D7) GN=PF10_0136 PE=3 SV=1 | 1 | 42.33 | | |
| tr\|Q8IJC4\|Q8IJC4_PLAF7 Methyltransferase, putative OS=Plasmodium falciparum (isolate 3D7) GN=PF10_0274 PE=4 SV=2 | 1 | 41.92 | | |
| tr\|Q8IDZ2\|Q8IDZ2_PLAF7 Uncharacterized protein OS=Plasmodium falciparum (isolate 3D7) GN=PF13_0184 PE=4 SV=1 | 1 | 39.50 | | |
| tr\|Q8IES1\|Q8IES1_PLAF7 Uncharacterized protein OS=Plasmodium falciparum (isolate 3D7) GN=PF13_0020 PE=4 SV=1 | 1 | 38.14 | | |
| tr\|Q8IJX2\|Q8IJX2_PLAF7 PPPDE peptidase, putative OS=Plasmodium falciparum (isolate 3D7) GN=PF10_0069 PE=4 SV=2 | 1 | 37.68 | | |
| tr\|C6KSV2\|C6KSV2_PLAF7 Uncharacterized protein OS=Plasmodium falciparum (isolate 3D7) GN=PFF0525w PE=4 SV=1 | 1 | 37.39 | | |
| tr\|Q8ILH0\|Q8ILH0_PLAF7 rRNA (Adenosine-2-O-)-methyltransferase, putative OS=Plasmodium falciparum (isolate 3D7) GN=PF14_0273 PE=4 SV=1 | 1 | 37.35 | | |

| | | | | |
|---|---|---|---|---|
| tr\|Q8IKQ4\|Q8IKQ4_PLAF7 Uncharacterized protein OS=Plasmodium falciparum (isolate 3D7) GN=PF14_0549 PE=4 SV=1 | 1 | 35.33 | | |
| tr\|Q8I427\|Q8I427_PLAF7 Cell differentiation protein rcd1, putative OS=Plasmodium falciparum (isolate 3D7) GN=PFE0375w PE=4 SV=1 | 1 | 31.11 | | |
| sp\|Q5THJ4-2\|VP13D_HUMAN Isoform 2 of Vacuolar protein sorting-associated protein 13D OS=Homo sapiens GN=VPS13D;sp\|Q5THJ4\|VP13D_HUMAN Vacuolar protein sorting-associated protein 13D OS=Homo sapiens GN=VPS13D PE=1 SV=2 | 1 | 28.27 | | |
| tr\|Q8IJ79\|Q8IJ79_PLAF7 Leucine-rich repeat protein 8, LRR8 OS=Plasmodium falciparum (isolate 3D7) GN=PF10_0320 PE=4 SV=2 | 1 | 27.37 | | |
| tr\|Q8IL46\|Q8IL46_PLAF7 Protein prenyltransferase alpha subunit, putative OS=Plasmodium falciparum (isolate 3D7) GN=PF14_0403 PE=4 SV=2 | 1 | 26.77 | | |
| tr\|Q8I508\|Q8I508_PLAF7 Conserved Plasmodium protein OS=Plasmodium falciparum (isolate 3D7) GN=PFL2025w PE=4 SV=1 | 1 | 23.02 | | |
| tr\|C6KT75\|C6KT75_PLAF7 Ribonuclease OS=Plasmodium falciparum (isolate 3D7) GN=PFF1150w PE=3 SV=1 | 1 | 22.48 | | |
| tr\|Q8I701\|Q8I701_PLAF7 Deoxyhypusine hydroxylase OS=Plasmodium falciparum (isolate 3D7) GN=PF13_0013 PE=3 SV=1 | 1 | 21.89 | | |
| tr\|F2Z393\|F2Z393_HUMAN Transaldolase OS=Homo sapiens GN=TALDO1 PE=1 SV=1;sp\|P37837\|TALDO_HUMAN Transaldolase OS=Homo sapiens GN=TALDO1 PE=1 SV=2 | 1 | 19.95 | | |
| tr\|Q8I2S2\|Q8I2S2_PLAF7 Putative uncharacterized protein OS=Plasmodium falciparum (isolate 3D7) GN=PFI1150w PE=4 SV=1 | 1 | 18.98 | | |
| tr\|Q8IK14\|Q8IK14_PLAF7 Uncharacterized protein OS=Plasmodium falciparum (isolate 3D7) GN=PF10_0026 PE=4 SV=1 | 1 | 18.13 | | |
| tr\|Q8IB20\|Q8IB20_PLAF7 Zinc finger protein, putative OS=Plasmodium falciparum (isolate 3D7) GN=PF08_0056 PE=4 SV=1 | 1 | 16.66 | | |
| tr\|Q8IKN3\|Q8IKN3_PLAF7 Uncharacterized protein OS=Plasmodium falciparum (isolate 3D7) GN=PF14_0571 PE=4 SV=2 | 1 | 14.00 | | |
| tr\|Q8IJ40\|Q8IJ40_PLAF7 Acetyl-CoA transporter, putative OS=Plasmodium falciparum (isolate 3D7) GN=PF10_0360 PE=4 SV=2 | 1 | 13.57 | | |
| tr\|C0H552\|C0H552_PLAF7 Putative uncharacterized protein OS=Plasmodium falciparum (isolate 3D7) GN=PFI1120c PE=4 SV=1 | 1 | 13.50 | | |
| sp\|C0H4X5\|DRE2_PLAF7 Anamorsin homolog OS=Plasmodium falciparum (isolate 3D7) GN=MAL8P1.31 PE=3 SV=1 | 1 | 12.94 | | |
| tr\|Q8IBA8\|Q8IBA8_PLAF7 Uncharacterized protein OS=Plasmodium falciparum (isolate 3D7) GN=MAL8P1.18 PE=4 SV=1 | 1 | 12.38 | | |
| tr\|Q8IKT8\|Q8IKT8_PLAF7 RNA binding protein, putative OS=Plasmodium falciparum (isolate 3D7) GN=PF14_0513 PE=4 SV=1 | 1 | 12.34 | | |
| tr\|C0H4N1\|C0H4N1_PLAF7 Uncharacterized protein OS=Plasmodium falciparum (isolate 3D7) GN=MAL7P1.83 PE=4 SV=1 | 1 | 11.86 | | |
| sp\|P61970\|NTF2_HUMAN Nuclear transport factor 2 OS=Homo sapiens GN=NUTF2 PE=1 SV=1 | 1 | 11.50 | | |
| tr\|Q8IE72\|Q8IE72_PLAF7 DEAD box helicase, putative OS=Plasmodium falciparum (isolate 3D7) GN=MAL13P1.134 PE=4 SV=1 | 1 | 10.66 | | |
| tr\|Q8IHN2\|Q8IHN2_PLAF7 Plasmodium exported protein OS=Plasmodium falciparum (isolate 3D7) GN=PF11_0508 PE=4 SV=1 | 1 | 10.33 | | |
| tr\|Q8ILW0\|Q8ILW0_PLAF7 SufC ATPase, putative OS=Plasmodium falciparum (isolate 3D7) GN=PF14_0133 PE=3 SV=1 | 1 | 9.07 | | |
| tr\|Q8IE15\|Q8IE15_PLAF7 Uncharacterized protein OS=Plasmodium falciparum (isolate 3D7) GN=PF13_0167 PE=4 SV=1 | 1 | 8.08 | | |
| tr\|Q8IE63\|Q8IE63_PLAF7 Tetratricopeptide repeat family protein, putative OS=Plasmodium falciparum (isolate 3D7) GN=MAL13P1.139 PE=4 SV=1 | 1 | 7.25 | | |
| tr\|Q8IAN1\|Q8IAN1_PLAF7 Uncharacterized protein OS=Plasmodium falciparum (isolate 3D7) GN=PF08_0127 PE=4 SV=1 | 1 | 6.91 | | |
| tr\|Q8IBG5\|Q8IBG5_PLAF7 Nucleolus BRIX protein, putative OS=Plasmodium falciparum (isolate 3D7) GN=PF07_0122 PE=4 SV=1 | 1 | 6.55 | | |
| tr\|Q8IDT8\|Q8IDT8_PLAF7 Uncharacterized protein OS=Plasmodium falciparum (isolate 3D7) GN=MAL13P1.202 PE=4 SV=1 | 1 | 6.42 | | |
| tr\|H7C368\|H7C368_HUMAN Oxysterol-binding protein (Fragment) OS=Homo sapiens GN=OSBP2 PE=1 SV=1 | 1 | 6.42 | | |
| tr\|Q8IBY9\|Q8IBY9_PLAF7 Uncharacterized protein OS=Plasmodium falciparum (isolate 3D7) GN=PF07_0041 PE=4 SV=1 | 1 | 6.42 | | |
| tr\|Q8IJV9\|Q8IJV9_PLAF7 Conserved Plasmodium membrane protein OS=Plasmodium falciparum (isolate 3D7) GN=PF10_0082 PE=4 SV=2 | 1 | 6.42 | | |
| tr\|Q8IID0\|Q8IID0_PLAF7 Uncharacterized protein OS=Plasmodium falciparum (isolate 3D7) GN=PF11_0244 PE=4 SV=1 | 1 | 6.42 | | |

| | | | | |
|---|---|---|---|---|
| tr\|Q8IM40\|Q8IM40_PLAF7 DNA mismatch repair protein, putative OS=Plasmodium falciparum (isolate 3D7) GN=PF14_0051 PE=4 SV=1 | 1 | 6.42 | | |
| tr\|Q8IKG0\|Q8IKG0_PLAF7 Uncharacterized protein OS=Plasmodium falciparum (isolate 3D7) GN=PF14_0645 PE=4 SV=1 | 1 | 6.42 | | |
| tr\|O77371\|O77371_PLAF7 Cleavage and polyadenylation specificity factor protein, putative OS=Plasmodium falciparum (isolate 3D7) GN=PFC0825c PE=4 SV=1 | 1 | 6.42 | | |
| tr\|O97299\|O97299_PLAF7 Putative uncharacterized protein OS=Plasmodium falciparum (isolate 3D7) GN=PFC1030w PE=4 SV=1 | 1 | 6.42 | | |
| tr\|Q8I1Z9\|Q8I1Z9_PLAF7 Regulator of chromosome condensation, putative OS=Plasmodium falciparum (isolate 3D7) GN=PFD0145c PE=4 SV=1 | 1 | 6.42 | | |
| tr\|Q8I1X0\|Q8I1X0_PLAF7 Uncharacterized protein OS=Plasmodium falciparum (isolate 3D7) GN=PFD0290w PE=4 SV=1 | 1 | 6.42 | | |
| tr\|Q8I2G6\|Q8I2G6_PLAF7 Cytoadherence-linked protein OS=Plasmodium falciparum (isolate 3D7) GN=PFI1710w PE=4 SV=1 | 1 | 6.42 | | |
| tr\|Q8I4T4\|Q8I4T4_PLAF7 rRNA processing protein, putative OS=Plasmodium falciparum (isolate 3D7) GN=PFL2400w PE=4 SV=1 | 1 | 6.42 | | |
| tr\|O96164\|O96164_PLAF7 Serine repeat antigen 4 (SERA-4) OS=Plasmodium falciparum (isolate 3D7) GN=SERA-4 PE=1 SV=1;tr\|O96166\|O96166_PLAF7 Serine repeat antigen 2 (SERA-2) OS=Plasmodium falciparum (isolate 3D7) GN=SERA-2 PE=3 SV=3 | 1 | 6.42 | | |
| tr\|Q8I3A3\|Q8I3A3_PLAF7 Ubiquitin specific protease, putative OS=Plasmodium falciparum (isolate 3D7) GN=PFI0225w PE=4 SV=1 | 1 | 5.99 | | |
| tr\|Q8IHV9\|Q8IHV9_PLAF7 Uncharacterized protein OS=Plasmodium falciparum (isolate 3D7) GN=PF11_0417 PE=4 SV=1 | 1 | 5.51 | | |
| tr\|Q8ILU6\|Q8ILU6_PLAF7 Uracil-DNA glycosylase OS=Plasmodium falciparum (isolate 3D7) GN=PF14_0148 PE=3 SV=1 | 1 | 5.39 | | |
| tr\|Q8IDV4\|Q8IDV4_PLAF7 Uncharacterized protein OS=Plasmodium falciparum (isolate 3D7) GN=PF13_0212 PE=4 SV=1 | 1 | 5.19 | | |
| sp\|Q5T1C6\|THEM4_HUMAN Acyl-coenzyme A thioesterase THEM4 OS=Homo sapiens GN=THEM4 PE=1 SV=1 | 1 | 4.69 | | |
| tr\|Q8ID74\|Q8ID74_PLAF7 Polynucleotide kinase, putative OS=Plasmodium falciparum (isolate 3D7) GN=PF13_0334 PE=4 SV=1 | 1 | 4.42 | | |
| tr\|Q9U0H9\|Q9U0H9_PLAF7 Uncharacterized protein OS=Plasmodium falciparum (isolate 3D7) GN=PFD0540c PE=4 SV=1 | 1 | 4.34 | | |
| tr\|Q9U0L3\|Q9U0L3_PLAF7 Transcription factor, putative OS=Plasmodium falciparum (isolate 3D7) GN=PFD0360w PE=4 SV=1 | 1 | 4.16 | | |
| tr\|Q8I6U9\|Q8I6U9_PLAF7 Cytochrome c1, putative OS=Plasmodium falciparum (isolate 3D7) GN=PF14_0597 PE=4 SV=1 | 1 | 4.04 | | |
| tr\|Q8IB63\|Q8IB63_PLAF7 Uncharacterized protein OS=Plasmodium falciparum (isolate 3D7) GN=PF08_0035 PE=4 SV=1 | 1 | 4.03 | | |
| tr\|Q8IBR1\|Q8IBR1_PLAF7 Uncharacterized protein OS=Plasmodium falciparum (isolate 3D7) GN=MAL7P1.98 PE=4 SV=1 | 1 | 3.83 | | |
| tr\|C6KTA7\|C6KTA7_PLAF7 Ankyrin-repeat protein, putative OS=Plasmodium falciparum (isolate 3D7) GN=PFF1315w PE=4 SV=1 | 1 | 3.70 | | |
| tr\|H3BQ06\|H3BQ06_HUMAN Uncharacterized protein OS=Homo sapiens PE=4 SV=1;sp\|Q9ULP9-2\|TBC24_HUMAN Isoform 2 of TBC1 domain family member 24 OS=Homo sapiens GN=TBC1D24;sp\|Q9ULP9\|TBC24_HUMAN TBC1 domain family member 24 OS=Homo sapiens GN=TBC1D24 PE=1 SV=2 | 1 | 3.57 | | |
| tr\|Q8IIC2\|Q8IIC2_PLAF7 Uncharacterized protein OS=Plasmodium falciparum (isolate 3D7) GN=PF11_0252 PE=4 SV=1 | 1 | 3.49 | | |
| tr\|Q8I1Y3\|Q8I1Y3_PLAF7 Uncharacterized protein OS=Plasmodium falciparum (isolate 3D7) GN=PFD0225w PE=4 SV=1 | 1 | 3.38 | | |
| tr\|Q8IKS5\|Q8IKS5_PLAF7 Uncharacterized protein OS=Plasmodium falciparum (isolate 3D7) GN=PF14_0527 PE=4 SV=1 | 1 | 2.94 | | |
| tr\|Q8I3J4\|Q8I3J4_PLAF7 Ubiquitin conjugating enzyme, putative OS=Plasmodium falciparum (isolate 3D7) GN=PFE1350c PE=1 SV=1 | 1 | 2.87 | | |
| tr\|Q8I249\|Q8I249_PLAF7 N-terminal acetyltransferase, putative OS=Plasmodium falciparum (isolate 3D7) GN=PFA_0465c PE=4 SV=1 | 1 | 2.85 | | |
| tr\|Q8I540\|Q8I540_PLAF7 Cell cycle control protein, putative OS=Plasmodium falciparum (isolate 3D7) GN=PFL1855w PE=4 SV=1 | 1 | 2.77 | | |
| tr\|Q8IE05\|Q8IE05_PLAF7 Sedlin, putative OS=Plasmodium falciparum (isolate 3D7) GN=PF13_0174 PE=4 SV=1 | 1 | 2.72 | | |
| tr\|Q8IK60\|Q8IK60_PLAF7 Uncharacterized protein OS=Plasmodium falciparum (isolate 3D7) GN=PF14_0746 PE=4 SV=2 | 1 | 2.65 | | |
| tr\|Q8ILX9\|Q8ILX9_PLAF7 GTP binding protein, putative OS=Plasmodium falciparum (isolate 3D7) GN=PF14_0114 PE=4 SV=1 | 1 | 2.63 | | |

| | | | | |
|---|---|---|---|---|
| tr\|Q8IJ27\|Q8IJ27_PLAF7 GDP dissociation inhibitor domain containing protein OS=Plasmodium falciparum (isolate 3D7) GN=PF10_0373 PE=4 SV=1 | 1 | 2.59 | | |
| tr\|Q8IET6\|Q8IET6_PLAF7 Uncharacterized protein OS=Plasmodium falciparum (isolate 3D7) GN=PF13_0015 PE=4 SV=1 | 1 | 2.49 | | |
| tr\|Q8IET0\|Q8IET0_PLAF7 Sodium/hydrogen exchanger, Na+, H+ antiporter OS=Plasmodium falciparum (isolate 3D7) GN=PF13_0019 PE=4 SV=1 | 1 | 2.49 | | |
| tr\|Q8ILL8\|Q8ILL8_PLAF7 Uncharacterized protein OS=Plasmodium falciparum (isolate 3D7) GN=PF14_0225 PE=4 SV=1 | 1 | 2.48 | | |
| tr\|Q8II07\|Q8II07_PLAF7 Conserved Plasmodium protein OS=Plasmodium falciparum (isolate 3D7) GN=PF11_0368 PE=4 SV=2 | 1 | 2.45 | | |
| tr\|Q8II47\|Q8II47_PLAF7 Uncharacterized protein OS=Plasmodium falciparum (isolate 3D7) GN=PF11_0327 PE=4 SV=1 | 1 | 2.41 | | |
| tr\|Q8I3J7\|Q8I3J7_PLAF7 Uncharacterized protein OS=Plasmodium falciparum (isolate 3D7) GN=PFE1335c PE=4 SV=1 | 1 | 2.41 | | |
| tr\|Q8IL63\|Q8IL63_PLAF7 Adaptor complexes medium subunit family OS=Plasmodium falciparum (isolate 3D7) GN=PF14_0386 PE=4 SV=1 | 1 | 2.41 | | |
| tr\|O77314\|O77314_PLAF7 Putative uncharacterized protein OS=Plasmodium falciparum (isolate 3D7) GN=PFC0145c PE=4 SV=1 | 1 | 2.38 | | |
| tr\|C6KT20\|C6KT20_PLAF7 Uncharacterized protein OS=Plasmodium falciparum (isolate 3D7) GN=PFF0870w PE=4 SV=1 | 1 | 2.36 | | |
| tr\|Q8I559\|Q8I559_PLAF7 Conserved Plasmodium protein OS=Plasmodium falciparum (isolate 3D7) GN=PFL1760w PE=4 SV=2 | 1 | 2.31 | | |
| tr\|Q8IDP0\|Q8IDP0_PLAF7 Uncharacterized protein OS=Plasmodium falciparum (isolate 3D7) GN=MAL13P1.228 PE=4 SV=1 | 1 | 2.15 | | |
| tr\|Q8IJG3\|Q8IJG3_PLAF7 Uncharacterized protein OS=Plasmodium falciparum (isolate 3D7) GN=PF10_0235 PE=4 SV=1 | 1 | 2.12 | | |
| sp\|C6KSQ6\|RAD50_PLAF7 Probable DNA repair protein RAD50 OS=Plasmodium falciparum (isolate 3D7) GN=PFF0285c PE=3 SV=1 | 1 | 2.08 | | |
| tr\|Q8IDA1\|Q8IDA1_PLAF7 Uncharacterized protein OS=Plasmodium falciparum (isolate 3D7) GN=PF13_0319 PE=4 SV=1 | 1 | 2.07 | | |
| tr\|Q8I362\|Q8I362_PLAF7 Putative uncharacterized protein OS=Plasmodium falciparum (isolate 3D7) GN=PFI0435c PE=4 SV=1 | 1 | 2.06 | | |
| tr\|Q8IEH3\|Q8IEH3_PLAF7 Uncharacterized protein OS=Plasmodium falciparum (isolate 3D7) GN=MAL13P1.73 PE=4 SV=1 | 1 | 1.99 | | |
| tr\|Q8IHN7\|Q8IHN7_PLAF7 Plasmodium exported protein (PHISTc) OS=Plasmodium falciparum (isolate 3D7) GN=PF11_0503 PE=4 SV=1 | 1 | 1.95 | | |
| tr\|Q8I3K7\|Q8I3K7_PLAF7 Membrane skeletal protein IMC1-related OS=Plasmodium falciparum (isolate 3D7) GN=PFE1285w PE=4 SV=1 | 1 | 1.84 | | |
| sp\|Q9H3N1\|TMX1_HUMAN Thioredoxin-related transmembrane protein 1 OS=Homo sapiens GN=TMX1 PE=1 SV=1 | 1 | 1.82 | | |
| tr\|Q8IL73\|Q8IL73_PLAF7 Uncharacterized protein OS=Plasmodium falciparum (isolate 3D7) GN=PF14_0375 PE=4 SV=1 | 1 | 1.76 | | |
| tr\|Q9U0H7\|Q9U0H7_PLAF7 Uncharacterized protein OS=Plasmodium falciparum (isolate 3D7) GN=PFD0550c PE=4 SV=1 | 1 | 1.76 | | |
| tr\|C6KSW2\|C6KSW2_PLAF7 Uncharacterized protein OS=Plasmodium falciparum (isolate 3D7) GN=PFF0575c PE=4 SV=1 | 1 | 1.74 | | |
| tr\|O77380\|O77380_PLAF7 CPSF (Cleavage and polyadenylation specific factor), subunit A, putative OS=Plasmodium falciparum (isolate 3D7) GN=PFC0780w PE=4 SV=2 | 1 | 1.72 | | |
| tr\|Q8I5W3\|Q8I5W3_PLAF7 Uncharacterized protein OS=Plasmodium falciparum (isolate 3D7) GN=PFL0425c PE=4 SV=1 | 1 | 1.70 | | |
| tr\|Q8IB48\|Q8IB48_PLAF7 Uncharacterized protein OS=Plasmodium falciparum (isolate 3D7) GN=MAL8P1.52 PE=4 SV=1 | 1 | 1.63 | | |
| tr\|Q8I3I0\|Q8I3I0_PLAF7 Cyclophilin, putative OS=Plasmodium falciparum (isolate 3D7) GN=PFE1430c PE=3 SV=1 | 1 | 1.63 | | |
| tr\|C0H598\|C0H598_PLAF7 Uncharacterized protein OS=Plasmodium falciparum (isolate 3D7) GN=MAL13P1.21 PE=4 SV=1 | 1 | 1.60 | | |
| tr\|Q8I592\|Q8I592_PLAF7 Elongation factor G, mitochondrial OS=Plasmodium falciparum (isolate 3D7) GN=PFL1590c PE=3 SV=1 | 1 | 1.56 | | |
| tr\|Q8IEN8\|Q8IEN8_PLAF7 Uncharacterized protein OS=Plasmodium falciparum (isolate 3D7) GN=PF13_0041 PE=4 SV=1 | 1 | 1.54 | | |
| tr\|Q8IJU3\|Q8IJU3_PLAF7 Conserved Plasmodium protein OS=Plasmodium falciparum (isolate 3D7) GN=PF10_0099 PE=4 SV=2 | 1 | 1.54 | | |
| tr\|Q8I5X8\|Q8I5X8_PLAF7 Eukaryotic translation initiation factor 5, putative OS=Plasmodium falciparum (isolate 3D7) GN=PFL0335c PE=4 SV=1 | 1 | 1.51 | | |
| tr\|C0H4P9\|C0H4P9_PLAF7 RNA binding protein, putative OS=Plasmodium falciparum (isolate 3D7) GN=MAL7P1.157a PE=4 SV=1 | 1 | 1.47 | | |

| | | | | |
|---|---|---|---|---|
| sp\|Q504Y2\|PKDCC_HUMAN Extracellular tyrosine-protein kinase PKDCC OS=Homo sapiens GN=PKDCC PE=2 SV=2 | 1 | 1.41 | | |
| tr\|Q8IL40\|Q8IL40_PLAF7 Uncharacterized protein OS=Plasmodium falciparum (isolate 3D7) GN=PF14_0409 PE=4 SV=1 | 1 | 1.40 | | |
| tr\|Q8IKV4\|Q8IKV4_PLAF7 Aminomethyltransferase, putative OS=Plasmodium falciparum (isolate 3D7) GN=PF14_0497 PE=4 SV=1 | 1 | 1.36 | | |
| tr\|O96158\|O96158_PLAF7 Conserved Plasmodium protein OS=Plasmodium falciparum (isolate 3D7) GN=PFB0285c PE=4 SV=1 | 1 | 1.34 | | |
| tr\|E5RID5\|E5RID5_HUMAN Carbonic anhydrase 2 OS=Homo sapiens GN=CA2 PE=1 SV=1;tr\|E5RK37\|E5RK37_HUMAN Carbonic anhydrase 2 OS=Homo sapiens GN=CA2 PE=1 SV=1;sp\|P00918\|CAH2_HUMAN Carbonic anhydrase 2 OS=Homo sapiens GN=CA2 PE=1 SV=2 | 1 | 1.32 | | |
| sp\|P28066-2\|PSA5_HUMAN Isoform 2 of Proteasome subunit alpha type-5 OS=Homo sapiens GN=PSMA5;sp\|P28066\|PSA5_HUMAN Proteasome subunit alpha type-5 OS=Homo sapiens GN=PSMA5 PE=1 SV=3 | 1 | 1.32 | | |
| tr\|Q8IBL1\|Q8IBL1_PLAF7 Uncharacterized protein OS=Plasmodium falciparum (isolate 3D7) GN=MAL7P1.129 PE=4 SV=1 | 1 | 1.30 | | |
| tr\|Q8I0W1\|Q8I0W1_PLAF7 mRNA processing protein, putative OS=Plasmodium falciparum (isolate 3D7) GN=PFI1600w PE=4 SV=1 | 1 | 1.30 | | |
| tr\|O97320\|O97320_PLAF7 Histone H2A OS=Plasmodium falciparum (isolate 3D7) GN=PFC0920w PE=3 SV=1;sp\|Q71UI9\|H2AV_HUMAN Histone H2A.V OS=Homo sapiens GN=H2AFV PE=1 SV=3;sp\|P0C0S5\|H2AZ_HUMAN Histone H2A.Z OS=Homo sapiens GN=H2AFZ PE=1 SV=2 | 1 | 1.26 | | |
| tr\|Q8IIY8\|Q8IIY8_PLAF7 Plasmodium falciparum Maurers Cleft 2 transmembrane domain protein 11.1, PfMC-2TM_11.1 OS=Plasmodium falciparum (isolate 3D7) GN=MC-2TM PE=4 SV=2 | 1 | 1.20 | | |
| sp\|P14209-3\|CD99_HUMAN Isoform 3 of CD99 antigen OS=Homo sapiens GN=CD99;sp\|P14209\|CD99_HUMAN CD99 antigen OS=Homo sapiens GN=CD99 PE=1 SV=1 | 1 | 1.17 | | |
| tr\|Q8I5N6\|Q8I5N6_PLAF7 Uncharacterized protein OS=Plasmodium falciparum (isolate 3D7) GN=PFL0830w PE=4 SV=1 | 1 | 1.17 | | |
| tr\|Q8I3F6\|Q8I3F6_PLAF7 Mitochondrial ribosomal protein S16, putative OS=Plasmodium falciparum (isolate 3D7) GN=PFE1560c PE=4 SV=1 | 1 | 1.16 | | |
| tr\|Q8IM76\|Q8IM76_PLAF7 Uncharacterized protein OS=Plasmodium falciparum (isolate 3D7) GN=PF14_0014 PE=4 SV=1 | 1 | 1.16 | | |
| tr\|Q8IKM6\|Q8IKM6_PLAF7 Uncharacterized protein OS=Plasmodium falciparum (isolate 3D7) GN=PF14_0578 PE=4 SV=1 | 1 | 1.14 | | |
| tr\|O97307\|O97307_PLAF7 Pfmc-2TM Maurers cleft two transmembrane protein OS=Plasmodium falciparum (isolate 3D7) GN=PfMC-2TM PE=4 SV=1 | 1 | 1.14 | | |
| sp\|P11021\|GRP78_HUMAN 78 kDa glucose-regulated protein OS=Homo sapiens GN=HSPA5 PE=1 SV=2 | 1 | 1.14 | | |
| tr\|Q8I5K7\|Q8I5K7_PLAF7 Uncharacterized protein OS=Plasmodium falciparum (isolate 3D7) GN=PFL0990w PE=4 SV=1 | 1 | 1.13 | | |
| tr\|Q8I1X5\|Q8I1X5_PLAF7 Pre-mRNA splicing factor, putative OS=Plasmodium falciparum (isolate 3D7) GN=PFD0265w PE=4 SV=1;sp\|Q6P2Q9\|PRP8_HUMAN Pre-mRNA-processing-splicing factor 8 OS=Homo sapiens GN=PRPF8 PE=1 SV=2 | 1 | 1.10 | | |
| tr\|Q8I523\|Q8I523_PLAF7 3-hydroxyisobutyryl-coenzyme A hydrolase, putative OS=Plasmodium falciparum (isolate 3D7) GN=PFL1940w PE=4 SV=1 | 1 | 1.10 | | |
| tr\|Q8IDQ4\|Q8IDQ4_PLAF7 Uncharacterized protein OS=Plasmodium falciparum (isolate 3D7) GN=MAL13P1.217 PE=4 SV=1 | 1 | 1.10 | | |
| sp\|P60709\|ACTB_HUMAN Actin, cytoplasmic 1 OS=Homo sapiens GN=ACTB PE=1 SV=1;sp\|P63261\|ACTG_HUMAN Actin, cytoplasmic 2 OS=Homo sapiens GN=ACTG1 PE=1 SV=1 | 1 | 1.09 | | |
| tr\|Q8IJY7\|Q8IJY7_PLAF7 Uncharacterized protein OS=Plasmodium falciparum (isolate 3D7) GN=PF10_0054 PE=4 SV=1 | 1 | 1.09 | | |
| tr\|K7EJB9\|K7EJB9_HUMAN Calreticulin (Fragment) OS=Homo sapiens GN=CALR PE=1 SV=1;sp\|P27797\|CALR_HUMAN Calreticulin OS=Homo sapiens GN=CALR PE=1 SV=1 | 1 | 1.08 | | |
| sp\|Q8IID4\|DYHC2_PLAF7 Dynein heavy chain-like protein PF11_0240 OS=Plasmodium falciparum (isolate 3D7) GN=PF11_0240 PE=3 SV=1 | 1 | 1.08 | | |
| tr\|Q8IBF5\|Q8IBF5_PLAF7 Uncharacterized protein OS=Plasmodium falciparum (isolate 3D7) GN=PF07_0127 PE=4 SV=1 | 1 | 1.07 | | |
| sp\|Q8IZ41-2\|RASEF_HUMAN Isoform 2 of Ras and EF-hand domain-containing protein OS=Homo sapiens GN=RASEF;sp\|Q8IZ41\|RASEF_HUMAN Ras and EF-hand domain-containing protein OS=Homo sapiens GN=RASEF PE=1 SV=1 | 1 | 1.07 | | |
| tr\|Q8I3L3\|Q8I3L3_PLAF7 Uncharacterized protein OS=Plasmodium falciparum (isolate 3D7) GN=PFE1255w PE=4 SV=1 | 1 | 1.07 | | |
| sp\|P32119\|PRDX2_HUMAN Peroxiredoxin-2 OS=Homo sapiens GN=PRDX2 PE=1 SV=5 | 1 | 1.06 | | |
| tr\|Q8IE74\|Q8IE74_PLAF7 Uncharacterized protein OS=Plasmodium falciparum (isolate 3D7) GN=MAL13P1.133 PE=4 SV=1 | 1 | 1.06 | | |

| | | | | |
|---|---|---|---|---|
| tr\|Q8ID89\|Q8ID89_PLAF7 Cytochrome c oxidase subunit 2, putative OS=Plasmodium falciparum (isolate 3D7) GN=PF13_0327 PE=4 SV=1 | 1 | 1.05 | | |
| sp\|Q9H1D9\|RPC6_HUMAN DNA-directed RNA polymerase III subunit RPC6 OS=Homo sapiens GN=POLR3F PE=1 SV=1 | 1 | 1.04 | | |
| sp\|Q9UL25\|RAB21_HUMAN Ras-related protein Rab-21 OS=Homo sapiens GN=RAB21 PE=1 SV=3 | 1 | 1.03 | | |
| tr\|O77360\|O77360_PLAF7 DEAD box helicase, putative OS=Plasmodium falciparum (isolate 3D7) GN=PFC0440c PE=4 SV=1 | 1 | 1.02 | | |
| tr\|Q8I1X1\|Q8I1X1_PLAF7 Lysine decarboxylase, putative OS=Plasmodium falciparum (isolate 3D7) GN=PFD0285c PE=4 SV=1 | 1 | 1.02 | | |
| tr\|Q8IK86\|Q8IK86_PLAF7 Uncharacterized protein OS=Plasmodium falciparum (isolate 3D7) GN=PF14_0720 PE=4 SV=1 | 1 | 1.01 | | |
| sp\|Q8ILR9\|YPF17_PLAF7 Protein PF14_0175 OS=Plasmodium falciparum (isolate 3D7) GN=PF14_0175 PE=3 SV=1 | 1 | 1.01 | | |
| tr\|Q8IEM1\|Q8IEM1_PLAF7 U4/U6 small nuclear ribonucleoprotein, putative OS=Plasmodium falciparum (isolate 3D7) GN=MAL13P1.45 PE=4 SV=1 | 1 | 1.00 | | |
| tr\|C6KTD0\|C6KTD0_PLAF7 Amino acid transporter, putative OS=Plasmodium falciparum (isolate 3D7) GN=PFF1430c PE=4 SV=1 | 1 | 1.00 | | |
| sp\|P48681\|NEST_HUMAN Nestin OS=Homo sapiens GN=NES PE=1 SV=2 | 1 | 1.00 | | |
| tr\|Q8IE49\|Q8IE49_PLAF7 DNA-directed RNA polymerase OS=Plasmodium falciparum (isolate 3D7) GN=PF13_0150 PE=3 SV=1 | 1 | 0.99 | | |
| tr\|Q8IIM9\|Q8IIM9_PLAF7 UDP-galactose transporter, putative OS=Plasmodium falciparum (isolate 3D7) GN=PF11_0141 PE=4 SV=1 | 1 | 0.98 | | |
| tr\|Q8I5D5\|Q8I5D5_PLAF7 NIMA-related protein kinase (Pfnek-1) OS=Plasmodium falciparum (isolate 3D7) GN=PFL1370w PE=4 SV=1 | 1 | 0.97 | | |
| tr\|Q8IK49\|Q8IK49_PLAF7 Uncharacterized protein OS=Plasmodium falciparum (isolate 3D7) GN=PF14_0758 PE=4 SV=1 | 1 | 0.97 | | |
| tr\|Q8IB83\|Q8IB83_PLAF7 Uncharacterized protein OS=Plasmodium falciparum (isolate 3D7) GN=PF08_0027 PE=4 SV=1 | 1 | 0.97 | | |
| tr\|Q8ILH5\|Q8ILH5_PLAF7 Uncharacterized protein OS=Plasmodium falciparum (isolate 3D7) GN=PF14_0268 PE=4 SV=2 | 1 | 0.97 | | |
| tr\|A0A087X1A9\|A0A087X1A9_HUMAN Vesicle-trafficking protein SEC22b (Fragment) OS=Homo sapiens GN=SEC22B PE=1 SV=1;sp\|O75396\|SC22B_HUMAN Vesicle-trafficking protein SEC22b OS=Homo sapiens GN=SEC22B PE=1 SV=4 | 1 | 0.97 | | |
| tr\|Q8IEL1\|Q8IEL1_PLAF7 Uncharacterized protein OS=Plasmodium falciparum (isolate 3D7) GN=PF13_0056 PE=4 SV=1 | 1 | 0.96 | | |
| tr\|Q8IEM0\|Q8IEM0_PLAF7 HORMA domain protein, putative OS=Plasmodium falciparum (isolate 3D7) GN=PF13_0050 PE=4 SV=1 | 1 | 0.96 | | |
| sp\|Q12789-3\|TF3C1_HUMAN Isoform 2 of General transcription factor 3C polypeptide 1 OS=Homo sapiens GN=GTF3C1;sp\|Q12789\|TF3C1_HUMAN General transcription factor 3C polypeptide 1 OS=Homo sapiens GN=GTF3C1 PE=1 SV=4 | 1 | 0.95 | | |
| tr\|Q8I5Q7\|Q8I5Q7_PLAF7 Uncharacterized protein OS=Plasmodium falciparum (isolate 3D7) GN=PFL0720w PE=4 SV=1 | 1 | 0.95 | | |
| tr\|Q8I4U1\|Q8I4U1_PLAF7 Uncharacterized protein OS=Plasmodium falciparum (isolate 3D7) GN=PFL2365w PE=4 SV=1 | 1 | 0.95 | | |
| tr\|Q8IDM0\|Q8IDM0_PLAF7 Uncharacterized protein OS=Plasmodium falciparum (isolate 3D7) GN=MAL13P1.239 PE=4 SV=1 | 1 | 0.95 | | |
| tr\|Q8I3X5\|Q8I3X5_PLAF7 Uncharacterized protein OS=Plasmodium falciparum (isolate 3D7) GN=PFE0655w PE=4 SV=1 | 1 | 0.94 | | |
| tr\|C0H592\|C0H592_PLAF7 REX2 protein OS=Plasmodium falciparum (isolate 3D7) GN=REX2 PE=4 SV=1 | 1 | 0.94 | | |
| tr\|Q8ILL6\|Q8ILL6_PLAF7 Calcium/calmodulin-dependent protein kinase, putative OS=Plasmodium falciparum (isolate 3D7) GN=PF14_0227 PE=4 SV=2 | 1 | 0.93 | | |
| tr\|C6KT12\|C6KT12_PLAF7 Alpha adaptin-like protein, putative OS=Plasmodium falciparum (isolate 3D7) GN=PFF0830w PE=4 SV=1 | 1 | 0.91 | | |
| sp\|P08107\|HSP71_HUMAN Heat shock 70 kDa protein 1A/1B OS=Homo sapiens GN=HSPA1A PE=1 SV=5;sp\|P08107-2\|HSP71_HUMAN Isoform 2 of Heat shock 70 kDa protein 1A/1B OS=Homo sapiens GN=HSPA1A | 1 | 0.91 | | |
| sp\|P00441\|SODC_HUMAN Superoxide dismutase [Cu-Zn] OS=Homo sapiens GN=SOD1 PE=1 SV=2 | 1 | 0.90 | | |
| tr\|Q8IL19\|Q8IL19_PLAF7 Serine/threonine kinase-1, PfLammer OS=Plasmodium falciparum (isolate 3D7) GN=LAMMER PE=1 SV=1 | 1 | 0.88 | | |
| tr\|Q8I239\|Q8I239_PLAF7 Phosphatidylinositol-4-phosphate-5-kinase OS=Plasmodium falciparum (isolate 3D7) GN=PfPIP5K/NCS PE=4 SV=1 | 1 | 0.88 | | |

| | | | | |
|---|---|---|---|---|
| tr\|Q8IIH1\|Q8IIH1_PLAF7 Uncharacterized protein OS=Plasmodium falciparum (isolate 3D7) GN=PF11_0203 PE=3 SV=1 | 1 | 0.87 | | |
| tr\|Q8IEL5\|Q8IEL5_PLAF7 Mitochondrial ATP synthase delta subunit, putative OS=Plasmodium falciparum (isolate 3D7) GN=MAL13P1.47 PE=3 SV=1 | 1 | 0.85 | | |
| tr\|Q8IL76\|Q8IL76_PLAF7 Uncharacterized protein OS=Plasmodium falciparum (isolate 3D7) GN=PF14_0372 PE=4 SV=2 | 1 | 0.85 | | |
| tr\|Q8IAQ5\|Q8IAQ5_PLAF7 DNAJ protein, putative OS=Plasmodium falciparum (isolate 3D7) GN=PF08_0115 PE=4 SV=1 | 1 | 0.84 | | |
| sp\|Q92508\|PIEZ1_HUMAN Piezo-type mechanosensitive ion channel component 1 OS=Homo sapiens GN=PIEZO1 PE=1 SV=4;tr\|E7EUT2\|E7EUT2_HUMAN Piezo-type mechanosensitive ion channel component 1 OS=Homo sapiens GN=PIEZO1 PE=1 SV=1 | 1 | 0.84 | | |
| tr\|Q8I4T3\|Q8I4T3_PLAF7 PFG377 protein OS=Plasmodium falciparum (isolate 3D7) GN=PFL2405c PE=4 SV=1 | 1 | 0.83 | | |
| sp\|C6KTB7\|ALTH1_PLAF7 Putative E3 ubiquitin-protein ligase protein PFF1365c OS=Plasmodium falciparum (isolate 3D7) GN=PFF1365c PE=3 SV=1 | 1 | 0.83 | | |
| sp\|Q96C34-2\|RUND1_HUMAN Isoform 2 of RUN domain-containing protein 1 OS=Homo sapiens GN=RUNDC1;sp\|Q96C34\|RUND1_HUMAN RUN domain-containing protein 1 OS=Homo sapiens GN=RUNDC1 PE=1 SV=3 | 1 | 0.82 | | |
| tr\|Q8II38\|Q8II38_PLAF7 Pre-mRNA splicing factor, putative OS=Plasmodium falciparum (isolate 3D7) GN=PF11_0336 PE=4 SV=1 | 1 | 0.81 | | |
| sp\|P17931\|LEG3_HUMAN Galectin-3 OS=Homo sapiens GN=LGALS3 PE=1 SV=5;tr\|G3V3R6\|G3V3R6_HUMAN Galectin OS=Homo sapiens GN=LGALS3 PE=1 SV=1 | 1 | 0.79 | | |
| tr\|Q8IID3\|Q8IID3_PLAF7 Uncharacterized protein OS=Plasmodium falciparum (isolate 3D7) GN=PF11_0241 PE=4 SV=1 | 1 | 0.79 | | |
| tr\|Q8IBP4\|Q8IBP4_PLAF7 Phosphoinositide-binding protein, putative OS=Plasmodium falciparum (isolate 3D7) GN=MAL7P1.108 PE=4 SV=2 | 1 | 0.79 | | |
| tr\|Q8I6U7\|Q8I6U7_PLAF7 Citrate synthase OS=Plasmodium falciparum (isolate 3D7) GN=PF10_0218 PE=3 SV=1 | 1 | 0.78 | | |
| tr\|E9PLD0\|E9PLD0_HUMAN Ras-related protein Rab-1B OS=Homo sapiens GN=RAB1B PE=1 SV=1;sp\|Q9H0U4\|RAB1B_HUMAN Ras-related protein Rab-1B OS=Homo sapiens GN=RAB1B PE=1 SV=1 | 1 | 0.78 | | |
| tr\|C6KSL5\|C6KSL5_PLAF7 Pfmc-2TM Maurers cleft two transmembrane protein OS=Plasmodium falciparum (isolate 3D7) GN=PfMC-2TM PE=4 SV=1;tr\|C6KTE8\|C6KTE8_PLAF7 Pfmc-2TM Maurers cleft two transmembrane protein OS=Plasmodium falciparum (isolate 3D7) GN=PFF1525 | 1 | 0.77 | | |
| tr\|Q8I2Y2\|Q8I2Y2_PLAF7 N-glycosylase/DNA lyase, putative OS=Plasmodium falciparum (isolate 3D7) GN=PFI0835c PE=4 SV=1 | 1 | 0.76 | | |
| sp\|O95236-2\|APOL3_HUMAN Isoform 2 of Apolipoprotein L3 OS=Homo sapiens GN=APOL3;sp\|O95236\|APOL3_HUMAN Apolipoprotein L3 OS=Homo sapiens GN=APOL3 PE=1 SV=3 | 1 | 0.76 | | |
| tr\|Q8IJU9\|Q8IJU9_PLAF7 Protein phosphatase, putative OS=Plasmodium falciparum (isolate 3D7) GN=PF10_0093 PE=4 SV=2 | 1 | 0.76 | | |
| tr\|Q8IIU1\|Q8IIU1_PLAF7 Conserved Plasmodium protein OS=Plasmodium falciparum (isolate 3D7) GN=PF11_0073 PE=4 SV=2 | 1 | 0.76 | | |
| tr\|Q8IKG1\|Q8IKG1_PLAF7 Uncharacterized protein OS=Plasmodium falciparum (isolate 3D7) GN=PF14_0644 PE=4 SV=1 | 1 | 0.76 | | |
| tr\|C0H494\|C0H494_PLAF7 Uncharacterized protein OS=Plasmodium falciparum (isolate 3D7) GN=PFD0350w PE=4 SV=1 | 1 | 0.76 | | |
| tr\|Q8I1N9\|Q8I1N9_PLAF7 Zinc finger protein, putative OS=Plasmodium falciparum (isolate 3D7) GN=PFD0970c PE=4 SV=1 | 1 | 0.76 | | |
| tr\|Q8I5H3\|Q8I5H3_PLAF7 Uncharacterized protein OS=Plasmodium falciparum (isolate 3D7) GN=PFL1175w PE=4 SV=1 | 1 | 0.76 | | |
| tr\|B9ZSH7\|B9ZSH7_PLAF7 Pfmc-2TM Maurers cleft two transmembrane protein OS=Plasmodium falciparum (isolate 3D7) GN=PfMC-2TM PE=4 SV=1 | 1 | 0.76 | | |
| sp\|Q8NHG7\|SVIP_HUMAN Small VCP/p97-interacting protein OS=Homo sapiens GN=SVIP PE=1 SV=1 | 1 | 0.76 | | |
| tr\|Q8IKX1\|Q8IKX1_PLAF7 Uncharacterized protein OS=Plasmodium falciparum (isolate 3D7) GN=PF14_0480 PE=4 SV=1 | 1 | 0.76 | | |
| tr\|I3L0N3\|I3L0N3_HUMAN Vesicle-fusing ATPase OS=Homo sapiens GN=NSF PE=1 SV=1;sp\|P46459\|NSF_HUMAN Vesicle-fusing ATPase OS=Homo sapiens GN=NSF PE=1 SV=3;tr\|I3L0L3\|I3L0L3_HUMAN Vesicle-fusing ATPase (Fragment) OS=Homo sapiens GN=NSF PE=1 SV=1 | 1 | 0.75 | | |
| tr\|Q9U0H5\|Q9U0H5_PLAF7 Uncharacterized protein OS=Plasmodium falciparum (isolate 3D7) GN=PFD0560w PE=4 SV=1 | 1 | 0.74 | | |
| tr\|Q8I3R5\|Q8I3R5_PLAF7 CCR4 OS=Plasmodium falciparum (isolate 3D7) GN=PFE0980c PE=4 SV=1 | 1 | 0.74 | | |

| | | | | |
|---|---|---|---|---|
| sp\|Q9H479\|FN3K_HUMAN Fructosamine-3-kinase OS=Homo sapiens GN=FN3K PE=1 SV=1 | 1 | 0.74 | | |
| tr\|C9JIF9\|C9JIF9_HUMAN Acylamino-acid-releasing enzyme OS=Homo sapiens GN=APEH PE=1 SV=1;sp\|P13798\|ACPH_HUMAN Acylamino-acid-releasing enzyme OS=Homo sapiens GN=APEH PE=1 SV=4 | 1 | 0.73 | | |
| tr\|Q8IEA7\|Q8IEA7_PLAF7 Uncharacterized protein OS=Plasmodium falciparum (isolate 3D7) GN=PF13_0120 PE=4 SV=1 | 1 | 0.73 | | |
| tr\|Q8IJ11\|Q8IJ11_PLAF7 Pfmc-2TM Maurers cleft two transmembrane protein OS=Plasmodium falciparum (isolate 3D7) GN=PF10_0390 PE=4 SV=2;tr\|Q8IIY1\|Q8IIY1_PLAF7 Uncharacterized protein OS=Plasmodium falciparum (isolate 3D7) GN=PF11_0025 PE=4 SV=1 | 1 | 0.72 | | |
| tr\|C0H4N5\|C0H4N5_PLAF7 Dynein heavy chain, putative OS=Plasmodium falciparum (isolate 3D7) GN=MAL7P1.89 PE=4 SV=1 | 1 | 0.72 | | |
| tr\|Q8I338\|Q8I338_PLAF7 Putative uncharacterized protein OS=Plasmodium falciparum (isolate 3D7) GN=PFI0555c PE=4 SV=1 | 1 | 0.70 | | |
| tr\|Q8I1N8\|Q8I1N8_PLAF7 RIO-like kinase OS=Plasmodium falciparum (isolate 3D7) GN=PfRIO2 PE=4 SV=1 | 1 | 0.70 | | |
| sp\|P02042\|HBD_HUMAN Hemoglobin subunit delta OS=Homo sapiens GN=HBD PE=1 SV=2;tr\|E9PFT6\|E9PFT6_HUMAN Hemoglobin subunit delta OS=Homo sapiens GN=HBD PE=1 SV=1 | 1 | 0.70 | | |
| tr\|Q8I248\|Q8I248_PLAF7 Cold-shock protein, putative OS=Plasmodium falciparum (isolate 3D7) GN=PFA_0470c PE=4 SV=1 | 1 | 0.70 | | |
| tr\|Q8IC51\|Q8IC51_PLAF7 Pfmc-2TM Maurers cleft two transmembrane protein OS=Plasmodium falciparum (isolate 3D7) GN=PfMC-2TM PE=4 SV=1;tr\|C6KTE8\|C6KTE8_PLAF7 Pfmc-2TM Maurers cleft two transmembrane protein OS=Plasmodium falciparum (isolate 3D7) GN=PFF1525 | 1 | 0.69 | | |
| tr\|Q8IET9\|Q8IET9_PLAF7 Uncharacterized protein OS=Plasmodium falciparum (isolate 3D7) GN=MAL13P1.13 PE=4 SV=1 | 1 | 0.69 | | |
| sp\|P06703\|S10A6_HUMAN Protein S100-A6 OS=Homo sapiens GN=S100A6 PE=1 SV=1;tr\|R4GN98\|R4GN98_HUMAN Protein S100 (Fragment) OS=Homo sapiens GN=S100A6 PE=1 SV=1 | 1 | 0.68 | | |
| tr\|Q8IJB7\|Q8IJB7_PLAF7 Uncharacterized protein OS=Plasmodium falciparum (isolate 3D7) GN=PF10_0281 PE=4 SV=1 | 1 | 0.66 | | |
| tr\|Q8IIS7\|Q8IIS7_PLAF7 Conserved Plasmodium protein OS=Plasmodium falciparum (isolate 3D7) GN=PF11_0088 PE=4 SV=2 | 1 | 0.66 | | |
| tr\|C0H5D9\|C0H5D9_PLAF7 Uncharacterized protein OS=Plasmodium falciparum (isolate 3D7) GN=PF13_0148 PE=4 SV=1 | 1 | 0.65 | | |
| sp\|O75131\|CPNE3_HUMAN Copine-3 OS=Homo sapiens GN=CPNE3 PE=1 SV=1 | 1 | 0.63 | | |
| tr\|C6KSZ7\|C6KSZ7_PLAF7 Uncharacterized protein OS=Plasmodium falciparum (isolate 3D7) GN=PFF0755c PE=4 SV=1 | 1 | 0.62 | | |
| tr\|G3V1D1\|G3V1D1_HUMAN Ferritin OS=Homo sapiens GN=FTH1 PE=1 SV=1;tr\|G3V192\|G3V192_HUMAN Ferritin OS=Homo sapiens GN=FTH1 PE=1 SV=1;sp\|P02794\|FRIH_HUMAN Ferritin heavy chain OS=Homo sapiens GN=FTH1 PE=1 SV=2 | 1 | 0.62 | | |
| tr\|Q9U0I8\|Q9U0I8_PLAF7 Uncharacterized protein OS=Plasmodium falciparum (isolate 3D7) GN=PFD0485w PE=4 SV=1 | 1 | 0.62 | | |
| tr\|O96183\|O96183_PLAF7 Sec61 gamma subunit, putative OS=Plasmodium falciparum (isolate 3D7) GN=PFB0450w PE=3 SV=1 | 1 | 0.60 | | |
| tr\|Q8IDL9\|Q8IDL9_PLAF7 Uncharacterized protein OS=Plasmodium falciparum (isolate 3D7) GN=MAL13P1.240 PE=4 SV=1 | 1 | 0.60 | | |
| sp\|Q96Q11-2\|TRNT1_HUMAN Isoform 2 of CCA tRNA nucleotidyltransferase 1, mitochondrial OS=Homo sapiens GN=TRNT1;sp\|Q96Q11\|TRNT1_HUMAN CCA tRNA nucleotidyltransferase 1, mitochondrial OS=Homo sapiens GN=TRNT1 PE=1 SV=2 | 1 | 0.60 | | |
| tr\|C6KSU4\|C6KSU4_PLAF7 Uncharacterized protein OS=Plasmodium falciparum (isolate 3D7) GN=PFF0480w PE=4 SV=1 | 1 | 0.59 | | |
| sp\|Q0ZLH3\|PJVK_HUMAN Pejvakin OS=Homo sapiens GN=DFNB59 PE=1 SV=1 | 1 | 0.56 | | |
| tr\|C6KT41\|C6KT41_PLAF7 Uncharacterized protein OS=Plasmodium falciparum (isolate 3D7) GN=PFF0980w PE=4 SV=1 | 1 | 0.55 | | |
| tr\|Q8IKT9\|Q8IKT9_PLAF7 Uncharacterized protein OS=Plasmodium falciparum (isolate 3D7) GN=PF14_0512 PE=4 SV=1 | 1 | 0.50 | | |
| tr\|C6KSP5\|C6KSP5_PLAF7 Glyoxalase I, putative OS=Plasmodium falciparum (isolate 3D7) GN=PFF0230c PE=4 SV=1 | 1 | 0.50 | | |
| tr\|Q8IEE7\|Q8IEE7_PLAF7 Sec20 homolog, putative OS=Plasmodium falciparum (isolate 3D7) GN=MAL13P1.87 PE=4 SV=1 | 1 | 0.48 | | |
| tr\|Q8IKJ5\|Q8IKJ5_PLAF7 Zinc finger protein, putative OS=Plasmodium falciparum (isolate 3D7) GN=PF14_0610 PE=4 SV=1 | 1 | 0.48 | | |

| | | | | |
|---|---|---|---|---|
| tr\|Q8IDE1\|Q8IDE1_PLAF7 Uncharacterized protein OS=Plasmodium falciparum (isolate 3D7) GN=PF13_0299 PE=4 SV=1 | 1 | 0.47 | | |
| tr\|O97295\|O97295_PLAF7 O-acyltransferase OS=Plasmodium falciparum (isolate 3D7) GN=PFC0995c PE=3 SV=1 | 1 | 0.46 | | |
| tr\|A8KAJ9\|A8KAJ9_HUMAN cDNA FLJ78342 OS=Homo sapiens GN=TYW5 PE=1 SV=1 | 1 | 0.46 | | |
| tr\|C0H5G7\|C0H5G7_PLAF7 RNA binding protein, putative OS=Plasmodium falciparum (isolate 3D7) GN=MAL13P1.385 PE=4 SV=1 | 1 | 0.45 | | |
| tr\|Q8I273\|Q8I273_PLAF7 2-C-methyl-D-erythritol 4-phosphate cytidylyltransferase, putative OS=Plasmodium falciparum (isolate 3D7) GN=PFA_0340w PE=4 SV=1 | 1 | 0.44 | | |
| tr\|C6S3I6\|C6S3I6_PLAF7 Uncharacterized protein OS=Plasmodium falciparum (isolate 3D7) GN=PF14_0783 PE=4 SV=1 | 1 | 0.43 | | |
| tr\|Q8I265\|Q8I265_PLAF7 Serine/threonine protein kinase, putative OS=Plasmodium falciparum (isolate 3D7) GN=PFA_0380w PE=4 SV=1 | 1 | 0.42 | | |
| tr\|Q8I576\|Q8I576_PLAF7 Uncharacterized protein OS=Plasmodium falciparum (isolate 3D7) GN=PFL1670c PE=4 SV=1 | 1 | 0.38 | | |
| tr\|C6S3F2\|C6S3F2_PLAF7 Serine esterase, putative OS=Plasmodium falciparum (isolate 3D7) GN=PF11_0168a PE=4 SV=1 | 1 | 0.37 | | |
| tr\|Q8IC44\|Q8IC44_PLAF7 STARP antigen OS=Plasmodium falciparum (isolate 3D7) GN=PF07_0006 PE=4 SV=1 | 1 | 0.35 | | |
| tr\|C0H539\|C0H539_PLAF7 Putative uncharacterized protein OS=Plasmodium falciparum (isolate 3D7) GN=PFI0805w PE=4 SV=1 | 1 | 0.32 | | |
| tr\|Q8I612\|Q8I612_PLAF7 Uncharacterized protein OS=Plasmodium falciparum (isolate 3D7) GN=PFL0165c PE=4 SV=1 | 1 | 0.25 | | |
| tr\|C0H499\|C0H499_PLAF7 Uncharacterized protein OS=Plasmodium falciparum (isolate 3D7) GN=PFD0415c PE=4 SV=1 | 1 | 0.25 | | |
| tr\|Q8IKB0\|Q8IKB0_PLAF7 Uncharacterized protein OS=Plasmodium falciparum (isolate 3D7) GN=PF14_0696 PE=4 SV=2 | 1 | 0.24 | | |
| tr\|Q8IE19\|Q8IE19_PLAF7 GPI transamidase subunit PIG-U, putative OS=Plasmodium falciparum (isolate 3D7) GN=MAL13P1.165 PE=4 SV=1 | 1 | 0.22 | | |
| tr\|Q8IID6\|Q8IID6_PLAF7 Uncharacterized protein OS=Plasmodium falciparum (isolate 3D7) GN=PF11_0238 PE=4 SV=1 | 1 | 0.17 | | |
| tr\|Q8I2N8\|Q8I2N8_PLAF7 Putative uncharacterized protein OS=Plasmodium falciparum (isolate 3D7) GN=PFI1330c PE=4 SV=1 | 1 | 0.14 | | |
| tr\|Q8IKY9\|Q8IKY9_PLAF7 SEL-1 protein, putative OS=Plasmodium falciparum (isolate 3D7) GN=PF14_0462 PE=4 SV=1 | 1 | 0.14 | | |
| tr\|Q8IKB7\|Q8IKB7_PLAF7 Protein YIPF OS=Plasmodium falciparum (isolate 3D7) GN=PF14_0689 PE=3 SV=2 | 1 | 0.13 | | |
| tr\|Q8ID99\|Q8ID99_PLAF7 Uncharacterized protein OS=Plasmodium falciparum (isolate 3D7) GN=PF13_0321 PE=4 SV=1 | 1 | 0.12 | | |
| tr\|Q8IKZ5\|Q8IKZ5_PLAF7 Uncharacterized protein OS=Plasmodium falciparum (isolate 3D7) GN=PF14_0456 PE=4 SV=1 | 1 | 0.11 | | |
| tr\|Q8I098\|Q8I098_PLAF7 Erythrocyte membrane protein 1, PfEMP1 OS=Plasmodium falciparum (isolate 3D7) GN=VAR PE=4 SV=1 | 1 | 0.10 | | |
| tr\|C0H4B0\|C0H4B0_PLAF7 Uncharacterized protein OS=Plasmodium falciparum (isolate 3D7) GN=MAL4P1.163 PE=4 SV=1 | 1 | 0.10 | | |
| tr\|C6S3G2\|C6S3G2_PLAF7 Alpha/beta hydrolase, putative OS=Plasmodium falciparum (isolate 3D7) GN=PF11_0441a PE=4 SV=1 | 1 | 0.08 | | |
| tr\|Q8I5R8\|Q8I5R8_PLAF7 RNA polymerase subunit 8c, putative OS=Plasmodium falciparum (isolate 3D7) GN=PFL0665c PE=4 SV=1 | 1 | 0.08 | | |
| tr\|C6KT61\|C6KT61_PLAF7 Uncharacterized protein OS=Plasmodium falciparum (isolate 3D7) GN=PFF1080w PE=4 SV=1 | 1 | 0.08 | | |
| tr\|F5H6I7\|F5H6I7_HUMAN Atlastin-3 OS=Homo sapiens GN=ATL3 PE=1 SV=1;sp\|Q6DD88\|ATLA3_HUMAN Atlastin-3 OS=Homo sapiens GN=ATL3 PE=1 SV=1 | 1 | 0.08 | | |
| tr\|C6KT97\|C6KT97_PLAF7 Oxidoreductase, short-chain dehydrogenase family, putative OS=Plasmodium falciparum (isolate 3D7) GN=PFF1265w PE=4 SV=1 | 1 | 0.06 | | |
| tr\|C0H4U9\|C0H4U9_PLAF7 Uncharacterized protein OS=Plasmodium falciparum (isolate 3D7) GN=MAL8P1.79 PE=4 SV=1 | 1 | 0.04 | | |
| tr\|Q8IBV2\|Q8IBV2_PLAF7 Transcription elongation factor s-II, putative OS=Plasmodium falciparum (isolate 3D7) GN=PF07_0057 PE=4 SV=1 | 1 | 0.04 | | |
| tr\|E9PBW4\|E9PBW4_HUMAN Hemoglobin subunit gamma-2 OS=Homo sapiens GN=HBG2 PE=1 SV=1;sp\|P69892\|HBG2_HUMAN Hemoglobin subunit gamma-2 OS=Homo sapiens GN=HBG2 PE=1 SV=2;sp\|P69891\|HBG1_HUMAN Hemoglobin subunit gamma-1 OS=Homo sapiens GN=HBG1 PE=1 SV=2 | 1 | 0.04 | | |
| sp\|P30041\|PRDX6_HUMAN Peroxiredoxin-6 OS=Homo sapiens GN=PRDX6 PE=1 SV=3 | 1 | 0.04 | | |
| sp\|P10599\|THIO_HUMAN Thioredoxin OS=Homo sapiens GN=TXN PE=1 SV=3 | 1 | 0.03 | | |

| | | | | |
|---|---|---|---|---|
| tr\|Q8IHY7\|Q8IHY7_PLAF7 Calcium-binding protein, putative OS=Plasmodium falciparum (isolate 3D7) GN=PF11_0389 PE=4 SV=1 | 1 | 0.02 | | |
| tr\|A0A087WVP1\|A0A087WVP1_HUMAN Protocadherin Fat 1 OS=Homo sapiens GN=FAT1 PE=1 SV=1;sp\|Q14517\|FAT1_HUMAN Protocadherin Fat 1 OS=Homo sapiens GN=FAT1 PE=1 SV=2;tr\|H0Y9H4\|H0Y9H4_HUMAN Protocadherin Fat 1 (Fragment) OS=Homo sapiens GN=FAT1 PE=1 SV=1 | 1 | 0.02 | | |
| tr\|Q8IJ82\|Q8IJ82_PLAF7 DER1-like protein, putative OS=Plasmodium falciparum (isolate 3D7) GN=PF10_0317 PE=4 SV=1 | 1 | 0.02 | | |
| tr\|Q8I514\|Q8I514_PLAF7 Uncharacterized protein OS=Plasmodium falciparum (isolate 3D7) GN=PFL1995c PE=4 SV=1 | 1 | 0.02 | | |
| tr\|E7ESF5\|E7ESF5_HUMAN Calcitonin gene-related peptide 2 OS=Homo sapiens GN=CALCB PE=4 SV=1 | 1 | 0.02 | | |
| tr\|A0A0B4J268\|A0A0B4J268_HUMAN Protein TRAV4 (Fragment) OS=Homo sapiens GN=TRAV4 PE=4 SV=1 | 1 | 0.01 | | |
| sp\|P00918\|CAH2_HUMAN Carbonic anhydrase 2 OS=Homo sapiens GN=CA2 PE=1 SV=2;tr\|E5RID5\|E5RID5_HUMAN Carbonic anhydrase 2 OS=Homo sapiens GN=CA2 PE=1 SV=1;tr\|E5RK37\|E5RK37_HUMAN Carbonic anhydrase 2 OS=Homo sapiens GN=CA2 PE=1 SV=1 | 1 | 0.00 | | |
| sp\|Q8I4V2\|RBM22_PLAF7 Pre-mRNA-splicing factor PFL2310w OS=Plasmodium falciparum (isolate 3D7) GN=PFL2310w PE=3 SV=1 | 1 | 0.00 | | |
| sp\|Q14587-2\|ZN268_HUMAN Isoform 2 of Zinc finger protein 268 OS=Homo sapiens GN=ZNF268;sp\|Q14587\|ZN268_HUMAN Zinc finger protein 268 OS=Homo sapiens GN=ZNF268 PE=1 SV=2 | 1 | 0.00 | | |
| sp\|Q15051-2\|IQCB1_HUMAN Isoform 2 of IQ calmodulin-binding motif-containing protein 1 OS=Homo sapiens GN=IQCB1;sp\|Q15051\|IQCB1_HUMAN IQ calmodulin-binding motif-containing protein 1 OS=Homo sapiens GN=IQCB1 PE=1 SV=1 | 1 | 0.00 | | |
| tr\|E7EWB4\|E7EWB4_HUMAN Dihydropyrimidinase-related protein 5 (Fragment) OS=Homo sapiens GN=DPYSL5 PE=1 SV=4;sp\|Q9BPU6\|DPYL5_HUMAN Dihydropyrimidinase-related protein 5 OS=Homo sapiens GN=DPYSL5 PE=1 SV=1 | 1 | 0.00 | | |

# Appendix 5

# Comparison of the proteins significantly altered in abundance following OZ277, OZ439 and DHA treatment of *Plasmodium falciparum* infected red blood cells (p-value ≤ 0.05 and fold-change ≥ 1.5) and the parasite proteins reported as peroxide antimalarial alkylation targets in chemical proteomics studies

| | | Significantly altered protein abundance | | | Protein alkylation targets | | |
|---|---|---|---|---|---|---|---|
| **Protein name** | **Uniprot ID** | **OZ277** | **OZ439** | **DHA** | **Ismail *et al.*[1]** | **Ismail *et al.*[2]** | **Wang *et al.*[3]** |
| 101 kDa malaria antigen (Acidic basic repeat antigen) | Q8I5D2 | | | ✓ | | ✓ | |
| 14-3-3 protein | C0H4V6 | | | ✓ | | | ✓ |
| 26S protease regulatory subunit 10B, putative | Q8IEQ1 | ✓ | ✓ | ✓ | | | |
| 26S protease regulatory subunit 4, putative | Q8IJW0 | | | ✓ | | | |
| 26S protease regulatory subunit 6A, putative | Q8II60 | | ✓ | ✓ | | | |
| 26S protease regulatory subunit 6B, putative | Q8I1V1 | | ✓ | ✓ | | | |
| 26S protease regulatory subunit 7, putative | Q8IEK3 | | ✓ | ✓ | | | |
| 26S protease regulatory subunit 8, putative | Q8I4U5 | | ✓ | ✓ | | | |
| 26S proteasome regulatory subunit p55, putative | Q8IJM0 | ✓ | | | | | |
| 26S proteasome regulatory subunit RPN1, putative | O96153 | ✓ | ✓ | ✓ | | | |
| 26S proteasome regulatory subunit RPN10, putative | Q8IAR6 | | | ✓ | | | |
| 26S proteasome regulatory subunit RPN11, putative | Q8ID28 | | | ✓ | | | |
| 26S proteasome regulatory subunit RPN13, putative | Q8ILV5 | | | ✓ | | | |
| 26S proteasome regulatory subunit RPN2, putative | Q8IKH3 | | ✓ | ✓ | | | |

| | | | | | | | |
|---|---|---|---|---|---|---|---|
| 26S proteasome regulatory subunit RPN3, putative | Q8IDV2 | ✓ | ✓ | | | | |
| 26S proteasome regulatory subunit RPN6 | Q8IM66 | | ✓ | ✓ | | | |
| 26S proteasome regulatory subunit RPN7, putative | Q8II71 | ✓ | ✓ | | | | |
| 26S proteasome regulatory subunit RPN8, putative | Q8I323 | ✓ | ✓ | ✓ | | | |
| 2-C-methyl-D-erythritol 2,4-cyclodiphosphate synthase | A0A143ZWM3 | | | | ✓ | ✓ | |
| 2-methoxy-6-polyprenyl-1,4-benzoquinol methylase, mitochondrial | O96145 | | | ✓ | | | |
| 2-oxoglutarate dehydrogenase E1 component | Q8I6S5 | | ✓ | ✓ | | | |
| 2-oxoisovalerate dehydrogenase subunit alpha | Q8IEJ6 | | | ✓ | | | |
| 40S ribosomal protein S10, putative | Q8IBQ5 | | | ✓ | | | |
| 40S ribosomal protein S11, putative | O77381 | | | ✓ | | | |
| 40S ribosomal protein S12 | O97249 | | | ✓ | ✓ | ✓ | |
| 40S ribosomal protein S15 | Q8IDB0 | | | ✓ | | | |
| 40S ribosomal protein S15A, putative | O77395 | ✓ | | ✓ | | | |
| 40S ribosomal protein S16, putative | Q8IAX5 | | | ✓ | | | |
| 40S ribosomal protein S19 | C0H5C2 | | | ✓ | | | ✓ |
| 40S ribosomal protein S19 | Q8IFP2 | | | ✓ | | | ✓ |
| 40S ribosomal protein S21 | Q8IHS5 | | | ✓ | | | ✓ |
| 40S ribosomal protein S23, putative | O97248 | | | ✓ | | | |

| | | | | | | | |
|---|---|---|---|---|---|---|---|
| 40S ribosomal protein S24 | Q8I3R6 | | | ✓ | | | |
| 40S ribosomal protein S25 | Q8ILN8 | | | ✓ | | | |
| 40S ribosomal protein S27 | Q8IEN2 | | | ✓ | | | |
| 40S ribosomal protein S28e, putative | Q8IKL9 | | | ✓ | | | |
| 40S ribosomal protein S3 | Q8IKH8 | ✓ | | ✓ | | | ✓ |
| 40S ribosomal protein S3a | O97313 | | | ✓ | ✓ | ✓ | ✓ |
| 40S ribosomal protein S4 | Q8IIU8 | | | ✓ | | | |
| 40S ribosomal protein S5 | Q8IL02 | | | ✓ | | | ✓ |
| 40S ribosomal protein S5, putative | Q8IBN5 | | | ✓ | | | ✓ |
| 40S ribosomal protein S6 | Q8IDR9 | ✓ | | ✓ | | | |
| 40S ribosomal protein S7 | Q8IET7 | | | ✓ | | | |
| 40S ribosomal protein S8 | Q8IM10 | | | ✓ | | | |
| 40S ribosomal protein S9, putative | Q8I3R0 | | | ✓ | | | |
| 40S ribosomal protein SA | A0A143ZZG2 | | | | ✓ | | |
| 40S ribosomal protein SA | Q8IJD4 | ✓ | | ✓ | | ✓ | |
| 60 kDa chaperonin | Q8I0V3 | | | | ✓ | ✓ | |
| 60S acidic ribosomal protein P0 | Q8II61 | | | ✓ | ✓ | ✓ | |
| 60S acidic ribosomal protein P1, putative | Q8IIX0 | | | ✓ | | | |

| | | | | | | | |
|---|---|---|---|---|---|---|---|
| 60S acidic ribosomal protein P2 | O00806 | | | ✓ | ✓ | ✓ | |
| 60S ribosomal export protein NMD3, putative | Q8IBG6 | ✓ | ✓ | ✓ | | | |
| 60S ribosomal protein L1, putative | Q8IL58 | | | ✓ | | | |
| 60S ribosomal protein L10, putative | Q8ILV2 | | | ✓ | | | ✓ |
| 60S ribosomal protein L11a, putative | Q8IBQ6 | | | ✓ | | | |
| 60S ribosomal protein L13 | Q8IAX6 | | | ✓ | | | |
| 60S ribosomal protein L13, putative | Q8IJZ7 | | | ✓ | | | |
| 60S ribosomal protein L14, putative | Q8ILE8 | | | | | | ✓ |
| 60S ribosomal protein L17, putative | Q8IDI5 | ✓ | | ✓ | | | ✓ |
| 60S ribosomal protein L18-2, putative | C0H5G3 | | | ✓ | | | |
| 60S ribosomal protein L18a | Q8IDS6 | ✓ | | ✓ | | | |
| 60S ribosomal protein L19 | C6KSY6 | ✓ | | ✓ | | | |
| 60S ribosomal protein L2 | Q8I3T9 | | | | | | ✓ |
| 60S ribosomal protein L21 | Q8ILK3 | | | ✓ | | | ✓ |
| 60S ribosomal protein L22, putative | Q8IB51 | ✓ | ✓ | ✓ | | | |
| 60S ribosomal protein L23, putative | Q8IE09 | | | | | | ✓ |
| 60S ribosomal protein L24, putative | Q8IEM3 | ✓ | | ✓ | | | ✓ |
| 60S ribosomal protein L26, putative | O77364 | | | ✓ | | | |

| | | | | | |
|---|---|---|---|---|---|
| 60S ribosomal protein L27 | Q8IKM5 | | | ✓ | ✓ |
| 60S ribosomal protein L27a, putative | C6KT23 | | | ✓ | |
| 60S ribosomal protein L29 | C6S3J6 | | | ✓ | |
| 60S ribosomal protein L3 | Q8IJC6 | | | ✓ | ✓ |
| 60S ribosomal protein L30e, putative | Q8IJK8 | | | ✓ | ✓ |
| 60S ribosomal protein L31 | Q8I463 | | | ✓ | |
| 60S ribosomal protein L32 | Q8I3B0 | | | ✓ | |
| 60S ribosomal protein L35ae, putative | Q8IHT9 | | | ✓ | |
| 60S ribosomal protein L36 | Q8I713 | | | ✓ | |
| 60S ribosomal protein L37a | O96184 | ✓ | | ✓ | |
| 60S ribosomal protein L38 | Q8II62 | | | ✓ | |
| 60S ribosomal protein L4 | Q8I431 | | | ✓ | ✓ |
| 60S ribosomal protein L44 | O97231 | | ✓ | ✓ | |
| 60S ribosomal protein L6, putative | Q8IE85 | | | ✓ | |
| 60S ribosomal protein L7, putative | O97250 | | | ✓ | |
| 60S ribosomal protein L7-3, putative | Q8ILL2 | | | ✓ | |
| 60S ribosomal subunit protein L24-2, putative | Q8I441 | | | ✓ | |
| ABC transporter E family member 1, putative | Q8I6Z4 | | ✓ | | |

| | | | | | | | |
|---|---|---|---|---|---|---|---|
| Acetyl-CoA synthetase, putative | C6KTB4 | ✓ | ✓ | | | | |
| Actin I | A0A144A1R5 | | | | ✓ | | ✓ |
| Actin-1 | Q8I4X0 | ✓ | ✓ | ✓ | | ✓ | |
| Actin-2 | Q8ILW9 | ✓ | | ✓ | | | |
| Acyl-CoA binding protein, isoform 2, ACBP2 | Q8IK24 | | ✓ | ✓ | | | |
| Acyl-CoA synthetase | Q8I535 | | ✓ | ✓ | | | |
| Acyl-CoA synthetase | Q8I3L4 | ✓ | ✓ | ✓ | | | ✓ |
| Acylphosphatase, putative | C6S3F0 | | | ✓ | | | |
| Adenosine deaminase | Q8IJA9 | | | | | | ✓ |
| Adenosylhomocysteinase | P50250 | | ✓ | ✓ | ✓ | ✓ | ✓ |
| Adenylosuccinate synthetase | Q8IDF6 | ✓ | ✓ | | ✓ | ✓ | |
| ADP-ribosylation factor | A0A143ZY58 | | | | ✓ | | |
| ADP-ribosylation factor 1 | Q7KQL3 | | ✓ | | | ✓ | |
| Alpha/beta hydrolase, putative | Q8IK20 | | | ✓ | | | |
| Alpha/beta-hydrolase, putative | Q8IE45 | ✓ | | ✓ | | | |
| Alternative splicing factor ASF-1, putative | Q8IIG9 | | | ✓ | | | |
| Anamorsin homologue | C0H4X5 | | | | | ✓ | ✓ |
| Annexin A7 | P20073 | | | ✓ | | | |

| | | | | | | | |
|---|---|---|---|---|---|---|---|
| AP2/ERF domain-containing protein PFD0985w | Q8I1N6 | | | ✓ | ✓ | | |
| AP-4 complex subunit mu, putative | Q8IIH2 | | | ✓ | | | |
| Asparagine and aspartate rich protein 1 | Q8I586 | ✓ | ✓ | ✓ | | | |
| Asparagine-rich protein, putative | Q8I5A3 | | ✓ | ✓ | | | |
| Aspartate aminotransferase | O96142 | ✓ | | | | | |
| Aspartate carbamoyltransferase | Q8IDP8 | | | | | | ✓ |
| Aspartate--tRNA ligase | Q8I2B1 | ✓ | ✓ | ✓ | | | |
| ATP synthase subunit alpha | O96252 | | | ✓ | | | |
| ATP synthase subunit beta | Q8I0V2 | | | ✓ | | | |
| ATPase ASNA1 homolog | Q8I1T8 | ✓ | ✓ | ✓ | | | |
| ATP-dependent Clp protease, putative | Q8IM28 | | | ✓ | | | |
| ATP-dependent RNA helicase DDX6 | O97285 | | | ✓ | | | |
| ATP-dependent RNA helicase DHR1, putative | Q8IET8 | | ✓ | ✓ | | | |
| ATP-dependent RNA helicase UAP56 | Q9TY94 | ✓ | | ✓ | | | ✓ |
| ATP-dependent zinc metalloprotease FTSH 1 | Q8I526 | | | ✓ | | | |
| ATP-dependent zinc metalloprotease FTSH, putative | Q8IKI9 | | ✓ | ✓ | | | |
| Autophagy-related protein 18, putative | Q8IJR6 | | | | | | ✓ |
| Bacterial histone-like protein | Q8I3A2 | | | ✓ | | | |

| | | | | | | | |
|---|---|---|---|---|---|---|---|
| Bax inhibitor 1, putative | Q8I4U9 | | | ✓ | | | |
| Bifunctional dihydrofolate reductase-thymidylate synthase | Q8I1R6 | | | | ✓ | ✓ | |
| Calcium-dependent protein kinase 1 | A0A143ZWW4 | | | | | | ✓ |
| Calcium-transporting ATPase | Q76NN8 | | | | | ✓ | ✓ |
| Calcyclin binding protein, putative | Q8I542 | | ✓ | ✓ | | | |
| Calmodulin | P62203 | | ✓ | ✓ | | | |
| Calponin homology domain-containing protein, putative | Q8IKZ7 | | ✓ | ✓ | | | |
| cAMP-dependent protein kinase regulatory subunit | Q7KQK0 | ✓ | ✓ | ✓ | | | ✓ |
| Carbamoyl phosphate synthetase | Q8IEN3 | | ✓ | ✓ | | | ✓ |
| Casein kinase 1 | C6S3F7 | | | ✓ | ✓ | ✓ | |
| Casein kinase 2, alpha subunit | Q8IIR9 | ✓ | | ✓ | | | ✓ |
| Casein kinase II subunit beta | Q8IDR5 | | ✓ | ✓ | | | |
| Catalase | P04040 | ✓ | | | | | |
| Cation transporting P-ATPase | Q8I461 | | | ✓ | | | |
| CCR4-NOT transcription complex subunit 1, putative | Q8IIW4 | | | ✓ | | | |
| Cdc2-related protein kinase 3 | Q8I1T4 | | | ✓ | | | |
| CDGSH iron-sulfur domain-containing protein, putative | C0H4A8 | | ✓ | ✓ | | | |
| Cell division cycle protein 48 homologue, putative | C6KT34 | | | ✓ | | | ✓ |

| | | | | | | | |
|---|---|---|---|---|---|---|---|
| Centrin-3 | Q8IJC7 | | | ✓ | | | |
| Cg1 protein | Q8IBZ8 | | | ✓ | | | |
| Chaperone binding protein, putative | Q8IDY6 | ✓ | | ✓ | | | |
| Choline-phosphate cytidylyltransferase | Q8IEE9 | | | ✓ | | | |
| Chromatin assembly factor 1 subunit, putative | Q8IE52 | | | ✓ | | | |
| Cleavage and polyadenylation specificity factor subunit 3, putative | Q8IL83 | | | ✓ | | | |
| Coatamer beta subunit, putative | Q8ILG6 | | | ✓ | | | |
| Coatomer alpha subunit, putative | C6KSR5 | | | | | | ✓ |
| Coatomer subunit beta | Q8I390 | ✓ | | ✓ | | | |
| Coatomer subunit delta | Q8II16 | | | ✓ | | | |
| Coatomer subunit gamma | Q8IHR6 | | | ✓ | | | |
| Cofilin/actin-depolymerizing factor homolog 1 | Q8I467 | | | | ✓ | ✓ | |
| Coproporphyrinogen-III oxidase | Q8IHU1 | ✓ | | | | | |
| CRAL/TRIO domain-containing protein, putative | Q8II87 | ✓ | | | | | |
| CTP synthase | Q8ILZ3 | ✓ | ✓ | | | | |
| CutA, putative | Q8I4T9 | ✓ | ✓ | | | | |
| Cysteine proteinase falcipain 2b | Q8I6U5 | | ✓ | | | | |
| Cysteine proteinase falcipain 3 | Q8IIL0 | | | ✓ | | | |

| | | | | | |
|---|---|---|---|---|---|
| Cysteine--tRNA ligase, putative | Q8IJP3 | | ✓ | | |
| Cytoadherence linked asexual protein 9 | Q8I2G2 | | | ✓ | |
| Cytochrome b5, putative | Q8I599 | | | ✓ | |
| Cytosolic glyoxalase II | C0H490 | ✓ | | | |
| DEAD/DEAH box helicase, putative | Q8I3B4 | | ✓ | ✓ | |
| Deoxyribose-phosphate aldolase, putative | Q8IJI7 | ✓ | ✓ | | |
| Deoxyuridine 5'-triphosphate nucleotidohydrolase | Q8II92 | ✓ | ✓ | ✓ | |
| Deubiquinating/deneddylating enzyme | Q8IIJ6 | | ✓ | ✓ | |
| Diacylglycerol kinase | Q8IKC5 | | ✓ | ✓ | |
| Dicarboxylate/tricarboxylate carrier | Q8IB73 | | ✓ | | |
| Dihydrolipoyl dehydrogenase | Q8I5A0 | ✓ | | ✓ | |
| Dihydroorotase, putative | Q8IKA9 | ✓ | | | |
| Dipeptidyl aminopeptidase 1 | A0A144A2G5 | | | | ✓ |
| DNA ligase | Q8IES4 | | | ✓ | |
| DNA mismatch repair protein MSH6, putative | Q8I447 | | ✓ | | |
| DNA polymerase epsilon catalytic subunit A, putative | C6KTD8 | | ✓ | ✓ | |
| DNA primase small subunit | Q7KQM1 | | ✓ | ✓ | |
| DNA replication licensing factor MCM3, putative | Q8I3J5 | | | ✓ | |

| | | | | | | | |
|---|---|---|---|---|---|---|---|
| DNA-(apurinic or apyrimidinic site) lyase | O97240 | ✓ | | | | | |
| DNA/RNA-binding protein Alba 2 | Q8IDN4 | | | ✓ | | | |
| DNA/RNA-binding protein Alba 4 | Q8IDM3 | ✓ | | ✓ | | | |
| DNA-binding chaperone, putative | Q8I5N9 | | ✓ | ✓ | | | |
| DNA-directed RNA polymerase subunit | O77375 | | | | ✓ | ✓ | |
| DNA-directed RNA polymerases I and III subunit RPAC1, putative | Q8IHT3 | ✓ | | ✓ | | | |
| DnaJ protein, putative | C0H5E9 | | ✓ | | | | |
| DnaJ protein, putative | C6KTC7 | | | | | | ✓ |
| DnaJ protein, putative | Q8IB72 | | | | | | ✓ |
| DnaJ protein, putative | Q8IKA6 | | | ✓ | | | |
| Dynein heavy chain, putative | A0A143ZY83 | | | | | ✓ | |
| Dynein heavy chain, putative | A0A143ZYP5 | | | | ✓ | ✓ | |
| E3 ubiquitin-protein ligase | C0H4K6 | | | ✓ | | | |
| Elongation factor 1 (EF-1), putative | O97319 | | ✓ | ✓ | | | |
| Elongation factor 1-alpha | Q8I0P6 | ✓ | ✓ | ✓ | ✓ | ✓ | ✓ |
| Elongation factor 1-beta | Q8I320 | ✓ | ✓ | | | | |
| Elongation factor 1-gamma, putative | Q8IDV0 | ✓ | ✓ | | | | ✓ |
| Elongation factor 2 | Q8IKW5 | ✓ | ✓ | | | | ✓ |

| | | | | | | | |
|---|---|---|---|---|---|---|---|
| Elongation factor Tu | Q8IE20 | ✓ | | | | | |
| Endoplasmin, putative | Q8I0V4 | | | | | | ✓ |
| Enolase | A0A143ZZ61 | | | | ✓ | | ✓ |
| Enolase | Q8IJN7 | | ✓ | ✓ | | ✓ | |
| Enoyl-CoA hydratase, putative | Q8ILL1 | | | ✓ | | | |
| ER lumen protein-retaining receptor | Q76NM1 | | | | | ✓ | |
| Erythrocyte binding antigen-175 | Q8IBE8 | | | | ✓ | ✓ | |
| Ethanolamine kinase | Q8IIB7 | ✓ | ✓ | ✓ | | | |
| Eukaryotic initiation factor 4A | Q8IKF0 | | ✓ | ✓ | | | ✓ |
| Eukaryotic initiation factor 4A-III, putative | Q8IFN9 | | | ✓ | | | |
| Eukaryotic translation initation factor 4 gamma | C0H5B1 | | | ✓ | | | |
| Eukaryotic translation initiation factor 2 subunit alpha, putative | Q8IBH7 | | | ✓ | | | |
| Eukaryotic translation initiation factor 2 subunit beta, putative | Q8IJT9 | | | ✓ | | | |
| Eukaryotic translation initiation factor 2 subunit gamma, putative | Q8ILY9 | | | ✓ | | | |
| Eukaryotic translation initiation factor 3 subunit C | Q8I5Y3 | | | | | | ✓ |
| Eukaryotic translation initiation factor 6 | Q8IE00 | | ✓ | ✓ | | | |
| Eukaryotic translation initiation factor subunit eIF2A, putative | Q8IJL2 | | ✓ | ✓ | | | |
| Exported protein 1 | Q8IIF0 | | | | ✓ | ✓ | |

| | | | | | | | |
|---|---|---|---|---|---|---|---|
| Exportin-1, putative | Q8IEF5 | ✓ | | ✓ | | | |
| Flap endonuclease 1 | Q7K734 | | | | | ✓ | |
| Folate transporter 2 | Q8IIK1 | | | ✓ | | | |
| Fructose-bisphosphate aldolase | A0A144A3T1 | | | | ✓ | | ✓ |
| Fructose-bisphosphate aldolase | Q7KQL9 | | | ✓ | | ✓ | |
| Gametocyte exported protein 19 | B9ZSI9 | | ✓ | ✓ | | | |
| Geranylgeranyl pyrophosphate synthase, putative | Q8II79 | ✓ | | | | | |
| Glideosome associated protein with multiple membrane spans 2 | Q8IFN1 | | | ✓ | | | |
| Glideosome-associated protein 40, putative | Q8I3V1 | | ✓ | ✓ | | | |
| Glucose-6-phosphate dehydrogenase-6-phosphogluconolactonase | A0A144A6N0 | | | | ✓ | ✓ | |
| Glucose-6-phosphate isomerase | Q8ILA4 | | ✓ | ✓ | ✓ | ✓ | |
| Glutamate dehydrogenase | Q8ILT0 | | | ✓ | | | ✓ |
| Glutamate dehydrogenase, putative | Q8IAM0 | | ✓ | | | | ✓ |
| Glutamate--tRNA ligase, putative | Q8IDK7 | | ✓ | | | | ✓ |
| Glutamine synthetase, putative | C0H551 | | | ✓ | | | ✓ |
| Glutamine--tRNA ligase, putative | Q8IE10 | ✓ | ✓ | | | | |
| Glutaredoxin 1 | Q9NLB2 | | ✓ | ✓ | | | |
| Glutathione peroxidase 1 | P07203 | | ✓ | | | | |

| | | | | | | | |
|---|---|---|---|---|---|---|---|
| Glutathione reductase | O15770 | | | ✓ | | | |
| Glutathione S-transferase | A0A144A1J6 | | | | ✓ | | |
| Glyceraldehyde-3-phosphate dehydrogenase | Q8IKK7 | ✓ | ✓ | | | | ✓ |
| Glycerol-3-phosphate dehydrogenase | Q8I5P5 | ✓ | ✓ | ✓ | | | |
| Glycine--tRNA ligase | Q8ILP6 | | ✓ | ✓ | | | |
| Glycogen synthase kinase 3 | O77344 | ✓ | | | | | |
| Glycophorin binding protein | A0A143ZWU2 | | | | | | ✓ |
| GTP-binding nuclear protein | Q7KQK6 | ✓ | | ✓ | ✓ | ✓ | |
| Haloacid dehalogenase-like hydrolase | Q8IJ74 | | ✓ | ✓ | | | ✓ |
| Haloacid dehalogenase-like hydrolase, putative | Q8I5F4 | ✓ | ✓ | | | | |
| Heat shock protein 110 | Q8IC01 | | | | | | ✓ |
| Heat shock protein 70 | Q8I2X4 | | | | ✓ | ✓ | |
| Heat shock protein 70 | Q8IB24 | ✓ | ✓ | ✓ | ✓ | ✓ | ✓ |
| Heat shock protein 90 | Q8IC05 | ✓ | ✓ | ✓ | ✓ | ✓ | ✓ |
| Heat shock protein DNAJ homologue Pfj4 | Q7KQK3 | | ✓ | | | | |
| High mobility group protein B1 | Q8I616 | | ✓ | ✓ | | | |
| High molecular weight rhoptry protein 2 | C0H571 | | | | | | ✓ |
| Histidine--tRNA ligase, putative | Q8IL22 | | ✓ | | | | |

| | | | | | | | |
|---|---|---|---|---|---|---|---|
| Histone H2A | C6KT18 | | | | ✓ | ✓ | |
| Histone H2B | Q8IIV1 | | | ✓ | | | |
| Histone H4 | Q8IIV2 | | | ✓ | | | |
| Histone S-adenosyl methyltransferase, putative | Q8I5E0 | | | ✓ | | | |
| Hsc70-interacting protein | Q8I3J0 | | ✓ | ✓ | | | |
| HSP40, subfamily A, putative | Q8IL88 | | ✓ | ✓ | | | ✓ |
| Hsp70/Hsp90 organizing protein | A0A144A2J9 | | | | ✓ | | |
| HVA22/TB2/DP1 family protein, putative | O77388 | ✓ | | ✓ | | | |
| Hydroxyethylthiazole kinase | Q8I527 | ✓ | | | | | |
| Hypoxanthine phosphoribosyltransferase | Q8IJS1 | | ✓ | ✓ | ✓ | ✓ | ✓ |
| Hypoxanthine-guanine phosphoribosyltransferase | P00492 | | ✓ | | | | |
| Importin beta, putative | Q8IAY9 | ✓ | ✓ | ✓ | | | |
| Importin subunit alpha | Q8IAW0 | | | ✓ | | | ✓ |
| Importin-7, putative | C0H4L1 | | ✓ | ✓ | | | ✓ |
| Inner membrane complex sub-compartment protein 3 | Q8IKM6 | | | | | | ✓ |
| Inosine-5'-monophosphate dehydrogenase | Q8I2U5 | | ✓ | ✓ | | | |
| Inositol-3-phosphate synthase | Q8I3Y8 | | | ✓ | | | |
| Insulinase, putative | Q8III5 | | ✓ | ✓ | | | ✓ |

| | | | | | | | |
|---|---|---|---|---|---|---|---|
| Isoleucine--tRNA ligase, putative | Q8IDZ9 | | ✓ | ✓ | | | ✓ |
| Karyopherin beta | Q8I3M5 | ✓ | ✓ | ✓ | | | |
| Knob-associated histidine-rich protein | Q9TY99 | | | | | | ✓ |
| Leucine--tRNA ligase, putative | C6KT64 | ✓ | ✓ | | | | |
| L-lactate dehydrogenase | Q76NM3 | ✓ | ✓ | | ✓ | ✓ | ✓ |
| Lysine decarboxylase-like protein, putative | Q8I1V0 | ✓ | ✓ | ✓ | | | |
| Lysine-rich membrane-associated PHISTb protein | Q8I3F0 | | | ✓ | | | |
| Lysine--tRNA ligase | Q8IDJ8 | | ✓ | ✓ | | | |
| Lysophospholipase, putative | Q8I4R0 | | | ✓ | | | |
| Lysophospholipase, putative | Q8IBZ2 | | | | | | ✓ |
| M17 leucyl aminopeptidase | Q8IL11 | | ✓ | ✓ | | | |
| M18 aspartyl aminopeptidase | Q8I2J3 | | ✓ | ✓ | | | |
| M1-family alanyl aminopeptidase | Q8IEK1 | ✓ | ✓ | ✓ | ✓ | ✓ | |
| Mago nashi protein homologue, putative | Q8IBJ9 | | | ✓ | | | |
| Mannose-6-phosphate isomerase, putative | Q8IAL6 | ✓ | ✓ | | | | |
| Mature parasite-infected erythrocyte surface antigen | Q8I492 | | | | | ✓ | ✓ |
| Memo-like protein | C0H4B1 | | ✓ | | | | |
| Merozoite surface protein 1 | Q8I0U8 | ✓ | | ✓ | ✓ | ✓ | ✓ |

| | | | | | | | |
|---|---|---|---|---|---|---|---|
| Merozoite surface protein 7 | Q8IDX8 | | ✓ | ✓ | | | |
| Merozoite surface protein 9 | A0A144A026 | | | | ✓ | | |
| Merozoite surface protein P41 | Q8I1Y0 | | | ✓ | | | |
| Merozoite surface protein P92 | Q8ID66 | ✓ | ✓ | ✓ | | | |
| Methionine--tRNA ligase | Q8IJ60 | ✓ | ✓ | ✓ | | | ✓ |
| Methyltransferase, putative | Q8IKS6 | ✓ | | ✓ | | | |
| Mitochondrial import inner membrane translocase subunit TIM10, putative | Q8I5W2 | | | ✓ | | | |
| Mitochondrial import inner membrane translocase subunit TIM8, putative | Q8ILN5 | | | ✓ | | | |
| Mitochondrial inner membrane TIM10 associated protein, putative | Q8I472 | | ✓ | ✓ | | | |
| Mitochondrial phosphate carrier protein | Q8I623 | | ✓ | ✓ | | | |
| Monocarboxylate transporter, putative | C0H564 | | | ✓ | | | |
| mRNA-decapping enzyme 2, putative | Q8IEM5 | | | ✓ | | | |
| MSP7-like protein | Q8IDY0 | | | ✓ | | | |
| MSP7-like protein | Q8IDY3 | | | ✓ | | | |
| Multidrug resistance protein 1 | Q7K6A5 | | | | ✓ | ✓ | ✓ |
| Multiprotein bridging factor type 1, putative | Q8II81 | | ✓ | ✓ | | | |
| MYND finger protein, putative | C6KSM2 | | ✓ | | | | |

| | | | | | | | |
|---|---|---|---|---|---|---|---|
| Myosin C | Q8IE50 | | | ✓ | | | |
| Myosin-A | Q8IDR3 | | | | ✓ | ✓ | |
| Nascent polypeptide-associated complex subunit alpha, putative | C6KT55 | | ✓ | ✓ | | | |
| Nascent polypeptide-associated complex subunit beta | Q8ILK2 | | ✓ | ✓ | | | |
| Nicotinate phosphoribosyltransferase, putative | C6KTC6 | | ✓ | ✓ | | | |
| Non-SERCA-type Ca2+-transporting P-ATPase | A0A143ZZK9 | | | | | | ✓ |
| Novel putative transporter 1 | Q8I291 | | | ✓ | | | |
| Nuclear protein localization protein 4, putative | Q8I426 | | ✓ | ✓ | | | |
| Nuclear transport factor 2, putative | Q8ILX1 | ✓ | ✓ | | | | |
| Nucleolar GTP-binding protein 2 | Q8ILM2 | | | ✓ | | | |
| Nucleolar preribosomal GTPase, putative | Q8I3H9 | | | ✓ | | | |
| Nucleolar protein 10, putative | Q8IAL3 | ✓ | | | | | |
| Nucleoside diphosphate kinase | Q8ID43 | | ✓ | ✓ | | | |
| Nucleoside transporter 1 | Q8IDM6 | | | ✓ | | | |
| Nucleoside transporter 2 | Q8IB78 | | | | | | ✓ |
| Nucleosome assembly protein | Q8I2W3 | | | ✓ | ✓ | ✓ | |
| Nucleosome assembly protein | Q8I608 | | | ✓ | | | |
| Obg-like ATPase 1 | Q8IBM9 | | | | | | ✓ |

| | | | | | | | |
|---|---|---|---|---|---|---|---|
| Organic anion transporter | C6KSY4 | | | ✓ | | | |
| Ornithine aminotransferase | Q6LFH8 | ✓ | ✓ | | ✓ | ✓ | ✓ |
| Pantothenate kinase, putative | Q8ILP4 | ✓ | | ✓ | | | |
| Pantothenate kinase, putative | Q8IL92 | ✓ | ✓ | | | | |
| Parasite-infected erythrocyte surface protein | O77361 | | | ✓ | | | |
| Parasite-infected erythrocyte surface protein | Q8I2A1 | | | ✓ | | | |
| Parasite-infected erythrocyte surface protein | Q8I488 | | | | | | ✓ |
| Parasitophorous vacuolar protein 1 | Q8II72 | ✓ | | ✓ | | | |
| Peptidase | Q8IKT5 | | ✓ | ✓ | | | |
| Peptidyl-prolyl cis-trans isomerase | Q76NN7 | | ✓ | ✓ | | | ✓ |
| Peptidyl-prolyl cis-trans isomerase | Q8I6S4 | | | ✓ | | | |
| Peptidyl-prolyl cis-trans isomerase | Q8ILM0 | | | ✓ | | | |
| Peroxiredoxin-2 | P32119 | ✓ | ✓ | | | | |
| Phosphoenolpyruvate/phosphate translocator | Q8I0U9 | | ✓ | ✓ | | | |
| Phosphoethanolamine N-methyltransferase | Q8IDQ9 | ✓ | ✓ | | | | ✓ |
| Phosphoglycerate kinase (EC 2.7.2.3) | P27362 | ✓ | ✓ | | ✓ | ✓ | |
| Phosphoglycerate mutase | Q8IIG6 | | | ✓ | | | |
| Phosphoribosylpyrophosphate synthetase | Q8IE67 | | | | | | ✓ |

| | | | | | | | |
|---|---|---|---|---|---|---|---|
| Phosphotransferase | C6KT76 | ✓ | ✓ | ✓ | ✓ | ✓ | ✓ |
| Plasmepsin I | A0A144A171 | | | | ✓ | ✓ | ✓ |
| Plasmepsin II | Q8I6V3 | ✓ | ✓ | ✓ | ✓ | ✓ | ✓ |
| Plasmepsin III | Q8IM15 | ✓ | | ✓ | | | ✓ |
| Plasmepsin IV | Q8IM16 | ✓ | | ✓ | | | ✓ |
| Plasmepsin-1 | Q7KQM4 | | | ✓ | | | |
| Poly(A) polymerase PAP, putative | C6KT92 | | ✓ | ✓ | | | |
| Polyadenylate-binding protein | Q8I5H4 | | | | | | ✓ |
| PRE-binding protein | Q8IJS7 | ✓ | | ✓ | | | |
| Prefoldin subunit 2, putative | Q8ILS7 | ✓ | ✓ | | | | |
| Prefoldin subunit 3 | Q8IBR6 | | ✓ | ✓ | | | |
| Prefoldin subunit 4 | Q8I3A4 | ✓ | ✓ | | | | |
| Pre-mRNA-splicing factor ATP-dependent RNA helicase PRP22, putative | Q8IJA4 | | | ✓ | | | |
| Pre-mRNA-splicing factor ATP-dependent RNA helicase PRP43, putative | Q8I2X7 | | | ✓ | | | |
| Pre-mRNA-splicing factor BUD31, putative | Q8I3N5 | | | ✓ | | | |
| Pre-mRNA-splicing factor CLF1, putative | Q8I1Z2 | | | ✓ | | | |
| Pre-mRNA-splicing factor CWF18, putative | Q8IKW1 | | | ✓ | | | |

| | | | | | | | |
|---|---|---|---|---|---|---|---|
| Pre-mRNA-splicing factor PRP46, putative | O97334 | | | ✓ | | | |
| Probable ATP-dependent 6-phosphofructokinase | Q8I2Z8 | ✓ | | ✓ | | | ✓ |
| Probable cathepsin C | Q8IIJ9 | | ✓ | ✓ | | ✓ | |
| Probable DNA repair protein RAD50 | C6KSQ6 | | | | ✓ | ✓ | |
| Profilin | Q8I2J4 | | ✓ | ✓ | | | |
| Proliferating cell nuclear antigen | P61074 | | | | ✓ | ✓ | |
| Proliferating cell nuclear antigen | Q7KQJ9 | | | ✓ | | | |
| Proline--tRNA ligase | A0A144A0G8 | | | | ✓ | ✓ | |
| Proline--tRNA ligase | Q8I5R7 | ✓ | ✓ | | | | |
| Proteasome endopeptidase complex | C6KST3 | | ✓ | ✓ | | | |
| Proteasome endopeptidase complex | Q8IK90 | | ✓ | ✓ | | | |
| Proteasome endopeptidase complex | Q8IAR3 | | ✓ | ✓ | | | |
| Proteasome maturation factor UMP1, putative | Q8I3I7 | | ✓ | | | | |
| Proteasome subunit alpha type | Q8IBI3 | | ✓ | ✓ | | | ✓ |
| Proteasome subunit alpha type | Q8IDG3 | | | ✓ | | | |
| Proteasome subunit alpha type | Q8IDG2 | | ✓ | ✓ | | | |
| Proteasome subunit alpha type-3, putative | O77396 | ✓ | | ✓ | | | |
| Proteasome subunit beta | Q7K6A9 | ✓ | | ✓ | | | |

| | | | | | | | |
|---|---|---|---|---|---|---|---|
| Proteasome subunit beta type | C0H4E8 | | ✓ | ✓ | | | |
| Proteasome subunit beta type | Q8IJT1 | ✓ | | ✓ | | | |
| Proteasome subunit beta type | Q8IKC9 | ✓ | ✓ | ✓ | | | |
| Proteasome subunit beta type | Q8I261 | | ✓ | ✓ | | | |
| Proteasome subunit beta type | Q8I6T3 | ✓ | ✓ | ✓ | | | |
| Proteasome subunit beta type-6, putative | Q8I0U7 | ✓ | ✓ | | | | |
| Protein arginine N-methyltransferase 1 | Q8ILK1 | ✓ | | | | | |
| Protein disulphide-isomerase | C0H4Y6 | | | | | | ✓ |
| Protein DJ-1 | C6KTB1 | | ✓ | ✓ | | | |
| Protein GCN20 | Q8IIE9 | ✓ | | | | | |
| Protein PFC0760c | O77384 | | | | ✓ | ✓ | |
| Protein phosphatase PPM2 | Q8IHY0 | ✓ | ✓ | | | | |
| Protein S100-A4 | P26447 | | | ✓ | | | |
| Protein S100-A7A | Q86SG5 | | | ✓ | | | |
| Protein SIS1 | O96212 | | ✓ | | | | |
| Protein transport protein SEC31 | O96221 | | ✓ | ✓ | | | ✓ |
| Protein transport protein SEC7, putative | Q8IL42 | | | ✓ | | | |
| Purine nucleoside phosphorylase | Q8I3X4 | ✓ | ✓ | | | | ✓ |

| | | | | | | | |
|---|---|---|---|---|---|---|---|
| Putative 50S ribosomal protein L18, apicoplastic | Q6LFD5 | | | | | ✓ | |
| Putative cell division cycle ATPase | P46468 | | | | ✓ | ✓ | |
| Putative chloroquine resistance transporter | Q8IBZ9 | | | | | ✓ | ✓ |
| Pyridoxal 5'-phosphate synthase subunit Pdx1 | C6KT50 | ✓ | | ✓ | | | ✓ |
| Pyridoxal 5'-phosphate synthase subunit Pdx2 | Q8IIK4 | ✓ | | | | | |
| Pyrroline-5-carboxylate reductase | Q8IDC6 | | | ✓ | | | |
| Pyruvate kinase | C6KTA4 | ✓ | ✓ | | | | ✓ |
| Rab GDP dissociation inhibitor | Q8I501 | ✓ | | | | | |
| Ran binding protein 1, putative | Q76NN6 | ✓ | ✓ | ✓ | | | |
| Ran-binding protein, putative | Q8IDG6 | ✓ | ✓ | ✓ | | | |
| Ras-related protein Rab-39A | Q14964 | | | ✓ | | | |
| Receptor for activated c kinase | Q8IBA0 | ✓ | | ✓ | | | |
| Repetitive organellar protein, putative | A0A144A0C5 | | | | ✓ | ✓ | |
| Replication factor C subunit 2, putative | O96260 | | | ✓ | | | |
| Replication factor C subunit 3, putative | Q8IKK4 | | | ✓ | | | |
| Replication factor C subunit 4, putative | Q8I512 | | | ✓ | | | |
| Replication protein A1, large subunit | Q9U0J0 | | ✓ | ✓ | | | |
| Reticulocyte-binding protein 3 | Q8I4R2 | | | | ✓ | ✓ | |

| | | | | | | | |
|---|---|---|---|---|---|---|---|
| Rhoptry neck protein 3 | Q8I4R5 | | | | | | ✓ |
| Rhoptry protein RHOP148 | Q8ID44 | | | ✓ | | | |
| Rhoptry-associated membrane antigen | C0H4M0 | | | | | ✓ | |
| Ribonuclease, putative | C6KSZ5 | | | ✓ | | | |
| Ribonucleoside-diphosphate reductase | Q8IL94 | | ✓ | ✓ | | | |
| Ribonucleotide reductase small subunit | Q8IM38 | | ✓ | ✓ | ✓ | ✓ | |
| Ribonucleotide reductase small subunit, putative | Q8IJN8 | | ✓ | ✓ | | | |
| Ribosomal protein L15 | C0H4A6 | | | ✓ | | | |
| Ribosome assembly protein 4, putative | Q8IHQ8 | | | ✓ | | | |
| Ribosome assembly protein RRB1, putative | Q8IAZ7 | | | ✓ | | | |
| Ribosome biogenesis protein BOP1 homolog | Q8IM36 | | | ✓ | | | |
| Ribosome production factor 1, putative | C0H549 | | ✓ | ✓ | | | |
| Ribosome-interacting GTPase 1, putative | Q8I3M1 | | ✓ | ✓ | | | |
| Ring-infected erythrocyte surface antigen | Q8I0U6 | | | | ✓ | ✓ | ✓ |
| RNA (Uracil-5-)methyltransferase, putative | Q8II27 | | ✓ | ✓ | | | |
| RNA lariat debranching enzyme, putative | Q8IDT0 | ✓ | ✓ | | | | |
| RNA-binding protein musashi, putative | Q8I2Y5 | | | ✓ | | | |
| RNA-binding protein, putative | Q8IAW1 | | ✓ | | | | |

| | | | | | | | |
|---|---|---|---|---|---|---|---|
| RNA-binding protein, putative | Q8IJI3 | ✓ | ✓ | | | | |
| rRNA adenine N(6)-methyltransferase | Q8ILT8 | | ✓ | ✓ | | | |
| RuvB-like helicase | Q8IIU3 | ✓ | | ✓ | | | |
| S-adenosylmethionine synthase | Q7K6A4 | | | | | | ✓ |
| S-antigen | A0A143ZZC7 | | | | ✓ | ✓ | |
| Secretory complex protein 62 | Q8IL86 | | | | | | ✓ |
| Serine hydroxymethyltransferase | Q8I566 | ✓ | ✓ | | | | |
| Serine repeat antigen 5 | A0A143ZWK2 | | | | | | ✓ |
| Serine repeat antigen 6 | Q9TY96 | | ✓ | ✓ | | | |
| Serine repeat antigen 7 | O96163 | | ✓ | ✓ | | | |
| Serine/threonine protein phosphatase 5 | Q8IDE7 | ✓ | | | | | |
| Serine/threonine protein phosphatase CPPED1, putative | Q8IM55 | ✓ | | | | | |
| Serine/threonine-protein phosphatase | Q8ILV1 | | | ✓ | | | |
| Serine-repeat antigen protein (111 kDa antigen) | Q9TY95 | | | ✓ | | ✓ | |
| Serine--tRNA ligase, putative | Q8IBS3 | | ✓ | ✓ | | | |
| Signal peptidase complex subunit SPC2, putative | Q9NFA0 | | | ✓ | | | |
| Signal peptidase I | Q8IE14 | | | ✓ | | | |
| Signal recognition particle 54 kDa protein | Q8IKX4 | | ✓ | | | | |

| | | | | | | | |
|---|---|---|---|---|---|---|---|
| Signal recognition particle receptor, beta subunit | Q8I4W4 | | | | | | ✓ |
| Signal recognition particle subunit SRP19 | Q8I5P4 | | | ✓ | | | |
| Signal recognition particle subunit SRP68, putative | C6KT56 | ✓ | ✓ | ✓ | | | |
| Signal recognition particle subunit SRP9 | C0H4Q0 | | | ✓ | | | |
| Single-stranded DNA-binding protein | Q8I415 | | | ✓ | | | |
| Skeleton-binding protein 1 | Q8I487 | | | | | | ✓ |
| Small GTP-binding protein sar1 | Q8I1S0 | | | ✓ | | | |
| Small heat shock protein, putative | Q8IES0 | | | ✓ | | | |
| Small ubiquitin-related modifier | Q8I444 | | | ✓ | | | |
| SNARE protein, putative | Q8I3G6 | ✓ | ✓ | | | | |
| SNARE protein, putative | Q8IET3 | | | ✓ | | | |
| Sortilin | Q8IKV8 | | | ✓ | | | |
| Spermidine synthase | Q8II73 | | | | | | ✓ |
| StAR-related lipid transfer protein | Q8I298 | | | ✓ | | | |
| Stearoyl-CoA desaturase | Q8I0W9 | | | ✓ | | | |
| STI1-like protein | Q8ILC1 | | | ✓ | | ✓ | |
| Succinate--CoA ligase [ADP-forming] subunit alpha, mitochondrial | Q8IIR8 | | | ✓ | | | |
| Succinyl-CoA ligase, putative | Q8IL89 | | | ✓ | | | |

| | | | | | | | |
|---|---|---|---|---|---|---|---|
| Superoxide dismutase [Cu-Zn] | H7BYH4 | ✓ | ✓ | | | | |
| Superoxide dismutase [Fe] | Q8IAY6 | | | ✓ | | | |
| Suppressor of kinetochore protein 1, putative | Q8ID38 | ✓ | | ✓ | | | |
| Syntaxin, Qa-SNARE family | Q8I4Z9 | | ✓ | ✓ | | | |
| T-complex protein 1 subunit alpha | Q8II43 | | ✓ | ✓ | | | |
| T-complex protein 1 subunit beta | O97247 | | ✓ | | | | |
| T-complex protein 1 subunit delta | C0H5I7 | | ✓ | | | | ✓ |
| T-complex protein 1 subunit epsilon | O97282 | | ✓ | | | | |
| T-complex protein 1 subunit eta | O77323 | | | | ✓ | ✓ | |
| T-complex protein 1 subunit gamma | Q8I5C4 | | ✓ | | | | |
| T-complex protein 1 subunit theta | O96220 | | ✓ | ✓ | | | |
| T-complex protein 1 subunit zeta | C6KST5 | | ✓ | | | | ✓ |
| Thioredoxin peroxidase 1 | Q8IL80 | | | ✓ | | | ✓ |
| Thioredoxin reductase | A0A143ZVU1 | | | | | ✓ | |
| Thioredoxin reductase 2 | P61076 | ✓ | ✓ | ✓ | | | |
| Thioredoxin-like protein, putative | Q8ILQ8 | | | | | | ✓ |
| Thioredoxin-related protein, putative | Q8IDH5 | | | | | | ✓ |
| Thioredoxin-related transmembrane protein 4 | Q9H1E5 | | ✓ | ✓ | | | |

| | | | | | | | |
|---|---|---|---|---|---|---|---|
| Threonine--tRNA ligase | Q8IIA4 | ✓ | | | | | ✓ |
| Thymidylate kinase | Q8I4S1 | ✓ | ✓ | | | | |
| Transcription factor with AP2 domain(S) | C6KSY0 | ✓ | | ✓ | | | |
| Transcription factor with AP2 domain(S) | Q8I531 | ✓ | | ✓ | | | |
| Transcription factor with AP2 domain(S) | Q8IBF6 | | | ✓ | | | |
| Transcription initiation factor TFIID subunit 7, putative | Q8I2M0 | | | ✓ | | | |
| Translation elongation factor EF-1, subunit alpha, putative | Q8IIC9 | ✓ | ✓ | ✓ | | | |
| Translation initiation factor SUI1, putative | Q8I375 | ✓ | ✓ | | | | |
| Translationally-controlled tumor protein homologue | Q8I3Z5 | | ✓ | ✓ | | | |
| Transmembrane emp24 domain-containing protein 9 | Q9BVK6 | | | ✓ | | | |
| Transporter, putative | Q8I611 | | | ✓ | | | |
| Triosephosphate isomerase | A0A144A4G4 | | | | ✓ | | |
| Triosephosphate isomerase | Q7KQM0 | | ✓ | ✓ | | ✓ | |
| tRNA binding protein, putative | Q8IL48 | | ✓ | ✓ | | | |
| Tubulin alpha chain | Q6ZLZ9 | | | | ✓ | ✓ | ✓ |
| Tubulin beta chain | A0A143ZWL7 | | | | ✓ | | ✓ |
| Tubulin beta chain | Q7KQL5 | ✓ | ✓ | ✓ | | ✓ | |
| Tubulin-specific chaperone A | Q8I250 | ✓ | ✓ | | | | |

| | | | | | | | |
|---|---|---|---|---|---|---|---|
| U4/U6 snRNA-associated-splicing factor, putative | Q8I2U4 | | | ✓ | | | |
| U6 snRNA-associated Sm-like protein LSm1, putative | Q8IIB9 | | ✓ | ✓ | | | |
| U6 snRNA-associated Sm-like protein LSm3, putative | C0H4W2 | | | ✓ | | | |
| U6 snRNA-associated Sm-like protein LSm4, putative | Q8IIT3 | | | ✓ | | | |
| U6 snRNA-associated Sm-like protein LSm6, putative | Q8IE68 | | | ✓ | | | |
| Ubiquinol-cytochrome c reductase iron-sulphur subunit, putative | Q8IL75 | | | ✓ | | | |
| Ubiquitin domain-containing protein DSK2, putative | Q8IIM8 | ✓ | ✓ | | | | |
| Ubiquitin fusion degradation protein UFD1, putative | Q8ILR6 | | ✓ | ✓ | | | |
| Ubiquitin-40S ribosomal protein S27a, putative | Q8IM64 | ✓ | | | | | |
| Ubiquitin-60S ribosomal protein L40 | Q8ID50 | | | ✓ | | | ✓ |
| Ubiquitin-activating enzyme E1 | Q8I5F9 | ✓ | ✓ | ✓ | | | |
| Ubiquitin-conjugating enzyme E2 | Q8I607 | ✓ | | | | | ✓ |
| Ubiquitin-like protein nedd8 homologue, putative | Q8IEI4 | | | ✓ | | | |
| Ubiquitin-related modifier 1 homologue | Q8IHY3 | | ✓ | ✓ | | | |
| UMP-CMP kinase, putative | Q8I231 | ✓ | | | | | |
| Uncharacterised protein | A0A143ZXZ0 | | | | | ✓ | |
| Uncharacterised protein | A0A144A431 | | | | ✓ | ✓ | |
| Uncharacterised protein | C0H488 | | | ✓ | | | |

| | | | | | | |
|---|---|---|---|---|---|---|
| Uncharacterised protein | C0H4C7 | ✓ | | | | |
| Uncharacterised protein | C0H4N9 | | | ✓ | | |
| Uncharacterised protein | C0H4U4 | | | ✓ | | ✓ |
| Uncharacterised protein | C0H4U5 | | ✓ | ✓ | | |
| Uncharacterised protein | C0H4W0 | ✓ | ✓ | | | |
| Uncharacterised protein | C0H579 | ✓ | | | | |
| Uncharacterised protein | C0H5A0 | | | ✓ | | ✓ |
| Uncharacterised protein | C0H5F2 | | ✓ | ✓ | | |
| Uncharacterised protein | C6KSQ8 | | | ✓ | | |
| Uncharacterised protein | C6KSR4 | | | ✓ | | |
| Uncharacterised protein | C6KSR6 | | | ✓ | | |
| Uncharacterised protein | C6KSV8 | | ✓ | ✓ | | |
| Uncharacterised protein | C6KT13 | | | ✓ | | |
| Uncharacterised protein | C6KTA3 | | ✓ | ✓ | | |
| Uncharacterised protein | C6KTE1 | | ✓ | ✓ | | |
| Uncharacterised protein | O96174 | | ✓ | ✓ | | |
| Uncharacterised protein | O96217 | | | ✓ | | |
| Uncharacterised protein | O96259 | | | ✓ | | |

| | | | | | | |
|---|---|---|---|---|---|---|
| Uncharacterised protein | O97238 | | | ✓ | | |
| Uncharacterised protein | O97269 | | | ✓ | | |
| Uncharacterised protein | Q8I1T0 | | ✓ | ✓ | | |
| Uncharacterised protein | Q8I202 | | | ✓ | | |
| Uncharacterised protein | Q8I259 | | ✓ | ✓ | | |
| Uncharacterised protein | Q8I294 | ✓ | | | | |
| Uncharacterised protein | Q8I2Q0 | ✓ | ✓ | ✓ | | |
| Uncharacterised protein | Q8I2X8 | | | ✓ | | |
| Uncharacterised protein | Q8I308 | | ✓ | ✓ | | |
| Uncharacterised protein | Q8I3Q8 | | | ✓ | | |
| Uncharacterised protein | Q8I403 | ✓ | | | | |
| Uncharacterised protein | Q8I490 | | | | | ✓ |
| Uncharacterised protein | Q8I506 | | | ✓ | | |
| Uncharacterised protein | Q8I546 | | | | | ✓ |
| Uncharacterised protein | Q8I547 | | ✓ | ✓ | | |
| Uncharacterised protein | Q8I573 | | | ✓ | | |
| Uncharacterised protein | Q8I5G0 | | | | | ✓ |
| Uncharacterised protein | Q8I5Q2 | | | ✓ | | |

| | | | | |
|---|---|---|---|---|
| Uncharacterised protein | Q8I5S3 | ✓ | ✓ | |
| Uncharacterised protein | Q8I5U3 | | ✓ | ✓ |
| Uncharacterised protein | Q8I5Y9 | ✓ | ✓ | ✓ |
| Uncharacterised protein | Q8IAL4 | | | ✓ |
| Uncharacterised protein | Q8IAV1 | | | ✓ |
| Uncharacterised protein | Q8IBL4 | | | ✓ |
| Uncharacterised protein | Q8IBL5 | | | ✓ |
| Uncharacterised protein | Q8IBM6 | | | ✓ |
| Uncharacterised protein | Q8IBP0 | | | ✓ |
| Uncharacterised protein | Q8IBT7 | | | ✓ |
| Uncharacterised protein | Q8IBT8 | | | ✓ |
| Uncharacterised protein | Q8IC27 | | | ✓ |
| Uncharacterised protein | Q8IDI7 | | | ✓ |
| Uncharacterised protein | Q8IDI8 | ✓ | | |
| Uncharacterised protein | Q8IDN2 | ✓ | | |
| Uncharacterised protein | Q8IDN9 | ✓ | | ✓ |
| Uncharacterised protein | Q8IE31 | | | ✓ |
| Uncharacterised protein | Q8IE43 | | | ✓ |

| | | | | | | |
|---|---|---|---|---|---|---|
| Uncharacterised protein | Q8IEC2 | | | ✓ | | |
| Uncharacterised protein | Q8IEJ0 | | ✓ | ✓ | | |
| Uncharacterised protein | Q8IEK8 | ✓ | | ✓ | | |
| Uncharacterised protein | Q8IEQ3 | | | ✓ | | |
| Uncharacterised protein | Q8IER6 | | | ✓ | | |
| Uncharacterised protein | Q8IHV2 | | | ✓ | | |
| Uncharacterised protein | Q8IHW3 | | | ✓ | | |
| Uncharacterised protein | Q8IHW7 | | | ✓ | | |
| Uncharacterised protein | Q8IHZ2 | | | | | ✓ |
| Uncharacterised protein | Q8IHZ8 | | | ✓ | | |
| Uncharacterised protein | Q8II41 | | | ✓ | | |
| Uncharacterised protein | Q8IIA5 | ✓ | ✓ | | | |
| Uncharacterised protein | Q8IIF6 | | ✓ | | | |
| Uncharacterised protein | Q8IIG8 | ✓ | | | | |
| Uncharacterised protein | Q8IIP3 | | ✓ | ✓ | | |
| Uncharacterised protein | Q8IIT1 | | ✓ | ✓ | | |
| Uncharacterised protein | Q8IIU5 | | | | | ✓ |
| Uncharacterised protein | Q8IJB8 | ✓ | ✓ | | | |

| | | | | | | | |
|---|---|---|---|---|---|---|---|
| Uncharacterised protein | Q8IJU4 | ✓ | | ✓ | | | |
| Uncharacterised protein | Q8IJX4 | | | ✓ | | | ✓ |
| Uncharacterised protein | Q8IKG9 | ✓ | | ✓ | | | |
| Uncharacterised protein | Q8IKL1 | | | | | | ✓ |
| Uncharacterised protein | Q8IKN7 | | | | | | ✓ |
| Uncharacterised protein | Q8IKP8 | | ✓ | ✓ | | | |
| Uncharacterised protein | Q8IKQ7 | ✓ | ✓ | | | | |
| Uncharacterised protein | Q8IKR2 | ✓ | | | | | ✓ |
| Uncharacterised protein | Q8IKT7 | | | ✓ | | | |
| Uncharacterised protein | Q8ILD4 | | | ✓ | | | |
| Uncharacterised protein | Q8ILG8 | | ✓ | ✓ | | | |
| Uncharacterised protein | Q8ILK4 | | | ✓ | | | |
| Uncharacterised protein | Q8ILR0 | | | ✓ | | | |
| Uncharacterised protein | Q8ILX3 | | | ✓ | | | |
| Uncharacterised protein | Q8ILY8 | | | ✓ | | | ✓ |
| Uncharacterised protein PFC0810c | O77374 | | | | ✓ | ✓ | |
| Vacuolar fusion protein MON1, putative | Q8IDH2 | | | ✓ | | | |
| Vacuolar protein sorting-associated protein 26 | Q8I4T1 | | | ✓ | | | |

| | | | | | | | |
|---|---|---|---|---|---|---|---|
| Vacuolar protein sorting-associated protein 35 | Q8IIQ6 | ✓ | | | | | |
| Variant-silencing SET domain-containing protein | Q8IE95 | | | | | ✓ | |
| Vesicle transport v-SNARE protein VTI1, putative | Q8I563 | | ✓ | ✓ | | | |
| Vesicle-associated membrane protein, putative | Q8IL71 | ✓ | | | | | |
| V-type H(+)-translocating pyrophosphatase, putative | Q8IKR1 | | | | | | ✓ |
| V-type proton ATPase catalytic subunit A | Q76NM6 | | | | ✓ | ✓ | ✓ |
| V-type proton ATPase subunit B | Q6ZMA8 | ✓ | | ✓ | ✓ | ✓ | |
| V-type proton ATPase subunit C | Q8I280 | | | ✓ | | | |
| V-type proton ATPase subunit F | Q8IHW4 | | | ✓ | | | |
| WD repeat-containing protein, putative | Q8I5B5 | | | ✓ | | | |
| Zinc finger protein, putative | Q8I3L5 | | | ✓ | | | |
| Zinc finger transcription factor, putative | Q7KQK4 | | | ✓ | | | |
| Zinc transporter, putative | Q8IBU1 | | | ✓ | | | |

[1] Protein alkylation targets identified by Ismail *et al*. using ozonide- and artemisinin-based click chemistry probes. See reference (1).

[2] Protein alkylation targets identified by Ismail *et al*. using artemisinin-based click chemistry probes. See reference (2).

[3] Protein alkylation targets identified by Wang *et al*. using artemisinin-based click chemistry probes. See reference (3).

## References


1. Ismail HM, Barton VE, Panchana M, Charoensutthivarakul S, Biagini GA, Ward SA, O'Neill PM. 2016. A click chemistry-based proteomic approach reveals that 1, 2, 4-trioxolane and artemisinin antimalarials share a common protein alkylation profile. Angew Chem Int Ed Engl 55:6401-6405.
2. Ismail HM, Barton V, Phanchana M, Charoensutthivarakul S, Wong MHL, Hemingway J, Biagini GA, O'Neill PM, Ward SA. 2016. Artemisinin activity-based probes identify multiple molecular targets within the asexual stage of the malaria parasites *Plasmodium falciparum* 3D7. Proc Natl Acad Sci U S A 113:2080-2085.
3. Wang J, Zhang C-J, Chia WN, Loh CC, Li Z, Lee YM, He Y, Yuan L-X, Lim TK, Liu M, Liew CX, Lee YQ, Zhang J, Lu N, Lim CT, Hua Z-C, Liu B, Shen H-M, Tan KSW, Lin Q. 2015. Haem-activated promiscuous targeting of artemisinin in *Plasmodium falciparum*. Nat Commun 6:10111.

# Appendix 6

# Chapter 5 – metabolomics supplementary material

| Mass | RT | FORMULA | Putative metabolite | Map | Cam3.II$^{R539T}$ | | | | | | Cam3.II$^{rev}$ | | | | | |
|---|---|---|---|---|---|---|---|---|---|---|---|---|---|---|---|---|
| | | | | | Fold change (vs DMSO) | | | ttest: | ttest: | ttest: | Fold change (vs DMSO) | | | ttest: | ttest: | ttest: |
| | | | | | OZ277 | OZ439 | DHA | OZ277 | OZ439 | DHA | OZ277 | OZ439 | DHA | OZ277 | OZ439 | DHA |
| 390.2769 | 4.1 | C24H38O4 | Bis(2-ethylhexyl)phthalate | Miscellaneous | 1.07 | 0.93 | 1.11 | 0.8151 | 0.7230 | 0.6940 | 1.99 | 1.41 | 1.05 | 0.4914 | 0.6334 | 0.8842 |
| 202.1430 | 21.0 | C8H18N4O2 | NG,NG-Dimethyl-L-arginine | Miscellaneous | 0.89 | 0.75 | 1.15 | 0.6004 | 0.2438 | 0.6250 | 1.38 | 1.32 | 1.15 | 0.4582 | 0.5579 | 0.4090 |
| 136.0373 | 16.0 | C4H8O5 | Erythronicacid | Miscellaneous | 1.02 | 0.86 | 0.89 | 0.9674 | 0.7568 | 0.8004 | 1.25 | 1.16 | 0.98 | 0.4355 | 0.5539 | 0.9554 |
| 381.0227 | 16.6 | C8H17NO12P2 | N-Acetyl-D-glucosamine 1,6-bisphosphate | Miscellaneous | 0.91 | 1.03 | 0.72 | 0.7666 | 0.9244 | 0.2452 | 1.03 | 1.34 | 0.82 | 0.9169 | 0.3677 | 0.1745 |
| 164.0321 | 12.4 | C5H8O6 | 2-Dehydro-D-xylonate | Miscellaneous | 0.93 | 0.81 | 1.00 | 0.6923 | 0.4377 | 0.9938 | 1.25 | 1.21 | 1.11 | 0.4877 | 0.2909 | 0.3322 |
| 148.1251 | 4.2 | C11H16 | Pentylbenzene | Miscellaneous | 0.42 | 0.57 | 0.76 | 0.1429 | 0.2798 | 0.5960 | 1.24 | 1.75 | 1.59 | 0.5617 | 0.2606 | 0.2858 |
| 213.1114 | 14.2 | C9H15N3O3 | Methyl 2-diazoacetamidohexonate | Miscellaneous | 1.07 | 0.82 | 0.97 | 0.8824 | 0.6367 | 0.9437 | 1.29 | 1.06 | 1.36 | 0.5297 | 0.8868 | 0.5663 |
| 173.1052 | 11.8 | C8H15NO3 | N-Acetyl-L-leucine | Miscellaneous | 0.84 | 0.98 | 0.90 | 0.7196 | 0.9622 | 0.8272 | 1.10 | 1.10 | 0.95 | 0.8609 | 0.8768 | 0.9473 |
| 679.1053 | 12.9 | C21H27N7O15P2 | nicotinamide guanine dinucleotide | Miscellaneous | 0.95 | 0.89 | 1.06 | 0.8339 | 0.5991 | 0.7631 | 1.30 | 1.18 | 1.12 | 0.6529 | 0.6978 | 0.6691 |
| 212.0085 | 13.2 | C5H9O7P | phosphinomethylisomalate | Miscellaneous | 0.99 | 1.06 | 1.09 | 0.9085 | 0.6578 | 0.4880 | 1.24 | 1.21 | 1.09 | 0.7319 | 0.7384 | 0.8815 |
| 189.1115 | 15.1 | C7H15N3O3 | L-Homocitrulline | Miscellaneous | 0.92 | 0.74 | 0.90 | 0.8804 | 0.4957 | 0.8068 | 1.22 | 1.12 | 1.01 | 0.3715 | 0.5416 | 0.9788 |
| 120.0938 | 4.2 | C9H12 | Cumene | Miscellaneous | 0.43 | 0.74 | 0.74 | 0.0925 | 0.5445 | 0.5410 | 1.26 | 1.60 | 1.43 | 0.4680 | 0.2566 | 0.3480 |
| 249.0307 | 18.4 | C8H11NO6S | Norepinephrinesulfate | Miscellaneous | 1.37 | 1.08 | 1.24 | 0.0822 | 0.7806 | 0.4655 | 2.96 | 2.47 | 1.49 | 0.5107 | 0.5337 | 0.6476 |
| 174.1368 | 21.0 | C8H18N2O2 | Ne,Ne dimethyllysine | Miscellaneous | 0.86 | 0.75 | 0.82 | 0.7255 | 0.4875 | 0.6356 | 1.31 | 1.15 | 0.98 | 0.3264 | 0.4383 | 0.9605 |
| 177.9975 | 11.1 | C5H11AsO2 | Arsenobetaine | Miscellaneous | 0.86 | 1.00 | 0.91 | 0.7943 | 0.9942 | 0.8768 | 1.26 | 1.22 | 0.91 | 0.5987 | 0.6527 | 0.8929 |
| 138.0430 | 7.9 | C6H6N2O2 | NicotinamideN-oxide | Miscellaneous | 0.35 | 0.89 | 0.41 | 0.3214 | 0.8704 | 0.3556 | 0.80 | 0.42 | 0.36 | 0.7026 | 0.2232 | 0.1793 |
| 151.0495 | 12.3 | C5H5N5O | 2-Hydroxyadenine | Miscellaneous | 0.83 | 1.24 | 0.61 | 0.5291 | 0.4214 | 0.1756 | 0.81 | 1.09 | 0.77 | 0.5767 | 0.8239 | 0.5132 |
| 179.0583 | 6.0 | C9H9NO3 | 4-oxo-4-(3-pyridyl)-butanoate | Miscellaneous | 1.08 | 0.99 | 1.07 | 0.7718 | 0.9334 | 0.7239 | 1.05 | 1.27 | 1.27 | 0.7941 | 0.4761 | 0.3148 |
| 302.1731 | 4.8 | C15H26O6 | Tributyrin | Miscellaneous | 0.88 | 0.80 | 1.35 | 0.6326 | 0.5014 | 0.2365 | 0.86 | 0.92 | 1.16 | 0.7539 | 0.8338 | 0.8086 |
| 129.0790 | 21.3 | C6H11NO2 | (R)-piperidine-3-carboxylate | Miscellaneous | 0.98 | 0.87 | 1.01 | 0.9416 | 0.6210 | 0.9790 | 1.10 | 1.01 | 0.95 | 0.6979 | 0.9549 | 0.8774 |
| 884.5440 | 3.8 | C55H72N4O6 | dihydrogeranylgeranyl-bacteriopheophytin | Miscellaneous | 1.04 | 1.41 | 0.86 | 0.8700 | 0.2112 | 0.1007 | 1.13 | 1.17 | 1.01 | 0.6507 | 0.5617 | 0.9623 |
| 186.0641 | 14.3 | C7H10N2O4 | (S)-AMPA | Miscellaneous | 0.90 | 0.92 | 0.79 | 0.6668 | 0.7143 | 0.3127 | 0.83 | 0.83 | 0.69 | 0.0826 | 0.0060 | 0.1164 |
| 244.1309 | 4.8 | C12H20O5 | Polyethylene, oxidized | Miscellaneous | 0.79 | 0.76 | 1.40 | 0.3946 | 0.3815 | 0.2757 | 0.71 | 0.81 | 1.07 | 0.5242 | 0.6358 | 0.9225 |
| 242.0192 | 15.0 | C6H11O8P | 6-deoxy-5-ketofructose-1-phosphate | Miscellaneous | 0.94 | 0.97 | 0.94 | 0.6567 | 0.8534 | 0.6942 | 1.05 | 1.07 | 0.96 | 0.9145 | 0.8518 | 0.8828 |
| 210.0293 | 21.8 | C6H11O6P | 3-propylphosphoenolpyruvate | Miscellaneous | 1.14 | 1.12 | 1.15 | 0.5765 | 0.6220 | 0.6036 | 1.19 | 0.93 | 1.26 | 0.5293 | 0.8310 | 0.3153 |
| 96.0213 | 13.8 | C5H4O2 | Furfural | Miscellaneous | 0.87 | 0.73 | 0.97 | 0.5715 | 0.1752 | 0.8670 | 0.91 | 1.15 | 1.60 | 0.5514 | 0.5809 | 0.1097 |
| 266.1549 | 3.8 | C12H26O4S | sodium dodecyl sulfate | Miscellaneous | 0.77 | 0.94 | 2.33 | 0.2535 | 0.8313 | 0.4370 | 1.05 | 0.75 | 1.05 | 0.8208 | 0.3027 | 0.9430 |
| 223.1209 | 10.3 | C12H17NO3 | Cerulenin | Miscellaneous | 0.92 | 0.75 | 0.91 | 0.8711 | 0.5673 | 0.8576 | 1.31 | 1.12 | 1.03 | 0.7624 | 0.8899 | 0.9774 |
| 276.0247 | 16.7 | C6H13O10P | 2-Carboxy-D-arabinitol 1-phosphate | Miscellaneous | 0.92 | 0.92 | 0.84 | 0.5851 | 0.5843 | 0.2276 | 0.82 | 1.16 | 0.90 | 0.4247 | 0.5342 | 0.4036 |
| 246.1367 | 8.8 | C14H18N2O2 | Hypaphorine | Miscellaneous | 0.98 | 1.07 | 1.16 | 0.7442 | 0.4190 | 0.2621 | 1.14 | 1.13 | 0.97 | 0.6962 | 0.6384 | 0.8998 |
| 222.0740 | 14.1 | C8H14O7 | 6-Acetyl-D-glucose | Miscellaneous | 0.78 | 0.92 | 0.92 | 0.0680 | 0.1270 | 0.5338 | 1.28 | 1.20 | 1.11 | 0.3081 | 0.2998 | 0.3589 |
| 712.3671 | 14.9 | C36H56O14 | Digitalin | Miscellaneous | 0.93 | 0.87 | 1.06 | 0.7911 | 0.5741 | 0.7854 | 1.06 | 0.90 | 0.88 | 0.8701 | 0.7187 | 0.4617 |
| 621.0274 | 17.7 | C15H22N5O16P3 | ADP ribose 1",2"-phosphate | Miscellaneous | 0.95 | 1.05 | 0.76 | 0.8561 | 0.8461 | 0.3926 | 0.71 | 0.93 | 0.92 | 0.3724 | 0.8182 | 0.7656 |
| 334.0667 | 15.9 | C9H19O11P | sn-glycero-3-Phospho-1-inositol | Miscellaneous | 0.90 | 0.85 | 0.90 | 0.6518 | 0.3189 | 0.4846 | 1.22 | 0.85 | 0.98 | 0.1444 | 0.2811 | 0.9161 |
| 179.0583 | 6.6 | C9H9NO3 | 3-Succinoylpyridine | Miscellaneous | 0.93 | 0.92 | 1.14 | 0.6616 | 0.2484 | 0.4673 | 1.02 | 1.03 | 1.15 | 0.8892 | 0.8211 | 0.4747 |

| | | | | | | | | | | | | | | | | | |
|---|---|---|---|---|---|---|---|---|---|---|---|---|---|---|---|---|---|
| 265.1311 | 8.4 | C14H19NO4 | N(alpha)-Benzyloxycarbonyl-L-leucine | Miscellaneous | 1.02 | 0.87 | 0.94 | 0.9625 | 0.6607 | 0.8786 | 1.17 | 1.17 | 0.99 | 0.5148 | 0.5082 | 0.9874 |
| 237.0849 | 12.5 | C8H15NO7 | N-Acetyl-D-glucosaminate | Miscellaneous | 0.96 | 1.08 | 1.11 | 0.8695 | 0.7795 | 0.7057 | 0.87 | 1.11 | 1.02 | 0.1985 | 0.5399 | 0.9339 |
| 145.0525 | 8.8 | C9H7NO | 3-Methyleneoxindole | Miscellaneous | 1.07 | 1.12 | 1.29 | 0.4781 | 0.1621 | 0.2460 | 1.06 | 1.24 | 1.04 | 0.8670 | 0.4087 | 0.8977 |
| 187.0633 | 8.8 | C11H9NO2 | Indoleacrylicacid | Miscellaneous | 1.03 | 1.09 | 1.28 | 0.7016 | 0.2861 | 0.1938 | 1.13 | 1.18 | 0.99 | 0.6948 | 0.5894 | 0.9841 |
| 163.0844 | 15.8 | C6H13NO4 | Deoxymannojirimycin | Miscellaneous | 0.94 | 0.91 | 1.01 | 0.7805 | 0.8005 | 0.9676 | 1.48 | 1.40 | 1.09 | 0.2845 | 0.4884 | 0.4712 |
| 258.1103 | 4.8 | C12H18O6 | 1,1'-(Tetrahydro-6a-hydroxy-2,3a,5-trimethylfuro[2,3-d]-1,3-dioxole-2,5-diyl)bis-ethanone | Miscellaneous | 0.96 | 0.84 | 1.31 | 0.8877 | 0.4045 | 0.1797 | 0.77 | 0.71 | 0.92 | 0.5485 | 0.4467 | 0.8835 |
| 212.0086 | 12.5 | C5H9O7P | P-DPD | Miscellaneous | 1.03 | 0.94 | 1.19 | 0.8849 | 0.8213 | 0.3666 | 1.17 | 1.18 | 1.12 | 0.7646 | 0.7097 | 0.7560 |
| 195.0744 | 11.8 | C6H13NO6 | D-Glucose oxime | Miscellaneous | 0.71 | 0.89 | 0.98 | 0.1845 | 0.3323 | 0.8686 | 1.01 | 1.11 | 0.89 | 0.9717 | 0.3329 | 0.1604 |
| 304.1022 | 15.8 | C10H16N4O7 | Vicine | Miscellaneous | 1.07 | 1.06 | 0.90 | 0.3520 | 0.7477 | 0.2176 | 0.91 | 1.02 | 0.92 | 0.5909 | 0.8982 | 0.7290 |
| 112.0161 | 12.4 | C5H4O3 | 2-Furoate | Miscellaneous | 0.97 | 0.83 | 0.90 | 0.8747 | 0.0940 | 0.3321 | 1.18 | 0.93 | 1.07 | 0.2219 | 0.4985 | 0.4650 |
| 336.0762 | 10.2 | C17H17ClO5 | 6-Methyl-griseofulvin | Miscellaneous | 0.96 | 0.99 | 0.89 | 0.7310 | 0.9694 | 0.7412 | 1.49 | 1.16 | 0.95 | 0.0310 | 0.3322 | 0.7528 |
| 179.0583 | 7.1 | C9H9NO3 | N-Acetylanthranilate | Miscellaneous | 0.88 | 1.42 | 1.90 | 0.3750 | 0.2284 | 0.1589 | 1.71 | 1.72 | 1.93 | 0.0845 | 0.0322 | 0.2342 |
| 423.3347 | 7.9 | C25H45NO4 | Linoelaidylcarnitine | Miscellaneous | 1.12 | 1.02 | 0.83 | 0.6236 | 0.7984 | 0.1243 | 0.96 | 1.01 | 1.00 | 0.5847 | 0.9282 | 0.9816 |
| 243.1471 | 8.5 | C12H21NO4 | Tiglylcarnitine | Miscellaneous | 0.71 | 0.79 | 0.81 | 0.0047 | 0.0244 | 0.0305 | 0.94 | 0.93 | 0.99 | 0.7933 | 0.7341 | 0.9403 |
| 200.0298 | 11.7 | C12H8OS | dibenzothiophene-5-oxide | Miscellaneous | 0.91 | 0.91 | 1.02 | 0.5724 | 0.5935 | 0.8644 | 1.05 | 1.27 | 0.95 | 0.8287 | 0.0195 | 0.7067 |
| 151.0301 | 10.5 | C4H9NO3S | methiin | Miscellaneous | 0.80 | 0.86 | 0.94 | 0.2672 | 0.4021 | 0.7815 | 1.00 | 1.22 | 1.22 | 0.9761 | 0.1114 | 0.3910 |
| 98.0367 | 12.6 | C5H6O2 | 2-Furanmethanol | Miscellaneous | 1.11 | 1.07 | 0.88 | 0.6863 | 0.6181 | 0.3892 | 1.30 | 1.41 | 1.02 | 0.1683 | 0.0588 | 0.9172 |
| 309.1060 | 14.7 | C11H19NO9 | O-Acetylneuraminic acid | Miscellaneous | 0.85 | 0.99 | 0.85 | 0.1931 | 0.8936 | 0.2982 | 0.92 | 1.18 | 0.99 | 0.4925 | 0.5013 | 0.9442 |
| 147.0895 | 12.2 | C6H13NO3 | N-hydroxyisoleucine | Miscellaneous | 0.94 | 0.87 | 0.93 | 0.9054 | 0.7985 | 0.9026 | 1.04 | 1.00 | 0.93 | 0.9420 | 0.9962 | 0.9237 |
| 261.1324 | 18.1 | C10H19N3O5 | Aspartylysine | Miscellaneous | 1.01 | 1.05 | 1.06 | 0.9047 | 0.7360 | 0.6408 | 0.82 | 0.80 | 1.00 | 0.3392 | 0.3052 | 0.9972 |
| 253.0852 | 23.5 | C14H11N3O2 | aeruginosin A | Miscellaneous | 1.06 | 1.07 | 1.07 | 0.7923 | 0.7950 | 0.8216 | 1.04 | 0.88 | 1.08 | 0.9044 | 0.6677 | 0.7404 |
| 201.1365 | 11.9 | C10H19NO3 | Capryloylglycine | Miscellaneous | 0.88 | 0.91 | 1.01 | 0.7552 | 0.8142 | 0.9796 | 1.01 | 0.99 | 1.02 | 0.9706 | 0.9828 | 0.9673 |
| 358.1111 | 15.0 | C12H22O12 | melibionate | Miscellaneous | 1.07 | 1.01 | 1.14 | 0.2277 | 0.9011 | 0.3083 | 1.03 | 1.00 | 1.04 | 0.8173 | 0.9932 | 0.5674 |
| 326.1215 | 16.0 | C12H22O10 | 2-O-alpha-L-Rhamnopyranosyl-D-glucopyranose | Miscellaneous | 1.05 | 0.99 | 0.99 | 0.7887 | 0.9075 | 0.9627 | 1.15 | 1.18 | 1.04 | 0.1465 | 0.1054 | 0.6015 |
| 122.0479 | 14.1 | C6H6N2O | Picolinamide | Miscellaneous | 1.15 | 1.13 | 1.09 | 0.1974 | 0.3233 | 0.0582 | 1.06 | 1.11 | 1.32 | 0.5179 | 0.2733 | 0.1611 |
| 348.1105 | 13.0 | C20H16N2O4 | Camptothecin | Miscellaneous | 1.34 | 1.00 | 1.01 | 0.4737 | 0.9868 | 0.9848 | 1.16 | 1.02 | 0.88 | 0.6553 | 0.9145 | 0.7094 |
| 378.1375 | 13.9 | C12H26O13 | Galactinoldihydrate | Miscellaneous | 1.07 | 1.10 | 1.04 | 0.5748 | 0.4660 | 0.7163 | 0.91 | 0.97 | 0.96 | 0.6620 | 0.8114 | 0.8364 |
| 259.0459 | 12.0 | C6H14NO8P | glycerophosphoserine | Miscellaneous | 1.12 | 0.81 | 0.90 | 0.3979 | 0.2061 | 0.7431 | 1.08 | 0.98 | 0.77 | 0.8141 | 0.9423 | 0.2724 |
| 614.3964 | 5.7 | C32H58N2O7S | CHAPS | Miscellaneous | 1.13 | 0.98 | 0.92 | 0.4344 | 0.9287 | 0.7067 | 0.97 | 1.00 | 0.95 | 0.7817 | 0.9936 | 0.4386 |
| 256.1213 | 4.8 | C15H16N2O2 | ancymidol | Miscellaneous | 0.90 | 1.02 | 1.03 | 0.6444 | 0.9590 | 0.8731 | 0.93 | 0.92 | 0.99 | 0.7169 | 0.6171 | 0.9479 |
| 149.0688 | 15.6 | C5H11NO4 | 4-amino-4-deoxy-L-arabinose | Miscellaneous | 1.16 | 0.81 | 1.20 | 0.4822 | 0.2453 | 0.4996 | 1.03 | 0.97 | 1.10 | 0.8928 | 0.7794 | 0.3520 |
| 374.1372 | 10.2 | C20H22O7 | Kievitone hydrate | Miscellaneous | 0.96 | 0.84 | 0.88 | 0.8660 | 0.3321 | 0.4425 | 0.90 | 1.08 | 1.14 | 0.3057 | 0.2625 | 0.4372 |
| 188.0144 | 5.2 | C7H8O4S | Benzyl sulfate | Miscellaneous | 1.00 | 0.69 | 1.13 | 0.9906 | 0.2259 | 0.0823 | 1.05 | 0.68 | 1.09 | 0.7141 | 0.1369 | 0.4437 |
| 206.1671 | 4.5 | C14H22O | alpha-Irone | Miscellaneous | 0.98 | 1.12 | 1.36 | 0.9159 | 0.6547 | 0.0426 | 1.04 | 1.12 | 1.10 | 0.7371 | 0.3245 | 0.3532 |
| 140.0474 | 12.8 | C7H8O3 | 2,3,5-Trihydroxytoluene | Miscellaneous | 0.94 | 1.08 | 1.03 | 0.6109 | 0.5539 | 0.8664 | 0.77 | 1.08 | 1.00 | 0.2338 | 0.6285 | 0.9857 |
| 98.0845 | 10.5 | C5H10N2 | xi-4,5-Dihydro-2,4(5)-dimethyl-1H-imidazole | Miscellaneous | 0.96 | 1.01 | 1.03 | 0.8636 | 0.9622 | 0.8521 | 0.91 | 1.09 | 1.08 | 0.3945 | 0.5011 | 0.5339 |
| 212.0087 | 15.2 | C5H9O7P | phosphinomethylmalate | Miscellaneous | 1.01 | 1.07 | 0.84 | 0.9572 | 0.6442 | 0.3253 | 0.98 | 0.97 | 0.88 | 0.8390 | 0.7901 | 0.4387 |

| | | | | | | | | | | | | | | | | | |
|---|---|---|---|---|---|---|---|---|---|---|---|---|---|---|---|---|---|
| 246.0504 | 12.5 | C6H15O8P | Glycerophosphoglycerol | Miscellaneous | 1.04 | 1.21 | 0.99 | 0.8160 | 0.3074 | 0.9400 | 1.00 | 1.06 | 1.01 | 0.9884 | 0.6985 | 0.9274 |
| 267.0955 | 16.8 | C9H17NO8 | Neuraminic acid | Miscellaneous | 0.99 | 1.02 | 0.93 | 0.9260 | 0.7852 | 0.4314 | 1.10 | 1.09 | 1.03 | 0.5560 | 0.4676 | 0.8780 |
| 166.0841 | 12.2 | C6H14O5 | 3-deoxy-D-galactose | Miscellaneous | 1.19 | 0.70 | 1.69 | 0.4840 | 0.2729 | 0.0395 | 0.94 | 0.74 | 1.42 | 0.7453 | 0.1768 | 0.2507 |
| 165.0426 | 5.0 | C8H7NO3 | 4-Nitroacetophenone | Miscellaneous | 1.00 | 1.05 | 1.01 | 0.9815 | 0.6614 | 0.9279 | 0.96 | 0.94 | 0.90 | 0.4475 | 0.3130 | 0.2339 |
| 150.0541 | 9.3 | C6H6N4O | 1-Methylhypoxanthine | Miscellaneous | 1.04 | 1.02 | 1.16 | 0.8462 | 0.8775 | 0.3519 | 0.97 | 1.09 | 1.04 | 0.7843 | 0.4846 | 0.7804 |
| 237.0848 | 16.1 | C8H15NO7 | N-Glycolyl-D-mannosamine | Miscellaneous | 0.97 | 1.00 | 0.98 | 0.7889 | 0.9840 | 0.8706 | 1.10 | 1.13 | 1.02 | 0.7408 | 0.6734 | 0.9191 |
| 371.3034 | 4.8 | C21H41NO4 | Tetradecanoylcarnitine | Miscellaneous | 0.93 | 1.00 | 0.98 | 0.6696 | 0.9736 | 0.8857 | 0.98 | 1.04 | 0.96 | 0.8937 | 0.8535 | 0.8049 |
| 189.1002 | 11.0 | C8H15NO4 | (2S)-2-{[1-(R)-Carboxyethyl]amino}pentanoate | Miscellaneous | 1.00 | 1.14 | 1.06 | 0.9838 | 0.2972 | 0.6956 | 1.00 | 1.00 | 0.96 | 0.9857 | 0.9566 | 0.8226 |
| 397.3190 | 4.8 | C23H43NO4 | trans-Hexadec-2-enoylcarnitine | Miscellaneous | 1.00 | 1.04 | 1.08 | 0.9757 | 0.6069 | 0.4653 | 0.94 | 0.91 | 0.95 | 0.5226 | 0.6463 | 0.5925 |
| 287.1118 | 15.3 | C11H17N3O6 | N-Ribosylhistidine | Miscellaneous | 1.01 | 1.18 | 1.07 | 0.9656 | 0.1327 | 0.6141 | 1.00 | 1.00 | 0.85 | 0.9321 | 0.9963 | 0.0112 |
| 420.1533 | 4.8 | C20H24N2O8 | 2-N,6-N-Bis(2,3-dihydroxy-N-benzoyl)-L-serine | Miscellaneous | 1.15 | 1.15 | 1.07 | 0.6997 | 0.5516 | 0.7468 | 0.94 | 0.96 | 1.05 | 0.6939 | 0.7812 | 0.7238 |
| 261.1213 | 12.1 | C11H19NO6 | Mycosporine | Miscellaneous | 1.11 | 1.08 | 1.09 | 0.4802 | 0.1623 | 0.5464 | 1.05 | 1.06 | 1.04 | 0.7731 | 0.6725 | 0.7825 |
| 169.9886 | 16.9 | C3H6O6S | Glycerone sulfate | Miscellaneous | 1.05 | 1.04 | 0.99 | 0.4665 | 0.3926 | 0.9196 | 0.85 | 1.03 | 0.99 | 0.0518 | 0.6995 | 0.9634 |
| 203.0795 | 8.0 | C8H13NO5 | 2-acetamidoglucal | Miscellaneous | 1.02 | 1.08 | 0.98 | 0.9503 | 0.7941 | 0.9636 | 0.97 | 0.81 | 0.80 | 0.8915 | 0.4054 | 0.3899 |
| 139.0634 | 7.9 | C7H9NO2 | 5-Acetyl-2,4-dimethyloxazole | Miscellaneous | 1.02 | 1.12 | 1.09 | 0.9387 | 0.6817 | 0.6078 | 0.95 | 1.01 | 1.01 | 0.7634 | 0.9220 | 0.9341 |
| 387.0409 | 18.6 | C10H17N3O9S2 | glutathione-sulfite | Miscellaneous | 0.74 | 1.04 | 1.27 | 0.4178 | 0.9065 | 0.6922 | 0.50 | 1.14 | 0.98 | 0.0944 | 0.6039 | 0.8979 |
| 145.0527 | 11.6 | C9H7NO | 1(2H)-Isoquinolinone | Miscellaneous | 1.05 | 1.10 | 1.07 | 0.6812 | 0.6010 | 0.4607 | 1.03 | 0.92 | 0.95 | 0.7828 | 0.5978 | 0.7007 |
| 326.1917 | 3.8 | C18H30O3S | 2-Dodecylbenzenesulfonic acid | Miscellaneous | 1.59 | 1.71 | 1.03 | 0.4618 | 0.0969 | 0.9160 | 0.60 | 0.81 | 0.72 | 0.1367 | 0.5104 | 0.2875 |
| 291.0954 | 12.4 | C11H17NO8 | 2-Deoxy-2,3-dehydro-N-acetylneuraminic acid | Miscellaneous | 1.06 | 1.12 | 1.11 | 0.6438 | 0.4587 | 0.6164 | 0.86 | 1.05 | 0.92 | 0.4176 | 0.6964 | 0.6968 |
| 268.1211 | 5.2 | C16H16N2O2 | N-Butyl-beta-carboline-3-carboxylate | Miscellaneous | 1.15 | 1.22 | 1.09 | 0.5033 | 0.6172 | 0.6989 | 1.22 | 0.97 | 0.98 | 0.4792 | 0.8595 | 0.9165 |
| 242.0192 | 16.4 | C6H11O8P | D-myo-Inositol 1,2-cyclic phosphate | Miscellaneous | 0.92 | 0.78 | 1.39 | 0.8137 | 0.4494 | 0.3552 | 0.66 | 0.78 | 1.12 | 0.1236 | 0.3035 | 0.6149 |
| 161.1052 | 11.0 | C7H15NO3 | (S)-Carnitine | Miscellaneous | 1.06 | 1.00 | 1.16 | 0.6570 | 0.9849 | 0.3159 | 0.93 | 0.91 | 1.09 | 0.7191 | 0.4975 | 0.6317 |
| 246.0853 | 10.3 | C9H14N2O6 | 5-6-Dihydrouridine | Miscellaneous | 0.92 | 0.84 | 1.17 | 0.5578 | 0.3464 | 0.5628 | 0.78 | 0.93 | 0.85 | 0.4675 | 0.7989 | 0.5790 |
| 246.0504 | 14.0 | C6H15O8P | 2-deoxyglucose-6-phosphate | Miscellaneous | 1.57 | 1.03 | 1.50 | 0.4260 | 0.8094 | 0.3268 | 1.07 | 1.22 | 1.17 | 0.8044 | 0.5544 | 0.6553 |
| 369.1933 | 10.7 | C22H27NO4 | Corydaline | Miscellaneous | 0.83 | 0.97 | 0.91 | 0.2138 | 0.7822 | 0.6876 | 0.80 | 1.06 | 1.07 | 0.0695 | 0.6801 | 0.7126 |
| 261.1212 | 12.9 | C11H19NO6 | Lotaustralin | Miscellaneous | 1.01 | 0.89 | 1.01 | 0.8784 | 0.0986 | 0.8490 | 0.81 | 0.89 | 0.91 | 0.1040 | 0.3615 | 0.4288 |
| 121.0528 | 4.8 | C7H7NO | 3-Acetylpyridine | Miscellaneous | 0.91 | 1.09 | 1.15 | 0.7443 | 0.7962 | 0.5014 | 0.91 | 0.92 | 1.06 | 0.5878 | 0.5708 | 0.8192 |
| 181.0964 | 10.2 | C7H11N5O | 6-methyltetrahydropterin | Miscellaneous | 1.31 | 1.03 | 1.03 | 0.0868 | 0.8401 | 0.8434 | 0.92 | 0.86 | 0.82 | 0.6500 | 0.1442 | 0.2801 |
| 283.3241 | 8.6 | C19H41N | CTAB | Miscellaneous | 0.98 | 1.05 | 0.94 | 0.9357 | 0.7946 | 0.7793 | 1.09 | 1.07 | 0.97 | 0.3929 | 0.4891 | 0.8962 |
| 228.0807 | 15.7 | C18H28N6O4S2 | Ovothiol disulfide | Miscellaneous | 1.02 | 0.48 | 0.73 | 0.9719 | 0.2458 | 0.6619 | 0.91 | 0.92 | 0.93 | 0.8744 | 0.9235 | 0.9286 |
| 234.1215 | 17.8 | C9H18N2O5 | 2,6-Diamino-7-hydroxy-azelaic acid | Miscellaneous | 0.94 | 1.05 | 1.16 | 0.5366 | 0.7387 | 0.3169 | 1.07 | 0.82 | 1.02 | 0.5398 | 0.1195 | 0.8934 |
| 125.0477 | 12.2 | C6H7NO2 | N-Ethylmaleimide | Miscellaneous | 1.00 | 1.08 | 1.02 | 0.9433 | 0.5069 | 0.7657 | 0.95 | 0.97 | 0.95 | 0.7710 | 0.9106 | 0.7524 |
| 428.3658 | 4.2 | C29H48O2 | (24R,24'R)-Fucosterol epoxide | Miscellaneous | 0.94 | 0.99 | 1.06 | 0.6741 | 0.9003 | 0.7549 | 1.35 | 1.13 | 1.13 | 0.0815 | 0.2843 | 0.6912 |
| 324.1530 | 16.6 | C12H24N2O8 | Procollagen 5-(D-galactosyloxy)-L-lysine | Miscellaneous | 1.18 | 1.13 | 1.12 | 0.1484 | 0.2363 | 0.4558 | 1.00 | 0.93 | 0.92 | 0.9952 | 0.6701 | 0.6318 |
| 130.1106 | 18.5 | C6H14N2O | ε-aminocaproamide | Miscellaneous | 1.05 | 1.06 | 1.14 | 0.6957 | 0.6952 | 0.3244 | 1.04 | 1.11 | 1.01 | 0.8064 | 0.6471 | 0.9134 |
| 185.1053 | 11.2 | C9H15NO3 | Otonecine | Miscellaneous | 0.88 | 0.90 | 0.87 | 0.4651 | 0.5760 | 0.5172 | 1.01 | 1.01 | 0.93 | 0.9367 | 0.9548 | 0.7458 |
| 256.1210 | 7.9 | C15H16N2O2 | 1-(9H-Pyrido[3,4-b]indol-1-yl)-1,4-butanediol | Miscellaneous | 0.93 | 1.08 | 0.98 | 0.6939 | 0.8164 | 0.8960 | 0.93 | 0.91 | 0.89 | 0.8013 | 0.7003 | 0.6751 |

| | | | | | | | | | | | | | | | | | |
|---|---|---|---|---|---|---|---|---|---|---|---|---|---|---|---|---|---|
| 300.1109 | 4.8 | C16H16N2O4 | 5-Nitro-2-(3-phenylpropylamino)benzoic acid | Miscellaneous | 0.91 | 1.14 | 1.05 | 0.7026 | 0.6603 | 0.8537 | 0.94 | 0.87 | 0.87 | 0.7116 | 0.4982 | 0.4865 |
| 251.1005 | 14.3 | C9H17NO7 | Muramic acid | Miscellaneous | 1.04 | 1.09 | 1.08 | 0.7893 | 0.3653 | 0.5955 | 0.96 | 0.97 | 1.12 | 0.5802 | 0.7932 | 0.4486 |
| 707.2477 | 16.5 | C26H45NO21 | Lacto-N-tetraose | Miscellaneous | 0.97 | 1.21 | 1.07 | 0.9395 | 0.6461 | 0.8606 | 0.68 | 0.75 | 1.01 | 0.1803 | 0.3492 | 0.9842 |
| 277.0912 | 15.6 | C9H15N3O7 | Lycomarasmine B | Miscellaneous | 1.10 | 1.11 | 1.07 | 0.3764 | 0.2946 | 0.5594 | 0.85 | 0.89 | 0.89 | 0.2062 | 0.4123 | 0.3742 |
| 192.0635 | 13.8 | C7H12O6 | 5D-5-O-Methyl-2,3,5/4,6-pentahydroxycyclohexanone | Miscellaneous | 0.87 | 0.90 | 1.05 | 0.7971 | 0.8315 | 0.9309 | 1.27 | 1.29 | 0.89 | 0.7226 | 0.7131 | 0.9069 |
| 342.1216 | 4.6 | C18H18N2O5 | Dictyoquinazol C | Miscellaneous | 1.12 | 0.90 | 1.10 | 0.7582 | 0.4453 | 0.5261 | 0.89 | 1.03 | 1.03 | 0.5542 | 0.6794 | 0.8070 |
| 84.0212 | 11.0 | C4H4O2 | 4-Hydroxy-2-butynal | Miscellaneous | 1.09 | 0.99 | 0.99 | 0.6527 | 0.9364 | 0.9557 | 0.90 | 0.85 | 1.13 | 0.6594 | 0.4447 | 0.4878 |
| 151.0634 | 4.8 | C8H9NO2 | N-Acetoxyarylamine | Miscellaneous | 1.03 | 0.94 | 0.88 | 0.8857 | 0.7831 | 0.5363 | 0.86 | 0.89 | 0.93 | 0.4330 | 0.5364 | 0.7580 |
| 220.0848 | 10.8 | C11H12N2O3 | 5-Hydroxytryptophan | Miscellaneous | 1.00 | 0.97 | 1.07 | 0.9949 | 0.9080 | 0.6973 | 0.87 | 0.92 | 0.96 | 0.4951 | 0.6312 | 0.8403 |
| 210.0740 | 13.7 | C7H14O7 | beta-D-Sedoheptulopyranose | Miscellaneous | 0.81 | 0.91 | 0.93 | 0.4738 | 0.3408 | 0.8022 | 1.11 | 1.14 | 0.99 | 0.5850 | 0.4743 | 0.9688 |
| 157.1102 | 10.1 | C8H15NO2 | Homostachydrine | Miscellaneous | 0.93 | 0.93 | 0.92 | 0.5191 | 0.4831 | 0.5482 | 1.02 | 0.92 | 0.93 | 0.9552 | 0.8594 | 0.8664 |
| 225.0637 | 11.5 | C10H11NO5 | 2-amino-2-deoxy-isochorismate | Miscellaneous | 1.05 | 1.05 | 1.27 | 0.8751 | 0.8358 | 0.4249 | 0.75 | 0.91 | 1.01 | 0.1015 | 0.5398 | 0.9505 |
| 312.1761 | 3.8 | C17H28O3S | N-Undecylbenzenesulfonic acid | Miscellaneous | 1.48 | 1.51 | 0.99 | 0.4947 | 0.1387 | 0.9787 | 0.56 | 0.73 | 0.60 | 0.1408 | 0.3759 | 0.1690 |
| 425.3504 | 7.8 | C25H47NO4 | Elaidiccarnitine | Miscellaneous | 0.97 | 0.94 | 0.89 | 0.8062 | 0.5293 | 0.3837 | 0.93 | 0.99 | 0.97 | 0.7171 | 0.9795 | 0.8045 |
| 369.0842 | 12.7 | C19H15NO7 | 7-Hydroxy-R-acenocoumarol | Miscellaneous | 0.55 | 1.31 | 0.74 | 0.4196 | 0.6996 | 0.6319 | 0.32 | 0.62 | 0.64 | 0.2877 | 0.5412 | 0.5708 |
| 242.1518 | 4.8 | C13H22O4 | 2-isocapryloyl-3R-hydroxymethyl-γ-butyrolactone | Miscellaneous | 1.29 | 0.91 | 1.10 | 0.3378 | 0.7371 | 0.6158 | 3.14 | 0.83 | 0.57 | 0.4592 | 0.2669 | 0.0166 |
| 218.0403 | 13.2 | C12H10O2S | cis-1,2-Dihydroxy-1,2-dihydrodibenzothiophene | Miscellaneous | 0.93 | 1.14 | 0.91 | 0.6639 | 0.3367 | 0.5124 | 1.05 | 1.15 | 0.94 | 0.4029 | 0.0246 | 0.7902 |
| 573.0878 | 12.5 | C16H25N5O14P2 | GDP-3,6-dideoxy-D-galactose | Miscellaneous | 1.23 | 0.92 | 0.80 | 0.4788 | 0.8035 | 0.5000 | 1.47 | 0.92 | 0.98 | 0.1582 | 0.7977 | 0.9480 |
| 347.1214 | 13.9 | C14H21NO9 | Dide-O-methylsimmondsin | Miscellaneous | 0.98 | 0.95 | 0.80 | 0.8382 | 0.6714 | 0.7018 | 1.20 | 1.13 | 0.94 | 0.3126 | 0.3687 | 0.6827 |
| 191.0795 | 12.7 | C7H13NO5 | Calystegine C1 | Miscellaneous | 1.02 | 1.20 | 0.98 | 0.9340 | 0.6475 | 0.9276 | 0.96 | 0.87 | 1.04 | 0.8075 | 0.5438 | 0.7947 |
| 173.0477 | 7.9 | C10H7NO2 | 2-Quinolinecarboxylic acid | Miscellaneous | 0.50 | 1.02 | 0.62 | 0.4962 | 0.9760 | 0.6006 | 0.34 | 0.83 | 0.65 | 0.2852 | 0.7580 | 0.5655 |
| 139.0634 | 5.2 | C7H9NO2 | Ethyl 2-pyrrolecarboxylate | Miscellaneous | 1.00 | 1.13 | 1.18 | 0.9948 | 0.7735 | 0.5404 | 0.85 | 0.86 | 1.01 | 0.4715 | 0.5437 | 0.9677 |
| 225.0637 | 4.6 | C10H11NO5 | 2-Hydroxy-4,7-dimethoxy-2H-1,4-benzoxazin-3(4H)-one | Miscellaneous | 0.87 | 1.11 | 0.96 | 0.6808 | 0.7994 | 0.8695 | 1.61 | 0.83 | 0.89 | 0.5859 | 0.2767 | 0.5216 |
| 194.0790 | 12.5 | C7H14O6 | 5-O-Methyl-myo-inositol | Miscellaneous | 1.12 | 1.08 | 0.97 | 0.5983 | 0.6793 | 0.8306 | 1.08 | 0.94 | 0.82 | 0.8815 | 0.8807 | 0.6413 |
| 255.1105 | 7.9 | C12H17NO5 | N-D-Glucosylarylamine | Miscellaneous | 0.88 | 1.31 | 1.21 | 0.1930 | 0.0027 | 0.2710 | 0.86 | 0.90 | 0.93 | 0.3470 | 0.2863 | 0.3116 |
| 245.1628 | 8.2 | C12H23NO4 | 2-Methylbutyroylcarnitine | Miscellaneous | 0.97 | 1.00 | 0.96 | 0.8049 | 0.9302 | 0.7746 | 0.91 | 0.90 | 0.90 | 0.7332 | 0.6272 | 0.6859 |
| 116.0837 | 4.8 | C6H12O2 | 4-Hydroxyhexan-3-one | Miscellaneous | 0.52 | 0.88 | 0.86 | 0.4819 | 0.8625 | 0.8367 | 0.39 | 0.69 | 0.81 | 0.2932 | 0.5990 | 0.7735 |
| 133.0739 | 16.2 | C5H11NO3 | 1-deoxyxylonojirimycin | Miscellaneous | 1.10 | 1.26 | 1.19 | 0.3109 | 0.3275 | 0.4827 | 0.86 | 0.88 | 0.97 | 0.2030 | 0.5114 | 0.7199 |
| 425.3505 | 4.6 | C25H47NO4 | Oleoylcarnitine | Miscellaneous | 1.05 | 0.97 | 1.07 | 0.6454 | 0.8329 | 0.7131 | 0.91 | 0.91 | 0.96 | 0.6125 | 0.6764 | 0.8049 |
| 383.1429 | 13.7 | C14H25NO11 | N-Acetyllactosamine | Miscellaneous | 1.21 | 1.01 | 1.19 | 0.2787 | 0.9285 | 0.3688 | 0.94 | 0.91 | 1.04 | 0.7346 | 0.7763 | 0.7783 |
| 199.1212 | 10.5 | C10H17NO3 | Tussilagine | Miscellaneous | 0.99 | 0.96 | 1.03 | 0.9554 | 0.9118 | 0.9019 | 0.89 | 0.90 | 0.77 | 0.5735 | 0.7370 | 0.4358 |
| 179.0583 | 4.8 | C9H9NO3 | Methyl n-formylanthranilate | Miscellaneous | 0.99 | 1.01 | 1.45 | 0.9783 | 0.9792 | 0.2712 | 0.85 | 0.85 | 1.02 | 0.6076 | 0.4979 | 0.8990 |
| 207.1108 | 13.3 | C8H17NO5 | N-Ethylglycocyamine | Miscellaneous | 0.96 | 1.06 | 0.85 | 0.7891 | 0.8585 | 0.3936 | 1.03 | 0.98 | 0.96 | 0.8893 | 0.8859 | 0.8608 |
| 268.0794 | 14.7 | C9H16O9 | 2(alpha-D-Mannosyl)-D-glycerate | Miscellaneous | 1.25 | 1.13 | 1.37 | 0.5894 | 0.6745 | 0.0719 | 0.94 | 1.12 | 1.10 | 0.6691 | 0.6598 | 0.4152 |
| 86.0367 | 13.9 | C4H6O2 | 1,4-Lactone | Miscellaneous | 2.09 | 1.09 | 2.31 | 0.3700 | 0.6778 | 0.3519 | 1.09 | 0.97 | 1.36 | 0.5547 | 0.8709 | 0.5665 |
| 223.1055 | 13.2 | C8H17NO6 | N-acetyl -D- glucosaminitol | Miscellaneous | 1.05 | 1.06 | 1.02 | 0.8304 | 0.7777 | 0.8826 | 1.02 | 0.97 | 1.04 | 0.9026 | 0.7832 | 0.8097 |
| 321.0695 | 19.4 | C11H15NO10 | beta-Citryl-L-glutamic acid | Miscellaneous | 0.97 | 1.02 | 0.82 | 0.8869 | 0.9245 | 0.1056 | 0.69 | 1.00 | 0.74 | 0.1240 | 0.9840 | 0.3744 |

| | | | | | | | | | | | | | | | | |
|---|---|---|---|---|---|---|---|---|---|---|---|---|---|---|---|---|
| 126.0251 | 14.7 | C5H6N2S | Pyrazinemethanethiol | Miscellaneous | 1.45 | 0.36 | 0.92 | 0.6177 | 0.2056 | 0.9273 | 1.01 | 0.65 | 0.85 | 0.9852 | 0.6145 | 0.8394 |
| 241.0950 | 4.8 | C11H15NO5 | Methocarbamol | Miscellaneous | 1.26 | 0.93 | 1.10 | 0.5755 | 0.9032 | 0.8524 | 1.41 | 0.68 | 0.93 | 0.3116 | 0.3788 | 0.8754 |
| 247.1420 | 11.4 | C11H21NO5 | Hydroxybutyrylcarnitine | Miscellaneous | 1.18 | 0.96 | 1.13 | 0.0585 | 0.5165 | 0.1148 | 0.98 | 0.89 | 1.15 | 0.9465 | 0.6643 | 0.4479 |
| 291.0954 | 12.9 | C11H17NO8 | 2,7-Anhydro-alpha-N-acetylneuraminic acid | Miscellaneous | 0.94 | 1.00 | 1.11 | 0.5993 | 0.9850 | 0.6679 | 0.69 | 0.96 | 0.93 | 0.0856 | 0.8952 | 0.7419 |
| 138.0428 | 12.3 | C6H6N2O2 | 4-Nitroaniline | Miscellaneous | 0.90 | 0.77 | 0.90 | 0.7400 | 0.4387 | 0.7556 | 1.01 | 0.98 | 0.93 | 0.9752 | 0.9628 | 0.8946 |
| 228.1474 | 10.2 | C11H20N2O3 | L-isoleucyl-L-proline | Miscellaneous | 1.13 | 1.06 | 1.17 | 0.4133 | 0.7314 | 0.4828 | 1.09 | 1.01 | 1.11 | 0.6436 | 0.9723 | 0.5626 |
| 350.0616 | 16.6 | C9H19O12P | nonulose 9-phosphate | Miscellaneous | 0.96 | 1.08 | 0.94 | 0.3605 | 0.3304 | 0.2098 | 0.85 | 1.00 | 0.88 | 0.3884 | 0.9837 | 0.5829 |
| 88.0160 | 14.7 | C3H4O3 | 3-Hydroxypropenoate | Miscellaneous | 1.51 | 1.22 | 1.23 | 0.3634 | 0.4876 | 0.2017 | 0.84 | 0.93 | 1.34 | 0.2197 | 0.6579 | 0.0591 |
| 195.0663 | 12.4 | C6H14NO4P | D,L-α-methylphosphinothricin | Miscellaneous | 0.85 | 0.97 | 0.84 | 0.6887 | 0.9427 | 0.6347 | 0.86 | 0.88 | 0.86 | 0.7806 | 0.7874 | 0.8473 |
| 167.9825 | 12.5 | C3H5O6P | hydroxypyruvaldehyde phosphate | Miscellaneous | 0.94 | 1.21 | 0.65 | 0.7860 | 0.2840 | 0.1059 | 0.75 | 0.99 | 0.79 | 0.4440 | 0.9806 | 0.4292 |
| 243.1041 | 10.6 | C10H17N3O2S | Biotin amide | Miscellaneous | 0.99 | 0.98 | 0.88 | 0.9787 | 0.9459 | 0.6280 | 1.02 | 0.99 | 0.92 | 0.9532 | 0.9912 | 0.8611 |
| 195.0897 | 4.9 | C10H13NO3 | Damascenine | Miscellaneous | 1.20 | 0.94 | 1.28 | 0.3229 | 0.8561 | 0.6160 | 1.21 | 0.68 | 0.80 | 0.5173 | 0.2484 | 0.5481 |
| 193.0410 | 10.9 | C6H11NO4S | γ-thiomethyl glutamate | Miscellaneous | 0.82 | 1.11 | 0.69 | 0.4962 | 0.7914 | 0.2307 | 0.86 | 0.95 | 0.87 | 0.6400 | 0.8272 | 0.7297 |
| 177.1002 | 13.4 | C7H15NO4 | N-Methyl-1-deoxynojirimycin | Miscellaneous | 0.99 | 1.04 | 0.97 | 0.8784 | 0.5164 | 0.7987 | 1.00 | 1.00 | 1.01 | 0.9900 | 0.9867 | 0.9340 |
| 461.3352 | 4.7 | C24H47NO7 | D-Glucosylsphingosine | Miscellaneous | 0.98 | 1.07 | 1.04 | 0.8110 | 0.6802 | 0.8472 | 0.90 | 0.90 | 0.91 | 0.6729 | 0.7305 | 0.6248 |
| 289.1274 | 13.3 | C11H19N3O6 | Ophthalmicacid | Miscellaneous | 1.21 | 0.95 | 1.25 | 0.3862 | 0.8349 | 0.2988 | 0.84 | 0.83 | 0.95 | 0.7742 | 0.7358 | 0.9213 |
| 427.3662 | 4.6 | C25H49NO4 | Stearoylcarnitine | Miscellaneous | 1.05 | 1.01 | 1.00 | 0.6607 | 0.9402 | 0.9979 | 0.87 | 0.99 | 0.89 | 0.7099 | 0.9896 | 0.7361 |
| 320.0510 | 16.2 | C8H17O11P | octulose 8-phosphate | Miscellaneous | 0.93 | 1.05 | 0.99 | 0.5238 | 0.6600 | 0.9400 | 0.80 | 1.00 | 0.86 | 0.5558 | 0.9967 | 0.6822 |
| 191.0794 | 12.0 | C7H13NO5 | 2-amino-3,7-dideoxy-D-threo-hept-6-ulosonate | Miscellaneous | 1.20 | 1.12 | 1.24 | 0.5961 | 0.8090 | 0.5317 | 0.79 | 0.94 | 0.98 | 0.6242 | 0.9087 | 0.9503 |
| 129.1518 | 14.5 | C8H19N | Octylamine | Miscellaneous | 1.71 | 1.98 | 0.90 | 0.4997 | 0.5291 | 0.7740 | 0.85 | 0.84 | 1.04 | 0.7534 | 0.3558 | 0.8247 |
| 159.1259 | 13.4 | C8H17NO2 | Methacholine | Miscellaneous | 1.08 | 1.02 | 1.18 | 0.5278 | 0.8093 | 0.2941 | 0.87 | 0.83 | 0.92 | 0.7045 | 0.6203 | 0.8011 |
| 265.0807 | 10.1 | C10H11N5O4 | 5'-Dehydroadenosine | Miscellaneous | 1.25 | 1.50 | 2.45 | 0.6955 | 0.3859 | 0.1825 | 0.97 | 0.79 | 0.79 | 0.7389 | 0.1359 | 0.1901 |
| 355.9912 | 16.6 | C6H14O13P2 | methanofuran biosynthesis intermediate MF1 | Miscellaneous | 0.86 | 1.15 | 0.52 | 0.6682 | 0.6073 | 0.0793 | 0.70 | 1.09 | 0.74 | 0.2893 | 0.8133 | 0.4953 |
| 171.0895 | 13.8 | C8H13NO3 | Crotanecine | Miscellaneous | 0.99 | 0.98 | 0.82 | 0.9728 | 0.9583 | 0.6200 | 0.91 | 0.97 | 0.87 | 0.8353 | 0.9425 | 0.6665 |
| 278.1882 | 4.0 | C17H26O3 | [6]-Paradol | Miscellaneous | 1.25 | 1.28 | 1.20 | 0.0326 | 0.4933 | 0.3806 | 0.91 | 0.83 | 0.95 | 0.7767 | 0.5992 | 0.8859 |
| 294.1833 | 4.1 | C17H26O4 | Phytuberin | Miscellaneous | 0.94 | 1.12 | 1.33 | 0.5216 | 0.5104 | 0.3333 | 2.40 | 1.19 | 0.73 | 0.5458 | 0.8391 | 0.5296 |
| 272.0299 | 16.0 | C7H13O9P | β-(2,6-anhydro-3-deoxy-D-arabino-heptulopyranosid)onate 7-phosphate | Miscellaneous | 0.89 | 0.96 | 0.92 | 0.6920 | 0.8400 | 0.7661 | 0.74 | 0.95 | 0.75 | 0.5516 | 0.9296 | 0.5010 |
| 205.0950 | 10.8 | C8H15NO5 | N-Acetyl-D-fucosamine | Miscellaneous | 1.19 | 1.17 | 1.22 | 0.5962 | 0.6457 | 0.5787 | 0.88 | 0.82 | 0.95 | 0.8552 | 0.7703 | 0.9421 |
| 288.0594 | 11.9 | C10H12N2O8 | Orotidine | Miscellaneous | 0.97 | 1.00 | 1.04 | 0.6889 | 0.9737 | 0.7163 | 0.94 | 0.94 | 0.85 | 0.9391 | 0.9401 | 0.8438 |
| 143.0946 | 10.7 | C7H13NO2 | 4-(Trimethylammonio)but-2-enoate | Miscellaneous | 0.95 | 0.91 | 0.89 | 0.8965 | 0.8158 | 0.7516 | 0.89 | 0.95 | 0.80 | 0.8959 | 0.9570 | 0.8048 |
| 590.0660 | 16.6 | C16H24N4O16P2 | IDP-D-mannose | Miscellaneous | 1.23 | 1.39 | 1.09 | NA | NA | NA | 0.62 | 0.84 | 0.76 | 0.5342 | 0.8299 | 0.7391 |
| 284.9645 | 7.9 | C6H8N3O4ClS2 | Chloraminophenamide | Miscellaneous | 0.00 | 0.00 | 0.00 | NA | NA | NA | 0.96 | 0.88 | 0.91 | NA | NA | NA |
| 145.0739 | 12.4 | C6H11NO3 | [FA oxo,amino(6:0)] 3-oxo-5S-amino-hexanoic acid | Amino Acid Metabolism | 0.91 | 0.78 | 0.87 | 0.8028 | 0.3922 | 0.6986 | 3.91 | 2.98 | 1.30 | 0.4698 | 0.5091 | 0.7409 |
| 141.0191 | 15.9 | C2H8NO4P | Ethanolamine phosphate | Amino Acid Metabolism | 0.98 | 1.27 | 0.78 | 0.8765 | 0.1175 | 0.1558 | 2.00 | 2.61 | 0.78 | 0.6009 | 0.5199 | 0.7909 |
| 129.0790 | 12.4 | C6H11NO2 | L-Pipecolate | Amino Acid Metabolism | 0.64 | 0.87 | 0.83 | 0.0935 | 0.5915 | 0.3214 | 1.07 | 1.03 | 0.91 | 0.9379 | 0.9534 | 0.9108 |
| 113.0589 | 9.8 | C4H7N3O | Creatinine | Amino Acid Metabolism | 0.66 | 0.25 | 2.85 | 0.5045 | 0.1767 | 0.0340 | 1.03 | 0.69 | 4.24 | 0.8519 | 0.0942 | 0.3785 |

| | | | | | | | | | | | | | | | | |
|---|---|---|---|---|---|---|---|---|---|---|---|---|---|---|---|---|
| 160.1211 | 22.0 | C7H17N2O2 | Putreanine | Amino Acid Metabolism | 0.79 | 0.74 | 1.03 | 0.6382 | 0.5341 | 0.9518 | 1.11 | 1.18 | 0.87 | 0.6442 | 0.4583 | 0.6705 |
| 169.0851 | 12.4 | C7H11N3O2 | N(pi)-Methyl-L-histidine | Amino Acid Metabolism | 0.87 | 0.60 | 1.42 | 0.7071 | 0.2233 | 0.3749 | 1.46 | 1.06 | 1.57 | 0.5436 | 0.8912 | 0.3031 |
| 264.1108 | 7.9 | C13H16N2O4 | alpha-N-Phenylacetyl-L-glutamine | Amino Acid Metabolism | 1.01 | 0.84 | 1.23 | 0.9798 | 0.5396 | 0.5832 | 1.93 | 1.74 | 1.43 | 0.4368 | 0.4815 | 0.5192 |
| 145.0739 | 14.2 | C6H11NO3 | 6-Amino-2-oxohexanoate | Amino Acid Metabolism | 0.83 | 0.72 | 0.96 | 0.7202 | 0.4973 | 0.9355 | 1.70 | 1.85 | 0.81 | 0.5150 | 0.4873 | 0.7889 |
| 264.1111 | 4.9 | C13H16N2O4 | Formyl-N-acetyl-5-methoxykynurenamine | Amino Acid Metabolism | 0.96 | 0.84 | 1.40 | 0.9099 | 0.6525 | 0.4379 | 1.56 | 1.33 | 1.37 | 0.6116 | 0.7006 | 0.5979 |
| 182.0580 | 8.7 | C9H10O4 | 3-(4-Hydroxyphenyl)lactate | Amino Acid Metabolism | 1.11 | 0.83 | 1.69 | 0.6925 | 0.5421 | 0.0577 | 1.40 | 0.81 | 1.78 | 0.6519 | 0.6929 | 0.4242 |
| 117.0539 | 15.7 | C3H7N3O2 | Guanidinoacetate | Amino Acid Metabolism | 1.10 | 0.74 | 1.47 | 0.6805 | 0.2626 | 0.1519 | 1.15 | 0.99 | 1.62 | 0.8186 | 0.9850 | 0.4816 |
| 103.0633 | 12.1 | C4H9NO2 | N,N-Dimethylglycine | Amino Acid Metabolism | 1.09 | 0.73 | 1.40 | 0.7913 | 0.2781 | 0.3429 | 1.20 | 1.06 | 1.15 | 0.5802 | 0.7083 | 0.4255 |
| 247.0690 | 13.8 | C9H13NO7 | N-Succinyl-L-glutamate | Amino Acid Metabolism | 1.26 | 0.92 | 1.38 | 0.3855 | 0.6973 | 0.3601 | 0.87 | 0.95 | 1.28 | 0.7284 | 0.8694 | 0.7459 |
| 192.0634 | 12.4 | C7H12O6 | Quinate | Amino Acid Metabolism | 0.79 | 0.81 | 0.99 | 0.6558 | 0.7054 | 0.9831 | 1.44 | 1.67 | 0.80 | 0.6283 | 0.4939 | 0.8236 |
| 217.1061 | 12.9 | C8H15N3O4 | N-Acetyl-L-citrulline | Amino Acid Metabolism | 0.73 | 1.07 | 0.66 | 0.5081 | 0.8818 | 0.3655 | 0.75 | 1.22 | 0.92 | 0.1815 | 0.2348 | 0.7119 |
| 398.1373 | 16.3 | C15H22N6O5S | S-Adenosyl-L-methionine | Amino Acid Metabolism | 0.95 | 0.88 | 1.10 | 0.4349 | 0.3348 | 0.1610 | 1.00 | 1.02 | 1.23 | 0.9976 | 0.9338 | 0.4989 |
| 188.1525 | 21.3 | C9H20N2O2 | N6,N6,N6-Trimethyl-L-lysine | Amino Acid Metabolism | 0.99 | 0.88 | 1.01 | 0.9805 | 0.6972 | 0.9709 | 1.22 | 1.12 | 0.95 | 0.4363 | 0.5301 | 0.8721 |
| 156.0535 | 10.9 | C6H8N2O3 | 4-Imidazolone-5-propanoate | Amino Acid Metabolism | 0.97 | 0.99 | 1.41 | 0.8497 | 0.9388 | 0.1052 | 1.29 | 1.05 | 1.54 | 0.6232 | 0.9087 | 0.4030 |
| 384.1217 | 13.6 | C14H20N6O5S | S-Adenosyl-L-homocysteine | Amino Acid Metabolism | 1.09 | 1.25 | 0.84 | 0.5726 | 0.2100 | 0.3629 | 0.98 | 1.08 | 1.02 | 0.9522 | 0.8113 | 0.8866 |
| 297.0894 | 7.9 | C11H15N5O3S | 5'-Methylthioadenosine | Amino Acid Metabolism | 0.88 | 0.77 | 1.39 | 0.6105 | 0.4095 | 0.1404 | 1.19 | 1.22 | 1.24 | 0.5802 | 0.4721 | 0.4259 |
| 172.0484 | 15.2 | C6H8N2O4 | Hydantoin-5-propionate | Amino Acid Metabolism | 0.95 | 0.91 | 0.90 | 0.7444 | 0.4735 | 0.6390 | 0.83 | 0.77 | 0.81 | 0.1880 | 0.1114 | 0.1722 |
| 167.9823 | 15.7 | C3H5O6P | 3-Phosphonopyruvate | Amino Acid Metabolism | 1.04 | 0.73 | 0.98 | 0.9012 | 0.1721 | 0.9374 | 2.77 | 2.19 | 0.96 | 0.4471 | 0.4730 | 0.9001 |
| 101.0840 | 11.1 | C5H11NO | Betaine aldehyde | Amino Acid Metabolism | 0.82 | 0.90 | 0.74 | 0.4078 | 0.3978 | 0.1059 | 1.34 | 1.00 | 1.00 | 0.1516 | 0.9928 | 0.9948 |
| 259.1170 | 11.2 | C10H17N3O5 | Linatine | Amino Acid Metabolism | 0.43 | 1.03 | 0.73 | 0.0572 | 0.9400 | 0.3672 | 0.46 | 1.05 | 0.84 | 0.2054 | 0.9097 | 0.7116 |
| 290.1227 | 16.7 | C10H18N4O6 | N-(L-Arginino)succinate | Amino Acid Metabolism | 0.99 | 1.01 | 0.86 | 0.9347 | 0.9305 | 0.1973 | 1.07 | 1.14 | 0.97 | 0.6699 | 0.5166 | 0.7796 |
| 177.0459 | 8.1 | C6H11NO3S | N-Formyl-L-methionine | Amino Acid Metabolism | 0.68 | 0.99 | 1.00 | 0.4997 | 0.9875 | 0.9959 | 1.35 | 1.54 | 1.24 | 0.1823 | 0.0276 | 0.4433 |
| 430.0654 | 15.2 | C11H20N4O10P2 | CMP-2-aminoethylphosphonate | Amino Acid Metabolism | 0.99 | 1.07 | 1.04 | 0.9468 | 0.6847 | 0.6312 | 0.95 | 0.88 | 1.02 | 0.8112 | 0.5412 | 0.9263 |
| 130.1106 | 10.4 | C6H14N2O | N-Acetylputrescine | Amino Acid Metabolism | 0.95 | 0.68 | 0.75 | 0.8469 | 0.1378 | 0.2540 | 1.35 | 1.07 | 1.20 | 0.1133 | 0.8450 | 0.5590 |
| 158.0579 | 7.9 | C7H10O4 | 2-Isopropylmaleate | Amino Acid Metabolism | 0.71 | 0.94 | 1.10 | 0.2860 | 0.7738 | 0.6857 | 0.89 | 0.89 | 1.01 | 0.6350 | 0.6359 | 0.9642 |
| 203.0582 | 8.9 | C11H9NO3 | Indolepyruvate | Amino Acid Metabolism | 0.87 | 0.94 | 0.97 | 0.5733 | 0.7782 | 0.8791 | 0.86 | 0.98 | 0.89 | 0.6670 | 0.9437 | 0.7542 |
| 173.0801 | 14.1 | C6H11N3O3 | 5-Guanidino-2-oxopentanoate | Amino Acid Metabolism | 0.92 | 1.20 | 0.87 | 0.7850 | 0.5602 | 0.6751 | 1.06 | 1.33 | 1.18 | 0.7576 | 0.2584 | 0.2985 |
| 211.0359 | 15.0 | C4H10N3O5P | Phosphocreatine | Amino Acid Metabolism | 0.96 | 1.04 | 1.02 | 0.8894 | 0.8794 | 0.9487 | 1.05 | 1.10 | 0.78 | 0.6635 | 0.5585 | 0.3520 |
| 189.0640 | 13.9 | C7H11NO5 | N-Acetyl-L-glutamate | Amino Acid Metabolism | 0.90 | 1.06 | 1.08 | 0.6486 | 0.7611 | 0.7245 | 1.01 | 1.05 | 0.88 | 0.9107 | 0.7301 | 0.5165 |
| 307.0837 | 14.0 | C10H17N3O6S | Glutathione | Amino Acid Metabolism | 1.22 | 0.98 | 1.02 | 0.4560 | 0.9334 | 0.9527 | 1.24 | 1.09 | 1.16 | 0.3415 | 0.6080 | 0.6083 |
| 253.0950 | 4.6 | C12H15NO5 | Dihydroferuloylglycine | Amino Acid Metabolism | 0.98 | 0.96 | 0.97 | 0.9394 | 0.8993 | 0.8631 | 1.15 | 0.96 | 1.11 | 0.4178 | 0.7738 | 0.5507 |
| 612.1515 | 17.2 | C20H32N6O12S2 | Glutathione disulfide | Amino Acid Metabolism | 0.77 | 1.07 | 0.93 | 0.1329 | 0.7645 | 0.7225 | 0.69 | 1.06 | 0.91 | 0.1910 | 0.8352 | 0.6093 |
| 87.0684 | 10.4 | C4H9NO | 4-Aminobutanal | Amino Acid Metabolism | 1.02 | 0.93 | 0.96 | 0.9333 | 0.6431 | 0.7802 | 0.97 | 1.22 | 1.07 | 0.7459 | 0.1230 | 0.7043 |
| 148.0372 | 14.8 | C5H8O5 | (R)-2-Hydroxyglutarate | Amino Acid Metabolism | 1.03 | 1.08 | 0.96 | 0.7489 | 0.4873 | 0.5724 | 1.11 | 1.02 | 0.94 | 0.6971 | 0.9299 | 0.8113 |
| 89.0477 | 14.6 | C3H7NO2 | L-Alanine | Amino Acid Metabolism | 0.99 | 0.94 | 1.06 | 0.8707 | 0.2338 | 0.1450 | 1.04 | 1.07 | 0.98 | 0.7258 | 0.3218 | 0.8554 |
| 117.0790 | 12.4 | C5H11NO2 | L-Valine | Amino Acid Metabolism | 0.94 | 0.95 | 0.93 | 0.3104 | 0.5420 | 0.3279 | 1.09 | 1.00 | 0.98 | 0.1759 | 0.9794 | 0.7471 |
| 155.0695 | 14.5 | C6H9N3O2 | L-Histidine | Amino Acid Metabolism | 0.90 | 1.08 | 0.94 | 0.1776 | 0.0242 | 0.3662 | 1.10 | 1.09 | 0.98 | 0.0992 | 0.1463 | 0.8412 |
| 115.0633 | 12.8 | C5H9NO2 | L-Proline | Amino Acid Metabolism | 1.12 | 1.12 | 1.02 | 0.2218 | 0.1747 | 0.8060 | 1.18 | 1.10 | 1.12 | 0.1011 | 0.1688 | 0.1202 |
| 129.0789 | 7.9 | C6H11NO2 | N4-Acetylaminobutanal | Amino Acid Metabolism | 0.38 | 0.95 | 0.71 | 0.2756 | 0.9298 | 0.6257 | 0.33 | 0.85 | 0.81 | 0.2627 | 0.7779 | 0.7981 |
| 146.0580 | 12.8 | C6H10O4 | (S)-2-Aceto-2-hydroxybutanoate | Amino Acid Metabolism | 1.03 | 1.00 | 0.96 | 0.7010 | 0.9974 | 0.8028 | 1.00 | 1.05 | 0.94 | 0.9719 | 0.5893 | 0.4612 |

| | | | | | | | | | | | | | | | | |
|---|---|---|---|---|---|---|---|---|---|---|---|---|---|---|---|---|
| 171.0532 | 7.9 | C7H9NO4 | 2,3,4,5-Tetrahydrodipicolinate | Amino Acid Metabolism | 0.69 | 0.99 | 0.95 | 0.3531 | 0.9647 | 0.8694 | 0.64 | 1.22 | 1.04 | 0.1373 | 0.2523 | 0.9077 |
| 149.0511 | 11.5 | C5H11NO2S | L-Methionine | Amino Acid Metabolism | 1.07 | 0.99 | 1.02 | 0.2456 | 0.9229 | 0.8156 | 1.08 | 1.05 | 1.15 | 0.3291 | 0.6463 | 0.1283 |
| 131.0946 | 11.3 | C6H13NO2 | L-Leucine | Amino Acid Metabolism | 0.92 | 0.95 | 1.06 | 0.1624 | 0.4203 | 0.1932 | 1.00 | 1.13 | 0.96 | 0.9945 | 0.0942 | 0.5017 |
| 119.0583 | 14.4 | C4H9NO3 | L-Threonine | Amino Acid Metabolism | 1.05 | 0.98 | 1.17 | 0.4968 | 0.7904 | 0.0139 | 0.95 | 1.02 | 1.02 | 0.5132 | 0.7264 | 0.7505 |
| 179.0583 | 8.0 | C9H9NO3 | Hippurate | Amino Acid Metabolism | 0.86 | 0.94 | 1.15 | 0.4135 | 0.8514 | 0.6434 | 0.89 | 1.04 | 1.17 | 0.2902 | 0.7505 | 0.4094 |
| 146.1055 | 22.6 | C6H14N2O2 | L-Lysine | Amino Acid Metabolism | 0.88 | 0.93 | 0.91 | 0.4571 | 0.6316 | 0.6805 | 0.97 | 1.06 | 0.96 | 0.8041 | 0.6985 | 0.8819 |
| 161.1052 | 13.3 | C7H15NO3 | L-Carnitine | Amino Acid Metabolism | 1.02 | 0.93 | 1.01 | 0.8825 | 0.3010 | 0.9256 | 1.06 | 1.01 | 1.06 | 0.8881 | 0.9750 | 0.8561 |
| 197.0690 | 7.9 | C9H11NO4 | N-Hydroxy-L-tyrosine | Amino Acid Metabolism | 0.84 | 1.24 | 1.03 | 0.6417 | 0.6900 | 0.9113 | 0.81 | 0.95 | 0.96 | 0.3750 | 0.8238 | 0.9209 |
| 113.0476 | 8.3 | C5H7NO2 | 1-Pyrroline-2-carboxylate | Amino Acid Metabolism | 1.44 | 1.44 | 0.92 | 0.4553 | 0.3359 | 0.6479 | 0.92 | 0.95 | 0.88 | 0.6531 | 0.8519 | 0.5884 |
| 237.0308 | 16.9 | C7H11NO6S | S-Cysteinosuccinic acid | Amino Acid Metabolism | 1.06 | 0.97 | 0.93 | 0.5129 | 0.5677 | 0.4508 | 0.99 | 1.07 | 0.98 | 0.9075 | 0.5415 | 0.9326 |
| 113.0477 | 15.9 | C5H7NO2 | (S)-1-Pyrroline-5-carboxylate | Amino Acid Metabolism | 0.93 | 1.04 | 0.91 | 0.5473 | 0.7694 | 0.4498 | 1.25 | 1.12 | 1.00 | 0.2448 | 0.2712 | 0.9950 |
| 146.0691 | 15.0 | C5H10N2O3 | L-Glutamine | Amino Acid Metabolism | 0.93 | 0.97 | 0.93 | 0.3709 | 0.7056 | 0.4252 | 0.96 | 0.96 | 1.02 | 0.5634 | 0.6312 | 0.8101 |
| 165.0462 | 13.3 | C5H11NO3S | L-Methionine S-oxide | Amino Acid Metabolism | 1.00 | 0.93 | 1.26 | 0.9952 | 0.7432 | 0.2810 | 0.78 | 1.04 | 1.06 | 0.3324 | 0.8756 | 0.8617 |
| 165.0790 | 10.2 | C9H11NO2 | L-Phenylalanine | Amino Acid Metabolism | 1.03 | 1.02 | 1.02 | 0.5783 | 0.8452 | 0.5234 | 0.99 | 1.02 | 0.97 | 0.6494 | 0.8575 | 0.6484 |
| 87.0320 | 15.5 | C3H5NO2 | 2-Aminoacrylate | Amino Acid Metabolism | 1.08 | 0.98 | 0.96 | 0.3892 | 0.7475 | 0.5519 | 1.21 | 1.01 | 1.02 | 0.0200 | 0.8040 | 0.9225 |
| 181.0739 | 7.9 | C9H11NO3 | 3-Amino-3-(4-hydroxyphenyl)propanoate | Amino Acid Metabolism | 0.80 | 1.23 | 1.13 | 0.4127 | 0.3456 | 0.3835 | 0.82 | 0.88 | 1.02 | 0.2484 | 0.3000 | 0.9294 |
| 218.1267 | 17.1 | C9H18N2O4 | N2-(D-1-Carboxyethyl)-L-lysine | Amino Acid Metabolism | 0.90 | 1.06 | 0.90 | 0.3777 | 0.6886 | 0.5223 | 0.87 | 1.00 | 0.87 | 0.5826 | 0.9801 | 0.3099 |
| 204.1474 | 19.9 | C9H20N2O3 | 3-Hydroxy-N6,N6,N6-trimethyl-L-lysine | Amino Acid Metabolism | 0.96 | 1.02 | 0.96 | 0.7445 | 0.9025 | 0.7169 | 1.02 | 1.25 | 0.98 | 0.8932 | 0.0233 | 0.8279 |
| 213.0638 | 12.5 | C9H11NO5 | N,N-Dihydroxy-L-tyrosine | Amino Acid Metabolism | 1.18 | 1.12 | 1.04 | 0.3596 | 0.5624 | 0.8171 | 1.03 | 1.03 | 1.08 | 0.7621 | 0.7642 | 0.5353 |
| 175.0481 | 14.3 | C6H9NO5 | N-Acetyl-L-aspartate | Amino Acid Metabolism | 0.86 | 0.99 | 0.94 | 0.6866 | 0.9212 | 0.8871 | 0.94 | 0.94 | 0.82 | 0.5348 | 0.5650 | 0.6283 |
| 131.0694 | 14.6 | C4H9N3O2 | Creatine | Amino Acid Metabolism | 1.02 | 1.05 | 1.04 | 0.8240 | 0.5302 | 0.6945 | 0.94 | 0.97 | 0.96 | 0.6639 | 0.8066 | 0.7468 |
| 204.0900 | 11.6 | C11H12N2O2 | L-Tryptophan | Amino Acid Metabolism | 1.23 | 1.06 | 1.19 | 0.1887 | 0.4903 | 0.0426 | 1.08 | 1.01 | 1.09 | 0.4085 | 0.9184 | 0.6350 |
| 131.0946 | 10.9 | C6H13NO2 | L-Isoleucine | Amino Acid Metabolism | 1.07 | 0.98 | 1.10 | 0.2434 | 0.8562 | 0.2152 | 0.97 | 0.97 | 0.94 | 0.4955 | 0.8170 | 0.4840 |
| 138.0317 | 7.9 | C7H6O3 | Gentisate aldehyde | Amino Acid Metabolism | 0.98 | 1.34 | 1.91 | 0.9645 | 0.6062 | 0.1955 | 0.77 | 0.77 | 0.79 | 0.5410 | 0.5241 | 0.5553 |
| 175.0957 | 15.8 | C6H13N3O3 | L-Citrulline | Amino Acid Metabolism | 0.98 | 1.01 | 1.00 | 0.8202 | 0.9583 | 0.9957 | 1.05 | 1.01 | 1.01 | 0.3868 | 0.8205 | 0.9545 |
| 203.0794 | 12.2 | C8H13NO5 | N2-Acetyl-L-aminoadipate | Amino Acid Metabolism | 1.13 | 1.10 | 1.08 | 0.0467 | 0.4111 | 0.4992 | 0.92 | 0.92 | 1.00 | 0.6265 | 0.6385 | 0.9867 |
| 135.0684 | 7.7 | C8H9NO | 2-Phenylacetamide | Amino Acid Metabolism | 0.86 | 1.16 | 0.93 | 0.3779 | 0.6776 | 0.6406 | 0.92 | 1.09 | 0.99 | 0.5517 | 0.5666 | 0.9455 |
| 246.1329 | 17.1 | C9H18N4O4 | N2-(D-1-Carboxyethyl)-L-arginine | Amino Acid Metabolism | 1.09 | 0.96 | 0.95 | 0.4390 | 0.7648 | 0.6787 | 0.99 | 1.00 | 0.97 | 0.9667 | 0.9943 | 0.8982 |
| 105.0426 | 15.7 | C3H7NO3 | L-Serine | Amino Acid Metabolism | 1.09 | 1.05 | 1.01 | 0.3206 | 0.5784 | 0.9328 | 1.10 | 1.03 | 0.96 | 0.0889 | 0.6190 | 0.7927 |
| 190.0954 | 17.2 | C7H14N2O4 | LL-2,6-Diaminoheptanedioate | Amino Acid Metabolism | 0.99 | 1.14 | 0.99 | 0.9201 | 0.3846 | 0.9179 | 1.13 | 0.84 | 1.03 | 0.6606 | 0.3310 | 0.8609 |
| 229.0585 | 14.5 | C9H11NO6 | 4-(L-Alanin-3-yl)-2-hydroxy-cis,cis-muconate 6-semialdehyde | Amino Acid Metabolism | 1.22 | 1.13 | 1.10 | 0.3687 | 0.4863 | 0.6677 | 0.89 | 1.02 | 1.06 | 0.5109 | 0.8366 | 0.4985 |
| 240.1222 | 14.2 | C10H16N4O3 | Homocarnosine | Amino Acid Metabolism | 0.97 | 1.08 | 0.95 | 0.9276 | 0.8596 | 0.8944 | 0.98 | 0.93 | 0.88 | 0.8385 | 0.6825 | 0.4157 |
| 203.1158 | 11.1 | C9H17NO4 | O-Acetylcarnitine | Amino Acid Metabolism | 1.07 | 0.99 | 1.09 | 0.6301 | 0.9574 | 0.5700 | 0.87 | 0.82 | 1.07 | 0.5601 | 0.4042 | 0.7522 |
| 209.0688 | 7.9 | C10H11NO4 | 4-Hydroxyphenylacetylglycine | Amino Acid Metabolism | 1.09 | 1.20 | 0.92 | 0.7082 | 0.1229 | 0.5828 | 0.73 | 0.96 | 0.96 | 0.0070 | 0.7288 | 0.6373 |
| 181.0739 | 12.9 | C9H11NO3 | L-Tyrosine | Amino Acid Metabolism | 0.96 | 0.97 | 1.11 | 0.5372 | 0.7590 | 0.1329 | 0.85 | 1.00 | 0.95 | 0.1250 | 0.9965 | 0.7285 |
| 102.0317 | 14.8 | C4H6O3 | 2-Oxobutanoate | Amino Acid Metabolism | 1.58 | 0.84 | 1.91 | 0.2447 | 0.6798 | 0.1218 | 0.67 | 0.81 | 1.22 | 0.0523 | 0.2139 | 0.3844 |
| 132.0535 | 15.2 | C4H8N2O3 | L-Asparagine | Amino Acid Metabolism | 1.03 | 1.11 | 1.07 | 0.5766 | 0.1296 | 0.2042 | 0.95 | 1.01 | 1.02 | 0.6305 | 0.9426 | 0.9265 |
| 132.0899 | 21.8 | C5H12N2O2 | L-Ornithine | Amino Acid Metabolism | 0.93 | 0.99 | 0.95 | 0.2537 | 0.8067 | 0.5610 | 0.85 | 0.96 | 0.86 | 0.3578 | 0.7555 | 0.5063 |
| 169.0738 | 13.8 | C8H11NO3 | L-Noradrenaline | Amino Acid Metabolism | 1.42 | 1.07 | 1.19 | 0.3408 | 0.4709 | 0.3837 | 1.08 | 1.00 | 1.16 | 0.7602 | 0.9776 | 0.1800 |

| | | | | | | | | | | | | | | | | |
|---|---|---|---|---|---|---|---|---|---|---|---|---|---|---|---|---|
| 174.1117 | 23.5 | C6H14N4O2 | L-Arginine | Amino Acid Metabolism | 0.94 | 1.00 | 1.03 | 0.1170 | 0.9652 | 0.4824 | 0.93 | 1.01 | 0.96 | 0.3566 | 0.9003 | 0.8670 |
| 161.0689 | 14.7 | C6H11NO4 | L-2-Aminoadipate | Amino Acid Metabolism | 1.47 | 1.15 | 1.20 | 0.3445 | 0.5488 | 0.4779 | 1.01 | 1.16 | 1.18 | 0.9435 | 0.6536 | 0.1602 |
| 190.0954 | 14.2 | C7H14N2O4 | meso-2,6-Diaminoheptanedioate | Amino Acid Metabolism | 0.87 | 0.92 | 1.01 | 0.1154 | 0.2539 | 0.9452 | 0.95 | 1.01 | 1.23 | 0.9053 | 0.9744 | 0.6168 |
| 131.0584 | 14.4 | C5H9NO3 | L-Glutamate 5-semialdehyde | Amino Acid Metabolism | 0.98 | 1.08 | 0.97 | 0.7713 | 0.3088 | 0.6741 | 0.93 | 1.06 | 0.93 | 0.4061 | 0.5560 | 0.7382 |
| 129.0426 | 9.5 | C5H7NO3 | L-1-Pyrroline-3-hydroxy-5-carboxylate | Amino Acid Metabolism | 0.92 | 0.97 | 1.09 | 0.4037 | 0.8243 | 0.4599 | 0.95 | 1.02 | 0.94 | 0.6480 | 0.8571 | 0.6319 |
| 322.1376 | 15.1 | C12H22N2O8 | Avenic acid A | Amino Acid Metabolism | 1.07 | 1.12 | 1.07 | 0.5085 | 0.4009 | 0.5126 | 1.01 | 0.93 | 0.96 | 0.9188 | 0.4606 | 0.5673 |
| 142.0742 | 13.0 | C6H10N2O2 | Ectoine | Amino Acid Metabolism | 1.03 | 1.27 | 1.13 | 0.8705 | 0.1521 | 0.5861 | 1.11 | 0.99 | 0.92 | 0.6820 | 0.9760 | 0.6550 |
| 129.0426 | 10.0 | C5H7NO3 | 5-Oxoproline | Amino Acid Metabolism | 0.84 | 0.91 | 1.20 | 0.3691 | 0.6654 | 0.2323 | 0.85 | 0.93 | 0.98 | 0.4277 | 0.7478 | 0.8696 |
| 103.0997 | 19.5 | C5H13NO | Choline | Amino Acid Metabolism | 1.09 | 1.23 | 1.14 | 0.8624 | 0.6670 | 0.7937 | 0.79 | 0.83 | 1.04 | 0.3800 | 0.5444 | 0.8214 |
| 229.0885 | 14.7 | C9H15N3O2S | Ergothioneine | Amino Acid Metabolism | 1.47 | 0.39 | 0.91 | 0.6081 | 0.2466 | 0.9228 | 1.03 | 0.73 | 0.86 | 0.9487 | 0.7149 | 0.8504 |
| 104.0110 | 14.3 | C3H4O4 | Hydroxypyruvate | Amino Acid Metabolism | 0.91 | 1.16 | 0.91 | 0.7588 | 0.4601 | 0.7798 | 0.81 | 0.86 | 0.90 | 0.0547 | 0.2335 | 0.7112 |
| 147.0531 | 14.5 | C5H9NO4 | L-Glutamate | Amino Acid Metabolism | 1.00 | 1.18 | 1.00 | 0.9844 | 0.4812 | 0.9899 | 0.88 | 0.90 | 1.00 | 0.6332 | 0.5514 | 0.9521 |
| 243.0855 | 13.7 | C9H13N3O5 | gamma-Glutamyl-beta-cyanoalanine | Amino Acid Metabolism | 1.03 | 1.06 | 0.92 | 0.8635 | 0.7141 | 0.6930 | 0.94 | 0.94 | 0.97 | 0.7055 | 0.8169 | 0.8751 |
| 117.0790 | 11.3 | C5H11NO2 | Betaine | Amino Acid Metabolism | 1.02 | 0.94 | 1.05 | 0.9540 | 0.8072 | 0.8000 | 0.97 | 0.94 | 0.95 | 0.9061 | 0.7751 | 0.6691 |
| 145.1103 | 13.3 | C7H15NO2 | 4-Trimethylammoniobutanoate | Amino Acid Metabolism | 1.11 | 1.07 | 1.22 | 0.6079 | 0.7518 | 0.2151 | 0.89 | 0.86 | 0.95 | 0.6038 | 0.4853 | 0.7906 |
| 197.1165 | 12.3 | C9H15N3O2 | Hercynine | Amino Acid Metabolism | 0.79 | 0.70 | 0.87 | 0.4251 | 0.2471 | 0.6372 | 0.98 | 1.02 | 1.08 | 0.9663 | 0.9587 | 0.9039 |
| 133.0375 | 14.8 | C4H7NO4 | L-Aspartate | Amino Acid Metabolism | 1.30 | 1.14 | 1.18 | 0.5486 | 0.7867 | 0.5228 | 0.95 | 0.96 | 1.06 | 0.8841 | 0.9315 | 0.8877 |
| 111.9924 | 14.3 | CH5O4P | Hydroxymethylphosphonate | Amino Acid Metabolism | 0.78 | 1.17 | 1.11 | 0.3685 | 0.6623 | 0.7401 | 0.69 | 0.82 | 0.94 | 0.0315 | 0.1477 | 0.8775 |
| 132.0423 | 14.5 | C5H8O4 | (S)-2-Acetolactate | Amino Acid Metabolism | 1.57 | 1.22 | 1.24 | 0.3514 | 0.5374 | 0.1568 | 0.83 | 0.87 | 1.12 | 0.2194 | 0.4551 | 0.6140 |
| 170.0147 | 14.7 | C6H6N2O2S | Thiourocanic acid | Amino Acid Metabolism | 1.48 | 0.21 | 0.91 | 0.6054 | NA | 0.9254 | 0.94 | 0.53 | 0.80 | 0.9027 | NA | 0.7810 |
| 125.9987 | 10.4 | C2H6O4S | 2-Hydroxyethanesulfonate | Amino Acid Metabolism | 0.88 | 0.80 | 1.66 | 0.7689 | 0.7046 | 0.2761 | 0.98 | 0.82 | 1.10 | 0.9370 | 0.5736 | 0.5901 |
| 159.0896 | 12.3 | C7H13NO3 | 5-Acetamidopentanoate | Amino Acid Metabolism | 1.04 | 0.97 | 0.99 | 0.9426 | 0.9472 | 0.9792 | 0.92 | 0.99 | 1.08 | 0.9009 | 0.9842 | 0.9266 |
| 312.0221 | 16.0 | C9H16N2O5Se | gamma-Glutamyl-Se-methylselenocysteine | Amino Acid Metabolism | 0.98 | 1.05 | 1.06 | 0.9407 | 0.7619 | 0.6579 | 0.95 | 0.93 | 0.88 | 0.9171 | 0.8660 | 0.6625 |
| 219.1108 | 8.6 | C9H17NO5 | Pantothenate | Amino Acid Metabolism | 0.96 | 1.06 | 1.05 | 0.7770 | 0.5788 | 0.5671 | 0.94 | 0.95 | 0.97 | 0.8596 | 0.8759 | 0.9357 |
| 114.0317 | 14.7 | C5H6O3 | 2-Hydroxy-2,4-pentadienoate | Amino Acid Metabolism | 1.94 | 1.31 | 1.31 | 0.3563 | 0.5377 | 0.1560 | 0.74 | 0.86 | 1.28 | 0.1125 | 0.4421 | 0.3186 |
| 336.1648 | 17.4 | C12H24N4O7 | N2-Fructopyranosylarginine | Amino Acid Metabolism | 1.95 | 1.61 | 1.56 | 0.3268 | 0.5128 | 0.3490 | 1.11 | 0.76 | 1.11 | 0.7005 | 0.3264 | 0.7736 |
| 306.0523 | 12.1 | C18H10O5 | Kinobscurinone | Biosynthesis of Polyketides and Nonribosomal Peptides | 1.14 | 1.18 | 1.00 | 0.3003 | 0.3645 | 0.9884 | 0.89 | 1.14 | 0.89 | 0.6399 | 0.6542 | 0.5250 |
| 199.0481 | 7.9 | C8H9NO5 | Clavulanic acid | Biosynthesis of Secondary Metabolites | 0.90 | 1.00 | 0.91 | 0.7945 | 0.9929 | 0.6987 | 0.60 | 0.88 | 1.22 | 0.1507 | 0.5540 | 0.4533 |
| 357.1571 | 15.0 | C20H23NO5 | deacetylcolchicine | Biosynthesis of Secondary Metabolites | 0.91 | 0.88 | 1.03 | 0.4092 | 0.2426 | 0.6847 | 1.01 | 1.29 | 0.95 | 0.8752 | 0.0024 | 0.4201 |
| 153.0790 | 7.9 | C8H11NO2 | vanillylamine | Biosynthesis of Secondary Metabolites | 0.92 | 1.23 | 1.05 | 0.7718 | 0.5710 | 0.8107 | 0.92 | 1.10 | 1.06 | 0.7031 | 0.6371 | 0.8496 |
| 365.0898 | 11.3 | C20H15NO6 | 6-Methylpretetramide | Biosynthesis of Secondary Metabolites | 0.93 | 0.90 | 1.10 | 0.7466 | 0.7258 | 0.6321 | 0.91 | 0.91 | 1.09 | 0.6050 | 0.5068 | 0.7536 |
| 331.0843 | 12.8 | C20H13NO4 | Sanguinarine | Biosynthesis of Secondary Metabolites | 0.89 | 1.07 | 1.13 | 0.4775 | 0.6322 | 0.5233 | 0.82 | 0.94 | 0.84 | 0.3528 | 0.7845 | 0.5305 |
| 168.1150 | 4.3 | C10H16O2 | Iridodial | Biosynthesis of Secondary Metabolites | 0.72 | 1.10 | 0.63 | NA | 0.8941 | NA | 0.51 | 1.20 | 1.13 | NA | 0.7049 | 0.8090 |

| | | | | | | | | | | | | | | | | | |
|---|---|---|---|---|---|---|---|---|---|---|---|---|---|---|---|---|---|
| 240.1474 | 11.1 | C12H20N2O3 | Slaframine | Biosynthesis of Secondary Metabolites | 1.02 | 0.95 | 1.01 | 0.7607 | 0.5351 | 0.8504 | 0.98 | 1.08 | 1.06 | 0.8534 | 0.6872 | 0.7279 |
| 192.0271 | 17.7 | C6H8O7 | Citrate | Carbohydrate Metabolism | 1.00 | 0.72 | 1.05 | 0.9987 | 0.4610 | 0.8825 | 6.28 | 4.69 | 3.00 | 0.4523 | 0.4704 | 0.4203 |
| 112.0160 | 17.6 | C5H4O3 | 2,3-Dihydroxy-2,4-cyclopentadien-1-one | Carbohydrate Metabolism | 0.94 | 0.70 | 0.93 | 0.8587 | 0.3748 | 0.8311 | 3.38 | 2.61 | 1.63 | 0.4939 | 0.5192 | 0.5822 |
| 174.0164 | 17.4 | C6H6O6 | cis-Aconitate | Carbohydrate Metabolism | 1.00 | 0.83 | 1.16 | 0.9795 | 0.3103 | 0.2968 | 1.74 | 1.54 | 1.73 | 0.6703 | 0.7243 | 0.6593 |
| 598.3571 | 15.2 | C28H54O13 | Sucrose monopalmitate | Carbohydrate Metabolism | 0.84 | 0.89 | 0.93 | 0.6432 | 0.7060 | 0.8174 | 0.81 | 0.53 | 0.87 | 0.8512 | 0.5760 | 0.8997 |
| 146.0216 | 15.2 | C5H6O5 | 2-Oxoglutarate | Carbohydrate Metabolism | 1.01 | 0.89 | 1.41 | 0.9759 | 0.7571 | 0.2646 | 0.88 | 0.55 | 1.71 | 0.9087 | 0.5938 | 0.6963 |
| 162.0529 | 8.0 | C6H10O5 | L-Rhamnono-1,4-lactone | Carbohydrate Metabolism | 1.24 | 0.70 | 1.43 | 0.6150 | 0.2472 | 0.3086 | 1.61 | 1.10 | 1.54 | 0.4938 | 0.7286 | 0.4357 |
| 118.0266 | 14.8 | C4H6O4 | Succinate | Carbohydrate Metabolism | 0.89 | 0.74 | 1.27 | 0.3313 | 0.0486 | 0.0812 | 1.01 | 0.88 | 1.32 | 0.9753 | 0.6686 | 0.5718 |
| 116.0109 | 15.5 | C4H4O4 | Fumarate | Carbohydrate Metabolism | 1.06 | 0.84 | 1.02 | 0.6307 | 0.0831 | 0.8860 | 1.04 | 1.03 | 1.10 | 0.9289 | 0.9429 | 0.8172 |
| 134.0216 | 15.6 | C4H6O5 | (S)-Malate | Carbohydrate Metabolism | 1.10 | 0.86 | 0.97 | 0.3909 | 0.1413 | 0.7593 | 1.01 | 0.99 | 1.08 | 0.9748 | 0.9705 | 0.8682 |
| 136.0373 | 12.2 | C4H8O5 | [FA trihydroxy(4:0)] 2,3,4-trihydroxy-butanoic acid | Carbohydrate Metabolism | 1.07 | 0.89 | 1.36 | 0.8015 | 0.6503 | 0.2479 | 1.21 | 0.91 | 1.18 | 0.3129 | 0.4725 | 0.5333 |
| 154.0032 | 11.1 | C3H7O5P | Propanoyl phosphate | Carbohydrate Metabolism | 48.17 | 1.24 | 48.42 | 0.4229 | 0.1084 | 0.4196 | 1.81 | 1.01 | 51.72 | 0.2544 | 0.9810 | 0.4239 |
| 607.0812 | 14.8 | C17H27N3O17P2 | UDP-N-acetyl-D-glucosamine | Carbohydrate Metabolism | 0.98 | 0.91 | 0.99 | 0.7326 | 0.0404 | 0.8348 | 0.88 | 0.96 | 1.02 | 0.7488 | 0.9203 | 0.9641 |
| 210.0376 | 16.7 | C6H10O8 | D-Glucarate | Carbohydrate Metabolism | 0.92 | 0.83 | 0.91 | 0.8137 | 0.5917 | 0.7415 | 1.48 | 1.57 | 0.96 | 0.5592 | 0.4357 | 0.9339 |
| 167.9824 | 17.1 | C3H5O6P | Phosphoenolpyruvate | Carbohydrate Metabolism | 0.97 | 1.10 | 0.58 | 0.8968 | 0.5245 | 0.0447 | 0.97 | 1.15 | 0.66 | 0.8756 | 0.5641 | 0.0700 |
| 319.0669 | 14.6 | C8H18NO10P | N-Gluconyl ethanolamine phosphate | Carbohydrate Metabolism | 2.81 | 1.39 | 2.50 | 0.4151 | 0.5454 | 0.4794 | 0.98 | 1.40 | 2.94 | 0.9182 | 0.0074 | 0.4373 |
| 185.9930 | 16.6 | C3H7O7P | 3-Phospho-D-glycerate | Carbohydrate Metabolism | 1.07 | 1.11 | 0.75 | 0.5979 | 0.4100 | 0.1258 | 0.84 | 1.11 | 0.77 | 0.5129 | 0.7122 | 0.2506 |
| 276.0247 | 17.3 | C6H13O10P | 6-Phospho-D-gluconate | Carbohydrate Metabolism | 1.02 | 0.91 | 0.94 | 0.8793 | 0.5251 | 0.6338 | 0.71 | 0.99 | 0.91 | 0.1877 | 0.9720 | 0.4186 |
| 90.0317 | 9.3 | C3H6O3 | (S)-Lactate | Carbohydrate Metabolism | 0.95 | 1.29 | 0.51 | 0.8484 | 0.3618 | 0.1014 | 0.87 | 1.09 | 0.59 | 0.6309 | 0.7430 | 0.1525 |
| 185.9929 | 17.6 | C3H7O7P | 2-Phospho-D-glycerate | Carbohydrate Metabolism | 0.86 | 1.05 | 0.57 | 0.6205 | 0.8904 | 0.1723 | 0.58 | 1.01 | 0.63 | 0.1749 | 0.9726 | 0.1740 |
| 244.0348 | 15.2 | C6H13O8P | L-Fuculose 1-phosphate | Carbohydrate Metabolism | 1.00 | 0.90 | 0.95 | 0.9945 | 0.4048 | 0.8202 | 1.29 | 1.02 | 1.04 | 0.2862 | 0.9581 | 0.8351 |
| 130.0267 | 11.6 | C5H6O4 | Mesaconate | Carbohydrate Metabolism | 1.08 | 0.96 | 1.08 | 0.2509 | 0.4204 | 0.4061 | 1.18 | 1.03 | 1.07 | 0.3708 | 0.7307 | 0.6374 |
| 265.9593 | 17.7 | C3H8O10P2 | 3-Phospho-D-glyceroyl phosphate | Carbohydrate Metabolism | 0.84 | 1.07 | 0.58 | 0.6241 | 0.8637 | 0.2435 | 0.49 | 0.95 | 0.60 | 0.1627 | 0.9247 | 0.1731 |
| 196.0583 | 14.1 | C6H12O7 | D-Mannonate | Carbohydrate Metabolism | 1.13 | 0.93 | 1.27 | 0.5224 | 0.8122 | 0.2664 | 1.17 | 1.29 | 1.14 | 0.5382 | 0.1350 | 0.3775 |
| 88.0160 | 11.7 | C3H4O3 | Pyruvate | Carbohydrate Metabolism | 1.09 | 1.03 | 1.13 | 0.3712 | 0.6668 | 0.4544 | 1.19 | 1.06 | 1.13 | 0.3387 | 0.5744 | 0.3711 |
| 178.0478 | 11.7 | C6H10O6 | D-Glucono-1,5-lactone | Carbohydrate Metabolism | 1.14 | 1.02 | 1.11 | 0.1869 | 0.7786 | 0.4628 | 1.18 | 1.04 | 1.12 | 0.3546 | 0.6457 | 0.4301 |
| 260.0296 | 15.0 | C6H13O9P | D-Glucose 1-phosphate | Carbohydrate Metabolism | 1.05 | 1.02 | 1.07 | 0.6947 | 0.8784 | 0.5260 | 0.97 | 1.03 | 0.98 | 0.9333 | 0.9229 | 0.9339 |
| 195.0744 | 17.0 | C6H13NO6 | 2-Amino-2-deoxy-D-gluconate | Carbohydrate Metabolism | 0.92 | 0.81 | 0.88 | 0.8649 | 0.6437 | 0.7781 | 0.96 | 1.09 | 0.87 | 0.9520 | 0.9090 | 0.8675 |
| 88.0160 | 12.4 | C3H4O3 | 3-Oxopropanoate | Carbohydrate Metabolism | 1.11 | 0.96 | 1.02 | 0.5694 | 0.4941 | 0.8570 | 1.07 | 1.15 | 1.07 | 0.7305 | 0.5240 | 0.7676 |
| 178.0478 | 12.4 | C6H10O6 | L-Galactono-1,4-lactone | Carbohydrate Metabolism | 1.12 | 0.99 | 1.06 | 0.4289 | 0.9051 | 0.6618 | 1.08 | 1.11 | 1.11 | 0.7354 | 0.3831 | 0.6261 |
| 194.0790 | 11.1 | C7H14O6 | 3-O-Methyl-myo-inositol | Carbohydrate Metabolism | 0.97 | 0.47 | 1.40 | 0.9484 | 0.1323 | 0.5337 | 1.42 | 1.34 | 0.92 | 0.4419 | 0.4867 | 0.8703 |
| 580.0345 | 18.5 | C15H22N2O18P2 | UDP-glucuronate | Carbohydrate Metabolism | 0.88 | 0.89 | 0.79 | 0.6227 | 0.5729 | 0.0895 | 0.64 | 1.01 | 0.67 | 0.1751 | 0.9823 | 0.0907 |
| 150.0529 | 12.3 | C5H10O5 | D-Xylose | Carbohydrate Metabolism | 1.04 | 0.90 | 1.09 | 0.7993 | 0.3350 | 0.3899 | 0.84 | 0.84 | 1.01 | 0.4770 | 0.3510 | 0.9408 |
| 254.1001 | 13.7 | C9H18O8 | 3-beta-D-Galactosyl-sn-glycerol | Carbohydrate Metabolism | 0.88 | 1.00 | 0.91 | 0.5864 | 0.9831 | 0.6208 | 1.03 | 1.05 | 0.90 | 0.6012 | 0.6427 | 0.5549 |
| 260.0298 | 16.0 | C6H13O9P | D-Mannose 6-phosphate | Carbohydrate Metabolism | 1.13 | 1.00 | 1.11 | 0.4110 | 0.9884 | 0.5992 | 0.91 | 1.06 | 0.72 | 0.5285 | 0.7471 | 0.1654 |
| 408.1534 | 4.8 | C19H24N2O8 | Melatonin glucuronide | Carbohydrate metabolism | 1.07 | 1.09 | 1.13 | 0.7793 | 0.6403 | 0.6207 | 0.91 | 1.02 | 0.93 | 0.6640 | 0.9152 | 0.7471 |
| 166.0477 | 12.6 | C5H10O6 | D-Xylonate | Carbohydrate Metabolism | 0.98 | 0.96 | 1.01 | 0.9280 | 0.7527 | 0.9778 | 1.21 | 1.13 | 0.97 | 0.2026 | 0.0896 | 0.6923 |
| 132.0423 | 12.5 | C5H8O4 | 2-Acetolactate | Carbohydrate Metabolism | 1.13 | 1.07 | 1.09 | 0.1089 | 0.5718 | 0.5895 | 1.24 | 1.18 | 1.05 | 0.1589 | 0.1434 | 0.5947 |
| 566.0552 | 16.0 | C15H24N2O17P2 | UDP-glucose | Carbohydrate Metabolism | 1.02 | 1.00 | 0.86 | 0.9213 | 0.9895 | 0.3369 | 0.97 | 1.07 | 0.87 | 0.9519 | 0.8844 | 0.7518 |

| | | | | | | | | | | | | | | | | | |
|---|---|---|---|---|---|---|---|---|---|---|---|---|---|---|---|---|---|
| 265.1161 | 11.1 | C10H19NO7 | D-1-[(3-Carboxypropyl)amino]-1-deoxyfructose | Carbohydrate Metabolism | 0.89 | 0.96 | 1.03 | 0.4448 | 0.7044 | 0.8776 | 0.92 | 0.92 | 1.05 | 0.7336 | 0.7164 | 0.8580 |
| 164.0686 | 11.3 | C6H12O5 | L-Rhamnose | Carbohydrate Metabolism | 1.19 | 1.04 | 1.17 | 0.1944 | 0.7905 | 0.5005 | 1.17 | 1.07 | 1.21 | 0.0368 | 0.2979 | 0.3011 |
| 342.1162 | 15.1 | C12H22O11 | Sucrose | Carbohydrate Metabolism | 0.96 | 1.07 | 1.04 | 0.8715 | 0.8172 | 0.8758 | 2.54 | 1.17 | 6.42 | 0.3804 | 0.6615 | 0.3858 |
| 196.0583 | 13.2 | C6H12O7 | D-Gluconic acid | Carbohydrate Metabolism | 1.04 | 1.01 | 1.11 | 0.5537 | 0.7890 | 0.0317 | 1.07 | 1.03 | 0.98 | 0.0430 | 0.6689 | 0.8253 |
| 162.0529 | 12.4 | C6H10O5 | 3-Ethylmalate | Carbohydrate Metabolism | 1.04 | 1.03 | 1.00 | 0.6065 | 0.8602 | 0.9782 | 1.07 | 1.10 | 1.03 | 0.5297 | 0.3163 | 0.8669 |
| 106.0266 | 11.6 | C3H6O4 | D-Glycerate | Carbohydrate Metabolism | 1.02 | 1.17 | 1.14 | 0.7601 | 0.4052 | 0.2809 | 0.97 | 0.92 | 1.02 | 0.6602 | 0.5042 | 0.6703 |
| 182.0791 | 13.9 | C6H14O6 | Mannitol | Carbohydrate Metabolism | 2.81 | 0.95 | 3.01 | 0.4241 | 0.5054 | 0.3999 | 1.17 | 1.18 | 2.24 | 0.2614 | 0.2172 | 0.3931 |
| 180.0634 | 12.5 | C6H12O6 | D-Glucose | Carbohydrate Metabolism | 1.06 | 1.07 | 1.03 | 0.2631 | 0.3321 | 0.6671 | 1.04 | 1.13 | 1.04 | 0.5182 | 0.1564 | 0.7636 |
| 230.0192 | 15.4 | C5H11O8P | D-Ribose 5-phosphate | Carbohydrate Metabolism | 0.85 | 1.02 | 0.70 | 0.7152 | 0.9509 | 0.4850 | 1.10 | 1.31 | 0.76 | 0.8022 | 0.4576 | 0.6391 |
| 150.0165 | 17.2 | C4H6O6 | (R,R)-Tartaric acid | Carbohydrate Metabolism | 1.05 | 0.98 | 0.96 | 0.6289 | 0.8971 | 0.7174 | 1.73 | 1.68 | 0.90 | 0.4551 | 0.4157 | 0.6207 |
| 309.9856 | 17.3 | C5H12O11P2 | D-Ribose 1,5-bisphosphate | Carbohydrate Metabolism | 0.87 | 1.34 | 0.40 | 0.7678 | 0.5118 | 0.1243 | 0.80 | 1.29 | 0.65 | 0.3162 | 0.3097 | 0.2757 |
| 221.0900 | 12.2 | C8H15NO6 | N-Acetyl-D-mannosamine | Carbohydrate Metabolism | 1.10 | 1.03 | 1.00 | 0.1358 | 0.8112 | 0.9545 | 0.92 | 0.91 | 0.99 | 0.7013 | 0.6679 | 0.9683 |
| 166.0477 | 13.1 | C5H10O6 | D-Arabinonate | Carbohydrate Metabolism | 1.05 | 1.02 | 0.82 | 0.8021 | 0.8647 | 0.2728 | 1.52 | 1.39 | 0.98 | 0.3490 | 0.3315 | 0.9086 |
| 84.0211 | 14.1 | C4H4O2 | 3-Butynoate | Carbohydrate Metabolism | 1.55 | 1.02 | 1.83 | 0.4029 | 0.9372 | 0.2510 | 0.92 | 1.07 | 1.41 | 0.6093 | 0.7947 | 0.1237 |
| 342.1163 | 16.2 | C12H22O11 | Lactose | Carbohydrate Metabolism | 1.02 | 0.86 | 1.50 | 0.8361 | 0.1563 | 0.4388 | 0.97 | 0.88 | 0.93 | 0.8617 | 0.5840 | 0.6479 |
| 260.0297 | 16.5 | C6H13O9P | D-Glucose 6-phosphate | Carbohydrate Metabolism | 0.98 | 0.86 | 1.35 | 0.9211 | 0.5078 | 0.3636 | 0.53 | 0.57 | 1.32 | 0.1831 | 0.2254 | 0.4789 |
| 180.0635 | 17.0 | C6H12O6 | D-Fructose | Carbohydrate Metabolism | 1.01 | 1.05 | 0.97 | 0.9074 | 0.7055 | 0.7708 | 0.94 | 0.95 | 0.95 | 0.7252 | 0.7551 | 0.7740 |
| 150.0529 | 11.7 | C5H10O5 | D-Ribose | Carbohydrate Metabolism | 1.21 | 1.05 | 1.15 | 0.2349 | 0.3972 | 0.2996 | 1.13 | 1.09 | 1.04 | 0.2745 | 0.3863 | 0.6745 |
| 240.0845 | 15.2 | C8H16O8 | D-glycero-L-galacto-Octulose | Carbohydrate Metabolism | 0.94 | 0.93 | 0.87 | 0.3958 | 0.4985 | 0.0935 | 1.04 | 1.07 | 1.00 | 0.7237 | 0.4572 | 0.9992 |
| 194.0427 | 14.3 | C6H10O7 | D-Galacturonate | Carbohydrate Metabolism | 0.72 | 1.11 | 0.89 | 0.4715 | 0.5767 | 0.7868 | 0.79 | 0.92 | 0.78 | 0.0054 | 0.3620 | 0.5639 |
| 605.0771 | 17.8 | C16H25N5O16P2 | GDP-mannose | Carbohydrate Metabolism | 0.95 | 0.92 | 1.02 | 0.6601 | 0.4377 | 0.8280 | 0.86 | 0.95 | 0.86 | 0.7159 | 0.9173 | 0.7026 |
| 177.0638 | 12.9 | C6H11NO5 | 4-Hydroxy-4-methylglutamate | Carbohydrate Metabolism | 0.81 | 0.99 | 1.10 | 0.1544 | 0.9596 | 0.7167 | 0.70 | 1.02 | 0.90 | 0.0036 | 0.9155 | 0.6496 |
| 120.0423 | 10.4 | C4H8O4 | D-Erythrose | Carbohydrate Metabolism | 0.82 | 0.78 | 1.04 | 0.1028 | 0.0689 | 0.7622 | 1.01 | 1.00 | 0.99 | 0.9820 | 0.9859 | 0.9447 |
| 589.0827 | 17.2 | C16H25N5O15P2 | GDP-L-fucose | Carbohydrate Metabolism | 0.92 | 0.94 | 0.96 | 0.4900 | 0.5623 | 0.8538 | 0.86 | 0.85 | 0.88 | 0.5498 | 0.6018 | 0.7304 |
| 262.0453 | 15.0 | C6H15O9P | D-Mannitol 1-phosphate | Carbohydrate Metabolism | 1.12 | 1.08 | 1.07 | 0.7140 | 0.8199 | 0.7927 | 0.70 | 0.81 | 0.91 | 0.1024 | 0.3723 | 0.3895 |
| 200.0087 | 12.5 | C4H9O7P | D-Erythrose 4-phosphate | Carbohydrate Metabolism | 0.98 | 1.31 | 0.65 | 0.9293 | 0.1012 | 0.0644 | 0.68 | 0.88 | 0.72 | 0.2477 | 0.6143 | 0.2681 |
| 169.9981 | 15.1 | C3H7O6P | Glycerone phosphate | Carbohydrate Metabolism | 0.76 | 1.07 | 0.64 | 0.5717 | 0.8531 | 0.3532 | 0.93 | 1.16 | 0.84 | 0.7801 | 0.5007 | 0.7335 |
| 259.0459 | 15.5 | C6H14NO8P | alpha-D-Glucosamine 1-phosphate | Carbohydrate Metabolism | 1.33 | 1.38 | 1.24 | 0.6852 | 0.6912 | 0.7641 | 0.60 | 0.82 | 0.87 | 0.0612 | 0.5433 | 0.4519 |
| 180.0634 | 14.7 | C6H12O6 | D-Galactose | Carbohydrate Metabolism | 1.98 | 1.30 | 1.27 | 0.3734 | 0.5746 | 0.2334 | 0.69 | 0.79 | 1.27 | 0.1297 | 0.3310 | 0.4820 |
| 260.0296 | 15.7 | C6H13O9P | D-Fructose 6-phosphate | Carbohydrate Metabolism | 0.84 | 0.91 | 0.85 | 0.2126 | 0.4671 | 0.2555 | 0.79 | 1.05 | 0.68 | 0.6574 | 0.9132 | 0.4597 |
| 290.0403 | 16.0 | C7H15O10P | D-Sedoheptulose 7-phosphate | Carbohydrate Metabolism | 0.95 | 0.96 | 1.01 | 0.8326 | 0.8578 | 0.9876 | 0.81 | 0.93 | 0.81 | 0.6870 | 0.8823 | 0.6169 |
| 152.0685 | 12.9 | C5H12O5 | Ribitol | Carbohydrate Metabolism | 0.97 | 0.80 | 1.57 | 0.9140 | 0.4546 | 0.2620 | 0.79 | 1.28 | 0.90 | 0.5745 | 0.7076 | 0.8227 |
| 179.0794 | 16.4 | C6H13NO5 | D-Glucosamine | Carbohydrate Metabolism | 1.02 | 0.94 | 1.05 | 0.8156 | 0.6287 | 0.5874 | 0.87 | 0.88 | 0.86 | 0.8339 | 0.8428 | 0.8117 |
| 339.9961 | 15.1 | C6H14O12P2 | beta-D-Fructose 2,6-bisphosphate | Carbohydrate Metabolism | 0.85 | 1.10 | 0.58 | 0.8130 | 0.8730 | 0.4525 | 0.90 | 1.21 | 0.87 | 0.8019 | 0.6034 | 0.8134 |
| 161.0688 | 11.1 | C6H11NO4 | 4-Methyl-L-glutamate | Carbohydrate Metabolism | 0.86 | 1.08 | 0.89 | 0.6937 | 0.7929 | 0.6731 | 0.64 | 0.98 | 0.93 | 0.2879 | 0.9658 | 0.8619 |
| 331.5547 | 14.1 | C21H27N7O14P2 | NAD+ | Energy Metabolism | 1.03 | 1.06 | 1.04 | 0.5838 | 0.6371 | 0.5326 | 1.00 | 1.11 | 1.20 | 0.9536 | 0.2504 | 0.3133 |
| 743.0762 | 16.5 | C21H28N7O17P3 | NADP+ | Energy Metabolism | 0.95 | 0.96 | 0.84 | 0.6911 | 0.6034 | 0.0500 | 0.80 | 0.96 | 0.84 | 0.2557 | 0.7755 | 0.0735 |
| 506.9960 | 15.9 | C10H16N5O13P3 | ATP | Energy Metabolism | 0.92 | 0.93 | 0.77 | 0.8101 | 0.4991 | 0.2895 | 0.81 | 0.99 | 0.78 | 0.4432 | 0.9739 | 0.4615 |
| 97.9768 | 17.3 | H3O4P | Orthophosphate | Energy Metabolism | 1.04 | 0.94 | 1.03 | 0.7753 | 0.5960 | 0.8561 | 1.03 | 1.04 | 0.94 | 0.8149 | 0.5310 | 0.5097 |
| 427.0294 | 14.8 | C10H15N5O10P2 | ADP | Energy Metabolism | 0.95 | 0.99 | 0.90 | 0.8061 | 0.9406 | 0.4479 | 0.74 | 0.95 | 0.87 | 0.0321 | 0.7375 | 0.3694 |

| | | | | | | | | | | | | | | | | | |
|---|---|---|---|---|---|---|---|---|---|---|---|---|---|---|---|---|---|
| 210.0741 | 11.6 | C7H14O7 | Sedoheptulose | Energy Metabolism | 0.81 | 0.77 | 1.12 | 0.3741 | 0.3332 | 0.6875 | 1.25 | 1.18 | 0.93 | 0.3947 | 0.4255 | 0.8507 |
| 339.9962 | 17.6 | C6H14O12P2 | D-Fructose 1,6-bisphosphate | Energy Metabolism | 0.85 | 1.02 | 0.59 | 0.6514 | 0.9652 | 0.1351 | 0.70 | 1.16 | 0.70 | 0.3337 | 0.6716 | 0.4820 |
| 370.0069 | 17.9 | C7H16O13P2 | D-Sedoheptulose 1,7-bisphosphate | Energy Metabolism | 0.84 | 1.09 | 0.52 | 0.6924 | 0.8419 | 0.1626 | 0.58 | 0.92 | 0.72 | 0.1989 | 0.8178 | 0.5286 |
| 318.0353 | 15.1 | C8H15O11P | 3-Deoxy-D-manno-octulosonate 8-phosphate | Glycan Biosynthesis and Metabolism | 0.89 | 0.95 | 1.01 | 0.6729 | 0.8760 | 0.9769 | 1.03 | 1.27 | 1.01 | 0.9458 | 0.5210 | 0.9820 |
| 446.0612 | 16.2 | C11H20N4O11P2 | CDP-ethanolamine | Lipid Metabolism | 1.01 | 1.23 | 0.83 | 0.9399 | 0.1792 | 0.1565 | 1.12 | 1.40 | 0.90 | 0.8797 | 0.6273 | 0.8857 |
| 216.0401 | 12.7 | C5H13O7P | 2-C-Methyl-D-erythritol 4-phosphate | Lipid Metabolism | 0.70 | 0.49 | 1.66 | 0.5106 | 0.2814 | 0.5243 | 1.12 | 1.09 | 1.43 | 0.6967 | 0.6290 | 0.2922 |
| 183.0661 | 14.9 | C5H14NO4P | Choline phosphate | Lipid Metabolism | 1.12 | 1.60 | 0.68 | 0.6283 | 0.0528 | 0.2310 | 1.53 | 2.08 | 0.90 | 0.6997 | 0.5012 | 0.9068 |
| 488.1081 | 15.2 | C14H26N4O11P2 | CDP-choline | Lipid Metabolism | 0.96 | 1.04 | 0.81 | 0.8040 | 0.8367 | 0.2177 | 1.11 | 1.17 | 1.08 | 0.8236 | 0.7038 | 0.8477 |
| 172.0137 | 14.7 | C3H9O6P | sn-Glycerol 3-phosphate | Lipid Metabolism | 5.39 | 1.25 | 5.47 | 0.3949 | 0.7541 | 0.4290 | 1.03 | 1.53 | 6.29 | 0.8998 | 0.4224 | 0.4119 |
| 257.1025 | 14.4 | C8H20NO6P | sn-glycero-3-Phosphocholine | Lipid Metabolism | 1.18 | 1.18 | 1.12 | 0.4629 | 0.3809 | 0.5540 | 0.91 | 1.02 | 1.05 | 0.7208 | 0.9339 | 0.8834 |
| 472.1127 | 14.3 | C14H26N4O10P2 | CMP-N-trimethyl-2-aminoethylphosphonate | Lipid Metabolism | 1.03 | 1.07 | 1.06 | 0.5430 | 0.3440 | 0.2300 | 1.15 | 1.15 | 0.97 | 0.7159 | 0.7109 | 0.9232 |
| 921.2494 | 14.1 | C31H54N7O17P3S | Decanoyl-CoA | Lipid Metabolism | 0.96 | 0.94 | 0.71 | 0.9525 | 0.8519 | 0.6398 | 1.41 | 1.18 | 0.87 | 0.3816 | 0.5554 | 0.8082 |
| 449.3146 | 4.7 | C26H43NO5 | Chenodeoxyglycocholate | Lipid Metabolism | 0.84 | 0.99 | 1.31 | 0.4732 | 0.9756 | 0.4590 | 1.00 | 1.29 | 1.40 | 0.9856 | 0.4503 | 0.4056 |
| 188.1049 | 4.8 | C9H16O4 | (+/-)-Methyl 5-acetoxyhexanoate | Lipid Metabolism | 1.41 | 1.46 | 1.47 | 0.7789 | 0.7508 | 0.7330 | 0.33 | 0.28 | 1.20 | 0.4197 | 0.3925 | 0.8746 |
| 102.0317 | 13.4 | C4H6O3 | Acetoacetate | Lipid Metabolism | 1.29 | 1.00 | 1.39 | 0.2823 | 0.9930 | 0.2418 | 1.03 | 1.02 | 0.96 | 0.9002 | 0.9630 | 0.8709 |
| 215.0559 | 15.6 | C5H14NO6P | sn-glycero-3-Phosphoethanolamine | Lipid Metabolism | 1.03 | 1.09 | 1.02 | 0.8251 | 0.6532 | 0.8934 | 0.93 | 0.93 | 0.94 | 0.5931 | 0.5559 | 0.5610 |
| 125.0146 | 14.7 | C2H7NO3S | Taurine | Lipid Metabolism | 1.07 | 0.93 | 1.12 | 0.7584 | 0.7434 | 0.7287 | 1.03 | 0.96 | 1.14 | 0.8889 | 0.8219 | 0.7558 |
| 384.3392 | 5.2 | C27H44O | Cholesta-5,7-dien-3beta-ol | Lipid Metabolism | 1.12 | 1.18 | 1.07 | 0.6742 | 0.5245 | 0.7286 | 0.94 | 0.96 | 1.09 | 0.6768 | 0.6499 | 0.1787 |
| 258.1831 | 4.2 | C14H26O4 | FA methyl(15:0) tridecanedioic acid | Lipids: Fatty Acyls | 0.21 | 0.75 | 0.84 | 0.0364 | 0.7082 | 0.8344 | 2.74 | 2.35 | 1.99 | 0.3401 | 0.3525 | 0.4869 |
| 214.1570 | 4.2 | C12H22O3 | 3-Oxododecanoic acid | Lipids: Fatty Acyls | 0.37 | 0.61 | 0.78 | 0.0677 | 0.4098 | 0.6498 | 1.29 | 1.82 | 1.57 | 0.5918 | 0.2108 | 0.4207 |
| 178.0300 | 7.9 | C6H10O4S | 3,3'-Thiobispropanoic acid | Lipids: Fatty Acyls | 1.15 | 0.89 | 1.45 | 0.6200 | 0.4775 | 0.0445 | 1.28 | 0.91 | 1.52 | 0.5048 | 0.7764 | 0.3967 |
| 314.2458 | 4.2 | C18H34O4 | FA hydroxy(18:1)] | Lipids: Fatty Acyls | 0.67 | 0.93 | 1.02 | 0.1993 | 0.8345 | 0.9617 | 1.35 | 1.05 | 1.18 | 0.2300 | 0.8829 | 0.7151 |
| 190.1722 | 4.2 | C14H22 | 3,5,7-Trimethyl-2E,4E,6E,8E-undecatetraene | Lipids: Fatty Acyls | 0.41 | 0.60 | 0.76 | 0.0600 | 0.3493 | 0.5642 | 1.27 | 1.67 | 1.41 | 0.4420 | 0.2366 | 0.4223 |
| 340.2984 | 3.7 | C21H40O3 | FA oxo(21:0) | Lipids: Fatty Acyls | 0.76 | 1.07 | 0.94 | 0.3364 | 0.7874 | 0.7711 | 1.06 | 1.12 | 0.89 | 0.9072 | 0.8734 | 0.8107 |
| 300.2665 | 4.0 | C18H36O3 | FA hydroxy(18:0) | Lipids: Fatty Acyls | 1.12 | 1.00 | 1.03 | 0.3117 | 0.9755 | 0.7961 | 1.18 | 3.13 | 0.94 | 0.6362 | 0.3680 | 0.7697 |
| 100.0888 | 4.3 | C6H12O | [FA (6:0)] hexanal | Lipids: Fatty Acyls | 0.51 | 0.75 | 0.91 | 0.0700 | 0.5607 | 0.8219 | 0.98 | 1.40 | 1.25 | 0.9293 | 0.1675 | 0.5430 |
| 280.2403 | 3.9 | C18H32O2 | Linoleate | Lipids: Fatty Acyls | 0.98 | 0.85 | 0.87 | 0.8392 | 0.1632 | 0.2610 | 1.21 | 1.16 | 1.07 | 0.3588 | 0.4882 | 0.6534 |
| 215.1157 | 12.5 | C10H17NO4 | 2-Amino-9,10-epoxy-8-oxodecanoic acid | Lipids: Fatty Acyls | 0.94 | 0.80 | 0.89 | 0.8566 | 0.5278 | 0.7357 | 1.17 | 1.00 | 1.03 | 0.5042 | 0.9805 | 0.9378 |
| 298.2511 | 4.0 | C18H34O3 | FA oxo(18:0) | Lipids: Fatty Acyls | 1.07 | 1.06 | 1.00 | 0.7598 | 0.7925 | 0.9942 | 1.25 | 0.91 | 0.81 | 0.6277 | 0.6929 | 0.5002 |
| 278.2246 | 4.0 | C18H30O2 | [FA (18:3)] 9Z,12Z,15Z-octadecatrienoic acid | Lipids: Fatty Acyls | 0.99 | 0.93 | 0.91 | 0.9023 | 0.5185 | 0.4268 | 1.07 | 1.13 | 1.03 | 0.7192 | 0.4727 | 0.8821 |
| 200.1777 | 4.1 | C12H24O2 | Dodecanoic acid | Lipids: Fatty Acyls | 0.97 | 0.85 | 0.98 | 0.7994 | 0.3597 | 0.8933 | 1.01 | 0.81 | 1.06 | 0.9118 | 0.0233 | 0.7297 |
| 306.2562 | 3.9 | C20H34O2 | Icosatrienoic acid | Lipids: Fatty Acyls | 0.91 | 0.91 | 0.90 | 0.3072 | 0.1813 | 0.1183 | 1.20 | 1.06 | 1.02 | 0.3069 | 0.2920 | 0.8599 |
| 126.1045 | 4.3 | C8H14O | FA (8:1) octenal | Lipids: Fatty Acyls | 0.66 | 0.77 | 0.85 | 0.3321 | 0.4890 | 0.6432 | 0.93 | 1.19 | 1.16 | 0.7786 | 0.2763 | 0.6335 |
| 272.2350 | 4.1 | C16H32O3 | FA hydroxy(16:0)] hexadecanoic acid | Lipids: Fatty Acyls | 1.06 | 0.99 | 1.07 | 0.6311 | 0.9203 | 0.5559 | 1.12 | 1.04 | 0.99 | 0.4188 | 0.8212 | 0.9487 |
| 296.2350 | 4.0 | C18H32O3 | [FA (18:1)] 9R,10S-epoxy-12Z-octadecenoic acid | Lipids: Fatty Acyls | 1.05 | 0.98 | 1.19 | 0.8138 | 0.9326 | 0.4408 | 1.99 | 1.10 | 1.04 | 0.4504 | 0.8228 | 0.8299 |

| | | | | | | | | | | | | | | | | |
|---|---|---|---|---|---|---|---|---|---|---|---|---|---|---|---|---|
| 270.2194 | 4.0 | C16H30O3 | FA oxo(16:0) | Lipids: Fatty Acyls | 1.10 | 1.11 | 1.19 | 0.6051 | 0.7266 | 0.4626 | 1.05 | 0.80 | 1.00 | 0.8670 | 0.4166 | 0.9910 |
| 330.2565 | 3.9 | C22H34O2 | [FA (22:5)] 7Z,10Z,13Z,16Z,19Z-docosapentaenoic acid | Lipids: Fatty Acyls | 0.91 | 0.87 | 0.99 | 0.2610 | 0.1253 | 0.9502 | 1.13 | 1.10 | 0.98 | 0.2330 | 0.2764 | 0.8636 |
| 252.2089 | 4.2 | C16H28O2 | FA (16:2) | Lipids: Fatty Acyls | 0.69 | 0.78 | 0.83 | 0.4066 | 0.4523 | 0.5802 | 1.01 | 1.23 | 1.11 | 0.9773 | 0.2626 | 0.6665 |
| 230.1517 | 4.7 | C12H22O4 | Dodecanedioic acid | Lipids: Fatty Acyls | 1.24 | 1.28 | 1.33 | 0.8034 | 0.7990 | 0.6877 | 0.72 | 0.45 | 1.15 | 0.5214 | 0.2323 | 0.8208 |
| 208.1827 | 4.2 | C14H24O | FA (14:2) tetradecadienal | Lipids: Fatty Acyls | 0.72 | 0.80 | 0.85 | 0.3389 | 0.4525 | 0.6215 | 1.06 | 1.23 | 1.12 | 0.7923 | 0.1246 | 0.5667 |
| 340.3342 | 3.8 | C22H44O2 | Docosanoic acid | Lipids: Fatty Acyls | 1.00 | 1.09 | 1.03 | 0.9656 | 0.4476 | 0.7336 | 1.05 | 0.99 | 0.99 | 0.6827 | 0.9526 | 0.9137 |
| 423.3349 | 4.7 | C25H45NO4 | O-9Z,12Z-Hexadecadienoyl-R-carnitine | Lipids: Fatty Acyls | 1.12 | 0.98 | 1.11 | 0.2316 | 0.8839 | 0.5398 | 0.94 | 1.05 | 1.00 | 0.4593 | 0.7706 | 0.9905 |
| 280.2401 | 7.8 | C18H32O2 | FA (18:2) | Lipids: Fatty Acyls | 1.03 | 0.97 | 0.98 | 0.9276 | 0.9029 | 0.9364 | 0.87 | 0.98 | 0.79 | 0.3377 | 0.9257 | 0.3392 |
| 282.2559 | 3.9 | C18H34O2 | [FA (18:1)] 9Z-octadecenoic acid | Lipids: Fatty Acyls | 1.07 | 1.05 | 1.06 | 0.0412 | 0.1868 | 0.1883 | 1.25 | 1.06 | 0.91 | 0.3550 | 0.5017 | 0.4660 |
| 254.2247 | 4.0 | C16H30O2 | FA(16:1) | Lipids: Fatty Acyls | 0.93 | 0.95 | 1.00 | 0.4182 | 0.5335 | 0.9957 | 1.56 | 1.05 | 0.87 | 0.5105 | 0.5927 | 0.3338 |
| 304.2406 | 3.9 | C20H32O2 | FA (20:4) | Lipids: Fatty Acyls | 1.03 | 1.16 | 1.10 | 0.7913 | 0.1908 | 0.4391 | 1.02 | 1.09 | 0.95 | 0.8911 | 0.0841 | 0.7754 |
| 282.2559 | 7.8 | C18H34O2 | FA (18:1) | Lipids: Fatty Acyls | 1.03 | 1.12 | 0.97 | 0.8368 | 0.5094 | 0.8209 | 1.24 | 1.22 | 1.11 | 0.0500 | 0.1875 | 0.6083 |
| 228.1362 | 4.7 | C12H20O4 | Traumatic acid | Lipids: Fatty Acyls | 0.59 | 0.78 | 0.79 | 0.4094 | 0.6472 | 0.6657 | 0.68 | 0.66 | 0.74 | 0.5434 | 0.5423 | 0.6600 |
| 242.2247 | 4.0 | C15H30O2 | FA methyl(14:0) | Lipids: Fatty Acyls | 0.93 | 1.01 | 0.99 | 0.3301 | 0.9065 | 0.9434 | 1.05 | 0.97 | 0.85 | 0.8391 | 0.7907 | 0.1301 |
| 268.2402 | 4.0 | C17H32O2 | FA methyl(16:1) | Lipids: Fatty Acyls | 0.94 | 0.94 | 0.90 | 0.4487 | 0.5414 | 0.2241 | 1.08 | 0.97 | 0.92 | 0.6982 | 0.7863 | 0.3092 |
| 312.3031 | 3.9 | C20H40O2 | FA (20:0) | Lipids: Fatty Acyls | 0.97 | 0.99 | 0.97 | 0.7141 | 0.9089 | 0.6259 | 0.95 | 0.93 | 0.83 | 0.6504 | 0.5665 | 0.1658 |
| 228.2089 | 4.0 | C14H28O2 | Tetradecanoic acid | Lipids: Fatty Acyls | 1.09 | 1.02 | 1.02 | 0.2144 | 0.8650 | 0.8116 | 1.08 | 1.02 | 0.91 | 0.6241 | 0.7253 | 0.2532 |
| 214.1933 | 4.1 | C13H26O2 | FA methyl(12:0) dodecanoic acid | Lipids: Fatty Acyls | 1.32 | 1.31 | 1.19 | 0.4857 | 0.4098 | 0.5187 | 1.15 | 0.87 | 0.87 | 0.3806 | 0.4321 | 0.6443 |
| 270.2558 | 3.9 | C17H34O2 | FA (17:0) | Lipids: Fatty Acyls | 0.97 | 0.97 | 1.04 | 0.3751 | 0.6945 | 0.6061 | 1.02 | 1.08 | 0.96 | 0.6988 | 0.1875 | 0.6981 |
| 279.2564 | 4.7 | C18H33NO | Linoleamide | Lipids: Fatty Acyls | 2.60 | 1.88 | 2.82 | 0.2778 | 0.4030 | 0.1745 | 4.10 | 0.86 | 1.95 | 0.0162 | 0.8293 | 0.4206 |
| 298.2872 | 3.9 | C19H38O2 | FA methyl(18:0) | Lipids: Fatty Acyls | 1.00 | 1.08 | 1.06 | 0.9625 | 0.2250 | 0.5487 | 0.96 | 0.81 | 0.90 | 0.6416 | 0.1771 | 0.0292 |
| 242.1003 | 15.5 | C8H18O8 | D-erythro-D-galacto-octitol | Lipids: Fatty Acyls | 1.03 | 1.12 | 1.16 | 0.6960 | 0.1626 | 0.3504 | 0.91 | 0.99 | 1.01 | 0.1758 | 0.8911 | 0.9450 |
| 130.0630 | 4.8 | C6H10O3 | [FA oxo(6:0)] 2-oxo-hexanoic acid | Lipids: Fatty Acyls | 1.00 | 1.07 | 1.04 | 0.9827 | 0.8518 | 0.8546 | 0.78 | 0.87 | 0.96 | 0.1700 | 0.5144 | 0.8609 |
| 98.0368 | 13.9 | C5H6O2 | [FA (5:2)] 2,4-pentadienoic acid | Lipids: Fatty Acyls | 2.16 | 0.96 | 2.57 | 0.4284 | 0.7679 | 0.3087 | 1.12 | 1.15 | 1.70 | 0.5797 | 0.4286 | 0.4598 |
| 150.1407 | 4.3 | C11H18 | 4,8-Dimethyl-1,3E,7-nonatriene | Lipids: Fatty Acyls | 0.63 | 0.73 | 1.03 | 0.4778 | 0.2265 | 0.9396 | 0.88 | 1.25 | 1.08 | 0.6686 | 0.1761 | 0.5731 |
| 142.0994 | 4.6 | C8H14O2 | FA (8:1) | Lipids: Fatty Acyls | 0.53 | 0.88 | 0.75 | 0.4140 | 0.8233 | 0.6586 | 0.43 | 0.79 | 0.77 | 0.2538 | 0.7127 | 0.6601 |
| 284.2715 | 3.9 | C18H36O2 | Octadecanoic acid | Lipids: Fatty Acyls | 1.18 | 1.17 | 1.09 | 0.0402 | 0.1196 | 0.2172 | 0.93 | 0.97 | 0.78 | 0.6401 | 0.8424 | 0.1547 |
| 217.1314 | 9.9 | C10H19NO4 | O-Propanoylcarnitine | Lipids: Fatty Acyls | 1.05 | 0.96 | 1.04 | 0.7282 | 0.5964 | 0.6685 | 1.09 | 0.91 | 1.02 | 0.7059 | 0.6801 | 0.9487 |
| 172.1464 | 4.3 | C10H20O2 | Decanoic acid | Lipids: Fatty Acyls | 1.08 | 1.09 | 1.08 | 0.8027 | 0.7849 | 0.7770 | 0.91 | 0.77 | 0.93 | 0.5347 | 0.0407 | 0.5757 |
| 256.2402 | 4.0 | C16H32O2 | FA(16:0) | Lipids: Fatty Acyls | 1.20 | 1.22 | 1.10 | 0.1236 | 0.1977 | 0.4102 | 0.85 | 0.95 | 0.76 | 0.4638 | 0.8462 | 0.2888 |
| 447.3351 | 4.6 | C27H45NO4 | N-stearoyl tyrosine | Lipids: Fatty Acyls | 0.91 | 0.93 | 1.14 | 0.6033 | 0.7578 | 0.5688 | 1.09 | 0.95 | 1.06 | 0.5821 | 0.8560 | 0.7784 |
| 231.1471 | 9.0 | C11H21NO4 | O-Butanoylcarnitine | Lipids: Fatty Acyls | 1.07 | 1.03 | 1.11 | 0.3396 | 0.4935 | 0.4393 | 0.96 | 1.03 | 0.95 | 0.8691 | 0.9198 | 0.8402 |
| 399.3348 | 4.7 | C23H45NO4 | O-Palmitoyl-R-carnitine | Lipids: Fatty Acyls | 0.99 | 1.05 | 1.12 | 0.9395 | 0.7456 | 0.4545 | 0.95 | 0.96 | 0.95 | 0.8436 | 0.8757 | 0.7916 |
| 287.2461 | 4.3 | C16H33NO3 | Lauroyl diethanolamide | Lipids: Fatty Acyls | 1.20 | 0.91 | 0.89 | 0.6950 | 0.7564 | 0.7342 | 0.71 | 0.88 | 0.87 | 0.1389 | 0.4648 | 0.4976 |
| 222.1620 | 4.1 | C14H22O2 | 7E,9E,11-Dodecatrienyl acetate | Lipids: Fatty Acyls | 1.04 | 1.01 | 1.17 | 0.8405 | 0.9757 | 0.4709 | 1.46 | 1.16 | 0.66 | 0.7422 | 0.8729 | 0.5490 |
| 668.4304 | 8.0 | C68H124N2O23 | Ganglioside GA1 (d18:1/24:1(15Z)) | Lipids: Gangliosides | 0.99 | 0.94 | 0.59 | 0.9826 | 0.8423 | 0.2566 | 0.90 | 0.94 | 0.70 | 0.6025 | 0.8397 | 0.1645 |
| 602.5267 | 3.7 | C39H70O4 | 1-(14-methyl-pentadecanoyl)-2-(8-[3]-ladderane-octanyl)-sn-glycerol | Lipids: Glycerolipids | 1.18 | 1.17 | 0.85 | 0.4110 | 0.3900 | 0.2152 | 1.64 | 1.74 | 1.03 | 0.5347 | 0.5302 | 0.9364 |
| 790.4891 | 7.9 | C41H74O12S | 1,2-Di-O-(8-hexadecenoyl)-3-O-(6-sulfoquinovopyranosyl)glycerol | Lipids: Glycerolipids | 0.82 | 0.84 | 0.82 | 0.4630 | 0.3878 | 0.4141 | 0.94 | 1.16 | 0.87 | 0.7484 | 0.3957 | 0.5598 |

| | | | | | | | | | | | | | | | | |
|---|---|---|---|---|---|---|---|---|---|---|---|---|---|---|---|---|
| 772.5259 | 3.7 | C42H77O10P | PG(36:3) | Lipids: Glycerophospholipids | 0.99 | 1.21 | 0.81 | 0.9334 | 0.2259 | 0.1577 | 1.49 | 1.64 | 1.04 | 0.6845 | 0.6301 | 0.9561 |
| 774.5424 | 3.8 | C42H79O10P | PG(36:2) | Lipids: Glycerophospholipids | 0.96 | 1.20 | 0.78 | 0.7197 | 0.2981 | 0.1134 | 1.38 | 1.64 | 0.97 | 0.7243 | 0.6259 | 0.9629 |
| 864.5735 | 3.8 | C45H85O13P | PI(36:1) | Lipids: Glycerophospholipids | 1.07 | 1.13 | 0.66 | 0.8102 | 0.4439 | 0.0608 | 1.43 | 1.52 | 1.21 | 0.5305 | 0.4721 | 0.5621 |
| 763.5349 | 3.7 | C40H78NO10P | PS(34:0) | Lipids: Glycerophospholipids | 1.22 | 1.20 | 0.85 | 0.3176 | 0.4769 | 0.3632 | 1.76 | 1.63 | 1.00 | 0.4172 | 0.5152 | 0.9912 |
| 862.5580 | 3.8 | C45H83O13P | PI(36:2) | Lipids: Glycerophospholipids | 1.00 | 1.35 | 0.73 | 0.9893 | 0.0184 | 0.0334 | 1.25 | 1.23 | 0.95 | 0.5757 | 0.6322 | 0.6804 |
| 600.3274 | 4.3 | C27H53O12P | [PI(18:0)] 1-octadecanoyl-sn-glycero-3-phospho-(1'-myo-inositol) | Lipids: Glycerophospholipids | 1.15 | 1.05 | 0.94 | 0.4659 | 0.7215 | 0.5427 | 1.24 | 0.96 | 1.10 | 0.5061 | 0.8462 | 0.6959 |
| 748.5246 | 3.8 | C40H77O10P | PG(34:1) | Lipids: Glycerophospholipids | 0.91 | 1.18 | 0.86 | 0.4500 | 0.3202 | 0.2248 | 1.33 | 1.65 | 0.95 | 0.6387 | 0.5534 | 0.8762 |
| 776.5566 | 3.8 | C42H81O10P | PG(36:1) | Lipids: Glycerophospholipids | 0.94 | 1.12 | 0.89 | 0.5151 | 0.4796 | 0.3257 | 1.10 | 1.21 | 1.10 | 0.8428 | 0.7113 | 0.8355 |
| 785.5214 | 3.8 | C42H76NO10P | PS(36:3) | Lipids: Glycerophospholipids | 1.11 | 1.35 | 0.95 | 0.6431 | 0.3027 | 0.8230 | 1.24 | 1.22 | 1.22 | 0.6861 | 0.7091 | 0.7075 |
| 912.5730 | 3.8 | C49H85O13P | PI(40:5) | Lipids: Glycerophospholipids | 1.25 | 1.22 | 0.83 | 0.4846 | 0.3360 | 0.3333 | 1.27 | 1.28 | 1.06 | 0.5230 | 0.3854 | 0.7106 |
| 787.5376 | 3.8 | C42H78NO10P | PS(36:2) | Lipids: Glycerophospholipids | 1.08 | 1.37 | 0.92 | 0.7012 | 0.3338 | 0.7317 | 1.47 | 1.38 | 1.19 | 0.5715 | 0.5815 | 0.7159 |
| 783.5769 | 4.5 | C44H82NO8P | PE(39:3) | Lipids: Glycerophospholipids | 0.92 | 0.84 | 1.27 | 0.6656 | 0.4711 | 0.2187 | 2.00 | 2.01 | 1.25 | 0.0348 | 0.1137 | 0.4768 |
| 789.5510 | 7.4 | C42H80NO10P | PS(18:0/18:1(9Z)) | Lipids: Glycerophospholipids | 0.99 | 1.19 | 0.75 | 0.9682 | 0.4259 | 0.1799 | 1.43 | 1.38 | 1.36 | 0.0874 | 0.3063 | 0.1602 |
| 807.5057 | 3.8 | C44H74NO10P | PS(38:6) | Lipids: Glycerophospholipids | 1.10 | 1.07 | 1.05 | 0.3092 | 0.7282 | 0.6488 | 1.36 | 1.26 | 1.18 | 0.3997 | 0.5744 | 0.4239 |
| 655.4215 | 7.9 | C35H62NO8P | PE(30:4) | Lipids: Glycerophospholipids | 0.80 | 1.14 | 1.25 | 0.5823 | 0.7992 | 0.7598 | 1.67 | 0.97 | 0.98 | 0.1590 | 0.9199 | 0.9420 |
| 831.5782 | 4.0 | C48H82NO8P | PC(40:7) | Lipids: Glycerophospholipids | 1.09 | 0.95 | 1.07 | 0.7120 | 0.7810 | 0.7761 | 1.43 | 1.17 | 1.05 | 0.4124 | 0.2711 | 0.6489 |
| 691.5139 | 7.3 | C37H74NO8P | PC(29:0) | Lipids: Glycerophospholipids | 1.13 | 0.92 | 0.92 | 0.6456 | 0.6815 | 0.7046 | 1.07 | 1.22 | 1.07 | 0.5327 | 0.4262 | 0.5651 |
| 773.5923 | 4.1 | C43H84NO8P | PE(38:1) | Lipids: Glycerophospholipids | 1.06 | 1.00 | 1.08 | 0.4343 | 0.9633 | 0.3743 | 1.30 | 1.24 | 1.07 | 0.4341 | 0.4560 | 0.5099 |
| 810.5272 | 7.2 | C41H79O13P | PI(32:0) | Lipids: Glycerophospholipids | 1.03 | 1.09 | 0.88 | 0.8959 | 0.4199 | 0.4449 | 1.27 | 1.40 | 1.17 | 0.0402 | 0.2686 | 0.1689 |
| 761.5209 | 3.8 | C40H76NO10P | PS(34:1) | Lipids: Glycerophospholipids | 1.00 | 1.06 | 0.86 | 0.9782 | 0.3643 | 0.0889 | 1.14 | 1.10 | 1.05 | 0.5511 | 0.6519 | 0.5961 |
| 720.4736 | 3.8 | C41H69O8P | PA(38:6) | Lipids: Glycerophospholipids | 0.89 | 0.97 | 1.00 | 0.6840 | 0.8402 | 0.9938 | 1.20 | 1.16 | 1.06 | 0.6193 | 0.6351 | 0.8758 |
| 805.5627 | 4.0 | C46H80NO8P | PC(38:6) | Lipids: Glycerophospholipids | 0.96 | 0.89 | 1.01 | 0.8749 | 0.6254 | 0.9637 | 1.36 | 1.09 | 0.95 | 0.3823 | 0.7447 | 0.8564 |
| 757.5620 | 4.5 | C42H80NO8P | PE(37:2) | Lipids: Glycerophospholipids | 0.68 | 0.74 | 1.16 | 0.1250 | 0.3574 | 0.4901 | 1.62 | 1.74 | 0.75 | 0.0462 | 0.0413 | 0.3064 |
| 860.5404 | 3.8 | C45H81O13P | PI(36:3) | Lipids: Glycerophospholipids | 1.05 | 1.38 | 0.83 | 0.6469 | 0.0750 | 0.1544 | 1.14 | 1.09 | 0.89 | 0.5594 | 0.7742 | 0.5541 |
| 705.5300 | 4.1 | C38H76NO8P | PC(30:0) | Lipids: Glycerophospholipids | 1.01 | 1.06 | 1.03 | 0.9423 | 0.5688 | 0.7191 | 1.24 | 0.99 | 0.94 | 0.4448 | 0.9815 | 0.7882 |
| 783.5053 | 3.8 | C42H74NO10P | PS(36:4) | Lipids: Glycerophospholipids | 1.01 | 1.04 | 0.99 | 0.8770 | 0.8068 | 0.9363 | 1.22 | 1.19 | 1.00 | 0.3509 | 0.3975 | 0.9655 |
| 689.4991 | 3.8 | C37H72NO8P | PE(32:1) | Lipids: Glycerophospholipids | 0.97 | 0.97 | 0.98 | 0.8784 | 0.9009 | 0.9353 | 1.22 | 1.18 | 1.02 | 0.3320 | 0.4921 | 0.9424 |
| 757.5620 | 6.0 | C42H80NO8P | 1-(9Z-hexadecenoyl)-2-(9Z-octadecenoyl)-sn-glycero-3-phosphocholine | Lipids: Glycerophospholipids | 1.07 | 0.97 | 0.87 | 0.7665 | 0.8756 | 0.3596 | 1.35 | 1.29 | 1.12 | 0.3274 | 0.4113 | 0.5447 |
| 836.5406 | 7.2 | C43H81O13P | PI(34:1) | Lipids: Glycerophospholipids | 1.09 | 1.11 | 0.77 | 0.7982 | 0.6159 | 0.4403 | 1.30 | 1.22 | 1.10 | 0.4626 | 0.5020 | 0.8266 |
| 809.5210 | 7.2 | C44H76NO10P | PS(18:1(9Z)/20:4(5Z,8Z,11Z,14Z)) | Lipids: Glycerophospholipids | 1.14 | 1.19 | 0.90 | 0.5167 | 0.0847 | 0.5032 | 1.29 | 1.20 | 1.15 | 0.1702 | 0.4993 | 0.4568 |
| 789.5528 | 3.8 | C42H80NO10P | PS(36:1) | Lipids: Glycerophospholipids | 1.05 | 1.30 | 0.79 | 0.7595 | 0.0109 | 0.1766 | 1.08 | 1.19 | 1.02 | 0.6448 | 0.2272 | 0.8521 |
| 763.5143 | 3.9 | C43H74NO8P | PE(38:6) | Lipids: Glycerophospholipids | 1.01 | 1.00 | 0.99 | 0.9736 | 0.9978 | 0.9775 | 1.47 | 1.10 | 1.11 | 0.1448 | 0.5805 | 0.7425 |
| 838.5571 | 7.2 | C43H83O13P | PI(34:0) | Lipids: Glycerophospholipids | 1.23 | 1.21 | 0.91 | 0.4390 | 0.2438 | 0.6189 | 1.32 | 1.21 | 1.07 | 0.1084 | 0.4516 | 0.7076 |
| 775.5502 | 3.9 | C45H78NO7P | PE(P-40:6) | Lipids: Glycerophospholipids | 1.06 | 0.94 | 0.97 | 0.8377 | 0.7985 | 0.9205 | 1.38 | 1.09 | 1.05 | 0.3753 | 0.7856 | 0.9092 |
| 809.5216 | 3.8 | C44H76NO10P | PS(38:5) | Lipids: Glycerophospholipids | 1.03 | 1.06 | 1.04 | 0.7810 | 0.7031 | 0.7740 | 1.10 | 1.05 | 1.00 | 0.0568 | 0.4952 | 0.9912 |
| 674.4898 | 3.8 | C37H71O8P | PA(34:1) | Lipids: Glycerophospholipids | 0.98 | 1.17 | 0.92 | 0.7886 | 0.3453 | 0.5773 | 1.05 | 1.04 | 0.96 | 0.5064 | 0.5817 | 0.7737 |
| 700.5045 | 3.8 | C39H73O8P | PA(36:2) | Lipids: Glycerophospholipids | 0.91 | 1.20 | 0.91 | 0.4458 | 0.3694 | 0.5685 | 1.04 | 0.97 | 0.95 | 0.7881 | 0.8320 | 0.7194 |
| 807.5772 | 4.0 | C46H82NO8P | PC(38:5) | Lipids: Glycerophospholipids | 0.99 | 0.96 | 1.02 | 0.9431 | 0.5082 | 0.8602 | 1.33 | 1.06 | 1.01 | 0.3124 | 0.4704 | 0.8426 |

| | | | | | | | | | | | | | | | | | |
|---|---|---|---|---|---|---|---|---|---|---|---|---|---|---|---|---|---|
| 691.5144 | 3.8 | C37H74NO8P | PE(32:0) | Lipids: Glycerophospholipids | 0.91 | 0.97 | 0.90 | 0.5203 | 0.8840 | 0.6519 | 1.12 | 1.00 | 0.91 | 0.3620 | 0.9685 | 0.5246 |
| 835.5361 | 3.8 | C46H78NO10P | PS(40:6) | Lipids: Glycerophospholipids | 1.08 | 1.03 | 0.90 | 0.8072 | 0.9084 | 0.7071 | 1.15 | 1.06 | 0.98 | 0.6129 | 0.8204 | 0.9503 |
| 523.2912 | 4.3 | C24H46NO9P | [PS(18:1)] 1-(9Z-octadecenoyl)-sn-glycero-3-phosphoserine | Lipids: Glycerophospholipids | 1.02 | 1.06 | 1.07 | 0.9173 | 0.7542 | 0.8311 | 0.93 | 0.94 | 0.67 | 0.7160 | 0.8318 | 0.2056 |
| 773.5361 | 3.9 | C45H76NO7P | PE(P-40:7) | Lipids: Glycerophospholipids | 0.99 | 0.89 | 0.99 | 0.9192 | 0.2719 | 0.9148 | 1.22 | 1.09 | 0.94 | 0.4188 | 0.7897 | 0.8039 |
| 837.5524 | 3.8 | C46H80NO10P | PS(40:5) | Lipids: Glycerophospholipids | 1.07 | 1.26 | 0.97 | 0.4501 | 0.0205 | 0.8109 | 1.10 | 1.04 | 1.03 | 0.5566 | 0.6023 | 0.7464 |
| 777.5677 | 3.9 | C45H80NO7P | PE(P-40:5) | Lipids: Glycerophospholipids | 1.09 | 1.00 | 1.02 | 0.5441 | 0.9914 | 0.9156 | 1.37 | 1.10 | 1.01 | 0.2083 | 0.5145 | 0.9611 |
| 785.5923 | 6.0 | C44H84NO8P | 1-(11Z-octadecenoyl)-2-(9Z-octadecenoyl)-sn-glycero-3-phosphocholine | Lipids: Glycerophospholipids | 1.05 | 0.97 | 0.83 | 0.8110 | 0.7851 | 0.1788 | 1.13 | 1.11 | 0.99 | 0.5557 | 0.6887 | 0.9011 |
| 785.5923 | 5.3 | C44H84NO8P | 1-(9Z-tetradecenoyl)-2-(13Z-docosenoyl)-sn-glycero-3-phosphocholine | Lipids: Glycerophospholipids | 1.14 | 1.14 | 0.98 | 0.5091 | 0.1893 | 0.8697 | 1.31 | 1.33 | 1.00 | 0.3764 | 0.3685 | 0.9632 |
| 757.5621 | 4.1 | C42H80NO8P | PC(34:2) | Lipids: Glycerophospholipids | 1.07 | 1.05 | 1.19 | 0.5597 | 0.7607 | 0.0701 | 1.17 | 1.05 | 0.98 | 0.3304 | 0.7549 | 0.7935 |
| 833.5940 | 4.0 | C48H84NO8P | PC(40:6) | Lipids: Glycerophospholipids | 0.97 | 0.97 | 1.04 | 0.8418 | 0.8620 | 0.8718 | 1.35 | 1.03 | 0.96 | 0.2016 | 0.8598 | 0.8695 |
| 759.5772 | 5.3 | C42H82NO8P | 1-(9Z-octadecenoyl)-2-hexadecanoyl-sn-glycero-3-phosphocholine | Lipids: Glycerophospholipids | 1.06 | 1.06 | 0.88 | 0.7456 | 0.7203 | 0.4755 | 1.27 | 1.29 | 0.93 | 0.3522 | 0.3318 | 0.4561 |
| 702.5207 | 3.8 | C39H75O8P | PA(36:1) | Lipids: Glycerophospholipids | 1.01 | 1.30 | 0.94 | 0.9658 | 0.2241 | 0.7220 | 1.11 | 1.02 | 1.00 | 0.4997 | 0.8816 | 0.9882 |
| 785.5928 | 4.1 | C44H84NO8P | PC(36:2) | Lipids: Glycerophospholipids | 1.06 | 1.02 | 1.12 | 0.3219 | 0.8345 | 0.1040 | 1.24 | 1.03 | 1.00 | 0.4379 | 0.8457 | 0.9791 |
| 855.5059 | 3.8 | C48H74NO10P | PS(42:10) | Lipids: Glycerophospholipids | 1.14 | 1.24 | 1.15 | 0.1542 | 0.4771 | 0.4816 | 1.08 | 1.12 | 1.18 | 0.6900 | 0.6124 | 0.2843 |
| 759.5771 | 6.5 | C42H82NO8P | PE(15:0/22:1(13Z)) | Lipids: Glycerophospholipids | 0.97 | 0.98 | 0.94 | 0.8287 | 0.8981 | 0.4304 | 1.21 | 1.19 | 1.09 | 0.2865 | 0.3848 | 0.2998 |
| 722.4887 | 3.7 | C41H71O8P | PA(38:5) | Lipids: Glycerophospholipids | 0.95 | 1.06 | 1.00 | 0.7802 | 0.7310 | 0.9984 | 1.06 | 0.98 | 0.97 | 0.7963 | 0.9124 | 0.8875 |
| 749.5354 | 4.0 | C43H76NO7P | PE(P-38:5) | Lipids: Glycerophospholipids | 1.02 | 1.02 | 1.05 | 0.8759 | 0.9098 | 0.7522 | 1.21 | 1.04 | 1.05 | 0.2341 | 0.7643 | 0.7670 |
| 733.5621 | 6.9 | C40H80NO8P | 1-octadecanoyl-2-tetradecanoyl-sn-glycero-3-phosphocholine | Lipids: Glycerophospholipids | 1.19 | 1.12 | 0.98 | 0.3533 | 0.3405 | 0.8298 | 1.15 | 1.13 | 1.00 | 0.3280 | 0.3115 | 0.9834 |
| 759.5772 | 6.0 | C42H82NO8P | 1-(11Z-octadecenoyl)-2-hexadecanoyl-sn-glycero-3-phosphocholine | Lipids: Glycerophospholipids | 1.06 | 0.95 | 0.88 | 0.7275 | 0.6426 | 0.3244 | 0.80 | 1.13 | 1.00 | 0.2768 | 0.5669 | 0.9737 |
| 831.5067 | 3.8 | C46H74NO10P | PS(40:8) | Lipids: Glycerophospholipids | 1.20 | 1.66 | 1.31 | 0.7259 | 0.4999 | 0.7060 | 1.12 | 0.92 | 1.35 | 0.8333 | 0.8489 | 0.6748 |
| 521.3477 | 7.9 | C26H52NO7P | PC(18:1) | Lipids: Glycerophospholipids | 1.20 | 0.93 | 1.26 | 0.3954 | 0.7451 | 0.2093 | 1.27 | 1.12 | 1.21 | 0.1649 | 0.4908 | 0.3552 |
| 783.5770 | 4.1 | C44H82NO8P | PC(36:3) | Lipids: Glycerophospholipids | 1.05 | 1.02 | 1.10 | 0.5095 | 0.8527 | 0.2508 | 1.16 | 1.00 | 1.02 | 0.3498 | 0.9639 | 0.6276 |
| 743.5478 | 4.1 | C41H78NO8P | PE(36:2) | Lipids: Glycerophospholipids | 1.01 | 1.09 | 1.00 | 0.7361 | 0.3229 | 0.9980 | 1.25 | 1.07 | 1.04 | 0.2952 | 0.6595 | 0.7739 |
| 731.5462 | 4.1 | C40H78NO8P | PC(32:1) | Lipids: Glycerophospholipids | 1.12 | 1.14 | 1.25 | 0.6495 | 0.6906 | 0.5282 | 1.03 | 0.97 | 0.98 | 0.9058 | 0.9004 | 0.9468 |
| 733.5622 | 6.2 | C40H80NO8P | 1-tetradecanoyl-2-octadecanoyl-sn-glycero-3-phosphocholine | Lipids: Glycerophospholipids | 1.11 | 1.04 | 0.90 | 0.4715 | 0.5697 | 0.1296 | 1.09 | 0.96 | 0.95 | 0.5489 | 0.6177 | 0.7319 |
| 759.5770 | 4.1 | C42H82NO8P | PC(34:1) | Lipids: Glycerophospholipids | 1.07 | 1.10 | 1.14 | 0.4652 | 0.5831 | 0.2556 | 1.11 | 1.01 | 0.99 | 0.5606 | 0.9407 | 0.9253 |
| 739.5142 | 4.0 | C41H74NO8P | PE(36:4) | Lipids: Glycerophospholipids | 1.01 | 0.92 | 1.01 | 0.9129 | 0.4304 | 0.9327 | 1.15 | 1.06 | 0.97 | 0.4666 | 0.5524 | 0.7851 |
| 696.4744 | 3.8 | C39H69O8P | PA(36:4) | Lipids: Glycerophospholipids | 0.92 | 1.13 | 1.00 | 0.3115 | 0.5320 | 0.9826 | 1.08 | 0.98 | 0.93 | 0.7814 | 0.9208 | 0.7867 |
| 477.2855 | 4.7 | C23H44NO7P | LysoPE(18:2) | Lipids: Glycerophospholipids | 1.15 | 1.12 | 1.53 | 0.3584 | 0.5103 | 0.1416 | 1.22 | 0.94 | 0.96 | 0.4647 | 0.8289 | 0.8975 |
| 495.3328 | 7.9 | C24H50NO7P | PE(19:0) | Lipids: Glycerophospholipids | 1.10 | 0.85 | 1.30 | 0.6094 | 0.2227 | 0.0176 | 1.17 | 1.06 | 1.19 | 0.2889 | 0.7222 | 0.1336 |
| 713.4997 | 3.8 | C39H72NO8P | PE(34:3) | Lipids: Glycerophospholipids | 1.10 | 1.05 | 1.06 | 0.5539 | 0.8495 | 0.7776 | 1.17 | 0.99 | 0.96 | 0.5671 | 0.9696 | 0.9107 |
| 785.5923 | 4.6 | C44H84NO8P | PE(39:2) | Lipids: Glycerophospholipids | 1.63 | 1.68 | 1.41 | 0.0074 | 0.0516 | 0.1936 | 1.65 | 1.08 | 1.39 | 0.0483 | 0.7144 | 0.0184 |
| 751.5514 | 4.0 | C43H78NO7P | PE(O-38:5) | Lipids: Glycerophospholipids | 1.06 | 1.13 | 1.09 | 0.6032 | 0.5269 | 0.5440 | 1.36 | 1.07 | 1.10 | 0.0133 | 0.4972 | 0.4661 |

| | | | | | | | | | | | | | | | | |
|---|---|---|---|---|---|---|---|---|---|---|---|---|---|---|---|---|
| 523.3641 | 7.9 | C26H54NO7P | PC(18:0) | Lipids: Glycerophospholipids | 1.06 | 0.89 | 1.26 | 0.6997 | 0.2629 | 0.0580 | 1.05 | 1.01 | 1.14 | 0.6425 | 0.9460 | 0.2292 |
| 839.5676 | 3.8 | C46H82NO10P | PS(40:4) | Lipids: Glycerophospholipids | 1.10 | 1.36 | 1.03 | 0.1039 | 0.1292 | 0.8715 | 1.00 | 1.03 | 1.04 | 0.9849 | 0.8482 | 0.7220 |
| 509.3481 | 7.9 | C25H52NO7P | LysoPC(17:0) | Lipids: Glycerophospholipids | 1.22 | 0.86 | 1.30 | 0.4331 | 0.3216 | 0.1241 | 0.98 | 1.12 | 0.93 | 0.9375 | 0.5818 | 0.6169 |
| 410.2431 | 7.9 | C19H39O7P | [PA(16:0/0:0)] 1-hexadecanoyl-2-sn-glycero-3-phosphate | Lipids: Glycerophospholipids | 1.31 | 1.13 | 1.40 | 0.3559 | 0.6626 | 0.1600 | 1.27 | 0.95 | 1.01 | 0.0518 | 0.8053 | 0.8999 |
| 525.3065 | 4.3 | C24H48NO9P | PS(18:0) | Lipids: Glycerophospholipids | 0.98 | 1.04 | 1.15 | 0.9250 | 0.8680 | 0.7062 | 0.95 | 1.00 | 0.78 | 0.7394 | 0.9906 | 0.2576 |
| 551.3956 | 4.6 | C28H58NO7P | LysoPC(20:0) | Lipids: Glycerophospholipids | 1.08 | 0.87 | 1.06 | 0.5736 | 0.3561 | 0.7406 | 1.09 | 1.05 | 1.08 | 0.5365 | 0.4894 | 0.5506 |
| 493.3174 | 4.8 | C24H48NO7P | LysoPC(16:1) | Lipids: Glycerophospholipids | 1.04 | 0.68 | 1.15 | 0.8350 | 0.0834 | 0.3558 | 1.55 | 0.83 | 1.26 | 0.1859 | 0.4967 | 0.1550 |
| 811.5377 | 7.0 | C44H78NO10P | [PS(18:0/20:4)] 1-octadecanoyl-2-(5Z,8Z,11Z,14Z-eicosatetraenoyl)-sn-glycero-3-phosphoserine | Lipids: Glycerophospholipids | 1.13 | 1.29 | 0.89 | 0.5401 | 0.0362 | 0.4341 | 1.19 | 1.10 | 1.06 | 0.3636 | 0.5881 | 0.7506 |
| 733.5623 | 4.2 | C40H80NO8P | PC(32:0) | Lipids: Glycerophospholipids | 1.19 | 1.11 | 1.03 | 0.1492 | 0.5007 | 0.8609 | 1.06 | 0.92 | 0.94 | 0.4723 | 0.2767 | 0.5695 |
| 479.3378 | 4.7 | C24H50NO6P | LysoPC(O-16:1) | Lipids: Glycerophospholipids | 1.12 | 1.01 | 1.07 | 0.0473 | 0.8965 | 0.5963 | 1.13 | 1.03 | 1.04 | 0.1818 | 0.7953 | 0.7252 |
| 811.5370 | 3.8 | C44H78NO10P | PS(38:4) | Lipids: Glycerophospholipids | 1.07 | 1.13 | 0.99 | 0.4628 | 0.3834 | 0.9594 | 1.10 | 1.03 | 1.01 | 0.2070 | 0.6564 | 0.9718 |
| 527.3002 | 4.6 | C27H46NO7P | LysoPE(22:5) | Lipids: Glycerophospholipids | 0.78 | 1.08 | 0.97 | 0.5934 | 0.8514 | 0.9395 | 0.53 | 0.74 | 0.81 | 0.2491 | 0.5477 | 0.6715 |
| 519.3328 | 4.7 | C26H50NO7P | PC(18:2) | Lipids: Glycerophospholipids | 1.19 | 0.96 | 1.64 | 0.3589 | 0.8357 | 0.1178 | 1.27 | 0.96 | 1.01 | 0.0910 | 0.7956 | 0.9710 |
| 545.3478 | 4.5 | C28H52NO7P | LysoPC(20:3) | Lipids: Glycerophospholipids | 0.62 | 1.05 | 0.85 | 0.3751 | 0.9147 | 0.7350 | 0.52 | 0.61 | 0.90 | 0.3116 | 0.4124 | 0.8418 |
| 509.3849 | 4.7 | C26H56NO6P | LysoPC(O-18:0) | Lipids: Glycerophospholipids | 1.01 | 1.03 | 1.05 | 0.8460 | 0.8392 | 0.8324 | 1.16 | 1.13 | 1.04 | 0.1020 | 0.4559 | 0.5574 |
| 723.5200 | 4.0 | C41H74NO7P | PE(P-36:4) | Lipids: Glycerophospholipids | 1.05 | 0.97 | 1.02 | 0.6558 | 0.8137 | 0.8940 | 1.29 | 1.01 | 0.95 | 0.1600 | 0.9137 | 0.7939 |
| 811.5377 | 6.0 | C44H78NO10P | PS(18:0/20:4(5Z,8Z,11Z,14Z)) | Lipids: Glycerophospholipids | 1.10 | 1.22 | 1.10 | 0.2162 | 0.2847 | 0.4411 | 1.05 | 0.93 | 1.00 | 0.5883 | 0.1913 | 0.9698 |
| 724.5053 | 3.8 | C41H73O8P | PA(38:4) | Lipids: Glycerophospholipids | 1.02 | 1.27 | 1.00 | 0.8742 | 0.4692 | 0.9902 | 0.96 | 0.91 | 0.94 | 0.9098 | 0.5576 | 0.8220 |
| 481.3532 | 4.8 | C24H52NO6P | [LysoPC(16:2)] 1-hexadecyl-sn-glycero-3-phosphocholine | Lipids: Glycerophospholipids | 1.10 | 0.95 | 1.06 | 0.5132 | 0.6138 | 0.7069 | 0.92 | 0.83 | 1.03 | 0.4007 | 0.3136 | 0.8382 |
| 523.3641 | 4.7 | C26H54NO7P | LysoPC(18:0) | Lipids: Glycerophospholipids | 1.24 | 0.92 | 1.15 | 0.2034 | 0.6360 | 0.4930 | 1.00 | 1.01 | 1.08 | 0.9698 | 0.9673 | 0.5689 |
| 479.3011 | 7.9 | C23H46NO7P | LysoPE(18:1) | Lipids: Glycerophospholipids | 1.12 | 1.10 | 1.32 | 0.5607 | 0.6029 | 0.4173 | 1.22 | 1.07 | 0.89 | 0.3781 | 0.7980 | 0.7227 |
| 766.5878 | 4.4 | C45H83O7P | PA(O-42:4) | Lipids: Glycerophospholipids | 1.26 | 0.99 | 0.98 | 0.1672 | 0.9798 | 0.9629 | 1.00 | 1.06 | 0.99 | 0.9724 | 0.5952 | 0.9444 |
| 759.5771 | 4.8 | C42H82NO8P | PE(37:1) | Lipids: Glycerophospholipids | 1.59 | 1.48 | 1.03 | 0.0030 | 0.0111 | 0.8119 | 1.22 | 1.33 | 1.09 | 0.2220 | 0.3048 | 0.5591 |
| 509.3486 | 4.7 | C25H52NO7P | LysoPE(20:0) | Lipids: Glycerophospholipids | 1.13 | 0.84 | 1.34 | 0.4286 | 0.3401 | 0.2721 | 1.12 | 0.95 | 1.11 | 0.5351 | 0.7886 | 0.5453 |
| 765.5303 | 4.0 | C43H76NO8P | PE(38:5) | Lipids: Glycerophospholipids | 1.11 | 1.04 | 1.16 | 0.3137 | 0.8100 | 0.4125 | 1.07 | 1.03 | 0.95 | 0.3502 | 0.6581 | 0.6874 |
| 809.5932 | 4.0 | C46H84NO8P | PC(38:4) | Lipids: Glycerophospholipids | 1.09 | 1.00 | 1.08 | 0.2995 | 0.9912 | 0.2979 | 1.16 | 0.95 | 0.92 | 0.0498 | 0.5259 | 0.4145 |
| 733.5622 | 4.8 | C40H80NO8P | 1,2-dihexadecanoyl-sn-glycero-3-phosphocholine | Lipids: Glycerophospholipids | 1.78 | 1.04 | 1.45 | 0.0067 | 0.7286 | 0.0029 | 1.25 | 0.85 | 1.20 | 0.1857 | 0.3405 | 0.3681 |
| 708.5092 | 3.7 | C41H73O7P | PA(O-38:5) | Lipids: Glycerophospholipids | 1.09 | 1.80 | 1.24 | 0.4568 | 0.2303 | 0.1195 | 1.11 | 0.96 | 0.99 | 0.4280 | 0.7078 | 0.9548 |
| 764.5712 | 4.4 | C45H81O7P | PA(P-20:0/22:4(7Z,10Z,13Z,16Z)) | Lipids: Glycerophospholipids | 1.19 | 1.05 | 1.01 | 0.2103 | 0.8128 | 0.9655 | 1.06 | 1.03 | 1.06 | 0.6700 | 0.7809 | 0.6543 |
| 517.3163 | 4.7 | C26H48NO7P | [PC(18:3)] | Lipids: Glycerophospholipids | 1.15 | 0.98 | 1.37 | 0.2197 | 0.8919 | 0.0911 | 0.97 | 0.89 | 1.09 | 0.8509 | 0.5067 | 0.7066 |
| 479.3012 | 4.7 | C23H46NO7P | PE(18:1) | Lipids: Glycerophospholipids | 0.99 | 1.05 | 1.30 | 0.9391 | 0.8175 | 0.4099 | 1.04 | 0.92 | 0.88 | 0.8811 | 0.7756 | 0.6883 |
| 767.5461 | 4.0 | C43H78NO8P | PE(38:4) | Lipids: Glycerophospholipids | 1.14 | 1.08 | 1.14 | 0.5033 | 0.6955 | 0.5999 | 1.11 | 1.02 | 1.01 | 0.4203 | 0.7567 | 0.9082 |
| 438.2738 | 4.7 | C21H43O7P | [PA(18:0)] 1-octadecanoyl-2-sn-glycero-3-phosphate | Lipids: Glycerophospholipids | 1.15 | 0.86 | 1.19 | 0.4402 | 0.4424 | 0.5326 | 0.99 | 0.96 | 1.05 | 0.9569 | 0.8601 | 0.7835 |
| 543.3326 | 4.7 | C28H50NO7P | LysoPC(20:4) | Lipids: Glycerophospholipids | 1.15 | 0.87 | 1.35 | 0.2674 | 0.4455 | 0.3869 | 1.19 | 0.90 | 0.90 | 0.2426 | 0.6168 | 0.5904 |
| 495.3328 | 4.8 | C24H50NO7P | LysoPC(16:0) | Lipids: Glycerophospholipids | 1.28 | 0.87 | 1.30 | 0.3089 | 0.3608 | 0.1579 | 1.14 | 0.90 | 1.00 | 0.5145 | 0.6806 | 0.9948 |

| | | | | | | | | | | | | | | | | |
|---|---|---|---|---|---|---|---|---|---|---|---|---|---|---|---|---|
| 501.2854 | 4.6 | C25H44NO7P | LysoPE(20:4) | Lipids: Glycerophospholipids | 0.72 | 0.99 | 1.03 | 0.4321 | 0.9804 | 0.9472 | 0.66 | 0.83 | 0.79 | 0.2835 | 0.6106 | 0.4917 |
| 481.3169 | 4.8 | C23H48NO7P | LysoPE(18:0) | Lipids: Glycerophospholipids | 1.24 | 0.93 | 1.18 | 0.2603 | 0.6898 | 0.3004 | 1.08 | 0.90 | 0.96 | 0.7306 | 0.6440 | 0.7866 |
| 521.3484 | 4.7 | C26H52NO7P | LysoPC(18:1) | Lipids: Glycerophospholipids | 1.21 | 0.95 | 1.40 | 0.0887 | 0.6744 | 0.0361 | 0.99 | 0.94 | 1.05 | 0.9345 | 0.7501 | 0.7832 |
| 436.2589 | 4.7 | C21H41O7P | PA(18:1(9Z)/0:0) | Lipids: Glycerophospholipids | 1.19 | 0.88 | 1.27 | 0.2649 | 0.3733 | 0.1118 | 1.00 | 0.79 | 1.12 | 0.9869 | 0.3762 | 0.5867 |
| 410.2431 | 4.8 | C19H39O7P | LysoPA(16:0) | Lipids: Glycerophospholipids | 1.28 | 0.83 | 1.24 | 0.2374 | 0.4062 | 0.3769 | 1.05 | 0.98 | 1.02 | 0.7868 | 0.9147 | 0.8735 |
| 545.2751 | 4.3 | C26H44NO9P | [PS(20:4)] 1-(5Z,8Z,11Z,14Z-eicosatetraenoyl)-sn-glycero-3-phosphoserine | Lipids: Glycerophospholipids | 1.30 | 1.10 | 1.55 | 0.2590 | 0.5379 | 0.3318 | 1.20 | 0.98 | 0.87 | 0.2744 | 0.9100 | 0.5922 |
| 727.5530 | 4.1 | C41H78NO7P | PE(P-36:2) | Lipids: Glycerophospholipids | 1.10 | 1.07 | 0.94 | 0.1855 | 0.7736 | 0.7219 | 1.01 | 0.88 | 0.93 | 0.9688 | 0.2594 | 0.6416 |
| 501.2851 | 7.9 | C25H44NO7P | LysoPE(0:0/20:4(5Z,8Z,11Z,14Z)) | Lipids: Glycerophospholipids | 0.75 | 1.27 | 0.97 | 0.3747 | 0.4531 | 0.9301 | 0.89 | 0.89 | 0.79 | 0.7431 | 0.7598 | 0.4296 |
| 733.5622 | 4.5 | C40H80NO8P | PE(35:0) | Lipids: Glycerophospholipids | 0.89 | 0.82 | 0.67 | 0.4507 | 0.2732 | 0.0579 | 1.04 | 1.02 | 0.51 | 0.8124 | 0.8033 | 0.0030 |
| 437.2909 | 4.7 | C21H44NO6P | LysoPE(P-16:0) | Lipids: Glycerophospholipids | 1.32 | 1.16 | 1.37 | 0.1152 | 0.4888 | 0.1040 | 1.11 | 0.87 | 0.88 | 0.4901 | 0.4111 | 0.5346 |
| 453.2875 | 4.8 | C28H39NO4 | Sambutoxin | Lipids: Prenols | 1.08 | 1.03 | 1.19 | 0.7202 | 0.8785 | 0.4842 | 1.34 | 1.05 | 0.91 | 0.1406 | 0.8773 | 0.7129 |
| 152.1200 | 4.3 | C10H16O | (1R,4S)-fenchan-2-one | Lipids: Prenols | 0.79 | 0.75 | 0.85 | 0.5251 | 0.1762 | 0.4665 | 0.93 | 1.17 | 1.09 | 0.7190 | 0.1556 | 0.6337 |
| 772.6459 | 7.8 | C44H89N2O6P | SM(d39:1) | Lipids: Sphingolipids | 0.92 | 1.09 | 0.86 | 0.7720 | 0.6359 | 0.5468 | 1.10 | 1.21 | 1.15 | 0.8542 | 0.6469 | 0.2289 |
| 800.6772 | 7.8 | C46H93N2O6P | SM(d41:1) | Lipids: Sphingolipids | 1.08 | 1.12 | 0.98 | 0.7597 | 0.4342 | 0.9570 | 1.51 | 1.18 | 1.11 | 0.3355 | 0.6619 | 0.4916 |
| 828.7099 | 7.7 | C48H97N2O6P | SM(d43:1) | Lipids: Sphingolipids | 1.28 | 1.04 | 0.87 | 0.5166 | 0.6892 | 0.6684 | 1.46 | 1.22 | 1.15 | 0.1698 | 0.6125 | 0.2843 |
| 798.6624 | 7.8 | C46H91N2O6P | SM(d41:2) | Lipids: Sphingolipids | 0.95 | 1.07 | 0.88 | 0.7414 | 0.6418 | 0.3992 | 1.24 | 1.22 | 1.14 | 0.2850 | 0.4091 | 0.1710 |
| 770.6303 | 7.8 | C44H87N2O6P | SM(d18:2/21:0) | Lipids: Sphingolipids | 1.10 | 1.11 | 0.92 | 0.7565 | 0.5916 | 0.7013 | 1.20 | 1.26 | 1.19 | 0.3874 | 0.2841 | 0.3944 |
| 758.6295 | 7.8 | C43H87N2O6P | SM(d38:1) | Lipids: Sphingolipids | 0.97 | 1.01 | 0.83 | 0.8998 | 0.9387 | 0.4337 | 1.21 | 1.10 | 1.06 | 0.1594 | 0.5509 | 0.6274 |
| 784.6465 | 7.8 | C45H89N2O6P | SM(d40:2) | Lipids: Sphingolipids | 0.97 | 1.06 | 0.88 | 0.8995 | 0.7003 | 0.4309 | 1.25 | 1.24 | 1.11 | 0.2570 | 0.3911 | 0.4945 |
| 786.6617 | 7.8 | C45H91N2O6P | SM(d40:1) | Lipids: Sphingolipids | 1.06 | 1.12 | 0.90 | 0.7896 | 0.2349 | 0.5885 | 1.27 | 1.13 | 1.03 | 0.2412 | 0.6277 | 0.6962 |
| 782.6301 | 7.8 | C45H87N2O6P | SM(d40:3) | Lipids: Sphingolipids | 1.08 | 1.26 | 0.97 | 0.7683 | 0.3089 | 0.8562 | 1.29 | 1.04 | 1.21 | 0.1892 | 0.8137 | 0.6115 |
| 826.6938 | 7.7 | C48H95N2O6P | SM(d43:2) | Lipids: Sphingolipids | 0.93 | 1.13 | 0.84 | 0.5363 | 0.4230 | 0.2514 | 1.27 | 1.07 | 1.14 | 0.1981 | 0.7116 | 0.0430 |
| 814.6917 | 7.8 | C47H95N2O6P | SM(d42:1) | Lipids: Sphingolipids | 1.47 | 1.19 | 1.12 | 0.3925 | 0.1615 | 0.7315 | 1.24 | 1.06 | 1.15 | 0.3122 | 0.7925 | 0.3456 |
| 744.6152 | 7.8 | C42H85N2O6P | SM(d37:1) | Lipids: Sphingolipids | 0.91 | 0.97 | 0.86 | 0.7367 | 0.8094 | 0.4384 | 1.23 | 1.08 | 1.21 | 0.3127 | 0.2881 | 0.3874 |
| 674.5358 | 7.8 | C37H75N2O6P | SM(d32:1) | Lipids: Sphingolipids | 0.91 | 0.91 | 0.96 | 0.6462 | 0.6094 | 0.8240 | 1.07 | 1.06 | 1.08 | 0.6987 | 0.5533 | 0.3823 |
| 810.6622 | 7.8 | C47H91N2O6P | SM(d42:3) | Lipids: Sphingolipids | 0.97 | 1.12 | 0.90 | 0.7942 | 0.1287 | 0.2859 | 1.16 | 1.12 | 1.06 | 0.1626 | 0.5280 | 0.4726 |
| 674.5360 | 4.4 | C37H75N2O6P | EPC(d35:1) | Lipids: Sphingolipids | 1.06 | 0.89 | 0.92 | 0.7538 | 0.5126 | 0.7617 | 1.19 | 1.17 | 1.05 | 0.1937 | 0.3761 | 0.8215 |
| 786.6623 | 4.5 | C45H91N2O6P | SM(d18:1/22:0) | Lipids: Sphingolipids | 1.13 | 1.08 | 0.89 | 0.6566 | 0.5085 | 0.7505 | 1.24 | 1.19 | 0.97 | 0.3651 | 0.4816 | 0.8709 |
| 784.6470 | 4.3 | C45H89N2O6P | SM(d18:1/22:1(13Z)) | Lipids: Sphingolipids | 1.05 | 1.12 | 0.85 | 0.8242 | 0.5672 | 0.5609 | 1.31 | 1.16 | 0.99 | 0.2180 | 0.4136 | 0.9500 |
| 756.6144 | 7.8 | C43H85N2O6P | SM(d38:2) | Lipids: Sphingolipids | 0.99 | 0.98 | 0.94 | 0.9784 | 0.8740 | 0.7496 | 1.17 | 1.18 | 1.10 | 0.0589 | 0.1209 | 0.5475 |
| 814.6914 | 4.6 | C47H95N2O6P | SM(d18:0/24:1(15Z)) | Lipids: Sphingolipids | 1.20 | 1.17 | 1.09 | 0.3276 | 0.2618 | 0.8504 | 1.44 | 1.22 | 1.08 | 0.0750 | 0.4938 | 0.4195 |
| 619.5900 | 3.9 | C40H77NO3 | Cer(d40:2) | Lipids: Sphingolipids | 1.17 | 0.99 | 0.78 | 0.5664 | 0.9484 | 0.3498 | 1.23 | 1.17 | 0.97 | 0.5381 | 0.6673 | 0.9509 |
| 756.6145 | 4.3 | C43H85N2O6P | SM(d16:1/22:1) | Lipids: Sphingolipids | 0.92 | 1.00 | 0.96 | 0.7464 | 0.9896 | 0.8933 | 1.23 | 1.51 | 1.06 | 0.1507 | 0.0950 | 0.8917 |
| 688.5521 | 7.8 | C38H77N2O6P | SM(d33:1) | Lipids: Sphingolipids | 0.91 | 0.80 | 1.00 | 0.4363 | 0.2211 | 0.9994 | 0.95 | 1.02 | 1.04 | 0.3897 | 0.8198 | 0.5326 |
| 840.7081 | 7.7 | C49H97N2O6P | SM(d44:2) | Lipids: Sphingolipids | 1.01 | 1.14 | 0.84 | 0.8968 | 0.3853 | 0.3792 | 1.12 | 0.93 | 0.83 | 0.0409 | 0.2506 | 0.5306 |
| 810.6629 | 4.3 | C47H91N2O6P | SM(d18:2/24:1) | Lipids: Sphingolipids | 1.08 | 1.05 | 0.95 | 0.5592 | 0.5851 | 0.8532 | 1.25 | 1.18 | 1.04 | 0.1637 | 0.1568 | 0.7872 |
| 716.5836 | 4.4 | C40H81N2O6P | EPC(d38:1) | Lipids: Sphingolipids | 1.14 | 0.89 | 0.87 | 0.5560 | 0.4463 | 0.6441 | 1.19 | 1.27 | 0.99 | 0.3101 | 0.1377 | 0.9727 |
| 727.5877 | 7.8 | C42H82NO6P | [SP (24:0)] N-(15Z-tetracosenoyl)-sphing-4-enine-1-phosphate | Lipids: Sphingolipids | 1.01 | 0.98 | 0.87 | 0.9136 | 0.9026 | 0.4067 | 1.13 | 0.99 | 1.07 | 0.2138 | 0.9156 | 0.5464 |

| | | | | | | | | | | | | | | | | | |
|---|---|---|---|---|---|---|---|---|---|---|---|---|---|---|---|---|---|
| 647.6213 | 3.9 | C42H81NO3 | [SP (24:0)] N-(15Z-tetracosenoyl)-sphing-4-enine | Lipids: Sphingolipids | 1.29 | 1.08 | 0.86 | 0.1309 | 0.7321 | 0.6914 | 1.68 | 1.11 | 1.13 | 0.3116 | 0.7933 | 0.7949 |
| 702.5679 | 4.9 | C39H79N2O6P | N-(tricosanoyl)-tetradecasphing-4-enine-1-phosphoethanolamine | Lipids: Sphingolipids | 0.99 | 1.11 | 0.83 | 0.9331 | 0.6380 | 0.1240 | 1.18 | 1.12 | 0.97 | 0.2054 | 0.5216 | 0.9169 |
| 617.4775 | 7.8 | C34H68NO6P | [SP (16:0)] N-(hexadecanoyl)-sphing-4-enine-1-phosphate | Lipids: Sphingolipids | 0.91 | 0.98 | 0.99 | 0.5536 | 0.8667 | 0.9451 | 1.16 | 1.04 | 1.07 | 0.3834 | 0.7899 | 0.1941 |
| 716.5839 | 7.8 | C40H81N2O6P | SM(d35:1) | Lipids: Sphingolipids | 0.90 | 1.08 | 1.00 | 0.3982 | 0.4202 | 0.9996 | 1.06 | 1.07 | 1.12 | 0.3329 | 0.5086 | 0.4575 |
| 379.2488 | 7.9 | C18H38NO5P | [SP] Sphing-4-enine-1-phosphate | Lipids: Sphingolipids | 0.72 | 0.80 | 0.99 | 0.3028 | 0.3987 | 0.9852 | 1.23 | 0.98 | 0.95 | 0.1553 | 0.8859 | 0.8208 |
| 688.5525 | 4.4 | C38H77N2O6P | EPC(d36:1) | Lipids: Sphingolipids | 1.09 | 1.09 | 0.97 | 0.5921 | 0.5599 | 0.9147 | 1.14 | 1.18 | 1.10 | 0.5044 | 0.2887 | 0.5800 |
| 730.5991 | 7.8 | C41H83N2O6P | SM(d36:1) | Lipids: Sphingolipids | 0.95 | 0.96 | 0.93 | 0.7375 | 0.5232 | 0.5688 | 1.06 | 1.01 | 1.04 | 0.4136 | 0.9481 | 0.8319 |
| 565.5439 | 4.1 | C36H71NO3 | Cer(d36:1) | Lipids: Sphingolipids | 1.13 | 0.99 | 0.92 | 0.6583 | 0.9369 | 0.7995 | 1.45 | 1.00 | 1.00 | 0.4759 | 0.9970 | 0.9941 |
| 700.5517 | 7.8 | C39H77N2O6P | SM(d34:2) | Lipids: Sphingolipids | 0.98 | 1.01 | 1.06 | 0.8099 | 0.9275 | 0.6502 | 1.03 | 0.98 | 1.07 | 0.6814 | 0.8364 | 0.4021 |
| 702.5675 | 7.8 | C39H79N2O6P | SM(d34:1) | Lipids: Sphingolipids | 0.97 | 1.02 | 1.06 | 0.7449 | 0.8645 | 0.6147 | 0.98 | 0.98 | 1.02 | 0.8011 | 0.8613 | 0.8205 |
| 700.5519 | 4.4 | C39H77N2O6P | EPC(d37:2) | Lipids: Sphingolipids | 1.13 | 1.02 | 0.99 | 0.1797 | 0.8559 | 0.9589 | 1.12 | 1.11 | 1.09 | 0.4735 | 0.4027 | 0.4320 |
| 728.5839 | 7.8 | C41H81N2O6P | SM(d36:2) | Lipids: Sphingolipids | 0.97 | 0.92 | 1.00 | 0.7938 | 0.2221 | 0.9992 | 1.00 | 1.02 | 1.01 | 0.9982 | 0.8348 | 0.9716 |
| 702.5677 | 4.4 | C39H79N2O6P | EPC(d37:1) | Lipids: Sphingolipids | 1.08 | 1.03 | 0.96 | 0.4497 | 0.8652 | 0.8742 | 1.15 | 1.15 | 1.08 | 0.3696 | 0.3424 | 0.5928 |
| 730.5996 | 4.4 | C41H83N2O6P | EPC(d39:1) | Lipids: Sphingolipids | 1.05 | 1.00 | 0.91 | 0.7309 | 0.9971 | 0.7596 | 1.12 | 1.10 | 0.98 | 0.4896 | 0.4828 | 0.9417 |
| 812.6778 | 4.8 | C47H93N2O6P | SM(d42:2) | Lipids: Sphingolipids | 1.07 | 1.11 | 0.88 | 0.3457 | 0.2621 | 0.4579 | 1.00 | 0.99 | 0.97 | 0.9811 | 0.9673 | 0.8272 |
| 461.3348 | 7.9 | C24H47NO7 | Psychosine | Lipids: Sphingolipids | 1.08 | 1.26 | 0.93 | 0.4725 | 0.5365 | 0.4814 | 1.16 | 1.07 | 1.05 | 0.5817 | 0.7483 | 0.8481 |
| 273.2670 | 7.1 | C16H35NO2 | Hexadecasphinganine | Lipids: Sphingolipids | 1.20 | 1.11 | 1.08 | 0.1565 | 0.1448 | 0.6517 | 1.02 | 1.01 | 0.92 | 0.9105 | 0.9616 | 0.7361 |
| 812.6778 | 4.4 | C47H93N2O6P | SM(d18:1/24:1(15Z)) | Lipids: Sphingolipids | 1.18 | 1.25 | 1.02 | 0.0831 | 0.1298 | 0.9259 | 1.15 | 1.01 | 1.06 | 0.2668 | 0.8820 | 0.6966 |
| 812.6778 | 7.1 | C47H93N2O6P | SM(d18:2/24:0) | Lipids: Sphingolipids | 1.22 | 1.15 | 1.03 | 0.1375 | 0.4408 | 0.8372 | 0.98 | 0.87 | 0.90 | 0.7284 | 0.2243 | 0.3818 |
| 537.5127 | 3.9 | C34H67NO3 | [SP (16:0)] N-(hexadecanoyl)-sphing-4-enine | Lipids: Sphingolipids | 1.28 | 1.13 | 0.93 | 0.0962 | 0.5416 | 0.7147 | 1.17 | 0.87 | 1.04 | 0.7527 | 0.7315 | 0.9450 |
| 315.2775 | 4.3 | C18H37NO3 | Dehydrophytosphingosine | Lipids: Sphingolipids | 1.50 | 0.97 | 1.65 | 0.5426 | 0.9636 | 0.3877 | 0.97 | 0.98 | 0.96 | 0.9192 | 0.8501 | 0.7385 |
| 381.2647 | 7.9 | C18H40NO5P | [SP] Sphinganine-1-phosphate | Lipids: Sphingolipids | 0.98 | 0.97 | 0.92 | 0.8999 | 0.8788 | 0.6578 | 1.14 | 0.98 | 0.84 | 0.8106 | 0.9662 | 0.7290 |
| 299.2825 | 5.0 | C18H37NO2 | [SP] Sphing-4-enine | Lipids: Sphingolipids | 1.04 | 1.08 | 0.80 | 0.8219 | 0.6543 | 0.2194 | 0.90 | 0.97 | 0.80 | 0.8653 | 0.9662 | 0.6903 |
| 392.2924 | 7.9 | C24H40O4 | Ursodiol | Lipids: Sterol lipids | 0.79 | 0.95 | 1.02 | 0.4435 | 0.8820 | 0.9354 | 1.07 | 1.34 | 1.01 | 0.7687 | 0.3212 | 0.9428 |
| 466.3119 | 3.7 | C27H46O4S | Cholesterolsulfate | Lipids: Sterol lipids | 1.06 | 1.13 | 0.99 | 0.4074 | 0.3855 | 0.9493 | 1.16 | 1.15 | 0.92 | 0.5225 | 0.3362 | 0.4254 |
| 408.2875 | 4.8 | C24H40O5 | Cholate | Lipids: Sterol lipids | 1.02 | 0.82 | 1.36 | 0.9379 | 0.1590 | 0.1729 | 1.04 | 0.97 | 1.15 | 0.6329 | 0.6614 | 0.4825 |
| 392.2925 | 4.8 | C24H40O4 | [ST hydrox] 3alpha,7alpha-Dihydroxy-5beta-cholan-24-oic Acid | Lipids: Sterol lipids | 0.89 | 1.03 | 1.20 | 0.6599 | 0.9298 | 0.1459 | 0.96 | 1.05 | 1.10 | 0.8406 | 0.7005 | 0.6170 |
| 382.3236 | 5.1 | C27H42O | [ST (3:0)] cholest-5Z,7Z,24-trien-3beta-ol | Lipids: Sterol lipids | 1.05 | 1.28 | 1.04 | 0.7571 | 0.4704 | 0.8587 | 1.05 | 1.02 | 1.07 | 0.1627 | 0.8298 | 0.3028 |
| 446.3759 | 4.0 | C29H50O3 | Nebrosteroid M | Lipids: Sterol lipids | 1.01 | 1.03 | 0.95 | 0.9563 | 0.9134 | 0.7523 | 1.09 | 0.79 | 1.00 | 0.5330 | 0.0852 | 0.9969 |
| 368.3444 | 3.8 | C27H44 | [ST] (5Z,7E)-9,10-seco-5,7,10(19)-cholestatriene | Lipids: Sterol lipids | 0.95 | 1.10 | 0.99 | 0.7149 | 0.6235 | 0.9361 | 0.91 | 0.99 | 1.05 | 0.6574 | 0.9685 | 0.7868 |
| 302.0607 | 14.0 | C8H18N2O6S2 | PIPES | Medium Component | 0.93 | 1.02 | 0.85 | 0.4706 | 0.8085 | 0.5712 | 1.04 | 1.12 | 0.93 | 0.8120 | 0.6177 | 0.5606 |
| 238.0985 | 10.4 | C8H18N2O4S | HEPES | Medium Component | 0.86 | 0.87 | 0.88 | 0.5614 | 0.4377 | 0.4966 | 0.84 | 1.02 | 1.13 | 0.2638 | 0.8858 | 0.6306 |
| 354.0563 | 7.9 | C19H14O5S | Phenolsulfonphthalein | Medium Component | 0.90 | 0.91 | 0.98 | 0.4127 | 0.4447 | 0.8618 | 1.04 | 1.11 | 1.02 | 0.6562 | 0.3578 | 0.8718 |
| 191.0254 | 14.7 | C6H9NO4S | a Cysteine adduct | Medium Contaminant | 1.47 | 0.56 | 1.71 | 0.2498 | 0.2552 | 0.2418 | 10.61 | 4.96 | 3.09 | 0.4401 | 0.4774 | 0.3516 |

| | | | | | | | | | | | | | | | | |
|---|---|---|---|---|---|---|---|---|---|---|---|---|---|---|---|---|
| 326.1226 | 12.8 | C13H18N4O6 | 6,7-Dimethyl-8-(1-D-ribityl)lumazine | Metabolism of Cofactors and Vitamins | 0.96 | 0.96 | 0.76 | 0.8072 | 0.8504 | 0.1137 | 1.59 | 1.54 | 1.25 | 0.6707 | 0.7047 | 0.8282 |
| 299.0770 | 14.9 | C9H18NO8P | D-4'-Phosphopantothenate | Metabolism of Cofactors and Vitamins | 0.86 | 0.98 | 0.69 | 0.5483 | 0.9076 | 0.1020 | 0.70 | 1.13 | 0.82 | 0.5712 | 0.8588 | 0.6370 |
| 249.0403 | 13.6 | C8H12NO6P | Pyridoxine phosphate | Metabolism of Cofactors and Vitamins | 0.92 | 0.97 | 1.21 | 0.5820 | 0.9064 | 0.1989 | 0.82 | 0.72 | 1.23 | 0.7007 | 0.5367 | 0.7062 |
| 214.1316 | 8.7 | C10H18N2O3 | Dethiobiotin | Metabolism of Cofactors and Vitamins | 0.81 | 0.84 | 0.75 | 0.0491 | 0.2779 | 0.0153 | 0.36 | 0.59 | 0.65 | 0.0978 | 0.2244 | 0.3874 |
| 144.0423 | 13.6 | C6H8O4 | 2,3-Dimethylmaleate | Metabolism of Cofactors and Vitamins | 0.53 | 0.57 | 2.00 | 0.3107 | 0.3475 | 0.1105 | 0.77 | 0.73 | 2.00 | 0.1308 | 0.2726 | 0.2932 |
| 169.0739 | 8.3 | C8H11NO3 | Pyridoxine | Metabolism of Cofactors and Vitamins | 1.08 | 1.01 | 1.15 | 0.4601 | 0.8994 | 0.1620 | 0.98 | 0.80 | 1.27 | 0.9404 | 0.5478 | 0.4930 |
| 264.1044 | 19.8 | C12H16N4OS | Thiamin | Metabolism of Cofactors and Vitamins | 0.95 | 1.07 | 0.90 | 0.7488 | 0.6202 | 0.5996 | 0.97 | 0.93 | 0.97 | 0.8608 | 0.7023 | 0.8936 |
| 239.1023 | 9.6 | C9H13N5O3 | Dihydrobiopterin | Metabolism of Cofactors and Vitamins | 0.85 | 0.92 | 0.84 | 0.3234 | 0.5695 | 0.3470 | 0.86 | 1.07 | 1.04 | 0.1793 | 0.4706 | 0.8020 |
| 183.0532 | 7.9 | C8H9NO4 | 4-Pyridoxate | Metabolism of Cofactors and Vitamins | 1.14 | 1.11 | 1.03 | 0.1856 | 0.6763 | 0.7739 | 1.00 | 0.95 | 1.08 | 0.9895 | 0.7531 | 0.5452 |
| 255.0738 | 11.4 | C11H13NO6 | Nicotinate D-ribonucleoside | Metabolism of Cofactors and Vitamins | 1.07 | 1.06 | 1.33 | 0.8214 | 0.8152 | 0.3603 | 0.83 | 0.96 | 1.05 | 0.2074 | 0.6793 | 0.8134 |
| 334.0568 | 15.2 | C11H15N2O8P | Nicotinamide D-ribonucleotide | Metabolism of Cofactors and Vitamins | 1.05 | 1.15 | 0.87 | 0.7169 | 0.3608 | 0.2253 | 0.95 | 0.97 | 0.94 | 0.7174 | 0.8336 | 0.7726 |
| 225.0637 | 12.9 | C10H11NO5 | 4-Amino-4-deoxychorismate | Metabolism of Cofactors and Vitamins | 0.87 | 1.02 | 1.13 | 0.4405 | 0.8834 | 0.4488 | 0.60 | 0.99 | 0.87 | 0.0476 | 0.9744 | 0.1509 |
| 122.0480 | 7.9 | C6H6N2O | Nicotinamide | Metabolism of Cofactors and Vitamins | 1.25 | 0.98 | 0.80 | 0.5689 | 0.9558 | 0.2338 | 0.94 | 1.02 | 1.06 | 0.8163 | 0.9204 | 0.7959 |
| 144.0423 | 14.3 | C6H8O4 | Methylitaconate | Metabolism of Cofactors and Vitamins | 1.62 | 1.32 | 1.27 | 0.2913 | 0.5515 | 0.3468 | 0.80 | 1.04 | 1.34 | 0.2287 | 0.8596 | 0.2937 |
| 115.0270 | 14.9 | C4H5NO3 | Maleamate | Metabolism of Cofactors and Vitamins | 1.40 | 1.42 | 1.07 | 0.4180 | 0.4614 | 0.8156 | 0.94 | 0.96 | 0.95 | 0.8041 | 0.8787 | 0.8529 |
| 167.0582 | 8.2 | C8H9NO3 | Pyridoxal | Metabolism of Cofactors and Vitamins | 0.92 | 1.09 | 0.83 | 0.7485 | 0.6652 | 0.3344 | 0.63 | 1.15 | 0.70 | 0.1601 | 0.7267 | 0.2332 |
| 187.1209 | 11.8 | C9H17NO3 | 8-Amino-7-oxononanoate | Metabolism of Cofactors and Vitamins | 1.08 | 1.24 | 1.13 | 0.5325 | 0.2266 | 0.4131 | 0.90 | 0.95 | 0.91 | 0.7449 | 0.8765 | 0.7530 |
| 323.0521 | 16.2 | C9H14N3O8P | CMP | Nucleotide Metabolism | 0.97 | 1.20 | 0.85 | 0.8425 | 0.3113 | 0.2860 | 1.71 | 2.28 | 1.26 | 0.6578 | 0.4560 | 0.8295 |
| 348.0472 | 15.2 | C10H13N4O8P | IMP | Nucleotide Metabolism | 0.78 | 0.76 | 1.33 | 0.4145 | 0.4426 | 0.3868 | 1.82 | 1.54 | 1.26 | 0.5732 | 0.6149 | 0.6750 |
| 176.0432 | 16.4 | C5H8N2O5 | N-Carbamoyl-L-aspartate | Nucleotide Metabolism | 0.73 | 0.69 | 0.95 | 0.0446 | 0.0358 | 0.7279 | 0.47 | 0.47 | 0.96 | 0.4155 | 0.4046 | 0.9623 |
| 135.0545 | 9.7 | C5H5N5 | Adenine | Nucleotide Metabolism | 1.05 | 0.92 | 1.40 | 0.7626 | 0.5872 | 0.2575 | 0.98 | 0.95 | 1.00 | 0.9319 | 0.8214 | 0.9781 |
| 307.0570 | 15.2 | C9H14N3O7P | dCMP | Nucleotide Metabolism | 1.02 | 1.06 | 0.93 | 0.6326 | 0.2530 | 0.2110 | 0.95 | 1.00 | 1.09 | 0.7060 | 0.9835 | 0.7008 |
| 158.0327 | 10.8 | C5H6N2O4 | (S)-Dihydroorotate | Nucleotide Metabolism | 0.77 | 0.90 | 1.12 | 0.2077 | 0.6846 | 0.4327 | 0.52 | 0.48 | 1.35 | 0.3970 | 0.3534 | 0.7668 |
| 97.9675 | 15.9 | H2O4S | Sulfate | Nucleotide Metabolism | 0.80 | 0.98 | 0.93 | 0.4276 | 0.9430 | 0.8203 | 0.89 | 1.15 | 0.56 | 0.7216 | 0.4513 | 0.0338 |
| 404.0023 | 16.0 | C9H14N2O12P2 | UDP | Nucleotide Metabolism | 0.99 | 1.04 | 0.88 | 0.9728 | 0.7807 | 0.4208 | 1.08 | 1.17 | 0.98 | 0.8661 | 0.7131 | 0.9711 |
| 347.0630 | 13.6 | C10H14N5O7P | AMP | Nucleotide Metabolism | 1.12 | 0.95 | 1.20 | 0.5809 | 0.7443 | 0.4970 | 1.01 | 1.05 | 1.05 | 0.9483 | 0.8088 | 0.8299 |
| 136.0385 | 10.2 | C5H4N4O | Hypoxanthine | Nucleotide Metabolism | 1.10 | 1.00 | 1.06 | 0.4285 | 0.9766 | 0.4655 | 0.93 | 0.94 | 0.94 | 0.2919 | 0.3170 | 0.5566 |
| 128.0586 | 14.8 | C5H8N2O2 | 5,6-Dihydrothymine | Nucleotide Metabolism | 1.02 | 0.94 | 1.09 | 0.8469 | 0.5339 | 0.5181 | 1.22 | 1.41 | 0.90 | 0.6488 | 0.4059 | 0.7199 |

| | | | | | | | | | | | | | | | | | |
|---|---|---|---|---|---|---|---|---|---|---|---|---|---|---|---|---|---|
| 267.0966 | 9.2 | C10H13N5O4 | Adenosine | Nucleotide Metabolism | 0.89 | 1.04 | 1.06 | 0.4867 | 0.9072 | 0.8292 | 0.90 | 0.91 | 0.89 | 0.5400 | 0.5548 | 0.4409 |
| 268.0808 | 10.9 | C10H12N4O5 | Inosine | Nucleotide Metabolism | 0.89 | 1.15 | 0.56 | 0.6714 | 0.5524 | 0.1241 | 0.84 | 0.99 | 0.64 | 0.5450 | 0.9593 | 0.2697 |
| 338.0622 | 15.5 | C9H15N4O8P | 1-(5'-Phosphoribosyl)-5-amino-4-imidazolecarboxamide | Nucleotide Metabolism | 0.90 | 1.09 | 0.93 | 0.1937 | 0.7098 | 0.5566 | 0.98 | 0.89 | 1.01 | 0.9020 | 0.6083 | 0.9788 |
| 428.0135 | 16.5 | C10H14N4O11P2 | IDP | Nucleotide Metabolism | 0.95 | 1.03 | 1.76 | NA | NA | 0.6425 | 0.58 | 0.82 | 0.77 | 0.4767 | 0.7993 | 0.7403 |
| 351.1577 | 9.8 | C20H21N3O3 | Phe-Trp | Peptide(di-) | 0.55 | 0.25 | 2.33 | 0.4667 | 0.2496 | 0.2491 | 1.03 | 0.77 | 4.42 | 0.8675 | 0.1645 | 0.3368 |
| 243.1583 | 15.2 | C11H21N3O3 | Lys-Pro | Peptide(di-) | 0.56 | 0.64 | 0.66 | 0.0111 | 0.0214 | 0.0814 | 0.42 | 0.42 | 0.44 | 0.2218 | 0.2256 | 0.1705 |
| 174.1004 | 13.5 | C7H14N2O3 | Val-Gly | Peptide(di-) | 0.95 | 0.85 | 1.05 | 0.8322 | 0.5039 | 0.8432 | 1.11 | 1.22 | 1.19 | 0.8050 | 0.7038 | 0.6752 |
| 216.1110 | 11.4 | C9H16N2O4 | Thr-Pro | Peptide(di-) | 0.58 | 0.57 | 0.67 | 0.0109 | 0.0058 | 0.0422 | 0.43 | 0.52 | 0.45 | 0.1612 | 0.2440 | 0.1834 |
| 212.0909 | 11.8 | C8H12N4O3 | Gly-His | Peptide(di-) | 0.76 | 0.74 | 0.68 | 0.1927 | 0.0875 | 0.1242 | 0.43 | 0.49 | 0.43 | 0.1573 | 0.1823 | 0.1788 |
| 186.1006 | 11.3 | C8H14N2O3 | Ala-Pro | Peptide(di-) | 0.67 | 0.61 | 0.62 | 0.1136 | 0.0648 | 0.1027 | 0.45 | 0.39 | 0.45 | 0.1231 | 0.0850 | 0.1469 |
| 176.0797 | 11.5 | C6H12N2O4 | Ala-Ser | Peptide(di-) | 0.88 | 0.80 | 0.74 | 0.4717 | 0.2889 | 0.2954 | 0.62 | 0.67 | 0.67 | 0.1057 | 0.1039 | 0.1216 |
| 247.0805 | 15.5 | C8H13N3O6 | Asn-Asp | Peptide(di-) | 0.79 | 0.81 | 0.60 | 0.2282 | 0.2435 | 0.0288 | 0.71 | 0.73 | 0.57 | 0.0911 | 0.0941 | 0.0219 |
| 204.0745 | 14.5 | C7H12N2O5 | Ala-Asp | Peptide(di-) | 0.80 | 0.81 | 0.68 | 0.4383 | 0.2859 | 0.2736 | 0.75 | 0.70 | 0.65 | 0.1010 | 0.0338 | 0.0885 |
| 244.1059 | 14.9 | C10H16N2O5 | Glu-Pro | Peptide(di-) | 0.89 | 0.72 | 0.85 | 0.4729 | 0.1041 | 0.3879 | 0.72 | 0.52 | 0.63 | 0.3598 | 0.0646 | 0.2990 |
| 232.1057 | 12.7 | C9H16N2O5 | Val-Asp | Peptide(di-) | 0.95 | 1.01 | 0.86 | 0.6714 | 0.9504 | 0.0227 | 0.91 | 0.98 | 1.01 | 0.4432 | 0.8736 | 0.9012 |
| 261.1324 | 16.4 | C10H19N3O5 | Lys-Asp | Peptide(di-) | 0.88 | 0.87 | 0.74 | 0.4209 | 0.3159 | 0.0805 | 0.93 | 0.88 | 0.84 | 0.5158 | 0.2492 | 0.1266 |
| 190.0590 | 15.2 | C6H10N2O5 | Asp-Gly | Peptide(di-) | 0.99 | 0.97 | 1.03 | 0.8780 | 0.7380 | 0.6441 | 0.90 | 0.95 | 0.78 | 0.1691 | 0.7442 | 0.1075 |
| 234.0851 | 15.3 | C8H14N2O6 | Glu-Ser | Peptide(di-) | 0.89 | 0.79 | 0.83 | 0.5062 | 0.2545 | 0.3045 | 0.70 | 0.79 | 0.75 | 0.0238 | 0.2222 | 0.0204 |
| 262.0803 | 16.8 | C9H14N2O7 | Glu-Asp | Peptide(di-) | 1.10 | 1.01 | 0.94 | 0.6258 | 0.9584 | 0.7053 | 0.75 | 0.93 | 0.96 | 0.0104 | 0.5075 | 0.6628 |
| 220.0695 | 15.5 | C7H12N2O6 | Asp-Ser | Peptide(di-) | 1.00 | 0.97 | 0.87 | 0.9816 | 0.7995 | 0.0783 | 0.85 | 0.98 | 0.86 | 0.1100 | 0.8242 | 0.0438 |
| 248.0645 | 17.0 | C8H12N2O7 | Asp-Asp | Peptide(di-) | 0.95 | 0.92 | 1.01 | 0.7815 | 0.6750 | 0.9660 | 0.82 | 0.95 | 0.92 | 0.0557 | 0.7580 | 0.4832 |
| 344.1371 | 4.6 | C18H20N2O5 | Tyr-Tyr | Peptide(di-) | 1.06 | 1.11 | 1.18 | 0.7968 | 0.7658 | 0.3567 | 1.31 | 1.08 | 1.06 | 0.1146 | 0.7274 | 0.6831 |
| 246.1214 | 13.6 | C10H18N2O5 | Glu-Val | Peptide(di-) | 1.12 | 1.03 | 1.15 | 0.1622 | 0.7076 | 0.2584 | 1.01 | 1.01 | 1.12 | 0.9044 | 0.9040 | 0.2476 |
| 229.1062 | 13.7 | C9H15N3O4 | Asn-Pro | Peptide(di-) | 1.23 | 0.98 | 1.27 | 0.1981 | 0.8697 | 0.2430 | 0.99 | 1.01 | 1.15 | 0.9315 | 0.9501 | 0.4925 |
| 231.1219 | 13.6 | C9H17N3O4 | Val-Asn | Peptide(di-) | 0.85 | 0.74 | 0.86 | 0.6982 | 0.4206 | 0.6740 | 1.06 | 0.99 | 0.91 | 0.8390 | 0.9617 | 0.8442 |
| 218.1268 | 13.0 | C9H18N2O4 | Leu-Ser | Peptide(di-) | 1.15 | 1.27 | 1.13 | 0.1567 | 0.2675 | 0.3285 | 1.37 | 1.25 | 1.12 | 0.2861 | 0.4528 | 0.6265 |
| 289.1386 | 16.4 | C10H19N5O5 | Asp-Arg | Peptide(di-) | 0.98 | 1.10 | 0.95 | 0.7875 | 0.1481 | 0.4699 | 0.99 | 0.97 | 0.98 | 0.9679 | 0.9074 | 0.9536 |
| 245.1739 | 21.8 | C11H23N3O3 | Lys-Val | Peptide(di-) | 1.12 | 1.15 | 1.23 | 0.7849 | 0.7590 | 0.6340 | 0.82 | 0.76 | 1.08 | 0.4217 | 0.3039 | 0.7140 |
| 248.1008 | 14.6 | C9H16N2O6 | Glu-Thr | Peptide(di-) | 1.01 | 1.10 | 0.96 | 0.9779 | 0.5968 | 0.8753 | 0.71 | 0.85 | 0.92 | 0.1596 | 0.3140 | 0.5113 |
| 277.1095 | 12.3 | C10H19N3O4S | Met-Gln | Peptide(di-) | 1.02 | 0.77 | 0.86 | 0.9585 | 0.5950 | 0.7361 | 1.00 | 0.84 | 0.93 | 0.9981 | 0.6503 | 0.9056 |
| 202.1318 | 12.8 | C9H18N2O3 | Leu-Ala | Peptide(di-) | 1.04 | 1.07 | 1.08 | 0.4983 | 0.2721 | 0.3233 | 1.03 | 1.06 | 1.03 | 0.9354 | 0.8577 | 0.9423 |
| 228.1474 | 13.1 | C11H20N2O3 | Leu-Pro | Peptide(di-) | 1.08 | 1.03 | 1.12 | 0.5581 | 0.8173 | 0.4497 | 0.93 | 0.96 | 0.93 | 0.5765 | 0.8108 | 0.4810 |
| 260.1372 | 10.9 | C11H20N2O5 | Glu-Leu | Peptide(di-) | 1.14 | 1.20 | 1.12 | 0.7138 | 0.6887 | 0.7648 | 0.79 | 0.88 | 0.95 | 0.4930 | 0.6996 | 0.8221 |
| 246.1215 | 12.2 | C10H18N2O5 | Leu-Asp | Peptide(di-) | 1.06 | 1.24 | 1.04 | 0.8352 | 0.6040 | 0.9056 | 0.75 | 0.90 | 0.86 | 0.4142 | 0.7506 | 0.3801 |
| 220.1061 | 13.0 | C8H16N2O5 | Thr-Thr | Peptide(di-) | 1.21 | 1.16 | 1.26 | 0.7232 | 0.7729 | 0.6696 | 0.79 | 0.88 | 0.89 | 0.5409 | 0.7676 | 0.5238 |
| 233.1375 | 13.0 | C9H19N3O4 | Lys-Ser | Peptide(di-) | 1.06 | 1.14 | 1.26 | 0.8723 | 0.7860 | 0.6063 | 0.87 | 0.87 | 0.94 | 0.7187 | 0.7232 | 0.8303 |
| 190.0954 | 11.9 | C7H14N2O4 | Thr-Ala | Peptide(di-) | 1.13 | 1.24 | 1.18 | 0.8077 | 0.6600 | 0.7232 | 0.78 | 0.92 | 0.91 | 0.6409 | 0.8874 | 0.7875 |
| 204.1109 | 11.9 | C8H16N2O4 | Val-Ser | Peptide(di-) | 1.23 | 1.24 | 1.27 | 0.6736 | 0.6450 | 0.6021 | 0.83 | 0.92 | 0.95 | 0.7190 | 0.8696 | 0.8866 |
| 188.1161 | 13.6 | C8H16N2O3 | Val-Ala | Peptide(di-) | 1.08 | 1.17 | 1.22 | 0.8487 | 0.7441 | 0.6545 | 0.74 | 0.92 | 0.88 | 0.4900 | 0.8670 | 0.7008 |
| 484.1925 | 15.2 | C19H28N6O9 | Ala-Glu-Glu-His | Peptide(tetra-) | 0.87 | 0.71 | 0.61 | 0.6395 | 0.2481 | 0.1176 | 0.48 | 0.50 | 0.48 | 0.0844 | 0.0889 | 0.0799 |

| | | | | | | | | | | | | | | | | |
|---|---|---|---|---|---|---|---|---|---|---|---|---|---|---|---|---|
| 520.1961 | 14.1 | C19H32N6O9S | Asp-Met-Gln-Gln | Peptide(tetra-) | 1.26 | 0.87 | 1.09 | 0.7332 | 0.7479 | 0.8907 | 1.36 | 1.09 | 1.05 | 0.4556 | 0.8348 | 0.9469 |
| 624.3495 | 14.7 | C30H44N10O5 | Arg-Phe-Phe-Arg | Peptide(tetra-) | 1.65 | 1.05 | 1.30 | 0.2966 | 0.9222 | 0.4840 | 1.13 | 1.46 | 1.95 | 0.6362 | 0.4068 | 0.3722 |
| 426.0876 | 16.8 | C13H22N4O8S2 | Asp-Cys-Cys-Ser | Peptide(tetra-) | 0.63 | 0.76 | 0.80 | 0.1972 | 0.3371 | 0.4255 | 0.83 | 1.36 | 1.62 | 0.5793 | 0.3982 | 0.3869 |
| 558.2554 | 14.7 | C25H34N8O7 | Gln-Phe-Gln-His | Peptide(tetra-) | 1.42 | 1.08 | 1.28 | 0.3960 | 0.8738 | 0.4893 | 1.11 | 1.39 | 1.37 | 0.6944 | 0.4649 | 0.4999 |
| 439.2431 | 10.9 | C20H33N5O6 | Asn-Leu-Pro-Pro | Peptide(tetra-) | 0.82 | 0.53 | 0.57 | 0.2882 | 0.0142 | 0.1790 | 0.47 | 0.35 | 0.15 | 0.0395 | 0.0050 | 0.0007 |
| 500.1765 | 10.2 | C21H32N4O6S2 | Cys-Met-Phe-Thr | Peptide(tetra-) | 1.11 | 0.99 | 0.91 | 0.5833 | 0.9404 | 0.6633 | 1.33 | 1.04 | 1.23 | 0.2153 | 0.9057 | 0.2511 |
| 498.1791 | 10.6 | C21H30N4O8S | Asp-Met-Phe-Ser | Peptide(tetra-) | 1.01 | 0.99 | 0.92 | 0.9634 | 0.9184 | 0.5039 | 1.22 | 1.13 | 1.02 | 0.3076 | 0.4731 | 0.6641 |
| 445.2542 | 13.4 | C19H35N5O7 | Ala-Leu-Lys-Asp | Peptide(tetra-) | 0.88 | 0.91 | 1.01 | 0.5657 | 0.5961 | 0.9853 | 1.08 | 1.04 | 0.83 | 0.7505 | 0.8855 | 0.6260 |
| 459.2075 | 9.2 | C17H29N7O8 | Asn-Val-Asn-Asn | Peptide(tetra-) | 0.83 | 1.06 | 0.77 | 0.1165 | 0.6266 | 0.3486 | 1.01 | 1.17 | 1.16 | 0.9515 | 0.0500 | 0.0611 |
| 471.2335 | 12.4 | C20H33N5O8 | Asn-Glu-Ile-Pro | Peptide(tetra-) | 0.91 | 0.93 | 0.98 | 0.5254 | 0.5441 | 0.8156 | 0.90 | 0.98 | 0.96 | 0.4457 | 0.9396 | 0.8349 |
| 374.2163 | 14.6 | C16H30N4O6 | Ala-Leu-Thr-Ala | Peptide(tetra-) | 1.01 | 1.10 | 0.98 | 0.9231 | 0.4636 | 0.7367 | 1.00 | 1.06 | 1.12 | 0.9900 | 0.7407 | 0.4501 |
| 390.1745 | 17.2 | C15H26N4O8 | Ala-Val-Asp-Ser | Peptide(tetra-) | 0.83 | 1.04 | 0.90 | 0.1557 | 0.8436 | 0.2092 | 0.88 | 0.93 | 1.02 | 0.4831 | 0.6354 | 0.8151 |
| 461.1866 | 17.8 | C16H27N7O9 | Arg-Asp-Asp-Gly | Peptide(tetra-) | 0.94 | 0.99 | 1.03 | 0.5294 | 0.9054 | 0.6992 | 0.80 | 0.92 | 0.95 | 0.0301 | 0.3503 | 0.5917 |
| 498.1791 | 9.7 | C21H30N4O8S | Asp-Val-Cys-Tyr | Peptide(tetra-) | 0.99 | 1.02 | 0.83 | 0.9411 | 0.9072 | 0.2520 | 1.07 | 1.01 | 0.95 | 0.6135 | 0.9236 | 0.7281 |
| 550.3109 | 15.7 | C26H42N6O7 | Gln-Leu-Lys-Tyr | Peptide(tetra-) | 0.89 | 0.77 | 0.95 | 0.0711 | 0.4061 | 0.6211 | 0.90 | 1.05 | 0.73 | 0.7727 | 0.7219 | 0.3282 |
| 376.1595 | 17.1 | C14H24N4O8 | Ala-Thr-Ala-Asp | Peptide(tetra-) | 1.01 | 1.05 | 0.97 | 0.9135 | 0.7233 | 0.5722 | 0.93 | 0.97 | 1.02 | 0.2121 | 0.6625 | 0.7806 |
| 716.2952 | 10.5 | C40H40N6O7 | Trp-Trp-Tyr-Tyr | Peptide(tetra-) | 0.81 | 0.89 | 0.88 | 0.3587 | 0.5533 | 0.6083 | 0.87 | 1.02 | 1.19 | 0.3327 | 0.8684 | 0.3298 |
| 424.1593 | 11.3 | C18H24N4O8 | Ala-Asp-Gly-Tyr | Peptide(tetra-) | 1.16 | 1.00 | 1.15 | 0.1328 | 0.9831 | 0.0192 | 1.04 | 1.12 | 1.06 | 0.8817 | 0.5868 | 0.8040 |
| 498.1790 | 10.2 | C21H30N4O8S | Ala-Met-Asp-Tyr | Peptide(tetra-) | 1.05 | 1.08 | 1.00 | 0.7967 | 0.6320 | 0.9936 | 1.18 | 1.08 | 0.99 | 0.2879 | 0.6654 | 0.9682 |
| 500.1772 | 9.9 | C21H32N4O6S2 | Cys-Leu-Cys-Tyr | Peptide(tetra-) | 1.12 | 1.15 | 1.02 | 0.6169 | 0.5000 | 0.9192 | 1.16 | 1.12 | 0.90 | 0.3654 | 0.4793 | 0.4426 |
| 489.2437 | 13.9 | C20H35N5O9 | Asp-Leu-Lys-Asp | Peptide(tetra-) | 0.99 | 1.02 | 1.10 | 0.9264 | 0.8546 | 0.4474 | 1.07 | 1.12 | 0.89 | 0.7987 | 0.6615 | 0.5879 |
| 318.1539 | 17.8 | C12H22N4O6 | Ala-Ala-Ala-Ser | Peptide(tetra-) | 1.00 | 1.01 | 1.15 | 0.9508 | 0.9411 | 0.2886 | 1.00 | 0.94 | 1.11 | 0.9260 | 0.3962 | 0.1088 |
| 382.1312 | 10.8 | C16H22N4O5S | Cys-Phe-Gly-Gly | Peptide(tetra-) | 0.49 | 1.19 | 0.75 | 0.2868 | 0.8353 | 0.6893 | 0.49 | 1.66 | 0.75 | 0.1094 | 0.4384 | 0.4916 |
| 318.1539 | 16.1 | C12H22N4O6 | Ala-Thr-Ala-Gly | Peptide(tetra-) | 1.06 | 1.04 | 1.00 | 0.2940 | 0.6548 | 0.9687 | 1.00 | 1.00 | 0.99 | 0.9963 | 0.9681 | 0.9194 |
| 348.1645 | 16.4 | C13H24N4O7 | Ala-Thr-Ala-Ser | Peptide(tetra-) | 1.09 | 1.13 | 1.03 | 0.2795 | 0.4789 | 0.8108 | 1.12 | 1.11 | 0.99 | 0.2521 | 0.2284 | 0.9193 |
| 251.1558 | 22.0 | C22H42N6O7 | Asp-Leu-Lys-Lys | Peptide(tetra-) | 1.02 | 1.04 | 1.08 | 0.8390 | 0.4511 | 0.2269 | 0.75 | 0.81 | 0.87 | 0.1846 | 0.3630 | 0.4155 |
| 374.1920 | 15.7 | C14H26N6O6 | Asn-Lys-Gly-Gly | Peptide(tetra-) | 1.00 | 1.28 | 1.10 | 0.9813 | 0.1155 | 0.4683 | 0.89 | 1.12 | 1.01 | 0.2923 | 0.5112 | 0.9511 |
| 556.2400 | 15.1 | C25H32N8O7 | Asn-Thr-Trp-His | Peptide(tetra-) | 0.94 | 1.13 | 0.79 | 0.8730 | 0.6736 | 0.6021 | 1.03 | 1.13 | 0.89 | 0.7694 | 0.5397 | 0.7398 |
| 213.6398 | 20.8 | C20H37N5O5 | Ala-Leu-Lys-Pro | Peptide(tetra-) | 1.11 | 0.95 | 1.12 | 0.2206 | 0.7091 | 0.4098 | 0.88 | 1.00 | 0.93 | 0.6626 | 0.9900 | 0.7862 |
| 394.1164 | 17.1 | C13H22N4O8S | Glu-Cys-Gly-Ser | Peptide(tetra-) | 1.10 | 1.09 | 0.89 | 0.4922 | 0.6651 | 0.5063 | 0.75 | 0.95 | 0.80 | 0.3719 | 0.8529 | 0.2761 |
| 376.1418 | 14.6 | C14H24N4O6S | Ala-Cys-Pro-Ser | Peptide(tetra-) | 1.41 | 0.00 | 0.75 | 0.6556 | NA | NA | 0.76 | 0.68 | 0.88 | 0.5709 | 0.6663 | 0.8564 |
| 243.1219 | 12.4 | C10H17N3O4 | Ala-Gly-Pro | Peptide(tri-) | 0.82 | 0.58 | 0.61 | 0.4719 | 0.0680 | 0.0600 | 0.26 | 0.26 | 0.39 | 0.1112 | 0.1111 | 0.2235 |
| 383.1802 | 10.9 | C16H25N5O6 | Glu-His-Val | Peptide(tri-) | 0.80 | 0.76 | 0.67 | 0.2587 | 0.1934 | 0.1631 | 0.46 | 0.49 | 0.35 | 0.1235 | 0.1108 | 0.0935 |
| 373.1483 | 16.6 | C15H23N3O8 | Glu-Glu-Pro | Peptide(tri-) | 0.81 | 0.74 | 0.45 | 0.4081 | 0.3097 | 0.0435 | 0.39 | 0.52 | 0.24 | 0.1076 | 0.1916 | 0.0540 |
| 229.1062 | 13.1 | C9H15N3O4 | Gly-Gly-Pro | Peptide(tri-) | 0.70 | 0.68 | 0.73 | 0.0339 | 0.1709 | 0.2775 | 0.45 | 0.47 | 0.47 | 0.0641 | 0.0553 | 0.0825 |
| 261.1329 | 13.2 | C10H19N3O5 | Val-Gly-Ser | Peptide(tri-) | 0.62 | 1.19 | 0.79 | 0.1033 | 0.7229 | 0.4850 | 0.46 | 1.12 | 0.92 | 0.2385 | 0.7980 | 0.8789 |
| 333.1539 | 11.2 | C13H23N3O7 | Glu-Ser-Val | Peptide(tri-) | 0.72 | 0.69 | 0.73 | 0.0314 | 0.0798 | 0.1754 | 0.41 | 0.51 | 0.36 | 0.0383 | 0.0826 | 0.0374 |
| 275.1484 | 11.5 | C11H21N3O5 | Leu-Gly-Ser | Peptide(tri-) | 0.50 | 1.03 | 0.76 | 0.1545 | 0.9457 | 0.5130 | 0.54 | 1.14 | 0.90 | 0.3078 | 0.7437 | 0.8565 |
| 319.1021 | 16.5 | C11H17N3O8 | Ala-Asp-Asp | Peptide(tri-) | 0.96 | 1.00 | 0.99 | 0.3812 | 0.9463 | 0.9205 | 0.92 | 1.02 | 0.92 | 0.2786 | 0.8944 | 0.5255 |
| 334.1856 | 15.4 | C13H26N4O6 | Lys-Thr-Ser | Peptide(tri-) | 0.99 | 0.98 | 1.01 | 0.9676 | 0.9177 | 0.9596 | 1.08 | 1.13 | 0.96 | 0.8378 | 0.7737 | 0.8940 |
| 348.2010 | 15.4 | C14H28N4O6 | Lys-Thr-Thr | Peptide(tri-) | 1.01 | 1.09 | 0.97 | 0.8811 | 0.4767 | 0.8381 | 1.11 | 1.00 | 0.92 | 0.7409 | 0.9872 | 0.7111 |

| | | | | | | | | | | | | | | | | | |
|---|---|---|---|---|---|---|---|---|---|---|---|---|---|---|---|---|---|
| 365.0890 | 16.1 | C12H19N3O8S | Glu-Asp-Cys | Peptide(tri-) | 0.90 | 1.03 | 0.88 | 0.3080 | 0.7317 | 0.2210 | 0.92 | 0.96 | 0.85 | 0.7756 | 0.9011 | 0.4832 |
| 408.2236 | 26.2 | C17H28N8O4 | Pro-Arg-His | Peptide(tri-) | 1.00 | 1.01 | 1.07 | 0.9576 | 0.8489 | 0.6631 | 1.16 | 1.09 | 1.04 | 0.2215 | 0.0395 | 0.6107 |
| 307.1015 | 16.8 | C10H17N3O8 | Asp-Ser-Ser | Peptide(tri-) | 0.73 | 1.07 | 0.84 | 0.4277 | 0.8362 | 0.6226 | 0.61 | 1.07 | 0.85 | 0.2043 | 0.8303 | 0.6416 |
| 408.1471 | 15.4 | C18H24N4O5S | Thr-Trp-Cys | Peptide(tri-) | 0.94 | 0.91 | 0.90 | 0.8794 | 0.8266 | 0.7985 | 1.10 | 1.14 | 0.94 | 0.6269 | 0.5809 | 0.8806 |
| 318.1177 | 15.3 | C11H18N4O7 | Ala-Asn-Asp | Peptide(tri-) | 1.03 | 1.11 | 1.08 | 0.8073 | 0.5893 | 0.5337 | 0.92 | 0.89 | 0.90 | 0.5430 | 0.4220 | 0.3760 |
| 305.0860 | 16.8 | C10H15N3O8 | Asp-Asp-Gly | Peptide(tri-) | 1.00 | 0.97 | 1.08 | 0.9461 | 0.5913 | 0.0761 | 0.84 | 0.88 | 0.94 | 0.1003 | 0.3319 | 0.6284 |
| 277.1096 | 12.7 | C10H19N3O4S | Met-Ala-Gly | Peptide(tri-) | 0.88 | 0.92 | 0.91 | 0.7095 | 0.8129 | 0.7776 | 1.58 | 1.34 | 1.25 | 0.5261 | 0.5682 | 0.7247 |
| 346.1599 | 17.7 | C12H22N6O6 | Asp-Gly-Arg | Peptide(tri-) | 1.00 | 0.99 | 0.98 | 0.9406 | 0.8846 | 0.6726 | 0.97 | 0.93 | 1.01 | 0.7502 | 0.5241 | 0.8997 |
| 351.1100 | 12.2 | C12H21N3O7S | Glu-Cys-Thr | Peptide(tri-) | 1.19 | 0.93 | 1.09 | 0.3572 | 0.7592 | 0.6710 | 0.88 | 0.86 | 1.01 | 0.5173 | 0.4339 | 0.8992 |
| 263.1119 | 15.2 | C9H17N3O6 | Ala-Ser-Ser | Peptide(tri-) | 1.04 | 1.13 | 1.26 | 0.8430 | 0.5283 | 0.3957 | 1.25 | 1.24 | 1.04 | 0.4732 | 0.2869 | 0.7844 |
| 261.0957 | 14.2 | C9H15N3O6 | Ala-Asp-Gly | Peptide(tri-) | 1.25 | 0.89 | 1.06 | 0.3419 | 0.4063 | 0.7923 | 1.02 | 1.01 | 0.95 | 0.9310 | 0.9276 | 0.7247 |
| 346.2212 | 17.5 | C15H30N4O5 | Leu-Lys-Ser | Peptide(tri-) | 0.93 | 1.16 | 1.01 | 0.4722 | 0.3603 | 0.9297 | 1.07 | 1.17 | 1.17 | 0.2243 | 0.2801 | 0.2315 |
| 317.1330 | 15.5 | C11H19N5O6 | Ala-Asn-Asn | Peptide(tri-) | 1.10 | 1.12 | 1.20 | 0.4942 | 0.3073 | 0.1622 | 0.85 | 1.18 | 0.97 | 0.0319 | 0.0594 | 0.7201 |
| 356.2423 | 21.1 | C17H32N4O4 | Leu-Lys-Pro | Peptide(tri-) | 1.02 | 0.98 | 1.03 | 0.7498 | 0.8397 | 0.4583 | 0.98 | 0.96 | 0.96 | 0.7974 | 0.7610 | 0.6653 |
| 291.1253 | 11.0 | C11H21N3O4S | Leu-Cys-Gly | Peptide(tri-) | 0.78 | 1.02 | 0.89 | 0.4875 | 0.9506 | 0.6654 | 0.80 | 1.03 | 0.83 | 0.5149 | 0.9119 | 0.6285 |
| 381.1721 | 8.8 | C18H27N3O4S | Leu-Phe-Cys | Peptide(tri-) | 1.02 | 1.09 | 0.84 | 0.9774 | 0.8860 | 0.6533 | 0.94 | 1.12 | 0.98 | 0.8250 | 0.7545 | 0.9719 |
| 335.1329 | 14.6 | C12H21N3O8 | Glu-Ser-Thr | Peptide(tri-) | 1.30 | 1.00 | 1.28 | 0.5934 | 0.9935 | 0.6417 | 1.03 | 1.21 | 1.19 | 0.9493 | 0.7369 | 0.7619 |
| 364.1203 | 9.3 | C16H20N4O4S | Trp-Cys-Gly | Peptide(tri-) | 0.78 | 1.25 | 1.08 | 0.4845 | 0.6511 | 0.8771 | 0.74 | 1.24 | 0.81 | 0.2040 | 0.5397 | 0.6447 |
| 317.1697 | 15.8 | C12H23N5O5 | Lys-Asn-Gly | Peptide(tri-) | 1.08 | 1.09 | 1.08 | 0.3639 | 0.3170 | 0.5066 | 0.73 | 0.73 | 0.88 | 0.1996 | 0.2091 | 0.5042 |
| 231.1217 | 12.9 | C9H17N3O4 | Ala-Ala-Ala | Peptide(tri-) | 0.79 | 0.68 | 0.75 | 0.6433 | 0.4553 | 0.4070 | 0.95 | 0.96 | 0.75 | 0.9126 | 0.8963 | 0.5554 |
| 275.0940 | 10.5 | C10H17N3O4S | Cys-Gly-Pro | Peptide(tri-) | 0.92 | 0.89 | 0.93 | 0.7938 | 0.7182 | 0.8081 | 1.09 | 1.07 | 0.84 | 0.8173 | 0.8589 | 0.7032 |
| 321.0996 | 12.7 | C11H19N3O6S | Glu-Ala-Cys | Peptide(tri-) | 0.99 | 1.07 | 1.18 | 0.9557 | 0.6348 | 0.2798 | 0.94 | 0.95 | 1.06 | 0.3838 | 0.7083 | 0.5033 |
| 335.1329 | 15.9 | C12H21N3O8 | Thr-Thr-Asp | Peptide(tri-) | 1.01 | 1.11 | 0.99 | 0.8266 | 0.4220 | 0.8647 | 1.01 | 1.04 | 1.00 | 0.9758 | 0.8684 | 0.9866 |
| 305.1224 | 14.8 | C11H19N3O7 | Glu-Ala-Ser | Peptide(tri-) | 1.33 | 1.42 | 1.50 | 0.4913 | 0.3104 | 0.3428 | 0.93 | 0.79 | 1.02 | 0.7276 | 0.1916 | 0.8288 |
| 291.1067 | 15.5 | C10H17N3O7 | Ala-Asp-Ser | Peptide(tri-) | 0.97 | 1.21 | 1.11 | 0.8814 | 0.3620 | 0.6513 | 0.86 | 0.85 | 0.93 | 0.5575 | 0.4278 | 0.5899 |
| 424.1896 | 14.3 | C18H28N6O4S | Phe-Cys-Arg | Peptide(tri-) | 0.66 | 0.60 | 0.73 | 0.4799 | 0.3810 | 0.5911 | 0.96 | 0.99 | 1.01 | 0.9539 | 0.9897 | 0.9935 |
| 365.1256 | 11.8 | C13H23N3O7S | Glu-Met-Ser | Peptide(tri-) | 1.57 | 1.67 | 1.45 | 0.1902 | 0.4326 | 0.4777 | 0.82 | 0.85 | 0.93 | 0.6770 | 0.7681 | 0.8713 |
| 188.1162 | 12.1 | C8H16N2O3 | Leucyl-Glycine | Peptides | 0.74 | 0.66 | 0.70 | 0.2593 | 0.1049 | 0.2991 | 0.95 | 0.89 | 0.95 | 0.8290 | 0.4922 | 0.7507 |
| 230.0902 | 15.2 | C9H14N2O5 | Aspartyl-Proline | Peptides | 1.33 | 0.97 | 1.09 | 0.3364 | 0.8723 | 0.7965 | 0.64 | 0.53 | 0.62 | 0.3775 | 0.2204 | 0.3699 |
| 178.0412 | 14.1 | C5H10N2O3S | Glycyl-Cysteine | Peptides | 1.10 | 1.06 | 1.08 | 0.3633 | 0.7523 | 0.4472 | 1.23 | 1.07 | 1.13 | 0.3529 | 0.7054 | 0.6083 |
| 289.1384 | 18.1 | C10H19N5O5 | Aspartyl-Arginine | Peptides | 0.90 | 1.13 | 1.01 | 0.6226 | 0.7399 | 0.9532 | 0.77 | 0.82 | 1.09 | 0.2204 | 0.3938 | 0.7470 |
| 245.1011 | 13.4 | C9H15N3O5 | Asparaginyl-Hydroxyproline | Peptides | 1.03 | 1.00 | 1.02 | 0.8371 | 1.0000 | 0.9203 | 0.85 | 1.10 | 1.05 | 0.0584 | 0.6752 | 0.4997 |
| 245.1010 | 12.5 | C9H15N3O5 | Hydroxyprolyl-Asparagine | Peptides | 1.08 | 1.13 | 1.10 | 0.5706 | 0.3388 | 0.7243 | 1.00 | 1.07 | 0.92 | 0.9624 | 0.6861 | 0.6322 |
| 114.0317 | 13.6 | C5H6O3 | cis-Acetylacrylate | Xenobiotics Biodegradation and Metabolism | 0.76 | 0.50 | 1.71 | 0.5441 | 0.2023 | 0.1403 | 0.94 | 1.00 | 1.44 | 0.6663 | 0.9975 | 0.3641 |
| 166.0267 | 14.9 | C8H6O4 | 4-Hydroxyphenylglyoxylate | Xenobiotics Biodegradation and Metabolism | 1.05 | 1.05 | 1.03 | 0.6346 | 0.6418 | 0.8692 | 1.11 | 1.10 | 0.97 | 0.3730 | 0.4233 | 0.7345 |
| 166.0266 | 14.0 | C8H6O4 | Phthalate | Xenobiotics Biodegradation and Metabolism | 1.09 | 1.05 | 1.05 | 0.5047 | 0.7615 | 0.8459 | 1.12 | 1.10 | 1.01 | 0.0731 | 0.4601 | 0.9524 |
| 137.0477 | 7.0 | C7H7NO2 | Anthranilate | Xenobiotics Biodegradation and Metabolism | 0.86 | 1.02 | 1.16 | 0.4152 | 0.9488 | 0.3896 | 1.06 | 1.07 | 1.06 | 0.5406 | 0.6582 | 0.6996 |

| | | | | | | | | | | | | | | | | | |
|---|---|---|---|---|---|---|---|---|---|---|---|---|---|---|---|---|---|
| 351.1099 | 12.8 | C12H21N3O7S | S-(2-Hydroxyethyl)glutathione | Xenobiotics Biodegradation and Metabolism | 0.99 | 0.81 | 1.01 | 0.9732 | 0.0937 | 0.9621 | 0.98 | 0.75 | 0.77 | 0.9230 | 0.0974 | 0.4064 |
| 137.0477 | 12.0 | C7H7NO2 | 4-Aminobenzoate | Xenobiotics Biodegradation and Metabolism | 2.46 | 2.27 | 2.71 | 0.1926 | 0.1484 | 0.1873 | 1.68 | 1.59 | 0.99 | 0.3751 | 0.3511 | 0.9664 |

# Appendix 7

# Comparison of the exposure time-dependence of the activities of synthetic ozonide antimalarials and dihydroartemisinin against K13 wild-type and mutant *Plasmodium falciparum* strains

Yang T, Xie SC, Cao P, Giannangelo C, McCaw J, Creek DJ, Charman SA, Klonis N, Tilley L. 2016. Comparison of the exposure time-dependence of the activities of synthetic ozonide antimalarials and dihydroartemisinin against K13 wild-type and mutant *Plasmodium falciparum* strains. Antimicrob Agents Chemother 60:4501-4510.

AMERICAN SOCIETY FOR MICROBIOLOGY | Antimicrobial Agents and Chemotherapy

# Comparison of the Exposure Time Dependence of the Activities of Synthetic Ozonide Antimalarials and Dihydroartemisinin against K13 Wild-Type and Mutant *Plasmodium falciparum* Strains

**Tuo Yang,[a] Stanley C. Xie,[a] Pengxing Cao,[b] Carlo Giannangelo,[c] James McCaw,[b,d,e] Darren J. Creek,[c] Susan A. Charman,[c] Nectarios Klonis,[a] Leann Tilley[a]**

Department of Biochemistry and Molecular Biology, Bio21 Molecular Science and Biotechnology Institute, The University of Melbourne, Melbourne, VIC, Australia[a]; School of Mathematics & Statistics, The University of Melbourne, Melbourne, VIC, Australia[b]; Monash Institute of Pharmaceutical Sciences, Faculty of Pharmacy and Pharmaceutical Sciences, Melbourne, VIC, Australia[c]; Centre for Epidemiology and Biostatistics, Melbourne School of Population and Global Health, The University of Melbourne, Melbourne, VIC, Australia[d]; Murdoch Childrens Research Institute, Royal Children's Hospital, Parkville, VIC, Australia[e]

**Fully synthetic endoperoxide antimalarials, namely, OZ277 (RBx11160; also known as arterolane) and OZ439 (artefenomel), have been approved for marketing or are currently in clinical development. We undertook an analysis of the kinetics of the *in vitro* responses of *Plasmodium falciparum* to the new ozonide antimalarials. For these studies we used a K13 mutant (artemisinin resistant) isolate from a region in Cambodia and a genetically matched (artemisinin sensitive) K13 revertant. We used a pulsed-exposure assay format to interrogate the time dependence of the response. Because the ozonides have physicochemical properties different from those of the artemisinins, assay optimization was required to ensure that the drugs were completely removed following the pulsed exposure. Like that of artemisinins, ozonide activity requires active hemoglobin degradation. Short pulses of the ozonides were less effective than short pulses of dihydroartemisinin; however, when early-ring-stage parasites were exposed to drugs for periods relevant to their *in vivo* exposure, the ozonide antimalarials were markedly more effective.**

*Plasmodium falciparum* caused 200 million malaria infections and 438,000 deaths in 2014 (1). While the rate is still very high, malaria deaths have in fact dropped steadily over the last decade, as countries where malaria is endemic have adopted World Health Organization (WHO)-recommended artemisinin-based combination therapies (ACTs) (2). The clinically used derivatives of artemisinin, such as artesunate and dihydroartemisinin (DHA), clear *P. falciparum* infections rapidly, providing prompt therapy for both uncomplicated and severe infections (3). A disadvantage of the artemisinins is their short *in vivo* half-lives (~1 h), with the consequent need for multidose treatment regimens (3) and coadministration with a longer-lived partner drug (4).

Because malaria treatment is so heavily reliant on artemisinin-based therapies, it is extremely concerning that resistance to this drug class is now evident in six Southeast Asian countries (5, 6). Resistance is associated with mutations in the β-propeller domain of a Kelch protein, K13 (PF3D7_1343700) (7). Resistance initially manifested as delayed parasite clearance, but reports of clinical failure (recrudescence of infections) are now increasing in areas with concomitant partner drug resistance (8, 9).

Another issue with the widespread application of the artemisinins is the difficulty of maintaining the supply. The parent compound is prepared by large-scale extraction from plants, and artemisinin derivatives are generated semisynthetically, with growth, harvest, and production processes taking about 18 months (10). Recent advances in production protocols (11) and heterologous production systems (12, 13) are helping to provide the >350 million artemisinin-based treatments supplied annually (14). Nonetheless, there is an urgent need for wholly synthetic endoperoxides that are as effective and as affordable as the currently used artemisinins. Preferably, these synthetic endoperoxides will show efficacy in shorter-course treatment regimens, and ideally, they will maintain activity against artemisinin-resistant strains (10).

Artemisinins have a 1,2,4-trioxane core incorporating an endoperoxide linkage that is essential for activity (15). In the early 1990s, fully synthetic symmetrical dispiro-1,2,4,5-tetraoxane compounds with promising antimalarial activity were generated (16). Further medicinal chemistry efforts revealed that the antimalarial activity is maximized when the steric environment of the peroxide bond is carefully controlled. Asymmetrical 1,2,4-trioxolanes, in which one side of the ozonide heterocycle is sterically hindered and the other is more accessible, exhibited excellent antimalarial activity along with good *in vivo* exposure, and they were developed for clinical use (17–20).

OZ277 (arterolane maleate; also called RBx11160) was the first synthetic ozonide to undergo clinical trials and is now marketed by Ranbaxy Pty. Ltd. in India (10, 21, 22). It has good activity

**Received** 13 March 2016 **Returned for modification** 28 March 2016
**Accepted** 3 May 2016

**Accepted manuscript posted online** 9 May 2016

**Citation** Yang T, Xie SC, Cao P, Giannangelo C, McCaw J, Creek DJ, Charman SA, Klonis N, Tilley L. 2016. Comparison of the exposure time dependence of the activities of synthetic ozonide antimalarials and dihydroartemisinin against K13 wild-type and mutant *Plasmodium falciparum* strains. Antimicrob Agents Chemother 60:4501–4510. doi:10.1128/AAC.00574-16.

Address correspondence to Leann Tilley, ltilley@unimelb.edu.au.

N.K. and L.T. contributed equally to this article.

Supplemental material for this article may be found at http://dx.doi.org/10.1128/AAC.00574-16.

against all asexual blood stages of *P. falciparum*; however, the half-life of OZ277 is only 2- to 3-fold longer than that of DHA, and plasma exposure is lower in malaria patients than in volunteers (23, 24). OZ439 (artefenomel) appears to be more promising, exhibiting a much longer *in vivo* elimination half-life (46 to 62 h) (25, 26), and is currently undergoing phase II clinical trials (10, 25). The extended exposure profile offers the possibility that it might be effective, in combination with a second agent, as a single-dose oral cure for malaria (10, 25).

As for the artemisinins, the peroxide bond is key to the antimalarial activity of the ozonides (27), consistent with the suggestion that they need to be activated by a reduced iron source in order to exert their activity. The involvement of carbon-centered radicals as the toxic species is supported by the observation that nitroxide radical spin trap compounds antagonize the activity of both artemisinins and OZ277 (28). Nonetheless, until now, it has not been demonstrated formally that the ozonides are activated via the same mechanism as that for the artemisinins, nor is it clear whether they offer improved efficacy against artemisinin-resistant parasites. We present here an analysis of the ability of ozonide antimalarials to prevent the multiplication of the laboratory strain 3D7 as well as that of a K13 mutant isolate from Cambodia and its genetically matched K13 revertant.

## MATERIALS AND METHODS

**Culture and tight synchronization of parasites.** 3D7, Cam3.II, and Cam3.II_rev parasite-infected red blood cells (RBCs) were cultured in complete medium containing RPMI 1640, 25 mM HEPES, pH 7.4, 2 g/liter sodium bicarbonate, 4 mM L-glutamine, 0.2% (wt/wt) D-glucose, 22 μg/ml gentamicin, and 0.5 mM hypoxanthine and supplemented with 5% (vol/vol) human serum and 0.25% AlbuMAX II. Cultures were incubated at 37°C in 1% $O_2$, 5% $CO_2$, and 94% $N_2$ (29).

To generate tightly synchronized parasites, cultures were presynchronized to a 5- to 10-h window with two sorbitol treatments, and schizonts were harvested using a 70% Percoll cushion (30) when the ring:schizont ratio was about 2:1 or when the flux of ring formation was judged to be sufficient for tight synchronization (31). The harvested schizonts were added to precultured RBCs (5% hematocrit) and incubated for 0.5 to 3 h on a shaker to maximize the generation of singly infected rings (32). Excess schizonts were removed by sorbitol treatment, and the tightly synchronized ring culture was adjusted to 1 to 2% parasitemia and incubated on a shaker to achieve the parasite age postinvasion needed for the drug pulse assay. The harvested schizonts were added to precultured RBCs (5% hematocrit) and incubated for 0.5 to 1.5 h on a shaker to maximize the generation of singly infected rings.

**Drug pulse assays, interaction assays, and washing protocols.** Drugs were serially diluted in complete medium, with or without 0.2% uninfected RBCs, in V-bottomed 96-well microplates. Culture was added to the drugs (0.2% final hematocrit, 1 to 2% final parasitemia) and incubated as required before washing four times with 200 μl of complete medium, with or without transferring the cultures to wells of a new plate (after the first wash). Unwashed samples containing drugs at >10× the 50% lethal concentration ($LC_{50}$) (standard extended-exposure assay) acted as controls for 100% parasite killing ($Pt_{kill}$). Parasitemia was also monitored in samples with no drug ($Pt_{control}$). Serial dilution factors were chosen in an effort to enable measurement of the minimum viability at high drug concentrations while giving good coverage of the concentration range resulting in 50% of the maximum killing effect. All assays were performed as technical duplicates.

Parasite viability was determined by measuring parasitemia in the cycle following drug treatment by flow cytometry using SYTO 61 (33). The culture medium was removed, and the cell pellets were resuspended in 20 μl SYTO 61 (2 μM in phosphate-buffered saline [PBS]), incubated for 15 min at room temperature, diluted to 200 μl, and incubated for 0.5 to 2 h before being measured. Viability was defined as the fraction of the parasite population that survived drug exposure and was able to multiply in the cycle following exposure to the drug with the same efficiency as that of the control. It is possible that some parasites enter a dormant state where they remain "viable" but unable to replicate within the period (>48 h) examined. Therefore, we used the term "viability (replication competence)" (*V*) to indicate that replication competence in the second cycle was measured. *V* was calculated using the measured parasitemias in the presence of zero drug ($Pt_{control}$) and in the presence of >10× the $LC_{50}$ ($Pt_{kill}$), as follows: $V = (Pt - Pt_{kill})/(Pt_{control} - Pt_{kill})$.

Nonlinear regression models were fitted to the data in Microsoft Excel by using the Solver add-in (34). $LC_{50}$ values correspond to the drug concentrations producing a 50% loss of parasite viability in a particular assay and were determined by fitting a simple sigmoidal function to the data.

For studies of drug activation, tightly synchronized parasites (1 to 1.5% parasitemia) were preincubated in the absence or presence of sublethal concentrations of BiPy (Sigma-Aldrich) or E64d (Sigma-Aldrich) for 1 h. Serial dilutions of DHA, OZ277, and OZ439 were prepared in separate plates and added to plates containing the preincubated parasites.

**Drug stability assays.** DHA, OZ277, and OZ439 (1 μM) were incubated for different times under the conditions used for standard assays in our laboratory (wells containing 200 μl RBCs at 0.2% hematocrit in V-bottomed plates) (31). The amount of drug activity remaining in the supernatant was determined by incubating serial dilutions of the supernatant with a parasite culture for >48 h under standard assay conditions before determinations of parasitemia and viability. The relative drug concentration was estimated from the supernatant dilution producing 50% viability, with reference to a parallel assay established using fresh drug.

## RESULTS

**A modified washing procedure is required to assess ozonide potency in pulsed-exposure assays.** We previously examined the responses of laboratory and field strains of *P. falciparum* to artemisinins by using drug assays designed to mimic *in vivo* exposure (31, 34). In this assay format, parasites are subjected to short drug pulses, and viability (replication competence) is monitored in the next life cycle. Parasites exhibit complex drug responses that depend on their age postinvasion, their genotype, and the duration of the drug exposure (34, 35).

In this work, we examined the responses of parasites to OZ277 and OZ439 pulses of different durations. Because the physicochemical properties of the ozonides are different from those of DHA, it was important to ensure complete removal of the drugs after the drug pulse to ensure that the activity was not overestimated. That is, the wash procedure needed to be sufficiently stringent to ensure that the drug was diluted to a level well below the inhibitory level.

Our standard protocol for performing pulse assays involves incubating cultures (200 μl; 0.2% hematocrit) with drugs in V-bottomed microplates for a specified period and then removing the drug by washing the cells four times with complete culture medium (containing 5% serum and 0.25% AlbuMax II) (31). In this procedure, the infected RBCs are maintained within the same microplate wells during the course of the assay. This approach is sufficient to dilute the concentration of highly soluble drugs present in the supernatant >10,000-fold. To test the efficiency of this procedure in removing the ozonides, suspensions of uninfected RBCs (0.1% hematocrit) were incubated for 3 h in the presence of drugs at concentrations of up to 2 μM, and the RBCs were washed using the standard protocol. In order to detect any drug activity remaining in the wells, we added aliquots of RBCs infected with

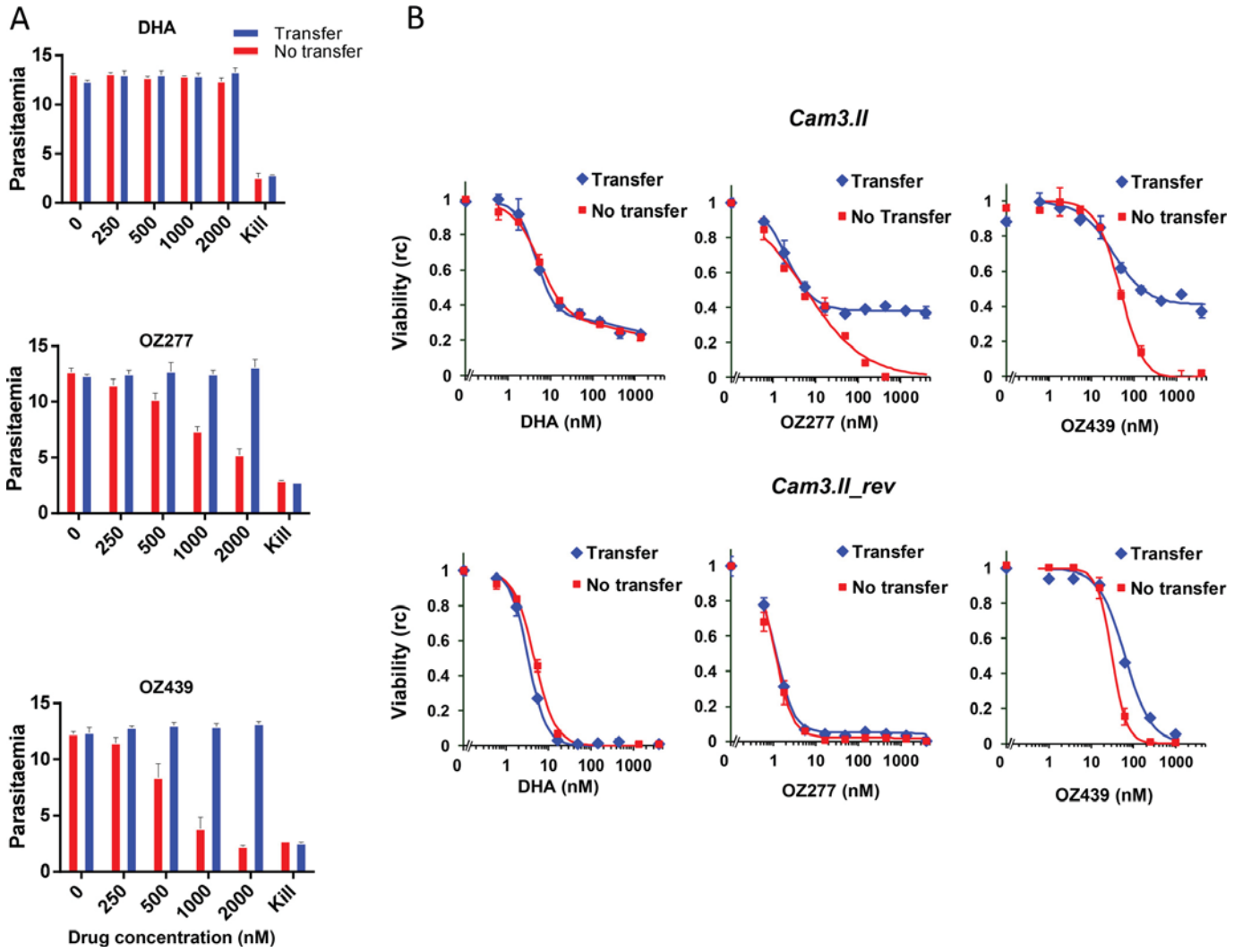


**FIG 1** Enhanced washing protocols are required for pulse assays of ozonide antimalarials. (A) The indicated concentrations of endoperoxides were incubated with RBCs (0.2% hematocrit) under standard culture conditions (complete medium, 37°C, V-bottomed microplate) for 3 h. The RBCs were washed using the standard protocol, with the cells maintained in their original well (red bars) or transferred to a fresh well (blue bars) prior to the addition of 200 μl of parasite-containing culture (0.1% hematocrit, 2 to 4% parasitemia, strain 3D7). The samples were then cultured for >48 h prior to determining viability (replication competence). Data represent the averages for two (OZ439) or one (DHA and OZ277) experiment, each with ≥2 technical replicates. (B) Early-ring-stage K13 mutant (Cam3.II) or revertant (Cam3.II_rev) cultures were incubated for 6 h with the indicated drugs. During a 4-step washing protocol, the cultures were maintained in their original wells (red symbols) or transferred to fresh wells (blue symbols). The samples were then cultured for >48 h prior to determination of viability (replication competence [rc]). Data represent a typical experiment of two independent experiments, each performed in duplicate.

the laboratory parasite 3D7 (2 to 4% parasitemia) to the washed uninfected RBCs and measured the parasitemia after culture for >48 h to allow the parasites to enter the next parasite cycle.

We found that DHA at concentrations of up to 2 μM was efficiently removed by the washing procedure, such that the parasitemia was unaffected (Fig. 1A, top panel). In contrast, wells incubated with ≥500 nM ozonides retained significant drug activity after the standard washing protocol, producing a reduction in the parasitemia during the postwash incubation period (Fig. 1A). For OZ439, 50% of parasites were rendered nonviable when the initial added concentration was between 500 and 1,000 nM. Given that the $LC_{50}$ for exposure times of >48 h ($LC_{50\_>48\ h}$) for OZ439 is ~9 nM (Table 1), this suggests that ~1% of the added OZ439 remained associated with the well. In contrast, when we modified the washing procedure so that the uninfected RBCs were transferred to fresh microplate wells after the first wash, there was little or no drug activity remaining (Fig. 1A). These results indicate that transferring the samples to fresh wells substantially improves the efficiency of washing.

**TABLE 1** Potencies of DHA and ozonides against different *P. falciparum* strains in standard assays (constant drug exposure for >48 h)

| Strain | $LC_{50>48\ h}$ (nM)[a] | | |
|---|---|---|---|
| | DHA | OZ277 | OZ439 |
| 3D7 | 2.6 ± 0.8 | 1.8 ± 0.7 | 8.7 ± 1.4 |
| Cam3.II | 2.3 ± 0.4 | 1.0 | 4.4 ± 0.7 |
| Cam3.II_rev | 2.4 ± 0.2 | 1.3 ± 0.1 | 6.1 ± 1.4 |

[a] Data are means ± standard deviations ($n = 3$).

Inefficient drug removal compromises the accuracy of determinations of drug potency, particularly under conditions where the concentration producing a 50% loss of viability is high, as in the case of the very early ring stage of artemisinin-resistant parasites from the field. To test this, we examined different washing protocols by using a laboratory-adapted field isolate from Cambodia (Cam3.II; K13 mutant) that was previously shown to exhibit reduced sensitivity to DHA (35, 36). We also employed a reverted transfectant in the same line (Cam3.II_rev), in which the *K13* wild-type genotype has been restored (36).

We added drugs at the least sensitive (very early ring) stage of the K13 mutant for a period of 6 h, washed the cultures, and examined viability after >48 h (Fig. 1B, top panels). The dose-response profile obtained with DHA was unaffected by the washing protocol, with both the standard and enhanced washing methods associated with residual viability values of about 30% at physiologically relevant drug doses (~700 nM) (Fig. 1B, top left panel; see Table S1 in the supplemental material). This failure to render all of the parasites nonviable, even at high drug concentrations, confirms the resistance phenotype, while the overlapping profiles show that DHA is efficiently diluted using the standard washing protocol. In contrast, the loss of viability following pulsed exposure to the ozonides was substantively dependent on the washing regimen. The standard washing regimen resulted in an almost complete loss of parasite viability (>95%) by OZ439 and OZ277 at the highest concentrations examined (Fig. 1B, top panels). In contrast, the residual viability was much higher when the transfer washing regimen was employed (~40% residual viability) (Fig. 1B, top panels). The problem was less obvious for the sensitive very early ring stage of the K13 revertant (Cam3.11_rev) (Fig. 1B, bottom panels), because the $LC_{50}$ values were much lower and inefficient washing was thus more difficult to detect.

Because OZ439 is lipophilic, there is the possibility that a substantial fraction of the added drug is associated with cell membranes and the walls of the wells during the initial incubation period. This would mean that the added concentration of ozonides would not reflect the concentration in the medium, which would influence the ability to compare the *in vitro* efficacies of different drugs and to extrapolate to an *in vivo* setting. We were therefore interested in determining whether OZ439 activity in the culture supernatant was significantly decreased as a result of binding to surfaces. To estimate the proportion of the drug activity that remains in the supernatant, we mixed different concentrations of OZ439 with uninfected RBCs in wells, recovered the supernatants, and serially diluted them in new wells, with the addition of fresh 3D7-infected RBCs (0.2% hematocrit, 1 to 2% parasitemia). The drug activities remaining in the supernatant, determined with reference to equivalent freshly prepared samples of OZ439, were found to be ~90% of the added concentration over a broad concentration range (see Fig. S1 in the supplemental material). This demonstrates that under the conditions of our assays, ~90% of the added drug is retained in the culture supernatant.

Another possible source of error in estimates of drug efficacy may arise due to degradation of the endoperoxide during the incubation pulse. To estimate degradation losses, we incubated drugs (1 μM) with uninfected RBCs under our culture conditions for different periods before serially diluting the supernatants, with the addition of fresh infected RBCs, and examining parasite viability after >48 h. The effective drug activity remaining was determined with reference to freshly prepared drugs by determining the drug dilution required to render 50% of the parasites nonviable. DHA lost activity with a half-life of ~8 h (Fig. 2). OZ277 lost activity more slowly, with a half-life of ~17 h. In contrast, OZ439 was stable under culture conditions, with a half-life of ≫48 h and <20% loss after 48 h (Fig. 2). The observed difference in the stabilities of OZ277 and OZ439 is broadly consistent with previously reported differences in stability in blood (19).

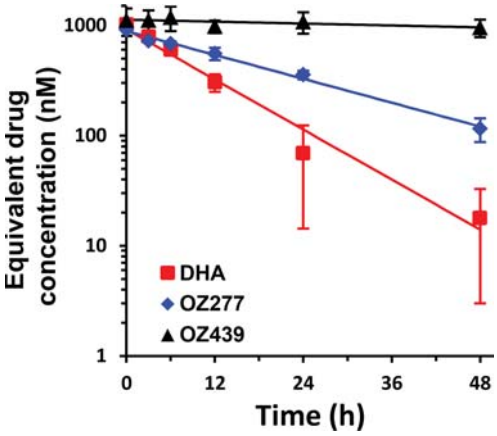


**FIG 2** Degradation of drugs under culture conditions. Drugs (1 μM) were incubated for different times under our standard conditions for drug assays (200 μl of RBCs at 0.2% hematocrit in V-bottomed plates), after which the supernatant was collected and transferred to a new well containing infected RBCs. Parasite viability (replication competence) was determined after >48 h and compared with the viability of parasites exposed to equivalent freshly prepared drug dilutions. The drug dilution required to render 50% of parasites nonviable was determined and used to estimate the effective drug concentration remaining in the supernatant. Data represent the averages for two independent experiments, with error bars representing the ranges for duplicates. Lines correspond to best fits, with half-lives of 8, 17, and 210 h for DHA, OZ277, and OZ439, respectively.

**Exposure time dependence of the response of parasites to ozonides.** We initially compared the activities of the ozonides and DHA against the K13 mutant and revertant parasites and against the laboratory strain 3D7 by using a "standard" assay format where ring-stage parasites (~20-h synchronization window) are left in contact with drug for more than one parasite life cycle (>48 h) before assessment of parasitemia. With extended exposure, the parasites exhibited very similar $LC_{50}$ values for all three drugs (1 to 9 nM) (Table 1 and Fig. 3), in agreement with previous work (17, 19). However, we previously showed that drug activity determined using a >48-h exposure is a poor predictor of the *in vivo* efficacy of artemisinins, as these drugs exhibit different (usually much shorter) exposure times *in vivo* (34, 35). We therefore used our improved washing protocols to compare the exposure time dependence of the parasite responses, focusing on the stages where parasites exhibit relatively low sensitivity.

We found that the very early ring stage of the Cam3.II strain showed markedly decreased sensitivity to a 3-h pulse of DHA compared with the Cam3.II_rev strain (Fig. 3A, left panels; see Table S1 in the supplemental material), as reported previously for other K13 mutant strains (35). In particular, >50% of Cam3.II parasites survived a 3-h 700 nM DHA pulse, compared to ~5% of Cam3.II_rev parasites. Similarly, the K13 mutant exhibited significantly lower sensitivities to 3-h and 6-h pulses of OZ277 and OZ439 (Fig. 3, top panels; see Table S1). It is important that the decreased efficacy (in a 6-h exposure) was less evident when the

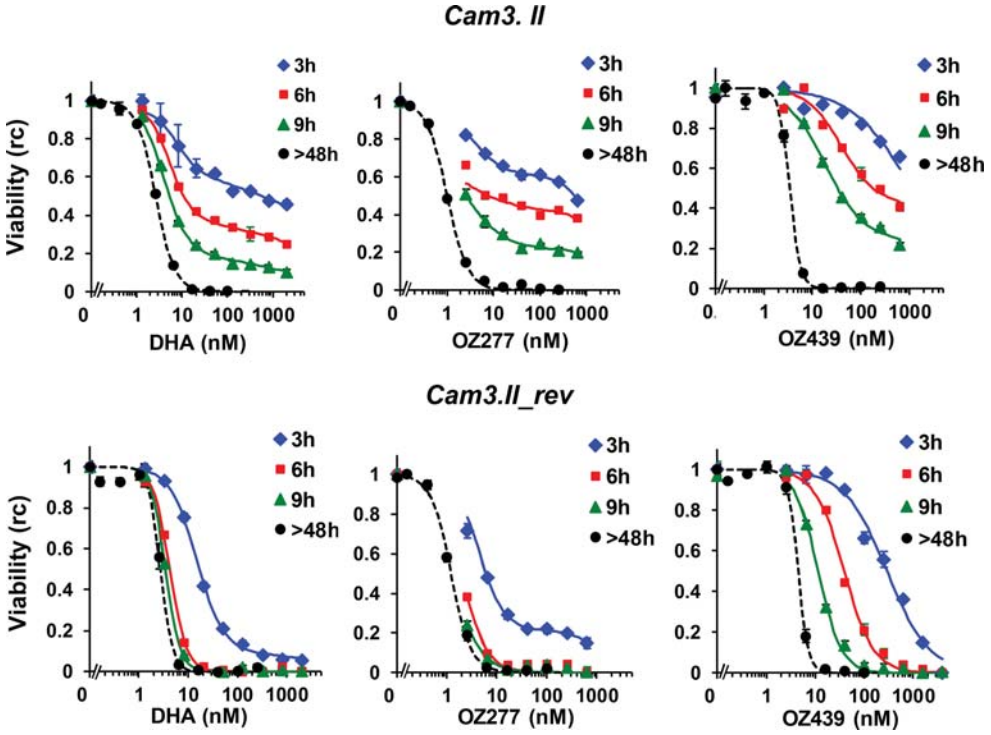


**FIG 3** Effects of pulse duration of different endoperoxides on viability (replication competence) of K13 mutant and revertant parasites. Very-early-ring-stage Cam3.II (top) and Cam3.II_rev (bottom) parasites were incubated with drugs for 3, 6, and 9 h (blue, red, and green symbols, respectively), or the drug pressure was maintained for >48 h (black symbols). For pulse assays, the drugs were removed using the enhanced washing protocols, and parasite viability (rc) was determined after >48 h. Data shown are representative of experimental replicates ($n = 2$ for pulse assays and $n = 3$ for >48-h assays). Error bars correspond to the ranges for technical replicates from the individual experiments. Solid curves correspond to the best fits obtained with the CED model, using the parameters for replicate 1 from Table 2. The dashed curves are included as a visual aid to illustrate the dose-response profiles of parasites exposed to drugs for >48 h.

standard (no transfer) washing procedure was employed (Fig. 1). This emphasizes the need for particular care in pulse assays of the efficacy of ozonides.

We also examined the mid-ring stage of 3D7 parasites, which we previously showed to exhibit relatively low sensitivity to artemisinins (34). In agreement with our previous report, the mid-ring stage showed low sensitivity to a 1.5-h pulse exposure to DHA ($LC_{50\_3\ h}$, 180 nM) but exhibited a marked increase in sensitivity at longer exposure times (see Fig. S2 in the supplemental material). We found that mid-ring-stage 3D7 parasites exhibited an even lower sensitivity to 1.5-h pulsed exposures to OZ277 and OZ439 ($LC_{50\_1.5\ h} > 1{,}000$ nM). Again, the parasites became sensitive to the ozonides as the exposure time was increased (see Fig. S2). When treatment was initiated at the trophozoite stage, the exposure time dependence of drug action was less dramatic but was still apparent (see Fig. S2).

The complex dependence of drug activity on different exposure factors makes it difficult to directly quantitate or compare the activities of different endoperoxides. We previously developed a cumulative effective dose (CED) model that is able to describe the complex concentration and exposure time dependence of artemisinin-mediated loss of viability and that facilitates comparisons of different drugs and their effects on different strains (34). According to this model, the extent to which a particular endoperoxide renders parasites nonviable (replication incompetent) is dependent on its "effective dose" (likely representing the amount of activated endoperoxide) rather than the administered concentration (37). The effective dose is a saturable function of the administered drug concentration, with the parameter $K_M$ representing the drug concentration that produces half the maximum effect (34). The minimum time required to render 50% of the parasites nonviable at saturating drug concentrations ($t^{\wedge}_{50}$) and the slope of the sigmoidal function that relates the effective dose to the parasite viability ($\gamma$) are also determined through application of the CED model to viability data. In performing this analysis, we do not explicitly take into account the changing drug concentrations over time (as revealed in Fig. 2), as the CED model can characterize only the cumulative effect on viability over an entire drug pulse, independently of any detailed changes in kinetics during that drug pulse. In the case of OZ277 and OZ439, this does not have a major influence on the analysis (i.e., parameter estimation), as the experimental observations occur over a period (9 h) much shorter than the *in vitro* half-lives of the drugs (Fig. 2). In the case of DHA (with a half-life of 8 h), drug instability will lead to an overestimation of $K_M$ values and will also influence the underlying slope of the dose-response curve ($\gamma$) but will not affect the magnitude of $t^{\wedge}_{50}$.

The CED model is able to describe the observed dependence of drug activity against early-ring-stage Cam3.II and Cam3.II_rev parasites on drug concentration and exposure time (Fig. 3, fitted solid lines [these provide good fits to the 3-, 6-, and 9-h exposure data]). Analysis of the fit parameters showed that the $K_M$ value is essentially independent of the strain but shows a more pronounced dependence on the identity of the drug (Table 2). It is interesting that the average $K_M$ value obtained for DHA treatment of the K13 revertant and mutant strains used in this work (mean ±

**TABLE 2** CED model parameters describing the actions of DHA and ozonides on early ring stages of strains Cam3.II_rev and Cam3.II

| | Values for R1, R2[a] | | | | | |
|---|---|---|---|---|---|---|
| | DHA | | OZ277 | | OZ439 | |
| Parameter | Cam3.II_rev | Cam3.II | Cam3.II_rev | Cam3.II | Cam3.II_rev | Cam3.II |
| $t^{\wedge}_{50}$ (h) | 1.4, 1.2 | 3.0, 3.3 | 1.4, 0.9 | 3.7, 4.1 | 2.6, 2.2 | 5.1, 5.2 |
| $K_M$ (nM) | 17, 18 | 11.5, 12.5 | 6, 30 | 4, 7 | 35, 100 | 28, 76 |
| γ | 3.2, 2.4 | 1.6, 1.8 | 2.2, 1.6 | 1.3, 1.5 | 3.2, 2.1 | 1.9, 2.2 |

[a] R1 and R2 correspond to the different experimental replicates.

standard error of the mean [SEM], 15 ± 2; $n = 4$; values were obtained by using the combined data for Cam3.II_rev and Cam3.II from Table 2) is similar to values reported earlier for another pair of wild-type and K13 mutant strains (14 and 19 nM for PL2 and PL7, respectively [35]). In contrast, the combined $K_M$ value for OZ439 (60 ± 20; $n = 4$) is markedly greater than that for DHA, while the value for OZ277 (12 ± 7; $n = 4$) is similar to that for DHA. Although the $K_M$ values determined in this analysis are macroscopic constants and are influenced by the different chemical properties of the drugs (including different levels of binding to proteins), the observed trends are broadly in agreement with their relative abilities to be activated by iron (38).

The CED analysis shows that sensitivity to endoperoxides is largely determined by the $t^{\wedge}_{50}$ value (34). The use of isogenic lines in the present study revealed that the K13 mutation (R539T) increased the $t^{\wedge}_{50}$ value for DHA from ~1.3 h to ~3.2 h (Table 2), a trend in general agreement with that previously reported for wild-type (PL2) and K13 mutant (PL7) field strains (values of 1.4 and 4.9 h, respectively [35]). Interestingly, early-ring-stage K13 revertant parasites exhibited similar $t^{\wedge}_{50}$ values when exposed to either OZ277 or DHA (Table 2). K13 mutant parasites exhibited larger $t^{\wedge}_{50}$ values, but again they were similar for OZ277 and DHA. OZ439 also showed an increased $t^{\wedge}_{50}$ value for the K13 mutant; however, in this case, the times required to render 50% of parasites nonviable ($t^{\wedge}_{50}$ values) were 1 to 2 h longer for both strains than the value for DHA.

**Simulation of *in vivo* parasite responses.** To consider the possible clinical implications of our findings, we modeled parasite responses to drug exposure at levels that might be expected to be achieved in patients. The different *in vivo* pharmacokinetic properties of the drugs, as well as their different pharmacodynamic behaviors, preclude a simple comparison using the observed *in vitro* concentration-response profiles shown in Fig. 3. Moreover, traditional approaches for assessing drug efficacy *in vivo*, such as measuring peak concentrations and areas under the curve (AUC), are inappropriate for drugs, such as the artemisinins, which exhibit short *in vivo* half-lives and lag times in their action.

In the present study, we investigated how efficiently a single dose of drug might reduce the parasite burden in an infection comprised of early-ring-stage parasites. We chose early rings because this is the stage at which K13 mutants exhibit the highest ability to survive drug treatment (7, 39). For this simulation, we took advantage of the fact that the reported pharmacokinetics of each drug (summarized in Table S2 in the supplemental material) indicate that saturating concentrations of all the drugs are achieved relatively quickly. That is, the time required (following drug administration) for drug concentrations to reach $K_M$ values is typically less than 20 min, and these saturating levels are maintained for many hours. As a result, the CED model predicts that the viability ($V$) will vary as a function of drug exposure time ($t^e$) according to the equation $V(t^e) = [1 + (t^e/t^{\wedge}_{50})^{\gamma}]^{-1}$ while these saturating conditions are maintained. That is, early killing events will be independent of the precise pharmacological concentration. In contrast, viability at longer times will depend on both the administered drug dose and the drug pharmacokinetics (i.e., how long it takes for the drug to decay to sublethal levels). In this work, we used the CED model parameters that describe the response of early rings to exposure times of up to 9 h (Table 2) and incorporated knowledge of the pharmacokinetic profile for each drug (see Table S2) (24, 25, 40) in order to generate simulations of parasite viability *in vivo* over the first 9 h following a single-dose exposure (Fig. 4).

One consequence of the fact that saturating drug concentrations are achieved rapidly and sustained for several hours *in vivo* is that the times required to achieve a 50% reduction in viability of early rings are well approximated by the $t^{\wedge}_{50}$ values shown in Table 2. Thus, the CED model analysis indicates that the much slower reduction of parasitemia observed for resistant strains *in vitro* will be reflected *in vivo*. The simulations show that a single-dose exposure to DHA would reduce the parasite load to a much smaller degree in the K13 mutant than in the revertant strain, leading to an ~20-fold greater parasite burden ~7 h after treatment (Fig. 4, top panel). There is no further substantial parasite killing at times longer than this, as the *in vivo* DHA concentrations become sublethal. As a result, a substantial fraction of the early ring population of the resistant Cam3.II strain (~20%) (Fig. 4, top panel) is able to survive a single-dose DHA exposure, which helps to explain the *in vivo* resistance phenotype. The simulations also show that, as with the trends observed *in vitro*, the times taken to reduce the parasite load by 50% are similar for OZ277 and DHA treatments but somewhat longer for OZ439 treatment (up to ~5 h for resistant strains). In the case of a short-lived drug, such as DHA (~1-h half-life), such an increase in the time taken to kill 50% of parasites would present a major disadvantage, further increasing the risk of treatment failure in a resistant infection. However, the much longer *in vivo* half-life of OZ439 (see Table S2) means that the *in vivo* drug concentration is maintained for >72 h at a level much greater than the $LC_{50}$ value observed in a standard kill assay (Table 1). This means that unlike the situation for DHA, where the drug is essentially depleted after 9 h, OZ439 will continue to efficiently kill both sensitive and resistant parasites well beyond 9 h, with anticipated activity for more than 72 h. (This is evident from Fig. 3, where a comparison is made of the loss of viability for parasites exposed to OZ439 for >48 h [black symbols] and the data for parasites exposed to DHA for 3 h [blue symbols] and 6 h [red symbols].) Thus, our analysis suggests that a single-dose exposure to OZ439 will reduce the parasite load in a resistant infection much more efficiently than a single dose of DHA.

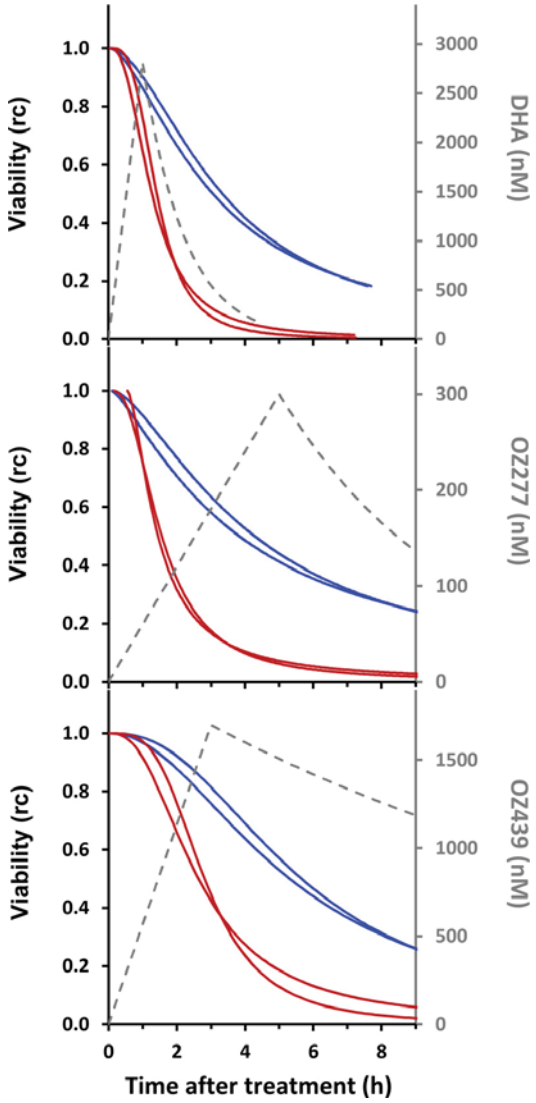


**FIG 4** Simulation of *in vivo*-like responses to single-dose treatments with different drugs. Viability profiles for K13 revertant (Cam3.II_rev; red curves) and K13 mutant (Cam3.II; blue curves) parasites in hypothetical patients following treatment at the very early ring stage with a single dose of DHA, OZ277, or OZ439 were calculated using the CED model parameters shown in Table 2 and the pharmacokinetic parameters shown in Table S2 in the supplemental material. Viability calculations were performed at times after treatment when the *in vivo* drug concentrations were greater than the $K_M$ value, with the assumption that these represent saturating drug concentrations. (See the text for further details.) The duplicate blue and red curves correspond to independent simulations performed using CED model parameters derived from the analysis of independent experimental replicates (Table 2). The dashed gray lines correspond to estimates of the *in vivo* drug concentrations based on reported values.

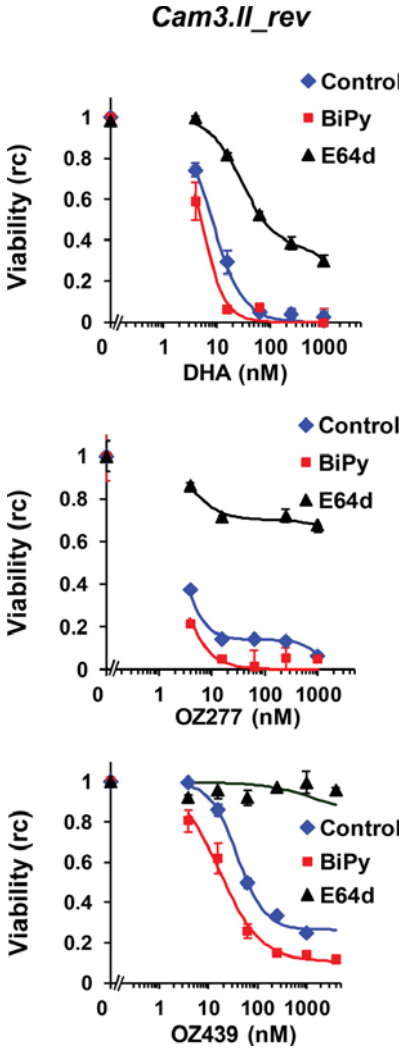


**FIG 5** Role of hemoglobin degradation in the action of ozonides against K13 revertant parasites. Tightly synchronized early-ring-stage Cam3.II_rev parasites (1 to 1.5% parasitemia) were preincubated in the absence or presence of a sublethal concentration (determined by an initial analysis of the cytotoxicity of the compounds alone) of E64d (5 μM) or BiPy (150 μM) for 1 h before exposure to serial dilutions of DHA, OZ277, or OZ439 for 3 h. The drugs were removed using the enhanced washing protocol, and parasite viability (rc) was determined after >48 h. Data represent a typical set of data from two independent experiments, each performed in duplicate.

**The activities of DHA and the ozonides are antagonized by a hemoglobinase inhibitor.** The activation of artemisinins via a reduced iron source is integral to their mode of action (34, 41). Recent work indicates that in the case of DHA, this iron source is heme generated during hemoglobin digestion, even when artemisinins are applied at the very early ring stage (34, 37). Accordingly, the falcipain inhibitor E64d exhibited significant antagonism of the action of a 3-h pulse of DHA against K13 revertant (Cam3.II_rev) parasites (Fig. 5). Like that of DHA, the activity of the ozonides was strongly antagonized by E64d (Fig. 5), indicating that their activity is dependent on hemoglobin degradation. In contrast, the iron chelator BiPy slightly synergized the activities of DHA and the ozonides, indicating that free iron makes little contribution to activation of the endoperoxides in very early rings (Fig. 5). Similar interactions were observed when E64d or BiPy was used in combination with a 6-h pulse of DHA or the ozonides against mid-ring-stage 3D7 parasites (see Fig. S3 in the supplemental material).

## DISCUSSION

In this work, we used a pulsed exposure assay to examine the activity of ozonides at different parasite stages. To achieve reliable estimates of efficacy, it was essential to ensure that the drugs were efficiently removed by the washing procedures employed at the

end of the exposure period. We found that significant levels of ozonides remained in the culture wells when a standard washing procedure was employed. This was particularly true for OZ439, the most lipophilic of the three compounds tested. While the adherent fraction is likely quite low (on the order of 1% at micromolar concentrations), killing is caused by the continued exposure of the culture to the remaining drug for the duration of the incubation (>48 h). This can result in overestimation of the efficacy, particularly for resistant strains subjected to short exposures, which need a high level of drug to effect killing. This is important because it could result in the mischaracterization of resistant parasites as sensitive.

Artemisinins are activated via a reduced iron source generated during hemoglobin digestion (34, 37). Recent work (42) confirmed earlier studies (43) suggesting that artemisinins exert their activity by alkylating multiple targets within the parasite. Like the artemisinins, the ozonide antimalarials harbor an endoperoxide bridge; however, it is still unclear whether they are activated in the same way and are subject to the same mechanisms of resistance.

In this work, we showed that, as for DHA, short pulses of ozonides are more active against the trophozoite stage than against the mid-ring stage of 3D7 parasites, consistent with an enhanced hemoglobin degradation flux. Moreover, we found that falcipain inhibitors markedly antagonized the activity of the ozonides, as would be anticipated upon disruption of the supply of heme. In contrast, the iron chelator BiPy had very little effect under the conditions of our experiments, indicating that, like artemisinins (37), the ozonides are dependent on hemoglobin-derived heme rather than free iron for activation.

There is evidence that the parasite mounts a proteostasis response that counteracts the artemisinin-induced insult and that killing is achieved only when this defense system is overwhelmed (35). As a result, the extent of killing is highly dependent on the duration of drug exposure (34, 35, 37). In this work, we found that the killing of parasites by both DHA and the ozonides is highly nonlinear with respect to exposure time. For example, mid-ring-stage 3D7 parasites are insensitive to a short (3 h) exposure to drugs, but exposure to double that time (6 h) results in 100% killing, with an $LC_{50}$ value that is not much higher than that observed for a 9-h pulse.

We demonstrated previously that in order for artemisinins to render parasites nonviable, the parasites need to be exposed to a sufficient concentration of activated endoperoxide for a sufficient time (34). This manifests as a delay following the application of endoperoxides before 50% of parasites are rendered nonviable. This delay is stage and strain dependent. The CED model predicts that killing will be more efficient if the endoperoxide is more efficiently activated (e.g., due to a higher level of activator or a more readily activated endoperoxide) (37). This is responsible for the particular sensitivity of trophozoite-stage parasites to endoperoxides (34).

The extent of killing will also be determined in part by stage- and strain-dependent differences in the ability of the parasite to deal with damaged proteins (34, 35, 37). This is expected to manifest as a change in the $t^{\wedge}_{50}$ (time required to render 50% of parasites nonviable at a saturating drug concentration). For example, the very early rings of strains with wild-type K13 are particularly sensitive to DHA, likely because their cellular defense systems are particularly weak (35, 44). Similarly, the early rings of K13 mutant strains are less sensitive to DHA than those of wild-type strains, likely because K13 mutants exhibit an enhanced cellular defense system (35, 44). In this work, we showed that the differential sensitivity of different stages and strains to DHA was matched by similar differences in sensitivity to the ozonides, consistent with the suggestion that the basic mechanism of action of ozonides is similar to that of DHA and that they are prone to the same resistance mechanisms.

We found that the $K_M$ and $t^{\wedge}_{50}$ values varied substantively depending on the chemical features of the endoperoxide, presumably due to differences in the efficiency of activation and/or the toxicity of the activated species. Access to the peroxide bond is more sterically restricted in OZ439 than in DHA (17, 18). We found that OZ439 exhibits moderately larger $t^{\wedge}_{50}$ values than those of DHA, leading to lower levels of parasite inactivation when the exposure time is short. One possible interpretation is that the higher stability of OZ439 results in slower heme-mediated activation in the parasite, requiring a longer exposure time to render parasites nonviable. It is also possible that differences in the physicochemical properties of OZ439 may slow the rate of accumulation of the drug in the parasite or lead to different protein target interactions. A combination of these factors may be responsible for the requirement for a slightly longer exposure time to render 50% of parasites nonviable.

In an effort to understand the potential *in vivo* consequence of the *in vitro* behavior of the ozonides, we used our estimates of drug pharmacodynamics (CED model parameters) to predict parasite behavior in a patient. Parasite viability was simulated for the first 9 h following a single drug dose administered at the very early ring stage to patients harboring wild-type or K13 mutant parasites. We did not attempt to extend the simulation beyond 9 h because stage-dependent differences in sensitivity complicate predictions of the behavior of surviving parasites at longer time points (35). We employed the available pharmacokinetic profiles for the different drugs in patients or volunteers to represent the drug concentrations likely experienced by the parasites. Our simulations indicate that following drug exposure, reduction of parasite numbers to 50% of initial levels may take 1 to 2 h longer when OZ439 is employed than when DHA is used. Indeed, in a retrospective analysis of phase II clinical data, OZ439 was assessed for efficacy in patients with K13 mutant and wild-type parasites (25). In that study, a trend toward an extension of the clearance half-life was observed for patients infected with K13 mutant compared with wild-type parasites (5.5 h versus 4.4 h), although the results were not statistically significant.

Despite the predicted lower initial levels of killing of very early rings, the longer *in vivo* half-life of OZ439 means that it will perform much more effectively than OZ277 or DHA at reducing parasite burdens in clinical infections, particularly in the case of K13 mutant parasites. Because the *in vivo* concentrations of OZ439 are maintained well above the $LC_{50\_>48\,h}$ value for more than a full life cycle, K13 mutant parasites that survive exposure at the very early ring stage will continue to be exposed to OZ439 in the more sensitive trophozoite stage. Thus, our work supports clinical trials that are under way to assess OZ439 for use (in combination with an effective partner drug) as a single-dose treatment and for multidose treatment of infections in areas with a high penetrance of K13 mutations.

Clearly, there are a number of factors that complicate comparisons of the activities of different drugs *in vitro*, as well as attempts to extrapolate from *in vitro* to *in vivo* behavior. In particular, the

differences in physicochemical properties between the three compounds suggest likely differences in protein binding both in the *in vitro* culture medium and *in vivo* in blood and plasma, leading to differences in unbound concentrations for the same total drug concentration. Since it is generally assumed that only unbound drug is available for permeating cell membranes and interacting with biological targets (45), these differences would be expected to affect the *in vitro* and *in vivo* activities. It also remains to be determined whether the ozonides induce dormancy in a subpopulation of parasites, as has been reported for the artemisinins (46, 47). Given these caveats, it will be critical to validate the predictions from our simulation by using detailed measurements of parasite killing and clearance times *in vivo*.

In summary, our data provide information about the mode of activation of the ozonides and show that a parasite harboring a K13 mutation exhibits reduced sensitivity to the ozonides. Despite this reduced sensitivity, the data strongly suggest that the longer half-life of OZ439 will result in significantly improved efficacy against K13 mutant parasites and that OZ439 will prove valuable in global efforts to battle artemisinin-resistant malaria. We anticipate that predictions of *in vivo* efficacy provided by our CED model will help to inform decisions about clinical use of the new endoperoxides.

## ACKNOWLEDGMENTS

We thank Shannon Kenny for technical assistance. We thank David Fidock, Columbia University, for providing Cam3.II and Cam3.II_rev parasites. We thank the Medicines for Malaria Venture for providing samples of OZ277 and OZ439.

## FUNDING INFORMATION

This work, including the efforts of Leann Tilley, was funded by Department of Health | National Health and Medical Research Council (NHMRC) (APP1092808). This work, including the efforts of Leann Tilley, was funded by Department of Health | National Health and Medical Research Council (NHMRC) (APP1060357). This work, including the efforts of Leann Tilley, was funded by Australian Research Council (ARC) (DP110100624).

## REFERENCES

1. **World Health Organization.** 2015. World malaria report, 2015. WHO, Geneva, Switzerland. http://www.who.int/malaria/publications/world-malaria-report-2015/report/en/.
2. **Enserink M.** 2010. Malaria's drug miracle in danger. Science **328:**844–846. http://dx.doi.org/10.1126/science.328.5980.844.
3. **White NJ, Pukrittayakamee S, Hien TT, Faiz MA, Mokuolu OA, Dondorp AM.** 2014. Malaria. Lancet **383:**723–735. http://dx.doi.org/10.1016/S0140-6736(13)60024-0.
4. **White NJ.** 2013. Pharmacokinetic and pharmacodynamic considerations in antimalarial dose optimization. Antimicrob Agents Chemother **57:**5792–5807. http://dx.doi.org/10.1128/AAC.00287-13.
5. **Lubell Y, Dondorp A, Guerin PJ, Drake T, Meek S, Ashley E, Day NP, White NJ, White LJ.** 2014. Artemisinin resistance—modelling the potential human and economic costs. Malar J **13:**452. http://dx.doi.org/10.1186/1475-2875-13-452.
6. **Tun KM, Imwong M, Lwin KM, Win AA, Hlaing TM, Hlaing T, Lin K, Kyaw MP, Plewes K, Faiz MA, Dhorda M, Cheah PY, Pukrittayakamee S, Ashley EA, Anderson TJ, Nair S, McDew-White M, Flegg JA, Grist EP, Guerin P, Maude RJ, Smithuis F, Dondorp AM, Day NP, Nosten F, White NJ, Woodrow CJ.** 2015. Spread of artemisinin-resistant *Plasmodium falciparum* in Myanmar: a cross-sectional survey of the K13 molecular marker. Lancet Infect Dis **15:**415–421. http://dx.doi.org/10.1016/S1473-3099(15)70032-0.
7. **Ariey F, Witkowski B, Amaratunga C, Beghain J, Langlois AC, Khim N, Kim S, Duru V, Bouchier C, Ma L, Lim P, Leang R, Duong S, Sreng S, Suon S, Chuor CM, Bout DM, Menard S, Rogers WO, Genton B, Fandeur T, Miotto O, Ringwald P, Le Bras J, Berry A, Barale JC, Fairhurst RM, Benoit-Vical F, Mercereau-Puijalon O, Menard D.** 2014. A molecular marker of artemisinin-resistant *Plasmodium falciparum* malaria. Nature **505:**50–55. http://dx.doi.org/10.1038/nature12876.
8. **Amaratunga C, Lim P, Suon S, Sreng S, Mao S, Sopha C, Sam B, Dek D, Try V, Amato R, Blessborn D, Song L, Tullo GS, Fay MP, Anderson JM, Tarning J, Fairhurst RM.** 2016. Dihydroartemisinin-piperaquine resistance in *Plasmodium falciparum* malaria in Cambodia: a multisite prospective cohort study. Lancet Infect Dis **16:**357–365. http://dx.doi.org/10.1016/S1473-3099(15)00487-9.
9. **Spring MD, Lin JT, Manning JE, Vanachayangkul P, Somethy S, Bun R, Se Y, Chann S, Ittiverakul M, Sia-ngam P, Kuntawunginn W, Arsanok M, Buathong N, Chaorattanakawee S, Gosi P, Ta-aksorn W, Chanarat N, Sundrakes S, Kong N, Heng TK, Nou S, Teja-isavadharm P, Pichyangkul S, Phann ST, Balasubramanian S, Juliano JJ, Meshnick SR, Chour CM, Prom S, Lanteri CA, Lon C, Saunders DL.** 2015. Dihydroartemisinin-piperaquine failure associated with a triple mutant including kelch13 C580Y in Cambodia: an observational cohort study. Lancet Infect Dis **15:**683–691. http://dx.doi.org/10.1016/S1473-3099(15)70049-6.
10. **Wells TN, Hooft van Huijsduijnen R, Van Voorhis WC.** 2015. Malaria medicines: a glass half full? Nat Rev Drug Discov **14:**424–442. http://dx.doi.org/10.1038/nrd4573.
11. **Patra N, Srivastava AK.** 2015. Use of model-based nutrient feeding for improved production of artemisinin by hairy roots of *Artemisia annua* in a modified stirred tank bioreactor. Appl Biochem Biotechnol **177:**373–388. http://dx.doi.org/10.1007/s12010-015-1750-8.
12. **Paddon CJ, Keasling JD.** 2014. Semi-synthetic artemisinin: a model for the use of synthetic biology in pharmaceutical development. Nat Rev Microbiol **12:**355–367. http://dx.doi.org/10.1038/nrmicro3240.
13. **Zhang Y, Nowak G, Reed DW, Covello PS.** 2011. The production of artemisinin precursors in tobacco. Plant Biotechnol J **9:**445–454. http://dx.doi.org/10.1111/j.1467-7652.2010.00556.x.
14. **UNITAID.** 2014. Demand forecast for artemisinin-based combination therapies (ACTs) in 2013–2014. UNITAID, Vernier, Switzerland.
15. **O'Neill PM, Barton VE, Ward SA.** 2010. The molecular mechanism of action of artemisinin. The debate continues. Molecules **15:**1705–1721. http://dx.doi.org/10.3390/molecules15031705.
16. **Vennerstrom JL, Fu HN, Ellis WY, Ager AL, Jr, Wood JK, Andersen SL, Gerena L, Milhous WK.** 1992. Dispiro-1,2,4,5-tetraoxanes: a new class of antimalarial peroxides. J Med Chem **35:**3023–3027. http://dx.doi.org/10.1021/jm00094a015.
17. **Vennerstrom JL, Arbe-Barnes S, Brun R, Charman SA, Chiu FC, Chollet J, Dong Y, Dorn A, Hunziker D, Matile H, McIntosh K, Padmanilayam M, Santo Tomas J, Scheurer C, Scorneaux B, Tang Y, Urwyler H, Wittlin S, Charman WN.** 2004. Identification of an antimalarial synthetic trioxolane drug development candidate. Nature **430:**900–904. http://dx.doi.org/10.1038/nature02779.
18. **Dong Y, Chollet J, Matile H, Charman SA, Chiu FC, Charman WN, Scorneaux B, Urwyler H, Santo Tomas J, Scheurer C, Snyder C, Dorn A, Wang X, Karle JM, Tang Y, Wittlin S, Brun R, Vennerstrom JL.** 2005. Spiro and dispiro-1,2,4-trioxolanes as antimalarial peroxides: charting a workable structure-activity relationship using simple prototypes. J Med Chem **48:**4953–4961. http://dx.doi.org/10.1021/jm049040u.
19. **Charman SA, Arbe-Barnes S, Bathurst IC, Brun R, Campbell M, Charman WN, Chiu FC, Chollet J, Craft JC, Creek DJ, Dong Y, Matile H, Maurer M, Morizzi J, Nguyen T, Papastogiannidis P, Scheurer C, Shackleford DM, Sriraghavan K, Stingelin L, Tang Y, Urwyler H, Wang X, White KL, Wittlin S, Zhou L, Vennerstrom JL.** 2011. Synthetic ozonide drug candidate OZ439 offers new hope for a single-dose cure of uncomplicated malaria. Proc Natl Acad Sci U S A **108:**4400–4405. http://dx.doi.org/10.1073/pnas.1015762108.
20. **Kaiser M, Wittlin S, Nehrbass-Stuedli A, Dong Y, Wang X, Hemphill A, Matile H, Brun R, Vennerstrom JL.** 2007. Peroxide bond-dependent antiplasmodial specificity of artemisinin and OZ277 (RBx11160). Antimicrob Agents Chemother **51:**2991–2993. http://dx.doi.org/10.1128/AAC.00225-07.
21. **Valecha N, Looareesuwan S, Martensson A, Abdulla SM, Krudsood S, Tangpukdee N, Mohanty S, Mishra SK, Tyagi PK, Sharma SK, Moehrle J, Gautam A, Roy A, Paliwal JK, Kothari M, Saha N, Dash AP, Bjorkman A.** 2010. Arterolane, a new synthetic trioxolane for treatment of uncomplicated Plasmodium falciparum malaria: a phase II, multicenter, randomized, dose-finding clinical trial. Clin Infect Dis **51:**684–691. http://dx.doi.org/10.1086/655831.

22. **Valecha N, Krudsood S, Tangpukdee N, Mohanty S, Sharma SK, Tyagi PK, Anvikar A, Mohanty R, Rao BS, Jha AC, Shahi B, Singh JP, Roy A, Kaur P, Kothari M, Mehta S, Gautam A, Paliwal JK, Arora S, Saha N.** 2012. Arterolane maleate plus piperaquine phosphate for treatment of uncomplicated *Plasmodium falciparum* malaria: a comparative, multicenter, randomized clinical trial. Clin Infect Dis **55:**663–671. http://dx.doi.org/10.1093/cid/cis475.
23. **Gautam A, Ahmed T, Sharma P, Varshney B, Kothari M, Saha N, Roy A, Moehrle JJ, Paliwal J.** 2011. Pharmacokinetics and pharmacodynamics of arterolane maleate following multiple oral doses in adult patients with *P. falciparum* malaria. J Clin Pharmacol **51:**1519–1528. http://dx.doi.org/10.1177/0091270010385578.
24. **Saha N, Moehrle JJ, Zutshi A, Sharma P, Kaur P, Iyer SS.** 2014. Safety, tolerability and pharmacokinetic profile of single and multiple oral doses of arterolane (RBx11160) maleate in healthy subjects. J Clin Pharmacol **54:**386–393. http://dx.doi.org/10.1002/jcph.232.
25. **Phyo AP, Jittamala P, Nosten FH, Pukrittayakamee S, Imwong M, White NJ, Duparc S, Macintyre F, Baker M, Mohrle JJ.** 2016. Antimalarial activity of artefenomel (OZ439), a novel synthetic antimalarial endoperoxide, in patients with *Plasmodium falciparum* and *Plasmodium vivax* malaria: an open-label phase 2 trial. Lancet Infect Dis **16:**61–69. http://dx.doi.org/10.1016/S1473-3099(15)00320-5.
26. **Moehrle JJ, Duparc S, Siethoff C, van Giersbergen PL, Craft JC, Arbe-Barnes S, Charman SA, Gutierrez M, Wittlin S, Vennerstrom JL.** 2013. First-in-man safety and pharmacokinetics of synthetic ozonide OZ439 demonstrates an improved exposure profile relative to other peroxide antimalarials. Br J Clin Pharmacol **75:**524–537. http://dx.doi.org/10.1111/j.1365-2125.2012.04368.x.
27. **Tang Y, Dong Y, Vennerstrom JL.** 2004. Synthetic peroxides as antimalarials. Med Res Rev **24:**425–448. http://dx.doi.org/10.1002/med.10066.
28. **Fugi MA, Wittlin S, Dong Y, Vennerstrom JL.** 2010. Probing the antimalarial mechanism of artemisinin and OZ277 (arterolane) with nonperoxidic isosteres and nitroxyl radicals. Antimicrob Agents Chemother **54:**1042–1046. http://dx.doi.org/10.1128/AAC.01305-09.
29. **Foley M, Deady LW, Ng K, Cowman AF, Tilley L.** 1994. Photoaffinity labeling of chloroquine-binding proteins in *Plasmodium falciparum*. J Biol Chem **269:**6955–6961.
30. **Ranford-Cartwright LC, Sinha A, Humphreys GS, Mwangi JM.** 2010. New synchronization method for *Plasmodium falciparum*. Malar J **9:**170. http://dx.doi.org/10.1186/1475-2875-9-170.
31. **Xie SC, Dogovski C, Kenny S, Tilley L, Klonis N.** 2014. Optimal assay design for determining the in vitro sensitivity of ring stage *Plasmodium falciparum* to artemisinins. Int J Parasitol **44:**893–899. http://dx.doi.org/10.1016/j.ijpara.2014.07.008.
32. **Klonis N, Crespo-Ortiz MP, Bottova I, Abu-Bakar N, Kenny S, Rosenthal PJ, Tilley L.** 2011. Artemisinin activity against *Plasmodium falciparum* requires hemoglobin uptake and digestion. Proc Natl Acad Sci U S A **108:**11405–11410. http://dx.doi.org/10.1073/pnas.1104063108.
33. **Fu Y, Tilley L, Kenny S, Klonis N.** 2010. Dual labeling with a far red probe permits analysis of growth and oxidative stress in *P. falciparum*-infected erythrocytes. Cytometry A **77:**253–263. http://dx.doi.org/10.1002/cyto.a.20856.
34. **Klonis N, Xie SC, McCaw JM, Crespo-Ortiz MP, Zaloumis SG, Simpson JA, Tilley L.** 2013. Altered temporal response of malaria parasites determines differential sensitivity to artemisinin. Proc Natl Acad Sci U S A **110:**5157–5162. http://dx.doi.org/10.1073/pnas.1217452110.
35. **Dogovski C, Xie SC, Burgio G, Bridgford J, Mok S, McCaw JM, Chotivanich K, Kenny S, Gnadig N, Straimer J, Bozdech Z, Fidock DA, Simpson JA, Dondorp AM, Foote S, Klonis N, Tilley L.** 2015. Targeting the cell stress response of *Plasmodium falciparum* to overcome artemisinin resistance. PLoS Biol **13:**e1002132. http://dx.doi.org/10.1371/journal.pbio.1002132.
36. **Straimer J, Gnadig NF, Witkowski B, Amaratunga C, Duru V, Ramadani AP, Dacheux M, Khim N, Zhang L, Lam S, Gregory PD, Urnov FD, Mercereau-Puijalon O, Benoit-Vical F, Fairhurst RM, Menard D, Fidock DA.** 2015. Drug resistance. K13-propeller mutations confer artemisinin resistance in *Plasmodium falciparum* clinical isolates. Science **347:**428–431. http://dx.doi.org/10.1126/science.1260867.
37. **Xie SC, Dogovski C, Hanssen E, Chiu F, Yang T, Crespo MP, Stafford C, Batinovic S, Teguh S, Charman S, Klonis N, Tilley L.** 2016. Haemoglobin degradation underpins the sensitivity of early ring stage *Plasmodium falciparum* to artemisinins. J Cell Sci **129:**406–416. http://dx.doi.org/10.1242/jcs.178830.
38. **Wang X, Creek DJ, Schiaffo CE, Dong Y, Chollet J, Scheurer C, Wittlin S, Charman SA, Dussault PH, Wood JK, Vennerstrom JL.** 2009. Spiroadamantyl 1,2,4-trioxolane, 1,2,4-trioxane, and 1,2,4-trioxepane pairs: relationship between peroxide bond iron(II) reactivity, heme alkylation efficiency, and antimalarial activity. Bioorg Med Chem Lett **19:**4542–4545. http://dx.doi.org/10.1016/j.bmcl.2009.07.013.
39. **Witkowski B, Khim N, Chim P, Kim S, Ke S, Kloeung N, Chy S, Duong S, Leang R, Ringwald P, Dondorp AM, Tripura R, Benoit-Vical F, Berry A, Gorgette O, Ariey F, Barale JC, Mercereau-Puijalon O, Menard D.** 2013. Reduced artemisinin susceptibility of *Plasmodium falciparum* ring stages in western Cambodia. Antimicrob Agents Chemother **57:**914–923. http://dx.doi.org/10.1128/AAC.01868-12.
40. **Dondorp AM, Nosten F, Yi P, Das D, Phyo AP, Tarning J, Lwin KM, Ariey F, Hanpithakpong W, Lee SJ, Ringwald P, Silamut K, Imwong M, Chotivanich K, Lim P, Herdman T, An SS, Yeung S, Singhasivanon P, Day NP, Lindegardh N, Socheat D, White NJ.** 2009. Artemisinin resistance in *Plasmodium falciparum* malaria. N Engl J Med **361:**455–467. http://dx.doi.org/10.1056/NEJMoa0808859.
41. **Meshnick SR.** 2003. Artemisinin and heme. Antimicrob Agents Chemother **47:**2712. http://dx.doi.org/10.1128/AAC.47.8.2712-2713.2003.
42. **Wang J, Zhang C-J, Chia W, Loh CCY, Li Z, Lee YM, He Y, Yuan L-X, Lim TK, Liu M, Liew CX, Lee YQ, Zhang J, Lu N, Lim CT, Hua Z-C, Liu B, Shen H-M, Tan KSW, Lin Q.** 2015. Haem-activated promiscuous targeting of artemisinin in *Plasmodium falciparum*. Nat Commun **6:**10111. http://dx.doi.org/10.1038/ncomms10111.
43. **Meshnick SR, Taylor TE, Kamchonwongpaisan S.** 1996. Artemisinin and the antimalarial endoperoxides: from herbal remedy to targeted chemotherapy. Microbiol Rev **60:**301–315.
44. **Mok S, Ashley EA, Ferreira PE, Zhu L, Lin Z, Yeo T, Chotivanich K, Imwong M, Pukrittayakamee S, Dhorda M, Nguon C, Lim P, Amaratunga C, Suon S, Hien TT, Htut Y, Faiz MA, Onyamboko MA, Mayxay M, Newton PN, Tripura R, Woodrow CJ, Miotto O, Kwiatkowski DP, Nosten F, Day NP, Preiser PR, White NJ, Dondorp AM, Fairhurst RM, Bozdech Z.** 2015. Population transcriptomics of human malaria parasites reveals the mechanism of artemisinin resistance. Science **347:**431–435. http://dx.doi.org/10.1126/science.1260403.
45. **Smith DA, Di L, Kerns EH.** 2010. The effect of plasma protein binding on in vivo efficacy: misconceptions in drug discovery. Nat Rev Drug Discov **9:**929–939. http://dx.doi.org/10.1038/nrd3287.
46. **Tucker MS, Mutka T, Sparks K, Patel J, Kyle DE.** 2012. Phenotypic and genotypic analysis of in vitro-selected artemisinin-resistant progeny of *Plasmodium falciparum*. Antimicrob Agents Chemother **56:**302–314. http://dx.doi.org/10.1128/AAC.05540-11.
47. **Hott A, Casandra D, Sparks KN, Morton LC, Castanares GG, Rutter A, Kyle DE.** 2015. Artemisinin-resistant *Plasmodium falciparum* parasites exhibit altered patterns of development in infected erythrocytes. Antimicrob Agents Chemother **59:**3156–3167. http://dx.doi.org/10.1128/AAC.00197-15.